

Signals, Systems, Transforms, and Digital Signal Processing with MATLAB[®]

Michael Corinthis

MATLAB[®]
examples



CRC Press
Taylor & Francis Group

**Signals,
Systems,
Transforms, and
Digital Signal
Processing
with MATLAB[®]**

This page intentionally left blank

Signals, Systems, Transforms, and Digital Signal Processing with MATLAB[®]

Michael Corinthis

**École Polytechnique de Montréal
Montréal, Canada**



CRC Press

Taylor & Francis Group

Boca Raton London New York

CRC Press is an imprint of the
Taylor & Francis Group, an **informa** business

MATLAB® is a trademark of The MathWorks, Inc. and is used with permission. The MathWorks does not warrant the accuracy of the text or exercises in this book. This book's use or discussion of MATLAB® software or related products does not constitute endorsement or sponsorship by The MathWorks of a particular pedagogical approach or particular use of the MATLAB® software.

CRC Press
Taylor & Francis Group
6000 Broken Sound Parkway NW, Suite 300
Boca Raton, FL 33487-2742

© 2009 by Taylor and Francis Group, LLC
CRC Press is an imprint of Taylor & Francis Group, an Informa business

No claim to original U.S. Government works

Printed in the United States of America on acid-free paper
10 9 8 7 6 5 4 3 2 1

International Standard Book Number: 978-1-4200-9048-2 (Hardback)

This book contains information obtained from authentic and highly regarded sources. Reasonable efforts have been made to publish reliable data and information, but the author and publisher cannot assume responsibility for the validity of all materials or the consequences of their use. The authors and publishers have attempted to trace the copyright holders of all material reproduced in this publication and apologize to copyright holders if permission to publish in this form has not been obtained. If any copyright material has not been acknowledged please write and let us know so we may rectify in any future reprint.

Except as permitted under U.S. Copyright Law, no part of this book may be reprinted, reproduced, transmitted, or utilized in any form by any electronic, mechanical, or other means, now known or hereafter invented, including photocopying, microfilming, and recording, or in any information storage or retrieval system, without written permission from the publishers.

For permission to photocopy or use material electronically from this work, please access www.copyright.com (<http://www.copyright.com/>) or contact the Copyright Clearance Center, Inc. (CCC), 222 Rosewood Drive, Danvers, MA 01923, 978-750-8400. CCC is a not-for-profit organization that provides licenses and registration for a variety of users. For organizations that have been granted a photocopy license by the CCC, a separate system of payment has been arranged.

Trademark Notice: Product or corporate names may be trademarks or registered trademarks, and are used only for identification and explanation without intent to infringe.

Library of Congress Cataloging-in-Publication Data

Corinthios, Michael.

Signals, systems, transforms, and digital signal processing with MATLAB / Michael Corinthios.
p. cm.

Includes bibliographical references and index.
ISBN 978-1-4200-9048-2 (hard back : alk. paper)

1. Signal processing--Digital techniques. 2. System analysis. 3. Fourier transformations. 4. MATLAB. I. Title.

TK5102.9.C64 2009
621.382'2--dc22

2009012640

Visit the Taylor & Francis Web site at
<http://www.taylorandfrancis.com>

and the CRC Press Web site at
<http://www.crcpress.com>

To Maria, Angela, Gisèle, John.

This page intentionally left blank

Contents

Preface	xxv
Acknowledgment	xxvii
1 Continuous-Time and Discrete-Time Signals and Systems	1
1.1 Introduction	2
1.2 Continuous-Time Signals	2
1.3 Periodic Functions	3
1.4 Unit Step Function	4
1.5 Graphical Representation of Functions	5
1.6 Even and Odd Parts of a Function	6
1.7 Dirac-Delta Impulse	7
1.8 Basic Properties of the Dirac-Delta Impulse	8
1.9 Other Important Properties of the Impulse	11
1.10 Continuous-Time Systems	11
1.11 Causality, Stability	12
1.12 Examples of Electrical Continuous-Time Systems	12
1.13 Mechanical Systems	13
1.14 Transfer Function and Frequency Response	14
1.15 Convolution and Correlation	15
1.16 A Right-Sided and a Left-Sided Function	20
1.17 Convolution with an Impulse and Its Derivatives	21
1.18 Additional Convolution Properties	21
1.19 Correlation Function	22
1.20 Properties of the Correlation Function	22
1.21 Graphical Interpretation	23
1.22 Correlation of Periodic Functions	25
1.23 Average, Energy and Power of Continuous-Time Signals	25
1.24 Discrete-Time Signals	26
1.25 Periodicity	27
1.26 Difference Equations	28
1.27 Even/Odd Decomposition	28
1.28 Average Value, Energy and Power Sequences	29
1.29 Causality, Stability	30
1.30 Problems	30
1.31 Answers to Selected Problems	40
2 Fourier Series Expansion	47
2.1 Trigonometric Fourier Series	47
2.2 Exponential Fourier Series	48
2.3 Exponential versus Trigonometric Series	50
2.4 Periodicity of Fourier Series	51

2.5	Dirichlet Conditions and Function Discontinuity	53
2.6	Proof of the Exponential Series Expansion	55
2.7	Analysis Interval versus Function Period	55
2.8	Fourier Series as a Discrete-Frequency Spectrum	56
2.9	Meaning of Negative Frequencies	58
2.10	Properties of Fourier Series	58
2.10.1	Linearity	58
2.10.2	Time Shift	60
2.10.3	Frequency Shift	60
2.10.4	Function Conjugate	61
2.10.5	Reflection	61
2.10.6	Symmetry	64
2.10.7	Half-Periodic Symmetry	65
2.10.8	Double Symmetry	67
2.10.9	Time Scaling	70
2.10.10	Differentiation Property	72
2.11	Differentiation of Discontinuous Functions	74
2.11.1	Multiplication in the Time Domain	74
2.11.2	Convolution in the Time Domain	75
2.11.3	Integration	75
2.12	Fourier Series of an Impulse Train	77
2.13	Expansion into Cosine or Sine Fourier Series	78
2.14	Deducing a Function Form from Its Expansion	81
2.15	Truncated Sinusoid Spectral Leakage	83
2.16	The Period of a Composite Sinusoidal Signal	86
2.17	Passage through a Linear System	88
2.18	Parseval's Relations	89
2.19	Use of Power Series Expansion	90
2.20	Inverse Fourier Series	91
2.21	Problems	92
2.22	Answers to Selected Problems	100
3	Laplace Transform	105
3.1	Introduction	105
3.2	Bilateral Laplace Transform	105
3.3	Conditions of Existence of Laplace Transform	107
3.4	Basic Laplace Transforms	110
3.5	Notes on the ROC of Laplace Transform	112
3.6	Properties of Laplace Transform	115
3.6.1	Linearity	116
3.6.2	Differentiation in Time	116
3.6.3	Multiplication by Powers of Time	116
3.6.4	Convolution in Time	117
3.6.5	Integration in Time	117
3.6.6	Multiplication by an Exponential (Modulation)	118
3.6.7	Time Scaling	118
3.6.8	Reflection	119
3.6.9	Initial Value Theorem	119
3.6.10	Final Value Theorem	119
3.6.11	Laplace Transform of Anticausal Functions	120
3.6.12	Shift in Time	121

3.7	Applications of the Differentiation Property	122
3.8	Transform of Right-Sided Periodic Functions	123
3.9	Convolution in Laplace Domain	124
3.10	Cauchy's Residue Theorem	125
3.11	Inverse Laplace Transform	128
3.12	Case of Conjugate Poles	129
3.13	The Expansion Theorem of Heaviside	131
3.14	Application to Transfer Function and Impulse Response	132
3.15	Inverse Transform by Differentiation and Integration	133
3.16	Unilateral Laplace Transform	134
	3.16.1 Differentiation in Time	135
	3.16.2 Initial and Final Value Theorem	137
	3.16.3 Integration in Time Property	137
	3.16.4 Division by Time Property	137
3.17	Gamma Function	138
3.18	Table of Additional Laplace Transforms	141
3.19	Problems	143
3.20	Answers to Selected Problems	149
4	Fourier Transform	153
4.1	Definition of the Fourier Transform	153
4.2	Fourier Transform as a Function of f	155
4.3	From Fourier Series to Fourier Transform	156
4.4	Conditions of Existence of the Fourier Transform	157
4.5	Table of Properties of the Fourier Transform	158
	4.5.1 Linearity	159
	4.5.2 Duality	160
	4.5.3 Time Scaling	161
	4.5.4 Reflection	161
	4.5.5 Time Shift	161
	4.5.6 Frequency Shift	161
	4.5.7 Modulation Theorem	162
	4.5.8 Initial Time Value	163
	4.5.9 Initial Frequency Value	163
	4.5.10 Differentiation in Time	164
	4.5.11 Differentiation in Frequency	164
	4.5.12 Integration in Time	164
	4.5.13 Conjugate Function	165
	4.5.14 Real Functions	165
	4.5.15 Symmetry	166
4.6	System Frequency Response	166
4.7	Even-Odd Decomposition of a Real Function	167
4.8	Causal Real Functions	168
4.9	Transform of the Dirac-Delta Impulse	169
4.10	Transform of a Complex Exponential and Sinusoid	169
4.11	Sign Function	171
4.12	Unit Step Function	172
4.13	Causal Sinusoid	172
4.14	Table of Fourier Transforms of Basic Functions	172
4.15	Relation between Fourier and Laplace Transforms	174
4.16	Relation to Laplace Transform with Poles on Imaginary Axis	175

4.17	Convolution in Time	176
4.18	Linear System Input–Output Relation	177
4.19	Convolution in Frequency	178
4.20	Parseval’s Theorem	178
4.21	Energy Spectral Density	179
4.22	Average Value versus Fourier Transform	180
4.23	Fourier Transform of a Periodic Function	181
4.24	Impulse Train	182
4.25	Fourier Transform of Powers of Time	182
4.26	System Response to a Sinusoidal Input	183
4.27	Stability of a Linear System	183
4.28	Fourier Series versus Transform of Periodic Functions	184
4.29	Transform of a Train of Rectangles	184
4.30	Fourier Transform of a Truncated Sinusoid	185
4.31	Gaussian Function Laplace and Fourier Transform	186
4.32	Inverse Transform by Series Expansion	187
4.33	Fourier Transform in ω and f	188
4.34	Fourier Transform of the Correlation Function	189
4.35	Ideal Filters Impulse Response	190
4.36	Time and Frequency Domain Sampling	191
4.37	Ideal Sampling	191
4.38	Reconstruction of a Signal from its Samples	193
4.39	Other Sampling Systems	195
	4.39.1 Natural Sampling	195
	4.39.2 Instantaneous Sampling	197
4.40	Ideal Sampling of a Bandpass Signal	200
4.41	Sampling an Arbitrary Signal	201
4.42	Sampling the Fourier Transform	203
4.43	Problems	204
4.44	Answers to Selected Problems	222
5	System Modeling, Time and Frequency Response	233
5.1	Transfer Function	233
5.2	Block Diagram Reduction	233
5.3	Galvanometer	234
5.4	DC Motor	237
5.5	A Speed-Control System	239
5.6	Homology	245
5.7	Transient and Steady-State Response	247
5.8	Step Response of Linear Systems	248
5.9	First Order System	248
5.10	Second Order System Model	249
5.11	Settling Time	250
5.12	Second Order System Frequency Response	253
5.13	Case of a Double Pole	254
5.14	The Over-Damped Case	255
5.15	Evaluation of the Overshoot	255
5.16	Causal System Response to an Arbitrary Input	256
5.17	System Response to a Causal Periodic Input	257
5.18	Response to a Causal Sinusoidal Input	259
5.19	Frequency Response Plots	260

5.20	Decibels, Octaves, Decades	260
5.21	Asymptotic Frequency Response	261
5.21.1	A Simple Zero at the Origin	261
5.21.2	A Simple Pole	262
5.21.3	A Simple Zero in the Left Plane	262
5.21.4	First Order System	264
5.21.5	Second Order System	264
5.22	Bode Plot of a Composite Linear System	267
5.23	Graphical Representation of a System Function	268
5.24	Vectorial Evaluation of Residues	269
5.25	Vectorial Evaluation of the Frequency Response	273
5.26	A First Order All-Pass System	275
5.27	Filtering Properties of Basic Circuits	275
5.28	Lowpass First Order Filter	277
5.29	Minimum Phase Systems	280
5.30	General Order All-Pass Systems	281
5.31	Signal Generation	283
5.32	Application of Laplace Transform to Differential Equations	284
5.32.1	Linear Differential Equations with Constant Coefficients	285
5.32.2	Linear First Order Differential Equation	285
5.32.3	General Order Differential Equations with Constant Coefficients	286
5.32.4	Homogeneous Linear Differential Equations	287
5.32.5	The General Solution of a Linear Differential Equation	288
5.32.6	Partial Differential Equations	291
5.33	Transformation of Partial Differential Equations	293
5.34	Problems	297
5.35	Answers to Selected Problems	314
6	Discrete-Time Signals and Systems	323
6.1	Introduction	323
6.2	Linear Time-Invariant Systems	324
6.3	Linear Constant-Coefficient Difference Equations	324
6.4	The z -Transform	325
6.5	Convergence of the z -Transform	327
6.6	Inverse z -Transform	330
6.7	Inverse z -Transform by Partial Fraction Expansion	336
6.8	Inversion by Long Division	337
6.9	Inversion by a Power Series Expansion	338
6.10	Inversion by Geometric Series Summation	339
6.11	Table of Basic z -Transforms	340
6.12	Properties of the z -Transform	340
6.12.1	Linearity	340
6.12.2	Time Shift	340
6.12.3	Conjugate Sequence	340
6.12.4	Initial Value	341
6.12.5	Convolution in Time	344
6.12.6	Convolution in Frequency	344
6.12.7	Parseval's Relation	347
6.12.8	Final Value Theorem	347
6.12.9	Multiplication by an Exponential	348
6.12.10	Frequency Translation	348

6.12.11	Reflection Property	349
6.12.12	Multiplication by n	349
6.13	Geometric Evaluation of Frequency Response	349
6.14	Comb Filters	351
6.15	Causality and Stability	353
6.16	Delayed Response and Group Delay	354
6.17	Discrete-Time Convolution and Correlation	355
6.18	Discrete-Time Correlation in One Dimension	357
6.19	Convolution and Correlation as Multiplications	360
6.20	Response of a Linear System to a Sinusoid	361
6.21	Notes on the Cross-Correlation of Sequences	361
6.22	LTI System Input/Output Correlation Sequences	362
6.23	Energy and Power Spectral Density	363
6.24	Two-Dimensional Signals	363
6.25	Linear Systems, Convolution and Correlation	366
6.26	Correlation of Two-Dimensional Signals	370
6.27	IIR and FIR Digital Filters	374
6.28	Discrete-Time All-Pass Systems	375
6.29	Minimum-Phase and Inverse System	378
6.30	Unilateral z -Transform	381
6.30.1	Time Shift Property of Unilateral z -Transform	383
6.31	Problems	384
6.32	Answers to Selected Problems	390
7	Discrete-Time Fourier Transform	395
7.1	Laplace, Fourier and z -Transform Relations	395
7.2	Discrete-Time Processing of Continuous-Time Signals	400
7.3	A/D Conversion	400
7.4	Quantization Error	403
7.5	D/A Conversion	404
7.6	Continuous versus Discrete Signal Processing	406
7.7	Interlacing with Zeros	407
7.8	Sampling Rate Conversion	409
7.8.1	Sampling Rate Reduction	410
7.8.2	Sampling Rate Increase: Interpolation	414
7.8.3	Rational Factor Sample Rate Alteration	417
7.9	Fourier Transform of a Periodic Sequence	419
7.10	Table of Discrete-Time Fourier Transforms	420
7.11	Reconstruction of the Continuous-Time Signal	424
7.12	Stability of a Linear System	425
7.13	Table of Discrete-Time Fourier Transform Properties	425
7.14	Parseval's Theorem	425
7.15	Fourier Series and Transform Duality	426
7.16	Discrete Fourier Transform	429
7.17	Discrete Fourier Series	433
7.18	DFT of a Sinusoidal Signal	434
7.19	Deducing the z -Transform from the DFT	436
7.20	DFT versus DFS	438
7.21	Properties of DFS and DFT	439
7.21.1	Periodic Convolution	441
7.22	Circular Convolution	443

7.23	Circular Convolution Using the DFT	445
7.24	Sampling the Spectrum	446
7.25	Table of Properties of DFS	447
7.26	Shift in Time and Circular Shift	448
7.27	Table of DFT Properties	449
7.28	Zero Padding	450
7.29	Discrete z -Transform	453
7.30	Fast Fourier Transform	455
7.31	An Algorithm for a Wired-In Radix-2 Processor	462
	7.31.1 Post-Permutation Algorithm	464
	7.31.2 Ordered Input/Ordered Output (OIIO) Algorithm	465
7.32	Factorization of the FFT to a Higher Radix	466
	7.32.1 Ordered Input/Ordered Output General Radix FFT Algorithm	469
7.33	Feedback Elimination for High-Speed Signal Processing	470
7.34	Problems	472
7.35	Answers to Selected Problems	478
8	State Space Modeling	483
8.1	Introduction	483
8.2	Note on Notation	483
8.3	State Space Model	484
8.4	System Transfer Function	488
8.5	System Response with Initial Conditions	489
8.6	Jordan Canonical Form of State Space Model	490
8.7	Eigenvalues and Eigenvectors	497
8.8	Matrix Diagonalization	498
8.9	Similarity Transformation of a State Space Model	499
8.10	Solution of the State Equations	501
8.11	General Jordan Canonical Form	507
8.12	Circuit Analysis by Laplace Transform and State Variables	509
8.13	Trajectories of a Second Order System	513
8.14	Second Order System Modeling	515
8.15	Transformation of Trajectories between Planes	519
8.16	Discrete-Time Systems	522
8.17	Solution of the State Equations	528
8.18	Transfer Function	528
8.19	Change of Variables	529
8.20	Second Canonical Form State Space Model	531
8.21	Problems	533
8.22	Answers to Selected Problems	538
9	Filters of Continuous-Time Domain	543
9.1	Lowpass Approximation	543
9.2	Butterworth Approximation	544
9.3	Denormalization of Butterworth Filter Prototype	547
9.4	Denormalized Transfer Function	550
9.5	The Case $\varepsilon \neq 1$	552
9.6	Butterworth Filter Order Formula	553
9.7	Nomographs	554
9.8	Chebyshev Approximation	556
9.9	Pass-Band Ripple	560

9.10	Transfer Function of the Chebyshev Filter	560
9.11	Maxima and Minima of Chebyshev Filter Response	563
9.12	The Value of ε as a Function of Pass-Band Ripple	564
9.13	Evaluation of Chebyshev Filter Gain	564
9.14	Chebyshev Filter Tables	565
9.15	Chebyshev Filter Order	567
9.16	Denormalization of Chebyshev Filter Prototype	568
9.17	Chebyshev's Approximation: Second Form	571
9.18	Response Decay of Butterworth and Chebyshev Filters	572
9.19	Chebyshev Filter Nomograph	575
9.20	Elliptic Filters	576
	9.20.1 Elliptic Integral	576
9.21	Properties, Poles and Zeros of the sn Function	577
	9.21.1 Elliptic Filter Approximation	580
9.22	Pole Zero Alignment and Mapping of Elliptic Filter	584
9.23	Poles of $H(s)$	589
9.24	Zeros and Poles of $G(\omega)$	591
9.25	Zeros, Maxima and Minima of the Magnitude Spectrum	591
9.26	Points of Maxima/Minima	591
9.27	Elliptic Filter Nomograph	592
9.28	$N = 9$ Example	597
9.29	Tables of Elliptic Filters	599
9.30	Bessel's Constant Delay Filters	611
9.31	A Note on Continued Fraction Expansion	612
9.32	Evaluating the Filter Delay	617
9.33	Bessel Filter Quality Factor and Natural Frequency	618
9.34	Maximal Flatness of Bessel and Butterworth Response	619
9.35	Bessel Filter's Delay and Magnitude Response	622
9.36	Denormalization and Deviation from Ideal Response	622
9.37	Bessel Filter's Magnitude and Delay	626
9.38	Bessel Filter's Butterworth Asymptotic Form	626
9.39	Delay of Bessel–Butterworth Asymptotic Form Filter	628
9.40	Delay Plots of Butterworth Asymptotic Form Bessel Filter	629
9.41	Bessel Filters Frequency Normalized Form	633
9.42	Poles and Zeros of Asymptotic and Frequency Normalized Bessel Filter Forms	634
9.43	Response and Delay of Normalized Form Bessel Filter	634
9.44	Bessel Frequency Normalized Form Attenuation Setting	635
9.45	Bessel Filter Nomograph	639
9.46	Frequency Transformations	639
9.47	Lowpass to Bandpass Transformation	641
9.48	Lowpass to Band-Stop Transformation	651
9.49	Lowpass to Highpass Transformation	653
9.50	Note on Lowpass to Normalized Band-Stop Transformation	657
9.51	Windows	661
9.52	Rectangular Window	662
9.53	Triangle (Bartlett) Window	663
9.54	Hanning Window	663
9.55	Hamming Window	664
9.56	Problems	665
9.57	Answers to Selected Problems	671

10	Passive and Active Filters	677
10.1	Design of Passive Filters	677
10.2	Design of Passive Ladder Lowpass Filters	677
10.3	Analysis of a General Order Passive Ladder Network	680
10.4	Input Impedance of a Single-Resistance Terminated Network	683
10.5	Evaluation of the Ladder Network Components	684
10.6	Matrix Evaluation of Input Impedance	689
10.7	Bessel Filter Passive Ladder Networks	693
10.8	Tables of Single-Resistance Ladder Network Components	694
10.9	Design of Doubly Terminated Passive LC Ladder Networks	695
10.9.1	Input Impedance Evaluation	695
10.10	Tables of Double-Resistance Terminated Ladder Network Components	701
10.11	Closed Forms for Circuit Element Values	703
10.12	Elliptic Filter Realization as a Passive Ladder Network	706
10.12.1	Evaluating the Elliptic LC Ladder Circuit Elements	707
10.13	Table of Elliptic Filter Passive Network Components	709
10.14	Element Replacement for Frequency Transformation	709
10.14.1	Lowpass to Bandpass Transformation	710
10.14.2	Lowpass to Highpass Transformation	711
10.14.3	Lowpass to Band-Stop Transformation	711
10.15	Realization of a General Order Active Filter	713
10.16	Inverting Integrator	713
10.17	Biquadratic Transfer Functions	714
10.18	General Biquad Realization	716
10.19	First Order Filter Realization	721
10.20	A Biquadratic Transfer Function Realization	723
10.21	Sallen–Key Circuit	725
10.22	Problems	728
10.23	Answers to Selected Problems	729
11	Digital Filters	733
11.1	Introduction	733
11.2	Signal Flow Graphs	733
11.3	IIR Filter Models	734
11.4	First Canonical Form	734
11.5	Transposition	734
11.6	Second Canonical Form	736
11.7	Transposition of the Second Canonical Form	737
11.8	Structures Based on Poles and Zeros	738
11.9	Cascaded Form	738
11.10	Parallel Form	739
11.11	Matrix Representation	739
11.12	Finite Impulse Response (FIR) Filters	740
11.13	Linear Phase FIR Filters	741
11.14	Conversion of Continuous-Time to Discrete-Time Filter	743
11.15	Impulse Invariance Approach	743
11.16	Shortcut Impulse Invariance Design	746
11.17	Backward-Rectangular Approximation	747
11.18	Forward Rectangular and Trapezoidal Approximations	749
11.19	Bilinear Transform	751
11.20	Lattice Filters	760

11.21	Finite Impulse Response All-Zero Lattice Structures	760
11.22	One-Zero FIR Filter	761
11.23	Two-Zeros FIR Filter	762
11.24	General Order All-Zero FIR Filter	764
11.25	All-Pole Filter	769
11.26	First Order One-Pole Filter	770
11.27	Second Order All-Pole Filter	771
11.28	General Order All-Pole Filter	772
11.29	Pole-Zero IIR Lattice Filter	775
11.30	All-Pass Filter Realization	781
11.31	Schur–Cohn Stability Criterion	782
11.32	Frequency Transformations	783
11.33	Least Squares Digital Filter Design	786
11.34	Padé Approximation	786
11.35	Error Minimization in Prony’s Method	790
11.36	FIR Inverse Filter Design	794
11.37	Impulse Response of Ideal Filters	798
11.38	Spectral Leakage	800
11.39	Windows	801
11.40	Ideal Digital Filters Rectangular Window	801
11.41	Hanning Window	802
11.42	Hamming Window	803
11.43	Triangular Window	804
11.44	Comparison of Windows Spectral Parameters	805
11.45	Linear-Phase FIR Filter Design Using Windows	807
11.46	Even- and Odd-Symmetric FIR Filter Design	808
11.47	Linear Phase FIR Filter Realization	810
11.48	Sampling the Unit Circle	810
11.49	Impulse Response Evaluation from Unit Circle Samples	814
11.49.1	Case I-1: Odd Order, Even Symmetry, $\mu = 0$	814
11.49.2	Case I-2: Odd Order, Even Symmetry, $\mu = 1/2$	815
11.49.3	Case II-1	815
11.49.4	Case II-2: Even Order, Even Symmetry, $\mu = 1/2$	815
11.49.5	Case III-1: Odd Order, Odd Symmetry, $\mu = 0$	816
11.49.6	Case III-2: Odd Order, Odd Symmetry, $\mu = 1/2$	816
11.49.7	Case IV-1: Even Order, Odd Symmetry, $\mu = 0$	816
11.49.8	Case IV-2: Even Order, Odd Symmetry, $\mu = 1/2$	816
11.50	Problems	817
11.51	Answers to Selected Problems	828
12	Energy and Power Spectral Densities	835
12.1	Energy Spectral Density	835
12.2	Average, Energy and Power of Continuous-Time Signals	838
12.3	Discrete-Time Signals	839
12.4	Energy Signals	840
12.5	Autocorrelation of Energy Signals	840
12.6	Energy Signal through Linear System	842
12.7	Impulsive and Discrete-Time Energy Signals	843
12.8	Power Signals	848
12.9	Cross-Correlation	848
12.9.1	Power Spectral Density	849

12.10	Power Spectrum Conversion of a Linear System	850
12.11	Impulsive and Discrete-Time Power Signals	852
12.12	Periodic Signals	854
12.12.1	Response of an LTI System to a Sinusoidal Input	855
12.13	Power Spectral Density of an Impulse Train	856
12.14	Average, Energy and Power of a Sequence	859
12.15	Energy Spectral Density of a Sequence	860
12.16	Autocorrelation of an Energy Sequence	860
12.17	Power Density of a Sequence	860
12.18	Passage through a Linear System	861
12.19	Problems	861
12.20	Answers to Selected Problems	869
13	Introduction to Communication Systems	875
13.1	Introduction	875
13.2	Amplitude Modulation (AM) of Continuous-Time Signals	876
13.2.1	Double Side-Band (DSB) Modulation	876
13.2.2	Double Side-Band Suppressed Carrier (DSB-SC) Modulation	877
13.2.3	Single Side-Band (SSB) Modulation	879
13.2.4	Vestigial Side-Band (VSB) Modulation	882
13.2.5	Frequency Multiplexing	882
13.3	Frequency Modulation	883
13.4	Discrete Signals	887
13.4.1	Pulse Modulation Systems	887
13.5	Digital Communication Systems	888
13.5.1	Pulse Code Modulation	888
13.5.2	Pulse Duration Modulation	890
13.5.3	Pulse Position Modulation	892
13.6	PCM-TDM Systems	893
13.7	Frequency Division Multiplexing (FDM)	893
13.8	Problems	894
13.9	Answers to Selected Problems	904
14	Fourier-, Laplace- and z-Related Transforms	911
14.1	Walsh Transform	911
14.2	Rademacher and Haar Functions	911
14.3	Walsh Functions	912
14.4	The Walsh (Sequency) Order	913
14.5	Dyadic (Paley) Order	914
14.6	Natural (Hadamard) Order	914
14.7	Discrete Walsh Transform	916
14.8	Discrete-Time Walsh Transform	917
14.9	Discrete-Time Walsh–Hadamard Transform	917
14.9.1	Natural (Hadamard) Order	917
14.9.2	Dyadic or Paley Order	918
14.9.3	Sequency or Walsh Order	919
14.10	Natural (Hadamard) Order Fast Walsh–Hadamard Transform	919
14.11	Dyadic (Paley) Order Fast Walsh–Hadamard Transform	920
14.12	Sequency Ordered Fast Walsh–Hadamard Transform	921
14.13	Generalized Walsh Transform	922
14.14	Natural Order	922

14.15	Generalized Sequency Order	923
14.16	Generalized Walsh–Paley (p-adic) Transform	923
14.17	Walsh–Kaczmarz Transform	923
14.18	Generalized Walsh Factorizations for Parallel Processing	924
14.19	Generalized Walsh Natural Order GWN Matrix	924
14.20	Generalized Walsh–Paley GWP Transformation Matrix	925
14.21	GWK Transformation Matrix	926
14.22	High Speed Optimal Generalized Walsh Factorizations	926
14.23	GWN Optimal Factorization	926
14.24	GWP Optimal Factorization	927
14.25	GWK Optimal Factorization	927
14.26	Karhunen Loève Transform	928
14.27	Hilbert Transform	931
14.28	Hilbert Transformer	934
14.29	Discrete Hilbert Transform	935
14.30	Hartley Transform	936
14.31	Discrete Hartley Transform	938
14.32	Mellin Transform	939
14.33	Mellin Transform of e^{jx}	941
14.34	Hankel Transform	943
14.35	Fourier Cosine Transform	945
14.36	Discrete Cosine Transform (DCT)	946
14.37	Fractional Fourier Transform	948
14.38	Discrete Fractional Fourier Transform	950
14.39	Two-Dimensional Transforms	950
14.40	Two-Dimensional Fourier Transform	951
14.41	Continuous-Time Domain Hilbert Transform Relations	953
14.42	$H_I(j\omega)$ versus $H_R(j\omega)$ with No Poles on Axis	953
14.43	Case of Poles on the Imaginary Axis	957
14.44	Hilbert Transform Closed Forms	958
14.45	Wiener–Lee Transforms	959
14.46	Discrete-Time Domain Hilbert Transform Relations	961
14.47	Problems	964
14.48	Answers to Selected Problems	967
15	Digital Signal Processors: Architecture, Logic Design	973
15.1	Introduction	973
15.2	Systems for the Representation of Numbers	973
15.3	Conversion from Decimal to Binary	974
15.4	Integers, Fractions and the Binary Point	974
15.5	Representation of Negative Numbers	975
15.5.1	Sign and Magnitude Notation	975
15.5.2	1’s and 2’s Complement Notation	976
15.6	Integer and Fractional Representation of Signed Numbers	978
15.6.1	1’s and 2’s Complement of Signed Numbers	979
15.7	Addition	982
15.7.1	Addition in Sign and Magnitude Notation	982
15.7.2	Addition in 1’s Complement Notation	984
15.7.3	Addition in 2’s Complement Notation	985
15.8	Subtraction	986
15.8.1	Subtraction in Sign and Magnitude Notation	987

15.8.2	Numbers in 1's Complement Notation	988
15.8.3	Subtraction in 2's Complement Notation	989
15.9	Full Adder Cell	990
15.10	Addition/Subtraction Implementation in 2's Complement	991
15.11	Controlled Add/Subtract (CAS) Cell	992
15.12	Multiplication of Unsigned Numbers	992
15.13	Multiplier Implementation	993
15.14	3-D Multiplier	995
15.14.1	Multiplication in Sign and Magnitude Notation	997
15.14.2	Multiplication in 1's Complement Notation	997
15.14.3	Numbers in 2's Complement Notation	998
15.15	A Direct Approach to 2's Complement Multiplication	1000
15.16	Division	1002
15.16.1	Division of Positive Numbers:	1003
15.16.2	Division in Sign and Magnitude Notation	1004
15.16.3	Division in 1's Complement	1004
15.16.4	Division in 2's Complement	1005
15.16.5	Nonrestoring Division	1006
15.17	Cellular Array for Nonrestoring Division	1009
15.18	Carry Look Ahead (CLA) Cell	1011
15.19	2's Complement Nonrestoring Division	1014
15.20	Convergence Division	1016
15.21	Evaluation of the n^{th} Root	1018
15.22	Function Generation by Chebyshev Series Expansion	1020
15.23	An Alternative Approach to Chebyshev Series Expansion	1026
15.24	Floating Point Number Representation	1027
15.24.1	Addition and Subtraction	1029
15.24.2	Multiplication	1029
15.24.3	Division	1030
15.25	Square Root Evaluation	1030
15.25.1	The Paper and Pencil Method	1030
15.25.2	Binary Square Root Evaluation	1031
15.25.3	Comparison Approach	1031
15.25.4	Restoring Approach	1032
15.25.5	Nonrestoring Approach	1032
15.26	Cellular Array for Nonrestoring Square Root Extraction	1033
15.27	Binary Coded Decimal (BCD) Representation	1033
15.28	Memory Elements	1037
15.28.1	Set-Reset (SR) Flip-Flop	1038
15.28.2	The Trigger or T Flip-Flop	1040
15.28.3	The JK Flip-Flop	1040
15.28.4	Master-Slave Flip-Flop	1041
15.29	Design of Synchronous Sequential Circuits	1042
15.29.1	Realization Using SR Flip-Flops	1044
15.29.2	Realization Using JK Flip-Flops.	1045
15.30	Realization of a Counter Using T Flip-Flops	1046
15.30.1	Realization Using JK Flip-Flops	1046
15.31	State Minimization	1048
15.32	Asynchronous Sequential Machines	1050
15.33	State Reduction	1051
15.34	Control Counter Design for Generator of Prime Numbers	1054

15.34.1	Micro-operations and States	1055
15.35	Fast Transform Processors	1059
15.36	Programmable Logic Arrays (PLAs)	1062
15.37	Field Programmable Gate Arrays (FPGAs)	1063
15.38	DSP with Xilinx FPGAs	1065
15.39	Texas Instruments TMS320C6713B Floating-Point DSP	1067
15.40	Central Processing Unit (CPU)	1069
15.41	CPU Data Paths and Control	1071
15.41.1	General-Purpose Register Files	1071
15.41.2	Functional Units	1072
15.41.3	Register File Cross Paths	1072
15.41.4	Memory, Load, and Store Paths	1073
15.41.5	Data Address Paths	1073
15.42	Instruction Syntax	1074
15.43	TMS320C6000 Control Register File	1074
15.44	Addressing Mode Register (AMR)	1075
15.44.1	Addressing Modes	1076
15.45	Syntax for Load/Store Address Generation	1076
15.45.1	Linear Addressing Mode	1077
15.46	Programming the T.I. DSP	1078
15.47	A Simple C Program	1079
15.48	The Generated Assembly Code	1080
15.48.1	Calling an Assembly Language Function	1083
15.49	Fibonacci Series in C Calling Assembly-Language Function	1087
15.50	Finite Impulse Response (FIR) Filter	1087
15.51	Infinite Impulse Response (IIR) Filter on the DSP	1088
15.52	Real-Time DSP Applications Using MATLAB–Simulink	1092
15.53	Detailed Steps for DSP Programming in C++ and Simulink	1094
15.53.1	Steps to Implement a C++ Program on the DSP Card	1094
15.53.2	Steps to Implement a Simulink Program on the DSP Card	1096
15.54	Problems	1098
15.55	Answers to Selected Problems	1101
16	Random Signal Processing	1105
16.1	Nonparametric Methods of Power Spectrum Estimation	1108
16.2	Correlation of Continuous-Time Random Signals	1109
16.3	Passage through an LTI System	1110
16.4	Wiener Filtering in Continuous-Time Domain	1113
16.5	Causal Wiener Filter	1116
16.6	Random Sequences	1118
16.7	From Statistical to Time Averages	1119
16.8	Correlation and Covariance in z -Domain	1120
16.9	Random Signal Passage through an LTI System	1121
16.10	PSD Estimation of Discrete-Time Random Sequences	1124
16.11	Fast Fourier Transform (FFT) Evaluation of the Periodogram	1128
16.12	Parametric Methods for PSD Estimation	1131
16.13	The Yule–Walker Equations	1132
16.14	System Modeling for Linear Prediction, Adaptive Filtering and Spectrum Estimation	1134
16.15	Wiener and Least-Squares Models	1134
16.16	Wiener Filtering	1135

16.17	Least-Squares Filtering	1138
16.18	Forward Linear Prediction	1138
16.19	Backward Linear Prediction	1140
16.20	Lattice MA FIR Filter Realization	1143
16.21	AR Lattice of Order p	1146
16.22	ARMA(p, q) Process	1146
16.23	Power Spectrum Estimation	1147
16.24	FIR Wiener Filtering of Noisy Signals	1148
16.25	Two-Sided IIR Wiener Filtering	1151
16.26	Causal IIR Wiener Filter	1152
16.27	Wavelet Transform	1154
16.28	Discrete Wavelet Transform	1157
16.29	Important Signal Processing MATLAB Functions	1164
16.30	lpc	1167
16.31	Yulewalk	1168
16.32	dfilt	1169
16.33	logspace	1170
16.34	FIR Filter Design	1170
16.35	fir2	1173
16.36	Power Spectrum Estimation Using MATLAB	1174
16.37	Parametric Modeling Functions	1174
16.38	prony	1175
16.39	Problems	1176
16.40	Answers to Selected Problems	1179
17	Distributions	1181
17.1	Introduction	1181
17.2	Distributions as Generalizations of Functions	1181
17.3	What is a Distribution?	1182
17.4	The Impulse as the Limit of a Sequence	1184
17.5	Properties of Distributions	1184
17.5.1	Linearity	1184
17.5.2	Time Shift	1185
17.5.3	Time Scaling	1185
17.5.4	Product with an Ordinary Function	1186
17.5.5	Symmetry	1186
17.5.6	Differentiation	1187
17.5.7	Multiplication Times an Ordinary Function	1187
17.5.8	Sequence of Distributions	1187
17.6	Approximating the Impulse	1187
17.7	Other Approximating Sequences and Functions of the Impulse	1190
17.8	Test Functions	1191
17.9	Convolution	1192
17.10	Multiplication by an Impulse Derivative	1193
17.11	The Dirac-Delta Impulse as a Limit of a Gaussian Function	1195
17.12	Fourier Transform of Unity	1196
17.13	The Impulse of a Function	1196
17.14	Multiplication by t	1199
17.15	Time Scaling	1199
17.16	Some Properties of the Dirac-Delta Impulse	1200
17.17	Additional Fourier Transforms	1201

17.18 Riemann–Lebesgue Lemma 1201
 17.19 Generalized Limits 1202
 17.20 Fourier Transform of Higher Impulse Derivatives 1204
 17.21 The Distribution t^{-k} 1204
 17.22 Initial Derivatives of the Transform 1206
 17.23 The Unit Step Function as a Limit 1207
 17.24 Inverse Fourier Transform and Gibbs Phenomenon 1208
 17.25 Ripple Elimination 1212
 17.26 Transforms of $|t|$ and $tu(t)$ 1213
 17.27 The Impulse Train as a Limit 1214
 17.28 Sequence of Distributions 1216
 17.29 Poisson’s Summation Formula 1218
 17.30 Moving Average 1219
 17.31 Problems 1220
 17.32 Answers to Selected Problems 1222

18 Generalization of Distributions Theory, Extending Laplace-, z - and Fourier-Related Transforms 1225

18.1 Introduction 1225
 18.2 An Anomaly 1225
 18.3 Generalized Distributions for Continuous-Time Functions 1226
 18.3.1 Properties of Generalized Distributions in s Domain 1226
 18.3.2 Linearity 1226
 18.3.3 Shift in s 1226
 18.3.4 Scaling 1227
 18.3.5 Convolution 1227
 18.3.6 Differentiation 1227
 18.3.7 Multiplication of Derivative by an Ordinary Function 1228
 18.4 Properties of the Generalized Impulse in s Domain 1228
 18.4.1 Shifted Generalized Impulse 1228
 18.4.2 Differentiation 1228
 18.4.3 Convolution 1228
 18.4.4 Convolution with an Ordinary Function 1229
 18.4.5 Multiplication of an Impulse Times an Ordinary Function 1230
 18.4.6 Multiplication by Higher Derivatives of the Impulse 1230
 18.5 Additional Generalized Impulse Properties 1230
 18.6 Generalized Impulse as a Limit of a Three-Dimensional Sequence 1232
 18.7 Discrete-Time Domain 1234
 18.8 3-D Test Function as a Possible Generalization 1235
 18.8.1 Properties of Generalized Distributions in z -Domain 1235
 18.8.2 Linearity 1236
 18.8.3 Scaling in z -Domain 1236
 18.8.4 Differentiation 1236
 18.8.5 Convolution 1237
 18.9 Properties of the Generalized Impulse in z -Domain 1237
 18.9.1 Differentiation 1237
 18.10 Generalized Impulse as Limit of a 3-D Sequence 1238
 18.10.1 Convolution of Generalized Impulses 1240
 18.10.2 Convolution with an Ordinary Function 1241
 18.11 Extended Laplace and z -Transforms 1242
 18.12 Generalization of Fourier-, Laplace- and z -Related Transforms 1242

18.13 Hilbert Transform Generalization	1245
18.14 Generalizing the Discrete Hilbert Transform	1247
18.15 Generalized Hartley Transform	1247
18.16 Generalized Discrete Hartley Transform	1248
18.17 Generalization of the Mellin Transform	1249
18.18 Multidimensional Signals and the Solution of Differential Equations	1251
18.19 Problems	1254
18.20 Answers to Selected Problems	1255
A Appendix	1257
A.1 Symbols	1257
A.2 Frequently Needed Expansions	1257
A.3 Important Trigonometric Relations	1259
A.4 Orthogonality Relations	1259
A.5 Frequently Encountered Functions	1260
A.6 Mathematical Formulae	1260
A.7 Frequently Encountered Series Sums	1261
A.8 Biographies of Pioneering Scientists	1262
A.9 Plato (428 BC–347 BC)	1262
A.10 Ptolemy (circa 90–168 AD)	1264
A.11 Euclid (circa 300 BC)	1265
A.12 Abu Ja’far Muhammad ibn Musa Al-Khwarizmi (780–850 AD)	1266
A.13 Nicolaus Copernicus (1473–1543)	1269
A.14 Galileo Galilei (1564–1642)	1272
A.15 Sir Isaac Newton (1643–1727)	1274
A.16 Guillaume-François-Antoine de L’Hôpital (1661–1704)	1278
A.17 Pierre-Simon Laplace (1749–1827)	1279
A.18 Gaspard Clair François Marie, Baron Riche de Prony (1755–1839)	1281
A.19 Jean Baptiste Joseph Fourier (1768–1830)	1285
A.20 Johann Carl Friedrich Gauss (1777–1855)	1289
A.21 Friedrich Wilhelm Bessel (1784–1846)	1290
A.22 Augustin-Louis Cauchy (1789–1857)	1292
A.23 Niels Henrik Abel (1802–1829)	1295
A.24 Johann Peter Gustav Lejeune Dirichlet (1805–1859)	1297
A.25 Pafnuty Lvovich Chebyshev (1821–1894)	1298
A.26 Paul A.M. Dirac	1300
References	1303
Index	1307

This page intentionally left blank

Preface

Simplification without compromise of rigor is the principal objective in this presentation of the subject of signal analysis, systems, transforms and digital signal processing. Graphics, the language of scientists and engineers, physical interpretation of subtle mathematical concepts and a gradual transition from basic to more advanced topics, are meant to be among the important contributions of this book.

Laplace transform, Fourier transform, Discrete-time signals and systems, z -transform and distributions, such as the Dirac-delta impulse, have become important topics of basic science and engineering mathematics courses. In recent years, an increasing number of students, from all specialties of science and engineering, have been attending courses on signals, systems and DSP. This book is addressed to undergraduate and graduate students, as well as scientists and engineers in practically all fields of science and engineering.

The book starts with an introduction to continuous-time and discrete-time signals and systems. It then presents Fourier series expansion and the decomposition of signals as a discrete spectrum. The decomposition process is illustrated by evaluating the signal's harmonic components and then effecting a step-by-step addition of the harmonics. The resulting sum is seen to converge incrementally toward the analyzed function. Such an early introduction to the concept of frequency decomposition is meant to provide a tangible notion of the basis of Fourier analysis. In later chapters, the student realizes the value of the knowledge acquired in studying Fourier series, a subject that is in a way more subtle than Fourier transform.

The Laplace transform is normally covered in basic mathematics university courses. In this book the bilateral Laplace transform is presented, followed by the unilateral transform and its properties.

The Fourier transform is subsequently presented, shown to be in fact a special case of the Laplace transform. Impulsive spectra are given particular attention. It is then applied to sampling techniques; ideal, natural and instantaneous, among others. In Chapter 5 we study the dynamics of physical systems, mathematical modeling, and time and frequency response.

Discrete time signals and systems, z -transform, continuous and discrete time filters, elliptic, Bessel and lattice filters, active and passive filters, and continuous time and discrete-time state space models are subsequently presented.

Fourier transform of sequences, the discrete Fourier transform and the Fast Fourier transform merit special attention. A unique Matrix–Equation–Matrix sequence of operations is presented as a means of simplifying considerably the Fast Fourier Transform algorithm.

Fourier-, Laplace- and z -related transforms such as Walsh–Hadamard, generalized Walsh, Hilbert, discrete cosine, Hartley, Hankel and Mellin transforms are subsequently covered.

The architecture and design of digital signal processors is given a special attention. The logic of compute arithmetic, modular design of logic circuits, the design of combinatorial logic circuits, synchronous and asynchronous sequential machines are among the topics discussed in Chapter 15. Parallel processing, wired-in design leading to addressing elimination and to optimal architecture up to massive parallelism are important topics of digital signal processor design. An overall view of present day logic circuit design tools, Programmable logic arrays, DSP technology with application to real-time processing follows.

Random signals and random signal processing in both the continuous and discrete time domains are studied in Chapter 16. The following chapter presents the important subject of distribution theory, with attention given to simplify the subject and present its practical results.

The book then presents a significant new development. It reveals a mathematical anomaly and sets out to undo it. Laplace and z -transforms and a large class of Fourier-, Laplace- and z -related transforms, are rewritten and their transform tables doubled in length. Such extension of transform domains is the result of a recently proposed generalization of the Dirac-delta impulse and distribution theory.

It is worthwhile noticing that students are able to use the Dirac-delta impulse and related singularities in solving problems in different scientific areas. They do so in general without necessarily learning the intricacies of the theory of distributions. They are taught the basic properties of the Dirac-delta impulse and its relatives, and that usually suffices for them to appreciate and use them. The proposed generalization of the theory of distributions may appear to be destined toward the specialist in the field. However, once taught the basic properties of the new generalized distributions, and of the generalized impulse in particular, it will be as easy for the student to learn the new expanded Laplace, z and related transforms, without the need to fall back on the theory of distributions for rigorous mathematical justification.

For the benefit of the reader, for a gradual presentation and more profound understanding of the subject, most of the chapters in the book present and apply Laplace and z -transforms in the usual form found in the literature. In writing the book I felt that the reader would benefit considerably from studying transforms as they are presently taught and as described in mathematics, physics and engineering books. By thus acquiring solid knowledge and background, the student would be well prepared to learn and better appreciate, in the last chapter, the value of the new extended transforms.

Throughout MATLAB refers to *MATLAB*[®] which, similarly to *Maple*[®] and *Simulink*[®] is a registered trademark of The MathWorks, Inc., 3 Apple Hill Drive, Natick, MA 01760; Phone: 508-647-7000. Web: www.mathworks.com

Mathematica, throughout this book, refers to *Mathematica*[®], a registered trademark of Wolfram Research Inc., web <http://www.wolfram.com> email: info@wolfram.com, Stephen Wolfram. Phone: 217-398-0700, 100 Trade Center Drive, Champaign, IL 61820.

Xilinx Inc. and Altera Inc. have copyright on all their products cited in Chapter 15.

TMS320C6713B Floating-Point DSP[®] is a registered trademark of Texas Instruments Inc. Code composer studio[®] is a registered trademark of Texas Instruments Inc. All related trademarks are the property of Texas Instruments, www.ti.com.

Michael J. Corinthios

Acknowledgment

The author is indebted to Michel Lemire for his valuable contribution in the form of many problems and his verification of some chapters.

Thanks are due to Clement Frappier for many helpful verifications and fruitful discussions, to Jules O'Shea for valuable suggestions regarding some chapters. Thanks to Flavio Mini for his valuable professional help with the book's graphics. Thanks to Jean Bouchard for his technical support.

The author is particularly grateful to Nora Konopka. Thanks to her vision and valuable support this book was adopted and published by CRC Press/Taylor & Francis. Many thanks to Jessica Vakili, Katy Smith and Iris Fahrer for the final phase of manuscript editing and production.

Some research results have been included in the different chapters of this book. The author is indebted to many professors and distinguished scientists for encouragement and valuable support during years of research. Special thanks are due to K.C. Smith, the late honorable J. L. Yen, M. Abu Zeid, James W. Cooley, the late honorable Ben Gold and his wife Sylvia, Charles Rader, Jim Kaiser, Mark Karpovsky, A. Constantinides, A. Tzafestas, A. N. Venetsanopoulos, Bede Liu, Fred J. Taylor, Rodger E. Ziemer, Simon Haykin, Ahmed Rao, John S. Thompson, Gérard Alengrin, Gérard Favier, Jacob Benesty, Michael Shalmon, A. Goneid and Michael Mikhail.

Thanks are due to my colleagues Mario Lefebvre, Roland Malhamé, Romano De Santis, Chahé Nerguizian, Cevdet Akyel and Maged Beshai for many enlightening observations and to André Bazergui and Christophe Guy for their encouragement and support.

Special thanks to Carole Malboeuf for encouragement and support.

Thanks are due to many students, technicians and secretaries who have contributed to the book over several years. In particular, thanks are due to Simon Boutin, Etienne Boutin, Kamal Jamaoui, Ghassan Aniba, Said Grami, Hicham Aissaoui, Zaher Dannaoui, André Lacombe, Patricia Gilbert, Mounia Berdai, Kai Liu, Anthony Ghannoum, Nabil El Ghali, Salam Benchikh and Emilie Labrèche.

This page intentionally left blank

1

Continuous-Time and Discrete-Time Signals and Systems

A General Note on Symbols and Notation

Throughout, whenever possible, we shall use lower case letters to designate time functions and upper case letters to designate their transforms.

We shall use the Meter-Kilogram-Second (MKS) System of units, so that length is measured in meters (m), mass in kilograms (k) and time in seconds (s). Electric potential is in volts (V), current in amperes (A), frequency in cycles/sec (Hz), angular or radian frequency in rad/sec (r/s), energy in joules (J), power in watts (W), etc.

A list of symbols used in this book is given in Chapter A. The following symbols will be used often and merit remembering

Centered rectangle of total width $2T$: $\Pi_T(t) = u(t+T) - u(t-T)$,

Centered triangle of height 1 and total base width $2T$: $\Lambda_T(t)$,

Rectangle of width T starting at $t = 0$: $R_T(t) = u(t) - u(t-T)$.

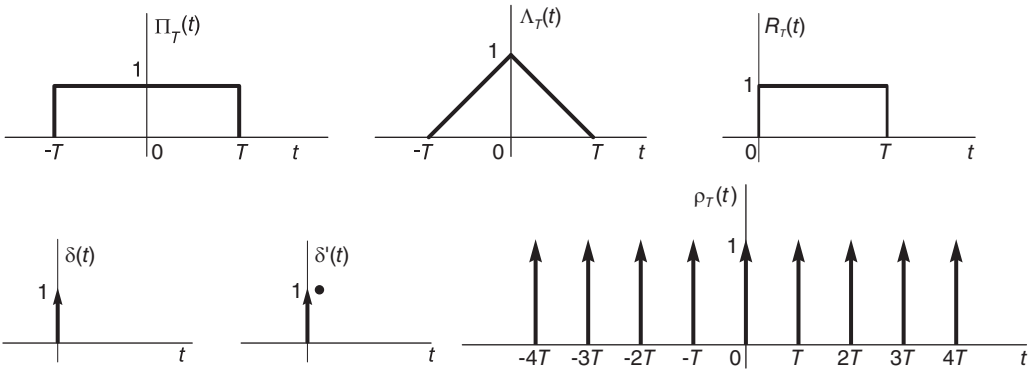


FIGURE 1.1 Centered rectangle, triangle, causal rectangle, impulse and its derivative.

These functions are represented graphically in Fig. 1.1. In this figure we see, moreover, the usual graphical representation of the Dirac-delta impulse $\delta(t)$ and a possible representation of its derivative $\delta'(t)$ as well as the impulse train of period T ,

$$\rho_T(t) = \sum_{n=-\infty}^{\infty} \delta(t - nT).$$

The function $Sh(x)$ is the hyperbolic generalization of the the usual (trigonometric) Sampling function $Sa(x) = \sin x/x$. The function $Sd_N(\Omega)$ is the discrete counterpart of the sampling function. It is given by $Sd_N(\Omega) = \sin[N\Omega]/\sin(\Omega)$ and is closely related to the Dirichlet function $dirich(x, N) = \sin(Nx/2)/N\sin(x/2)$. In fact,

$$dirich(x, N) = \frac{1}{N}Sd_N(x/2) \tag{1.1}$$

$$Sd_N(\Omega) = N \text{ dirich}(2\Omega, N) \tag{1.2}$$

These functions are depicted schematically in Chapter A.

1.1 Introduction

Engineers and scientists spend considerable time and effort exploring the behavior of dynamic physical systems. Whether they are unraveling laws governing mechanical motion, wave propagation, seismic tremors, structural vibrations, biomedical imaging, socio-economic tendencies or spatial communication, they search for mathematical models representing the physical systems and study their responses to pertinent input signals.

In this chapter, a brief summary of basic notions of continuous-time and discrete-time signals and systems is presented. A more detailed treatment of these subjects is contained in the following chapters. The student is assumed to have basic knowledge of Laplace and Fourier transform as taught in a university first-year mathematics course. The subject of signals and systems is covered by many excellent books in the literature [47] [57] [62].

1.2 Continuous-Time Signals

A continuous-time signal $f(t)$ is a function of time, defined for all values of the independent time variable t . More generally it may be a function $f(x)$ where x may be a variable such as distance and not necessarily t for time. The function $f(t)$ is generally continuous but may have a discontinuity; a sudden jump, at a point $t = t_0$ for example.

Example 1.1 *The function $f(t) = t$ shown in Fig. 1.2, is defined for all values of t , i.e. for $-\infty < t < \infty$, and has no discontinuities.*

Example 1.2 *The function $f(t) = e^{-|t|}$ shown in Fig. 1.3 is defined for all values of t and is continuous everywhere.*

Its derivative $f'(t) = df/dt$, however, given by

$$f'(t) = \begin{cases} -e^{-t}, & t > 0 \\ e^t, & t < 0 \end{cases}$$

and shown in the figure is discontinuous at $t = 0$ due to the sudden change of slope of $f(t)$ at $t = 0$ where the derivative jumps from 1 at $t = 0^-$ to -1 at $t = 0^+$, a jump of -2 . The figure also shows the function $f''(t) = d^2f/dt^2 = e^{-|t|} - 2\delta(t)$. The impulse $-2\delta(t)$ is due to the differentiation of the jump discontinuity, as we shall see shortly and in more detail later on.

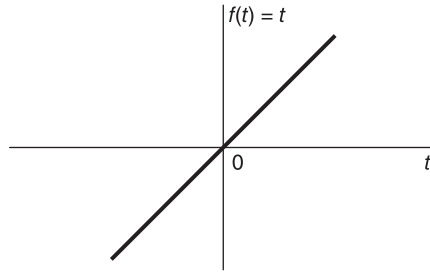


FIGURE 1.2 Continuous time function defined for all values of time.

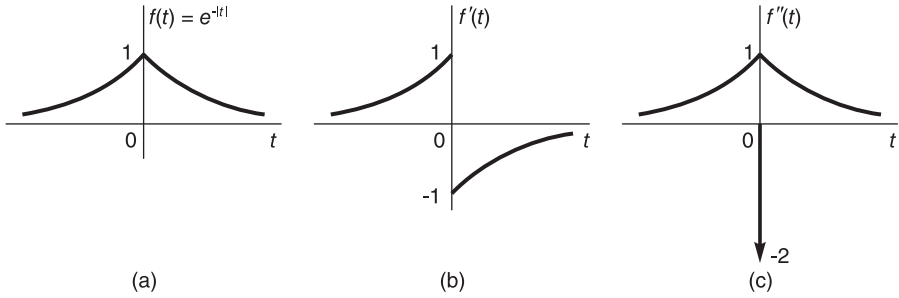


FIGURE 1.3 A function and its derivatives.

Note: The notation t_0^- and t_0^+ mean, with $\varepsilon > 0$, the limit, $t_0^- = \lim_{\varepsilon \rightarrow 0} (t_0 - \varepsilon)$, and $t_0^+ = \lim_{\varepsilon \rightarrow 0} (t_0 + \varepsilon)$.

1.3 Periodic Functions

A periodic function $f(t)$ is one that repeats periodically over the whole time axis $t \in (-\infty, \infty)$, that is, for all values of t where $-\infty < t < \infty$. A periodic function $f(t)$ of period T satisfies the relation

$$f(t + kT) = f(t), \quad k = \pm 1, \pm 2, \dots \tag{1.3}$$

as shown in Fig. 1.4.

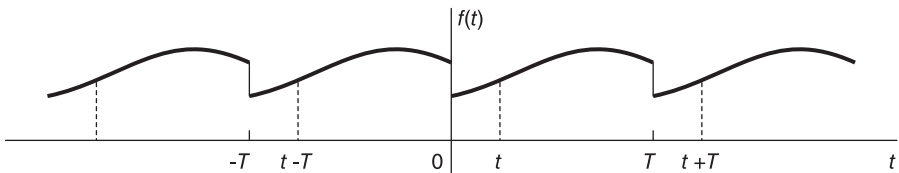


FIGURE 1.4 Periodic function.

Example 1.3 A sinusoid $v(t) = \cos(\beta t)$ where $\beta = 2\pi f_0$ rad/s, and $f_0 = 100$ Hz has a period $T = 1/f_0 = 2\pi/\beta = 0.01$ sec since $\cos[\beta(t + T)] = \cos(\beta t)$.

1.4 Unit Step Function

The Heaviside or unit step function $u(t)$, also often denoted $u_{-1}(t)$, shown in Fig. 1.5, is defined by

$$u(t) = \begin{cases} 1, & t > 0 \\ 0, & t < 0 \end{cases} \tag{1.4}$$

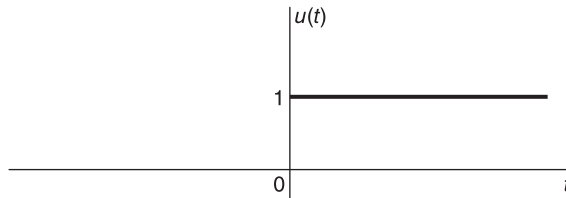


FIGURE 1.5 Heaviside unit step function.

It has a discontinuity at $t = 0$, and is thus undefined for $t = 0$. It may be assigned the value $1/2$ at $t = 0$ as we shall see in discussing distributions. It is an important function which, when multiplied by a general function $f(t)$, produces a *causal* function $f(t)u(t)$ which is nil for $t < 0$.

A general function $f(t)$ defined for $t \in (-\infty, \infty)$ will be called a *two-sided* function, being well defined for $t < 0$ and $t \geq 0$. A *right-sided* function $f(t)$ is one that is defined for all values $t \geq t_0$ and is nil for $t < t_0$ where t_0 is a finite value. A *left-sided* function $f(t)$ is one that is defined for $t \leq t_0$ and is nil for $t > t_0$.

Example 1.4 The function $f(t) = e^{-t}u(t)$ shown in Fig. 1.6 is a *right-sided* function and is *causal*, being nil for $t < 0$.

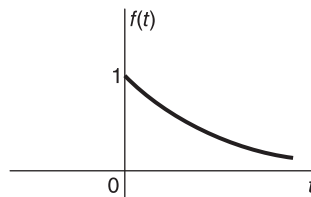


FIGURE 1.6 Causal exponential.

1.5 Graphical Representation of Functions

Graphical representation of functions is of great importance to engineers and scientists. As we shall see shortly, the evaluation of convolutions and correlations is often made simpler through a graphical representation of the operations involved. The following example illustrates some basic signal transformations and their graphical representation.

Example 1.5 *The sign function $\text{sgn}(t)$ is equal to 1 for $t > 0$ and to -1 for $t < 0$, i.e.,*

$$\text{sgn}(t) = u(t) - u(-t).$$

Sketch the sign and related functions

$$y_1(t) = \text{sgn}(2t + 2), \quad y_2(t) = 2\text{sgn}(-3t + 6), \quad y_3(t) = 2\text{sgn}(-3 - t/3).$$

To draw $y_1(t)$ we apply a time compression to $\text{sgn}(t)$ by a factor of 2, which simply produces the same function, then displace the result with its axis to the point $2t + 2 = 0$, i.e., $t = -1$. The function $y_2(t)$ is an amplification by 2, a time compression by 3 and a reflection of $\text{sgn}(t)$ followed by a shift of the axis to the point $-3t + 6 = 0$, i.e., $t = 2$. The function $y_3(t)$ is the same as $y_2(t)$ except shifted to the point $-3 - t/3 = 0$, i.e., $t = -9$, as shown in Fig. 1.7. Note that, alternatively, we may sketch the functions by rewriting them in the forms

$$y_1 = \text{sgn}[2(t + 1)], \quad y_2(t) = 2\text{sgn}[-3(t - 2)], \quad y_3(t) = 2\text{sgn}\left[-\frac{1}{3}(t + 9)\right]$$

putting into evidence the time shift to be applied.

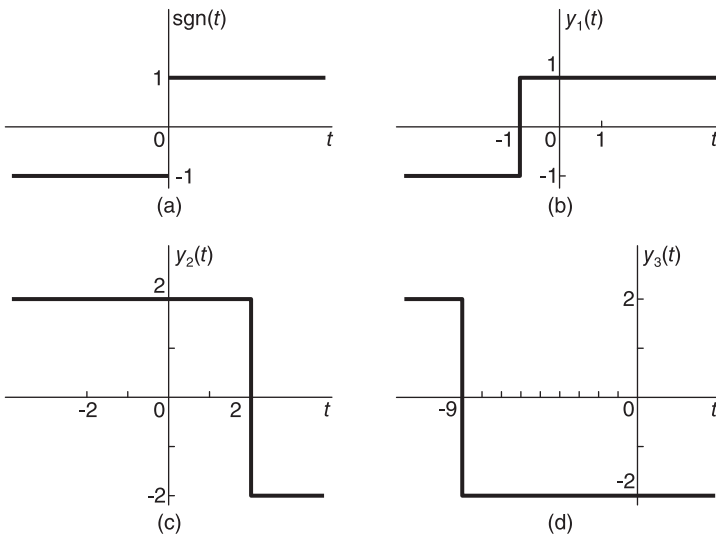


FIGURE 1.7 Sign and related functions.

Example 1.6 Given the function $f(t)$ shown in Fig. 1.8, sketch the functions $g(t) = f[-(1/3)t - 1]$ and $y(t) = f[-(1/3)t + 1]$.

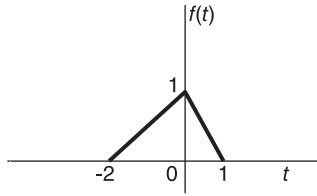


FIGURE 1.8 Given function $f(t)$.

Proceeding as in the last example we obtain the functions shown in Fig. 1.9.

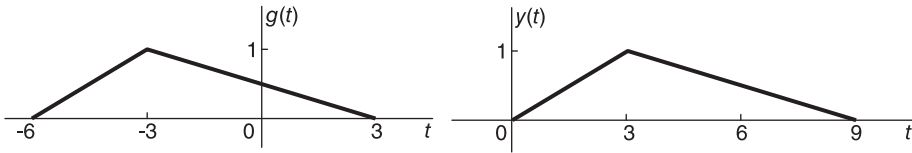


FIGURE 1.9 Reflection, shift, expansion, ... of a function.

1.6 Even and Odd Parts of a Function

A signal $f(t)$ can be decomposed into a part $f_e(t)$ of even symmetry, and another $f_o(t)$ of odd symmetry. In fact,

$$\begin{aligned} f_e(t) &= \{f(t) + f(-t)\} / 2 \\ f_o(t) &= \{f(t) - f(-t)\} / 2. \end{aligned} \tag{1.5}$$

The inverse relations expressing $f(t)$ and $f(-t)$ as functions of $f_e(t)$ and $f_o(t)$ are

$$\begin{aligned} f(t) &= \{f_e(t) + f_o(t)\} \\ f(-t) &= \{f_e(t) - f_o(t)\}. \end{aligned} \tag{1.6}$$

Example 1.7 Evaluate the even and odd parts of the function

$$f(t) = e^{-t}u(t) + e^{4t}u(-t).$$

We have

$$\begin{aligned} f_e(t) &= \{e^{-t}u(t) + e^{4t}u(-t) + e^t u(-t) + e^{-4t}u(t)\} / 2 \\ f_o(t) &= \{e^{-t}u(t) + e^{4t}u(-t) - e^t u(-t) - e^{-4t}u(t)\} / 2. \end{aligned}$$

The function $f(t)$ and its even and odd parts $f_e(t)$ and $f_o(t)$, respectively, are shown in Fig. 1.10.

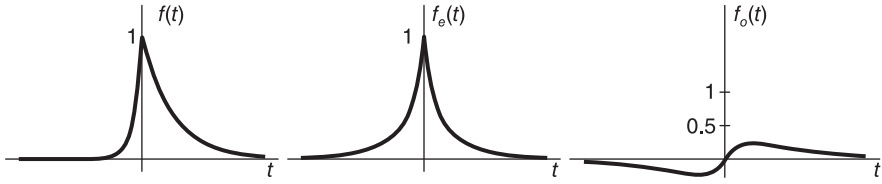


FIGURE 1.10 A function and its even and odd parts.

Example 1.8 Find the even and odd parts of

$$f(t) = \cos t + 0.5 \sin 2t \cos 3t + 0.3t^2 - 0.4t^3.$$

Since the sine function is odd and the cosine function is even we can write $f_e(t) = \cos t + 0.3t^2$, $f_o(t) = 0.5 \sin 2t \cos 3t - 0.4t^3$.

The function $f(t)$ and its even and odd parts $f_e(t)$ and $f_o(t)$, respectively, are shown in Fig. 1.11.

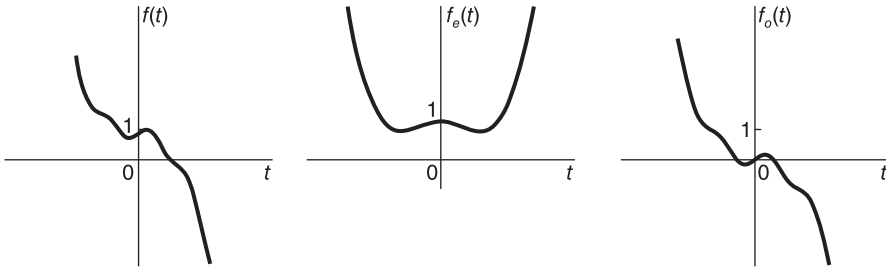


FIGURE 1.11 Even and odd parts of a function.

1.7 Dirac-Delta Impulse

The Dirac-delta impulse is an important member of a family known as “Generalized functions,” or “Distributions.” In the following we study this generalized function by relating it to the unit step function and viewing it as a limit of an ordinary function.

The Dirac-delta impulse $\delta(t)$ represented schematically in Fig. 1.1 above can be viewed as the result of differentiating the unit step function $u(t)$. Conversely, the integral of the Dirac-delta impulse is the unit step function.

We note that the derivative of the unit step function $u(t)$, Fig. 1.5, is nil for $t > 0$, the function being a constant equal to 1 for $t > 0$. Similarly, the derivative is nil for $t < 0$. At $t = 0$, the derivative is infinite.

The Dirac-delta impulse $\delta(t)$ is not an ordinary function, being nil for all $t \neq 0$, and yet its integral is not zero. The integral can be non-nil if and only if the value of the impulse is infinite at $t = 0$. We shall see that by modeling the step function as a limit of a sequence, its derivative tends in the limit to the impulse $\delta(t)$.

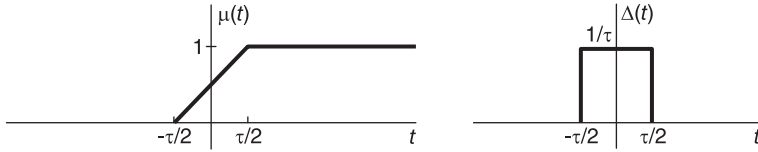


FIGURE 1.12 Approximation of the unit step function and its derivative.

A simple sequence and the limiting process are shown in Fig.1.12. Consider the function $\mu(t)$, which is an approximation of the step function $u(t)$, and its derivative $\Delta(t)$ shown in Fig. 1.12. We have

$$\mu(t) = \begin{cases} t/\tau + 0.5, & -\tau/2 \leq t \leq \tau/2 \\ 0, & t \leq -\tau/2 \\ 1, & t \geq \tau/2. \end{cases} \tag{1.7}$$

As $\tau \rightarrow 0$ the function $\mu(t)$ tends to $u(t)$. As long as $\tau > 0$ the function $\mu(t)$ is continuous and its derivative is

$$\Delta(t) = \begin{cases} 1/\tau, & -\tau/2 < t < \tau/2 \\ 0, & t < -\tau/2, t > \tau/2. \end{cases} \tag{1.8}$$

As $\tau \rightarrow 0$ the function $\Delta(t)$ becomes progressively narrower and of greater height. Its area, however, is always equal to 1. In the limit as τ becomes zero the function $\Delta(t)$ tends to $\delta(t)$, which satisfies the conditions

$$\delta(t) = 0, \quad t \neq 0 \tag{1.9}$$

$$\int_{-\infty}^{\infty} \delta(t) dt = 1. \tag{1.10}$$

1.8 Basic Properties of the Dirac-Delta Impulse

One of the basic properties of the Dirac-delta impulse $\delta(t)$ is known as the sampling property, namely,

$$f(t) \delta(t) = f(0)\delta(t) \tag{1.11}$$

where $f(t)$ is a continuous function, hence well defined at $t = 0$.

Using the simple model of the impulse as the limit of a rectangle, as we have just seen, the product $f(t) \Delta(t)$ may be represented as shown in Fig.1.13. We may write

$$g(t) = f(t) \delta(t) = \lim_{\tau \rightarrow 0} f(t) \Delta(t) = f(0) \delta(t). \tag{1.12}$$

Note that the area under $g(t)$ tends to $f(0)$. Another important property is written

$$\int_{-\infty}^{\infty} f(t) \delta(t) dt = f(0). \tag{1.13}$$

This property results directly from the previous one since

$$\int_{-\infty}^{\infty} f(t) \delta(t) dt = \int_{-\infty}^{\infty} f(0)\delta(t) dt = f(0) \int_{-\infty}^{\infty} \delta(t) dt = f(0). \tag{1.14}$$

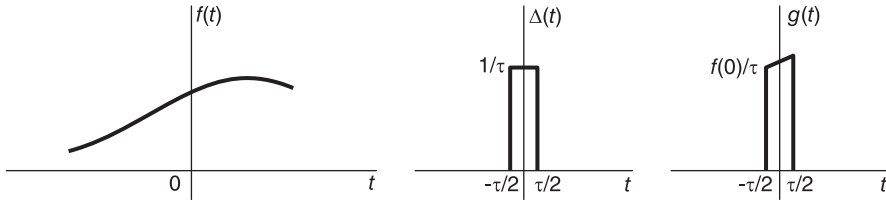


FIGURE 1.13 Multiplication of a function by a narrow pulse.

Other properties include the time shifted impulse, namely,

$$f(t) \delta(t - t_0) = f(t_0) \delta(t - t_0) \tag{1.15}$$

$$\int_{-\infty}^{\infty} f(t) \delta(t - t_0) dt = f(t_0) \int_{-\infty}^{\infty} \delta(t - t_0) dt = f(t_0). \tag{1.16}$$

The time-scaling property of the impulse is written

$$\delta(at) = \frac{1}{|a|} \delta(t). \tag{1.17}$$

We can verify its validity when the impulse is modeled as the limit of a rectangle. This is illustrated in Fig. 1.14 which shows, respectively, the rectangles $\Delta(t)$, $\Delta(3t)$ and the more general $\Delta(at)$, which tend in the limit to $\delta(t)$, $\delta(3t)$ and $\delta(at)$, respectively, as $\tau \rightarrow 0$. Note that as shown in the figure, with $a = 3$ or a is a general positive value, the function $\Delta(at)$ is but a compression of $\Delta(t)$ by an amount equal to a . In the limit as $\tau \rightarrow 0$ the rectangle $\Delta(3t)$ becomes of zero width and infinite height, but its area remains $(1/\tau) \cdot (\tau/3) = 1/3$. In the limit we have $\delta(3t) = (1/3)\delta(t)$ and similarly, $\delta(at) = (1/a)\delta(t)$, in agreement with the stated property.

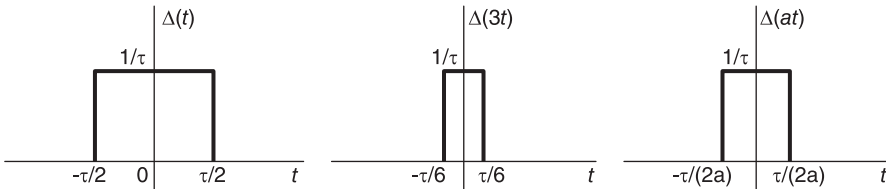


FIGURE 1.14 Compression of a rectangle.

We can, alternatively, establish this relation using the basic properties of the impulse. Consider the integral

$$I = \int_{-\infty}^{\infty} f(t) \delta(at) dt. \tag{1.18}$$

With $a > 0$, let $\tau = a t$. We have

$$I = \int_{-\infty}^{\infty} f\left(\frac{\tau}{a}\right) \delta(\tau) \cdot \frac{1}{a} d\tau = \frac{1}{a} f(0) = \frac{1}{a} \int_{-\infty}^{\infty} f(t) \delta(t) dt. \tag{1.19}$$

The last two equations imply (1.17). With $a < 0$ let $a = -\alpha$ where $\alpha > 0$. Writing $\tau = at = -\alpha t$ we have

$$I = \int_{-\infty}^{-\infty} f\left(\frac{-\tau}{\alpha}\right) \delta(\tau) \cdot \frac{d\tau}{(-\alpha)} = \frac{1}{\alpha} f(0) = \frac{1}{|a|} \int_{-\infty}^{\infty} f(t) \delta(t) dt \quad (1.20)$$

confirming the general validity of (1.17). Dirac-delta impulses arise whenever differentiation is performed on functions that have discontinuities. This is illustrated in the following example.

Example 1.9 A function $f(t)$ that has discontinuities at $t = 12$ and $t = 17$, and has “corner points” at $t = 5$ and $t = 9$, whereat its derivative is discontinuous, is shown in Fig. 1.15, together with its derivative. In particular the function $f(t)$ and its derivative $f'(t)$ are given by

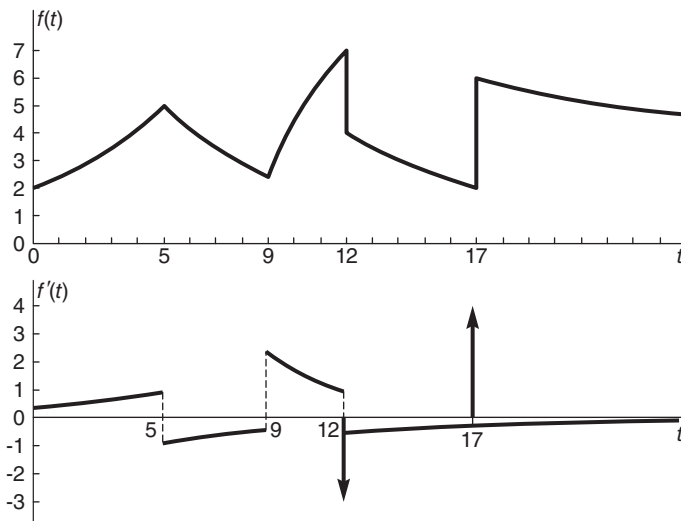


FIGURE 1.15 Function with discontinuities and its derivative.

$$f(t) = \begin{cases} 2e^{0.1833t}, & 0 \leq t \leq 5 \\ 12.5026e^{-0.1833t}, & 5 \leq t \leq 9 \\ 10 - 123.4840e^{-0.3098t}, & 9 \leq t < 12 \\ 21.1047e^{-0.1386t}, & 12 < t < 17 \\ 4 + 21.1047e^{-0.1386t}, & t > 17 \end{cases}$$

$$f'(t) = \begin{cases} 0.3667e^{0.1833t}, & 0 \leq t < 5 \\ -2.2917e^{-0.1833t}, & 5 < t < 9 \\ 38.2553e^{-0.3098t}, & 9 < t < 12 \\ -2.9251e^{-0.1386t}, & 12 < t < 17 \\ -2.9251e^{-0.1386t}, & t > 17. \end{cases}$$

As the figure shows, in addition the derivative $f'(t)$ has two impulses, namely, $-3\delta(t - 12)$ and $4\delta(t - 17)$. The function $f(t)$ at $t = 12$ has both a discontinuity and a corner point, leading to an impulse and a discontinuous derivative $f'(t)$ at $t = 12$. This is due to the fact that if the section of the function $f(t)$ between $t = 12$ and $t = 17$ is moved upwards until the “jump” discontinuity at $t = 12$ is reduced to zero, the function will still display a corner; hence the discontinuous derivative at $t = 12$. It is interesting to note that at $t = 17$ the function has a discontinuity but no corner point. The reason here is that apart from the jump, due to the addition of the constant value 4, for $t \geq 17$, the function is the same for $t \geq 17$ as it is for $12 \leq t \leq 17$. The student should notice that in the expression of $f(t)$, as well as that of $f'(t)$ above, the function is undefined at each discontinuity. This is stated by using the inequalities $<$ and $>$ instead of \leq and \geq .

1.9 Other Important Properties of the Impulse

In Chapter 17, Section 17.16, we list important properties of the Dirac-delta impulse for future reference. The subject is dealt with at length and all these properties are justified in Chapter 18.

1.10 Continuous-Time Systems

In this book we deal exclusively with linear time invariant (LTI) systems. A system may be viewed as a collection of components which, receiving an *excitation force*, called *input*, $x(t)$, produces a *response* $y(t)$ called the *output*, as shown in Fig. 1.16.

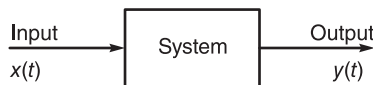


FIGURE 1.16 System with input and output.

A system is called *dynamic* if its response $y(t)$ to an input $x(t)$ applied at time t depends not only on the value of the input at that instant, but also on the history preceding the instant t . This property implies that a dynamic system can memorize its past history. A

dynamic system has therefore *memory* and is generally described by differential equations.

1.11 Causality, Stability

To be physically realizable a system has to be causal. The name stems from the fact that a physically realizable system should reflect a cause-effect relation. The system input is the “cause,” its output the “effect,” and the effect has to follow the cause and cannot precede it. If the input to the system is an impulse $\delta(t)$, its output is called the “impulse response,” denoted $h(t)$. The symbol $h(t)$ is due to the fact that the Laplace transform of the system impulse response is the system transfer function $H(s)$, that is,

$$H(s) = \mathcal{L}[h(t)]. \quad (1.21)$$

where the symbol \mathcal{L} stands for ‘Laplace transform’. Since the input $\delta(t)$ is nil for $t < 0$, a physically realizable system would produce an impulse response that is nil for $t < 0$, and non-nil for solely $t \geq 0$. Such an impulse response is called “causal.” On the other hand, if the impulse response $h(t)$ of a system is not nil for $t < 0$ then it is not causal and the system would not be physically realizable since it would respond to the input $\delta(t)$ before the input is applied. A noncausal impulse response is an abstract mathematical concept that is nevertheless useful for analysis. We shall see in Chapter 4 that a system is stable if the Fourier transform $H(j\omega)$ of its impulse response $h(t)$ exists.

1.12 Examples of Electrical Continuous-Time Systems

A simple example of a system *without* memory is the simple electric resistance shown in Fig. 1.17(a). A voltage $v(t)$ volts applied across an ideal resistor of resistance R ohms produces a current

$$i(t) = \frac{v(t)}{R} \text{ Ampere.} \quad (1.22)$$

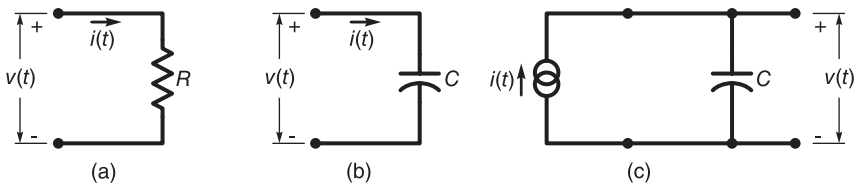


FIGURE 1.17 Resistor and capacitor as linear systems.

The output $i(t)$ is function of the input $v(t)$ and is not function of any previous value of the input. The resistor is therefore a *memory-less* system.

An electric capacitor, on the other hand, is a dynamic system; a system the response of which depends on the past and not only on the value of the input $v(t)$ applied at a time t .

The charge stored by the capacitor shown in Fig. 1.17(b) is given by

$$q(t) = C v(t) \tag{1.23}$$

and the current $i(t)$ is the derivative of the charge

$$i(t) = \frac{dq(t)}{dt} = C \frac{dv}{dt}. \tag{1.24}$$

The capacitor memorizes the past through its accumulated charge. We note that if the input is a current source, Fig. 1.17(c), the output would be the voltage $v(t)$ across the capacitor. The input–output relation is written

$$v(t) = \frac{q(t)}{C} = \frac{1}{C} \int_{-\infty}^t i(\tau) d\tau. \tag{1.25}$$

We see that the output $v(t)$ at time t is a function of the accumulated input rather than only the value of the input $i(t)$ at an instant t .

Example 1.10 Evaluate the current $i(t)$ in the capacitor, Fig. 1.17(b), in response to a step function input voltage $v(t) = u(t)$ volts.

We have

$$i(t) = C \frac{dv}{dt} = C \frac{d}{dt} u(t) = C \delta(t) \text{ ampere.}$$

An electric circuit containing an inductor is similarly a dynamic system that memorizes its past.

Example 1.11 Consider the electric circuit shown in Fig. 1.18. Write the relation between the output current $i(t)$ and the input voltage $v(t)$.

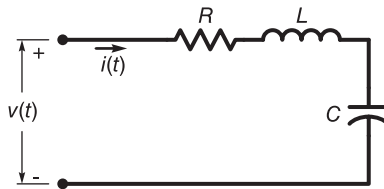


FIGURE 1.18 R-L-C electric circuit.

We have

$$R i(t) + L \frac{di}{dt} + \frac{1}{C} \int i dt = v(t)$$

The derivative and integral reflect the memorization of the past values of $i(t)$ in determining the output.

1.13 Mechanical Systems

We shall see later on that a homology exists that relates a mechanical system to an equivalent electrical system and electric circuits in particular. Similarly, homologies exist between

hydraulic, heat transfer and other systems on the one hand and electric circuits on the other. Such homologies may be used to convert the model of any physical system into its equivalent electrical homologue, solve the equivalent electric circuit, and convert the results to the original system.

1.14 Transfer Function and Frequency Response

The transfer function $H(s)$ of a linear system, assuming zero initial conditions, is defined by

$$H(s) = \frac{Y(s)}{X(s)} \quad (1.26)$$

where $X(s) = \mathcal{L}[x(t)]$ and $Y(s) = \mathcal{L}[y(t)]$. We shall use the notation \mathcal{L} and \mathcal{L}^{-1} to denote the direct and inverse Laplace transform, respectively, so that $X(s)$ is the Laplace transform of the input $x(t)$, Fig. 1.19, and $Y(s)$ is the transform of the output $y(t)$, respectively. Conversely, if the transfer function $H(s)$ of a system is known and if the system is “at

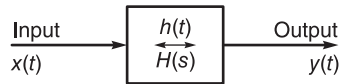


FIGURE 1.19 Linear system with input and output.

rest”, meaning zero initial conditions, its output $y(t)$ is such that $Y(s) = X(s)H(s)$. This means that in the time domain the output $y(t)$ is the convolution of the input $x(t)$ with the system’s impulse response $h(t)$. We write

$$y(t) = x(t) * h(t) \quad (1.27)$$

where the asterisk symbol $*$ denotes the convolution operation. As we shall see in more detail in Chapter 3, the Laplace variable s is a generally complex variable. We shall throughout write $s = \sigma + j\omega$, so that $\sigma = \Re[s]$ and $\omega = \Im[s]$. The Laplace s plane has $s = \sigma$ as its horizontal axis and $s = j\omega$ as its vertical axis. The transfer function $H(s)$ is generally well defined over only a limited region of the s plane. This is called the *region of convergence* (ROC) of $H(s)$. If this ROC includes the $j\omega$ axis, then the substitution $s = j\omega$ is permissible, resulting in $H(s) = H(j\omega)$ which is referred to as the system *frequency response*.

The frequency response $H(j\omega)$ is in fact the Fourier transform of the impulse response $h(t)$, in as much as the transfer function $H(s)$ is its Laplace transform. As we shall see in Chapter 4 the Fourier transform of any function of time is simply the Laplace transform evaluated on the $j\omega$ axis of the s plane, if such substitution is permissible, i.e. if the ROC of the Laplace transform contains the $j\omega$ axis.

When the frequency response $H(j\omega)$ exists, the system input–output relation is the same input–output relation given above with s replaced by $j\omega$, that is, $Y(j\omega) = X(j\omega)H(j\omega)$, and the frequency response is given by

$$H(j\omega) = Y(j\omega)/X(j\omega). \quad (1.28)$$

Example 1.12 Consider a linear system having the transfer function

$$H(s) = \frac{1}{s + 3}, \quad \Re[s] > -3.$$

Evaluate the frequency response $H(j\omega)$. Does such system behave as a highpass or lowpass filter?

Since the ROC of $H(s)$ is $\sigma = \Re[s] > -3$, i.e. the line $\sigma = 0$, which is the vertical axis $s = j\omega$ of the s plane, is in the ROC, the frequency response exists and is given by

$$H(j\omega) = H(s)|_{s=j\omega} = \frac{1}{j\omega + 3} = \frac{3 - j\omega}{\omega^2 + 9} = \frac{1}{\sqrt{\omega^2 + 9}} e^{j \arctan[-\omega/3]}$$

$$|H(j\omega)| = \frac{1}{\sqrt{\omega^2 + 9}}, \quad \arg [H(j\omega)] = \arctan [-\omega/3].$$

The modulus $|H(j\omega)|$, which is the Fourier amplitude spectrum, and the phase spectrum $\arg [H(j\omega)]$ of the frequency response are shown in Fig.1.20. The amplitude spectrum of the output $y(t)$ is related to that of the input $x(t)$ by the equation

$$|Y(j\omega)| = |X(j\omega)| |H(j\omega)|.$$

The higher frequency components of $X(j\omega)$ are attenuated by the drop in value of $|H(j\omega)|$ as $\omega > 0$ increases.. The system acts therefore as a lowpass filter.

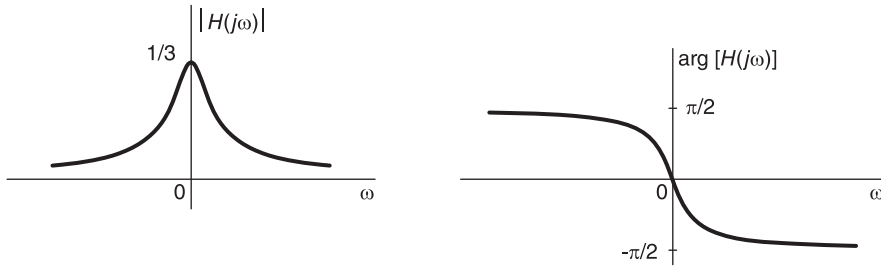


FIGURE 1.20 Modulus and phase of frequency response.

1.15 Convolution and Correlation

Convolution and correlation are important mathematical tools that are encountered in evaluating the response of linear systems and in signal spectral analysis. In this section we study properties of the convolution and correlation integrals. The convolution $y(t)$ of two general functions $x(t)$ and $v(t)$, denoted symbolically

$$y(t) = x(t) * v(t) \tag{1.29}$$

is given by

$$y(t) = \int_{-\infty}^{\infty} x(\tau) v(t - \tau) d\tau = \int_{-\infty}^{\infty} v(\tau) x(t - \tau) d\tau \tag{1.30}$$

The convolution integral is commutative, distributive and associative, that is,

$$x(t) * v(t) = v(t) * x(t) \quad (1.31)$$

$$x(t) * [v_1(t) + v_2(t)] = x(t) * v_1(t) + x(t) * v_2(t) \quad (1.32)$$

$$x(t) * [v_1(t) * v_2(t)] = [x(t) * v_1(t)] * v_2(t) = [x(t) * v_2(t)] * v_1(t). \quad (1.33)$$

In evaluating the convolution integral, as in Equation (??), it is instructive to visualize the two functions in the integrand, namely, $x(\tau)$ and $v(t - \tau)$ versus the integral variable τ as they relate to the given functions $x(t)$ and $v(t)$, respectively. We first note that the function $x(\tau)$ versus τ is the same as $x(t)$ versus t apart from a change of label of the horizontal axis. We need next to deduce the shape of $v(t - \tau)$ versus τ . To this end consider the simple

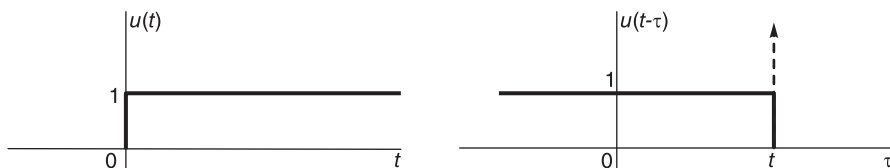


FIGURE 1.21 Step function and its mobile reflection.

step function $u(t)$ shown in Fig. 1.21 and its reflection and shifting leading to the function $u(t - \tau)$, which we shall call the “mobile function,” and which is plotted versus τ in the same figure. This mobile function is plotted as shown since by definition it should equal 1 if and only if $\tau < t$ and 0 otherwise. Note that the value t has to be a fixed value on the τ axis, and that the position of the mobile function $u(t - \tau)$ depends on the value of t . As shown in the figure a vertical dashed axis with an arrow head, which we shall call the *mobile axis*, is drawn at the point $\tau = t$. If t is varied the mobile axis moves, dragging with it the mobile function $u(t - \tau)$. The function $u(t - \tau)$ is thus the reflected function $u(-\tau)$ frozen as an image then slid by its mobile axis to the point $\tau = t$. Similarly, the signal $v(t - \tau)$ is obtained by reflecting the signal $v(t)$ and then sliding the result as a frozen image by its mobile axis to the point $\tau = t$.

Example 1.13 Let

$$x(t) = 3\{u(t + 4) - u(t - 7)\}$$

$$v(t) = e^{\alpha t}\{u(t + 2) - u(t - 6)\}, \quad \alpha = 0.1831.$$

Evaluate the convolution $y(t) = x(t) * v(t)$.

The two functions are shown in Fig. 1.22 (a) and (b), respectively. To evaluate the integral

$$y(t) = \int_{-\infty}^{\infty} x(\tau) v(t - \tau) d\tau$$

we start with the reflection $v(-\tau)$ of $v(\tau)$ versus τ shown in Fig. 1.22 (c). The rest of Fig. 1.22 shows the function $v(t - \tau)$ versus τ for $t = -3$, $t = 4$ and $t = 10$, respectively. As seen in the figure, the mobile function $v(t - \tau)$, in the interval where it is non-nil, is simply the function $v(t)$ with t replaced by $t - \tau$, so that $v(t - \tau) = e^{\alpha(t - \tau)}$. Figures 1.22 (d), (e), (f) show the three distinct positions of the function $v(t - \tau)$, which produce three distinct integrals that need be evaluated.

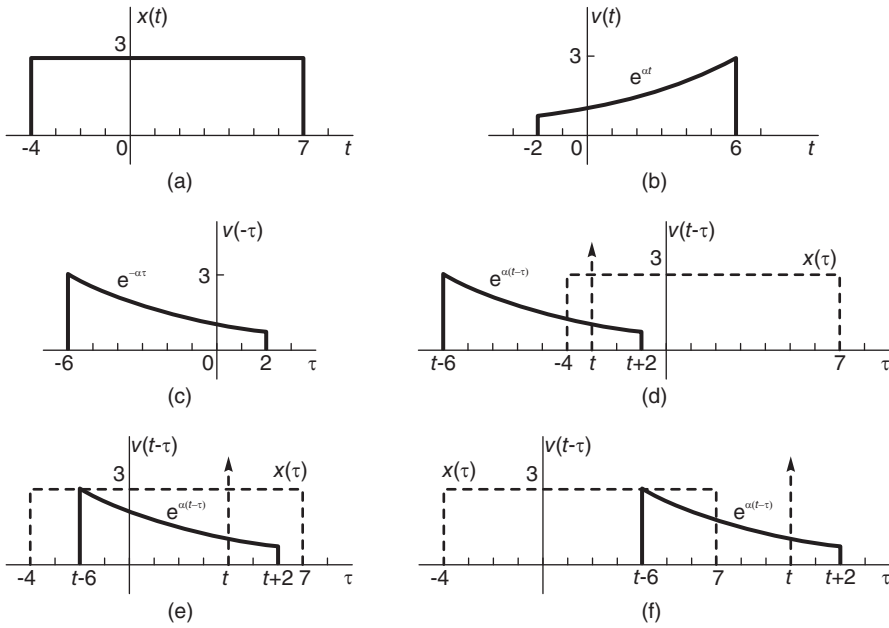


FIGURE 1.22 Step by step convolution of two functions.

As Fig. 1.22 (d) shows, if $t + 2 < -4$, i.e. $t < -6$, then the two functions $x(\tau)$ and $v(t - \tau)$ do not overlap, their product is therefore nil and $y(t) = 0$. If on the other hand $t + 2 > -4$ and $t - 6 < -4$, that is, for $-6 < t < 2$

$$y(t) = \int_{-4}^{t+2} 3e^{\alpha(t-\tau)} d\tau = 3e^{\alpha t} \left. \frac{e^{-\alpha\tau}}{\alpha} \right|_{t+2}^{-4} = \frac{3}{\alpha} e^{\alpha t} \left\{ e^{4\alpha} - e^{-\alpha(t+2)} \right\}.$$

Referring to Fig. 1.22 (e), we have for $t - 6 > -4$ and $t + 2 < 7$, that is, for $2 < t < 5$

$$y(t) = \int_{t-6}^{t+2} 3e^{\alpha(t-\tau)} d\tau = 3e^{\alpha t} \left. \frac{e^{-\alpha\tau}}{\alpha} \right|_{t+2}^{t-6} = \frac{3}{\alpha} e^{\alpha t} \left\{ e^{-\alpha(t-6)} - e^{-\alpha(t+2)} \right\}.$$

From Fig. 1.22 (f), for $t - 6 < 7$ and $t + 2 > 7$, that is, for $5 < t < 13$,

$$y(t) = \int_{t-6}^7 3e^{\alpha(t-\tau)} d\tau = 3e^{\alpha t} \left. \frac{e^{-\alpha\tau}}{\alpha} \right|_7^{t-6} = (3/\alpha) e^{\alpha t} \left\{ e^{-\alpha(t-6)} - e^{-7\alpha} \right\}.$$

With $t - 6 > 7$, i.e. $t > 13$, the mobile function $v(t - \tau)$ does not overlap with $x(\tau)$ so that the product is nil and we have $y(t) = 0$. The function $y(t)$ is shown in Fig. 1.23.

Example 1.14 Using MATLAB[®] verify the result of the convolution $y(t) = x(t) * v(t)$ of the last example.

```
We may write
alpha=0.1831
x(1:110)=3
for n=1:80
v(n)=exp(alpha*(n-20)*0.1)
end
```

`y=conv(x,v)`

`plot(y)`

The result is the same as that obtained above.

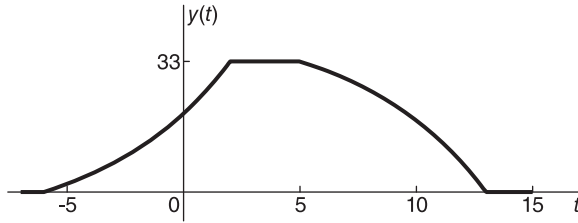


FIGURE 1.23 Result of the convolution of two functions.

Analytic Approach

In the analytic approach we write

$$\begin{aligned} y(t) &= \int_{-\infty}^{\infty} x(\tau)v(t-\tau)d\tau \\ &= \int_{-\infty}^{\infty} 3[u(\tau+4) - u(\tau-7)]e^{\alpha(t-\tau)}[u(t-\tau+2) - u(t-\tau-6)]d\tau. \end{aligned}$$

This is the sum of four integrals. Consider the first integral, namely,

$$I_1 = \int_{-\infty}^{\infty} 3u(\tau+4)e^{\alpha(t-\tau)}u(t-\tau+2)d\tau.$$

In the integrand the step function $u(\tau+4)$ is non-nil if and only if $\tau > -4$, and the step function $u(t-\tau+2)$ is non-nil if and only if $\tau < t+2$. The limits of integration are therefore to be replaced by -4 and $t+2$, the interval wherein the integrand is non-nil. Moreover, the two inequalities $\tau > -4$ and $\tau < t+2$ imply that $t > \tau - 2 > -6$. We therefore write

$$I_1 = \left\{ \int_{-4}^{t+2} 3e^{\alpha(t-\tau)} d\tau \right\} u(t+6) = \frac{3}{\alpha} (e^{4\alpha} e^{\alpha t} - e^{-2\alpha}) u(t+6).$$

The three other integrals are similarly evaluated obtaining

$$I_2 = - \int_{-\infty}^{\infty} 3u(\tau+4)e^{\alpha(t-\tau)}u(t-\tau-6)d\tau = -3 \int_{-4}^{t-6} e^{\alpha(t-\tau)} d\tau u(t-2).$$

$$I_2 = -\frac{3}{\alpha} (e^{4\alpha} e^{\alpha t} - e^{6\alpha}) u(t-2).$$

$$I_3 = -3 \int_7^{t+2} e^{\alpha(t-\tau)} d\tau u(t-5) = -\frac{3}{\alpha} (e^{-7\alpha} e^{\alpha t} - e^{-2\alpha}) u(t-5)$$

$$I_4 = 3 \int_7^{t-6} e^{\alpha(t-\tau)} d\tau u(t-13) = \frac{3}{\alpha} (e^{-7\alpha} e^{\alpha t} - e^{6\alpha}) u(t-13).$$

$$y(t) = I_1 + I_2 + I_3 + I_4.$$

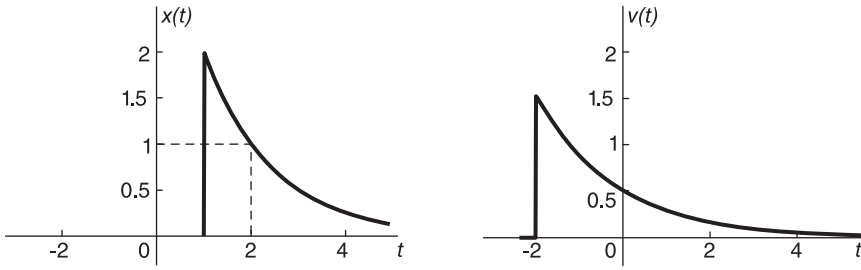


FIGURE 1.24 Two right-sided exponentials.

Using *Mathematica* we can verify the result by plotting the function $y(t)$, obtaining the same result as found above.

Example 1.15 Evaluate the convolution of the two exponential functions shown in Fig. 1.24.

From the function forms we can write $x(t) = 4e^{-0.69t}u(t-1)$, $v(t) = 0.5e^{-0.55t}u(t+2)$. We may start by drawing the function $x(\tau)$ and the mobile one $v(t-\tau)$ as shown in Fig. 1.25.

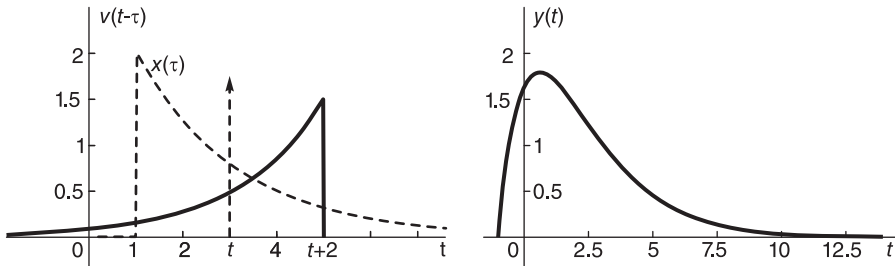


FIGURE 1.25 The functions $x(\tau)$, $v(t-\tau)$ and the convolution $y(t)$.

From the figure we note that $y(t) = 0$ for $t+2 < 1$, i.e. $t < -1$ and that for $t > -1$

$$y(t) = x(t) * v(t) = \int_1^{t+2} 4e^{-0.69\tau} 0.5e^{-0.55(t-\tau)} d\tau$$

$$y(t) = (12.43e^{-0.55t} - 10.8e^{-0.69t}), \quad t > -1.$$

Alternatively we proceed analytically by writing

$$y(t) = \int_{-\infty}^{\infty} 4e^{-0.69\tau} u(\tau-1) 0.5e^{-0.55(t-\tau)} u(t-\tau+2) d\tau$$

$$y(t) = 2 \left\{ \int_1^{t+2} e^{-0.69\tau - 0.55t + 0.55\tau} d\tau \right\} u(t+1)$$

$$= (12.43e^{-0.55t} - 10.8e^{-0.69t}) u(t+1)$$

The following *Mathematica* program plots $y(t)$ as can be seen in Fig. 1.25.

Clear

```
y[t_]:= (12.43*Exp[-0.55 t] - 10.8 Exp[-0.69t]) UnitStep[t+1]
```

```
Plot[y[t],{t,-2,15}, AxesLabel -> {t,y}, PlotRange -> {0,2}]
```

1.16 A Right-Sided and a Left-Sided Function

The convolution, analytically, of two opposite-sided functions requires special attention as the following example illustrates.

Example 1.16 Evaluate the convolution of the two exponential functions $x(t)$ and $v(t)$ shown in Fig. 1.26.

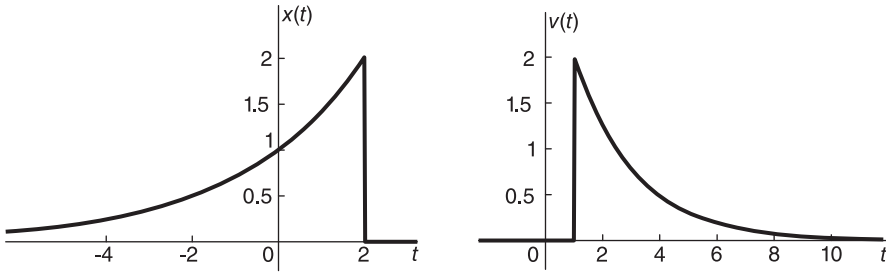


FIGURE 1.26 Left-sided and right-sided exponential.

We have, from the forms of the functions, $x(t) = e^{\alpha t}$, $t \leq 2$, where $\alpha = 0.35$. Similarly, $v(t) = Be^{-\beta t}$, $t \geq 1$, where $B = 3.2$ and $\beta = 0.47$. The convolution is given by

$$y(t) = \int_{-\infty}^{\infty} e^{0.35\tau} u(2-\tau) 3.2e^{-0.47(t-\tau)} u(t-\tau-1) d\tau.$$

The product of the step functions is non-nil if and only if $\tau < 2$ and $\tau < t-1$. These conditions do not imply an upper and a lower bound for the variable τ . Instead, these are two upper bounds. We note in particular that the product of the two step-functions is non-nil if $\tau < 2$ in the case where $2 \leq t-1$, i.e. $t \geq 3$ and that, on the other hand, the product is non-nil if $\tau < t-1$ in the case where $t-1 \leq 2$, i.e. $t \leq 3$. We can therefore write

$$y(t) = \left\{ \int_{-\infty}^2 e^{0.35\tau} 3.2e^{-0.47(t-\tau)} d\tau \right\} u(t-3) + \left\{ \int_{-\infty}^{t-1} e^{0.35\tau} 3.2e^{-0.47(t-\tau)} d\tau \right\} u(3-t).$$

$$y(t) = 20.11e^{-0.47t} u(t-3) + 1.72e^{0.35t} u(3-t).$$

The result can be verified graphically as seen in Fig. 1.27. The figure confirms that in the case where $t-1 \leq 2$, i.e. $t \leq 3$ we have

$$y(t) = \left\{ \int_{-\infty}^{t-1} e^{0.35\tau} 3.2e^{-0.47(t-\tau)} d\tau \right\}$$

and that for the case where $t-1 \geq 2$, i.e. $t \geq 3$ we have

$$y(t) = \left\{ \int_{-\infty}^2 e^{0.35\tau} 3.2e^{-0.47(t-\tau)} d\tau \right\}$$

The function $y(t)$ is shown in Fig. 1.28.

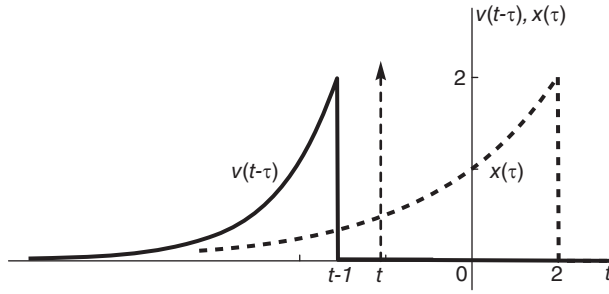


FIGURE 1.27 Convolution detail of left-sided and right-sided exponential.

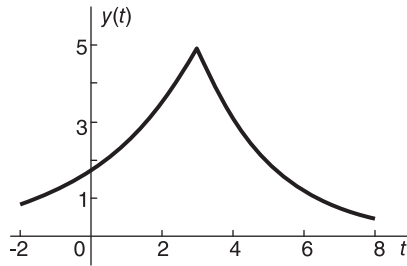


FIGURE 1.28 Convolution result $y(t)$.

1.17 Convolution with an Impulse and Its Derivatives

The properties of Distributions such as the Dirac-delta impulse and its derivatives are discussed at length in Chapter 17. We summarize here some properties of the convolution with an impulse and its derivatives.

$$f(t) * \delta(t) = \int_{-\infty}^{\infty} f(\tau)\delta(t - \tau)d\tau = f(t). \tag{1.34}$$

$$f(t) * \delta(t - t_0) = \int_{-\infty}^{\infty} f(\tau)\delta(t - \tau - t_0)d\tau = f(t - t_0). \tag{1.35}$$

$$f(t) * \delta'(t) = \int_{-\infty}^{\infty} f(\tau)\delta'(t - \tau)d\tau = - \int_{-\infty}^{\infty} f'(\tau)\delta(t - \tau)d\tau = -f'(t). \tag{1.36}$$

$$f(t) * \delta^{(n)}(t) = (-1)^n \int_{-\infty}^{\infty} f^{(n)}(\tau)\delta(t - \tau)d\tau = (-1)^n f^{(n)}(t). \tag{1.37}$$

1.18 Additional Convolution Properties

The following properties of the convolution integral are worthwhile remembering

$$v(t) * x'(t) = v'(t) * x(t) = [v(t) * x(t)]'. \tag{1.38}$$

If $z(t) = v(t) * x(t)$ then

$$v(t) * x(t - t_0) = \int_{-\infty}^{\infty} v(\tau) x(t - t_0 - \tau) d\tau = z(t - t_0). \quad (1.39)$$

1.19 Correlation Function

The correlation function measures the resemblance between two signals or the periodicity of a given signal. Operating on two aperiodic, generally complex, functions $x(t)$ and $v(t)$, it is called the cross-correlation function denoted by the symbol $r_{xv}(t)$ and defined by

$$r_{xv}(t) \triangleq x(t) \star v(t) = \int_{-\infty}^{\infty} x(t + \tau) v^*(\tau) d\tau \quad (1.40)$$

where the star symbol \star will be used to denote correlation and the asterisk $*$ stands for the complex conjugate. The autocorrelation of a function $x(t)$ is given by

$$r_{xx}(t) \triangleq x(t) \star x(t) = \int_{-\infty}^{\infty} x(t + \tau) x^*(\tau) d\tau. \quad (1.41)$$

Replacing $t + \tau$ by λ and then replacing λ by τ we obtain the equivalent forms

$$r_{xv}(t) = \int_{-\infty}^{\infty} x(\tau) v^*(\tau - t) d\tau \quad (1.42)$$

$$r_{xx}(t) = \int_{-\infty}^{\infty} x(\tau) x^*(\tau - t) d\tau \quad (1.43)$$

and the same without the asterisk if the functions are real.

1.20 Properties of the Correlation Function

The correlation function can be expressed as a convolution. In fact,

$$r_{xv}(t) = \int_{-\infty}^{\infty} x(\tau) v^*(\tau - t) d\tau = \int_{-\infty}^{\infty} x(\tau) v^*[-(t - \tau)] d\tau = x(t) * v^*(-t). \quad (1.44)$$

In other words, *the cross correlation $r_{xv}(t)$ is but the convolution of $x(t)$ with the reflection of $v^*(t)$* . For real functions

$$r_{xv}(t) = x(t) * v(-t). \quad (1.45)$$

The cross-correlation function is *not* commutative. In fact, for generally complex functions,

$$r_{vx}(t) \triangleq v(t) \star x(t) = \int_{-\infty}^{\infty} v(t + \tau) x^*(\tau) d\tau. \quad (1.46)$$

By replacing $t + \tau$ by λ and then replacing λ by τ we can write using (Equation 1.40)

$$r_{vx}(t) = \int_{-\infty}^{\infty} v(\lambda) x^*(\lambda - t) d\lambda = \int_{-\infty}^{\infty} v(\tau) x^*(\tau - t) d\tau = r_{xv}^*(-t). \quad (1.47)$$

In other words the correlation of $v(t)$ with $x(t)$ is equal to the conjugate of the reflection about $t = 0$ of the correlation of $x(t)$ with $v(t)$. Moreover, $r_{xx}(-t) = r_{xx}^*(t)$. For real functions it follows that $r_{vx}(t) = r_{xv}(-t)$, and $r_{xx}(-t) = r_{xx}(t)$. We deduce that the autocorrelation function of a real signal is real and even, while that of a complex one has an even modulus and an odd argument.

1.21 Graphical Interpretation

We assume for simplicity the two functions $v(t)$ and $x(t)$ to be real. Consider the cross-correlation $r_{vx}(t)$. We have

$$r_{vx}(t) = \int_{-\infty}^{\infty} v(t + \tau) x(\tau) d\tau. \tag{1.48}$$

Similarly to the convolution operation we should represent graphically the two functions in the integrand, $x(\tau)$ and $v(t + \tau)$. To deduce the effect of replacing the variable t by $t + \tau$ we visualize the effect on a step function $u(t)$ and compare it with $u(t + \tau)$, as shown in Fig. 1.29.

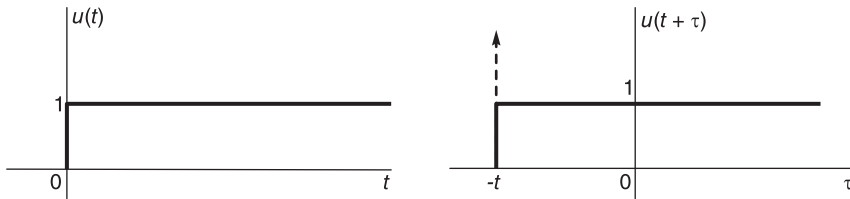


FIGURE 1.29 Unit step function and its mobile form $u(t + \tau)$.

We note that the effect of replacing t by $t + \tau$ is to simply displace the function to the point $\tau = -t$. Note that contrary to the convolution the function is not folded around the vertical axis but rather simply displaced. Moreover, the *mobile axis* represented by a dashed vertical line with an arrowhead is now at $\tau = -t$ instead of $\tau = t$.

Example 1.17 Evaluate the cross-correlation $r_{gf}(t)$ of the two causal functions

$$f(t) = e^{\alpha t} u(t), \quad g(t) = e^{\beta t} u(t)$$

where $\alpha, \beta < 0$.

We have

$$r_{gf}(t) = \int_{-\infty}^{\infty} g(t + \tau) f(\tau) d\tau.$$

The two functions are shown in Fig. 1.30.

Referring to Fig. 1.31 showing the stationary and mobile functions versus the τ axis we can write:

For $-t < 0$, i.e. $t > 0$

$$r_{gf}(t) = \int_0^{\infty} e^{\beta(t+\tau)} e^{\alpha\tau} d\tau = e^{\beta t} \left. \frac{e^{(\alpha+\beta)\tau}}{\alpha + \beta} \right|_0^{\infty} = \frac{-e^{\beta t}}{\alpha + \beta}, \quad (\alpha + \beta) < 0.$$

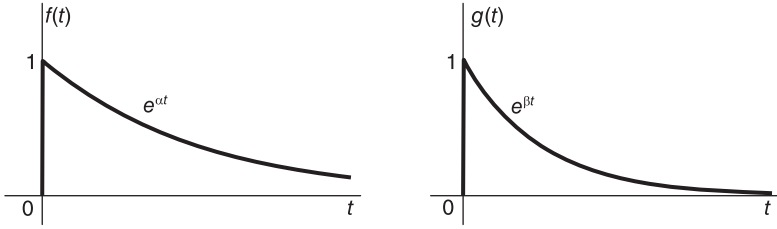


FIGURE 1.30 Two causal exponentials.

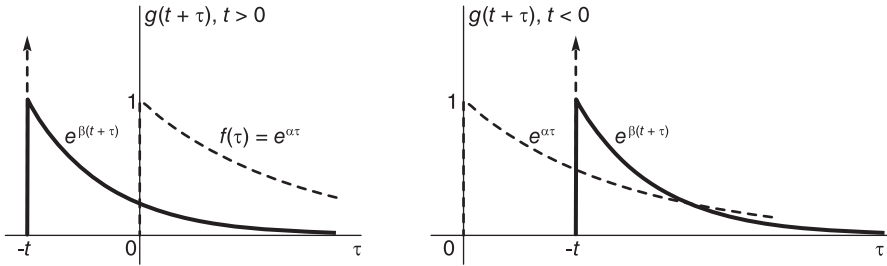


FIGURE 1.31 Correlation steps of two causal exponentials.

For $-t > 0$, i.e. $t < 0$

$$r_{gf}(t) = \int_{-t}^{\infty} e^{\alpha\tau} e^{\beta(t+\tau)} d\tau = e^{\beta t} \frac{e^{(\alpha+\beta)\tau}}{\alpha + \beta} \Big|_{-t}^{\infty} = \frac{-e^{-\alpha t}}{\alpha + \beta}, \quad (\alpha + \beta) < 0.$$

Analytic Approach

Alternatively we may employ an analytic approach. We have

$$r_{gf}(t) = \int_{-\infty}^{\infty} e^{\beta(t+\tau)} u(t+\tau) e^{\alpha\tau} u(\tau) d\tau.$$

The step functions in the integrand are non-nil if and only if $\tau > 0$ and $\tau > -t$, wherefrom the integrand is non-nil if $\tau > 0$ and $0 > -t$, i.e. $t > 0$, or if $\tau > -t$ and $-t > 0$, i.e. $t < 0$. We can therefore write

$$r_{gf}(t) = \int_0^{\infty} e^{\alpha\tau} e^{\beta(t+\tau)} d\tau u(t) + \int_{-t}^{\infty} e^{\alpha\tau} e^{\beta(t+\tau)} d\tau u(-t).$$

We note that these two integrals are identical to those deduced using the graphic approach. We thus obtain the equivalent result

$$r_{gf}(t) = \frac{-e^{\beta t}}{\alpha + \beta} u(t) - \frac{e^{-\alpha t}}{\alpha + \beta} u(-t), \quad (\alpha + \beta) < 0$$

which is shown in Fig. 1.32 for the case $\alpha = -0.5$ and $\beta = -1$.

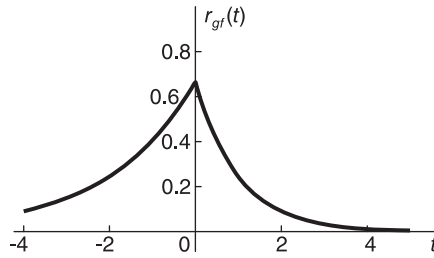


FIGURE 1.32 Correlation result $r_{gf}(t)$.

1.22 Correlation of Periodic Functions

The cross-correlation function $r_{vx}(t)$ of two periodic generally complex signals $v(t)$ and $x(t)$ of the same period of repetition T_0 is given by

$$r_{vx}(t) = \frac{1}{T_0} \int_{-T_0/2}^{T_0/2} v(t + \tau) x^*(\tau) d\tau. \quad (1.49)$$

The integral is evaluated over one period, for example, between $t = 0$ and $t = T_0$, the functions being periodic. The autocorrelation function is similarly given by

$$r_{xx}(t) = \frac{1}{T_0} \int_{-T_0/2}^{T_0/2} x(t + \tau) x^*(\tau) d\tau. \quad (1.50)$$

The auto- and cross-correlation functions are themselves periodic of the same period as can easily be seen through a graphical representation.

1.23 Average, Energy and Power of Continuous-Time Signals

The average or d-c value of a real signal $f(t)$ is by definition

$$\bar{f}(t) \triangleq \lim_{T \rightarrow \infty} \frac{1}{2T} \int_{-T}^T f(t) dt. \quad (1.51)$$

The *normalized energy*, or simply *energy*, E is given by

$$E = \int_{-\infty}^{\infty} f^2(t) dt. \quad (1.52)$$

A signal of finite energy is called an *energy signal*. The *normalized power* of an aperiodic signal is defined by

$$\bar{f^2}(t) \triangleq \lim_{T \rightarrow \infty} \frac{1}{2T} \int_{-T}^T f^2(t) dt. \quad (1.53)$$

A signal of finite normalized power is called a power signal. If the signal $f(t)$ is periodic of period T , its normalized power is given by

$$P = \bar{f^2}(t) = \frac{1}{T} \int_T f^2(t) dt \quad (1.54)$$

Note that a power signal has infinite energy; an energy signal has zero power. If the signal $f(t)$ is in volts, the power is in watts and the energy in joules.

Example 1.18 Evaluate the average value of the unit step function $f(t) = u(t)$.

We have

$$\bar{f}(t) = \lim_{T \rightarrow \infty} \frac{1}{2T} \int_{-T}^T f(t) dt = \lim_{T \rightarrow \infty} \frac{1}{2T} \int_0^T dt = 0.5$$

It is interesting to note that the average power of a sinusoid of amplitude A , such as $v(t) = A \sin(\beta t + \theta)$, is

$$\overline{v^2}(t) = \frac{A^2}{T} \int_0^T \sin^2(\beta t + \theta) dt \quad (1.55)$$

and since its period is $T = 2\pi/\beta$, the average power simplifies to $\overline{v^2}(t) = A^2/2$.

1.24 Discrete-Time Signals

Discrete-time signals will be dealt with at length in Chapter 6. We consider here only some basic properties of such signals. By convention, square brackets are used to designate sequences, for example, $v[n]$, $x[n]$, $f[n]$, \dots , in contrast with the usual parentheses used in designating continuous-time functions, such as $v(t)$, $x(t)$, $f(t)$, \dots . A discrete-time signal $x[n]$ is a *sequence* of values that are functions of the integer values $n = 0, \pm 1, \pm 2, \dots$ (See Fig. 1.33.) A sequence $x[n]$ may be the sampling of a continuous-time function $x_c(t)$ with a sampling interval of T seconds. In this case we have

$$x[n] = x_c(t) |_{t=nT} = x_c(nT). \quad (1.56)$$

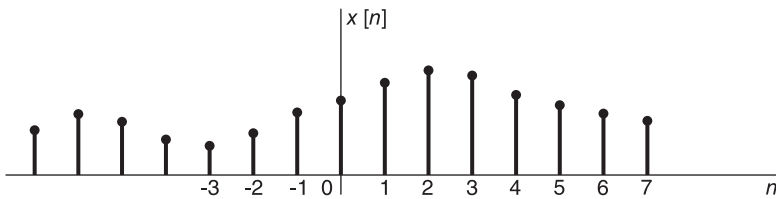


FIGURE 1.33 Discrete time signal.

Unit Step Sequence or Discrete Step The unit step sequence or discrete step is defined by

$$u[n] = \begin{cases} 1, & n \geq 0 \\ 0, & \text{otherwise} \end{cases} \quad (1.57)$$

and is shown in Fig. 1.34. We note that the unit step sequence is simpler in concept than the continuous-time Heaviside unit step function, being well defined, equal to 1, for $n = 0$.

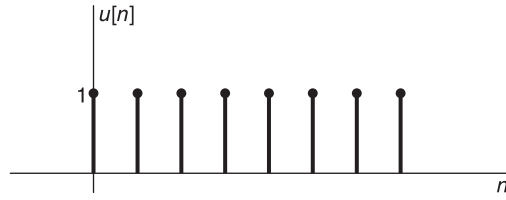


FIGURE 1.34 Unit step sequence.

Discrete impulse or unit sample sequence The discrete impulse, also referred to as the unit sample sequence, shown in Fig. 1.35, is defined by

$$\delta[n] = \begin{cases} 1, & n = 0 \\ 0, & \text{otherwise.} \end{cases} \quad (1.58)$$

We note, similarly, that the discrete impulse $\delta[n]$ is a much simpler concept than the continuous-time Dirac-delta function $\delta(t)$, the former being well defined equal to 1 at $n = 0$.

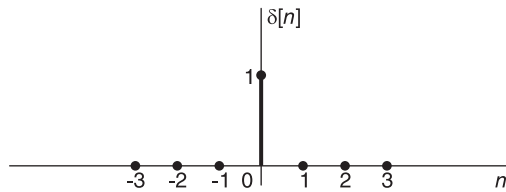


FIGURE 1.35 Discrete-time impulse or unit sample sequence.

1.25 Periodicity

Similarly to continuous-time functions a periodic sequence $x[n]$ of period N satisfies

$$x[n + kN] = x[n], \quad k = \pm 1, \pm 2, \pm 3, \dots \quad (1.59)$$

Example 1.19 Let $x[n] = \cos \gamma n$, $\gamma = \pi/8$. The period N of $x[n]$ is evaluated as the least value satisfying $x[n + N] = x[n]$, that is, $\cos[\gamma(n + N)] = \cos \gamma n$ or $\gamma N = 2k\pi$, k integer. The period N is the least value satisfying this condition, namely, $N = 2\pi/\gamma = 16$.

Sequences that have the form of periodic ones in the continuous-time domain may not be periodic in the discrete time domain.

Example 1.20 Is the sequence $x[n] = \cos n$ periodic?

To be periodic with period N it should satisfy the condition $\cos n = \cos(n + N)$. This implies that the value N should be a multiple of 2π , i.e. $N = 2k\pi$, k integer. Since π is an

irrational number, however, no value for k exists that would produce an integer value for N . The sequence is therefore not periodic.

The sum of two periodic sequences is in general periodic. Let $y[n] = v[n] + x[n]$, where $v[n]$ and $x[n]$ are periodic with periods K and M , respectively. The period N of the sum $y[n]$ is the least common multiple of K and M , i.e.

$$N = lcm(K, M). \quad (1.60)$$

If $y[n] = v[n]x[n]$, the value $N = lcm(K, M)$ is the period or a multiple of the period of $y[n]$.

1.26 Difference Equations

Similarly to continuous-time systems a dynamic discrete-time linear system is a system that has memory. Its response is not only function of the input but also of past inputs and outputs. A discrete-time dynamic linear system is in general described by one or more linear difference equations relating its input $x[n]$ and output $y[n]$, such as the equation

$$\sum_{k=0}^N d_k y[n-k] = \sum_{k=0}^M c_k x[n-k]. \quad (1.61)$$

We can extract the first term of the left-hand side in order to evaluate the output $y[n]$. We have

$$d_0 y[n] = - \sum_{k=1}^N d_k y[n-k] + \sum_{k=0}^M c_k x[n-k] \quad (1.62)$$

$$y[n] = - \sum_{k=1}^N a_k y[n-k] + \sum_{k=0}^M b_k x[n-k] \quad (1.63)$$

where

$$a_k = d_k/d_0, \quad b_k = c_k/d_0. \quad (1.64)$$

We note that the response $y[n]$ is a function of the past values $y[n-k]$ and $x[n-k]$, and not only of the input $x[n]$.

1.27 Even/Odd Decomposition

Similarly to continuous-time systems a given sequence may be decomposed into an even and an odd component as the following example illustrates.

Example 1.21 Given the sequence $h[n]$ defined by $h[n] = (1 + n^2)u[n] + e^{\alpha n}u[-n]$ with $\alpha > 0$, evaluate and sketch its even and odd parts.

We have, as depicted in Fig. 1.36.

$$h_e[n] = (1/2) [1 + n^2 + e^{-\alpha|n|}] \quad (1.65)$$

$$\begin{aligned}
 h_o(n) &= \frac{1}{2} [1 + n^2 - e^{-\alpha n}], \quad n \geq 0 \\
 &= \frac{1}{2} [e^{\alpha n} - 1 - n^2], \quad n \leq 0
 \end{aligned}
 \tag{1.66}$$

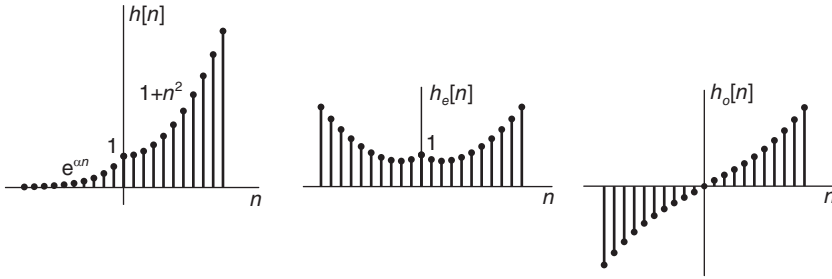


FIGURE 1.36 Even and odd parts of a general sequence.

1.28 Average Value, Energy and Power Sequences

The average value of a sequence $x[n]$ which may be denoted $\overline{x[n]}$ is by definition

$$\overline{x[n]} = \lim_{M \rightarrow \infty} \frac{1}{2M+1} \sum_{n=-M}^M x[n].
 \tag{1.67}$$

As we shall see in more detail in Chapter 12, a real sequence $x[n]$ is an energy sequence if it has a finite energy E which can be defined as

$$E = \sum_{n=-\infty}^{\infty} x[n]^2.
 \tag{1.68}$$

A real aperiodic sequence $x[n]$ is a power sequence if it has a finite average power P which may be defined as

$$P = \overline{x[n]^2} = \lim_{M \rightarrow \infty} \frac{1}{2M+1} \sum_{n=-M}^M x[n]^2.
 \tag{1.69}$$

If the sequence is periodic of period N it is a power sequence and its average power may be defined as

$$P = \overline{x[n]^2} = \frac{1}{N} \sum_{n=0}^{N-1} x[n]^2.
 \tag{1.70}$$

Note that an energy sequence has zero power and a power sequence has infinite energy.

1.29 Causality, Stability

Similarly to continuous-time systems, a discrete-time system is causal if its impulse response, also called unit sample response, $h[n]$ is causal, that is, if the impulse response is nil for $n < 0$. Moreover, a discrete-time system is stable if its impulse response is right-sided and $\lim_{n \rightarrow \infty} h[n] = 0$, or if its impulse response is left-sided and $\lim_{n \rightarrow -\infty} h[n] = 0$. We shall see in Chapter 6 that a system is stable if the Fourier transform $H(e^{j\Omega})$ of its impulse response $h[n]$ exists; otherwise the system is unstable. If the poles of the system transfer function $H(z)$ are on the unit circle in the z -plane, the system is critically stable.

Example 1.22 A causal system is described by the difference equation

$$y[n] - ay[n-1] = x[n].$$

Evaluate the system impulse response.

Since the system is causal its impulse response is nil for $n < 0$. To evaluate the impulse response we assume the input $x[n] = \delta[n]$, that is, $x[0] = 1$ and $x[n] = 0$, otherwise. With $n = 0$ we have $y[0] = x[0] = 1$ since $y[-1] = 0$, the system being causal. With $n = 1$ we have $x[1] = 0$ and $y[1] = ay[0] = a$. With $n = 2$ we have $y[2] = ay[1] = a^2$. Repeating this process for $n = 2, 3, \dots$ we deduce that the impulse response is given by

$$h[n] = y[n] = \begin{cases} a^n, & n = 1, 2, 3, \dots \\ 0, & \text{otherwise.} \end{cases}$$

which can be written in the form

$$h[n] = a^n u[n]$$

The z transform that is presented in Chapter 6 simplifies the evaluation of a system response $y[n]$ to a general input sequence $x[n]$, and its impulse response among others. The following chapters deal with continuous time and discrete time systems, their Fourier, Laplace and z transforms, signal and system mathematical models and solutions to their differential and difference equations.

1.30 Problems

Problem 1.1 What are the even and odd parts of the signal $v(t) = 10 \sin(3\pi t + \pi/5)$?

Problem 1.2 Let

$$f(t) = \begin{cases} 1, & 0 \leq t < 1 \\ 0.5t + 1, & -2 \leq t \leq 0 \\ 0, & \text{otherwise.} \end{cases}$$

Sketch the function $f(t)$ and

- $g(t) = f(-2t + 4)$
- $y(t) = f(-t/2 - 1)$.

Problem 1.3 Given the signals

$$f(t) = \begin{cases} t-1, & 1 \leq t \leq 2 \\ e^{-(t-2)}, & t \geq 2 \\ 0, & t \leq 1 \end{cases}$$

and $g(t) = f(t+3)$.

Draw the signals

a) $f(t)$ and $g(t)$

b) $f(-t)$ and $g(-t)$

c) $v(t) = f(2t)$, $w(t) = g(2t)$

d) $x(t) = f(2t+4)$, $y(t) = f(t/2+2)$

e) $p(t) = g(-2t+4)$, $r(t) = g(-t/2-2)$.

Re-do using Mathematica.

Problem 1.4 Let $f(t)$ be the function shown in Fig. 1.37 which is nil for $|t| > 2$.

Sketch

a) $f_1(t) = f(-t) - 2$, b) $f_2(t) = 2 - f(t+3)$, c) $f_3(t) = f(2t)$, d) $f_4(t) = f(t/3)$, e) $f_5(t) = f(-2t - 6)$, f) $f_6(t) = f(-2t + 8)$.

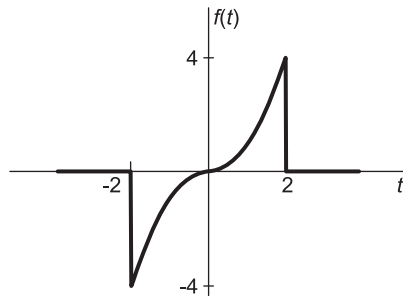


FIGURE 1.37 Function $f(t)$ of Problem 1.4

Problem 1.5 Sketch the functions $f_1(t) = u(-t-2)$, $f_2(t) = -u(-t+2)$, $f_3(t) = te^{-t}u(t)$, $f_4(t) = (t+2)e^{-(t+2)}u(t+2)$, $f_5(t) = (2t^2 - 12t + 22)u(3-t)$.

Problem 1.6 Sketch the functions

$u(t-1)$, $u(t+2)$, $u(1-t)$, $u(-2-t)$,

$e^{-t}u(t)$, $e^{-(t-1)}u(t-1)$, $e^{2t}u(2-t)$,

$\delta(t+2)$, $e^{-t}\delta(t+2)$, $e^{2t}d\delta(t)/dt$, $e^{2(t-3)}d\delta(t-3)/dt$

$\cos(8\pi t - \pi/3)$, $e^{-t}\cos(4\pi t + \pi/4)u(t)$

$\delta(2t)$, $e^t[\delta(t) + \delta(t-1)]$, $Sa(\pi t)$, $Sa[\pi(t-1)]$, $Sa(\pi t - 1)$, $x(2t)$ where $x(t) = AR_T(t)$.

Note that $x(t) d\delta(t)/dt = x(0) d\delta(t)/dt - \delta(t) dx(t)/dt|_{t=0}$

Problem 1.7 Given that $x(t) = 2(t+2)R_1(t+2) + 1.5e^{-0.2877t}u(t+1)$, sketch the functions $x(t-3)$, $x(t+3)$, $x(3-t)$, $x(-t)$, $x(-t-3)$, $x(t)\delta(t-1)$, $\int_{-\infty}^{\infty} x(\tau)\delta(\tau-t-1)d\tau$.

Problem 1.8 Let $f(t) = u(t)$. Represent graphically the functions $f(\tau)$, $f(t-\tau)$, $f(t+\tau)$ versus τ , assuming a) $t = 3$ and b) $t = -4$. Describe in words the kind of operations, such as reflection, shift, etc. that need be applied on $f(t)$ to produce each of these functions. Re-do the solution for the case $f(t) = e^{-t}u(t)$.

Problem 1.9 Sketch the signals

- a) $\delta(t) + \delta(t - 3)$ b) $e^t [\delta(t) + \delta(t - 1)]$ c) $e^t u(t - 2)$ d) $Sa(\pi t)$ e) $Sa[\pi(t - 1)]$
 f) $Sa[\pi t - 1]$

Problem 1.10 Evaluate the autocorrelation of the periodic function

$$x(t) = e^{-a|t|}, \quad -T_0/2 \leq t \leq T_0/2.$$

Problem 1.11 Evaluate and sketch the convolution

$$z(t) = x(t) * v(t)$$

and the cross-correlation $r_{vx}(t)$ of the two functions $v(t)$ and $x(t)$ given by :

$$v(t) = v_0(t) + 2\delta(t + 1)$$

where

$$v_0(t) = \begin{cases} 3, & 1 \leq t \leq 2 \\ 1, & 2 \leq t \leq 3 \\ 2, & 3 \leq t \leq 4 \\ 0, & \text{elsewhere,} \end{cases}$$

$$x(t) = \begin{cases} 1, & -5 \leq t \leq -3 \\ 2, & -3 \leq t \leq -2 \\ 3, & -2 \leq t \leq -1 \\ 0, & \text{elsewhere.} \end{cases}$$

Problem 1.12 Given the signals

$$v(t) = u(t + 2) - u(t - 1)$$

$$x(t) = (2 - t) \{u(t) - u(t - 2)\}$$

$$y(t) = y_1(t) + 2\delta(t - 1)$$

where

$$y_1(t) = \begin{cases} 1, & -3 \leq t \leq -2 \\ 2, & -2 \leq t \leq -1 \\ 0, & \text{otherwise} \end{cases}$$

evaluate the convolutions $z(t) = v(t) * x(t)$, $g(t) = v(t) * y(t)$ and the correlations $r_{xv} = x(t) \star v(t)$ and $r_{yv} = y(t) \star v(t)$. Verify the correlation results by comparing them with the corresponding convolutions.

Problem 1.13 Evaluate the cross-correlation $r_{vx}(t)$ of the two signals

$$v(t) = u(5 - t) \quad \text{and} \quad x(t) = e^{\alpha t} \{u(t + 5) - u(t - 5)\}.$$

Problem 1.14 Evaluate the cross-correlation $r_{vx}(t)$ of the two signals

$$x(t) = e^{1-t} u(t + 5) \quad \text{and} \quad v(t) = e^{-t-2} u(t - 5).$$

Problem 1.15 Let

$$x_0(t) = \begin{cases} 1, & 0 < t < T \\ -1, & T < t < 2T \\ 0, & \text{otherwise} \end{cases}$$

$$x(t) = \sum_{n=-\infty}^{\infty} x_0(t - 3nT)$$

$$y(t) = \Pi_{T/2}(t) = u(t + T/2) - u(t - T/2).$$

Sketch the convolution $z(t) = x(t) * y(t)$.

Problem 1.16 Evaluate the cross correlation $r_{vx}(t)$ of the two signals

$$x(t) = u(t - 2) \quad \text{and} \quad v(t) = \sin tu(4\pi - t).$$

Problem 1.17 Given $v(t) = \Pi_{\lambda/2}(t)$ and $x(t) = \sin \beta t$, with $\beta = 2\pi/T$

- a) evaluate the cross-correlation $r_{vx}(t)$ of the two signals $v(t)$ and $x(t)$.
- b) Under what condition would the cross-correlation $r_{vx}(t)$ be nil?

Problem 1.18 Evaluate and sketch the convolution $y(t)$ and the cross-correlation $r_{vx}(t)$ of the two functions

$$v(t) = \begin{cases} 3, & 1 \leq t \leq 4 \\ 3e^{-(t-4)}, & 4 \leq t \leq 7 \\ 0, & \text{otherwise} \end{cases}$$

$$x(t) = \begin{cases} t - 1, & 1 \leq t \leq 4 \\ (t - 7)^2 / 3, & 4 \leq t \leq 7 \\ 0, & \text{otherwise.} \end{cases}$$

Problem 1.19 Evaluate the convolution $z(t)$ and the cross correlation $r_{vx}(t)$ of the two signals

$$v(t) = e^{-\beta t}u(t - 4)$$

$$x(t) = e^{\alpha t}u(-t - 3)$$

with $\alpha > 0$ and $\beta > 0$. Sketch $z(t)$ and $r_{vx}(t)$ assuming that $x(-3) = v(4) = 0.5$.

Problem 1.20 Evaluate the period and the fundamental frequency of the signals

- (a) $2 \cos(t)$, (b) $5 \sin(2000\pi t + \pi/4)$, (c) $\cos(2000\pi t) + \sin(4000\pi t)$, (d) $\cos(2000\pi t) + \sin(3000\pi t)$, (e) $\sum_{n=-\infty}^{\infty} v(t - n/10)$, where $v(t) = R_{0.12}(t)$.

Problem 1.21 A system has the impulse response $g(t) = R_T(t - T)$. Sketch the impulse response and evaluate the system response $y(t)$ if its input $x(t)$ is given by

- a) $x(t) = \delta(t - T)$
- b) $x(t) = K$
- c) $x(t) = \sin(2\pi t/T)$
- d) $x(t) = \cos(\pi t/T)$
- e) $x(t) = u(t)$
- f) $x(t) = u(t) - u(-t)$.

Problem 1.22 Sketch the functions $x(t) = \Pi_2(t)$ and $y(t) = (1 - t)R_2(t)$ and evaluate

- a) $x(t) * x(t)$
- b) $x(t) * y(t)$
- c) $y(t) * y(t)$
- d) $r_{xy}(t)$
- e) $r_{yx}(t)$
- f) $r_{yy}(t)$.

Problem 1.23 A system has an impulse response $h(t) = 3e^{-t}R_{4.2}(t) + \delta(t - 4.2)$. Evaluate the system response to the input $x(t) = 2R_{3.5}(t)$

Evaluate the convolutions $z(t) = v(t) * x(t)$ and $w(t) = v(t) * y(t)$ where

$$x(t) = (2 - t)R_2(t)$$

$$y(t) = y_1(t) + 2\delta(t - 1)$$

and

$$y_1(t) = \begin{cases} 1, & -3 < t < -2 \\ 2, & -2 < t < -1 \\ 0, & \text{elsewhere} \end{cases}$$

Problem 1.24 Evaluate

- $2e^{-0.46t}u(t+2) * u(t-3)$
- $e^{0.55t}u(2-t) * e^{0.9t}u(1-t)$
- $0.25e^{-0.46t}u(t+3) * u(1-t)$
- $x(t)u(t) * y(t)u(t-T)$
- $y(t)u(t) \star x(t)u(t)$
- $y(t)u(-t) \star x(t)u(t)$
- $\sin(\pi t) \star \sin(\pi t)R_1(t)$.

Problem 1.25 Evaluate the convolution $z(t) = x(t) * v(t)$

where

$$x(t) = \begin{cases} 1, & 0 < t < 2 \\ -1, & 2 < t < 4 \\ 0, & \text{elsewhere} \end{cases}$$

and $v(t)$ is a periodic signal of period $T = 4$ sec. such that

$$v(t) = \begin{cases} 1 & 0 < t < 1 \\ 0 & 1 < t < 4 \end{cases}.$$

Problem 1.26 Evaluate the convolution

$$z(t) = v(t)x(t)$$

where

$$\begin{aligned} v(t) &= tR_T(t) \\ x(t) &= t^2R_{2T}(t) \end{aligned}$$

where $T = 1$ sec.

Problem 1.27 A system has the impulse response

$$h(t) = (1-t)\{u(t) - u(t-1)\}.$$

Evaluate the system output if the input is

$$x(t) = t\{u(t) - u(t-1)\}.$$

Problem 1.28 a) Evaluate the convolution

$$z(t) = x(t) * v(t)$$

and the cross-correlation $r_{xv}(t)$ of the two signals

$$\begin{aligned} x(t) &= \begin{cases} t, & 0 \leq t \leq 1 \\ 0, & \text{elsewhere} \end{cases} \\ v(t) &= \begin{cases} t, & 0 \leq t \leq 1 \\ 2-t, & 1 \leq t \leq 2 \\ 0, & \text{elsewhere.} \end{cases} \end{aligned}$$

b) Show that if the convolution $z(t)$ is known then the correlation $r_{xv}(t)$ for this example can be deduced directly thereof.

Problem 1.29 Let

$$x(t) = tR_T(t)$$

$$v(t) = 10e^{-t}R_T(t)$$

where

$$R_T(t) = u(t) - u(t - T)$$

and $T = 10$ sec. Evaluate and plot the convolution $v(t) * x(t)$ and the correlation $r_{xv}(t)$. Use Mathematica to evaluate the integrals. Verify the results using MATLAB.

Problem 1.30 a) Evaluate the cross-correlation $r_{wv}(t)$ of the signals

$$w(t) = (1 - t)u(t) + (t - 1)u(t - 1)$$

$$v(t) = tu(t) - 2(t - 1)u(t - 1) + (t - 2)u(t - 2).$$

Note : A graphic approach may simplify the solution.

b) Evaluate the convolution $z(t) = w(t) * v(t)$.

Problem 1.31 Evaluate the response of the system of which the impulse response is

$$h(t) = (e^{-t} - e^{-3t})u(t)$$

to the input

$$x(t) = e^{-t}u(t).$$

Problem 1.32 Evaluate the convolution of the signals $h(t)$ and $x(t)$ where

$$x(t) = h(t) = (1 - t)R_1(t) = (1 - t)\{u(t) - u(t - 1)\}.$$

Problem 1.33 Evaluate the impulse response of the electric circuit shown in Fig. 1.38.

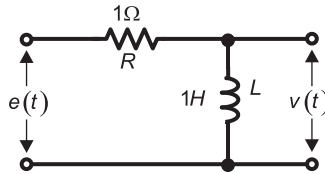


FIGURE 1.38 R-L circuit.

Deduce by convolution the response of the circuit to the input

$$e(t) = e^{-t}R_T(t) = e^{-t}[u(t) - u(t - T)], \text{ with } T = 1.$$

Verify the result T using a solution in Laplace domain.

Problem 1.34 Evaluate the convolution

$$z(t) = x(t) * y(t)$$

where

$$x(t) = e^{-at}R_T(t) = e^{-at}\{u(t) - u(t - T)\}$$

$T = 1$, and

$$y(t) = -R_2(t) = u(t) - u(t - 2).$$

Problem 1.35 Evaluate and sketch the convolution $z(t)$ and correlation $r_{xv}(t)$ of the signals $v(t)$ and $x(t)$ for the three cases :

a) $v(t) = \{2 - |t|\} \Pi_2(t) = \{2 - |t|\} \{u(t+2) - u(t-2)\}$

$$x(t) = 2 \sum_{n=-\infty}^{\infty} \delta(t - 1.5n).$$

b) $v(t)$ and $x(t)$ are periodic with period $T = 4$ sec, and

$$v(t) = x(t) = \begin{cases} 2, & |t| < 1 \\ 0, & 1 < |t| \leq 2. \end{cases}$$

c) $v(t)$ and $x(t)$ are periodic with period $T = 1$ sec, with

$$v(t) = \begin{cases} 1, & 0 < t < 0.5 \\ 0, & 0.5 < t < 1 \end{cases}$$

$$x(t) = e^{-2t}, \quad 0 < t < 1.$$

Problem 1.36 Show the correlation transition from simple correlation to cyclic by evaluating and plotting the autocorrelation of the signal.

$$f(t) = \Pi_{\tau/2}(t) = u(t + \tau/2) - u(t - \tau/2)$$

and that of

$$g(t) = \sum_{n=-\infty}^{\infty} f(t - nT)$$

with a) $T > 2\tau$ and b) $T = 1.5\tau$.

Problem 1.37 Evaluate and sketch the cross-correlation $r_{vx}(t)$ of the two signals

$$x(t) = -(t+10) \{u(-10-t) - u(-20-t)\} + 250e^{0.16t}u(-20-t)$$

and

$$v(t) = 1.64e^{-0.06t}u(t+30).$$

Problem 1.38 Evaluate the cross-correlation $r_{vx}(t)$ of the two signals

$$v(t) = u(t+3)$$

$$x(t) = 2\delta(t-6) + (0.5 - e^{2-t}) [u(t-2) - u(t-6)].$$

Problem 1.39 The objective is to evaluate the convolution $z(t)$ of the two functions $x(t) = 1 + \Pi_1(t)$ and $y(t) = \Pi_1(t)$.

a) Sketch the two functions.

b) Consider the result of evaluating dz/dt as the convolution of $[dx(t)/dt] * y(t)$ and then integrating the result to deduce $z(t)$.

Is this the proper value of convolution $z(t)$ of the two functions? If not, evaluate the true value and state the reason the suggested approach produces the wrong result.

Problem 1.40 A weak signal $s(t)$ that is of a finite duration $(0, 10^{-3})$ sec and zero elsewhere is transmitted at $t = 0$. It is then received with appreciable added noise after undergoing a delay of an unknown amount τ_0 . A radar-type receiver should evaluate the delay. It is proposed to apply the received signal, namely, the noise plus the delayed signal $s(t - \tau_0)$, to the input of a filter the impulse response of which is $h(t) = s(10^{-3} - t)$, that is, an impulse response corresponding to an inverted but realizable version of the signal $s(t)$.

State if the filter output does reveal the delay of the signal. Explain.

Problem 1.41 The video black and white signal $v(t)$ is a periodic signal of period $T = 1/15750$ sec defined by

$$v(t) = \begin{cases} 1.0, & 0 < t < 0.02T \\ 1.4, & 0.02T < t < 0.1T \\ 1.0, & 0.1T < t < 0.16T \\ 0, & 0.16T < t < T \end{cases}$$

Sketch the signal $v(t)$. Evaluate

- a) The average value $\overline{v(t)}$ of $v(t)$
- b) The average power $\overline{v^2(t)}$ of $v(t)$
- c) The energy E of $v(t)$ over one period.

Problem 1.42 Evaluate the average value, the average power and the total energy of each of the following signals

- a) $v_a(t) = 1 + 2 \cos(50\pi t) + 5 \sin(200\pi t + \pi/8)$
- b) $v_b(t) = 2R_5(t)$
- c) $v_c(t) = \sum_{n=-\infty}^{\infty} v_2(t - 10n)$
- d) The periodic ramp $v_d(t)$ shown in Fig. 1.39.

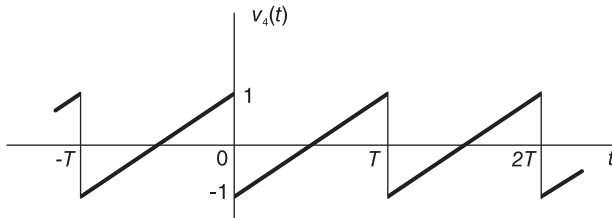


FIGURE 1.39 Periodic ramp.

Problem 1.43 Given the two signals

$x(t) = A_1 \cos(2\pi f_1 t + \theta_1)$ and $y(t) = A_2 \cos(2\pi f_2 t + \theta_2)$, where $0 \leq \theta_1 \leq 2\pi$, $0 \leq \theta_2 \leq 2\pi$, $f_1 > 0$ and $f_2 > 0$.

- 1. Let $v(t) = x(t) + y(t)$. Evaluate the average power $\overline{v^2(t)}$ of $v(t)$ for the two cases $f_1 = f_2$ and $f_1 \neq f_2$.
- 2. Let $z(t) = x(t) y(t)$. Evaluate the average power $\overline{z^2(t)}$ of $z(t)$ for the two cases $f_1 = f_2$ and $f_1 \neq f_2$.

Problem 1.44 Sketch each of the following periodic signals of period T and evaluate the average value and average power.

$$a) v(t) = \begin{cases} \sin 4\pi t/T, & 0 \leq t \leq T/4 \\ 0, & T/4 \leq t \leq T \end{cases}$$

$$b) w(t) = \sin \pi t/T, \quad 0 \leq t \leq T$$

$$c) x(t) = \begin{cases} -\sin 6\pi t/T, & 0 \leq t \leq T/3 \\ 0, & T/3 \leq t \leq T \end{cases}$$

$$d) y(t) = 4 - 2 \sin 2\pi t/T$$

e) With $T = 1$ and $t_0 = 0.0796$

$$z(t) = \begin{cases} \sin [2\pi(t - t_0)], & 0 < t < 2t_0, T/2 < t < T/2 + 2t_0 \\ 0 & 2t_0 \leq t \leq T/2, T/2 + 2t_0 < t < T. \end{cases}$$

Problem 1.45 Given the periodic signal $x(t)$ of period T

$$x(t) = \begin{cases} 6 - 15t/T, & 0 < t < T/5 \\ 3, & T/5 < t < 2T/5 \\ 0, & 2T/5 < t < T \end{cases}$$

Sketch the signal $x(t)$. Evaluate a) its average value, b) its average power, c) its total energy, d) its energy over one period.

Problem 1.46 The signal $x(t) = R_{0.001}(t)$ represents an electric potential given in volts versus the time t in seconds. Let

$$v(t) = \sum_{n=-\infty}^{\infty} x(t - nT).$$

Evaluate the period T ensuring that the average power of $v(t)$ be a) 0,8 watt, b) 8 Watt.

Problem 1.47 Given a periodic signal

$$x(t) = \begin{cases} 5, & 0 < t < 0.01, 0.03 < t < 0.04, 0.06 < t < 0.07 \\ -5, & 0.01 < t < 0.02, 0.05 < t < 0.06, 0.08 < t < 0.09 \\ 0, & 0.02 < t < 0.03, 0.04 < t < 0.05, 0.07 < t < 0.08, 0.09 < t < 0.1 \end{cases}$$

of which the values are given in volts versus t in seconds, with a period $T = 0.1$ sec.

1. Sketch the signal.
2. Evaluate the average value $\overline{x(t)}$ in volts .
3. Evaluate the average power $\overline{x^2(t)}$ in watts.
4. Evaluate the energy in joules over a one period.

Problem 1.48 Let $v(t) = x(t) + y(t)$, where $x(t)$ is the signal defined in Problem 1.47 and $y(t)$ is a periodic signal of period $T = 0.05$ sec,

$$y(t) = \begin{cases} 5, & 0 < t < 0.04 \\ 0, & 0.04 < t < 0.05 \end{cases}$$

1. Sketch $v(t)$ and evaluate its average value $\overline{v(t)}$.
2. Evaluate the average power $\overline{v^2(t)}$.
3. Evaluate the energy over a one period.

Problem 1.49 Let $z(t) = y(t) \sin(200\pi t)$, where $y(t)$ is the signal defined Problem 1.48.

1. Evaluate the average value $\overline{z(t)}$ in volts .
2. Evaluate the average power $\overline{z^2(t)}$ in watts.
3. Evaluate the energy in joules over a one period.

Problem 1.50 Given a periodic signal $x(t)$ with period T sec.

$$x(t) = \begin{cases} At/T, & 0 < t < \tau_0 \\ 0, & \tau_0 < t < T \end{cases}$$

where $\tau_0 = 0.75T$. Evaluate the average value $\overline{x(t)}$. A clipping of $x(t)$ produces the signal

$$y(t) = \begin{cases} At/T, & 0 < t < t_a \\ a_0 & t_a < t < \tau_0 \\ 0 & \tau_0 < t < T \end{cases}$$

with, $\tau_0 = 0.5T$ and $A = 1$. Sketch the signal $y(t)$ for $a_0 = 0.3A$. Find the value(s) of a_0 producing an average signal value of 0.1 Volt.

Problem 1.51 Consider the sequence $x[n] = u[n + 4]$.

- a) Sketch $x[m]$, $x[n - m]$ and $x[n + m]$ versus m for $n = 3$ and for $n = -5$.
- b) Repeat a) if $x[n] = 0.9^n u[n - 3]$.

Problem 1.52 a) Show that the sum of the energy of the even part $x_e[n]$ plus that of the odd part $x_o[n]$ of a sequence $x[n]$ is equal to the energy of the sequence itself.

b) Given the sequence $x[n] = 3a^n u[-n] - a^{-n} u[n]$, evaluate the even and odd parts x_e and x_o and their energies E_e and E_o , respectively, and compare the sum to the energy E of $x[n]$.

Problem 1.53 Evaluate the average values of the two sequences $x[n] = a^{-n} u[n]$, $a > 1$ and $y[n] = u[n]$.

Problem 1.54 Evaluate the energy of the sequence $x[n] = na^n u[-n]$, $a > 1$.

Problem 1.55 Evaluate the period of each the following sequences if it is periodic and show why it is aperiodic otherwise.

- a) $\sin(0.25\pi n - \pi/3)$
- b) $x[n] = \cos(0.5n + \pi/4)$
- c) $x[n] = \sin[(\pi/13)n + \pi/3] + \cos[(\pi/17)n - \pi/8]$
- d) $x[n] = \cos[(\pi/105)n + \pi/3] \sin[(\pi/133)n + \pi/4]$

Problem 1.56 A system is described by the difference equation

$$y[n] = ay[n - 1] + x[n]$$

Assuming zero initial conditions evaluate the impulse response $h[n]$ of the system, that is, the response $y[n]$ if the input is the impulse $x[n] = \delta[n]$.

1.31 Answers to Selected Problems

Problem 1.1

$$v_e(t) = 10 \sin(\pi/5) \cos 3\pi t = 5.878 \cos 3\pi t$$

$$v_o(t) = 10 \cos(\pi/5) \sin 3\pi t = 8.090 \sin 3\pi t$$

Problem 1.2 See Fig. 1.40.

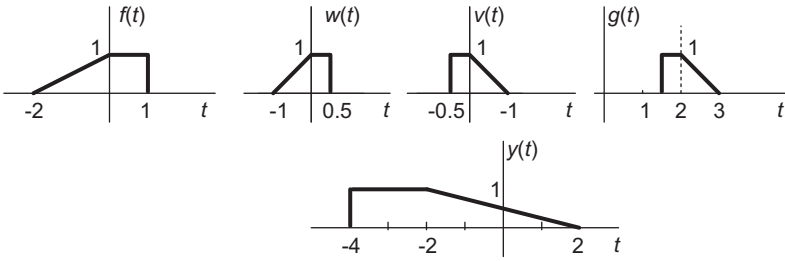


FIGURE 1.40 Functions of Problem 1.2.

Problem 1.3 See Fig. 1.41.

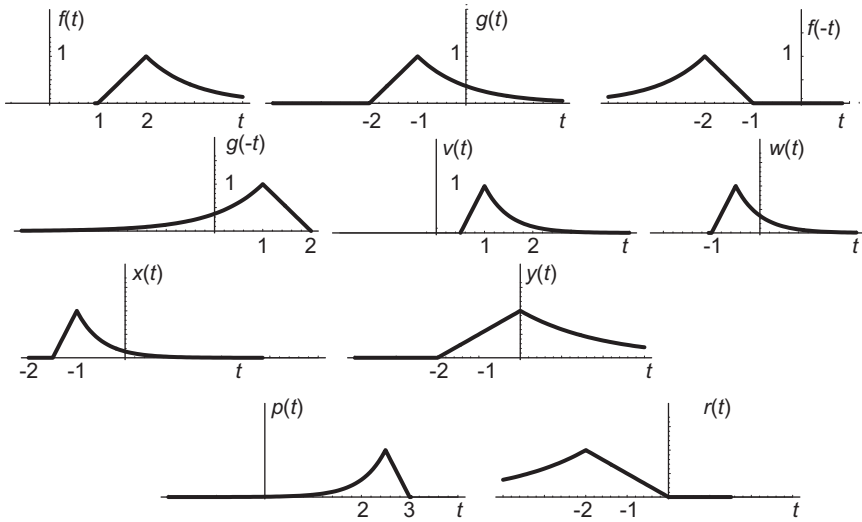


FIGURE 1.41 Functions of Problem 1.3.

Problem 1.4 See Fig. 1.42.

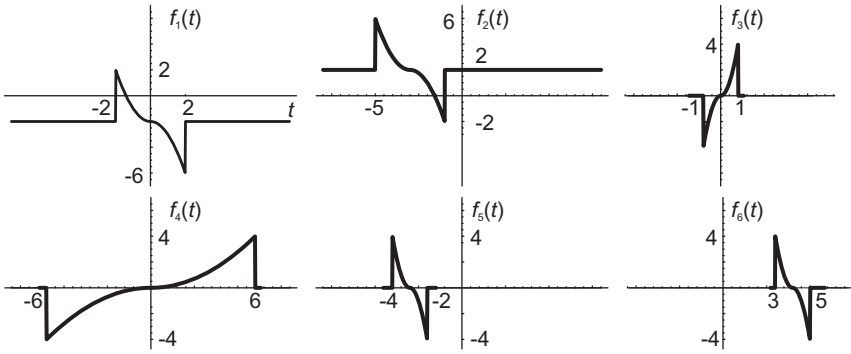


FIGURE 1.42 Functions of Problem 1.4.

Problem 1.5 See Fig. 1.43.

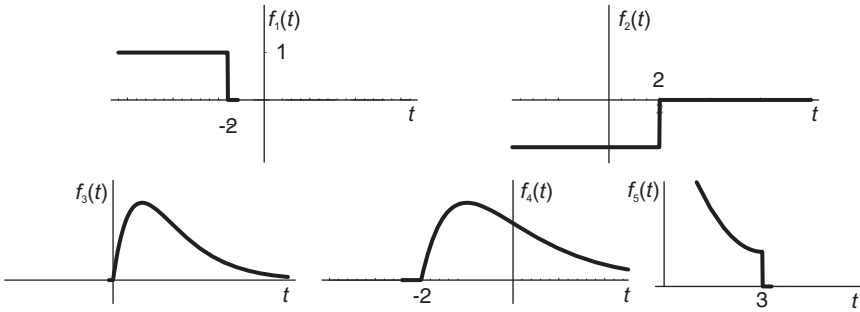


FIGURE 1.43 Functions of Problem 1.5.

Problem 1.6 See Fig. 1.44.

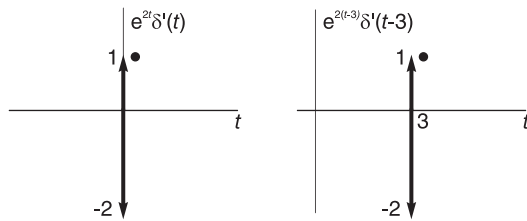


FIGURE 1.44 Partial answer to Problem 1.6.

Problem 1.8 See Fig. 1.45.

Problem 1.10

$$r_{xx}(t) = e^{at} \left[\frac{e^{-2at} - e^{-aT_0}}{2aT_0} \right] + (t/T_0) e^{-at} + e^{-at} \frac{1 - e^{2a(t-T_0/2)}}{2aT_0} + (t/T_0) e^{-aT_0+at}, \quad \text{for}$$

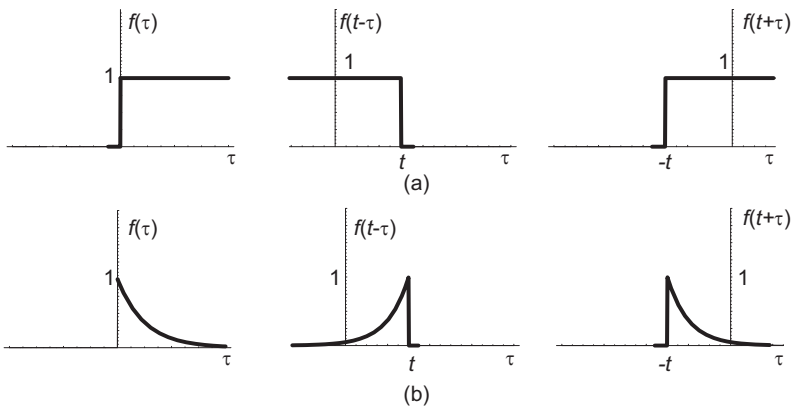


FIGURE 1.45 Functions of Problem 1.8.

$0 < t < T_0/2$. and $r_{xx}(-t) = r_{xx}(t)$, as shown in Fig. 1.46.

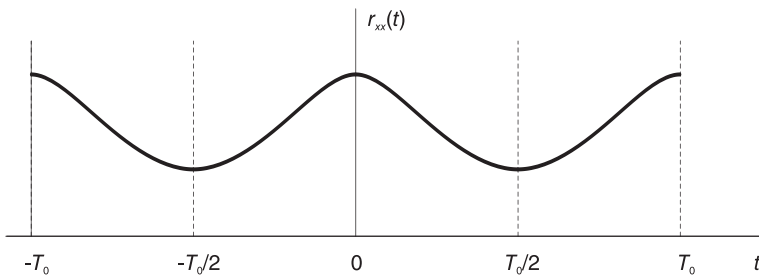


FIGURE 1.46 A periodic function for autocorrelation evaluation.

Problem 1.11 See Fig. 1.47.

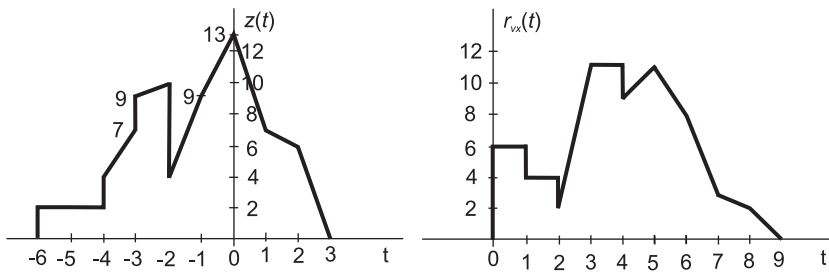


FIGURE 1.47 Results of Problem 1.11.

Problem 1.12 See Fig. 1.48.

Problem 1.15 See Fig. 1.49.

Problem 1.17

a) $r_{vx}(t) = -\lambda S_a(\lambda\beta/2) \sin \beta t$. b) $r_{vx}(t) = 0$ if $\lambda = kT$.

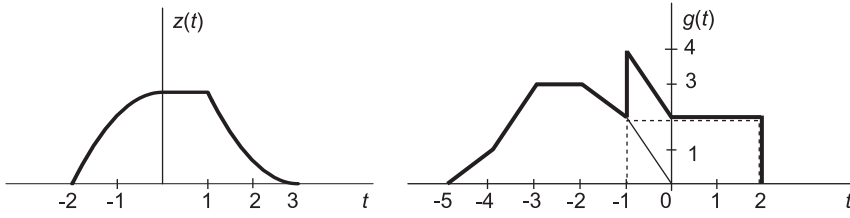


FIGURE 1.48 Functions of Problem 1.12.

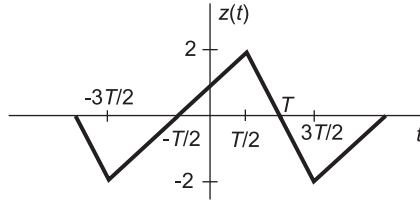


FIGURE 1.49 Functions of Problem 1.15.

Problem 1.18 See Fig. 1.50.

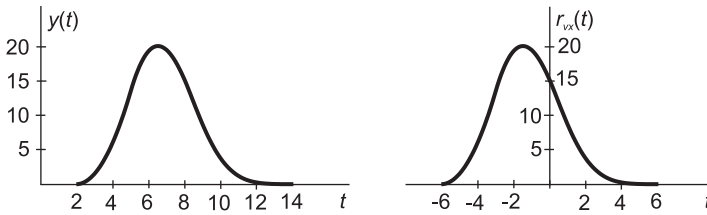


FIGURE 1.50 Functions of Problem 1.18.

Problem 1.20

- a) 6.283 s, 0.159 Hz. b) 1 ms, 1 kHz. c) 1 ms, 1 kHz. d) 2 ms, 500 Hz. e) 0.1 s, 10 Hz.

Problem 1.21

- a) $g(t - T)$, b) KT , c) 0, d) $(-2T/\pi) \sin(\pi t/T)$, e) 0 for $t \leq T$; $t - T$ for $T \leq t \leq 2T$; T for $t \geq 2T$, f) $-T$ for $t \leq T$; $2t - 3T$ for $T \leq t \leq 2T$; T for $t \geq 2T$.

Problem 1.22

- a) $t + 4$ for $-4 \leq t \leq 0$; $4 - t$ for $0 \leq t \leq 4$; 0 otherwise. b) $t^2/2 - t$ for $-2 \leq t \leq 0$; $t^2/2 - 3t + 4$ for $2 \leq t \leq 4$; 0 otherwise. c) $t^3/6 - t^2 + t$ for $0 \leq t \leq 2$; $-t^3/6 + t^2 - t - 4/3$ for $2 \leq t \leq 4$; 0 otherwise. d) $-t^2/2 + t$ for $0 \leq t \leq 2$; $t^2/2 + 3t + 4$ for $-4 \leq t \leq -2$; 0 otherwise. e) See part b). f) $-t^3/6 + t + 2/3$ for $-2 \leq t \leq 0$; $t^3/6 - t + 2/3$ for $0 \leq t \leq 2$; 0 otherwise.

Problem 1.23

- 0 for $t \leq 0$; $6 - 6e^{-t}$ for $0 \leq t \leq 3.5$; $192.7e^{-t}$ for $3.5 \leq t \leq 4.2$; $198.7e^{-t} + 1.91$ for $4.2 \leq t \leq 7.7$; 0 for $t > 7.7$.

Problem 1.24

- a) $\{10.91 - 4.35e^{-0.46(t-3)}\} u(t - 1)$, b) $\{4.05e^{0.55t} - 1.42e^{0.9t}\} u(3 - t)$, c) $2.16u(-2 - t) +$

$$0.86e^{-0.46t}u(t+2), \quad \text{d) } \left\{ \int_0^{t-T} x(\tau)y(t-\tau)d\tau \right\} u(t-T), \quad \text{e) } \left\{ \int_0^{\infty} x(\tau)y(t+\tau)d\tau \right\} u(t) + \left\{ \int_{-t}^{\infty} x(\tau)y(t+\tau)d\tau \right\} u(-t), \quad \text{f) } \left\{ \int_0^t x(\tau)y(t+\tau)d\tau \right\} u(-t), \quad \text{g) } (1/2)\cos(\pi t).$$

Problem 1.25 See Fig. 1.51.

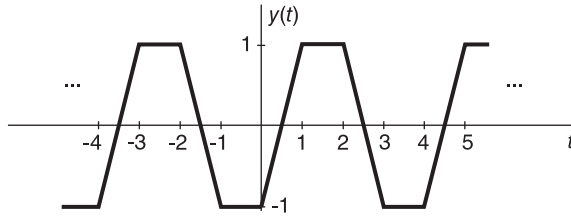


FIGURE 1.51 Convolution result of Problem 1.25.

Problem 1.38

0 for $t < 9$; $5.52 + t/2 - 148.4e^t$ for $-9 < t \leq -5$; 2.018 for $t \geq -5$.

Problem 1.39

See Fig.1.52.

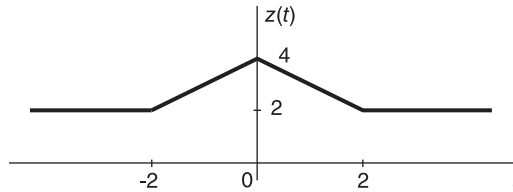


FIGURE 1.52 Convolution result of Problem 1.39.

Problem 1.40

$t = \tau_0 + 10^{-3}$ sec.

Problem 1.41

a) 0.192 V, b) 0.237 W, c) 15×10^{-6} J.

Problem 1.42

a) 1 V, 15.5 W, ∞ J. b) 0 V, 0 W, 20 J. c) 1 V, 2 W, ∞ J. d) 0 V, 0.33 W, ∞ J.

Problem 1.43

a) $0.5A_1^2 + 0.5A_2^2$ for $f_1 \neq f_2$; $0.5A_1^2 + 0.5A_2^2 + A_1A_2 \cos(\theta_1 - \theta_2)$, for $f_1 = f_2$. b) $0.25A_1^2A_2^2$ for $f_1 \neq f_2$; $0.25A_1^2A_2^2 + 0.125A_1^2A_2^2 \cos(2[\theta_1 - \theta_2])$ for $f_1 = f_2$.

Problem 1.44

a) 0.159 V, 0.125 W. b) 0.637 V, 0.5 W. c) 0 V, 0.167 W. d) 4 V, 18 W. e) 0 V, 28.8×10^{-3} W.

Problem 1.45

a) 1.5 V, b) 6 W, c) ∞ J, d) 2.4 J.

Problem 1.46

a) 5×10^{-3} s b) 0.75×10^{-3} s.

Problem 1.47

a) $\overline{x(t)} = 0$ volt, b) $\overline{x^2(t)} = 15$ watts, c) $E_x = 1.5$ joule.

Problem 1.48

a) $v(t) = x(t) + y(t)$, $\overline{v(t)} = 4$ V, b) $\overline{v^2(t)} = 35$ W, c) $E_v = 3.5$ J.

Problem 1.49

a) $\overline{z(t)} = 0$ V, b) $\overline{z^2(t)} = 10$ W, c) $E_z = 0.5$ J.

Problem 1.50

a) $A\tau_0^2/(2T^2)$. b) $a_0 = 0.2764$ or 0.7236 .

Problem 1.51

See Fig. 1.53.

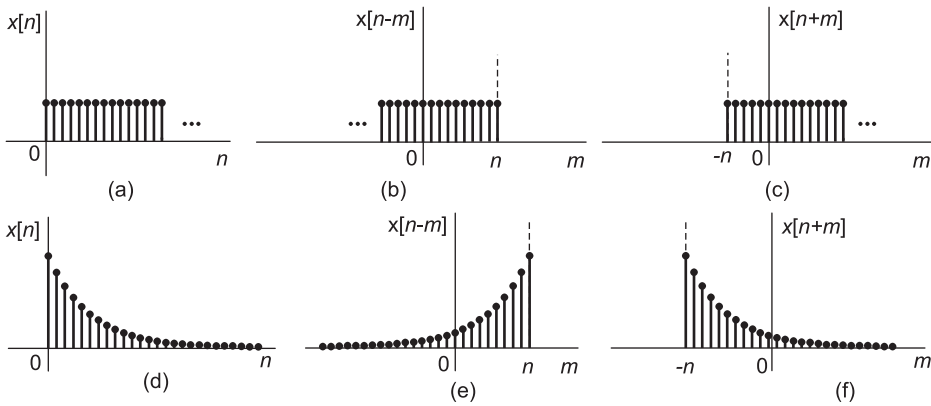


FIGURE 1.53 Sequences of Problem 1.51.

Problem 1.52

$$E = \sum_{n=1}^{\infty} a^{-2n} + \sum_{n=-\infty}^{-1} 9a^{2n} + 4 = (10a^{-2}/(1 - a^{-2})) + 4$$

$$E_e = \sum_{n=1}^{\infty} a^{-2n} + \sum_{n=-\infty}^{-1} a^{2n} + 4 = (2a^{-2}/(1 - a^{-2})) + 4$$

$$E_o = \sum_{n=1}^{\infty} 4a^{-2n} + \sum_{n=-\infty}^{-1} 4a^{2n} = 8a^{-2}/(1 - a^{-2}).$$

Problem 1.53

$$\overline{x[n]} = 0$$

$$\overline{y[n]} = 0.5$$

Problem 1.54

$$E = \sum_{m=0}^{\infty} m^2 b^m = b(1 + b)/(1 - b)^3 = a^{-2}(1 + a^{-2})/(1 - a^{-2})^3.$$

Problem 1.55

- a) $N = 8$. N is rational. The signal is periodic
- b) $N = 4\pi$. N is not rational. The signal is aperiodic
- c) $x[n]$ is periodic with a period $N = 442$.
- d) $x[n]$ is a product of two periodic signals, is periodic with a period $N = 3990$.

Problem 1.56

$$y[n] = a^n, \quad n \geq 0.$$

2

Fourier Series Expansion

A *finite duration*, or *periodic*, function $f(t)$ can in general be decomposed into a sum of trigonometric or complex exponential functions called Fourier series [31] [57] [71]. The Fourier series, which is then referred to as the *expansion* of the given function $f(t)$, will be denoted by the symbol $\hat{f}(t)$, in order to distinguish the expansion from the expanded function. The Fourier series $\hat{f}(t)$ is said to *represent* the given function $f(t)$ over its interval of definition.

In proving many properties of Fourier series there arises the need to interchange the order of integration or differentiation and summation. The property of infinite series or infinite integrals that ensures the validity of interchanging the order of integration and summation is *uniform convergence*. Throughout this book uniform convergence will be assumed, thus allowing the reversal of order of such operations.

2.1 Trigonometric Fourier Series

Let $f(t)$ be a time function defined for all values of the real variable t , that is, for $t \in (-\infty, \infty)$ such as the function shown in Fig. 2.1.

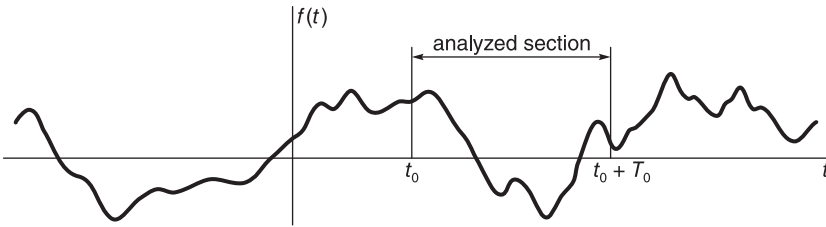


FIGURE 2.1 A function and an analysis interval.

A section of $f(t)$ of finite duration T_0 spanning the interval $(t_0, t_0 + T_0)$ can be *represented* as a trigonometric series $\hat{f}(t)$ such that

$$\hat{f}(t) = f(t), \quad t_0 < t < t_0 + T_0. \quad (2.1)$$

The Fourier series $\hat{f}(t)$ is given by:

$$\hat{f}(t) = a_0/2 + \sum_{n=1}^{\infty} (a_n \cos n\omega_0 t + b_n \sin n\omega_0 t) \quad (2.2)$$

where $\omega_0 = 2\pi/T_0$ and

$$a_n = \frac{2}{T_0} \int_{t_0}^{t_0+T_0} f(t) \cos n\omega_0 t \, dt$$

$$b_n = \frac{2}{T_0} \int_{t_0}^{t_0+T_0} f(t) \sin n\omega_0 t \, dt.$$
(2.3)

The part of $f(t)$ defined over the interval $(t_0, t_0 + T_0)$ which is analyzed in a Fourier series will be referred to as the *analysis section*. Physically, the coefficient $a_0/2$ measures the zero-frequency component of $f(t)$. The coefficients a_n and b_n are the amplitudes of the components $\cos n\omega_0 t$ and $\sin n\omega_0 t$ respectively, the n^{th} harmonics, of frequency $n\omega_0$, that is, n times the *fundamental frequency* $\omega_0 = 2\pi/T_0$, corresponding to the analysis interval of $f(t)$.

Note on Notation In referring to the trigonometric series coefficients of two functions such as $f(t)$ and $g(t)$ we shall use the symbols $a_{n,f}$ and $b_{n,f}$ to denote the coefficients of $f(t)$, and $a_{n,g}$ and $b_{n,g}$ for those of $g(t)$. When, however, only one function $f(t)$ is being discussed or when it is clear from the context that the function in question is $f(t)$ then for simplicity of notation we shall refer to them as a_n and b_n , respectively.

An alternative expression of the trigonometric Fourier series may be obtained by rewriting Equation (2.2) in the form

$$\begin{aligned} \hat{f}(t) &= a_0/2 + \sum_{n=1}^{\infty} \sqrt{a_n^2 + b_n^2} \left\{ \frac{a_n \cos n\omega_0 t}{\sqrt{a_n^2 + b_n^2}} + \frac{b_n \sin n\omega_0 t}{\sqrt{a_n^2 + b_n^2}} \right\} \\ &= a_0/2 + \sum_{n=1}^{\infty} \sqrt{a_n^2 + b_n^2} \cos \left\{ n\omega_0 t - \arctan \left(\frac{b_n}{a_n} \right) \right\} \\ &= C_0 + \sum_{n=1}^{\infty} C_n \cos(n\omega_0 t - \phi_n) \end{aligned}$$
(2.4)

$$C_0 = a_0/2, \quad C_n = \sqrt{a_n^2 + b_n^2} \quad \text{and} \quad \phi_n = \arctan(b_n/a_n).$$
(2.5)

These relations between the Fourier series coefficients are represented vectorially in Fig. 2.2.

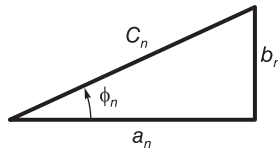


FIGURE 2.2 Fourier series coefficient C_n as a function of a_n and b_n .

2.2 Exponential Fourier Series

The section of the function $f(t)$ defined over the same interval $(t_0, t_0 + T_0)$ can alternatively be represented by an exponential Fourier series $\hat{f}(t)$ such that

$$\hat{f}(t) = f(t), \quad t_0 < t < t_0 + T_0$$
(2.6)

the exponential series having the form

$$\hat{f}(t) = \sum_{n=-\infty}^{\infty} F_n e^{jn\omega_0 t} \tag{2.7}$$

so that

$$f(t) = \sum_{n=-\infty}^{\infty} F_n e^{jn\omega_0 t}, \quad t_0 < t < t_0 + T_0 \tag{2.8}$$

where $\omega_0 = 2\pi/T_0$ and the coefficients F_n are given by

$$F_n = \frac{1}{T_0} \int_{t_0}^{t_0+T_0} f(t) e^{-jn\omega_0 t} dt. \tag{2.9}$$

The value T_0 is the Fourier series expansion *analysis interval* and $\omega_0 = 2\pi/T_0$ is the *fundamental frequency of the expansion*.

We note that the coefficient F_0 , given by

$$F_0 = \frac{1}{T_0} \int_{t_0}^{t_0+T_0} f(t) dt \tag{2.10}$$

is the average value (d-c component) of $f(t)$ over the interval $(t_0, t_0 + T_0)$. Moreover, we note that if the function $f(t)$ is real we have

$$F_{-n} = \frac{1}{T_0} \int_{t_0}^{t_0+T_0} f(t) e^{jn\omega_0 t} dt = F_n^*, \quad f(t) \text{ real} \tag{2.11}$$

where F_n^* is the conjugate of F_n . In other words

$$|F_{-n}| = |F_n|, \quad \arg[F_{-n}] = -\arg[F_n], \quad f(t) \text{ real.} \tag{2.12}$$

The phase angle $\arg[F_n]$ may be alternatively written $\angle[F_n]$. We shall adopt the notation

$$f(t) \xleftrightarrow{FSC} F_n \tag{2.13}$$

or simply

$$f(t) \longleftrightarrow F_n \tag{2.14}$$

to denote by F_n the exponential Fourier series coefficients (FSC) of $f(t)$. The notation $F_n = FSC[f(t)]$ will also be used occasionally. The following example shows that for basic functions we may deduce the exponential coefficients without having to perform an integration.

Example 2.1 Evaluate the exponential coefficients of $v(t) = A \sin(\beta t)$, $x(t) = A \cos(\beta t)$ and $y(t) = A \sin(\beta t + \theta)$ with an analysis interval equal to the function period.

The period of $v(t)$ is $T = 2\pi/\beta$. The analysis interval is the same value T and the fundamental frequency of the analysis is $\omega_0 = 2\pi/T = \beta$. We may write

$$v(t) = A \sin(\beta t) = A(e^{j\beta t} - e^{-j\beta t})/(2j) = \sum_{n=-\infty}^{\infty} V_n e^{jn\omega_0 t} = \sum_{n=-\infty}^{\infty} V_n e^{jn\beta t}. \tag{2.15}$$

Equating the coefficients of the exponentials in both sides we obtain the exponential series coefficients of $v(t) = A \sin(\beta t)$, namely,

$$V_n = \begin{cases} \mp jA/2, & n = \pm 1 \\ 0, & \text{otherwise} \end{cases}$$

Similarly, we obtain the exponential series coefficients of $x(t) = A \cos(\beta t)$

$$X_n = \begin{cases} A/2, & n = \pm 1 \\ 0, & \text{otherwise} \end{cases}$$

and those of $y(t) = \sin(\beta t + \theta)$

$$Y_n = \begin{cases} \mp(jA/2)e^{-j\pm\theta}, & n = \pm 1 \\ 0, & \text{otherwise} \end{cases}$$

These results are often employed and are thus worth remembering.

2.3 Exponential versus Trigonometric Series

To establish the relations between the exponential and trigonometric Series coefficients for a real function $f(t)$, we write

$$\hat{f}(t) = F_0 + (F_1 e^{j\omega_0 t} + F_{-1} e^{-j\omega_0 t}) + (F_2 e^{2j\omega_0 t} + F_{-2} e^{-2j\omega_0 t}) + \dots \quad (2.16)$$

$$F_n = |F_n| e^{j \arg[F_n]} \quad (2.17)$$

$$\begin{aligned} \hat{f}(t) = & F_0 + (|F_1| e^{j \arg[F_1]} e^{j\omega_0 t} + |F_1| e^{-j \arg[F_1]} e^{-j\omega_0 t}) \\ & + (|F_2| e^{j \arg[F_2]} e^{j2\omega_0 t} + |F_2| e^{-j \arg[F_2]} e^{-j2\omega_0 t}) + \dots \end{aligned} \quad (2.18)$$

$$\hat{f}(t) = F_0 + \sum_{n=1}^{\infty} 2 |F_n| \cos(n\omega_0 t + \arg[F_n]). \quad (2.19)$$

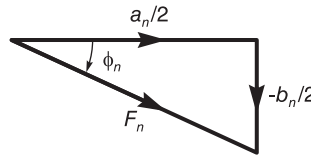


FIGURE 2.3 Fourier series coefficient F_n as a function of a_n and b_n .

Comparing this expression with (2.4) we have $F_0 = C_0 = a_0/2$; $|F_n| = C_n/2 = \sqrt{a_n^2 + b_n^2}/2$, $n > 0$; $\arg[F_n] = -\phi_n = -\arctan(b_n/a_n)$, $n > 0$. This relation can be represented vectorially as in Fig. 2.3. We can also write

$$F_n = (C_n/2)e^{-j\phi_n} = (1/2)(a_n - j b_n), \quad n > 0 \quad (2.20)$$

$$F_{-n} = (C_n/2)e^{j\phi_n} = (1/2)(a_n + j b_n), \quad n > 0. \quad (2.21)$$

as can be seen in Fig. 2.4.

The inverse relations are $C_0 = 2F_0$; $C_n = 2 |F_n|$, $n > 0$; $\phi_n = -\arg[F_n]$, $n > 0$; $a_0 = 2F_0$; $a_n = 2 \Re[F_n]$, $n > 0$; $b_n = -2 \Im[F_n]$, $n > 0$.

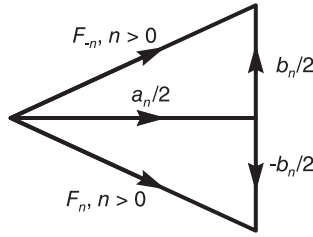


FIGURE 2.4 Fourier series coefficients F_n and F_{-n} as functions of a_n and b_n .

2.4 Periodicity of Fourier Series

As shown in Fig. 2.1 the function $f(t)$ outside the analysis interval is assumed to have any shape unrelated to its form within the interval. How then does the Fourier series $\hat{f}(t)$ compare with $f(t)$ outside the analysis interval? The answer to this question is straightforward. The Fourier series is periodic with period T_0 , and is none other than a *periodic extension*, that is, a periodic repetition, of the analysis section of $f(t)$. In fact

$$\hat{f}(t + kT_0) = \sum_{n=-\infty}^{\infty} F_n e^{jn\omega_0(t+kT_0)} = \sum_{n=-\infty}^{\infty} F_n e^{jn\omega_0 t} = \hat{f}(t) \tag{2.22}$$

since $e^{j2\pi nk} = 1$, n and k integers. The Fourier series $\hat{f}(t)$ appears as in Fig. 2.5 where it is simply the periodic extension of the analysis section shown in Fig. 2.1.

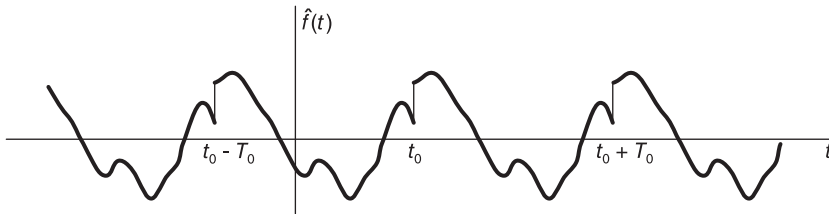


FIGURE 2.5 Periodic extension induced by Fourier series.

We note that if the function $f(t)$ is itself periodic with period T_0 then its Fourier series $\hat{f}(t)$, evaluated over one period as an analysis interval, is identical to the function $f(t)$ over the entire time axis t , and this is the case whatever the value of the starting point t_0 of the analysis interval. We therefore write

$$\hat{f}(t) = f(t), \quad -\infty < t < \infty, \quad f(t) \text{ periodic.} \tag{2.23}$$

$$F_n = \frac{1}{T_0} \int_{T_0} f(t) e^{-in\omega_0 t} dt \tag{2.24}$$

It is important to note that the Fourier series “sees” the given finite duration function as if it were periodically extended. In other words, the Fourier series is simply an expansion

of the periodic extension of the given function. In what follows, a periodic extension of the analyzed function is applied throughout, in order to view the function as the Fourier series sees it. We shall occasionally use the symbol $\tilde{f}(t)$ to denote the periodically extended version of the finite duration function $f(t)$. For a periodic function, the analysis interval is assumed to be, by default, equal to the function period.

We also note that we have assumed the function $f(t)$ to be continuous. If the function has finite discontinuities then in the neighborhoods of a discontinuity there exists what is called “Gibbs phenomenon.” which will be dealt with in Chapter 16. Suffice it to say that if $f(t)$ has a finite discontinuity at time $t = t_1$, say, then its Fourier series converges to the average value at the “jump” at $t = t_1$. In other words $\hat{f}(t_1) = \{f(t_1^+) + f(t_1^-)\} / 2$.

Example 2.2 For the function $f(t)$ given by

$$f(t) = \begin{cases} A(t - 0.5), & 0 < t \leq 1 \\ A/2, & t \leq 0 \text{ and } t \geq 1 \end{cases}$$

shown in Fig. 2.6 evaluate (a) the trigonometric and (b) the exponential Fourier series expansions $\hat{f}(t)$ of $f(t)$ on the interval $(0, 1)$.

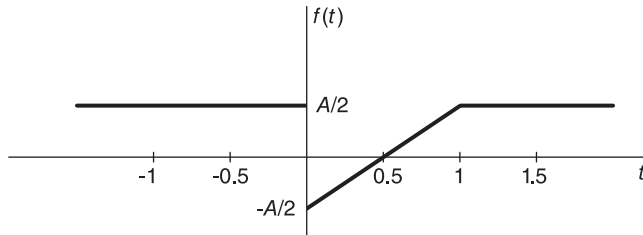


FIGURE 2.6 Function $f(t)$.

By performing a periodic extension we obtain a periodic ramp of a period equal to 1 second, which is the form of the sought expansion $\hat{f}(t)$.

(a) Trigonometric series

$$a_n = 2A \int_0^1 (t - 0.5) \cos n\omega_0 t \, dt = 0$$

$$b_n = 2A \int_0^1 (t - 0.5) \sin(2\pi n t) \, dt = -\frac{A}{\pi n}.$$

Hence

$$\hat{f}(t) = \sum_{n=1}^{\infty} \left(\frac{-A}{\pi n} \right) \sin 2\pi n t.$$

$$f(t) = A(t - 0.5) = \frac{-A}{\pi} \sum_{n=1}^{\infty} \frac{\sin 2\pi n t}{n}, \quad 0 < t < 1.$$

Moreover, if $\tilde{f}(t)$ refers to the periodic extension of $f(t)$ then it has discontinuities at $t = 0, \pm 1, \pm 2, \dots$ wherefrom

$$\hat{f}(0) = \hat{f}(1) = \left\{ \tilde{f}(0^+) + \tilde{f}(0^-) \right\} / 2 = (A/2 - A/2) = 0.$$

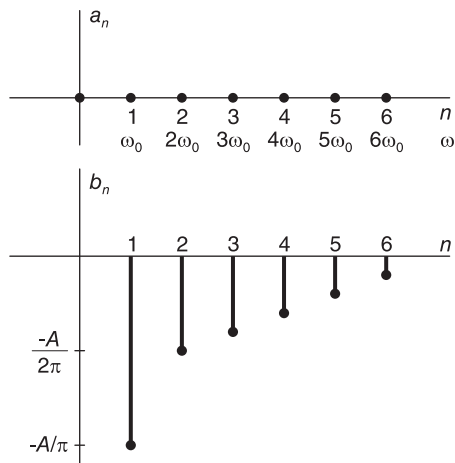


FIGURE 2.7 Fourier series coefficient a_n and b_n of Example 2.2.

The coefficients a_n and b_n are represented graphically in Fig. 2.7.

(b) Exponential series

$$F_n = \int_0^1 A(t - 0, 5) e^{-j2\pi nt} dt = jA/(2\pi n), \quad n \neq 0$$

$$|F_n| = A/(2\pi |n|), \quad n \neq 0; \quad \arg[F_n] = \begin{cases} \pi/2, & n > 0 \\ -\pi/2, & n < 0. \end{cases}$$

$$F_0 = \int_0^1 A(t - 0, 5) dt = 0.$$

$$\hat{f}(t) = \frac{jA}{2\pi} \sum_{n = -\infty, n \neq 0}^{\infty} \frac{1}{n} e^{j2\pi nt}$$

and

$$\hat{f}(t) = \begin{cases} f(t) = A(t - 0, 5), & 0 < t < 1 \\ 0, & t = 0 \text{ and } t = 1. \end{cases}$$

The exponential coefficients are shown in Fig. 2.8.

The form of $\hat{f}(t)$, identical to the periodic extension $\tilde{f}(t)$ of $f(t)$, is shown in Fig. 2.9.

As we shall see shortly, the periodic ramp has odd symmetry about the origin $t = 0$, which explains the fact that the coefficients a_n are nil and the exponential coefficients F_n are pure imaginary.

2.5 Dirichlet Conditions and Function Discontinuity

A function $f(t)$ that is of finite duration, and equivalently its periodic extension $\tilde{f}(t)$, which satisfies the Dirichlet conditions, can be expanded in a Fourier series. To satisfy the Dirichlet conditions the function has to be bounded in value, and be single-valued, that is,

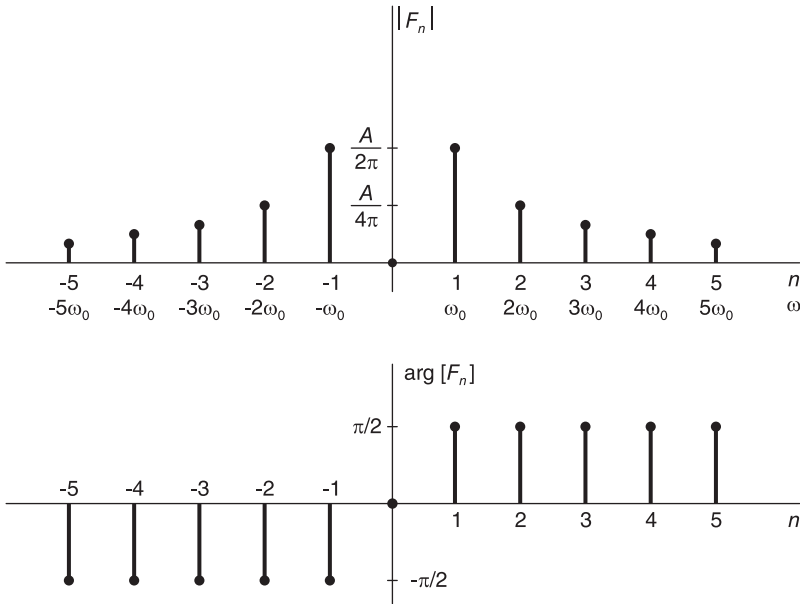


FIGURE 2.8 Fourier series coefficient F_n of Example.

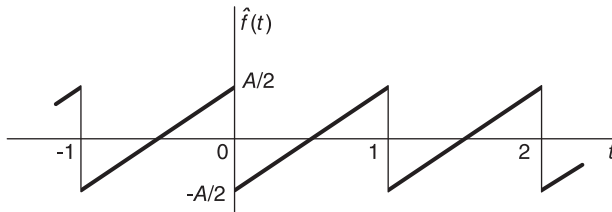


FIGURE 2.9 Periodic extension of the analysis section as seen by Fourier series.

continuous, or else have a finite number of finite jump discontinuities, and should have at most a finite number of maxima and minima. Consider three functions, assuming that the interval of analysis is, say, $(-1, 1)$, thus containing the point of origin, $t = 0$. The first, $f_1(t) = Ae^{-t}u(t)$, shown in Fig. 2.10, is discontinuous at $t = 0$. Since the jump discontinuity A is finite the function does not tend to infinity for any value of t and is therefore *bounded* in value, thus satisfying the Dirichlet conditions.

The second function $f_2(t) = 1/t$ not only has a discontinuity at $t = 0$, it is *not bounded* at $t = 0$, tending to $+\infty$ if t is positive and $t \rightarrow 0$, and to $-\infty$ if t is negative and $t \rightarrow 0$. This function does not, therefore, satisfy the Dirichlet conditions. The third function $f_3(t) = \cos(1/t)$, as can be seen in the figure, tends to unity as $t \rightarrow \pm\infty$. However, as $t \rightarrow 0$ through positive or negative values, the argument $1/t$ increases rapidly so that $f_3(t)$ increases in frequency indefinitely producing an infinite number of Maxima and minima. This function does not, therefore, satisfy the Dirichlet conditions.

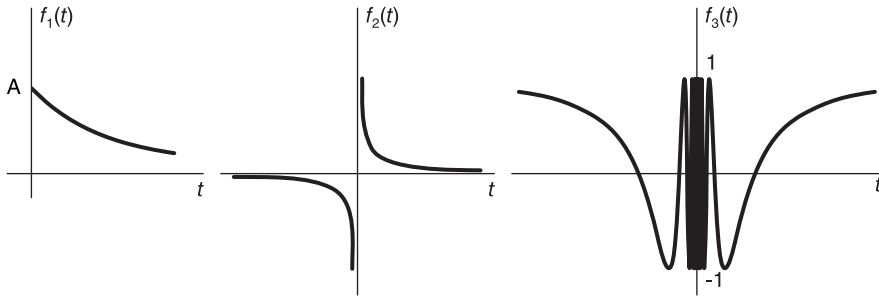


FIGURE 2.10 Functions illustrating Dirichlet conditions.

2.6 Proof of the Exponential Series Expansion

To prove that the Fourier series coefficients are given by Equation (2.7) multiply both sides of the equation by $e^{-jk\omega_0 t}$, obtaining

$$\hat{f}(t) e^{-jk\omega_0 t} = \sum_{n=-\infty}^{\infty} F_n e^{jn\omega_0 t} e^{-jk\omega_0 t}. \tag{2.25}$$

Integrating both sides over the interval $(t_0, t_0 + T_0)$ and using Equation (2.8) we have

$$\int_{t_0}^{t_0+T_0} \hat{f}(t) e^{-jk\omega_0 t} dt = \int_{t_0}^{t_0+T_0} f(t) e^{-jk\omega_0 t} dt = \int_{t_0}^{t_0+T_0} \sum_{n=-\infty}^{\infty} F_n e^{j(n-k)\omega_0 t} dt.$$

Interchanging the order of integration and summation and using the property

$$\int_{t_0}^{t_0+T_0} e^{jm\omega_0 t} dt = \begin{cases} 0, & m \neq 0 \\ T_0, & m = 0. \end{cases} \tag{2.26}$$

we have

$$\int_{t_0}^{t_0+T_0} f(t) e^{-jk\omega_0 t} dt = T_0 F_k \tag{2.27}$$

and a replacement of k by n completes the proof.

2.7 Analysis Interval versus Function Period

Given a periodic signal, we consider the effect of performing an expansion using an analysis interval that is a multiple of the signal period. The fundamental frequency of a periodic function $f(t)$ of period τ_0 will be denoted ω_0 , i.e. $\omega_0 = 2\pi/\tau_0$. If a Fourier series expansion, with analysis interval T_0 equal to the function period τ_0 as usual, is performed, the Fourier series has a fundamental frequency of analysis equal to the signal fundamental frequency ω_0 . The Fourier series coefficients in this case are the usual coefficients F_n . In particular, we have

$$f(t) = \sum_{n=-\infty}^{\infty} F_n e^{jn\omega_0 t} \tag{2.28}$$

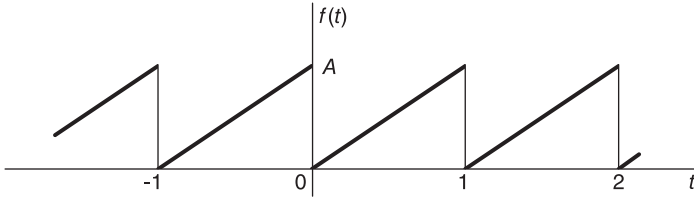


FIGURE 2.11 Periodic ramp.

Consider now the Fourier series expansion using an analysis interval $T_1 = m\tau_0$. In this case let us denote by Ω_0 this Fourier series fundamental frequency of analysis, and by G_n the Fourier series coefficients. We have $\Omega_0 = 2\pi/T_1 = \omega_0/m$ and we may write

$$f(t) = \sum_{n=-\infty}^{\infty} F_n e^{jn\omega_0 t} = \sum_{k=-\infty}^{\infty} G_k e^{jk\Omega_0 t} = \sum_{k=-\infty}^{\infty} G_k e^{jk\omega_0 t/m}. \quad (2.29)$$

Comparing the powers of the exponentials on both sides we note that the equation is satisfied if and only if $G_0 = F_0$, $G_m = F_1$, $G_{2m} = F_2$, \dots , $G_{rm} = F_r$, r integer, i.e.

$$G_n = \begin{cases} F_{n/m}, & n = r m, \text{ i.e. } n = 0, \pm m, \pm 2m, \dots \\ 0, & \text{otherwise.} \end{cases} \quad (2.30)$$

In other words

$$G_n = \begin{cases} F_{n/m} |_{n \rightarrow n/m}, & n = 0, \pm m, \pm 2m, \dots \\ 0, & \text{otherwise.} \end{cases} \quad (2.31)$$

The coefficients G_n are therefore all nil except for those where n is a multiple of m . Moreover, $G_0 = F_0$, $G_{\pm m} = F_{\pm 1}$, $G_{\pm 2m} = F_{\pm 2}$, \dots

Example 2.3 Evaluate the Fourier series coefficients of the function $f(t)$ shown in Fig. 2.11 over an analysis interval i) $T_0 = 1$ second and ii) $T_0 = 3$ seconds. i) We note that the analysis section of $f(t)$, which we can take as that bounded between $t = 0$ and $t = 1$, is the same as that of $f(t)$ of Example 2.2 (Fig. 2.9) except for a vertical shift of $A/2$.

We may therefore write

$$F_n = \begin{cases} A/2, & n = 0 \\ jA/(2\pi n), & n \neq 0. \end{cases}$$

The modulus $|F_n|$ and phase $\arg[F_n]$ are shown in Fig. 2.12.

ii) We have $T_0 = 3\tau_0$ and, from Equation (2.31),

$$G_n = \begin{cases} A/2, & n = 0 \\ F_{n/m} |_{n \rightarrow n/3} = j3A/(2\pi n), & n = \pm 3, \pm 6, \pm 9, \dots \\ 0, & \text{otherwise} \end{cases}$$

The modulus $|G_n|$ and phase $\arg[G_n]$ are shown in Fig. 2.13.

2.8 Fourier Series as a Discrete-Frequency Spectrum

The Fourier series exponential coefficients $|F_n|$ and $\arg[F_n]$, or trigonometric ones, a_n and b_n , as seen plotted versus the index n represent the frequency spectrum of the function $f(t)$.

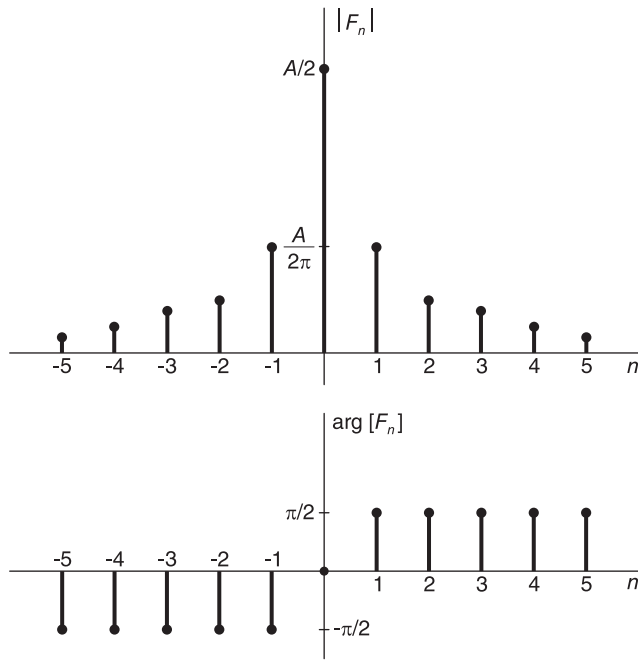


FIGURE 2.12 Fourier series coefficients of the periodic ramp.

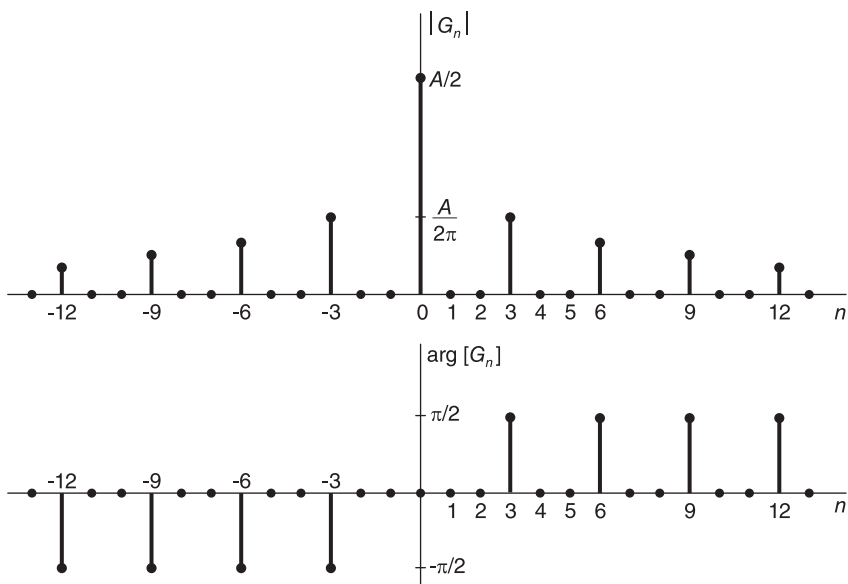


FIGURE 2.13 Fourier series coefficients of periodic ramp with analysis interval triple its period.

The abscissa of the graph represents, in fact, the frequency ω in r/sec, such that the values $n = \pm 1$ correspond to $\omega = \pm\omega_0$, the values $n = \pm 2$ correspond to $\omega = \pm 2\omega_0$, and so on. The student may have noticed such labeling of the abscissa in Fig. 2.8 in relation to Example 2.2. We note, moreover, that the Fourier series spectrum is defined only for multiples of the fundamental frequency ω_0 . The Fourier series thus describes a *discrete spectrum*.

Example 2.4 Show that the result of adding the fundamental and a few harmonics of Example 2.2 converges progressively toward the analyzed ramp.

We have found the expansion of a ramp

$$f(t) = -\frac{A}{\pi} \sum_{n=1}^{\infty} \frac{\sin 2\pi n t}{n}.$$

We note that the fundamental component is $-(A/\pi) \sin 2\pi t$, of period 1 sec., the period of repetition T_0 of $f(t)$, as it should be. The second harmonic, $-A/(2\pi) \sin 4\pi t$, has a period equal to 0.5 sec., that is $T_0/2$, and amplitude $A/(2\pi)$, that is, half that of the fundamental component. Similarly, the third harmonic $-A/(3\pi) \sin 6\pi t$, has a period $1/3$ sec. = $T_0/3$ and has an amplitude $1/3$ of that of the fundamental; and so on. All these facts are described, albeit in different forms, by the frequency spectra shown in Fig. 2.14. Part (a) of the figure shows the first four and the 20th harmonic of the Fourier series expansion of $f(t)$. Part (b) shows the results of cumulative additions of these spectral components up to 20 components. In this figure, every graph shows the result of adding one or more harmonics to the previous one. We see that the Fourier series converges rapidly toward the periodic ramp $f(t)$.

2.9 Meaning of Negative Frequencies

We encounter negative frequencies only when we evaluate the exponential form of Fourier series. To represent a sinusoid in complex exponential form we need to add the conjugate $e^{-jk\omega_0 t}$ to each exponential $e^{jk\omega_0 t}$ to form the sinusoid. Neither the positive frequencies $k\omega_0$ nor the negative ones $-k\omega_0$ have any meaning by themselves. Only the combination of the two produces a sinusoid of a meaningful frequency $k\omega_0$.

2.10 Properties of Fourier Series

Table 2.1 summarizes basic properties of the exponential Fourier series, but can be rewritten in a slightly different form for the trigonometric series, as we shall shortly see. The properties are stated with reference to a function $f(t)$ that is periodic of period T_0 and fundamental frequency $\omega_0 = 2\pi/T$.

2.10.1 Linearity

This property states that the Fourier series coefficients of the (weighted) sum of two functions is the sum of the (weighted) coefficients of the two functions. i.e. $a_1 f(t) + a_2 g(t) \longleftrightarrow a_1 F_n + a_2 G_n$ where a_1 and a_2 are constants.

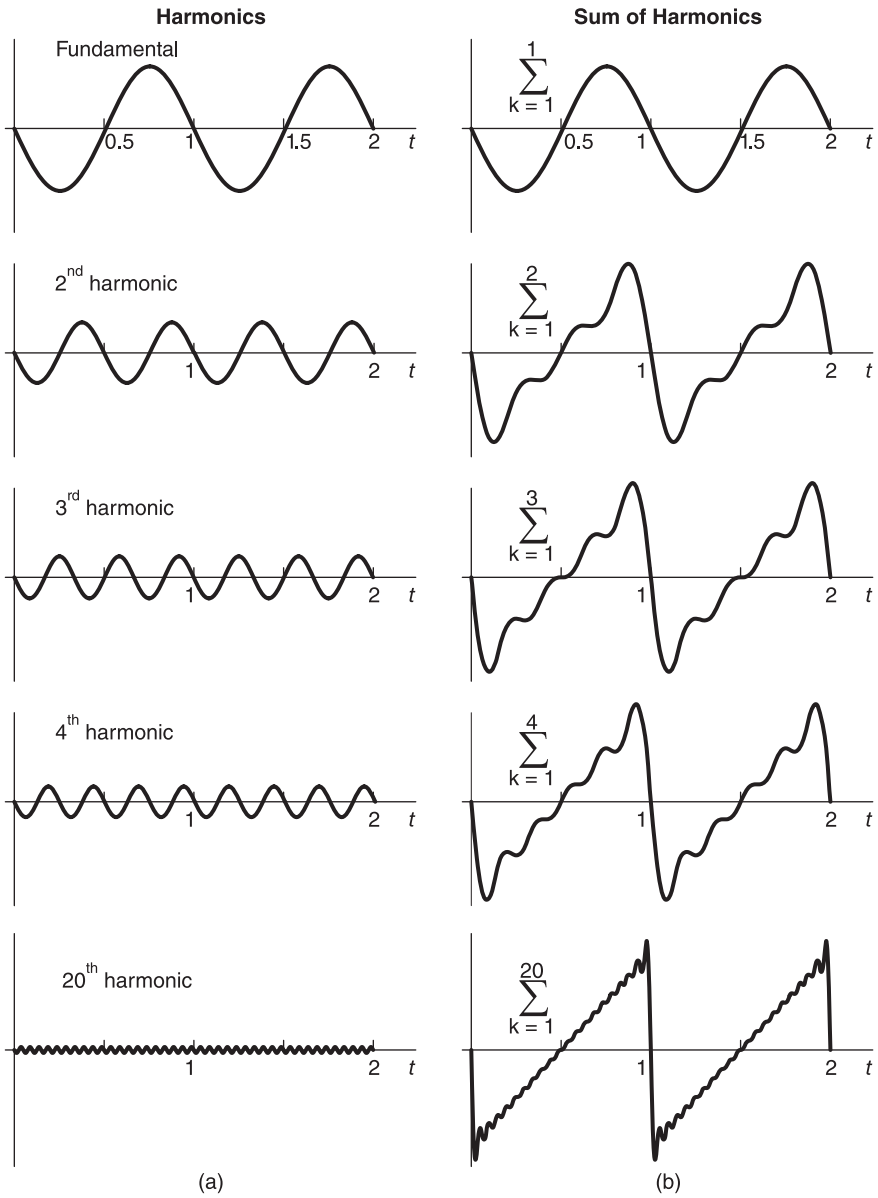


FIGURE 2.14 Result of cumulative addition of harmonics.

TABLE 2.1 Properties of Fourier series of a periodic function with analysis interval T_0 equal to the function period, and $\omega_0 = 2\pi/T_0$

Function $f(t)$	Fourier series coefficients
$af(t) + bg(t)$	$aF_n + bG_n$
$f(t - t_0)$	$F_n e^{-jn\omega_0 t_0}$
$e^{jm\omega_0 t} f(t)$	F_{n-m}
$f^*(t)$	F_{-n}^*
$f(-t)$	F_{-n}
$f(at), a > 0, \left(\text{period } \frac{T_0}{a}\right)$	F_n
$\frac{1}{T_0} \int_{T_0} f(\tau)g(t - \tau)d\tau$	$F_n G_n$
$f(t)g(t)$	$\sum_{m=-\infty}^{\infty} F_m G_{n-m}$
$f(t)$ real	$F_{-n} = F_n^*$
$\frac{df(t)}{dt}$	$j n \omega_0 F_n$
$\int_{-\infty}^t f(t)dt, F_0 = 0$	$\frac{1}{jn\omega_0} F_n$

2.10.2 Time Shift

The time shift property states that $g(t) = f(t - t_0) \longleftrightarrow F_n e^{-jn\omega_0 t_0}$.

Proof For simplicity the amount of time shift t_0 is taken to be not more than one period T_0 ; see Fig. 2.15. The more general case directly follows. We have

$$G_n = \frac{1}{T_0} \int_{t_0}^{t_0+T_0} f(t - t_0) e^{-jn\omega_0 t} dt. \quad (2.32)$$

Setting $t - t_0 = u$ completes the proof. The trigonometric coefficients are

$$a_{n,g} = a_{n,f} \cos n\omega_0 t_0 - b_{n,f} \sin n\omega_0 t_0, \quad b_{n,g} = b_{n,f} \cos n\omega_0 t_0 + a_{n,f} \sin n\omega_0 t_0. \quad (2.33)$$

2.10.3 Frequency Shift

To show that

$$g(t) = f(t) e^{jk\omega_0 t} \longleftrightarrow F_{n-k}, \quad k \text{ integer}. \quad (2.34)$$

We have

$$G_n = \frac{1}{T_0} \int_{t_0}^{t_0+T_0} f(t) e^{jk\omega_0 t} e^{-jn\omega_0 t} dt = F_{n-k} \quad (2.35)$$

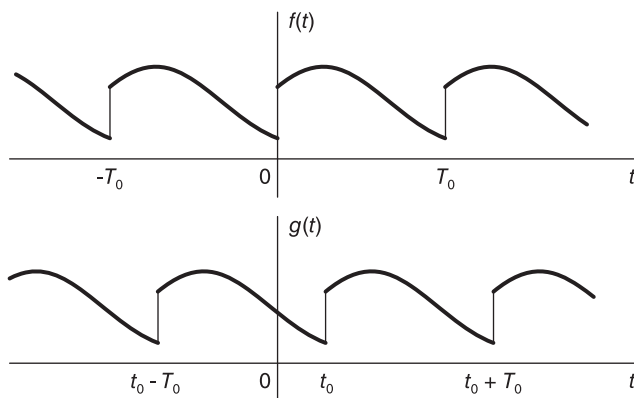


FIGURE 2.15 Periodic function and its time-shifted version.

$$a_{n,g} = 2\Re [G_n] = 2\Re [F_{n-k}] = a_{n-k,f}, \quad b_{n,g} = -2\Im [G_n] = -2\Im [F_{n-k}] = b_{n-k,f}. \quad (2.36)$$

2.10.4 Function Conjugate

If the function $f(t)$ is complex then its conjugate $f^*(t)$ has Fourier series coefficients equal to F_{-n}^* .

Proof We have

$$F_n = \frac{1}{T_0} \int_{T_0} f(t) e^{-jn\omega_0 t} dt \quad (2.37)$$

$$F_{-n}^* = \frac{1}{T_0} \int_{T_0} f^*(t) e^{-jn\omega_0 t} dt = FSC[f^*(t)]. \quad (2.38)$$

2.10.5 Reflection

If $f(t) \xleftrightarrow{FSC} F_n$ then $f(-t) \xleftrightarrow{FSC} F_{-n}$.

Proof With reference to Fig. 2.16,

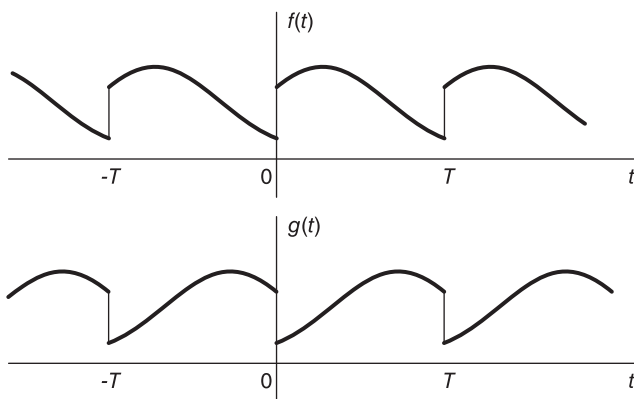


FIGURE 2.16 A function and its reflection.

let $g(t) = f(-t)$ and $\omega_0 = 2\pi/T$,

$$G_n = \frac{1}{T} \int_0^T g(t)e^{-jn\omega_0 t} dt = \frac{1}{T} \int_0^T f(-t)e^{-jn\omega_0 t} dt. \tag{2.39}$$

Let $\tau = -t$.

$$G_n = \frac{-1}{T} \int_0^{-T} f(\tau)e^{jn\omega_0 \tau} d\tau = \frac{1}{T} \int_{-T}^0 f(\tau)e^{jn\omega_0 \tau} d\tau = F_{-n} \tag{2.40}$$

Example 2.5 Consider the function $f(t) = e^{\alpha t} \{u(t) - u(t - T)\}$, where $T = 2\pi$, shown in Fig. 2.17 for a value $\alpha < 0$.

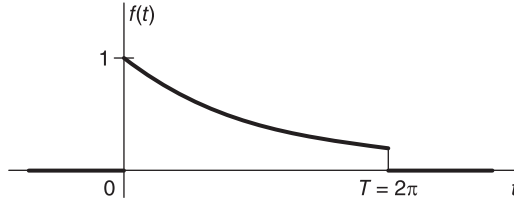


FIGURE 2.17 Function $f(t)$.

- a) Evaluate the exponential Fourier series expansion of $f(t)$ with a general analysis interval $(0, T)$.
- b) Deduce the exponential and trigonometric series expansion of the exponential function $w(t)$ shown in Fig. 2.18.

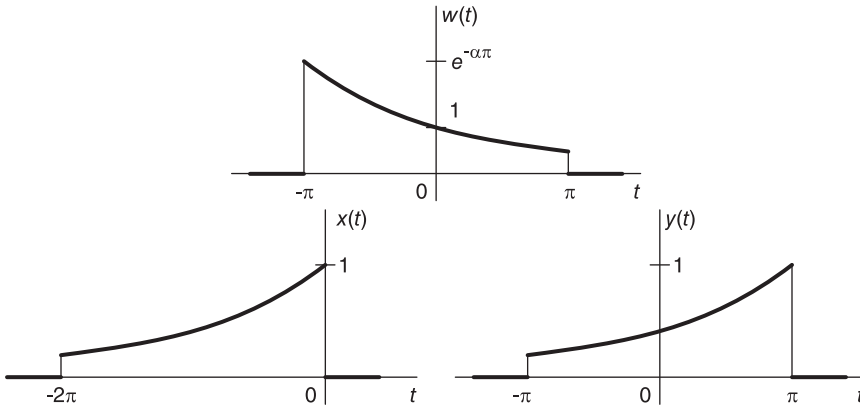


FIGURE 2.18 Three related functions.

- c) Using the reflection and shifting properties deduce the expansions of the functions $x(t)$ and $y(t)$ shown in the figure. d) As a verification deduce the expansion of $z(t) = e^t$, $-\pi < t < \pi$.

From the function forms in the figure we note that $x(t) = f(-t)$ and $y(t) = x(t - T/2)$.

a) We have, with $\omega_0 = 2\pi/T$,

$$F_n = \frac{1}{T} \int_0^T e^{\alpha t} e^{-jn\omega_0 t} dt = \frac{1}{T} \frac{e^{\alpha T} - 1}{\alpha - jn2\pi/T}$$

The expansion can be written in the form

$$e^{\alpha t} = \sum_{n=-\infty}^{\infty} F_n e^{jn\omega_0 t} = \sum_{n=-\infty}^{\infty} \frac{1}{T} \frac{e^{\alpha T} - 1}{\alpha - jn2\pi/T} e^{jn(2\pi/T)t}, \quad 0 < t < T.$$

With $T = 2\pi$, $\omega_0 = 1$,

$$e^{\alpha t} = \frac{1}{2\pi} \sum_{n=-\infty}^{\infty} \frac{e^{2\pi\alpha} - 1}{(\alpha - jn)} e^{jnt}, \quad 0 < t < 2\pi$$

and the trigonometric series is given by

$$a_{n,f} = \frac{\alpha (e^{2\pi\alpha} - 1)}{\pi (\alpha^2 + n^2)}, \quad n \geq 0, \quad b_{n,f} = \frac{-(e^{2\pi\alpha} - 1)n}{\pi (\alpha^2 + n^2)}, \quad n \geq 1$$

$$e^{\alpha t} = \frac{(e^{2\alpha\pi} - 1)}{2\alpha\pi} + \sum_{n=1}^{\infty} \frac{\alpha (e^{2\alpha\pi} - 1)}{\pi (\alpha^2 + n^2)} \cos nt - \sum_{n=1}^{\infty} \frac{(e^{2\alpha\pi} - 1)n}{\pi (\alpha^2 + n^2)} \sin nt$$

for $0 < t < 2\pi$.

b) We have $w(t) = e^{\alpha t}$, $-\pi < t < \pi$; $w(t) = f(t + \pi)e^{-\alpha\pi}$,

$$W_n = e^{-\alpha\pi} F_n e^{jn\omega_0\pi} = e^{-\alpha\pi} F_n e^{jn\pi} = e^{-\alpha\pi} \frac{(-1)^n (e^{2\alpha\pi} - 1)}{2\pi(\alpha - jn)} = \frac{(-1)^n \sinh(\alpha\pi)(\alpha + jn)}{\pi(\alpha^2 + n^2)}$$

$$a_{n,w} = 2 \Re[W_n] = \frac{(-1)^n 2\alpha \sinh(\alpha\pi)}{\pi(\alpha^2 + n^2)}, \quad b_{n,w} = -2 \Im[W_n] = \frac{(-1)^n 2n \sinh(\alpha\pi)}{\pi(\alpha^2 + n^2)}$$

$$e^{\alpha t} = \frac{2 \sinh \alpha\pi}{\pi} \left\{ \frac{1}{2\alpha} + \sum_{n=1}^{\infty} (-1)^n \frac{\alpha}{\alpha^2 + n^2} \cos nt - \sum_{n=1}^{\infty} (-1)^n \frac{n}{\alpha^2 + n^2} \sin nt \right\}$$

for $-\pi < t < \pi$.

c) Since $x(t) = f(-t)$, $x(t) = e^{-\alpha t}$, $-T < t < 0$,

$$X_n = F_{-n} = \frac{1}{T} \frac{e^{\alpha T} - 1}{(\alpha + jn2\pi/T)}.$$

$$y(t) = x(t - T/2) \stackrel{FSC}{\leftarrow} X_n e^{-jn\omega_0(T/2)} = X_n e^{-jn\pi} = (-1)^n X_n$$

$$Y_n = (-1)^n \frac{e^{\alpha T} - 1}{T(\alpha + jn2\pi/T)}.$$

The trigonometric coefficients, $a_{n,y}$ and $b_{n,y}$, of $y(t)$ are given by

$$a_{0,y} = \frac{e^{2\alpha\pi} - 1}{2\pi\alpha}$$

$$a_{n,y} = 2 \Re[Y_n] = (-1)^n \frac{\alpha (e^{2\alpha\pi} - 1)}{\pi (\alpha^2 + n^2)}, \quad b_{n,y} = -2 \Im[Y_n] = (-1)^n \frac{(e^{2\alpha\pi} - 1)n}{\pi (\alpha^2 + n^2)}$$

$$e^{-\alpha(t-\pi)} = \frac{(e^{2\alpha\pi} - 1)}{2\alpha\pi} + \sum_{n=1}^{\infty} (-1)^n \frac{\alpha(e^{2\alpha\pi} - 1)}{\pi(\alpha^2 + n^2)} \cos nt \\ + \sum_{n=1}^{\infty} (-1)^n \frac{(e^{2\alpha\pi} - 1)n}{\pi(\alpha^2 + n^2)} \sin nt, \quad -\pi < t < \pi$$

which agrees with the result obtained in the expansion of $w(t)$. Note that $y(t) = e^{\alpha\pi} \times w(t)|_{\alpha \rightarrow -\alpha}$.

$$d) z(t) = e^{-\pi} y(-t)|_{\alpha=1},$$

$$Z_n = (-1)^n \frac{e^{\pi} - e^{-\pi}}{2\pi(1 - jn)}$$

which agrees with $W_n|_{\alpha=1}$.

2.10.6 Symmetry

Given a general *aperiodic* function $f(t)$, defined over a finite interval $(t_0, t_0 + T_0)$, to study its Fourier series properties we extend it periodically in order to view it as it is seen by Fourier series. Symmetry properties are revealed by observing a given periodic or periodically extended function over the interval of one period, such as the interval $(-T_0/2, T_0/2)$, or $(0, T_0)$. We have, with $\omega_0 = 2\pi/T_0$,

$$F_n = \frac{1}{T_0} \left\{ \int_{-T_0/2}^{T_0/2} f(t) \cos n\omega_0 t - j \int_{-T_0/2}^{T_0/2} f(t) \sin n\omega_0 t \right\} dt. \quad (2.41)$$

Even Function

Let $f(t)$ be even over the interval $(-T_0/2, T_0/2)$, Fig. 2.19.

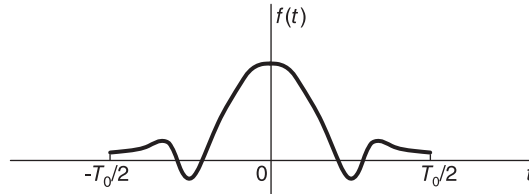


FIGURE 2.19 A periodic function and its time-shifted version.

$$f(-t) = f(t), \quad -T_0/2 < t < T_0/2. \quad (2.42)$$

In this case the second integral vanishes and we have

$$F_n = \frac{2}{T_0} \int_0^{T_0/2} f(t) \cos n\omega_0 t dt \quad (2.43)$$

$$f(t) = \sum_{n=-\infty}^{\infty} F_n e^{jn\omega_0 t} = F_0 + \sum_{n=1}^{\infty} 2F_n \cos n\omega_0 t \quad (2.44)$$

wherefrom an *even (and real) function has a real spectrum*.

The trigonometric coefficients are given by

$$a_n = 2 \Re[F_n] = 2F_n = \frac{4}{T_0} \int_0^{T_0/2} f(t) \cos n\omega_0 t \, dt, \quad n \geq 0. \quad (2.45)$$

$$f(t) = a_0/2 + \sum_{n=1}^{\infty} a_n \cos n\omega_0 t \quad (2.46)$$

Odd Function

Let $f(t)$ be an odd function over the interval $(-T_0/2, T_0/2)$, as shown in Fig. 2.20.

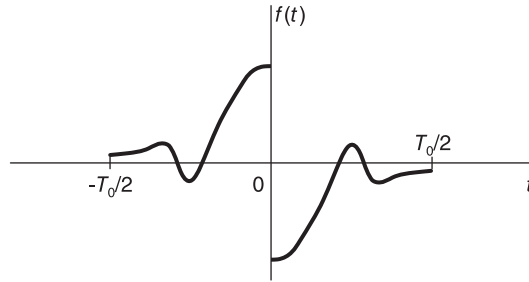


FIGURE 2.20 A function with odd symmetry.

We have

$$f(-t) = -f(t), \quad -T_0/2 < t < T_0/2. \quad (2.47)$$

The first integral vanishes and we have $\Re[F_n] = 0$,

$$F_n = \frac{-2j}{T_0} \int_0^{T_0/2} f(t) \sin n\omega_0 t \, dt \quad (2.48)$$

$$b_n = j2F_n = \frac{4}{T_0} \int_0^{T_0/2} f(t) \sin n\omega_0 t \, dt, \quad a_n = 0, \quad n \geq 0 \quad (2.49)$$

and the expansion has the form

$$f(t) = \sum_{n=1}^{\infty} b_n \sin n\omega_0 t = \sum_{n=1}^{\infty} (j2F_n) \sin n\omega_0 t. \quad (2.50)$$

We deduce that *an odd (and real) function has an imaginary exponential Fourier series spectrum.*

2.10.7 Half-Periodic Symmetry

There are two types of symmetry over half a period:

Even Half-Periodic Symmetry

A function $f(t)$ satisfying the condition

$$f(t \pm T_0/2) = f(t) \quad (2.51)$$

is said to have *even half-periodic symmetry*. The form of such a function is shown in Fig. 2.21. We notice that $f(t)$ in fact has a period of $T_0/2$, half the analysis period T_0 . Half-periodic symmetry, therefore, means symmetry over half the *analysis period*, rather than half the *function period*. We have already treated in the above such a case where the analysis interval was assumed to be a multiple of the signal period. We have with $\omega_0 = 2\pi/T_0$

$$F_n = \frac{1}{T_0} \left[\int_0^{T_0/2} f(t) e^{-jn\omega_0 t} dt + \int_{T_0/2}^{T_0} f(t) e^{-jn\omega_0 t} dt \right]. \quad (2.52)$$

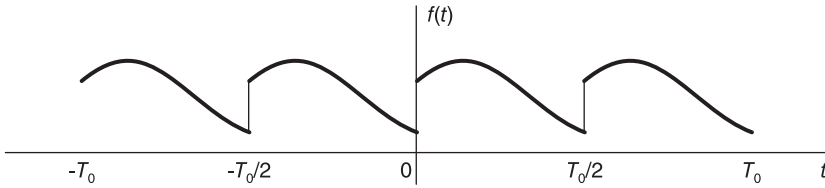


FIGURE 2.21 A function with even half-periodic symmetry.

Denoting by I_2 the second integral and letting $\tau = t - T_0/2$ we have

$$I_2 = \int_0^{T_0/2} f(\tau + T_0/2) e^{-jn\omega_0(\tau + T_0/2)} d\tau = (-1)^n \int_0^{T_0/2} f(\tau) e^{-jn\omega_0\tau} d\tau \quad (2.53)$$

since $f(t)$ is periodic of period $T_0/2$, and since $e^{-jn\omega_0(\tau + T_0/2)} = e^{-jn\omega_0\tau - jn\pi} = (-1)^n e^{-jn\omega_0\tau}$. Hence

$$F_n = \begin{cases} \frac{2}{T_0} \int_0^{T_0/2} f(t) e^{-jn\omega_0 t} dt, & n \text{ even} \\ 0, & n \text{ odd.} \end{cases} \quad (2.54)$$

Moreover

$$F_0 = \frac{2}{T_0} \int_0^{T_0/2} f(t) dt \quad (2.55)$$

$$a_n = 2\Re[F_n] = \begin{cases} \frac{4}{T_0} \int_0^{T_0/2} f(t) \cos n\omega_0 t dt, & n = 0, 2, 4, \dots \\ 0, & n \text{ odd} \end{cases} \quad (2.56)$$

$$b_n = -2\Im[F_n] = \begin{cases} \frac{4}{T_0} \int_0^{T_0/2} f(t) \sin n\omega_0 t dt, & n = 2, 4, 6, \dots \\ 0, & n \text{ odd} \end{cases} \quad (2.57)$$

$$f(t) = \sum_{\substack{n = -\infty \\ n \text{ even}}}^{\infty} F_n e^{jn\omega_0 t} \quad (2.58)$$

$$f(t) = a_0/2 + \sum_{n=2, 4, 6, \dots}^{\infty} (a_n \cos n\omega_0 t + b_n \sin n\omega_0 t) \quad (2.59)$$

wherefrom a function that has even half-periodic symmetry has only even harmonics.

Odd Half-Periodic Symmetry

A function satisfying the condition

$$f(t \pm T_0/2) = -f(t) \tag{2.60}$$

is said to have *odd half-periodic symmetry*. Fig. 2.22 shows the general form of such a function.

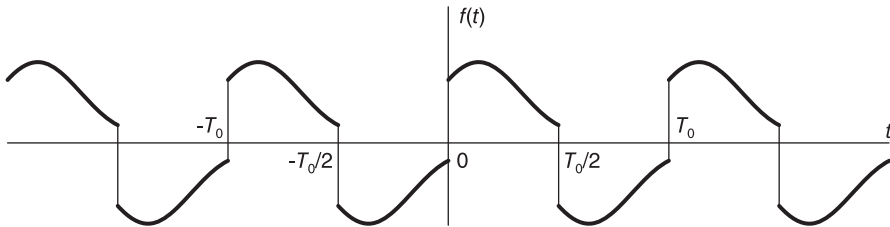


FIGURE 2.22 A function with odd half-periodic symmetry.

We can similarly show that

$$F_n = \begin{cases} \frac{2}{T_0} \int_0^{T_0/2} f(t) e^{-jn\omega_0 t} dt, & n \text{ odd} \\ 0, & n \text{ even} \end{cases} \tag{2.61}$$

$$a_n = 2\Re[F_n] = \begin{cases} \frac{4}{T_0} \int_0^{T_0/2} f(t) \cos n(2\pi/T_0)t dt, & n \text{ odd} \\ 0, & n \text{ even} \end{cases} \tag{2.62}$$

$$b_n = -2\Im[F_n] = \begin{cases} \frac{4}{T_0} \int_0^{T_0/2} f(t) \sin n(2\pi/T_0)t dt, & n \text{ odd} \\ 0, & n \text{ even} \end{cases} \tag{2.63}$$

$$f(t) = \sum_{\substack{n = -\infty \\ n \text{ odd}}}^{\infty} F_n e^{jn\omega_0 t} \tag{2.64}$$

$$f(t) = \sum_{\substack{n = 1 \\ n \text{ odd}}}^{\infty} (a_n \cos n\omega_0 t + b_n \sin n\omega_0 t) \tag{2.65}$$

wherefrom a function that has odd half-periodic symmetry has only odd harmonics.

2.10.8 Double Symmetry

We consider here a case of double symmetry, namely double odd symmetry, such as the one shown in Fig. 2.23.

Other cases of double symmetry can be similarly considered. We note that this function is odd and has odd half-periodic symmetry. We have $f(-t) = -f(t)$ and $f(t \pm T_0/2) = -f(t)$. Since the function is odd we can write

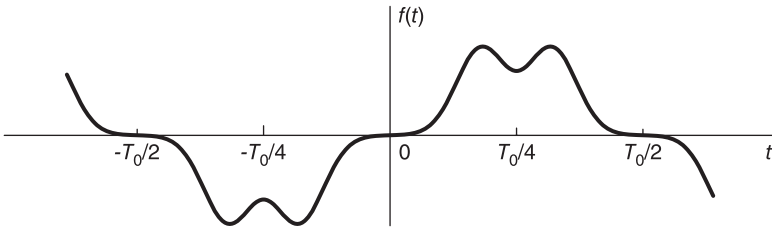


FIGURE 2.23 Double symmetry.

$$\begin{aligned}
 F_n &= \frac{-2j}{T_0} \int_0^{T_0/2} f(t) \sin n\omega_0 t \, dt \\
 &= \frac{-2j}{T_0} \left\{ \int_0^{T_0/4} f(t) \sin n\omega_0 t + \int_{T_0/4}^{T_0/2} f(t) \sin n\omega_0 t \right\} dt = \frac{-2j}{T_0} \{I_1 + I_2\}
 \end{aligned} \tag{2.66}$$

where I_1 and I_2 denote the first and second integral, respectively. Letting $t = T_0/2 - \tau$ we have

$$I_2 = - \int_{T_0/4}^0 f\left(\frac{T_0}{2} - \tau\right) \sin n\omega_0 \left(\frac{T_0}{2} - \tau\right) d\tau = \int_0^{T_0/4} f(\tau) \sin(n\pi - n\omega_0\tau) d\tau \tag{2.67}$$

$$I_2 = \int_0^{T_0/4} f(\tau) \sin n\omega_0\tau (-1)^{n+1} d\tau = (-1)^{n+1} I_1 \tag{2.68}$$

wherefrom

$$F_n = \frac{-2j}{T_0} [1 + (-1)^{n+1}] I_1 \tag{2.69}$$

i.e.

$$F_n = \begin{cases} (-4j/T_0) \int_0^{T_0/4} f(t) \sin n\omega_0 t \, dt, & n \text{ odd} \\ 0, & n \text{ even.} \end{cases} \tag{2.70}$$

Figure 2.24 shows functions with different types of symmetry, with an analysis interval assumed equal to T in each case.

We notice that the function $f_1(t)$ is even and has odd symmetry over half the period T , while $f_2(t)$ is odd and has odd half-periodic symmetry. To verify function symmetry its average d-c value should be rendered zero by a vertical shift which affects only its zeroth coefficient.

Removing the d-c average value reveals any hidden symmetry. The function $f_3(t)$ is identical in appearance apart from a vertical shift to $f_2(t)$, wherefrom it too is odd and has odd half-periodic symmetry. The function $f_4(t)$ is similar to $f_1(t)$ and is therefore even and has odd half-periodic symmetry.

The function $f_5(t)$ is identical in form to $f_2(t)$, but has even half-periodic symmetry. The reason for the difference is that half-periodic symmetry means symmetry over half the analysis period rather than the function period.

Example 2.6 Assuming an analysis interval equal to the period, evaluate the exponential and the trigonometric series expansions of the function $f(t)$, shown in Fig. 2.25.

To reveal the symmetry we effect a vertical shift of -1 , rendering the average value of the function equal to zero, thus obtaining the function $g(t) = f(t) - 1$.

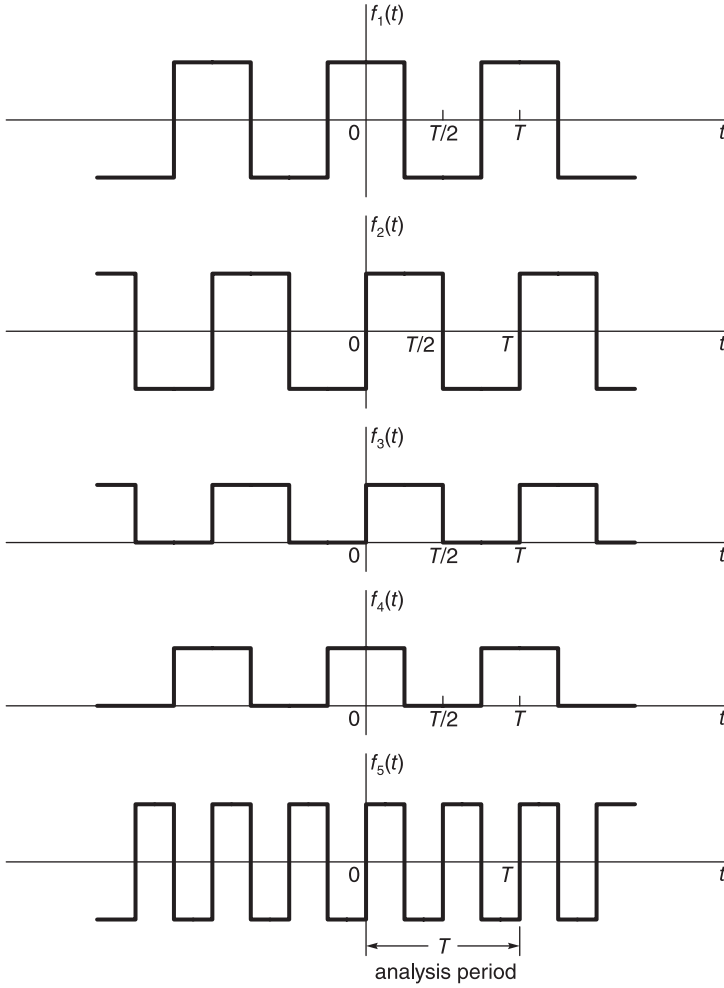


FIGURE 2.24 Functions with different types of symmetry.

The function $g(t)$ has a period $\tau = 4$ seconds. It is odd and has odd half-periodic symmetry; hence double symmetry. We have

$$\begin{aligned}
 G_n &= \frac{-4j}{T_0} \int_0^{T_0/4} g(t) \sin n\omega_0 t \, dt = -j \int_0^1 t \sin n\frac{\pi}{2}t \, dt, \quad n \text{ odd} \\
 &= -j \left\{ \frac{\sin(n\pi t/2)}{(n^2\pi^2)/4} - \frac{t \cos(n\pi t/2)}{n\pi/2} \right\}, \quad n \text{ odd.}
 \end{aligned}$$

Simplifying and noticing that $F_n = G_n$, $n \neq 0$ and $F_0 = 1$ we obtain

$$F_n = \begin{cases} \frac{(-1)^{(n+1)/2} j 4}{\pi^2 n^2}, & n = \pm 1, \pm 3, \pm 5, \dots \\ 1, & n = 0 \\ 0, & \text{otherwise} \end{cases}$$

and

$$f(t) = 1 + \sum_{n=\pm 1, \pm 3, \pm 5, \dots}^{\infty} \frac{(-1)^{(n+1)/2} j 4}{\pi^2 n^2} e^{jn(\pi/2)t}.$$

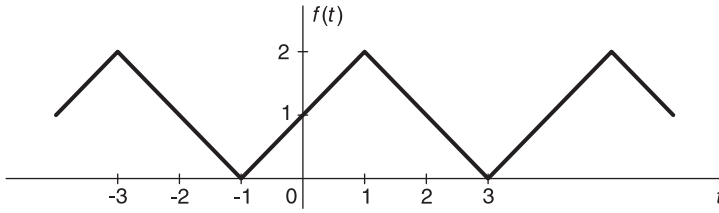


FIGURE 2.25 Function with double symmetry.

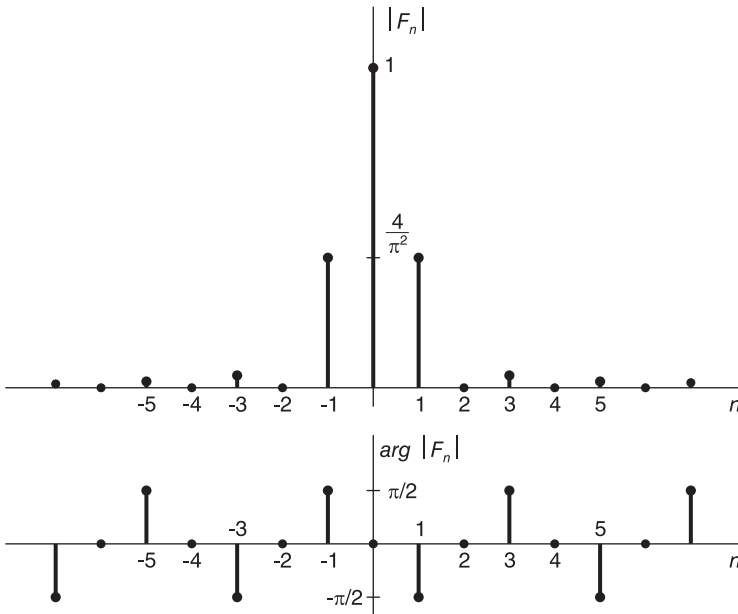


FIGURE 2.26 Discrete spectrum of Example 2.6.

The coefficients F_n are shown in Fig. 2.26. The trigonometric coefficients are given by:

$$a_{n,f} = 2 \Re[F_n] = 0, \quad n \neq 0, \quad a_{0,f} = 2$$

$$b_{n,f} = -2 \Im[F_n] = \begin{cases} \frac{8}{\pi^2 n^2}, & n = 1, 5, 9, \dots \\ \frac{-8}{\pi^2 n^2}, & n = 3, 7, 11, \dots \end{cases}$$

$$f(t) = 1 + \frac{8}{\pi^2} \left(\sin \frac{\pi}{2}t - \frac{1}{3^2} \sin \frac{3\pi}{2}t + \frac{1}{5^2} \sin \frac{5\pi}{2}t - \dots \right)$$

$$= 1 + \frac{8}{\pi^2} \sum_{n=1}^{\infty} (-1)^{n-1} \frac{\sin (2n-1) (\pi/2)t}{(2n-1)^2}$$

2.10.9 Time Scaling

Let a function $f(t)$ be periodic of a period T_0 . Let $g(t) = f(\alpha t)$, $\alpha > 0$.

A function $f(t)$ and the corresponding time scaled version $g(t) = f(\alpha t)$ with $\alpha = 2.5$ are shown in Fig. 2.27.

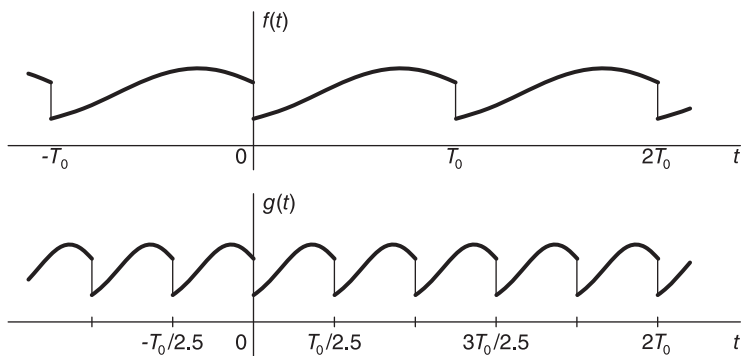


FIGURE 2.27 A function and its compressed form.

The function $g(t)$ is periodic with period $T_0/\alpha = 0.4T_0$. We show that the Fourier series coefficients G_n of the expansion of $g(t)$ over its period (T_0/α) are equal to the coefficients F_n of the expansion of $f(t)$ over its period T_0 . We have

$$g(t) = \sum_{n=-\infty}^{\infty} G_n e^{jn \frac{2\pi}{(T_0/\alpha)} t} \tag{2.71}$$

$$G_n = \frac{1}{(T_0/\alpha)} \int_{T_0/\alpha} g(t) e^{-jn \frac{2\pi}{(T_0/\alpha)} t} dt. \tag{2.72}$$

Letting $\alpha t = \tau$, $\alpha dt = d\tau$ we have

$$G_n = \frac{\alpha}{T_0} \frac{1}{\alpha} \int_{T_0} g\left(\frac{\tau}{\alpha}\right) e^{-jn2\pi\tau/T_0} d\tau = \frac{1}{T_0} \int_{T_0} f(\tau) e^{-jn2\pi\tau/T_0} d\tau = F_n. \tag{2.73}$$

We conclude that if $g(t) = f(\alpha t)$, $\alpha > 0$, then $G_n = F_n$. The trigonometric coefficients of $g(t)$ are therefore also equal to those of $f(t)$. The difference between the two expansions is in the values of the fundamental frequency in both cases, i.e. $2\pi/T_0$ versus $5\pi/T_0$.

Example 2.7 Let $f(t) = t^2$, $0 < t < 1$. Deduce the exponential and trigonometric Fourier series expansions of $f(t)$ using the fact that the expansion of the function $g(t) = t^2$, $0 < t < 2\pi$ is given by

$$t^2 = \frac{4\pi^2}{3} + \sum_{n=1}^{\infty} \left(\frac{4}{n^2} \cos nt - \frac{4\pi}{n} \sin nt \right), \quad 0 < t < 2\pi.$$

We note that apart from a factor $4\pi^2$ the function $f(t)$ is a compressed version of the function $g(t)$, as can be seen in Fig. 2.28. In fact

$$f(t) = \frac{1}{4\pi^2} g(2\pi t)$$

The trigonometric coefficients of $f(t)$ are therefore given by

$$a_{0,f} = \frac{1}{4\pi^2} a_{0,g} = \frac{2}{3}, \quad a_{n,f} = \frac{1}{4\pi^2} a_{n,g} = \frac{1}{\pi^2 n^2}, \quad b_{n,f} = \frac{1}{4\pi^2} b_{n,g} = \frac{-1}{\pi n}.$$

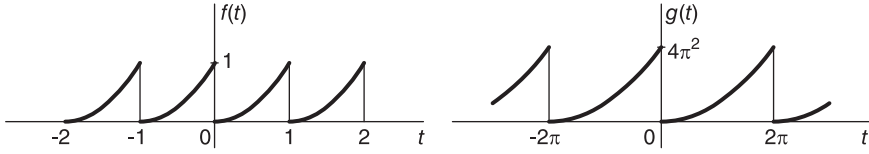


FIGURE 2.28 Function and stretched and amplified version thereof.

We can write

$$t^2 = \frac{1}{3} + \sum_{n=1}^{\infty} \frac{1}{\pi^2 n^2} \cos 2\pi n t - \sum_{n=1}^{\infty} \frac{1}{\pi n} \sin 2\pi n t, \quad 0 < t < 1.$$

The exponential coefficients of $g(t)$ are $G_0 = a_{0,g}/2 = 4\pi^2/3$,

$$G_n = \frac{1}{2}(a_{n,g} - j b_{n,g}) = \frac{1}{2} \left(\frac{4}{n^2} + j \frac{4\pi}{n} \right) = \frac{2(1 + j\pi n)}{n^2}, \quad n > 0$$

wherefrom $F_0 = 1/3$,

$$F_n = \frac{1}{4\pi^2} G_n = \frac{1 + j\pi n}{2\pi^2 n^2}, \quad n > 0$$

and the exponential series expansion is

$$f(t) = t^2 = \frac{1}{3} + \sum_{n=-\infty}^{\infty} \frac{1 + j\pi n}{2\pi^2 n^2} e^{jn2\pi t}, \quad 0 < t < 1.$$

2.10.10 Differentiation Property

The differentiation property states that $f'(t) \xleftrightarrow{FSC} (jn\omega_0) F_n$. To prove this property let $g(t) = f'(t)$. We may write with $\omega_0 = 2\pi/T$,

$$f(t) = \sum_{n=-\infty}^{\infty} F_n e^{jn\omega_0 t} \quad (2.74)$$

and differentiating both sides we have

$$g(t) = f'(t) = \frac{d}{dt} \sum_{n=-\infty}^{\infty} F_n e^{jn\omega_0 t} = \sum_{n=-\infty}^{\infty} jn\omega_0 F_n e^{jn\omega_0 t} \quad (2.75)$$

wherefrom $G_n = jn\omega_0 F_n$ as stated. Repeated differentiation leads to the more general form

$$f^{(m)}(t) = \frac{d^m f(t)}{dt^m} \xleftrightarrow{FSC} (jn\omega_0)^m F_n. \quad (2.76)$$

Similarly, the trigonometric series expansion of $f(t)$ is given by

$$f(t) = a_{0,f}/2 + \sum_{n=1}^{\infty} (a_{n,f} \cos n\omega_0 t + b_{n,f} \sin n\omega_0 t). \quad (2.77)$$

Differentiating both sides of the expansion we have

$$g(t) = f'(t) = \omega_0 \sum_{n=1}^{\infty} n (b_{n,f} \cos n\omega_0 t - a_{n,f} \sin n\omega_0 t) \quad (2.78)$$

wherefrom $a_{n,g} = n\omega_0 b_{n,f}$ and $b_{n,g} = -n\omega_0 a_{n,f}$.

Example 2.8 Let $f(t) = (t^2 - t)$, $0 \leq t \leq 1$ be the periodic parabola shown in Fig. 2.29. Evaluate the Fourier series of $f(t)$ using the differentiation property.

Since $f(t)$ is continuous everywhere its derivative $f'(t)$ has at most finite discontinuities and hence satisfies the Dirichlet conditions, as can be seen in the figure.

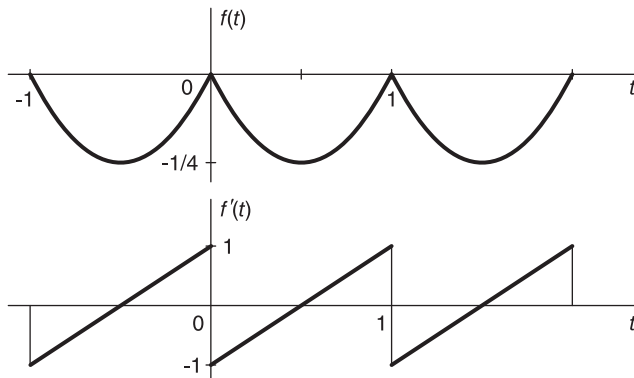


FIGURE 2.29 Repeated parabola and its derivative.

Let $g(t) \triangleq f'(t) = 2t - 1$, $0 < t < 1$. The derivative function $f'(t)$ is thus the periodic ramp shown in the figure. From Example 2.2 the series coefficients of the ramp are given by $G_n = j/(\pi n)$, $n \neq 0$ and $G_0 = 0$, so that with $\omega_0 = 2\pi$

$$F_n = G_n / (jn\omega_0) = \frac{1}{2\pi^2 n^2}, \quad n \neq 0$$

$$F_0 = \int_0^1 (t^2 - t) dt = [t^3/3 - t^2/2]_0^1 = \frac{-1}{6}.$$

The trigonometric coefficients are given by

$$a_{n,f} = 2 \Re[F_n] = \frac{1}{\pi^2 n^2}, \quad n \neq 0$$

$a_{0,f} = 2F_0 = -1/3$ and $b_{n,f} = -2 \Im[F_n] = 0$. We can therefore write

$$t^2 - t = \frac{-1}{6} + \frac{1}{2\pi^2} \sum_{n=-\infty}^{\infty} \frac{e^{j2\pi nt}}{n^2} = \frac{-1}{6} + \sum_{n=1}^{\infty} \frac{\cos 2\pi nt}{\pi^2 n^2}, \quad 0 \leq t \leq 1.$$

Note that by putting $t = 0$ we obtain

$$\sum_{n=1}^{\infty} \frac{1}{n^2} = \frac{\pi^2}{6},$$

which is a special case of the Euler sum of powers of reciprocals of natural numbers

$$\sum_{k=1}^{\infty} \frac{1}{k^{2n}} = \frac{2^{2n-1} \pi^{2n}}{(2n)!} |B_{2n}|$$

where B_{2n} is the Bernoulli number of index $2n$, and $B_2 = 1/6$.

2.11 Differentiation of Discontinuous Functions

As noted earlier, in manipulating expressions containing infinite series and infinite integrals we often need to interchange the order of differentiation or integration and summation. As an example that illustrates that such is not always the case we have obtained the Fourier series expansion for the function $f(t) = t$, $0 < t < 1$

$$F_n = j/(2\pi n), \quad n \neq 0, \quad F_0 = 0.5 \quad (2.79)$$

$$t = 0.5 - \frac{1}{\pi} \sum_{n=1}^{\infty} \frac{\sin 2\pi nt}{n}, \quad 0 < t < 1. \quad (2.80)$$

The derivative of the left-hand side of this equation is equal to 1. The derivative of the sum on the right-hand side evaluated as a sum of derivatives produces

$$\frac{d}{dt} \left\{ 0.5 - \frac{1}{\pi} \sum_{n=1}^{\infty} \frac{\sin 2\pi nt}{n} \right\} = -\frac{1}{\pi} \sum_{n=1}^{\infty} \frac{d}{dt} \left(\frac{\sin 2\pi nt}{n} \right) = -\sum_{n=1}^{\infty} 2 \cos(2\pi nt) \quad (2.81)$$

which is divergent since $\lim_{n \rightarrow \infty} \cos(2\pi nt) \neq 0$ implying nonuniform convergence of the sum of derivatives. We note therefore that a simple differentiation of the Fourier series expansion by interchanging the order of differentiation and summation is not always possible. The problem is due to the jump-discontinuities of the periodic extension of the function $f(t)$ at each period boundary; discontinuities that lead to impulses when differentiated. The differentiation property holds true as long as we take into consideration such impulses.

2.11.1 Multiplication in the Time Domain

Let $x(t)$ and $f(t)$ be two periodic functions of period T_0 . Let their Fourier series coefficients with an interval of analysis T_0 be X_n and F_n , respectively. Consider their product $g(t) = x(t)f(t)$. We assume that $x(t)$, $f(t)$ and hence $g(t)$ satisfy the Dirichlet conditions. The Fourier series coefficients of $g(t)$ are

$$G_n = \frac{1}{T_0} \int_{-T_0/2}^{T_0/2} g(t) e^{-jn\omega_0 t} dt = \frac{1}{T_0} \int_{-T_0/2}^{T_0/2} x(t) f(t) e^{-jn\omega_0 t} dt. \quad (2.82)$$

Replacing $f(t)$ by its Fourier series expansion we have

$$G_n = \frac{1}{T_0} \int_{-T_0/2}^{T_0/2} x(t) \left\{ \sum_{k=-\infty}^{\infty} F_k e^{jk\omega_0 t} \right\} e^{-jn\omega_0 t} dt. \quad (2.83)$$

Interchanging the order of integration and summation, we have

$$G_n = \frac{1}{T_0} \sum_{k=-\infty}^{\infty} F_k \int_{-T_0/2}^{T_0/2} x(t) e^{j(k-n)\omega_0 t} dt. \quad (2.84)$$

Now using the definition of the Fourier series coefficients of $x(t)$, namely,

$$X_n = \frac{1}{T_0} \int_{-T_0/2}^{T_0/2} x(t) e^{-jn\omega_0 t} dt \quad (2.85)$$

we have

$$X_{n-k} = \frac{1}{T_0} \int_{-T_0/2}^{T_0/2} x(t) e^{-j(n-k)\omega_0 t} dt \quad (2.86)$$

$$G_n = \sum_{k=-\infty}^{\infty} F_k X_{n-k}. \quad (2.87)$$

The relation states that *multiplication in the time domain corresponds to convolution in the frequency domain*.

2.11.2 Convolution in the Time Domain

Let $x(t)$ and $f(t)$ be two periodic functions of period T_0 . Let $g(t)$ be the convolution of $x(t)$ and $f(t)$, defined as

$$g(t) = x(t) * f(t) = \frac{1}{T_0} \int_{-T_0/2}^{T_0/2} x(\tau) f(t - \tau) d\tau = \frac{1}{T_0} \int_{-T_0/2}^{T_0/2} x(t - \tau) f(\tau) d\tau. \quad (2.88)$$

The Fourier series coefficients G_n are given by

$$G_n = \frac{1}{T_0} \int_{-T_0/2}^{T_0/2} g(t) e^{-jn\omega_0 t} dt = \frac{1}{T_0^2} \int_{-T_0/2}^{T_0/2} \int_{-T_0/2}^{T_0/2} x(\tau) f(t - \tau) d\tau e^{-jn\omega_0 t} dt.$$

Interchanging the order of the two integrals

$$G_n = \frac{1}{T_0^2} \int_{-T_0/2}^{T_0/2} x(\tau) \int_{-T_0/2}^{T_0/2} f(t - \tau) e^{-jn\omega_0 t} dt d\tau. \quad (2.89)$$

Let $t - \tau = u$

$$\begin{aligned} G_n &= \frac{1}{T_0^2} \int_{-T_0/2}^{T_0/2} x(\tau) \int_{-T_0/2}^{T_0/2} f(u) e^{-jn\omega_0(\tau-u)} du d\tau \\ &= \frac{1}{T_0^2} \int_{-T_0/2}^{T_0/2} x(\tau) e^{-jn\omega_0\tau} \int_{-T_0/2}^{T_0/2} f(u) e^{-jn\omega_0 u} du d\tau. \end{aligned} \quad (2.90)$$

We note however that the second integrand is periodic with period T_0 since $f(u)$ is periodic and $e^{-jn\omega_0(T_0+u)} = e^{-jn\omega_0 u}$ is also periodic of period T_0 . The second integrand could thus be written as

$$\int_{-T_0/2}^{T_0/2} f(u) e^{-jn\omega_0 u} du = T_0 F_n. \quad (2.91)$$

Substituting we have

$$G_n = X_n F_n. \quad (2.92)$$

This is the dual important relation to the one just seen. It states that *convolution in the time domain corresponds to multiplication in the frequency domain*.

2.11.3 Integration

We evaluate the effect of integration of a function $f(t)$ and its Fourier series expansion

$$f(t) = F_0 + \sum_{n=-\infty, n \neq 0}^{\infty} F_n e^{jn\omega_0 t}, \quad \omega_0 = 2\pi/T \quad (2.93)$$

$$\int f(t)dt = F_0t + \sum_{n=-\infty, n \neq 0}^{\infty} F_n \frac{e^{jn\omega_0 t}}{jn\omega_0} + C \quad (2.94)$$

where C is a constant. Let $g(t) = \int f(t)dt - F_0t$ and G_n its Fourier series coefficients. We deduce that

$$g(t) = \sum_{n=-\infty, n \neq 0}^{\infty} F_n \frac{e^{jn\omega_0 t}}{jn\omega_0} + C \quad (2.95)$$

$$G_n = \frac{F_n}{jn\omega_0}, \quad n \neq 0, \quad G_0 = C. \quad (2.96)$$

Similarly, for the trigonometric coefficients,

$$f(t) = a_{0,f}/2 + \sum_{n=1}^{\infty} a_{n,f} \cos n\omega_0 t + b_{n,f} \sin n\omega_0 t. \quad (2.97)$$

Let $g(t) = \int f(t)dt - (a_{0,f}/2)t$.

$$\begin{aligned} g(t) &= \sum_{n=1}^{\infty} a_{n,f} \frac{\sin n\omega_0 t}{n\omega_0} - b_{n,f} \frac{\cos n\omega_0 t}{n\omega_0} + C \\ &= (a_{0,g}/2) + \sum_{n=1}^{\infty} a_{n,g} \cos n\omega_0 t + b_{n,g} \sin n\omega_0 t. \end{aligned} \quad (2.98)$$

Hence $a_{0,g}/2 = C$, $a_{n,g} = -b_{n,f}/(n\omega_0)$, $b_{n,g} = a_{n,f}/(n\omega_0)$.

Example 2.9 Show the result of integrating the Fourier series expansion of the periodic function $f(t)$ of period $T = 1$, where $f(t) = At$, $0 < t < 1$.

From Example 2.3

$$f(t) = At = F_0 + \sum_{n=-\infty, n \neq 0}^{\infty} F_n e^{jn\omega_0 t} = A/2 + \sum_{n=-\infty, n \neq 0}^{\infty} \frac{jA}{2\pi n} e^{jn2\pi t}$$

$$\int f(t)dt = At^2/2 = At/2 + \sum_{n=-\infty, n \neq 0}^{\infty} \frac{A}{4\pi^2 n^2} e^{jn2\pi t} + C$$

$$g(t) = At^2/2 - At/2 = C + \sum_{n=-\infty, n \neq 0}^{\infty} \frac{A}{4\pi^2 n^2} e^{jn2\pi t}$$

$$C = G_0 = \int g(t)dt = \int_0^1 (At^2 - At/2) dt = \frac{-A}{12}.$$

We obtain the expansion

$$At^2/2 - At/2 = \frac{-A}{12} + \sum_{n=-\infty, n \neq 0}^{\infty} \frac{A}{4\pi^2 n^2} e^{jn2\pi t}, \quad 0 < t < 1$$

and we note that $G_n = F_n/(jn\omega_0) = A/(4\pi^2 n^2)$ as expected.

2.12 Fourier Series of an Impulse Train

Let the function $f(t)$ be the impulse train $\rho_T(t)$ shown in Fig. 2.30. The Fourier series expansion is given by

$$\rho_T(t) = \sum_{n=-\infty}^{\infty} F_n e^{jn\omega_0 t} \tag{2.99}$$

where

$$F_n = \frac{1}{T} \int_{-T/2}^{T/2} \rho_T(t) e^{-jn\omega_0 t} dt = \frac{1}{T} \int_{-T/2}^{T/2} \delta(t) e^{-jn\omega_0 t} dt = \frac{1}{T} \tag{2.100}$$

wherefrom the coefficients are all equal to the reciprocal $1/T$ of the period T leading to the comb-like spectrum shown in the same figure.

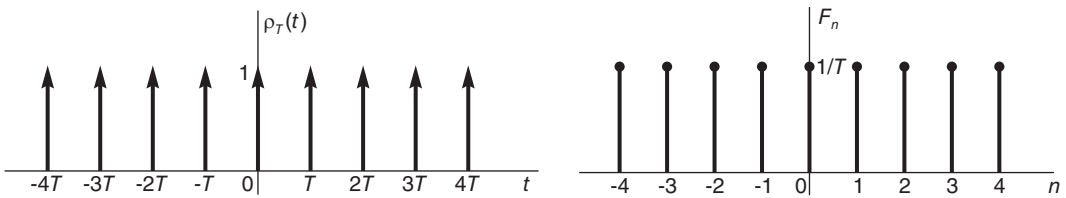


FIGURE 2.30 Impulse train and its Fourier series coefficients

Example 2.10 Half-Wave Rectification Evaluate the Fourier series over an interval $(0, 2\pi)$ of the function

$$f(t) = \begin{cases} \sin t, & 0 \leq t \leq \pi \\ 0, & \pi \leq t \leq 2\pi. \end{cases}$$

Effecting a periodic extension we obtain the function and its derivative $f'(t)$ shown in Fig. 2.31. The second derivative $x(t) = f''(t)$, is also shown in the figure.

$$x(t) = f''(t) = -f(t) + \sum_{n=-\infty}^{\infty} \delta(t - 2n\pi) + \sum_{n=-\infty}^{\infty} \delta(t - \pi - 2n\pi)$$

Since the analysis interval is 2π the function $x(t)$ has two impulse trains of period 2π each, with a time shift of π separating them. The coefficients of each train is the reciprocal of its period, wherefrom

$$X_n = -n^2 F_n = -F_n + 1/(2\pi) + 1/(2\pi) e^{-jn\pi}$$

$$F_n = \frac{1}{2\pi} \frac{1 + (-1)^n}{1 - n^2}, \quad n \neq \pm 1 = \begin{cases} \frac{-1}{\pi(n^2 - 1)}, & n \text{ even} \\ 0, & n \text{ odd} \\ \mp j/4, & n = \pm 1 \end{cases}$$

where L'Hopital's rule was used by writing

$$F_1 = \lim_{n \rightarrow 1} \left\{ \frac{1}{2\pi} \frac{1 + e^{-jn\pi}}{1 - n^2} \right\} = \frac{1}{2\pi} \lim_{n \rightarrow 1} \left\{ \frac{-j\pi e^{-jn\pi}}{-2n} \right\} = \frac{-j}{4}.$$

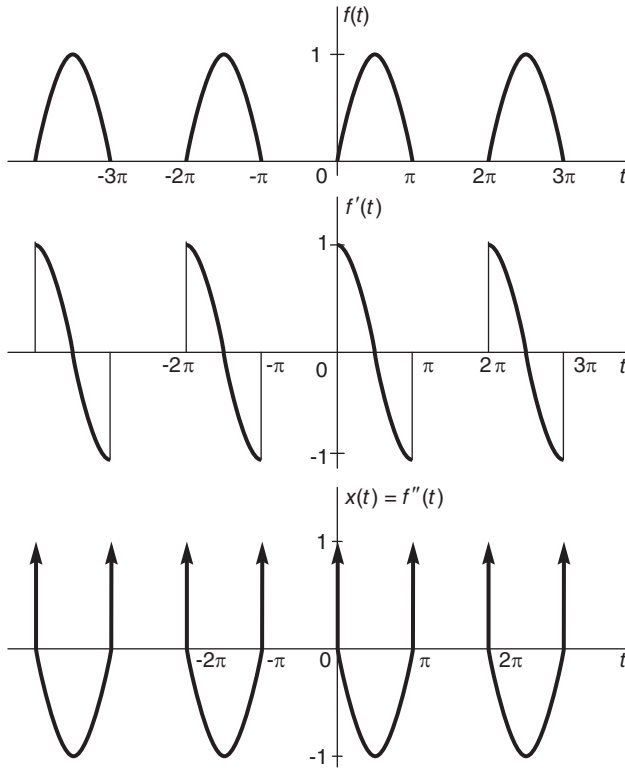


FIGURE 2.31 Half-wave rectified sinusoid.

2.13 Expansion into Cosine or Sine Fourier Series

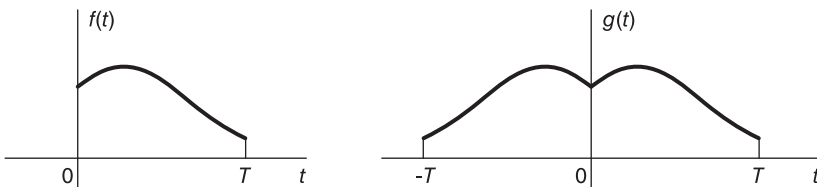


FIGURE 2.32 A function, made even by reflection.

Given a function $f(t)$ defined in the interval $(0, T)$ we can expand it into a *cosine Fourier series* by reflecting it into the vertical axis, as shown in Fig. 2.32, establishing even symmetry. In particular, we write

$$g(t) = \begin{cases} f(t), & 0 < t < T \\ f(-t), & -T < t < 0 \end{cases} \quad (2.101)$$

so that $g(-t) = g(t)$, $-T < t < T$, and extend $g(t)$ periodically with a period $2T$, that is,

$g(t + 2kT) = g(t)$, k integer. The function $g(t)$ being even, the coefficients are given by

$$G_n = \frac{1}{2T} \int_0^{2T} g(t)e^{jn\omega_0 t} dt = \frac{1}{T} \int_0^T g(t) \cos n\omega_0 t dt \quad (2.102)$$

where $\omega_0 = 2\pi/2T = \pi/T$.

$$a_{n,g} = 2G_n = \frac{2}{T} \int_0^T f(t) \cos n\omega_0 t dt, \quad n \geq 0, \quad b_{n,g} = 0 \quad (2.103)$$

$$\begin{aligned} g(t) &= \sum_{n=-\infty}^{\infty} G_n e^{jn\omega_0 t} = G_0 + 2 \sum_{n=1}^{\infty} G_n \cos n\omega_0 t, \quad -T < t < T \\ &= a_{0,g}/2 + \sum_{n=1}^{\infty} a_{n,g} \cos n\omega_0 t, \quad -T < t < T \end{aligned} \quad (2.104)$$

and since $g(t) = f(t)$ for $0 < t < T$ we can write

$$f(t) = a_{0,g}/2 + \sum_{n=1}^{\infty} a_{n,g} \cos n(\pi/T)t, \quad 0 < t < T. \quad (2.105)$$

We have thus expanded the given function $f(t)$ into a Fourier series containing only cosine terms.

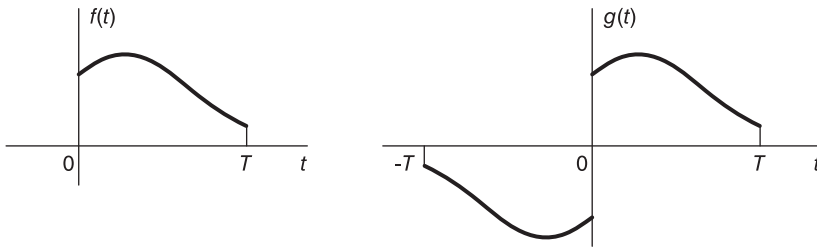


FIGURE 2.33 A function made odd by reflection.

Similarly, we can expand the function into a *sine Fourier series* by reflecting it in the origin, as shown in Fig. 2.33, establishing odd symmetry. We write

$$g(t) = \begin{cases} f(t), & 0 < t < T \\ -f(-t), & -T < t < 0 \end{cases} \quad (2.106)$$

so that $g(t)$ and its periodic extension, with period $2T$, are odd, $g(-t) = -g(t)$. We obtain, with $\omega_0 = \pi/T$,

$$G_n = \frac{-j}{T} \int_0^T g(t) \sin n\omega_0 t dt = \frac{-j}{T} \int_0^T f(t) \sin n\omega_0 t dt \quad (2.107)$$

$$b_{n,g} = -2\Im[G_n] = \frac{2}{T} \int_0^T f(t) \sin n\omega_0 t dt \quad (2.108)$$

$$g(t) = 2j \sum_{n=1}^{\infty} G_n \sin n\omega_0 t = \sum_{n=1}^{\infty} b_{n,g} \sin n(\pi/T)t, \quad -T < t < T \quad (2.109)$$

We have thus obtained the expansion as the sine series

$$f(t) = g(t) = \sum_{n=1}^{\infty} b_{n,g} \sin n(\pi/T)t, \quad 0 < t < T. \quad (2.110)$$

Example 2.11 Consider a function $f(t)$ which over the time interval $(0, \theta)$ is given by $f(t) = e^{\alpha t}$, $0 \leq t < \theta$, with $\alpha = -1$. Show how to obtain cosine and sine Fourier series expansions of $f(t)$.

(a) Cosine series

The given function $f(t)$ is shown in Fig. 2.34. To obtain a cosine series of the function we establish even symmetry, with

$$g(t) = \begin{cases} f(t), & 0 \leq t < \theta \\ f(-t), & -\theta < t < 0 \end{cases}$$

as shown in the figure, i.e.

$$g(t) = \begin{cases} e^{-t}, & 0 \leq t < \theta \\ e^t, & -\theta < t < 0. \end{cases}$$

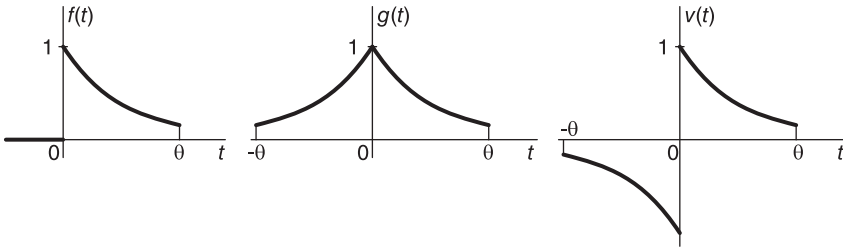


FIGURE 2.34 A function rendered even and odd, respectively.

Since $g(t)$ is an even function and its periodic extension is of a period equal to $T = 2\theta$, writing $\omega_0 = 2\pi/T = \pi/\theta$, we have

$$\begin{aligned} G_n &= \frac{1}{\theta} \int_0^\theta e^{\alpha t} \cos n\omega_0 t \, dt = \frac{1}{\theta} \int_0^\theta \Re[e^{\alpha t} e^{-jn\omega_0 t}] \, dt \\ &= \frac{1}{\theta} \Re \int_0^\theta e^{\alpha t} e^{-jn\omega_0 t} \, dt = \frac{\alpha}{\theta} \frac{[(-1)^n e^{\alpha\theta} - 1]}{(\alpha^2 + n^2\pi^2/\theta^2)}. \end{aligned}$$

The trigonometric series coefficients of $g(t)$ are given by

$$\begin{aligned} a_{n,g} &= 2 \Re[G_n] = \frac{2\alpha}{\theta} \frac{(-1)^n e^{\alpha\theta} - 1}{\alpha^2 + n^2\pi^2/\theta^2}, \quad n \geq 0 \\ b_{n,g} &= 0 \end{aligned}$$

wherefrom we can write the expansion

$$e^{\alpha|t|} = \frac{1}{\alpha\theta} (e^{\alpha\theta} - 1) + \sum_{n=1}^{\infty} \frac{2\alpha}{\theta} \frac{[(-1)^n e^{\alpha\theta} - 1]}{(\alpha^2 + n^2\pi^2/\theta^2)} \cos(n\pi t/\theta), \quad -\theta \leq t \leq \theta.$$

The expansion of the given function $f(t)$ can be written, noticing that $f(t) = g(t)$, $0 < t < \theta$, so that

$$e^{\alpha t} = \frac{(e^{\alpha\theta} - 1)}{\alpha\theta} + \sum_{n=1}^{\infty} \frac{2\alpha}{\theta} \frac{[(-1)^n e^{\alpha\theta} - 1]}{(\alpha^2 + n^2\pi^2/\theta^2)} \cos(n\pi t/\theta), \quad 0 < t < \theta.$$

We have thus obtained a cosine series expansion of the function $f(t)$.

(b) Sine series

A sine series expansion can be obtained if an odd function is constructed from $f(t)$, as shown in the figure. We write

$$v(t) = \begin{cases} f(t), & 0 < t < \theta \\ -f(-t), & -\theta < t < 0 \end{cases} = \begin{cases} e^{-t}, & 0 < t < \theta \\ -e^t, & -\theta < t < 0. \end{cases}$$

The coefficients V_n of $v(t)$ are pure imaginary due to the odd symmetry. We have, with $\omega_0 = 2\pi/T = \pi/\theta$,

$$V_n = \frac{-j}{\theta} \int_0^\theta e^{\alpha t} \sin(n\omega_0 t) dt = \frac{-j}{\theta} \int_0^\theta e^{\alpha t} \Im [e^{jn\omega_0 t}] dt = \frac{-j}{\theta} \Im \left[\int_0^\theta e^{\alpha t} e^{jn\omega_0 t} dt \right].$$

Integrating we obtain

$$V_n = j \frac{n\pi}{\theta^2} \frac{(-1)^n e^{\alpha\theta} - 1}{(\alpha^2 + n^2\pi^2/\theta^2)}.$$

The trigonometric series coefficients are given by $a_n, v = 0, n \geq 0$,

$$b_n, v = -2 \Im[V_n] = \frac{2n\pi}{\theta^2} \frac{1 - (-1)^n e^{\alpha\theta}}{(\alpha^2 + n^2\pi^2/\theta^2)}.$$

We can therefore write the expansion

$$v(t) = \sum_{n=1}^{\infty} \frac{2n\pi}{\theta^2} \frac{1 - (-1)^n e^{\alpha\theta}}{(\alpha^2 + n^2\pi^2/\theta^2)} \sin(n\pi t/\theta), \quad -\theta < t < \theta$$

and

$$e^{\alpha t} = \sum_{n=1}^{\infty} \frac{2n\pi}{\theta^2} \frac{1 - (-1)^n e^{\alpha\theta}}{(\alpha^2 + n^2\pi^2/\theta^2)} \sin(n\pi t/\theta), \quad 0 < t < \theta.$$

2.14 Deducing a Function Form from Its Expansion

If we are given a Fourier series expansion of an interval of a function $f(t)$ we can deduce the function overall periodic form using the symmetry property reflected in its expansion, as the following examples illustrate.

Example 2.12 Deduce the overall form of the function $f(t)$ of which the Fourier series expansion is given by

$$\sum_{n=0}^{\infty} \frac{\sin(2n+1)t}{2n+1} = \frac{\pi}{4}, \quad 0 < t < \pi.$$

We note that the expansion is a sum of sine functions of the form $\sin kt$, $k = 2n + 1$. We can write the trigonometric expansion

$$f(t) = \sum_{k=1, 3, 5, \dots}^{\infty} b_k \sin k\omega_0 t$$

where $\sin \omega_0 t = \sin t$, $\sin 3\omega_0 t = \sin 3t$, \dots . The fundamental frequency $\omega_0 = 1 = 2\pi/T$, that is, $T = 2\pi$. The expanded function is therefore of period $T = 2\pi$. It is odd since its expansion is a sine series. Moreover, since it has only odd harmonics it has odd half-periodic symmetry, that is, $f(t + T/2) = -f(t)$. These results are summarized in Fig. 2.35.

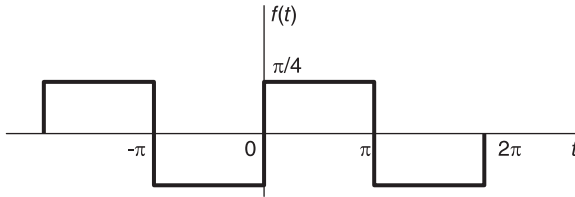


FIGURE 2.35 Function form deduced from Fourier series expansion.

Example 2.13 Deduce the overall form of the function $f(t)$ which has the Fourier series expansion

$$\sum_{n=0}^{\infty} (-1)^n \frac{\cos(2n+1)t}{2n+1} = \frac{\pi}{4}, \quad -\frac{\pi}{2} < t < \frac{\pi}{2}.$$

Similarly to the previous example we have $\cos k\omega_0 t = \cos kt$, $k = (2n + 1)$ so that the fundamental frequency is $\omega_0 = 1$, that is, $\omega_0 = 2\pi/T = 1$ or $T = 2\pi$. The periodically extended function $f(t)$ is therefore of period $T = 2\pi$. Since the expansion is a cosine series the function is even. Since it contains only odd harmonics the function has odd half-periodic symmetry. The function $f(t)$, shown in Fig. 2.36, has double symmetry, being even and having half-periodic odd symmetry.

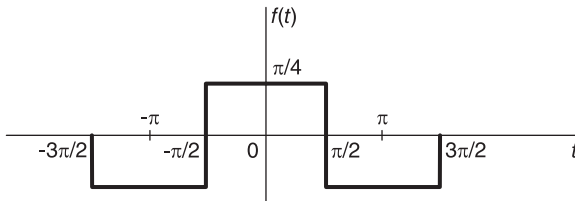


FIGURE 2.36 Function form deduced from Fourier series expansion.

2.15 Truncated Sinusoid Spectral Leakage

In this section we study a phenomenon referred to as *spectral leakage*. This phenomenon is observed if a Fourier series expansion of a sinusoid is performed with an analysis interval that is not related to the function period. Instead of a sharp spectral line at the signal frequency, the result is “spectral leakage” as we shall shortly see. We start by evaluating the Fourier series of a sinusoid with an analysis interval that is a multiple of its period.

Example 2.14 Evaluate the expansion of $f(t) = \cos(\beta t)$ over an analysis interval T_0 that is five times the period.

We have $\omega_0 = 2\pi/T_0 = 2\pi/5\tau = \beta/5$, and the expansion has the form

$$f(t) = \cos(\beta t) = (e^{j\beta t} + e^{-j\beta t})/2 = \sum_{n=-\infty}^{\infty} F_n e^{jn\omega_0 t} = \sum_{n=-\infty}^{\infty} F_n e^{jn(\beta/5)t}.$$

Equating coefficients of similar terms we obtain $F_n = 1/2$, for $n = \pm 5$ and $F_n = 0$ otherwise, as expected.

We consider now the more general problem of the analysis of a sinusoid $f(t) = \sin(\beta t + \theta)$ with an arbitrary analysis interval unrelated to its period. Writing

$$f(t) = \sin(\beta t + \theta) = \left\{ e^{j(\theta + \beta t)} - e^{-j(\theta + \beta t)} \right\} / (2j) \tag{2.111}$$

we note that since the analysis interval T_0 is not a multiple of or equal to the period τ_0 the series depends on the starting point t_0 of the analysis interval ($t_0, t_0 + T_0$). For simplicity we assume $t_0 = 0$. We have $\omega_0 = 2\pi/T_0$,

$$\begin{aligned} F_n &= \frac{1}{T_0} \int_0^{T_0} f(t) e^{-jn\omega_0 t} dt \\ &= \frac{1}{T_0 2j} \left\{ e^{j\theta} \int_0^{T_0} e^{j\beta t} e^{-jn\omega_0 t} dt - e^{-j\theta} \int_0^{T_0} e^{-j\beta t} e^{-jn\omega_0 t} dt \right\} \\ &= \frac{-1}{2} \left\{ e^{j\theta} \frac{e^{j(\beta T_0 - 2\pi n)} - 1}{(\beta T_0 - 2\pi n)} + e^{-j\theta} \frac{e^{-j(\beta T_0 + 2\pi n)} - 1}{(\beta T_0 + 2\pi n)} \right\} \end{aligned} \tag{2.112}$$

which can be rewritten in the form

$$F_n = -\frac{1}{2} \left\{ j e^{j(\beta T_0/2 - \pi n + \theta)} \frac{\sin(\beta T_0/2 - \pi n)}{(\beta T_0/2 - \pi n)} - j e^{-j(\beta T_0/2 + \pi n + \theta)} \frac{\sin(\beta T_0/2 + \pi n)}{(\beta T_0/2 + \pi n)} \right\}. \tag{2.113}$$

We shall use the *sampling function* defined by $Sa(x) = (\sin x)/x$, noticing that $Sa(0) = \lim_{x \rightarrow 0} (\sin(x))/x = 1$ using l’Hopital’s rule. We also note in passing that $\text{sinc} \lambda = \sin(\pi \lambda)/(\pi \lambda) = Sa(\pi \lambda)$, and conversely $Sa(x) = \text{sinc}(x/\pi)$. The Sa function is shown schematically in Fig. 2.37. We can rewrite the equation of F_n in the form

$$F_n = -\frac{j}{2} \left\{ e^{j(\beta T_0/2 - \pi n + \theta)} Sa(\beta T_0/2 - n\pi) - e^{-j(\beta T_0/2 + \pi n + \theta)} Sa(\beta T_0/2 + n\pi) \right\} \tag{2.114}$$

i.e.

$$F_n = \frac{1}{2} \left\{ e^{j[(T_0/\tau_0 - n - 0.5)\pi + \theta]} Sa[\pi(T_0/\tau_0 - n)] + e^{-j[(T_0/\tau_0 + n - 0.5)\pi + \theta]} Sa[\pi(T_0/\tau_0 + n)] \right\}. \tag{2.115}$$

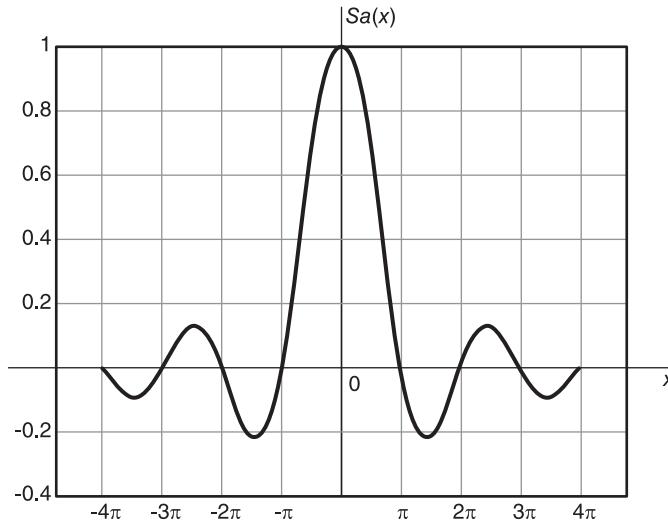


FIGURE 2.37 Sampling function $Sa(x)$.

Having found the coefficients we can write the expansion in the form

$$\begin{aligned} \sin(\beta t + \theta) = & \sum_{n=-\infty}^{\infty} \left\{ \frac{1}{2} e^{j\left\{\left(\frac{\pi}{\tau_0} - n - 0.5\right)\pi + \theta\right\}} Sa \left[\pi \left(\frac{T_0}{\tau_0} - n \right) \right] \right. \\ & \left. + \frac{1}{2} e^{-j\left\{\left(\frac{\pi}{\tau_0} + n - 0.5\right)\pi + \theta\right\}} Sa \left[\pi \left(\frac{T_0}{\tau_0} + n \right) \right] \right\} e^{j\frac{2\pi}{T_0}nt}, \quad 0 < t < T_0. \end{aligned} \quad (2.116)$$

As may be expected, in the case $T_0 = m\tau_0$, m positive integer, the expression of the coefficients should reduce to the simple form corresponding to that of a pure sinusoid with an analysis interval that is multiple of its period. In fact, substituting we obtain

$$F_n = \begin{cases} \frac{1}{2} e^{j(\theta - \pi/2)}, & n = m \\ \frac{1}{2} e^{-j(\theta - \pi/2)}, & n = -m \\ 0, & \text{otherwise.} \end{cases} \quad (2.117)$$

Example 2.15 For the signal $f(t) = \sin(6t + \pi/4)$ evaluate the Fourier series over the interval $(0, T_0)$ with (a) $T_0 = 15\pi/6$ s (b) $T_0 = 3\pi$ s Represent graphically the series coefficients.

The period of $f(t)$ is given by $\tau_0 = 2\pi/6 = \pi/3$.

(a) $T_0/\tau_0 = 7.5$.

The analysis interval T_0 is not a multiple of τ_0 . Substituting in Equation (2.115) we have

$$F_n = \frac{1}{2} e^{j(7.25-n)\pi} Sa[(7.5\pi - n)\pi] + \frac{1}{2} e^{-j(7.25+n)\pi} Sa[(7.5 + n)\pi].$$

The modulus $|F_n|$ and argument $\arg[F_n]$, that is, the amplitude and phase spectrum, are represented graphically in Fig. 2.38. We note that the amplitude spectrum rises to a maximum that lies between $n = \pm 7$ and $n = \pm 8$ respectively. Each sampling function $Sa(\cdot)$ peaks when its argument is equal to zero, that is, at $n \pm 7.5$ but these true peaks are not seen since the coefficients F_n are defined only for integer values of n .

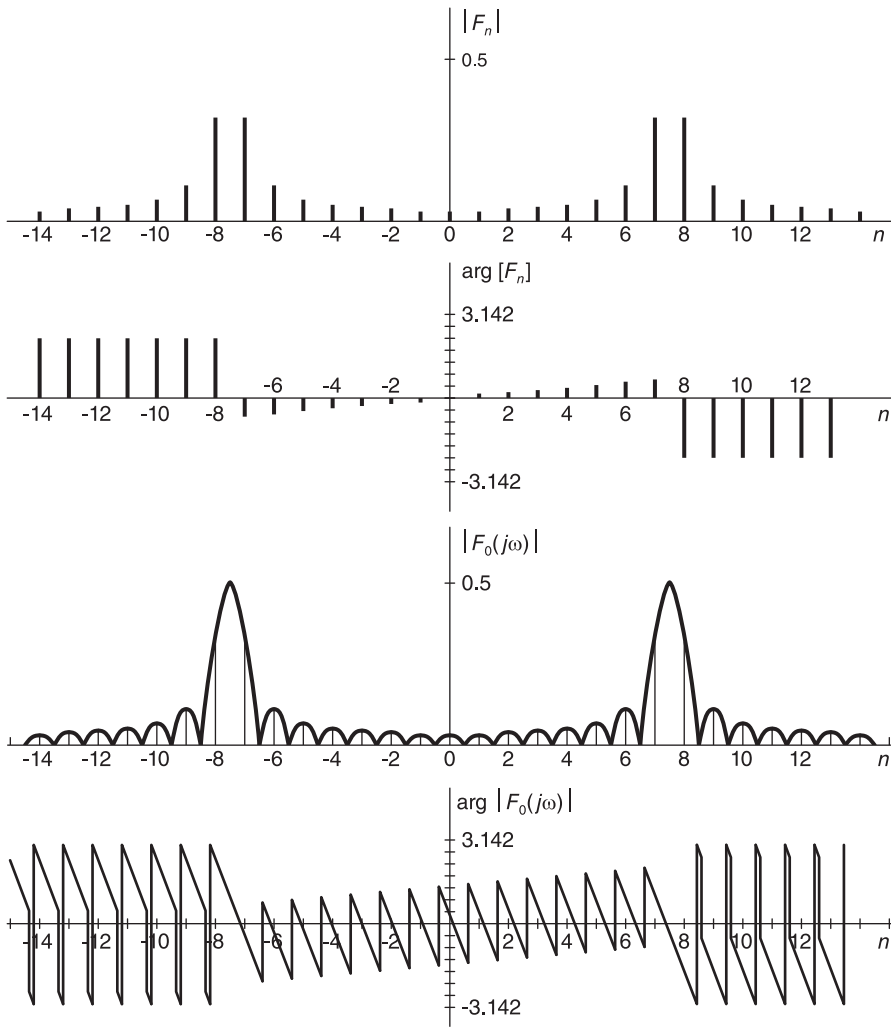


FIGURE 2.38 Fourier series coefficients of truncated sinusoid and corresponding Fourier transform spectrum.

If n is made to vary as a real (continuous) variable ω we would see the continuous form of the curve of coefficients as defined by this last equation. The resulting curves are shown in the figure. The exponential coefficients F_n are in fact the discrete functions resulting from sampling at integer values of n these continuous functions, which are none other than the Fourier transform spectra, as we shall see in Chapter 4.

(b) We have $T_0/\tau_0 = 3\pi/(\pi/3) = 9$. Since T_0 is a multiple of τ_0 , the coefficients F_n are given by

$$F_n = \frac{1}{2} e^{j(8.75-n)\pi} \text{Sa}[(9-n)\pi] + \frac{1}{2} e^{-j(8.75+n)\pi} \text{Sa}[(9+n)\pi]$$

$$F_n = \begin{cases} 0, & n \neq \pm 9 \\ \frac{1}{2} e^{\mp j\pi/4}, & n = \pm 9 \end{cases}$$

$|F_9| = |F_{-9}| = 1/2$, $\arg[F_9] = -\arg[F_{-9}] = -\pi/4$, as shown in Fig. 2.39.

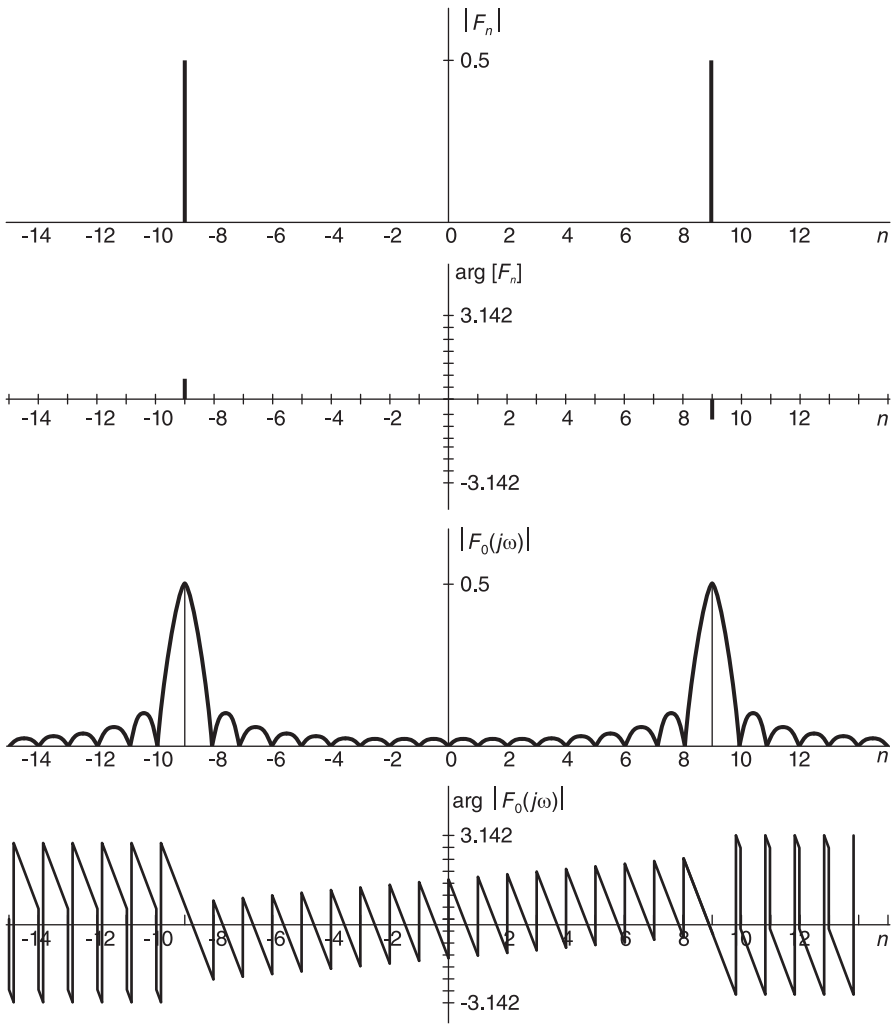


FIGURE 2.39 Fourier series coefficients of a properly truncated sinusoid and corresponding Fourier transform spectrum.

The corresponding continuous functions, of which the coefficients F_n are but samples taken at discrete values of n , as we have just seen, are shown in the figure. As will be noted in Chapter 4 this continuous function is none other than the Fourier transform of the analysis section of the sinusoid.

2.16 The Period of a Composite Sinusoidal Signal

Let $f(t)$ be the sum of several sinusoidal components of different frequencies. To effect a Fourier series expansion of $f(t)$ while avoiding spectral leakage we need to evaluate the period of $f(t)$ or, equivalently, its fundamental frequency. We note that the fundamental

frequency of $f(t)$ is the highest frequency of which each of the frequencies of the different components is a multiple. The fundamental frequency of $f(t)$ can thus be found by evaluating the *greatest common divisor (GCD)* of the frequencies of its components. Equivalently, the period of $f(t)$ is the *least common multiple (LCM)* of the periods of its components.

Example 2.16 Given a signal $x(t)$ defined by

$$x(t) = A \sin \beta_1 t + B \cos \beta_2 t$$

with $\beta_1 = 23100\pi$ r/s and $\beta_2 = 8820\pi$ r/s.

- a) Evaluate the fundamental frequency of $x(t)$.
- b) Evaluate the Fourier series coefficients of $x(t)$ with an analysis interval $T_0 = 4.8$ ms.
- c) Evaluate the Fourier series coefficients with an analysis interval $T_0 = 48$ ms.

a) Let $x(t) = x_1(t) + x_2(t)$, where $x_1(t) = A \sin \beta_1 t$ and $x_2(t) = B \cos \beta_2 t$. The value of the fundamental frequency Ω_0 is the GCD of β_1 and β_2 . By successive simplification of the ratio β_1/β_2 , eliminating common factors, we obtain $\Omega_0 = 420\pi$ r/s.

It is worthwhile noticing that in general the GCD may be evaluated by decomposing each of β_1 and β_2 into the product of its prime numbers. We have

$$\beta_1 = 2^2 \times 3 \times 5^2 \times 7 \times 11 \times \pi, \quad \beta_2 = 2^2 \times 3^2 \times 5 \times 7^2 \times \pi.$$

The intersection of the corresponding two sets of prime numbers, that is,

$$\{2, 2, 3, 5, 5, 7, 11\} \cap \{2, 2, 3, 3, 5, 7, 7\} = \{2, 2, 3, 5, 7\}$$

is the set of elements of which the product forms the greatest common divisor. The GCD of the prime numbers is thus given by $2 \times 2 \times 3 \times 5 \times 7 = 420$, and $\Omega_0 = 420 \pi$.

b) With an analysis interval $T_0 = 0.0048 = \tau_0$ the Fourier series fundamental frequency is $\omega_0 = 2\pi/T_0 = \Omega_0$, $\beta_1 = 55\omega_0$, $\beta_2 = 21\omega_0$. Hence

$$X_n = \begin{cases} (A/2) e^{\mp j\pi/2} = \mp jA/2, & n = \pm 55 \\ B/2, & n = \pm 21 \\ 0, & \text{otherwise.} \end{cases}$$

c) With an analysis interval $T_0 = 0.048 = 10\tau_0$ that is, with a Fourier series fundamental frequency of $\omega_0 = 2\pi/(10\tau_0) = 0.1\Omega_0$, $\beta_1 = 55\Omega_0 = 550\omega_0$, $\beta_2 = 21\Omega_0 = 210\omega_0$ and

$$X_n = \begin{cases} (A/2) e^{\mp j\pi/2}, & n = \pm 550 \\ B/2, & n = \pm 210 \\ 0, & \text{otherwise.} \end{cases}$$

Example 2.17 Find the fundamental frequency and period of the signal

$$x(t) = \cos \beta_1 t \sin \beta_2 t$$

where $\beta_1 = 2\pi f_1$, $\beta_2 = 2\pi f_2$, $f_1 = 19053144$ Hz, $f_2 = 57499200$ Hz.

We may write the two frequencies as products of prime numbers

$$f_1 = 2^3 \cdot 3^9 \cdot 11^2$$

$$f_2 = 2^6 \cdot 3^3 \cdot 5^2 \cdot 11^3$$

wherefrom $f_0 = \text{GCD}(f_1, f_2) = 2^3 \cdot 3^3 \cdot 11^2 = 26136$, $\tau_0 = 1/f_0 = 3.8261 \times 10^{-5}$ s. We note that we may also write $x(t) = \frac{1}{2} [\sin \gamma_1 t - \sin \gamma_2 t]$, where $\gamma_1 = \beta_1 + \beta_2 = 2\pi \times 76552344$, $\gamma_2 = \beta_2 - \beta_1 = 2\pi \times 38446056$ and $f_0 = \text{GCD}(\gamma_1/(2\pi), \gamma_2/(2\pi)) = 26136$, as found.

The GCD of two numbers m and n can be evaluated using the MATLAB® function `gcd(m, n)`. Decomposition into prime numbers of a number n can be effected using the MATLAB function `factor(n)`. For three numbers m, n, k the GCD can be evaluated by writing

$$\text{gcd}\{\text{gcd}(m, n), k\}.$$

Note that for the sum or product of two sinusoids of frequencies f_1 and f_2 Hz to be periodic the ratio f_1/f_2 of their frequencies should be a rational value, i.e. can be expressed as the ratio of two integers. If the ratio is irrational the sum or product of the sinusoids is not periodic.

The period of a signal $x(t)$ that is the sum of two sinusoids $x_1(t)$ and $x_2(t)$ may be evaluated as the least common multiple LCM of the periods of $x_1(t)$ and of $x_2(t)$. The LCM is obtained as the union of the two prime number sets corresponding to the two periods.

Example 2.18 A signal is the sum of two sinusoids of periods $T_1 = 2063.698$ sec and $T_2 = 60.605$ sec. Evaluate its period.

Let

$$\tau_1 = T_1 \times 10^3 = 2063698 = 2 \times 7 \times 13 \times 17 \times 23 \times 29, \quad (2.118)$$

$$\tau_2 = T_2 \times 10^3 = 60605 = 5 \times 17 \times 23 \times 31. \quad (2.119)$$

Now

$$\{2, 7, 13, 17, 23, 29\} \cup \{5, 17, 23, 31\} = \{2, 5, 7, 13, 17, 23, 29, 31\} \quad (2.120)$$

$$\tau = 2 \times 5 \times 7 \times 13 \times 17 \times 23 \times 29 \times 31 = 319873190. \quad (2.121)$$

Hence the period is $T = 319873.190$ sec.

The LCM of two numbers m and n can be evaluated using the MATLAB instruction `lcm(m, n)`.

2.17 Passage through a Linear System

Let $x(t)$ and $y(t)$ be the input and output of a linear time invariant (LTI) system. As stated in Chapter 1 we may write, with zero initial conditions,

$$Y(s) = X(s)H(s) \quad (2.122)$$

$$Y(j\omega) = X(j\omega)H(j\omega) \quad (2.123)$$

where the transfer function $H(j\omega)$ is referred to as the *system frequency response*. Let the input $x(t)$ be periodic of period T . We can write the Fourier series expansion

$$x(t) = \sum_{n=-\infty}^{\infty} X_n e^{jn\omega_0 t}, \quad \omega_0 = 2\pi/T. \quad (2.124)$$

As we shall see in Chapter 4 the Fourier transform of 1 is $2\pi\delta(\omega)$ and using the shift in frequency property, the transform of $e^{jn\omega_0 t}$ is $2\pi\delta(\omega - n\omega_0)$. If the input to the system is $x(t) = e^{jn\omega_0 t}$ then the input output relation is

$$Y(j\omega) = X(j\omega)H(j\omega) = 2\pi\delta(\omega - n\omega_0)H(j\omega) = 2\pi H(jn\omega_0)\delta(\omega - n\omega_0). \quad (2.125)$$

Hence

$$y(t) = H(jn\omega_0)e^{jn\omega_0 t}. \tag{2.126}$$

The response of the system to each complex exponential $e^{jn\omega_0 t}$ is therefore $H(jn\omega_0)e^{jn\omega_0 t}$, and the response to the sum of such exponentials is the sum of the responses to each of them. The output of the system is thus given by

$$y(t) = \sum_{n=-\infty}^{\infty} X_n H(jn\omega_0) e^{jn\omega_0 t}. \tag{2.127}$$

This last equation has the form of a Fourier series expansion of the output $y(t)$

$$y(t) = \sum_{n=-\infty}^{\infty} Y_n e^{jn\omega_0 t} \tag{2.128}$$

where the coefficients are given by

$$Y_n = X_n H(jn\omega_0). \tag{2.129}$$

In other words the output (discrete) spectrum is equal to the multiplication of the input spectrum by the frequency response “sampled” at multiples of the fundamental frequency.

2.18 Parseval’s Relations

As observed in Chapter 1, the “normalized energy” or simply energy of a real signal $f(t)$ expressed in volts is given by

$$E = \int_{-\infty}^{\infty} f^2(t) dt \text{ joules} \tag{2.130}$$

If $f(t)$ is a periodic signal of period T then the average power dissipated in one period T is given by

$$P = \overline{f^2}(t) = \frac{1}{T} \int_T f^2(t) dt \text{ watts.} \tag{2.131}$$

Let F_n be the Fourier series coefficients of the periodic function $f(t)$. Parseval’s relation states that

$$\frac{1}{T} \int_T f(t)^2 dt = \sum_{n=-\infty}^{\infty} |F_n|^2. \tag{2.132}$$

Proof We have

$$\begin{aligned} \frac{1}{T} \int_T |f(t)|^2 dt &= \frac{1}{T} \int_T f(t) f^*(t) dt = \frac{1}{T} \int_T f(t) \left\{ \sum_{n=-\infty}^{\infty} F_n e^{jn\omega_0 t} \right\}^* dt \\ &= \frac{1}{T} \sum_{n=-\infty}^{\infty} F_n^* \int_T f(t) e^{-jn\omega_0 t} dt = \sum_{n=-\infty}^{\infty} F_n^* F_n = F_0^2 + 2 \sum_{n=1}^{\infty} |F_n|^2. \end{aligned}$$

In terms of the trigonometric Fourier series, since $F_0 = a_0/2$, and $F_n = (a_n - jb_n)/2$, i.e. $|F_n| = \sqrt{a_n^2 + b_n^2}/2$, $n \geq 1$, Parseval’s relation takes the form

$$\frac{1}{T} \int_T f(t)^2 dt = a_0^2/4 + \frac{1}{2} \sum_{n=1}^{\infty} (a_n^2 + b_n^2). \tag{2.133}$$

2.19 Use of Power Series Expansion

For certain functions the Fourier series can be evaluated using a power series expansion as the following example demonstrates.

Example 2.19 Evaluate the expansions of $f(t) = \ln[2 \cos(t/2)]$ and $g(t) = \ln[2 \sin(t/2)]$.

The functions are depicted in Fig. 2.40.

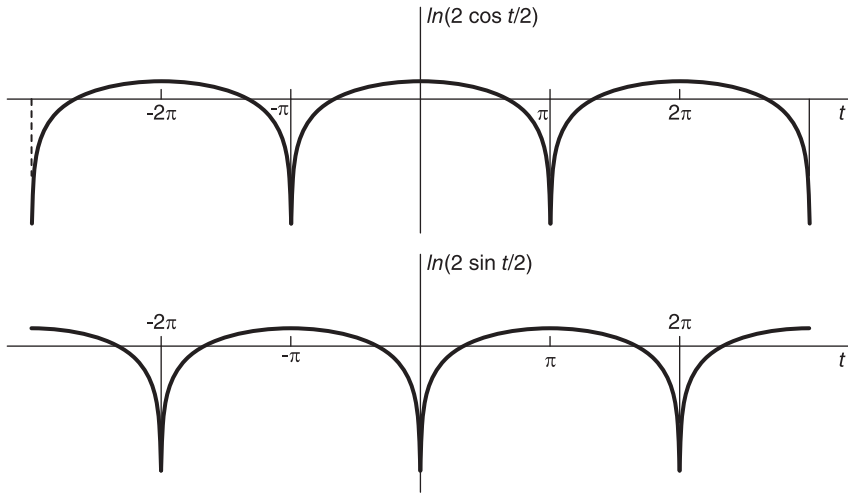


FIGURE 2.40 Log-cosine and log-sine functions.

We make use of the power series expansion

$$\ln(1+z) = \sum_{n=1}^{\infty} \frac{(-1)^{n-1}}{n} z^n$$

$$\ln(1+e^{jt}) = \sum_{n=1}^{\infty} \frac{(-1)^{n-1}}{n} e^{jnt}.$$

We note that $f(t)$ is finite if and only if $2 \cos(t/2) > 0$ i.e. $-\pi < t < \pi$ so that

$$|2 \cos(t/2)| = |e^{jt/2} + e^{-jt/2}| = |e^{-jt/2}(e^{jt} + 1)| = |e^{jt} + 1|, \quad -\pi < t < \pi$$

and if $z = re^{j\theta}$ then

$$\ln(z) = \ln(re^{j\theta}) = \ln(re^{j\theta} e^{j2k\pi}) = \ln(r) + j(\theta + 2k\pi) = \ln(|z|) + j\{\arg(z) + 2k\pi\}$$

i.e. $\ln(|z|) = \Re[\ln z]$.

We may therefore write

$$\ln[2 \cos(t/2)] = \ln[|1 + e^{jt}|] = \Re[\ln[(1 + e^{jt})]], \quad -\pi < t < \pi$$

$$\ln [2 \cos(t/2)] = \Re \left[\sum_{n=1}^{\infty} \frac{(-1)^{n-1}}{n} e^{jnt} \right] = \sum_{n=1}^{\infty} \frac{(-1)^{n-1}}{n} \cos(nt), \quad -\pi < t < \pi$$

which is the trigonometric Fourier series expansion. The coefficients are

$$a_0 = 0, \quad a_n = (-1)^{n-1}/n, \quad n \neq 0; \quad b_n = 0, \quad F_n = a_n/2 = (-1)^{n-1}/(2n).$$

The exponential coefficients F_n are shown in Fig. 2.41.

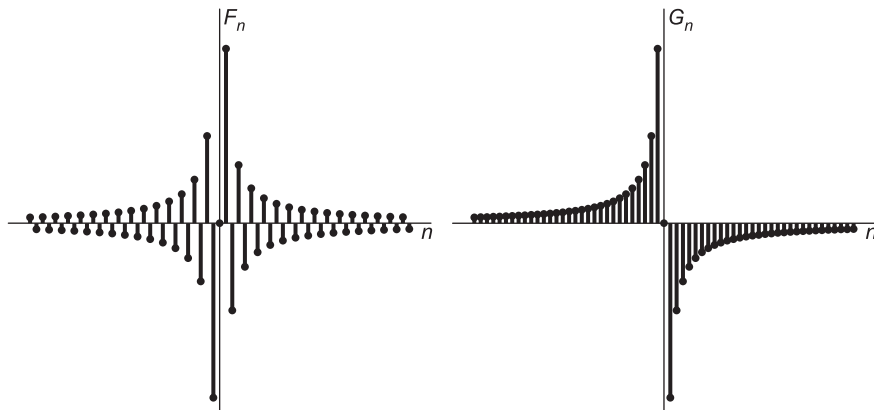


FIGURE 2.41 Discrete spectra of log-cosine and log-sine functions.

Similarly,

$$2 \sin(t/2) = | -j(e^{jt/2} - e^{-jt/2}) | = |1 - e^{jt}|, \quad 0 < t < 2\pi$$

$$\ln [2 \sin (t/2)] = \Re [\ln \{ 1 + e^{j(t+\pi)} \}] = \Re \left[\sum_{n=1}^{\infty} (-1)^{n-1} \frac{e^{j(t+\pi)n}}{n} \right] = - \sum_{n=1}^{\infty} \frac{\cos nt}{n}, \quad 0 < t < 2\pi$$

which is the trigonometric Fourier series expansion. The coefficients are

$$a_0 = 0, \quad a_n = -1/n, \quad n \neq 0; \quad b_n = 0, \quad G_0 = 0, \quad G_n = -1/(2n).$$

The exponential Coefficients G_n are shown in the figure.

2.20 Inverse Fourier Series

In some applications that call for the evaluation of infinite summations it is sometimes possible to obtain solutions which may be viewed as evaluations of an *inverse Fourier series*. The following example illustrates the approach.

Example 2.20 Evaluate the function described by the expansion

$$\sum_{n=1}^{\infty} (-1)^n \frac{\sin nt}{n}, \quad -\pi < t < \pi.$$

Let

$$S = \sum_{n=1}^{\infty} (-1)^n \frac{\sin nt}{n} = \Im \left[\sum_{n=1}^{\infty} (-1)^n \frac{e^{jnt}}{n} \right].$$

We note that

$$\begin{aligned} \ln(1+z) &= \sum_{n=1}^{\infty} (-1)^{n-1} \frac{z^n}{n} \\ S &= -\Im \left[\sum_{n=1}^{\infty} (-1)^{n-1} \frac{e^{jnt}}{n} \right] = -\Im[\ln(1+e^{jt})]. \end{aligned}$$

Writing $\ln(re^{j\theta}) = \ln r + j\theta$, $-\pi < \theta \leq \pi$, we have

$$\begin{aligned} 1 + e^{jt} &= e^{jt/2} \left[e^{-jt/2} + e^{jt/2} \right] = 2e^{jt/2} \cos(t/2) = re^{j\theta} \\ r &= 2 \cos(t/2), \quad \theta = t/2, \quad -\pi < t < \pi \\ \ln(1 + e^{jt}) &= \ln r + j\theta = \ln \{2 \cos(t/2)\} + jt/2, \quad -\pi < t < \pi \\ S &= -t/2, \quad -\pi < t < \pi. \end{aligned}$$

2.21 Problems

Problem 2.1 Consider a periodic signal $f(t)$ of period $T = 2$

$$f(t) = 4t, \quad 0 < t < 1$$

and

$$f(t + T/2) = -f(t).$$

Sketch the signal $f(t)$. Evaluate the Fourier series expansion over one period $T = 2$, by integrating over the intervals a) $(0, 2)$, b) $(-1, 1)$ and c) $(0, 1)$ successively, comparing the results obtained with those produced by Mathematica or Maple.

Problem 2.2 Consider the periodic signal $y(t)$ of period $T = 16\tau$ such that

$$y(t) = \begin{cases} 1, & 0 < t < \tau, \quad 6\tau < t < 10\tau, \quad 15\tau < t < 16\tau \\ 0, & \tau < t < 6\tau, \quad 10\tau < t < 15\tau. \end{cases}$$

Evaluate the Fourier series coefficients of $y(t)$ with an analysis interval a) $(-4\tau, 4\tau)$, b) $(0, 16\tau)$.

Problem 2.3 Let $f(t)$ be periodic with period $T = 2$ sec. With $f(t) = t^k$, $0 < t < 1$

i) If $k = 2$, sketch the function and evaluate the Fourier series expansion of $f(t)$ for the cases:

- $f(t) = t^k$, $-1 < t < 0$
- $f(t) = -t^k$, $-1 < t < 0$
- $f(t+1) = -f(t)$.

ii) Repeat the above if $k = 3$.

Problem 2.4 Consider the periodic signal

$$x(t) = C_0 + \sum_{n=1}^{+\infty} C_n \cos(20\pi nt - \phi_n)$$

For each of the following functions evaluate the coefficients C_n and ϕ_n . Note that the amplitude coefficients C_n cannot be negative and that the phase coefficients are such that $0 \leq \phi_n < 2\pi$.

a) $x(t) = 5$

b) $x(t) = \cos(40\pi[t - 0.02])$

c) $x(t) = \sin(60\pi t)$

d) $x(t) = 3 + 3 \cos(20\pi t) + 4 \sin(20\pi t) + 0.5 \sin\left(40\pi t - \frac{\pi}{4}\right)$

e) $x(t) = \cos(40\pi t) \cos(60\pi t)$

Problem 2.5 The Fourier series expansion of a periodic signal $x(t)$ with an analysis interval equal to the signal period T sec is given by

$$x(t) = C_0 + \sum_{n=1}^{+\infty} C_n \cos(20\pi nt - \phi_n).$$

Evaluate in terms of C_0 , C_n and ϕ_n , the corresponding coefficients of the signals :

a) $5x(t)$, b) $x(t) + 5$, c) $x(t + 5T)$, d) $x(t + T/5)$, e) $dx(t)/dt$.

Problem 2.6 Let $v(t) = \sum_{n=-\infty}^{\infty} v_0(t - 2n\pi)$ where $v_0(t) = \sin(t) R_\pi(t)$.

a) Sketch the signal $v(t)$ and evaluate its exponential Fourier series coefficients V_n with an analysis interval of $T = 2\pi$.

b) Let $y(t) = [\sin(t) R_\pi(t)] * \rho_\pi(t)$. Evaluate the Fourier series coefficients Y_n with the same analysis interval $T = 2\pi$, in terms of the coefficients V_n .

Problem 2.7 Evaluate as a sum of trigonometric functions the signal $v(t)$, given that its exponential Fourier series coefficients, with an analysis interval equal to T , are given by

$$V_n = \begin{cases} 1, & n = 0 \\ 2e^{+j\pi/4} + je^{-j20\pi/T}, & n = +1 \\ 2e^{-j\pi/4} - je^{+j20\pi/T}, & n = -1. \end{cases}$$

Problem 2.8 For each of the following signals

$$f(t) = 6, \quad g(t) = \cos(2\pi t/T), \quad h(t) = \sin(6\pi t/T)$$

$$s(t) = h(t) + 2g(t) + 3, \quad v(t) = g(t + 2T), \quad w(t) = dg(t)/dt$$

$$x(t) = \cos[4\pi(t - 1)/T], \quad y(t) = \sin(6\pi t/T + \pi/4).$$

a) Evaluate the trigonometric Fourier series coefficients with an analysis interval equal to T .

b) Repeat the above, evaluating instead the exponential coefficients.

Problem 2.9 Let a_n and b_n be the trigonometric Fourier series coefficients of a signal $v(t)$, with an analysis interval T . For the same analysis interval, evaluate the trigonometric series coefficients of the following signals expressed in terms of the coefficients a_n and b_n .

a) $y(t) = \alpha_0 v(t) + \alpha_1$, where α_0 and α_1 are real constants

b) $y(t) = dv(t)/dt$

c) $y(t) = v(t - t_0)$, where t_0 is a constant delay

Problem 2.10 Evaluate the exponential Fourier series coefficients of the two periodic following signals $x(t)$ and $y(t)$ with an analysis interval equal to one period

a) $x(t) = A\rho_{0.1}(t)$ b) $y(t) = 4\rho_3(t) - 2\rho_3(t+1)$

Problem 2.11 Consider the periodic signal $x(t) = \sum_n v(t - 3n)$ where $v(t) = (A/3)t R_3(t)$.

a) Evaluate the trigonometric Fourier series coefficients of the signal $y(t) = dx(t)/dt$, with an analysis interval of 3 seconds.

b) Deduce from the result obtained in part a) the trigonometric coefficients of the signal $x(t)$ with the same analysis interval.

Problem 2.12 Evaluate the exponential Fourier series coefficients of each of the following signals with an analysis interval equal to T .

a) $x(t) = \sum_n A\Pi_{d/2}\left(t - \frac{T}{2} - nT\right)$, where $d \leq T$

b) $y(t) = 3x\left(t + \frac{T}{4}\right) - 1$

c) The signal $z(t)$ obtained after the component of frequency $2/T$ Hz is removed from the signal $x(t)$

Problem 2.13 Let the signal $v(t) = \sin(t) \sum_n R_{2\pi}(t - 4\pi n)$.

a) Evaluate the exponential Fourier series coefficients V_n of $v(t)$ with an analysis interval equal to 4π .

b) Given that the exponential coefficients X_n , of a signal $x(t)$ have the values

$$X_n = \begin{cases} 0, & n = \pm 2 \\ V_n, & \text{otherwise.} \end{cases}$$

Sketch $x(t)$.

c) Let $y(t) = v(t - \pi) - v(t + \pi)$.

Deduce the exponential coefficients of $y(t)$ with an analysis interval of 4π in terms of the coefficients V_n .

d) Redo part c) with an analysis interval of 8π .

Problem 2.14 Let $x(t)$ be a periodic signal of period $T = 10^{-3}$ seconds having exponential Fourier series coefficients X_n , with an analysis interval 10^{-3} seconds, given by

$$X_n = 0.25Sa(\pi n/4)$$

a) What is the average value of $x(t)$?

b) What is the amplitude of the signal component of frequency 9 kHz ?

Problem 2.15 A periodic signal $v(t)$ of period T has exponential Fourier series coefficients V_n , evaluated with an analysis interval $2T$, given by

$$V_n = \begin{cases} 1, & n = 0 \\ 0, & n = \pm 1 \\ \frac{(-1)^{n+1}}{2\pi(1-n^2)}, & \text{otherwise.} \end{cases}$$

a) Evaluate the exponential Fourier series coefficients of the signal $v(t)$ if the analysis interval is T .

b) Let $x(t) = v(t) + 3$. Evaluate the exponential Fourier series coefficients X_n of the signal $x(t)$ if the analysis interval is $2T$.

c) Let $y(t) = v(t) + \cos(\pi t/T)$. Evaluate the exponential Fourier series coefficients Y_n of the signal $y(t)$ if the analysis interval is $2T$.

d) Let $z(t) = v(t - T)$. Evaluate the exponential Fourier series coefficients Z_n of the signal $z(t)$ if the analysis interval is $2T$.

Problem 2.16 Given the periodic signal $v(t) = \sum_{n=-\infty}^{\infty} V_n e^{j200\pi nt}$ where the coefficients V_n are given by

$$V_n = \begin{cases} 5, & n = 0 \\ 3, & n = \pm 1 \\ 1, & n = \pm 3 \\ 0, & \text{otherwise.} \end{cases}$$

a) What is the average value of $v(t)$? b) What is the fundamental frequency of $v(t)$?

Problem 2.17 A periodic signal is given by $v(t) = \sum_{n=-\infty}^{\infty} V_n e^{j200\pi nt}$ where

$$V_n = \begin{cases} 3, & n = \pm 3 \\ 1, & n = \pm 6 \\ 0, & \text{otherwise.} \end{cases}$$

a) What is the signal average value?

b) What is the fundamental frequency of the signal $v(t)$?

Problem 2.18 A periodic signal is given by $v(t) = \sum_{n=-\infty}^{\infty} V_n e^{j200\pi nt}$ where

$$V_n = \begin{cases} 3, & n = \pm 2 \\ 1, & n = \pm 3 \\ 0, & \text{otherwise.} \end{cases}$$

a) What is the signal average value?

b) What is its fundamental frequency?

Problem 2.19 Consider the periodic signal $v(t)$ of period $T = 2$ sec such that

$$v(t) = \begin{cases} t^2, & 0 < t < 1 \\ 0, & 1 < t < 2. \end{cases}$$

Evaluate and plot the Fourier series coefficients of $v(t)$ and of the signal $x(t)$ that is the modulation of $v(t)$ such that

$$x(t) = v(t) \cos(2m\pi/T).$$

Problem 2.20 A linear system receives an input signal $v(t)$ and produces an output signal $x(t)$. The system output $x(t)$ is then filtered by an ideal lowpass filter of frequency response $G(j\omega)$, where

$$G(j\omega) = \Pi_{9\pi}(\omega) = u(\omega + 9\pi) - u(\omega - 9\pi).$$

Given that the system impulse response is

$$h(t) = e^{-2|t|}$$

evaluate and sketch the exponential Fourier series coefficients, with analysis interval of $T = 1$ sec, of the system input $v(t)$ and output $x(t)$, and of the filter output $y(t)$ for the following cases :

- i) $v(t) = \sin 2\pi t$,
- ii) $v(t) = \sin 11\pi t$,
- iii) $v(t) = \sum_{n=-\infty}^{\infty} \delta(t - nT)$.

Problem 2.21 Given the signal

$$x(t) = A \sin \beta_1 t + B \cos \beta_2 t$$

where

$$\beta_1 = 2000\pi, \quad \beta_2 = 5000\pi$$

- a) What is the signal fundamental frequency?
- b) Evaluate the exponential Fourier series coefficients X_n of $x(t)$ with an analysis interval of 0.002 sec.
- c) What are the values of the coefficients if the analysis interval is 0.01 sec?

Problem 2.22 Given the signal

$$x(t) = 5 + 2 \sin(2.5\pi t + \pi/4) + 3 \cos\{5\pi(t - 0.02)\}.$$

- a) Evaluate the trigonometric Fourier series coefficients with an analysis interval of 0.8 sec.
- b) Evaluate the exponential Fourier series coefficients with an analysis interval of 2.4 sec.

Problem 2.23 For the signal

$$x(t) = \sum_{n=-\infty}^{\infty} x_0(t - 0.4n)$$

where

$$x_0(t) = \begin{cases} 2 + 10t, & -0.1 \leq t \leq 0.1 \\ 4 - 10t, & 0.1 \leq t \leq 0.3 \\ 0, & \text{otherwise.} \end{cases}$$

- a) Sketch the signal $x(t)$.
- b) Using differentiation evaluate the exponential Fourier series coefficients X_n of $x(t)$.
- c) If a filter suppresses all components of $x(t)$ of amplitude less than 1% of that of its fundamental, what is the maximum frequency contained in the filtered signal?

Problem 2.24 A signal $x(t)$ is given by

$$x(t) = \sum_{n=-\infty}^{\infty} x_0(t - nT)$$

where

$$x_0(t) = \begin{cases} A - 2At/T, & 0 < t < T \\ 0, & \text{otherwise.} \end{cases}$$

- a) State the kind of symmetry that $x(t)$ has, deducing whether its exponential Fourier series coefficients X_n are real or imaginary and whether they are nil for even or odd values of n .
- b) Evaluate the coefficients X_n and sketch the amplitude spectrum in dB relative to the fundamental component, versus the positive frequency in Hz, with $T = 0.01$ sec.
- c) Let ξ_n be the exponential Fourier series coefficients obtained with an analysis interval of $T_1 = 0.05$ sec. Write the value of ξ_n in terms of X_n .

Problem 2.25 Given the signal

$$v(t) = 3 + 4 \sin(0.5\pi t + \pi/4) + 3 \cos[\pi(t - 0.2)].$$

- a) Evaluate the trigonometric Fourier series coefficients of $v(t)$ with an analysis interval $T_1 = 4$ sec.
 b) Evaluate the exponential series coefficients V_n with analysis interval $T_2 = 12$ sec.

Problem 2.26 Consider the signal

$$v(t) = \sum_{n=-\infty}^{\infty} v_0(t - nT)$$

where

$$v_0(t) = \{2At/T - (A/3) \sin(6\pi t/T)\} \Pi_{T/2}(t)$$

- a) Sketch the signal $v(t)$.
 b) By symmetry consideration state whether its exponential Fourier series coefficients V_n are real, imaginary, nil or non-nil for only even or only odd n .
 c) Evaluate the coefficients V_n and plot the amplitude spectrum in dB relative to the fundamental component versus the positive frequency in Hz, given that the period $T = 10^{-3}$ sec.

Problem 2.27 A signal $v(t)$ has exponential Fourier series coefficients V_n evaluated with an analysis interval of 10^{-6} sec, where

$$V_n = \begin{cases} 1, & n = 0 \\ 1 \pm j, & n = \pm 1 \\ 0.5, & n = \pm 3. \end{cases}$$

- a) Evaluate the signal $v(t)$ as a sum of real functions.
 b) Let $y(t) = 3 + 2v(t - 0.2 \times 10^{-6})$. Evaluate the Fourier series coefficients Y_n of $y(t)$ with the same analysis interval 10^{-6} sec.
 c) Let $z(t)$ be a signal having exponential Fourier series coefficients Z_n with the same analysis interval, such that

$$Z_n = \begin{cases} 1, & n = \pm 1 \\ 0, & n \neq \pm 1. \end{cases}$$

Can the signal $z(t)$ be obtained by feeding the signal $v(t)$ to a linear system of frequency response $H(j\omega)$? If yes, specify the value of $H(j\omega)$.

- d) Repeat part c) for the case where

$$Z_n = \begin{cases} 1, & n = 0 \\ 0.5, & n = \pm 1 \\ 3, & n = \pm 4. \end{cases}$$

Problem 2.28 Given the signal $f(t) = 15 + 2 \cos(40\pi t - \pi/8) + 8 \sin(70\pi t + 2\pi/7)$, evaluate the exponential Fourier series coefficients F_n of $f(t)$ using an appropriate analysis interval.

Problem 2.29 A finite duration section of a signal $x(t)$ is obtained by multiplying it by a rectangular window. Let $f(t)$ be the finite-duration signal thus obtained

$$f(t) = x(t) R_T(t).$$

Let F_n be the exponential Fourier series coefficients of $f(t)$ evaluated with an analysis interval $(0, T)$.

a) With $x(t)$ periodic of frequency β rad/sec, state the conditions under which the expansion

$$x(t) = \sum_{n=-\infty}^{\infty} F_n e^{j(2\pi n/T)t}$$

is valid.

b) If $x(t) = A \cos \beta t$ evaluate the Fourier transform $F(j\omega)$ of $f(t)$. Sketch the amplitude spectrum $|F(j\omega)|$ assuming $A = 1$ and $\beta \gg 2\pi/T$. Sketch and describe the effect of reducing the window width T to $\beta < 2\pi/T$.

Problem 2.30 The two periodic signals $x(t)$ and $y(t)$ have periods $T_1 = 0.05$ sec and $T_2 = 0.025$ sec, respectively, and complex exponential Fourier series coefficients with analysis intervals T_1 and T_2 , respectively, given by

$$X_n = \begin{cases} 1, & n = 0 \\ \pm j, & n = \pm 1 \\ 1/4, & n = \pm 4 \\ 0, & \text{otherwise} \end{cases}$$

$$Y_n = \begin{cases} \pm 2j, & n = \pm 1 \\ 1/2, & n = \pm 2 \\ 0, & \text{otherwise.} \end{cases}$$

a) Evaluate the Fourier series coefficients V_n of the signal $v(t) = x(t) + y(t)$ over an analysis interval of one period.

b) Evaluate the coefficients Z_n of the signal $z(t) = x(t) \cos(80\pi t)$ over an appropriately chosen analysis interval.

Problem 2.31 Given the signal

$$v(t) = \sum_{n=-\infty}^{\infty} v_0(t - n\pi)$$

where

$$v_0(t) = \sin t R_\pi(t) = \sin t [u(t) - u(t - \pi)]$$

show that by differentiating twice $v(t)$ it is possible to evaluate its exponential Fourier series coefficients V_n with an analysis interval equal to π . To which frequency in Hz does the coefficient V_n correspond?

Problem 2.32 Consider the derivative $\rho_T'(t)$ of an impulse train. a) Evaluate the coefficients of the exponential Fourier series expansion of ρ_T' with an analysis interval equal to the period T .

b) Given the signal

$$f(t) = \sum_{n=-\infty}^{\infty} f_0(t - 2n)$$

where

$$f_0(t) = t^2 R_1(t) = t^2 [u(t) - u(t - 1)].$$

By differentiating $f(t)$ twice evaluate the exponential Fourier series coefficients F_n of $f(t)$ with an analysis interval equal to its period T . Deduce the trigonometric series coefficients.

- c) Verify the results obtained in part a) by direct evaluation of the integrals of the Fourier series coefficients or using Mathematica or Maple.
 d) As another verification evaluate and sketch the sum

$$a_0 + \sum_{n=1}^M \{a_n \cos(n2\pi t/T) + b_n \sin(n2\pi t/T)\}$$

with $M = 30$, showing that it is an approximation of $f(t)$.

Problem 2.33 Given the signal

$$v(t) = \begin{cases} A \sin(\beta t + \theta), & 0 \leq t \leq t_1 \\ A \sin \theta e^{0.2t}, & t \leq 0 \\ 0.2t - t_1, & t \geq t_1 \end{cases}$$

where $A = 2$, $\theta = \pi/4$, $\beta = 2\pi/T$ and $t_1 = 5T/2 - \theta/\beta$.

- a) Represent graphically the signal $v(t)$, assuming $T = 8$ sec.
 b) Evaluate the exponential Fourier series coefficients of $v(t)$ over the interval $(0, t_1)$.
 c) Evaluate the exponential Fourier series coefficients of $v(t)$ over the interval $(0, 2T)$.
 d) The signal $w(t)$ is the truncation in time of the signal $v(t)$ by multiplying $v(t)$ by a rectangular window, so that

$$w(t) = v(t)R_{2T}(t)$$

where $R_{2T}(t) = u(t) - u(t - 2T)$.

The signal $w(t)$ is then applied to the input of a filter having the frequency response

$$|H(j\omega)| = 8\Lambda_{4\beta}(\omega)$$

Recall that $\Lambda_x(\omega)$ is a triangle centered about the origin of total width $2x$ and a height of one.

$$\arg [H(j\omega)] = -\pi/(4\beta)$$

Evaluate the exponential Fourier series coefficients of the filter input $w(t)$ and output $y(t)$ with an analysis interval $(0, 2T)$.

Problem 2.34 Evaluate the fundamental frequency f_0 and the period T of each of the following signals

- a) $f(t) = \sin 42\pi t + 2 \cos 105\pi t$
 b) $g(t) = 5 \sin 294\pi t \sin 126\pi t$
 c) $v(t) = \sin 12t + \cos 20\pi t$
 d) $x(t) = 5 \sin 15\pi t + 7 \cos 15\pi t$
 e) $w(t) = 5 \sin 60\pi t + 7 \cos 140\pi t + 3 \cos(180\pi t + \pi/3)$

Problem 2.35 Determine the types of symmetry and evaluate the trigonometric and exponential Fourier series of the function

$$f(t) = \begin{cases} t, & 0 \leq t \leq \pi \\ -t, & -\pi \leq t \leq 0. \end{cases}$$

Problem 2.36 State the types of symmetry and evaluate the trigonometric and exponential Fourier series with analysis interval 2π of the function

$$f(t) = \begin{cases} \cos t, & 0 < t < \pi \\ -\cos t, & -\pi < t < 0. \end{cases}$$

Problem 2.37 Show that, by differentiation twice, the Fourier series coefficients of the function

$$f(t) = \begin{cases} \cos t, & 0 < t < \pi \\ -\cos t, & -\pi < t < 0 \end{cases}$$

with an analysis interval of 2π can be deduced without integration.

Problem 2.38 Sketch the function $y(t) = |\sin t|$ and evaluate its exponential Fourier series coefficients over an analysis interval $T = 2\pi$.

2.22 Answers to Selected Problems

Problem 2.1 $V_n = 0$, n even; $V_n = -8/(n^2\pi^2) - j4/(n\pi)$, n odd.

Problem 2.2

a) $Y_n = (1/4)Sa(n\pi/4)$, b) $Y_n = (1/8)Sa(n\pi/8) + (-1)^n(1/4)Sa(n\pi/4)$.

Problem 2.3

ii) $k=3$ c) $V_n = \begin{cases} [12 - 3n^2\pi^2 + j(6n\pi - n^3\pi^3)]/(n^4\pi^4), & n \text{ odd} \\ 0, & n \text{ even} \end{cases}$

Problem 2.4

a) $C_n = 5$, $n = 0$; $C_n = 0$, otherwise

b) $C_n = 1$, $n = 2$; $C_n = 0$, otherwise. $\phi_n = 0.8\pi$, $n = 2$

c) $C_n = 1$, $n = 3$; $C_n = 0$, otherwise. $\phi_n = \pi/2$, $n = 3$

d) $C_n = 3$, $n = 0$; $C_n = 5$, $n = 1$; $C_n = 0.5$, $n = 2$; $C_n = 0$, otherwise. $\phi_n = 0.927$, $n = 1$; $\phi_n = 3\pi/4$, $n = 2$.

e) $C_n = 0.5$, $n = 1, 5$; $C_n = 0$, otherwise. $\phi_n = 0$, $n = 1, 5$

Problem 2.5

a) $5x(t) = 5C_0 + \sum_{n=1}^{\infty} 5C_n \cos(2\pi nt/T - \phi_n)$

b) $x(t) + 5 = (C_0 + 5) + \sum_{n=1}^{\infty} C_n \cos(2\pi nt/T - \phi_n)$

c) $x(t + 5T) = C_0 + \sum_{n=1}^{\infty} C_n \cos(2\pi nt/T - \phi_n)$

d) $x(t + T/5) = C_0 + \sum_{n=1}^{\infty} C_n \cos\{2\pi nt/T - (\phi_n - 2\pi n/5)\}$

e) $(d/dt)[x(t)] = \sum_{n=1}^{\infty} (2\pi n/T) C_n \cos\{2\pi nt/T - (\phi_n - \pi/2)\}$.

Problem 2.6

a) $V_n = \frac{1 + e^{-j\pi n}}{2\pi(1 - n^2)}$, $n \neq \pm 1$, $V_{\pm 1} = \mp j/4$

b) $Y_n = \frac{1 + e^{-j\pi n}}{\pi(1 - n^2)}$, $n \neq \pm 1$, $V_{\pm 1} = 0$.

Problem 2.7 $v(t) = 1 + 4 \cos(2\pi t/T + \pi/4) - 2 \sin(2\pi t/T - 20\pi/T)$.

Problem 2.8

a) $a_{0,f} = 12$; $a_{n,f} = b_{n,f} = 0$. $a_{0,g} = b_{n,g} = 0$; $a_{n,g} = 1$, $n = 1$; 0 otherwise. $a_{0,h} = a_{n,h} = 0$; $b_{n,h} = 1$, $n = 3$; 0 otherwise. $a_{0,s} = 6$, $a_n = 2$, $n = 1$; 0 otherwise, $b_n = 1$, $n = 3$; 0 otherwise.

$a_{0,v} = b_{n,v} = 0$; $a_{n,v} = 1$, $n = 1$; 0 otherwise. $a_{0,w} = a_{n,w} = 0$, $b_{n,w} = -2\pi/T$, $n = 1$; 0 otherwise.

$a_{0,x} = 0, a_{n,x} = \cos(4\pi/T)$, $n = 2$; 0 otherwise, $b_n = \sin(4\pi/T)$, $n = 2$; 0 otherwise.

$a_{0,y} = 0, a_{n,y} = 1/\sqrt{2}$, $n = 3$; 0 otherwise, $b_{n,y} = 1/\sqrt{2}$, $n = 3$; 0 otherwise.

b) $F_n = 6$, $n = 0$; 0 otherwise. $G_n = 1/2$, $n = \pm 1$; 0 otherwise. $H_n = \mp j/2$, $n = \pm 3$; 0 otherwise. $S_n = 3$, $n = 0$; $S_n = 1$, $n = \pm 1$; $S_n = \mp j/2$, $n = \pm 3$; 0 otherwise.

$V_n = 1/2$; $n = \pm 1$; 0 otherwise. $W_n = \pm j\pi/T$, $n = \pm 1$; 0 otherwise, $X_n = (1/2)e^{\mp j4\pi T}$ $n = \pm 2$; 0 otherwise. $Y_n = (\mp j/2)e^{\mp j\pi/4}$ for $n = \pm 3$; 0 otherwise.

Problem 2.9

a) $a_{0,y} = \alpha_0 a_0 + 2\alpha_1$, $a_{n,y} = \alpha_0 a_n$ and $b_{n,y} = \alpha_0 b_n$

b) $a_{0,y} = 0$, $a_{n,y} = 2\pi n b_n / T$ and $b_{n,y} = -2\pi a_n / T$

c) $a_{0,y} = a_0$, $a_{n,y} = a_n \cos(2\pi n t_0 / T) - b_n \sin(2\pi n t_0 / T)$,
 $b_{n,y} = b_n \cos(2\pi n t_0 / T) + a_n \sin(2\pi n t_0 / T)$.

Problem 2.10

a) $X_n = 10A$, b) $Y_n = (4/3) - (2/3)e^{+j2\pi n/3}$.

Problem 2.11

a) $Y_n = 0$, $n = 0, Y_n = -A/3$, otherwise. a) $X_n = A/2$, $n = 0$, $X_n = j(A/2\pi n)$, otherwise.

Problem 2.13

a) $V_n = (1 - e^{-j\pi n}) / [4\pi(1 - n^2/4)]$, $n \neq \pm 2$; $V_{\pm 2} = \mp j/4$.

c) $Y_n = j(e^{-j\pi n} - 1) \sin(\pi n/2) / 2\pi(1 - n^2/4)$, $n \neq \pm 2$; $Y_{\pm 2} = 0$

d) $Y_n = j[(-1)^n - 1] \sin(\pi n/4) / 2\pi(1 - n^2/16)$, $n = \text{even}$; $Y_n = 0$, $n = \text{odd}$.

Problem 2.14

a) $\overline{x(t)} = X_0 = 0.25$. b) $2|X_{\pm 9}| = 0.05$.

Problem 2.15

a) $V_n = 1$, $n = 0$; 0 otherwise.

b) $X_n = 4$, $n = 0, Y_n = [(-1)^n + 1] / 2\pi(1 - n^2)$ otherwise.

c) $Y_n = 1$, $n = 0, Y_n = 0.5$, $n = \pm 1; Y_n = [(-1)^n + 1] / 2\pi(1 - n^2)$, otherwise.

d) $Z_n = V_n$.

Problem 2.16 a) $\overline{v(t)} = V_0 = 5$. b) $\text{gcd}(100, 300) = 100$ Hz.

Problem 2.17 a) $\overline{v(t)} = V_0 = 0$. b) $\text{gcd}(300, 600) = 300$ Hz.

Problem 2.18 a) $\overline{v(t)} = V_0 = 0$. b) $\text{gcd}(200, 300) = 100$ Hz.

Problem 2.21 $x(t) = A \sin \beta_1 t + B \cos \beta_2 t \triangleq x_1 + x_2$.

a) $\omega_0 = 1000\pi$.

b) $X_n = \begin{cases} (A/2)e^{\mp j\pi/2} = \mp j(A/2), & n = \pm 2 \\ B/2, & n = \pm 5 \\ 0, & \text{otherwise} \end{cases}$

c) $X_n = \begin{cases} \mp jA/2, & n = \pm 10 \\ B/2, & n = \pm 25 \\ 0, & \text{otherwise} \end{cases}$

Problem 2.23

$X_n = \frac{j 100 \sin n\pi/2}{-n^2} \left(\frac{0.4}{2\pi}\right)^2 = \frac{-j4}{\pi^2 n^2} \sin(n\pi/2)$, $n \neq 0$, $X_0 = \overline{x(t)} = 2$. See Fig.

2.42. The maximum frequency is $\omega = 9 \times \text{fundamental} = 9\omega_0 = 9 \times \frac{2\pi}{T}$ r/s, $f = 22.5$ Hz..

Problem 2.24 See Fig. 2.43

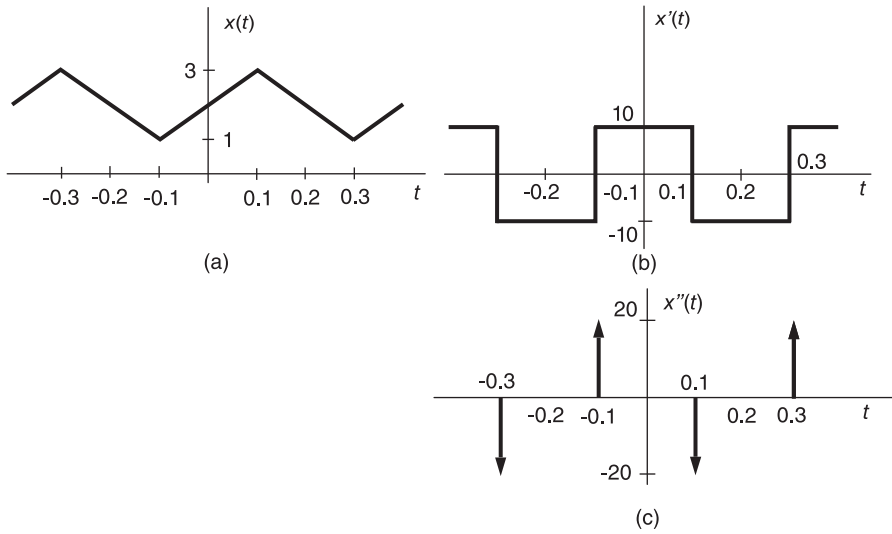


FIGURE 2.42 Function and derivatives, Problem 2.23.

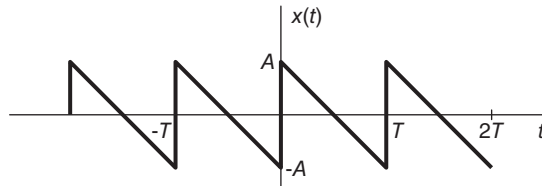


FIGURE 2.43 Figure for Problem 2.24.

$$|X_n| = \frac{A}{|n|\pi}, \quad |X_1| = A/\pi$$

$$\xi_n = \begin{cases} 0, & n \neq k5, \quad k \text{ integer} \\ X_{n/5}, & n = k5, \quad k \text{ integer} \end{cases}$$

Problem 2.29

a) $T = k2\pi/\beta$, k integer. b) See Fig. 2.44.

Problem 2.32 See Figs. 2.45 and 2.46.

a) $\rho'_T(t) \xrightarrow{\text{FSC}} (jn\omega_0)/T$.

b) $a_n = (-1)^n 2/(n^2\pi^2)$, $b_n = -[2 - 2(-1)^n + (-1)^n n^2\pi^2]/(n^3\pi^3)$.

Problem 2.34

a) $T = 1/f_0 = 0.0952$ sec.

b) $f_0 = 42$ Hz, $T = 0.0238$ sec.

c) $v(t)$ is not periodic since the ratio of the two frequencies is not rational.

d) $f_0 = 7.5$ Hz, $T = 0.1333$ sec.

e) $f_0 = 10$ Hz, $T = 0.1$ sec.

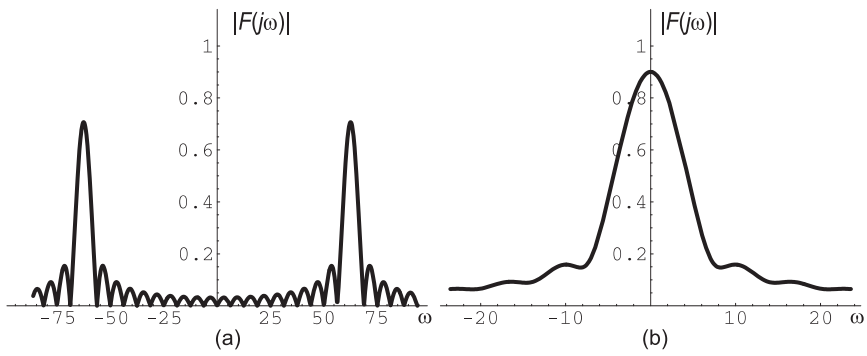


FIGURE 2.44 Figure for Problem 2.29.

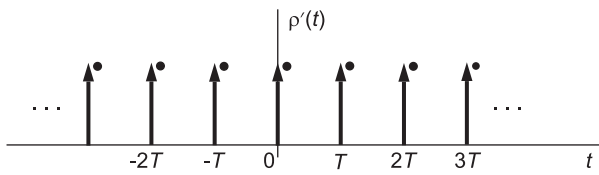


FIGURE 2.45 Derivative of the impulse train.

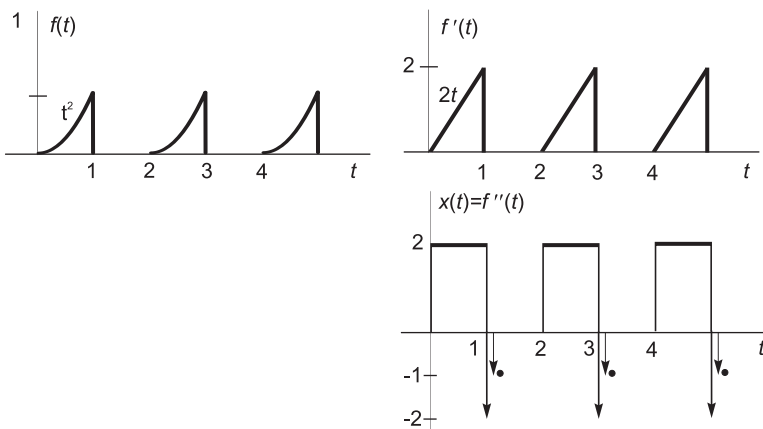


FIGURE 2.46 Derivatives of the parabola train.

This page intentionally left blank

3

Laplace Transform

3.1 Introduction

The Laplace transform, named after the French mathematician Pierre Simon Laplace (see Appendix), is a major tool for the analysis of continuous time signals and systems and the solution of differential equations. In fact the Fourier transform, one of the most important signal analysis tools is, as we shall see in the next chapter, but a special case of the Laplace transform.

In this chapter we study the most general form of the Laplace transform, also referred to as the *Bilateral Laplace transform*, followed by the one-sided transform known as the *unilateral transform*. We shall see that the bilateral Laplace transform is in principle applicable to general two-sided functions. We shall learn, however, that according to the current literature the bilateral Laplace transforms of the simplest of two sided functions, such as unity or a simple pure sinusoid, do not exist even though their Fourier transforms do, [1] [30] [45] [57] [63] [64] [70]. In fact, the bilateral Laplace transform, according to the present literature, exists only for right-sided functions or left-sided functions, but the transforms of two-sided functions such as 1 , $\sin t$, e^t , ... do not exist, and if they are expressed as the sum of a causal and an anticausal part then their conditions of existence are mutually exclusive, hence the transforms cannot be added to produce the overall transform.

The fact that Fourier transform can operate on basic two-sided functions such as 1 , $\sin t$, $\cos t$ and t while the more general Laplace transform cannot may be viewed as a mathematical anomaly.

The key to resolving the anomaly and extending the domain of existence of Laplace transform to cover these and a much larger class of functions, including functions that have no Fourier transform, is a generalization of the Dirac-delta impulse introduced in [21]. The result as we shall see later on is a significant expansion of the domains of existence of Laplace and z -transform and other related transforms such as Hilbert, Hartley and Mellin transform [19] [23] [27].

For the benefit of the student and a gradual understanding of the subject this chapter presents the Laplace transform in the usual form found in the literature. The new recent developments extending the domains of existence of Laplace, z and related transforms constitutes a slightly more advanced topic and is deferred to Chapter 18.

3.2 Bilateral Laplace Transform

Let $f(t)$ be a two-sided piecewise continuous time function, that is, a time function that is either continuous for all t or is composed of a succession of continuous sections. The Laplace

transform of such a function, also known as the bilateral Laplace transform, is defined by

$$F(s) = \int_{-\infty}^{\infty} f(t)e^{-st} dt \quad (3.1)$$

where s is a complex variable $s = \sigma + j\omega$ called the *complex frequency*. The integral in the definition is referred to as the “Laplace integral.” Integrals having infinite limits are known as “improper integrals.” The infinite limits imply that the transform exists if and only if the integral is convergent. The variable ω is the *angular or radian frequency* measured in radians per second. The variable σ is called the *damping factor*. The s plane with abscissa σ and ordinate $j\omega$ is called the complex s plane. We write symbolically $F(s) = \mathcal{L}[f(t)]$ or, alternatively, $f(t) \xleftrightarrow{\mathcal{L}} F(s)$ meaning that $F(s)$ is the Laplace transform of $f(t)$. The inverse relation $f(t) = \mathcal{L}^{-1}[F(s)]$ stating that the function $f(t)$ is the inverse transform of $F(s)$ is given by the *inversion formula*

$$f(t) = \frac{1}{2\pi j} \int_{\sigma-j\infty}^{\sigma+j\infty} F(s)e^{st} ds. \quad (3.2)$$

As we shall see, the contour of integration, the vertical line extending from the point $s = \sigma - j\infty$ to $s = \sigma + j\infty$ in the complex s plane, has to be in the *region of convergence* (ROC) of the transform $F(s)$, that is, in the region where the transform exists. Before exploring the conditions of existence of the Laplace transform we study two basic but revealing examples of the Laplace transform of simple exponentials.

Example 3.1 Evaluate the Laplace transform of the right-sided (causal) function.

$$f(t) = e^{\alpha t}u(t).$$

We have

$$F(s) = \mathcal{L}[f(t)] = \int_0^{\infty} e^{\alpha t}e^{-st} dt = \left[\frac{e^{-(s-\alpha)t}}{s-\alpha} \right]_{\infty}^0 = \frac{1}{s-\alpha} \left\{ 1 - \lim_{t \rightarrow \infty} e^{-(\sigma+j\omega-\alpha)t} \right\}.$$

The limit in question is zero if $\sigma > \alpha$ and infinity if $\sigma < \alpha$. If $\sigma = \alpha$ the integral is not convergent. We conclude that the Laplace transform exists if and only if $\sigma > \alpha$ and therefore

$$F(s) = \frac{1}{s-\alpha}, \quad \sigma > \alpha.$$

The condition of existence $\sigma > \alpha$ is the ROC of the Laplace transform, and the boundary value α of the ROC is called the abscissa of convergence. In what follows we shall see that the point $s = \alpha$ in the complex s plane is the pole of the function $F(s)$, since with $s = \alpha$ the value of $F(s)$ is infinite. The function $f(t)$ is shown in Fig. 3.1, together with its pole $s = \alpha$ denoted by \times in the complex s plane, for the two cases $\alpha > 0$ and $\alpha < 0$, respectively. We see that the ROC of the Laplace transform $F(s)$, shown hatched in the figure, of this *right-sided* exponential extends in the s plane to the *right* of the pole.

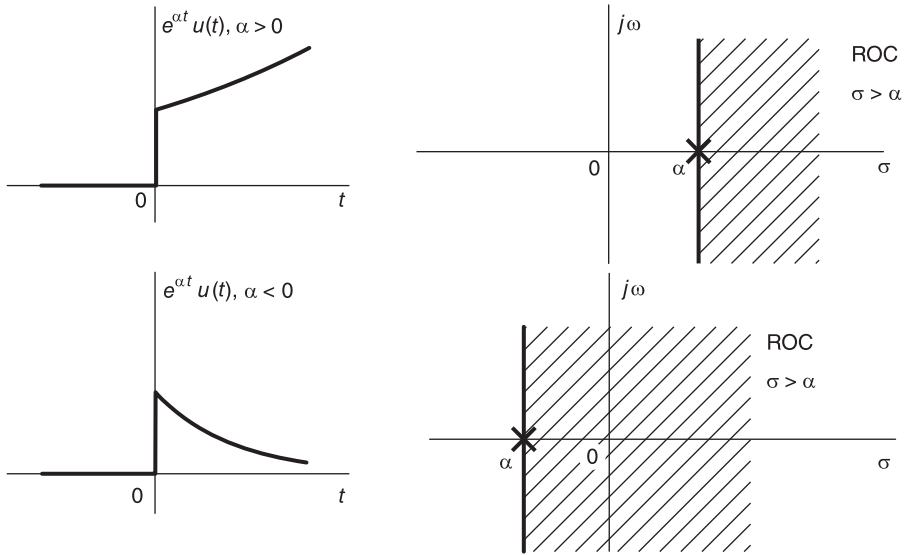


FIGURE 3.1 Functions and regions of convergence.

Example 3.2 Evaluate the Laplace transform of the left-sided (anticausal) function.

$$f(t) = e^{\alpha t} u(-t).$$

We have

$$F(s) = \mathcal{L}[f(t)] = \int_{-\infty}^0 e^{\alpha t} e^{-st} dt = \left[\frac{e^{-(s-\alpha)t}}{s-\alpha} \right]_0^{-\infty} = \frac{1}{s-\alpha} \left\{ \lim_{t \rightarrow -\infty} e^{-(\sigma+j\omega-\alpha)t} - 1 \right\}.$$

In this case the limit in question is zero if $\sigma < \alpha$ and infinity if $\sigma > \alpha$. If $\sigma = \alpha$ the integral is not convergent. We conclude that the Laplace transform is given by

$$F(s) = \frac{-1}{s-\alpha}, \quad \sigma < \alpha.$$

The pole $s = \alpha$ and the ROC $\sigma < \alpha$ can be seen in Fig. 3.2 for the cases $\alpha > 0$ and $\alpha < 0$, respectively.

We see that the ROC of the Laplace transform $F(s)$ of this left-sided function extends in the s plane to the left of the pole.

In what follows, these important basic properties of the Laplace transform and its conditions of existence will be seen to be applicable in general.

3.3 Conditions of Existence of Laplace Transform

A sufficient condition for existence of the Laplace transform

$$F(s) = \int_{-\infty}^{\infty} f(t) e^{-st} dt \tag{3.3}$$

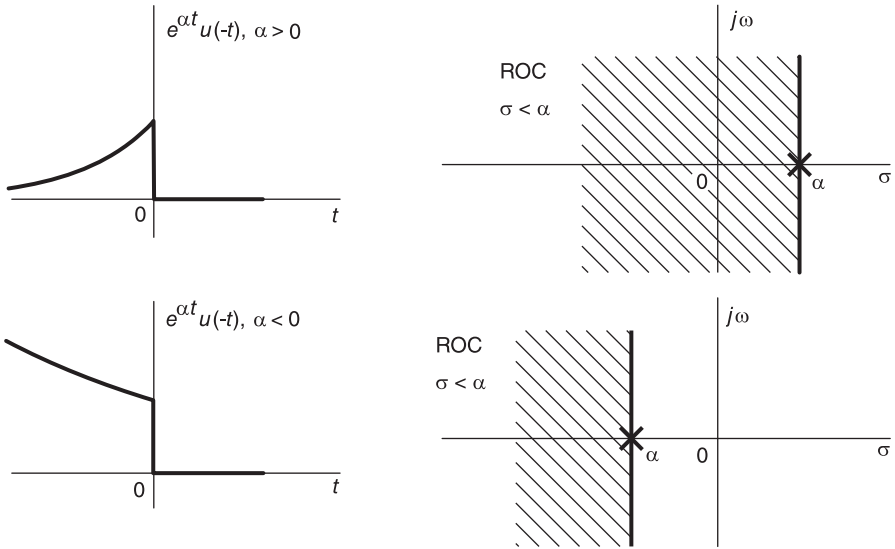


FIGURE 3.2 Functions and regions of convergence.

is that the integral be absolutely convergent, that is, it converges when the integrand is replaced by its absolute value. We can write

$$\int_{-\infty}^{\infty} f(t)e^{-st} dt \leq \int_{-\infty}^{\infty} |f(t)e^{-st}| dt = \int_{-\infty}^{\infty} |f(t)| e^{-\sigma t} dt. \tag{3.4}$$

If we can find a positive value M and real values α and β such that

$$|f(t)| \leq \begin{cases} Me^{\beta t}, & t \leq 0 \\ Me^{\alpha t}, & t \geq 0 \end{cases} \tag{3.5}$$

as shown in Fig. 3.3, then the function $f(t)$ is said to be of *exponential order*. The right-sided part is referred to as a function of “*exponential order* α .” The left-sided part of $f(t)$ is referred to as a function of “*exponential order* β .” We can write

$$\int_{-\infty}^{\infty} |f(t)| e^{-\sigma t} dt \leq \int_{-\infty}^0 Me^{(\beta-\sigma)t} dt + \int_0^{\infty} Me^{(\alpha-\sigma)t} dt. \tag{3.6}$$

The first integral reduces to

$$\int_{-\infty}^0 Me^{(\beta-\sigma)t} dt = M \frac{e^{(\beta-\sigma)t}}{\beta-\sigma} \Big|_{-\infty}^0 = \frac{M}{\beta-\sigma} \left\{ 1 - \lim_{t \rightarrow -\infty} e^{(\beta-\sigma)t} \right\}. \tag{3.7}$$

The limit in this equation is equal to zero if $\sigma < \beta$, and infinity if $\sigma > \beta$. For $\sigma = \beta$ the integral is not convergent. Similarly, the second integral reduces to

$$\int_0^{\infty} Me^{(\alpha-\sigma)t} dt = M \frac{e^{(\alpha-\sigma)t}}{\alpha-\sigma} \Big|_0^{\infty} = \frac{M}{\alpha-\sigma} \left\{ \lim_{t \rightarrow \infty} e^{(\alpha-\sigma)t} - 1 \right\} \tag{3.8}$$

and the limit in this equation is equal to zero if $\sigma > \alpha$, and to infinity if $\sigma < \alpha$. The integral does not converge in the case $\sigma = \alpha$.

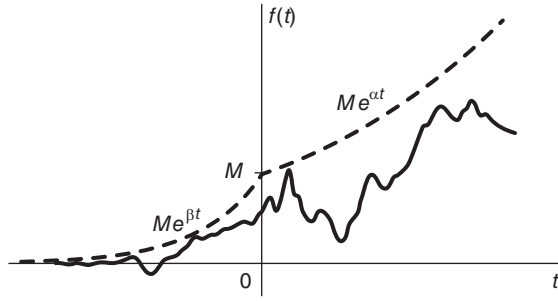


FIGURE 3.3 Bounding exponentials.

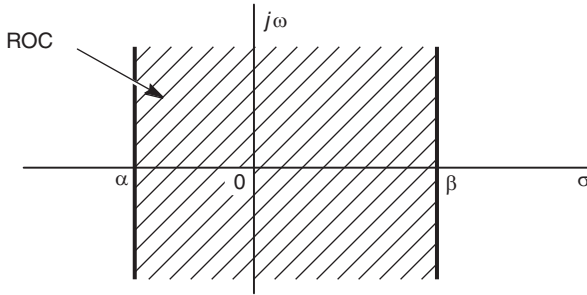


FIGURE 3.4 Strip of convergence of two-sided function.

We conclude that the transform exists if and only if $\alpha < \sigma < \beta$. This ROC appears therefore as a vertical strip in the complex s plane. As an illustration the vertical strip of convergence is depicted in Fig. 3.4 for the case $\alpha < 0$ and $\beta > 0$. It may be worthwhile adding a few remarks regarding exponential order. A right-sided function $f(t)$ which satisfies the condition that $\lim_{t \rightarrow \infty} |f(t)| e^{-\sigma t} = 0$ if $\sigma > \alpha$ is called a function of exponential order α . For example, the function $f(t) = u(t)$ is of exponential order zero since $\lim_{t \rightarrow \infty} u(t)e^{-\sigma t} = 0$ if $\sigma > 0$. If as in the above the function $f(t)$ satisfies the condition $|f(t)| \leq Me^{\alpha t}$ then $|f(t)| e^{-\sigma t} \leq Me^{\alpha t} e^{-\sigma t}$. Hence

$$\lim_{t \rightarrow \infty} |f(t)| e^{-\sigma t} = 0 \text{ if } \sigma > \alpha \tag{3.9}$$

so that $f(t)$ is of exponential order α as stated above. Another simple example of a function of exponential order is the simple causal exponential $f(t) = e^{\alpha t} u(t)$. Since $|f(t)| e^{-\sigma t} = e^{(\alpha - \sigma)t} u(t) \rightarrow 0$ as $t \rightarrow \infty$ if $\sigma > \alpha$, this is simply a function of exponential order α .

A function $f(t) = t^n e^{\alpha t} u(t)$ is of exponential order α since $\lim_{t \rightarrow \infty} |f(t)| e^{-\sigma t} = \lim_{t \rightarrow \infty} t^n e^{-(\sigma - \alpha)t} = 0$ if $\sigma > \alpha$. A function such as $f(t) = e^{t^2}$ is not of exponential order since $\lim_{t \rightarrow \infty} e^{t^2} e^{-\sigma t}$ is infinite.

Finally, note that if a function $f(t)$ is a right-sided function and is of exponential order α , i.e. $|f(t)| \leq Me^{\alpha t}$, $t \geq 0$, then from the above we conclude that the Laplace transform exists for $\sigma > \alpha$. The ROC is therefore a half plane, that is, the part of the s plane extending to the right of the point $s = \alpha$, as depicted in Fig. 3.5 for two cases $\alpha > 0$ and $\alpha < 0$, respectively.

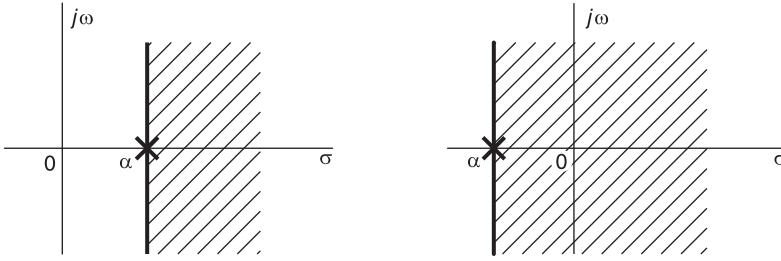


FIGURE 3.5 Regions of convergence of right-sided functions.

3.4 Basic Laplace Transforms

The following are examples of Laplace transforms of some basic functions.

Example 3.3 Evaluate the Laplace transform of $f(t) = \delta(t)$.

We have

$$F(s) = \int_{-\infty}^{\infty} f(t)e^{-st} dt = \int_{-\infty}^{\infty} \delta(t)e^{-st} dt = e^0 = 1.$$

Example 3.4 Evaluate the Laplace transform of the step function

$$f(t) = u(t).$$

$$F(s) = \int_{-\infty}^{\infty} u(t)e^{-st} dt = \int_0^{\infty} e^{-st} dt = \frac{1}{s}, \quad \sigma > 0.$$

The function, its pole marked by an \times and the ROC of its transform are shown in Fig. 3.6.

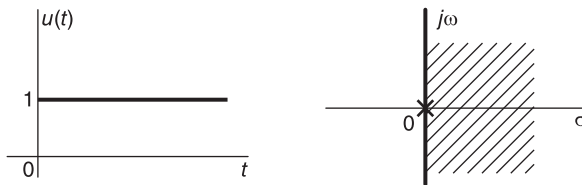


FIGURE 3.6 Unit step function and its ROC.

Example 3.5 Evaluate the Laplace transform of the function

$$f(t) = \sin \beta t u(t).$$

We may write

$$F(s) = \int_0^{\infty} \sin \beta t e^{-st} dt = \frac{1}{2j} \int_0^{\infty} (e^{j\beta t} - e^{-j\beta t}) e^{-st} dt$$

$$F(s) = \frac{1}{2j} \left[\frac{1}{s - j\beta} - \frac{1}{s + j\beta} \right] = \frac{\beta}{s^2 + \beta^2}, \quad \sigma > 0.$$

Table 3.1 lists the Laplace transform of some common basic functions.

TABLE 3.1 Laplace transforms of common functions

$f(t) = \mathcal{L}^{-1}[F(s)]$	$F(s) = \mathcal{L}[f(t)]$
$\delta(t)$	1
$\delta(t - t_0)$	e^{-st_0}
$u(t)$	$\frac{1}{s}$
$tu(t)$	$\frac{1}{s^2}$
$t^n u(t)$	$\frac{n!}{s^{n+1}}$
$\frac{t^{n-1}}{(n-1)!} u(t)$	$\frac{1}{s^n}$
$\frac{t^{n-1}}{(n-1)!} e^{-\alpha t} u(t)$	$\frac{1}{(s + \alpha)^n}$
$e^{at} u(t)$	$\frac{1}{s - a}$
$te^{at} u(t)$	$\frac{1}{(s - a)^2}$
$t^n e^{at} u(t)$	$\frac{n!}{(s - a)^{n+1}}$
$\sin(\omega_0 t) u(t)$	$\frac{\omega_0}{(s^2 + \omega_0^2)}$
$\cos(\omega_0 t) u(t)$	$\frac{s}{(s^2 + \omega_0^2)}$
$e^{-at} \sin(\omega_0 t) u(t)$	$\frac{\omega_0}{[(s + a)^2 + \omega_0^2]}$
$e^{-at} \cos(\omega_0 t) u(t)$	$\frac{(s + a)}{[(s + a)^2 + \omega_0^2]}$
$t \cos(\beta_0 t) u(t)$	$\frac{(s^2 - \beta_0^2)}{(s^2 + \beta_0^2)^2}$
$(1/\sqrt{t}) u(t)$	$\sqrt{\frac{\pi}{s}}$
$t^\nu u(t), \nu > -1$	$\frac{\Gamma(\nu + 1)}{s^{\nu+1}}$
$\cosh(at) u(t)$	$\frac{s^2 - a^2}{s^2 - a^2}$
$\sinh(at) u(t)$	$\frac{a}{s^2 - a^2}$

3.5 Notes on the ROC of Laplace Transform

Some exponential and damped sinusoidal functions and their convergence regions are shown in Fig. 3.7 and Fig. 3.8, respectively. The following remarks can be made:

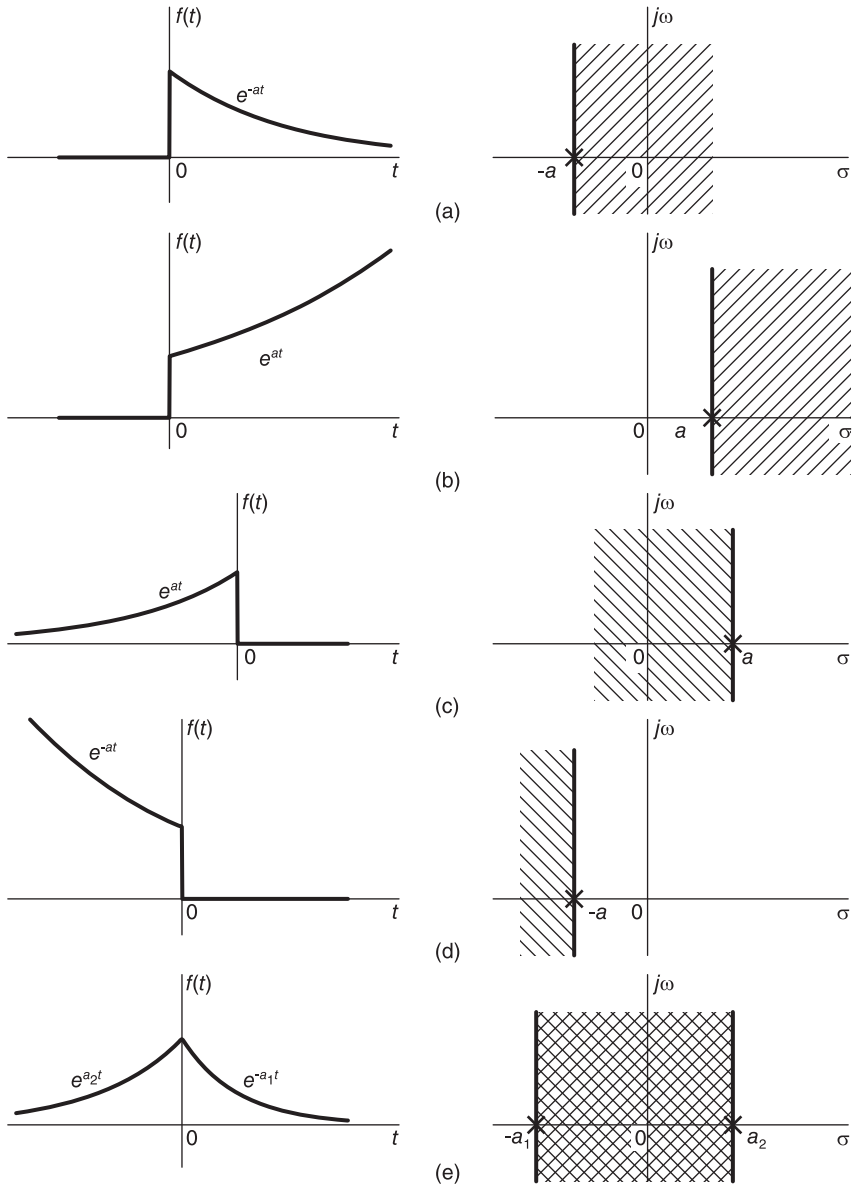


FIGURE 3.7 One-sided and two-sided functions and their regions of convergence.

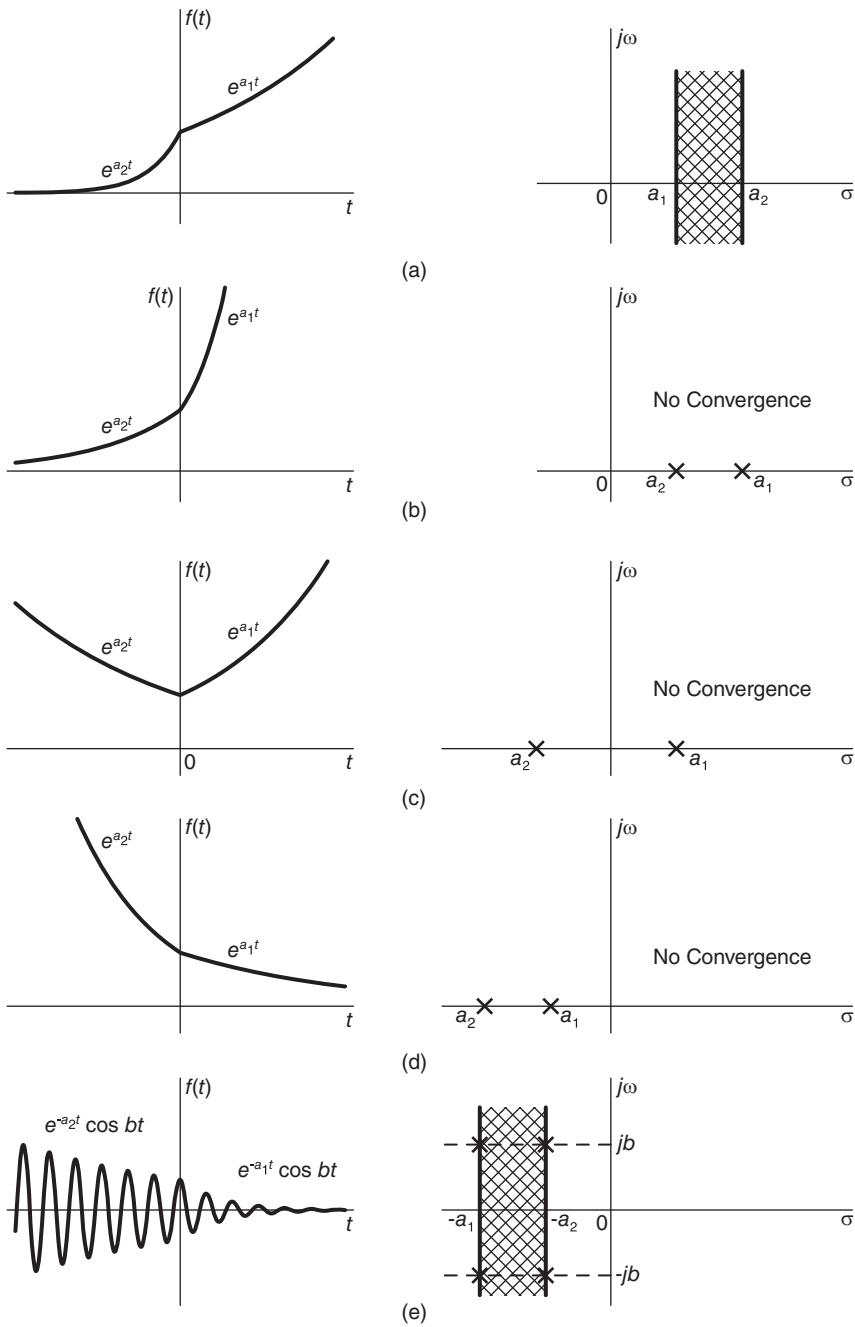


FIGURE 3.8 Two-sided functions and their regions of convergence.

a) A *right-sided* exponential $e^{-at}u(t)$ having a Laplace transform $1/(s + a)$, i.e. a pole at $s = -a$, has a ROC that extends in the s plane to the *right* of the pole.

b) A *left-sided* exponential $e^{at}u(-t)$ has a Laplace transform

$$\int_{-\infty}^0 e^{at} e^{-st} dt = \frac{-1}{s-a}, \quad \sigma < a \quad (3.10)$$

and a convergence region that extends to the *left* of the pole $s = a$.

c) A two-sided exponential has as ROC a vertical strip in the s plane extending to the *right* of the pole of the *right-sided* component and to the *left* of the pole of the *left-sided* component, if such region exists.

d) These properties apply equally to damped sinusoids, the deciding factor on their convergence being their bounding exponential; hence the real parts of their poles.

e) For two-sided exponential function the transform exists if and only if the entire two-sided function, over the whole time axis $t \in (-\infty, \infty)$, can be bounded by a *single exponential* as can be seen in Fig. 3.9. If no bounding exponential exists, such as in the case shown in Fig. 3.10, then the Laplace transform does not exist.

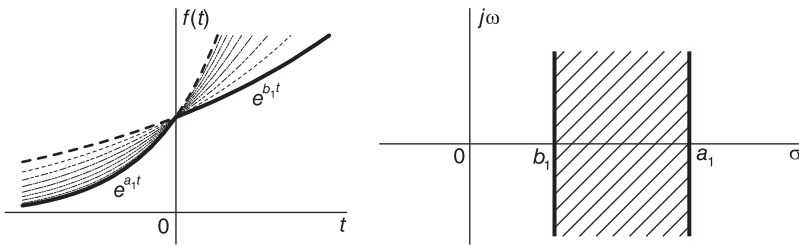


FIGURE 3.9 Set of bounding exponentials and corresponding ROC.

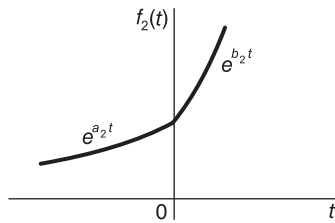


FIGURE 3.10 Absence of transform due to absence of bounding exponential.

f) The Laplace transform of a function composed of a sum of *right-sided* exponentials and *left-sided* exponentials has a convergence region which extends to the *right* of the *rightmost* pole(s) of the *right-sided* function and to the *left* of the *leftmost* pole(s) of the *left-sided* function, if such a region exists.

g) The ROC of the Laplace transform of a finite duration function is the entire s plane since the integral converges absolutely.

h) As we shall see in the next chapter, the Fourier transform $F(j\omega)$ of a function $f(t)$ is but a special case of its Laplace transform $F(s)$ and may be obtained by simply substituting $s = j\omega$, *if such a substitution is permissible*, meaning that the $j\omega$ axis is in the ROC, or is itself the boundary of the ROC, of Laplace transform.

3.6 Properties of Laplace Transform

Table 3.2 lists basic properties of the Laplace transform. Some of the proofs of these properties are given in what follows.

TABLE 3.2 Basic properties of Laplace transform

Operation	Time domain	Laplace Domain
Linearity	$a_1f_1(t) + a_2f_2(t)$	$a_1F_1(s) + a_2F_2(s)$
Differentiation in time	$\frac{d^n f(t)}{dt^n}$	$s^n F(s)$
Multiplication by time	$-tf(t)$	$\frac{dF(s)}{ds}$
Integration	$\int_{-\infty}^t f(t)dt$	$\frac{F(s)}{s}$
Time shift	$f(t - t_0)$	$F(s)e^{-st_0}$
Modulation	$f(t)e^{s_0t}$	$F(s - s_0)$
Time scale	$f(at)$	$\frac{1}{ a }F\left(\frac{s}{a}\right)$
Reflection	$f(-t)$	$F(-s)$
Convolution in frequency	$f_1(t)f_2(t)$	$\frac{1}{2\pi j} \int_{c-j\infty}^{c+j\infty} G(p)F(s - p)dp$
Initial value theorem		$f(0^+) = \lim_{s \rightarrow \infty} [sF(s)]$
Final value theorem		$f(\infty) = \lim_{s \rightarrow 0} [sF(s)]$

3.6.1 Linearity

Let

$$f(t) = a_1 f_1(t) + a_2 f_2(t) + \dots + a_n f_n(t) = \sum_{i=1}^n a_i f_i(t) \quad (3.11)$$

where the values a_i are constants and $f_i(t) \xleftrightarrow{\mathcal{L}} F_i(s)$. The linearity property states that the Laplace transform of $f(t)$ is given by

$$F(s) = \mathcal{L}\{f(t)\} = \sum_{i=1}^n a_i F_i(s). \quad (3.12)$$

3.6.2 Differentiation in Time

If $f(t)$ is a continuous two-sided function and $g(t)$ its derivative $g(t) = f'(t)$ then $G(s) = sF(s)$.

Proof We recall the inversion formula

$$f(t) = \frac{1}{2\pi j} \int_{\sigma-j\infty}^{\sigma+j\infty} F(s) e^{st} ds. \quad (3.13)$$

Differentiating both sides we obtain

$$f'(t) = \frac{1}{2\pi j} \int_{\sigma-j\infty}^{\sigma+j\infty} sF(s) e^{st} ds \quad (3.14)$$

implying that $\mathcal{L}[f'(t)] = sF(s)$ as stated. Repeating we obtain

$$f''(t) = \{f'(t)\}' \xleftrightarrow{\mathcal{L}} s \{sF(s)\} = s^2 F(s) \quad (3.15)$$

$$f^{(n)}(t) \triangleq \frac{d^n}{dt^n} f(t) = s^n F(s). \quad (3.16)$$

Example 3.6 Evaluate the Laplace transform of $\delta'(t)$ and $\delta^{(n)}(t)$.

We have $\delta(t) \longleftrightarrow 1$, hence $\delta'(t) \xleftrightarrow{\mathcal{L}} s$, and $\delta^{(n)}(t) \xleftrightarrow{\mathcal{L}} s^n$.

3.6.3 Multiplication by Powers of Time

To prove the multiplication by time t property of Laplace transform listed in Table 3.2 we differentiate the Laplace transform of the function $f(t)$, obtaining

$$F'(s) = \int_{-\infty}^{\infty} (-t) f(t) e^{-st} dt \quad (3.17)$$

so that $(-t) f(t) \longleftrightarrow F'(s)$, as stated. Repeated differentiation produces

$$t^n f(t) \longleftrightarrow (-1)^n F^{(n)}(s). \quad (3.18)$$

Example 3.7 Evaluate $\mathcal{L}[t^n u(t)]$.

$$u(t) \longleftrightarrow \frac{1}{s}, \quad \sigma > 0$$

$$t^n u(t) \longleftrightarrow (-1)^n \left[\frac{n!}{s^{n+1}} (-1)^n \right] = \frac{n!}{s^{n+1}}, \quad \sigma > 0.$$

Example 3.8 Evaluate $\mathcal{L}[te^{\alpha t} \cos \beta t u(t)]$.

We have

$$\begin{aligned}\mathcal{L}[e^{\alpha t} \cos \beta t u(t)] &= \frac{(s - \alpha)}{(s - \alpha)^2 + \beta^2}, \quad \sigma > \alpha \\ \mathcal{L}[te^{\alpha t} \cos \beta t u(t)] &= \frac{(s - \alpha)^2 - \beta^2}{[(s - \alpha)^2 + \beta^2]^2}, \quad \sigma > \alpha.\end{aligned}$$

Example 3.9 Evaluate $\mathcal{L}[t^n e^{\alpha t} u(t)]$ and $\mathcal{L}[t^{n-1} e^{\alpha t} / (n-1)! u(t)]$.

Let $f(t) = e^{\alpha t} u(t)$. We have

$$\begin{aligned}F(s) &= \frac{1}{s - \alpha}, \quad \sigma > \alpha \\ F^{(n)}(s) &= \frac{d^n}{ds^n} \frac{1}{s - \alpha} = (-1)^n \frac{n!}{(s - \alpha)^{n+1}}, \quad \sigma > \alpha \\ \mathcal{L}[t^n e^{\alpha t} u(t)] &= (-1)^n F^{(n)}(s) = \frac{n!}{(s - \alpha)^{n+1}}, \quad \sigma > \alpha \\ \frac{t^{n-1}}{(n-1)!} e^{\alpha t} u(t) &\stackrel{\mathcal{L}}{\longleftrightarrow} \frac{1}{(s - \alpha)^n}, \quad \sigma > \alpha.\end{aligned}$$

3.6.4 Convolution in Time

$$f_1 * f_2 \triangleq \int_{-\infty}^{\infty} f_1(\tau) f_2(t - \tau) d\tau \stackrel{\mathcal{L}}{\longleftrightarrow} F_1(s) F_2(s). \quad (3.19)$$

Proof

$$\mathcal{L}\left[\int_{-\infty}^{\infty} f_1(\tau) f_2(t - \tau) d\tau\right] = \int_{-\infty}^{\infty} \int_{-\infty}^{\infty} f_1(\tau) f_2(t - \tau) d\tau e^{-st} dt. \quad (3.20)$$

Reversing the order integration assuming uniform convergence

$$\mathcal{L}[f_1 * f_2] = \int_{-\infty}^{\infty} f_1(\tau) \int_{-\infty}^{\infty} f_2(t - \tau) e^{-st} dt d\tau. \quad (3.21)$$

Letting $t - \tau = \lambda$

$$\mathcal{L}[f_1 * f_2] = \int_{-\infty}^{\infty} f_1(\tau) e^{-s\tau} d\tau \int_{-\infty}^{\infty} f_2(\lambda) e^{-s\lambda} d\lambda = F_1(s) F_2(s). \quad (3.22)$$

3.6.5 Integration in Time

According to this property

$$\mathcal{L}\left[\int_{-\infty}^t f(\tau) d\tau\right] = \frac{1}{s} F(s). \quad (3.23)$$

Proof Let $g(t) = \int_{-\infty}^t f(\tau) d\tau$. We have $f(t) = g'(t)$, $F(s) = sG(s)$ wherefrom $G(s) = F(s)/s$, as stated.

Example 3.10 Show that integration of a function $f(t)$ is equivalent to its convolution with a unit step function; deducing the transform of the integral.

We may write

$$f(t) * u(t) = \int_{-\infty}^{\infty} f(\tau)u(t - \tau)d\tau = \int_{-\infty}^t f(\tau)d\tau$$

confirming the fact that the integration is equivalent to a convolution with the step function.

Since $u(t) \xleftrightarrow{\mathcal{L}} 1/s$

$$\mathcal{L} \left[\int_{-\infty}^t f(\tau)d\tau \right] = \frac{1}{s}F(s).$$

3.6.6 Multiplication by an Exponential (Modulation)

$$e^{at}f(t) \xleftrightarrow{\mathcal{L}} F(s - a). \quad (3.24)$$

Proof

$$\mathcal{L} [e^{at}f(t)] = \int_{-\infty}^{\infty} f(t)e^{-(s-a)t}dt = F(s - a). \quad (3.25)$$

Example 3.11 Evaluate the transform of $f(t) = e^{\alpha t} \cos \beta t u(t)$.

We may write

$$\cos \beta t u(t) \xleftrightarrow{\mathcal{L}} \frac{s}{s^2 + \beta^2}, \quad \sigma > 0$$

$$e^{\alpha t} \cos \beta t u(t) \xleftrightarrow{\mathcal{L}} \frac{(s - \alpha)}{(s - \alpha)^2 + \beta^2}, \quad \sigma > \alpha.$$

Note that multiplication by a real exponential $e^{\alpha t}$ shifts the poles, hence the boundary of the ROC in the s plane, from the line $\sigma = 0$ to the line $\sigma = \alpha$.

3.6.7 Time Scaling

$$f(at) \xleftrightarrow{\mathcal{L}} \frac{1}{|a|}F\left(\frac{s}{a}\right) \quad (3.26)$$

where a is a constant.

Proof We may write $g(t) = f(at)$

$$G(s) = \int_{-\infty}^{\infty} f(at)e^{-st}dt.$$

If $a > 0$, let $at = \tau$

$$G(s) = \int_{-\infty}^{\infty} f(\tau)e^{-s\tau/a} \frac{d\tau}{a} = \frac{1}{a}F\left(\frac{s}{a}\right).$$

If $a < 0$ we put $a = -\alpha$ where $\alpha > 0$

$$G(s) = \int_{-\infty}^{\infty} f(-\alpha t)e^{-st}dt$$

and with $\tau = -\alpha t$ we have

$$G(s) = \int_{\infty}^{-\infty} f(\tau)e^{s\tau/\alpha} \frac{d\tau}{(-\alpha)} = \frac{1}{\alpha} \int_{-\infty}^{\infty} f(\tau)e^{-s\tau/(-\alpha)}d\tau = \frac{1}{|a|}F\left(\frac{s}{a}\right)$$

as stated.

3.6.8 Reflection

Using the time scaling property with $a = -1$ we have

$$f(-t) \xleftrightarrow{\mathcal{L}} F(-s). \quad (3.27)$$

Note that if $f(t)$ is right-sided and its transform has a ROC $\sigma > \alpha$ then its reflection $f(-t)$, has a ROC $\sigma < -\alpha$, and vice versa.

3.6.9 Initial Value Theorem

The initial value theorem states that if a function $f(t)$ is a causal function, being nil for $t < 0$, and if $F(s)$ is its Laplace transform then

$$f(0^+) = \lim_{s \rightarrow \infty} sF(s). \quad (3.28)$$

Proof The Taylor series expansion of $f(t)$ can be written in the form

$$f(t) = \left[f(0^+) + f'(0^+)t + f''(0^+)\frac{t^2}{2!} + f'''(0^+)\frac{t^3}{3!} + \dots \right] u(t) = \sum_{k=0}^{\infty} f^{(k)}(0^+) \frac{t^k}{k!} u(t). \quad (3.29)$$

Using the transform $\mathcal{L}[t^n u(t)] = n!/s^{n+1}$ obtained above we have

$$F(s) = \sum_{k=0}^{\infty} f^{(k)}(0^+) \frac{1}{s^{k+1}} = \frac{f(0^+)}{s} + \frac{f'(0^+)}{s^2} + \frac{f''(0^+)}{s^3} + \dots \quad (3.30)$$

$$sF(s) = f(0^+) + \frac{f'(0^+)}{s} + \frac{f''(0^+)}{s^2} + \dots \quad (3.31)$$

wherefrom $f(0^+) = \lim_{s \rightarrow \infty} sF(s)$.

Example 3.12 Using Laplace transform find the initial value of the function

$$f(t) = Ae^{\alpha t} \cos(\beta t + \theta)u(t).$$

We have

$$f(t) = Ae^{\alpha t} \{ \cos \theta \cos \beta t - \sin \theta \sin \beta t \} u(t)$$

$$F(s) = A \frac{\cos \theta (s - \alpha) - \beta \sin \theta}{(s - \alpha)^2 + \beta^2}, \quad \sigma > \alpha$$

$$f(0^+) = \lim_{s \rightarrow \infty} sF(s) = \lim_{s \rightarrow \infty} A \frac{\cos \theta (1 - \alpha/s) - \beta \sin \theta/s}{(1 - \alpha/s)^2 + \beta^2/s^2} = A \cos \theta$$

which is the same value obtained by letting $t \rightarrow 0^+$ in the expression of $f(t)$.

3.6.10 Final Value Theorem

If a function $f(t)$ is causal

$$\lim_{s \rightarrow 0} sF(s) = f(\infty). \quad (3.32)$$

Proof From the differentiation property we have $\mathcal{L}[f'(t)] = \int_{0^+}^{\infty} f'(t)e^{-st} dt = sF(s) - f(0^+)$ wherefrom

$$\lim_{s \rightarrow 0} \int_{0^+}^{\infty} f'(t)e^{-st} dt = \int_{0^+}^{\infty} f'(t) \lim_{s \rightarrow 0} e^{-st} dt = \lim_{s \rightarrow 0} sF(s) - f(0^+) \quad (3.33)$$

$$\int_{0^+}^{\infty} f'(t)dt = f(t)|_{0^+}^{\infty} = f(\infty) - f(0^+) = \lim_{s \rightarrow 0} sF(s) - f(0^+). \tag{3.34}$$

Hence $\lim_{s \rightarrow 0} sF(s) = f(\infty)$ as stated.

Example 3.13 Verify the final value of the function

$$f(t) = Ae^{\alpha t} \cos \beta t u(t).$$

We have

$$F(s) = A \frac{s - \alpha}{(s - \alpha)^2 + \beta^2}, \quad \sigma > \alpha.$$

If $\alpha \geq 0$, applying the stated property we obtain $f(\infty) = \lim_{s \rightarrow 0} sF(s) = 0$, which is not true since with $\alpha \geq 0$ the function does not tend to zero as $t \rightarrow \infty$. The reason for the false conclusion is the fact that the ROC of $sF(s)$, i.e. that of $F(s)$, does not include the point $s = 0$ as can be seen in Fig. 3.11. We cannot therefore let s tend toward zero as required by the final value theorem. If $\alpha < 0$, as can be seen in Fig. 3.12 the ROC of $sF(s)$ does include the point $s = 0$ and the property produces the expected result $f(\infty) = 0$.

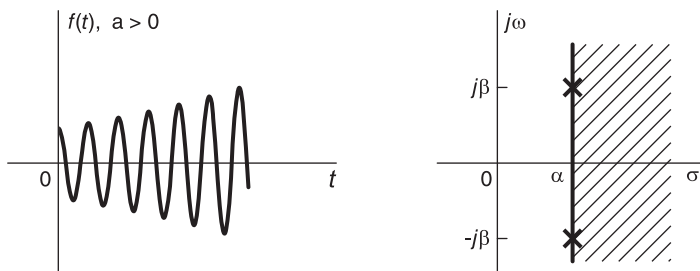


FIGURE 3.11 Growing causal exponential.

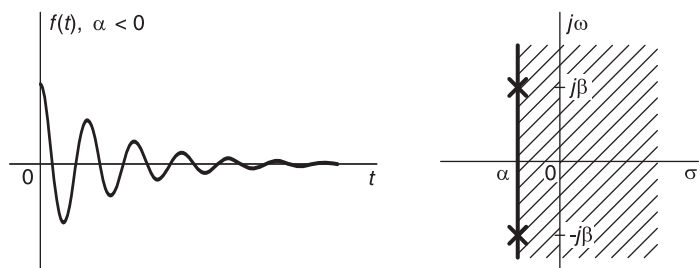


FIGURE 3.12 Decaying causal exponential.

3.6.11 Laplace Transform of Anticausal Functions

Applying the reflection property $f(-t) \xleftrightarrow{\mathcal{L}} F(-s)$ we obtain the transforms of basic left-sided functions listed in Table 3.3.

TABLE 3.3 Laplace transforms of anticausal functions

$f(t) = \mathcal{L}^{-1}[F(s)]$	$F(s) = \mathcal{L}[f(t)]$
$u(-t)$	$\frac{-1}{s}$
$-tu(-t)$	$\frac{1}{s^2}$
$t^n u(-t)$	$\frac{-n!}{s^{n+1}}$
$e^{-at}u(-t)$	$\frac{-1}{s+a}$
$te^{-at}u(-t)$	$\frac{-1}{(s+a)^2}$
$t^n e^{-at}u(-t)$	$\frac{-n!}{(s+a)^{n+1}}$
$\sin(\omega_0 t)u(-t)$	$\frac{-\omega_0}{s^2 + \omega_0^2}$
$\cos(\omega_0 t)u(-t)$	$\frac{-s}{s^2 + \omega_0^2}$
$e^{at} \sin(\omega_0 t)u(-t)$	$\frac{-\omega_0}{(s-a)^2 + \omega_0^2}$
$e^{at} \cos(\omega_0 t)u(-t)$	$\frac{-(s-a)}{(s-a)^2 + \omega_0^2}$

It is worthwhile remembering that the pole location of the transform of the anticausal function $e^{at}u(-t)$ is $s = a$, the same as that of the causal counterpart $e^{at}u(t)$, and that the ROC of the first is to the left of the pole while that of the second is to the right. Similarly, the poles of the anticausal functions $e^{at} \sin(\omega_0 t)u(-t)$ and $e^{at} \cos(\omega_0 t)u(-t)$ are at $s = -a \pm j\omega_0$, the same locations as those of the causal counterparts $e^{at} \sin(\omega_0 t)u(t)$ and $e^{at} \cos(\omega_0 t)u(t)$.

3.6.12 Shift in Time

If $f(t) \xrightarrow{\mathcal{L}} F(s)$ then $f(t - t_0) \xrightarrow{\mathcal{L}} e^{-t_0 s} F(s)$.

Proof

$$\mathcal{L}[f(t - t_0)] = \int_{-\infty}^{\infty} f(t - t_0)e^{-st} dt. \tag{3.35}$$

Let $t - t_0 = \tau$. We have

$$\mathcal{L}[f(t - t_0)] = \int_{-\infty}^{\infty} f(\tau)e^{-s(t_0+\tau)} d\tau = e^{-t_0 s} \int_{-\infty}^{\infty} f(\tau)e^{-s\tau} d\tau = e^{-t_0 s} F(s) \tag{3.36}$$

as stated.

Example 3.14 Evaluate the Laplace transform of $f(t) = \sin(\beta t)u(t - T)$.

We have

$$f(t) = \sin\{\beta(t - T + T)\}u(t - T) = [\sin\{\beta(t - T)\} \cos(\beta T) + \cos\{\beta(t - T)\} \sin(\beta T)]u(t - T)$$

$$F(s) = \cos(\beta T) \frac{\beta e^{-sT}}{s^2 + \beta^2} + \sin(\beta T) \frac{se^{-sT}}{s^2 + \beta^2} = \frac{\beta \cos(\beta T) + \sin(\beta T)s}{s^2 + \beta^2} e^{-sT}, \quad \sigma > 0.$$

3.7 Applications of the Differentiation Property

It is often possible to evaluate the Laplace transform by successive differentiation as the following examples illustrate.

Example 3.15 Evaluate by differentiation the Laplace transform of

$$f(t) = e^{\alpha t}u(-t).$$

We have $f'(t) = -e^{\alpha t}\delta(t) + \alpha e^{\alpha t}u(-t) = -\delta(t) + \alpha f(t)$, $sF(s) = -1 + \alpha F(s)$ wherefrom $F(s) = -1/(s - \alpha)$, $\sigma < \alpha$.

Example 3.16 Let $v(t) = \cos \beta t u(t)$. Evaluate the Laplace transform $V(s)$ by evaluating the two first derivatives of $v(t)$.

$$v'(t) = \cos \beta t \delta(t) - \beta \sin \beta t u(t) = \delta(t) - \beta \sin \beta t u(t)$$

$$v''(t) = \delta'(t) - \beta \{\sin \beta t \delta(t) + \beta \cos \beta t u(t)\} = \delta'(t) - \beta^2 v(t).$$

$$s^2 V(s) = s - \beta^2 V(s); \text{ hence } V(s) = s/(s^2 + \beta^2).$$

Example 3.17 Let $f(t)$ be the truncated sinusoid

$$f(t) = \sin(\beta t + \theta)R_T(t).$$

Evaluate the Laplace transform of $f(t)$ through successive differentiation.

We have

$$\begin{aligned} f'(t) &= \sin(\beta t + \theta)R'_T + \beta \cos(\beta t + \theta)R_T(t) \\ &= \sin(\beta t + \theta) \{\delta(t) - \delta(t - T)\} + \beta \cos(\beta t + \theta)R_T(t) \\ &= \sin \theta \delta(t) - \sin(\beta t + \theta)\delta(t - T) + \beta \cos(\beta t + \theta)R_T(t) \end{aligned}$$

$$f''(t) = \sin \theta \delta'(t) - \sin(\beta T + \theta)\delta'(t - T) + \beta \cos \theta \delta(t) - \beta \cos(\beta T + \theta)\delta(t - T) - \beta^2 f(t)$$

$$s^2 F(s) = -\beta^2 F(s) + \beta \cos \theta - \beta \cos(\beta T + \theta)e^{-Ts} + \sin \theta s - \sin(\beta T + \theta)se^{-Ts}$$

$$F(s) = \frac{\beta \cos \theta + \sin \theta s - \{\beta \cos(\beta T + \theta) + \sin(\beta T + \theta)s\}e^{-Ts}}{s^2 + \beta^2}.$$

Since the function $f(t)$ is of finite duration, the ROC of its Laplace transform $F(s)$ is the entire s plane.

3.8 Transform of Right-Sided Periodic Functions

Consider a right-sided periodic function $f(t)$ of period T , as the one shown in Fig. 3.13, which is a repetition to the right of a base function $f_0(t)$. We can write

$$f(t) = \sum_{n=0}^{\infty} f_0(t - nT). \tag{3.37}$$

Let $F_0(s) = \mathcal{L}[f_0(t)]$. We have

$$F(s) = \sum_{n=0}^{\infty} F_0(s)e^{-nTs} = \frac{F_0(s)}{1 - e^{-Ts}}, \quad \sigma = \Re[s] > 0. \tag{3.38}$$

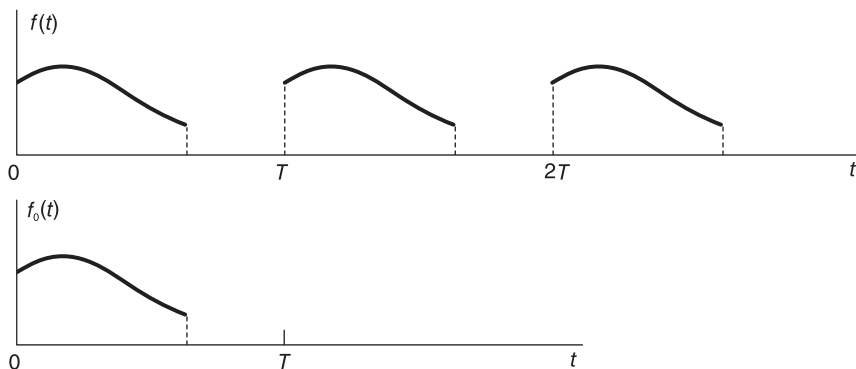


FIGURE 3.13 Causal periodic function and its base period.

Example 3.18 Evaluate the Laplace transform of the causal periodic function shown in Fig. 3.14

The transform of the base period is

$$F_0(s) = \int_0^{\tau} e^{-st} dt = \frac{1}{s}(1 - e^{-\tau s})$$

$$F(s) = \frac{1}{s} \frac{(1 - e^{-\tau s})}{(1 - e^{-Ts})}.$$

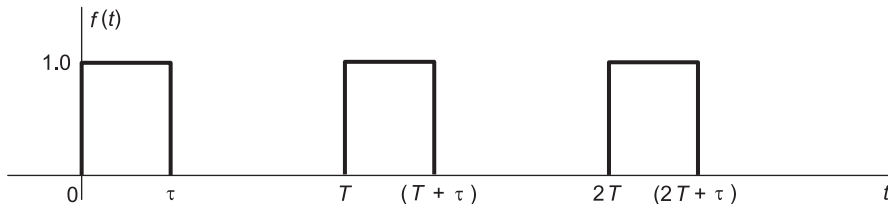


FIGURE 3.14 Causal train of rectangular pulses.

Example 3.19 Evaluate by differentiation the Laplace transform of the function $f(t) = \Pi_\tau(t)$. Show that the transform can be written using the hyperbolic sampling function $Sh(x) = \sinh(x)/x$. Deduce the transform of the function $g(t) = \sum_{n=0}^{\infty} f(t - 4n\tau)$.

We have $f'(t) = \delta(t + \tau) - \delta(t - \tau)$, $sF(s) = e^{\tau s} - e^{-\tau s}$.

$$F(s) = \frac{e^{\tau s} - e^{-\tau s}}{s} = \tau \frac{2 \sinh(\tau s)}{\tau s} = 2\tau Sh(\tau s)$$

$$G(s) = \sum_{n=0}^{\infty} F(s)e^{-4n\tau s} = \frac{F(s)}{1 - e^{-4\tau s}} = \frac{2\tau Sh(\tau s)}{1 - e^{-4\tau s}}.$$

Example 3.20 Evaluate the Laplace transform of the causal periodic ramp

$$v(t) = \sum_{n=0}^{\infty} v_0(t - nT)$$

where $v_0(t) = AtR_T(t)$ and $R_T(t) = u(t) - u(t - T)$.

Let

$$x_0 = v_0'(t) = \frac{A}{T}R_T(t) - A\delta(t - T)$$

$$X_0(s) = \frac{A}{T} \int_0^T e^{-st} dt - Ae^{-sT} = \frac{A}{T} \frac{1 - e^{-sT}}{s} - Ae^{-sT} = A \left\{ \frac{1 - e^{-Ts} - Tse^{-Ts}}{Ts} \right\}$$

$$V_0(s) = \frac{X_0(s)}{s} = \frac{A}{T} \frac{1 - e^{-Ts} - Tse^{-Ts}}{s^2}$$

$$V(s) = \frac{V_0(s)}{1 - e^{-Ts}} = \frac{A}{T} \frac{1 - e^{-Ts} - Tse^{-Ts}}{s^2(1 - e^{-Ts})}.$$

Example 3.21 Evaluate the inverse transform of

$$V(s) = \frac{1}{(s + a)(1 - e^{-bs})}.$$

Let $V(s) = V_0(s)/(1 - e^{-bs})$ where $V_0(s) = 1/(s + a)$, $v_0(t) = e^{-at}u(t)$,

$$v(t) = \sum_{n=0}^{\infty} v_0(t - nb) = \sum_{n=0}^{\infty} e^{-a(t-nb)}u(t - nb).$$

We note that in the interval $(kb, (k + 1)b)$ the function $v(t)$ is given by

$$v(t) = e^{-at} + e^{-a(t-b)} + \dots + e^{-a(t-kb)} = e^{-at} \sum_{m=0}^k e^{mab} = e^{-at} \frac{1 - e^{ab(k+1)}}{1 - e^{ab}}.$$

3.9 Convolution in Laplace Domain

Let $f(t)$ and $g(t)$ be two functions having Laplace transforms $F(s)$ and $G(s)$ with converge regions $\sigma_{f_1} < \sigma < \sigma_{f_2}$ and $\sigma_{g_1} < \sigma < \sigma_{g_2}$, respectively, and let $x(t)$ be their product $x(t) = f(t)g(t)$. The Laplace transform of $x(t)$ is given by

$$X(s) = \mathcal{L}[f(t)g(t)] = \frac{1}{2\pi j} \int_{c-j\infty}^{c+j\infty} G(p)F(s-p)dp, \quad (3.39)$$

$$\sigma_{f_1} + \sigma_{g_1} < \sigma \triangleq \Re[s] < \sigma_{f_2} + \sigma_{g_2}. \quad (3.40)$$

The path of integration being in the convergence region of the integrand, namely, $\max[\sigma_{g_1}, \sigma - \sigma_{f_2}] < \Re[p] < \min[\sigma_{g_2}, \sigma - \sigma_{f_1}]$.

Proof We can write

$$X(s) = \int_{-\infty}^{\infty} f(t)g(t)e^{-st} dt = \int_{-\infty}^{\infty} f(t)e^{-st} \frac{1}{2\pi j} \int_{c-j\infty}^{c+j\infty} G(p)e^{pt} dp dt. \quad (3.41)$$

Replacing $g(t)$ by its value as the inverse transform of $G(s)$ we can write

$$X(s) = \int_{-\infty}^{\infty} f(t)e^{-st} \frac{1}{2\pi j} \int_{c-j\infty}^{c+j\infty} G(p)e^{pt} dp dt \quad (3.42)$$

where the contour integral has to be in the ROC of $G(p)$, namely, $\sigma_{g_1} < \Re[p] < \sigma_{g_2}$. Interchanging the order of integration

$$\begin{aligned} X(s) &= \frac{1}{2\pi j} \int_{c-j\infty}^{c+j\infty} G(p) \int_{-\infty}^{\infty} f(t)e^{-(s-p)t} dt dp \\ &= \frac{1}{2\pi j} \int_{c-j\infty}^{c+j\infty} G(p)F(s-p)dp. \end{aligned} \quad (3.43)$$

The function $F(s-p)$ in the integrand implies that for convergence $\sigma_{f_1} < \Re[s-p] < \sigma_{f_2}$, i.e.

$$\sigma - \sigma_{f_2} < \Re[p] < \sigma - \sigma_{f_1} \quad (3.44)$$

and since the region of conversion of the function $G(p)$ in the integrand is $\sigma_{g_1} < \Re[p] < \sigma_{g_2}$, the overall region of conversion of the integrand in the p plane is

$$\max[\sigma_{g_1}, \{\sigma - \sigma_{f_2}\}] < \Re[p] < \min[\sigma_{g_2}, \{\sigma - \sigma_{f_1}\}]. \quad (3.45)$$

The p plane line integral in the definition of $X(s)$ has to lie in this ROC. In other words the value of c should satisfy the condition

$$\max[\sigma_{g_1}, \{\sigma - \sigma_{f_2}\}] < c < \min[\sigma_{g_2}, \{\sigma - \sigma_{f_1}\}]. \quad (3.46)$$

This completes the proof. Convolution in Laplace domain is often evaluated using the theory of residues.

3.10 Cauchy's Residue Theorem

This important theorem states that if $f(p)$ is a function of the complex variable p , which is analytic inside and on a closed contour Γ except at a finite number of poles inside Γ , then

$$\oint_{\Gamma} f(p)dp = 2\pi j [\text{sum of residues of } f(p) \text{ at its poles inside } \Gamma]. \quad (3.47)$$

Example 3.22 Using the complex convolution theorem evaluate the Laplace transform $X(s)$ of the function $x(t) = f(t)g(t)$ where

$$f(t) = e^t u(-t) + e^{-4(t-2)} u(t-2)$$

and $g(t) = e^{3t}u(-t) + e^{-5t}u(t)$.

We have

$$F(s) = \frac{1}{-s+1} + \frac{e^{-2s}}{s+4} = \frac{-1}{s-1} + \frac{e^{-2s}}{s+4}, \quad -4 < \sigma < 1$$

$$G(s) = \frac{1}{-s+3} + \frac{1}{s+5} = \frac{-1}{s-3} + \frac{1}{s+5}, \quad -5 < \sigma < 3.$$

The regions of convergence of $F(s)$ and $G(s)$ are shown in Fig. 3.15(a) and (b), respectively. We note that they are bounded by the poles at $\sigma_{f_1} = -4$, $\sigma_{f_2} = 1$ and $\sigma_{g_1} = -5$, $\sigma_{g_2} = 3$, respectively. The ROC of $X(s)$ is $\sigma_{f_1} + \sigma_{g_1} < \sigma < \sigma_{f_2} + \sigma_{g_2}$, i.e. $-9 < \sigma < 4$.

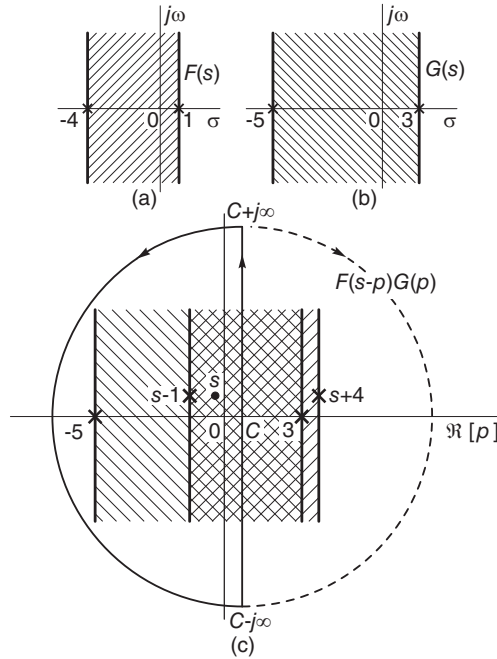


FIGURE 3.15 Convolution in Laplace domain.

Let $P(s) = G(p)F(s-p)$. The ROC of the product $P(s)$ is shown in Fig. 3.15(c), together with the contour of integration. As stated in the theorem the ROC of the product $P(s)$ is seen in the figure bounded such that

$$\max[-5, \sigma - 1] < \Re[p] < \min[3, \sigma + 4].$$

The ROC of $P(s)$ is the cross-hatched region $\sigma - 1 < \Re[p] < 3$. The contour of integration of the complex convolution integral has to lie within this region. It is closed by drawing a semicircle to the left or, alternatively, by a semicircle to the right. In the first case, shown in the figure, the poles enclosed are seen to be those at $p = -5$ and $p = s - 1$.

We have

$$P(s) = \left\{ \frac{-1}{p-3} + \frac{1}{p+5} \right\} \left\{ \frac{-1}{s-p-1} + \frac{e^{-2(s-p)}}{s-p+4} \right\}$$

or

$$P(s) = \frac{8(s-p+4) - 8e^{-2(s-p)}(s-p-1)}{(p-3)(p+5)(p-s+1)(p-s-4)}$$

$$X(s) = \mathcal{L}[x(t)] = \sum [\text{residues of } P(s) \text{ at the poles } p = -5 \text{ and } p = s - 1]$$

i.e.

$$X(s) = \frac{8(s+9) - 8e^{-2(s+5)}(s+4)}{-8(-4-s)(-9-s)} + \frac{8(5)}{(s-4)(s+4)(-5)}.$$

Using a partial fraction expansion we obtain

$$X(s) = \frac{-1}{s-4} + \frac{e^{-2(s+5)}}{s+9}.$$

We note that the inverse transform of $X(s)$ is given by

$$x(t) = \mathcal{L}^{-1}[X(s)] = e^{4t}u(-t) + e^{(-9t+8)}u(t-2)$$

which agrees with the value $x(t) = f(t)g(t)$.

Example 3.23 Evaluate the Laplace transform of $te^{-at}u(t)$ using the complex convolution property.

Writing $w(t) = te^{-at}u(t) = tu(t)e^{-at}u(t)$, we have $tu(t) \xrightarrow{\mathcal{L}} 1/s^2, \sigma > 0; e^{-at}u(t) \xrightarrow{\mathcal{L}} 1/(s+a), \sigma > -a..$

$$W(s) = \frac{1}{2\pi j} \int_{c-j\infty}^{c+j\infty} \frac{1}{p^2} \frac{1}{s-p+a} dp, \sigma > (-a), 0 < c < \sigma + a.$$

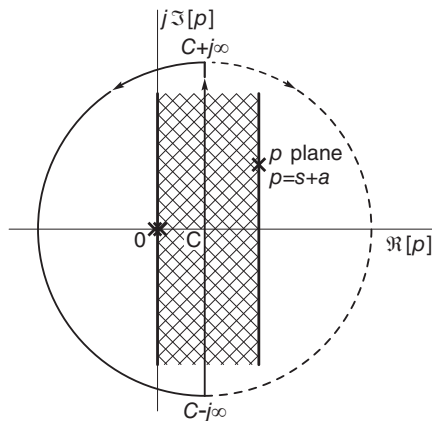


FIGURE 3.16 Closing the contour of integration in the complex s plane.

Referring to Fig. 3.16 we note that if the contour of integration is taken as the vertical line, extending from $c - j\infty$ to $c + j\infty$, followed by the counterclockwise arc then the closed contour contains the double pole at $p = 0$. If on the other hand the vertical line is followed by the clockwise arc, shown dotted in the figure, the enclosed pole would be the simple one at $p = s + a$. Choosing the first contour we have

$$\begin{aligned} W(s) &= \text{Res} \left[\frac{1}{p^2(s-p+a)} \text{ at } p = 0 \right] \\ &= \lim_{p \rightarrow 0} \frac{d}{ds} \left\{ \frac{1}{s-p+a} \right\} = \left[\frac{1}{(s-p+a)^2} \right]_{p=0} = \frac{1}{(s+a)^2}, \quad \sigma > (-a). \end{aligned}$$

a result that can be found alternatively using the property

$$tf(t) \xleftrightarrow{\mathcal{L}} \frac{-dF(s)}{ds}$$

with $f(t) = e^{-at}u(t)$. If instead the second, clockwise, contour is chosen, we obtain

$$W(s) = -\text{Res} \left[\frac{-1}{p^2(s-p-a)} \quad \text{at } p = s+a \right] = \frac{1}{(s+a)^2}, \quad \sigma > -a.$$

3.11 Inverse Laplace Transform

Given a Laplace transform $F(s)$ we recall the inversion formula, Equation (3.2), which produces $f(t)$. If $F(s)$ is rational, that is, a ratio of two polynomials in s , $F(s) = N(s)/D(s)$, the inverse transform can be evaluated by first effecting a partial fraction expansion of $F(s)$ into a sum of simple terms, followed by the use of tables of transforms to find the inverse of each term. We assume $F(s)$ to be a “proper fraction,” that is, the order of the numerator polynomial $N(s)$ is less than that of the denominator, $D(s)$, otherwise a long division is effected to obtain a proper fraction.

Example 3.24 Evaluate the inverse transform of $F(s) = (s^2 + 5s + 10)/(s + 2)$. Using long division we have $F(s) = s + 3 + 4/(s + 2)$, wherefrom $f(t) = \delta'(t) + 3\delta(t) + 4e^{-2t}u(t)$.

Effecting a partial fraction expansion assuming simple poles p_i of $F(s)$ we obtain

$$F(s) = \sum_{i=1}^n \frac{C_i}{s - p_i} \quad (3.48)$$

having as inverse transform

$$f(t) = \sum_{i=1}^n C_i e^{p_i t} u(t). \quad (3.49)$$

The residues C_i associated with the poles p_i are given by

$$C_i = (s - p_i)F(s)|_{s=p_i}. \quad (3.50)$$

A multiple pole p_i of order m_i appears as a factor of the form $(s - p_i)^{m_i}$ in the denominator. Such a multiple pole produces m_i terms in the decomposition

$$\frac{C_{i1}}{(s - p_i)} + \frac{C_{i2}}{(s - p_i)^2} + \dots + \frac{C_{im_i}}{(s - p_i)^{m_i}} = \sum_{j=1}^{m_i} \frac{C_{ij}}{(s - p_i)^j}. \quad (3.51)$$

The residues C_{ij} are given by

$$C_{ij} = \frac{1}{(m_i - j)!} \frac{d^{m_i - j}}{ds^{m_i - j}} [(s - p_i)^{m_i} F(s)]|_{s=p_i}, \quad i = 1, 2, \dots, m_i \quad (3.52)$$

wherefrom

$$F(s) = \sum_{i=1}^n \sum_{j=1}^{m_i} \frac{C_{ij}}{(s - p_i)^j}. \quad (3.53)$$

Now

$$e^{\alpha t} \frac{t^{n-1}}{(n-1)!} \xleftrightarrow{\mathcal{L}} \frac{1}{(s-\alpha)^n}, \quad \sigma > \alpha \quad (3.54)$$

so that

$$f(t) = \sum_{i=1}^n e^{p_i t} \sum_{j=1}^{m_i} C_{ij} \frac{t^{j-1}}{(j-1)!}. \quad (3.55)$$

Example 3.25 Evaluate the inverse transform of

$$F(s) = \frac{9s^2 - 38s + 55}{(s+3)(s-2)^3}, \quad \sigma > 2.$$

We write

$$\begin{aligned} F(s) &= \frac{A}{s+3} + \frac{C_3}{(s-2)^3} + \frac{C_2}{(s-2)^2} + \frac{C_1}{(s-2)} \\ A &= (s+3)F(s)|_{s=-3} = \frac{9s^2 - 38s + 55}{(s-2)^3} \Big|_{s=-3} = -2 \\ C_3 &= (s-2)^3 F(s)|_{s=2} = \frac{9s^2 - 38s + 55}{(s+3)} \Big|_{s=2} = 3. \end{aligned}$$

To evaluate C_1 and C_2 we may differentiate obtaining

$$\begin{aligned} C_2 &= \frac{1}{(3-2)!} \frac{d}{ds} [(s-2)^3 F(s)]|_{s=2} \\ &= \lim_{s \rightarrow 2} \frac{d}{ds} \frac{9s^2 - 38s + 55}{(s+3)} = \lim_{s \rightarrow 2} \frac{9s^2 + 54s - 169}{(s+3)^2} = -1 \\ C_1 &= \frac{1}{2!} \frac{d^2}{ds^2} [(s-2)^3 F(s)]|_{s=2} = \frac{1}{2} \frac{d}{ds} \left[\frac{9s^2 + 54s - 169}{(s+3)^2} \right] = 2. \end{aligned}$$

Alternatively, using the values of A and C_3 we have

$$F(s) = \frac{9s^2 - 38s + 55}{(s+3)(s-2)^3} = \frac{-2}{s+3} + \frac{3}{(s-2)^3} + \frac{C_2}{(s-2)^2} + \frac{C_1}{(s-2)}.$$

Putting $s = 0$ we obtain $-5 = C_2 - 2C_1$. Putting $s = 1$ we have $-3 = C_2 - C_1$. Solving we find $C_1 = 2$ and $C_2 = -1$, wherefrom

$$f(t) = \left[-2e^{-3t} + \frac{3}{2}t^2 e^{2t} - te^{2t} + 2e^{2t} \right] u(t).$$

3.12 Case of Conjugate Poles

A rational Laplace transform $F(s)$, a ratio of real coefficient polynomials, has as inverse transform a real function $f(t)$. Each complex root of each of the two polynomials is accompanied by its conjugate. It is useful to develop the form that results from combining the expressions of each such pair and use it in deducing the inverse transform. If $f(t) = Ae^{\alpha t} \cos(\beta t + \theta) u(t)$ then

$$F(s) = A \frac{\cos \theta (s - \alpha) - \sin \theta \beta}{(s - \alpha)^2 + \beta^2}, \quad \sigma > \alpha. \quad (3.56)$$

If we rewrite $F(s)$ in this form we can deduce the values of α , β , A and θ , hence directly the inverse transform. We can also rewrite $f(t)$ in the form

$$\begin{aligned} f(t) &= (A/2) \{e^{(\alpha+j\beta)t}e^{j\theta} + e^{(\alpha-j\beta)t}e^{-j\theta}\} u(t) \\ &= (A/2) \{e^{pt}e^{j\theta} + e^{p^*t}e^{-j\theta}\} u(t) = \{Ce^{pt} + C^*e^{p^*t}\} u(t) \end{aligned} \quad (3.57)$$

where $p = \alpha + j\beta$ and $C = (A/2)e^{j\theta}$, i.e. $A = 2|C|$ and $\theta = \arg[C]$, so that

$$F(s) = \frac{C}{s-p} + \frac{C^*}{s-p^*}, \quad \sigma > \alpha \quad (3.58)$$

and, conversely, if this is the value of $F(s)$ then

$$f(t) = \{Ce^{pt} + C^*e^{p^*t}\} = 2|C|e^{\alpha t} \cos(\beta t + \arg[C]) u(t). \quad (3.59)$$

It is worthwhile memorizing this form as the inverse transform of the given $F(s)$. Other forms are worth remembering. Writing $C = a + jb$, i.e. $a = (A/2)\cos\theta$, $b = (A/2)\sin\theta$, then $A = 2\sqrt{a^2 + b^2}$ and $\theta = \arctan(b/a)$,

$$F(s) = \frac{2a(s-\alpha) - 2b\beta}{(s-\alpha)^2 + \beta^2}, \quad \sigma > \alpha \quad (3.60)$$

so that the inverse transform is directly written as $f(t) = Ae^{\alpha t} \cos(\beta t + \theta) u(t)$.

Example 3.26 Evaluate the Inverse transform of

$$F(s) = \frac{4s^2 + s - 1}{(s+1)(s^2+1)}.$$

We write

$$\begin{aligned} F(s) &= \frac{A}{(s+1)} + \frac{C}{(s-j)} + \frac{C^*}{(s+j)} \\ A &= (s+1)F(s)|_{s=-1} = 1 \end{aligned}$$

$$C = \lim_{s \rightarrow j} (s-j)F(s) = \lim_{s \rightarrow j} \frac{4s^2 + s - 1}{(s+1)(s+j)} = 3/2 + j.$$

Note that for the pole $p = \alpha + j\beta = j$, we have $\alpha = 0$ and $\beta = 1$. Writing $C = a + jb$, we have $a = 3/2$ and $b = 1$, wherefrom

$$F(s) = \frac{1}{(s+1)} + \frac{3s-2}{s^2+1}.$$

Alternatively, having evaluated A we can write

$$F(s) = \frac{4s^2 + s - 1}{(s+1)(s^2+1)} = \frac{1}{(s+1)} + \frac{Bs+C}{(s^2+1)}.$$

Multiplying both sides by the common denominator of $F(s)$ we have

$$4s^2 + s - 1 = s^2 + 1 + (Bs+C)(s+1)$$

$$3s^2 + s - 2 = B(s^2 + s) + C(s+1).$$

Equating the coefficients of equal powers of s , that is, s^i , $i = 1, 2, \dots$ we obtain $B = 3$, $B + C = 1$, wherefrom $C = -2$ as just found. We can write

$$f(t) = [e^{-t} + 3 \cos t - 2 \sin t] u(t)$$

or, still,

$$f(t) = [e^{-t} + \sqrt{13} \cos(t + \arctan(2/3))] u(t).$$

Example 3.27 Evaluate $\mathcal{L}^{-1}[F(s)]$ where

$$F(s) = \frac{4s + 16}{(s^2 + 4s + 15)(s^2 + 6s + 13)}.$$

We write

$$F(s) = \frac{As + B}{(s^2 + 4s + 15)} + \frac{Cs + D}{(s^2 + 6s + 13)}.$$

Multiplying both sides by the denominator of $F(s)$

$$4s + 16 = (As + B)(s^2 + 6s + 13) + (Cs + D)(s^2 + 4s + 15).$$

Equating the coefficients of the same powers of s

$$A + C = 0$$

$$6A + B + 4C + D = 0$$

$$13A + 6B + 5C + 4D = 4$$

$$13B + 5D = 16.$$

By successive elimination of variables we obtain $A = C = 0$, $B = 2$, $D = -2$ wherefrom

$$F(s) = \frac{2}{(s+2)^2 + 1} - \frac{2}{(s+3)^2 + 4}$$

$$f(t) = [2e^{-2t} \sin t - e^{-3t} \sin 2t] u(t).$$

3.13 The Expansion Theorem of Heaviside

According to the expansion theorem of Heaviside if $F(s)$ is a proper fraction, i.e.

$$F(s) = \frac{N(s)}{D(s)} \tag{3.61}$$

with $N(s)$ of lower order than $D(s)$, and if the poles p_i of $F(s)$ are simple then

$$F(s) = \sum_{i=1}^n \frac{N(p_i)}{D'(p_i)} \frac{1}{(s - p_i)} \tag{3.62}$$

and

$$f(t) = \sum_{i=1}^n \frac{N(p_i)}{D'(p_i)} e^{p_i t}. \tag{3.63}$$

Proof An expansion in partial fractions of $F(s)$, assuming simple poles can be written in the form

$$F(s) = \sum_{i=1}^n \frac{C_i}{s - p_i} \tag{3.64}$$

where

$$C_i = \lim_{s \rightarrow p_i} (s - p_i)F(s) = \lim_{s \rightarrow p_i} \frac{(s - p_i)N(s)}{D(s)} = N(p_i) \lim_{s \rightarrow p_i} \frac{(s - p_i)}{D(s)}. \quad (3.65)$$

Using l'Hopital's rule

$$C_i = N(p_i) \frac{1}{D'(p_i)} \quad (3.66)$$

wherefrom

$$F(s) = \sum_{i=1}^n \frac{N(p_i)}{D'(p_i)} \frac{1}{s - p_i} \quad (3.67)$$

and the inverse transform $f(t)$ follows.

Example 3.28 Evaluate the inverse transform of

$$F(s) = \frac{-2s^2 - 9s + 11}{(s - 2)(s + 3)(s + 1)} \triangleq \frac{N(s)}{D(s)}.$$

We have

$$D(s) = (s - 2)(s + 3)(s + 1) = s^3 + 2s^2 - 5s - 6$$

$$D'(s) = 3s^2 + 4s - 5$$

$$\frac{N(p_1)}{D'(p_1)} = \frac{N}{D'} \Big|_{s \rightarrow 2} = -1$$

$$\frac{N(p_2)}{D'(p_2)} = \frac{N}{D'} \Big|_{s \rightarrow -3} = 2$$

$$\frac{N(p_3)}{D'(p_3)} = \frac{N}{D'} \Big|_{s \rightarrow -1} = -3$$

so that

$$f(t) = [-e^{2t} + 2e^{-3t} - 3e^{-t}] u(t).$$

3.14 Application to Transfer Function and Impulse Response

If the input $x(t)$ of a linear time invariant LTI system with zero initial is the impulse $x(t) = \delta(t)$ then $Y(s) = X(s)H(s) = H(s)$, and the output is called the *system impulse response*, denoted $h(t)$, being the inverse of $H(s)$

$$h(t) = \mathcal{L}^{-1}[H(s)]. \quad (3.68)$$

The system *frequency response* $H(j\omega)$ of a system is simply the Fourier transform of its impulse response $h(t)$

$$H(j\omega) = \mathcal{F}[h(t)] \quad (3.69)$$

and it may be deduced directly from the transfer function $H(s)$ by the substitution $s = j\omega$, if the ROC of $H(s)$ includes the imaginary axis $s = j\omega$.

In the time domain the output is the convolution of the input with the impulse response, $y(t) = x(t) * h(t)$. Moreover, if the input $x(t)$ is the unit step function $u(t)$ then the output is called the *unit step response*, and $Y(s) = X(s)H(s) = H(s)/s$, implying that the unit step response is simply the integral of the impulse response. These are important system response properties that will be often used in what follows.

3.15 Inverse Transform by Differentiation and Integration

Given a function $F(s)$ its inverse Laplace transform $f(t)$ may be formed by evaluating the inverse transform $g(t)$ of $G(s) = F(s)/s$, so that $F(s) = sG(s)$ and $f(t) = dg(t)/dt$.

Example 3.29 Knowing that $\mathcal{L}[\sqrt{t}u(t)] = (\sqrt{\pi}/2)s^{-3/2}$ evaluate the inverse transform of $F(s) = \sqrt{\pi}/\sqrt{s}$.

Let $G(s) = F(s)/s = \sqrt{\pi}/s^{3/2}$. We have $g(t) = 2\sqrt{t}u(t)$; hence $f(t) = g'(t) = (1/\sqrt{t})u(t)$.

Similarly, given a function $F(s)$ its inverse transform may be found by evaluating the inverse $g(t)$ of $G(s) = sF(s)$, so that $F(s) = G(s)/s$ and $f(t) = \int_0^t g(t)dt$.

Example 3.30 Evaluate $f(t)$ given that

$$F(s) = \frac{2a^2}{s(s^2 - 4a^2)}.$$

Let

$$G(s) = sF(s) = \frac{2a^2}{s^2 - 4a^2} = \frac{a \times 2a}{s^2 - (2a)^2}.$$

We have

$$\begin{aligned} \sinh bt u(t) &\longleftrightarrow \frac{b}{s^2 - b^2} \\ g(t) &= a \sinh 2at u(t) \end{aligned}$$

$$f(t) = \int_0^t a \sinh 2at dt = a \cosh 2at / (2a)|_0^t u(t) = (1/2) [\cosh 2at - 1] = \sinh^2 at.$$

We have seen that $tf(t) \longleftrightarrow -F'(s)$. Given a transform $F(s)$, to evaluate its inverse $f(t)$ we may start by letting $G(s) = -F'(s)$ of which the inverse transform is $g(t) = tf(t)$. Hence $f(t)$ is deduced as $f(t) = g(t)/t$.

Example 3.31 Evaluate the inverse transform of $F(s) = \ln[(s-a)/(s-b)]$.

Let

$$G(s) = -F'(s) = - \left\{ \frac{(s-b)}{(s-a)} \frac{(s-b) - (s-a)}{(s-b)^2} \right\} = \frac{b-a}{(s-a)(s-b)} = \frac{-1}{s-a} + \frac{1}{s-b}$$

$$g(t) = (e^{bt} - e^{at}) u(t) \quad \text{and} \quad f(t) = (e^{bt}/t - e^{at}/t) u(t).$$

The dual of this approach stems from the property that

$$f(t)/t \longleftrightarrow \int_0^\infty F(s)ds. \quad (3.70)$$

Using this property, given a transfer function $F(s)$, to evaluate its inverse $f(t)$ we let $G(s) = \int_s^\infty F(s)ds$. Its inverse transform is $g(t) = f(t)/t$. We thus deduce $f(t)$ as $f(t) = tg(t)$.

Example 3.32 Find the inverse transform of

$$F(s) = \frac{as}{(s^2 - a^2)^2}.$$

We write

$$G(s) = \int_s^\infty \frac{as \, ds}{(s^2 - a^2)^2} = \frac{1}{2} \frac{a}{s^2 - a^2}$$

$g(t) = (1/2) \sinh at u(t)$; hence $f(t) = (t/2) \sinh at u(t)$.

3.16 Unilateral Laplace Transform

The *unilateral Laplace transform* is closely related to the bilateral Laplace transform studied above. Its *raison d'être* is the solution of boundary value problems and in particular linear constant coefficients differential equations with nonzero initial conditions. In such problems an input is usually applied at a time instant such as $t = 0$, to a causal system and the solution of the differential equations describing the system is sought for $t > 0$. The unilateral Laplace transform of a function $f(t)$, which will be denoted $F_I(s)$, is by definition

$$F_I(s) = \mathcal{L}_{\mathcal{I}}[f(t)] = \int_{0^+}^{\infty} f(t)e^{-st} dt. \quad (3.71)$$

Symbolically we may write $F_I(s) = \mathcal{L}_{\mathcal{I}}[f(t)]$; $f(t) \xleftrightarrow{\mathcal{L}_{\mathcal{I}}} F_I(s)$. The unilateral transform thus views the function starting from the instant $t = 0^+$. Note that if the function $f(t)$ is nil for $t < 0$, such as the function $f(t) = e^{\alpha t}u(t)$, its unilateral transform is identical to the bilateral transform. The transforms differ if and only if the function is non-nil for any $t < 0$. Moreover, in contrast with the bilateral Laplace transform, the unilateral transform ignores any value of the function at $t = 0$, and therefore ignores any impulse or derivatives of an impulse that the function may have at $t = 0$.

The inverse unilateral Laplace transform is given by

$$f(t) = \frac{1}{2\pi j} \int_{\sigma-j\infty}^{\sigma+j\infty} F_I(s)e^{st} ds, \quad t > 0 \quad (3.72)$$

$$f(t) = 0, \quad t \leq 0 \quad (3.73)$$

where the line integral has to be in the ROC of $F_I(s)$.

Example 3.33 Evaluate the unilateral Laplace transform of the function $f(t) = e^{-\alpha t}u(t)$.

We have

$$F_I(s) = \mathcal{L}_{\mathcal{I}}[f(t)] = \int_{0^+}^{\infty} e^{-\alpha t} e^{-st} dt = \frac{1}{s + \alpha}, \quad \sigma > -\alpha$$

which is identical to the bilateral transform $F(s)$ of $f(t)$.

Example 3.34 Evaluate the unilateral Laplace transform of the function $f(t) = \delta(t) + e^{-\alpha t}u(t)$.

We have

$$F_I(s) = \int_{0^+}^{\infty} e^{-\alpha t} e^{-st} dt = \frac{1}{s + \alpha}, \quad \sigma > -\alpha$$

which is not the same as the bilateral transform $F(s)$ of $f(t)$ given by

$$F(s) = \int_{-\infty}^{\infty} \{\delta(t) + e^{-\alpha t}u(t)\}e^{-st} dt = 1 + \frac{1}{s + \alpha}, \quad \sigma > -\alpha.$$

Example 3.35 Compare the unilateral and bilateral Laplace transforms of the function $f(t) = e^{\beta t}u(-t) + e^{-\alpha t}u(t)$, $\alpha > 0$, $\beta > 0$.

We have, as obtained above,

$$F_I(s) = \mathcal{L} [e^{-\alpha t}u(t)] = \frac{1}{s + \alpha}, \quad \sigma > -\alpha$$

which is not the same as the bilateral transform $F(s)$ of $f(t)$ given by

$$F(s) = \frac{-1}{s - \beta} + \frac{1}{s + \alpha}, \quad -\alpha < \sigma < \beta.$$

Most properties of the bilateral transform apply with slight modification to the unilateral transform as will be seen in what follows. Only the properties of differentiation, integration, initial and final value theorems need be rewritten to incorporate the initial values of the transformed function and its derivatives and integrals.

Example 3.36 Show that $\mathcal{L}_I[1] = \mathcal{L}_I[u(t)] = \mathcal{L}[u(t)]$.

We have

$$\mathcal{L}_I[1] = \int_{0^+}^{\infty} e^{-st} dt = \frac{e^{-st}}{s} \Big|_{\infty}^{0^+} = \frac{1}{s}, \quad \sigma > 0 = \mathcal{L}[u(t)]$$

$$\mathcal{L}_I[u(t)] = \int_{0^+}^{\infty} u(t)e^{-st} dt = \int_0^{\infty} e^{-st} dt = \frac{e^{-st}}{s} \Big|_{\infty}^0 = \frac{1}{s}, \quad \sigma > 0 = \mathcal{L}_I[1].$$

Example 3.37 Evaluate the unilateral transform of $f(t) = \cos \beta t$ using the bilateral transform. We have

$$\mathcal{L}_I[\cos \beta t] = \mathcal{L}[\cos \beta t u(t)] = \frac{s}{s^2 + \beta^2}, \quad \sigma > 0.$$

3.16.1 Differentiation in Time

Given a function $f(t)$ and its unilateral Laplace transform $F_I(s)$, let the function $g(t)$ be its derivative

$$g(t) = df(t)/dt = f'(t). \quad (3.74)$$

The unilateral Laplace transform of $g(t)$ is given by

$$G_I(s) = sF_I(s) - f(0^+) \quad (3.75)$$

i.e.

$$\mathcal{L}_I[f'(t)] = sF_I(s) - f(0^+). \quad (3.76)$$

Proof

$$G_I(s) = \int_{0^+}^{\infty} g(t)e^{-st} dt = \int_{0^+}^{\infty} f'(t)e^{-st} dt. \quad (3.77)$$

Integrating by parts, with $u' = f'(t)$, $v = e^{-st}$, $u = f(t)$, $v' = -se^{-st}$,

$$G_I(s) = uv - \int uv' = f(t)e^{-st} \Big|_{0^+}^{\infty} + s \int_{0^+}^{\infty} f(t)e^{-st} dt. \quad (3.78)$$

Since $f(t)$ is assumed to be of exponential order we have $\lim_{t \rightarrow \infty} f(t)e^{-st} = 0$ and

$$G_I(s) = -f(0^+) + sF_I(s) \quad (3.79)$$

as asserted.

Similarly, let $x(t) = dg(t)/dt = f''(t)$. We have

$$X_I(s) = \int_{0^+}^{\infty} x(t)e^{-st} dt = \int_{0^+}^{\infty} f''(t)e^{-st} dt. \quad (3.80)$$

Integrating by parts, with $u' = f''(t)$, $v = e^{-st}$, $u = f'(t)$, $v' = -se^{-st}$,

$$\begin{aligned} X_I(s) &= uv - \int uv' = f'(t)e^{-st}|_{0^+}^{\infty} + s \int_{0^+}^{\infty} f'(t)e^{-st} dt \\ &= sG_I(s) - f'(0^+) = s\{sF_I(s) - f(0^+)\} - f'(0^+) \\ &= s^2F_I(s) - sf(0^+) - f'(0^+). \end{aligned} \quad (3.81)$$

Summarizing we write

$$f'(t) \xleftrightarrow{\mathcal{L}_I} sF_I(s) - f(0^+) \quad (3.82)$$

$$f''(t) \xleftrightarrow{\mathcal{L}_I} s^2F_I(s) - sf(0^+) - f'(0^+). \quad (3.83)$$

It can be shown that more generally

$$f^{(n)}(t) \xleftrightarrow{\mathcal{L}_I} s^n F_I(s) - \sum_{i=1}^n s^{n-i} f^{(i-1)}(0^+) \quad (3.84)$$

i.e.

$$f^{(n)}(t) \xleftrightarrow{\mathcal{L}_I} s^n F_I(s) - s^{n-1} f(0^+) - s^{n-2} f^{(1)}(0^+) - \dots - s f^{(n-2)}(0^+) - f^{(n-1)}(0^+). \quad (3.85)$$

Example 3.38 Evaluate $\mathcal{L}_I[t^n]$ using the differentiation theorem.

Let $f(t) = t^n$. We note that $f^{(n)}(t) = n!$ and $f^{(n+1)}(t) = 0$. We can therefore write

$$\mathcal{L}_I[f^{(n+1)}(t)] = 0 = s^{n+1}F_I(s) - \sum_{i=1}^{n+1} s^{n+1-i} f^{(i-1)}(0^+)$$

$$0 = s^{n+1}F_I(s) - s^n f(0^+) - s^{n-1} f^{(1)}(0^+) - \dots - f^{(n)}(0^+).$$

Now $f(0^+) = f'(0^+) = f^{(2)}(0^+) = \dots = f^{(n-1)}(0^+) = 0$, $f^{(n)}(0^+) = n!$ and $f^{(n+1)}(0^+) = 0$, wherefrom

$$s^{n+1}F_I(s) = n!$$

$$F_I(s) = \frac{n!}{s^{n+1}}, \quad \sigma > 0.$$

Note that this is equal to the bilateral transform of its causal component $t^n u(t)$.

Example 3.39 Evaluate $\mathcal{L}_I[\sin^2 \beta t]$. Let $f(t) = \sin^2 \beta t$ and $g(t) = f'(t)$. We have

$$g(t) = 2\beta \sin \beta t \cos \beta t$$

$$G_I(s) = sF_I(s) - f(0^+) = sF_I(s)$$

$$F_I(s) = \frac{G_I(s)}{s} = \frac{2\beta^2}{s(s^2 + 4\beta^2)}.$$

3.16.2 Initial and Final Value Theorem

The initial value of the function $f(t)$ is given by

$$f(0^+) = \lim_{s \rightarrow \infty} sF_I(s). \quad (3.86)$$

Proof We have already shown that if $g(t) = f'(t)$ then

$$G_I(s) = sF_I(s) - f(0^+). \quad (3.87)$$

We also know that the existence of $G_I(s)$ implies that as $s \rightarrow \infty$ in the ROC, $\lim_{s \rightarrow \infty} G_I(s) = 0$. We can therefore write

$$\lim_{s \rightarrow \infty} G_I(s) = 0 = \lim_{s \rightarrow \infty} sF_I(s) - f(0^+) \quad (3.88)$$

$$f(0^+) = \lim_{s \rightarrow \infty} sF_I(s) \quad (3.89)$$

as stated. The Final Value theorem is proved in a similar way as was done in relation with the bilateral Laplace transform.

3.16.3 Integration in Time Property

This property states that if a function $f(t)$ is piecewise continuous and of exponential order then

$$\int_{-\infty}^t f(\tau) d\tau \xleftrightarrow{\mathcal{L}_I} \frac{1}{s} [F(s) + f^{(-1)}(0^+)] \quad (3.90)$$

where the symbol $f^{(-1)}(\cdot)$ stands for the integral of the function.

Proof With $g(t) = \int_{-\infty}^t f(\tau) d\tau$, which is a continuous function of exponential order, we have $f(t) = g'(t)$, wherefrom

$$F_I(s) = sG_I(s) - g(0^+) \quad (3.91)$$

$$G_I(s) = \frac{1}{s} [F_I(s) + g(0^+)] = \frac{1}{s} \left[F_I(s) + \int_{-\infty}^{0^+} f(\tau) d\tau \right] \quad (3.92)$$

i.e.

$$G_I(s) = \frac{1}{s} [F_I(s) + f^{(-1)}(0^+)] \quad (3.93)$$

as stated.

3.16.4 Division by Time Property

If $\mathcal{L}_I[f(t)] = F_I(s)$, $\sigma > \alpha$ and if $\lim_{t \rightarrow 0^+} f(t)/t$ exists, then

$$\frac{f(t)}{t} \xleftrightarrow{\mathcal{L}} \int_s^\infty F_I(y) dy. \quad (3.94)$$

Consider the integral

$$I = \int_s^\infty F_I(y) dy = \int_s^\infty \int_{0^+}^\infty f(t) e^{-yt} dt dy. \quad (3.95)$$

Interchanging the order of integration we have

$$I = \int_{0^+}^{\infty} f(t) \int_s^{\infty} e^{-yt} dy dt = \int_{0^+}^{\infty} f(t) \left. \frac{e^{-yt}}{-t} \right|_s^{\infty} dt = \int_{0^+}^{\infty} \frac{f(t)}{t} e^{-st} dt, \quad \sigma > \alpha \quad (3.96)$$

i.e.

$$\int_s^{\infty} F_I(y) dy = \mathcal{L}_I \left[\frac{f(t)}{t} \right] \quad (3.97)$$

as stated.

3.17 Gamma Function

The Gamma function is given by

$$\Gamma(x) = \int_0^{\infty} e^{-t} t^{x-1} dt. \quad (3.98)$$

Integrating by parts with $u = e^{-t}$, $v' = t^{x-1}$, $u' = -e^{-t}$, $v = t^x/x$, we have

$$\Gamma(x) = e^{-t} \frac{t^x}{x} \Big|_0^{\infty} + \frac{1}{x} \int_0^{\infty} e^{-t} t^x dt. \quad (3.99)$$

If $x > 0$ we have

$$\Gamma(x) = \frac{1}{x} \int_0^{\infty} e^{-t} t^x dt = \frac{\Gamma(x+1)}{x}. \quad (3.100)$$

We have, therefore, the recursive relation

$$\Gamma(x+1) = x \Gamma(x). \quad (3.101)$$

Since $\Gamma(1) = 1$ we deduce that $\Gamma(2) = 1$, $\Gamma(3) = 2!$, $\Gamma(4) = 3!$ and

$$\Gamma(n+1) = n!, \quad n = 1, 2, 3, \dots \quad (3.102)$$

It can be shown that $\Gamma(1/2) = \sqrt{\pi}$. Indeed,

$$\Gamma(1/2) = \int_0^{\infty} t^{-1/2} e^{-t} dt. \quad (3.103)$$

Letting $t = x^2$ we have $\Gamma(1/2) = \int_0^{\infty} e^{-x^2} 2x dx = 2 \frac{\sqrt{\pi}}{2} = \sqrt{\pi}$.

Example 3.40 Evaluate the Laplace transform of $f(t) = t^\nu u(t)$.

We have

$$F(s) = \int_{-\infty}^{\infty} t^\nu u(t) e^{-st} dt = \int_0^{\infty} t^\nu e^{-st} dt.$$

The integral has the form of the Gamma function. Writing $t = y/s$ we have

$$F(s) = \frac{1}{s} \int_0^{\infty} \left(\frac{y}{s}\right)^\nu e^{-y} dy = \frac{1}{s^{\nu+1}} \int_0^{\infty} y^\nu e^{-y} dy = \frac{\Gamma(\nu+1)}{s^{\nu+1}}, \quad \nu > -1.$$

If ν is an integer, $\nu = n$, we have $f(t) = t^n u(t)$, $\Gamma(n+1) = n!$, $n = 1, 2, 3, \dots$ wherefrom

$$F(s) = \frac{n!}{s^{n+1}}, \quad \sigma > 0$$

as found earlier.

Example 3.41 Evaluate $\mathcal{L}_I \left[\frac{1}{\sqrt{t}} u(t) \right]$.

We have

$$\mathcal{L}_I \left[t^{-1/2} \right] = \frac{\Gamma(1/2)}{s^{1/2}} = \sqrt{\frac{\pi}{s}}.$$

Note that the function $1/\sqrt{t}$ is not of exponential order. Yet its Laplace transform exists. As noted earlier the condition that the function be of exponential order is a sufficient but not necessary condition for the existence of the transform.

Example 3.42 Evaluate $\mathcal{L}_I[Si(t)]$ using the transformation

$$\mathcal{L}_I \left[\frac{\sin t}{t} \right] = \arctan \frac{1}{s}.$$

Using the integration in time property we have

$$\mathcal{L}_I [Si(t)] = \mathcal{L}_I \left[\int_0^\infty \frac{\sin \tau}{\tau} d\tau \right] = \frac{\arctan(1/s)}{s}.$$

Example 3.43 Evaluate the impulse response of the system characterized by the differential equation

$$\frac{d^2 y}{dt^2} + 3 \frac{dy}{dt} + 2y = \frac{1}{2} \frac{dx}{dt} + x$$

if $y'(0) = 2$, $y(0) = 1$, $x(0) = 0$. We have

$$\frac{d^2 y}{dt^2} + 3 \frac{dy}{dt} + 2y = \frac{1}{2} \frac{dx}{dt} + x.$$

Using the differentiation property of the unilateral Laplace transform, in transforming both sides of the equation, we obtain

$$s^2 Y(s) - sy(0^+) - \frac{dy(0^+)}{dt} + 3sY(s) - 3y(0^+) + 2Y(s) = \frac{1}{2}sX(s) - \frac{1}{2}x(0^+) + X(s).$$

Substituting the initial conditions $y(0^+) = 1$ and $\frac{dy(0^+)}{dt} = 2$, we have

$$(s^2 + 3s + 2)Y(s) - s - 2 - 3 = \left(\frac{s}{2} + 1 \right) X(s).$$

If $x(t) = \delta(t)$, $X(s) = 1$

$$Y(s) = \frac{(s+2)}{2(s^2+3s+2)} + \frac{(s+5)}{(s^2+3s+2)}$$

The second term of $y(t)$ is due to the initial conditions. The first term is the impulse response, being the response of the system to an impulse with zero initial conditions. Writing $Y(s) = H(s) + Y_{I.C.}(s)$ we have

$$Y_{I.C.}(s) = \frac{s+5}{s^2+3s+2} = \frac{4}{s+1} - \frac{3}{s+2}.$$

The impulse response is given by $h(t) = \mathcal{L}^{-1}[H(s)] = \frac{1}{2}e^{-t}u(t)$, $y(t) = h(t) + y_{I.C.}(t)$ and

$$y_{I.C.}(t) = \mathcal{L}^{-1}[Y_{I.C.}(s)] = (4e^{-t} - 3e^{-2t})u(t).$$

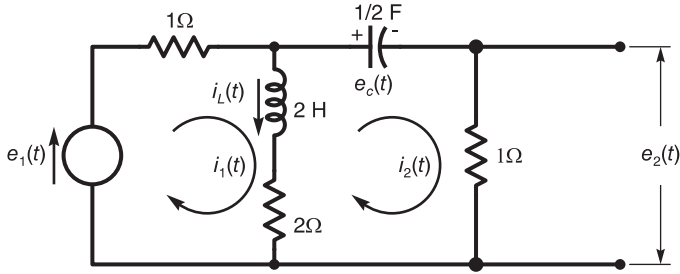


FIGURE 3.17 Electric circuit with voltage source.

Example 3.44 Determine the expression of $E_2(s) = \mathcal{L}\{e_2(t)\}$ as a function of $E_1(s)$ for the electric circuit shown in Fig. 3.17 if $e_c(0) \neq 0$.

The loop equations are given by

$$\begin{aligned} \left(\frac{2di_1}{dt} + 3i_1\right) - \left(\frac{2di_2}{dt} + 2i_2\right) &= e_1 \\ -\left(\frac{2di_1}{dt} + 2i_1\right) + \left(\frac{2di_2}{dt} + 3i_2 + 2 \int i_2 dt\right) &= 0. \end{aligned}$$

Laplace transforming the equations we have

$$(2s + 3)I_1(s) - (2s + 2)I_2(s) = E_1(s) + 2[i_1(0^+) - i_2(0^+)]$$

$$\begin{aligned} -(2s + 2)I_1(s) + (2s + 3 + 2/s)I_2(s) &= -(2/s)i_2^{(-1)}(0^+) - 2[i_1(0^+) - i_2(0^+)] \\ &= -\frac{e_c(0^+)}{s} - 2i_L(0^+) \end{aligned}$$

with $i_L(0^+) = 0$. Eliminating $I_1(s)$, we obtain

$$E_2(s) = I_2(s) = \frac{(2s^2 + 2s)E_1(s) - (2s + 3)e_c(0^+)}{4s^2 + 9s + 6}.$$

Example 3.45 Evaluate the Laplace transform of the alternating rectangles causal function $f(t)$ shown in Fig. 3.18. Evaluate the transform for the case $a = 1$. The base function for

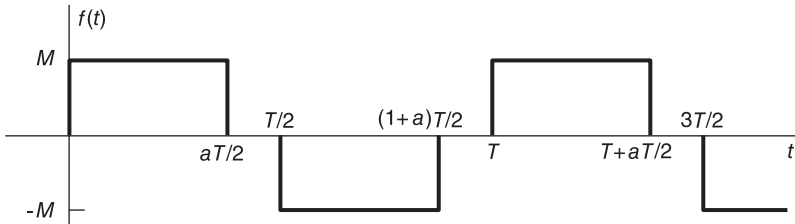


FIGURE 3.18 Causal periodic function with alternating sign rectangles.

this causal periodic function is given by

$$f_T(t) = M \left[u(t) - u\left(t - \frac{a}{2}T\right) - u\left(t - \frac{T}{2}\right) + u\left\{t - \frac{T}{2}(1+a)\right\} \right].$$

The Laplace transform of $f_T(t)$ is given by

$$F_T(s) = \frac{M}{s} \left[1 - e^{-aTs/2} - e^{-Ts/2} + e^{-T(1+a)s/2} \right].$$

We deduce that the transform of $f(t)$ is given by

$$F(s) = \frac{M}{s} \frac{(1 - e^{-aTs/2} - e^{-Ts/2} + e^{-T(a+1)s/2})}{(1 - e^{-Ts})}.$$

With $a = 1$

$$F(s) = \frac{M}{s} \frac{(1 - 2e^{-Ts/2} + e^{-Ts})}{(1 - e^{-Ts})} = \frac{M}{s} \frac{(1 - e^{-Ts/2})^2}{(1 - e^{-Ts/2})(1 + e^{-Ts/2})} = \frac{M}{s} \frac{(1 - e^{-Ts/2})}{(1 + e^{-Ts/2})}.$$

3.18 Table of Additional Laplace Transforms

Additional Laplace transforms are listed in Tables 3.4 and 3.5. New extended bilateral Laplace transforms thanks to a recent generalization of the Dirac-delta impulse are presented in Chapter 18.

TABLE 3.4 Additional Laplace transforms

$f(t)$	$F(s)$
$t^{\nu-1}e^{\alpha t}u(t), \Re[\nu] > 0$	$\frac{\Gamma(\nu)}{(s-\alpha)^\nu}$
$(\beta e^{\beta t} - \alpha e^{\alpha t})u(t)$	$\frac{(\beta-\alpha)s}{(s-\alpha)(s-\beta)}$
$t \sin \beta t u(t)$	$\frac{2\beta s}{(s^2 + \beta^2)^2}$
$(\sin \beta t + \beta t \cos \beta t)u(t)$	$\frac{2\beta s^2}{(s^2 + \beta^2)^2}$
$t \cos \beta t u(t)$	$\frac{s^2 - \beta^2}{(s^2 + \beta^2)^2}$
$t \cosh \beta t u(t)$	$\frac{s^2 + \beta^2}{(s^2 - \beta^2)^2}$
$t^2 \sin \beta t u(t)$	$\frac{2\beta(3s^2 - \beta^2)}{(s^2 + \beta^2)^3}$
$t^2 \cos \beta t u(t)$	$\frac{2(s^3 - 3\beta^2 s)}{(s^2 + \beta^2)^3}$
$t^2 \cosh \beta t u(t)$	$\frac{2(s^3 + 3\beta^2 s)}{(s^2 - \beta^2)^3}$
$t^2 \sinh \beta t u(t)$	$\frac{2\beta(3s^2 + \beta^2)}{(s^2 - \beta^2)^3}$
$\cos \beta t \cosh \beta t u(t)$	$\frac{s^3}{s^4 + 4\beta^4}$
$(\cos \beta t + \cosh \beta t)u(t)$	$\frac{2s^3}{s^4 - \beta^4}$
$e^{-ae^t}u(t), \Re[a] > 0$	$a^s \Gamma(-s, a)$
$\sin 2\sqrt{at}u(t)$	$\sqrt{\pi a} s^{-3/2} e^{-a/s}$
$\frac{\cos 2\sqrt{at}}{\sqrt{\pi t}}u(t)$	$\frac{e^{-a/s}}{\sqrt{s}}$

TABLE 3.5 Additional Laplace transforms (contd.)

$f(t)$	$F(s)$
$\sin 2\sqrt{at} u(t)$	$\sqrt{\pi a} \frac{e^{-a/s}}{s^{3/2}}$
$\frac{e^{-a^2/(4t)}}{\sqrt{\pi t}} u(t)$	$\frac{e^{-a\sqrt{s}}}{\sqrt{s}}$
$\frac{a}{2\sqrt{\pi t^3}} e^{-a^2/(4t)} u(t)$	$e^{-a\sqrt{s}}$
$\operatorname{erf}\left(\frac{a}{2\sqrt{t}}\right) u(t)$	$\frac{1 - e^{-a\sqrt{s}}}{s}$
$\operatorname{erfc}\left(\frac{a}{2\sqrt{t}}\right) u(t)$	$\frac{e^{-a\sqrt{s}}}{s}$
$\frac{e^{-2\sqrt{at}}}{\sqrt{\pi t}} u(t)$	$\frac{e^{-a/s}}{\sqrt{s}} \operatorname{erfc}[s/(2a)]$
$\frac{2a}{\sqrt{\pi}} e^{-a^2 t^2} u(t)$	$\frac{e^{s^2/(4a^2)} \operatorname{erfc}[s/(2a)]}{s}$
$\frac{1}{t} u(t)$	$\operatorname{Ei}(as)$
$\frac{1}{t^2 + a^2} u(t)$	$[\cos as \{\pi/2 - \operatorname{Si}(as)\} - \sin as \operatorname{Ci}(as)] / a$
$\frac{t}{t^2 + a^2} u(t)$	$\sin as \{\pi/2 - \operatorname{Si}(as)\} + \cos as \operatorname{Ci}(as)$

3.19 Problems

Problem 3.1 For the filter shown in Fig. 3.19, let the initial charge on the capacitor be $v(0) = v_0$. and let the input be the causal signal $e(t) = \sum_{n=0}^{\infty} e_0(t - 2n)$ where $e_0 = tR_1(t) = t[u(t) - u(t - 1)]$. Evaluate the transient and steady-state components of the output $v(t)$. Set v_0 so that the transient response be nil. Evaluate and sketch the output that results.

Problem 3.2

- a) Evaluate the impulse response $h(t)$ of the filter shown in Fig. 3.20.
- b) Without Laplace transform evaluate the filter unit step response
- c) Deduce the response $y(t)$ of the filter to the input

$$x(t) = u(t) - u(t - 1).$$

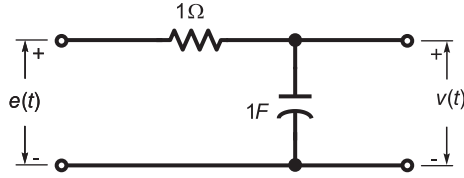


FIGURE 3.19 R-C electric circuit.

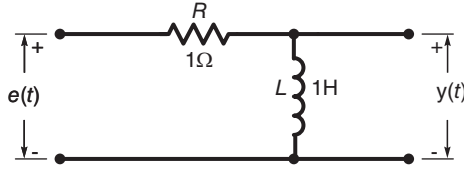


FIGURE 3.20 R-L circuit.

d) Using Laplace transform and the filter transfer function evaluate the response of the system to the input

$$x(t) = \sum_{n=0}^{\infty} \delta(t - n).$$

Problem 3.3 Given a system with impulse response $h(t) = e^{-t}u(t)$, evaluate the response $y_1(t)$ and $y_2(t)$ of this system to the inputs $x_1(t)$ and $x_2(t)$ where

$$x_1(t) = (1/k)[u(t) - u(t - k)]$$

$$x_2(t) = (t/k^2)u(t) - 2\{(t - k)/k^2\}u(t - k) + \{(t - 2k)/k^2\}u(t - 2k).$$

a) Sketch $x_1(t)$ and $x_2(t)$.

b) Confirm that as $k \rightarrow 0$ the inputs $x_1(t)$ and $x_2(t)$ tend to the Dirac-delta impulse $\delta(t)$ by showing that the responses $y_1(t)$ and $y_2(t)$ tend to the impulse response $h(t)$.

Problem 3.4 Let

$$h(t) = \begin{cases} t, & 0 \leq t \leq 1 \\ 2 - t, & 1 \leq t \leq 2 \\ 0, & \text{otherwise} \end{cases}$$

be the impulse response of a filter. Without using Laplace transform:

a) sketch the unit step response of the filter

b) sketch the response of the filter to the input

$$x(t) = u(t) - u(t - 4)$$

c) sketch its response to

$$v(t) = \sum_{n=0}^{\infty} nT \delta(t - nT), \quad T = 1.$$

Problem 3.5 Evaluate the response $y(t)$ of a system of transfer function

$$H(s) = \frac{4s + 2}{s^3 + 4s^2 + 6s + 4}$$

to the input

$$x(t) = e^{-(t-1)}u(t - 1).$$

Problem 3.6 Evaluate the transfer function of a system of which the impulse response is $u(t-1)$. Sketch the step response of the system.

Problem 3.7 For the circuit shown in Fig. 3.20

a) Evaluate the transfer function $H(s)$ between the input $e(t)$ and output $v(t)$

b) Evaluate the system impulse response.

c) Evaluate the response of the circuit to the inputs

i) $e_1(t) = R_T(t) = u(t) - u(t-1)$

ii) $e_2(t) = \sum_{n=-\infty}^{\infty} \delta(t-n)$

iii) $e_3(t) = \sum_{n=0}^{\infty} \delta(t-n)$

Problem 3.8 Let $x(t) = x_1(t) + x_2(t)$, $v(t) = v_1(t) + v_2(t)$ where $x_1(t) = u(t)$, $x_2(t) = u(-t)$

$$v_1(t) = \sin \beta t u(t), \quad v_2(t) = \sin \beta t u(-t).$$

Evaluate Laplace and Fourier transform of $x(t)$ and $v(t)$ if they exist, stating the regions of convergence and the reason if nonexistent.

Problem 3.9 Given the transfer function of a system

$$H(s) = \frac{s+13}{s^2+s-6}.$$

For all possible regions of convergence of $H(s)$ state whether the system is realizable and/or stable.

Problem 3.10 Evaluate the inverse Laplace transform of $F(s) = \frac{as+b}{s^2+\beta^2}$.

Problem 3.11 Given $v(t) = \cos(t) R_\tau(t)$, where $\tau > 0$,

a) evaluate by successive differentiation the Laplace transform $V(s)$ of $v(t)$. State its ROC.

b) deduce the Laplace transform of $\cos tu(t)$ by evaluating $\lim_{\tau \rightarrow \infty} V(s)$.

Problem 3.12 Evaluate the Laplace transform of each of the following signals, specifying its ROC.

a) $v_a(t) = -e^{\alpha t} u(\beta - t)$, $\alpha > 0$

b) $v_b(t) = (t/2)[u(t) - u(t-2)]$

c) $v_c(t) = e^{-2t} u(-t) + e^{4t} u(t)$

Problem 3.13 Evaluate the impulse response $h(t)$ of the systems having the following transfer functions:

a) $H(s) = \frac{1}{s+1}$, ROC: $\Re[s] > -1$.

b) $H(s) = \frac{1}{s+1}$, ROC: $\Re[s] < -1$.

c) $H(s) = \frac{s}{s+1}$, ROC: $\Re[s] > -1$.

d) $H(s) = \frac{s+1}{s^2+6s+8}$, ROC: $\Re[s] > -2$.

e) $H(s) = \frac{2s}{s^2-s-6}$, ROC: $-2 < \Re[s] < +3$.

$$f) H(s) = \frac{1}{(s+1)^2}, \text{ ROC: } \Re[s] > -1.$$

$$g) H(s) = \frac{1}{(s+1)^2(s+2)}, \text{ ROC: } \Re[s] > -1.$$

Problem 3.14 Given the Laplace transform

$$X(s) = \frac{5}{s+4} - \frac{2}{s}.$$

Evaluate the inverse transform $x(t)$ for all possible regions of convergence of $X(s)$.

Problem 3.15 For a given signal $x(t)$ the Laplace transform $X(s)$ has poles at $s = -10$ and $s = +10$ and a zero at $s = -2$. Determine the ROC of $X(s)$ under each of the following conditions

a) $x(t) = 0$ for $t < 5$

b) $x(t) = 0$ for $t > 0$

c) The Fourier transform $X(j\omega)$ of $x(t)$ exists

d) The Fourier transform of $x(t+10)$ exists

e) The Fourier transform of $e^{-t}x(t)$ exists

f) The Fourier transform of $e^{-12t}x(t)$ exists

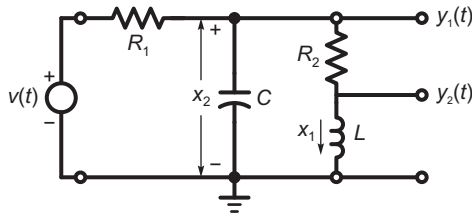


FIGURE 3.21 RLC circuit.

Problem 3.16 For the circuit shown in Fig. 3.21, with $v(t)$ the input, and $y_1(t)$ and $y_2(t)$ the outputs

a) With $R_1 = 10^3 \Omega$, $R_2 = 10^2 \Omega$, $L = 10 \text{ H}$ and $C = 10^{-3} \text{ F}$ evaluate the transfer function $H(s)$ and the impulse response.

b) Assuming the initial conditions $x_1(0) = 0.1 \text{ Amp}$, $x_2(0) = 10 \text{ volts}$ evaluate the response of the circuit to the input $v(t) = 100u(t) \text{ volts}$.

Problem 3.17 The switch S in the electric circuit depicted in Fig. 8.35 is closed at $t = 0$, the circuit having zero initial conditions.

Evaluate the voltage drop x_1 across the capacitor C and the current x_2 through the inductance L once the switch is closed.

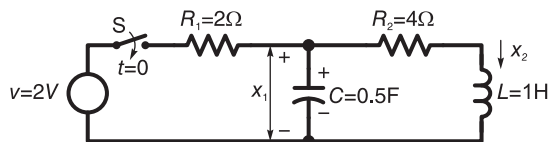


FIGURE 3.22 RLC electric circuit

Problem 3.18 For each of the following cases specify the values of the parameter α ensuring the existence of the Laplace transform and that of the Fourier transform of $x(t)$.

- $x(t) = e^{4t}u(-t) + e^{\alpha t}u(t)$
- $x(t) = u(t) + e^{-\alpha t}u(-t)$
- $x(t) = e^{3t}u(t) - e^{\alpha t}u(t)$
- $x(t) = u(t - \alpha) - e^{-3t}u(t)$
- $x(t) = e^{-3t}u(t) + e^{-4t}u(\alpha t)$, where $\alpha \neq 0$
- $x(t) = \cos(20\pi t)u(t) + \alpha u(t)$

Problem 3.19 For the function

$$f(t) = \sum_{i=1}^M A_i e^{\alpha_i t} \sin(\beta_i t + \theta_i) u(t)$$

where

$$\beta_1 > \beta_2 > \dots > \beta_M > 0$$

represent graphically the poles in the s plane, evaluate the Laplace transform and state if the Fourier transform exists for the following three cases:

- $\alpha_1 > \alpha_2 > \dots > \alpha_M > 0$, ii) $\alpha_1 < \alpha_2 < \dots < \alpha_M < 0$,
- $\alpha_1 = \alpha_2 = \dots = \alpha_M = 0$.

Problem 3.20 For each of the following signals evaluate the Laplace transform, the poles with the ROC, and state whether or not the Fourier transform exists.

- $v_1(t) = \sum_{i=1}^P A_i e^{-a_i t} \cos(b_i t + \theta_i) u(t) + \sum_{i=1}^P B_i e^{c_i t} \cos(d_i t + \phi_i) u(-t)$, where the a_i , b_i and c_i are distinct and $b_i > 0$, $d_i > 0$, $a_i > 0$, $c_i > 0$, $\forall i$
- The same function $v_1(t)$ but with the conditions:

$$b_i > 0, \quad d_i > 0, \quad a_i > 0, \quad c_i < 0, \quad \forall i$$

- The same function $v_1(t)$ but with the conditions:

$$b_i > 0, \quad a_i = 0, \quad B_i = 0, \quad \forall i$$

- $v_2(t) = A \cos(bt + \theta)$, $-\infty < t < \infty$
- $v_3(t) = Ae^{-t}$, $-\infty < t < \infty$

Problem 3.21 Given the transfer function

$$H(s) = \frac{2s + 2}{s^2 + 2s + 5}$$

- Evaluate and sketch the zeros and poles in the complex s plane.
- Assuming that $H(s)$ is the transfer function of an unstable system evaluate the system impulse response $h(t)$.
- Assuming the frequency response $H(j\omega)$ exists, state the ROC of $H(s)$ and evaluate $h(t)$ and $H(j\omega)$.

Problem 3.22 The signals $f_1(t)$, $f_2(t)$, \dots , $f_{12}(t)$ shown in Fig. 3.23 are composed of exponentials and exponentially damped sinusoids. For each of these signals

- Without evaluating the Laplace transform nor referring to the ROC state whether or not the signal has a Laplace transform and the basis for such conclusion.
- Draw the ROC and deduce whether or not the Fourier transform exists.

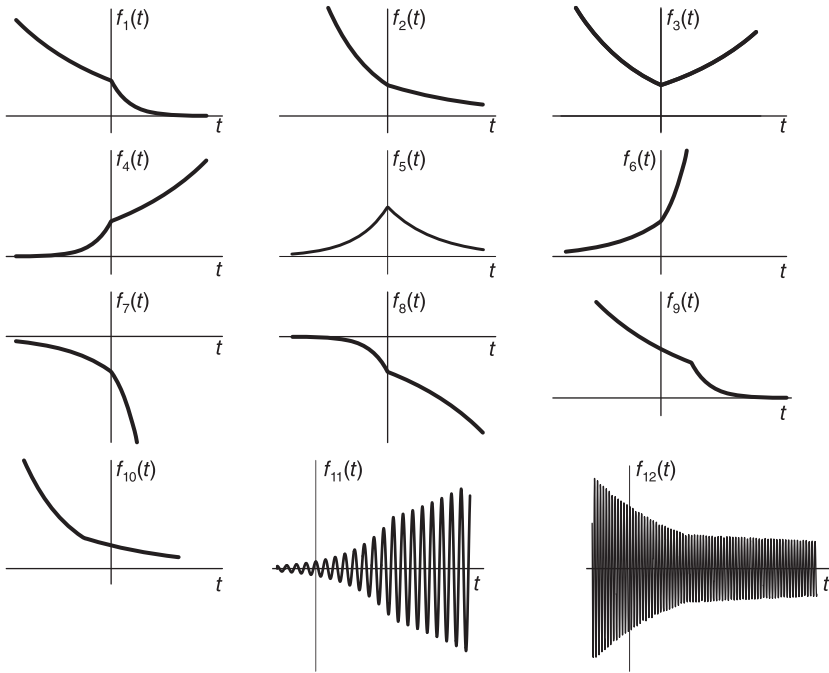


FIGURE 3.23 Exponential and damped sinusoidal signals.

Problem 3.23 Let $X(s)$ be the Laplace transform of a signal $x(t)$, where

$$X(s) = \frac{1}{s+1} + \frac{1}{s-3}.$$

- Given that the ROC of $X(s)$ is $\Re[s] > 3$, evaluate $x(t)$. Evaluate the Fourier transform $X(j\omega)$ of $x(t)$.
- Redo part a) if the ROC is $\Re[s] < -1$ instead.
- Redo part a) if the ROC is, instead, $-1 < \Re[s] < 3$.

Problem 3.24 Given the system transfer function

$$H(s) = \frac{7s^3 - s^2 + 3s - 1}{s^4 - 1} \quad (3.104)$$

- Evaluate the poles and zeros of $H(s)$.
- Specify the different possible ROC's of $H(s)$.
- Evaluate the system impulse response $h(t)$, assuming that i) the system is causal, ii) the system is anticausal, and iii) the system impulse response is two-sided.
- Evaluate $H(j\omega)$ the Fourier transform of $h(t)$ if it exists. If it does not, explain why.

Problem 3.25 A causal linear system has an input $v(t)$, and output $y(t)$ and an impulse response $h(t)$. Assuming that the input $v(t)$ is anticausal, i.e. $v(t) = 0$ for $t > 0$, that

$$V(s) = \frac{s+2}{s-2}$$

and that the output is given by $y(t) = e^{-t}u(t) - 2e^{2t}u(-t)$.

a) Evaluate and sketch the poles and zeros and the regions of convergence of $V(s)$, $H(s)$ and $Y(s)$.

b) Evaluate $h(t)$.

c) Evaluate the system frequency response $H(j\omega)$ and its output $y(t)$ in response to the input $v(t) = \cos(2t - \pi/3)$.

3.20 Answers to Selected Problems

Problem 3.1 See Fig. 3.24.

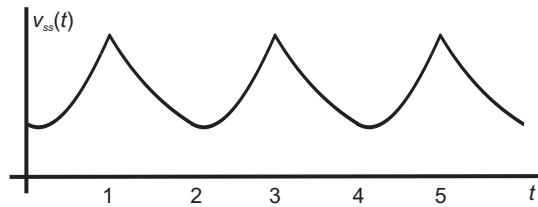


FIGURE 3.24 System total response.

Problem 3.2 a) $h(t) = \delta(t) - e^{-t}u(t)$; b) $y(t) = e^{-t}u(t) - e^{-(t-1)}u(t-1)$; c) $X(s) = (1/1 - e^{-s})$; d) $y_{ss}(t) = \delta(t) - e^{-t}u(t) - C_1 e^{-t}u(t) + C_1 e^{-(t-1)}u(t-1)$, $y_{tr.}(t) = C_1 e^{-t}u(t)$.

Problem 3.3 See Fig. 3.25. $\lim_{k \rightarrow 0} Y_2(s) = \frac{1}{s+1}$

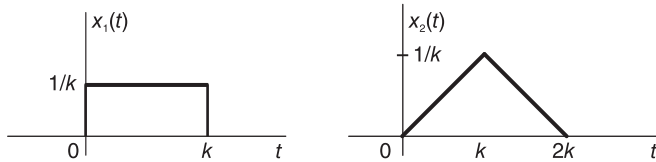


FIGURE 3.25 Two input signals, Problem 3.3.

Problem 3.4 See Fig. 3.26 and Fig. 3.27.

Problem 3.5 $y(t) = \{3 e^{-2(t-1)} + 3.162 e^{-(t-1)} \cos(t - 2.893) - 2 e^{-(t-1)}\} u(t - 1)$. See Fig. 3.28

Problem 3.7 ii) $v_2(t) = \sum_{n=-\infty}^{\infty} h(t-n) = \sum_{n=-\infty}^{\infty} \{\delta(t-n) - e^{-(t-n)}u(t-n)\}$. iii) $v_3(t) = \sum_{n=0}^{\infty} \{\delta(t-n) - e^{-(t-n)}u(t-n)\}$.

Problem 3.8 $X(s)$ and $V(s)$ do not exist. $X(j\omega) = \mathcal{F}[1] = 2\pi\delta(\omega)$. $V(j\omega) = V_1(j\omega) + V_2(j\omega) = (\pi/j) \{\delta(\omega - \beta) - \delta(\omega + \beta)\} = \mathcal{F}[\sin \beta t]$.

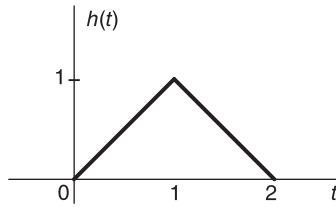


FIGURE 3.26 Impulse response of Problem 3.4.

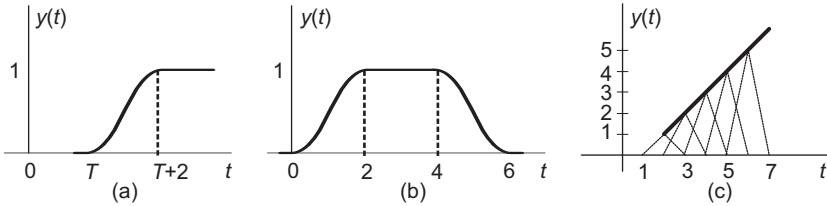


FIGURE 3.27 Results of Problem 3.4.

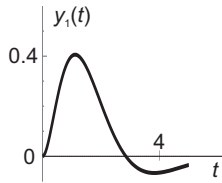


FIGURE 3.28 Figure for Problem 3.5.

Problem 3.9 1. $\sigma > 2$. Realizable, unstable. 2. $\sigma < -3$. Not realizable, unstable. 3. $-3 < \sigma < 2$. Not realizable. Stable.

Problem 3.11 a) $V(s) = (s + \sin \tau e^{-\tau s} - s \cos \tau e^{-\tau s}) / (s^2 + 1)$. ROC entire plane. b) $\lim_{\tau \rightarrow \infty} V(s) = s / (s^2 + 1)$, $\sigma \Rightarrow 0$

Problem 3.12 c) $v_a(t) = -e^{\alpha t} u(\beta - t) = -e^{\alpha \beta} e^{\alpha[t-\beta]} u(-[t-\beta])$ $V_a(s) = (e^{\alpha \beta} e^{-\beta s}) / (s - \alpha)$, ROC: $\sigma = \Re[s] < \alpha$ b) $V_b(s) = (1/2) \frac{1}{s^2} - (1/2) e^{-2s} \frac{1}{s^2} - e^{-2s} \frac{1}{s}$, ROC: entire s plane. c) No Laplace transform.

Problem 3.13 a) $h(t) = e^{-t} u(t)$; b) $h(t) = -e^{-t} u(t) + \delta(t)$; d) $h(t) = 1.5e^{-4t} u(t) - 0.5e^{-2t} u(t)$; e) $h(t) = 0.8e^{-2t} u(t) - 1.6e^{+3t} u(-t)$; f) $h(t) = te^{-t} u(t)$; g) $h(t) = -e^{-t} u(t) + te^{-t} u(t) + e^{-2t} u(t)$

Problem 3.14 1. ROC $\Re[s] < -4$: $h(t) = -5e^{-4t} u(-t) + 2u(-t)$. ROC $-4 < \Re[s] < 0$: $h(t) = 5e^{-4t} u(t) + 2u(-t)$. ROC $\Re[s] > 0$: $h(t) = 5e^{-4t} u(t) - 2u(t)$

Problem 3.15 ROC's: $\Re[s] < -10$, $-10 < \Re[s] < +10$ and $\Re[s] > 10$. a) $\Re[s] > 10$; b) $\Re[s] < -10$; c) $-10 < \Re[s] < +10$; d) $-10 < \Re[s] < +10$; e) $-10 < \Re[s] < +10$ f) $\Re[s] > 10$.

Problem 3.16 a) $H(s) = (s + 10) / (s^2 + 11s + 110)$,
 $h(t) = 1.119 e^{-5.5t} \cos(8.93t - 0.467) u(t)$.
 b) $y(t) = 11.74 e^{-5.5t} \cos(8.93t + 0.552) u(t)$.

Problem 3.17 $x_2(t) = 2[(1/2)(1 - e^{-2t}) - (1/3)(1 - e^{-3t})]u(t)$.

Problem 3.18

- a) $x(t) = e^{4t}u(-t) + e^{\alpha t}u(t)$ ROC of $X(s) : \alpha < \sigma < 4$, $X(s)$ exists iff $\alpha < 4$, $X(j\omega)$ exists iff $\alpha \leq 0$
- b) $x(t) = u(t) + e^{-\alpha t}u(-t)$ ROC of $X(s) : 0 < \sigma < -\alpha$, $X(s)$ exists iff $\alpha < 0$, $X(j\omega)$ exists if $\alpha \leq 0$.
- c) $x(t) = e^{3t}u(t) - e^{\alpha t}u(t)$ ROC: $\sigma > \max(3, \alpha)$, $X(s)$ exists for $\forall \alpha$, $X(j\omega)$ does not exist.
- d) $x(t) = u(t-\alpha) - e^{-3t}u(t)$ ROC: $\sigma > 0$, $X(s)$ exists for $\forall \alpha$, $X(j\omega)$ exists for $\forall \alpha$.
- e) $x(t) = e^{-3t}u(t) + e^{-4t}u(\alpha t)$, where $\alpha \neq 0$. ROC: $\sigma > -3$ if $\alpha > 0$, $X(s)$ exists iff $\alpha > 0$, $X(j\omega)$ exists iff $\alpha > 0$.
- f) $x(t) = \cos(20\pi t)u(t) + \alpha u(-t)$ ROC: $\sigma > 0$ iff $\alpha = 0$, $X(s)$ exists iff $\alpha = 0$, $X(j\omega)$ exists for $\forall \alpha$

Problem 3.21

- a) Zero: $s = -1$. Poles: $s = -1 \pm j2$
- b) $h(t) = -2e^{-t} \cos 2t u(-t)$.
- c) $h(t) = 2e^{-t} \cos 2t u(t)$.

Problem 3.22

- a) $f_1(t)$: Transform exists, $f_2(t)$: No transform. $f_3(t)$: No transform. $f_4(t)$: Transform exists. $f_5(t)$: Transform exists. $f_6(t)$: No transform. $f_7(t)$: No transform. $f_8(t)$: Transform exists. $f_9(t)$: Transform exists. $f_{10}(t)$: No transform. $f_{11}(t)$: Transform exists. $f_{12}(t)$: No transform.
- b) $f_1(t)$: No Fourier transform. $f_2(t)$: No Fourier transform. $f_3(t)$: No Fourier transform. $f_4(t)$: No Fourier transform. $f_5(t)$: Transform exists. $f_6(t)$: No Fourier transform. $f_7(t)$: No Fourier transform. $f_8(t)$: No Fourier transform. $f_9(t)$: No Fourier transform. $f_{10}(t)$: No Fourier transform. $f_{11}(t)$: No Fourier transform. $f_{12}(t)$: No Fourier transform.

Problem 3.23

- a) $x(t) = e^{-t}u(t) + e^{3t}u(t)$. $X(j\omega)$ does not exist
- b) $x(t) = -e^{-t}u(-t) - e^{3t}u(-t)$. $X(j\omega)$ does not exist
- c) $x(t) = e^{-t}u(t) - e^{3t}u(-t)$.

$$X(j\omega) = \frac{1}{j\omega + 1} + \frac{1}{j\omega - 3}$$

Problem 3.24 See Fig. 3.29

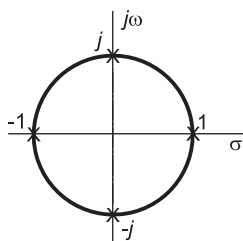


FIGURE 3.29 System poles, Problem 3.24.

- b)
 - i) $h(t) = (2e^t + 3e^{-t} + 2 \cos t) u(t)$ (3.105)
 - ii) $h(t) = \{-2e^t - 3e^{-t} - 2 \cos t\} u(-t)$ (3.106)

iii) Case A: The ROC is $0 < \sigma < 1$

$$h(t) = (3e^{-t} + 2 \cos t) u(t) - 2e^t u(-t) \tag{3.107}$$

See Fig. 3.30.

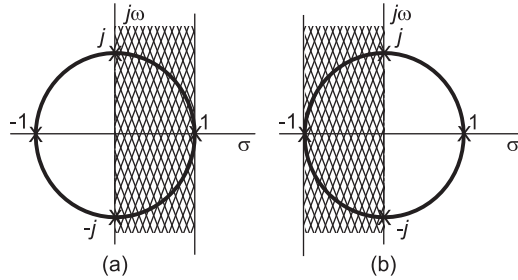


FIGURE 3.30 Problem 3.24. Two possible ROCs.

Case B: The ROC is $-1 < \sigma < 0$

$$h(t) = 3e^{-t}u(t) - \{2e^t + 2 \cos t\} u(-t)$$

d)

Case A: $H(j\omega) = \frac{3}{j\omega+1} + 2 \mathcal{F}[\cos t u(t)] - \frac{2}{j\omega-1}$

and $\mathcal{F}[\cos t u(t)] = (1/2) \left[\frac{1}{j(\omega-1)} + \pi \delta(\omega-1) + \frac{1}{j(\omega+1)} + \pi \delta(\omega+1) \right]$.

Case B: $H(j\omega) = \frac{3}{j\omega+1} - \frac{2}{j\omega-1} - 2 \mathcal{F}[\cos t u(-t)]$,

$$\cos t u(-t) \longleftrightarrow \frac{1}{2} \left[-1/[j(\omega-1)] - 1/[j(\omega+1)] + \pi \delta(\omega-1) + \pi \delta(\omega+1) \right].$$

Problem 3.25

a) See Fig. 3.31.

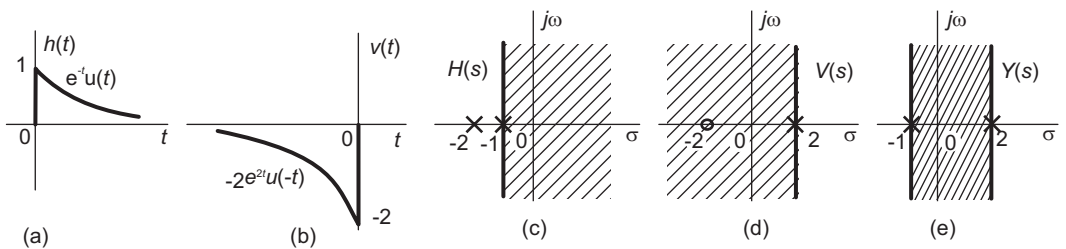


FIGURE 3.31 Figure for Problem 3.25.

b) $h(t) = (-3e^{-t} + 6e^{-2t}) u(t)$

c) $y(t) = 0.9487 \cos(2t + 1.7726)$.

4

Fourier Transform

In Chapter 3 we have studied the Laplace transform and noted that a special case thereof is the Fourier transform. As we shall note in this chapter, the Fourier transform, similarly to the bilateral Laplace transform, decomposes general two-sided functions, those defined over the entire time axis $-\infty < t < \infty$. We shall also note that by introducing distributions, and in particular, impulses, their derivatives and integrals, we can evaluate Fourier transforms of functions that have no transform in the ordinary sense, such as infinite duration two-sided periodic functions.

4.1 Definition of the Fourier Transform

The Fourier transform of a generally complex function $f(t)$, when it exists, is given by

$$F(j\omega) = \int_{-\infty}^{\infty} f(t) e^{-j\omega t} dt. \quad (4.1)$$

We write $F(j\omega) = \mathcal{F}[f(t)]$ and $f(t) \xleftrightarrow{\mathcal{F}} F(j\omega)$. The inverse Fourier transform $f(t) = \mathcal{F}^{-1}[F(j\omega)]$ is written:

$$f(t) = \frac{1}{2\pi} \int_{-\infty}^{\infty} F(j\omega) e^{j\omega t} d\omega. \quad (4.2)$$

As in the previous chapter, in what follows the Laplace complex frequency variable is written as $s = \sigma + j\omega$. We note that when it exists, the Fourier transform $F(j\omega)$ can be written in the form

$$F(j\omega) = \int_{-\infty}^{\infty} f(t) e^{-st} dt \Big|_{s=j\omega} = F(s) \Big|_{s=j\omega}. \quad (4.3)$$

The Fourier transform is thus the Laplace transform evaluated on the vertical axis $s = j\omega$ in the s plane. The substitution $s = j\omega$ is permissible and produces the Fourier transform *if and only if the $s = j\omega$ axis is in the ROC of $F(s)$* . We shall see shortly that in addition the Fourier transform exists if the $s = j\omega$ axis is the boundary line of the ROC of Laplace transform.

Example 4.1 Evaluate $F(j\omega)$ if $f(t) = e^{-\alpha t} u(t)$, $\alpha > 0$.

We have

$$F(s) = \frac{1}{s + \alpha}, \quad \sigma = \Re[s] > -\alpha.$$

The ROC of $F(s)$ includes the $j\omega$ axis, as seen in Fig. 4.1; hence

$$F(j\omega) = F(s) \Big|_{s=j\omega} = \frac{1}{\alpha + j\omega} = \frac{1}{\sqrt{\alpha^2 + \omega^2}} e^{-j \arctan(\omega/\alpha)}.$$

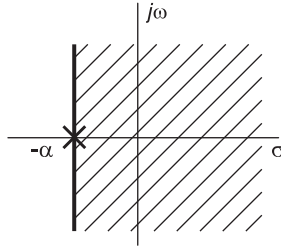


FIGURE 4.1 Laplace transform ROC.

Example 4.2 Evaluate $F(j\omega)$ given that $f(t) = e^{-\alpha|t|}$.

Referring to Fig. 4.2 we have

$$F(s) = \frac{1}{s + \alpha} + \frac{1}{-s + \alpha}, \quad -\alpha < \sigma < \alpha.$$

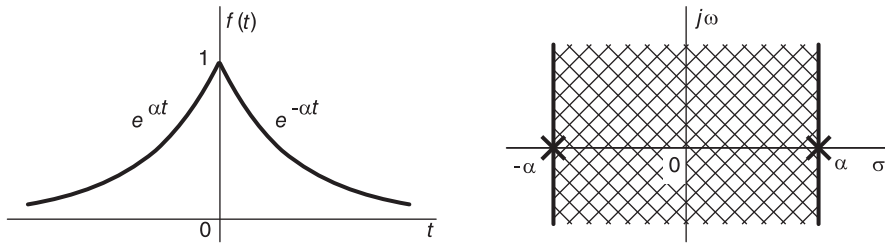


FIGURE 4.2 Two-sided exponential and ROC.

The ROC of $F(s)$ exists if and only if $\alpha > 0$ in which case it includes the axis $\sigma = 0$ in the s plane, the Fourier transform $F(j\omega)$ exists and is given by

$$F(j\omega) = \frac{1}{j\omega + \alpha} - \frac{1}{j\omega - \alpha} = \frac{2\alpha}{\alpha^2 + \omega^2}, \quad \alpha > 0.$$

NOTE: If $\alpha = 0$ the function $f(t)$ becomes the unity two-sided function, $f(t) = 1$, the region of convergence (ROC) strip shrinks to a line, the $j\omega$ axis itself, and as we shall subsequently see the Fourier transform is given by $F(j\omega) = 2\pi\delta(\omega)$. In this case according to the current literature the Laplace transform does not exist. As observed in the previous chapter a recent development [19] [21] [23] [27] extends the domains of Laplace and z -transform. Among the results is that the Laplace transform of $f(t) = 1$ and more complex two-sided functions are made to exist, and that the Fourier transform can be directly deduced thereof, as we shall see in Chapter 18.

4.2 Fourier Transform as a Function of f

In this section we focus our attention on a variant of the definition of the Fourier transform which defines the transform as a function of the frequency f in Hz rather than the angular frequency ω in r/s.

In what follows, using the notation $F(f)$, which employs the special *sans serif* font F , rather than the usual roman F , to designate the Fourier transform of a function $f(t)$ expressed as a function of f in Hz, we have

$$F(f) = F(j\omega)|_{\omega=2\pi f} = F(j2\pi f) = \int_{-\infty}^{\infty} f(t) e^{-j2\pi ft} dt. \quad (4.4)$$

Since $\omega = 2\pi f$, $d\omega = 2\pi df$ the inverse transform is given by

$$f(t) = \frac{1}{2\pi} \int_{-\infty}^{\infty} F(j2\pi f) e^{j2\pi ft} 2\pi df = \int_{-\infty}^{\infty} F(f) e^{j2\pi ft} df. \quad (4.5)$$

To simplify the notation the transform may be denoted $F(j\omega)$ meaning $F(f)$. In describing relations between $F(f)$ and $F(j\omega)$ it would be judicious to use the more precise notation, namely, $F(f)$.

Example 4.3 Let

$$f(t) = e^{-\alpha t} u(t), \quad \alpha > 0.$$

Evaluate the Fourier transform expressed in ω r/s and in f Hz.

We have

$$F(j\omega) = \frac{1}{j\omega + \alpha}$$

$$F(f) = \frac{1}{j2\pi f + \alpha}.$$

It is worthwhile noticing that in the case of transforms containing distributions such as impulses and their derivatives, or integrals, which we shall study shortly, the expression of a transform $F(f)$ will be found to differ slightly from that of $F(j\omega)$. The following example illustrates this point. It uses material to be studied in more detail shortly, but is included at this point since it is pertinent in the present context.

Example 4.4 Let $f(t) = \cos(\beta t)$, where $\beta = 2\pi f_0$ and $f_0 = 100$ Hz. Evaluate $F(j\omega)$ and $F(f)$.

We shall see shortly that the Fourier transform $F(j\omega)$ is given by

$$F(j\omega) = \pi [\delta(\omega - \beta) + \delta(\omega + \beta)] = \pi [\delta(\omega - 200\pi) + \delta(\omega + 200\pi)].$$

To evaluate $F(f)$ we can write:

$$F(f) = F(j\omega)|_{\omega=2\pi f} = \pi [\delta(2\pi f - \beta) + \delta(2\pi f + \beta)].$$

Using the scaling property $\delta(ax) = (1/|a|)\delta(x)$ we have

$$F(f) = (1/2) \left[\delta\left(f - \frac{\beta}{2\pi}\right) + \delta\left(f + \frac{\beta}{2\pi}\right) \right]$$

i.e.

$$F(f) = (1/2) [\delta(f - f_0) + \delta(f + f_0)].$$

4.3 From Fourier Series to Fourier Transform

Let $f(t)$ be a finite duration function defined over the interval $(-T/2, T/2)$. We have seen in Chapter 2 that the function $f(t)$, or equivalently its periodic extension, can be expanded into a Fourier series with exponential coefficients F_n that represent a discrete spectrum, function of the harmonic frequencies $\omega = n\omega_0$ r/s, $n = 0, \pm 1, \pm 2, \pm 3, \dots$, where $\omega_0 = 2\pi/T$. For our present purpose we shall write $F(jn\omega_0)$ to designate $T F_n$

$$F(jn\omega_0) \triangleq T F_n = \int_{-T/2}^{T/2} f(t) e^{-jn\omega_0 t} dt. \quad (4.6)$$

We now view the effect of starting with a finite duration function and its Fourier series and see the effect of increasing its duration T toward infinity. We note that by increasing the finite duration T of the function until $T \rightarrow \infty$ the fundamental frequency ω_0 tends toward a small value $\Delta\omega$ which ultimately tends to zero:

$$\omega_0 \rightarrow \Delta\omega \rightarrow 0. \quad (4.7)$$

Meanwhile the Fourier series sum tends to an integral, the spacing ω_0 between the coefficients tending to zero and the discrete spectrum tending to a function of a continuous variable ω . We can write

$$\lim_{T \rightarrow \infty} F(jn\omega_0) = \lim_{\Delta\omega \rightarrow 0} F(jn\Delta\omega) = \lim_{T \rightarrow \infty} \int_{-T/2}^{T/2} f(t) e^{-jn\Delta\omega t} dt. \quad (4.8)$$

With $\Delta\omega \rightarrow 0$, $n\Delta\omega \rightarrow \omega$ and under favorable conditions such as Dirichlet's we may write in the limit

$$F(j\omega) = \int_{-\infty}^{\infty} f(t) e^{-j\omega t} dt. \quad (4.9)$$

This is none other than the definition of the Fourier transform of $f(t)$. We conclude that with the increase of the signal duration the Fourier series ultimately becomes the Fourier transform.

Example 4.5 For the function $f(t)$ shown in the Fig. 4.3 (a) evaluate the coefficients F_n of Fourier series for a general value τ , and for $\tau = 1$, with:

i) $T = 2\tau$, ii) $T = 4\tau$, iii) $T = 8\tau$, iv) $T \rightarrow \infty$.

Represent schematically the discrete spectrum $F(jn\omega_0) = T F_n$ as a function of $\omega = n\omega_0$ for the first three cases, and the spectrum $F(j\omega)$ for the fourth case.

We have

$$F_n = \frac{1}{T} \int_{-\tau/2}^{\tau/2} e^{-jn\omega_0 t} dt = \frac{\tau}{T} \frac{e^{jn\omega_0 \frac{\tau}{2}} - e^{-jn\omega_0 \frac{\tau}{2}}}{2jn\omega_0 \frac{\tau}{2}} = \frac{\tau}{T} \text{Sa}\left(n\pi \frac{\tau}{T}\right).$$

$$i) F_n = \frac{1}{2} \text{Sa}\left(n \frac{\pi}{2}\right), \quad ii) F_n = \frac{1}{4} \text{Sa}\left(n \frac{\pi}{4}\right), \quad iii) F_n = \frac{1}{8} \text{Sa}\left(n \frac{\pi}{8}\right).$$

In the fourth case, as $T \rightarrow \infty$ the function becomes the centered rectangle of total width τ shown in Fig. 4.3 (b).

This function will be denoted by the symbol $\Pi_{\tau/2}(t)$. As $T \rightarrow \infty$, therefore, the function becomes

$$f(t) = \Pi_{\tau/2}(t) = u(t + \tau/2) - u(t - \tau/2)$$

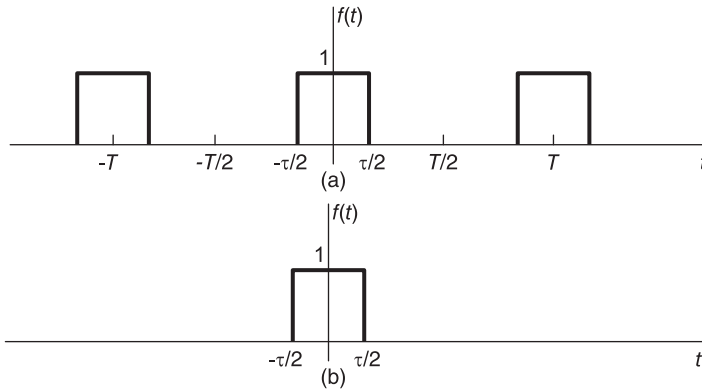


FIGURE 4.3 (a) Train of rectangular pulses, (b) its limit as $T \rightarrow \infty$.

The Fourier transform of $f(t)$ is $F(j\omega) = \tau Sa(\omega\tau/2)$. The spectra $F(jn\omega_0) = TF_n$ are given by

- i) $F(jn\omega_0) = Sa\left(n \frac{\pi}{2}\right)$, ii) $F(jn\omega_0) = Sa\left(n \frac{\pi}{4}\right)$,
- iii) $F(jn\omega_0) = Sa\left(n \frac{\pi}{8}\right)$, iv) $F(j\omega) = \tau Sa(\tau\omega/2) = Sa(\omega/2)$.

These spectra, shown in Fig. 4.4, illustrate the transition from the Fourier series discrete spectrum to the continuous Fourier transform spectrum as the function period T tends to infinity.

4.4 Conditions of Existence of the Fourier Transform

The following Dirichlet conditions, are sufficient for the existence of the Fourier transform of a function $f(t)$

1. The function $f(t)$ has a single value for every value t , it has a finite number of maxima and minima and a finite number of discontinuities in every finite interval.
2. The function $f(t)$ is absolutely integrable, i.e.

$$\int_{-\infty}^{\infty} |f(t)| dt < \infty. \tag{4.10}$$

Since the Fourier transform $F(j\omega)$ is generally complex we may write

$$F(j\omega) = F_r(j\omega) + jF_i(j\omega) \tag{4.11}$$

where $F_r(j\omega) \triangleq \Re[F(j\omega)]$, $F_i(j\omega) \triangleq \Im[F(j\omega)]$ and in polar notation

$$F(j\omega) = A(\omega) e^{j\phi(\omega)} \tag{4.12}$$

so that the *amplitude spectrum* $A(\omega)$ is given by $A(\omega) = |F(j\omega)|$ and the *phase spectrum* $\phi(\omega)$ is given by $\phi(\omega) = \arg[F(j\omega)]$.

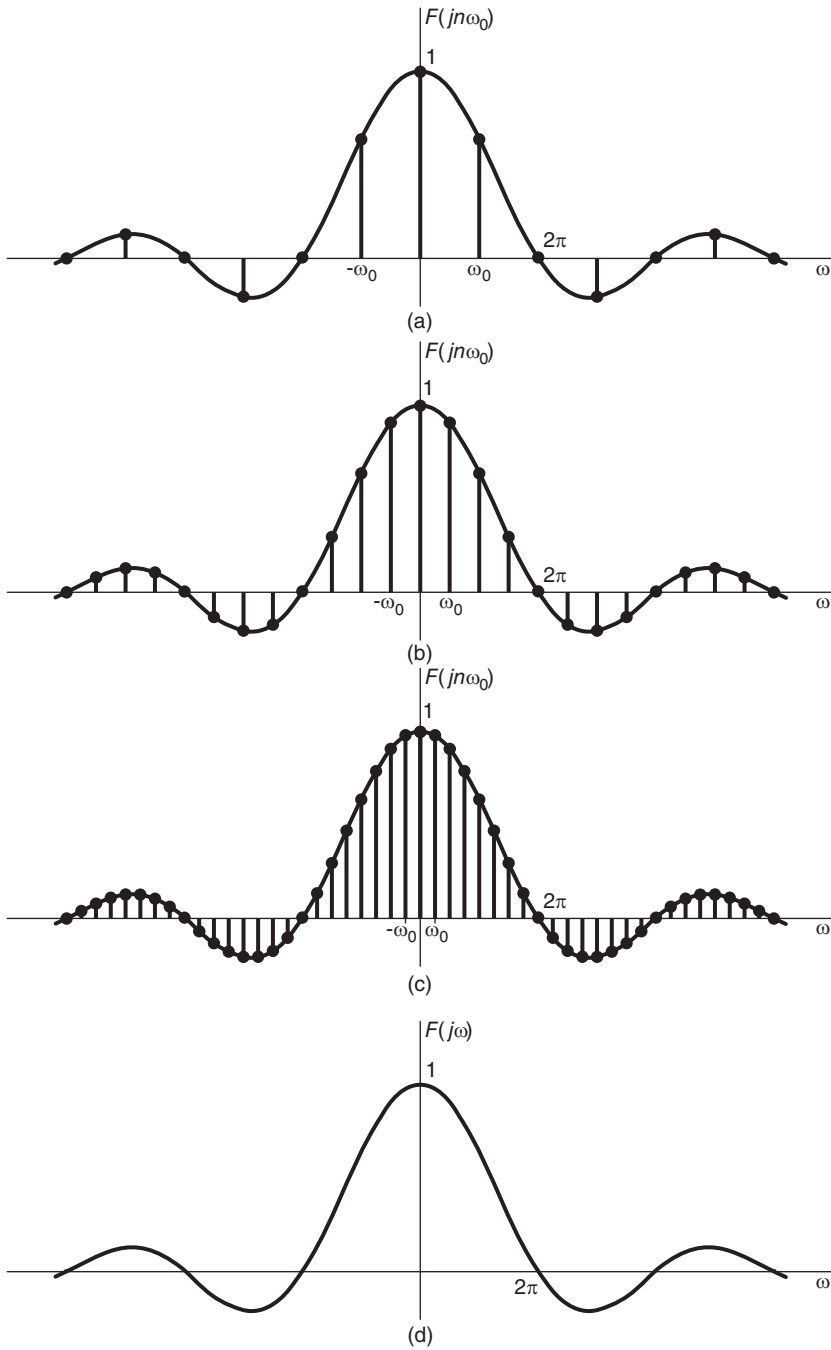


FIGURE 4.4 Effect of the pulse train period on its discrete spectrum.

4.5 Table of Properties of the Fourier Transform

Table 4.1 lists basic properties of the Fourier transform. In the following we state and prove some of these properties.

TABLE 4.1 Properties of Fourier transform

Property	Function	Transform
Linearity	$\alpha f_1(t) + \beta f_2(t)$, α and β constants	$\alpha F_1(j\omega) + \beta F_2(j\omega)$
Duality	$F(jt)$	$2\pi f(-\omega)$
Time Scale	$f(at)$, a constant	$\frac{1}{ a } F\left(j\frac{\omega}{a}\right)$
Reflection	$f(-t)$	$F(-j\omega)$
Time shift	$f(t - t_0)$	$F(j\omega) e^{-jt_0\omega}$
Frequency shift	$e^{j\omega_0 t} f(t)$	$F[j(\omega - \omega_0)]$
Initial value in time	$f(0)$	$\frac{1}{2\pi} \int_{-\infty}^{\infty} F(j\omega) d\omega$
Initial value in frequency	$\int_{-\infty}^{\infty} f(t) dt$	$F(0)$
Differentiation in time	$f^{(n)}(t)$	$(j\omega)^n F(j\omega)$
Differentiation in frequency	$t^n f(t)$	$j^n F^{(n)}(j\omega)$
Integration in time	$\int_{-\infty}^t f(\tau) d\tau$	$\frac{F(j\omega)}{j\omega} + \pi F(0) \delta(\omega)$
Conjugate functions	$f^*(t)$	$F^*(-j\omega)$
Multiplication in time	$f_1(t) f_2(t)$	$\frac{1}{2\pi} \int_{-\infty}^{\infty} F_1(jy) F_2\{j(\omega - y)\} dy$
Multiplication in frequency	$\int_{-\infty}^{\infty} f_1(\tau) f_2(t - \tau) d\tau$	$F_1(j\omega) F_2(j\omega)$

Parseval Relation

$$\int_{-\infty}^{\infty} |f(t)|^2 dt = \frac{1}{2\pi} \int_{-\infty}^{\infty} |F(j\omega)|^2 d\omega$$

4.5.1 Linearity

$$a_1 f_1(t) + \dots + a_n f_n(t) \xleftrightarrow{\mathcal{F}} a_1 F_1(j\omega) + \dots + a_n F_n(j\omega). \tag{4.13}$$

4.5.2 Duality

$$F(jt) \longleftrightarrow 2\pi f(-\omega). \quad (4.14)$$

Proof Since

$$f(t) = \frac{1}{2\pi} \int_{-\infty}^{\infty} F(j\omega) e^{j\omega t} d\omega$$

if we write $t = -\tau$ we have

$$2\pi f(-\tau) = \int_{-\infty}^{\infty} F(j\omega) e^{-j\omega\tau} d\omega.$$

Replacing ω by t

$$2\pi f(-\tau) = \int_{-\infty}^{\infty} F(jt) e^{-jt\tau} dt$$

and replacing τ by ω

$$2\pi f(-\omega) = \int_{-\infty}^{\infty} F(jt) e^{-j\omega t} dt = \mathcal{F}[F(jt)].$$

Example 4.6 Apply the duality property to the function of Example 4.2, with $\alpha = 1$, i.e. $f(t) = e^{-|t|}$.

Since $F(j\omega) = 2/(\omega^2 + 1)$, the transform of $g(t) = F(jt) = 2/(t^2 + 1)$ is $G(j\omega) = 2\pi f(-\omega) = 2\pi e^{-|\omega|}$, as shown in Fig. 4.5.

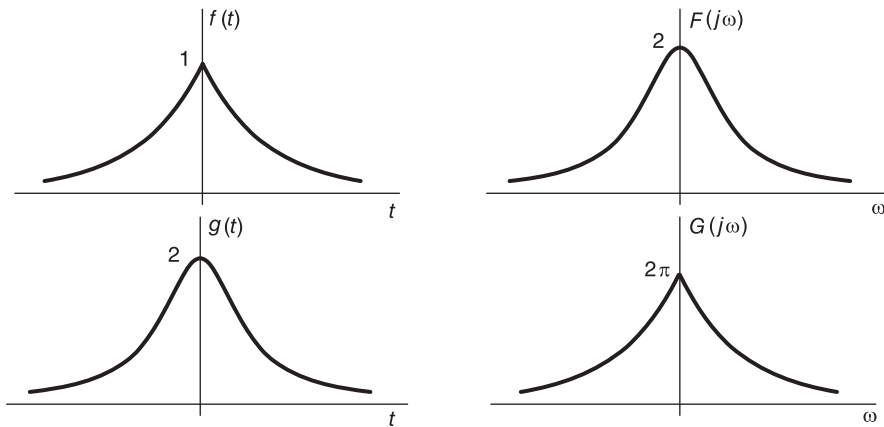


FIGURE 4.5 Duality property of the Fourier transform.

Example 4.7 Apply the duality property to the Fourier transform of the function $f(t) = e^{-t}u(t) + e^{2t}u(-t)$.

$$F(j\omega) = \frac{1}{j\omega + 1} - \frac{1}{j\omega - 2} = \frac{3(\omega^2 + 2 - j\omega)}{\omega^4 + 5\omega^2 + 4}.$$

From the duality property, with

$$g(t) = F(jt) = \frac{3(t^2 + 2 - jt)}{t^4 + 5t^2 + 4},$$

$$G(j\omega) = \mathcal{F}[F(jt)] = 2\pi f(-\omega) = 2\pi \{e^{\omega}u(-\omega) + e^{-2\omega}u(\omega)\}.$$

4.5.3 Time Scaling

If a is a real constant then

$$f(at) \xleftrightarrow{\mathcal{F}} \frac{1}{|a|} F\left(\frac{j\omega}{a}\right). \tag{4.15}$$

The proof is the same as seen in the context of Laplace transform.

Example 4.8 Using $\mathcal{F}[f(t)]$ where $f(t) = \Pi_{T/2}(t)$ evaluate the transform of $f(10t)$.

We have $F(j\omega) = T \text{Sa}(T\omega/2)$. For $g(t) = f(10t) = u(t + T/20) - u(t - T/20) = \Pi_{T/20}(t)$, Fig. 4.6, we have $G(j\omega) = (T/10)\text{Sa}(T\omega/20)$ as can be obtained by direct evaluation.

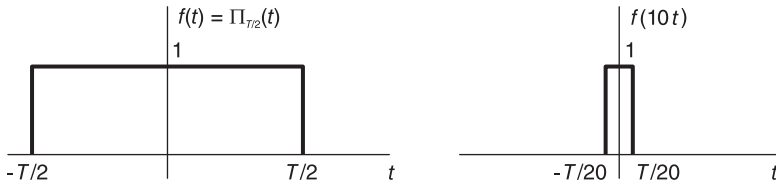


FIGURE 4.6 Compression of a rectangular function.

4.5.4 Reflection

$$f(-t) \xleftrightarrow{\mathcal{F}} F(-j\omega). \tag{4.16}$$

This property follows from the time scaling property with $a = -1$.

4.5.5 Time Shift

$$f(t - t_0) \xleftrightarrow{\mathcal{F}} F(j\omega) e^{-jt_0\omega}. \tag{4.17}$$

With $F(j\omega) = A(\omega) e^{j\phi(\omega)}$, the property means that

$$f(t - t_0) \xleftrightarrow{\mathcal{F}} A(\omega) e^{j[\phi(\omega) - t_0\omega]}$$

so that if $f(t)$ is shifted in time by an interval t_0 then its Fourier amplitude spectrum remains the same while its phase spectrum is altered by the linear term $-t_0\omega$.

Proof Letting $x = t - t_0$ we have

$$\int_{-\infty}^{\infty} f(t - t_0) e^{-j\omega t} dt = \int_{-\infty}^{\infty} f(x) e^{-j\omega(t_0+x)} dx = F(j\omega) e^{-jt_0\omega}.$$

4.5.6 Frequency Shift

$$e^{j\omega_0 t} f(t) \xleftrightarrow{\mathcal{F}} F[j(\omega - \omega_0)]. \tag{4.18}$$

Indeed

$$\int_{-\infty}^{\infty} f(t) e^{j\omega_0 t} e^{-j\omega t} dt = \int_{-\infty}^{\infty} f(t) e^{-j(\omega - \omega_0)t} dt = F[j(\omega - \omega_0)].$$

4.5.7 Modulation Theorem

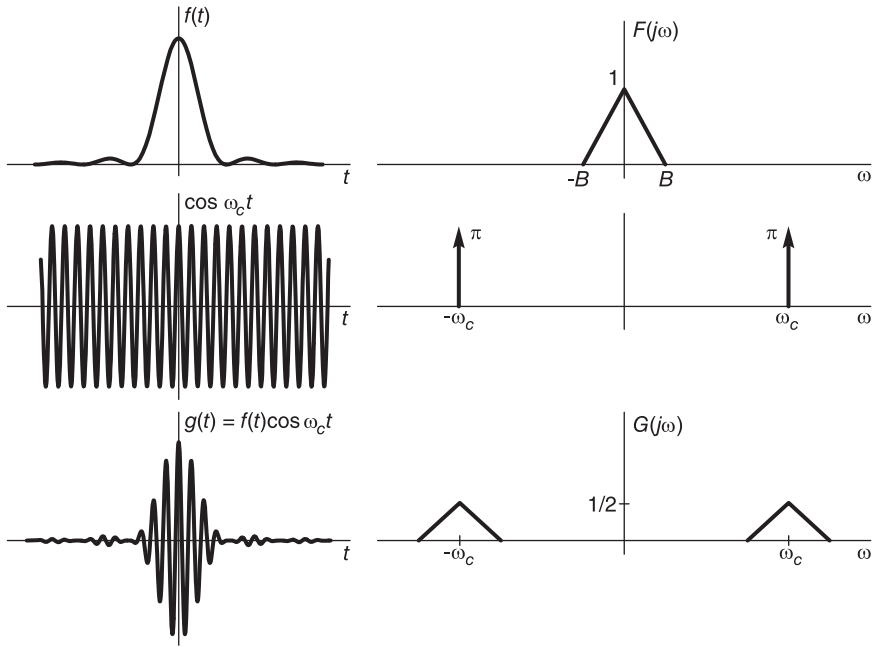


FIGURE 4.7 Modulation and the resulting spectrum.

Consider a system where a signal $f(t)$ is *modulated* by being multiplied by the sinusoid $\cos(\omega_c t)$ usually referred to as the *carrier signal*, producing the signal $g(t) = f(t) \cos(\omega_c t)$. The angular frequency ω_c is called the *carrier frequency*. According to this property, if $f(t) \xleftrightarrow{\mathcal{F}} F(j\omega)$ then

$$f(t) \cos \omega_c t \longleftrightarrow \frac{1}{2} [F\{j(\omega + \omega_c)\} + F\{j(\omega - \omega_c)\}]. \quad (4.19)$$

Proof We have

$$f(t) \cos(\omega_c t) = \frac{1}{2} [f(t) e^{j\omega_c t} + f(t) e^{-j\omega_c t}].$$

From the frequency shift property

$$G(j\omega) = \mathcal{F}[f(t) \cos(\omega_c t)] = \frac{1}{2} [F\{j(\omega + \omega_c)\} + F\{j(\omega - \omega_c)\}].$$

Similarly, we can show that

$$f(t) \sin(\omega_c t) \xleftrightarrow{\mathcal{F}} \frac{-j}{2} [F\{j(\omega - \omega_c)\} - F\{j(\omega + \omega_c)\}]. \quad (4.20)$$

The spectra $F(j\omega)$ and $G(j\omega)$ of a function $f(t)$ and its modulated version $g(t)$ are shown in Fig. 4.7. For example if $f(t) = e^{-t}u(t)$ and $g(t) = f(t) \cos \omega_0 t$, where $\omega_0 = 10\pi$, the spectra $F(j\omega) = 1/(j\omega + 1)$ and $G(j\omega)$ are shown in Fig. 4.8

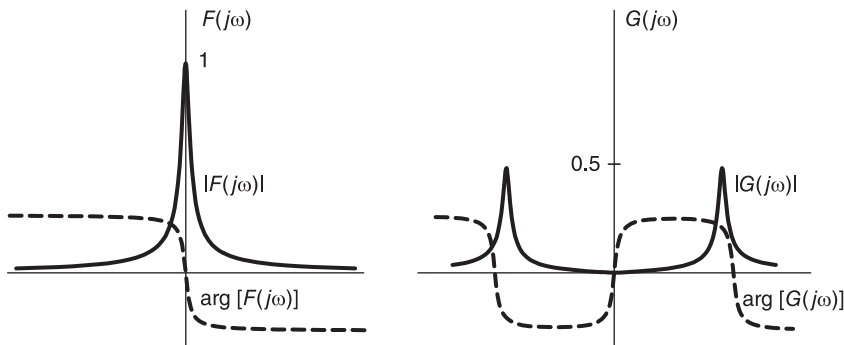


FIGURE 4.8 Spectrum of a function before and after modulation.

Example 4.9 Evaluate the Fourier transform of

$$f(t) = \Pi_{T/2}(t) \cos(\omega_0 t).$$

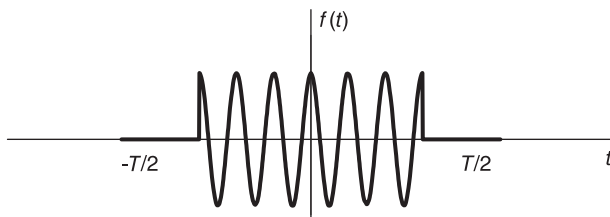


FIGURE 4.9 Modulated rectangle.

The function $f(t)$ is shown in Fig. 4.9. The Fourier transform of the centered rectangle function $\Pi_{T/2}(t)$ is $\mathcal{F}[\Pi_{T/2}(t)] = T \text{Sa}(\omega T/2)$, wherefrom

$$\Pi_{T/2}(t) \cos(\omega_0 t) \xrightarrow{\mathcal{F}} (T/2) [\text{Sa}\{(\omega - \omega_0) T/2\} + \text{Sa}\{(\omega + \omega_0) T/2\}].$$

4.5.8 Initial Time Value

From Equation (4.2)

$$f(0) = \frac{1}{2\pi} \int_{-\infty}^{\infty} F(j\omega) d\omega. \tag{4.21}$$

4.5.9 Initial Frequency Value

From Equation (4.1)

$$F(0) = \int_{-\infty}^{\infty} f(t) dt. \tag{4.22}$$

4.5.10 Differentiation in Time

If $f(t)$ is a continuous function, then

$$\mathcal{F}\left[\frac{df(t)}{dt}\right] = j\omega F(j\omega). \quad (4.23)$$

Proof We have

$$\begin{aligned} f(t) &= \frac{1}{2\pi} \int_{-\infty}^{\infty} F(j\omega) e^{j\omega t} d\omega \\ \frac{df(t)}{dt} &= \frac{1}{2\pi} \frac{d}{dt} \int_{-\infty}^{\infty} F(j\omega) e^{j\omega t} d\omega \\ \frac{df(t)}{dt} &= \frac{1}{2\pi} \int_{-\infty}^{\infty} \frac{d}{dt} F(j\omega) e^{j\omega t} d\omega = \frac{1}{2\pi} \int_{-\infty}^{\infty} j\omega F(j\omega) e^{j\omega t} d\omega \\ &= \mathcal{F}^{-1}[j\omega F(j\omega)] \end{aligned}$$

as asserted. Similarly we can show that the Fourier transform of the function

$$f^{(n)} \triangleq \frac{d^n}{dt^n} f(t) \quad (4.24)$$

when it exists, is given by

$$\mathcal{F}[f^{(n)}] = (j\omega)^n F(j\omega). \quad (4.25)$$

4.5.11 Differentiation in Frequency

$$\frac{d}{d\omega} F(j\omega) = \int_{-\infty}^{\infty} -jt f(t) e^{-j\omega t} dt = \mathcal{F}[-jt f(t)] \quad (4.26)$$

so that $(-jt) f(t) \xleftrightarrow{\mathcal{F}} dF(j\omega)/d\omega$. Differentiating further we obtain

$$(-jt)^n f(t) \xleftrightarrow{\mathcal{F}} \frac{d^n}{d\omega} F(j\omega). \quad (4.27)$$

4.5.12 Integration in Time

$$\mathcal{F}\left[\int_{-\infty}^t f(\tau) d\tau\right] = \frac{F(j\omega)}{j\omega}, \quad F(0) = 0. \quad (4.28)$$

Proof Let

$$w(t) = \int_{-\infty}^t f(\tau) d\tau.$$

For $w(t)$ to have a Fourier transform it should tend to 0 as $t \rightarrow \infty$, i.e.

$$\int_{-\infty}^{\infty} f(\tau) d\tau = F(0) = 0.$$

and since $f(t) = dw(t)/dt$, we have $F(j\omega) = j\omega W(j\omega)$ so that, as stated,

$$W(j\omega) = F(j\omega)/j\omega.$$

An n -fold integration leads to $F(j\omega)/(j\omega)^n$. We shall shortly see that the transform of the unit step function $u(t)$ is

$$\mathcal{F}[u(t)] = \pi\delta(\omega) + \frac{1}{j\omega}. \quad (4.29)$$

If $F(0) \neq 0$, i.e. if $w(t) = \int_{-\infty}^{\infty} f(\tau) d\tau \neq 0$ we can express the function $w(t)$ as a convolution of $f(t)$ with the unit step function $u(t)$

$$w(t) = f(t) * u(t) \triangleq \int_{-\infty}^{\infty} f(\tau) u(t - \tau) d\tau \quad (4.30)$$

since the right-hand side can be rewritten as $\int_{-\infty}^t f(\tau) d\tau$. Using the property that convolution in the time domain corresponds to multiplication in the frequency domain we may write

$$W(j\omega) = \mathcal{F}[w(t)] = F(j\omega) \cdot \mathcal{F}[u(t)] = F(j\omega) \left\{ \pi\delta(\omega) + \frac{1}{j\omega} \right\} \quad (4.31)$$

$$\mathcal{F} \left[\int_{-\infty}^t f(\tau) d\tau \right] = \frac{F(j\omega)}{j\omega} + \pi F(0) \delta(\omega) \quad (4.32)$$

which is a more general result.

4.5.13 Conjugate Function

Let $w(t) = f^*(t)$, i.e. $w(t)$ is the conjugate of $f(t)$. We have

$$W(j\omega) = \int_{-\infty}^{\infty} f^*(t) e^{-j\omega t} dt = \left\{ \int_{-\infty}^{\infty} f(t) e^{j\omega t} dt \right\}^* = F^*(-j\omega) \quad (4.33)$$

i.e. $\mathcal{F}[f^*(t)] = F^*(-j\omega)$.

4.5.14 Real Functions

We have so far assumed the function $f(t)$ to be generally complex. If $f(t)$ is real we may write

$$F(-j\omega) = \int_{-\infty}^{\infty} f(t) e^{j\omega t} dt = \left\{ \int_{-\infty}^{\infty} f(t) e^{-j\omega t} dt \right\}^* = F^*(j\omega) \quad (4.34)$$

i.e. $|F(-j\omega)| = |F(j\omega)|$; $\arg |F(-j\omega)| = -\arg |F(j\omega)|$. With

$$F_r(j\omega) \triangleq \Re[F(j\omega)] = \int_{-\infty}^{\infty} f(t) \cos \omega t dt \quad (4.35)$$

$$F_i(j\omega) \triangleq \Im[F(j\omega)] = - \int_{-\infty}^{\infty} f(t) \sin \omega t dt \quad (4.36)$$

we have $F_r(-j\omega) = F_r(j\omega)$, $F_i(-j\omega) = -F_i(j\omega)$, that is, $F_r(j\omega)$ is an even function and $F_i(j\omega)$ is odd. The inverse transform is written

$$f(t) = \frac{1}{2\pi} \int_{-\infty}^{\infty} F(j\omega) e^{j\omega t} d\omega = \frac{1}{2\pi} \left\{ \int_{-\infty}^{\infty} F(j\omega) \cos \omega t d\omega + j \int_{-\infty}^{\infty} F(j\omega) \sin \omega t d\omega \right\}$$

wherefrom using the symmetry property of $F_r(j\omega)$ and $F_i(j\omega)$,

$$f(t) = \frac{1}{\pi} \left\{ \int_0^{\infty} F_r(j\omega) \cos \omega t d\omega - \int_0^{\infty} F_i(j\omega) \sin \omega t d\omega \right\}. \quad (4.37)$$

We can also write $F(j\omega) = |F(j\omega)| e^{j \arg[F(j\omega)]} = A(\omega) e^{j\phi(\omega)}$

$$\begin{aligned} f(t) &= \frac{1}{\pi} \left\{ \int_0^{\infty} [A(\omega) \cos \{\phi(\omega)\} \cos \omega t - A(\omega) \sin \{\phi(\omega)\} \sin \omega t] d\omega \right\} \\ &= \frac{1}{\pi} \int_0^{\infty} A(\omega) \cos \{\omega t + \phi(\omega)\} d\omega. \end{aligned} \quad (4.38)$$

4.5.15 Symmetry

We have seen that the Fourier transform of a real function has conjugate symmetry. We now consider the effect of time function symmetry on its transform.

i) Real Even Function

Let $f(t)$ be a real and even function, i.e. $f(-t) = f(t)$. We have

$$F(j\omega) = \int_{-\infty}^{\infty} f(t) (\cos \omega t - j \sin \omega t) dt \quad (4.39)$$

$$F_r(j\omega) = 2 \int_0^{\infty} f(t) \cos \omega t dt \quad (4.40)$$

$F_r(-j\omega) = F_r(j\omega)$, $F_i(j\omega) = 0$, that is, the transform of a real and even function is real (and even). The inverse transform is written

$$f(t) = \frac{1}{2\pi} \int_{-\infty}^{\infty} F_r(j\omega) e^{j\omega t} d\omega = \frac{1}{\pi} \int_0^{\infty} F_r(j\omega) \cos \omega t d\omega. \quad (4.41)$$

ii) Real Odd Function

Let $f(t)$ be real and odd, i.e. $f(-t) = -f(t)$. We have $F_r(j\omega) = 0$

$$F_i(j\omega) = -2 \int_0^{\infty} f(t) \sin \omega t dt \quad (4.42)$$

$F_i(-j\omega) = -F_i(j\omega)$, that is, the transform of a real and odd function is imaginary (and odd). The inverse transform is written

$$f(t) = \frac{1}{2\pi} \int_{-\infty}^{\infty} jF_i(j\omega) e^{j\omega t} d\omega = \frac{1}{\pi} \int_0^{\infty} F_i(j\omega) \sin \omega t d\omega. \quad (4.43)$$

4.6 System Frequency Response

Given a linear system with impulse response $h(t)$ we have seen that its transfer function, also called system function, is given by $H(s) = \mathcal{L}[h(t)]$. As stated earlier, the frequency response of the system is $H(j\omega) = \mathcal{F}[h(t)]$. We deduce that the frequency response exists if the transfer function exists for $s = j\omega$, and may be evaluated as its value on the $j\omega$ axis in the s plane.

Example 4.10 Evaluate the transfer function and the frequency response of the system of which the impulse response is given by $h(t) = e^{-\alpha t} \sin(\beta t) u(t)$, $\alpha > 0$.

The frequency response is

$$H(j\omega) = \mathcal{F}[h(t)] = H(s)|_{s=j\omega} = \frac{\beta}{(j\omega + \alpha)^2 + \beta^2} = A(\omega)e^{j\phi(\omega)}.$$

The impulse response $h(t)$, the amplitude and phase spectra $A(\omega)$ and $\phi(\omega)$ are shown in Fig. 4.10.

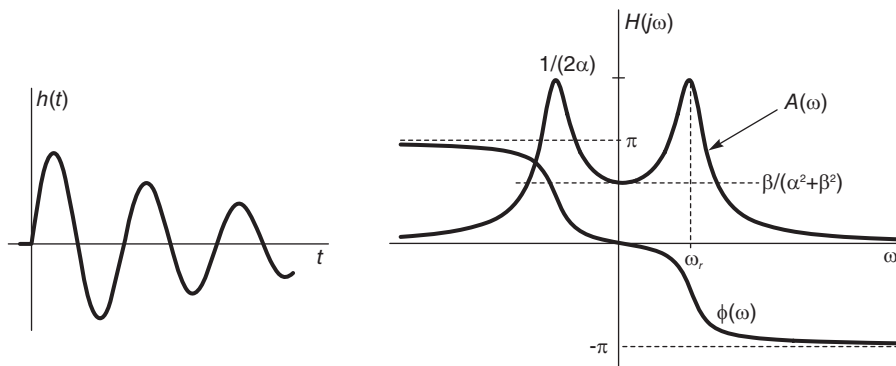


FIGURE 4.10 Damped sinusoid and its spectrum.

4.7 Even–Odd Decomposition of a Real Function

Let $f(t)$ be a real function. As we have seen in Chapter 1, we can decompose $f(t)$ into a sum of an even component $f_e(t) = (f(t) + f(-t))/2$, and an odd one $f_o(t) = (f(t) - f(-t))/2$, so that

$$F_e(j\omega) = \mathcal{F}[f_e(t)] = 2 \int_0^\infty f_e(t) \cos \omega t \, dt \tag{4.44}$$

$$F_o(j\omega) = \mathcal{F}[f_o(t)] = -j \int_{-\infty}^\infty f_o(t) \sin \omega t \, dt = -2j \int_0^\infty f_o(t) \sin \omega t \, dt. \tag{4.45}$$

Since $f_e(t)$ and $f_o(t)$ are real even and real odd respectively their transforms $F_e(j\omega)$ and $F_o(j\omega)$ are real and imaginary respectively. Now $F(j\omega) = F_e(j\omega) + F_o(j\omega)$, and by definition $F(j\omega) = F_r(j\omega) + jF_i(j\omega)$, wherefrom $F_r(j\omega) = F_e(j\omega)$, and $F_i(j\omega) = F_o(j\omega)/j$, i.e.

$$F_r(j\omega) = 2 \int_0^\infty f_e(t) \cos \omega t \, dt \tag{4.46}$$

$$F_i(j\omega) = -2 \int_0^\infty f_o(t) \sin \omega t \, dt \tag{4.47}$$

and recalling that for $f(t)$ real, $F_r(j\omega)$ and $F_i(j\omega)$ are even and odd respectively we have the inverse relations

$$f_e(t) = \mathcal{F}^{-1}[F_r(j\omega)] = \frac{1}{\pi} \int_0^\infty F_r(j\omega) \cos \omega t \, d\omega \tag{4.48}$$

$$f_o(t) = \mathcal{F}^{-1}[jF_i(j\omega)] = -\frac{1}{\pi} \int_0^\infty F_i(j\omega) \sin \omega t \, d\omega. \tag{4.49}$$

4.8 Causal Real Functions

We show that a causal function $f(t)$ can be expressed as a function of $F_r(j\omega)$ alone or $F_i(j\omega)$ alone. For $t > 0$ we have $f(-t) = 0$, wherefrom

$$f(t) = \begin{cases} 2f_e(t) = 2f_o(t), & t > 0 \\ f_e(0), & t = 0 \\ 0, & \text{otherwise.} \end{cases} \quad (4.50)$$

Using the equations of $f_e(t)$ and $f_o(t)$

$$f(t) = \frac{2}{\pi} \int_0^\infty F_r(j\omega) \cos \omega t \, d\omega = -\frac{2}{\pi} \int_0^\infty F_i(j\omega) \sin \omega t \, d\omega, \quad t > 0 \quad (4.51)$$

and

$$f(0) = \frac{1}{\pi} \int_0^\infty F_r(j\omega) \, d\omega = \frac{f(0^+)}{2} \quad (\text{Gibbs phenomenon}). \quad (4.52)$$

Knowing $F_r(j\omega)$ we can deduce $f(t)$, using

$$f(t) = \frac{2}{\pi} \int_0^\infty F_r(j\omega) \cos \omega t \, d\omega, \quad t > 0 \quad (4.53)$$

and $F_i(j\omega)$ can be evaluated using $f(t)$ or directly from $F_r(j\omega)$

$$F_i(j\omega) = -\int_0^\infty f(t) \sin \omega t \, dt = -\frac{2}{\pi} \int_0^\infty \int_0^\infty F_r(jy) \cos(yt) \sin \omega t \, dy \, dt. \quad (4.54)$$

Similarly $F_r(j\omega)$ can be deduced knowing $F_i(j\omega)$

$$F_r(j\omega) = \int_0^\infty f(t) \cos \omega t \, dt = -\frac{2}{\pi} \int_0^\infty \int_0^\infty F_i(jy) \sin(yt) \cos \omega t \, dy \, dt. \quad (4.55)$$

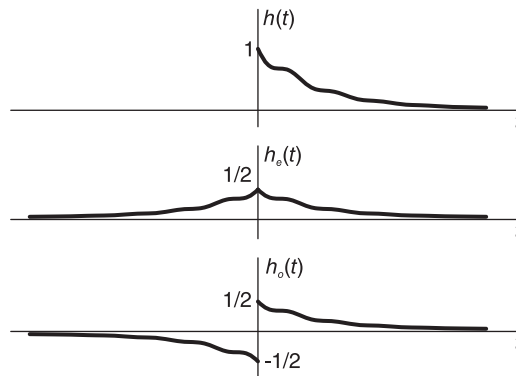


FIGURE 4.11 Causal function, even and odd components.

We conclude that if a system impulse response $h(t)$ is a causal function, as shown in Fig. 4.11, we may write the following relations, where $H(j\omega) = H_R(j\omega) + jH_I(j\omega)$

$$h(0) = \frac{1}{2\pi} \int_{-\infty}^\infty H(j\omega) \, d\omega \quad (4.56)$$

$$[h(0^+) + h(0^-)] / 2 = \frac{1}{2\pi} \int_{-\infty}^{\infty} H(j\omega) d\omega \tag{4.57}$$

$$h(0^+) = \frac{1}{\pi} \int_{-\infty}^{\infty} H_R(j\omega) d\omega = \frac{2}{\pi} \int_0^{\infty} H_R(j\omega) d\omega \tag{4.58}$$

$$h(t) = h_e(t) + h_o(t). \tag{4.59}$$

Since $h_e(t) \longleftrightarrow H_R(j\omega)$, $h_o(t) \longleftrightarrow jH_I(j\omega)$

$$\int_{-\infty}^{\infty} h_e^2(t) dt = \frac{1}{2\pi} \int_{-\infty}^{\infty} H_R^2(j\omega) d\omega \tag{4.60}$$

$$\int_{-\infty}^{\infty} h_o^2(t) dt = \frac{1}{2\pi} \int_{-\infty}^{\infty} H_I^2(j\omega) d\omega \tag{4.61}$$

$$\int_0^{\infty} h^2(t) dt = \frac{2}{\pi} \int_0^{\infty} H_R^2(j\omega) d\omega. \tag{4.62}$$

More formal relations between the real and imaginary parts of the spectrum, known as Hilbert transforms, will be derived in Chapter 14.

4.9 Transform of the Dirac-Delta Impulse

For $f(t) = \delta(t)$,

$$F(j\omega) = \int_{-\infty}^{\infty} \delta(t) e^{-j\omega t} dt = 1 \tag{4.63}$$

as shown in Fig. 4.12. $\delta(t) \xleftrightarrow{\mathcal{F}} 1$.

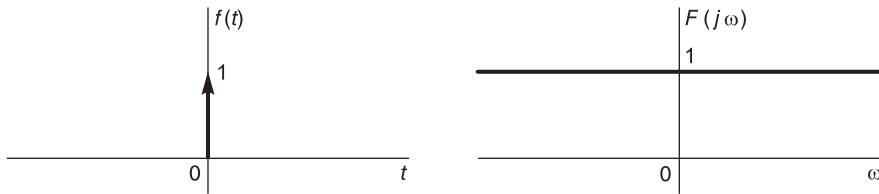


FIGURE 4.12 Impulse and transform.

We deduce from the time shifting property that $\delta(t - t_0) \xleftrightarrow{\mathcal{F}} e^{-j\omega t_0}$, as represented in Fig. 4.13.

4.10 Transform of a Complex Exponential and Sinusoid

The transform of unity is given by

$$\mathcal{F}[1] = \int_{-\infty}^{\infty} e^{-j\omega t} dt = 2\pi\delta(\omega). \tag{4.64}$$

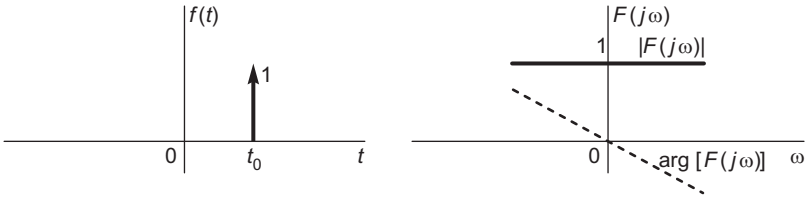


FIGURE 4.13 Delayed impulse and transform.

Note that since $\delta(t) \xrightarrow{\mathcal{F}} 1$, using duality, $1 \xrightarrow{\mathcal{F}} 2\pi\delta(-\omega) = 2\pi\delta(\omega)$, as shown in Fig. 4.14.

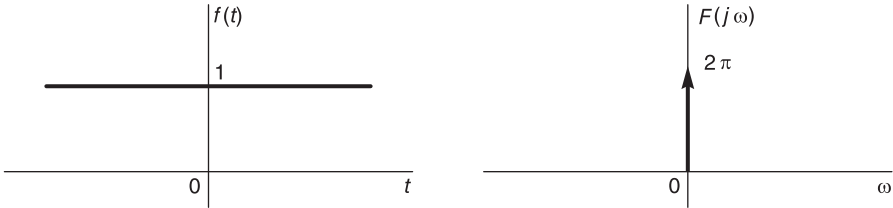


FIGURE 4.14 Unit constant and its Fourier transform.

Using the shift-in frequency property,

$$e^{j\omega_0 t} \xrightarrow{\mathcal{F}} 2\pi\delta(\omega - \omega_0).$$

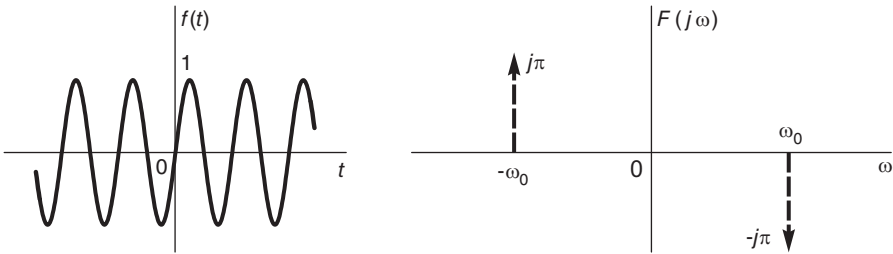


FIGURE 4.15 Sine function and its transform.

For $f(t) = \sin(\omega_0 t) = \frac{1}{2j}(e^{j\omega_0 t} - e^{-j\omega_0 t})$

$$F(j\omega) = j\pi [\delta(\omega + \omega_0) - \delta(\omega - \omega_0)] \tag{4.65}$$

as shown in Fig. 4.15. For $f(t) = \cos(\omega_0 t) = \frac{1}{2}(e^{j\omega_0 t} + e^{-j\omega_0 t})$,

$$F(j\omega) = \pi [\delta(\omega + \omega_0) + \delta(\omega - \omega_0)] \tag{4.66}$$

as shown in Fig. 4.16.

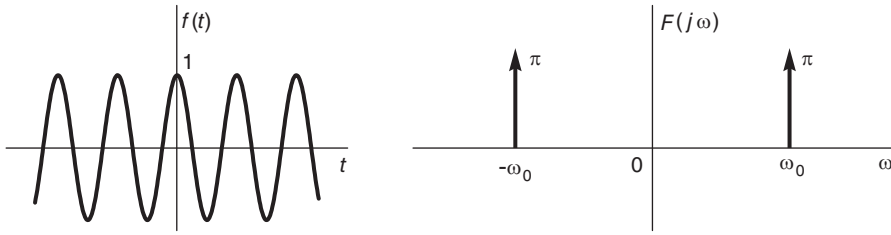


FIGURE 4.16 Cosine function and its transform.

4.11 Sign Function

The sign function $f(t) = \text{sgn}(t)$, seen in Fig. 4.17, is equal to 1 for $t > 0$ and -1 for $t < 0$. With K a constant, we can write $(d/dt)[\text{sgn}(t) + K] = 2\delta(t)$,

$$\mathcal{F} \left[\frac{d}{dt} \{ \text{sgn}(t) + K \} \right] = j\omega \mathcal{F} [\text{sgn}(t) + K] = 2 \tag{4.67}$$

$$j\omega \mathcal{F} [\text{sgn}(t)] + j\omega 2\pi K \delta(\omega) = 2 \tag{4.68}$$

$$\mathcal{F} [\text{sgn}(t)] = 2/(j\omega) - 2\pi K \delta(\omega). \tag{4.69}$$

The value of K should be such that

$$\text{sgn}(t) + \text{sgn}(-t) = 0 \tag{4.70}$$

i.e.

$$[2/(j\omega) - 2\pi K \delta(\omega)] + [2/(-j\omega) - 2\pi K \delta(\omega)] = 0 \tag{4.71}$$

wherefrom $K = 0$ and, as depicted in Fig. 4.17,

$$\mathcal{F} [\text{sgn}(t)] = 2/(j\omega). \tag{4.72}$$

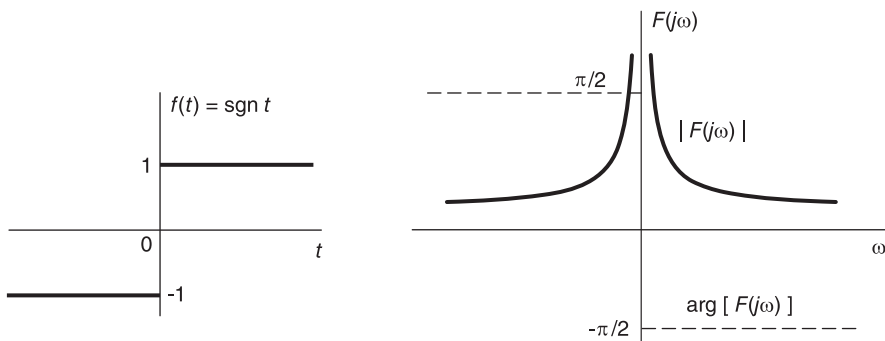


FIGURE 4.17 Signum function and its transform.

4.12 Unit Step Function

Let $f(t) = u(t)$. Writing $u(t) = 1/2 + (1/2) \operatorname{sgn}(t)$, we have

$$u(t) \xleftrightarrow{\mathcal{F}} \pi\delta(\omega) + 1/(j\omega).$$

Now $F(s) = \mathcal{L}[u(t)] = \frac{1}{s}$, $\sigma > 0$. The pole is on the $s = j\omega$ axis; the boundary of the ROC. The Fourier transform is thus equal to the value of the Laplace transform on the $j\omega$ axis plus an impulse due to the pole.

4.13 Causal Sinusoid

Let $f(t) = \cos(\omega_0 t) u(t)$. Using the modulation theorem we can write

$$\begin{aligned} \cos(\omega_0 t) u(t) &\xleftrightarrow{\mathcal{F}} \frac{\pi}{2} [\delta(\omega - \omega_0) + \delta(\omega + \omega_0)] + \frac{1}{2j(\omega - \omega_0)} + \frac{1}{2j(\omega + \omega_0)} \\ &\xleftrightarrow{\mathcal{F}} \frac{\pi}{2} [\delta(\omega - \omega_0) + \delta(\omega + \omega_0)] + \frac{j\omega}{(\omega_0^2 - \omega^2)}. \end{aligned} \tag{4.73}$$

The function, its poles and Fourier transform are shown in Fig. 4.18. Similarly,

$$\sin(\omega_0 t) u(t) \xleftrightarrow{\mathcal{F}} \frac{\pi}{2j} [\delta(\omega - \omega_0) - \delta(\omega + \omega_0)] + \frac{\omega_0}{(\omega_0^2 - \omega^2)}. \tag{4.74}$$

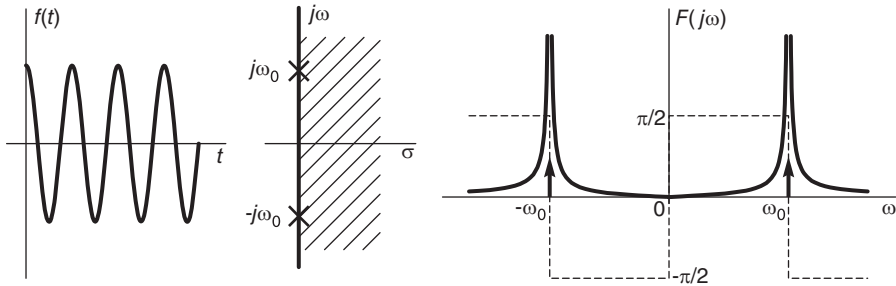


FIGURE 4.18 Causal sinusoid and its transform.

4.14 Table of Fourier Transforms of Basic Functions

Table 4.2 shows Fourier transforms of some basic functions.

TABLE 4.2 Fourier Transforms of some basic functions

$f(t)$	$F(j\omega)$
$\text{sgn } t$	$2/(j\omega)$
$e^{-\alpha t}u(t), \alpha > 0$	$\frac{1}{\alpha + j\omega}$
$te^{-\alpha t}u(t), \alpha > 0$	$\frac{1}{(\alpha + j\omega)^2}$
$ t $	$-2/\omega^2$
$\delta(t)$	1
$\delta^{(n)}(t)$	$(j\omega)^n$
1	$2\pi\delta(\omega)$
$e^{j\omega_0 t}$	$2\pi\delta(\omega - \omega_0)$
t^n	$2\pi j^n \delta^{(n)}(\omega)$
$1/t$	$-j\pi \text{sgn}(\omega)$
$u(t)$	$\pi\delta(\omega) + \frac{1}{j\omega}$
$t^n u(t)$	$n!/(j\omega)^{n+1} + \pi j^n \delta^{(n)}(\omega)$
$tu(t)$	$j\pi\delta'(\omega) - 1/\omega^2$
$t^2 u(t)$	$-\pi\delta''(\omega) + j2/\omega^3$
$t^3 u(t)$	$-j\pi\delta^{(3)}(\omega) + 3!/\omega^4$
$\cos \omega_0 t$	$\pi [\delta(\omega - \omega_0) + \delta(\omega + \omega_0)]$
$\sin \omega_0 t$	$j\pi [\delta(\omega + \omega_0) - \delta(\omega - \omega_0)]$
$\cos \omega_0 t u(t)$	$\frac{\pi}{2} [\delta(\omega - \omega_0) + \delta(\omega + \omega_0)] + \frac{j\omega}{\omega_0^2 - \omega^2}$
$\sin \omega_0 t u(t)$	$\frac{\pi}{2j} [\delta(\omega - \omega_0) - \delta(\omega + \omega_0)] + \frac{\omega_0}{\omega_0^2 - \omega^2}$
$e^{-\alpha t} \sin \omega_0 t u(t), \alpha > 0$	$\frac{\omega_0}{(\alpha + j\omega)^2 + \omega_0^2}$
$\Pi_\tau(t)$	$2\tau \text{Sa}[\omega\tau]$
$\frac{W}{\pi} \text{Sa}[Wt]$	$\Pi_W(\omega)$
$\Lambda_\tau(t) = \begin{cases} 1 - \frac{ t }{\tau}, & t < \tau \\ 0, & t \geq \tau \end{cases}$	$\tau \left[\text{Sa}\left(\frac{\omega\tau}{2}\right) \right]^2$
$\frac{W}{2\pi} \left[\text{Sa}\left(\frac{Wt}{2} t\right) \right]^2$	$\Lambda_W(\omega)$
$e^{-\alpha t }, \alpha > 0$	$\frac{2\alpha}{\alpha^2 + \omega^2}$
$e^{-t^2/(2\sigma^2)}$	$\sigma\sqrt{2\pi}e^{-\sigma^2\omega^2/2}$
$\rho_T(t) = \sum_{n=-\infty}^{\infty} \delta(t - nT)$	$\omega_0 \rho_{\omega_0} = \omega_0 \sum_{n=-\infty}^{\infty} \delta(\omega - n\omega_0), \omega_0 = 2\pi/T$

4.15 Relation between Fourier and Laplace Transforms

Consider a simple example relating Fourier to Laplace transform.

Example 4.11 Let $f(t) = e^{-\alpha t} \cos(\beta t) u(t)$, $\alpha > 0$. We have

$$F(s) = \frac{(s + \alpha)}{(s + \alpha)^2 + \beta^2}, \quad \sigma = \Re[s] > -\alpha.$$

Since $-\alpha < 0$ the Laplace transform $F(s)$ converges for $\sigma = 0$, i.e., for $s = j\omega$; hence

$$F(j\omega) = F(s)|_{s=j\omega} = \frac{j\omega + \alpha}{(j\omega + \alpha)^2 + \beta^2}.$$

The poles of $F(s)$, that is, the zeros of the denominator $(s + \alpha)^2 + \beta^2$ of $F(s)$, are given by $s = -\alpha \pm j\beta$. If the s plane is seen as a horizontal plane the modulus $|F(s)|$ of $F(s)$ would appear as a surface on the plane containing two mountain peaks that rise to infinity at the poles as shown in Fig. 4.19(a). The poles and the ROC of the Laplace transform are also shown in the figure.

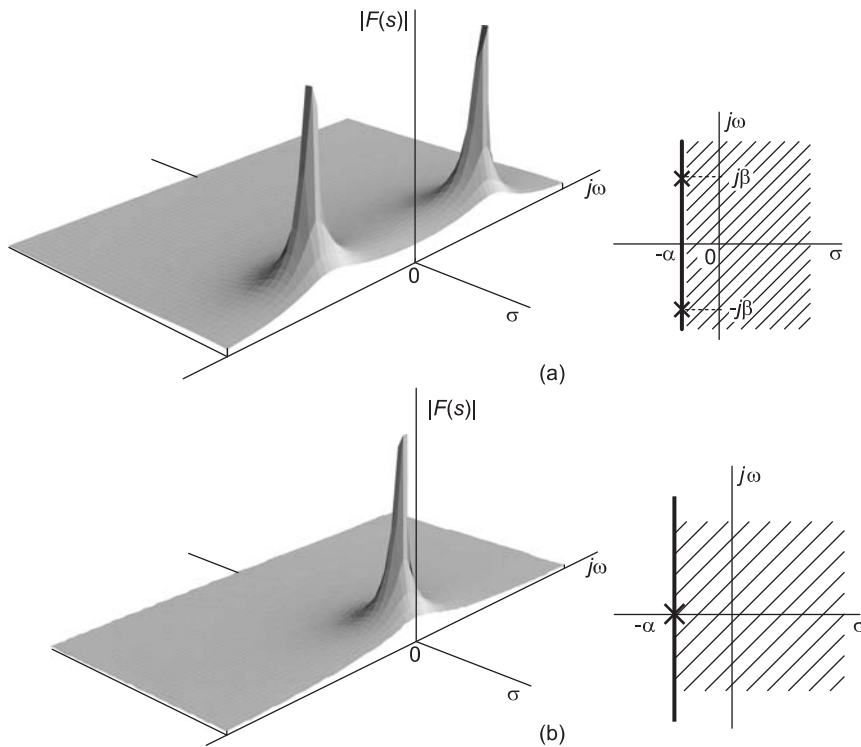


FIGURE 4.19 Fourier spectrum seen along the imaginary axis of Laplace transform plane.

The following observations summarize the relations between Fourier transform and Laplace transform:

1. The mountain peak of a pole in the s plane at a point, say, $s = -\alpha + j\beta$, as in the last example, Fig. 4.19 (a), leads to a corresponding valley along the $s = j\omega$ axis. The general form of the Fourier transform amplitude spectrum $|F(j\omega)|$ thus can be deduced from knowledge of the locations of the poles and zeros of the Laplace transform $F(s)$. The peaks in the Fourier transform amplitude spectrum resulting from two conjugate poles are not exactly at the points $s = j\beta$ and $s = -j\beta$ due to the superposition of the two surfaces, which tends to result in a sum that has higher peaks and drawn closer together than those of the separate individual peaks. The two Fourier transform peaks are thus closer to the point of origin $\omega = 0$, at frequencies $\pm\omega_r$, where $|\omega_r|$ is slightly less than β as we shall see later on in Chapter 5. The closer the poles are to the $s = j\omega$ axis the higher and more pointed the peaks of the Fourier transform. Ultimately, if the poles are on the axis itself, the function has pure sinusoids, a step function or a constant. Such cases lead to impulses along the axis. In the case $\beta = 0$ the function is given by $f(t) = e^{-\alpha t}u(t)$ and its transform by $F(s) = 1/(s + \alpha)$, as shown in Fig. 4.19(b). The transform has one real pole at $s = -\alpha$, a single peak appears on the s plane, and the Fourier transform seen along the $j\omega$ axis is a bell shape centered at the frequency $j\omega = 0$.
2. In the case $\alpha = 0$ the function is given by $f(t) = \cos \beta t u(t)$ and

$$F(s) = \frac{s}{s^2 + \beta^2}, \quad \Re[s] > 0. \tag{4.75}$$

The transform $F(s)$ contains two poles at $s = \pm j\beta$ and a zero at $s = 0$. In this case a slice by a vertical plane applied onto the horizontal s plane taken along the $j\omega$ axis would show that the Fourier transform has two sharp peaks mounting to infinity on the axis itself, and drops to zero at the origin. The Fourier transform in this special case, where the poles are on the axis itself, contains two impulses at the points $s = j\beta$ and $s = -j\beta$. Due to the presence of the poles on the axis, the Laplace transform exists only to the right of the $j\omega$ axis, i.e. for $\sigma > 0$. The Fourier transform $F(j\omega)$ exists as a distribution. It is equal to the Laplace transform with $s = j\omega$ plus two impulses. It is in fact given by

$$F(j\omega) = F(s)|_{s=j\omega} + \frac{\pi}{2} \{ \delta(\omega - \beta) + \delta(\omega + \beta) \} = \frac{j\omega}{\beta^2 - \omega^2} + \frac{\pi}{2} \{ \delta(\omega - \beta) + \delta(\omega + \beta) \}.$$

3. For *two-sided* periodic functions such as $\cos \beta t$, the Fourier transform exists in the limit, as a distribution, expressed using impulses. The Fourier transform of $\sin(\beta t)$ e.g., is given by

$$\mathcal{F}[\sin(\beta t)] = -j\pi\delta(\omega - \beta) + j\pi\delta(\omega + \beta). \tag{4.76}$$

For such two-sided infinite duration functions the Laplace transform does not exist according to present literature, even if the Fourier transform, a special case thereof exists, as mentioned above.

4. A function of which the Laplace transform does not converge on the $j\omega$ axis, and of which the ROC boundary line is not the $j\omega$ axis, has no Fourier transform.

4.16 Relation to Laplace Transform with Poles on Imaginary Axis

If poles are on the imaginary axis the Laplace transform ROC excludes the axis. In such a case the Fourier transform is equal to the Laplace transform plus impulsive components as

the following example illustrates.

Example 4.12 Evaluate the Fourier transform of the function

$$f(t) = \sum_{i=1}^n A_i \cos(\omega_i t + \theta_i) u(t).$$

We can rewrite the function in the form

$$f(t) = \sum_{i=1}^n \{ (a_i e^{j\omega_i t} + a_i^* e^{-j\omega_i t}) / 2 \} u(t)$$

where $a_i = A_i e^{j\theta_i}$, obtaining its Fourier transform

$$F(j\omega) = F(s)|_{s=j\omega} + (\pi/2) \sum_{i=1}^n \{ a_i \delta(\omega - \omega_i) + a_i^* \delta(\omega + \omega_i) \}$$

where

$$F(s) = A_i \frac{\cos \theta_i s - \omega_i \sin \theta_i}{s^2 + \omega_i^2}, \quad \sigma > 0.$$

As mentioned earlier, we shall see in Chapter 18 that thanks to a recent generalization of the Dirac-delta impulse and the consequent extension of the Laplace domain, the Laplace transform is made to exist on the $j\omega$ axis itself. Its value includes generalized impulses on the axis, and the Fourier transform can be obtained thereof by a straight forward substitution $s = j\omega$, impulse and all. The Fourier transform is thus deduced by such simple substitution rather being equal to a part from Laplace transform and another, the impulsive component, which is foreign to the Laplace transform and has to be evaluated separately, as is presently the case.

4.17 Convolution in Time

Theorem: The Fourier transform of the convolution of two functions $f_1(t)$ and $f_2(t)$ is equal to the product of their transforms, that is,

$$f_1 * f_2 \triangleq \int_{-\infty}^{\infty} f_1(\tau) f_2(t - \tau) d\tau \xrightarrow{\mathcal{F}} F_1(j\omega) F_2(j\omega). \quad (4.77)$$

The proof is straightforward and is similar to that employed in the Laplace domain.

Example 4.13 Evaluate the forward and inverse transform of the triangle

$$\Lambda_\tau(t) = \begin{cases} 1 - \frac{|t|}{\tau}, & |t| < \tau \\ 0, & |t| > \tau \end{cases}$$

shown in Fig. 4.20, using the convolution in time property.

We note that the rectangle $f(t) = \Pi_T(t)$ shown in Fig. 4.21 has a Fourier transform $F(j\omega) = 2T \text{Sa}(\omega T)$. The “auto-convolution” of $f(t)$ gives the triangle $w(t) = f(t) * f(t) = 2T \Lambda_{2T}(t)$. Therefore $W(j\omega) = \{F(j\omega)\}^2 = 4T^2 \text{Sa}^2(\omega T)$. Substituting $\tau = 2T$

$$\mathcal{F}[\Lambda_\tau(t)] = \frac{1}{\tau} W(j\omega) = \tau \text{Sa}^2\left(\frac{\omega\tau}{2}\right)$$

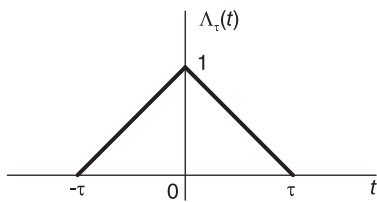


FIGURE 4.20 Triangular signal.

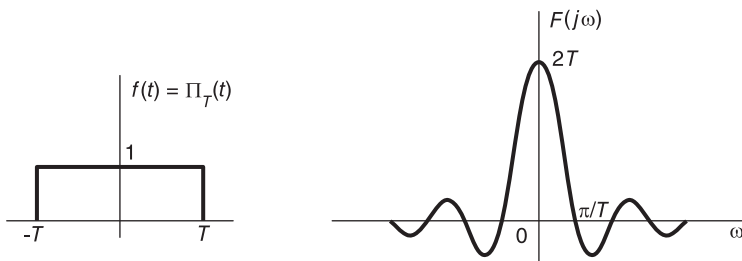


FIGURE 4.21 Rectangle and spectrum.

as shown in Fig. 4.22.

Using the duality property and replacing τ by B we obtain

$$\frac{B}{2\pi} Sa^2 \left\{ \frac{B}{2}t \right\} \xleftrightarrow{\mathcal{F}} \Lambda_B(\omega)$$

as shown in Fig. 4.23. The transform of the square of the sampling function is therefore a triangle as expected.

4.18 Linear System Input–Output Relation

As stated earlier, the frequency response $H(j\omega)$ of a linear system is the transform of the impulse response $h(t)$

$$H(j\omega) = \int_{-\infty}^{\infty} h(t) e^{-j\omega t} dt \triangleq A(\omega) e^{j\phi(\omega)} \tag{4.78}$$

where $A(\omega) = |H(j\omega)|$ and $\phi(\omega) = \arg[H(j\omega)]$. The response $y(t)$ of the system to an input $x(t)$ is the convolution

$$y(t) = x(t) * h(t) = \int_{-\infty}^{\infty} x(\tau) h(t - \tau) d\tau \tag{4.79}$$

and by the convolution theorem $Y(j\omega) = X(j\omega) H(j\omega)$.

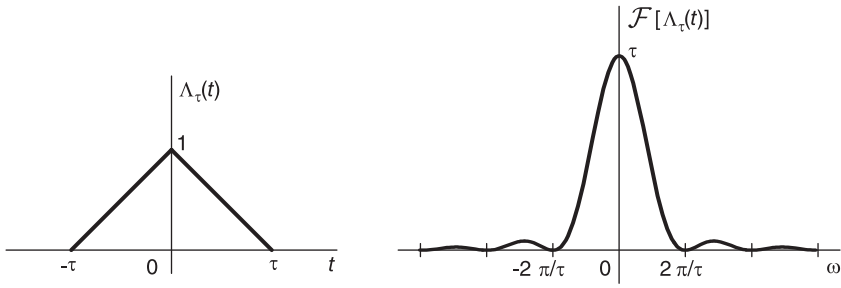


FIGURE 4.22 Triangle and spectrum.

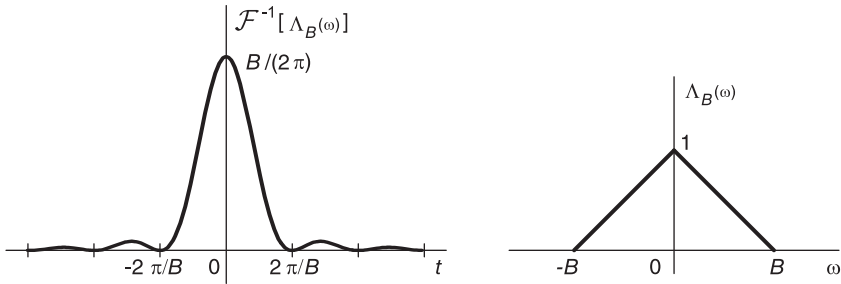


FIGURE 4.23 Inverse transform of a triangular spectrum.

4.19 Convolution in Frequency

The duality property of the Fourier transform has as a consequence the fact that multiplication in time corresponds to convolution in frequency.

$$f_1(t) f_2(t) \xleftrightarrow{\mathcal{F}} \frac{1}{2\pi} \int_{-\infty}^{\infty} F_1(jy) F_2[j(\omega - y)] dy. \tag{4.80}$$

4.20 Parseval's Theorem

Parseval's theorem states that

$$\int_{-\infty}^{\infty} |f(t)|^2 dt = \frac{1}{2\pi} \int_{-\infty}^{\infty} |F(j\omega)|^2 d\omega. \tag{4.81}$$

Proof

$$\int_{-\infty}^{\infty} |f(t)|^2 dt = \int_{-\infty}^{\infty} f^*(t) f(t) dt = \int_{-\infty}^{\infty} f^*(t) \frac{1}{2\pi} \int_{-\infty}^{\infty} F(j\omega) e^{j\omega t} d\omega dt$$

i.e.

$$\int_{-\infty}^{\infty} |f(t)|^2 dt = \frac{1}{2\pi} \int_{-\infty}^{\infty} F(j\omega) \int_{-\infty}^{\infty} f^*(t) e^{j\omega t} dt d\omega = \frac{1}{2\pi} \int_{-\infty}^{\infty} F(j\omega) F^*(j\omega) d\omega$$

which is the same as stated in (4.81). If $f(t)$ is real then

$$\int_{-\infty}^{\infty} f(t)^2 dt = \frac{1}{2\pi} \int_{-\infty}^{\infty} |F(j\omega)|^2 d\omega = \frac{1}{\pi} \int_0^{\infty} |F(j\omega)|^2 d\omega.$$

4.21 Energy Spectral Density

The spectrum

$$\varepsilon(\omega) \triangleq |F(j\omega)|^2 \tag{4.82}$$

is called the *energy spectral density*. The name is justified by Parseval's theorem stating that the integral of $|F(j\omega)|^2$ is equal to the signal energy. If $f(t)$ is an electric potential in volts applied across a resistance of 1 ohm then the quantity $\int_{-\infty}^{\infty} f^2(t) dt$ is equal to the energy in joules dissipated in the resistance. A function $f(t)$ having a finite energy

$$E = \int_{-\infty}^{\infty} f^2(t) dt = \frac{1}{2\pi} \int_{-\infty}^{\infty} \varepsilon(\omega) d\omega \tag{4.83}$$

is called an *energy signal*. If a signal is periodic of period T , its energy is infinite. Such a signal is called a *power signal*. Its power is finite and is evaluated as the energy over one period divided by the period T . As seen in Chapter 2, Parseval's relation gives the same in terms of the Fourier series coefficients. This topic will be dealt with at length in Chapter 12.

Example 4.14 *Let*

$$f(t) = A \Pi_{\tau/2}(t) = A [u(t + \tau/2) - u(t - \tau/2)].$$

Evaluate the signal energy spectral density.

We have $F(j\omega) = A\tau Sa(\tau\omega/2)$. The energy density spectrum is given by $\varepsilon(\omega) = |F(j\omega)|^2 = A^2\tau^2 Sa^2(\tau\omega/2)$. From Parseval's theorem the area under this density spectrum is equal to 2π times the energy of $f(t)$, that is, equal to $2\pi A^2 \times \tau$.

We can measure the energy in a frequency band ω_1, ω_2 , as shown in Fig. 4.24. We write

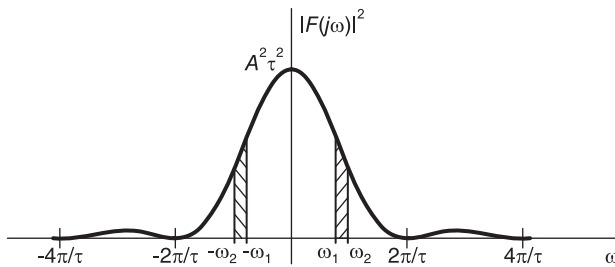


FIGURE 4.24 Energy density spectrum.

$$E(\omega_1, \omega_2) = 2 \times \frac{1}{2\pi} \int_{\omega_1}^{\omega_2} |F(j\omega)|^2 d\omega = \frac{1}{\pi} \int_{\omega_1}^{\omega_2} \varepsilon(\omega) d\omega$$

where the multiplication by 2 accounts for the negative frequencies part of the spectrum.

4.22 Average Value versus Fourier Transform

We shall see in Chapter 12 that signals of finite energy are called energy signals and those of finite power are called power signals. In this section we consider closely related properties and in particular the relation between the signal average value and its Fourier transform.

The average value, also referred to as the d-c average value, of a signal $x(t)$ is by definition

$$\bar{x}(t) = \lim_{T \rightarrow \infty} \frac{1}{2T} \int_{-T}^T x(t) dt. \quad (4.84)$$

Consider the case where the value of the Fourier transform $X(j\omega)$ at zero frequency exists. Since

$$X(j\omega) = \int_{-\infty}^{\infty} x(t) e^{-j\omega t} dt \quad (4.85)$$

implies that

$$X(0) = \int_{-\infty}^{\infty} x(t) dt \quad (4.86)$$

the signal average value is given by

$$\bar{x}(t) = \lim_{T \rightarrow \infty} \frac{1}{2T} \int_{-T}^T x(t) dt = \lim_{T \rightarrow \infty} \frac{1}{2T} X(0) = 0. \quad (4.87)$$

In other words if the Fourier transform $X(j\omega)$ at zero frequency has a finite value the signal has a zero average value $\bar{x}(t)$.

Consider now the case where the Fourier transform $X(j\omega)$ at zero frequency does not exist. This occurs if the transform has an impulse at zero frequency. The transform of a constant, a unit step function and related signals are examples of such signals. To evaluate the signal average value under such conditions consider the case where the Fourier transform is the sum of a continuous nonimpulsive transform $X_c(j\omega)$ and an impulse of intensity C , i.e.

$$X(j\omega) = X_c(j\omega) + C\delta(\omega). \quad (4.88)$$

The inverse transform of $X(j\omega)$ is given by

$$x(t) = \mathcal{F}^{-1}[X(j\omega)] = \mathcal{F}^{-1}[X_c(j\omega)] + C/(2\pi). \quad (4.89)$$

The signal average value is

$$\bar{x}(t) = \lim_{T \rightarrow \infty} \frac{1}{2T} \int_{-T}^T x(t) dt = \frac{C}{2\pi} + \lim_{T \rightarrow \infty} \frac{1}{2T} \int_{-T}^T \frac{1}{2\pi} \int_{-\infty}^{\infty} X_c(j\omega) e^{j\omega t} d\omega dt. \quad (4.90)$$

We may write

$$\bar{x}(t) = \frac{C}{2\pi} + I \quad (4.91)$$

where

$$I = \frac{1}{2\pi} \lim_{T \rightarrow \infty} \frac{1}{2T} \int_{-\infty}^{\infty} X_c(j\omega) \int_{-T}^T e^{j\omega t} d\omega dt \quad (4.92)$$

i.e.

$$I = \frac{1}{2\pi} \lim_{T \rightarrow \infty} \frac{1}{2T} \int_{-\infty}^{\infty} X_c(j\omega) 2T \text{Sa}(\omega T) d\omega. \tag{4.93}$$

Using the sampling function limit property Equation (17.179) proven in Chapter 17, we can write

$$\lim_{T \rightarrow \infty} T \text{Sa}(T\omega) = \pi \delta(\omega). \tag{4.94}$$

Hence

$$I = \lim_{T \rightarrow \infty} \frac{1}{2T} \int_{-\infty}^{\infty} X_c(j\omega) \delta(\omega) d\omega \tag{4.95}$$

i.e.

$$I = \lim_{T \rightarrow \infty} \frac{1}{2T} X_c(0) = 0 \tag{4.96}$$

$$\bar{x}(t) = C / (2\pi). \tag{4.97}$$

Example 4.15 Evaluate the average value of the signal $x(t) = 10u(t)$.

We have

$$X(j\omega) = 10 / (j\omega) + 10\pi\delta(\omega)$$

wherefrom $\bar{x}(t) = 5$, which can be confirmed by direct integration of $x(t)$.

Example 4.16 Evaluate the average value of the signal $x(t) = 5$.

We have

$$X(j\omega) = 10\pi\delta(\omega)$$

wherefrom $\bar{x}(t) = 10\pi / (2\pi) = 5$, as expected.

4.23 Fourier Transform of a Periodic Function

A periodic function $f(t)$ of period T , being not absolutely integrable it has no Fourier transform in the ordinary sense. Its transform exists only in the limit. Its Fourier series can be written

$$f(t) = \sum_{n=-\infty}^{\infty} F_n e^{jn\omega_0 t}, \quad \omega_0 = 2\pi/T \tag{4.98}$$

$$F(j\omega) = \mathcal{F} \left[\sum_{n=-\infty}^{\infty} F_n e^{jn\omega_0 t} \right] = 2\pi \sum_{n=-\infty}^{\infty} F_n \delta(\omega - n\omega_0). \tag{4.99}$$

This is an important relation that gives the value of the Fourier transform as a function of the Fourier series coefficients. We note that the spectrum of a periodic function is composed of impulses at the harmonic frequencies, equally spaced by the fundamental frequency ω_0 , the intensity of the n^{th} harmonic impulse being equal to $2\pi \times$ the Fourier series coefficient F_n .

4.24 Impulse Train

We have found that the Fourier series expansion an impulse train of period T , with $\omega_0 = 2\pi/T$ is

$$f(t) = \rho_T(t) = \frac{1}{T} \sum_{n=-\infty}^{\infty} e^{jn\omega_0 t} \quad (4.100)$$

Hence

$$\mathcal{F}[\rho_T(t)] = \frac{2\pi}{T} \sum_{n=-\infty}^{\infty} \delta(\omega - n\omega_0) = \omega_0 \rho_{\omega_0}(\omega) \quad (4.101)$$

$$\rho_{\omega_0}(\omega) \triangleq \sum_{n=-\infty}^{\infty} \delta(\omega - n\omega_0) \quad (4.102)$$

as shown in Fig. 4.25

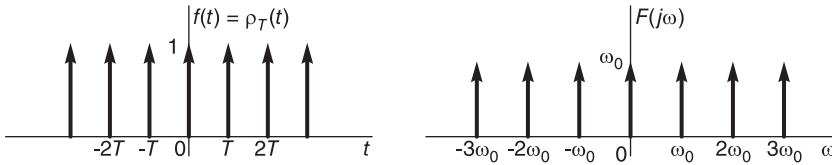


FIGURE 4.25 Impulse train and spectrum.

4.25 Fourier Transform of Powers of Time

Since $1 \xleftrightarrow{\mathcal{F}} 2\pi\delta(\omega)$, using the property $(-jt)^n f(t) \xleftrightarrow{\mathcal{F}} F^{(n)}(j\omega)$, i.e. $t^n f(t) \xleftrightarrow{\mathcal{F}} j^n F^{(n)}(j\omega)$, we deduce that

$$t^n \xleftrightarrow{\mathcal{F}} 2\pi j^n \delta^{(n)}(\omega). \quad (4.103)$$

In particular

$$t \xleftrightarrow{\mathcal{F}} 2\pi j \delta'(\omega). \quad (4.104)$$

Moreover,

$$|t| = t \operatorname{sgn}(t) \quad (4.105)$$

and since $\operatorname{sgn}(t) \xleftrightarrow{\mathcal{F}} 2/(j\omega)$,

$$|t| \xleftrightarrow{\mathcal{F}} \frac{1}{2\pi} [2\pi j \delta'(\omega)] * 2/(j\omega) = 2\delta(\omega) * \left[\frac{1}{\omega}\right]' = \frac{-2}{\omega^2}. \quad (4.106)$$

We also note that

$$|t| + t = 2tu(t) \quad (4.107)$$

i.e.

$$tu(t) = (|t| + t)/2 \quad (4.108)$$

$$tu(t) \xleftrightarrow{\mathcal{F}} j\pi\delta'(\omega) - \frac{1}{\omega^2}. \quad (4.109)$$

4.26 System Response to a Sinusoidal Input

Consider a linear system of frequency response $H(j\omega)$. We study the two important cases of its response to a complex exponential and to a pure sinusoid.

1. Let $x(t)$ be the complex exponential of a frequency β

$$x(t) = Ae^{j\beta t}. \quad (4.110)$$

We have

$$X(j\omega) = A \times 2\pi\delta(\omega - \beta). \quad (4.111)$$

The Transform of the output $y(t)$ is given by

$$Y(j\omega) = 2\pi A\delta(\omega - \beta)H(j\omega) = 2\pi AH(j\beta)\delta(\omega - \beta) = X(j\omega)H(j\beta). \quad (4.112)$$

wherefrom

$$y(t) = H(j\beta)x(t) = Ae^{j\beta t}H(j\beta) = A|H(j\beta)|e^{j(\beta t + \arg[H(j\beta)])}. \quad (4.113)$$

The output is therefore the same as the input simply multiplied by the value of the frequency response at the frequency of the input.

2. Let

$$x(t) = A \cos(\beta t) = A(e^{j\beta t} + e^{-j\beta t})/2 \quad (4.114)$$

$$Y(j\omega) = A\pi H(j\beta)\delta(\omega - \beta) + A\pi H(-j\beta)\delta(\omega + \beta) \quad (4.115)$$

$$y(t) = (A/2)e^{j\beta t}H(j\beta) + (A/2)e^{-j\beta t}H(-j\beta) \quad (4.116)$$

and since $H(-j\beta) = H^*(j\beta)$ we have

$$y(t) = A|H(j\beta)|\cos\{\beta t + \arg[H(j\beta)]\}. \quad (4.117)$$

The response to a sinusoid of frequency β is therefore a sinusoid of the same frequency, of which the amplitude is multiplied by $|H(j\beta)|$ and the phase increased by $\arg[H(j\beta)]$.

4.27 Stability of a Linear System

A linear system is stable if its frequency response $H(j\omega)$ exists, otherwise it is unstable. In other words the existence of the Fourier transform of the impulse response implies that the system is stable. For a causal system this implies that no pole exists in the right half of the s plane. For an anticausal (left-sided) system it means that no pole exists in the left half of the s plane. A system of which the poles are on the $j\omega$ axis is called critically stable.

4.28 Fourier Series versus Transform of Periodic Functions

Let $f(t)$ be a periodic function of period T_0 and $f_0(t)$ its “base period” taken as that defined over the interval $(-T_0/2, T_0/2)$. We note that $f(t)$ is the periodic extension of $f_0(t)$. We can write

$$f(t) = \sum_{n=-\infty}^{\infty} f_0(t - nT_0) \quad (4.118)$$

and

$$f_0(t) = f(t) \Pi_{T_0/2}(t). \quad (4.119)$$

We can express $f(t)$ as the convolution of $f_0(t)$ with an impulse train

$$f(t) = f_0(t) * \sum_{n=-\infty}^{\infty} \delta(t - nT_0) \quad (4.120)$$

$$F(j\omega) = \omega_0 \sum_{n=-\infty}^{\infty} F_0(jn\omega_0) \delta(\omega - n\omega_0) \quad (4.121)$$

$$F_0(j\omega) = \int_{-T_0/2}^{T_0/2} f_0(t) e^{-j\omega t} dt = \int_{-T_0/2}^{T_0/2} f(t) e^{-j\omega t} dt \quad (4.122)$$

$$F_0(jn\omega_0) = \int_{-T_0/2}^{T_0/2} f_0(t) e^{-jn\omega_0 t} dt = T_0 F_n \quad (4.123)$$

$$F_n = \frac{1}{T_0} F_0(jn\omega_0) \quad (4.124)$$

which when substituted into Equation (4.121) gives the same relation, Equation (4.99), found above. These same relations hold if the base period is taken as the value of $f(t)$ over the interval $(0, T_0)$ so that $f_0(t) = f(t) R_{T_0}(t)$.

4.29 Transform of a Train of Rectangles

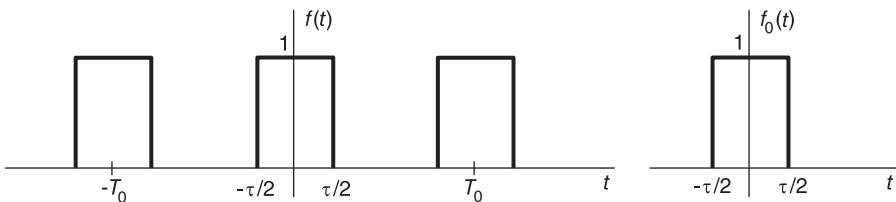


FIGURE 4.26 Train of rectangles and base period.

The problem of evaluating the Fourier transform of a train of rectangles is often encountered. It is worthwhile solving for possible utilization elsewhere.

Consider the function $f(t)$ shown in Fig. 4.26 wherein $T_0 \geq \tau$, ensuring that the successive rectangles do not touch. Let $\omega_0 = 2\pi/T_0$. We have

$$f(t) = \Pi_{\tau/2}(t) * \rho_T(t). \tag{4.125}$$

$$F(j\omega) = \omega_0 \rho_{\omega_0}(\omega) \tau Sa\left(\frac{\tau}{2}\omega\right) \tag{4.126}$$

i.e.

$$F(j\omega) = \omega_0 \tau \sum_{n=-\infty}^{\infty} Sa\left(\frac{n\omega_0\tau}{2}\right) \delta(\omega - n\omega_0). \tag{4.127}$$

Moreover, $F(j\omega) = 2\pi \sum_{n=-\infty}^{\infty} F_n \delta(\omega - n\omega_0)$, where

$$F_n = \frac{\tau}{T_0} Sa\left(n\pi \frac{\tau}{T_0}\right). \tag{4.128}$$

4.30 Fourier Transform of a Truncated Sinusoid

Consider a sinusoid of frequency β , truncated by a rectangular window of duration T , namely,

$$f(t) = \sin(\beta t + \theta) R_T(t).$$

We have evaluated the Laplace transform of this signal in Chapter 3, Example 3.17. We may replace s by $j\omega$ in that expression, obtaining its Fourier transform. Alternatively, to better visualize the effect on the spectrum of the truncation of the sinusoid, we may write

$$F(s) = \frac{1}{2j} \int_0^T \left\{ e^{j(\beta t + \theta)} - e^{-j(\beta t + \theta)} \right\} e^{-st} dt = \frac{1}{2j} \left\{ e^{j\theta} \frac{1 - e^{-(s-j\beta)T}}{s - j\beta} - e^{-j\theta} \frac{1 - e^{-(s+j\beta)T}}{s + j\beta} \right\}.$$

Using the generalized hyperbolic sampling function $Sh(z) = \sinh(z)/z$ we can write

$$F(s) = \frac{1}{2j} \left\{ e^{j\theta} e^{-(s-j\beta)T/2} \frac{2 \sinh[(s-j\beta)T/2]}{s - j\beta} - e^{-j\theta} e^{-(s+j\beta)T/2} \frac{2 \sinh[(s+j\beta)T/2]}{s + j\beta} \right\} \\ = [T/(2j)] \left\{ e^{j\theta} e^{-(s-j\beta)T/2} Sh[(s-j\beta)T/2] - e^{-j\theta} e^{-(s+j\beta)T/2} Sh[(s+j\beta)T/2] \right\}.$$

We note that for x real,

$$Sh(jx) = \sinh(jx)/(jx) = (e^{jx} - e^{-jx})/(2jx) = \sin(x)/x = Sa(x).$$

We can therefore write

$$F(j\omega) = [T/(2j)] \left\{ e^{-j(\omega-\beta)T/2+j\theta} Sa[(\omega-\beta)T/2] - e^{-j(\omega+\beta)T/2-j\theta} Sa[(\omega+\beta)T/2] \right\} \\ F(j\omega) = \frac{T}{2} \left\{ e^{-j\{(\omega-\beta)T/2-\theta+\pi/2\}} Sa[(\omega-\beta)\frac{T}{2}] - e^{-j\{(\omega+\beta)T/2+\theta+\pi/2\}} Sa[(\omega+\beta)\frac{T}{2}] \right\}.$$

The Fourier series coefficients F_n in the expansion

$$f(t) = \sum_{n=-\infty}^{\infty} F_n e^{jn\omega_0 t}, \quad 0 < t < T \tag{4.129}$$

where $\omega_0 = 2\pi/T$, can be deduced from the Fourier transform. We write

$$F_n = (1/T)F(jn\omega_0) = (1/2) \left\{ e^{-j\{(n\omega_0 - \beta)T/2 - \theta + \pi/2\}} Sa[(n\omega_0 - \beta)T/2] - e^{-j\{(n\omega_0 + \beta)T/2 + \theta + \pi/2\}} Sa[(n\omega_0 + \beta)T/2] \right\} \quad (4.130)$$

which is identical to the expression obtained in Chapter 2 by direct evaluation of the coefficients. In fact, referring to Fig. 2.38 and Fig. 2.39 of Chapter 2 we can see now that the continuous curves in the lower half of each of these figures are the Fourier transform spectra of which the discrete spectra of the Fourier series coefficients are but sampling at intervals multiple of ω_0 .

We finally notice that if $w(t)$ is the periodic extension of $f(t)$, we may write

$$w(t) = \sum_{n=-\infty}^{\infty} f(t - nT) = \sum_{n=-\infty}^{\infty} W_n e^{jn\omega_0 t} = \sum_{n=-\infty}^{\infty} F_n e^{jn\omega_0 t}, \quad \forall t \quad (4.131)$$

since $W_n = F_n$,

$$W(j\omega) = 2\pi \sum_{n=-\infty}^{\infty} W_n \delta(\omega - n\omega_0) = 2\pi \sum_{n=-\infty}^{\infty} F_n \delta(\omega - n\omega_0). \quad (4.132)$$

$$W(j\omega) = \pi \sum_{n=-\infty}^{\infty} \left\{ e^{-j\{(n\omega_0 - \beta)T/2 - \theta + \pi/2\}} Sa[(n\omega_0 - \beta)T/2] - e^{-j\{(n\omega_0 + \beta)T/2 + \theta + \pi/2\}} Sa[(n\omega_0 + \beta)T/2] \right\} \delta(\omega - n\omega_0).$$

If $T = m\tau$, where $\tau = 2\pi/\beta$ is the function period, this expression reduces to

$$W(j\omega) = \pi \left\{ e^{j(\theta - \pi/2)} \delta(\omega - \beta) + e^{-j(\theta - \pi/2)} \delta(\omega + \beta) \right\} \quad (4.133)$$

which is indeed the transform of $w(t) = \sin(\beta t + \theta)$.

4.31 Gaussian Function Laplace and Fourier Transform

The Gaussian function merits special attention. It is often encountered in studying properties of distributions and sequences leading to the Dirac-delta impulse among other important applications.

We evaluate the transform of the Gaussian function

$$f(x) = e^{-x^2/2} \quad (4.134)$$

$$F(j\omega) \triangleq \mathcal{F}[f(x)] = \int_{-\infty}^{\infty} e^{-x^2/2} e^{-j\omega x} dx. \quad (4.135)$$

Consider the integral

$$I = \int_C e^{-z^2/2} dz \quad (4.136)$$

where $z = x + jy$ and C is the rectangular contour of width 2ξ and height ω in the z plane shown in Fig. 4.27. Since the function $e^{-z^2/2}$ has no singularities inside the enclosed region, the integral around the contour is zero. We have

$$I = \left\{ \int_{-\xi+j0}^{\xi+j0} + \int_{\xi+j0}^{\xi+j\omega} + \int_{\xi+j\omega}^{-\xi+j\omega} + \int_{-\xi+j\omega}^{-\xi+j0} \right\} e^{-z^2/2} dz = 0.$$

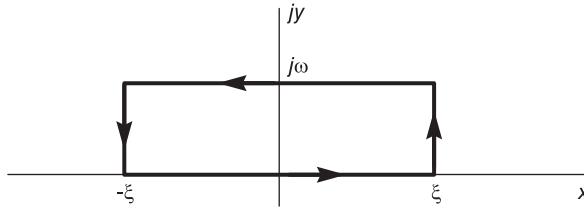


FIGURE 4.27 Integration on a contour in the complex plane.

Consider the second integral.

With $z = \xi + jy$, $dz = jdy$,

$$\begin{aligned} \left| \int_{\xi+j0}^{\xi+j\omega} e^{-z^2/2} dz \right| &= \left| j \int_0^\omega e^{-\xi^2/2} e^{-jy\xi} e^{y^2/2} dy \right| \\ &\leq e^{-\xi^2/2} \int_0^\omega e^{y^2/2} dy \leq e^{-\xi^2/2} \int_0^\omega e^{\omega^2/2} dy = e^{-\xi^2/2} \omega e^{\omega^2/2} \end{aligned}$$

which tends to zero as $\xi \rightarrow \infty$. Similarly, the fourth integral can be shown to tend in the limit to zero. Now in the first integral we have $z = x$ and in the third $z = x + j\omega$ so that

$$I = \int_{-\xi}^{\xi} e^{-x^2/2} dx + \int_{\xi}^{-\xi} e^{-(x+j\omega)^2/2} dx. \tag{4.137}$$

Taking the limit as $\xi \rightarrow \infty$ we have

$$\int_{-\infty}^{\infty} e^{-(x+j\omega)^2/2} dx = \int_{-\infty}^{\infty} e^{-x^2/2} dx \tag{4.138}$$

The right-hand side of this equation is equal to $\sqrt{2\pi}$ since

$$\int_{-\infty}^{\infty} e^{-\alpha x^2} dx = \sqrt{\pi/\alpha}. \tag{4.139}$$

We may therefore write

$$e^{\omega^2/2} \int_{-\infty}^{\infty} e^{-x^2/2} e^{-j\omega x} dx = \sqrt{2\pi}. \tag{4.140}$$

Replacing x by t we have

$$e^{-t^2/2} \longleftrightarrow \sqrt{2\pi} e^{-\omega^2/2}. \tag{4.141}$$

Therefore apart from the factor $\sqrt{2\pi}$ the Gaussian function is its own transform. Similarly, we obtain

$$e^{-\alpha t^2} \xleftrightarrow{\mathcal{L}} \sqrt{\pi/\alpha} e^{s^2/(4\alpha)}. \tag{4.142}$$

4.32 Inverse Transform by Series Expansion

Consider the Fourier transform

$$F(j\omega) = (\alpha + \beta e^{-j\omega})^m. \tag{4.143}$$

To evaluate the inverse transform we may use the expansion

$$F(j\omega) = \sum_{i=0}^m \binom{m}{i} \alpha^{m-i} \beta^i e^{-j\omega i} \tag{4.144}$$

$$f(t) = \mathcal{F}^{-1}[F(j\omega)] = \sum_{i=0}^m \binom{m}{i} \alpha^{m-i} \beta^i \delta(t - i). \tag{4.145}$$

In probability theory this represents the probability density of a lattice-type random variable, with $\alpha + \beta = 1$, referred to as a binomial distribution.

4.33 Fourier Transform in ω and f

Table 4.3 lists some properties of the Fourier transform written as a function of ω and of f .

TABLE 4.3 Fourier Transform Properties in ω and f

Time domain	Time domain	Transform in ω	Transform in f
Inverse transform	$f(t)$	$\frac{1}{2\pi} \int_{-\infty}^{\infty} F(j\omega) e^{j\omega t} d\omega$	$\int_{-\infty}^{\infty} F(f) e^{j2\pi f t} df$
Time shift	$f(t - t_0)$	$e^{-jt_0\omega} F(j\omega)$	$e^{-j2\pi f t_0} F(f)$
Frequency shift	$e^{j2\pi f_0 t} f(t)$	$F[j(\omega - \omega_0)]$	$F(f - f_0)$
Time scaling	$f(at)$	$\frac{1}{ a } F\left[j\left(\frac{\omega}{a}\right)\right]$	$\frac{1}{ a } F\left(\frac{f}{a}\right)$
Convolution in time	$f(t) * g(t)$	$F(j\omega) G(j\omega)$	$F(f) G(f)$
Multiplication in time	$f(t) g(t)$	$\frac{1}{2\pi} \{F(j\omega) * G(j\omega)\}$	$F(f) * G(f)$
Differentiation in time	$f^{(n)}(t)$	$(j\omega)^n F(j\omega)$	$(j2\pi f)^n F(f)$
Differentiation in frequency	$(-jt)^n f(t)$	$F^{(n)}(j\omega)$	$\frac{1}{(2\pi)^n} F^{(n)}(f)$
Integration	$\int_{-\infty}^t f(\tau) d\tau$	$\frac{F(j\omega)}{j\omega} + \pi F(0) \delta(\omega)$	$\frac{F(f)}{j2\pi f} + \frac{F(0)}{2} \delta(f)$

Table 4.4 lists basic Fourier transforms as functions of the radian (angular) frequency ω in rad/sec and of the frequency f in Hz.

TABLE 4.4 Fourier transforms in ω and f

$f(t)$	$F(j\omega)$	$F(f)$
$\delta(t)$	1	1
$\delta(t - t_0)$	$e^{-jt_0\omega}$	$e^{-jt_02\pi f}$
1	$2\pi\delta(\omega)$	$\delta(f)$
$e^{j\omega_0 t}$	$2\pi\delta(\omega - \omega_0)$	$\delta(f - f_0)$
$sgn(t)$	$2/(j\omega)$	$1/(j\pi f)$
$u(t)$	$1/(j\omega) + \pi\delta(\omega)$	$1/(j2\pi f) + (1/2)\delta(f)$
$\cos\omega_0 t$	$\pi[\delta(\omega - \omega_0) + \delta(\omega + \omega_0)]$	$(1/2)[\delta(f - f_0) + \delta(f + f_0)]$
$\sin\omega_0 t$	$-j\pi[\delta(\omega - \omega_0) - \delta(\omega + \omega_0)]$	$(-1/2)[\delta(f - f_0) - \delta(f + f_0)]$
$\delta^{(n)}(t)$	$(j\omega)^n$	$(j2\pi f)^n$
t^n	$j^n 2\pi\delta^{(n)}(\omega)$	$\left(\frac{j}{2\pi}\right)^n \delta^{(n)}(f)$
$\cos\omega_0 t u(t)$	$\frac{\pi}{2}[\delta(\omega - \omega_0) + \delta(\omega + \omega_0)] + \frac{j\omega}{\omega_0^2 - \omega^2}$	$\frac{1}{4}[\delta(f - f_0) + \delta(f + f_0)] + \frac{jf}{2\pi(f_0^2 - f^2)}$
$\sin\omega_0 t u(t)$	$\frac{-j\pi}{2}[\delta(\omega - \omega_0) - \delta(\omega + \omega_0)] + \frac{\omega_0}{\omega_0^2 - \omega^2}$	$\frac{-j}{4}[\delta(f - f_0) - \delta(f + f_0)] + \frac{f_0}{2\pi(f_0^2 - f^2)}$

4.34 Fourier Transform of the Correlation Function

Since the cross correlation of two signals $f(t)$ and $g(t)$ can be written as the convolution

$$r_{fg}(t) = f(t) * g(-t). \tag{4.146}$$

We have

$$R_{fg}(j\omega) = F(j\omega)G^*(j\omega). \tag{4.147}$$

$$R_{ff}(j\omega) = F(j\omega)F^*(j\omega) = |F(j\omega)|^2. \tag{4.148}$$

This subject will be viewed in more detail in Chapter 12.

4.35 Ideal Filters Impulse Response

The impulse response of an ideal filter may be evaluated as the inverse transform of its frequency response.

Ideal Lowpass Filter

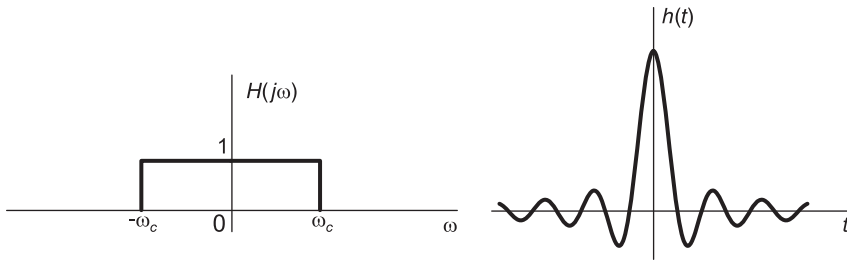


FIGURE 4.28 Ideal lowpass filter frequency and impulse response.

The frequency response $H(j\omega)$ of an ideal lowpass filter is given by

$$H(j\omega) = \Pi_{\omega_c}(\omega) \tag{4.149}$$

as depicted in Fig. 4.28, which also shows its impulse response

$$h(t) = \frac{\omega_c}{\pi} Sa(\omega_c t). \tag{4.150}$$

Ideal Bandpass Filter

Let $G(j\omega)$ be the frequency response of an ideal lowpass filter of cut-off frequency $\omega_c = B/2$ and gain 2. Referring to Fig. 4.29 we note that the bandpass filter frequency response $H(j\omega)$ can be obtained if modulation is applied to the impulse response of the lowpass filter. We can write the frequency response $H(j\omega)$ as a function of the lowpass filter frequency response $G(j\omega)$.

$$H(j\omega) = (1/2) [G\{j(\omega - \omega_0)\} + G\{j(\omega + \omega_0)\}]. \tag{4.151}$$

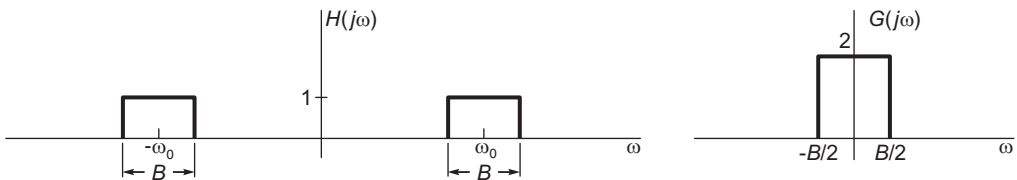


FIGURE 4.29 Ideal bandpass filter frequency response.

The impulse response of the lowpass filter is

$$g(t) = \mathcal{F}^{-1} [G(j\omega)] = \frac{2B}{2\pi} Sa\left(\frac{B}{2}t\right) = \frac{B}{\pi} Sa\left(\frac{B}{2}t\right) \tag{4.152}$$

Hence the impulse response of the bandpass filter is

$$h(t) = g(t) \cos \omega_0 t = \frac{B}{\pi} \text{Sa} \left(\frac{B}{2} t \right) \cos \omega_0 t \quad (4.153)$$

and is shown in Fig. 4.30

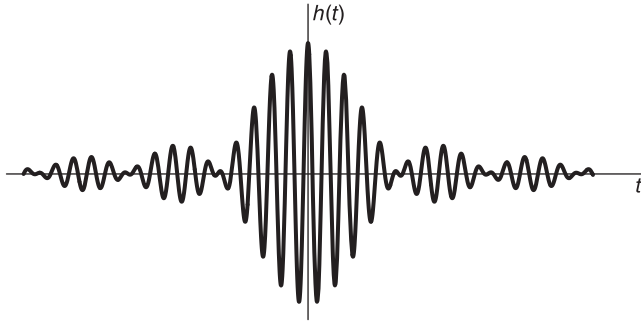


FIGURE 4.30 Ideal bandpass filter impulse response.

Ideal Highpass Filter

The frequency response of an ideal highpass filter may be written in the form

$$H(j\omega) = 1 - \Pi_{\omega_c}(\omega) \quad (4.154)$$

and its impulse response is

$$h(t) = \delta(t) - \frac{\omega_c}{\pi} \text{Sa}(\omega_c t). \quad (4.155)$$

4.36 Time and Frequency Domain Sampling

In the following we study Shanon's Sampling Theorem, Ideal, Natural and Instantaneous sampling techniques, both in time and frequency domains.

4.37 Ideal Sampling

A band-limited signal having no spectral energy at frequencies greater than or equal to f_c cycles per second is uniquely determined by its values at equally spaced intervals T if $T \leq \frac{1}{2f_c}$ seconds.

This theorem, known as the Nyquist-Shannon sampling theorem, implies that if the Fourier spectrum of a signal $f(t)$ is nil at frequencies equal to or greater than a cut-off frequency $\omega_c = 2\pi f_c$ r/s, then all the information in $f(t)$ is contained in its values at multiples

of the interval T if $T \leq \frac{1}{2f_c}$ seconds, that is, if the sampling frequency is $f_s = (1/T) \geq 2f_c$ Hz.

Proof Consider a signal $f(t)$ of which the Fourier transform $F(j\omega)$ is nil for frequencies equal to or greater than $\omega_c = 2\pi f_c$ r/s.

$$F(j\omega) = 0, \quad |\omega| \geq \omega_c. \quad (4.156)$$

Ideal Sampling of a continuous function $f(t)$ is represented mathematically as a multiplication of the function by an impulse train $\rho_T(t)$.

$$\rho_T(t) = \sum_{n=-\infty}^{\infty} \delta(t - nT) \quad (4.157)$$

where T is the sampling period. The ideally sampled signal $f_s(t)$, Fig. 4.31, is thus given by:

$$f_s(t) = f(t)\rho_T(t) = \sum_{n=-\infty}^{\infty} f(nT)\delta(t - nT). \quad (4.158)$$

The sampling frequency will be denoted f_s in Hz and ω_s in rad/sec, that is, $f_s = 1/T$ and $\omega_s = 2\pi f_s = 2\pi/T$. The sampling frequency symbol f_s , should not to be confused with the symbol $f_s(t)$ designating the ideally sampled signal.

The Fourier Transform $\mathcal{F}[\rho_T(t)]$ of the impulse train is given by

$$\rho_T(t) \xrightarrow{\mathcal{F}} \omega_s \sum_{k=-\infty}^{\infty} \delta(\omega - k\omega_s) = \omega_s \rho_{\omega_s}(\omega) \quad (4.159)$$

so that,

$$F_s(j\omega) = \mathcal{F}[f_s(t)] = \frac{1}{2\pi} F(j\omega) * \omega_s \sum_{k=-\infty}^{\infty} \delta(\omega - k\omega_s) = \frac{1}{T} \sum_{k=-\infty}^{\infty} F[j(\omega - k\omega_s)]. \quad (4.160)$$

As can be seen in Fig. 4.31. Since the convolution of a function with an impulse produces the same function displaced to the position of the impulse, the result of the convolution of $F(j\omega)$ with the impulse train is a periodic repetition of $F(j\omega)$. From the figure we notice that the replicas of $F(j\omega)$ along the frequency axis ω will not overlap if and only if the sampling frequency ω_s satisfies the condition

$$\omega_s \geq 2\omega_c \quad (4.161)$$

or

$$\frac{2\pi}{T} \geq 4\pi f_c \quad (4.162)$$

that is,

$$T \leq \frac{1}{2f_c}. \quad (4.163)$$

In other words, the sampling frequency $f_s = 1/T$ must be greater than or equal to twice the signal bandwidth,

$$f_s = \frac{1}{T} \geq 2f_c. \quad (4.164)$$

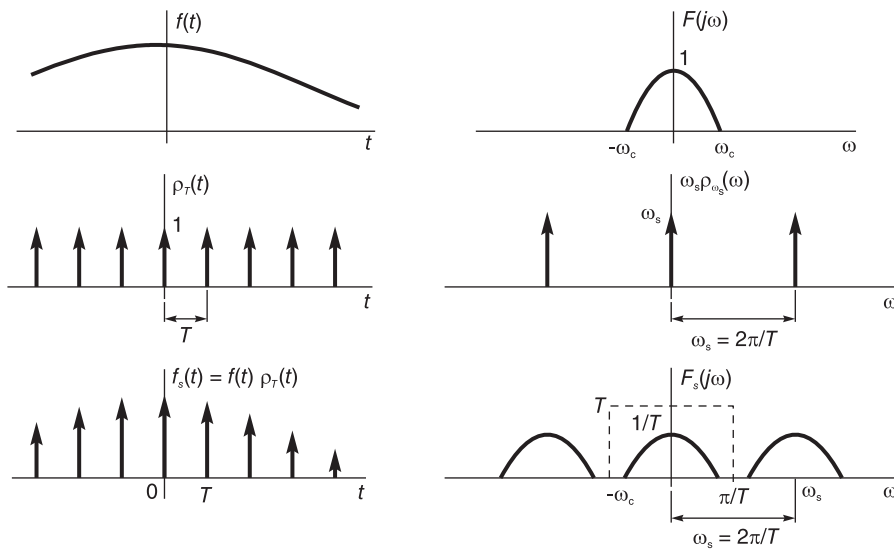


FIGURE 4.31 Ideal sampling in time and frequency domains.

If the condition $f_s \geq 2f_c$ is satisfied then it is possible to reconstruct $f(t)$ from $f_s(t)$. If it is not satisfied then spectra overlap and add up, a condition called *aliasing*. If spectra are aliased due to *undersampling* then it is not possible to reconstruct $f(t)$ from its sampled version $f_s(t)$. The minimum allowable sampling rate $f_{s,\min} = 2f_c$ is called the *Nyquist rate*. The maximum allowable sampling interval $T_{\max} = 1/(2f_c)$ seconds is called the *Nyquist interval*. It is common to call half the sampling frequency the *Nyquist frequency*, denoting the maximum allowable bandwidth for a given sampling frequency.

The continuous-time signal $f(t)$ can be recovered from the ideally sampled signal $f_s(t)$ if we can reconstruct the Fourier transform $F(j\omega)$ from the transform $F_s(j\omega)$. As shown by a dotted line in the figure, this can be done by simply applying to $f_s(t)$ an ideal lowpass filter of gain equal to T , which would let pass the main base period of $F_s(j\omega)$ and cut off all repetitions thereof. The resulting spectrum is thus $F(j\omega)$, which means that the filter output is simply $f(t)$. The filter’s pass-band may be $(-\omega_c, \omega_c)$ or $(-\omega_s/2, \omega_s/2) = (-\pi/T, \pi/T)$. In fact, as Fig. 4.31 shows, the filter can have a bandwidth B r/s, where $\omega_c \leq B < \omega_s - \omega_c$. Let $H(j\omega)$ be the frequency response of the filter. We can write

$$H(j\omega) = T \Pi_B(\omega). \tag{4.165}$$

It is common to choose $B = \pi/T$. As Fig. 4.32 shows, if the sampling period is greater than $1/(2f_c)$ seconds then spectral aliasing, that is, superposition caused by overlapped spectra, occurs. The result is that the original signal $f(t)$ cannot be recovered from the ideally sampled signal $f_s(t)$.

4.38 Reconstruction of a Signal from its Samples

As we have seen, given a proper sampling rate, the signal $f(t)$ may be reconstructed from the ideally sampled signal $f_s(t)$ by applying to the latter ideal lowpass filtering. The signal

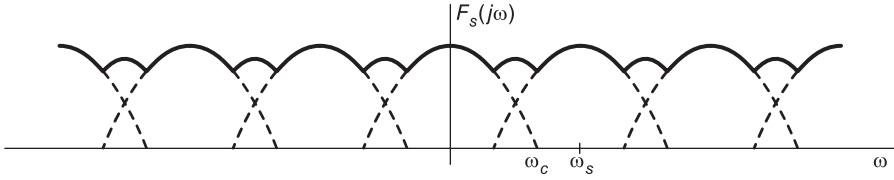


FIGURE 4.32 Spectral aliasing.

$f(t)$ may be reconstructed using a filter of a bandwidth equal to half the sampling frequency $\omega_s/2 = \pi/T$

$$H(j\omega) = T \Pi_{\omega_s/2}(\omega) = T \{u(\omega + \pi/T) - u(\omega - \pi/T)\}. \tag{4.166}$$

The filter input, as shown in Fig. 4.33, is given by $x(t) = f_s(t)$. Its output is denoted by $y(t)$.

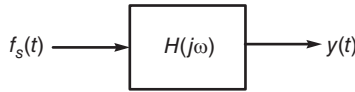


FIGURE 4.33 Reconstruction filter.

We have

$$Y(j\omega) = X(j\omega)H(j\omega) = F_s(j\omega)H(j\omega) = F(j\omega) \tag{4.167}$$

wherefrom $y(t) = f(t)$.

It is interesting to visualize the process of the construction of the continuous-time signal $f(t)$ from the sampled signal $f_s(t)$. We have

$$y(t) = f_s(t) * h(t) \tag{4.168}$$

where $h(t) = \mathcal{F}^{-1}[H(j\omega)]$ is the filter impulse response, that is,

$$h(t) = \mathcal{F}^{-1}[T \Pi_{\pi/T}(\omega)] = Sa(\pi t/T). \tag{4.169}$$

We have

$$y(t) = f(t) = f_s(t) * Sa\{(\pi/T)t\}. \tag{4.170}$$

We can write

$$f_s(t) = \sum_{n=-\infty}^{\infty} f(nT) \delta(t - nT) \tag{4.171}$$

$$f(t) = \left\{ \sum_{n=-\infty}^{\infty} f(nT) \delta(t - nT) \right\} * Sa(\pi t/T) = \sum_{n=-\infty}^{\infty} f(nT) Sa\left[\frac{\pi}{T}(t - nT)\right]. \tag{4.172}$$

In terms of the signal bandwidth ω_c , with $T = \frac{\pi}{\omega_c}$ (Nyquist interval), if the filter pass-band is $(-\omega_c, \omega_c)$ then

$$H(j\omega) = T \Pi_{\omega_c}(\omega) \tag{4.173}$$

$$h(t) = \mathcal{F}^{-1}[H(j\omega)] = \frac{\omega_c T}{\pi} Sa(\omega_c t) \tag{4.174}$$

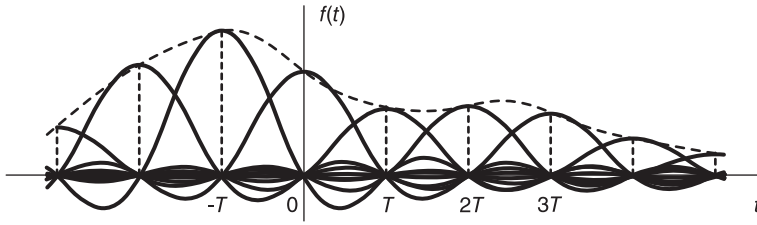


FIGURE 4.34 Reconstruction as convolution with sampling function.

$$f(t) = f_s(t) * h(t) = \frac{\omega_c T}{\pi} \sum_{n=-\infty}^{\infty} f(nT) Sa[\omega_c(t - nT)]. \tag{4.175}$$

If T equals the Nyquist interval, $T = \pi/\omega_c$ then

$$f(t) = \sum_{n=-\infty}^{\infty} f\left(\frac{n\pi}{\omega_c}\right) Sa(\omega_c t - n\pi). \tag{4.176}$$

The signal $f(t)$ can thus be reconstructed from the sampled signal if a convolution between the sampled signal and the sampling function $Sa\{(\pi/T)t\}$ is effected, as shown in Fig. 4.34. The convolution of the sampling function $Sa\{(\pi/T)t\}$ with each successive impulse of the sampled function $f_s(t)$ produces the same sampling function displaced to the location of the impulse. The sum of all the shifted versions of the sampling function produces the continuous time function $f(t)$. It should be noted that such a process is theoretically possible but not physically realizable. The ideal lowpass filter having a noncausal impulse response is not realizable. In practice, therefore, an approximation of the ideal filter is employed, leading to approximate reconstruction of the continuous-time signal.

4.39 Other Sampling Systems

As we have noted above the type of sampling studied so far is called “ideal sampling.” Such sampling was performed by multiplying the continuous signal by an ideal impulse train. In practice impulses and ideal impulse trains can only be approximated. In what follows we study mathematical models for sampling systems that do not necessitate the application of an ideal impulse train.

4.39.1 Natural Sampling

Natural sampling refers to a type of sampling where a continuous-time signal is multiplied by a train of square pulses which may be narrow to approximate ideal impulses. Referring to Fig. 4.35, we note that a continuous signal $f(t)$ is multiplied by the train $q_\tau(t)$ of period T , composed of square pulses of width τ . The function $f_n(t)$ produced by such natural sampling is given by

$$f_n(t) = f(t)q_\tau(t). \tag{4.177}$$

We note that the pulse train $q_\tau(t)$ may be expressed as the convolution of a rectangular pulse $\Pi_{\tau/2}(t)$ with the ideal impulse train $\rho_T(t)$

$$q_\tau(t) = \Pi_{\tau/2}(t) * \rho_T(t). \tag{4.178}$$

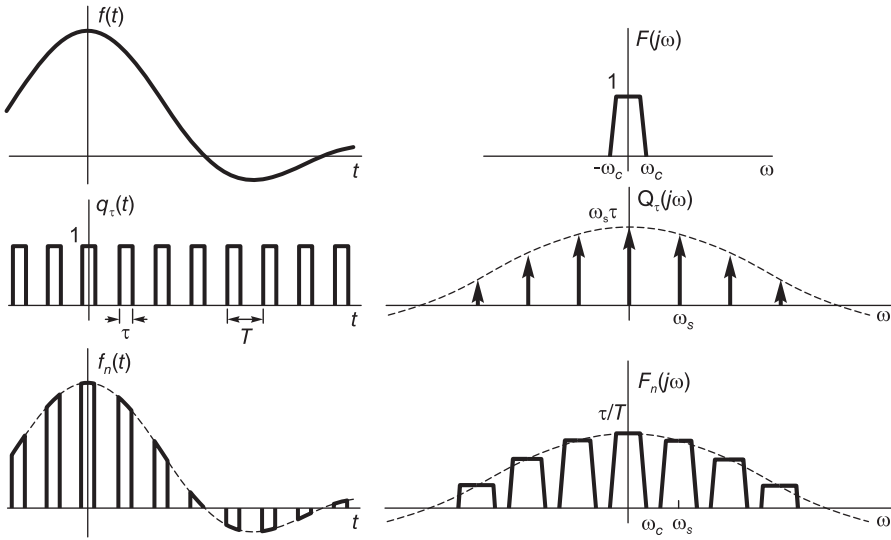


FIGURE 4.35 Natural sampling in time and frequency.

We can write

$$Q_{\tau}(j\omega) = \mathcal{F}[\rho_T(t)] \mathcal{F}[\Pi_{\tau/2}(t)] = \omega_s \rho_{\omega_s}(\omega) \tau Sa\left(\frac{\tau}{2}\omega\right) \tag{4.179}$$

where $\omega_s = 2\pi/T$, i.e.

$$Q_{\tau}(j\omega) = \omega_s \tau \sum_{n=-\infty}^{\infty} \delta(\omega - n\omega_s) Sa\left(\frac{\tau}{2}\omega\right) = \omega_s \tau \sum_{n=-\infty}^{\infty} Sa\left(\frac{n\omega_s \tau}{2}\right) \delta(\omega - n\omega_s). \tag{4.180}$$

The spectrum $Q_{\tau}(j\omega)$ shown in Fig. 4.35 has thus the form of an ideal impulse train modulated in intensity by the sampling function. The transform of $f_n(t)$ is given by

$$F_n(j\omega) = \frac{1}{2\pi} F(j\omega) * Q_{\tau}(j\omega) = \frac{\tau}{T} \sum_{n=-\infty}^{\infty} Sa(n\pi\tau/T) F[j(\omega - n\omega_s)]. \tag{4.181}$$

Referring to Fig. 4.35, which shows the form of $F_n(j\omega)$, we note that, similarly to what we have observed above, if the spectrum $F(j\omega)$ is band-limited to a frequency ω_c , i.e.

$$F(j\omega) = 0, \quad |\omega| \geq \omega_c \tag{4.182}$$

and if the Nyquist sampling frequency is respected, i.e.,

$$\omega_s = \frac{2\pi}{T} \geq 2\omega_c \tag{4.183}$$

then there is no aliasing of spectra. We would then be able to reconstruct $f(t)$ by feeding $f_n(t)$ into an ideal lowpass filter with a pass-band $(-B, B)$ where $\omega_c < B < \omega_s - \omega_c$ as seen above in relation to ideal sampling. Again, we can simply choose $B = \omega_s/2 = \pi/T$. The filter gain has to be $G = T/\tau$, as can be deduced from Fig. 4.35. The frequency response is given by

$$H(j\omega) = (T/\tau)\Pi_{\pi/T}(\omega) = (T/\tau)\{u(\omega + \pi/T) - u(\omega - \pi/T)\}. \tag{4.184}$$

The transform of the filter's output is given by

$$Y(j\omega) = F_n(j\omega) (T/\tau)\Pi_{\pi/T}(\omega) = F(j\omega). \tag{4.185}$$

Hence the filter time-domain output is $y(t) = f(t)$.

4.39.2 Instantaneous Sampling

In a natural sampling system, as we have just seen, the sampled function $f_n(t)$ is composed of pulses of width τ each and of height that follows the form of $f(t)$ during the duration τ of each successive pulse. We now study another type of sampling known as *instantaneous sampling*, where all the pulses of the sampled function are identical in shape, modulated only in height by the values of $f(t)$ at the sampling instants $t = nT$.

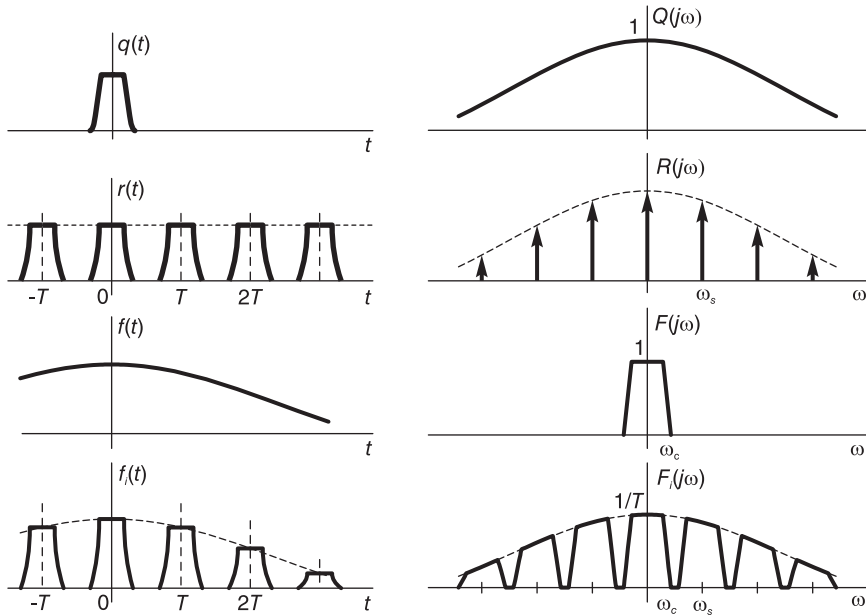


FIGURE 4.36 Instantaneous sampling in time and frequency.

Let $q(t)$ be an arbitrary finite duration function, i.e. a narrow pulse, as shown in Fig. 4.36, and let $r(t)$ be a train of pulses which is a periodic repetition of the pulse $q(t)$ with a period of repetition T , as seen in the figure.

The instantaneously sampled function $f_i(t)$ may be viewed as the result of applying the continuous-time function $f(t)$ to the input of a system such as that shown in Fig. 4.37. As the figure shows, the function $f(t)$ is first ideally sampled, through multiplication by an ideal impulse train $\rho_T(t)$. The result is the ideally sampled signal $f_s(t)$. This signal is then fed to the input of a linear system, of which the impulse response $h(t)$ is the function $q(t)$

$$h(t) = q(t). \tag{4.186}$$

The system output is the instantaneously sampled signal $f_i(t)$

$$f_i(t) = f_s(t) * q(t) = \sum_{n=-\infty}^{\infty} f(nT) \delta(t - nT) * q(t) = \sum_{n=-\infty}^{\infty} f(nT) q(t - nT). \tag{4.187}$$

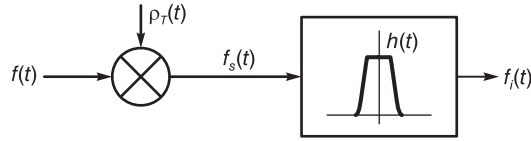


FIGURE 4.37 Instantaneous sampling model.

We have, with $\omega_s = 2\pi/T$, and using Equation (4.160)

$$\begin{aligned} F_i(j\omega) &= F_s(j\omega)Q(j\omega) = \frac{1}{T}Q(j\omega) \sum_{n=-\infty}^{\infty} F[j(\omega - n\omega_s)] \\ &= \frac{1}{T} \sum_{n=-\infty}^{\infty} Q(j\omega) F[j(\omega - n\omega_s)]. \end{aligned} \quad (4.188)$$

as seen in Fig. 4.36. If $F(j\omega)$ is band-limited to a frequency $\omega_c = 2\pi f_c$ r/s, i.e.

$$F(j\omega) = 0, \quad |\omega| \geq \omega_c \quad (4.189)$$

we can avoid spectral aliasing if

$$\omega_s = \frac{2\pi}{T} \geq 2\omega_c \quad (4.190)$$

i.e.

$$\frac{1}{T} \geq 2f_c. \quad (4.191)$$

The minimum sampling frequency is therefore $f_{s,min} = 2f_c$, that is, the same Nyquist rate $2f_c$ which applied to ideal sampling. Note, however, that the spectrum $F_i(j\omega)$ is no more a simple periodic repetition of $F(j\omega)$. It is the periodic repetition of $F(j\omega)$ but its amplitude is modulated by that of $Q(j\omega)$, as shown in Fig. 4.36. We deduce that the spectrum $F(j\omega)$, and hence $f(t)$, cannot be reconstructed by simple ideal lowpass filtering, even if the Nyquist rate is respected. In fact the filtering of $f_i(t)$ by an ideal lowpass filter produces at the filter output the spectrum

$$Y(j\omega) = F_i(j\omega) \Pi_{\pi/T}(\omega) = \frac{1}{T}Q(j\omega)F(j\omega). \quad (4.192)$$

To reconstruct $f(t)$ the filter should have instead the frequency response

$$H(j\omega) = \frac{T}{Q(j\omega)} \Pi_{\pi/T}(\omega) \quad (4.193)$$

for the output to equal

$$Y(j\omega) = F_i(j\omega)H(j\omega) = \frac{1}{T}Q(j\omega)F(j\omega) \frac{T}{Q(j\omega)} = F(j\omega). \quad (4.194)$$

Example 4.17 *Flat-top sampling.* Let $q(t) = \Pi_{\tau/2}(t)$. Evaluate $F_i(j\omega)$.

We have $Q(j\omega) = \tau Sa(\tau\omega/2)$

$$F_i(j\omega) = \frac{\tau}{T} \sum_{n=-\infty}^{\infty} Sa(\tau\omega/2) F[j(\omega - n\omega_s)].$$

Example 4.18 *Sample and hold.* Evaluate $F_i(j\omega)$ in the case of “sample and hold” type of sampling where, as in Fig. 4.38,

$$q(t) = R_\tau(t) = u(t) - u(t - \tau).$$

We have

$$Q(j\omega) = \tau Sa(\tau\omega/2) e^{-j\tau\omega/2}.$$

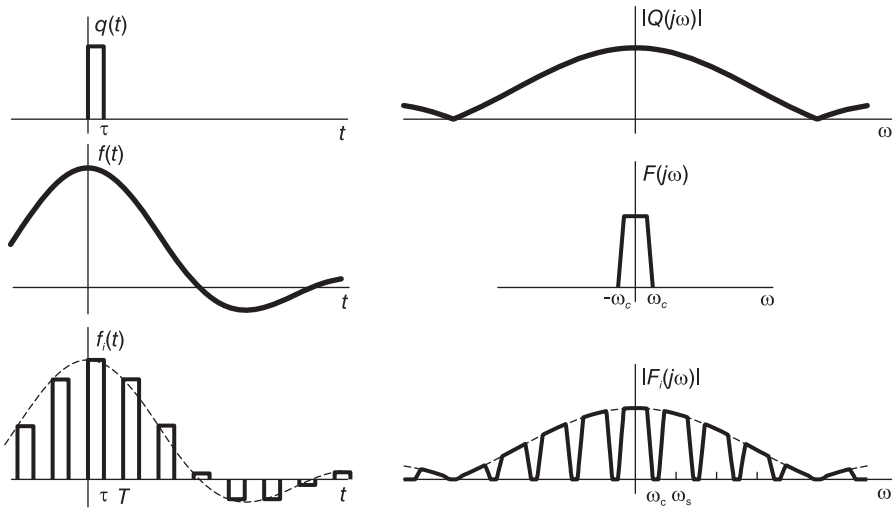


FIGURE 4.38 Sample and hold type of instantaneous sampling.

Such instantaneous sampling is represented in Fig. 4.38. We have

$$\begin{aligned} F_i(j\omega) &= \frac{\tau}{T} \sum_{n=-\infty}^{\infty} Sa(\tau\omega/2) e^{-j\tau\omega/2} F[j(\omega - n\omega_s)] \\ &= (\tau/T) e^{-j\tau\omega/2} \sum_{n=-\infty}^{\infty} F[j(\omega - n\omega_s)] Sa(\tau\omega/2). \end{aligned} \tag{4.195}$$

The reconstruction of $f(t)$ may be effected using an equalizing lowpass filter as shown in Fig. 4.39.

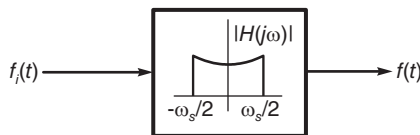


FIGURE 4.39 Reconstruction filter.

4.40 Ideal Sampling of a Bandpass Signal

Consider a signal that is a “bandpass” type, that is, a signal of which the spectrum occupies a frequency band that does not extend down to zero frequency, such as that shown in Fig. 4.40.

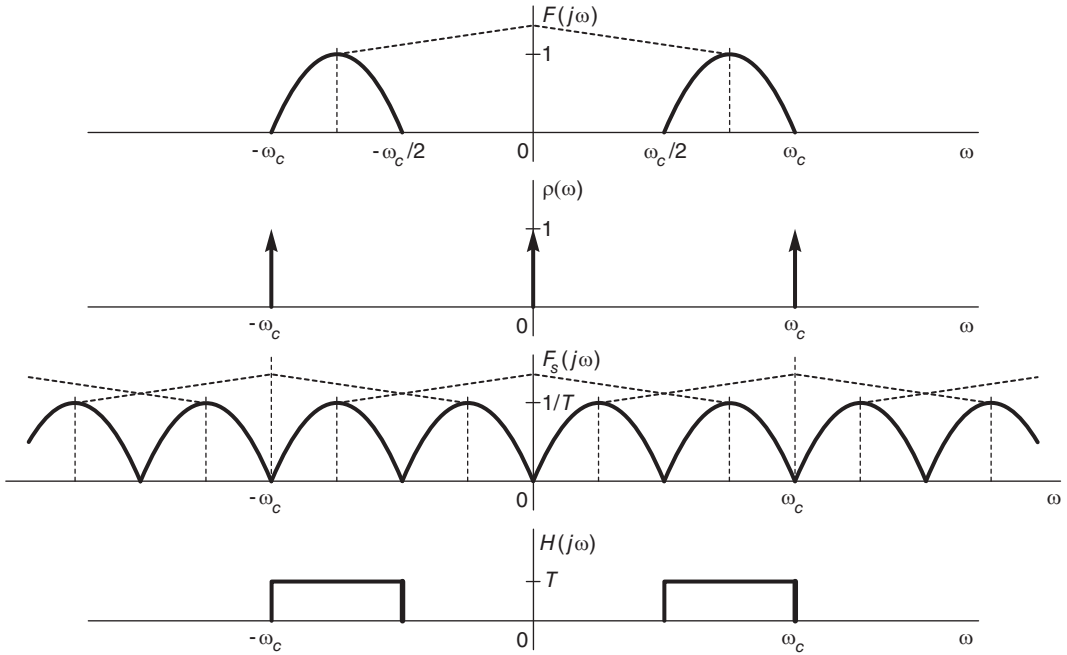


FIGURE 4.40 Ideal sampling of a bandpass signal.

It may be possible to sample such a signal without loss of information at a frequency that is lower than twice the maximum frequency ω_c of its spectrum. To illustrate the principle consider the example shown in the figure, where the spectrum $F(j\omega)$ of a signal $f(t)$ extends over the frequency band $\omega_c/2 < |\omega| < \omega_c$ and is zero elsewhere. As shown in the figure, the signal may be sampled at a sampling frequency ω_s equal to ω_c instead of $2\omega_c$, the Nyquist rate

$$\omega_s = 2\pi/T = \omega_c. \tag{4.196}$$

The sampling impulse train is

$$\rho_T(t) = \sum_{n=-\infty}^{\infty} \delta(t - nT), \quad T = 2\pi/\omega_c \tag{4.197}$$

and the ideally sampled signal is given by

$$f_s(t) = f(t) \sum_{n=-\infty}^{\infty} \delta(t - nT) \tag{4.198}$$

having a transform

$$F_s(j\omega) = \frac{1}{2\pi} F(j\omega) * \omega_s \sum_{n=-\infty}^{\infty} \delta(\omega - n\omega_s) = \frac{1}{T} \sum_{n=-\infty}^{\infty} F[j(\omega - n\omega_s)]. \quad (4.199)$$

As the figure shows no aliasing occurs and therefore the signal $f(t)$ can be reconstructed from $f_s(t)$ through bandpass filtering. The filter frequency response $H(j\omega)$ is shown in the figure.

We note therefore that for bandpass signals it may be possible to sample a signal at frequencies less than the Nyquist rate without loss of information.

4.41 Sampling an Arbitrary Signal

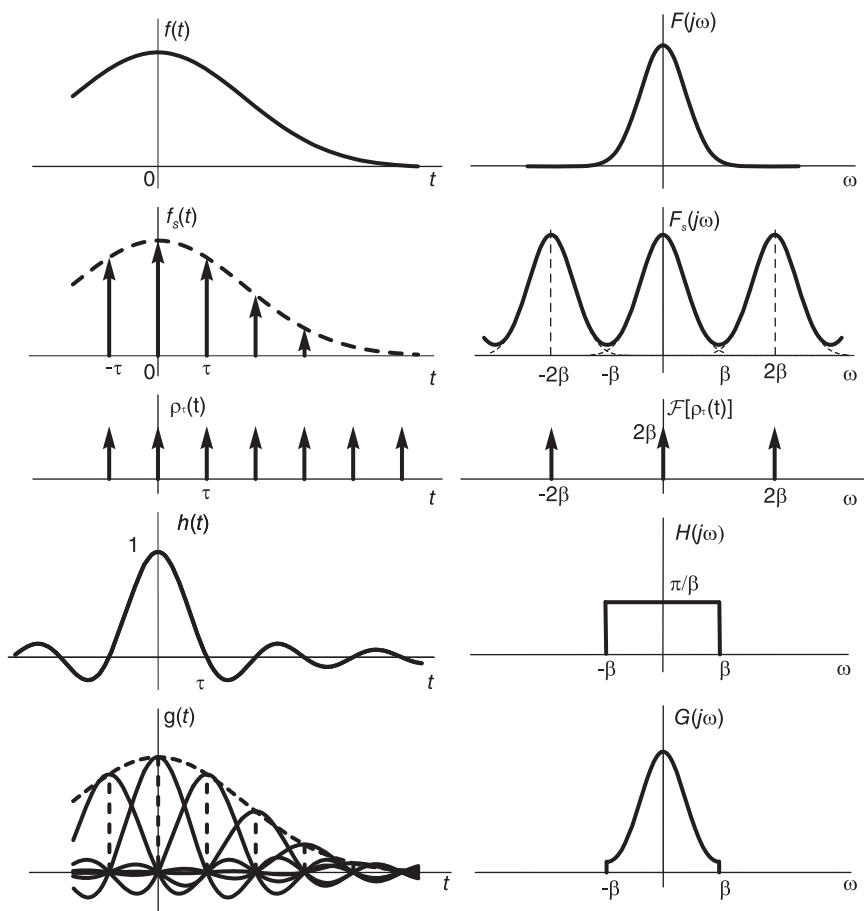


FIGURE 4.41 Sampling an arbitrary signal.

It is interesting to study the effect of sampling a general signal $f(t)$ that is not necessarily of limited bandwidth, or a signal of which the bandwidth exceeds half the sampling frequency, thus leading to aliasing. Such a signal and its spectrum are shown in Fig. 4.41, where we notice that the signal spectrum extends beyond a given frequency β that is half the sampling frequency $\omega_s = 2\beta$. The sampling period is $\tau = \pi/\beta$. The sampled signal is given by

$$f_s(t) = f(t) \rho_\tau(t) = f(t) \sum_{n=-\infty}^{\infty} \delta(t - n\tau) = \sum_{n=-\infty}^{\infty} f(n\tau) \delta(t - n\tau) \quad (4.200)$$

$$\begin{aligned} F_s(j\omega) &= \frac{1}{2\pi} F(j\omega) * \frac{2\pi}{\tau} \sum_{n=-\infty}^{\infty} \delta\left(\omega - n\frac{2\pi}{\tau}\right) = \frac{1}{\tau} \sum_{n=-\infty}^{\infty} F\left[j\left(\omega - n\frac{2\pi}{\tau}\right)\right] \\ &= \frac{\beta}{\pi} \sum_{n=-\infty}^{\infty} F[j(\omega - n2\beta)]. \end{aligned} \quad (4.201)$$

As the figure shows this is an *aliased* spectrum. The original signal $f(t)$ cannot be reconstructed from $f_s(t)$ since the spectrum $F(j\omega)$ cannot be recovered, by filtering say, from $F_s(j\omega)$. Assume now that we do apply on $F_s(j\omega)$ a lowpass filter, as shown in the figure, of a cut-off frequency β . The output of the filter is a signal $g(t)$ such that

$$G(j\omega) = F_s(j\omega)H(j\omega) \quad (4.202)$$

where $H(j\omega)$ is the frequency response of the lowpass filter, which we take as

$$H(j\omega) = \frac{\pi}{\beta} \Pi_\beta(\omega) = \frac{\pi}{\beta} [u(\omega + \beta) - u(\omega - \beta)]. \quad (4.203)$$

The impulse response of the lowpass filter is $h(t) = \mathcal{F}^{-1}[H(j\omega)] = Sa(\beta t)$. The spectrum $G(j\omega)$ of the filter output is, as shown in the figure, the aliased version of $F(j\omega)$ as it appears in the frequency interval $(-\beta, \beta)$. The filter output $g(t)$ can be written

$$\begin{aligned} g(t) &= f_s(t) * h(t) = \sum_{n=-\infty}^{\infty} f(n\tau) \delta(t - n\tau) * Sa(\beta t) \\ &= \sum_{n=-\infty}^{\infty} f\left(n\frac{\pi}{\beta}\right) Sa(\beta t - n\pi). \end{aligned} \quad (4.204)$$

We note that $g(t) \neq f(t)$ due to aliasing. However,

$$g(k\tau) = \sum_{n=-\infty}^{\infty} f\left(n\frac{\pi}{\beta}\right) Sa(\beta k\tau - n\pi) = \sum_{n=-\infty}^{\infty} f(n\tau) Sa[(k - n)\pi] = f(k\tau) \quad (4.205)$$

since $Sa[(k - n)\pi] = 1$ if and only if $n = k$ and is zero otherwise. This type of sampling therefore produces a signal $g(t)$ that is identical to $f(t)$ at the sampling instants. Between the sampling points the resulting signal $g(t)$ is an interpolation of those values of $f(t)$ which depends on the chosen sampling frequency (2β). If, and only if, the spectrum $F(j\omega)$ is band-limited to a frequency $\omega_c < \beta$, the reconstructed signal $g(t)$ is equal for all t to $f(t)$.

4.42 Sampling the Fourier Transform

In a manner similar to sampling in the time domain we can consider the problem of sampling the transform domain. Time and frequency simply reverse roles. In fact, the Fourier transform of a periodic signal, as we have seen earlier, is but a sampling of that of the base period. As shown in Fig. 4.42, given a function $f(t)$ that is limited in duration to the interval $|t| < T$ its Fourier Transform $F(j\omega)$ may be ideally sampled by multiplying it by an impulse train in the frequency domain. If the sampling interval is β r/s then the signal $f(t)$ can be recovered from $f_s(t)$ by a simple extraction of its base period, if and only if the sampling interval β satisfies the condition

$$\tau = \frac{2\pi}{\beta} > 2T, \text{ i.e. } \beta < \frac{\pi}{T}. \tag{4.206}$$

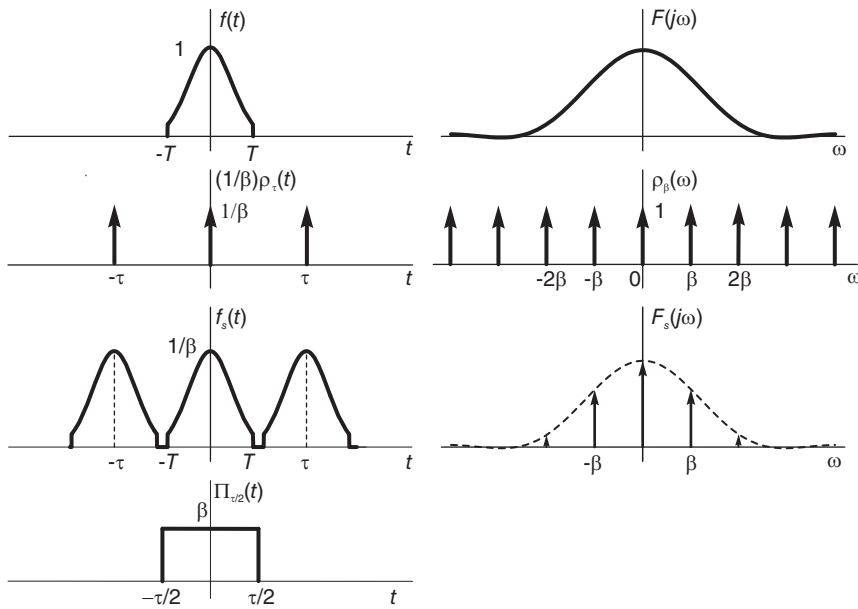


FIGURE 4.42 Sampling the transform domain.

This is the Nyquist rate that should be applied to sampling the transform. To show that this is the case we refer to the figure and note that the impulse train in the frequency domain is the transform of an impulse train in the time domain. We may write

$$\sum_{n=-\infty}^{\infty} \delta(t - n\tau) \longleftrightarrow \frac{2\pi}{\tau} \sum_{n=-\infty}^{\infty} \delta\left(\omega - n\frac{2\pi}{\tau}\right) = \beta \sum_{n=-\infty}^{\infty} \delta(\omega - n\beta) \tag{4.207}$$

$$F_s(j\omega) = F(j\omega) \sum_{n=-\infty}^{\infty} \delta(\omega - n\beta) = \sum_{n=-\infty}^{\infty} F(jn\beta) \delta(\omega - n\beta). \tag{4.208}$$

The effect of multiplication by an impulse train in the frequency domain is a convolution by an impulse train in the time domain. We have

$$f_s(t) = f(t) * \frac{1}{\beta} \sum_{n=-\infty}^{\infty} \delta(t - n\tau) = \frac{1}{\beta} \sum_{n=-\infty}^{\infty} f\left(t - n\frac{2\pi}{\beta}\right). \quad (4.209)$$

When the Nyquist rate is satisfied we have

$$f(t) = f_s(t) \beta \Pi_{\tau/2}(t) \quad (4.210)$$

$$\begin{aligned} F(j\omega) &= \beta \frac{1}{2\pi} F_s(j\omega) * \mathcal{F}[\Pi_{\tau/2}(t)] = \frac{1}{\tau} \sum_{n=-\infty}^{\infty} F(jn\beta) \delta(\omega - n\beta) * \tau Sa\left(\frac{\tau}{2}\omega\right) \\ &= \sum_{n=-\infty}^{\infty} F(jn\beta) Sa\left(\frac{\pi}{\beta}\omega - n\pi\right). \end{aligned} \quad (4.211)$$

Similarly to sampling in the time domain, the continuous spectrum is reconstructed from the sampled one through a convolution with a sampling function. Note that given a function $f(t)$ of finite duration, sampling its transform leads to its periodic repetition. This is the dual of the phenomenon encountered in sampling the time domain.

Note, moreover, that in the limit case $\beta = \pi/T$ i.e. $\tau = 2T$ the Fourier series expansion of the periodic function $f_s(t)$ with an analysis interval equal to its period τ may be written

$$f_s(t) = \sum_{n=-\infty}^{\infty} F_{s,n} e^{jn(2\pi/\tau)t} \quad (4.212)$$

$$F_{s,n} = \frac{1}{\tau} \int_{-\tau/2}^{\tau/2} \frac{1}{\beta} f(t) e^{-jn(2\pi/\tau)t} dt = \frac{1}{\beta\tau} F(jn2\pi/\tau) = \frac{1}{2\pi} F(jn2\pi/\tau) \quad (4.213)$$

$$F_s(j\omega) = 2\pi \sum_{n=-\infty}^{\infty} F_{s,n} \delta(\omega - n2\pi/\tau) = \sum_{n=-\infty}^{\infty} F(jn\beta) \delta(\omega - n\beta) \quad (4.214)$$

as expected, being the transform of the periodic function $f_s(t)$ of period τ and fundamental frequency β . The periodic repetition of a finite duration function leads to the Fourier series discrete spectrum and to sampling of its Fourier transform.

4.43 Problems

Problem 4.1 Consider a function $x(t)$ periodic with period $T = 2\tau$ and defined by

$$x(t) = \begin{cases} A, & |t| < \tau/2 \\ -A, & \tau/2 < |t| \leq \tau. \end{cases}$$

- Evaluate the Fourier transform $X(j\omega)$ of $x(t)$
- Sketch the function

$$y(t) = \sin(4\pi t/\tau) x(t)$$

and evaluate its Fourier transform

- Evaluate the Fourier transform of the causal function $v(t) = y(t) u(t)$

Problem 4.2 Evaluate Laplace and Fourier transform of the signals

- a) $f_1(t) = (t - 1)u(t - 1)$
- b) $f_2(t) = tu(t) - (t - t_0)u(t - t_0), \quad t_0 > 0$

Problem 4.3 Evaluate the Fourier transform of the following functions:

- a) The even function defined by

$$x(t) = \begin{cases} 2 - t, & 0 \leq t \leq 1 \\ 1, & 1 \leq t < 2 \\ 0, & t > 2 \end{cases}$$

and $x(-t) = x(t)$.

- b) The two-sided periodic function $y(t)$ defined by $y(t) = \sum_{n=-\infty}^{\infty} x(t - 5n)$.
- c) The causal function $z(t) = y(t)u(t)$.

Problem 4.4 a) Evaluate the Fourier transform of the triangle $\Lambda_\tau(t)$.

- b) Deduce the Fourier transform and the Fourier series expansion of the function

$$y(t) = \sum_{n=-\infty}^{\infty} x(t - nT)$$

where $T > 2\tau$ and $x(t) = \tau\Lambda_\tau(t)$.

Problem 4.5 Evaluate the Fourier series and Fourier transform of the periodic signal $y(t)$ of period $T = 2$ defined by:

$$y(t) = e^{-t}, \quad 0 < t < 1$$

and the three cases

- a) $y(-t) = y(t), \quad -1 < t < 1$
- b) $y(-t) = -y(t), \quad -1 < t < 1$
- c) $y(t + 1) = -y(t), \quad 0 < t < 2$

Problem 4.6 Let $f(t)$ be a periodic signal of period $T = 2$ sec., and

$$f(t) = \begin{cases} t^2, & 0 \leq t < 1 \\ 0, & 1 < t \leq 2. \end{cases}$$

a) Evaluate the Fourier series coefficients and the Fourier transform over the interval $(-1, 1)$ of $f(t)$.

- b) The causal function $g(t) = \sum_{n=0}^{\infty} f_0(t - nT)$ where $f_0(t) = f(t)R_T(t)$.

Problem 4.7 Consider the signal

$$v(t) = (1 + \cos m\omega_0 t) \Pi_{T/2}(t)$$

where m is an integer and $\omega_0 = 2\pi/T$.

- a) Evaluate the Fourier transform $V(j\omega)$ of $v(t)$.
- b) Plot $v(t)$ and $|V(j\omega)|$ for the cases $m = 1, m = 2$ and $m = 10$ showing the fusion on the two spectral peaks for positive and negative frequencies $\pm m\omega_0$ in the case $m = 1$.

c) Evaluate the Fourier transform of the signal

$$x(t) = \sum_{n=-\infty}^{\infty} v(t - nT).$$

d) Evaluate the transform of the causal signal

$$w(t) = x(t)u(t).$$

Problem 4.8 Given the signals

$$v(t) = 2\Lambda_2(t) \triangleq \begin{cases} 2 - |t|, & |t| \leq 2 \\ 0, & |t| \geq 2 \end{cases}$$

and

$$x(t) = \sum_{n=-\infty}^{\infty} \{\delta(t - 2n) + 2\delta[t - (2n + 1)]\}.$$

a) Evaluate and sketch the convolution

$$z(t) = v(t) * x(t)$$

and its Fourier transform $Z(j\omega)$ and Fourier series coefficients Z_n . Verify the result using $V(j\omega)$ and $X(j\omega)$.

b) Evaluate and sketch the Fourier transform of

$$y(t) = v(t) \cos^2(2\pi t).$$

Problem 4.9 a) Evaluate the Fourier transform of the function

$$f(t) = a_0 + 2 \sum_{i=1}^M A_i \cos(\omega_i t + \theta_i).$$

b) Let $g(t) = f(t)u(t)$. Evaluating the Laplace transform $G(s)$ and the Fourier transform $G(j\omega)$ of $g(t)$ show that the latter is the same as the first except for added impulses.

Problem 4.10 Let

$$f(t) = A_1 \sin(\omega_1 t + \theta_1)$$

$$g(t) = A_2 \cos(\omega_2 t + \theta_2)$$

where $\omega_2 > \omega_1$.

Evaluate the Fourier series and Fourier transform of the functions

a) $x(t) = f(t) + g(t)$

b) $y(t) = f(t)g(t)$

Problem 4.11 A periodic signal $f(t)$ of period $T = 0.01$ sec. has the Fourier series coefficients F_n given by

$$F_n = \begin{cases} 5/(2\pi), & n = \pm 1 \\ 3/(2\pi), & n = \pm 3 \\ 0, & \text{otherwise.} \end{cases}$$

The signal $f(t)$ has been recorded using a magnetic-tape recorder at a speed of 15 in./sec.

a) Let $v(t)$ be the signal obtained by reading the magnetic tape at a speed of 30 in./sec. Evaluate the Fourier transform $V(j\omega)$ of $v(t)$.

b) Let $w(t)$ be the signal obtained by reading backward the magnetic tape at a speed of 15 in./sec. Evaluate $W(j\omega) = \mathcal{F}[w(t)]$.

Problem 4.12 The Fourier transform $X(j\omega)$ of a signal $x(t)$ is given by

$$X(j\omega) = 2\delta(\omega) + 2\delta(\omega - 200\pi) + 2\delta(\omega + 200\pi) + 3\delta(\omega - 500\pi) + 3\delta(\omega + 500\pi).$$

- Is the signal $x(t)$ periodic? If yes, what is its period? If no, explain why.
- The signal $x(t)$ is multiplied by $w(t) = \sin 200\pi t$. Evaluate the Fourier transform $V(j\omega)$ of the result $v(t) = w(t)x(t)$.
- The signal $z(t)$ is the convolution of $x(t)$ with $y(t) = e^{-t}u(t)$. Evaluate the Fourier transform $Z(j\omega)$ of $z(t)$.

Problem 4.13 Given the finite duration signal $v(t) = e^{-t}R_T(t)$.

- Evaluate its Laplace transform $V(s)$, stating its ROC.
- Evaluate its Fourier transform $V(j\omega)$.
- Let

$$f(t) = \sum_{n=-\infty}^{\infty} v(t - nT).$$

Sketch $f(t)$. Evaluate its exponential Fourier series coefficients F_n with an analysis interval equal to T .

- Deduce the Fourier series coefficients V_n of $v(t)$ with the same analysis interval.
- Evaluate the Fourier transform $F(j\omega)$ of $f(t)$.

Problem 4.14 Let $z(t) = \sum_{n=0}^{\infty} \delta(t - nT)$.

- Evaluate the Fourier transform $Z(j\omega)$ and the Laplace transform $Z(s)$.
- The signal $z(t)$ is applied to the input of a system of impulse response

$$h(t) = e^{-t}R_T(t) = e^{-t}[u(t) - u(t - T)]$$

Evaluate the system output $y(t)$, its Laplace transform $Y(s)$, its Fourier transform $Y(j\omega)$ and the exponential Fourier series coefficients Y_n evaluated over the interval $(0, T)$.

- Deduce the Fourier transform $Y_p(j\omega)$ of the system response $y_p(t)$ to the input $x(t) = \rho_T(t)$.

Problem 4.15 Given the system transfer function

$$H(s) = \frac{2s - 96}{s^2 + 2s + 48}.$$

- Assuming that the point $s = 4\sqrt{2} e^{j3\pi/4}$ is in the ROC of $H(s)$, evaluate the system impulse response $h(t)$.
- Assuming that the point $s = 12.2e^{j\pi/6}$ is in the ROC of $H(s)$, evaluate $h(t)$.
- Assuming that the point $s = (8.2)\sqrt{2} e^{-j3\pi/4}$ is in the ROC of $H(s)$, evaluate $h(t)$.
- Assuming that the system is stable and receives the input $x(t) = \sin(2.5t + \pi/4)$, evaluate its output $y(t)$.
- The system output $y(t)$ in part d) is truncated by a rectangular window of width T . The result is the signal $z_0(t) = y(t)R_T(t)$. Evaluate the Fourier transform $Z_0(j\omega)$ of $z_0(t)$, the Fourier transform of the signal

$$z(t) = \sum_{n=-\infty}^{\infty} z_0(t - nT)$$

and the Fourier series coefficients Z_n over analysis interval $(0, T)$ for the two cases i) $T = 3.2\pi$ sec., ii) $T = 6\pi$ sec.

Problem 4.16 A signal $v(t)$ has the Fourier transform

$$V(j\omega) = 100Sa^2(50\omega).$$

The signal $x(t)$ has the transform

$$X(j\omega) = 100 \{Sa^2(50\omega - 10\pi) + Sa^2(50\omega + 10\pi)\}.$$

- Evaluate and plot the signal $v(t)$.
- Suggest a simple system which upon receiving the signal $v(t)$ would produce the signal $x(t)$. Plot the signal $x(t)$ and its spectrum $X(j\omega)$.
- The signal $y(t)$ is given by

$$y(t) = \sum_{n=-\infty}^{\infty} x(t - 200n).$$

Sketch $y(t)$. Evaluate the spectrum $Y(j\omega) = \mathcal{F}[y(t)]$ and plot it for $0.16\pi < \omega < 0.24\pi$.

Problem 4.17 Consider the signal:

$$v_T(t) = v(t)R_T(t)$$

where

$$v(t) = 10 + 10 \cos \beta_1(t - 4) + 5 \sin \beta_2(t - 1/8) + 10 \cos \beta_3(t - 3/8)$$

and $\beta_1 = \pi$, $\beta_2 = 2\pi$, $\beta_3 = 4\pi$, $T = 4$ sec.

- Evaluate the exponential Fourier series coefficients V_n of $v_T(t)$ over the interval $(0, T)$.
- Let

$$x(t) = \sum_{n=-\infty}^{\infty} v_T(t - nT).$$

Is $v(t)$ periodic? What is its period and relation to $x(t)$?

- Evaluate the Fourier transform of $x(t)$.

Problem 4.18 Given a signal $x(t)$, of which the Fourier transform is given by

$$X(j\omega) = [\delta(\omega + 440\pi) + \delta(\omega - 440\pi)] + 0.5 [\delta(\omega + 880\pi) + \delta(\omega - 880\pi)]$$

and the signal $y(t)$ given by $y(t) = x(t)[1 + \cos(\pi t)]$.

- Sketch the spectrum $Y(j\omega)$, the Fourier transform of $y(t)$.
- Is the signal $y(t)$ periodic? If yes evaluate its expansion as an exponential Fourier series with an analysis interval equal to its period.

Problem 4.19 Given a periodic signal $x(t)$ described by its exponential Fourier series

$$x(t) = \sum_{n=-\infty}^{\infty} X_n e^{j200\pi n t} \quad \text{where} \quad X_n = \begin{cases} 2, & n = 0 \\ 3 \pm j, & n = \pm 2 \\ 2.5, & n = \pm 4 \\ 0, & \text{otherwise} \end{cases} \quad \text{and} \quad y(t) = x(t) \cos(400\pi t).$$

- Sketch $Y(j\omega)$, the Fourier transform of $y(t)$.
- What is the average value of the signal $y(t)$?
- What is the amplitude of the sinusoidal component of $y(t)$ that is of frequency 400 Hz?

Problem 4.20 Given a signal $v(t)$ and its Fourier transform $V(j\omega)$, can we deduce that $V(0)$ is the average of the signal? Justify your answer.

Problem 4.21 Evaluate the Fourier transform of each of the following signals

a) The even function

$$v_a(t) = \begin{cases} 2-t, & 0 < t < 3 \\ t-4, & 3 < t < 4 \\ 0, & t > 4 \end{cases}$$

b) $v_b(t) = \sum_{n=-\infty}^{\infty} \delta(t - 2n - 1)$

c) $v_c(t) = \sum_{n=-\infty}^{\infty} \delta(t - 2nT) - \sum_{n=-\infty}^{\infty} \delta(t - 2nT - T)$.

Problem 4.22 Given a periodic signal $x(t)$ that when expanded in an exponential Fourier series with an analysis interval equal to its period T produces the coefficients

$$X_n = 0.25 \text{Sa}(\pi n/4),$$

and a signal $z(t) = x(t)y(t)$ where $y(t)$ has a Fourier transform given by

$$Y(j\omega) = \frac{1}{j\omega + 4}.$$

- Evaluate the Fourier transform $X(j\omega)$ of $x(t)$.
- Evaluate the Fourier transform $Z(j\omega)$ of $z(t)$.
- Is the signal $z(t)$ periodic? Justify your answer.

Problem 4.23 Let $x(t)$ be a periodic signal of period 5×10^{-2} seconds having exponential Fourier series coefficients X_n , with an analysis interval equal to the signal period, given by

$$X_n = \begin{cases} 1, & n = 0 \\ \pm j, & n = \pm 1 \\ 1/4, & n = \pm 4 \\ 0, & \text{otherwise.} \end{cases}$$

The signal $y(t)$, be a periodic signal of period 2.5×10^{-2} seconds, having Fourier series coefficients Y_n , with an analysis interval equal to its period, given by

$$Y_n = \begin{cases} 2, & n = \pm 1 \\ 0, & \text{otherwise} \end{cases}$$

and the signal $v(t)$ given by $v(t) = x(t)y(t)$.

- Evaluate the Fourier transform $V(j\omega)$ of $v(t)$.
- Evaluate the exponential Fourier series coefficients V_n , of the signal $v(t)$ with an analysis interval that would be considered pertinent.

Problem 4.24 The Fourier transform $X(j\omega)$ of a signal $x(t)$ is given by

$$X(j\omega) = 3[\delta(\omega + 500\pi) + \delta(\omega - 500\pi)] + 2[\delta(\omega + 200\pi) + \delta(\omega) + \delta(\omega - 200\pi)].$$

- Is the signal $x(t)$ periodic? If yes, what is its period in seconds?
- The signal $v(t)$ is obtained by multiplying $x(t)$ by the carrier $\sin(200\pi t)$. Evaluate the fourier transform $V(j\omega)$ of $v(t)$.
- The signal $z(t)$ is obtained as the convolution of $x(t)$ with $e^{tu}(t)$. Evaluate the Fourier transform $Z(j\omega)$ of $z(t)$.

Problem 4.25 A given signal $x(t)$ has a Fourier transform $X(j\omega) = [10 + |\omega|/4\pi] \Pi_{20\pi}(\omega)$.

a) Let $y(t) = x(2t)$. Sketch the Fourier transform of $y(t)$.

b) Let $z(t) = x(T-t)$, where T is a real constant. Sketch the amplitude spectrum $|Z(j\omega)|$ of the signal $z(t)$.

Problem 4.26 A signal $f(t)$ band limited to a frequency B is sampled by the pulse train $g(t)$ shown in Fig.4.43). The Fourier transform $F(j\omega)$ of the signal is assumed to have the form shown in the figure.

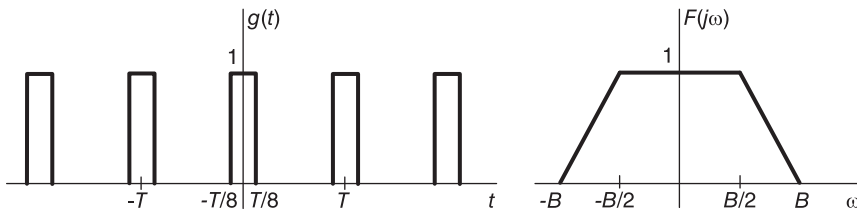


FIGURE 4.43 Pulse train $g(t)$ and the spectrum of the signal $f(t)$.

a) Evaluate the spectrum $G(j\omega)$ of the function $g(t)$.

b) Evaluate and sketch the spectrum of the sampled function $f_s(t) = f(t)g(t)$, with i) $T = \pi/(2B)$ and ii) $T = 2\pi/B$.

c) Specify the filter needed to reconstruct $f(t)$ from $f_s(t)$ if such reconstruction is possible.

Problem 4.27 A system has the impulse response

$$h(t) = u(t) - 2u(t-1) + u(t-2).$$

Sketch the response of the system to the inputs

i) $x_1(t) = \delta(t) + \delta(t+1)$ and

ii) $x_2(t) = \delta(t) + \delta(t-1)$

iii) $x_3(t) = \sum_{n=-\infty}^{\infty} \delta(t-2n)$

Problem 4.28 A band-limited signal $v(t)$ has a Fourier spectrum $V(j\omega)$ which may be approximated as $V(j\omega) = \begin{cases} 2 - |\omega|/(2\pi), & |\omega| < 2\pi \\ 0, & |\omega| > 2\pi. \end{cases}$

The signal $v(t)$ is sampled by the pulse train $x(t)$ defined by $x(t) = \sum_{n=-\infty}^{\infty} x_0(t-nT)$,

where $x_0(t)$ is the triangle

$$x_0(t) = \begin{cases} 8t/T, & 0 < t < T/8 \\ 2 - 8t/T, & T/8 < t < T/4 \\ 0, & t < 0, t > T/4. \end{cases}$$

a) Evaluate and sketch the Fourier spectrum $V_s(j\omega)$ of the sampled signal $v_s(t) = v(t)x(t)$.

b) State whether this is ideal, natural or instantaneous sampling. Can the original signal $v(t)$ be reconstructed without distortion from $v_s(t)$ using ideal filtering with: i) $T = 2/3$ sec and ii) $T = 0.25$ sec? If yes, specify the filter's required frequency response.

Problem 4.29 In an instantaneous sampling system a continuous-time signal $v(t)$ is multiplied by the impulse train $\rho_T(t) = \sum_{n=-\infty}^{\infty} \delta(t - nT)$ and the resulting signal $w(t) = v(t)\rho_T(t)$ is the input of a system of which the impulse response $h(t)$ is given by $h(t) = R_{T/2}(t - \tau)$, where $0 \leq \tau < T/2$ and $R_{T/2}(t)$ is the rectangle

$$R_{T/2}(t) = u(t) - u(t - T/2).$$

a) Evaluate $Y(j\omega)$, the Fourier transform of the system output $y(t)$, as a function of $V(j\omega)$, the transform of $v(t)$.

b) Evaluate the filter frequency response $H_0(j\omega)$ which would reconstruct the original signal $v(t)$ from the sampling system output $y(t)$ assuming that $v(t)$ is band-limited to a frequency ω_m . What is the maximum permissible value of T to allow such reconstruction?

c) To reconstruct an approximation of the original signal $v(t)$ the system output $y(t)$ is fed to an ideal lowpass filter of frequency response $H_2(j\omega)$ defined by

$$H_2(j\omega) = \begin{cases} e^{j\pi/4}, & -\pi/T < \omega < 0 \\ e^{-j\pi/4}, & 0 < \omega < \pi/T \\ 0, & |\omega| > \pi/T. \end{cases}$$

Let $T = 10^{-3}$ sec., $\tau = 0$ and $v(t) = \sin 200\pi t$. Evaluate the filter output $z(t)$.

Problem 4.30 An ideal lowpass filter of frequency response $G(j\omega) = \Pi_{\omega_m}(\omega)$, receives an input signal $v(t)$ given by

$$v(t) = e^{-2t}u(t) + e^{2t}u(-t).$$

The filter output $x(t)$ is sampled by an alternating-sign impulse train $r(t)$

$$r(t) = \sum_{n=-\infty}^{\infty} (-1)^n \delta(t - nT).$$

The sampled signal $w(t) = x(t)r(t)$ is then filtered by a bandpass filter of frequency response

$$H(j\omega) = \begin{cases} 1, & \pi/T < |\omega| < 3\pi/T \\ 0, & \text{elsewhere} \end{cases}$$

producing the output $y(t)$. Assuming that the sampling interval T is given by

$$T = \pi / (2\omega_m).$$

a) Evaluate and sketch the Fourier transforms $V(j\omega)$, $X(j\omega)$, $R(j\omega)$ and $W(j\omega)$ of $v(t)$, $x(t)$, $r(t)$ and $w(t)$, respectively.

b) How can the signal $v(t)$ be reconstructed from $w(t)$ and from $y(t)$?

c) What is the maximum value of T for such reconstruction to be possible?

Problem 4.31 A signal $v(t)$ is sampled by an impulse train $r(t)$ resulting in the sampled signal $y(t) = v(t)r(t)$.

Evaluate and sketch to $\omega = 7$ r/s the spectrum $Y(j\omega)$ of $y(t)$ given that

i) $v(t) = \cos t$ and

a) $r(t) = \sum_{n=-\infty}^{\infty} e^{j2nt}$.

$$b) \quad r(t) = \sum_{n=-\infty}^{\infty} \Pi_{\pi/6}(t - \pi n).$$

$$c) \quad r(t) = \sum_{n=-\infty}^{\infty} \Pi_{\pi/6}(t - 4\pi n/3).$$

Repeat the above given that

ii) $v(t) = Sa^2(t/2)$ instead.

Problem 4.32 In an instantaneous sampling system two input signals $x_1(t)$ and $x_2(t)$ are sampled by the two impulse trains

$$p_1(t) = \sum_{n=-\infty}^{\infty} \delta(t - nT)$$

and

$$p_2(t) = p_1(t - T/2)$$

respectively. The sum of the two sampled signals $v_1(t) = x_1(t)p_1(t)$ and $v_2(t) = x_2(t)p_2(t)$ is fed as the input of a system of impulse response $h(t)$

$$h(t) = u(t) - u(t - T/8)$$

and output $v(t)$.

a) Sketch the system output $v(t)$ if $x_1(t) = 1$, $x_2(t) = 4$ and $T = 8$.

b) Can the two sampled signals be separated from the system output $v(t)$? How?

Problem 4.33 A periodic signal $v(t)$ has the exponential Fourier series coefficients,

$$V_n = \begin{cases} 1, & n = \pm 1 \\ \pm j4, & n = \pm 5 \\ 0, & \text{otherwise} \end{cases}$$

with an analysis interval T . The signal $v(t)$ is sampled naturally by the impulse train

$$p(t) = \sum_{n=-\infty}^{\infty} p_0(t - nT/8)$$

where

$$p_0(t) = \Pi_{T/32}(t).$$

The sampled signal $v_s(t) = v(t)p(t)$ is applied to the input of a filter of frequency response

$$H(j\omega) = \begin{cases} A, & |\omega| \leq 8\pi/T \\ \frac{-AT}{2\pi}(t - 10\pi/T), & \frac{8\pi}{T} \leq |\omega| \leq \frac{10\pi}{T} \\ 0, & \text{otherwise} \end{cases}$$

producing an output $y(t)$. Evaluate $V(j\omega)$, $P(j\omega)$, $V_s(j\omega)$, $Y(j\omega)$ and $y(t)$, stating whether or not aliasing results.

Problem 4.34 A signal $x(t)$ is band-limited to the frequency range $-B < \omega < B$ r/s. The signal $x_s(t)$ is obtained by sampling the signal $x(t)$

$$x_s(t) = x(t)p(t)$$

where

$$p(t) = \sum_{n=-\infty}^{\infty} p_0(t - nT)$$

$$p_0(t) = \Pi_{T/20}(t) = u(t + T/20) - u(t - T/20)$$

and $T = \pi/B$.

- a) Evaluate $X_s(j\omega) = \mathcal{F}[x_s(t)]$ as a function of $X(j\omega)$.
- b) To reconstruct $x(t)$ from $x_s(t)$ a filter of frequency response $H(j\omega)$ is used. Determine $H(j\omega)$. Is such filter physically realizable? Explain why.

Problem 4.35 A signal $x(t)$ is band-limited in frequency to the band $0 < |\omega| < B$, being zero elsewhere. The signal is ideally sampled by the impulse train $\rho_T(t) = \sum_{n=-\infty}^{\infty} \delta(t - nT)$ where $T = \pi/B$. The resulting sampled signal $x_s(t) = x(t)\rho_T(t)$ is fed as the input of a linear system of impulse response

$$h(t) = Sa(\pi t/T) \sum_{n=-\infty}^{\infty} \delta(t - nT/4)$$

and output $y(t)$.

- a) Evaluate $X_s(j\omega)$ the Fourier spectrum of the sampled signal $x_s(t)$, and $H(j\omega)$ the system frequency response.
- b) Evaluate $Y(j\omega)$, the Fourier transform of the system output $y(t)$.
- c) Can the overall system be replaced by an equivalent simple ideal sampling system? If so, specify the required sampling frequency and period.

Problem 4.36 In an instantaneous sampling system a signal $x(t)$ is first ideally sampled with a sampling period of $T = 10^{-3}$ sec. The ideally sampled signal

$$x_s(t) = x(t) \sum_{n=-\infty}^{\infty} \delta(t - nT)$$

thus obtained is applied to a system of impulse response

$$h(t) = R_\tau(t) = u(t) - u(t - \tau)$$

and output $y(t)$. To reconstruct the original signal from $y(t)$ an ideal lowpass filter of frequency response

$$H(j\omega) = \Pi_{1000\pi}(\omega) = u(\omega + 1000\pi) - u(\omega - 1000\pi)$$

is used, with $y(t)$ as its input and $z(t)$ its output. Let $x(t)$ be a sinusoid of frequency 400 Hz and amplitude of 1. Describe the form, frequency and amplitude of $z(t)$ for the two cases

- a) $\tau = T = 10^{-3}$ sec
- b) $\tau = T/2 = 0.5 \times 10^{-3}$ sec

Problem 4.37 A signal $x(t)$ is to be sampled. To avoid aliasing the signal $x(t)$ is fed to a lowpass-type filter of frequency response $H(j\omega)$

$$H(j\omega) = \begin{cases} 1, & |\omega| \leq \omega_c \\ -10(|\omega| - 1.6\omega_c)/(6\omega_c), & \omega_c \leq |\omega| \leq 1.6\omega_c \\ 0, & \text{otherwise.} \end{cases}$$

See Fig. 4.44.

The signal $x_f(t)$ at the filter output is then ideally sampled by the impulse train $\rho_T(t) = \sum_{n=-\infty}^{\infty} \delta(t - nT)$. The sampled signal $x_s(t) = x_f(t) \rho_T(t)$ is fed to a lowpass filter of frequency response $G(j\omega) = \Pi_{\pi/T}(\omega) = u(\omega + \pi/T) - u(\omega - \pi/T)$, and output $x_g(t)$.

a) What value of ω_c would ensure the absence of aliasing?

Letting $\omega_c = 10\pi$ rad/s, $T = 0.1$ sec. and $x(t) = \sum_{n=-\infty}^{\infty} x_0(t - 0.4n)$

where

$$x_0(t) = \begin{cases} 1, & |t| < 0.1 \\ -1, & 0.1 < |t| \leq 0.2 \\ 0, & \text{otherwise.} \end{cases}$$

b) Sketch $x(t)$. Evaluate $X_f(j\omega)$ the Fourier transform of the filter output $x_f(t)$, and $X_s(j\omega)$, the transform of $x_s(t)$.

c) Evaluate $X_g(j\omega)$ the spectrum of the second filter output $x_g(t)$.

d) Evaluate $x_g(t)$.

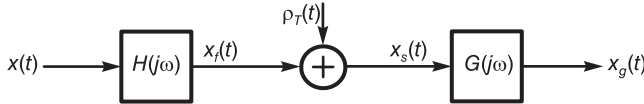


FIGURE 4.44 Filtering-sampling system.

Problem 4.38 A signal $v(t)$ is obtained by the natural sampling of a continuous-time signal $x(t)$, such that

$$v(t) = x(t) p(t)$$

where $p(t)$ is a periodic signal of period T .

a) What conditions should be placed on $X(j\omega)$ the spectrum of $x(t)$ to avoid aliasing?

b) Evaluate $V(j\omega) = \mathcal{F}[v(t)]$ expressed as a function of $X(j\omega)$ and P_n the Fourier series coefficients of $p(t)$.

c) Show that to reconstruct $x(t)$ from $v(t)$ the average value of $p(t)$ should not be nil.

Problem 4.39 A sampled signal $x_s(t)$ is obtained by multiplying a continuous-time signal $x(t)$ by a train of narrow rectangular pulses, with a sampling frequency of 48 kHz, as shown in Fig.4.45.

$$x_s(t) = x(t) p(t).$$

For each of the following signals $x(t)$ state whether or not the Nyquist rate is satisfied to avoid spectral aliasing, explaining why.

a) $x(t) = A \cos(35\pi \times 10^3 t)$

b) $x(t) = R_T(t) = u(t) - u(t - T)$, $T = 1/48000$

c) $x(t) = e^{-0.001t} u(t)$

d) $x(t) = A_1 \cos(300\pi t) + A_2 \sin(4000\pi t) + A_3 \cos(3 \times 10^4 \pi t)$

e) $x(t) = \sum_{n=-\infty}^{\infty} x_0(t - n\tau)$

where $\tau = 0.5 \times 10^{-3}$ sec. and

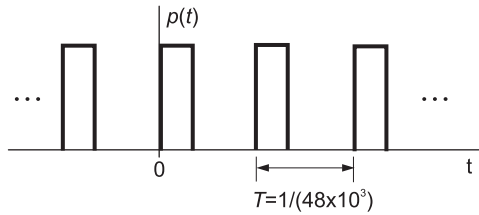


FIGURE 4.45 Pulses train.

$$x_0(t) = 3\Pi_{0.1}(t) = 3[u(t + 0.1) - u(t - 0.1)]$$

f) $x(t) = \sin(4 \times 10^3\pi t) \sin(4 \times 10^4\pi t)$

Problem 4.40 In an instantaneous sampling system a signal $x(t)$ is ideally sampled by an impulse train $p(t)$. The resulting signal $x_i(t) = x(t)p(t)$ is applied to a system of impulse response $h(t)$ and output $y(t)$. Due to extraneous interference the impulse train is in fact an ideal impulse train $\rho_T(t)$ plus noise in the form of a 60 Hz interference such that

$$p(t) = \rho_T(t) [1 + 0.1 \cos(120\pi t)]$$

where $T = 0.005$ sec and

$$\rho_T(t) = \sum_{n=-\infty}^{\infty} \delta(t - nT).$$

- a) Sketch the Fourier transform $P(j\omega)$ for $-600\pi < \omega < 600\pi$.
- b) To avoid spectral aliasing and to be able to reconstruct $x(t)$ from the system output $y(t)$, to what frequency should the spectrum of $x(t)$ be limited?

Problem 4.41 A signal $x(t)$ is sampled by the impulse train

$$\rho_T(t) = \sum_{n=-\infty}^{\infty} \delta(t - nT)$$

where $T = 1/16000$ sec., producing the sampled signal $x_s(t) = x(t)\rho_T(t)$. For each of the following three cases state the frequency band outside of which the Fourier transform $X(j\omega)$ of $x(t)$ is nil. Deduce whether or not it is possible to reconstruct $x(t)$ from $x_s(t)$,

- a) $x(t)$ is the product of two signals $v(t)$ and $y(t)$ band-limited to $|\omega| < 2000\pi$ and $|\omega| < 10000\pi$, respectively.
- b) $x(t)$ is the product of a signal $y(t)$ that is band-limited to $|\omega| < 6000\pi$ and the signal $\cos(24000\pi t)$.
- c) $x(t)$ is the convolution of two signals $w(t)$ and $z(t)$ which are band-limited to $|\omega| < 20000\pi$ and $|\omega| < 14000\pi$, respectively.

Problem 4.42 In a sampling system the input signal $v(t)$ is multiplied by the impulse train

$$\rho_T(t) = \sum_{n=-\infty}^{\infty} \delta(t - nT).$$

The sampled signal $v_s(t) = v(t)\rho_T(t)$ is then fed to an ideal lowpass filter of frequency response

$$H(j\omega) = T \Pi_{2\pi/(3T)}(\omega)$$

and output $y(t)$. Sketch the Fourier transforms $V(j\omega)$, $V_s(j\omega)$ and $Y(j\omega)$ of the signals $v(t)$, $v_s(t)$ and $y(t)$, respectively, given that

- $V(j\omega) = \left[1 - \{6T/(5\pi)\}^2 \omega^2\right] \Pi_{2\pi/(3T)}(\omega)$
- $V(j\omega) = \Lambda_{3\pi/(2T)}(\omega)$
- $v(t)$ is the signal

$$v(t) = 3 \cos \beta_1 t + 2 \cos \beta_2 t - \cos \beta_3 t$$

where $\beta_1 = \pi/(2T)$, $\beta_2 = 5\pi/(4T)$, $\beta_3 = 3\pi/(2T)$. Evaluate $y(t)$.

Problem 4.43 A signal $v(t)$ is sampled by the impulse train of “doublets”

$$r(t) = \rho_T(t) + \rho_T(t - T/6)$$

a) Evaluate the Fourier transform $R(j\omega)$ and the exponential Fourier series coefficients R_n of the impulse train $r(t)$.

b) Given that the Fourier transform $V(j\omega)$ of $v(t)$ is given by

$$V(j\omega) = (1 - \omega^2/\pi^2) \Pi_\pi(\omega)$$

evaluate the sampling period T that would ensure the absence of spectral aliasing and hence the possible reconstruction of $v(t)$ from the sampled function

$$v_s(t) = v(t) r(t).$$

c) Sketch the amplitude spectrum $|V_s(j\omega)|$ of $v_s(t)$ assuming $T = 1$.

Problem 4.44 A signal $f(t)$ that has the Fourier transform

$$F(j\omega) = (1 - \omega^2/W^2) \Pi_W(\omega)$$

is modulated by a carrier $\cos \beta t$, where β is much larger than W . The modulated signal $g(t) = f(t) \cos \beta t$ is then fed to a lowpass filter of frequency response

$$H_1(j\omega) = \Pi_\beta(\omega)$$

and output $v(t)$.

a) Sketch $F(j\omega)$, $G(j\omega)$ and $V(j\omega)$.

b) The signal $v(t)$ is sampled by the impulse train $\rho_T(t)$ where $T = 2\pi/\beta$ and the result $v_s(t) = v(t) \rho_T(t)$ is fed to a filter, of which the output should be the signal $v(t)$. Evaluate the filter frequency response $H_2(j\omega)$.

Problem 4.45 Given the signal

$$v(t) = \cos \beta_1 t - \cos \beta_2 t + \cos \beta_3 t$$

where

$$\beta_1 = 800\pi, \quad \beta_2 = 2400\pi, \quad \beta_3 = 3200\pi.$$

Let $v_s(t)$ be the signal obtained by ideal sampling of the signal $v(t)$ with an impulse train of period T , so that $v_s(t) = v(t) \rho_T(t)$.

a) Evaluate and sketch the spectrum $V(j\omega)$. Evaluate $V_s(j\omega)$ as a function of T .

b) The sampled signal $v_s(t)$ is fed to ideal lowpass filter of frequency response

$$H(j\omega) = \Pi_B(\omega)$$

where $B = 2000\pi$. For the three cases

$$T = T_1, \quad T = T_2 \quad \text{and} \quad T = T_3$$

where

$$T_1 = 2\pi / (4000\pi), \quad T_2 = 2\pi / (4800\pi) \quad \text{and} \quad T_3 = 2\pi / (7200\pi)$$

sketch the Fourier transforms $R_1(j\omega)$, $R_2(j\omega)$ and $R_3(j\omega)$ of the impulse trains $\rho_{T_1}(t)$, $\rho_{T_2}(t)$ and $\rho_{T_3}(t)$, respectively, and the corresponding spectra $V_{s_1}(j\omega)$, $V_{s_2}(j\omega)$ and $V_{s_3}(j\omega)$ of the sampled signals.

c) Sketch the spectra $Y_1(j\omega)$, $Y_2(j\omega)$ and $Y_3(j\omega)$ and the corresponding signals $y_1(t)$, $y_2(t)$ and $y_3(t)$, at the filter output for the three cases, respectively.

Problem 4.46 Let $f(t) = e^{-\alpha t} R_{\tau/2}(t) = e^{-\alpha t} \{u(t) - u(t - \tau/2)\}$.

- a) Show that by differentiating $f(t)$ it is possible to evaluate its Laplace transform $F(s)$.
- b) Let $v(t) = e^{-\alpha|t|} \Pi_{\tau/2}(t)$. Express $V(s) = \mathcal{L}[v(t)]$ as a function of $F(s)$.
- c) Evaluate $V(j\omega) = \mathcal{F}[v(t)]$ from $V(s)$ if possible. If not, state why and evaluate alternatively $V(j\omega)$. Simplify and plot $V(j\omega)$. With $\alpha = \tau = 0.1$ evaluate the first zero of $V(j\omega)$. You may use Mathematica command `FindRoot` for this purpose.
- d) A signal $x(t)$ is sampled instantaneously by the train of pulses

$$p_T(t) = \sum_{n=-\infty}^{\infty} v(t - nT)$$

with $\alpha = \tau = 0.1$. The signal has the spectrum

$$X(j\omega) = \begin{cases} 1, & 0 < |\omega| < \pi \\ 2 - |\omega|/\pi, & \pi < |\omega| < 2\pi \\ 0, & \text{otherwise.} \end{cases}$$

Evaluate and plot the spectrum $X_i(j\omega)$ of the instantaneously sampled signal $x_i(t)$.

e) What is the required value of T to avoid aliasing? Specify the frequency response of the required filter that would reconstruct $x(t)$ from $x_i(t)$.

Problem 4.47 Given the function of duration $\tau/2$

$$f(t) = (4/\tau^2) (t - \tau/2)^2 R_{\tau/2}(t).$$

- a) By differentiating $f(t)$ twice, deduce its Laplace transform without evaluating integrals.
- b) Let $v(t) = f(t) + f(-t)$. Evaluate $V(s) = \mathcal{L}[v(t)]$. Plot the spectrum $V(j\omega)$ assuming $\tau = 0.1$.
- c) A train of pulses $p_T(t)$ of period T is constructed by repeating $v(t)$ so that

$$p_T(t) = \sum_{n=-\infty}^{\infty} v(t - nT).$$

Sketch the spectrum $P_T(j\omega) = \mathcal{F}[p_T(t)]$.

d) A signal $x_c(t)$ has the spectrum

$$X_c(j\omega) = \begin{cases} 1, & 0 < |\omega| < \pi f_c \\ 2 - |\omega| / (\pi f_c), & \pi f_c < |\omega| < 2\pi f_c \\ 0, & \text{otherwise.} \end{cases}$$

Natural sampling is applied to the signal $x_c(t)$ using the train of pulses $p_T(t)$. Evaluate the spectrum $X_n(j\omega)$ of the naturally sampled signal $x_n(t)$ thus obtained. What is the minimum value of the sampling frequency f_s to avoid aliasing assuming that $f_c = 1$ Hz. Plot the spectrum $X_n(j\omega)$ for the case of maximum possible sampling frequency.

e) Repeat part d) assuming now instantaneous instead of natural sampling. Specify the frequency response $H(j\omega)$ of the filter that would reconstruct $x_c(t)$ from $x_i(t)$.

Problem 4.48 In a sampling system signals are sampled ideally at a frequency of 5 kHz and transmitted over a communication channel. At the receiving end the signal is reconstructed using an ideal lowpass filter of cut-off frequency equal to half the sampling frequency. Assuming that the input signal is given by

$$x_c(t) = 10 + 10 \cos(3000\pi t) + 15 \sin(6000\pi t).$$

Is the reconstructed signal $y_c(t)$ at the receiving end equal to $x_c(t)$? If not what is its value? Justify your answer in the time domain and by evaluating and sketching the corresponding spectrum $X_c(j\omega)$.

Problem 4.49 Consider the signal $v(t) = x(t)y(t)$, where $x(t)$ is a band limited signal such that its Fourier transform $X(j\omega)$ is nil for $|\omega| > 10^4\pi$, and $y(t)$ is a periodic signal of frequency of repetition 10 kHz.

a) Express the Fourier transform $V(j\omega)$ of the signal $v(t)$ as a function of $X(j\omega)$.

b) Under what condition can the signal $x(t)$ be reconstructed from $v(t)$ using a simple ideal filter? Specify the requirements of such a filter.

Problem 4.50 A signal $x(t)$ is ideally sampled by the impulse train $p_T(t)$ of period $T = 125 \times 10^{-6}$. The sampled signal $x(t)p_T(t)$ is applied to the input of a linear system of which the impulse response is $g(t)$ and frequency response is $G(j\omega) = 125 \times 10^{-6} \Pi_{8000\pi}(\omega)$.

a) Describe the system output $v(t)$ (form, frequency, amplitude) if $x(t)$ is a sinusoid of frequency 3.6 kHz and amplitude 1 volt.

b) Describe the system output $v(t)$ (form, frequency, amplitude) if $x(t)$ is a sinusoid of frequency 4.8 kHz and amplitude 1 volt.

c) Sketch the Fourier transform $V(j\omega)$ of the output signal $v(t)$ if $x(t)$ is a signal of which the Fourier transform is $3\Lambda_{\pi \times 10^4}(\omega)$. Does the signal $v(t)$ contain all the information necessary to reconstruct the original signal $x(t)$?

Problem 4.51 A signal $x(t)$ having a Fourier transform

$$X(j\omega) = \begin{cases} 1 - \frac{|\omega|}{2\pi}, & |\omega| \leq 2\pi \\ 0, & |\omega| > 2\pi \end{cases}$$

is the input of a filter of which the frequency response is

$$H(j\omega) = \begin{cases} |\omega|/\pi, & |\omega| \leq \pi \\ 0, & |\omega| > \pi. \end{cases}$$

a) Evaluate the mean value of $x(t)$.

b) Evaluate the filter response $y(t)$.

c) Evaluate the energy of the signal at the filter output.

Problem 4.52 A signal $x(t)$ has a Fourier transform

$$X(j\omega) = \begin{cases} 4, & |\omega| < 1 \\ 2, & 1 < |\omega| < 2 \\ 0, & \text{elsewhere.} \end{cases}$$

This signal is multiplied by a signal $y(t)$ where

$$y(t) = v(t) + \frac{4}{\pi} \cos 4t$$

and $v(t)$ has a Fourier transform

$$V(j\omega) = 2\Pi_2(\omega) = 2\{u(\omega + 2) - u(\omega - 2)\}.$$

The multiplier output $z(t) = x(t)y(t)$ is applied as the input to a filter of frequency response

$$H(j\omega) = \begin{cases} 1, & 1 < |\omega| < 3 \\ 0, & \text{elsewhere} \end{cases}$$

and output $w(t)$.

a) Evaluate the spectra $Z(j\omega)$ and $W(j\omega)$ at the input and output of the filter, respectively.

b) Evaluate the energies of the signals $z(t)$ and $w(t)$, in the frequency band $1 < |\omega| < 2$.

Problem 4.53 A periodic signal $v(t)$ of period $T = 1$ sec. has a Fourier series expansion

$$v(t) = \sum_{n=-\infty}^{\infty} V_n e^{jn2\pi t}$$

$$\text{where } V_n = \begin{cases} 4.5(1 + \cos \pi n/4), & 0 \leq |n| \leq 4 \\ 0, & |n| > 4. \end{cases}$$

The signal $v(t)$ is multiplied by the signal

$$x(t) = Sa^2(\pi t).$$

The result $g(t) = v(t)x(t)$ is applied to the input of an ideal lowpass filter of frequency response

$$H(j\omega) = \Pi_{2\pi}(\omega) = u(\omega + 2\pi) - u(\omega - 2\pi).$$

a) Evaluate and sketch the Fourier transforms $V(j\omega)$ and $X(j\omega)$ of the signals $x(t)$ and $v(t)$, as well as $G(j\omega)$ and $Y(j\omega)$ the transforms of the input and output $g(t)$ and $y(t)$ of the filter, respectively.

b) Evaluate $y(t)$.

Problem 4.54 A system is constructed as a cascade of four systems of transfer functions $H_1(s)$, $H_2(s)$, $H_3(s)$ and $H_4(s)$ with impulse responses $h_1(t)$, $h_2(t)$, $h_3(t)$ and $h_4(t)$, where

$$h_1(t) = \delta(t - 2\pi/\beta)$$

$$h_2(t) = \beta Sa(\beta t)$$

$$H_3(j\omega) = j\omega\Pi_{2\beta}(\omega) = j\omega\{u(\omega + 2\beta) - u(\omega - 2\beta)\}$$

$$h_4(t) = 2 + \text{sgn}(t).$$

a) Evaluate the frequency response $H(j\omega)$ of the system, and its impulse response.

b) Evaluate the response $y(t)$ of the system if $\beta = 100\pi$ and

i) $x(t) = \sin(20\pi t)$ and ii) $x(t) = \sin(200\pi t)$.

Problem 4.55 For each of the following signals evaluate the Laplace transform, the poles with the region of convergence, and state whether or not the Fourier transform exists.

$$a) \quad v_1(t) = \sum_{i=1}^P A_i e^{-a_i t} \cos(b_i t + \theta_i) u(t) + \sum_{i=1}^P B_i e^{c_i t} \cos(d_i t + \phi_i) u(-t)$$

where the a_i , b_i and c_i are distinct and $b_i > 0$, $d_i > 0$, $a_i > 0$, $c_i > 0$, $\forall i$.

b) The same function $v_1(t)$ but with the conditions:

$$b_i > 0, \quad d_i > 0, \quad a_i > 0, \quad c_i < 0, \quad \forall i.$$

c) The same function $v_1(t)$ but with the conditions:

$$b_i > 0, \quad a_i = 0, \quad B_i = 0, \quad \forall i.$$

$$d) \quad v_2(t) = A \cos(bt + \theta), \quad -\infty < t < \infty.$$

$$e) \quad v_3(t) = A e^{-t}, \quad -\infty < t < \infty.$$

Problem 4.56 A periodic signal $v(t)$ of period $T = 10^{-3}$ sec has the Fourier series coefficients

$$V_n = \begin{cases} 1, & n = 0 \\ \mp j, & n = \pm 1 \\ 1/8, & n = \pm 3 \\ 0, & \text{otherwise.} \end{cases}$$

This signal is applied as the input to a system of frequency response $H(j\omega)$ and output $y(t)$, where

$$|H(j\omega)| = \begin{cases} |\omega| / (2000\pi), & 0 \leq |\omega| \leq 2000\pi \\ 1, & 2000\pi \leq |\omega| < 4000\pi \\ 0, & |\omega| > 4000\pi \end{cases}$$

$$\arg[H(j\omega)] = \begin{cases} -\omega/4000, & |\omega| < 3000\pi \\ 0, & |\omega| > 3000\pi. \end{cases}$$

a) Evaluate the Fourier transform $V(j\omega)$ of $v(t)$.

b) Evaluate the Fourier transform $Y(j\omega)$ of $y(t)$.

c) Evaluate $y(t)$.

Problem 4.57 A periodic signal $x(t)$ is given by its expansion over one period

$$x(t) = \sum_{n=-\infty}^{\infty} X_n e^{j100\pi n t}$$

where $X_n = (-1)^n \text{Sa}(n\pi/4)$.

a) What is the period of $x(t)$? What is its average value? What is the amplitude of the sinusoidal component of frequency 150 Hz?

b) The signal $x(t)$ is applied to a filter of frequency response $H(j\omega)$ and output $y(t)$, where

$$|H(j\omega)| = \Lambda_{200\pi}(\omega - 300\pi) + \Lambda_{200\pi}(\omega + 300\pi)$$

$$\arg[H(j\omega)] = \begin{cases} -\pi/2, & 100\pi < \omega < 500\pi \\ \pi/2, & -500\pi < \omega < -100\pi \\ 0, & \text{otherwise.} \end{cases}$$

Evaluate the filter output $y(t)$ as a sum of solely real functions.

Problem 4.58 A periodic signal $v(t)$ of period 5 msec has a Fourier transform

$$V(j\omega) = \sum_{k=-7}^7 \alpha_k \delta(\omega - 400n\pi)$$

where $\alpha_{-k} = \alpha_k^*$ and for $k = 0, 1, \dots, 7$ the coefficients α_k are given by $\alpha_k = 6\pi, 10\pi, 0, 0, 2\pi, 0, 0, j\pi$.

a) Evaluate the trigonometric Fourier series coefficients of $v(t)$ over one period and $v(t)$ as a sum of real trigonometric functions.

b) A signal $x(t)$ is obtained by applying the signal $v(t)$ to the input of a filter of impulse response $h(t)$. Evaluate the signal $x(t)$ knowing that

$$H(j\omega) = 8\Lambda_{3200\pi}(\omega).$$

c) A signal $y(t)$ is obtained by modulating the signal $v(t)$ using the carrier $v_c(t) = \cos 3200\pi t$ and the result $v_m(t) = v(t)v_c(t)$ is applied to an ideal lowpass filter of frequency response

$$H_2(j\omega) = \Pi_{2000\pi}(\omega)$$

and output $y(t)$. Evaluate $y(t)$.

d) A signal $z(t)$ is the sum

$$z(t) = v(t) + v(t) * h_3(t)$$

where

$$h_3(t) = \mathcal{F}^{-1}[H_3(j\omega)] \quad \text{and} \quad H_3(j\omega) = e^{-j\omega/1600}.$$

Evaluate $Z(j\omega)$ and $z(t)$.

Problem 4.59 The signal $f(t) = \cos \beta_1 t - \sin \beta_2 t$ is multiplied by the ideal impulse train

$$\rho_T(t) = \sum_{n=-\infty}^{\infty} \delta(t - nT)$$

where $T = 2\pi/(\beta_1 + \beta_2)$. To reconstruct the signal $f(t)$ from the product signal $g(t) = f(t)\rho_T(t)$ a filter is proposed. If this is possible specify the filter frequency response $H(j\omega)$.

Problem 4.60 The signals $x(t)$, $y(t)$ and $z(t)$ have the Fourier transforms, expressed with respect to the frequency f in Hz,

$$X(f) = 0, \quad |f| < 500 \text{ or } |f| \geq 8000$$

$$Y(f) = 0, \quad |f| \geq 12000$$

$$Z(f) = 0, \quad |f| \geq 16000$$

The following related signals should be sampled with no loss of information. Find for each signal the minimum required sampling rate:

a) $x(t)$

b) $x(t) + z(t)$

c) $x(t) + y(t) \cos(44000\pi t)$

d) $x(t) \cos^2(17000\pi t)$

e) $y(t)z(t)$

Problem 4.61 In a sampling system the input signal $x(t)$ is multiplied by the ideal impulse train $\rho_{0.1}(t)$. The result is applied to the input of an ideal lowpass filter of cut-off frequency $f_c = 5$ Hz and a gain of 0.5.

With $x(t) = A \cos(6\pi t) + B \sin(12\pi t)$, evaluate the filter output $y(t)$.

Problem 4.62 In a natural sampling system the input signal $m(t)$ is multiplied by the train of rectangles $p(t) = \sum_{n=-\infty}^{\infty} \Pi_{0.05T}(t - nT)$ where $T = 10^{-4}$ s producing the product $y(t)$.

Given that the signal $m(t)$ is limited in frequency to 7 kHz, suggest a simple operation to apply to the signal $y(t)$ in order to restore $m(t)$. Specify the required restoring element. If it is not possible to fully restore $m(t)$ suggest how to recover the maximum bandwidth of the signal without distortion, and specify the information loss incurred.

Problem 4.63 In a sampling system the input signal $x(t)$ is multiplied by the train of rectangles $p(t) = \sum_{n=-\infty}^{\infty} \Pi_{T/6}(t - nT)$ of frequency of repetition $f_p = 1/T$ Hz. The product $w(t) = p(t)x(t)$ is applied to the input of an ideal lowpass filter of frequency response $H(f) = \Pi_{f_c}(f)$ producing the output $v(t)$.

a) Given that $f_c = 250$ Hz and $x(t) = \cos(200\pi t)$, what should be the values of the frequency f_p (excluding $f_p = 0$) to obtain an output signal $v(t) = \alpha \cos(2\pi f_0 t)$? Specify the values of α and f_0 .

b) With $f_c = 250$ Hz and $x(t) = \cos(200\pi t)$, what should be the values of the frequency f_p (excluding $f_p = 0$) to obtain an output signal $v(t) = \alpha \cos(2\pi f_0 t) + \beta \cos(2\pi f_1 t)$? Specify the values of α , β , f_0 and f_1 .

c) With $f_p = 150$ Hz and $x(t) = \cos(200\pi t)$, what should be the values of the cut-off frequency f_c to obtain an output of nil, i.e. $v(t) = 0$?

Problem 4.64 Sketch the two signals $x(t) = \text{sint}$ and $y(t) = 2\pi\Lambda_{2\pi}(t - 3\pi)$. By differentiating $y(t)$ twice evaluate the convolution $v(t) = x(t) * y(t)$. Plot the result indicating the expression that applies to each section.

Problem 4.65 Consider the cross-correlation functions $r_{xy}(t) = x(t) \star y(t)$ and $r_{yx}(t) = y(t) \star x(t)$, where $x(t)$ and $y(t)$ are real functions.

a) Express the Fourier transforms of $r_{xy}(t)$ and $r_{yx}(t)$ as functions of $X(j\omega)$ and $Y(j\omega)$.

b) Given that $x(t) \neq y(t)$, $x(t) \neq 0$ and $y(t) \neq 0$, state a sufficient condition in the time domain and one in the frequency domain which ensure that $r_{xy}(t) = r_{yx}(t)$.

4.44 Answers to Selected Problems

Problem 4.1

$$\text{a) } X(j\omega) = W(j\omega) - A2\pi\delta(\omega) = 2\pi A \sum_{n=-\infty, n \neq 0}^{\infty} \text{Sa}(n\pi/2)\delta(\omega - n\pi/\tau).$$

$$\text{b) } Y(j\omega) = (j/2)[X\{j(\omega + \omega_c)\} - X\{j(\omega - \omega_c)\}].$$

$$\text{c) } V(j\omega) = [1/(2\pi)]Y(j\omega) * \{1/(j\omega) + \pi\delta(\omega)\}.$$

Problem 4.2

$$\text{a) } (t-1)u(t-1) \xrightarrow{\mathcal{F}} (j\pi\delta'(\omega) - \frac{1}{\omega^2})e^{-j\omega} = j\pi\delta'(\omega) - \pi\delta(\omega) - e^{-j\omega/\omega^2}.$$

$$\text{b) } F_2(j\omega) = \pi t_0\delta(\omega) + \frac{e^{-jt_0\omega}}{\omega^2} - \frac{1}{\omega^2}.$$

Problem 4.3

$$\text{a) } X(j\omega) = 4\text{Sa}(2\omega) + \text{Sa}^2(0.5\omega)$$

$$\text{b) } Y(j\omega) = 0.4\pi \sum_{n=-\infty}^{\infty} \{4\text{Sa}(0.8\pi n) + \text{Sa}^2(0.2\pi n)\} \delta(\omega - 0.4\pi n)$$

c)

$$Z(j\omega) = \left[0.2 \sum_{n=-\infty}^{\infty} \{4Sa(0.8\pi n) + Sa^2(0.2\pi n)\} \frac{1}{j(\omega - 0.4\pi n)} \right] \\ + 0.2\pi \sum_{n=-\infty}^{\infty} \{4Sa(0.8\pi n) + Sa^2(0.2\pi n)\} \delta(\omega - 0.4\pi n)$$

Problem 4.4

$$Y(j\omega) = \omega_0 \sum_{n=-\infty}^{\infty} \tau^2 Sa^2(\tau n \omega_0 / 2) \delta(\omega - n\omega_0) \\ y(t) = \sum_{n=-\infty}^{\infty} Y_n e^{jn\omega_0 t}, \quad Y_n = (\tau^2 / T) Sa^2(\tau n \omega_0 / 2)$$

Problem 4.5

$$Y(j\omega) = 2\pi \sum V_n \delta(\omega - n\omega_0), \quad \omega_0 = \pi$$

a) $V_n = \frac{e - (-1)^n}{e(1 + n^2\pi^2)}$, $V_0 = 1 - e^{-1}$. b) $V_n = \frac{-jn\pi[e - (-1)^n]}{e(n^2\pi^2 + 1)}$
 c) $V_n = 0$, n even

$$V_n = \frac{e + 1}{e(1 + jn\pi)}, \quad n \text{ odd}$$

Problem 4.6

a) $F_n = \begin{cases} \frac{2 + jn\pi}{2n^2\pi^2}, & n \text{ even}, \quad n \neq 0 \\ \frac{-2n\pi - j(n^2\pi^2 - 4)}{2n^3\pi^3}, & n \text{ odd} \end{cases}$

b) $G(j\omega) = \sum_{n=-\infty}^{\infty} \left\{ F_n \frac{1}{j(\omega - n\pi)} + \pi F_n \delta(\omega - n\pi) \right\}$

Problem 4.7

a) $V(j\omega) = T Sa(T\omega/2) + (T/2) Sa[T(\omega - \omega_0)/2] + (T/2) Sa[T(\omega + \omega_0)/2]$

c) $X(j\omega) = 2\pi\delta(\omega) + \pi \{ \delta(\omega - m\omega_0) + \delta(\omega + m\omega_0) \}$

d)

$$W(j\omega) = \left\{ \frac{1}{j\omega} + \pi\delta(\omega) \right\} + \frac{1}{2} \left\{ \frac{1}{j(\omega - m\omega_0)} + \frac{1}{j(\omega + m\omega_0)} \right\} \\ + \frac{\pi}{2} \{ \delta(\omega - m\omega_0) + \delta(\omega + m\omega_0) \}$$

Problem 4.8 See Fig. 4.46. $z(t) = 6$, $Z(j\omega) = 12\pi\delta(\omega)$,

$$Z_n = \begin{cases} 6, & n = 0 \\ 0, & n \neq 0 \end{cases}$$

b) See Fig. 4.47.

$$Y(j\omega) = \frac{1}{2\pi} V(j\omega) * \frac{\pi}{2} \{ \delta(\omega - 4\pi) + 2\delta(\omega) + \delta(\omega + 4\pi) \} \\ = \frac{1}{2} V(j\omega) + \frac{1}{4} V[j(\omega - 4\pi)] + \frac{1}{4} V[j(\omega + 4\pi)] \\ = Sa^2(\omega - 4\pi) + 2 Sa^2(\omega) + Sa^2(\omega + 4\pi)$$

Problem 4.9

$$G(j\omega) = G(s)|_{s=j\omega} + \pi a_0 \delta(\omega) + \pi \sum_{i=1}^M \{ a_i \delta(\omega - \omega_i) + a_i^* \delta(\omega + \omega_i) \}$$

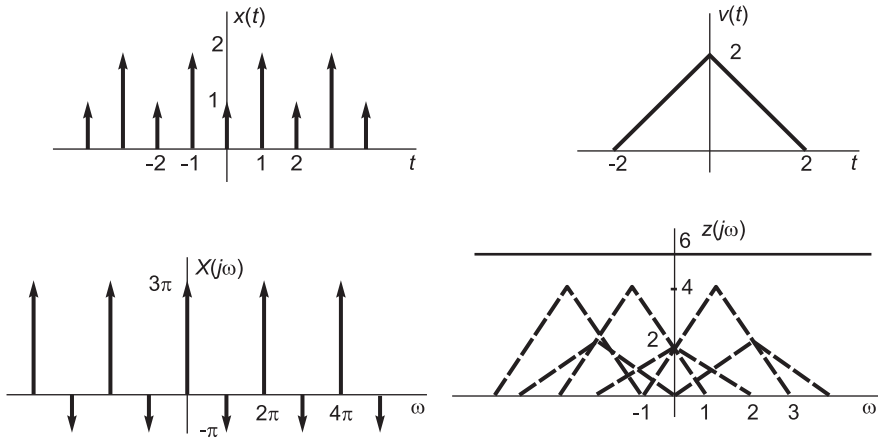


FIGURE 4.46 Figure for Problem 4.8.

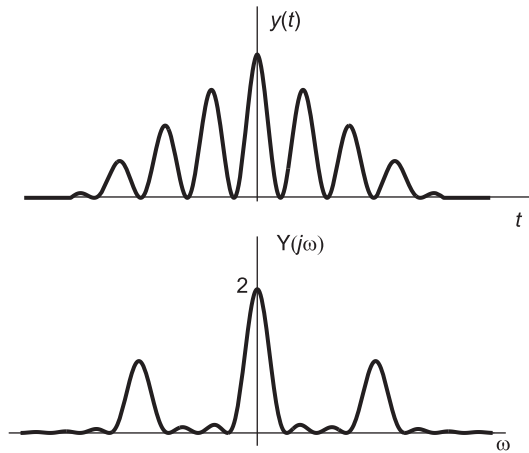


FIGURE 4.47 Figure for Problem 4.8 b).

Problem 4.10

$$X(j\omega) = \pi[-jA_1e^{j\theta_1}\delta(\omega - \omega_1) + jA_1e^{-j\theta_1}\delta(\omega + \omega_1)] + \pi[A_2e^{j\theta_2}\delta(\omega - \omega_2) + A_2e^{-j\theta_2}\delta(\omega + \omega_2)]$$

b) See Fig. 4.48.

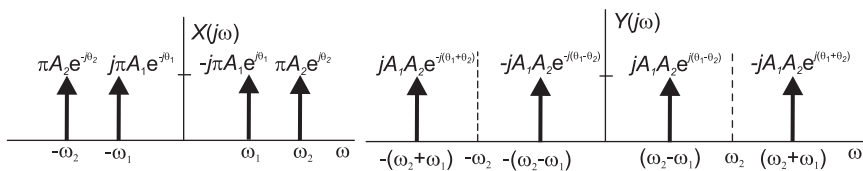


FIGURE 4.48 Figure for Problem 4.10.

$$Y_n = \begin{cases} \pm (jA_1A_2/4) e^{\pm j(\theta_2 - \theta_1)}, & n = \pm(m - k) \\ \mp (jA_1A_2/4) e^{\pm j(\theta_1 + \theta_2)}, & n = \pm(m + k) \\ 0, & \text{otherwise} \end{cases}$$

Problem 4.11

$$V(j\omega) = 5\{\delta(\omega - 400\pi) + \delta(\omega + 400\pi)\} + 3\{\delta(\omega - 1200\pi) + \delta(\omega + 1200\pi)\}$$

b) $W(j\omega) = F(j\omega)$

Problem 4.12

a) $T = 1/50 = 0.02 \text{ sec.}$

b) $W(j\omega) = (-j/2)\{2\delta(\omega - 200\pi) - 3\delta(\omega - 300\pi) + 2\delta(\omega - 400\pi) + 3\delta(\omega - 700\pi) - 2\delta(\omega + 200\pi) + 3\delta(\omega + 300\pi) - 2\delta(\omega + 400\pi) - 3\delta(\omega + 700\pi)\}$

c) $Z(j\omega) = 2\delta(\omega) + \frac{2}{1 + j200\pi}\delta(\omega - 200\pi) + \frac{2}{1 - j200\pi}\delta(\omega + 200\pi) + \frac{3}{1 + j500\pi}\delta(\omega - 500\pi) + \frac{3}{1 - j500\pi}\delta(\omega + 500\pi)$

Problem 4.13

a) $V(s) = \int_0^T e^{-t} e^{-st} dt = \frac{e^{-(s+1)t}}{(s+1)} \Big|_0^T = \frac{1 - e^{-(s+1)T}}{s+1}, \quad \forall s$

b) $V(j\omega) = \frac{1 - e^{-(j\omega+1)T}}{j\omega+1}$

c) $F_n = \frac{1 - e^{-T}}{T(jn\omega_0 + 1)}$ d) $V_n = F_n$ e) $F(j\omega) = \frac{2\pi}{T} (1 - e^{-T}) \sum_{n=-\infty}^{\infty} \frac{1}{(jn\omega_0 + 1)} \delta(\omega - n\omega_0)$

Problem 4.14

a) $Z(j\omega) = 0.5 + \frac{\omega_0}{2} \sum_{n=-\infty}^{\infty} \delta(\omega - n\omega_0) + \frac{1}{T} \sum_{n=-\infty}^{\infty} \frac{1}{j(\omega - n\omega_0)}$

$$Z(s) = \frac{1}{1 - e^{-Ts}}$$

b) $y(t) = \sum_{n=0}^{\infty} e^{-\alpha(t-nT)} R_T(t - nT)$

$$Y(s) = \frac{[1 - e^{-(s+\alpha)T}]}{(s + \alpha)(1 - e^{-Ts})}$$

$$Y_n = \frac{1}{T} Y_0(jn\omega_0) = \frac{1}{T} \frac{1 - e^{-\alpha T}}{\alpha + jn\omega_0}$$

c) $Y_p(j\omega) = \omega_0 \sum_{n=-\infty}^{\infty} \frac{1 - e^{-\alpha T}}{\alpha + jn\omega_0} \delta(\omega - n\omega_0)$

$$Y_p(j\omega) = \omega_0 \sum_{n=-\infty}^{\infty} \frac{1 - e^{-\alpha T}}{\alpha + jn\omega_0} \delta(\omega - n\omega_0).$$

Problem 4.15

a) $h(t) = 8e^{-8t}u(t) + 6e^{6t}u(-t)$

b) $h(t) = (8e^{-8t} - 6e^{6t})u(t)$

c) $h(t) = (-8e^{-8t} + 6e^{6t})u(-t)$

- d) $y(t) = 1.7645 \sin(2.5t + 0.8253)$
 e) $Z_n = (-jA/2) \{e^{j\theta} e^{-j(n\pi - T\pi/\tau)} \text{Sa}[n\pi - (T/\tau)\pi]\}$
 $+ (jA/2) \{e^{-j\theta} e^{-j(n\pi + T\pi/\tau)} \text{Sa}[n\pi + (T/\tau)\pi]\}$
 i) $Z(j\omega) = \pi A \{e^{j(\theta - \pi/2)} \delta(\omega - 4\omega_0) + e^{-j(\theta - \pi/2)} \delta(\omega + 4\omega_0)\}$
 ii) Z_n same, with $T/\tau = 7.5$, $Z(j\omega) = 2\pi \sum_{n=-\infty}^{\infty} Z_n \delta(\omega - n\omega_0)$

Problem 4.16

- b) $x(t) = 2v(t) \cos 0.2\pi t$
 c) $Y(j\omega) = 0.01\pi \sum_{n=-\infty}^{\infty} X(j0.01n\pi) \delta(\omega - 0.01n\pi)$

Problem 4.17

- a) $V_0 = 10$, $V_2 = 5$, $V_4 = \frac{-j5}{2} e^{-j\pi/4}$, $V_8 = 5e^{-j3\pi/2}$, $V_{-n} = V_n^*$,
 $V_n = 0$ otherwise c) $X(j\omega) = 2\pi \sum_{n=-\infty}^{\infty} V_n \delta(\omega - n\omega_0)$.

Problem 4.18

$$y(t) = \sum_{n=-\infty}^{\infty} Y_n e^{j\pi n t} \text{ where } Y_n = \begin{cases} 1/(2\pi), & n = \pm 440 \\ 1/(4\pi), & n = \pm 439, \pm 441, \pm 880 \\ 1/(8\pi), & n = \pm 879, \pm 881 \\ 0, & \text{otherwise} \end{cases}$$

Problem 4.19

- a) $Y(j\omega) = (1/2) X[j(\omega - 400\pi)] + (1/2) X[j(\omega + 400\pi)]$; b) $\overline{y(t)} = [1/(2\pi)] \times 6\pi = 3$ volt.
 c) $[1/(2\pi)] \times 2 |3\pi \pm \pi j| = |3 \pm j| = 3.16$ volt.

$$\text{Problem 4.20 } V(0) = \int_{-\infty}^{+\infty} v(t) e^{-j\omega t} dt \Big|_{\omega=0} = \int_{-\infty}^{+\infty} v(t) dt \neq \overline{v(t)}.$$

Problem 4.21

- a) $V_a(j\omega) = (-2 + 4 \cos 3\omega - 2 \cos 4\omega) / \omega^2$
 b) $V_b(j\omega) = \pi \sum_{n=-\infty}^{\infty} (-1)^n \delta(\omega - n\pi)$
 c) $V_c(j\omega) = (\pi/T) \sum_{n=-\infty}^{\infty} [1 - (-1)^n] \delta(\omega - n\pi/T)$

Problem 4.22

- a) $X(j\omega) = 2\pi \sum_n 0.25 \text{Sa}(\pi n/4) \delta(\omega - 2\pi n/T)$
 b) $Z(j\omega) = \sum_n \frac{0.25 \text{Sa}(\pi n/4)}{j(\omega - 2\pi n/T) + 4}$
 c) No. $Z(j\omega)$ is not impulsive

Problem 4.23

- a) $V(j\omega) = \pi \delta(\omega + 240\pi) - 4\pi j \delta(\omega + 120\pi) + 5\pi \delta(\omega + 80\pi) + 4\pi j \delta(\omega + 40\pi)$
 $- 4\pi j \delta(\omega - 40\pi) + 5\pi \delta(\omega - 80\pi) + 4\pi j \delta(\omega - 120\pi) + \pi \delta(\omega - 240\pi)$

$$\text{b) } V_n = \begin{cases} \mp 2j, & n = \pm 1 \\ 2.5, & n = \pm 2 \\ \pm 2j, & n = \pm 3 \\ 0.5, & n = \pm 6 \\ 0, & \text{otherwise} \end{cases}$$

- Problem 4.24** c) $Z(j\omega) = \frac{3}{1-j500\pi} \delta(\omega + 500\pi) + \frac{3}{1+j500\pi} \delta(\omega - 500\pi)$

$$+ \frac{2}{1-j200\pi} \delta(\omega + 200\pi) + \frac{2}{1+j200\pi} \delta(\omega - 200\pi) + 2\delta(\omega)$$

Problem 4.25 b) $z(t) = x(T - t)$, $Z(j\omega) = X^*(j\omega) e^{-j\omega T}$, $|Z(j\omega)| = |X(j\omega)|$

Problem 4.28 a) $V_s(j\omega) = (1/8) \sum_{n=-\infty}^{\infty} Sa^2(n\pi/8) e^{-jn\pi/4} V[j(\omega - n2\pi/T)]$ i) $T_0 = 2/3$ sec, $\omega_0 = 2\pi/T = 3\pi$. Aliasing. Reconstruction not possible.

ii) $T = 0.25$, $\omega_0 = 2\pi/0.25 = 8\pi$. No aliasing. An ideal lowpass filter of cut-off frequency B , $2\pi < B < 6\pi$ and gain $G = 8$.

Problem 4.29 a) $Y(j\omega) = (1/2) Sa(T\omega/4) e^{-j(\tau+T/4)\omega} \sum_{n=-\infty}^{\infty} V[j(\omega - n\omega_0)]$ b) $(2\pi/T) >$

$2\omega_m$, i.e. $T < \frac{\pi}{\omega_m} = \frac{\pi}{2\pi f_m} = \frac{1}{2f_m}$

c) $z(t) = 0.4979 \sin(200\pi t - 0.30\pi)$.

Problem 4.30 See Figs. 4.49 and 4.50.

$$T < (\pi/\omega_m).$$

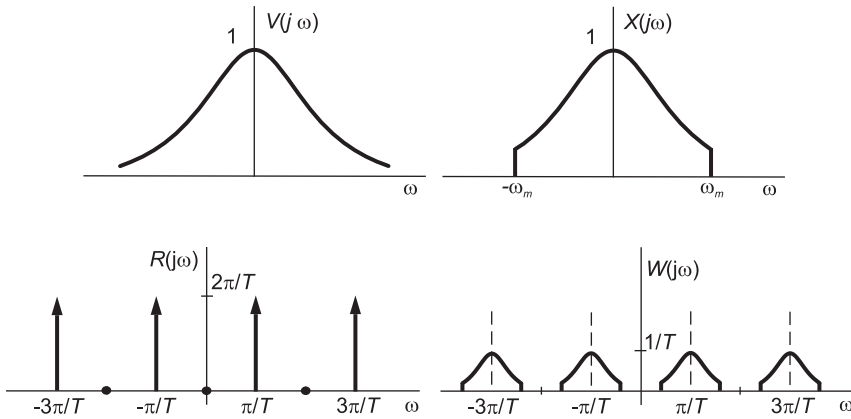


FIGURE 4.49 Figure for Problem 4.30.

Problem 4.31

i)

a) $Y(j\omega) = 2\pi \sum_{n=-\infty}^{\infty} \delta(\omega - 2n - 1)$.

b) $Y(j\omega) = (2\pi/3) \sum_{n=-\infty}^{\infty} Sa(n\pi/3) \delta(\omega - 2n - 1)$.

See Fig. 4.51.

c) $Y(j\omega) = (\pi/4) \sum_{n=-\infty}^{\infty} Sa(\pi n/4) \{ \delta(\omega - 1.5n - 1) + \delta(\omega - 1.5n + 1) \}$.

ii)

a) $Y(j\omega) = 2\pi \sum_{n=-\infty}^{\infty} \Lambda_1(\omega - 2n)$

b) $Y(j\omega) = (2\pi/3) \sum_{n=-\infty}^{\infty} Sa(n\pi/3) \Lambda_1(\omega - 2n)$

See Fig. 4.52.

c) See Fig. 4.53. $Y(j\omega) = (\pi/2) \sum_{n=-\infty}^{\infty} Sa(n\pi/4) \Lambda_1(\omega - 1.5n)$.

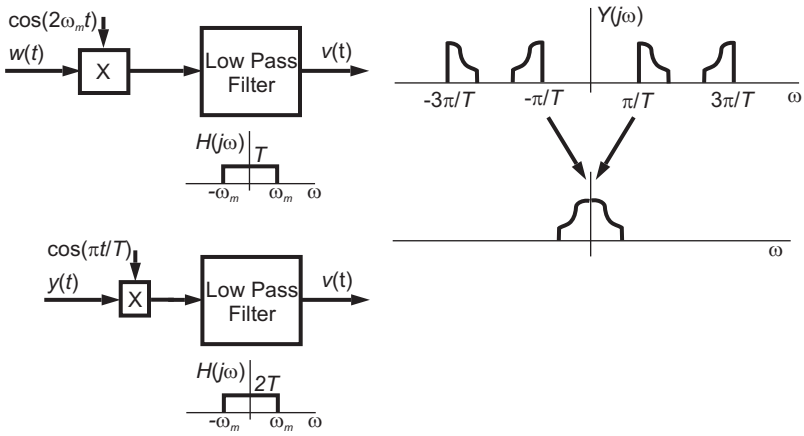


FIGURE 4.50 Figure for Problem 4.30.

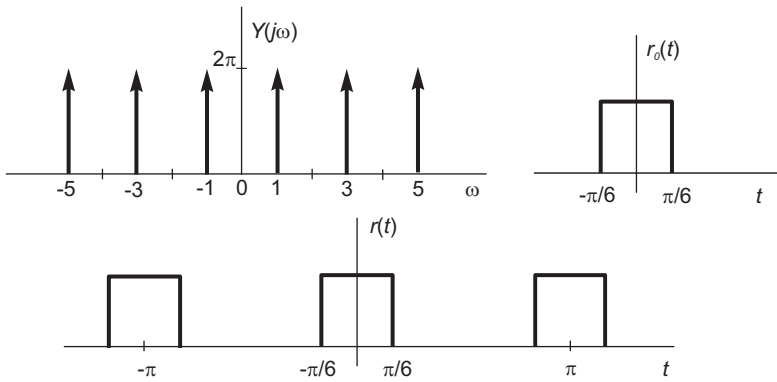


FIGURE 4.51 Figure for Problem 4.31.

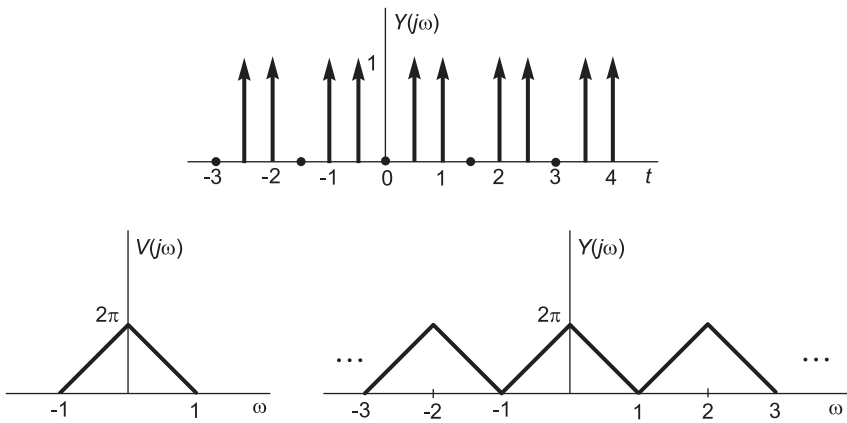


FIGURE 4.52 Figure for Problem 4.31.

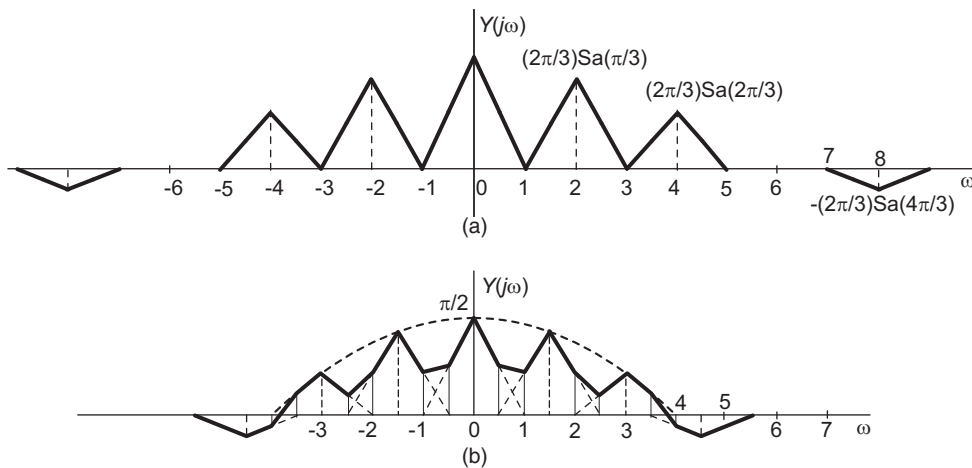


FIGURE 4.53 Figure for Problem 4.31.

Problem 4.32 See Fig. 4.54.

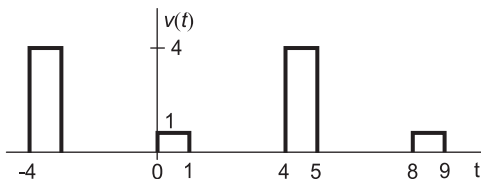


FIGURE 4.54 Figure for Problem 4.32.

b) By de-multiplexing with a repetition period of 8 sec and a delay between the first and second signal of 4 seconds.

Problem 4.33 See Fig. 4.55.

$y(t) = A \cos(2\pi t/T) + \frac{8A}{\pi} \sin(6\pi t/T)$. Yes. Aliasing results due to inadequate sampling rate.

Problem 4.34 $X_s(j\omega) = (1/10) \sum_{n=-\infty}^{\infty} Sa(n\pi/10) X[j(\omega - 2nB)]$, $B = \pi/T$.

b) $H(j\omega) = \Pi_B(\omega) = u(\omega + B) - u(\omega - B)$.

Problem 4.35 See Fig. 4.56.

$y(t) = x(t) \sum_{n=-\infty}^{\infty} \delta(t - nT/4)$, which is ideal sampling of $x(t)$ with a sampling frequency $\omega_s = 8B$, i.e. a sampling period of $2\pi/(8B) = T/4$.

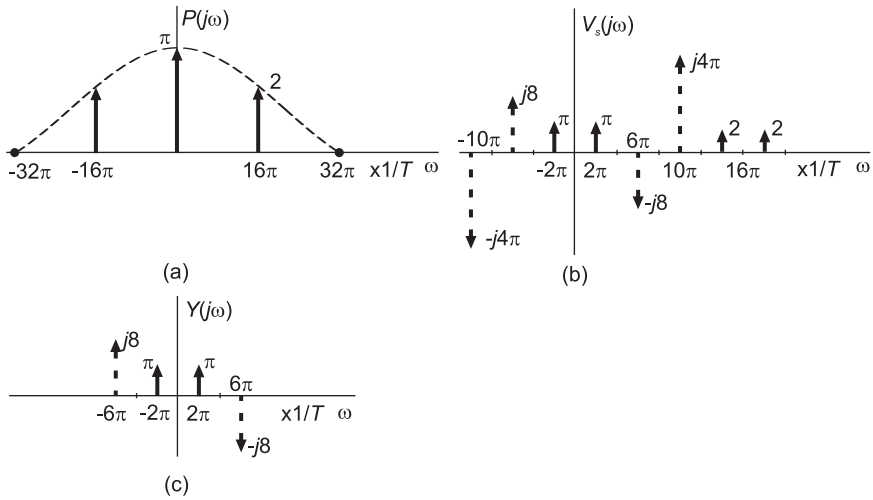


FIGURE 4.55 Figure for Problem 4.33.

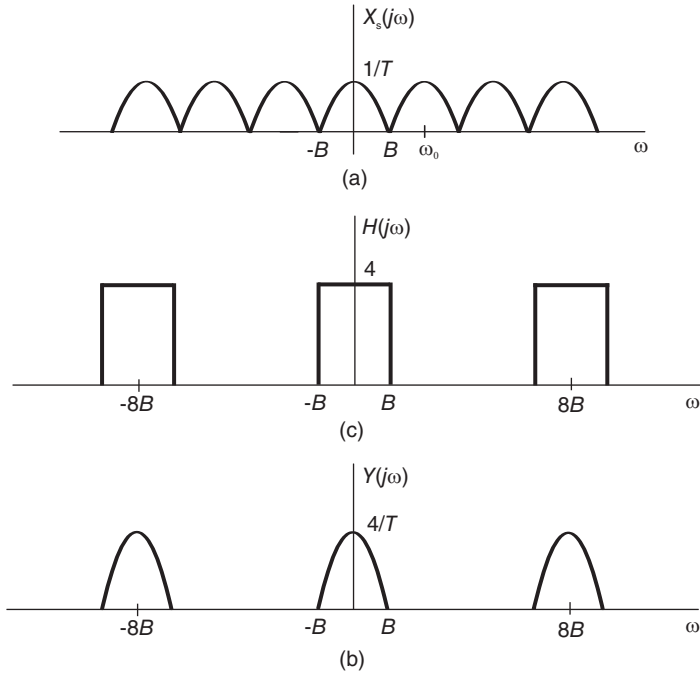


FIGURE 4.56 Figure for Problem 4.35.

Problem 4.36

- a) $\tau = T = 10^{-3}$ sec
- b) $\tau = 0.5T$. The output $z(t)$ is a sinusoid of frequency 400 Hz and amplitude 0.468.

Problem 4.37 See Fig. 4.57.

- a) $\omega_s = 2\pi/T$.

$$\begin{aligned}
 X(j\omega) &= 2\pi Sa(0.5\pi) \{ \delta(\omega - 5\pi) + \delta(\omega + 5\pi) \} \\
 &+ 2\pi(1/6) Sa(1.5\pi) \{ \delta(\omega - 15\pi) + \delta(\omega + 15\pi) \}
 \end{aligned}$$

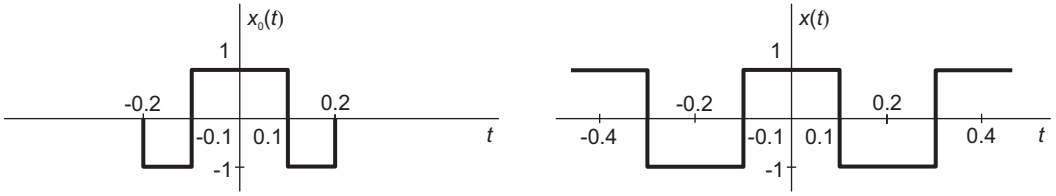


FIGURE 4.57 Figure for Problem 4.37.

See Fig. 4.58.

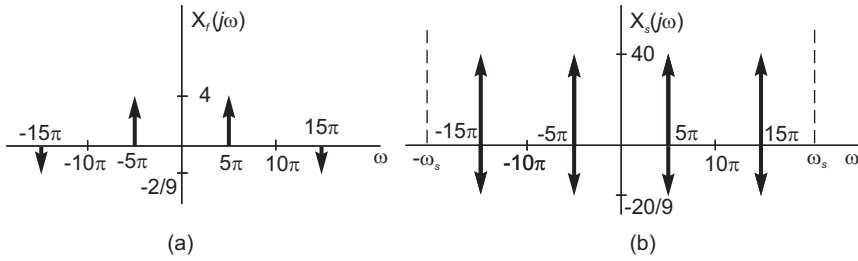


FIGURE 4.58 Figure for Problem 4.37.

- b) $X_f(j\omega) = 4\{\delta(\omega - 5\pi) + \delta(\omega + 5\pi)\} - (2/9)\{\delta(\omega - 15\pi) + \delta(\omega + 15\pi)\}$.
- c) $X_g(j\omega) = (40 - 20/9)\{\delta(\omega - 5\pi) + \delta(\omega + 5\pi)\}$.
- d) $x_g(t) = (37.778/\pi)\cos 5\pi t = 12.03\cos 5\pi t$.

Problem 4.60 a) 16 kHz, b) 32 kHz, c) 68 kHz, d) 50 kHz, e) 56 kHz

Problem 4.61

$$5A\cos(6\pi t) - 5B\sin(8\pi t).$$

Problem 4.62 The lower frequencies of $m(t)$ are recovered by applying $y(t)$ to the input of a lowpass filter of cut-off frequency of 3 kHz and a gain of 10. Loss of information for frequencies higher than 3 kHz.

Problem 4.63

- a) $f_p - 100 > 250$ or $f_p - 100 = 100$, i.e. $f_p > 350$, or $f_p = 200$, $f_0 = 100$, $\alpha = 1/3 = 0.333$ if $f_p > 350$; d $\alpha = 1/3 + (1/3)\text{Sa}(\pi/3) = 0.609$ if $f_p = 200$.
- b) $175 < f_p < 350$, $f_p \neq 200$, $\alpha = 0.333$ $f_0 = 100$, $\beta = (1/3)\text{Sa}(\pi/3) = 0.276$ and $f_1 = f_p - 100$.
- c) $f_c < 50$.

Problem 4.64

The convolution result $z(t)$ is shown in Fig. 4.59.

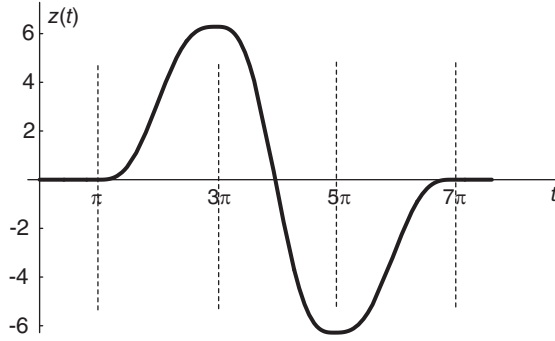


FIGURE 4.59 Convolution result.

System Modeling, Time and Frequency Response

The behavior of dynamic physical systems can generally be described or approximated using linear differential equations [34]. Whether the system is electrical, mechanical, biomedical or even socioeconomic, its mathematical model can usually be approximated using differential or difference equations. Once the differential or difference equations have been determined the system transfer function and its response to different inputs can be evaluated. The objective in this chapter is to learn about modeling of linear systems, the evaluation of their transfer functions and properties of their time and frequency response.

5.1 Transfer Function

Consider a linear time invariant (LTI) system described by the linear differential equation

$$\frac{d^n y}{dt^n} + a_{n-1} \frac{d^{n-1} y}{dt^{n-1}} + \dots + a_0 y = b_m \frac{d^m v}{dt^m} + b_{m-1} \frac{d^{m-1} v}{dt^{m-1}} + \dots + b_0 v \quad (5.1)$$

where $v(t)$ is the system input and $y(t)$ its output. Assuming zero initial conditions we can evaluate through Laplace transformation its transfer function $H(s)$. We write

$$(s^n + a_{n-1}s^{n-1} + a_{n-2}s^{n-2} + \dots + a_0) Y(s) = (b_m s^m + b_{m-1}s^{m-1} + \dots + b_0) V(s) \quad (5.2)$$

$$H(s) = \frac{Y(s)}{V(s)} = \frac{b_m s^m + b_{m-1}s^{m-1} + \dots + b_0}{s^n + a_{n-1}s^{n-1} + \dots + a_0} \triangleq \frac{N(s)}{D(s)}. \quad (5.3)$$

A partial fraction expansion can be applied to decompose $H(s)$ into the sum of first or second order fractions. If the order of the numerator polynomial $N(s)$ is greater than or equal to that of the denominator polynomial $D(s)$ a long division may be performed to reduce the expression of $H(s)$ into a polynomial in s plus a proper fraction.

5.2 Block Diagram Reduction

A block diagram describing the model of a physical system can be reduced by applying basic rules governing transfer functions. We consider the following cases:

1. Cascade Connection: A system composed of a cascade of two blocks G and H of transfer functions $G(s)$ and $H(s)$ is shown in Fig. 5.1(a). Referring to this figure we can deduce the overall transfer function $H_o(s)$. We can write

$$H_o(s) = \frac{Y(s)}{X(s)} = \frac{Y(s)}{W(s)} \cdot \frac{W(s)}{X(s)} = G(s) H(s). \quad (5.4)$$

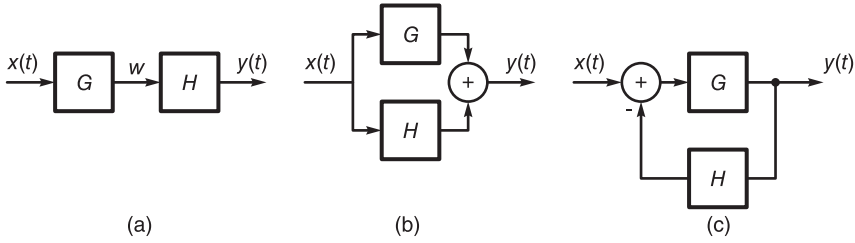


FIGURE 5.1 Block diagrams of (a) cascade, (b) parallel and (c) feedback systems.

We deduce that the cascade of two systems of transfer functions G and H leads to an overall transfer function

$$H_o = GH. \quad (5.5)$$

2. Parallel Connection: A system consisting of two subsystems connected in parallel is shown in Fig. 5.1(b). From this figure we can write

$$X(s)G(s) + X(s)H(s) = Y(s) \quad (5.6)$$

$$H_o(s) = \frac{Y(s)}{X(s)} = G(s) + H(s). \quad (5.7)$$

3. Feedback Loop: A system that includes a subsystem of transfer function $G(s)$ and another in the feedback path of transfer function $H(s)$ is shown Fig. 5.1(c). The input to the system is $x(t)$ and the output $y(t)$. The block diagram can be reduced by opening the loop and the overall transfer function evaluated by writing the input–output relation. We have

$$[X(s) - Y(s)H(s)]G(s) = Y(s) \quad (5.8)$$

wherefrom the overall transfer function is given by

$$H_o(s) = \frac{Y(s)}{X(s)} = \frac{G(s)}{1 + G(s)H(s)}. \quad (5.9)$$

The relation

$$H_o = \frac{G}{1 + GH} \quad (5.10)$$

is an important one for reducing a block diagram containing a feedback loop.

5.3 Galvanometer

Evaluating the mathematical model of a given dynamic physical system requires generally basic knowledge of the physical laws governing the system behavior. In this section an example is given to illustrate the modeling of a simple electromechanical system.

In modeling mechanical systems it should be noticed that the force F in a spring is equal to kx where k is the spring stiffness and x is the compression or extension of the spring. Viscous friction between two surfaces produces a force F equal to $b\dot{x}$, where b is the coefficient of friction and \dot{x} is the relative speed between the moving surfaces generating the friction.

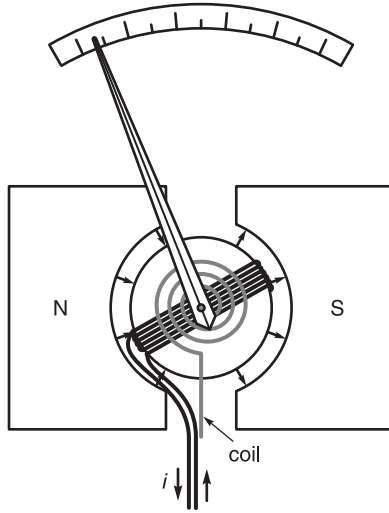


FIGURE 5.2 Galvanometer.

The galvanometer, represented schematically in Fig. 5.2, is a moving coil electric current detector. It employs a coil wound around a cylinder of length l and radius r free to rotate in the magnetic field of a permanent magnet as seen in the figure. When a current passes through the coil its interaction with the magnetic field produces a force on each rod of the coil producing a torque causing the cylinder to turn. As seen in the figure, a restraining coil-type spring is employed so that the amount of deflection of a needle attached to the coil is made proportional to the current passing through the coil. In what follows we analyze this electromechanical system in order to deduce its mathematical model and transfer function. Let $v(t)$ be the voltage input and $i(t)$ the current through the moving coil, which has a resistance R ohm and inductance L henry. When the coil rotates an electromotive force called *back emf* $e_c(t)$ is developed opposing the current flow. The equivalent circuit is shown in Fig. 5.3. The back emf $e_c(t)$ is given by the known expression “ Blv ,” where B is the magnetic field, l stands for the coil length which in the present case is replaced by $2nl$ for a coil of n windings, each winding having two opposite rods of length l each, moving across the magnetic field. The speed of rotation of the cylinder is $v = r\dot{\theta}$, where θ is the angle of rotation. In other words,

$$e_c = 2nBlr\dot{\theta} \triangleq k_1\dot{\theta} \tag{5.11}$$

where $k_1 = 2nBlr$. The voltage current equation is

$$e(t) = Ri + L\frac{di}{dt} + e_c = Ri + L\frac{di}{dt} + k_1\dot{\theta}. \tag{5.12}$$

The torque is produced by the force F on each rod of the coil, given by the know rule “ $Bl i$.” In the present case the overall torque is the couple

$$C = n \times F \times 2r = 2nBlri = k_1i. \tag{5.13}$$

The rotation is opposed by viscous friction which is proportional to the rotational speed. The friction couple is $b\dot{\theta}$. The rotor movement is also opposed by the couple produced by the coil spring, which is proportional to the angle of rotation θ , i.e., the coil spring exerts a couple given by $k\theta$. Assuming the rotor has an inertia J (kg/m^2), we may write the

equilibrium of couples as depicted in Fig. 5.3.

$$C = k_1 i = J\ddot{\theta} + b\dot{\theta} + k\theta. \tag{5.14}$$

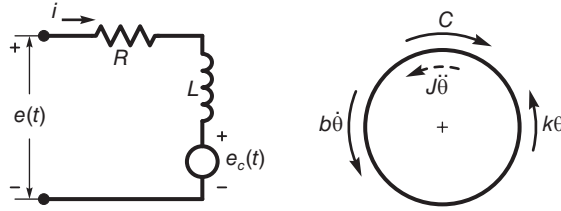


FIGURE 5.3 Galvanometer circuit and balance of couples.

We have thus obtained two differential equations that describe the system. To draw a block diagram representing it we first note that the current i is determined by the input $e(t)$ and $k_1\dot{\theta}$ which is a differentiation of the system output θ . Hence the system has feedback. We apply the Laplace transform obtaining

$$E(s) = (R + Ls) I(s) + k_1 s \Theta(s) \tag{5.15}$$

$$E(s) - k_1 s \Theta(s) \triangleq E_1(s) = (R + Ls) I(s) \tag{5.16}$$

$$I(s) = \frac{1}{R + Ls} E_1(s) \tag{5.17}$$

$$C(s) = k_1 I(s) = (Js^2 + bs + k) \Theta(s) \tag{5.18}$$

$$\Theta(s) = \frac{k_1}{Js^2 + bs + k} I(s). \tag{5.19}$$

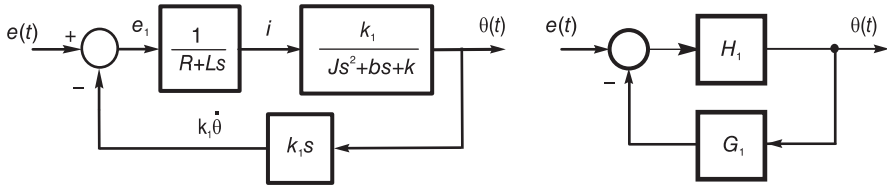


FIGURE 5.4 Galvanometer block diagram.

The block diagram is shown in Fig. 5.4. It can be redrawn as shown on the right in the same figure, where

$$H_1 = \frac{k_1}{(R + Ls)(Js^2 + bs + k)} \tag{5.20}$$

$$G_1 = k_1 s. \tag{5.21}$$

The overall transfer function is given by

$$H(s) = \frac{\Theta(s)}{E(s)} = \frac{H_1}{1 + G_1 H_1} \tag{5.22}$$

$$H(s) = \frac{k_1}{(R + Ls)(Js^2 + bs + k) + k_1^2 s} \tag{5.23}$$

5.4 DC Motor

A DC motor is represented schematically in Fig.5.5.

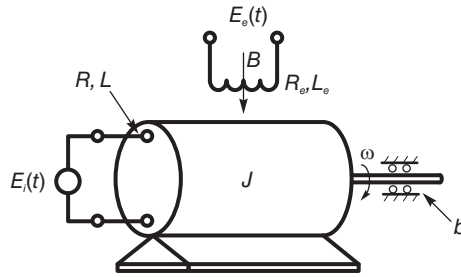


FIGURE 5.5 DC Motor.

A coil of resistance R_e and inductance L_e in the inductor circuit receives a voltage $E_e(t)$ creating a magnetic field B through which the rotor is free to turn with an angular velocity ω r/s. A voltage $E_i(t)$ is applied to the armature coil, of resistance R and Inductance L wound around the rotor, as seen in the figure and in more detail in Fig. 5.6.

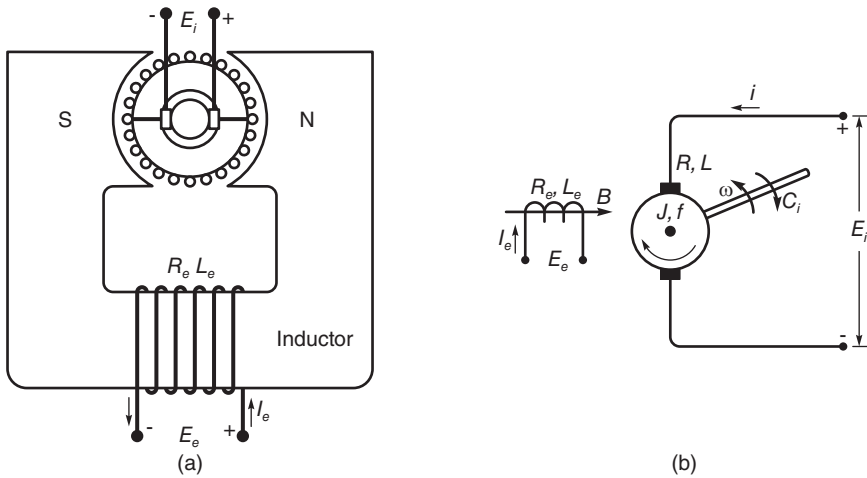


FIGURE 5.6 DC motor (a) armature and inductor, (b) inductor circuit.

The rotor is in the form of a cylinder of length l and radius r around which is wound a coil of n windings. One such winding is shown in Fig. 5.7.

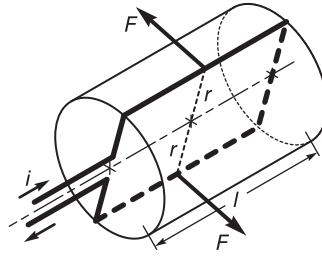


FIGURE 5.7 One winding of DC motor coil.

The following are the major component values:

- e_c : back emf in the rotor armature
- R_e, L_e : resistance in ohms and inductance in henry of the inductor circuit
- R, L : resistance and inductance in the armature circuit.
- $2n$: number of rods in the rotor armature circuit
- n_e : number of turns in the inductor coil

We may write relative to the inductor circuit

$$E_e = R_e i_e + L_e \frac{di_e}{dt}. \quad (5.24)$$

The magnetic field B is the product of the permeability μ and the magnetic intensity H and

$$B = \mu H = \mu n_e i_e \text{ Weber/m}^2. \quad (5.25)$$

In relation to the armature circuit we have

$$E_i = Ri + L \frac{di}{dt} + e_c \quad (5.26)$$

where e_c is the back emf evaluated using the “ Bli ” rule

$$e_c = 2nBlr\omega = 2nlr\mu n_e i_e \omega = k_1 i_e \omega. \quad (5.27)$$

The torque in the armature circuit is the couple evaluated using the “ Bli ” rule, i.e. a force $F = Bli$ per rod. Referring to Fig 5.7, we have

$$C = 2nBlri = 2n\mu Hlri = k_1 i_e i \text{ Newton meter}. \quad (5.28)$$

Let $C_i(t)$ be a couple acting on the load, opposing its rotation. We have, assuming the rotor has inertia J and viscous friction coefficient b ,

$$C = C_i(t) + J\dot{\omega} + b\omega. \quad (5.29)$$

We note that the differential equations are nonlinear, containing the products $i_e \omega$ and $i_e i$. The operation is simplified by fixing one of the two variables i_e or i . As an example, consider the case where i_e is a constant, $i_e = K_e$ and the control effected by the input voltage $E_i(t)$. In this case we have

$$E_i(t) = Ri + L \frac{di}{dt} + k_1 K_e \omega \quad (5.30)$$

$$k_1 K_e i = J\dot{\omega} + b\omega + C_i(t) \quad (5.31)$$

$$E_i(s) = (R + Ls) I(s) + k_1 K_e \omega \tag{5.32}$$

$$E_1(s) \triangleq E_i(s) - k_1 K_e \omega = (R + Ls) I(s) \tag{5.33}$$

$$I(s) = \frac{1}{R + Ls} E_1(s) \tag{5.34}$$

$$k_1 K_e I(s) = (Js + b) \Omega(s) + C_i(s) \tag{5.35}$$

$$C_1(s) \triangleq k_1 K_e I(s) - C_i(s) = (Js + b) \Omega(s) \tag{5.36}$$

$$\Omega(s) = \frac{1}{Js + b} C_1(s) \tag{5.37}$$

as represented by the block diagram in Fig. 5.8.

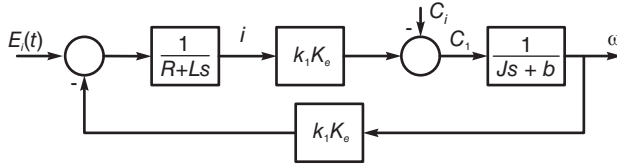


FIGURE 5.8 DC motor block diagram.

Usually the armature inductance L is negligible. Writing

$$G_1 = \frac{k_1 K_e}{R + Ls} = \frac{k_1 K_e}{R}, \quad G_2 = \frac{1}{Js + B}, \quad G_3 = k_1 K_e \tag{5.38}$$

and referring to the redrawn block diagram in the form shown in Fig. 5.9(a) with the input labeled x , output labeled y and the output of the G_1 block labeled x_1 , we may write

$$X_1 = (X - G_3 Y) G_1 = X G_1 - G_3 G_1 Y \tag{5.39}$$

which allows us to displace the left adder to the right, leading to the diagram of Fig. 5.9(b) which upon opening the feedback loop leads to that shown in Fig. 5.9(c) where

$$H_1(s) = \frac{\frac{1}{Js + b}}{1 + \frac{1}{Js + b} \times \frac{k_1^2 K_e^2}{R}} = \frac{1}{Js + b + \frac{k_1^2 K_e^2}{R}} = \frac{R}{(Js + b) R + k_1^2 K_e^2} \tag{5.40}$$

The system transfer function, if the couple $C_i(t)$ is nil, is given by $H(s) = G_1 H_1(s)$.

5.5 A Speed-Control System

We consider a system which regulates rotational speed. As shown in Fig. 5.10, the system includes a rotary potentiometer at its input, the angular position of which, shown as the angle θ , determines the speed Ω of the rotary load at its output. The system includes a differential amplifier, a DC motor, gears for speed conversion and a flywheel representing the rotary load.

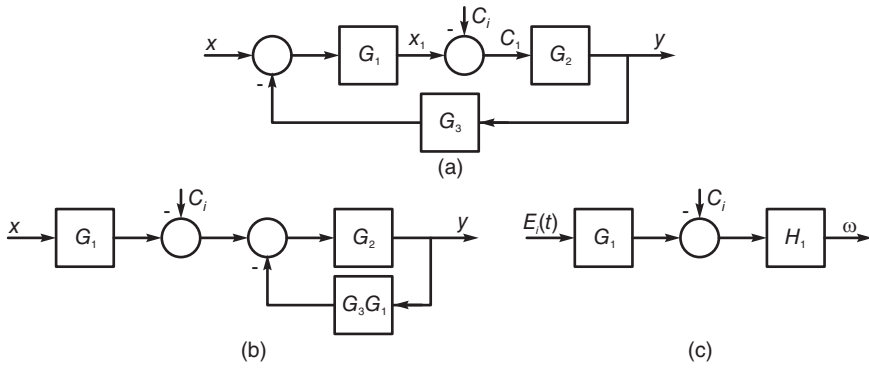


FIGURE 5.9 DC motor block diagram simplification steps.

It also includes a dynamo used as a tachometer measuring the load rotational speed and producing an electric signal e_t that is fed back to the differential amplifier input.

We start by making the following observations:

1. The potentiometer output in volts denoted e_i in the figure is given by $e_i = \theta E / (2\pi)$ volts.
2. The amplifier has a gain A . Its output voltage is given by $v = A(e_i - e_t)$ volts.
3. The electric motor is assumed to have a rotor in the form of a cylinder of radius r and length l , similarly to the one described in the last section and shown in Fig. 5.7, which rotates in the magnetic field B of a magnet. The figures shows the flow of current i in one winding around the rotor. There are n such windings for a total of $2n$ rods that rotate in the magnetic field, with total coil resistance of R ohm and inductance L henry. The rotor is assumed to have a rotational speed Ω_m and a back electromotive force (emf) of $e_c = k_m \Omega_m$ volts.

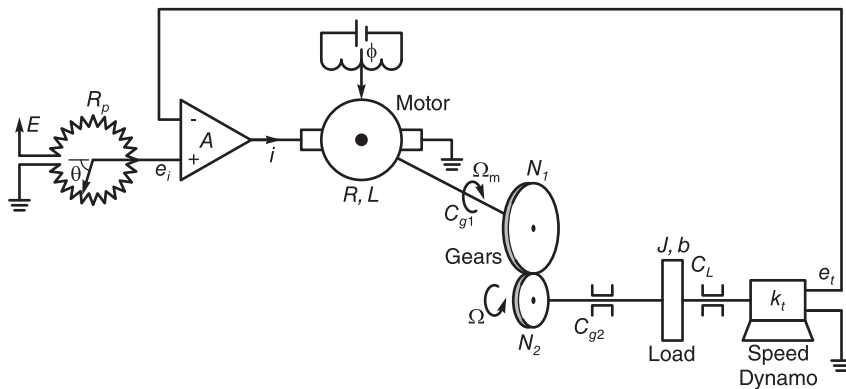


FIGURE 5.10 A system for speed control.

We can therefore write

$$v = iR + L \frac{di}{dt} + e_c. \tag{5.41}$$

4. The current i flowing in the magnitic field B Weber/m² of the motor's permanent

magnet, produces a rotational couple C . The couple is proportional to the current. The force on each rod of the n windings is given by, $Bl i$, the couple per winding is $2Bl r i$ and the total couple C is thus given by

$$C = 2n Bl r i = k_m i \text{ Newton Meter} \tag{5.42}$$

where

$$k_m = 2n Bl r. \tag{5.43}$$

5. This couple C works against the opposing couples, namely, the couple $J_m \dot{\Omega}_m$ due to the moment of inertia of the rotor (J_m is in kgm^2), viscous friction couple $b_m \Omega_m$, the coefficient b_m being in $\text{Nm}/(\text{r/s})$, and a couple C_{g1} that is the effect of the load reflected through the gears. These couples are depicted in Fig. 5.11. We can therefore write

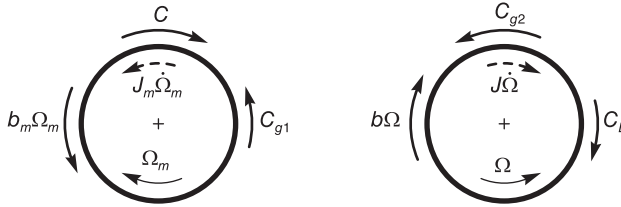


FIGURE 5.11 Equilibrium of couples in rotating systems.

$$C = J_m \dot{\Omega}_m + b_m \Omega_m + C_{g1}. \tag{5.44}$$

6. Considering a gear ratio N_1/N_2 , as shown in Fig. 5.11, the following relations apply between the couple C_{g1} due to the load, opposing the rotation of the the motor shaft and C_{g2} its value on the load side; as well as the rotational speeds Ω_m and Ω at the two sides respectively of the gears

$$\frac{C_{g1}}{C_{g2}} = \frac{N_1}{N_2} \tag{5.45}$$

$$\frac{\Omega_m}{\Omega} = \frac{N_2}{N_1}. \tag{5.46}$$

Assuming as shown in Fig. 5.10 a load in the form of a flywheel of inertia J and an external couple $C_L(t)$ resisting its rotation, together with viscous friction of coefficient b we can represent the equilibrium of couples as shown in Fig. 5.11, writing

$$C_{g2} = J \dot{\Omega} + b \Omega + C_L. \tag{5.47}$$

As detailed in what follows, using these equations we can construct the block diagram shown in Fig. 5.12. We apply the Laplace transform to each equation, assuming zero initial conditions, thus obtaining the transfer function of each subsystem. In particular, starting by the equation relating v and i we write

$$v - e_c = v_d = Ri + L \frac{di}{dt} \tag{5.48}$$

$$V_d(s) = (R + Ls) I(s) \tag{5.49}$$

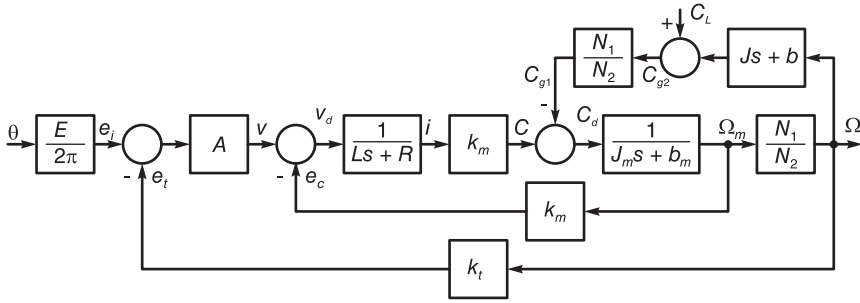


FIGURE 5.12 System block diagram.

$$H_1(s) = \frac{I(s)}{V_d(s)} = \frac{1}{R + Ls}. \tag{5.50}$$

This subsystem appears as part of the block diagram shown in Fig. 5.12. The diagram is then extended by adding the block representing the relation

$$C = k_m I. \tag{5.51}$$

Writing

$$C_d = C - C_{g1i} = J_m \dot{\Omega}_m + b_m \Omega_m \tag{5.52}$$

we have

$$C_d(s) = (J_m s + b_m) \Omega_m(s) \tag{5.53}$$

$$H_2(s) = \frac{\Omega_m(s)}{C_d(s)} = \frac{1}{J_m s + b_m} \tag{5.54}$$

which represents another section of the overall block diagram of Fig. 5.12. We subsequently use the relation

$$\Omega = (N_1/N_2)\Omega_m \tag{5.55}$$

$$C_{g2}(s) = (Js + b)\Omega(s) + C_L \tag{5.56}$$

$$C_{g1i}(s) = (N_1/N_2)C_{g2}(s) \tag{5.57}$$

thus closing the loop to C_{g1i} . We also have the relations $e_c = k_m \Omega_m$ and $e_t = k_t \Omega$ as shown in the figure. Assuming the motor inductance L to be negligibly small, we may write

$$C = (v - e_c)(k_m/R) = vk_m/R - k_m^2 \Omega_m/R \triangleq x_1 - x_2 \tag{5.58}$$

as shown in Fig. 5.13.

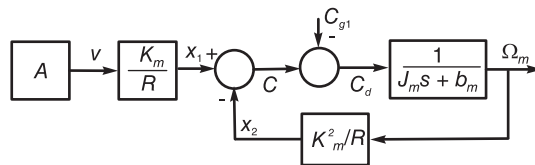


FIGURE 5.13 Block diagram of a system component.

We can displace the second adder in this figure to the left of the first by writing

$$C_2 = C - C_{g1i} = x_1 - x_2 - C_{g1i} = (x_1 - C_{g1i}) - x_2 \tag{5.59}$$

as shown in Fig. 5.14,

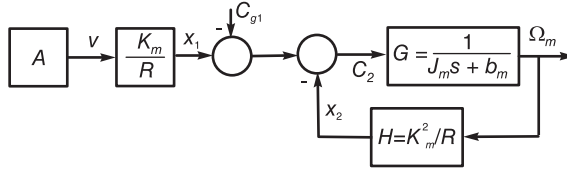


FIGURE 5.14 Subsystem block diagram.

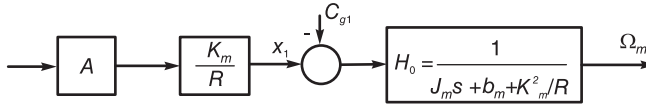


FIGURE 5.15 Reduced block diagram.

Letting $G = 1/(J_m s + b_m)$ and $H = k_m^2/R$, we evaluate the transfer function of the loop with feedback, obtaining

$$H_0 = \frac{G}{1 + GH} = \frac{1}{J_m s + b_m + k_m^2/R} \tag{5.60}$$

as shown in Fig. 5.15. Replacing the section between the amplifier output v and the rotational speed Ω_m in the overall system, Fig. 5.12, by its equivalent system of Fig. 5.15 we obtain the block diagram shown in Fig. 5.16.

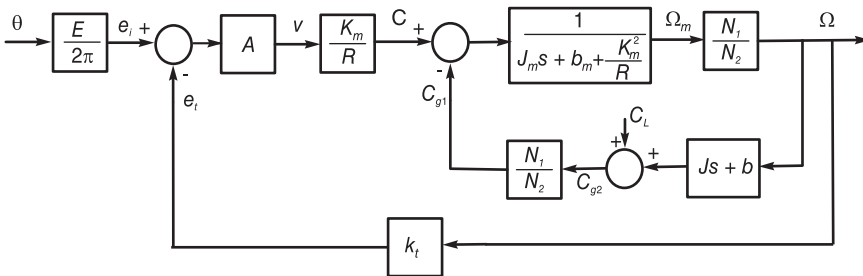


FIGURE 5.16 Overall block diagram.

To obtain the overall system transfer function with load torque $C_L = 0$ we follow similar steps, replacing the subsystem with a feedback loop by its open loop equivalent.

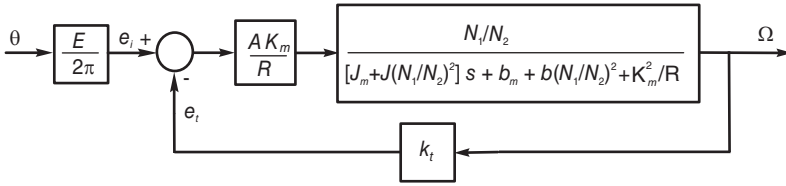


FIGURE 5.17 Block diagram simplification step.

The result is shown in Fig. 5.17, which can in turn be reduced to Fig. 5.18, wherein

$$H_1 = E_i(s)/\Theta(s) = E/(2\pi) \tag{5.61}$$

and

$$H_2 = \frac{A(k_m/R)(N_1/N_2)}{[J_m + J(N_1/N_2)^2]s + b_m + b(N_1/N_2)^2 + k_m^2/R + A(k_m k_t/R)(N_1/N_2)} \tag{5.62}$$

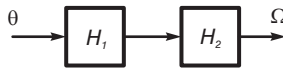


FIGURE 5.18 Two systems in cascade.

and the overall system transfer function is $H(s) = H_1(s)H_2(s)$. The system may be simulated using MATLAB®–Simulink, by connecting appropriate blocks as shown in Fig. 5.19.

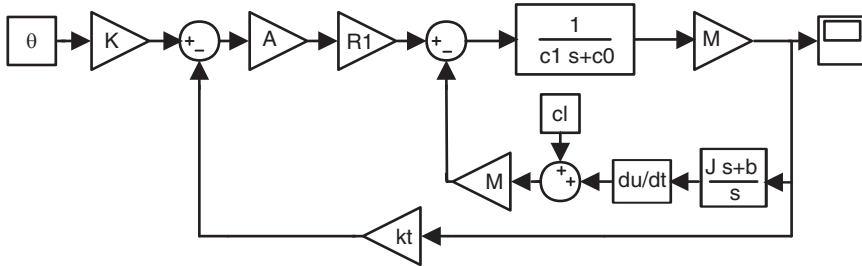


FIGURE 5.19 Simulink system block diagram.

Alternatively, a simplified block diagram may be used, as shown in Fig. 5.20. The system step response appears as the oscilloscope output shown in the figure.

The program parameters are:

```
% Simulink parameters for speed control simulation
theta=pi/2;
Cl=0;
```

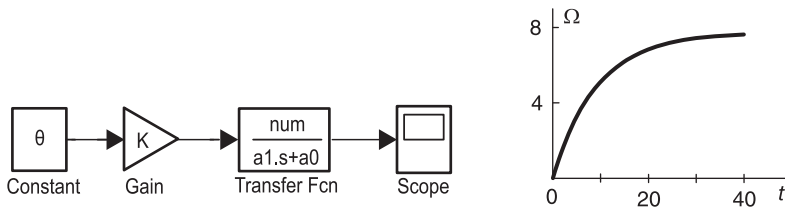


FIGURE 5.20 Simplified Simulink system block diagram.

```

E=10;
A=10;
L=0;
R=1;
km=1;
kt=0.3;
R1=km/R;
Jm=100;
bm=0.5;
M=10;
J=2;
b=0.01;
c1=Jm;
c0=bm+(km^2)/R
num=A*km*M/R;
a1=Jm+J*M^2;
a0=bm+b*M^2+(km^2)/R+A*km*kt*M/R;
plot(ScopeData(:,1), ScopeData(:,2))
grid;
title('Step response of speed control system');
ylabel('omega');
xlabel('t');

```

5.6 Homology

Homology may be used to model a physical system by constructing a homologous, equivalent, system in a different medium. As an illustration, we focus our attention on homologies that allow us to study a mechanical system by analyzing its equivalent electrical system. The same approach may be used to convert other systems such as, for example, hydraulic, acoustic and heat transfer systems into electrical circuit equivalents. An electro-mechanical homology can be deduced by observing a simple mechanical system and its electrical equivalent. Consider the system of a mass and attached spring shown in Fig. 5.21 (a).

The force in the spring is proportional to its deformation from its rest position. Let the stiffness of the spring be k (Newton/meter or n/m) and assume that the force F is applied with the system at rest, so that if the mass m travels a distance x then the force in the spring is kx . We also assume, as shown in the figure, that there is viscous friction between

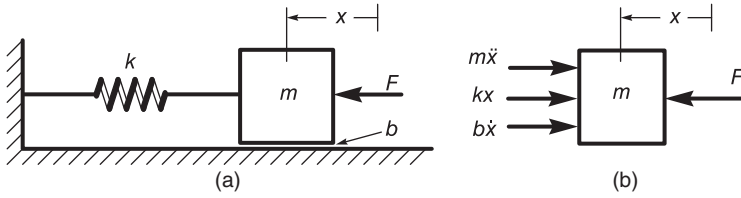


FIGURE 5.21 (a) A mechanical translational system, (b) Equilibrium of forces on a free-body diagram.

the mass and the support, with coefficient of friction b . The equilibrium of forces are shown on an isolated free-body diagram in Fig. 5.21 (b).

We note that the force of inertia $m\ddot{x}$ is opposite to the displacement direction x . The equation describing the balance of forces is given by

$$F = m\ddot{x} + b\dot{x} + kx. \tag{5.63}$$

Consider the electric circuit shown in Fig. 5.22, having as input a current source of $i(t)$ amperes (A) and has an output of v volts.

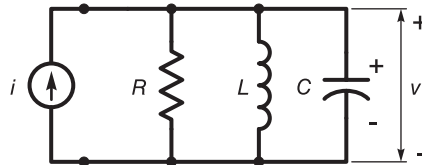


FIGURE 5.22 Electric circuit as a homologue of a mechanical system.

We have

$$i = C \frac{dv}{dt} + \frac{1}{R}v + \frac{1}{L} \int v dt. \tag{5.64}$$

Rewriting the mechanical system equation as a function of the speed $V = \dot{x}$ we have

$$F = m \frac{dV}{dt} + bV + k \int V dt. \tag{5.65}$$

Comparing the two last equations we note that the electric circuit homology implies the following correspondence of variables

Mechanical	Electrical homology
F	i
V	v
m	C
b	$1/R$
k	$1/L$

(5.66)

5.7 Transient and Steady-State Response

Let $H(s)$ be the transfer function of a linear time-invariant system having an input $v(t)$ and output $y(t)$, Fig. 5.23. We can write the transfer function $H(s)$ as a ratio of two polynomials

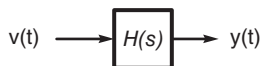


FIGURE 5.23 System with input and output.

$$H(s) = \frac{N(s)}{D(s)}. \quad (5.67)$$

Let the poles of $H(s)$ be p_1, p_2, \dots, p_n , i.e.

$$H(s) = \frac{N(s)}{(s-p_1)(s-p_2)\dots(s-p_n)} \quad (5.68)$$

and the input $v(t)$ to the system to be such that

$$V(s) = \frac{N_i(s)}{(s-q_1)(s-q_2)\dots(s-q_m)}. \quad (5.69)$$

We have

$$\begin{aligned} Y(s) &= V(s)H(s) \\ &= \frac{N(s)N_i(s)}{(s-p_1)(s-p_2)\dots(s-p_n)(s-q_1)(s-q_2)\dots(s-q_m)}. \end{aligned} \quad (5.70)$$

For simplicity we assume distinct poles. Using a partial fraction expansion of $Y(s)$ we may write

$$Y(s) = \frac{A_1}{s-p_1} + \frac{A_2}{s-p_2} + \dots + \frac{A_n}{s-p_n} + \frac{B_1}{s-q_1} + \frac{B_2}{s-q_2} + \dots + \frac{B_m}{s-q_m} \quad (5.71)$$

wherefrom

$$y(t) = \mathcal{L}^{-1}[Y(s)] = \left\{ \sum_{i=1}^n A_i e^{p_i t} + \sum_{i=1}^m B_i e^{q_i t} \right\} u(t) = y_n(t) + y_s(t) \quad (5.72)$$

where

$$y_n(t) = \sum_{i=1}^n A_i e^{p_i t} u(t) \quad (5.73)$$

is called the system *natural response*, also called the *complementary* or *homogeneous solution*, and

$$y_s(t) = \sum_{i=1}^m B_i e^{q_i t} u(t) \quad (5.74)$$

is called the *steady-state response*, the *forced response* or the *particular solution*. For a stable system the poles p_1, p_2, \dots, p_n are all in the left half of the s plane, that is,

$$\Re[p_i] < 0, \quad i = 1, 2, \dots, n. \quad (5.75)$$

The natural response $y_n(t)$ is thus transient in nature, vanishing as $t \rightarrow \infty$. The forced response $y_s(t)$ depends on the input excitation force $v(t)$ and constitutes the steady state response. If in particular the input $v(t)$ has a pure sinusoidal component then two poles q_i and $q_j = q_i^*$ lie on the $j\omega$ axis of the s plane. The steady-state output will thus have a pure sinusoidal component that lasts in the form of a steady-state output as $t \rightarrow \infty$.

5.8 Step Response of Linear Systems

We have noted that the transfer function $H(s)$ of a linear system can be decomposed using a partial fraction expansion into the sum of first order systems. Moreover, by adding two terms in the case of two conjugate poles, we can combine their contributions into one of a second order system. Analyzing the time and frequency response of first and second order systems is thus of interest, an important step in the study of the behavior of general order linear systems.

5.9 First Order System

To study the step response of a first order system let

$$H(s) = \frac{1}{s\tau + 1} \quad (5.76)$$

be the system transfer function, and let the input $v(t)$ be the unit step function and $y(t)$ be the output. We have

$$Y(s) = V(s)H(s) = \frac{1}{s(s\tau + 1)} = \frac{1}{s} - \frac{\tau}{s\tau + 1} \quad (5.77)$$

$$y(t) = \left\{ 1 - e^{-t/\tau} \right\} u(t). \quad (5.78)$$

The *system response time* is often taken to be the time after which the response $y(t)$ reaches 5% of its final value. It is then referred to as the *5% response time*. Since the final value of the response, the value of $y(t)$ as $t \rightarrow \infty$, is 1, the response time is the value of t for which

$$y(t) = 1 - e^{-t/\tau} = 1 - 0.05 \quad (5.79)$$

i.e. $e^{-t/\tau} = 0.05$. Now $0.05 \cong e^{-3}$, so that $e^{-t/\tau} \cong e^{-3}$, or $t \cong 3\tau$. The *5% response time* may therefore be taken equal to 3τ .

We can similarly find the *2% response time*. In this case noticing that $0.02 \cong e^{-4}$ we write $e^{-t/\tau} = e^{-4}$, wherefrom the *time response within 2%* is given by $t \cong 4\tau$.

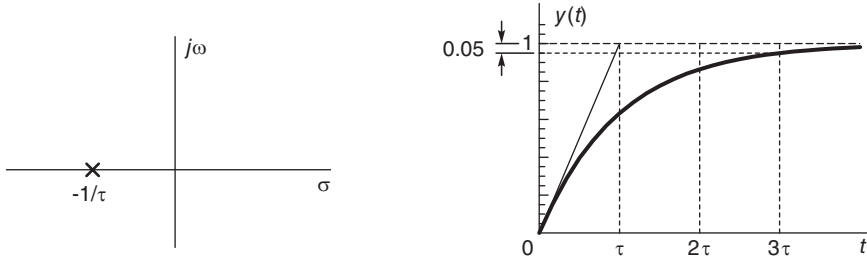


FIGURE 5.24 First order system pole and step response.

The system pole and its step response $y(t)$ are shown in Fig. 5.24. Note that the derivative of $y(t)$ at $t = 0^+$ is

$$\frac{dy}{dt} \Big|_{t=0^+} = \frac{1}{\tau} e^{-t/\tau} u(t) \Big|_{t=0^+} = \frac{1}{\tau}. \tag{5.80}$$

This initial slope is shown in the figure, where the tangent line at $t = 0$ has an abscissa of τ and ordinate of one. The 5% response time is shown in the figure to be equal to three times the value τ .

5.10 Second Order System Model

The transfer function $H(s)$ of a second order system is commonly written in the form

$$H(s) = \frac{\omega_0^2}{s^2 + 2\omega_0\zeta s + \omega_0^2}. \tag{5.81}$$

We can write

$$H(s) = \frac{\omega_0^2}{(s - p_1)(s - p_2)} \tag{5.82}$$

$$p_1, p_2 = \begin{cases} -\omega_0\zeta \pm \omega_0\sqrt{\zeta^2 - 1}, & \zeta > 1 \\ -\omega_0\zeta \pm j\omega_0\sqrt{1 - \zeta^2}, & 0 < \zeta < 1 \\ -\omega_0\zeta, & \zeta = 1 \\ \pm j\omega_0, & \zeta = 0. \end{cases} \tag{5.83}$$

The positions of the two poles for the different values of ζ , namely, $\zeta = 0$, $0 < \zeta < 1$, $\zeta = 1$ and $\zeta > 1$ and a constant ω_0 are shown in Fig. 5.25. We note that with ω_0 constant the poles move from the values $\pm j\omega_0$ on the $j\omega$ axis, along a circle of radius ω_0 until they coincide for $\zeta = 1$. Subsequently, for $\zeta > 1$ and increasing they split and move along the real axis as shown in the figure.

The value ω_0 is called the *natural frequency*. The imaginary part of the pole position for the case $0 < \zeta < 1$ is called the *damped natural frequency* ω_p , that is,

$$\omega_p = \omega_0\sqrt{1 - \zeta^2}. \tag{5.84}$$

We shall see later on that the peak of the frequency response amplitude spectrum $|H(j\omega)|$ for this same case $0 < \zeta < 1$ is at a frequency, known as the *resonance frequency*, given by

$$\omega_r = \omega_0\sqrt{1 - 2\zeta^2}. \tag{5.85}$$

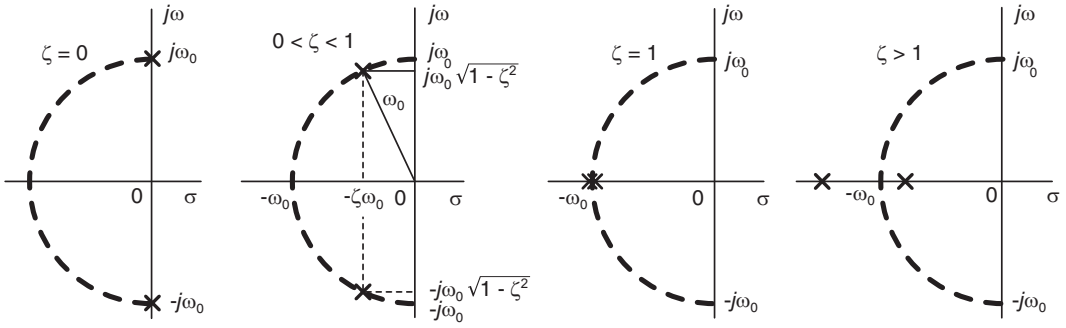


FIGURE 5.25 Poles of second order system as damping increases.

If the input $v(t)$ is the unit step function $v(t) = u(t)$ the output is given by

$$Y(s) = V(s)H(s) = \frac{\omega_0^2}{s(s^2 + 2\omega_0\zeta s + \omega_0^2)}. \quad (5.86)$$

For the case $0 < \zeta < 1$ the two complex conjugate poles to the left of the $j\omega$ axis lead to a damped sinusoidal system response. In particular, writing $p = \alpha + j\beta$ where $\alpha = -\omega_0\zeta$ and $\beta = \omega_0\sqrt{1-\zeta^2}$ we have $\omega_0 = \sqrt{\alpha^2 + \beta^2}$ and

$$Y(s) = \frac{\omega_0^2}{s(s-p)(s-p^*)} = \frac{A}{s} + \frac{B}{s-p} + \frac{B^*}{s-p^*} \quad (5.87)$$

$$A = \frac{\omega_0^2}{pp^*} = 1 \quad (5.88)$$

$$B = \frac{\omega_0^2}{p(p-p^*)} = \frac{-\omega_0^2}{2\beta} \frac{(\beta + j\alpha)}{\alpha^2 + \beta^2} \quad (5.89)$$

$$Y(s) = \frac{1}{s} - \frac{\omega_0^2}{2\beta(\alpha^2 + \beta^2)} \left\{ \frac{\beta + j\alpha}{s-p} + \frac{\beta - j\alpha}{s-p^*} \right\} \quad (5.90)$$

$$y(t) = 1 - \frac{1}{2\omega_0\sqrt{1-\zeta^2}} \left\{ (\beta + j\alpha)e^{pt} + (\beta - j\alpha)e^{p^*t} \right\}. \quad (5.91)$$

Writing

$$\beta + j\alpha = \omega_0 e^{j \tan^{-1}(\alpha/\beta)} = \omega_0 e^{-j \tan^{-1}(\zeta/\sqrt{1-\zeta^2})} = \omega_0 e^{-j(\pi/2 - \cos^{-1} \zeta)} = -j\omega_0 e^{j \cos^{-1} \zeta} \quad (5.92)$$

we obtain

$$y(t) = \left\{ 1 - \frac{1}{\sqrt{1-\zeta^2}} e^{-\zeta\omega_0 t} \sin\left(\omega_0\sqrt{1-\zeta^2} t + \cos^{-1} \zeta\right) \right\} u(t). \quad (5.93)$$

5.11 Settling Time

Similarly to the response time, the *settling time* t_s is the time after which the system step response deviates by less than 5% of its steady-state value as measured from the instant the input unit step function is applied. The concept is illustrated schematically in Fig. 5.26(a).

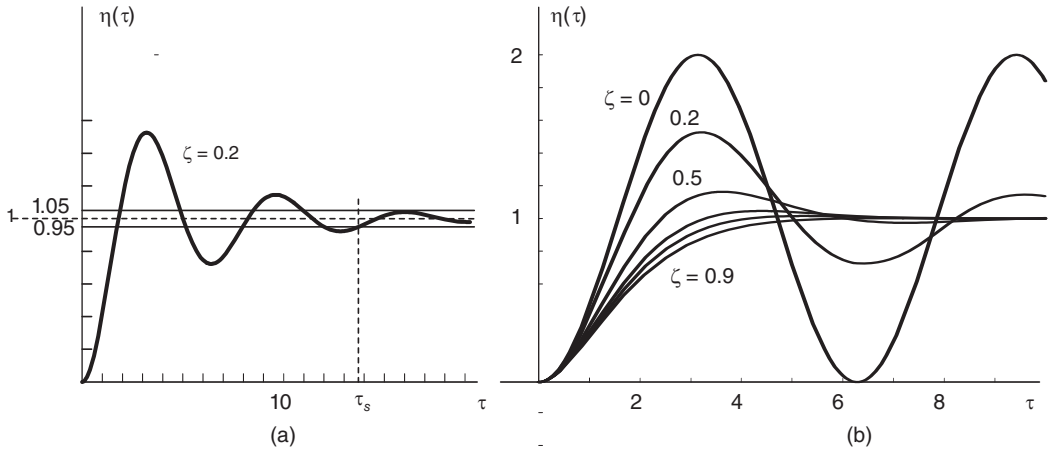


FIGURE 5.26 Step response of second order system and effect of varying damping coefficient.

In order to plot the response versus t for different values of the damping coefficient ζ the value of the natural frequency ω_0 would need to be specified. Instead of producing a plot corresponding to each value assigned to ω_0 we can produce normalized plots by writing $\tau = \omega_0 t$ and plotting the response as a function of τ . We may write for $t > 0$

$$\eta(\tau) = y(t)|_{t=\tau/\omega_0} = 1 - \frac{1}{\sqrt{1-\zeta^2}} e^{-\zeta\tau} \sin\left(\sqrt{1-\zeta^2} \tau + \cos^{-1} \zeta\right). \quad (5.94)$$

The normalized response $\eta(\tau)$ is shown in Fig. 5.26 (b) for different values of the damping coefficient ζ . Note the diminishing of the overshoot of $\eta(\tau)$ as ζ increases from $\zeta = 0$ toward $\zeta = 1$. In fact, the overshoot vanishes for $\zeta \geq 0.707$.

If $\zeta = 0$ the poles are on the $j\omega$ axis. The system response has a pure sinusoidal component. As ζ increases from 0, the response becomes more damped. With $\zeta = 1$, the case of double pole, the response reaches its final value displaying no overshoot. For $\zeta > 1$ the system is over-damped, the poles are both real on both sides of the point $\sigma = -\omega_0$ and the response rises slowly to its final value of 1.

By varying ζ while keeping ω_0 constant and evaluating the corresponding settling time t_s we obtain the relation shown in Fig. 5.27, where $\tau_s = \omega_0 t_s$ is plotted versus ζ . As the figure shows, the minimum settling time corresponds to $\zeta = 0.707$. This is called the *optimal damping coefficient*.

Example 5.1 Consider the resistance R inductance L capacitance C (R - L - C) circuit shown in Fig. 5.28. Evaluate the natural frequency ω_0 and the damping coefficient ζ . We have

$$v_i(t) = Ri + L \frac{di}{dt} + \frac{1}{C} \int i dt$$

$$v_0(t) = \frac{1}{C} \int i dt.$$

Assuming zero initial conditions we write

$$V_i(s) = RI(s) + LsI(s) + \frac{1}{Cs}I(s)$$

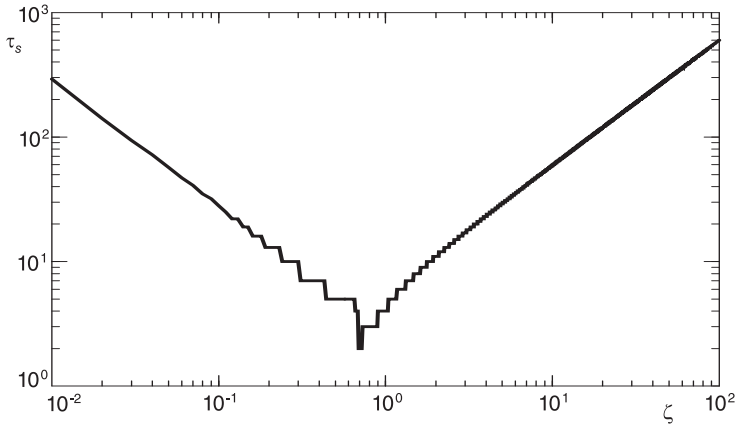


FIGURE 5.27 Settling time as a function of damping coefficient.

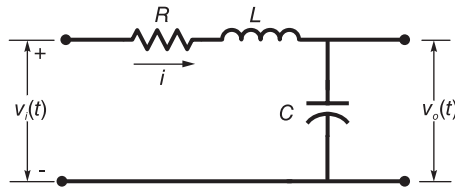


FIGURE 5.28 R-L-C circuit.

$$V_o(s) = \frac{1}{Cs} I(s)$$

$$H(s) = \frac{V_o(s)}{V_i(s)} = \frac{1/(Cs)}{R + Ls + 1/(Cs)} = \frac{1/(LC)}{s^2 + (R/L)s + 1/(LC)} = \frac{\omega_0^2}{s^2 + 2\zeta\omega_0s + \omega_0^2}$$

$$\omega_0 = 1/\sqrt{LC}, \quad 2\zeta\omega_0 = R/L, \quad \zeta = R\sqrt{LC}/(2L) = (R/2)\sqrt{C/L}.$$

Example 5.2 A mechanical translation system is shown in Fig. 5.29. A force f is applied to the mass m , which moves against a spring of stiffness k , a damper of viscous friction coefficient b_1 and viscous friction with the support of coefficient b_2 .

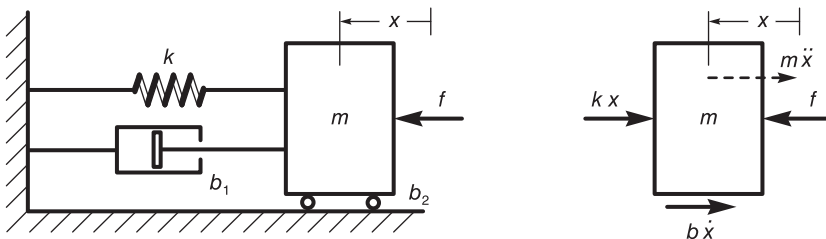


FIGURE 5.29 Mechanical translation system and mass equilibrium of forces.

The force $f(t)$ is opposed by the force $m\ddot{x}$, which acts in a direction that is opposite to the

direction x of movement x . We can write

$$f = m\ddot{x} + b\dot{x} + kx.$$

where $b = b_1 + b_2$. Laplace transforming we have

$$F(s) = (ms^2 + bs + k) X(s).$$

The transfer function is given by

$$H(s) = \frac{X(s)}{F(s)} = \frac{1}{ms^2 + bs + k} = \frac{1/m}{s^2 + (b/m)s + k/m} = \frac{\omega_0^2/k}{s^2 + 2\zeta\omega_0s + \omega_0^2}$$

$$\omega_0 = \sqrt{k/m}, \quad 2\zeta\omega_0 = b/m, \quad \zeta = b/(2\sqrt{km}).$$

A rotational mechanical system shown in Fig. 5.30 represents a rotating shaft with as input an angular displacement θ_1 and as output the angle of rotation θ_2 of the load of inertia J . The balance of couples is shown in the figure.

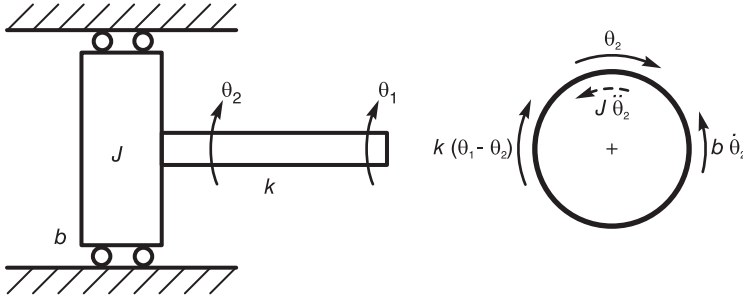


FIGURE 5.30 Rotational system.

The shaft is assumed to be of stiffness k so that the torque applied to the load is given by $k(\theta_1 - \theta_2)$. This torque is opposed by the moment of inertia $J\ddot{\theta}_2$ and the viscous friction $b\dot{\theta}_2$

$$k(\theta_1 - \theta_2) = J\ddot{\theta}_2 + b\dot{\theta}_2. \tag{5.95}$$

Laplace transforming the equations, assuming zero initial conditions, we have

$$k[\Theta_1(s) - \Theta_2(s)] = Js^2\Theta_2(s) + bs\Theta_2(s) \tag{5.96}$$

$$H(s) = \frac{\Theta_2(s)}{\Theta_1(s)} = \frac{k}{Js^2 + bs + k} = \frac{k/J}{s^2 + (b/J)s + k/J} = \frac{\omega_0^2}{s^2 + 2\zeta\omega_0s + \omega_0^2} \tag{5.97}$$

$$\omega_0 = \sqrt{k/J}, \quad 2\zeta\omega_0 = b/J, \quad \zeta = b/(2\sqrt{Jk}).$$

5.12 Second Order System Frequency Response

The frequency response $H(j\omega)$ of a second order system is given by

$$H(j\omega) = \frac{1}{(j\omega/\omega_0)^2 + j2\zeta(\omega/\omega_0) + 1}. \tag{5.98}$$

Let $\Omega = \omega/\omega_0$ be a normalized frequency and $G(j\Omega)$ be the corresponding normalized frequency response

$$G(j\Omega) = H(j\omega)|_{\omega=\omega_0\Omega} = \frac{1}{(1 - \Omega^2) + j2\zeta\Omega}. \tag{5.99}$$

The absolute value and phase of the normalized frequency response are shown in Fig. 5.31 for different values of the parameter ζ . We note the resonance-type phenomenon that appears in the curve of $|G(j\Omega)|$. The resonance peak disappears for values of ζ greater than $\zeta = 0.707$.

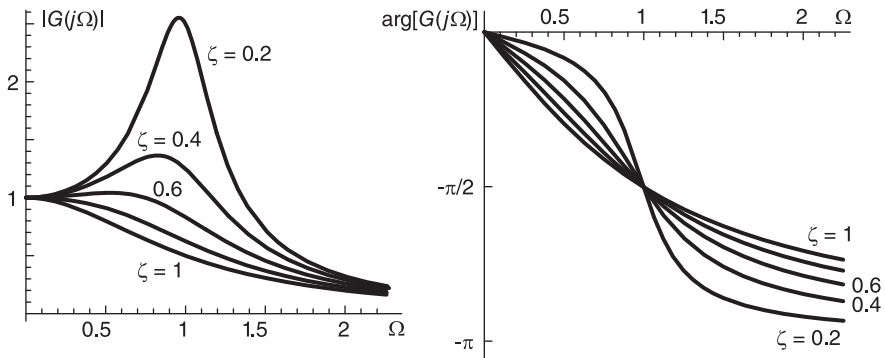


FIGURE 5.31 Effect of damping coefficient on second order system amplitude and phase response.

5.13 Case of a Double Pole

With the damping coefficient $\zeta = 1$ the poles coincide so that $p, p^* = -\omega_0$. The step response is given by

$$Y(s) = \frac{\omega_0^2}{s(s^2 + 2\omega_0s + \omega_0^2)} = \frac{\omega_0^2}{s(s + \omega_0)^2}. \tag{5.100}$$

Effecting a partial fraction expansion we obtain

$$Y(s) = \frac{1}{s} - \frac{1}{s + \omega_0} - \frac{\omega_0}{(s + \omega_0)^2} \tag{5.101}$$

$$y(t) = \{1 - e^{-\omega_0 t} - \omega_0 t e^{-\omega_0 t}\} u(t). \tag{5.102}$$

We can write

$$\eta_2(\tau) = y(t)|_{t=\tau/\omega_0} = \{1 - e^{-\tau} - \tau e^{-\tau}\} u(t). \tag{5.103}$$

The response is sketched in Fig. 5.32.

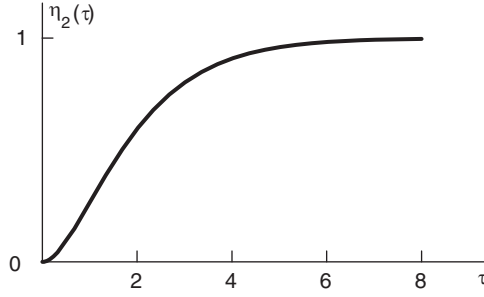


FIGURE 5.32 Step response of a double pole second order system.

5.14 The Over-Damped Case

With $\zeta > 1$ we have two distinct real poles given by

$$p_1, p_2 = -\zeta\omega_0 \pm \omega_0\sqrt{\zeta^2 - 1} \tag{5.104}$$

$$Y(s) = \frac{\omega_0^2}{s(s-p_1)(s-p_2)} = \frac{A}{s} + \frac{B}{s-p_1} + \frac{C}{s-p_2} \tag{5.105}$$

$$y(t) = \{A + Be^{p_1 t} + Ce^{p_2 t}\} u(t) \tag{5.106}$$

$$A = \frac{\omega_0^2}{p_1 p_2} = 1, \quad B = \frac{1}{p_1(p_1 - p_2)} = \frac{1}{2(\zeta^2 - 1) - 2\zeta\sqrt{\zeta^2 - 1}} \tag{5.107}$$

$$C = \frac{1}{p_2(p_2 - p_1)} = \frac{1}{2(\zeta^2 - 1) + 2\zeta\sqrt{\zeta^2 - 1}}. \tag{5.108}$$

5.15 Evaluation of the Overshoot

Differentiating the expression of the step response $y(t)$ and equating the derivative to zero we find the maxima/minima of the response, wherefrom the overshoot. With $\theta = \cos^{-1} \zeta$

$$\frac{dy}{dt} = -\omega_0 e^{-\zeta\omega_0 t} \cos(\omega_0\sqrt{1-\zeta^2} t + \theta) + \frac{\zeta\omega_0 e^{-\zeta\omega_0 t}}{\sqrt{1-\zeta^2}} \sin(\omega_0\sqrt{1-\zeta^2} t + \theta) = 0.$$

$$\tan(\omega_0\sqrt{1-\zeta^2} t + \theta) = \frac{\sqrt{1-\zeta^2}}{\zeta} = \tan \theta \tag{5.109}$$

$$\omega_0\sqrt{1-\zeta^2} t = 0, \pi, 2\pi, \dots \tag{5.110}$$

The overshoot occurs therefore at a time t_0 given by

$$t_0 = \pi / [\omega_0\sqrt{1-\zeta^2}]. \tag{5.111}$$

At the peak point of the overshoot the value of the response is

$$y(t_0) = 1 + \frac{1}{\sqrt{1-\zeta^2}} e^{-\zeta\pi/\sqrt{1-\zeta^2}} \sin(\pi + \theta) = 1 + e^{-\zeta\pi/\sqrt{1-\zeta^2}} \tag{5.112}$$

and the overshoot, denoted r is given by

$$r = y(t_0) - 1 = e^{-\zeta\pi/\sqrt{1-\zeta^2}}. \quad (5.113)$$

The effect of varying ζ on the amount r of overshoot is shown in Fig. 5.33.

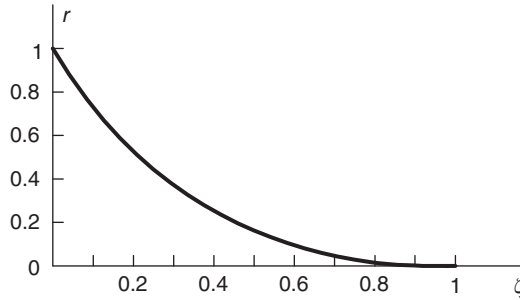


FIGURE 5.33 Effect of damping coefficient on overshoot.

5.16 Causal System Response to an Arbitrary Input

In this section we evaluate the response of a causal system to an arbitrary input as well as to a causal input. Let $h(t) = h_g(t)u(t)$ be the causal impulse response of a linear system, which is expressed as the causal part of a general function $h_g(t)$. The system response $y(t)$ to a general input signal $x(t)$ is given by

$$y(t) = x(t) * h(t) = \int_{-\infty}^{\infty} x(\tau) h_g(t - \tau) u(t - \tau) d\tau = \int_{-\infty}^t x(\tau) h_g(t - \tau) d\tau \quad (5.114)$$

or, alternatively,

$$y(t) = \int_{-\infty}^{\infty} x(t - \tau) h_g(\tau) u(\tau) d\tau = \int_0^{\infty} x(t - \tau) h_g(\tau) d\tau = \int_0^{\infty} x(t - \tau) h(\tau) d\tau. \quad (5.115)$$

Consider now the case of a causal input. With $x(t) = x_g(t)u(t)$, a causal input to the causal system we obtain

$$y(t) = \left\{ \int_0^t x(\tau) h(t - \tau) d\tau \right\} u(t) = \left\{ \int_0^t h(\tau) x(t - \tau) d\tau \right\} u(t). \quad (5.116)$$

5.17 System Response to a Causal Periodic Input

To evaluate the response of a stable linear system to a general (not sinusoidal) causal periodic input let the system transfer function be given by

$$H(s) = \frac{N(s)}{(s - p_1)(s - p_2) \dots (s - p_n)} \tag{5.117}$$

and the input be denoted $v(t)$, as shown in Fig. 5.34. We assume distinct poles to simplify the presentation.

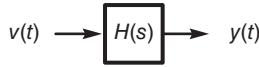


FIGURE 5.34 A system with input and output.

A causal periodic signal $v(t)$ is but a repetition for $t > 0$ of a base period $v_0(t)$, as shown in Fig. 5.35. We have, as seen in Chapter 3,

$$V(s) = \frac{V_0(s)}{1 - e^{-Ts}}, \quad \sigma = \Re[s] > 0 \tag{5.118}$$

where $V_0(s) = \mathcal{L}[v_0(t)]$. The system response $y(t)$ is described by

$$Y(s) = V(s)H(s) = \frac{V_0(s)N(s)}{(1 - e^{-Ts})(s - p_1)(s - p_2) \dots (s - p_n)}. \tag{5.119}$$

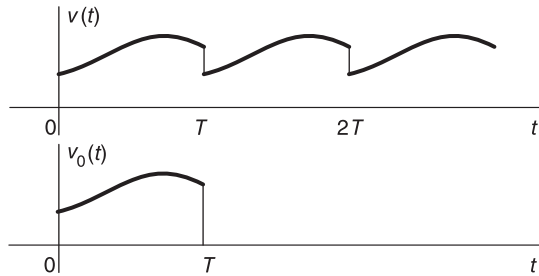


FIGURE 5.35 Causal periodic signal and its base period.

The expression of $Y(s)$ can be decomposed into the form

$$Y(s) = V(s)H(s) = \frac{A_1}{s - p_1} + \frac{A_2}{s - p_2} + \dots + \frac{A_n}{s - p_n} + \frac{F_0(s)}{1 - e^{-Ts}}. \tag{5.120}$$

We note that the function $F_0(s)$ satisfies the equation

$$F_0(s) = (1 - e^{-Ts}) \left[V(s)H(s) - \sum_{i=1}^n \frac{A_i}{s - p_i} \right] \tag{5.121}$$

and that the system response $y(t)$ is composed of a transient component $y_{tr}(t)$ due to the poles p_i on the left of the $j\omega$ axis and a steady-state component $y_{ss}(t)$ due to the periodic input. In particular, we can write

$$Y_{tr}(s) = \sum_{i=1}^n \frac{A_i}{s - p_i} \tag{5.122}$$

$$Y_{ss}(s) = \frac{F_0(s)}{1 - e^{-Ts}} \tag{5.123}$$

$$y_{tr}(t) = \sum_{i=1}^n C_i e^{p_i t} u(t) \tag{5.124}$$

$$y_{ss}(t) = f_0(t) + f_0(t - T) + f_0(t - 2T) + \dots = \sum_{n=0}^{\infty} f_0(t - nT) \tag{5.125}$$

$$y(t) = y_{tr}(t) + y_{ss}(t). \tag{5.126}$$

Example 5.3 Evaluate the response of the first order system of transfer function

$$H(s) = \frac{1}{s + 1}$$

to the input $v(t)$ shown in Fig. 5.36.

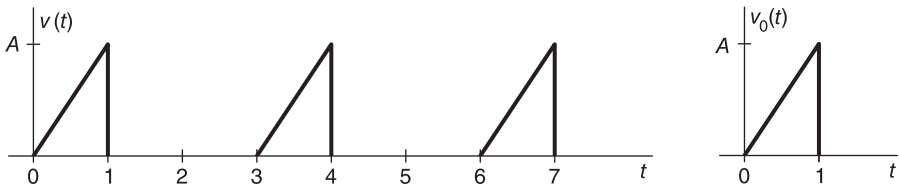


FIGURE 5.36 A periodic signal composed of ramps.

We can write

$$v_0(t) = At[u(t) - u(t - 1)] = Atu(t) - A(t - 1)u(t - 1) - Au(t - 1)$$

$$Y(s) = \frac{A(1 - e^{-s} - se^{-s})}{s^2(s + 1)(1 - e^{-3s})} = \frac{A_1}{s + 1} + \frac{F_0(s)}{(1 - e^{-3s})}$$

$$A_1 = (s + 1) Y(s)|_{s=-1} = \frac{A}{(1 - e^3)} = \frac{-A}{(e^3 - 1)} = -0.0524A.$$

$$y_{tr}(t) = \mathcal{L}^{-1} \left[\frac{A_1}{s + 1} \right] = A_1 e^{-t} u(t)$$

$$y_{ss}(t) = \mathcal{L}^{-1} [F_0(s) / (1 - e^{-3s})] = f_0(t) + f_0(t - 3) + f_0(t - 6) + \dots$$

$$F_0(s) = \frac{A(1 - e^{-s} - se^{-s})}{s^2(s + 1)} - \frac{A_1(1 - e^{-3s})}{s + 1} = A \left[\left(\frac{1}{s^2} - \frac{1}{s} + \frac{1}{s + 1} \right) e^{-s} \left(\frac{1}{s^2} - \frac{1}{s} + \frac{1}{s + 1} \right) - se^{-s} \left(\frac{1}{s^2} - \frac{1}{s} + \frac{1}{s + 1} \right) \right] - \frac{A_1}{s + 1} + \frac{A_1}{s + 1} e^{-3s}.$$

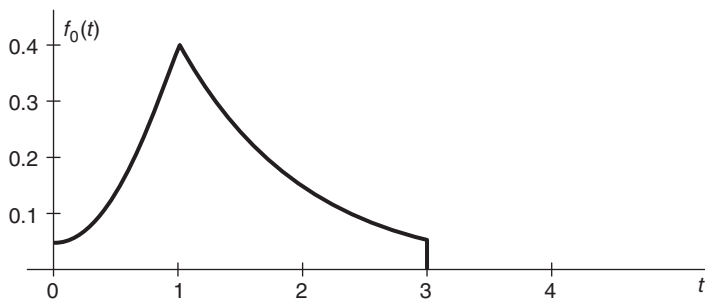


FIGURE 5.37 System response over one period.

Note that the third term can be rewritten in the form

$$se^{-s} \left(\frac{1}{s^2} - \frac{1}{s} + \frac{1}{s+1} \right) = e^{-s} \left(\frac{1}{s} - 1 + \frac{s}{s+1} \right) = e^{-s} \left(\frac{1}{s} - \frac{1}{s+1} \right)$$

wherefrom

$$f_0(t) = A [\{tu(t) - u(t) + e^{-t}u(t)\} - (t-1)u(t-1)] - A_1e^{-t}u(t) + A_1e^{-(t-3)}u(t-3)$$

which is depicted in Fig. 5.37. The periodic component of the output is

$$y_{ss}(t) = \sum_{n=0}^{\infty} f_0(t-3n)$$

and is represented, for the case $A = 1$ together with the overall output $y(t) = y_{tr}(t) + y_{ss}(t)$ in Fig. 5.38.

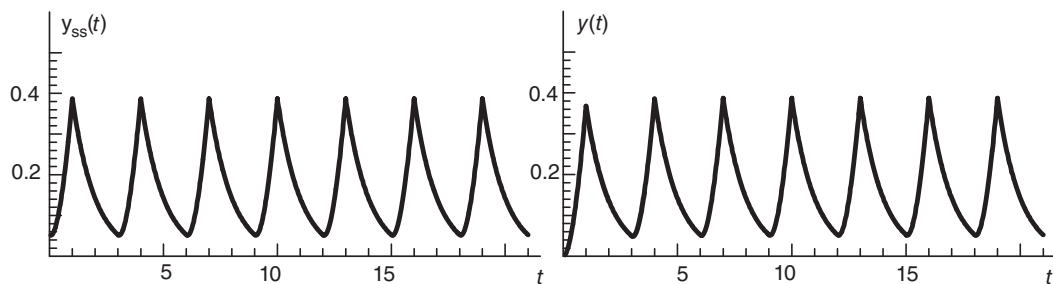


FIGURE 5.38 Periodic component of system response and overall response.

5.18 Response to a Causal Sinusoidal Input

Let the input to a linear system be a causal sinusoidal input $v(t)$

$$v(t) = A \cos \beta t u(t) \tag{5.127}$$

$$V(s) = A \frac{s}{s^2 + \beta^2}, \quad \sigma > 0. \quad (5.128)$$

The system response $y(t)$ has the transform

$$Y(s) = H(s) \frac{As}{s^2 + \beta^2} = \frac{N(s)}{(s - p_1)(s - p_2) \dots (s - p_n)(s^2 + \beta^2)} \quad (5.129)$$

which can be decomposed into the form

$$Y(s) = \frac{A_1}{s - p_1} + \frac{A_2}{s - p_2} + \dots + \frac{A_n}{s - p_n} + \frac{B}{s - j\beta} + \frac{B^*}{s + j\beta} \quad (5.130)$$

where distinct poles are assumed in order to simplify the presentation. Assuming a stable system, having its poles p_i to the left of the $j\omega$ axis in the s plane, the first n terms lead to a transient output

$$y_{tr}(t) = \sum_{i=1}^n A_i e^{p_i t} u(t) \quad (5.131)$$

which tends to zero as $t \rightarrow \infty$. The steady state output is therefore due to the last two terms. We note that

$$B = (s - j\beta) Y(s)|_{s=j\beta} = H(j\beta) \frac{Aj\beta}{2j\beta} = AH(j\beta)/2 \quad (5.132)$$

$$B^* = AH(-j\beta)/2. \quad (5.133)$$

The steady state response $y_{ss}(t)$ for $t > 0$ is given by

$$y_{ss}(t) = (A/2) H(j\beta) e^{j\beta t} + (A/2) H(-j\beta) e^{-j\beta t} = A |H(j\beta)| \cos\{\beta t + \arg[H(j\beta)]\}.$$

The steady state output is therefore also a sinusoid amplified by $|H(j\beta)|$ and has a phase shift equal to $\arg[H(j\beta)]$.

5.19 Frequency Response Plots

Several kinds of plots are used for representing a system frequency response $H(j\omega)$, namely,

1. Bode Plot: In this plot the horizontal axis is a logarithmic scale frequency ω axis. The vertical axis is either the magnitude $20 \log_{10} |H(j\omega)|$ in decibels or the phase $\arg[H(j\omega)]$.

2. Nyquist Plot: In this plot the frequency response $H(j\omega)$ is plotted in polar form as a vector of length $|H(j\omega)|$ and angle $\arg[H(j\omega)]$. As ω increases, the vector tip produces a polar plot that is the frequency response Nyquist plot.

3. Black's Diagram: In this plot the vertical axis is the magnitude $|H(j\omega)|$ in decibels. The horizontal axis is the phase $\arg[H(j\omega)]$. The plot shows the evolution of $H(j\omega)$ as ω increases.

5.20 Decibels, Octaves, Decades

The number of decibels and the slope in decibel/octave or decibel/decade in a Bode Plot are defined as follows:

Number of decibels = $20 \log_{10}(\text{output}/\text{input})$.
 Octave = The range between two frequencies ω_1 and ω_2 where $\omega_2 = 2\omega_1$.
 Decade = The range between ω_1 and ω_2 where $\omega_2 = 10\omega_1$.
 Number of octaves = $\log_2(\omega_2/\omega_1)$.
 Number of decades = $\log_{10}(\omega_2/\omega_1)$.
 Number of decades corresponding to one octave = $\log_{10} 2 = 0.3$
 that is, 1 octave = 0.3 decade.

5.21 Asymptotic Frequency Response

In the following we analyze the frequency response of basic transfer functions and in particular those of first and second order systems.

5.21.1 A Simple Zero at the Origin

For a simple zero at the origin $H(s) = s$, $H(j\omega) = j\omega$, $|H(j\omega)| = |\omega|$,

$$\arg H(j\omega) = \begin{cases} \pi/2, & \omega > 0 \\ -\pi/2, & \omega < 0. \end{cases} \quad (5.134)$$

The zero on the s plane, and the magnitude and phase spectra, are shown, respectively, in Fig. 5.39.

Consider the variation in decibels of $|H(j\omega)|$ in one decade, that is, between a frequency ω and another 10ω . We have

$$20 \log_{10}(|H(j\omega_2)|/|H(j\omega_1)|) = 20 \log_{10}(10|\omega_1|/|\omega_1|) = 20 \text{ dB}. \quad (5.135)$$

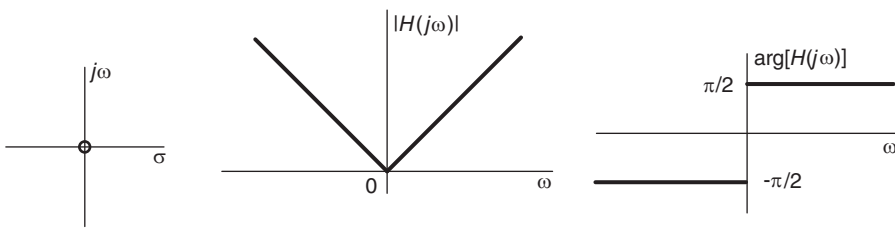


FIGURE 5.39 Simple zero, amplitude and phase response.

The Bode plot is therefore a straight line of slope 20 dB/decade. In one octave, that is, from a frequency ω to another 2ω the slope is

$$20 \log_{10}(2|\omega|/|\omega|) = 6 \text{ dB/octave}. \quad (5.136)$$

The Bode plot shows the magnitude spectrum in decibels and the phase spectrum versus a logarithmic scale of ω , as shown in Fig. 5.40.

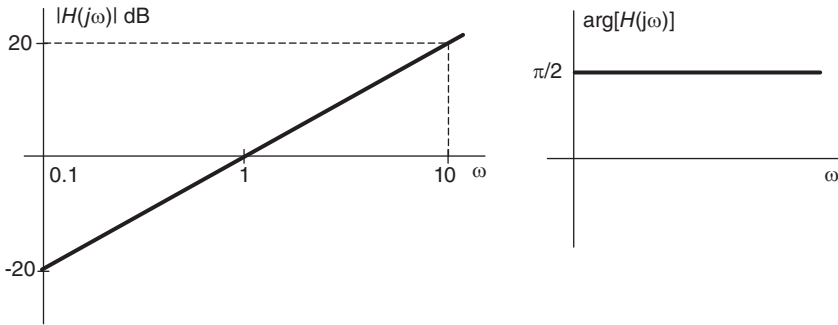


FIGURE 5.40 Asymptotic magnitude and phase response.

5.21.2 A Simple Pole

Let $H(s) = 1/s$. We have $H(j\omega) = 1/(j\omega) = -j/\omega$, $|H(j\omega)| = 1/|\omega|$,

$$\arg[H(j\omega)] = \begin{cases} -\pi/2, & \omega > 0 \\ \pi/2, & \omega < 0 \end{cases} \tag{5.137}$$

as shown in Fig. 5.41.

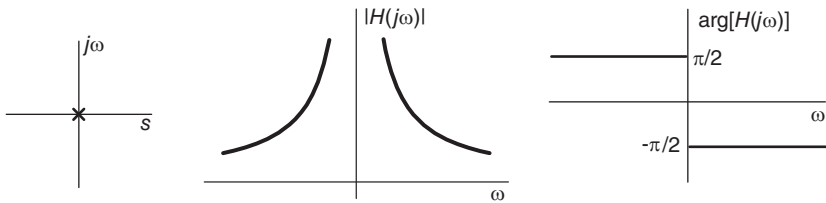


FIGURE 5.41 Simple pole, magnitude and phase response.

The slope in one decade is given by

$$20 \log_{10} \frac{1/(10|\omega|)}{1/|\omega|} = -20 \text{ dB/decade} = -6 \text{ dB/octave} \tag{5.138}$$

as represented in Fig. 5.42.

5.21.3 A Simple Zero in the Left Plane

Consider the case of the transfer function

$$H(s) = s\tau + 1 \tag{5.139}$$

and the corresponding frequency response $H(j\omega) = j\omega\tau + 1$. We have

$$|H(j\omega)| = \sqrt{1 + \omega^2\tau^2} \tag{5.140}$$

$$\arg[H(j\omega)] = \tan^{-1}[\omega\tau] \tag{5.141}$$

as represented schematically in Fig. 5.43.

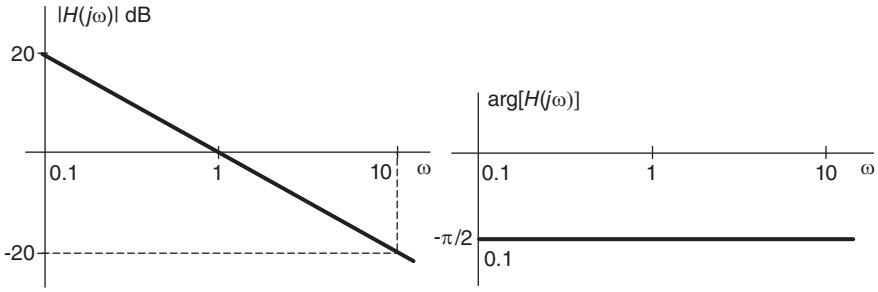


FIGURE 5.42 Simple pole, asymptotic magnitude and phase response.

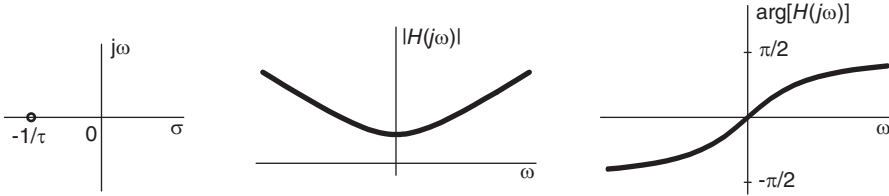


FIGURE 5.43 A zero, amplitude and phase response.

Asymptotic Behavior

By studying the behavior of the amplitude spectrum $H(j\omega)$ for both small and large values of ω we can draw the two asymptotes in a Bode plot. If $\omega \rightarrow 0$ we have

$$20 \log_{10} |H(j\omega)| \approx 20 \log_{10} 1 = 0 \text{ dB}, \quad \arg [H(j\omega)] \approx 0. \tag{5.142}$$

If $\omega \rightarrow \infty$ the change of gain in one decade is given by

$$20 \log_{10} \frac{10\omega\tau}{\omega\tau} = 20 \text{ dB/decade}, \quad \arg [H(j\omega)] \approx \pi/2. \tag{5.143}$$

The intersection of the asymptotes is the point satisfying $20 \log_{10} \omega\tau = 0$, i.e., $\omega\tau = 1$ or $\omega = 1/\tau$ as shown in Fig. 5.44.

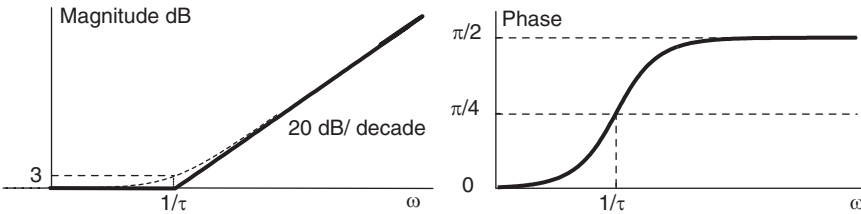


FIGURE 5.44 A zero and asymptotic response.

The true value of the gain at $\omega = 1/\tau$ is

$$20 \log_{10} |H(j\omega)|_{\omega=1/\tau} = 20 \log_{10} \sqrt{1 + \omega^2\tau^2} \Big|_{\omega=1/\tau} = 10 \log_{10} 2 = 3 \text{ dB} \tag{5.144}$$

and the phase ϕ at $\omega = 1/\tau$ is given by

$$\phi = \tan^{-1} 1 = \pi/4 \tag{5.145}$$

as shown in the figure.

5.21.4 First Order System

Consider the first order system having the transfer function

$$H(s) = \frac{1}{s\tau + 1} \tag{5.146}$$

and the frequency response is

$$H(j\omega) = \frac{1}{j\omega\tau + 1} \tag{5.147}$$

$$|H(j\omega)| = \frac{1}{\sqrt{1 + \omega^2\tau^2}}, \quad \arg[H(j\omega)] = -\tan^{-1}[\omega\tau] \tag{5.148}$$

as shown in Fig. 5.45. Following the same steps we obtain the Bode plot shown in Fig. 5.46. We note that the asymptote for large ω has a slope of -20 dB/decade and meets the 0 dB asymptote at the point $\omega = 1/\tau$.

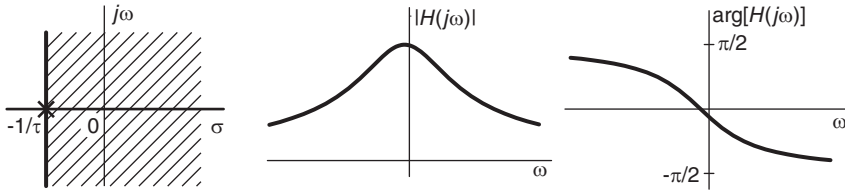


FIGURE 5.45 A pole, amplitude and phase response.

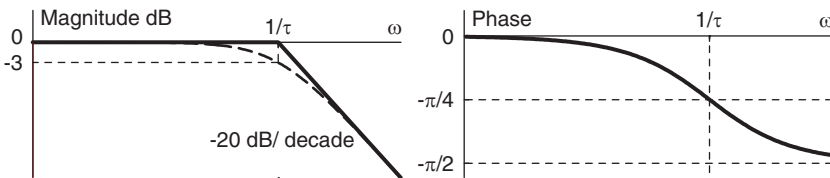


FIGURE 5.46 Asymptotic response.

5.21.5 Second Order System

Consider the transfer function $H(s)$ of the second order system

$$H(s) = \frac{\omega_0^2}{s^2 + 2\omega_0\zeta s + \omega_0^2}. \tag{5.149}$$

The frequency response is given by

$$H(j\omega) = \frac{\omega_0^2}{-\omega^2 + j2\omega_0\zeta\omega + \omega_0^2} = \frac{\omega_0^2 \{(\omega_0^2 - \omega^2) - j2\omega_0\zeta\omega\}}{(\omega_0^2 - \omega^2)^2 + 4\omega_0^2\zeta^2\omega^2} \tag{5.150}$$

$$|H(j\omega)| = \frac{\omega_0^2}{\sqrt{(\omega_0^2 - \omega^2)^2 + 4\omega_0^2\zeta^2\omega^2}}, \quad \arg[H(j\omega)] = -\arctan\left[\frac{2\omega_0\zeta\omega}{\omega_0^2 - \omega^2}\right]. \quad (5.151)$$

If $\omega \rightarrow 0$, $|H(j\omega)| \rightarrow 1$ Gain = $20 \log_{10} 1 = 0$ dB, and $\arg[H(j\omega)] \rightarrow 0$. If $\omega \rightarrow \infty$, $|H(j\omega)| \rightarrow \omega_0^2/\omega^2$

$$\text{Gain per decade} = 20 \log_{10} \left\{ \frac{\omega_0^2/(10\omega_1)^2}{\omega_0^2/\omega_1^2} \right\} = 20 \log(10^{-2}) = -40\text{dB/decade}. \quad (5.152)$$

The slope of the asymptote is therefore -40 dB/decade or -12 dB/octave. As $\omega \rightarrow \infty$, $H(j\omega) \rightarrow -\omega_0^2/\omega^2$ wherefrom $\arg[H(j\omega)] \rightarrow -\pi$. The Magnitude and phase responses are shown in Fig. 5.47 for the case $\zeta = 0.01$.

The two asymptotes meet at a point such that $20 \log_{10} \{\omega_0^2/\omega^2\} = 0$, i.e. $\omega = \omega_0$. This may be referred to as the *cut-off frequency* $\omega_c = \omega_0$. The true gain at $\omega = \omega_c$ is given by

$$\text{Gain} = 20 \log_{10} [|H(j\omega_0)|] = 20 \log_{10} \{1/(2\zeta)\} = -20 \log(2\zeta). \quad (5.153)$$

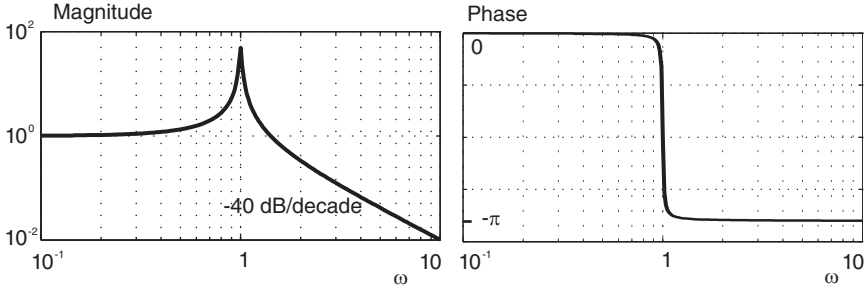


FIGURE 5.47 Bode plot of amplitude and frequency response.

For example if $\zeta = 1$ the gain is -6 dB. If $\zeta = 1/2$ the gain = 0 dB. The peak point of the magnitude frequency response $|H(j\omega)|$ can be found by differentiating the expression $|H(j\omega)|^2$. Writing

$$\frac{d}{d\omega} |H(j\omega)|^2 = \frac{d}{d\omega} \frac{\omega_0^4}{(\omega_0^2 - \omega^2)^2 + 4\omega_0^2\zeta^2\omega^2} = 0 \quad (5.154)$$

we obtain $-4(\omega_0^2 - \omega^2) + 8\omega_0^2\zeta^2 = 0$, wherefrom the frequency of the peak, which shall be denoted ω_r , is given by

$$\omega_r = \omega_0 \sqrt{1 - 2\zeta^2}. \quad (5.155)$$

A geometric construction showing the relations among the different frequencies leading to the resonance frequency of a second order system is shown in Fig. 5.48.

The poles are shown at positions given by

$$p_1, p_2 = -\zeta\omega_0 \pm \omega_0 \sqrt{\zeta^2 - 1}. \quad (5.156)$$

As can be seen from this figure, the peak frequency ω_r can be found by drawing a circle centered at the point $\sigma = -\zeta\omega_0$, of radius $\omega_p = \omega_0 \sqrt{1 - \zeta^2}$. The intersection of the circle

with the vertical axis is a point on the $j\omega$ axis given by $j\omega = j\omega_r$ that is, a point above the origin by the resonance frequency ω_r . Note that as can be seen in the figure

$$\omega_r^2 = \omega_p^2 - \zeta^2 \omega_0^2 = \omega_0^2 (1 - \zeta^2) - \zeta^2 \omega_0^2 = \omega_0^2 - 2\zeta^2 \omega_0^2 \tag{5.157}$$

$$\omega_r = \omega_0 \sqrt{1 - 2\zeta^2} \tag{5.158}$$

as expected.

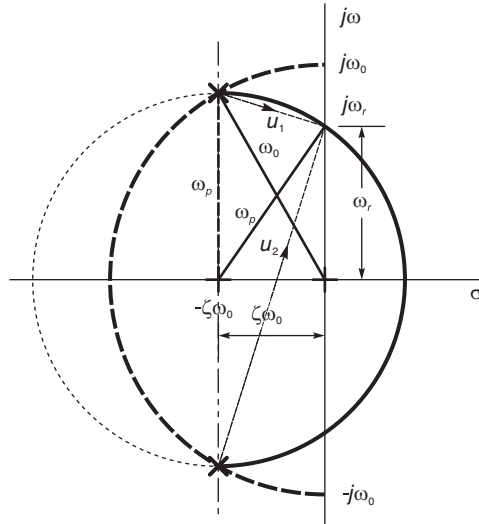


FIGURE 5.48 A construction leading to the resonance frequency of a second order system.

Note that the value of $|F(j\omega)|$ is given by

$$|F(j\omega)| = \frac{1}{|u_1| |u_2|} \tag{5.159}$$

where u_1 and u_2 are the vectors extending from the poles to the point on the vertical axis $s = j\omega$, as shown in the figure. The value of $|F(j\omega)|$ is a maximum when $|u_1| |u_2|$ is minimum, which can be shown to occur when u_1 and u_2 are at right angles; hence meeting on that circle centered at the point $\sigma = -\zeta\omega_0$ and joining the poles. The value of the peak of $|H(j\omega)|$ at the resonance frequency ω_r is given by

$$P(\zeta) = |H(j\omega_r)| = \frac{\omega_0^2}{\sqrt{[\omega_0^2 - \omega_0^2(1 - 2\zeta^2)]^2 + 4\omega_0^4\zeta^2(1 - 2\zeta^2)}} = \frac{1}{2\zeta\sqrt{1 - \zeta^2}} \tag{5.160}$$

a relation depicted as a function of ζ in Fig. 5.49.

We note from Fig. 5.31 that if $\zeta > 0.5$ the magnitude spectrum resembles that of a lowpass filter. On the other hand if $\zeta \rightarrow 0$ then the poles approach the $j\omega$ axis, producing resonance, and the resonance frequency ω_r approaches the natural frequency ω_0 and the spectrum has a sharp peak as shown in the figure. The quality Q describing the degree of selectivity of such a second order system is usually taken as

$$Q = \frac{1}{2\zeta} \tag{5.161}$$

and gives a measure of the sharpness of the magnitude spectral peak. We note that, as expected, the lower the value of ζ the higher the selectivity.

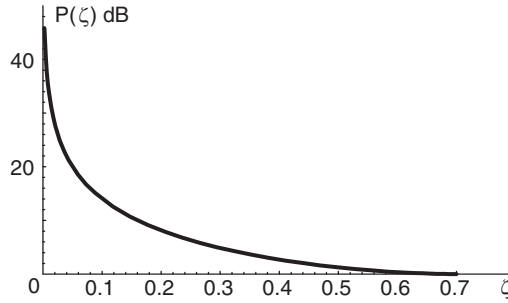


FIGURE 5.49 The resonance peak as a function of damping coefficient.

5.22 Bode Plot of a Composite Linear System

The transfer function of a linear system can be in general factored into a product of basic first and second order systems. Since the logarithm of a product is the sum of logarithms the overall Bode plot can be deduced by adding the Bode plots of those basic components. The resulting amplitude spectrum in decibels is thus the sum of the amplitude spectra of the individual components. Similarly, the overall phase spectrum may be deduced by adding the individual phase spectra. The following example illustrates the approach.

Example 5.4 Deduce and verify the Bode plot of the system transfer function

$$H(s) = \frac{As}{(s + a)(s^2 + 2\zeta\omega_0s + \omega_0^2)}$$

with $a = 1.5$, $\zeta = 0.1$, $\omega_0 = 800$. Set the value of A so that the magnitude of the response at the frequency 1 rad/sec be equal to 20 dB.

Letting $\tau = 1/a$ we have

$$H(s) = \frac{As}{(s + 1/\tau)(s^2 + 2\zeta\omega_0s + \omega_0^2)} = \frac{(A\tau/\omega_0^2)s}{(s\tau + 1)(s^2/\omega_0^2 + 2\zeta s/\omega_0 + 1)}$$

$$H(j\omega) = \frac{(A\tau/\omega_0^2)j\omega}{(j\omega\tau + 1)(-\omega^2/\omega_0^2 + j2\zeta\omega/\omega_0 + 1)}$$

The value of the magnitude spectrum $|H(j\omega)|$ at $\omega = 1$ may be shown equal to $1.554710^{-7}A$. To obtain a spectrum magnitude of 20 dB, we should have $20 \log_{10} |H(j1)| = 20$, i.e. $|H(j1)| = 10$, wherefrom $A = 10/1.554710^{-7} = 6.4319 \cdot 10^7$. The Bode plot of the amplitude and phase spectra of the successive components of $H(s)$ are shown in Fig. 5.50. Note that the command **bode** of MATLAB may be used to display such plots. The left side of these figures shows the amplitude spectra in decibels while those on the right show the phase

spectra. The addition of the amplitude spectra in the figure produces the overall amplitude spectrum. Similarly the addition of the right parts of the figure produces the overall phase spectrum. The sum of these plots, the Bode plot of the composite system transfer function $H(s)$, is shown in Fig. 5.51.

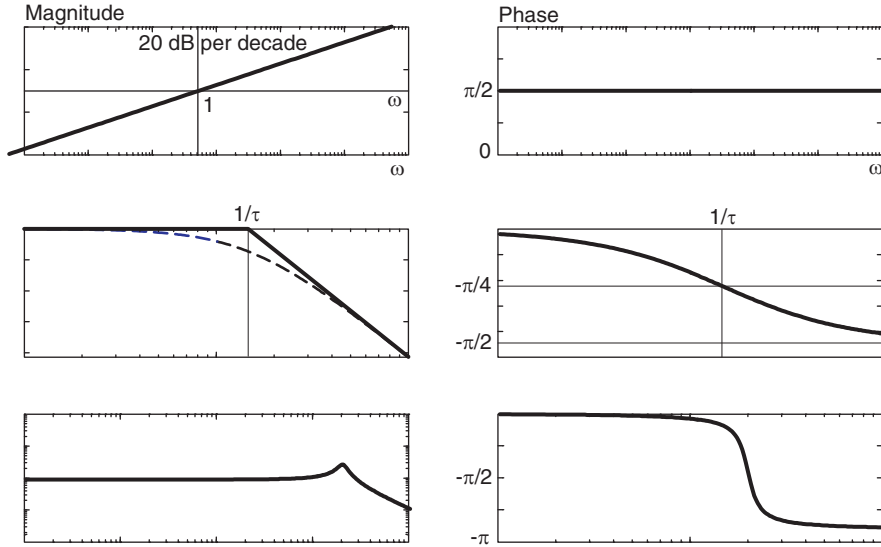


FIGURE 5.50 Bode plot of amplitude and phase spectra of system components.

5.23 Graphical Representation of a System Function

A rational system function $H(s)$, as we have seen, can be expressed in the form

$$H(s) = K \frac{\prod_{i=1}^M (s - z_i)}{\prod_{i=1}^N (s - p_i)} \tag{5.162}$$

in which z_i and p_i are its zeros and poles, respectively. We have also seen that the zeros and poles can be represented graphically in the s plane. For the system function $H(s)$ to be graphically represented in the s plane it only remains to indicate the value K , the gain factor, on the pole-zero diagram. The gain factor K may be added, for example, next to the origin of the s plane.

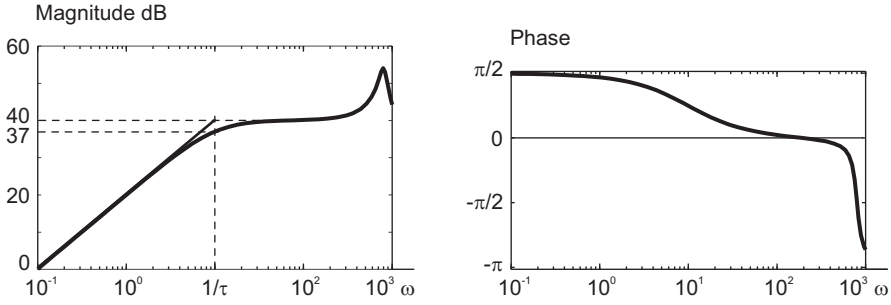


FIGURE 5.51 Overall system Bode plot.

5.24 Vectorial Evaluation of Residues

The evaluation of the inverse Laplace transform of a function $F(s)$ necessitates often evaluating the residues at its poles. Such evaluation may be performed vectorially. To show how vectors may be used to evaluate a function in the s plane, let

$$F(s) = \frac{s - z_1}{(s - p_1)(s - p_2)}. \tag{5.163}$$

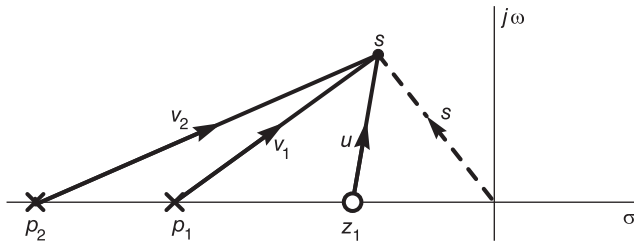


FIGURE 5.52 Vectors in s plane.

Assuming that the function $F(s)$ needs be evaluated at a point s in the complex plane as shown in Fig. 5.52, we note that using the vectors shown in the figure we can write $u = s - z_1$, $v_1 = s - p_1$, $v_2 = s - p_2$. Hence

$$F(s) = \frac{u}{v_1 v_2}. \tag{5.164}$$

Consider now the transfer function

$$F(s) = 10 \frac{(s + 2)}{(s + 1)(s + 4)(s^2 + 4s + 8)}. \tag{5.165}$$

Let $p_1 = -1$, $p_2 = -4$. A partial fraction expansion of $F(s)$ has the form

$$F(s) = \frac{r_1}{s + 1} + \frac{r_2}{s + 4} + \frac{r_3}{s - p_3} + \frac{r_3^*}{s - p_3^*} \tag{5.166}$$

where $p_3, p_3^* = -2 \pm j2$. The residue r_1 associated with the pole $s = -1$ is given by

$$r_1 = (s + 1)F(s)|_{s=-1} = 10 \frac{(s + 2)}{(s + 4)(s^2 + 4s + 8)} \Big|_{s=-1} \tag{5.167}$$

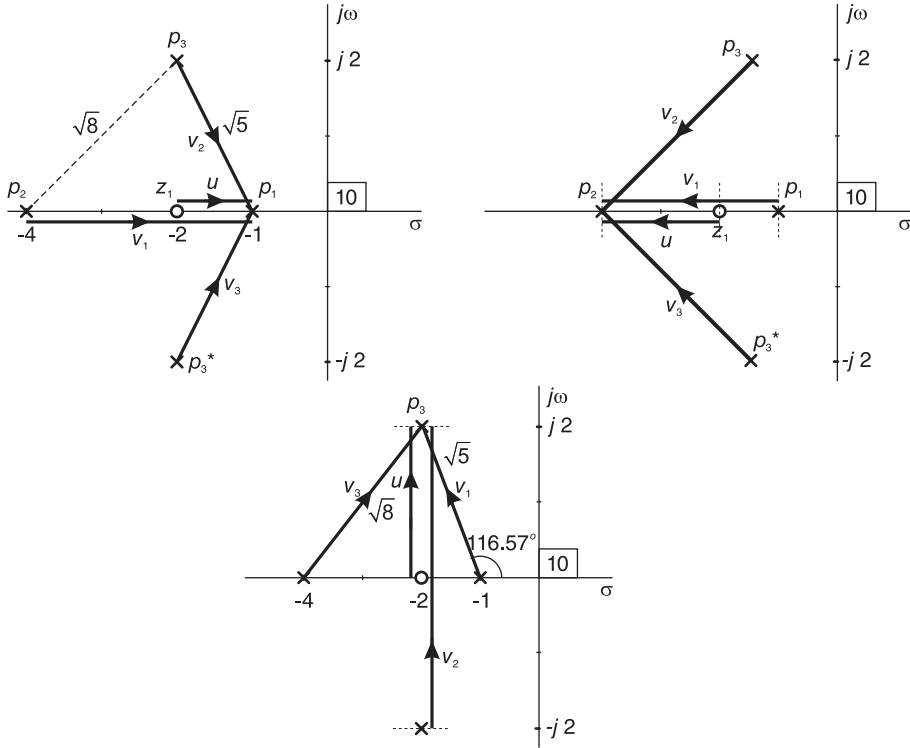


FIGURE 5.53 Graphic evaluation of residues.

The poles and zeros are plotted in Fig. 5.53 where, moreover, the gain factor 10 of the transfer function can be seen marked near the point of origin. We note that the residue r_1 can be evaluated as $r_1 = 10u/(v_1v_2v_3)$, where u is the vector extending from the zero at $s = -2$ to the pole $s = -1$ and v_1, v_2 and v_3 are the vectors extending from the poles p_2, p_3 and p_3^* to the pole $s = -1$, as shown in the figure. We obtain

$$r_1 = 10 \frac{1}{3 \times \sqrt{5} \times \sqrt{5}} = \frac{2}{3} \tag{5.168}$$

Similarly, referring to the figure, the residue r_2 associated with the pole $s = -4$ is given by

$$r_2 = 10 \frac{u}{v_1v_2v_3} = 10 \frac{(-2)}{(-3)\sqrt{8}\sqrt{8}} = \frac{5}{6} \tag{5.169}$$

and the residue r_3 associated with the pole $s = -2 + j2$ is given by

$$\begin{aligned} r_3 &= 10 \frac{u}{v_1v_2v_3} = 10 \frac{2\angle 90^\circ}{\sqrt{5}\angle 116.57^\circ 4\angle 90^\circ \sqrt{8}\angle 45^\circ} = 0.7906\angle -161.57^\circ \\ &= 0.7906e^{-j2.8199} = -0.75 - j0.25 \end{aligned} \tag{5.170}$$

$$r_3^* = -0.75 + j0.25, \tag{5.171}$$

$$f(t) = \mathcal{L}^{-1} [F(s)] = [(2/3)e^{-t} + (5/6)e^{-4t} + 1.5812e^{-2t} \cos(2t - 161.57^\circ)]u(t). \tag{5.172}$$

To summarize, for the case of simple poles, the residue at pole $s = p_i$ is equal to the gain factor multiplied by the product of the vectors extending from the zeros to the pole p_i , divided by the product of the vectors extending from the poles to the pole p_i . In other words the residue r_i associated with the pole $s = p_i$ is given by

$$r_i = K \frac{u_1 u_2 \dots u_M}{v_1 v_2 \dots v_{N-1}} = K \frac{\prod_{i=1}^M u_i}{\prod_{i=1}^{N-1} v_i} \tag{5.173}$$

where K is the gain factor, u_1, u_2, \dots, u_M are the vectors extending from the M zeros of $F(s)$ to the pole $s = p_i$, and v_1, v_2, \dots, v_{N-1} are the vectors extending from all other poles to the pole $s = p_i$.

Case of double pole

We now consider the vectorial evaluation of residues in the case of a double pole. Let $F(s)$ be given by

$$F(s) = K \frac{(s - z_1)(s - z_2) \dots (s - z_M)}{(s - p_1)^2 (s - p_2)(s - p_3) \dots (s - p_N)} \tag{5.174}$$

having a double pole at $s = p_1$. A partial fraction expansion of $F(s)$ has the form

$$F(s) = \frac{r_1}{(s - p_1)^2} + \frac{\rho_1}{s - p_1} + \frac{r_2}{s - p_2} + \frac{r_3}{s - p_3} + \dots + \frac{r_N}{s - p_N}. \tag{5.175}$$

The residues $r_i, i = 1, 2, \dots, N$ are evaluated as in the case of simple poles, that is, as the gain factor multiplied by the product of vectors extending from the zeros to the pole $s = p_i$ divided by those extending from the other poles to $s = p_i$. The residue ρ_1 is given by

$$\rho_1 = \left\{ \frac{d}{ds} \left[(s - p_1)^2 F(s) \right] \right\}_{s=p_1} = \left\{ \frac{d}{ds} \left[K \frac{(s - z_1)(s - z_2) \dots (s - z_M)}{(s - p_2)(s - p_3) \dots (s - p_N)} \right] \right\}_{s=p_1}.$$

Using the relation

$$\frac{d}{ds} \{ \log X(s) \} = \frac{1}{X(s)} \frac{d}{ds} X(s) \tag{5.176}$$

$$\frac{d}{ds} X(s) = X(s) \frac{d}{ds} \{ \log X(s) \} \tag{5.177}$$

we can write

$$\rho_1 = K \left\{ \left[\frac{(s - z_1)(s - z_2) \dots (s - z_M)}{(s - p_2)(s - p_3) \dots (s - p_N)} \right] \frac{d}{ds} [\log(s - z_1) + \log(s - z_2) + \dots + \log(s - z_M) - \log(s - p_2) - \log(s - p_3) - \dots - \log(s - p_N)] \right\}_{s=p_1}.$$

Since

$$r_1 = (s - p_1)^2 F(s) \Big|_{s=p_1} = K \frac{(s - z_1)(s - z_2) \dots (s - z_M)}{(s - p_2)(s - p_3) \dots (s - p_N)} \Big|_{s=p_1}$$

we have

$$\begin{aligned} \rho_1 &= r_1 \left[\frac{1}{s - z_1} + \frac{1}{s - z_2} + \dots + \frac{1}{s - z_M} - \frac{1}{s - p_2} \right. \\ &\quad \left. - \frac{1}{s - p_3} - \dots - \frac{1}{s - p_N} \right] \Bigg|_{s=p_1} \\ &= r_1 \left[\frac{1}{p_1 - z_1} + \frac{1}{p_1 - z_2} + \dots + \frac{1}{p_1 - z_M} - \frac{1}{p_1 - p_2} \right. \\ &\quad \left. - \frac{1}{p_1 - p_3} - \dots - \frac{1}{p_1 - p_N} \right]. \end{aligned}$$

Vectorially we write

$$\rho_1 = r_1 \left[\sum_i \frac{1}{u_i} - \sum_k \frac{1}{v_k} \right] \tag{5.178}$$

where $u_i = p_1 - z_i$, $v_i = p_1 - p_i$. The residue ρ_1 is therefore the product of the residue r_1 and the difference between the sum of the reciprocals of the vectors extending from the zeros to the pole $s = p_1$ and those extending from the other poles to $s = p_1$.

Example 5.5 Evaluate vectorially the partial fraction expansion of

$$F(s) = 12 \frac{(s + 2)}{(s + 1)(s + 3)^2(s + 4)}.$$

The poles and zeros of $F(s)$ are shown in Fig. 5.54. We have

$$F(s) = \frac{r_1}{(s + 3)^2} + \frac{\rho_1}{s + 3} + \frac{r_2}{s + 1} + \frac{r_3}{s + 4}.$$

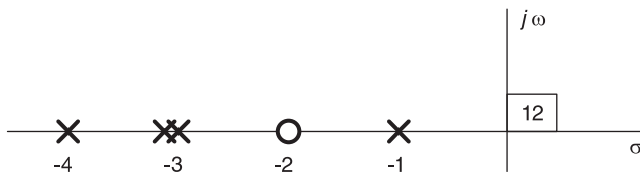


FIGURE 5.54 Poles and zero on real axis.

Referring to Fig. 5.55 we have

$$r_1 = 12 \frac{u}{v_1 v_2} = 12 \frac{(-1)}{(-2)(-1)} = 6, \quad r_2 = 12 \frac{u}{v_1^2 v_2} = 12 \frac{(1)}{(2^2)(3)} = 1$$

$$r_3 = 12 \frac{u}{v_1 v_2^2} = 12 \frac{(-2)}{(-3)(-1)^2} = 8, \quad \rho_1 = r_1 \left[\frac{1}{(-1)} - \left\{ \frac{1}{(-2)} + \frac{1}{1} \right\} \right] = -9.$$

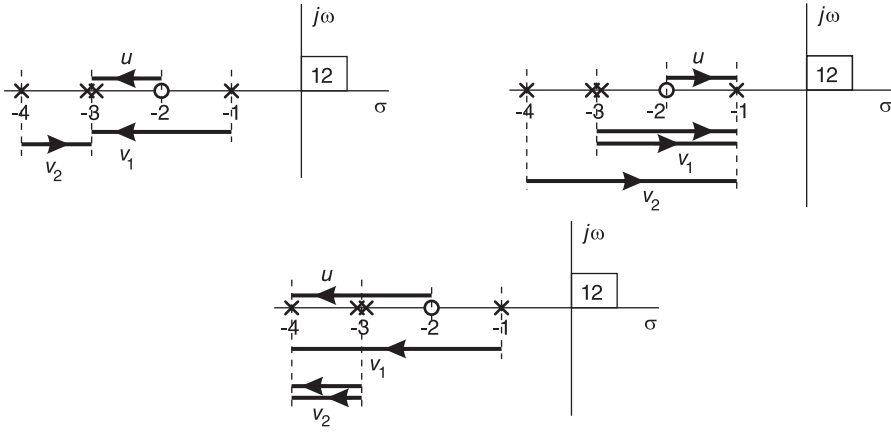


FIGURE 5.55 Vectorial evaluation of residues.

5.25 Vectorial Evaluation of the Frequency Response

Given a system function

$$H(s) = K \frac{(s - z_1)(s - z_2) \dots (s - z_M)}{(s - p_1)(s - p_2) \dots (s - p_N)} = K \frac{\prod_{k=1}^M (s - z_k)}{\prod_{k=1}^N (s - p_k)} \tag{5.179}$$

the system frequency response is

$$H(j\omega) = K \frac{(j\omega - z_1)(j\omega - z_2) \dots (j\omega - z_M)}{(j\omega - p_1)(j\omega - p_2) \dots (j\omega - p_N)} = K \frac{\prod_{k=1}^M (j\omega - z_k)}{\prod_{k=1}^N (j\omega - p_k)} \tag{5.180}$$

Similarly to the vectorial evaluation of residues, the value of $H(j\omega)$ at any frequency, say $\omega = \omega_0$, can be evaluated vectorially as the product of the gain factor and the product of the vectors extending from the zeros to the point $s = j\omega_0$ divided by the product of the vectors extending from the poles to the point $s = j\omega_0$.

Example 5.6 For the system of transfer function

$$H(s) = \frac{10(s + 2)}{(s + 1)(s + 4)}$$

Evaluate $|H(j\omega)|$ and $\arg[H(j\omega)]$ for $\omega = 2$ r/s. From Fig. 5.56 we can write

$$H(j2) = 10 \frac{2\sqrt{2} \angle 45^\circ}{\sqrt{5} \angle 63.435^\circ \sqrt{20} \angle 26.57^\circ}$$

$$|H(j2)| = \sqrt{8} = 2.8284, \quad \arg[H(j2)] = -45^\circ = -0.7854$$

wherefrom $H(j2) = 2.8284e^{-j0.7854}$.

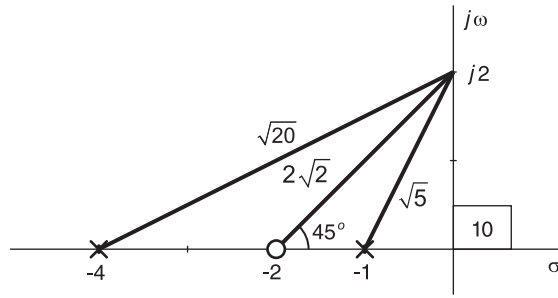


FIGURE 5.56 Vectors from zero and poles to a point on imaginary axis.

Example 5.7 Evaluate the frequency response of the third order system having the transfer function

$$H(s) = \frac{10(s + 1)}{s^3 + 5s^2 + 6s}$$

and the system response to the input

$$x(t) = 5 \sin(2t + \pi/3).$$

We can write

$$H(s) = \frac{10(s + 1)}{s(s^2 + 5s + 6)} = \frac{10(s + 1)}{s(s + 2)(s + 3)}.$$

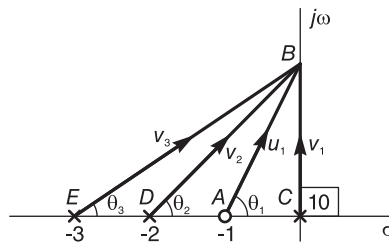


FIGURE 5.57 Vectors to a frequency point.

Referring to Fig. 5.57 we have

$$H(j\omega) = 10 \frac{(j\omega + 1)}{j\omega(j\omega + 2)(j\omega + 3)}.$$

We note that numerator is the vector u_1 extending from the point $s = -1$ to the point $s = j\omega$, i.e. from point A to point B. The denominator, similarly, is the product of the vectors v_1, v_2 and v_3 extending from the points C, D, and E, respectively to the point B in the figure. We can therefore write

$$H(j\omega) = 10 \frac{u_1}{v_1 v_2 v_3} = 10 \frac{\sqrt{1 + \omega^2} e^{j\theta_1}}{\omega e^{j\pi/2} \sqrt{4 + \omega^2} e^{j\theta_2} \sqrt{9 + \omega^2} e^{j\theta_3}} = 10 \frac{\sqrt{1 + \omega^2}}{\omega \sqrt{4 + \omega^2} \sqrt{9 + \omega^2}} e^{j\phi}$$

where

$$\phi = \arg [H(j\omega)] = \theta_1 - \pi/2 - \theta_2 - \theta_3 = \tan^{-1}(\omega) - \pi/2 - \tan^{-1}(\omega/2) - \tan^{-1}(\omega/3).$$

The system response to the sinusoid $x(t) = 5 \sin(\beta t + \pi/3)$, where $\beta = 2$ is given by

$$y(t) = 5 |H(j\beta)| \sin\{\beta t + \pi/3 + \arg[H(j\beta)]\}.$$

Now

$$|H(j\beta)| = 10 \frac{\sqrt{1 + \beta^2}}{\beta \sqrt{4 + \beta^2} \sqrt{9 + \beta^2}} = 10 \frac{\sqrt{5}}{2\sqrt{8}\sqrt{13}} = 1.0963$$

$$\arg[H(j\beta)] = \tan^{-1} 2 - \pi/2 - \tan^{-1} 1 - \tan^{-1} (1/3) = -\pi/2$$

wherefrom

$$y(t) = 5.4816 \sin(2t - \pi/6).$$

5.26 A First Order All-Pass System

The vectorial evaluation of the frequency response provides a simple visualization of the response of an allpass system. Such a system acts as an allpass filter that has a constant gain of 1 for all frequencies. Let the system function $H(s)$ have a zero and a pole at $s = \alpha$ and $s = -\alpha$, respectively, as shown in Fig. 5.58.

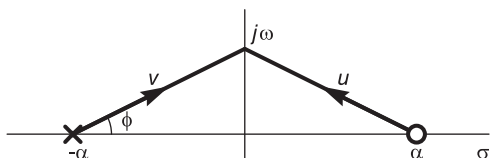


FIGURE 5.58 Allpass system pole-zero-symmetry property.

We note that at any frequency ω the value of $H(j\omega)$ is given by

$$H(j\omega) = \frac{u}{v} = \frac{\sqrt{\alpha^2 + \omega^2} \angle(\pi - \phi)}{\sqrt{\alpha^2 + \omega^2} \angle\phi} = 1 \angle(\pi - 2\phi) \tag{5.181}$$

where u and v are the vectors shown in in Fig. 5.58, and $\phi = \tan^{-1}(\omega/\alpha)$. The amplitude and phase spectra $|H(j\omega)|$ and $\arg[H(j\omega)]$ are shown in Fig. 5.59. We shall view shortly allpass systems in more detail.

5.27 Filtering Properties of Basic Circuits

In this section we study the filtering properties of first and second order linear systems in the form of basic electric circuits. Consider the circuit shown in Fig. 5.60(a). We have

$$V_0(s) = V_i(s) \frac{R}{R + \frac{1}{Cs}} = V_i(s) \frac{RCs}{1 + RCs} \tag{5.182}$$

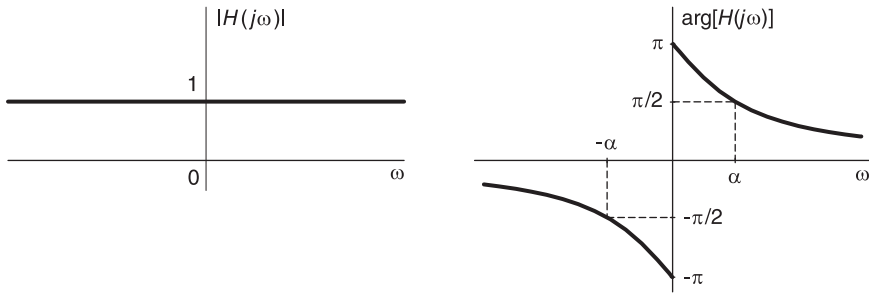


FIGURE 5.59 Frequency response of an allpass system.

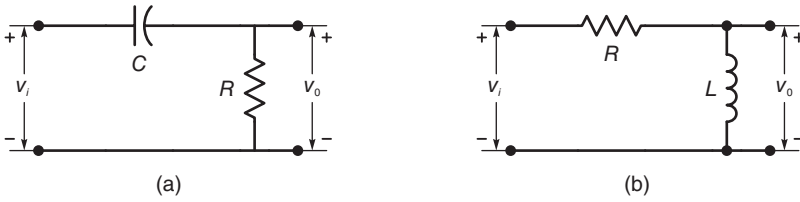


FIGURE 5.60 Two electric circuits.

$$H(s) = \frac{V_0(s)}{V_i(s)} = \frac{\tau s}{1 + \tau s} = \frac{s}{s + 1/\tau}, \quad \tau = RC. \tag{5.183}$$

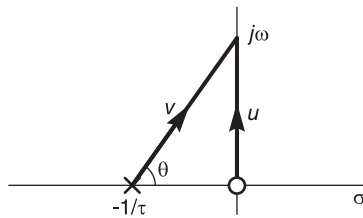


FIGURE 5.61 Vectors to a frequency point.

Referring to Fig. 5.61 we have

$$H(j\omega) = \frac{u}{v} = \frac{\omega e^{j\pi/2}}{\sqrt{\omega^2 + 1/\tau^2} e^{j\theta}} \tag{5.184}$$

where

$$\theta = \tan^{-1}(\omega\tau) \tag{5.185}$$

$$|H(j\omega)| = \frac{|\omega|}{\sqrt{\omega^2 + 1/\tau^2}} \tag{5.186}$$

$$\arg\{H(j\omega)\} = \pi/2 - \tan^{-1}(\omega\tau). \tag{5.187}$$

See Fig. 5.62. Similarly consider the circuit shown in Fig. 5.60(b).

$$V_0(s) = V_i(s) \frac{Ls}{R + Ls} = V_i(s) \frac{(L/R)s}{1 + (L/R)s} = V_i(s) \frac{\tau s}{1 + \tau s} \tag{5.188}$$

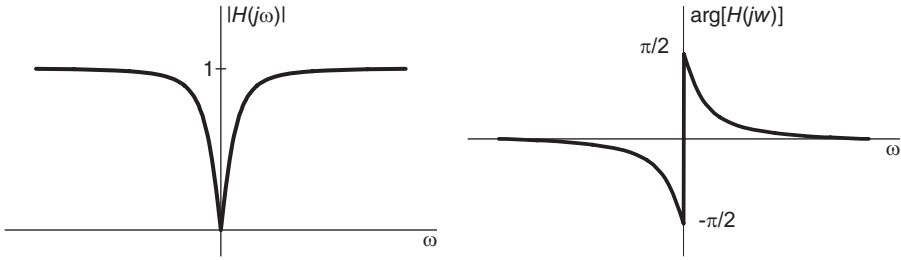


FIGURE 5.62 Frequency response of a first order system.

where $\tau = L/R$. This circuit has the same transfer function as that of Fig. 5.60(a). Having a zero at $s = 0$, i.e. at $\omega = 0$, these two circuits behave as highpass filters. At zero frequency the capacitor has infinite impedance, acting as a series open circuit blocking any current flow, leading to a zero output. At infinite frequency the capacitor has zero impedance, behaves as a short circuit so that $v_0 = v_i$. The same remarks can be made in relation with Fig. 5.60(b) where the inductor at zero frequency is a short circuit leading to zero output and at infinite frequency is an open circuit so that $v_0 = v_i$.

5.28 Lowpass First Order Filter

Consider the circuit shown in Fig. 5.63(a).

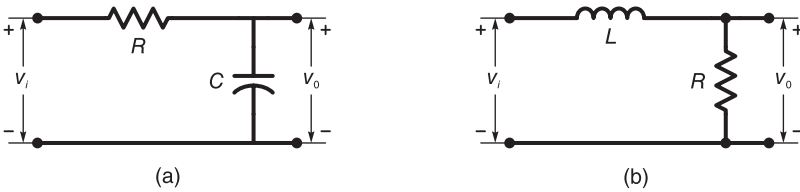


FIGURE 5.63 Two electric circuits.

We have

$$H(s) = \frac{V_0(s)}{V_i(s)} = \frac{1/(Cs)}{R + 1/(Cs)} = \frac{1}{1 + RCs} = \frac{1}{1 + \tau s} \tag{5.189}$$

where $\tau = RC$. Similarly consider the circuit shown in Fig. 5.63(b). The transfer function is given by

$$H(s) = \frac{V_0(s)}{V_i(s)} = \frac{R}{R + Ls} = \frac{1}{1 + (L/R)s} = \frac{1}{1 + \tau s} \tag{5.190}$$

$$H(j\omega) = 1 / (1 + j\omega\tau) \tag{5.191}$$

where $\tau = L/R$. We have

$$H(s) = (1/\tau) / (s + 1/\tau). \tag{5.192}$$

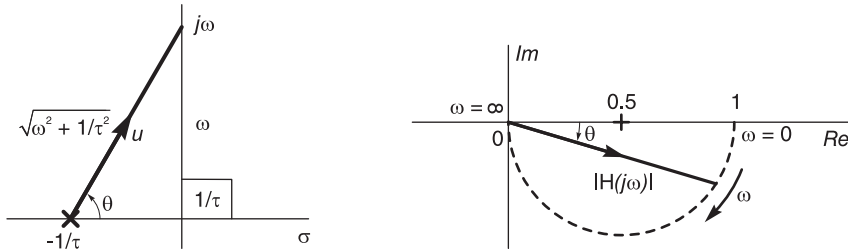


FIGURE 5.64 Vector to a frequency point and the evolution of magnitude spectrum in the phase plane.

Referring to Fig. 5.64(a) we have $H(j\omega) = 1/u$,

$$|H(j\omega)| = (1/\tau) / \sqrt{\omega^2 + (1/\tau)^2} = 1 / \sqrt{1 + \omega^2\tau^2}, \quad \theta = \arg [H(j\omega)] = -\tan^{-1}(\omega\tau).$$

The polar plot showing the evolution in the complex plane with the frequency ω increasing from 0 to ∞ of $H(j\omega)$ is shown in Fig. 5.64(b). This can be verified geometrically and confirmed by the MATLAB command polar (Hangle, Habs).

We note that each of these two circuits acts as a lowpass filter. At zero frequency the capacitor has infinite impedance, appearing as an open circuit, and the inductor has zero impedance acting as a short circuit, wherefrom $v_0 = v_i$. At infinite frequency the reverse occurs, the capacitor is a short circuit and the inductor an open circuit, so that $v_0 = 0$. A second order system with a zero in its transfer function $H(s)$ at $s = 0$ behaves as a bandpass filter. Consider the circuit shown in Fig. 5.65.

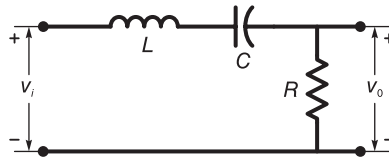


FIGURE 5.65 R-L-C electric circuit.

We have

$$H(s) = \frac{V_o(s)}{V_i(s)} = \frac{R}{R + Ls + 1/(Cs)} = \frac{(R/L)s}{s^2 + (R/L)s + 1/(LC)} = \frac{2\zeta\omega_0 s}{s^2 + 2\zeta\omega_0 s + \omega_0^2}$$

where

$$\omega_0 = \frac{1}{\sqrt{LC}}, \quad 2\zeta\omega_0 = R/L, \text{ i.e. } \zeta = \frac{R}{2L\omega_0} = \frac{R}{2} \sqrt{\frac{C}{L}} \tag{5.193}$$

$$H(j\omega) = j2\zeta\omega_0\omega / (\omega_0^2 - \omega^2 + j2\zeta\omega_0\omega). \tag{5.194}$$

The general outlook of the amplitude and phase spectra of $H(j\omega)$ are shown in Fig. 5.66 for the case $\omega_0 = 1$ and $\zeta = 0.2$.

We note that the system function $H(s)$ has a zero at $s = 0$ and at both $H(0)$ and $H(j\infty)$ are equal to zero, implying a bandpass property of this second order system.

At zero frequency the inductor is a short circuit but the capacitor is an open one, wherefrom the output voltage is zero. At infinite frequency the inductor is an open circuit and

the capacitor a short circuit; hence the output is again zero. At the resonance frequency $\omega_0 = 1/\sqrt{LC}$ the output voltage v_0 reaches a peak. Note that the impedance of the $L - C$ component is given by

$$Z(s) = Ls + \frac{1}{Cs} = \frac{LCs^2 + 1}{Cs} = L \frac{s^2 + 1/(LC)}{s}. \tag{5.195}$$

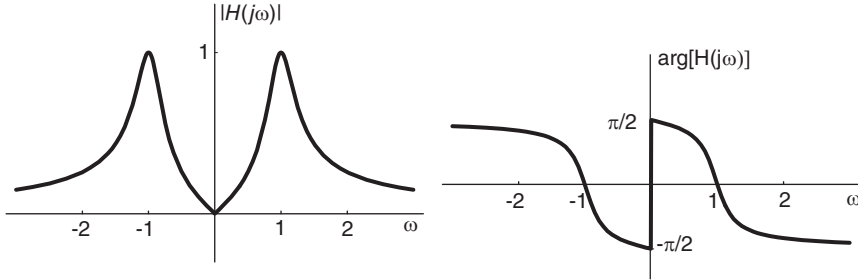


FIGURE 5.66 Amplitude and phase spectra of a second order system.

Referring to Fig. 5.67, we note that $Z(s)$ has two zeros on the $j\omega$ axis, and one pole at $s = 0$.

The zeros of $Z(s)$ are given by $LCs^2 = -1$, i.e.

$$-\omega^2 + \frac{1}{LC} = 0 \tag{5.196}$$

$$\omega^2 = \frac{1}{LC}, \text{ i.e. } \omega = \frac{1}{\sqrt{LC}}. \tag{5.197}$$

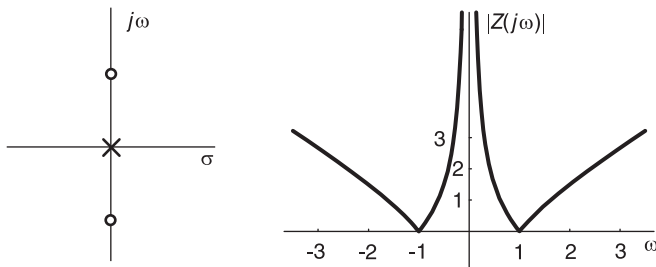


FIGURE 5.67 Transfer function with a pole and two zeros and its frequency spectrum.

Let $L = C = 1$

$$Z(j\omega) = \frac{1 - \omega^2}{j\omega} = \frac{j(\omega^2 - 1)}{\omega}, \quad |Z(j\omega)| = \frac{|\omega^2 - 1|}{|\omega|} \tag{5.198}$$

as represented graphically in the figure.

5.29 Minimum Phase Systems

We have seen that a causal system is stable if and only if its poles are all in the left half of the s plane. For stability there is no restriction on the location of zeros in the plane. The location of a zero, whether it is in the left half or right half of the s plane, has an effect, however, on the phase of the frequency response. The following example illustrates the effect of reflecting a zero into the s -plane's $j\omega$ axis on the phase of the system frequency response.

Example 5.8 Evaluate the magnitude and phase of a system frequency response $H_1(j\omega)$ for a general value ω given that

$$H_1(s) = \frac{10(s + 3)}{(s - p_1)(s - p_1^*)(s + 5)}$$

where $p_1 = -2 + j2$. Repeat for the case of the same system but where the zero is reflected into the $j\omega$ axis, so that the system transfer function is given by

$$H_2(s) = \frac{10(s - 3)}{(s - p_1)(s - p_1^*)(s + 5)}$$

Compare the magnitude and phase response in both cases.

We have

$$H_1(j\omega) = \frac{10(j\omega + 3)}{(j\omega - p_1)(j\omega - p_1^*)(j\omega + 5)}, \quad H_2(j\omega) = \frac{10(j\omega - 3)}{(j\omega - p_1)(j\omega - p_1^*)(j\omega + 5)}$$

Referring to Fig. 5.68 we can rewrite the frequency responses in the form

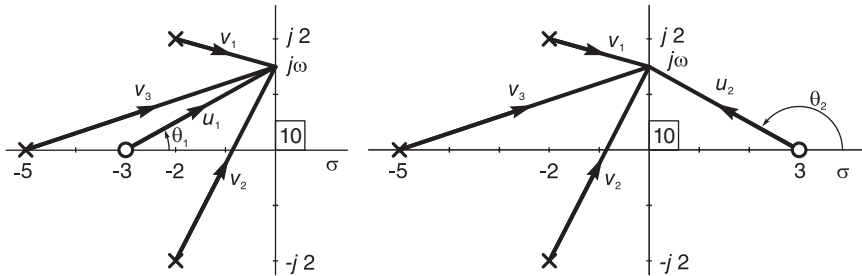


FIGURE 5.68 Vectorial evaluation of frequency response.

$$H_1(j\omega) = \frac{10u_1}{v_1v_2v_3}, \quad H_2(j\omega) = \frac{10u_2}{v_1v_2v_3}$$

We note that

$$|H_1(j\omega)| = \frac{10|u_1|}{|v_1||v_2||v_3|} = \frac{10|u_2|}{|v_1||v_2||v_3|} = |H_2(j\omega)|$$

The magnitude responses are therefore the same for both cases. Regarding the phase, however, we have

$$\begin{aligned} \phi_1 &\triangleq \arg [H_1(j\omega)] = \arg [u_1] - \arg [v_1 v_2 v_3] = \theta_1 - \arg [v_1 v_2 v_3] \\ \phi_2 &\triangleq \arg [H_2(j\omega)] = \arg [u_2] - \arg [v_1 v_2 v_3] = \theta_2 - \arg [v_1 v_2 v_3] \end{aligned}$$

where θ_1 and θ_2 are the angles of the vectors u_1 and u_2 as shown in the figure.

We note that for $\omega > 0$ the phase angle θ_1 of $H_1(j\omega)$ is smaller in value than the angle θ_2 of $H_2(j\omega)$. A zero in the left half of the s plane thus contributes a lesser phase angle to the phase spectrum than does its reflection into the $j\omega$ axis. The same applies to complex zeros. If the input to the system is a sinusoid of frequency β rad/sec, the system output, as we have seen, is the same sinusoid amplified by $|H(j\omega)|_{\omega=\beta} = |H(j\beta)|$ and delayed by $\arg \{H(j\omega)\}_{\omega=\beta} = \arg \{H(j\beta)\}$.

The phase lag, hence the delay, of the system output increases with the increase of the phase $\arg \{H(j\omega)\}$ of the frequency response. Since a zero in the left half plane contributes less phase to the value of the phase spectrum $\arg \{H(j\omega)\}$ at any frequency ω than does a zero in the right half of the s plane, it causes less phases lag in the system response. It is for this reason that a causal system of which all zeros are located in the left half of the s plane is referred to as a “minimum phase” system in addition to being stable. We note, moreover, that the inverse $1/H(s)$ of the system function $H(s)$ is also causal, stable and minimum phase. If, on the other hand, a zero of $H(s)$ exists in the right half of the s plane, the inverse $1/H(s)$ would have a pole at that location, and is therefore an unstable system.

5.30 General Order All-Pass Systems

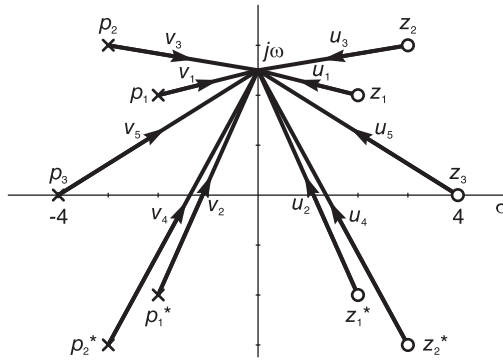


FIGURE 5.69 Vectors from allpass system poles and zeros to a frequency point.

Consider a transfer function

$$H(s) = K \frac{\prod_i (s - z_i)}{\prod_i (s - p_i)} \tag{5.199}$$

having the pole-zero pattern in the s plane shown in Fig. 5.69. Each pole p_i has an image in the form of a zero z_i by reflection into the $j\omega$ axis. The magnitude spectrum of such a system can be written in the form

$$|H(j\omega)| = \frac{K \prod_{i=1}^5 |u_i|}{\prod_{i=1}^5 |v_i|} \tag{5.200}$$

Referring to the figure we notice that

$$|u_i| = |v_i|, \quad i = 1, 2, \dots, 5. \tag{5.201}$$

We deduce that

$$|H(j\omega)| = K. \tag{5.202}$$

Since the magnitude spectrum is a constant for all frequencies this is called an allpass system. An allpass system, therefore, has poles in the left half of the s plane only, and zeros in the right half which are reflections thereof into the $s = j\omega$ axis. The transfer function is denoted $H_{ap}(s)$. We note that an allpass system, having its zeros in the right half s -plane, is not minimum phase. Any causal and stable system can be realized as a cascade of an allpass system and a minimum phase system

$$H(s) = H_{\min}(s) H_{ap}(s). \tag{5.203}$$

The allpass system's transfer function $H_{ap}(s)$ has the right half s plane zeros of $H(s)$ and has, in the left half of the s plane, their reflections into the $j\omega$ axis as poles. The transfer function $H_{\min}(s)$ has poles and zeros only in the left half of the s plane. The poles are the same as those of $H(s)$. The zeros are the same as the left half plane zeros of $H(s)$ plus additional zeros that are at the same positions of the poles of $H_{ap}(s)$. These additional zeros are there so as to cancel the new poles of $H_{ap}(s)$ in the product $H_{\min}(s) H_{ap}(s)$.

Example 5.9 Decompose the transfer function $H(s)$ shown in Fig. 5.70 into an allpass and minimum phase functions.

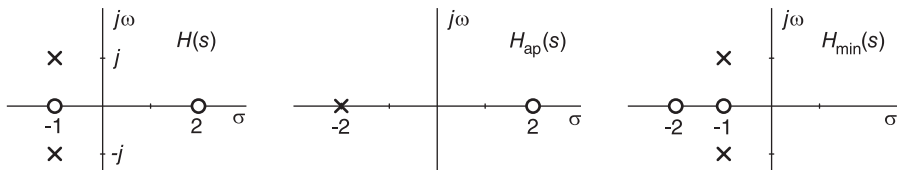


FIGURE 5.70 Transfer function decomposition into allpass and minimum phase factors.

The required allpass and minimum phase functions are shown in the figure.

Example 5.10 Given the transfer function $H(s)$ shown in Fig. 5.71 derive the transfer functions $H_{ap}(s)$ and $H_{\min}(s)$ of which $H(s)$ is the product.

The required allpass and minimum phase transfer functions are shown in the figure.

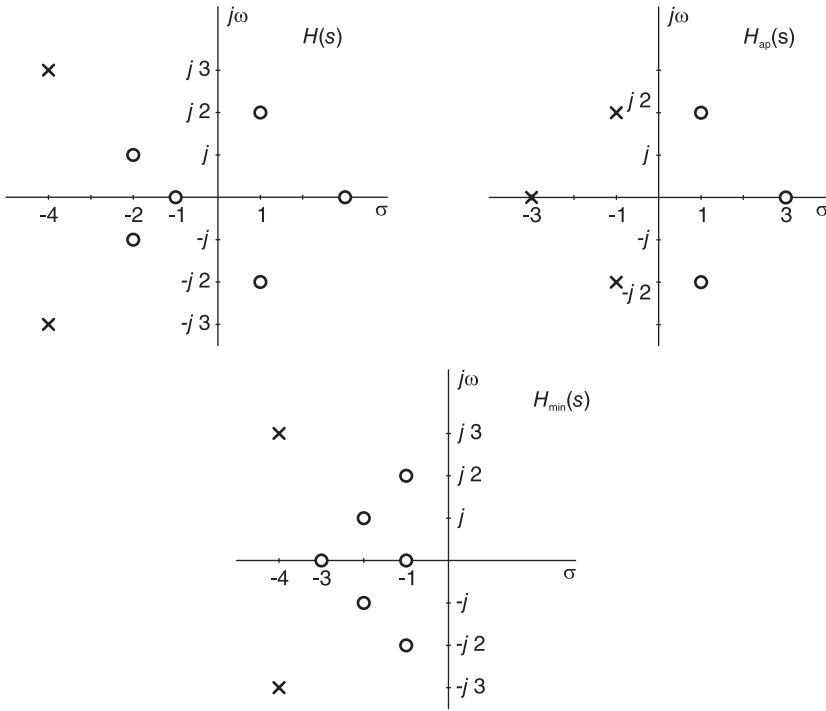


FIGURE 5.71 Decomposition into allpass and minimum phase system.

5.31 Signal Generation

As we have seen, dynamic linear systems may be modeled by linear constant-coefficient differential equations. Conversely, it is always possible to construct, using among others integrators, a physical system of which the behavior mirrors a model given in the form of differential equations. This concept can be extended as a means of constructing signal generators. A linear system can be constructed using integrators, adders, constant multipliers,... effectively simulating any system described by a particular differential equation. By choosing a differential equation of which the solution is a sinusoid, an exponential or a damped sinusoid, for example, such a system can be constructed ensuring that its output is the desired signal to be generated. The following example illustrates the approach.

Example 5.11 Show a block diagram using integrators, adders, ... of a signal generator producing the function

$$y(t) = Ae^{-\alpha t} \sin \beta t u(t).$$

Set the integrators' initial conditions to ensure generating the required signal.

To generate the function $y(t)$ consider the second order system transfer function

$$H(s) = \frac{\omega_0^2}{s^2 + 2\zeta\omega_0 s + \omega_0^2}.$$

Assuming zero input, i.e.

$$\ddot{y} + 2\zeta\omega_0\dot{y} + \omega_0^2 y = 0$$

$$s^2Y(s) - s y(0^+) - \dot{y}(0^+) + 2\zeta\omega_0 \{s Y(s) - y(0^+)\} + \omega_0^2 Y(s) = 0$$

i.e.

$$Y(s) = \frac{s y(0^+) + \dot{y}(0^+) + 2\zeta\omega_0 y(0^+)}{s^2 + 2\zeta\omega_0 s + \omega_0^2}.$$

Now

$$y(0^+) = 0$$

and

$$\dot{y}(0^+) = [Ae^{-\alpha t} \beta \cos \beta t - A\alpha e^{-\alpha t} \sin \beta t]_{t=0} = A\beta$$

wherefrom

$$Y(s) = \frac{A\beta}{s^2 + 2\zeta\omega_0 s + \omega_0^2} = A\beta \left[\frac{C_1}{s - p_1} + \frac{C_1^*}{s - p_1^*} \right]$$

$$p_1 = -\zeta\omega_0 + j\omega_0 \sqrt{1 - \zeta^2} = -\zeta\omega_0 + j\omega_p$$

$$y(t) = 2A\beta |C_1| e^{-\zeta\omega_0 t} \cos(\omega_p t + \arg[C_1])$$

$$|C_1| = \frac{1}{2\omega_p}, \quad \arg[C_1] = -90^\circ$$

$$y(t) = \frac{A\beta}{\omega_p} e^{-\zeta\omega_0 t} \sin \omega_p t$$

$\beta/\omega_p = 1$ i.e. $\omega_0 \sqrt{1 - \zeta^2} = \beta$, $\zeta\omega_0 = \alpha$, $\omega_0^2 = \alpha^2 + \beta^2$, and $\zeta = \alpha/\omega_0$

$$\ddot{y} = -2\zeta\omega_0 \dot{y} - \omega_0^2 y = -2\alpha \dot{y} - (\alpha^2 + \beta^2) y.$$

See Fig. 5.72. Note that if we set $\alpha = 0$ we would obtain an oscillator generating a pure sinusoid.

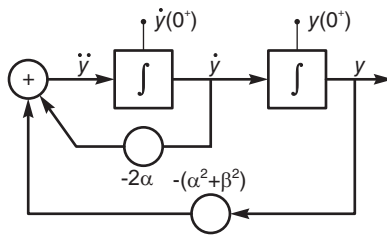


FIGURE 5.72 Sinusoid generator.

5.32 Application of Laplace Transform to Differential Equations

We have seen several examples of the solution of differential equations using the Laplace transform. This subject is of great importance and constitutes one of the main applications of the Laplace transform. In what follows we review the basic properties of linear constant coefficient differential equations with boundary and initial conditions followed by their solutions and those of partial differential equations using Laplace transform.

5.32.1 Linear Differential Equations with Constant Coefficients

We shall review basic linear differential equations and general forms of their solutions. Subsequently, we study the application of Laplace and Fourier transform to the solution of these equations. Partial differential equations and their solutions using transforms extend the scope of the applications to a larger class of models of physical systems.

5.32.2 Linear First Order Differential Equation

Consider the linear first order differential equation

$$y' + P(t)y = Q(t). \quad (5.204)$$

The solution of this equation employs the **integrating factor** $f(t) = e^{\int P(t)dt}$. Multiplying both sides of the differential equation by the integrating factor we have

$$y'e^{\int P(t)dt} + P(t)ye^{\int P(t)dt} = Q(t)e^{\int P(t)dt} \quad (5.205)$$

which may be rewritten in the form

$$\frac{d}{dt} \left\{ ye^{\int P(t)dt} \right\} = Q(t)e^{\int P(t)dt}. \quad (5.206)$$

Hence

$$ye^{\int P(t)dt} = \int Q(t)e^{\int P(t)dt} dt + C. \quad (5.207)$$

where C is a constant. We deduce that

$$y(t) = e^{-\int P(t)dt} \int Q(t)e^{\int P(t)dt} dt + Ce^{-\int P(t)dt}. \quad (5.208)$$

Example 5.12 Solve the equation

$$y' - 2ty = t.$$

We have $P(t) = -2t$, $Q(t) = t$. The integrating factor is $f(t) = e^{\int -2tdt} = e^{-t^2}$

$$e^{-t^2}y' - 2te^{-t^2}y = te^{-t^2}$$

$$\frac{d}{dt} (ye^{-t^2}) = te^{-t^2}$$

$$ye^{-t^2} = \int te^{-t^2} dt + C$$

$$y = e^{t^2} \left(\frac{-1}{2} \right) e^{-t^2} + Ce^{t^2} = Ce^{t^2} - 1/2.$$

Example 5.13 Given

$$f(t) = \int_0^\infty \frac{e^{-w}e^{-t/w}}{\sqrt{w}} dw.$$

Evaluate $f'(t)$ and relate it to $f(t)$. Write a differential equation in f and f' and solve it to evaluate $f(t)$.

We have

$$f'(t) = \int_0^\infty \frac{e^{-w}e^{-t/w}}{\sqrt{w}} \left(\frac{-1}{w} \right) dw = - \int_0^\infty \frac{e^{-w}e^{-t/w}}{w^{3/2}} dw.$$

Let $\frac{t}{w} = u$, $w = \frac{t}{u}$, $dw = -\frac{t}{u^2} du$

$$f'(t) = \int_{\infty}^0 \frac{e^{-t/u} e^{-u}}{(t/u)^{3/2}} \frac{t}{u^2} du = - \int_0^{\infty} \frac{e^{-u} e^{-t/u}}{\sqrt{t} \sqrt{u}} du = -\frac{1}{\sqrt{t}} f(t)$$

$$f'(t) + \frac{1}{\sqrt{t}} f(t) = 0$$

which has the form

$$f'(t) + P(t)f(t) = 0.$$

The integrating factor is

$$I = e^{\int P(t)dt} = e^{\int \frac{1}{\sqrt{t}} dt} = e^{2\sqrt{t}}.$$

Multiplying the differential equation by I

$$e^{2\sqrt{t}} f'(t) + \frac{1}{\sqrt{t}} e^{2\sqrt{t}} f(t) = 0$$

$$\frac{d}{dt} [e^{2\sqrt{t}} f(t)] = 0.$$

Integrating we have

$$e^{2\sqrt{t}} f(t) = C$$

$$f(t) = C e^{-2\sqrt{t}}.$$

To evaluate the constant C we use the initial condition

$$f(0) = C = \int_0^{\infty} \frac{e^{-w}}{\sqrt{w}} dw$$

$$C = \int_0^{\infty} e^{-w} w^{-1/2} dw = \Gamma(1/2) = \sqrt{\pi}.$$

We conclude that

$$f(t) = \int_0^{\infty} \frac{e^{-w} e^{-t/w}}{\sqrt{w}} dw = \sqrt{\pi} e^{-2\sqrt{t}}.$$

5.32.3 General Order Differential Equations with Constant Coefficients

An n^{th} order linear differential equation with constant coefficients has the form

$$a_0 y^{(n)} + a_1 y^{(n-1)} + \dots + a_n y = f(t) \quad (5.209)$$

where $y^{(k)} = \frac{d^k}{dt^k} y(t)$. The equation

$$a_0 y^{(n)} + a_1 y^{(n-1)} + \dots + a_n y = 0 \quad (5.210)$$

is called the corresponding *homogeneous equation*, while the first equation is the *nonhomogeneous equation* and the function $f(t)$ is called the *forcing function* or the *nonhomogeneous term*. The solution of the homogeneous equation may be denoted $y_h(t)$. The solution of the nonhomogeneous equation is the particular solution denoted $y_p(t)$. The general solution of the nonhomogeneous equation with general nonzero initial conditions is given by

$$y(t) = y_h(t) + y_p(t). \quad (5.211)$$

5.32.4 Homogeneous Linear Differential Equations

From the above the n^{th} order homogeneous linear differential equation with constant coefficients may be written in the form

$$y^{(n)} + a_1 y^{(n-1)} + \dots + a_n y = 0 \quad (5.212)$$

where the coefficients a_1, a_2, \dots, a_n are constants. The solution of the homogeneous equation is obtained by first writing the corresponding characteristic equation, namely

$$\lambda^n + a_1 \lambda^{n-1} + \dots + a_{n-1} \lambda + a_n = 0 \quad (5.213)$$

which is formed by replacing each derivative $y^{(i)}$ by λ^i in the equation.

Let the roots of the characteristic equation be $\lambda_1, \lambda_2, \dots, \lambda_n$. If the roots are distinct the solution of the homogeneous equation has the form

$$y = C_1 e^{\lambda_1 t} + C_2 e^{\lambda_2 t} + \dots + C_n e^{\lambda_n t}. \quad (5.214)$$

If some roots are complex the solution may be rewritten using sine and cosine terms. For example, if $\lambda_2 = \lambda_1^*$, let $\lambda_1 = \alpha + j\beta$, $\lambda_2 = \alpha - j\beta$, the solution includes the terms

$$C_1 e^{\lambda_1 t} + C_2 e^{\lambda_1^* t} = C_1 e^{(\alpha + j\beta)t} + C_1^* e^{(\alpha - j\beta)t}. \quad (5.215)$$

Writing $C_1 = A_1 e^{j\theta_1}$, the terms may be rewritten as

$$A_1 e^{j\theta_1} e^{(\alpha + j\beta)t} + A_1 e^{-j\theta_1} e^{(\alpha - j\beta)t} = 2A_1 e^{\alpha t} \cos(\beta t + \theta_1) \quad (5.216)$$

which may be rewritten in the form

$$K_1 e^{\alpha t} \cos \beta_1 t + K_2 e^{\alpha t} \sin \beta_1 t. \quad (5.217)$$

Similarly, if two roots, such as λ_1 and λ_2 , are real and $\lambda_2 = -\lambda_1$ then the contribution to the solution may be written in the form

$$\begin{aligned} C_1 e^{\lambda_1 t} + C_2 e^{-\lambda_1 t} &= C_1 (\cosh \lambda_1 t - \sinh \lambda_1 t) + C_2 (\cosh \lambda_1 t + \sinh \lambda_1 t) \\ &= (C_1 + C_2) \cosh \lambda_1 t + (C_2 - C_1) \sinh \lambda_1 t = K_1 \cosh \lambda_1 t + K_2 \sinh \lambda_1 t. \end{aligned}$$

If one of the roots is repeated, i.e. a multiple zero, the characteristic equation has the factor $(\lambda - \lambda_i)^m$. The corresponding terms in the solution are

$$K_0 e^{\lambda_i t} + K_1 t e^{\lambda_i t} + K_2 t^2 e^{\lambda_i t} + \dots + K_{m-1} t^{m-1} e^{\lambda_i t}. \quad (5.218)$$

Example 5.14 Evaluate the solution of the homogeneous equation

$$y^{(6)} - 13y^{(4)} + 54y^{(3)} + 198y^{(2)} - 216y^{(1)} - 648y = 0.$$

The characteristic equation is

$$\lambda^6 - 13\lambda^4 + 54\lambda^3 + 198\lambda^2 - 216\lambda - 648 = 0.$$

Its roots are

$$\lambda_1 = 2, \quad \lambda_2 = -2, \quad \lambda_3 = -3, \quad \lambda_4 = -3, \quad \lambda_5 = 3 + j3, \quad \lambda_6 = 3 - j3.$$

$$y(t) = K_1 \cosh 2t + K_2 \sinh 2t + K_3 e^{-3t} + K_4 t e^{-3t} + K_5 e^{3t} \cos 3t + K_6 e^{3t} \sin 3t.$$

5.32.5 The General Solution of a Linear Differential Equation

As stated above, given an n^{th} order linear differential equation of constant coefficient

$$y^{(n)} + a_1y^{(n-1)} + \dots + a_ny = f(t) \quad (5.219)$$

the solution is the sum of the solution $y_h(t)$ of the homogeneous equation

$$y^{(n)} + a_1y^{(n-1)} + \dots + a_ny = 0 \quad (5.220)$$

and the particular solution $y_p(t)$, i.e.

$$y(t) = y_h(t) + y_p(t). \quad (5.221)$$

In what follows, we study the evaluation of the particular solution $y_p(t)$ from the form of the homogeneous solution $y_h(t)$. As we shall see, the solution $y_p(t)$ is in general a sum of terms of the form $C_1e^{\alpha t}$, $C_2te^{\alpha t}$, $C_3t^2e^{\alpha t}$, ... or these terms multiplied by sines and cosines.

The constants C_1 , C_2 , C_3 , ... are found by substituting the solution into the differential equation and equating the coefficients of like powers of t . Once the general solution $y(t)$ is determined the unknown constants of the homogeneous solution are determined by making use of the given initial conditions. The approach is called the method of undetermined coefficients. The form of the particular solution is deduced from the nonhomogeneous term $f(t)$. Let $P_m(t)$ represent an m^{th} order polynomial in powers of t .

1. If $f(t) = P_m(t)$ then $y_p(t) = A_mt^m + A_{m-1}t^{m-1} + \dots + A_0$, where the coefficients A_0, A_1, \dots, A_m are constants to be determined.
2. If $f(t) = e^{\alpha t}P_m(t)$ then $y_p(t) = e^{\alpha t}(A_mt^m + A_{m-1}t^{m-1} + \dots + A_0)$.
3. If $f(t) = e^{\alpha t}P_m(t)\sin\beta t$ or $f(t) = e^{\alpha t}P_m(t)\cos\beta t$ then

$$y_p(t) = e^{\alpha t}\sin\beta t(A_mt^m + A_{m-1}t^{m-1} + \dots + A_0) + e^{\alpha t}\cos\beta t(B_mt^m + B_{m-1}t^{m-1} + \dots + B_0). \quad (5.222)$$

A special condition may arise necessitating multiplying the polynomial in $y_p(t)$ by a power of t . This condition occurs if any term of the assumed solution $y_p(t)$ (apart from the multiplication constant) is the same as a term in the homogeneous solution $y_h(t)$. In this case the assumed solution $y_p(t)$ should be multiplied by t^k where k is the least positive power needed to eliminate such common factors between $y_p(t)$ and $y_h(t)$.

Example 5.15 Solve the differential equation

$$y'' + 2y' - 3y = 7t^2.$$

The homogeneous equation $y'' + 2y' - 3y = 0$ has the characteristic equation $(\lambda - 1)(\lambda + 3) = 0$ and the solution $y_h = C_1e^{-3t} + C_2e^t$.

The nonhomogeneous term $f(t) = 7t^2$ is a polynomial of order 2. We therefore assume a particular solution of the form $y_p(t) = A_2t^2 + A_1t + A_0$

$$y_p' = 2A_2t + A_1, \quad y_p'' = 2A_2.$$

Substituting in the differential equation

$$2A_2 + 4A_2t + 2A_1 - 3A_2t^2 - 3A_1t - 3A_0 = 7t^2.$$

Equating the coefficients of equal powers of t we obtain

$$A_2 = -7/3, \quad A_1 = -28/9, \quad A_0 = -98/27$$

so that

$$y_p(t) = -(7/3)t^2 - (28/9)t - 98/27$$

and

$$y(t) = C_1 e^{-3t} + C_2 e^t - (7/3)t^2 - (28/9)t - (98/27).$$

Example 5.16 Solve the equation

$$y' - 3y = t(\cos 2t + \sin 2t) - 2(\cos 2t - \sin 2t).$$

We have

$$y' - 3y = (t - 2) \cos 2t + (t + 2) \sin 2t.$$

The solution of the homogeneous equation is $y_h = C_1 e^{3t}$. The assumed particular solution is $y_p = (K_1 t + K_0) \cos 2t + (L_1 t + L_0) \sin 2t$.

$$\begin{aligned} y_p' &= (K_1 t + K_0)(-2 \sin 2t) + K_1 \cos 2t + (L_1 t + L_0)(2 \cos 2t) + L_1 \sin 2t \\ &= (L_1 - 2K_1 t - 2K_0) \sin 2t + (K_1 + 2L_1 t + 2L_0) \cos 2t. \end{aligned}$$

Substituting into the differential equation

$$\begin{aligned} (L_1 - 2K_0 - 2K_1 t) \sin 2t + (K_1 + 2L_0 + 2L_1 t) \cos 2t - (3L_1 t + 3L_0) \sin 2t \\ - (3K_1 t + 3K_0) \cos 2t = (t - 2) \cos 2t + (t + 2) \sin 2t. \end{aligned}$$

Equating the coefficients of same terms

$$2L_1 - 3K_1 = 1$$

$$K_1 + 2L_0 - 3K_0 = -2$$

$$-2K_1 - 3L_1 = 1$$

$$L_1 - 2K_0 - 3L_0 = 2.$$

Solving we obtain

$$K_1 = -5/13, \quad L_1 = -1/13, \quad K_0 = 9/169, \quad L_0 = -123/169.$$

We deduce that

$$y = y_h + y_p = C_1 e^{3t} + \left(\frac{-5}{13}t + \frac{9}{169} \right) \cos 2t + \left(-\frac{1}{13}t - \frac{123}{169} \right) \sin 2t.$$

Example 5.17 Solve the differential equation $y'' = 4t^2 - 3t + 1$, with the initial conditions $y(0) = 1$ and $y'(0) = -1$.

We first note that the homogeneous equation $y'' = 0$ implies the characteristic equation $\lambda^2 = 0$ i.e. $\lambda_1, \lambda_2 = 0, 0$; hence the homogeneous solution

$$y_h(t) = C_1 t e^{\lambda_1 t} + C_2 e^{\lambda_1 t} = C_1 t + C_2.$$

The assumed particular solution is $y_p(t) = A_2 t^2 + A_1 t + A_0$. We note however that apart from the multiplying constants the last two terms are the same as those of the homogeneous

solution $y_h(t)$. We therefore multiply the assumed particular solution by t^2 obtaining $y_p(t) = A_2t^4 + A_1t^3 + A_0t^2$. Now

$$y_p'(t) = 4A_2t^3 + 3A_1t^2 + 2A_0t$$

$$y_p''(t) = 12A_2t^2 + 6A_1t + 2A_0.$$

Substituting in the differential equation we have

$$12A_2t^2 + 6A_1t + 2A_0 = 4t^2 - 3t + 1.$$

Equating the coefficients of equal powers of t we have $12A_2 = 4$, i.e. $A_2 = 1/3$; $6A_1 = -3$, $A_1 = 0.5$; $2A_0 = 1$, $A_0 = 0.5$. so that

$$y_p(t) = (1/3)t^4 - (1/2)t^3 + (1/2)t^2.$$

The general solution is therefore

$$y(t) = C_1t + C_2 + (1/3)t^4 - (1/2)t^3 + (1/2)t^2.$$

Applying the initial conditions we have $y(0) = 1 = C_2$, $y'(t) = C_1 + \frac{4}{3}t^3 - \frac{3}{2}t^2 + t$, $y'(0) = C_1 = -1$, i.e.

$$y(t) = -t + 1 + (1/3)t^4 - (1/2)t^3 + (1/2)t^2.$$

Example 5.18 Newton's law of cooling states that the rate of cooling of an object is proportional to the difference between its temperature and that of its surroundings. Let T denote the object's temperature and T_s that of its surroundings. The cooling process, with the time t in minutes, is described by the differential equation

$$\frac{dT}{dt} = k(T - T_s).$$

An object in a surrounding temperature of 20°C cools from 100°C to 50°C in 30 minutes. (a) How long would it take to cool to 30°C ? (b) What is its temperature 10 minutes after it started cooling?

We have $T_s = 20^\circ$,

$$\frac{dT}{dt} - kT = -20k.$$

The integrating factor is $f = e^{-\int kdt} = e^{-kt}$. Multiplying both sides by the integrating factor we obtain

$$\begin{aligned} \frac{d}{dt}\{Te^{-kt}\} &= -20ke^{-kt} \\ Te^{-kt} &= -20k \int e^{-kt} dt = 20e^{-kt} + C \\ T &= 20 + Ce^{kt} \end{aligned}$$

$T(0) = 100$ implies that $100 = 20 + C$, i.e. $C = 80$. Moreover, $T(30) = 50 = 20 + 80e^{30k}$, so that $e^k = (3/8)^{1/30}$ and

$$T = 20 + 80(3/8)^{t/30}.$$

(a) To find the value t so that $T = 30^\circ\text{C}$ we write $30 = 20 + 80(3/8)^{t/30}$. Solving we have

$$t = 30 \ln(1/8) / \ln(3/8) = 30(-2.0794) / (-0.9808) = 63.60 \text{ minutes.}$$

(b) Putting $t = 10$ we find $T = 77.69^\circ\text{C}$. Alternatively, we may apply the unilateral Laplace transform to the differential equation obtaining, with $T(0^+) = 100$,

$$sT(s) - T(0^+) - kT(s) = -20k/s$$

$$T(s) = \frac{100}{s-k} - \frac{20k}{s(s-k)} = \frac{20}{s} + \frac{80}{s-k}$$

$$T(t) = (20 + 80e^{kt})u(t)$$

as obtained above.

5.32.6 Partial Differential Equations

We have seen methods for solving ordinary linear differential equations with constant coefficients using the method of undetermined coefficients and using in particular Laplace transform. Models of dynamic physical systems are sometimes known in the form of partial differential equations. In this section a brief summary is given on the solution of such equations using Laplace and Fourier transform. The equation

$$\frac{\partial^2 y(x, t)}{\partial t^2} - 2 \frac{\partial^2 y(x, t)}{\partial x^2} = 0 \quad (5.223)$$

is a partial differential equation since the unknown variable y is a function of two variables; x and t . In general if the unknown function y in the differential equation is a function of more than one variable then the equation is a partial differential equation.

Consider a semiinfinite thin rod extending from $x = 0$ to $x = \infty$. The problem of evaluating the potential $v(x, t)$ of any point x at any instant t , assuming zero voltage leakage and zero inductance, is described by the partial differential equation

$$\frac{\partial^2 v}{\partial x^2} = a^2 \frac{\partial v}{\partial t} \quad (5.224)$$

with $a^2 = RC$, that is, the product of the rod resistance per unit length R and the capacitance to the ground per unit length C . This same partial differential equation is also referred to as the one dimensional heat equation, in which case $v(x, t)$ is the heat of point x at instant t of a thin insulated rod. The following example can therefore be seen as either an electric potential or heat conduction problem

Example 5.19 Solve the differential equation

$$\frac{\partial^2 v}{\partial x^2} = a^2 \frac{\partial v}{\partial t}, \quad 0 < x < \infty, \quad t > 0$$

with the initial condition

$$v(x, 0) = 0, \quad 0 < x < \infty$$

and the boundary conditions $v(0, t) = f(t)$, $\lim_{x \rightarrow \infty} |v(x, t)| < \infty$, $t > 0$. Find next the value $v(x, t)$ if $f(t) = u(t)$.

The Laplace transform of $\partial v / \partial t$ is given by

$$\mathcal{L} \left[\frac{\partial}{\partial t} v(x, t) \right] = sV(x, s) - v(x, 0).$$

The transform of $\partial^2 v / \partial x^2$ is found by writing

$$\mathcal{L} \left[\frac{\partial}{\partial x} v(x, t) \right] = \frac{d}{dx} \mathcal{L} [v(x, t)] = \frac{d}{dx} V(x, s)$$

$$\mathcal{L} \left[\frac{\partial^2}{\partial x^2} v(x, t) \right] = \frac{d}{dx} \left\{ \frac{d}{dx} \mathcal{L}[v(x, t)] \right\} = \frac{d^2}{dx^2} V(x, s).$$

The Laplace transform of the partial differential equation is therefore

$$\frac{d^2}{dx^2} V(x, s) = a^2 s V(x, s) - a^2 v(x, 0).$$

Substituting with the initial condition $v(x, 0) = 0$ we have

$$\frac{d^2}{dx^2} V(x, s) = a^2 s V(x, s).$$

We have thus obtained an ordinary differential equation that can be readily solved for $V(x, s)$. The equation has the form

$$V'' - a^2 s V = 0.$$

The solution has the form, with $s > 0$,

$$V(x, s) = C_1(s)e^{a\sqrt{s}x} + C_2(s)e^{-a\sqrt{s}x}.$$

Laplace transforming the boundary conditions we have

$$V(0, s) = F(s), \quad \lim_{x \rightarrow \infty} |V(x, s)| < \infty.$$

The second condition implies that $C_1 = 0$, so that

$$V(0, s) = C_2(s) = F(s)$$

and

$$V(x, s) = F(s)e^{-a\sqrt{s}x}.$$

The inverse Laplace transform of this equation is written

$$v(x, t) = f(t) * \mathcal{L}^{-1} \left[e^{-a\sqrt{s}x} \right].$$

Let $b = ax$. From the table of Laplace transform of causal functions

$$\frac{be^{-b^2/(4t)}}{2\sqrt{\pi}t^{3/2}} \longleftrightarrow e^{-b\sqrt{s}}.$$

We can therefore write

$$v(x, t) = f(t) * \frac{be^{-b^2/(4t)}}{2\sqrt{\pi}t^{3/2}} = \frac{ax}{2\sqrt{\pi}} \int_0^t \frac{e^{-a^2x^2/(4\tau)}}{\tau^{3/2}} f(t - \tau) d\tau$$

since $f(t)$ is causal. If $f(t) = u(t)$ we have

$$v(x, t) = \frac{ax}{2\sqrt{\pi}} \int_0^t \frac{e^{-a^2x^2/(4\tau)}}{\tau^{3/2}} d\tau.$$

$$\text{Let } \frac{a^2x^2}{4\tau} = u^2, \quad d\tau = -\frac{a^2x^2}{2u^3} du$$

$$\begin{aligned} v(x, t) &= \frac{ax}{2\sqrt{\pi}} \int_{ax/(2\sqrt{t})}^{ax/(2\sqrt{t})} \frac{e^{-u^2} 8u^3}{a^3x^3} \left(-\frac{a^2x^2}{2u^3} \right) du = \frac{-ax}{2\sqrt{\pi}} \int_{\infty}^{ax/(2\sqrt{t})} \frac{4e^{-u^2}}{ax} du \\ &= \frac{2}{\sqrt{\pi}} \int_{ax/(2\sqrt{t})}^{\infty} e^{-u^2} du = \frac{2}{\sqrt{\pi}} \left\{ \int_0^{\infty} e^{-u^2} du - \int_0^{ax/(2\sqrt{t})} e^{-u^2} du \right\} \\ &\triangleq I_1 + I_2. \end{aligned}$$

Let, in I_1 , $u^2 = y$, $2u du = dy$, $du = \frac{dy}{2u} = \frac{dy}{2\sqrt{y}}$

$$I_1 = \frac{2}{\sqrt{\pi}} \left\{ \int_0^\infty \frac{e^{-y}}{2\sqrt{y}} dy \right\} = \frac{1}{\sqrt{\pi}} \int_0^\infty e^{-y} y^{1/2-1} dy = \frac{1}{\sqrt{\pi}} \Gamma\left(\frac{1}{2}\right) = 1$$

$$v(x, t) = 1 - \operatorname{erf}\left(\frac{ax}{2\sqrt{t}}\right)$$

where

$$\operatorname{erf}z = \frac{2}{\sqrt{\pi}} \int_0^z e^{-t^2} dt.$$

5.33 Transformation of Partial Differential Equations

In the following we study the solution of partial differential equations using Laplace and Fourier transform.

$$\frac{\partial v}{\partial t} - \frac{\partial^2 v}{\partial x^2} = 1, \quad 0 < x < 1, \quad t > 0. \tag{5.225}$$

Boundary conditions $v(0, t) = v(1, t) = 0$. Initial conditions $v(x, 0) = 0$

$$\mathcal{L}[v_t(x, t)] \equiv \mathcal{L}\left[\frac{\partial v}{\partial t}\right] = sV(x, s) - v(x, 0) \tag{5.226}$$

$$\mathcal{L}[v_x(x, t)] \triangleq \mathcal{L}\left[\frac{\partial v}{\partial x}\right] = \frac{d}{dx}V(x, s) \tag{5.227}$$

$$\mathcal{L}[v_{xx}(x, t)] \equiv \mathcal{L}\left[\frac{\partial^2 v}{\partial x^2}\right] = \frac{d^2}{dx^2}\mathcal{L}[v] = \frac{d^2}{dx^2}V(x, s) \tag{5.228}$$

$$sV(x, s) - v(x, 0) - \frac{d^2}{dx^2}V(x, s) = \frac{1}{s} \tag{5.229}$$

$$\frac{d^2}{dx^2}V(x, s) - sV(x, s) = -\frac{1}{s}. \tag{5.230}$$

Boundary condition $V(0, s) = V(1, s) = 0$

$$\lambda^2 - s = 0, \quad \lambda = \pm\sqrt{s}. \tag{5.231}$$

Solution of homogeneous equation $\frac{d^2}{dx^2}V(x, s) - sV(x, s) = 0$ is

$$V_h = k_1 \cosh \sqrt{s}x + k_2 \sinh \sqrt{s}x. \tag{5.232}$$

The forcing function, the nonhomogeneous term, is $\phi(x) = 1$, a polynomial of order zero. $V_p = A_0$ (V_p is the particular solution). To evaluate A_0 we substitute into the differential equation

$$-sV_p(x, s) = -\frac{1}{s}, \quad -A_0s = -\frac{1}{s}, \quad A_0 = \frac{1}{s^2} \tag{5.233}$$

$$V(x, s) = V_h(x, s) + V_p(x, s) = k_1 \cosh \sqrt{s}x + k_2 \sinh \sqrt{s}x + \frac{1}{s^2}. \tag{5.234}$$

Substituting with the boundary conditions $v(0, t) = v(1, t) = 0$, i.e. $V(0, s) = V(1, s) = 0$

$$k_1 + \frac{1}{s^2} = 0, \quad k_1 = -\frac{1}{s^2} \quad (5.235)$$

$$k_1 \cosh \sqrt{s} + k_2 \sinh \sqrt{s} + \frac{1}{s^2} = 0 \quad (5.236)$$

$$-\frac{1}{s^2} \cosh \sqrt{s} + k_2 \sinh \sqrt{s} + \frac{1}{s^2} = 0 \quad (5.237)$$

$$k_2 \sinh \sqrt{s} - \frac{1}{s^2} (\cosh \sqrt{s} - 1) = 0 \quad (5.238)$$

$$k_2 = \frac{\cosh \sqrt{s} - 1}{s^2 \sinh \sqrt{s}} \quad (5.239)$$

$$\begin{aligned} V(x, s) &= -\frac{1}{s^2} \cosh \sqrt{sx} + \frac{(\cosh \sqrt{s} - 1) \sinh \sqrt{sx}}{s^2 \sinh \sqrt{s}} + \frac{1}{s^2} \\ &= \frac{1 - \cosh \sqrt{sx}}{s^2} + \frac{(\cosh \sqrt{s} - 1) \sinh \sqrt{sx}}{s^2 \sinh \sqrt{s}}. \end{aligned} \quad (5.240)$$

The singularity points are found by writing

$$s^2 \sinh \sqrt{s} = 0 \quad (5.241)$$

$$\sinh \sqrt{s} = (e^{\sqrt{s}} - e^{-\sqrt{s}}) / 2 = 0 \quad (5.242)$$

$$e^{\sqrt{s}} = e^{-\sqrt{s}} \quad (5.243)$$

$$e^{2\sqrt{s}} = 1 = e^{j2\pi k}, \quad k = 0, 1, 2, \dots \quad (5.244)$$

$$2\sqrt{s} = j2\pi k, \quad \sqrt{s} = j\pi k \quad (5.245)$$

$$s = -\pi^2 k^2, \quad k = 0, 1, 2, \dots \quad (5.246)$$

The function $V(x, s)$ can be factored into the form

$$V(x, s) = \frac{1 - \cosh [0.5\sqrt{s}(2x-1)] / \cosh(\sqrt{s}/2)}{s^2} \quad (5.247)$$

i.e.

$$V(x, s) = \frac{1}{s^2} \left\{ 1 - \frac{e^{\frac{\sqrt{s}}{2}(2x-1)} + e^{-\frac{\sqrt{s}}{2}(2x-1)}}{e^{\sqrt{s}/2} + e^{-\sqrt{s}/2}} \right\} \quad (5.248)$$

and it is assumed that

$$\lim_{|s| \rightarrow \infty} V(x, s) = 0, \quad 0 < x < 1. \quad (5.249)$$

Referring to Fig. 5.73 we note that the inverse transform is given by

$$v(x, t) = \frac{1}{2\pi j} \int_{c-j\infty}^{c+j\infty} V(x, s) e^{st} ds \quad (5.250)$$

where c is such that $V(x, s)$ converges along the contour of integration. To use the theory of residues, we rewrite the equation in the form

$$v(x, t) = \frac{1}{2\pi j} \left\{ \oint V(x, s) e^{st} ds - \int_D V(x, s) e^{st} ds \right\} \quad (5.251)$$

which is true if and only if

$$\int_D V(x, s) e^{st} ds = 0 \tag{5.252}$$

i.e. we have to show that with

$$s = c + Re^{j\theta}, \quad \frac{-\pi}{2} < \theta < \frac{\pi}{2} \tag{5.253}$$

$$\lim_{R \rightarrow \infty} \int_D V(x, s) e^{st} ds = 0. \tag{5.254}$$

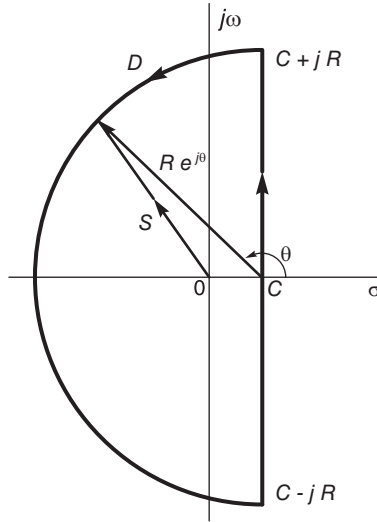


FIGURE 5.73 Integration on a closed contour.

For the case $Re[\sqrt{s}] < 0$. Multiplying by $e^{\sqrt{s}/2}$ the numerator and denominator of $V(x, s)$ we have

$$V(x, s) = \left\{ 1 - \frac{e^{x\sqrt{s}} + e^{(1-x)\sqrt{s}}}{e^{\sqrt{s}} + 1} \right\} / s^2 \tag{5.255}$$

which tends to zero as $|s| \rightarrow \infty$. For the case $Re[\sqrt{s}] > 0$ we multiply the numerator and denominator by $e^{-\sqrt{s}/2}$ obtaining

$$V(x, s) = \left\{ 1 - \frac{e^{\sqrt{s}(x-1)} + e^{-x\sqrt{s}}}{1 + e^{-\sqrt{s}}} \right\} / s^2 \tag{5.256}$$

which also tends to zero as $|s| \rightarrow \infty$. We conclude that the integral along the section D vanishes as $R \rightarrow \infty$ and we may write

$$v(x, t) = \frac{1}{2\pi j} \oint V(x, s) e^{st} ds. \tag{5.257}$$

Using Cauchy's residue theorem we have

$$v(x, t) = \sum \text{residues of } V(x, s) e^{st} \text{ at the poles.} \tag{5.258}$$

Writing

$$V(x, s) = \sum_{k=0}^{\infty} \frac{r_k}{s + \pi^2 k^2} = \frac{r_0}{s} + \sum_{k=1}^{\infty} \frac{r_k}{s + \pi^2 k^2} \quad (5.259)$$

$$v(x, t) = \left\{ r_0 + \sum_{k=1}^{\infty} r_k e^{-\pi^2 k^2 t} \right\} u(t). \quad (5.260)$$

We find the residues r_0, r_1, \dots by evaluating

$$\lim_{s \rightarrow -k^2 \pi^2} \left\{ (s + k^2 \pi^2) \frac{1 - \cosh[0.5\sqrt{s}(2x-1)] / \cosh(\sqrt{s})}{s^2} \right\}. \quad (5.261)$$

We obtain (using *Mathematica*®) $r_0 = -(x-1)x/2 = x(1-x)/2$, $r_1 = -(4/\pi^3) \sin(\pi x)$, $r_2, r_4, r_6, \dots = 0$, $r_3 = -[4/(27\pi^3)] \sin(3\pi x)$, $r_5 = -[4/(125\pi^3)] \sin(5\pi x)$

$$v(x, t) = x(1-x)/2 + \sum_{k=1,3,5,\dots}^{\infty} \frac{4}{\pi^3} \frac{\sin k\pi x}{k^3} e^{-\pi^2 k^2 t}. \quad (5.262)$$

Example 5.20 Solve the heat equation

$$\frac{\partial v(x, t)}{\partial t} = a^2 \frac{\partial^2 v(x, t)}{\partial x^2}, \quad -\infty < x < \infty, \quad t > 0$$

with the initial condition

$$v(x, 0) = Ae^{-\gamma^2 x^2}$$

and the boundary conditions $v(x, t) \rightarrow 0$, $\partial v(x, t)/\partial x \rightarrow 0$ as $|x| \rightarrow \infty$. The Fourier transform of $v(x, t)$ from the domain of the distance x to the frequency Ω is by definition

$$V(j\Omega, t) = \mathcal{F}[v(x, t)] = \int_{-\infty}^{\infty} v(x, t) e^{-j\Omega x} dx.$$

Fourier transforming the heat equation we have, taking into consideration the boundary condition

$$\mathcal{F}\left[\frac{\partial v(x, t)}{\partial t}\right] = a^2 \mathcal{F}\left[\frac{\partial^2 v(x, t)}{\partial x^2}\right]$$

$$\frac{d}{dt} \mathcal{F}[v(x, t)] = -a^2 \Omega^2 \mathcal{F}[v(x, t)]$$

$$\frac{d}{dt} V(j\Omega, t) = -a^2 \Omega^2 V(j\Omega, t)$$

$$\frac{dV}{dt} + a^2 \Omega^2 V = 0.$$

The characteristic equation is

$$\lambda + a^2 \Omega^2 = 0.$$

The solution is

$$V(j\Omega, t) = Ce^{-a^2 \Omega^2 t}.$$

From the initial condition we may write

$$V(j\Omega, 0) = C = \mathcal{F}\left[Ae^{-\gamma^2 x^2}\right]$$

The Fourier transform of the Gaussian function is

$$e^{-x^2/(2\sigma^2)} \longleftrightarrow \sigma\sqrt{2\pi} e^{-\sigma^2\Omega^2/2}.$$

Letting $1/(2\sigma^2) = \gamma^2$ we have

$$C = A \frac{\sqrt{\pi}}{\gamma} e^{-\Omega^2/(4\gamma^2)}$$

$$V(j\Omega, t) = A \frac{\sqrt{\pi}}{\gamma} e^{-\Omega^2\{1/(4\gamma^2)+a^2t\}}.$$

Using the same transform of the Gaussian function with

$$\{1/(4\gamma^2) + a^2t\} = \sigma^2/2$$

we obtain

$$e^{-x^2/(1/\gamma^2+4a^2t)} \longleftrightarrow 2\sqrt{\pi}\sqrt{1/(4\gamma^2) + a^2t} e^{-\Omega^2\{1/(4\gamma^2)+a^2t\}}$$

$$\frac{1}{\sqrt{1+4\gamma^2a^2t}} e^{-x^2/(1/\gamma^2+4a^2t)} \longleftrightarrow (\sqrt{\pi}/\gamma) e^{-\Omega^2\{1/(4\gamma^2)+a^2t\}}$$

$$v(x, t) = \frac{A}{\sqrt{1+4\gamma^2a^2t}} e^{-\gamma^2x^2/(1+4\gamma^2a^2t)}.$$

Note that the boundary condition has been employed implicitly in evaluating

$$\mathcal{F}[\partial^2v(x, t)/\partial x^2].$$

In fact letting

$$I = \mathcal{F}\left[\frac{\partial^2v(x, t)}{\partial x^2}\right] = \int_{-\infty}^{\infty} \frac{\partial^2v}{\partial x^2} e^{-j\Omega x} dx$$

and integrating by parts with $u = e^{-j\Omega x}$ and $w' = \partial^2v/\partial x^2$ we have

$$I = \int uw' = uw - \int u'w = \frac{\partial v}{\partial x} e^{-j\Omega x} \Big|_{-\infty}^{\infty} + j\Omega \int e^{-j\Omega x} \frac{\partial v}{\partial x} dx$$

$$= \frac{\partial v}{\partial x} e^{-j\Omega x} \Big|_{-\infty}^{\infty} + j\Omega \left\{ e^{-j\Omega x} \Big|_{-\infty}^{\infty} + j\Omega \int_{-\infty}^{\infty} v e^{-j\Omega x} dx \right\}$$

$$= \left(\frac{\partial v}{\partial x} + j\Omega v \right) e^{-j\Omega x} \Big|_{-\infty}^{\infty} - \Omega^2 \int_{-\infty}^{\infty} v e^{-j\Omega x} dx.$$

Using the boundary condition $v(x, t) \rightarrow 0$ and $\partial v(x, t)/\partial x \rightarrow 0$ as $|x| \rightarrow \infty$

$$I = \mathcal{F}\left[\frac{\partial^2v(x, t)}{\partial x^2}\right] = -\Omega^2 \mathcal{F}[v(x, t)]$$

which is the usual Fourier transform property of differentiation twice in the “time” domain.

5.34 Problems

Problem 5.1 Consider a stable system of transfer function

$$H(s) = \frac{\omega_0^2}{s^2 + 2\zeta\omega_0s + \omega_0^2}$$

where $\zeta < 1$. The input to the system, with zero initial conditions, is the signal

$$x(t) = \sin \omega_1 t.$$

- a) Draw the poles and zeros of the output $Y(s)$ in the complex s plane.
- b) Evaluate graphically the residues and deduce $y(t)$.
- c) What is the steady state output of the system under these conditions? What is the transient response $y_{tr}(t)$?
- d) Evaluate graphically the frequency response of the system at the frequency ω_0 .

Problem 5.2 Consider the system having the transfer function

$$H(s) = \frac{1}{(s - p_1)(s^2 + 2\zeta\omega_0 s + \omega_0^2)}$$

with $\zeta = 0.707$ and p_1 real.

a) Show the effect of moving the pole p_1 along the real axis on the system step response. Show the effective order of the system for the three cases

- i) $p_1 = -0.01\zeta\omega_0$, ii) $p_1 = -\zeta\omega_0$, iii) $p_1 = -10\zeta\omega_0$.

b) Show that if a zero z_1 is very close to the pole p_1 the effect is a virtual cancellation of the pole.

Problem 5.3 Evaluate the impulse response of the system represented by its poles and zeros as shown in Fig. 5.74, assuming a gain of unity.

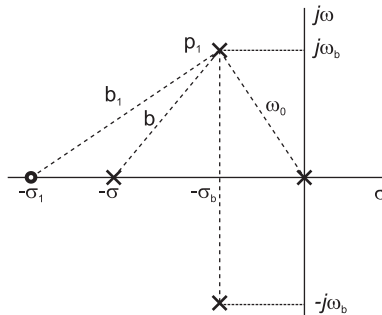


FIGURE 5.74 Pole-zero plot in s plane.

Problem 5.4 Consider the system having a transfer function

$$H(s) = \frac{64}{s^3 + 8s^2 + 32s + 64}.$$

- a) Evaluate the transfer function poles.
- b) Find the system unit step response by evaluating the residues graphically.

Problem 5.5 A system has the transfer function

$$H(s) = \frac{10(s + 2\zeta\omega_0)}{s^2 + 2\zeta\omega_0 s + \omega_0^2}$$

where $\zeta = 0.5$, $\omega_0 = 2$ rad/sec. Using a graphic evaluation of residues evaluate the system output $y(t)$ in response to the input $x(t) = \sin \beta t u(t)$, where $\beta = \omega_0 \sqrt{1 - \zeta^2}$ assuming zero initial conditions.

Problem 5.6 Consider the unit step response of the second order system

$$H(s) = \omega_0^2 / (s^2 + 2\zeta\omega_0s + \omega_0^2).$$

a) Determine the value of ζ which leads to a minimal 2% response time. If $\omega_0 = 10$ rad/sec, what is that minimal response time? and what is the time of the overshoot peak?

b) For the series R-L-C circuit shown in Fig. 5.75, evaluate the value of the resistor R which produces a 2% minimum unit step response time. What is the minimum time thus obtained?

Problem 5.7 Consider the series R-L-C circuit shown in Fig. 5.75.

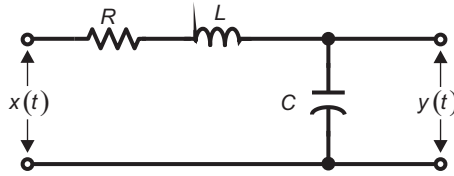


FIGURE 5.75 R-L-C circuit.

a) Evaluate the circuit transfer function in the form

$$H(s) = \omega_0^2 / (s^2 + 2\zeta\omega_0s + \omega_0^2).$$

b) Evaluate the values of ζ and ω_0 so that the overshoot of the unit step response is 40%, and the 5% response time is $t_s = 0.01$ sec.

c) If $C = 1 \mu F$ evaluate R and L so that ζ and ω_0 have the values thus obtained.

Problem 5.8 Evaluate the transfer function $H(s)$ of the positive feedback system described by the block diagram shown in Fig. 5.76.

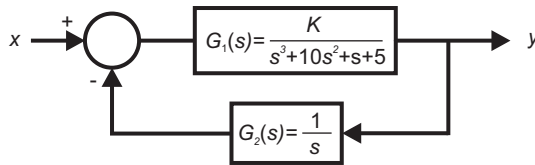


FIGURE 5.76 System block diagram.

Problem 5.9 For the system having the transfer function

$$H(s) = \frac{50(s + 4)}{s^3 + 4s^2 + 29s}$$

a) Evaluate the amplitude and phase of the steady state response to the input

$$x(t) = \sin 5t$$

b) For the second order subsystem, evaluate the peak in dB and its frequency.

c) Show as a bode diagram the system frequency response.

Problem 5.10 Assuming that the capacitor in the electric circuit shown in Fig.5.77 is $v_c(0) = v_0$ evaluate the circuit response to the input

$$e(t) = \sum_{n=0}^{\infty} e_0(t - 4n)$$

where

$$e_0 = u(t) - u(t - 1).$$

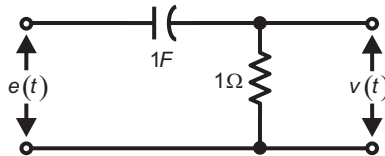


FIGURE 5.77 R-C electric circuit.

Identify the transient and steady-state components of the response. Choose the value v_0 which would annul the transient component. Show that the steady-state response is then periodic.

Problem 5.11 Given the system with the transfer function

$$H(s) = \frac{s^2 + 4s + 5}{s^2 + 4s + 8}.$$

a) Evaluate the system response $y_1(t)$ to the input

$$x(t) = e^{-3t}u(t).$$

b) Deduce the system response $y_2(t)$ to the input

$$v(t) = e^{-3t+5}u(t - 2).$$

Problem 5.12 Consider the electric circuit shown in Fig. 5.78.

a) State whether this circuit is a lowpass or highpass filter by describing its behavior as a function of frequency.

b) Evaluate the circuit transfer function $H(s)$, its impulse response $h(t)$ and its frequency response in modulus and argument. Plot the frequency response.

c) Deduce the unit step response of the circuit and its response to the input

$$x(t) = e^{-7(t/2-3)}u(t - 5).$$

d) Evaluate the response of the circuit to the causal impulse train

$$x(t) = \sum_{t=0}^{\infty} \delta(t - n).$$

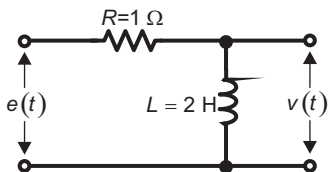


FIGURE 5.78 R-L electric circuit.

Problem 5.13 The signal

$$x(t) = \cos(4t - \pi/3) u(t)$$

is applied to a system of which the transfer function has the form

$$H(s) = \frac{\omega_0^2 s}{s^2 + 2\zeta\omega_0 s + \omega_0^2}$$

and of which the poles and zeros are shown in Fig. 5.79.

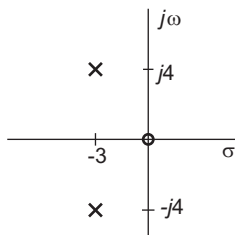


FIGURE 5.79 Pole-zero diagram in Laplace plane.

a) Evaluate the response $y(t)$ of the system to the input $x(t)$.

b) Evaluate the system response $y(t)$ if the system is cascaded with a system of transfer function

$$G(s) = e^{-3s}.$$

Problem 5.14 A system has a unit gain, a zero at $s = 0$ and the poles $s = -2 \pm j2$.

a) Evaluate the system steady-state response $y_1(t)$ if the input is

$$x(t) = \sin(2t - \pi/3) u(t - 2).$$

b) The system is cascaded with a system of impulse response $\delta(t - 3)$. For the same input $x(t)$ to the first system, what is the overall system output?

Problem 5.15 Sketch the response of a filter of which the transfer function is given by

$$H(s) = \frac{1 - e^{-Ts}}{s}, \quad T > 0$$

to the inputs a) $x(t) = \sum_{n=0}^3 n \delta(t - nT)$, b) $v(t) = \sum_{n=0}^3 n \delta(t - nT/2)$.

Problem 5.16 A system is constructed as a cascade of two systems of impulse responses $h_1(t)$ and $h_2(t)$, where

$$h_1(t) = A_1 e^{-\alpha t} u(t)$$

$$h_2(t) = A_2 e^{-\beta(t-1)} u(t-1).$$

Evaluate the response of the system to the inputs : a) $\delta(t)$, b) $\delta(t-2)$.

Problem 5.17 The impulse response of a system is $h(t) = R_1(t)$. Using the convolution integral evaluate the response of the system to the input $x(t) = t u(t)$. Verify your answer using Laplace transform.

Problem 5.18 A system is constructed as a cascade of two systems with transfer functions

$$H_1(s) = \frac{s+2}{s^2+2s+2}$$

and

$$H_2(s) = \frac{1}{s+1}.$$

Evaluate the system response $y(t)$ to the input $10\delta(t-2)$.

Problem 5.19 The causal impulse train

$$e(t) = \sum_{n=0}^{\infty} \delta(t-nT)$$

is applied as the input to the electric circuit shown in Fig. 5.80. Assuming zero initial conditions, evaluate the transient and steady-state components of the circuit output $v(t)$.

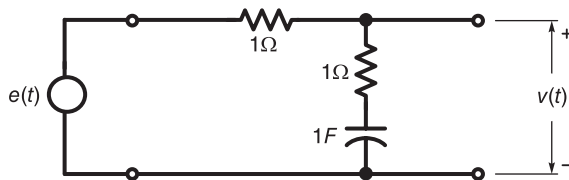


FIGURE 5.80 R-C circuit.

Problem 5.20 a) Identify the transfer function $H(s)$ of a system of which the frequency response has the bode plot shown in Fig. 5.81.

b) Show a block diagram of a filter structure which is a model for such a system.

Problem 5.21 For the second order system, of transfer function $H(s)$,

$$H(s) = \frac{\omega_0^2}{s^2 + 2\zeta\omega_0 s + \omega_0^2}$$

with $\zeta = 0.707$

a) Evaluate the response $y_1(t)$ of the system to the input

$$x(t) = e^{-\alpha t} \cos \omega_1 t u(t)$$

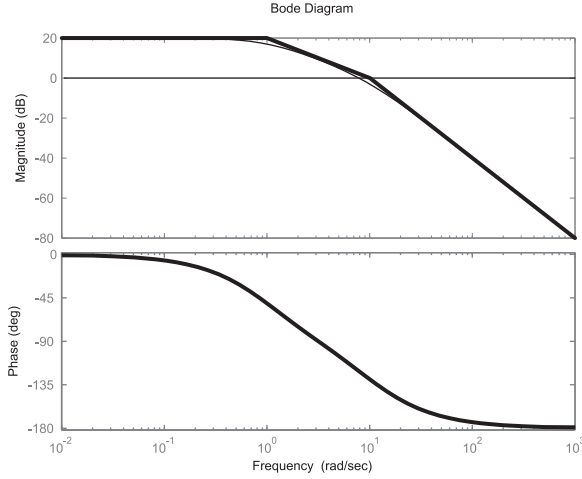


FIGURE 5.81 Bode plot.

$$\alpha = \zeta\omega_0/2$$

$$\omega_1 = \omega_0\sqrt{1 - \zeta^2}.$$

and zero initial conditions.

b) Evaluate the system output for zero-input assuming the initial conditions $y(0) = y_0$ and $y'(0) = y'_0$.

Problem 5.22 For the DC current motor shown in Fig. 5.82 assuming a constant voltage E_e in the inductor circuit, a negligible inductance of the induit circuit and negligible load $C_i(t) \cong 0$.

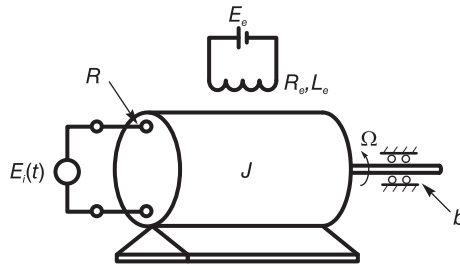


FIGURE 5.82 DC motor.

- a) Draw an equivalent electric circuit of the system.
- b) Show that the transfer function $H(s)$ from $E_i(t)$ to the angular rotation speed $\Omega(t)$ has the form

$$H(s) = b_0 / (s + a_0).$$

c) Let $b_0 = a_0 = 1$. Evaluate the response of the motor to the input

$$x(t) = \sum_{n=0}^{\infty} \delta(t - nT)$$

with $T = 1$ sec. Sketch the periodic component of the response.

Problem 5.23 A system has the impulse response

$$h(t) = e^{-\alpha t} \sin \beta t u(t).$$

a) Write the transfer function $H(s)$ of the system in the normalized form

$$H(s) = K\omega_0^2 / (s^2 + 2\zeta\omega_0s + \omega_0^2)$$

giving the values of ω_0 , ζ and K as functions of α and β .

b) Evaluate the resonance frequency ω_r of the amplitude spectrum $|H(j\omega)|$ of the frequency response. Plot the amplitude and phase spectra of the system frequency response.

c) The system is followed, in cascade, by a filter of frequency response

$$G(j\omega) = \Pi_{\omega_r}(\omega) = u(\omega + \omega_r) - u(\omega - \omega_r).$$

Plot the amplitude spectrum at the system output if the input is the Dirac-delta impulse $\delta(t)$.

Problem 5.24 A system for setting the tension T in a string, by adjusting the angle θ in the rotary potentiometer at the input, is shown in Fig. 5.83. The voltage difference $(e_1 - e_2)$ is the input of the amplifier of gain A . The amplifier output is connected to the DC motor inductor that, as shown in the figure, is assumed to have a resistance R ohm and inductance L henry, respectively. As shown in the figure, the motor armature has a constant current I_0 (supplied by a current source). The current in the inductor is denoted $i(t)$ and produces a magnetic field $B(t)$ that is proportional to it, i.e. $B(t) = k_1 i(t)$, so that the motor torque C is also proportional to it, i.e. $C = k_2 i$.

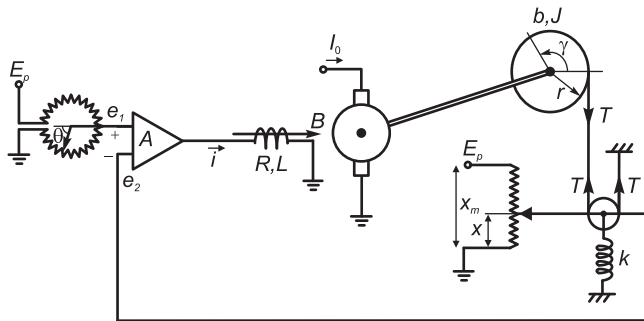


FIGURE 5.83 Tension regulation system.

The motor applied the torque to a rotating wheel which turns by an angle γ , resulting in an increase in its tension T . The small pulley, shown in the figure, is thus pulled upward a distance x against the stiffness k of a spring.

The voltage e_2 is seen in the figure to be proportional to the displacement x . The maximum value of x is the length x_m of the potentiometer. It may be assumed that $x = \gamma r/2$, where r is the radius of the wheel. When the tension T is zero, the angle γ and the displacement x are both zero. Assuming that the small pulley and the spring have negligible inertia, while the wheel has inertia J and rotates against viscous friction of coefficient b .

a) Write the differential equations that may lead to finding the output tension T as a function of the input θ . Assume constants of proportionality k_1, k_2, \dots if needed.

b) If θ is a constant, $\theta = \theta_0$, what is the steady state value of T ?

Problem 5.25 The support of the mechanical system shown in Fig. 5.84 is displaced upward by a distance $x(t)$ and speed $\dot{x}(t)$.

a) Show that the equation of movement $\dot{y}(t)$ of the mass M can be put in the form

$$a_1 \dot{v} + a_0 v = a_2 (e - v) + a_3 \int (e - v) dt$$

where

$$v(t) = \dot{y}(t) \quad \text{and} \quad e(t) = \dot{x}(t).$$

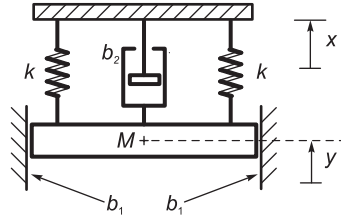


FIGURE 5.84 Mechanical system with springs.

b) Show the homolog electric circuit equivalent of the system.

The coefficient of viscous friction b_1 and b_2 and the spring stiffness k are shown in the figure.

Problem 5.26 A system has the impulse response

$$h(t) = \begin{cases} 2t/T, & 0 \leq t \leq T/2 \\ 2 - 2t/T, & T/2 \leq t \leq T \\ 0, & \text{otherwise.} \end{cases}$$

Evaluate the step response.

Problem 5.27 For the R - L - C electric circuit shown in Fig. 5.85 assuming $L = 1$ H and $C = 1$ F.

a) Show the trajectory of the poles of the circuit transfer function as R varies

b) Evaluate the resistance R so that the overshoot of the step response be 10%. Sketch the resulting poles in the s plane.

Problem 5.28 Given the transfer function

$$H(s) = \frac{50(s + 4)}{s(s^2 + 4s + 100)}.$$

Decomposing the system function into a cascade of a simple pole, a zero and a second order transfer function

a) Show the Bode plot of each component transfer function drawing the asymptotes thereof. For the second order system function evaluate and show on the bode plot the peak value and peak frequency ω_r .

b) Show the Bode plot and asymptotes of the overall system frequency response.

c) If the input is $\sin 5t$ evaluate the system response.

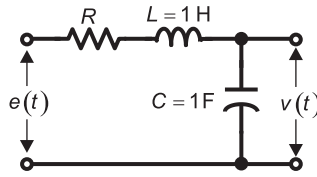


FIGURE 5.85 R-L-C circuit.

Problem 5.29 Consider the speed-regulation system shown in Fig. 5.86. The DC motor, on the right in the figure, has a constant magnetic field. The motor speed is controlled by the voltage output of the amplifier (of gain A) which is applied to its armature. The motor armature is assumed to have a resistance R_m ohms and a negligible inductance. The motor drives a load of inertia J against viscous friction of coefficient b and the load couple C . The same motor axle that rotates the load also rotates the axle of the tachometer, a voltage generator which converts positive rotation speed ω into a corresponding voltage $e_T = k_T\omega$ with the polarity shown in the figure. The armature of the tachometer has resistance and inductance R_g ohm and L_g henry, respectively, as shown in the figure. The potentiometer on the left is of length l and resistance R_p . The amplifier can be assumed to have infinite input impedance.

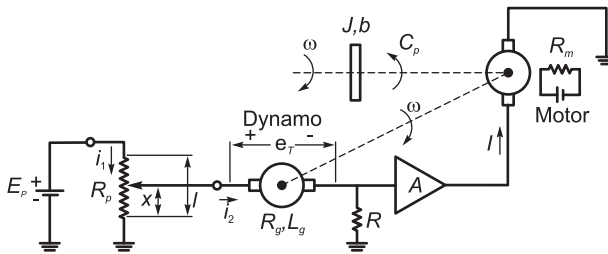


FIGURE 5.86 Speed regulation system.

- Explain in a few words how the feedback in the system tends to stabilize the output rotational speed.
- Write the differential equations describing the dynamics of the system between its input x and output ω .
- Show that if $R \gg R_p$ the system transfer function can be evaluated using Laplace transform.
- Draw a block diagram representing the system.
- Show the input-output steady-state relation and the role the amplifier gain A plays in speed regulation.

Problem 5.30 In the mechanical system shown in Fig. 5.87, the upper support is displaced upwards a distance x . The mass m is thus pulled up a distance y measured from its position of static equilibrium whereat $x = 0$. In the figure each spring has stiffness $k/2$, and b_1 and b_2 are coefficients of viscous friction.

- Write the differential equations describing the dynamics of the system between its input $x(t)$ and output $y(t)$.

b) Let $m = 1 \text{ Kg}$, $b_1 = 0.7 \text{ n/(m/sec)}$,

$$b_2 = 1.5 \text{ n/(m/sec)}$$

$$k = 15 \text{ n/m}, \quad y(0) = 1 \text{ m}$$

and $x(t) = e^{-3t} \cos(4t + \pi/3) u(t)$.

Evaluate and plot the response $y(t)$ of the system.

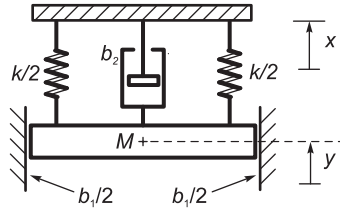


FIGURE 5.87 Suspended mechanical system.

Problem 5.31 The electromechanical system shown in Fig. 5.88 has an input voltage $e(t)$ and an output voltage $v(t)$. The armature of the electric motor is fed a current i , which is the output of a current amplifier of gain K , so that the current i is equal to K times the voltage v_{c_1} at the amplifier input, as shown in the figure. The amplifier may be assumed to have infinite input impedance. The magnetic field ϕ of the motor is constant, so that the motor couple C applied to the load is proportional to the current i . The generator (dynamo) is on the same axle as the load and produces the output signal $v(t)$ which is proportional to Ω , the speed of rotation of the load. The load has an inertia J and its rotation is opposed by viscous friction of coefficient b .

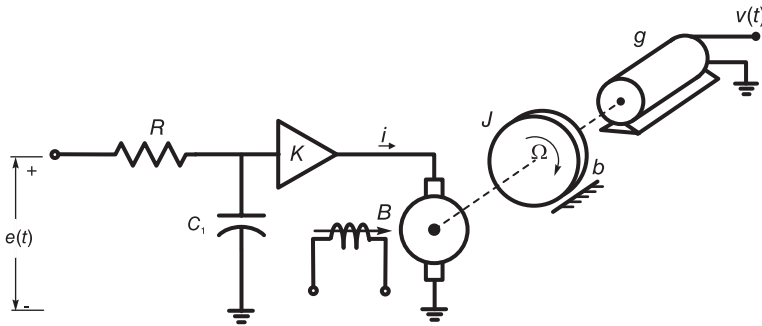


FIGURE 5.88 Speed control system.

a) Write the differential equations describing the system, assuming constants of proportionality k_1, k_2, \dots , if needed.

b) Evaluate the system transfer function between the input and output.

c) Let k_m be the constant of proportionality relating C and i , that is, $C = k_m i$. Evaluate the unit step response of the system assuming

$$k_m = 0.5 \text{ Nm/A}, \quad K = 10, \quad q = 1$$

$$b = 1 \text{ Nm}/(\text{rad}/\text{sec}), \quad J = 1 \text{ kg m}^2$$

$$R = 10 \text{ k}\Omega, \quad C_1 = 50 \text{ }\mu\text{F}.$$

- d) Evaluate the 5% setting time t_s of the unit step response.
 e) Evaluate the system response if the input is given by

$$e(t) = \sum_{n=0}^{\infty} E\delta(t-n)$$

and zero initial conditions.

Problem 5.32 Evaluate the Fourier transforms and the cross-correlation $r_{vf}(t)$ of the two functions

$$v(t) = u(t - 3T/2) - u(t - 7T/2)$$

$$f(t) = R_T(t) = u(t) - u(t - T).$$

Evaluate the Fourier transform $R_{vf}(j\omega)$ of the cross-correlation $r_{vf}(t)$ using the transforms $V(j\omega)$ and $F(j\omega)$.

Problem 5.33 Given a general periodic signal $v(t)$ of period T , show that by cross-correlating the signal with a sinusoid of a given frequency it is possible to reveal the amplitude and phase of the signal component of that frequency. To this end evaluate the cross correlation $r_{vf}(t)$ of the signal $v(t)$ with the sinusoid $f(t) = \cos k\omega_0 t$, where k is an integer and $\omega_0 = 2\pi/T$, and the function $v(t)$ which is periodic with period T .

Problem 5.34 Consider the two signals

$$v(t) = t^2\Pi_1(t) = t^2[u(t+1) - u(t-1)]$$

$$x(t) = e^{-|t|}\Pi_1(t).$$

- a) Evaluate the Fourier transforms $V(j\omega)$ and $X(j\omega)$ of $v(t)$ and $x(t)$ respectively.
 b) Evaluate the Fourier transform of the cross-correlation $r_{vx}(t)$ of the two signals.

Problem 5.35 Consider the system described by the block diagram shown in Fig. 5.89. This system receives the input

$$x(t) = e^{-\gamma|t|}, \quad \gamma > 0.$$

a) Evaluate the transfer function $H(s)$ and the impulse response $h(t)$ of the system assuming that $h(t) = 0$ for $t < 0$.

b) Assuming $\alpha = 0.5$ and $\gamma = 0.2$ evaluate the system output $y(t)$ using the convolution integral. Verify the result using the Laplace transform.

Problem 5.36 The suspended mass in Fig. 5.90 weighs $M = 10 \text{ kg}$. It moves downward a distance $x(t)$ by its own weight $w = Mg$, where $g = 9.8 \text{ m}/\text{sec}^2$ is the gravity acceleration, and its movement induces an opposing force kx in each of the springs of stiffness $k = 500 \text{ Newton}/\text{m}$ and a viscous friction $b\dot{x}$ in the shown damper of coefficient of viscous friction $b = 150 \text{ Newton sec}/\text{m}$. Let $x = 0$ be the position of the mass at rest with no tension or compression in the spring. Evaluate and sketch the displacement $x(t)$ of the mass assuming it is released to move under its own weight at $t = 0$ with $\dot{x}(0) = -5 \text{ cm}/\text{sec}$. Evaluate the natural frequency ω_n and damping coefficient ζ of the system. Evaluate $\lim_{t \rightarrow \infty} x(t)$. Let $x = 0$ be the position of the mass at rest with no tension or compression in the spring. Evaluate and sketch the displacement $x(t)$ of the mass assuming it is released to move under its own weight at $t = 0$ with $x(0) = -10 \text{ cm}$ and $\dot{x}(0) = -5 \text{ cm}/\text{sec}$. Evaluate the natural frequency ω_n and damping coefficient ζ of the system. Evaluate $\lim_{t \rightarrow \infty} x(t)$.

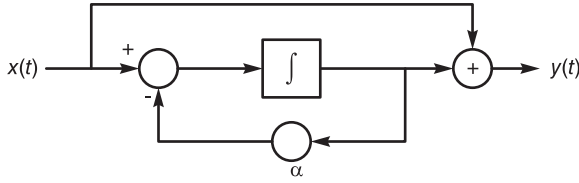


FIGURE 5.89 Block diagram with integrator.

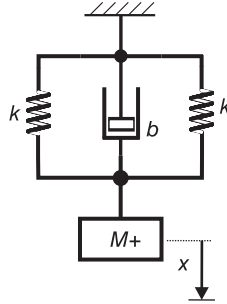


FIGURE 5.90 Suspended mechanical system.

Problem 5.37 Given the system transfer function

$$H(s) = \frac{A(s + s_0)}{s(s^2 + 2\zeta\omega_0s + \omega_0^2)}$$

where $A = 10$, $s_0 = 1.5$, $\omega_0 = 100$, $\zeta = 0.1$. Plot the bode diagram of the different system components and deduce that of the overall bode diagram of the system.

Problem 5.38 Plot the bode diagram of the different components and the overall response of the following system transfer functions:

a) $H(s) = \frac{s\tau_1 + 1}{s\tau_2 + 1}$, where $\tau_1 = 0.01$, $\tau_2 = 0.2$.

b) $H(s) = \frac{A}{(s + \alpha)(s^2 + 2\zeta\omega_0s + \omega_0^2)}$, where $\alpha = 0.5$, $\zeta = 0.05$, $\omega_0 = 30$.

Evaluate A so that the system gain at zero frequency is 0 dB. Evaluate the peak at resonance and the approximate resonance frequency.

Problem 5.39 A linear system has the impulse response

$$h(t) = [\alpha + e^{-t} - e^{\beta t}] u(t)$$

where α and β are real values.

- a) Evaluate $H(s)$, the system transfer function. Assuming $\alpha \neq 0$, specify the ROC.
- b) For which values of α and β is the system stable?
- c) For which values of α and β is the system physically realizable?

Problem 5.40 A signal $x(t)$ is the periodic repetition of rectangles of width $T/10$ seconds,

$$x(t) = 3.2 \sum_{n=-\infty}^{\infty} \Pi_{T/10}(t - nT)$$

where $T = 0.015$ seconds.

The signal is applied to the input of a filter of frequency response $H(j\omega)$ and output $y(t)$.

a) What conditions should $H(j\omega)$ satisfy so that the filter output $y(t)$ be a DC voltage equal to 2 volts ?

b) What conditions should $H(j\omega)$ satisfy so that the filter output $y(t)$ be a sinusoid of frequency 200 Hz and amplitude 0.6 volt?

c) What conditions should $H(j\omega)$ satisfy so that the filter output $y(t)$ be a sinusoid of frequency 1 kHz and amplitude 0.2 volt?

Problem 5.41 A signal $x(t)$ is applied to the input of two filters connected in parallel having the impulse responses $h_1(t) = 8u(t - 0.02)$ and $h_2(t) = -8u(t - 0.06)$.

The sum of the filters' outputs is the system output $y(t)$.

a) Sketch the impulse response $h(t)$ of the overall system, having an input $x(t)$ and output $y(t)$.

b) Evaluate the frequency response of the system.

The signal $x(t) = 2 \cos(40\pi t + 2\pi/5)$ is applied to the system input. Evaluate the system output $y(t)$ and the delay of the sinusoid caused by passage through the system.

Problem 5.42 A linear system has the impulse response $g(t) = u(t - T) - u(t - 2T)$ where T is a positive real constant.

a) Evaluate the system frequency response $G(j\omega)$.

b) Evaluate the system output signal $y(t)$ if the input is $x(t) = \delta(t - T)$.

c) Evaluate the system output if the input is $x(t) = K$.

d) Evaluate the output if $x(t) = \sin(2\pi t/T)$.

e) Evaluate the output if $x(t) = \cos(\pi t/T)$.

Problem 5.43 Let $h(t) = e^{-10t} \cos(2\pi t) u(t)$ be the impulse response of a linear system. A signal $x(t)$ of average value 5 volts is applied to the input of the system. What is the average value of the signal at the system output?

Problem 5.44 The impulse response of a linear system is given by

$$h(t) = [h_1(t) - h_1(t)h_2(t)] * h_3(t) * h_4(t)$$

where $h_1(t) = d[\omega_c Sa(\omega_c t)/2\pi]/dt$, $h_2(t)$ is a function of which the Fourier transform is given by $H_2(j\omega) = e^{-j2\pi\omega/\omega_c}$, $h_3(t) = 3\omega_c Sa(3\omega_c t)/\pi$ and $h_4(t) = u(t)$.

a) Evaluate the frequency response of the system.

b) The signal $x(t) = \sin(2\omega_c t) + \cos(\omega_c t/2)$ is applied to the linear system input. Evaluate the system output signal $y(t)$.

Problem 5.45 Referring to Fig. 5.48 showing the relations among the different frequencies leading to the resonance frequency of a second order system, show that the value of $|F(j\omega)|$ is a maximum when u_1 and u_2 are at right angles; hence meeting on the circle joining the poles.

Problem 5.46 A linear system is described by the block diagram shown in Fig. 5.91. The integrator output $v(t)$ is the integral of its input $y(t)$, that is, $v(t) = \int_{-\infty}^t y(\tau) d\tau$. Evaluate the system impulse response and frequency response.

Problem 5.47 The system shown in Fig. 5.92 is used to produce an echo sound.

a) Evaluate and sketch its impulse response $h(t)$.

b) Describe the form, frequency and amplitude of the output signal $y(t)$ when the input $x(t)$ is a pure sinusoid of frequency 440 Hz and amplitude 1V.

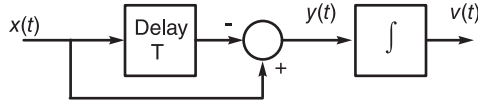


FIGURE 5.91 System block diagram.

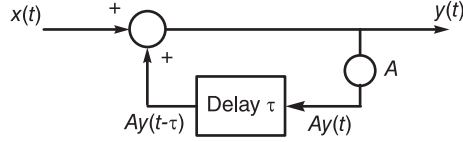


FIGURE 5.92 System block diagram.

Problem 5.48 To eliminate some frequency components, a system that receives an input $x(t)$ uses a delay element of delay T . The system output is $y(t) = x(t) + x(t - T)$. Evaluate the delay T required to eliminate any component of frequency 60 Hz. Which other components will also be eliminated by the system?

Problem 5.49 A periodic signal $x(t)$ of period $T = 2 \times 10^{-3}$ sec is defined by

$$x(t) = \begin{cases} 1 - t/T & , \quad 0 < t < T/2 \\ t/T - 3/2 & , \quad T/2 < t < T \end{cases}$$

The signal is applied as input to a filter of frequency response

$$H(j\omega) = \begin{cases} 5, & 0 < \omega < 2\pi \times 10^3 \\ \frac{-5(\omega - 3\pi \times 10^3)}{\pi \times 10^3}, & 2\pi \times 10^3 < \omega < 3\pi \times 10^3 \\ 0 & \omega > 3\pi \times 10^3 \end{cases}$$

and $H(-j\omega) = H^*(j\omega)$. Evaluate the system output $y(t)$ expressed using trigonometric functions.

Problem 5.50 Sketch the frequency response of a system that receives an input $x(t)$ and generates an output $y(t) = x(t) - x_1(t)$ where

$$X_1(j\omega) = \mathcal{F}[x_1(t)] = X(j\omega)H_0(j\omega).$$

- a) $H_0(j\omega) = \Pi_{\omega_c}(\omega)$
- b) $H_0(j\omega) = \begin{cases} 1, & \omega_1 < |\omega| < \omega_2 \\ 0, & \text{otherwise} \end{cases}$

Problem 5.51 Given $v(t) = 1 + 3 \sin(800\pi t)$, $X(j\omega) = V(j\omega)H(j\omega)$, where

$$|H(j\omega)| = \begin{cases} 1, & 500\pi < |\omega| < 1000\pi \\ 0, & \text{otherwise.} \end{cases}$$

$$\arg[H(j\omega)] = -10^{-3}\omega$$

$$y(t) = 2v(t) \cos(1000\pi t)$$

$$z(t) = 5v(t) \cos(1000\pi t + \pi/4).$$

- a) Evaluate $x(t)$.
- b) Evaluate or sketch $Y(j\omega)$.
- c) Evaluate the exponential Fourier series coefficients Z_n of $z(t)$ with an analysis interval of 0.02 sec.

Problem 5.52 A sinusoidal signal $x(t) = \cos 700t$ in the system shown in Fig. 5.93 is applied to a delay element which effects a phase delay of 45° before being added to the signals $y(t) = 2$ and $z(t) = \sin 500t$ to produce the system output $v(t)$.

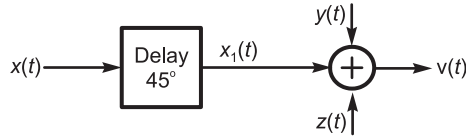


FIGURE 5.93 System including a delay element.

- a) Sketch the Fourier transform $V(j\omega)$ of $v(t)$.
- b) What is the fundamental frequency of $v(t)$. The signal $v(t)$ is applied to the input of a system of frequency response $H(j\omega)$ and output $y(t)$, where

$$|H(j\omega)| = \begin{cases} 0.01 |\omega|, & 0 \leq |\omega| \leq 10^3 \\ 10, & |\omega| \geq 10^3 \end{cases}$$

$$\arg [H(j\omega)] = \begin{cases} (\pi/1600) \omega, & |\omega| \leq 400 \\ \pi/4, & |\omega| \geq 400. \end{cases}$$

- c) Evaluate $y(t)$ the system output.

Problem 5.53 A train of square pulses

$$x(t) = \sum_{n=-\infty}^{\infty} x_0(t - nT)$$

where $T = 1/220$ sec and $x_0(t) = R_{T/6}(t)$ is applied as the input to a filter of frequency response $H(j\omega)$ and output $y(t)$. The objective is that the signal $y(t)$ is made to resemble the 440-Hz musical note “A” (La), which has the amplitude spectrum shown in Fig. 5.94, i.e.

$$|Z(j\omega)| = \{\delta(\omega - \beta) + \delta(\omega + \beta)\} + \{\delta(\omega - 2\beta) + \delta(\omega + 2\beta)\} \\ + 0.1 \{\delta(\omega - 3\beta) + \delta(\omega + 3\beta)\} + 0.18 \{\delta(\omega - 4\beta) \\ + \delta(\omega + 4\beta)\} + 0.14 \{\delta(\omega - 5\beta) + \delta(\omega + 5\beta)\}$$

where $\beta = 2\pi \times 440$ rad/sec.

- a) Evaluate $|X(j\omega)|$ the amplitude spectrum of $x(t)$.
- b) Is it possible to obtain an amplitude spectrum $|Y(j\omega)|$ which is identical to $|Z(j\omega)|$? If yes, specify the filter frequency response $H(j\omega)$. If not show how to ensure that $|Y(j\omega)|$ approximate at best the spectrum $|Z(j\omega)|$.

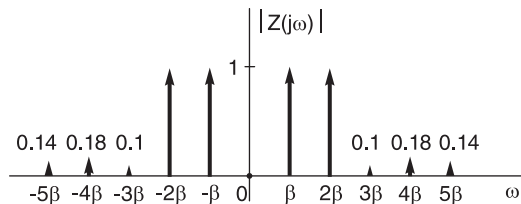


FIGURE 5.94 Signal impulsive amplitude spectrum.

Problem 5.54 Given the system transfer function

$$H(s) = \frac{3s^2 + 12s + 48}{s^3 + 3s^2 + 4s + 12}, \quad -3 < \Re[s] < 0.$$

- a) Evaluate the impulse response $h(t)$.
- b) Evaluate the frequency response $H(j\omega)$ if it exists.
- c) Is this system physically realizable? Justify your answer.
- d) The system is followed by a differentiator, a system that receiving a signal $x(t)$ produces an output dx/dt . Evaluate the frequency response $G(j\omega)$ of the overall cascade of the two systems and its impulse response $g(t)$, stating whether this overall system is physically realizable.

Problem 5.55 In an amphitheater sound system a microphone is placed relative to a speaker on stage as shown in Fig. 5.95. The speaker's audio signal $x(t)$ reaches the microphone directly as well as indirectly by reflection from the stage floor. The signal received by the microphone may be modeled in the form

$$y(t) = \alpha x(t - t_a) + \beta x(t - t_b)$$

where t_a is the propagation delay along the direct path and t_b is that along the indirect one.

- a) Given that the speed of sound is 343 m/s, determine the transfer function $H(s)$ from the input $x(t)$ to the output $y(t)$.
- b) Sketch the system magnitude squared frequency response $|H(j\omega)|^2$.
- c) Repeat the above for the case shown in Fig 5.96. Considering that the speech signal frequency band extends to about 5kHz, which setup of microphone placement among these two produces less sound interference? Explain why?

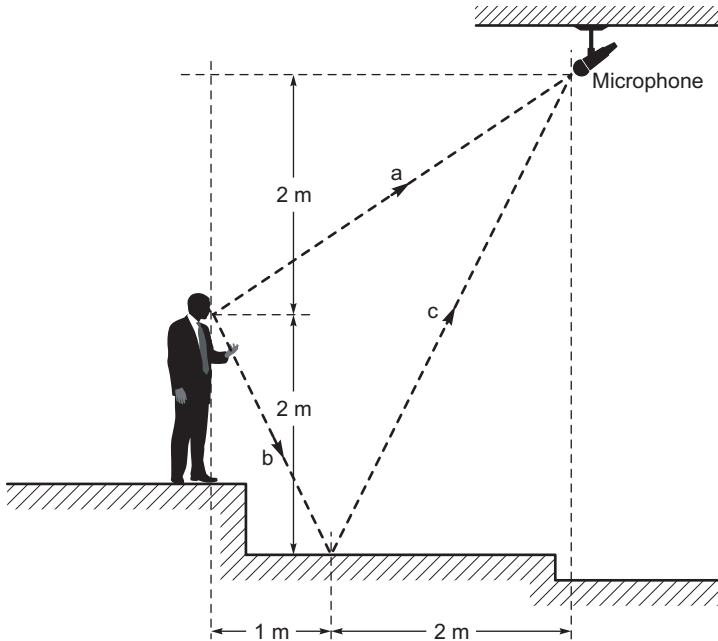


FIGURE 5.95 Signal with interference caption.

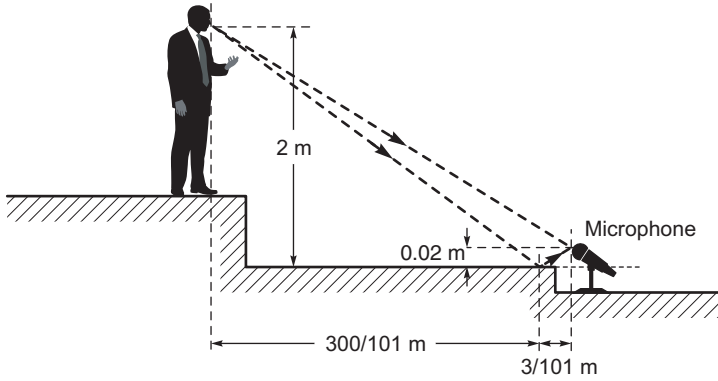


FIGURE 5.96 Signal with interference alternative approach.

5.35 Answers to Selected Problems

Problem 5.1 a) See Fig. 5.97.

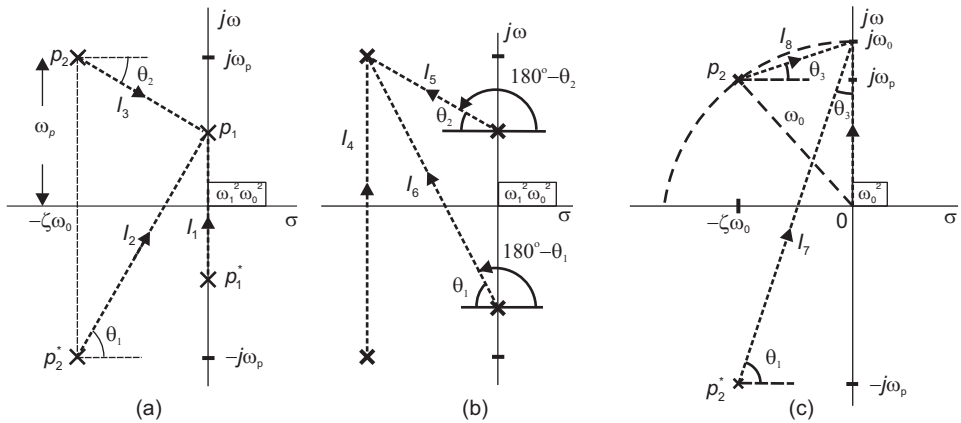


FIGURE 5.97 Figure for Problem 5.1.

$$\omega_p = \omega_0 \sqrt{1 - \zeta^2}.$$

b)

$$y(t) = 2|C_1| \cos(\omega_1 t + \underline{C_1}) u(t) + 2|C_2| e^{-\zeta\omega_0 t} \cos(\omega_p t + \underline{C_2}) u(t)$$

$$|C_1| = \frac{\omega_1^2 \omega_0^2}{2\omega_1 \sqrt{(\zeta\omega_0)^2 + (\omega_1 + \omega_p)^2} \sqrt{(\zeta\omega_0)^2 + (\omega_p - \omega_1)^2}}$$

$$\underline{C_1} = - \left\{ \pi/2 + \tan^{-1} \frac{\omega_1 + \omega_p}{\zeta\omega_0} - \tan^{-1} \frac{\omega_p - \omega_1}{\zeta\omega_0} \right\}$$

$$|C_2| = \frac{\omega_1^2 \omega_0^2}{2\omega_p \sqrt{(\zeta\omega_0)^2 + (\omega_p - \omega_1)^2} \sqrt{(\zeta\omega_0)^2 + (\omega_p + \omega_1)^2}}$$

$$\underline{C_2} = - \left\{ \left(\pi - \tan^{-1} \frac{\omega_p - \omega_1}{\zeta\omega_0} \right) + \left(\pi - \tan^{-1} \frac{\omega_p + \omega_1}{\zeta\omega_0} \right) + \pi/2 \right\}$$

c)

$$y_{ss}(t) = 2|C_1| \cos(\omega_1 t + \underline{C_1}) u(t)$$

$$y_{tr, I.C.0} = 2|C_2| e^{-\zeta\omega_0 t} \cos(\omega_p t + \underline{C_2}) u(t)$$

d) $|H(j\omega_0)| = 1/(2\zeta)$, $H(j\omega_0) = -\pi/2$.

Problem 5.2

$$Y(s) = \frac{K_0}{s} + \frac{K_1}{s - p_1} + \frac{K_2}{s - p_2} + \frac{K_2^*}{s - p_2^*}$$

See Fig. 5.98.

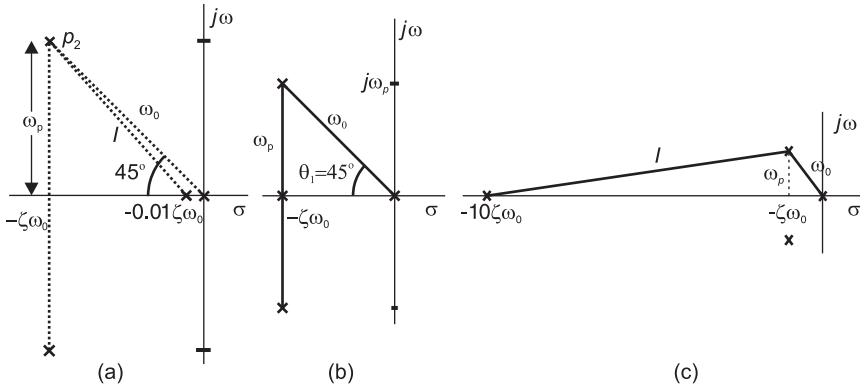


FIGURE 5.98 Figure for Problem 5.2.

case (i)

$$y(t) \cong K_0 u(t) + K_1 e^{p_1 t} u(t) = \frac{141}{\omega_0^3} (1 - e^{-0.01 \zeta \omega_0 t}) u(t)$$

case (ii)

$$y(t) = K_0 u(t) + K_1 e^{-\zeta\omega_0 t} u(t) + 2|K_2| e^{-\zeta\omega_0 t} \cos(\omega_p t + \underline{K_2}) u(t)$$

$$= \frac{1}{\omega_0^3} \{ 1.41 - 2.83 e^{-\zeta\omega_0 t} + 2e^{-\zeta\omega_0 t} \cos(0.7 \omega_0 t + 45^\circ) \} u(t)$$

case (iii)

$$y(t) \cong \frac{1}{\omega_0^3} \{ 0.14 + 0.22 e^{-\zeta\omega_0 t} \cos(0.7 \omega_0 t - 231^\circ) \} u(t)$$

b) See Fig. 5.99.

For an arbitrary position of pole p_1 : $K_0 \cong \frac{\ell_2}{\ell_2 \ell_1^2} = \frac{1}{\ell_1^2}$, $K_1 \cong \frac{0}{-\ell_2 \ell_3^2} \cong 0$, $K_2 \cong \frac{\ell_3}{\ell_3 \ell_1 \times 2\ell_4} = \frac{1}{2\ell_1 \ell_4}$; the same residue values had the pole p_1 been absent.

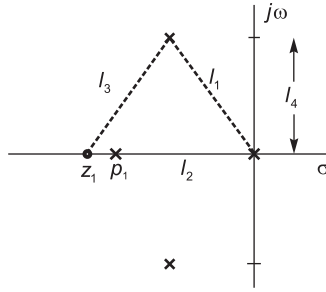


FIGURE 5.99 Figure for Problem 5.2b).

Problem 5.3 See Fig. 5.100.

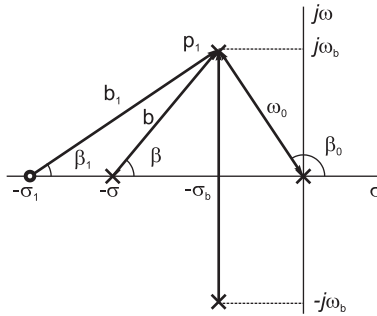


FIGURE 5.100 Figure for Problem 5.3.

$$h(t) = \frac{\sigma_1}{\sigma \omega_0^2} - \frac{\sigma_1 - \sigma}{\sigma b^2} e^{-\sigma t} + 2 \frac{b_1}{2\omega_0 \omega_b b} e^{-\sigma_b t} \cos(\omega_b t + \beta_1 - \beta_0 - \beta - 90^\circ)$$

Problem 5.4 See Fig. 5.101.

$$y(t) = (1 - e^{-4t} - 1.16 e^{-2t} \sin 3.46 t) u(t)$$

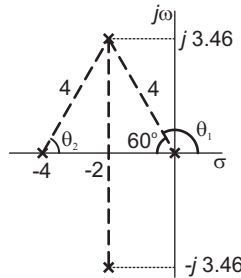


FIGURE 5.101 Figure for Problem 5.4.

Problem 5.5 $y(t) = [2.165e^{-2t} \cos(1.73t + 60^\circ) + 3.3 \cos(1.73t - 109.1^\circ)] u(t)$.

Problem 5.6 $\omega_0 t_s = 3.5793$ and $t_s = 0.35793$ sec. Overshoot peak time $t_p = 0.5060$.

b) $R = 1.56 \Omega$

Problem 5.7 c) $R = 520 \Omega$.

Problem 5.8 $H = Ks/(s^4 + 10s^3 + s^2 + 5s - K)$.

Problem 5.9 $y(t) = 3.14 \sin(5t - 117.35^\circ)$.

b) $\omega_p = \omega_0 \sqrt{1 - 2\zeta^2} = 5.39 \sqrt{1 - 2(0.37)^2} = 4.59$. The peak value at ω_p is $P = 1/(2\zeta\sqrt{1 - \zeta^2}) = 3.25$ db.

Problem 5.10

$\phi(t)$ is the periodic repetition of the function $\phi(t)$ shown in Fig. 5.102, with a period of 4 sec.

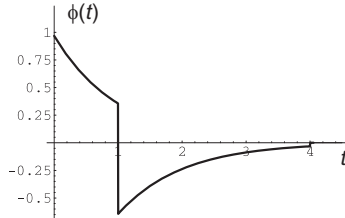


FIGURE 5.102 Figure for Problem 5.10.

Problem 5.11

a) $y_1(t) = 0.4 e^{-3t} u(t) + 0.671 e^{-2t} \cos(2t + 0.4636) u(t)$

b) $y_2(t) = e^{-1} y_1(t - 2)$
 $= 0.4 e^{-1} e^{-3(t-2)} u(t - 2)$
 $+ 0.671 e^{-1} e^{-2(t-2)} \cos(2t - 1.536) u(t - 2)$

Problem 5.12

$$\phi(t) = \delta(t) - 0.5 e^{-0.5 t} u(t) - 0.77 e^{-0.5 t} u(t) + 0.77 e^{-(t-1)/2} u(t - 1)$$

which is the periodic steady-state component of the response.

Problem 5.13 a) $y(t) = 3.901 \cos(4t - 0.6884) u(t)$.

b) $y(t) = 3.901 \cos(4t - 0.1221) u(t - 3)$

Problem 5.14 a) $y_1(t) = 0.2236 \sin(2t - 3.8846) u(t - 2)$.

b) $y_2(t) = 0.2236 \sin[2(t - 3) - 3.8846] u(t - 5)$.

Problem 5.19

$$\phi(t) = 0.5 \delta(t) + 0.25 e^{-0.5 t} u(t) + 0.38 e^{-0.5 t} u(t) - 0.38 e^{-0.5(t-1)} u(t - 1)$$

$$= 0.5 \delta(t) + 0.63 e^{-0.5 t} u(t) - 0.38 e^{-0.5(t-1)} u(t - 1)$$

The steady-state response $y_{ss}(t)$ is the periodic repetition of $\phi(t)$.

$$y_{tr}(t) = -0.38 e^{-0.5 t} u(t)$$

Problem 5.20 a)

$$H(s) = \frac{100}{s^2 + 11s + 10}$$

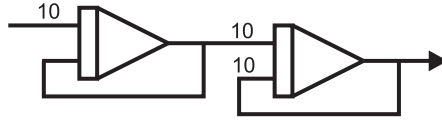


FIGURE 5.103 Figure for Problem 5.20.

b) See Fig. 5.103

Problem 5.22

a) See Fig. 5.104.

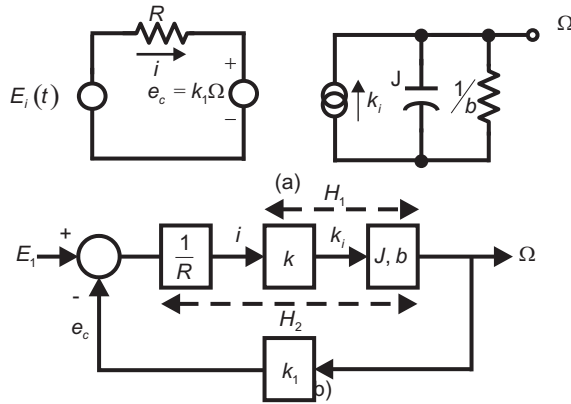


FIGURE 5.104 Figure for Problem 5.22.

b)

$$H(s) = \frac{k/RJ}{s + (b/J + k_1 k/RJ)} = \frac{b_0}{s + a_0}$$

c)

$$y_{tr}(t) = C_1 e^{-t} = -0.5 e^{-t}$$

y_{ss} is the periodic repetition of $\phi(t)$, where

$$\phi(t) = 1.58 e^{-t} u(t) - 0.58 e^{-(t-1)} u(t-1)$$

Problem 5.31

$$H(s) = \frac{Kk_m q}{RC_1 J \left(s + \frac{1}{RC_1}\right) \left(s + \frac{b}{J}\right)}$$

b)

$$y(t) = (5 - 10e^{-t} + 5e^{-2t}) u(t)$$

c) $t_s = 3.676$.

d)

$$\phi(t) = 10E (e^{-t} - e^{-2t}) u(t) + 5.82E [e^{-t} u(t) - e^{-(t-1)} u(t-1)] - 1.57E [e^{-2t} u(t) - e^{-2(t-1)} u(t-1)]$$

$$y(t) = -5.82E e^{-t}u(t) + 1.57E e^{-2t}u(t) + \sum_{n=0}^{\infty} \phi(t-n)$$

Problem 5.33

$$r_{vf}(t) = |V(jk\omega_0)| \cos \{k\omega_0 t + \arg [V(jk\omega_0)]\}$$

Problem 5.34

$$V(j\omega) = 2Sa(\omega) - 4 \frac{Sa(\omega)}{\omega^2} + \frac{4 \cos \omega}{\omega^2}$$

$$X(j\omega) = 2 \frac{1 - e^{-1} \cos \omega + e^{-1} \omega \sin \omega}{1 + \omega^2}$$

$$R_{vx}(j\omega) = V(j\omega) X^*(j\omega)$$

Problem 5.35 See Fig. 5.105.

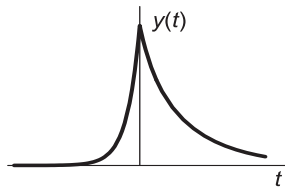


FIGURE 5.105 Figure for Problem 5.35.

$$y(t) = 1.4e^{2t}u(-t) + \{1.067e^{-0.5t} + 0.333e^{-2t}\}u(t)$$

Problem 5.36

$$x_1(t) = 0.098 \{1 - 1.5119e^{-7.5t} \sin(6.6144t + 0.7227)\}u(t)$$

$$x_2(t) = 0.1569e^{-7.5t} \cos(6.6144t - 0.934)u(t)$$

$$x(t) = x_1(t) - x_2(t)$$

$$\lim_{t \rightarrow \infty} x(t) = 0.098 \text{ m} = 9.8 \text{ cm}$$

Problem 5.39

a) $H(s) = \frac{\alpha}{s} + \frac{1}{s+1} - \frac{1}{s-\beta}$, ROC : $\begin{cases} \Re[s] > \beta, & \beta \geq 0 \\ \Re[s] > 0, & \beta \leq 0 \end{cases}$

b) $\alpha = 0$ and $\beta < 0$; so that the $j\omega$ axis is in the ROC of $H(s)$.

c) $\forall \alpha, \beta$ (since $h(t) = 0, t < 0$, for all values of α and β).

Problem 5.40

a) $H(j\omega) = \begin{cases} 0 & \text{for } \omega = 2\pi n/0.015, \text{ where } |n| \geq 1 \text{ and } n \text{ not multiple of } 5 \\ 2/0.64 = 3.125 & \text{for } \omega = 0 \end{cases}$

b) $H(j\omega) = \begin{cases} 0 & \text{for } \omega = 2\pi n/0.015, \text{ for all } n \text{ other than } n = \pm 3 \text{ and } n \text{ multiple of } 5 \\ 0.6/[2 \times 0.64\text{Sa}(3\pi/5)] = 0.929 & \text{for } \omega = \pm 400\pi \end{cases}$

c) It is not possible to satisfy the requirement.

Problem 5.41

b) $H(j\omega) = (8e^{-j0.02\omega} - 8e^{-j0.06\omega})/(j\omega) = 0.32\text{Sa}(0.02\omega) e^{-j0.04\omega}$

c) $y(t) = 0.15 \cos(40\pi t + \frac{2\pi}{5} - \frac{8\pi}{5}) = 0.15 \cos(40\pi t - \frac{6\pi}{5})$. Delay: 0.04 seconds.

Problem 5.42 c) $y(t) = KT$.

d) $y(t) = 0$

e) $y(t) = (2T/\pi) \cos(\pi t/T - 3\pi/2)$

Problem 5.43 Output's average = 0.358.**Problem 5.44**

$$H(j\omega) = [1 - e^{-j2\pi\omega/\omega_c}] \Pi_{\omega_c}(\omega) / 2$$

b) $y(t) = \cos(\omega_c t/2)$.

Problem 5.45

Referring to Fig. 5.106, we differentiate the product $u^2 v^2$ and find the value of x for which the derivative is zero. The result is found to be $x_{min} = -1 \pm \sqrt{1 - k^2} = -1 \pm \xi$ as required.

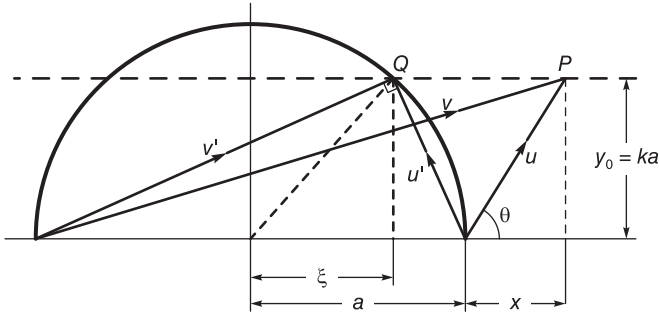


FIGURE 5.106 Figure for Problem 5.45.

Problem 5.46 $H(j\omega) = T\text{Sa}(\omega T/2) e^{-j\omega T/2}$ **Problem 5.47**

a) $h(t) = \sum_{n=0}^{\infty} A^n \delta(t - n\tau)$.

b) $H(j\omega) = \frac{1}{1 - Ae^{-j\omega\tau}}$. Output: sinusoid, 440Hz, $|H(j\omega)|_{\omega=880\pi} = 1.67$ volts.

Problem 5.48 $H(j2\pi \times 60) = 1 + e^{-j120\pi T} = 0$ for $T = n/120$, n odd. $H(j\omega) = 1 + e^{-j\omega n/120}$, n odd. Suppresses all odd harmonics of frequencies $60/n$ Hz.

Problem 5.49

$$y(t) = (15/\pi) \sin(2\pi t/T) + (10/\pi^2) \cos(2\pi t/T) = 4.88 \cos(2\pi t/T - 1.36).$$

Problem 5.50 See Fig. 5.107.**Problem 5.51**

a) $H(j800\pi) = e^{-j0.001\omega}$

$x(t) = 3 \sin[800\pi(t - 10^{-3})]$ or $x(t) = 3 \sin(800\pi t - 0.8\pi)$.

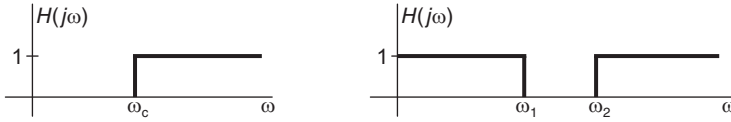


FIGURE 5.107 Figure for Problem 5.50.

b) Let $y(t) = v(t)w(t)$, where $w(t) = 2 \cos 1000\pi t$. $Y(j\omega) = [1/(2\pi)] V(j\omega) * W(j\omega)$. See Fig. 5.108.

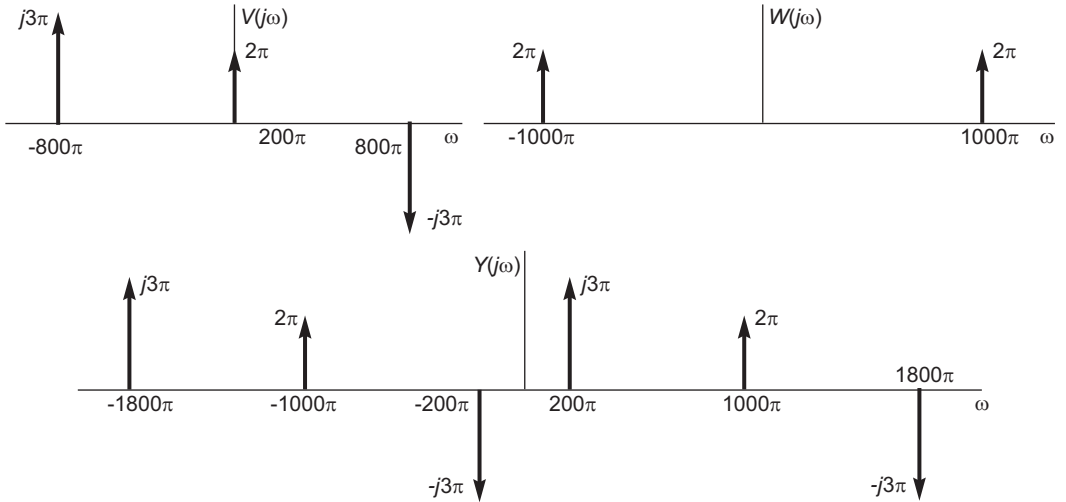


FIGURE 5.108 Figure for Problem 5.51

c) $z(t) = \sum_{n=-\infty}^{\infty} Z_n e^{j2\pi n t/T}$, where $T = 0.02$,

$$Z_n = \begin{cases} 1, & n = 0 \\ \mp 3j/2, & n = \pm 8 \\ 5/2 e^{\pm j\pi/4}, & n = \pm 10 \end{cases}$$

$$Z_n = \begin{cases} 1, & n = 0 \\ \mp 3j/2, & n = \pm 8 \\ 5/2 e^{\pm j\pi/4}, & n = \pm 10 \end{cases}$$

Problem 5.52

- a) $X_1(j\omega) = (1/2) \{e^{-j\pi/4} 2\pi\delta(\omega) + e^{j\pi/4} 2\pi\delta(\omega)\} = \pi \{e^{-j\pi/4}\delta(\omega - 700) + e^{j\pi/4}\delta(\omega + 700)\}$
 $V(j\omega) = 4\pi\delta(\omega) - j\pi \{\delta(\omega - 500) - \delta(\omega + 500)\} + \pi \{e^{-j\pi/4}\delta(\omega - 700) + e^{j\pi/4}\delta(\omega + 700)\}$.
 See Fig. 5.109.
- b) $\omega_0 = 100$ r/s and $f_0 = 50/\pi$ Hz
- c) $y(t) = 5 \cos(500t - \pi/4) + 7 \cos 700t$.

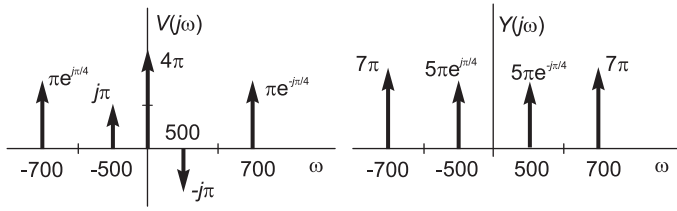


FIGURE 5.109 Figure for Problem 5.52.

Problem 5.53

$$|X(j\omega)| = (\pi/3) \sum_{n=-\infty}^{\infty} |Sa(n\pi/6)| \delta(\omega - n\omega_0)$$

We should have $|H(0)| = 0$, $|H(j\beta)| = 1.15$, $|H(j2\beta)| = 2.31$, $|H(j4\beta)| = 0.831$, $|H(j5\beta)| = 0.808$, $|H(j\omega)| = 0$, $\omega = k\omega_0$; $k = 1, 3, 5, 7, 9$ and $k > 10$.

Problem 5.54

a)

$$h(t) = 3e^{-3t}u(t) - 6 \sin 2t u(-t)$$

b)

$$H(j\omega) = \frac{3}{j\omega + 3} - j3 \left\{ \frac{-1}{j(\omega + 2)} + \pi \delta(\omega + 2) + \frac{1}{j(\omega - 2)} - \pi \delta(\omega - 2) \right\}$$

c) The system is not physically realizable, being noncausal.

d)

$$G(j\omega) = 3 - \frac{9}{j\omega + 3} - 6 \left\{ \frac{-1}{j(\omega + 2)} + \pi \delta(\omega + 2) - \frac{1}{j(\omega - 2)} + \pi \delta(\omega - 2) \right\}$$

$g(t)$ being noncausal the system is not physically realizable.

Problem 5.55

a) $t_a = 10.512 \times 10^{-3}$

b) $t_b = 19.557 \times 10^{-3}$, $|H(j\omega)|^2 = 1.04 + 0.4 \cos(9.0456 \times 10^{-3}\omega)$

c) $t_a = 10.480 \times 10^{-3}$, $t_b = 10.544 \times 10^{-3}$, $|H(j\omega)|^2 = 1.04 + 0.4 \cos(64.69 \times 10^{-3}\omega)$

d) The second setup is preferable, causing less interference in the audio range extending to 10000π r/s

6

Discrete-Time Signals and Systems

6.1 Introduction

As we have seen in Chapter 1, a discrete-time signal is a sequence $v[n]$ which is defined for every integer value n . A discrete-time signal has the general appearance of the sequence $v[n]$ shown in Fig. 6.1.

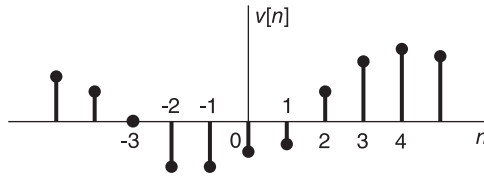


FIGURE 6.1 Discrete time signal.

A sequence $x[n]$ may be obtained by sampling a continuous-time signal $x_c(t)$. The process may be represented as shown in Fig. 6.2, where the switch is closed periodically every T seconds producing at the output a discrete-time signal, namely, the sequence

$$x[n] = x_c(t)|_{t=nT} = x_c(nT) \quad (6.1)$$

and the sampling frequency is $f_s = 1/T$.

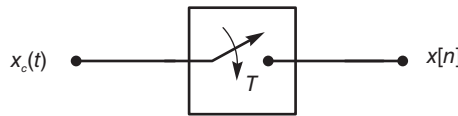


FIGURE 6.2 Sampling of a continuous-time signal.

If the input is a sinusoid such as $x_c(t) = \sin(\beta t)$ the resulting sequence is $x[n] = \sin(\beta nT) \triangleq \sin(\gamma nT)$. In other words, a continuous-time signal of frequency β results in a sequence of frequency $\gamma = \beta T$. This relation is an important one. If the frequency in the continuous-time domain is denoted by ω and that in the discrete-time domain is denoted Ω then the relation between the frequencies in the two domains is

$$\Omega = \omega T. \quad (6.2)$$

Example 6.1 Evaluate the frequency of the sequence that is the discrete-time sampling of the continuous-time signal $x_c(t) = \cos(1000\pi t + 0.1\pi)$, with a sampling frequency of $f_s = 2000$ Hz.

Let the frequency of $x_c(t)$ be denoted β rad/sec or $f_c = \beta/(2\pi)$ Hz. We have $\beta = 1000\pi$ rad/sec and $f_c = 500$ Hz. The sampling period is $T = 1/f_s = 0.0005$ sec. The corresponding discrete time sequence is $x[n] = x_c(nT) = \cos(1000\pi n 0.0005 + 0.1\pi) = \cos(0.5\pi n + 0.1\pi)$, of frequency $\gamma = 0.5\pi$, which is simply $\gamma = \beta T$.

A discrete signal $v[n]$ can be written as the sum of delayed impulses

$$v[n] = \dots + v[-2]\delta[n+2] + v[-1]\delta[n+1] + v[0]\delta[n] + v[1]\delta[n-1] + \dots \quad (6.3)$$

$$v[n] = \sum_{k=-\infty}^{\infty} v[k]\delta[n-k]. \quad (6.4)$$

6.2 Linear Time-Invariant Systems

Let $y_1[n]$ be the response of a discrete-time system to an input $v_1[n]$ and $y_2[n]$ be its response to an input $v_2[n]$. The system is linear if its response to $\alpha v_1[n] + \beta v_2[n]$ is $\alpha y_1[n] + \beta y_2[n]$; α and β being constant values. The system is *linear time-invariant* (LTI), *shift invariant* or *stationary*, if its response to $v_1[n-k]$ is $y_1[n-k]$.

Let $h[n]$ be the impulse response of an LTI system, that is, its response to an impulse $\delta[n]$. Being stationary, its response to a delayed impulse $\delta[n-k]$ is $h[n-k]$ and to the delayed impulse $v[k]\delta[n-k]$ is $v[k]h[n-k]$, and from (6.4) if $v[n]$ is the input to the system then, by superposition, its output is

$$y[n] = \sum_{k=-\infty}^{\infty} v[k]h[n-k] = v[n] * h[n]. \quad (6.5)$$

The system response is therefore, as expected, the *discrete convolution* of the input with the impulse response.

6.3 Linear Constant-Coefficient Difference Equations

LTI discrete-time systems are characterized by linear constant-coefficient difference equations of the form

$$\sum_{k=0}^N d_k y[n-k] = \sum_{k=0}^M c_k v[n-k] \quad (6.6)$$

where $v[n]$ is the system input and $y[n]$ its response. We can write

$$\begin{aligned} y[n] &= -\sum_{k=1}^N (d_k/d_0) y[n-k] + \sum_{k=0}^M (c_k/d_0) v[n-k] \\ &= -\sum_{k=1}^N a_k y[n-k] + \sum_{k=0}^M b_k v[n-k] \end{aligned} \quad (6.7)$$

where $a_k = d_k/d_0$ and $b_k = c_k/d_0$.

Example 6.2 Assuming zero initial condition, evaluate the impulse response of the system defined by the linear constant-coefficients difference equation

$$y[n] = 2a \cos b y[n-1] - a^2 y[n-2] + v[n] - a \cos b v[n-1].$$

To evaluate the impulse response $h[n]$ we assume an input $v[n] = \delta[n]$ and, with zero initial conditions, $y[n] = 0$ for $n < 0$. Substituting for n the values 0, 1, 2, ... we obtain $y[0] = 1$, $y[1] = a \cos b$, $y[2] = 2a^2 \cos^2 b - a^2 = a^2 \cos 2b$, etc., and, in general, we have

$$y[n] = \begin{cases} a^n \cos b n, & n \geq 0 \\ 0, & n < 0 \end{cases}$$

wherefrom $h[n] = a^n \cos b n u[n]$.

We shall subsequently see how the z -transform simplifies the evaluation of the impulse response as well as the solution of difference equations.

6.4 The z -Transform

The *bilateral* or *two-sided* z -transform of a sequence $v[n]$ is defined by

$$V(z) = \sum_{n=-\infty}^{\infty} v[n] z^{-n} \quad (6.8)$$

where z is a complex variable and $v[n]$ is assumed to be a general two-sided sequence, that is, a sequence defined over the entire interval $-\infty < n < \infty$. The bilateral z -transform of a sequence $v[n]$ will be denoted $V(z)$. It will alternatively be denoted $V_{II}(z)$ to put into evidence the fact that it is the two-sided transform.

For the bilateral transform we may write

$$V_{II}(z) = \mathcal{Z}(v[n]) \quad (6.9)$$

and

$$v[n] \xleftrightarrow{\mathcal{Z}} V_{II}(z) \quad (6.10)$$

meaning that $V_{II}(z)$ is the z -transform of $v[n]$.

As we shall see shortly, similarly to Laplace transform a *unilateral* or *one-sided* z -transform also exists and is particularly useful for the solution of linear constant-coefficient difference equations with initial conditions. The following remarks parallel those made in the context of Laplace transform.

We shall see below that the bilateral z -transform is in principle applicable to general two-sided sequences, that is, sequences defined for $-\infty < n < \infty$. In the current literature the transform of a two-sided sequence is expressed as the sum of the transform of the right-sided part of the sequence and that of its left-sided part. However, this approach fails to transform the most basic of two-sided sequences, such as 1, $\sin n$, $\cos n$, a^n , n and na^n , among others.

According to the current literature such basic two-sided sequences have no z -transform. In fact the bilateral z -transform, according to the present literature, exists only for right-sided sequences or else left-sided sequences and if a true two-sided sequence, such as 1, $\sin n$ or

e^n is expressed as the sum of a causal and anticausal part then their respective transforms are mutually exclusive and cannot be added to produce the overall transform.

In recent papers [21] [23] [27], it has been pointed out that the fact that basic two-sided sequences such as 1 , $\sin n$ and $\cos n$ have a Fourier transform but no z -transform, that the more general z -transform, of which Fourier is but a special case, does not exist while Fourier does, may be viewed as a mathematical anomaly.

The key to resolving the anomaly and extending the domain of existence of z -transform to cover these and a much larger class of sequences that have heretofore had no transform, be it Fourier, Laplace or z -transform, is in a generalization of the Dirac-delta impulse introduced in [21] and [23]. The result is a significant expansion of the domains of existence of Laplace and z -transform and other related ones such as Hilbert, Hartley and Mellin transforms, extending considerably the domains of their applications. In the present chapter, however, to familiarize the student with basic bilateral and unilateral z -transform we follow the same approach commonly used in the current literature. The new extended transforms are deferred to Chapter 18.

Using polar coordinates we can write

$$z = re^{j\Omega} \quad (6.11)$$

where z is viewed as a vector of length r and angle Ω in the complex z -plane. The z -transform is thus written

$$V(re^{j\Omega}) = \sum_{n=-\infty}^{\infty} v[n]r^{-n}e^{-j\Omega n}. \quad (6.12)$$

We note that if $r = r_0$, a constant, we have $z = r_0e^{j\Omega}$ which by varying Ω defines a circle of radius r_0 in the z plane as shown in Fig. 6.3.

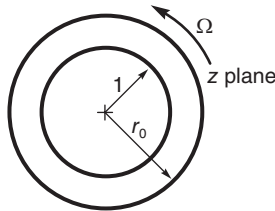


FIGURE 6.3 Unit circle and a larger circle in z -plane.

If $r = 1$, the circle of unit radius shown in the figure is called the “unit circle.” The z -transform on the unit circle is given by

$$V(e^{j\Omega}) = \sum_{n=-\infty}^{\infty} v[n]e^{-j\Omega n} \quad (6.13)$$

and is in fact, by definition the Fourier transform of the sequence $v[n]$. It is referred to as the *discrete-time Fourier transform* (DTFT). This is the discrete-time counter part of the continuous-time property stating that the Fourier transform is but a special case of the Laplace transform, being the value of the Laplace transform on the $s = j\omega$ axis in the complex s plane. We also note in passing from (6.12) that the z -transform of a sequence $v[n]$ can be viewed as the Fourier transform of a weighted sequence, namely, the sequence $v[n]$ multiplied by r^{-n} .

6.5 Convergence of the z -Transform

The Fourier transform $V(e^{j\Omega})$ is given by an infinite sum of a power series. This series converges uniformly if the sequence is absolutely summable. Similarly, the z -transform in polar form is given by an infinite sum that is absolutely convergent if the sequence $v[n]r^{-n}$ is absolutely summable, i.e.,

$$\sum_{n=-\infty}^{\infty} |v[n]r^{-n}| < \infty. \tag{6.14}$$

In general, this condition is satisfied in an annular region in the z -plane, referred to as the region of convergence (ROC), namely, the region:

$$r_1 < |z| < r_2. \tag{6.15}$$

The radii r_1 and r_2 are functions of the sequence $v[n]$ and may thus be also denoted r_{v_1} and r_{v_2} . In particular, we have the following four cases.

Case 1: Finite Duration Sequence

For a sequence $v[n]$ of finite duration $[n_1, n_2]$ and nil elsewhere which is of finite value over the interval, i.e., $|v[n]| < \infty$ for $n_1 \leq n \leq n_2$. We have

$$V(z) = \sum_{n=n_1}^{n_2} v[n]z^{-n} = v[n_1]z^{-n_1} + v[n_1 + 1]z^{-(n_1+1)} + \dots + v[n_2]z^{-n_2}. \tag{6.16}$$

The ROC is therefore the whole z -plane, except $z = \infty$ if $n_1 < 0$ and except $z = 0$ if $n_2 > 0$, so that, the ROC is $0 < z < \infty$ and may include $z = 0$ or $z = \infty$. The sequence and its ROC are shown in Fig. 6.4.

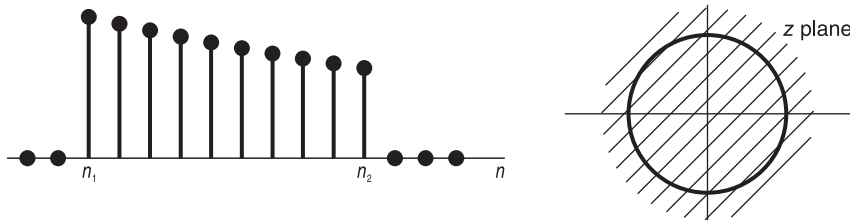


FIGURE 6.4 Finite duration sequence and its ROC.

Case 2: Right-Sided Sequence

A right-sided sequence $v[n]$ is one that extends to the right on the n axis as $n \rightarrow \infty$, starting from a finite value n_1 . In other words it is nil for $n < n_1$. In this case we have

$$V(z) = \sum_{n=n_1}^{\infty} v[n]z^{-n} = v[n_1]z^{-n_1} + v[n_1 + 1]z^{-(n_1+1)} + v[n_1 + 2]z^{-(n_1+2)} + \dots \tag{6.17}$$

The ROC is the exterior of a circle, i.e. $|z| > r_1$, except $z = \infty$ if $n_1 < 0$; see Fig. 6.5.

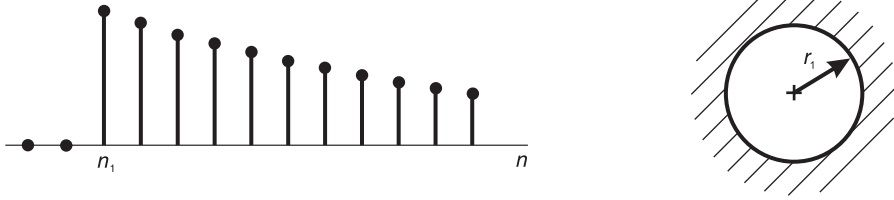


FIGURE 6.5 Right-sided sequence and its ROC.

If the sequence is causal, $n_1 \geq 0$, the ROC includes $z = \infty$.

Case 3: Left-Sided Sequence

A left-sided sequence $v[n]$ is one that extends to the left on the n axis as $n \rightarrow -\infty$, starting from a finite value n_2 . In other words it is nil for $n > n_2$. We have

$$\begin{aligned} V(z) &= \sum_{n=-\infty}^{n_2} v[n] z^{-n} = \sum_{m=-n_2}^{\infty} v[-m] z^m \\ &= v[n_2]z^{-n_2} + v[n_2 - 1]z^{-(n_2-1)} + v[n_2 - 2]z^{-(n_2-2)} + \dots \end{aligned}$$

which is the same as the expression of $V(z)$ in the previous case except for the replacement of n by $-n$ and z by z^{-1} . The ROC is therefore $|z| < r_2$, except $z = 0$ if $n_2 > 0$; see Fig. 6.6.

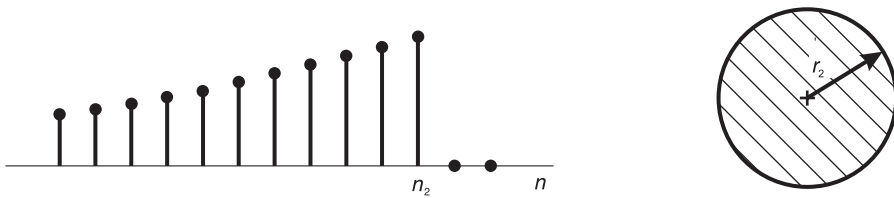


FIGURE 6.6 Left-sided sequence and its ROC.

We note that the z -transform of an anticausal sequence, a sequence that is nil for $n > 0$, converges for $z = 0$.

Case 4: General Two-Sided Sequence

Given a general two-sided sequence $v[n]$ we have

$$V(z) = \sum_{n=-\infty}^{\infty} v[n] z^{-n} = \sum_{n=0}^{\infty} v[n] z^{-n} + \sum_{n=-\infty}^{-1} v[n] z^{-n}. \tag{6.18}$$

The first term converges for $|z| > r_1$, the second term for $|z| < r_2$, wherefrom there is convergence if and only if $r_1 < r_2$ and the ROC is the annular region

$$r_1 < |z| < r_2. \tag{6.19}$$

Example 6.3 Evaluate the z -transform and the Fourier transform of the sequence

$$v(n) = e^{\alpha n}u[n] + e^{\beta n}u[-1 - n]$$

we have

$$\begin{aligned} V(z) &= \sum_{n=0}^{\infty} e^{\alpha n} z^{-n} + \sum_{n=-\infty}^{-1} e^{\beta n} z^{-n} \\ &= \frac{1}{1 - e^{\alpha} z^{-1}} + \sum_{m=1}^{\infty} e^{-\beta m} z^m, \quad |z| > e^{\alpha} \\ &= \frac{1}{1 - e^{\alpha} z^{-1}} + e^{-\beta} z \frac{1}{1 - e^{-\beta} z}, \quad e^{\alpha} < |z| < e^{\beta}. \end{aligned}$$

We note that the sequence has two poles $z = e^{\alpha}$ and $z = e^{\beta}$. The ROC is a ring bounded by the two poles as shown in Fig. 6.7.

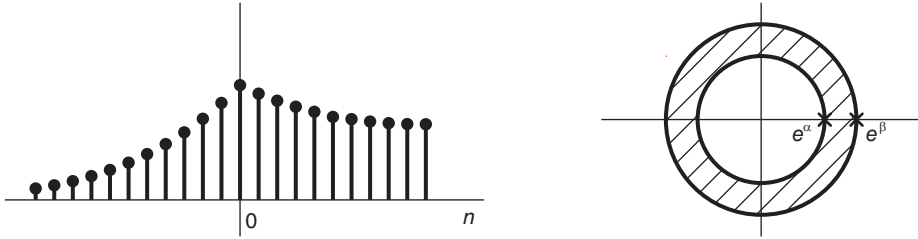


FIGURE 6.7 Two-sided sequence and its ROC.

The Fourier transform exists if the unit circle is in the ROC, i.e. if and only if $e^{\alpha} < 1 < e^{\beta}$ in which case it is given by

$$V(e^{j\Omega}) = \frac{1}{1 - e^{\alpha} e^{-j\Omega}} + \frac{e^{-\beta} e^{j\Omega}}{1 - e^{-\beta} e^{j\Omega}}.$$

Example 6.4 Evaluate the z-transform of $v[n] = a^n \sin bn u[n]$, where a and b are real.

We have

$$\begin{aligned} V(z) &= \sum_{n=0}^{\infty} a^n \sin bn z^{-n} = \frac{1}{2j} \sum_{n=0}^{\infty} (a^n e^{jbn} z^{-n} - a^n e^{-jbn} z^{-n}) \\ &= \frac{1}{2j} \left[\sum_{n=0}^{\infty} (ae^{jb} z^{-1})^n - \sum_{n=0}^{\infty} (ae^{-jb} z^{-1})^n \right] \\ &= \frac{-j/2}{1 - ae^{jb} z^{-1}} - \frac{-j/2}{1 - ae^{-jb} z^{-1}}. \end{aligned}$$

The ROC is given by $|ae^{\pm jb} z^{-1}| < 1$, i.e. $|z| > |a|$. The expression can be rewritten in the form

$$V(z) = \frac{a \sin b z^{-1}}{1 - 2a \cos b z^{-1} + a^2 z^{-2}}, \quad |z| > |a|.$$

The poles of $V(z)$ and its ROC are shown in Fig. 6.8.

Similarly, we can show that

$$\begin{aligned} a^n u[n] &\xrightarrow{z} \frac{1}{1 - az^{-1}}, \quad |z| > |a| \\ a^n \cos bn u[n] &\xrightarrow{z} \frac{1 - a \cos b z^{-1}}{1 - 2a \cos b z^{-1} + a^2 z^{-2}}, \quad |z| > |a| \end{aligned}$$

$$a^n u[-n] \xleftrightarrow{z} \sum_{n=-\infty}^0 a^n z^{-n} = \sum_{m=0}^{\infty} a^{-m} z^m = \frac{1}{1 - a^{-1}z}, \quad |z| < |a|.$$

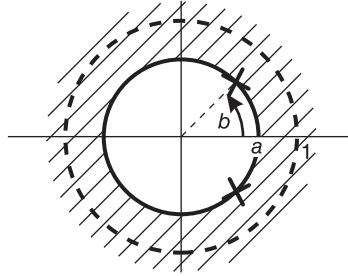


FIGURE 6.8 ROC of a right-sided sequence.

We note that the transform of a real exponential $e^{\alpha n} u[n]$ has the pole in the z plane at $z = e^{\alpha}$ on the real axis. The transform of the sequence $a^n u[n]$, where a is generally complex, has a pole at $z = a$. The transform of the sequence $e^{\alpha n} \cos \beta n u[n]$ has two conjugate poles, at $z = e^{\alpha + j\beta}$ and $z = e^{\alpha - j\beta}$.

In all of these cases the domain of convergence is the region in the z -plane that is exterior to the circle that passes through the pole or pair of conjugate poles. If a sequence is the sum of two such right-sided sequences the ROC is the exterior of the “poles” circle of larger radius. We recall similar rules associated with Laplace transform.

The same remarks apply to left-sided sequences. The z -transform of the sum of left-sided sequences has a ROC that is the interior of the circle that passes through the pole(s) of least radius.

For illustration purposes some basic one-sided sequences are shown together with their ROC in the Laplace s plane and in the z -plane in Fig. 6.9. Two-sided sequences are similarly shown with their regions of convergence in the s and z -plane, in Fig. 6.10.

6.6 Inverse z -Transform

The inverse z -transform can be derived as follows. We have by definition

$$V(z) = \sum_{n=-\infty}^{\infty} v[n] z^{-n}. \quad (6.20)$$

Multiplying both sides by z^{k-1} and integrating we have

$$\oint V(z) z^{k-1} dz = \oint \sum_{n=-\infty}^{\infty} v[n] z^{-n+k-1} dz \quad (6.21)$$

where the integration sign denotes a counterclockwise circular contour centered at the origin.

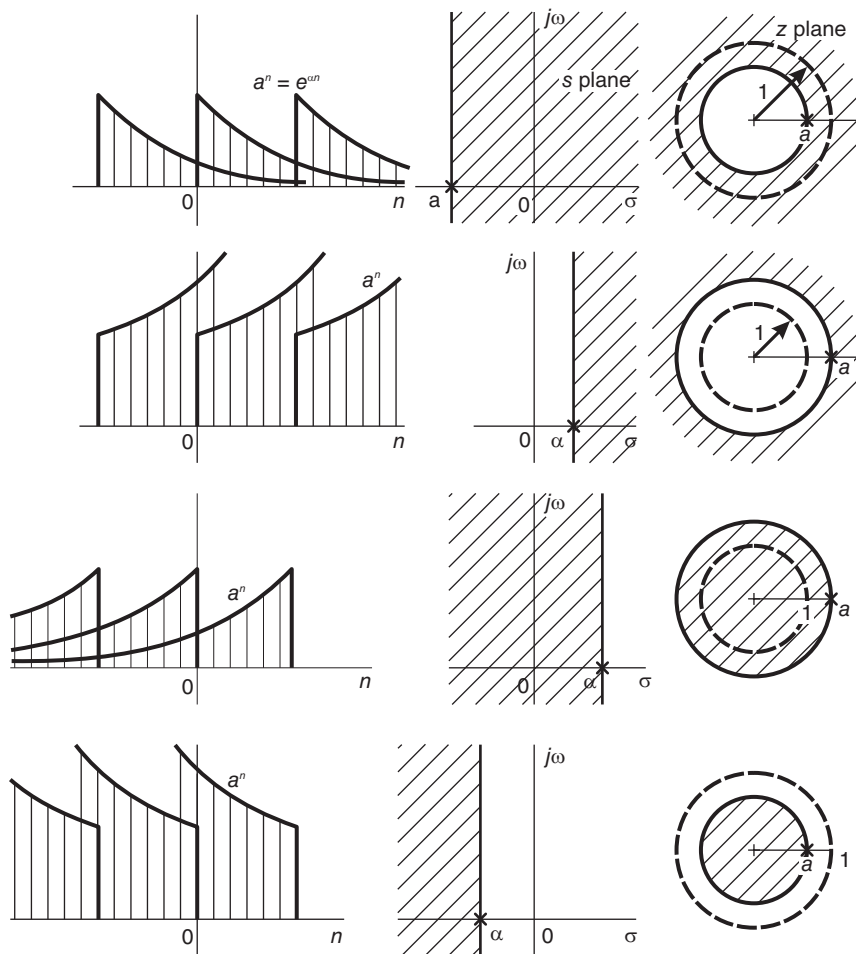


FIGURE 6.9 Right- and left-sided sequences and ROC.

Assuming uniform convergence, the order of summation and integration can be reversed, wherefrom

$$\oint V(z) z^{k-1} dz = \sum_{n=-\infty}^{\infty} \oint v[n] z^{-n+k-1} dz. \tag{6.22}$$

Now, according to Cauchy’s integration theorem

$$\oint_C z^{k-1} dz = \begin{cases} 2\pi j, & k = 0 \\ 0, & k \neq 0 \end{cases} \tag{6.23}$$

where C is a counterclockwise circular contour that is centered at the origin, wherefrom

$$\oint_C V(z) z^{k-1} dz = 2\pi j v[k] \tag{6.24}$$

and replacing k by n

$$v[n] = \frac{1}{2\pi j} \oint_C V(z) z^{n-1} dz \tag{6.25}$$

where the contour C is in the ROC of $V(z)$ and encircles the origin. This is the inverse z -transform. Replacing z by $e^{j\Omega}$ we obtain the inverse Fourier transform

$$v[n] = \frac{1}{2\pi} \int_{-\pi}^{\pi} V(e^{j\Omega}) e^{j\Omega n} d\Omega. \tag{6.26}$$

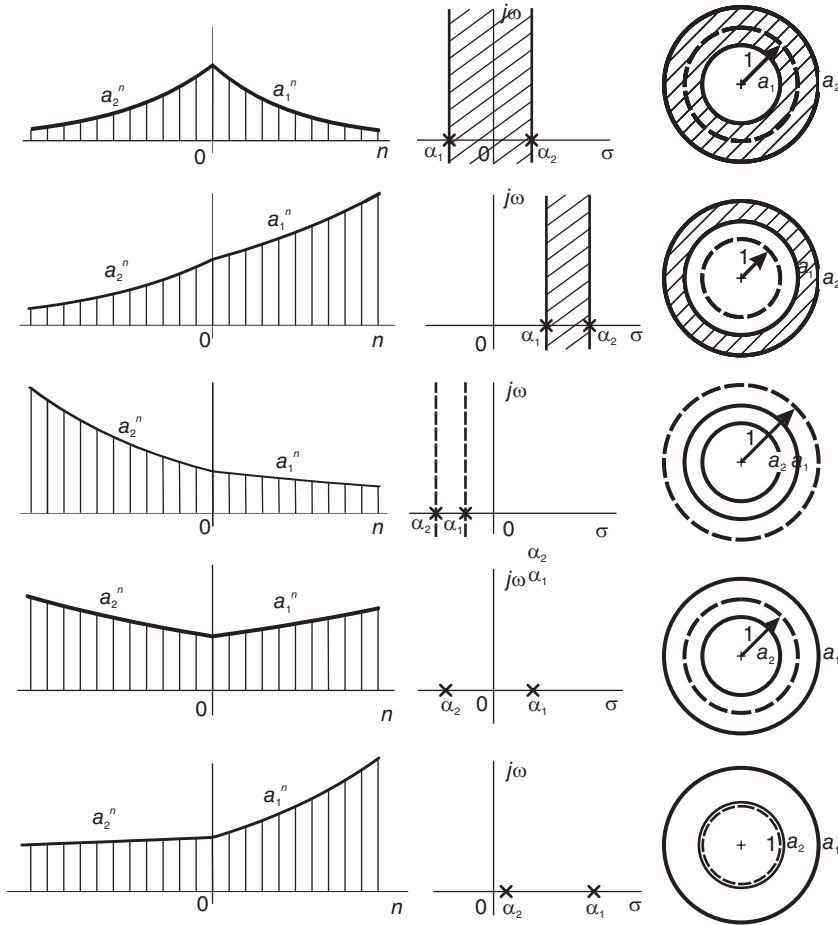


FIGURE 6.10 Two-sided sequences and ROC.

If $V(z)$ is rational, the ratio of two polynomials, the residue theorem may be applied to evaluate Equation (6.25). We can write

$$v[n] = \sum [\text{residues of } V(z) z^{n-1} \text{ at its poles inside } C]. \tag{6.27}$$

If $V(z) z^{n-1}$ is a rational function in z and has a pole of order m at $z = z_0$ we can write

$$V(z) z^{n-1} = \frac{F(z)}{(z - z_0)^m} \tag{6.28}$$

where $F(z)$ has no poles at $z = z_0$. The residue of $V(z)z^{n-1}$ at $z = z_0$ is given by

$$\text{Res} [V(z)z^{n-1} \text{ at } z = z_0] = \frac{1}{(m-1)!} \left[\frac{d^{m-1}F(z)}{dz^{m-1}} \right]_{z=z_0}. \tag{6.29}$$

In particular, for the case of a simple pole ($m = 1$)

$$\text{Res} [V(z)z^{n-1} \text{ at } z = z_0] = F(z_0). \tag{6.30}$$

Example 6.5 Let

$$V(z) = \frac{2 - 1.25z^{-1}}{1 - 1.25z^{-1} + 0.375z^{-2}}, \quad |z| > 0.75.$$

Evaluate the inverse transform of $V(z)$.

We have

$$V(z) = \frac{2 - 1.25z^{-1}}{(1 - 0.5z^{-1})(1 - 0.75z^{-1})}, \quad |z| > 0.75$$

$$v[n] = \frac{1}{2\pi j} \oint_C \frac{(2 - 1.25z^{-1})z^{n-1}dz}{(1 - 0.5z^{-1})(1 - 0.75z^{-1})} = \frac{1}{2\pi j} \oint_C \frac{(2z - 1.25)z^n dz}{(z - 0.5)(z - 0.75)}.$$

The ROC implies a right-sided sequence. Moreover, $V(z)|_{z=\infty} = 2$ wherefrom the sequence is causal, i.e., $v[n] = 0$ for $n < 0$. With $n \geq 0$ the circle C contains two poles as seen in Fig. 6.11. Therefore

$$\begin{aligned} v[n] &= \left[\text{Res of } \frac{(2z - 1.25)z^n}{(z - 0.5)(z - 0.75)} \text{ at } z = 0.5 + \text{Res of } \frac{(2z - 1.25)z^n}{(z - 0.5)(z - 0.75)} \text{ at } z = 0.75 \right] \\ &= \left\{ \frac{(2 \times 0.5 - 1.25)(0.5)^n}{0.5 - 0.75} + \frac{(2 \times 0.75 - 1.25)(0.75)^n}{0.75 - 0.5} \right\} u[n] = \{(0.5)^n + (0.75)^n\} u[n]. \end{aligned}$$

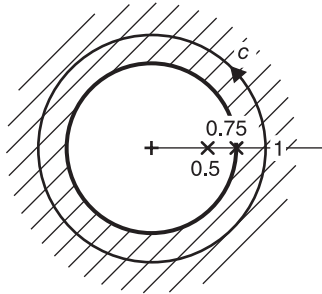


FIGURE 6.11 Contour of integration in ROC.

Example 6.6 Let

$$V(z) = \frac{-1.5z}{z^2 - 2.5z + 1}, \quad 0.5 < |z| < 2.$$

The ROC implies a two-sided sequence. The poles are shown in Fig. 6.12.

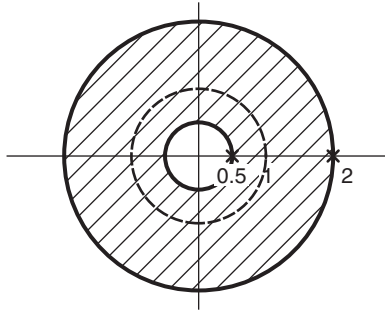


FIGURE 6.12 Annular ROC.

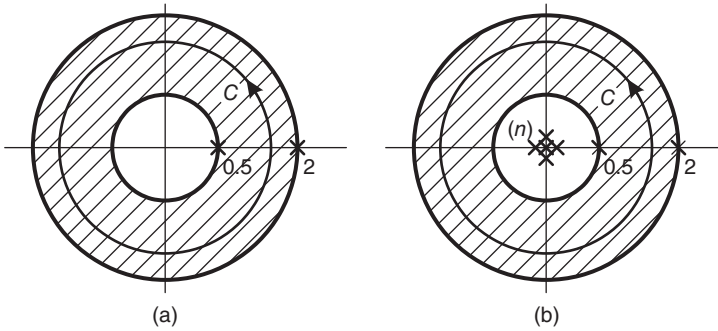


FIGURE 6.13 Contour of integration in ROC (a) with $n \geq 0$; (b) with $n < 0$.

We have

$$v[n] = \frac{1}{2\pi j} \oint \frac{-1.5z^n}{(z-2)(z-0.5)} dz.$$

For $n \geq 0$ the circle C encloses the pole $z = 0.5$, as shown in Fig. 6.13(a).

$$v[n] = \text{Res} \left[\frac{-1.5z^n}{(z-2)(z-0.5)} \text{ at } z = 0.5 \right] = \frac{-1.5(0.5)^n}{0.5-2} = (0.5)^n.$$

For $n < 0$ the circle C encloses a simple pole at $z = 0.5$ and a pole of order n at $z = 0$, as shown in Fig. 6.13(b). Writing $m = -n$ we have

$$\begin{aligned} v[n] &= \text{Res} \left[\frac{-1.5}{(z-2)(z-0.5)} z^m \text{ at } z = 0.5 \right] + \text{Res} \left[\frac{-1.5}{(z-2)(z-0.5)} z^m \text{ at } z = 0 \right] \\ &= (0.5)^{-m} + \frac{1}{(m-1)!} \left[\frac{d^{m-1}}{dz^{m-1}} \frac{-1.5}{(z-2)(z-0.5)} \right]_{z=0} \triangleq (0.5)^n + v_2[n]. \end{aligned}$$

Now if $m = 1$, i.e. $n = -1$,

$$v_2[n] = \frac{-1.5}{-2(-0.5)} = -1.5$$

and

$$v[n] = (0.5)^{-1} - 1.5 = 0.5.$$

For $m = 2$, i.e. $n = -2$

$$v_2[n] = -1.5 \frac{d}{dz} \frac{1}{z^2 - 2.5z + 1} \Big|_{z=0} = \frac{1.5(2z - 2.5)}{(z^2 - 2.5z + 1)^2} \Big|_{z=0}$$

$$v[n] = (0.5)^{-2} - 1.5 \times 2.5 = 2^{-2}.$$

For $m = 3$ we obtain

$$v_2[n] = \frac{-1.5}{2} \times \frac{d^2}{dz^2} \frac{1}{z^2 - 2.5z + 1} = \frac{-1.5}{2} \times \left\{ (z^2 - 2.5z + 1)^2 [-(2)] + (2z - 2.5) \times 2(z^2 - 2.5z + 1)(2z - 2.5) \right\} / \left\{ (z^2 - 2.5z + 1)^4 \right\} \Big|_{z=0} = -63/8$$

$$v[n] = (0.5)^{-3} - 63/8 = 8 - 63/8 = 2^{-3}.$$

Repeating we deduce that for $n < 0$, $v[n] = 2^n$ so that

$$v[n] = \begin{cases} 2^{-n}, & n \geq 0 \\ 2^n, & n < 0. \end{cases}$$

The successive differentiation is needed due to the multiple pole at $z = 0$. We can avoid such complication by using the substitution

$$z = 1/x$$

in

$$v[n] = \frac{1}{2\pi j} \oint_C V(z) z^{n-1} dz$$

obtaining

$$v[n] = \frac{-1}{2\pi j} \oint_{C_2} V\left(\frac{1}{x}\right) x^{-n-1} dx$$

where the contour of integration C_2 is now clockwise. Reversing the contour direction we have

$$v[n] = \frac{1}{2\pi j} \oint_{C_2} V\left(\frac{1}{x}\right) x^{-n-1} dx$$

where the direction of integration is now counterclockwise. We note that if the circle C is of radius r , the circle C_2 is of radius $1/r$. Moreover the poles of $V(z)$ that are inside C are moved by this transformation to outside the new contour.

Example 6.7 Evaluate the inverse transform of the last example for $n < 0$ using the transformation $z = 1/x$.

We write

$$v[n] = \frac{1}{2\pi j} \oint_{C_2} \frac{-1.5x^{-1}x^{-n-1}}{(x^{-1} - 2)(x^{-1} - 0.5)} dx = \frac{-1}{2\pi j} \oint \frac{1.5x^{-n}}{(x - 0.5)(x - 2)} dx.$$

$$v[n] = \text{Res} \left[\frac{-1.5x^{-n}}{(x - 0.5)(x - 2)} \text{ at } x = 0.5 \right] = \frac{-1.5(0.5)^{-n}}{-1.5} = 2^n, \quad n \leq 0.$$

The contour C_2 is shown in Fig. 6.14. The contour encloses a pole at $x = 0.5$ for $n \leq 0$.

Example 6.8 Given

$$X(z) = \frac{z^2}{(z - a)^2(1 - az)^2}, \quad a < |z| < a^{-1}$$

where a is real and $0 < a < 1$, show that $X(e^{j\Omega})$ is real implying that $x[n]$ is even-symmetric, and evaluate $x[n]$.

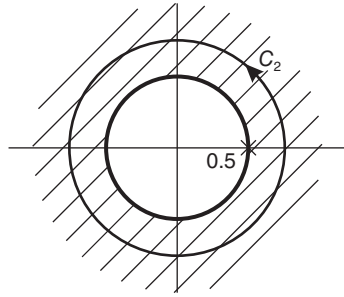


FIGURE 6.14 Circular contour in z plane.

We may write

$$X(e^{j\Omega}) = \frac{e^{j2\Omega}}{(e^{j\Omega} - a)^2(1 - ae^{j\Omega})^2} = \frac{1}{(1 - 2a \cos \Omega + a^2)^2}$$

which is real. Hence $x[-n] = x[n]$.

$$x[n] = \frac{1}{2\pi j} \oint_C \frac{z^{n+1}}{(z - a)^2(1 - az)^2} dz$$

With $n \geq 0$ the contour C encloses a pole at $z = a$.

$$x[n] = [\text{residue at } z = a] = \frac{d}{dz} \frac{z^{n+1}}{a^2(z - a^{-1})^2} \Big|_{z=a} = \frac{(1 - a^2)(n + 1)a^n + 2a^{n+2}}{(1 - a^2)^3}, \quad n \geq 0.$$

6.7 Inverse z -Transform by Partial Fraction Expansion

Given a z -transform $X(z)$ which is a rational function of z .

$$X(z) = \frac{\sum_{k=0}^M b_k z^{-k}}{1 + \sum_{k=0}^N a_k z^{-k}} = K \frac{\prod_{k=1}^M (1 - z_k z^{-1})}{\prod_{k=1}^N (1 - p_k z^{-1})} \tag{6.31}$$

a common way to evaluate the inverse transform $x[n]$ is to effect a partial fraction expansion. In the case $N > M$ and simple poles p_k , we obtain the expansion

$$X(z) = \sum_{k=1}^N \frac{A_k}{1 - p_k z^{-1}} \tag{6.32}$$

where

$$A_k = [(1 - p_k z^{-1})X(z)]_{z=p_k} \tag{6.33}$$

If $N \leq M$, we may perform a long division so that the expansion will include a polynomial of order $M - N$ in z^{-1} . For the case of multiple order poles a differentiation is called for. For example if $X(z)$ has a double pole at $z = p_k$ the expansion will include the two terms

$$\frac{B_1}{1 - p_k z^{-1}} + \frac{B_2}{(1 - p_k z^{-1})^2} \tag{6.34}$$

$$B_1 = p_k \left[\frac{d}{dz} (1 - p_k z^{-1})^2 X(z) \right]_{z=p_k}, \quad B_2 = [(1 - p_k z^{-1})^2 X(z)]_{z=p_k}.$$

Example 6.9 Evaluate the sequence $x[n]$ given that its z -transform is

$$X(z) = \frac{1 - (9/4)z^{-1} - (3/2)z^{-2}}{1 - (5/4)z^{-1} + (3/8)z^{-2}}.$$

Effecting a long division

$$X(z) = 4 - \frac{3 - (11/4)z^{-1}}{1 - (5/4)z^{-1} + (3/8)z^{-2}} = 4 - \left[\frac{A}{1 - (3/4)z^{-1}} + \frac{B}{1 - (1/2)z^{-1}} \right]$$

$$A = \frac{3 - 11/3}{1 - (1/2)(4/3)} = -2, \quad B = \frac{3 - 11/2}{1 - (3/4)(2)} = 5$$

$$X(z) = 4 + \frac{2}{1 - \frac{3}{4}z^{-1}} - \frac{5}{1 - \frac{1}{2}z^{-1}}$$

$$x[n] = 4\delta[n] + [2 \times (3/4)^n - 5 \times (1/2)^n] u[n].$$

6.8 Inversion by Long Division

Another approach to evaluate the inverse z -transform is the use of a long division.

Example 6.10 Evaluate the inverse transform of

$$V(z) = \frac{az^{-1}}{1 - a^{-1}z}, \quad |z| < |a|.$$

The ROC implies a left-sided sequence. The result of the division should reflect this fact as having increasing powers of z . We write

$$\begin{array}{r} 1 - a^{-1}z \overline{) az^{-1} + 1 + a^{-1}z + a^{-2}z^2 \dots} \\ \underline{az^{-1}} \phantom{+ 1 + a^{-1}z + a^{-2}z^2 \dots} \\ 1 \phantom{+ a^{-1}z + a^{-2}z^2 \dots} \\ \underline{1 - a^{-1}z} \phantom{+ a^{-2}z^2 \dots} \\ a^{-1}z \phantom{+ a^{-2}z^2 \dots} \\ \underline{a^{-1}z - a^{-2}z^2} \\ \dots \end{array}$$

wherefrom

$$V(z) = az^{-1} + 1 + a^{-1}z + a^{-2}z^2 + \dots = \sum_{n=-\infty}^1 a^n z^{-n}$$

$$v[n] = a^n u[1 - n].$$

6.9 Inversion by a Power Series Expansion

If $V(z)$ can be expressed as a power series in powers of z^{-1} we would be able to identify the sequence $v[n]$.

Example 6.11 Using a power series expansion, evaluate the inverse z -transform of

$$V(z) = \frac{1}{(1 + az^{-1})^2}.$$

We have the expansion

$$(1 + x)^{-2} = 1 - 2x + 3x^2 - 4x^3 + 5x^4 - \dots, \quad -1 < x < 1.$$

We can therefore write

$$V(z) = (1 + az^{-1})^{-2} = \sum_{n=0}^{\infty} (-1)^n (n+1) a^n z^{-n}, \quad |z| > |a|.$$

By definition

$$V(z) = \sum_{n=-\infty}^{\infty} v[n] z^{-n}$$

wherefrom $v[n]$ is the sequence

$$v[n] = (-1)^n (n+1) a^n u[n].$$

Example 6.12 Using a power series expansion evaluate the inverse z -transform of

$$X(z) = \log(1 + az^{-1}), \quad |z| > |a|.$$

Using the power series expansion of the log function we can write

$$X(z) = \sum_{n=1}^{\infty} \frac{(-1)^{n+1} a^n z^{-n}}{n}$$

$$x[n] = (-1)^{n+1} \frac{a^n}{n} u[n-1].$$

The sequence is shown in Fig. 6.15.

Example 6.13 Evaluate the inverse transform of

$$V(z) = \frac{1}{2} \ln \left(\frac{1 + az^{-1}}{1 - az^{-1}} \right), \quad |z| > |a|.$$

We have

$$\frac{1}{2} \ln \left(\frac{1 + az^{-1}}{1 - az^{-1}} \right) = az^{-1} + \frac{a^3 z^{-3}}{3} + \frac{a^5 z^{-5}}{5} + \frac{a^7 z^{-7}}{7} + \dots = \sum_{n=1, 3, 5, \dots}^{\infty} \frac{a^n}{n} z^{-n}, \quad |z| > |a|$$

wherefrom

$$v[n] = \begin{cases} a^n/n, & n = 1, 3, 5, \dots \\ 0, & \text{otherwise.} \end{cases}$$

The sequence $v[n]$ is shown in Fig. 6.16.

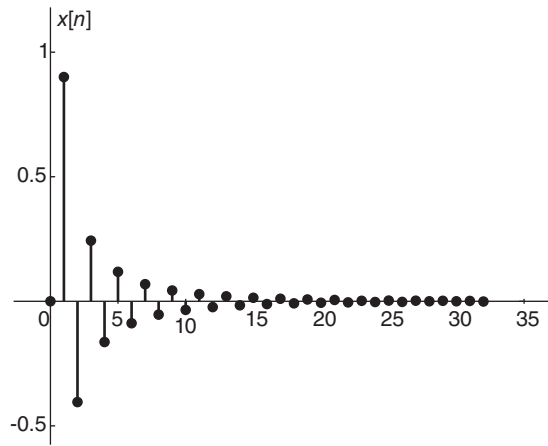


FIGURE 6.15 Inverse transform of a logarithmic transform.

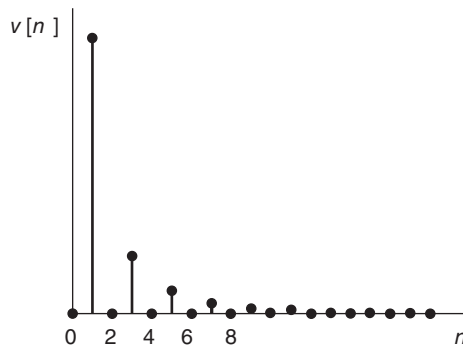


FIGURE 6.16 Inverse transform of a logarithmic $V(z)$.

6.10 Inversion by Geometric Series Summation

Recalling the geometric series summation

$$\sum_{n=n_1}^{n_2} x^n = x^{n_1} \frac{1 - x^{n_2 - n_1 + 1}}{1 - x}, \quad |x| < 1 \tag{6.35}$$

if we can express the given transform $V(z)$ in the form of the right-hand side of this equation we can deduce the sequence $v[n]$ using the left-hand side.

Example 6.14 Find the inverse transform of

$$V(z) = \frac{e^{2\alpha} z^3}{z - e^{-\alpha}} + \frac{e^{3\beta} z^{-3}}{1 - e^{-\beta} z}, \quad e^{-\alpha} < |z| < e^{\beta}.$$

We may write

$$V(z) = e^{2\alpha} z^2 \frac{1}{1 - e^{-\alpha} z^{-1}} + e^{3\beta} z^{-3} \frac{1}{1 - e^{-\beta} z} = \sum_{n=-2}^{\infty} (e^{-\alpha} z^{-1})^n + \sum_{n=-3}^{\infty} (e^{-\beta} z)^n$$

$$V(z) = \sum_{n=-2}^{\infty} e^{-\alpha n} z^{-n} + \sum_{m=-\infty}^3 (e^{-\beta} z)^{-m}, \quad e^{-\alpha} < |z| < e^{\beta}$$

$$v[n] = e^{-\alpha n} u[n+2] + e^{\beta n} u[3-n].$$

6.11 Table of Basic z -Transforms

Table 6.1 lists z -transforms of some basic sequences.

6.12 Properties of the z -Transform

Table 6.2 lists basic properties of z -transform. In the following, some of these properties are proved.

6.12.1 Linearity

The z -transform is linear, that is, if a_1 and a_2 are constants then

$$a_1 v_1[n] + a_2 v_2[n] \longleftrightarrow a_1 V_1(z) + a_2 V_2(z) \quad (6.36)$$

6.12.2 Time Shift

$$v[n-m] \longleftrightarrow z^{-m} V(z). \quad (6.37)$$

Proof

$$\sum_{n=-\infty}^{\infty} v[n-m] z^{-n} = \sum_{k=-\infty}^{\infty} v[k] z^{-(m+k)} = z^{-m} V(z) \quad (6.38)$$

having let $n-m = k$.

6.12.3 Conjugate Sequence

$$v^*[n] \xrightarrow{z} V^*(z^*). \quad (6.39)$$

Proof

$$Z(v^*[n]) = \sum v^*[n] z^{-n} = \left\{ \sum v[n] [z^*]^{-n} \right\}^* = V^*(z^*). \quad (6.40)$$

TABLE 6.1 Transforms of basic sequences

Sequence	Transform	R.O.C.
$\delta[n]$	1	All z
$u[n]$	$\frac{1}{1-z^{-1}}$	$ z > 1$
$u[n-m]$	$\frac{z^{-m}}{1-z^{-1}}$	$ z > 1$
$u[-n-1]$	$\frac{-1}{1-z^{-1}}$	$ z < 1$
$\delta[n-m]$	z^{-m}	All z -plane except $z = 0$ (if $m > 0$) or $z = \infty$ (if $m < 0$)
$\alpha^n u[n]$	$\frac{1}{1-\alpha z^{-1}}$	$ z > \alpha $
$-\alpha^n u[-n-1]$	$\frac{1}{1-\alpha z^{-1}}$	$ z < \alpha $
$n \alpha^n u[n]$	$\frac{\alpha z^{-1}}{(1-\alpha z^{-1})^2}$	$ z > \alpha $
$n^2 u[n]$	$\frac{z^2+z}{(z-1)^3}$	$ z > 1$
$-n \alpha^n u[-n-1]$	$\frac{\alpha z^{-1}}{(1-\alpha z^{-1})^2}$	$ z < \alpha $
$[\cos \Omega_0 n] u[n]$	$\frac{1-[\cos \Omega_0] z^{-1}}{1-[2 \cos \Omega_0] z^{-1}+z^{-2}}$	$ z > 1$
$[\sin \Omega_0 n] u[n]$	$\frac{[\sin \Omega_0] z^{-1}}{1-[2 \cos \Omega_0] z^{-1}+z^{-2}}$	$ z > 1$
$[r^n \cos \Omega_0 n] u[n]$	$\frac{1-[r \cos \Omega_0] z^{-1}}{1-[2r \cos \Omega_0] z^{-1}+r^2 z^{-2}}$	$ z > r$
$[r^n \sin \Omega_0 n] u[n]$	$\frac{[r \sin \Omega_0] z^{-1}}{1-[2r \cos \Omega_0] z^{-1}+r^2 z^{-2}}$	$ z > r$
$\cosh(n\alpha) u[n]$	$\frac{z[z-\cosh(\alpha)]}{z^2-2z \cosh(\alpha)+1}$	
$\sinh(n\alpha) u[n]$	$\frac{z \sinh(\alpha)}{z^2-2z \cosh(\alpha)+1}$	
$n a^{n-1} u[n]$	$\frac{z}{(z-a)^2}$	
$\frac{n(n-1)\dots(n-m+1)}{m!} a^{n-m} u[n]$	$\frac{z}{(z-a)^{m+1}}$	

6.12.4 Initial Value

Let $v[n]$ be a causal sequence. We have

$$V(z) = \sum_{n=0}^{\infty} v[n] z^{-n} \tag{6.41}$$

$$V(z) = v[0] + v[1]z^{-1} + v[2]z^{-2} + \dots \tag{6.42}$$

TABLE 6.2 Basic properties of z -transform

$a v[n] + b x(n)$	$aV(z) + bX(z)$
$v[n - n_0]$	$z^{-n_0}V(z)$
$\sum_{m=0}^n v[m]x[n - m]$	$V(z)X(z)$
$v[n]x[n]$	$\frac{1}{2\pi j} \oint_C V(y)X(z/y)y^{-1}dy$
$n v[n]$	$-z \frac{dV(z)}{dz}$
$v^*[n]$	$V^*(z^*)$
$a^n v[n]$	$V(a^{-1}z)$
$\lim_{n \rightarrow \infty} v[n]$	$\lim_{z \rightarrow 1} (1 - 1/z)V(z)$
$\Re\{v[n]\}$	$\frac{1}{2}[V(z) + V^*(z^*)]$
$\Im\{v[n]\}$	$\frac{1}{2j}[V(z) - V^*(z^*)]$
$v[-n]$	$V(1/z)$
$\sum_{k=-\infty}^n v[k]$	$\frac{1}{1 - z^{-1}}V(z)$
$v[0]$	$\lim_{z \rightarrow \infty} V(z), \quad v[n] = 0, \quad n < 0$
$\sum_{n=-\infty}^{\infty} v_1[n]v_2^*[n]$	$\frac{1}{2\pi j} \oint_C V_1(y)V_2^*(1/y^*)y^{-1}dy$

We note that

$$v[0] = V(\infty). \quad (6.43)$$

Right-Sided Sequence

Let $v[n]$ be a right-sided sequence that is non-nil for $n \geq N$, where N is a positive or negative integer and nil for $n < N$, as shown in Fig. 6.17.

We can write

$$V(z) = v[N]z^{-N} + v[N+1]z^{-(N+1)} + \dots \quad (6.44)$$

$$z^k V(z) = v[N]z^{-N+k} + v[N+1]z^{-(N+1)+k} + \dots \quad (6.45)$$

obtaining

$$\lim_{z \rightarrow \infty} z^k V(z) = \begin{cases} 0, & k < N \\ v[N], & k = N \\ \infty, & k > N. \end{cases} \tag{6.46}$$

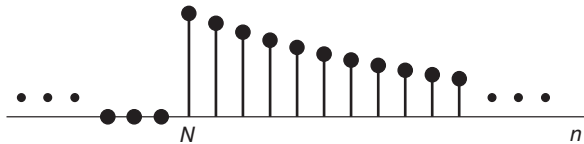


FIGURE 6.17 Right-sided sequence.

We conclude that for a right-sided sequence that is non-nil for $n \geq N$ the limit $\lim_{z \rightarrow \infty} z^k V(z)$ is equal to the initial value $v[N]$ if $k = N$; is zero if $k < N$; and is infinite if $k > N$. By evaluating this limit we may determine the sequence’s initial value

$$\lim_{z \rightarrow \infty} z^N V(z) = v[N]. \tag{6.47}$$

Left-Sided Sequence

For a left-sided sequence that is non-nil for $n \leq N$ and nil for $n > N$, as the sequence shows in Fig. 6.18, we write

$$z^k V(z) = v[N]z^{-N}z^k + v[N - 1]z^{-(N-1)}z^k + \dots \tag{6.48}$$

obtaining

$$\lim_{z \rightarrow 0} z^k V(z) = \begin{cases} 0, & k > N \\ v[N], & k = N \\ \infty, & k < N. \end{cases} \tag{6.49}$$

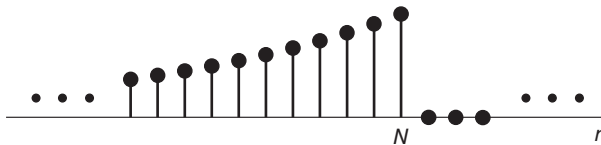


FIGURE 6.18 Left-sided sequence.

We conclude that for a left-sided sequence that is non-nil for $n \leq N$ the limit $\lim_{z \rightarrow 0} z^k V(z)$ is equal to $v[N]$ if $k = N$, is zero if $k > N$ and is infinite if $k < N$. By evaluating the limit we may thus deduce the sequence’s right-most value

$$\lim_{z \rightarrow 0} z^N V(z) = v[N]. \tag{6.50}$$

Example 6.15 Evaluate the initial value of

$$V(z) = \frac{az^{-5}}{1 - a^{-1}z}, \quad |z| < |a|.$$

We note that

$$\lim_{z \rightarrow 0} z^5 V(z) = a$$

$$\lim_{z \rightarrow 0} z^k V(z) = \begin{cases} 0, & k > 5 \\ \infty, & k < 5 \end{cases}$$

wherefrom $v[5] = a$ and $v[n] = 0$ for $n > 5$. This result can be easily verified by evaluating $v[n]$. We obtain

$$v[n] = a^{n-4}u[5-n].$$

6.12.5 Convolution in Time

The convolution in time property states that if $v_1[n] \longleftrightarrow V_1(z)$, $a_1 < |z| < b_1$, and $v_2[n] \longleftrightarrow V_2(z)$, $a_2 < |z| < b_2$, then the convolution

$$v_1[n] * v_2[n] = \sum_{k=-\infty}^{\infty} v_1[k]v_2[n-k] = \sum_{k=-\infty}^{\infty} v_1[n-k]v_2[k]. \quad (6.51)$$

has the transform

$$v_1[n] * v_2[n] \longleftrightarrow V_1(z)V_2(z), \quad \max(a_1, a_2) < |z| < \min(b_1, b_2) \quad (6.52)$$

Proof Let $w[n] = v_1[n] * v_2[n]$. We have

$$W(z) = \sum_{n=-\infty}^{\infty} \sum_{k=-\infty}^{\infty} v_1[k]v_2[n-k]z^{-n}. \quad (6.53)$$

Interchanging the order of summations we have

$$W(z) = \sum_{k=-\infty}^{\infty} v_1[k] \sum_{n=-\infty}^{\infty} v_2[n-k]z^{-n}. \quad (6.54)$$

Writing $n - k = m$ we have

$$W(z) = \sum_{k=-\infty}^{\infty} v_1[k]z^{-k} \sum_{m=-\infty}^{\infty} v_2[m]z^{-m} = V_1(z)V_2(z) \quad (6.55)$$

and the ROC includes the intersection of the ROC's of $V_1(z)$ and $V_2(z)$. If a pole is the border of the ROC of one of the two z -transforms and is canceled by a zero of the other transform then the ROC of the product $W(z)$ may extend farther in the plane.

6.12.6 Convolution in Frequency

We show that if $x[n] \longleftrightarrow X(z)$ and $v[n] \longleftrightarrow V(z)$ then

$$x[n]v[n] \longleftrightarrow \frac{1}{2\pi j} \oint_{C_1} X\left(\frac{z}{y}\right) V(y) y^{-1} dy \quad (6.56)$$

where C_1 is a contour in the common ROC of $X(z/y)$ and $V(y)$, that is, multiplication in the time domain corresponds to convolution in the z domain.

Proof Let $w[n] = x[n]v[n]$. We have

$$W(z) = \sum_{n=-\infty}^{\infty} x[n]v[n]z^{-n} = \sum_{n=-\infty}^{\infty} x[n] \frac{1}{2\pi j} \oint_{C_1} V(y) y^{n-1} dy z^{-n} \tag{6.57}$$

where C_1 is in the ROC of $V(y)$.

$$W(z) = \frac{1}{2\pi j} \sum_{n=-\infty}^{\infty} x[n] \oint_{C_1} V(y) \left(\frac{z}{y}\right)^{-n} y^{-1} dy. \tag{6.58}$$

Interchanging the order of summation and integration

$$W(z) = \frac{1}{2\pi j} \oint_{C_1} \sum_{n=-\infty}^{\infty} x[n] \left(\frac{z}{y}\right)^{-n} V(y) y^{-1} dy = \frac{1}{2\pi j} \oint_{C_1} X\left(\frac{z}{y}\right) V(y) y^{-1} dy \tag{6.59}$$

as stated. The transforms $X(z/y)$ and $V(y)$ have, respectively, the regions of convergence

$$r_{x_1} < \left|\frac{z}{y}\right| < r_{x_2} \quad \text{and} \quad r_{v_1} < |y| < r_{v_2} \tag{6.60}$$

wherefrom $W(z)$ has the ROC

$$r_{x_1} r_{v_1} < |z| < r_{x_2} r_{v_2}. \tag{6.61}$$

Equivalently,

$$W(z) = \frac{1}{2\pi j} \oint_{C_1} X(y) V\left(\frac{z}{y}\right) y^{-1} dy \tag{6.62}$$

with ROCs

$$r_{x_1} < |y| < r_{x_2} \quad \text{and} \quad r_{v_1} < \left|\frac{z}{y}\right| < r_{v_2} \tag{6.63}$$

and $W(z)$ has the same above stated ROC. Using polar representation we write

$$z = r e^{j\Omega}, \quad y = \rho e^{j\phi} \tag{6.64}$$

$$W(re^{j\Omega}) = \frac{1}{2\pi} \int_{-\pi}^{\pi} X(\rho e^{j\phi}) V\left\{\frac{r}{\rho} e^{j(\Omega-\phi)}\right\} d\phi. \tag{6.65}$$

The right-hand side shows the convolution of two spectra. If r and ρ are constants these spectra are z -transforms evaluated on two circles in the z -plane, of radii ρ and r/ρ respectively. For the particular case $r = 1$ we have the Fourier transform

$$W(e^{j\Omega}) = \frac{1}{2\pi} \int_{-\pi}^{\pi} X(\rho e^{j\phi}) V\left[\frac{1}{\rho} e^{j(\Omega-\phi)}\right] d\phi \tag{6.66}$$

wherein if ρ is constant the convolution is that of two z spectra, namely, those evaluated on a circle of radius ρ and another of radius $1/\rho$, respectively. If $\rho = 1$ we have the z -transform.

$$W(re^{j\Omega}) = \frac{1}{2\pi} \int_{-\pi}^{\pi} X(e^{j\phi}) V\left[re^{j(\Omega-\phi)}\right] d\phi \tag{6.67}$$

and the Fourier transform

$$W(e^{j\Omega}) = \frac{1}{2\pi} \int_{-\pi}^{\pi} X(e^{j\phi}) V[e^{j(\Omega-\phi)}] d\phi \quad (6.68)$$

which is simply the convolution of the two Fourier transforms $X(e^{j\Omega})$ and $V(e^{j\Omega})$ on the unit circle.

Example 6.16 Given $v_1[n] = n u[n]$, $v_2[n] = a^n u[n]$, evaluate the z -transform of $v[n] = v_1[n]v_2[n]$.

We have

$$V_1(z) = \sum_{n=0}^{\infty} n z^{-n}.$$

To evaluate this sum we note that

$$\sum_{n=0}^{\infty} z^{-n} = \frac{1}{1-z^{-1}}, \quad |z| > 1.$$

Differentiating we have

$$\sum_{n=0}^{\infty} (-n) z^{-n-1} = \frac{-z^{-2}}{(1-z^{-1})^2}, \quad |z| > 1$$

wherefrom

$$V_1(z) = \sum_{n=0}^{\infty} n z^{-n} = \frac{z^{-1}}{(1-z^{-1})^2}, \quad |z| > 1.$$

Since

$$V_2(z) = \frac{1}{1-az^{-1}}, \quad |z| > |a|$$

we have

$$\begin{aligned} V(z) &= \frac{1}{2\pi j} \oint V_1\left(\frac{z}{y}\right) V_2(y) y^{-1} dy = \frac{1}{2\pi j} \oint \frac{z^{-1}y}{(1-z^{-1}y)^2} \frac{y^{-1}}{1-ay^{-1}} dy \\ &= \frac{1}{2\pi j} \oint_C \frac{zy}{(y-z)^2(y-a)} dy. \end{aligned}$$

The contour of integration C must be in the ROC common to $V_1(z/y)$ and $V_2(y)$, that is,

$$\left| \frac{z}{y} \right| > 1 \quad \text{and} \quad |y| > |a|, \quad |a| < |y| < |z|.$$

The integrand has two poles in the y plane, namely, a double pole at $y = z$, z being a constant through the integration, and a simple one at $y = a$. The contour of integration is a circle which lies in the region between these two poles, thus enclosing the poles $y = a$, as shown in Fig. 6.19.

We deduce that

$$V(z) = \left[\text{Res of } \frac{zy}{(y-z)^2(y-a)} \text{ at } y = a \right] = \frac{za}{(z-a)^2} = \frac{az^{-1}}{(1-az^{-1})^2}, \quad |z| > |a|.$$

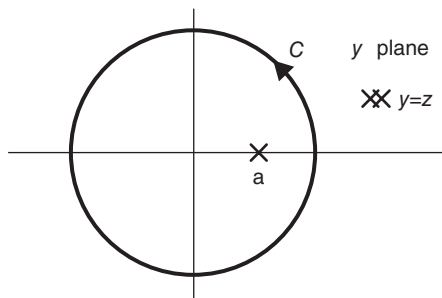


FIGURE 6.19 Contour of integration.

6.12.7 Parseval’s Relation

Parseval’s relation states that

$$\sum_{n=-\infty}^{\infty} v[n]x^*[n] = \frac{1}{2\pi j} \oint V(z) X^*(1/z^*) z^{-1} dz \tag{6.69}$$

the contour of integration being in the ROC common to $V(z)$ and $X^*(1/z^*)$.

Proof Let

$$w[n] = v[n]x^*[n]. \tag{6.70}$$

Using the complex convolution theorem we have

$$W(z) = \sum_{n=-\infty}^{\infty} w[n]z^{-n} = \frac{1}{2\pi j} \oint V(y) X^*\left(\frac{z^*}{y^*}\right) y^{-1} dy. \tag{6.71}$$

Now

$$\sum_{n=-\infty}^{\infty} w[n] = W(z)|_{z=1}. \tag{6.72}$$

Hence

$$\sum_{n=-\infty}^{\infty} v[n]x^*[n] = \frac{1}{2\pi j} \oint V(y) X^*(1/y^*) y^{-1} dy. \tag{6.73}$$

Replacing y by z completes the proof. We note that if the unit circle is in the ROC common to $V(z)$ and $X(z)$ the Fourier transforms $V(e^{j\Omega})$ and $X(e^{j\Omega})$ exist. Parseval’s relation with $z = e^{j\Omega}$ takes the forms

$$\sum_{n=-\infty}^{\infty} v[n]x^*[n] = \frac{1}{2\pi} \int_{-\pi}^{\pi} V(e^{j\Omega}) X^*(e^{j\Omega}) d\Omega \tag{6.74}$$

$$\sum_{n=-\infty}^{\infty} |v[n]|^2 = \frac{1}{2\pi} \int_{-\pi}^{\pi} |V(e^{j\Omega})|^2 d\Omega. \tag{6.75}$$

6.12.8 Final Value Theorem

The final value theorem for a right-sided sequence states that

$$\lim_{n \rightarrow \infty} v[n] = \lim_{z \rightarrow 1} (1 - z^{-1}) V(z). \tag{6.76}$$

Proof Let $v[n]$ be a right-sided sequence that extends from $n = M$ to ∞ and is nil otherwise and let

$$x[n] = v[n] - v[n - 1]. \quad (6.77)$$

We have

$$X(z) = (1 - z^{-1}) V(z) \quad (6.78)$$

$$X(z) = \sum_{n=M}^{\infty} x[n]z^{-n} = \lim_{N \rightarrow \infty} \sum_{n=M}^N \{v[n] - v[n - 1]\}z^{-n} \quad (6.79)$$

$$\begin{aligned} \lim_{z \rightarrow 1} X(z) &= \lim_{N \rightarrow \infty} \sum_{n=M}^N \{v[n] - v[n - 1]\} \\ &= \lim_{N \rightarrow \infty} [\{v[M] - v[M - 1]\} + \dots + \{v[0] - v[-1]\} + \{v[1] - v[0]\} \\ &\quad + \{v[2] - v[1]\} + \dots + \{v[N] - v[N - 1]\}] = \lim_{N \rightarrow \infty} v[N] = v[\infty] \end{aligned} \quad (6.80)$$

Example 6.17 Evaluate the z -transform of

$$v[n] = \{n0.5^n + 2 - 4(0.3)^n\} u[n]$$

and verify the result by evaluating its initial and final values. Using Table 6.1 we can write the z -transform of $v[n]$

$$V(z) = \frac{0.5z^{-1}}{(1 - 0.5z^{-1})^2} + \frac{2}{1 - z^{-1}} - \frac{4}{1 - 0.3z^{-1}}, \quad |z| > 1.$$

Applying the initial value theorem we have

$$v[0] = \lim_{z \rightarrow \infty} V(z) = -2.$$

Applying the final value theorem we have

$$v[\infty] = \lim_{z \rightarrow 1} (1 - z^{-1}) V(z) = \lim_{z \rightarrow 1} \left\{ \frac{0.5z^{-1}(1 - z^{-1})}{(1 - 0.5z^{-1})^2} + 2 - \frac{4(1 - z^{-1})}{1 - 0.3z^{-1}} \right\} = 2$$

as can be verified by direct evaluation of the sequence limits.

6.12.9 Multiplication by an Exponential

The multiplication by an exponential property states that

$$a^n v[n] \longleftrightarrow V(a^{-1}z). \quad (6.81)$$

In fact

$$\mathcal{Z}[a^n v[n]] = \sum_{n=0}^{\infty} a^n v[n] z^{-n} = \sum_{n=0}^{\infty} v[n] \{a^{-1}z\}^{-n} = V(a^{-1}z). \quad (6.82)$$

6.12.10 Frequency Translation

As a special case of the multiplication by an exponential property we have the frequency translation property, namely,

$$v[n]e^{j\beta n} \longleftrightarrow V(e^{-j\beta}z). \quad (6.83)$$

This property is also called the modulation by a complex exponential property.

6.12.11 Reflection Property

Let

$$v[n] \longleftrightarrow V(z), \quad \text{ROC} : r_{v1} < |z| < r_{v2}. \quad (6.84)$$

The reflection property states that

$$v[-n] \longleftrightarrow V\left(\frac{1}{z}\right), \quad \text{ROC} : 1/r_{v2} < |z| < 1/r_{v1}. \quad (6.85)$$

Indeed

$$\mathcal{Z}[v[-n]] = \sum_{n=-\infty}^0 v[-n]z^{-n} = \sum_{m=0}^{\infty} v[m]z^m = V(z^{-1}). \quad (6.86)$$

6.12.12 Multiplication by n

This property states that

$$n v[n] \longleftrightarrow -z \frac{dV(z)}{dz}. \quad (6.87)$$

Since

$$V(z) = \sum_{n=-\infty}^{\infty} v[n]z^{-n} \quad (6.88)$$

we have

$$\frac{dV(z)}{dz} = \sum_{n=-\infty}^{\infty} v[n](-n)z^{-n-1} \quad (6.89)$$

$$-z \frac{dV(z)}{dz} = \sum_{n=-\infty}^{\infty} n v[n]z^{-n} = \mathcal{Z}[n v[n]]. \quad (6.90)$$

6.13 Geometric Evaluation of Frequency Response

The general form of the system function $H(z)$ of a linear time-invariant (LTI) system may be written as

$$H(z) = \frac{Y(z)}{X(z)} = \frac{\sum_{k=0}^N b_k z^{-k}}{\sum_{k=0}^M a_k z^{-k}} = \frac{\sum_{k=0}^M b_k z^{-k}}{1 + \sum_{k=1}^N a_k z^{-k}}. \quad (6.91)$$

where $a_0 = 1$. We have

$$Y(z) + \sum_{k=1}^N a_k z^{-k} Y(z) = \sum_{k=0}^M b_k z^{-k} X(z). \quad (6.92)$$

Inverse transforming both sides we have the corresponding constant-coefficients linear difference equation

$$y[n] + \sum_{k=1}^N a_k y[n-k] = \sum_{k=0}^M b_k x[n-k]. \quad (6.93)$$

By factoring the numerator and denominator polynomials of the system function $H(z)$ we may write

$$H(z) = K \frac{\prod_{k=1}^M (1 - z_k z^{-1})}{\prod_{k=1}^N (1 - p_k z^{-1})}. \quad (6.94)$$

A factor of the numerator can be written

$$1 - z_k z^{-1} = \frac{z - z_k}{z} \quad (6.95)$$

contributing to $H(z)$ a zero at $z = z_k$ and a pole at $z = 0$. A factor in the denominator is similarly given by

$$1 - p_k z^{-1} = \frac{z - p_k}{z}. \quad (6.96)$$

The frequency response $H(e^{j\Omega})$ of the system is the Fourier transform of its impulse response. Putting $z = e^{j\Omega}$ in $H(z)$ we have

$$H(e^{j\Omega}) = \frac{\sum_{k=0}^N b_k e^{-j\Omega k}}{1 + \sum_{k=1}^M a_k e^{-j\Omega k}} = K \frac{\prod_{k=1}^M (1 - z_k e^{-j\Omega})}{\prod_{k=1}^N (1 - p_k e^{-j\Omega})}. \quad (6.97)$$

If the impulse response is real we have

$$H(e^{-j\Omega}) = H^*(e^{j\Omega}). \quad (6.98)$$

More generally

$$H(z^*) = H^*(z). \quad (6.99)$$

Each complex pole is accompanied by its complex conjugate. Similarly, zeros of $H(z)$ occur in complex conjugate pairs.

Similarly to continuous-time systems, the frequency response at any frequency Ω may be evaluated as the gain factor K times the product of vectors extending from the zeros to the point $z = e^{j\Omega}$ on the unit circle divided by the product of the vectors extending from the poles to the same point.

Example 6.18 The transfer function $H(z)$ of an LTI system has two zeros at $z = \pm j$ and poles at $z = 0.5e^{\pm j\pi/2}$ and $z = 0.5e^{\pm j3\pi/4}$. Evaluate the gain factor b_0 so that the system frequency response at $\Omega = 0$ be equal to 10.

Let u_1 and u_1^* be the vectors from the zeros to the point $z = 1$ on the unit circle, and let v_1 , v_1^* , v_2 , and v_2^* be the vectors extending from the poles to the same point $z = 1$, as shown in Fig. 6.20. We have

$$H(e^{j0}) = b_0 \frac{u_1 u_1^*}{v_1 v_1^* v_2 v_2^*} = b_0 \frac{|u_1|^2}{|v_1|^2 |v_2|^2} = \frac{b_0 (\sqrt{2})^2}{1.25 [(1 + \frac{0.5}{\sqrt{2}})^2 + (\frac{0.5}{\sqrt{2}})^2]} = 0.8175 b_0$$

$$b_0 = 10/0.8175 = 12.2324$$

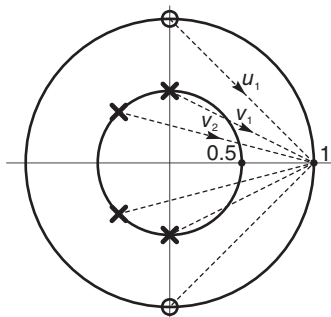


FIGURE 6.20 Geometric evaluation of frequency response.

6.14 Comb Filters

In general a comb filter adds to a signal a delayed replica thereof, leading to constructive and destructive interference. The resulting filter frequency response has in general uniformly spaced spikes; hence the name comb filter. Comb filters are used in anti-aliasing for interpolation and decimation sampling operations, 2-D and 3-D NTSC television decoders, and audio signal processing such as echo, flanging, and digital wave guide synthesis. Comb filters are either of the feedforward or feedback type and can be either analog or digital.

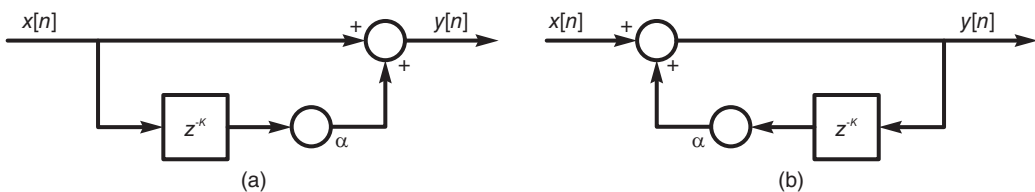


FIGURE 6.21 Comb filter model, (a) feedforward, (b) feedback.

In the feedforward form, the comb filter has the form shown in Fig. 6.21(a). We note that a delay of K samples is applied to the input sequence $x[n]$, followed by a weighting by a factor α . The output is given by

$$y[n] = x[n] + \alpha x[n - K] \tag{6.100}$$

$$Y(z) = X(z) + \alpha z^{-K} X(z) \tag{6.101}$$

$$H(z) = \frac{Y(z)}{X(z)} = 1 + \alpha z^{-K} = \frac{z^K + \alpha}{z^K} \tag{6.102}$$

The transfer function $H(z)$ has therefore a pole of order K at the origin and zeros given by

$$z^K = -\alpha = e^{j\pi} e^{j2m\pi} \alpha \tag{6.103}$$

$$z = \alpha^{1/K} e^{j(2m+1)\pi/K}, m = 0, 1, \dots, K - 1 \tag{6.104}$$

The pole-zero pattern is shown in Fig. 6.22(a) for the case $K = 8$, where the zeros can be seen to be uniformly spaced around a circle of radius $r = \alpha^{1/K}$.

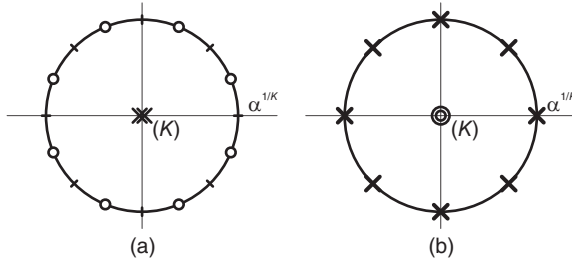


FIGURE 6.22 The pole-zero pattern of a comb filter, (a) feedforward, (b) feedback.

The magnitude and phase of the frequency response

$$H(e^{j\Omega}) = 1 + \alpha e^{-jK\Omega} \tag{6.105}$$

of such a comb filter, with $K = 8$ and $\alpha = 0.9$ can be seen in Fig. 6.23(a).

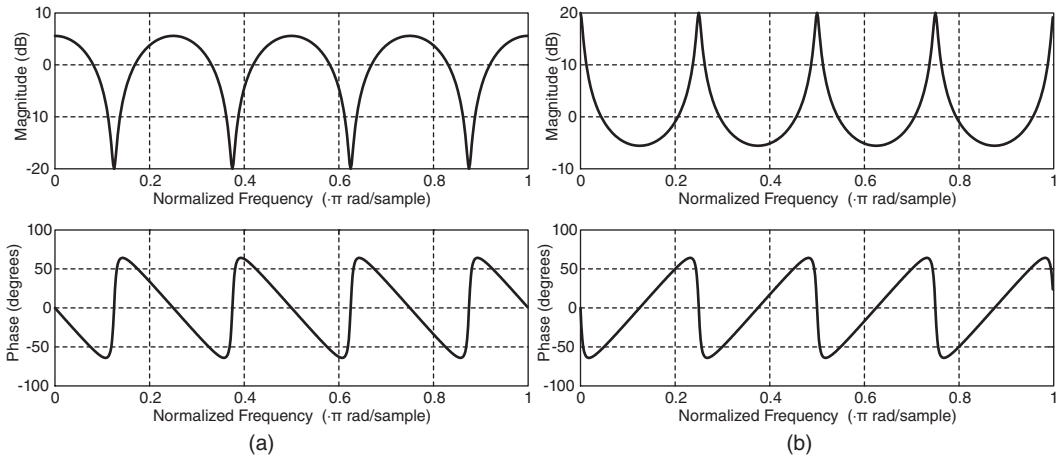


FIGURE 6.23 Magnitude and phase response of a comb filter, (a) feedforward, (b) feedback.

The feedback form of the comb filter is shown in Fig. 6.21(b). We may write

$$y[n] = x[n] + \alpha y[n - K] \tag{6.106}$$

$$Y(z) = X(z) + \alpha z^{-K} Y(z) \tag{6.107}$$

$$H(z) = \frac{Y(z)}{X(z)} = \frac{1}{1 - \alpha z^{-K}} = \frac{z^K}{z^K - \alpha} \tag{6.108}$$

In this case the transfer function has a zero of order K at the origin and K poles uniformly spaced around the unit circle. The poles are deduced from

$$z^K = \alpha e^{j2m\pi} \tag{6.109}$$

$$z = \alpha^{1/K} e^{j2m\pi/K}, m = 0, 1, \dots, K - 1 \tag{6.110}$$

as seen in Fig. 6.22(b) for the case $K = 8$. The magnitude and phase of the frequency response

$$H(e^{j\Omega}) = \frac{1}{1 - \alpha e^{-jK\Omega}} \quad (6.111)$$

are shown in Fig. 6.23(b).

6.15 Causality and Stability

Similarly to continuous-time systems a discrete-time system is causal if its impulse response $h[n]$ is zero for $n < 0$. It is stable if and only if

$$\sum_{n=-\infty}^{\infty} |h[n]| < \infty. \quad (6.112)$$

It is therefore stable if and only if

$$\sum_{n=-\infty}^{\infty} |h[n] z^{-n}| < \infty \quad (6.113)$$

and $|z| = 1$. In other words a system is stable if the Fourier transform, $H(e^{j\Omega})$ of its impulse response, that is, its frequency response, exists. If the system impulse response $h[n]$ is causal the Fourier transform $H(e^{j\Omega})$ exists, and the system is therefore stable, if and only if all the poles are inside the unit circle.

Example 6.19 For the system described by the linear difference equation

$$y[n] - 0.7y[n-1] + 2.25y[n-2] - 1.575y[n-3] = x[n]$$

evaluate the system function $H(z)$ and its conditions for causality and stability.

Transforming both sides we have

$$H(z) = \frac{Y(z)}{X(z)} = \frac{1}{1 - 0.7z^{-1} + 2.25z^{-2} - 1.575z^{-3}} = \frac{z^3}{(z^2 + 2.25)(z - 0.7)}.$$

The zeros and poles are shown in Fig. 6.24. We note that neither the difference equation nor the system function $H(z)$ implies a particular ROC, and thence whether or not the system is causal or stable. In fact there are three distinct possibilities for the ROC, namely, $|z| < 0.7$, $0.7 < |z| < 1.5$ and $|z| > 1.5$.

These correspond respectively to a left-sided, two-sided and right-sided impulse response. Since the system is stable if and only if the Fourier transform $H(e^{j\Omega})$ exists, only the second possibility, namely, the ROC $0.7 < |z| < 1.5$ corresponds to a stable system. In this case the system is stable but not causal. Note that the third possibility, $|z| > 1.5$, corresponds to a causal but unstable system.

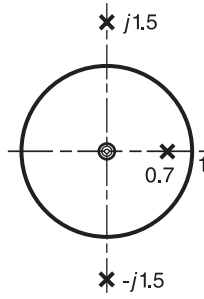


FIGURE 6.24 Poles and zeros in z -plane.

6.16 Delayed Response and Group Delay

An ideal lowpass filter has a frequency response $H(e^{j\Omega})$ defined by

$$H(e^{j\Omega}) = \begin{cases} 1, & |\Omega| < \Omega_c \\ 0, & \Omega_c < |\Omega| \leq \pi \end{cases} \tag{6.114}$$

and has zero phase

$$\arg[H(e^{j\Omega})] = 0. \tag{6.115}$$

The impulse response of this ideal filter is given by

$$h[n] = \frac{1}{2\pi} \int_{-\pi}^{\pi} H(e^{j\Omega}) e^{j\Omega n} d\Omega = \frac{1}{2\pi} \int_{-\Omega_c}^{\Omega_c} e^{j\Omega n} d\Omega = \frac{\sin(n\Omega_c)}{\pi n} = \frac{\Omega_c}{\pi} Sa(\Omega_c n). \tag{6.116}$$

The ideal lowpass filter is not realizable since the impulse response $h[n]$ is not causal. To obtain a realizable filter we can apply an approximation. If we shift the impulse response $h[n]$ to the right by M samples obtaining the impulse response $h[n - M]$, and if M is sufficiently large, most of the impulse response will be causal, and will be a close approximation of $h[n]$ except for the added delay.

An ideal filter with added delay M has the frequency response shown in Fig. 6.25.

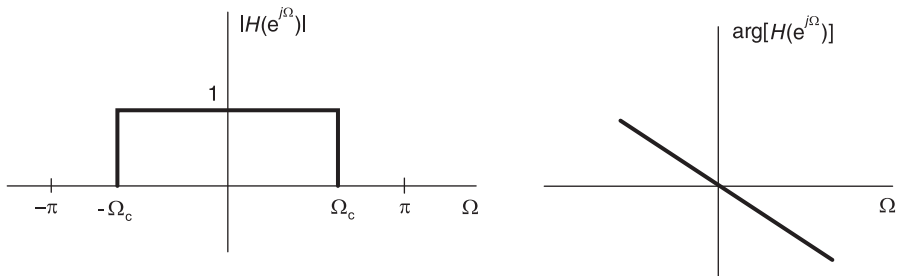


FIGURE 6.25 Ideal lowpass filter with linear phase.

Its frequency response $H(e^{j\Omega})$ is defined by

$$H(e^{j\Omega}) = \begin{cases} e^{-jM\Omega}, & |\Omega| < \Omega_c \\ 0, & \Omega_c < |\Omega| \leq \pi \end{cases} \quad (6.117)$$

that is,

$$|H(e^{j\Omega})| = \begin{cases} 1, & |\Omega| < \Omega_c \\ 0, & \Omega_c < |\Omega| \leq \pi \end{cases} \quad (6.118)$$

$$\arg[H(e^{j\Omega})] = -M\Omega, \quad |\Omega| < \pi \quad (6.119)$$

and its impulse response is

$$h[n] = \frac{\sin[(n-M)\Omega_c]}{\pi(n-M)}. \quad (6.120)$$

As shown in the figure, the resulting filter has a linear phase ($-M\Omega$) corresponding to the pure delay by M samples. Such a delay does not cause distortion to the signal and constitutes a practical solution to the question of causality and realizability of ideal filters.

Phase linearity is a quality that is often sought in the realization of continuous-time as well as digital filters. A measure of phase linearity is obtained by differentiating it, leading to a constant equal to the delay if the phase is truly linear. The measure is called the *group delay* and is defined as

$$\tau(\Omega) = -\frac{d}{d\Omega} [\arg[H(e^{j\Omega})]]. \quad (6.121)$$

Before differentiating the phase any discontinuities are eliminated first by adding integer multiples of π , thus leading to a phase $\arg[H(e^{j\Omega})]$ that is continuous without the discontinuities caused by crossing the boundary points $\pm\pi$ on the unit circle.

Example 6.20 For the first-order system of transfer function

$$H(z) = \frac{1}{1 - az^{-1}}$$

where a is real, evaluate the group delay of its frequency response.

We have

$$H(e^{j\Omega}) = \frac{1}{1 - ae^{-j\Omega}} = \frac{1 - ae^{j\Omega}}{1 - 2a \cos \Omega + a^2}$$

$$\arg[H(e^{j\Omega})] = \tan^{-1} \frac{-a \sin \Omega}{1 - a \cos \Omega}$$

$$\begin{aligned} \tau(\Omega) &= -\frac{d}{d\Omega} \left[\tan^{-1} \frac{-a \sin \Omega}{1 - a \cos \Omega} \right] \\ &= \frac{1}{1 + \left\{ \frac{a \sin \Omega}{1 - a \cos \Omega} \right\}^2} \frac{a [(1 - a \cos \Omega) \cos \Omega - a \sin^2 \Omega]}{(1 - a \cos \Omega)^2} = \frac{a \cos \Omega - a^2}{1 - 2a \cos \Omega + a^2}. \end{aligned}$$

6.17 Discrete-Time Convolution and Correlation

As seen above, the discrete convolution of two sequences $v[n]$ and $x[n]$ is given by

$$y[n] = \sum_{m=-\infty}^{\infty} v[m]x[n-m]. \quad (6.122)$$

The discrete correlation $r_{vx}[n]$ is given by

$$r_{vx}[n] = \sum_{m=-\infty}^{\infty} v[n+m]x[m]. \quad (6.123)$$

The same analytic and graphic approaches used in the convolution and correlation of continuous-time systems can be used in evaluating discrete convolutions and correlations. The approach is best illustrated by examples.

Example 6.21 Let $h[n] = e^{-0.1n}u[n]$, $x[n] = 0.1n R_N[n]$, where $R_N[n] = u[n] - u[n-N]$. Evaluate the convolution $y[n] = h[n] * x[n]$.

Analytic solution

$$\begin{aligned} y[n] &= \sum_{k=-\infty}^{\infty} x[k]h[n-k] \\ &= \sum_{k=-\infty}^{\infty} 0.1k \{u[k] - u[k-N]\} e^{-0.1(n-k)} u[n-k] \\ &= \left\{ \sum_{k=0}^n 0.1k e^{-0.1(n-k)} \right\} u[n] - \left\{ \sum_{k=N}^n 0.1k e^{-0.1(n-k)} \right\} u[n-N] \end{aligned}$$

i.e.

$$y[n] = \left\{ 0.1e^{-0.1n} \sum_{k=0}^n k e^{0.1k} \right\} u[n] - \left\{ 0.1e^{-0.1n} \sum_{k=N}^n k e^{0.1k} \right\} u[n-N].$$

Letting $a = e^{0.1}$ and using the Weighted Geometric Series (WGS) Sum $\mathcal{S}(a, n_1, n_2)$ as evaluated in the Appendix we may write

$$y[n] = \{0.1a^{-n} \mathcal{S}(a, 0, n)\} u[n] - \{0.1a^{-n} \mathcal{S}(a, N, n)\} u[n-N].$$

This expression can be simplified manually, using Mathematica® or MATLAB®.

In particular, the sum of a weighted geometric series can be coded as a the following MATLAB function:

```
function [summ] = wtdsum(a,n1,n2)
sum=0;
for k=n1:n2
sum=sum+k .* a ^k;
end
summ=sum;
```

The sequences $h[n]$, $x[n]$, $h[n-m]$ for $0 \leq n \leq N-1$, $h[n-m]$ for $0 \leq n \leq N-1$, $h[n-m]$ for $n \geq N$ and $y[n]$, respectively, are shown in Fig. 6.26 for the case $N = 50$.

Graphic Approach

For $n < 0$, $y[n] = 0$. For $0 \leq n \leq N-1$, $y[n] = \sum_{m=0}^n 0.1m e^{-0.1(n-m)}$.

For $n \geq N$, $y[n] = \sum_{m=0}^{N-1} 0.1m e^{-0.1(n-m)}$.

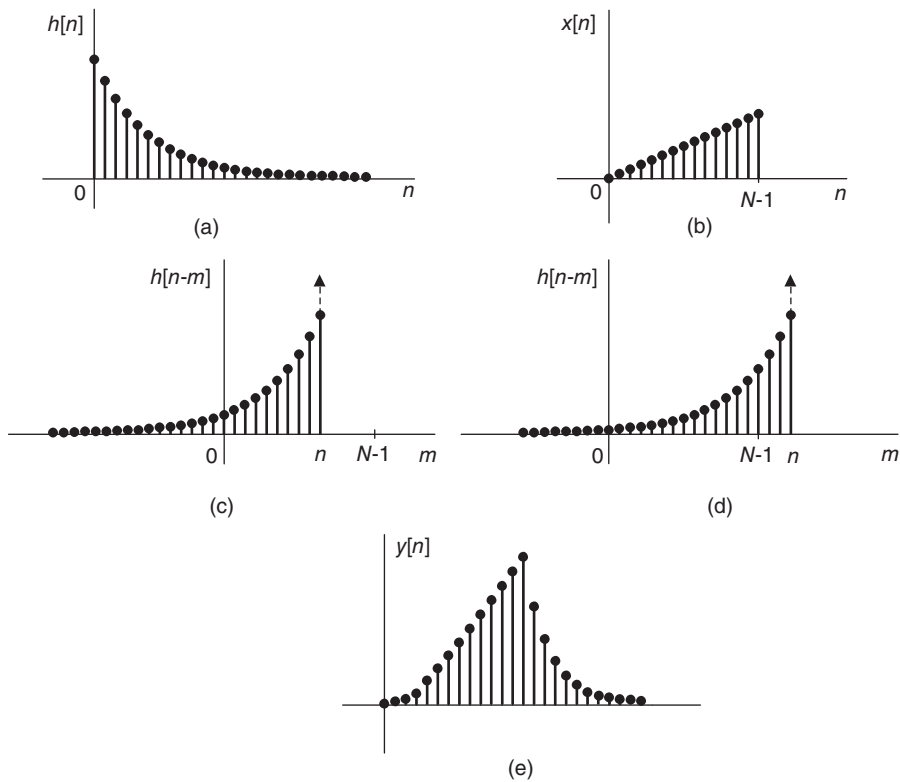


FIGURE 6.26 Convolution of two sequences.

6.18 Discrete-Time Correlation in One Dimension

The following example illustrates discrete correlation for one-dimensional signals followed by a faster approach to its analytic evaluation.

Example 6.22 Evaluate the cross-correlation $r_{xh}[n]$ of the two sequences $x[n] = u[n] - u[n - N]$ and $h[n] = e^{-\alpha n}u[n]$.

We start with the usual analytic approach. We have

$$r_{xh}[n] = \sum_{m=-\infty}^{\infty} \{u[n+m] - u[n+m-N]\} e^{-\alpha m} u[m]$$

$$u[m] u[n+m] \neq 0 \text{ iff } m \geq 0 \text{ and } m \geq -n$$

$$\text{i.e. } m \geq 0 \text{ if } 0 \geq -n \text{ or } n \geq 0$$

$$m \geq -n \text{ if } n \leq 0$$

$$u[n+m-N] u[m] \neq 0 \text{ iff } m \geq 0 \text{ and } m \geq N-n$$

$$\text{i.e. } m \geq 0 \text{ if } 0 \geq N-n \text{ or } n \geq N$$

$$m \geq N-n \text{ if } N-n \geq 0 \text{ or } n \leq N$$

$$r_{xh}[n] = \left\{ \sum_{m=0}^{\infty} e^{-\alpha m} \right\} u[n] + \left\{ \sum_{m=-n}^{\infty} e^{-\alpha m} \right\} u[-n-1] - \left\{ \sum_{m=0}^{\infty} e^{-\alpha m} \right\} u[n-N] - \left\{ \sum_{m=N-n}^{\infty} e^{-\alpha m} \right\} u[N-1-n].$$

The graphic approach proceeds with reference to Fig. 6.27(a-d):

For $-n + N - 1 < 0$ i.e. $n > N - 1$, $r_{xh}[n] = 0$.

For $-n + N - 1 \geq 0$ and $-n \leq 0$ i.e. $0 \leq n \leq N - 1$

$$r_{xh}[n] = \sum_{m=0}^{-n+N-1} e^{-\alpha m} = \frac{1 - e^{-\alpha(N-n)}}{1 - e^{-\alpha}}.$$

For $-n \geq 0$ i.e. $n \leq 0$, $r_{xh}[n] = \sum_{m=-n}^{-n+N-1} e^{-\alpha m} = e^{\alpha n} \frac{1 - e^{-\alpha N}}{1 - e^{-\alpha}}$.

The sequence $r_{xh}[n]$ is shown in Fig. 6.27(e) for the case $N = 50$.

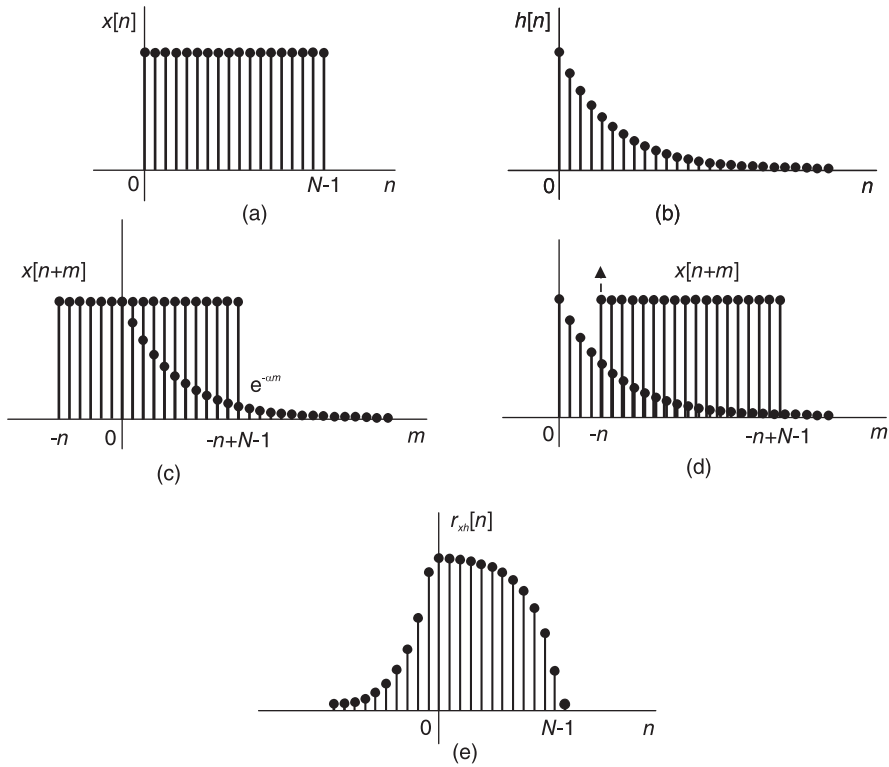


FIGURE 6.27 Cross-correlation of two sequences.

A Shortcut Analytic Approach

To avoid the decomposition of the correlation expression into four sums as just seen, a simpler shortcut approach consists of referring to the rectangular sequence $x[n]$ by the rectangle symbol R rather than decomposing it into the sum of two step functions.

To this end we define a mobile rectangular window $R_{n_0,N}[n]$, which starts at $n = n_0$ and is of duration N

$$R_{n_0,N}[n] = u[n - n_0] - u[n - (n_0 + N)].$$

Using this window we can write

$$\begin{aligned} r_{xh}[n] &= \sum_{m=-\infty}^{\infty} e^{-\alpha m} u[m] \{u[n+m] - u[n+m-N]\} \\ &= \sum_{m=-\infty}^{\infty} e^{-\alpha m} u[m] R_{-n,N}[m] \triangleq \sum_{m=-\infty}^{\infty} e^{-\alpha m} p. \end{aligned}$$

Referring to Fig. 6.27 we draw the following conclusions.

If $-n + N - 1 < 0$, $r_{xh}[n] = 0$.

If $-n \leq 0$ and $-n + N - 1 \geq 0$ i.e. $0 \leq n \leq N - 1$, the product $p \neq 0$ iff $0 \leq m \leq -n + N - 1$.

If $-n \geq 0$ i.e. $n \leq 0$ then $p \neq 0$ iff $-n \leq m \leq -n + N - 1$.

$$r_{xh}[n] = \left\{ \sum_{m=0}^{-n+N-1} e^{-\alpha m} \right\} \{u[n] - u[n-N]\} + \left\{ \sum_{m=-n}^{-n+N-1} e^{-\alpha m} \right\} u[-n-1].$$

Example 6.23 Evaluate the cross-correlation $r_{xv}[n]$ of the two sequences $x[n] = \beta n \{u[n] - u[n-N]\}$ and $v[n] = e^{-\alpha n} u[n]$.

The sequences are shown in Fig. 6.28(a) and (b), respectively.

$$r_{xv}(n) = \sum_{m=-\infty}^{\infty} \beta[n+m] \{u[n+m] - u[n+m-N]\} e^{-\alpha m} u[m].$$

Referring to Fig. 6.28(c) and (d) we may write

For $-n + N - 1 < 0$ i.e. $n > N - 1$, $r_{xv}(n) = 0$.

For $0 \leq -n + N - 1 \leq N - 1$ i.e. $0 \leq n \leq N - 1$

$$r_{xv}[n] = \sum_{m=0}^{N-n-1} e^{-\alpha m} \beta(n+m).$$

For $-n \geq 0$ i.e. $n \leq 0$

$$r_{xv}[n] = \sum_{m=-n}^{N-n-1} e^{-\alpha m} \beta(n+m).$$

Letting $a = e^{-\alpha}$ we can write this result using the WGS Sum $\mathcal{S}(a, n_1, n_2)$ evaluated in the Appendix. We obtain for $0 \leq n \leq N - 1$

$$\begin{aligned} r_{xv}[n] &= \beta n \left\{ \sum_{m=0}^{N-n-1} e^{-\alpha m} \right\} + \beta \left\{ \sum_{m=0}^{N-n-1} m e^{-\alpha m} \right\} \\ &= \beta n (1 - e^{-\alpha(N-n)}) / (1 - e^{-\alpha}) + \beta \mathcal{S}(a, 0, N - n - 1) \end{aligned}$$

and for $n \leq 0$

$$\begin{aligned} r_{xv}[n] &= \beta n \left\{ \sum_{m=-n}^{N-n-1} e^{-\alpha m} \right\} + \beta \left\{ \sum_{m=-n}^{N-n-1} m e^{-\alpha m} \right\} \\ &= \beta n e^{\alpha n} (1 - e^{-\alpha N}) / (1 - e^{-\alpha}) + \beta \mathcal{S}(a, -n, N - n - 1). \end{aligned}$$

The cross-correlation sequence $r_{xv}[n]$ is shown in Fig. 6.28(e). The result can be confirmed using the cross-correlation MATLAB command `xcorr(x,v)`.

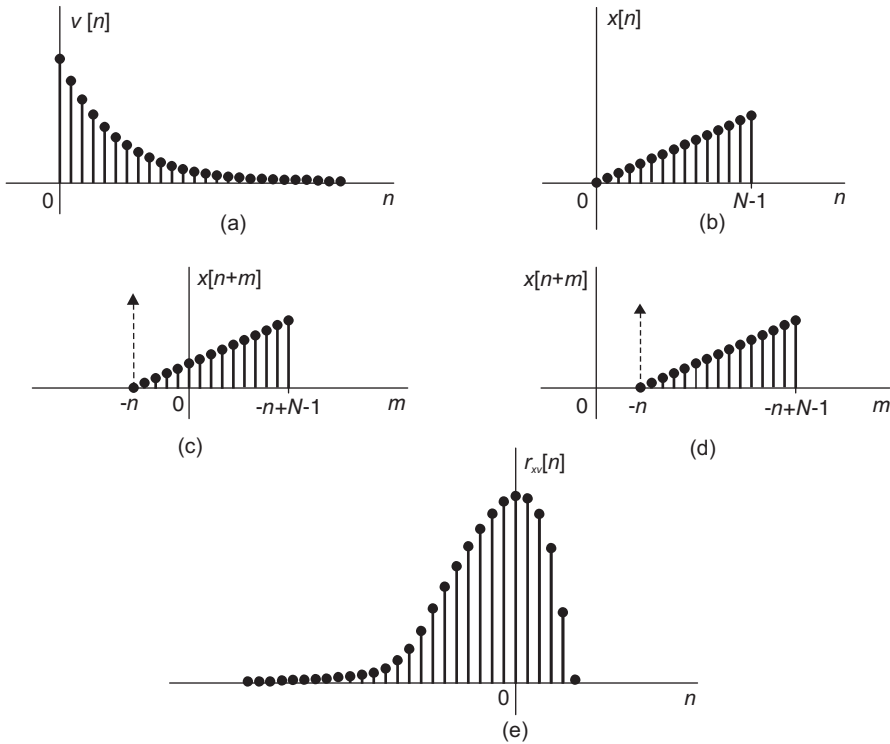


FIGURE 6.28 Discrete cross-correlation.

6.19 Convolution and Correlation as Multiplications

Given a finite duration sequence its z -transform is a polynomial in z^{-1} . The convolution in time of two finite duration sequences corresponds to multiplication of the two polynomials in the z -domain. As the following examples illustrate it is possible to use this property to evaluate convolutions and correlations as simple spatial multiplications.

Example 6.24 Evaluate the convolution $z[n]$ of the two sequences defined by: $x[n] = \{2, 3, 4\}$ and $y[n] = \{1, 2, 3\}$, for $n = 0, 1, 2$ and zero elsewhere.

The following multiplication structure evaluates the convolution, where x_k stands for $x[k]$ and y_k stands for $y[k]$. As in hand multiplication, each value $z[k]$ is deduced by adding the elements above it. The result is $z[n] = \{2, 7, 16, 17, 12\}$, for $n = 0, 1, 2, 3, 4$, respectively.

$$\begin{array}{r}
 x[2] \ x[1] \ x[0] \\
 y[2] \ y[1] \ y[0] \\
 \hline
 y_0x_2 \ y_0x_1 \ y_0x_0 \\
 y_1x_2 \ y_1x_1 \ y_1x_0 \\
 \hline
 y_2x_2 \ y_2x_1 \ y_2x_0 \\
 \hline
 z[4] \ z[3] \ z[2] \ z[1] \ z[0]
 \end{array}$$

Example 6.25 Evaluate the correlation $r_{vx}[n]$ of the two sequences defined by: $v[n] = \{1, 2, 3\}$ and $x[n] = \{2, 3, 4\}$, for $n = 0, 1, 2$ and zero elsewhere.

The following multiplication structure evaluates the correlation, where again v_k stands for $v[k]$ and x_k stands for $x[k]$.

$$\begin{array}{r}
 \begin{array}{ccc}
 x[2] & x[1] & x[0] \\
 v[0] & v[1] & v[2]
 \end{array} \\
 \hline
 \begin{array}{ccc}
 v_2x_2 & v_2x_1 & v_2x_0 \\
 v_1x_2 & v_1x_1 & v_1x_0 \\
 v_0x_2 & v_0x_1 & v_0x_0
 \end{array} \\
 \hline
 r_{vx}[-2] & r_{vx}[-1] & r_{vx}[0] & r_{vx}[1] & r_{vx}[2]
 \end{array}$$

The result is $r_{vx}[n] = 4, 11, 20, 13, 6$, for $n = -2, -1, 0, 1, 2$, respectively.

6.20 Response of a Linear System to a Sinusoid

As with continuous-time systems if the input to a discrete-time linear system of transfer function $H(z)$ is

$$x[n] = A \sin(\beta n + \theta) \tag{6.124}$$

then the system output can be shown to be given by

$$y[n] = A |H(e^{j\beta})| \sin(\beta n + \theta + \arg[H(e^{j\beta})]) \tag{6.125}$$

6.21 Notes on the Cross-Correlation of Sequences

Given two real energy sequences $x[n]$ and $y[n]$, that is, sequences of finite energy, the cross-correlation of x and y may be written in the form

$$r_{xy}[k] = \sum_{n=-\infty}^{\infty} x[n+k]y[n], \quad k = 0, \pm 1, \pm 2, \dots \tag{6.126}$$

The symbol $r_{xy}[k]$ stands for the cross-correlation of x with y at a ‘lag’ k , and the lag or shift k is an integer which has values extending from $-\infty$ to ∞ . The autocorrelation $r_{xx}[k]$ has the same expression as $r_{xy}[k]$ with y replaced by x . Similarly to continuous-time signals, it is easy to show that

$$r_{yx}[k] = r_{xy}[-k] \tag{6.127}$$

and that the correlation may be written as a convolution :

$$r_{xy}[k] = x[k] * y[-k] \tag{6.128}$$

Moreover, for power sequences of infinite energy but finite power, the cross-correlation is written

$$r_{xy}[k] = \lim_{M \rightarrow \infty} \frac{1}{2M+1} \sum_{n=-M}^M x[n+k]y[n] \tag{6.129}$$

and the autocorrelation $r_{xx}[k]$ is this same expression with y replaced by x .

6.22 LTI System Input/Output Correlation Sequences

Consider the relation between the input and output correlations of an LTI system receiving an input sequence $x[n]$ and producing a response $y[n]$, as shown in Fig. 6.29.

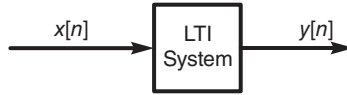


FIGURE 6.29 Input and output of an LTI system.

We have

$$y[n] = h[n] * x[n] = \sum_{m=-\infty}^{\infty} h[m]x[n - m] \quad (6.130)$$

$$r_{yx}[k] = y[k] * x[-k] = h[k] * x[k] * x[-k] = h[k] * r_{xx}[k] \quad (6.131)$$

This relation may be represented as shown in Fig. 6.30, where the input is $r_{xx}[k]$, the LTI system unit pulse response is $h[k]$ and the system produces the input–output cross-correlation $r_{yx}[k]$. The index k can also be replaced by n , the usual time sequence index.

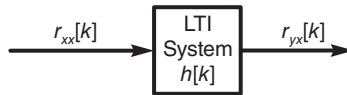


FIGURE 6.30 Correlations at input and output of an LTI system.

Moreover, if we replace k by $-k$ in Equation (6.131) we obtain, using Equation (6.127)

$$r_{xy}[k] = h[-k] * r_{xx}[k]. \quad (6.132)$$

The autocorrelation of the output is similarly found by replacing x by y . We have

$$r_{yy}[k] = y[k] * y[-k] = h[k] * x[k] * h[-k] * x[-k] = r_{hh}[k] * r_{xx}[k] = \sum_{m=-\infty}^{\infty} r_{hh}[m]r_{xx}[k - m].$$

The energy of the output sequence is given by

$$\sum_{n=-\infty}^{\infty} y[n]^2 = r_{yy}[0] = \sum_{m=-\infty}^{\infty} r_{hh}[m]r_{xx}[m] \quad (6.133)$$

wherein the autocorrelation $r_{hh}[k]$ of the unit step response exists if and only if the system is stable.

6.23 Energy and Power Spectral Density

The energy of a sequence $x[n]$, if finite, is given by

$$E_x = \sum_{n=-\infty}^{\infty} |x[n]|^2. \quad (6.134)$$

We may write

$$E_x = \sum_{n=-\infty}^{\infty} x[n]x^*[n] = \sum_{n=-\infty}^{\infty} x[n] \frac{1}{2\pi} \int_{-\pi}^{\pi} X^*(e^{j\Omega})e^{-j\Omega n} d\Omega \quad (6.135)$$

$$= \frac{1}{2\pi} \int_{-\pi}^{\pi} X^*(e^{j\Omega}) \sum_{n=-\infty}^{\infty} x[n]e^{-j\Omega n} d\Omega = \frac{1}{2\pi} \int_{-\pi}^{\pi} |X(e^{j\Omega})|^2 d\Omega \quad (6.136)$$

Similarly to the case of continuous-time signals the “energy spectral density” is by definition

$$S_{xx}(\Omega) = |X(e^{j\Omega})|^2 \quad (6.137)$$

so that the energy is given by

$$E_x = \frac{1}{2\pi} \int_{-\pi}^{\pi} S_{xx}(\Omega) d\Omega. \quad (6.138)$$

A periodic sequence $x[n]$ of period N has infinite energy. Its average power is by definition

$$P_x = \frac{1}{N} \sum_{n=0}^{N-1} |x[n]|^2. \quad (6.139)$$

We may write

$$P_x = \frac{1}{N} \sum_{n=0}^{N-1} x[n] \frac{1}{N} \sum_{k=0}^{N-1} X^*[k]e^{-\frac{j2\pi k n}{N}} = \frac{1}{N^2} \sum_{k=0}^{N-1} X^*[k] \sum_{n=0}^{N-1} x[n]e^{-\frac{j2\pi k n}{N}} = \frac{1}{N^2} \sum_{k=0}^{N-1} |X[k]|^2$$

and the energy of $x[n]$ over one period is $E = NP_x$. The “power spectral density” of the sequence $x[n]$ may be defined as

$$P_{xx}[k] = |X[k]|^2. \quad (6.140)$$

6.24 Two-Dimensional Signals

Let $x[n_1, n_2]$ be a two-dimensional sequence representing an image, two-dimensional data or any other signal. The z -transform of the sequence is given by

$$X(z_1, z_2) = \sum_{n_1=-\infty}^{\infty} \sum_{n_2=-\infty}^{\infty} x[n_1, n_2] z_1^{-n_1} z_2^{-n_2}. \quad (6.141)$$

In polar notation $z_1 = r_1 e^{j\Omega_1}$, $z_2 = r_2 e^{j\Omega_2}$,

$$X(r_1 e^{j\Omega_1}, r_2 e^{j\Omega_2}) = \sum_{n_1=-\infty}^{\infty} \sum_{n_2=-\infty}^{\infty} x[n_1, n_2] r_1^{-n_1} r_2^{-n_2} e^{-j\Omega_1 n_1} e^{-j\Omega_2 n_2}. \quad (6.142)$$

If $r_1 = r_2 = 1$ we have the two-dimensional Fourier transform

$$X(e^{j\Omega_1}, e^{j\Omega_2}) = \sum_{n_1=-\infty}^{\infty} \sum_{n_2=-\infty}^{\infty} x[n_1, n_2] e^{-j\Omega_1 n_1} e^{-j\Omega_2 n_2}. \quad (6.143)$$

Convergence:

The z -transform converges if

$$\sum_{n_1=-\infty}^{\infty} \sum_{n_2=-\infty}^{\infty} |x[n_1, n_2] z_1^{-n_1} z_2^{-n_2}| < \infty. \quad (6.144)$$

The inverse transform is given by

$$x[n_1, n_2] = \left(\frac{1}{2\pi j}\right)^2 \oint_{C_1} \oint_{C_2} X(z_1, z_2) z_1^{n_1-1} z_2^{n_2-1} dz_1 dz_2 \quad (6.145)$$

where the contours C_1 and C_2 are closed contours encircling the origin and lie in the ROC of the integrands. The inverse Fourier transform is written

$$x[n_1, n_2] = \left(\frac{1}{2\pi}\right)^2 \int_{-\pi}^{\pi} \int_{-\pi}^{\pi} X(e^{j\Omega_1}, e^{j\Omega_2}) e^{j\Omega_1 n_1} e^{j\Omega_2 n_2} d\Omega_1 d\Omega_2. \quad (6.146)$$

If a sequence is separable, i.e.

$$x[n_1, n_2] = x_1[n_1] x_2[n_2] \quad (6.147)$$

then

$$X(z_1, z_2) = X_1(z_1) X_2(z_2) \quad (6.148)$$

since

$$X(z_1, z_2) = \sum_{n_1} \sum_{n_2} x_1[n_1] x_2[n_2] z_1^{-n_1} z_2^{-n_2} = \sum_{n_1} x_1[n_1] z_1^{-n_1} \sum_{n_2} x_2[n_2] z_2^{-n_2}. \quad (6.149)$$

Properties

If

$$x[n_1, n_2] \longleftrightarrow X(z_1, z_2) \quad (6.150)$$

then

$$x[n_1 + m, n_2 + k] \longleftrightarrow z_1^m z_2^k X(z_1, z_2) \quad (6.151)$$

$$a^{n_1} b^{n_2} x[n_1, n_2] \longleftrightarrow X(a^{-1} z_1, b^{-1} z_2) \quad (6.152)$$

$$n_1 n_2 x[n_1, n_2] \longleftrightarrow \frac{d^2 X(z_1, z_2)}{dz_1 dz_2} \quad (6.153)$$

$$x^*[n_1, n_2] \longleftrightarrow X^*(z_1^*, z_2^*) \quad (6.154)$$

$$x[-n_1, -n_2] \longleftrightarrow X(z_1^{-1}, z_2^{-1}) \tag{6.155}$$

$$x[n_1, n_2] * y[n_1, n_2] \longleftrightarrow X(z_1, z_2)Y(z_1, z_2) \tag{6.156}$$

$$x[n_1, n_2]y[n_1, n_2] \longleftrightarrow \left(\frac{1}{2\pi j}\right)^2 \oint_{C_1} \oint_{C_2} X\left(\frac{z_1}{w_1}, \frac{z_2}{w_2}\right)Y(w_1)w_1^{-1}w_2^{-1}dw_1dw_2. \tag{6.157}$$

A two-dimensional system having input $x[n_1, n_2]$ and output $y[n_1, n_2]$ may be described by a difference equation of the general form

$$\sum_{k=0}^M \sum_{m=0}^N a_{km}y[n_1 - k, n_2 - m] = \sum_{k=0}^P \sum_{m=0}^Q b_{km}x[n_1 - k, n_2 - m]. \tag{6.158}$$

The system function $H(z)$ may be evaluated by applying the z -transform, obtaining

$$\sum_{k=0}^M \sum_{m=0}^N a_{km}z_1^{-k}z_2^{-m}Y(z_1, z_2) = \sum_{k=0}^P \sum_{m=0}^Q b_{km}z_1^{-k}z_2^{-m}X(z_1, z_2) \tag{6.159}$$

wherefrom

$$H(z_1, z_2) = \frac{Y(z_1, z_2)}{X(z_1, z_2)} = \frac{\sum_{k=0}^P \sum_{m=0}^Q b_{km}z_1^{-k}z_2^{-m}}{\sum_{k=0}^M \sum_{m=0}^N a_{km}z_1^{-k}z_2^{-m}}. \tag{6.160}$$

Examples of basic two-dimensional sequences follow.

Impulse

The 2-D impulse is defined by

$$\delta[n_1, n_2] = \begin{cases} 1, & n_1 = n_2 = 0 \\ 0, & \text{otherwise.} \end{cases} \tag{6.161}$$

The impulse is represented graphically in Fig. 6.31(a).

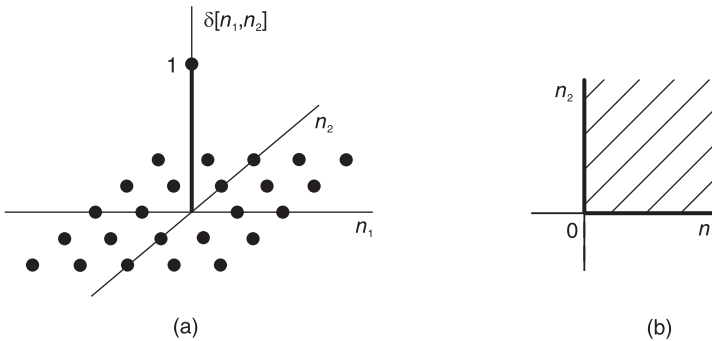


FIGURE 6.31 (a) Two-dimensional impulse, (b) representation of unit step 2-D sequence.

Unit Step 2-D Sequence

$$u[n_1, n_2] = \begin{cases} 1, & n_1, n_2 \geq 0 \\ 0, & \text{otherwise.} \end{cases} \tag{6.162}$$

In what follows, the area in the $n_1 - n_2$ plane wherein a sequence is non-nil will be hatched. The unit step function is non-nil, equal to 1 in the first quarter of the plane. Its support being the first quarter plane, we may represent it graphically, as depicted in Fig. 6.31(b).

Causal Exponential

$$x[n_1, n_2] = \begin{cases} a_1^{n_1} a_2^{n_2}, & n_1, n_2 \geq 0 \\ 0, & \text{otherwise.} \end{cases} \quad (6.163)$$

Complex Exponential

$$x[n_1, n_2] = e^{j(\Omega_1 n_1 + \Omega_2 n_2)}, \quad -\infty \leq n_1 \leq \infty, \quad -\infty \leq n_2 \leq \infty. \quad (6.164)$$

Sinusoid

$$x[n_1, n_2] = \sin(\Omega_1 n_1 + \Omega_2 n_2). \quad (6.165)$$

6.25 Linear Systems, Convolution and Correlation

Similarly to one-dimensional systems the system impulse response $h[n_1, n_2]$ is the inverse z -transform of the system transfer function $H(z_1, z_2)$. The system response is the convolution of the input $x[n_1, n_2]$ with the impulse response.

$$y[n_1, n_2] = x[n_1, n_2] * h[n_1, n_2] = \sum_{m_1=-\infty}^{\infty} \sum_{m_2=-\infty}^{\infty} h[m_1, m_2] x[n_1 - m_1, n_2 - m_2].$$

The correlation of two 2-D sequences $x[n_1, n_2]$ and $y[n_1, n_2]$ is defined by

$$r_{xy}[n_1, n_2] = x[n_1, n_2] \star y[n_1, n_2] = \sum_{m_1=-\infty}^{\infty} \sum_{m_2=-\infty}^{\infty} x[n_1 + m_1, n_2 + m_2] y[m_1, m_2].$$

The convolution and correlation of images and in general two-dimensional sequences are best illustrated by examples.

Example 6.26 Evaluate the convolution $z[n_1, n_2]$ of the two sequences

$$x[n_1, n_2] = e^{-\alpha(n_1+n_2)} u[n_1, n_2]$$

$$y[n_1, n_2] = e^{-\beta(n_1+n_2)} u[n_1, n_2].$$

The sequences $x[n_1, n_2]$ and $y[n_1, n_2]$ are represented graphically by hatching the region in the $n_1 - n_2$ plane wherein they are non-nil. The two sequences are thus represented by the hatched regions in Fig. 6.32(a) and (b).

Let

$$p[m_1, m_2] = e^{-\alpha(m_1+m_2)} e^{-\beta(n_1-m_1+n_2-m_2)}.$$

We have

$$z[n_1, n_2] = \sum_{m_1=-\infty}^{\infty} \sum_{m_2=-\infty}^{\infty} p[m_1, m_2] u[m_1, m_2] u[n_1 - m_1, n_2 - m_2].$$

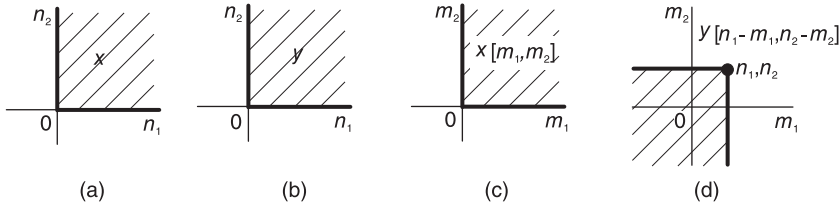


FIGURE 6.32 Convolution of 2-D sequences.

The analytic solution is obtained by noticing that the product of the step functions is non-nil if and only if

$$m_1 \geq 0, \quad m_2 \geq 0, \quad m_1 \leq n_1, \quad m_2 \leq n_2, \quad \text{i.e. } n_1 \geq 0, \quad n_2 \geq 0$$

wherefrom

$$z[n_1, n_2] = \sum_{m_1=0}^{n_1} \sum_{m_2=0}^{n_2} p[m_1, m_2] u[n_1, n_2].$$

Simplifying we obtain

$$\begin{aligned} z[n_1, n_2] &= \left\{ e^{-\beta(n_1+n_2)} \sum_{m_1=0}^{n_1} e^{(\beta-\alpha)m_1} \sum_{m_2=0}^{n_2} e^{(\beta-\alpha)m_2} \right\} u[n_1, n_2] \\ &= e^{-\beta(n_1+n_2)} \frac{\{1 - e^{-(\alpha-\beta)(n_1+1)}\} \{1 - e^{-(\alpha-\beta)(n_2+1)}\}}{\{1 - e^{-(\alpha-\beta)}\}^2} u[n_1, n_2]. \end{aligned}$$

The graphic solution is obtained by referring to Fig. 6.32(c) and (d). Similarly to the one-dimensional sequences case, the sequence $x[m_1, m_2]$ is shown occupying the first quarter of the $m_1 - m_2$ plane, while the sequence $y[n_1 - m_1, n_2 - m_2]$ is a folding around the point of origin of the sequence $y[m_1, m_2]$ followed by a displacement of the point of origin, referred to as the ‘mobile axis’, shown in the figure as an enlarged dot, to the point n_1, n_2 in the $m_1 - m_2$ plane. The figure shows that if $n_1 < 0$ or $n_2 < 0$ then $z[n_1, n_2] = 0$. If $n_1 \geq 0$ and $n_2 \geq 0$ then

$$z[n_1, n_2] = \sum_{m_1=0}^{n_1} \sum_{m_2=0}^{n_2} p[m_1, m_2]$$

in agreement with the results obtained analytically.

Example 6.27 Let a system impulse response be the causal exponential

$$h[n_1, n_2] = e^{-\alpha(n_1+n_2)} u[n_1, n_2]$$

and the input be an L-shaped image of width N , namely,

$$x[n_1, n_2] \triangleq L_N[n_1, n_2] \triangleq u[n_1, n_2] - u[n_1 - N, n_2 - N].$$

Evaluate the system output $y[n_1, n_2]$.

The non-nil regions of the sequences, respectively, are shown in Fig. 6.33(a) and (b). In what follows, for simplifying the expressions, we shall write

$$p \equiv p[m_1, m_2] = e^{-\alpha(m_1+m_2)}$$

where we use alternatively the symbols p or $p[m_1, m_2]$. We have

$$y[n_1, n_2] = \sum_{m_1=-\infty}^{\infty} \sum_{m_2=-\infty}^{\infty} p u[m_1, m_2] \{u[n_1 - m_1, n_2 - m_2] - u[n_1 - m_1 - N, n_2 - m_2 - N]\}.$$

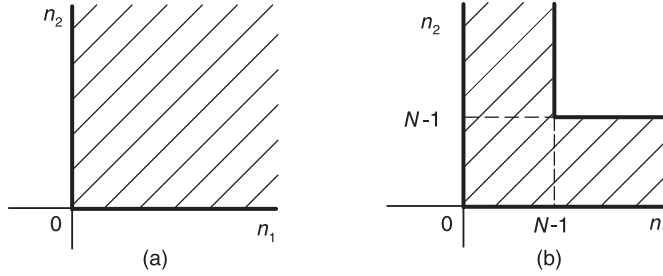


FIGURE 6.33 Two 2-D sequences.

Analytic approach:

The analytic approach, redefining the limits of summation based on the range of variable values for which the products of step functions are non-nil, shows that

$$y[n_1, n_2] = \left\{ \sum_{m_1=0}^{n_1} \sum_{m_2=0}^{n_2} p u[n_1, n_2] \right\} - \left\{ \sum_{m_1=0}^{n_1-N} \sum_{m_2=0}^{n_2-N} p u[n_1 - N, n_2 - N] \right\} \\ = S_1 u[n_1, n_2] - S_2 u[n_1 - N, n_2 - N]$$

where

$$S_1 = \frac{(1 - e^{-\alpha(n_1+1)}) (1 - e^{-\alpha(n_2+1)})}{(1 - e^{-\alpha})^2}, \quad S_2 = \frac{\{1 - e^{-\alpha(n_1-N+1)}\} \{1 - e^{-\alpha(n_2-N+1)}\}}{(1 - e^{-\alpha})^2}.$$

Graphic approach:

As mentioned above, in the graphic approach the sequence $x[n_1, n_2]$ is folded about the point of origin and the point of origin becomes a mobile axis that has the coordinates (n_1, n_2) , dragging the folded quarter-plane to the point (n_1, n_2) in the $m_1 - m_2$ plane.

Referring to Fig. 6.34(a-c) we have

For $n_1 < 0$ or $n_2 < 0$, $y[n_1, n_2] = 0$.

The Region of Validity, $n_1 < 0$ and $n_2 < 0$, of this result will be denoted as the area A, covering all quarters except the first of the $n_1 - n_2$ plane, as shown in Fig. 6.35(a).

Referring again to Fig. 6.34(a-c) we deduce the following:

For $\{n_1 \geq 0$ and $0 \leq n_2 \leq N - 1\}$ or $\{n_2 \geq 0$ and $0 \leq n_1 \leq N - 1\}$ we have

$$y[n_1, n_2] = \sum_{m_1=0}^{n_1} \sum_{m_2=0}^{n_2} p[m_1, m_2] = \frac{(1 - e^{-\alpha(n_1+1)}) (1 - e^{-\alpha(n_2+1)})}{(1 - e^{-\alpha})^2}.$$

The region of validity of this result, namely, $\{n_1 \geq 0$ and $0 \leq n_2 \leq N - 1\}$ or $\{n_2 \geq 0$ and $0 \leq n_1 \leq N - 1\}$, is shown as the area B in Fig. 6.35(b).

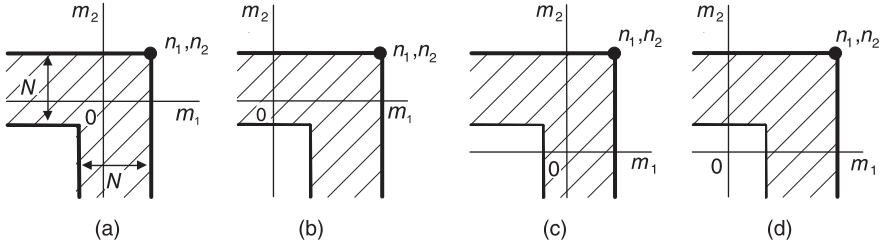


FIGURE 6.34 Convolution of two 2-D sequences.

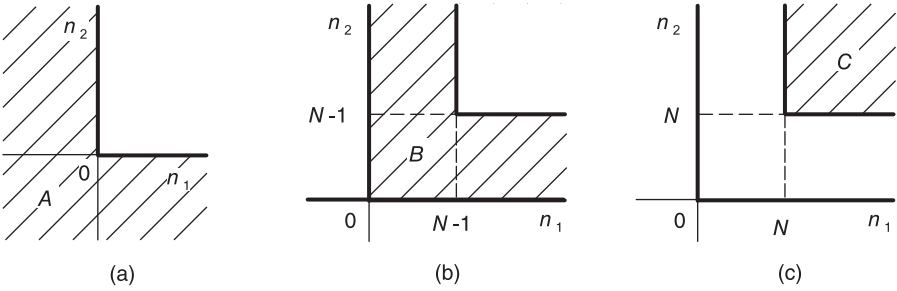


FIGURE 6.35 Regions of validity A, B, C of convolution expressions.

For the case $n_1 \geq N$ and $n_2 \geq N$, shown as the area C in Fig. 6.35(c) we have

$$y[n_1, n_2] = \sum_{m_1=n_1-N+1}^{n_1} \sum_{m_2=n_2-N+1}^{n_2} p + \sum_{m_1=n_1-N+1}^{n_1} \sum_{m_2=0}^{n_2-N} p + \sum_{m_2=n_2-N+1}^{n_2} \sum_{m_1=0}^{n_1-N} p$$

or, equivalently,

$$y[n_1, n_2] = \sum_{m_1=0}^{n_1} \sum_{m_2=0}^{n_2} p[m_1, m_2] - \sum_{m_1=0}^{n_1-N} \sum_{m_2=0}^{n_2-N} p[m_1, m_2].$$

The region of validity of this result, namely, $n_1 \geq N$ and $n_2 \geq N$, is shown as the Area C in Fig. 6.35(c). Combining these results we may write, corresponding to the region of validity B

$$y_B[n_1, n_2] = \sum_{m_1=0}^{n_1} \sum_{m_2=0}^{n_2} p[m_1, m_2] \{u[n_1, n_2] - u[n_1 - N, n_2 - N]\}$$

and for the region of validity C

$$y_C[n_1, n_2] = \left\{ \sum_{m_1=0}^{n_1} \sum_{m_2=0}^{n_2} p - \sum_{m_1=0}^{n_1-N} \sum_{m_2=0}^{n_2-N} p \right\} u[n_1 - N, n_2 - N]$$

so that the overall result may be written in the form

$$y[n_1, n_2] = y_B[n_1, n_2] + y_C[n_1, n_2].$$

6.26 Correlation of Two-Dimensional Signals

The cross-correlation of two continuous-domain images is written

$$r_{xy}(s, t) = \int_{-\infty}^{\infty} \int_{-\infty}^{\infty} x(s + \sigma, t + \tau) y(\sigma, \tau) d\sigma d\tau. \tag{6.166}$$

The cross-correlation of two discrete-domain 2-D sequences is written

$$r_{xy}[n_1, n_2] = \sum_{m_1=-\infty}^{\infty} \sum_{m_2=-\infty}^{\infty} x[n_1 + m_1, n_2 + m_2] y[m_1, m_2]. \tag{6.167}$$

Example 6.28 Evaluate the cross-correlation $r_{xh}[n_1, n_2]$ of the L-shaped sequence

$$x[n_1, n_2] = L_N[n_1, n_2] \triangleq u[n_1, n_2] - u[n_1 - N, n_2 - N]$$

and

$$h[n_1, n_2] = e^{-\alpha(n_1+n_2)} u[n_1, n_2].$$

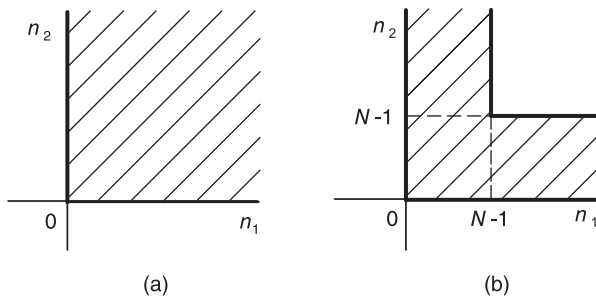


FIGURE 6.36 Two 2-D sequences.

The regions of nonzero values of the two sequences, respectively, are shown in Fig. 6.36. We may write

$$p \equiv p[m_1, m_2] = e^{-\alpha(m_1+m_2)}.$$

$$r_{xh}[n_1, n_2] = \sum_{m_1=-\infty}^{\infty} \sum_{m_2=-\infty}^{\infty} p u[m_1, m_2] \{u[n_1 + m_1, n_2 + m_2] - u[n_1 + m_1 - N, n_2 + m_2 - N]\}.$$

The graphic approach to the evaluation of the cross-correlation sequence is written with reference to Fig. 6.37(a-f).

In these figures the mobile axis is shown as the enlarged dot at $(-n_1, -n_2)$ in the $m_1 - m_2$ plane. The inner corner of the L-section has the coordinates $(-n_1 + N - 1, -n_2 + N - 1)$. Referring to Fig. 6.37(a) we can write:

For $-n_1 + N - 1 < 0$ and $-n_2 + N - 1 < 0$, i.e. $n_1 \geq N$ and $n_2 \geq N$, the region of validity A shown in Fig. 6.37(d), denoting the cross-correlation by $r_{xh,1}[n_1, n_2]$ we have

$$r_{xh,1}[n_1, n_2] = 0.$$

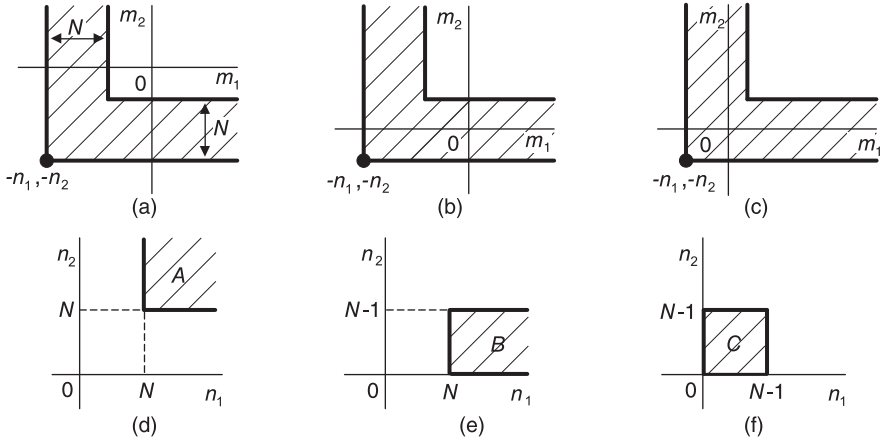


FIGURE 6.37 Cross-correlation of two 2-D sequences.

Referring to Fig. 6.37(b) we can write:

For $0 \leq -n_2 + N - 1 \leq N - 1$ and $-n_1 + N - 1 < 0$, i.e. $0 \leq n_2 \leq N - 1$ and $n_1 \geq N$, the region of validity B as in Fig. 6.37(e), we have

$$r_{xh}[n_1, n_2] = \sum_{m_1=0}^{\infty} \sum_{m_2=0}^{-n_2+N-1} p[m_1, m_1].$$

Given the region of validity of this expression we can rewrite it in the form

$$r_{xh,2}[n_1, n_2] = \sum_{m_1=0}^{\infty} \sum_{m_2=0}^{-n_2+N-1} p[m_1, m_1] \{u[n_1 - N, n_2] - u[n_1 - N, n_2 - N]\}.$$

Referring to Fig. 6.37(c) we can write:

For $0 \leq -n_1 + N - 1 \leq N - 1$ and $0 \leq -n_2 + N - 1 \leq N - 1$, i.e. $0 \leq n_1 \leq N - 1$ and $0 \leq n_2 \leq N - 1$, the region of validity C, Fig. 6.37(f), we have

$$r_{xh}[n_1, n_2] = \sum_{m_1=0}^{\infty} \sum_{m_2=0}^{-n_2+N-1} p[m_1, m_2] + \sum_{m_1=0}^{-n_1+N-1} \sum_{m_2=-n_2+N}^{\infty} p[m_1, m_2]$$

or equivalently

$$r_{xh}[n_1, n_2] = \sum_{m_1=0}^{\infty} \sum_{m_2=0}^{\infty} p[m_1, m_2] + \sum_{m_1=-n_1+N}^{\infty} \sum_{m_2=-n_2+N}^{\infty} p[m_1, m_2]$$

and given the region of validity of this expression we can rewrite it in the form

$$r_{xh,3}[n_1, n_2] = \left\{ \sum_{m_1=0}^{\infty} \sum_{m_2=0}^{\infty} p + \sum_{m_1=-n_1+N}^{\infty} \sum_{m_2=-n_2+N}^{\infty} p \right\} \cdot \{u[n_1, n_2] u[-n_1 + N - 1, -n_2 + N - 1]\}$$

wherein the product of step functions defines the region of validity as the area C in the $n_1 - n_2$ plane as required. Two subsequent steps are shown in Fig. 6.38(a-d).

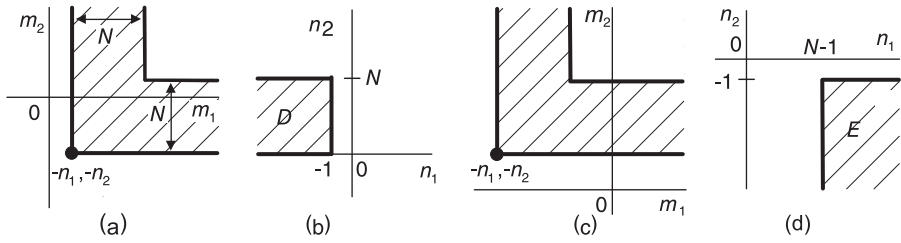


FIGURE 6.38 Correlation steps and corresponding regions of validity.

Referring to Fig. 6.38(a) we can write:

For $-n_1 > 0$ and $0 \leq -n_2 + N - 1 \leq N - 1$, i.e. $n_1 \leq -1$ and $0 \leq n_2 \leq N - 1$, the region of validity D , Fig. 6.38(b), we have

$$r_{xh,4}[n_1, n_2] = \left\{ \sum_{m_1=-n_1}^{\infty} \sum_{m_2=0}^{-n_2+N-1} p + \sum_{m_1=-n_1}^{-n_1+N-1} \sum_{m_2=-n_2+N}^{\infty} p \right\} \cdot \{u[-1-n_1, n_2] - u[-1-n_1, n_2-N]\}.$$

Referring to Fig. 6.38(c) we can write:

For $-n_2 > 0$ and $-n_1 + N - 1 < 0$, i.e. $n_1 \geq N$ and $n_2 \leq -1$, the region of validity E shown in Fig. 6.38(d), we have

$$r_{xh,5}[n_1, n_2] = \left\{ \sum_{m_1=0}^{\infty} \sum_{m_2=-n_2}^{-n_2+N-1} p[m_1, m_2] \right\} u[n_1 - N, -1 - n_2].$$

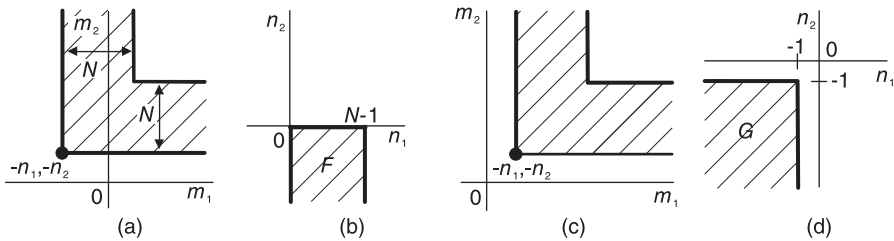


FIGURE 6.39 Correlation steps and corresponding regions of validity.

Referring to Fig. 6.39(a) we may write for the region of validity F shown in Fig. 6.39(b):

$$r_{xh,6}[n_1, n_2] = \left\{ \sum_{m_1=0}^{\infty} \sum_{m_2=-n_2}^{-n_2+N-1} p + \sum_{m_1=0}^{-n_1+N-1} \sum_{m_2=-n_2+N}^{\infty} p \right\} \cdot \{u[n_1, -1-n_2] - u[n_1-N, -1-n_2]\}.$$

Similarly, referring to Fig. 6.39(c) we may write

$$r_{xh,7}[n_1, n_2] = \left\{ \sum_{m_1=-n_1}^{\infty} \sum_{m_2=-n_2}^{\infty} p - \sum_{m_1=-n_1+N}^{\infty} \sum_{m_2=-n_2+N}^{\infty} p \right\} \cdot u[-1-n_1, -1-n_2].$$

which has the region of validity G shown in Fig. 6.39(d).

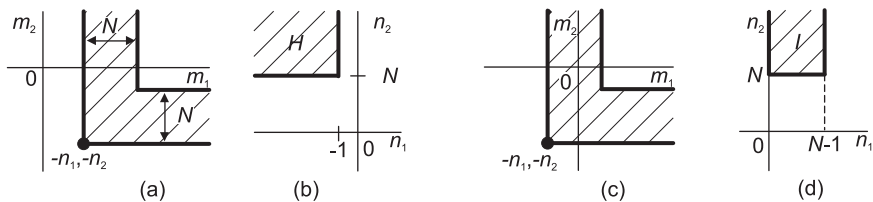


FIGURE 6.40 Correlation steps and regions of validity.

Referring to Fig. 6.40(a-d) we have
 For the region of validity H shown in Fig. 6.40(b):

$$r_{xh,8}[n_1, n_2] = \left\{ \sum_{m_1=-n_1}^{-n_1+N-1} \sum_{m_2=0}^{\infty} p[m_1, m_2] \right\} u[-1-n_1, n_2-N]$$

and over region I shown in Fig. 6.40(d)

$$r_{xh,9}[n_1, n_2] = \left\{ \sum_{m_1=0}^{-n_1+N-1} \sum_{m_2=0}^{\infty} p[m_1, m_2] \right\} \cdot \{u[n_1, n_2-N] - u[n_1-N, n_2-N]\}$$

and the cross-correlation over the entire $n_1 - n_2$ plane is given by

$$r_{xh}[n_1, n_2] = \sum_{i=1}^9 r_{xh,i}[n_1, n_2].$$

The regions of validity A, B, \dots, I , over the entire plane, of the cross-correlations $r_{xh,1}[n_1, n_2], r_{xh,2}[n_1, n_2], \dots, r_{xh,9}[n_1, n_2]$, are shown in Fig. 6.41.

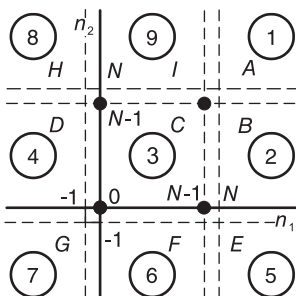


FIGURE 6.41 Correlation regions of validity.

6.27 IIR and FIR Digital Filters

A digital filter may be described by a difference equation of the form

$$\sum_{k=0}^N a_k y[n-k] = \sum_{k=0}^M b_k v[n-k] \quad (6.168)$$

where $a_0 = 1$, $v[n]$ is its input and $y[n]$ is its response. We can rewrite this equation in the form

$$y[n] = - \sum_{k=1}^N a_k y[n-k] + \sum_{k=0}^M b_k v[n-k]. \quad (6.169)$$

Applying the z -transform to the two sides of this equation we have

$$Y(z) = - \sum_{k=1}^N a_k z^{-k} Y(z) + \sum_{k=0}^M b_k z^{-k} V(z). \quad (6.170)$$

The filter transfer function is therefore given by

$$H(z) = \frac{Y(z)}{V(z)} = \frac{\sum_{k=0}^M b_k z^{-k}}{1 + \sum_{k=1}^N a_k z^{-k}} = \frac{b_0 + b_1 z^{-1} + b_2 z^{-2} + \dots + b_M z^{-M}}{1 + a_1 z^{-1} + a_2 z^{-2} + \dots + a_N z^{-N}}. \quad (6.171)$$

The impulse response $h[n]$ is the inverse z -transform of the the rational transfer function $H(z)$ and is therefore in general a sum of infinite-duration exponentials or time-weighted exponentials. It is for this reason that such filters are referred to as infinite impulse response (IIR) filters.

A finite impulse response (FIR) filter is a filter the impulse response of which is of finite duration. Such a filter is also called non-recursive as well as an all-zero filter. Since the impulse response $h[n]$ is of finite duration the transfer function $H(z)$ of an FIR filter has no poles, other than a multiple pole at the origin. The impulse response is often a truncation, or a windowed finite duration section, of an infinite impulse response $h_\infty[n]$. In such a case it is an approximation of an IIR filter. Let the input to the filter be $x[n]$ and its output be $y[n]$. We can write

$$H(z) = \sum_{n=0}^{N-1} h[n] z^{-n} \quad (6.172)$$

$$Y(z) = H(z)X(z) = \sum_{k=0}^{N-1} h[k] z^{-k} X(z) \quad (6.173)$$

$$y[n] = \sum_{k=0}^{N-1} h[k] x[n-k]. \quad (6.174)$$

In Chapter 11 we study different structures for the implementation of IIR and FIR filters.

6.28 Discrete-Time All-Pass Systems

As with continuous-time systems an allpass system has a magnitude spectrum that is constant for all frequencies. To be causal and stable the system’s poles should be inside the unit circle. Similarly to continuous-time systems every pole has an “image” which in the present case is reflected into the unit circle producing a zero outside the unit circle. In fact a pole $z = p_1$ and its conjugate $z = p_1^*$ are accompanied by their reflections, the zeros $z_1 = 1/p_1^*$ and $z_1^* = 1/p_1$, respectively. A pole $z = p_0$ where p_0 is real is accompanied by its reciprocal, the zero $z = 1/p_0$.

Such relations are illustrated for the case of a third order system with two complex conjugate poles and a real one in Fig. 6.42, where the poles p_1 , p_2 and p_3 are seen to be accompanied by the three zeros z_1 , z_2 and z_3 . To illustrate the evaluation of the system frequency response, the figure also shows vectors u_1 , u_2 and u_3 , extending from the zeros to an arbitrary point $z = e^{j\Omega}$ on the z -plane unit circle and vectors v_1 , v_2 and v_3 , extending from the poles to the same point.

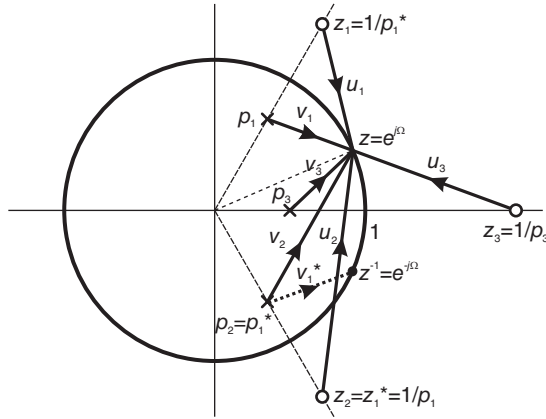


FIGURE 6.42 Vectors from poles and zeros to a point on unit circle.

The transfer function of a first order allpass system, having a single generally complex pole $z = p$, has the form

$$H(z) = \frac{z^{-1} - p^*}{1 - pz^{-1}} \tag{6.175}$$

An allpass system of a higher order is a cascade of such first order systems. The transfer function of the third order system shown in the figure is given by

$$H(z) = \frac{z^{-1} - p_1^*}{1 - p_1 z^{-1}} \frac{z^{-1} - p_2^*}{1 - p_2 z^{-1}} \frac{z^{-1} - p_3^*}{1 - p_3 z^{-1}} \tag{6.176}$$

where $p_2 = p_1^*$ and $p_3^* = p_3$. To show that the system is in fact allpass with $|H(e^{j\Omega})| = 1$ consider a single component, the i^{th} component, in the cascade. We may write

$$H_i(z) = \frac{z^{-1} - p_i^*}{1 - p_i z^{-1}} = \frac{1 - p_i^* z}{z - p_i} \tag{6.177}$$

Note that the vectors v_i , $i = 1, 2, 3$ in the figure are given by $v_i = e^{j\Omega} - p_i$. We may therefore write

$$H_i(e^{j\Omega}) = \frac{e^{-j\Omega} - p_i^*}{1 - p_i e^{-j\Omega}} = e^{j\Omega} \frac{v_i^*}{v_i} \quad (6.178)$$

wherefrom

$$|H_i(e^{j\Omega})| = 1. \quad (6.179)$$

The general expression of $H(z)$ may be written in the form

$$H(z) = \prod_{i=1}^n \frac{z^{-1} - p_i^*}{1 - p_i z^{-1}} \quad (6.180)$$

It is interesting to note that the transfer function of an allpass filter may be written in the form

$$H(z) = \frac{B(z)}{A(z)} = \frac{z^{-K} A(z^{-1})}{A(z)}. \quad (6.181)$$

Indeed, for a real pole the filter component has the form

$$H(z) = \frac{z^{-1} - p}{1 - pz^{-1}} \triangleq \frac{B(z)}{A(z)}$$

$$B(z) = z^{-1} - p = z^{-1}(1 - pz) = z^{-1}A(z^{-1}).$$

For two conjugate complex poles p_1 and $p_2 = p_1^*$ we have

$$H(z) = \frac{z^{-1} - p_1}{1 - p_1 z^{-1}} \frac{z^{-1} - p_2}{1 - p_2 z^{-1}} = \frac{B(z)}{A(z)}$$

$$A(z) = (1 - p_1 z^{-1})(1 - p_2 z^{-1})$$

$$B(z) = (z^{-1} - p_1)(z^{-1} - p_2) = z^{-2}(1 - p_1 z)(1 - p_2 z) = z^{-2}A(z^{-1}).$$

For a system of general order K , we have

$$H(z) = \prod_{i=1}^K \frac{z^{-1} - p_i}{1 - p_i z^{-1}} = \frac{B(z)}{A(z)} \quad (6.182)$$

$$A(z) = \prod_{i=1}^K (1 - p_i z^{-1}) \quad (6.183)$$

$$B(z) = \prod_{i=1}^K (z^{-1} - p_i) = z^{-K} \prod_{i=1}^K (1 - p_i z) = z^{-K} A(z^{-1}) \quad (6.184)$$

$$H(z) = \frac{z^{-K} A(z^{-1})}{A(z)}. \quad (6.185)$$

The allpass filter transfer function may thus be written in the form

$$H(z) = \prod_{i=1}^{n_1} \frac{z^{-1} - p_i}{1 - p_i z^{-1}} \prod_{i=1}^{n_2} \frac{b_i + a_i z^{-1} + z^{-2}}{1 + a_i z^{-1} + b_i z^{-2}} \quad (6.186)$$

where the first product covers the real poles and the second covers the complex conjugate ones. Equivalently the transfer function may be written in the form

$$H(z) = \frac{a_n + a_{n-1}z^{-1} + \dots + a_2z^{-(n-2)} + a_1z^{-(n-1)} + z^{-n}}{1 + a_1z^{-1} + a_2z^{-2} + \dots + a_{n-1}z^{-(n-1)} + a_nz^{-n}}. \quad (6.187)$$

Example 6.29 The transfer function of a system is given by

$$H(z) = \frac{1 - 0.3z^{-1}}{1 - 0.7z^{-1}}.$$

We need to obtain a cascade of the system with an allpass one, resulting in a transfer function $G(z) = H(z)H_{ap}(z)$ of a stable system. Evaluate $H_{ap}(z)$ and $G(z)$.

Since $G(z)$ should be the transfer function of a stable system, the pole $z = 0.7$ should be maintained. The allpass filter transfer function is given by

$$H_{ap}(z) = \frac{z^{-1} - 0.3}{1 - 0.3z^{-1}}$$

and

$$G(z) = H(z)H_{ap}(z) = \frac{z^{-1} - 0.3}{1 - 0.7z^{-1}}.$$

Since $|H_{ap}(e^{j\Omega})| = 1$, we have $|G(e^{j\Omega})| = |H(e^{j\Omega})|$. The poles and zeros of the three transfer functions are shown in Fig. 6.43(a-c), respectively.

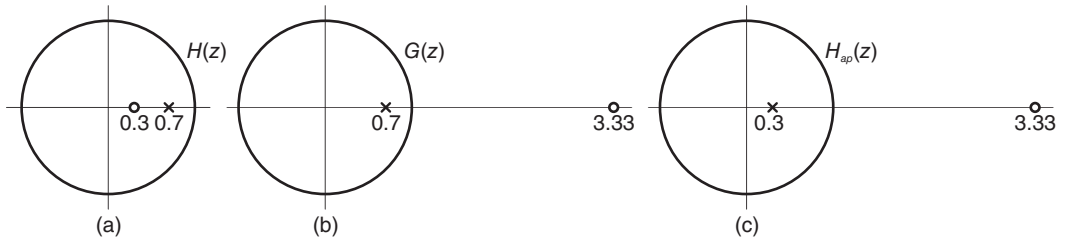


FIGURE 6.43 Poles and zeros of (a) $H(z)$, (b) $G(z)$ and (c) $H_{ap}(z)$.

Example 6.30 Evaluate the transfer function of an allpass filter given that its denominator polynomial is

$$A(z) = 1 - 0.75z^{-1} + 0.25z^{-2} - 0.1875z^{-3}.$$

The transfer function of the allpass filter is $H(z) = B(z)/A(z)$ where

$$B(z) = z^{-3}A(z^{-1}).$$

Hence

$$H(z) = \frac{-0.1875 + 0.25z^{-1} - 0.75z^{-2} + z^{-3}}{1 - 0.75z^{-1} + 0.25z^{-2} - 0.1875z^{-3}}.$$

Consider a first order component of an allpass filter

$$H(z) = \frac{z^{-1} - p^*}{1 - pz^{-1}} \tag{6.188}$$

With $p = re^{j\theta}$ the group delay of each such component is given by

$$\tau(\Omega) = \frac{1 - r^2}{|1 - re^{j\theta}e^{-j\Omega}|^2} > 0 \tag{6.189}$$

The group delay of a general order allpass filter is the sum of such expressions and is thus non-negative. Allpass filters are often employed for group delay equalization to counter phase nonlinearities. Cascading a filter with an allpass filter keeps the magnitude response unchanged. If the allpass filter has a pole that coincides with the filter's zero, the zero is canceled and the overall result is a flipping of the zero to its image at the conjugate location in the z -plane. As we shall see, such an approach is employed in designing minimum-phase systems.

6.29 Minimum-Phase and Inverse System

A system transfer function may be expressed in the form

$$H(z) = \frac{\sum_{k=0}^M b_k z^{-k}}{1 + \sum_{k=1}^N a_k z^{-k}} = K \frac{\prod_{k=1}^M (1 - z_k z^{-1})}{\prod_{k=1}^N (1 - p_k z^{-1})} \quad (6.190)$$

where z_k and p_k are the zeros and poles, respectively. A causal stable LTI system has all its poles p_k inside the unit circle. The zeros z_k may be inside or outside the unit circle. As with continuous-time systems, to be minimum phase the system function zeros must be inside the unit circle. A stable causal minimum phase system has a causal and stable inverse $G(z) = 1/H(z)$ since its poles and zeros also lie inside the unit circle. If the system is not minimum phase, that is, if it has zeros outside the unit circle, then the inverse system has poles outside the unit circle and is therefore not stable.

A causal stable LTI discrete-time system can always be expressed as the cascade of a minimum-phase system and an allpass system

$$H(z) = H_{\min}(z) H_{\text{ap}}(z). \quad (6.191)$$

To perform such factorization we start by defining $H_{\text{ap}}(z)$ as the transfer function which has each "offending" zero of $H(z)$, that is, each zero outside the unit circle, coupled with a pole at the reciprocal conjugate location. Each such zero z_k is thus combined with a pole p_k , with $z_k = 1/p_k^*$, producing the factor

$$\frac{z^{-1} - p_k^*}{1 - p_k z^{-1}} \quad (6.192)$$

The allpass $H_{\text{ap}}(z)$ is a product of such factors. The minimum phase transfer function $H_{\min}(z)$ has all its poles and zeros inside the unit circle and can be deduced as $H_{\min}(z) = H(z)/H_{\text{ap}}(z)$. The approach is analogous to that studied in the context of continuous-time systems, as the following example illustrates.

Example 6.31 Given the system function $H(z)$ depicted in Fig. 6.44 evaluate and sketch the poles and zeros in the z -plane of the corresponding system functions $H_{\min}(z)$ and $H_{\text{ap}}(z)$.

The cascade system components $H_{\text{ap}}(z)$ and $H_{\min}(z)$ are shown in Fig. 6.45. The figure shows that the zeros z_1 and z_1^* of $H_{\text{ap}}(z)$ are made equal to those of $H(z)$, and the poles q_1 and q_1^* of $H_{\text{ap}}(z)$ are deduced as the reflections of those zeros. $H_{\min}(z)$ has the two

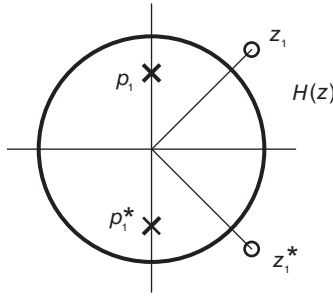


FIGURE 6.44 System’s poles and zeros.

poles p_1 and p_1^* of $H(z)$. The zeros ζ_1 and its conjugate ζ_1^* of $H_{min}(z)$ are then made to coincide in position with q_1 and q_1^* so that in the product $H_{ap}(z)H_{min}(z)$ the poles of $H_{ap}(z)$ cancel out with the zeros of $H_{min}(z)$, ensuring that $H_{ap}(z)H_{min}(z) = H(z)$. The resulting system function $H_{min}(z)$ is a minimum phase function, having its poles and zeros inside the unit circle, as desired.

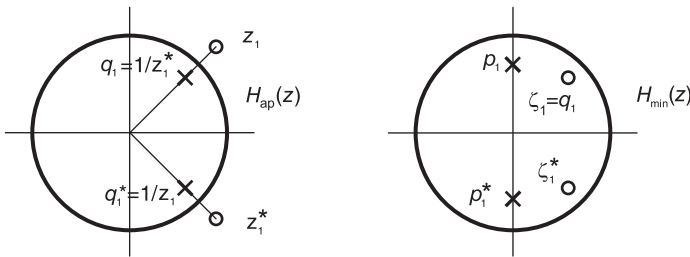


FIGURE 6.45 Allpass and minimum-phase components of a transfer function.

We can write

$$H(z) = \frac{(z - z_1)(z - z_1^*)}{(z - p_1)(z - p_1^*)}$$

$$H_{ap}(z) = \frac{(z^{-1} - q_1^*)(z^{-1} - q_1)}{(1 - q_1 z^{-1})(1 - q_1^* z^{-1})}$$

where $q_1 = 1/z_1^*$, $q_1^* = 1/z_1$ as shown in the figure.

$$H_{min}(z) = K \frac{(z - \zeta_1)(z - \zeta_1^*)}{(z - p_1)(z - p_1^*)}$$

where $\zeta_1 = 1/z_1^*$, $\zeta_1^* = 1/z_1$. Multiplying $H_{min}(z)$ by $H_{ap}(z)$ and equating the product to $H(z)$ we obtain $K = |z_1^2|$.

Given a desired magnitude response $|H(e^{j\Omega})|$ it is always possible to evaluate the corresponding minimum phase system function $H(z)$. We may write

$$H(z)H(z^{-1}) = H(e^{j\Omega})H(e^{-j\Omega})\Big|_{e^{j\Omega} \rightarrow z} = |H(e^{j\Omega})|^2\Big|_{e^{j\Omega} \rightarrow z} \tag{6.193}$$

By replacing $e^{j\Omega}$ by z in the magnitude squared response $|H(e^{j\Omega})|^2$ we thus obtain the function $F(z) = H(z)H(z^{-1})$. The required system function $H(z)$ is deduced by simply selecting thereof the poles and zeros which lie inside the unit circle. To thus factor the function $F(z) = H(z)H(z^{-1})$ into its two components $H(z)$ and $H(z^{-1})$ it would help to express it in the form

$$F(z) = H(z)H(z^{-1}) = K^2 \frac{\prod_{k=1}^M (1 - z_k z^{-1})(1 - z_k z)}{\prod_{k=1}^N (1 - p_k z^{-1})(1 - p_k z)}. \quad (6.194)$$

Example 6.32 Given the magnitude squared spectrum

$$|H(e^{j\Omega})|^2 = \frac{1.25 - \cos \Omega}{1.5625 - 1.5 \cos \Omega}$$

evaluate the corresponding minimum phase transfer function $H(z)$.

We can write

$$|H(e^{j\Omega})|^2 = H(e^{j\Omega})H(e^{-j\Omega}) = \frac{1.25 - (e^{j\Omega} + e^{-j\Omega})/2}{1.5625 - 1.5(e^{j\Omega} + e^{-j\Omega})/2}$$

$$F(z) = H(z)H(z^{-1}) = H(e^{j\Omega})H(e^{-j\Omega})|_{e^{j\Omega} \rightarrow z} = \frac{1.25 - 0.5(z + z^{-1})}{1.5625 - 0.75(z + z^{-1})}.$$

To identify the poles and zeros we note that the function $F(z)$ may be written in the form

$$F(z) = K^2 \frac{(1 - az^{-1})(1 - az)}{(1 - bz^{-1})(1 - bz)} = K^2 \frac{1 - a(z + z^{-1}) + a^2}{1 - b(z + z^{-1}) + b^2}$$

so that here a is a zero and b is a pole of $F(z)$. We deduce that $a = 0.5$, $b = 0.75$, $K = 1$ and the transfer function of the minimum phase system is given by

$$H(z) = \frac{1 - 0.5z^{-1}}{1 - 0.75z^{-1}}$$

having a pole and a zero inside the unit circle.

Example 6.33 Let

$$H(z) = (1 - 0.4z^{-1})(1 - 1.25z^{-1})$$

Evaluate $H_{ap}(z)$ and $H_{min}(z)$ so that

$$H(z) = H_{min}(z)H_{ap}(z), \quad H_{ap} = \frac{z^{-1} - 0.8}{(1 - 0.8z^{-1})}$$

$$H_{min}(z) = \frac{H(z)}{H_{ap}(z)} = \frac{(1 - 0.4z^{-1})(1 - 1.25z^{-1})(1 - 0.8z^{-1})}{(z^{-1} - 0.8)} = 1.25(1 - 0.4z^{-1})(1 - 0.8z^{-1})$$

as can be seen in Fig. 6.46. We note that the impulse response $h[n]$ of this filter is of a finite length; hence the name finite impulse response or FIR filter.

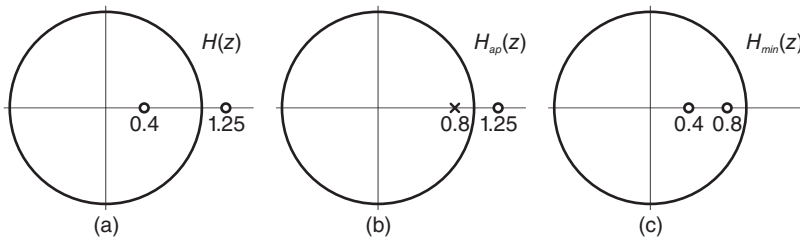


FIGURE 6.46 Zeros and poles of (a) $H(z)$, (b) $H_{ap}(z)$ and (c) $H_{min}(z)$.

Example 6.34 Given

$$H(z) = \frac{(1 - 2e^{j0.25\pi} z^{-1})(1 - 2e^{-j0.25\pi} z^{-1})}{(1 - 0.3z^{-1})(1 - 0.9z^{-1})}$$

Evaluate $H_{ap}(z)$ and $H_{min}(z)$.

The transfer function $H(z)$ is represented graphically in Fig. 6.47(a). We construct $H_{ap}(z)$ as in Fig. 6.47(b) by reflecting the offending zeros of $H(z)$. We may write

$$H_{ap}(z) = \frac{(z^{-1} - 0.5e^{-j0.25\pi})(z^{-1} - 0.5e^{j0.25\pi})}{(1 - 0.5e^{j0.25\pi} z^{-1})(1 - 0.5e^{-j0.25\pi} z^{-1})}$$

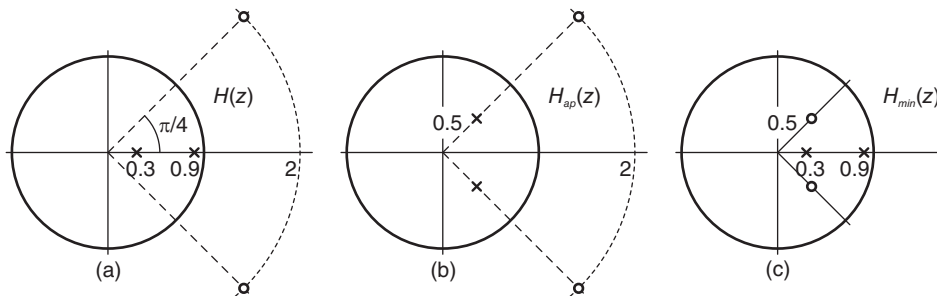


FIGURE 6.47 Zeros and poles of (a) $H(z)$, (b) $H_{ap}(z)$ and (c) $H_{min}(z)$.

$$H_{min}(z) = \frac{H(z)}{H_{ap}(z)} = \frac{(2 - e^{j0.25\pi} z^{-1})(2 - e^{-j0.25\pi} z^{-1})}{(1 - 0.3z^{-1})(1 - 0.9z^{-1})}$$

as can be seen in Fig. 6.47(c).

6.30 Unilateral z -Transform

The *unilateral z -transform* is a special form of the z -transform that is an important tool for the solution of linear difference equations with nonzero initial conditions. It is applied

in the analysis of dynamic discrete-time linear systems in the same way that the unilateral Laplace transform is used in the analysis of continuous-time dynamic LTI systems. Similarly to the unilateral Laplace transform, the unilateral z -transform of a sequence $x[n]$ is the z -transform of the *causal* part of the sequence. It disregards any value of the sequence for $n < 0$. Denoting by $X_I(z)$ the unilateral z -transform of a general sequence $x[n]$ we have

$$X_I[z] = \sum_{n=0}^{\infty} x[n]z^{-n} = Z_I[x[n]] \tag{6.195}$$

and we may write $x[n] = Z_I^{-1}[X_I[z]]$, and $x[n] \xleftrightarrow{Z_I} X_I[z]$. We note that if the sequence $x[n]$ is causal, its unilateral transform $X_I(z)$ is identical to its bilateral z -transform $X(z)$.

Example 6.35 Compare the unilateral and bilateral z -transforms of the sequences

- a) $v[n] = \delta[n] + na^n u[n]$
- b) $x[n] = a^n u[n - 2]$
- c) $y[n] = a^n u[n + 5]$

The sequences are shown in Fig. 6.48, assuming a value $a = 0.9$ as an illustration.

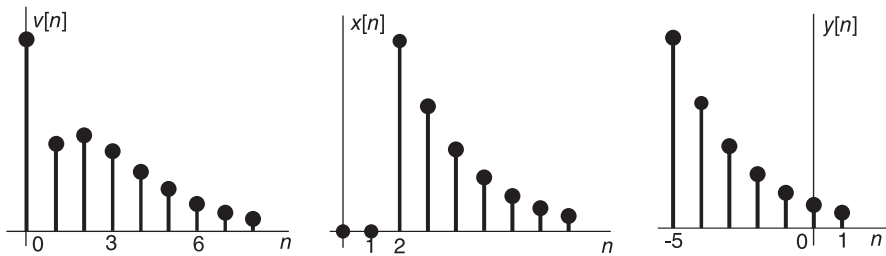


FIGURE 6.48 Three sequences of example.

a) We have

$$\begin{aligned} V_I[z] &= Z_I[v[n]] = \sum_{n=0}^{\infty} \{\delta[n] + na^n u[n]\}z^{-n} \\ &= V_{II}[z] = 1 + \frac{az^{-1}}{(1 - az^{-1})^2}, \quad |z| > |a|. \end{aligned}$$

The unilateral transform $V_I(z)$ is equal to the bilateral transform $V_{II}(z)$; the sequence $v[n]$ being causal.

b) The sequence $x[n]$ is causal. Its unilateral transform $X_I(z)$ is therefore equal to the bilateral transform $X_{II}(z)$. Writing

$$\begin{aligned} x[n] &= a^2 a^{n-2} u[n - 2] \\ X_I[z] &= X_{II}[z] = a^2 z^{-2} Z[a^n u[n]] = a^2 \frac{z^{-2}}{1 - az^{-1}}, \quad |z| > |a|. \end{aligned}$$

c) The sequence $y[n] = a^n u[n + 5]$ is not causal. Its bilateral transform $Y_{II}(z)$ is given by

$$\begin{aligned} Y_{II}(z) &= \sum_{n=-\infty}^{\infty} a^n u[n + 5]z^{-n} = \sum_{n=-5}^{\infty} a^n z^{-n} \\ &= \frac{a^{-5} z^5}{1 - az^{-1}}, \quad |z| > |a| \end{aligned}$$

whereas its unilateral transform is equal to

$$Y_I(z) = \sum_{n=0}^{\infty} a^n z^{-n} = \frac{1}{1 - az^{-1}}, \quad |z| > |a|.$$

6.30.1 Time Shift Property of Unilateral z -Transform

The unilateral z -transform has almost identical properties to those of the bilateral z -transform. An important distinction exists, however, between the time-shift properties of the two transforms. We have seen that the time shift property of the bilateral z -transform is simply given by

$$x[n - n_0] \xleftrightarrow{Z_{II}} z^{-n_0} X_{II}(z). \tag{6.196}$$

We now view the same property as it applies to the unilateral transform $X_I(z)$. Consider the three sequences $x[n]$, $v[n]$ and $y[n]$ shown in Fig. 6.49.

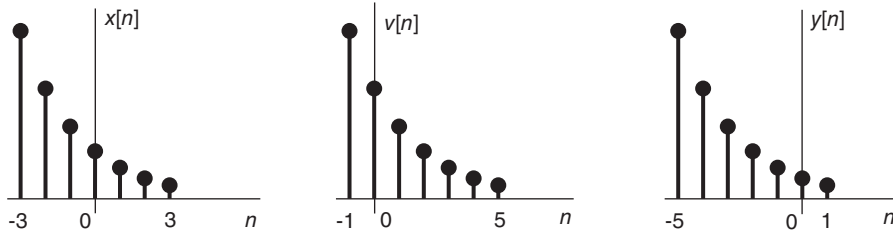


FIGURE 6.49 A sequence shifted right and left.

The first, $x[n]$, extends from $n = -3$ to $n = 3$. The sequence $v[n]$ is a right shift of $x[n]$ by two points and $y[n]$ is a left shift by two points, i.e. $v[n] = x[n - 2]$ and $y[n] = x[n + 2]$. We may write

$$\begin{aligned} V_I[z] &= x[-2] + x[-1]z^{-1} + x[0]z^{-2} + x[1]z^{-3} + x[2]z^{-4} + x[3]z^{-5} \\ &= x[-2] + x[-1]z^{-1} + z^{-2}X_I[z] \end{aligned} \tag{6.197}$$

$$Y_I[z] = x[2] + x[3]z^{-1} = z^2 [X_I[z] - x[0] - z^{-1}x[1]]. \tag{6.198}$$

More generally, if $n_0 > 0$ then

$$x[n - n_0] \xleftrightarrow{Z_I} z^{-n_0} \left[\sum_{k=1}^{n_0} x[-k]z^k + X_I[z] \right] \tag{6.199}$$

and

$$x[n + n_0] \xleftrightarrow{Z_I} z^{n_0} \left[X_I[z] - \sum_{k=0}^{n_0-1} z^{-k} x[k] \right]. \tag{6.200}$$

In particular

$$x[n - 1] \xleftrightarrow{Z_I} z^{-1} [x[-1]z + X_I[z]] = x[-1] + z^{-1}X_I[z] \tag{6.201}$$

$$x[n + 1] \xleftrightarrow{Z_I} z [X_I[z] - x[0]] \tag{6.202}$$

$$x[n - 2] \xleftrightarrow{Z_I} z^{-2} [x[-1]z + x[-2]z^2 + X_I[z]] \tag{6.203}$$

$$x[n + 2] \xleftrightarrow{Z_I} z^2 [X_I[z] - x[0] - z^{-1}x[1]]. \tag{6.204}$$

Example 6.36 Evaluate the response $y[n]$ of the system described by the difference equation

$$y[n] - \frac{3}{4}y[n-1] + \frac{1}{8}y[n-2] = x[n]$$

if the input is a unit pulse $\delta[n]$ and the initial conditions are $y[-1] = -1$ and $y[-2] = 2$. Since $x[n] = \delta[n]$ we have $X_I(z) = 1$. Applying the unilateral z -transform to both sides of the difference equation we have

$$Y_I[z] - \frac{3}{4}z^{-1}[y[-1]z + Y_I[z]] + \frac{1}{8}z^{-2}[y[-1]z + y[-2]z^2 + Y_I[z]] = 1$$

$$\frac{Y_I[z]}{z} = \frac{\left[1 + \frac{3}{4}y[-1] - \frac{1}{8}y[-2]\right]z - \frac{1}{8}y[-1]}{(z - 1/4)(z - 1/2)} = \frac{1/8}{(z - 1/4)(z - 1/2)}.$$

Using a partial fraction expansion we obtain

$$Y_I[z] = \frac{1}{2} \left[\frac{1}{(1 - (1/2)z^{-1})} - \frac{1}{(1 - (1/4)z^{-1})} \right]$$

$$y[n] = \frac{1}{2} [(0.5)^n - (0.25)^n] u[n].$$

6.31 Problems

Problem 6.1 A system has an impulse response

$$h[n] = 3^{-n} \cos(\pi n/8) u[n]$$

receives the input

$$x[n] = 10\delta[n - 5].$$

Evaluate the system output $y[n]$. Verify the result using the z -transform.

Problem 6.2 In the sampling system shown in Fig. 6.50 the continuous-time signal $x_c(t)$ is sampled by an analog to digital (A/D) converter with a sampling frequency of 48 kHz. The resulting discrete-time signal $x[n] = x_c(nT)$, where T is the sampling interval, is applied to a filter of transfer function $H(z)$ the output of which, $y[n]$, is then converted to a continuous time signal $y(t)$ using a digital to analog (D/A) converter, as shown in the figure. The filter amplitude spectrum $|H(e^{j\Omega})|$ is given by

$$|H(e^{j\Omega})| = \begin{cases} 3|\Omega|/\pi, & |\Omega| \leq \pi/3 \\ -3(|\Omega| - \pi)/\pi, & 2\pi/3 \leq |\Omega| \leq \pi \\ 1, & \pi/3 \leq |\Omega| \leq 2\pi/3 \\ 0, & \text{otherwise.} \end{cases}$$

a) Given that the input signal $x_c(t)$ is a sinusoid of frequency 6 kHz and amplitude 1 volt, describe the output signal $y(t)$ in form, amplitude and frequency content.

b) If $x(t)$ is a sinusoid of frequency 28 kHz, what is the frequency of the output signal $y(t)$?

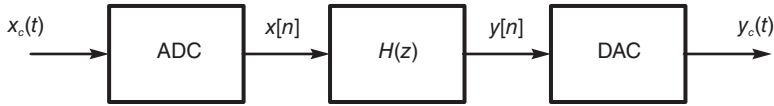


FIGURE 6.50 Signal sampling, digital filtering and reconstruction.

Problem 6.3 For the two sequences $x[n]$ and $y[n]$ given in the following tables

n	≤ -2	-1	0	1	2	3	4	≥ 5
$x[n]$	0	2	1	0	-1	-2	-1	0

n	≤ 87	88	98	90	≥ 91
$y[n]$	0	1	1	1	0

- a) Evaluate the convolution $z[n] = x[n] * y[n]$.
- b) Evaluate the cross-correlation $r_{yx}[n]$.

Problem 6.4 Evaluate the z-transform of

$$x[n] = 10^{0.05n} n u[n + 15].$$

Problem 6.5 Evaluate the transfer function $H(z)$ of a system that has the impulse response

$$h[n] = (n + 1) 3^{-(n+1)/3} u[n].$$

Problem 6.6 Consider the system shown in Fig.6.51, where a continuous-time signal $x(t)$ is applied to a system of impulse response $h(t)$ and to the input of an analog to digital A/D converter. The converter's output $x[n]$ is applied to a discrete-time linear system of impulse response $g[n]$ and output $v[n]$.

The sampling frequency of the A/D converter is 10 Hz and sampling starts at $t = 0$. The signal $x(t)$ and the impulse responses $h(t)$ and $g[n]$ are given by

$$x(t) = \begin{cases} 3, & 0.05 < t < 0.25 \\ 7, & 0.25 < t < 0.45 \\ 0, & \text{otherwise} \end{cases}$$

$$h(t) = \begin{cases} 5, & 0 < t < 0.2 \\ 3, & 0.2 < t < 0.4 \\ 0, & \text{otherwise} \end{cases}$$

$$g[n] = \begin{cases} 4, & 0 \leq n \leq 1 \\ 4, & 4 \leq n \leq 5 \\ 0, & \text{otherwise} \end{cases}$$

- a) Evaluate $y(t)$ using the convolution integral.
- b) Evaluate $v[n]$ by effecting a discrete-time convolution.

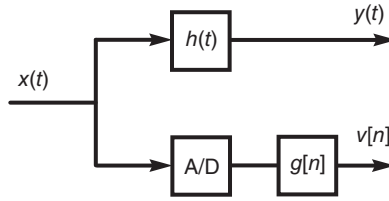


FIGURE 6.51 System block diagram.

Problem 6.7 For each of the following sequences sketch the ROC in the z -plane with the unit circle shown as a circle of reference.

- a) $s[n] = \alpha^n u[n], |\alpha| < 1$
- b) $v[n] = \alpha^n u[n] + \beta^n u[n], |\alpha| < 1$ and $|\beta| > 1$
- c) $w[n] = \alpha^n u[n - 3], |\alpha| < 1$
- d) $x[n] = \alpha^n u[-n], |\alpha| < 1$
- e) $y[n] = \alpha^n u[-n] + \beta^n u[n], |\alpha| < 1$ and $|\beta| > 1$
- f) $z[n] = \alpha^n u[n] + \beta^n u[-n], |\alpha| < 1$ and $|\beta| > 1$

Problem 6.8 A signal $x_c(t) = \cos(375\pi t - \pi/3)$ is converted to a sequence $x[n]$ by an A/D converter at a rate of 1000 samples/sec. The sequence $x[n]$ is fed to an FIR digital filter of impulse response

$$h[n] = a^n R_N[n] = a^n \{u[n] - u[n - N]\}.$$

The filter output $y[n]$ is then converted back to a continuous-time signal $y_c(t)$.

- a) Write the difference equation describing the filter.
- b) Let $a = 0.9, N = 16$. Evaluate the system output $y_c(t)$.

Problem 6.9 Evaluate the impulse response of the system of transfer function

$$H(z) = \frac{4z - 12}{z^2 - 8z + 12}, \quad 2 < |z| < 6.$$

Problem 6.10 The sequence $x[n] = a^n R_N[n]$ is applied to the input of a system of transfer function

$$H(z) = \frac{1}{1 - b^{-1}z^{-1}} - z^{-N} \frac{b^{-N}}{1 - b^{-1}z^{-1}}$$

and output $y[n]$.

- a) Evaluate the z -transform $Y(z)$ of the system output.
- b) Evaluate the inverse transform of $Y(z)$ to obtain the system response $y[n]$.
- c) Rewrite the system response using the sequences $R_N[n], R_N[n - N], \dots$
- d) Evaluate the system impulse response $h[n]$.
- e) Evaluate the convolution $w[n] = x[n] * h[n]$. Compare the result with $y[n]$.

Problem 6.11 Let

$$S_1(r, n_1, n_2) = \sum_{n=n_1}^{n_2} r^n$$

and

$$S_2(r, n_1, n_2) = \sum_{n=n_1}^{n_2} nr^n.$$

- a) Evaluate $S_1(r, n_1, n_2)$ and $S_2(r, n_1, n_2)$.
 b) Evaluate the cross-correlation $r_{vx}[n]$ of the two sequences

$$v[n] = nR_N[n]$$

$$x[n] = e^{-n}u[n]$$

expressing the result in terms of S_1 and S_2 .

Problem 6.12 A system is described by the difference equation

$$y[n] = 0.75y[n-1] - 0.125y[n-2] + 2x[n-1] + 2x[n-2].$$

- a) Evaluate the system impulse response
 b) Evaluate the system response if the input is the ramp

$$x[n] = n u[n].$$

Problem 6.13 Given two sequences $x_{-2}, x_{-1}, x_0, x_1, x_2, x_3$ and $v_{-2}, v_{-1}, v_0, v_1, v_2, v_3$, where x_n denotes $x[n]$ and v_n denotes $v[n]$.

a) Show the structure of a multiplication that would produce the convolution $z[n]$ of the two sequences. Show the order of the values of the convolution sequence $z[n]$ in the multiplication result.

b) Show the structure of a multiplication that would produce the cross-correlation $r_{vx}[n]$ of the two sequences. Show the order of the values of the correlation sequence $r_{vx}[n]$ in the multiplication result. Using the z -transform show that the structure of the multiplier does produce the expected cross-correlation $r_{vx}[n]$.

Problem 6.14 Evaluate the transfer function $H(z)$ of a system that has an impulse response $h[n]$ defined by

$$h[n] = \sum_{m=-2}^{\infty} \{2^{-8m+1}\delta[n-8m] - 2^{-8m}\delta[n-8m-1]\}.$$

Problem 6.15 The impulse response of a discrete-time linear system is given by

$$h[n] = \alpha^n u[n] + \lambda \beta^n u[-n] + \rho \cos(\pi n/8) u[n]$$

where α, β, λ and ρ are real constants.

a) For which values of α, λ, β and ρ is the system stable? State the ROC of the system transfer function $H(z)$ in the z -plane.

b) For which values of α, λ, β and ρ is the system physically realizable? State the ROC of the system transfer function $H(z)$ in the z -plane.

c) For which values of α, λ, β and ρ is the system stable and physically realizable?

Problem 6.16 A digital filter is described by the difference equation

$$v[n] = x[n] - x[n-1] + 5v[n-1]$$

where $x[n]$ is the filter input and $v[n]$ its output. The filter output is applied to a second filter described by the difference equation

$$y[n] = v[n] + 3v[n-1]$$

where $y[n]$ is its output.

a) Evaluate the transfer function $H(z)$ of the overall system, between the input $x[n]$ and the output $y[n]$. Specify its ROC.

b) Assuming the filter to be a causal system, state whether or not it is stable, explaining the reason justifying your conclusion. Evaluate the filter impulse response $h[n]$.

Problem 6.17 Design a digital oscillator using the a discrete-time system which generates a sinusoid upon receiving the impulse $\delta[n]$. The oscillator should employ a D/A converter with a frequency of 10,000 samples per second, to generate a sinusoid $y(t)$ of frequency 440 Hz. Evaluate the difference equation describing the system. Specify the filter employed by the D/A converter to generate the continuous-time signal $y(t)$.

Problem 6.18 A sequence $x[n]$ is applied to the input of a filter which is composed of two linear systems connected in parallel, the outputs of which are added up producing the filter output $y[n]$.

a) Evaluate the difference equation describing this filter given that the two constituent systems' transfer functions are physically realizable and are given by

$$H(z) = z^{-2}/(5 - z^{-1}), \quad G(z) = 4/(2 + z^{-1}).$$

b) Evaluate the filter output $y[n]$ if the input sequence is $x[n] = 5$.

Problem 6.19 Let

$$v[n] = n R_N[n],$$

$N > 0$ and

$$x[n] = e^{-\alpha n} R_N[n]$$

Let

$$y[n] = \sum_{m=-\infty}^{\infty} v[m] x[n+m]$$

a) Evaluate the sum

$$S(n_1, n_2) = \sum_{n=n_1}^{n_2} n a^n$$

b) Evaluate $y[n]$. Express the result in terms of $S(n_1, n_2)$

c) Evaluate the transform $Y(z)$ of $y[n]$.

Problem 6.20 Consider a general sequence $x[n]$ defined over $-\infty < n < \infty$ with z -transform $X(z)$ and a sequence $y[n]$ of z -transform $Y(z)$. Assuming that

$$Y(z) = X(z^M), \quad M \text{ integer}$$

a) Evaluate $y[n]$ as a function of $x[n]$.

b) If

$$x[n] = a^n u[n+K]$$

evaluate $y[n]$.

Problem 6.21 A system has an input $v[n]$, an output $x[n]$ and the frequency response

$$H(e^{j\Omega}) = 1 - 0.7e^{-j8\Omega}.$$

a) Evaluate the system impulse response $h[n]$.

b) A system having a frequency response $G(e^{j\Omega})$ receives the sequence $x[n]$ and produces a sequence $y[n]$ which should equal the original sequence $v[n]$, i.e. $y[n] = v[n]$.

Evaluate $G(e^{j\Omega})$.

Evaluate and sketch the poles and zeros of the system transfer function $G(z)$.

c) For every possible ROC of $G(z)$ state whether or not the system is stable.

d) Let $g[n]$ be the sequence defined by the convolution

$$y[n] = g[n] * x[n].$$

Evaluate the sequence $g[n]$.

Problem 6.22 Consider the sequence

$$x[n] = 4^{-|n|}.$$

Evaluate the z -transform $X(z)$, and the Fourier transform $X(e^{j\Omega})$ of the sequence $x[n]$.

Problem 6.23 a) Evaluate the cross-correlation $r_{vx}(n)$ of the two sequences

$$v[n] = e^{-n-3}u[n-4]$$

$$x[n] = e^{2-n}u[n+3].$$

b) Evaluate the convolution and the correlation $r_{vx}(n)$ of the two causal sequences

$$v[n] = \{5, 3, 1, -2, -3, 1\}; 0 \leq n \leq 5$$

$$x[n] = \{2, 3, -1, -5, 1, 4\}; 0 \leq n \leq 5.$$

Problem 6.24 A system transfer function has poles at $z = 0.5e^{\pm j\pi/2}$ and $z = e^{\pm j\pi/2}$, and two zeros at $z = e^{\pm j\pi/4}$. Determine the gain factor K so that the frequency response at $\Omega = 0$ be equal to 10.

Problem 6.25 The denominator polynomial of the system function of an allpass filter is

$$A(z) = 1 + a_1z^{-1} + a_2z^{-2} + \dots + a_nz^{-n}.$$

Show that its numerator polynomial is given by

$$B(z) = a_n + a_{n-1}z^{-1} + a_{n-2}z^{-2} + \dots + a_1z^{-(n-1)} + z^{-n}.$$

Problem 6.26 Given

$$H(z) = (1 - 0.7e^{j0.2\pi}z^{-1})(1 - 0.7e^{-j0.2\pi}z^{-1})(1 - 2e^{j0.4\pi}z^{-1})(1 - 2e^{-j0.4\pi}z^{-1}).$$

Evaluate $H_{ap}(z)$ and $H_{min}(z)$ in the decomposition $H(z) = H_{ap}(z)H_{min}(z)$.

Problem 6.27 Evaluate the unilateral z -transforms of the sequences (a) $x[n] = 0.5^{n+2}u[n+5]$, (b) $x[n] = 0.7^{n-3}u[n-3]$, (c) $x[n] = \delta[n] + \delta[n+3] + 3\delta[n-3] - 2^{n-2}u[1-n]$.

Problem 6.28 Solve the difference equation

$$y[n] = 0.75y[n-2] + x[n]$$

where $x[n] = \delta[n-1]$, given the initial conditions $y[-1] = y[-2] = 1$.

Problem 6.29 A system has the transfer function

$$H(z) = \frac{Y(z)}{X(z)} = \frac{1}{1/(9/16)z^{-2}}.$$

What initial conditions of $y[n]$ for $n < 0$ would produce a system output $y[n]$ of zero for $n \geq 0$?

6.32 Answers to Selected Problems

Problem 6.1 $y[n] = 10 \cdot 3^{-(n-5)} \cos \{ \pi (n - 5) / 8 \} u[n - 5]$.

Problem 6.2 See Fig. 6.52

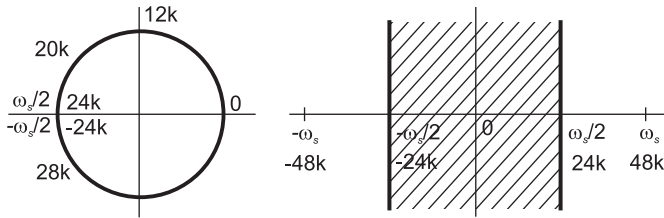


FIGURE 6.52 Figure for Problem 6.2.

a) $f = 48 \times 10^3$, $T = 1/f = \frac{10^{-3}}{48}$, $\omega = 2\pi \times 6000$ r/s, $\Omega = \omega T = \pi/4$, $|H(e^{j\Omega})|_{\Omega=\pi/4} = 3/4$. The output $y(t)$ is a sinusoid of frequency 6 kHz and amplitude $3/4$ volt.

b) Aliasing has the effect that the output is a sinusoid of frequency 20 kHz .

Problem 6.3 a) The values of $z[n]$ are listed in the following table

n	< 87	87	88	89	90	91	92	93	94	≥ 95
$z[n]$	0	2	3	3	0	-3	-4	-3	-1	0

b) The values of $r_{xy}[n]$ are listed in the following table

n	≤ 83	84	85	86	87	88	89	90	91	≥ 92
$r_{xy}[n]$	0	-1	-3	-4	-3	0	3	3	2	0

Problem 6.4

$$X(z) = z^{15} V(z) = 10^{-0.75} \left\{ \frac{a z^{14}}{(1 - a z^{-1})^2} - \frac{15 z^{15}}{1 - a z^{-1}} \right\}, \quad 1.122 < |z| < \infty$$

Problem 6.5

$$H(z) = z \frac{3^{-1/3} z^{-1}}{(1 - 3^{-1/3} z^{-1})^2} = \frac{3^{-1/3}}{(1 - 3^{-1/3} z^{-1})^2}, \quad |z| > 3^{-1/3} = 0.69$$

See Fig. 6.53.

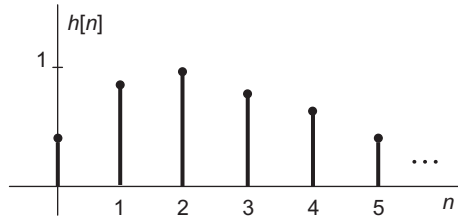


FIGURE 6.53 Figure for Problem 6.5.

Problem 6.6 a) See Fig. 6.54 and Fig. 6.55.

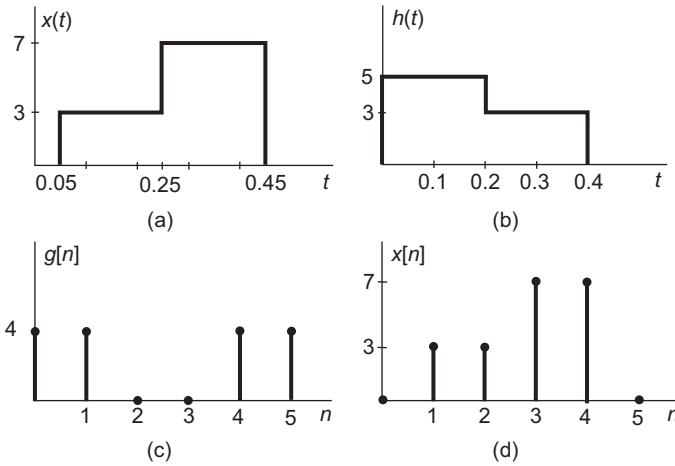


FIGURE 6.54 Figure for Problem 6.6.

b) We effect the discrete convolution in the form of a multiplication as shown in the table below.

See Fig. 6.56.

Problem 6.7

- a) $|z| > |\alpha|$, $|\alpha| < 1$
- b) $|z| > |\beta| > 1$
- c) $|z| > |\alpha|$ same as a)
- d) $|z| < |\alpha| < 1$
- e) No convergence
- f) $|\alpha| < |z| < |\beta|$

Problem 6.8

$$y[n] - a y[n - 1] = x[n] - a^N x[n - N]$$

b)

$$y_c(t) = 0.7694 \cos(375\pi t - 1.9503)$$

Problem 6.9

$$h[n] = 2^{n-1}u[n - 1] - 0.56^n u[-n]$$

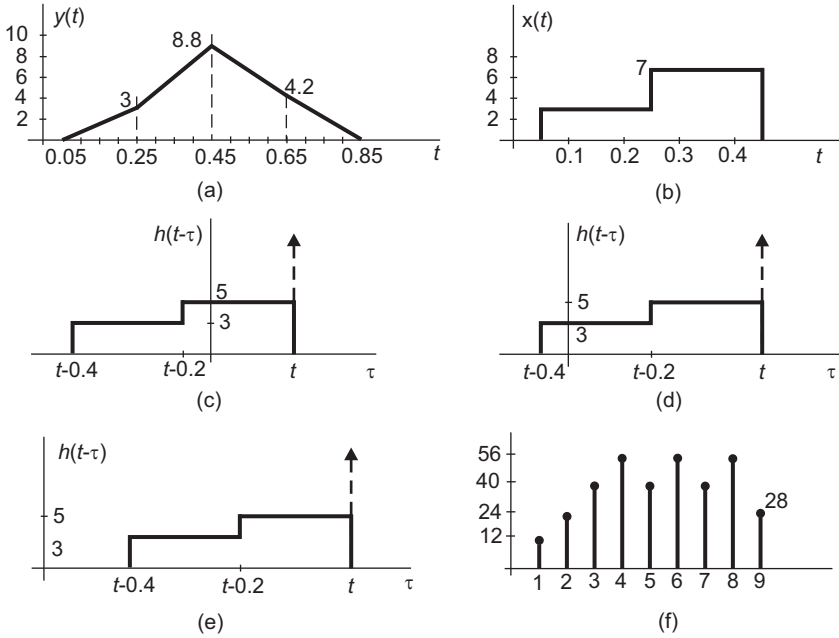


FIGURE 6.55 Figure for Problem 6.6.

			4	4	0	0	4	4
					3	3	7	7
			28	28	0	0	28	28
		28	28	0	0	28	28	
	12	12	0	0	12	12		
	12	12	0	0	12	12		
	12	24	40	56	40	24	40	28

FIGURE 6.56 Figure for Problem 6.6.

Problem 6.10

- c) $y[n] = \{(b^{-n} - ba^{n+1}) / (1 - ab)\} R_N[n] + \{(a^{n-N+1}b^{-N+1} - a^N b^{N-n}) / (1 - ab)\} R_N[n - N]$.
- d) $h[n] = b^{-n} R_N[n]$.
- e) $w[n] = y[n]$.

Problem 6.11

Let $r = e^{-1}$

$$S_1(r, n_1, n_2) = \sum_{n=n_1}^{n_2} r^n = r^{n_1} \frac{1 - r^{n_2 - n_1 + 1}}{1 - r}$$

$$S_2 = \frac{n_1 r^{n_1} + (1 - n_1) r^{n_1 + 1} - (n_2 + 1) r^{n_2 + 1} + n_2 r^{n_2 + 2}}{(1 - r)^2}$$

For $0 \leq n \leq N - 1$, with $r = e^{-1}$

$$r_{vx}[n] = n \sum_{m=0}^{-n+N-1} e^{-m} + \sum_{m=0}^{-n+N-1} m e^{-m} = n S_1(r, 0, -n + N - 1) + S_2(r, 0, -n + N - 1)$$

For $n \leq 0$, $r_{vx}[n] = n S_1(r, -n, -n + N - 1) + S_2(r, -n, -n + N - 1)$.

Problem 6.12

- a) $h[n] = 2 \left\{ 6(0.5)^{n-1} - 5(0.25)^{n-1} \right\} u[n-1]$.
- b) $y[n] = \left\{ 5.333 - 8(0.5)^{n-1} + 2.667(0.25)^{-1} \right\} u[n-1]$.

Problem 6.13

a)

	x_3	x_2	x_1	x_0	x_{-1}	x_{-2}						
	v_3	v_2	v_1	v_0	v_{-1}	v_{-2}						
	$v_{-2}x_3$	$v_{-2}x_2$	$v_{-2}x_1$	$v_{-2}x_0$	$v_{-2}x_{-1}$	$v_{-2}x_{-2}$						
	$v_{-1}x_3$	$v_{-1}x_2$	$v_{-1}x_1$	$v_{-1}x_0$	$v_{-1}x_{-1}$	$v_{-1}x_{-2}$						
	v_0x_3	v_0x_2	v_0x_1	v_0x_0	v_0x_{-1}	v_0x_{-2}						
	v_1x_3	v_1x_2	v_1x_1	v_1x_0	v_1x_{-1}	v_1x_{-2}						
	v_2x_3	v_2x_2	v_2x_1	v_2x_0	v_2x_{-1}	v_2x_{-2}						
	v_3x_3	v_3x_2	v_3x_1	v_3x_0	v_3x_{-1}	v_3x_{-2}						
	$z[6]$	$z[5]$	$z[4]$	$z[3]$	$z[2]$	$z[1]$	$z[0]$	$z[-1]$	$z[-2]$	$z[-3]$	$z[-4]$	

b)

				x_3	x_2	x_1	x_0	x_{-1}	x_{-2}			
				v_{-2}	v_{-1}	v_0	v_1	v_2	v_3			
				v_3x_3	v_3x_2	v_3x_1	v_3x_0	v_3x_{-1}	v_3x_{-2}			
				v_2x_3	v_2x_2	v_2x_1	v_2x_0	v_2x_{-1}	v_2x_{-2}			
				v_1x_3	v_1x_2	v_1x_1	v_1x_0	v_1x_{-1}	v_1x_{-2}			
				v_0x_3	v_0x_2	v_0x_1	v_0x_0	v_0x_{-1}	v_0x_{-2}			
				$v_{-1}x_3$	$v_{-1}x_2$	$v_{-1}x_1$	$v_{-1}x_0$	$v_{-1}x_{-1}$	$v_{-1}x_{-2}$			
	$v_{-2}x_3$	$v_{-2}x_2$	$v_{-2}x_1$	$v_{-2}x_0$	$v_{-2}x_{-1}$	$v_{-2}x_{-2}$						
	$r_{vx}[-5]$	$r_{vx}[-4]$	$r_{vx}[-3]$	$r_{vx}[-2]$	$r_{vx}[-1]$	$r_{vx}[0]$	$r_{vx}[1]$	$r_{vx}[2]$	$r_{vx}[3]$	$r_{vx}[4]$	$r_{vx}[5]$	

Problem 6.14 $H(z) = 2^{17}z^{16} (1 - 2^{-1}z^{-1}) / (1 - 2^{-8}z^{-8})$.

Problem 6.15 ROCs: $|z| > |\alpha|$, $|z| < |\beta|$ and $|z| > 1$.

- a) 1. $|\alpha| < 1$. 2. $|\beta| > 1$ if $\lambda \neq 0$ and 3. $\rho = 0$ should be satisfied.
- b) $\lambda = 0$.
- c) $\lambda = 0$, $|\alpha| < 1$, and $\rho = 0$.

Problem 6.16

- a) Filter 1 : $\frac{1-z^{-1}}{1-5z^{-1}}$, Filter 2 : $1 + 3z^{-1}$. Hence $H(z) = \frac{(1-z^{-1})(1+3z^{-1})}{(1-5z^{-1})}$ Two possible ROCs $|z| > 5$ or $|z| < 5$, excluding $z = 0$.
- b) The system is unstable.

Problem 6.17 $y[n] = \sin(\Omega_0)x[n-1] + 2\cos(\Omega_0)y[n-1] - y[n-2]$.

Problem 6.18 a) The output $y[n] = 7.9$ volts .

Problem 6.20 b) $y[n] = \begin{cases} a^{n/M}, & n = kM, \quad k \geq -K \\ 0, & \text{otherwise} \end{cases}$.

Problem 6.21 $h[n] = \frac{1}{2}\delta[n-1] + \frac{1}{2}\delta[n+1] + \frac{(-1)^n n}{\sqrt{2\pi(n^2-1/16)}}$.

Problem 6.23

n	0	1	2	3	4	5	6	7	8	9	10
$z[n]$	10	21	6	-29	-23	13	29	16	-16	-11	4

Convolution

n	-10	-9	-8	-7	-6	-5	-4	-3	-2	-1	0
$r_{vx}[n]$	20	17	-18	-27	-7	29	27	-6	-14	-3	2

Correlation**Problem 6.24**

$K = 42.677$.

Problem 6.26

$$H_{min}(z) = (2 - 1.4e^{j0.2\pi}z^{-1})(2 - 1.4e^{-j0.2\pi}z^{-1})(1 - 0.5e^{j0.4\pi}z^{-1})(1 - 0.5e^{-j0.4\pi}z^{-1}).$$

$$H_{ap}(z) = \frac{(z^{-1} - 0.5e^{-j0.4\pi})(z^{-1} - 0.5e^{j0.4\pi})}{(1 - 0.5e^{j0.4\pi}z^{-1})(1 - 0.5e^{-j0.4\pi}z^{-1})}.$$

Problem 6.27 (a) $X_I(z) = 0.25/(1 - 0.25z^{-1})$, (b) $X_I(z) = z^{-3}/(1 - 0.7z^{-1})$,
 (c) $X_I(z) = 0.75 - 2^{-1}z^{-1} + 3z^{-3}$.

Problem 6.28 $y[n] = \{1.3854 \times 0.866^n - 0.6354(-0.866^n)\}u[n]$.

Problem 6.29 $y[-1] = 0$, $y[-2] = -16/9$.

Discrete-Time Fourier Transform

The Fourier transform of a discrete signal, which is referred to as the discrete-time Fourier transform (DTFT) is a special case of the z -transform in as much as the Fourier transform of a continuous signal is a special case of the Laplace transform. In the present discrete-time context we write for simplicity Fourier transform to mean the DTFT. We will, moreover, see in this chapter that the discrete Fourier transform (DFT) is a sampled version of the DTFT, in as much as the Fourier series is a sampled version of the Fourier transform of a continuous signal. The chapter ends with a simplified presentation of the fast Fourier transform (FFT), an efficient algorithm for evaluating the DFT.

7.1 Laplace, Fourier and z -Transform Relations

Let $v_c(t)$ be a continuous time function having a Laplace transform $V_c(s)$ and a Fourier transform $V_c(j\omega)$. Let $v_s(t)$ be the corresponding ideally sampled function

$$v_s(t) = v_c(t)\rho_T(t) = v_c(t) \sum_{n=-\infty}^{\infty} \delta(t - nT) = \sum_{n=-\infty}^{\infty} v_c(nT)\delta(t - nT). \quad (7.1)$$

Its Laplace transform $V_s(s)$ is given by

$$V_s(s) = \mathcal{L}[v_s(t)] = \sum_{n=-\infty}^{\infty} v_c(nT)e^{-nTs} \quad (7.2)$$

and its Fourier transform as already obtained in Chapter 4 is

$$V_s(j\omega) = \{1/(2\pi)\}V_c(j\omega) * \mathcal{F}[\rho_T(t)] = \frac{1}{T} \sum_{n=-\infty}^{\infty} V_c \left[j \left(\omega - n\frac{2\pi}{T} \right) \right] \quad (7.3)$$

wherefrom the Laplace transform of $v_s(t)$ may be also written in the form

$$V_s(s) = V_s(j\omega)|_{\omega=s/j} = \frac{1}{T} \sum_{n=-\infty}^{\infty} V_c \left(s - jn\frac{2\pi}{T} \right). \quad (7.4)$$

It is to be noted that such an extension of the transform from the $j\omega$ axis to the s plane, the common practice in the current literature, is not fully justified since it implies that the multiplication in the time domain $v_c(t)\rho_T(t)$ corresponds to a convolution of $V_c(s)$ with the Laplace transform of the two-sided impulse train $\rho_T(t)$. Since the Laplace transform of such an impulse train does not exist, according to the current literature, the last equation is simply not justified. A rigorous justification based on a generalization of the Dirac-delta impulse and the resulting extension of Laplace transform domain leads to a large class of

new distributions that now have a Laplace transform. Among these is the transform of the two sided impulse train, and is included in Chapter 18 dedicated to distributions. For now therefore we accept such extension from the Fourier axis to the Laplace plane without presenting a rigorous justification.

Now consider a sequence $v[n] = v_c(nT)$. We have

$$V(z) = \sum_{n=-\infty}^{\infty} v[n]z^{-n} = \sum_{n=-\infty}^{\infty} v_c(nT)z^{-n}. \quad (7.5)$$

Its Fourier transform DTFT is

$$V(e^{j\Omega}) = \sum_{n=-\infty}^{\infty} v[n]e^{-j\Omega n} = \sum_{n=-\infty}^{\infty} v_c(nT)e^{-j\Omega n} \quad (7.6)$$

and as we have seen, the inverse Fourier transform is

$$v[n] = \frac{1}{2\pi} \int_{-\pi}^{\pi} V(e^{j\Omega}) e^{j\Omega n} d\Omega. \quad (7.7)$$

Comparing $V(z)$ with the Laplace transform $V_s(s)$ we note that the two transforms are related by a simple change of variables. In particular, letting

$$z = e^{Ts} \quad (7.8)$$

we have

$$V(z)|_{z=e^{Ts}} = V(e^{Ts}) = \sum_{n=-\infty}^{\infty} v_c(nT)e^{-nTs} = V_s(s) \quad (7.9)$$

and conversely

$$V_s(s)|_{s=(1/T)\ln z} = V(z). \quad (7.10)$$

This is an important relation establishing the equivalence of the Laplace transform of an ideally sampled continuous-time function $v_c(t)$ at intervals T and the z -transform of its discrete-time sampling as a sequence, $v[n]$.

We note that the substitution $z = e^{Ts}$ transforms the axis $s = j\omega$ into the unit circle

$$z = e^{j\omega T} = e^{j\Omega} \quad (7.11)$$

where

$$\Omega \triangleq \omega T \quad (7.12)$$

which is the relation between the discrete-time domain angular frequency Ω in radians and the angular frequency of the continuous-time domain frequency ω in radians/sec. The vertical line $s = \sigma_0 + j\omega$ in the s plane is transformed into a circle $z = e^{\sigma_0 T} e^{jT\omega}$ of radius $e^{\sigma_0 T}$ in the z -plane. In fact a pole at $s = \alpha + j\beta$ is transformed into a pole $z = e^{(\alpha + j\beta)T}$ of radius $r = e^{\alpha T}$ and angle $\Omega = \beta T$ in the z -plane.

We may also evaluate the Fourier transform $V(e^{j\Omega})$ as a function of $V_c(j\omega)$. We have

$$\begin{aligned} V(e^{j\Omega}) &= \sum_{n=-\infty}^{\infty} v[n]e^{-j\Omega n} = V_s(j\omega)|_{\omega=\Omega/T} = \frac{1}{T} \sum_{n=-\infty}^{\infty} V_c \left[j \left(\omega - n \frac{2\pi}{T} \right) \right] \Big|_{\omega=\Omega/T} \\ &= \frac{1}{T} \sum_{n=-\infty}^{\infty} V_c \left[j \left(\frac{\Omega - 2\pi n}{T} \right) \right]. \end{aligned} \quad (7.13)$$

The spectra in the continuous and discrete time domains are shown in Fig. 7.1 assuming an abstract triangular shaped spectrum $V_c(j\omega)$ and absence of aliasing.

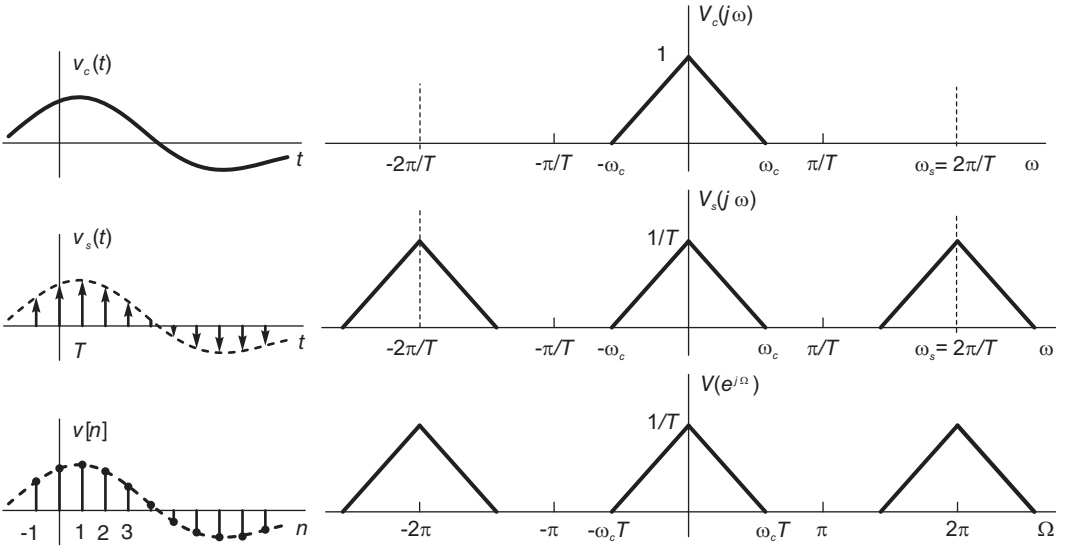


FIGURE 7.1 Spectra in continuous- and discrete-time domains.

Example 7.1 Let $v_c(t) = e^{-\alpha t}u(t)$. Compare the Laplace transform of its ideally sampled form $v_s(t)$ and the z-transform of its sampling $v[n] = v_c(nT)$, n integer.

We have

$$v_s(t) = v_c(t) \sum_{n=-\infty}^{\infty} \delta(t - nT) = \sum_{n=0}^{\infty} v_c(nT)\delta(t - nT) = \frac{1}{2}\delta(t) + \sum_{n=1}^{\infty} e^{-\alpha nT}\delta(t - nT)$$

where we have used the step function property that $u(0) = 1/2$. We may write

$$v_s(t) = \sum_{n=0}^{\infty} e^{-\alpha nT}\delta(t - nT) - \frac{1}{2}\delta(t)$$

$$\begin{aligned} V_s(s) &= \sum_{n=0}^{\infty} e^{-\alpha nT}e^{-snT} - \frac{1}{2} = \frac{1}{1 - e^{-(\alpha+s)T}} - \frac{1}{2} = \frac{1 + e^{-(s+\alpha)T}}{2[1 - e^{-(s+\alpha)T}]} \\ &= (1/2) \coth[(s + \alpha)T/2], \quad |e^{-(\alpha+s)T}| < 1 \text{ i.e. } e^{\sigma T} > e^{-\alpha T}, \text{ or } \sigma > -\alpha. \end{aligned}$$

Let

$$v[n] = v_c(nT) = e^{-\alpha nT}u[n] - \frac{1}{2}\delta[n]$$

$$V(z) = \sum_{n=0}^{\infty} e^{-\alpha nT}z^{-n} = \frac{1}{1 - e^{-\alpha T}z^{-1}} - \frac{1}{2}, \quad |e^{-\alpha T}z^{-1}| < 1 \text{ i.e. } |z| > e^{-\alpha T}.$$

We note that

$$V(z)|_{z=e^{sT}} = \frac{1}{1 - e^{-\alpha T}e^{-sT}} - \frac{1}{2} = V_s(s).$$

From this example we can draw several conclusions. Let us write

$$V_c(s) \triangleq \mathcal{L}[v_c(t)] = \frac{1}{s + \alpha}, \quad \text{Re}(s) > -\alpha. \tag{7.14}$$

We have

$$V_s(s) = \frac{1}{T} \sum_{n=-\infty}^{\infty} V_c \left(s - jn \frac{2\pi}{T} \right) = \frac{1}{T} \sum_{n=-\infty}^{\infty} \frac{1}{s - j2\pi n/T + \alpha}. \tag{7.15}$$

Comparing these results, we have the relation

$$\frac{1}{T} \sum_{n=-\infty}^{\infty} \frac{1}{s + \alpha - j2\pi n/T} = \frac{1}{2} \coth \left[(s + \alpha) \frac{T}{2} \right]. \tag{7.16}$$

It is interesting to note that the pole $s = -\alpha$ of $V_c(s)$ in the s plane is mapped as the pole $z = e^{-\alpha T}$ of $V(z)$ in the z -plane. Moreover, the expression of the Laplace transform $V_s(s)$ of the sampled function $v_s(t)$ shows that the transform has an infinite number of poles on the line $s = -\alpha + j2\pi n/T$, $n = 0, \pm 1, \pm 2, \dots$ with a uniform spacing equal to the sampling frequency $\omega_0 = 2\pi/T$, as shown in Fig. 7.2. Since the vertical line $s = -\alpha + j\omega$ is mapped onto the circle $z = e^{-\alpha T} e^{j\omega T}$, of radius $e^{-\alpha T}$, all the poles $s = -\alpha + jn\omega_0$ are mapped onto the single point $z = e^{-\alpha T} e^{jn\omega_0 T} = e^{-\alpha T}$.

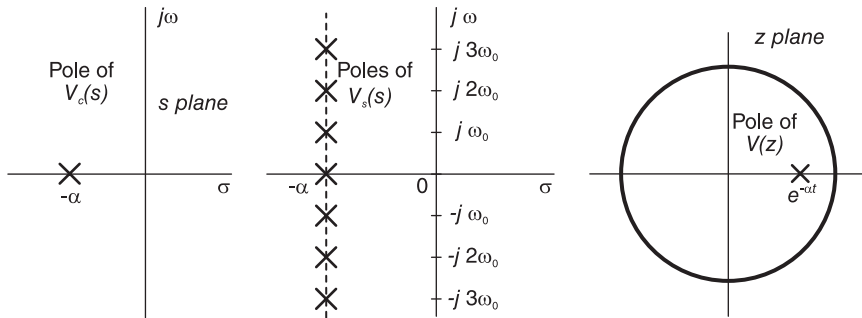


FIGURE 7.2 Poles in s and z -planes.

We can obtain this last equation alternatively by performing a partial fraction expansion of the transform $V_s(s)$. Noticing that it has an infinite number of poles, we write the expansion as an infinite sum of terms. Denoting by A_n the residue of the n^{th} term, we write

$$V_s(s) = \frac{1}{2} \coth \left[(s + \alpha) \frac{T}{2} \right] = \frac{1}{2} \sum_{n=-\infty}^{\infty} \frac{A_n}{s + \alpha - j2\pi n/T} \tag{7.17}$$

the n^{th} residue is given by

$$A_n = \lim_{s \rightarrow -\alpha + j2\pi n/T} \frac{(s + \alpha - j2\pi n/T) \cosh \left[(s + \alpha) \frac{T}{2} \right]}{\sinh \left[(s + \alpha) \frac{T}{2} \right]}. \tag{7.18}$$

The substitution leads to an indeterminate quantity. Using L'Hopital's rule we obtain

$$A_n = \lim_{s \rightarrow -\alpha + j2\pi n/T} \frac{(s + \alpha - j2\pi n/T)(T/2) \sinh \left[(s + \alpha) T/2 \right] + \cosh \left[(s + \alpha) T/2 \right]}{(T/2) \cosh \left[(s + \alpha) T/2 \right]} = \frac{2}{T}$$

wherefrom

$$V_s(s) = \frac{1}{2} \coth \left[(s + \alpha) \frac{T}{2} \right] = \frac{1}{T} \sum_{n=-\infty}^{\infty} \frac{1}{s + \alpha - j2\pi n/T} \tag{7.19}$$

as expected. We may also add that

$$V(z) = V_s(s)|_{s=\frac{1}{T} \ln z} \tag{7.20}$$

wherefrom

$$\frac{1}{T} \sum_{n=-\infty}^{\infty} \frac{1}{\frac{1}{T} \ln z + \alpha - j \frac{2\pi n}{T}} = \frac{1}{1 - e^{-\alpha T} z^{-1}} - \frac{1}{2}. \tag{7.21}$$

We notice further that by putting $\alpha = 0$ we obtain the relation

$$\sum_{n=-\infty}^{\infty} \frac{1}{\ln z - j2\pi n} = \frac{1}{1 - z^{-1}} - \frac{1}{2}. \tag{7.22}$$

We note that the evaluation of residues in the case of an infinite number of poles is an area known as Mittag-Leffler expansions. Moreover, the sum

$$\frac{1}{T} \sum_{n=-\infty}^{\infty} \frac{1}{s + \alpha - j2\pi n/T} \tag{7.23}$$

is divergent. It can be evaluated, however, using a Cauchy approach as the limit of the sum of a finite number of terms with positive index n plus the same number of terms with negative n . As a verification, therefore, we write

$$\frac{1}{T} \sum_{n=-\infty}^{\infty} \frac{1}{s + \alpha - j2\pi n/T} = \frac{1}{T} \frac{1}{s + \alpha} + \frac{1}{T} \left[\sum_{n=-\infty}^{-1} \frac{1}{s + \alpha - j2\pi n/T} + \sum_{n=1}^{\infty} \frac{1}{s + \alpha - j2\pi n/T} \right] \tag{7.24}$$

$$\frac{1}{T} \sum_{n=-\infty}^{\infty} \frac{1}{s + \alpha - j2\pi n/T} = \frac{1}{T} \frac{1}{s + \alpha} + \frac{1}{T} \sum_{n=1}^{\infty} \frac{2(s + \alpha)}{(s + \alpha)^2 + 4\pi^2 n^2/T^2} \tag{7.25}$$

Using the expansion

$$\coth z = \frac{1}{z} + \sum_{n=1}^{\infty} \frac{2z}{z^2 + n^2\pi^2} \tag{7.26}$$

with the substitution $z = (s + \alpha)T/2$, we obtain the same expression (7.16) found above.

Example 7.2 An ideal analog to digital (A/D) converter operating at a sampling frequency of $f_s = 1$ kHz receives a continuous-time signal $x_c(t) = \cos 100\pi t$ and produces the corresponding sequence $x[n]$. Evaluate the Fourier transform of the discrete-time signal at the output of the A/D converter.

The sampling period is $T = 1/f_s = 0.001$ sec, so that

$$\begin{aligned} x[n] &= x_c(nT) = x_c(0.001n) = \cos 0.1\pi n \\ X_c(j\omega) &= \pi [\delta(\omega - 100\pi) + \delta(\omega + 100\pi)] \\ X(e^{j\Omega}) &= \frac{1}{T} \sum_{n=-\infty}^{\infty} X_c \left[j \left(\frac{\Omega - 2\pi n}{T} \right) \right] \\ &= \frac{\pi}{T} \left\{ \sum_{n=-\infty}^{\infty} \delta \left(\frac{\Omega - 2\pi n}{T} - 100\pi \right) + \delta \left(\frac{\Omega - 2\pi n}{T} + 100\pi \right) \right\} \\ &= \pi \sum_{n=-\infty}^{\infty} \delta(\Omega - \pi/10 - 2\pi n) + \delta(\Omega + \pi/10 - 2\pi n). \end{aligned}$$

Note that

$$X(e^{j\Omega}) = \pi [\delta(\Omega - \pi/10) + \delta(\Omega + \pi/10)], \quad -\pi < \Omega < \pi.$$

The spectra are shown in Fig. 7.3.

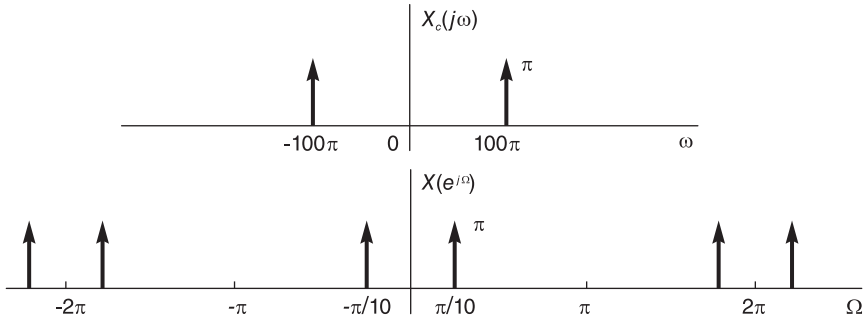


FIGURE 7.3 Spectra in continuous- and discrete-time domains.

7.2 Discrete-Time Processing of Continuous-Time Signals

As depicted in Fig. 7.4, a discrete-time signal processing system may be modeled in general as a pre-filtering unit such as a lowpass filter for limiting the signal spectral bandwidth in preparation for sampling, and ideal A/D converter also known as continuous-time to discrete-time (C/D) converter, a digital signal processor such as a digital filter or a digital spectrum analyzer, an ideal digital to analog (D/A) converter also known as discrete-time to continuous-time (D/C) converter and a post-filtering unit for eliminating any residual effects that may occur through aliasing. In what follows we shall study the relations between the inputs and outputs of each block in the system, both in time and in frequency domain.



FIGURE 7.4 Discrete-time processing using ideal A/D and D/A converters.

7.3 A/D Conversion

As seen in Fig. 7.5, a true A/D converter consists of a C/D converter followed by a quantizer and an encoder.

The C/D converter samples the analog, continuous-time, signal $x_c(t)$ by a C/D converter, producing the sequence $x[n] = x_c(nT)$. The quantizer converts each value $x[n]$, into one of a set of permissible levels. The resulting value $\hat{x}[n]$ is then encoded it into a corresponding binary representation. The binary coded output $\xi[n]$ may be in sign and magnitude, 1's complement, 2's complement or offset binary representation, among others. The process that the C/D converter employs to generate $x[n]$ may be viewed as shown in Fig. 7.6, where

the continuous-time signal is ideally sampled by an impulse train $\rho_T(t)$ and the result

$$x_s(t) = x_c(t)\rho_T(t) = \sum_{n=-\infty}^{\infty} x_c(nT)\delta(t - nT) \tag{7.27}$$

is converted to a sequence of samples. This conversion maps the successive impulses of intensities $x_c(nT)$ into the sequence $x[n] = x_c(nT)$.

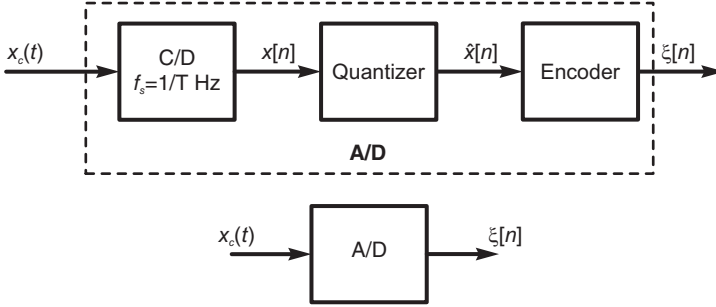


FIGURE 7.5 A/D conversion.

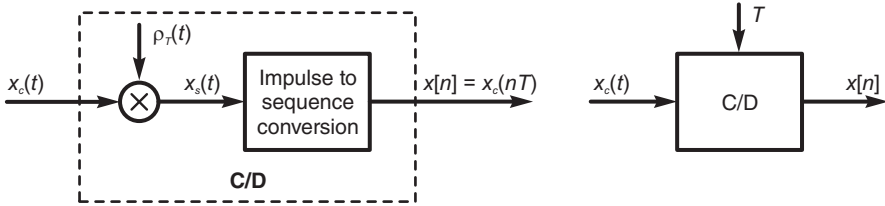


FIGURE 7.6 Analog signal to sequence conversion.

The quantizer receives the sequence $x[n]$ and produces a set of values $\hat{x}[n] = Q[x[n]]$. It employs $M + 1$ *decision levels* l_1, l_2, \dots, l_{M+1} where $M = 2^{b+1}$; $(b + 1)$ being the number of bits of quantization plus the sign bit. The amplitude of $x[n]$ is thus divided into M intervals, as can be seen in Fig. 7.7 for the case $M = 8, l_1 = -\infty, l_9 = \infty$.

The interval

$$\Delta_k = [l_{k+1} - l_k] \tag{7.28}$$

is the quantization step. In a uniform quantizer this is a constant $\Delta = \Delta_k$ referred to as the *quantization step size* or *resolution*. The *range* of such quantizer is

$$R = M\Delta = 2^{b+1}\Delta \tag{7.29}$$

and the maximum amplitude of $x[n]$ should be limited to

$$x_{max} = 2^b\Delta \tag{7.30}$$

otherwise clipping occurs.

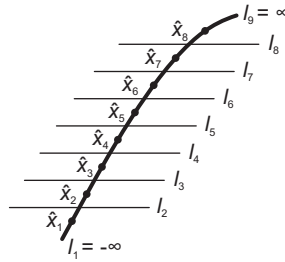


FIGURE 7.7 Signal level quantization.

The quantization error is

$$e[n] = Q[x[n]] - x[n] \tag{7.31}$$

and is bounded by

$$|e[n]| < \Delta/2, \tag{7.32}$$

apart from a high error that may result if clipping occurs.

The case of $M = 4$ bit uniform quantization, that is, the case of 3-bit magnitude plus a sign bit, where the quantizer output is rounded to the nearest quantization level is shown in Fig. 7.8.

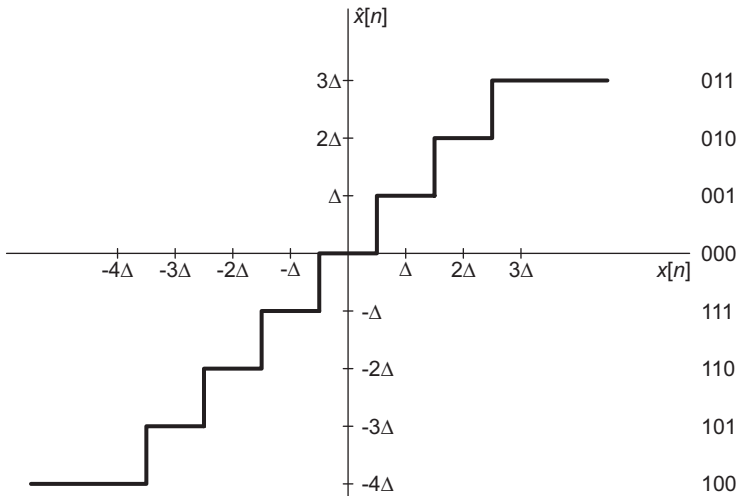


FIGURE 7.8 A/D quantization steps and their 2's complement code.

The values of the output in the case of 2's complement are shown in the figure.

As seen in Chapter 15, in fractional representation a number in 2's complement which has $(b + 1)$ bits in the form $x_0, x_1, x_2, \dots, x_b$ has the decimal value

$$-x_0 + x_1 2^{-1} + x_2 2^{-2} + \dots + x_b 2^{-b}. \tag{7.33}$$

For example, referring to the figure, the decimal value of 011 is $0 + 2^{-1} + 2^{-2} = 1/2 + 1/4 = 3/4$ and that of 110 is $-1 + 2^{-1} + 0 = -1 + 1/2 = -2/4$. In integer number representation

the same number is viewed as $x_b, x_{b-1}, \dots, x_1, x_0$ and has the decimal value

$$-x_b 2^b + x_{b-1} 2^{b-1} + \dots + x_1 2^1 + x_0 2^0 \tag{7.34}$$

so that the decimal value of 011 is $0 + 2 + 2^0 = 3$ and that of 110 is $-2^2 + 2 + 0 = -2$. In other words the two numbers are seen as $3/4$ and $-2/4$ in fractional representation, and as 3 and -2 in integer representation. These values are confirmed in the figure as corresponding to the levels 3Δ and -2Δ , respectively in either fractional or integer representation. In general, a integer number of decimal value a represented by $b + 1$ bits is viewed as simply the integer value a itself in integer representation, and as $a/2^b$ in fractional representation. The two representations are different ways of describing the same values; the fractional representation being more commonly used in signal processing literature.

7.4 Quantization Error

As we have seen, quantization is an approximation process of signal levels. The error of quantization $e[n]$ may be modeled as an additive noise such that

$$\hat{x}[n] = x[n] + e[n] \tag{7.35}$$

as shown in Fig. 7.9.

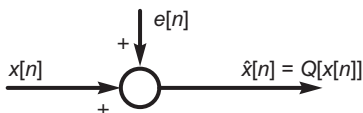


FIGURE 7.9 Additive quantization error.

Since the error is typically unknown it is defined in statistical terms. It is assumed to be a stationary white noise sequence that is uniformly distributed over the range $-\Delta/2 < e[n] < \Delta/2$. The values $e[n]$ and $e[k]$, where $k \neq n$ are therefore statistically uncorrelated. Moreover, it is assumed that the error sequence $e[n]$ is uncorrelated with the input sequence $x[n]$, which is assumed to be zero-mean and also stationary.

The signal to quantization noise ratio (SQNR) is defined as

$$\text{SQNR} = 10 \log_{10} \frac{P_x}{P_e} = 10 \log_{10} \frac{\sigma_x^2}{\sigma_e^2} \tag{7.36}$$

where P_x is the signal power

$$P_x = \sigma_x^2 = E[x^2[n]] \tag{7.37}$$

and P_e is the quantization power

$$P_e = \sigma_e^2 = E[e^2[n]]. \tag{7.38}$$

In the case where the quantization error is uniformly distributed with a probability density $p(e)$, as depicted in Fig. 7.10, we have

$$P_e = \sigma_e^2 = \int_{-\Delta/2}^{\Delta/2} p(e)e^2 de = \frac{1}{\Delta} \int_{-\Delta/2}^{\Delta/2} e^2 de = \frac{\Delta^2}{12} \tag{7.39}$$

Hence

$$\begin{aligned} \text{SQNR} &= 10 \log \frac{\sigma_x^2}{\sigma_e^2} = 20 \log_{10} \left(\frac{\sqrt{12}\sigma_x}{\Delta} \right) = 20 \log_{10} \left(\frac{\sqrt{12}\sigma_x 2^{b+1}}{R} \right) \\ &= 16.818 + 6.02b + 20 \log_{10} \frac{\sigma_x}{R} \text{ dB.} \end{aligned}$$

The SQNR can thus be seen to increase by about 6 dB for every increase of 1 bit.

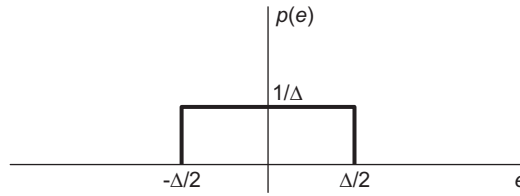


FIGURE 7.10 Quantization error probability density.

7.5 D/A Conversion

In D/A conversion, as represented in Fig. 7.11, the sequence $x[n]$ is converted to a succession of impulses so that each value $x[n]$ is converted to an impulse of intensity $x[n]$. The resulting signal is the ideally sampled signal $x_s(t)$. This in turn is applied to the input of a reconstruction ideal lowpass filter of frequency response $H_r(j\omega)$ to produce the continuous-time signal $x_c(t)$.

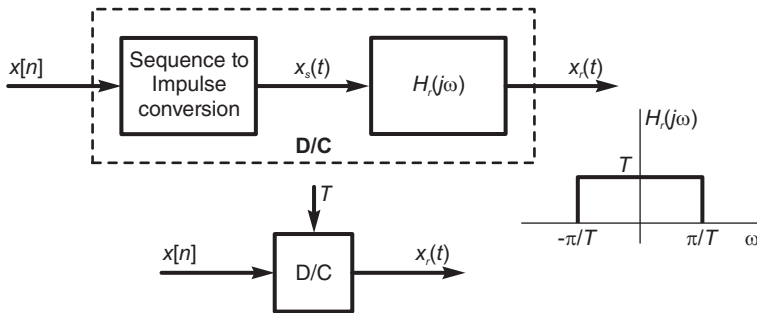


FIGURE 7.11 D/C conversion.

We may write

$$x_s(t) = \sum_{n=-\infty}^{\infty} x[n]\delta(t - nT) \tag{7.40}$$

$$X_s(j\omega) = \sum_{n=-\infty}^{\infty} x[n]e^{-jnT\omega} = X(e^{j\omega T}) = X(e^{j\Omega})|_{\Omega=\omega T} \tag{7.41}$$

The ideal lowpass reconstruction filter has the frequency response

$$H_r(j\omega) = T\Pi_{\pi/T}(\omega) \tag{7.42}$$

and its impulse response is

$$h_r(t) = Sa(\pi t/T) \tag{7.43}$$

The continuous-time signal $x_c(t)$ is assumed to be bandlimited so that $X_c(j\omega) = 0$ for $|\omega| > \omega_c = 2\pi f_c$ and the sampling period $T < \pi/\omega_c$ so that the sampling frequency $f_s = 1/T > 2f_c$. Aliasing is therefore absent. The filter output is

$$x_r(t) = x_s(t) * h_r(t) = \sum_{n=-\infty}^{\infty} x[n]\delta(t - nT) * h_r(t) = \sum_{n=-\infty}^{\infty} x[n]Sa[(\pi/T)(t - nT)] \tag{7.44}$$

which, as we have seen in Chapter 4, is the interpolation formula that reconstructs $x_c(t)$ from its sampled version. The filter output is therefore $x_r(t) = x_c(t)$ and the reconstruction produces the original continuous-time signal.

In the frequency domain we have

$$X_r(j\omega) = X_s(j\omega)H_r(j\omega) = X(e^{j\omega T})H_r(j\omega) \tag{7.45}$$

i.e.

$$X_r(j\omega) = \begin{cases} TX(e^{j\omega T}), & |\omega| < \pi/T \\ 0, & \text{otherwise.} \end{cases} \tag{7.46}$$

Since an ideal lowpass filter is not physically realizable, D/A converters use a zero-order hold that converts the ideally sampled signal $x_s(t)$ to a naturally sampled signal $x_n(t)$. The impulse response of the zero order hold is

$$h_z(t) = R_T(t) \tag{7.47}$$

and its frequency response is

$$H_z(j\omega) = Te^{-jT\omega/2}Sa(T\omega/2). \tag{7.48}$$

The result is a special case of natural sampling and produces a staircase-like signal as shown in Fig. 7.12.

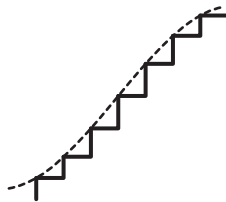


FIGURE 7.12 Natural sampling with zero-order hold.

As we have seen in Chapter 4 the reconstruction of such a signal may be effected using an equalizer filter of frequency response

$$H(j\omega) = \frac{e^{jT\omega/2}}{Sa(T\omega/2)}\Pi_{\pi/T}(\omega). \tag{7.49}$$

7.6 Continuous versus Discrete Signal Processing

In this section we consider two dual approaches to signal processing. In the first, depicted in Fig. 7.13(a) a continuous-time signal $x_c(t)$ is sampled by a C/D converter producing the sequence $x[n]$. The sequence is processed by a discrete-time system such as a digital filter of transfer function $H(z)$ and frequency response $H(e^{j\Omega})$.

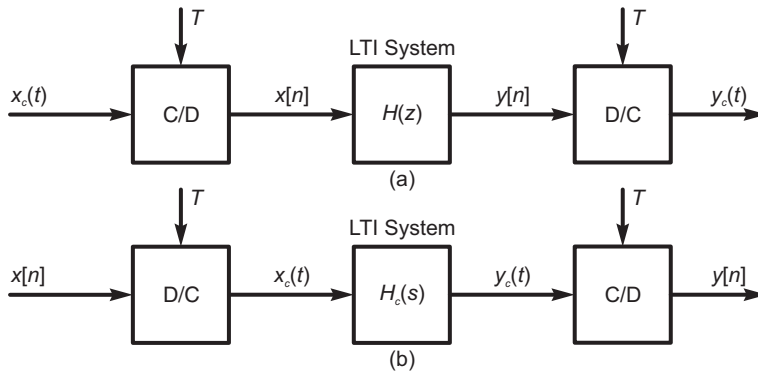


FIGURE 7.13 C/D and D/C signal processing: (a) discrete-time processing of analog signal, (b) continuous-time processing of discrete-time signal.

The output $y[n]$ is then converted back to the continuous-time domain as the signal $y_c(t)$. In Fig. 7.13(b) a sequence $x[n]$ is applied to a D/C converter producing a continuous-time signal $x_c(t)$. This is applied to the input of a continuous-time system such as an analog filter of transfer function $H(s)$ and frequency response $H(j\omega)$. The output $y_c(t)$ is then sampled by a C/D converter, producing the sequence $y[n]$. We note that the overall system shown in Fig. 7.13(a) acts as continuous-time system with input $x_c(t)$ and output $y_c(t)$, while that of Fig. 7.13(b) acts as a discrete-time system with input $x[n]$ and output $y[n]$. In what follows we develop the relations between the successive signals and in these two systems. Referring to Fig. 7.13(a) we may write

$$X(e^{j\Omega}) = \mathcal{F}[x[n]] = \frac{1}{T} \sum_{n=-\infty}^{\infty} X_c \left(j\frac{\Omega}{T} - j\frac{2\pi n}{T} \right) \tag{7.50}$$

$$Y(e^{j\Omega}) = X(e^{j\Omega})H(e^{j\Omega}) \tag{7.51}$$

The D/C converter reconstructs the continuous-time signal corresponding to the sequence $y[n]$ using a lowpass filter of frequency response

$$H_r(j\omega) = T\Pi_{\pi/T}(\omega) \tag{7.52}$$

so that

$$y_c(t) = \sum_{n=-\infty}^{\infty} y[n]h_r(t - nT) = \sum_{n=-\infty}^{\infty} y[n]Sa[(\pi/T)(t - nT)] \tag{7.53}$$

$$Y_c(j\omega) = H_r(j\omega)Y(e^{jT\omega}) = H_r(j\omega)X(e^{jT\omega})H(e^{jT\omega}) \quad (7.54)$$

$$= H_r(j\omega)H(e^{jT\omega})\frac{1}{T}\sum_{n=-\infty}^{\infty}X_c\left(j\omega - j\frac{2\pi n}{T}\right). \quad (7.55)$$

Since there is no aliasing we have

$$Y_c(j\omega) = H(e^{jT\omega})X_c(j\omega)\Pi_{\pi/T}(\omega) \quad (7.56)$$

$$Y_c(j\omega) = \begin{cases} H(e^{j\omega T})X_c(j\omega), & |\omega| \leq \pi/T \\ 0, & \text{otherwise.} \end{cases} \quad (7.57)$$

The overall digital signal processing (DSP) system of Fig. 7.13(a) acts therefore as a linear time invariant (LTI) continuous-time system of frequency response

$$H_c(j\omega) = \begin{cases} H(e^{j\omega T}), & |\omega| \leq \pi/T \\ 0, & \text{otherwise} \end{cases} \quad (7.58)$$

Referring to Fig. 7.13(b) we may write in the absence of aliasing

$$x_c(t) = \sum_{n=-\infty}^{\infty}x[n]Sa[(\pi/T)(t - nT)] \quad (7.59)$$

$$X_c(j\omega) = \begin{cases} TX(e^{j\omega T}), & |\omega| \leq \pi/T \\ 0, & \text{otherwise} \end{cases} \quad (7.60)$$

$$Y_c(j\omega) = \begin{cases} H_c(j\omega)X_c(j\omega), & |\omega| \leq \pi/T \\ 0, & \text{otherwise} \end{cases} \quad (7.61)$$

$$Y(e^{j\Omega}) = \sum_{n=-\infty}^{\infty}y[n]e^{-jn\Omega} = \sum_{n=-\infty}^{\infty}y_c(nT)e^{-jn\Omega} = \frac{1}{T}\sum_{n=-\infty}^{\infty}Y_c\left(j\frac{\Omega}{T} - j\frac{2\pi n}{T}\right) \quad (7.62)$$

$$Y(e^{j\Omega}) = \frac{1}{T}Y_c\left(j\frac{\Omega}{T}\right) = \frac{1}{T}X_c\left(j\frac{\Omega}{T}\right)H_c\left(j\frac{\Omega}{T}\right), |\Omega| < \pi \quad (7.63)$$

and

$$H(e^{j\Omega}) = H_c\left(j\frac{\Omega}{T}\right), |\Omega| < \pi \quad (7.64)$$

which is the equivalent overall system frequency response. The system output is

$$y_c(t) = \sum_{n=-\infty}^{\infty}y[n]Sa[(\pi/T)(t - nT)]. \quad (7.65)$$

7.7 Interlacing with Zeros

We have studied in Chapter 2 the case where the analysis interval of the Fourier series expansion is a multiple m of the function period. We have concluded that the discrete Fourier series spectrum is the same as that obtained if the analysis interval is equal to the function period but with $(m - 1)$ zeros inserted between the spectral lines.

Thanks to duality between the Fourier series (discrete spectrum) of a continuous-time function and the (continuous) Fourier transform of a discrete time function we have the same phenomenon that can be observed in discrete-time signals. The following example shows that by inserting $(M - 1)$ zeros between time-sequence samples the spectrum around the unit circle displays M repetitions of the signal spectrum.

Example 7.3 Let $x[n]$ be a given sequence and $x_1[n]$ be the sequence defined by

$$x_1[n] = \begin{cases} x[n/3], & n \text{ multiple of } 3 \\ 0, & \text{otherwise.} \end{cases}$$

Compare the spectra $X(e^{j\Omega})$ and $X_1(e^{j\Omega})$.

We can write

$$x_1[n] = \dots, x[-2], 0, 0, x[-1], 0, 0, x[0], 0, 0, x[1], 0, 0, x[2], 0, 0, \dots$$

$$X_1(z) = \sum_{n=-\infty}^{\infty} x[n]z^{-3n} = X(z^3)$$

$$X_1(e^{j\Omega}) = \sum_{n=-\infty}^{\infty} x[n]e^{-j\Omega 3n} = X(e^{j3\Omega}).$$

See Fig. 7.14.

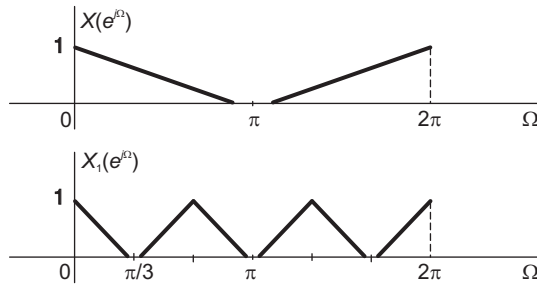


FIGURE 7.14 Spectral compression.

The generalization of this example is that if a sequence $x_1[n]$ is obtained from $x[n]$ such that

$$x_1[n] = \begin{cases} x[n/M], & n = \text{multiple of } M \\ 0, & \text{otherwise} \end{cases} \quad (7.66)$$

by interlacing with $M - 1$ zeros, an operation referred to as *upsampling* by a factor M as we shall see in the following section then

$$X_1(z) = \sum_{n=-\infty}^{\infty} x[n]z^{-Mn} = X(z^M)$$

$$X_1(e^{j\Omega}) = X(e^{jM\Omega}) \quad (7.67)$$

and the spectrum along the unit circle displays M periods instead of one period of $X(e^{j\Omega})$.

Here we have the duality to the case of Fourier series analysis with a multiple-period analysis interval. In the present case, insertion of $M - 1$ zeros in the time domain between the samples of $x[n]$ produces in the frequency domain, in the interval $(0, 2\pi)$, the spectrum $X_1(e^{j\Omega})$ which has M periods instead of the single period of the spectrum $X(e^{j\Omega})$ of $x[n]$.

Downsampling is the case when a sequence $y[n]$ is obtained from a sequence $x[n]$ by picking every M^{th} sample.

Example 7.4 Evaluate the z -transform and the Fourier transform of the sequence down-sampled sequence $y[n] = x[Mn]$ as a function of those of $x[n]$.

We have

$$Y(z) = \sum_{n=-\infty}^{\infty} y[n] z^{-n} = \sum_{n=-\infty}^{\infty} x[Mn] z^{-n}. \quad (7.68)$$

Letting $m = Mn$ we have

$$Y(z) = \sum_{m=0, \pm M, \pm 2M, \dots} x[m] z^{-m/M}. \quad (7.69)$$

We note that

$$\frac{1}{M} \sum_{k=0}^{M-1} e^{j\frac{2\pi}{M}km} = \begin{cases} 1, & m = 0, \pm M, \pm 2M, \dots \\ 0, & \text{otherwise.} \end{cases} \quad (7.70)$$

$$\begin{aligned} Y(z) &= \sum_{m=-\infty}^{\infty} x[m] z^{-m/M} \frac{1}{M} \sum_{k=0}^{M-1} e^{j\frac{2\pi}{M}km} = \frac{1}{M} \sum_{k=0}^{M-1} \sum_{m=-\infty}^{\infty} x[m] z^{-m/M} e^{j(2\pi/M)km} \\ &= \frac{1}{M} \sum_{k=0}^{M-1} \sum_{m=-\infty}^{\infty} x[m] \{z^{1/M} e^{-j2\pi k/M}\}^{-m} = \frac{1}{M} \sum_{k=0}^{M-1} X\{z^{1/M} e^{-j2\pi k/M}\}. \end{aligned} \quad (7.71)$$

Substituting $z = e^{j\Omega}$ we have the Fourier transform

$$Y(e^{j\Omega}) = \frac{1}{M} \sum_{k=0}^{M-1} X\{e^{j\Omega/M} e^{-j2\pi k/M}\} = \frac{1}{M} \sum_{k=0}^{M-1} X\{e^{j(\Omega-2\pi k)/M}\}. \quad (7.72)$$

Note that for $|\Omega| \leq \pi$

$$Y(e^{j\Omega}) = \frac{1}{M} X(e^{j\Omega/M}). \quad (7.73)$$

7.8 Sampling Rate Conversion

We often need to alter the sampling rate of a signal. For example we may need to convert signals from digital audio tapes (DAT) which are sampled at 48 kHz rate to the CD sampling rate of 44.1 kHz. Other applications include converting video signals between systems that use different sampling rates. Sample rate conversion may be performed by reconstructing the continuous-time domain signal followed by resampling at the desired rate. We consider here the rate conversion when performed entirely in the discrete-time domain. In what follows, we study rate reduction by an integer, rate increase by an integer and rate alteration by a rational factor.

7.8.1 Sampling Rate Reduction

In this section we study the problem of sample rate reduction by an integer factor. Let $x_c(t)$ be a continuous-time signal and $x_s(t)$ be its ideally sampled version with a sampling interval of T seconds, that is,

$$x_s(t) = x_c(t) \rho_T(t) = x_c(t) \sum_{n=-\infty}^{\infty} \delta(t - nT). \quad (7.74)$$

Let $x[n]$ be the corresponding discrete-time signal $x[n] = x_c(nT)$. We consider the case of reducing the sampling rate by increasing the sampling interval by an integer multiple M , so that the sampling interval is $\tau = MT$. This operation is called *down-sampling*. The resulting ideally sampled signal and corresponding sequence will be denoted by $x_{s,r}(t)$ and $x_r[n]$, respectively.

We have

$$x_{s,r}(t) = x_c(t) \sum_{n=-\infty}^{\infty} \delta(t - nMT) \quad (7.75)$$

$$x_r[n] = x_c(nMT). \quad (7.76)$$

Below, we evaluate the Fourier transform and the z -transform of these signals. The Fourier spectra of $x_c(t)$, $x_s(t)$, $x[n]$, $x_{s,r}(t)$ and $x_r[n]$ are sketched in Fig. 7.15 assuming an idealized trapezoidal shaped spectrum $X_c(j\omega)$ representing that of a bandlimited signal. The equations defining these spectra follow. For now, however, note that these spectra can be drawn without recourse to equations. From our knowledge of ideal sampling we note that the spectrum $X_s(j\omega)$ is a periodic repetition of the trapeze, which may be referred to as the basic “lobe,” $X_c(j\omega)$, with a period of $\omega_s = 2\pi/T$ and a gain factor of $1/T$. The spectrum $X(e^{j\Omega})$ versus Ω is identical to the spectrum $X_s(j\omega)$ after the scale change $\Omega = \omega T$. The spectrum $X_{s,r}(j\omega)$ of the sequence $x_r[n]$ is a periodic repetition of $X_c(j\omega)$ with a period of $\omega_{s,2} = 2\pi/(MT)$ and a gain factor of $1/(MT)$. In the figure the value M is taken equal to 3 for illustration, and the spectrum is drawn for the critical case where the successive spectra barely touch; just prior to aliasing. Finally, the spectrum $X_r(e^{j\Omega})$ is but a rescaling of $X_{s,r}(j\omega)$ with the substitution $\Omega = \omega MT$.

We note from Fig. 7.15 that by applying a sampling interval $\tau = MT$ instead of T , that is, by reducing the sampling frequency from $2\pi/T$ to $2\pi/(MT)$, aliasing may occur in $X_{s,r}(j\omega)$ and hence $X_r(e^{j\Omega})$ due to the fact that the lobe centered at the sampling frequency $\omega_{s,2} = 2\pi/(MT)$ is M times closer to the main lobe than in the case of ordinary sampling leading to $X_s(j\omega)$.

Assuming

$$X_c(j\omega) = 0, \quad |\omega| \geq \omega_c \quad (7.77)$$

to avoid aliasing, the sampling frequency should satisfy the condition

$$\frac{2\pi}{MT} \geq 2\omega_c \quad (7.78)$$

i.e.,

$$\omega_c \leq \frac{\pi}{MT}. \quad (7.79)$$

Let $\Omega_c = \omega_c T$. For the normal rate of sampling producing $x[n]$ the constraint on the signal bandwidth to avoid aliasing is

$$X(e^{j\Omega}) = 0, \quad \Omega_c \leq |\Omega| < \pi \quad (7.80)$$

whereas for the reduced sampling rate, producing $x_r[n]$, it is

$$X(e^{j\Omega}) = 0, \quad M\Omega_c \leq |\Omega| < \pi, \quad \text{i.e. } \Omega_c < \pi/M. \tag{7.81}$$

Therefore the bandwidth of the sequence $x[n]$ has to be reduced by a factor M before down-sampling in order to avoid aliasing due to the reduced sampling rate.

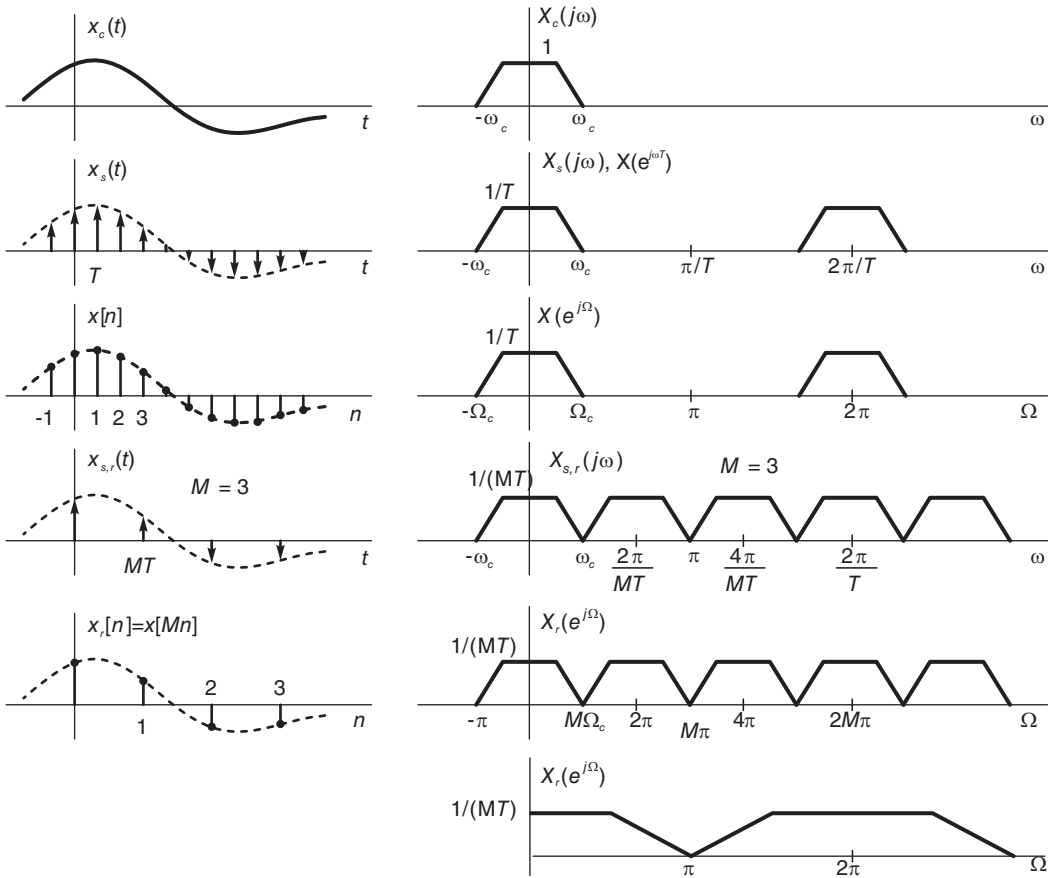


FIGURE 7.15 Sample rate reduction.

Down-sampling by a factor M is usually denoted by a down arrow and the letter M written next to it, as can be seen in Fig. 7.16(a).

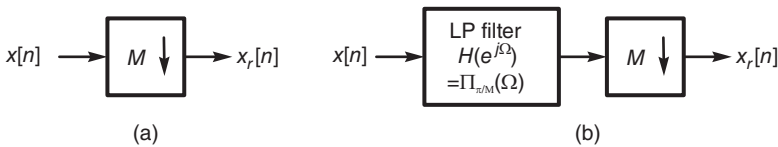


FIGURE 7.16 Sample rate reduction: (a) down-sampling, (b) decimation.

Aliasing can thus be avoided by passing the sequence through a prefiltering lowpass filter of bandwidth equal to π/M and a gain of one, that is, of frequency response

$$H(e^{j\Omega}) = \Pi_{\pi/M}(\Omega) = u[\Omega + \pi/M] - u[\Omega - \pi/M], \quad |\Omega| < \pi \quad (7.82)$$

prior to the sampling rate reduction, as seen in Fig. 7.16(b). Such prefiltering followed by sample-rate reduction is referred to as *decimation*.

We proceed now to write the pertinent equations assuming that the reduced sampling rate is adequate, producing no aliasing, as shown in the figure. From our knowledge of ideal sampling, the Fourier spectrum $X_s(j\omega) = \mathcal{F}[x_s(t)]$ is given by

$$X_s(j\omega) = \frac{1}{T} \sum_{m=-\infty}^{\infty} X_c[j(\omega - m2\pi/T)]. \quad (7.83)$$

The spectrum of the sequence $x[n]$ is given by

$$X(e^{j\Omega}) = X_s\left(j\frac{\Omega}{T}\right) = \frac{1}{T} \sum_{m=-\infty}^{\infty} X_c\left[j\left(\frac{\Omega}{T} - \frac{m2\pi}{T}\right)\right]. \quad (7.84)$$

With a sampling interval MT instead of T we have the spectrum $X_{s,r}(j\omega) = \mathcal{F}[x_{s,r}(t)]$ equal to

$$X_{s,r}(j\omega) = \frac{1}{MT} \sum_{m=-\infty}^{\infty} X_c\left[j\left(\omega - \frac{m2\pi}{MT}\right)\right]. \quad (7.85)$$

The spectrum of $x_r[n]$ is given by

$$X_r(e^{j\Omega}) = X_{s,r}(j\omega)|_{\omega=\Omega/(MT)} = \frac{1}{MT} \sum_{m=-\infty}^{\infty} X_c\left[j\left(\frac{\Omega - 2m\pi}{MT}\right)\right]. \quad (7.86)$$

An alternative form of the spectrum $X_{s,r}(j\omega)$ may be written by noticing from Fig. 7.15 that it is a periodic repetition with period $2\pi/T$ of a set of lobes, namely those centered at

$$\omega = 0, 2\pi/(MT), 4\pi/(MT), \dots, (M-1)2\pi/(MT).$$

In other words the spectrum is a repetition of the base period

$$X_{s,r,0}(j\omega) = \frac{1}{MT} \sum_{k=0}^{M-1} X_c\left[j\left(\omega - k\frac{2\pi}{MT}\right)\right] \quad (7.87)$$

so that we can write

$$X_{s,r}(j\omega) = \sum_{n=-\infty}^{\infty} X_{s,r,0}\left[j\left(\omega - \frac{2\pi n}{T}\right)\right]. \quad (7.88)$$

$$X_{s,r}(j\omega) = \frac{1}{MT} \sum_{n=-\infty}^{\infty} \sum_{k=0}^{M-1} X_c\left[j\left(\omega - \frac{2\pi k}{MT} - \frac{2\pi n}{T}\right)\right]. \quad (7.89)$$

Note that this second form can be obtained from the first by the simple substitution $m = Mn + k$, where $-\infty \leq n \leq \infty$ and $k = 0, 1, 2, \dots, M-1$. Using this second form we can write a second form for $X_r(e^{j\Omega})$, namely,

$$X_r(e^{j\Omega}) = X_{s,r}\left(\frac{j\Omega}{MT}\right) = \frac{1}{MT} \sum_{n=-\infty}^{\infty} \sum_{k=0}^{M-1} X_c\left[j\left(\frac{\Omega - 2\pi k}{MT} - \frac{2\pi n}{T}\right)\right] \quad (7.90)$$

$$X_r(e^{j\Omega}) = \frac{1}{M} \sum_{k=0}^{M-1} \frac{1}{T} \sum_{n=-\infty}^{\infty} X_c \left[j \left(\frac{\Omega - 2\pi k}{MT} - \frac{2\pi n}{T} \right) \right] \quad (7.91)$$

$$X_r(e^{j\Omega}) = \frac{1}{M} \sum_{k=0}^{M-1} X \left\{ e^{j(\Omega - 2\pi k)/M} \right\}. \quad (7.92)$$

Note that

$$X_r(e^{j\Omega}) = \frac{1}{M} X(e^{j\Omega/M}), \quad |\Omega| \leq \pi. \quad (7.93)$$

We may obtain the same result by noticing that

$$X_r(z) = \sum_{n=-\infty}^{\infty} x_r[n] z^{-n} = \sum_{n=-\infty}^{\infty} x[Mn] z^{-n} \quad (7.94)$$

and by proceeding as in Example 7.4, to arrive at the same result

$$X_r(e^{j\Omega}) = \frac{1}{M} \sum_{k=0}^{M-1} X \left\{ e^{j(\Omega - 2\pi k)/M} \right\}. \quad (7.95)$$

Example 7.5 A sequence $x[n]$ is bandlimited such that

$$X(e^{j\Omega}) = 0, \quad |\Omega| < 0.23\pi.$$

A sequence $y[n]$ is formed such that $y[n] = x[Mn]$. What is the maximum value M that ensures that the sequence $x[n]$ can be fully recovered from $y[n]$?

In Fig. 7.17 the spectrum $X(e^{j\Omega})$ is graphically sketched. The sequence $x[n]$ may be viewed as a sampling of a continuous time sequence $x_c(t)$ with a sampling interval T so that $x[n] = x_c(nT)$. The corresponding spectrum $X_s(j\omega)$ of the corresponding ideally sampled sequence

$$x_s(t) = x_c(t)\rho_T(t) = x_c(t) \sum_{n=-\infty}^{\infty} \delta(t - nT)$$

is shown next in the figure, where the sampling frequency is written $\omega_{s0} = 2\pi/T$. The sequence $y[n]$ corresponds to sampling the same continuous time sequence $x_c(t)$ but with a sampling interval MT , so that $y[n] = x[Mn] = x_c(MTn)$. In this case the sampling frequency is $\omega_s = 2\pi/(MT) = \omega_{s0}/M$, and the corresponding ideally sampled signal is

$$y_s(t) = x_c(t)\rho_{MT}(t) = x_c(t) \sum_{n=-\infty}^{\infty} \delta(t - nMT)$$

The spectrum $Y_s(j\omega)$ is periodic and its period is $\omega_s = \omega_{s0}/M$. The spectrum $Y(e^{j\Omega})$ of the sequence $y[n]$ is also shown in the figure. We note that the maximum value of M can have is $M = 4$, otherwise aliasing would occur. Alternatively, we note that bandwidth of the signal is $B = 0.23\pi/T$ so that the minimum sampling frequency that avoids aliasing is $\omega_s = 2B = 0.46\pi/T = 0.23\omega_{s0}$, i.e. we should have $\omega_s \geq 0.23\omega_{s0}$. Since $\omega_s = \omega_{s0}/M$, the maximum allowable value of M is $M = 4$ as stated.

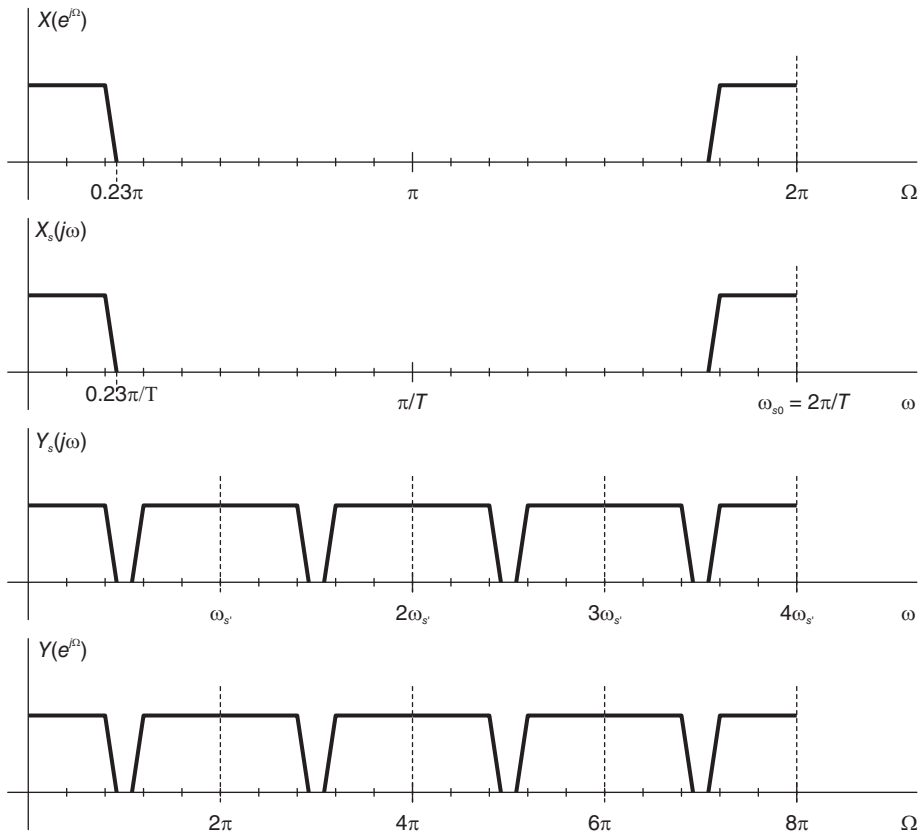


FIGURE 7.17 Maximum rate reduction example.

7.8.2 Sampling Rate Increase: Interpolation

Let $x[n]$ be the sampling of a continuous function $x_c(t)$ such that $x[n] = x_c(nT)$. Consider the effect of inserting $L - 1$ zeros between the successive samples of $x[n]$ as shown in Fig. 7.18. We obtain the sequence $x_z[n]$ such that

$$x_z[n] = \begin{cases} x[n/L], & n = mL, \quad m \text{ integer} \\ 0, & \text{otherwise.} \end{cases} \tag{7.96}$$

We have

$$X_z(z) = \sum_{n=-\infty}^{\infty} x_z[nL] z^{-nL} = \sum_{n=-\infty}^{\infty} x[n] z^{-nL} = X(z^L) \tag{7.97}$$

and

$$X_z(e^{j\Omega}) = X(e^{jL\Omega}). \tag{7.98}$$

The spectrum $X_z(e^{j\Omega})$ is shown in Fig. 7.18, where L is taken equal to 3, together with an assumed spectrum $X_c(j\omega)$ and the corresponding transform $X(e^{j\Omega})$. If a lowpass filter having the frequency response $H(e^{j\Omega})$, shown in the figure, with a gain of L and cut-off frequency π/L , is applied to $X_z(e^{j\Omega})$ the result is the spectrum $X_i(e^{j\Omega})$, also shown in the figure. The resulting sequence $x_i[n]$, of which the Fourier transform is $X_i(e^{j\Omega})$ is in fact an interpolation of $x[n]$.

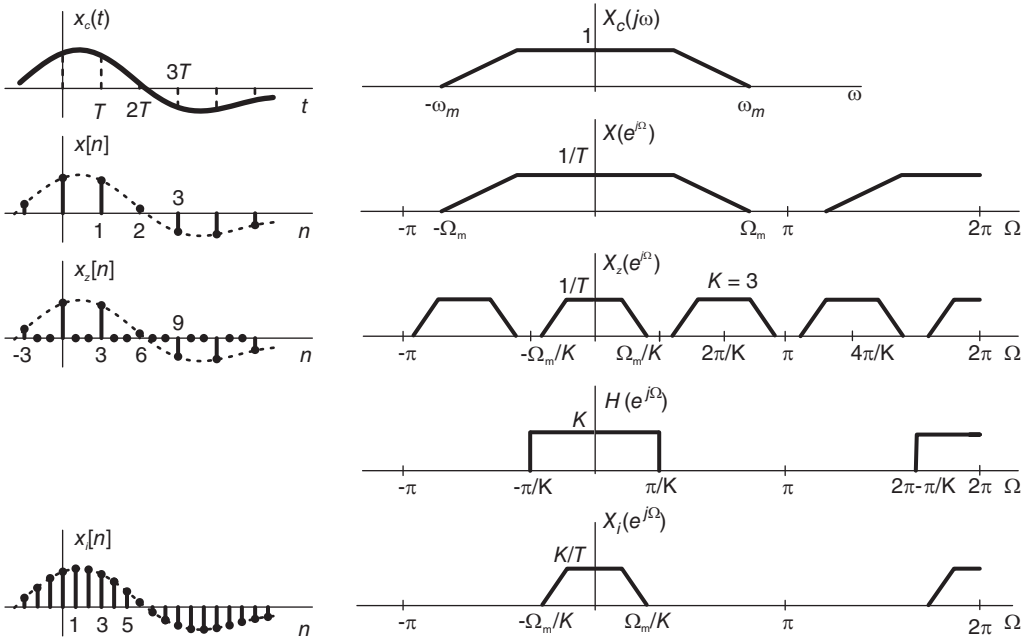


FIGURE 7.18 Interpolation spectra.

Note that

$$x_i[n] = x_z[n], \quad n = 0, \pm L, \pm 2L, \dots \tag{7.99}$$

The spectrum $X_i(e^{j\Omega})$ is, as desired, the spectrum that would be obtained if $x_c(t)$ were sampled with a sampling period of T/L . The insertion of zeros followed by the lowpass filtering thus leads to multiplying the sampling rate by a factor L or, equivalently, performing an L -point interpolation between the samples of $x[n]$ in the form of the sequence $x_i[n]$.

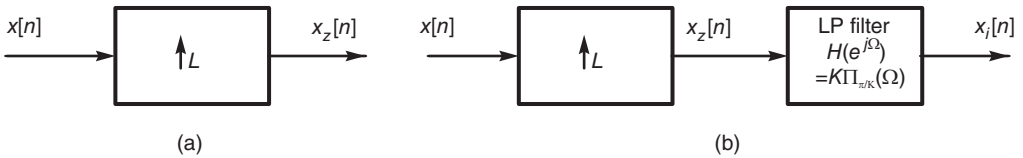


FIGURE 7.19 Sampling rate increase by a factor L : (a) upsampling, (b) interpolation.

As seen in Fig. 7.19(a) the upsampling operation by an integer factor L is denoted by an up arrow with the letter L written next to it. It interlaces $L-1$ zeros between samples. The interpolator, seen in Fig. 7.19(b), consists of the upsampling unit followed by the lowpass filter of frequency response

$$H(e^{j\Omega}) = K\Pi_{\pi/K}(\Omega) =, \quad |\Omega| < \pi. \tag{7.100}$$

Example 7.6 A sequence $x[n]$ is obtained by sampling the sinusoid $\cos(5000t)$ at a sampling frequency of 20000 Hz. It is then applied to the input of a system which interlaces with zeros by adding three zeros between each two consecutive samples. The sequence $y[n]$ is applied to

the input of a bandpass filter of unit gain and frequency response

$$H(e^{j\Omega}) = \begin{cases} 1, & \pi/4 < |\Omega| < 3\pi/4 \\ 0, & \text{otherwise.} \end{cases}$$

Evaluate the output $v[n]$ of the bandpass filter.

The sequence $y[n]$ is given by

$$y[n] = \begin{cases} x[n/4], & n \text{ multiple of } 4 \\ 0, & \text{otherwise.} \end{cases}$$

We have $f_s = 20 \text{ kHz}$. The sampling period is $T_s = 1/f_s$,

$$x_c(t) = \cos(\omega_0 t), \quad \omega_0 = 5000\pi$$

$f_0 = 2500 \text{ Hz}$, $\Omega_0 = \omega_0 T_s = 5000\pi/20000 = \pi/4$. $Y(z) = X(z^4)$, $Y(e^{j\Omega}) = X(e^{j4\Omega})$. The system performs upsampling by a factor of 4 as seen in Fig. 7.20.

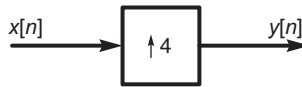


FIGURE 7.20 Upsampling by a factor of 4.

The spectra $X_s(j\omega)$, $X(e^{j\Omega})$, and $Y(e^{j\Omega})$ are depicted in in Fig. 7.21. The figure also shows the filter frequency response $H(e^{j\Omega})$ and the spectrum $V(e^{j\Omega})$ at the filter output. In evaluating $Y(e^{j\Omega})$ we use the impulse property

$$\delta(ax) = \frac{1}{|a|} \delta(x).$$

From the value of $V(e^{j\Omega})$, as seen in the figure, we conclude that the filter output is

$$v[n] = 0.25[\cos[(7\pi/16)n] + \cos[(9\pi/16)n]].$$

Example 7.7 In the up-down rate conversion-filtering system shown in Fig. 7.22 the C/D converter operates at a sampling frequency $f_s = 1/T$, the output of the upsampler is applied to the input of an LTI system of impulse response

$$h[n] = K \text{Sa}[\pi(n - m)/M]$$

where m is an integer.

Assuming that the input signal $x_c(t)$ is bandlimited so that $X_c(j\omega) = 0$ for $|\omega| \geq 1/(2T)$. Evaluate the system output $z[n]$ in terms of its input $x_c(t)$.

We have

$$v[n] = \begin{cases} x[n/L] = x_c(nT/L), & n = kL, \quad k \text{ integer} \\ 0, & \text{otherwise} \end{cases} \tag{7.101}$$

$$H(e^{j\Omega}) = KL \Pi_{\pi/L}(\Omega) e^{-jm\Omega}$$

$$w[n] = K v[n - m] = K x_c[(n - m)T/L]$$

$$z[n] = w[Ln] = K x_c[(Ln - m)T/L]$$

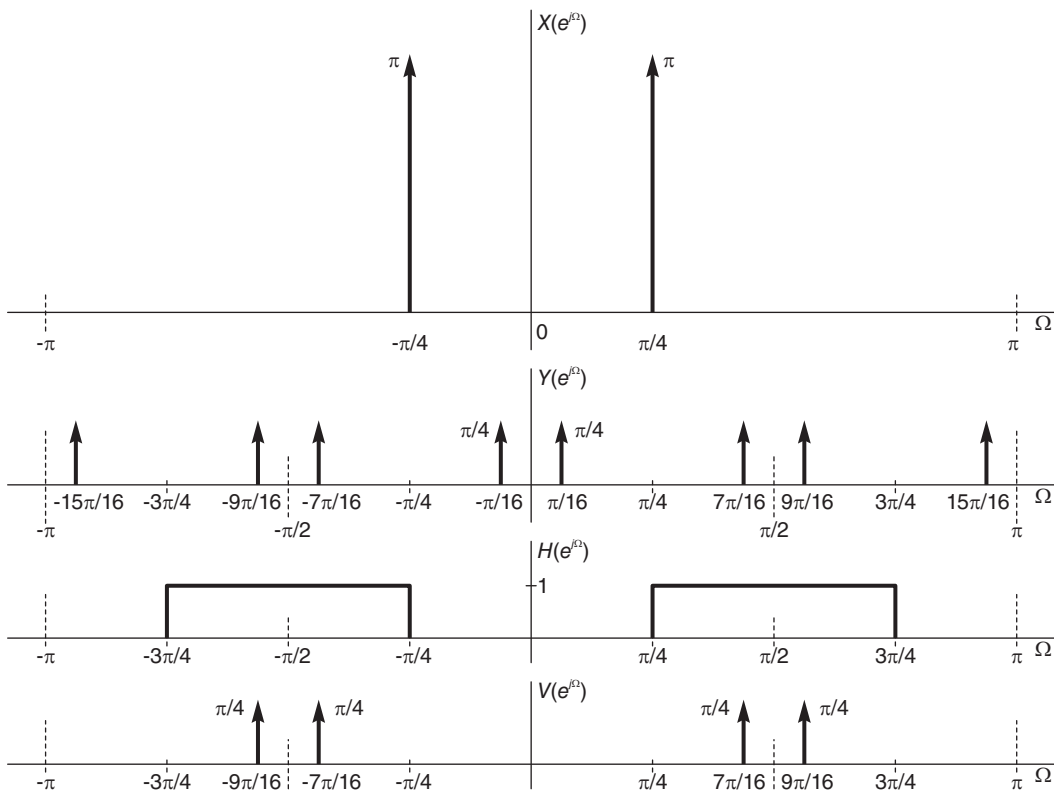


FIGURE 7.21 Spectra of an upsampling system.

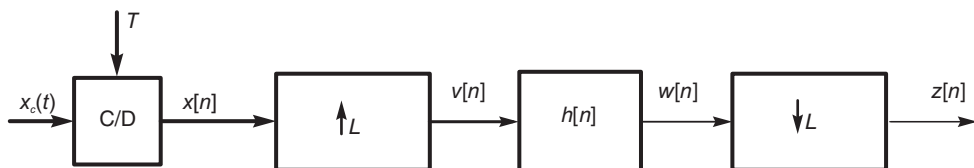


FIGURE 7.22 Rate conversion-filtering system.

7.8.3 Rational Factor Sample Rate Alteration

If the sampling rate of a sequence needs to be increased or decreased by a rational factor $F = K/M$, the sample rate alteration can be effected by cascading an interpolator which increases the sample rate by a factor L , followed by a decimator which reduces the resulting rate by a factor M . Such sample-rate converter is shown in Fig. 7.23(a).

The sequence $x[n]$ is applied to an interpolator followed by a decimator resulting in the altered-rate sequence $x_c[n]$. Note that the two cascaded lowpass filters of cut-off frequencies π/L and π/M , respectively, can be combined into a single lowpass filter, as shown in Fig. 7.23(b), of cut-off frequency π/B , where $B = \max(M, L)$, and a gain of L .

Example 7.8 A sequence $x[n]$ is obtained in a DAT recorder by sampling audio signals at a frequency of 48 kHz. We need to convert the sampling rate to that of CD players, namely 44.1 kHz. Show how to perform the rate conversion.

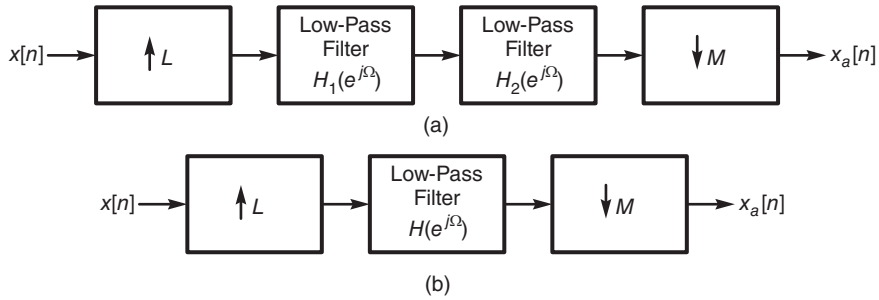


FIGURE 7.23 Sample rate rational factor alteration.

We may employ the rate conversion system shown in Fig. 7.24. We note that $48,000 = 2^7 \times 3 \times 5^3$ and $44,100 = 2^2 \times 3^2 \times 5^2 \times 7^2$. so that $48,000/44,100 = 2^5 \times 3^{-1} \times 5 \times 7^2 = 160/147$.

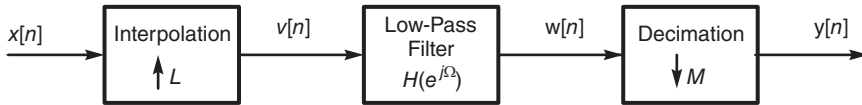


FIGURE 7.24 Sample rate conversion by a rational factor.

Note that decomposition into prime numbers can be performed using the MATLAB® function **factor**.

The system would therefore perform a sampling increase, interpolation, by the factor $L = 160$, filtering, as shown in the figure, and then sampling rate reduction, decimation, by a factor $M = 147$. The lowpass filter should have a cut frequency of $\pi/160$ and a gain of $L = 160$.

MATLAB's multirate processing function **upfirdn** may be called to change a signal sampling rate from 44.1 kHz to 48 kHz using a filter of a finite impulse response (FIR), which will be studied in detail in Chapter 11. We may write

```
g = gcd(48000,44100)
p = 48000/g
q = 44100/g
y = upfirdn(x,h,p,q)
```

We obtain $p = 160$, $q = 147$. The output result y is the response of the FIR filter, of impulse response h , to the input x .

Other related MATLAB functions are **decimate**, **interp** and **resample**.

7.9 Fourier Transform of a Periodic Sequence

Given a continuous-time periodic signal $v_c(t)$ and its discrete time sampling $v[n] = v_c(nT)$, we can evaluate its DTFT using the Fourier transform of its continuous-time counterpart.

$$V(e^{j\Omega}) = \frac{1}{T} \sum_{k=-\infty}^{\infty} V_c \left[j \left(\frac{\Omega - 2\pi k}{T} \right) \right] = \frac{1}{T} \sum_{k=-\infty}^{\infty} V_c(j\omega) \Big|_{\omega = \frac{\Omega - 2\pi k}{T}} \tag{7.102}$$

where

$$V(e^{j\Omega}) = \mathcal{F}[v[n]] \quad \text{and} \quad V_c(j\omega) = \mathcal{F}[v_c(t)]. \tag{7.103}$$

Example 7.9 Let $v[n] = 1$. Evaluate $V(e^{j\Omega})$.

With $v_c(t) = 1$ we have $V_c(j\omega) = 2\pi\delta(\omega)$, wherefrom

$$V(e^{j\Omega}) = \frac{1}{T} \sum_{k=-\infty}^{\infty} 2\pi\delta \left(\frac{\Omega - 2\pi k}{T} \right) = \sum_{k=-\infty}^{\infty} 2\pi\delta(\Omega - 2\pi k).$$

Example 7.10 Let $v_c(t) = \cos(\beta t + \theta)$. Evaluate $V_c(j\omega)$ and $V(e^{j\Omega})$ for $v[n] = v_c(nT)$.

We may write

$$\begin{aligned} V_c(j\omega) &= \pi \{ e^{j\theta} \delta(\omega - \beta) + e^{-j\theta} \delta(\omega + \beta) \} \\ v[n] = v_c(nT) &= \cos(\beta nT + \theta) = \cos(\gamma n + \theta), \quad \gamma = \beta T \\ V(e^{j\Omega}) &= \frac{1}{T} \sum_{k=-\infty}^{\infty} V_c \left[j \left(\frac{\Omega - 2\pi k}{T} \right) \right] \\ &= \frac{1}{T} \sum_{k=-\infty}^{\infty} \pi \left\{ e^{j\theta} \delta \left(\frac{\Omega - 2\pi k}{T} - \beta \right) + e^{-j\theta} \delta \left(\frac{\Omega - 2\pi k}{T} + \beta \right) \right\} \\ &= \sum_{k=-\infty}^{\infty} \pi \{ e^{j\theta} \delta(\Omega - 2\pi k - \beta T) + e^{-j\theta} \delta(\Omega - 2\pi k + \beta T) \}. \end{aligned}$$

We have established the transformation:

$$\cos(\gamma n + \theta) \xleftrightarrow{\mathcal{F}} \sum_{k=-\infty}^{\infty} \pi \{ e^{j\theta} \delta(\Omega - 2\pi k - \gamma) + e^{-j\theta} \delta(\Omega - 2\pi k + \gamma) \}.$$

The spectrum appears as two impulses on the unit circle as represented in 3-D in Fig. 7.25.

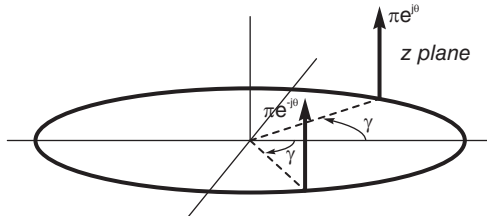


FIGURE 7.25 Impulses on unit circle.

7.10 Table of Discrete-Time Fourier Transforms

Table 7.1 lists discrete-time Fourier transforms of basic discrete-time functions.

TABLE 7.1 Discrete-time Fourier transforms of basic sequences

Sequence $x[n]$	Fourier Transform $X(e^{j\Omega})$
$\delta[n]$	1
$\delta[n - k]$	$e^{-jk\Omega}$
1	$\sum_{k=-\infty}^{\infty} 2\pi\delta(\Omega + 2k\pi)$
$u[n]$	$\frac{1}{1 - e^{-j\Omega}} + \sum_{k=-\infty}^{\infty} \pi\delta(\Omega + 2k\pi)$
$a^n u[n], a < 1$	$\frac{1}{1 - ae^{-j\Omega}}$
$(n + 1)a^n u[n], a < 1$	$\frac{1}{(1 - ae^{-j\Omega})^2}$
$R_N[n] = u[n] - u[n - N]$	$e^{-j(N-1)\Omega/2} Sd_N(\Omega/2)$
$\frac{\sin Bn}{\pi n}$	$\Pi_B(\Omega), -\pi \leq \Omega \leq \pi$
e^{jbn}	$2\pi \sum_{k=-\infty}^{\infty} \delta(\Omega - b + 2k\pi)$
$\cos(bn + \phi)$	$\pi \sum_{k=-\infty}^{\infty} e^{j\phi} \delta(\Omega - b + 2k\pi) + e^{-j\phi} \delta(\Omega + b + 2k\pi)$
$\sum_{k=-\infty}^{\infty} \delta[n - kN]$	$\frac{2\pi}{N} \sum_{k=-\infty}^{\infty} \delta\left(\Omega - \frac{2\pi k}{N}\right)$
$\frac{(n + r - 1)!}{n!(r - 1)!} a^n u[n], a < 1$	$\frac{1}{(1 - ae^{-j\Omega})^r}$
$nu[n]$	$\frac{e^{-j\Omega}}{(1 - e^{-j\Omega})^2} + j\pi \sum_{k=-\infty}^{\infty} \delta'(\Omega + 2k\pi)$

Example 7.11 Given $v_c(t) = \cos(2\pi \times 1000t)$. Let $T = 1/1500$ sec be the sampling period of $v_c(t)$ producing the discrete-time sampling $v[n] = v_c(nT)$. Evaluate $V(e^{j\Omega})$.

$$v[n] = v_c(nT) = \cos\left(2\pi \times 1000 \times \frac{1}{1500}n\right) = \cos\left(\frac{4\pi}{3}n\right) \triangleq \cos \gamma n, \quad \gamma = \frac{4\pi}{3}$$

$$V(e^{j\Omega}) = \sum_{k=-\infty}^{\infty} \pi \left\{ \delta\left(\Omega - 2k\pi - \frac{4\pi}{3}\right) + \delta\left(\Omega - 2k\pi + \frac{4\pi}{3}\right) \right\}.$$

The spectrum consists of two impulses within the interval $-\pi$ to π , shown as a function of the frequency Ω , and around the unit circle in Fig. 7.26. The impulses are located at angles $\Omega = 4\pi/3$ and $\Omega = -4\pi/3$, respectively, i.e. at $\Omega = 2\pi/3$ and $\Omega = -2\pi/3$. Under-sampling has caused a folding of the frequency around the point $\Omega = \pi$. The sinusoid appears as being equal to $\cos(2\pi n/3)$ which corresponds to a continuous-time signal of $v_c(t) = \cos(1000\pi t)$, rather than the original $v_c(t) = \cos(2000\pi t)$. This is not surprising, for we note that

$$\cos(4\pi n/3) = \cos(4\pi n/3 - 2\pi n) = \cos(2\pi n/3).$$

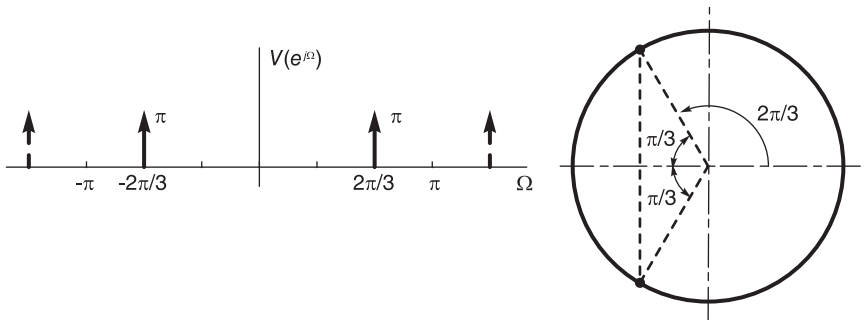


FIGURE 7.26 Impulses versus frequency and as seen on unit circle.

Example 7.12 A periodic signal $v_c(t)$ is applied to the input of an A/D converter of a sampling frequency of $f_s = 10000$ samples per second. The converter produces the output $v[n] = v_c(nT)$ where $T = 1/f_s$. Given that

$$v_c(t) = 4 + 2 \cos(4000\pi t) + \cos(12000\pi t + \pi/4).$$

Evaluate and sketch $V_c(j\omega)$ and $V(e^{j\Omega})$, the Fourier transforms of $v_c(t)$ and $v[n]$, respectively.

$$V_c(j\omega) = 8\pi \delta(\omega) + 2\pi \{ \delta(\omega - 4000\pi) + \delta(\omega + 4000\pi) \} + \pi \{ e^{j\pi/4} \delta(\omega - 12000\pi) + e^{-j\pi/4} \delta(\omega + 12000\pi) \}$$

See Fig. 7.27(a).

We have $\Omega = \omega T$. For $\omega = 4000\pi, 12000\pi, \Omega = 0.4\pi, 1.2\pi$, respectively. The frequency $\Omega = 1.2\pi$ folds back to

$$\Omega = 2\pi - 1.2\pi = 0.8\pi$$

as shown in Fig. 7.27(b).

$$\begin{aligned}
 V(e^{j\Omega}) &= (1/T) \sum_{k=-\infty}^{\infty} V_c \left[j \left\{ \frac{\Omega - 2k\pi}{T} \right\} \right] \\
 &= \sum_{n=-\infty}^{\infty} 8\pi \delta(\Omega - 2k\pi) + 2\pi \{ \delta(\Omega - 0.4\pi - 2k\pi) + \delta(\Omega + 0.4\pi - 2k\pi) \} \\
 &\quad + \pi \{ e^{j\pi/4} \delta(\Omega - 1.2\pi - 2k\pi) + e^{-j\pi/4} \delta(\Omega + 1.2\pi - 2k\pi) \} \\
 V(e^{j\Omega}) &= 8\pi \delta(\Omega) + 2\pi \{ \delta(\Omega - 0.4\pi) + \delta(\Omega + 0.4\pi) \} \\
 &\quad + \pi \{ e^{j\pi/4} \delta(\Omega + 0.8\pi) + e^{-j\pi/4} \delta(\Omega - 0.8\pi) \}, \quad -\pi \leq \Omega \leq \pi
 \end{aligned}$$

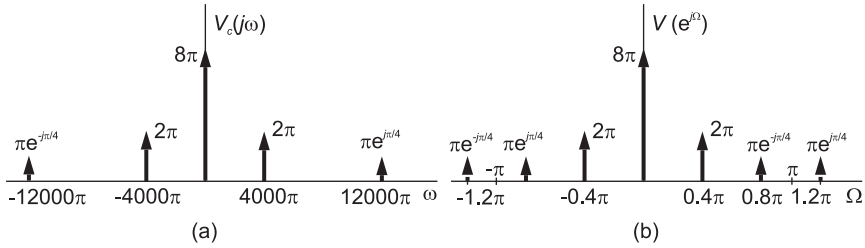


FIGURE 7.27 Fourier transform in continuous- and discrete-time domains.

Example 7.13 Given

$$x[n] = \cos \beta n = (e^{j\alpha n} + e^{-j\beta n}) / 2$$

we have

$$\begin{aligned}
 X(e^{j\Omega}) &= \pi \left[\sum_{k=-\infty}^{\infty} \delta(\Omega - \beta - 2k\pi) + \delta(\Omega + \beta - 2k\pi) \right] \\
 &\quad \pi \sum_{k=-\infty}^{\infty} \delta(t - \beta - 2k\pi) + \delta(t + \beta - 2k\pi) \xleftrightarrow{F.S.C.} \cos \beta n
 \end{aligned}$$

i.e. in terms of the base period we have

$$\begin{aligned}
 &\pi \{ \delta(t - \beta) + \delta(t + \beta) \}, \quad -\pi < t < \pi \xleftrightarrow{F.S.C.} \cos \beta n \\
 &\pi \left\{ \sum_{k=-\infty}^{\infty} \delta(t - \beta - 2k\pi) + \delta(t + \beta - 2k\pi) \right\} \xleftrightarrow{\mathcal{F}} 2\pi \sum_{n=-\infty}^{\infty} \cos \beta n \delta(\omega - n).
 \end{aligned}$$

Example 7.14 An A/D converter receives a continuous-time signal $x_c(t)$, samples it at a frequency of 1 kHz converting it into a sequence $x[n] = x_c(nT)$.

a) Evaluate the Fourier transform $X(e^{j\Omega})$ of the sequence $x[n]$ if

$$x_c(t) = 3 \cos 300\pi t + 5 \cos 700\pi t + 2 \cos 900\pi t.$$

b) A sequence $y[n]$ is obtained from $x[n]$ such that $y[n] = x[2n]$. Evaluate or sketch the Fourier transform $Y(e^{j\Omega})$ of $y[n]$.

c) A sequence $v[n]$ is obtained by sampling the sequence $x[n]$ such that

$$v[n] = \begin{cases} x[n], & n \text{ even} \\ 0, & n \text{ odd.} \end{cases}$$

Evaluate or sketch the Fourier transform $V(e^{j\Omega})$ of $v[n]$.

a)

$$X_c(j\omega) = 3\pi \{ \delta(\omega - 300\pi) + \delta(\omega + 300\pi) \} + 5\pi \{ \delta(\omega - 700\pi) + \delta(\omega + 700\pi) \} + 2\pi \{ \delta(\omega - 900\pi) + \delta(\omega + 900\pi) \}$$

$$\Omega = \omega T = 10^{-3}\omega.$$

The frequencies $\omega = 300\pi, 700\pi, 900\pi$ correspond to $\Omega = 0.3\pi, 0.7\pi, 0.9\pi$.

$$x[n] = 3 \cos 0.3\pi n + 5 \cos 0.7\pi n + 2 \cos 0.9\pi n$$

$$X(e^{j\Omega}) = (1/T) \sum_{k=-\infty}^{\infty} X_c(j\omega)|_{\omega=(\Omega-2\pi k)/T}$$

$$X(e^{j\Omega}) = \sum_{k=-\infty}^{\infty} 3\pi [\delta(\Omega - 0.3\pi - 2\pi k) + \delta(\Omega + 0.3\pi - 2\pi k)] + 5\pi [\delta(\Omega - 0.7\pi - 2\pi k) + \delta(\Omega + 0.7\pi - 2\pi k)] + 2\pi [\delta(\Omega - 0.9\pi - 2\pi k) + \delta(\Omega + 0.9\pi - 2\pi k)].$$

The spectrum $X(e^{j\Omega})$ is shown in Fig. 7.28.

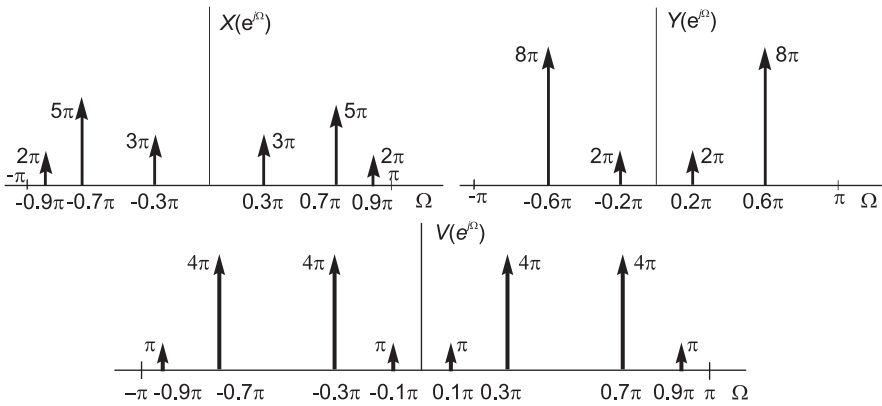


FIGURE 7.28 Spectra in discrete-time domain.

b) The sequence $y[n]$ is equivalent to sampling $x_c(t)$ with double the sampling period (half the original sampling frequency) i.e. with $T = 2 \times 10^{-3}$ sec.

$$Y(e^{j\Omega}) = 1/T \sum_{k=-\infty}^{\infty} X_c(j\omega)|_{\omega=(\Omega-2\pi k)/T}, \quad T = 2 \times 10^{-3}$$

$$= \sum_{k=-\infty}^{\infty} 3\pi [\delta(\Omega - 0.6\pi - 2\pi k) + \delta(\Omega + 0.6\pi - 2\pi k)] + 5\pi [\delta(\Omega - 1.4\pi - 2\pi k) + \delta(\Omega + 1.4\pi - 2\pi k)] + 2\pi [\delta(\Omega - 1.8\pi - 2\pi k) + \delta(\Omega + 1.8\pi - 2\pi k)].$$

The frequency 1.4π folds back to the frequency $(1 - 0.4)\pi = 0.6\pi$. The frequency 1.8π folds back to the frequency $(1 - 0.8)\pi = 0.2\pi$. The spectrum $Y(e^{j\Omega})$ is shown in the figure.

As a confirmation of these results note that we can write

$$y[n] = x[2n] = 3 \cos 0.6\pi n + 5 \cos 1.4\pi n + 2 \cos 1.8\pi n$$

i.e.

$$y[n] = 3 \cos 0.6\pi n + 5 \cos[(2\pi - 0.6\pi)n] + 2 \cos[(2\pi - 0.2\pi)n]$$

or

$$y[n] = 8 \cos 0.6\pi n + 2 \cos 0.2\pi n$$

as found.

c)

$$V(z) = \sum_{n=-\infty}^{\infty} v[n] z^{-n} = \sum_{n \text{ even}} v[n] z^{-n} = \sum_{n \text{ even}} x[n] z^{-n}.$$

We can write

$$V(z) = \frac{1}{2} \sum_{n=-\infty}^{\infty} x[n] \{1 + (-1)^n\} z^{-n} = \frac{1}{2} \{X(z) + X(-z)\}$$

$$V(e^{j\Omega}) = \frac{1}{2} \{X(e^{j\Omega}) + X(-e^{j\Omega})\} = \frac{1}{2} \{X(e^{j\Omega}) + X[e^{j(\Omega+\pi)}]\}.$$

The spectrum $V(e^{j\Omega})$ is shown in Fig. 7.28. Alternatively, we can write

$$V(z) = x[0] + x[2]z^{-2} + x[4]z^{-4} + \dots + x[-2]z^2 + \dots = \sum_{n=-\infty}^{\infty} x[2n]z^{-2n}$$

$$V(e^{j\Omega}) = \sum_{n=-\infty}^{\infty} y[n]e^{-j\Omega 2n} = Y(e^{j2\Omega})$$

confirming the obtained results.

7.11 Reconstruction of the Continuous-Time Signal

Let $v_c(t)$ be a band-limited signal having a spectrum $V_c(j\omega)$ which is nil for $|\omega| \geq \omega_c$. Let $v_s(t)$ be the ideal sampling of $v_c(t)$ with a sampling interval T and

$$v[n] = v_c(nT). \quad (7.104)$$

Assuming no aliasing, the sampling frequency ω_s satisfies

$$\omega_s = 2\pi/T > 2\omega_c. \quad (7.105)$$

We have seen that the continuous signal $v_c(t)$ can be recovered from the ideally sampled signal using a lowpass filter. It is interesting to view the mathematical operation needed to recover $v_c(t)$ from $v[n]$. We can recover the spectrum $V_c(j\omega)$ from $V(e^{j\omega T}) = V(e^{j\Omega})$ if we

multiply $V(e^{j\omega T})$ by a rectangular gate function of width $(-\pi/T, \pi/T)$, that is by passing the sequence $v[n]$ through an ideal lowpass filter of a cut-off frequency π/T :

$$V_c(j\omega) = T V(e^{j\omega T}) \Pi_{\pi/T}(\omega). \tag{7.106}$$

We can therefore write

$$\begin{aligned} v_c(t) &= \frac{1}{2\pi} \int_{-\infty}^{\infty} V_c(j\omega) e^{jt\omega} d\omega = \frac{1}{2\pi} \int_{-\pi/T}^{\pi/T} V_c(j\omega) e^{jt\omega} d\omega \\ &= \frac{T}{2\pi} \int_{-\pi/T}^{\pi/T} V(e^{j\omega T}) e^{jt\omega} d\omega = \frac{T}{2\pi} \int_{-\pi/T}^{\pi/T} \sum_{n=-\infty}^{\infty} v[n] e^{-jnT\omega} e^{jt\omega} d\omega \\ &= \frac{T}{2\pi} \sum_{n=-\infty}^{\infty} v[n] \int_{-\pi/T}^{\pi/T} e^{j(t-nT)\omega} d\omega = \sum_{n=-\infty}^{\infty} v[n] \frac{\sin(t-nT)\pi/T}{(t-nT)\pi/T} \end{aligned} \tag{7.107}$$

$$v_c(t) = \sum_{n=-\infty}^{\infty} v[n] \text{Sa}\{(t/T - n)\pi\}. \tag{7.108}$$

This is the same relation obtained above through analysis confined to the continuous-time domain. We have thus obtained an “interpolation formula” that reconstructs $v_c(t)$ given the discrete time version $v[n]$. It has the form of a convolution. It is, however, part continuous, part discrete, type of a convolution.

7.12 Stability of a Linear System

Similarly to continuous-time systems, a discrete-time linear system is stable if its frequency response $H(e^{j\Omega})$, the Fourier transform of its impulse response $h[n]$, exists. For a causal system this implies that its transfer function $H(z)$ has no poles outside the unit circle. If the poles are on the unit circle the system is called “critically stable.” An anticausal system, of which $h[n]$ is nil for $n > 0$ is stable if $H(z)$ has no pole inside the unit circle.

7.13 Table of Discrete-Time Fourier Transform Properties

Table 7.2 lists discrete-time Fourier transform (DTFT) properties.

7.14 Parseval’s Theorem

Parseval’s theorem states that

$$\sum_{n=-\infty}^{\infty} |x[n]|^2 = \frac{1}{2\pi} \int_{-\pi}^{\pi} |X(e^{j\Omega})|^2 d\Omega \tag{7.109}$$

TABLE 7.2 Discrete-time Fourier transform properties

Sequence	Fourier Transform
$ax[n] + by[n]$	$aX(e^{j\Omega}) + bY(e^{j\Omega})$
$x[n - n_0]$	$e^{-j\Omega n_0} X(e^{j\Omega})$
$e^{j\Omega_0 n} x[n]$	$X(e^{j(\Omega - \Omega_0)})$
$x[-n]$	$X(e^{-j\Omega}), x[n]$ real $X^*(e^{j\Omega})$
$x^*[n]$	$X^*(e^{-j\Omega})$
$x^*[-n]$	$X^*(e^{j\Omega})$
$nx[n]$	$j \frac{dX(e^{j\Omega})}{d\Omega}$
$x[n] * y[n]$	$X(e^{j\Omega}) Y(e^{j\Omega})$
$x[n] y[n]$	$\frac{1}{2\pi} \int_{-\pi}^{\pi} X(e^{j\theta}) Y(e^{j(\Omega - \theta)}) d\theta$
$r_{vx}[n] = v[n] * x[-n]$	$S_{vx}(\Omega) = V(e^{j\Omega}) X^*(e^{j\Omega})$
$x[n] \cos \Omega_0 n$	$(1/2) \{ X(e^{j(\Omega + \Omega_0)}) + X(e^{j(\Omega - \Omega_0)}) \}$

$$\sum_{\pi=-\infty}^{\infty} x[n] y^*[n] = \frac{1}{2\pi} \int_{-\pi}^{\pi} X(e^{j\Omega}) Y^*(e^{j\Omega}) d\Omega. \tag{7.110}$$

7.15 Fourier Series and Transform Duality

Below, we study the duality property relating Fourier series and transform in the continuous time domain to the Fourier transform in the discrete-time domain. Consider an even sequence $x[n]$ and suppose we know its Fourier transform $X(e^{j\Omega})$, i.e.

$$X(e^{j\Omega}) = \sum_{n=-\infty}^{\infty} x[n] e^{-j\Omega n} \tag{7.111}$$

$$x[n] = \frac{1}{2\pi} \int_{-\pi}^{\pi} X(e^{j\Omega}) e^{j\Omega n} d\Omega. \tag{7.112}$$

The spectrum $X(e^{j\Omega})$ is periodic with period 2π . We now show that if a continuous-time periodic function $x_c(t)$ has the same form as $X(e^{j\Omega})$, i.e. the same function but with Ω replaced by t ,

$$x_c(t) = X(e^{jt}) \tag{7.113}$$

then its Fourier series coefficients X_n are a simple reflection of the sequence $x[n]$,

$$X_n = x[-n]. \tag{7.114}$$

To show that such a duality property holds consider the Fourier series expansion of the periodic function $x_c(t) = X(e^{jt})$. The expansion takes the form

$$X(e^{jt}) = \sum_{n=-\infty}^{\infty} X_n e^{jn\omega_0 t} = \sum_{n=-\infty}^{\infty} X_n e^{jnt} \tag{7.115}$$

where we have noted that $\omega_0 = 1$. Comparing this equation with Equation (7.111) we have

$$X_n = x[-n] \tag{7.116}$$

as asserted. We also note that knowing the Fourier series coefficients X_n of the periodic function $x_c(t) = X(e^{jt})$ we also have the Fourier transform as

$$X_c(j\omega) = 2\pi \sum_{n=-\infty}^{\infty} x[-n] \delta(\omega - n). \tag{7.117}$$

Summarizing, we have the duality property:

If $x[n] \xleftrightarrow{\mathcal{F}} X(e^{j\Omega})$ then $x_c(t) = X(e^{jt}) \xleftrightarrow{FSC} X_n = x[-n]$ and

$$x_c(t) \xleftrightarrow{\mathcal{F}} 2\pi \sum_{n=-\infty}^{\infty} X_n \delta(\omega - n) = 2\pi \sum_{n=-\infty}^{\infty} x[-n] \delta(\omega - n). \tag{7.118}$$

Note that the Fourier series coefficients refer to the Fourier series expansion over one period of the periodic function $x_c(t) = X(e^{jt})$, namely, $-\pi \leq t \leq \pi$.

The converse of this property holds as well. In this case the property takes the form: If a function $x_c(t)$ is periodic with period 2π and its Fourier series coefficients X_n or equivalently its Fourier transform $X(j\omega)$ is known then the Fourier transform of the sequence $x[n] = X_{-n}$ is simply equal to $x_c(t)$ with t replaced by Ω . In other words:

If $x_c(t) \xleftrightarrow{FSC} X_n$ then $x[n] = X_{-n} \xleftrightarrow{\mathcal{F}} X(e^{j\Omega}) = x_c(\Omega)$.

The following examples illustrate the application of this property.

Example 7.15 Evaluate the Fourier transform $X(e^{j\Omega})$ of the sequence

$$x[n] = u[n + N] - u[n - (N + 1)].$$

Use the duality property to evaluate the Fourier transform of the continuous-time function $x_c(t) = X(e^{jt})$.

We have

$$X(z) = \sum_{n=-N}^N z^{-n} = z^N \frac{1 - z^{-(2N+1)}}{1 - z^{-1}}$$

$$X(e^{j\Omega}) = e^{jN\Omega} \frac{1 - e^{-j\Omega(2N+1)}}{1 - e^{-j\Omega}} = \frac{\sin[(2N + 1)\Omega/2]}{\sin(\Omega/2)}.$$

The sequence $x[n]$ and its Fourier transform $X(e^{j\Omega})$ are shown in Fig. 7.29.

Using duality we may write

$$x_c(t) = \frac{\sin[(2N + 1)t/2]}{\sin(t/2)} \xleftrightarrow{FSC} X_n = x[-n] = \begin{cases} 1, & -N \leq n \leq N \\ 0, & \text{otherwise} \end{cases}$$

and

$$x_c(t) \xleftrightarrow{\mathcal{F}} 2\pi \sum_{n=-\infty}^{\infty} X_n \delta(\omega - n) = 2\pi \sum_{n=-N}^N \delta(\omega - n).$$

The function $v_c(t)$ and its Fourier series coefficients are shown in the figure.

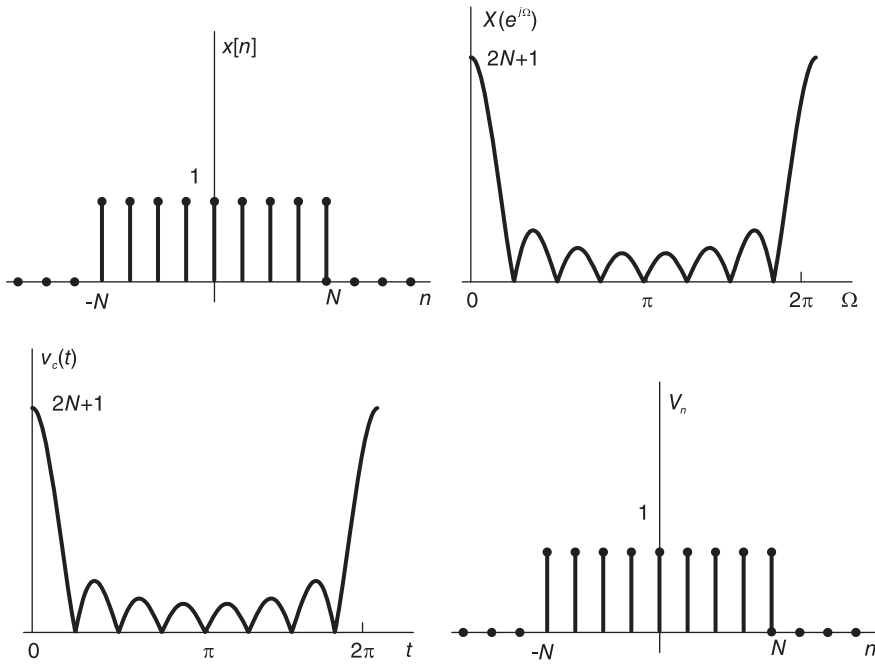


FIGURE 7.29 Duality between Fourier series and DFT.

Example 7.16 Let

$$x[n] = a^{-|n|}.$$

We have

$$X(z) = \mathcal{Z} [a^{-n}u[n] + a^n u[-n] - \delta[n]] = \frac{1}{1 - a^{-1}z^{-1}} + \frac{1}{1 - a^{-1}z} - 1$$

$$X(e^{j\Omega}) = \frac{1}{1 - a^{-1}e^{-j\Omega}} + \frac{1}{1 - a^{-1}e^{j\Omega}} - 1 = \frac{1 - a^{-2}}{1 - 2a^{-1} \cos \Omega + a^{-2}}.$$

Using the duality property, we may write

$$X(e^{jt}) = \frac{1 - a^{-2}}{1 - 2a^{-1} \cos t + a^{-2}} \xleftrightarrow{FSC} a^{-|n|}.$$

Example 7.17 Let

$$f_0(t) = \Pi_\tau(t)$$

and with $T > 2\tau$

$$f_c(t) = \sum_{n=-\infty}^{\infty} f_0(t - nT).$$

We have

$$F_0(j\omega) = 2\tau Sa(\tau\omega)$$

$$F_n = (1/T)F_0(jn\omega_0) = (2\tau/T) Sa(2n\pi\tau/T).$$

With $T = 2\pi$ and $\tau = B$ we may write

$$f[n] = F_{-n} = (B/\pi) Sa(nB) \xleftrightarrow{\mathcal{F}} \sum_{n=-\infty}^{\infty} \Pi_B(\Omega - 2n\pi)$$

i.e. $F(e^{j\Omega}) = \mathcal{F}[f[n]]$ is periodic with period 2π and its base period is given by

$$\Pi_B(\Omega) = u(\Omega + B) - u(\Omega - B), \quad -\pi \leq \Omega \leq \pi.$$

Example 7.18 Let $x[n] = 1$. We have

$$X(e^{j\Omega}) = \sum_{n=-\infty}^{\infty} e^{-j\Omega n} = 2\pi \sum_{k=-\infty}^{\infty} \delta(\Omega - 2k\pi).$$

From the duality property we may write

$$2\pi \sum_{n=-\infty}^{\infty} \delta(t - 2n\pi) \xleftrightarrow{F.S.C.} 1$$

$$\sum_{n=-\infty}^{\infty} \delta(t - 2n\pi) \xleftrightarrow{F.S.C.} 1/(2\pi)$$

which are the expected Fourier series coefficients of the impulse train.

7.16 Discrete Fourier Transform

Let $x[n]$ be an N -point finite sequence that is generally non-nil for $0 \leq n \leq N - 1$ and nil otherwise. The z -transform of $x[n]$ is given by

$$X(z) = \sum_{n=0}^{N-1} x[n]z^{-n}. \tag{7.119}$$

Its Fourier transform is given by

$$X(e^{j\Omega}) = \sum_{n=0}^{N-1} x[n]e^{-j\Omega n}. \tag{7.120}$$

We note that being the z -transform evaluated on the unit circle, $X(e^{j\Omega})$ is periodic in Ω with period 2π . In fact, for k integer

$$X(e^{j(\Omega+2k\pi)}) = \sum_{n=0}^{N-1} x[n]e^{-j(\Omega+2k\pi)n} = \sum_{n=0}^{N-1} x[n]e^{-j\Omega n} = X(e^{j\Omega}). \tag{7.121}$$

Similarly to the analysis of finite duration or periodic signals by Fourier series, the analysis of finite duration or periodic sequences is the role of the DFT. Moreover, in the same way that for continuous time signals the Fourier series is a sampling of the Fourier transform, for discrete-time signals the DFT is a sampling of their Fourier transform. In particular, for an N -point finite duration sequence or a sequence that is periodic with a period N , the DFT is in fact a uniform sampling of the Fourier transform such that the unit circle is sampled into N points with an angular spacing of $2\pi/N$, as shown in Fig. 7.30 for the case $N = 16$. The continuous angular frequency Ω is replaced by the discrete N values $\Omega_k = 2\pi k/N$, $k = 0, 1, \dots, N - 1$. Denoting the DFT by the symbol $X[k]$ we have its definition in the form

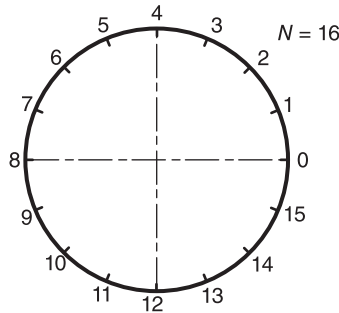


FIGURE 7.30 Unit circle divided into 16 points.

$$X[k] = X\left(e^{j2\pi k/N}\right) = \sum_{n=0}^{N-1} x[n]e^{-j2\pi nk/N}, \quad k = 0, 1, 2, \dots, N - 1 \quad (7.122)$$

Note that if T_s is the sampling period, the discrete domain frequency Ω , that is, the angle around the unit circle, is related to the continuous domain frequency ω by the equation

$$\Omega = \omega T_s, \quad (7.123)$$

and vice versa

$$\omega = \Omega/T_s = \Omega f_s \quad (7.124)$$

The fundamental frequency is the first sample of $X[k]$ on the unit circle. It appears at an angle $\Omega = 2\pi/N$. If $0 \leq k \leq N/2$, the k^{th} sample on the unit circle is the k^{th} harmonic of $x[n]$ and lies at an angle

$$\Omega = k \frac{2\pi}{N}. \quad (7.125)$$

It corresponds to a continuous-time domain frequency

$$\omega = \Omega f_s = k \frac{2\pi}{N} f_s \quad \text{r/s} \quad (7.126)$$

that is

$$f = \frac{k}{N} f_s \quad \text{Hz}. \quad (7.127)$$

If $k > N/2$ then the true frequency is f_s minus the frequency f thus evaluated, i.e.

$$f_{\text{true}} = f_s - \frac{k}{N} f_s = (N - k) \frac{f_s}{N} \quad \text{Hz}. \quad (7.128)$$

In other words, the index k is replaced by $N - k$ to produce the true frequency.

Example 7.19 Given that the sampling frequency is $f_s = 10$ kHz and an $N = 500$ -point DFT, evaluate the continuous-time domain frequency corresponding to the k^{th} sample on the unit circle, with (a) $k = 83$ and (b) $k = 310$. (c) To what continuous-time domain frequency corresponds the interval between samples on the unit circle.

(a) $f = (83/500)f_s = (83/500)10000 = 1660$ Hz.

(b) $f = (500 - 310/500)f_s = (190/500)10000 = 3800$ Hz.

(c) The frequency interval Δf corresponds to a spacing of $k = 1$, i.e. $\Delta f = (1/500)f_s = 10000/500 = 20$ Hz.

We also note that the DFT is periodic in k with period N . This is the case since it's a sampling of the Fourier transform around the unit circle and

$$e^{j2\pi(k+mN)/N} = e^{j2\pi k/N}. \tag{7.129}$$

The periodic sequence that is the periodic repetition of the DFT

$$X[k], \quad k = 0, 1, 2, \dots \tag{7.130}$$

is called the *Discrete Fourier Series* (DFS) and may be denoted by the symbol $\tilde{X}[k]$. The DFT is therefore only one period of the DFS as obtained by setting $k = 0, 1, \dots, N - 1$.

From the definition of the DFT:

$$X[k] = \sum_{n=0}^{N-1} x[n]e^{-j2\pi nk/N}, \quad k = 0, 1, \dots, N - 1 \tag{7.131}$$

the inverse transform can be evaluated by multiplying both sides of the equation by $e^{j2\pi kr/N}$. We obtain

$$X[k]e^{j2\pi kr/N} = \sum_{n=0}^{N-1} x[n]e^{-j2\pi k(n-r)/N}. \tag{7.132}$$

Effecting the sum of both sides with respect to k

$$\sum_{k=0}^{N-1} X[k]e^{j2\pi kr/N} = \sum_{k=0}^{N-1} \sum_{n=0}^{N-1} x[n]e^{-j2\pi k(n-r)/N} = \sum_{n=0}^{N-1} x[n] \sum_{k=0}^{N-1} e^{-j2\pi k(n-r)/N}. \tag{7.133}$$

For integer m we have

$$\sum_{k=0}^{N-1} e^{-j2\pi km/N} = \begin{cases} N, & \text{for } m = pN, \quad p \text{ integer} \\ 0, & \text{otherwise} \end{cases} \tag{7.134}$$

whence

$$\sum_{k=0}^{N-1} e^{-j2\pi k(n-r)/N} = \begin{cases} N, & \text{for } n = r + pN, \quad p \text{ integer} \\ 0, & \text{otherwise} \end{cases} \tag{7.135}$$

i.e.

$$\sum_{k=0}^{N-1} X[k]e^{j2\pi kr/N} = Nx[r]. \tag{7.136}$$

Replacing r by n we have the inverse transform

$$x[n] = \frac{1}{N} \sum_{k=0}^{N-1} X[k]e^{j2\pi nk/N}. \tag{7.137}$$

Example 7.20 Evaluate the DTFT and the DFT of the sequence

$$x[n] = \cos Bn R_N(n)$$

The z-transform is given by

$$X(z) = \sum_{n=0}^{N-1} \cos nBz^{-n} = \frac{1}{2} \sum_{n=0}^{N-1} (e^{jBn} + e^{-jBn})z^{-n}.$$

Let $a = e^{jB}$

$$X(z) = \sum_{n=0}^{N-1} (a^n z^{-n} + a^{*n} z^{-n}) = \frac{1}{2} \left(\frac{1 - a^N z^{-N}}{1 - az^{-1}} + \frac{1 - a^{*N} z^{-N}}{1 - a^* z^{-1}} \right).$$

The transform $X(z)$ can be rewritten

$$X(z) = \frac{1 - \cos B z^{-1} - \cos NB z^{-N} + \cos [(N-1)B] z^{-(N+1)}}{1 - 2 \cos B z^{-1} + z^{-2}}.$$

The Fourier transform is written

$$X(e^{j\Omega}) = \frac{1}{2} \left[\frac{1 - a^N e^{-jN\Omega}}{1 - ae^{-j\Omega}} + \frac{1 - a^{*N} e^{-jN\Omega}}{1 - a^* e^{-j\Omega}} \right].$$

The student can verify that $X(e^{j\Omega})$ can be written in the form

$$X(e^{j\Omega}) = 0.5 \{ e^{-j(B-\Omega)(N-1)/2} Sd_N[(B-\Omega)/2] + e^{-j(B+\Omega)(N-1)/2} Sd_N[(B+\Omega)/2] \}$$

or, alternatively,

$$X(e^{j\Omega}) = \frac{N}{2} \{ \Phi(\Omega - B) + \Phi(\Omega + B) \}$$

where

$$\Phi(\Omega) = \frac{\sin(N\Omega/2)}{N \sin(\Omega/2)} e^{-j(N-1)\Omega/2}.$$

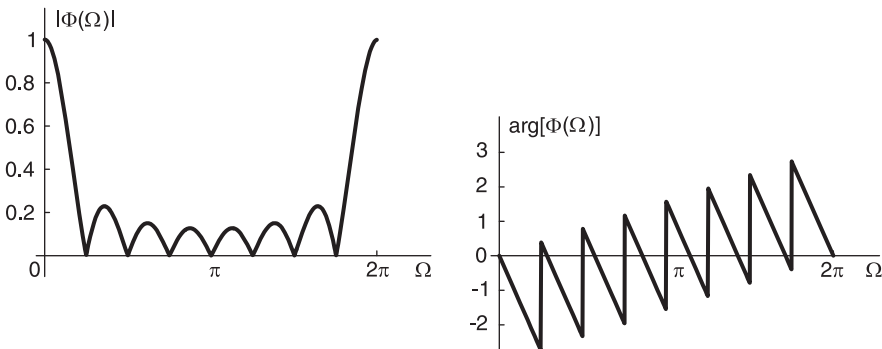


FIGURE 7.31 The Sd_N function and transform.

The absolute value and phase angle of the function $\Phi(\Omega)$ are shown in Fig. 7.31 for $N = 8$.

We note that the Fourier transform $X(e^{j\Omega})$ closely resembles the transform of a continuous time truncated sinusoid. The DFT is given by

$$X[k] = X\left(e^{j2\pi k/N}\right) = \frac{N}{2} \left\{ \Phi\left(\frac{2\pi}{N}k - B\right) + \Phi\left(\frac{2\pi}{N}k + B\right) \right\}.$$

For the special case where the interval N contains an integer number of cycles we have

$$B = \frac{2\pi}{N}m, \quad m = 0, 1, 2, \dots$$

$$X[k] = (N/2) \left[\Phi\left\{\frac{2\pi}{N}(k - m)\right\} + \Phi\left\{\frac{2\pi}{N}(k + m)\right\} \right] = \begin{cases} N/2, & k = m \text{ and } k = N - m \\ 0, & \text{otherwise.} \end{cases}$$

The DFT is thus composed of two discrete impulses, one at $k = m$, the other at $k = N - m$. Note that in the “well behaved” case $B = 2\pi m/N$ we can evaluate the DFT directly by writing

$$\cos(Bn) = \frac{1}{2} \left\{ e^{j\frac{2\pi}{N}mn} + e^{-j\frac{2\pi}{N}mn} \right\} = \frac{1}{N} \sum_{k=0}^{N-1} X[k] e^{j\frac{2\pi}{N}nk}, \quad n = 0, 1, \dots, N - 1..$$

Equating the coefficients of the exponentials we have

$$X[k] = \begin{cases} N/2, & k = m, \quad k = N - m \\ 0, & \text{otherwise.} \end{cases}$$

We recall from Chapter 2 that the Fourier series of a truncated continuous-time sinusoid contains in general two discrete sampling functions and that when the analysis interval is equal to the period of the sinusoid or to a multiple thereof the discrete Fourier series spectrum contains only two impulses. We see the close relation between the Fourier series of continuous-time signals and the DFT of discrete-time signals.

7.17 Discrete Fourier Series

We shall use the notation $\tilde{x}[n]$ to denote a periodic sequence of period N , i.e.

$$\tilde{x}[n] = \tilde{x}[n + kN], \quad k \text{ integer.} \tag{7.138}$$

We shall write $\tilde{X}[k] = DFS[\tilde{x}[n]]$ meaning $\tilde{x}[n] \xleftrightarrow{DFS} \tilde{X}[k]$. Let $x[n]$ be an aperiodic sequence. A periodic sequence $\tilde{x}[n]$ may be formed thereof in the form

$$\tilde{x}[n] = x[n] * \sum_{k=-\infty}^{\infty} \delta[n + kN] = \sum_{k=-\infty}^{\infty} x[n + kN], \quad k \text{ integer.} \tag{7.139}$$

If $x[n]$ is of finite duration $0 \leq n \leq N - 1$, i.e. a sequence of length N the added shifted versions thereof, forming $\tilde{x}[n]$, do not overlap, and we have

$$\tilde{x}[n] = x[n \bmod N] \tag{7.140}$$

where $n \bmod N$ means n modulo N ; meaning the remainder of the integer division $n \div N$. For example, $70 \bmod 32 = 6$. In what follows, we shall use the shorthand notation

$$\tilde{x}[n] = x[[n]]_N. \tag{7.141}$$

If the sequence $x[n]$ is of length $L < N$, again no overlapping occurs and in the range $0 \leq n \leq N - 1$ the value of $\tilde{x}[n]$ is the same as $x[n]$ followed by $(N - L)$ zeros. If on the other hand the length of the sequence $x[n]$ is $L > N$, overlap occurs leading to superposition (“aliasing”) and we cannot write $\tilde{x}[n] = x[n \bmod N]$.

7.18 DFT of a Sinusoidal Signal

Given a finite-duration sinusoidal signal $x_c(t) = \sin(\beta t + \theta)R_T(t)$ of frequency β and duration T , sampled with a sampling interval T_s and sampling frequency $f_s = 1/T_s$ Hz, i.e. $\omega_s = 2\pi/T_s$ r/s and the signal period is $\tau = 2\pi/\beta$. For simplicity of presentation we let $\theta = 0$, the more general case of $\theta \neq 0$ being similarly developed. We presently consider the particular case where the window duration T is a multiple m of the signal period τ i.e. $T = m\tau$, as can be seen in Fig. 7.32 for the case $m = 3$.

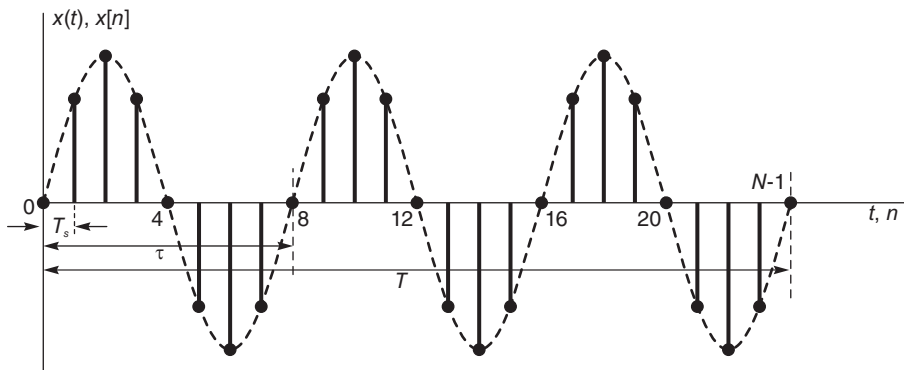


FIGURE 7.32 Sinusoid with three cycles during analysis window.

The discrete-time signal is given by $x[n] = x_c(nT_s) = \sin(Bn)R_N[n]$, where $B = \beta T_s$. We also note that the N -point DFT analysis corresponds to the signal window duration

$$T = m\tau = NT_s. \tag{7.142}$$

We may write

$$B = \beta T_s = \frac{2\pi}{\tau} T_s = \frac{2\pi}{N} m. \tag{7.143}$$

$$\sin(Bn) = \frac{1}{2j} \left\{ e^{j\frac{2\pi}{N} mn} - e^{-j\frac{2\pi}{N} mn} \right\} = \frac{1}{N} \sum_{k=0}^{N-1} X[k] e^{j2\pi nk/N}, \quad n = 0, 1, \dots, N - 1.$$

Hence

$$X[k] = \begin{cases} \mp jN/2, & k = m, \quad k = N - m \\ 0, & \text{otherwise.} \end{cases}$$

We note that the fundamental frequency of analysis in the continuous-time domain, which may be denoted by ω_0 is given by $\omega_0 = 2\pi/T$. The sinusoidal signal frequency β is a multiple m of the fundamental frequency ω_0 . In particular $\beta = 2\pi/\tau = m\omega_0$ and $B = \beta T_s = 2\pi m/N$. The unit circle is divided into N samples denoted $k = 0, 1, 2, \dots, N - 1$ corresponding to the frequencies $\Omega = 0, 2\pi/N, 4\pi/N, \dots, (N - 1)\pi/N$. The $k = 1$ point is the fundamental frequency $\Omega_0 = 2\pi/N$. Since $B = m2\pi/N$ it falls on the m^{th} point of the circle as the m^{th} harmonic. Its conjugate falls on the point $k = N - m$. The following example illustrates these observations.

Example 7.21 Given the signal $x_c(t) = \sin \beta t R_T(t)$, where $\beta = 250\pi$ r/s and $T = 24$ ms. A C/D converter samples this signal at a frequency of 1000 Hz. At what values of k does the DFT $X[k]$ display its spectral peaks?

The signal period is $\tau = 2\pi/\beta = 8$ ms. The rectangular window of duration T contains $m = T/\tau = 24/8 = 3$ cycles of the signal as can be seen in Fig. 7.32. The sampling period is $T_s = 1$ ms. The sampled signal is the sequence $x[n] = \sin Bn R_N[n]$, where $B = \beta T_s = \pi/4$ and $N = T/T_s = 24$. The fundamental frequency of analysis is $\omega_0 = 2\pi/T$, and the signal frequency is $\beta = 2\pi/\tau = (T/\tau)\omega_0 = m\omega_0$. In the discrete-time domain

$$B = \beta T_s = \frac{2\pi}{\tau} T_s = \frac{2\pi}{T/m} T_s = \frac{2\pi}{N} m = m\Omega_0.$$

The spectral peak occurs at $k = m = 3$ and at $k = N - m = 24 - 3 = 21$, which are the pole positions of the corresponding infinite duration signal, as can be seen in Fig. 7.33.

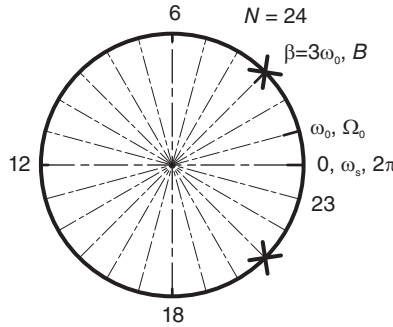


FIGURE 7.33 Unit circle divided into 24 points.

Example 7.22 Let

$$v(t) = \cos(25\pi t) R_T(t)$$

Assuming a sampling frequency f_s of 100 samples per second, evaluate the DFT if $T = 1.28$ sec.

Let T_s be the sampling interval. $f_s = 100$ Hz, $T_s = \frac{1}{f_s} = 0.01$ sec, $N = \frac{T}{T_s} = \frac{1.28}{0.01} = 128$.

$$v[n] = \cos(25\pi \times nT_s) R_N(n) = \cos(0.25\pi n) R_N(n) \triangleq \cos(Bn) R_N(n).$$

Writing $B = 0.25\pi = (2\pi/N)m$, we have $m = 16$. The DFT $X[k]$ has a peak on the unit circle at $k = 16$ and $k = 128 - 16 = 112$.

$$V[k] = \begin{cases} N/2 = 64, & k = 16, \quad k = 112 \\ 0, & \text{otherwise.} \end{cases}$$

as seen in Fig. 7.34

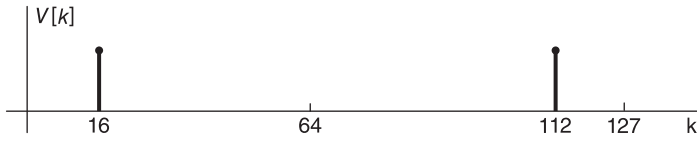


FIGURE 7.34 DFT of a sequence.

7.19 Deducing the z -Transform from the DFT

Consider a finite duration sequence $x[n]$ that is in general non-nil for $0 \leq n \leq N-1$ and nil otherwise, and its periodic extension $\tilde{x}[n]$ with a period of repetition N

$$\tilde{x}[n] = \sum_{k=-\infty}^{\infty} x[n + kN]. \quad (7.144)$$

Since $x[n]$ is of length N its periodic repetition with period N produces no overlap; hence $\tilde{x}[n] = x[n]$, $0 \leq n \leq N-1$. The z -transform of the sequence $x[n]$ is given by

$$X(z) = \sum_{n=0}^{N-1} x[n] z^{-n} \quad (7.145)$$

and its DFS is given by

$$\tilde{X}[k] = \sum_{n=0}^{N-1} \tilde{x}[n] e^{-j2\pi kn/N} \triangleq \sum_{n=0}^{N-1} x[n] W_N^{kn} \quad (7.146)$$

where $W_N = e^{-j2\pi/N}$ is the N^{th} root of unity. The inverse DFS is

$$x[n] = \tilde{x}[n] = \frac{1}{N} \sum_{k=0}^{N-1} \tilde{X}[k] e^{j2\pi kn/N} \triangleq \frac{1}{N} \sum_{k=0}^{N-1} \tilde{X}[k] W_N^{-kn}, \quad 0 \leq n \leq N-1 \quad (7.147)$$

and the z -transform may thus be deduced from the DFS and hence from the DFT. We have

$$\begin{aligned} X(z) &= \sum_{n=0}^{N-1} x[n] z^{-n} = \sum_{n=0}^{N-1} \frac{1}{N} \sum_{k=0}^{N-1} \tilde{X}[k] W_N^{-kn} z^{-n} \\ &= \frac{1}{N} \sum_{k=0}^{N-1} \tilde{X}[k] \sum_{n=0}^{N-1} W_N^{-kn} z^{-n} = \frac{1-z^{-N}}{N} \sum_{k=0}^{N-1} \frac{\tilde{X}[k]}{1-W_N^{-k} z^{-1}} \\ &= \frac{1-z^{-N}}{N} \sum_{k=0}^{N-1} \frac{X[k]}{1-W_N^{-k} z^{-1}} \end{aligned} \quad (7.148)$$

which is an interpolation formula reconstructing the z -transform from the N -point DFT on the z -plane unit circle. We can similarly obtain an interpolation formula reconstructing the transform $X(e^{j\Omega})$ from the DFT. To this end we replace z by $e^{j\Omega}$ in the above obtaining

$$\begin{aligned}
 X(e^{j\Omega}) &= \frac{1}{N} \sum_{k=0}^{N-1} \tilde{X}[k] \frac{1 - W_N^{-kN} e^{-j\Omega N}}{1 - W_N^{-k} e^{-j\Omega}} \\
 &= \frac{1}{N} \sum_{k=0}^{N-1} \tilde{X}[k] \frac{1 - e^{j(2\pi/N)kN} e^{-j\Omega N}}{1 - W_N^{-k} e^{-j\Omega}} \\
 &= \frac{1}{N} \sum_{k=0}^{N-1} \tilde{X}[k] e^{-j(\Omega - 2\pi k/N)(N-1)/2} \frac{\sin\{(\Omega - 2\pi k/N) N/2\}}{\sin\{(\Omega - 2\pi k/N)/2\}} \\
 &= \frac{1}{N} \sum_{k=0}^{N-1} \tilde{X}[k] e^{-j(\Omega - 2\pi k/N)(N-1)/2} Sd_N[(\Omega - 2\pi k/N)/2]
 \end{aligned}
 \tag{7.149}$$

The function $Sd_N(\Omega/2) = \sin(N\Omega/2) / \sin(\Omega/2)$ is depicted in Fig. 7.35 for the case $N = 8$. Note that over one period the function has zeros at values of Ω which are multiples of $2\pi/N = 2\pi/8$. In fact

$$Sd_N(r\pi/N) = \frac{\sin(r\pi)}{\sin(r\pi/N)} = \begin{cases} N, & r = 0 \\ 0, & r = 1, 2, \dots, N - 1. \end{cases}
 \tag{7.150}$$

Hence

$$\begin{aligned}
 X(e^{j\Omega})|_{\Omega=2\pi m/N} &= \frac{1}{N} \sum_{k=0}^{N-1} \tilde{X}[k] e^{-j(2\pi/N)(m-k)(N-1)/2} \\
 &\quad \cdot Sd_N[\pi(m-k)/N] = \tilde{X}[m]
 \end{aligned}
 \tag{7.151}$$

confirming that the Fourier transform $X(e^{j\Omega})$ curve passes through the N points of the DFT.

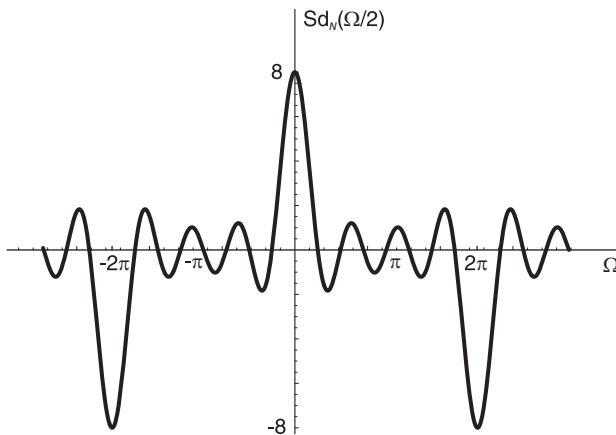


FIGURE 7.35 The function $Sd_N(\Omega/2)$.

7.20 DFT versus DFS

The DFS is but a periodic repetition of the DFT. Consider a finite duration sequence $x[n]$ of length N , i.e. a sequence that is nil except in the interval $0 \leq n \leq N-1$, we may extend it periodically with period N , obtaining the sequence

$$\tilde{x}[n] = \sum_{k=-\infty}^{\infty} x[n+kN]. \quad (7.152)$$

The DFS of $\tilde{x}[n]$ is $\tilde{X}[k]$ and the DFT is simply

$$X[k] = \tilde{X}[k], \quad 0 \leq k \leq N-1. \quad (7.153)$$

In other words the DFT is but the base period of the DFS. We may write the DFT in the form

$$X[k] = \sum_{n=0}^{N-1} \tilde{x}[n] e^{-j\frac{2\pi}{N}nk} = \sum_{n=0}^{N-1} x[n] e^{-j\frac{2\pi}{N}nk}, \quad 0 \leq k \leq N-1. \quad (7.154)$$

The inverse DFT is

$$x[n] = \frac{1}{N} \sum_{k=0}^{N-1} X[k] e^{j\frac{2\pi}{N}nk}, \quad n = 0, 1, \dots, N-1. \quad (7.155)$$

In summary, as we have seen in Chapter 2, here again in evaluating the DFT of a sequence $x[n]$ we automatically perform a periodic extension of $x[n]$ obtaining the sequence $\tilde{x}[n]$. This in effect produces the sequence “seen” by the DFS. We then evaluate the DFS and deduce the DFT by extracting the DFS coefficients in the base interval $0 \leq k \leq N-1$. It is common in the literature to emphasize the fact that

$$X[k] = \tilde{X}[k] R_N[k] \quad (7.156)$$

where $R_N[k]$ is the N -point rectangle $R_N[k] = u[k] - u[k-N]$, that is, the DFT $X[k]$ is an N -point rectangular window truncation of the periodic DFS $\tilde{X}[k]$. The result is an emphasis on the fact that $X[k]$ is nil for values of k other than $0 \leq k \leq N-1$. Such distinction, however, adds no new information than that provided by the DFS, and is therefore of little significance. In deducing and applying properties of the DFT a judicious approach is to perform a periodic extension, evaluate the DFS and finally deduce the DFT as its base period.

Example 7.23 Let $x[n]$ be the rectangle $x[n] = R_4[n]$. Evaluate the Fourier transform, the 8-point DFS and 8-point DFT of the sequence and its periodic repetition.

Referring to Fig. 7.36 we have

$$X(e^{j\Omega}) = \sum_{n=0}^3 e^{-j\Omega n} = \frac{1 - e^{-j4\Omega}}{1 - e^{-j\Omega}} = \frac{e^{-j2\Omega}}{e^{-j\Omega/2}} \frac{\sin(4\Omega/2)}{\sin \Omega/2} = e^{-j3\Omega/2} Sd_4(\Omega/2)$$

The DFS, with $N = 8$, of the periodic sequence $\tilde{x}[n] = \sum_{k=-\infty}^{\infty} x[n+8k]$ is

$$\tilde{X}[k] = X(e^{j\Omega}) \Big|_{\Omega=(2\pi/N)k} = \sum_{n=0}^3 e^{-j\frac{2\pi}{N}kn} = e^{-j3(\pi/8)k} Sd_4(\pi k/8).$$

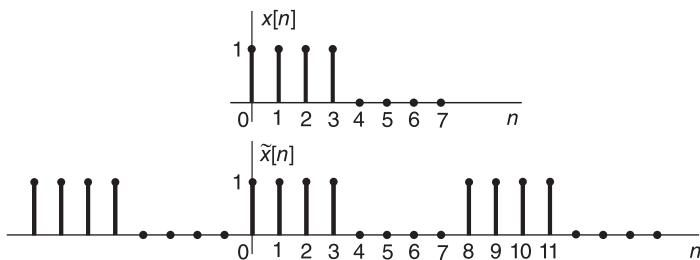


FIGURE 7.36 Rectangular sequence and periodic repetition.

The magnitude spectrum is

$$|\tilde{X}[k]| = \begin{cases} 4, & k = 0 \\ 2.613, & k = 1, 7 \\ 0, & k = 2, 4, 6 \\ 1.082, & k = 3, 5 \end{cases}$$

which is plotted in Fig. 7.37. The DFT is the base period of the DFS, i.e.

$$X[k] = \tilde{X}[k] R_N[k] = e^{-j3\pi k/8} Sd_4(\pi k/8), \quad k = 0, 1, \dots, 7.$$

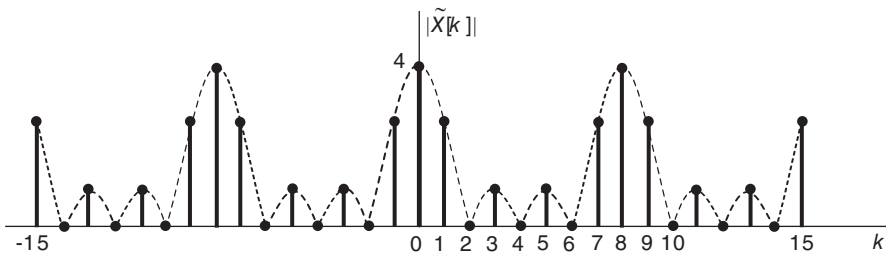


FIGURE 7.37 Periodic discrete amplitude spectrum.

7.21 Properties of DFS and DFT

The following are basic properties of DFS.

Linearity The linearity property states that if $\tilde{x}_1[n]$ and $\tilde{x}_2[n]$ are periodic sequences of period N each then

$$\tilde{x}_1[n] + \tilde{x}_2[n] \xleftrightarrow{DFS} \tilde{X}_1[k] + \tilde{X}_2[k]. \tag{7.157}$$

Shift in Time The shift in time property states that

$$\tilde{x}[n - m] \xleftrightarrow{DFS} W_N^{km} \tilde{X}[k]. \tag{7.158}$$

Shift in Frequency The dual of the shift in time property states that

$$\tilde{x}[n] W_N^{-nm} \xleftrightarrow{DFS} \tilde{X}[n - m]. \tag{7.159}$$

Duality From the definition of the DFS and its inverse we may write

$$\tilde{x}[-n] = \frac{1}{N} \sum_{k=0}^{N-1} \tilde{X}[k] W_N^{nk}. \tag{7.160}$$

Replacing n by k and vice versa we have

$$\tilde{x}[-k] = \frac{1}{N} \sum_{n=0}^{N-1} \tilde{X}[n] W_N^{nk} = \frac{1}{N} DFS [\tilde{X}[n]]. \tag{7.161}$$

In other words if $\tilde{x}[n] \xleftrightarrow{DFS} \tilde{X}[k]$ then $\tilde{X}[n] \xleftrightarrow{DFS} N\tilde{x}[-k]$. This same property applies to the DFT where, as always, operations such as reflection are performed on the periodic extensions of the time and frequency sequences. The DFT is then simply the base period of the periodic sequence, extending from index 0 to index $N - 1$.

Example 7.24 We have evaluated the DFT $X[k]$ and DFS $\tilde{X}[k]$ of the rectangular sequence $x[n]$ of Example 7.23 and its periodic extension $\tilde{x}[n]$ with a period $N = 8$, respectively, shown in Fig. 7.36. From the duality property we deduce that given a sequence

$$y[n] = X[n] = \tilde{X}[n] R_N[n] = e^{-j3\pi n/8} Sd_4(\pi n/8) R_N[n]$$

i.e.

$$y[n] = e^{-j3\pi n/8} Sd_4(\pi n/8), \quad n = 0, 1, \dots, 7$$

and its periodic repetition $\tilde{y}[n]$, the DFS of the latter is $\tilde{Y}[k] = N\tilde{x}[-k]$ and the DFT of $y[n]$ is

$$Y[k] = N\tilde{x}[-k] R_N[k].$$

To visualize these sequences note that the complex periodic sequence

$$\tilde{y}[n] = \tilde{X}[n] = e^{-j3\pi n/8} Sd_4(\pi n/8),$$

of which the absolute value is $|\tilde{y}[n]| = |\tilde{X}[n]|$, has the same absolute value as the spectrum shown in Fig. 7.37 with the index k replaced by n . The sequence $y[n]$ has an absolute value which is the base $N = 8$ -point period of this sequence and is shown in Fig. 7.38

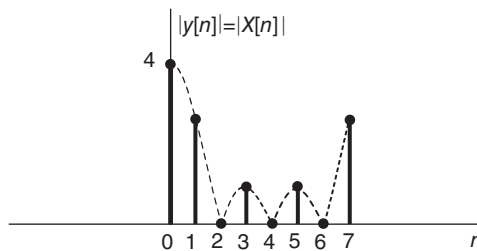


FIGURE 7.38 Base-period $|y[n]|$ of periodic absolute value sequence $\tilde{y}[n]$

The transform $\tilde{Y}[k] = N\tilde{x}[-k]$ is visualized by reflecting the sequence $\tilde{x}[n]$ of Fig. 7.36 about the vertical axis and replacing the index n by k . The transform $Y[k]$ is simply the N -point base period of $\tilde{Y}[k]$, as shown in Fig. 7.39

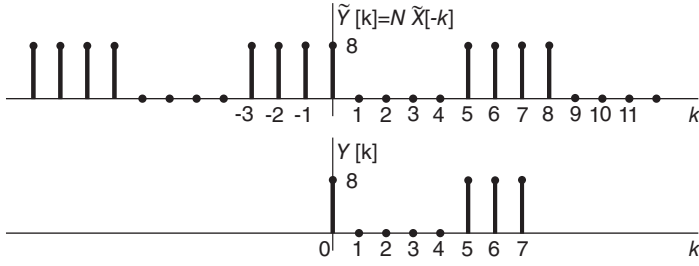


FIGURE 7.39 Reflection of a periodic sequence and base-period extraction.

7.21.1 Periodic Convolution

Given two periodic sequences $\tilde{x}[n]$ and $\tilde{v}[n]$ of period N each, multiplication of their DFS $\tilde{X}[k]$ and $\tilde{V}[k]$ corresponds to periodic convolution of $\tilde{x}[n]$ and $\tilde{v}[n]$. Let $w[n]$ denote the periodic convolution, written in the form

$$\tilde{w}[n] = \tilde{x}[n] \otimes \tilde{v}[n] = \sum_{m=0}^{N-1} \tilde{x}[m] \tilde{v}[n - m]. \tag{7.162}$$

The DFS of $\tilde{w}[n]$ is given by

$$\tilde{W}[k] = \sum_{n=0}^{N-1} \left\{ \sum_{m=0}^{N-1} \tilde{x}[m] \tilde{v}[n - m] \right\} e^{-j(2\pi/N)nk} = \sum_{m=0}^{N-1} \tilde{x}[m] \sum_{n=0}^{N-1} \tilde{v}[n - m] e^{-j(2\pi/N)nk}. \tag{7.163}$$

Let $n - m = r$

$$\begin{aligned} \tilde{W}[k] &= \sum_{m=0}^{N-1} \tilde{x}[m] \sum_{r=-m}^{-m+N-1} \tilde{v}[r] e^{-j(2\pi/N)(r+m)k} \\ &= \sum_{m=0}^{N-1} \tilde{x}[m] e^{-j(2\pi/N)mk} \sum_{r=0}^{N-1} \tilde{v}[r] e^{-j(2\pi/N)rk} = \tilde{X}[k] \tilde{V}[k]. \end{aligned} \tag{7.164}$$

In other words

$$\tilde{x}[n] \otimes \tilde{v}[n] \xleftrightarrow{DFS} \tilde{X}[k] \tilde{V}[k]. \tag{7.165}$$

The dual of this property states that

$$\tilde{x}[n] \tilde{v}[n] \xleftrightarrow{DFS} (1/N) \tilde{X}[k] \otimes \tilde{V}[k]. \tag{7.166}$$

Example 7.25 Evaluate the periodic convolution $\tilde{z}[n] = \tilde{x}[n] \otimes \tilde{v}[n]$ for the two sequences $\tilde{x}[n]$ and $\tilde{v}[n]$ shown in Fig.7.40

Proceeding graphically as shown in the figure we fold the sequence $\tilde{v}[n]$ about its axis and slide the resulting sequence $\tilde{v}[n - m]$ to the point $m = n$ along the m axis evaluating successively the sum of the product $\tilde{x}[m] \tilde{v}[n - m]$ for each value of n . We obtain the value of $\tilde{z}[n]$, of which the base period has the form shown in the following table.

n	0	1	2	3	4	5	6	7
$\tilde{z}[n]$	16	12	7	3	6	10	13	17

The periodic sequence $\tilde{z}[n]$ is depicted in Fig. 7.41

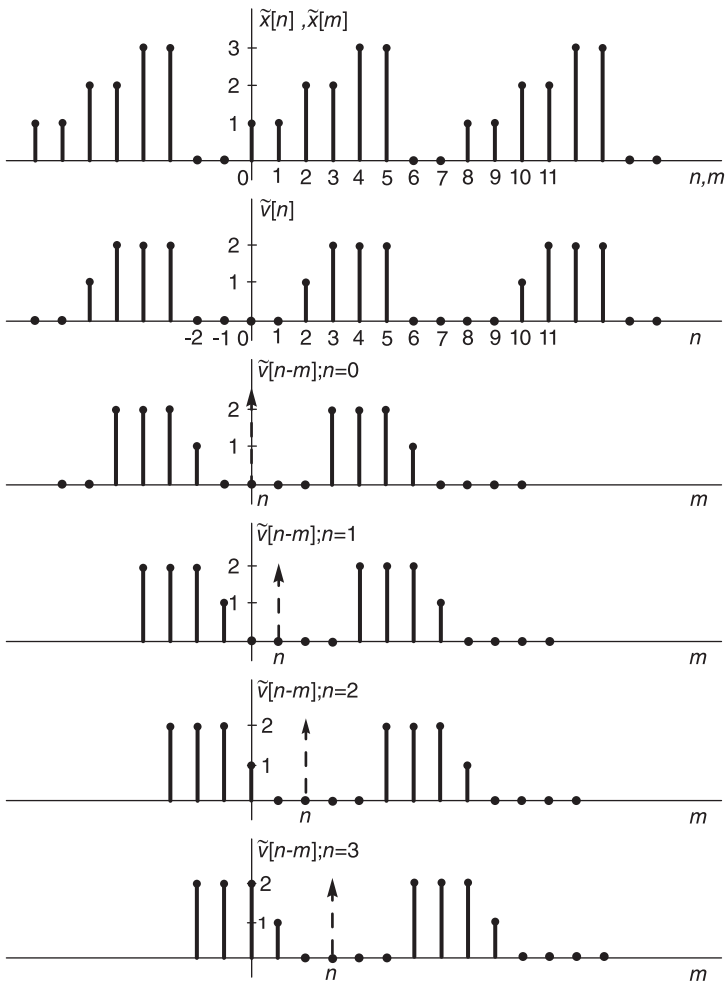


FIGURE 7.40 Example of periodic convolution.

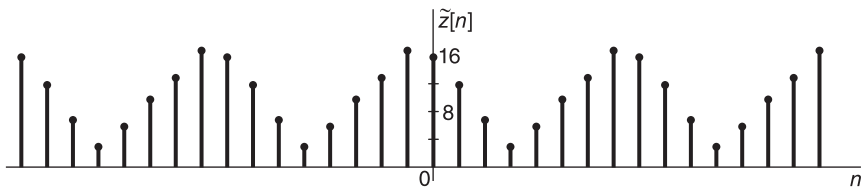


FIGURE 7.41 Circular convolution result.

7.22 Circular Convolution

Circular convolution of two finite duration sequences, each N points long, is simply periodic convolution followed by retaining only the base period. Symbolically we may write for N -point circular convolution

$$x[n] \circledast v[n] = \{\tilde{x}[n] \circledast \tilde{v}[n]\} R_N[n]. \tag{7.167}$$

$$x[n] \circledast v[n] \xleftrightarrow{DFT} X[k] V[k] \tag{7.168}$$

$$x[n] v[n] \xleftrightarrow{DFT} (1/N) X[k] \circledast V[k]. \tag{7.169}$$

The practical approach is therefore to simply perform periodic convolution then extract the base period, obtaining the circular convolution.

In other words, circular convolution is given by

$$x[n] \circledast v[n] = \left[\sum_{m=0}^{N-1} \tilde{x}[m] \tilde{v}[n-m] \right] R_N[n] = \left[\sum_{m=0}^{N-1} \tilde{v}[m] \tilde{x}[n-m] \right] R_N[n] \tag{7.170}$$

For the case of the two sequences defined in the last example, circular convolution would be evaluated identically as periodic convolution $\tilde{z}[n]$, followed by retaining only its base period, i.e.

$$x[n] \circledast v[n] = \tilde{z}[n] R_N[n]$$

$$x[n] \circledast v[n] = \{16, 12, 7, 3, 6, 10, 13, 17\}, \text{ for } \{n = 0, 1, 2, 3, 4, 5, 6, 7.\}$$

Circular convolution can be related to the usual linear convolution. Let $y[n]$ be the N -point linear convolution of two finite length sequences $x[n]$ and $v[n]$

$$y[n] = x[n] * v[n]. \tag{7.171}$$

Circular convolution is given by

$$z[n] = x[n] \circledast v[n] = \left\{ \sum_{k=-\infty}^{\infty} y[n+kN] \right\} R_N[n]. \tag{7.172}$$

which can be written in the matrix form

$$\begin{bmatrix} z[0] \\ z[1] \\ \vdots \\ z[N-2] \\ z[N-1] \end{bmatrix} = \begin{bmatrix} x[0] & x[N-1] & x[N-2] & \dots & x[1] \\ x[1] & x[0] & x[N-1] & \dots & x[2] \\ \vdots & \vdots & \vdots & \vdots & \vdots \\ x[N-2] & x[N-3] & x[N-4] & \dots & x[N-1] \\ x[N-1] & x[N-2] & x[N-3] & \dots & x[0] \end{bmatrix} \begin{bmatrix} v[0] \\ v[1] \\ \vdots \\ v[N-2] \\ v[N-1] \end{bmatrix} \tag{7.173}$$

to be compared with linear convolution which with $N = 6$ for example, for better visibility, can be written in the form

$$\begin{bmatrix} y[0] \\ y[1] \\ y[2] \\ y[3] \\ y[4] \\ y[N-1] \\ y[N] \\ y[N+1] \\ y[N+2] \\ y[N+3] \\ y[2N-2] \end{bmatrix} = \begin{bmatrix} x[0] & & & & & & & & & & \\ & x[1] & & & & & & & & & \\ & & x[0] & & & & & & & & \\ & & & x[1] & & & & & & & \\ & & & & x[0] & & & & & & \\ & & & & & x[1] & & & & & \\ x[N-1] & & & & & & x[0] & & & & \\ & x[N-1] & & & & & & x[1] & & & \\ & & x[N-1] & & & & & & x[2] & & \\ & & & x[N-1] & & & & & & x[3] & \\ & & & & x[N-1] & & & & & & x[4] \\ & & & & & x[N-1] & & & & & \\ & & & & & & x[N-1] & & & & \\ & & & & & & & x[N-1] & & & \\ & & & & & & & & x[N-1] & & \end{bmatrix} \begin{bmatrix} v[0] \\ v[1] \\ v[2] \\ v[3] \\ v[4] \\ v[N-1] \end{bmatrix} \tag{7.174}$$

We note that in the linear convolution matrix of Equation (7.174) if the lower triangle, starting at the $N + 1^{st}$ row (giving the value of $y[n]$) is moved up to cover the space of the upper vacant triangle we would obtain the same matrix of the circular convolution matrix (7.173). We may therefore write

$$\begin{bmatrix} z[0] \\ z[1] \\ \vdots \\ z[N-2] \\ z[N-1] \end{bmatrix} = \begin{bmatrix} y[0] + y[N] \\ y[1] + y[N+1] \\ \vdots \\ y[N-2] + y[2N-2] \\ y[N-1] \end{bmatrix} \tag{7.175}$$

Circular convolution is therefore an aliasing of the linear convolution sequence $y[n]$. We also note that if the sequences $x[n]$ and $v[n]$ are of lengths N_1 and N_2 , the linear convolution sequence $y[n]$ is of length $N_1 + N_2 - 1$. If an N -point circular convolution is effected the result would be the same as linear convolution if and only if $N \geq N_1 + N_2 - 1$.

Example 7.26 Evaluate the linear convolution $y[n] = x[n] * v[n]$ of the sequences $x[n]$ and $v[n]$ which are the base periods of $\tilde{x}[n]$ and $\tilde{v}[n]$ of the last example. Deduce the value of circular convolution $z[n]$ from $y[n]$.

Proceeding similarly, as shown in Fig. 7.42, we obtain the linear convolution $y[n]$ which may be listed in the form of the following table.

n	0	1	2	3	4	5	6	7	8	9	10
$y[n]$	0	0	1	3	6	10	13	17	16	12	6

The sequence $y[n]$ is depicted in Fig. 7.43. To deduce the value of circular convolution $z[n]$ from the linear convolution $y[n]$ we construct the following table, where $z[n] = y[n] + y[n + 8]$, obtaining the circular convolution $z[n]$ as found above.

$y[n]$	0	0	1	3	6	10	13	17	16	12	6	0	0	0
$y[n + 8]$	16	12	6	0	0	0	0	0	0	0	0	0	0	0
$z[n]$	16	12	7	3	6	10	13	17	0	0	0	0	0	0

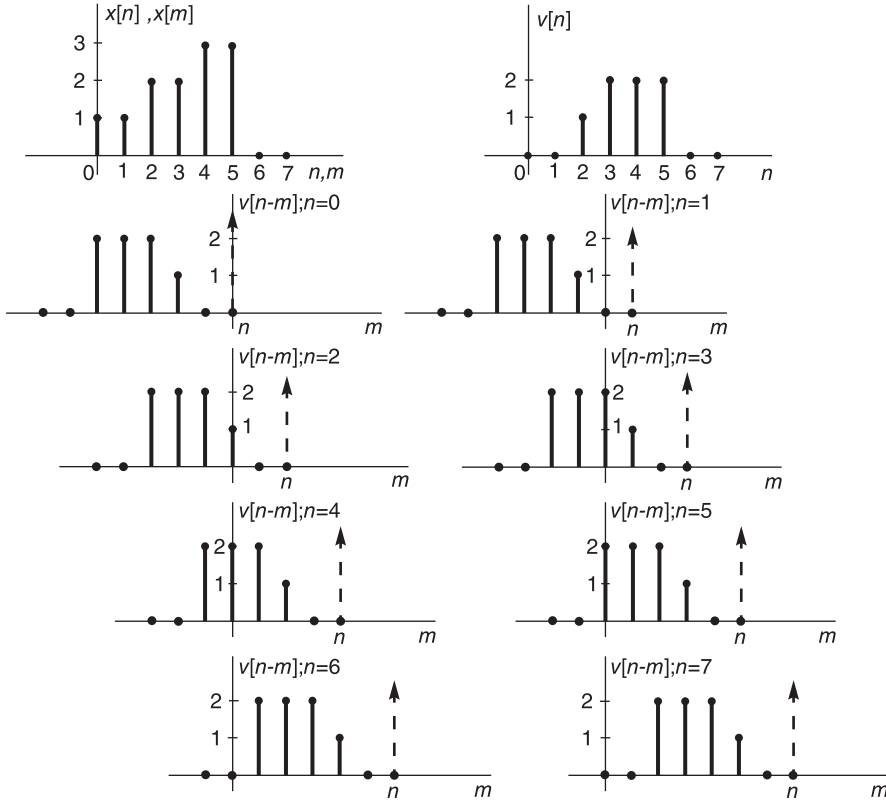


FIGURE 7.42 Linear convolution of two sequences.

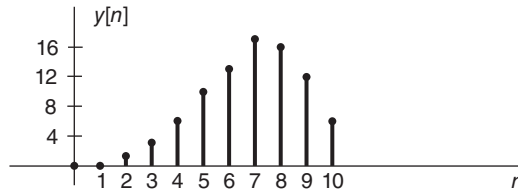


FIGURE 7.43 Linear convolution results.

7.23 Circular Convolution Using the DFT

The following example illustrates circular convolution using the DFT.

Example 7.27 Consider the circular convolution of the two sequences $\tilde{x}[n]$ and $\tilde{v}[n]$ of the last example. We evaluate $\tilde{X}[k]$, $\tilde{V}[k]$ and their product and verify that the circular convolution $\tilde{z}[n] = \tilde{x}[n] \circledast \tilde{v}[n]$ has the DFS $\tilde{X}[k] = \tilde{X}[k] \tilde{V}[k]$. By extracting the N -point base period we conclude that the DFT relation $Z[k] = X[k] V[k]$ also holds.

The sequences $\tilde{x}[n]$ and $\tilde{v}[n]$ are periodic with period $N = 8$. For $0 \leq n \leq 7$ we have

$$\begin{aligned} \tilde{x}[n] &= \delta[n] + \delta[n - 1] + 2\delta[n - 2] + 2\delta[n - 3] + 3\delta[n - 4] + 3\delta[n - 5] \\ \tilde{v}[n] &= \delta[n - 2] + 2\{\delta[n - 3] + 2\delta[n - 4] + 2\delta[n - 5]\} \end{aligned}$$

$$\begin{aligned}\tilde{X}[k] &= \sum_{n=0}^{N-1} \tilde{x}[n] e^{-j(2\pi/N)nk} \\ &= 1 + e^{-j(2\pi/8)k} + 2e^{-j(2\pi/8)2k} + 2e^{-j(2\pi/8)3k} + 3e^{-j(2\pi/8)4k} + 3e^{-j(2\pi/8)5k}\end{aligned}$$

$$X[k] = \tilde{X}[k] R_N[k] = \tilde{X}[k], \quad k = 0, 1, \dots, N-1$$

$$\tilde{V}[k] = e^{-j(2\pi/8)2k} + 2 \left\{ e^{-j(2\pi/8)3k} + e^{-j(2\pi/8)4k} + e^{-j(2\pi/8)5k} \right\}$$

$$V[k] = \tilde{V}[k] R_N[k] = \tilde{V}[k], \quad k = 0, 1, \dots, N-1.$$

Letting $w = e^{-j(2\pi/8)k}$ we have

$$\tilde{X}[k] = 1 + w + 2w^2 + 2w^3 + 3w^4 + 3w^5$$

$$\tilde{V}[k] = w^2 + 2w^3 + 2w^4 + 2w^5.$$

Multiplying the two polynomials noticing that $w^k = w^{k \bmod 8}$, we have

$$\tilde{Z}[k] = \tilde{X}[k] \tilde{V}[k] = 16 + 12w + 7w^2 + 3w^3 + 6w^4 + 10w^5 + 13w^6 + 17w^7, \quad 0 \leq k \leq N-1$$

$$X[k] V[k] = \tilde{Z}[k] R_N[k] = \tilde{Z}[k], \quad 0 \leq k \leq 7.$$

The inverse transform of $\tilde{Z}[k]$ is

$$\begin{aligned}\tilde{z}[n] &= 16\delta[n] + 12\delta[n-1] + 7\delta[n-2] + 3\delta[n-3] + 6\delta[n-4] \\ &\quad + 10\delta[n-5] + 13\delta[n-6] + 17\delta[n-7], \quad 0 \leq n \leq N-1\end{aligned}$$

and

$$z[n] = \tilde{z}[n], \quad 0 \leq n \leq N-1.$$

This is the same result obtained above by performing circular convolution directly in the time domain. Similarly, the N -point Circular correlation of two sequences $v[n]$ and $x[n]$ may be written

$$c_{vx}[n] = v[n] \circledast x[-n]. \quad (7.176)$$

and its DFT is

$$C_{vx}[k] = V[k] X^*[k]. \quad (7.177)$$

7.24 Sampling the Spectrum

Let $x[n]$ be an aperiodic sequence with z -transform $X(z)$ and Fourier transform $X(e^{j\Omega})$.

$$X(z) = \sum_{n=-\infty}^{\infty} x[n] z^{-n} \quad (7.178)$$

$$X(e^{j\Omega}) = \sum_{n=-\infty}^{\infty} x[n] e^{-j\Omega n}. \quad (7.179)$$

Sampling the z -transform on the unit circle uniformly into N points, that is at $\Omega = [2\pi/N]k$, $k = 0, 1, \dots, N-1$ we obtain the periodic DFS

$$\tilde{X}[k] = \sum_{n=-\infty}^{\infty} x[n] e^{-j(2\pi/N)nk}. \quad (7.180)$$

We recall, on the other hand, that the same DFS

$$\tilde{X}[k] = \sum_{n=0}^{N-1} \tilde{x}[n] e^{-j(2\pi/N)nk} \tag{7.181}$$

is the expansion of a periodic sequence $\tilde{x}[n]$ of period N . To show that $\tilde{x}[n]$ is but an aliasing of the aperiodic sequence $x[n]$ we use the inverse relation

$$\begin{aligned} \tilde{x}[n] &= \frac{1}{N} \sum_{k=0}^{N-1} \tilde{X}[k] e^{j(2\pi/N)nk} = \frac{1}{N} \sum_{k=0}^{N-1} \sum_{m=-\infty}^{\infty} x[m] e^{-j(2\pi/N)mk} e^{j(2\pi/N)nk} \\ &= \frac{1}{N} \sum_{m=-\infty}^{\infty} x[m] \sum_{k=0}^{N-1} e^{j(2\pi/N)(n-m)k}. \end{aligned} \tag{7.182}$$

Now

$$\frac{1}{N} \sum_{k=0}^{N-1} e^{j(2\pi/N)(n-m)k} = \begin{cases} 1, & m - n = lN \\ 0, & \text{otherwise} \end{cases} \tag{7.183}$$

wherefrom

$$\tilde{x}[n] = \sum_{l=-\infty}^{\infty} x[n + lN] \tag{7.184}$$

confirming that sampling the Fourier transform of an aperiodic sequence $x[n]$, leading to the DFS, has for effect aliasing in time of the sequence $x[n]$, which results in a periodic sequence $\tilde{x}[n]$ that can be quite different from $x[n]$. If on the other hand $x[n]$ is of length N or less the resulting sequence $\tilde{x}[n]$ is a simple periodic extension of $x[n]$. Since the DFT is but the base period of the DFS these same remarks apply directly to the DFT.

7.25 Table of Properties of DFS

Table 7.3 summarizes basic properties of the DFS expansion. Since the DFT of an N -point sequence $x[n]$ is but the base period of the DFS expansion of $\tilde{x}[n]$, the periodic extension of $x[n]$, the same properties apply to the DFT. We simply replace the sequence $x[n]$ by its periodic extension $\tilde{x}[n]$, apply the DFS property and extract the base period of the resulting DFS. A table of DFT properties is included in Section 7.27. The following example illustrates the approach in applying the shift in time property, which states that if $\tilde{x}[n] \longleftrightarrow \tilde{X}[k]$ then $\tilde{x}[n - m] \longleftrightarrow e^{-j(2\pi/N)km} \tilde{X}[k]$.

Proof of Shift in Time Property Let $\tilde{v}[n] = \tilde{x}[n - m]$

$$\tilde{V}[k] = \sum_{n=0}^{N-1} \tilde{x}[n - m] e^{-j(2\pi/N)km}. \tag{7.185}$$

Let $n - m = r$

$$\tilde{V}[k] = \sum_{r=-m}^{-m+N-1} \tilde{x}[r] e^{-j(2\pi/N)k(r+m)} = e^{-j(2\pi/N)km} \sum_{r=0}^{N-1} \tilde{x}[r] e^{-j(2\pi/N)kr} = e^{-j(2\pi/N)km} \tilde{X}[k]$$

as stated. Note that if the amount of shift m is greater than N the resulting shift is by $m \bmod N$ since the sequence $\tilde{x}[n]$ is periodic of period N .

TABLE 7.3 DFS properties

Time n	Frequency k
$\tilde{x}[n]$	$\tilde{X}[k]$
$\tilde{x}^*[n]$	$\tilde{X}^*[-k]$
$\tilde{x}^*[-n]$	$\tilde{X}^*[k]$
$\tilde{x}_e[n]$	$\Re[\tilde{X}[k]]$
$\tilde{x}_o[n]$	$j\Im[\tilde{X}[k]]$
$\tilde{x}[n-m]$	$e^{-j(2\pi/N)km} \tilde{X}[k]$
$e^{j(2\pi/N)mn} \tilde{x}[n]$	$\tilde{X}[k-m]$
$\tilde{x}[n] \otimes \tilde{v}[n]$	$\tilde{X}[k] \tilde{V}[k]$
$\tilde{x}[n] \tilde{v}[n]$	$(1/N) \tilde{X}[k] \otimes \tilde{V}[k]$

7.26 Shift in Time and Circular Shift

Given a periodic sequence $\tilde{x}[n]$ of period N the name circular shift refers to shifting the sequence by say, m samples followed by extracting the base period, that is, the period $0 \leq n \leq N-1$. If we consider the result of the shift on the base period before and after the shift we deduce that the result is a rotation, a circular shift, of the N samples. For example consider a periodic sequence $\tilde{x}[n]$ of period $N=8$, which has the values $\{\dots, 2, 9, 8, 7, 6, 5, 4, 3, 2, 9, 8, 7, 6, 5, 4, 3, \dots\}$. Its base period $\tilde{x}[n] = 2, 9, 8, 7, 6, 5, 4, 3$ for $n = 0, 1, 2, \dots, 7$, as shown in Fig. 7.44(a).

If the sequence is shifted one point to the right the resulting base period is $\tilde{x}[n-1] = 3, 2, 9, 8, 7, 6, 5, 4$ as shown in Fig. 7.44(b). If it is shifted instead by one point to the left, the resulting sequence is $\tilde{x}[n+1] = 9, 8, 7, 6, 5, 4, 3, 2$, as shown in Fig. 7.44(c). We note that the effect is a simple rotation to the left by the number of shifts. If the shift of $\tilde{x}[n]$ is to the right by three point the result is $\tilde{x}[n-3] = 5, 4, 3, 2, 9, 8, 7, 6$, as shown in Fig. 7.44(d). The base period of $\tilde{x}[n]$ is given by $\tilde{x}[n]R_N[n]$, that of $\tilde{x}[n-m]$ is $\tilde{x}[n-m]R_N[n]$ as shown in the figure. The arrow in the figure is the reference point. Shifting the sequence $\tilde{x}[n]$ to the right by k points corresponds to the unit circle as a wheel turning counterclockwise k steps and reading the values starting from the reference point and vice versa.

Note: The properties listed are those of the DFS, but apply equally to the DFT with the proper interpretation that $\tilde{x}[n]$ and $\tilde{X}[k]$ are periodic extensions of the N -point sequences $x[n]$ and $X[k]$, that $X[k] = \tilde{X}[k]R_N[k]$ and $x[n] = \tilde{x}[n]R_N[n]$. The shift in time producing $\tilde{x}[n-m]$ is equivalent to circular shift and the periodic convolution $\tilde{x}[n] \otimes \tilde{v}[n]$ is equivalent to cyclic convolution in the DFT domain.

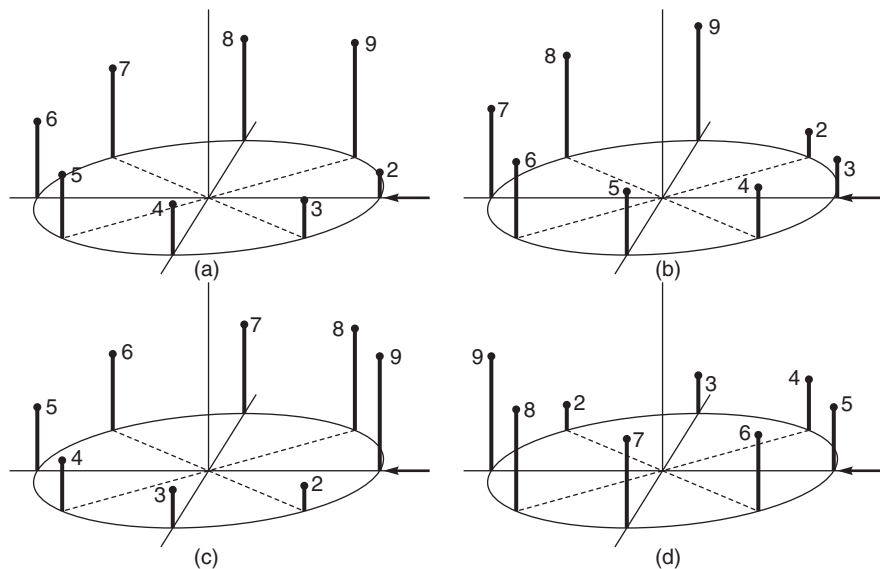


FIGURE 7.44 Circular shift operations.

7.27 Table of DFT Properties

TABLE 7.4 DFT properties

Time n	Frequency k
$x[n]$	$X[k]$
$x^*[n]$	$X^* [[-k]]_N R_N[k]$
$x^* [[-n]]_N R_N[k]$	$X^*[k]$
$x [[n - m]]_N R_N[k]$	$e^{-j(2\pi/N)km} X[k]$
$e^{j(2\pi/N)mn} x[n]$	$X [[k - m]]_N R_N[k]$
$x[n] \otimes v[n]$	$X[k] V[k]$
$x[n] v[n]$	$(1/N) X[k] \otimes V[k]$
$\sum_{n=0}^{N-1} v[n] x^*[n]$	$\frac{1}{N} \sum_{k=0}^{N-1} V[k] X^*[k]$

Properties of the DFT are listed in Table 7.4. As noted above, the properties are the

same as those of the DFS except for a truncation of a periodic sequence to extract its base period.

7.28 Zero Padding

Consider a sequence of $x[n]$ of length N defined over the interval $0 \leq n \leq N-1$ and zero elsewhere, and its periodic repetition $\tilde{x}[n]$. We study the effect on the DFT of annexing N zeros, called padding with zeros leading to a sequence $x_2[n]$ of length $2N$. More generally, we consider padding the sequence $x[n]$ with zeros leading to a sequence $x_4[n]$ say of length $4N$, $x_8[n]$ of length $8N$ and higher.

The addition of N zeros to the sequence implies that the new periodic sequence $\tilde{x}_2[n]$ is equivalent to a convolution of the original N -point sequence $x[n]$ with an impulse train of period $2N$. The result is a sequence of a period double the original period N of the sequence $\tilde{x}[n]$, which is but a convolution of the sequence $x[n]$ with an impulse train of period N . The effect of doubling the period is that in the frequency domain the DFS $\tilde{X}_2[k]$ and the DFT $X_2[k]$ are but finer sampling of the unit circle; into $2N$ points rather than N points. Similarly zero padding leading to a sequence $x_4[n]$ of length $4N$ produces a DFT $X_4[k]$ that is a still finer sampling of the unit circle into $4N$ points, and so on. We conclude that zero padding leads to finer sampling of the Fourier transform $X(e^{j\Omega})$, that is, to an interpolation between the samples of $X[k]$.

The duality between time and frequency domains implies moreover that given a DFT $X[k]$ and DFS $\tilde{X}[k]$ of a sequence $x[n]$, zero padding of the $X[k]$ and, equivalently, $\tilde{X}[k]$, leading to a DFT sequence $X_2[k]$ corresponds to convolution in the frequency domain of $X[k]$ with an impulse train of period $2N$. This implies multiplication in the time domain of the sequence $x[n]$ by an impulse train of double the frequency such that the resulting sequence $x_2[n]$ is a finer sampling, by a factor of two, of the original sequence $x[n]$. Similarly, zero padding $X[k]$ leading to a sequence $X_4[k]$ of length $4N$ has for effect a finer sampling, by a factor of 4, i.e. interpolation, of the original sequence $x[n]$.

Example 7.28 Let $x[n] = R_N[n]$

$$\begin{aligned} X(e^{j\Omega}) &= \sum_{n=0}^{N-1} e^{-j\Omega n} = \frac{1 - e^{-j\Omega N}}{1 - e^{-j\Omega}} = \frac{e^{-j\Omega N/2}}{e^{-j\Omega/2}} \frac{2j \sin(\Omega N/2)}{2j \sin(\Omega/2)} \\ &= e^{-j\Omega(N-1)/2} \frac{\sin(N\Omega/2)}{\sin(\Omega/2)} = e^{-j\Omega(N-1)/2} Sd_N(\Omega/2). \end{aligned}$$

We consider the case $N = 4$ so that $x[n] = R_4[n]$ and then the case of padding $x[n]$ with zeros obtaining the 16 point sequence

$$y[n] = \begin{cases} x[n], & n = 0, 1, 2, 3 \\ 0, & n = 4, 5, \dots, 15. \end{cases}$$

We have

$$X[k] = \sum_{n=0}^3 e^{-j(2\pi/4)nk} = X(e^{j\Omega}) \Big|_{\Omega=(2\pi/4)k} = e^{-j(3/2)(\pi/2)k} Sd_4(k\pi/4) = \begin{cases} N = 4, & k = 0 \\ 0, & k = 1, 2, 3 \end{cases}$$

$$\begin{aligned}
 Y[k] &= \sum_{n=0}^3 e^{-j(2\pi/16)nk} = \frac{1 - e^{-j(2\pi/16)4k}}{1 - e^{-j(2\pi/16)k}} \\
 &= \frac{e^{-j(2\pi/16)2k}}{e^{-j(2\pi/16)k/2}} \frac{\sin[(2\pi/16)2k]}{\sin[(2\pi/16)k/2]} = e^{-j(2\pi/16)(3k/2)} S_{d_4}(k\pi/16)
 \end{aligned}$$

which is a four times finer sampling of $X(e^{j\Omega})$ than in the case of $X[k]$.

Example 7.29 Consider a sinusoid $x_c(t) = \sin(\omega_1 t)$, where $\omega_1 = 2\pi f_1$, sampled at a frequency $f_s = 25600$ Hz. The sinusoid is sampled for a duration of $\tau = 2.5$ msec into N_1 samples. The frequency f_1 of $x_c(t)$ is such that in the time interval $(0, \tau)$ there are 8.5 cycles of the sinusoid.

a) Evaluate the 64-point FFT of the sequence $x[n] = x_c(nT_s)$, where T_s is the sampling interval $T_s = 1/f_s$.

b) Apply zero padding by annexing 192 zeros to the samples of the sequence $x[n]$. Evaluate the 256-point FFT of the padded signal vector. Observe the interpolation and the higher spectral peaks that appear thanks to zero padding.

The following MATLAB program evaluates the FFT of the signal $x[n]$ and subsequently that of the zero-padded vector $x_z[n]$.

```

% Zero-padding-example. Corinthians 2008
fs=25600 % sampling frequency
Ts=1/fs % sampling period Ts = 3.9063x10(-5)
tau=0.0025 % duration of sinusoid
N1=0.0025/Ts % N1=64
t=(0:N1-1)*Ts % time in seconds
% tau contains 8.5 cycles of sinusoid and 64 samples.
tau1=tau/8.5 % tau1 is the period of the sinusoid.
% f1 is the frequency of the sinusoid in Hz.
f1=1/tau1
w1=2*pi*f1
x=sin(w1*t);
figure(1)
stem(t,x)
title('x[n]')
X=fft(x);
% N1=64 samples on unit circle cover the range 0 to fs Hz
freq=(0:63)*fs/64;
Xabs=abs(X);
figure(2)
stem(freq,Xabs)
title('Xabs[k]')
% Add 28 - 64 = 192 zeros.
N = 28
T = N * Ts % Duration of zero-padded vector.
xz=[x zeros(1,192)]; % xz is x with zero padding
t = (0 : N - 1) * Ts % t=(0:255)*Ts
figure(3)
stem(t,xz)
title('Zero-padded vector xz[n]')
Xz=fft(xz);

```

```

Xzabs=abs(Xz);
freqf = (0 : 255) * fs/256; % frequency finer-sampling vector
figure(4)
stem(freqf,Xzabs)
title('Xzabs[k]')
    
```

The signal $x[n]$ is depicted in Fig. 7.45(a). The modulus $|X[k]|$ of its DFT can be seen in Fig. 7.45(b). We note that the signal frequency falls in the middle between two samples on the unit circle. Hence the peak of the spectrum $|X[k]|$ which should equal $N_1/2 = 32$ falls between two samples and cannot be seen. The zero-padded signal $x_z[n]$ is shown in Fig. 7.45(c). The modulus $|X_z[k]|$ of the DFT of the zero padded signal can be seen in Fig. 7.45(d).

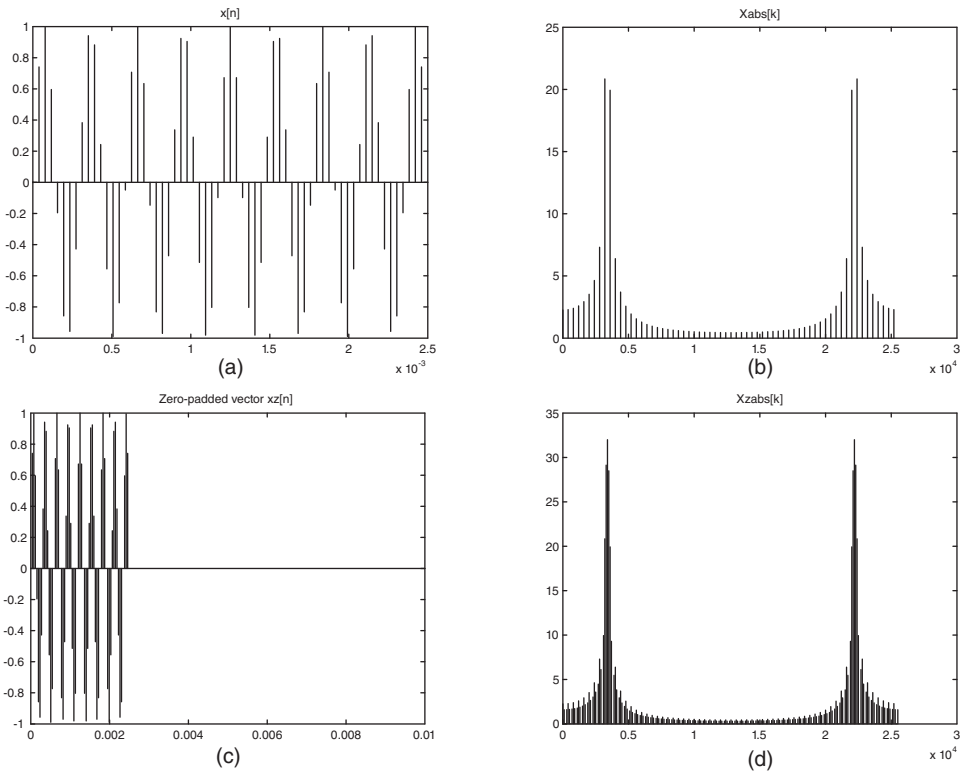


FIGURE 7.45 Zero-padding: (a) A sinusoidal sequence, (b) 64-point DFT, (c) zero-padded sequence to 256 points, (d) 256-point DFT of padded sequence.

We note that interpolation has been effected, revealing the spectral peak of $N_1/2 = 32$, which now falls on one of the $N = 256$ samples around the unit circle. By increasing the sequence length through zero padding to $N = 4N_1$ an interpolation of the DFT spectrum by a factor of 4 has been achieved.

7.29 Discrete z -Transform

A *discrete z -transform* (DZT) may be defined as the result of sampling a circle in the z -plane centered about the origin. Note that the DFT is a special case of the DZT obtained if the radius of the circle is unity. An approach to system identification pole-zero modeling employing DZT evaluation and a weighting of z -transform spectra has been proposed as an alternative to Prony's approach. A system is given as a black box and the objective is to evaluate its poles and zeros by applying a finite duration input sequence or an impulse and observing its finite duration output. The approach is based on the fact that knowing only a finite duration of the impulse response the evaluation of the DZT on a circle identifies fairly accurately the frequency of the least damping poles.

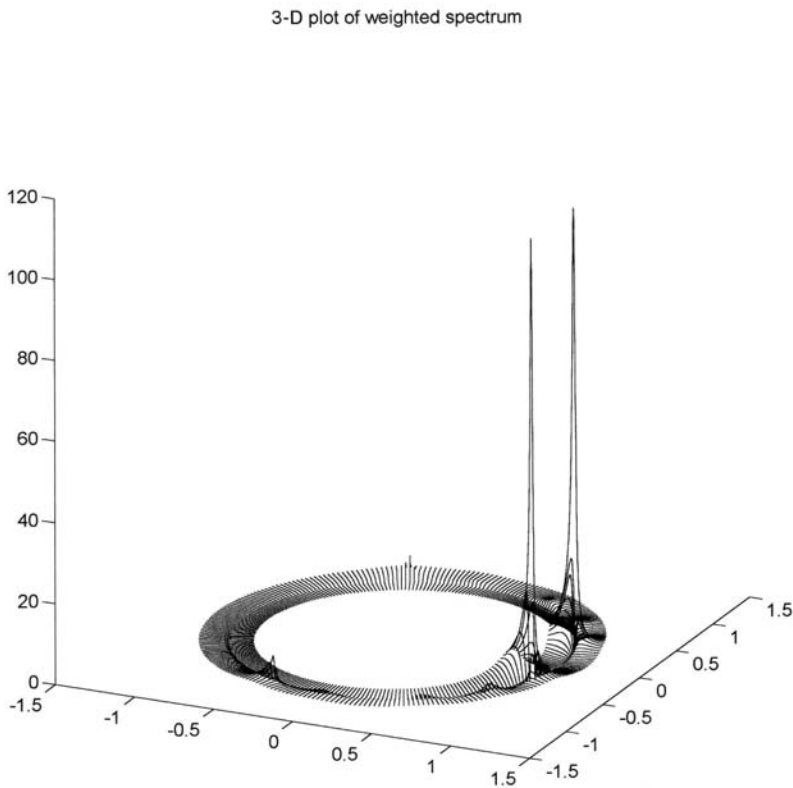


FIGURE 7.46 3-D plot of weighted z -spectrum unmasking a pole pair.

However, identification of the components' damping coefficients, i.e. the radius of the pole

or pole-pair, cannot be deduced through radial z -transforms since spectra along a radial contour passing through the pole-zero rises exponentially toward the origin of the z -plane due to a multiple pole at the origin of the transform of such a finite duration sequence. The proposed weighting of spectra unmask the poles identifying their location in the z -plane both in angle and radius as shown in Fig. 7.46 [26]. Once the pole locations and their residues are found the zeros are deduced. The least damped poles are thus deleted “deflating” the system, i.e. reducing its order. The process is repeated identifying the new least damped poles and so on until all the poles and zeros have been identified. In [26] an example is given showing the identification of a system of the 14th order.

Example 7.30 Given the sequence

$$x[n] = a^n \{u[n] - u[n - N]\}$$

with $a = 0.7$ and $N = 16$.

- a) Evaluate the z -transform $X(z)$ of $x[n]$, stating its region of convergence (ROC).
- b) Evaluate and sketch the poles and zeros of $X(z)$ in the z -plane.
- c) Evaluate the z -transform on a circle of radius a in the z -plane.
- d) Evaluate $X_a[k]$, the DZT along the circle of radius a , by sampling the z -transform along the circle at frequencies $\Omega = 0, 2\pi/N, 3\pi/N, \dots, (N - 1)\pi/N$, similarly to the sampling the DFT effects along the unit circle.

We have

$$x[n] = a^n R_N[n]$$

a)

$$\begin{aligned} X(z) &= \sum_{n=0}^{N-1} a^n z^{-n} = \frac{1 - a^N z^{-N}}{1 - az^{-1}}, \quad z \neq 0 \\ &= \frac{z^N - a^N}{z^{N-1}(z - a)}. \end{aligned}$$

b) Zeros

$$\begin{aligned} a^N z^{-N} &= 1 = e^{-j2\pi k} \\ z^N &= a^N e^{j2\pi k} \\ z &= ae^{j2\pi k/N} = 0.7e^{j2\pi k/16} \end{aligned}$$

implying a coincidence pole-zero at $z = a$, pole of order $N - 1$ at $z = 0$. See Fig. 7.47.

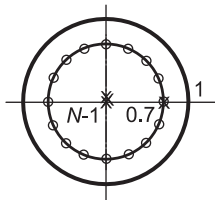


FIGURE 7.47 Sampling a circle of general radius.

c)

$$\begin{aligned} X(ae^{j\Omega}) &= \frac{1 - e^{-j\Omega N}}{1 - e^{-j\Omega}} = e^{-j\Omega(N-1)/2} \frac{\sin(N\Omega/2)}{\sin(\Omega/2)} \\ &= e^{-j\Omega(N-1)/2} Sd_N(\Omega/2). \end{aligned}$$

d)

$$X_a[k] = \frac{1 - e^{-j2\pi k}}{1 - e^{-j2\pi k/N}} = \begin{cases} N, & k = 0 \\ 0, & k = 1, 2, \dots, N-1. \end{cases}$$

Example 7.31 Evaluate the Fourier transform of the sequence

$$x[n] = \begin{cases} 1 - \frac{|n|}{N}, & -N \leq n \leq N \\ 0, & \text{otherwise} \end{cases}$$

where N is odd. Using duality deduce the corresponding Fourier series expansion and Fourier transform. Evaluate the Fourier transform of the sequence $x_1[n] = x[n - N]$. We may write

$$x[n] = v[n] * v[n]$$

where

$$v[n] = \Pi_{(N-1)/2}[n]$$

$$X(e^{j\Omega}) = [V(e^{j\Omega})]^2 = Sd_N^2(\Omega/2) = \left\{ \frac{\sin(N\Omega/2)}{\sin(\Omega/2)} \right\}^2.$$

Using duality we have

$$Sd_N^2(t/2) \xleftrightarrow{FSC} V_n = \begin{cases} 1 - \frac{|n|}{N}, & -N \leq n \leq N \\ 0, & \text{otherwise} \end{cases}$$

and

$$Sd_N^2(t/2) \xleftrightarrow{\mathcal{F}} V(j\omega) = 2\pi \sum_{n=-N}^N (1 - |n|/N) \delta(\omega - n).$$

$$X_1(e^{j\Omega}) = e^{-j\Omega N} Sd_N^2(\Omega/2).$$

7.30 Fast Fourier Transform

The FFT is an efficient algorithm that reduces the computations required for the evaluation of the DFT. In what follows, the derivation of the FFT is developed starting with a simple example of the DFT of $N = 8$ points. The DFT can be written in matrix form. This form is chosen because it makes it easy to visualize the operations in the DFT and its conversion to the FFT.

To express the DFT in matrix form we define an input *data vector* x of dimension N the elements of which are the successive elements of the input sequence $x[n]$. Similarly we define a vector X of which the elements are the coefficients $X[k]$ of the DFT. The DFT

$$X[k] = \sum_{n=0}^{N-1} x[n] e^{-j2\pi nk/N} \quad (7.186)$$

can thus be written in the matrix form as $X = F_N x$ where F_N is an $N \times N$ matrix of which the elements are given by $[F_N]_{rs} = w^{rs}$ and

$$w = e^{-j\frac{2\pi}{N}}. \quad (7.187)$$

The inverse relation is written

$$x = \frac{1}{N} F_N^* X. \tag{7.188}$$

Note that premultiplication of a square matrix A by a diagonal matrix D producing the matrix $C = D A$ may be obtained by multiplying the successive elements of the diagonal matrix D by the successive rows of A . Conversely, postmultiplication of a square matrix A by a diagonal matrix D producing the matrix $C = A D$ may be obtained by multiplying the successive elements of the diagonal matrix D by the successive columns of A . The following example shows the factorization of the matrix F_N , which leads to the FFT.

Example 7.32 Let $N = 8$. The unit circle is divided as shown in Fig. 7.48. Since $w^4 = -w^0$, $w^5 = -w^1$, $w^6 = -w^2$, and $w^7 = -w^3$, we have

$$\begin{aligned}
 X &= \begin{bmatrix} w^0 & w^0 & w^0 & w^0 & w^0 & w^0 & w^0 & w^0 \\ w^0 & w^1 & w^2 & w^3 & w^4 & w^5 & w^6 & w^7 \\ w^0 & w^2 & w^4 & w^6 & w^0 & w^2 & w^4 & w^6 \\ w^0 & w^3 & w^6 & w^1 & w^4 & w^7 & w^2 & w^5 \\ w^0 & w^4 & w^0 & w^4 & w^0 & w^4 & w^0 & w^4 \\ w^0 & w^5 & w^2 & w^7 & w^4 & w^1 & w^6 & w^3 \\ w^0 & w^6 & w^4 & w^2 & w^0 & w^6 & w^4 & w^2 \\ w^0 & w^7 & w^6 & w^5 & w^4 & w^3 & w^2 & w^1 \end{bmatrix} \begin{bmatrix} x_0 \\ x_1 \\ x_2 \\ x_3 \\ x_4 \\ x_5 \\ x_6 \\ x_7 \end{bmatrix} \\
 &= \begin{bmatrix} w^0 & w^0 & w^0 & w^0 & w^0 & w^0 & w^0 & w^0 \\ w^0 & w^1 & w^2 & w^3 & -w^0 & -w^1 & -w^2 & -w^3 \\ w^0 & w^2 & -w^0 & -w^2 & w^0 & w^2 & -w^0 & -w^2 \\ w^0 & w^3 & -w^2 & w^1 & -w^0 & -w^3 & w^2 & -w^1 \\ w^0 & -w^0 & w^0 & -w^0 & w^0 & -w^0 & w^0 & -w^0 \\ w^0 & -w^1 & w^2 & -w^3 & -w^0 & w^1 & -w^2 & w^3 \\ w^0 & -w^2 & -w^0 & w^2 & w^0 & -w^2 & -w^0 & w^2 \\ w^0 & -w^3 & -w^2 & -w^1 & -w^0 & w^3 & w^2 & w^1 \end{bmatrix} \begin{bmatrix} x_0 \\ x_1 \\ x_2 \\ x_3 \\ x_4 \\ x_5 \\ x_6 \\ x_7 \end{bmatrix}.
 \end{aligned}$$

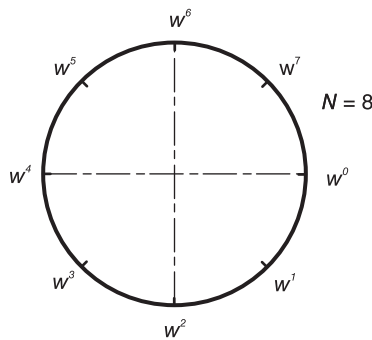


FIGURE 7.48 Unit circle divided into $N = 8$ points.

We may rewrite this matrix relation as the set of equations

$$\begin{aligned}
 X_0 &= x_0 + x_1 + \dots + x_7 \\
 X_1 &= (x_0 - x_4)w^0 + (x_1 - x_5)w^1 + (x_2 - x_6)w^2 + (x_3 - x_7)w^3 \\
 X_2 &= (x_0 + x_4)w^0 + (x_1 + x_5)w^2 - (x_2 + x_6)w^0 - (x_3 + x_7)w^2 \\
 X_3 &= (x_0 - x_4)w^0 + (x_1 - x_5)w^3 - (x_2 - x_6)w^2 + (x_3 - x_7)w^1 \\
 X_4 &= (x_0 + x_4)w^0 - (x_1 + x_5)w^0 + (x_2 + x_6)w^0 - (x_3 + x_7)w^0 \\
 X_5 &= (x_0 - x_4)w^0 - (x_1 - x_5)w^1 + (x_2 - x_6)w^2 - (x_3 - x_7)w^3 \\
 X_6 &= (x_0 + x_4)w^0 - (x_1 + x_5)w^2 - (x_2 + x_6)w^0 + (x_3 + x_7)w^2 \\
 X_7 &= (x_0 - x_4)w^0 - (x_1 - x_5)w^3 - (x_2 - x_6)w^2 - (x_3 - x_7)w^1.
 \end{aligned}$$

These operations can be expressed back in matrix form:

$$X = \begin{bmatrix} w^0 & w^0 & w^0 & w^0 & & & & \\ & w^0 & w^2 & -w^0 & -w^2 & & & \\ & & w^0 & w^3 & -w^2 & w^1 & & \\ w^0 & -w^0 & w^0 & -w^0 & & & & \\ & & w^0 & -w^1 & w^2 & -w^3 & & \\ w^0 & -w^2 & -w^0 & w^2 & & & & \\ & & & w^0 & -w^3 & -w^2 & -w^1 & \end{bmatrix} \underbrace{\begin{bmatrix} x_0 + x_4 \\ x_1 + x_5 \\ x_2 + x_6 \\ x_3 + x_7 \\ x_0 - x_4 \\ x_1 - x_5 \\ x_2 - x_6 \\ x_3 - x_7 \end{bmatrix}}_g.$$

Calling the vector on the right g , we can rewrite this equation in the form:

$$X = \begin{bmatrix} w^0 & w^0 & w^0 & w^0 & & & & \\ & w^0 & w^2 & -w^0 & -w^2 & & & \\ & & w^0 & w^3 & -w^0 & -w^2 & & \\ w^0 & -w^0 & w^0 & -w^0 & & & & \\ & & w^0 & -w^0 & w^0 & -w^0 & & \\ w^0 & -w^2 & -w^0 & w^2 & & & & \\ & & & w^0 & -w^2 & -w^0 & w^2 & \end{bmatrix} \text{diag}(w^0, w^0, w^0, w^0, w^0, w^1, w^2, w^3)g.$$

Let

$$h = \text{diag}(w^0, w^0, w^0, w^0, w^0, w^1, w^2, w^3)g.$$

A graphical representation of this last equation is shown on the left side of Fig. 7.49. We can write

$$\begin{aligned}
 X_0 &= (h_0 + h_2)w^0 + (h_1 + h_3)w^0 \\
 X_1 &= (h_4 + h_6)w^0 + (h_5 + h_7)w^0 \\
 X_2 &= (h_0 - h_2)w^0 + (h_1 - h_3)w^2 \\
 X_3 &= (h_4 - h_6)w^0 + (h_5 - h_7)w^2 \\
 X_4 &= (h_0 + h_2)w^0 - (h_1 + h_3)w^0 \\
 X_5 &= (h_4 + h_6)w^0 - (h_5 + h_7)w^0 \\
 X_6 &= (h_0 - h_2)w^0 - (h_1 - h_3)w^2 \\
 X_7 &= (h_4 - h_6)w^0 - (h_5 - h_7)w^2
 \end{aligned}$$

which can be rewritten in the form

$$X = \begin{bmatrix} w^0 & w^0 & & & & & & & \\ & & w^0 & w^2 & w^0 & & & & \\ & & & & & w^0 & w^2 & & \\ w^0 & -w^0 & & & & & & & \\ & & & w^0 & -w^0 & & & & \\ & & w^0 & -w^2 & & & & & \\ & & & & & w^0 & -w^2 & & \\ & & & & & & & & \end{bmatrix} \underbrace{\begin{bmatrix} h_0 + h_2 \\ h_1 + h_3 \\ h_0 - h_2 \\ h_1 - h_3 \\ h_4 + h_6 \\ h_5 + h_7 \\ h_4 - h_6 \\ h_5 - h_7 \end{bmatrix}}_l$$

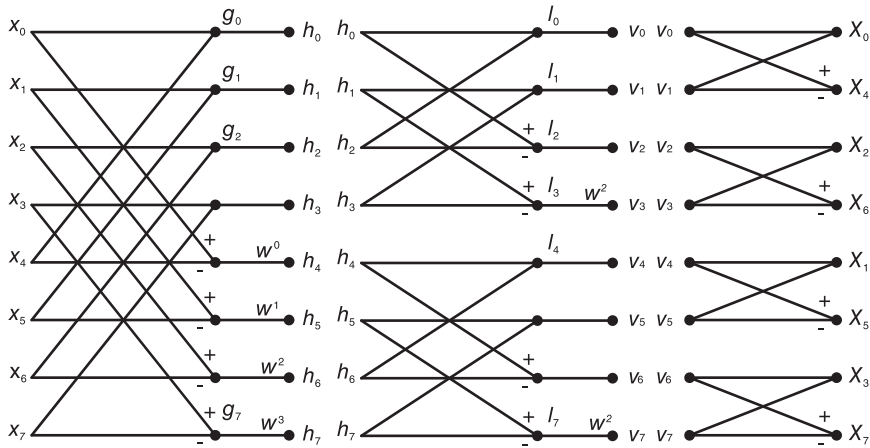


FIGURE 7.49 Steps in factorization of the DFT.

Denoting by l the vector on the right, the relation between the vectors h and l can be represented graphically as shown in the figure. We can write

$$X = \begin{bmatrix} w^0 & w^0 & & & & & & & \\ & & w^0 & w^0 & w^0 & w^0 & & & \\ & & & & & & w^0 & w^0 & \\ w^0 & -w^0 & & & & & & & \\ & & & w^0 & -w^0 & & & & \\ & & w^0 & -w^0 & & & & & \\ & & & & & w^0 & -w^0 & & \\ & & & & & & & & \end{bmatrix} \text{diag}(w^0, w^0, w^0, w^2, w^0, w^0, w^0, w^2) l.$$

Let

$$v = \text{diag}(w^0, w^0, w^0, w^2, w^0, w^0, w^0, w^2) l.$$

We have

$$\begin{aligned}
 X_0 &= (v_0 + v_1) \\
 X_1 &= (v_4 + v_5) \\
 X_2 &= (v_2 + v_3) \\
 X_3 &= (v_6 + v_7) \\
 X_4 &= (v_0 - v_1) \\
 X_5 &= (v_4 - v_5) \\
 X_6 &= (v_2 - v_3) \\
 X_7 &= (v_6 - v_7).
 \end{aligned}$$

These relations are represented graphically in the figure. The overall factorization diagram is shown in Fig. 7.50.

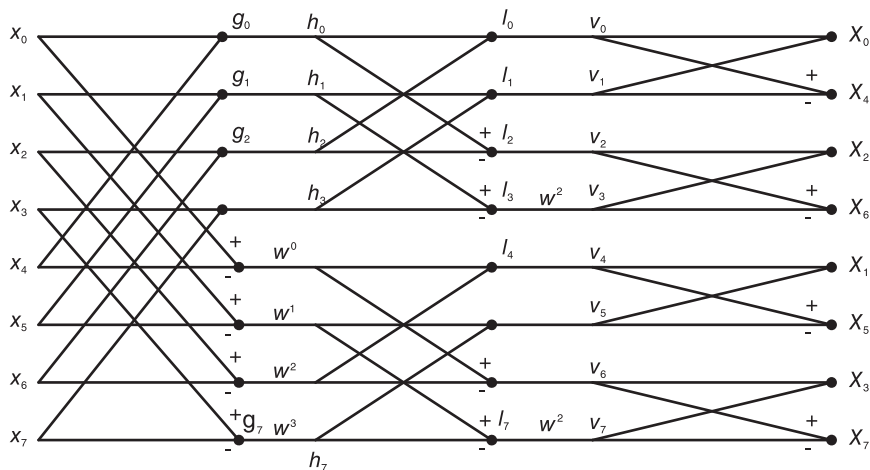


FIGURE 7.50 An FFT factorization of the DFT.

We note that the output of the diagram is not the vector X in normal order. The output vector is in fact a vector X' which is the same as X but is in “reverse bit order.”

We now write this factorization more formally in order to obtain a factorization valid for an input sequence of a general length of N elements. Let

$$T_2 = \begin{bmatrix} 1 & 1 \\ 1 & -1 \end{bmatrix}. \tag{7.189}$$

The Kronecker product $A \times B$ of two matrices A and B result in a matrix having the elements b_{ij} of B replaced by the product Ab_{ij} . For example, let

$$A = \begin{bmatrix} a_{00} & a_{01} \\ a_{10} & a_{11} \end{bmatrix} \tag{7.190}$$

and

$$B = \begin{bmatrix} b_{00} & b_{01} \\ b_{10} & b_{11} \end{bmatrix}. \tag{7.191}$$

shown in Fig. 7.50. The factorization of the matrix F_8' is given by

$$F_8' = \begin{bmatrix} 1 & 1 & & & & & & \\ 1 & -1 & & & & & & \\ & & 1 & 1 & & & & \\ & & 1 & -1 & & & & \\ & & & & 1 & 1 & & \\ & & & & 1 & -1 & & \\ & & & & & & 1 & 1 \\ & & & & & & 1 & -1 \end{bmatrix} \begin{bmatrix} 1 & & & & & & & \\ & 1 & & & & & & \\ & & w^0 & & & & & \\ & & & w^2 & & & & \\ & & & & 1 & & & \\ & & & & & 1 & & \\ & & & & & & w^0 & \\ & & & & & & & w^2 \end{bmatrix} \begin{bmatrix} 1 & 1 & & & & & & \\ & 1 & 1 & & & & & \\ 1 & -1 & & & & & & \\ & & 1 & -1 & & & & \\ & & & & 1 & 1 & & \\ & & & & & & 1 & 1 \\ & & & & & & 1 & -1 \\ & & & & & & & 1 & -1 \end{bmatrix} \tag{7.203}$$

and may be written in the closed form

$$F_8' = \prod_{i=1}^3 (D_{2^i} \times I_{2^{3-i}}) (I_{2^{i-1}} \times T_2 \times I_{2^{3-i}}). \tag{7.204}$$

This form can be generalized. For $N = 2^n$, writing [17]

$$K_{2^i} = \text{diag}(w^0, w^{2^i}, w^{2 \times 2^i}, w^{3 \times 2^i}, \dots) \tag{7.205}$$

and

$$D_{2^{n-i}} = \text{Quasidiag}(I_{2^{n-i-1}}, K_{2^i}). \tag{7.206}$$

A matrix

$$X = \text{Quasidiag}(A, B, C, \dots) \tag{7.207}$$

is one which has the matrices A, B, C, \dots along its diagonal and zero elements elsewhere. We can write the factorization in the general form

$$F_N' = \prod_{i=1}^n (D_{2^i} \times I_{2^{n-i}}) (I_{2^{i-1}} \times T_2 \times I_{2^{n-i}}). \tag{7.208}$$

As noted earlier from factorization diagram, Fig. 7.50, the coefficients X_i' of the transform are in reverse bit order. For $N = 8$, the normal order (0, 1, 2, 3, 4, 5, 6, 7) in 3-bit binary is written:

$$(000, 001, 010, 011, 100, 101, 110, 111). \tag{7.209}$$

The bit reverse order is written:

$$(000, 100, 010, 110, 001, 101, 011, 111) \tag{7.210}$$

which is in decimal: (0, 4, 2, 6, 1, 5, 3, 7). The DFT coefficients $X[k]$ in the diagram, Fig. 7.50 can be seen to be in this reverse bit order.

We note that the DFT coefficients $X[k]$ are evaluated in $\log_2 8 = 3$ iterations, each iteration involving 4 operations (multiplications). For a general value $N = 2^n$ the FFT

factorization includes $\log_2 N = n$ iterations, each containing $N/2$ operations for a total of $(N/2) \log_2 N$ operations. This factorization is a base-2 factorization applicable if $N = 2^n$, as mentioned above. If the number of points N of the finite duration input sequence satisfies that $N = r^n$ where r , called the radix or base, is an integer, then the FFT reduces the number of complex multiplications needed to evaluate the DFT from N^2 to $(N/r) \log_r N$. For $N = 1024$ and $r = 2$, the number of complex multiplications is reduced from about 10^6 to about $500 \times 10 = 5000$. With $r = 4$ this is further reduced to $256 \times 5 = 1280$.

7.31 An Algorithm for a Wired-In Radix-2 Processor

The following is a summary description of an algorithm and a wired-in processor for radix-2 FFT implementation [17].

Consider the DFT $F[k]$ of an N -point sequence $f[k]$

$$F[k] = \sum_{n=0}^{N-1} f[n] e^{-j2\pi nk/N}. \tag{7.211}$$

Writing $f_n \equiv f[n]$, $F_k \equiv F[k]$ and constructing the vectors

$$f = \text{col}(f_0, f_1, \dots, f_{N-1}) \tag{7.212}$$

$$F = \text{col}(F_0, F_1, \dots, F_{N-1}). \tag{7.213}$$

The TDF may be written in the matrix form

$$F = T_N f. \tag{7.214}$$

where the elements of the matrix T_N are given by

$$(T_N)_{nk} = \exp(-2\pi jnk/N). \tag{7.215}$$

Letting

$$w = e^{-j2\pi/N} = \cos(2\pi/N) - j \sin(2\pi/N) \tag{7.216}$$

$$(T_N)_{nk} = w^{nk} \tag{7.217}$$

$$T_N = \begin{bmatrix} w^0 & w^0 & w^0 & w^0 & \dots & w^0 \\ w^0 & w^1 & w^2 & w^3 & \dots & w^{N-1} \\ w^0 & w^2 & w^4 & w^6 & \dots & w^{2(N-1)} \\ \vdots & \vdots & \vdots & \vdots & \vdots & \vdots \\ w^0 & w^{N-1} & w^{2(N-1)} & w^{3(N-1)} & \dots & w^{(N-1)^2} \end{bmatrix}. \tag{7.218}$$

To reveal the symmetry in the matrix T_N we rearrange its rows by writing

$$T_N = P_N P_N^{-1} T_N = P_N T'_N \tag{7.219}$$

where in general P_K is the “perfect shuffle” permutation matrix which is defined by its operation on a vector of dimension K by the relation

$$P_K \text{col}(x_0, x_1, \dots, x_{K-1}) = \text{col}(x_0, x_{K/2}, x_1, x_{K/2+1}, x_2, x_{K/2+2}, \dots, x_{K-1}) \tag{7.220}$$

and therefore P_K^{-1} is a permutation operator which applied on a vector of dimension K would group the even and odd-ordered elements together, i.e.,

$$P_K^{-1} \cdot \text{col}(x_0, x_1, x_2, \dots, x_{K-1}) = \text{col}(x_0, x_2, x_4, \dots, x_1, x_3, x_5, \dots) \tag{7.221}$$

and

$$T'_N = P_N^{-1} T_N. \tag{7.222}$$

For example, for $N = 8$, T'_N can be written using the property of w

$$w^k = w^{k \bmod N} \tag{7.223}$$

$$T'_N = \begin{bmatrix} w^0 & w^0 & w^0 & w^0 & w^0 & w^0 & w^0 & w^0 \\ w^0 & w^2 & w^4 & w^6 & w^0 & w^2 & w^4 & w^6 \\ w^0 & w^4 & w^0 & w^4 & w^0 & w^4 & w^0 & w^4 \\ w^0 & w^6 & w^4 & w^2 & w^0 & w^6 & w^4 & w^2 \\ w^0 & w^1 & w^2 & w^3 & w^4 & w^5 & w^6 & w^7 \\ w^0 & w^3 & w^6 & w^1 & w^4 & w^7 & w^2 & w^5 \\ w^0 & w^5 & w^2 & w^7 & w^4 & w^1 & w^6 & w^3 \\ w^0 & w^7 & w^6 & w^5 & w^4 & w^3 & w^2 & w^1 \end{bmatrix}. \tag{7.224}$$

The matrix T'_N can be factored in the form

$$T'_N = \begin{bmatrix} Y_{N/2} & Y_{N/2} \\ Y_{N/2}K_1 & -Y_{N/2}K_1 \end{bmatrix} \tag{7.225}$$

$$\begin{aligned} T_N &= P_N \cdot \begin{bmatrix} Y_{N/2} & \phi \\ \phi & Y_{N/2} \end{bmatrix} \begin{bmatrix} I_{N/2} & I_{N/2} \\ K_1 & -K_1 \end{bmatrix} \\ &= P_N \cdot \begin{bmatrix} Y_{N/2} & \phi \\ \phi & Y_{N/2} \end{bmatrix} \begin{bmatrix} I_{N/2} & \phi \\ \phi & K_1 \end{bmatrix} \begin{bmatrix} I_{N/2} & I_{N/2} \\ I_{N/2} & -I_{N/2} \end{bmatrix} \end{aligned} \tag{7.226}$$

where, $K_1 = \text{diag}(w^0, w^1, w^2, w^3)$ and ϕ indicates the null matrix of appropriate dimension.

This process can be repeated, partitioning and factoring the matrix $Y_{N/2}$. Carrying the process to completion yields the FFT. This process can be described algebraically as follows.

We rewrite the last factored matrix equation in the form

$$T_N = P_N (Y_{N/2} \times I_2) D_N (I_{N/2} \times T_2) \tag{7.227}$$

where D_N is an $N \times N$ diagonal matrix, $\text{Quasidiag}(I_{N/2}, K_1)$, and in general I_k is the identity matrix of dimension k . The “core matrix” T_2 is given by

$$T_2 = \begin{bmatrix} 1 & 1 \\ 1 & -1 \end{bmatrix}. \tag{7.228}$$

If we continue this process further we can factor the $N/2 \times N/2$ matrix $Y_{N/2}$ in the form

$$Y_{N/2} = P_{N/2} (Y_{N/4} \times I_2) D_{N/2} (I_{N/4} \times T_2) \tag{7.229}$$

where $D_{N/2} = \text{Quasidiag}(I_{N/4}, K_2)$ and $K_2 = \text{diag}(w^0, w^2, w^4, w^6, \dots)$.

In general, if we write $k = 2^i$, $i = 0, 1, 2, 3, \dots$ then

$$Y_{N/k} = P_{N/k} (Y_{N/2k} \times I_2) D_{N/k} (I_{N/2k} \times T_2) \tag{7.230}$$

where

$$D_{N/k} = \text{Quasidiag} (I_{N/2k}, K_k) \quad (7.231)$$

and

$$K_k = \text{diag} (0, k, 2k, 3k, \dots). \quad (7.232)$$

Carrying this iterative procedure to the end and substituting into the original factored form of T_N we obtain the complete factorization

$$T_N = P_N \left[\left\{ P_{N/2} \left[\left\{ \dots P_{N/k} \left[\left\{ \dots \left\{ P_4 (T_2 \times I_2) D_4 (I_2 \times T_2) \right\} \times I_2 \right\} \dots \right\} \right. \right. \right. \\ \left. \left. \left. \times I_2 \right\} D_{N/k} (I_{N/2k} \times T_2) \dots \right\} \times I_2 \right\} D_{N/2} (I_{N/4} \times T_2) \right\} \times I_2 \right] D_N (I_{N/2} \times T_2). \quad (7.233)$$

7.31.1 Post-Permutation Algorithm

A useful relation between the Kronecker product and matrix multiplication is the transformation of a set A, B, C, \dots of dimensionally equal square matrices, described by

$$(ABC\dots) \times I = (A \times I) (B \times I) (C \times I) \dots \quad (7.234)$$

Applying this property we obtain

$$T_N = P_N (P_{N/2} \times I_2) \dots (P_{N/k} \times I_k) \dots (P_4 \times I_{N/4}) \cdot (T_2 \times I_{N/2}) (D_4 \times I_{N/4}) \\ (I_2 \times T_2 \times I_{N/4}) \dots (D_{N/k} \times I_k) (I_{N/2k} \times T_2 \times I_k) \dots \\ \cdot (D_{N/2} \times I_2) (I_{N/4} \times T_2 \times I_2) D_N (I_{N/2} \times T_2). \quad (7.235)$$

The product of the permutation matrices in this factorization is a reverse-bit ordering permutation matrix. The rest of the right-hand side is the computational part.

In building a serial machine (serial-word, parallel-bit), it is advantageous to implement a design that allows dynamic storage of the data in long dynamic shift registers, and which does not call for accessing data except at the input or output of these registers. To achieve this goal, a transformation should be employed that expresses the different factors of the computation part of the factorization in terms of the first operator applied to the data, i.e., $(I_{N/2} \times T_2)$, since this operator adds and subtracts data that are $N/2$ points apart, the longest possible distance. This form thus allows storage of data into two serially accessed long streams.

The transformation utilizes the perfect shuffle permutation matrix $P = P_N$ having the property

$$P^{-1} (I_{N/2} \times T_2) P = I_{N/4} \times T_2 \times I_2, \quad (7.236)$$

$$P^{-2} (I_{N/2} \times T_2) P^2 = I_{N/8} \times T_2 \times I_4. \quad (7.237)$$

and similar expressions for higher powers of P . If we write

$$S = (I_{N/2} \times T_2) \quad (7.238)$$

then in general

$$P^{-i} S P^i = I_{N/2^{i+1}} \times T_2 \times I_{2^i}. \quad (7.239)$$

Substituting we obtain

$$T_N = Q_1 Q_2 \dots Q_{n-1} P^{-(n-1)} S P^{(n-1)} M_2 P^{-(n-2)} S P^{(n-2)} \dots P^{-2} S P^2 M_{n-1} P^{-1} S P M_n S$$

where

$$Q_i = P_{N/2^{i-1}} \times I_{2^{i-1}} \quad (7.240)$$

$$M_i = D_{N/2^{n-i}} \times I_{2^{n-i}}. \tag{7.241}$$

Note that $P^n = I_N$ so that $P^{n-i} = P^{-i}$ and $P^{-(n-1)} = P$. Letting

$$\mu_i = P^{n-i} M_i P^{-(n-i)} = I_{2^{n-i}} \times D_{2^i} \tag{7.242}$$

$$\mu_1 = M_1 = I_N, \quad \mu_n = M_n = D_N. \tag{7.243}$$

We have

$$T_N = Q_1 Q_2 \dots Q_{n-1} P S P \mu_2 S P \mu_3 S \dots P \mu_{n-2} S P \mu_{n-1} S P \mu_n S = \prod_{i=1}^{n-1} (Q_i) \prod_{m=1}^n (P \mu_m S) \tag{7.244}$$

7.31.2 Ordered Input/Ordered Output (OIOO) Algorithm

The permutation operations can be merged into the iterative steps if we use the property

$$P_k (A_{k/2} \times I_2) P_k^{-1} = I_2 \times A_{k/2} \tag{7.245}$$

and

$$P_k (ABC \dots) P_k^{-1} = (P_k A P_k^{-1}) (P_k B P_k^{-1}) (P_k C P_k^{-1}) \dots \tag{7.246}$$

where the matrices A, B, C, \dots are of the same dimension as P_k . Applying these transformations we obtain

$$\begin{aligned} T_N &= [I_2 \times \{I_2 \times \{ \dots I_2 \times \{ \dots I_2 \times \{I_2 \times \{(I_2 \times T_2) P_4 D_4 (I_2 \times T_2)\} \\ &\dots \} P_{N/k} D_{N/k} (I_{N/(2k)} \times T_2) \dots P_{N/2} D_{N/2} (I_{N/4} \times T_2)\} \}}] \cdot P_N D_N (I_{N/2} \times T_2) \\ &= (I_{N/k} \times T_2) (I_{N/4} \times P_4) (I_{N/4} \times D_4) (I_{N/2} \times T_2) \dots (I_k \times P_{N/k}) (I_k \times D_{N/k}) \\ &\quad (I_{N/2} \times T_2) \dots (I_2 \times P_{N/2}) (I_2 \times D_{N/2}) (I_{N/2} \times T_2) P_N D_N (I_{N/2} \times T_2). \end{aligned} \tag{7.247}$$

which can be rewritten in the form

$$T_N = S p_2 \mu_2 S p_3 \mu_3 \dots S p_{n-1} \mu_{n-1} S p_n \mu_n S = \prod_{m=1}^n (p_m \mu_m S) \tag{7.248}$$

where

$$p_i = I_{2^{n-i}} \times P_{2^i} \tag{7.249}$$

$p_1 = I_N$ and μ_i is as given above.

Example 7.33 For $N = 8$

$$F = S p_2 \mu_2 S p_3 \mu_3 S f$$

$$F = \begin{bmatrix} 1 & & & & \\ & 1 & & & \\ & & 1 & & \\ & & & 1 & \\ 1 & & & & \\ & 1 & & & \\ & & 1 & & \\ & & & 1 & \\ & & & & 1 \end{bmatrix} \begin{bmatrix} 1 & & & & \\ & 1 & & & \\ & & 1 & & \\ & & & 1 & \\ 1 & & & & \\ & 1 & & & \\ & & 1 & & \\ & & & 1 & \\ & & & & 1 \end{bmatrix} \begin{bmatrix} 1 & & & & \\ & 1 & & & \\ & & 1 & & \\ & & & 1 & \\ & & & & w^0 \\ & & & & w^0 \\ & & & & w^2 \\ & & & & w^2 \end{bmatrix} \begin{bmatrix} 1 & & & & \\ & 1 & & & \\ & & 1 & & \\ & & & 1 & \\ & & & & 1 \\ & & & & w^0 \\ & & & & w^1 \\ & & & & w^2 \\ & & & & w^3 \end{bmatrix} \begin{bmatrix} 1 & & & & \\ & 1 & & & \\ & & 1 & & \\ & & & 1 & \\ 1 & & & & \\ & 1 & & & \\ & & 1 & & \\ & & & 1 & \\ & & & & 1 \end{bmatrix} \begin{bmatrix} f_0 \\ f_1 \\ f_2 \\ f_3 \\ f_4 \\ f_5 \\ f_6 \\ f_7 \end{bmatrix}.$$

The post-permutation algorithm and the OIOO machine-oriented algorithm lead to optimal wired-in architecture where no addressing is required and where data are to be operated upon are optimally spaced. We shall see later in this chapter that by slightly relaxing the condition on wired-in architecture we can eliminate the the feedback permutation phase, attaining higher processing speeds. For now, however, we consider the possibility of reducing the number of iterations, through parallelism, by employing a higher radix FFT factorization. The resulting processor architectures, both for radix 2 and for higher radices FFT factorizations will be discussed in Chapter 15.

7.32 Factorization of the FFT to a Higher Radix

Factorizations to higher radices $r = 4, 8, 16, \dots$ reduce the number of operations to $(N/r) \log_r(N)$, $N = r^n$. References [20] [22] [24] [28] [41] proposed parallel higher radix OIOO factorizations of the FFT. They employ a general radix perfect shuffle matrix introduced in [24] and has applications that go beyond the FFT [69]. These factorizations are optimal, leading to parallel wired-in processors eliminating the need for addressing, minimizing the number of required memory partitions and produce coefficients in the normal ascending order. A summary presentation of the higher radix matrix factorization follows. As stated above the DFT $X[k]$ of an N -point sequence $x[n]$ may be written in the matrix form $X = T_N x$ and T_N the $N \times N$ DFT matrix. To obtain higher radix versions of the FFT, we first illustrate the approach on a radix-4 FFT. Consider the DFT matrix with $N = 16$. The DFT matrix is

$$T_{16} = \begin{bmatrix} w^0 & w^0 & w^0 & \dots & w^0 \\ w^0 & w^1 & w^2 & \dots & w^{15} \\ w^0 & w^2 & w^4 & \dots & w^{14} \\ \vdots & \vdots & \vdots & \vdots & \vdots \\ w^0 & w^{15} & w^{14} & \dots & w^1 \end{bmatrix} \tag{7.250}$$

where $w = e^{-j2\pi/N}$. We start, similarly to the radix-2 case seen above, by applying the base-4 perfect shuffle permutation matrix of a 16-point vector, P_N with $N = 16$ defined by

$$P_{16} \{x_0, x_1, x_2, x_3, x_4, x_5, x_6, x_7, x_8, x_9, x_{10}, x_{11}, x_{12}, x_{13}, x_{14}, x_{15}\} = \{x_0, x_4, x_8, x_{12}, x_1, x_5, x_9, x_{13}, x_2, x_6, x_{10}, x_{14}, x_3, x_7, x_{11}, x_{15}\}. \tag{7.251}$$

and its inverse $P'_{16} \triangleq P_{16}^{-1} = P_{16}$. Writing $T_{16} = P_{16}T'_{16}$, i.e. $T'_{16} = P_{16}^{-1}T_{16} = P_{16}T_{16}$ we obtain

$$T'_{16} = \begin{bmatrix} w^0 & w^0 & w^0 & w^0 & w^0 & w^0 & w^0 & w^0 & w^0 & w^0 & w^0 & w^0 & w^0 & w^0 & w^0 & w^0 \\ w^0 & w^4 & w^8 & w^{12} & w^0 & w^4 & w^8 & w^{12} & w^0 & w^4 & w^8 & w^{12} & w^0 & w^4 & w^8 & w^{12} \\ w^0 & w^8 & w^0 & w^8 & w^0 & w^8 & w^0 & w^8 & w^0 & w^8 & w^0 & w^8 & w^0 & w^8 & w^0 & w^8 \\ w^0 & w^{12} & w^8 & w^4 & w^0 & w^{12} & w^8 & w^4 & w^0 & w^{12} & w^8 & w^4 & w^0 & w^{12} & w^8 & w^4 \\ w^0 & w^1 & w^2 & w^3 & w^4 & w^5 & w^6 & w^7 & w^8 & w^9 & w^{10} & w^{11} & w^{12} & w^{13} & w^{14} & w^{15} \\ w^0 & w^5 & w^{10} & w^{15} & w^4 & w^9 & w^{14} & w^3 & w^8 & w^{13} & w^2 & w^7 & w^{12} & w^1 & w^6 & w^{11} \\ w^0 & w^9 & w^2 & w^{11} & w^4 & w^{13} & w^6 & w^{15} & w^8 & w^1 & w^{10} & w^3 & w^{12} & w^5 & w^{14} & w^7 \\ w^0 & w^{13} & w^{10} & w^7 & w^4 & w^1 & w^{14} & w^{11} & w^8 & w^5 & w^2 & w^{15} & w^{12} & w^9 & w^6 & w^3 \\ w^0 & w^2 & w^4 & w^6 & w^8 & w^{10} & w^{12} & w^{14} & w^0 & w^2 & w^4 & w^6 & w^8 & w^{10} & w^{12} & w^{14} \\ w^0 & w^6 & w^{12} & w^2 & w^8 & w^{14} & w^4 & w^{10} & w^0 & w^6 & w^{12} & w^2 & w^8 & w^{14} & w^4 & w^{10} \\ w^0 & w^{10} & w^4 & w^{14} & w^8 & w^2 & w^{12} & w^6 & w^0 & w^{10} & w^4 & w^{14} & w^8 & w^2 & w^{12} & w^6 \\ w^0 & w^{14} & w^{12} & w^{10} & w^8 & w^6 & w^4 & w^2 & w^0 & w^{14} & w^{12} & w^{10} & w^8 & w^6 & w^4 & w^2 \\ w^0 & w^3 & w^6 & w^9 & w^{12} & w^{15} & w^2 & w^5 & w^8 & w^{11} & w^{14} & w^1 & w^4 & w^7 & w^{10} & w^{13} \\ w^0 & w^7 & w^{14} & w^5 & w^{12} & w^3 & w^{10} & w^1 & w^8 & w^{15} & w^6 & w^{13} & w^4 & w^{11} & w^2 & w^9 \\ w^0 & w^{11} & w^6 & w^1 & w^{12} & w^7 & w^2 & w^{13} & w^8 & w^3 & w^{14} & w^9 & w^4 & w^{15} & w^{10} & w^5 \\ w^0 & w^{15} & w^{14} & w^{13} & w^{12} & w^{11} & w^{10} & w^9 & w^8 & w^7 & w^6 & w^5 & w^4 & w^3 & w^2 & w^1 \end{bmatrix}$$

$$= \begin{bmatrix} Y_{N/4} & Y_{N/4} & Y_{N/4} & Y_{N/4} \\ Y_{N/4}K_1 & -jY_{N/4}K_1 & -Y_{N/4}K_1 & jY_{N/4}K_1 \\ Y_{N/4}K_2 & -Y_{N/4}K_2 & Y_{N/4}K_2 & -Y_{N/4}K_2 \\ Y_{N/4}K_3 & jY_{N/4}K_3 & -Y_{N/4}K_3 & -jY_{N/4}K_3 \end{bmatrix}$$

where

$$K_1 = \text{diag}(w^0, w^1, w^2, w^3), \quad K_2 = \text{diag}(w^0, w^2, w^4, w^6), \quad K_3 = \text{diag}(w^0, w^3, w^6, w^9)$$

$$T_{16} = P_{16} \begin{bmatrix} Y_{N/4} & & & \\ & Y_{N/4} & & \\ & & Y_{N/4} & \\ & & & Y_{N/4} \end{bmatrix} \begin{bmatrix} I_4 & I_4 & I_4 & I_4 \\ K_1 & -jK_1 & -K_1 & jK_1 \\ K_2 & -K_2 & K_2 & -K_2 \\ K_3 & jK_3 & -K_3 & -jK_3 \end{bmatrix}$$

$$= P_{16} \begin{bmatrix} Y_{N/4} & & & \\ & Y_{N/4} & & \\ & & Y_{N/4} & \\ & & & Y_{N/4} \end{bmatrix} \begin{bmatrix} I_4 & & & \\ & K_1 & & \\ & & K_2 & \\ & & & K_3 \end{bmatrix} \begin{bmatrix} I_4 & I_4 & I_4 & I_4 \\ I_4 & -jI_4 & -I_4 & jI_4 \\ I_4 & -I_4 & I_4 & -I_4 \\ I_4 & jI_4 & -I_4 & -jI_4 \end{bmatrix}$$

$$T_4 = \begin{bmatrix} 1 & 1 & 1 & 1 \\ 1 & -j & -1 & j \\ 1 & -1 & 1 & -1 \\ 1 & j & -1 & -j \end{bmatrix} \tag{7.252}$$

is the radix-4 core matrix. We may therefore write

$$T_N = P_N (Y_{N/4} \times I_4) D_N (I_4 \times T_4). \tag{7.253}$$

More generally, with a general radix r and $N = r^n$ the factorization takes the form

$$T_N = P_N (Y_{N/r} \times I_r) D_N (I_r \times T_r) \tag{7.254}$$

where the base- r perfect shuffle permutation matrix is written $P_N \equiv P_N^{(r)}$. Operating on a column vector x of dimension K , the base- p perfect shuffle permutation matrix of dimension $K \times K$ divides the vector into p consecutive subvectors, K/p elements each and selects successively one element of each subvector so that

$$P_K^{(p)} x = [x_0, x_{K/p}, x_{2K/p}, \dots, x_{(p-1)K/p}, x_1, x_{K/p+1}, \dots, x_2, x_{K/p+2}, \dots, x_{K-1}] \tag{7.255}$$

Following similar steps to the radix-2 we obtain a post-permutation factorization and in particular OIOO factorization [24].

Asymmetric Algorithms

For the case $N = r^n$, where n is integer, we can write

$$T_N = P_N^{(r)} T'_N \tag{7.256}$$

where,

$$T'_N = P_N'^{(r)} T_N \tag{7.257}$$

and

$$P_N^{(r)'} = P_N^{(r)-1} \tag{7.258}$$

$$Y_{N/k} = P_{N/k}^{(r)} (Y_{N/r^k} \times I_r) D_{N/k}^{(r)} (I_{N/r^k} \times T_r) \tag{7.259}$$

where

$$D_{N/k}^{(r)} = \text{quasi-diag}(I_{N/r^k}, K_k, K_{2k}, K_{3k}, \dots, K_{(r-1)k}) \tag{7.260}$$

$$K_m = \text{diag}\{0, m, 2m, 3m, \dots, (N/rk - 1)m\} \tag{7.261}$$

for any integer m ,

$$T_r = \begin{bmatrix} w^0 & w^0 & & & & & \\ w^0 & w^{N/r} & & & & & \\ w^0 & w^{2N/r} & & & & & \\ \vdots & \vdots & \vdots & \vdots & \vdots & \vdots & \\ w^0 & w^{(r-1)N/r} & \dots & \dots & \dots & w^{(r-1)^2 N/r} \end{bmatrix} \tag{7.262}$$

and I_k is the unit matrix of dimension k .

By starting with the matrix T_N and replacing in turn every matrix $Y_{N/k}$ by its value in terms of Y_{N/r^k} according to the recursive relation described by Equation (7.259), we arrive at the complete factorization. If we then apply the relation between the Kronecker product and matrix multiplication, namely,

$$(ABC \dots) \times I = (A \times I)(B \times I)(C \times I) \dots \tag{7.263}$$

where A, B, C, \dots, I are all square matrices of the same dimension, we arrive at the general radix- r FFT

$$\begin{aligned} T_N &= P_N^{(r)} (P_{N/r}^{(r)} \times I_r) \dots (P_{N/r}^{(r)} \times I_k) \dots (P_{r^2}^{(r)} \times I_{N/r^2}) \\ &\cdot (T_r \times I_{N/r})(D_{r^2} \times I_{N/r^2})(I_r \times T_r \times I_{N/r^2}) \dots \\ &\cdot (D_{N/r}^{(r)} \times I_r)(I_{N/r^k} \times T_r \times I_k) \dots \\ &\cdot (D_{N/r}^{(r)} \times I_r)(I_{N/r^2} \times T_r \times I_k) D_N^{(r)} (I_{N/r} \times T_r) \end{aligned} \tag{7.264}$$

To obtain algorithms that allow wired-in design we express each of the factors in the computation part of this equation (that is, those factors not including the permutation matrices) in terms of the least factor. If we denote this factor by

$$S^{(r)} = (I_{N/r} \times T_r) \tag{7.265}$$

and utilize the property of the powers of shuffle operators, namely,

$$\left\{ P_N^{(r)} \right\}^{-i} S_N^{(r)} \left\{ P_N^{(r)} \right\}^i = I_{N/r^{i+1}} \times T_r \times I_{r^i}. \tag{7.266}$$

We obtain the post-permutation machine-oriented FFT algorithm;

$$T_N = \prod_{i=1}^{n-1} Q_i^{(r)} \prod_{m=1}^n \left(P^{(r)} \mu_m^{(r)} S^{(r)} \right) \tag{7.267}$$

where

$$Q_i = P_{N/r^{i-1}}^{(r)} \times I_{r^{i-1}} \tag{7.268}$$

$$\mu_i^{(r)} = I_{r^{n-i}} \times D_{r^i}^{(r)} \tag{7.269}$$

and $P^{(r)}$ denotes the permutation matrix $P_N^{(r)}$.

The algorithm described by Equation (7.267) is suitable for the applications which do not call for ordered coefficients. In these applications, only the computation matrix

$$T_c = \prod_{m=1}^n \left(P^{(r)} \mu_m^{(r)} S^{(r)} \right) \tag{7.270}$$

is performed.

7.32.1 Ordered Input/Ordered Output General Radix FFT Algorithm

We can eliminate the post-permutation iterations [the operators $Q_i^{(r)}$] if we merge the permutation operators into the computation ones. An ordered set of coefficients would thus be obtained at the output. We thus use the transformations

$$P_k^{(r)} (A_{k/r} \times I_r) \left\{ P_k^{(r)} \right\}^{-1} = I_r \times A_{k/r}. \tag{7.271}$$

and hence

$$P_k^{(r)} (AB \dots) \left\{ P_k^{(r)} \right\}^{-1} = \left[P_k^{(r)} A \left\{ P_k^{(r)} \right\}^{-1} \right] \left[P_k^{(r)} B \left\{ P_k^{(r)} \right\}^{-1} \right] \dots \tag{7.272}$$

where A, B, \dots are of the same dimension as P_k . In steps similar to those followed in the case of the radix-2 case we arrive at the OIOO algorithm:

$$T_N = \prod_{m=1}^n \left(P_m^{(r)} \mu_m^{(r)} S^{(r)} \right) \tag{7.273}$$

where

$$P_i^{(r)} = I_{r^{n-i}} \times P_{r^i}^{(r)} \tag{7.274}$$

and

$$P_1 = \mu_1 = I_N. \tag{7.275}$$

The other matrices have been previously defined. As an illustration, the 16-point radix 4 FFT factorization for parallel wired-in architecture takes the form

$$F = \begin{bmatrix} 1 & 1 & 1 & 1 \\ 1 & 1 & 1 & 1 \\ 1 & -j & -1 & j \\ 1 & -j & -1 & j \\ 1 & -1 & 1 & -1 \\ 1 & -1 & 1 & -1 \\ 1 & j & -1 & -j \\ 1 & j & -1 & -j \\ 1 & 1 & 1 & 1 \\ 1 & 1 & 1 & 1 \\ 1 & -j & -1 & j \\ 1 & -j & -1 & j \\ 1 & -1 & 1 & -1 \\ 1 & -1 & 1 & -1 \\ 1 & j & -1 & -j \\ 1 & j & -1 & -j \end{bmatrix} \begin{bmatrix} 1 \\ 1 \\ 1 \\ 1 \\ 1 \\ 1 \\ 1 \\ 1 \\ 1 \\ 1 \\ 1 \\ 1 \\ 1 \\ 1 \\ 1 \\ 1 \end{bmatrix} \tag{7.276}$$

$$\begin{bmatrix} 1 \\ 1 \\ 1 \\ \omega^0 \\ \omega^1 \\ \omega^2 \\ \omega^3 \\ \omega^0 \\ \omega^2 \\ \omega^4 \\ \omega^6 \\ \omega^0 \\ \omega^3 \\ \omega^6 \\ \omega^9 \end{bmatrix} \begin{bmatrix} 1 & 1 & 1 & 1 \\ 1 & 1 & 1 & 1 \\ 1 & -j & -1 & j \\ 1 & -j & -1 & j \\ 1 & -1 & 1 & -1 \\ 1 & -1 & 1 & -1 \\ 1 & j & -1 & -j \\ 1 & j & -1 & -j \\ 1 & 1 & 1 & 1 \\ 1 & 1 & 1 & 1 \\ 1 & -j & -1 & j \\ 1 & -j & -1 & j \\ 1 & -1 & 1 & -1 \\ 1 & -1 & 1 & -1 \\ 1 & j & -1 & -j \\ 1 & j & -1 & -j \\ 1 & j & -1 & -j \end{bmatrix} \begin{bmatrix} f_0 \\ f_1 \\ f_2 \\ f_3 \\ f_4 \\ f_5 \\ f_6 \\ f_7 \\ f_8 \\ f_9 \\ f_{10} \\ f_{11} \\ f_{12} \\ f_{13} \\ f_{14} \\ f_{15} \end{bmatrix} \tag{7.277}$$

Symmetric algorithms lead to symmetric processors so that a radix-4 processor employs four complex multipliers operating in parallel instead of three. Such algorithms and the corresponding processor architectures can be seen in [24] [28].

7.33 Feedback Elimination for High-Speed Signal Processing

We have seen factorizations of the DFT leading to fully wired-in processors. In these parallel general radix processors, after each iteration data are fed back from the output memory to the input memory, the following iteration is performed. In this section we explore the possibility of eliminating the feedback cycle after following each iteration. We therefore need

to eliminate the permutation cycle that follows each iteration. In what follows we see that this is possible if we relax slightly the condition that the processor should be fully wired in. The approach is illustrated with reference to the OIOO algorithm. The modification is simply performed as follows [22].

We have

$$T_N = S^{(r)} P_2^{(\mu_2^{(r)})} S^{(r)} \dots P_{n-1}^{(\mu_{n-1}^{(r)})} S^{(r)} P_n^{(\mu_n^{(r)})} S^{(r)} \tag{7.278}$$

which can be rewritten as

$$T_N = S_1^{(\mu_2^{(r)})} S_2^{(\mu_3^{(r)})} \dots S_{n-2}^{(\mu_{n-1}^{(r)})} S_{n-1}^{(\mu_n^{(r)})} S_n^{(r)} \tag{7.279}$$

that is,

$$T_N = \prod_{m=1}^n \left(\mu_m^{(r)} S_m^{(r)} \right) \tag{7.280}$$

where

$$S_{m-1}^{(r)} = S^{(r)} P_m^{(r)}, \quad m = 2, 3, \dots, n, \quad S_n^{(r)} = S^{(r)}, \quad \mu_1 = I_N. \tag{7.281}$$

We now show that the pre-weighting operator $S_m^{(r)}$ calls always for combining data that are at least N/r^2 words apart. We have for m not equal to 1

$$S_{m-1} = S P_m = (I_{N/r} \times T_r) P_m = P_m P_m^{-1} (I_{N/r} \times T_r) P_m. \tag{7.282}$$

and we can easily show that

$$P_m^{-1} (I_{N/r} \times T_r) P_m = (I_{N/r^2} \times T_r \times I_r). \tag{7.283}$$

and therefore

$$S_{m-1} = P_m (I_{N/r^2} \times T_r \times I_r). \tag{7.284}$$

Thus we can see that the matrix I_{N/r^2} in the second factor causes the operator S_{m-1} to operate on data that are always N/r^2 words apart. In the first iteration, however, the operator S_n operates on data which are N/r words apart. The permutation operators have thus been absorbed in the operator S with the result that they are effected as part of the new operators S_i , thus eliminating the separate permutation operations.

As an illustration, the radix-2 FFT factorization for OIOO high speed processing is represented graphically in Fig. 7.51 for the case $N = 8$.

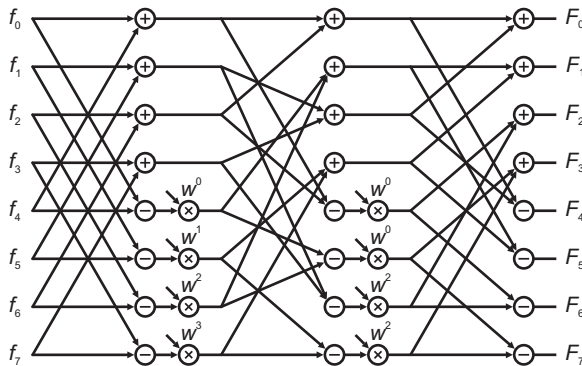


FIGURE 7.51 Radix-2 FFT factorization for high speed processing.

We shall see the resulting processor architecture, where feedback is eliminated, in Chapter 15.

7.34 Problems

Problem 7.1 The A/D converter seen in Fig. 7.52 operates at a sampling frequency of 48,000 samples per second. The input signal $m(t)$ is bandlimited to the frequency range 12 to 35 kHz, i.e. $M(j\omega) = 0$ for $|\omega| < 24000$ r/s and $|\omega| > 70000$ r/s.

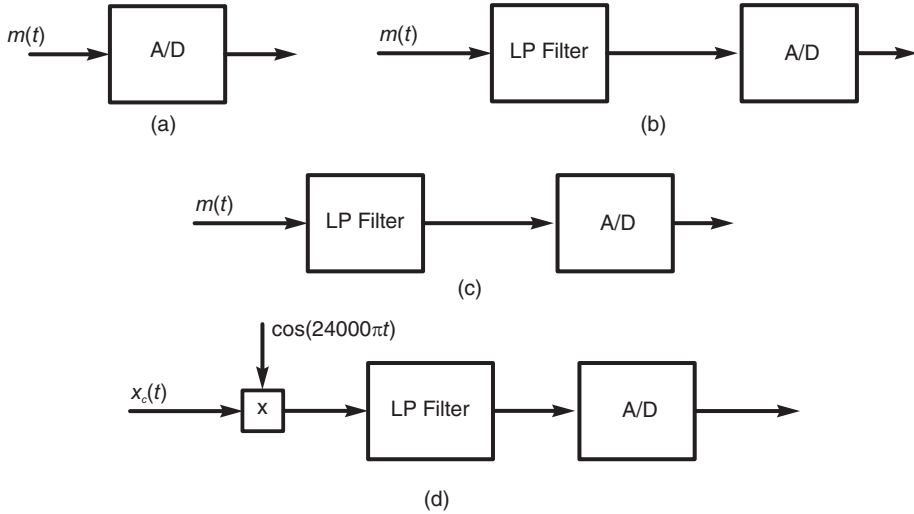


FIGURE 7.52 Alternative sampling systems.

Compare the performance of the systems shown in Fig. 7.52(a-d) in sampling the signal $m(t)$, given that the lowpass filter in Fig. 7.52(b) has a cut-off frequency of 60000π r/s, while those of Fig. 7.52(c) and Fig. 7.52(d) have a cut-off frequency of 46000π . Specify in each case which part of the signal is theoretically preserved through sampling.

Problem 7.2 In the DSP system shown in Fig. 7.13(a) we consider the case where the C/D and D/C converters operate with sampling periods T_1 and T_2 , respectively. The input signal $x_c(t)$ has the spectrum $X_c(j\omega)$ depicted in Fig. 7.53, where $\omega_x = 20000\pi$ r/s, and the LTI system is a filter of frequency response

$$H(e^{j\Omega}) = \Pi_{3\pi/4}.$$

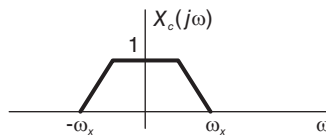


FIGURE 7.53 Spectrum of $x_c(t)$.

Let $f_1 = 1/T_1$ and $f_2 = 1/T_2$. Sketch the spectra of $x[n]$, $y[n]$ and $y_c(t)$ and deduce the resulting value of $Y_c(0)$ and the cut-off frequency f_y in Hz of $Y_c(j\omega)$ for each of the following cases: a) $f_1 = f_2 = 20$ kHz, b) $f_1 = 20$ kHz, $f_2 = 40$ kHz, c) $f_1 = 40$ kHz, $f_2 = 20$ kHz.

Problem 7.3 In the DSP system shown in Fig. 7.13(a) consider the case where the LTI system is a finite impulse response (FIR) filter of impulse response

$$h[n] = 0.5^n R_N[n]$$

and $N = 16$. Assuming that the input signal $x_c(t)$ is bandlimited to the frequency $\omega_c = \pi/T$, evaluate the equivalent overall frequency response $H_c(j\omega)$ of the system between its input $x_c(t)$ and its output $y_c(t)$.

Problem 7.4 A signal $x_c(t)$ has the spectrum $X_c(j\omega)$ depicted in Fig. 7.53. Let $x[n] = x_c(nT)$,

$$x_M[n] = x[n] \sum_{k=-\infty}^{\infty} \delta[n - kM]$$

$$x_r[n] = x_M[Mn] = x[Mn].$$

Sketch the spectra $X(e^{j\Omega})$, $X_M(e^{j\Omega})$ and $X_r(e^{j\Omega})$ of $x[n]$, $x_M[n]$ and $x_r[n]$, respectively, given that $M = 3$, $T = 1/1500$ sec and $\omega_x = 300\pi$ r/s. Repeat for the case $\omega_x = 600\pi$ r/s.

Problem 7.5 A signal $x_c(t)$, of which the spectrum $X_c(j\omega)$ is depicted in Fig. 7.53, where $\omega_x = 10000\pi$ r/s, is applied to the input of the system shown in Fig.7.54. In this system the C/D and D/C converters operate at sampling frequencies $f_1 = 1/T_1$ and $f_2 = 1/T_2$, respectively.

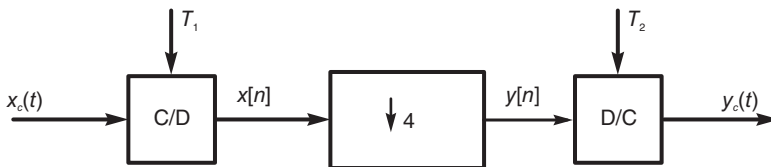


FIGURE 7.54 A down-sampling system.

- a) Sketch the spectra of $x[n]$ and $y[n]$ when T_1 has the maximum permissible value of to ensure absence of aliasing. What is this maximum value?
- b) Sketch $Y(e^{j\Omega})$ and $Y_c(j\omega)$ in the absence of aliasing and evaluate T_1 and T_2 so that $y_c(t) = x_c(t)$.
- c) In the case $T_1 = T_2$ evaluate $y_c(t)$ as a function of $x_c(t)$.

Problem 7.6 A signal $x_c(t)$ is the sum of four continuous-time signals, namely, a constant of 5 volts and three pure sinusoids of amplitudes 4, 6 and 10 volts, and frequencies 125, 375 and 437.5 Hz, respectively. The signal $x_c(t)$ is sampled at a rate of 1000 samples per sec, for a total interval of 4.096 sec. An FFT algorithm is applied to the sequence $x[n]$ thus obtained in order to evaluate the DFT $X[k]$ of the sequence $x[n]$. Evaluate $|X[k]|$.

Problem 7.7 In the wave synthesizer shown in Fig. 7.55, a 4096-point inverse FFT (IFFT) is applied to an input sequence $X[k]$. The resulting sequence $x[n]$ is repeated periodically

and continuously applied to a D/A converter at a rate of 512 points per second to generate the required continuous-time signal $x_c(t)$.

Assuming that the required continuous-time signal $x_c(t)$ is a sum of four sinusoids of amplitudes 2, 1, 0.5 and 0.25 volts and frequencies 117, 118, 119 and 120 Hz, respectively, specify the input sequence $X[k]$ that would lead to such output.

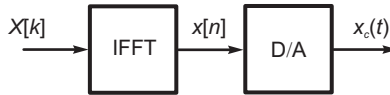


FIGURE 7.55 Inverse FFT followed by D/A conversion.

Problem 7.8 A periodic signal $v_c(t)$ is applied to the input of an A/D converter of a sampling frequency of $f_s = 10000$ samples per second. The converter produces the output $v[n] = v_c(nT)$ where $T = 1/f_s$. Given that

$$v_c(t) = 4 + 2 \cos(4000\pi t) + \cos(12000\pi t + \pi/4). \quad (7.285)$$

Evaluate and sketch $V_c(j\omega)$ and $V(e^{j\Omega})$, the Fourier transforms of $v_c(t)$ and $v[n]$, respectively.

Problem 7.9 Given the sequence

$$x[n] = 6 + 0.5 \sin(0.6\pi n - \pi/4) \quad (7.286)$$

which is applied to the input of a discrete-time system of transfer function

$$H(z) = \frac{2}{4 - 3z^{-1}}. \quad (7.287)$$

- Evaluate the system output $y[n]$.
- A sequence $v[n]$ is obtained from $x[n]$ such that $v[n] = x[n]$ for $0 \leq n \leq 99$. Evaluate the discrete Fourier transform $V[k]$ of $v[n]$.

Problem 7.10 Consider the sequence

$$x[n] = 3 \cos(2\pi n/12) + 5 \sin(2\pi n/6). \quad (7.288)$$

- Evaluate the Fourier transform $X(e^{j\Omega})$ of $x[n]$.
- The 48-point sequence $y[n]$ is given by $y[n] = x[n]$, $0 \leq n \leq 47$. Evaluate the discrete Fourier transform $Y[k]$ of $y[n]$.

Problem 7.11 Given the sequence

$$x[n] = a^n \{u[n] - u[n - N]\} \quad (7.289)$$

with $a = 0.7$ and $N = 16$.

- Evaluate the z-transform $X(z)$ of $x[n]$, stating its ROC.
- Evaluate and sketch the poles and zeros of $X(z)$ in the z-plane.
- Evaluate the z-transform on a circle of radius a in the z-plane.
- Evaluate $X_a[k]$, the DZT along the circle of radius a , by sampling the z-transform along the circle at frequencies $\Omega = 0, 2\pi/N, 3\pi/N, \dots, (N-1)\pi/N$, similarly to the sampling the DFT effects along the unit circle.

Problem 7.12 The continuous-time signal

$$x_c(t) = \cos \beta_1 t + \sin \beta_2 t + \cos \beta_3 t \tag{7.290}$$

where $\beta_1 = 3000\pi$, $\beta_2 = 6000\pi$ and $\beta_3 = 7000\pi$ r/s is sampled using an A/D converter operating at a sampling frequency $f_s = 5$ kHz, producing the output $x[n] = x_c(n/f_s)$.

- a) Evaluate $x[n]$.
- b) Evaluate and sketch the spectrum $X(e^{j\Omega})$ of the sequence $x[n]$.
- c) The sequence $x[n]$ is fed to a filter of frequency response

$$H(e^{j\Omega}) = \begin{cases} 1, & 7\pi/10 < |\Omega| < \pi \\ 0, & 0 < |\Omega| < 7\pi/10. \end{cases} \tag{7.291}$$

Evaluate the filter output $y[n]$.

Problem 7.13 A sequence $x[n]$ is composed of 8192 samples obtained from a continuous-time signal $x_a(t)$ band limited to 4 kHz by sampling it at a rate of 8000 samples/second.

$$x[n] = x_a(n/8000), \quad 0 \leq n \leq 8191. \tag{7.292}$$

An 8192-point FFT of the sequence $x[n]$ is evaluated and its absolute value is shown in Fig. 7.56.

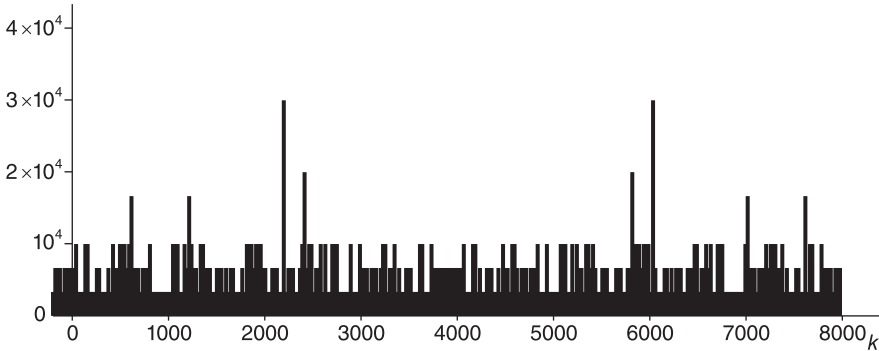


FIGURE 7.56 DFT coefficients.

Deduce from the figure an approximate value of the amplitude in volts and the frequency in Hz of the dominant component of the signal $x_a(t)$.

Problem 7.14 Let

$$T_3 = \begin{bmatrix} w^0 & w^0 & w^0 \\ w^0 & w^1 & w^2 \\ w^0 & w^2 & w^1 \end{bmatrix} \tag{7.293}$$

where $w = e^{-j2\pi/3}$, and $T_9 = T_3 \times T_3$ (Kronecker product of T_3 with itself).

Show that T_9 can be factored into a simple product of matrices expressed uniquely in terms of T_3 and I_3 . Show how to subsequently obtain a factorization in terms of uniquely $C_9 = I_3 \times T_3$ and the perfect shuffle matrix P_9 to result in an algorithm leading to hard-wired architecture using the minimum of memory partitions.

Problem 7.15 Evaluate the impulse response $h[n]$ of a filter which should have the frequency response $H(e^{j\Omega}) = \cos \Omega + j \sin(\Omega/4)$.

Problem 7.16 Given the sequence

$$x[n] = \begin{cases} \pm j, & n = 2, 14 \\ 2, & n = 4, 12 \\ 1, & n = 7, 9 \end{cases} \quad (7.294)$$

evaluate the DFT $X[k]$ of $x[n]$ with $N = 16$.

Problem 7.17 a) Evaluate the impulse response $h[n]$ of a filter knowing that its 16-point DFT $H[k]$ is given by

$$H[k] = j2 \sin(\pi k/4) + 4 \cos(\pi k/2) + 2 \cos(7\pi k/8). \quad (7.295)$$

b) Evaluate the impulse response $h[n]$ if its 16-point DFT $H[k]$ is given by

$$H[k] = \begin{cases} \cos(k\pi/7), & 2 \leq k \leq 9 \\ 0, & k = 0, 1, 10, 11, \dots, 15. \end{cases} \quad (7.296)$$

Problem 7.18 Given the 16-point DFT $X[k]$ of a sequence $x[n]$, namely,

$$X[k] = (k - 8)^2, \quad k = 0, 1, \dots, 15 \quad (7.297)$$

evaluate the sequence $x[n]$.

Problem 7.19 Given the sequence

$$x[n] = 3 + 5 \sin\left(\frac{6\pi}{N}n\right) + 10 \sin^2\left(\frac{2\pi}{N}n\right), \quad n = 0, 1, \dots, N - 1 \quad (7.298)$$

evaluate its N -point DFT $X[k]$ for $k = 0, 1, \dots, N - 1$.

Problem 7.20 Given the sequence

$$x[n] = \delta[n + K] + \delta[n - K], \quad K \text{ integer}. \quad (7.299)$$

Evaluate its Fourier transform $X(e^{j\Omega})$. Apply the duality property to deduce the Fourier series expansion and the Fourier transform of the function $v_c(t) = X(e^{jt})$.

Problem 7.21 Evaluate the periodic function $v(t)$ of period 2π which has the Fourier series coefficients

$$V_n = \Pi_N[n] = u[n + N] - u[n - N]. \quad (7.300)$$

Using duality, deduce $\mathcal{F}[\Pi_N[n]]$.

Problem 7.22 In a sampling system signals are sampled by an A/D converter at a frequency of 5 kHz and transmitted over a communication channel. At the receiving end the signal is reconstructed. Assuming the input signal is given by

$$x_c(t) = 10 + 10 \cos(3000\pi t) + 15 \sin(6000\pi t).$$

Is the reconstructed signal $y_c(t)$ at the receiving end equal to $x_c(t)$? If not what is its value? Justify your answer in the time domain and by evaluating and sketching the corresponding spectra $X_c(j\omega)$ and $X(e^{j\Omega})$.

Problem 7.23 Given the sequence $x[n] = R_N[n]$, where N is even.
 a) Sketch the sequences

$$v[n] = \begin{cases} x[n/2], & n, \text{ even}, 0 \leq n \leq 2N - 1 \\ 0, & n, \text{ odd}, 0 \leq n \leq 2N - 1 \end{cases}$$

$$w[n] = x[N - 1 - n]$$

$$y[n] = (-1)^n x[n]$$

b) Evaluate, as a function of $X\left(e^{j\frac{2\pi}{2N}k}\right)$, the $2N$ point DFT of $v[n]$, and the N -point DFTs of $y[n]$ and $w[n]$.

Problem 7.24 Evaluate the sequence $x[n]$ given that its $N = 16$ -point DFT is

$$X[k] = 2, \quad 1 \leq k \leq N - 1$$

and $X[0] = 15$.

Problem 7.25 A sequence $y[n]$ has a 12-point DFT $Y[k] = X[k]V[k]$, where $X[k]$ and $V[k]$ are the 12-point DFTs of the sequences

$$x[n] = 2\delta[n] + 4\delta[n - 7]$$

$$v[n] = [2 \ 2 \ 2 \ 0 \ 2 \ 2 \ 2 \ 0 \ 0 \ 0 \ 0 \ 0].$$

Evaluate $y[n]$.

Problem 7.26 Given the sequences

$$x[n] = \delta[n] + 2\delta[n - 1] + 4\delta[n - 2] + 8\delta[n - 3] + 4\delta[n - 4] + 2\delta[n - 5]$$

$$v[n] = \begin{cases} 1, & 0 \leq n \leq 4 \\ 0, & \text{otherwise} \end{cases}$$

let $X[k]$ and $V[k]$ be the 7-point DFT of $x[n]$ and $v[n]$, respectively. Given that a sequence $y[n]$ has the 7-point DFT $Y[k] = X[k]V[k]$, evaluate $y[n]$.

Problem 7.27 With $y[n]$ the linear convolution $x[n] * v[n]$, write the matrix equation that gives the values of $y[n]$ in terms of $x[n]$ and $v[n]$. Deduce from this equation and Equation (7.173), how circular convolution can be evaluated from linear convolution.

Problem 7.28 The two signals $v_c(t) = \cos 500\pi t$ and $x_c(t) = \sin 500\pi t$ are sampled by a C/D converter at a frequency $f_s = 1$ kHz producing the two sequences $v[n]$ and $x[n]$.

- (a) Evaluate the $N = 16$ -point circular convolution $z[n] = v[n] \circledast x[n]$.
- (b) Evaluate the $N = 16$ -point circular autocorrelation of $v[n]$.
- (c) Evaluate the $N = 16$ -point circular cross-correlation of $v[n]$ and $x[n]$.

Problem 7.29 A causal filter has the transfer function

$$H(z) = z/(z - a)$$

The filter frequency response is sampled uniformly into N samples producing the sequence

$$V[k] = H(e^{j2\pi k/N})$$

Evaluate the inverse DFT $v[n]$, with $a = 0.95$ and $N = 64$.

Problem 7.30 Prove that multiplication of two finite duration sequences in the time domain corresponds to a circular convolution in the DFT domain.

Problem 7.31 Prove that for two N -point sequences $v[n]$ and $x[n]$ with DFTs $V[k]$ and $X[k]$

$$\sum_{n=0}^{N-1} v[n]x^*[n] = \frac{1}{N} \sum_{k=0}^{N-1} V[k]X^*[k]$$

Problem 7.32 Let $y[n] = \cos(2r\pi n/N) \cos(2s\pi n/N)$ where r and s are integers, evaluate the sum

$$\sum_{n=0}^{N-1} y[n].$$

Problem 7.33 The real part of the frequency response of a causal system is given by

$$H_R(e^{j\Omega}) = 1 + a^4 \cos(4\Omega) + a^8 \cos(8\Omega) + a^{12} \cos(12\Omega) + a^{16} \cos(16\Omega)$$

where $a = 0.95$. Knowing that the system unit sample response is real valued, deduce the imaginary part of the frequency response $H_I(e^{j\Omega})$ and the system impulse response.

7.35 Answers to Selected Problems

Problem 7.1 a) Only the frequency band 12 – 13 kHz preserved. b) Only the frequency band 12 – 18 kHz preserved. c) The frequency band 12 – 23 kHz preserved. No aliasing, but the frequency band 23 – 35 kHz lost. d) No aliasing, spectrum shifted, but all information preserved. See Fig. 7.57.

Problem 7.2 a) $Y_c(0) = 1$, $f_y = 7.5$ kHz; b) $Y_c(0) = 0.5$, $f_y = 15$ kHz; c) $Y_c(0) = 2$, $f_y = 5$ kHz.

Problem 7.3 $H_c(j\omega) = \begin{cases} (1 - 1.526 \times 10^{-5} e^{-j16T\omega}) / (1 - 0.5e^{-jT\omega}), & |\omega| < \pi/T \\ 0, & \text{otherwise.} \end{cases}$

Problem 7.4 See Fig. 7.58.

Problem 7.5

- $f_1 \geq 40$ kHz.
- $T_1 \leq 1/40000$, $T_2 = MT_1$.
- $y_c(t) = x_c(4t)$.

Problem 7.6

$$|X[k]| = \begin{cases} 5N=20480, & k=0 \\ 4N/2=8192, & k=512, 3584 \\ 6N/2=12288, & k=1536, 2560 \\ 10N/2=20480, & k=1792, 2304 \\ 0, & \text{otherwise} \end{cases}$$

Problem 7.7

$$|X[k]| = \begin{cases} N=4096, & k=936, 3160 \\ N/2=2048, & k=944, 3152 \\ N/4=1024, & k=952, 3144 \\ N/8=512, & k=960, 3136 \\ 0, & \text{otherwise} \end{cases}$$

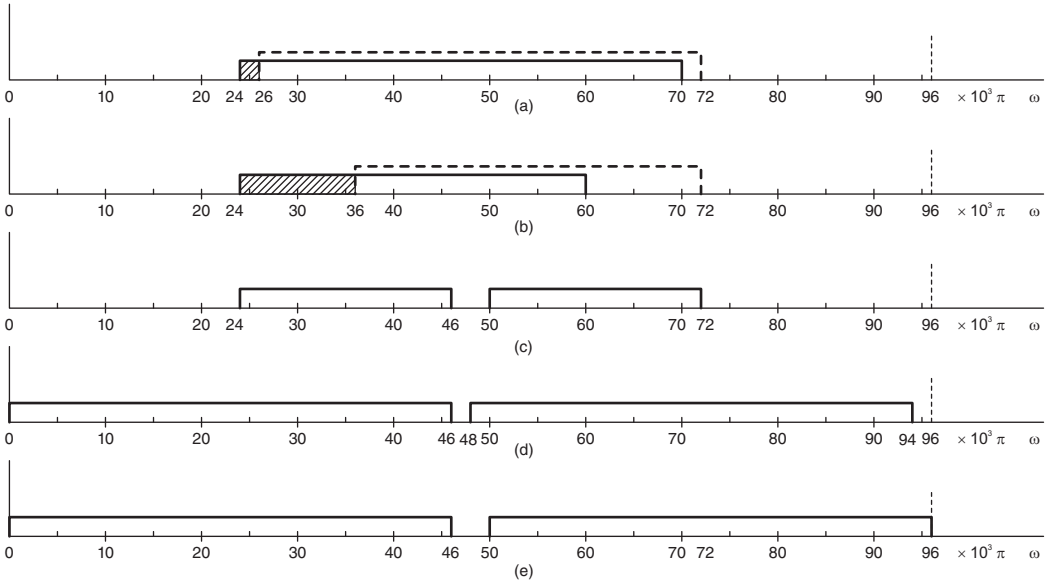


FIGURE 7.57 Comparison of different sampling approaches.

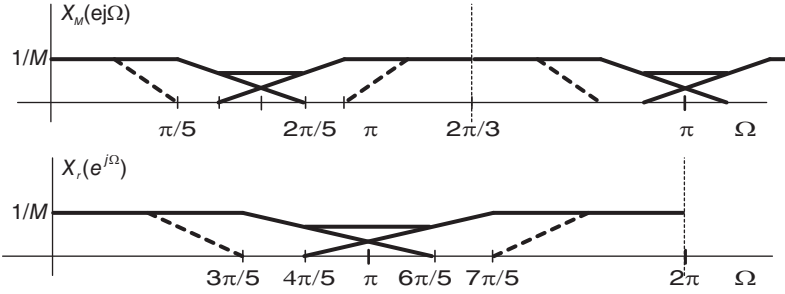


FIGURE 7.58 Spectra $X_M(e^{j\Omega})$ and $X_r(e^{j\Omega})$.

The phase values $arg[X[k]]$ are arbitrary.

Problem 7.8 See Fig. 7.59.

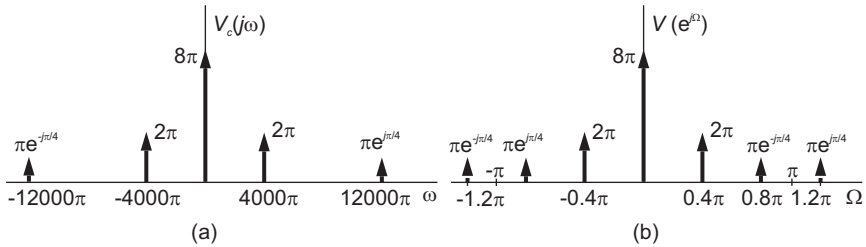


FIGURE 7.59 Figure for Problem 7.8.

Problem 7.9

- a) $y[n] = 12 + 0.175 \sin(0.6\pi n - 1.310)$.
- b) $V[0] = 600, V[30] = 25e^{-j3\pi/4}, V[70] = 25e^{j3\pi/4}, V[k] = 0$, otherwise..

Problem 7.10

$$Y[k] = \begin{cases} 3N/2 = 72, & n = 4, 44 \\ \mp j5N/2 = \mp j120, & n = 8, 40 \\ 0, & otherwise \end{cases}$$

Problem 7.11

- c) $X(ae^{j\Omega}) = \frac{1 - e^{-j\Omega N}}{1 - e^{-j\Omega}} = e^{-j\Omega(N-1)/2} \frac{\sin(N\Omega/2)}{\sin(\Omega/2)} = e^{-j\Omega(N-1)/2} Sd_N(\Omega/2)$
- d) $X_a[k] = \frac{1 - e^{-j2\pi k}}{1 - e^{-j2\pi k/N}} = \begin{cases} N, & k=0 \\ 0, & k=1, 2, \dots, N-1 \end{cases}$ · See Fig. 7.60

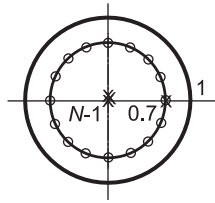


FIGURE 7.60 Figure for Problem 7.11.

Problem 7.12

- b) $X(e^{j\Omega}) = 2\pi \{ \delta(\Omega - 3\pi/5) + \delta(\Omega + 3\pi/5) \} + j\pi \{ \delta(\Omega - 4\pi/5) - \delta(\Omega + 4\pi/5) \}$,
- $$-\pi \leq \Omega \leq \pi$$

- c) $y[n] = -\sin(4\pi n/5)$.

Problem 7.13 The main component is a sinusoidal component of amplitude 7.3 volt and frequency 2.15 kHz.

Problem 7.14 $T_9 = P^{-1}S_9PS_9 = PS_9PS_9, S_9 = (I_3 \times T_3)$.

Problem 7.15 $h[n] = \frac{1}{2}\delta[n-1] + \frac{1}{2}\delta[n+1] + (-1)^n n / [\sqrt{2}\pi(n^2 - 1/16)]$.

Problem 7.16 $X[k] = 2 \sin(\pi k/4) + 4 \cos(\pi k/2) + 2 \cos(7\pi k/8)$.

Problem 7.17

- a) $h[n] = \begin{cases} -1, & n = 2 \\ 2, & n = 4, 12 \\ 1, & n = 7, 9, 14 \end{cases}$.
- b) $h[n] = \frac{1}{16} \cos(11\pi n/16 + 11\pi/14) \frac{\sin\{4(\pi/7 + \pi n/8)\}}{\sin(\pi/14 + \pi n/16)} R_{16}[n]$.

Problem 7.18

$$x[n] = \frac{1}{16} \{ 64 + 98 \cos(\pi n/8) + 72 \cos(\pi n/4) + 50 \cos(3\pi n/8) + 32 \cos(\pi n/2) \\ + 18 \cos(5\pi n/8) + 8 \cos(3\pi n/4) + 2 \cos(7\pi n/8) \}$$

Problem 7.19

$$X[k] = \begin{cases} 8N, & k = 0 \\ -5N/2, & k = 2, \quad N - 2 \\ \mp j5N/2, & k = 2, \quad N - 3 \\ 0, & \end{cases}$$

Problem 7.20

$$v_c(t) = 2 \cos Kt \xleftrightarrow{FSC} V_n = \begin{cases} 1, & n = \pm K \\ 0, & \text{otherwise.} \end{cases}$$

Problem 7.21

$$Sd_{2N+1}(t/2) \xleftrightarrow{FSC} \Pi_N[n], \quad \Pi_N[n] \xleftrightarrow{\mathcal{F}} Sd_{2N+1}(\Omega/2).$$

Problem 7.22

$$y_c(t) = 10 + 10 \cos(300\pi t) - 15 \sin(4000\pi t)$$

The spectra $X_s(j\omega)$ and $X(e^{j\Omega})$ are shown in Fig. 7.61.

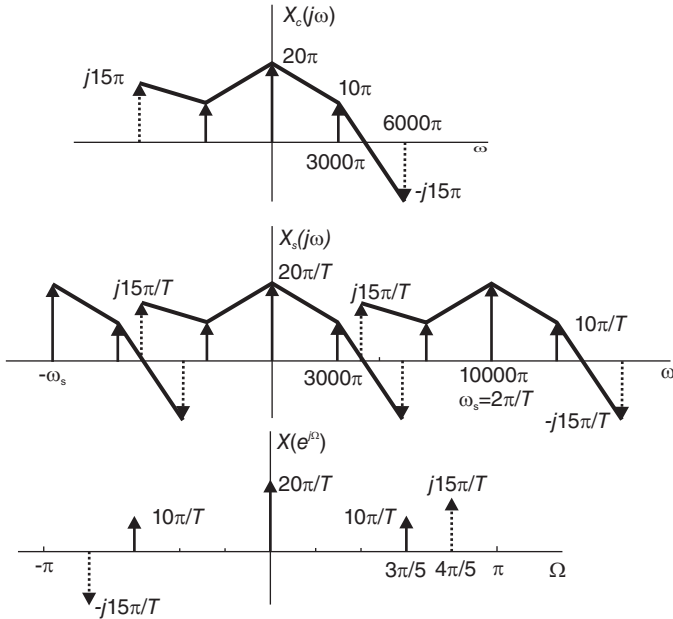


FIGURE 7.61 Spectra $X_s(j\omega)$ and $X(e^{j\Omega})$.

Problem 7.24 $x[n] = 2\delta[n] + 13/16$.

Problem 7.25 $y[n] = [12 \ 12 \ 4 \ 0 \ 4 \ 4 \ 4 \ 8 \ 8 \ 8 \ 0 \ 8]$.

Problem 7.26 $y[n] = \{15 \ 9 \ 9 \ 15 \ 19 \ 20 \ 18\}$.

Problem 7.27

- (a) $z[n] = 8 \sin(\pi n/2)$.
- (b) $c_{vv}[n] = 8 \cos(\pi n/2)$.
- (b) $c_{vx}[n] = -8 \sin(\pi n/2)$.

Problem 7.28 $v[n] = 1.039 \times 0.95^n R_{64}[n]$.

Problem 7.31 $\sum_{n=0}^{N-1} y[n] = N/2$, if $r = s$ or $r = N - s$, otherwise 0.

Problem 7.32 $h[n] = \delta[n] + 0.8145\delta[n-4] + 0.6634\delta[n-8] + 0.5404\delta[n-12] + 0.4401\delta[n-16]$.

8.1 Introduction

A *state space model* is a matrix-based approach to describe linear systems. In this chapter we study how *state variables* are used to construct a state space model of a linear system described by an n^{th} order linear differential equation. State space models of discrete-time systems are subsequently explored.

8.2 Note on Notation

In this chapter, to conform to the usual notation on state space modeling in the literature, we shall in general use the symbol $u(t)$ to denote the input signal to a system. This is not to be confused with the same symbol we have so far used to denote the unit step function. The student should easily deduce from the context that the symbol $u(t)$ denotes the input signal here. As is usual in automatic control literature the unit step function will be denoted $u_{-1}(t)$, to be distinguished from the input $u(t)$.

The state space approach is based on the fact that a linear time invariant (LTI) system may be modeled as a set of first order equations in the matrix form

$$\dot{x}(t) = Ax(t) + Bu(t) \tag{8.1}$$

where in general x is an n -element vector, A is an $n \times n$ matrix, u is an m -element vector, m being the number of inputs, and B is an $n \times m$ matrix.

In the homogeneous case where $u(t) = 0$ and with initial conditions $x(0)$ the equation

$$\dot{x}(t) = Ax(t) \tag{8.2}$$

is a first order differential equation having the solution

$$x(t) = e^{At}x(0) \triangleq \phi(t)x(0). \tag{8.3}$$

The matrix

$$\phi(t) = e^{At} \tag{8.4}$$

is called the *state transition matrix*.

8.3 State Space Model

Consider the n^{th} order LTI system described by the linear differential equation

$$\alpha_n y^{(n)} + \alpha_{n-1} y^{(n-1)} + \dots + \alpha_0 y = \beta_n u^{(n)} + \beta_{n-1} u^{(n-1)} + \dots + \beta_0 u \tag{8.5}$$

where $u(t)$ is the system input and $y(t)$ is its output and

$$y^{(i)} = \frac{d^i}{dt^i} y(t), \quad u^{(i)} = \frac{d^i}{dt^i} u(t). \tag{8.6}$$

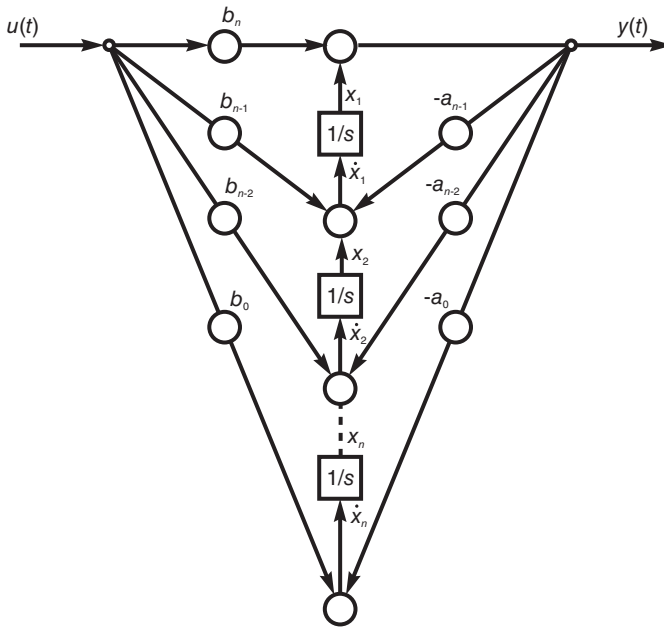


FIGURE 8.1 First canonical form realization.

Dividing both sides by α_n and letting $a_i = \alpha_i/\alpha_n$ and $b_i = \beta_i/\alpha_n$ we have

$$\frac{d^n y}{dt^n} + a_{n-1} \frac{d^{n-1} y}{dt^{n-1}} + \dots + a_0 y = b_n \frac{d^n u}{dt^n} + b_{n-1} \frac{d^{n-1} u}{dt^{n-1}} + \dots + b_0 u. \tag{8.7}$$

Laplace transforming both sides assuming zero initial conditions

$$(s^n + a_{n-1} s^{n-1} + \dots + a_0) Y(s) = (b_n s^n + b_{n-1} s^{n-1} + \dots + b_0) U(s). \tag{8.8}$$

The system transfer function is given by

$$H(s) = \frac{Y(s)}{U(s)} = \frac{b_n s^n + b_{n-1} s^{n-1} + \dots + b_0}{s^n + a_{n-1} s^{n-1} + \dots + a_0}. \tag{8.9}$$

To construct the state space model we divide both sides of (8.8) by s^n

$$\begin{aligned}
 Y(s) &= -a_{n-1} \frac{Y(s)}{s} - a_{n-2} \frac{Y(s)}{s^2} - \dots - a_0 \frac{Y(s)}{s^n} \\
 &\quad + b_n U(s) + b_{n-1} \frac{U(s)}{s} + \dots + b_0 \frac{U(s)}{s^n} \\
 &= b_n U(s) + \{b_{n-1} U(s) - a_{n-1} Y(s)\} (1/s) + \{b_{n-2} U(s) \\
 &\quad - a_{n-2} Y(s)\} (1/s^2) + \dots + \{b_0 U(s) - a_0 Y(s)\} (1/s^n).
 \end{aligned}
 \tag{8.10}$$

We can translate the input–output relation as the flow diagram shown in Fig. 8.1.

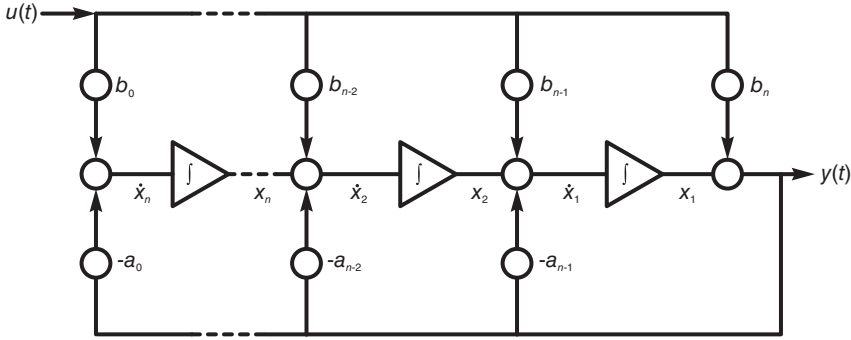


FIGURE 8.2 Equivalent representation of first canonical form.

In the figure, circles with coefficients next to them stand for multiplication by the coefficient. A circle is an adder if it receives more than one arrow and issues one arrow as its output. We note that the diagram includes boxes having a transfer function equal to $1/s$. Each box is an integrator. The diagram is redrawn in Fig. 8.2, showing the integrators that would be employed to construct a physical model. Both equivalent flow diagrams are referred to as the first canonical model form of the system model.

The state space model is obtained by labeling the output of each integrator as a state variable. An n^{th} order system has n integrators acting as the n memory elements storing the state of the system at any moment. Calling the state variables x_1, x_2, \dots, x_n as shown in the figures, the inputs to the integrators are given by $\dot{x}_1, \dot{x}_2, \dots, \dot{x}_n$, respectively, where $\dot{x}_i \triangleq dx_i/dt$. Referring to Fig. 8.1 or Fig. 8.2 we can write

$$y = x_1 + b_n u \tag{8.11}$$

$$\dot{x}_1 = b_{n-1} u - a_{n-1} y + x_2 = -a_{n-1} x_1 + x_2 + (b_{n-1} - a_{n-1} b_n) u \tag{8.12}$$

$$\dot{x}_2 = b_{n-2} u - a_{n-2} y + x_3 = -a_{n-2} x_1 + x_3 + (b_{n-2} - a_{n-2} b_n) u \tag{8.13}$$

$$\dot{x}_{n-1} = -a_1 x_1 + x_n + (b_1 - a_1 b_n) u \tag{8.14}$$

$$\dot{x}_n = -a_0 x_1 + (b_0 - a_0 b_n) u. \tag{8.15}$$

Using matrix notation these equations can be written in the form

$$\dot{x}(t) = Ax(t) + Bu(t) \tag{8.16}$$

$$y(t) = Cx(t) + Du(t) \tag{8.17}$$

$$\begin{bmatrix} \dot{x}_1 \\ \dot{x}_2 \\ \vdots \\ \dot{x}_{n-1} \\ \dot{x}_n \end{bmatrix} = \begin{bmatrix} -a_{n-1} & 1 & 0 & \dots & 0 & 0 \\ -a_{n-2} & 0 & 1 & & 0 & 0 \\ \vdots & & & & & \\ -a_1 & 0 & 0 & & 0 & 1 \\ -a_0 & 0 & 0 & & 0 & 0 \end{bmatrix} \begin{bmatrix} x_1 \\ x_2 \\ \vdots \\ x_{n-1} \\ x_n \end{bmatrix} + \begin{bmatrix} b_{n-1} - a_{n-1}b_n \\ b_{n-2} - a_{n-2}b_n \\ \vdots \\ b_1 - a_1b_n \\ b_0 - a_0b_n \end{bmatrix} u(t) \quad (8.18)$$

$$y(t) = [1 \ 0 \ 0 \ \dots \ 0 \ 0] \begin{bmatrix} x_1 \\ x_2 \\ \vdots \\ x_{n-1} \\ x_n \end{bmatrix} + b_n u(t) \quad (8.19)$$

where we identify A as a matrix of dimension $(n \times n)$, B as a column vector of dimension $(n \times 1)$, C a row vector of dimension $(1 \times n)$ and D a scalar. This is referred to as the first canonical form of the state equations.

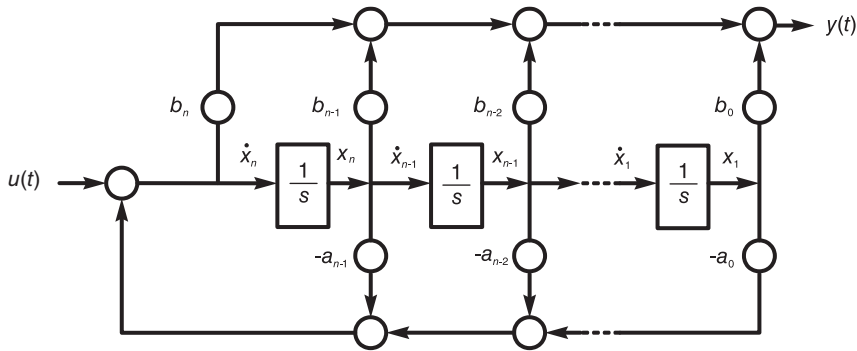


FIGURE 8.3 Second canonical form realization.

A fundamental linear systems property is that reversing all arrows in a system flow diagram produces the same system transfer function. This is effected on Fig. 8.2 resulting in Fig. 8.3. Note that converging arrows to a point must lead to an adder, whereas diverging arrows from a point means that the point is a branching point. This is the second canonical form of the system state equations.

The second canonical form is obtained by writing the state equations corresponding to this flow diagram. We have

$$\dot{x}_1 = x_2 \quad (8.20)$$

$$\dot{x}_2 = x_3 \quad (8.21)$$

$$\dot{x}_{n-1} = x_n \quad (8.22)$$

$$\dot{x}_n = -a_0x_1 - a_1x_2 - \dots - a_{n-2}x_{n-1} - a_{n-1}x_n + u \quad (8.23)$$

$$\begin{aligned} y &= b_0x_1 + \dots + b_{n-2}x_{n-1} + b_{n-1}x_n \\ &+ b_n \{-a_0x_1 - a_1x_2 - \dots - a_{n-2}x_{n-1} - a_{n-1}x_n + u(t)\} \\ &= (b_0 - b_n a_0) x_1 + \dots + (b_{n-2} - b_n a_{n-2}) x_{n-1} + (b_{n-1} - b_n a_{n-1}) x_n + b_n u \end{aligned} \quad (8.24)$$

that is,

$$\begin{bmatrix} \dot{x}_1 \\ \dot{x}_2 \\ \vdots \\ \dot{x}_{n-1} \\ \dot{x}_n \end{bmatrix} = \begin{bmatrix} 0 & 1 & 0 & \dots & 0 \\ 0 & 0 & 1 & \dots & 0 \\ \vdots & & & & \\ 0 & 0 & 0 & \dots & 1 \\ -a_0 & -a_1 & -a_2 & \dots & -a_{n-1} \end{bmatrix} \begin{bmatrix} x_1 \\ x_2 \\ \vdots \\ x_{n-1} \\ x_n \end{bmatrix} + \begin{bmatrix} 0 \\ 0 \\ \vdots \\ 0 \\ 1 \end{bmatrix} u \tag{8.25}$$

$$y = [b_0 - b_n a_0 \quad \dots \quad b_{n-2} - b_n a_{n-2} \quad \dots \quad b_{n-1} - b_n a_{n-1}] \begin{bmatrix} x_1 \\ x_2 \\ \vdots \\ x_{n-1} \\ x_n \end{bmatrix} + [b_n] u. \tag{8.26}$$

The second canonical form can be obtained directly from the system differential equation or transfer function as the following example illustrates.

Example 8.1 Given the system transfer function:

$$H(s) = \frac{3s^3 + 2s^2 + 5s}{5s^4 + 3s^3 + 2s^2 + 1}.$$

Show how to directly deduce the second canonical state space model which was obtained above by reversing the arrows of the first canonical model flow diagram.

We have

$$H(s) = \frac{Y(s)}{U(s)} = \frac{(3/5)s^3 + (2/5)s^2 + s}{s^4 + (3/5)s^3 + (2/5)s^2 + 1/5}.$$

We write $H(s) = H_1(s)H_2(s)$; see Fig. 8.4.

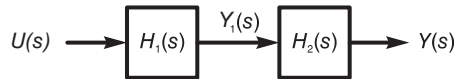


FIGURE 8.4 A cascade of two systems.

$$H_1(s) = \frac{Y_1(s)}{U(s)} = \frac{1}{s^4 + (3/5)s^3 + (2/5)s^2 + 1/5}$$

$$H_2(s) = \frac{Y(s)}{Y_1(s)} = (3/5)s^3 + (2/5)s^2 + s$$

i.e. $y_1^{(4)} + (3/5)y_1^{(3)} + (2/5)\dot{y}_1 + (1/5)y_1 = u$. Let $y_1 = x_1$, $\dot{x}_1 = x_2$, $\dot{x}_2 = x_3$, $\dot{x}_3 = x_4$ as shown in Fig. 8.5, i.e. $x_2 = \dot{y}_1$, $x_3 = \dot{y}_1^{(2)}$, $x_4 = y_1^{(3)}$ and $\dot{x}_4 = y_1^{(4)} = -(3/5)x_4 - (2/5)x_3 - (1/5)x_1 + u$.

$$y(t) = (3/5)y_1^{(3)} + (2/5)\ddot{y}_1 + \dot{y}_1 = (3/5)x_4 + (2/5)x_3 + x_2.$$

The state space model is therefore

$$\begin{bmatrix} \dot{x}_1 \\ \dot{x}_2 \\ \dot{x}_3 \\ \dot{x}_4 \end{bmatrix} = \begin{bmatrix} 0 & 1 & 0 & 0 \\ 0 & 0 & 1 & 0 \\ 0 & 0 & 0 & 1 \\ -1/5 & 0 & -2/5 & -3/5 \end{bmatrix} \begin{bmatrix} x_1 \\ x_2 \\ x_3 \\ x_4 \end{bmatrix} + \begin{bmatrix} 0 \\ 0 \\ 0 \\ 1 \end{bmatrix} u \tag{8.27}$$

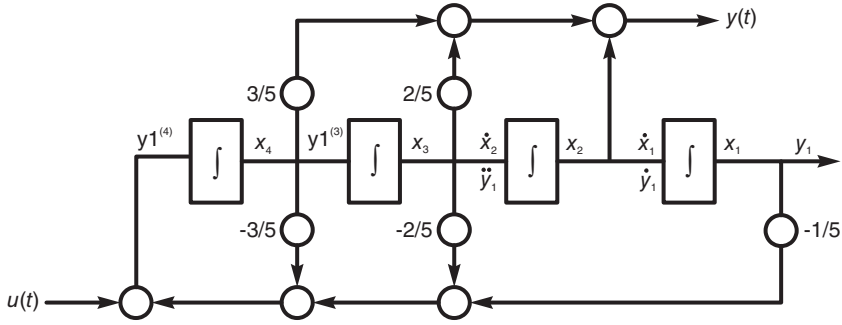


FIGURE 8.5 Direct evaluation of second canonical form.

$$y = [0 \ 1 \ 2/5 \ 3/5] \begin{bmatrix} x_1 \\ x_2 \\ x_3 \\ x_4 \end{bmatrix}. \tag{8.28}$$

For a given dynamic physical system there is no unique state space model. A variety of equivalent models that describe the system behavior can be found. The power of the state space model lies in the fact that the matrix representation makes possible the modeling of a system with multiple inputs and multiple outputs. In this case the input is a vector $u(t)$ representing i inputs and the output is a vector $y(t)$, representing k outputs. The matrices are: A of dimension $(n \times n)$, B of dimension $(n \times i)$, C of dimension $(k \times n)$ and D of dimension $(k \times i)$. The initial conditions may be introduced as the vector $x(0)$. In what follows we shall focus our attention mainly on single input, single output systems. However, the obtained results can be easily extended to the multiinput multioutput case.

8.4 System Transfer Function

Applying the Laplace transform to both sides of the state equations assuming zero initial conditions we have

$$sX(s) = A X(s) + B U(s) \tag{8.29}$$

$$Y(s) = C X(s) + D U(s) \tag{8.30}$$

where $X(s) = \mathcal{L}[x(t)]$, $U(s) = \mathcal{L}[u(t)]$ and $Y(s) = \mathcal{L}[y(t)]$. We can write

$$(sI - A) X(s) = B U(s) \tag{8.31}$$

$$X(s) = (sI - A)^{-1} B U(s) \tag{8.32}$$

$$Y(s) = \{C (sI - A)^{-1} B + D\} U(s) \tag{8.33}$$

wherefrom the transfer function is given by

$$H(s) = Y(s) \{U(s)\}^{-1} = C (sI - A)^{-1} B + D. \tag{8.34}$$

Writing

$$\Phi(s) = (sI - A)^{-1} = \frac{adj(sI - A)}{det(sI - A)} \tag{8.35}$$

we have

$$H(s) = C \Phi(s) B + D. \quad (8.36)$$

Hence the poles of the system are the roots of $\det(sI - A)$, known as the *characteristic polynomial*. The matrix $(sI - A)$ is thus known as the *characteristic matrix*. The matrix $\phi(t) = \mathcal{L}^{-1}[\Phi(s)]$ is the state transition matrix seen above in Equation (8.4). It can be shown that the transfer function thus obtained is the same as that evaluated by Laplace transforming the system's n^{th} order differential equation.

8.5 System Response with Initial Conditions

The following relations apply in general to multiinput multioutput systems and as a special case to single input single output ones. Assuming the initial conditions $x(0) = x_0$ we can write

$$sX(s) - x_0 = A X(s) + B U(s) \quad (8.37)$$

$$X(s) = (sI - A)^{-1} x_0 + (sI - A)^{-1} B U(s) \quad (8.38)$$

$$Y(s) = C (sI - A)^{-1} x_0 + \{C (sI - A)^{-1} B + D\} U(s) \quad (8.39)$$

$$X(s) = \Phi(s) x_0 + \Phi(s) B U(s) \quad (8.40)$$

$$Y(s) = C \Phi(s) x_0 + \{C \Phi(s) B + D\} U(s). \quad (8.41)$$

In the time domain these equations are written

$$x(t) = \phi(t) x_0 + \int_0^t \phi(t - \tau) B u(\tau) d\tau \quad (8.42)$$

where

$$\phi(t) = \mathcal{L}^{-1}[\Phi(s)] \quad (8.43)$$

$$\begin{aligned} y(t) &= C \phi(t) x_0 + \int_0^t C \phi(t - \tau) B u(\tau) d\tau + D u(t) \\ &= C \phi(t) x_0 + \int_0^t h(t - \tau) u(\tau) d\tau \end{aligned} \quad (8.44)$$

and

$$h(t) = C \phi(t) B + D \delta(t) \quad (8.45)$$

is the system impulse response. In electric circuits, state variables are normally taken as the voltage across a capacitor and a current through an inductor, that is, the electrical quantities that resist instantaneous change and therefore determine the behavior of the electric circuit. In general, however, such choice of physical state variables does not lead to a canonical form of the state space model.

8.6 Jordan Canonical Form of State Space Model

The Jordan or diagonal form is more symmetric in matrix structure than the canonical forms we have just seen. There are two ways to obtain the Jordan form. The first is to effect a partial fraction expansion of the transfer function $H(s)$. The second is to effect a matrix diagonalization using a similarity transformation. We have

$$H(s) = \frac{Y(s)}{U(s)} = \frac{b_n s^n + b_{n-1} s^{n-1} + \dots + b_0}{s^n + a_{n-1} s^{n-1} + \dots + a_0}. \quad (8.46)$$

Effecting a long division we have

$$Y(s) = \left\{ b_n + [(b_{n-1} - b_n a_{n-1}) s^{n-1} + (b_{n-2} - b_n a_{n-2}) s^{n-2} + \dots + (b_0 - b_n a_0)] / [s^n + a_{n-1} s^{n-1} + \dots + a_0] \right\} U(s) = b_n U(s) + F(s) U(s).$$

Assuming at first simple poles $\lambda_1, \lambda_2, \dots, \lambda_n$, for simplicity, we can write

$$Y(s) = b_n U(s) + \left\{ \frac{r_1}{s - \lambda_1} + \frac{r_2}{s - \lambda_2} + \dots + \frac{r_n}{s - \lambda_n} \right\} U(s) \quad (8.47)$$

$$r_i = (s - \lambda_i) F(s) |_{s=\lambda_i}. \quad (8.48)$$

Consider the i^{th} term. Writing

$$\dot{x}_i = \lambda_i x_i + u \quad (8.49)$$

$$y_i = r_i x_i \quad (8.50)$$

we have

$$sX_i(s) = \lambda_i X_i(s) + U(s) \quad (8.51)$$

$$H_i(s) = \frac{X_i(s)}{U(s)} = \frac{1}{s - \lambda_i} \quad (8.52)$$

$$Y_i(s) = r_i X_i(s) = \frac{r_i}{s - \lambda_i} U(s). \quad (8.53)$$

The corresponding flow diagram is shown in Fig. 8.6. By labeling the successive integrator outputs x_1, x_2, \dots, x_n we deduce the state equations

$$\begin{bmatrix} \dot{x}_1 \\ \dot{x}_2 \\ \vdots \\ \dot{x}_n \end{bmatrix} = \begin{bmatrix} \lambda_1 & 0 & 0 & \dots & 0 \\ 0 & \lambda_2 & 0 & \dots & 0 \\ \vdots & \vdots & \vdots & \ddots & \vdots \\ 0 & 0 & 0 & \dots & \lambda_n \end{bmatrix} \begin{bmatrix} x_1 \\ x_2 \\ \vdots \\ x_n \end{bmatrix} + \begin{bmatrix} 1 \\ 1 \\ \vdots \\ 1 \end{bmatrix} u \quad (8.54)$$

$$y = [r_1 \ r_2 \ \dots \ r_n] \begin{bmatrix} x_1 \\ x_2 \\ \vdots \\ x_n \end{bmatrix} + b_n u. \quad (8.55)$$

We consider next the case of multiple poles. To simplify the presentation we assume one multiple pole. Generalization to more than one such pole is straightforward. In this case we write

$$\begin{aligned} Y(s) &= \beta_n U(s) + F(s) U(s) \\ &= \beta_n U(s) + \left\{ \left[\frac{r_{1,1}}{(s - \lambda_1)^m} + \frac{r_{1,2}}{(s - \lambda_1)^{m-1}} + \dots + \frac{r_{1,m}}{(s - \lambda_1)} \right] \right. \\ &\quad \left. + \frac{r_{m+1}}{s - \lambda_{m+1}} + \frac{r_{m+2}}{s - \lambda_{m+2}} + \dots + \frac{r_n}{s - \lambda_n} \right\} U(s). \end{aligned} \quad (8.56)$$

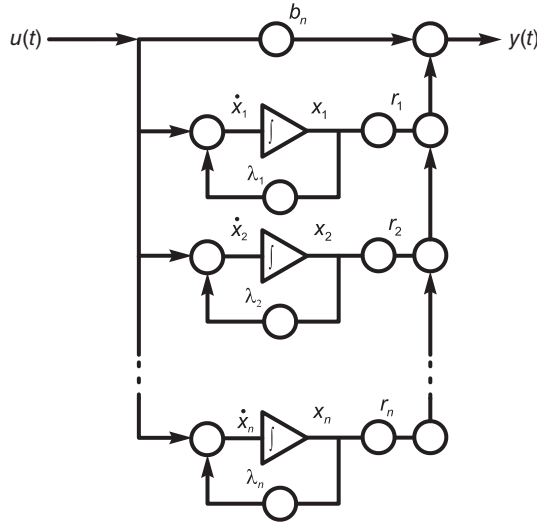


FIGURE 8.6 Jordan parallel form realization.

We recall that the residues of the pole of order m are given by

$$r_{1,i} = \frac{1}{(i-1)!} \frac{d^{i-1}}{ds^{i-1}} (s - \lambda_1)^m F(s) |_{s=\lambda_1}, \quad i = 1, 2, \dots, m. \tag{8.57}$$

The corresponding flow diagram is shown in Fig. 8.7. The state equations can be deduced thereof. We obtain

$$\dot{x}_1 = \lambda_1 x_1 + x_2 \tag{8.58}$$

$$\dot{x}_2 = \lambda_1 x_2 + x_3 \tag{8.59}$$

⋮

$$\dot{x}_{m-1} = \lambda_1 x_{m-1} + x_m \tag{8.60}$$

$$\dot{x}_m = \lambda_1 x_m + u \tag{8.61}$$

$$\dot{x}_{m+1} = \lambda_{m+1} x_{m+1} + u \tag{8.62}$$

⋮

$$\dot{x}_n = \lambda_n x_n + u \tag{8.63}$$

$$y = r_{1,1}x_1 + r_{1,2}x_2 + \dots + r_{1,m}x_m + r_{m+1}x_{m+1} + \dots + r_n x_n + b_n u. \tag{8.64}$$

The state space model in matrix form is therefore

$$\begin{bmatrix} \dot{x}_1 \\ \dot{x}_2 \\ \vdots \\ \dot{x}_{m-1} \\ \dot{x}_m \\ \dot{x}_{m+1} \\ \vdots \\ \dot{x}_n \end{bmatrix} = \begin{bmatrix} \lambda_1 & 1 & 0 & \dots & 0 & 0 & 0 & \dots & 0 \\ 0 & \lambda_1 & 1 & \dots & 0 & 0 & 0 & \dots & 0 \\ \vdots & & & \dots & & & & \dots & 0 \\ 0 & 0 & 0 & \dots & \lambda_1 & 1 & 0 & \dots & 0 \\ 0 & 0 & 0 & \dots & 0 & \lambda_1 & 0 & \dots & 0 \\ 0 & 0 & 0 & \dots & 0 & 0 & \lambda_{m+1} & \dots & 0 \\ \vdots & & & \dots & & & & \dots & \\ 0 & 0 & 0 & \dots & 0 & 0 & 0 & \dots & \lambda_n \end{bmatrix} \begin{bmatrix} x_1 \\ x_2 \\ \vdots \\ x_{m-1} \\ x_m \\ x_{m+1} \\ \vdots \\ x_n \end{bmatrix} + \begin{bmatrix} 0 \\ 0 \\ \vdots \\ 0 \\ 1 \\ 1 \\ \vdots \\ 1 \end{bmatrix} u \tag{8.65}$$

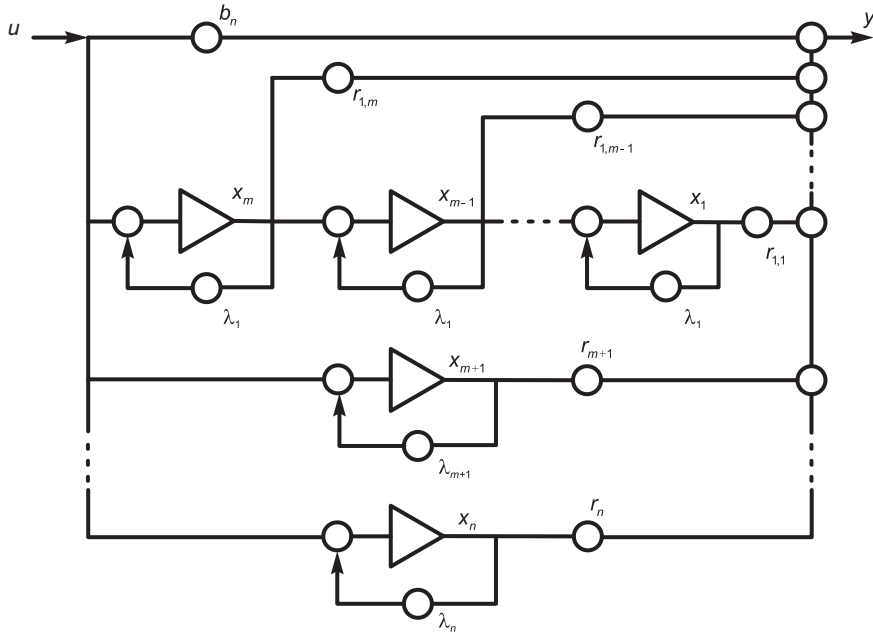


FIGURE 8.7 Jordan parallel form with multiple pole.

$$y = [r_{1,1} \ r_{1,2} \ \dots \ r_{1,m} \ r_{m+1} \ \dots \ r_n] \begin{bmatrix} x_1 \\ x_2 \\ \vdots \\ x_{m-1} \\ x_m \\ x_{m+1} \\ \vdots \\ x_n \end{bmatrix} + [b_n] u. \tag{8.66}$$

The $m \times m$ submatrix the diagonal elements of which are all the same pole λ_1 is called a *Jordan block* of order m .

Example 8.2 Consider the electric circuit shown in Fig. 8.8.

Evaluate the state space model. Let $R_1 = R_2 = 1 \ \Omega$, $L = 1 \ H$ and $C = 1 \ F$. Compare the transfer function obtained from the state space model with that obtained by direct evaluation. Evaluate the circuit impulse response, the response to the input $u(t) = e^{-\alpha t} u_{-1}(t)$ and the circuit unit step response.

Introducing the state variables x_1 volts and x_2 ampere shown in Fig. 8.8, we have

$$\begin{aligned} u &= R_1(C\dot{x}_1 + x_2) + x_1 \\ L\dot{x}_2 + R_2x_2 &= x_1 \\ \dot{x}_1 &= -\frac{1}{C}x_2 - \frac{x_1}{R_1C} + \frac{u}{R_1C} \\ \dot{x}_2 &= \frac{1}{L}x_1 - \frac{R_2}{L}x_2 \\ y &= x_1 \end{aligned}$$

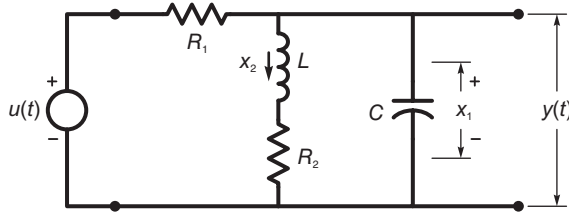


FIGURE 8.8 Electric circuit.

$$\begin{pmatrix} \dot{x}_1 \\ \dot{x}_2 \end{pmatrix} = \begin{pmatrix} -\frac{1}{R_1 C} & -\frac{1}{C} \\ \frac{1}{L} & -\frac{R_2}{L} \end{pmatrix} \begin{pmatrix} x_1 \\ x_2 \end{pmatrix} + \begin{pmatrix} \frac{1}{R_1 C} \\ 0 \end{pmatrix} u$$

$$y = (1 \ 0) \begin{pmatrix} x_1 \\ x_2 \end{pmatrix}.$$

With $R_1 = R_2 = 1 \ \Omega$, $L = 1 \ H$ and $C = 1 \ F$, we have

$$A = \begin{bmatrix} -1 & -1 \\ 1 & -1 \end{bmatrix}, \quad B = \begin{pmatrix} 1 \\ 0 \end{pmatrix}, \quad C = (1 \ 0), \quad D = 0$$

$$\begin{bmatrix} \dot{x}_1 \\ \dot{x}_2 \end{bmatrix} = \begin{bmatrix} -1 & -1 \\ 1 & -1 \end{bmatrix} \begin{bmatrix} x_1 \\ x_2 \end{bmatrix} + \begin{bmatrix} 1 \\ 0 \end{bmatrix} u(t)$$

$$y = [1 \ 0] \begin{bmatrix} x_1 \\ x_2 \end{bmatrix}.$$

Alternatively, Laplace transforming the differential equations, assuming zero initial conditions, we have

$$sX_1(s) = -\frac{1}{C}X_2(s) - \frac{1}{R_1 C}X_1(s) + \frac{1}{R_1 C}U(s)$$

$$sX_2(s) = \frac{1}{L}X_1(s) - \frac{R_2}{L}X_2(s)$$

$$Y(s) = X_1(s).$$

Solving for $X_1(s)$ and $X_2(s)$ we obtain

$$X_1(s) = \frac{(Ls + R_2)}{R_1 + (1 + R_1Cs)(Ls + R_2)}U(s)$$

$$Y(s) = \frac{Ls + R_2}{R_1 + (1 + R_1Cs)(Ls + R_2)}U(s)$$

$$H(s) = \frac{Y(s)}{U(s)} = \frac{Ls + R_2}{R_1 + (1 + R_1Cs)(Ls + R_2)}.$$

With the given values of R_1 , R_2 , L and C we have

$$H(s) = \frac{s + 1}{1 + (1 + s)(s + 1)} = \frac{s + 1}{(s + 1)^2 + 1}$$

$$\Phi(s) = (sI - A)^{-1} = \left[\begin{pmatrix} s & 0 \\ 0 & s \end{pmatrix} - \begin{pmatrix} -1 & -1 \\ 1 & -1 \end{pmatrix} \right]^{-1} = \left[\begin{matrix} s + 1 & 1 \\ -1 & s + 1 \end{matrix} \right]^{-1} = \frac{adj(sI - A)}{det(sI - A)}$$

$$\begin{aligned}
 \text{adj}(sI - A) &= \text{Transpose of the matrix of cofactors} = (-1)^{i+j} m_{ij} \\
 &= \begin{pmatrix} s+1 & 1 \\ -1 & s+1 \end{pmatrix}^T = \begin{pmatrix} s+1 & -1 \\ 1 & s+1 \end{pmatrix} \\
 \det(sI - A) &\equiv |sI - A| = (s+1)^2 + 1 \\
 \Phi(s) &= \frac{\begin{pmatrix} s+1 & -1 \\ 1 & s+1 \end{pmatrix}}{[(s+1)^2 + 1]} = \begin{bmatrix} \frac{s+1}{(s+1)^2 + 1} & \frac{-1}{(s+1)^2 + 1} \\ \frac{1}{(s+1)^2 + 1} & \frac{s+1}{(s+1)^2 + 1} \end{bmatrix} \\
 \phi(t) &= \begin{bmatrix} e^{-t} \cos t & -e^{-t} \sin t \\ e^{-t} \sin t & e^{-t} \cos t \end{bmatrix} u(t).
 \end{aligned}$$

The transfer function $H(s)$ is given by

$$\begin{aligned}
 H(s) &= C \Phi(s) B + D \\
 &= (1 \ 0) \left\{ (s+1)^2 + 1 \right\}^{-1} \begin{bmatrix} s+1 & -1 \\ 1 & s+1 \end{bmatrix} \begin{pmatrix} 1 \\ 0 \end{pmatrix} = \frac{s+1}{(s+1)^2 + 1}.
 \end{aligned}$$

The impulse response is given by

$$h(t) = \mathcal{L}^{-1}[H(s)] = e^{-t} \cos t u(t).$$

Alternatively, we have

$$\begin{aligned}
 h(t) &= C \phi(t) B + D \delta(t) \\
 &= (1 \ 0) \begin{bmatrix} \cos t & -\sin t \\ \sin t & \cos t \end{bmatrix} e^{-t} u(t) \begin{pmatrix} 1 \\ 0 \end{pmatrix} \\
 &= (\cos t - \sin t) e^{-t} u(t) \begin{pmatrix} 1 \\ 0 \end{pmatrix} = e^{-t} \cos t u(t)
 \end{aligned}$$

$$y(t) = h * v + Dv(t) = v(t) * e^{-t} \cos t u(t).$$

With

$$v(t) = e^{-\alpha t} u(t)$$

$$\begin{aligned}
 y &= \int_{-\infty}^{\infty} e^{-\alpha \tau} u(\tau) e^{-(t-\tau)} \cos(t-\tau) u(t-\tau) d\tau = \int_0^t e^{-\alpha \tau} e^{-t} \cos(t-\tau) d\tau u(t) \\
 &= \Re \left[e^{-t} \int_0^t e^{-(\alpha-1)\tau} e^{j(t-\tau)} d\tau \right] = \frac{e^{-t} \{ (\alpha-1) \cos t + \sin t - (\alpha-1) e^{-(\alpha-1)t} \}}{(\alpha-1)^2 + 1} u(t).
 \end{aligned}$$

If $\alpha = 0$

$$y = \frac{e^{-t}}{2} (-\cos t + \sin t + e^t) u(t)$$

which is the system unit step response.

Example 8.3 Evaluate the state space model of a system of transfer function

$$H(s) = \frac{Y(s)}{U(s)} = \frac{3s^3 + 10s^2 + 5s + 4}{(s+1)(s+2)(s^2+1)}.$$

Using a partial fraction expansion we have

$$Y(s) = H(s)U(s) = \left(\frac{3}{s+1} - \frac{2}{s+2} + \frac{1}{s+j} + \frac{1}{s-j} \right) U(s).$$

Writing

$$Y(s) = 3X_1(s) - 2X_2(s) + X_3(s) + X_4(s)$$

we obtain

$$\begin{aligned} X_1(s) &= \frac{U(s)}{s+1}, & \dot{x}_1 + x_1 &= u, & \dot{x}_1 &= -x_1 + u \\ X_2(s) &= \frac{U(s)}{s+2}, & \dot{x}_2 + 2x_2 &= u, & \dot{x}_2 &= -2x_2 + u \\ X_3(s) &= \frac{U(s)}{s+j}, & \dot{x}_3 + jx_3 &= u, & \dot{x}_3 &= -jx_3 + u \\ X_4(s) &= \frac{U(s)}{s-j}, & \dot{x}_4 - jx_4 &= u, & \dot{x}_4 &= jx_4 + u. \end{aligned}$$

We have obtained the state space model

$$\begin{pmatrix} \dot{x}_1 \\ \dot{x}_2 \\ \dot{x}_3 \\ \dot{x}_4 \end{pmatrix} = \begin{bmatrix} -1 & 0 & 0 & 0 \\ 0 & -2 & 0 & 0 \\ 0 & 0 & -j & 0 \\ 0 & 0 & 0 & j \end{bmatrix} \begin{bmatrix} x_1 \\ x_2 \\ x_3 \\ x_4 \end{bmatrix} + \begin{bmatrix} 1 \\ 1 \\ 1 \\ 1 \end{bmatrix} u$$

$$y = [3 \ -2 \ 1 \ 1] \begin{bmatrix} x_1 \\ x_2 \\ x_3 \\ x_4 \end{bmatrix}.$$

This is the Jordan canonical form.

Example 8.4 Consider the multiple-input multiple-output system of which the inputs are $u_1(t)$ and $u_2(t)$ and the transforms of the outputs $y_1(t)$ and $y_2(t)$ are given by

$$\begin{aligned} Y_1(s) &= \frac{3s^3 + 10s^2 + 5s + 4}{(s+1)(s+2)(s^2+1)} \{3U_1(s) + 5U_2(s)\} \\ Y_2(s) &= 2 \frac{s^3 + 10s^2 + 26s + 19}{(s+1)(s+2)^2} U_1(s) + 4 \frac{s+1}{(s+1)^2 + 1} U_2(s). \end{aligned}$$

Let $U_T = 3U_1 + 5U_2$. We may write

$$\begin{aligned} Y_1 &= \frac{3}{s+1} U_T - \frac{2}{s+2} U_T + \frac{1}{s+j} U_T + \frac{1}{s-j} U_T \\ &= 3X_1 - 2X_2 + X_3 + X_4 \\ X_1 &= \frac{U_T}{s+1}, \quad X_2 = \frac{U_T}{s+2}, \quad X_3 = \frac{U_T}{s+j}, \quad X_4 = \frac{U_T}{s-j} \\ \dot{x}_1 &= -x_1 + u_T, \quad \dot{x}_2 = -2x_2 + u_T, \quad \dot{x}_3 = -jx_3 + u_T, \quad \dot{x}_4 = jx_4 + u_T \\ \begin{bmatrix} \dot{x}_1 \\ \dot{x}_2 \\ \dot{x}_3 \\ \dot{x}_4 \end{bmatrix} &= \begin{bmatrix} -1 & & & \\ & -2 & & \\ & & -j & \\ & & & j \end{bmatrix} \begin{bmatrix} x_1 \\ x_2 \\ x_3 \\ x_4 \end{bmatrix} + \begin{bmatrix} 3 & 5 \\ 3 & 5 \\ 3 & 5 \\ 3 & 5 \end{bmatrix} \begin{bmatrix} u_1 \\ u_2 \end{bmatrix} \\ y_1 &= [3 \ -2 \ 1 \ 1] \begin{bmatrix} x_1 \\ x_2 \\ x_3 \\ x_4 \end{bmatrix}. \end{aligned}$$

Let $Y_2(s) \triangleq Y_{21}(s) + Y_{22}(s)$ and $U_{i2} \triangleq 2U_1$

$$Y_{21}(s) = \left[\frac{U_{i2}}{(s+2)^2} + \frac{3U_{i2}}{s+2} + \frac{2U_{i2}}{s+1} + U_{i2} \right] \triangleq X_5 + 3X_6 + 2X_7 + U_{i2}$$

$$X_5 = \frac{U_{i2}}{(s+2)^2}, \quad X_6 = \frac{U_{i2}}{s+2}, \quad X_7 = \frac{U_{i2}}{s+1}, \quad X_5 = \frac{X_6}{s+2}$$

$$\dot{x}_5 = -2x_5 + x_6, \quad \dot{x}_6 = -2x_6 + u_{i2}, \quad \dot{x}_7 = -x_7 + u_{i2}$$

$$\begin{bmatrix} \dot{x}_5 \\ \dot{x}_6 \\ \dot{x}_7 \end{bmatrix} = \begin{bmatrix} -2 & 1 & \\ & -2 & \\ & & -1 \end{bmatrix} \begin{bmatrix} x_5 \\ x_6 \\ x_7 \end{bmatrix} + \begin{bmatrix} 0 \\ 2 \\ 2 \end{bmatrix} u_1$$

$$y_{21} = [1 \ 3 \ 2] \begin{bmatrix} x_5 \\ x_6 \\ x_7 \end{bmatrix} + [2] u_1$$

$$Y_{22}(s) = \frac{s+1}{(s+1)^2+1} 4U_2(s) = \frac{s+1}{(s+1)^2+1} U_{i3}(s)$$

where $U_{i3}(s) = 4U_2(s)$. With $p = -1 + j$ we have

$$Y_{22}(s) = \frac{0.5U_{i3}}{s-p} + \frac{0.5U_{i3}}{s-p^*} = 0.5X_8 + 0.5X_9$$

$$X_8 = \frac{U_{i3}}{s-p}, \quad X_9 = \frac{U_{i3}}{s-p^*}$$

$$\dot{x}_8 = (-1 + j)x_8 + u_{i3}, \quad \dot{x}_9 = (-1 - j)x_9 + u_{i3}$$

$$\begin{bmatrix} \dot{x}_8 \\ \dot{x}_9 \end{bmatrix} = \begin{bmatrix} -1 + j & \\ & -1 - j \end{bmatrix} \begin{bmatrix} x_8 \\ x_9 \end{bmatrix} + \begin{bmatrix} 4 \\ 4 \end{bmatrix} u_2$$

$$y_{22} = [0.5 \ 0.5] \begin{bmatrix} x_8 \\ x_9 \end{bmatrix}.$$

Combining we have

$$\begin{bmatrix} \dot{x}_1 \\ \dot{x}_2 \\ \dot{x}_3 \\ \dot{x}_4 \\ \dot{x}_5 \\ \dot{x}_6 \\ \dot{x}_7 \\ \dot{x}_8 \\ \dot{x}_9 \end{bmatrix} = \begin{bmatrix} -1 & & & & & & & & \\ & -2 & & & & & & & \\ & & -j & & & & & & \\ & & & j & & & & & \\ & & & & -2 & 1 & & & \\ & & & & & -2 & & & \\ & & & & & & -1 & & \\ & & & & & & & -1 + j & \\ & & & & & & & & -1 - j \end{bmatrix} \begin{bmatrix} x_1 \\ x_2 \\ x_3 \\ x_4 \\ x_5 \\ x_6 \\ x_7 \\ x_8 \\ x_9 \end{bmatrix} + \begin{bmatrix} 3 \ 5 \\ 3 \ 5 \\ 3 \ 5 \\ 3 \ 5 \\ 0 \ 0 \\ 2 \ 0 \\ 2 \ 0 \\ 0 \ 4 \\ 0 \ 4 \end{bmatrix} \begin{bmatrix} u_1 \\ u_2 \end{bmatrix}$$

$$\begin{bmatrix} y_1 \\ y_2 \end{bmatrix} = \begin{bmatrix} 3 & -2 & 1 & 1 & 0 & 0 & 0 & 0 & 0 \\ 0 & 0 & 0 & 0 & 1 & 3 & 2 & 0.5 & 0.5 \end{bmatrix} \begin{bmatrix} x_1 \\ x_2 \\ x_3 \\ x_4 \\ x_5 \\ x_6 \\ x_7 \\ x_8 \\ x_9 \end{bmatrix} + \begin{bmatrix} 0 & 0 \\ 2 & 0 \end{bmatrix} \begin{bmatrix} u_1 \\ u_2 \end{bmatrix}.$$

We have seen in constructing the Jordan state equations form that the system poles were used to obtain a partial fraction expansion of the system transfer function. We will now see that the poles are but the system eigenvalues. In fact, eigenvalues and eigenvectors play an important role in a system state space representation as will be seen below.

8.7 Eigenvalues and Eigenvectors

Given a matrix A and a vector $v \neq 0$, the eigenvalues of A are the set of scalar values λ for which the equation

$$Av = \lambda v \quad (8.67)$$

has a nontrivial solution.

Rewriting this equation in the form

$$(A - \lambda I)v = 0 \quad (8.68)$$

we note that a nontrivial solution exists if and only if the *characteristic equation*

$$\det(A - \lambda I) = 0 \quad (8.69)$$

is satisfied.

Example 8.5 Find the eigenvalues of the matrix

$$A = \begin{bmatrix} 1 & -1 \\ 2 & 4 \end{bmatrix}$$

we have

$$(A - \lambda I)v = 0$$

i.e.

$$\left\{ \begin{bmatrix} 1 & -1 \\ 2 & 4 \end{bmatrix} - \begin{bmatrix} \lambda & 0 \\ 0 & \lambda \end{bmatrix} \right\} \begin{bmatrix} v_{1,1} \\ v_{2,1} \end{bmatrix} = \begin{bmatrix} 0 \\ 0 \end{bmatrix}$$

$$\begin{bmatrix} 1 - \lambda & -1 \\ 2 & 4 - \lambda \end{bmatrix} \begin{bmatrix} v_{1,1} \\ v_{2,1} \end{bmatrix} = \begin{bmatrix} 0 \\ 0 \end{bmatrix}.$$

The characteristic equation is given by

$$\det(A - \lambda I) = 0 = \begin{bmatrix} 1 - \lambda & -1 \\ 2 & 4 - \lambda \end{bmatrix} = (1 - \lambda)(4 - \lambda) + 2 = 0$$

i.e.

$$|A - \lambda I| = \lambda^2 - 5\lambda + 6 = (\lambda - 2)(\lambda - 3) = 0.$$

The eigenvalues, the roots of this polynomial, are given by

$$\lambda_1 = 2, \quad \lambda_2 = 3.$$

As with poles the eigenvalues can be *distinct* (simple) or *repeated* (multiple). There are n eigenvalues in all for an $(n \times n)$ matrix.

Let λ_i , $i = 1, 2, \dots, n$ be the n eigenvalues of a matrix A of dimension $n \times n$. Assuming that the eigenvalues are all distinct, corresponding to each eigenvalue λ_i there is an eigenvector v_i defined by

$$Av_i = \lambda_i v_i. \quad (8.70)$$

Example 8.6 Evaluate the eigenvectors of the matrix A given in the previous example.

We write for $\lambda_1 = 2$

$$\begin{bmatrix} 1 & -1 \\ 2 & 4 \end{bmatrix} \begin{bmatrix} v_{1,1} \\ v_{1,2} \end{bmatrix} = 2 \begin{bmatrix} v_{1,1} \\ v_{1,2} \end{bmatrix}$$

$$v_{1,1} - v_{1,2} = 2v_{1,1}$$

$$2v_{1,1} + 4v_{1,2} = 2v_{1,2}, \text{ i.e. } v_{1,1} = -v_{1,2}$$

wherefrom the eigenvector associated with $\lambda_1 = 2$ is given by

$$v_1 = \begin{bmatrix} 1 \\ -1 \end{bmatrix} k_1$$

where k_1 is any multiplying constant. With $\lambda_2 = 3$ we have

$$\begin{bmatrix} 1 & -1 \\ 2 & 4 \end{bmatrix} \begin{bmatrix} v_{2,1} \\ v_{2,2} \end{bmatrix} = 3 \begin{bmatrix} v_{2,1} \\ v_{2,2} \end{bmatrix}$$

$$v_{2,1} - v_{2,2} = 3v_{2,1}$$

$$2v_{2,1} - 4v_{2,2} = 3v_{2,2}, \text{ i.e. } 2v_{2,1} = -v_{2,2}.$$

The eigenvector associated with the eigenvalue $\lambda_2 = 3$ is thus given by

$$v_2 = \begin{bmatrix} 1 \\ -2 \end{bmatrix} k_2$$

where k_2 is any scalar.

The definition of the eigenvector implies that an eigenvector v_i of a matrix A is a vector that is transformed by A onto itself except for a change in length λ_i . Moreover, as the last example shows, an eigenvector remains one even if its length is multiplied by a scalar factor k , for

$$A(kv) = kAv = k\lambda v = \lambda(kv). \quad (8.71)$$

The eigenvector can be normalized to unit length by dividing each of its elements by its norm

$$\|v\| = \sqrt{v_1^2 + v_2^2 + \dots + v_n^2}. \quad (8.72)$$

8.8 Matrix Diagonalization

Given a square matrix A , the matrix $S = T^{-1}AT$ is said to be similar to A . A special case of similarity transformations is one that diagonalizes the matrix A . In this case the transformation matrix is known as the *Modal matrix* usually denoted M , so that the transformed matrix $S = M^{-1}AM$ is diagonal.

Eigenvectors play an important role in matrix diagonalization. The modal matrix M has as successive columns the eigenvectors v_1, v_2, \dots, v_n of the matrix A assuming distinct eigenvalue. We may write this symbolically in the form

$$M = [v_1 \ v_2 \ \dots \ v_n] \quad (8.73)$$

and

$$\begin{aligned} A M &= A [v_1 \ v_2 \ \dots \ v_n] = [Av_1 \ Av_2 \ \dots \ Av_n] = [\lambda_1 v_1 \ \lambda_2 v_2 \ \dots \ \lambda_n v_n] \\ &= [v_1 \ v_2 \ \dots \ v_n] \begin{bmatrix} \lambda_1 & 0 & 0 & \dots \\ & \lambda_2 & 0 & \dots \\ & & \vdots & \\ 0 & 0 & 0 & \lambda_n \end{bmatrix} = M \Lambda \end{aligned} \quad (8.74)$$

where

$$\Lambda = \text{diag}(\lambda_1, \lambda_2, \dots, \lambda_n). \quad (8.75)$$

We have thus obtained

$$M^{-1} A M = \Lambda. \quad (8.76)$$

The matrix M having as columns the eigenvectors of the matrix A can thus transform the matrix A into a diagonal one.

Example 8.7 Verify that the matrix M constructed using the eigenvectors in the last example diagonalizes the matrix A .

Writing

$$M = \begin{bmatrix} 1 & 1 \\ -1 & -2 \end{bmatrix}$$

we have

$$\begin{aligned} M^{-1} &= \frac{\text{adj}[M]}{|M|} = \frac{\begin{bmatrix} -2 & -1 \\ 1 & 1 \end{bmatrix}}{-1} = \begin{bmatrix} 2 & 1 \\ -1 & -1 \end{bmatrix} \\ M^{-1} A M &= \begin{bmatrix} 2 & 1 \\ -1 & -1 \end{bmatrix} \begin{bmatrix} 1 & -1 \\ 2 & 4 \end{bmatrix} \begin{bmatrix} 1 & 1 \\ -1 & -2 \end{bmatrix} = \begin{bmatrix} 2 & 0 \\ 0 & 3 \end{bmatrix} = \begin{bmatrix} \lambda_1 & 0 \\ 0 & \lambda_2 \end{bmatrix}. \end{aligned}$$

The matrix A is thus diagonalized by the matrix M as expected.

8.9 Similarity Transformation of a State Space Model

The state equation with zero input, $u = 0$, is given by

$$\dot{x} = Ax \quad (8.77)$$

Let

$$x = Tz. \quad (8.78)$$

We have

$$\dot{x} = T\dot{z} = A Tz \quad (8.79)$$

$$\dot{z} = T^{-1} A Tz = Sz. \quad (8.80)$$

where

$$S = T^{-1} A T. \quad (8.81)$$

With nonzero input we write

$$\dot{x} = T\dot{z} = A Tz + Bu \quad (8.82)$$

$$\dot{z} = T^{-1}A Tz + T^{-1}Bu = Sz + T^{-1}Bu = Sz + B_Tu \quad (8.83)$$

where $B_T = T^{-1}B$, and

$$y = Cx + Du = C Tz + Du = C_Tz + D_Tu \quad (8.84)$$

where $C_T = C T$, $D_T = D$. Similarly to the above, Laplace transforming the equations we have

$$(sI - S) Z(s) = B_T U(s) \quad (8.85)$$

$$Z(s) = (sI - S)^{-1} B_T U(s) \quad (8.86)$$

$$Y(s) = \left\{ C_T (sI - S)^{-1} B_T + D_T \right\} U(s) \quad (8.87)$$

wherefrom the transfer function is given by

$$H(s) = Y(s) \{U(s)\}^{-1} = C_T (sI - S)^{-1} B_T + D_T. \quad (8.88)$$

Writing

$$Q(s) = (sI - S)^{-1} \quad (8.89)$$

we have

$$H(s) = C_T Q(s) B_T + D_T. \quad (8.90)$$

The matrix $Q(s)$ and its inverse $Q(t) = \mathcal{L}^{-1}[Q(s)]$ are the state transition matrix of the transformed model.

Letting

$$Q(t) = e^{St} \quad (8.91)$$

we may write

$$\phi(t) = e^{At} = T Q(t) T^{-1} = T e^{St} T^{-1}. \quad (8.92)$$

Example 8.8 Evaluate the state transition matrix $\phi(t)$ for the matrix A of the previous example.

$$A = \begin{bmatrix} 1 & -1 \\ 2 & 4 \end{bmatrix}$$

$$\phi(t) = e^{At} = \sum_{n=0}^{\infty} A^n t^n / n! = I + At + A^2 t^2 / 2 + \dots$$

$$\begin{aligned} \Phi(s) &= (sI - A)^{-1} = \left\{ \begin{bmatrix} s & 0 \\ 0 & s \end{bmatrix} - \begin{bmatrix} 1 & -1 \\ 2 & 4 \end{bmatrix} \right\}^{-1} = \begin{bmatrix} s-1 & 1 \\ -2 & s-4 \end{bmatrix}^{-1} \\ &= \frac{\text{adj} \begin{bmatrix} s-1 & 1 \\ -2 & s-4 \end{bmatrix}}{(s-1)(s-4) + 2} = \frac{\begin{bmatrix} s-4 & -1 \\ 2 & s-1 \end{bmatrix}}{s^2 - 5s + 6} = \begin{bmatrix} \frac{2}{s-2} - \frac{1}{s-3} & \frac{1}{s-2} - \frac{1}{s-3} \\ \frac{-2}{s-2} + \frac{1}{s-3} & \frac{-1}{s-2} + \frac{2}{s-3} \end{bmatrix} \end{aligned}$$

$$\phi(t) = \begin{bmatrix} 2e^{2t} - e^{3t} & e^{2t} - e^{3t} \\ -2e^{2t} + 2e^{3t} & -e^{2t} + 2e^{3t} \end{bmatrix} u(t)$$

$$\phi_{11}(t) = 2 \left(1 + 2t + \frac{4t^2}{2} + \dots \right) - \left(1 + 3t + \frac{9t^2}{2} + \dots \right) = 1 + t - \frac{t^2}{2} + \dots$$

$$\phi_{12}(t) = \left(1 + 2t + \frac{4t^2}{2} + \dots \right) - \left(1 + 3t + \frac{9t^2}{2} + \dots \right) = -t - \frac{5t^2}{2} - \dots$$

$$\phi_{21}(t) = -2(1 + 2t + 2t^2 + \dots) + 2\left(1 + 3t + \frac{9t^2}{2} + \dots\right) = 2t + 5t^2 + \dots$$

$$\phi_{22}(t) = -(1 + 2t + 2t^2 + \dots) + 2\left(1 + 3t + \frac{9t^2}{2} + \dots\right) = 1 + 4t + 7t^2 + \dots$$

Alternatively, since

$$A^2 = \begin{bmatrix} 1 & -1 \\ 2 & 4 \end{bmatrix} \begin{bmatrix} 1 & -1 \\ 2 & 4 \end{bmatrix} = \begin{bmatrix} -1 & -5 \\ 10 & 14 \end{bmatrix}$$

we may write

$$\begin{aligned} \phi(t) &= I + At + A^2t^2/2 + A^3t^3/3! + \dots = \begin{bmatrix} 1 & 0 \\ 0 & 1 \end{bmatrix} + \begin{bmatrix} t & -t \\ 2t & 4t \end{bmatrix} + \frac{1}{2} \begin{bmatrix} -t^2 & -5t^2 \\ 10t^2 & 14t^2 \end{bmatrix} + \dots \\ &= \begin{bmatrix} 1 + t - t^2/2 + \dots & -t - 5t^2/2 - \dots \\ 2t + 5t^2 + \dots & 1 + 4t + 7t^2 + \dots \end{bmatrix} \end{aligned}$$

which agrees with the result just obtained.

8.10 Solution of the State Equations

The solution of the state equation

$$\dot{x} = Ax \tag{8.93}$$

can be found by Laplace transformation. We have

$$sX(s) - x(0) = A X(s) \tag{8.94}$$

$$(sI - A) X(s) = x(0) \tag{8.95}$$

$$X(s) = (sI - A)^{-1} x(0) = \Phi(s) x(0) \tag{8.96}$$

$$x(t) = \phi(t) x(0) \tag{8.97}$$

$$\phi(t) = \mathcal{L}^{-1} [(sI - A)^{-1}] = e^{At}. \tag{8.98}$$

Note that the usual exponential function properties apply to the exponential of a matrix.

For example, it is easy to show that

$$e^{At_1} e^{At_2} = e^{A(t_1+t_2)} \tag{8.99}$$

$$e^{At} e^{-At} = e^{A \cdot 0} = I \tag{8.100}$$

$$e^{-At} = \{e^{At}\}^{-1} \tag{8.101}$$

$$\frac{d}{dt} e^{At} = A e^{At}. \tag{8.102}$$

From Equation (8.42) with nonzero initial conditions and input $u(t)$ we have

$$x(t) = \phi(t) x(0) + \phi(t) * Bu(t). \tag{8.103}$$

We can write

$$x(t) = e^{At} x(0) + e^{At} * Bu(t) = e^{At} x(0) + \int_0^t e^{A\tau} Bu(t - \tau) d\tau \tag{8.104}$$

$$h(t) = Ce^{At}Bu(t) + D\delta(t) \quad (8.105)$$

$$\begin{aligned} y(t) &= \{C\phi(t)B + D\delta(t)\} * u = \{Ce^{At}B\} * u + Du \\ &= \int_0^t Ce^{A(t-\tau)}Bu(\tau) d\tau + Du(t). \end{aligned} \quad (8.106)$$

Example 8.9 Find the matrix e^{At} and the response of the electric circuit of Example 8.1.

We have

$$\dot{x} = Ax + Bu$$

$$y = Cx + Du$$

$$A = \begin{bmatrix} -1 & -1 \\ 1 & -1 \end{bmatrix}, \quad B = \begin{bmatrix} 1 \\ 0 \end{bmatrix}, \quad C = [1 \ 0], \quad D = 0.$$

The eigenvalues are the roots of the characteristic equation

$$\det(\lambda I - A) = 0$$

$$\begin{vmatrix} \lambda + 1 & 1 \\ -1 & \lambda + 1 \end{vmatrix} = 0$$

$$(1 + \lambda)^2 + 1 = 0$$

$$\lambda^2 + 2\lambda + 2 = 0$$

$$\lambda_1 = -1 + j1, \quad \lambda_2 = -1 - j1.$$

$$Av_1 = \lambda_1 v_1$$

$$(A - \lambda_1 I)v_1 = 0$$

$$\left\{ \begin{bmatrix} -1 & -1 \\ 1 & -1 \end{bmatrix} - \begin{bmatrix} \lambda_1 & 0 \\ 0 & \lambda_1 \end{bmatrix} \right\} v_1 = 0$$

$$\begin{bmatrix} -1 - \lambda_1 & -1 \\ 1 & -1 - \lambda_1 \end{bmatrix} \begin{bmatrix} v_{11} \\ v_{21} \end{bmatrix} = 0$$

$$(-1 - \lambda_1)v_{11} - v_{21} = 0$$

$$v_{11} - (1 + \lambda_1)v_{21} = 0$$

$$v_{21} = -(1 + \lambda_1)v_{11}$$

$$v_{11} = (1 + \lambda_1)v_{21}$$

$$v_{21} = \frac{1}{1 + \lambda_1}v_{11}$$

$$-(1 + \lambda_1)v_{11} = \frac{1}{1 + \lambda_1}v_{11}$$

$$-1 + \lambda_1 = -1 - 1 + j1 = -2 + j1$$

$$\frac{1}{1 + \lambda_1} = \frac{1}{1 - 1 + j1} = \frac{1}{j1} = -j$$

$$v_{21} = -(1 + \lambda_1)^2 v_{21} = -(1 + \lambda_1)v_{11}.$$

Say

$$v_{11} = 1$$

$$v_{21} = -(1 + \lambda_1) = -(1 - 1 + j1) = -j$$

$$v_1 = [1 \quad -j]^T.$$

With $v_{21} = 1$ we have

$$v_{11} = (1 + \lambda_1) = j$$

i.e.

$$v_1 = [j \quad 1]^T.$$

With eigenvalue λ_2 we have

$$v_{22} = -(1 + \lambda_2) v_{12}$$

$$v_{12} = -(1 + \lambda_2) v_{22}$$

with $v_{12} = 1$

$$v_{22} = -(1 - 1 - j1) v_{12} = j$$

i.e.

$$v_2 = [1 \quad j]^T$$

with $v_{22} = 1$

$$v_{12} = (-j) v_{22} = -j$$

i.e.

$$v_2 = [-j \quad 1]^T.$$

Taking $v_1 = [1 \quad -j]^T$ and $v_2 = [1 \quad j]^T$ we have

$$M = \begin{bmatrix} 1 & 1 \\ -j & j \end{bmatrix}$$

$$M^{-1} = \begin{bmatrix} j & j \\ -1 & 1 \end{bmatrix}^T / (j + j) = \begin{pmatrix} j & -1 \\ j & 1 \end{pmatrix} / j2 = \begin{pmatrix} 1/2 & j/2 \\ 1/2 & -j/2 \end{pmatrix}$$

$$\begin{aligned} M^{-1} A M &= \frac{1}{2} \begin{pmatrix} 1 & j \\ 1 & -j \end{pmatrix} \begin{bmatrix} -1+j & -1-j \\ 1+j & 1-j \end{bmatrix} \\ &= \frac{1}{2} \begin{bmatrix} -1+j+j-1 & -1-j+j+1 \\ -1+j-j+1 & -1-j-j-1 \end{bmatrix} \\ &= \frac{1}{2} \begin{pmatrix} -2+j2 & 0 \\ 0 & -2-j2 \end{pmatrix} = \begin{bmatrix} -1+j & 0 \\ 0 & -1-j \end{bmatrix} = J \end{aligned}$$

$$\begin{aligned} e^{At} &= M e^{Jt} M^{-1} \\ &= \begin{bmatrix} 1 & 1 \\ -j & j \end{bmatrix} \begin{bmatrix} e^{-t+jt} & 0 \\ 0 & e^{-t-jt} \end{bmatrix} \begin{bmatrix} 1 & j \\ 1 & -j \end{bmatrix} / 2 \\ &= \frac{1}{2} \begin{bmatrix} e^{-t+jt} + e^{-t-jt} & j e^{-t+jt} - j e^{-t-jt} \\ -j e^{-t+jt} + j e^{-t-jt} & e^{-t+jt} + e^{-t-jt} \end{bmatrix} \\ &= \begin{bmatrix} e^{-t} \cos t & -e^{-t} \sin t \\ e^{-t} \sin t & e^{-t} \cot t \end{bmatrix}, \quad t > 0 \end{aligned}$$

which is in agreement with what we found earlier as the value of $\phi(t)$.

Note that with

$$J = \begin{bmatrix} \lambda_1 & & & \\ & \lambda_2 & & \\ & & \ddots & \\ & & & \lambda_n \end{bmatrix} \tag{8.107}$$

$$e^{Jt} = \begin{bmatrix} e^{\lambda_1 t} & & & \\ & e^{\lambda_2 t} & & \\ & & \ddots & \\ & & & e^{\lambda_n t} \end{bmatrix}. \quad (8.108)$$

We conclude that the exponential of a diagonal matrix J is a diagonal matrix the elements of which are the exponentials of the elements of J .

Example 8.10 Evaluate and verify the transformation between the canonical and Jordan state space models of the system of Example 8.4 and transfer function

$$H(s) = \frac{Y(s)}{U(s)} = \frac{s^3 + 10s^2 + 26s + 19}{(s+1)(s+2)^2}.$$

We have found

$$\begin{bmatrix} \dot{x}_1 \\ \dot{x}_2 \\ \dot{x}_3 \end{bmatrix} = \begin{bmatrix} -2 & 1 & 0 \\ 0 & -2 & 0 \\ 0 & 0 & -1 \end{bmatrix} \begin{bmatrix} x_1 \\ x_2 \\ x_3 \end{bmatrix} + \begin{bmatrix} 0 \\ 1 \\ 1 \end{bmatrix} u$$

$$y = [1 \ 3 \ 2] \begin{bmatrix} x_1 \\ x_2 \\ x_3 \end{bmatrix} + u$$

$$J = \begin{bmatrix} -2 & 1 & 0 \\ 0 & -2 & 0 \\ 0 & 0 & -1 \end{bmatrix}$$

$$B_J = [0 \ 1 \ 1]^T, \quad C_J = [1 \ 3 \ 2]$$

and

$$D_J = D.$$

To find the transformation matrix T and its inverse and the transition matrix $Q(s)$ of the Jordan model directly from the Jordan matrix J and from the canonical form matrix A we note that

$$Q(t) \triangleq e^{Jt} = \begin{bmatrix} e^{-2t} & te^{-2t} & 0 \\ 0 & e^{-2t} & 0 \\ 0 & 0 & e^{-t} \end{bmatrix}$$

$$H(s) = \frac{s^3 + 10s^2 + 26s + 19}{(s+1)(s^2 + 4s + 4)} = \frac{s^3 + 10s^2 + 26s + 19}{s^3 + 5s^2 + 8s + 4}$$

$$b_0 = 19, \quad b_1 = 26, \quad b_2 = 10, \quad b_3 = 1$$

$$a_0 = 4, \quad a_1 = 8, \quad a_2 = 5, \quad a_3 = 1 = a_n$$

$$\dot{x} = Ax + Bu$$

$$y = Cx + Du$$

$$A = \begin{bmatrix} -5 & 1 & 0 \\ -8 & 0 & 1 \\ -4 & 0 & 0 \end{bmatrix}$$

$$B = [5 \ 18 \ 15]^T, \quad C = [1 \ 0 \ 0]$$

and $D = 1$. We may also evaluate the transition matrix $Q(t)$ by writing

$$Q(s) = (sI - J)^{-1} = \left[\begin{bmatrix} s & & \\ & s & \\ & & s \end{bmatrix} - \begin{bmatrix} -2 & 1 & 0 \\ 0 & -2 & 0 \\ 0 & 0 & -1 \end{bmatrix} \right]^{-1} = \frac{\text{adj}(sI - J)}{|sI - J|}$$

$$= \begin{bmatrix} \frac{1}{s+2} & \frac{1}{(s+2)^2} & 0 \\ 0 & \frac{1}{s+2} & 0 \\ 0 & 0 & \frac{1}{s+1} \end{bmatrix}$$

of which the inverse transform is indeed $Q(t)$ found above. The eigenvalues are $\lambda_i = -2, -2, -1$.

$$(A - \lambda_1 I)x_1 = 0, \text{ i.e. } (A + 2I)x_1 = 0.$$

Let $x_1 = [x_{11} \ x_{12} \ x_{13}]^T$. We have

$$\left(\begin{bmatrix} -5 & 1 & 0 \\ -8 & 0 & 1 \\ -4 & 0 & 0 \end{bmatrix} + \begin{bmatrix} 2 & & \\ & 2 & \\ & & 2 \end{bmatrix} \right) \begin{bmatrix} x_{11} \\ x_{12} \\ x_{13} \end{bmatrix} = \begin{bmatrix} -3 & 1 & 0 \\ -8 & 2 & 1 \\ -4 & 0 & 2 \end{bmatrix} \begin{bmatrix} x_{11} \\ x_{12} \\ x_{13} \end{bmatrix} = \begin{bmatrix} 0 \\ 0 \\ 0 \end{bmatrix}$$

$$-3x_{11} + x_{12} = 0, \quad x_{12} = 3x_{11}$$

$$-8x_{11} + 2x_{12} + x_{13} = 0$$

$$-4x_{11} + 2x_{13} = 0, \quad x_{13} = 2x_{11}$$

$$-8x_{11} + 6x_{11} + 2x_{11} = 0.$$

Take $x_1 = (\alpha \ 3\alpha \ 2\alpha)^T = \alpha(1 \ 3 \ 2)^T$.

$$(A - \lambda I)t_1 = x_1, \text{ i.e. } (A + 2I)t_1 = x_1.$$

Let $t_1 = [t_{11} \ t_{12} \ t_{13}]^T$.

$$\begin{bmatrix} -3 & 1 & 0 \\ -8 & 2 & 1 \\ -4 & 0 & 2 \end{bmatrix} \begin{bmatrix} t_{11} \\ t_{12} \\ t_{13} \end{bmatrix} = \begin{bmatrix} \alpha \\ 3\alpha \\ 2\alpha \end{bmatrix}$$

$$-3t_{11} + t_{12} = \alpha, \quad t_{12} = \alpha + 3t_{11}$$

$$-8t_{11} + 2t_{12} + t_{13} = 3\alpha$$

$$-4t_{11} + 2t_{13} = 2\alpha, \quad t_{13} = \alpha + 2t_{11}$$

$$-8t_{11} + 2\alpha + 6t_{11} + \alpha + 2t_{11} = 3\alpha.$$

Take $t_{11} = \beta$ so that $t_1 = [\beta \ \alpha + 3\beta \ \alpha + 2\beta]^T$

$$(A - \lambda_2 I)x_2 = 0, \quad (A + I)x_2 = 0.$$

With $x_2 = [x_{21} \ x_{22} \ x_{23}]^T$

$$\begin{bmatrix} -4 & 1 & 0 \\ -8 & 1 & 1 \\ -4 & 0 & 1 \end{bmatrix} \begin{bmatrix} x_{21} \\ x_{22} \\ x_{23} \end{bmatrix} = 0$$

$$-4x_{21} + x_{22} = 0, \quad x_{22} = 4x_{21}$$

$$-8x_{21} + x_{22} + x_{23} = 0$$

$$\begin{aligned} -4x_{21} + x_{23} &= 0, & x_{23} &= 4x_{21} \\ -8x_{21} + 4x_{21} + 4x_{21} &= 0. \end{aligned}$$

Take $x_{21} = \gamma$ so that $x_2 = [\gamma \ 4\gamma \ 4\gamma]$.

$$T = [x_1 \ t_1 \ x_2] = \begin{bmatrix} \alpha & \beta & \gamma \\ 3\alpha & \alpha + 3\beta & 4\gamma \\ 2\alpha & \alpha + 2\beta & 4\gamma \end{bmatrix}.$$

Taking $\alpha = 1$, $\beta = 0$, $\gamma = 1$

$$T = \begin{bmatrix} 1 & 0 & 1 \\ 3 & 1 & 4 \\ 2 & 1 & 4 \end{bmatrix}, \quad |T| = 1$$

$$T^{-1} = \text{adj}[T] / 1 = \begin{bmatrix} 0 & -4 & 1 \\ 1 & 2 & -1 \\ -1 & -1 & 1 \end{bmatrix}^T = \begin{bmatrix} 0 & 1 & -1 \\ -4 & 2 & -1 \\ 1 & -1 & 1 \end{bmatrix}$$

$$T^{-1} A T = \begin{bmatrix} 0 & 1 & -1 \\ -4 & 2 & -1 \\ 1 & -1 & 1 \end{bmatrix} \begin{bmatrix} -2 & 1 & -1 \\ -6 & 1 & -4 \\ -4 & 0 & -4 \end{bmatrix} = \begin{bmatrix} -2 & 1 & 0 \\ 0 & -2 & 0 \\ 0 & 0 & -1 \end{bmatrix} = J.$$

Example 8.11 The transformation to the Jordan form assuming distinct eigenvalues $\lambda_1, \lambda_2, \dots, \lambda_n$ produces

$$A_w = J = M^{-1} A M = \begin{bmatrix} \lambda_1 & & & \\ & \lambda_2 & & \\ & & \ddots & \\ & & & \lambda_n \end{bmatrix}$$

where the matrix M in this case is the one diagonalizing the matrix A , having as columns the eigenvectors of A corresponding to $\lambda_1, \lambda_2, \dots, \lambda_n$ respectively.

The state transition matrix of the transformed model can be similarly evaluated by Laplace transforming the equations. We obtain

$$sW(s) - A_w W(s) = B_w U(s)$$

$$(sI - A_w) W(s) = B_w U(s)$$

$$W(s) = (sI - A_w)^{-1} B_w U(s) = Q(s) B_w U(s)$$

where

$$Q(s) = (sI - A_w)^{-1} = (sI - M^{-1} A M)^{-1}$$

$$Y(s) = C_w (sI - A_w)^{-1} B_w U(s) + D_w U(s).$$

The transfer function is given by

$$H(s) = Y(s) U^{-1}(s) = C_w (sI - A_w)^{-1} B_w + D_w$$

and has to be the same as the transfer function of the system, that is,

$$H(s) = C (sI - A)^{-1} B + D$$

and since $D_w = D$ we have

$$C_w (sI - A_w)^{-1} B_w = C (sI - A)^{-1} B.$$

To show this we recall the property

$$(F G)^{-1} = G^{-1}F^{-1}.$$

Now

$$\begin{aligned} C_w (sI - A_w)^{-1} B_w &= C M (sI - A_w)^{-1} M^{-1} B \\ &= C M \{M (sI - M^{-1} A M)\}^{-1} B \\ &= C M (sM - A M)^{-1} B \\ &= C \{(sM - A M) M^{-1}\}^{-1} B = C (sI - A)^{-1} B. \end{aligned}$$

We may write

$$C_w Q(s) B_w = C \Phi(s) B$$

i.e.

$$C M Q(s) M^{-1} B = C \Phi(s) B$$

or

$$\begin{aligned} \Phi(s) &= M Q(s) M^{-1} \\ \phi(t) &= M Q M^{-1} \end{aligned}$$

and in particular, if $J = A_w = M^{-1} A M$, i.e. $Q(t) = e^{Jt}$ then

$$\phi(t) = M e^{Jt} M^{-1}$$

as stated earlier.

We also note that

$$\begin{aligned} \det(\lambda I - A_w) &= \det(\lambda I - M^{-1} A M) = \det(\lambda M^{-1} M - M^{-1} A M) \\ &= \det[M^{-1} (\lambda I - A) M]. \end{aligned}$$

Recalling that

$$\det(X Y) = \det(X) \det(Y)$$

and that

$$\det(M^{-1}) = (\det M)^{-1}$$

we have

$$\det(\lambda I - A_w) = (\det M)^{-1} \det(\lambda I - A) \det(M) = \det(\lambda I - A).$$

8.11 General Jordan Canonical Form

As noted above, a transformation from the state variables $x(t)$ to the variables $w(t)$ may be obtained using a transformation matrix M . We write

$$x(t) = M w(t) \tag{8.109}$$

i.e.

$$w(t) = M^{-1} x(t). \tag{8.110}$$

The matrix M must be a $n \times n$ nonsingular matrix for its inverse to exist. Substituting in the state space equations

$$\dot{x} = Ax + Bu \tag{8.111}$$

$$y = Cx + Du \tag{8.112}$$

we have

$$M\dot{w} = A Mw + Bu \tag{8.113}$$

$$\dot{w} = M^{-1}A Mw + M^{-1}Bu. \tag{8.114}$$

Writing

$$\dot{w} = A_w w + B_w u \tag{8.115}$$

we have $A_w = M^{-1}A M$ and $B_w = M^{-1}B$. Moreover

$$y = Cx + Du = C Mw + Du. \tag{8.116}$$

Writing

$$y = C_w w + D_w u \tag{8.117}$$

we have $C_w = C M$ and $D_w = D$.

The similarity transformation relating the similar matrices A and A_w has the following properties:

The eigenvalues $\lambda_1, \lambda_2, \dots, \lambda_n$ of A_w are the same as those of A . In other words

$$\det(sI - A_w) = \det(sI - A) = (s - \lambda_1)(s - \lambda_2)\dots(s - \lambda_n). \tag{8.118}$$

Substituting $s = 0$ we have

$$(-1)^n \det A_w = (-1)^n \det A = (-1)^n \lambda_1 \lambda_2 \dots \lambda_n \tag{8.119}$$

$$\det A_w = \det A = \lambda_1 \lambda_2 \dots \lambda_n. \tag{8.120}$$

If the eigenvalues of the matrix M are distinct, we have

$$M^{-1}A M = \Lambda = \text{diag}(\lambda_1, \lambda_2, \dots, \lambda_n) \tag{8.121}$$

where the diagonal matrix is the diagonal Jordan Matrix J . If corresponding to every eigenvalue λ_i that is repeated m times a set of m linearly independent eigenvectors can be found then again

$$M^{-1}A M = \Lambda = \text{diag}(\lambda_1, \lambda_2, \dots, \lambda_n). \tag{8.122}$$

In most cases of repeated roots the product $M^{-1}A M$ is not a diagonal matrix but rather a matrix close to a diagonal one in which 1's appear above the diagonal, thus forming what is called a Jordan block.

$$B_{ik}(\lambda_k) = \begin{bmatrix} \lambda_k & 1 & 0 & \dots & 0 \\ 0 & \lambda_k & 1 & \dots & 0 \\ 0 & 0 & \lambda_k & \dots & 0 \\ \vdots & & & & \\ 0 & 0 & 0 & \dots & 1 \\ 0 & 0 & 0 & \dots & \lambda_k \end{bmatrix}. \tag{8.123}$$

The matrix $M^{-1}A M$ is then the general Jordan form, $M^{-1}A M = J$ where in the case of an eigenvalue λ_1 repeated m times and the rest are distinct eigenvalues

$$J = \begin{bmatrix} B_{11}(\lambda_1) & & & & & & \\ & B_{21}(\lambda_1) & & & & & \\ & & \ddots & & & & \\ & & & B_{m1}(\lambda_1) & & & \\ & & & & B_{12}(\lambda_2) & & \\ & & & & & \ddots & \\ & & & & & & B_{rs}(\lambda_s) \end{bmatrix}. \tag{8.124}$$

We note that the Jordan block corresponding to a *distinct* eigenvalue λ_i reduces to one element, namely, λ_i along the diagonal, so that the matrix J is simply the diagonal matrix

$$J = \Lambda = \text{diag}(\lambda_1, \lambda_2, \dots, \lambda_n). \tag{8.125}$$

Example 8.12 *Identify the Jordan blocks of the matrix*

$$J = \begin{bmatrix} \lambda_1 & 1 & & & & \\ & \lambda_1 & 1 & & & \\ & & \lambda_1 & 0 & & \\ & & & \lambda_1 & 0 & \\ & & & & \lambda_2 & 0 \\ & & & & & \lambda_3 \end{bmatrix}.$$

We have two triangular matrices, each including a 1 on the off diagonal. The Jordan blocks are therefore

$$B_{11}(\lambda_1) = \begin{bmatrix} \lambda_1 & 1 \\ & \lambda_1 & 1 \\ & & \lambda_1 \end{bmatrix}, \quad B_{21}(\lambda_1) = \lambda_1$$

$$B_{12}(\lambda_2) = \lambda_2, \quad B_{13}(\lambda_3) = \lambda_3.$$

We have already seen above this Jordan form for the case of repeated eigenvalues and the corresponding flow diagram. Let x_i, t_2, \dots, t_n denote the column vectors of the matrix M , where x_i is the linearity independent eigenvector associated with the Jordan block $B_{ji}(\lambda_i)$ of the repeated eigenvalue λ_i . We have

$$M = [x_i \mid t_1 \mid t_2 \mid \dots \mid t_k \mid \dots] \tag{8.126}$$

$$A M = A[x_i \mid t_1 \mid t_2 \mid \dots \mid t_k \mid \dots] \tag{8.127}$$

$$M B_{ji}(\lambda_i) = [x_i \mid t_1 \mid t_2 \mid \dots \mid t_k \mid \dots] \begin{bmatrix} \lambda_i & 1 & & & & \\ & \lambda_i & 1 & & & \\ & & \lambda_i & 1 & & \\ & & & \ddots & \ddots & \\ & & & & \lambda_i & 1 \\ & & & & & \lambda_i \end{bmatrix} \tag{8.128}$$

$$= [\lambda_i x_i \mid \lambda_i t_1 + x_i \mid \lambda_i t_2 + t_1 \mid \dots \mid \lambda_i t_k + t_{k-1} \mid \dots]$$

$$M^{-1} A M = J = B_{ji}(\lambda_i), \text{ i.e. } A M = M B_{ji}(\lambda_i). \tag{8.129}$$

Hence

$$A x_i = \lambda_i x_i, \quad A t_1 = \lambda_i t_1 + x_i, \quad A t_2 = \lambda_i t_2 + t_1, \quad \dots, \quad A t_k = \lambda_i t_k + t_{k-1}. \tag{8.130}$$

The column vectors x_i, t_1, t_2, \dots are thus successively evaluated.

8.12 Circuit Analysis by Laplace Transform and State Variables

The following example illustrates circuit analysis by Laplace transform and state space representation.

Example 8.13 Referring to the electric circuit shown in Fig. 8.9, switch S_1 is closed at $t = 0$ with $v_c(0) = v_{c0} = 7$ volts. At $t = t_1 = 3s$ switch S_2 is closed. The voltage source $v_1(t)$ applies a constant voltage of $K = 10$ volts. Evaluate and plot the circuit outputs $y_1 = x_1$ and $y_2 = x_2$.

At $t = 0$, with S_1 closed and S_2 open, the voltage v_c across the capacitor is $v_{c0} = 7$ and the current i_2 is zero. $x_1(0) = v_{c0}$, $x_2(0) = 0$, $\dot{x}_2(0) = v_{c0}/L = v_{c0}/2$.

$$x_1 = (R_2 + R_3)x_2 + L\dot{x}_2 \tag{8.131}$$

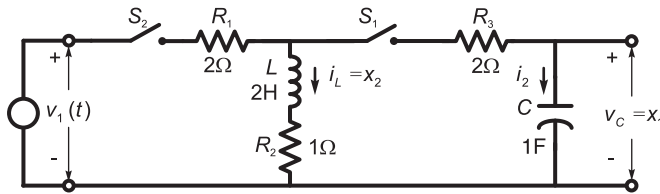


FIGURE 8.9 Electric circuit with two independent switches.

$$x_2 = -Cx_1 \tag{8.132}$$

$$\dot{x}_2 = \frac{1}{L}x_1 - \frac{(R_2 + R_3)}{L}x_2 \tag{8.133}$$

$$y_2 = i_L = x_2 \tag{8.134}$$

$$y_1 = v_c = x_1 \tag{8.135}$$

$$\begin{pmatrix} \dot{x}_1 \\ \dot{x}_2 \end{pmatrix} = \begin{pmatrix} 0 & -\frac{1}{C} \\ \frac{1}{L} & -\frac{(R_2 + R_3)}{L} \end{pmatrix} \begin{pmatrix} x_1 \\ x_2 \end{pmatrix} \tag{8.136}$$

$$y_2 = (0 \ 1) \begin{pmatrix} x_1 \\ x_2 \end{pmatrix} \tag{8.137}$$

$$y_1 = (1 \ 0) \begin{pmatrix} x_1 \\ x_2 \end{pmatrix} \tag{8.138}$$

$$A = \begin{bmatrix} 0 & -1 \\ 0.5 & -1.5 \end{bmatrix}$$

$$B = 0$$

$$C_1 = [1 \ 0], \quad C_2 = [0 \ 1]$$

$$\Phi(s) = (sI - A)^{-1} = \begin{bmatrix} s & 1 \\ -0.5 & s + 1.5 \end{bmatrix}^{-1} = \begin{bmatrix} s + 1.5 & -1 \\ 0.5 & s \end{bmatrix} / (s^2 + 1.5s + 0.5)$$

$$\begin{bmatrix} x_1(t) \\ x_2(t) \end{bmatrix} = \begin{bmatrix} \phi_{11}(t) & \phi_{12}(t) \\ \phi_{21}(t) & \phi_{22}(t) \end{bmatrix} \begin{bmatrix} x_1(0) \\ x_2(0) \end{bmatrix}$$

so that

$$\begin{aligned} x_1(t) &= \phi_{11}(t) x_1(0) = v_{c0} (2e^{-0.5t} - e^{-t}) u(t) \\ x_2(t) &= \phi_{21}(t) x_1(0) = v_{c0} (e^{-0.5t} - e^{-t}) u(t). \end{aligned}$$

Substituting $t = 3$ we obtain $v_C = x_1 = 4.8409$ volt, and $i_L = x_2 = 2.6492$ ampere. These are the initial conditions at the moment Switch S_2 is closed., which is now considered the instant $t = 0$. We write the new circuit equations. For $t > 0$ the output is the sum of the response due to the initial conditions plus that due to the input $v_1(t)$ applied at $t = 0$. We may write $v_1(t) = Ku(t)$.

The equations describing the voltage $v_c(t)$ and current $i_L(t)$ are

$$v_1(t) = R_1 i_1 + R_2 i_L + L \frac{di_L}{dt} \tag{8.139}$$

where

$$i_L = i_1 - i_2 \tag{8.140}$$

$$R_3 i_2 - R_2 i_L - L \frac{di_L}{dt} = -v_c(t). \tag{8.141}$$

With

$$x_1 = v_c(t), \quad x_2 = i_L(t) \tag{8.142}$$

we have

$$\begin{aligned} v_1(t) &= R_1 (i_L + i_2) + R_2 i_L + L \frac{di_L}{dt} = (R_1 + R_2) i_L + R_1 C \frac{dv_c}{dt} + L \frac{di_L}{dt} \\ &= (R_1 + R_2) x_2 + R_1 C \dot{x}_1 + L \dot{x}_2 \end{aligned} \tag{8.143}$$

and

$$R_3 C \dot{x}_1 - R_2 x_2 - L \dot{x}_2 + x_1 = 0. \tag{8.144}$$

The two equations imply that

$$\dot{x}_2 = \frac{1}{(R_1 + R_3)L} \{R_1 x_1 - (R_1 R_3 + R_2 R_3 + R_1 R_2) x_2 + R_3 v_1(t)\} \tag{8.145}$$

$$\dot{x}_1 = \frac{1}{(R_1 + R_3)C} \{-x_1 - R_1 x_2 + v_1(t)\} \tag{8.146}$$

$$\begin{pmatrix} \dot{x}_1 \\ \dot{x}_2 \end{pmatrix} = \begin{pmatrix} \frac{-1}{(R_1 + R_3)C} & \frac{-R_1}{(R_1 + R_3)C} \\ \frac{R_1}{(R_1 + R_3)L} & \frac{-(R_1 R_3 + R_2 R_3 + R_1 R_2)}{(R_1 + R_3)L} \end{pmatrix} \begin{pmatrix} x_1 \\ x_2 \end{pmatrix} + \begin{pmatrix} \frac{1}{(R_1 + R_3)C} \\ \frac{R_3}{(R_1 + R_3)L} \end{pmatrix} v_1(t)$$

$$y_1(t) = v_c(t) = x_1 \tag{8.147}$$

$$y_2 = i_L = x_2. \tag{8.148}$$

$$A = \begin{bmatrix} -0.25 & -0.5 \\ 0.25 & -1 \end{bmatrix}$$

$$B = \begin{bmatrix} 0.25 \\ 0.25 \end{bmatrix}, \quad C_1 = [1 \ 0], \quad C_2 = [0 \ 1], \quad D = 0.$$

We may write

$$\begin{bmatrix} \dot{x}_1(t) \\ \dot{x}_2(t) \end{bmatrix} = \begin{bmatrix} b_1 & b_2 \\ a_1 & a_2 \end{bmatrix} \begin{bmatrix} x_1(t) \\ x_2(t) \end{bmatrix} + \begin{bmatrix} b_3 \\ a_3 \end{bmatrix} v_1(t) = Ax + Bv_1$$

where $b_1 = a_{11}$, $b_2 = a_{12}$, $b_3 = b_{11}$, $a_1 = a_{21}$, $a_2 = a_{22}$, $a_3 = b_{21}$

$$X(s) = \Phi(s)x(0) + \Phi(s)BU(s)$$

$$\Phi(s) = (sI - A)^{-1} = \begin{bmatrix} s - a_2 & b_2 \\ a_1 & s - b_1 \end{bmatrix} / [s^2 - (a_2 + b_1)s + a_1b_2]$$

obtaining

$$X_1(s) = \frac{b_2x_2(0^+) + (s - a_2)x_1(0^+)}{(s - p_1)(s - p_2)} + \frac{b_2a_3 + (s - a_2)b_3}{(s - p_1)(s - p_2)}U_1(s) \quad (8.149)$$

where

$$p_1, p_2 = \left[a_2 + b_1 \pm \sqrt{a_2^2 + 2a_2b_1 + b_1^2 - 4a_1b_2} \right] / 2. \quad (8.150)$$

With $v_1(t) = Ku(t)$, $U_1(s) = K/s$

$$X_1(s) = \frac{F}{s - p_1} + \frac{G}{s - p_2} + \left\{ \frac{H}{s} + \frac{I}{s - p_1} + \frac{J}{s - p_2} \right\} K \quad (8.151)$$

$$F = [b_2x_2(0^+) + (p_1 - a_2)x_1(0^+)] / [p_1 - p_2] \quad (8.152)$$

$$G = [b_2x_2(0^+) + (p_2 - a_2)x_1(0^+)] / [p_2 - p_1] \quad (8.153)$$

$$H = [b_2a_3 - a_2b_3] / [p_1p_2] \quad (8.154)$$

$$I = [b_2a_3 + (p_1 - a_2)b_3] / [p_1(p_1 - p_2)] \quad (8.155)$$

$$J = [b_2a_3 + (p_2 - a_2)b_3] / [p_2(p_2 - p_1)] \quad (8.156)$$

$$X_2(s) = \frac{(s - b_1)x_2(0^+) + a_1x_1(0^+)}{(s - p_1)(s - p_2)} + \frac{(s - b_1)a_3 + a_1b_3}{(s - p_1)(s - p_2)}U_1(s). \quad (8.157)$$

With $U_1(s) = K/s$

$$X_2(s) = \frac{A}{s - p_1} + \frac{B}{s - p_2} + \left\{ \frac{C}{s} + \frac{D}{s - p_1} + \frac{E}{s - p_2} \right\} K \quad (8.158)$$

where

$$A = [(p_1 - b_1)x_2(0^+) + a_1x_1(0^+)] / [p_1 - p_2] \quad (8.159)$$

$$B = [(p_2 - b_1)x_2(0^+) + a_1x_1(0^+)] / [p_2 - p_1] \quad (8.160)$$

$$C = [-b_1a_3 + a_1b_3] / [p_1p_2] \quad (8.161)$$

$$D = [(p_1 - b_1)a_3 + a_1b_3] / [p_1(p_1 - p_2)] \quad (8.162)$$

$$E = [(p_2 - b_1)a_3 + a_1b_3] / [p_2(p_2 - p_1)]. \quad (8.163)$$

$$y_1(t) = x_1(t) = [\{Fe^{p_1t} + Ge^{p_2t}\} + \{H + Ie^{p_1t} + Je^{p_2t}\}K]u(t) \quad (8.164)$$

$$y_2(t) = x_2(t) = [\{Ae^{p_1t} + Be^{p_2t}\} + \{C + De^{p_1t} + Ee^{p_2t}\}K]u(t). \quad (8.165)$$

The following MATLAB[®] program illustrates the solution of the state space model from the moment switch S_2 is closed, taking into account the initial conditions of the capacitor voltage and the inductor current at that moment.

```
x10=vc0=4.8409
x20=iL0=2.6492
a11=-1/((R1+R3)*C)
a12=-R1/((R1+R3)*C)
a21=R1/((R1+R3)*L)
a22=-(R1*R3+R2*R3+R1*R2)/((R1+R3)*L)
A=[a11 a12; a21 a22]
b11=1/((R1+R3)*C)
b21=R3/((R1+R3)*L)
B=[b11 ; b21]
CC1=[1 0]
CC2=[0 1]
D=0
x0=[x10,x20]
t=0:0.01:10;
K=10
u=K*ones(length(t),1);
y1=lsim(A,B,CC1,D,u,t,x0);
y2=lsim(A,B,CC2,D,u,t,x0);
```

The state variables' evolution of state variables $x_1(t)$ and $x_2(t)$ once switch S_2 is closed is shown in Fig. 8.10.

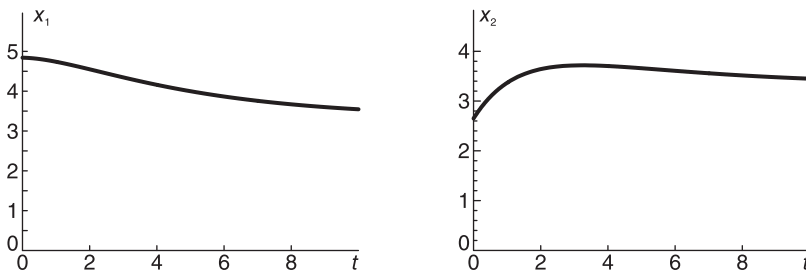


FIGURE 8.10 State variables $x_1(t)$ and $x_2(t)$ as a function of time.

8.13 Trajectories of a Second Order System

The trajectory of a system can be represented as a plot of state variable x_2 versus x_1 in the phase plane $x_1 - x_2$ or z_2 versus z_1 in the $z_1 - z_2$ phase plane as t increases as an implicit parameter from an initial value t_0 . The form of the trajectory depends on whether the eigenvalues are real or complex, of the same or opposite sign, and on their relative values.

As we have seen the matrix J has an off-diagonal element if $\lambda_1 = \lambda_2$, i.e.

$$\begin{bmatrix} \dot{z}_1 \\ \dot{z}_2 \end{bmatrix} = \begin{bmatrix} \lambda & 1 \\ 0 & \lambda \end{bmatrix} \begin{bmatrix} z_1 \\ z_2 \end{bmatrix} \quad (8.166)$$

if λ_1 and λ_2 are complex, we may write:

$$\lambda_{1,2} = -\zeta\omega_0 \pm j\omega_0\sqrt{1-\zeta^2}. \quad (8.167)$$

Below we view the trajectories that result in each of these cases.

Example 8.14 The matrices of a system state space model $\dot{x} = Ax + Bv$, $y = Cx + Dv$ are given by

$$A = \begin{bmatrix} 0 & 1 \\ -20 & -9 \end{bmatrix}, \quad B = \begin{bmatrix} 0 \\ 1 \end{bmatrix}, \quad C = [0 \ 1].$$

a) Assuming the initial conditions $x(0) = \begin{bmatrix} 1 \\ 0 \end{bmatrix}$ and $v(t) = u(t-2)$, evaluate the system output $y(t)$.

b) With the initial conditions $x(0) = \begin{bmatrix} 1 \\ 1 \end{bmatrix}$ and $v(t) = 0$ sketch the system trajectory in the $z_1 - z_2$ plane of the same system equivalent model

$$\dot{z} = Jz$$

where $x = Tz$ and

$$J = T^{-1}AT = \begin{bmatrix} \lambda_1 & 0 \\ 0 & \lambda_2 \end{bmatrix}.$$

$$\Phi(s) = (sI - A)^{-1} = \begin{bmatrix} s & -1 \\ 20 & s+9 \end{bmatrix}^{-1} = \frac{\begin{bmatrix} s+9 & 1 \\ -20 & s \end{bmatrix}}{s^2 + 9s + 20}$$

$$\phi(t) = \begin{bmatrix} \phi_{11}(t) & \phi_{12}(t) \\ \phi_{21}(t) & \phi_{22}(t) \end{bmatrix}$$

$$\begin{aligned} y(t) &= C\phi(t)x(0) + C\phi(t)B * v(t) = [0 \ 1] \phi(t) \begin{bmatrix} 1 \\ 0 \end{bmatrix} + [0 \ 1] \phi(t) \begin{bmatrix} 0 \\ 1 \end{bmatrix} * u(t-2) \\ &= [0 \ 1] \begin{bmatrix} \phi_{11}(t) \\ \phi_{21}(t) \end{bmatrix} + \phi_{22}(t) * u(t-2) = \phi_{21}(t) + \phi_{22}(t) * u(t-2) \end{aligned}$$

$$\phi_{21}(t) = \mathcal{L}^{-1} \left[\frac{-20}{s^2 + 9s + 20} \right] = \mathcal{L}^{-1} \left[\frac{-20}{(s+4)(s+5)} \right] = (20e^{-5t} - 20e^{-4t})u(t)$$

$$\phi_{22}(t) = \mathcal{L}^{-1} \left[\frac{s}{(s+4)(s+5)} \right] = (5e^{-5t} - 4e^{-4t})u(t)$$

$$\begin{aligned} \phi_{22}(t) * u(t-2) &= \int_{-\infty}^{\infty} (5e^{-5\tau} - 4e^{-4\tau})u(\tau)u(t-\tau-2)d\tau \\ &= \left\{ \int_0^{t-2} (5e^{-5\tau} - 4e^{-4\tau})d\tau \right\} u(t-2) = \{e^{-4(t-2)} - e^{-5(t-2)}\} u(t-2) \end{aligned}$$

$$y(t) = (20e^{-5t} - 20e^{-4t})u(t) + \{e^{-4(t-2)} - e^{-5(t-2)}\}u(t-2).$$

b) $z = T^{-1}x$, $J = T^{-1}AT$

$$\det(\lambda I - A) = 0, \quad \lambda(\lambda + 9) + 20 = 0; \quad \text{hence } \lambda_1 = -5, \quad \lambda_2 = -4$$

$$J = \begin{bmatrix} -5 & 0 \\ 0 & -4 \end{bmatrix}, \quad T = \begin{bmatrix} t_{11} & t_{12} \\ t_{21} & t_{22} \end{bmatrix}$$

where $\begin{bmatrix} t_{11} \\ t_{21} \end{bmatrix}$ and $\begin{bmatrix} t_{12} \\ t_{22} \end{bmatrix}$ are the eigenvectors of A , i.e.

$$A \begin{bmatrix} t_{11} \\ t_{21} \end{bmatrix} = \lambda_1 \begin{bmatrix} t_{11} \\ t_{21} \end{bmatrix}, \quad (\lambda_1 I - A) \begin{bmatrix} t_{11} \\ t_{21} \end{bmatrix} = 0$$

$$\begin{bmatrix} -5 & -1 \\ 20 & 4 \end{bmatrix} \begin{bmatrix} t_{11} \\ t_{21} \end{bmatrix} = 0, \quad \text{i.e.} \quad \begin{bmatrix} t_{11} \\ t_{21} \end{bmatrix} = \begin{bmatrix} 1 \\ -5 \end{bmatrix}$$

$$\begin{bmatrix} -4 & -1 \\ 20 & 5 \end{bmatrix} \begin{bmatrix} t_{12} \\ t_{22} \end{bmatrix} = 0, \quad \text{i.e.} \quad \begin{bmatrix} t_{12} \\ t_{22} \end{bmatrix} = \begin{bmatrix} 1 \\ -4 \end{bmatrix}.$$

Therefore $T = \begin{bmatrix} 1 & 1 \\ -5 & 4 \end{bmatrix}$, $T^{-1} = \begin{bmatrix} -4 & -1 \\ 5 & 1 \end{bmatrix}$

$$\dot{z} = Jz = \begin{bmatrix} -5 & 0 \\ 0 & -4 \end{bmatrix} z, \quad \begin{bmatrix} \dot{z}_1 \\ \dot{z}_2 \end{bmatrix} = \begin{bmatrix} -5 & 0 \\ 0 & -4 \end{bmatrix} \begin{bmatrix} z_1 \\ z_2 \end{bmatrix}$$

$$z(0) = T^{-1}x(0) = \begin{bmatrix} -4 & -1 \\ 5 & 1 \end{bmatrix} \begin{bmatrix} 1 \\ 1 \end{bmatrix} = \begin{bmatrix} -5 \\ 6 \end{bmatrix}$$

$$\dot{z}_1 + 5z_1 = 0, \quad sZ_1(s) - z_1(0) + 5Z_1(s) = 0,$$

$$Z_1(s) = \frac{z_1(0)}{s + 5}, \quad z_1(t) = z_1(0)e^{-5t}u(t) = -5e^{-5t}u(t)$$

$$z_2(t) = z_2(0)e^{-4t}u(t) = 6e^{-4t}u(t).$$

See Fig. 8.11.

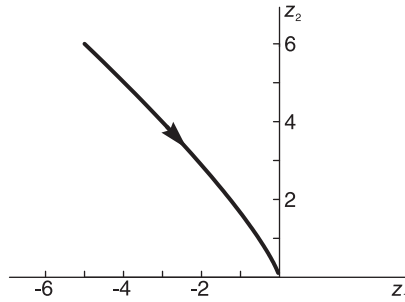


FIGURE 8.11 Trajectory in $z_1 - z_2$ plane.

8.14 Second Order System Modeling

A second order system, as we have seen, may be described by the system function:

$$H(s) = \frac{Y(s)}{U(s)} = \frac{1}{s^2 + 2\zeta\omega_0 s + \omega_0^2} \tag{8.168}$$

$$s^2Y(s) = -2\zeta\omega_0sY(s) - \omega_0^2Y(s) + U(s). \tag{8.169}$$

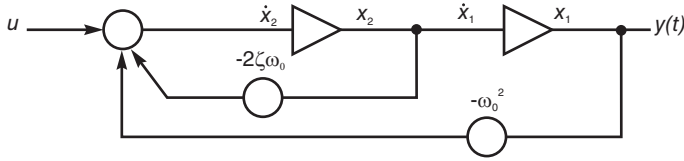


FIGURE 8.12 Second order system.

We shall use a simple triangle as a symbol denoting an integrator. Connecting two integrators in cascade and labeling their outputs x_1 and x_2 , we obtain Fig. 8.12. We may write

$$x_1 = y, \quad \dot{x}_1 = x_2, \quad \dot{x}_2 = \ddot{y} = -2\zeta\omega_0\dot{y} - \omega_0^2y + u \tag{8.170}$$

$$\dot{x}_2 = -2\zeta\omega_0\dot{x}_1 - \omega_0^2x_1 + u = -2\zeta\omega_0x_2 - \omega_0^2x_1 + u. \tag{8.171}$$

The state space equations are therefore

$$\begin{bmatrix} \dot{x}_1 \\ \dot{x}_2 \end{bmatrix} = \begin{bmatrix} 0 & 1 \\ -\omega_0^2 & -2\zeta\omega_0 \end{bmatrix} \begin{bmatrix} x_1 \\ x_2 \end{bmatrix} + \begin{bmatrix} 0 \\ 1 \end{bmatrix} u = Ax + Bu \tag{8.172}$$

$$y = [1 \ 0] \begin{bmatrix} x_1 \\ x_2 \end{bmatrix} = Cx. \tag{8.173}$$

The system poles are the eigenvalues, that is, the roots of the equation

$$|A - \lambda I| = 0 \tag{8.174}$$

$$\begin{vmatrix} -\lambda & 1 \\ -\omega_0^2 & -2\zeta\omega_0 - \lambda \end{vmatrix} = \lambda^2 + 2\zeta\omega_0\lambda + \omega_0^2 = 0 \tag{8.175}$$

$$\lambda_1, \lambda_2 = \left\{ -2\zeta\omega_0 \pm \sqrt{4\zeta^2\omega_0^2 - 4\omega_0^2} \right\} / 2 = -\zeta\omega_0 \pm \omega_0\sqrt{\zeta^2 - 1} = -\zeta\omega_0 \pm \omega_p \tag{8.176}$$

where $\omega_p = \omega_0\sqrt{\zeta^2 - 1}$. To evaluate the eigenvectors, we have the following cases:

Case 1: Distinct real poles $\lambda_1 \neq \lambda_2$.

Let $p^{(1)}$ and $p^{(2)}$ be the eigenvectors. By definition

$$\lambda_1 p^{(1)} = Ap^{(1)}, \quad \lambda_2 p^{(2)} = Ap^{(2)} \tag{8.177}$$

$$\lambda_1 \begin{bmatrix} p_1^{(1)} \\ p_2^{(1)} \end{bmatrix} = \begin{bmatrix} 0 & 1 \\ -\omega_0^2 & -2\zeta\omega_0 \end{bmatrix} \begin{bmatrix} p_1^{(1)} \\ p_2^{(1)} \end{bmatrix} \tag{8.178}$$

$\lambda_1 p_1^{(1)} = p_2^{(1)}$. Choosing $p_1^{(1)} = 1$ we have $p_2^{(1)} = \lambda_1$

$$\lambda_1 p_2^{(1)} = -\omega_0^2 p_1^{(1)} - 2\zeta\omega_0 p_2^{(1)} \tag{8.179}$$

i.e. $\lambda_1^2 + 2\zeta\omega_0\lambda_1 + \omega_0^2 = 0$ as it should. Similarly, $p_1^{(2)} = 1$ and $p_2^{(2)} = \lambda_2$. The equivalent Jordan form is $\dot{z} = Jz$ where J is the diagonal matrix

$$J = T^{-1}AT \tag{8.180}$$

$$T = [p^{(1)} \ p^{(2)}] = \begin{bmatrix} 1 & 1 \\ \lambda_1 & \lambda_2 \end{bmatrix}, \quad T^{-1} = \begin{bmatrix} \lambda_2 & -1 \\ -\lambda_1 & 1 \end{bmatrix} \frac{1}{(\lambda_2 - \lambda_1)} \quad (8.181)$$

$$J = \begin{bmatrix} \lambda_1 & 0 \\ 0 & \lambda_2 \end{bmatrix}, \quad \begin{bmatrix} \dot{z}_1 \\ \dot{z}_2 \end{bmatrix} = \begin{bmatrix} \lambda_1 & 0 \\ 0 & \lambda_2 \end{bmatrix} \begin{bmatrix} z_1 \\ z_2 \end{bmatrix}, \quad Q(t) = \begin{bmatrix} e^{\lambda_1 t} & 0 \\ 0 & e^{\lambda_2 t} \end{bmatrix} \quad (8.182)$$

$$\begin{aligned} \phi(t) &= T Q T^{-1} = \begin{bmatrix} 1 & 1 \\ \lambda_1 & \lambda_2 \end{bmatrix} \begin{bmatrix} e^{\lambda_1 t} & 0 \\ 0 & e^{\lambda_2 t} \end{bmatrix} \begin{bmatrix} \lambda_2 & -1 \\ -\lambda_1 & 1 \end{bmatrix} \frac{1}{(\lambda_2 - \lambda_1)} \\ &= \begin{bmatrix} \lambda_2 e^{\lambda_1 t} - \lambda_1 e^{\lambda_2 t} & -e^{\lambda_1 t} + e^{\lambda_2 t} \\ \lambda_1 \lambda_2 e^{\lambda_1 t} - \lambda_1 \lambda_2 e^{\lambda_2 t} & -\lambda_1 e^{\lambda_1 t} + \lambda_2 e^{\lambda_2 t} \end{bmatrix} \frac{1}{(\lambda_2 - \lambda_1)} \end{aligned} \quad (8.183)$$

which can alternatively be evaluated as

$$\phi(t) = \mathcal{L}^{-1}[\Phi(s)], \quad \Phi(s) = (sI - A)^{-1}. \quad (8.184)$$

Case 2: Equal eigenvalues $\lambda_1 = \lambda_2$ (double pole).

If $\zeta = 1$, $\lambda_1, \lambda_2 = -\omega_0$. The eigenvectors denoted p and q should satisfy the equations

$$Ap = \lambda p \quad (8.185)$$

$$Aq = \lambda q + p \quad (8.186)$$

$$\begin{bmatrix} 0 & 1 \\ -\omega_0^2 & -2\omega_0 \end{bmatrix} \begin{bmatrix} p_1 \\ p_2 \end{bmatrix} = -\omega_0 \begin{bmatrix} p_1 \\ p_2 \end{bmatrix} \quad (8.187)$$

$p_2 = -\omega_0 p_1$. Taking $p_1 = 1$ we have $p_2 = -\omega_0$.

$$q_2 = -\omega_0 q_1 + p_1 = -\omega_0 q_1 + 1. \quad (8.188)$$

Choosing $q_1 = 0$ we have $q_2 = 1$, wherefrom

$$T = [p \ q] = \begin{bmatrix} 1 & 0 \\ -\omega_0 & 1 \end{bmatrix}, \quad T^{-1} = \begin{bmatrix} 1 & 0 \\ \omega_0 & 1 \end{bmatrix} \quad (8.189)$$

$$J = T^{-1} A T = \begin{bmatrix} -\omega_0 & 1 \\ 0 & -\omega_0 \end{bmatrix} = \begin{bmatrix} \lambda & 1 \\ 0 & \lambda \end{bmatrix} \quad (8.190)$$

$$\begin{aligned} Q(s) &= (sI - J)^{-1} = \begin{bmatrix} s - \lambda & -1 \\ 0 & s - \lambda \end{bmatrix}^{-1} = \begin{bmatrix} s - \lambda & 1 \\ 0 & s - \lambda \end{bmatrix} \frac{1}{(s - \lambda)^2} \\ &= \begin{bmatrix} 1/(s - \lambda) & 1/(s - \lambda)^2 \\ 0 & 1/(s - \lambda) \end{bmatrix} = \begin{bmatrix} e^{\lambda t} & t e^{\lambda t} \\ 0 & e^{\lambda t} \end{bmatrix} u(t) \end{aligned} \quad (8.191)$$

and

$$\phi(t) = \mathcal{L}^{-1} [(sI - A)^{-1}] = T Q T^{-1}. \quad (8.192)$$

Case 3: Complex poles (complex eigenvalues) i.e. $\zeta < 1$.

$$\lambda_1, \lambda_2 = -\zeta \omega_0 \pm j \omega_p \triangleq -\alpha \pm j \omega_p, \quad \alpha = \zeta \omega_0, \quad \omega_p = \omega_0 \sqrt{1 - \zeta^2} \quad (8.193)$$

$$\lambda_2 = \lambda_1^*. \quad (8.194)$$

As found above we have

$$T = \begin{bmatrix} 1 & 1 \\ \lambda_1 & \lambda_2 \end{bmatrix}, \quad T^{-1} = \begin{bmatrix} \lambda_2 & -1 \\ -\lambda_1 & 1 \end{bmatrix} \frac{1}{(\lambda_2 - \lambda_1)} = \begin{bmatrix} \lambda_2 & -1 \\ -\lambda_1 & 1 \end{bmatrix} \frac{1}{-j2\omega_p} \quad (8.195)$$

$$J = \begin{bmatrix} \lambda_1 & 0 \\ 0 & \lambda_2 \end{bmatrix}, \quad Q(t) = \begin{bmatrix} e^{\lambda_1 t} & 0 \\ 0 & e^{\lambda_2 t} \end{bmatrix} \quad (8.196)$$

$$\phi(t) = T Q T^{-1}. \quad (8.197)$$

With zero input and initial conditions $x(0)$

$$x(t) = \phi(t)x(0) \quad (8.198)$$

$$z(t) = Q(t)z(0) \quad (8.199)$$

$$z(t) = T^{-1}x(t) \quad (8.200)$$

$$z(0) = T^{-1}x(0) \quad (8.201)$$

$$\phi = T Q T^{-1} = \begin{bmatrix} \lambda_2 e^{\lambda_1 t} - \lambda_1 e^{\lambda_2 t} & -e^{\lambda_1 t} + e^{\lambda_2 t} \\ \lambda_1 \lambda_2 e^{\lambda_1 t} - \lambda_1 \lambda_2 e^{\lambda_2 t} & -\lambda_1 e^{\lambda_1 t} + \lambda_2 e^{\lambda_2 t} \end{bmatrix} \frac{1}{-j2\omega_p}. \quad (8.202)$$

Writing $\lambda_1 = |\lambda_1| e^{j\angle\lambda_1} = \omega_0 e^{j(\pi-\theta)}$ where $\theta = \cos^{-1} \zeta$, $\lambda_2 = \omega_0 e^{-j\angle\lambda_1} = \omega_0 e^{-j(\pi-\theta)}$

$$\begin{aligned} \phi_{11}(t) &= \left\{ \omega_0 e^{-j(\pi-\theta)} e^{(-\alpha+j\omega_p)t} - \omega_0 e^{j(\pi-\theta)} e^{(-\alpha-j\omega_p)t} \right\} \frac{1}{-j2\omega_p} \\ &= \frac{\omega_0 e^{-\alpha t}}{j2\omega_p} \left\{ e^{j(\omega_p t + \theta)} - e^{-j(\omega_p t + \theta)} \right\} = \frac{\omega_0}{\omega_p} e^{-\alpha t} \sin(\omega_p t + \theta). \end{aligned} \quad (8.203)$$

Similarly,

$$\phi_{12}(t) = (1/\omega_p) e^{-\alpha t} \sin \omega_p t \quad (8.204)$$

$$\phi_{21}(t) = (-\omega_0^2/\omega_p) e^{-\alpha t} \sin \omega_p t \quad (8.205)$$

$$\phi_{22}(t) = (-\omega_0/\omega_p) e^{-\alpha t} \sin(\omega_p t - \theta) \quad (8.206)$$

$$\phi(t) = \begin{bmatrix} (\omega_0/\omega_p) e^{-\alpha t} \sin(\omega_p t + \theta) & (1/\omega_p) e^{-\alpha t} \sin \omega_p t \\ (-\omega_0^2/\omega_p) e^{-\alpha t} \sin \omega_p t & (-\omega_0/\omega_p) e^{-\alpha t} \sin(\omega_p t - \theta) \end{bmatrix} u(t). \quad (8.207)$$

Trajectories

We have found that in case 1, where λ_1 and λ_2 are real and distinct, we have

$$z_1 = z_1(0) e^{\lambda_1 t} \quad (8.208)$$

$$z_2 = z_2(0) e^{\lambda_2 t}. \quad (8.209)$$

If $\lambda_2 < \lambda_1 < 0$ then z_2 decays faster than z_1 and the system trajectories appear as in Fig. 8.13. Each trajectory corresponds to and has as initial point a distinct initial condition.

If the two poles are closer so that λ_2 approaches λ_1 then z_1 and z_2 decay at about the same rate. With $\lambda_1 = \lambda_2$ the trajectories appear as in Fig. 8.14.

If on the other hand $\lambda_1 > 0$ and $\lambda_2 < 0$ then z_1 grows while z_2 decays and the trajectories appear as in Fig. 8.15.

The case of complex conjugate poles leads to z_1 and z_2 expressed in terms of complex exponentials. The trajectories are instead plotted in the $x_1 - x_2$ plane. We have

$$x(t) = \phi(t)x(0) = \begin{bmatrix} \phi_{11} & \phi_{12} \\ \phi_{21} & \phi_{22} \end{bmatrix} \begin{bmatrix} x_1(0) \\ x_2(0) \end{bmatrix}. \quad (8.210)$$

Substituting the values of ϕ_{11} , ϕ_{12} , ϕ_{21} and ϕ_{22} given above it can be shown that $x_1(t)$ and $x_2(t)$ can be expressed in the form

$$x_1(t) = A_1 x_1(0) e^{-\alpha t} \cos(\omega_p t + \gamma_1) \quad (8.211)$$

$$x_2(t) = A_2 x_2(0) e^{-\alpha t} \cos(\omega_p t + \gamma_2) \quad (8.212)$$

where A_1 and A_2 are constants.

The trajectory has in general the form of a spiral, converging toward the origin if $0 < \zeta < 1$, as shown in Fig. 8.16, and diverging outward if $\zeta < 0$ as shown in Fig. 8.17. If $\zeta = 0$ the trajectories have in general the form of ellipses as shown in Fig. 8.18, and become circles if the phase difference $\gamma_1 - \gamma_2 = \pm\pi/2$.

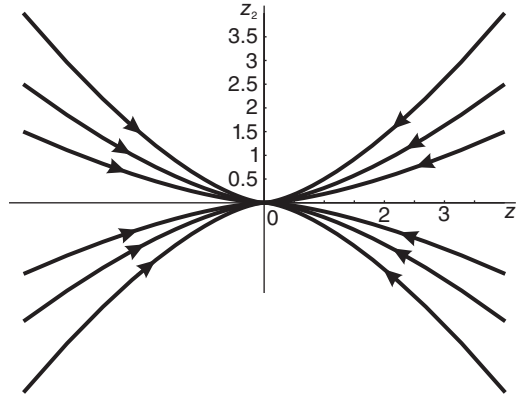


FIGURE 8.13 Set of trajectories in $z_1 - z_2$ plane.

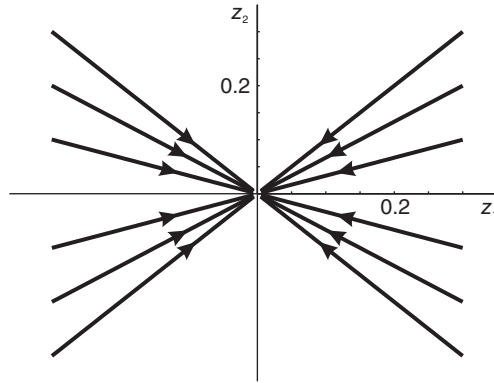


FIGURE 8.14 Trajectories in the case $\lambda_1 = \lambda_2$.

8.15 Transformation of Trajectories between Planes

Knowing the form of the system trajectories in the $z_1 - z_2$ plane we can deduce their form in the $x_1 - x_2$ plane. To this end, in the $x_1 - x_2$ plane we draw the two straight lines, passing through the origin that represent the axes z_1 and z_2 . The trajectories are then skewed to appear as they should be on skewed axes z_1 and z_2 which are not perpendicular to each other in the $x_1 - x_2$ plane. The following example illustrates the approach.

Example 8.15 For the system described by the state equations $\dot{x} = Ax + Bu$, where

$$A = \begin{bmatrix} -3 & -1 \\ 2 & 0 \end{bmatrix}, \quad B = \begin{bmatrix} -2 \\ 0 \end{bmatrix}$$

sketch the trajectories with zero input $u(t)$ in the $z_1 - z_2$ plane of the equivalent Jordan model $\dot{z} = Jz$. Show how the z_1 and z_2 axes appear in the $x_1 - x_2$ plane and sketch the trajectories as they are transformed from the $z_1 - z_2$ plane to the $x_1 - x_2$ plane.

We have

$$|\lambda I - A| = 0, \quad \lambda^2 + 3\lambda + 2 = (\lambda + 1)(\lambda + 2) = 0$$

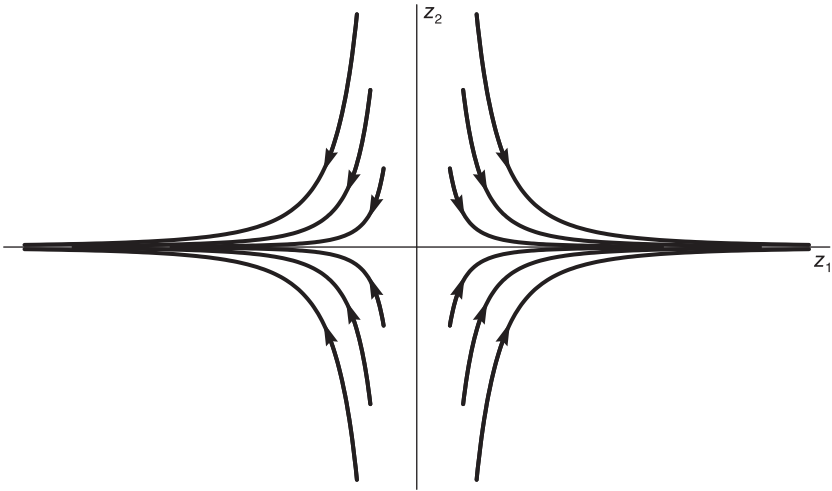


FIGURE 8.15 Trajectories in the case $\lambda_1 > 0$ and $\lambda_2 < 0$.

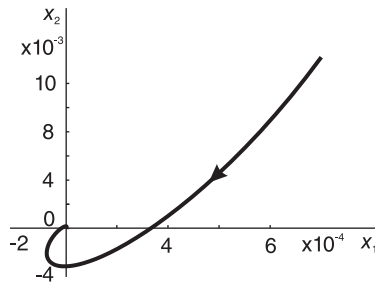


FIGURE 8.16 A trajectory in the case of complex conjugate poles and $0 < \zeta < 1$.

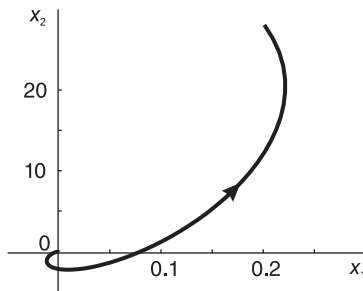


FIGURE 8.17 Diverging spiral-type trajectory.

$$\lambda_1, \lambda_2 = -1, -2$$

$$J = \begin{bmatrix} -1 & 0 \\ 0 & -2 \end{bmatrix}, \quad \dot{z} = Jz = \begin{bmatrix} -1 & 0 \\ 0 & -2 \end{bmatrix} \begin{bmatrix} z_1 \\ z_2 \end{bmatrix}$$

$$z_1 = z_1(0)e^{-t}, \quad z_2 = z_2(0)e^{-2t}.$$

The trajectories are shown in Fig. 8.19.

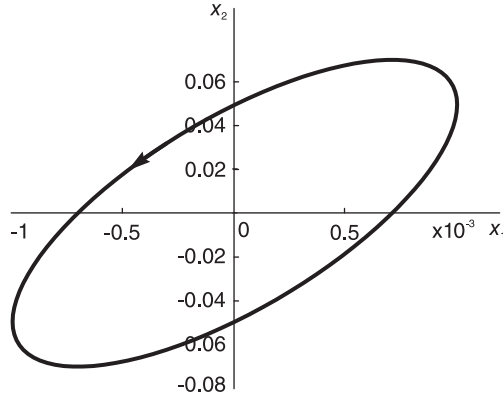


FIGURE 8.18 Trajectory in the case of complex conjugate poles and $\zeta = 0$.

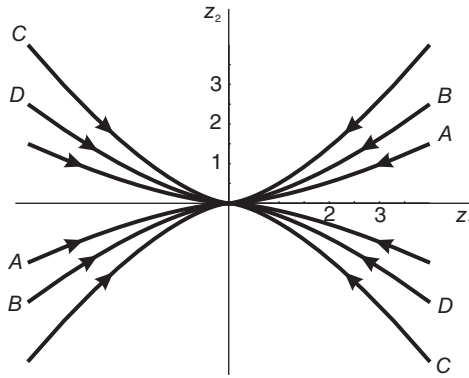


FIGURE 8.19 Trajectories in $z_1 - z_2$ plane.

The eigenvectors $p^{(1)}$ and $p^{(2)}$ are reduced from $\lambda_1 p^{(1)} = Ap^{(1)}$, $\lambda_2 p^{(2)} = Ap^{(2)}$. We obtain

$$p^{(1)} = \begin{bmatrix} 1 \\ -2 \end{bmatrix}, \quad p^{(2)} = \begin{bmatrix} 1 \\ -1 \end{bmatrix} \tag{8.213}$$

wherefrom

$$T = [p^{(1)} \ p^{(2)}] = \begin{bmatrix} 1 & 1 \\ -2 & -1 \end{bmatrix}, \quad T^{-1} = \begin{bmatrix} -1 & -1 \\ 2 & 1 \end{bmatrix} \tag{8.214}$$

and

$$T^{-1}AT = J \tag{8.215}$$

as it should.

For the axes transformation to the $x_1 - x_2$ plane we have $z = T^{-1}x$

$$\begin{bmatrix} z_1 \\ z_2 \end{bmatrix} = \begin{bmatrix} -1 & -1 \\ 2 & 1 \end{bmatrix} \begin{bmatrix} x_1 \\ x_2 \end{bmatrix} \tag{8.216}$$

$$z_1 = -x_1 - x_2 \tag{8.217}$$

$$z_2 = 2x_1 + x_2. \tag{8.218}$$

For the axis z_1 we set $z_2 = 0$ obtaining the straight line equation $x_2 = -2x_1$. For the axis z_2 we set $z_1 = 0$ obtaining the straight line equation $x_2 = -x_1$.

The transformed axes are shown in the $x_1 - x_2$ plane in Fig. 8.20. The $z_1 - z_2$ plane trajectories are now skewed to fit into the four sectors created by the two inclined z_1 and z_2 axes in the $x_1 - x_2$ plane, as seen in the figure. In particular the trajectories in the $z_1 - z_2$ plane, labeled A–A, B–B, C–C and D–D in Fig. 8.19 are transformed into the same labeled trajectories, respectively, in the $x_1 - x_2$ plane, Fig. 8.20.

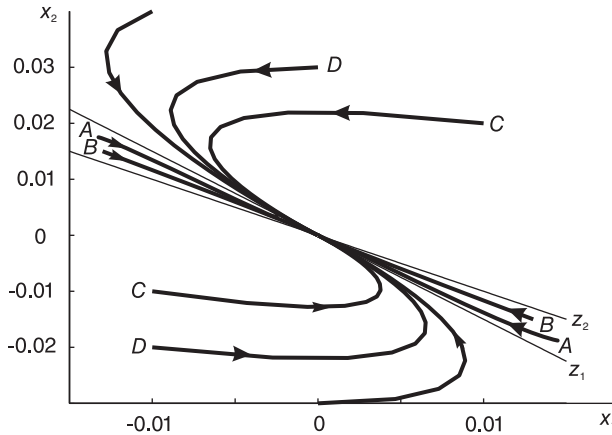


FIGURE 8.20 Trajectories in $x_1 - x_2$ plane.

8.16 Discrete-Time Systems

Similarly, a state space model is defined for discrete-time systems. Consider the system described by the linear difference equation with constant coefficients

$$\sum_{k=0}^N a_k y[n - k] = \sum_{k=0}^N b_k u[n - k] \tag{8.219}$$

and assume $a_0 = 1$ without loss of generality.

The system transfer function is obtained by z -transforming both sides. We have

$$\sum_{k=0}^N a_k z^{-k} Y(z) = \sum_{k=0}^N b_k z^{-k} U(z) \tag{8.220}$$

$$H(z) = \frac{Y(z)}{U(z)} = \frac{\sum_{k=0}^N b_k z^{-k}}{\sum_{k=0}^N a_k z^{-k}} = \frac{b_0 + b_1 z^{-1} + \dots + b_N z^{-N}}{a_0 + a_1 z^{-1} + \dots + a_N z^{-N}} = \frac{b_0 z^N + b_1 z^{N-1} + \dots + b_N}{a_0 z^N + a_1 z^{N-1} + \dots + a_N}$$

We can write

$$y[n] = - \sum_{k=1}^N a_k y[n-k] + \sum_{k=0}^N b_k u[n-k] \tag{8.221}$$

$$Y(z) = - \sum_{k=1}^N a_k z^{-k} Y(z) + \sum_{k=0}^N b_k z^{-k} U(z). \tag{8.222}$$

The flow diagram corresponding to these equations is shown in Fig. 8.21. The structure is referred to as the first canonical form. We will encounter similar structures in connection with digital filters.

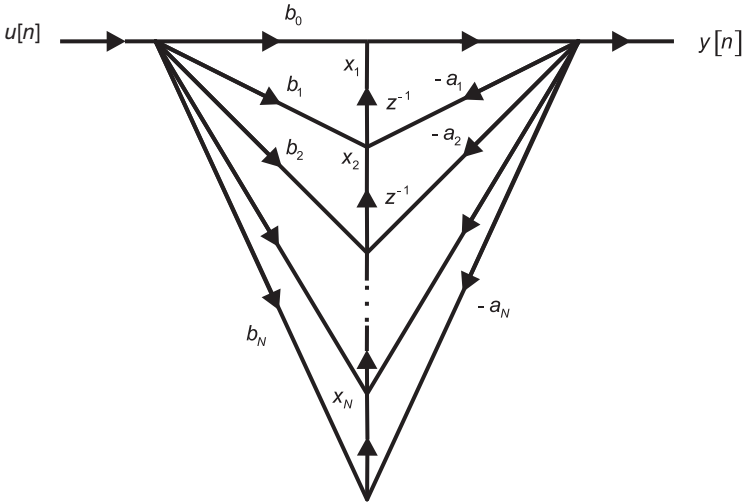


FIGURE 8.21 Discrete-time system state space model.

$$x_1[n+1] = x_2[n] + b_1 u[n] - a_1 y[n] \tag{8.223}$$

$$x_2[n+1] = x_3[n] + b_2 u[n] - a_2 y[n] \tag{8.224}$$

⋮

$$x_{N-1}[n+1] = x_N[n] + b_{N-1} u[n] - a_{N-1} y[n] \tag{8.225}$$

$$x_N[n+1] = - a_N y[n] + b_N u[n] \tag{8.226}$$

$$y[n] = x_1[n] + b_0 u[n] \tag{8.227}$$

$$\begin{aligned} x_1[n+1] &= x_2[n] + b_1 u[n] - a_1 x_1[n] - a_1 b_0 u[n] \\ &= - a_1 x_1[n] + x_2[n] + (b_1 - a_1 b_0) u[n] \end{aligned} \tag{8.228}$$

$$\begin{aligned} x_2[n+1] &= x_3[n] + b_2 u[n] - a_2 x_1[n] - a_2 b_0 u[n] \\ &= - a_2 x_1[n] + x_3[n] + (b_2 - a_2 b_0) u[n] \end{aligned} \tag{8.229}$$

⋮

$$\begin{aligned} x_{N-1}[n+1] &= x_N[n] + b_{N-1} u[n] - a_{N-1} x_1[n] - a_{N-1} b_0 u[n] \\ &= - a_{N-1} x_1[n] + x_N[n] + (b_{N-1} - a_{N-1} b_0) u[n] \end{aligned} \tag{8.230}$$

$$x_N[n+1] = -a_N x_1[n] - a_N b_0 u[n] + b_N u[n] = -a_N x_1[n] + (b_N - a_N b_0) u[n] \quad (8.231)$$

$$y[n] = x_1[n] + b_0 u[n] \quad (8.232)$$

$$\begin{bmatrix} x_1[n+1] \\ x_2[n+1] \\ \vdots \\ x_{N-1}[n+1] \\ x_N[n+1] \end{bmatrix} = \begin{bmatrix} -a_1 & 1 & 0 & \dots & 0 \\ -a_2 & 0 & 1 & \dots & 0 \\ \vdots & & & & \\ -a_{N-1} & 0 & 0 & \dots & 1 \\ -a_N & 0 & 0 & \dots & 0 \end{bmatrix} \begin{bmatrix} x_1[n] \\ x_2[n] \\ \vdots \\ x_{N-1}[n] \\ x_N[n] \end{bmatrix} + \begin{bmatrix} b_1 - a_1 b_0 \\ b_2 - a_2 b_0 \\ \vdots \\ b_{N-1} - a_{N-1} b_0 \\ b_N - a_N b_0 \end{bmatrix} u[n] \quad (8.233)$$

$$y[n] = [1 \ 0 \ 0 \ \dots \ 0] \begin{bmatrix} x_1[n] \\ x_2[n] \\ \vdots \\ x_N[n] \end{bmatrix} + b_0 u[n]. \quad (8.234)$$

The state equations take the form

$$x[n+1] = Ax[n] + Bu[n] \quad (8.235)$$

$$y[n] = Cx[n] + Du[n]. \quad (8.236)$$

Example 8.16 Evaluate the transfer function and a state space model of the system described by the difference equation

$$y[n] - 1.2y[n-1] + 0.35y[n-2] = 3u[n-1] - 1.7u[n-2].$$

Applying the z-transform we obtain

$$Y(z) - 1.2z^{-1}Y(z) + 0.35z^{-2}Y(z) = 3z^{-1}U(z) - 1.7z^{-2}U(z)$$

$$H(z) = \frac{Y(z)}{U(z)} = \frac{3z^{-1} - 1.7z^{-2}}{1 - 1.2z^{-1} + 0.35z^{-2}} = \frac{3z - 1.7}{z^2 - 1.2z + 0.35}.$$

Writing $H(z)$ in the form

$$H(z) = \frac{\sum_{k=0}^2 b_k z^{-k}}{\sum_{k=0}^2 a_k z^{-k}}$$

we identify the coefficients a_k and b_k as

$$a_0 = 1, \quad a_1 = -1.2, \quad a_2 = 0.35$$

$$b_0 = 0, \quad b_1 = 3, \quad b_2 = -1.7.$$

See Fig. 8.22. The second canonical form state equations have the form

$$\begin{bmatrix} x_1[n+1] \\ x_2[n+1] \end{bmatrix} = \begin{bmatrix} 1.2 & 1 \\ -0.35 & 0 \end{bmatrix} \begin{bmatrix} x_1[n] \\ x_2[n] \end{bmatrix} + \begin{bmatrix} 3 \\ -1.7 \end{bmatrix} u[n]$$

$$y[n] = [1 \ 0] \begin{bmatrix} x_1[n] \\ x_2[n] \end{bmatrix}.$$

The first canonical form gives the state equations

$$\begin{bmatrix} x_1[n+1] \\ x_2[n+1] \end{bmatrix} = \begin{bmatrix} 0 & 1 \\ -0.35 & 1.2 \end{bmatrix} \begin{bmatrix} x_1[n] \\ x_2[n] \end{bmatrix} + \begin{bmatrix} 0 \\ 1 \end{bmatrix} u[n]$$

$$y[n] = [-1.7 \ 3] \begin{bmatrix} x_1[n] \\ x_2[n] \end{bmatrix}.$$

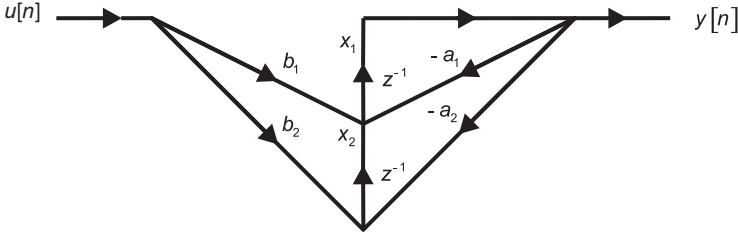


FIGURE 8.22 Second order system model with state variables.

Example 8.17 *Effect a partial fraction expansion and show the Jordan flow diagram of the system transfer function*

$$H(z) = \frac{z^2 - 5}{(z - 1)(z - 2)^3}$$

We have

$$H(z) = A + \frac{Bz^3}{(z - 2)^3} + \frac{Cz^2}{(z - 2)^2} + \frac{Dz}{z - 2} + \frac{Ez}{z - 1}$$

$$A = H(z)|_{z=0} = \frac{-5}{(-1)(-8)} = -\frac{5}{8}$$

$$E = \frac{H(z)(z - 1)}{z} \Big|_{z=1} = \frac{z^2 - 5}{z(z - 2)^3} \Big|_{z=1} = \frac{-4}{-1} = 4$$

$$B = \frac{H(z)(z - 2)^3}{z^3} \Big|_{z=2} = \frac{z^2 - 5}{z^3(z - 1)} = \frac{4 - 5}{8(1)} = -\frac{1}{8}$$

To find C and D we substitute $z = 3$ obtaining

$$\frac{9 - 5}{2 \times 1} = \frac{-5}{8} + \frac{4 \times 3}{3 - 1} + \frac{D \times 3}{1} + \frac{C \times 9}{1} - \frac{1}{8} \cdot \frac{27}{1}$$

i.e.

$$3D + 9C = 0.$$

Substituting $z = -1$

$$\frac{1 - 5}{-2 \times -27} = \frac{-5}{8} + \frac{4(-1)}{-2} + \frac{D(-1)}{-3} + \frac{C}{9} + \frac{(-1)}{8} \cdot \frac{(-1)}{(-27)}$$

$$3D + C + 13 = 0$$

wherefrom $C = 13/8$ and $D = -39/8$.

We may write

$$Y(z) = A U(z) + Bz^3 X_1(z) + Cz^2 X_2(z) + Dz X_3(z) + Ez X_4(z)$$

where

$$X_1(z) = \frac{U(z)}{(z - 2)^3}$$

$$X_2(z) = \frac{U(z)}{(z - 2)^2}$$

$$X_3(z) = \frac{U(z)}{(z-2)}$$

$$X_4(z) = \frac{U(z)}{(z-1)}$$

$$X_1(z) = \frac{1}{(z-2)^3}U(z) = \frac{1}{z-2}X_2(z) = \frac{z^{-1}}{1-2z^{-1}}X_2(z)$$

$$x_1[n] - 2x_1[n-1] = x_2[n-1]$$

$$x_1[n+1] = 2x_1[n] + x_2[n]$$

$$X_2(z) = \frac{1}{(z-2)^2}U(z) = \frac{1}{z-2}X_3(z) = \frac{z^{-1}}{1-2z^{-1}}X_3(z)$$

$$x_2[n] - 2x_2[n-1] = x_3[n-1]$$

$$x_2[n+1] = 2x_2[n] + x_3[n]$$

$$X_3(z) = \frac{1}{z-2}U(z) = \frac{z^{-1}}{1-2z^{-1}}U(z)$$

$$x_3[n] - 2x_3[n-1] = u[n-1]$$

$$x_3[n+1] = 2x_3[n] + u[n]$$

$$X_4(z) = \frac{1}{z-1}U(z) = \frac{z^{-1}}{1-z^{-1}}U(z)$$

$$x_4[n] - x_4[n-1] = u[n-1]$$

$$x_4[n+1] = x_4[n] + u[n].$$

With $\lambda_1 = 2$ and $\lambda_2 = 1$ we have

$$x_1[n+1] = \lambda_1 x_1[n] + x_2[n]$$

$$x_2[n+1] = \lambda_1 x_2[n] + x_3[n]$$

$$x_3[n+1] = \lambda_1 x_3[n] + u[n]$$

$$x_4[n+1] = \lambda_2 x_4[n] + u[n]$$

$$\begin{bmatrix} x_1[n+1] \\ x_2[n+1] \\ x_3[n+1] \\ x_4[n+1] \end{bmatrix} = \begin{bmatrix} \lambda_1 & 1 & 0 & 0 \\ 0 & \lambda_1 & 1 & 0 \\ 0 & 0 & \lambda_1 & 0 \\ 0 & 0 & 0 & \lambda_2 \end{bmatrix} \begin{bmatrix} x_1[n] \\ x_2[n] \\ x_3[n] \\ x_4[n] \end{bmatrix} + \begin{bmatrix} 0 \\ 0 \\ 1 \\ 1 \end{bmatrix} u[n]$$

$$y[n] = Au[n] + Bx_1[n+3] + Cx_2[n+2] + Dx_3[n+1] + Ex_4[n+1].$$

Now

$$x_4[n+1] = \lambda_2 x_4[n] + u[n]$$

$$x_3[n+1] = \lambda_1 x_3[n] + u[n]$$

$$\begin{aligned} x_2[n+2] &= \lambda_1 x_2[n+1] + x_3[n+1] = \lambda_1 \{ \lambda_1 x_2[n] + x_3[n] + \lambda_1 x_3[n] + u[n] \} \\ &= \lambda_1^2 x_2[n] + 2\lambda_1 x_3[n] + u[n] \end{aligned}$$

$$x_1[n+3] = \lambda_1 x_1[n+2] + x_2[n+2] = \lambda_1^3 x_1[n] + 3\lambda_1^2 x_2[n] + 3\lambda_1 x_3[n] + u[n].$$

Hence

$$\begin{aligned}
 y[n] &= Au[n] + B\{\lambda_1^3 x_1[n] + 3\lambda_1^2 x_2[n] + 3\lambda_1 x_3[n] + u[n]\} \\
 &= [8B \ 12B + 4C \ 6B + 4C + 2D \ E] x[n] \\
 &\quad + (A + B + C + D + E) u[n] \\
 &= [-1 \ 5 \ -4 \ 4] x[n] = [r_1 \ r_2 \ r_3 \ E] \begin{bmatrix} x_1[n] \\ x_2[n] \\ x_3[n] \\ x_4[n] \end{bmatrix}
 \end{aligned}$$

where

$$r_1 = 8B, \quad r_2 = 12B + 4C, \quad r_3 = 6B + 4C + 2D$$

which is represented graphically in Fig. 8.23. We note that with a transfer function

$$H(z) = \frac{Y(z)}{U(z)} = \frac{b_0 + b_1 z^{-1} + \dots + b_N z^{-N}}{1 + a_1 z^{-1} + a_2 z^{-2} + \dots + a_N z^{-N}}.$$

The corresponding difference equation is given by

$$y[n] + a_1 y[n-1] + \dots + a_N y[n-N] = b_0 u[n] + b_1 u[n-1] + \dots + b_N u[n-N].$$

If we replace n by $n + N$ in this difference equation we obtain

$$y[n+N] + a_1 y[n+N-1] + \dots + a_N y[n] = b_0 u[n+N] + b_1 u[n+N-1] + \dots + b_N u[n]$$

which corresponds to the equivalent transfer function

$$H(z) = \frac{Y(z)}{U(z)} = \frac{b_0 z^N + b_1 z^{N-1} + \dots + b_N}{z^N + a_1 z^{N-1} + a_2 z^{N-2} + \dots + a_N}.$$

It is common practice in state space modeling to write the difference equation in terms of unit advances as in the last difference equation instead of delays as in the first one.

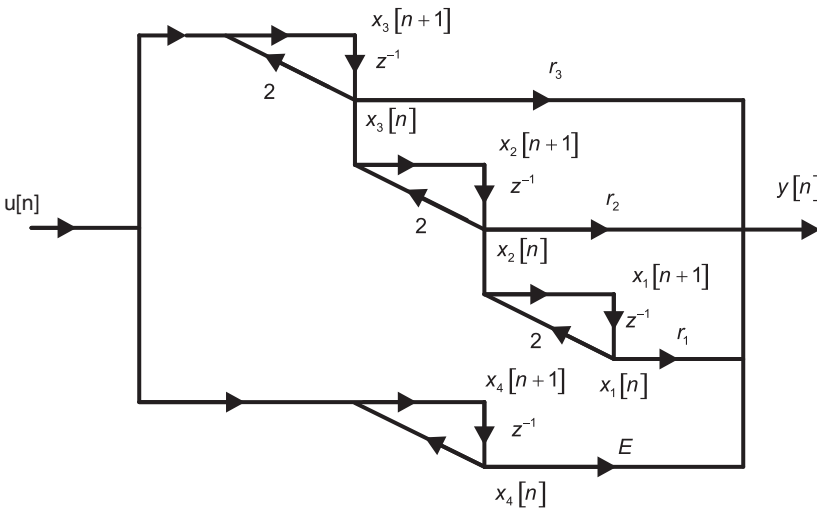


FIGURE 8.23 Jordan flow diagram.

8.17 Solution of the State Equations

We have found the state model in the form

$$x[n+1] = Ax[n] + Bu[n] \quad (8.237)$$

$$y[n] = Cx[n] + Du[n]. \quad (8.238)$$

We assume a causal input $u[n]$ and the initial conditions given as the state vector $x[0]$. The i^{th} state equation is given by

$$x_i[n+1] = a_{i1}x_1[n] + a_{i2}x_2[n] + \dots + a_{iN}x_N[n] + b_{i1}u_1[n] + b_{i2}u_2[n] + \dots + b_{iN}u_N[n]$$

where a_{ij} are the elements of A and b_{ij} those of B and where for generality multiple input is assumed. Applying the z -transform to this equation we have

$$zX_i(z) - zx_i(0) = a_{i1}X_1(z) + a_{i2}X_2(z) + \dots + a_{iN}X_N(z) + b_{i1}U_1(z) + b_{i2}U_2(z) + \dots + b_{iN}U_N(z). \quad (8.239)$$

The result of applying the z -transform to the state equations can be written in the matrix form

$$zX(z) - zx(0) = AX(z) + BU(z) \quad (8.240)$$

wherefrom

$$(zI - A)X(z) = zx(0) + BU(z) \quad (8.241)$$

$$X(z) = z(zI - A)^{-1}x(0) + (zI - A)^{-1}BU(z). \quad (8.242)$$

Similarly to the continuous-time case we define the discrete-time transition matrix $\phi(n)$ as the inverse transform of

$$\Phi(z) = z(zI - A)^{-1} \quad (8.243)$$

$$\phi(n) = \mathcal{Z}^{-1}[\Phi(z)] \quad (8.244)$$

so that

$$X(z) = \Phi(z)x(0) + z^{-1}\Phi(z)BU(z) \quad (8.245)$$

$$\begin{aligned} Y(z) &= Cz(zI - A)^{-1}x(0) + \{C(zI - A)^{-1}B + D\}U(z) \\ &= C\Phi(z)x(0) + \{Cz^{-1}\Phi(z)B + D\}U(z). \end{aligned} \quad (8.246)$$

8.18 Transfer Function

To evaluate the transfer function we set the initial conditions $x[0] = 0$. We have

$$X(z) = (zI - A)^{-1}BU(z) \quad (8.247)$$

$$Y(z) = CX(z) + DU(z) = [C(zI - A)^{-1}B + D]U(z) \quad (8.248)$$

$$H(z) = Y(z)\{U(z)\}^{-1} = C(zI - A)^{-1}B + D. \quad (8.249)$$

We have found that

$$X(z) = \Phi(z)x(0) + z^{-1}\Phi(z)BU(z). \quad (8.250)$$

Inverse z -transformation produces

$$x[n] = \phi[n]x[0] + \phi[n-1] * Bu[n] = \phi[n]x[0] + \sum_{k=0}^{n-1} \phi[n-k-1]Bu[k] \quad (8.251)$$

$$Y(z) = C\Phi(z)x(0) + \{Cz^{-1}\Phi(z)B + D\}U(z) \quad (8.252)$$

$$y[n] = C\phi[n]x(0) + C\sum_{k=0}^{n-1} \phi[n-k-1]Bu[k] + Du[n]. \quad (8.253)$$

Similarly to the continuous-time case we can express the transition matrix $\phi[n]$ as a power of the A matrix. To show this we may substitute recursively into the equation

$$x[n+1] = Ax[n] + Bu[n] \quad (8.254)$$

with

$$n = 0, 1, 2, \dots$$

obtaining

$$x[1] = Ax[0] + Bu[0] \quad (8.255)$$

$$x[2] = Ax[1] + Bu[1] = A^2x[0] + ABu[0] + Bu[1] \quad (8.256)$$

$$x[3] = Ax[2] + Bu[2] = A^3x[0] + A^2Bu[0] + ABu[1] \quad (8.257)$$

$$x[4] = Ax[3] + Bu[3] = A^4x[0] + A^3Bu[0] + A^2Bu[1] + Bu[3]. \quad (8.258)$$

We deduce that

$$x[n] = A^n x[0] + \sum_{k=0}^{n-1} A^{n-k-1} Bu[k]. \quad (8.259)$$

Comparing this with Equation (8.251) above we have

$$\phi[n] = A^n \quad (8.260)$$

which is another expression for the value of the transition matrix $\phi(n)$. We deduce the following properties

$$\phi[n_1 + n_2] = A^{n_1 + n_2} = \phi(n_1)\phi(n_2) \quad (8.261)$$

$$\phi[0] = A^0 = I \quad (8.262)$$

$$\phi^{-1}[n] = A^{-n} = \phi[-n]. \quad (8.263)$$

8.19 Change of Variables

As with continuous-time systems if we apply the change of variables

$$x[n] = Tw[n] \quad (8.264)$$

then the state equations

$$x[n+1] = Ax[n] + Bu[n] \quad (8.265)$$

$$y[n] = Cx[n] + Du[n] \quad (8.266)$$

take the form

$$Tw[n+1] = ATw[n] + Bu[n] \quad (8.267)$$

$$y[n] = CTw[n] + Du[n] \quad (8.268)$$

$$w[n+1] = T^{-1}ATw[n] + T^{-1}Bu[n] = A_w w[n] + B_w u[n] \quad (8.269)$$

where

$$A_w = T^{-1}AT, \quad B_w = T^{-1}B \quad (8.270)$$

$$y[n] = C_w w[n] + D_w u[n] \quad (8.271)$$

where

$$C_w = CT, \quad D_w = D. \quad (8.272)$$

Similarly to continuous time systems it can be shown that

$$\det(zI - A_w) = \det(zI - A) = (z - \lambda_1)(z - \lambda_2) \dots (z - \lambda_N) \quad (8.273)$$

$\lambda_1, \lambda_2, \dots, \lambda_N$ being the eigenvalues of A .

$$\det(A_w) = \det(A) = \lambda_1, \lambda_2, \dots, \lambda_N \quad (8.274)$$

$$H(z) = C_w(zI - A_w)^{-1}B_w + D_w = C(zI - A)^{-1}B + D. \quad (8.275)$$

The following examples illustrates the computations involved in these relations. MATLAB®, Mathematica® and Maple® prove to be powerful tools for the solution of state space equations.

Example 8.18 Evaluate the transfer function of a discrete-time system given that its state space matrices are given by

$$A = \begin{bmatrix} 2 & 1 & 0 & 0 \\ 0 & 2 & 1 & 0 \\ 0 & 0 & 2 & 0 \\ 0 & 0 & 0 & 1 \end{bmatrix}, \quad B = \begin{bmatrix} 0 \\ 0 \\ 1 \\ 1 \end{bmatrix}, \quad C = [-1 \quad 5 \quad -4 \quad 4], \quad D = 0.$$

We have

$$H(z) = C \Phi(z) z^{-1}B + D = C(zI - A)^{-1}B + D$$

$$zI - A = \begin{bmatrix} z-2 & 1 & 0 & 0 \\ 0 & z-2 & 1 & 0 \\ 0 & 0 & z-2 & 0 \\ 0 & 0 & 0 & z-1 \end{bmatrix}$$

$$(zI - A)^{-1} = \frac{\text{adj}[zI - A]}{\det[zI - A]}$$

$$\det[zI - A] = (z - 2)^3 (z - 1)$$

$$\text{adj}[zI - A] = \begin{bmatrix} (z-2)^2(z-1) & 0 & 0 & 0 \\ (z-2)(z-1) & (z-2)^2(z-1) & (z-2)^2(z-1) & 0 \\ z-1 & (z-2)(z-1) & (z-2)^2(z-1) & 0 \\ 0 & 0 & 0 & (z-2)^3 \end{bmatrix}$$

$$(zI - A)^{-1} = \begin{bmatrix} (z-2)^2(z-1) & (z-2)(z-1) & z-1 & 0 \\ 0 & (z-2)^2(z-1) & (z-2)(z-1) & 0 \\ 0 & (z-2)^2(z-1) & (z-2)^2(z-1) & 0 \\ 0 & 0 & 0 & (z-2)^3 \end{bmatrix}$$

$$(zI - A)^{-1} = \begin{bmatrix} \frac{1}{z-2} & \frac{1}{(z-2)^2} & \frac{1}{(z-2)^3} & 0 \\ 0 & \frac{1}{z-2} & \frac{1}{(z-2)^2} & 0 \\ 0 & \frac{1}{z-2} & \frac{1}{z-2} & 0 \\ 0 & 0 & 0 & \frac{1}{z-1} \end{bmatrix}$$

$$\begin{aligned} H(z) &= C(zI - A)^{-1}B + D \\ &= [-1 \ 5 \ -4 \ 4] \begin{bmatrix} \frac{1}{z-2} & \frac{1}{(z-2)^2} & \frac{1}{(z-2)^3} & 0 \\ 0 & \frac{1}{z-2} & \frac{1}{(z-2)^2} & 0 \\ 0 & \frac{1}{z-2} & \frac{1}{z-2} & 0 \\ 0 & 0 & 0 & \frac{1}{z-1} \end{bmatrix} \begin{bmatrix} 0 \\ 0 \\ 1 \\ 1 \end{bmatrix} \\ &= \left[\left(\frac{-1}{z-2} \right) \left(\frac{-1}{(z-2)^2} + \frac{1}{z-2} \right) \left(\frac{-1}{(z-2)^3} + \frac{5}{(z-2)^2} - \frac{4}{z-2} \right) \left(\frac{4}{z-1} \right) \right] \begin{bmatrix} 0 \\ 0 \\ 1 \\ 1 \end{bmatrix} \\ &= \frac{-1}{(z-2)^3} + \frac{5}{(z-2)^2} - \frac{4}{z-2} + \frac{4}{z-1}. \\ &H(z) = \frac{z^2 - 5}{(z-1)(z-2)^3}. \end{aligned} \tag{8.276}$$

8.20 Second Canonical Form State Space Model

The following example illustrates an approach for evaluating the state space model of a discrete-time system.

Example 8.19 Evaluate the state space model of a system, given its transfer function

$$H(z) = \frac{Y(z)}{U(z)} = \frac{\beta_0 + \beta_1 z^{-1} + \beta_2 z^{-2} + \beta_3 z^{-3}}{1 + \alpha_1 z^{-1} + \alpha_2 z^{-2} + \alpha_3 z^{-3}}.$$

We have

$$H(z) = \frac{\beta_0 z^3 + \beta_1 z^2 + \beta_2 z + \beta_3}{z^3 + \alpha_1 z^2 + \alpha_2 z + \alpha_3}.$$

Let us write

$$H(z) = \frac{Y_1(z)}{U(z)} \frac{Y(z)}{Y_1(z)} = H_1(z) H_2(z)$$

where

$$H_1(z) = \frac{Y_1(z)}{U(z)} = \frac{1}{z^3 + \alpha_1 z^2 + \alpha_2 z + \alpha_3}$$

$$H_2(z) = \frac{Y(z)}{Y_1(z)} = \beta_0 z^3 + \beta_1 z^2 + \beta_2 z + \beta_3$$

wherefrom

$$z^3 Y_1(z) = -\alpha_1 z^2 Y_1(z) - \alpha_2 z Y_1(z) - \alpha_3 Y_1(z) + U(z).$$

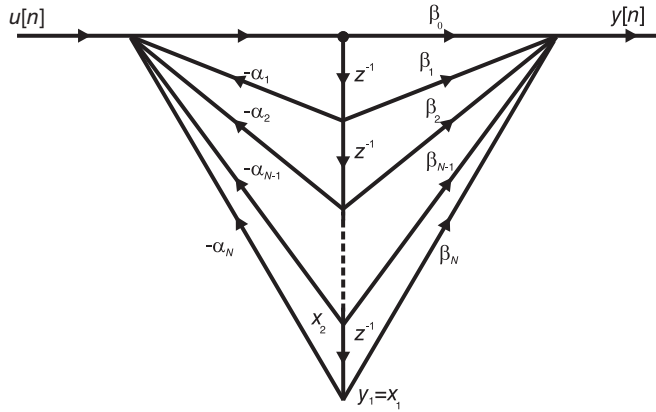


FIGURE 8.24 Second canonical form state space model.

This relation can be represented in a flow diagram form as shown in Fig. 8.24 where delay elements, denoted z^{-1} , are connected in series. The state variables x_1 , x_2 and x_3 are the outputs of these delay elements as shown in the figure, wherefrom we can write

$$y_1[n] = x_1[n], \quad x_1[n+1] = x_2[n], \quad x_2[n+1] = x_3[n]$$

$$x_2[n] = y_1[n+1], \quad x_3[n] = y_1[n+2], \quad x_3[n+1] = y_1[n+3]$$

$$\begin{aligned} z^3 Y_1(z) &= z X_3(z) = -\alpha_1 z^2 Y_1(z) - \alpha_2 z Y_1(z) - \alpha_3 Y_1(z) + U(z) \\ &= -\alpha_1 X_3(z) - \alpha_2 X_2(z) - \alpha_3 X_1(z) + U(z). \end{aligned}$$

This relation defines the value at the input of the left-most delay element, and is thus represented schematically as shown in the figure. The figure is completed by noticing that

$$\begin{aligned} Y(z) &= \beta_0 z^3 Y_1(z) + \beta_1 z^2 Y_1(z) + \beta_2 z Y_1(z) + \beta_3 Y_1(z) \\ &= \beta_0 z X_3(z) + \beta_1 X_3(z) + \beta_2 X_2(z) + \beta_3 X_1(z). \end{aligned}$$

We therefore found $x_3[n+1] = -\alpha_1 x_3[n] - \alpha_2 x_2[n] - \alpha_3 x_1[n] + u[n]$

$$y[n] = \beta_0 x_3[n+1] + \beta_1 x_3[n] + \beta_2 x_2[n] + \beta_3 x_1[n].$$

The state space equations are therefore given by:

$$\begin{bmatrix} x_1[n+1] \\ x_2[n+1] \\ x_3[n+1] \end{bmatrix} = \begin{bmatrix} 0 & 1 & 0 \\ 0 & 0 & 1 \\ -\alpha_3 & -\alpha_2 & -\alpha_1 \end{bmatrix} \begin{bmatrix} x_1[n] \\ x_2[n] \\ x_3[n] \end{bmatrix} + \begin{bmatrix} 0 \\ 0 \\ 1 \end{bmatrix} u[n]$$

$$\begin{aligned} y[n] &= \beta_0 \{-\alpha_1 x_3[n] - \alpha_2 x_2[n] - \alpha_3 x_1[n] + u[n]\} + \beta_1 x_3[n] + \beta_2 x_2[n] + \beta_3 x_1[n] \\ &= (\beta_3 - \beta_0 \alpha_3) x_1[n] + (\beta_2 - \beta_0 \alpha_2) x_2[n] + (\beta_1 - \beta_0 \alpha_1) x_3[n] + \beta_0 u[n] \end{aligned}$$

$$y[n] = [(\beta_3 - \beta_0 \alpha_3) \quad (\beta_2 - \beta_0 \alpha_2) \quad (\beta_1 - \beta_0 \alpha_1)] \begin{bmatrix} x_1[n] \\ x_2[n] \\ x_3[n] \end{bmatrix} + \beta_0 u[n].$$

8.21 Problems

Problem 8.1 For the two-input two-output electric circuit shown in Fig. 8.25 let x_1 , x_2 and x_3 be the currents through the inductors, and x_4 and x_5 the voltages across the capacitors, as shown in the figure. The inputs to the system are the voltages v_1 and v_2 . The outputs are voltages across the capacitors y_1 and y_2 . Evaluate the matrices A , B , C and D of the state space model describing the circuit.

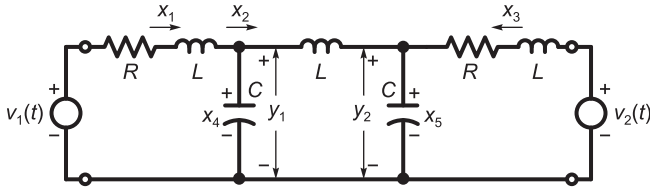


FIGURE 8.25 Two-input two-output system.

Problem 8.2 The force $f(t)$ is applied to the mass on the left in Fig. 8.26, which is connected through a spring of stiffness k to the mass on the right. Each mass is m kg. The movement encounters viscous friction of coefficient b between the masses and the support. By choosing state variable x_1 as the speed of the left mass, x_2 the force in the spring and x_3 the speed of the right mass and, as shown in the figure, and with the outputs y_1 and y_2 the speeds of the masses, evaluate the state space model.

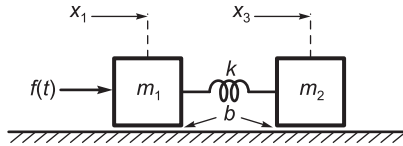


FIGURE 8.26 Two masses and a spring.

Problem 8.3 With x_1 the current in the inductor and x_2 the voltage across the capacitor in the circuit shown in Fig. 8.27, with $v(t)$ the input and y_1 and y_2 the outputs of the circuit

- a) Evaluate the state space model.
- b) With $R_1 = 10^3 \Omega$, $R_2 = 10^2 \Omega$, $L = 10 H$ and $C = 10^{-3} F$ evaluate the transition matrix $\Phi(s)$, the transfer function matrix $H(s)$ and the impulse response matrix.
- c) Assuming the initial conditions

$$x_1(0) = 0.1 \text{ amp}, \quad x_2(0) = 10 \text{ volt}$$

evaluate the response of the circuit to the input $v(t) = 100u(t)$ volts.

Problem 8.4 For the circuit shown in Fig. 8.28 evaluate the state space model, choosing state variables x_1 and x_2 as the voltages across the capacitors and x_3 the current through the inductor, as shown in the figure.

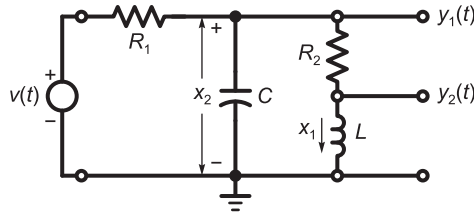


FIGURE 8.27 R-L-C circuit with two outputs.

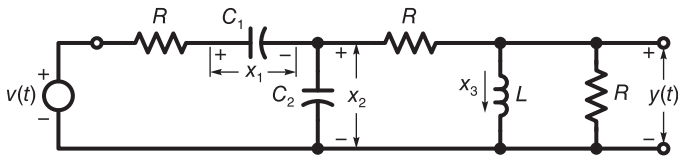


FIGURE 8.28 R-L-C electric circuit.

Problem 8.5 The matrices of a state space model are

$$A = \begin{bmatrix} 0 & 1 \\ -5000 & -50 \end{bmatrix}, \quad B = \begin{bmatrix} 0 & 0 \\ 5000 & -74 \end{bmatrix}, \quad C = [1 \ 0], \quad D = 0.$$

- a) Evaluate the transition matrix $\phi(t)$ and the transfer function $H(s)$.
- b) Evaluate the unit step response given the initial conditions $x_1(0) = 2$ and $x_2(0) = 4$, where x_1 and x_2 are the state variables.

Problem 8.6 Consider the system represented by the block diagram shown in Fig. 8.29

- a) Evaluate the system state model.
- b) Evaluate the transfer function from the input $u(t)$ to the output $y(t)$.

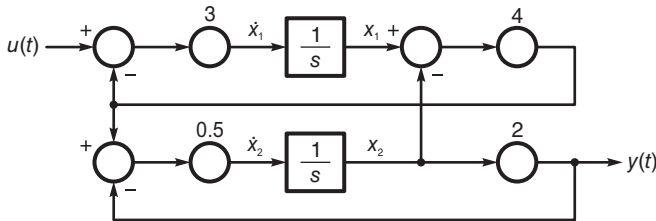


FIGURE 8.29 System block diagram.

Problem 8.7 Evaluate the state space model of the circuit shown in Fig. 8.30 with x_1 and x_2 the state variables equal to the voltage across the capacitor and the current through the inductor, respectively. Draw the block diagram representing the system structure.

Problem 8.8 Consider the two-input electric circuit shown in Fig. 8.31. Assuming the initial conditions in the capacitor C and inductor L to be v_0 and i_0 , respectively,

- a) Evaluate the state space model of the system.
- b) Draw the block diagram representing the circuit.

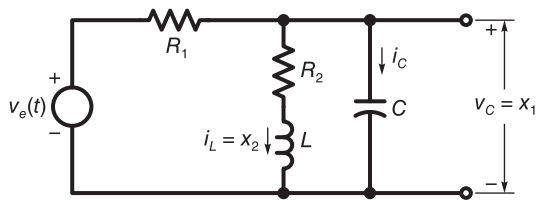


FIGURE 8.30 R–L–C electric circuit.

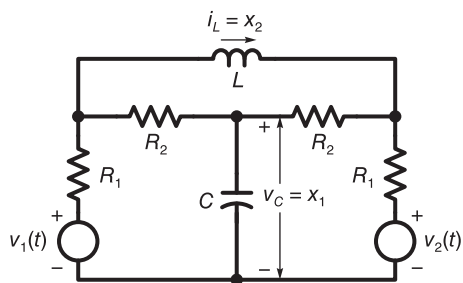


FIGURE 8.31 R–L–C Electric circuit.

Problem 8.9 Consider the block diagram of the system shown in Fig. 8.32.

- Write the state space equations describing the system.
- Write the third order differential equation relating the input $u(t)$ and the output $y(t)$.
- Evaluate the transfer function from the input to the output. Verify the result using MATLAB.

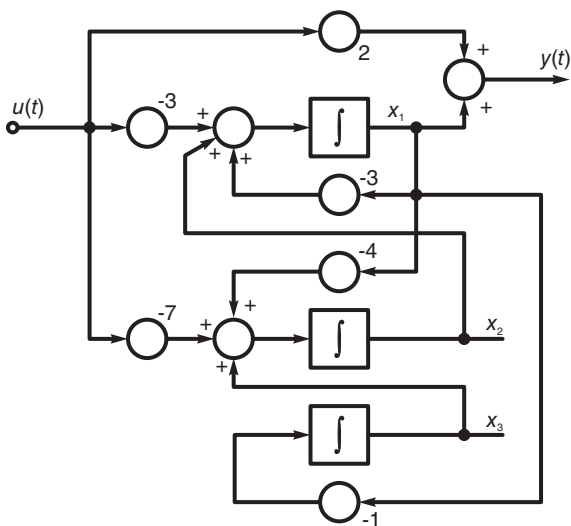


FIGURE 8.32 System block diagram.

Problem 8.10 Evaluate the state space model of the system of transfer function:

$$H(s) = \frac{s^2 + s + 2}{4s^3 + 3s^2 + 2s + 1}$$

Problem 8.11 Consider the electric circuit shown in Fig. 8.33 where the two switches close at $t = 0$, the state variables x_1 and x_2 are the current through and voltage across the inductor and capacitor, respectively, and where the output is the current i_1 through the resistor R_1 . Assuming the initial conditions $x_1(0) = 1$ ampere and $x_2(0) = 2$ volt, evaluate

- a) The state space model matrices A , B , C and D , the transition matrix $\phi(t)$; the state space vector x ; and the output $i_1(t)$,
- b) The equivalent Jordan form, the equivalent system $\dot{z} = Jz$ and the system trajectories.
- c) Repeat if $R_2 = 2.5\Omega$.

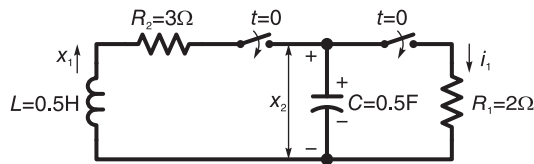


FIGURE 8.33 R–L–C electric circuit.

Problem 8.12 Consider the system represented by the block diagram shown in Fig. 8.34, with state variables x_1 and x_2 as shown in the figure.

- a) Write the state space equations describing the system.
- b) From the system eigenvalues and assuming $\alpha > 0$, state under what conditions would the system be unstable?
- c) With $\alpha = 5$, $k_1 = 2$, $k_2 = 3$ evaluate the system output in response to the input $v(t) = u(t)$ and with zero initial conditions.
- d) For the same values of α , k_1 and k_2 in part c) evaluate the equivalent Jordan diagonalized model $\dot{z} = Jz$ and sketch the system trajectories in the $x_1 - x_2$ and $z_1 - z_2$ planes, assuming zero input, and initial conditions $x_1(0) = x_2(0) = 1$. Show how the axes z_1 and z_2 of the $z_1 - z_2$ plane appear in the $x_1 - x_2$ plane.

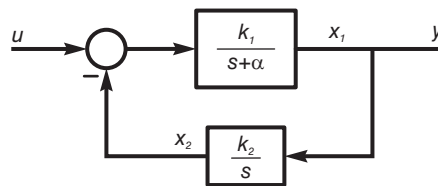


FIGURE 8.34 System block diagram.

Problem 8.13 The switch S in the electric circuit depicted in Fig. 8.35 is closed at $t = 0$, the circuit having zero initial conditions.

Evaluate the matrices A , B , C and D of the state space equations, the state variables $x_1(t)$ and $x_2(t)$ for $t > 0$, where x_1 is the voltage across C and x_2 the current through L as shown in the figure.

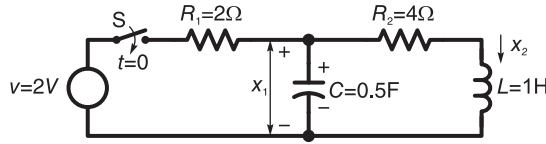


FIGURE 8.35 R–L–C electric circuit.

Problem 8.14 Evaluate the state space model and the state space variables $x_1(t)$ and $x_2(t)$ for the electric circuit shown in Fig. 8.36.

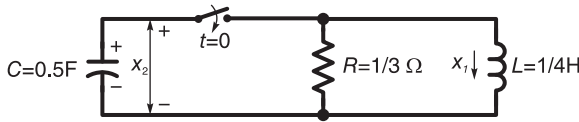


FIGURE 8.36 R–L–C electric circuit.

Problem 8.15 Evaluate the transfer function of the system of which the space model is given by

$$\dot{x}(t) = \begin{bmatrix} 1 & 4 & 0 \\ -2 & 0 & 2 \\ 0 & 2 & 1 \end{bmatrix} x(t) + \begin{bmatrix} 1 \\ 1 \\ 0 \end{bmatrix} u$$

$$y = [1 \ 0 \ 2] x(t) + 3u(t).$$

Problem 8.16 The state space model of a system is given by $\dot{x} = Ax + Bv$, where

$$A = \begin{bmatrix} 0 & -3 \\ 3 & 0 \end{bmatrix}, \quad B = \begin{bmatrix} 2 \\ 0 \end{bmatrix}, \quad x(0) = \begin{bmatrix} 3 \\ 0 \end{bmatrix}, \quad v(t) = 2u(t).$$

Evaluate the state variables $x_1(t)$ and $x_2(t)$, the transition matrices $Q(t)$ and $\phi(t)$, and plot the system trajectory.

Problem 8.17 Consider the electric circuit shown in Fig. 8.37.

a) Evaluate the state space model assuming that the state space variables are the current and voltage in the inductor and capacitor, respectively, as shown in the figure.

b) Evaluate the transition matrices $\phi(t)$ and $Q(t)$.

c) Assuming the initial condition $x_1(0) = 2$ ampere, $x_2(0) = 3$ volt, evaluate $x_1(t)$ and $x_2(t)$ and draw the system trajectories.

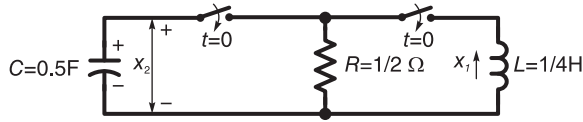


FIGURE 8.37 R-L-C electric circuit.

8.22 Answers to Selected Problems

Problem 8.1

$$\begin{bmatrix} \dot{x}_1 \\ \dot{x}_2 \\ \dot{x}_3 \\ \dot{x}_4 \\ \dot{x}_5 \end{bmatrix} = \begin{bmatrix} -R/L & 0 & 0 & -1/L & 0 \\ 0 & 0 & 0 & 1/L & -1/L \\ 0 & 0 & -R/L & 0 & -1/L \\ 1/C & -1/C & 0 & 0 & 0 \\ 0 & 1/C & 1/C & 0 & 0 \end{bmatrix} \begin{bmatrix} x_1 \\ x_2 \\ x_3 \\ x_4 \\ x_5 \end{bmatrix} + \begin{bmatrix} 1/L & 0 \\ 0 & 0 \\ 0 & 1/L \\ 0 & 0 \\ 0 & 0 \end{bmatrix} \begin{bmatrix} u_1 \\ u_2 \end{bmatrix}$$

$$\begin{bmatrix} y_1 \\ y_2 \end{bmatrix} = \begin{bmatrix} 0 & 0 & 0 & 1 & 0 \\ 0 & 0 & 0 & 0 & 1 \end{bmatrix} \begin{bmatrix} x_1 \\ x_2 \\ x_3 \\ x_4 \\ x_5 \end{bmatrix}$$

Problem 8.2

$$\begin{bmatrix} \dot{x}_1 \\ \dot{x}_2 \\ \dot{x}_3 \end{bmatrix} = \begin{bmatrix} -b/m & -1/m & 0 \\ k & 0 & -k \\ 0 & 1/m & -b/m \end{bmatrix} \begin{bmatrix} x_1 \\ x_2 \\ x_3 \end{bmatrix} + \begin{bmatrix} 1/m \\ 0 \\ 0 \end{bmatrix} f(t)$$

Problem 8.3

c)

$$y(t) = \begin{bmatrix} 11.74 e^{-5.5t} \cos(8.93t + 0.552) u(t) \\ 12.318 e^{-5.5t} \cos(8.93t - 7.571) u(t) \end{bmatrix}$$

Problem 8.4

$$\begin{bmatrix} \dot{x}_1 \\ \dot{x}_2 \\ \dot{x}_3 \end{bmatrix} = \begin{bmatrix} -1/(RC_1) & -1/(RC_1) & 0 \\ -1/(RC_2) & -3/(2RC_2) & -1/(2C_2) \\ 0 & 1/(2L) & -R/(2L) \end{bmatrix} \begin{bmatrix} x_1 \\ x_2 \\ x_3 \end{bmatrix} + \begin{bmatrix} 1/(RC_1) \\ 1/(RC_2) \\ 0 \end{bmatrix} u$$

$$y = [0 \quad 1/2 \quad -R/2] \begin{bmatrix} x_1 \\ x_2 \\ x_3 \end{bmatrix}$$

Problem 8.5

$$\Delta = s^2 + 50s + 5000$$

$$H(s) = [10000/\Delta \quad -148/\Delta].$$

b)

$$y_{\text{I.C.}}(t) = 4.3319e^{-25t} \cos(66.144t - 0.394) u(t)$$

$$y_{\text{zero I.C.}}(t) = [0.1704 + 0.1822e^{-25t} \cos(66.144t + 2.780)] u(t)$$

$$y(t) = y_{\text{I.C.}}(t) + y_{\text{zero I.C.}}(t)$$

Problem 8.6

$$H(s) = \frac{12}{s^2 + 15s + 12}$$

Problem 8.7

$$\begin{pmatrix} \dot{x}_1 \\ \dot{x}_2 \end{pmatrix} = \begin{pmatrix} -\frac{1}{CR_1} & -\frac{1}{C} \\ \frac{1}{L} & -\frac{R_2}{L} \end{pmatrix} \begin{pmatrix} x_1 \\ x_2 \end{pmatrix} + \begin{pmatrix} \frac{1}{CR_1} \\ 0 \end{pmatrix} v_e$$

$$y = (1 \ 0) \begin{pmatrix} x_1 \\ x_2 \end{pmatrix} + 0 v_e$$

Problem 8.8

$$\begin{bmatrix} \dot{x}_1 \\ \dot{x}_2 \end{bmatrix} = \begin{bmatrix} \frac{-2}{(R_1+R_2)C} & 0 \\ 0 & \frac{-2R_1R_2}{L(R_1+R_2)} \end{bmatrix} \begin{bmatrix} x_1 \\ x_2 \end{bmatrix} + \begin{bmatrix} \frac{1}{(R_1+R_2)C} & \frac{1}{(R_1+R_2)C} \\ \frac{R_2}{L(R_1+R_2)} & \frac{-R_2}{L(R_1+R_2)} \end{bmatrix} \begin{bmatrix} u_1 \\ u_2 \end{bmatrix}$$

$$\dot{x} = Ax + Bu$$

Problem 8.9

$$H(s) = \frac{Y(s)}{U(s)} = \frac{2s^3 + 3s^2 + s + 2}{s^3 + 3s^2 + 4s + 1}$$

Problem 8.10

$$\begin{bmatrix} \dot{x}_1 \\ \dot{x}_2 \\ \dot{x}_3 \end{bmatrix} = \begin{bmatrix} 0 & 1 & 0 \\ 0 & 0 & 1 \\ -1/4 & -1/2 & -3/4 \end{bmatrix} \begin{bmatrix} x_1 \\ x_2 \\ x_3 \end{bmatrix} + \begin{bmatrix} 0 \\ 0 \\ 1 \end{bmatrix} u$$

$$y = [1/2 \ 1/4 \ 1/4] \begin{bmatrix} x_1 \\ x_2 \\ x_3 \end{bmatrix}$$

Problem 8.11

See Fig. 8.38.

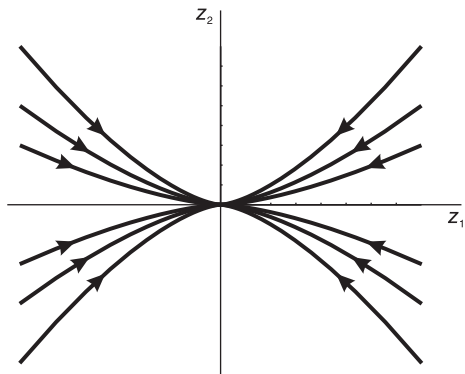


FIGURE 8.38 Figure for Problem 8.11.

a)

$$\phi(t) = \frac{1}{3} \begin{bmatrix} 4e^{-5t} - e^{-2t} & 2e^{-5t} - 2e^{-2t} \\ 2e^{-2t} - 2e^{-5t} & 4e^{-2t} - e^{-5t} \end{bmatrix} u(t)$$

$$x(t) = \phi(t)x(0) = \phi(t) \begin{bmatrix} 1 \\ 2 \end{bmatrix} = \frac{1}{3} \begin{bmatrix} 8e^{-5t} - 5e^{-2t} \\ 10e^{-2t} - 4e^{-5t} \end{bmatrix} u(t)$$

$$i_1 = (1/R_1)x_2 = 0.5x_2 = [(5/3)e^{-2t} - (2/3)e^{-5t}] u(t)$$

b) $z_1(t) = z_1(0)e^{-2t}u(t)$, $z_2(t) = z_2(0)e^{-5t}u(t)$.

c) $i_1 = (3te^{-3t} + e^{-3t})u(t)$, $z_1(t) = z_1(0)e^{-3t}u(t) + z_2(0)te^{-3t}u(t)$.

Problem 8.12

a) $A = \begin{bmatrix} -\alpha & -k_1 \\ k_2 & 0 \end{bmatrix}$, $B = \begin{bmatrix} k_1 \\ 0 \end{bmatrix}$, $C = [1 \ 0]$, $D = 0$.

See Fig. 8.39 and Fig. 8.40.

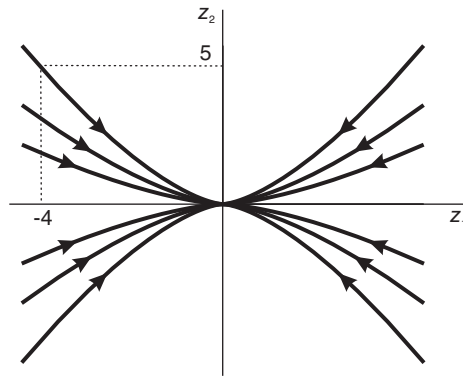


FIGURE 8.39 Figure for Problem 8.12.

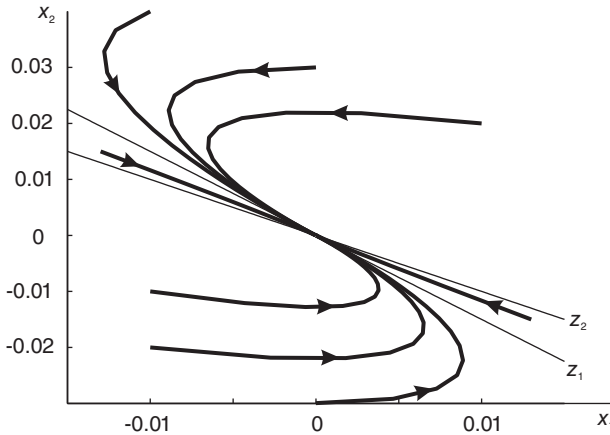


FIGURE 8.40 Figure for Problem 8.12.

b) The system is unstable if $\lambda_2 > 0$ i.e. if $\text{sign}(k_1) \neq \text{sign}(k_2)$.

c)

$$x(t) = \begin{bmatrix} 2e^{-2t} - 2e^{-3t} \\ 1 - 3e^{-2t} + 2e^{-3t} \end{bmatrix} u(t)$$

$$\begin{aligned} \text{d) } x_1(t) &= (-2e^{-2t} + 3e^{-3t} - 2e^{-2t} + 2e^{-3t})u(t) = (-4e^{-2t} + 5e^{-3t})u(t) \\ x_2(t) &= (3e^{-2t} - 3e^{-3t} + 3e^{-2t} - 2e^{-3t})u(t) = (6e^{-2t} - 5e^{-3t})u(t) \\ z_1 &= -2x_1 - 2x_2, \quad z_2 = 3x_1 + 2x_2. \end{aligned}$$

Problem 8.13

$$A = \begin{bmatrix} -1 & -2 \\ 1 & -4 \end{bmatrix}, \quad B = \begin{bmatrix} 1 \\ 0 \end{bmatrix}, \quad C = [0 \ 1], \quad D = 0.$$

$$\phi(t) = \begin{bmatrix} 2e^{-2t} - e^{-3t} & -2e^{-2t} + 2e^{-3t} \\ e^{-2t} - e^{-3t} & -e^{-2t} + 2e^{-3t} \end{bmatrix} u(t)$$

$$x_1(t) = \left\{ 2 \int_0^t (2e^{-\tau} - e^{-3\tau}) d\tau \right\} u(t) = 2[2(1 - e^{-t}) - \frac{1}{3}(1 - e^{-3t})]u(t)$$

$$x_2(t) = \phi_{21}(t) * 2u(t) = \left\{ 2 \int_0^t (2e^{-2\tau} - e^{-3\tau}) d\tau \right\} u(t) = 2[(1/2)(1 - e^{-2t}) - (1/3)(1 - e^{-3t})]u(t)$$

Problem 8.14

$$A = \begin{bmatrix} 0 & 1/L \\ -1/C & -1/(RC) \end{bmatrix} = \begin{bmatrix} 0 & 4 \\ -2 & -6 \end{bmatrix}$$

$$\phi(t) = \begin{bmatrix} 2e^{-2t} - e^{-4t} & 2e^{-2t} - 2e^{-4t} \\ -e^{-2t} + e^{-4t} & -e^{-2t} + 2e^{-4t} \end{bmatrix} u(t)$$

$$x(t) = \phi(t)x(0) = \begin{bmatrix} \phi_{11}x_1(0) & \phi_{12}x_2(0) \\ \phi_{21}x_1(0) & \phi_{22}x_2(0) \end{bmatrix}$$

Problem 8.15

$$H(s) = \frac{3s^3 - 5s^2 + 22s - 40}{s^3 - 2s^2 + 5s - 4}$$

Problem 8.16

$$x_1(t) = [3 \cos 3t + (4/3) \sin 3t] u(t)$$

$$x_2(t) = [3 \sin 3t + (4/3) \{1 - \cos 3t\}] u(t)$$

Problem 8.17

$$Q(t) = \begin{bmatrix} e^{-\lambda_1 t} & 0 \\ 0 & e^{\lambda_2 t} \end{bmatrix} = \begin{bmatrix} e^{(-2+j2)t} & 0 \\ 0 & e^{(-2-j2)t} \end{bmatrix}$$

$$\phi(t) = e^{-2t} \begin{bmatrix} \sin 2t + \cos 2t & -2 \sin 2t \\ \sin 2t & -2 \sin 2t + \cos 2t \end{bmatrix} u(t)$$

$$x(t) = \phi(t) x(0)$$

$$\begin{bmatrix} x_1(t) \\ x_2(t) \end{bmatrix} = \begin{bmatrix} 2e^{-2t} (\cos 2t - \sin 2t) \\ 2e^{-2t} \cos 2t \end{bmatrix}$$

This page intentionally left blank

9

Filters of Continuous-Time Domain

In this chapter we study different approaches to the design of continuous-time filters, also referred to as analog filters. An important application is the design of a filter of which the frequency response best matches that of a given spectrum. This is referred to as a problem of *approximation*. It has many applications in science and engineering.

Filters are often used to eliminate or reduce noise that contaminates a signal. For example, a bandpass filter may remove from a signal a narrow-band extraneous added noise. Filters are also used to limit the frequency spectrum of a signal before sampling, thus avoiding aliasing. They may be used as equalizers to compensate for spectral distortion inherent in a communication channel. Many excellent books treat the subject of continuous-time filters [4] [12] [48] [60].

In what follows we study approximation techniques for ideal filters. Lowpass, bandpass, highpass and bandstop ideal filters are approximated by models known as Butterworth, Chebyshev, elliptic and Bessel–Thomson.

9.1 Lowpass Approximation

Consider the magnitude-squared spectrum $|H(j\omega)|^2$ of an ideal lowpass filter with a cut-off frequency of 1, shown in Fig. 9.1.

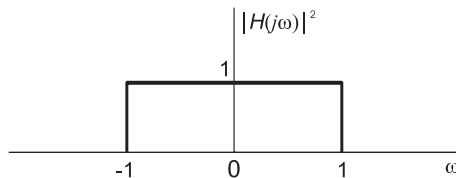


FIGURE 9.1 Ideal lowpass filter frequency response.

Our objective is to find a rational transfer function, a ratio of two polynomials, which has the same as or is an approximation of this frequency spectrum.

9.2 Butterworth Approximation

A rational function, a ratio of two polynomials in ω , which approximates the given ideal magnitude-squared spectrum is the Butterworth approximation given by

$$|H(j\omega)|^2 = \frac{1}{1 + \varepsilon^2 \omega^{2n}}. \quad (9.1)$$

The value of ε is often taken equal to 1, so that the magnitude spectrum is given by

$$|H(j\omega)|^2 = \frac{1}{1 + \omega^{2n}}. \quad (9.2)$$

To simplify the presentation, we follow this approach by setting $\varepsilon = 1$ and defer the discussion of the case $\varepsilon \neq 1$, to a following section. The amplitude spectrum $|H(j\omega)|$ of the Butterworth approximation

$$|H(j\omega)| = \frac{1}{\sqrt{1 + \omega^{2n}}} \quad (9.3)$$

is shown in Fig. 9.2 for different values of the filter order n .

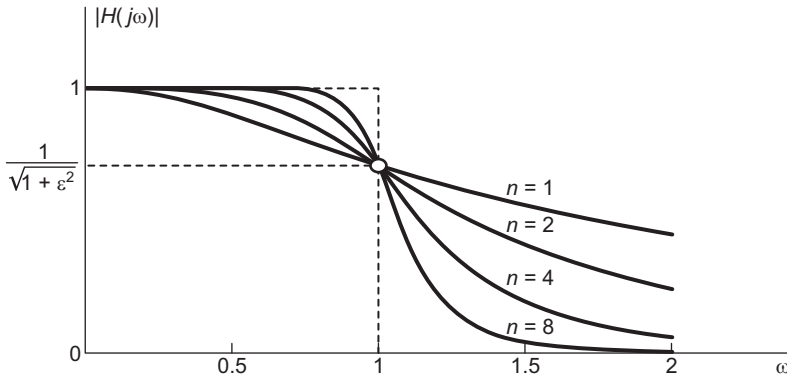


FIGURE 9.2 Butterworth filter frequency response.

We note that the amplitude spectrum $|H(j\omega)|$, similarly to the magnitude-squared spectrum $|H(j\omega)|^2$, is written in a *normalized* form, the frequency ω being a *normalized frequency*, such that the frequency $\omega = 1$ is the *cut-off frequency* of the spectrum, also referred to as the *pass-band edge frequency*, whereat the amplitude spectrum $|H(j\omega)|$ drops to a value of $1/\sqrt{2}$, corresponding to a 3 dB drop from its value of 1 at $\omega = 0$. Such a normalized lowpass filter is referred to as a *prototype*, since it serves as a basis for obtaining thereof denormalized and other types of filters.

We can rewrite the amplitude spectrum $|H(j\omega)|$ using the binomial expansion in the form

$$|H(j\omega)| = (1 + \omega^{2n})^{-1/2} = 1 - \frac{1}{2}\omega^{2n} + \frac{3}{8}\omega^{4n} - \frac{5}{16}\omega^{6n} + \dots \quad (9.4)$$

Hence the $2n - 1$ first derivatives of $|H(j\omega)|$ are nil at $\omega = 0$. The spectrum in the neighborhood of $\omega = 0$ is therefore as flat as possible for a given order n . The Butterworth amplitude spectrum thus produces what is known as a “maximally flat” approximation.

To evaluate the transfer function $H(s)$ corresponding to the given power magnitude-squared $|H(j\omega)|^2$ we first note that

$$|H(j\omega)|^2 = H(j\omega)H^*(j\omega) = H(j\omega)H(-j\omega) = H(s)H(-s)|_{s=j\omega} \tag{9.5}$$

that is,

$$H(s)H(-s) = |H(j\omega)|^2|_{\omega=s/j} = \frac{1}{1+(-js)^{2n}} = \frac{1}{1+(-s^2)^n} = \frac{1}{1+(-1)^n s^{2n}}. \tag{9.6}$$

We set out to deduce the value of $H(s)$ from this product. The poles of the product $H(s)H(-s)$ are found by writing

$$(-1)^n s^{2n} = -1 \tag{9.7}$$

$$s^{2n} = (-1)^{n-1} = e^{j(n-1)\pi} e^{j2k\pi}, \quad k = 1, 2, \dots \tag{9.8}$$

The poles are therefore given by

$$s_k = e^{j\pi(2k+n-1)/(2n)}, \quad k = 1, 2, \dots, 2n. \tag{9.9}$$

We note that there are $2n$ poles equally spaced around the unit circle $|s| = 1$ in the s plane, as shown in Fig. 9.3 for different values of n .

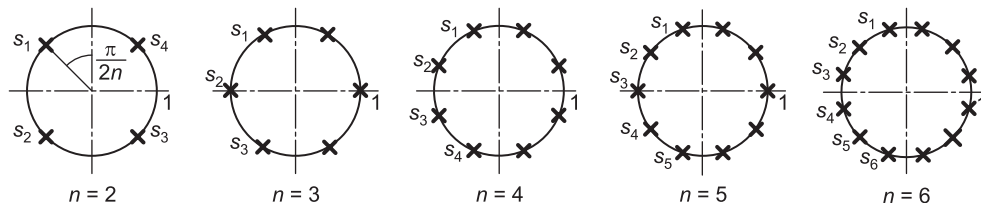


FIGURE 9.3 Poles of Butterworth filter for different orders.

We also note that the n poles s_1, s_2, \dots, s_n are in the left half of the s plane as shown in the figure. We can therefore select these as the poles of $H(s)$ thus ensuring a stable system. The transfer function sought is therefore

$$H(s) = \frac{1}{\prod_{i=1}^n (s - s_i)} \tag{9.10}$$

where

$$s_i = e^{j\pi(2i+n-1)/(2n)} = \cos \pi \left(\frac{2i+n-1}{2n} \right) + j \sin \pi \left(\frac{2i+n-1}{2n} \right). \tag{9.11}$$

Writing

$$H(s) \triangleq \frac{1}{A(s)} = \frac{1}{s^n + a_{n-1}s^{n-1} + \dots + a_2s^2 + a_1s + 1} \tag{9.12}$$

where $A(s)$ is the ‘‘Butterworth polynomial,’’ we can evaluate the coefficients a_1, a_2, \dots, a_{n-1} . The result is shown in Table 9.1.

TABLE 9.1 Butterworth filter coefficients of the denominator polynomial $s^n + a_1s^{n-1} + a_2s^{n-2} + \dots + a_2s^2 + a_1s + 1$

n	a_1	a_2	a_3	a_4	a_5
2	1.414214				
3	2				
4	2.613126	3.414214			
5	3.236068	5.236068			
6	3.863703	7.464102	9.141620		
7	4.493959	10.097834	14.591794		
8	5.125831	13.137071	21.846150	25.688356	
9	5.758770	16.581719	31.163437	41.986385	
10	6.392453	20.431729	42.802061	64.882396	74.233429

TABLE 9.2 Butterworth lowpass filter prototype poles and residues

n	Poles	Residues
2	$-0.7071 \pm j0.7071$	$\mp j0.7071$
3	$-1.0000, -0.5000 \pm j0.8660$	$1.0000, -0.5000 \mp j0.2887$
4	$-0.9239 \pm j0.3827, -0.3827 \pm j0.9239$	$0.4619 \mp j1.1152, -0.4619 \pm j0.1913$
5	$-0.8090 \pm j0.5878, -0.3090 \pm j0.9511, -1.0000$	$-0.8090 \mp j1.1135, -0.1382 \pm j0.4253, 1.8944$
6	$-0.2588 \pm j0.9659, -0.9659 \pm j0.2588, -0.7071 \pm j0.7071$	$0.2041 \pm j0.3536, 1.3195 \mp j2.2854, -1.5236, -1.5236$
7	$-0.9010 \pm j0.4339, -0.2225 \pm j0.9749, -0.6235 \pm j0.7818, -1.0000$	$-1.4920 \mp j3.0981, 0.3685 \pm j0.0841, -1.0325 \pm j1.2947, 4.3119$
8	$-0.8315 \pm j0.5556, -0.1951 \pm j0.9808, -0.9808 \pm j0.1951, -0.5556 \pm j0.8315$	$-4.2087 \mp j0.8372, 0.2940 \mp j0.1964, 3.5679 \mp j5.3398, 0.3468 \pm j1.7433$
9	$-1.0000, -0.7660 \pm j0.6428, -0.1736 \pm j0.9848, -0.5000 \pm j0.8660, -0.9397 \pm j0.3420$	$10.7211, -3.9788 \pm j3.3386, 0.0579 \mp j0.3283, 1.6372 \pm j0.9452, -3.0769 \mp j8.4536$
10	$-0.8910 \pm j0.4540, -0.4540 \pm j0.8910, -0.1564 \pm j0.9877, -0.9877 \pm j0.1564, -0.7071 \pm j0.7071$	$-11.4697 \mp j3.7267, 1.8989 \mp j0.6170, -0.1859 \mp j0.2558, 9.7567 \mp j13.4290, \pm j6.1449$

We note that the coefficients are symmetric about the polynomial center, that is,

$$a_1 = a_{n-1}, \quad a_2 = a_{n-2}, \quad \dots \tag{9.13}$$

a symmetry resulting from the uniform spacing of the poles about the unit circle. Note also that with each complex pole s_i there is a conjugate pole s_i^* so that

$$s_i s_i^* = |s_i|^2 = 1. \tag{9.14}$$

The poles s_i of such a normalized prototype filter are function of only the order n . Hence, given the order n , the poles s_i are directly implied, as given in Table 9.2.

The Butterworth transfer function denominator polynomial coefficients may be evaluated recursively. We have $a_n = a_0 = 1$ and

$$a_k = a_{k-1} \frac{\cos[(k-1)\pi/(2n)]}{\sin[k\pi/(2n)]}, \quad k = 1, 2, \dots, n \tag{9.15}$$

wherefrom we may write

$$a_k = \prod_{m=1}^k \frac{\cos[(m-1)\pi/(2n)]}{\sin[m\pi/(2n)]}, \quad k = 1, 2, \dots, n \tag{9.16}$$

The MATLAB[®] function **Butter**($n, W_n, 's'$), where the argument ' s' ' means *continuous-time* filter, accepts the value of the order n and the cut-off frequency W_n . If the cut-off frequency W_n is set equal to 1, the resulting filter has $\varepsilon = 1$ and a 3 dB attenuation at the cut-off frequency $\omega = 1$. The MATLAB function $(B, A) = \mathbf{Butter}(n, W_n, 's')$ returns the coefficients of the numerator $B(s)$ and denominator $A(s)$ of the transfer function. The function $(z, p, K) = \mathbf{Butter}(n, W_n, 's')$ returns the filter zeros z_i as elements of the vector z , the poles p_i as elements of the vector p and the “gain” K , so that the filter transfer function is expressed in the form

$$H(s) = K \frac{\prod_{i=1}^n (s - z_i)}{\prod_{i=1}^n (s - p_i)}. \quad (9.17)$$

With $W_n = 1$ the results A, B, z, p, K are those of the normalized filter and are the same as those listed in the tables. To determine the filter order n , the function

$$[N, W_n] = \mathbf{buttord}(W_p, W_s, R_p, R_s, 's') \quad (9.18)$$

is used. In this case the arguments W_p and R_p are the edge frequency at the end of the pass-band and the corresponding attenuation, respectively. The arguments W_s and R_s are the stop-band edge frequency and the corresponding attenuation. The results N and W_n are the filter order and the 3 dB cut-off frequency ω_c , respectively.

The maximum value of the filter response occurs at zero frequency

$$|H(j\omega)|_{\max} = |H(j0)| = K. \quad (9.19)$$

To obtain a maximum response of M dB we write

$$20 \log_{10} K = M \quad (9.20)$$

$$K = 10^{M/20}. \quad (9.21)$$

For example, if $M = 0$ dB, $K = 1$ and if $M = 10$ dB, $K = 10^{0.5} = 3.1623$.

9.3 Denormalization of Butterworth Filter Prototype

To convert the normalized filter into a denormalized one with a true cut-off frequency of f_c Hz, that is, $\omega_c = 2\pi f_c$ radians/second, the filter transfer function is denormalized by the substitution

$$\omega \longrightarrow \omega/\omega_c \quad (9.22)$$

meaning that we replace ω by ω/ω_c .

The magnitude-squared spectrum of the denormalized filter is therefore

$$|H(j\omega)|^2 = \frac{1}{1 + (\omega/\omega_c)^{2n}} \quad (9.23)$$

a function of two parameters, the cut-off frequency ω_c and the order n .

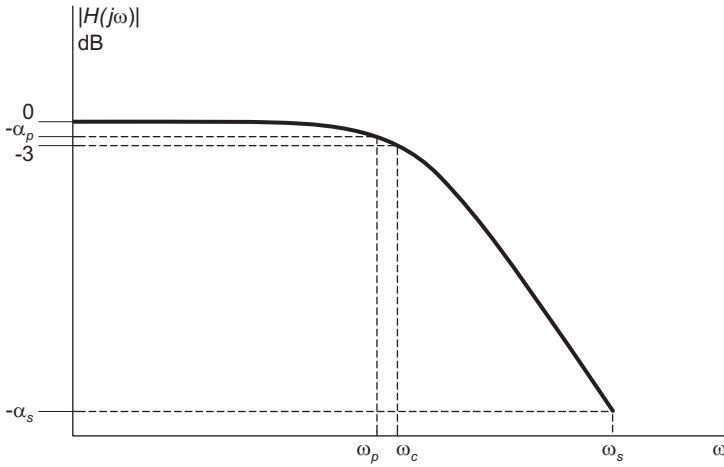


FIGURE 9.4 Butterworth filter frequency response.

As Fig. 9.4 shows, the attenuation at the end of the pass-band, at $\omega = \omega_p$, is α_p dB. At the beginning of the stop-band, at $\omega = \omega_s$ it is α_s dB. The region between the pass-band and the stop-band is the *transition-band*.

We note that at the *cut-off frequency* $\omega = \omega_c$ r/s the magnitude-squared spectrum is given by $|H(j\omega_c)|^2 = 0.5$, $|H(j\omega_c)| = 0.707$ and the attenuation by

$$\alpha_c = 10 \log_{10} \frac{|H(j0)|^2}{|H(j\omega_c)|^2} = 10 \log_{10} \frac{1}{0.5} = 3 \text{ dB.} \quad (9.24)$$

Moreover

$$20 \log_{10} \frac{|H(j0)|}{|H(j\omega_p)|} = \alpha_p \quad (9.25)$$

i.e.

$$\alpha_p = 10 \log_{10} \left\{ 1 + (\omega_p/\omega_c)^{2n} \right\} \quad (9.26)$$

$$(\omega_p/\omega_c)^{2n} = 10^{\alpha_p/10} - 1. \quad (9.27)$$

Similarly

$$20 \log_{10} \left\{ \frac{1}{1/\sqrt{1 + (\omega_s/\omega_c)^{2n}}} \right\} = \alpha_s \quad (9.28)$$

i.e.

$$1 + (\omega_s/\omega_c)^{2n} = 10^{\alpha_s/10} \quad (9.29)$$

$$(\omega_s/\omega_c)^{2n} = 10^{\alpha_s/10} - 1. \quad (9.30)$$

Hence

$$\left(\frac{\omega_p}{\omega_s} \right)^{2n} = \frac{10^{\alpha_p/10} - 1}{10^{\alpha_s/10} - 1}. \quad (9.31)$$

Example 9.1 Evaluate the transfer function of a lowpass Butterworth filter that satisfies the following specifications: a 3-dB cut-off frequency of 2 kHz, attenuation of at least 50 dB

at 4 kHz. Evaluate the pass-band edge frequency ω_p whereat the attenuation should equal 0.5 dB.

With cut-off frequency 2 kHz, i.e. $\omega_c = 2\pi \times 2000$ r/s, taken as normalized frequency $\omega = 1$, the stop-band frequency (4 kHz) corresponds to $\omega = 2$. We should have

$$10 \log_{10} \frac{1}{1 + 2^{2n}} = -50 \tag{9.32}$$

i.e. $(1 + 2^{2n}) = 10^5$, or $n = 8.3$. We choose for the filter order the next higher integer $n = 9$. From Butterworth filter tables we obtain the normalized (prototype) transfer function with order $n = 9$. The denormalized transfer function is then

$$H_{denorm}(s) = H_{norm}(s)|_{s \rightarrow s/(2\pi \times 2000)} \tag{9.33}$$

Substituting $\omega_c = 2\pi \times 2000$ and $\alpha_p = 0.5$ we obtain

$$\omega_p = \omega_c(10^{0.05} - 1)^{1/18} = 2\pi \times 1779.4 \text{ r/s}$$

so that the pass-band edge frequency is $f_p = 1.7794$ kHz.

Example 9.2 Evaluate the order of a Butterworth filter having the specifications: at the frequency 10 kHz the attenuation should at most be 1 dB; at the frequency 15 kHz the attenuation should be not less than 60 dB.

We have $\alpha_p = 1$ dB, $\alpha_s = 60$ dB, $\omega_p = 2\pi \times 10 \times 10^3 = 6.2832 \times 10^4$ r/s and $\omega_s = 2\pi \times 15 \times 10^3 = 9.4248 \times 10^4$ r/s

$$\left(\frac{\omega_p}{\omega_s}\right)^{2n} = \left(\frac{10}{15}\right)^{2n} = \frac{10^{0.1} - 1}{10^6 - 1} = 2.5893 \times 10^{-7}$$

wherefrom $n = 18.7029$. We choose the next higher integer, the ceiling of n , $[n] = 19$, as the filter order. If we maintain fixed the values ω_s , α_p and α_s then the cut-off frequency ω_c may be evaluated by writing

$$\omega_c = \frac{\omega_s}{(10^{\alpha_s/10} - 1)^{1/38}} = \frac{9.4248 \times 10^4}{(10^6 - 1)^{1/38}} = 6.5521 \times 10^4 \text{ r/s}$$

$$f_c = \omega_c/(2\pi) = 10.4280 \text{ kHz.}$$

The fourth value ω_p will increase slightly due to the increase in the value of n to the next higher integer. Let ω'_p denote this updated value of the pass-band edge frequency. We have

$$\left(\frac{\omega'_p}{\omega_s}\right)^{2n} = \frac{10^{\alpha_p/10} - 1}{10^{\alpha_s/10} - 1} = 2.5893 \times 10^{-7}$$

$$\frac{\omega'_p}{\omega_s} = (2.5893 \times 10^{-7})^{1/38} = 0.6709$$

$$\omega'_p = 0.6709 \omega_s = 0.6709 \times 2\pi \times 15 \times 10^3$$

$$= 2\pi \times 1.0064 \times 10^4 = 6.3232 \times 10^4.$$

The same result is obtained by writing the MATLAB command

$$[N, W_n] = \mathbf{buttord}(W_p, W_s, R_p, R_s, 's')$$

where $W_p = \omega_p$, $W_s = \omega_s$, $R_p = \alpha_p$, $R_s = \alpha_s$ resulting in the order $N = n = 19$ and $W_n = \omega_c$, the cutoff frequency found above.

Using MATLAB we obtain the order $n = 19$ and the value W_n , the cut-off frequency. We can also obtain the numerator and denominator coefficients of the transfer function's polynomials $B(s)$ and $A(s)$ as well as the poles and zeros.

9.4 Denormalized Transfer Function

As we have seen above, the denormalized filter magnitude-squared spectrum has the form

$$|H(j\omega)|^2 = \frac{1}{1 + (\omega/\omega_c)^{2n}} = \frac{\omega_c^{2n}}{\omega^{2n} + \omega_c^{2n}} \quad (9.34)$$

where ω is the true denormalized frequency in rad/sec. The transfer function is denormalized by replacing s by s/ω_c . We may write

$$H(s)H(-s) = \frac{1}{1 + (s/j\omega_c)^{2n}} = \frac{\omega_c^{2n}}{\omega_c^{2n} + (-1)^n s^{2n}}. \quad (9.35)$$

The true, denormalized, poles are found by writing

$$(-1)^n s^{2n} = -\omega_c^{2n} \quad (9.36)$$

$$s^{2n} = \omega_c^{2n} e^{j(n-1)\pi} e^{j2k\pi}. \quad (9.37)$$

Denoting by q_k the denormalized poles we have

$$q_k = \omega_c e^{j\pi(2k+n-1)/(2n)} = \omega_c s_k, \quad k = 1, 2, \dots, 2n. \quad (9.38)$$

These are the same values of the poles obtained above for the normalized form except that now the poles are on a circle of radius ω_c rather than the unit circle. The transfer function has the denormalized form

$$H(s) = \frac{\omega_c^n}{\prod_{i=1}^n (s - q_i)} \quad (9.39)$$

where we note that its numerator is given by ω_c^n instead of 1. The poles in the last example may thus be evaluated. We have

$$q_k = 2.0856 \times 10^4 \pi e^{j\pi(2k+18)/38} = 6.5520 \times 10^4 e^{j\pi(2k+18)/38}, \quad k = 1, 2, \dots, 19. \quad (9.40)$$

The transfer function $H(s)$ is given by

$$H(s) = \frac{\omega_c^{19}}{\prod_{i=1}^{19} (s - q_i)} = \frac{(6.5520 \times 10^4)^{19}}{\prod_{i=1}^{19} (s - q_i)} = \frac{3.2445 \times 10^{91}}{\prod_{i=1}^{19} (s - q_i)}. \quad (9.41)$$

The amplitude spectrum is shown in Fig. 9.5

As we have seen in Chapter 8, knowing the filter transfer function we can construct the filter in structures known as canonical or direct forms as well as cascade or parallel forms. As an illustration, the filter of this last example can be realized as a cascade of a first order filter, corresponding to the single real pole, and nine second order filters, corresponding to the complex conjugate poles, as shown in Fig. 9.6

We can alternatively evaluate the 19th order polynomial $A(s)$, thus writing $H(s)$ in the form

$$H(s) = \frac{1}{A(s)} = \frac{(2.0856 \times 10^4 \pi)^{19}}{s^{19} + \alpha_{18}s^{18} + \alpha_{17}s^{17} + \dots + \alpha_1 s + \alpha_0}. \quad (9.42)$$

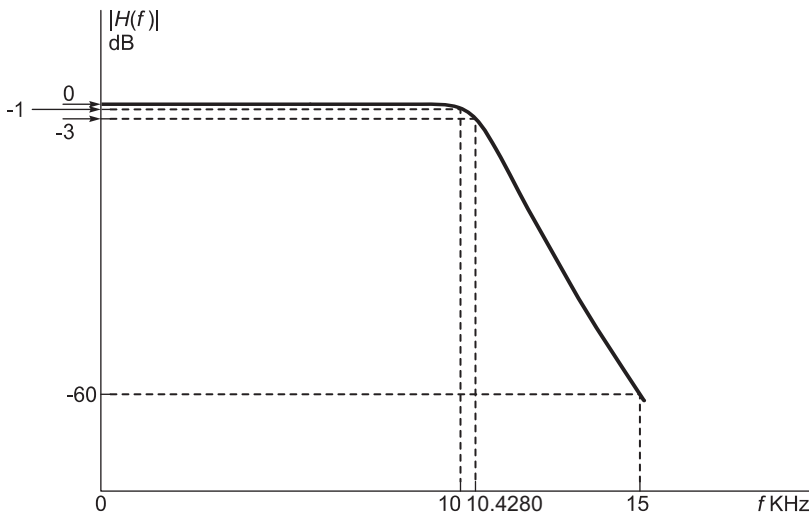


FIGURE 9.5 Butterworth filter frequency response.

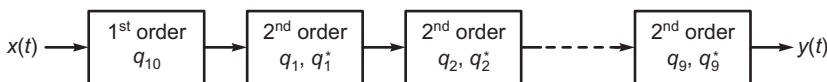


FIGURE 9.6 System cascade realization.

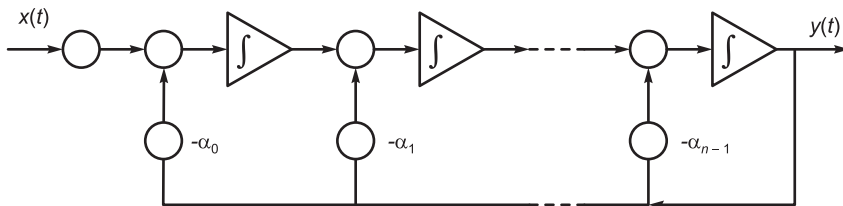


FIGURE 9.7 Possible filter realization.

The filter may be realized for example in a direct (canonical) form as described in Chapter 8, obtaining the structure shown in Fig. 9.7 with $n = 19$.

A parallel form of realization can be obtained by applying a partial fraction expansion. We obtain the form

$$H(s) = \sum_{i=1}^{19} \frac{A_i}{s - q_i} = \frac{A_{10}}{s - q_{10}} + \sum_{i=1}^9 \frac{A_i s + B_i}{s^2 - 2\Re[q_i]s + |q_i|^2}. \tag{9.43}$$

The filter may thus be realized as a parallel structure containing one first order and nine second order filters.

9.5 The Case $\varepsilon \neq 1$

For the Butterworth approximation with $\varepsilon \neq 1$ we may write

$$|H_\varepsilon(j\omega)|^2 = \frac{H^2}{1 + \varepsilon^2\omega^{2n}} \tag{9.44}$$

and with

$$|H(j\omega)|^2 = \frac{H^2}{1 + \omega^{2n}} \tag{9.45}$$

we note that

$$|H_\varepsilon(j\omega)|^2 = |H(j\omega)|^2 \Big|_{\omega \rightarrow \varepsilon^{1/n}\omega} \tag{9.46}$$

and that the magnitude-squared spectrum $|H_\varepsilon(j\omega)|^2$ can be written as a denormalized spectrum with the cut-off frequency ω_c appearing explicitly by letting $\varepsilon^2 = 1/\omega_c^{2n}$, or $\varepsilon = 1/\omega_c^n$, and conversely $\omega_c = \varepsilon^{-1/n}$.

The transfer function $H_\varepsilon(s)$ can be determined from $H(s)$ by replacing s by $\varepsilon^{1/n}s$, or equivalently by s/ω_c .

$$H_\varepsilon(s) = H(s) \Big|_{s \rightarrow \varepsilon^{1/n}s} = \frac{1}{\prod_{i=1}^n (s - s_i)} \Big|_{s \rightarrow \sqrt[n]{\varepsilon}s} = \frac{1}{\prod_{i=1}^n (\sqrt[n]{\varepsilon}s - s_i)} = \frac{\varepsilon^{-1}}{\prod_{i=1}^n (s - q_i)} \tag{9.47}$$

The poles of $H_\varepsilon(s)$ are thus given by

$$q_i = \varepsilon^{-1/n} s_i \tag{9.48}$$

and are therefore on a circle in the s plane of radius $\varepsilon^{-1/n}$ as shown in Fig. 9.8.

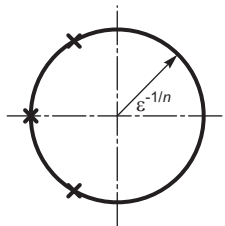


FIGURE 9.8 Third order system poles in the case $\varepsilon \neq 1$.

Example 9.3 Starting from the prototype of a third order Butterworth filter, evaluate the parameter ε needed to produce an attenuation of 2 dB at the frequency $\omega = 1$. Evaluate the filter transfer function obtained using this value of ε and the filter poles.

The third order Butterworth filter prototype transfer function is

$$H(s) = \frac{1}{s^3 + 2s^2 + 2s + 1}$$

Writing

$$10 \log_{10} (1 + \varepsilon^2) = 2$$

we obtain

$$1 + \varepsilon^2 = 10^{0.2} = 1.5849.$$

Hence $\varepsilon^2 = 0.5849$ and $\varepsilon = 0.7648$.

$$\begin{aligned} H_\varepsilon(s) &= H(s)|_{s \rightarrow \varepsilon^{1/3}s} = \frac{1}{\varepsilon s^3 + 2\varepsilon^{2/3}s^2 + 2\varepsilon^{1/3}s + 1} \\ &= \frac{\varepsilon^{-1}}{s^3 + 2\varepsilon^{-1/3}s^2 + 2\varepsilon^{-2/3}s + \varepsilon^{-1}} \\ &= \frac{1.3076}{s^3 + 2.1870s^2 + 2.3915s + 1.3076}. \end{aligned}$$

The poles are

$$q_i = \varepsilon^{-1/3}s_i = \varepsilon^{-1/3}(-0.5 \pm j0.866) \quad \text{and} \quad -\varepsilon^{-1/3}.$$

The attenuation at $\omega = 1$ is given by

$$20 \log_{10} \frac{|H(j0)|}{|H(j1)|} = 20 \log_{10} \frac{1}{1/\sqrt{1 + \varepsilon^2}} = 10 \log_{10} (1 + \varepsilon^2) = 2 \text{ dB}$$

as required.

9.6 Butterworth Filter Order Formula

As with the case $\varepsilon = 1$, let the pass-band edge frequency of a Butterworth filter be $\omega = \omega_p$. Let the required corresponding drop in magnitude spectrum be at most R_p dB. Let the stop-band edge frequency be $\omega = \omega_s$ and the corresponding magnitude attenuation be at least R_s dB. The filter order can be evaluated by writing

$$|H(j\omega)|^2 = \frac{K^2}{1 + \varepsilon^2 \omega^{2n}} \tag{9.49}$$

$$10 \log_{10} \left[\frac{|H(j0)|^2}{|H(j\omega_p)|^2} \right] = 10 \log_{10} \left[\frac{K^2}{\{K^2/(1 + \varepsilon^2 \omega_p^{2n})\}} \right] = R_p \tag{9.50}$$

i.e.

$$\varepsilon^2 \omega_p^{2n} = 10^{0.1R_p} - 1. \tag{9.51}$$

Similarly

$$\varepsilon^2 \omega_s^{2n} = 10^{0.1R_s} - 1 \tag{9.52}$$

$$\frac{\omega_s^{2n}}{\omega_p^{2n}} = \frac{10^{0.1R_s} - 1}{10^{0.1R_p} - 1} \tag{9.53}$$

$$2n \log_{10} \left(\frac{\omega_s}{\omega_p} \right) = \log_{10} \left(\frac{10^{0.1R_s} - 1}{10^{0.1R_p} - 1} \right) \tag{9.54}$$

$$n = 0.5 \log_{10} \left(\frac{10^{0.1R_s} - 1}{10^{0.1R_p} - 1} \right) / \log_{10} \left(\frac{\omega_s}{\omega_p} \right). \tag{9.55}$$

A MATLAB function may effect such an evaluation. Calling it **butterorder.m** we can write the function in the form

```
function [n] = butterorder (wp,ws,Rp,Rs)
n=0.5*log10((10^(Rs/10)-1)/(10^(Rp/10)-1))/log10(ws/wp).
```

Note that MATLAB has the built-in function **Buttord** which evaluates the Butterworth filter order.

9.7 Nomographs

A nomograph for deducing the order of a Butterworth filter to meet given specifications is shown in Fig. 9.9.

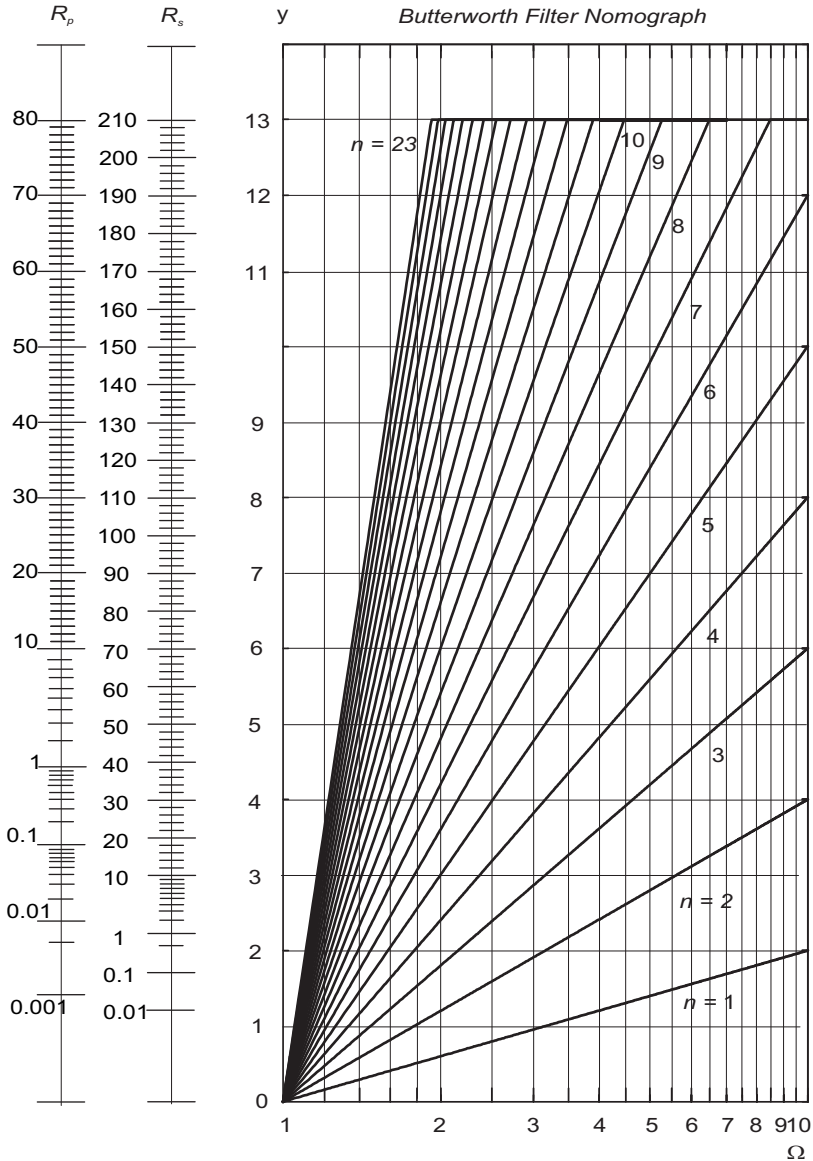


FIGURE 9.9 Butterworth filter nomograph.

Nomographs can be used whatever the value of ε , in contrast with the tables of filter transfer function coefficients and poles which are given for $\varepsilon = 1$. The following example

shows that knowing the pass-band and stop-band attenuation or simply the attenuation at two given frequencies the filter order can be determined using the nomograph.

Example 9.4 Design a Butterworth filter prototype having an attenuation of at most 1 dB in the pass-band i.e. at $\omega = 1$ and at least 30 dB at $\omega = 3$. Evaluate the filter transfer function if the cut-off frequency should equal 2 kHz.

Since the pass-band attenuation at $\omega = 1$ is not 3 dB the value of ϵ is not 1. We have

$$20 \log \frac{1}{1/\{1 + \epsilon^2\}^{1/2}} = 1$$

$$\sqrt{1 + \epsilon^2} = 10^{0.05} = 1.122$$

$$1 + \epsilon^2 = 1.26 \text{ i.e. } \epsilon^2 = 0.26, \text{ or } \epsilon = 0.51$$

$$20 \log \{|H(j0)| / |H(j3)|\} \geq 30.$$

Writing

$$\frac{|H(j0)|}{|H(j3)|} = \frac{1}{1/\sqrt{1 + \epsilon^2} 3^{2n}} = 10^{1.5} = 31.6228$$

$$n = 3.76.$$

We take the filter order as the ceiling $\lceil n \rceil = 4$.

Nomograph Approach

As shown in Fig. 9.10 a filter nomograph has two vertical scales labeled R_p and R_s on the left of a chart labeled y versus Ω containing a set of curves. Let α_p denote pass-band attenuation or the attenuation at a frequency ω_1 and α_s denote stop-band attenuation or the attenuation at a higher frequency ω_2 .

The chart is used by marking the value α_p on the left vertical scale R_p and the value α_s on the vertical scale R_s , as shown in the figure.

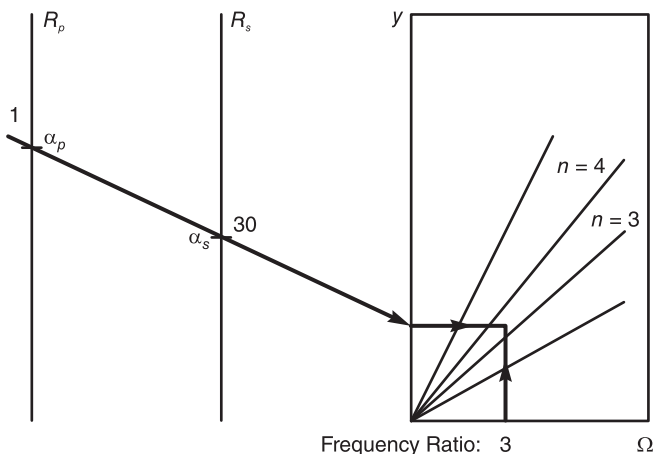


FIGURE 9.10 Evaluating the filter order using the nomograph.

A straight-line is drawn joining the point $R_p = \alpha_p = 1$ on the left-hand vertical scale to the point $R_s = \alpha_s = 30$ on the second vertical line and is extended until it intersects

the vertical axis y of the attenuation versus Ω chart. As shown in the figure, a horizontal line is subsequently drawn to the right. On the Ω axis a vertical line is drawn at the value of $\Omega = \omega_2/\omega_1 = 3/1 = 3$, that is, the ratio of the two given frequencies. The intersection point of the two lines is noted. The filter order, $n = 4$ in the present example, is read on the nomograph curve that is closest to and not lower than the intersection point.

Denormalization: From the tables the normalized filter transfer function is given by

$$H(s) = \frac{1}{s^4 + 2.613s^3 + 3.414s^2 + 2.613s + 1}.$$

To obtain a filter of cut-off frequency $\omega_c = 2\pi \times 2000$ r/s, we replace ω by ω/ω_c and s by s/ω_c , wherefrom the denormalized transfer function $H_d(s)$ is given by

$$\begin{aligned} H_d(s) &= H(s)|_{s \rightarrow s/\omega_c} \\ &= \frac{1}{(s/\omega_c)^4 + 2.613(s/\omega_c)^3 + 3.414(s/\omega_c)^2 + 2.613(s/\omega_c) + 1} \\ &= \frac{\omega_c^4}{s^4 + 2.613\omega_c s^3 + 3.414\omega_c^2 s^2 + 2.613\omega_c^3 s + \omega_c^4} \\ &= 2.4937 \times 10^{16}/D(s) \end{aligned}$$

$$D(s) = s^4 + 3.2838 \times 10^4 s^3 + 5.3915 \times 10^8 s^2 + 5.1855 \times 10^{12} s + 2.4937 \times 10^{16}.$$

A MATLAB program containing the statements

$$Wn = 2\pi \times 2000, \quad N = 4, \quad [b, a] = \mathbf{Butter}(N, Wn, 's')$$

produces the same results.

9.8 Chebyshev Approximation

The Butterworth approximation being maximally flat at $\omega = 0$ is the best approximation of the ideal filter's pass-band. However for a given filter it does not necessarily lead to the best overall approximation of the ideal filter spectrum, as seen in Fig. 9.1. In fact a narrower transition band can be obtained if the approximation allowed ripple variations in the pass-band. This is what the Chebyshev approximation sets out to do, and is referred to also as Chebyshev Type I. A dual form, Chebyshev Type II, will be studied later on in this chapter.

The magnitude-squared spectrum of the Chebyshev approximation of the ideal lowpass filter is given by

$$|H(j\omega)|^2 = \frac{1}{1 + \varepsilon^2 C_n^2(\omega)} \quad (9.56)$$

where $C_n(\omega)$ denotes the Chebyshev polynomials of order n . These are defined by the equation

$$C_n(\omega) = \cos(n \cos^{-1} \omega), \quad 0 \leq \omega \leq 1 \quad (9.57)$$

or, equivalently,

$$C_n(\omega) = \cosh(n \cosh^{-1} \omega), \quad \omega \geq 1. \quad (9.58)$$

By direct substitution we have

$$C_1(\omega) = \cos(\cos^{-1} \omega) = \omega \quad (9.59)$$

$$C_2(\omega) = \cos(2 \cos^{-1} \omega). \tag{9.60}$$

Writing

$$\cos^{-1} \omega = \theta \text{ i.e. } \omega = \cos \theta \tag{9.61}$$

we have

$$C_2(\omega) = \cos(2\theta) = 2 \cos^2 \theta - 1 = 2\omega^2 - 1 \tag{9.62}$$

$$C_3(\omega) = \cos 3\theta = 4(\cos \theta)^3 - 3 \cos \theta = 4\omega^3 - 3\omega. \tag{9.63}$$

We can obtain a recursive relation for generating these polynomials.

$$C_{n+1}(\omega) = \cos[(n+1)\theta] = \cos n\theta \cos \theta - \sin n\theta \sin \theta \tag{9.64}$$

$$C_{n-1}(\omega) = \cos n\theta \cos \theta + \sin n\theta \sin \theta. \tag{9.65}$$

$$C_{n+1}(\omega) + C_{n-1}(\omega) = 2 \cos \theta \cos n\theta = 2\omega C_n(\omega) \tag{9.66}$$

i.e.

$$C_{n+1}(\omega) = 2\omega C_n(\omega) - C_{n-1}(\omega). \tag{9.67}$$

For example

$$C_4(\omega) = 2\omega(4\omega^3 - 3\omega) - (2\omega^2 - 1) = 8\omega^4 - 8\omega^2 + 1 \tag{9.68}$$

$$C_5(\omega) = 16\omega^5 - 20\omega^3 + 5\omega. \tag{9.69}$$

We note, moreover, that

$$C_n(1) = \cos(n \cos^{-1} 1) = \cos(n2k\pi), \quad k = 0, 1, 2, \dots \tag{9.70}$$

i.e.

$$C_n(1) = 1 \tag{9.71}$$

and that

$$C_n(0) = \begin{cases} 0, & n = 1, 3, 5, \dots \\ -1, & n = 2, 6, 10, \dots \\ 1, & n = 0, 4, 8, \dots \end{cases} \tag{9.72}$$

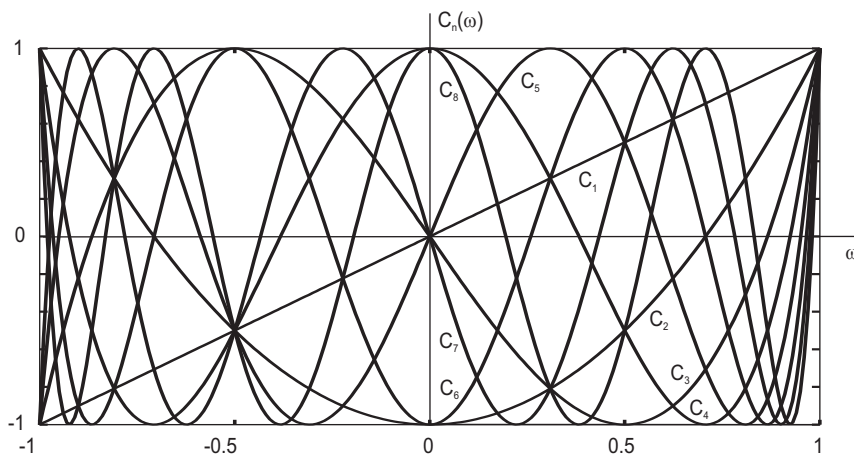


FIGURE 9.11 Chebyshev polynomials.

Chebyshev polynomials $C_n(\omega)$ for $n = 1$ to 8 are shown in Fig. 9.11. We may write

$$\cos^{-1} \omega = \theta, \quad \omega = \cos \theta \quad (9.73)$$

$$\sin \theta = \sqrt{1 - \omega^2} \quad (9.74)$$

$$e^{j\theta} = \cos \theta + j \sin \theta = \omega + j\sqrt{1 - \omega^2} \quad (9.75)$$

$$e^{jn\theta} = \left(\omega + j\sqrt{1 - \omega^2}\right)^n \quad (9.76)$$

so that

$$\begin{aligned} C_n(\omega) &= \cos(n \cos^{-1} \omega) = \cos n\theta = (e^{jn\theta} + e^{-jn\theta})/2 \\ &= \left\{ \left(\omega + j\sqrt{1 - \omega^2}\right)^n + \left(\omega + j\sqrt{1 - \omega^2}\right)^{-n} \right\} / 2. \end{aligned} \quad (9.77)$$

Since

$$e^{-j\theta} = \cos \theta - j \sin \theta = \omega - j\sqrt{1 - \omega^2} \quad (9.78)$$

we have, alternatively,

$$e^{-jn\theta} = \left(\omega - j\sqrt{1 - \omega^2}\right)^n \quad (9.79)$$

so that we can also write the equivalent alternative form

$$C_n(\omega) = \left\{ \left(\omega + j\sqrt{1 - \omega^2}\right)^n + \left(\omega - j\sqrt{1 - \omega^2}\right)^n \right\} / 2. \quad (9.80)$$

We can, moreover, use the more general hyperbolic functions, thus allowing $|\omega|$ to have values greater than 1. We write

$$\cosh^{-1} \omega = \gamma, \quad \omega = \cosh \gamma \quad (9.81)$$

$$\sinh \gamma = \sqrt{\omega^2 - 1} \quad (9.82)$$

$$e^\gamma = \cosh \gamma + \sinh \gamma = \omega + \sqrt{\omega^2 - 1} \quad (9.83)$$

$$e^{-\gamma} = \cosh \gamma - \sinh \gamma = \omega - \sqrt{\omega^2 - 1} \quad (9.84)$$

$$\begin{aligned} C_n(\omega) &= \cosh(n \cosh^{-1} \omega) = \cosh(n\gamma) = (e^{n\gamma} + e^{-n\gamma})/2 \\ &= \left\{ \left(\omega + \sqrt{\omega^2 - 1}\right)^n + \left(\omega + \sqrt{\omega^2 - 1}\right)^{-n} \right\} / 2 \end{aligned} \quad (9.85)$$

and since

$$e^{-n\gamma} = \left(\omega - \sqrt{\omega^2 - 1}\right)^n \quad (9.86)$$

we have, alternatively,

$$C_n(\omega) = \left\{ \left(\omega + \sqrt{\omega^2 - 1}\right)^n + \left(\omega - \sqrt{\omega^2 - 1}\right)^n \right\} / 2. \quad (9.87)$$

The magnitude-squared spectrum

$$|H(j\omega)|^2 = \frac{1}{1 + \varepsilon^2 C_n^2(\omega)} \quad (9.88)$$

is shown in Fig. 9.12 for $n = 1$ to 4 . Having a uniform amplitude of oscillations in the pass-band, this filter is known as an *equiripple* approximation. We note that for n odd, $H(j0) = 1$, whereas for n even

$$|H(0)| = \frac{1}{\sqrt{1 + \varepsilon^2}} \quad (9.89)$$

and that for all n

$$|H(j1)| = \frac{1}{\sqrt{1 + \varepsilon^2}}. \tag{9.90}$$

To denormalize the filter we use the replacement $\omega \rightarrow \omega/\omega_c$. We may write

$$|H_{\text{denorm}}(j\omega)|^2 = \frac{1}{1 + \varepsilon^2 C_n^2(\omega/\omega_c)}. \tag{9.91}$$

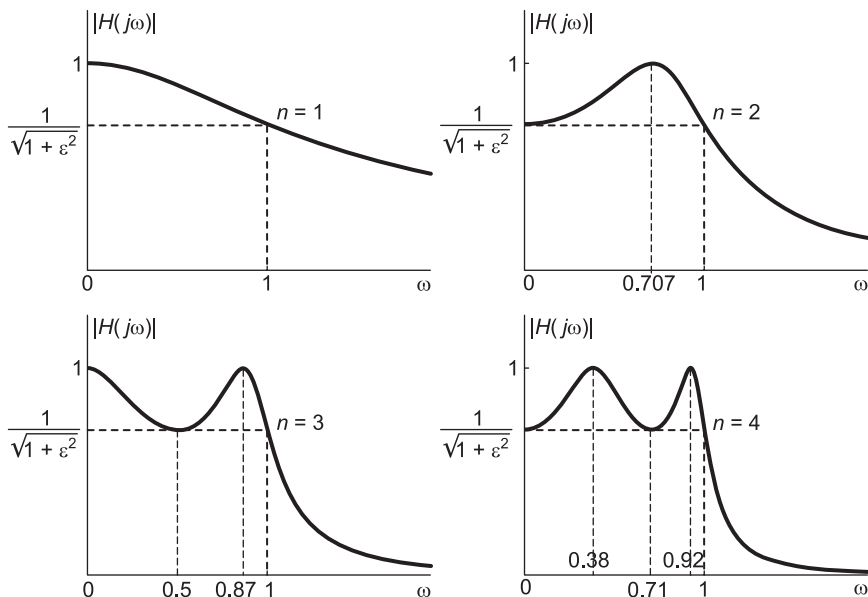


FIGURE 9.12 Chebyshev filter response for different orders.

Example 9.5 Evaluate the expression $H(s)H(-s)$ for a Chebyshev filter of the fifth order which has a maximum pass-band attenuation of 0.3 dB.

The maximum attenuation in the pass-band occurs at $\omega = 1$. We have

$$10 \log_{10} [1 + \varepsilon^2 C_n^2(1)] = 10 \log_{10} (1 + \varepsilon^2) = 0.3 \tag{9.92}$$

$$1 + \varepsilon^2 = 10^{0.03}, \quad \varepsilon^2 = 0.0715, \quad \varepsilon = 0.2674 \tag{9.93}$$

$$|H(j\omega)|^2 = \frac{1}{1 + 0.0715 C_5^2(\omega)} = \frac{1}{1 + 0.0715 (16\omega^5 - 20\omega^3 + 5\omega)^2} \tag{9.94}$$

$$\begin{aligned} |H(j\omega)|^2 &= \frac{1}{1 + 0.0715 (25\omega^2 - 20\omega^4 + 560\omega^6 - 640\omega^8 + 256\omega^{10})} \\ &= \frac{1}{1 + 1.7880\omega^2 - 14.304\omega^4 + 40.051\omega^6 - 45.772\omega^8 + 18.309\omega^{10}} \end{aligned} \tag{9.95}$$

$$H(s)H(-s) = |H(j\omega)|^2 \Big|_{\omega=-js} = \frac{1}{D(s)} \tag{9.96}$$

where

$$\begin{aligned} D(s) &= 1 + 1.7880(-js)^2 - 14.304(-js)^4 + 40.051(-js)^6 - 45.772(-js)^8 \\ &\quad + 18.309(-js)^{10} \\ &= 1 - 1.7880s^2 - 14.304s^4 - 40.051s^6 - 45.772s^8 - 18.309s^{10}. \end{aligned} \quad (9.97)$$

9.9 Pass-Band Ripple

Since the magnitude-squared spectrum

$$|H(j\omega)|^2 = \frac{1}{1 + \varepsilon^2 C_n^2(\omega)} \quad (9.98)$$

is a function of $C_n^2(\omega)$, and since $0 \leq C_n^2(\omega) \leq 1$ in the pass-band $0 \leq |\omega| \leq 1$ we have

$$|H(j\omega)|_{\max}^2 = 1 \quad (9.99)$$

and

$$|H(j\omega)|_{\min}^2 = \frac{1}{1 + \varepsilon^2}. \quad (9.100)$$

It is worthwhile noticing that

$$C_n^2(0) = \begin{cases} 1, & n, \text{ even} \\ 0, & n, \text{ odd} \end{cases} \quad (9.101)$$

and

$$|H(0)|^2 = \begin{cases} 1/(1 + \varepsilon^2), & n \text{ even} \\ 1, & N \text{ odd.} \end{cases} \quad (9.102)$$

9.10 Transfer Function of the Chebyshev Filter

The transfer function $H(s)$ is found by writing

$$H(s)H(-s) = |H(j\omega)|^2|_{\omega=-js} = \frac{1}{1 + \varepsilon^2 C_n^2(-js)}. \quad (9.103)$$

The poles of the product $H(s)H(-s)$ are the roots of the equation

$$1 + \varepsilon^2 C_n^2(-js) = 0 \quad (9.104)$$

i.e.

$$C_n(-js) = \pm j/\varepsilon \quad (9.105)$$

$$\cos[n \cos^{-1}(-js)] = \pm j/\varepsilon. \quad (9.106)$$

Writing

$$\phi = \phi_1 + j\phi_2 = \cos^{-1}(-js) \quad (9.107)$$

we have

$$-js = \cos \phi = \cos \phi_1 \cosh \phi_2 - j \sin \phi_1 \sinh \phi_2 \quad (9.108)$$

$$s = \sin \phi_1 \sinh \phi_2 + j \cos \phi_1 \cosh \phi_2. \tag{9.109}$$

We proceed to evaluate ϕ_1 and ϕ_2 . We have

$$\cos [n (\phi_1 + j\phi_2)] = \pm j/\varepsilon \tag{9.110}$$

$$\cos n\phi_1 \cosh n\phi_2 - j \sin n\phi_1 \sinh n\phi_2 = \pm j/\varepsilon \tag{9.111}$$

wherefrom

$$\cos n\phi_1 \cosh n\phi_2 = 0 \tag{9.112}$$

$$\sin n\phi_1 \sinh n\phi_2 = \pm 1/\varepsilon \tag{9.113}$$

i.e.

$$\cos n\phi_1 = 0 \tag{9.114}$$

$$n\phi_1 = \pm (2k - 1) \pi/2, \quad k = 1, 2, 3, \dots, 2n. \tag{9.115}$$

Let

$$\phi_1 = (2k - 1) \pi/(2n), \quad k = 1, 2, 3, \dots, 2n \tag{9.116}$$

$$\sin n\phi_1 = \pm 1 \tag{9.117}$$

and

$$\sinh n\phi_2 = 1/\varepsilon \tag{9.118}$$

that is,

$$\cosh n\phi_2 = \sqrt{1 + \frac{1}{\varepsilon^2}} \tag{9.119}$$

or

$$e^{n\phi_2} = \cosh n\phi_2 + \sinh n\phi_2 = \sqrt{1 + \frac{1}{\varepsilon^2}} \pm \frac{1}{\varepsilon}. \tag{9.120}$$

Note that if

$$e^{n\phi_2} = \sqrt{1 + \frac{1}{\varepsilon^2}} + \frac{1}{\varepsilon} \tag{9.121}$$

then

$$e^{-n\phi_2} = \frac{1}{\sqrt{1 + \frac{1}{\varepsilon^2}} + \frac{1}{\varepsilon}} = \sqrt{1 + \frac{1}{\varepsilon^2}} - \frac{1}{\varepsilon} \tag{9.122}$$

wherefrom

$$e^{\phi_2} = \left\{ \sqrt{1 + \frac{1}{\varepsilon^2}} + \frac{1}{\varepsilon} \right\}^{1/n} \tag{9.123}$$

$$e^{-\phi_2} = \left\{ \sqrt{1 + \frac{1}{\varepsilon^2}} + \frac{1}{\varepsilon} \right\}^{-1/n} = \left\{ \sqrt{1 + \frac{1}{\varepsilon^2}} - \frac{1}{\varepsilon} \right\}^{1/n} \tag{9.124}$$

$$\cosh \phi_2 = \left[\left(\sqrt{1 + \frac{1}{\varepsilon^2}} + \frac{1}{\varepsilon} \right)^{1/n} + \left(\sqrt{1 + \frac{1}{\varepsilon^2}} - \frac{1}{\varepsilon} \right)^{-1/n} \right] / 2 \tag{9.125}$$

$$\sinh \phi_2 = \left[\left(\sqrt{1 + \frac{1}{\varepsilon^2}} + \frac{1}{\varepsilon} \right)^{1/n} - \left(\sqrt{1 + \frac{1}{\varepsilon^2}} - \frac{1}{\varepsilon} \right)^{-1/n} \right] / 2. \tag{9.126}$$

The poles coordinates, are, therefore,

$$s = s_k = \sigma_k + j\omega_k \tag{9.127}$$

$$\sigma_k = \sin \phi_1 \sinh \phi_2 = -\sin \left[\left(\frac{2k-1}{2n} \right) \pi \right] \sinh \phi_2, \quad k = 1, 2, \dots, 2n \tag{9.128}$$

$$\omega_k = \cos \phi_1 \cosh \phi_2 = \cos \left[\left(\frac{2k-1}{2n} \right) \pi \right] \cosh \phi_2, \quad k = 1, 2, \dots, 2n. \tag{9.129}$$

These equations satisfy the relation

$$\frac{\sigma_k^2}{\sinh^2 \phi_2} + \frac{\omega_k^2}{\cosh^2 \phi_2} = 1 \tag{9.130}$$

which is the equation of an ellipse having major and minor axes of lengths $a = \cosh \phi_2$ and $b = \sinh \phi_2$, respectively, as shown for the case $n = 6$ in Fig. 9.13.

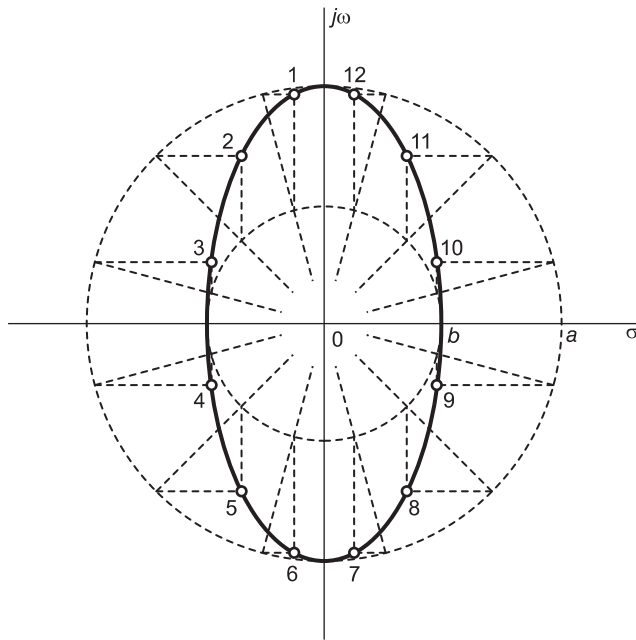


FIGURE 9.13 Poles' ellipse for a sixth order Chebyshev filter.

The poles therefore lie on this elliptic contour in the s plane and those n poles that are in the left half of the s plane, namely, $s_k = \sigma_k + j\omega_k$, where

$$\sigma_k = -\sin \left[\left(\frac{2k-1}{2n} \right) \pi \right] \sinh \phi_2, \quad k = 1, 2, \dots, n \tag{9.131}$$

$$\omega_k = \cos \left[\left(\frac{2k-1}{2n} \right) \pi \right] \cosh \phi_2, \quad k = 1, 2, \dots, n \tag{9.132}$$

are those of $H(s)$.

The figure is constructed by drawing two concentric circles of radii a and b , and radial lines from the origin at angles $\pi/12, 3\pi/12, 5\pi/12, \dots$ from the horizontal axis. From the point of intersection of a radial line with the small circle a vertical line is drawn. From the point of intersection of the same radial line with the big circle, a horizontal line is drawn. As shown in the figure, the intersection of the vertical and horizontal lines is the pole location on the ellipse.

The filter transfer function can thus be written in the form

$$H(s) = \frac{1}{\prod_{i=0}^{n-1} (s - s_i)} \tag{9.133}$$

which can also be written

$$H(s) = \frac{1}{s^n + a_{n-1}s^{n-1} + \dots + a_1s + a_0}. \tag{9.134}$$

The poles and the coefficients a_i of the denominator polynomial of $H(s)$ can be easily evaluated for any order n . Using MATLAB functions such as

$$[B, A] = \text{cheby1}(N, R, Wn, 's') \tag{9.135}$$

$$[Z, P, K] = \text{cheby1}(N, R, Wn, 's') \tag{9.136}$$

$$[N, Wn] = \text{cheb1ord}(Wp, Ws, Rp, Rs, 's') \tag{9.137}$$

such evaluations can be simplified.

9.11 Maxima and Minima of Chebyshev Filter Response

The magnitude frequency response $|H(j\omega)|$ of the Chebyshev filter is maximum equal to K when $C_n(\omega) = 0$, i.e.

$$C_n(\omega) = \cos(n \cos^{-1} \omega) = 0 \tag{9.138}$$

$$n \cos^{-1} \omega = (2k + 1)\pi/2, \quad k = 0, 1, 2, \dots \tag{9.139}$$

For $0 < \omega < 1$

$$\cos^{-1} \omega = (2k + 1)\pi/(2n) \tag{9.140}$$

$$\omega = \cos[(2k + 1)\pi/(2n)]. \tag{9.141}$$

The frequency values of the maxima are thus summarized as follows:

$n = 1: \omega = 0; n = 2: \omega = 0.707; n = 3: \omega = 0, 0.866; n = 4: \omega = 0.3827, 0.9239; n = 5: \omega = 0, 0.5878, 0.9511.$

The minima of $|H(j\omega)|$ occur when $|C_n(\omega)| = 1$

$$C_n(\omega) = \cos(n \cos^{-1} \omega) = \pm 1 \tag{9.142}$$

$$n \cos^{-1} \omega = \cos^{-1} 1 = k\pi, \quad k = 0, 1, 2, \dots \tag{9.143}$$

i.e. $\cos^{-1} \omega = k\pi/n, \quad \omega = \cos(k\pi/n).$

We deduce that a minimum occurs for $n = 1$ at $\omega = 1$, for $n = 2$ at $\omega = 0, 1$, for $n = 3$ at $\omega = 0.5, 1$ and for $n = 4$ at $\omega = 0, 0.707, 1.$

The points of maxima/minima are show in Fig. 9.12.

9.12 The Value of ε as a Function of Pass-Band Ripple

Let R_p dB be the desired Chebyshev filter peak-to-peak ripple, i.e. between the minimum and maximum of the filter response in the pass-band.

$$\text{We write } 20 \log_{10} \left(\frac{K}{K/\sqrt{1+\varepsilon^2}} \right) = R_p \text{ dB}$$

$$10 \log_{10} (1 + \varepsilon^2) = R_p \quad (9.144)$$

wherefrom

$$\varepsilon = \sqrt{10^{R_p/10} - 1}. \quad (9.145)$$

For example, for the ripple values $R_p = 0.5, 1, 2$ dB, the corresponding ε values are $\varepsilon = 0.3493, 0.5088, 0.7648$, respectively.

9.13 Evaluation of Chebyshev Filter Gain

For Chebyshev filters the squared magnitude spectrum is given by

$$|H(j\omega)|^2 = \frac{K^2}{1 + \varepsilon^2 C_n^2(\omega)} \quad (9.146)$$

and the transfer function has the form

$$H(s) = \frac{b_0}{s^n + a_{n-1}s^{n-1} + \dots + a_1s + a_0}. \quad (9.147)$$

The constants K and b_0 produce the desired filter gain. The maximum values $|H(j\omega)|_{\max}$ of filter frequency response occur at values of ω such that $C_n(\omega) = 0$, hence $|H(j\omega)|_{\max} = K$. The minimum values of the magnitude response in the pass-band occur at values of ω such that $|C_n(\omega)|$ is maximum, equal to 1, $|C_n(\omega)| = 1$, hence $|H(j\omega)|_{\min} = K/\sqrt{1+\varepsilon^2}$. If the filter order n is odd, therefore, the response is maximum equal to K at zero frequency. We can therefore write

$$H(0) = |H(j\omega)|_{\max} = K = b_0/a_0, \quad n \text{ odd}. \quad (9.148)$$

For n even the response at zero frequency is a pass-band minimum equal to $K/\sqrt{1+\varepsilon^2}$, so that

$$H(0) = |H(j\omega)|_{\min} = K/\sqrt{1+\varepsilon^2} = b_0/a_0, \quad n \text{ even}. \quad (9.149)$$

To obtain $|H(j\omega)|_{\max} = M$ dB, we write $20 \log_{10} |H(j\omega)|_{\max} = 20 \log_{10} K = M$, hence $K = 10^{M/20}$.

For n odd we have

$$b_0 = K a_0 = 10^{M/20} a_0. \quad (9.150)$$

For n even

$$b_0 = K a_0 / \sqrt{1 + \varepsilon^2} = 10^{M/20} a_0 / \sqrt{1 + \varepsilon^2}. \quad (9.151)$$

For example, if the filter is to have maximum gain equal to 1, we have $M = 0$ dB, so that for n odd, $K = 1$ and $b_0 = a_0$, whereas for n even, $K = 1$ and $b_0 = a_0/\sqrt{1+\varepsilon^2}$. If the filter is to have $M = 10$ dB then $20 \log_{10} K = 10$ dB, so that $K = 10^{1/2} = 3.1623$. Hence for n odd $b_0 = 3.1623 a_0$ and for n even $b_0 = 3.1623 a_0 / \sqrt{1 + \varepsilon^2}$.

9.14 Chebyshev Filter Tables

Lowpass prototype Chebyshev filter denominator polynomial coefficients for different pass-band ripples are given in Table 9.3 to Table 9.5. The corresponding poles and their residues are given in Table 9.6 to Table 9.8.

TABLE 9.3 Chebyshev filter polynomial coefficients with ripple $R = 0.5$ dB, denominator polynomial $A(s) = s^n + a_{n-1}s^{n-1} + \dots + a_2s^2 + a_1s + a_0$, numerator polynomial $B(s) = b_0$ and 0 dB maximum gain

n	b_0	a_{n-1}	a_{n-2}	a_{n-3}	a_{n-4}	a_{n-5}	a_{n-6}	a_{n-7}	a_{n-8}
2	1.4314	1.4256	1.5162						
3	0.7157	1.2529	1.5349	0.7157					
4	0.3578	1.1974	1.7169	1.0255	0.3791				
5	0.1789	1.1725	1.9374	1.3096	0.7525	0.1789			
6	0.0895	1.1592	2.1718	1.5898	1.1719	0.4324	0.0948		
7	0.0447	1.1512	2.4127	1.8694	1.6479	0.7557	0.2821	0.0447	
8	0.0224	1.1461	2.6567	2.1492	2.1840	1.1486	0.5736	0.1525	0.0237

TABLE 9.4 Chebyshev polynomial coefficients with ripple $R = 1$ dB, denominator polynomial $A(s) = s^n + a_{n-1}s^{n-1} + \dots + a_2s^2 + a_1s + a_0$, numerator polynomial $B(s) = b_0$ and 0 dB maximum gain

n	b_0	a_{n-1}	a_{n-2}	a_{n-3}	a_{n-4}	a_{n-5}	a_{n-6}	a_{n-7}	a_{n-8}
2	0.9826	1.0977	1.1025						
3	0.4913	0.9883	1.2384	0.4913					
4	0.2457	0.9528	1.4539	0.7426	0.2756				
5	0.1228	0.9368	1.6888	0.9744	0.5805	0.1228			
6	0.0614	0.9283	1.9308	1.2021	0.9393	0.3071	0.0689		
7	0.0307	0.9231	2.1761	1.4288	1.3575	0.5486	0.2137	0.0307	
8	0.0224	0.9198	2.4230	1.6552	1.8369	0.8468	0.4478	0.1073	0.0172

TABLE 9.5 Chebyshev polynomial coefficients with ripple $R = 3$ dB, denominator polynomial $A(s) = s^n + a_{n-1}s^{n-1} + \dots + a_2s^2 + a_1s + a_0$, numerator polynomial $B(s) = b_0$ and 0 dB maximum gain

n	b_0	a_{n-1}	a_{n-2}	a_{n-3}	a_{n-4}	a_{n-5}	a_{n-6}	a_{n-7}	a_{n-8}
2	0.5012	0.6449	0.7079						
3	0.2506	0.5972	0.9283	0.2506					
4	0.1253	0.5816	1.1691	0.4048	0.1770				
5	0.0626	0.5745	1.4150	0.5489	0.4080	0.0626			
6	0.0313	0.5707	1.6628	0.6906	0.6991	0.1634	0.0442		
7	0.0157	0.5684	1.9116	0.8314	1.0518	0.3000	0.1462	0.0157	
8	0.0078	0.5669	2.1607	0.9719	1.4667	0.4719	0.3208	0.0565	0.0111

TABLE 9.6 Chebyshev lowpass prototype poles and residues; ripple $R = 0.5$ dB

n	Poles	Residues
2	$-0.7128 \pm j1.0040$	$0 \mp j0.7128$
3	$-0.3132 \pm j1.0219, -0.6265$	$-0.3132 \mp j0.0960, 0.6265$
4	$-0.1754 \pm j1.0163, -0.4233 \pm j0.4209$	$-0.1003 \mp j0.1580, 0.1003 \mp j0.4406$
5	$-0.1120 \pm j1.0116, -0.2931 \pm j0.6252, -0.3623$	$0.0849 \pm j0.0859, -0.2931 \mp j0.1374, 0.4165$
6	$-0.0777 \pm j1.0085, -0.2121 \pm j0.7382, -0.2898 \pm j0.2702$	$0.0701 \mp j0.0467, -0.1400 \pm j0.1935, 0.0698 \mp j0.3394$
7	$-0.0570 \pm j1.0064, -0.1597 \pm j0.8071, -0.2308 \pm j0.4479, -0.2562$	$-0.0254 \mp j0.0566, 0.1280 \pm j0.1292, -0.2624 \mp j0.1042, 0.3196$
8	$-0.0436 \pm j1.0050, -0.1242 \pm j0.8520, -0.1859 \pm j0.5693, -0.2193 \pm j0.1999$	$-0.0458 \pm j0.0130, 0.1146 \mp j0.0847, -0.1167 \pm j0.1989, 0.0479 \mp j0.2764$
9	$-0.0345 \pm j1.0040, -0.0992 \pm j0.8829, -0.1520 \pm j0.6553, -0.1864 \pm j0.3487, -0.1984$	$0.0056 \pm j0.0373, -0.0556 \mp j0.1000, 0.1498 \pm j0.1174, -0.2301 \mp j0.0760, 0.2606$
10	$-0.0279 \pm j1.0033, -0.0810 \pm j0.9051, -0.1261 \pm j0.7183, -0.1589 \pm j0.4612, -0.1761 \pm j0.1589$	$0.0305 \mp j0.0010, -0.0866 \pm j0.0357, 0.1124 \mp j0.1125, -0.0905 \pm j0.1881, 0.0342 \mp j0.2328$

TABLE 9.7 Chebyshev lowpass prototype poles and residues; ripple $R = 1$ dB

n	Poles	Residues
2	$-0.5489 \pm j0.8951$	$0 \mp j0.5489$
3	$-0.2471 \pm j0.9660, -0.4942$	$-0.2471 \mp j0.0632, 0.4942$
4	$-0.1395 \pm j0.9834, -0.3369 \pm j0.4073$	$-0.0663 \pm j0.1301, 0.0663 \mp j0.3463$
5	$-0.0895 \pm j0.9901, -0.2342 \pm j0.6119, -0.2895$	$0.0748 \pm j0.0574, -0.2342 \mp j0.0896, 0.3189$
6	$-0.0622 \pm j0.9934, -0.1699 \pm j0.7272, -0.2321 \pm j0.2662$	$0.0477 \mp j0.0453, -0.0913 \pm j0.1600, 0.0436 \mp j0.2588$
7	$-0.0457 \pm j0.9953, -0.1281 \pm j0.7982, -0.1851 \pm j0.4429, -0.2054$	$-0.0284 \mp j0.0393, 0.1113 \pm j0.0848, -0.2024 \mp j0.0647, 0.2390$
8	$-0.0350 \pm j0.9965, -0.0997 \pm j0.8448, -0.1492 \pm j0.5644, -0.1760 \pm j0.1982$	$-0.0325 \pm j0.0181, 0.0761 \mp j0.0787, -0.0726 \pm j0.1569, 0.0290 \mp j0.2062$
9	$-0.0277 \pm j0.9972, -0.0797 \pm j0.8769, -0.1221 \pm j0.6509, -0.1497 \pm j0.3463, -0.1593$	$0.0116 \pm j0.0270, -0.0564 \mp j0.0672, 0.1219 \pm j0.0734, -0.1730 \mp j0.0459, 0.1918$
10	$-0.0224 \pm j0.9978, -0.0650 \pm j0.9001, -0.1013 \pm j0.7143, -0.1277 \pm j0.4586, -0.1415 \pm j0.1580$	$0.0227 \mp j0.0073, -0.0591 \pm j0.0408, 0.0708 \mp j0.0952, -0.0547 \pm j0.1436, 0.0204 \mp j0.1710$

TABLE 9.8 Chebyshev lowpass prototype poles and residues; ripple $R = 3$ dB

n	Poles	Residues
2	$-0.3224 \pm j0.7772$	$\mp j0.3224$
3	$-0.1493 \pm j0.9038, -0.2986$	$-0.1493 \mp j0.0247, 0.2986$
4	$-0.0852 \pm j0.9465, -0.2056 \pm j0.3920$	$-0.0260 \pm j0.0828, 0.0260 \mp j0.2080$
5	$-0.0549 \pm j0.9659, -0.1436 \pm j0.5970,$ -0.1775	$0.0512 \pm j0.0228, -0.1436 \mp j0.0346,$ 0.1848
6	$-0.0382 \pm j0.9764, -0.1044 \pm j0.7148,$ $-0.1427 \pm j0.2616$	$0.0193 \mp j0.0340, -0.0352 \pm j0.1021,$ $0.0159 \mp j0.1493$
7	$-0.0281 \pm j0.9827, -0.0789 \pm j0.7881,$ $-0.1140 \pm j0.4373, -0.1265$	$-0.0238 \mp j0.0163, 0.0748 \pm j0.0330,$ $-0.1183 \mp j0.0234, 0.1346$
8	$-0.0216 \pm j0.9868, -0.0614 \pm j0.8365,$ $-0.0920 \pm j0.5590, -0.1085 \pm j0.1963$	$-0.0138 \pm j0.0173, 0.0299 \mp j0.0564,$ $-0.0263 \pm j0.0941, 0.0102 \mp j0.1157$
9	$-0.0171 \pm j0.9896, -0.0491 \pm j0.8702,$ $-0.0753 \pm j0.6459, -0.0923 \pm j0.3437,$ -0.0983	$0.0130 \pm j0.0118, -0.0435 \mp j0.0268,$ $0.0756 \pm j0.0267, -0.0980 \mp j0.0160,$ 0.1060
10	$-0.0138 \pm j0.9915, -0.0401 \pm j0.8945,$ $-0.0625 \pm j0.7099, -0.0788 \pm j0.4558,$ $-0.0873 \pm j0.1570$	$0.0101 \mp j0.0099, -0.0240 \pm j0.0342,$ $0.0260 \mp j0.0614, -0.0192 \pm j0.0827,$ $0.0070 \mp j0.0943$

9.15 Chebyshev Filter Order

The pass-band edge frequency of a Chebyshev filter is also referred to as the cut-off frequency. We write $\omega_c = \omega_p$. Let the required peak-to-peak ripple in the pass-band be not more than R_p dB, the stop-band edge frequency be $\omega = \omega_s$ and the corresponding attenuation be at least R_s dB. The filter order can be evaluated by writing

$$|H(j\omega)|^2 = \frac{K^2}{1 + \varepsilon^2 C_n^2(\omega/\omega_p)} \tag{9.152}$$

$$10 \log_{10} \left[\frac{|H(j\omega)|_{\max}^2}{|H(j\omega_p)|^2} \right] = 10 \log_{10} \left[\frac{K^2}{K^2/[1 + \varepsilon^2 C_n^2(1)]} \right] = R_p \tag{9.153}$$

i.e. $1 + \varepsilon^2 = 10^{0.1R_p}$, or $\varepsilon = \sqrt{10^{0.1R_p} - 1}$ as obtained above. Similarly

$$1 + \varepsilon^2 C_n^2(\omega_s/\omega_p) = 10^{0.1R_s} \tag{9.154}$$

$$C_n^2(\omega_s/\omega_p) = (10^{0.1R_s} - 1)/\varepsilon^2 \tag{9.155}$$

$$C_n(\omega_s/\omega_p) = \cosh \{ n \cosh^{-1}(\omega_s/\omega_p) \} = \sqrt{10^{0.1R_s} - 1}/\varepsilon. \tag{9.156}$$

Hence

$$n = \frac{\cosh^{-1} \left[\frac{\sqrt{10^{0.1R_s} - 1}}{\varepsilon} \right]}{\cosh^{-1}(\omega_s/\omega_p)}. \tag{9.157}$$

A MATLAB function may effect such an evaluation. Calling it **cheby1order.m** we can write the function in the form

```
function [n] = cheby1order (wp,ws,Rp,Rs)
eps=sqrt(10^(0.1*Rp)-1)
n=acosh(sqrt(10^(0.1*Rs)-1)/eps)/acosh(ws/wp)
```

Note that MATLAB has the built-in function *Cheb1ord* which evaluates the Chebyshev (Type I) filter order.

9.16 Denormalization of Chebyshev Filter Prototype

As with the Butterworth case, to denormalize the filter we replace ω by ω/ω_c where ω_c is the desired cut-off frequency in rad/sec. We therefore write

$$\omega \longrightarrow \omega/\omega_c, \quad s \longrightarrow s/\omega_c. \quad (9.158)$$

The poles after denormalization are given by

$$q_k = \Sigma_k + j\Omega_k = \omega_c s_k = \omega_c \sigma_k + j\omega_c \omega_k \quad (9.159)$$

i.e.

$$\Sigma_k = -\omega_c \sin \left[\frac{(2k-1)}{2n} \right] \sinh \phi_2 \quad (9.160)$$

$$\Omega_k = \omega_c \cos \left[\frac{(2k-1)\pi}{2n} \right] \cosh \phi_2. \quad (9.161)$$

The equation of the ellipse takes the form

$$\frac{\Sigma_k^2}{\omega_c^2 \sinh^2 \phi_2} + \frac{\Omega_k^2}{\omega_c^2 \cosh^2 \phi_2} \quad (9.162)$$

Example 9.6 Evaluate the transfer function $H(s)$ of a prototype Chebyshev filter of order $n = 7$ and a pass-band attenuation of 0.5 dB. Evaluate the filter poles and zeros.

We may use the tables or the MATLAB function call

$$[B, A] = \mathbf{cheby1}(N, R, Wn, 's')$$

with $N = 7$, $R = 0.5$ dB and the 3 dB cut-off frequency $Wn = 1$ we obtain

$$H(s) = \frac{0.0447}{s^7 + 1.151s^6 + 2.413s^5 + 1.869s^4 + 1.648s^3 + 0.756s^2 + 0.282s + 0.0447}$$

which agrees with the values listed in the 0.5 dB of Table 9.3.

The poles and zeros of the filter may be obtained from the tables or using the MATLAB command

$$[Z, P, K] = \mathbf{cheby1}(N, R, Wn, 's').$$

We obtain

$$P = \{-0.057 \pm j1.0064, -0.1597 \pm j0.8071, -0.231 \pm j0.448, -0.256\}$$

$$Z = \emptyset.$$

The filter transfer function has no zeros and has a gain factor $K = 0.0447$.

Example 9.7 Using MATLAB find the order and the 3 dB cut-off frequency of a Chebyshev filter having the following specifications: pass-band frequency $\omega_p = 2\pi \times 1000$ r/s, stop-band edge frequency $\omega_s = 2\pi \times 2500$ r/s, Pass-band maximum attenuation $\alpha_p = 1$ dB, Stop-band minimum attenuation $\alpha_s = 40$ dB. Evaluate the transfer function, the poles, zeros and gain.

We can use the function `cheby1order` as developed in the last section to evaluate the filter order. We write: $w_p = 2\pi \times 1000$, $w_s = 2\pi \times 2500$, $R_p = 1$, $R_s = 40$, and the function call `cheby1order(wp, ws, Rp, Rs)`, obtaining $n = 3.8128$, thus choosing $n = 4$. Alternatively, we may use MATLAB's built-in functions, writing

$$[N, Wn] = \mathbf{cheb1ord}(Wp, Ws, Rp, Rs, 's')$$

where $Wp = \omega_p$, $Ws = \omega_s$, $Rp = \alpha_p = 1$, $Rs = \alpha_s = 40$, i.e. $\omega_c = 6.2832 \times 10^3$ r/s. The program results are: $N = 4$, $Wn = 6.2832 \times 10^3$, that is, $\omega_c = 6.2832 \times 10^3$ r/s. The transfer function's numerator and denominator polynomial coefficients are found using the MATLAB function call

$$[B, A] = \mathbf{cheby1}(N, R, Wn, 's')$$

where $R = Rp$, the pass-band ripple. We obtain

$$H(s) = N(s)/D(s).$$

where $N(s) = 3.8287 \times 10^{14}$,

$$D(s) = s^4 + 5986.7s^3 + 5.7399 \times 10^7s^2 + 1.8421 \times 10^{11}s + 4.2958 \times 10^{14}.$$

The transfer function $H(s)$ has no zeros. The poles are

$$P = \{-2.1166 \pm j2.5593, -0.8767 \pm j6.1788\}$$

and the gain is $K = 3.8287 \times 10^{14}$.

Example 9.8 Design a Chebyshev filter having the specifications given in the following table and a response of 0 dB at zero frequency.

Frequency	Attenuation
10 kHz	≤ 1 dB
15 kHz	≥ 60 dB

Let $\omega_p = 2\pi \times 10^4$ r/s, $\omega_s = 2\pi \times 15 \times 10^3$ r/s.

In the prototype filter let the attenuation at $\omega = 1$ be 1 dB. The normalized frequency $\omega = 1$ corresponds, therefore, to the true pass-band edge frequency $\omega_p = 2\pi \times 10^4$ r/s. The normalized frequency $\omega = 1.5$ corresponds to the true stop-band edge frequency $\omega_s = 2\pi \times 15 \times 10^3$ r/s. We have

$$10 \log [1 + \varepsilon^2] = 1$$

wherefrom $\varepsilon^2 = 10^{0.1} - 1 = 0.259$, i.e. $\varepsilon = 0.51$

$$10 \log_{10} \frac{1}{|H(j1.5)|^2} = 60$$

$$10 \log_{10} [1 + \varepsilon^2 C_n^2(1.5)] = 60$$

$$C_n^2(1.5) = \frac{10^6 - 1}{\varepsilon^2} = 3.86 \times 10^6$$

$$C_n(1.5) = \cosh(n \cosh^{-1} 1.5) = 1.963 \times 10^3$$

$$\cosh(n \times 0.9624) = 1.963 \times 10^3$$

$$n \times 0.9624 = \cosh^{-1} 1.963 \times 10^3 = 8.275$$

i.e. $n = 8.6$. We choose $n = 9$.

$$\phi_2 = \ln \left(\sqrt{1 + 1/\varepsilon^2} + 1/\varepsilon \right)^{1/n} = 0.1587$$

$$\sinh \phi_2 = 0.1594, \quad \cosh \phi_2 = 1.013.$$

The normalized filter poles are given by

$$s_k = \sigma_k + j\omega_k$$

$$\sigma_k = -\sin \left(\frac{2k-1}{9} \frac{\pi}{2} \right) \times 0.1594, \quad k = 0, 1, 2, \dots, n-1$$

$$\omega_k = \cos \left(\frac{2k-1}{9} \frac{\pi}{2} \right) \times 1.013, \quad k = 1, 2, \dots, n.$$

To denormalize the filter we replace s by s/ω_c . The true (denormalized) filter poles are thus given by

$$q_k \triangleq \Sigma_k + j\Omega_k$$

where

$$\Sigma_k = -0.319 \times 10^4 \pi \sin \left(\frac{2k-1}{9} \frac{\pi}{2} \right)$$

$$\Omega_k = 2.029 \times 10^4 \pi \cos \left(\frac{2k-1}{9} \frac{\pi}{2} \right).$$

The ellipse's minor axis has a length given by

$$\alpha = \omega_c \sinh \phi_2 = 0.319 \times 10^4 \pi.$$

Its major axis is given by

$$\beta = \omega_c \cosh \phi_2 = 2.029 \times 10^4 \pi$$

$$H(s) = \frac{K}{\prod_{i=0}^8 (s - q_i)}$$

where the gain K is taken equal to the product

$$K = \prod_{i=1}^9 (-q_i)$$

so that the zero-frequency gain $H(0) = 1$.

Example 9.9 Design the filter having the specifications given in the last example using MATLAB.

We write the program

```

Wp = 2π × 104
Ws = 2π × 15 × 103
Rp = 1
Rs = 60
[N, Wn] = cheb1ord(Wp, Ws, Rp, Rs, 's')
[B, A] = cheby1(N, Rp, Wn, 's')
[Z, P, K] = cheby1(N, Rp, Wn, 's')..

```

We obtain $N = 9$. The coefficients' vectors B and A define a transfer function given by

$$H(s) = \frac{1.1716 \times 10^4}{D(s)}$$

where

$$\begin{aligned}
 D(s) = & s^9 + 5.765 \times 10^4 s^8 + 1.054 \times 10^{10} s^7 + 4.667 \times 10^4 s^6 \\
 & + 3.706 \times 10^{19} s^5 + 1.177 \times 10^{24} s^4 + 4.838 \times 10^{28} s^3 \\
 & + 9.440 \times 10^{32} s^2 + 1.715 \times 10^{37} s + 1.1716 \times 10^{41}.
 \end{aligned}$$

The poles and zeros are

$$\begin{aligned}
 P = \{ & -0.1738 \pm j6.2658, -0.5006 \pm j5.5100, -0.7669 \pm j4.0897, \\
 & -0.9407 \pm j2.1761, -1.0011 \}
 \end{aligned}$$

$$Z = \emptyset \quad (\text{no zeros})$$

and the gain is $K = 1.1716 \times 10^{41}$ so that $H(0) = 1$.

9.17 Chebyshev's Approximation: Second Form

By replacing ω by $1/\omega$ the Chebyshev filter spectrum is made to have ripples in the stop-band and none in the pass-band. The lowpass approximation, referred to often as Chebyshev Type II takes the form

$$|H(j\omega)|^2 = \frac{\varepsilon^2 C_n^2(1/\omega)}{1 + \varepsilon^2 C_n^2(1/\omega)}. \quad (9.163)$$

To show this, let, $|H_I(j\omega)|^2$ be the spectrum of the Chebyshev approximation studied above, which we shall now call *Type I approximation*. We start by evaluating the spectrum

$$G(j\omega) = 1 - |H_I(j\omega)|^2 = 1 - \frac{1}{1 + \varepsilon^2 C_n^2(\omega)} \quad (9.164)$$

as can be seen in Fig. 9.14 for a fourth order filter. We next replace ω by $1/\omega$ to obtain the Chebyshev Type II spectrum

$$|H_{II}(j\omega)|^2 = G(j/\omega) = 1 - \frac{1}{1 + \varepsilon^2 C_n^2(1/\omega)} = \frac{\varepsilon^2 C_n^2(1/\omega)}{1 + \varepsilon^2 C_n^2(1/\omega)}. \quad (9.165)$$

The amplitude spectrum of the fourth order Chebyshev Type II filter is shown in Fig. 9.14. Poles, zeros and the transfer function of such filters can be readily evaluated using the MATLAB function *Cheby2*.

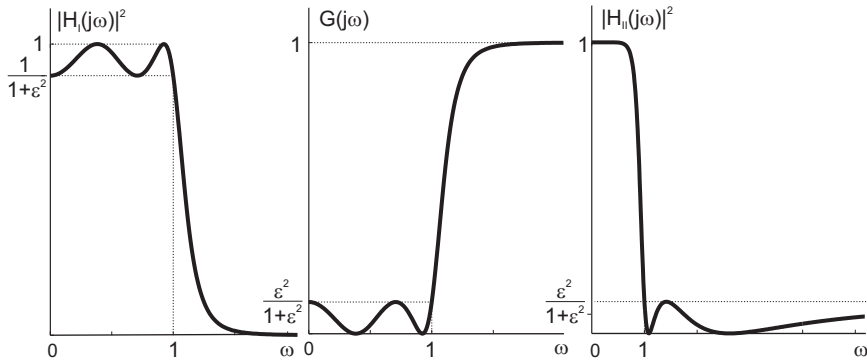


FIGURE 9.14 Amplitude spectrum of a fourth order Chebyshev Type II filter.

9.18 Response Decay of Butterworth and Chebyshev Filters

Plotting the amplitude spectrum in decibels versus a logarithmic scale of the frequency ω axis we can readily compare the rate of decay of the responses of different orders of Butterworth and Chebyshev filters. We may thus obtain and plot the response asymptotes. Consider the Butterworth filter amplitude spectrum with $\epsilon = 1$

$$|H(j\omega)| = \frac{1}{\sqrt{1 + \omega^{2n}}}. \tag{9.166}$$

The magnitude of the spectrum at $\omega = 0$ is given by

$$20 \log_{10} |H(j0)| = 20 \log_{10} 1 = 0 \text{ dB}. \tag{9.167}$$

The attenuation at a general value ω is given by

$$10 \log_{10} [|H(j0)|^2 / |H(j\omega)|^2] = 10 \log_{10} (1 + \omega^{2n}) \text{ dB}. \tag{9.168}$$

We now evaluate the two asymptotes of the attenuation curve, namely, the asymptote for ω below the cut-off frequency $\omega = 1$ and that for ω above the cut-off frequency, $\omega > 1$. Letting $\omega \ll 1$ we obtain $|H(j\omega)| \approx 1$ so that the attenuation is given by the asymptote

$$\alpha_1 = 20 \log_{10} 1 = 0 \text{ dB}. \tag{9.169}$$

With $\omega \gg 1$ we have

$$|H(j\omega)| \approx \frac{1}{\sqrt{\omega^{2n}}} = \frac{1}{\omega^n} \tag{9.170}$$

so that the asymptote for frequencies above the cut-off frequency $\omega = 1$ is given by

$$\alpha_2 = -20 \log_{10} \frac{1}{\omega^n} = 20n \log_{10} \omega \text{ dB}. \tag{9.171}$$

The asymptote α_2 as a function of ω can be converted into the equation of a straight line by rewriting it in terms of a logarithmic frequency scale. In w octaves the asymptote above $\omega = 1$ is given by

$$\alpha_2 = 20n \log_{10} 2^w = 20nw \times 0.3 = 6nw \text{ dB.} \tag{9.172}$$

The asymptote has a slope of $6n$ dB/octave. If instead we write $\omega = 10^v$ then v is the number of frequency decades, and

$$\alpha_2 = 20n \log_{10} 10^v = 20nv \text{ dB} \tag{9.173}$$

that is, a slope of $m_d = 20n$ dB/decade. The attenuation in the stop-band is therefore $6n$ dB per octave or, equivalently, $20n$ dB per decade. For a first order Butterworth filter, it is 6 dB/octave (20 dB/decade) as shown in Fig. 9.15. For a second order filter, it is 12 dB/octave (40 dB/decade) and so on.

In the pass-band with $\omega \ll 1$ the attenuation α_1 , as we found, is given by the asymptote $\alpha_1 = 0$. In the vicinity of $\omega = 1$ i.e. $w = 0$, the true relation of the attenuation α differs slightly from the asymptotes α_1 and α_2 , as shown by the dotted line in the figure. In particular, at $\omega = 1$, the value of the attenuation is

$$-20 \log_{10} |H(j1)| = -20 \log_{10} \frac{1}{\sqrt{2}} = 10 \log_{10} 2 = 3 \text{ dB} \tag{9.174}$$

independently of the filter order n .

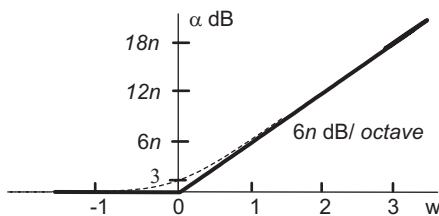


FIGURE 9.15 First order Butterworth filter attenuation.

For the Chebyshev approximation we have

$$|H(j\omega)| = \frac{1}{\sqrt{1 + \varepsilon^2 C_n^2(\omega)}}. \tag{9.175}$$

The ripple amplitude in the frequency range $0 < |\omega| < 1$ is given by

$$r = 1 - \frac{1}{\sqrt{1 + \varepsilon^2}} = 1 - (1 + \varepsilon^2)^{-1/2} = 1 - [1 - (1/2)\varepsilon^2 + (3/8)\varepsilon^4 - \dots]. \tag{9.176}$$

For small ε we have

$$r \approx \varepsilon^2/2. \tag{9.177}$$

In the stop-band where $\omega \gg 1$ and $\varepsilon^2 C_n^2(\omega) \gg 1$ we have

$$|H(j\omega)| = \frac{1}{\varepsilon C_n(\omega)}. \tag{9.178}$$

The attenuation in the pass-band is given by

$$\alpha_1 = -20 \log_{10} \varepsilon^2/2 \tag{9.179}$$

and that in the stop-band is given by

$$\alpha_2 = -20 \log_{10} \frac{1}{\varepsilon C_n(\omega)} = 20 \log \varepsilon C_n(\omega). \quad (9.180)$$

From Equation (9.87), for $\omega \gg 1$ we have

$$C_n(\omega) \approx 2^{n-1} \omega^n \quad (9.181)$$

so that

$$\alpha_2 = 20 \log_{10} \varepsilon 2^{n-1} \omega^n = 20 \log_{10} \varepsilon + 20n \log_{10} \omega + 20 \log 2^{n-1}. \quad (9.182)$$

Writing $\omega = 2^w$ we have

$$\alpha_2 = 20 \log_{10} \varepsilon + 20n \log_{10} 2^w + 20 \log_{10} 2^{n-1} = 20 \log_0 \varepsilon + 6nw + 6(n-1). \quad (9.183)$$

We note that ε is usually less than 1, so that the first term, $20 \log \varepsilon$ is negative, reducing the value of the attenuation α_2 . If $\varepsilon = 1$ the ripple amount is given by $20 \log_{10} \sqrt{1 + \varepsilon^2} = 3$ dB. In this case $20 \log_{10} \varepsilon = 0$ and

$$\alpha_2 = 6nw + 6(n-1) \quad (9.184)$$

which is the same as the Butterworth asymptote except for an increase of the constant $6(n-1)$ for a given n .

9.19 Chebyshev Filter Nomograph

A nomograph for Chebyshev filters is shown in Fig. 9.16.

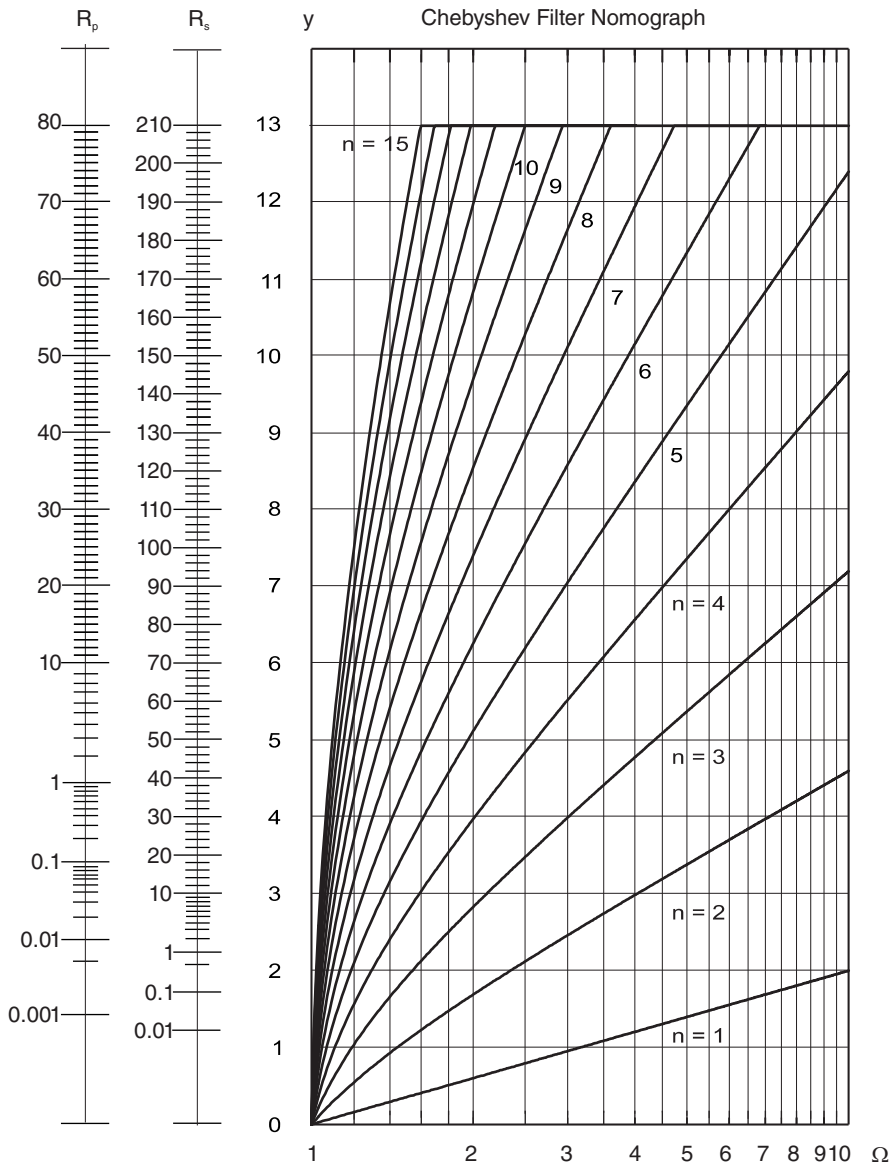


FIGURE 9.16 Chebyshev filter nomograph.

To evaluate the required filter order for a given specification using the nomograph we follow the same approach illustrated above in Fig. 9.10.

9.20 Elliptic Filters

By allowing ripples to occur in both the pass-band and stop-band, the elliptic, or “Cauer,” filter approximation attains a faster rate of attenuation in the transition band. We start with a brief summary of properties of elliptic integrals.

9.20.1 Elliptic Integral

The *incomplete elliptic integral of the first kind, in the Legendre Form*, is defined as

$$u(\varphi, k) = \int_0^\varphi \frac{d\theta}{\sqrt{1 - k^2 \sin^2 \theta}}. \quad (9.185)$$

The parameter k is called the modulus of the integral, $k = \text{mod } u$. The related parameter $k' = \sqrt{1 - k^2}$ is called the complementary modulus. The complete elliptic integral, denoted $K(k)$, or simply K , is given by

$$K(k) \equiv K = u(\pi/2, k) \quad (9.186)$$

and

$$K(k') = K'(k) \equiv K'. \quad (9.187)$$

The variables k and k' are assumed to be real and $0 < k, k' < 1$.

In the incomplete elliptic integral the upper limit φ is a function of u , called the amplitude of u

$$\varphi = \text{am } u. \quad (9.188)$$

The inverse relation may be written

$$u = \arg \varphi \quad (9.189)$$

that is, u is argument of φ . The sine of the amplitude,

$$\sin \varphi = \sin(\text{am } u) \quad (9.190)$$

is given the symbol sn which stands for the *sine-amplitude function*, also called the *Jacobian elliptic sine function*

$$sn \, u = \sin \varphi = \sin \text{am } u \quad (9.191)$$

which is also written

$$sn(u, k) = \sin[\varphi(u, k)]. \quad (9.192)$$

Related functions are the cosine amplitude function

$$cn \, u = \cos \varphi = \cos \text{am } u \quad (9.193)$$

and the delta amplitude function

$$dn \, u = \Delta \varphi = \sqrt{1 - k^2 \sin^2 \varphi} = \frac{d\varphi}{du}. \quad (9.194)$$

The name *elliptic integral* is due to the fact that such an integral appears when the circumference of an ellipse is evaluated. Differentiation of the elliptic functions leads to the relations

$$\frac{d}{du}(sn \, u) = cn \, u \, dn \, u \quad (9.195)$$

$$\frac{d}{du} (cn u) = -sn u dn u \tag{9.196}$$

$$\frac{d}{du} (dn u) = -k^2 sn u cn u. \tag{9.197}$$

The following relations can be readily established

$$sn(0) = 0, \quad cn(0) = 1, \quad dn(0) = 1 \tag{9.198}$$

$$sn(-u) = -sn u, \quad cn(-u) = cn u, \quad dn(-u) = dn u, \quad tn(-u) = -tn u \tag{9.199}$$

where $tn u = sn u / cn u = x / \sqrt{1 - x^2}$.

9.21 Properties, Poles and Zeros of the *sn* Function

The *sn*(*u*) function resembles the trigonometric sine but is in general more rounded and flat near its peak. With $k = 0$ the function

$$sn(u, 0) = \sin(u). \tag{9.200}$$

As k increases toward 1 the function becomes progressively more flat about its peak and with a progressively longer period, as seen in Fig. 9.17.

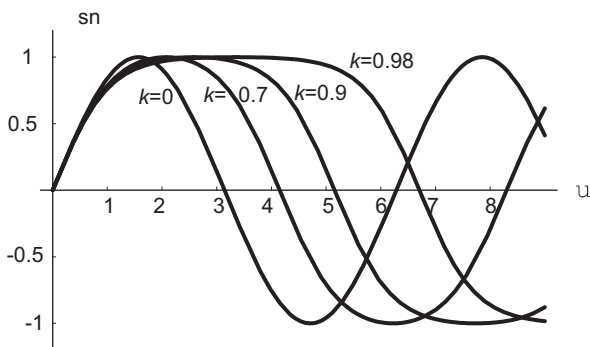


FIGURE 9.17 The *sn* function for different values of k .

With $k = 1$ it equals

$$sn(u, 1) = \tanh(u) \tag{9.201}$$

becoming flat-topped and of infinite period.

Note that in Mathematica instead of the variable k a variable m is used, where $m = k^2$. The elliptic function $sn(u, k)$ is a generalization of the trigonometric sine function. Related elliptic functions are

$$cn(u) = \cos[\varphi(u)] \tag{9.202}$$

$$sc(u) = \tan[\varphi(u)] \tag{9.203}$$

$$cs(u) = \cot[\varphi(u)] \tag{9.204}$$

$$nc(u) = \sec[\varphi(u)] \quad (9.205)$$

$$ns(u) = \csc[\varphi(u)]. \quad (9.206)$$

Among the important properties of the sn function relate to its operation on a complex argument. In particular we have

$$sn(ju, k) = j sc(u, k') \quad (9.207)$$

$$cn(ju, k) = nc(u, k'). \quad (9.208)$$

The following relations are among the important properties of elliptic integrals and Jacobi elliptic functions

$$K(k) = u(\pi/2, k) = \int_0^{\pi/2} \frac{d\theta}{\sqrt{1 - k^2 \sin^2 \theta}} = K'(k') \quad (9.209)$$

$$u(-\phi, k) = -u(\phi, k) \quad (9.210)$$

$$sn K(k) = 1 \quad (9.211)$$

$$sn^2 u + cn^2 u = 1 \quad (9.212)$$

$$dn^2 u + k^2 sn^2 u = 1 \quad (9.213)$$

$$sn(u \pm v) = \frac{sn u cn v dn v \pm sn v cn u dn u}{1 - k^2 sn^2 u sn^2 v} \quad (9.214)$$

$$sn(u + K) = \frac{cn u}{dn u}. \quad (9.215)$$

Using this last relation we can write

$$\begin{aligned} sn(K + jK') &= \frac{cn jK'}{dn jK'} = \frac{1/cn(K', k')}{dn(K', k')/cn(K', k')} = \frac{1}{dn(K', k')} \\ &= \frac{1}{\sqrt{1 - k'^2 sn^2 K'(k')}} = \frac{1}{\sqrt{1 - k'^2 sn^2 K(k)}} = \frac{1}{k}. \end{aligned} \quad (9.216)$$

The following relations can be established

$$sn(u + 2K) = -sn u, \quad cn(u + 2K) = -cn u \quad (9.217)$$

$$sn(2K + j2K') = 0, \quad cn(2K + j2K') = 1, \quad dn(2K + j2K') = -1 \quad (9.218)$$

$$dn(u + 2K) = dn u, \quad tn(u + 2K) = tn u. \quad (9.219)$$

By replacing u by $u + 2K$ we also have

$$sn(u + 4K) = sn u \quad (9.220)$$

$$cn(u + 4K) = cn u. \quad (9.221)$$

The Jacobian elliptic functions $sn u$, $cn u$ and $dn u$ are doubly periodic, that is, periodic along horizontal, vertical or oblique lines in the u plane. The following relations can be established

$$sn(u + j2K') = sn u \quad (9.222)$$

$$cn(u + 2K + j2K') = cn u \quad (9.223)$$

$$dn(u + j4K') = dn u. \quad (9.224)$$

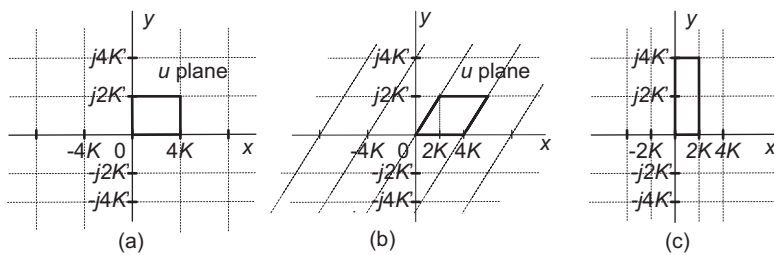


FIGURE 9.18 Period parallelograms of Jacobian elliptic functions.

These periodicity relations may be represented graphically by drawing a grid on the complex u plane. This is illustrated in Fig. 9.18.

In particular, the grids of periodicity of the sn and dn functions are shown respectively in Fig. 9.18(a) and (c) and appear as repetitions of rectangular “cells” in the u plane. On the other hand, the grid corresponding to the cn function, shown in Fig. 9.18(b) is a repetition of parallelograms. Such cells are in fact referred to as *period parallelograms*.

For our present purpose the periodicity, the poles, and the zeros of the function $sn u$ are of particular interest. We have just seen that with m and n integers, the function $sn u$ has the periods $4mK + j2nK'$ and the zeros $2mK + j2nK'$. It can be shown that it has the poles $2mK + j(2n + 1)K'$ with their residues $(-1)^m / k$. The pole-zero pattern thus appears as shown in Fig. 9.19 where the poles with their residues written next to them in parentheses, and the zeros are shown on the complex u plane, where $u = x + jy$.

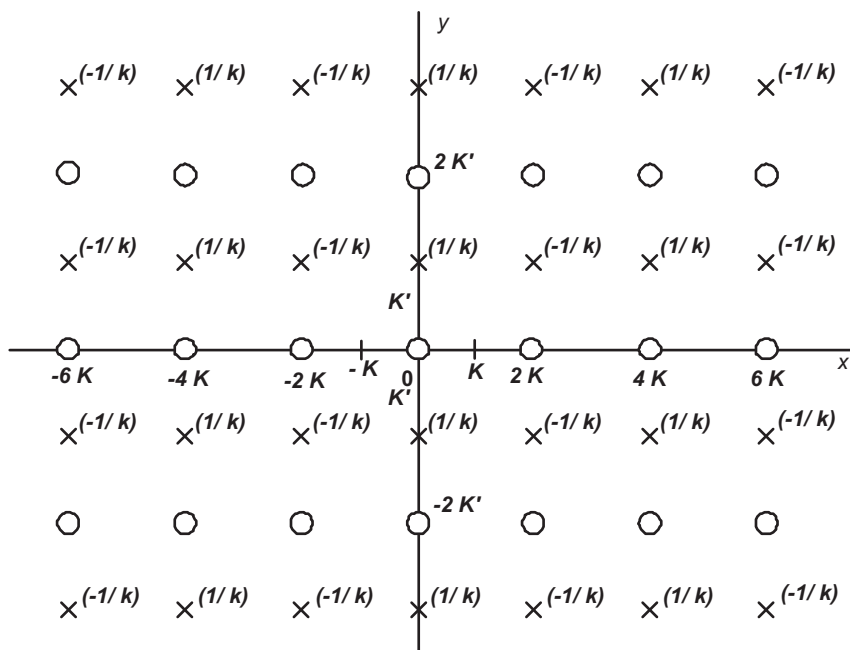


FIGURE 9.19 Pole-zero pattern of the sn function.

The complete elliptic integral K can be evaluated using MATLAB or *Mathematica*®, as we shall see. It has the series expansion

$$K = \frac{\pi}{2} \left\{ 1 + \left(\frac{1}{2}\right)^2 k^2 + \left(\frac{1.3}{2.4}\right)^2 k^4 + \dots + \left[\frac{(2n-1)!!}{2^n n!}\right]^2 k^{2n} + \dots \right\} \quad (9.225)$$

where the notation $(2n-1)!!$ stands for

$$(2n-1)!! = 1, 3, 5, \dots, (2n-1). \quad (9.226)$$

A plot of the complete elliptic integral $K(k)$ as a function of its argument k is shown in Fig. 9.20.

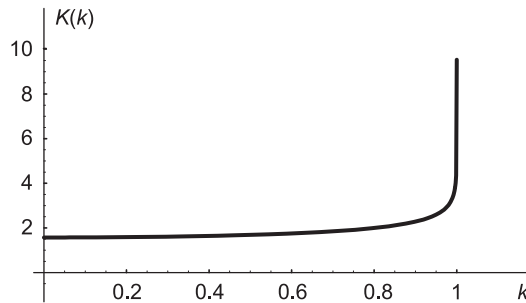


FIGURE 9.20 Complete elliptic integral $K(k)$ as a function of k .

9.21.1 Elliptic Filter Approximation

The squared-magnitude spectrum of the elliptic filter approximation is written

$$|H(j\omega)|^2 = \frac{1}{1 + \varepsilon^2 G^2(\omega)}. \quad (9.227)$$

As an illustration the desired form of the squared-magnitude spectrum $|H(j\omega)|^2$ is shown for an elliptic filter of the seventh order in Fig. 9.21, where we notice the ripples in both the pass-band and the stop-band. We recall that in the Chebyshev approximation the function $|H(j\omega)|^2$ has the same expression except for the replacement of $G^2(\omega)$ by $C_n^2(\omega)$ where

$$C_n(\omega) = \cos(n \cos^{-1} \omega). \quad (9.228)$$

In the elliptic filter approximation the trigonometric cosine is replaced with a Jacobian elliptic sine function. The exact form of this function depends on whether the filter order, denoted N , is even or odd. If N is odd the function $G(\omega)$ is given by

$$G(\omega) = sn[n \operatorname{sn}^{-1}(\omega, k), k_1]. \quad (9.229)$$

If N is even then

$$G(\omega) = sn[n \operatorname{sn}^{-1}(\omega, k) + K_1, k_1] \quad (9.230)$$

where k and k_1 are deduced from the desired filter specifications.

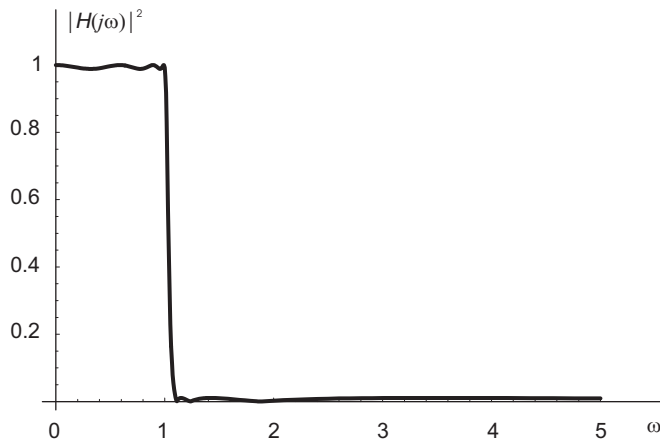


FIGURE 9.21 Elliptic filter magnitude-squared spectrum.

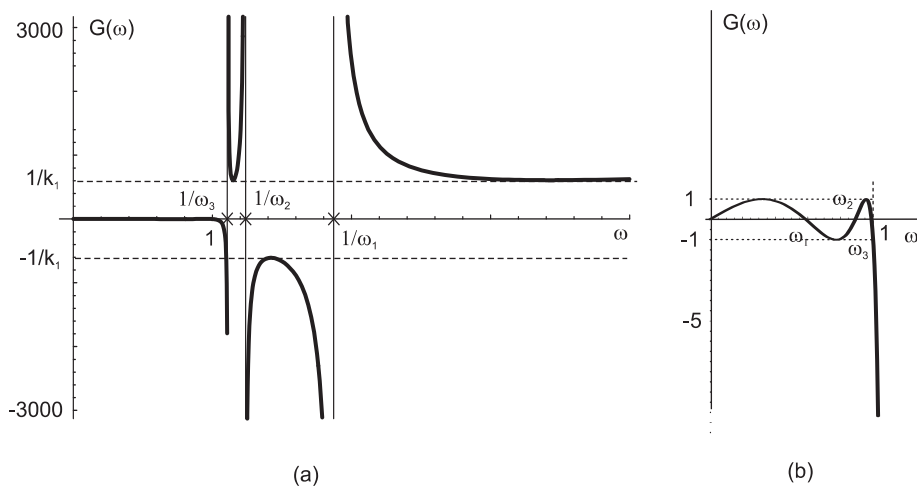


FIGURE 9.22 Function $G(\omega)$.

The function $G(\omega)$ is called the *Chebyshev rational function*. As an illustration this function is shown for the case $N = 7$ in Fig. 9.22(a) and (b). In Fig. 9.22(a) the form of the function over the entire frequency range is shown. In Fig. 9.22(b) the form of the function, mainly in the pass-band, is slightly magnified for better visibility.

The parameters that appear in the figure, namely, ω_1 , ω_2 , ω_3 and k_1 are to be explained in what follows.

As the figure shows, the function is equal to zero at $\omega = 0, \omega_1, \omega_2$ and ω_3 . It has poles, where it tends to infinity, at $\omega = 1/\omega_3, 1/\omega_2, 1/\omega_1$ and ∞ . The function displays equal local minima between the poles at $\omega = 1/\omega_3$ and $1/\omega_2$, as well as between $1/\omega_1$ and ∞ , where it equals $1/k_1$. It displays a local maximum equal to $-1/k_1$ between the poles at $\omega = 1/\omega_2$ and $1/\omega_1$. In Fig. 9.23 the low frequency range, namely, the pass-band and transition band of the same function $G(\omega)$ are redrawn for better visibility of function form in these bands. We shall shortly define a parameter k , and its reciprocal, the stop-band edge frequency $\omega_s = 1/k$ which appears in the figure. Note that in the figure the value of

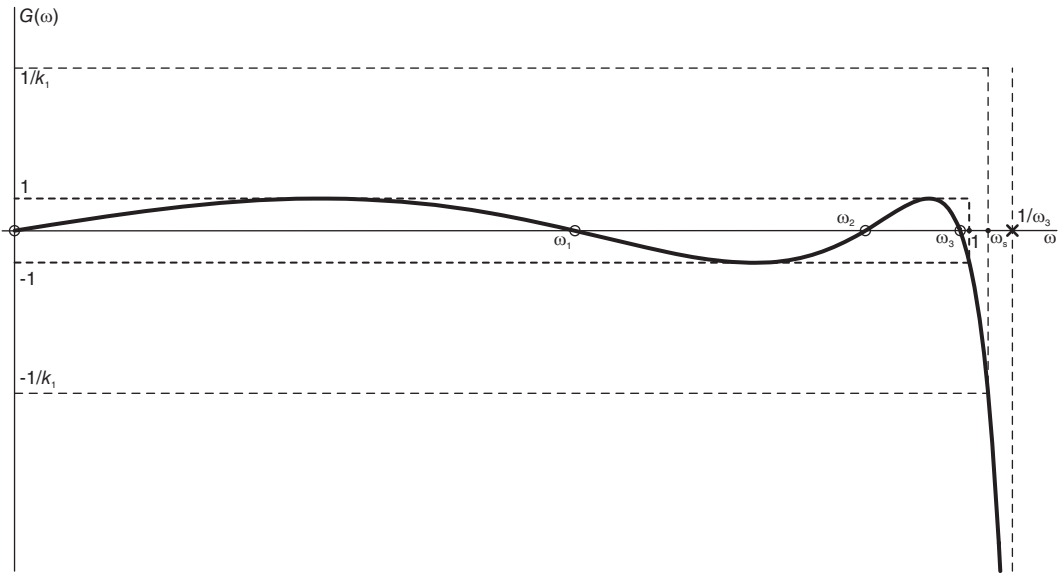


FIGURE 9.23 Function $G(\omega)$ over the pass-band and transition band.

$G(\omega)$ at $\omega = 1$ is -1 and that its value at $\omega = \omega_s$ is $-1/k_1$. The function tends to $-\infty$ at $\omega = 1/\omega_3$.

An important property that results in this particular shape of the function $G(\omega)$ is the reciprocity of its values between the pass-band and stop-band. The relation has the form

$$G(\omega) G\left(\frac{\omega_s}{\omega}\right) = \frac{1}{k_1}. \tag{9.231}$$

We note from the figure that in the pass-band the function $G(\omega)$ oscillates between -1 and 1 . In the stop-band, as implied by the last relation, its absolute value has a minimum of $1/k_1$. The magnitude-squared spectrum $|H(j\omega)|^2$ therefore oscillates between $1/(1 + \varepsilon^2)$ and 1 in the pass-band and between 0 and $1/(1 + \varepsilon^2/k_1^2)$ in the stop-band.

The following relations apply

$$\omega_s = \frac{\omega_p}{k} \tag{9.232}$$

where ω_s is the stop-band edge frequency and ω_p is the pass-band edge frequency which is normalized to 1 , that is,

$$\omega_p = 1, \quad k = 1/\omega_s, \quad k' = \sqrt{1 - k^2}. \tag{9.233}$$

Filter design specifications are commonly given as in Fig. 9.24, which shows the amplitude spectrum of a third order filter as an illustration. As seen in the figure for this case the filter gain at zero frequency is a maximum equal to 1 . The pass-band ripple of the amplitude spectrum $|H(j\omega)|$ is denoted δ_1 , so that the minimum of the amplitude spectrum in the pass-band is $(1 - \delta_1)$ which, as will be seen, is also equal to $1/\sqrt{1 + \varepsilon^2}$ as shown. The pass-band edge frequency is $\omega_c \equiv \omega_p = 1$, and that of the stop band is $\omega_s = 1/k$.

The relations between $G(\omega)$ and $H(j\omega)$, summarized in Table 9.9 can be readily established.

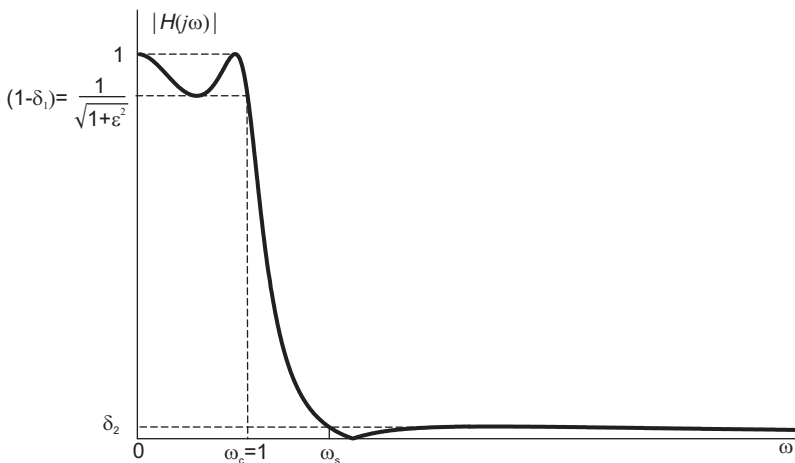


FIGURE 9.24 Elliptic filter specifications.

TABLE 9.9 The relation between $G(\omega)$ and $H(j\omega)$

	$G(\omega)$	$ H(j\omega) $
Pass-band	0 (max/min) = ± 1	1 $\sqrt{1/(1+\epsilon^2)} = 1 - \delta_1$
Stop-band	(max/min) = $\pm 1/k_1$ $\pm \infty$	$1/\sqrt{1+\epsilon^2/k_1^2} = \delta_2$ 0

We have

$$\delta_2^2 = \frac{1}{1 + \epsilon^2/k_1^2} \tag{9.234}$$

wherefrom

$$k_1 = \delta_2 \epsilon / \sqrt{1 - \delta_2^2}, \quad k_1' = \sqrt{1 - k_1^2}. \tag{9.235}$$

In the pass-band

$$(1 - \delta_1)^2 = \frac{1}{1 + \epsilon^2} \tag{9.236}$$

wherefrom

$$\epsilon^2 = \frac{1}{(1 - \delta_1)^2} - 1 = \frac{2\delta_1 - \delta_1^2}{(1 - \delta_1)^2} \tag{9.237}$$

$$\epsilon = \frac{\sqrt{2\delta_1 - \delta_1^2}}{(1 - \delta_1)}. \tag{9.238}$$

Letting the ripple in the pass-band be R_p dB and that in the stop-band be R_s dB we deduce the following useful relations.

$$20 \log_{10} [1/(1 - \delta_1)] = R_p \tag{9.239}$$

$$\delta_1 = 1 - 10^{-0.05R_p} \tag{9.240}$$

$$20 \log_{10} (1/\delta_2) = R_s \tag{9.241}$$

$$\delta_2 = 10^{-0.05R_s} \tag{9.242}$$

$$\varepsilon = \sqrt{10^{0.1R_p} - 1} \quad (9.243)$$

$$k_1 = \sqrt{(10^{0.1R_p} - 1) / (10^{0.1R_s} - 1)}. \quad (9.244)$$

9.22 Pole Zero Alignment and Mapping of Elliptic Filter

In this section we evaluate the positions of the poles and zeros of the function $|H(j\omega)|^2$ in the complex u plane. A transformation in two steps is then applied to map these poles and zeros to the Laplace s plane in such a way as to obtain the desired elliptic filter magnitude spectrum.

To evaluate the filter transfer function $H(s)$ and its poles and zeros we start by considering the squared magnitude spectrum given by

$$|H(j\omega)|^2 = H(j\omega)H(-j\omega) = \frac{1}{1 + \varepsilon^2 G^2(\omega)}. \quad (9.245)$$

Letting $\psi = sn^{-1}(\omega, k)$, i.e. $\omega = sn(\psi, k)$, and

$$u = n\psi = n sn^{-1}(\omega, k) \quad (9.246)$$

we have

$$G(\omega) = \begin{cases} sn(n\psi, k_1) = sn(u, k_1), & N \text{ odd} \\ sn(n\psi + K_1, k_1) = sn(u + K_1, k_1), & N \text{ even} \end{cases} \quad (9.247)$$

and

$$|H(j\omega)|^2 = \begin{cases} \frac{1}{1 + \varepsilon^2 sn^2(u, k_1)}, & N \text{ odd} \\ \frac{1}{1 + \varepsilon^2 sn^2(u + K_1, k_1)}, & N \text{ even.} \end{cases} \quad (9.248)$$

Writing

$$H(j\omega)H(-j\omega) = H(s)H(-s)|_{s=j\omega} \quad (9.249)$$

we have

$$H(s)H(-s) = \begin{cases} \frac{1}{1 + \varepsilon^2 sn^2(u, k_1)}, & N \text{ odd} \\ \frac{1}{1 + \varepsilon^2 sn^2(u + K_1, k_1)}, & N \text{ even} \end{cases} \quad (9.250)$$

where

$$u = n\psi = n sn^{-1}(\omega, k) = n sn^{-1}(s/j, k). \quad (9.251)$$

The poles are obtained by writing

$$1 + \varepsilon^2 sn^2(u, k_1) = 0, \quad N \text{ odd} \quad (9.252)$$

$$1 + \varepsilon^2 sn^2(u + K_1, k_1) = 0, \quad N \text{ even} \quad (9.253)$$

i.e.

$$sn(u, k_1) = \pm j/\varepsilon, \quad N \text{ odd} \quad (9.254)$$

$$sn(u + K_1, k_1) = \pm j/\varepsilon, \quad N \text{ even.} \quad (9.255)$$

From the periodicity of the sn function we can write

$$sn(u + mK_1, k_1) = \pm j/\varepsilon, \begin{cases} m \text{ even for } N \text{ odd} \\ m \text{ odd for } N \text{ even} \end{cases} \tag{9.256}$$

$$u = \pm sn^{-1}(j/\varepsilon, k_1) - mK_1, \begin{cases} m \text{ even for } N \text{ odd} \\ m \text{ odd for } N \text{ even.} \end{cases} \tag{9.257}$$

Letting

$$u_0 = sn^{-1}(j/\varepsilon, k_1) \tag{9.258}$$

the position of the poles are given by

$$u = \pm u_0 - mK_1, \begin{cases} m \text{ even for } N \text{ odd} \\ m \text{ odd for } N \text{ even.} \end{cases} \tag{9.259}$$

The zeros and poles of the magnitude squared spectrum $|H(j\omega)|^2$ on the complex u plane, with $u = x + jy$, are shown in Fig. 9.25 which is plotted for illustration for an odd filter order. Note that the zeros of $|H(j\omega)|^2$ are double zeros, being the poles of $sn^2(u, k_1)$. The value $u_0 = sn^{-1}(j/\varepsilon, k_1)$ appears in the figure. Note the repetition of the poles along the real axis with a spacing of $2K_1$. Note, moreover, the periodicity along the imaginary axis. This is due to the periodicity of the sn function along the imaginary axis.

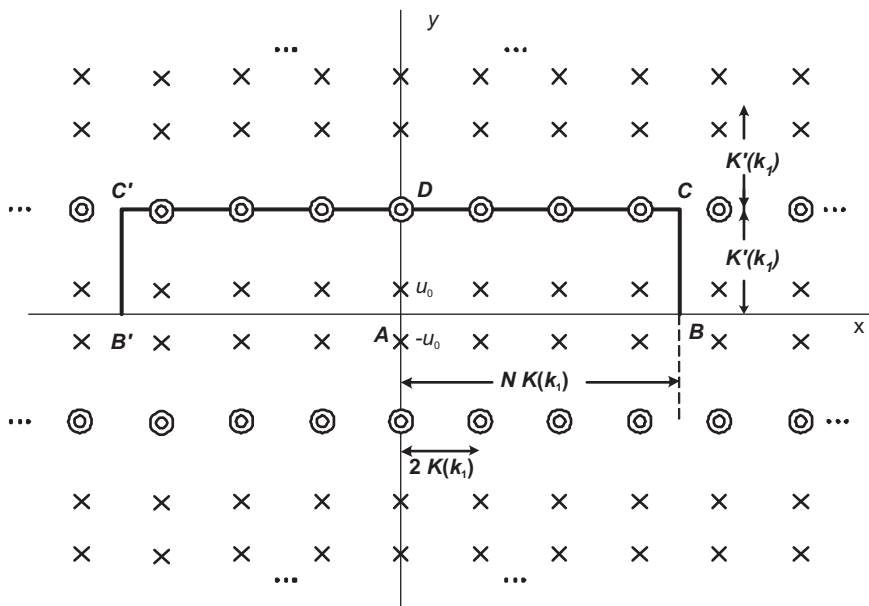


FIGURE 9.25 Zeros and poles on the complex u plane.

The periodic repetition of the poles with a spacing of $2K'_1$ is seen in the figure. The figure shows a rectangle drawn to enclose poles and zeros for the case $N = 7$ as an illustration. We note that if we travel around the rectangle $ABCD$ in the u plane, as shown in the figure, we would readily observe maxima and minima created by the presence of the poles and zeros. In fact, the rectangle $ABCDC'B'A$ is drawn to include seven poles and accompanying seven

zeros, in order to obtain the desired frequency response $|H(j\omega)|^2$ shown in Fig. 9.21. The portion AB of the path corresponds to the positive frequency pass-band. The portion CD corresponds to the positive frequency stop-band. The line BC is the transition between the pass-band and stop-band.

Note that the negative-frequencies portion of $|H(j\omega)|^2$ are taken into account by following the path $ABCDC'B'A$ shown in the figure. Also note that the ripples in the pass-band are due to the existence of the poles adjacent to this path. The ripples in the stop-band are due to the zeros along the path.

The present objective is to convert the rectangle shown in the u plane to the left half s plane in such a way that the zeros lie on the $s = j\omega$ axis, the point B is transformed to the point $s = j\omega_c = j$, the point C is transformed to $s = j\omega_s = j/k$ and the point D is transformed to $s = \pm j\infty$. These objectives are summarized in Table 9.10.

TABLE 9.10 Transformation objectives

Point	u	s
A	0	0
B	NK_1	$j\omega_c = j$
C	$NK_1 + jK'_1$	$j\omega_s = j/k$
D	jK'_1	$j\infty$

A conformal mapping is used to effect such a transformation. The mapping is given by

$$s = j \operatorname{sn} \left(\frac{K}{NK_1} u, k \right) \tag{9.260}$$

such that with

$$u = n \operatorname{sn}^{-1} (\omega, k) \tag{9.261}$$

if

$$\frac{K}{NK_1} = \frac{1}{n} = \frac{K'}{K'_1} \tag{9.262}$$

then

$$s = j \operatorname{sn} (u/n, k) = j\omega \tag{9.263}$$

and the four points are mapped as required. In particular we obtain the results shown in Table 9.11.

TABLE 9.11 Mapping of four points from u to s plane

Point	u	s
A	0	$j \operatorname{sn} (0, k) = 0$
B	NK_1	$j \operatorname{sn} (K, k) = j$
C	$NK_1 + jK'_1$	$j \operatorname{sn} (K + jK', k) = j/k$
D	jK'_1	$j \operatorname{sn} (jK', k) = j\infty$

The order of the filter is given by

$$N = \frac{KK'_1}{K'K_1}. \tag{9.264}$$

The transformation from the u plane to the s plane may be viewed as the result of a

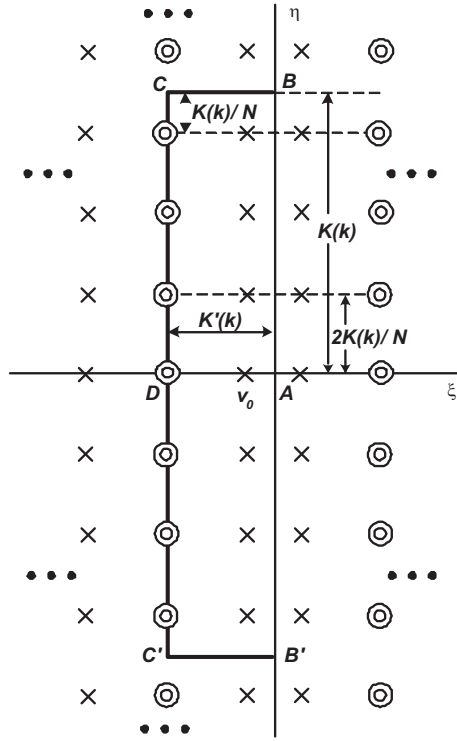


FIGURE 9.26 Poles and zeros in the v plane.

rotation of the u plane by 90° resulting in a v plane followed by one from the v plane to the s plane. The first transformation is written

$$v = j \frac{K(k)}{NK(k_1)} u. \tag{9.265}$$

The poles and zeros in the v plane are shown in Fig. 9.26. The value u_0 in the u plane is transformed to v_0 shown in the figure in the v plane, where

$$v_0 = j \frac{K(k)}{NK(k_1)} u_0 = j \frac{K(k)}{NK(k_1)} sn^{-1}(j/\varepsilon, k_1). \tag{9.266}$$

The transformation from the v plane to the s plane is therefore

$$s = j\omega_c sn(-jv, k) = j sn(-jv, k). \tag{9.267}$$

The points A , B , C and D of the u plane (Fig. 9.24) correspond to the similarly labeled points in the v plane, where the successive coordinates are

$$v = 0, \quad jK(k), \quad -K'(k) + jK(k) \quad \text{and} \quad -K'(k). \tag{9.268}$$

These are transformed respectively, as expected, to

$$s = j\omega_c sn 0 = 0, \quad j\omega_c sn [K(k)] = j\omega_c = j \tag{9.269}$$

$$j\omega_c sn [K(k) + jK'(k)] = j\omega_c/k = j\omega_s = j/k \tag{9.270}$$

and

$$j\omega_c sn [jK'(k)] = j\infty. \tag{9.271}$$

The negative frequencies are similarly transformed. The successive transformations from the u plane to the v plane and thence to the s plane are listed in Table 9.12 which shows the four points A , B , C and D in the three different planes.

TABLE 9.12 Transformations from u to v and s plane

Point	u	v	s
A	0	0	0
B	NK_1	jK	j
C	$NK_1 + jK'_1$	$-K' + jK$	j/k
D	jK'_1	$-K'$	$j\infty$

As stated above we have

$$|H(j\omega)|^2 = \frac{1}{1 + \varepsilon^2 G^2(\omega)} \tag{9.272}$$

so that

$$G(\omega) = sn(u, k_1) = sn(n sn^{-1}(\omega, k), k_1). \tag{9.273}$$

Given any point $v = \xi + j\eta$ in the v plane we can evaluate the corresponding point $s = \sigma + j\omega$ in the s plane. We can thus deduce the positions of the poles and zeros in the s plane using their known coordinates in the v plane. We have

$$\begin{aligned} s = \sigma + j\omega &= j sn(-jv, k) = sn(-j\xi + \eta, k) \\ &= j\omega_c \frac{sn \eta \ cn j\xi \ dn j\xi - sn j\xi \ cn \eta \ dn \eta}{1 - k^2 sn^2 \eta \ sn^2 j\xi}. \end{aligned} \tag{9.274}$$

Now

$$cn(jv, k) = nc(v, k') \tag{9.275}$$

$$sn(ju, k) = j \frac{sn(u, k')}{cn(u, k')} \tag{9.276}$$

$$cn(ju, k) = \frac{1}{cn(u, k')} \tag{9.277}$$

$$dn(ju, k) = \frac{dn(u, k')}{cn(u, k')}. \tag{9.278}$$

Writing

$$s = j\omega_c \frac{N}{D} \tag{9.279}$$

we have

$$\begin{aligned} N &= sn \eta \frac{1}{cn(\xi, k')} \frac{dn(\xi, k')}{cn(\xi, k')} - j \frac{sn(\xi, k')}{cn(\xi, k')} \ cn \eta \ dn \eta \\ &= \frac{sn \eta \ dn(\xi, k') - j \ sn(\xi, k') \ cn \eta \ dn \eta \ cn(\xi, k')}{cn^2(\xi, k')} \end{aligned} \tag{9.280}$$

$$D = 1 + k^2 sn^2 \eta \frac{sn^2(\xi, k')}{cn^2(\xi, k')} = \frac{cn^2(\xi, k') + k^2 sn^2 \eta \ sn^2(\xi, k')}{cn^2(\xi, k')} \tag{9.281}$$

$$s = \frac{j\omega_c sn \eta \operatorname{dn}(\xi, k') + \omega_c sn(\xi, k') cn \eta \operatorname{dn} \eta cn(\xi, k')}{cn^2(\xi, k') + k^2 sn^2 \eta sn^2(\xi, k')} \triangleq \frac{N_1}{D_1} \tag{9.282}$$

$$\begin{aligned} D_1 &= 1 - sn^2(\xi, k') + k^2 sn^2 \eta sn^2(\xi, k') \\ &= 1 - sn^2(\xi, k') [1 - k^2 sn^2 \eta] = 1 - sn^2(\xi, k') d_n^2(\eta, k) \end{aligned} \tag{9.283}$$

wherefrom

$$\sigma = \frac{\omega_c sn(\xi, k') cn(\eta, k) \operatorname{dn}(\eta, k) cn(\xi, k')}{1 - sn^2(\xi, k') \operatorname{dn}^2(\eta, k)} \tag{9.284}$$

$$\omega = \frac{\omega_c sn(\eta, k) \operatorname{dn}(\xi, k')}{1 - sn^2(\xi, k') \operatorname{dn}^2(\eta, k)}. \tag{9.285}$$

The poles may be found by substituting for their ξ and η coordinates in the v plane, as shown in Fig. 9.26, namely,

$$v = \xi + j\eta = v_0 \pm j2 \frac{K(k)}{N} i, \quad i = 0, 1, \dots, (N - 1)/2. \tag{9.286}$$

The zeros are found by substituting

$$v = \xi + j\eta = -K'(k) \pm j2 \frac{K(k)}{N} i, \quad i = 0, 1, \dots, (N - 1)/2. \tag{9.287}$$

We can, alternatively, obtain the poles' and zeros' locations in the s plane by transforming their coordinates in the u plane using Table 9.11 or 9.12.

Part of the above analysis was carried out assuming N to be odd. The same analysis with minor differences can be applied for the case of N even [4] [60].

9.23 Poles of $H(s)$

In this section we effect a direct evaluation of the poles of $H(s)$. We first note that we can write

$$v_0 = j \frac{u_0}{n} = j \frac{K}{NK_1} u_0. \tag{9.288}$$

Using the relation

$$sn(jv, k) = j sc(v, k') \tag{9.289}$$

we can write

$$j sc(nv_0, k'_1) = sn(jnv_0, k_1) = sn(\pm u_0, k_1) = \pm j/\varepsilon \tag{9.290}$$

i.e.

$$v_0 = \frac{sc^{-1}(\pm 1/\varepsilon, k'_1)}{n} = \pm \frac{K}{NK_1} sc^{-1}(1/\varepsilon, k'_1) \tag{9.291}$$

which is another expression giving the value of v_0 .

As found above the poles are at $u = \pm u_0 - mK_1$, i.e. at values of s given by

$$s = j sn \left(\frac{K}{NK_1} u, k \right) = j sn \left(\pm \frac{K}{NK_1} u_0 - m \frac{K}{N}, k \right), \tag{9.292}$$

m even for N odd; m odd for N even

or equivalently

$$s = j \operatorname{sn} \left(\mp jv_0 - m \frac{K}{N}, k \right), \quad m \text{ even for } N \text{ odd; } m \text{ odd for } N \text{ even.} \quad (9.293)$$

The poles in the left half of the s plane are found by writing

$$s = j \operatorname{sn} \left(jv_0 - m \frac{K}{N}, k \right), \quad m \text{ even for } N \text{ odd; } m \text{ odd for } N \text{ even.} \quad (9.294)$$

Using the summation formula

$$\operatorname{sn}(u \pm v) = \frac{\operatorname{sn} u \operatorname{cn} v \operatorname{dn} v \pm \operatorname{cn} u \operatorname{sn} v \operatorname{dn} u}{1 - k^2 \operatorname{sn}^2 u \operatorname{sn}^2 v} \quad (9.295)$$

we have

$$\begin{aligned} s = j & \left[\operatorname{sn}(jv_0, k) \operatorname{cn} \left(\frac{mK}{N}, k \right) \operatorname{dn} \left(\frac{mK}{N}, k \right) \right. \\ & \left. \pm \operatorname{cn}(jv_0, k) \operatorname{sn} \left(\frac{mK}{N}, k \right) \operatorname{dn}(jv_0, k) \right] \\ & / \left[1 - k^2 \operatorname{sn}^2(jv_0, k) \operatorname{sn}^2 \left(\frac{mK}{N}, k \right) \right]. \end{aligned} \quad (9.296)$$

Letting

$$\mu = mK/N, \quad \begin{cases} m \text{ odd for } N \text{ even} \\ m \text{ even for } N \text{ odd} \end{cases} \quad (9.297)$$

and using the relations

$$\operatorname{sn}(jv, k) = j \operatorname{sc}(v, k') \quad (9.298)$$

$$\operatorname{cn}(jv, k) = \operatorname{nc}(v, k') \quad (9.299)$$

$$\operatorname{dn}(jv, k) = \frac{\operatorname{dn}(v, k')}{\operatorname{cn}(v, k')} \quad (9.300)$$

we have the poles

$$\begin{aligned} s = j & [j \operatorname{sc}(v_0, k') \operatorname{cn}(\mu, k) \operatorname{dn}(\mu, k) \\ & \pm \operatorname{nc}(v_0, k') \operatorname{sn}(\mu, k) \operatorname{dn}(v_0, k') / \operatorname{cn}(v_0, k')] \\ & / [1 + k^2 \operatorname{sc}^2(v_0, k') \operatorname{sn}^2(\mu, k)]. \end{aligned} \quad (9.301)$$

Now

$$\operatorname{dn}^2(\mu, k) = 1 - k^2 \operatorname{sn}^2(\mu, k) \quad (9.302)$$

$$\operatorname{sc}(v_0, k') = \operatorname{sn}(v_0, k') / \operatorname{cn}(v_0, k') \quad (9.303)$$

$$\operatorname{nc}(v_0, k') = 1 / \operatorname{cn}(v_0, k') \quad (9.304)$$

wherefrom the poles are given by

$$\begin{aligned} s & = \frac{-\operatorname{sn}(v_0, k') \operatorname{cn}(\mu, k) \operatorname{dn}(\mu, k) \operatorname{cn}(v_0, k') \pm j \operatorname{sn}(\mu, k) \operatorname{dn}(v_0, k')}{\operatorname{cn}^2(v_0, k') + k^2 \operatorname{sn}^2(v_0, k') \operatorname{sn}^2(\mu, k)} \\ & = \frac{-\operatorname{sn}(v_0, k') \operatorname{cn}(\mu, k) \operatorname{dn}(\mu, k) \operatorname{cn}(v_0, k') \pm j \operatorname{sn}(\mu, k) \operatorname{dn}(v_0, k')}{1 - \operatorname{dn}^2(\mu, k) \operatorname{sn}^2(v_0, k')}. \end{aligned} \quad (9.305)$$

9.24 Zeros and Poles of $G(\omega)$

The Chebyshev rational function $G(\omega)$ is zero if

$$G(\omega) = \begin{cases} sn(n\psi, k_1) = 0, & N \text{ odd} \\ sn(n\psi + K_1, k_1) = 0, & N \text{ even} \end{cases} \quad (9.306)$$

and from the periodicity of the sn function we can write, similarly to the above,

$$sn(n\psi + mK_1, k_1) = 0, \quad \begin{cases} m \text{ even for } N \text{ odd} \\ m \text{ odd for } N \text{ even} \end{cases} \quad (9.307)$$

i.e.

$$n\psi + mK_1 = 0 \quad (9.308)$$

$$\psi = sn^{-1}(\omega, k) = -mK_1/n = -mK/N. \quad (9.309)$$

The frequency values (for $\omega > 0$) at which $G(\omega) = 0$, which may be denoted $\omega_{m,z,G}$, are therefore given by

$$\omega_{m,z,G} = sn(mK/N, k), \quad \begin{cases} m \text{ even for } N \text{ odd} \\ m \text{ odd for } N \text{ even.} \end{cases} \quad (9.310)$$

Since

$$G(\omega) G\left(\frac{1}{k\omega}\right) = \frac{1}{k_1} \quad (9.311)$$

if $G(\omega) = 0$ then $G\left(\frac{1}{k\omega}\right) = \infty$. The poles of $G(\omega)$ are therefore at frequencies given by

$$\omega_{m,p,G} = \frac{1}{k\omega_{m,z}} = \frac{1}{k sn(mK/N, k)}, \quad \begin{cases} m \text{ even for } N \text{ odd} \\ m \text{ odd for } N \text{ even.} \end{cases} \quad (9.312)$$

9.25 Zeros, Maxima and Minima of the Magnitude Spectrum

As noted above the zeros of $H(j\omega)$ are the poles of $G(\omega)$, wherefrom the zeros of $H(j\omega)$ (for $\omega > 0$) are given by

$$\omega_{m,z,H} = \frac{1}{k sn(mK/N, k)}, \quad \begin{cases} m \text{ even for } N \text{ odd} \\ m \text{ odd for } N \text{ even.} \end{cases} \quad (9.313)$$

9.26 Points of Maxima/Minima

In the pass-band region the maxima of $|H(j\omega)|$ are equal to 1 and occur at the zeros of $G(\omega)$, i.e. at the frequencies, which may be denoted $\omega_{m,z,G}$

$$\omega_{m,z,G} = sn(mK/N, k), \quad \begin{cases} m, \text{ even for } N \text{ odd} \\ m \text{ odd for } N \text{ even.} \end{cases} \quad (9.314)$$

The minima of $|H(j\omega)|$ in the pass-band correspond to the maxima of $G^2(\omega)$, that is, the points of maxima or minima of

$$G(\omega) = \begin{cases} sn(n\psi, k_1) = 0, & N \text{ odd} \\ sn(n\psi + K_1, k_1) = 0, & N \text{ even.} \end{cases} \tag{9.315}$$

They can be deduced by noticing the locations of the zeros of the sn function along the real axis, Fig. 9.19, and that by symmetry the function has its maxima/minima halfway between these zeros. The frequencies of the maxima/minima of $G(\omega)$ in the pass-band, denoted $\omega_{m,mx,p,G}$, are therefore given by

$$\omega_{m,mx,p,G} = sn(mK/N, k), \quad \begin{cases} m \text{ odd for } N \text{ odd} \\ m \text{ even for } N \text{ even} \end{cases} \tag{9.316}$$

and those of maxima/minima in the stop band, denoted $\omega_{m,mx,s,G}$, are given by

$$\omega_{m,mx,s,G} = \frac{1}{k\omega_{m,mx,p,G}} = \frac{1}{ksn(mK/N, k)}, \quad \begin{cases} m \text{ odd for } N \text{ odd} \\ m \text{ even for } N \text{ even.} \end{cases} \tag{9.317}$$

9.27 Elliptic Filter Nomograph

The nomograph of elliptic filters is shown in Fig. 9.27. As stated above in connection with Butterworth and Chebyshev filters, the elliptic filter in order to meet certain desired specifications may be evaluated using the nomograph.

Example 9.10 *Design an elliptic filter having an attenuation of 1% in the pass-band and a minimum of 40 dB in the stop-band, with pass-band edge frequency $\omega_p = 1$ and stop-band edge frequency $\omega_s = 1.18$. Evaluate the filter order N , the poles and zeros of $G(\omega)$, $|H(j\omega)|$ and $H(s)$. Plot $G(\omega)$ and $|H(j\omega)|^2$.*

We have $\delta_1 = 0.01$ and

$$20 \log_{10} \delta_2 = -40$$

$$\delta_2 = 0.01$$

$$k = 1/\omega_s = 0.84746, \quad k' = \sqrt{1 - k^2} = 0.53086.$$

The pass-band cut-off frequency ω_c is

$$\omega_c = \omega_p = 1.$$

We may evaluate $K(k)$ using *Mathematica*, noticing that *Mathematica*, requires using $m = k^2$ as an argument rather than k . We write

$$K(k) = \mathbf{EllipticK}[m] = 2.10308.$$

Similarly

$$K' = K(k') = \mathbf{EllipticK}[(k')^2] = \mathbf{EllipticK}[1 - k^2] = 1.7034$$

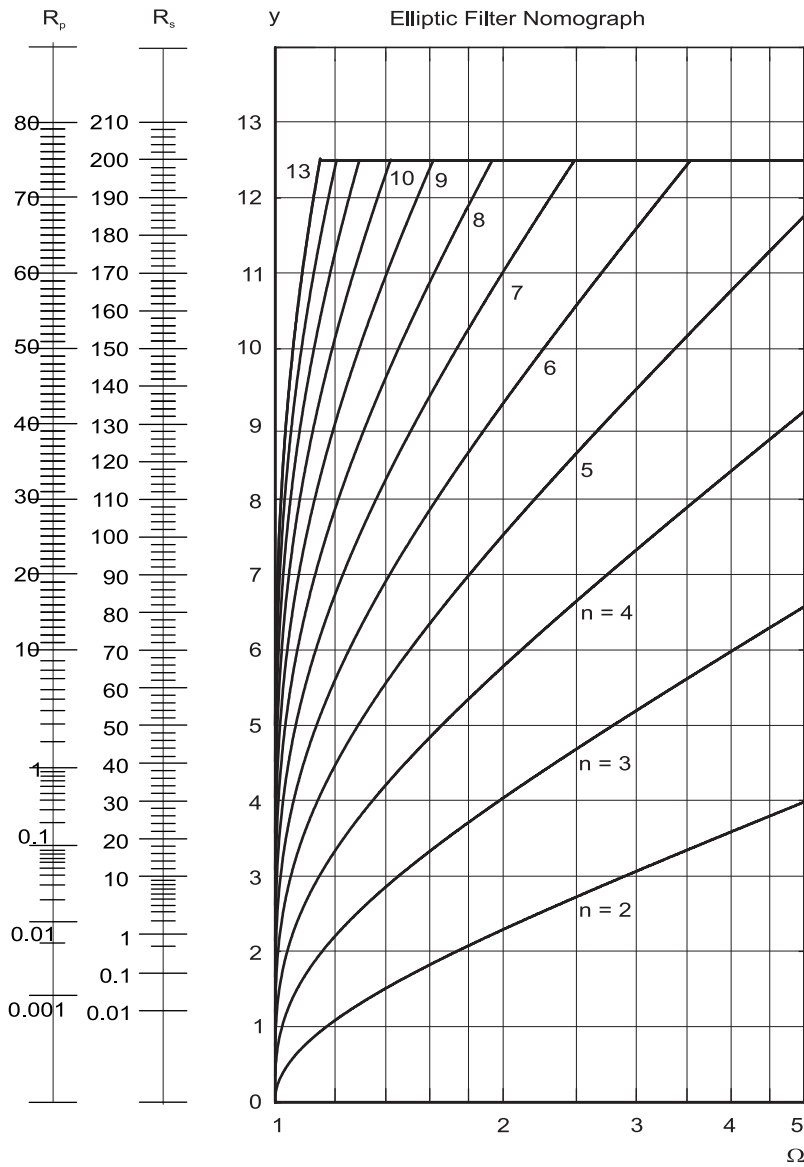


FIGURE 9.27 Elliptic filter nomograph.

$$\varepsilon = \frac{\sqrt{2\delta_1 - \delta_1^2}}{(1 - \delta_1)} = 0.14249$$

$$k_1 = \delta_2 \varepsilon / \sqrt{1 - \delta_2^2} = 0.001425, \quad k'_1 = \sqrt{1 - k_1^2} = 0.99999$$

$$K_1 = K(k_1) = \mathbf{EllipticK}[k_1^2] = 1.5708$$

$$K'_1 = K(k'_1) = \mathbf{EllipticK}[(k'_1)^2] = 7.93989.$$

The order of the filter N should be the least integer value that is greater than or equal to, i.e. the “ceiling,” of

$$\frac{K'_1 K}{K_1 K'} = 6.2407$$

wherefrom

$$N = \mathbf{Ceiling}[6.2407] = 7.$$

This may be referred to as the “first iteration” in the filter design process. Having forced the filter order to the integer value $N = 7$ it no longer equals the ratio $(K'_1 K) / (K_1 K')$. To reconcile the value $N = 7$ with this ratio we reevaluate the parameter k so that the ratio $K(k)/K'(k)$ is equal to the ratio

$$r = \frac{NK(k_1)}{K'(k_1)} = \frac{7 \times 1.15708}{7.93989} = 1.38485.$$

The function $K(k)/K'(k)$ as a function of k is shown in Fig. 9.28.

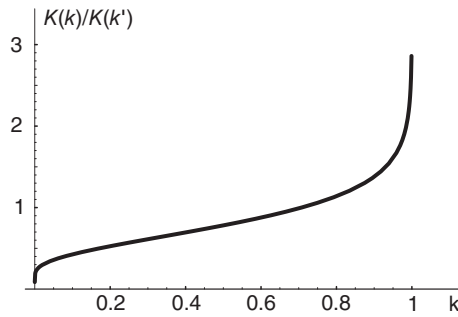


FIGURE 9.28 K/K' as a function of k .

The required value of k is that producing $K/K' = r = 1.38485$. Note that $\omega_s = 1/k$. Altering k means altering ω_s . The given stop-band edge frequency ω_s is thus altered to $\omega_{s,2}$. Since, however, the filter order N is made higher than the required ratio the result is a filter with lower value of ω_s and hence better than the given specifications. We may find the value of k using a root-finding numerical analysis algorithm, or by using the Mathematica instructions

$$\mathbf{ratio}[k_]:= \mathbf{EllipticK}[k^2] / \mathbf{EllipticK}[1 - k^2]$$

and

$$ktrue = \mathbf{FindRoot}[\mathbf{ratio}[k] = r, \{k, 0.5\}]$$

we obtain

$$ktrue = 0.901937$$

wherefrom

$$\omega_{s,2} = 1/ktrue = 1.10872.$$

The second iteration is thus started with this value of stop-band edge frequency $\omega_s = 1.10872$. The updated values are

$$K = 2.289, \quad K' = 1.65289.$$

The value v_0 may be found by writing

$$v_0 = -I(K/(N K1)) \mathbf{InverseJacobiSN}[I/\varepsilon, k1^2]$$

where $I = j$. Alternatively,

$$v_0 = K/(N K1) \mathbf{InverseJacobiSC}[1/\varepsilon, k1p^2]$$

where $k_1 p = k_1'$. We obtain

$$v_0 = 0.550962.$$

The poles p_0, p_1, p_2 and p_3 are found by writing

$$\begin{aligned} p_0 &= I \text{ JacobiSN}[I v_0, k^2] \\ p_1 &= I \text{ JacobiSN}[I v_0 + 2K/N, k^2] \\ &\dots \\ p_3 &= I \text{ JacobiSN}[I v_0 + 6K/N, k^2]. \end{aligned}$$

We obtain

$$\begin{aligned} p_0 &= -0.607725 \\ p_1, p_1^* &= -0.382695 \pm j0.703628 \\ p_2, p_2^* &= -0.135675 \pm j0.957725 \\ p_3, p_3^* &= -0.0302119 \pm j1.02044. \end{aligned}$$

The poles can be alternatively evaluated by converting the ξ and η coordinates in the v plane to the s plane. The resulting poles and zeros in the s plane are shown in Fig. 9.29.

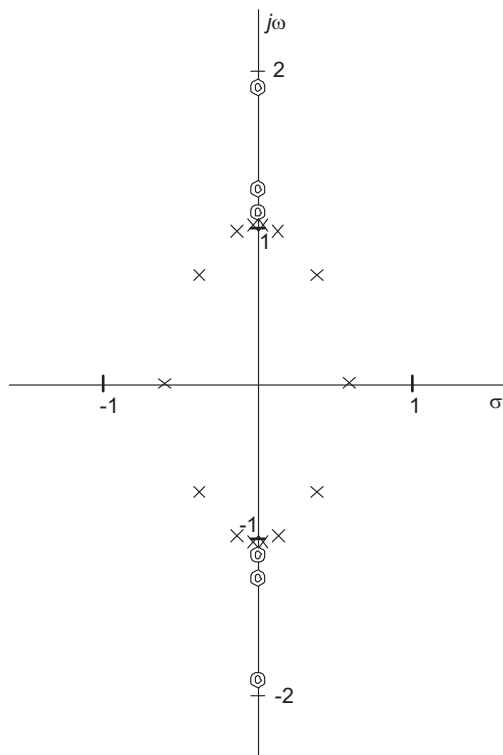


FIGURE 9.29 Elliptic filter poles and zeros in s plane.

These coordinates are given by

$$(\xi, \eta) = (-v_0, 0), (-v_0, 2K/N), (-v_0, 4K/N), (-v_0, 6K/N)$$

i.e.

$$\xi_0 = \xi_1 = \xi_2 = \xi_3 = -v_0 = -0.550962$$

and we find

$$\eta_0 = 0, \quad \eta_1 = 0.654001, \quad \eta_2 = 1.308, \quad \eta_3 = 1.962.$$

The pole coordinates as found above are coded in Mathematica by writing

$$\begin{aligned} \sigma[\xi_-, \eta_-, k_-] := & \text{JacobiSN}[\xi, (1 - k^2)] \\ & \text{JacobiCN}[\eta, k^2] \text{JacobiDN}[\eta, k^2] \\ & \text{JacobiCN}[\xi, (1 - k^2)] / \\ & (1 - ((\text{JacobiSN}[\xi, (1 - k^2)]))^2) \\ & ((\text{JacobiDN}[\eta, k^2])^2) \end{aligned}$$

and

$$\begin{aligned} \omega[\xi_-, \eta_-, k_-] := & \text{JacobiSN}(\eta, k^2) \\ & ((\text{JacobiDN}(\xi, (1 - k^2)))^2) / \\ & (1 - ((\text{JacobiSN}[\xi, (1 - k^2)]))^2) \\ & ((\text{JacobiDN}[\eta, k^2])^2). \end{aligned}$$

The same values of the poles are obtained as

$$p_i = \sigma_i + j\omega_i.$$

The functions $G(\omega)$ and $|H(j\omega)|$ are plotted by observing that

$$n = K'_1/K' = NK_1/K = 4.80365$$

and writing

$$G[\omega_-, n_-, k_-, k1_-, K1_-] := \text{JacobiSN}[n \text{InverseJacobiSN}[\omega, k^2], k1^2].$$

This function is coded in Mathematica as complex-valued even though it has a zero imaginary component, except for rounding off computational errors. To visualize $G(\omega)$ we therefore plot the real part of $G(\omega)$. The result is shown in Fig. 9.22(a) and (b), where the overall spectrum and the pass-band, enlarged, are shown, respectively. The zeros of $G(\omega)$ are evaluated by writing

$$\begin{aligned} \omega z0 &= \text{JacobiSN}[0, k^2] \\ \omega z1 &= \text{JacobiSN}[2K/N, k^2] \\ &\dots \\ \omega z3 &= \text{JacobiSN}[6K/N, k^2]. \end{aligned}$$

We obtain

$$\omega_{z0} = 0, \quad \omega_{z1} = 0.580704, \quad \omega_{z2} = 0.887562, \quad \omega_{z3} = 0.989755.$$

The poles of $G(\omega)$ are given by $\omega_{pi} = 1/(k \omega_{zi})$. We obtain

$$\omega_{p0} = \infty, \quad \omega_{p1} = 1.90928, \quad \omega_{p2} = 1.24918, \quad \omega_{p3} = 1.1202.$$

The points of maxima/minima in $G(\omega)$ and $|H(j\omega)|$ are given in the pass-band by

$$\begin{aligned} \omega_{m0} &= \text{JacobiSN}[K/N, k^2] = 0.31682 \\ \omega_{m1} &= \text{JacobiSN}[3K/N, k^2] = 0.76871 \end{aligned}$$

$$\omega_{m2} = \mathbf{JacobiSN}[5K/N, k^2] = 0.95568$$

and in the stop band by $1/(k\omega_{mi})$, that is,

$$\omega_{ms0} = 3.4995, \quad \omega_{ms1} = 1.44232, \quad \omega_{ms2} = 1.16014.$$

The function $|H(j\omega)|^2$ is written as

$$Hsq[\omega_-, n_-, k_-, k1_-, \epsilon_-, K1_-] := 1 / (1 + \epsilon^2 (\text{Re}[\mathbf{JacobiSN}[n \mathbf{InverseJacobiSN}[\omega, k^2], k1^2]])^2).$$

The magnitude-squared spectrum $|H(j\omega)|^2$ is shown in Fig. 9.21. The pole zero pattern in the u plane is seen in Fig. 9.30.

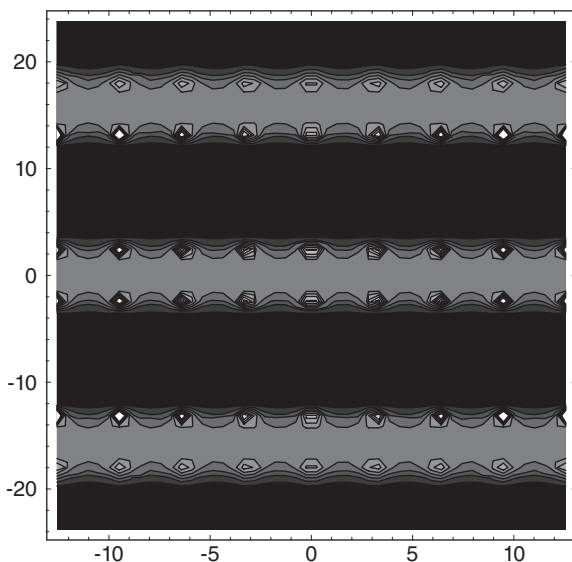


FIGURE 9.30 Pole-zero pattern of $n = 7$ elliptic filter example.

The N even case is similarly treated and is dealt with in a problem at the chapter's end.

9.28 $N = 9$ Example

Example 9.11 Design a lowpass elliptic filter having a maximum response of 0 dB, a maximum pass-band ripple of $R_p = 0.1$ dB, a stop-band ripple of at least $R_s = 55$ dB, a normalized pass-band edge frequency of $\omega_p = 1$ and a stop-band edge frequency $\omega_s = 1.1$. Evaluate the filter transfer function, its poles and zeros and the poles and zeros of the function $G(\omega)$ in its frequency response.

From the filter specifications we obtain:

$$\epsilon = 0.15262, \quad k = 0.909091, \quad K = 2.32192, \quad K' = 1.64653, \quad k_1 = 0.00027140,$$

$$k'_1 = 1, \quad K_1 = 1.5708, \quad K'_1 = 9.5982, \quad N_1 = (K'_1 K) / (K_1 K') = 8.616.$$

The least higher integer is $N = \text{Ceil}[8.616] = 9$. Replacing the real value N_1 by integer $N = 9$ improves slightly the specifications altering in the process some parameters. The next step is to ensure that the rational-Chebyshev function condition, namely, $NK_1/K'_1 = K/K'$, is satisfied. We can either re-evaluate R_s or ω_s to satisfy this condition.

In the previous example of $N = 7$ we chose to update the value of k , hence modifying ω_s . In the present example, for illustration purposes, to validate the condition we shall choose to keep the value k and hence ω_s unchanged, and instead update the value k_1 and hence the attenuation R_s .

A numeric solution by iterative evaluation of the two ratios for successive values of k_1 , starting with the present value $k_1 = 0.00027140$, would produce an estimate of the value k_1 . Alternatively, we may use the Mathematica command *FindRoot*. We write

$$\text{ratio1} = K/K', \quad \text{ratio2}[N_, k_1] := NK_1/K'_1$$

$$k_1 \text{true} = \mathbf{FindRoot}[\text{ratio2}[N, k_1] == \text{ratio2}, \{k_1, 0.00027140\}].$$

We obtain the new value

$$k_1 = 0.000177117$$

$$R_s = 10 \log_{10} [1 + (10^{0.1R_p} - 1) / k_1^2] = 58.707$$

$$k'_1 = 1, \quad K_1 = 1.5708, \quad K'_1 = 10.025, \quad n = K'_1/K' = 6.08856, \quad v_0 = -0.423536.$$

The poles are given by

$$p_m = -j \operatorname{sn}(jv_0 + mK/N, k), \quad m = 0, 1, 2, 3, 4.$$

We obtain

$$p_0 = -0.448275, \quad p_1, p_1^* = -0.341731 \mp j0.544813$$

$$p_2, p_2^* = -0.173149 \mp j0.847267$$

$$p_3, p_3^* = -0.0695129 \mp j0.969793.$$

$$p_4, p_4^* = -0.0178438 \mp j1.01057.$$

The zeros are $z_i = \{j2.30201, j1.3902, j1.1706, j1.1065\}$ and their conjugates. The zeros of $G(\omega)$ are $\{0, 0.477843, 0.790219, 0.939686\}$. The poles are $\{2.30201, 1.39202, 1.1706, \infty\}$. The rational Chebyshev function $G(\omega)$ is shown in Fig. 9.31.

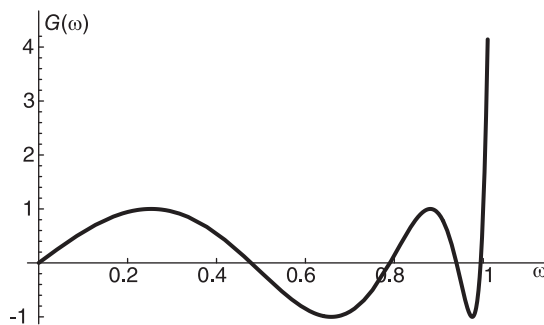


FIGURE 9.31 Function $G(\omega)$ for elliptic filter of order $N = 9$.

The filter transfer function is given by $H(s) = N(s)/D(s)$ where

$$N(s) = 0.1339 + 0.301452s^2 + 0.23879s^4 + 0.07642s^6 + 0.00777s^8$$

$$D(s) = 0.133901 + 0.606346s + 1.6165s^2 + 3.23368s^3 + 4.5243s^4 \\ + 5.71909s^5 + 4.69624s^6 + 4.08983s^7 + 1.65275s^8 + s^9.$$

The filter magnitude response $|H(j\omega)|$ is shown in Fig. 9.32.

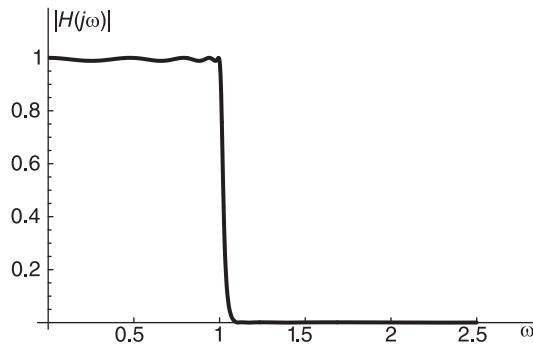


FIGURE 9.32 Magnitude spectrum function $|G(\omega)|$ of ninth order elliptic filter.

It is worthwhile noticing that MATLAB uses the approach followed in the previous $N = 7$ example; updating the value k and hence ω_s , instead of updating k_1 and hence R_s as was done in the present example. To reconcile the values of the poles and zeros found in this example with those that result from using MATLAB we should specify to MATLAB that $R_s = 58.707$. Doing so we obtain identical results as found above.

The following short MATLAB program may be used for such verification.

```
Rp=0.1
Rs=58.707
Wp=1
Ws=1.1
[Nm, Wpm] = ellipord(Wp, Ws, Rp, Rs, 's')
[Z,P,K]=ellipap(N,Rp,Rs)
[B,A]=ellip(N,Rp,Rs,Wp,'s')
```

The student will note that the poles and zeros, and the transfer function, produced by MATLAB are identical with the results obtained above.

9.29 Tables of Elliptic Filters

The transfer function coefficients, the poles and zeros of elliptic filters are listed in Table 9.13 to Table 9.22 for different values of the filter order N , the pass-band ripple R_p dB, the stop-band edge frequency ω_s , and the stop-band ripple R_s dB.

TABLE 9.13 Elliptic filter denominator polynomial $a_0 + a_1s + \dots + a_{n-1}s^{n-1} + s^n$ and numerator polynomial $b_0 + b_2s^2 + b_4s^4 + \dots$ coefficients, poles and zeros, with $R_p = 0.1$ dB and $\omega_s = 1.05$

	$N = 2$	$N = 3$	$N = 4$	$N = 5$	$N = 7$	$N = 9$
R_s	0.3426455	1.7477711	6.3969941	13.8413868	30.4700260	47.2761726
a_0	1.3990302	3.2826436	1.8508723	1.3173786	0.5256578	0.2097217
a_1	0.1508135	1.4193116	1.4822580	1.8794136	1.3811996	0.8052803
a_2		2.9026725	2.8780944	3.1068871	2.7719512	2.0212569
a_3			1.3123484	2.8637648	3.9831910	3.8129189
a_4				1.7228910	3.9074600	5.0952301
a_5					3.5962977	6.2421799
a_6					1.6550949	4.9331746
a_7						4.2336178
a_8						1.6490642
b_0	1.3830158	3.2826436	1.8296856	1.3173786	0.5256578	0.2097217
b_2	0.9613194	2.7232585	2.1383746	1.9050150	1.0658098	0.5467436
b_4			0.4787958	0.6552837	0.6808319	0.5077885
b_6					0.1324515	0.1943523
b_8						0.0245867
Zeros						
	$\pm j1.1994432$	$\pm j1.0979117$	$\pm j1.8200325$	$\pm j1.3318177$	$\pm j1.6475352$	$\pm j1.9984177$
			$\pm j1.0740734$	$\pm j1.0646230$	$\pm j1.1438273$	$\pm j1.2626443$
					$\pm j1.0571288$	$\pm j1.0979117$
						$\pm j1.0542324$
Poles						
	-0.0754068	-0.0448535	-0.6185761	-0.2669018	-0.3623864	-0.3552567
	$\pm j1.1804000$	$\pm j1.0793319$	$\pm j1.1432441$	$\pm j1.0158871$	$\pm j0.7912186$	$\pm j0.6169914$
		-2.8129654	-0.0375981	-0.0301146	-0.0979300	-0.1495512
			$\pm j1.0459484$	$\pm j1.0280395$	$\pm j0.9794960$	$\pm j0.8930736$
				-1.1288581	-0.0182745	-0.0508626
					$\pm j1.0129061$	$\pm j0.9820104$
					-0.6979132	-0.0117722
						$\pm j1.0073711$
						-0.5141787

TABLE 9.14 Elliptic filter denominator polynomial $a_0 + a_1s + \dots + a_{n-1}s^{n-1} + s^n$ and numerator polynomial $b_0 + b_2s^2 + b_4s^4 + \dots$ coefficients, poles and zeros, with $R_p = 0.1$ dB and $\omega_s = 1.1$

	$N = 2$	$N = 3$	$N = 4$	$N = 5$	$N = 7$	$N = 9$
R_s	0.5588853	3.3742719	10.7205944	20.0502491	39.3573265	58.7070427
a_0	1.6258769	2.8365345	1.6533079	1.0268282	0.3708066	0.1339013
a_1	0.2589655	1.6486701	1.7995999	1.8610135	1.1739773	0.6063457
a_2		2.4116752	2.7778502	2.8331900	2.4108458	1.6164997
a_3			1.5410995	2.8724523	3.6754971	3.2336819
a_4				1.6905622	3.7156317	4.5243044
a_5					3.4943247	5.7190928
a_6					1.6596349	4.6962447
a_7						4.0898266
a_8						1.6527468
b_0	1.607235	2.8365345	1.6343826	1.0268282	0.3708066	0.1339013
b_2	0.937700	2.0699894	1.6417812	1.2835929	0.6492805	0.3014518
b_4			0.2910518	0.3717959	0.3518730	0.2387967
b_6					0.0560947	0.0764154
b_8						0.0077724
Zeros						
	$\pm j1.3092301$	$\pm j1.1706040$	$\pm j2.0856488$	$\pm j1.4809093$	$\pm j1.8747718$	$\pm j2.3020096$
			$\pm j1.1361890$	$\pm j1.1221945$	$\pm j1.2344811$	$\pm j1.3920196$
					$\pm j1.1109130$	$\pm j1.1706040$
						$\pm j1.1065024$
Poles						
	-0.1294827	-0.0854214	-0.7038162	-0.3296916	-0.3726059	-0.3417307
	$\pm j1.2685075$	$\pm j1.1218480$	$\pm j0.9764946$	$\pm j0.9532986$	$\pm j0.7068694$	$\pm j0.5448126$
		-2.2408323	-0.0667335	-0.0495333	-0.1291176	-0.1731486
			$\pm j1.0661265$	$\pm j1.0393462$	$\pm j0.9574274$	$\pm j0.8472668$
				-0.9321125	-0.0282791	-0.0695129
					$\pm j1.0182745$	$\pm j0.9697934$
					-0.5996296	-0.0178438
						$\pm j1.0105669$
						-0.4482749

TABLE 9.15 Elliptic filter denominator polynomial $a_0 + a_1s + \dots + a_{n-1}s^{n-1} + s^n$ and numerator polynomial $b_0 + b_2s^2 + b_4s^4 + \dots$ coefficients, poles and zeros, with $R_p = 0.1$ dB and $\omega_s = 1.20$

	$N = 2$	$N = 3$	$N = 4$	$N = 5$	$N = 7$	$N = 9$
R_s	1.0747750	6.6912446	17.0510120	28.3031082	50.9628677	73.6290512
a_0	1.9986240	2.4314215	1.3903317	0.7920082	0.2577848	0.0839041
a_1	0.4725369	1.9409142	1.9870989	1.7790993	0.9701640	0.4439832
a_2		2.0576346	2.6737130	2.6525514	2.0995352	1.2791656
a_3			1.6706022	2.8478775	3.3690655	2.7163413
a_4				1.6920280	3.5413387	4.0003653
a_5					3.3943024	5.2264667
a_6					1.6671665	4.4675741
a_7						3.9510615
a_8						1.6574275
b_0	1.9757459	2.4314215	1.3744167	0.7920082	0.2577848	0.0839041
b_2	0.8836113	1.4305701	1.0948827	0.7874882	0.3588836	0.1501842
b_4			0.1404266	0.1754069	0.1515365	0.0932849
b_6					0.0180661	0.0228895
b_8						0.0017088
Zeros						
	$\pm j1.4953227$	$\pm j1.3036937$	$\pm j2.4948752$	$\pm j1.7228950$	$\pm j2.2286088$	$\pm j2.7662959$
			$\pm j1.2539659$	$\pm j1.2333397$	$\pm j1.3933201$	$\pm j1.6059589$
					$\pm j1.2164999$	$\pm j1.3036937$
						$\pm j1.2098579$
Poles						
	-0.2362685	-0.1567661	-0.7268528	-0.3791553	-0.3711948	-0.3235983
	$\pm j1.3938440$	$\pm j1.1702591$	$\pm j0.7981539$	$\pm j0.8753982$	$\pm j0.6271909$	$\pm j0.4807398$
		-1.7441024	-0.1084483	-0.0754299	-0.1614480	-0.1928080
			$\pm j1.0868686$	$\pm j1.0516452$	$\pm j0.9285520$	$\pm j0.7970691$
				-0.7828577	-0.0410804	-0.0903314
					$\pm j1.0244980$	$\pm j0.9539840$
					-0.5197204	-0.0254899
						$\pm j1.0143603$
						-0.3929724

TABLE 9.16 Elliptic filter denominator polynomial $a_0 + a_1s + \dots + a_{n-1}s^{n-1} + s^n$ and numerator polynomial $b_0 + b_2s^2 + b_4s^4 + \dots$ coefficients, poles and zeros, with $R_p = 0.1$ dB and $\omega_s = 1.50$

	$N = 2$	$N = 3$	$N = 4$	$N = 5$	$N = 7$	$N = 9$
R_s	3.2103367	14.8477592	29.06367	43.41521	72.12859	100.84222
a_0	2.7450464	2.0172143	1.0930740	0.5794907	0.1664555	0.0478134
a_1	1.0682132	2.3059034	2.0598156	1.6299865	0.7556445	0.3003893
a_2		1.8774745	2.6121931	2.5107679	1.7825338	0.9609295
a_3			1.7447219	2.8060758	3.0337298	2.1981611
a_4				1.7120869	3.3540711	3.4522831
a_5					3.2864916	4.7003198
a_6					1.6783862	4.2156830
a_7						3.7991598
a_8						1.6640812
b_0	2.7136242	2.0172143	1.0805616	0.5794907	0.1664555	0.0478134
b_2	0.6910082	0.7188895	0.5154718	0.3454847	0.1389352	0.0513107
b_4			0.0352222	0.0439371	0.0342428	0.0187645
b_6					0.0022557	0.0026331
b_8						0.0001063517
Zeros						
	$\pm j1.9816788$	$\pm j1.6751162$	$\pm j3.4784062$	$\pm j2.3318758$	$\pm j3.0870824$	$\pm j3.8748360$
			$\pm j1.5923420$	$\pm j1.5574064$	$\pm j1.8204368$	$\pm j2.1532161$
					$\pm j1.5285687$	$\pm j1.6751167$
						$\pm j1.5171083$
Poles						
	-0.5341066	-0.2896462	-0.6987343	-0.4170375	-0.3594736	-0.2996915
	$\pm j1.5683675$	$\pm j1.2124279$	$\pm j0.6169485$	$\pm j0.7757661$	$\pm j0.5431284$	$\pm j0.4158787$
		-1.2981820	-0.1736266	-0.1141294	-0.1983054	-0.2101821
			$\pm j1.1081139$	$\pm j1.0661507$	$\pm j0.8873446$	$\pm j0.7358851$
				-0.6497532	-0.0595590	-0.1163022
					$\pm j1.0325530$	$\pm j0.9312235$
					-0.4437103	-0.0363620
						$\pm j1.0194213$
						-0.3390055

TABLE 9.17 Elliptic filter denominator polynomial $a_0 + a_1s + \dots + a_{n-1}s^{n-1} + s^n$ and numerator polynomial $b_0 + b_2s^2 + b_4s^4 + \dots$ coefficients, poles and zeros, with $R_p = 0.1$ dB and $\omega_s = 2.00$

	$N = 2$	$N = 3$	$N = 4$	$N = 5$	$N = 7$	$N = 9$
R_s	7.4183841	24.0103645	41.44714	58.90077	93.80865	128.71700
a_0	3.2140923	1.8193306	0.9529442	0.4878087	0.1307924	0.0350682
a_1	1.6868869	2.4820001	2.0536783	1.5354161	0.6536626	0.2408231
a_2		1.8804820	2.6104007	2.4510162	1.6278777	0.8186090
a_3			1.7733949	2.7860096	2.8652318	1.9547179
a_4				1.7269419	3.2595117	3.1841259
a_5					3.2332163	4.4386373
a_6					1.6854397	4.0871892
a_7						3.7222681
a_8						1.6681999
b_0	3.1773009	1.8193306	0.9420359	0.4878087	0.1307924	0.0350682
b_2	0.4256776	0.3530481	0.2439743	0.1579160	0.0592773	0.0204342
b_4			0.0084653	0.0105752	0.0078078	0.0040145
b_6					0.0002660873	0.0002974799
b_8						0.0000061483
Zeros						
	$\pm j2.7320509$	$\pm j2.2700682$	$\pm j4.9221134$	$\pm j3.2508049$	$\pm j4.3544307$	$\pm j5.4955812$
			$\pm j2.1431894$	$\pm j2.0892465$	$\pm j2.4903350$	$\pm j2.9870205$
					$\pm j2.0445139$	$\pm j2.2700801$
						$\pm j2.0266929$
Poles						
	-0.8434435	-0.3818585	-0.6704431	-0.4290917	-0.3501695	-0.2863379
	$\pm j1.5819910$	$\pm j1.2179047$	$\pm j0.5356388$	$\pm j0.7213293$	$\pm j0.5019931$	$\pm j0.3848209$
		-1.1167650	-0.2162544	-0.1389126	-0.2171252	-0.2171315
			$\pm j1.1168200$	$\pm j1.0735674$	$\pm j0.8622670$	$\pm j0.7025610$
				-0.5909334	-0.0711239	-0.1307105
					$\pm j1.0371404$	$\pm j0.9171293$
					-0.4086024	-0.0430916
						$\pm j1.0223918$
						-0.3136567

TABLE 9.18 Elliptic filter denominator polynomial $a_0 + a_1s + \dots + a_{n-1}s^{n-1} + s^n$ and numerator polynomial $b_0 + b_2s^2 + b_4s^4 + \dots$ coefficients, poles and zeros, with $R_p = 1$ dB and $\omega_s = 1.05$

	$N = 2$	$N = 3$	$N = 4$	$N = 5$	$N = 7$	$N = 9$
R_s	2.8161201	8.1342306	15.8403254	24.1345406	40.9259720	57.7355919
a_0	1.1672218	0.9845755	0.6921654	0.3951263	0.1576625	0.0629026
a_1	0.3141664	1.1629654	0.8610367	0.9765996	0.6017573	0.3248769
a_2		1.0788120	1.7548053	1.3156878	1.1064552	0.7644661
a_3			0.8757772	1.9993536	2.2500968	1.9224738
a_4				0.9212833	1.8620958	2.2301505
a_5					2.6510124	3.8865836
a_6					0.9125805	2.4398959
a_7						3.2892845
a_8						0.9111509
b_0	1.0402875	0.9845755	0.6168931	0.3951263	0.1576625	0.0629026
b_2	0.7230927	0.8167971	0.7209700	0.5713782	0.3196723	0.1639868
b_4			0.1614298	0.1965417	0.2042045	0.1523029
b_6					0.0397267	0.0582928
b_8						0.0073744
Zeros						
	$\pm j1.1994432$	$\pm j1.0979117$	$\pm j1.8200325$	$\pm j1.3318177$	$\pm j1.6475352$	$\pm j1.9984177$
			$\pm j1.0740734$	$\pm j1.0646230$	$\pm j1.1438273$	$\pm j1.2626443$
					$\pm j1.0571288$	$\pm j1.0979117$
						$\pm j1.0542324$
Poles						
	-0.1570832	-0.0655037	-0.4009260	-0.1811854	-0.2062934	-0.1952473
	$\pm j1.0688998$	$\pm j1.0171063$	$\pm j0.7239584$	$\pm j0.8584824$	$\pm j0.6815526$	$\pm j0.5518380$
		-0.9478046	-0.0369626	-0.0235591	-0.0619527	-0.0875141
			$\pm j1.0046415$	$\pm j1.0011643$	$\pm j0.9376404$	$\pm j0.8504819$
				-0.5117943	-0.0119201	-0.0306968
					$\pm j0.9997520$	$\pm j0.9644962$
					-0.3522483	-0.0071783
						$\pm j0.9996399$
						-0.2698779

TABLE 9.19 Elliptic filter denominator polynomial $a_0 + a_1s + \dots + a_{n-1}s^{n-1} + s^n$ and numerator polynomial $b_0 + b_2s^2 + b_4s^4 + \dots$ coefficients, poles and zeros, with $R_p = 1$ dB and $\omega_s = 1.10$

	$N = 2$	$N = 3$	$N = 4$	$N = 5$	$N = 7$	$N = 9$
R_s	4.0254035	11.4797106	20.8316784	30.4704971	49.8163643	69.1665344
a_0	1.2099342	0.8507724	0.5725316	0.3079804	0.1112174	0.0401615
a_1	0.4582576	1.2018049	0.8679778	0.8917965	0.4903824	0.2379754
a_2		1.0114629	1.6637303	1.2198991	0.9529513	0.6027271
a_3			0.9074267	1.9296353	2.0209396	1.5925974
a_4				0.9200925	1.7563342	1.9553030
a_5					2.5363598	3.4938834
a_6					0.9141089	2.3051746
a_7						3.1400957
a_8						0.9121705
b_0	1.0783550	0.8507724	0.5102693	0.3079804	0.1112174	0.0401615
b_2	0.6291147	0.6208596	0.5125793	0.3849928	0.1947411	0.0904156
b_4			0.0908691	0.1115141	0.1055386	0.0716232
b_6					0.0168247	0.0229195
b_8						0.0023312
Zeros						
	$\pm j1.3092301$	$\pm j1.1706040$	$\pm j2.0856488$	$\pm j1.4809093$	$\pm j1.8747718$	$\pm j2.3020096$
			$\pm j1.1361890$	$\pm j1.1221945$	$\pm j1.2344811$	$\pm j1.3920196$
					$\pm j1.1109130$	$\pm j1.1706040$
						$\pm j1.1065024$
Poles						
	-0.2291288	-0.0976508	-0.3992289	-0.2021446	-0.2067972	-0.1867364
	$\pm j1.0758412$	$\pm j1.0163028$	$\pm j0.6384812$	$\pm j0.8047847$	$\pm j0.6212643$	$\pm j0.4973284$
		-0.8161613	-0.0544844	-0.0346207	-0.0776460	-0.0987919
			$\pm j1.0033507$	$\pm j1.0002208$	$\pm j0.9117621$	$\pm j0.8075584$
				-0.4465618	-0.0175239	-0.0407234
					$\pm j0.9992438$	$\pm j0.9490941$
					-0.3101749	-0.0105628
						$\pm j0.9993268$
						-0.2385414

TABLE 9.20 Elliptic filter denominator polynomial $a_0 + a_1s + \dots + a_{n-1}s^{n-1} + s^n$ and numerator polynomial $b_0 + b_2s^2 + b_4s^4 + \dots$ coefficients, poles and zeros, with $R_p = 1$ dB and $\omega_s = 1.20$

	$N = 2$	$N = 3$	$N = 4$	$N = 5$	$N = 7$	$N = 9$
R_s	6.1502934	16.2089367	27.4318619	38.7567558	61.4223289	84.0885468
a_0	1.2358198	0.7292653	0.4667410	0.2375500	0.0773183	0.0251657
a_1	0.6411310	1.2304325	0.8489720	0.7997738	0.3916809	0.1703283
a_2		0.9749216	1.5872189	1.1386032	0.8165457	0.4690942
a_3			0.9252886	1.8562533	1.8052552	1.3064655
a_4				0.9228818	1.6546732	1.7041823
a_5					2.4244421	3.1289227
a_6					0.9162023	2.1740050
a_7						2.9947217
a_8						0.9134463
b_0	1.1014256	0.7292653	0.4159834	0.2375500	0.0773183	0.0251657
b_2	0.4925897	0.4290762	0.3313791	0.2361943	0.1076413	0.0450453
b_4			0.0425018	0.0526104	0.0454509	0.0279793
b_6					0.0054186	0.0068653
b_8						0.00051253
Zeros						
	$\pm j1.4953227$	$\pm j1.3036937$	$\pm j2.4948752$	$\pm j1.7228950$	$\pm j2.2286088$	$\pm j2.7662959$
			$\pm j1.2539659$	$\pm j1.2333397$	$\pm j1.3933201$	$\pm j1.6059589$
					$\pm j1.2164999$	$\pm j1.3036937$
						$\pm j1.2098579$
Poles						
	-0.3205655	-0.1364613	-0.3869712	-0.2175678	-0.2033161	-0.1765779
	$\pm j1.0644518$	$\pm j1.0100591$	$\pm j0.5604469$	$\pm j0.7481667$	$\pm j0.5641533$	$\pm j0.4475963$
		-0.7019989	-0.0756731	-0.0480837	-0.0933708	-0.1080689
			$\pm j1.0002558$	$\pm j0.9984784$	$\pm j0.8818856$	$\pm j0.7622858$
				-0.3915787	-0.0243799	-0.0516555
					$\pm j0.9984710$	$\pm j0.9308186$
					-0.2740688	-0.0147112
						$\pm j0.9988877$
						-0.2114193

TABLE 9.21 Elliptic filter denominator polynomial $a_0 + a_1s + \dots + a_{n-1}s^{n-1} + s^n$ and numerator polynomial $b_0 + b_2s^2 + b_4s^4 + \dots$ coefficients, poles and zeros, with $R_p = 1$ dB and $\omega_s = 1.50$

	$N = 2$	$N = 3$	$N = 4$	$N = 5$	$N = 7$	$N = 9$
R_s	11.1938734	25.1758442	39.51826	53.87453	82.58809	111.30172
a_0	1.2144312	0.6050306	0.3638481	0.1738088	0.0499256	0.0143409
a_1	0.8794183	1.2455788	0.8051777	0.6915782	0.2954669	0.1127507
a_2		0.9664114	1.5155253	1.0556664	0.6773588	0.3453196
a_3			0.9387957	1.7725538	1.5764157	1.0278672
a_4				0.9286768	1.5422249	1.4440999
a_5					2.3004806	2.7442405
a_6					0.9192135	2.0283818
a_7						2.8334117
a_8						0.9152431
b_0	1.0823629	0.6050306	0.3242800	0.1738088	0.0499256	0.0143409
b_2	0.2756172	0.2156192	0.1546947	0.1036225	0.0416713	0.0153898
b_4			0.0105703	0.0131782	0.0102706	0.0056281
b_6					0.0006765593	0.00078975
b_8						0.000031898
Zeros						
	$\pm j1.9816788$	$\pm j1.6751162$	$\pm j3.4784062$	$\pm j2.3318758$	$\pm j3.0870824$	$\pm j3.8748360$
			$\pm j1.5923420$	$\pm j1.5574064$	$\pm j1.8204368$	$\pm j2.1532161$
					$\pm j1.5285687$	$\pm j1.6751167$
						$\pm j1.5171083$
Poles						
	-0.4397091	-0.1876980	-0.3649884	-0.2288747	-0.1957901	-0.1637814
	$\pm j1.0104885$	$\pm j0.9942250$	$\pm j0.4806919$	$\pm j0.6816781$	$\pm j0.5027540$	$\pm j0.3956954$
		-0.5910153	-0.1044094	-0.0665406	-0.1108784	-0.1162305
			$\pm j0.9939365$	$\pm j0.9952536$	$\pm j0.8432065$	$\pm j0.7084979$
				-0.3378462	-0.0338441	-0.0650214
					$\pm j0.9971886$	$\pm j0.9064133$
					-0.2381883	-0.0204507
						$\pm j0.9982014$
						-0.1842750

TABLE 9.22 Elliptic filter denominator polynomial $a_0 + a_1s + \dots + a_{n-1}s^{n-1} + s^n$ and numerator polynomial $b_0 + b_2s^2 + b_4s^4 + \dots$ coefficients, poles and zeros, with $R_p = 1$ dB and $\omega_s = 2.00$

	$N = 2$	$N = 3$	$N = 4$	$N = 5$	$N = 7$	$N = 9$
R_s	17.0952606	34.4541321	51.90635	69.36026	104.26816	139.17599
a_0	1.1700772	0.5456786	0.3170348	0.1463103	0.0392291	0.0105182
a_1	0.9989416	1.2449721	0.7753381	0.6350259	0.2518903	0.0894842
a_2		0.9740258	1.4831116	1.0142939	0.6104009	0.2910073
a_3			0.9455027	1.7296971	1.4634978	0.9001004
a_4				0.9325243	1.4845004	1.3181715
a_5					2.2370582	2.5551229
a_6					0.9210811	1.9536068
a_7						2.7506700
a_8						0.9163475
b_0	1.0428325	0.5456786	0.2825575	0.1463103	0.0392291	0.0105182
b_2	0.1397131	0.1058910	0.0731785	0.0473643	0.0177792	0.0061290
b_4			0.0025391	0.0031719	0.0023418	0.0012041
b_6					0.00007980855	0.000089228
b_8						0.0000018442
Zeros						
	$\pm j2.7320509$	$\pm j2.2700682$	$\pm j4.9221134$	$\pm j3.2508049$	$\pm j4.3544307$	$\pm j5.4955468$
			$\pm j2.1431894$	$\pm j2.0892465$	$\pm j2.4903350$	$\pm j2.9870026$
					$\pm j2.0445139$	$\pm j2.2700672$
						$\pm j2.0266819$
Poles						
	-0.4994708	-0.2170337	-0.3512729	-0.2323381	-0.1906844	-0.1567457
	$\pm j0.9594823$	$\pm j0.9815753$	$\pm j0.4424977$	$\pm j0.6464399$	$\pm j0.4720468$	$\pm j0.3702247$
		-0.5399584	-0.1214784	-0.0776246	-0.1197249	-0.1195047
			$\pm j0.9891761$	$\pm j0.9929136$	$\pm j0.8210439$	$\pm j0.6795733$
				-0.3125989	-0.0395660	-0.0723407
					$\pm j0.9963087$	$\pm j0.8920580$
					-0.2211307	-0.0239280
						$\pm j0.9977474$
						-0.1713093

The following are useful MATLAB elliptic filter functions.

ellipap, ellipord, ellipdeg, ellip, ellipj, ellipk.

Moreover, MATLAB's Maple allows the user to call *Mathematica* functions such as

JacobiSN and **InverseJacobiSN**.

9.30 Bessel’s Constant Delay Filters

A filter of frequency response $H(j\omega)$, having a magnitude spectrum $|H(j\omega)|$ and phase $\arg[H(j\omega)]$ amplifies and delays in general the signals it receives. Amplification and simple delay do not change signal form. If the amplification and delay are constant, independent of the input signal frequency, the filter output is as desired amplified and delayed with no distortion. This is referred to as “distortionless transmission.” The present objective is to obtain a filter that acts as a pure delay, say t_0 seconds. The filter input signal $x(t)$ produces the filter output $y(t) = K x(t - t_0)$; an amplification of K and delay t_0 . In reality only an approximation is obtained, similarly to the deviation from the ideally flat magnitude response $|H(j\omega)|$ in the pass-band in Butterworth approximation. The filter response in both cases is shown in Fig. 9.33. The filter magnitude response $|H(j\omega)|$ and delay, denoted $\tau(\omega)$, are the required values only at d-c and fall off with the increase in frequency ω .

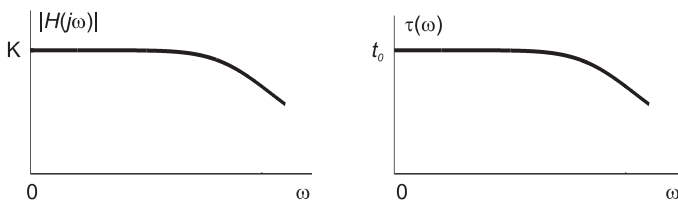


FIGURE 9.33 Butterworth filter magnitude response and Bessel filter delay response.

The objective that the filter response to the input signal $x(t)$ be $y(t) = K x(t - t_0)$, $t_0 \geq 0$ means that with an input Fourier transform spectrum $X(j\omega)$ the output should be

$$Y(j\omega) = K e^{-jt_0\omega} X(j\omega). \tag{9.318}$$

A filter effecting such distortionless transmission should therefore have the frequency response

$$H(j\omega) = Y(j\omega) / X(j\omega) = K e^{-jt_0\omega} \tag{9.319}$$

so that the amplitude spectrum, denoted $A(\omega)$,

$$A(\omega) \triangleq |H(j\omega)| = K \tag{9.320}$$

is a constant at all frequencies, and the phase spectrum, denoted $\phi(\omega)$,

$$\phi(\omega) = \arg [H(j\omega)] = -\omega t_0 \tag{9.321}$$

is proportional to frequency. The group delay $\tau(\omega)$ is given by

$$\tau(\omega) = -\frac{d}{d\omega} \arg [H(j\omega)] = t_0. \tag{9.322}$$

The Bessel filter, also referred to as the Thomson filter sets out to approximate such a linear-phase frequency response. We note that the desired filter transfer function is given by

$$H(s) = K e^{-st_0} \tag{9.323}$$

and may be rewritten in the form

$$H(s) = Ke^{-s} \quad (9.324)$$

where s is a normalized complex frequency producing a delay of unity. We thus obtain a normalized form that can be denormalized by replacing s by t_0s to obtain a particular delay t_0 . The objective is to find a rational function that approximates this exponential form. We can write $H(s)$ in the form

$$H(s) = \frac{K}{e^s} = \frac{K}{f(s) + g(s)} \quad (9.325)$$

$$f(s) = \cosh s \quad \text{and} \quad g(s) = \sinh s. \quad (9.326)$$

Using the power series expansions

$$\cosh(s) = 1 + \frac{s^2}{2!} + \frac{s^4}{4!} + \frac{s^6}{6!} + \dots \quad (9.327)$$

$$\sinh(s) = s + \frac{s^3}{3!} + \frac{s^5}{5!} + \frac{s^7}{7!} + \dots \quad (9.328)$$

we can write

$$\frac{f(s)}{g(s)} = \coth s = \frac{1 + s^2/2! + s^4/4! + s^6/6! + \dots}{s + s^3/3! + s^5/5! + s^7/7! + \dots}. \quad (9.329)$$

In what follows we convert this ratio into a series of integer multiples of $(1/s)$ using a “continued fraction expansion” thereof.

9.31 A Note on Continued Fraction Expansion

In the Theory of Numbers the continued fraction expansion is a basic tool that serves, among others, to convert fractional numbers into a series of integers. Consider the simple example of finding the continued fraction expansion of π . We may write

$$\begin{aligned} \pi &= 3.141592\dots = 3 + \frac{1}{7.0625} = 3 + \frac{1}{7 + \frac{1}{15.9966}} \\ &= 3 + \frac{1}{7 + \frac{1}{15 + \frac{1}{1 + 0.0034}}} = 3 + \frac{1}{7 + \frac{1}{15 + \frac{1}{1 + \frac{1}{292.6346}}}} \\ &= 3 + \frac{1}{7 + \frac{1}{15 + \frac{1}{1 + \frac{1}{292 + \frac{1}{1.5758}}}}} = \dots \end{aligned} \quad (9.330)$$

We have thus converted the value π into a series of integers: $\{3, 7, 15, 1, 292, 1, \dots\}$. The inverse operation of the set $\{3, 7, 15, 1, 292, 1\}$ is

$$\begin{aligned} \pi &\simeq 3 + \frac{1}{7 + \frac{1}{15 + \frac{1}{1 + \frac{1}{292 + \frac{1}{1 + 0}}}}} = 3 + \frac{1}{7 + \frac{1}{15 + \frac{1}{1 + \frac{1}{293}}}} \\ &= 3 + \frac{1}{7 + \frac{1}{15 + \frac{1}{1 + 0.0034}}} = \dots \end{aligned} \tag{9.331}$$

Mathematica has an instruction that evaluates the continued fraction of a number, to any number of integers. Writing **ContinuedFraction** $[\pi, 25]$ we obtain the result as the 25 integers $\{3, 7, 15, 1, 292, 1, 1, 1, 2, 1, 3, 1, 14, 2, 1, 1, 2, 2, 2, 1, 84, 2, 1, 1\}$. Returning to our Bessel filter approximation problem the presentation is simplified by effecting the continued fraction expansion of the function $\coth s$ after truncating the numerator and denominator polynomials $f(s)$ and $g(s)$ to say $n = 5$ terms. As shown in the table,

$n \equiv \text{numerator}, d \equiv \text{denominator}$		Q
$d = s + \frac{s^3}{3!} + \frac{s^5}{5!} + \frac{s^7}{7!} + \frac{s^9}{9!}$	$n = 1 + \frac{s^2}{2!} + \frac{s^4}{4!} + \frac{s^6}{6!} + \frac{s^8}{8!}$ $1 + \frac{s^2}{3!} + \frac{s^4}{5!} + \frac{s^6}{7!} + \frac{s^8}{9!}$	$1/s$
$n = s + \frac{s^3}{3!} + \frac{s^5}{5!} + \frac{s^7}{7!} + \frac{s^9}{9!}$ $s + \frac{s^3}{10} + \frac{s^5}{280} + \frac{s^7}{15120}$	$d = \frac{s^2}{3} + \frac{s^4}{30} + \frac{s^6}{840} + \frac{s^8}{45360}$	$3/s$
$d = \frac{s^3}{15} + \frac{s^5}{210} + \frac{s^7}{7560}$	$n = \frac{s^2}{3} + \frac{s^4}{30} + \frac{s^6}{840} + \frac{s^8}{45360}$ $\frac{s^2}{3} + \frac{s^4}{42} + \frac{s^6}{1512}$	$5/s$
$n = \frac{s^3}{15} + \frac{s^5}{210} + \frac{s^7}{7560}$ $\frac{s^3}{15} + \frac{s^5}{270}$	$d = \frac{s^4}{105} + \frac{s^6}{1890}$	$7/s$
$d = \frac{s^5}{945}$	$n = \frac{s^4}{105} + \frac{s^6}{1890}$ $\frac{s^4}{105}$	$9/s$
$\frac{s^6}{1890}$		

we first divide the numerator $n = f(s)$ by the denominator $d = g(s)$ obtaining the quotient $Q = n \div d = 1/s$. Next we effect the subtraction $n - Qd$. This “remainder” is now the new denominator $d = s^2/3 + s^4/30 + s^6/840 + s^8/45360$. The previous d descends becoming the new n . Again we effect the division $Q = n \div d$, obtaining the new quotient $Q = 3/s$. Next we effect the subtraction $n - Qd$ and this remainder is now the new denominator $d = s^3/15 + s^5/210 + s^7/7560$. The previous d now becomes the new numerator $n = s^2/3 + s^4/30 + s^6/840 + s^8/45360$, so that $Q = 5/s$, and the process is repeated as shown. The alternating numerator-denominator division process produces the

series of quotients Q as the result of the continued fraction expansion

$$Q = \{1/s, 3/s, 5/s, 7/s, 9/s\}. \quad (9.332)$$

It can be shown that for higher values of the polynomial truncation length n the same pattern applies, that is,

$$Q = \{1/s, 3/s, 5/s, 7/s, 9/s, 11/s, 13/s, \dots\}. \quad (9.333)$$

We have therefore obtained the approximation

$$\frac{f(s)}{g(s)} = \coth s = \frac{1}{s} + \frac{1}{\frac{3}{s} + \frac{1}{\frac{5}{s} + \frac{1}{\frac{7}{s} + \frac{1}{\frac{9}{s} + \frac{1}{\frac{11}{s} + \frac{1}{\dots}}}}}}}. \quad (9.334)$$

With $n = 5$ we have

$$\begin{aligned} \frac{f(s)}{g(s)} = \coth s &\approx \frac{1}{s} + \frac{1}{\frac{3}{s} + \frac{1}{\frac{5}{s} + \frac{1}{\frac{7}{s} + \frac{1}{\frac{9}{s}}}}} = \frac{1}{s} + \frac{1}{\frac{3}{s} + \frac{1}{\frac{5}{s} + \frac{9s}{63 + s^2}}} \\ &= \frac{1}{s} + \frac{1}{\frac{3}{s} + \frac{s(63 + s^2)}{315 + 14s^2}} = \frac{1}{s} + \frac{315s + 14s^3}{945 + 105s^2 + s^4} \\ &= \frac{945 + 420s^2 + 15s^4}{945s + 105s^3 + s^5} \end{aligned} \quad (9.335)$$

wherefrom

$$f(s) = \cosh s \approx 945 + 420s^2 + 15s^4 \quad (9.336)$$

$$g(s) = \sinh s \approx 945s + 105s^3 + s^5 \quad (9.337)$$

and write the approximation

$$H(s) = \frac{K}{f(s) + g(s)} = \frac{K}{945 + 945s + 420s^2 + 105s^3 + 15s^4 + s^5}. \quad (9.338)$$

In the present case of $n = 5$, to have a gain $H(0)$ equal to unity we set $K = 945$ obtaining

$$H(s) = \frac{945}{945 + 945s + 420s^2 + 105s^3 + 15s^4 + s^5}. \quad (9.339)$$

The process of evaluation of the continued fraction expansion can be coded as a MATLAB program.

```
N=5
for i=1:N
e(i)=factorial(2*(i-1))
o(i)=factorial(2*i-1)
end
a=1./ e
```

```

b=1./ o
nm=a
d=b
for i=1:N
xx=i
r(i)=nm(1)/d(1)
r2=r(i)*d
onebr2=1./r2
r2e=nm(2: N-i+1)-r2(2:N-i+1)
onebr2=1./ r2e
nm=d
onebnm=1./ nm
d=r2e(1:N-i)
onebd=1./ d
end

```

The program verifies the values of the successive quotients, $\{1/s, 3/s, 5/s, \dots\}$ by evaluating the successive numerator–denominator alternating division. To construct and simplify the function $H(s)$ from the result of the continued fraction expansion for any value n a *Mathematica* program can be written. The following program produces the result of simplifying the continued fraction expansion for the case $n = 5$.

```

b = 0
c = 9/p + b
d = 1/c
e = 7/p + d
f = 1/e
g = 5/p + f
h = 1/g
i = 3/p + h
j = 1/i
H = 1/p + j
Cothx = Together[H]
num = Numerator[Cothx]
den = Denominator[Cothx]
exppap = Expand[num + den]
K = Coefficient[exppap, p, 0]
H = K (1/exppap)

```

An observation of the denominator polynomial of the transfer function $H(s)$, namely

$$B(s) = s^5 + 15s^4 + 105s^3 + 420s^2 + 945s + 945 \quad (9.340)$$

reveals the fact that it is none other than the Bessel polynomial of order 5. This is generally the case. For a general order n the denominator of the transfer function $H(s)$ is the n^{th} order Bessel polynomial $B_n(s)$. Table 9.23 shows the first six such polynomials. Bessel polynomials can be evaluated using the recursive relation

$$B_n(s) = (2n - 1) B_{n-1}(s) + s^2 B_{n-2}(s). \quad (9.341)$$

In fact the coefficient a_k in the Bessel polynomial

$$B_n(s) = s^n + a_{n-1}s^{n-1} + a_{n-2}s^{n-2} + \dots + a_1s + a_0 \quad (9.342)$$

TABLE 9.23 Bessel polynomials

n	$B_n(s)$
0	1
1	$s + 1$
2	$s^2 + 3s + 3$
3	$s^3 + 6s^2 + 15s + 15$
4	$s^4 + 10s^3 + 45s^2 + 105s + 105$
5	$s^5 + 15s^4 + 105s^3 + 420s^2 + 945s + 945$
6	$s^6 + 21s^5 + 210s^4 + 1260s^3 + 4725s^2 + 10395s + 10395$

is given by

$$a_k = \frac{(2n-k)!}{2^{(n-k)}k!(n-k)!}, \quad k = 0, 1, \dots, n. \quad (9.343)$$

The filter transfer function is $H(s) = a_0/B_n(s)$. As seen above, the transfer function of Bessel filter general order n is derived directly from Bessel's polynomials. In fact we can write the transfer function in the form

$$H(s) = \frac{b_0}{A_n(s)} \quad (9.344)$$

where the denominator polynomial $A_n(s)$ is Bessel's polynomial $B_n(s)$ of order n

$$A_n(s) = B_n(s) = \sum_{k=0}^n a_k s^k \quad (9.345)$$

$$b_0 = a_0 = \frac{(2n)!}{(2^n)(n!)}. \quad (9.346)$$

The squared-magnitude spectrum is given by

$$|H(j\omega)|^2 = H(s)H(-s)|_{s=j\omega} = \frac{b_0^2}{A_n(j\omega)A_n(-j\omega)} = \frac{b_0^2}{D_n(\omega^2)}. \quad (9.347)$$

It can be shown that

$$D_n(\omega^2) = \sum_{k=0}^n d_{n,k} \omega^{2(n-k)} \quad (9.348)$$

where

$$d_{n,k} = \frac{(n+k)!(2k!)}{(n-k)![k!2^k]^2}. \quad (9.349)$$

This model of Bessel filter will be referred to henceforth as the delay normalized form of Bessel filter to distinguish it from two other closely related forms that we shall see shortly. The poles of the delay normalized Bessel filter can be evaluated as the roots of the Bessel polynomial $B_n(s)$. Using MATLAB for $n = 5$, for example, we evaluate the function roots (A) where A is the vector representing the denominator polynomial of $H(s)$

$$A = [1 \ 15 \ 105 \ 420 \ 945 \ 945]. \quad (9.350)$$

We obtain the poles $p_1, p_1^* = -2.3247 \pm j3.5710$, $p_2 = -3.6467$, $p_3, p_3^* = -3.3520 \pm j1.7427$. Similarly the poles of a Bessel filter of order $n = 10$ say can be plotted using the instructions

$A = [1 \ 55 \ 1485 \ 25740 \ 315315 \ 2837835 \ 18918900 \ 91891800 \ 310134825 \ 654729075 \ 654729075]$
 $B = [654729075]$

`pzmap(B, A)`

Figure 9.34 shows the filter’s poles for the case $n = 10$.

The Bessel filter transfer function denominator coefficients and poles are listed in Table 9.24.

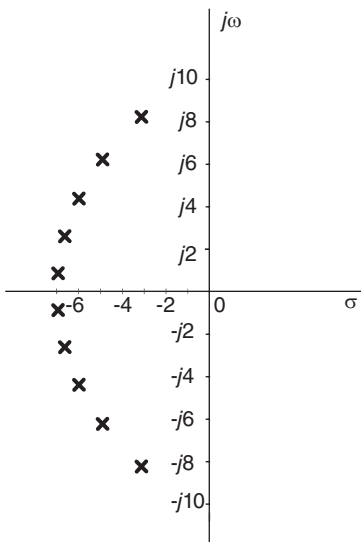


FIGURE 9.34 Poles of delay normalized Bessel filter model.

9.32 Evaluating the Filter Delay

Given a filter in general, Bessel or otherwise, of transfer function $H(s)$ and frequency response $H(j\omega) = H(s)|_{s=j\omega}$ it is interesting to find a form deducing thereof its group delay $\tau(\omega)$. To this end let us separate the real and imaginary parts, writing

$$H(j\omega) = X(j\omega) + jY(j\omega) \tag{9.351}$$

where

$$X(j\omega) = \Re[H(j\omega)] \quad \text{and} \quad Y(j\omega) = \Im[H(j\omega)]. \tag{9.352}$$

We can write

$$H(j\omega) = |H(j\omega)| e^{j\phi(\omega)} \tag{9.353}$$

where

$$|H(j\omega)| = \sqrt{[X(j\omega)]^2 + [Y(j\omega)]^2} \tag{9.354}$$

$$\phi(\omega) = \tan^{-1}[Y(j\omega)/X(j\omega)]. \tag{9.355}$$

TABLE 9.24 Bessel filter delay normalized model denominator coefficients

	$N=2$	$N=3$	$N=4$	$N=5$	$N=6$	$N=7$	$N=8$	$N=9$	$N=10$
a_0	3	15	105	945	10395	135135	2027025	34459425	654729075
a_1	3	15	105	945	10395	135135	2027025	34459425	654729075
a_2	1	6	45	420	4725	62370	945945	16216200	310134825
a_3	0	1	10	105	1260	17325	270270	4729725	91891800
a_4	0	0	1	15	210	3150	51975	945945	18918900
a_5	0	0	0	1	21	378	6930	135135	2837835
a_6	0	0	0	0	1	28	630	13860	315315
a_7	0	0	0	0	0	1	36	990	25740
a_8	0	0	0	0	0	0	1	45	1485
a_9	0	0	0	0	0	0	0	1	55
a_{10}	0	0	0	0	0	0	0	0	1

Poles									
-1.5000	-1.8389	-2.1038	-2.3247	-2.5159	-2.6857	-2.8390	-2.9793	-3.1089	
$\pm j0.8660$	$\pm j1.7544$	$\pm j2.6574$	$\pm j3.5710$	$\pm j4.4927$	$\pm j5.4207$	$\pm j6.3539$	$\pm j7.2915$	$\pm j8.2327$	
	-2.3222	-2.8962	-3.3520	-3.7357	-4.0701	-4.3683	-4.6384	-4.8862	
		$\pm j0.8672$	$\pm j1.7427$	$\pm j2.6263$	$\pm j3.5172$	$\pm j4.4144$	$\pm j5.3173$	$\pm j6.2250$	
			-3.6467	-4.2484	-4.7583	-5.2048	-5.6044	-5.9675	
				$\pm j0.8675$	$\pm j1.7393$	$\pm j2.6162$	$\pm j3.4982$	$\pm j4.3849$	
					-4.9718	-5.5879	-6.1294	-6.6153	
						$\pm j0.8676$	$\pm j1.7378$	$\pm j2.6116$	
							-6.2970	-6.9220	
									$\pm j0.8677$

The group delay is by definition

$$\begin{aligned}
 \tau(\omega) &= -\frac{d\phi(\omega)}{d\omega} = -\frac{d}{d\omega} \left\{ \tan^{-1} [Y(j\omega) / X(j\omega)] \right\} \\
 &= \frac{-1}{1 + Y^2(j\omega) / X^2(j\omega)} \frac{X(j\omega) Y'(j\omega) - X'(j\omega) Y(j\omega)}{X^2(j\omega)} \\
 &= \frac{X'(j\omega) Y(j\omega) - X(j\omega) Y'(j\omega)}{|H(j\omega)|^2}.
 \end{aligned}
 \tag{9.356}$$

Note that $H(-j\omega) = H^*(j\omega)$, that is, $X(-j\omega) = X(j\omega)$ and $Y(-j\omega) = -Y(j\omega)$; hence $X(j\omega)$ is even and $Y(j\omega)$ is odd and their derivatives $X'(j\omega)$ and $Y'(j\omega)$ are odd and even, respectively. The group delay is therefore a ratio of two even functions of ω . In fact the group delay will be shown next to be a ratio of two polynomials in powers of ω^2 , similarly to the expression of the frequency spectrum $|H(j\omega)|^2$.

9.33 Bessel Filter Quality Factor and Natural Frequency

We note that the transfer function of the Bessel filter may be factored into a product of first and second order system transfer functions. In other words the Bessel filter may be expressed as a cascade of first and second order systems. We recall that a typical second order system transfer function may be written in the form

$$H(s) = \frac{\omega_0^2}{s^2 + 2\zeta\omega_0s + \omega_0^2} \triangleq \frac{1}{D(s)}.
 \tag{9.357}$$

The denominator $D(s)$ is often written in the form

$$D(s) = s^2 + (\omega_0/Q)s + \omega_0^2 \quad (9.358)$$

where Q is referred to as the *quality factor* $Q = 1/(2\zeta)$. The poles have the form

$$s = -\alpha \pm j\beta = -\zeta\omega_0 \pm j\omega_0\sqrt{1-\zeta^2}, \quad (9.359)$$

$$\alpha = \zeta\omega_0 = \omega_0/(2Q), \quad \beta = \omega_0\sqrt{1-\zeta^2} \quad (9.360)$$

i.e. $\beta = \omega_0\sqrt{1-1/(4Q^2)}$ and $\omega_0 = \sqrt{\alpha^2 + \beta^2}$. Moreover, $Q = \omega_0/(2\alpha) = \sqrt{\alpha^2 + \beta^2}/(2\alpha)$. For a Bessel filter of order $n = 2$, for example,

$$H(s) = \frac{3}{s^2 + 3s + 3} \quad (9.361)$$

$$\omega_0 = \sqrt{3}. \quad (9.362)$$

The poles are $s = -1.5 \pm j\sqrt{3}/2 = -\alpha \pm j\beta$,

$$\alpha = 1.5, \quad \beta = \sqrt{3}/2, \quad Q = \omega_0/(2\alpha) = 1/\sqrt{3} = 0.577. \quad (9.363)$$

For a fifth order filter by evaluating the quadratic factors of the transfer function we find

$$H(s) = 945/D(s) \quad (9.364)$$

where

$$D(s) = (s^2 + 6.7039s + 14.2725)(s^2 + 4.6493s + 18.1563)(s + 3.64674). \quad (9.365)$$

For the first two quadratic factors of $D(s)$ the values of ω_0 are respectively $\omega_{01} = \sqrt{14.2725} = 3.778$ and $\omega_{02} = \sqrt{18.1563} = 4.261$. Their quality factors are $Q_1 = \omega_{01}/6.7039 = 0.564$ and $Q_2 = \omega_{02}/4.6493 = 0.916$. The third factor of $D(s)$ is a first order expression showing a pole of $H(s)$ at $s = -3.64674$.

9.34 Maximal Flatness of Bessel and Butterworth Response

In this section we consider the problem of attaining a maximally flat frequency response such as the one encountered in the Butterworth filter magnitude spectrum $|H(j\omega)|$ and Bessel filter group delay $\tau(\omega)$. Consider the general form of a system transfer function $H(s)$

$$H(s) = \frac{B(s)}{A(s)}. \quad (9.366)$$

We can write the transfer function in the form

$$H(s) = \frac{m_1(s) + n_1(s)}{m_2(s) + n_2(s)} \quad (9.367)$$

where $m_1(s)$ is the polynomial of even powers of s in the numerator and $n_1(s)$ is that of odd powers. Similarly $m_2(s)$ and $n_2(s)$ are the even-powered and odd-powered in s polynomials

of the denominator $A(s)$, respectively. The magnitude spectrum $|H(j\omega)|$ of the system is given by

$$|H(j\omega)|^2 = H(s)H(-s)|_{s=j\omega}. \quad (9.368)$$

Let $F(s) = H(s)H(-s)$. We have

$$F(s) = \frac{m_1(s) + n_1(s)}{m_2(s) + n_2(s)} \frac{m_1(s) - n_1(s)}{m_2(s) - n_2(s)} = \frac{m_1^2(s) - n_1^2(s)}{m_2^2(s) - n_2^2(s)} \quad (9.369)$$

and

$$|H(j\omega)|^2 = F(j\omega) = \frac{m_1^2(j\omega) - n_1^2(j\omega)}{m_2^2(j\omega) - n_2^2(j\omega)}. \quad (9.370)$$

We note that $m_1^2(s)$, $n_1^2(s)$, $m_2^2(s)$ and $n_2^2(s)$ are polynomials in powers of s^2 . Similarly, $m_1^2(j\omega)$, $n_1^2(j\omega)$, $m_2^2(j\omega)$ and $n_2^2(j\omega)$ are polynomials in powers of ω^2 .

Example 9.12 Let

$$H(s) = \frac{s^3 + 11s^2 + 36s + 36}{s^4 + 17s^3 + 99s^2 + 223s + 140}.$$

By separating the even and odd polynomials in the numerator and the denominator, evaluate $|H(j\omega)|^2$.

We have $m_1(s) = 11s^2 + 36$, $n_1(s) = s^3 + 36s$, $m_2(s) = s^4 + 99s^2 + 140$, $n_2(s) = 17s^3 + 223s$

$$\begin{aligned} F(s) &= H(s)H(-s) = \frac{(11s^2 + 36)^2 - (s^3 + 36s)^2}{(s^4 + 99s^2 + 140)^2 - (17s^3 + 223s)^2} \\ &= \frac{1296 - 504s^2 + 49s^4 - s^6}{19600 - 22009s^2 + 2499s^4 - 91s^6 + s^8} \\ |H(j\omega)|^2 &= \frac{1296 + 504\omega^2 + 49\omega^4 + \omega^6}{19600 + 22009\omega^2 + 2499\omega^4 + 91\omega^6 + \omega^8}. \end{aligned}$$

We note that the magnitude-squared spectrum can be written in the general form

$$|H(j\omega)|^2 = \frac{K [1 + d_2\omega^2 + d_4\omega^4 + d_6\omega^6 + \dots + d_{2m}\omega^{2m}]}{1 + c_2\omega^2 + c_4\omega^4 + c_6\omega^6 + \dots + c_{2n}\omega^{2n}} \quad (9.371)$$

with $n = m + 1$. The function $|H(j\omega)|^2$ is analytic at $\omega = 0$ and can thus be expanded into a Maclaren series. This can be obtained simply by performing a long division. We obtain

$$|H(j\omega)|^2 = K + K(d_2 - c_2)\omega^2 + K[(d_4 - c_4) - c_2(d_2 - c_2)]\omega^4 + \dots \quad (9.372)$$

To obtain a flat spectrum equal to unity at $\omega = 0$, we first set $|H(j0)|^2 = K = 1$. Note that the successive terms of this Maclaren expansion of $|H(j\omega)|^2$ are the successive derivatives of $|H(j\omega)|^2$ at the origin. For maximum flatness we set each of these successively to zero; except for evidently, the last one, otherwise we end up with $|H(j\omega)|^2$ equal to 1. We thus set the first $(n - 1)$ derivatives with respect to ω^2 to zero. Setting the first term to zero we have $d_2 = c_2$. Setting the second to zero we obtain

$$d_4 - c_4 - c_2(d_2 - c_2) = d_4 - c_4 = 0, \quad (9.373)$$

i.e., $d_4 = c_4$; and so on. We conclude that for maximum flatness the coefficients of the same powers of ω^2 in the numerator and denominator have to be the same. The maximally flat magnitude-squared spectrum has therefore the general form

$$|H(j\omega)|^2 = \frac{K(1 + d_2\omega^2 + d_4\omega^4 + \dots + d_{2m}\omega^{2m})}{1 + d_2\omega^2 + d_4\omega^4 + \dots + d_{2m}\omega^{2m} + c_{2n}\omega^{2n}}. \tag{9.374}$$

In the Butterworth approximation a condition is added to maximal flatness, namely, that the transfer function should have no zeros on the $s = j\omega$ axis except at $s = \infty$, so that the spectrum would not fall to zero along the $j\omega$ axis except at infinite frequency. The numerator should therefore have no powers of ω , and if we put $K = 1$

$$|H(j\omega)|^2 = \frac{1}{1 + c_{2n}\omega^{2n}} \tag{9.375}$$

which we write as the Butterworth filter form

$$|H(j\omega)|^2 = \frac{1}{1 + \varepsilon^2\omega^{2n}}. \tag{9.376}$$

We can thus see the basis of the Butterworth approximation. The Bessel–Thomson filter is maximally flat as far as the group delay $\tau(\omega)$ is concerned. The expression of $\tau(\omega)$ has the same form as that we just obtained for the magnitude spectrum $|H(j\omega)|^2$, namely

$$\tau(\omega) = \frac{K(1 + d_2\omega^2 + d_4\omega^4 + \dots + d_{2m}\omega^{2m})}{1 + d_2\omega^2 + d_4\omega^4 + \dots + d_{2m}\omega^{2m} + c_{2n}\omega^{2n}}. \tag{9.377}$$

For example, for $n = 3$

$$H(s) = \frac{15}{s^3 + 6s^2 + 15s + 15} \tag{9.378}$$

and by differentiation, as given in the last section, we find that the delay is given by

$$\tau(\omega) = \frac{1 + 0.2\omega^2 + 0.0267\omega^4}{1 + 0.2\omega^2 + 0.0267\omega^4 + 0.0044\omega^6}. \tag{9.379}$$

Note the equality of corresponding numerator and denominator coefficients. For $n = 5$

$$H(s) = \frac{945}{s^5 + 15s^4 + 105s^3 + 420s^2 + 945s + 945} \tag{9.380}$$

the delay is similarly found to be

$$\tau(\omega) = N(\omega) / D(\omega) \tag{9.381}$$

where

$$N(\omega) = \{1 + 0.1111\omega^2 + 0.0071\omega^4 + 3.5273 \times 10^{-4}\omega^6 + 1.6797 \times 10^{-5}\omega^8\} \tag{9.382}$$

$$D(\omega) = \{1 + 0.1111\omega^2 + 0.0071\omega^4 + 3.5273 \times 10^{-4}\omega^6 + 1.6797 \times 10^{-5}\omega^8 + 1.198 \times 10^{-6}\omega^{10}\}. \tag{9.383}$$

9.35 Bessel Filter's Delay and Magnitude Response

The Bessel filter's magnitude response $|H(j\omega)|$ and magnitude square response $|H(j\omega)|^2$ can be readily evaluated from its transfer function $H(s)$. The magnitude response for filter orders $n = 1$ to $n = 10$ is shown in Fig. 9.35. The magnitude response in decibels can also be deduced as $10 \log_{10}(|H(j\omega)|^2)$ and is shown in Fig. 9.36 for filter orders $n = 3$ to $n = 10$. The magnitude response versus a logarithmic frequency axis is shown in Fig. 9.37. The attenuation $\alpha(\omega)$ in dB is $\alpha(\omega) = -10 \log_{10}(|H(j\omega)|^2)$ and is shown in Fig. 9.38. The filter delay $\tau(\omega)$ is evaluated through differentiation of the real and imaginary parts of its frequency response $H(j\omega)$ as given above. It is also convenient to evaluate the percentage error deviation ε of the filter delay, as a function of frequency, from its zero-frequency nominal value. The results for filter orders $n = 1$ to $n = 10$ are shown in Fig. 9.39 and Fig. 9.40, respectively.

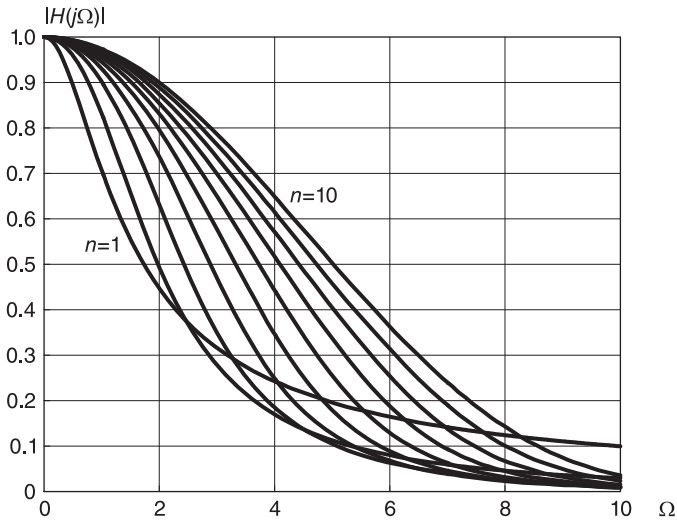


FIGURE 9.35 Bessel filter's magnitude versus frequency response.

9.36 Denormalization and Deviation from Ideal Response

In order to obtain a filter transfer function that is normalized, to be valid for any value of nominal delay t_0 , we have replaced t_0s by s , noting that s becomes a normalized complex frequency. We could have replaced t_0s by p , in which case the symbol p is the normalized complex frequency. In this case the normalized filter transfer function may be denoted $H_n(p)$. For example for a first order filter we have

$$H_n(p) = \frac{1}{p+1}. \quad (9.384)$$

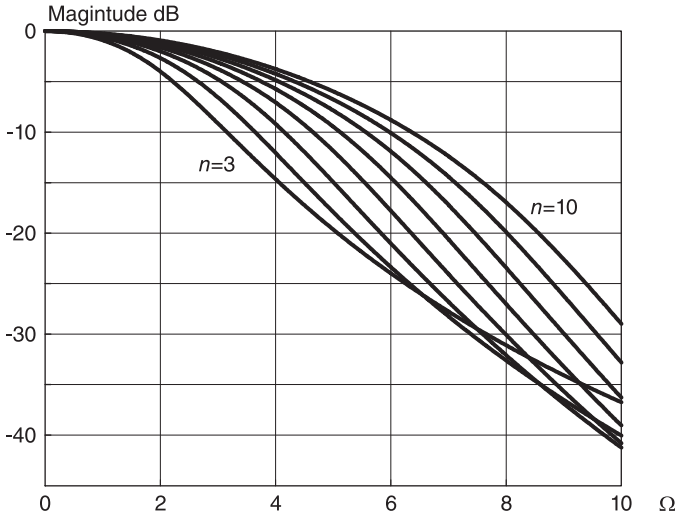


FIGURE 9.36 Bessel filter magnitude in dB response for different filter orders.

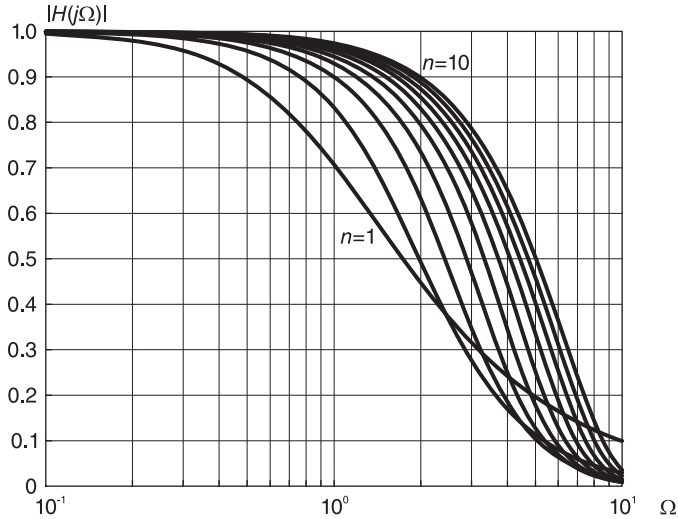


FIGURE 9.37 Bessel's magnitude spectrum versus logarithmic frequency scale.

Writing $p = j\Omega$ we recognize Ω as a normalized frequency in as much as p is a normalized complex frequency and

$$H_n(j\Omega) = \frac{1}{j\Omega + 1}. \tag{9.385}$$

To denormalize the filter to achieve a specific delay t_0 we use the substitutions $p = t_0s$ and with $s = j\omega$, $p = t_0j\omega = j\Omega$, i.e. $\Omega = t_0\omega$. The denormalized filter has the transfer function and frequency response given respectively by

$$H(s) = H_n(p)|_{p=t_0s} = H_n(t_0s) = \frac{1}{t_0s + 1} \tag{9.386}$$

$$H(j\omega) = H_n(j\Omega)|_{\Omega=t_0\omega} = H_n(jt_0\omega) = \frac{1}{jt_0\omega + 1}. \tag{9.387}$$

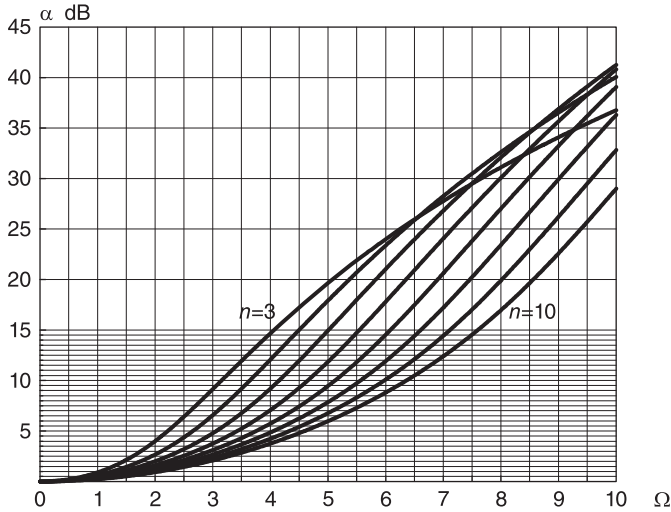


FIGURE 9.38 Bessel filter attenuation.

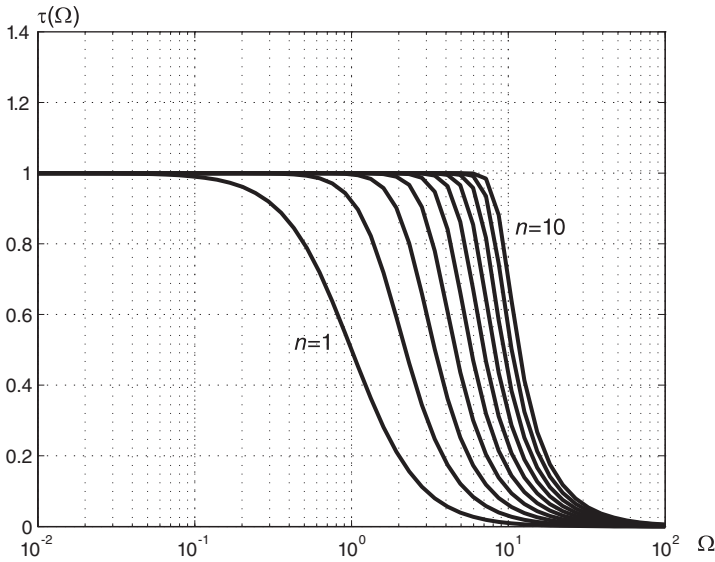


FIGURE 9.39 Bessel filter’s delay response for different filter orders.

The phase angle of the normalized “prototype” filter frequency response is $\phi_n(\Omega) = \arg[H_n(j\Omega)]$. Similarly, the phase angle of the denormalized filter frequency response is $\phi(\omega) = \arg[H(j\omega)]$.

The delay of the normalized filter is $\tau_n(\Omega) = -d\phi_n(\Omega)/d\Omega$, and that of the denormalized filter is

$$\tau(\omega) = -\frac{d\phi(\omega)}{d\omega} = -\frac{d\phi_n(\Omega)}{d\Omega} \frac{d\Omega}{d\omega} = t_0\tau_n(\Omega) = t_0\tau_n(t_0\omega). \tag{9.388}$$

Applying the approach to the first order Bessel filter we have

$$\phi_n(\Omega) \triangleq \arg[H_n(j\Omega)] = -\tan^{-1}\Omega. \tag{9.389}$$

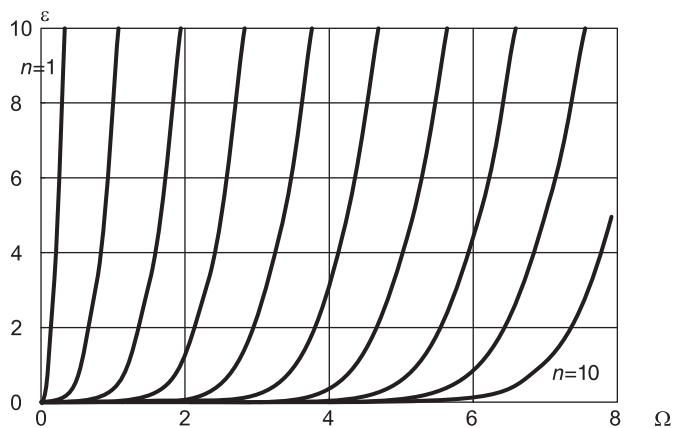


FIGURE 9.40 Bessel filter’s percent delay error for different filter orders.

The delay of the prototype is given by

$$\tau_n(\Omega) = -\frac{d}{d\Omega}\phi_n(\Omega) = \frac{1}{1 + \Omega^2}. \tag{9.390}$$

The delay of the denormalized filter is

$$\tau(\omega) = -\frac{d}{d\omega}\phi(\omega) = \frac{t_0}{1 + (t_0\omega)^2}. \tag{9.391}$$

Alternatively,

$$\tau(\omega) = -\frac{d\phi_n(\Omega)}{d\Omega} \frac{d\Omega}{d\omega} = t_0\tau_n(t_0\omega) = \frac{t_0}{1 + (t_0\omega)^2}. \tag{9.392}$$

Let for example $t_0 = 1$ ms. The nominal delay at zero frequency is $\tau(0) = t_0 = 1$ ms as required. Note that this Bessel filter of order 1 is far from ideal. Instead of a constant nominal delay of 1 ms, the delay at a frequency of say, $f = 100$ Hz, i.e. $\omega = 200\pi$ rad/sec, is $\tau(\omega) = 10^{-3} / [1 + (200\pi \cdot 10^{-3})^2] = 0.7170 \times 10^{-3}$ sec = 0.7170 ms. If the filter input is say a sinusoid of frequency $f = 500$ Hz the filter would delay it by $\tau(1000\pi) = 10^{-3} / [1 + (1000\pi \cdot 10^{-3})^2] = 0.0920$ ms.

The normalized Bessel filter of order 3 has the transfer function

$$H_n(p) = \frac{15}{p^3 + 6p^2 + 15p + 15} \tag{9.393}$$

and its delay can be shown to be given by

$$\tau_n(\Omega) = \frac{225 + 45\Omega^2 + 6\Omega^4}{225 + 45\Omega^2 + 6\Omega^4 + \Omega^6}. \tag{9.394}$$

Denormalized, this filter produces a delay of

$$\tau(\omega) = t_0\tau_n(t_0\omega) = \frac{t_0 [225 + 45(t_0\omega)^2 + 6(t_0\omega)^4]}{225 + 45(t_0\omega)^2 + 6(t_0\omega)^4 + (t_0\omega)^6}. \tag{9.395}$$

With a nominal delay of $t_0 = 1$ ms, this third order filter produces the desired nominal delay of $t_0 = 1$ ms at zero frequency. At a frequency $f = 100$ Hz, substituting $\omega = 200\pi$

we find the delay equal to 0.9998 ms. At a frequency $f = 500$ Hz, the delay is 0.5660 ms, and at the frequency $f = 1000$ Hz, its delay is 0.1558 ms. It is worthwhile noticing that the normalized filter prototype is often written in the complex frequency variable s rather than p . For example, the first order filter transfer function is written

$$H_n(s) = \frac{1}{s+1} \quad (9.396)$$

and

$$H_n(j\omega) = \frac{1}{j\omega+1}. \quad (9.397)$$

Such notation implies that the frequency variables s and p are normalized. With s the normalized frequency, the denormalization takes the form $s \rightarrow t_0s$ and $\omega \rightarrow t_0\omega$, leading to the same results just obtained.

9.37 Bessel Filter's Magnitude and Delay

Let the required nominal delay at d-c be given by $t_0 = 10 \mu\text{s}$, and the required attenuation at $f = 80$ kHz, i.e. $\omega = 5.0265 \times 10^5$ rad/sec, be at most 10 dB. We have $\Omega = \omega t_0 = 5.0265$. From Figs. 9.37 and 9.39 we note that with $\Omega = 5.03$ the required filter order is $n = 7$. Note that the required 10 dB attenuation of $|H(j\Omega)|$ means that $20 \log |H(j\Omega)| = -10$, i.e. $|H(j\Omega)| = 0.3162$ (see Fig. 9.38). In fact we have with $n = 6$, $|H(j5)| = 11.85$ dB and with $n = 7$, $|H(j5)| = 9.46$ dB.

The percent delay versus the normalized frequency $\Omega = \omega t_0$ is shown in Fig. 9.40. For the same case $t_0 = 10 \mu\text{s}$ suppose that the deviation from the value t_0 at the same frequency $\omega = 5.0265 \times 10^5$ rad/sec should not exceed 2%. We have $\Omega = \omega t_0 = 5.0265$. The required filter order as seen in Fig. 9.40 is $n = 8$. To satisfy the specifications on both magnitude and delay error we choose the higher of the two values; hence $n = 8$.

9.38 Bessel Filter's Butterworth Asymptotic Form

Another form of a Bessel filter model, which may be referred to as the Butterworth asymptotic form, or for brevity the asymptotic form, is derived by requiring the magnitude squared response to be asymptotically equivalent to the Butterworth filter response both at zero frequency and at high frequencies. The result is a normalization of the Bessel filter by applying a frequency transformation that causes its magnitude frequency response to be asymptotically equivalent to that of Butterworth filter at high frequencies, while maintaining its asymptotic equivalence to the same filter at low frequencies. The normalized Butterworth filter magnitude-squared response at zero frequency is unity, the same as Bessel's. Its high-frequency, magnitude-squared response tends to

$$\lim_{\omega \rightarrow \infty} |H(j\omega)|^2 = \frac{1}{\omega^{2n}}. \quad (9.398)$$

For Bessel filter we have

$$\lim_{\omega \rightarrow \infty} |H(j\omega)|^2 = \frac{b_0^2}{\omega^{2n}}. \quad (9.399)$$

To equate the two limits we normalize ω by using the replacement

$$\omega \longrightarrow b_0^{1/n} \omega, \quad s \longrightarrow b_0^{1/n} s. \tag{9.400}$$

The frequency scaling constant shall be denoted p_0 , i.e. $p_0 = b_0^{1/n}$. We obtain the normalized transfer function

$$H_{II}(s) = \frac{b_0}{A_n \left(b_0^{1/n} s \right)} = \frac{b_0}{\sum_{k=0}^n a_k b_0^{k/n} s^k} = \frac{1}{\sum_{k=0}^n a_k b_0^{(k/n-1)} s^k} \tag{9.401}$$

and the magnitude squared response

$$|H_{II}(j\omega)|^2 = \frac{b_0^2}{\sum_{k=0}^n d_{n,k} b_0^{2(1-k/n)} \omega^{2(n-k)}} = \frac{1}{\sum_{k=0}^n d_{n,k} b_0^{-2k/n} \omega^{2(n-k)}}. \tag{9.402}$$

It can be shown that the group delay at zero frequency is

$$\tau(\omega)|_{\omega=0} = b_0^{1/n}. \tag{9.403}$$

Example 9.13 With $n = 3$,

$$b_0 = \frac{(2n)!}{(2^n)(n!)} = 15$$

$$a_k = \frac{(2n-k)!}{2^{n-k} k! (n-k)!}, \quad k = 0, 1, \dots, n$$

$$H(s) = \frac{15}{s^3 + 6s^2 + 15s + 15}, \quad |H(j\omega)|^2 = \frac{225}{\omega^6 + 6\omega^4 + 45\omega^2 + 225}.$$

With

$$p_0 = b_0^{1/3} = 2.4662, \quad p_0^3 = 15$$

$$H_{II}(s) = H(s)|_{s \rightarrow p_0 s} = \frac{15}{s^3 p_0^3 + 6s^2 p_0^2 + 15s p_0 + 15}$$

$$= \frac{1}{s^3 + (6/p_0) s^2 + (15/p_0^2) s + 1} = \frac{1}{s^3 + 2.433s^2 + 2.466s + 1}.$$

MATLAB has the commands **besselap** and **besself** which produce the Bessel asymptotic form transfer function, poles and zeros, as the following short program illustrates.

```
n=5
Wo=1
[z,p,k]=besselap(n)
[b,a] = besself(n,Wo)
sys=tf(b,a) pzmap(sys)
```

The Bessel filter Butterworth asymptotic form transfer function coefficients and poles are listed in Table 9.25.

TABLE 9.25 Bessel–Butterworth asymptotic form filter coefficients

	$N=2$	$N=3$	$N=4$	$N=5$	$N=6$	$N=7$	$N=8$	$N=9$	$N=10$
a_0	1	1	1	1	1	1	1	1	1
a_1	1.7321	2.4662	3.2011	3.9363	4.6717	5.4071	6.1427	6.8783	7.6139
a_2	1	2.4329	4.3916	6.8864	9.9202	13.494	17.608	22.264	27.46
a_3	0	1	3.1239	6.7767	12.358	20.268	30.904	44.665	61.949
a_4	0	0	1	3.8107	9.6223	19.926	36.506	61.443	97.109
a_5	0	0	0	1	4.4952	12.929	29.899	60.374	110.91
a_6	0	0	0	0	1	5.1783	16.697	42.592	93.825
a_7	0	0	0	0	0	1	5.8606	20.926	58.316
a_8	0	0	0	0	0	0	1	6.5424	25.616
a_9	0	0	0	0	0	0	0	1	7.22365
a_{10}	0	0	0	0	0	0	0	0	1

Poles									
-0.8660	-0.7456	-0.6572	-0.8516	-0.9094	-0.8800	-0.9097	-0.8911	-0.9091	
$\pm j0.5$	$\pm j0.7114$	$\pm j0.8302$	$\pm j0.4427$	$\pm j0.1857$	$\pm j0.3217$	$\pm j0.1412$	$\pm j0.2527$	$\pm j0.1140$	
	-0.9416	-0.9048	-0.5906	-0.7997	-0.7527	-0.8473	-0.8148	-0.8688	
		$\pm j0.2709$	$\pm j0.9072$	$\pm j0.5622$	$\pm j0.6505$	$\pm j0.4259$	$\pm j0.5086$	$\pm j0.3430$	
			-0.9264	-0.5386	-0.4967	-0.7111	-0.6744	-0.7838	
				$\pm j0.9617$	$\pm j1.0025$	$\pm j0.7187$	$\pm j0.7731$	$\pm j0.5759$	
					-0.9195	-0.4622	-0.4331	-0.6418	
						$\pm j1.0344$	$\pm j1.0601$	$\pm j0.8176$	
							-0.9155	-0.4083	
								$\pm j1.0813$	

9.39 Delay of Bessel–Butterworth Asymptotic Form Filter

Consider the Bessel–Butterworth asymptotic form transfer function

$$H(s) = \frac{1}{1 + a_1s + a_2s^2 + \dots + a_{n-1}s^{n-1} + s^n}. \tag{9.404}$$

We show that the nominal delay of this filter, that is, the d-c delay, is simply equal to the coefficient of s , i.e. $\tau(0) = a_1$.

We can obtain a MacLauren series expansion of $H(s)$ by performing a long division, obtaining

$$H(s) = 1 - a_1s - (a_2 + a_1^2)s^2 - \dots \tag{9.405}$$

which can be written in the form

$$H(s) = 1 - b_1s - b_2s^2 - b_3s^3 - \dots \tag{9.406}$$

where in particular $b_1 = a_1$. We can write

$$H(s)H(-s) = (1 - b_1s - b_2s^2 - b_3s^3 - \dots)(1 + b_1s - b_2s^2 + b_3s^3 - \dots) \tag{9.407}$$

which can be written in the form

$$H(s)H(-s) = 1 - c_2s^2 + c_4s^4 - c_6s^6 + \dots \tag{9.408}$$

$$|H(j\omega)|^2 = H(s)H(-s)|_{s=j\omega} = 1 + c_2\omega^2 + c_4\omega^4 + c_6\omega^6 + \dots \tag{9.409}$$

$$H(j\omega) = (1 + b_2\omega^2 + b_4\omega^4 + \dots) - j(b_1\omega + b_3\omega^3 + b_5\omega^5 + \dots) \tag{9.410}$$

$$X(j\omega) = 1 + b_2\omega^2 + b_4\omega^4 + \dots \tag{9.411}$$

$$Y(j\omega) = -(b_1\omega + b_3\omega^3 + b_5\omega^5 + \dots) \tag{9.412}$$

$$X'(j\omega) = 1 + 2b_2\omega + 4b_4\omega^3 + \dots \tag{9.413}$$

$$Y'(j\omega) = -(b_1 + 3b_3\omega^2 + 5b_5\omega^4 + \dots) \tag{9.414}$$

$$\begin{aligned} \tau(\omega) &= \frac{X'(j\omega)Y(j\omega) - X(j\omega)Y'(j\omega)}{|H(j\omega)|^2} \\ &= \left\{ \left[-(1 + 2b_2\omega + 4b_4\omega^3 + \dots) (b_1\omega + b_3\omega^3 + b_5\omega^5 + \dots) \right] \right. \\ &\quad \left. + \left[(1 + b_2\omega^2 + b_4\omega^4 + \dots) \right] \right\} / (1 + c_2\omega^2 + c_4\omega^4 + \dots). \end{aligned} \tag{9.415}$$

Hence the d-c delay is simply

$$t_0 \triangleq \tau(0) = b_1 = a_1 \tag{9.416}$$

as we set out to prove.

If a nominal delay of t_1 seconds is desired the required transfer function can be evaluated by replacing the frequency variable s in the transfer function by $(t_1/a_1)s$. In other words we apply the replacement $s \rightarrow cs$, where $c = t_1/a_1$. For example, with $n = 5$ we have

$$H(s) = 1 / (1 + 3.9363s + 6.8864s^2 + 6.7767s^3 + 3.8107s^4 + s^5). \tag{9.417}$$

The nominal delay of this Bessel-Butterworth-Asymptotic Form filter is therefore the coefficient of s , i.e. $t_0 = \tau(0) = 3.9363$ sec. To design a filter with a delay at d-c of $t_1 = 39.3628$ sec we use the replacement $s \rightarrow cs$ where $c = t_1/t_0 = 10$, obtaining the required denormalized transfer function

$$H_{\text{denorm}}(s) = 1 / (1 + 39.363s + 688.64s^2 + 6776.7s^3 + 38107s^4 + 10^5s^5) \tag{9.418}$$

which has the required d-c delay as seen by the coefficient of s .

9.40 Delay Plots of Butterworth Asymptotic Form Bessel Filter

The delay of the Butterworth asymptotic form Bessel filter as a function of normalized frequency Ω is shown in Fig. 9.41.

The percentage error of deviation of the delay from the nominal d-c value of the Butterworth asymptotic form Bessel filter is shown in Fig. 9.42. The magnitude response in dB is shown in Fig. 9.43.

Let $\tau_n(\Omega)$ denote the delay of the n^{th} order Butterworth asymptotic form filter, and t_0 be its d-c delay. With $n = 2$, as can be seen in Fig. 9.42 the d-c delay is

$$t_0 = \tau_2(0) = 1.73205 \tag{9.419}$$

$$\Omega = t_0\omega = 1.73205\omega \tag{9.420}$$

and

$$H(s) = \frac{1}{s^2 + 1.73205s + 1}. \tag{9.421}$$

With $n = 10$, the nominal delay is $\tau_{10}(0) = 7.61388$.

Assume a required d-c delay of $t_0 = 10 \mu\text{s}$. With $n = 1$ and s the normalized complex frequency.

$$H(s) = \frac{1}{s + 1} \tag{9.422}$$

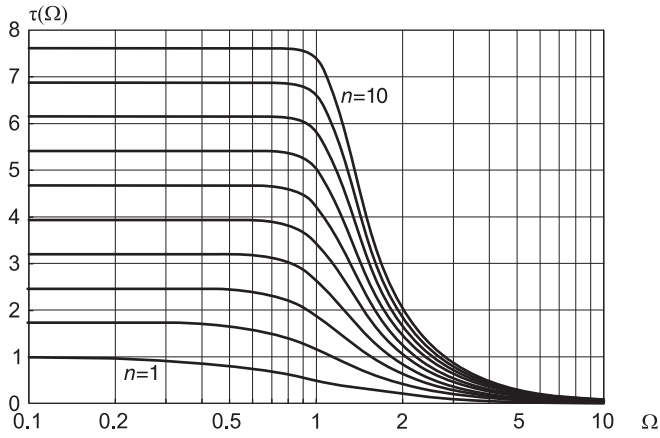


FIGURE 9.41 Bessel-Butterworth asymptotic filter delay response.

$$\tau(\omega) = \frac{1}{1 + \omega^2} \tag{9.423}$$

$$H(j\omega) = \frac{1}{1 + j\omega} = \frac{1 - j\omega}{1 + \omega^2} \tag{9.424}$$

$$|H(j\omega)|^2 = \frac{1}{1 + \omega^2} \tag{9.425}$$

$$\arg[H(j\omega)] = \phi(\omega) = \tan^{-1}(-\omega) = -\tan^{-1}\omega \tag{9.426}$$

$$\tau(\omega) = \frac{-d}{d\omega}\phi(\omega) = \frac{1}{1 + \omega^2} \tag{9.427}$$

same as the delay normalized Bessel model.

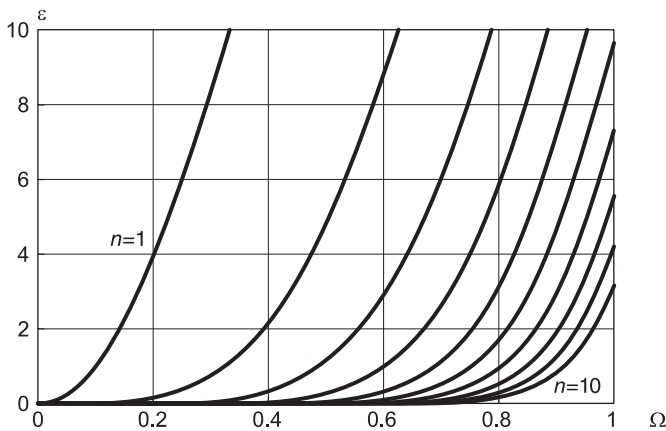


FIGURE 9.42 Bessel-Butterworth asymptotic filter percent delay error.

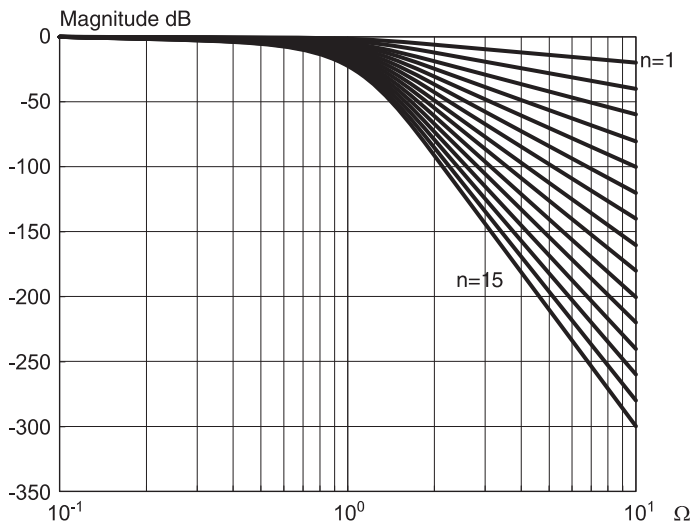


FIGURE 9.43 Magnitude dB response of Butterworth asymptotic form Bessel filter.

With $n = 2$

$$\begin{aligned} \tau_2(\omega) &= \frac{1.73205(1 + \omega^2)}{(1 - \omega + \omega^2)(1 + \omega + \omega^2)} = \frac{1.73205(1 + \omega^2)}{(1 + \omega^2)^2 - \omega^2} \\ &= \frac{1.73205(1 + \omega^2)}{\omega^4 + 2\omega^2 + 1 - \omega^2} = \frac{1.73205(1 + \omega^2)}{\omega^4 + \omega^2 + 1}. \end{aligned} \tag{9.428}$$

We have $\tau_2(0) = 1.73205$, and at $\omega = 1$,

$$\tau_2(\omega)|_{\omega=1} = 1.73205 \times \frac{2}{3} = \frac{2}{3}\tau_2(0). \tag{9.429}$$

For $n = 1$,

$$\tau_1(1) = 0.5 = 0.5\tau_1(0). \tag{9.430}$$

The specifications would for example require at $\Omega = 0.8$ a max error of 2% which implies that $n = 6$ or more. If at $\omega = 0.8$, the max error has to be 5% the required filter order is $n = 5$. With $n = 5$, $\tau_5(0) = 3.93628$.

Note that if the prototype filter frequency response is written as a function of frequency denoted Ω , so that if its phase is denoted $\phi(\Omega) = \arg[H(j\Omega)]$ then the delay is given by $\tau(\Omega) = -d\phi(\Omega)/d\Omega$. If we apply the frequency transformation $\Omega = c\omega$ and $s \rightarrow cs$ then the resulting filter delay is $\tau(\omega)$, where $\tau(\omega) = -d\phi(\omega)/d\omega = -(d\phi(\Omega)/d\Omega)d\Omega/d\omega = c\tau(\Omega)$. The filter delay is thus multiplied by the scaling constant c .

Example 9.14 With $c = 10$ we write $s \rightarrow 10s$

$$H(s) = \frac{a_0}{10^n a_n s^n + \dots + 10^2 a_2 s^2 + 10 a_1 s + a_0}.$$

With $n = 5$

$$H(s) = \frac{1}{10^5 s^5 + 38107 s^4 + 6776.67 s^3 + 688.64 s^2 + 39.363 s + 1}.$$

The resulting delay at d-c is $\tau_5(0) = 39.3628 \text{ sec} = 10\tau_{5,\text{prot}}(0)$ where $\tau_{5,\text{prot}}(\omega)$ is the prototype model d-c delay.

Suppose now that the Butterworth asymptotic form filter should satisfy the condition that the error deviation from the nominal d-c value $\tau_n(0)$ should be at most 0.5% at $\Omega = 0.6$. From Fig. 9.43 we deduce that the filter order should be $n = 5$.

With $n = 5$ the prototype nominal delay is $\tau_5(0) = 3.93628$. If the required delay is $t_1 = 100$ sec then the required time scaling constant is $c = \tau_r/\tau_5(0) = 100/3.93628 = 25.405$. If the prototype filter normalized frequency variable is denoted Ω we use the substitution $\Omega = c\omega$. If it is denoted ω we write $\omega \rightarrow c\omega$. The true denormalized frequency is therefore $\omega = \Omega/c$. The denormalized transfer function is obtained by writing $s \rightarrow cs$.

$$H_{denorm}(s) = H(s)|_{s \rightarrow cs}$$

Example 9.15 Design a Bessel–Butterworth asymptotic filter prototype that should have an attenuation of 0 dB at $\omega = 0$ and less than 5 dB for frequencies below $\Omega = 0.7$ and attenuation of at least 60 dB at $\Omega = 3$. At $\Omega = 0.7$ the percent delay error compared to its nominal d-c value should not exceed 0.3%. Convert the prototype to obtain a delay at d-c of $t_0 = 100$ sec.

Referring to Fig. 9.44 we may make the following observations.

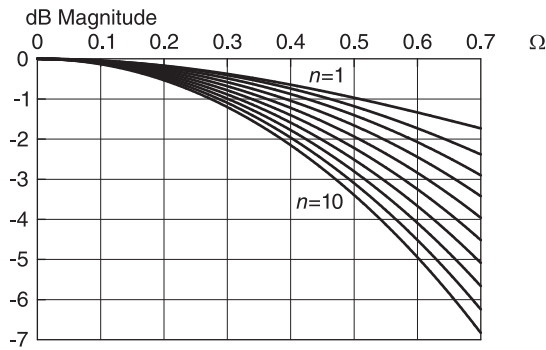


FIGURE 9.44 Bessel–Butterworth asymptotic filter, detail, magnitude dB response for different filter orders.

With $\Omega = 0.7$ and maximum attenuation $\alpha \leq 5$ dB we find $n \leq 6$. With $\omega = 3$ and attenuation $\alpha = 60$ dB or more we find from Fig. 9.49 that the filter order n should be $n = 7$. From Fig. 9.43 we see that with $\Omega = 0.7$ r/s and percent delay error of 0.3% the filter order should be at least $n = 7$. Placing priority on the delay percentage error we choose $n = 7$. With $n = 7$ the normalized filter delay at d-c is $t_0 = \tau_7(0) = 5.40713$.

Since the required delay is $\tau_r = 100$ sec, we have $c = 100/5.40713 = 18.4941$. The transfer function is given by

$$H(s) = H_{norm}(s)|_{s \rightarrow cs} = 1 / (7.4 \times 10^8 s^7 + 2.072 \times 10^8 s^6 + 2.797 \times 10^7 s^5 + 2.331 \times 10^6 s^4 + 12.8205 \times 10^4 s^3 + 4.615 \times 10^3 s^2 + 100s + 1)$$

and the filter d-c delay is 100 sec as required. Note that with the frequency scaling thus applied the resulting filter should satisfy the condition that the attenuation at the frequency $\omega = 0.7/c = 0.03785$ is given by 5.08372 dB as expected, having taken $n = 7$ rather than the value $n \leq 6$ required to yield an attenuation of at most 5 dB. Moreover, with the

transfer function thus obtained the delay error at the same frequency is given by 0.2103%, which is an admissible error.

9.41 Bessel Filters Frequency Normalized Form

Bessel filter’s frequency normalized form is the same as the asymptotic form, but with a 3 dB cut-off frequency of 1 r/s. The magnitude response in dB is shown in Fig. 9.45.

Table 9.26 gives the attenuation in dB of this filter prototype at frequencies $\Omega = 2, 5, 10$ with 0 dB attenuation at $\Omega = 0$. These values are confirmed by the figure.

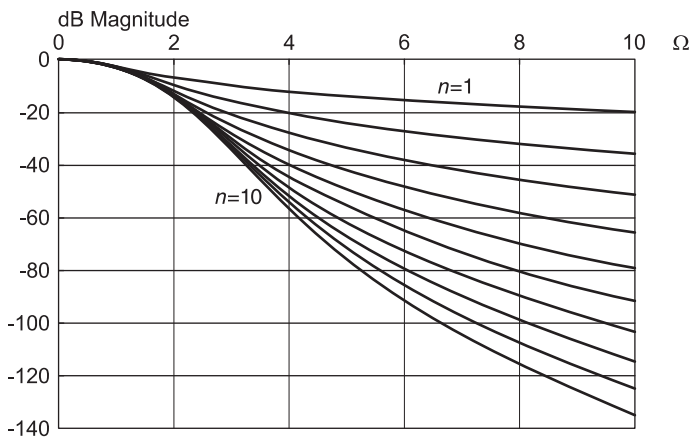


FIGURE 9.45 Magnitude response in dB of Bessel filter’s frequency normalized form.

TABLE 9.26 Bessel filter frequency normalized form attenuation at three frequencies

Filter order n	Attenuation in dB		
	$\Omega = 2$	$\Omega = 5$	$\Omega = 10$
1	6.99	14.15	20.04
2	9.82	24.07	35.89
3	12.00	33.44	51.23
4	13.41	41.92	65.68
5	14.06	49.39	79.12
6	14.17	55.93	91.62
7	13.98	61.69	103.34
8	13.68	66.80	114.40
9	13.38	71.35	124.91
10	13.14	75.41	134.92

9.42 Poles and Zeros of Asymptotic and Frequency Normalized Bessel Filter Forms

As we have seen, the Bessel–Thomson filter transfer function is an all-pole transfer function. The poles of the different Bessel filter forms and filter orders n ranging from 0 to 10 are given in the above table. As an illustration, the poles' pattern in the complex s plane for the Bessel filter asymptotic form is shown in Fig. 9.46 for filter order $n = 10$. By using the same scales for the vertical and horizontal axes, this figure is redrawn, where it appears together with the frequency normalized form, in Fig. 9.47(a) and (b), respectively. It can be shown that the poles lie in general on close to circular contours of greater radius than the unit circle and with centers displaced to the right of the origin, as can be seen in the figure.

9.43 Response and Delay of Normalized Form Bessel Filter

The frequency normalized form Bessel filter transfer function coefficients and poles are listed in Table 9.27. The delay of the frequency normalized form Bessel filter as a function of normalized frequency Ω is shown in Fig. 9.48. The percentage delay deviation error from the nominal d-c value of this filter is shown in Fig. 9.49.

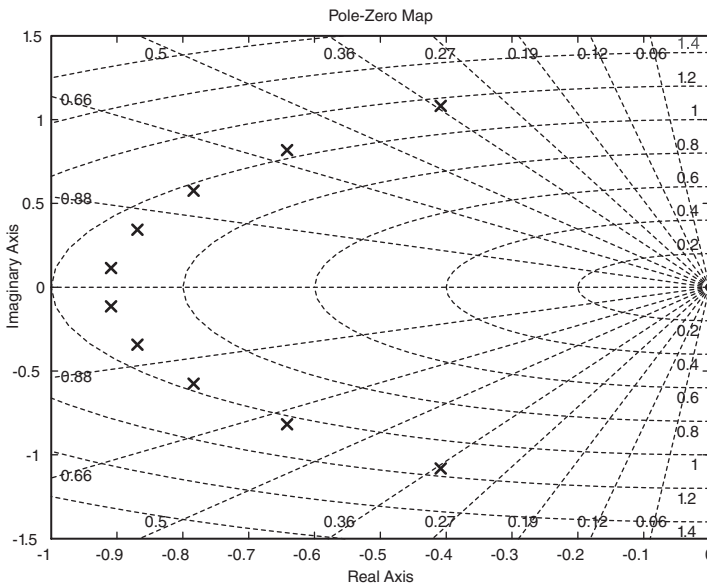


FIGURE 9.46 Bessel filter asymptotic form poles' pattern in the s plane.

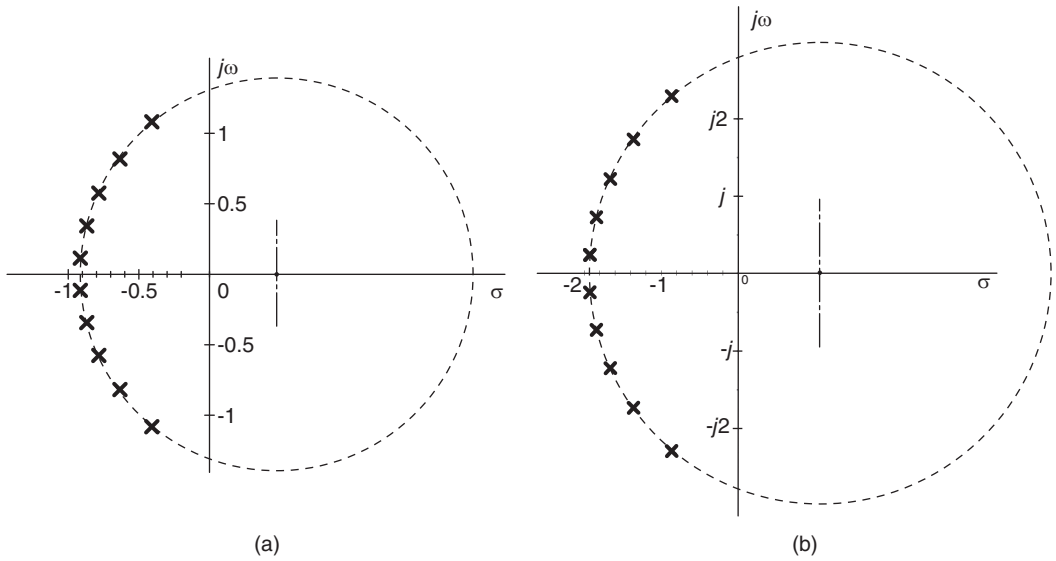


FIGURE 9.47 Bessel filter poles' pattern for: (a) the asymptotic form, (b) the frequency normalized form.

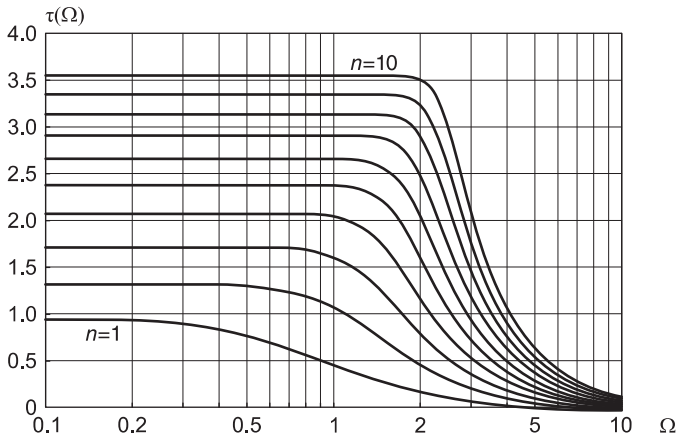


FIGURE 9.48 Delay versus frequency response of the frequency normalized form Bessel filter.

9.44 Bessel Frequency Normalized Form Attenuation Setting

As observed earlier, the frequency variable of the filter prototype may be denoted Ω or the lower case ω . In either case it should be remembered that the frequency in question is a normalized one. If the attenuation at unit frequency $\omega = 1$ is to be a general value α dB instead of the prototype attenuation 3 dB, we need to apply a frequency conversion of the form $\omega \rightarrow c_n \omega$, i.e. $\Omega = c_n \omega$. The denormalized frequency is thus given by

$$\omega = \Omega / c_n. \tag{9.431}$$

TABLE 9.27 Frequency normalized form Bessel filter coefficients

	$N=2$	$N=3$	$N=4$	$N=5$	$N=6$	$N=7$	$N=8$	$N=9$	$N=10$
a_0	1.6180	2.7718	5.2582	11.2128	26.630	69.221	194.026	580.175	1836.25
a_1	2.2032	4.8664	11.1154	27.2182	71.991	204.322	616.929	1967.78	6593.93
a_2	1.0000	3.4175	10.0702	29.3643	88.463	278.355	915.412	3140.75	11216.21
a_3	0	1.0000	4.7306	17.8198	63.774	228.229	831.618	3106.97	11933.98
a_4	0	0	1.0000	6.1794	28.734	122.485	508.505	2107.58	8823.03
a_5	0	0	0	1.0000	7.768	43.3851	215.58	1021.18	4752.50
a_6	0	0	0	0	1.000	9.48599	62.3148	355.233	1896.24
a_7	0	0	0	0	0	1.000	11.3221	86.0601	555.865
a_8	0	0	0	0	0	0	1.000	13.2677	115.16
a_9	0	0	0	0	0	0	0	1.000	15.3162
a_{10}	0	0	0	0	0	0	0	0	1.000
Poles									
	-1.1016	-1.0474	-99524	-0.95768	-0.93066	-0.90987	-0.89287	-0.8784	-0.86576
	$\pm j0.63601$	$\pm j0.99927$	$\pm j1.2571$	$\pm j1.4711$	$\pm j1.6619$	$\pm j1.8365$	$\pm j1.9983$	$\pm j2.1498$	$\pm j2.2926$
		-1.3227	-1.37	-1.3809	-1.3819	-1.3789	-1.3738	-1.3676	-1.3607
			$\pm j0.41031$	$\pm j0.71791$	$\pm j0.97147$	$\pm j1.1916$	$\pm j1.3884$	$\pm j1.5677$	$\pm j1.7335$
				-1.5023	-1.5715	-1.612	-1.6369	-1.6524	-1.6618
					$\pm j0.3209$	$\pm j0.58924$	$\pm j0.8228$	$\pm j1.0314$	$\pm j1.2211$
						-1.6844	-1.7574	-1.8072	-1.8422
							$\pm j0.27287$	$\pm j0.51238$	$\pm j0.72726$
								-1.8566	-1.9276
									$\pm j0.24162$

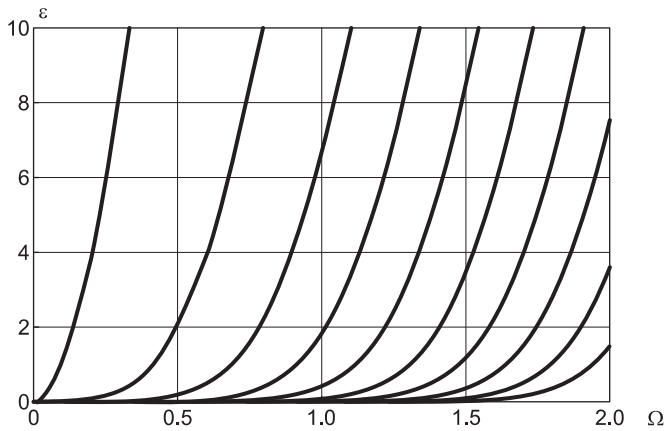


FIGURE 9.49 Delay deviation percentage error of the frequency normalized form Bessel filter.

To evaluate the scaling constant c_n we apply the transformation to the prototype magnitude squared spectrum $|H(j\omega)|^2$ replacing ω by $c_n\omega$. We then evaluate the dB value of the magnitude squared spectrum at $\omega = 1$ and equate it with the required value α dB. We obtain an n^{th} order equation in the unknown c_n , which is found by solving the equation. With the value of c_n determined we apply the transformation

$$s \longrightarrow c_n s \tag{9.432}$$

to the transfer function $H(s)$.

The following examples illustrate the approach.

Example 9.16 Evaluate the transfer function of a second order lowpass Bessel Typ3 filter which should have an attenuation of 1.5 dB rather than the prototype's 3 dB at the edge of the pass-band frequency $\omega = 1$.

The prototype filter transfer function is given by

$$H(s) = \frac{1.61803}{1.61803 + 2.203s + s^2} = \frac{1}{1 + 1.361656s + 0.618036s^2}.$$

Its squared-magnitude frequency response is given by

$$|H(j\omega)|^2 = \frac{1}{1 + a_2\omega^2 + a_4\omega^4}$$

where $a_2 = 0.6180$, $a_4 = 0.3820$. The required frequency transformation is written $\omega \rightarrow c_2\omega$, where c_2 is the scaling constant for the second order filter which is to be evaluated. The resulting denormalized magnitude squared response is written.

$$|H_d(j\omega)|^2 = \frac{1}{1 + a_2c_2^2\omega^2 + a_4c_2^4\omega^4}.$$

The attenuation at $\omega = 1$ should be $\alpha = 1.5$ dB, meaning that

$$10 \log_{10} (1 + a_2c_2^2 + a_4c_2^4) = \alpha = 1.5$$

$$1 + 0.6180c_2^2 + 0.3820c_2^4 = 10^{0.1\alpha} = 10^{0.15} = 1.4125.$$

Letting $c_2^2 = x$ we have a quadratic equation in x , which solved produces the value $c_2^2 = x = 0.50798$, i.e. $c_2 = 0.7127$. The required frequency transformation is therefore $\omega \rightarrow 0.7127\omega$, i.e. $s \rightarrow 0.7127s$.

The required denormalized transfer function is therefore

$$H_d(s) = \frac{1}{1 + 1.361656 \times c_2s + 0.618036 \times c_2^2s^2} = \frac{1}{1 + 0.9705s + 0.3139s^2}$$

which has a squared-magnitude spectrum given by

$$|H_d(j\omega)|^2 = \frac{1}{1 + a_2c_2^2\omega^2 + a_4c_2^4\omega^4} = \frac{1}{1 + 0.3139\omega^2 + 0.0986\omega^4}.$$

Example 9.17 Repeat the above example given that the required filter is of order $n = 3$.

The prototype third order filter transfer function is given by

$$H(s) = \frac{1}{1 + 1.755674s + 1.232954s^2 + 0.360778s^3}.$$

Its squared-magnitude frequency response is given by

$$|H(j\omega)|^2 = \frac{1}{1 + a_2\omega^2 + a_4\omega^4 + a_6\omega^6}$$

where $a_2 = 0.6165$, $a_4 = 0.2534$, $a_6 = 0.1303$. The required frequency transformation is $\omega \rightarrow c_3\omega$. The denormalized magnitude squared response is

$$|H_d(j\omega)|^2 = \frac{1}{1 + a_2c_3^2\omega^2 + a_4c_3^4\omega^4 + a_6c_3^6\omega^6}.$$

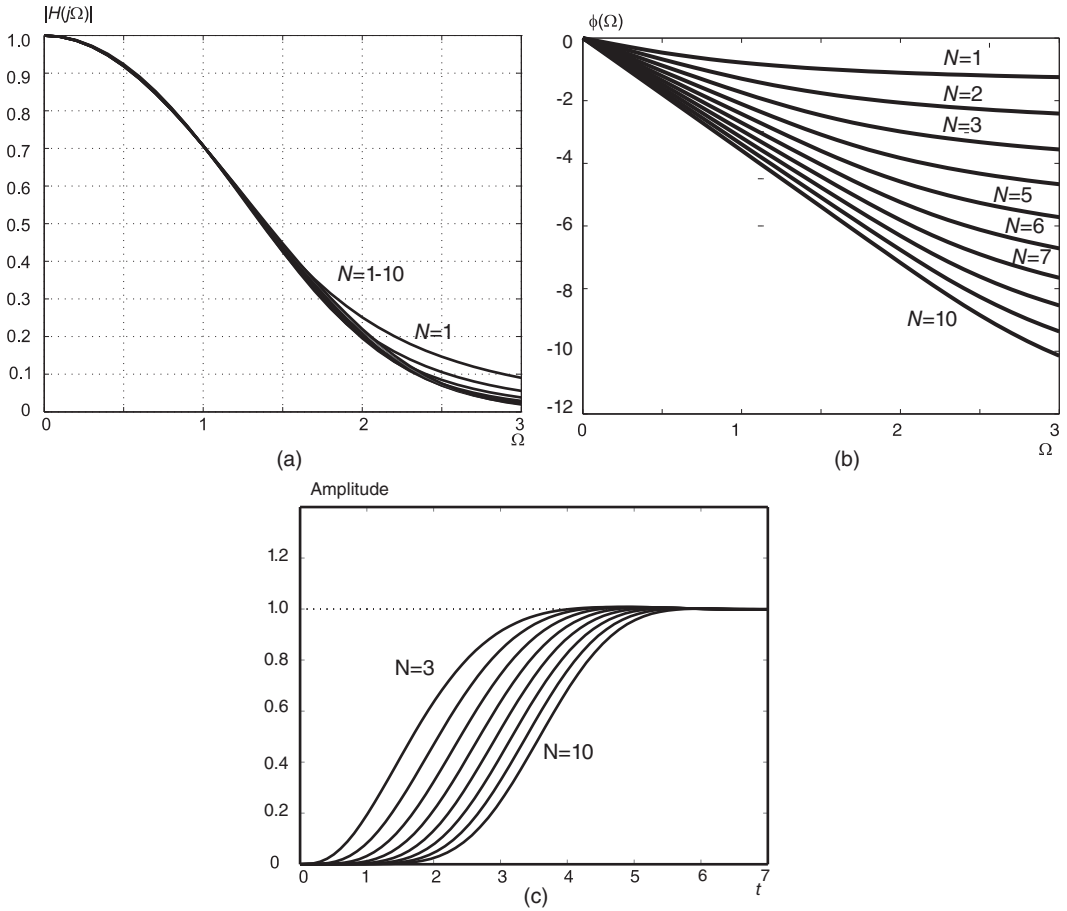


FIGURE 9.50 Bessel filter’s frequency normalized form: (a) amplitude, (b) phase and (c) step response.

For an attenuation at $\omega = 1$ of $\alpha = 1.5$ dB, we have

$$10 \log_{10} (1 + a_2 c_3^2 + a_4 c_3^4 + a_6 c_3^6) = \alpha = 1.5.$$

Letting $c_3^2 = x$ we have

$$1 + a_2 x + a_4 x^2 + a_6 x^3 = 10^{0.15} = 1.4125.$$

The solution of this cubic equation is $c_3^2 = x = 0.525184$, i.e. $c_3 = 0.724696$. The required frequency transformation is therefore $\omega \rightarrow 0.724696\omega$, i.e. $s \rightarrow 0.724696s$. The required denormalized transfer function is therefore

$$H_d(s) = \frac{1}{1 + 1.27237s + 0.647574s^2 + 0.13733s^3}.$$

Plots of the magnitude and unwrapped phase and step responses of the frequency normalized form Bessel filter are shown in Fig. 9.50(a-c). Unwrapping the phase may be effected using the MATLAB function **unwrap**.

9.45 Bessel Filter Nomograph

A nomograph for evaluating the frequency normalized form Bessel filter order is shown in Fig. 9.51.

Example 9.18 Evaluate the order of a frequency normalized form Bessel filter which should have an attenuation of at least 30 dB at $\Omega = 1$ and 80 dB at $\Omega = 5$. Suppose that in addition the filter should have a delay at $\Omega = 1.5$ that is not more than 2% off its d-c delay value, which should be $t_1 = 10$ sec. Evaluate the filter transfer function.

We may use the table or the Bessel nomograph, deducing that $n = 6$. We can see from Fig. 9.49, which displays the percentage delay error, that the filter order should be $n = 7$. Placing priority on the delay error requirement we may choose $n = 7$. The seventh order filter delay at d-c is equal to $\tau_7(0) = 2.95172$. The required scaling constant is $c = t_1/2.95172 = 3.38785$. Using the seventh order frequency normalized form filter transfer function $H_{prototype}(s)$ from the frequency normalized form table we have

$$\begin{aligned}
 H(s) &= H_{prototype}(s)|_{s \rightarrow cs} \\
 &= 69.2213 / (5122.38s^7 + 14342.7s^6 + 19362.6s^5 + 16135.5s^4 \\
 &\quad + 8874.52s^3 + 3194.83s^2 + 692.213s + 69.2213).
 \end{aligned}$$

The d-c delay is as desired equal to 10 sec.

9.46 Frequency Transformations

Given the transfer function of a lowpass filter, such as a prototype normalized lowpass filter transfer function we can convert the filter into a bandpass, bandstop or highpass filter.

Let $H(s)$ be the transfer function of the prototype lowpass filter. The required transformation from the lowpass to the bandpass, highpass, ... transfer function is effected by a change of variable, and in particular by a transformation of the variable s of the form

$$s \longrightarrow R(s) \tag{9.433}$$

where $R(s)$ is a rational function of the general form

$$R(s) = \frac{s(s^2 + \omega_2^2)(s^2 + \omega_4^2)(s^2 + \omega_6^2) \dots}{(s^2 + \omega_1^2)(s^2 + \omega_3^2)(s^2 + \omega_5^2) \dots} \tag{9.434}$$

To this end we shall associate the variable p with the lowpass prototype filter transfer function and the variable s with the desired filter transfer function. The change of variables is thus written

$$p = R(s) = \frac{s(s^2 + \omega_2^2)(s^2 + \omega_4^2)(s^2 + \omega_6^2) \dots}{(s^2 + \omega_1^2)(s^2 + \omega_3^2)(s^2 + \omega_5^2) \dots} \tag{9.435}$$

If, moreover, we write $p = j\Omega$ and $s = j\omega$ then in what follows the variable Ω will denote the frequency variable of the prototype filter, and the variable ω will denote that of the desired filter, and we have

$$j\Omega = \frac{j\omega(\omega_2^2 - \omega^2)(\omega_4^2 - \omega^2) \dots}{(\omega_1^2 - \omega^2)(\omega_3^2 - \omega^2) \dots} \tag{9.436}$$

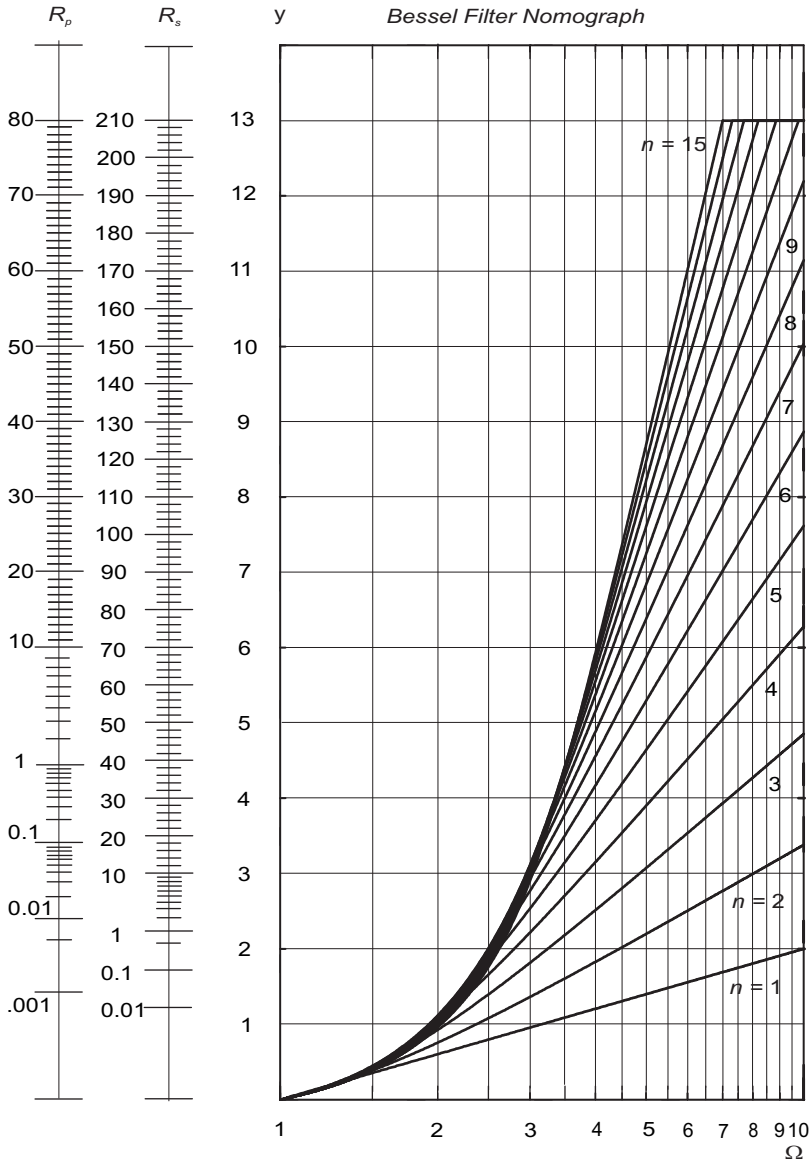


FIGURE 9.51 Bessel filter nomograph.

$$\Omega = \frac{\omega (\omega_2^2 - \omega^2) (\omega_4^2 - \omega^2) \dots}{(\omega_1^2 - \omega^2) (\omega_3^2 - \omega^2) \dots} \tag{9.437}$$

As illustration Fig. 9.52 shows, the frequency transformation resulting from writing

$$p = R(s) = \frac{s (s^2 + \omega_2^2) (s^2 + \omega_4^2)}{(s^2 + \omega_1^2) (s^2 + \omega_3^2)} \tag{9.438}$$

so that

$$\Omega = \frac{\omega (\omega_2^2 - \omega^2) (\omega_4^2 - \omega^2)}{(\omega_1^2 - \omega^2) (\omega_3^2 - \omega^2)} \tag{9.439}$$

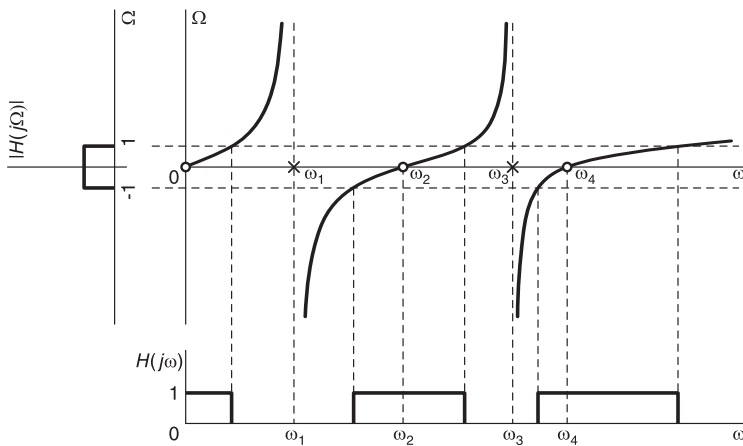


FIGURE 9.52 Frequency transformation.

The construction shown by dotted lines in the figure starts by plotting $H(j\Omega)$, the frequency response of the lowpass filter, versus Ω . Two dotted horizontal lines are then drawn at $\Omega = -1$ and $\Omega = 1$. The points of intersection of these two horizontal lines with the successive sections of the Ω versus ω curve indicate the successive values of ω corresponding to $\Omega = 1$ and $\Omega = -1$. Vertical dotted lines are drawn at these ω values. The $H(j\omega)$ plot corresponding to the lowpass response $H(j\Omega)$ is then drawn by setting $H(j\omega) = 1$ at all points of the axis ω which correspond to points on the axis Ω whereat $H(j\Omega) = 1$.

The resulting frequency response $H(j\omega)$, for this particular transformation, is seen to have both a lowpass region and two bandpass regions. It is to be noted that in this figure, and in most of those to follow, to simplify the figure only the positive axis of the frequency ω is drawn. In reality there is the negative ω axis, and the amplitude spectrum $|H(j\omega)|$ is symmetric about the point $\omega = 0$. In what follows, we study lowpass to bandpass, lowpass to bandstop and lowpass to highpass transformations.

9.47 Lowpass to Bandpass Transformation

Consider the transformation of a prototype lowpass filter transfer function, which will be referred to as $H_{LP}(s)$ to a bandpass one, denoted $H_{BP}(s)$. The desired bandpass filter should have a low and high pass-band edge frequencies of ω_L and ω_H rad/sec, respectively. Alternatively, the desired filter may be required to have a bandwidth B rad/sec and a central frequency ω_0 , where $B = \omega_H - \omega_L$ and $\omega_0 = \sqrt{\omega_1\omega_2}$.

The transformation is given by

$$p = R(s) = \frac{s^2 + \omega_0^2}{Bs} \tag{9.440}$$

that is,

$$s \longrightarrow \frac{s^2 + \omega_0^2}{Bs} \tag{9.441}$$

With $s = j\omega$ we have

$$p = j\Omega = \frac{-\omega^2 + \omega_0^2}{jB\omega} = \frac{j(\omega^2 - \omega_0^2)}{B\omega}. \quad (9.442)$$

The relation Ω versus ω and the resulting transformation from the prototype frequency response $H(j\Omega)$ to the bandpass frequency response are shown in Fig. 9.53. We have

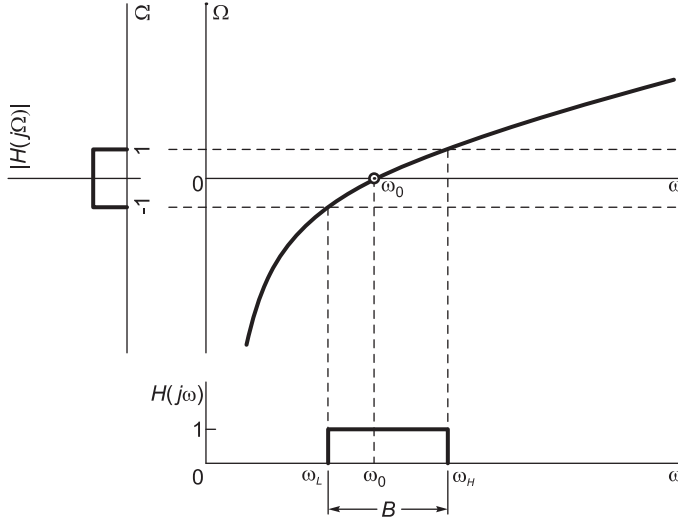


FIGURE 9.53 Lowpass to bandpass frequency transformation.

$$\omega^2 - B\Omega\omega - \omega_0^2 = 0 \quad (9.443)$$

$$\omega = \frac{B\Omega \pm \sqrt{B^2\Omega^2 + 4\omega_0^2}}{2}. \quad (9.444)$$

We note that if $\Omega = 0$ then $\omega = \pm\omega_0$. If $\Omega = \pm\infty$ then $\omega = 0, \pm\infty$. The normalized pass-band cut-off edge frequency $\Omega = 1$ and its negative frequency image $\Omega = -1$ are transformed to the low and high edge frequencies ω_L and ω_H . These may also be denoted ω_{p1} and ω_{p2} respectively, being the two pass-band edge frequencies; a notation used by MATLAB. Similarly, the stop-band edge frequencies will be denoted ω_{s1} and ω_{s2} .

$$\omega_H = \frac{B + \sqrt{B^2 + 4\omega_0^2}}{2} \quad (9.445)$$

$$\omega_L = \frac{-B + \sqrt{B^2 + 4\omega_0^2}}{2} \quad (9.446)$$

$$\omega_H - \omega_L = B \quad (9.447)$$

$$\omega_H\omega_L = \omega_0^2 \quad (9.448)$$

as required. We thus obtain the bandpass filter transfer function

$$H_{BP}(s) = H_{LP}\left(\frac{s^2 + \omega_0^2}{Bs}\right). \quad (9.449)$$

We note in passing that we can obtain a normalized form of the bandpass filter transfer function, where the central frequency is 1 and the bandwidth is a normalized bandwidth $\beta = B/\omega_0$ by using the transformation

$$p = \frac{s^2 + 1}{\beta s}. \tag{9.450}$$

Proceeding similarly we find that if $\Omega = 0$ then $\omega = 1$, and substituting $\Omega = 1$ and $\Omega = -1$ respectively we obtain

$$\omega_H = \frac{\beta + \sqrt{\beta^2 + 4}}{2} \tag{9.451}$$

$$\omega_L = \frac{-\beta + \sqrt{\beta^2 + 4}}{2} \tag{9.452}$$

$$\omega_H - \omega_L = \beta \tag{9.453}$$

$$\omega_0^2 = \omega_H \omega_L = 1. \tag{9.454}$$

The advantage of this form of normalized bandwidth is that it is the form listed in filter tables, which can therefore be used for verification.

Example 9.19 Design a bandpass Butterworth filter having a maximum pass-band gain = 0 dB, pass-band edge frequencies $\omega_{p1} = 2\pi \times 1000$ r/s, $\omega_{p2} = 2\pi \times 2000$ r/s. pass-band maximum attenuation 3 dB, stop-band edge frequencies $\omega_{s1} = 2\pi \times 500$, $\omega_{s2} = 2\pi \times 3000$, and stop-band minimum attenuation 25 dB.

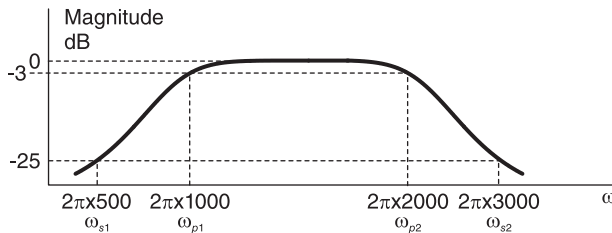


FIGURE 9.54 Bandpass filter response.

- a) Evaluate the transfer function $H(s)$ of the bandpass filter by first evaluating a lowpass prototype and then converting it to a bandpass filter.
- b) Evaluate the transfer function $H(s)$ of the bandpass filter by constructing it as a lowpass filter cascaded with a highpass one.
- c) Which of the two filters is simpler to realize?

The filter specifications may be sketched as in Fig. 9.54. We note that the lowpass to bandpass transformation is

$$s \longrightarrow \frac{s^2 + \omega_0^2}{Bs}$$

With $s = j\Omega$ the frequency variable in the lowpass prototype we have

$$j\Omega = \frac{-\omega^2 + \omega_0^2}{Bj\omega}, \text{ i.e. } \Omega = \frac{\omega^2 - \omega_0^2}{B\omega}$$

$$B = 2\pi \times 1000$$

$$\omega_0 = \sqrt{2\pi \times 1000 \times 2\pi \times 2000} = 2\pi\sqrt{2} \times 10^3.$$

With $\omega = \omega_{p_1} = 2\pi \times 1000$ and $\omega = \omega_{p_2} = 2\pi \times 2000$ we find $\Omega = \pm 1$ as expected. With $\omega = \omega_{s_1} = 2\pi \times 500$ we have $\Omega_{s_1} = -3.5$. With $\omega = \omega_{s_2} = 2\pi \times 3000$ we have $\Omega_{s_2} = 2.33$

$$10 \log_{10} (1 + 2.33^{2n}) = 25 \text{ dB}$$

$$2.33^{2n} = 10^{2.5} - 1$$

$$2n \log 2.33 = \log_{10} (10^{2.5} - 1)$$

$$n = \log_{10} (10^{2.5} - 1) / (2 \log_{10} 2.33) = 3.4.$$

We take $n = 4$. From the tables or MATLAB command

$$[B, A] = \mathbf{butter}(N, Wn, 's'), \quad N = 4, \quad Wn = 1$$

$$\begin{aligned} H(s) &= \frac{1}{s^4 + 2.613s^3 + 3.414s^2 + 2.613s + 1} \Big|_{s \rightarrow \frac{s^2 + \omega_0^2}{Bs}} \\ &= \frac{1}{s^4 + 2.613s^3 + 3.414s^2 + 2.613s + 1} \Big|_{s \rightarrow \frac{s^2 + \omega_0^2}{Bs}} \\ &= 1.56 \times 10^{15} s^4 / D(s) \end{aligned}$$

where

$$\begin{aligned} D(s) &= s^8 + 1.64 \times 10^4 s^7 + 4.5 \times 10^8 s^6 + 4.54 \times 10^{12} s^5 + 6.02 \times 10^{16} s^4 \\ &\quad + 3.58 \times 10^{20} s^3 + 2.8 \times 10^{24} s^2 + 8.08 \times 10^{27} s + 3.89 \times 10^{31}. \end{aligned}$$

b) For the lowpass part with $\omega = \omega_{p_2} = 2\pi \times 2000$, $\Omega = 1$. With $\omega = \omega_{s_2} = 2\pi \times 3000$, $\Omega = 1.5$, $10 \log_{10} (1 + 1.5^{2n}) = 25 \text{ dB}$.

$$1.5^{2n} = 10^{2.5} - 1$$

$$2n \log_{10} (1.5) = \log_{10} (10^{2.5} - 1)$$

$$n = \log_{10} (10^{2.5} - 1) / (2 \log_{10} 1.5) = 7.095.$$

We choose $n = 8$.

For the highpass part, with $\omega = \omega_{p_1} = 2\pi \times 1000\Omega = 1$ so that $\omega = \omega_{s_1} = 2\pi \times 500$ corresponds to $\Omega = 2$.

$$10 \log_{10} (1 + 2^{2n}) = 25 \text{ dB}$$

$$2^{2n} = 10^{2.5} - 1$$

$$2n \log_{10} 2 = \log_{10} (10^{2.5} - 1)$$

$$n = \log_{10} (10^{2.5} - 1) / (2 \log_{10} 2) = 4.15.$$

We take $n = 5$

$$H(s) = H_1(s) \Big|_{s \rightarrow 2\pi \times 1000/s} \times H_2(s) \Big|_{s \rightarrow s/2\pi \times 2000}$$

where

$$H_1(s) = \frac{1}{s^5 + 3.236 s^4 + 5.236 s^3 + 5.236 s^2 + 3.236 s + 1}$$

$$H_2(s) = 1/D_2(s)$$

where

$$D_2(s) = s^8 + 5.13s^7 + 13.14s^6 + 21.85s^5 + 25.69s^4 + 21.85s^3 + 13.14s^2 + 5.13s + 1.$$

c) Solution a) produces numerator order 4, denominator order 8. Solution b) produces numerator order 0, denominator order 13. Solution a) is simpler to realize.

MATLAB produces the same result obtained above.

$$Wp = 1$$

$$Ws = 2.3$$

$$Rp = 3$$

$$Rs = 25$$

$$[N, Wn] = \text{buttord}(Wp, Ws, Rp, Rs, 's')$$

producing $N = 4$, $Wn = 1.1205$

$$Wn = [2 * pi * 1000 \quad 2 * pi * 2000].$$

The function call

$$[B, A] = \text{butter}(4, Wn, 's')$$

yields the same transfer function $H(s)$ of the bandpass filter obtained above in part a).

The results may also be obtained using Mathematica:

$$\omega 1 = 2\pi \cdot 1000$$

$$\omega 2 = 2\pi \cdot 2000$$

$$B = \omega 2 - \omega 1$$

$$\omega 0sq = \omega 1 \omega 2$$

$$H[s_-] := 1 / (s^4 + 2.6131 s^3 + 3.4142 s^2 + 2.6131 s + 1)$$

$$Hbp[s_-] := H[(s^2 + \omega 0sq) / (Bs)].$$

$$\text{Factor}[Hbp[s]].$$

Example 9.20 a) Evaluate the transfer function $H(s)$ of a lowpass Butterworth filter having a magnitude characteristic of zero dB at zero frequency, maximum attenuation of 3 dB at frequency $\omega = 1$ and maximum attenuation of 40 dB at $\omega = 4$.

b) Convert the prototype lowpass filter thus obtained into a bandpass filter with lower and upper 3-dB cut-off frequencies of 1400 Hz and 2000 Hz. Show the transformation required to convert the lowpass filter of part a) to this bandpass filter and the transfer function of the bandpass filter.

As can be seen in Fig. 9.55, at $\omega = 1$ the attenuation is 3 dB; hence $\varepsilon = 1$.

$$20 \log_{10} \left\{ \frac{H(j0)}{H(j4)} \right\} = 20 \log_{10} \left\{ \frac{1}{1/\sqrt{1+4^{2n}}} \right\} = 40$$

i.e. $10 \log_{10} (1 + 4^{2n}) = 40$

$$4^{2n} = 10^4 - 1, \quad n = \frac{\log_{10}(10^4 - 1)}{2 \log_{10} 4} = 3.3219.$$

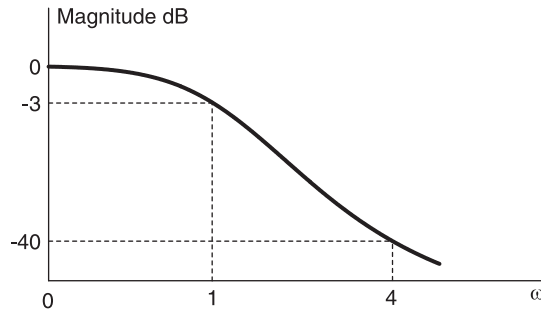


FIGURE 9.55 Lowpass Butterworth filter frequency response in dB

The filter order is the ceiling of this value, i.e. $n = 4$. We note that having replaced the value $n = 3.3219$ by the integer value $n = 4$, we have effectively altered (improved on) the given filter specifications. The resulting filter cannot have exactly 3 dB attenuation at $\omega = 1$ and 40 dB attenuation at $\omega = 4$.

To evaluate precisely the resulting filter specifications we can fix the 3-dB frequency ω_c to one and evaluate the true attenuation of the $n = 4$ filter at $\omega = 4$. In this case, the attenuation is given by substituting $n = 4$, obtaining $\alpha = 20 \log_{10}(\sqrt{1 + 4^8}) = 48.165$ dB.

The filter specifications have been exceeded as expected. If, on the other hand, we fix the attenuation to 40 dB at $\omega = 4$, then the 3-dB frequency ω_c cannot equal 1; hence ε cannot equal one.

To evaluate the 3 dB cut-off frequency ω_c in this case, which is called Wn by MATLAB, we write

$$|H(j\omega)| = \frac{1}{\sqrt{1 + \varepsilon^2 \omega^{2n}}}$$

and we have the two equations

$$20 \log_{10} \sqrt{1 + \varepsilon^2 \omega_c^8} = 3$$

$$20 \log_{10} \sqrt{1 + \varepsilon^2 4^8} = 40$$

wherefrom

$$1 = \varepsilon^2 4^8 = 10^4, \quad \varepsilon^2 = (10^4 - 1) / 4^8 = 0.1526, \quad \varepsilon = 0.3906$$

$$1 + \varepsilon^2 \omega_c^8 = 10^{0.3}, \quad \omega_c = \left[\frac{(10^{0.3} - 1)}{\varepsilon^2} \right]^{1/8} = 1.2642.$$

MATLAB follows this approach, producing $Wn = 1.2649$ as a result of the instruction $[N, Wn] = \text{Buttord}(Wp, Ws, Rs, 's')$, with $Wp = 1$, $Ws = 4$, $Rp = 3$, $Rs = 40$, which is very close to this value of ω_c . See Fig. 9.56. Note that the attenuation at $\omega = 1$ is $20 \log_{10}(\sqrt{1 + \varepsilon^2}) = 0.6167$, which is within the given specifications.

In the present case we have $N = 4$ and denoting by $H_T(s)$ the transfer function as given by the tables we have

$$H_T(s) = \frac{1}{s^4 + 2.613s^3 + 3.414s^2 + 2.613s + 1}.$$

As we have just noted, this transfer function produces an attenuation of 3 dB at $\omega = 1$ and 48.165 dB at $\omega = 4$. The MATLAB instruction $[B, A] = \text{Butter}(N, Wn, 's')$ with $Wn = 1.2649$ (as produced by `Buttord`) results in

$$H(s) = \frac{2.5601}{s^4 + 3.3054s^3 + 5.4629s^2 + 5.2888s + 2.5601}.$$

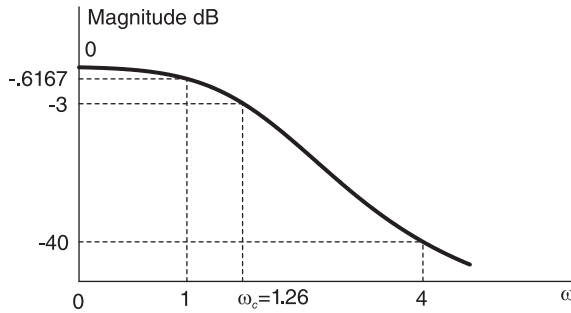


FIGURE 9.56 Butterworth filter as obtained by MATLAB.

We note that the transfer function $H(s)$ produced by MATLAB can be deduced from the normalized ($\omega_c = 1$) transfer function $H_T(s)$ given by the tables by writing.

$$H(s) = H_T(s) \Big|_{s \rightarrow \varepsilon^{1/n} s = \varepsilon^{1/4} s = 0.7906s}$$

as can be easily verified.

b) The bandpass filter can be obtained by writing:

$$B = \omega_2 - \omega_1 = 1200\pi = 3769.9$$

$$\omega_0 = \sqrt{\omega_1 \omega_2} = 10514.$$

The bandpass filter transfer function may be obtained from the table transfer function by writing:

$$H_{BP}(s) = H_T(s) \Big|_{s \rightarrow \frac{s^2 + \omega_0^2}{Bs}} = \frac{2.01987 \times 10^{14} s^4}{D(s)}$$

where

$$D(s) = s^8 + 9851.2s^7 + 4.9068 \times 10^8 s^6 + 3.4068 \times 10^{12} s^5 + 8.4244 \times 10^{16} s^4 + 3.7659 \times 10^{20} s^3 + 5.9956 \times 10^{24} s^2 + 1.3306 \times 10^{28} s + 1.49304 \times 10^{32}.$$

Alternatively, if $H(s)$ is the filter transfer function obtained with $\omega_c = 1.2642$ and $\varepsilon = 0.3906$ then we may write:

$$H_{BP}(s) = H(s) \Big|_{s \rightarrow \frac{\omega_c}{B} \frac{s^2 + \omega_0^2}{s}}$$

We obtain the same transfer function as the one just found.

The MATLAB instruction $[B, A] = \mathbf{Butter}(N, Wn2, 's')$ with $Wn2 = [w1, w2]$ and $w1 = \omega_1, w2 = \omega_2$ produces the same transfer function except for a small difference due to the fact that MATLAB evaluates the 3-dB frequency as $Wn = 1.2649$, rather than $\omega_c = 1.2642$, the value found above analytically.

Example 9.21 Evaluate the transfer function, the poles and the zeros of a third order bandpass Butterworth filter with 0 dB maximum gain, 3 dB maximum attenuation in the pass-band, a central frequency of 50 kHz and a bandwidth of 5 kHz.

$$\omega_0 = 2\pi \times 50 \times 10^3 = 3.1416 \times 10^5$$

$$n = 3$$

$$B = 2\pi \times 5 \times 10^3 = 3.1416 \times 10^4$$

$$H_{LP}(s) = \frac{1}{s^3 + 2s^2 + 2s + 1}$$

$$H_{BP}(s) = H_{LP}\left(\frac{s^2 + \omega_0^2}{Bs}\right) = \frac{B^3 s^3}{D(s)}$$

where

$$D(s) = s^6 + 2Bs^5 + (3\omega_0^2 + 2B^2)s^4 + (4B\omega_0^2 + B^3)s^3 + (3\omega_0^4 + 2B^2\omega_0^2)s^2 + 2B\omega_0^4s + \omega_0^6.$$

Let c_i be the coefficient of s^i in the denominator polynomial. We have

$$c_5 = 2B = 2\pi \times 10^4 = 6.2832 \times 10^4$$

$$c_4 = 3\omega_0^2 + 2B^2 = 2.9806 \times 10^{11}$$

$$c_3 = 1.2434 \times 10^{16}$$

$$H_{BP}(s) = 3.1006 \times 10^{13} s^3 / D(s)$$

where

$$D(s) = s^6 + 6.2832 \times 10^4 s^5 + 2.9806 \times 10^{11} s^4 + 1.2434 \times 10^{16} s^3 + 2.9418 \times 10^{22} s^2 + 6.1204 \times 10^{26} s + 9.6139 \times 10^{32}.$$

Verification by MATLAB: We need to evaluate the two frequencies ω_L and ω_H at the two edges of the pass-band

$$\omega_H = \frac{B + \sqrt{B^2 + 4\omega_0^2}}{2} = 3.3026 \times 10^5$$

$$\omega_L = \frac{-B + \sqrt{B^2 + 4\omega_0^2}}{2} = 2.9884 \times 10^5$$

$$\omega_H - \omega_L = 3.1416 \times 10^4 = B.$$

This is verified by the MATLAB program:

```
N = 3
Wn = [w1 w2]
[b, a] = butter(N, Wn, 's')
[z, p, k] = butter(N, Wn, 's')
pzmap[b, a].
```

The last instruction plots the filter poles and zeros. The poles are given by

$$p = \left\{ -0.0819 \times 10^5 \pm j3.2796 \times 10^5, -0.1571 \times 10^5 \right. \\ \left. \pm j3.1377 \times 10^5, -0.0751 \times 10^5 \pm j3.0075 \times 10^5 \right\}.$$

The transfer function has a triple zero at $s = 0$. Writing $\omega_L = 2\pi f_1$ and $\omega_H = 2\pi f_2$ we have $f_1 = 47.562$ kHz, $f_2 = 52.562$ kHz, and the bandwidth is equal to $f_2 - f_1 = 50$ kHz as required.

Example 9.22 Repeat the last example using a Chebyshev filter with an attenuation of 1 dB in the pass-band.

Referring to the Chebyshev tables of coefficients, or alternatively, using MATLAB, we evaluate the third order, 1 dB, lowpass prototype (normalized) Chebyshev filter using the instructions

$$N = 3, \quad Wn = 1, \quad R = 1$$

$$[b, a] = \mathbf{cheby1}(N, R, Wn, 's')$$

obtaining

$$H_{LP}(s) = \frac{0.4913}{s^3 + 0.9883s^2 + 1.2384s + 0.4913}$$

wherefrom

$$H_{BP}(s) = H_{LP}\left(\frac{s^2 + \omega_0^2}{Bs}\right) = \frac{0.4913B^3s^3}{D(s)}$$

where

$$D(s) = (s^6 + 3s^4\omega_0^2 + 3s^2\omega_0^4 + \omega_0^6) + 0.9883Bs(s^4 + 2s^2\omega_0^2 + \omega_0^4) + 1.2384B^2s^2(s^2 + \omega_0^2) + 0.4913B^3s^3$$

i.e.

$$H_{BP}(s) = 1.5234 \times 10^{13}s^3/D(s)$$

where

$$D(s) = s^6 + 3.1048 \times 10^4s^5 + 2.9731 \times 10^{11}s^4 + 6.1439 \times 10^{15}s^3 + 2.9343 \times 10^{22}s^2 + 3.0244 \times 10^{26}s + 9.6139 \times 10^{32}.$$

A simple MATLAB program may be written to verify these results and evaluate and plot the poles and zero, by using in particular the functions

(with $N = 3$, $R = 1$, $Wn = [\omega_L, \omega_H]$)
 $[b, a] = \mathbf{cheby1}(N, R, Wn, 's')$
 $[z, p, k] = \mathbf{cheby1}(N, R, Wn, 's')$
 $\mathbf{pzmap}(b, a)$.

The poles are given by

$$p = \{-0.0407 \times 10^5 \pm j3.2968 \times 10^5, -0.0369 \times 10^5 \pm j2.9933 \times 10^5, -0.0776 \times 10^5 \pm j3.1406 \times 10^5\}$$

and there is a zero of order 3 at $s = 0$.

Example 9.23 Evaluate the transfer function, poles and zeros of a bandpass elliptic filter which has a ripple of at most 1 dB in the pass-band and at least 30 dB in the stopband and which has a pass-band with edge frequencies 1.5 kHz and 3 kHz and a stopband with edge frequencies of 1.0 kHz and 4 kHz.

We have $\omega_L = 2\pi \times 1.5 \times 10^3 = 9424.78$ r/s, $\omega_H = 2\pi \times 3 \times 10^3 = 1.885 \times 10^4$ r/s, $Rp = 1$ dB, $Rs = 30$ dB, $\omega_{s_1} = 2\pi \times 10^3$ r/s, $\omega_{s_2} = 2\pi \times 4 \times 10^3$ r/s.

To first evaluate the transfer function of the lowpass prototype we need to find the filter order n that would suffice to meet the given specifications. To this end we do an inverse transformation in order to evaluate the pass-band cut-off frequency Ω_p and stop-band edge frequency Ω_s of the prototype, corresponding to those of the given bandpass filter specifications.

We have

$$B = \omega_H - \omega_L = 2\pi \times 1.5 \times 10^3 = 9424.78 \text{ r/s}$$

$$\omega_0 = \sqrt{\omega_L\omega_H} = 2\pi\sqrt{4.5 \times 10^6} = 2\pi \times 1.7321 \times 10^3 = 13328.6 \text{ r/s}$$

$$\Omega = \frac{\omega^2 - \omega_0^2}{B\omega}.$$

Now

$$\omega = \omega_0 \text{ implies that } \Omega = 0$$

$$\omega = \pm\omega_L \text{ and } \omega = \pm\omega_H \text{ imply that } \Omega_p = \pm 1$$

$$\omega = \pm\omega_{s_1} = \pm 2\pi \times 10^3 \text{ imply that } \Omega_{s_1} = \pm 4$$

$$\omega = \pm\omega_{s_2} = \pm 2\pi \times 4 \times 10^3 \text{ imply that } \Omega_{s_2} = \pm 6.5.$$

Taking the positive values of the frequency Ω of the lowpass prototype we retain the narrower transition interval from $\Omega = 1$ to Ω_s , namely, $\Omega_s = 4$ thus satisfying the more stringent of the two conditions. For the lowpass prototype we therefore have the frequencies $\Omega_p = 1$ and $\Omega_s = 4$ and the corresponding attenuation limits $R_p = 1$ dB and $R_s = 30$ dB.

The filter order can be found as shown above in the section dealing with the design of lowpass elliptic filters. Alternatively, using MATLAB with $Wp = 1$ and $Ws = 4$, the function

$$[N, Wn] = \text{ellipord}(Wp, Ws, Rp, Rs, 's')$$

produces the values $N = 3$ and $Wn = 1$.

The filter order being known to equal 3 we may evaluate the MATLAB function

$$[b, a] = \text{ellip}(N, Rp, Rs, Wn, 's').$$

We obtain the lowpass prototype transfer function

$$H_{LP}(s) = \frac{0.1490s^2 + 0.5687}{s^3 + 0.9701s^2 + 1.2460s + 0.5687}.$$

and thence the bandpass transfer function

$$H_{BP}(s) = H_{LP}\left(\frac{s^2 + \omega_0^2}{Bs}\right).$$

We obtain

$$H_{BP}(s) = N(s)/D(s)$$

where

$$N(s) = 4.43202 \times 10^{19}s + 9.75051 \times 10^{11}s^3 + 1404.29s^5$$

$$D(s) = 5.60682 \times 10^{24} + 2.88557 \times 10^{20}s + 1.14344 \times 10^{17}s^2 \\ + 3.72465 \times 10^{12}s^2 + 6.43636 \times 10^8s^4 + 9142.98s^5 + s^6.$$

The result is in agreement with the results produced by MATLAB upon execution of the instructions, with $N = 3$,

$$Wn = [\omega_L \ \omega_H]$$

$$[b, a] = \text{ellip}(N, Rp, Rs, Wn, 's').$$

The filter's poles and zeros are also evaluated and plotted by the functions

$$[z, p, k] = \text{ellip}(N, Rp, Rs, Wn, 's')$$

$$\text{pzmap}(b, a).$$

The poles and zeros pattern is shown in Fig. 9.57.

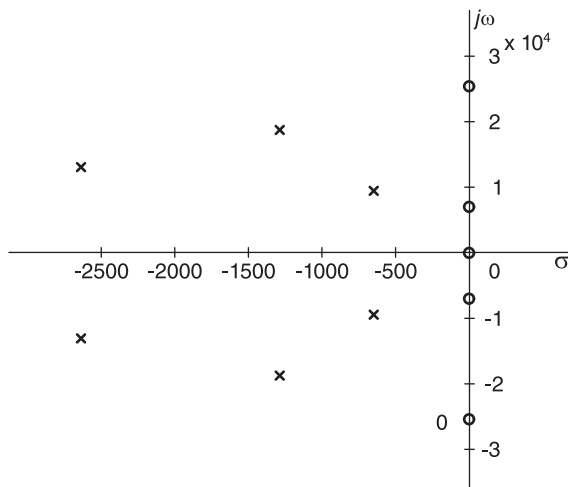


FIGURE 9.57 Elliptic bandpass filter poles and zeros.

9.48 Lowpass to Band-Stop Transformation

We consider now the transformation from a prototype (normalized) lowpass filter to a bandstop filter transfer function. The desired bandstop filter should have a low and high stop-band edge frequencies of ω_1 and ω_2 rad/sec, respectively. Alternatively, the desired filter may be required to have a stop-band width B rad/sec and a central frequency ω_0 , where $B = \omega_2 - \omega_1$ and $\omega_0 = \sqrt{\omega_1\omega_2}$. The transformation is

$$p = \frac{Bs}{s^2 + \omega_0^2}. \tag{9.455}$$

The transfer function of the bandstop filter is thus given by

$$H_{BS}(s) = H_{LP}\left(\frac{Bs}{s^2 + \omega_0^2}\right) \tag{9.456}$$

and substituting $p = j\Omega$ and $s = j\omega$, we obtain

$$\Omega = B\omega/(\omega_0^2 - \omega^2) \tag{9.457}$$

$$\Omega\omega^2 + B\omega - \Omega\omega_0^2 = 0 \tag{9.458}$$

$$\omega = \frac{-B \pm \sqrt{B^2 + 4\Omega^2\omega_0^2}}{2\Omega}. \tag{9.459}$$

The overall transformation, including positive and negative frequencies, of a normalized “prototype” lowpass Chebyshev filter spectrum to a bandstop filter is illustrated in Fig. 9.58. We adopt the following notation. In the lowpass prototype we assign to the critical points of maxima/minima on the positive frequency axis the letters A, B, C, \dots and their negative-frequency images A^-, B^-, C^-, \dots . As the figure shows, the positive frequency points A, B, C, \dots are transformed to the set A^-, B^-, C^-, \dots on the positive axis and to A^+, B^+, C^+, \dots on the negative axis.

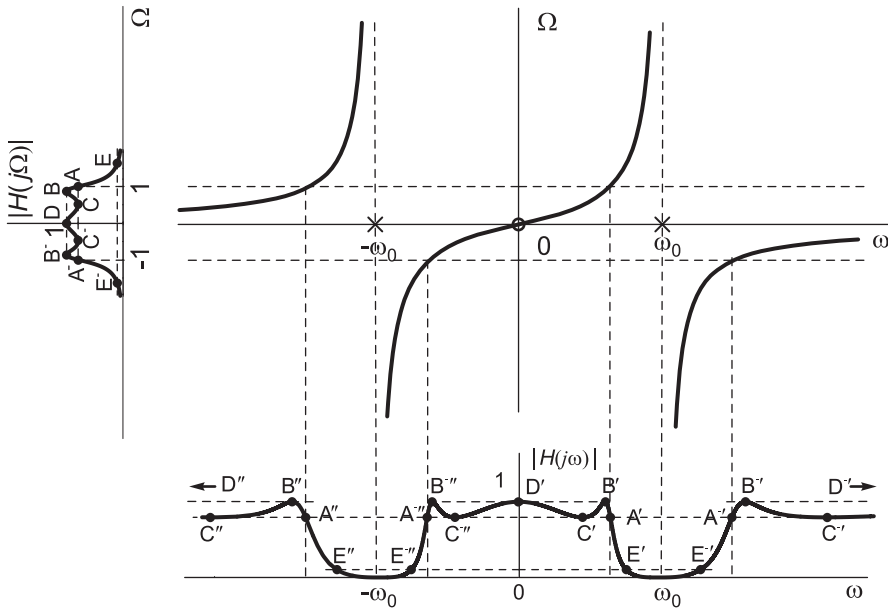


FIGURE 9.58 Lowpass to bandstop transformation.

Similarly the negative frequency points A^-, B^-, C^-, \dots are transformed to the set A'^-, B'^-, C'^-, \dots on the positive axis and to A'', B'', C'', \dots on the negative axis. This notation will be used in what follows.

We note that if $\Omega = 0$ then $\omega = 0, \pm\infty$. If $\Omega = \pm\infty$ then $\omega = \pm\omega_0$. With $\Omega = 1$ and -1 respectively we have

$$\omega_H = \frac{B + \sqrt{B^2 + 4\omega_0^2}}{2} \tag{9.460}$$

$$\omega_L = \frac{-B + \sqrt{B^2 + 4\omega_0^2}}{2} \tag{9.461}$$

wherefrom

$$\omega_H - \omega_L = B \tag{9.462}$$

$$\omega_L \omega_H = \omega_0^2 \tag{9.463}$$

as required.

Example 9.24 Design a bandstop Chebyshev filter with the following specifications: (1) pass-band ripple 3 dB, (2) stop-band attenuation: minimum 25 dB, (3) pass-band cut-off edge frequencies 500 Hz and 5 kHz, (4) stop-band cut-off edge frequencies 1 kHz and 3 kHz.

We use the substitution

$$s \longrightarrow \frac{Bs}{s^2 + \omega_0^2}.$$

We write

$$\omega_{p1} = 2\pi \times 500, \quad \omega_{p2} = 2\pi \times 5000, \quad \omega_{s1} = 2\pi \times 1000, \quad \omega_{s2} = 2\pi \times 3000$$

$$B = \omega_{p2} - \omega_{p1} = 2\pi \times 4500 = 2.8274 \times 10^4 \text{ r/s}$$

$$\omega_0 = \sqrt{\omega_{p1} \omega_{p2}} = 9.9346 \times 10^3 = 2\pi \times 1581.1 \text{ r/s}$$

$$\Omega_{s1} = \frac{B\omega_{s1}}{|\omega_{s1}^2 - \omega_0^2|} = 3$$

$$\Omega_{s2} = \frac{B\omega_{s2}}{|\omega_{s2}^2 - \omega_0^2|} = 2.0769.$$

We choose the lowpass prototype stop-band edge frequency $\Omega_s = 2.0769$ to ensure satisfying the minimum requirement. As in the last example the 3 dB pass-band attenuation means $10 \log_{10} \{1 + \varepsilon^2 C_n^2(1)\} = 3 \text{ dB}$ wherefrom $\varepsilon = 0.9976$.

At $\Omega = \Omega_s = 2.0769$ the attenuation should be 25 dB, i.e. $10 \log_{10} \{1 + \varepsilon^2 C_n^2(2.0769)\} = 25$, obtaining $n = 2.6237$. We therefore choose $n = 3$. The lowpass prototype transfer function $H_{LP}(s)$, from the 3-dB Chebyshev table, is thus the same as in the last example. The required system function $H_{BS}(s)$ of the bandstop filter is given by

$$H_{BS}(s) = \frac{0.2506}{s^3 + 0.5972s^2 + 0.9283s + 0.2506} \Big|_{s \rightarrow \frac{Bs}{s^2 + \omega_0^2}}.$$

Mathematica produces the required transfer function

$$H_{BS}(s) = N(s) / D(s).$$

where

$$N(s) = 9.61389 \times 10^{23} + 2.92227 \times 10^{16} s^2 + 2.96088 \times 10^8 s^4 + s^6$$

$$D(s) = 9.61389 \times 10^{23} + 1.02023 \times 10^{21} s + 2.17251 \times 10^{17} s^2 + 1.10872 \times 10^{14} s^3 + 2.20121 \times 10^9 s^4 + 104737 s^5 + s^6.$$

The result can be confirmed by MATLAB.

$$N = 3$$

$$R = 3$$

$$Wn = [2 * pi * 5002 * pi * 5000]$$

$$[B2, A2] = \mathbf{cheby1}(N, R, Wn, 'stop', 's')$$

$$Hmat = tf(B2, A2)$$

produces similar results.

9.49 Lowpass to Highpass Transformation

Given a prototype lowpass filter to obtain a highpass filter with a pass-band edge frequency, i.e. cut-off frequency, ω_c , the transformation is written

$$p = R(s) = \omega_c / s \tag{9.464}$$

and writing $s = j\omega$ we have $j\Omega = -j\omega_c / \omega$, i.e. $\Omega = -\omega_c / \omega$.

The relation Ω versus ω and the resulting transformation from the prototype frequency response $H(j\Omega)$ to the highpass frequency response is shown in Fig. 9.59.

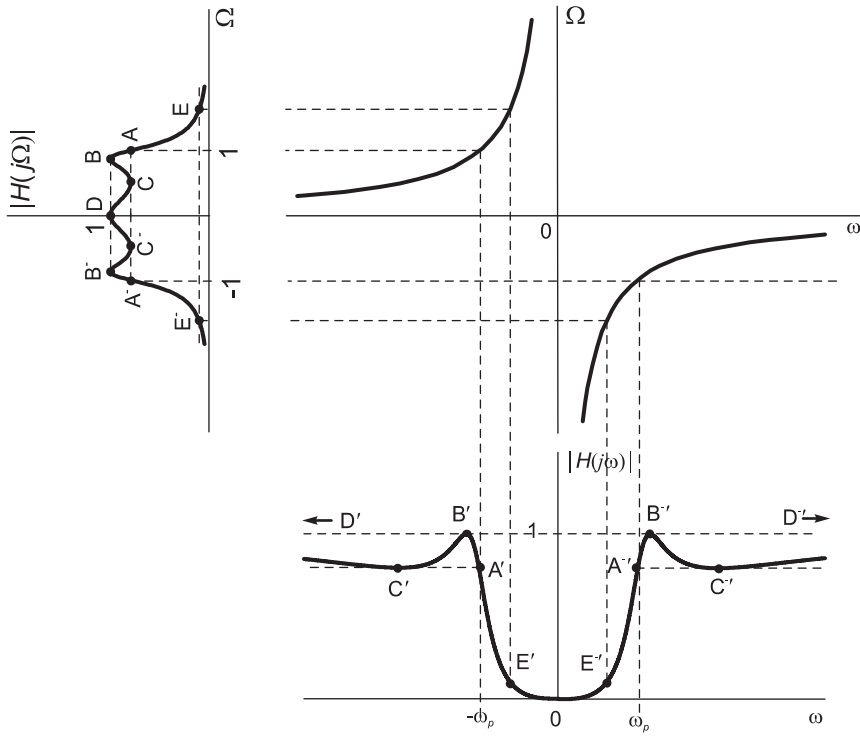


FIGURE 9.59 Lowpass to highpass transformation.

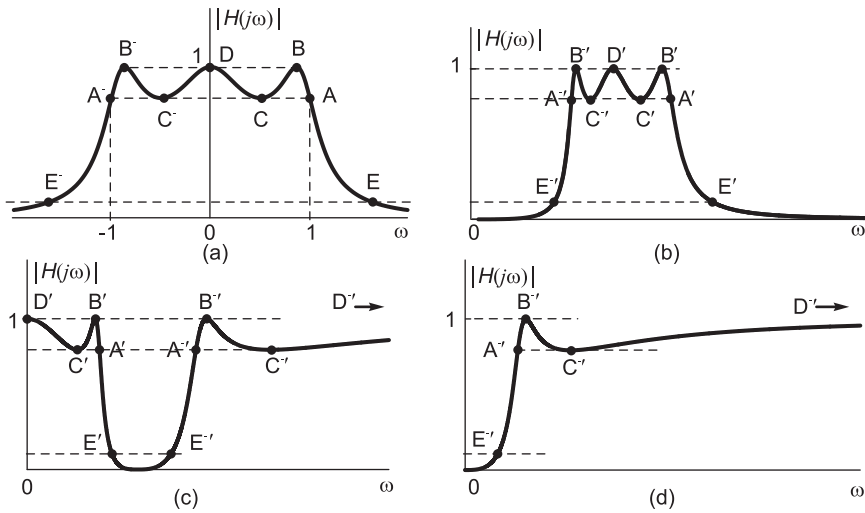


FIGURE 9.60 Transformation of salient points from lowpass to bandpass, bandstop and high transformation.

The result of such transformation on the frequency magnitude response $|H(j\Omega)|$ is shown as an illustration for a Chebyshev filter.

To summarize, the transformations of maxima/minima and edge frequencies, from the lowpass filter prototype to bandpass, bandstop and highpass filters, are grouped together in Fig. 9.60.

Example 9.25 Design a highpass Butterworth filter having a maximum response of 10 dB, a pass-band edge frequency of 1000 Hz, a maximum pass-band attenuation of 1 dB, a stop-band edge frequency of 500 Hz and a stop-band attenuation of at least 30 dB below the maximum response.

The desired spectrum is shown in Fig. 9.61.

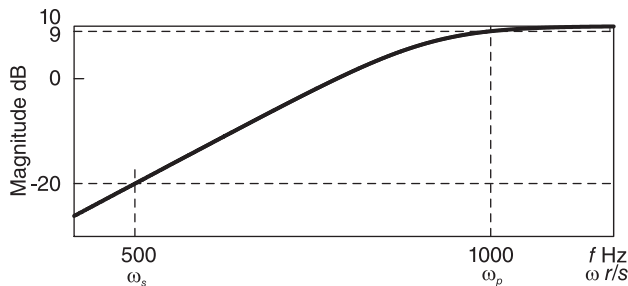


FIGURE 9.61 Desired highpass filter frequency response.

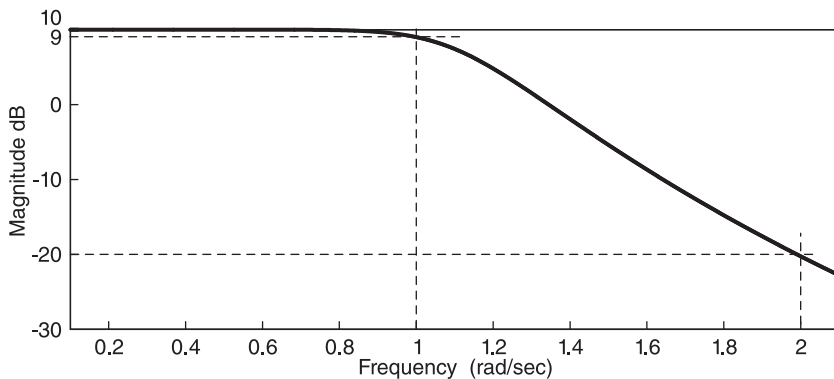


FIGURE 9.62 Lowpass (LP) prototype with 1 dB pass-band attenuation.

We start by evaluating the corresponding prototype shown in Fig. 9.62. We note that the specified pass-band edge frequency $\omega_p = 2\pi \times 1000$ r/s corresponds to 1 dB attenuation from the maximum value of the response. The value ϵ in the prototype lowpass filter is thus not equal to 1. We write, using the variable Ω for the lowpass prototype frequency,

$$|H(j\Omega)| = \frac{K}{\sqrt{1 + \epsilon^2 \Omega^{2n}}}$$

We have with $\Omega = 0$

$$10 \log K = 10 \text{ dB}, \quad K = 10^{0.5} = 3.162.$$

The lowpass to highpass transformation is written

$$s \longrightarrow \omega_p/s, \text{ i.e. by replacement } p = \omega_p/s$$

where ω_p is the required cut-off frequency

$$\omega_p = 2\pi \times 1000 \text{ r/s.}$$

Writing $p = j\Omega$ and $s = j\omega$

$$j\Omega = \frac{\omega_p}{j\omega}, \quad \Omega = -\frac{\omega_p}{\omega}$$

$$\Omega = -\frac{2\pi \times 1000}{\omega}.$$

The frequency $\Omega = 1$ in the prototype thus corresponds to the frequency $\omega = 2\pi \times 1000$ r/s in the highpass filter, as desired. Note that the absolute value of the frequency is taken; thus evaluating the positive frequency value. We write

$$\Omega_s = \frac{\omega_p}{\omega_s} = \frac{2\pi \times 1000}{2\pi \times 500} = 2.$$

The attenuation at $\Omega = 1$ is 1 dB relative to that at zero frequency

$$20 \log_{10} \left\{ \frac{K}{K/\sqrt{1+\varepsilon^2}} \right\} = 1$$

$$1 + \varepsilon^2 = 10^{0.1} = 1.2589$$

$$\varepsilon^2 = 0.2589, \quad \varepsilon = 0.5088.$$

The attenuation at $\Omega_s = 2$ should be 30 dB below that at zero frequency

$$20 \log \left\{ \frac{K}{K/\sqrt{1+\varepsilon^2 2^{2n}}} \right\} = 30 \text{ dB}$$

$$1 + \varepsilon^2 4^n = 10^3$$

$$0.2589 \times 4^n = 999$$

$$4^n = 3.8586 \times 10^3$$

$$n \log 4 = 3 \log (3.8586)$$

$$n = 5.95.$$

We choose $n = 6$ to ensure meeting the specifications. Since $\varepsilon \neq 1$ we may find the lowpass filter system function $H_\varepsilon(s)$ by first finding the normalized $\varepsilon = 1$ system function $H(s)$ and then replace s by $\varepsilon^{1/n}s$. From the filter tables or the MATLAB call `[B, A] = butter(6, 1, 's')` %n = 6, cut-off frequency = 1, continuous filter

$$H_{LP}(s) = \frac{K}{s^6 + 3.864s^5 + 7.464s^4 + 9.142s^3 + 7.464s^2 + 3.864s + 1}.$$

Note that this is the tables prototype, characterized by an attenuation of 3 dB at $\omega = 1$. To obtain a 1 dB pass-band attenuation we evaluate ε and thus convert the lowpass prototype.

$$H_\varepsilon(s) = H_{LP}(s) \Big|_{s \rightarrow \varepsilon^{1/6} s = 0.894s} \\ = \frac{3.162}{0.5088s^6 + 2.200s^5 + 4.758s^4 + 6.521s^3 + 5.959s^2 + 3.452s + 1}$$

and the highpass system function is given by

$$H_{HP}(s) = H_\varepsilon(s) \Big|_{s \rightarrow \omega_p/s = 2\pi \times 1000/s}.$$

We obtain

$$H_{HP}(s) = N(s)/D(s)$$

where

$$N(s) = 3.162s^6$$

$$D(s) = 3.131 \times 10^{22} + 2.154 \times 10^{19}s + 7.416 \times 10^{15}s^2 \\ + 1.618 \times 10^{12}s^3 + 2.353 \times 10^8s^4 + 2.169 \times 10^4s^5 + s^6.$$

To verify this result using MATLAB we should find the 3 dB frequencies Ω_c and ω_c in the prototype lowpass and highpass, respectively. We write

$$20 \log \sqrt{1 + \varepsilon^2 \Omega_c^{2n}} = 3 \text{ dB}$$

$$1 + \varepsilon^2 \Omega_c^{12} = 10^{0.3}$$

$$\Omega_c^{12} = (10^{0.3} - 1) / \varepsilon^2 = 3.8438$$

$$\Omega_c = 1.1187$$

and

$$\Omega_c = \frac{\omega_p}{\omega_c}$$

$$\omega_c = \frac{\omega_p}{\Omega_c} = \frac{2\pi \times 1000}{1.9606} = 2\pi \times 893.86 \text{ r/s}.$$

A MATLAB program including the statement

$$[B, A] = \mathbf{butter}(6, \omega_c, 'high', 's')$$

where $\omega_c = \omega_c$ produces the same system function $H_{HP}(s)$ as obtained above.

9.50 Note on Lowpass to Normalized Band-Stop Transformation

We note here again that a transformation from the prototype lowpass filter to a *normalized* bandstop filter is of interest for generating filter tables. With a normalized bandwidth $\beta = B/\omega_0$ the transformation is written

$$s \longrightarrow \frac{\beta s}{s^2 + 1}. \quad (9.465)$$

Writing

$$p = \frac{\beta s}{s^2 + 1} \quad (9.466)$$

and substituting $p = j\Omega$ and $s = j\omega$, we obtain

$$\Omega\omega^2 + \beta\omega - \Omega = 0 \quad (9.467)$$

$$\omega = \frac{-\beta \pm \sqrt{\beta^2 + 4\Omega^2}}{2}. \quad (9.468)$$

Letting $\Omega = 1$ and -1 respectively we have

$$\omega_H = \frac{\sqrt{\beta^2 + 4} + \beta}{2} \quad (9.469)$$

$$\omega_L = \frac{\sqrt{\beta^2 + 4} - \beta}{2} \quad (9.470)$$

wherefrom

$$\omega_H - \omega_L = \beta \quad (9.471)$$

$$\omega_L\omega_H = 1 \quad (9.472)$$

that is, the central frequency is 1 and the bandwidth is the normalized β . The filter can be subsequently denormalized so that the central frequency be made equal to an arbitrary value ω_0 by writing

$$s \longrightarrow \frac{s}{\omega_0}. \quad (9.473)$$

The overall transformation is

$$s \longrightarrow \frac{\beta s}{s^2 + 1} \xrightarrow{s \rightarrow s/\omega_0} \frac{Bs}{s^2 + \omega_0^2} \quad (9.474)$$

as expected. We note that in the literature the filter tables are often given in terms of the normalized bandwidth β .

Example 9.26 Using MATLAB's instruction

$$[b, a] = \text{cheby1}(n, R, Wn, 's')$$

the transfer function of a bandpass Chebyshev filter of order n , attenuation in the pass-band R dB and pass-band cut-off edge frequencies ω_L and ω_H , can be determined. Assuming a normalized bandwidth of $\beta = 0.1$, $n = 8$ and $R = 0.5$ dB, the argument Wn is a vector the elements of which are $\omega_L \equiv \omega_{p1}$ and $\omega_H \equiv \omega_{p1}$. We shall therefore write $Wn = [\omega_L \ \omega_H]$.

Note that the argument 's' in the MATLAB instruction signifies that the desired filter is an analog (continuous-domain) filter. To evaluate ω_L and ω_H we note that $\omega_0 = 1$ so that $\omega_L\omega_H = \omega_0^2 = 1$. Moreover, $\beta = 0.1 = \omega_L - \omega_H$. Solving we have $\omega_L = 0.9512$, $\omega_H = 1.0512$. The execution of the MATLAB command yields the transfer function

$$H(s) = N(s)/D(s)$$

where

$$N(s) = 2.237 \times 10^{-10} s^8$$

where

$$\begin{aligned} D(s) = & s^{16} + 0.1146s^{15} + 8.026s^{14} + 0.8043s^{13} + 28.15s^{12} + 2.417s^{11} \\ & + 56.38s^{10} + 4.032s^9 + 70.5s^8 + 4.031s^7 + 56.37s^6 + 2.416s^5 \\ & + 28.14s^4 + 0.8039s^3 + 8.021s^2 + 0.1145s + 0.9992. \end{aligned}$$

To obtain a central frequency $\omega_0 = 2\pi \times 1000$ r/s we write

$$s \longrightarrow \frac{s}{\omega_0} = \frac{s}{2\pi \times 1000}$$

and the bandwidth thus obtained is given by

$$B = \beta\omega_0 = 2\pi \times 100 \text{ r/s.}$$

Example 9.27 Design a bandpass Chebyshev filter with the following specifications: (1) pass-band ripple 3 dB, (2) stop-band attenuation: minimum 25 dB, (3) pass-band cut-off edge frequencies 1 kHz and 3 kHz, (4) stop-band cut-off edge frequencies 500 Hz and 5 kHz.

We have the pass-band 3 dB edge frequencies

$$\omega_L \equiv \omega_{p1} = 2\pi \times 1000, \quad \omega_H \equiv \omega_{p2} = 2\pi \times 3000$$

and the stop-band edge frequencies $\omega_{s1} = 2\pi \times 500$ and $\omega_{s2} = 2\pi \times 5000$.

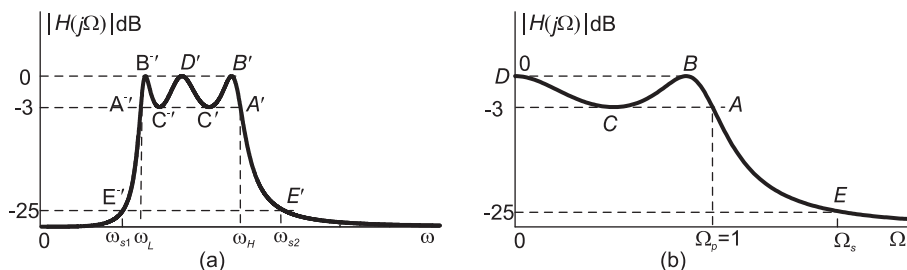


FIGURE 9.63 Bandpass response points and corresponding lowpass ones.

The bandpass frequency response points and the corresponding points of the lowpass prototype can be seen in Fig. 9.63. Point A maps to points A^{-} and A^{+} . Point B maps to points B^{-} and B^{+} as shown in the figure. We have

$$\begin{aligned} \omega_0^2 &= \omega_L \omega_H = 4\pi^2 \times 3 \times 10^6 \\ \omega_0 &= \sqrt{\omega_L \omega_H} = 2\pi\sqrt{3} \times 10^3 \text{ r/s} \\ B &= \omega_H - \omega_L = 2\pi \times 2000 \text{ r/s.} \end{aligned}$$

To evaluate the positive frequency Ω_s , i.e. point E in the lowpass prototype corresponding to the points E^{-} and E^{+} in the bandpass filter we write

$$\begin{aligned} \Omega_{s1} &= \frac{|\omega_{s1}^2 - \omega_0^2|}{B\omega_{s1}} = \frac{4\pi^2 |500^2 - 3 \times 10^6|}{2\pi \times 2000 \times 2\pi \times 500} = 2.75 \\ \Omega_{s2} &= \frac{|\omega_{s2}^2 - \omega_0^2|}{B\omega_{s2}} = \frac{4\pi^2 |25 \times 10^6 - 3 \times 10^6|}{2\pi \times 2000 \times 2\pi \times 5000} = 2.2. \end{aligned}$$

The stop-band edge frequencies therefore map to the frequencies $\Omega_s = 2.2$ and $\Omega_s = 2.75$ in the lowpass prototype.

To meet the given specifications we choose $\Omega_s = 2.2$ since it produces the higher selectivity; hence the higher filter order. In the lowpass prototype the attenuation at $\Omega = 1$ is 3 dB, wherefrom

$$10 \log_{10} \{1 + \varepsilon^2 C_n^2(1)\} = 3 \text{ dB}$$

$$1 + \varepsilon^2 = 10^{0.3} = 1.9953, \quad \varepsilon^2 = 0.9953, \quad \varepsilon = 0.9976.$$

At $\Omega = \Omega_s = 2.2$ the attenuation should be 25 dB, wherefrom

$$10 \log_{10} \{1 + \varepsilon^2 C_n^2(2.2)\} = 25 \text{ dB}$$

$$1 + 0.9953 C_n^2(2.2) = 10^{2.5}, \quad C_n^2(2.2) = 315.2230, \quad C_n(2.2) = 17.7545$$

$$\cosh(n \cosh^{-1} 2.2) = 17.7545$$

$$\cosh(n \times 1.4254) = 17.7545$$

$$1.4254n = \cosh^{-1}(17.7545) = 3.569$$

$$n = 2.51.$$

We choose $n = 3$. The filter spectrum is represented graphically in Fig. 9.63(a). The corresponding lowpass prototype is shown in Fig. 9.63(b).

To obtain the coefficients for Chebyshev with attenuation of 1 dB in pass-band for say $n = 3$ we may write

$$[B, A] = \mathbf{cheby1}(n, R, Wn, 's') = \mathbf{cheby1}(3, 1, 1, 's') \quad (9.475)$$

We obtain the lowpass filter prototype system function

$$H_{LP}(s) = \frac{0.2506}{s^3 + 0.5972s^2 + 0.9283s + 0.2506} \quad (9.476)$$

and deduce the bandpass filter system function by replacing s by $(s^2 + \omega_0^2) / (Bs)$, obtaining

$$H_{BP}(s) = H_{LP}(s) \Big|_{s \rightarrow \frac{s^2 + 4\pi^2 \times 3 \times 10^6}{2\pi \times 2000 s}} \quad (9.477)$$

Using *Mathematica* we have

$$H_{BP}(s) = 4.9729 \times 10^{11} s^3 / D(s) \quad (9.478)$$

where

$$D(s) = 1.661 \times 10^{24} + 1.053 \times 10^{20} s + 5.944 \times 10^{16} s^2 \\ + 2.275 \times 10^{12} s^3 + 5.019 \times 10^8 s^4 + 7.505 \times 10^3 s^5 + s^6.$$

The MATLAB statements

$$Wn = [2 * pi * 1000, 2 * pi * 3000] \quad (9.479)$$

$$[B, A] = \mathbf{cheby1}(3, 3, Wn, 's') \quad (9.480)$$

produce the same system function $H_{BP}(s)$ we just obtained. The general appearance of the frequency response of such a bandpass filter is shown in Fig. 9.64. In the same figure we see a corresponding bandstop filter response.

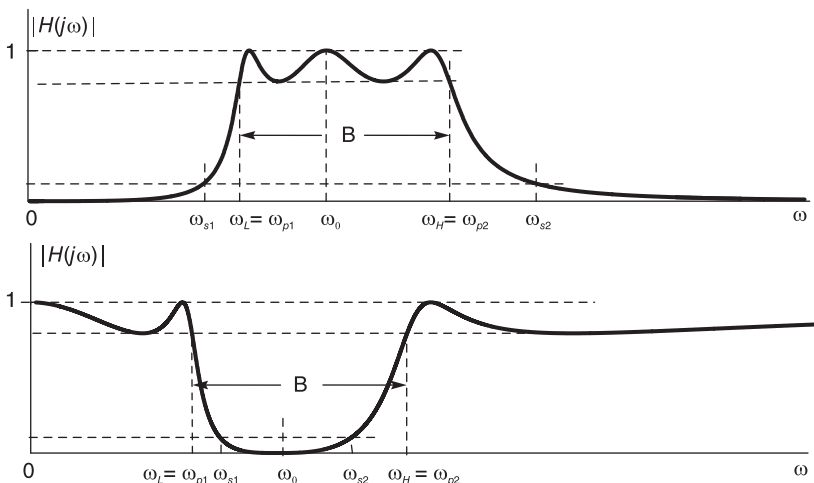


FIGURE 9.64 Bandpass and bandstop responses.

9.51 Windows

We have seen in Chapter 2 the “spectral leakage” phenomenon that results from the truncation of a pure infinite duration sinusoid. We have noted in Chapters 2 and 4 that the side lobes and ripples that appear in the spectrum of a pure sinusoid are due to the fact that the truncation extracting a finite-duration sinusoid is a multiplication in time by a rectangular window.

If $x(t)$ denotes an infinite duration signal then the finite duration truncation thereof $x_f(t)$ may be written

$$x_f(t) = x(t) w(t) \tag{9.481}$$

where $w(t)$ is the rectangular window. For example, $w(t)$ may be the centered rectangle

$$w(t) = \Pi_T(t) = u(t + T) - u(t - T). \tag{9.482}$$

The result of the truncation in the frequency domain is a convolution of the spectrum $X(j\omega)$ with the transform $W(j\omega)$ of the rectangular window. We may write

$$X_f(j\omega) = \mathcal{F}[x_f(t)] = \frac{1}{2\pi} X(j\omega) * W(j\omega). \tag{9.483}$$

Now

$$W(j\omega) = \mathcal{F}[\Pi_T(t)] = 2T Sa(T\omega) \tag{9.484}$$

so that

$$X_f(j\omega) = \frac{T}{\pi} X(j\omega) * Sa(T\omega). \tag{9.485}$$

To observe the effect of the convolution with the sampling function, consider a signal with a finite bandwidth of which the spectrum $X(j\omega)$ is idealized as a rectangle. The convolution of this spectrum with the sampling function leads to a spectrum $X_r(j\omega)$ having overshoot and ripples, caused by the main lobe and side lobes of the sampling function. This illustrated in Fig. 9.65, where both the sampling function $Sa(T\omega)$ and the resulting spectrum $X_f(j\omega)$ can be seen.

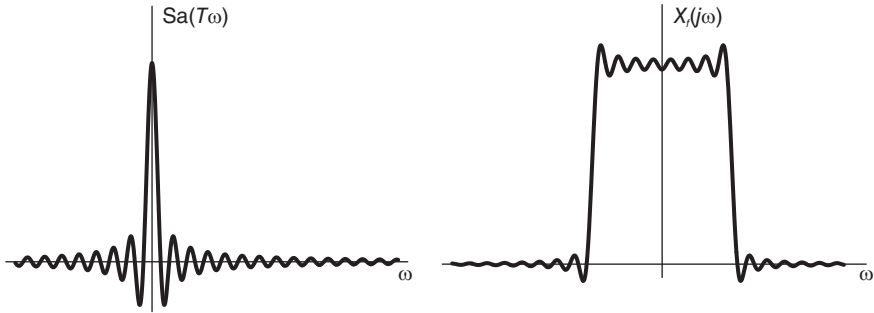


FIGURE 9.65 Ripples caused by rectangular window truncation.

This is the same Gibbs phenomenon that is observed by truncating the Fourier series of a periodic function.

If a softer transition window is used instead of the rectangular window then the ripples are reduced. On the other hand, the main lobe of the spectrum becomes wider than that of the rectangular window reducing the resolution and increasing the transition width at signal discontinuities. For example the corresponding result of the spectral convolution if the rectangular window is replaced by a triangular one is shown in Fig. 9.66. In what follows, we study several forms of basic windows and evaluate their spectra.

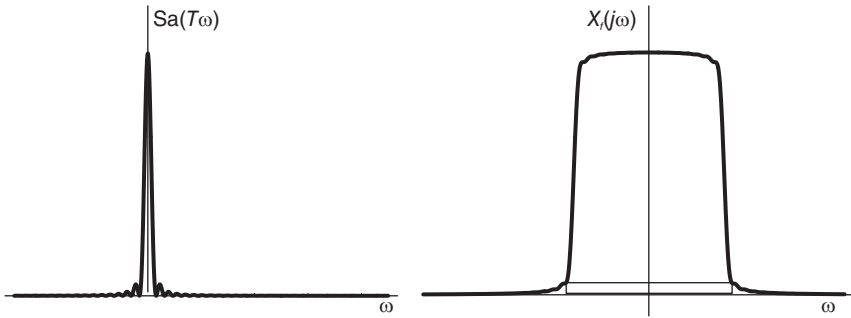


FIGURE 9.66 Ripples caused by triangular window truncation.

9.52 Rectangular Window

$$v(t) = u(t + T/2) - u(t - T/2) = \Pi_{T/2}(t) \tag{9.486}$$

$$V(j\omega) = T Sa\left(\frac{T}{2}\omega\right) = T Sa(\pi fT) = T \frac{\sin(\pi fT)}{(\pi fT)}. \tag{9.487}$$

A rectangular window and its magnitude spectrum are shown in Fig. 9.67.

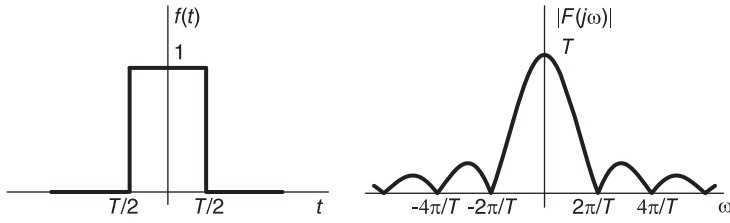


FIGURE 9.67 Rectangular window and transform.

9.53 Triangle (Bartlett) Window

$$v(t) = \left\{ 1 - \frac{2|t|}{T} \right\} \Pi_{T/2}(t) \tag{9.488}$$

$$V(j\omega) = (T/2)Sa^2(T\omega/4) \tag{9.489}$$

$$V_f(f) = \frac{T}{2}Sa^2\left(\frac{T}{2}\pi f\right) = \frac{T}{2} \frac{\sin^2(T\pi f/2)}{(T\pi f/2)^2}. \tag{9.490}$$

A triangular (Bartlett) window and its spectrum are shown in Fig. 9.68.

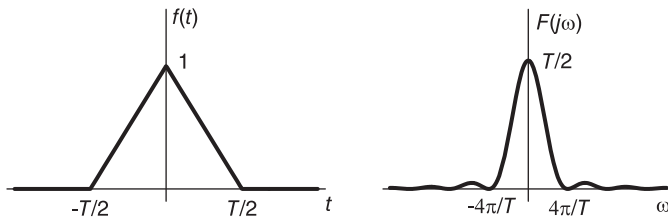


FIGURE 9.68 Triangle (Bartlett) window and transform.

9.54 Hanning Window

$$v(t) = A \left(\cos^2 \frac{\pi t}{T} \right) \Pi_{T/2} = \frac{A}{2} \left\{ 1 + \cos \frac{2\pi t}{T} \right\} \Pi_{T/2}(t) \triangleq v_1(t) \Pi_{T/2}(t) \tag{9.491}$$

$$v_1(t) = \frac{A}{2} \left\{ 1 + \cos \frac{2\pi}{T} t \right\} \tag{9.492}$$

$$V_1(j\omega) = \frac{A}{2} \times 2\pi\delta(\omega) + \frac{A}{2} \times \pi \left\{ \delta\left(\omega - \frac{2\pi}{T}\right) + \delta\left(\omega + \frac{2\pi}{T}\right) \right\} \tag{9.493}$$

$$\begin{aligned}
 V(j\omega) &= \frac{1}{2\pi} V_1(j\omega) * T \text{Sa}\left(\frac{T}{2}\omega\right) \\
 &= \frac{AT}{4} \left\{ 2\text{Sa}\left(\frac{T}{2}\omega\right) + \text{Sa}\left[\frac{T}{2}\omega - \pi\right] + \text{Sa}\left[\frac{T}{2}\omega + \pi\right] \right\}
 \end{aligned} \tag{9.494}$$

$$\begin{aligned}
 V_f(f) &= \frac{AT}{4} \{ 2\text{Sa}(T\pi f) + \text{Sa}[\pi T f - \pi] + \text{Sa}[\pi T f + \pi] \} \\
 &\quad - \sin(\pi T f) T f (T f - 1) \} / \{ T\pi f (T f - 1) (T f + 1) \} \\
 &\triangleq \frac{AT}{4} \frac{N(f)}{D(f)}
 \end{aligned} \tag{9.495}$$

$$\begin{aligned}
 N(f) &= 2T^2 f^2 \sin(T\pi f) - 2 \sin T\pi f - T^2 f^2 \sin(T\pi f) \\
 &\quad - T f \sin(T\pi f) - T^2 f^2 \sin(T\pi f) + T f \sin(T\pi f) = -2 \sin T\pi f
 \end{aligned} \tag{9.496}$$

$$V_f(f) = \frac{AT}{2} \frac{\sin(T\pi f)}{T\pi f (1 - T^2 f^2)} = \frac{A}{2} \frac{\sin(T\pi f)}{\pi f (1 - T^2 f^2)}. \tag{9.497}$$

The Hanning window spectrum can also be rewritten in the form

$$V(j\omega) = \frac{4\pi^2 \sin(T\omega/2)}{4\pi^2\omega - T^2\omega^3}. \tag{9.498}$$

With $A = 1$ and $T = 1$ the form of the window and its spectrum are shown in Fig. 9.69.

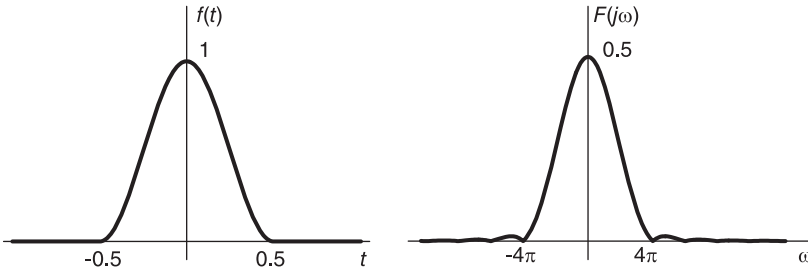


FIGURE 9.69 Hanning window and transform.

9.55 Hamming Window

$$v(t) = \left\{ 0.54 + 0.46 \cos \frac{2\pi t}{T} \right\} / P_{i_{T/2}}(t) = v_1(t) / P_{i_{T/2}}(t) \tag{9.499}$$

$$v_1(t) = 0.54 + 0.46 \cos(2\pi t/T) \tag{9.500}$$

$$V_1(j\omega) = 0.54 \times 2\pi \delta(\omega) + 0.46\pi \left\{ \delta\left(\omega - \frac{2\pi}{T}\right) + \delta\left(\omega + \frac{2\pi}{T}\right) \right\} \tag{9.501}$$

$$\begin{aligned}
 V(j\omega) &= \frac{1}{2\pi} V_1(j\omega) * T \text{Sa}\left(\frac{T}{2}\omega\right) \\
 &= \frac{T}{2} \left\{ 1.08 \text{Sa}\left(\frac{T}{2}\omega\right) + 0.46 \text{Sa}\left[\frac{T}{2}\left(\omega - \frac{2\pi}{T}\right)\right] \right. \\
 &\quad \left. + 0.46 \text{Sa}\left[\frac{T}{2}\left(\omega + \frac{2\pi}{T}\right)\right] \right\}
 \end{aligned}
 \tag{9.502}$$

which can be rewritten in the form

$$V(j\omega) = \frac{(0.16T^2\omega^2 - 4.32\pi^2) \sin(\omega T/2)}{T^2\omega^3 - 4\pi^2\omega}
 \tag{9.503}$$

$$\begin{aligned}
 V_f(f) &= \frac{T}{2} \left\{ 1.08 \frac{\sin(\pi f T)}{\pi f T} + 0.46 \frac{\sin(\pi f T - \pi)}{\pi f T - \pi} + 0.46 \frac{\sin(\pi f T + \pi)}{\pi f T + \pi} \right\} \\
 &= \frac{T}{2} \left\{ 1.08 (f^2 T^2 - 1) \sin \pi f T - 0.46 f T (f T + 1) \sin \pi f T \right. \\
 &\quad \left. - 0.46 f T (f T - 1) \sin \pi f T \right\} / \left\{ \pi f T (f T - 1) (f T + 1) \right\} \\
 &\triangleq \frac{T}{2} \left\{ \frac{N_1(f)}{\pi f T (f^2 T^2 - 1)} \right\}
 \end{aligned}
 \tag{9.504}$$

$$\begin{aligned}
 N_1(f) &= 1.08 f^2 T^2 \sin \pi f T - 1.08 \sin \pi f T - 0.46 f^2 T^2 \sin \pi f T \\
 &\quad - 0.46 f T \sin \pi f T - 0.46 f^2 T^2 \sin \pi f T + 0.46 f T \sin \pi f T \\
 &= \sin \pi f T \{ 0.16 f^2 T^2 - 1.08 \}
 \end{aligned}
 \tag{9.505}$$

$$V_f(f) = \frac{1}{2} \frac{\sin \pi f T \{ 0.16 f^2 T^2 - 1.08 \}}{\pi f (f^2 T^2 - 1)} = \frac{\sin \pi f T (0.54 - 0.08 f^2 T^2)}{\pi f (1 - f^2 T^2)}.
 \tag{9.506}$$

The form of the Hamming window with $A = 1$ and $T = 1$ and its spectrum are shown in Fig. 9.70.

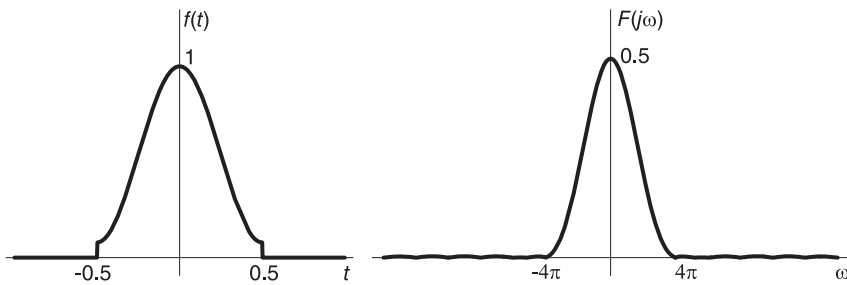


FIGURE 9.70 Hamming window and transform.

9.56 Problems

Problem 9.1 a) Evaluate analytically the transfer function $H(s)$ of a lowpass Butterworth filter given the following specifications:

Gain at zero frequency = R dB; a constant. At normalized frequency $\omega = 1$ the gain is $(R - 3)$ dB at $\omega = 4$ the gain is less than or equal to $(R - 48)$ dB.

b) The objective is to design a bandpass Butterworth filter with a maximum gain G dB and lower and upper 3-dB cut-off frequencies 1500 Hz and 2000 Hz. Show the transformation required to convert the lowpass filter of part a) to this bandpass filter.

Problem 9.2 a) Evaluate the transfer function of a filter, given the following specification:

Frequency	Attenuation
0	0dB
1	-1.5dB
2	-12dB

b) Rewrite the transfer function if the attenuations are 10, 8.5, and -2 , respectively.

Problem 9.3 Use the lowpass filter designed in Problem 9.2 to evaluate the transfer function of a bandpass and bandstop filters with edge frequencies

$$\omega_1 = 2\pi \times 750 \text{ r/s}, \quad \omega_2 = 2\pi \times 1200 \text{ r/s}.$$

Evaluate the transfer function of a highpass filter of cut-off frequency of $2\pi \times 500$ r/s.

Problem 9.4 Evaluate the transfer function $H_{BS}(s)$ of a bandstop Chebyshev filter having the following specifications:

Maximum gain in pass-band 0 dB. Attenuation in pass-band ≤ 1 dB. Stop-band attenuation ≥ 40 dB. Pass-band edge frequencies

$$\omega_l = 2\pi \times 900 \text{ r/s}$$

$$\omega_h = 2\pi \times 4000 \text{ r/s}.$$

Stop-band edge frequencies

$$\omega_2 = 2\pi \times 2200 \text{ r/s}$$

$$\omega_3 = 2\pi \times 2900 \text{ r/s}.$$

Problem 9.5 Evaluate the transfer function $H_{LP}(s)$ of a prototype lowpass fifth order Butterworth filter of maximal gain 0 dB and attenuation of 3 dB at normalized frequency $\omega = 1$. Show the transformation needed to convert this filter into a bandstop filter of 3 dB edge frequencies $\omega_l = 2\pi \times 90$ r/s and $\omega_h = 2\pi \times 110$ r/s.

Problem 9.6 Let $H_{LP}(s)$ be the lowpass prototype sixth order filter transfer function (having an attenuation of 3 dB at $\omega = 1$). The objective is to design a sixth order highpass filter having an attenuation of 1.5 dB at $\omega = 1$ and a maximum gain of 0 dB.

What transformation is needed to convert the lowpass transfer function $H_{LP}(s)$ into the transfer function $H_{HP}(s)$ of the highpass filter?

Problem 9.7 Evaluate the transfer function $H_{BS}(s)$ of a bandstop Butterworth filter having the following specifications.

Frequency	Gain
0, ∞	10 dB
$2\pi \times 500$, $2\pi \times 1500$	≥ 9 dB
$2\pi \times 800$, $2\pi \times 930$	≤ 0 dB

Problem 9.8 Repeat the last problem where now the specifications are

Frequency	Gain
0, ∞	10 dB
$2\pi \times 500$, $2\pi \times 1500$	≥ 7 dB
$2\pi \times 800$, $2\pi \times 930$	≤ 0 dB

Problem 9.9 Evaluate the transfer function $H(s)$ of a Butterworth lowpass filter having the following specifications.

Frequency	Gain
0	5 dB
1	2 dB
1.5	≤ -9 dB

Problem 9.10 Starting from an eighth order Butterworth lowpass filter prototype with gain 0 dB at zero frequency and 3 dB attenuation at the cut-off frequency $\omega = 1$, what transformation is needed to obtain a Butterworth highpass filter with maximum gain 0 dB and a 1.5 dB attenuation at the cut-off frequency $\omega = 1$?

Problem 9.11 Given

$$|H(j\omega)|^2 = (\omega^2 + 4) / (\omega^2 + 1).$$

a) Sketch the amplitude squared response $|H(j\omega)|^2$ in dB versus the frequency ω indicating the frequency values corresponding to 4, 3.5, 1.5, and 1 dB gain levels.

b) Evaluate the transfer function $H(s)$ of a filter having $|H(j\omega)|^2$ as the amplitude-squared spectrum.

c) Sketch the amplitude spectrum $|G(j\omega)|$ of the frequency response $G(j\omega)$ of the filter of which the transfer function is given by

$$G(s) = H(s)|_{s \rightarrow 8\pi \times 10^6 / s}.$$

Problem 9.12 Consider the design of a bandpass Butterworth filter having the following specifications:

a) Evaluate the filter transfer function using a lowpass to bandpass transformation.
 b) Evaluate the filter transfer function by realizing the filter as a cascade of lowpass and a highpass filters.

c) Considering the orders of the numerator and denominator polynomials of the transfer functions obtained in the two approaches a) and b) which filter would be simpler to realize.

Frequency	Gain
Pass-band	Maximum 0 dB
$2\pi \times 1000$ and $2\pi \times 2000$	≥ -1 dB
$2\pi \times 500$ and $2\pi \times 3000$	≤ -25 dB

Problem 9.13 To generate a sinusoid of frequency 1 kHz a train $p(t)$ of alternating rectangles is used. The train has a frequency of repetition of $f = 1$ kHz and can be written in the form

$$p(t) = \sum_{n=-\infty}^{\infty} p_0(t - nT), \quad T = 1/f$$

where

$$p_0(t) = \begin{cases} 1, & |t| < T/4 \\ -1, & T/4 < |t| < T/2 \\ 0, & \text{otherwise} \end{cases}$$

This train is applied to the input of a lowpass Butterworth filter which should attenuate all frequency components above the fundamental frequency, thus leading to an approximation of the sinusoid.

Evaluate and sketch the Fourier transform $P(j\omega)$ of the train $p(t)$. Evaluate the transfer function $H(s)$ of the lowest-order Butterworth filter ensuring that the resulting 1 kHz sinusoid have an amplitude of at least 1 volt, and that all higher harmonics do not exceed 0.03 volt in amplitude.

Problem 9.14 Evaluate the transfer function $H(s)$ of a Butterworth lowpass filter of order 4 of a maximum response of 0 dB and a gain of -1.5 dB at the frequency $f = 100$ kHz. At what frequency does the filter have a gain of -3 dB?

Problem 9.15 Consider the continuous-time rectangular, triangular (Bartlett), Hanning and Hamming windows.

a) Plot these windows spectra on the same frequency axis with their peaks normalized to the same value showing their first three lobes (on a normal, not logarithmic scale) thus allowing a visual comparison of their lobe widths and the decay of the side lobes. Which of the windows has the narrowest main lobe and which has the widest? The width of the lobe being the frequency corresponding to the point that is 3 dB below the maximum point. Which window has the biggest first side-lobe?

b) Plot the same spectra with the vertical axis now expressed in decibels.

Problem 9.16 Verify the spectra of the continuous time Hanning and Hamming windows by evaluating and plotting their Fourier transforms using Mathematica or Maple and comparing them with those obtained analytically.

Problem 9.17 Consider the signal

$$v(t) = \cos \beta t + \cos \gamma t$$

where

$$\beta = 7 \times 2\pi/T$$

and

$$\gamma = 9 \times 2\pi/T.$$

The signal $v(t)$ is multiplied by a window $w(t)$ of overall width T . Evaluate and sketch the spectrum $W(j\omega)$ and that of the product $z(t) = v(t)w(t)$ assuming $T = 1$ s for the four different windows: rectangular, triangular (Bartlett), Hanning and Hamming. Repeat the above if $\gamma = 8 \times 2\pi/T$ instead. What conclusions can be made regarding the possibility of detecting the signal frequency components. How can such detection be improved irrespective of the kind of window used?

Problem 9.18 Design an elliptic filter having a ripple of $\delta_1 = 0.01$ in the pass-band and $\delta_2 = 0.01$ in the stop-band, with a pass-band edge frequency of 1 kHz and a stop-band edge frequency of 1.3 kHz. Evaluate the filter order N , the poles and zeros of its transfer function $H(s)$. Evaluate and plot the Chebyshev rational function $G(\omega)$ and the magnitude squared spectrum $|H(j\omega)|^2$. Evaluate the zeros and poles of $G(\omega)$ and the maxima/minima of $G(\omega)$ and $|H(j\omega)|$ in the pass-band and the stop-band.

Problem 9.19 Let

$$x = Ae^{j\theta}$$

and

$$w(x) = \operatorname{sn}(x, k).$$

a) Evaluate w_r , the real part of $w(x)$, and w_i , the imaginary part, as function of A , θ and k .

b) Knowing that $\operatorname{cn}(u + 2K) = -\operatorname{cn} u$, show that $\operatorname{cn} u$ has a period $4K$.

Problem 9.20 A lowpass filter of cut-off frequency 3 kHz is required. The attenuation should be at least 30 dB at 6 kHz and not more than 1.5 dB in the pass-band, where the maximum response should be 0 dB.

a) Evaluate the minimum Butterworth filter order.

b) Evaluate the minimum Chebyshev filter order.

Problem 9.21 Evaluate the filter transfer function meeting the following specifications:

a) Butterworth, lowpass, – cut-off frequency 100 r/s

– maximum response 0 dB

– attenuation at the cut-off frequency: 1 dB

– attenuation of at least 30 dB at 300 r/s

b) Chebyshev, lowpass, – cut-off frequency: 2 kHz

– maximum response: 0 dB

– maximum attenuation in the pass-band 1 dB

– attenuation of at least 30 dB at 4 kHz

Problem 9.22 Evaluate the transfer function $H(s)$ of a filter satisfying the following specifications:

– Chebyshev highpass

– Cut-off frequency 300 Hz

– Maximal response +20 dB

– Response at cut-off frequency +19 dB

– Response less than -22 dB in the frequency band 0 to 100 Hz

Problem 9.23 Evaluate the transfer function $H(s)$ of a filter satisfying the following specifications:

– Chebyshev highpass

– Cut-off frequency 300 Hz

- Maximal response +20 dB
- Response at cut-off frequency +19 dB
- Response less than -22 dB in the frequency band 0 to 100 Hz

Problem 9.24 The objective is to design for an audio system a tonality controller of three frequency bands. The controller has three filters, namely, a lowpass, a bandpass and a high-pass filter for the corresponding frequency ranges, and have the following properties:

Filter 1

- Butterworth, lowpass
- Cut-off frequency: 500 Hz
- Maximum response: 0 dB
- Attenuation at the cut-off frequency: 3 dB
- Attenuation at 1 kHz: 20 dB minimum

Filter 2

- Butterworth bandpass
- Edge frequencies: 500 Hz and 2 kHz
- Maximum response: 0 dB
- Attenuation at the edge frequencies: 3 dB
- Attenuation at 200 Hz and 2 kHz: 20 dB minimum

Filter 3

- Butterworth highpass
- Cut-off frequency: 2 kHz
- Maximum response: 0 dB
- Attenuation at the cut-off frequency: 3 dB
- Attenuation at 1 kHz: 20 dB minimum

- a) Evaluate the transfer function of each of the three filters.
- b) If the frequency responses of these filters should be increased or reduced by 10 dB, how should the transfer function be altered?

Problem 9.25 Evaluate the transfer function $H(s)$ of a least-order filter satisfying the following specifications:

- Butterworth bandpass
- Cut-off frequency 697 Hz and 852 Hz
- Maximum response: 0 dB
- Attenuation at pass-band edge frequencies: 10 dB

Problem 9.26 To prevent illegal copying of analog audio signals it is proposed to use a coder which employs a filter to cut off the frequency band (3715 to 3965 Hz). Signal recorders would be so constructed as to detect a gap in the spectrum and stop illegal recording.

The proposed filter would have the following properties:

- Butterworth, bandstop
- Cut-off edge frequencies 3715 Hz and 3965 Hz
- Maximal response 0 dB
- Attenuation at cut-off frequencies: 3 dB
- Minimum attenuation of 60 dB at 3800 Hz and 3880 Hz

Evaluate the transfer function of the coding filter.

Problem 9.27 Given the transfer function of a filter

$$H(s) = \frac{3}{s^2 + 3s + 3},$$

show how to evaluate the group delay of the filter as a function of the frequency ω . Deduce from the delay expression obtained the filter's delay at frequencies $\omega = 0$ and $\omega = 2$. Verify the result by referring to the filter's delay figures.

Problem 9.28 a) For a Bessel type 1 filter of order 2 specify the transfer function and evaluate the group delay and the value of its delay at frequency $\omega = 1$ relative to its zero-frequency delay. Evaluate the filter order so that the delay at frequency $\omega = 5$ be greater than or equal to half its value at zero frequency.

b) Evaluate the transfer function and poles of a type 1 Bessel filter of the second order producing an attenuation of 0 dB at $\omega = 0$. Evaluate the filter impulse response $h(t)$.

9.57 Answers to Selected Problems

Problem 9.1

a) $H(s) = 10^{R/20} / (s^4 + 2.613s^3 + 3.414s^2 + 2.613s + 1)$.

b) $B = 2\pi(2000 - 1500) = 2\pi \cdot 500$, $\omega_0 = 2\pi \times 1732.1$ r/s,

$$H_{BP}(s) = \frac{10^{R/20}}{s^4 + 2.613s^3 + 3.414s^2 + 2.613s + 1} \Big|_{s \rightarrow \frac{s^2 + \omega_0^2}{Bs}}$$

Problem 9.2

$$H(s) = \frac{2.0761}{s^3 + 2.5514s^2 + 3.2548s + 2.0761}$$

$$H(s) = \frac{5.4962 \times 10^{12}}{s^3 + 2.4046 \times 10^4 s^2 + 2.8911 \times 10^8 s + 1.738 \times 10^{12}}$$

Problem 9.3 $H_{HP}(s) = s^3 / (s^3 + 1.885 \times 10^4 s^2 + 1.777s + 8.372 \times 10^{11})$.

Problem 9.4 See Fig. 9.71 $H_{BS}(s) = N(s) / D(s)$ where

$$N(s) = s^{10} + 7.106 \times 10^8 s^8 + 2.020 \times 10^{17} s^6 + 2.871 \times 10^{25} s^4 + 2.04 \times 10^{33} s^2 + 5.798 \times 10^{40}$$

$$D(s) = s^{10} + 92075s^9 + 3.720 \times 10^9 s^8 + 1.54 \times 10^{14} s^7 + 2.583 \times 10^{18} s^6 + 6.288 \times 10^{22} s^5 + 3.671 \times 10^{26} s^4 + 3.11 \times 10^{30} s^3 + 1.068 \times 10^{34} s^2 + 3.757 \times 10^{37} s + 5.798 \times 10^{40}$$

We obtain the same results as just found.

Problem 9.5

$$H(s) = \frac{1}{s^5 + 3.236s^4 + 5.236s^3 + 5.236s^2 + 3.236s + 1}$$

$$H_{BS}(s) = H_{LP}(s) \Big|_{s \rightarrow Bs / (s^2 + \omega_0^2)}$$

Problem 9.6

$$H_{HP}(s) = \frac{1}{s^6 + 3.86s^5 + 7.46s^4 + 9.14s^3 + 7.46s^2 + 3.86s + 1} \Big|_{s \rightarrow 0.9289/s}$$

Problem 9.7 See Fig. 9.72.

$$H_{BS}(s) = K \frac{s^2 + b_3}{s^2 + a_2s + a_3}$$

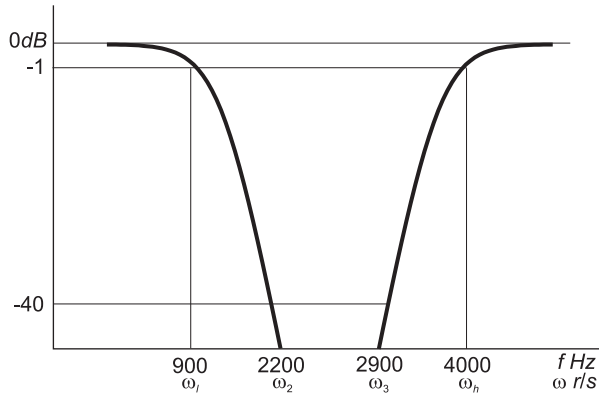


FIGURE 9.71 Figure for Problem 9.4.

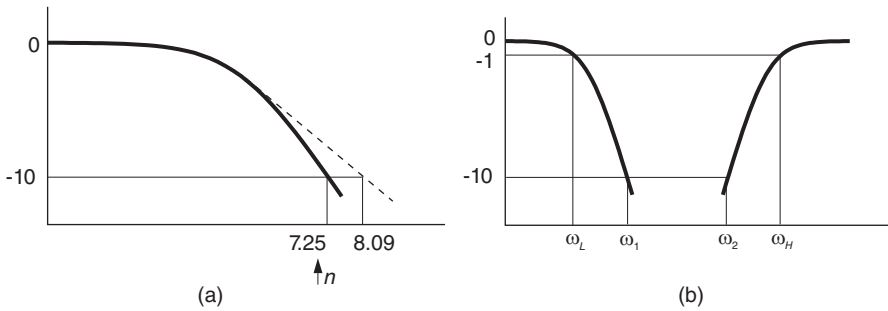


FIGURE 9.72 Figure for Problem 9.7.

where $K = 3.1623$, $a_3 = b_3 = \omega_0^2 = 2.96 \times 10^7$, $a_2 = \varepsilon B = 3.1972 \times 10^3$

Problem 9.8

$$H_{BS}(s) = 3.1623 \frac{s^2 + 2.96 \times 10^7}{s^2 + 6.28 \times 10^3 s + 2.96 \times 10^7}$$

Problem 9.9 $H(s) = K/(s^4 + 2 \cdot 613s^3 + 3 \cdot 414s^2 + 2 \cdot 613s + 1)$, $10 \log_{10} K^2 = 5$, $K = 1 \cdot 7783$.

Problem 9.10

$$s \xrightarrow{\varepsilon^{1/n}} \varepsilon^{1/n} s \xrightarrow{1/\varepsilon} \varepsilon^{1/n} / s$$

Problem 9.11

- b) $H(s) = (s - 2)/(s + 1)$
- c) See Fig. 9.73.

Problem 9.13 See Figs. 9.74 and 9.75.

$$H(s) = \frac{1}{1 + 0.00029s + 4.237 \cdot 10^{-8}s^2 + 3.083 \cdot 10^{-12}s^3}$$

Problem 9.14

$$H(s) = \frac{1}{s^4 + 2.613s^3 + 3.414s^2 + 2.613s + 1}$$

$H_{\varepsilon, \text{denorm}}(s) = 1/D(s)$

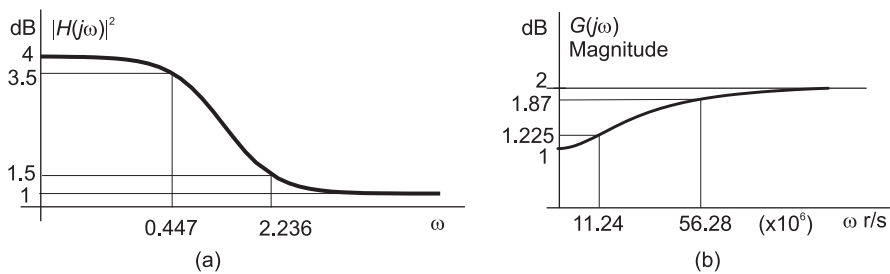


FIGURE 9.73 Filter responses of Problem 9.11.

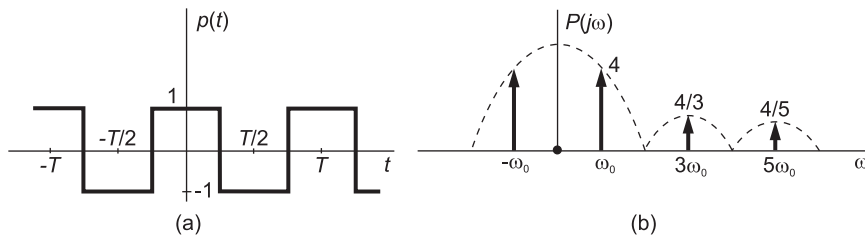


FIGURE 9.74 A train and spectrum of Problem 9.13.

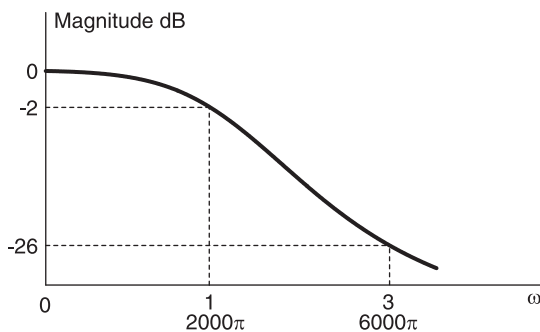


FIGURE 9.75 Filter response, Problem 9.13.

$$D(s) = 1 + 3.72 \times 10^{-6}s + 6.93 \times 10^{-12}s^2 + 7.56 \times 10^{-18}s^3 + 4.12 \times 10^{-24}s^4$$

Problem 9.15

The rectangular window has the narrowest main lobe. The Hanning window has the widest main lobe. The rectangular window has the biggest first side lobe.

Problem 9.17

Increasing the window width T improves the resolution, the spectrum of a truncated sinusoid becoming sharper, tending toward an impulse. See Fig. 9.76.

Problem 9.19

$$w = w_r + jw_i = \frac{sn a dn(b, k') + j cn a dn a sn(b, k') cn(b, k')}{1 - dn^2 a sn^2(b, k')}$$

Problem 9.20

- c) $h_a(t) = e^{-t}u(t) - e^{-0.5t} \cos 8.66t u(t) + 0.5e^{-0.5t} \sin 8.66t u(t)$.
- d) $h[n] = [a^n - b^n \cos \beta n + 0.5b^n \sin \beta n] u[n]$, where $a = e^{-1}$, $b = e^{-0.5}$, $\beta = 8.66$.

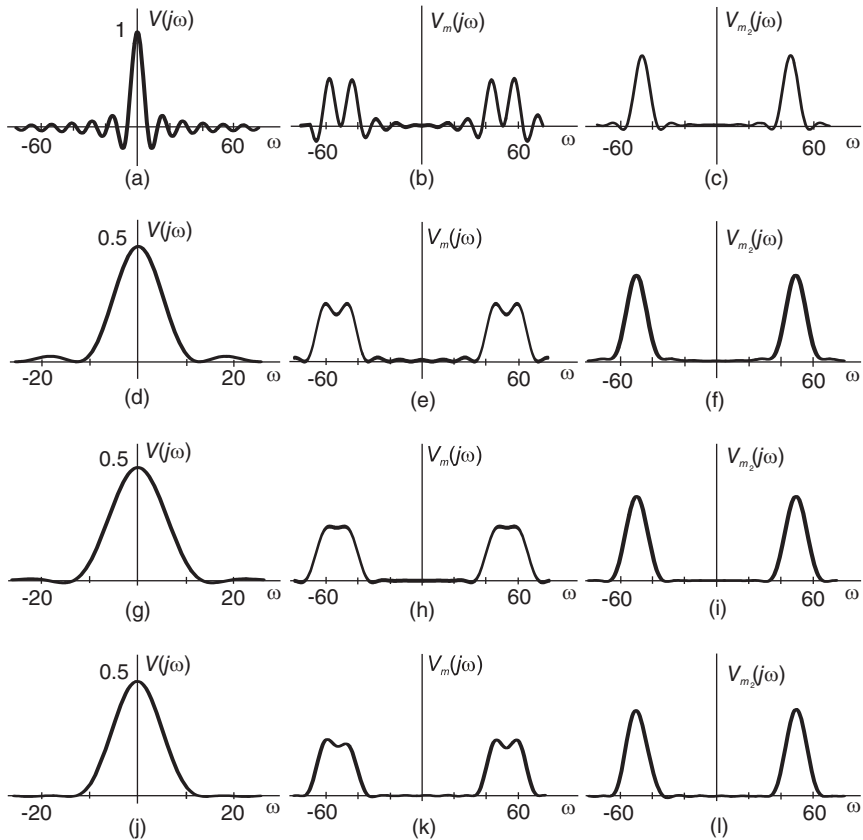


FIGURE 9.76 Figure for Problem 9.17.

$$e) H(z) = \frac{1}{1 - az^{-1}} - \frac{1 - bz^{-1} \cos \beta}{1 - 2bz^{-1} \cos \beta + b^2z^{-2}} + 0.5 \frac{bz^{-1} \sin \beta}{1 - 2bz^{-1} \cos \beta + b^2z^{-2}}$$

Problem 9.21

- a) $n \geq 6$.
- b) $n \geq 4$.

Problem 9.22

$$a) H_{\text{denorm}}(s) = \frac{1}{s^4 + 2.61s^3 + 3.41s^2 + 2.61s + 1} \Big|_{s \rightarrow \frac{\varepsilon^{1/4}s}{100} = 8.446 \times 10^{-3}s}$$

$$b) H_{\text{denorm}}(s) = \frac{0.25}{s^4 + 0.95s^3 + 1.45s^2 + 0.74s + 0.28} \Big|_{s \rightarrow s/4000\pi}$$

Problem 9.23

$$H_{\text{HPdenorm}}(s) = \frac{2.5}{s^4 + 0.95s^3 + 1.45s^2 + 0.74s + 0.28} \Big|_{s \rightarrow 600\pi/s}$$

Problem 9.24

$$a) \text{Filter 1 } H_{\text{denorm}}(s) = \frac{1}{s^4 + 2.61s^3 + 3.41s^2 + 2.61s + 1} \Big|_{s \rightarrow s/(1000\pi)}$$

$$\text{Filter 2 } H_{\text{BPF}}(s) = \frac{1}{s^3 + 2s^2 + 2s + 1} \Big|_{s \rightarrow (s^2 + \omega_0^2)/(Bs)}, \text{ where } \omega_0^2 = 4\pi^2 \times 10^6 \text{ and } B = 3000\pi.$$

Filter 3 $H_{\text{HPdenorm}}(s) = \frac{1}{s^4 + 0.95s^3 + 1.45s^2 + 0.74s + 0.28} \Big|_{s \rightarrow 4000\pi/s}$.

b) The transfer functions should be multiplied by the factor 3.16 and 0.316, respectively.

Problem 9.25

$$H_{\text{bandpass}}(s) = \frac{1}{3s + 1} \Big|_{s \rightarrow (s^2 + \omega_0^2)/(Bs)}$$

where $\omega_0^2 = (2\pi)^2 \times 697 \times 852 = 2.375\pi^2 \times 10^6$, $B = 2\pi(852 - 697) = 310\pi$.

Problem 9.26 The stopband filter transfer function is

$$H_{\text{stopband}}(s) = \frac{1}{s^7 + 4.5s^6 + 10.1s^5 + 14.6s^4 + 14.6s^3 + 10.1s^2 + 4.5s + 1} \Big|_{s \rightarrow Bs/(s^2 + \omega_0^2)}$$

where $\omega_0^2 = 58,92\pi^2 \times 10^6$, $B = 500\pi$.

Problem 9.27

$$\tau = \frac{3(3 + w^2)}{9 + 3w^2 + w^4}$$

The delay at $\omega = 0$ is $\tau = 1$, and at $\omega = 2$ is $\tau = 0.5675$.

Problem 9.28

a) order is $n \geq 5$. b) $h(t) = 3.4642 e^{-1.5t} \sin(0.866t) u(t)$.

This page intentionally left blank

10

Passive and Active Filters

In this chapter we study the design of passive and active continuous-time domain filters.

10.1 Design of Passive Filters

This chapter explores passive and active circuit realization of continuous-time filters. We have seen how to evaluate the transfer function of a filter such as Butterworth, Chebyshev, elliptic or Bessel–Thomson, given frequency response specifications. Having evaluated the filter transfer function $H(s)$ we have also seen how to realize it as an active filter using integrators, constant multipliers and adders.

In this section we consider the problem of realizing lowpass filters as passive networks, that is, electric circuits made up of resistors, inductors and capacitors without the need for integrators. Converting these to bandpass, bandstop and highpass filters can be subsequently effected by well-known circuit elements transformation techniques, as seen later on in this chapter. In high frequency and microwave applications in particular, passive filters are of great importance. In integrated circuit technology means exist, moreover, for realizing inductances by equivalent components.

From network theory, ladder networks such as those shown in Fig. 10.1, are well suited for implementing Butterworth, Chebyshev and Bessel–Thomson filters. Figures 10.1(a) and (b) show voltage driven and current driven networks, respectively, terminated in a 1 ohm resistor, which are suitable for realizing even-ordered lowpass filters. For odd-ordered lowpass filters, Figures 10.1(c) and (d) show current driven and voltage driven networks, respectively, similarly terminated in a 1 ohm resistor. We shall also see other ladder networks well suited for implementing Caueer elliptic filters.

10.2 Design of Passive Ladder Lowpass Filters

In this section we study an approach to the design of general order lowpass filters in the form of passive ladder networks. Consider the current-driven inductance capacitance (LC) passive circuit terminated in a 1 ohm resistance shown in Fig. 10.1(c) and redrawn with components replaced by their impedances in Fig. 10.2. We shall determine the recursive relations describing the voltage and current values $v_1, v_2, i_0, i_1, \dots$, the circuit input impedance and its transfer function.

By starting from the right side of the circuit we can deduce a recursive relation giving the value of each voltage v_k as a function of the voltage v_{k-1} and each current i_k as a function of the current i_{k-1} .

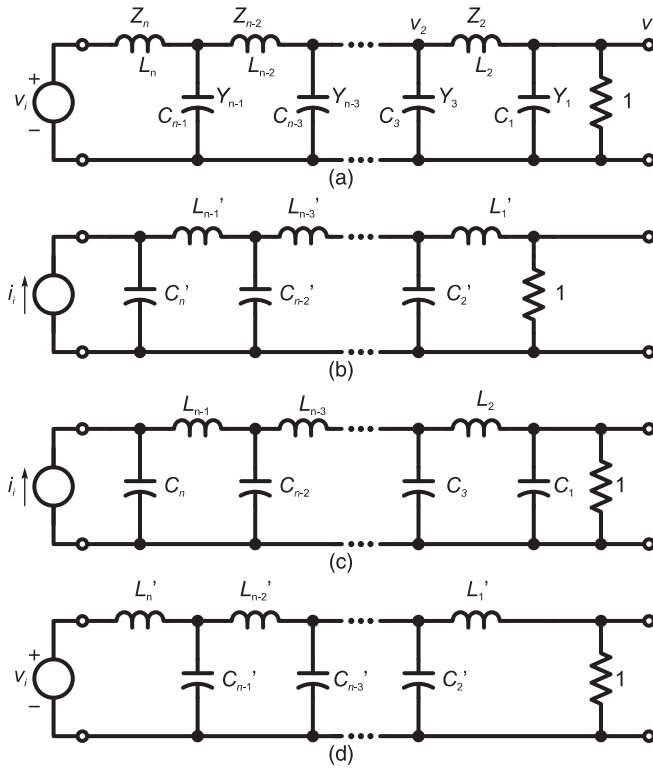


FIGURE 10.1 (a) Voltage-driven passive ladder network for even-ordered lowpass filters (LP), (b) current-driven network for even-ordered lowpass filters, (c) current-driven network for odd-ordered LP filter, (d) voltage-driven network for odd-ordered LP filter.

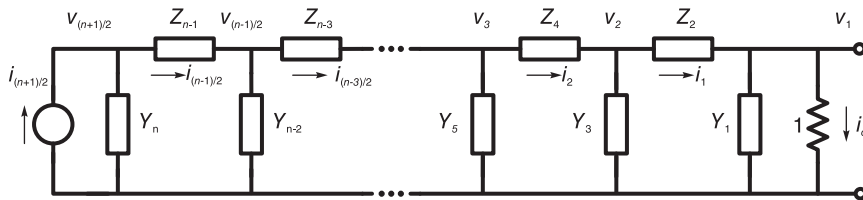


FIGURE 10.2 Ladder network with impedances.

We can write the voltage and current equations

$$V_1(s) = I_0(s) \tag{10.1}$$

$$I_1(s) = I_0(s) + V_1(s) Y_1(s) \tag{10.2}$$

$$V_2(s) = V_1(s) + I_1(s) Z_2(s) \tag{10.3}$$

$$I_2(s) = I_1(s) + V_2(s) Y_3(s) \tag{10.4}$$

and in general

$$V_k(s) = V_{k-1}(s) + I_{k-1}(s) Z_{2(k-1)}(s), \quad k = 2, 3, \dots, (n+1)/2 \tag{10.5}$$

$$I_k(s) = I_{k-1}(s) + V_k(s) Y_{2k-1}(s), \quad k = 1, 2, \dots, (n+1)/2. \tag{10.6}$$

As an example consider the ladder network containing $n = 3$ components C_1, L_2 and C_3 shown in Fig. 10.3(a), where $C_1 = 1/2, L_2 = 4/3$ and $C_3 = 3/2$. We shall see that this passive ladder network is in fact a realization of a third order Butterworth filter.

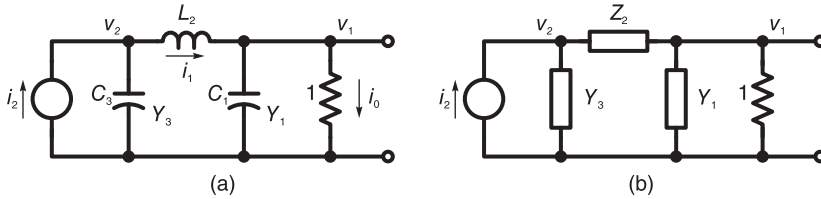


FIGURE 10.3 Third order network and its impedance representation.

To proceed as in the analysis of general ladder networks as given above we redraw the circuit with the impedance $Z_2 = L_2s$ and admittances $Y_1(s) = C_1s$ and $Y_3(s) = C_3s$ as shown in Fig. 10.3(b). The voltage-current equations are

$$V_1(s) = I_0(s) \tag{10.7}$$

$$V_2(s) = V_1(s) + I_1(s) Z_2(s) \tag{10.8}$$

$$I_2(s) = I_1(s) + V_2(s) Y_3(s) \tag{10.9}$$

$$I_1(s) = I_0(s) + V_1(s) Y_1(s) = I_0(s) + I_0(s) C_1s = I_0(s) (1 + C_1s) \tag{10.10}$$

$$\begin{aligned} V_2(s) &= V_1(s) + I_1(s) Z_2(s) = I_0(s) + I_0(s) (1 + C_1s) L_2s \\ &= I_0(s) (1 + L_2s + C_1L_2s^2) \triangleq I_0(s)P(s) \end{aligned} \tag{10.11}$$

$$\begin{aligned} I_2(s) &= I_1(s) + V_2(s) Y_3(s) \\ &= I_0(s) (1 + C_1s) + C_3sI_0(s) (1 + L_2s + C_1L_2s^2) \\ &= I_0(s) (1 + C_1s + C_3s + C_2L_2s^2 + C_1C_3L_2s^3) \triangleq I_0(s)Q(s). \end{aligned} \tag{10.12}$$

The input impedance is given by

$$Z(s) \equiv Z_{in}(s) = \frac{V_2(s)}{I_2(s)} = \frac{1 + L_2s + C_1L_2s^2}{1 + (C_1 + C_3)s + C_3L_2s^2 + C_1C_3L_2s^3}. \tag{10.13}$$

Substituting for C_1, L_2 and C_3

$$Z(s) = \frac{1 + (4/3)s + (2/3)s^2}{1 + 2s + 2s^2 + s^3}. \tag{10.14}$$

We now proceed to establish a relation between the circuit input impedance $Z(s) \equiv Z_{in}(s)$ and its transfer function $H(s)$. We may rewrite the impedance in the form

$$Z(s) = \frac{m_1(s) + n_1(s)}{m_2(s) + n_2(s)} \tag{10.15}$$

where $m_1(s)$ is the even polynomial and $n_1(s)$ the odd one of the numerator, and $m_2(s)$ and $n_2(s)$ are the even and odd polynomials, respectively, of the denominator.

$$m_1(s) = 1 + \frac{2}{3}s^2, \quad n_1(s) = \frac{4}{3}s \tag{10.16}$$

$$m_2(s) = 1 + 2s^2, \quad n_2(s) = 2s + s^3. \tag{10.17}$$

The transfer function is given by

$$\begin{aligned} H(s) &= \frac{V_1(s)}{I_2(s)} = \frac{1}{1 + (C_1 + C_3)s + C_3L_2s^2 + C_1C_3L_2s^3} \\ &= \frac{1}{1 + 2s + 2s^2 + s^3} = \frac{1}{m_2(s) + n_2(s)}. \end{aligned} \quad (10.18)$$

which is the third order Butterworth filter transfer function. We note that the impedance and transfer function expressions have the same denominator $m_2(s) + n_2(s)$. This simple example will serve to illustrate the more general approach that follows.

10.3 Analysis of a General Order Passive Ladder Network

Consider now a general order passive ladder network. As the last example shows we can evaluate the equations recursively and thus deduce the value of the input impedance and that of the transfer function. In particular, for a general order n passive ladder network we obtain

$$V_1(s) = I_o(s)P(s) \quad (10.19)$$

and

$$I_i(s) = I_o(s)Q(s) \quad (10.20)$$

where $P(s)$ and $Q(s)$ are polynomials in s ; hence

$$Z(s) \equiv Z_{in}(s) = \frac{V_1(s)}{I_i(s)} = \frac{P(s)}{Q(s)} \quad (10.21)$$

$$H(s) = \frac{V_o(s)}{I_i(s)} = \frac{I_o(s)}{I_i(s)} = \frac{1}{Q(s)}. \quad (10.22)$$

The polynomials $P(s)$ and $Q(s)$ can be written in the form

$$P(s) = 1 + a_1s + a_2s^2 + \dots + a_{n-1}s^{n-1} \quad (10.23)$$

$$Q(s) = 1 + b_1s + b_2s^2 + \dots + b_ns^n. \quad (10.24)$$

Letting as before $m_1(s)$ and $n_1(s)$ be the even polynomial and odd polynomial components, respectively, of the polynomial $P(s)$, and let $m_2(s)$ and $n_2(s)$ be the even and odd polynomial components of the polynomial $Q(s)$, we can write

$$Z(s) = \frac{P(s)}{Q(s)} = \frac{1 + a_1s + a_2s^2 + \dots + a_{n-1}s^{n-1}}{1 + b_1s + b_2s^2 + \dots + b_ns^n} = \frac{m_1(s) + n_1(s)}{m_2(s) + n_2(s)} \quad (10.25)$$

$$H(s) = \frac{1}{Q(s)} = \frac{1}{m_2(s) + n_2(s)} \quad (10.26)$$

$$m_1(s) = 1 + a_2s^2 + a_4s^4 + \dots + a_{n-1}s^{n-1} \quad (10.27)$$

$$n_1(s) = a_1s + a_3s^3 + a_5s^5 + \dots + a_{n-2}s^{n-2} \quad (10.28)$$

$$m_2(s) = 1 + b_2s^2 + b_4s^4 + \dots + b_{n-1}s^{n-1} \quad (10.29)$$

$$n_2(s) = b_1s + b_3s^3 + b_5s^5 + \dots + b_ns^n. \quad (10.30)$$

To deduce the input impedance $Z(s)$ from a given transfer function $H(s)$ we note that

$$\begin{aligned} Z(s) + Z(-s) &= \frac{m_1(s) + n_1(s)}{m_2(s) + n_2(s)} + \frac{m_1(s) - n_1(s)}{m_2(s) - n_2(s)} \\ &= \frac{2\{m_1(s)m_2(s) - n_1(s)n_2(s)\}}{m_2^2(s) - n_2^2(s)}. \end{aligned} \tag{10.31}$$

We shall show in the following section, through power transfer considerations, that the factor $m_1m_2 - n_1n_2$ is equal to 1. For now let us verify this by direct evaluation in the context of the Butterworth filter example of Fig. 10.3 considered above. We can write

$$m_1(s)m_2(s) = 1 + c_2s^2 + c_4s^4 + \dots + c_{2n-2}s^{2n-2} \tag{10.32}$$

$$n_1(s)n_2(s) = d_2s^2 + d_4s^4 + d_6s^6 + \dots + d_{2n-2}s^{2n-2} \tag{10.33}$$

where

$$c_2 = a_2 + b_2 \tag{10.34}$$

$$c_4 = a_2b_2 + a_4 + b_4 \tag{10.35}$$

$$c_6 = a_2b_4 + a_4b_2 + a_6 + b_6 \tag{10.36}$$

...

$$d_2 = a_1b_1 \tag{10.37}$$

$$d_4 = a_1b_3 + a_3b_1 \tag{10.38}$$

$$d_6 = a_1b_5 + a_5b_1 + a_3b_3. \tag{10.39}$$

With $n = 3$ we have

$$a_1 = L_2, \quad a_2 = C_1L_2, \quad b_1 = C_1 + C_3, \quad b_2 = C_3L_2, \quad b_3 = C_1C_3L_2. \tag{10.40}$$

Hence

$$c_2 = a_2 + b_2 = C_1L_2 + C_3L_2 = a_1b_1 = d_2 \tag{10.41}$$

and

$$c_4 = a_2b_2 = C_1C_3L_2^2 = a_1b_3 = d_4 \tag{10.42}$$

and for a general order n

$$c_i = d_i, \quad i = 2, 4, 6, \dots \tag{10.43}$$

We can therefore write

$$n_1(s)n_2(s) = c_2s^2 + c_4s^4 + \dots + c_{2n-2}s^{2n-2} = 1 + m_1(s)m_2(s) \tag{10.44}$$

i.e.

$$m_1(s)m_2(s) - n_1(s)n_2(s) = 1 \tag{10.45}$$

as stated above. Hence

$$Z(s) + Z(-s) = \frac{2}{m_2^2(s) - n_2^2(s)}. \tag{10.46}$$

We may therefore write

$$Z(s) + Z(-s) = 2H(s)H(-s). \tag{10.47}$$

Knowing the filter transfer function $H(s)$ the required input impedance $Z(s)$ may be evaluated using this equation. Let

$$F(s) \triangleq H(s)H(-s) \tag{10.48}$$

i.e.

$$Z(s) + Z(-s) = 2F(s). \quad (10.49)$$

By effecting a partial fraction expansion we may write $F(s)$ in the form

$$F(s) = \sum_{i=1}^{2n} \frac{r_i}{(s - p_i)} \quad (10.50)$$

where r_i is the residue at the pole p_i . Suppose the poles are written such that p_1, p_2, \dots, p_n are located in the left-half s plane. The value of the input impedance $Z(s)$ is simply given by

$$Z(s) = 2 \sum_{i=1}^n \frac{r_i}{(s - p_i)} \quad (10.51)$$

where the pole locations in the left-half s plane ensures filter stability.

Given a filter magnitude-squared spectrum $|H(j\omega)|^2$, therefore, we write

$$H(s)H(-s) = |H(j\omega)|^2 \Big|_{\omega=-js} \quad (10.52)$$

thus deducing the value of $F(s) = H(s)H(-s)$, wherefrom the value of the filter transfer function $H(s)$ can be deduced. The required circuit input impedance may be found by effecting a partial fraction expansion of $F(s)$ and collecting the terms associated with the left-half s plane poles. We may put the result obtained above in the form

$$\begin{aligned} \frac{1}{2} \{Z(s) + Z(-s)\} &\triangleq F(s) = H(s)H(-s) = \frac{A(-s^2)}{B(-s^2)} \\ &= \frac{A_0 - A_1s^2 + A_2s^4 - \dots + (-1)^n A_n s^{2n}}{B_0 - B_1s^2 + B_2s^4 - \dots + (-1)^n B_n s^{2n}}. \end{aligned} \quad (10.53)$$

With $s = j\omega$ we have

$$\Re\{Z(j\omega)\} = \frac{1}{2} \{Z(j\omega) + Z(-j\omega)\} = |H(j\omega)|^2 = \frac{A(\omega^2)}{B(\omega^2)}. \quad (10.54)$$

The following example illustrates the approach.

Example 10.1 Evaluate the passive ladder network input impedance $Z(s)$ corresponding to a lowpass Butterworth filter of order $n = 3$.

We have

$$\begin{aligned} |H(j\omega)|^2 &= \frac{1}{1 + \omega^6} \\ \Re\{Z(j\omega)\} &= \frac{1}{1 + \omega^6} = \frac{A(\omega^2)}{B(\omega^2)} \\ A(\omega^2) &= 1, \quad B(\omega^2) = 1 + \omega^6 \\ F(s) &= \frac{1}{2} \{Z(s) + Z(-s)\} = \frac{A(-s^2)}{B(-s^2)} = \frac{1}{1 - s^6} = \frac{-1}{s^6 - 1}. \end{aligned}$$

The poles of $F(s)$ are given by $s^6 = 1 = e^{j2\pi k}$, $s_k = e^{j2\pi k/6}$, $k = 0, 1, 2, \dots, 5$. The poles in the left-half plane are given by $p_1 = s_2 = e^{j2\pi/3}$, $p_2 = -1$, $p_3 = e^{-j2\pi/3}$. The residue at p_1 is given by

$$r_1 = \frac{-1}{(s - p_2)(s - p_3) \dots (s - p_6)} \Big|_{s=p_1} = \frac{-1}{v_1 v_2 v_3 v_4 v_5}$$

where v_1, v_2, \dots, v_5 are the vectors shown in Fig. 10.4(a).

$$v_1 = -1,$$

$$|v_2| = \sqrt{(1.5)^2 + (\sqrt{3}/2)^2} = 1.7321, \quad \arg[v_2] = \tan^{-1}\left(\frac{\sqrt{3}/2}{-1.5}\right) = 2.6180,$$

$$|v_3| = 2, \quad \arg[v_3] = 2.0944, \quad v_4 = j\sqrt{3}, \quad |v_5| = 1, \quad \arg[v_5] = \pi/3 = 1.0472.$$

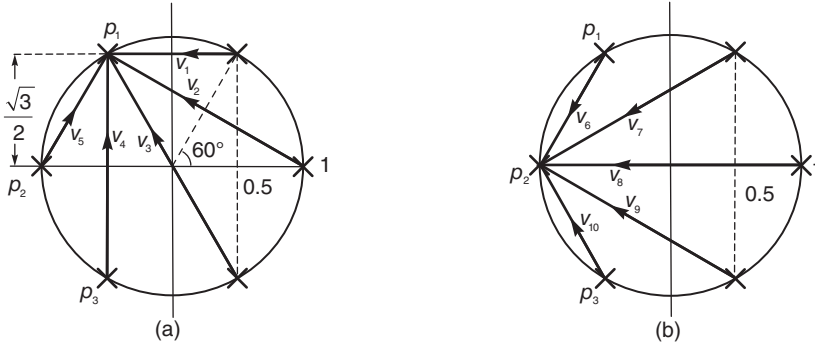


FIGURE 10.4 Vectorial evaluation of residues.

We obtain $r_1 = -0.1667e^{j2.094} = 0.1667e^{-j1.0472}$, $r_3 = r_1^* = 0.1667e^{j1.0472}$. From Fig. 10.4(b)

$$r_2 = \frac{1}{|v_6|^2 |v_7|^2 v_8} = \frac{1}{1 \cdot (1.5^2 + 0.75) (-2)} = -0.1667.$$

We deduce the value of $Z(s)$ by writing

$$\begin{aligned} Z(s) &= \frac{2r_1}{s - p_1} + \frac{2r_2}{s - p_2} + \frac{2r_3}{s - p_3} \\ &= \frac{0.333e^{-j1.0472}}{s - e^{j2\pi/3}} + \frac{-0.333}{s + 1} + \frac{0.333e^{j1.0472}}{s - e^{-j2\pi/3}} = \frac{(2/3)s^2 + (4/3)s + 1}{s^3 + 2s^2 + 2s + 1}. \end{aligned}$$

Note that for higher order systems a MATLAB[®] program using the instruction “residue” may be employed to expand $F(s)$ into partial fractions by evaluating the residues r_1, r_2, r_3 at the poles p_1, p_2, p_3 . The same instruction “residue” can subsequently be used to effect the inverse of the partial fraction expansion needed to evaluate the impedance $Z(s)$ as the ratio of two polynomials.

10.4 Input Impedance of a Single-Resistance Terminated Network

A short-cut approach to input impedance evaluation for the realization of a given transfer function may be formulated by referring to Fig. 10.5. This figure may serve as a model for the lossless network terminated in a resistor.

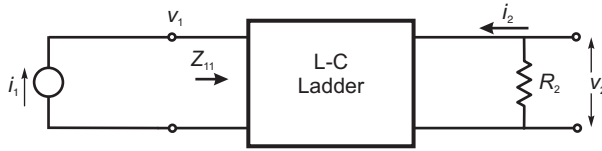


FIGURE 10.5 Resistance terminated two-port network.

For simplicity of presentation the resistor is taken to be $R_2 = 1$ ohm. By proper scaling the case of a general value of R_2 can be subsequently dealt with. As seen in the figure the input impedance of the lossless network is denoted Z_{11} . Since the two-port is lossless the average input power to the network from the source is equal to that delivered to the load. We may therefore write

$$|I_1(j\omega)|^2 \Re[Z_{11}(j\omega)] = |V_2(j\omega)|^2 \tag{10.55}$$

With $H(j\omega) = V_2(j\omega)/I_1(j\omega)$ we may write

$$\Re[Z_{11}(j\omega)] = |V_2(j\omega)|^2 / |I_1(j\omega)|^2 = |H(j\omega)|^2 \tag{10.56}$$

If $Z(s)$ denotes the input impedance, i.e. $Z \triangleq Z_{11}$, we may write

$$\Re[Z(j\omega)] = \frac{1}{2}[Z(j\omega) + Z(-j\omega)] = |H(j\omega)|^2 \tag{10.57}$$

and if Z_e denotes the even part of Z we may write

$$Z_e(s) = \frac{1}{2}[Z(s) + Z(-s)] = H(s)H(-s) \tag{10.58}$$

as asserted above in the context of the particular LC ladder networks shown in Fig. 10.1. Similar relations can be derived for the input admittance $Y(s) = 1/Z(s)$.

10.5 Evaluation of the Ladder Network Components

Having evaluated the input impedance $Z(s)$ we should evaluate the inductance (L) and capacitance (C) values of the ladder network. Consider the circuit shown in Fig. 10.6. The input impedance Z is given by

$$Z = Z_1 + Z_{1,2} \tag{10.59}$$

$$\frac{1}{Z_{1,2}} = \frac{1}{Z_2} + \frac{1}{Z_3 + Z_{3,4}}, \quad Z_{1,2} = \frac{1}{\frac{1}{Z_2} + \frac{1}{Z_3 + Z_{3,4}}} \tag{10.60}$$

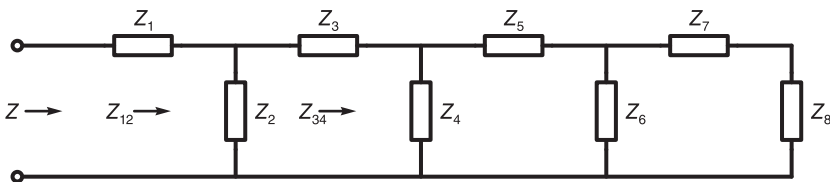


FIGURE 10.6 Ladder network with impedances.

$$\frac{1}{Z_{3,4}} = \frac{1}{Z_4} + \frac{1}{Z_5 + Z_{5,6}}, \quad Z_{3,4} = \frac{1}{\frac{1}{Z_4} + \frac{1}{Z_5 + Z_{5,6}}} \tag{10.61}$$

$$\frac{1}{Z_{5,6}} = \frac{1}{Z_6} + \frac{1}{Z_7 + Z_8}, \quad Z_{5,6} = \frac{1}{\frac{1}{Z_6} + \frac{1}{Z_7 + Z_8}}. \tag{10.62}$$

We conclude that

$$Z = Z_1 + \frac{1}{\frac{1}{Z_2} + \frac{1}{Z_3 + \frac{1}{\frac{1}{Z_4} + \frac{1}{Z_5 + \frac{1}{\frac{1}{Z_6} + \frac{1}{Z_7 + Z_8}}}}}} \tag{10.63}$$

which is the impedance written in a continued fraction expansion.

Example 10.2 Write in the form of a continued fraction expansion the input impedance of the circuit shown in Fig. 10.7.

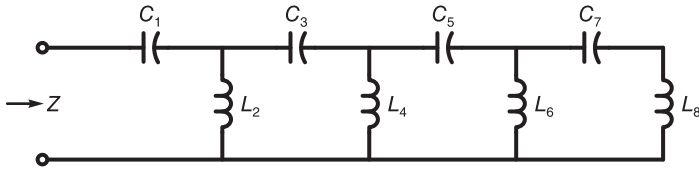


FIGURE 10.7 LC type ladder network.

We recall an approach to the evaluation of the continued fraction expansion that we encountered in connection with the design of constant-delay Bessel filters. In the present context we may write

$$Z = \frac{1}{C_1 s} + \frac{1}{\frac{1}{L_2 s} + \frac{1}{\frac{1}{C_3 s} + \frac{1}{\frac{1}{L_4 s} + \frac{1}{\frac{1}{C_5 s} + \frac{1}{\frac{1}{L_6 s} + \frac{1}{\frac{1}{C_7 s} + L_8 s}}}}}}.$$

As observed in Chapter 9 the process of continued fraction expansion can be written as an alternating long division. The following example illustrates the approach.

Example 10.3 Consider the ladder network of Fig. 10.2. (a) Write the circuit input impedance in a continued fraction expansion form. (b) Starting from the input impedance $Z(s)$ as a ratio of two polynomials show the continued fraction expansion, deducing the circuit elements values.

a) The input impedance of the circuit shown in this figure can be written in the form

$$Z(s) = Y_3 + \frac{1}{Z_2 + \frac{1}{Y_1 + 1}}$$

$$Y_3 = C_3s, \quad Z_2 = L_2s \quad \text{and} \quad Y_1 = C_1s$$

so that

$$Z(s) = C_3s + \frac{1}{L_2s + \frac{1}{C_1s + 1}} = 1.5s + \frac{1}{\frac{4}{3}s + \frac{1}{0.5s + 1}}$$

b) We first write the value of the input admittance $Y(s)$

$$Y(s) = \frac{1}{Z(s)} = \frac{s^3 + 2s^2 + 2s + 1}{(2/3)s^2 + (4/3)s + 1}$$

We next perform the continued fraction expansion as an alternating long division where at every new iteration the preceding denominator becomes the new numerator that is divided by the remainder just obtained. The operation takes the form shown in Fig. 10.8. The first term of the numerator ($s^3 + 2s^2 + 2s + 1$) is first divided by that of the denominator ($2/3 s^2 + 4/3 s + 1$). The result $(3/2)s$ is recorded as the first quotient and multiplied by the denominator producing $(s^3 + 2s^2 + 3/2 s)$. This product is subtracted from the numerator. The result is the remainder $(1/2) s + 1$.

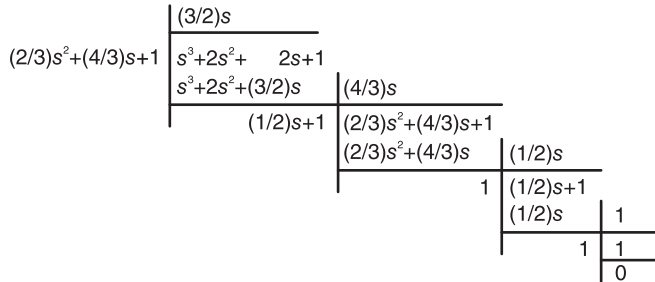


FIGURE 10.8 Continued fraction expansion.

Now starts the second iteration. The past denominator $(2/3 s^2 + 4/3 s + 1)$ now becomes the new numerator to be divided by the remainder $(1/2) s + 1$. The process is thus repeated dividing the first term of $2/3 s^2$ of the numerator by that $(1/2) s$ of the denominator the result is recorded as the second quotient $4/3 s$.

The process is repeated leading to a third quotient of $1/2 s$ as seen above. The final step produces the fourth quotient equal to 1.

The four quotients thus evaluated are none other than the successive impedances Z_1, Z_2, Z_3 and the 1 ohm resistor. We deduce that

$$Z_1 = (3/2)s, \quad Z_2 = (4/3)s, \quad Z_3 = (1/2)s \quad \text{and} \quad R = 1 \Omega$$

i.e.

$$L_1 = 1.5 H, \quad C_2 = 4/3 F \quad \text{and} \quad L_3 = 0.5 H$$

as desired.

We have therefore seen how the continued partial fraction expansion using this alternating type of long division yields the values of the ladder elements. It is interesting to note that the same four quotients $3/2 s$, $4/3 s$, $1/2 s$ and 1 can be interpreted as $Z_3 = L'_3 s$, $Y_2 = C'_2 s$, $Z_1 = L'_1 s$ and R , thus leading to the ladder circuit driven by a voltage source, shown in Fig. 10.9

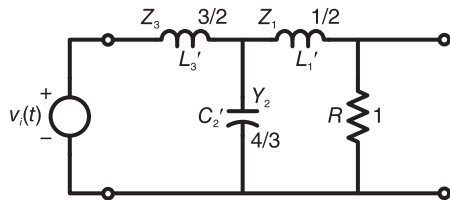


FIGURE 10.9 Third order ladder network.

In what follows we shall see how the values of the different circuit elements for a given desired filter realization can be determined. We shall note that the two networks shown in Fig. 10.1(a) and (b) are equivalent forms, and that the same is true for the two networks shown in Figs. 10.1 (c) and (d). We shall also note in what follows that the component values $C_1, L_2, C_3, L_4, \dots$ are the same as the values $L'_1, C'_2, L'_3, C'_4, \dots$ in the equivalent circuit.

In voltage-driven ladder networks the voltage and current equations are the same as those of the current and voltage equations, respectively, of the corresponding current driven network. Impedances are replaced by admittances and vice versa. We obtain with

$$Z_1 = L'_1 s, \quad Y_2 = C'_2 s \quad \text{and} \quad Z_3 = L'_3 s \tag{10.64}$$

$$I_1(s) = V_0(s) \tag{10.65}$$

$$I_2(s) = I_1(s) + V_1(s) Y_2(s) \tag{10.66}$$

$$V_2(s) = V_1(s) + I_2(s) Z_3(s) \tag{10.67}$$

and in general

$$I_k(s) = I_{k-1}(s) + V_{k-1}(s) Y_{2(k-1)}(s), \quad k = 2, 3, \dots, (n+1)/2 \tag{10.68}$$

$$V_k(s) = V_{k-1}(s) + I_k(s) Z_{2k-1}(s), \quad k = 1, 2, \dots, (n+1)/2 \tag{10.69}$$

$$V_1(s) = V_0(s) + I_1(s) Z_1(s) = V_0(s) (1 + L'_1 s) \tag{10.70}$$

$$\begin{aligned} I_2(s) &= I_1(s) + V_1(s) Y_2(s) = V_0(s) + V_0(s) (1 + L'_1 s) C'_2 s \\ &= V_0(s) (1 + C'_2 s + C'_2 L'_1 s^2) \end{aligned} \tag{10.71}$$

$$\begin{aligned} V_2(s) &= V_1(s) + I_2(s) Z_3(s) \\ &= V_0(s) (1 + L'_1 s) + L'_3 s V_0(s) (1 + C'_2 s + C'_2 L'_1 s^2) \\ &= V_0(s) \{1 + (L'_1 + L'_3) s + C'_2 L'_3 s^2 + C'_2 L'_1 L'_3 s^3\}. \end{aligned} \tag{10.72}$$

The input impedance is given by

$$Z(s) = \frac{V_2(s)}{I_2(s)} = \frac{1 + (L'_1 + L'_3) s + C'_2 L'_3 s^2 + C'_2 L'_1 L'_3 s^3}{1 + C'_2 s + C'_2 L'_1 s^2} \tag{10.73}$$

as found above. Moreover, substituting we have

$$Y(s) = \frac{(2/3)s^2 + (4/3)s + 1}{s^3 + 2s^2 + 2s + 1} \tag{10.74}$$

and

$$H(s) = \frac{V_0(s)}{V_2(s)} = \frac{1}{s^3 + 2s^2 + 2s + 1} \tag{10.75}$$

which, as expected, is the Butterworth filter third order transfer function.

We have just seen how to obtain two passive ladder networks, current driven and voltage driven, respectively, which are lowpass Butterworth filters of the third order $n = 3$. The same principle applies to the realization of lowpass Butterworth, Chebyshev and Bessel-Thomson filters of a general order.

Continued partial-fractions expansion has been shown to generate as successive quotients the values of the inductor and capacitor elements. Before ending this section it is worthwhile noticing that the alternating long division illustrated above can be rewritten in a form that saves horizontal space. This is accomplished by rewriting it in the form shown in Table 10.1

TABLE 10.1 Continued fraction expansion

D, N, D, ...	N, D, N, ...	Q
$D_1: \frac{2}{3}s^2 + \frac{4}{3}s + 1$	$N_1: s^3 + 2s^2 + 2s + 1$ $Q_1D_1: s^3 + 2s^2 + \frac{3}{2}s$	$Q_1: \frac{3}{2}s$
$N_2: \frac{2}{3}s^2 + \frac{4}{3}s + 1$ $Q_2D_2: \frac{2}{3}s^2 + \frac{4}{3}s$	$D_2: \frac{1}{2}s + 1$	$Q_2: \frac{4}{3}s$
$D_3: 1$	$N_3: \frac{1}{2}s + 1$ $Q_3D_3: \frac{1}{2}s$	$Q_3: \frac{1}{2}s$
$N_4: 1$	$D_4: 1$ $Q_4D_4: 1$	$Q_4: 1$
		0

Note:

N : numerator

D : denominator

N_1, N_2, N_3, \dots are successive numerators

D_1, D_2, D_3, \dots are successive denominators

Q_1, Q_2, Q_3, \dots are quotients

R_1, R_2, R_3, \dots are remainders

$$D_2 = R_1 = N_1 - Q_1D_1 \tag{10.76}$$

$$N_2 = D_1 \tag{10.77}$$

$$Q_2 = \text{Quotient } [N_2/D_2] \tag{10.78}$$

$$D_3 = R_2 = N_2 - Q_2D_2 \tag{10.79}$$

$$N_3 = D_2 \tag{10.80}$$

$$Q_3 = \text{Quotient } [N_3/D_3] \tag{10.81}$$

$$N_4 = D_3. \tag{10.82}$$

10.6 Matrix Evaluation of Input Impedance

An alternative approach to the evaluation of the input impedance $Z(s)$ from the magnitude-squared spectrum $|H(j\omega)|^2$ is one that is visually appealing, being readily described in matrix form. We deduce from Equation 10.51 that the impedance $Z(s)$ of the ladder network has the form

$$Z(s) = \frac{a_0 + a_1s + a_2s^2 + \dots + a_ns^n}{b_0 + b_1s + b_2s^2 + \dots + b_ns^n} = \frac{P(s)}{Q(s)} \tag{10.83}$$

where the denominator polynomial $Q(s)$ may be directly deduced from the left-hand plane poles p_i of $F(s) \triangleq H(s)H(-s)$, i.e. $Q(s) = \prod_{i=1}^n (s - p_i)$. In fact, if the filter transfer function $H(s)$ is known, then polynomial $Q(s)$ is simply its denominator. The coefficients b_k of the impedance denominator $Q(s)$ are therefore known. To evaluate the impedance $Z(s)$ we therefore need to evaluate the coefficients a_k of the numerator polynomial $P(s)$.

To this end we start by expressing each of the two polynomials $P(s)$ and $Q(s)$ as a sum of a polynomial of even powers and another of odd powers,

$$P(s) = (a_0 + a_2s^2 + a_4s^4 + \dots) + (a_1s + a_3s^3 + a_5s^5 + \dots) = m_1 + n_1 \tag{10.84}$$

$$Q(s) = (b_0 + b_2s^2 + b_4s^4 + \dots) + (b_1s + b_3s^3 + b_5s^5 + \dots) = m_2 + n_2 \tag{10.85}$$

so that

$$Z(s) = \frac{P(s)}{Q(s)} = \frac{m_1 + n_1}{m_2 + n_2} = \frac{P(s)Q(-s)}{Q(s)Q(-s)} = \frac{(m_1 + n_1)(m_2 - n_2)}{m_2^2 - n_2^2} \tag{10.86}$$

and if we put $s = j\omega$ then

$$Q(j\omega) = m_2 + n_2 = (b_0 - b_2\omega^2 + b_4\omega^4 - \dots) + j\omega b_1 - j\omega^3 b_3 + j\omega^5 b_5 - \dots \tag{10.87}$$

and

$$Z(j\omega) = \frac{(m_1 + n_1)(m_2 - n_2)}{(m_2 + n_2)(m_2 - n_2)} \Big|_{s=j\omega} = \frac{m_1m_2 - m_1n_2 + m_2n_1 - n_1n_2}{m_2^2 - n_2^2} \Big|_{s=j\omega}. \tag{10.88}$$

We note that with $s = j\omega$ the products m_1m_2 and n_1n_2 are real while m_1n_2 and m_2n_1 are imaginary, Hence

$$\Re \{Z(j\omega)\} = \frac{m_1m_2 - n_1n_2}{m_2^2 - n_2^2} \Big|_{s=j\omega}. \tag{10.89}$$

The numerator and denominator polynomials are seen to be even having even powers of ω . We can write

$$\Re \{Z(j\omega)\} = \frac{A_0 + A_1\omega^2 + \dots + A_n\omega^{2n}}{B_0 + B_1\omega^2 + \dots + B_n\omega^{2n}} \triangleq \frac{A(\omega^2)}{B(\omega^2)} = |H(j\omega)|^2. \tag{10.90}$$

We note that the denominator $B(\omega^2)$ of $\Re\{Z(j\omega)\}$ is the same as that of $|H(j\omega)|^2$. As for the numerator $A(\omega^2)$ we may write

$$A(\omega^2) = (m_1 m_2 - n_1 n_2)|_{s=j\omega} \tag{10.91}$$

Now the right-hand side is given by

$$(m_1 m_2 - n_1 n_2) = (a_0 + a_2 s^2 + \dots + a_n s^{2n})(b_0 + b_2 s^2 + \dots + b_n s^{2n}) - (a_1 s + a_3 s^3 + a_5 s^5 + \dots)(b_1 s + b_3 s^3 + b_5 s^5 + \dots) \tag{10.92}$$

so that

$$A(\omega^2) = A_0 + A_1 \omega^2 + A_2 \omega^4 + \dots + A_n \omega^{2n} = (m_1 m_2 - n_1 n_2)|_{s=j\omega} = (a_0 - a_2 \omega^2 + a_4 \omega^4 - \dots)(b_0 - b_2 \omega^2 + b_4 \omega^4 - \dots) + \omega^2 (a_1 - a_3 \omega^2 + a_5 \omega^4 - \dots)(b_1 - b_3 \omega^2 + b_5 \omega^4 - \dots) \tag{10.93}$$

In this equation the coefficients A_k are known since the polynomial $A(\omega^2)$ is the numerator of $|H(j\omega)|^2$, the b_k are known as stated above. To solve for the unknown coefficients a_k we equate the coefficients of equal power. We have

$$A_0 = a_0 b_0 \tag{10.94}$$

$$A_1 = -a_0 b_2 + a_1 b_1 - a_2 b_0 \tag{10.95}$$

$$A_2 = a_0 b_4 - a_1 b_3 + a_2 b_2 - a_3 b_1 + a_4 b_0 \tag{10.96}$$

⋮

More generally, we can write

$$A_k = \sum_{i=-k}^k (-1)^i a_{i+k} b_{k-i} \tag{10.97}$$

These relations can be put in the matrix form :

$$\begin{bmatrix} A_0 \\ A_1 \\ A_2 \\ A_3 \\ \vdots \end{bmatrix} = \begin{bmatrix} b_0 & 0 & 0 & 0 & 0 & 0 & 0 & 0 & \dots \\ -b_2 & b_1 & -b_0 & 0 & 0 & 0 & 0 & 0 & \\ b_4 & -b_3 & b_2 & -b_1 & b_0 & 0 & 0 & 0 & \\ -b_6 & b_5 & -b_4 & b_3 & -b_2 & b_1 & -b_0 & 0 & \\ \vdots & & & & & & & & \end{bmatrix} \begin{bmatrix} a_0 \\ a_1 \\ a_2 \\ a_3 \\ a_4 \\ a_5 \\ a_6 \\ \vdots \end{bmatrix} \tag{10.98}$$

Evaluating a_0, a_1, a_2, \dots we find $P(s)$. Since as seen above

$$\begin{aligned} \frac{1}{2} \{Z(s) + Z(-s)\} &= H(s)H(-s) = |H(j\omega)|^2|_{\omega=-js} = \frac{A(-s^2)}{B(-s^2)} \\ &= \frac{A_0 - A_1 s^2 + A_2 s^4 - \dots + (-1)^n A_n s^{2n}}{B_0 - B_1 s^2 + B_2 s^4 - \dots + (-1)^n B_n s^{2n}} \end{aligned} \tag{10.99}$$

the denominator $B(-s^2)$ is directly evaluated as the denominator of $|H(j\omega)|^2$ with ω replaced by s/j , and since

$$B(-s^2) = m_2^2 - n_2^2 = Q(s)Q(-s) \tag{10.100}$$

the value of $Q(s)$ is simply the product

$$Q(s) = (s - p_1)(s - p_2) \dots (s - p_n) \tag{10.101}$$

where p_1, p_2, \dots, p_n are the roots of $B(-s^2)$ in the left half of the s plane, i.e. the poles of $F(s)$. Having found $P(s)$ and $Q(s)$ we have evaluated

$$Z(s) = P(s)/Q(s). \tag{10.102}$$

Example 10.4 Evaluate the input impedance $Z(s)$ of the passive ladder network corresponding to a lowpass Butterworth filter of order $n = 4$.

The magnitude-squared spectrum of a Butterworth filter is given by

$$|H(j\omega)|^2 = \frac{1}{1 + \omega^{2n}} = \frac{1}{1 + \omega^8}$$

$$\frac{1}{2} \{Z(s) + Z(-s)\} = F(s) = \frac{A(-s^2)}{B(-s^2)} = |H(j\omega)|^2 \Big|_{\omega=-js} = \frac{1}{1 + s^8}$$

that is, $A(-s^2) = 1, B(-s^2) = 1 + s^8$.

The poles of $F(s)$ are given by $s^8 = -1 = e^{-j\pi} e^{j2k\pi}, s_k = e^{j(2k-1)\pi/8}, k = 1, 2, 3, \dots$. The roots of $Q(s)$ are the poles of $F(s)$ which are in the left-half plane, i.e.,

$$p_1 = s_3 = e^{j5\pi/8}, p_2 = s_4 = e^{j7\pi/8}, p_3 = p_1^*, p_4 = p_2^*.$$

Hence

$$Q(s) = (s - p_1)(s - p_2)(s - p_3)(s - p_4) = s^4 + 2.6131s^3 + 3.4142s^2 + 2.6131s + 1.$$

Since

$$Q(s) = b_0 + b_1s + b_2s^2 + \dots + b_ns^n$$

we have

$$b_0 = 1, b_1 = 2.6131, b_2 = 3.4142, b_3 = 2.6131, b_4 = 1.$$

Since

$$A(-s^2) = A_0 - A_1s^2 + A_2s^4 - A_3s^6 + A_4s^8 = 1$$

we have

$$A_0 = 1 \text{ and } A_1 = A_2 = A_3 = A_4 = 0.$$

We can thus construct the matrix form :

$$\begin{bmatrix} 1 \\ 0 \\ 0 \\ 0 \\ 0 \end{bmatrix} = \begin{bmatrix} b_0 & 0 & 0 & 0 & 0 \\ -b_2 & b_1 & -b_0 & 0 & 0 \\ b_4 & -b_3 & b_2 & -b_1 & b_0 \\ 0 & 0 & -b_4 & b_3 & -b_2 \\ 0 & 0 & 0 & 0 & b_4 \end{bmatrix} \begin{bmatrix} a_0 \\ a_1 \\ a_2 \\ a_3 \\ a_4 \end{bmatrix}.$$

Note that the values b_5, b_6, b_7 and b_8 are all zero, simplifying the matrix structure. Substituting with the values of b_0, b_1, \dots, b_4 we have

$$1 = a_0$$

$$0 = -3.4142a_0 + 2.6131a_1 - a_2 = -3.4142 + 2.6131a_1 - a_2$$

$$0 = 1 - 2.6131a_1 + 3.4142a_2 - 2.6131a_3 + a_4$$

$$0 = - a_2 + 2.6131a_3 - 3.4142a_4$$

$$0 = a_4.$$

Simplifying we have

$$0 = - a_2 + 2.6131a_3$$

$$0 = - 2.4142 + 2.4142a_2 - 2.6131a_3$$

which when added produce $a_2 = 1.7071$. Hence $a_3 = 0.6533$ and $a_1 = 1.9599$. The value of $Z(s)$ is thus given by

$$\begin{aligned} Z(s) &= \frac{P(s)}{Q(s)} = \frac{a_0 + a_1s + \dots + a_n s^n}{b_0 + b_1s + \dots + b_n s^n} \\ &= \frac{1 + 1.9599s + 1.7071s^2 + 0.6533s^3}{1 + 2.6131s + 3.4142s^2 + 2.6131s^3 + s^4} \end{aligned}$$

and

$$Y(s) = \frac{1}{Z(s)} = \frac{1 + 2.6131s + 3.4142s^2 + 2.6131s^3 + s^4}{1 + 1.9599s + 1.7071s^2 + 0.6533s^3}$$

We perform a continued fraction expansion as shown in Table 10.2 which leads to the realization shown in Fig. 10.10, with

$$C'_4 = 1.531, \quad L'_3 = 1.577, \quad C'_2 = 1.083 \quad \text{and} \quad L'_1 = 0.3827.$$

TABLE 10.2 Continued fraction expansion

D, N, D	N, D, N	Q
$0.653s^3 + 1.707s^2 + 1.959s + 1$	$s^4 + 2.613s^3 + 3.414s^2 + 2.613s + 1$ $s^4 + 2.613s^3 + 3s^2 + 1.531s$	1.531s
$0.653s^3 + 1.707s^2 + 1.959s + 1$ $0.653s^3 + 1.707s^2 + 1.577s$	$0.414s^2 + 1.082s + 1$	1.577s
$0.383s + 1$	$0.414s^2 + 1.082s + 1$ $0.414s^2 + 1.082s$	1.083s
$0.383s + 1$ $0.383s$		1 0.383s
1		1 1
		0

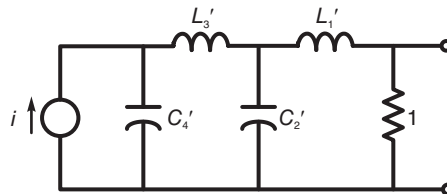


FIGURE 10.10 Resulting passive circuit realization.

Alternatively we identify the successive quotients and corresponding elements as

$$Q_1 = L_4s, \quad L_4 = 1.531, \quad Q_2 = C_3s, \quad C_3 = 1.577 \quad (10.103)$$

$$Q_3 = L_2s, \quad L_2 = 1.083, \quad Q_4 = C_1s, \quad C_1 = 0.383. \quad (10.104)$$

as seen in Fig. 10.11.

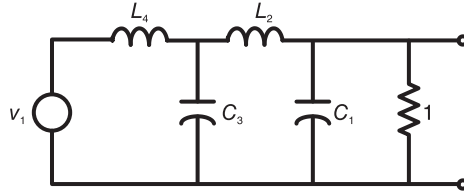


FIGURE 10.11 Fourth order ladder network.

10.7 Bessel Filter Passive Ladder Networks

The same approach of designing Butterworth and Chebyshev filter passive ladder networks applies to Bessel–Thomson ladder networks. The following example illustrates the approach.

Example 10.5 Show the realizations of a third order prototype lowpass Bessel filter type 1 as a passive ladder network. Evaluate the LC values if the filter is of the fourth, instead of the third, order.

The prototype lowpass Bessel filter of order $n = 3$ has the transfer function

$$H(s) = \frac{15}{s^3 + 6s^2 + 15s + 15}.$$

We have

$$F(s) = H(s)H(-s) = \frac{-225}{s^6 - 6s^4 + 45s^2 - 225}.$$

Decomposing using partial fractions we write

$$F(s) = \sum_{i=1}^{2n} \frac{r_i}{(s - s_i)}$$

such that the poles s_1, s_2 and s_3 are in the left-hand half of the s plane. We find $s_1, s_3 = -1.8389 \pm j1.7544, s_2 = -2.3222$ and their residues

$$r_1, r_3 = -0.0587 \mp j0.4133, \quad r_2 = -0.7174$$

so that the network input impedance is given by

$$Z(s) = \sum_{i=1}^n \frac{2r_i}{(s - s_i)} = \frac{1.2s^2 + 7.2s + 15}{s^3 + 6s^2 + 15s + 15}$$

and $Y(s) = 1/Z(s)$. A continued fraction expansion produces the circuit element values $C_3 = 0.833$, $L_2 = 0.48$, $C_1 = 0.1667$, which apply to the current-driven circuit shown in Fig. 10.1(c). Alternatively we write $L'_3 = 0.833$, $C'_2 = 0.48$, $L'_1 = 0.1667$, which apply to the voltage driven circuit shown in Fig. 10.1(d). For a Bessel filter of order $n = 4$ we have

$$H(s) = \frac{105}{s^4 + 10s^3 + 45s^2 + 105s + 105}$$

Proceeding as in the last example we obtain the ladder network input impedance

$$Z(s) = \frac{1.408163s^3 + 14.081632s^2 + 59.081633s + 105}{s^4 + 10s^3 + 45s^2 + 105s + 105}$$

Effecting a continued fraction expansion of the admittance $Y(s) = 1/Z(s)$ we obtain $L_4 = 0.7101449$, $C_3 = 0.462682$, $L_2 = 0.289855$, and $C_1 = 0.1$, which apply to the voltage driven passive ladder network shown in Fig. 10.1(a).

For higher order filters, computations of the passive ladder network circuit components should be automated by writing simple computer programs to evaluate the required filter input impedance, and the continued fraction expansion, which produces the circuit elements.

10.8 Tables of Single-Resistance Ladder Network Components

Tables for Butterworth, Chebyshev, and Bessel–Thomson filter passive ladder networks having the single-resistance structures seen above in Fig. 10.1 are given below. Elliptic filter tables follow shortly.

Table 10.3 lists Butterworth passive ladder components.

TABLE 10.3 Butterworth passive ladder components

n	C ₁	L ₂	C ₃	L ₄	C ₅	L ₆	C ₇	L ₈	C ₉	L ₁₀
2	0.7071	1.4142	0	0	0	0	0	0	0	0
3	0.5	1.3333	1.5	0	0	0	0	0	0	0
4	0.3827	1.0824	1.5772	1.5307	0	0	0	0	0	0
5	0.3090	0.8944	1.382	1.6944	1.5451	0	0	0	0	0
6	0.2588	0.7579	1.2016	1.5529	1.7593	1.5529	0	0	0	0
7	0.2225	0.6560	1.055	1.3972	1.6588	1.7988	1.5576	0	0	0
8	0.1951	0.5776	0.9370	1.2588	1.5283	1.7287	1.8246	1.5607	0	0
9	0.1737	0.5156	0.8414	1.1408	1.4037	1.6202	1.7772	1.8424	1.5628	0
10	0.1564	0.4654	0.7627	1.0406	1.2921	1.51	1.6869	1.8121	1.8552	1.5643

Tables 10.4 and 10.5 list Chebyshev passive ladder components with pass-band ripples of 0.5 and 1 dB, respectively. Table 10.6 lists the delay-normalized Bessel–Thomson filter form passive ladder components.

TABLE 10.4 Chebyshev 0.5 dB passive ladder components

n	C ₁	L ₂	C ₃	L ₄	C ₅	L ₆	C ₇	L ₈	C ₉	L ₁₀
2	0.7014	0.9403	0	0	0	0	0	0	0	0
3	0.7981	1.3001	1.3465	0	0	0	0	0	0	0
4	0.8352	1.3916	1.7279	1.3138	0	0	0	0	0	0
5	0.8529	1.4291	1.8142	1.6426	1.5388	0	0	0	0	0
6	0.8627	1.4483	1.8494	1.7101	1.9018	1.4042	0	0	0	0
7	0.8687	1.4595	1.8677	1.7369	1.9713	1.7252	1.5983	0	0	0
8	0.8725	1.4666	0.8786	1.7508	1.998	1.7838	1.9871	1.4379	0	0
9	0.8752	1.4714	0.8856	1.7591	2.0116	1.8055	2.0203	1.7571	1.6238	0
10	0.8771	1.4748	0.8905	1.7645	2.0197	1.8165	2.0432	1.8119	1.9816	1.4539

TABLE 10.5 Chebyshev 1 dB passive ladder components

n	C ₁	L ₂	C ₃	L ₄	C ₅	L ₆	C ₇	L ₈	C ₉	L ₁₀
2	0.9110	0.9957	0	0	0	0	0	0	0	0
3	1.0118	1.3332	1.5088	0	0	0	0	0	0	0
4	1.0495	1.4126	1.9093	1.2817	0	0	0	0	0	0
5	1.0674	1.4441	1.9938	1.5908	1.6652	0	0	0	0	0
6	1.0773	1.4601	2.027	1.6507	2.0491	1.3457	0	0	0	0
7	1.0833	1.4692	2.0438	1.6735	2.1194	1.6488	1.712	0	0	0
8	1.0872	1.4751	2.0537	1.685	2.1453	1.7021	2.0922	1.3691	0	0
9	1.0899	1.479	2.0601	1.6918	2.1582	1.7213	2.1574	1.6707	1.7317	0
10	1.0918	1.4817	2.0645	1.6962	2.1658	1.7307	2.1803	1.7215	2.1111	1.3801

10.9 Design of Doubly Terminated Passive LC Ladder Networks

As noted above, there are two types of passive lowpass lossless ladder networks, namely, the single-resistance terminated networks studied above and double-resistance terminated networks on which we presently focus our attention. For Butterworth, Chebyshev and Bessel filters, the networks shown in Fig. 10.12 are suitable structures. We shall shortly see structures suitable for the realization of elliptic filters.

10.9.1 Input Impedance Evaluation

Each of the double-resistance terminated networks of Fig. 10.12 is a passive LC circuit receiving its input from a source of resistance R_1 and terminated into a resistive load R_2 , as represented schematically in Fig. 10.13.

In the present context a *transmission coefficient* is defined as the ratio of the power delivered to the load P_L to the maximum available power from the source P_a . We write

$$|T(j\omega)|^2 = \frac{P_L}{P_a} \tag{10.105}$$

The maximum available power from a source of resistance R_1 is obtained if the load resistance is equal to that of the source. To show this we refer to Fig. 10.14, where the load resistance is written $R_2 = x$. The power dissipated in the resistance is given by

$$P_L(x) = I^2 x = \left(\frac{v_s}{R_1 + x} \right)^2 x \tag{10.106}$$

TABLE 10.6 Bessel–Thomson passive ladder components

n	C ₁	L ₂	C ₃	L ₄	C ₅	L ₆	C ₇	L ₈	C ₉	L ₁₀
2	0.3333	1.000	0	0	0	0	0	0	0	0
3	0.1667	0.48	0.8333	0	0	0	0	0	0	0
4	0.1	0.2899	0.4627	0.7101	0	0	0	0	0	0
5	0.0667	0.1948	0.3103	0.4215	0.6231	0	0	0	0	0
6	0.0476	0.14	0.2247	0.3005	0.3821	0.5595	0	0	0	0
7	0.0357	0.1055	0.1704	0.2288	0.2827	0.3487	0.5111	0	0	0
8	0.0278	0.0823	0.1338	0.1806	0.2227	0.2639	0.3212	0.4732	0	0
9	0.0222	0.0660	0.1077	0.1463	0.1811	0.2129	0.2465	0.2986	0.4424	0
10	0.0182	0.0543	0.0887	0.1209	0.1504	0.1770	0.2021	0.2311	0.2797	0.4161

Differentiating $P_L(x)$ with respect to x and equating the derivative to zero we obtain $R_2 = R_1$, as stated, and note that the corresponding maximum available power is given by

$$P_a = v_s^2 / (4R_1). \tag{10.107}$$

The voltage transfer function is given by

$$H(s) = V_2(s)/V_s(s) \tag{10.108}$$

and

$$|H(j\omega)|^2 = |V_2(j\omega)|^2 / |V_s(j\omega)|^2 \tag{10.109}$$

We may therefore write

$$|T(j\omega)|^2 = \frac{P_L}{P_a} = \frac{|V_2(j\omega)|^2 / R_2}{|V_s(j\omega)|^2 / (4R_1)} = \frac{4R_1}{R_2} |H(j\omega)|^2 \tag{10.110}$$

A related function is the *reflection coefficient*, denoted $|\rho(j\omega)|^2$, which is defined as the ratio of the missed, or “reflected,” power to the available power. We may therefore write

$$|\rho(j\omega)|^2 = \frac{P_a - P_L}{P_a} = 1 - |T(j\omega)|^2 \tag{10.111}$$

$$|\rho(j\omega)|^2 = 1 - \frac{4R_1}{R_2} |H(j\omega)|^2 \tag{10.112}$$

$$\rho(s)\rho(-s) = 1 - \frac{4R_1}{R_2} H(s)H(-s). \tag{10.113}$$

Since the LC ladder network is lossless the power P_i at its input is the same as the power P_o at its output. Let z_0 denote the input impedance of the LC ladder, that seen past the source resistance R_1 , as shown in Fig. 10.13. Writing

$$Z_0(j\omega) = R_0 + jX_0(j\omega) \tag{10.114}$$

we have

$$P_i = |I_1(j\omega)|^2 R_0 = \frac{|V_s(j\omega)|^2}{|R_1 + Z_0(j\omega)|^2} R_0 \tag{10.115}$$

$$P_o = \frac{|V_2(j\omega)|^2}{R_2}. \tag{10.116}$$

$$\frac{|V_s(j\omega)|^2 R_0}{|R_1 + Z_0(j\omega)|^2} = \frac{|V_2(j\omega)|^2}{R_2} \tag{10.117}$$

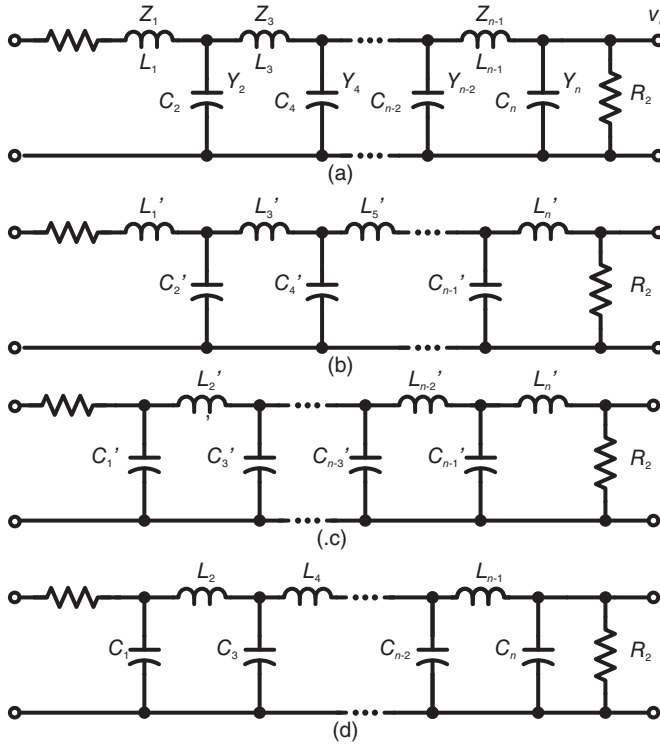


FIGURE 10.12 Double-resistance-terminated passive ladder networks for Butterworth, Chebyshev and Bessel filters: (a) LC ladder, even order; (b) odd order; (c) dual form, even order; (d) odd order.

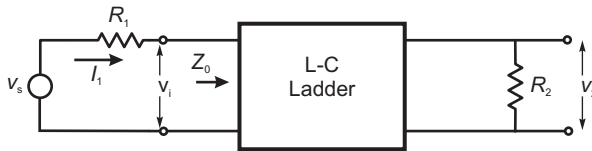


FIGURE 10.13 Double-resistance terminated network model.

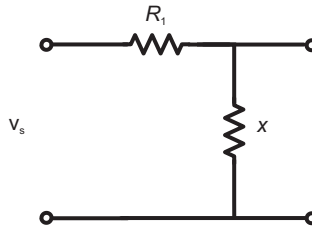


FIGURE 10.14 Electric circuit model for evaluating maximum deliverable power.

$$|T(j\omega)|^2 = \frac{4R_1}{R_2} |H(j\omega)|^2 = \frac{4R_1 R_0}{|R_1 + Z_0(j\omega)|^2} \tag{10.118}$$

$$|\rho(j\omega)|^2 = 1 - |T(j\omega)|^2 = \frac{|R_1 + Z_0(j\omega)|^2 - 4R_1R_0}{|R_1 + Z_0(j\omega)|^2} \quad (10.119)$$

$$|\rho(j\omega)|^2 = \frac{(R_1 + R_0)^2 + X_0^2(j\omega) - 4R_1R_0}{|R_1 + Z_0(j\omega)|^2} \quad (10.120)$$

$$|\rho(j\omega)|^2 = \frac{(R_1 - R_0)^2 + X_0^2(j\omega)}{|R_1 + Z_0(j\omega)|^2} = \frac{|R_1 - Z_0(j\omega)|^2}{|R_1 + Z_0(j\omega)|^2} \quad (10.121)$$

$$\rho(s)\rho(-s) = \frac{[R_1 - Z_0(s)][R_1 - Z_0(-s)]}{[R_1 + Z_0(s)][R_1 + Z_0(-s)]} \quad (10.122)$$

$$\rho(s) = \pm \frac{Z_0(s) - R_1}{Z_0(s) + R_1} \quad (10.123)$$

The function $F(s) \triangleq \rho(s)\rho(-s)$ should have quadrantal symmetry, each pole and each zero in the left half of the s plane having a mirror image in the right half. The function $\rho(s)$ is chosen by grouping the poles in the left half plane and as a minimum phase function also having its zeros in the left half of the plane, otherwise negative inductance and capacitance values may result. The input impedance is therefore given by

$$Z_0(s) = R_1 \frac{1 - \rho(s)}{1 + \rho(s)} \quad (10.124)$$

or

$$Z_0(s) = R_1 \frac{1 + \rho(s)}{1 - \rho(s)}. \quad (10.125)$$

and the input admittance is $Y_0(s) = 1/Z_0(s)$.

In applying these results to an n^{th} order Butterworth, Chebyshev and Bessel filters we note that the transfer function has the form

$$H(s) = \frac{K}{A(s)} = \frac{K}{s^n + a_{n-1}s^{n-1} + a_{n-2}s^{n-2} + \dots + a_0} \quad (10.126)$$

where K is an arbitrary gain value. The dc response is given by $H(0) = K/a_0$. For the general case where the source and load resistances are R_1 and R_2 , respectively, we note that the network response at dc is given by

$$H(0) = (V_2/V_s)|_{s=0} = \frac{R_2}{R_1 + R_2}. \quad (10.127)$$

since at dc all inductances are short circuits and all capacitors are open circuits. To reconcile the values of the resulting network transfer function with that of the desired filter we write

$$H(0) = \frac{K}{a_0} = \frac{R_2}{R_1 + R_2} \quad (10.128)$$

wherefrom

$$K = a_0 \frac{R_2}{R_1 + R_2}. \quad (10.129)$$

Having evaluated the network input impedance from knowledge of its transfer function, the next step in the design is to evaluate the successive L and C circuit elements. The following examples illustrate the approach.

Example 10.6 Design a passive LC ladder network for Butterworth filter of the third order with $R_1 = 1$ and $R_2 = 0.5$ ohm.

We have

$$H(s) = \frac{K}{s^3 + 2s^2 + 2s + 1}$$

$$K = \frac{R_2}{R_1 + R_2} a_0 = (0.5/1.5)a_0 = 0.3333$$

$$H(s) = \frac{0.3333}{s^3 + 2s^2 + 2s + 1}$$

$$H(s)H(-s) = \frac{-0.1111}{s^6 - 1}$$

$$\rho(s)\rho(-s) = \frac{s^6 - 0.1111}{s^6 - 1}$$

$$\rho(s) = \frac{s^3 + 1.387s^2 + 0.9615s + 0.3333}{s^3 + 2s^2 + 2s + 1}$$

$$Z_0(s) = \left[\frac{2s^3 + 3.387s^2 + 2.961s + 1.333}{0.6133s^2 + 1.039s + 0.6667} \right]_{\pm 1}$$

We may write

$$Y_0(s) = 1/Z_0(s) = \frac{2s^3 + 3.387s^2 + 2.961s + 1.333}{0.6133s^2 + 1.039s + 0.6667}$$

A continued fraction expansion of $Y_0(s)$ produces

$$Y_0(s) = 3.2611s + \frac{1}{0.7788s + \frac{1}{1.1811s + \frac{1}{0.5}}} = C_1s + \frac{1}{L_2s + \frac{1}{C_3s + \frac{1}{R_2}}}$$

i.e.

$$C_1 = 3.2611 F, \quad L_2 = 0.7788 H, \quad C_3 = 1.1811 F$$

which refer to the element values in Fig. 10.12(d), with order $n = 3$, redrawn in Fig. 10.15.

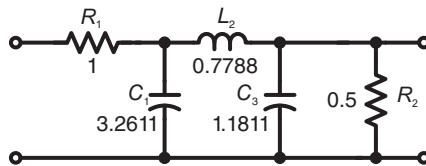


FIGURE 10.15 Butterworth third order filter with $R_1 = 1$ and $R_2 = 0.5$ ohm.

Example 10.7 Design a passive lowpass Chebyshev filter having a pass-band edge frequency of 1, a ripple of $R_p = 1$ dB in the pass-band, a stop-band edge frequency of 2 and an attenuation of at least 40 dB in the stop band. The passive filter should have a source resistance $R_1 = 1$ ohm and a load resistance $R_2 = 0.5$ ohm.

Using the Chebyshev filter nomograph or by direct evaluation, we find the filter order $n = 5$, and the transfer function has the form

$$H(s) = \frac{K}{s^5 + 0.9368s^4 + 1.689s^3 + 0.9744s^2 + 0.5805s + 0.1228}$$

$$K = \frac{0.5}{1 + 0.5} a_0 = 0.1228/3 = 0.04094$$

$$H(s) = \frac{0.04094}{s^5 + 0.9368s^4 + 1.689s^3 + 0.9744s^2 + 0.5805s + 0.1228}$$

$$H(s)H(-s) = \frac{-0.001676}{s^{10} + 2.5s^8 + 2.188s^6 + 0.7813s^4 + 0.09766s^2 - 0.01509}$$

$$\rho(s)\rho(-s) = N(s)/D(s)$$

where

$$N(s) = s^{10} + 2.5s^8 + 2.188s^6 + 0.7813s^4 + 0.09766s^2 - 0.001676$$

$$D(s) = s^{10} + 2.5s^8 + 2.188s^6 + 0.7813s^4 + 0.09766s^2 - 0.01509$$

$$\rho(s) = N_r(s)/D_r(s)$$

$$N_r(s) = s^5 + 0.3994s^4 + 1.33s^3 + 0.3711s^2 + 0.3578s + 0.04094$$

$$D_r(s) = s^5 + 0.9368s^4 + 1.689s^3 + 0.9744s^2 + 0.5805s + 0.1228$$

$$Y_0(s) = N_0(s)/D_0(s)$$

where

$$N_0(s) = 2s^5 + 1.336s^4 + 3.019s^3 + 1.345s^2 + 0.9384s + 0.1638$$

$$D_0(s) = 0.5375s^4 + 0.3591s^3 + 0.6033s^2 + 0.2227s + 0.08188.$$

A continued fraction expansion of the impedance $Y_0(s)$ produces the values $C_1 = 3.7211$, $L_2 = 0.6949$, $C_3 = 4.7448$, $L_4 = 0.6650$, $C_5 = 2.9936$ with reference to Fig. 10.12(d).

Example 10.8 Design a passive lowpass Bessel filter of the fifth order, with a source resistance $R_1 = 1$ ohm and a load resistance $R_2 = 1$ ohm.

The filter transfer function is given by

$$H(s) = \frac{K}{s^5 + 15s^4 + 105s^3 + 420s^2 + 945s + 945}$$

$$H(0) = K = \frac{R_2}{R_1 + R_2} a_0 = \frac{1}{2} 945 = 472.5.$$

$$H(s)H(-s) = \frac{-223300}{s^{10} - 15s^8 + 315s^6 - 6300s^4 + 99225s^2 - 893025}$$

$$\rho(s)\rho(-s) = \frac{s^{10} - 15s^8 + 315s^6 - 6300s^4 + 99225s^2}{s^{10} - 15s^8 + 315s^6 - 6300s^4 + 99225s^2 - 893025}$$

$$\rho(s) = \frac{s^5 + 12.85s^4 + 75.06s^3 + 231.5s^2 + 315s}{s^5 + 15s^4 + 105s^3 + 420s^2 + 945s + 945}$$

obtaining

$$Y_0(s) = \frac{2s^5 + 27.85s^4 + 180.1s^3 + 651.5s^2 + 1260s + 945}{2.15s^4 + 29.94s^3 + 188.5s^2 + 630s + 945}$$

Continued fraction expansion produces

$$Y_0(s) = 0.9302987s + \frac{1}{0.4577030s + \frac{1}{0.3312217s + \frac{1}{0.2089637s + \frac{1}{0.0718129s + 1}}}}$$

$$Y_0(s) = C_1s + \frac{1}{L_2s + \frac{1}{C_3s + \frac{1}{L_4s + \frac{1}{C_5s + 1}}}}$$

$C_1 = 0.9302987 F$, $L_2 = 0.4577030 H$, $C_3 = 0.3312217 F$, $L_4 = 0.2089637 H$, $C_5 = 0.0718129 F$, with reference to Fig. 10.12(d).

It is important to recall that the input impedance is given by

$$Z_0(s) = R_1 \left[\frac{1 + \rho(s)}{1 - \rho(s)} \right]^{\pm 1} \tag{10.130}$$

In these examples we have chosen the negative exponent so that

$$Y_0(s) = R_1 \frac{1 + \rho(s)}{1 - \rho(s)} \tag{10.131}$$

and proceeded with a continued fraction expansion on $Y_0(s)$. We may write instead

$$Z_0(s) = R_1 \frac{1 + \rho(s)}{1 - \rho(s)} \tag{10.132}$$

and perform the expansion on $Z_0(s)$ instead of $Y_0(s)$ we would obtain a dual circuit realization. In the case of the Bessel filter of the last example the result of the continued fraction expansion would be written in the form

$$Z_0(s) = 0.9302987s + \frac{1}{0.4577030s + \frac{1}{0.3312217s + \frac{1}{0.2089637s + \frac{1}{0.0718129s + 1}}}}$$

$$Z_0(s) = L'_1s + \frac{1}{C'_2s + \frac{1}{L'_3s + \frac{1}{C'_4s + \frac{1}{L'_5s + 1}}}}$$

i.e. $L'_1 = 0.9302987 F$, $C'_2 = 0.4577030 H$, $L'_3 = 0.3312217 F$, $C'_4 = 0.2089637 H$, $L'_5 = 0.0718129 F$, with reference to Fig. 10.12(b) which is the dual network for the same filter. The same approach yields a dual network realization for any given passive filter.

10.10 Tables of Double-Resistance Terminated Ladder Network Components

Tables for Butterworth, Chebyshev, and Bessel–Thomson filter passive ladder networks, having the double-resistance structures seen above in Fig. 10.12 are given below.

The table depicted in Fig. 10.7 lists the LC components of Butterworth filter, Chebyshev filter with Ripple $R_p = 0.5$ dB and $R_p = 1$ dB, respectively, and Bessel filter, given a source and load resistances $R_1 = R_2 = 1$ Ohm.

TABLE 10.7 LC components of Butterworth, Chebyshev, and Bessel filter with $R_1 = 1$ and $R_2 = 1$ ohm

Butterworth										
n	L1	C2	L3	C4	L5	C6	L7	C8	L9	C10
2	1.4142135	1.4142135								
3	1	2	1							
4	0.7653669	1.8477590	1.8477590	0.7653669						
5	0.6180340	1.6180340	2.0000000	1.6180340	0.6180340					
6	0.5176381	1.4142135	1.9318516	1.9318516	1.4142135	0.5176381				
7	0.4450419	1.2469796	1.8019377	2.0000000	1.8019377	1.2469796	0.4450419			
8	0.3901806	1.1111405	1.6629392	1.9615705	1.9615705	1.6629392	1.1111405	0.3901806		
9	0.3472964	1.0000000	1.5320889	1.8793852	2.0000000	1.8793852	1.5320889	1.0000000	0.3472964	
10	0.3128689	0.9079810	1.4142135	1.7820131	1.9753767	1.9753767	1.7820131	1.4142135	0.9079810	0.3128689

Chebyshev , Rp=0.5 dB										
n	L1	C2	L3	C4	L5	C6	L7	C8	L9	C10
3	1.5962801	1.0966917	1.5962801							
5	1.7057701	1.2296268	2.5408273	1.2296268	1.7057701					
7	1.7372911	1.2582365	2.6382923	1.3443341	2.6382923	1.2582365	1.7372911			
9	1.7504390	1.2690431	2.6677804	1.3673258	2.7239041	1.3673258	2.6677804	1.2690431	1.7504390	

Chebyshev , Rp=1 dB										
n	L1	C2	L3	C4	L5	C6	L7	C8	L9	C10
3	2.0235927	0.9941024	2.0235927							
5	2.1348815	1.0911072	3.0009229	1.0911072	2.1348815					
7	2.1665573	1.1115092	3.0936420	1.1735204	3.0936420	1.1115092	2.1665573			
9	2.1797233	1.1191769	3.1214337	1.1896729	3.1746340	1.1896729	3.1214337	1.1191769	2.1797233	

Bessel										
n	L1	C2	L3	C4	L5	C6	L7	C8	L9	C10
2	1.5773503	0.4226497								
3	1.2550243	0.5527864	0.1921893							
4	1.0598230	0.5116169	0.3181414	0.1104186						
5	0.9302987	0.4577030	0.3312217	0.2089637	0.0718129					
6	0.8376592	0.4115725	0.3158199	0.2364269	0.1480323	0.0504892				
7	0.7676538	0.3744134	0.2944135	0.2378304	0.1778259	0.1104061	0.0374569			
8	0.7125409	0.3445570	0.2734607	0.2296681	0.1866805	0.1386715	0.0855168	0.0289046		
9	0.6677724	0.3202778	0.2547027	0.2183962	0.1859234	0.1505970	0.1111501	0.0681938	0.0229871	
10	0.6305036	0.3002230	0.2383952	0.2066336	0.1808241	0.1539468	0.1240671	0.0912645	0.0561304	0.0185163

TABLE 10.8 LC components of Butterworth, Chebyshev, and Bessel filter with $R_1 = 1$ and $R_2 = 0.5$ ohm

Butterworth										
n	L1	C2	L3	C4	L5	C6	L7	C8	L9	C10
2	3.3460653	0.4482877								
3	3.2611668	0.7788752	1.1810828							
4	3.1868467	0.8826236	2.4523757	0.2174541						
5	3.1331182	0.9237115	3.0509586	0.4955220	0.6856601					
6	3.0937600	0.9422967	3.3686848	0.6542407	1.6531422	0.1412241				
7	3.0640011	0.9513154	3.5532126	0.7511913	2.2726419	0.3535574	0.4798938			
8	3.0408158	0.9557860	3.6677780	0.8139274	2.6862726	0.5003356	1.2340633	0.1042324		
9	3.0222850	0.9579226	3.7425926	0.8564643	2.9733922	0.6046270	1.7846375	0.2734546	0.3684670	
10	3.0071540	0.9587976	3.7933960	0.8864170	3.1794882	0.6807837	2.1942642	0.4021408	0.9817598	0.0825094

Chebyshev, Rp=0.5 dB										
n	L1	C2	L3	C4	L5	C6	L7	C8	L9	C10
2	1.5132107	0.6537845								
3	2.9430563	0.6502766	2.1902683							
4	1.8158209	1.1328121	2.4881477	0.7731912						
5	3.2227516	0.7645139	4.1228442	0.7115762	2.3196552					
6	1.8786346	1.1884230	2.7588890	1.2403497	2.5976038	0.7976077				
7	3.3055162	0.7898839	4.3574743	0.8132132	4.2418938	0.7251586	2.3565648			
8	1.9011692	1.2053467	2.8152432	1.2863656	2.8478560	1.2628261	2.6310105	0.8063372		
9	3.3403423	0.7994794	4.4282985	0.8341056	4.4545779	0.8235114	4.2795486	0.7303722	2.3719165	
10	1.9116981	1.2127421	2.8365641	1.2999451	2.8964415	1.3054066	2.8743703	1.2713919	2.6456409	0.8104105

Chebyshev, Rp=1 dB										
n	L1	C2	L3	C4	L5	C6	L7	C8	L9	C10
3	3.4774134	0.6152597	2.8539989							
5	3.7211404	0.6949039	4.7448044	0.6649843	2.9936297					
7	3.7915926	0.7118456	4.9425006	0.7347578	4.8636122	0.6756758	3.0331428			
9	3.8210182	0.7181986	5.0012693	0.7485135	5.0411592	0.7428651	4.9003520	0.6797411	3.0495369	

Bessel										
n	L1	C2	L3	C4	L5	C6	L7	C8	L9	C10
2	2.6180339	0.1909830								
3	2.1156411	0.2612603	0.3618383							
4	1.7892765	0.2460610	0.6126817	0.0529598						
5	1.5686426	0.2216998	0.6456386	0.1015338	0.1392515					
6	1.4101563	0.1999287	0.6196482	0.1158268	0.2894014	0.0246416				
7	1.2904471	0.1820671	0.5797060	0.1171184	0.3496505	0.0541818	0.0734617			
8	1.1963962	0.1675869	0.5394835	0.1134693	0.3685235	0.0683360	0.1683743	0.0142190		
9	1.1201822	0.1557589	0.5029773	0.1081238	0.3680418	0.0744407	0.2195165	0.0336405	0.0453487	
10	1.0568831	0.1459684	0.4709930	0.1024330	0.3586335	0.0762694	0.2456387	0.0451692	0.1113216	0.0091111

Similarly, the table depicted in Fig. 10.8 lists the LC components of Butterworth filter, Chebyshev filter with Ripple $R_p = 0.5$ dB and $R_p = 1$ dB, respectively, and Bessel filter, given a source resistance of $R_1 = 1$ Ohm and a load resistance of $R_2 = 0.5$ Ohm.

Similarly, Table 10.8 lists the LC components of Butterworth filter, Chebyshev filter with ripple $R_p = 0.5$ dB and $R_p = 1$ dB, respectively, and Bessel filter, given a source resistance of $R_1 = 1$ ohm and a load resistance of $R_2 = 0.5$ ohm.

10.11 Closed Forms for Circuit Element Values

There exist closed forms of the inductance and capacitance values for lowpass filter LC passive ladder networks. For a Butterworth filter of order n , the filter transfer function has

the form

$$H(s) = \frac{K}{s^n + a_{n-1}s^{n-1} + \dots + a_1s + a_0} \quad (10.133)$$

where the denominator coefficients are given by Equation (9.16) in Chapter 9. Let r_{21} denote the ratio of the load resistance R_2 to the source resistance R_1 , $r_{21} = R_2/R_1$. We have

$$\alpha = \left[\frac{1 + r_{21}}{1 - r_{21}} \right]^{\pm 1/n} \quad (10.134)$$

where the plus and minus sign apply for $r_{21} \geq 1$ and $r_{21} \leq 1$, respectively. The input impedance may be expanded in the form

$$Z_0(s) = L_1s + \frac{1}{C_2s + \frac{1}{L_3s + \frac{1}{\dots + \frac{1}{X}}}} \quad (10.135)$$

where X is a resistance or a conductance, and letting

$$\gamma_m = m\pi/(2n) \quad (10.136)$$

we have

$$L_1 = \frac{2R_1 \sin \gamma_1}{(1 - \alpha)\omega_c} \quad (10.137)$$

where ω_c is the cut-off frequency, which is equal to one for a normalized prototype filter.

$$L_{2m-1}C_{2m} = \frac{4 \sin \gamma_{4m-3} \sin \gamma_{4m-1}}{\omega_c^2(1 - 2\alpha \cos \gamma_{4m-2} + \alpha^2)} \quad (10.138)$$

$$L_{2m+1}C_{2m} = \frac{4 \sin \gamma_{4m-1} \sin \gamma_{4m+1}}{\omega_c^2(1 - 2\alpha \cos \gamma_{4m} + \alpha^2)}. \quad (10.139)$$

The last elements in the ladder are given by

$$L_n = \frac{2R_2 \sin \gamma_1}{(1 + \alpha)\omega_c} \quad (10.140)$$

for n odd, and

$$C_n = \frac{2 \sin \gamma_1}{R_2(1 + \alpha)\omega_c} \quad (10.141)$$

for n even.

Similar forms exist for expansions in the form

$$Y_0(s) = C_1s + \frac{1}{L_2s + \frac{1}{C_3s + \frac{1}{L_4s + \frac{1}{\dots + \frac{1}{X}}}}} \quad (10.142)$$

Note that the first term C_1s is an admittance same as the expanded $Y_0(s)$. Since each term after the first is in the form of $1/D$, its denominator D represents successively an impedance, an admittance, an impedance, and so on. Note also that each new term $1/D$ reflects the role reversal in the continued fraction expansion, where the last denominator becomes the new numerator. The final term X is therefore a resistance or a conductance depending on whether n is even or odd.

$$C_1 = \frac{2 \sin \gamma_1}{R_1(1 - \alpha)\omega_c} \quad (10.143)$$

$$C_{2m-1}L_{2m} = \frac{4 \sin \gamma_{4m-3} \sin \gamma_{4m-1}}{\omega_c^2(1 - 2\alpha \cos \gamma_{4m-2} + \alpha^2)} \tag{10.144}$$

$$C_{2m+1}L_{2m} = \frac{4 \sin \gamma_{4m-1} \sin \gamma_{4m+1}}{\omega_c^2(1 - 2\alpha \cos \gamma_{4m} + \alpha^2)}. \tag{10.145}$$

The last elements in the ladder are given by

$$L_n = \frac{2R_2 \sin \gamma_1}{(1 + \alpha)\omega_c} \tag{10.146}$$

for n odd, and

$$C_n = \frac{2 \sin \gamma_1}{R_2(1 + \alpha)\omega_c} \tag{10.147}$$

for n even, which lead to the dual circuit forms.

For Chebyshev passive filters similar closed forms have been proposed. We have, with R_p denoting pass-band ripple,

$$\varepsilon = \sqrt{10^{R_p/10} - 1} \tag{10.148}$$

$$K = 1 - \left(\frac{1 - r_{21}}{1 + r_{21}} \right)^2, \quad n \text{ odd} \tag{10.149}$$

$$K = (1 + \varepsilon^2) \left[1 - \left(\frac{1 - r_{21}}{1 + r_{21}} \right)^2 \right] = 10^{0.1R_p} \left[1 - \left(\frac{1 - r_{21}}{1 + r_{21}} \right)^2 \right], \quad n \text{ even} \tag{10.150}$$

$$\hat{a} = \frac{1}{n} \sinh^{-1} \left(\frac{\sqrt{1 - K}}{\varepsilon} \right). \tag{10.151}$$

The continued fraction expansion of the input impedance $Z_0(s)$ leads to the inductances and capacitances values given in the following:

$$L_1 = \frac{2R_1 \sin \gamma_1}{(\sinh a - \sinh \hat{a})\omega_c}. \tag{10.152}$$

Let

$$\phi_m(a, \hat{a}) = \sinh^2 a + \sinh^2 \hat{a} + \sin^2 \gamma_{2m} - 2 \sinh a \sinh \hat{a} \cos \gamma_{2m} \tag{10.153}$$

$$L_{2m-1}C_{2m} = \frac{4 \sin \gamma_{4m-3} \sin \gamma_{4m-1}}{\omega_c^2 \phi_{2m-1}(a, \hat{a})} \tag{10.154}$$

$$L_{2m+1}C_{2m} = \frac{4 \sin \gamma_{4m-1} \sin \gamma_{4m+1}}{\omega_c^2 \phi_{2m}(a, \hat{a})}. \tag{10.155}$$

The continued fraction expansion of the input admittance $Y_0(s)$ leads to the inductances and capacitances values given in the following:

$$C_1 = \frac{2 \sin \gamma_1}{\omega_c R_1 (\sinh a - \sinh \hat{a})} \tag{10.156}$$

$$C_{2m-1}L_{2m} = \frac{4 \sin \gamma_{4m-3} \sin \gamma_{4m-1}}{\omega_c^2 \phi_{2m-1}(a, \hat{a})} \tag{10.157}$$

$$C_{2m+1}L_{2m} = \frac{4 \sin \gamma_{4m-1} \sin \gamma_{4m+1}}{\omega_c^2 \phi_{2m}(a, \hat{a})} \tag{10.158}$$

Example 10.9 Design a fourth order passive lowpass Chebyshev filter having a pass-band edge frequency of 1500 Hz and a maximum pass-band ripple of $R_p = 0.5$ dB. The passive filter should have a source resistance $R_1 = 100$ ohm and a load resistance $R_2 = 200$ ohm.

We have $\omega_c = 3000\pi = 9424.8$ r/s, $\varepsilon = \sqrt{10^{0.1R_p} - 1} = 0.34931$, $K = 0.99735$, $\hat{a} = 0.036712$, $a = 0.44353$, wherefrom we obtain the set of component values $L_1 = 0.019266$ H, $C_2 = 1.202 \mu F$, $L_3 = 0.0264$ H, $C_4 = 0.82038 \mu F$, with reference to Fig. 10.12(a) redrawn in Fig. 10.16.

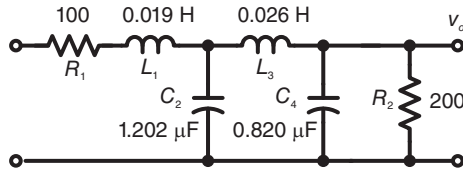


FIGURE 10.16 Chebyshev fourth order double-resistance terminated filter example.

10.12 Elliptic Filter Realization as a Passive Ladder Network

We now consider the design of double-resistance terminated elliptic filters, having a source resistance R_1 and load resistance R_2 , such as the passive elliptic filter of general odd order n seen in Fig. 10.17(a), and its dual form, 10.17(b).

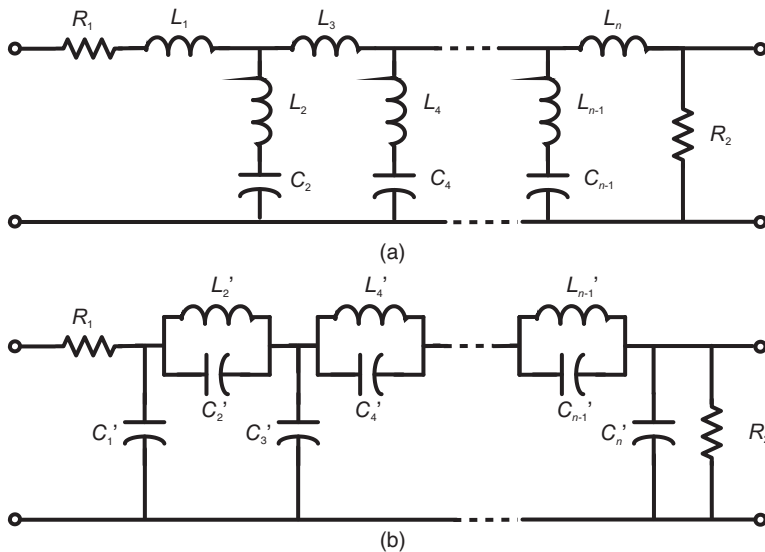


FIGURE 10.17 Elliptic filter passive ladder network of odd order employing (a) series LC resonance circuits; (b) the dual form employing parallel resonance circuits.

The particular circuit shown in the figure is suitable for the realization of lowpass elliptic filters of *odd* order. A similar structure with a slight change would be used for even order filters. However, elliptic filters of even order require that the filter frequency response have a finite value at infinite frequency. Ordinary passive ladder networks of the type seen so far cannot have such properties. In fact a passive RLC network would have to employ coupled coils, that is, transformers, in order to produce such a response. To avoid the added complexity, and the difficulty in obtaining precise element values, it is common to simply implement a filter of odd order $N + 1$ when the minimum requirements call for a filter of even order N . The passive network thus obtained has higher selectivity than the minimum required.

We have just seen how to evaluate the input impedance of a double-resistance terminated passive ladder network knowing its required transfer function. We now apply the approach to the case of elliptic filters and then proceed to evaluate the L and C circuit elements.

10.12.1 Evaluating the Elliptic LC Ladder Circuit Elements

Elliptic filter transfer functions contain zeros on the $s = j\omega$ axis. These are implemented by including an inductance in series with a capacitance as shunt circuits in the ladder as can be seen in Fig. 10.18 for the case of a fifth order filter.

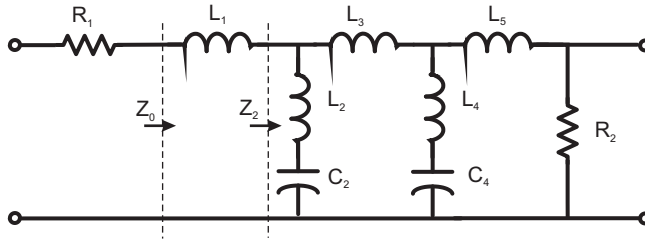


FIGURE 10.18 Fifth order elliptic, passive, double-resistance terminated, network.

Alternatively, they may be implemented as an inductance in parallel with a capacitance as series circuits along the ladder network structure, seen in Fig. 10.17(b). The impedance of an LC series combination is given by

$$Z(s) = Ls + 1/(Cs) \tag{10.159}$$

i.e

$$Z(j\omega) = j\omega L + 1/(j\omega C) \tag{10.160}$$

which has a zero value if $j\omega L = -1/(j\omega C)$ i.e $\omega^2 = 1/(LC)$, or $\omega = \pm 1/\sqrt{LC}$.

This is the circuit resonance frequency, at which the series LC circuit becomes a short circuit annulling the output, whence the zero of the transfer function. Similarly, the parallel LC circuit at that same resonance frequency has zero admittance, thus acting as an open circuit annulling the output. The zeros of elliptic filter transfer function $H(s)$ are therefore the resonance frequencies at which the LC combination circuits become short circuits.

Knowledge of the zeros of the filter transfer function is the key to dissecting the passive ladder network into successive simple sections of which the elements can be identified. Referring to Fig. 10.18, we note that the input impedance, labeled Z_0 in the figure, seen to the right of the source resistance R_1 , may be written

$$Z_0(s) = L_1s + Z_2(s) \tag{10.161}$$

where $Z_2(s)$ is the impedance looking to the right past the impedance L_1 . At the $L_2 - C_2$ shunt circuit resonance frequency $\omega = \pm 1/\sqrt{L_2C_2}$ the series combination become a short circuit, so that $Z_0(s) = L_1s$ and $Z_0(j\omega) = j\omega L_1$. From the value of desired input impedance $Z_0(s)$ we may evaluate $Z_0(j\omega)$ and thereof $L_1 = Z_0(j\omega)/(j\omega)$. We have thus identified the first circuit component, L_1 , by short circuiting the rest of the ladder circuit. We now deduce the value of $Z_2(s)$ as $Z_2(s) = Z_0(s) - L_1s$. This process, together with partial fraction expansions applied successively, produces the ladder circuit elements.

Example 10.10 As an illustration, let us consider the design of a passive lowpass fifth order elliptic filter with pass-band ripple $R_p = 0.1\text{dB}$ and $\omega_s = 1.20$ and with both source and load resistances equal to 1 ohm. From the tables, the required transfer function is

$$H(s) = \frac{K(0.17544s^4 + 0.787581s^2 + 0.79205)}{s^5 + 1.69203s^4 + 2.84788s^3 + 2.65258s^2 + 1.77912s + 0.79205} \triangleq \frac{KN(s)}{D(s)}$$

$$H(0) = K = \frac{R_2}{R_1 + R_2} = 0.5$$

$$|H(j\omega)|^2 = \frac{1}{4} \frac{|N(j\omega)|^2}{|D(j\omega)|^2} \quad (10.162)$$

Referring to Fig. 10.18 and proceeding as in the above we write

$$|T(j\omega)|^2 = \frac{4R_1}{R_2} |H(j\omega)|^2 = \frac{|N(j\omega)|^2}{|D(j\omega)|^2} \quad (10.163)$$

$$|\rho(j\omega)|^2 = 1 - |T(j\omega)|^2 = \frac{|D(j\omega)|^2 - |N(j\omega)|^2}{|D(j\omega)|^2} \quad (10.164)$$

$$\rho(s)\rho(-s) = \frac{G(s)}{D(s)D(-s)} \triangleq \frac{P(s)P(-s)}{D(s)D(-s)} \quad (10.165)$$

$$G(s) = P(s)P(-s) = -s^{10} - 2.8636s^8 - 2.96856s^6 - 1.31513s^4 - 0.210917s^2$$

$$P(s) = s^5 + 1.43117s^3 + 0.458157s$$

$$\rho(s) = \pm \frac{P(s)}{D(s)}$$

$$Z_0(s) = R_1 \frac{1 \mp \rho(s)}{1 \pm \rho(s)}$$

obtaining, for the case of $R_1 = 1$ ohm,

$$Z_0(s) = \frac{1.18202s^5 + s^4 + 2.52895s^3 + 1.5677s^2 + 1.32225s + 0.468103}{s^4 + 0.837288s^3 + 1.5677s^2 + 0.7807s + 0.468109}$$

We presently, set out to evaluate the ladder circuit elements

L_1 , C_2 , L_2 , L_3 , C_4 , L_4 , and L_5 .

As observed above we start by evaluating the zeros of $H(s)$, obtaining the purely imaginary value $s_{Z,1} = \pm j1.72283$ and $s_{Z,2} = \pm j1.233307$.

Since at the resonance frequency $\omega_{Z,1}$, the L_2 - C_2 circuit is a short circuit, leading to the transfer function zero, the input impedance reduces to simply

$$Z_0(s_{Z,1}) = Z_0(j\omega_{Z,1}) = j\omega_{Z,1}L_1$$

wherefrom $L_1 = 0.91439$ H. Having identified the value of L_1 we advance one step to the right toward the load resistance. We have $Z_2(s) = Z_0(s) - L_1s$, where $Z_2(s)$ is the impedance seen past the inductance L_1 as shown in Fig. 10.18.

Referring to Fig. 10.19 we next effect a partial fraction expansion of $Y_2(s) = 1/Z_2(s) = Y_{2,1}(s) + Y_{2,2}(s) = \frac{C_2s}{L_2C_2s^2+1} + Y_{2,2}(s)$ obtaining

$$Y_{2,1}(s) = \frac{1.0651s}{0.3369s^2 + 1}$$

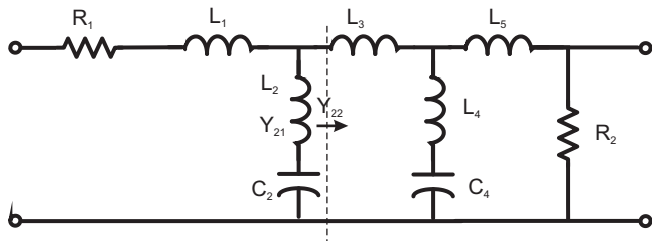


FIGURE 10.19 Admittances Y_{21} and Y_{22} .

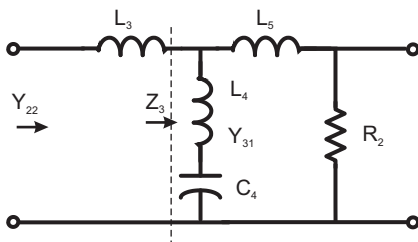


FIGURE 10.20 Impedance Z_3 as seen past inductance L_3 .

$C_2 = 1.0651f$, $L_2 = 0.3163 H$. We next write $Y_{2,2}(s) = Y_2(s) - Y_{2,1}(s)$, which is the admittance seen past the same shunt circuit, as seen in Fig. 10.20.

Next, we repeat the same steps followed above, using the zero $s_{Z,2}$ to deduce that $L_3 = Z_{2,2}(j\omega_{Z,2}) / (j\omega_{Z,2}) = 1.3819 H$. The impedance seen to the right of the inductance L_3 is $Z_3(s) = Z_{2,2}(s) - L_3s$. Proceeding similarly we obtain $C_4 = 0.6009F$, $L_4 = 1.0942H$ and $L_5 = 0.5299 H$. These are the same values within round-off errors as those obtained above through solution of simultaneous nonlinear equations.

The same approach may be used to evaluate the circuit components of double-resistance terminated Butterworth, Chebyshev and Bessel filters.

10.13 Table of Elliptic Filter Passive Network Components

Table 10.9 lists the ladder network component values for different orders and ripple specifications of elliptic filters.

10.14 Element Replacement for Frequency Transformation

In this section we study an approach to filter band frequency transformation by direct replacement of circuit elements.

TABLE 10.9 Tables of elliptic filter passive ladder network components

Rp = 0.1 dB																
n	ω_c	R_1	L_1	C_2	L_2	L_3	C_4	L_4	L_5	C_6	L_6	L_7	C_8	L_8	L_9	
3	1.05	1.74777	0.355497	0.153744	5.395955	0.355497										
	1.10	3.37427	0.446263	0.269928	2.703534	0.446263										
	1.20	6.69124	0.573361	0.449805	1.308052	0.573361										
	1.50	14.84776	0.770308	0.745610	0.477968	0.770308										
	2.00	24.01036	0.895444	0.937589	0.206971	0.895444										
5	1.05	13.84139	0.708128	0.766300	0.735718	1.127606	0.201381	4.381161	0.049847							
	1.10	20.05025	0.812964	0.924184	0.493384	1.224451	0.371933	2.135006	0.291249							
	1.20	28.30311	0.914410	1.065159	0.316277	1.382011	0.601310	1.093292	0.529738							
	1.50	43.41521	1.027894	1.215166	0.151340	1.631785	0.935251	0.440827	0.815488							
	2.00	58.90077	1.087578	1.293218	0.073172	1.793867	1.143296	0.200384	0.977198							
7	1.05	30.47003	0.919372	1.076593	0.342199	1.096230	0.405179	2.208500	0.843355	0.503420	1.518268	0.410979				
	1.10	39.35733	0.988208	1.167261	0.243745	1.277432	0.597201	1.356812	1.040294	0.678807	0.966685	0.582816				
	1.20	50.96287	1.050289	1.248717	0.161238	1.483773	0.828694	0.815420	1.287231	0.874278	0.589181	0.753949				
	1.50	72.12860	1.115931	1.335541	0.078568	1.756865	1.151737	0.371601	1.638271	1.125017	0.268219	0.955875				
	2.00	93.80866	1.149100	1.379787	0.038223	1.920258	1.352206	0.176920	1.856642	1.270227	0.126941	1.067202				
9	1.05	47.27617	1.025971	1.216541	0.205826	1.298028	0.606744	1.367286	0.761141	0.447452	0.210858	0.941339	0.743116	0.844075	0.639189	
	1.10	58.70704	1.072265	1.277415	0.147725	1.464031	0.790466	0.923202	1.001541	0.635744	1.284733	1.149562	0.895439	0.576332	0.770143	
	1.20	73.62905	1.112943	1.331389	0.098152	1.642565	0.999643	0.588578	1.290496	0.865383	0.789447	1.392296	1.051430	0.368766	0.896971	
	1.50	100.8422	1.154932	1.387608	0.047998	1.867654	1.276112	0.279268	1.690553	1.189602	0.365229	1.720367	1.236936	0.174372	1.041301	
	2.00	128.7170	1.175763	1.415677	0.023389	1.997615	1.440553	0.134707	1.936384	1.392257	0.174866	1.919004	1.338872	0.083711	1.118424	
Rp = 1 dB																
n	ω_c	R_1	L_1	C_2	L_2	L_3	C_4	L_4	L_5	C_6	L_6	L_7	C_8	L_8	L_9	
3	1.05	8.13423	1.055070	0.252230	3.289041	1.055070										
	1.10	11.47971	1.225248	0.374713	1.947518	1.225248										
	1.20	16.20894	1.424504	0.525437	1.119769	1.424504										
	1.50	25.17584	1.692004	0.733400	0.485925	1.692004										
	2.00	34.45413	1.851994	0.859035	0.225898	1.851994										
5	1.05	24.13454	1.561908	0.675600	0.834490	1.554596	0.265843	3.318816	0.885281							
	1.10	30.47050	1.696907	0.775115	0.588271	1.798923	0.399221	1.989070	1.121089							
	1.20	38.75676	1.828121	0.870048	0.387204	2.090947	0.563467	1.166719	1.380937							
	1.50	53.87453	1.976867	0.976938	0.188245	2.491606	0.793618	0.519499	1.718891							
	2.00	69.36026	2.055944	1.033918	0.091523	2.735670	0.935610	0.244865	1.919394							
7	1.05	40.9260	1.821564	0.863434	0.426679	1.676318	0.343810	2.602712	1.236956	0.467786	1.633923	1.223619				
	1.10	49.81636	1.910406	0.926617	0.307046	1.935794	0.480164	1.687526	1.552761	0.592772	1.106990	1.419933				
	1.20	61.42233	1.991676	0.984742	0.204461	2.228038	0.644442	1.048557	1.927241	0.730117	0.705514	1.625385				
	1.50	82.58809	2.078817	1.047610	0.100162	2.613715	0.873931	0.489726	2.440208	0.904835	0.333487	1.877166				
	2.00	104.2681	2.123292	1.079929	0.048836	2.844461	1.016380	0.235377	2.753060	1.005667	0.160336	2.019236				
9	1.05	57.73559	1.954712	0.956725	0.261722	1.948870	0.469508	1.766941	1.126045	0.353925	2.542240	1.409785	0.630984	0.994075	1.478983	
	1.10	69.16653	2.015030	0.999760	0.188751	2.180479	0.600620	1.215011	1.473389	0.489292	1.669271	1.716911	0.737640	0.699624	1.637800	
	1.20	84.08855	2.068669	1.038333	0.125854	2.430219	0.749854	0.784644	1.885305	0.653764	1.044986	2.068104	0.846524	0.458028	1.795801	
	1.50	111.3017	2.124688	1.078952	0.061729	2.746013	0.946963	0.376337	2.450792	0.885313	0.490761	2.536252	0.975847	0.221026	1.979582	
	2.00	139.1760	2.152745	1.099420	0.030117	2.928713	1.064150	0.182356	2.796797	1.029789	0.236418	2.817483	1.046885	0.107061	2.079170	

10.14.1 Lowpass to Bandpass Transformation

The transformation from a lowpass filter to a bandpass is written

$$s \rightarrow \frac{s^2 + \omega_0^2}{Bs}$$

$$\omega_0^2 = \omega_1\omega_2$$

$$B = \omega_2 - \omega_1.$$

The transformation of an inductance L is deduced by writing

$$LS \rightarrow L \frac{s^2 + \omega_0^2}{Bs} = L \left(\frac{s}{B} + \frac{\omega_0^2}{Bs} \right) = L' s + \frac{1}{C' B},$$

where

$$L' = \frac{L}{B}, \quad C' = \frac{B}{L\omega_0^2}$$

We deduce the transformation of the inductance show in Fig. 10.21(a).

The transformation of the a capacitor C is deduced by writing

$$\frac{1}{Cs} \leftrightarrow \frac{1}{C(s^2 + \omega_0^2)/Bs} = \frac{1}{C \left(\frac{s}{B} + \frac{\omega_0^2}{Bs} \right)} = \frac{1}{\frac{Cs}{B} + \frac{C\omega_0^2}{Bs}}.$$

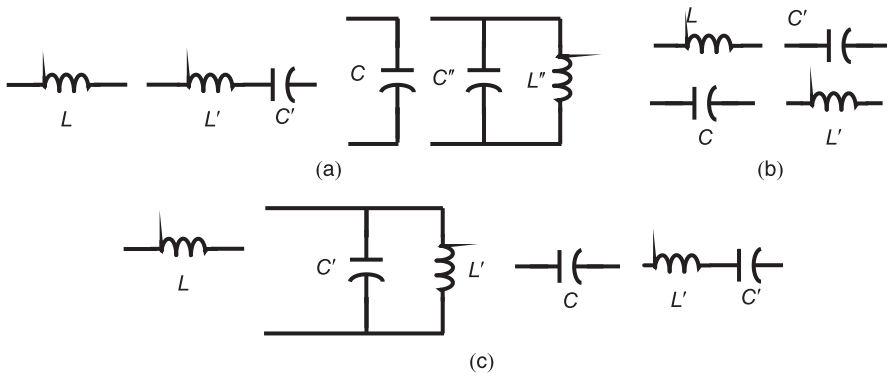


FIGURE 10.21 Component replacement for frequency transformation.

We thus obtain a parallel combination of a capacitor $C'' = C/B$ and an inductor $L'' = B/(C\omega_0^2)$. We deduce the transformation of the capacitance C shown in the figure.

10.14.2 Lowpass to Highpass Transformation

The lowpass to highpass transformation is written

$$s \rightarrow \frac{\omega_0}{s}$$

The inductance transformation is deduced by writing

$$Ls \longleftrightarrow L \frac{\omega_0}{s} = \frac{1}{\frac{1}{L\omega_0} s} = \frac{1}{C' s}$$

$$C' = \frac{1}{L\omega_0}$$

We deduce the transformation shown in Fig. 10.21(b).

The capacitance transformation is deduced by writing

$$\frac{1}{Cs} \longleftrightarrow \frac{s}{C\omega_0} = L' s$$

$$L' = \frac{1}{L\omega_0}$$

We deduce the transformation of the capacitance C into the inductance L' shown in the same figure.

10.14.3 Lowpass to Band-Stop Transformation

The transformation from lowpass (LP) to bandstop (BS) is written in the form

$$s \rightarrow \frac{Bs}{s^2 + \omega_0^2}$$

Proceeding similarly we obtain the transformations of an inductance L and a capacitance C to the parallel connection of an inductance L' and a capacitor C' where

$$L' = \frac{LB}{\omega_0^2}, \quad C' = 1/(LB)$$

and the transformation of a capacitor C into the series connection of an inductance L' and a capacitor C' , where

$$L' = \frac{1}{CB} \quad , \quad C' = \frac{CB}{\omega_0^2}$$

as can be seen in Fig. 10.21(c).

Example 10.11 Given the lowpass ladder-type Butterworth filter shown in Fig. 10.22, show how to obtain thereof a bandpass filter having pass-band edge frequencies $\omega_1 = 10^3 r/s$ and $\omega_2 = 2 \times 10^3 r/s$.

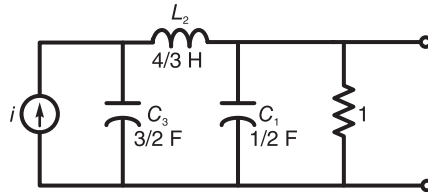


FIGURE 10.22 Component replacement for frequency transformation.

We have $B = \omega_2 - \omega_1 = 10^3 r/s$, $\omega_0^2 = \omega_2 \omega_1 = 2 \times 10^6$, $\omega_0 = 1.4142 \times 10^3$, wherefrom the inductor L_2 is replaced by the element in series. $L'_2 = L_2/B = (4/3)/10^3 = 1.333 \times 10^{-3} H$ and $C'_2 = B/(L_2 \omega_0^2) = 10^3 / [(4/3)2 \times 10^6] = 3.75 \times 10^{-4} F$ The capacitance C_1 is replaced by the parallel combination of $C''_1 = C_1/B = 0.5/10^3 = 0.5 \times 10^{-3} F$ and $L''_1 = B/(C_1 \omega_0^2) = 10^3 / (0.5 \times 2 \times 10^6) = 10^{-3} H$ Similarly the capacitance C_3 is replaced by the parallel combination

$$C''_3 = C_3/B = 1.5/10^3 = 1.5 \times 10^{-3} F$$

and

$$L''_3 = B/(C_3 \omega_0^2) = 10^3 / (1.5 \times 2 \times 10^6) = 0.3333 \times 10^{-3} H$$

The resulting circuit is shown in Fig. 10.23.

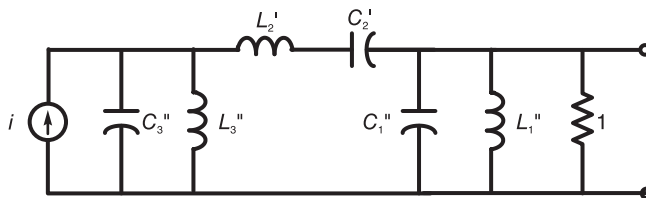


FIGURE 10.23 Component replacement for frequency transformation.

It can be shown that the filter transfer function is given by

$$H(s) = \frac{10^9 s^3}{s^6 + 2 \times 10^3 s^5 + 8 \times 10^6 s^4 + 9 \times 10^9 s^3 + 1.6 \times 10^{13} s^2 + 8 \times 10^{15} s + 8 \times 10^{18}}$$

10.15 Realization of a General Order Active Filter

There are several approaches to the realization of active filters of general order n . In one approach, referred to as the cascade approach, the transfer function is factored into the product of second order transfer functions if the filter order is even. If it is odd, one more first order factor representing a real pole results from the factorization. The problem then reduces to realizing a second order model for the second order factors and a first order model for the first order one. It is important in designing these filter models to ensure that there is enough isolation, provided by the employed operational amplifiers, to ensure that they can be cascaded without loading effects that would alter the behavior of each individual model.

A second approach to filter realization is referred to as the direct approach. The approach referred to as the state variables approach implements an n^{th} order filter directly using n integrators. We have encountered this approach in Chapter 8 in connection with the state space representation of linear systems. In the following we start by considering some details of this approach with the purpose of realizing filter prototypes to use in implementing filters of general order. Subsequently, we shall study methods for realizing second order models, referred to as *biquadratic transfer functions*, and means of realizing general order filters.

10.16 Inverting Integrator

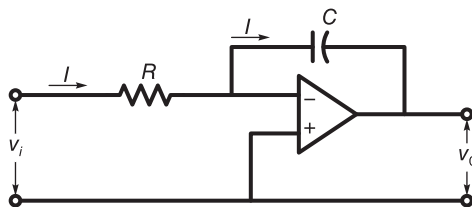


FIGURE 10.24 Inverting integrator.

A possible implementation of an inverting integrator is shown in Fig. 10.24. Under ideal conditions, operational amplifiers have an infinite input impedance, implying that the current into the amplifier input terminals is nil. This in turn implies that the current I through the resistance R is the same as that through the capacitor C , as shown in the figure. The voltage between the ideal operational amplifier's input terminals tends to zero. A second assumption is that the circuit has a zero output impedance, thus acting as an ideal voltage source; providing the necessary isolation if a load is connected to the circuit output. We can write

$$I = \frac{V_i}{R} = (0 - V_o)Cs = -V_oCs \quad (10.166)$$

$$\frac{V_o}{V_i} = -\frac{1}{RCs}. \quad (10.167)$$

If $RC = 1$ the output is simply the negative of the integral of the input. We have seen in Chapter 8 bloc diagrams showing the structures of filters of general order. The same structures can be used using inverting instead of noninverting integrators as the following examples illustrate. We note that if a fourth order system is to be realized as a cascade of two second order filters we may simply multiply each of the two transfer functions by a minus sign to account for the inversion of sign of the inverting integral. If the system order is odd a single amplifier may ultimately be needed to do a sign inversion.

Example 10.12 Show the realization using inverting integrals of a filter having the transfer function

$$H(s) = \frac{Y(s)}{V(s)} = \frac{-Ks}{s^2 + a_1s + a_0}.$$

We have

$$\begin{aligned} Y(s)(s^2 + a_1s + a_0) &= -Ks V(s) \\ s^2Y(s) &= -a_1s Y(s) - a_0Y(s) - Ks V(s) \\ Y(s) &= -a_1\frac{1}{s}Y(s) - a_0\frac{1}{s^2}Y(s) - K\frac{1}{s}V(s) \\ &= -\frac{1}{s}(a_1Y + KV) - \frac{1}{s^2}a_0Y = -\frac{1}{s} \left[(a_1Y + KV) - \frac{1}{s}a_0Y \right]. \end{aligned}$$

The filter realization is shown in Fig. 10.25.

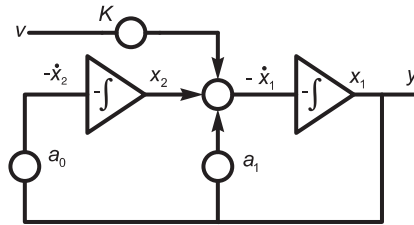


FIGURE 10.25 Filter realization using inverting integrals.

$$\begin{aligned} Y(s) &= K [-W(s) / s] = -K X_1(s) \\ X_1 &= W(s) / s, \quad X_2 = X_1 / s \\ W(s) &= V(s) - a_1X_1(s) - a_0X_2(s). \end{aligned}$$

The filter structure is shown in Fig. 10.26.

10.17 Biquadratic Transfer Functions

The transfer function of a general order filter may be factored as a product of second order transfer functions, each representing a pair of complex conjugate poles or a pair of real poles and, if the filter order is odd, a first order factor representing a real pole.

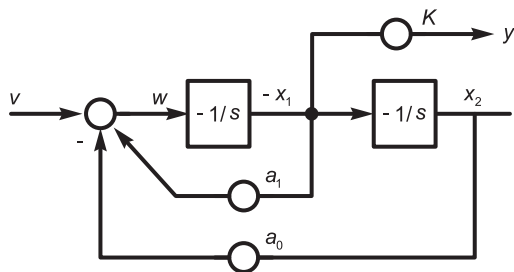


FIGURE 10.26 An alternative realization.

The general form of a second order transfer function may be written

$$H(s) = \frac{b_2s^2 + b_1s + b_0}{a_2s^2 + a_1s + a_0} \tag{10.168}$$

This is referred to as the general biquadratic form. A normalized lowpass Butterworth filter of the fourth order, for example, may be constructed as a cascade of two second order filters, each having a biquadratic transfer function with $a_2 = 1$ and $b_2 = b_1 = 0$. In general the biquadratic function of a lowpass filter such as Butterworth, Chebyshev or Bessel-Thomson may be put in the form

$$H(s) = K \frac{b_0}{s^2 + a_1s + a_0} = K \frac{\omega_0^2}{s^2 + (\omega_0/Q)s + \omega_0^2} \tag{10.169}$$

where ω_0 is the undamped natural frequency and Q the quality factor. We note that

$$Q = \frac{1}{2\zeta} \tag{10.170}$$

$$b_0 = a_0 = \omega_0^2, \quad a_2 = 1, \quad a_1 = 2\zeta\omega_0 = \frac{\omega_0}{Q}, \quad Q = \frac{\omega_0}{a_1} \tag{10.171}$$

The poles are at

$$s = -\alpha \pm j\beta = -\zeta\omega_0 \pm j\omega_0\sqrt{1 - \zeta^2} \tag{10.172}$$

where

$$\alpha = \zeta\omega_0 = \omega_0 / (2Q) \tag{10.173}$$

$$\beta = \omega_0\sqrt{1 - \zeta^2} = \omega_0\sqrt{1 - 1/(4Q^2)} \tag{10.174}$$

$$\omega_0 = \sqrt{\alpha^2 + \beta^2} \tag{10.175}$$

$$Q = \frac{\omega_0}{2\alpha} = \sqrt{\alpha^2 + \beta^2} / (2\alpha) \tag{10.176}$$

Replacing s by $1/s$ we obtain the corresponding highpass filter transfer function, which may be written in the form

$$H(s) = K \frac{s^2}{s^2 + a_1s + a_0} = K \frac{s^2}{s^2 + (\omega_0/Q)s + \omega_0^2} \tag{10.177}$$

A bandpass filter transfer function can be factored into biquadratic expressions of the form

$$H(s) = K \frac{b_1s}{s^2 + a_1s + a_0} = K \frac{(\omega_0/Q)s}{s^2 + (\omega_0/Q)s + \omega_0^2} \tag{10.178}$$

A band-elimination transfer function may be factored into biquadratic transfer functions of the form

$$H(s) = \frac{s^2 + b_0}{s^2 + a_1s + a_0} = K \frac{s^2 + \omega_0^2}{s^2 + (\omega_0/Q)s + \omega_0^2}. \quad (10.179)$$

An allpass transfer function may be factored into biquadratic functions of the form

$$H(s) = K \frac{s^2 - a_1s + a_0}{s^2 + a_1s + a_0} = K \frac{s^2 - (\omega_0/Q)s + \omega_0^2}{s^2 + (\omega_0/Q)s + \omega_0^2}. \quad (10.180)$$

10.18 General Biquad Realization

A general biquadratic transfer function having the form

$$H(s) = K \frac{b_2s^2 + b_1s + b_0}{s^2 + a_1s + a_0} \quad (10.181)$$

may be realized using a single operational amplifier as shown in Fig. 10.27. This negative feedback RC amplifier network, known as a Single Amplifier Biquad (SAB) was proposed by Friend, Harris and Hilberman [38], and is related to that of Delyiannis.

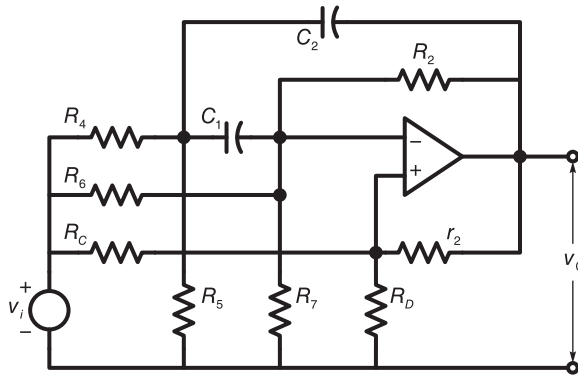


FIGURE 10.27 General biquad realization.

Using Thevenin's theorem the circuit may be replaced by its equivalent shown in Fig. 10.28(a) where

$$K_1 = \frac{R_5}{R_4 + R_5}, \quad K_2 = \frac{R_D}{R_C + R_D}, \quad K_3 = \frac{R_7}{R_6 + R_7}, \quad (10.182)$$

$$R_1 = \frac{R_4 R_5}{R_4 + R_5}, \quad r_1 = \frac{R_C R_D}{R_C + R_D}, \quad R_3 = \frac{R_6 R_7}{R_6 + R_7}. \quad (10.183)$$

With $K_1 v_{in}$ as the only source, and the other two replaced by short circuits, as shown in Fig. 10.28(b) we may write

$$V_1 = V_0 \frac{r_1}{r_1 + r_2} \quad (10.184)$$

$$V_2 - V_1 = I_1 \frac{1}{C_1 s} \quad (10.185)$$

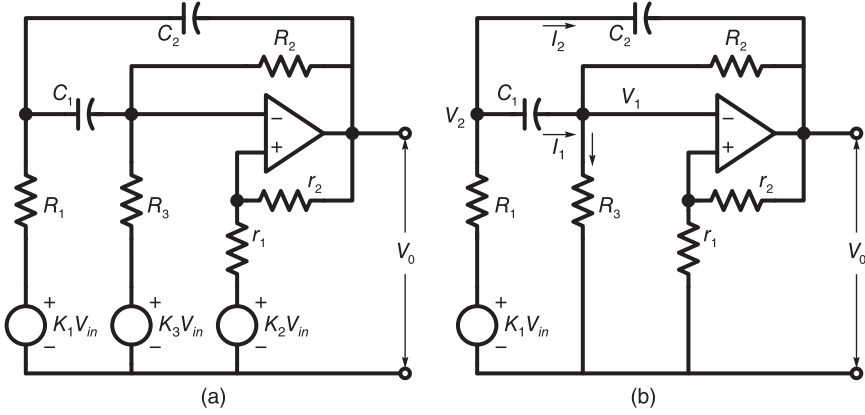


FIGURE 10.28 (a) Thevenin equivalent; (b) equivalent circuit with $K_1 v_{in}$ as the only source.

$$V_2 - V_0 = I_2 \frac{1}{C_2 s} \tag{10.186}$$

$$K_1 V_{in} = (I_1 + I_2) R_1 + V_2 \tag{10.187}$$

$$I_1 + (V_0 - V_1) / R_2 = V_1 / R_3. \tag{10.188}$$

Simplifying these equations we obtain

$$K_1 V_{in} = \left[\left(\frac{R_1}{R_3} + \frac{R_1}{R_2} + R_1 C_2 s + \frac{R_1 C_2}{R_3 C_1} + \frac{R_1 C_2}{R_2 C_1} + 1 + \frac{1}{R_3 C_1 s} + \frac{1}{R_2 C_1 s} \right) \frac{r_1}{r_1 + r_2} - \left(\frac{R_1}{R_2} - \frac{R_1 C_2}{R_2 C_1} - R_1 C_2 s - \frac{1}{R_2 C_1 s} \right) \right] V_0 \tag{10.189}$$

and the transfer function is given by

$$H_1(s) = \frac{V_0}{K_1 V_{in}}. \tag{10.190}$$

With $K_3 v_{in}$ as the only source, as shown in Fig. 10.29(a) we may write

$$V_1 = V_0 \frac{r_1}{r_1 + r_2} \tag{10.191}$$

$$(V_1 - V_0) = R_2 I_2 \tag{10.192}$$

$$V_1 - V_2 = I_3 \frac{1}{C_1 s} \tag{10.193}$$

$$K_3 V_{in} - I_1 R_3 = V_1 \tag{10.194}$$

$$I_1 = I_2 + I_3 \tag{10.195}$$

$$V_0 - V_2 = I_4 \frac{1}{C_2 s} \tag{10.196}$$

$$I_3 + I_4 = V_2 / R_1. \tag{10.197}$$

Solving these equations we obtain the transfer function in the form

$$H_3(s) = V_0 / (K_3 V_{in}) = \frac{1}{D_3(s)}. \tag{10.198}$$

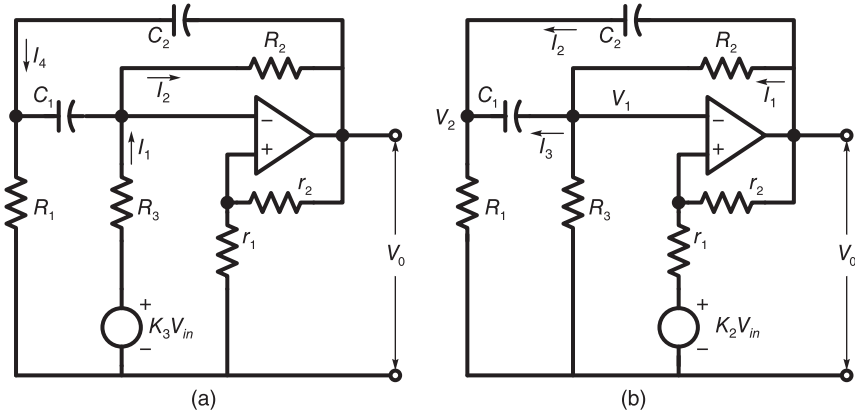


FIGURE 10.29 Equivalent circuit with (a) K_3v_{in} as only source; (b) K_2v_{in} as only source.

The denominator $D_3(s)$ is given by

$$D_3(s) = \left(\frac{R_3}{R_2} + C_1R_2s + 1 - \frac{R_3C_1^2s^2}{C_1s + C_2s + 1/R_1} \right) \frac{r_1}{(r_1 + r_2)} - \frac{R_3}{R_2} - \frac{R_3C_1C_2s^2}{C_1s + C_2s + 1/R_1}. \tag{10.199}$$

With K_2v_{in} as the only source, as shown in Fig. 10.29(b) we have

$$V_0 - V_1 = I_1R_2 \tag{10.200}$$

$$V_0 - V_2 = I_2 \frac{1}{C_2s} \tag{10.201}$$

$$V_1 - V_2 = I_3 \frac{1}{C_1s} \tag{10.202}$$

$$I_1 = I_3 + V_1/R_3 \tag{10.203}$$

$$I_2 + I_3 = V_2/R_1 \tag{10.204}$$

$$(V_0 - K_2V_{in}) \left(\frac{r_1}{r_1 + r_2} \right) + K_2V_{in} = V_1. \tag{10.205}$$

By successive elimination of intermediate variables we obtain the transfer function in the form

$$H_2(s) = V_0/(K_2V_{in}) = N_2(s)/D(s) \tag{10.206}$$

where

$$N_2(s) = r_1 [R_2 + R_3 + (C_1r_1R_1R_2 + C_2R_1R_2 + C_1R_1R_3 + C_2R_1R_3 + C_1R_2R_3)s + C_1C_2R_1R_2R_3s^2] \tag{10.207}$$

and

$$D(s) = r_1R_2 - r_2R_3 + (C_1r_1R_1R_2 + C_2r_1R_1R_2 - C_1R_1r_2R_3 - C_2R_1r_2R_3 + C_1r_1R_2R_3)s - C_1C_2R_1r_2R_2R_3s^2. \tag{10.208}$$

Combining these results we obtain the overall transfer function, which can be written in the form

$$H(s) = \frac{\beta_2s^2 + \beta_1s + \beta_0}{\alpha_2s^2 + \alpha_1s + \alpha_0} \tag{10.209}$$

and, equivalently, the form

$$H(s) = \frac{b_2s^2 + b_1s + b_0}{s^2 + a_1s + a_0}. \tag{10.210}$$

With $\rho = r_1/r_2$ the numerator and denominator coefficients are given by

$$\alpha_2 = -C_1C_2R_1r_2R_2R_3 \tag{10.211}$$

$$b_2 = \beta_2/\alpha_2 = K_2 \tag{10.212}$$

$$b_1 = \beta_1/\alpha_2 = -(C_1K_3\rho R_1R_2 + C_2K_3\rho R_1R_2 - C_1K_2R_1R_2 - C_2K_2R_1R_2 + C_1K_3R_1R_2 + C_2K_3R_1R_2 - C_1K_2R_1R_3 - C_2K_2R_1R_3 + C_1K_1\rho R_2R_3 + C_1K_1R_2R_3 - C_1K_2R_2R_3) / (C_1C_2R_1R_2R_3) \tag{10.213}$$

$$b_0 = \beta_0/\alpha_2 = -(K_3\rho R_2 - K_2R_2 + K_3R_2 - K_2R_3) / (C_1C_2R_1R_2R_3) \tag{10.214}$$

$$a_1 = \alpha_1/\alpha_2 = -(C_1\rho R_1R_2 + C_2\rho R_1R_2 - C_1R_1R_3 - C_2R_1R_3 + C_1\rho R_2R_3) / (C_1C_2R_1R_2R_3) \tag{10.215}$$

$$a_0 = \alpha_0/\alpha_2 = (R_3 - \rho R_2) / (C_1C_2R_1R_2R_3). \tag{10.216}$$

To realize a given quadratic transfer function we solve these equations, obtaining

$$R_1 = \frac{a_1C_2 + \sqrt{a_1^2C_2^2 + 4a_0C_2(C_1 + C_2)}\rho}{2a_0C_2(C_1 + C_2)} \tag{10.217}$$

$$R_2 = \frac{(b_2 - K_3)(1 + \rho)}{C_1C_2R_1(a_0b_2 - a_0K_3 + b_0\rho - a_0K_3\rho)} \tag{10.218}$$

$$R_3 = \frac{(b_2 - K_3)(1 + \rho)}{(b_0 - a_0b_2)C_1C_2R_1}. \tag{10.219}$$

To evaluate K_1 we write

$$(C_1C_2R_1R_2R_3)b_1 + C_1K_3\rho R_1R_2 + C_2K_3\rho R_1R_2 - C_1K_2R_1R_2 - C_2K_2R_1R_2 + C_1K_3R_1R_2 + C_2K_3R_1R_2 - C_1K_2R_1R_3 - C_2K_2R_1R_3 - C_1K_2R_2R_3 = -(C_1\rho R_2R_3 + C_1R_2R_3)K_1 \tag{10.220}$$

obtaining

$$K_1 = \frac{b_2 - b_1C_2R_1 + b_0C_1C_2R_1^2 + b_0C_2^2R_1^2}{1 + \rho}. \tag{10.221}$$

Example 10.13 Design an active elliptic filter with the following specifications

1. Ripple of 1 dB or less in pass-band $0 \leq \omega \leq 1$.
 2. At $\omega = 2.00$ the attenuation should be at least 17 dB.
- Redo the above to obtain a pass-band cut-off frequency of 1 kHz.
From elliptic tables

$$H(s) = K \prod_i \frac{s^2 + c_i}{s^2 + a_i s + b_i}.$$

With $n = 2$, $R_p = 1$ dB, $R_s = 17.095$ dB, $\omega_s = 2.00$.

$$H_{norm}(s) = \frac{0.1397s^2 + 1.0427}{s^2 + 0.998942s + 1.170077} = 0.1397 \frac{s^2 + 7.464102}{s^2 + 0.998942s + 1.170077}.$$

Denormalization: We have

$$\omega_c = 2\pi f_c = 2\pi \times 1000 = 2000\pi \text{ r/s.}$$

Replacing s by $s/(2000\pi)$ we have

$$H(s) = K \frac{[s/(2000\pi)]^2 + 7.464102}{[s/(2000\pi)]^2 + 0.998942s/(2000\pi) + 1.170077}$$

$$H(s) = \frac{0.1397s^2 + 4.1166 \times 10^7}{s^2 + 6.2765 \times 10^3s + 4.6193 \times 10^7}$$

i.e.

$$b_2 = 0.1397, \quad b_1 = 0, \quad b_0 = 4.1166 \times 10^7,$$

$$a_1 = 6.2765 \times 10^3, \quad a_0 = 4.6193 \times 10^7.$$

We deduce that $K_2 = b_2 = 0.1397$ and we have four nonlinear equations in the eight unknowns $C_1, C_2, K_1, K_3, \rho, R_1, R_2, R_3$. We let $C_1 = C_2 = 1 F$, and note that we should have $0 \leq K_1 \leq 1$ and $0 \leq K_3 \leq 1$.

For the normalized transfer function we obtain with $K_3 = 0.1$, $C_1 = C_2 = 1 F$ and $\rho = 0.8$

$$R_1 = 0.83586 \Omega, \quad R_2 = 0.108627 \Omega, \quad R_3 = 0.097231 \Omega$$

$$K_1 = 0.887076, \quad K_2 = 0.1397.$$

For the denormalized transfer function with the same values of K_3, C_1, C_2 and ρ we find

$$R_1 = 1.33031 \times 10^{-5} \Omega, \quad R_2 = 1.72883 \times 10^{-5} \Omega, \quad R_3 = 1.54747 \times 10^{-5} \Omega$$

$$K_1 = 0.887076, \quad K_2 = 0.1397.$$

If instead we let $C_1 = C_2 = 1\mu F$ we would obtain for the normalized prototype $R_1 = 835.86 k \Omega$, $R_2 = 108.627 k \Omega$, $R_3 = 97.231 k \Omega$, $K_1 = 0.887076$, $K_2 = 0.1397$ and for the denormalized filter the values $R_1 = 133.031\Omega$, $R_2 = 17.2883\Omega$, $R_3 = 15.4747\Omega$, and the same values of K_1 and K_2 .

Example 10.14 Design an active bandpass fourth order Chebyshev filter with pass-band ripple of 1 dB and pass-band edge-frequencies $\omega_L = 1 r/s$ and $\omega_H = 3 r/s$.

The bandpass filter transfer function is given by

$$H(s) = \frac{3.9305s^2}{s^4 + 2.1955s^3 + 10.4100s^2 + 6.5864s + 9}.$$

Factoring $H(s)$ we can write

$$H(s) = \frac{-1.9825s}{(s^2 + 1.6180s + 8.4048)} \frac{-1.9825s}{s^2 + 0.5775s + 1.0708}.$$

Writing $H(s) = H_1(s)H_2(s)$ we have

$$b_2 = 0, \quad b_1 = -1.9825, \quad b_0 = 0$$

for both transfer functions $H_1(s)$ and $H_2(s)$. The denominator coefficients are $a_1 = 1.6180$, $a_0 = 8.4048$ for $H_1(s)$ and $a_1 = 0.5775$, $a_0 = 1.0708$ for $H_2(s)$. We obtain for the realization of $H_1(s)$

$$R_1 = 0.13904\Omega, \quad R_2 = 0.855719\Omega, \quad K_1 = 0.250589$$

and for $H_2(s)$

$$R_1 = 0.38953\Omega, \quad R_2 = 2.39745\Omega, \quad K_1 = 0.702041.$$

10.19 First Order Filter Realization

As noted earlier if the filter has a real pole, there may arise the need for a simple realization of first order filter section. A possible passive circuit realization is shown in Fig. 10.30(a,b). The transfer functions of these circuits are, respectively,

$$H_1(s) = \frac{1/(RC)}{s + 1/(RC)}$$

and

$$H_2(s) = \frac{s}{s + 1/(RC)}$$

the second having a zero at $s = 0$.

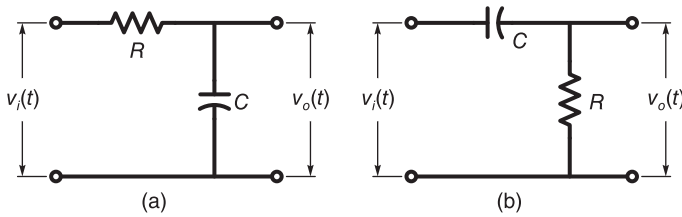


FIGURE 10.30 Two circuit realizations of first order filters.

We note that the first is a lowpass filter while the second is a highpass one. It is noted that if such a filter section is included as the last stage of a cascade of second order active networks then the preceding stage output will provide the required loading isolation between stages.

Active first order filters using one operation amplifier are easy to realize. Consider the circuit with two impedances shown in Fig. 10.31.

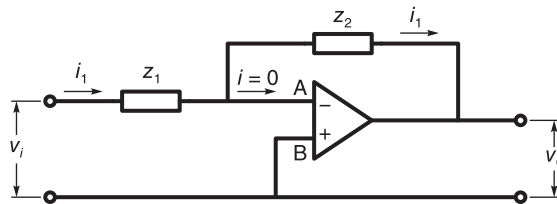


FIGURE 10.31 Active first order filter.

We can write

$$I_1(s) = V_i(s) / Z_1(s) = [0 - V_o(s)] / Z_2(s). \tag{10.222}$$

The circuit transfer function is

$$H(s) = \frac{V_o(s)}{V_i(s)} = -\frac{Z_2(s)}{Z_1(s)}. \tag{10.223}$$

If $Z_1(s) = Z_2(s) = R$ we have an inverter with

$$H(s) = \frac{V_o(s)}{V_i(s)} = -1. \quad (10.224)$$

If $Z_1(s) = R$ and $Z_2(s) = \frac{1}{Cs}$ then

$$H(s) = -\frac{1}{RCs} \quad (10.225)$$

$$V_o(s) = -\frac{1}{RCs} V_i(s) \quad (10.226)$$

i.e.

$$v_o(t) = -\frac{1}{RC} \int v_i dt \quad (10.227)$$

and the circuit is a simple integrator as seen earlier.

To realize a transfer function $H(s)$ that serves as a general first order filter we seek a solution leading to the general first order transfer function

$$H(s) = -K \frac{s + b_0}{s + a_0}. \quad (10.228)$$

The negative sign is due to the fact that the circuit produces negative gain. Writing

$$H(s) = \frac{-Z_2(s)}{Z_1(s)} = \frac{-K}{s + a_0} (s + b_0) \quad (10.229)$$

we can write

$$Z_2(s) = \frac{K}{s + a_0} \quad (10.230)$$

$$Z_1(s) = \frac{1}{s + b_0} = \frac{1}{\frac{1}{s} + b_0} \quad (10.231)$$

$$Y_1(s) = 1/Z_1(s) = \frac{1}{1/s} + b_0 = Y_{11} + Y_{12} = 1/Z_{11} + 1/Z_{12} \quad (10.232)$$

$Z_{11} = \frac{1}{s}$, $Z_{12} = 1/b_0$, i.e. $Z_1(s)$ is a capacitor $C_1 = 1$ in parallel with a resistor $R_1 = 1/b_0 \Omega$. Similarly

$$Z_2 = \frac{K}{s + a_0} = \frac{1}{s/K + a_0/K} = \frac{1}{\frac{1}{K/s} + a_0/K} \quad (10.233)$$

$$Y_2 = \frac{1}{K/s} + a_0/K = Y_{21} + Y_{22} \quad (10.234)$$

$$Z_{21} = 1/Y_{21} = \frac{K}{s} = \frac{1}{(1/K)s} = \frac{1}{Cs} \quad (10.235)$$

$$Y_{22} = a_0/K, \quad Z_{22} = K/a_0 \quad (10.236)$$

i.e. Z_2 is a capacitor $C_2 = 1/K$ F, in parallel with a resistor $R_2 = K/a_0 \Omega$. The circuit is shown in Fig. 10.32.

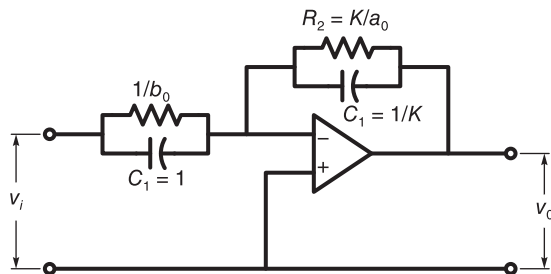


FIGURE 10.32 Realization of a first order filter.

10.20 A Biquadratic Transfer Function Realization

An approach to the realization of biquadratic functions is shown in Fig. 10.33. In this figure, the R-C circuit has the two inputs v_i and v_o . Its output v_1 , provides positive feedback to the operational amplifier being connected to its positive input terminal. A negative feedback to the operational amplifier is provided by the resistors R_A and R_B through a connection to the operational amplifier's negative input terminal.

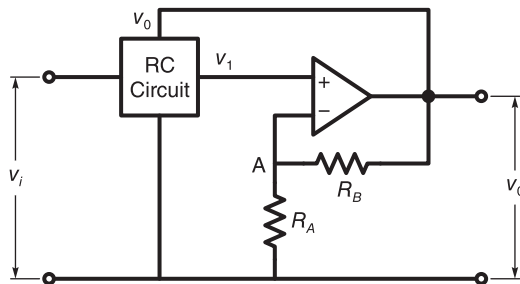


FIGURE 10.33 Biquadratic transfer function realization.

Assuming that the operational amplifier has infinite gain, the voltage between its terminals and the current through them are assumed to be zero. The voltage at point A in the figure is therefore equal to v_1 . We can write

$$V_1(s) = V_0(s) \frac{R_A}{R_A + R_B}. \tag{10.237}$$

Letting $\rho = R_A/R_B$ we have

$$V_1(s) = V_0(s) \frac{\rho}{1 + \rho}. \tag{10.238}$$

Let $H_{i,1}(s)$ be the feed forward transfer function $H_f(s)$ of the RC circuit and $H_{o,1}(s)$ be its feedback transfer function $H_b(s)$. We have

$$H_f(s) = H_{i,1}(s) = \left. \frac{V_1(s)}{V_i(s)} \right|_{V_o(s)=0} \tag{10.239}$$

$$H_b(s) = H_{o,1}(s) = \left. \frac{V_1(s)}{V_o(s)} \right|_{V_i(s)=0} \tag{10.240}$$

Using a common denominator $D(s)$, we can write $H_f(s)$ and $H_b(s)$ in the form

$$H_f(s) = N_f(s)/D(s), \quad H_b(s) = N_b(s)/D(s) \tag{10.241}$$

and we have

$$V_1(s) = H_f(s) V_i(s) + H_b(s) V_o(s) \tag{10.242}$$

i.e.

$$\frac{\rho}{1+\rho} V_o(s) = H_f(s) V_i(s) + H_b(s) V_o(s) \tag{10.243}$$

$$[\rho/(1+\rho) - H_b(s)] V_o(s) = H_f(s) V_i(s). \tag{10.244}$$

The overall transfer function is

$$\begin{aligned} H(s) &= \frac{V_o(s)}{V_i(s)} = \frac{H_f(s)}{[\rho/(1+\rho)] - H_b(s)} = \frac{N_f(s)/D(s)}{[\rho/(1+\rho)] - N_b(s)/D(s)} \\ &= \frac{(1+1/\rho) N_f(s)}{D(s) - (1+1/\rho) N_b(s)}. \end{aligned} \tag{10.245}$$

Among the many possible choices of the R-C circuit an example is shown in Fig. 10.34. The feed forward and feedback transfer functions $H_f(s)$ and $H_b(s)$ are found by grounding the terminals marked (1) and (2), resulting in the two circuits shown in Fig. 10.35(a,b) respectively.

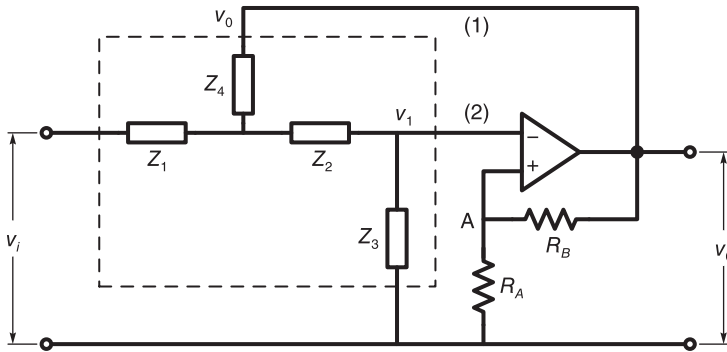


FIGURE 10.34 Possible R-C circuit for biquadratic transfer function realization.

Let the outputs of these two circuits be labeled v'_1 and v''_1 as shown in the figure. We have, from Fig. 10.35(a)

$$H_f(s) = \frac{V'_1(s)}{V_i(s)} = \frac{z_3 z_4}{z_1 z_4 + z_1 z_2 + z_1 z_3 + z_2 z_4 + z_3 z_4} \tag{10.246}$$

$$H_b(s) = \frac{z_1 z_3}{z_1 z_4 + z_1 z_2 + z_1 z_3 + z_2 z_4 + z_3 z_4}. \tag{10.247}$$

With

$$H_f(s) = N_f(s)/D(s) \tag{10.248}$$

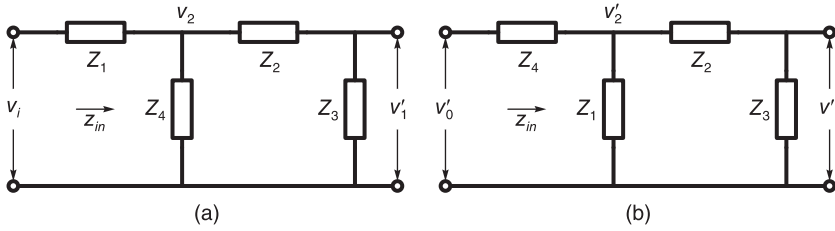


FIGURE 10.35 Result of grounding the terminals marked (1) and (2).

$$H_b(s) = N_b(s) / D(s) \tag{10.249}$$

$$\begin{aligned}
 H(s) &= \frac{(1 + 1/\rho)N_f(s)}{D(s) - (1 + 1/\rho)N_b(s)} \\
 &= \frac{(1 + 1/\rho)z_3z_4}{z_1z_4 + z_1z_2 + z_1z_3 + z_2z_4 + z_3z_4 - (1 + 1/\rho)z_1z_3}.
 \end{aligned}
 \tag{10.250}$$

Letting $z_1 = R_1$, $z_2 = R_2$, $z_3 = \frac{1}{C_2s}$, $z_4 = \frac{1}{C_1s}$ we obtain the circuit shown in Fig. 10.34 known as the lowpass Sallen–Key circuit.

10.21 Sallen–Key Circuit

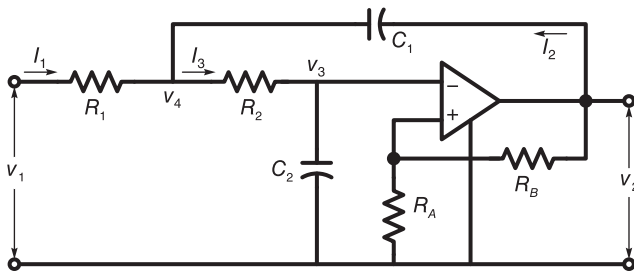


FIGURE 10.36 Sallen Key circuit.

The Sallen Key circuit is shown in Fig. 10.36. We can write the circuit equations

$$V_2 = KV_1 \tag{10.251}$$

$$V_1v_i = V_2 \frac{R_1}{R_1 + R_2} \tag{10.252}$$

$$v_2 = Av_3, \quad v_3 = v_2 \frac{R_A}{R_A + R_B} \tag{10.253}$$

Let

$$\alpha = \frac{R_A + R_B}{R_A} = 1 + \frac{R_B}{R_A} \quad (10.254)$$

$$V_2(s) - V_4(s) = \frac{1}{C_1 s} I_2 \quad (10.255)$$

$$(V_1 - V_4) = R_1 V_1 \quad (10.256)$$

$$(I_1 + I_2) R_2 = V_4 - V_3 \quad (10.257)$$

$$V_3 = (I_1 + I_2) \frac{1}{C_2 s} = \frac{V_4 - V_3}{R_2} \frac{1}{C_2 s} = V_2 \times \frac{R_A}{R_A + R_B} \quad (10.258)$$

$$V_3 \left(1 + \frac{1}{R_2} \right) = \frac{V_4}{R_2 C_2 s} \quad (10.259)$$

$$V_4 = (R_2 C_2 s + C_2 s) V_3 = (R_2 C_2 s + C_2 s) V_2 / \alpha \quad (10.260)$$

$$V_4 = V_1 - R_1 I_1 \quad (10.261)$$

$$I_1 = I_3 - I_2 \quad (10.262)$$

$$\frac{V_1 - V_4}{R_1} = \frac{V_4}{R_2 + \frac{1}{C_2 s}} - (V_2 - V_4) C_1 s \quad (10.263)$$

$$\begin{aligned} \frac{V_1 - V_4}{R_1} &= \frac{V_4}{R_2 + \frac{1}{C_2 s}} - (V_2 - V_4) C_1 s = \frac{V_4 C_2 s}{1 + R_2 C_2 s} - (V_2 - V_4) C_1 s \\ &= \frac{V_4 C_2 s - (V_2 - V_4) C_1 s (1 + R_2 C_2 s)}{1 + R_2 C_2 s} \\ &= \frac{V_4 C_2 s - V_2 C_1 s (1 + R_2 C_2 s) + V_4 C_1 s (1 + R_2 C_2 s)}{1 + R_2 C_2 s} \\ &= \frac{V_4 [C_2 s + C_1 s (1 + R_2 C_2 s)] - V_2 C_1 s (1 + R_2 C_2 s)}{1 + R_2 C_2 s} \end{aligned} \quad (10.264)$$

$$\begin{aligned} (V_1 - V_4) (1 + R_2 C_2 s) &= V_4 [R_1 C_2 s + R_1 C_1 s (1 + R_2 C_2 s)] \\ &\quad - V_2 R_1 C_1 s (1 + R_2 C_2 s) \end{aligned} \quad (10.265)$$

$$\begin{aligned} V_1 (1 + R_2 C_2 s) &= V_4 [(1 + R_2 C_2 s) + R_1 C_2 s + R_1 C_1 s (1 + R_2 C_2 s)] \\ &\quad - V_2 R_1 C_1 s (1 + R_2 C_2 s) \\ &= \frac{(R_2 C_2 s + C_2 s)}{A} V_2 [(1 + R_2 C_2 s) + R_1 C_2 s \\ &\quad + R_1 C_1 s (1 + R_2 C_2 s)] - V_2 R_1 C_1 s (1 + R_2 C_2 s) \end{aligned} \quad (10.266)$$

$$\begin{aligned} V_1 &= \frac{V_2}{\alpha} [1 + R_2 C_2 s + R_1 C_2 s + R_1 C_1 s (1 + R_2 C_2 s)] - V_2 R_1 C_1 s \\ &= V_2 \left[\frac{1 + R_2 C_2 s + R_1 C_2 s + R_1 C_1 s + R_1 R_2 C_1 C_2 s^2}{\alpha} - R_1 C_1 s \right] \\ &= V_2 \left[\frac{1 + (R_2 C_2 + R_1 C_2 + R_1 C_1) s + R_1 R_2 C_1 C_2 s^2 - R_1 C_1 \alpha s}{\alpha} \right] \end{aligned} \quad (10.267)$$

$$\begin{aligned}
 H(s) &= \frac{V_2}{V_1} = \frac{\alpha}{1 + (R_2C_2 + R_1C_2 + R_1C_1)s + R_1R_2C_1C_2s^2 - R_1C_1\alpha s} \\
 &= \frac{\alpha / (R_1R_2)}{\frac{1}{R_1R_2} + \left(\frac{C_2}{R_1} + \frac{C_2}{R_2} + \frac{C_1}{R_2}\right)s + C_1C_2s^2 - \frac{C_1\alpha}{R_2}s} \\
 &= \frac{\alpha G_1G_2}{G_1G_2 + (C_2G_1 + C_2G_2 + C_1G_2)s + C_1C_2s^2 - C_1G_2\alpha s} \tag{10.268}
 \end{aligned}$$

which has the form

$$H(s) = \frac{K}{s^2 + a_1s + a_0} = \frac{K}{s^2 + (\omega_0/Q)s + \omega_0^2} \tag{10.269}$$

with

$$K = \alpha / (R_1R_2C_1C_2) \tag{10.270}$$

$$a_1 = \frac{1}{C_1R_1} + \frac{1}{C_1R_2} + \frac{1}{C_2R_2} - \frac{\alpha}{C_2R_2} \tag{10.271}$$

$$a_0 = \frac{1}{R_1R_2C_1C_2} \tag{10.272}$$

$$\alpha = 1 + R_B/R_A \tag{10.273}$$

$$\omega_0 = \sqrt{a_0}, \quad Q = \omega_0/a_1 = \sqrt{a_0}/a_1. \tag{10.274}$$

We have two equations in a_0 and a_1 and the five unknowns C_1, C_2, R_1, R_2 and α . We may arbitrarily set $C_1 = C_2 = C$ obtaining

$$K = \alpha / (R_1R_2C^2) \tag{10.275}$$

$$a_0 = \frac{1}{R_1C} + \frac{2 - \alpha}{R_2C}, \tag{10.276}$$

Example 10.15 Show the active filter realization of a fourth order Butterworth filter prototype using the Sallen-Key configuration. Repeat to obtain the same filter with a cut-off frequency of 1 kHz.

The prototype filter transfer function can be factored into quadratic forms

$$H(s) \triangleq H_1(s)H_2(s) = \frac{1}{s^2 + 0.7654s + 1} \frac{1}{s^2 + 0.8478s + 1}.$$

For

$$H_1(s), \quad K = 1, \quad a_1 = 0.7654, \quad a_0 = 1.$$

For

$$H_2(s), \quad K = 1, \quad a_1 = 1.8478, \quad a_0 = 1.$$

Taking $C_1 = C_2 = 1 \text{ F}$ and $R_A = R_B$, i.e.

$$\alpha = 2$$

we have for $H_1(s)$

$$R_1 = 1/0.7654 = 1.3066 \text{ } \Omega, \quad R_2 = a_1/a_0 = 0.7654 \text{ } \Omega.$$

For $H_2(s)$ we have

$$R_1 = 1/1.8478 = 0.5412 \text{ } \Omega, \quad R_2 = 1.8478 \text{ } \Omega.$$

Replacing ω by $\omega / (2\pi \times 1000)$ we obtain the denormalized transfer function

$$H(s) = \frac{1.5585 \times 10^{15}}{s^4 + 1.6419 \times 10^4 s^3 + 1.3479 \times 10^8 s^2 + 6.4819 \times 10^{11} s + 1.5585 \times 10^{15}}$$

$$H_1(s) = \frac{K_1}{s^2 + 1.161 \times 10^4 s + 3.9478 \times 10^7}$$

$$H_2(s) = \frac{K_1}{s^2 + 4.8089 \times 10^3 s + 3.9478 \times 10^7}$$

where

$$K_1 = 3.9478 \times 10^7.$$

For $H_1(s)$ and $H_2(s)$ we have $a_0 = b_0 = 3.9478 \times 10^7$ and $a_1 = 1.161 \times 10^4$ and $a_1 = 4.8089 \times 10^3$, respectively. We obtain for $H_1(s)$:

$$R_1 = 8.6134 \times 10^{-5} \Omega$$

$$R_2 = 2.9408 \times 10^{-4} \Omega$$

and for $H_2(s)$

$$R_1 = 2.0795 \times 10^{-4} \Omega$$

$$R_2 = 1.2181 \times 10^{-4} \Omega.$$

10.22 Problems

Problem 10.1 A system is described by the differential equation

$$a_1 \dot{y} + a_0 y = b_0 x$$

and has a transfer function $H_1(s)$. A second system is described by the equation

$$a_2 \ddot{y} + a_1 \dot{y} + a_0 y = b_1 \dot{x} + b_0 x$$

and has a transfer function $H_2(s)$.

Using these two systems we need to obtain a third order filter which should have the transfer function

$$H(s) = \frac{K(s - z_1)}{(s - p_1)(s - p_1^*)(s - p_3)}$$

where

$$z_1 = -\gamma, \quad p_1 = -\alpha_1 + j\beta_1, \quad p_3 = -\alpha_2$$

Draw the block diagram of this filter and evaluate the coefficients a_0 , a_1 , a_2 , b_0 and b_1 which produce the desired filter.

Problem 10.2 Consider a Butterworth filter of order $n = 5$. Write its magnitude-squared spectrum $|H(j\omega)|^2$. Deduce thereof the function $F(s) = H(s)H(-s)$. Deduce the required input impedance $Z(s)$ for a passive ladder network realization. Sketch the ladder network. Perform a continued-fraction expansion and deduce the values of the passive ladder network components.

Problem 10.3 Find the input impedance $Z(s)$ of a passive ladder network corresponding to a lowpass Butterworth filter of order $n = 5$ using the matrix evaluation approach.

Problem 10.4 Evaluate the required input impedance $Z(s)$ of a passive ladder network for a Chebyshev filter of order $n = 10$ and pass-band ripple of 1 dB. Perform a continued-fraction expansion deducing the values of the circuit components.

Problem 10.5 For a delay normalized Bessel lowpass filter prototype of order $n = 5$ write the value of the transfer function $H(s)$ and the input impedance $Z(s)$ of a corresponding passive ladder network. Show a continued-fraction expansion and deduce the circuit components with reference to a sketch of the circuit.

Problem 10.6 For an elliptic filter lowpass prototype of order $n = 7$, a pass-band ripple of $R_p = 0.1$ dB, a stop band edge frequency of $W_s = 1.05$, sketch a realization as a passive ladder network and deduce its components.

Problem 10.7 Design an active elliptic filter using the SAB circuit of Fig. 10.27 with the following specifications

1. Ripple of 1 dB or less in the pass-band $0 \leq \omega \leq 1$.
2. At $\omega = 1.5$ the attenuation should be at least 11 dB.

Assume $C_1 = C_2 = 1$ F, $K_3 = 0.1$ and $\rho = 0.8$.

Re-do the above to obtain a pass-band cut off frequency of 200 Hz. Assume $C_1 = C_2 = 1\mu\text{F}$, $K_3 = 0.1$ and $\rho = 0.8$.

Problem 10.8 Using the Sallen Key circuit design an active lowpass Chebyshev filter with pass-band ripple of 1 dB, a minimum attenuation in the stop band of 50 dB and with pass-band edge frequency $\omega = 1$ and stop band edge frequency of $\omega = 4$.

10.23 Answers to Selected Problems

Problem 10.1 See Fig. 10.37.

$$H(s) = H_1(s)H_2(s)$$

where

$$H_1(s) = \frac{K}{s + \alpha_2} = \frac{b_0}{a_1s + a_0}$$

$$H_2(s) = \frac{s + \gamma}{s^2 + s c_1 + c_0} = \frac{b_1s + b_0}{a_2s^2 + a_1s + a_0}$$

For $H_2(s)$:

$$b_1 = 1, \quad b_0 = \gamma, \quad a_2 = 1, \quad a_1 = c_1, \quad a_0 = c_0$$

For $H_1(s)$:

$$b_0 = K, \quad a_1 = 1, \quad a_0 = \alpha_2$$

Problem 10.2

$$Z(s) = 2 \sum_{i=1}^5 \frac{r_i}{s - p_i} = \frac{0.6472s^4 + 2.094s^3 + 3.142s^2 + 2.589s + 1}{s^5 + 3.236s^4 + 5.236s^3 + 5.236s^2 + 3.236s + 1}$$

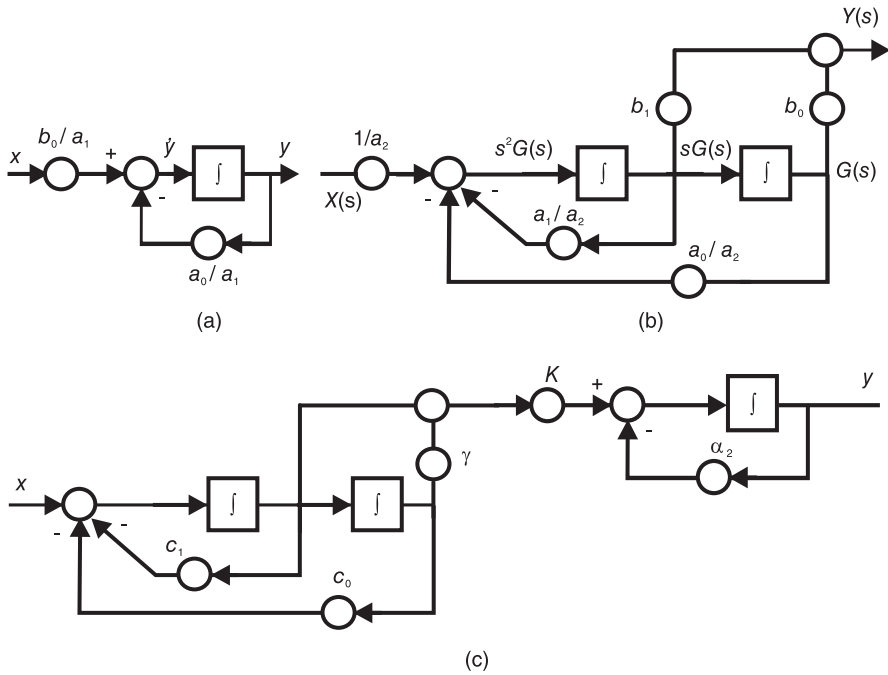


FIGURE 10.37 Block diagram, Problem 10.1.

The input admittance of the fifth order ladder network is $Y(s) = 1/Z(s)$. Performing a continued partial fraction expansion we obtain the successive quotients:

$Q = \{1.5451s, 1.6944s, 1.3820s, 0.8944s, 0.3090s\}$. The successive element values of the ladder network shown in Fig. 10.1 (c), which should be re-drawn for $n = 5$, are therefore $C_1 = 0.3090$, $L_2 = 0.8944$, $C_3 = 1.3820$, $L_4 = 1.6944$, $C_5 = 1.5451$.

Problem 10.3

$$Z(s) = \frac{0.6472s^4 + 2.0944s^3 + 3.1416s^2 + 2.5889s + 1}{s^5 + 3.236s^4 + 5.236s^3 + 5.236s^2 + 3.236s + 1}$$

The input admittance of the fifth order ladder network is $Y(s) = 1/Z(s)$. Performing a continued partial fraction expansion we obtain the successive quotients:

$Q = \{1.5451s, 1.6944s, 1.3820s, 0.8944s, 0.3090s\}$. The successive element values of the ladder network shown in Fig. 10.1 (c), which should be re-drawn for $n = 5$, are therefore $C_1 = 0.3090$, $L_2 = 0.8944$, $C_3 = 1.3820$, $L_4 = 1.6944$, $C_5 = 1.5451$.

Problem 10.4

The filter transfer function to be realized has the form $H(s) = K/D(s)$, where

$$D(s) = s^{10} + 0.9159s^9 + 2.919s^8 + 2.108s^7 + 2.982s^6 + 1.613s^5 + 1.244s^4 + 0.4554s^3 + 0.1825s^2 + 0.0345s + 0.004307$$

and $K = 0.004307$. The coefficient a_0 to a_9 are given, respectively, by $a_k = \{0.0043067, 0.041402, 0.14919, 0.4959, 0.78538, 1.5881, 1.2995, 1.8667, 0.66366, 0.72457\}$. The denominator polynomial of the input impedance is the same denominator polynomial $D(s)$ of the transfer function. We effect a continued fraction expansion, obtaining the same circuit component values as listed in Chapter 10, Table 10.14.

Problem 10.5

$$H(s) = 945/(s^5 + 15s^4 + 105s^3 + 420s^2 + 945s + 945).$$

The coefficient a_0 to a_9 are given, respectively, by $a_k = \{945, 582.41, 162.41, 24.074, 1.6049, \dots\}$. The denominator polynomial of the input impedance is the same denominator polynomial $D(s)$ of the transfer function. We effect a continued fraction expansion, obtaining the same circuit component values as listed in Chapter 10, Table 10.15.

Problem 10.6

$$Z_0 = Z_{in} - 1 \triangleq N_z(s)/D_z(s)$$

where

$$N_z(s) = 0.3176 + 0.630497s + 1.6748s^2 + 1.45543s^3 + 2.36087s^4 + 0.822248s^5 + s^6$$

and

$$D_z(s) = 0.3176 + 1.03853s + 1.6748s^2 + 3.35783s^3 + 2.36087s^4 + 3.52349s^5 + 1.s^6 + 1.20839s^7$$

and evaluating the zeros of $H(s)$ we apply the same approach as in the example to short circuit the remainder of the network, deducing successively the series inductances, applying a partial fraction, deducing the shunt circuits' L and C components. We obtain the values $L_1, C_2, L_2, L_3, C_4, L_4, L_5, C_6, L_6, L_7$ equal respectively to

$$0.9194, 1.0766, 0.3422, 1.0962, 0.4052, 2.2085, 0.8434, 0.50342, 1.5183, 0.4110.$$

Problem 10.7

$$H(s) = \frac{0.2756s^2 + 1.0823629}{s^2 + a_1s + a_0} = \frac{b_2s^2 + b_0}{s^2 + a_1s + a_0}$$

$$K = b_2 = 0.2756172.$$

With $C_1 = C_2 = 1$ F, $K_3 = 0.1$, $\rho = 0.8$. we obtain $K_2 = 0.2756172$, $R_1 = 0.782821$, $R_3 = 0.54011$, $R_2 = 0.411207$, $K_1 = 0.890099$.

The denormalized filter transfer function is given by

$$H(s) = \frac{427300 + 0.275617s^2}{479438 + 552.555 + s^2}$$

With $C_1 = C_2 = 10^{-6}$ F we obtain $K_2 = 0.2756172$, $R_1 = 1245.9$, $R_3 = 859.611$, $R_2 = 654.457$, $K_1 = 0.890099$.

Problem 10.8 For $H_1(s)$: $K = b_0 = 0.4956$, $b_1 = b_2 = 0$, $a_0 = 0.2794$, $a_1 = 0.6737$, $a_2 = 1$, $K = b_0 = 0.4956$, $R_2 = 1/a_1 = 1.4843$, $R_1 = 1/(a_0 * R_2 * C_1 * C_2) = 2.4112$, $\alpha = 1.7739$, $R_B/R_A = 0.7739$.

For $H_2(s)$: Taking $K = 1$ we have $b_0 = 0.4956$, $b_1 = b_2 = 0$, $a_0 = 0.9865$, $a_1 = 0.2791$, $a_2 = 1$, $K = b_0 = 0.4956$, $R_2 = 1/a_1 = 3.5829$, $R_1 = 1/(a_0 * R_2 * C_1 * C_2) = 0.2829$, $\alpha = 1.0137$, $R_B/R_A = 0.0137$. We have used the value $K = 1$ for the realization of the second transfer function $H_2(s)$ rather than $K = b_0 = 0.4956$ to avoid obtaining negative value for the ration R_B/R_A . Such replacement of the gain value does not affect the desired frequency response characteristic response.

This page intentionally left blank

11.1 Introduction

In this chapter we study different approaches to the design of digital filters. There are in general three types of structures of digital filters. As we shall see in what follows, finite impulse response (FIR) filters are nonrecursive in structure and are all-zero, no poles, filters. They are also referred to as moving average (MA) type filters. All-pole, no zero, filters are recursive in structure and are also referred to as autoregressive (AR) type filters. Infinite impulse response (IIR) filters are recursive in structure and are pole-zero filters, also referred to as autoregressive moving average (ARMA) type filters. We shall study methods for deducing the required transfer function from the continuous filter counterpart or otherwise. Lattice type filter structures are subsequently introduced. Least squares approaches to the design of digital filters are subsequently presented.

11.2 Signal Flow Graphs

Similarly to continuous-time systems a discrete-time system may be represented by a *signal flow graph*. Such a graph is composed of nodes and directed branches. If a system of transfer function $H(z)$ receives an input $v[n]$ and has an output $y[n]$, then

$$Y(z) = V(z)H(z) \tag{11.1}$$

a relation that can be represented by a directed branch labeled $H(z)$, with input node marked $v[n]$ and output node $y[n]$. If the system simply multiplies the input $v[n]$ by a constant α , i.e. $y[n] = \alpha v[n]$ the relation can be represented by a directed branch with an associated *weighting coefficient*, or *weighting constant* equal to α , as shown in Fig. 11.1(a). The input node is called a *source node*. The output node is a *sink node*. A node from which directed branches emanate is a *branch point*. A node to which more than one directed branch converge is an *adder*, as shown in Fig. 11.1(b), where the output is the weighted sum $y[n] = av_1[n] + bv_2[n]$.

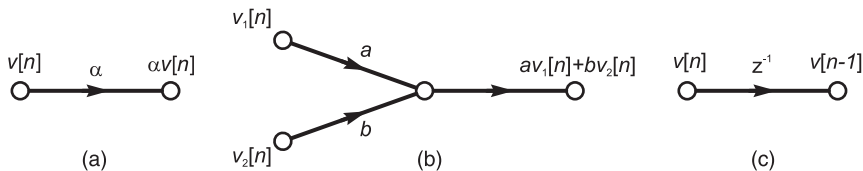


FIGURE 11.1 Flow diagram symbols for weighting, addition and delay.

An important element of a signal flow graph is the *delay element*. We note that the transfer function of a system that applies a unit delay to its input is $H(z) = z^{-1}$. If the input is $v[n]$, the output is $y[n] = v[n-1]$ since in the z -domain this means that $Y(z) = z^{-1}V(z)$. The signal flow graph is therefore a directed branch of weighting constant z^{-1} as shown in Fig. 11.1(c).

11.3 IIR Filter Models

We have seen in Chapter 6 that the input–output relation of an IIR filter may be written in the form

$$y[n] = - \sum_{k=1}^N a_k y[n-k] + \sum_{k=0}^M b_k v[n-k]. \quad (11.2)$$

and in the z -domain

$$Y(z) = - \sum_{k=1}^N a_k z^{-k} Y(z) + \sum_{k=0}^M b_k z^{-k} V(z). \quad (11.3)$$

The transfer function may be written in the form

$$H(z) = \frac{Y(z)}{V(z)} = \frac{\sum_{k=0}^M b_k z^{-k}}{1 + \sum_{k=1}^N a_k z^{-k}} = \frac{b_0 + b_1 z^{-1} + b_2 z^{-2} + \dots + b_M z^{-M}}{1 + a_1 z^{-1} + a_2 z^{-2} + \dots + a_N z^{-N}}. \quad (11.4)$$

In what follows we study different structures for the implementation of IIR filters.

11.4 First Canonical Form

The input–output relation as described by the difference Equation (11.2), or the z -domain Equation (11.4), can be represented graphically by a signal flow graph as shown in Fig. 11.2. The diagram is constructed by drawing the input line $v[n] \longleftrightarrow V(z)$ and the output line $y[n] \longleftrightarrow Y(z)$. By adding delay elements, of transfer function z^{-1} , the flow graph generates $v[n-1] \longleftrightarrow z^{-1}V(z)$, $v[n-2] \longleftrightarrow z^{-2}V(z)$, ... as delayed values of the input $v[n]$. Similarly, $y[n-1] \longleftrightarrow z^{-1}Y(z)$, $y[n-2]$, ... are generated as delayed versions of $y[n]$, as shown in the figure. The filter structure shown in Fig. 11.2 is known as the *first canonical form*, or *direct-form I*.

11.5 Transposition

From system theory if all arrows of a signal flow graph are reversed the resulting flow graph has the same transfer function as that of the original one.

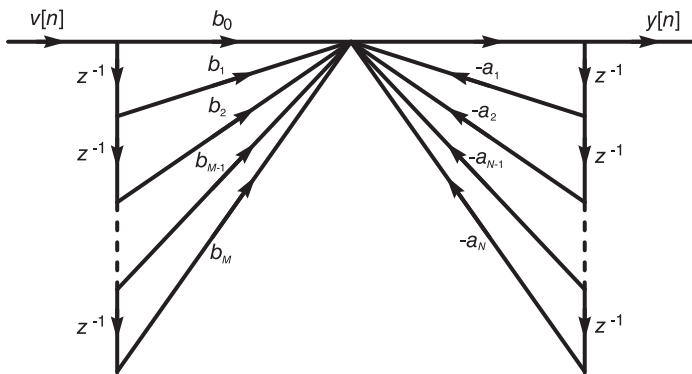


FIGURE 11.2 Digital IIR filter first canonical form.

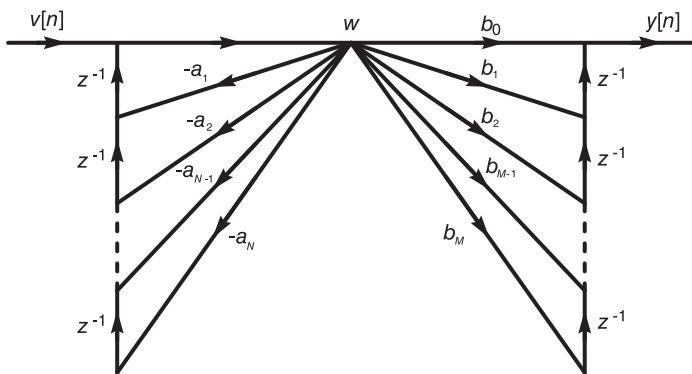


FIGURE 11.3 First canonical form with order of poles and zeros reversed.

If such process of arrow-reversal is applied to the flow graph of Fig. 11.2 the result is the flow graph shown in Fig. 11.3. Note that arrow-reversal implies that branch points become summing points and vice versa. The resulting structure is also known as the *transposed direct-form I*. Alternatively, we can obtain the structure shown in Fig. 11.3 by writing

$$H(z) = \frac{\sum_{k=0}^M b_k z^{-k}}{1 + \sum_{k=1}^N a_k z^{-k}} = H_1(z)H_2(z) \tag{11.5}$$

where

$$H_1(z) \triangleq \frac{1}{1 + \sum_{k=1}^N a_k z^{-k}} \tag{11.6}$$

$$H_2(z) \triangleq \sum_{k=0}^M b_k z^{-k}. \tag{11.7}$$

Let

$$H_1(z) = \frac{W(z)}{V(z)} \quad (11.8)$$

and

$$H_2(z) = \frac{Y(z)}{W(z)}. \quad (11.9)$$

We have

$$W(z) + W(z) \sum_{k=1}^N a_k z^{-k} = V(z) \quad (11.10)$$

i.e.

$$W(z) = - \sum_{k=1}^N \{a_k W(z)\} z^{-k} + V(z) \quad (11.11)$$

$$w[n] = - \sum_{k=1}^N a_k w[n-k] + v[n] \quad (11.12)$$

$$Y(z) = \sum_{k=0}^M \{b_k W(z)\} z^{-k} \quad (11.13)$$

and

$$y[n] = \sum_{k=0}^M b_k w[n-k]. \quad (11.14)$$

Denoting by w the central branch point in Fig. 11.3 we note that these equations are well described by this figure.

11.6 Second Canonical Form

Equations (11.11) and (11.13) can be rewritten in the forms

$$W(z) = V(z) - \sum_{k=1}^N a_k \{W(z)z^{-k}\} \quad (11.15)$$

and

$$Y(z) = \sum_{k=0}^M b_k \{W(z)z^{-k}\}. \quad (11.16)$$

These equations lead to the structure shown in Fig. 11.4 which is drawn for the case $M = N$. This form, known as the second canonical form or the *direct-form II*, can also be obtained from the first canonical form of Fig. 11.2 by viewing the structure as the cascade of two systems linked together by the middle point of the structure. By simply reversing the order of these two systems the second canonical form is obtained. We note that this form is optimal in the sense that it employs the least number of delay elements (z^{-1}), equal to the system order.

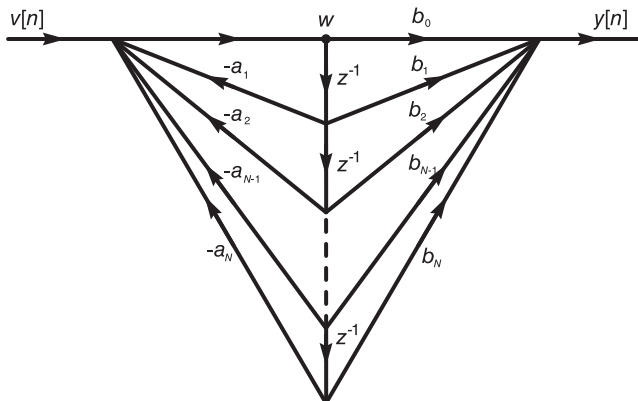


FIGURE 11.4 Second canonical form.

11.7 Transposition of the Second Canonical Form

Rewriting Equation (11.3) in the form

$$Y(z) = \sum_{k=1}^N \{b_k V(z) - a_k Y(z)\} z^{-k} + b_0 V(z) \tag{11.17}$$

$$y[n] = \sum_{k=1}^N \{b_k v[n-k] - a_k y[n-k]\} + b_0 v[n] \tag{11.18}$$

we obtain the filter structure shown in Fig. 11.5.

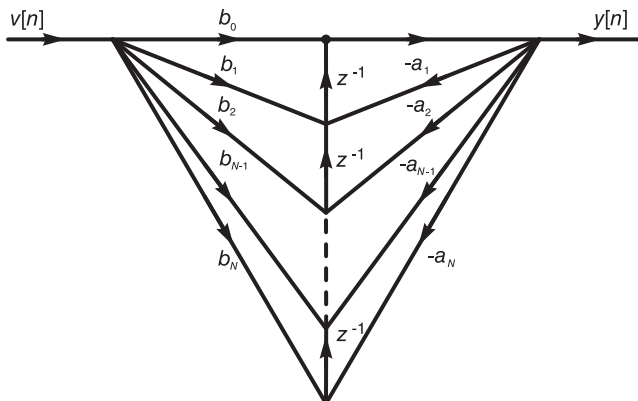


FIGURE 11.5 Second canonical form with orders of poles and zeros reversed.

This structure can also be obtained by the transposition (arrow-reversal) of the structure of Fig. 11.4. It is also known as the *transposed direct-form II*.

11.8 Structures Based on Poles and Zeros

A given rational transfer function $H(z)$ may be factored into the product of simple first and/or second order systems, or decomposed into the sum of such systems.

11.9 Cascaded Form

The transfer function $H(z)$ given by Equation (11.4) may be factored into the form

$$H(z) = G \prod_i H_i(z) \tag{11.19}$$

where G is the gain factor. Each $H_i(z)$ is a first or second order system transfer function. Real poles lead to first order systems; complex conjugate poles combine to form second order systems.

If $z = p_i$ is a real pole the resulting transfer function has the general form

$$H_i(z) = \frac{1 - z_i z^{-1}}{1 - p_i z^{-1}}. \tag{11.20}$$

Employing the second canonical form we obtain the structure of this first order filter shown in Fig. 11.6(a).

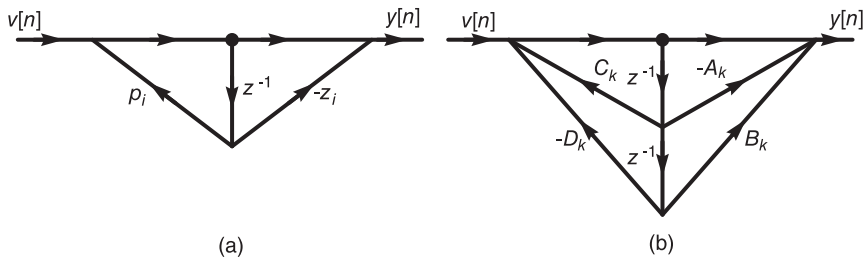


FIGURE 11.6 First and second order filter prototypes.

Note that if $H_i(z)$ has no zero, that is, if the value z_i in the numerator of $H_i(z)$ is zero, the branch having a coefficient $-z_i$ in the figure is eliminated.

A transfer function $H_k(z)$ having two conjugate zeros z_k and z_k^* , and two conjugate poles p_k and p_k^* may be written in the form

$$H_k(z) = \frac{1 - A_k z^{-1} + B_k z^{-2}}{1 - C_k z^{-1} + D_k z^{-2}}. \tag{11.21}$$

This second order filter structure is shown in Fig. 11.6(b).

In general a system transfer function may be decomposed in the form

$$H(z) = G \prod_i \frac{1 - z_i z^{-1}}{1 - p_i z^{-1}} \prod_k \frac{1 - A_k z^{-1} + B_k z^{-2}}{1 - C_k z^{-1} + d_k z^{-2}} \tag{11.22}$$

and has the form of a cascade of first and second order systems as those shown in Fig. 11.6.

11.10 Parallel Form

A partial fraction expansion of the filter transfer function $H(z)$ leads to a parallel filter structure. If the order of the numerator of $H(z)$ is greater than that of the denominator, a long division is performed. The result is the decomposition

$$H(z) = \sum_i e_i z^{-i} + \sum_j \frac{A_j}{1 - p_j z^{-1}} + \sum_k \frac{E_k (1 - z_k z^{-1})}{1 - c_k z^{-1} + D_k z^{-2}}. \tag{11.23}$$

A filter having such parallel structure is shown in Fig. 11.7.

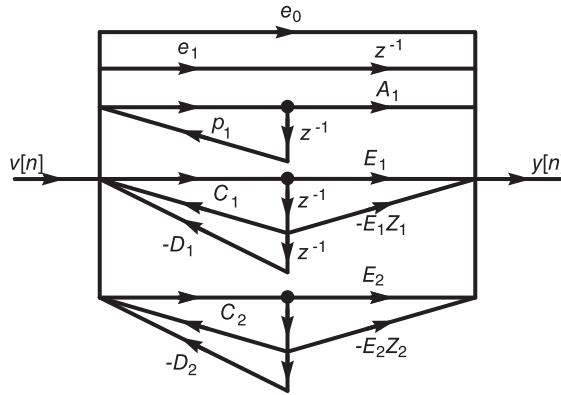


FIGURE 11.7 Parallel filter realization.

11.11 Matrix Representation

Another distinct model of such discrete-time systems is the state space model.

The approach may be illustrated using for example the IIR second canonical form which is reproduced in Fig. 11.8.

This state space model and alternative ones as well as matrix state space equations that can be deduced thereof are described and can be viewed in Chapter 8.

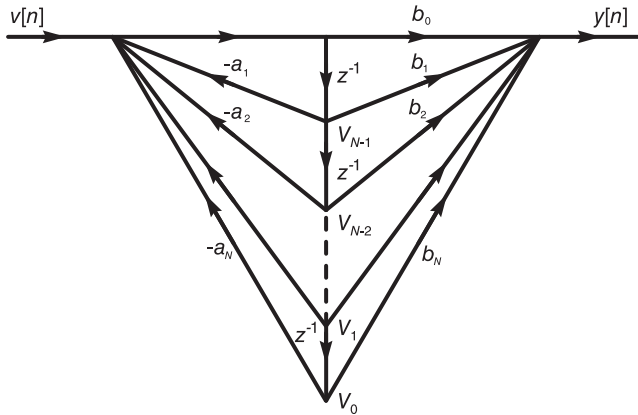


FIGURE 11.8 Matrix representation using state variable assignment.

11.12 Finite Impulse Response (FIR) Filters

As we have seen in Chapter 6, if the input to an FIR filter is $x[n]$ and its output is $y[n]$ we have

$$H(z) = Y(z)/X(z) = \sum_{n=0}^{N-1} h[n]z^{-n} \tag{11.24}$$

$$y[n] = \sum_{k=0}^{N-1} h[k]x[n-k]. \tag{11.25}$$

The filter can be realized using the structure shown in Fig. 11.9, obtaining a dual structure.

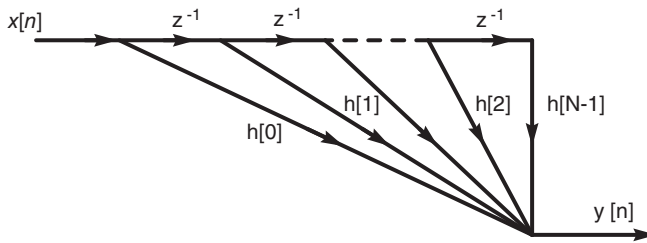


FIGURE 11.9 Finite impulse response filter structure.

Example 11.1 Show the structure of an FIR filter of which the impulse response is a 10-point truncation of

$$h_{\infty}[n] = (0.5)^n u[n].$$

We have

$$h[n] = h_{\infty}[n] R_{10}[n]$$

where

$$R_{10}[n] = u[n] - u[n - 10]$$

$$h[n] = (0.5)^n R_{10}[n].$$

The filter structure is the same as shown in Fig. 11.9, with the coefficients given by

$$\begin{aligned} h[0] &= 1, & h[1] &= 0.5, & h[2] &= 0.5^2 = 0.25 \\ h[3] &= 0.5^3 = 0.125, & h[4] &= 0.5^4 = 0.0625, & h[5] &= 0.0313 \\ h[6] &= 0.0157, & h[7] &= 0.0079, & h[8] &= 0.0039, & h[9] &= 0.0019. \end{aligned}$$

We note that if an FIR filter’s transfer function is factored by evaluating its roots then it can be expressed in the general form

$$H(z) = G \prod_i (1 - z_i z^{-1}) \prod_i (1 - A_k z^{-1} + B_k z^{-2}) \tag{11.26}$$

and can be realized as a cascade of first and second order zeros-only sections.

11.13 Linear Phase FIR Filters

FIR filters can be so designed as to have a linear phase frequency response. Note that if the impulse response is even-symmetric, the system frequency response is real. If the same symmetric impulse response is time-delayed, the system frequency response will have linear phase. Therefore, establishing even symmetry we write

$$h(n) = h(N - 1 - n). \tag{11.27}$$

The symmetry around the center of $h[n]$ is shown for the odd and even cases, $N = 7$ and $N = 8$, respectively, in Fig. 11.10. The case of odd symmetry is similarly analyzed and will be dealt with in Section 11.46.

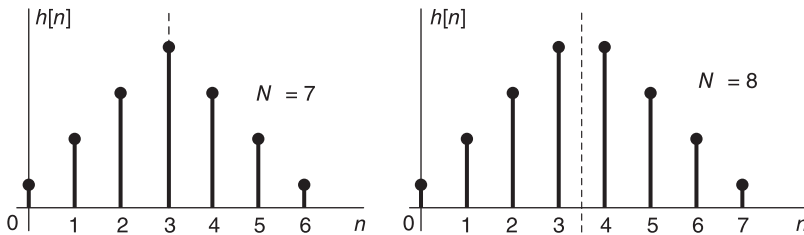


FIGURE 11.10 Symmetric impulse response for odd and even order.

Note that the center of symmetry is the point $n = (N - 1)/2$ for N odd and the midpoint between $n = (N/2) - 1$ and $N/2$ for N even. Such a shift to the right of $h[n]$ by

about $N/2$ point leads to causal impulse response that is nil for $n < 0$, hence to a realizable filter. We have

$$H(z) = \sum_{n=0}^{N-1} h(n)z^{-n}. \tag{11.28}$$

For even N

$$\begin{aligned} H(z) &= h[0] (z^0 + z^{-(N-1)}) + h[1] (z^{-1} + z^{-(N-2)}) + \dots \\ &\quad + h[N/2 - 1] (z^{-(N/2-1)} + z^{-N/2}) \\ &= \sum_{n=0}^{N/2-1} h[n] (z^{-n} + z^{-(N-1-n)}). \end{aligned} \tag{11.29}$$

For odd N

$$\begin{aligned} H(z) &= h[0] (z^0 + z^{-(N-1)}) + \dots + h[(N-1)/2 - 1] \\ &\quad \times \{z^{-(N-3)/2} + z^{-(N+1)/2}\} + h[(N-1)/2] (z^{-(N-1)/2}) \\ &= \sum_{n=0}^{(N-3)/2} h[n] (z^{-n} + z^{-(N-1-n)}) + h[(N-1)/2] z^{-(N-1)/2} \end{aligned} \tag{11.30}$$

and $Y(z) = X(z)H(z)$. The filter structure may be represented as shown in Fig. 11.11. For the odd N case the structure is shown in Fig. 11.12.

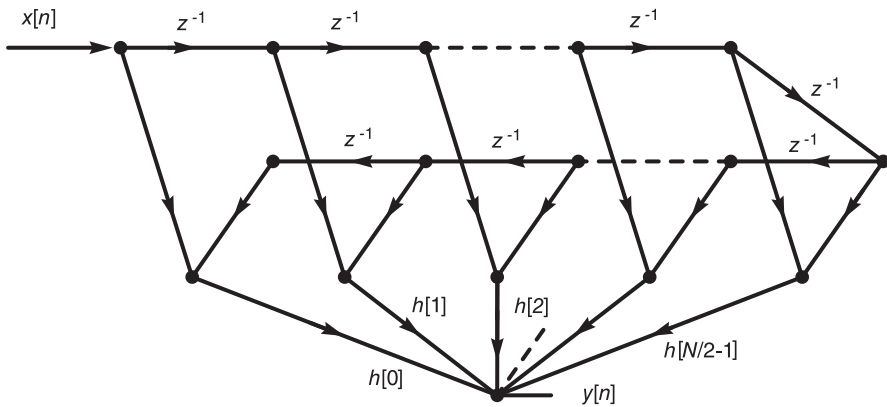


FIGURE 11.11 Linear phase FIR filter of even order.

The symmetry of the impulse response leads to a particular symmetry of the zeros' positions in the z -plane. In fact, if $H(z)$ has a zero $z = z_i$ it has a companion zero at $z = 1/z_i$. To show that this is the case note that the condition $h(n) = h(N - 1 - n)$ implies that

$$H(z) = h[N - 1] + h[N - 2]z^{-1} + \dots + h[0]z^{-(N-1)} = z^{-(N-1)}H(z^{-1}). \tag{11.31}$$

If $z = z_i$ is a zero then $z_i^{-(N-1)}H(z_i^{-1})=0$, i.e. $H(1/z_i) = 0$, wherefrom $1/z_i$ is also a zero. If $h[n]$ is real, its transform $H(z)$ has, moreover, with every complex zero $z = z_i$ a conjugate zero $z = z_i^*$, as shown in Fig. 11.13. A complex zero $z = z_i$ is thus accompanied by its conjugate $z = z_i^*$, the inverse $z = 1/z_i$ and the conjugate inverse $z = 1/z_i^*$. A complex zero that is not on the unit circle comes therefore in a group of four. A real zero z_i that is not on the unit circle is accompanied by its inverse $1/z_i$.

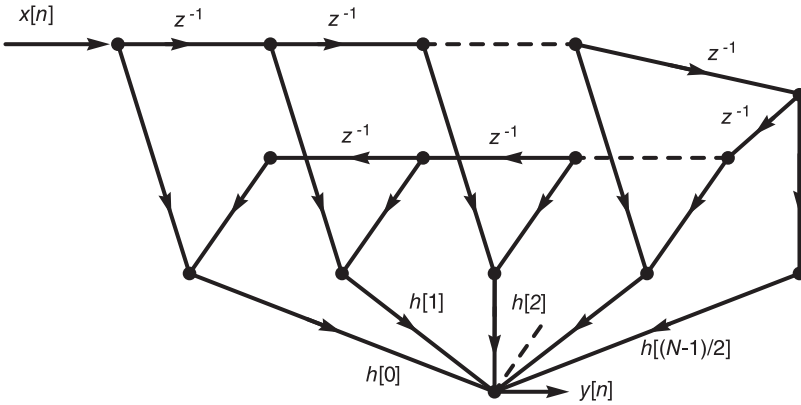


FIGURE 11.12 Linear phase FIR filter of odd order.

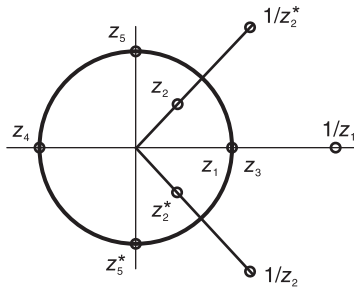


FIGURE 11.13 Sets of zeros of linear phase FIR filter.

As shown in the figure, a zero on the unit circle has its conjugate as its inverse. The system function $H(z)$ can thus be factored into first, second and fourth order components.

11.14 Conversion of Continuous-Time to Discrete-Time Filter

To derive a digital filter from a corresponding continuous-time analog filter either of two approaches are commonly used, namely, the *impulse invariance* approach, and the *bilinear transform* approach.

11.15 Impulse Invariance Approach

Let $H_c(s)$ be the transfer function of the continuous-time filter. Our objective is to evaluate a transfer function $H(z)$ of the digital filter that is the discrete-time domain counterpart.

The approach of impulse invariance consists of sampling the impulse response $h_c(t)$ of the continuous-time filter. The result is taken to be the impulse response (the unit-sample response) $h[n]$ of the digital filter. With $h[n]$ evaluated the system function $H(z)$ can be

deduced. An infinite impulse response IIR or an FIR filter can therefore be constructed. We have

$$h_c(t) = \mathcal{L}^{-1}[H_c(s)]. \quad (11.32)$$

The impulse response of the digital filter is given by

$$h[n] = T h_c(nT) \quad (11.33)$$

where T is the sampling period. The system function is given by

$$H(z) = \mathcal{Z}[h[n]]. \quad (11.34)$$

Using partial fractions, assuming simple poles we can write

$$H_c(s) = \sum_{k=1}^n \frac{A_k}{s - s_k} \quad (11.35)$$

wherefrom

$$h_c(t) = \sum_{k=1}^n A_k e^{s_k t} u(t) \quad (11.36)$$

and

$$h[n] = T \sum_{k=1}^n A_k e^{s_k nT} u[n] \quad (11.37)$$

$$H(z) = \sum_{k=1}^n \frac{T A_k}{1 - e^{s_k T} z^{-1}}. \quad (11.38)$$

Such sampling leads to the frequency domain relation, as found in Chapter 7,

$$H(e^{j\Omega}) = T \frac{1}{T} \sum_{n=-\infty}^{\infty} H_c \left[j \left(\frac{\Omega - 2\pi n}{T} \right) \right] = \sum_{n=-\infty}^{\infty} H_c \left[j \left(\frac{\Omega - 2\pi n}{T} \right) \right]. \quad (11.39)$$

We note that aliasing would occur if the filter bandwidth exceeds half the sampling frequency $f_s = 1/T$. In the absence of aliasing, on the other hand, we have

$$H(e^{j\Omega}) = H_c \left(j \frac{\Omega}{T} \right), \quad |\Omega| < \pi. \quad (11.40)$$

The multiplication by T of the impulse response is arbitrary and has no effect other than adjusting the digital filter gain. If the sampling frequency is high the filter gain is high. Multiplication by T is usually applied to bring down the gain to an acceptable level.

Example 11.2 *Let*

$$H_c(s) = \frac{s + c_0}{s^2 + b_1 s + b_0}$$

and let p and p^* be the poles of $H_c(s)$ and let $p = -\alpha + j\beta$. We have

$$H_c(s) = \frac{s + c_0}{(s - p)(s - p^*)} = \frac{A}{s - p} + \frac{A^*}{s - p^*}$$

$$A = \frac{p + c_0}{p - p^*}$$

wherefrom

$$\begin{aligned}
 h_c(t) &= Ae^{pt} + A^*e^{p^*t} = 2|A|e^{-\alpha t} \cos(\beta t + \arg[A])u(t) \\
 h[n] &= T \left(Ae^{pnT} + A^*e^{p^*nT} \right) = 2T|A|e^{-\alpha nT} \cos(\beta nT + \arg[A])u[n] \\
 H(z) &= T \left(\frac{A}{1 - e^{pT}z^{-1}} + \frac{A^*}{1 - e^{p^*T}z^{-1}} \right).
 \end{aligned}$$

Writing $a = e^{pT} = e^{(-\alpha + j\beta)T}$ we have

$$H(z) = T \left(\frac{A}{1 - az^{-1}} + \frac{A^*}{1 - a^*z^{-1}} \right) = T \frac{(A + A^*) - (Aa^* + A^*a)z^{-1}}{(1 - az^{-1})(1 - a^*z^{-1})}$$

which can be rewritten as

$$H(z) = \frac{T[2A_r - 2|A||a| \cos(\arg[A] + \arg[a])z - 1]}{1 - 2a_r z^{-1} + |a|^2 z^{-2}}$$

where

$$A_r = \Re[A].$$

Now

$$\begin{aligned}
 a_r &= \Re[a] = e^{-\alpha T} \cos \beta T \\
 |a| &= e^{-\alpha T}, \quad \arg[a] = \beta T
 \end{aligned}$$

wherefrom

$$H(z) = \frac{2|A|T \cos(\arg[A]) - 2|A|Te^{-\alpha T} \cos(\arg[A] + \beta T)z^{-1}}{1 - 2e^{-\alpha T} \cos \beta T z^{-1} + e^{-2\alpha T} z^{-2}}.$$

Higher order filters can be constructed using such a second order filter. A few observations may be added regarding the impulse invariance approach.

If the transfer function of the lowpass normalized (prototype) filter is $H_c(s)$ and if the required cut-off (pass-band edge) frequency is ω_c we can denormalize the filter by using the substitution

$$s \longrightarrow s/\omega_c. \tag{11.41}$$

The resulting denormalized filter transfer function is then

$$H_{c,\text{denorm}}(s) = H_c(s)|_{s \longrightarrow s/\omega_c}. \tag{11.42}$$

The impulse response is then

$$h_{c,\text{denorm}}(t) = \mathcal{L}^{-1}[H_{c,\text{denorm}}(s)] = \mathcal{L}^{-1}[H_c(s/\omega_c)]. \tag{11.43}$$

The digital filter impulse response is then

$$h[n] = T h_{c,\text{denorm}}(nT) \tag{11.44}$$

and the digital filter transfer function is

$$H(z) = \mathcal{Z}[h[n]]. \tag{11.45}$$

Assuming that the lowpass continuous-time prototype filter transfer function can be expressed in the form

$$H_c(s) = \sum_{i=1}^M \frac{A_i}{s - s_i} \tag{11.46}$$

we have

$$H_{c,\text{denorm}}(s) = \sum_{i=1}^M \frac{A_i}{s/\omega_c - s_i} = \sum_{i=1}^M \frac{A_i \omega_c}{s - \omega_c s_i} \quad (11.47)$$

$$h_{c,\text{denorm}}(t) = \sum_{i=1}^M A_i \omega_c e^{\omega_c s_i t} u[t] \quad (11.48)$$

$$h[n] = T \sum_{i=1}^M A_i \omega_c e^{\omega_c s_i n T} u[n] \quad (11.49)$$

$$H(z) = T \sum_{i=1}^M \frac{A_i \omega_c}{1 - e^{\omega_c T s_i} z^{-1}}. \quad (11.50)$$

Since $\Omega_c = \omega_c T$

$$H(z) = \sum_{i=1}^M \frac{A_i \Omega_c}{1 - e^{\Omega_c s_i} z^{-1}}. \quad (11.51)$$

We note that we can follow a shortcut to this procedure by the transformation from $H_c(s)$ to $H(z)$ in the form

$$\sum_{i=1}^M \frac{A_i}{s - s_i} \longrightarrow \sum_{i=1}^M \frac{A_i \Omega_c}{1 - e^{\Omega_c s_i} z^{-1}}. \quad (11.52)$$

Note also that the sampling period T determines the value Ω_c in the transformation.

11.16 Shortcut Impulse Invariance Design

We can implement the impulse invariance approach by normalizing the prototype lowpass filter directly to Ω_c . With

$$H_c(s) = \sum_{i=1}^M \frac{A_i}{s - s_i} \quad (11.53)$$

we write

$$H_{c,\text{denorm}}(s) = H_c(s)|_{s \rightarrow s/\Omega_c} = \sum_{i=1}^M \frac{A_i}{s/\Omega_c - s_i} = \sum_{i=1}^M \frac{A_i \Omega_c}{s - \Omega_c s_i} \quad (11.54)$$

$$h_{c,\text{denorm}}(t) = \sum_{i=1}^M A_i \Omega_c e^{\Omega_c s_i t} u(t). \quad (11.55)$$

In this case, however, the resulting analog filter has the same cut-off frequency as the desired digital filter cut-off frequency implying that now we should substitute $T = 1$, so that

$$h[n] = h_{c,\text{denorm}}(n) = \sum_{i=1}^M A_i \Omega_c e^{\Omega_c s_i n} u[n] \quad (11.56)$$

and

$$H(z) = \sum_{i=1}^M \frac{A_i \Omega_c}{1 - e^{\Omega_c s_i} z^{-1}} \quad (11.57)$$

which is the same result obtained above. In practice we can write, by inspection, Equation (11.57) directly from Equation (11.54)

11.17 Backward-Rectangular Approximation

We consider the discrete-time approximation of the constant-coefficients linear differential equation having the general form

$$\sum_{k=0}^N a_k \frac{d^k}{dt^k} y_c(t) = \sum_{k=0}^M b_k \frac{d^k}{dt^k} x_c(t). \tag{11.58}$$

In particular, we approximate the derivative dy/dt by the first backward difference denoted $\nabla^{(1)}$ defined by

$$\nabla^{(1)} [y[n]] = \frac{y[n] - y[n-1]}{T} \tag{11.59}$$

where (see Fig. 11.14)

$$y[n] = y_c(nT). \tag{11.60}$$

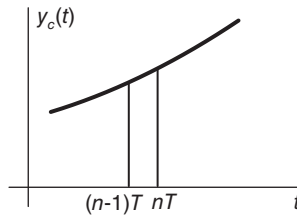


FIGURE 11.14 Approximation of the integral of a function.

The second derivative d^2y/dt^2 is similarly approximated by the second backward difference $\nabla^{(2)}$, as shown in Fig. 11.15

$$\begin{aligned} \nabla^{(2)} [y[n]] &= \nabla^{(1)} \left[\nabla^{(1)} y[n] \right] = \frac{\frac{y[n] - y[n-1]}{T} - \frac{y[n-1] - y[n-2]}{T}}{T} \\ &= \frac{y[n] - 2y[n-1] + y[n-2]}{T^2} \end{aligned} \tag{11.61}$$

$$H_1(z) = \frac{\mathcal{Z} [\nabla^{(1)} y[n]]}{Y(z)} = \frac{1 - z^{-1}}{T} \tag{11.62}$$

$$\mathcal{Z} \left[\nabla^{(2)} [y[n]] \right] = H_1^2(z) Y(z) = \left(\frac{1 - z^{-1}}{T} \right)^2 Y(z) \tag{11.63}$$

$$\mathcal{Z} \left[\nabla^{(k)} [y[n]] \right] = \left(\frac{1 - z^{-1}}{T} \right)^k Y(z) \tag{11.64}$$

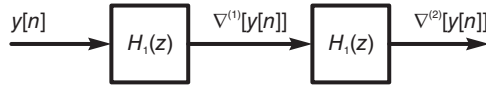


FIGURE 11.15 Backward derivative approximation block diagram.

$$\sum_{k=0}^N a_k \nabla^{(k)} [y [n]] = \sum_{k=0}^M b_k \nabla^{(k)} [x [n]] \tag{11.65}$$

$$\sum_{k=0}^N a_k \left(\frac{1 - z^{-1}}{T} \right)^k Y (z) = \sum_{k=0}^M b_k \left(\frac{1 - z^{-1}}{T} \right)^k X (z) \tag{11.66}$$

$$H (z) = \frac{Y (z)}{X (z)} = \frac{\sum_{k=0}^M b_k \left(\frac{1 - z^{-1}}{T} \right)^k}{\sum_{k=0}^N a_k \left(\frac{1 - z^{-1}}{T} \right)^k} \tag{11.67}$$

We note that

$$H_c (s) = \frac{\sum_{k=0}^M b_k s^k}{\sum_{k=0}^N a_k s^k} \tag{11.68}$$

Comparing $H (z)$ with $H_c (s)$ we note that

$$H (z) = H_c (s) \Big|_{s = \frac{1 - z^{-1}}{T}}$$

The Laplace variable s is thus related to z by writing $s = \frac{1 - z^{-1}}{T}$, i.e.

$$z^{-1} = 1 - sT, \quad z = \frac{1}{1 - sT} \tag{11.69}$$

Setting $s = j\omega$ we have

$$z = \frac{1}{1 - j\omega T} \tag{11.70}$$

If $\omega = 0$, then $z = 1$; if $\omega = \infty$, then $z = 0$; and if $\omega = -\infty$, then $z = 0$. The transformation $z = \frac{1}{1 - sT}$ is a conformal mapping converting circles into circles. The $j\omega$ axis of the s plane is transformed into a circle passing through the points $z = 1$ and $z = 0$. Its center is at $z = \frac{1}{2}$, which can be verified by writing

$$z = \frac{1}{2} + \frac{1}{1 - j\omega T} - \frac{1}{2} = \frac{1}{2} + \frac{1}{2} \frac{(1 + j\omega T)}{(1 - j\omega T)} = \frac{1}{2} + \frac{1}{2} e^{j2\theta} \tag{11.71}$$

$$\theta = \tan^{-1} \omega T \tag{11.72}$$

The $j\omega$ axis is thus transformed into the circle of radius $1/2$ and center $z = 1/2$ as shown in Fig. 11.16. We note that a stable system of which the transfer function’s ROC is to the left of the $j\omega$ axis, is transformed into a stable system, since the ROC is mapped into the inside of that circle. If the sampling period T is small the spectrum is concentrated close to $z = 1$ resulting in a good approximation, and vice versa.

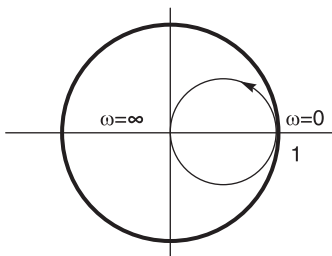


FIGURE 11.16 Transformation of the $j\omega$ axis.

11.18 Forward Rectangular and Trapezoidal Approximations

Consider the first order linear differential equation with constant coefficients

$$y' + ay = bx \tag{11.73}$$

$$y' = bx - ay \tag{11.74}$$

$$(s + a)Y(s) = bX(s) \tag{11.75}$$

$$Y(s) = \frac{b}{s + a}X(s) \tag{11.76}$$

$$y = \int y' dt = \int (bx - ay) dt \triangleq \int y_1 dt \tag{11.77}$$

where

$$y_1 = bx - ay \tag{11.78}$$

$$y = \int_{-\infty}^{(n-1)T} y_1 dt + \int_{(n-1)T}^{nT} y_1 dt. \tag{11.79}$$

In *forward rectangular approximation*, as seen in Fig. 11.17, each new increment is approximated as a rectangle. We have

$$y(nT) = y[(n-1)T] + Ty_1[(n-1)T]. \tag{11.80}$$

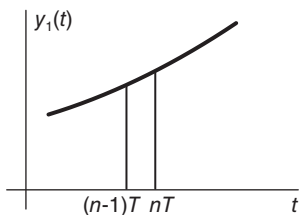


FIGURE 11.17 Forward rectangular approximation.

In *trapezoidal approximation* each new increment is approximated as a trapezoid. We write

$$y(nT) = y[(n-1)T] + \frac{T}{2} [y_1[(n-1)T] + y_1(nT)]. \tag{11.81}$$

For the rectangular approximation we have

$$Y(z) = z^{-1}Y(z) + Tz^{-1}Y_1(z) = z^{-1}Y(z) + Tz^{-1}[bX(z) - aY(z)] \tag{11.82}$$

$$Y(z) [1 - z^{-1} + aTz^{-1}] = Tz^{-1}bX(z) \tag{11.83}$$

$$H(z) = \frac{Y(z)}{X(z)} = \frac{bTz^{-1}}{1 - z^{-1} + aTz^{-1}} = \frac{b}{\frac{1}{T} \frac{1 - z^{-1}}{z^{-1}} + a} = H(s)|_{s=\frac{1}{T}(z-1)} \tag{11.84}$$

i.e. if $H(s) = \sum \frac{b_i}{s + a_i}$ then $H(z) = \sum \frac{b_i}{\frac{1}{T}(z-1) + a_i}$.

We note that $z = 1 + sT$, which is a vertical line going through $z = 1$ as shown in Fig. 11.18.

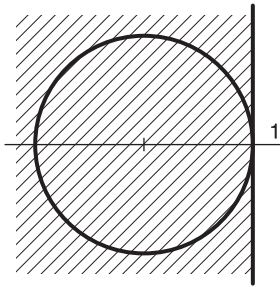


FIGURE 11.18 Forward rectangular approximation.

If $s = j\omega$, then $z = 1 + j\omega T$; if $\omega = 0$, then $z = 1$; if $\omega = \infty$, then $z = 1 + j\infty$; and if $\omega = -\infty$, then $z = 1 - j\infty$. A stable system may thus be transformed into an unstable one. For the trapezoidal approximation we write

$$Y(z) = z^{-1}Y(z) + \frac{T}{2} \{ [bX - aY] z^{-1} + bX - aY \} \tag{11.85}$$

$$Y(z) - z^{-1}Y(z) = \frac{T}{2} \{ bXz^{-1} - aYz^{-1} + bX - aY \} \tag{11.86}$$

$$Y(z) \left[1 - z^{-1} + a\frac{T}{2}z^{-1} + a\frac{T}{2} \right] = \frac{T}{2} bX(z) (1 + z^{-1}) \tag{11.87}$$

$$H(z) = \frac{Y(z)}{X(z)} = \frac{b\frac{T}{2}(1 + z^{-1})}{(1 - z^{-1}) + \frac{aT}{2}(1 + z^{-1})} = \frac{b}{\frac{2}{T} \frac{1 - z^{-1}}{1 + z^{-1}} + a} = H(s)|_{s=\frac{2}{T} \frac{1-z^{-1}}{1+z^{-1}}}$$

Such continuous domain to discrete domain transformation is known as the bilinear transformation, and will be discussed in the following section.

11.19 Bilinear Transform

We have seen that an ideal filter having an impulse response that is not causal is not realizable. We have also seen that analog classic filters, namely Butterworth, Chebyshev, elliptic and Bessel have a spectrum that extends to $\omega = \pm\infty$. Sampling the impulse response $h_c(t)$ to obtain a digital counterpart, according to the impulse invariance approach, will therefore always lead to spectral aliasing causing distortion. The trapezoidal approximation just seen is a conformal mapping called the *bilinear transform*. It converts the entire $j\omega$ axis of the s plane to one turn around the unit circle in the z -plane.

The bilinear transform has the form

$$s = \frac{2}{T} \frac{1 - z^{-1}}{1 + z^{-1}} \quad (11.88)$$

i.e.

$$z = \frac{1 + (T/2)s}{1 - (T/2)s}. \quad (11.89)$$

Writing

$$s = j\omega \quad \text{and} \quad z = re^{j\Omega} \quad (11.90)$$

we have

$$z = re^{j\Omega} = \frac{1 + j(T/2)\omega}{1 - j(T/2)\omega}. \quad (11.91)$$

We note, as stated above, that the point $\omega = 0$ is mapped to the point $z = 1$ and that the points $\omega = \pm\infty$ are mapped to the point $z = -1$, and, equating the magnitude and phase angle, we obtain

$$r = |z| = 1 \quad (11.92)$$

and that

$$e^{j\Omega} = e^{2j \tan^{-1}(T \omega/2)} \quad (11.93)$$

wherefrom

$$\Omega = 2 \tan^{-1}(T \omega/2) \quad (11.94)$$

and

$$\omega = (2/T) \tan(\Omega/2). \quad (11.95)$$

The relation of the analog frequency ω versus the digital frequency Ω is shown in Fig. 11.19, with T taken equal to 1. We note that this nonlinear relation compresses the ω axis such that as $\omega \rightarrow \pm\infty$, $\Omega \rightarrow \pm\pi$. Such nonlinearity causes a distortion in the form of a compression of the spectrum. The figure also shows that a lowpass filter of bandwidth ω_c is transformed to one with bandwidth Ω_c where

$$\Omega_c = 2 \tan^{-1}(T \omega_c/2) \quad (11.96)$$

instead of the usual relation where ω_c is normally transformed to $\Omega_c = \omega_c T$. The nonlinearity of the bilinear transform results in a different cut-off frequency than the expected one. To counteract such distortion a “prewarping,” is applied by altering the analog frequency to a value that when converted by the bilinear transform it produces the desired cut-off frequency. To this end we set

$$\omega_c = \frac{2}{T} \tan(\Omega_c/2). \quad (11.97)$$

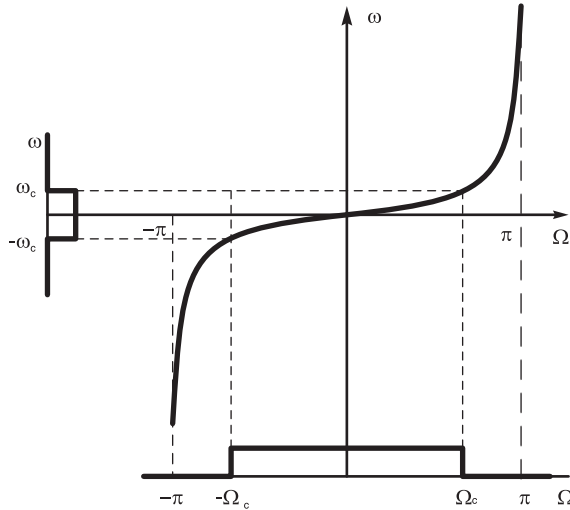


FIGURE 11.19 Bilinear transform continuous-time versus discrete-time frequency.

An analog filter having a transfer function

$$H(s) = \frac{\sum_{i=1}^n a_i s^i}{\sum_{i=1}^m b_i s^i} \tag{11.98}$$

is transformed into a digital filter with transfer function

$$H(z) = \frac{\sum_{i=1}^n a_i \left[\frac{2}{T} \frac{(1 - z^{-1})}{(1 + z^{-1})} \right]^i}{\sum_{i=1}^m b_i \left[\frac{2}{T} \frac{(1 - z^{-1})}{(1 + z^{-1})} \right]^i} \tag{11.99}$$

Example 11.3 A continuous-time signal $x_a(t)$ is limited in frequency to 2 kHz. It is sampled at the rate of 5000 samples/sec to produce the sequence $x[n] = x_a(n/5000)$ which is applied to the input of a digital filter. The filter output $y[n]$ is in turn applied to the input of a digital to analog D/A converter, producing the continuous-time signal $y_a(t)$. A digital is required so that the signal $y_a(t)$ correspond to filtering of the signal $x_a(t)$ by a lowpass first order Butterworth filter, with $\varepsilon = 1$, cut-off frequency 200 Hz and maximum gain 0 dB.

- a) Evaluate $H(z)$ using impulse invariance.
- b) Evaluate $H(z)$ using the bilinear transformation.

a) The continuous-time domain frequency is $\omega = 2\pi \times 200 = 400\pi$ r/s. The corresponding discrete-time domain frequency is $\Omega = \omega T = 400\pi/5000 = 0.08\pi$. The analog filter transfer function is

$$H_a(s) = \frac{1}{s + 1} \Bigg|_{s \rightarrow s/0.08\pi} = \frac{0.08\pi}{s + 0.08\pi} \tag{11.100}$$

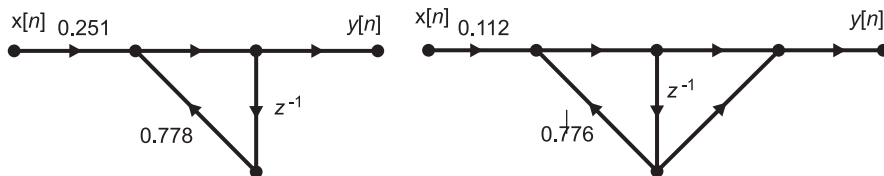


FIGURE 11.20 Digital filter structures by impulse invariance and bilinear transform.

The digital filter transfer function using impulse invariance is

$$H(z) = \frac{0.08\pi}{1 - e^{-0.08\pi}z^{-1}} = \frac{0.251}{1 - 0.778z^{-1}}. \tag{11.101}$$

b) Applying prewarping we have $\omega_0 = 2 \tan(0.08\pi/2) = 0.2527$. The denormalized analog filter transfer function is

$$H_a(s) = \frac{1}{s + 1} \Big|_{s \rightarrow s/\omega_0} = \frac{1}{s/0.2527 + 1}. \tag{11.102}$$

The digital filter transfer function using the bilinear transform is

$$H(z) = H_a(s) \Big|_{s = \frac{2(1-z^{-1})}{1+z^{-1}}} = \frac{0.112(1+z^{-1})}{1 - 0.776z^{-1}}. \tag{11.103}$$

The filter structures using impulse invariance and the bilinear transform, respectively, are shown in Fig. 11.20.

The MATLAB[®] commands

```
[Bm,Am]=butter(1,0.08)
filtMATLAB=filt(Bm,Am)
```

produce the same result we obtained using the bilinear transform.

Example 11.4 Apply the bilinear transformation to a first order Butterworth filter to obtain the transfer function $H(z)$ of a digital filter having the following specifications:

- Lowpass
- Cut-off frequency $\pi/4$
- Maximum response 0 dB
- Attenuation at cut-off frequency 3 dB

Applying prewarping we have $\omega_c = 2 \tan(0.25\pi/2) = 0.8284$. The denormalized continuous-domain transfer function is

$$H_a(s) = \frac{1}{s + 1} \Big|_{s \rightarrow s/\omega_c} = \frac{1}{s/0.8284 + 1} \tag{11.104}$$

The digital filter transfer function is

$$H(z) = H_a(s) \Big|_{s = \frac{2(1-z^{-1})}{1+z^{-1}}} = \frac{0.293(1+z^{-1})}{1 - 0.414z^{-1}}. \tag{11.105}$$

The filter structure is shown in Fig. 11.19.

The MATLAB commands

```
[Bm,Am]=butter(1,0.25)
filtMATLAB=filt(Bm,Am)
```

produce the same result.

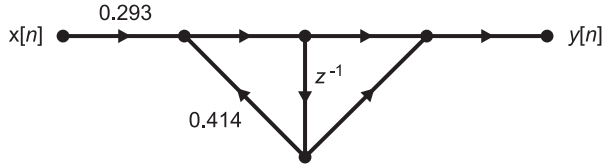


FIGURE 11.21 Digital filter structure using the bilinear transform.

Example 11.5 Design a second order Butterworth lowpass digital filter with a 3 dB cut off frequency of 125 Hz and a sampling frequency of 2000 Hz, using the bilinear transform.

We have a sampling frequency of $f_s = 2000$ i.e. a sampling period $T = 1/2000$ and a required cut-off frequency of $f_c = 125$ Hz meaning a digital filter cut-off frequency

$$\Omega_c = \omega_c T = \frac{2\pi \times 125}{2000} = \pi/8.$$

Prewarping: The true required analog filter cut off frequency is

$$\omega_c = \frac{2}{T} \tan\left(\frac{\Omega_c}{2}\right) = \frac{2}{T} \tan\left(\frac{\pi}{16}\right) = \frac{c}{T} = 0.3978/T.$$

For second order

$$H_c(s) = \frac{c^2}{T^2 s^2 + 1.4142cT + c^2} = \frac{0.1583}{T^2 s^2 + 0.5626Ts + 0.1583}$$

$$H(z) = H_c(s) \Big|_{s=\frac{2}{T} \frac{1-z^{-1}}{1+z^{-1}}} = \frac{0.1583 + 0.3165z^{-1} + 0.1583z^{-2}}{5.2835 - 7.6835z^{-1} + 3.0331z^{-2}}.$$

Example 11.6 Design a lowpass Chebyshev digital filter of the second order, which receives an input sequence $x[n]$ that is the result of A/D conversion of a continuous-time signal $x_c(t)$ at a frequency of 2000 samples per second. The signal $x_c(t)$ is band limited to $|\omega| < 1$ kHz. The filter should have a maximum gain of 15 dB and a gain of 13.5 dB at the cut-off frequency of 100 Hz.

a) Design a suitable lowpass continuous-time prototype filter, evaluating its poles and transfer function. Compare the transfer function thus obtained with MATLAB's. Plot the filter frequency response. Verify the resulting filter gain.

b) Convert the prototype into the required filter using impulse invariance. Verify if the gain versus frequency of the resulting filter is as required. If not, explain why?

c) Repeat b) using the bilinear transform.

$$a) |H_c(j\omega)|^2 = \frac{K^2}{1 + \varepsilon^2 C_2^2(\omega)} = \frac{K^2}{1 + \varepsilon^2 (2\omega^2 - 1)^2}$$

$$|H_c(j\omega)|_{\max} = K \quad (\text{at } \omega = \pm 1/\sqrt{2})$$

$$|H_c(j\omega)|^2 = K^2 / (1 + \varepsilon^2) \quad \text{at } \omega = 0, \pm 1$$

$$10 \log_{10} K^2 = 15$$

$$K = 10^{15/20} = 5.6234.$$

Note that MATLAB gives $H(s)$ as $H(s) = G/A(s)$ where G is chosen such that $|H(j\omega)|_{\max} = 1$, i.e. 0 dB.

In the present case of $n = 2$

$$|H(j0.707)| = 1$$

since $|H(j\omega)|$ is maximum for $\omega = 1/\sqrt{2}$.

$$10 \log_{10} (1 + \varepsilon^2) = 1.5 \text{ dB}$$

$$\varepsilon = \sqrt{10^{0.15} - 1} = 0.6423$$

$$\sigma_k = -b \sin [(2k + 1) \pi/4], \quad k = 0, 1$$

$$\omega_k = a \cos [(2k + 1) \pi/4], \quad k = 0, 1.$$

Hence the poles are

$$s = -0.4611 \pm j0.8442$$

$$H(s) = \frac{G}{s^2 + 0.922177s + 0.925206}.$$

The value G in the prototype is chosen so that $|H(j\omega)|_{\max} = 1$. We note that $H(j0) = |H(j\omega)|_{\max}/\sqrt{1 + \varepsilon^2}$. Hence $G/0.925206 = |H(j\omega)|_{\max}/\sqrt{1 + \varepsilon^2}$

$$G = \frac{0.925206}{\sqrt{1 + \varepsilon^2}} = 0.7785.$$

This agrees with MATLAB wherein the command $[B, A] = \text{cheby1}(N, R, Wn, 's')$ with $N = 2$, $R = 1.5 \text{ dB}$ and $Wn = 1$ produces the same result

$$H_c(s) = \frac{0.7785}{s^2 + 0.9222s + 0.9252}.$$

The prototype transfer function is therefore

$$H_c(s) = \frac{K \cdot 0.7785}{s^2 + 0.9222s + 0.9252} = \frac{4.37762}{s^2 + 0.9222s + 0.9252}.$$

Denormalization: Using the substitution $s \rightarrow s/200\pi$ we obtain

$$H_{c,denorm}(s) = \frac{1.7282 \times 10^6}{s^2 + 579.435s + 3.6525 \times 10^5} = \frac{3258.36\beta}{(s + \alpha)^2 + \beta^2}$$

where

$$\alpha = 289.718, \quad \beta = 530.394$$

$$h_c(t) = 3258.36e^{-\alpha t} \sin \beta t u(t).$$

b) $h[n] = Th_c(nT) = 1.62918a^n \sin bn u[n]$

where

$$a = 0.86514, \quad b = 0.265197$$

$$H(z) = \frac{1.62918a \sin bz^{-1}}{1 - 2a \cos bz^{-1} + a^2 z^{-2}} = \frac{0.3694z^{-1}}{1 - 1.6698z^{-1} + 0.7485z^{-2}}.$$

See Fig. 11.22.

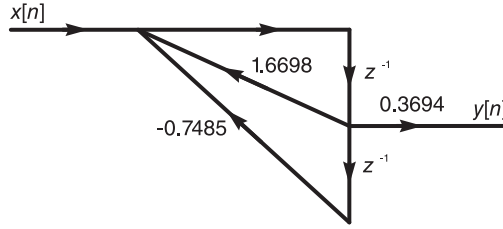


FIGURE 11.22 Digital filter.

To verify the resulting filter specifications we may use MATLAB, writing the commands

```
B = [0 0.3694 0]
A = [1 -1.6698 0.7485]
w = [0 0.1π]
H = freqz(B, A, w)
```

```
Habs = abs(H)
gain1 = 20 * log10(Habs(1))
gain2 = 20 * log10(Habs(2)).
We obtain gain1 = 13.43
gain2 = 14.96
```

which are the gains at $\Omega = 0$ and $\Omega = 0.1\pi$, respectively, and are close to the desired values 13.5 and 15 dB, respectively.

c) To use the bilinear transform we note that the desired cut-off frequency of 100 Hz, i.e. 200π corresponds to $\Omega_c = 200\pi T = 0.1\pi$.

Prewarping is effected by writing

$$\omega_c = (2/T) \tan(0.1\pi/2) = 633.538 \text{ r/s.}$$

To denormalize therefore we use the substitution

$$s \longrightarrow s/633.538$$

obtaining

$$H_{c,denorm}(s) = \frac{4.37762}{s^2 + 0.9222s + 0.9252} \Big|_{s \rightarrow s/633.538} = \frac{1.75705 \times 10^6}{s^2 + 584.2342s + 3.7135 \times 10^5}$$

$$H(z) = H_{c,denorm}(s) \Big|_{s \rightarrow \frac{1-z^{-1}}{1+z^{-1}}} = \frac{0.09392 + 0.18784z^{-1} + 0.0939z^{-2}}{1 - 1.67077z^{-1} + 0.75017z^{-2}}.$$

Example 11.7 Design a Chebyshev lowpass digital filter. The sampling frequency is 400 Hz. The filter should have 0 dB attenuation at zero frequency, a pass-band edge frequency of 40 Hz with a corresponding attenuation of at most 1 dB and a stop-band edge frequency of 60 Hz with at least 20 dB attenuation. Derive first the continuous-time prototype filter and then show its conversion to the required digital filter using impulse invariance and the bilinear transform.

The pass-band cut-off frequency, that is, the pass-band edge frequency is

$$\omega_c \equiv \omega_p = 80\pi \text{ r/s.}$$

The stop-band edge frequency is

$$\omega_s = 120\pi \text{ r/s,}$$

$$|H(j\omega)|^2 = \frac{1}{1 + \varepsilon^2 C_n^2(\omega/\omega_c)}$$

$$20 \log_{10} |H(j\omega_c)| \geq -1, \text{ i.e. } |H(j\omega_c)| \geq 0.8913.$$

Setting

$$10 \log_{10} \frac{1}{1 + \varepsilon^2} = -1$$

$$\varepsilon^2 = 10^{0.1} - 1, \text{ i.e. } \varepsilon = 0.5088$$

$$\omega_s = 1.5\omega_p = 1.5\omega_c$$

$$20 \log_{10} |H(j\omega_s)| \leq -20, \text{ i.e. } |H(j\omega_s)| \leq 10^{-1}.$$

Writing

$$10 \log_{10} \frac{1}{1 + \varepsilon^2 C_n^2(1.5)} = -20$$

we have

$$1 + \varepsilon^2 C_n^2(1.5) = 100$$

$$C_n(1.5) = \cosh(n \cosh^{-1} 1.5) = 19.5538$$

$$n \cosh^{-1} 1.5 = \cosh^{-1} 19.5538, \quad n = 3.809.$$

We take $n = 4$

$$H(s) = \frac{K}{s^4 + 0.9528s^3 + 1.4539s^2 + 0.7426s + 0.2756}.$$

To obtain a maximum gain of 1, for 0 dB magnitude response, we set

$$H(0) = \frac{K}{0.2756} = \frac{1}{\sqrt{1 + \varepsilon^2}}$$

$$K = \frac{0.2756}{\sqrt{1 + \varepsilon^2}} = 0.2457$$

in agreement with MATLAB using the command $[B, A] = \mathbf{cheby1}(4, 1, 1, 's')$.

This prototype has the required attenuation of 1 dB in the pass-band. However, its pass-band edge frequency (cut-off frequency) is normalized to unity. To convert it using impulse invariance to the required digital filter there are two possible approaches:

In the first approach we first denormalize this filter to obtain a true cut-off frequency of $\omega_p = 2\pi \times 40 = 80\pi$ r/s by writing $s \rightarrow s/80\pi$ obtaining the denormalized transfer function

$$H_d(s) = \frac{9.801 \times 10^8}{s^4 + 239.5s^3 + 9.184 \times 10^4 s^2 + 1.179 \times 10^7 s + 1.1 \times 10^9}.$$

The same may be obtained by writing the MATLAB command $[B, A] = \mathbf{cheby1}(4, 1, 80\pi, 's')$. The frequency response is shown in Fig. 11.23.

Using partial fraction expansion the transfer function $H_d(s)$ is expressed in the form

$$H_d(s) = \sum_{k=1}^4 \frac{R_k}{s - p_k}.$$

The poles p_i and the residues R_i may be obtained using the MATLAB command $[R, P, K] = \mathbf{residue}(B, A)$. The poles and their residues are given respectively by

$$P = \{-35.07 \pm j247.15, \quad -84.66 \pm j102.37\},$$

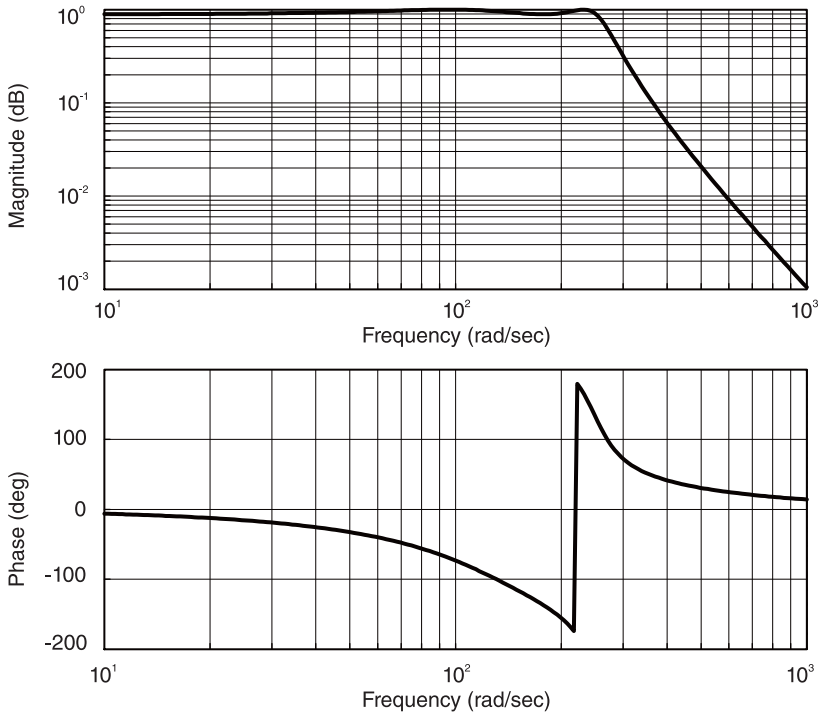


FIGURE 11.23 Chebyshev filter frequency response.

$$R = \{-16.654 \pm j32.71, 16.654 \mp 87.028\}.$$

The required transfer function is then given by

$$H(z) = T \sum_{k=1}^4 \frac{R_k}{1 - e^{p_k T} z^{-1}}.$$

The poles of $H(z)$ are given by

$$q_k = e^{p_k T} = \{0.747 \pm j0.531, 0.783 \pm j0.205\}$$

where $T = 1/400$ sec. We obtain

$$H(z) = \frac{0.00537z^{-1} + 0.0181z^{-2} + 0.00399z^{-3}}{1 - 3.059z^{-1} + 3.832z^{-2} - 2.292z^{-3} + 0.5495z^{-4}}$$

The frequency response using the MATLAB command `freqz(B, A)` is shown in Fig. 11.24.

In the second approach we denormalize the lowpass prototype directly to the frequency $\Omega_p = \omega_p T = 80\pi/4000 = 0.2\pi$. We thus use the substitution $s \rightarrow s/(0.2\pi)$ obtaining

$$H_{d,2}(s) = \frac{0.03829}{s^4 + 0.599s^3 + 0.574s^2 + 0.184s + 0.043}.$$

A partial fraction expansion of $H_{d,2}(s)$ produces

$$H_{d,2}(s) = \sum_{k=1}^4 \frac{\rho_k}{s - r_k}$$

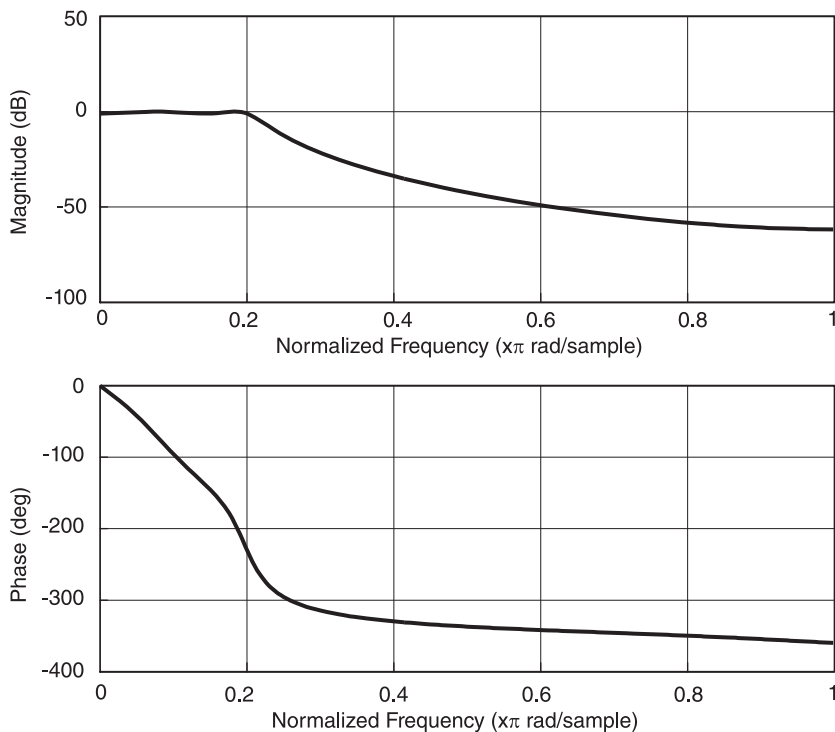


FIGURE 11.24 Chebyshev filter frequency response as obtained using MATLAB.

where the residues and poles are given, respectively, by

$$\rho = \{-0.042 \pm j0.082, \quad 0.042 \mp j0.218\}$$

$$r = \{-0.088 \pm j0.618, \quad -0.212 \pm j0.256\}.$$

We note that these are the same values as obtained above, multiplied by T . The digital filter transfer function is obtained as in the above but with T omitted. We write

$$H(z) = \sum_{k=1}^4 \frac{\rho_k}{1 - e^{r_k} z^{-1}} = \sum_{k=1}^4 \frac{\rho_k}{1 - q_k z^{-1}}$$

obtaining the same poles q_k and same transfer function $H(z)$ found above.

To convert the filter using the bilinear transform we first apply prewarping by writing

$$\omega_p = 2 \tan\left(\frac{\Omega_p}{2}\right) = 2 \tan\left(\frac{0.2\pi}{2}\right) = 0.6498$$

$$\omega_s = 2 \tan\left(\frac{\Omega_s}{2}\right) = 1.0191$$

$$20 \log_{10} |H_a(j\omega_p)| = 20 \log_{10} |H_a(j0.6498)| \geq -1$$

$$|H_a(j0.6498)| \geq 10^{-1/20}$$

$$\frac{1}{\sqrt{1+\varepsilon^2}} = 10^{-0.05}, \quad \frac{1}{1+\varepsilon^2} = 10^{-0.1}, \quad \varepsilon^2 = 10^{0.1} - 1, \quad \varepsilon = 0.5088$$

$$|H(j\omega)|^2 = \frac{1}{1 + \varepsilon^2 C_n^2(\omega/\omega_c)}$$

$$\omega_c = \omega_p = 0.6498.$$

With $\omega = \omega_s = 1.0191$

$$10 \log \left[\frac{1}{1 + \varepsilon^2 C_n^2(1.0191/0.6498)} \right] \leq -20$$

$$C_n(1.5683) = \cosh(n \cosh^{-1} 1.5683) = 19.5538$$

$$n \cosh^{-1} 1.5683 = \cosh^{-1} 19.5538, \quad n = \frac{\cosh^{-1}(19.5538)}{\cosh^{-1}(1.5683)} = 3.5897.$$

Take $n = 4$. As before we replace s by $s/(0.6498)$ or using $[B, A] = \text{cheby1}(4, 1, 0.6498, 's')$ we obtain

$$H_d(s) = \frac{0.0438}{s^4 + 0.6192s^3 + 0.61402s^2 + 0.20379s + 0.04916}.$$

Using the substitution $s \rightarrow 2 \frac{1-z^{-1}}{1+z^{-1}}$ we obtain

$$H(z) = \frac{0.00184 + 0.00734z^{-1} + 0.01101z^{-2} + 0.00734z^{-3} + 0.00184z^{-4}}{1 - 3.05434z^{-1} + 3.829z^{-2} - 2.29245z^{-3} + 0.55075z^{-4}}$$

which is in agreement with the result obtained using the MATLAB command $[B, A] = \text{cheby1}(4, 1, 0.2)$.

11.20 Lattice Filters

Lattice filters have received special attention due to their symmetric structures, their modularity and their resemblance to physical models such as those representing the human vocal tract for speech analysis and synthesis. Finite impulse response (FIR), all-zero, all-pole as well as pole-zero IIR filters can be realized as lattice structures as seen in what follows.

11.21 Finite Impulse Response All-Zero Lattice Structures

An FIR filter is a cascade of two-port networks such as the one shown in Fig. 11.25. The coefficients k_i shown in the figure are called the “reflection coefficients.”

We shall write the input-output relations and transfer function for one simple basic section, then proceed to do the same for a cascade of two and then three sections. Such simplified presentation should help explain and justify the same relations as they apply to a general order filter.

11.22 One-Zero FIR Filter

A simple one-zero FIR lattice filter section is shown in Fig. 11.25(a). In what follows the output of a first order filter will be denoted $y_1[n]$, that of a second order filter $y_2[n]$, and so on. Referring to this figure we can write the following equations.

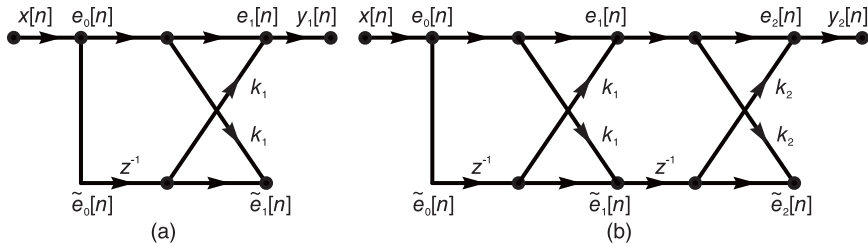


FIGURE 11.25 First and second order all-zero FIR lattice filter.

$$e_1[n] = e_0[n] + k_1 \tilde{e}_0[n-1] \tag{11.106}$$

$$\tilde{e}_1[n] = k_1 e_0[n] + \tilde{e}_0[n-1] \tag{11.107}$$

with the boundary conditions

$$e_0[n] = \tilde{e}_0[n] = x[n] \tag{11.108}$$

$$e_1[n] = y_1[n]. \tag{11.109}$$

Applying the z -transform to the equations we have

$$E_1(z) = E_0(z) + k_1 z^{-1} \tilde{E}_0(z) \tag{11.110}$$

$$\tilde{E}_1(z) = k_1 E_0(z) + z^{-1} \tilde{E}_0(z). \tag{11.111}$$

Two transfer functions, $H_1(z)$ and $\tilde{H}_1(z)$ relate the input $x[n]$ to the outputs $e_1[n]$ and $\tilde{e}_1[n]$, respectively. We write

$$H_1(z) = E_1(z)/X(z) = Y_1(z)/X(z) \tag{11.112}$$

$$\tilde{H}_1(z) = \tilde{E}_1(z)/X(z). \tag{11.113}$$

Applying the initial conditions we have

$$Y_1(z) = X(z) + k_1 z^{-1} X(z) \tag{11.114}$$

$$H_1(z) = Y_1(z)/X(z) = 1 + k_1 z^{-1} = 1 + a_1^{(1)} z^{-1} \tag{11.115}$$

where $a_1^{(1)} = k_1$.

The transfer function $H_1(z)$ of the first order all-zero filter is, as expected, a first order polynomial in z^{-1} which will be denoted $A_1(z)$.

$$H_1(z) = A_1(z) = 1 + a_1^{(1)} z^{-1}. \tag{11.116}$$

As we shall see shortly, the transfer function of a first order all-pole filter will be written $H_1(z) = 1/A_1(z)$, where $A_1(z)$ is this same polynomial.

Regarding the lower outputs we have

$$\tilde{E}_1(z) = (k_1 + z^{-1})X(z) \quad (11.117)$$

$$\tilde{H}_1(z) = \tilde{E}_1(z)/X(z) = k_1 + z^{-1} = a_1^{(1)} + z^{-1} = z^{-1}H_1(z^{-1}). \quad (11.118)$$

We shall also write

$$\tilde{A}_1(z) \triangleq \tilde{H}_1(z) = z^{-1}A_1(z^{-1}). \quad (11.119)$$

11.23 Two-Zeros FIR Filter

The transfer function of a single one-zero section was denoted $H_1(z)$. The transfer function of a cascade of two such sections is denoted $H_2(z)$, and for a cascade of i sections it is denoted $H_i(z)$. As we shall see shortly, we will find that $H_i(z)$ has the general form

$$H_i(z) = 1 + a_1^{(i)}z^{-1} + a_2^{(i)}z^{-2} + \dots + a_i^{(i)}z^{-i} = 1 + \sum_{k=1}^i a_k^{(i)}z^{-k} \triangleq A_i(z). \quad (11.120)$$

The superscript (i) of the coefficients $a_k^{(i)}$ specifies that the coefficients are associated with the i^{th} order transfer function $H_i(z)$. For example, for a cascade of two sections, such as the one shown in Fig. 11.25(b) we have

$$H_2(z) = E_2(z)/X(z) = Y_2(z)/X(z) = 1 + a_1^{(2)}z^{-1} + a_2^{(2)}z^{-2} \triangleq A_2(z). \quad (11.121)$$

As Fig. 11.25(b) shows the upper nodes are designated $e_0[n]$, $e_1[n]$ and $e_2[n]$, while the lower ones $\tilde{e}_0[n]$, $\tilde{e}_1[n]$ and $\tilde{e}_2[n]$. We note that the same equations found for the first order filter apply to each of the two cascaded sections, that is, for $s = 1, 2$, where s designates the section number, we have

$$e_s[n] = e_{s-1}[n] + k_s \tilde{e}_{s-1}[n-1] \quad (11.122)$$

$$\tilde{e}_s[n] = k_s e_{s-1}[n] + \tilde{e}_{s-1}[n-1] \quad (11.123)$$

with the boundary conditions

$$e_0[n] = \tilde{e}_0[n] = x[n] \quad (11.124)$$

$$e_2[n] = y_2[n]. \quad (11.125)$$

We note that the first section is described by the same equations written above for the case of one section. We can therefore write

$$E_1(z) = E_0(z) + k_1 z^{-1} \tilde{E}_0(z) = X(z) + k_1 z^{-1} X(z) \quad (11.126)$$

$$\tilde{E}_1(z) = k_1 E_0(z) + z^{-1} \tilde{E}_0(z) = k_1 X(z) + z^{-1} X(z). \quad (11.127)$$

Let $H_1(z)$ denote the transfer function between the input $x[n]$ and the first section upper output $e_1[n]$, and $\tilde{H}_1(z)$ that between the input and its lower output $\tilde{e}_1[n]$, that is,

$$H_1(z) = E_1(z)/X(z) \quad (11.128)$$

$$\tilde{H}_1(z) = \tilde{E}_1(z) / X(z). \tag{11.129}$$

The overall transfer functions between the input $x[n]$ and the upper and lower final outputs are similarly denoted $H_2(z)$ and $\tilde{H}_2(z)$

$$H_2(z) = E_2(z) / X(z) = Y_2(z) / X(z) \tag{11.130}$$

$$\tilde{H}_2(z) = \tilde{E}_2(z) / X(z). \tag{11.131}$$

We may now use the above results to evaluate the transfer functions of this second order filter. We have

$$H_1(z) = E_1(z) / X(z) = 1 + k_1 z^{-1} = 1 + a_1^{(1)} z^{-1} = A_1(z) \tag{11.132}$$

where $A_1(z)$ is the first order polynomial defined above. Moreover,

$$\tilde{H}_1(z) = \tilde{E}_1(z) / X(z) = k_1 + z^{-1} = z^{-1} H_1(z^{-1}) = \tilde{A}_1(z). \tag{11.133}$$

From the equations describing the second section we can write

$$E_2(z) = E_1(z) + k_2 z^{-1} \tilde{E}_1(z) \tag{11.134}$$

$$Y_2(z) = E_2(z) = \{H_1(z) + k_2 z^{-1} \tilde{H}_1(z)\} X(z) \tag{11.135}$$

$$H_2(z) = Y_2(z) / X(z) = H_1(z) + k_2 z^{-1} \tilde{H}_1(z) = A_1(z) + k_2 z^{-1} \tilde{A}_1(z) = A_2(z) \tag{11.136}$$

where

$$\begin{aligned} A_2(z) &= A_1(z) + k_2 z^{-2} A_1(z^{-1}) = 1 + a_1^{(1)} z^{-1} + k_2 z^{-2} (1 + a_1^{(1)} z) \\ &= 1 + k_1 z^{-1} + k_2 z^{-2} (1 + k_2 z) = 1 + (k_1 + k_1 k_2) z^{-1} + k_2 z^{-2} \end{aligned} \tag{11.137}$$

i.e.

$$a_1^{(2)} = k_1 + k_1 k_2 \tag{11.138}$$

$$a_2^{(2)} = k_2 \tag{11.139}$$

$$H_2(z) = H_1(z) + k_2 z^{-2} H_1(z^{-1}). \tag{11.140}$$

Moreover, from the equation

$$\tilde{e}_2[n] = k_2 e_1[n] + \tilde{e}_1[n-1] \tag{11.141}$$

we can write

$$\tilde{E}_2(z) = k_2 E_1(z) + z^{-1} \tilde{E}_1(z) = \{k_2 H_1(z) + z^{-1} \tilde{H}_1(z)\} X(z) \tag{11.142}$$

$$\tilde{H}_2(z) = \tilde{E}_2(z) / X(z) = k_2 H_1(z) + z^{-1} \tilde{H}_1(z) = k_2 H_1(z) + z^{-2} H_1(z^{-1}) \tag{11.143}$$

$$\tilde{A}_2(z) = k_2 A_1(z) + z^{-1} \tilde{A}_1(z) = k_2 A_1(z) + z^{-2} A_1(z^{-1}) \tag{11.144}$$

$$\tilde{H}_2(z) = z^{-2} H_2(z^{-1}) \tag{11.145}$$

$$\tilde{A}_2(z) = z^{-2} A_2(z^{-1}). \tag{11.146}$$

Following the same steps we can now write the equations for the third order all-zero filter shown in Fig. 11.26. Denoting again the section number by the variable s , we obtain

$$H_3(z) = Y_3(z) / X(z) = H_2(z) + k_3 z^{-1} \tilde{H}_2(z) = H_2(z) + k_3 z^{-3} H_2(z^{-1}) \tag{11.147}$$

$$A_3(z) = A_2(z) + k_3 z^{-3} A_2(z^{-1}) \tag{11.148}$$

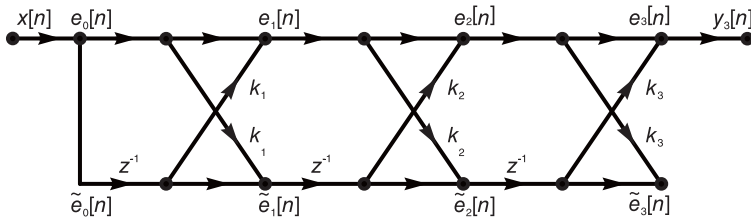


FIGURE 11.26 Third order all-zero FIR lattice filter.

$$H_3(z) = H_2(z) + k_3 z^{-3} H_2(z^{-1}) \tag{11.149}$$

$$\begin{aligned} H_3(z) = A_3(z) &= \{1 + a_1^{(2)} z^{-1} + a_2^{(2)} z^{-2}\} + k_3 z^{-3} \{1 + a_1^{(2)} z + a_2^{(2)} z^2\} \\ &= 1 + \{a_1^{(2)} + k_3 a_2^{(2)}\} z^{-1} + \{a_2^{(2)} + k_3 a_1^{(2)}\} z^{-2} + k_3 z^{-3} \\ &= 1 + a_1^{(3)} z^{-1} + a_2^{(3)} z^{-2} + a_3^{(3)} z^{-3} \end{aligned} \tag{11.150}$$

$$a_3^{(3)} = k_3 \tag{11.151}$$

$$a_1^{(3)} = a_1^{(2)} + k_3 a_2^{(2)} = k_1 + k_1 k_2 + k_2 k_3 \tag{11.152}$$

$$a_2^{(3)} = a_2^{(2)} + k_3 a_1^{(2)} = k_2 + k_3 (k_1 + k_1 k_2). \tag{11.153}$$

These relations can be written in matrix form. We have $a_3^{(3)} = k_3$ and

$$\begin{bmatrix} a_1^{(3)} \\ a_2^{(3)} \end{bmatrix} = \begin{bmatrix} a_1^{(2)} \\ a_2^{(2)} \end{bmatrix} + k_3 \begin{bmatrix} a_2^{(2)} \\ a_1^{(2)} \end{bmatrix} \tag{11.154}$$

$$\tilde{H}_3(z) = z^{-3} H_3(z^{-1}) \tag{11.155}$$

$$\tilde{A}_3(z) = z^{-3} A_3(z^{-1}). \tag{11.156}$$

11.24 General Order All-Zero FIR Filter

We are now in a position to deduce from the above the input–output relations and transfer functions $H_s(z)$ and $\tilde{H}_s(z)$ of the first to last section $s = 1, 2, 3, \dots, i$, of a general all-zero filter of order i . We have

$$H_s(z) = E_s(z) / X(z) = A_s(z), \quad s = 1, 2, \dots, i \tag{11.157}$$

$$\tilde{H}_s(z) = \tilde{E}_s(z) / X(z) = \tilde{A}_s(z), \quad s = 1, 2, \dots, i \tag{11.158}$$

$$e_s[n] = e_{s-1}[n] + k_s \tilde{e}_{s-1}[n-1] \tag{11.159}$$

$$\tilde{e}_s[n] = k_s e_{s-1}[n] + \tilde{e}_{s-1}[n-1] \tag{11.160}$$

with the boundary conditions

$$e_0[n] = \tilde{e}_0[n] = x[n] \tag{11.161}$$

$$e_i[n] = y[n]. \tag{11.162}$$

Each transfer function $H_s(z)$ can be deduced from the lower order $H_{s-1}(z)$ using the upward recursive relations

$$H_s(z) = H_{s-1}(z) + k_s z^{-1} \tilde{H}_{s-1}(z) = H_{s-1}(z) + k_s z^{-s} H_{s-1}(z^{-1}) \tag{11.163}$$

$$\tilde{H}_s(z) = z^{-s} H_s(z^{-1}). \tag{11.164}$$

From the upward recursion

$$H_s(z) = H_{s-1}(z) + k_s z^{-s} H_{s-1}(z^{-1}) \tag{11.165}$$

we can find the inverse, downward recursion. We write

$$H_{s-1}(z) = H_s(z) - k_s z^{-s} H_{s-1}(z^{-1}) \tag{11.166}$$

$$H_{s-1}(z^{-1}) = H_s(z^{-1}) - k_s z^s H_{s-1}(z) \tag{11.167}$$

$$\begin{aligned} H_s(z) &= H_{s-1}(z) + k_s z^{-s} \{H_s(z^{-1}) - k_s z^s H_{s-1}(z)\} \\ &= (1 - k_s^2) H_{s-1}(z) + k_s z^{-s} H_s(z^{-1}) \end{aligned} \tag{11.168}$$

$$H_{s-1}(z) = \frac{1}{(1 - k_s^2)} \{H_s(z) - k_s z^{-s} H_s(z^{-1})\} \tag{11.169}$$

$$A_s(z) = H_s(z) = A_{s-1}(z) + k_s z^{-i} A_{s-1}(z^{-1}) \tag{11.170}$$

$$\tilde{A}_s(z) = \tilde{H}_s(z) = z^{-s} A_s(z^{-1}) \tag{11.171}$$

$$A_s(z) = 1 + \sum_{m=1}^s a_m^{(s)} z^{-m} \tag{11.172}$$

$$\tilde{A}_s(z) = z^{-s} A_s(z^{-1}) = z^{-s} + z^{-s} \sum_{m=1}^s a_m^{(s)} z^m = z^{-s} + \sum_{m=1}^s a_m^{(s)} z^{m-s}. \tag{11.173}$$

The coefficients of the polynomial $A_s(z)$ are related by the upward recursion

$$a_s^{(s)} = k_s \tag{11.174}$$

$$a_m^{(s)} = a_m^{(s-1)} + k_s a_{s-m}^{(s-1)}, \quad m = 1, 2, \dots, s-1 \tag{11.175}$$

and we can deduce thereof the inverse, downward recursion. Replacing m by $s - m$ we have

$$a_{s-m}^{(s)} = a_{s-m}^{(s-1)} + k_s a_m^{(s-1)} \tag{11.176}$$

wherefrom

$$\begin{aligned} a_m^{(s-1)} &= a_m^{(s)} - k_s a_{s-m}^{(s-1)} = a_m^{(s)} - k_s \{a_{s-m}^{(s)} - k_s a_m^{(s-1)}\} \\ &= a_m^{(s)} - k_s a_{s-m}^{(s)} + k_s^2 a_m^{(s-1)} \end{aligned} \tag{11.177}$$

$$a_m^{(s-1)} (1 - k_s^2) = a_m^{(s)} - k_s a_{s-m}^{(s)}. \tag{11.178}$$

We have thus obtained the downward recursion

$$a_m^{(s-1)} = \frac{a_m^{(s)} - k_s a_{s-m}^{(s)}}{1 - k_s^2}, \quad m = 1, 2, \dots, s-1. \tag{11.179}$$

In both recursions $a_s^{(s)} = k_s$. The upward recursion can be written in the matrix form

$$\begin{bmatrix} a_1^{(s)} \\ a_2^{(s)} \\ \vdots \\ a_{s-1}^{(s)} \end{bmatrix} = \begin{bmatrix} a_1^{(s-1)} \\ a_2^{(s-1)} \\ \vdots \\ a_{s-1}^{(s-1)} \end{bmatrix} + k_s \begin{bmatrix} a_{s-1}^{(s-1)} \\ a_{s-2}^{(s-1)} \\ \vdots \\ a_1^{(s-1)} \end{bmatrix} \tag{11.180}$$

and the downward recursion can be written in the form

$$\begin{bmatrix} a_1^{(s-1)} \\ a_2^{(s-1)} \\ \vdots \\ a_{s-1}^{(s-1)} \end{bmatrix} = \frac{1}{(1 - k_s^2)} \left\{ \begin{bmatrix} a_1^{(s)} \\ a_2^{(s)} \\ \vdots \\ a_{s-1}^{(s)} \end{bmatrix} - k_s \begin{bmatrix} a_{s-1}^{(s)} \\ a_{s-2}^{(s)} \\ \vdots \\ a_1^{(s)} \end{bmatrix} \right\}. \tag{11.181}$$

Example 11.8 Show the lattice filter corresponding to the FIR filter shown in Fig. 11.27.

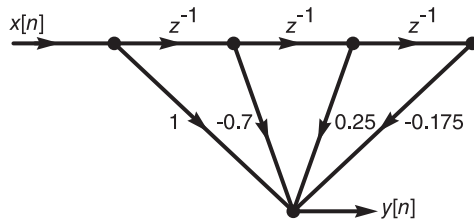


FIGURE 11.27 FIR filter.

From the figure we have

$$H_3(z) = 1 - 0.7z^{-1} + 0.25z^{-2} - 0.175z^{-3} = 1 + a_1^{(3)}z^{-1} + a_2^{(3)}z^{-2} + a_3^{(3)}z^{-3}$$

i.e.

$$a_1^{(3)} = -0.7, \quad a_2^{(3)} = +0.25, \quad a_3^{(3)} = -0.175.$$

We have $k_3 = a_3^{(3)} = -0.175$. Applying the downward recursion, starting with $s = 3$, we obtain the transfer function coefficients and hence the reflection coefficients for the successive sections $s = 2$ and $s = 1$. We write

$$\begin{aligned} \begin{bmatrix} a_1^{(2)} \\ a_2^{(2)} \end{bmatrix} &= \frac{1}{(1 - k_3^2)} \left\{ \begin{bmatrix} a_1^{(3)} \\ a_2^{(3)} \end{bmatrix} - k_3 \begin{bmatrix} a_2^{(3)} \\ a_1^{(3)} \end{bmatrix} \right\} \\ a_1^{(2)} &= \frac{a_1^{(3)} - k_3 a_2^{(3)}}{1 - k_3^2} = \frac{-0.7 + 0.175(0.25)}{1 - (0.175)^2} = -0.6770 \\ a_2^{(2)} &= \frac{a_2^{(3)} - k_3 a_1^{(3)}}{1 - k_3^2} = \frac{0.25 + 0.175 \times (-0.7)}{1 - (0.175)^2} = 0.1315 \end{aligned}$$

wherefrom $k_2 = a_2^{(2)} = 0.1315$. Setting $s = 2$ we have the downward recursion

$$\begin{bmatrix} a_1^{(1)} \end{bmatrix} = \frac{1}{(1 - k_2^2)} \left\{ \begin{bmatrix} a_1^{(2)} \end{bmatrix} - k_2 \begin{bmatrix} a_1^{(2)} \end{bmatrix} \right\}$$

$$a_1^{(1)} = \frac{a_1^{(2)} - k_2 a_1^{(2)}}{1 - k_2^2} = \frac{-0.6770 - 0.1315 \times (-0.6770)}{1 - (0.1315)^2} = -0.5983 = k_1.$$

The lattice filter thus obtained is shown in Fig. 11.28.

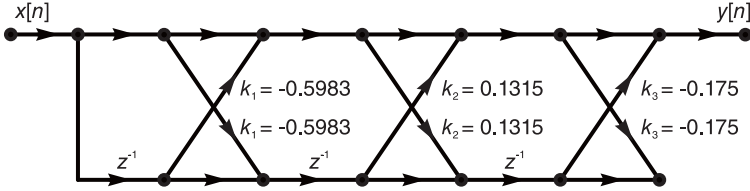


FIGURE 11.28 Third order all-zero FIR lattice filter.

Equivalently, we can evaluate the transfer functions $H_1(z), H_2(z), H_3(z), \dots$ from the input $x[n]$ to the outputs of the successive sections of the filter, and hence the successive reflection coefficients, as the following example illustrates.

Example 11.9 Let $h[n] = Aa^{-n}R_N[n]$ with $A = 1, a = 4$ and $N = 5$. Show a lattice realization of a filter having $h[n]$ as its unit sample (impulse) response. We have

$$H(z) = \sum_{n=0}^4 4^{-n} z^{-n} = (1 + 4^{-1} z^{-1} + 4^{-2} z^{-2} + 4^{-3} z^{-3} + 4^{-4} z^{-4}).$$

We have

$$\begin{aligned} H_4(z) &= 1 + 4^{-1} z^{-1} + 4^{-2} z^{-2} + 4^{-3} z^{-3} + 4^{-4} z^{-4} \\ &= 1 + 0.25z^{-1} + 0.0625z^{-2} + 0.0156z^{-3} + 0.0039z^{-4} \\ k_4 &= 4^{-4} = 39.06 \times 10^{-4}. \end{aligned}$$

We use the downward recursion

$$H_{s-1}(z) = \frac{1}{1 - k_s^2} \{H_s(z) - k_s z^{-s} H_s(z^{-1})\}$$

and note that since $H_s(z) = A_s(z)$ for all values of s , we can write this recursion alternatively as

$$A_{s-1}(z) = \frac{1}{1 - k_s^2} \{A_s(z) - k_s z^{-s} A_s(z^{-1})\}.$$

With $s = 4$ we write

$$\begin{aligned} H_3(z) &= \frac{1}{1 - k_4^2} \{H_4(z) - k_4 z^{-4} (1 + 4^{-1} z + 4^{-2} z^2 + 4^{-3} z^3 + 4^{-4} z^4)\} \\ &= \frac{1}{1 - 4^{-8}} \times (1 + 4^{-1} z^{-1} + 4^{-2} z^{-2} + 4^{-3} z^{-3} + 4^{-4} z^{-4} \\ &\quad - 4^{-4} z^{-4} - 4^{-5} z^{-3} - 4^{-6} z^{-2} - 4^{-7} z^{-1} - 4^{-8}) \\ &= 1 + \frac{4^{-1} - 4^{-7}}{1 - 4^{-8}} z^{-1} + \frac{4^{-2} - 4^{-6}}{1 - 4^{-8}} z^{-2} + \frac{4^{-3} - 4^{-5}}{1 - 4^{-8}} z^{-3} \\ &= 1 + 0.2499z^{-1} + 0.0623z^{-2} + 0.0146z^{-3} \end{aligned}$$

wherefrom $k_3 = 0.0146$.

Repeating, with $s = 3$, we have

$$H_2(z) = \frac{1}{1 - (0.0146)^2} \times \{1 + 0.2499z^{-1} + 0.0623z^{-2} + 0.0146z^{-3} - 0.0146z^{-3}(1 + 0.2499z + 0.0623z^2 + 0.0146z^3)\}$$

$$= 1 + 0.2490z^{-1} + 0.0587z^{-2}$$

wherefrom $k_2 = 0.0587$. With $s = 2$

$$H_1(z) = \frac{1}{1 - (0.0587)^2} \{1 + 0.249z^{-1} + 0.0587z^{-2} - 0.0587z^{-2}(1 + 0.249z + 0.0587z^2)\} = 1 + 0.2352z^{-1}$$

$$k_1 = 0.2352.$$

Alternatively we may write with

$$k_4 = a_4^{(4)} = 4^{-4} = 0.0039$$

$$\begin{bmatrix} a_1^{(3)} \\ a_2^{(3)} \\ a_3^{(3)} \end{bmatrix} = \frac{1}{(1 - k_4^2)} \left\{ \begin{bmatrix} a_1^{(4)} \\ a_2^{(4)} \\ a_3^{(4)} \end{bmatrix} - k_4 \begin{bmatrix} a_3^{(4)} \\ a_2^{(4)} \\ a_1^{(4)} \end{bmatrix} \right\} = \begin{bmatrix} 0.2499 \\ 0.0623 \\ 0.0146 \end{bmatrix}$$

$$k_3 = a_3^{(3)} = 0.0146$$

$$\begin{bmatrix} a_1^{(2)} \\ a_2^{(2)} \end{bmatrix} = \frac{1}{(1 - k_3^2)} \left\{ \begin{bmatrix} a_1^{(3)} \\ a_2^{(3)} \end{bmatrix} - k_3 \begin{bmatrix} a_2^{(3)} \\ a_1^{(3)} \end{bmatrix} \right\} = \begin{bmatrix} 0.2491 \\ 0.0586 \end{bmatrix}$$

$$k_2 = a_2^{(2)} = 0.0586$$

$$\begin{bmatrix} a_1^{(1)} \end{bmatrix} = \frac{1}{(1 - k_2^2)} \left\{ \begin{bmatrix} a_1^{(2)} \end{bmatrix} - k_2 \begin{bmatrix} a_1^{(2)} \end{bmatrix} \right\} = 0.2353 = k_1.$$

The resulting lattice filter is shown in Fig. 11.29.

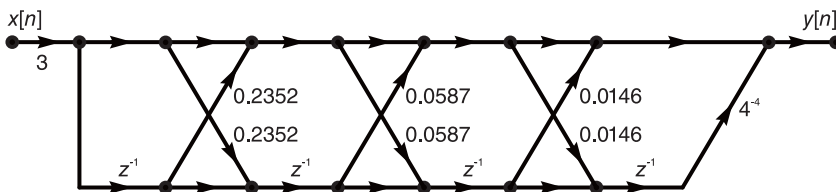


FIGURE 11.29 Fourth order all-zero FIR lattice filter.

Example 11.10 Given the lattice filter shown in the last figure evaluate its transfer function $H(z)$. Compare the result with that of the previous example.

From the figure we have

$$k_1 = 0.2352, \quad k_2 = 0.0587, \quad k_3 = 0.0146 \quad \text{and} \quad k_4 = 4^{-4}.$$

We evaluate the coefficients $a_m^{(s)}$ of the transfer functions $H_s(z)$ for the successive sections $s = 1, 2, \dots, 4$ using the upward recursion. We write

$$a_1^{(1)} = k_1$$

i.e. $a_1^{(1)} = 0.2352$. The coefficients $a_1^{(2)}$ and $a_2^{(2)}$ of $H_2(z)$ are evaluated by writing $a_2^{(2)} = k_2 = 0.0587$ and

$$\begin{bmatrix} a_1^{(2)} \end{bmatrix} = \begin{bmatrix} a_1^{(1)} \end{bmatrix} + k_2 \begin{bmatrix} a_1^{(1)} \end{bmatrix} = [0.2352] + 0.0587 [0.2352] = [0.2490].$$

Repeating the process we have $a_3^{(3)} = k_3 = 0.0146$ and

$$\begin{bmatrix} a_1^{(3)} \\ a_2^{(3)} \end{bmatrix} = \begin{bmatrix} a_1^{(2)} \\ a_2^{(2)} \end{bmatrix} + k_3 \begin{bmatrix} a_2^{(2)} \\ a_1^{(2)} \end{bmatrix} = \begin{bmatrix} 0.2490 \\ 0.0587 \end{bmatrix} + 0.0146 \begin{bmatrix} 0.0587 \\ 0.2490 \end{bmatrix} = \begin{bmatrix} 0.2499 \\ 0.0623 \end{bmatrix}$$

i.e. $a_1^{(3)} = 0.2499$, $a_2^{(3)} = 0.0623$ and

$$H_3(z) = 1 + 0.2499z^{-1} + 0.0623z^{-2} + 0.0146z^{-3}$$

$$a_4^{(4)} = k_4 = 0.0039$$

and

$$\begin{bmatrix} a_1^{(4)} \\ a_2^{(4)} \\ a_3^{(4)} \end{bmatrix} = \begin{bmatrix} a_1^{(3)} \\ a_2^{(3)} \\ a_3^{(3)} \end{bmatrix} + k_4 \begin{bmatrix} a_3^{(3)} \\ a_2^{(3)} \\ a_1^{(3)} \end{bmatrix} = \begin{bmatrix} 0.25 \\ 0.0625 \\ 0.0156 \end{bmatrix}$$

wherefrom

$$H_4(z) = 1 + 0.25z^{-1} + 0.0625z^{-2} + 0.0156z^{-3} + 0.0039z^{-4}$$

as expected.

11.25 All-Pole Filter

An all-pole filter of order i has a transfer function $H_i(z)$ of the form

$$H_i(z) = \frac{1}{1 + \sum_{m=1}^i a_m^{(i)} z^{-m}} \triangleq \frac{1}{A_i(z)} \tag{11.182}$$

where $A_i(z)$ is the same polynomial defined above in the context of the all-zero filter. The transfer function of the all-pole filter is therefore the inverse of the transfer function of the all-zero FIR filter studied above. For example, a first order filter has a transfer function designated $H_1(z)$ where

$$H_1(z) = \frac{1}{1 + a_1^{(1)} z^{-1}} = \frac{1}{1 + k_1 z^{-1}}. \tag{11.183}$$

A second order filter has a transfer function

$$H_2(z) = \frac{1}{1 + a_1^{(2)} z^{-1} + a_2^{(2)} z^{-2}} = \frac{1}{1 + (k_1 + k_1 k_2) z^{-1} + k_2 z^{-2}}. \tag{11.184}$$

Similarly to the all-zero FIR lattice filter, the all-pole filter may be realized as a cascade of two-port first order sections. An all-pole filter of order i is thus composed of i first-order stages.

Similarly to the all-zero filter case we write the input–output relations and transfer functions starting from the basic one-pole section followed by successively higher orders.

A single-stage first-order one-pole lattice filter is shown in Fig. 11.30(a). Referring to this figure we can write the input–output relations.

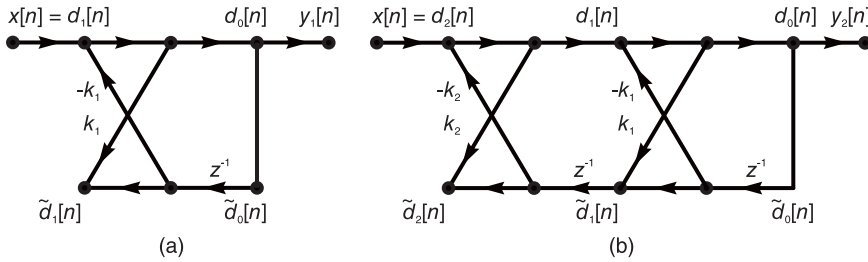


FIGURE 11.30 First and second order all-pole FIR lattice filter.

11.26 First Order One-Pole Filter

We have

$$d_0 [n] = d_1 [n] - k_1 \tilde{d}_0 [n - 1] \tag{11.185}$$

$$\tilde{d}_1 [n] = \tilde{d}_0 [n - 1] + k_1 d_0 [n] \tag{11.186}$$

with the boundary conditions

$$d_1 [n] = x[n] \tag{11.187}$$

$$d_0 [n] = \tilde{d}_0 [n] = y_1[n]. \tag{11.188}$$

Substituting, we have

$$d_0 [n] = y_1 [n] = x[n] - k_1 y_1 [n - 1] \tag{11.189}$$

$$Y_1 (z) + k_1 z^{-1} Y_1 (z) = X (z) \tag{11.190}$$

$$H_1 (z) = \frac{Y_1 (z)}{X (z)} = \frac{1}{1 + k_1 z^{-1}} = \frac{1}{1 + a_1^{(1)} z^{-1}} = \frac{1}{A_1 (z)} \tag{11.191}$$

where, as defined above, $a_1^{(1)} = k_1$. We write

$$\tilde{H}_1 (z) = Y_1 (z) / \tilde{D}_1 (z) \tag{11.192}$$

$$\tilde{d}_1 [n] = y_1 [n - 1] + k_1 y_1 [n] \tag{11.193}$$

$$\tilde{D}_1 (z) = z^{-1} Y_1 (z) + k_1 Y_1 (z) \tag{11.194}$$

$$\tilde{H}_1(z) = \frac{1}{z^{-1} + k_1} = \frac{1}{z^{-1} + a_1^{(1)}} = \frac{1}{z^{-1}A_1(z^{-1})} = zH_1(z^{-1}) = 1/\tilde{A}_1(z) \quad (11.195)$$

$$\tilde{A}_1(z) = zA_1(z^{-1}). \quad (11.196)$$

11.27 Second Order All-Pole Filter

Consider now the second order all-pole filter shown in Fig. 11.30(b). We can write, for $s = 1, 2$,

$$d_{s-1}[n] = d_s[n] - k_s \tilde{d}_{s-1}[n-1], \quad s = 1, 2 \quad (11.197)$$

$$\tilde{d}_s[n] = \tilde{d}_{s-1}[n-1] + k_s d_{s-1}[n], \quad s = 1, 2. \quad (11.198)$$

We note that $s = 1$ thus refers to the right section of the cascade, and $s = 2$ refers to the left section. The boundary conditions are

$$d_2[n] = x[n] \quad (11.199)$$

$$d_0[n] = \tilde{d}_0[n] = y_2[n] \quad (11.200)$$

$$D_1(z) = \{1 + k_1 z^{-1}\}Y_2(z) = \left(1 + a_1^{(1)} z^{-1}\right)Y_2(z) = A_1(z)Y_2(z). \quad (11.201)$$

Note that the last section is identical to the single one-pole section just analyzed. It has therefore the same transfer function $H_1(z)$.

$$H_1(z) = \frac{Y_2(z)}{D_1(z)} = \frac{1}{1 + a_1^{(1)} z^{-1}} = \frac{1}{A_1(z)} \quad (11.202)$$

$$\tilde{d}_1[n] = \tilde{d}_0[n-1] + k_1 d_0[n] = y_2[n-1] + k_1 y_2[n] \quad (11.203)$$

$$\tilde{D}_1(z) = \{(z^{-1} + k_1)\}Y_2(z) = \tilde{A}_1(z)Y_2(z) \quad (11.204)$$

$$\tilde{H}_1(z) = Y_2(z)/\tilde{D}_1(z) = 1/\tilde{A}_1(z) = zH_1(z^{-1}) \quad (11.205)$$

where, as established in the all-zero filter case,

$$\tilde{A}_1(z) = z^{-1}A_1(z^{-1}). \quad (11.206)$$

The left section is described by the equations

$$d_2[n] = x[n] = d_1[n] + k_2 \tilde{d}_1[n-1] \quad (11.207)$$

$$D_2(z) = D_1(z) + k_2 z^{-1} \tilde{D}_1(z) = \{A_1(z) + k_2 z^{-1} \tilde{A}_1(z)\}Y_2(z) = A_2(z)Y_2(z) \quad (11.208)$$

where

$$A_2(z) = A_1(z) + k_2 z^{-1} \tilde{A}_1(z) = 1 + a_1^{(2)} z^{-1} + a_2^{(2)} z^{-2} \quad (11.209)$$

as in the above

$$H_2(z) = Y_2(z)/D_2(z) = Y_2(z)/X(z) = 1/A_2(z) \quad (11.210)$$

$$\tilde{H}_2(z) = Y_2(z)/\tilde{D}_2(z) \quad (11.211)$$

$$\tilde{d}_2[n] = \tilde{d}_1[n-1] + k_2 d_1[n] \quad (11.212)$$

$$\tilde{D}_2(z) = z^{-1} \tilde{D}_1(z) + k_2 D_1(z) = \{z^{-1} \tilde{A}_1(z) + k_2 A_1(z)\}Y_2(z) = \tilde{A}_2(z)Y_2(z) \quad (11.213)$$

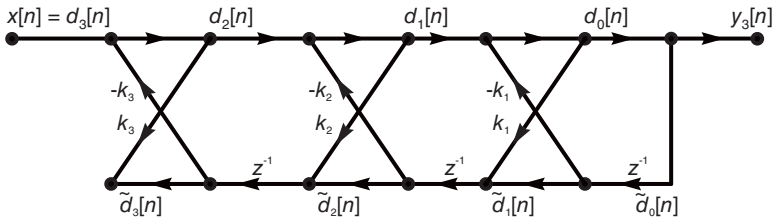


FIGURE 11.31 Third order all-pole FIR lattice filter.

$$\tilde{A}_2(z) = z^{-1}\tilde{A}_1(z) + k_2A_1(z) = z^{-2}A_2(z^{-1}) \tag{11.214}$$

$$\begin{aligned} \tilde{H}_2(z) &= Y_2(z)/\tilde{D}_2(z) = 1/\tilde{A}_2(z) = 1/\{z^{-2}A_2(z^{-1})\} \\ &= z^2/\{1 + a_1^{(2)}z + a_2^{(2)}z^2\}. \end{aligned} \tag{11.215}$$

Similarly, referring to the third order all-pole filter shown in Fig. 11.31, we have for $s = 1, 2, 3$, where $s = 1$ refers to the right-most, last, section, $s = 2$, to the middle section, and $s = 3$ to the left-most, first section,

$$H_s(z) = Y_3(z)/D_s(z) = 1/A_s(z), \quad s = 1, 2, 3 \tag{11.216}$$

$$\tilde{H}_s(z) = Y_3(z)/\tilde{D}_s(z), \quad s = 1, 2, 3 \tag{11.217}$$

$$H_1(z) = \frac{Y_3(z)}{D_1(z)} = \frac{1}{1 + a_1^{(1)}z^{-1}} = \frac{1}{A_1(z)} \tag{11.218}$$

$$\tilde{H}_1(z) = Y_3(z)/\tilde{D}_1(z) = 1/\tilde{A}_1(z) = zH_1(z^{-1}) \tag{11.219}$$

$$\tilde{A}_1(z) = z^{-1}A_1(z^{-1}) \tag{11.220}$$

$$\tilde{A}_3(z) = z^{-3}A_3(z^{-1}) \tag{11.221}$$

$$\tilde{H}_3(z) = Y_3(z)/\tilde{D}_3(z) = 1/\tilde{A}_3(z) = z^3/\{1 + a_1^{(3)}z + a_2^{(3)}z^2 + a_3^{(3)}z^3\}. \tag{11.222}$$

11.28 General Order All-Pole Filter

We deduce that for a general all-pole filter of order i the input-output transfer function $H_i(z) = Y_i(z)/X(z)$ is simply the inverse of that of the all-zero filter of the same order, and that for each section s of the filter, i.e. for $s = 1, 2, 3, \dots, i$, the transfer function $H_s(z) = Y_i(z)/D_s(z) = 1/A_s(z)$ where $A_s(z)$ is the corresponding polynomial of the all-zero filter. We can therefore write

$$H_i(z) = Y_i(z)/D_i(z) = 1/A_i(z) \tag{11.223}$$

$$\tilde{H}_i(z) = Y_i(z)/\tilde{D}_i(z) = 1/\tilde{A}_i(z). \tag{11.224}$$

The intermediate transfer functions between the intermediate upper nodes $d_1[n], d_2[n], \dots$, as well as the lower ones $\tilde{d}_1[n], \tilde{d}_2[n], \dots$ and the output $y_i[n]$ are given by

$$H_s(z) = Y_i(z)/D_s(z) = 1/A_s(z), \quad s = 1, 2, \dots, i \tag{11.225}$$

$$\tilde{H}_s(z) = Y_i(z)/\tilde{D}_s(z) = 1/\tilde{A}_s(z), \quad s = 1, 2, \dots, i \tag{11.226}$$

where again

$$A_s(z) = 1 + \sum_{m=1}^s a_m^{(s)} z^{-m} \tag{11.227}$$

$$\tilde{A}_s(z) = z^{-s} A_s(z^{-1}) = z^{-s} + z^{-s} \sum_{m=1}^s a_m^{(s)} z^m = z^{-s} + \sum_{m=1}^s a_m^{(s)} z^{m-s}. \tag{11.228}$$

The upward and downward recursions of the polynomial $A_i(z)$ and its coefficients, deduced above in studying the all-zero filter, can be used to evaluate the all-pole transfer functions. In particular we recall that

$$A_s(z) = A_{s-1}(z) + k_s z^{-s} A_{s-1}(z^{-1}) \tag{11.229}$$

$$\tilde{A}_s(z) = z^{-s} A_s(z^{-1}) \tag{11.230}$$

$$A_{s-1}(z) = \frac{1}{(1 - k_s^2)} \{A_s(z) - k_s z^{-s} A_s(z^{-1})\}. \tag{11.231}$$

The same downward recursion governing the relation between the coefficients may be used, namely,

$$\begin{bmatrix} a_1^{(s-1)} \\ a_2^{(s-1)} \\ \vdots \\ a_{i-1}^{(s-1)} \end{bmatrix} = \frac{1}{(1 - k_s^2)} \left\{ \begin{bmatrix} a_1^{(s)} \\ a_2^{(s)} \\ \vdots \\ a_{i-1}^{(s)} \end{bmatrix} - k_s \begin{bmatrix} a_{i-1}^{(s)} \\ a_{i-2}^{(s)} \\ \vdots \\ a_1^{(s)} \end{bmatrix} \right\} \tag{11.232}$$

and $k_s = a_s^{(s)}$.

Example 11.11 Consider the filter transfer function

$$H(z) = \frac{1}{1 - 2.4z^{-1} + 2.06z^{-2} - 0.744z^{-3} + 0.0945z^{-4}}.$$

Show a lattice realization of this filter. Verify the results by evaluating the system function of the resulting filter. Writing

$$H_4(z) = H(z) = \frac{1}{A_4(z)}$$

where

$$A_4(z) = 1 - 2.4z^{-1} + 2.06z^{-2} - 0.744z^{-3} + 0.0945z^{-4}$$

we have $k_4 = 0.0945$. Applying the “downward recursion”

$$A_3(z) = \frac{1}{1 - k_4^2} \{A_4(z) - k_4 z^{-4} A_4(z^{-1})\}$$

we have

$$\begin{aligned} A_3(z) &= \frac{1}{1 - (0.0945)^2} \{1 - 2.4z^{-1} + 2.06z^{-2} - 0.744z^{-3} + 0.0945z^{-4} \\ &\quad - 0.0945z^{-4}(1 - 2.4z + 2.06z^2 - 0.744z^3 + 0.0945z^4)\} \\ &= 1 - 2.3507z^{-1} + 1.8821z^{-2} - 0.5219z^{-3} \end{aligned}$$

wherefrom $k_3 = -0.5219$

Repeating we have

$$A_2(z) = \frac{1}{1 - (0.5219)^2} \{ 1 - 2.3507z^{-1} + 1.8821z^{-2} - 0.5219z^{-3} + 0.5219z^{-3}(1 - 2.3507z + 1.8821z^2 + 0.5219z^3) \}$$

$$= 1 - 1.8807z^{-1} + 0.9006z^{-2}$$

$$k_2 = 0.9006$$

$$A_1(z) = \frac{1}{1 - (0.9006)^2} \{ 1 - 1.8807z^{-1} + 0.9006z^{-2} - 0.9006z^{-2}(1 - 1.8807z + 0.9006z^2) \} = 1 - 0.9895z^{-1}$$

$$k_1 = -0.9895.$$

Alternatively we may write

With $a_1^{(4)} = -2.4, 2.06, \dots$

$$k_4 = a_4^{(4)} = 0.0945$$

$$\begin{bmatrix} a_1^{(3)} \\ a_2^{(3)} \\ a_3^{(3)} \end{bmatrix} = \frac{1}{(1 - k_4^2)} \left\{ \begin{bmatrix} a_1^{(4)} \\ a_2^{(4)} \\ a_3^{(4)} \end{bmatrix} - k_4 \begin{bmatrix} a_3^{(4)} \\ a_2^{(4)} \\ a_1^{(4)} \end{bmatrix} \right\} = \begin{bmatrix} -2.3507 \\ 1.8821 \\ -0.5219 \end{bmatrix}$$

$$k_3 = a_3^{(3)} = -0.5219$$

$$\begin{bmatrix} a_1^{(2)} \\ a_2^{(2)} \end{bmatrix} = \frac{1}{(1 - k_3^2)} \left\{ \begin{bmatrix} a_1^{(3)} \\ a_2^{(3)} \end{bmatrix} - k_3 \begin{bmatrix} a_2^{(3)} \\ a_1^{(3)} \end{bmatrix} \right\} = \begin{bmatrix} -1.8806 \\ 0.9007 \end{bmatrix}$$

$$k_2 = a_2^{(2)} = 0.9007$$

$$\begin{bmatrix} a_1^{(1)} \end{bmatrix} = \frac{1}{(1 - k_2^2)} \left\{ \begin{bmatrix} a_1^{(2)} \end{bmatrix} - k_2 \begin{bmatrix} a_1^{(2)} \end{bmatrix} \right\} = -0.9894 = k_1.$$

The structure shown in Fig. 11.32 is thus obtained. Note that the transfer functions $H_s(z)$, $s = 1, 2, 3, 4$ from the successive upper nodes $d_1[n], d_2[n], d_3[n]$ and $d_4[n] = x[n]$ to the output $d_0[n] = y_4[n]$ are given by $H_s(z) = 1/A_s(z)$.

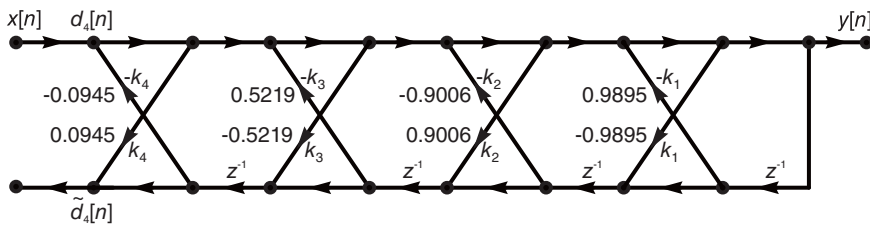


FIGURE 11.32 Fourth order all-pole FIR filter.

To verify the results we evaluate $A_4(z)$. We have

$$a_1^{(1)} = k_1$$

i.e. $a_1^{(1)} = -0.9895$ and

$$A_1(z) = 1 - 0.9895z^{-1}.$$

Since $k_2 = 0.9006$ we have

$$\begin{bmatrix} a_1^{(2)} \\ a_2^{(2)} \end{bmatrix} = \begin{bmatrix} a_1^{(1)} \\ 0 \end{bmatrix} + k_2 \begin{bmatrix} a_1^{(1)} \\ 1 \end{bmatrix} = \begin{bmatrix} -1.8807 \\ 0.9006 \end{bmatrix}$$

or $a_1^{(2)} = -1.8807$, $a_2^{(2)} = 0.9006$ and

$$A_2(z) = 1 - 1.8807z^{-1} + 0.9006z^{-2}.$$

With $k_3 = -0.5219$ we have

$$\begin{bmatrix} a_1^{(3)} \\ a_2^{(3)} \\ a_3^{(3)} \end{bmatrix} = \begin{bmatrix} a_1^{(2)} \\ a_2^{(2)} \\ 0 \end{bmatrix} + k_3 \begin{bmatrix} a_2^{(2)} \\ a_1^{(2)} \\ 1 \end{bmatrix} = \begin{bmatrix} -2.3507 \\ 1.8821 \\ -0.5219 \end{bmatrix}$$

so that

$$A_3(z) = 1 - 2.3507z^{-1} + 1.8821z^{-2} - 0.5219z^{-3}.$$

With $k_4 = 0.0945$ we have

$$\begin{bmatrix} a_1^{(4)} \\ a_2^{(4)} \\ a_3^{(4)} \\ a_4^{(4)} \end{bmatrix} = \begin{bmatrix} a_1^{(3)} + k_4 a_3^{(3)} \\ a_2^{(3)} + k_4 a_2^{(3)} \\ a_3^{(3)} + k_4 a_1^{(3)} \\ k_4 \end{bmatrix} = \begin{bmatrix} -2.4 \\ 2.06 \\ -0.744 \\ 0.0945 \end{bmatrix}$$

i.e.

$$A_4(z) = 1 - 2.4z^{-1} + 2.06z^{-2} - 0.744z^{-3} + 0.0945z^{-4}$$

and $H_4(z) = 1/A_4(z)$.

11.29 Pole-Zero IIR Lattice Filter

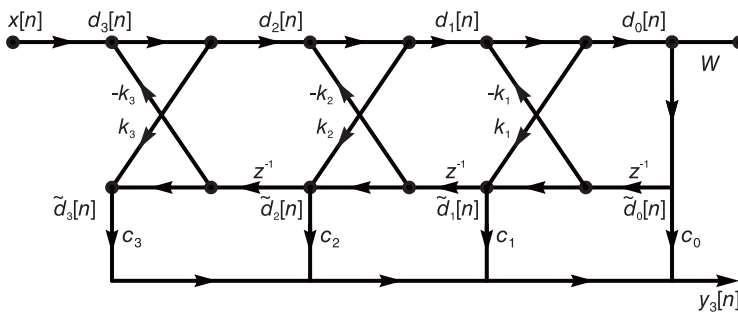


FIGURE 11.33 Third order pole-zero lattice filter.

The structure of a pole-zero IIR filter is shown in Fig. 11.33. The IIR lattice structure has the form of an all-pole lattice filter in cascade with a tapped delay line. The transfer

function from the input to the output of the all-pole filter is

$$H(z) = \frac{1}{A(z)}. \quad (11.233)$$

This is in cascade with the transfer function from the all-pole output to the taps of the delay line. The transfer function from the input to the successive taps of the delay line is therefore

$$\begin{aligned} H_k(z) &= H_1(z) \tilde{H}_k(z) \\ &= \frac{1}{A(z)} z^{-k} A_k(z^{-1}). \end{aligned} \quad (11.234)$$

The overall transfer function from the input $x[n]$ to the output $y[n]$ is therefore, with $c_k \equiv c_k^{(i)}$,

$$H(z) = \sum_{k=0}^i c_k H_k(z) = \frac{1}{A(z)} \sum_{k=0}^i c_k z^{-k} A_k(z^{-1}) = \frac{B(z)}{A(z)}. \quad (11.235)$$

In other words

$$B(z) = \sum_{k=0}^i c_k z^{-k} A_k(z^{-1}). \quad (11.236)$$

Now

$$A_k(z) = 1 + a_1^{(k)} z^{-1} + a_2^{(k)} z^{-2} + \cdots + a_k^{(k)} z^{-k} \quad (11.237)$$

$$A_k(z^{-1}) = 1 + a_1^{(k)} z + a_2^{(k)} z^2 + \cdots + a_k^{(k)} z^k \quad (11.238)$$

$$z^{-k} A_k(z^{-1}) = z^{-k} + a_1^{(k)} z^{-k+1} + a_2^{(k)} z^{-k+2} + \cdots + a_k^{(k)} \quad (11.239)$$

$$\begin{aligned} B(z) &= c_0 + c_1 \left\{ z^{-1} + a_1^{(1)} \right\} + c_2 \left\{ z^{-2} + a_1^{(2)} z^{-1} + a_2^{(2)} \right\} \\ &\quad + c_3 \left\{ z^{-3} + a_1^{(3)} z^{-2} + a_2^{(3)} z^{-1} + a_3^{(3)} \right\} \\ &\quad + \cdots \\ &\quad + c_i \left\{ z^{-i} + a_1^{(i)} z^{-(i-1)} + \cdots + a_{i-1}^{(i)} z^{-1} + a_i^{(i)} \right\} \end{aligned} \quad (11.240)$$

and since

$$B(z) = \sum_{k=0}^i b_k^{(i)} z^{-k} \quad (11.241)$$

we have

$$b_0^{(i)} = c_0 + c_1 a_1^{(1)} + c_2 a_2^{(2)} + \cdots + c_i a_i^{(i)} \quad (11.242)$$

$$b_1^{(i)} = c_1 + c_2 a_1^{(2)} + c_3 a_2^{(3)} + \cdots + c_i a_{i-1}^{(i)} \quad (11.243)$$

$$b_2^{(i)} = c_2 + c_3 a_1^{(3)} + c_4 a_2^{(4)} + \cdots + c_i a_{i-2}^{(i)} \quad (11.244)$$

$$b_i^{(i)} = c_i \quad (11.245)$$

We conclude that

$$b_k^{(i)} = \sum_{m=k}^i c_m^{(i)} a_{m-k}^{(m)}, \quad k = 0, 1, \dots, i. \quad (11.246)$$

$$b_k^{(i)} = c_k^{(i)} + \sum_{m=k+1}^i c_m^{(i)} a_{m-k}^{(m)}, \quad k = 0, 1, \dots, i \tag{11.247}$$

with the initial value $b_i^{(i)} = c_i^{(i)}$, which may also be rewritten

$$c_k^{(i)} = b_k^{(i)} - \sum_{m=k+1}^i c_m^{(i)} a_{m-k}^{(m)}, \quad k = 0, 1, \dots, i \tag{11.248}$$

with the initial value

$$c_i^{(i)} = b_i^{(i)}. \tag{11.249}$$

Example 11.12 Write the equations relating the coefficients of a third order pole-zero IIR filter in matrix form.

We have $i = 3$. The coefficients $b_k^{(3)}$ are given by $b_3^{(3)} = c_3^{(3)}$ and

$$b_0^{(3)} = c_0^{(3)} + c_1^{(3)} a_1^{(1)} + c_2^{(3)} a_2^{(2)} + c_3^{(3)} a_3^{(3)} \tag{11.250}$$

$$b_1^{(3)} = c_1^{(3)} + c_2^{(3)} a_1^{(2)} + c_3^{(3)} a_2^{(3)} \tag{11.251}$$

$$b_2^{(3)} = c_2^{(3)} + c_3^{(3)} a_1^{(3)} \tag{11.252}$$

or in matrix form

$$\begin{bmatrix} b_0^{(3)} \\ b_1^{(3)} \\ b_2^{(3)} \end{bmatrix} = \begin{bmatrix} c_0^{(3)} \\ c_1^{(3)} \\ c_2^{(3)} \end{bmatrix} + \begin{bmatrix} c_1^{(3)} & & & & \\ & c_2^{(3)} & & & \\ & & c_3^{(3)} & & \\ & & & c_3^{(3)} & \\ & & & & c_3^{(3)} \end{bmatrix} \begin{bmatrix} a_1^{(1)} \\ a_1^{(2)} \\ a_1^{(3)} \\ a_2^{(2)} \\ a_2^{(3)} \\ a_3^{(3)} \end{bmatrix} \tag{11.253}$$

where the blanks signify zero-elements. These same equations defining the $b_k^{(3)}$ coefficients can be rewritten in a form defining the c_k coefficients:

$$c_3^{(3)} = b_3^{(3)} \tag{11.254}$$

$$c_0^{(3)} = b_0^{(3)} - c_1^{(3)} a_1^{(1)} - c_2^{(3)} a_2^{(2)} - c_3^{(3)} a_3^{(3)} \tag{11.255}$$

$$c_1^{(3)} = b_1^{(3)} - c_2^{(3)} a_1^{(2)} - c_3^{(3)} a_2^{(3)} \tag{11.256}$$

$$c_2^{(3)} = b_2^{(3)} - c_3^{(3)} a_1^{(3)}. \tag{11.257}$$

The last three equations are solved in reverse order, that is, $c_2^{(3)}$ is deduced from $c_3^{(3)}$, whence $c_1^{(3)}$, and finally $c_0^{(3)}$. To this end we may reverse the order of the equations and obtain the corresponding matrix form. We have

$$\begin{bmatrix} c_2^{(3)} \\ c_1^{(3)} \\ c_0^{(3)} \end{bmatrix} = \begin{bmatrix} b_2^{(3)} \\ b_1^{(3)} \\ b_0^{(3)} \end{bmatrix} - \begin{bmatrix} & & & & \\ & & & & c_3^{(3)} \\ & & c_2^{(3)} & & \\ & c_1^{(3)} & & & \\ & & & c_2^{(3)} & \\ & & & & c_3^{(3)} \\ & & & & & c_3^{(3)} \end{bmatrix} \begin{bmatrix} a_1^{(1)} \\ a_1^{(2)} \\ a_1^{(3)} \\ a_2^{(2)} \\ a_2^{(3)} \\ a_3^{(3)} \end{bmatrix}. \tag{11.258}$$

Example 11.13 *Let*

$$H(z) = \frac{1 - 1.6z^{-1} + 1.18z^{-2} - 0.38z^{-3} + 0.04z^{-4}}{1 - 2.4z^{-1} + 2.06z^{-2} - 0.744z^{-3} + 0.0945z^{-4}} = \frac{B_4(z)}{A_4(z)} = \frac{\sum_{i=0}^4 b_i^{(4)} z^{-i}}{1 + \sum_{i=1}^4 a_i^{(4)} z^{-i}}.$$

Show the lattice filter realization.

We note that the denominator polynomial is the same as that of the previous all-pole filter example. As found above we have $k_4 = a_4^{(4)} = 0.0945$

$$\begin{bmatrix} a_1^{(3)} \\ a_2^{(3)} \\ a_3^{(3)} \end{bmatrix} = \frac{1}{(1 - k_4^2)} \left\{ \begin{bmatrix} a_1^{(4)} \\ a_2^{(4)} \\ a_3^{(4)} \end{bmatrix} - k_4 \begin{bmatrix} a_3^{(4)} \\ a_2^{(4)} \\ a_1^{(4)} \end{bmatrix} \right\} = \begin{bmatrix} -2.3507 \\ 1.8821 \\ -0.5219 \end{bmatrix} \tag{11.259}$$

$$k_3 = a_3^{(3)} = -0.5219 \tag{11.260}$$

$$\begin{bmatrix} a_1^{(2)} \\ a_2^{(2)} \end{bmatrix} = \frac{1}{(1 - k_3^2)} \left\{ \begin{bmatrix} a_1^{(3)} \\ a_2^{(3)} \end{bmatrix} - k_3 \begin{bmatrix} a_2^{(3)} \\ a_1^{(3)} \end{bmatrix} \right\} = \begin{bmatrix} -1.8806 \\ 0.9007 \end{bmatrix} \tag{11.261}$$

$$k_2 = a_2^{(2)} = 0.9007 \tag{11.262}$$

$$\begin{bmatrix} a_1^{(1)} \end{bmatrix} = \frac{1}{(1 - k_2^2)} \left\{ \begin{bmatrix} a_1^{(2)} \end{bmatrix} - k_2 \begin{bmatrix} a_1^{(2)} \end{bmatrix} \right\} = -0.9894 = k_1. \tag{11.263}$$

We also have from the numerator polynomial of $H(z)$

$$b_0^{(4)} = 1, \quad b_1^{(4)} = -1.6, \quad b_2^{(4)} = 1.18, \quad b_3^{(4)} = -0.38, \quad b_4^{(4)} = 0.04. \tag{11.264}$$

The matrix form with $i = 4$ is written

$$c_4^{(4)} = b_4^{(4)} \tag{11.265}$$

$$\begin{bmatrix} c_3^{(4)} \\ c_2^{(4)} \\ c_1^{(4)} \\ c_0^{(4)} \end{bmatrix} = \begin{bmatrix} b_3^{(4)} \\ b_2^{(4)} \\ b_1^{(4)} \\ b_0^{(4)} \end{bmatrix} - \begin{bmatrix} & & & c_4^{(4)} \\ & & c_4^{(4)} & \\ & c_2^{(4)} & & c_4^{(4)} \\ c_1^{(4)} & & c_3^{(4)} & \\ & c_2^{(4)} & & c_4^{(4)} \\ & & c_3^{(4)} & \\ & & & c_4^{(4)} \\ & & & & c_4^{(4)} \end{bmatrix} \begin{bmatrix} a_1^{(1)} \\ a_1^{(2)} \\ a_1^{(3)} \\ a_1^{(4)} \\ a_2^{(2)} \\ a_2^{(3)} \\ a_2^{(4)} \\ a_3^{(3)} \\ a_3^{(4)} \\ a_4^{(4)} \end{bmatrix} \tag{11.266}$$

i.e.

$$c_4^{(4)} = b_4^{(4)} = 0.04 \tag{11.267}$$

$$c_3^{(4)} = b_3^{(4)} - c_4^{(4)} a_1^{(4)} = -0.38 - 0.04(-2.4) = -0.284 \tag{11.268}$$

$$c_2^{(4)} = b_2^{(4)} - c_3^{(4)} a_1^{(3)} - c_4^{(4)} a_2^{(4)} \quad (11.269)$$

$$c_1^{(4)} = b_1^{(4)} - c_2^{(4)} a_1^{(2)} - c_3^{(4)} a_2^{(3)} - c_4^{(4)} a_3^{(4)} \quad (11.270)$$

$$c_0^{(4)} = b_0^{(4)} - c_1^{(4)} a_1^{(1)} - c_2^{(4)} a_2^{(2)} - c_3^{(4)} a_3^{(3)} - c_4^{(4)} a_4^{(4)}. \quad (11.271)$$

The following MATLAB program evaluates the lattice filter coefficients of the pole zero filter. The first part of the program would evaluate the coefficients of an all-zero or all-pole filter. The second part deals with the tapped delay line filter coefficients. The program deals with a fourth order filter. It can be easily extended to a general filter order.

% Lattice filt pole-zero example M.CORINTHIOS

% The all-pole part

a14=-2.4

a24=2.06

a34=-0.744

a44=0.0945

k4=a44

a13=(1/(1-k4^2))(a14-k4*a34)*

a23=(1/(1-k4^2))(a24-k4*a24)*

a33=(1/(1-k4^2))(a34-k4*a14)*

k3=a33

%

a12=(1/(1-k3^2))(a13-k3*a23)*

a22=(1/(1-k3^2))(a23-k3*a13)*

k2=a22

%

a11=(1/(1-k2^2))(a12-k2*a12)*

k1=a11

% The tapped delay line part

b04=1

b14=-1.6

b24=1.18

b34=-0.38

b44=0.04

c44=b44

*c34=b34-c44*a14*

*c24=b24-c34*a13-c44*a24*

*c14=b14-c24*a12-c34*a23-c44*a34*

*c04=b04-c14*a11-c24*a22-c34*a33-c44*a44*

We obtain

$$c_4^{(4)} = 0.04, \quad c_3^{(4)} = -0.284, \quad c_2^{(4)} = 0.43, \quad c_1^{(4)} = -0.227, \quad c_0^{(4)} = 0.2361$$

as can be seen in Fig. 11.34.

Example 11.14 Verify this last result by evaluating the numerator coefficients $b_k^{(i)}$.

For the case $i = 4$ we have

Since $k_2 = 0.17$ we have

$$\begin{bmatrix} a_1^{(2)} \\ a_2^{(2)} \end{bmatrix} = \begin{bmatrix} a_1^{(1)} \\ 0 \end{bmatrix} + k_2 \begin{bmatrix} a_1^{(1)} \\ 1 \end{bmatrix} = \begin{bmatrix} -0.9126 \\ 0.17 \end{bmatrix}$$

or $a_1^{(2)} = -0.9126$, $a_2^{(2)} = 0.17$. With $k_3 = -0.67$ we have

$$\begin{bmatrix} a_1^{(3)} \\ a_2^{(3)} \\ a_3^{(3)} \end{bmatrix} = \begin{bmatrix} a_1^{(2)} \\ a_2^{(2)} \\ 0 \end{bmatrix} + k_3 \begin{bmatrix} a_2^{(2)} \\ a_1^{(2)} \\ 1 \end{bmatrix} = \begin{bmatrix} -1.0265 \\ 0.7814 \\ -0.67 \end{bmatrix}$$

The coefficients $b_k^{(3)}$ are given by

$$b_0^{(3)} = c_0^{(3)} + c_1^{(3)} a_1^{(1)} + c_2^{(3)} a_2^{(2)} + c_3^{(3)} a_3^{(3)} \tag{11.272}$$

$$b_1^{(3)} = c_1^{(3)} + c_2^{(3)} a_1^{(2)} + c_3^{(3)} a_2^{(3)} \tag{11.273}$$

$$b_2^{(3)} = c_2^{(3)} + c_3^{(3)} a_1^{(3)} \tag{11.274}$$

and $b_3^{(3)} = c_3^{(3)}$. We obtain $b_0 = 0.6178$, $b_1 = 2.2385$, $b_2 = 3.1735$, $b_3 = 1$. Hence

$$H(z) = \frac{0.6178 + 2.2385z^{-1} + 3.1735z^{-2} + z^{-3}}{1 - 1.0265z^{-1} + 0.7814z^{-2} - 0.67z^{-3}}$$

11.30 All-Pass Filter Realization

In a K^{th} order all-zero FIR lattice filter the transfer function between the input $x[n]$ and the lower output terminal $e_K[n]$ is

$$H_{ap}(z) = \frac{\tilde{E}(z)}{X(z)} = \frac{z^{-K} A_K(z^{-1})}{A_K(z)}. \tag{11.275}$$

Similarly, in a K^{th} order all-pole FIR lattice filter the transfer function between the input $x[n]$ and the lower terminal $\tilde{d}_K[n]$ is

$$H_{ap}(z) = \frac{\tilde{D}_K(z)}{X(z)} = \frac{z^{-K} A_K(z^{-1})}{A_K(z)}. \tag{11.276}$$

We recall from Equation (6.187) that these are but general forms of allpass filters.

Example 11.16 Design an allpass lattice filter of transfer function $H_{ap}(z)$ of which the denominator should equal $A_K(z) = 1 - 2.4z^{-1} + 2.06z^{-2} - 0.744z^{-3} + 0.0945z^{-4}$

The required transfer function is

$$H_{ap}(z) = \frac{z^{-K} A_K(z^{-1})}{A_K(z)} = \frac{0.0945 - 0.744z^{-1} + 2.06z^{-2} - 2.4z^{-3} + z^{-4}}{1 - 2.4z^{-1} + 2.06z^{-2} - 0.744z^{-3} + 0.0945z^{-4}}$$

The same all-pole filter lattice filter obtained in the last example and shown in Fig. 11.32 may be employed, its transfer function denominator being the same as the present one. The allpass filter has its input $x[n]$, and its output taken as $\tilde{d}_4[n]$, as shown in the figure.

In the all-zero filter we found that

$$H_i(z) = \frac{Y_i(z)}{X(z)} = \frac{E_i(z)}{X(z)} \quad (11.277)$$

i.e.

$$E_i(z) = H_i(z) X(z) = A_i(z) X(z). \quad (11.278)$$

We also note that

$$\tilde{H}_i(z) = \frac{\tilde{E}_i(z)}{X(z)} \quad (11.279)$$

i.e.

$$\tilde{E}_i(z) = \tilde{H}_i(z) X(z) = \tilde{A}_i(z) X(z) = z^{-i} A_i(z^{-1}) X(z) \quad (11.280)$$

wherefrom, letting $H_{12}(z) = E_i(z) / \tilde{E}_i(z)$ we have

$$H_{12}(z) = \frac{E_i(z)}{\tilde{E}_i(z)} = \frac{z^i A_i(z)}{A_i(z^{-1})} = z^i \frac{1 + \sum_{k=1}^i a_k^{(i)} z^{-i}}{1 + \sum_{k=1}^i a_k^{(i)} z^i}. \quad (11.281)$$

Letting $z = e^{j\Omega}$ we have

$$H_{12}(e^{j\Omega}) = e^{ji\Omega} \frac{1 + \sum_{k=1}^i a_k^{(i)} e^{-ji\Omega}}{1 + \sum_{k=1}^i a_k^{(i)} e^{ji\Omega}}. \quad (11.282)$$

Writing

$$H_{12}(e^{j\Omega}) = e^{ji\Omega} \frac{N(\Omega)}{D(\Omega)} \quad (11.283)$$

we note that $D(\Omega) = N^*(\Omega)$. Therefore $|H_{12}(e^{j\Omega})| = 1$. The transfer function $H_{12}(z)$ relating $E_i(z)$ and $\tilde{E}_i(z)$ is therefore an allpass network.

11.31 Schur–Cohn Stability Criterion

The Schur–Cohn stability criterion states that a digital filter of system function

$$H(z) = \frac{B(z)}{A(z)} \quad (11.284)$$

is stable if and only if the reflection coefficients k_j associated with the denominator polynomial $A(z)$ are all of absolute value less than one, i.e.

$$|k_j| < 1, \text{ for all } j. \quad (11.285)$$

11.32 Frequency Transformations

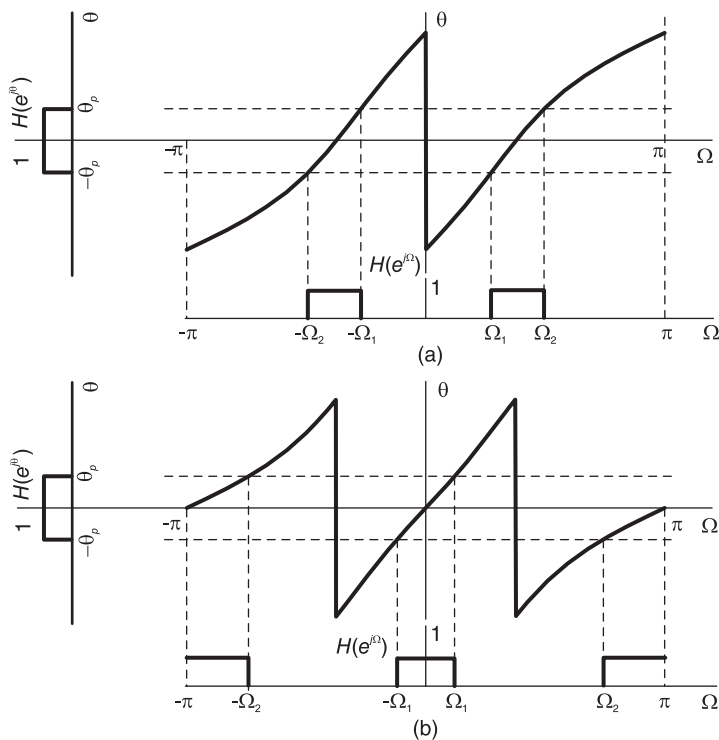


FIGURE 11.36 Lowpass to bandpass and bandstop frequency transformation.

We have seen how to convert a prototype lowpass continuous-time filter into a bandpass, bandstop and highpass filters. Corresponding discrete-time domain digital filters can be obtained in general from the continuous-time domain filters by using the bilinear transform approach as seen above.

Alternatively, as seen above, impulse invariance may be used to convert a continuous-time bandpass filter into a bandpass digital filter. Impulse invariance, based on sampling the continuous-time filter impulse response, cannot be used however to convert a highpass or bandstop filter into discrete time filter counter part since aliasing would occur, however high the sampling frequency.

Another distinct approach to designing discrete-time bandpass, bandstop and highpass filters is to apply a direct transformation which converts a discrete-time lowpass system function $H_{LP}(z)$ into the desired system function. Similarly to the continuous-time domain where the variable s in the lowpass system function $H_{LP}(s)$ was replaced by a function $w(s)$, written

$$s \longrightarrow w(s) \tag{11.286}$$

in the present context the variable z^{-1} in the prototype lowpass filter is replaced by a

function $w(z^{-1})$, written

$$z^{-1} \longrightarrow w(z^{-1}). \tag{11.287}$$

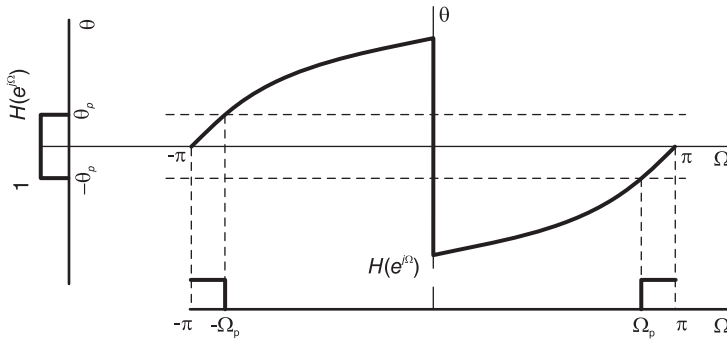


FIGURE 11.37 Lowpass to highpass frequency transformation.

Table 11.1 shows the appropriate transformation which would convert a lowpass IIR filter into a lowpass filter of different cut-off frequency, into a bandpass filter, a bandstop filter and a highpass filter, respectively. The frequency transformation that takes place can be visualized by replacing the lowpass filter variable z^{-1} by $e^{-j\theta}$ and replacing the resulting filter variable z^{-1} by $e^{-j\Omega}$.

The resulting relation of θ versus Ω for the transformations to bandpass, bandstop, and highpass filters are shown in Fig. 11.36(a-b) and Fig. 11.37, respectively.

In each of these figures is shown the lowpass filter frequency response $H_{LP}(e^{j\theta})$ with a cut-off frequency $\theta_c = \theta_p$ and the resulting desired filter response $H(e^{j\Omega})$. The approach is similar to the corresponding one we have seen in the context of continuous-time filters.

$$\theta_c = \theta_p$$

Example 11.17 Design a bandpass Chebyshev filter of order 3 of cut-off frequency 0.2π and 0.6π and 0.5 dB ripple by starting from a prototype lowpass filter of cut-off frequency $\Omega_c = 0.5\pi$ and then converting it into the desired bandpass filter.

The simple MATLAB program

$N = 3$ % filter order.

$R = 0.5$ % 0.5 dB ripple.

$Wn = 0.5$ % LP filter cut-off frequency 0.5π .

$[A, B] = cheby1(N, R, Wn)$

upon execution produces the coefficients vectors

$$B = [0.1589 \ 0.4768 \ 0.4768 \ 0.1589]$$

$$A = [1 \ -0.1268 \ 0.5239 \ -0.1257]$$

i.e.

$$H_{LP}[z] = \frac{0.1589 + 0.4768z^{-1} + 0.4768z^{-2} + 0.1589z^{-3}}{1 - 0.1268z^{-1} + 0.5239z^{-2} - 0.1257z^{-3}}.$$

With cut-off frequencies $\Omega_1 = 0.2\pi$ and $\Omega_2 = 0.6\pi$ of the desired bandpass filter and a cut-off frequency $\theta_c = 0.5\pi$ of the lowpass prototype, the parameters α and γ given in the table can be evaluated followed by the replacement of the variable z^{-1} in $H_{LP}(z)$ by

TABLE 11.1 Frequency transformations of a lowpass filter

Desired filter	Desired cut-off frequencies	Filter parameters	z^{-1} replaced by
Lowpass	Ω_c	$\alpha = \frac{\sin\left(\frac{\theta_p - \Omega_c}{2}\right)}{\sin\left(\frac{\theta_p + \Omega_c}{2}\right)}$	$\frac{z^{-1} - \alpha}{1 - \alpha z^{-1}}$
Bandpass	Ω_1, Ω_2	$\alpha = \frac{\cos\left(\frac{\Omega_2 + \Omega_1}{2}\right)}{\cos\left(\frac{\Omega_2 - \Omega_1}{2}\right)}$	$\frac{-z^{-2} + \frac{2\alpha\gamma}{\gamma+1}z^{-1} - \frac{\gamma-1}{\gamma+1}}{\frac{\gamma-1}{\gamma+1}z^{-2} - \frac{2\alpha\gamma}{\gamma+1}z^{-1} + 1}$
Bandstop	Ω_1, Ω_2	$\alpha = \frac{\cos\left(\frac{\Omega_2 + \Omega_1}{2}\right)}{\cos\left(\frac{\Omega_2 - \Omega_1}{2}\right)}$	
Highpass	Ω_c	$\alpha = \frac{\cos\left(\frac{\theta_p + \Omega_c}{2}\right)}{\cos\left(\frac{\theta_p - \Omega_c}{2}\right)}$	$\frac{-z^{-1} - \alpha}{1 + \alpha z^{-1}}$

the expression of the lowpass to bandpass transformation given in the table. To this end Mathematica may be used producing the result

$$H_{BP}[z] = \frac{b_0 + b_1z^{-1} + b_2z^{-2} + b_3z^{-3} + b_4z^{-4} + b_5z^{-5} + b_6z^{-6}}{a_0 + a_1z^{-1} + a_2z^{-2} + a_3z^{-3} + a_4z^{-4} + a_5z^{-5} + a_6z^{-6}}$$

where the numerator coefficient b_i and denominator coefficient a_i are given respectively by

$$b_i = [0.0916, 0, -0.2749, 0, 0.2749, 0, -0.0916]$$

$$a_i = [1, -1.4362, 1.5221, -1.2660, 1.1093, -0.5075, 0.2088].$$

The results thus obtained are identical to those produced by MATLAB.

The simple MATLAB program:

$N = 3$ % filter order $R = 0.5\%$ 0.5 dB ripple.

$W1 = 0.2$ % First cut-off frequency 0.5π .

$W2 = 0.6$ % Second filter cut-off frequency 0.5π .

$Wn = [W1 W2]$.

$[B2, A2] = \text{cheby1}(N, R, Wn)\%$

produces the same numerator and denominator coefficients, thus the same system function $H_{BP}(z)$.

Example 11.18 Show a realization of an allpass system of the first order having a real pole at $z = p$ using one multiplier, and a realization of a second order system with a complex pole $z = p$ and its conjugate using two multipliers.

1. One real pole

$$H(z) = \frac{z^{-1} - p}{1 - pz^{-1}} = \frac{-p + z^{-1}}{1 - pz^{-1}}$$

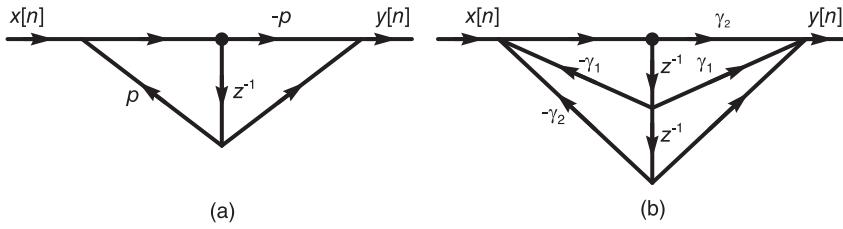


FIGURE 11.38 Allpass filter prototypes.

which leads to a possible filter structure as that shown in Fig. 11.38(a).

2. Two conjugate poles

$$p = \alpha + j\beta$$

$$\begin{aligned}
 H(z) &= \frac{z^{-1} - p^*}{1 - pz^{-1}} \frac{z^{-1} - p}{1 - p^*z^{-1}} = \frac{z^{-2} - (p + p^*)z^{-1} + |p|^2}{1 - (p + p^*)z^{-1} + |p|^2 z^{-2}} \\
 &= \frac{z^{-2} - 2\alpha z^{-1} + \alpha^2 + \beta^2}{1 - 2\alpha z^{-1} + (\alpha^2 + \beta^2) z^{-2}} = \frac{(\alpha^2 + \beta^2) - 2\alpha z^{-1} + z^{-2}}{1 - 2\alpha z^{-1} + (\alpha^2 + \beta^2) z^{-2}} = \frac{\gamma_2 + \gamma_1 z^{-1} + z^{-2}}{1 + \gamma_1 z^{-1} + \gamma_2 z^{-2}} \\
 &\qquad \qquad \qquad \gamma_1 = -2\alpha, \quad \gamma_2 = \alpha^2 + \beta^2
 \end{aligned}$$

realized as shown in Fig. 11.38(b).

11.33 Least Squares Digital Filter Design

We have seen how a digital filter may be obtained by applying the z -transform to a corresponding analog filter. We presently study methods wherein a digital filter is directly specified and designed with no reference to the analog filter continuous-time domain. In what follows, we study two methods in which the design is carried out in the time domain and two where it is effected in the frequency domain and the z -domain, respectively.

11.34 Padé Approximation

In the Padé approximation approach the objective is to evaluate a filter transfer function $H(z)$ such that the filter impulse response $h[n] = Z^{-1}[H(z)]$ best matches a given desired impulse response $h_d[n]$ given as a sequence of numerical values. Writing

$$H(z) = \frac{\sum_{k=0}^M b_k z^{-k}}{1 + \sum_{k=1}^N a_k z^{-k}} = \frac{B(z)}{A(z)} = \sum_{n=0}^{\infty} h[n] z^{-n} \tag{11.288}$$

the objective is therefore to evaluate the filter coefficients a_k and b_k which would minimize the sum-of-squares error

$$\varepsilon = \sum_{n=0}^K \{h[n] - h_d[n]\}^2 \tag{11.289}$$

where $K \geq M + N$, that is, K may be equal to or greater than the number of unknown coefficients a_k and b_k .

The minimization of the sum-of-squares error ε generally involves the solution of nonlinear equations. If, on the other hand, we choose $K = M + N$ the number of equations equals the number of unknowns a_k and b_k .

We may then write

$$B(z) = A(z)H(z) \tag{11.290}$$

$$b_n = a_n * h[n], \quad 0 \leq n \leq M \tag{11.291}$$

and note that $b_n = 0$ for $n < 0$ and $n > M$, and $a_n = 0$ for $n < 0$ and $n > N$. We may write

$$\sum_{k=0}^N a_k h[n-k] = \begin{cases} b_n, & 0 \leq n \leq M \\ 0, & n < 0, n > M. \end{cases} \tag{11.292}$$

$$h[n] = -a_1 h[n-1] - a_2 h[n-2] - \dots - a_N h[n-N] + b_n, \quad 0 \leq n \leq M \tag{11.293}$$

$$h[n] = -a_1 h[n-1] - a_2 h[n-2] - \dots - a_N h[n-N], \quad n < 0, n > M. \tag{11.294}$$

If we let $h[n] = h_d[n]$ for $0 \leq n \leq M + N$ we may write the last equation in matrix form

$$\begin{bmatrix} h_d[M] & h_d[M-1] & \dots & h_d[M+1-N] \\ h_d[M+1] & h_d[M] & \dots & h_d[M+2-N] \\ \vdots & \vdots & \ddots & \vdots \\ h_d[M+N-1] & h_d[M+N-2] & \dots & h_d[M] \end{bmatrix} \begin{bmatrix} a_1 \\ a_2 \\ \vdots \\ a_N \end{bmatrix} = - \begin{bmatrix} h_d[M+1] \\ h_d[M+2] \\ \vdots \\ h_d[M+N] \end{bmatrix}$$

We have $M + N$ linear equations that should be linearly independent, leading to a unique solution. Solving them we obtain the coefficients a_k . Substituting into Equation (11.292) we obtain with n replaced by k the values of the coefficients b_k .

$$b_k = h[k] + a_1 h[k-1] + a_2 h[k-2] + \dots + a_N h[k-N], \quad k = 0, 1, \dots, M \tag{11.295}$$

which can be written in the form

$$\begin{bmatrix} b_0 \\ b_1 \\ b_2 \\ \vdots \\ b_M \end{bmatrix} = \begin{bmatrix} h[0] & 0 & 0 & \dots & 0 \\ h[1] & h[0] & 0 & \dots & 0 \\ h[2] & h[1] & h[0] & \dots & 0 \\ \vdots & \vdots & \vdots & \ddots & \vdots \\ h[M] & h[M-1] & h[M-2] & \dots & h[M-N] \end{bmatrix} \begin{bmatrix} 1 \\ a_1 \\ a_2 \\ \vdots \\ a_N \end{bmatrix} \tag{11.296}$$

A perfect match $h[n] = h_d[n]$ is thus obtained for $n = 0, 1, \dots, M + N$. For $n > M + N$ however, no condition is imposed on $h[n]$ and the approximation may deviate considerably from $h_d[n]$. Such is the weakness of the Padé approximation.

Example 11.19 Given the desired impulse response

$$h_d[n] = \{10(0.75)^n + 20(0.6)^n\} u[n] \tag{11.297}$$

deduce the coefficients of the filter transfer function $H(z)$ such that $h[n] = h_d[n]$, using the Padé approximation.

We note that with $h[n] = h_d[n]$ we have

$$\begin{aligned} H(z) &= \frac{10}{1 - 0.75z^{-1}} + \frac{20}{1 - 0.6z^{-1}} = \frac{10 - 6z^{-1} + 20 - 15z^{-1}}{(1 - 0.75z^{-1})(1 - 0.6z^{-1})} \\ &= \frac{30 - 21z^{-1}}{1 - 1.35z^{-1} + 0.45z^{-2}} = \frac{b_0 + b_1z^{-1}}{1 + a_1z^{-1} + a_2z^{-2}}. \end{aligned}$$

To verify that Padé approximation produces the same result we proceed as given above with $M = 1$ and $N = 2$ so that $K = M + N = 3$

$$\begin{bmatrix} h_d[1] & h_d[0] \\ h_d[2] & h_d[1] \end{bmatrix} \begin{bmatrix} a_1 \\ a_2 \end{bmatrix} = - \begin{bmatrix} h_d[2] \\ h_d[3] \end{bmatrix} \tag{11.298}$$

$$\begin{bmatrix} 19.5 & 30 \\ 12.825 & 19.5 \end{bmatrix} \begin{bmatrix} a_1 \\ a_2 \end{bmatrix} = - \begin{bmatrix} 12.825 \\ 8.5388 \end{bmatrix}. \tag{11.299}$$

Solving, we obtain $a_1 = -1.350$ and $a_2 = 0.45$ as expected. Writing the matrix equation in the form $AX = B$ we may obtain the solution using the MATLAB function $\mathbf{X} = \mathbf{A} \setminus \mathbf{B}$. This is a very useful MATLAB command, and particularly powerful when we are dealing with systems of higher orders.

The coefficients b_k are given by

$$\begin{aligned} \begin{bmatrix} b_0 \\ b_1 \end{bmatrix} &= \begin{bmatrix} h[0] & 0 \\ h[1] & h[0] \end{bmatrix} \begin{bmatrix} 1 \\ a_1 \end{bmatrix} \\ &= \begin{bmatrix} 30 & 0 \\ 19.5 & 30 \end{bmatrix} \begin{bmatrix} 1 \\ -1.35 \end{bmatrix} = \begin{bmatrix} 30 \\ -21 \end{bmatrix}. \end{aligned} \tag{11.300}$$

Example 11.20 Use the Padé approximation to evaluate the transfer function $H_d(z)$ that models a Chebyshev Type 1 filter of the fourth order with 1 dB pass-band ripple and a pass-band edge frequency which is one quarter of the sampling frequency.

The filter transfer function is given by

$$H(z) = \frac{0.05552 + 0.2221z^{-1} + 0.3331z^{-2} + 0.2221z^{-3} + 0.05552z^{-4}}{1 - 0.7498z^{-1} + 1.073z^{-2} - 0.5598z^{-3} + 0.2337z^{-4}}. \tag{11.301}$$

The impulse response $h[n]$ is found as the inverse Z transform of $H(z)$. We obtain

$$h[n] = \{0.0555, 0.2637, 0.4713, 0.3237, -0.0726, -0.1994, -0.0006, 0.0971, -0.0212, -0.0738, 0.0219, 0.0610, \dots\} \tag{11.302}$$

By setting the desired impulse response $h_d[n]$ equal to the system impulse response $h[n]$ we obtain the matrix equation $AX = B$ where X is the vector of unknown a_k coefficients. With $M = 4$ and $N = 4$ we obtain

$$\begin{bmatrix} -0.0726 & 0.3237 & 0.4713 & 0.2637 \\ -0.1994 & -0.0726 & 0.3237 & 0.4713 \\ -0.0006 & -0.1994 & -0.0726 & 0.3237 \\ 0.0971 & -0.0006 & -0.1994 & -0.0726 \end{bmatrix} \begin{bmatrix} a_1 \\ a_2 \\ a_3 \\ a_4 \end{bmatrix} = \begin{bmatrix} 0.1994 \\ 0.0006 \\ -0.0971 \\ 0.0212 \end{bmatrix} \tag{11.303}$$

Using MATLAB we write $X = A \setminus B$ obtaining the solution X with the coefficients $a_1 = -0.7498$, $a_2 = 1.0725$, $a_3 = -0.5598$ and $a_4 = 0.2337$ as expected. The b_k coefficients are given by

$$B = \begin{bmatrix} 0.0555 & 0 & 0 & 0 & 0 \\ 0.2637 & 0.0555 & 0 & 0 & 0 \\ 0.4713 & 0.2637 & 0.0555 & 0 & 0 \\ 0.3237 & 0.4713 & 0.2637 & 0.0555 & 0 \\ -0.0726 & 0.3237 & 0.4713 & 0.2637 & 0.0555 \end{bmatrix} \begin{bmatrix} 1 \\ -0.7498 \\ 1.0725 \\ -0.5598 \\ 0.2337 \end{bmatrix} = \begin{bmatrix} 0.0555 \\ 0.2221 \\ 0.3331 \\ 0.2221 \\ 0.0555 \end{bmatrix}$$

where B is the vector of b_k coefficients, as expected.

It is important to note that in this example we assumed knowledge of the number of zeros M and poles N of the filter model. We were thus able to write $M + N$ equations and obtain an exact solution. If, on the other hand, we are given only the impulse response $h_d[n]$ and no knowledge of the number of zeros and poles M and N , the number of equations would not match those of the coefficients and the Padé approximation would not produce reliable results.

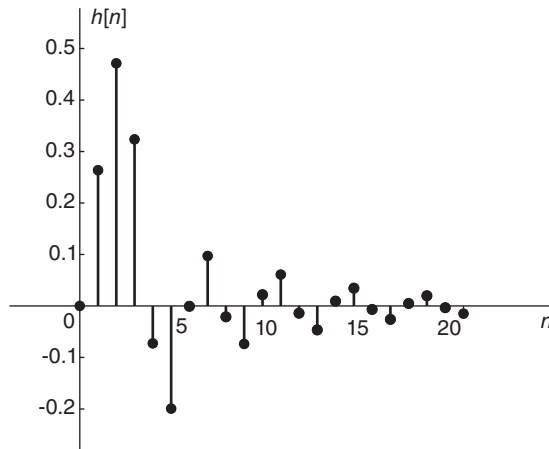


FIGURE 11.39 Desired impulse response.

Figure 11.39 shows the desired impulse response $h[n]$. The effect on the response of assuming a number of zeros $M = 5$ and poles $N = 5$ is shown in Fig. 11.40. In this figure, we see the true desired response $h[n]$ together with the erroneous response $\hat{h}[n]$ produced by the Padé approximation. We see that a slight deviation from the true numerator and denominator orders M and N of $H(z)$ leads to unreliable results.

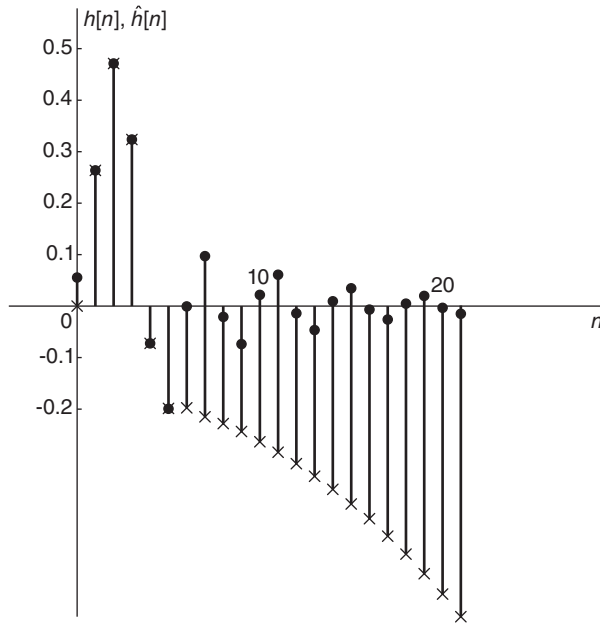


FIGURE 11.40 Desired filter response and erroneous Padé approximation.

11.35 Error Minimization in Prony’s Method

We have seen that a true minimization of the sum of squares error ε necessitates the solution of nonlinear equations. To avoid such difficulty we note that with $h[n]$ replaced by $h_d[n]$ the condition in Equation (11.294) should be as closely as possible approximated; i.e. we should aim for satisfying as closely as possible the condition

$$h_d[n] + a_1 h_d[n - 1] + a_2 h_d[n - 2] + \dots + a_N h_d[n - N] = 0, \quad n > M. \tag{11.304}$$

We may view the approximation error as the sum of squares

$$\varepsilon = \sum_{n=M+1}^{\infty} \left\{ h_d[n] + \sum_{m=1}^N a_m h_d[n - m] \right\}^2. \tag{11.305}$$

The coefficients a_k are found by setting

$$\frac{\partial \varepsilon}{\partial a_k} = 0, \quad k = 0, 1, \dots, N \tag{11.306}$$

$$\frac{\partial \varepsilon}{\partial a_k} = 2 \sum_{n=M+1}^{\infty} \left\{ h_d[n] + \sum_{m=1}^N a_m h_d[n - m] \right\} \{ h_d[n - k] \} = 0 \tag{11.307}$$

$$\sum_{n=M+1}^{\infty} \left\{ h_d[n] h_d[n - k] + \sum_{m=1}^N a_m h_d[n - m] h_d[n - k] \right\} = 0 \tag{11.308}$$

$$\sum_{m=1}^N \sum_{n=M+1}^{\infty} h_d[n-m] h_d[n-k] a_m = - \sum_{n=M+1}^{\infty} h_d[n] h_d[n-k] \tag{11.309}$$

$$\sum_{m=1}^N r[k, m] a_m = -r[k, 0], \quad k = 1, 2, \dots, N \tag{11.310}$$

where $r[k, m]$ is the autocorrelation

$$r[k, m] = \sum_{n=M+1}^{\infty} h_d[n-m] h_d[n-k]. \tag{11.311}$$

The result may be written in the matrix form

$$\begin{bmatrix} r[1, 1] & r[1, 2] & \dots & r[1, N] \\ r[2, 1] & r[2, 2] & \dots & r[2, N] \\ \vdots & \vdots & \ddots & \vdots \\ r[N, 1] & r[N, 2] & \dots & r[N, N] \end{bmatrix} \begin{bmatrix} a_1 \\ a_2 \\ \vdots \\ a_N \end{bmatrix} = - \begin{bmatrix} r[1, 0] \\ r[2, 0] \\ \vdots \\ r[N, 0] \end{bmatrix} \tag{11.312}$$

The b_k coefficients are then deduced using the values of the a_k coefficients as was done above. We have

$$b_k = h_d[k] + \sum_{i=1}^k a_i h_d[k-i], \quad k = 0, 1, \dots, M \tag{11.313}$$

which can be written in matrix form as seen above.

$$b_0 = h_d[0] \tag{11.314}$$

$$b_1 = h_d[1] + a_1 h_d[0] \tag{11.315}$$

$$b_2 = h_d[2] + a_1 h_d[1] + a_2 h_d[0] \tag{11.316}$$

...

$$b_k = h_d[k] + a_1 h_d[k-1] + a_2 h_d[k-2] + \dots + a_N h_d[k-N]. \tag{11.317}$$

$$b_M = h_d[M] + a_1 h_d[M-1] + a_2 h_d[M-2] + \dots + a_N h_d[0] \tag{11.318}$$

Shanks' approach introduced in 1967 concerns the estimation of the b_k coefficients. Let $H_p(z)$ be an all-pole filter

$$H_p(z) = \frac{1}{1 + \sum_{k=1}^N \hat{a}_k z^{-k}} \tag{11.319}$$

where the coefficients \hat{a}_k are those found as seen above. Let

$$H_z(z) = \sum_{k=0}^M b_k z^{-k} \tag{11.320}$$

and consider the cascade shown in Fig. 11.41.

Let the input to the cascade system be the unit pulse $\delta[n]$. The output of the first system is $h_p[n]$ as seen in the figure. The output $y[n]$ of the second system should be as closely as possible equal to the desired unit pulse response $h_d[n]$. The objective is to evaluate the coefficients b_k leading to such approximation. We have

$$Y(z) = H_z(z) H_p(z) = H_p(z) \sum_{k=0}^M b_k z^{-k} \tag{11.321}$$

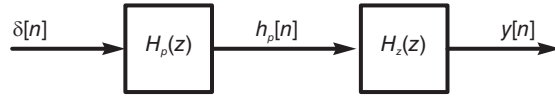


FIGURE 11.41 A cascade of an all-pole and an all-zero filters.

$$y[n] = h_p[n] * \sum_{k=0}^M b_k \delta[n - k] = \sum_{k=0}^M b_k h_p[n - k] \tag{11.322}$$

$$e[n] = h_d[n] - y[n] = h_d[n] - \sum_{k=0}^M b_k h_p[n - k] \tag{11.323}$$

$$\varepsilon = \sum_{n=0}^{\infty} \left\{ h_d[n] - \sum_{m=0}^M b_m h_p[n - m] \right\}^2 \tag{11.324}$$

$$\frac{\partial \varepsilon}{\partial b_k} = 2 \sum_{n=0}^{\infty} \left\{ h_d[n] - \sum_{m=0}^M b_m h_p[n - m] \right\} \{-h_p[n - k]\} = 0. \tag{11.325}$$

$$\sum_{m=0}^M b_m \sum_{n=0}^{\infty} h_p[n - k] h_p[n - m] = \sum_{n=0}^{\infty} h_p[n - k] h_d[n]. \tag{11.326}$$

Let

$$r_{h_p h_p}[k, m] = \sum_{n=0}^{\infty} h_p[n - k] h_p[n - m] \tag{11.327}$$

$$r_{h_p h_d}[k] = \sum_{n=0}^{\infty} h_p[n - k] h_d[n] \tag{11.328}$$

We have

$$\sum_{m=0}^M b_m r_{h_p h_p}[k, m] = r_{h_p h_d}[k], \quad k = 0, 1, \dots, M \tag{11.329}$$

$$\begin{bmatrix} r_{h_p h_p}[0, 0] & r_{h_p h_p}[0, 1] & \dots & r_{h_p h_p}[0, M] \\ r_{h_p h_p}[1, 0] & r_{h_p h_p}[1, 1] & \dots & r_{h_p h_p}[1, M] \\ \vdots & \vdots & \ddots & \vdots \\ r_{h_p h_p}[M, 0] & r_{h_p h_p}[M, 1] & \dots & r_{h_p h_p}[M, M] \end{bmatrix} \begin{bmatrix} b_0 \\ b_1 \\ \vdots \\ b_M \end{bmatrix} = \begin{bmatrix} r_{h_p h_d}[0] \\ r_{h_p h_d}[1] \\ \vdots \\ r_{h_p h_d}[M] \end{bmatrix} \tag{11.330}$$

which may be solved for the coefficients b_k .

Example 11.21 Using Prony’s method estimate the denominator coefficients a_k , and then the numerator coefficients b_k , of a system transfer function to approximate a desired unit pulse response of $N = 256$ points given by

$$h_d[n] = \sum_{i=1}^4 A_i a_i^n \cos(\gamma_i^n + \theta_i) u[n]$$

where for $n = 1, 2, 3, 4$, respectively, $A_i = 5, 10, 5, 8$, $a_i = 0.9, 0.7, 0.6, 0.5$, $\gamma_i = 32\pi/N, 64\pi/N, 96\pi/N, 128\pi/N$, and $\theta_i = \pi/3, \pi/5, \pi/4, 0.2\pi$. Prony’s method receives

the sequence $h_d[n]$ as a succession of N values but the analytical value of $h_d[n]$ is assumed to be unknown. Prony's method evaluates the parameters a_k and b_k of the transfer function

$$H(z) = \frac{\sum_{k=0}^M b_k z^{-k}}{1 + \sum_{k=1}^N a_k z^{-k}}$$

based solely on the those $N = 256$ values of $h_d[n]$.

A plot of the first seventy points of the sequence is shown in Fig. 11.42.

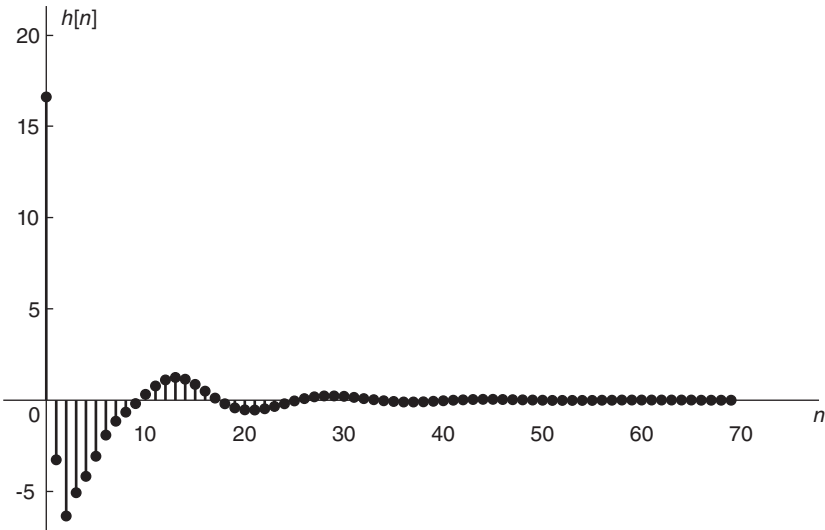


FIGURE 11.42 Given finite duration impulse response.

Applying Prony's method we write

$$\begin{bmatrix} r[1,1] & r[1,2] & \dots & r[1,N] \\ r[2,1] & r[2,2] & \dots & r[2,N] \\ \vdots & \vdots & \ddots & \vdots \\ r[N,1] & r[N,2] & \dots & r[N,N] \end{bmatrix} \begin{bmatrix} a_1 \\ a_2 \\ \vdots \\ a_N \end{bmatrix} = - \begin{bmatrix} r[1,0] \\ r[2,0] \\ \vdots \\ r[N,0] \end{bmatrix}$$

$$\begin{bmatrix} 7.6779 & 7.4925 & 6.3322 & 4.4969 & 1.9237 & -1.4702 & -5.2506 & -12.2434 \\ 7.4925 & 9.0091 & 9.7005 & 9.8727 & 9.3090 & 7.7721 & 5.8520 & -1.4780 \\ 6.3322 & 9.7005 & 12.6716 & 15.5732 & 17.8545 & 19.0098 & 19.9176 & 12.1098 \\ 4.4969 & 9.8727 & 15.5732 & 22.0883 & 28.3718 & 33.4095 & 38.4848 & 29.9518 \\ 1.9237 & 9.3090 & 17.8545 & 28.3718 & 39.4833 & 49.5130 & 59.8786 & 52.1225 \\ -1.4702 & 7.7721 & 19.0098 & 33.4095 & 49.5130 & 65.1775 & 81.6826 & 76.4534 \\ -5.2506 & 5.8520 & 19.9176 & 38.4848 & 59.8786 & 81.6826 & 105.4543 & 102.4345 \\ -12.2434 & -1.4780 & 12.1098 & 29.9518 & 52.1225 & 76.4534 & 102.4345 & 116.1464 \end{bmatrix} \begin{bmatrix} a_1 \\ a_2 \\ a_3 \\ a_4 \\ a_5 \\ a_6 \\ a_7 \\ a_8 \end{bmatrix} = - \begin{bmatrix} -6.7315 \\ -5.0701 \\ -2.4731 \\ 0.8269 \\ 4.8133 \\ 9.4361 \\ 14.3999 \\ 20.4411 \end{bmatrix}$$

We obtain the estimates of the coefficients a_1, a_2, \dots respectively, namely,

$$a_k = \{-3.1122, 4.7745, -4.7028, 3.3311, -1.7455, 0.6929, -0.1911, 0.0357\}$$

and then obtain the estimates of the coefficients b_0, b_1, b_2, \dots , namely,

$$b_k = \{16.5978, -54.9249, 83.0771, -78.9865, 51.9704, -24.3083, 7.6284, -1.4800\}$$

The estimates are accurate with maximum percentage error of 2.3×10^{-7} . MATLAB has the function **prony** which performs this same evaluation.

11.36 FIR Inverse Filter Design

The problem of inverse filtering, also referred to as “deconvolution” is encountered, for example, when an equalizer is sought to counteract the effect of a distorting filter. Let $G(z)$ be the transfer function of an linear time invariant (LTI) system and $g[n]$ be its impulse response. We seek a filter of transfer function $H(z)$, as seen in Fig. 11.43, such that

$$H(z) = 1/G(z) \quad (11.331)$$

and unit sample response $h[n]$. We note that $G(z)H(z) = 1$ implies that $g[n] * h[n] = \delta[n]$. If $G(z)$ has zeros outside the unit circle in the z -plane, the resulting inverse filter $H(z)$ is unstable. For a stable inverse filter the system $G(z)$ should therefore be minimum-phase.

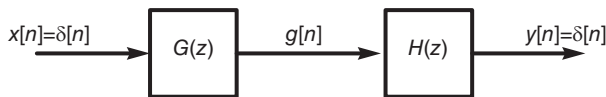


FIGURE 11.43 Cascade of a filter and its inverse.

Note, moreover, that if and only if $G(z)$ is an all-pole filter, the resulting filter $H(z)$ may be realized as an FIR filter; otherwise an FIR filter realization would be at best an approximation of the required true inverse filter.

With the inverse filter realized as an FIR filter of length N we obtain an approximation

$$g[n] * h[n] = d[n] \approx \delta[n]. \quad (11.332)$$

The error $e[n]$ of the approximation, as seen in Fig. 11.44, is given by

$$e[n] = \delta[n] - d[n] \quad (11.333)$$

and

$$d[n] = \sum_{k=0}^{N-1} h[k] g[n-k]. \quad (11.334)$$

The overall error is

$$\varepsilon = \sum_{n=0}^{\infty} |e[n]|^2 = \sum_{n=0}^{\infty} \left\{ \delta[n] - \sum_{m=0}^{N-1} h[m] g[n-m] \right\}^2 \quad (11.335)$$

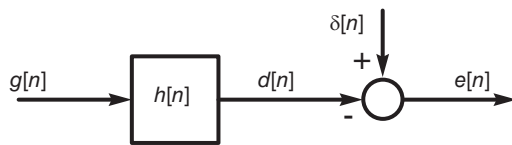


FIGURE 11.44 Approximation error model.

$$\frac{\partial \varepsilon}{\partial h[k]} = 2 \sum_{n=0}^{\infty} \left\{ \delta[n] - \sum_{m=0}^{N-1} h[m] g[n-m] \right\} g[n-k] = 0 \tag{11.336}$$

$$\sum_{m=0}^{N-1} h[m] \sum_{n=0}^{\infty} g[n-m] g[n-k] = \sum_{n=0}^{\infty} g[n-k] \delta[n]. \tag{11.337}$$

Letting $n - m = r$, the left-hand side takes the form

$$\sum_{m=0}^{N-1} h[m] \sum_{r=0}^{\infty} g[r] g[r-k+m] = \sum_{m=0}^{N-1} h[m] \sum_{n=0}^{\infty} g[n] g[n-k+m] = \sum_{m=0}^{N-1} h[m] r_{gg}[k-m]$$

where

$$r_{gg}[k] = \sum_{n=0}^{\infty} g[n] g[n-k] = g[n] * g[-n] \tag{11.338}$$

is the autocorrelation of $g[n]$. The filter is thus obtained as the solution of the equation

$$\sum_{m=0}^{N-1} h[m] r_{gg}[k-m] = \sum_{n=0}^{\infty} g[n-k] \delta[n] = \begin{cases} g[0], & k = 0 \\ 0, & k = 1, 2, \dots, N-1 \end{cases} \tag{11.339}$$

We may write in matrix form

$$\begin{bmatrix} r_{gg}[0] & r_{gg}[1] & \dots & r_{gg}[N-1] \\ r_{gg}[1] & r_{gg}[0] & \dots & r_{gg}[N-2] \\ \vdots & \vdots & \ddots & \vdots \\ r_{gg}[N-1] & r_{gg}[N-2] & \dots & r_{gg}[0] \end{bmatrix} \begin{bmatrix} h[0] \\ h[1] \\ \vdots \\ h[N-1] \end{bmatrix} = \begin{bmatrix} g[0] \\ 0 \\ \vdots \\ 0 \end{bmatrix} \tag{11.340}$$

which are N linear equations in the n unknowns $h[0], h[1], \dots, h[N-1]$.

In practice, if a delay of K samples is allowed so that

$$g[n] * h[n] \approx \delta[n-K] \tag{11.341}$$

instead of $g[n] * h[n] \approx \delta[n]$ a better approximation may result. In this case the filter is obtained by solving the equations

$$\sum_{m=0}^{N-1} h[m] r_{gg}[k-m] = \begin{cases} g[K-k], & k = 0, 1, \dots, K \\ 0, & k = K+1, \dots, N \end{cases} \tag{11.342}$$

Example 11.22 Evaluate the least-squares FIR inverse filter, with length $N = 16$, of a system with unit sample response

$$g[n] = a^n \cos \beta n \tag{11.343}$$

where $a = 0.5$ and $\beta = \pi/4$. Evaluate the least sum of squares error of the approximation.

We solve the matrix equation $Ah = y$ where A is the matrix of autocorrelations $r_{gg}[k]$ shown in Table 11.2, and $y = [g[0], 0, 0, \dots, 0]'$; the prime meaning transpose. The unit sample response $g[n]$ is shown in Fig. 11.45. The autocorrelation $r_{gg}[n]$ of $g[n]$ is shown in Fig. 11.46. We obtain the required unit sample response $h[n]$, shown in Fig. 11.47,

$$h[n] = \{0.99999, -0.35355, 0.12499, 0.04419, 0.01562, 0.00552, 0.00195, 0.00069, 0.00024, 0.00009, 0.00003, 0.00001, 0.000004, 0.000001, -0.000001, 0.000005\}. \tag{11.344}$$

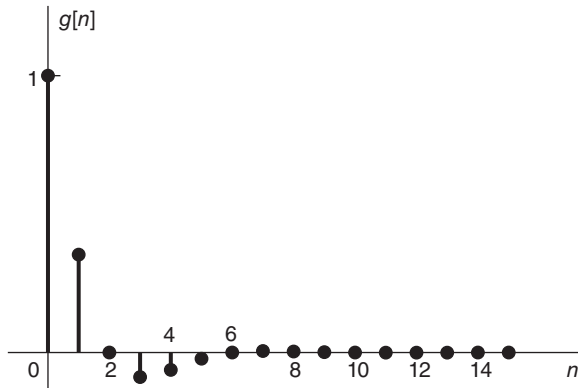


FIGURE 11.45 Given unit sample response.

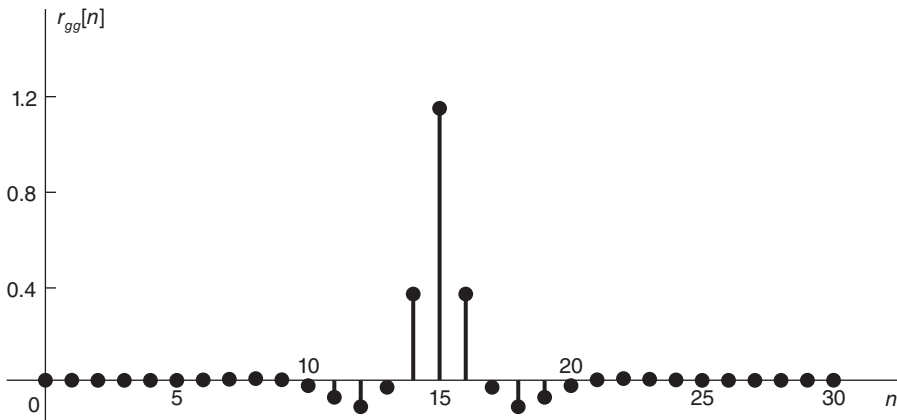


FIGURE 11.46 Autocorrelation $r_{gg}[n]$ of $g[n]$.

TABLE 11.2 Matrix of Correlations

1.1373	0.3605	-0.0294	-0.1109	-0.0711	-0.0225	0.0018	0.0069	0.0044	0.0014	-0.0001	-0.0004	-0.0003	-0.0001	0.0000	0.0000
0.3605	1.1373	0.3605	-0.0294	-0.1109	-0.0711	-0.0225	0.0018	0.0069	0.0044	0.0014	-0.0001	-0.0004	-0.0003	-0.0001	0.0000
-0.0294	0.3605	1.1373	0.3605	-0.0294	-0.1109	-0.0711	-0.0225	0.0018	0.0069	0.0044	0.0014	-0.0001	-0.0004	-0.0003	-0.0001
-0.1109	-0.0294	0.3605	1.1373	0.3605	-0.0294	-0.1109	-0.0711	-0.0225	0.0018	0.0069	0.0044	0.0014	-0.0001	-0.0004	-0.0003
-0.0711	-0.1109	-0.0294	0.3605	1.1373	0.3605	-0.0294	-0.1109	-0.0711	-0.0225	0.0018	0.0069	0.0044	0.0014	-0.0001	-0.0004
-0.0225	-0.0711	-0.1109	-0.0294	0.3605	1.1373	0.3605	-0.0294	-0.1109	-0.0711	-0.0225	0.0018	0.0069	0.0044	0.0014	-0.0001
0.0018	-0.0225	-0.0711	-0.1109	-0.0294	0.3605	1.1373	0.3605	-0.0294	-0.1109	-0.0711	-0.0225	0.0018	0.0069	0.0044	0.0014
0.0069	0.0018	-0.0225	-0.0711	-0.1109	-0.0294	0.3605	1.1373	0.3605	-0.0294	-0.1109	-0.0711	-0.0225	0.0018	0.0069	0.0044
0.0044	0.0069	0.0018	-0.0225	-0.0711	-0.1109	-0.0294	0.3605	1.1373	0.3605	-0.0294	-0.1109	-0.0711	-0.0225	0.0018	0.0069
0.0014	0.0044	0.0069	0.0018	-0.0225	-0.0711	-0.1109	-0.0294	0.3605	1.1373	0.3605	-0.0294	-0.1109	-0.0711	-0.0225	0.0018
-0.0001	0.0014	0.0044	0.0069	0.0018	-0.0225	-0.0711	-0.1109	-0.0294	0.3605	1.1373	0.3605	-0.0294	-0.1109	-0.0711	-0.0225
-0.0004	-0.0001	0.0014	0.0044	0.0069	0.0018	-0.0225	-0.0711	-0.1109	-0.0294	0.3605	1.1373	0.3605	-0.0294	-0.1109	-0.0711
-0.0003	-0.0004	-0.0001	0.0014	0.0044	0.0069	0.0018	-0.0225	-0.0711	-0.1109	-0.0294	0.3605	1.1373	0.3605	-0.0294	-0.1109
-0.0001	-0.0003	-0.0004	-0.0001	0.0014	0.0044	0.0069	0.0018	-0.0225	-0.0711	-0.1109	-0.0294	0.3605	1.1373	0.3605	-0.0294
0.0000	-0.0001	-0.0003	-0.0004	-0.0001	0.0014	0.0044	0.0069	0.0018	-0.0225	-0.0711	-0.1109	-0.0294	0.3605	1.1373	0.3605
0.0000	0.0000	-0.0001	-0.0003	-0.0004	-0.0001	0.0014	0.0044	0.0069	0.0018	-0.0225	-0.0711	-0.1109	-0.0294	0.3605	1.1373

The estimation error is given by

$$\varepsilon = \sum_{n=0}^{\infty} |e[n]|^2 = \sum_{n=0}^{\infty} \left\{ \delta[n] - \sum_{m=0}^{N-1} h[m] g[n-m] \right\}^2 = 2.52 \times 10^{-11}. \quad (11.345)$$

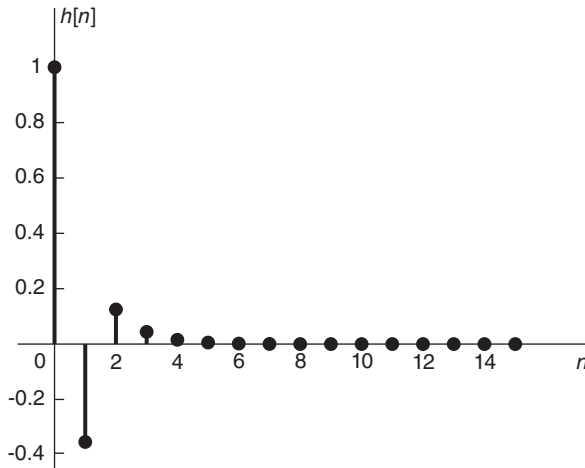


FIGURE 11.47 Required unit sample response.

11.37 Impulse Response of Ideal Filters

Figure 11.48 shows the frequency response of the ideal lowpass, highpass and bandpass digital filters, namely, $H_{LP}(e^{j\Omega})$, $H_{HP}(e^{j\Omega})$ and $H_{BP}(e^{j\Omega})$, respectively.

The impulse response $h_{LP}[n]$ of the ideal lowpass filter is given by the inverse Fourier transform of $H_{LP}(e^{j\Omega})$, namely,

$$h_{LP}[n] = \frac{1}{2\pi} \int_{-\Omega_c}^{\Omega_c} e^{j\Omega n} d\Omega = \frac{1}{2\pi} \left\{ \frac{e^{j\Omega_c n} - e^{-j\Omega_c n}}{jn} \right\} = \frac{1}{\pi} \frac{\sin(\Omega_c n)}{n} = \frac{\Omega_c}{\pi} Sa(\Omega_c n)$$

which is depicted in Fig. 11.49. The frequency response $H_{HP}(e^{j\Omega})$ of the highpass filter may be written in the form

$$H_{HP}(e^{j\Omega}) = 1 - H_{LP}(e^{j\Omega}). \quad (11.346)$$

Its impulse response $h_{HP}[n]$ may therefore be written in the form

$$h_{HP}[n] = \mathcal{F}^{-1}[H_{HP}(e^{j\Omega})] = \delta[n] - h_{LP}[n] = \begin{cases} -\frac{\Omega_c}{\pi} Sa(\Omega_c n), & n \neq 0 \\ 1 - \frac{\Omega_c}{\pi}, & n = 0. \end{cases} \quad (11.347)$$

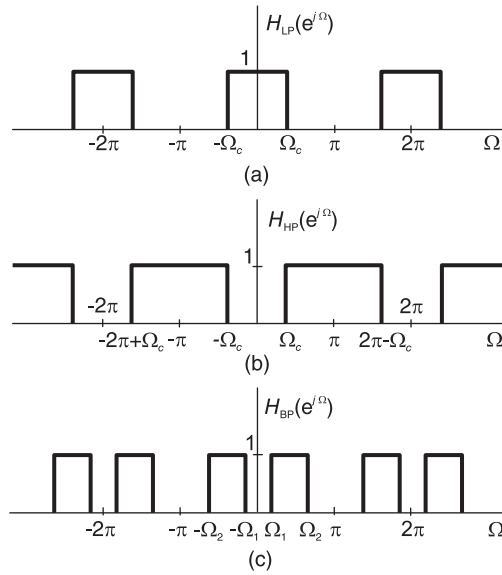


FIGURE 11.48 Ideal filters frequency responses.

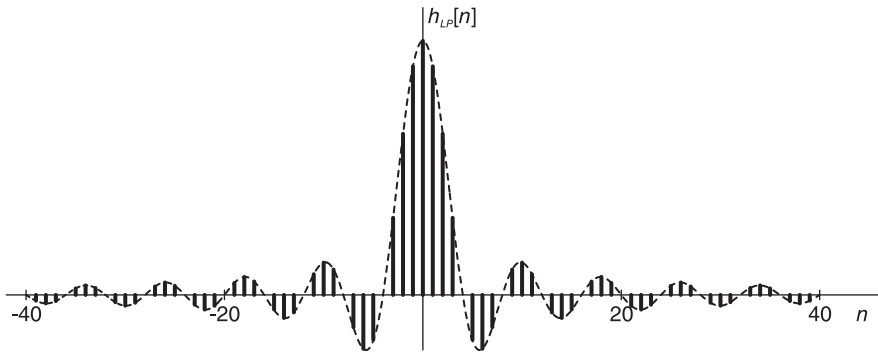


FIGURE 11.49 Ideal filter impulse responses.

The impulse response of the bandpass filter is given by

$$\begin{aligned}
 h_{BP}[n] &= \mathcal{F}^{-1} [H_{BP}(e^{j\Omega})] = \frac{1}{2\pi} \left\{ \int_{-\Omega_2}^{-\Omega_1} e^{j\Omega n} d\Omega + \int_{\Omega_1}^{\Omega_2} e^{j\Omega n} d\Omega \right\} \\
 &= \frac{1}{2\pi} \left\{ \frac{e^{j\Omega_2 n} - e^{-j\Omega_2 n}}{jn} - \frac{e^{j\Omega_1 n} - e^{-j\Omega_1 n}}{jn} \right\} = \frac{1}{\pi} \left\{ \frac{\sin \Omega_2 n}{n} - \frac{\sin \Omega_1 n}{n} \right\} \\
 &= \frac{1}{\pi} \{ \Omega_2 Sa(\Omega_2 n) - \Omega_1 Sa(\Omega_1 n) \} \tag{11.348}
 \end{aligned}$$

$$h_{BP}[0] = (\Omega_2 - \Omega_1) / \pi. \tag{11.349}$$

The impulse response $h_{BS}[n]$ of the bandstop filter is similarly found to be

$$h_{BS}[n] = \delta[n] - h_{BP}[n] = \begin{cases} (1/\pi) \{ \Omega_1 Sa(\Omega_1 n) - \Omega_2 Sa(\Omega_2 n) \}, & n \neq 0 \\ 1 - (\Omega_2 - \Omega_1) / \pi, & n = 0. \end{cases} \tag{11.350}$$

11.38 Spectral Leakage

We have seen in Fig. 11.49 the impulse response $h_{LP}[n]$ of the ideal lowpass filter. We note that the impulse response is a two-sided infinite duration sequence. To obtain a finite impulse response FIR filter realization we have to truncate the sequence $h_{LP}[n]$ obtaining a finite-duration sequence. Such truncation may be viewed as multiplying the sequence $h_{LP}[n]$ by a rectangular window $w[n]$ so that the resulting FIR sequence may be written in the form

$$h[n] = h_{LP}[n] w[n] \quad (11.351)$$

with the rectangular window $w[n]$ given by

$$w[n] = \Pi_N[n] = u[n + N] - u[n - N - 1]. \quad (11.352)$$

We thus retain $2N + 1$ points of the impulse response and discard the rest. The effect is certainly deviation from the desired ideal filter response. In fact the multiplication of $h_{LP}[n]$ by the window $w[n]$ corresponds to the convolution of the desired lowpass frequency response $H_{LP}(e^{j\Omega})$ shown in Fig. 11.48(a) above, with the Fourier transform $W(e^{j\Omega})$ of the rectangular sequence $w[n]$, given by,

$$W(e^{j\Omega}) = \sum_{n=-N}^N e^{-jn\Omega}. \quad (11.353)$$

Letting $m = n + N$, we have

$$\begin{aligned} W(e^{j\Omega}) &= \sum_{m=0}^{2N} e^{-j(m-N)\Omega} = e^{jN\Omega} \sum_{m=0}^{2N} e^{-jm\Omega} = e^{jN\Omega} \frac{1 - e^{-j(2N+1)\Omega}}{1 - e^{-j\Omega}} \\ &= \frac{\sin[(2N+1)\Omega/2]}{\sin(\Omega/2)} \triangleq Sd_{2N+1}(\Omega/2). \end{aligned} \quad (11.354)$$

The convolution in the frequency domain means that the resulting frequency response is given by

$$H(e^{j\Omega}) = \frac{1}{2\pi} H_{LP}(e^{j\Omega}) * W(e^{j\Omega}) = \frac{1}{2\pi} \int_{-\pi}^{\pi} H_{LP}(e^{j\Phi}) W[e^{j(\Omega-\Phi)}] d\Phi. \quad (11.355)$$

The spectrum $W(e^{j\Omega})$ is shown in Fig. 11.50

It is as expected composed of main and side lobes displaying a “ringing” phenomenon. The convolution of the spectrum $W(e^{j\Omega})$ with the ideal lowpass response $H_{LP}(e^{j\Omega})$ results therefore in overshoot and ripples that extend beyond the pass-band of the ideal lowpass filter response.

If the rectangular truncating window is replaced by one that applies the truncation in a progressive gradual transition, the result is a reduction of the side lobe peak ripple. Windows such as Hamming, Hanning, Triangular-Bartlett, Blackman, and Kaiser are examples of such windows that produce truncation with a softer transition than the rectangular window. In the following, basic windows are defined and their spectra are evaluated and displayed.

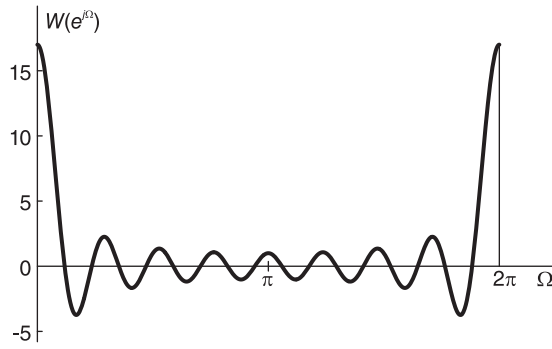


FIGURE 11.50 Transform of the rectangular sequence $w[n]$.

11.39 Windows

Similarly to the Continuous-time domain the subject of Windows has its importance in reducing spectral leakage, a phenomenon often encountered in analyzing truncated sinusoidal signals. Simultaneous plots of common windows Bartlett, Hanning, Hamming, Blackman and Kaiser with $\beta = 7$ are shown in Fig. 11.51. Amplitude spectra for Bartlett, Hanning, Hamming, Blackman and Kaiser with $\beta = 9$ can be seen in Fig. 11.52. In what follows we evaluate the spectra of common discrete-time windows.

11.40 Ideal Digital Filters Rectangular Window

The centered rectangular window has the transform

$$\begin{aligned} X(e^{j\Omega}) &= \sum_{n=-N}^N e^{-j\Omega n} = e^{j\Omega N} \frac{1 - e^{-j\Omega(2N+1)}}{1 - e^{-j\Omega}} \\ &= e^{j\Omega N} \frac{e^{-j\Omega(\frac{2N+1}{2})}}{e^{-j\Omega/2}} \frac{\sin[\Omega(\frac{2N+1}{2})]}{\sin(\Omega/2)} = \frac{\sin[\Omega(\frac{2N+1}{2})]}{\sin(\Omega/2)} = Sd_{2N+1}(\Omega/2). \end{aligned} \tag{11.356}$$

The causal rectangular window is given by

$$x[n] = R_N[n] = u[n] - u[n - N]. \tag{11.357}$$

Its z -transform is given by

$$X(z) = \frac{1 - z^{-N}}{1 - z^{-1}} \tag{11.358}$$

and its Fourier transform by

$$X(e^{j\Omega}) = \frac{1 - e^{-j\Omega N}}{1 - e^{-j\Omega}} = \frac{e^{-j\Omega N/2} \sin N\Omega/2}{e^{-j\Omega} \sin \Omega/2} = e^{-j\Omega(N-1)/2} Sd_N(\Omega/2) \tag{11.359}$$

The rectangular window and its amplitude and phase spectra are shown in Fig. 11.53.

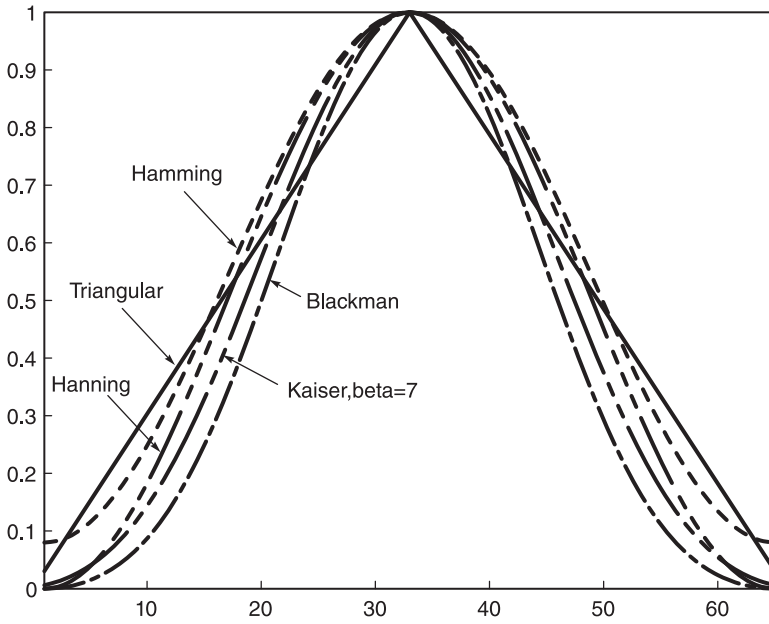


FIGURE 11.51 Common windows.

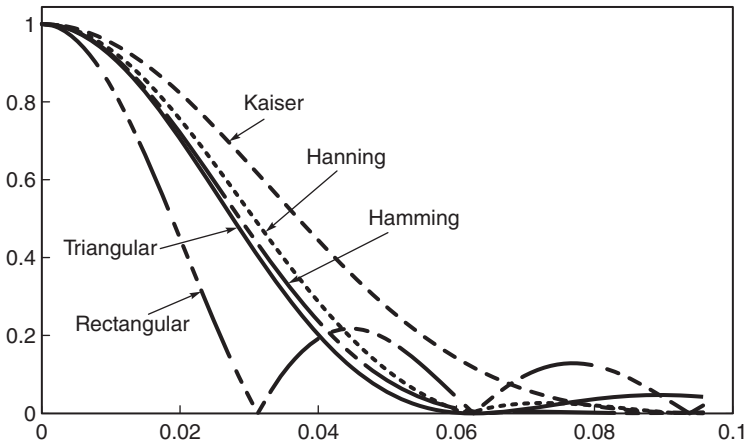


FIGURE 11.52 Common windows amplitude spectra.

11.41 Hanning Window

$$v[n] = \frac{1}{2} \left[1 - \cos \frac{2\pi n}{N} \right] R_N[n] = \frac{1}{2} R_N[n] - \frac{1}{4} \left\{ e^{j \frac{2\pi n}{N}} + e^{-j \frac{2\pi n}{N}} \right\} R_N[n]. \quad (11.360)$$

Let

$$x[n] = R_N[n] \longleftrightarrow X(e^{j\Omega}) = e^{-j\Omega(N-1)/2} Sd_N(\Omega/2). \quad (11.361)$$

We have

$$e^{j \frac{2\pi}{N} n} x[n] \longleftrightarrow X \left[e^{j(\Omega - 2\pi/N)} \right] \quad (11.362)$$

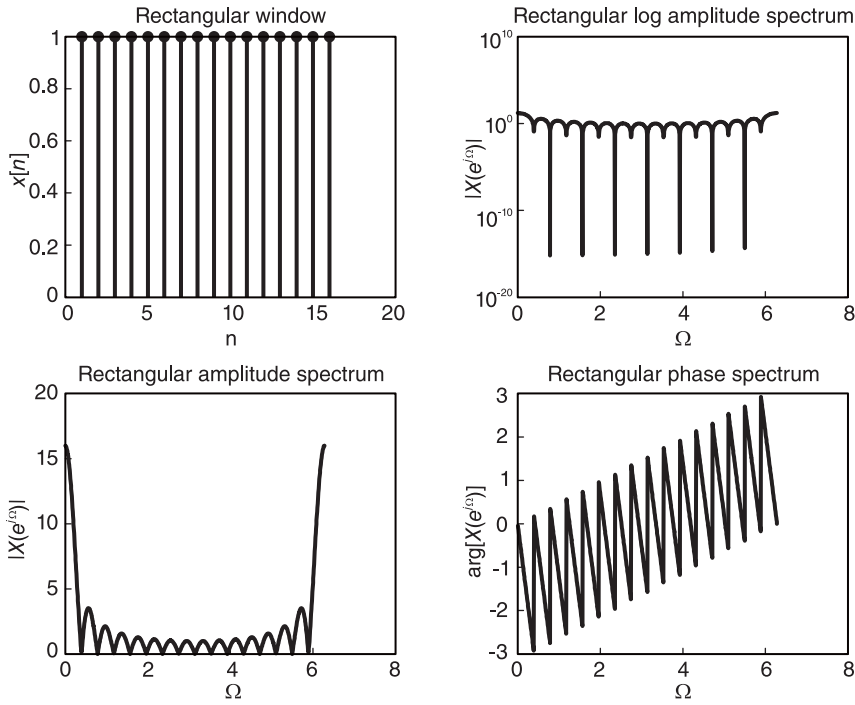


FIGURE 11.53 Rectangular window and spectrum.

$$\begin{aligned}
 V(e^{j\Omega}) &= \frac{1}{2}X(e^{j\Omega}) - \frac{1}{2}X[e^{j(\Omega-2\pi/N)}] - \frac{1}{2}X[e^{j(\Omega+2\pi/N)}] = \frac{1}{2}e^{-j\Omega(N-1)/2}Sd_N(\Omega/2) \\
 &\quad - \frac{1}{4}e^{-j(\Omega-2\pi/N)(N-1)/2}Sd_N[(\Omega-2\pi/N)/2] \\
 &\quad - \frac{1}{4}e^{-j(\Omega+2\pi/N)(N-1)/2}Sd_N[(\Omega+2\pi/N)/2].
 \end{aligned}
 \tag{11.363}$$

The Hanning window and its amplitude and phase spectra are shown in Fig. 11.54. The Hanning window spectrum can be rewritten in the form

$$V(j\omega) = \frac{4\pi^2 \sin(T\omega/2)}{4\pi^2\omega - T^2\omega^3}.$$

The Hamming window spectrum can be rewritten in the form

$$V(j\omega) = \frac{(0.16T^2\omega^2 - 4.32\pi^2) \sin(\omega T/2)}{T^2\omega^3 - 4\pi^2\omega}.$$

11.42 Hamming Window

$$\begin{aligned}
 w[n] &= \left\{ 0.54 - 0.46 \cos \frac{2\pi n}{N} \right\} R_N[n] \\
 &= 0.54R_N[n] - 0.23e^{j\frac{2\pi}{N}n}R_N[n] - 0.23e^{-j\frac{2\pi}{N}n}R_N[n]
 \end{aligned}
 \tag{11.364}$$

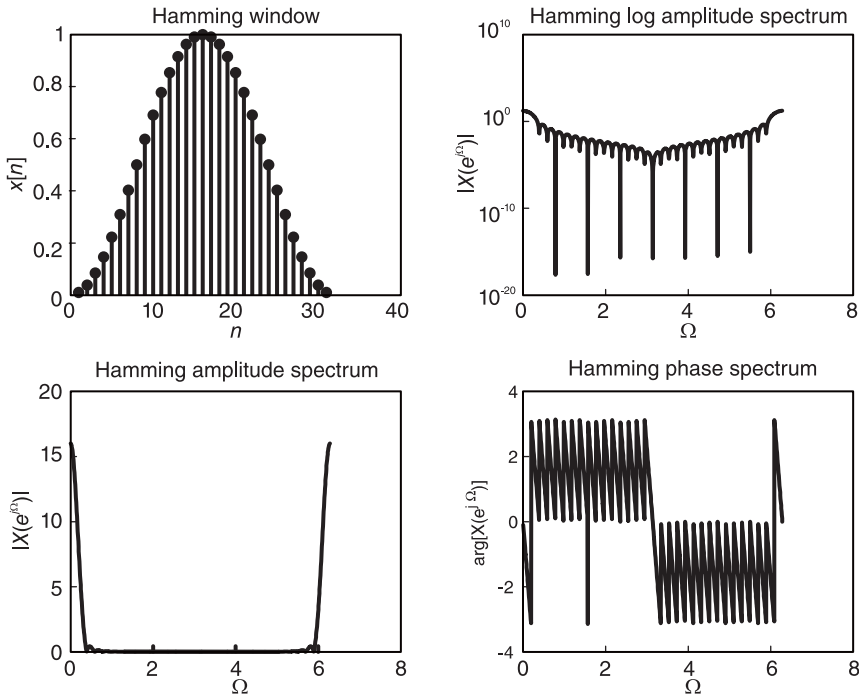


FIGURE 11.54 Hamming window and spectrum.

$$\begin{aligned}
 W(e^{j\Omega}) &= 0.54X(e^{j\Omega}) - 0.23X[e^{j(\Omega-2\pi/N)}] - 0.23X[e^{j(\Omega+2\pi/N)}] \\
 &= 0.54e^{-j\Omega(N-1)/2}Sd_N(\Omega/2) - 0.23e^{-j(\Omega/2-\pi/N)(N-1)}Sd_N(\Omega/2 - \pi/N) \\
 &\quad - 0.23e^{-j(\Omega/2+\pi/N)(N-1)}Sd_N(\Omega/2 + \pi/N).
 \end{aligned}$$

The Hamming window and its amplitude and phase spectra are show in Fig. 11.55.

11.43 Triangular Window

Consider the case of a triangular window with a total width of N points, where N is odd., as can be seen in Fig. 11.56.

$$t[n] = \begin{cases} n, & 0 \leq n \leq (N + 1) / 2 \\ N + 1 - n, & (N + 1) / 2 \leq n \leq N. \end{cases} \tag{11.365}$$

Let

$$s[n] = R_{(N+1)/2}[n] * R_{(N+1)/2}[n] \tag{11.366}$$

$$t[n] = s[n - 1] \tag{11.367}$$

$$S(e^{j\Omega}) = [F\{R_{(N+1)/2}[n]\}]^2 \tag{11.368}$$

$$\begin{aligned}
 F\{R_{(N+1)/2}[n]\} &= e^{-j\Omega\{(N+1)/2-1\}/2}Sd_{(N+1)/2}(\Omega/2) \\
 &= e^{-j\Omega(N-1)/4}Sd_{(N+1)/2}(\Omega/2) \\
 &= e^{-j\Omega(N-1)/4} \frac{\sin[(N + 1)\Omega/4]}{\sin(\Omega/2)} \tag{11.369}
 \end{aligned}$$

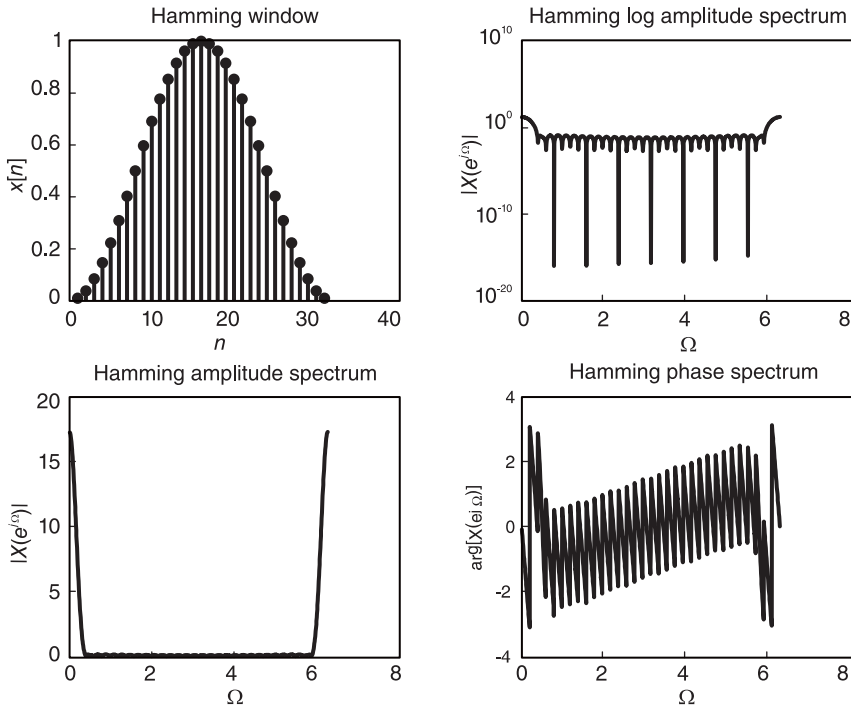


FIGURE 11.55 Hamming window and spectrum.

$$S(e^{j\Omega}) = e^{-j\Omega(N-1)/2} S_{d_{(N+1)/2}^2}(\Omega/2) = e^{-j\Omega(N-1)/2} \frac{\sin^2[(N+1)\Omega/4]}{\sin^2(\Omega/2)} \quad (11.370)$$

$$T(e^{j\Omega}) = S(e^{j\Omega}) e^{-j\Omega} = e^{-j\Omega(N+1)/2} \frac{\sin^2[(N+1)\Omega/4]}{\sin^2(\Omega/2)}. \quad (11.371)$$

The triangular or Bartlett window and its spectrum are shown in Fig. 11.56.

11.44 Comparison of Windows Spectral Parameters

Given a long duration sequence to evaluate the discrete Fourier transform (DFT), a truncation may be applied to extract a finite duration sequence. In speech analysis for example, given a long duration sequence we often need to analyze a short duration section thereof. Truncation is therefore called for. To avoid spectral leakage a rectangular window is usually replaced by a Hamming, Hanning, Bartlett or Kaiser Window.

The choice of an appropriate window constitutes usually a trade-off between different parameters. Reducing the side lobe peak, for example, leads in general to a widening of the main lobe, which when convolved with the ideal filter response leads to a wider transition region than that obtained using a rectangular window. Table 11.3 lists the properties of transition width, side lobe and stop-band attenuation of the different windows with N the window length.

As mentioned in discussing FIR filters, in practice, to obtain a physically realizable filter the impulse response should be made causal, by introducing a delay such that the impulse

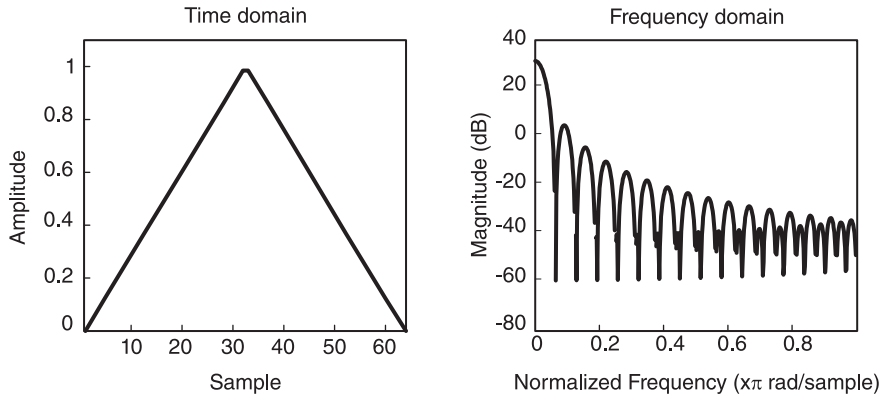


FIGURE 11.56 Triangular or Bartlett window and spectrum.

TABLE 11.3 Table of properties of some windows

Window	Transition width Δf Hz	Side lobe peak relative to main lobe (dB)	Stop-band attenuation (dB)
Rectangular	$0.9/N$	-13	-21
Hanning	$3.1/N$	-31	-44
Hamming	$3.3/N$	-41	-53
Blackman	$5.5/N$	-57	-74

response starts at $n = 0$ and extends to $n = N$. Such delay has the effect of introducing a linear phase in the frequency response. The window thus extends from $n = 0$ to $n = N$ and is symmetric about its middle point, i.e.

$$w[n] = w[N - n]. \quad (11.372)$$

An increase in the window length N leads to sharper peaks and narrower lobes and, consequently, to a narrower transition region between the pass-band and stop band. The relation between the window length N and the transition width Δf in Hz may be expressed in the form

$$N\Delta f = C \quad (11.373)$$

where C is a constant which depends on the window $w[n]$, as shown in the table. The transition width Δf is about equal to the width of the main lobe.

Example 11.23 Evaluate the order and impulse response of a lowpass FIR Filter using a suitable window with the following specifications: Attenuation at zero frequency is 0 dB. The pass-band edge frequency is $\Omega_p = 0.2\pi$. The stop-band edge frequency is $\Omega_s = 0.262\pi$ such that in the stop band

$$|H(e^{i\Omega})| \leq 0.01.$$

We note that the stop-band attenuation is $\alpha_s = 20 \log_{10} 0.01 = -40$ dB. The Hanning window suffices for such stop-band attenuation while having the least main lobe width. The required transition width is $\Delta\Omega = \Omega_s - \Omega_p = 0.062\pi$, i.e. $\Delta f = 0.031$ Hz. The filter order N is given by

$$N = \frac{3.1}{\Delta f} = \frac{3.1}{0.031} = 100.$$

The ideal impulse response of the filter should produce a cut-off frequency

$$\Omega_c = \frac{\Omega_p + \Omega_s}{2} = \frac{0.462\pi}{2} = 0.231\pi.$$

It should be delayed by $N/2 = 50$ samples before being multiplied by the Hanning window. It is therefore given by

$$h[n] = \frac{\Omega_c}{\pi} \text{Sa}[\Omega_c(n - 50)] = \frac{\sin[0.231\pi(n - 50)]}{\pi(n - 50)}, \quad 0 \leq n \leq N.$$

Another type of window that concentrates most of the energy in the main lobe for a given side lobe amplitude is the Kaiser window. In this regard the Kaiser window is nearly optimal and is in fact a family of windows dependent on a parameter β that controls its form. It is given by

$$w[n] = \frac{I_0 \left[\beta \sqrt{1 - \{(2n/N) - 1\}^2} \right]}{I_0(\beta)}, \quad 0 \leq n \leq N$$

where I_0 denotes the zeroth order modified Bessel function of the first kind, which can be evaluated using the power series expansion

$$I_0(x) = 1 + \sum_{k=1}^{\infty} \left\{ \frac{(x/2)^k}{k!} \right\}^2$$

11.45 Linear-Phase FIR Filter Design Using Windows

Given a desired frequency response $H_d(e^{j\Omega})$ a linear-phase FIR filter may be designed by first evaluating the filter unit sample response

$$h_d[n] = \mathcal{F}^{-1}[H_d(e^{j\Omega})] = \frac{1}{2\pi} \int_{-\pi}^{\pi} H_d(e^{j\Omega}) e^{j\Omega n} d\Omega. \tag{11.374}$$

Since the unit sample response $h_d[n]$ is of infinite duration we have to truncate it to deduce the required filter's finite impulse response $h[n]$. Such truncation may be effected by multiplying $h_d[n]$ by a window $w[n]$, so that

$$h[n] = h_d[n]w[n]. \tag{11.375}$$

The window $w[n]$ may be a simple rectangular window, or another window selected to reduce spectral leakage due to such truncation. Since the FIR filter should be causal and of finite length of say, M samples, we should introduce a delay such that in the case of a rectangular window for example $w[n] = R_M[n]$

$$h[n] = h_d[n]w[n] = \begin{cases} h_d[n], & n = 0, 1, \dots, M - 1 \\ 0, & \text{otherwise.} \end{cases} \tag{11.376}$$

By choosing an appropriate window we can effect a trade-off between the amount of spectral leakage ripple and the resulting frequency resolution.

11.46 Even- and Odd-Symmetric FIR Filter Design

We have seen that if the unit sample response $h[n]$ of an FIR filter is symmetric about its middle point, the resulting frequency response has linear phase. We now study a class of filters referred to as *generalized linear phase* filters. Consider the case of an FIR filter of length M , of which the unit sample response $h[n]$ has even or odd symmetry about its middle point. The unit sample response satisfies the relation

$$h[n] = \pm h[M - 1 - n], \quad n = 0, 1, \dots, M - 1. \tag{11.377}$$

as illustrated for the cases of M odd and even in Fig. 11.57.

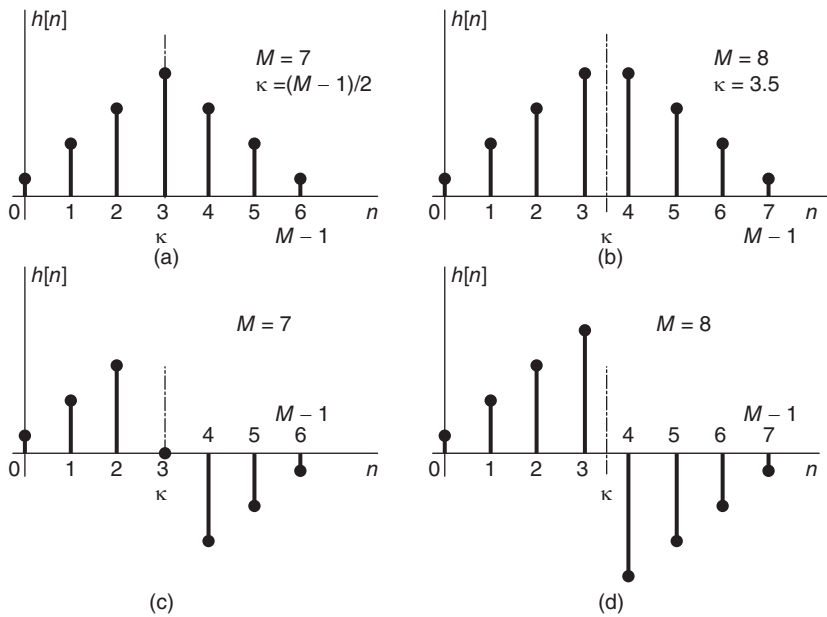


FIGURE 11.57 FIR filter impulse response with (a) Type I, odd order, even symmetry; (b) Type II, even order, even symmetry; (c) Type III, odd order, odd symmetry; and (d) Type IV, even order, odd symmetry.

The filter transfer function is given by

$$H(z) = \sum_{n=0}^{M-1} h[n]z^{-n} = h[0] + h[1]z^{-1} + \dots + h[M - 1]z^{-(M-1)} \tag{11.378}$$

Let $\kappa = (M - 1)/2$ be the middle point as shown in the figure. We may write, using the fact that $\kappa - M + 1 = -\kappa$

$$H(z) = z^{-\kappa} \left\{ h[0]z^{\kappa} + h[1]z^{(\kappa-1)} + \dots + h[M - 1]z^{\kappa-M+1} \right\}$$

$$H(e^{j\Omega}) = e^{-j\kappa\Omega} \left\{ h[0]e^{j\kappa\Omega} + h[1]e^{j(\kappa-1)\Omega} + \dots + h[M - 2]e^{-j(\kappa-1)\Omega} + h[M - 1]e^{-j\kappa\Omega} \right\}$$

For the case of Type I, even symmetry and M odd,

$$H(e^{j\Omega}) = e^{-j\kappa\Omega} \left\{ 2 \sum_{n=0}^{\kappa-1} h[n] \cos[(\kappa - n)\Omega] + h[\kappa] \right\}. \quad (11.379)$$

For Type II, even symmetry, $h[n] = h[M - 1 - n]$, and M even we have

$$H(e^{j\Omega}) = 2e^{-j\kappa\Omega} \left\{ \sum_{n=0}^{(M-2)/2} h[n] \cos[(\kappa - n)\Omega] \right\}. \quad (11.380)$$

For Type III, odd symmetry, $h[n] = -h[M - 1 - n]$, and M odd we have

$$H(e^{j\Omega}) = j2e^{-j\kappa\Omega} \left\{ \sum_{n=0}^{\kappa-1} h[n] \sin[(\kappa - n)\Omega] \right\} \quad (11.381)$$

and for Type IV, odd symmetry and M even, we may write

$$H(e^{j\Omega}) = j2e^{-j\kappa\Omega} \left\{ \sum_{n=0}^{(M-2)/2} h[n] \sin[(\kappa - n)\Omega] \right\}. \quad (11.382)$$

As noted in Section 11.13 the impulse response symmetry condition leads to groups of zeros in the z -plane. In particular, the condition $h[n] = \pm h[M - 1 - n]$ implies that

$$H(z) = \pm z^{-(M-1)} H(z^{-1}). \quad (11.383)$$

leading to a pattern of zeros in the z -plane as seen above in Fig. 11.13. The values of $H(z)$ at $z = 1$ and $z = -1$ can be readily established for Types II, III and IV. For Type II FIR filter we have

$$H(-1) = (-1)^{-(M-1)} H(-1) = -H(-1) \quad (11.384)$$

i.e. $H(e^{j\pi}) = H(-1) = 0$. Similarly, for a Type III filter $H(e^{j0}) = H(1) = 0$ and $H(e^{j\pi}) = H(-1) = 0$, and for a Type IV filter, $H(e^{j0}) = H(1) = 0$, as can be seen in Fig. 11.58.

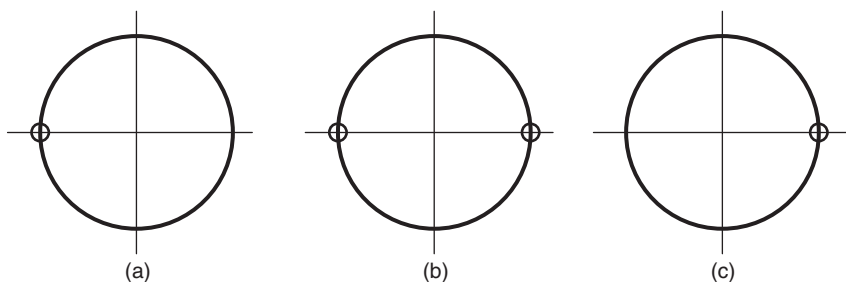


FIGURE 11.58 Linear phase FIR filter zeros at $\Omega = 0$ and $\Omega = \pi$: (a) Type II; (b) Type III; (c) Type IV.

11.47 Linear Phase FIR Filter Realization

The approach to realizing linear phase FIR filters starts by evaluating the desired filter impulse response $h_d[n]$ from the given desired frequency response $H_d(e^{j\Omega})$. We have

$$H_d(e^{j\Omega}) = \sum_{n=-\infty}^{\infty} h_d[n]e^{-j\Omega n} \quad (11.385)$$

and

$$h_d[n] = \frac{1}{2\pi} \int_{-\pi}^{\pi} H_d(e^{j\Omega n})e^{j\Omega n} d\Omega. \quad (11.386)$$

Since the theoretical impulse response is two sided and of infinite duration, a realization as an FIR filter necessitates truncating the impulse response to M points and applying the shift of $\kappa = (M - 1)/2$ samples as discussed above.

The truncation of the unit sample response $h_d[n]$ leads to spectral leakage in the form of ripples and side lobes as stated in the context of continuous-time signals. To reduce the size of lobes a window other than the rectangular one may be used. The effect however is to increase the width of the main lobe, which results in lower resolution and a wider transition range between the pass-band and the stop band. In the following we study the properties of well-known windows, which are important in reducing spectral leakage.

11.48 Sampling the Unit Circle

In uniform sampling of the z -plane unit circle into M uniformly spaced points, four cases merit consideration. There are the two possibilities of M even and M odd. Moreover, with the same sampling interval along the unit circle of $\Delta\Omega = 2\pi/M$, the first sample may be taken at $\Omega = 0$ or at $\Omega = \Delta\Omega/2 = \pi/M$. In other words the values of z in the z -plane are in the first case

$$z = 1, e^{j2\pi/M}, e^{j4\pi/M}, \dots, e^{j(M-1)2\pi/M} \quad (11.387)$$

and in the second case

$$z = e^{j\pi/M}, e^{j3\pi/M}, \dots, e^{j(2M-1)\pi/M}. \quad (11.388)$$

The sampling points are therefore

$$z_k = e^{j2\pi(k+\mu)/M} \quad (11.389)$$

where $\mu = 0$ in the first case and $\mu = 1/2$ in the second. The four sampling possibilities, M even and odd, $\mu = 0$ and $\mu = 1/2$, are illustrated in Figs. 11.59 and 11.60. In particular, Fig. 11.59(a-b) shows the case of M even, $M = 8$, with $\mu = 0$ and $\mu = 1/2$, respectively. Fig. 11.60(a-b) shows the case of M odd, $M = 7$, and with $\mu = 0$ and $\mu = 1/2$, respectively.

We have seen that there are four types of linear-phase FIR filter unit sample response, namely, Types I to IV. With a given number of points M of the unit sample response the unit circle is sampled into the same M points but with an initial rotation of $\mu = 0$ or $\mu = 1/2$. In all therefore we have eight cases to consider. We may refer to the first as Type

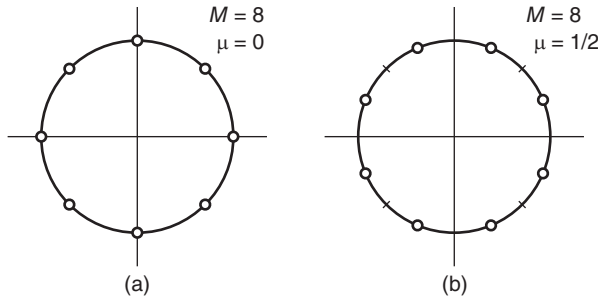


FIGURE 11.59 Unit circle sampling with an even number of M samples: (a) $\mu = 0$, (b) $\mu = 1/2$.

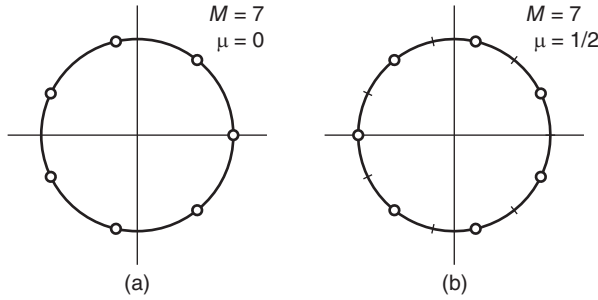


FIGURE 11.60 Unit circle sampling with an odd number of M samples: (a) $\mu = 0$, (b) $\mu = 1/2$.

I-1 and Type I-2 for the two cases $\mu = 0$ and $\mu = 1/2$ of Type I filter. Similarly, for Types II, III and IV, we have the sub-types Type II-1, II-2, Type III-1, III-2 and Type IV-1, IV-2, corresponding to the two cases $\mu = 0$ and $\mu = 1/2$, respectively.

In the following the symmetry in the time and frequency domains is used to reduce the computations needed to evaluate the filter impulse response $h[n]$ from samples of the frequency response.

To design a linear-phase FIR filter given a desired frequency response $H(e^{j\Omega})$ we may start by sampling the unit circle uniformly into M points. We thus obtain the DFT

$$H[k] = H(e^{j\Omega})|_{\Omega=2\pi k/M} = H(e^{j2\pi k/M}). \tag{11.390}$$

Since

$$H[k] = \sum_{n=0}^{M-1} h[n]e^{-j2\pi kn/M} \tag{11.391}$$

we can do an inverse DFT obtaining the unit sample response

$$h[n] = \frac{1}{M} \sum_{k=0}^{M-1} H[k]e^{j2\pi kn/M}. \tag{11.392}$$

As seen above, we may start the sampling at $\Omega = \pi/M$, which is the case $\mu = 1/2$, instead of $\Omega = 0$, the case of $\mu = 0$. The sampling frequencies are therefore $\Omega_k = (k + \mu)2\pi/M$. In

the case $\mu = 1/2$ we have

$$H[k + 1/2] = H(e^{j\Omega})|_{\Omega=\pi/M+2\pi k/M} \quad (11.393)$$

$$= H(e^{j(k+1/2)\pi/M}). \quad (11.394)$$

We may write

$$H[k + 1/2] = \sum_{n=0}^{M-1} h[n]e^{-j(2k+1)n\pi/M}. \quad (11.395)$$

Multiplying both sides of this equation by $e^{j2\pi kr/M}$ and effecting the summation over k we obtain

$$\sum_{k=0}^{M-1} e^{j2\pi kr/M} H[k + 1/2] = \sum_{k=0}^{M-1} e^{j2\pi kr/M} \sum_{n=0}^{M-1} h[n]e^{-j(k+1/2)2n\pi/M} \quad (11.396)$$

$$= \sum_{n=0}^{M-1} h[n] \sum_{k=0}^{M-1} e^{j\frac{2\pi}{M}(kr - kn - \frac{n}{2})} \quad (11.397)$$

$$= \sum_{n=0}^{M-1} h[n]e^{-\frac{j\pi n}{M}} \sum_{k=0}^{M-1} e^{j(2\pi/M)(r-n)k} \quad (11.398)$$

$$= Mh[r]e^{-j\pi r/M} \quad (11.399)$$

$$h[r] = \frac{1}{M}e^{j\pi r/M} \sum_{k=0}^{M-1} e^{j2\pi kr/M} H[k + 1/2] = \frac{1}{M} \sum_{k=0}^{M-1} H[k + 1/2]e^{j2\pi(k+1/2)r/M}.$$

Replacing r by n

$$h[n] = \frac{1}{M} \sum_{k=0}^{M-1} H[k + 1/2]e^{j2\pi(k+1/2)n/M}. \quad (11.400)$$

The fast Fourier transform (FFT) and the symmetry properties can be used to improve computation efficiency.

We note that an interpolation formula producing $H(z)$ for a given $H[k + 1/2]$ can be easily deduced. We have

$$H(z) = \sum_{n=0}^{M-1} h[n]z^{-n} \quad (11.401)$$

$$= \sum_{n=0}^{M-1} \frac{1}{M} \sum_{k=0}^{M-1} H[k + 1/2]e^{j2\pi(k+1/2)n/M} z^{-n} \quad (11.402)$$

$$= \frac{1}{M} \sum_{k=0}^{M-1} H[k + 1/2] \sum_{n=0}^{M-1} e^{j2\pi(k+1/2)n/M} z^{-n} \quad (11.403)$$

$$= \frac{1}{M} \sum_{k=0}^{M-1} H[k + 1/2] \frac{1 - e^{j\pi} z^{-M}}{1 - e^{j2\pi(k+1/2)/M} z^{-1}} \quad (11.404)$$

$$= \frac{1}{M} (1 + z^{-M}) \sum_{k=0}^{M-1} \frac{H[k + 1/2]}{1 - e^{j2\pi(k+1/2)/M} z^{-1}} \quad (11.405)$$

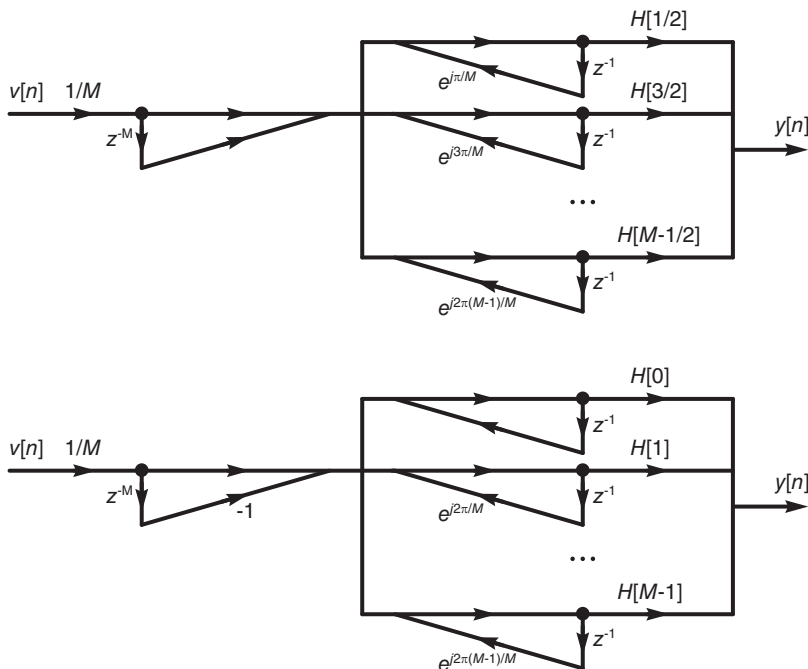


FIGURE 11.61 FIR filter unit circle sampling structure: (a) the case $\mu = 1/2$, (b) $\mu = 0$.

For the case $\mu = 1/2$ the filter can therefore be realized as shown in Fig. 11.61(a). For the case $\mu = 0$ the interpolation formula is

$$H(z) = \frac{1}{M}(1 - z^{-M}) \sum_{k=0}^{M-1} \frac{H[k]}{1 - e^{j2\pi k/M} z^{-1}} \tag{11.406}$$

and may be realized as seen in Fig. 11.61(b). By combining each pair of complex conjugate poles using the spectrum symmetry we can obtain a structure using real, instead of complex, multiplications.

It should be noted that the transfer function has coincident poles and zeros on the unit circle. With cumulative computation errors instability may occur. Such a problem may be avoided by sampling the transfer function $H(z)$ on a circle of radius r that is slightly less than unity. For the case $\mu = 0$, for example, the interpolation formula takes the form

$$H(z) = \frac{1}{M}(1 - r^M z^{-M}) \sum_{k=0}^{M-1} \frac{H_r[k]}{1 - r e^{j2\pi k/M} z^{-1}} \tag{11.407}$$

where

$$H_r[k] = H(re^{j2\pi k/M}), \tag{11.408}$$

and a similar expression applies for the case of filter Types 2 and 3. The circuit realization is modified accordingly.

As noted, the z -plane unit circle may be sampled in the usual DFT pattern, into M points

$$z_k = e^{j\frac{2\pi}{M}k} \tag{11.409}$$

or into the shifted by half a sample spacing points

$$z_k = e^{j\frac{2\pi}{M}} e^{j\frac{2\pi}{M}k} = e^{j\frac{2\pi}{M}(k+1/2)}. \tag{11.410}$$

The unit circle is therefore sampled at the points

$$z_k = e^{j\frac{2\pi}{M}(k+\mu)} \quad (11.411)$$

where $\mu = 0$, or $\mu = 1/2$. The sampling produces the discrete spectrum

$$H[k + \mu] = H(e^{j2\pi(k+\mu)/M}) = \sum_{n=0}^{M-1} h[n]e^{-j2\pi(k+\mu)n/M}, \quad k = 0, 1, \dots, M-1 \quad (11.412)$$

and the unit sample response is given by

$$h[n] = \frac{1}{M} \sum_{k=0}^{M-1} H[k + \mu]e^{j2\pi(k+\mu)n/M}, \quad n = 0, 1, \dots, M-1. \quad (11.413)$$

The filter may be realized, as seen above, by interpolation from the unit circle to the general z -plane. We may also do an interpolation along the unit circle itself to deduce $H(e^{j\Omega})$. We may write

$$\begin{aligned} H(z) &= \sum_{n=0}^{M-1} h[n]z^{-n} \\ &= \sum_{n=0}^{M-1} \frac{1}{M} \sum_{k=0}^{M-1} H[k + \mu]e^{j2\pi(k+\mu)n/M} z^{-n} \\ H(e^{j\Omega}) &= \frac{1}{M} \sum_{k=0}^{M-1} H[k + \mu] \frac{1 - e^{-j\Omega M + j2\pi(k+\mu)M/M}}{1 - e^{-j\Omega} e^{j2\pi(k+\mu)/M}} \\ &= \frac{1}{M} \sum_{k=0}^{M-1} H[k + \mu] e^{-j[\Omega - 2\pi(k+\mu)/M](M-1)/2} \frac{\sin [\{\Omega - 2\pi(k + \mu)/M\} / M/2]}{\sin [\{\Omega - 2\pi(k + \mu)/M\} / 2]} \\ &= \frac{1}{M} \sum_{k=0}^{M-1} H[k + \mu] e^{-j[\{\Omega - 2\pi(k+\mu)/M\} / M/2]} Sd_M [\{\Omega - 2\pi(k + \mu)/M\} / 2] \end{aligned}$$

The filter frequency response as a function of the continuous variable Ω may thus be deduced.

11.49 Impulse Response Evaluation from Unit Circle Samples

In what follows we evaluate the impulse response of linear phase FIR filters using symmetry properties in the time and frequency domains.

11.49.1 Case I-1: Odd Order, Even Symmetry, $\mu = 0$

Referring to Fig. 11.57(a) and Fig. 11.59(a) we may obtain

$$h[n] = \frac{2}{M} \left\{ \sum_{k=0}^{(M-1)/2} |H[k]| \cos [(2\pi kn/M) + \arg [H[k]]] \right\}, \quad n = 0, \dots, (M-1)/2.$$

and $h[n] = h[M-1-n]$, $n = 0, 1, \dots, M-1$.

11.49.2 Case I-2: Odd Order, Even Symmetry, $\mu = 1/2$

Referring to Fig. 11.57(a) and Fig. 11.59(b) we may write

$$h[n] = \frac{1}{M} \left[2 \sum_{k=0}^{(M-3)/2} |H[k + 1/2]| \cos\{2\pi(k + 1/2)n/M + \arg[H[k + 1/2]]\} + (-1)^n H[M/2] \right]$$

for $n = 0, 1, \dots, (M - 1)/2$ and $h[n] = h[M - 1 - n]$, $n = 0, 1, \dots, M - 1$.

11.49.3 Case II-1

In the case of FIR filter Type II-1, that is, even order, even symmetry with $\mu = 0$, referring to Fig. 11.57(b) and Fig. 11.59(a) we may write

$$\begin{aligned} h[n] &= \frac{1}{M} \sum_{k=0}^{M-1} H[k] e^{j2\pi kn/M}, \quad n = 0, 1, \dots, M - 1 \\ &= \frac{1}{M} \left[H[0] + \left\{ H[1] e^{j2\pi n/M} + H[M - 1] e^{j2\pi(M-1)n/M} \right\} \right. \\ &\quad + \left\{ H[2] e^{j2\pi 2n/M} + H[M - 2] e^{j2\pi(M-2)n/M} \right\} \\ &\quad + \dots \\ &\quad \left. + \left\{ H[M/2 - 1] e^{j2\pi(M/2-1)n/M} + H[M/2 + 1] e^{j2\pi(M/2+1)n/M} \right\} \right] \end{aligned}$$

having noted that

$$H[M/2] = \sum_{n=0}^{M-1} h[n] e^{-j\pi n} = \sum_{n=0}^{M-1} (-1)^n h[n] = 0.$$

We may therefore write

$$h[n] = \frac{1}{M} \left\{ H[0] + 2 \sum_{k=1}^{M/2-1} |H[k]| \cos[(2\pi kn/M) + \arg[H[k]]] \right\}, \quad n = 0, 1, \dots, M/2 - 1.$$

and $h[n] = h[M - 1 - n]$, $n = 0, 1, \dots, M - 1$.

11.49.4 Case II-2: Even Order, Even Symmetry, $\mu = 1/2$

Referring to Fig. 11.57(b) and Fig. 11.59(b), we may write

$$H[k + 1/2] = H(e^{j2\pi(k+1/2)/M}) = \sum_{n=0}^{M-1} h[n] e^{-j2\pi(k+1/2)n/M}, \quad k = 0, 1, \dots, M - 1.$$

The unit sample response is given by

$$h[n] = \frac{1}{M} \sum_{k=0}^{M-1} H[k + 1/2] e^{j2\pi(k+1/2)n/M}, \quad n = 0, 1, \dots, M - 1. \tag{11.414}$$

Combining conjugate terms we obtain

$$h[n] = \frac{2}{M} \sum_{k=0}^{M/2-1} |H[k+1/2]| \cos \left[2\pi(k + 1/2)n/M + \arg \left[H[k + 1/2] \right] \right], \quad n = 0, 1, \dots, M/2 - 1$$

and $h[n] = h[M - 1 - n]$, $n = 0, 1, \dots, M - 1$.

11.49.5 Case III-1: Odd Order, Odd Symmetry, $\mu = 0$

Referring to Fig. 11.57(c) and Fig. 11.59(a), we have

$$h[n] = \frac{2}{M} \left\{ \sum_{k=0}^{(M-1)/2} |H[k]| \cos[(2\pi kn/M) + \arg[H[k]]], n = 0, \dots, (M-3)/2. \right.$$

and $h[n] = -h[M-1-n]$, $n = 0, 1, \dots, M-1$.

11.49.6 Case III-2: Odd Order, Odd Symmetry, $\mu = 1/2$

Referring to Fig. 11.57(c) and Fig. 11.59(b), we have

$$h[n] = \frac{2}{M} \left[\sum_{k=0}^{(M-3)/2} |H[k+1/2]| \cos\{2\pi(k+1/2)n/M + \arg[H[k+1/2]]\} \right]$$

for $n = 0, 1, \dots, (M-3)/2$ and $h[n] = -h[M-1-n]$, $n = 0, 1, \dots, M-1$.

11.49.7 Case IV-1: Even Order, Odd Symmetry, $\mu = 0$

Referring to Fig. 11.57(d) and Fig. 11.59(a), we have

$$h[n] = \frac{1}{M} \left[2 \sum_{k=1}^{M/2-1} |H[k]| \cos\{2\pi kn/M + \arg[H[k]]\} + (-1)^n H[M/2] \right]$$

for $n = 0, 1, \dots, M/2-1$ and $h[n] = -h[M-1-n]$, $n = 0, 1, \dots, M-1$.

11.49.8 Case IV-2: Even Order, Odd Symmetry, $\mu = 1/2$

Referring to Fig. 11.57(d) and Fig. 11.59(b), we have

$$h[n] = \frac{2}{M} \sum_{k=0}^{M/2-1} |H[k+1/2]| \cos\left[2\pi(k+1/2)n/M + \arg\left[H[k+1/2]\right]\right], n = 0, 1, \dots, M/2-1$$

and $h[n] = -h[M-1-n]$, $n = 0, 1, \dots, M-1$.

Example 11.24 Consider a sequence $x[n]$ of length $M = 64$ defined by

$$x[n] = \begin{cases} 1.2^n, & n = 0, 1, \dots, 31 \\ -1.2^n, & n = 32, 33, \dots, 63 \end{cases} \quad (11.415)$$

Evaluate the transform $X[k]$ defined by

$$x[k] = x(e^{j2\pi(k+1/2)/M}), k = 0, 1, \dots, M-1 \quad (11.416)$$

Using the symmetries in the time and frequency domain show how to evaluate efficiently the unit sample response $h[n]$ from the transform $X[k]$ and obtaining $h[n] = x[n]$.

Evaluating the inverse transform of $X[k]$ using the Case III-2 equation of $h[n]$ we obtain the values of $x[n]$ for $n = 0$ to 31. Applying the symmetry condition $x[n] = -x[M-1-n]$, $n = 0, 1, \dots, M-1$ we obtain the required unit pulse response $h[n]$ which is equal to the negation of the given sequence $x[n]$ for $n = 0, 1, \dots, M-1$ as expected.

Example 11.25 Consider Case I-2 FIR filter of order $M = 8$. Let impulse response be

$$h[n] = [1 \ 2 \ 3 \ 4 \ 4 \ 3 \ 2 \ 1].$$

Show how to deduce its $\mu = 1/2$ -shifted DFT $H[k + 1/2]$ from its DFT $H[k]$. Show how to deduce the impulse response from the shifted DFT $H[k + 1/2]$.

The DFT of the sequence $h[n]$ is $H[k]$, $k = 0, 1, \dots, M-1$. The samples on the unit circle of $H[k]$ start at frequency $\Omega = 0$ and are spaced by the interval $\Delta\Omega = 2\pi/M$, as usual. The shifted spectrum $H[k + 1/2]$ corresponds to sampling the unit circle with the same sampling interval but starting at the angle $\Omega_0 = \pi/M$. To deduce the values of the shifted spectrum from $H[k]$ we may apply zero padding to $h[n]$ obtaining the sequence

$$h_z[n] = [1 \ 2 \ 3 \ 4 \ 4 \ 3 \ 2 \ 1 \ 0 \ 0 \ 0 \ 0 \ 0 \ 0 \ 0].$$

Such zero padding affects interpolation along the unit circle revealing the values of $H[k]$ half way between its samples. The DFT $H_z[k]$ of $h_z[n]$ is the same as $H[k]$ for even k , and is the interpolations between the samples of $H[k]$ for odd k . The odd samples of $H_z[k]$ are the shifted by $\mu = 1/2$ samples of the spectrum of $h[n]$. The spectrum $H_z[k]$ has in addition, however, its even samples which are those at frequencies multiple of the usual interval $\Omega_0 = 2\pi/M$.

We may now conserve the values of only the odd samples of $H_z[k]$ and reset to zero the even ones. We thus construct the spectrum $B[k] = H_z[k]$, k odd, $B[k] = 0$, k even. Note that such suppression of the even samples on the unit circle is in fact a multiplication by a comb filter of frequency response $G[k] = [0 \ 1 \ 0 \ 1 \ 0 \ 1 \ \dots]$. From the above remarks on the two-spiked sequence we note that the suppression of the even samples in the frequency domain corresponds to a convolution in the time domain of the sequence $h[n]$ with the two-spiked sequence

$$x[n] = 0.5[1 \ 0 \ 0 \ 0 \ 0 \ 0 \ 0 \ 0 \ 0 \ -1 \ 0 \ 0 \ 0 \ 0 \ 0 \ 0 \ 0]$$

producing the sequence

$$v[n] = 0.5[1 \ 2 \ 3 \ 4 \ 4 \ 3 \ 2 \ 1 \ -1 \ -2 \ -3 \ -4 \ -4 \ -3 \ -2 \ -1]$$

and we note that

$$h[n] = 2[v[n], n = 0, 1, \dots, M].$$

The value of $h[n]$ is therefore two times the inverse DFT of $H[k + 1/2]$. Since $h[n]$ is symmetric, we need only evaluate the first $M/2$ values and deduce the second half of $h[n]$ by symmetry.

These remarks illustrate the relations between the linear phase FIR filter impulse response, its DFT, the DFT of its zero-padded extension, its $\mu = 1/2$ -shifted spectrum and the $2M$ -point inverse DFT obtained after interlacing the samples of the M -point shifted spectrum with zeros.

11.50 Problems

Problem 11.1 Given the difference equation

$$y[n] - 0.8y[n-1] + 0.15y[n-2] = -x[n] + 0.7x[n-1].$$

- Evaluate the transfer function $H(z)$ of a filter described by this equation.
- Show a canonical-form structure of the filter using a minimum number of delay elements.
- Show a parallel realization of the filter.

Problem 11.2 Show the structure of an IIR filter having the impulse response

$$h[n] = n 3^{-n/2} u[n].$$

Problem 11.3 Show the structure of a digital filter of impulse response

$$h[n] = u[n] - u[n - 8].$$

Problem 11.4 A digital filter has a causal impulse response $h[n]$ and is described by the difference equation

$$y[n] = 0.2y[n - 2] + 0.1y[n - 1] + 2x[n] + 0.5x[n - 1]$$

where $x[n]$ is its input and $y[n]$ its output.

- Evaluate the filter system function $H(z)$.
- Is this filter stable? Why?
- Show an IIR realization of the filter, which uses a minimum number of delay elements.
- Evaluate the filter impulse response $h[n]$.
- Show a finite impulse response realization of the filter which utilizes $N = 8$ delay elements. Indicate the values of the filter coefficients in this realization.

Problem 11.5 In the sampling-filtering-reconstruction system shown in the Fig. 11.62 the input continuous-time signal $x(t)$ is sampled by the A/D converter at a frequency of 100 kHz.

a) The objective is to evaluate $H(z)$, the transfer function of the highpass digital filter shown in the figure. The filter should have a gain of 0 dB at $\Omega = \pi$ and -3 dB at $\Omega = 3\pi/8$. Show how $H(z)$ can be found by applying the bilinear transform to the highpass analog filter of transfer function

$$H_a(s) = \frac{1}{s + 1} \Big|_{s \rightarrow \omega/s}.$$

b) If $x(t)$ is a sinusoid of amplitude 1 volt and frequency 18.75 kHz, what is the system output $y(t)$?

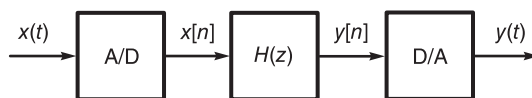


FIGURE 11.62 Signal sampling, filtering, and reconstruction.

Problem 11.6 In a system shown in Fig. 11.63 a signal $x(t)$ is sampled by an A/D converter at a frequency of $f_s = 32$ kHz. The converter output $x[n]$ is applied to a digital filter of impulse response $h[n]$. Its output $y[n]$ is fed to a D/A converter to effect an ideal reconstruction, producing an output $y(t)$.

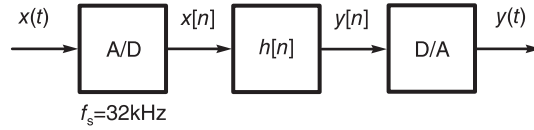


FIGURE 11.63 A/D conversion, filtering, and D/A conversion.

The impulse response $h[n]$ of the digital filter is given by

$$h[n] = \begin{cases} 3 - n, & 0 \leq n \leq 3 \\ 0, & \text{otherwise.} \end{cases}$$

- a) Evaluate the transfer function $H(z)$ of the digital filter.
- b) Deduce the difference equation describing the digital filter and sketch the filter structure.
- c) Given that the input signal $x(t)$ is a sinusoid of amplitude 1 volt and frequency 8 kHz, describe the output signal $y(t)$ (form, frequency, amplitude).

Problem 11.7 In the A/D conversion system shown in Fig. 11.64, the transfer function $H(z)$ of the digital filter is given by

$$H(z) = \frac{z}{4z + 3}$$

- a) Given that the digital filter of which the transfer function is $H(z)$ is causal specify the ROC of $H(z)$.
- b) Evaluate the frequency response $H(e^{j\Omega})$ of the digital filter and find the filter 3-dB cut-off frequency Ω_c .
- c) Assuming $x_c(t) = \sin 5\pi t$, $-\infty < t < \infty$ and the sampling frequency is 10 Hz evaluate the filter input $x[n]$, its output $y[n]$ and the D/A converter output $y(t)$.



FIGURE 11.64 Signal sampling, filtering and D/A conversion.

Problem 11.8 A finite impulse response (FIR) filter has the impulse response $h[n]$, $n = 0, 1, 2$. The filter receives as input a sequence $x[n]$ which is the result of sampling a signal $x_c(t)$ at a frequency of 1 kHz. The filter output $y[n]$ is fed to a D/A converter producing the corresponding continuous-time signal $y_c(t)$.

Given that the signal $y_c(t)$ should have the same average value as $x_c(t)$ and that it should contain no component of frequency 60 Hz, evaluate the filter impulse response.

Problem 11.9 Consider a digital filter of a structure shown in Fig. 11.65, where

$$a = -2, \quad b = -1, \quad c = 1, \quad d = 0.2.$$

- a) Redraw the filter structure minimizing the number of delay elements (z^{-1}).
- b) Write the difference equation describing the filter structure as shown in the figure.

- c) Evaluate the filter impulse response $h[n]$.
- d) Given that the average value of the input sequence $x[n]$ is equal to 1, what is the average value of the output $y[n]$?
- e) Redraw the filter structure as a cascade of first-order filters.

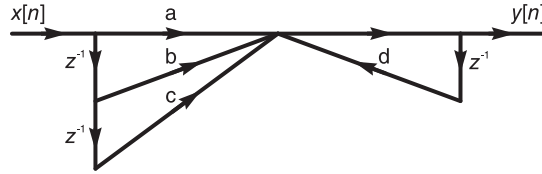


FIGURE 11.65 A digital filter structure.

Problem 11.10 A signal $x_c(t)$, band-limited to 5 kHz, is contaminated by an additive noise in the form of a sinusoid of amplitude 1 volt and frequency 7 kHz. The sum $v_c(t)$ is applied to an A/D converter operating at a sampling frequency of $f_s = 16$ kHz, producing the output $v[n] = v_c[nT]$, where $T = 1/f_s$. To reduce the effect of noise the sequence $v[n]$ is fed to a digital filter of transfer function

$$H(z) = H(s) \Big|_{s \rightarrow \frac{2}{T} \frac{1-z^{-1}}{1+z^{-1}}}, \quad T = 1/16000$$

where

$$H(s) = \frac{1}{s + 1} \Big|_{s \rightarrow s/(10^4 \pi)}$$

Evaluate the resulting attenuation of the noise component.

Problem 11.11 A digital filter has the structure shown in Fig. 11.66.

- a) Evaluate the transfer function $H(z)$ and the difference equation describing the filter.
- b) Given that $x[n] = x_1[n] - 4$, where $x_1[n]$ is a sinusoidal sequence of amplitude 2 and frequency $\Omega_0 = \pi/2$, evaluate $y[n]$.

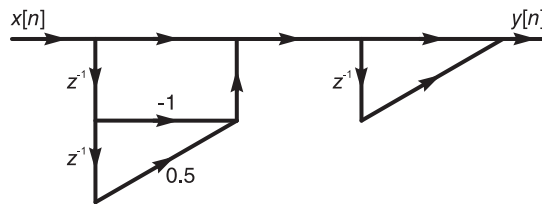


FIGURE 11.66 A digital filter structure.

Problem 11.12 A system is described by the difference equation

$$y[n] - 0.5y[n - 1] + 0.06y[n - 2] = -x[n] + 0.4x[n - 1].$$

- a) Evaluate the system transfer function $H(z)$ and show the filter structure using a minimum of delay elements.
- b) Evaluate the system impulse response $h[n]$. Show an FIR filter realization using the first $N = 7$ points of $h[n]$.
- c) Given that the discrete time system is obtained by sampling a continuous-time system with a sampling frequency of 10 samples/sec, evaluate the impulse response $h_c(t)$ of the corresponding continuous-time system.

Problem 11.13 A system has the transfer function

$$H(z) = \frac{z^2 + 2az + a^2}{z^2 + a^2}$$

where a is a real variable, $a > 0$.

- a) Evaluate the zeros and poles of $H(z)$ and its different possible regions of convergence.
- b) Assuming the filter is causal, evaluate its impulse response $h[n]$ as a sum of real expressions.
- c) What values of a ensure that the causal system is stable?
- d) Assuming $a = 0.5$ find the 3-dB cut-off frequency of the system frequency response $|H(e^{j\Omega})|$. What sampling frequency is needed so that this cut-off frequency should correspond to a continuous-time frequency of 100 Hz?

Problem 11.14 A Butterworth digital filter of first order should be obtained from a continuous-time filter using impulse invariance. The sampling period is $T = 0.1$ sec. The digital filter should have a gain of 10 dB at $\Omega = 0$ and 9 dB at $\Omega = 0.2$. Evaluate the transfer function $H_c(s)$ and $H(z)$ of the continuous-time and digital filter, respectively.

Problem 11.15 Consider the digital filter transfer function

$$H(z) = \frac{z^2 + \beta^2}{z^2 - 0.25}$$

where β is real and $\beta > 0$.

- a) Evaluate and sketch the poles and zeros of $H(z)$.
- b) What is the ROC of $H(z)$ if the filter is i) realizable, ii) unstable, iii) stable.
- c) Draw the filter structure using a minimum number of delay elements.
- d) Evaluate the filter impulse response $h[n]$ assuming the filter is causal.
- e) Evaluate and sketch the frequency response $H(j\omega)$ assuming it exists and $\beta = 1$. Does this filter behave as a lowpass, bandpass, highpass, or another type of filter? Explain.
- f) What is the value of β that would lead to a filter d-c gain of 4? If this is the case, what is the 3-dB frequency?

Problem 11.16 Consider the discrete-time rectangular, triangular and Kaiser windows. Using the MATLAB commands for these windows plot the first three lobes of their spectra normalized so that they have the same value of the peak.

Repeat the above for the Hanning and Hamming windows. Deduce from the plots which of the windows has the narrowest and which the widest main lobe at the 3 dB point. Which window produces the highest first side lobe peak?

Repeat the above, plotting now the spectra in decibels versus frequency.

Problem 11.17 Consider the causal system represented by the flow diagram shown in Fig. 11.67 where $a = 1/8$, $b = 1$, $c = 3$, $k = 4$, $m = 3$.

- a) Evaluate the system transfer function between its input $x[n]$ and output $y[n]$.
- b) Evaluate the system impulse response.
- c) Show a realization of the system employing a single delay element.

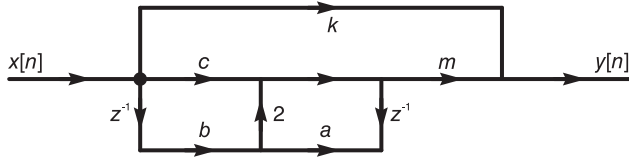


FIGURE 11.67 System flow diagram.

Problem 11.18 Consider the system given by the flow diagram shown in Fig. 11.68. With $a = 2, b = 3, c = 0.5, d = 1, e = -2, f = 0.25, g = 5, h = 0.2, k = 5, m = 2$.

- a) Evaluate the system transfer function.
- b) Show a realization of the same filter using a minimum number of delay elements.

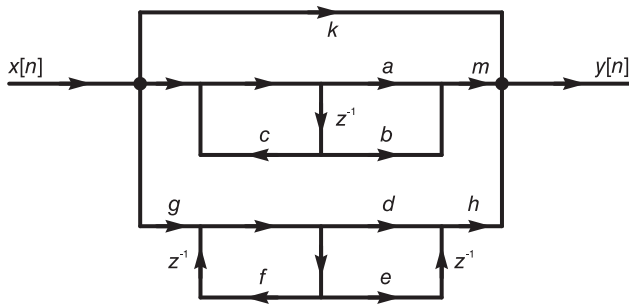


FIGURE 11.68 Digital filter structure.

Problem 11.19 Evaluate the transfer function $H(z)$ of a lowpass digital Chebyshev filter. The sampling frequency is 400 Hz with the following specifications

Frequency	Magnitude
0Hz	0Hz
40Hz	$\geq -1\text{ dB}$
70Hz	$\leq -20\text{ dB}$

Derive first the lowpass analog prototype then show the conversion to the digital filter using a) impulse invariance and b) the bilinear transformation. Show how to use MATLAB to verify the results.

Problem 11.20 Design a lattice filter having the transfer function

$$H(z) = \frac{12 - 5z^{-1} + 1.5z^{-2} - 0.5z^{-3}}{1 - 0.5z^{-1} + 0.25z^{-2} - 0.125z^{-3}}$$

Verify the design by evaluating the transfer function of the lattice filter.

Problem 11.21 Design a lattice filter having a transfer function

$$H(z) = 27 + 9z^{-1} + 3z^{-2} + z^{-3}$$

Verify the design by evaluating the lattice filter transfer function.

Problem 11.22 Evaluate the transfer function between the input $x[n]$ and the output $y[n]$, and that to the second output $w[n]$. With the input $x[n]$ and output $y[n]$ is the filter minimum phase?

Problem 11.23 A continuous-time linear system has the impulse response

$$h_c(t) = 2^{-10t}u(t).$$

A digital filter is constructed by impulse invariance where the impulse response is sampled at frequency of 10 Hz.

- Evaluate the digital filter impulse response $h[n]$ and its transfer function $H(z)$.
- The digital filter receives the input signal $x[n]$ and produces the response $y[n]$. Evaluate the response $y[n]$ if the input is
 - $x[n] = \cos(\pi n/8)$.
 - $x[n] = u[n]$.

Problem 11.24 A system has an impulse response $h[n]$ given by

$$h[n] = \begin{cases} 1, & n = 0 \\ 2, & n = 1 \\ 3, & n = 2 \\ 2, & n = 3 \\ 0, & \text{otherwise.} \end{cases}$$

- Express $h[n]$ for $-\infty \leq n \leq \infty$ as a sum of scaled and shifted versions of the unit step sequence $u[n]$. Recall that the unit step sequence $u[n]$ is equal to 1 for $n \geq 0$ and zero otherwise.
- Evaluate the system transfer function $H(z)$ and its frequency response $H(e^{j\Omega})$.
- Evaluate the four-point discrete Fourier transform $H[k]$ of the sequence $h[n]$. Represent $H[k]$ graphically for $0 \leq k \leq 8$.
- Draw the structure of a filter that has $h[n]$ as its impulse response, in the form of a block diagram showing adders, multipliers and delay elements.

Problem 11.25 Consider a causal system given by the difference equation

$$y[n] - y[n-1] - y[n-2] = x[n].$$

- Evaluate the system transfer function $H(z)$ and impulse response $h[n]$.
- Draw the structure of a filter having the same transfer function and using a minimum of delay elements.
- Evaluate the system response $y[n]$ if the input is $x[n] = \delta[n-1]$.
- Is this system stable?
- Does the Fourier transform of the system impulse response $h[n]$ exist? If yes, evaluate the system frequency response. If not state why not?

Problem 11.26 Show the structure of a lattice filter having the transfer function

$$H(z) = \frac{1 + 2z^{-1} + 3z^{-2} + 2z^{-3} + z^{-4}}{1 + 1.63z^{-1} + 1.75z^{-2} + 1.53z^{-3} + 0.5z^{-4}}.$$

Problem 11.27 Evaluate the order and the impulse response of a realizable FIR filter by choosing an appropriate window to obtain the following specifications:

- Attenuation at zero frequency: 0 dB.
- Pass-band and stop-band edge frequencies $\Omega_p = 0.2\pi$, $\Omega_s = 0.233\pi$.
- Stop band frequency response $|H(e^{j\Omega})| \leq 0.005$.

Problem 11.28 Design a first order Butterworth lowpass digital filter with a 3-dB cut-off frequency of $\Omega_c = 0.125\pi$ using the Bilinear transform.

Problem 11.29 A continuous-time signal $x_a(t)$ is limited in frequency to 2 kHz. It is sampled at the rate of 5000 samples/sec to produce the sequence $x[n] = x_a(n/5000)$ which is applied to the input of a digital filter. The filter output $y[n]$ is in turn applied to the input of a D/A converter, producing the continuous-time signal $y_a(t)$.

The objective is to evaluate the required digital filter transfer function $H(z)$ so that the signal $y_a(t)$ would correspond to filtering of the signal $x_a(t)$ by a lowpass first order Butterworth filter, with $\varepsilon = 1$, cut-off frequency 200 Hz and maximum gain 0 dB.

a) Evaluate $H(z)$ using impulse invariance.

b) Evaluate $H(z)$ using the bilinear transformation.

Sketch the filter structure in both cases, using a minimal number of delay elements.

Problem 11.30 A signal $x_a(t)$, band limited in frequency to 5 kHz, is sampled at the rate of 10 kHz. The resulting sequence $x[n]$ is applied to the input of a digital filter. The filter output $y[n]$ is applied to the input of a D/A converter, producing the continuous-time signal $y_a(t)$. It is required that the signal $y_a(t)$ be the result of filtering of the signal $x_a(t)$ by a lowpass first order Chebyshev filter, with pass-band ripple of $R_p = 1$ dB, cut-off frequency 500 Hz and maximum gain 0 dB. Evaluate the filter transfer function $H(z)$

a) Using impulse invariance.

b) Using the bilinear transform.

Sketch the filter structure in both cases, using a minimal number of delay elements.

Problem 11.31 Evaluate the transfer function $H(z)$ of a digital filter satisfying the following requirements.

– Lowpass

– Cut-off frequency 0.2

– Maximum response 15 dB

– Minimum attenuation at cut-off frequency 14 dB

a) Use the impulse invariance approach on a Butterworth filter of the first order to obtain the transfer function $H(z)$ and sketch the filter structure.

b) A sequence $x[n]$ is obtained by sampling an analog signal $x_a(t)$ at a rate of 50000 samples/s, so that $x[n] = x_a(n/50000)$. If the sequence $x[n]$ is applied to the input of the digital filter of transfer function $H(z)$ what is the effective cut-off frequency that has been applied to the analog signal $x_a(t)$.

Problem 11.32 A signal $x_a(t)$, band-limited in frequency to 20 kHz, is sampled at a rate of 48000 samples/s to form the sequence $x[n] = x_a(n/48000)$. This sequence is applied to the input of a digital filter, of which the output $y[n]$ is applied to the input of a D/A converter at the same rate 48000 samples/s producing the analog signal output $y_a(t)$.

The signal $y_a(t)$ should correspond to the filtering of the signal $x_a(t)$ by a highpass first order Butterworth ($\varepsilon = 1$) filter which should have a gain of 17 dB at a cut-off frequency of 2 kHz.

Evaluate the digital filter transfer function $H(z)$ using the bilinear transform, and sketch the filter structure using a minimum number of delay elements.

Problem 11.33 A signal $x_a(t)$ band-limited in frequency to 45 kHz is sampled at a rate of 100×10^3 samples/s to produce the sequence $x[n] = x_a(n/10^5)$. The sequence $x[n]$ is applied to the input of a digital filter of which the output $y[n]$ is applied at the same rate 100×10^3 values/s to the input of a D/A converter producing the output $y_a(t)$. The signal $y_a(t)$ should correspond to the filtering of the signal $x_a(t)$ by a lowpass first order Butterworth ($\varepsilon = 1$)

filter, which should have a maximum gain of 0 dB and a cut-off frequency of 5 kHz. Evaluate the digital filter transfer function $H(z)$ using

- a) Impulse invariance
- b) The bilinear transform

Sketch in both cases the filter structure using a minimum of delay elements.

Problem 11.34 Evaluate the transfer functions of the digital filters obtained by applying the bilinear transform to the following analog filters.

- a) Butterworth ($\varepsilon = 1$) highpass first order, cut-off frequency $\pi/2$, maximum gain 0 dB.
- b) Butterworth ($\varepsilon = 1$) highpass first order, cut-off frequency $\pi/8$, maximum gain 0 dB.
- c) Butterworth ($\varepsilon = 1$) highpass, second order, cut-off frequency $\pi/2$, maximum gain 0 dB.

For each case sketch the filter structure using a minimum of delay elements.

Problem 11.35 The transfer function of a digital filter is obtained using the bilinear transformation by writing

$$H(z) = H_a(s) \Big|_{s = \frac{2(1-z^{-1})}{T(1+z^{-1})}}$$

where $T = 0.25 \times 10^{-3}$ sec, and

$$H_a(s) = \frac{1}{s^2 + \sqrt{2}s + 1} \Big|_{s \rightarrow 2000\pi/s}$$

Evaluate

- a) The maximum gain of the digital filter and the frequency at which it occurs
- b) The minimal gain of the digital filter and the frequency at which it occurs
- c) The frequency at which the filter gain is 3 dB below the maximum gain

Problem 11.36 Let $g[n]$ and $h[n]$ be the impulse responses of two digital filters. The transfer function $H(z)$ has linear phase. If $g[n] = h[n - N]$, where N is an integer value, does the filter characterized by $g[n]$ produce linear phase? Justify your answer.

Problem 11.37 An FIR digital filter should have the impulse response

$$h[n] = \delta[n] - 0.5\delta[n - 1] + 0.4\delta[n - 2] - 0.25\delta[n - 3]$$

- a) Show the structure of a direct implementation of the filter.
- b) Evaluate the reflection coefficients and sketch the lattice structure implementation of the filter.

Problem 11.38 a) For a Bessel Type 1 filter of order 2, specify the transfer function and evaluate the group delay and the value of its delay at frequency $\omega = 1$ relative to its zero-frequency delay. Evaluate the filter order so that the delay at frequency $\omega = 5$ will be greater than or equal to half its value at zero frequency.

b) Evaluate the transfer function and poles of a Type 1 Bessel filter of the second order producing an attenuation of 0 dB at $\omega = 0$. Evaluate the filter impulse response $h(t)$.

c) Convert this filter to a digital one with a sampling interval of 0.1 sec, using impulse invariance. Determine the value of the digital filter transfer function and draw the filter structure using a minimal number of delay elements.

Problem 11.39 The objective is to design by impulse invariance a digital Butterworth lowpass filter of which the magnitude spectrum response is 0 dB at zero frequency. The attenuation is 3 dB at $\omega = 1$ and at least 18 dB at $\omega = 2$.

a) Evaluate the minimum order of the corresponding analog filter to meet these specifications.

b) Deduce the analog filter transfer function $H_a(s)$.

c) Evaluate the analog filter impulse response $h_a(t)$.

d) Evaluate the corresponding digital filter impulse response $h[n]$ as obtained by impulse invariance and assuming a sampling period $T = 1$ sec.

e) Evaluate the digital filter transfer function $H(z)$.

Problem 11.40 Design a highpass Chebyshev digital filter having a maximum frequency response of 0 dB, maximum ripple of 1 dB in the frequency band $0.3\pi \leq \Omega \leq \pi$ and such that $0 \leq |H(e^{j\Omega})| \leq 0.1$, in the band $0 \leq \Omega \leq 0.1\pi$, using the bilinear transform. Verify the result by plotting the frequency response and evaluating the response at $\Omega = 0.1\pi$ and $\Omega = 0.3\pi$.

Problem 11.41 Design a highpass Chebyshev digital filter with a frequency response that has a maximum of 0 dB and such that $0.9 \leq |H(e^{j\Omega})| \leq 1$, in the band $0.4\pi \leq \Omega \leq \pi$, and an attenuation of at least 19 dB in the frequency range $0 \leq \Omega \leq 0.14\pi$, using the bilinear transform. Verify the result by plotting the frequency response and evaluating the response at $\Omega = 0.14\pi$ and $\Omega = 0.4\pi$.

Problem 11.42 Show that if an $N + 1$ -point impulse response $h[n]$, $n = 0, 1, \dots, N$, where N is even, satisfies the condition

$$h[n] = h[n - N], \quad 0 \leq n \leq N$$

then its frequency response may be written in the form

$$H(e^{j\Omega}) = e^{-jN\Omega/2} \sum_{n=0}^{N/2} b[n] \cos[n\Omega]$$

where $b[n] = 2h[N/2 - n]$, $n = 1, 2, \dots, N/2$ and $b[0] = h[N/2]$.

Problem 11.43 Show that if an $N + 1$ -point impulse response $h[n]$, $n = 0, 1, \dots, N$, where N is even, satisfies the condition

$$h[n] = -h[n - N], \quad 0 \leq n \leq N$$

then its frequency response may be written in the form

$$H(e^{j\Omega}) = je^{-jN\Omega/2} \sum_{n=1}^{N/2} b[n] \sin[n\Omega]$$

where $b[n] = 2h[N/2 - n]$, $n = 1, 2, \dots, N/2$.

Problem 11.44 Show that if an $N + 1$ -point impulse response $h[n]$, $n = 0, 1, \dots, N$, where N is odd, satisfies the condition

$$h[n] = h[n - N], \quad 0 \leq n \leq N$$

then its frequency response may be written in the form

$$H(e^{j\Omega}) = e^{-jN\Omega/2} \sum_{n=1}^{(N+1)/2} b[n] \cos[(n - 1/2)\Omega]$$

where

$$b[n] = 2h[(N + 1)/2 - n], \quad n = 1, 2, \dots, (N + 1)/2.$$

Problem 11.45 Show that if an $N + 1$ -point impulse response $h[n]$, $n = 0, 1, \dots, N$, where N is odd, satisfies the condition

$$h[n] = -h[n - N], \quad 0 \leq n \leq N$$

then its frequency response may be written in the form

$$H(e^{j\Omega}) = je^{-jN\Omega/2} \sum_{n=1}^{(N+1)/2} b[n] \sin[(n - 1/2)\Omega]$$

where

$$b[n] = 2h[(N + 1)/2 - n], \quad n = 1, 2, \dots, (N + 1)/2.$$

Problem 11.46 Use the Padé approximation to evaluate the parameters of

$$H(z) = \frac{b_0 + b_1z^{-1}}{1 + a_1z^{-1} + a_2z^{-2}}$$

which would approximate the desired impulse response

$$h_d[n] = 10 \times 0.5^n (\cos \pi n/5 + \sin \pi n/5) u[n].$$

Problem 11.47 Use the Padé approximation to evaluate the parameters of

$$H(z) = \frac{b_0 + b_1z^{-1} + b_2z^{-2}}{1 + a_1z^{-1} + a_2z^{-2}}$$

which would approximate the desired impulse response

$$h_d[n] = Ar^n \cos(\gamma n) u[n] + BA r^{n-1} \cos[\gamma(n - 1)] u[n - 1]$$

where $A = 10$, $B = 2$, $r = 0.5$, $\gamma = 0.2\pi$.

Problem 11.48 Use the Padé approximation to evaluate the parameters of

$$H(z) = \frac{\sum_{k=0}^M b_k z^{-k}}{1 + \sum_{k=1}^N a_k z^{-k}}$$

with $M = 3$ and $N = 4$, to approximate the desired impulse response

$$h_d[n] = \sum_{k=1}^4 r_k^n u[n]$$

where $r_1 = 0.4$, $r_2 = 0.5$, $r_3 = 0.7$, $r_4 = 0.9$.

11.51 Answers to Selected Problems

Problem 11.1 See Fig. 11.69

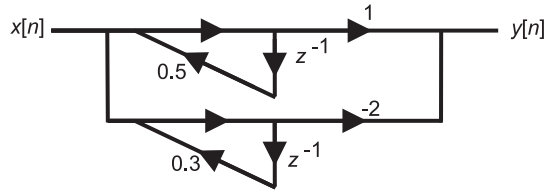


FIGURE 11.69 Figure for Problem 11.1.

Problem 11.2 See Fig. 11.70.

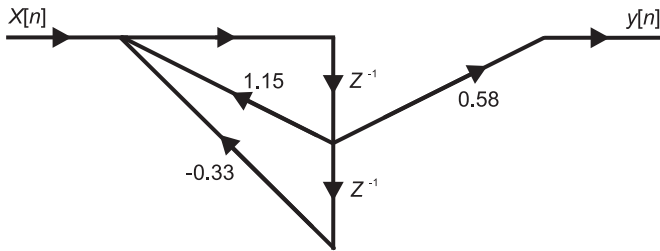


FIGURE 11.70 Figure for Problem 11.2.

Problem 11.3 See Fig. 11.71.

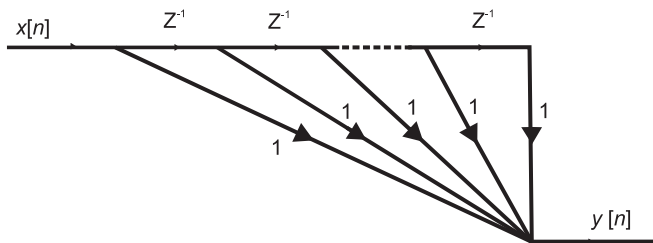


FIGURE 11.71 Figure for Problem 11.3.

Problem 11.4 d) $h[n] = (5/3)0.5^n u[n] + (1/3)(-0.4)^n u[n]$. e) The filter coefficients are listed in the following table:

n	0	1	2	3	4	5	6	7
$h[n]$	2	0.7000	0.4700	0.1870	0.1127	0.0487	0.0274	0.0125

Problem 11.5

$$H(z) = \frac{2(1 - z^{-1})}{3.336 - 0.664z^{-1}}$$

b) The output is a sinusoid of frequency 18.75 kHz and amplitude 0.707 volt .

Problem 11.6

b) See Fig. 11.72.

c) The output $y(t)$ is a sinusoid of amplitude 2.828 volts and frequency 8 kHz.

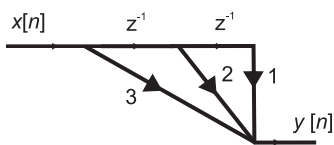


FIGURE 11.72 Figure for Problem 11.6.

Problem 11.7

c) $y[n] = 0.2 \sin(0.5\pi n + 0.6435)$, $y(t) = 0.2 \sin(5\pi t + 0.6435)$.

Problem 11.8

$$h[2] = h[0] = 7.117, \quad h[1] = -13.235$$

Problem 11.9 See Figs. 11.73 and 11.74.

c) $h[n] = -2(0.2)^n u[n] - (0.2)^{n-1} u[n-1] + (0.2)^{n-2} u[n-2]$.

d) $y[n] = x[n]H(e^{j0}) = 1(-2.5) = -2.5$.

e) $H(z) = \frac{(1+z^{-1})(-2+z^{-1})}{1-0.2z^{-1}}$.

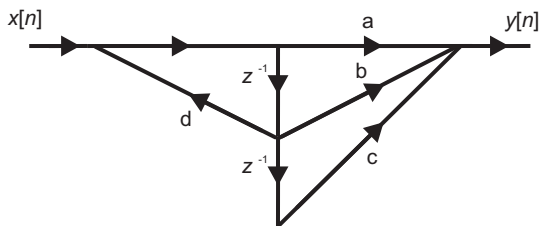


FIGURE 11.73 Figure for Problem 11.9.

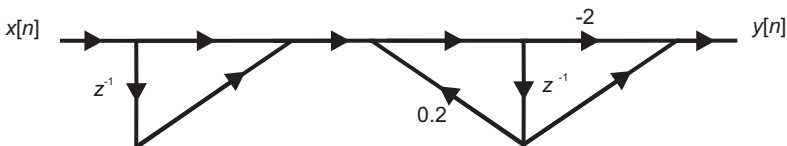


FIGURE 11.74 Figure for Problem 11.9.

Problem 11.10

The disturbance frequency $\omega = 2\pi \times 7000$ corresponds to the discrete-domain frequency $\Omega = \omega T = 7\pi/8$. The frequency $\Omega = 7\pi/8$ in the digital filter corresponds to a frequency

$\omega = 32 \times 10^3 \tan(7\pi/16)$ in the Continuous-time domain, and to a normalized frequency of 5.12 in the normalized filter. The attenuation level is 14.35 dB.

Problem 11.11

b) $y[n] = y_1[n] - 8$, where $y_1[n]$ is a sinusoid of amplitude = 7.07, and frequency $\pi/2$.

Problem 11.12 See Figs. 11.75 and 11.76.

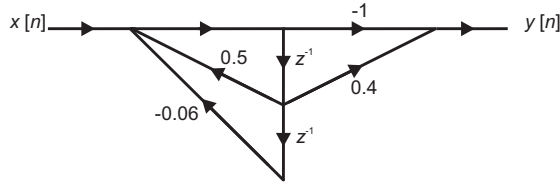


FIGURE 11.75 Figure for Problem 11.12.

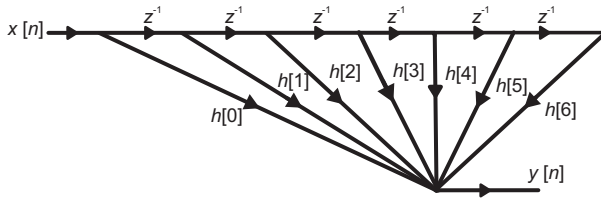


FIGURE 11.76 Figure for Problem 11.12.

c) $h_c(t) = -2(0.2)^{t/T}u(t) + (0.3)^{t/T}u(t) = -2(1.024 \times 10^{-7})^t u(t) + (5.905 \times 10^{-6})^t u(t)$.

Problem 11.13 $T = 2.895 \times 10^{-3}$ sec, The sampling frequency is $f_s = 1/T = 345.443$ samples/sec.

Problem 11.14

$$H(z) = 2.486 / (1 - 0.456z^{-1})$$

Problem 11.15 See Fig. 11.77 and Fig. 11.78.

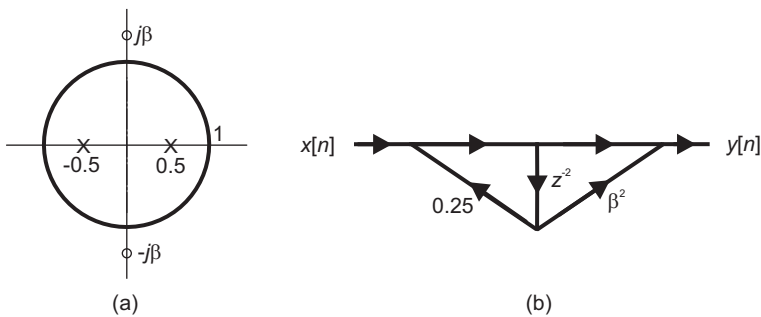


FIGURE 11.77 Figure for Problem 11.15.

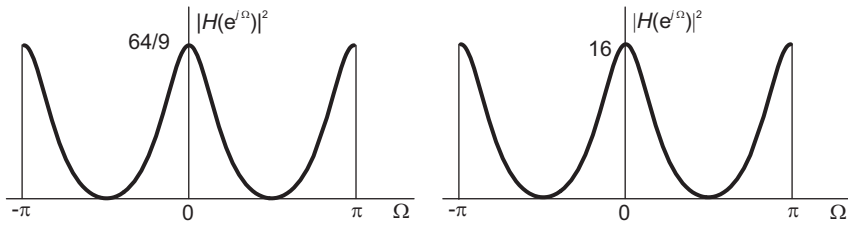


FIGURE 11.78 Figure for Problem 11.15.

e) $H(e^{j\Omega}) = (e^{j2\Omega} + \beta^2)/(e^{j2\Omega} - 0.25)$.

The filter acts as a bandstop filter. f) $\beta = \sqrt{2}$, $\Omega = \pm 0.5589, \pm 2.5826$.

Problem 11.17

$H(z) = (13 + 5z^{-1})/(1 - \frac{1}{4}z^{-1})$.

Problem 11.18

See Fig. 11.79 and Fig. 11.80.

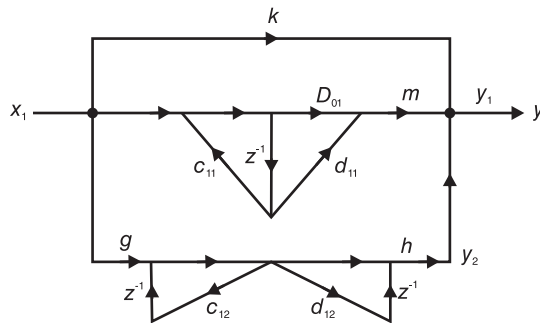


FIGURE 11.79 Figure for Problem 11.18.

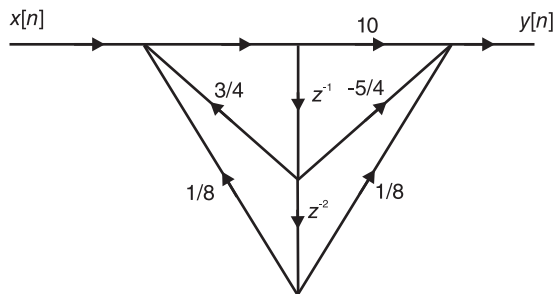


FIGURE 11.80 Figure for Problem 11.18.

Problem 11.19

$$H(z) = \frac{0.0114747 + 0.0344z^{-1} + 0.0344z^{-2} + 0.0115z^{-3}}{1 - 2.1378z^{-1} + 1.7694z^{-2} - 0.5398z^{-3}}$$

Problem 11.20 $k_3 = -0.125, k_2 = 0.1905, k_1 = -0.4$.

Problem 11.21 $k_3 = 1/27, k_2 = 0.0989, k_1 = 0.3$,

Problem 11.22 $H(z) = 0.9 + 1.159z^{-1} + 1.14z^{-2} + z^{-3}$. The filter is minimum phase.

Problem 11.23

ii) $y[n] = 2u[n] - 2^{-n}u[n]$.

Problem 11.24

d) $Y(z) = [1 + 2z^{-1} + 3z^{-2} + 2z^{-3}] X(z), y[n] = x[n] + 2x[n-1] + 3x[n-2] + 2x[n-3]$.

Problem 11.26 $k_4 = 0.5, k_3 = 0.9533, k_2 = 0.7373, k_1 = 0.2593, c_4(4) = 1, c_4(3) = 0.37, c_4(2) = 0.8233, c_4(1) = -0.3325, c_4(0) = -0.3735$.

Problem 11.27 $N = 200, h[n] = 0.2165 Sa[0.2165\pi(n - 100)], 0 \leq n \leq 200$.

Problem 11.28 $H(z) = (0.1659(1 + z^{-1})) / (1 - 0.6682z^{-1})$.

Problem 11.29 $H(z) = H_a(s) \Big|_{s = \frac{2(1-z^{-1})}{1+z^{-1}}} = \frac{0.112(1+z^{-1})}{1-0.776z^{-1}}$.

Problem 11.31

a) $H(z) = 2.209 / (1 - 0.675z^{-1})$.

b) The digital frequency $\Omega = 0.2$ corresponds to the analog frequency $f = 0.2 \times 50000 / (2\pi) = 1592$ Hz.

Problem 11.32 See Fig. 11.81. $H(z) = \frac{8.84(1-z^{-1})}{1-0.768z^{-1}}$.

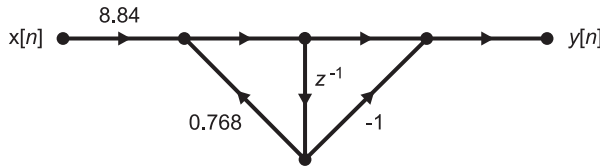


FIGURE 11.81 Figure for Problem 11.32.

Problem 11.33

a) $H(z) = 0.314 / (1 - 0.730z^{-1})$.

b) $H(z) = 0.137(1 + z^{-1}) / (1 - 0.727z^{-1})$. See Fig. 11.82.

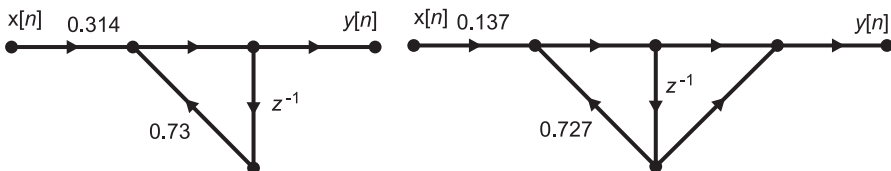


FIGURE 11.82 Figure for Problem 11.33.

Problem 11.34 See Fig. 11.83.

a) $H(z) = 1 - z^{-1}/2$.

$$H(z) = \frac{0.834(1 - z^{-1})}{1 - 0.668z^{-1}}, \frac{0.29 - 0.59z^{-1} + 0.29z^{-2}}{1 + 0.17z^{-2}}, \frac{0.29 - 0.59z^{-1} + 0.29z^{-2}}{1 + 0.17z^{-2}}.$$

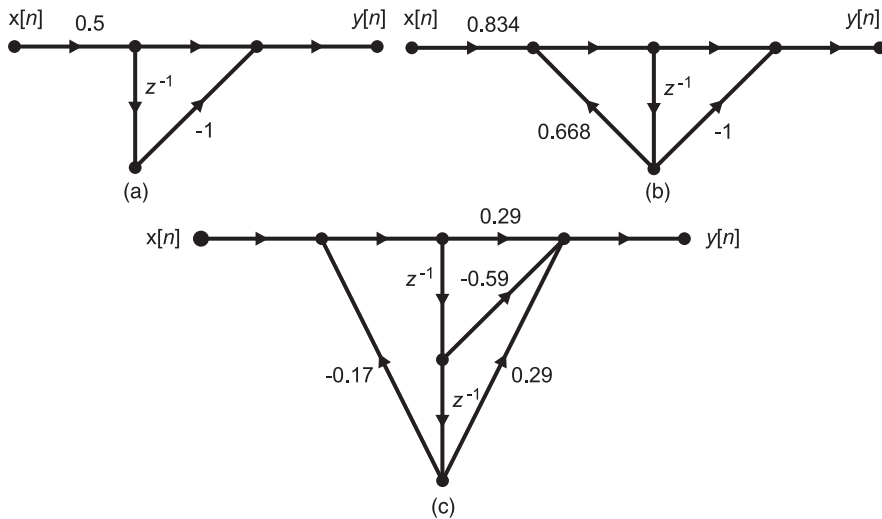


FIGURE 11.83 Figure for Problem 11.34.

Problem 11.35 b) The minimum gain of the analog filter is 0 and occurs at $\omega = 0$ since this is a highpass filter. The minimum gain of the digital filter is thus 0 dB and occurs at $\Omega = 0$.

c) The cut-off frequency (-3 dB point) of the analog filter is $\omega = 2000\pi$. The bilinear transform converts this point to the digital frequency $\Omega = 2 \arctan(\frac{1}{2} \times 2000\pi T) = 1.33$.

Problem 11.36 $G(e^{j\Omega}) = H(e^{j\Omega})e^{-j\Omega N} = |H(e^{j\Omega})|e^{-j\Omega[n_0+N]}$

Problem 11.37

The lattice structure is shown in Fig. 11.84

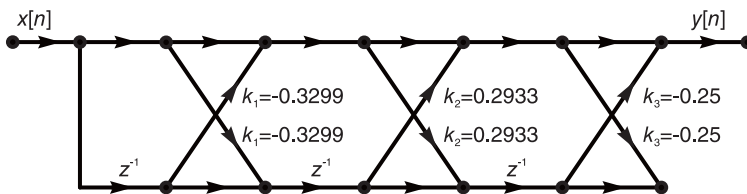


FIGURE 11.84 Figure for Problem 11.37.

Problem 11.40 $H(z) = 0.511389(1 - z^{-1})^2/(1 - 0.8773z^{-1} + 0.4178z^{-2})$.

Problem 11.41 $H(z) = 0.412687(1 - 2z^{-1} + z^{-2})/1 - 0.49503z^{-1} + 0.33914z^{-2}$.

Problem 11.46 $b_0 = 10$, $b_1 = -1.1062$, $a_1 = -0.809$, $a_2 = 0.25$.

Problem 11.47 $b_0 = 10$, $b_1 = 15.9549$, $b_2 = -80902$, $a_1 = -0.809$, $a_2 = 0.25$.

Problem 11.48 $b_0 = 4$, $b_1 = -7.5$, $b_2 = 4.54$, $b_3 = -0.8870$, $a_1 = -2.5$, $a_2 = 2.27$, $a_3 = -0.887$, $a_4 = 0.1260$.

12

Energy and Power Spectral Densities

In this chapter we study energy and power spectra and their relations to signal duration, periodicity and correlation functions.

12.1 Energy Spectral Density

Let $f(t)$ be an electric potential in volts applied across a resistance of $R = 1$ ohm. The total energy dissipated in such a resistance is given by

$$E = \int_{-\infty}^{\infty} \{f^2(t)/R\} dt. \quad (12.1)$$

Since the resistance value is unity the dissipated energy may be also be referred to as *normalized energy*. In what follows we shall refer to it simply as the dissipated energy, with the implicit assumption that it is the energy dissipated into a resistance of 1 ohm.

We recall Parseval's theorem which states that if a function $f(t)$ is generally complex and if $F(j\omega)$ is the Fourier transform of $f(t)$ then

$$\int_{-\infty}^{\infty} |f(t)|^2 dt = \frac{1}{2\pi} \int_{-\infty}^{\infty} |F(j\omega)|^2 d\omega. \quad (12.2)$$

The energy in the resistance may therefore be written in the form

$$E = \int_{-\infty}^{\infty} f^2(t) dt = \frac{1}{2\pi} \int_{-\infty}^{\infty} |F(j\omega)|^2 d\omega. \quad (12.3)$$

The function $|F(j\omega)|^2$ is called the *energy spectral density*, or simply the energy density, of $f(t)$. It is attributed the special symbol $\varepsilon_{ff}(\omega)$, that is,

$$\varepsilon_{ff}(\omega) \triangleq |F(j\omega)|^2. \quad (12.4)$$

We note that its integral is equal to 2π times the signal energy

$$E = \frac{1}{2\pi} \int_{-\infty}^{\infty} \varepsilon_{ff}(\omega) d\omega \quad (12.5)$$

hence the name "spectral density."

Given two signals $f_1(t)$ and $f_2(t)$, where $f_1(t)$ represent a current source and $f_2(t)$ the voltage that the current source produces across a resistance R of 1 ohm, the *normalized cross-energy* or simply *cross-energy* is given by

$$E_{f_1 f_2} = \int_{-\infty}^{\infty} f_1(t) f_2(t) dt. \quad (12.6)$$

Parseval's or Rayleigh's theorem is written

$$\int_{-\infty}^{\infty} f_1(t) f_2(t) dt = \frac{1}{2\pi} \int_{-\infty}^{\infty} F_1(-j\omega) F_2(j\omega) d\omega. \quad (12.7)$$

If $f_1(t)$ and $f_2(t)$ are real

$$F_1(-j\omega) = F_1^*(j\omega), \quad F_2(-j\omega) = F_2^*(j\omega). \quad (12.8)$$

the cross-energy is therefore given by

$$E_{f_1 f_2} = \int_{-\infty}^{\infty} f_1(t) f_2(t) dt = \frac{1}{2\pi} \int_{-\infty}^{\infty} F_1^*(j\omega) F_2(j\omega) d\omega. \quad (12.9)$$

The function

$$\varepsilon_{f_1 f_2}(\omega) \triangleq F_1^*(j\omega) F_2(j\omega) \quad (12.10)$$

is called the *cross-energy spectral density*. The cross-energy of the two signals is then given by

$$E = \frac{1}{2\pi} \int_{-\infty}^{\infty} \varepsilon_{f_1 f_2}(\omega) d\omega. \quad (12.11)$$

Example 12.1 Consider the ideal lowpass filter frequency response shown in Fig. 12.1.

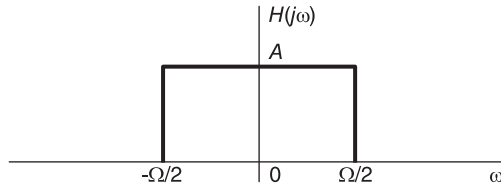


FIGURE 12.1 Ideal lowpass filter frequency response.

We have

$$H(j\omega) = A\Pi_{\Omega/2}(\omega) = A\{u(\omega + \Omega/2) - u(\omega - \Omega/2)\}.$$

The filter's impulse response is given by

$$h(t) = \mathcal{F}^{-1}[H(j\omega)] = \frac{A\Omega}{2\pi} \text{Sa}(\Omega t/2).$$

The energy spectral density of $h(t)$ is given by

$$\varepsilon_{hh}(\omega) = |H(j\omega)|^2 = A^2\Pi_{\Omega/2}(\omega).$$

We may evaluate the energy of $h(t)$ in a finite band of frequency, say, $\Omega/4 < |\omega| < \Omega/2$, as shown in Fig. 12.2.

$$E(\Omega/4, \Omega/2) = \frac{2}{2\pi} \int_{\Omega/4}^{\Omega/2} A^2 d\omega = \frac{A^2\Omega}{4\pi}. \quad (12.12)$$

The total energy of $h(t)$ is given by

$$E = \int_{-\infty}^{\infty} h^2(t) dt = \frac{A^2}{4\pi^2} \Omega^2 \int_{-\infty}^{\infty} \text{Sa}^2(\Omega t/2) dt. \quad (12.13)$$

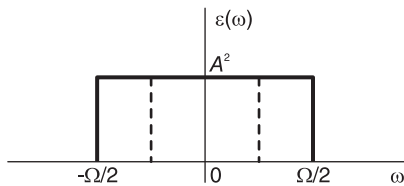


FIGURE 12.2 A frequency band of lowpass filter response.

It is easier, however, to evaluate the energy using Rayleigh’s theorem. We write

$$E = \frac{2}{2\pi} \int_0^{\Omega/2} \varepsilon_{hh}(\omega) d\omega = \frac{A^2\Omega}{2\pi}. \tag{12.14}$$

We note in passing that we have thus evaluated the integral of the square of the sampling function. In particular, we found that

$$E = \frac{A^2\Omega^2}{4\pi^2} \int_{-\infty}^{\infty} Sa^2(\Omega t/2) dt = \frac{A^2\Omega}{2\pi}. \tag{12.15}$$

Substituting $\Omega t/2 = x$, we have

$$\int_{-\infty}^{\infty} Sa^2(x) dx = \pi. \tag{12.16}$$

Example 12.2 Let

$$v(t) = A \cos \omega_c t$$

and

$$v_T(t) = v(t) \Pi_{T/2}(t) = v(t) \{u(t + T/2) - u(t - T/2)\}.$$

Evaluate the energy spectral density of this truncated sinusoid shown in Fig. 12.3.

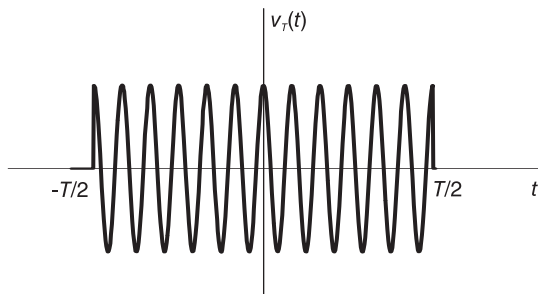


FIGURE 12.3 Truncated sinusoid.

We have

$$\Pi_{T/2}(t) \xleftrightarrow{\mathcal{F}} T Sa(\omega T/2)$$

$$V_T(j\omega) \triangleq \mathcal{F}[v_T(t)] = \frac{AT}{2} \{Sa[(\omega - \omega_c) T/2] + Sa[(\omega + \omega_c) T/2]\}$$

wherefrom the energy spectral density is given by

$$\varepsilon_{v_T v_T}(\omega) = |V_T(j\omega)|^2 = (A^2 T^2 / 4) \{ Sa^2 [(\omega - \omega_c) T / 2] + Sa^2 [(\omega + \omega_c) T / 2] + 2 Sa [(\omega - \omega_c) T / 2] Sa [(\omega + \omega_c) T / 2] \}$$

and is shown graphically in Fig. 12.4.

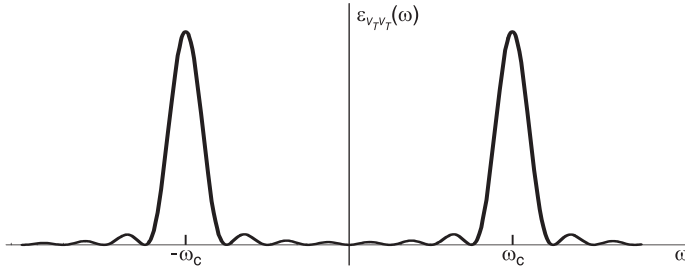


FIGURE 12.4 Energy spectral density.

12.2 Average, Energy and Power of Continuous-Time Signals

The *average normalized power*, or simply *average power*, of a signal $f(t)$ is defined by

$$\overline{f^2}(t) \triangleq \lim_{T \rightarrow \infty} \frac{1}{2T} \int_{-T}^T |f(t)|^2 dt. \quad (12.17)$$

The energy E , as seen above, is given by

$$E = \int_{-\infty}^{\infty} f^2(t) dt = \frac{1}{2\pi} \int_{-\infty}^{\infty} |F(j\omega)|^2 d\omega. \quad (12.18)$$

A signal that has a finite energy E has an average power $\overline{f^2}(t)$ of zero. Such a signal is called an *energy signal*.

A *power signal* is one that has infinite energy and finite non-nil average power, i.e. $0 < \overline{f^2}(t) < \infty$. A periodic signal is a power signal. Its average power P is evaluated as its power over one period.

Let $f(t)$ be periodic of period T_0 . Its average normalized power, or simply average power, is given by

$$P = \overline{f^2}(t) = \frac{1}{T_0} \int_{-T_0/2}^{T_0/2} |f(t)|^2 dt = \frac{1}{T_0} \int_{-T_0/2}^{T_0/2} f(t) f^*(t) dt. \quad (12.19)$$

From Parseval's relation for periodic functions

$$\frac{1}{T_0} \int_{-T_0/2}^{T_0/2} |f(t)|^2 dt = \sum_{n=-\infty}^{\infty} |F_n|^2. \quad (12.20)$$

The average power of a periodic signal is thus given by the sum

$$P = \overline{f^2(t)} = \sum_{n=-\infty}^{\infty} |F_n|^2. \tag{12.21}$$

12.3 Discrete-Time Signals

For discrete-time signals the energy and average power are similarly defined. If a sequence $f[n]$ has finite energy, defined as

$$E = \sum_{n=-\infty}^{\infty} f^2[n] \tag{12.22}$$

it is called an *energy signal*. If it has a finite average power, defined as

$$P = \lim_{M \rightarrow \infty} \frac{1}{2M+1} \sum_{n=-M}^M f^2[n] \tag{12.23}$$

it is called a power signal.

If the sequence is periodic with period M its average power over one period is

$$P = \frac{1}{M} \sum_{n=0}^{M-1} f^2[n]. \tag{12.24}$$

An impulsive signal

$$f(t) = \sum_{n=-\infty}^{\infty} f_n \delta(t - nT) \tag{12.25}$$

such as the one shown in Fig. 12.5, and that can be an ideal sampling of a continuous-time signal, is considered to be an energy signal if its average power defined as

$$\lim_{M \rightarrow \infty} \frac{1}{2MT} \sum_{n=-M}^M |f_n|^2 \tag{12.26}$$

is zero, otherwise it is a power signal.

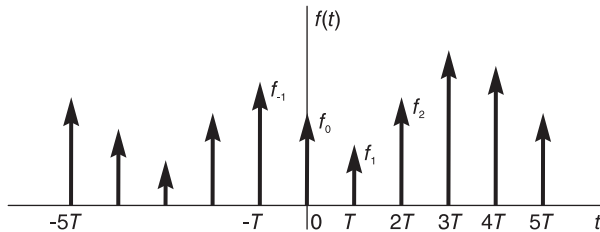


FIGURE 12.5 Impulsive signal.

12.4 Energy Signals

Let $f(t)$ and $g(t)$ be two real energy signals. We show that the Fourier transform of their cross-correlation function $r_{fg}(t)$ is equal to the cross-spectral density $\varepsilon_{fg}(\omega)$.

We have already seen that correlation can be written as a convolution

$$r_{fg}(t) = \int_{-\infty}^{\infty} f(t + \tau) g(\tau) d\tau = f(t) * g(-t) \quad (12.27)$$

$$r_{fg}(-t) = r_{gf}(t). \quad (12.28)$$

The Fourier transform of $r_{fg}(t)$ is therefore given by

$$R_{fg}(j\omega) = F(j\omega) G^*(j\omega) = \varepsilon_{fg}(\omega) \quad (12.29)$$

i.e. the Fourier transform of the cross-correlation function of two energy signals is equal to their cross-energy spectral density.

Moreover, we note that if the functions $f(t)$ and $g(t)$ are complex then

$$r_{fg}(t) = \int_{-\infty}^{\infty} f(t + \tau) g^*(\tau) d\tau \quad (12.30)$$

$$R_{fg}(j\omega) \triangleq \mathcal{F}[r_{fg}(t)] = F(j\omega) G^*(j\omega) = \varepsilon_{fg}(\omega). \quad (12.31)$$

and

$$r_{fg}(-t) = r_{fg}^*(t). \quad (12.32)$$

12.5 Autocorrelation of Energy Signals

The Fourier transform of the autocorrelation function $r_{ff}(t)$ of an energy signal $f(t)$ is given by

$$R_{ff}(j\omega) = \mathcal{F}[r_{ff}(t)] = F(j\omega) F^*(j\omega) = |F(j\omega)|^2 = \varepsilon_{ff}(\omega) \quad (12.33)$$

i.e.

$$r_{ff}(t) \xleftrightarrow{\mathcal{F}} |F(j\omega)|^2 = \varepsilon_{ff}(\omega) \quad (12.34)$$

$$\varepsilon_{ff}(\omega) = R_{ff}(j\omega) \quad (12.35)$$

so that the Fourier transform of the autocorrelation function of an energy signal is equal to the energy spectral density of the signal.

We note that the Fourier transform $F(j\omega)$ of a complex function $f(t)$ is not in general symmetric about origin, that is, $F(-j\omega) \neq F^*(j\omega)$. The energy spectral density $\varepsilon_{ff}(\omega) \triangleq |F(j\omega)|^2$ is real but not symmetric about the origin. Being real, however, its inverse transform is symmetric, that is, $r_{ff}(-t) = r_{ff}^*(t)$, as already established.

We note on the other hand that if the function $f(t)$ is real then $F(-j\omega) = F^*(j\omega)$ wherefrom the function $\varepsilon_{ff}(\omega) = |F(j\omega)|^2$ is even and its inverse transform $r_{ff}(t)$ is real (and even); $r_{ff}(-t) = r_{ff}(t)$.

Let $f(t)$ be generally complex. Writing

$$r_{ff,R}(t) \triangleq \Re[r_{ff}(t)], \quad r_{ff,I}(t) \triangleq \Im[r_{ff}(t)] \quad (12.36)$$

$$r_{ff,R}(t) = r_{ff,R}(-t) \tag{12.37}$$

$$r_{ff,I}(t) = -r_{ff,I}(-t) \tag{12.38}$$

$$\begin{aligned} \varepsilon_{ff}(\omega) &= \int_{-\infty}^{\infty} r_{ff}(t) e^{-j\omega t} dt \\ &= \int_{-\infty}^{\infty} [r_{ff,R}(t) + jr_{ff,I}(t)] (\cos \omega t - j \sin \omega t) dt \\ &= 2 \int_0^{\infty} (r_{ff,R}(t) \cos \omega t + r_{ff,I}(t) \sin \omega t) dt \end{aligned} \tag{12.39}$$

$$\begin{aligned} r_{ff}(t) &= \frac{1}{2\pi} \int_{-\infty}^{\infty} \varepsilon_{ff}(\omega) e^{j\omega t} d\omega \\ &= \frac{1}{2\pi} \left\{ \int_{-\infty}^{\infty} \varepsilon_{ff}(\omega) \cos \omega t d\omega + j \int_{-\infty}^{\infty} \varepsilon_{ff}(\omega) \sin \omega t d\omega \right\} \end{aligned} \tag{12.40}$$

i.e.

$$r_{ff,R}(t) = \frac{1}{2\pi} \int_{-\infty}^{\infty} \varepsilon_{ff}(\omega) \cos \omega t d\omega \tag{12.41}$$

$$r_{ff,I}(t) = \frac{1}{2\pi} \int_{-\infty}^{\infty} \varepsilon_{ff}(\omega) \sin \omega t d\omega. \tag{12.42}$$

We note that

$$r_{ff}(0) = \frac{1}{2\pi} \int_{-\infty}^{\infty} \varepsilon_{ff}(\omega) d\omega. \tag{12.43}$$

If the function $f(t)$ is real we have

$$r_{ff}(-t) = r_{ff}(t), \quad r_{ff,I}(t) = 0 \tag{12.44}$$

$$\varepsilon_{ff}(\omega) = |F(j\omega)|^2 = 2 \int_0^{\infty} r_{ff}(t) \cos \omega t dt \tag{12.45}$$

$$r_{ff}(t) = \frac{1}{\pi} \int_0^{\infty} \varepsilon_{ff}(\omega) \cos \omega t d\omega \tag{12.46}$$

and

$$r_{ff}(t) \leq r_{ff}(0) = E \tag{12.47}$$

E being the energy of $f(t)$.

Example 12.3 Show that $R_{ff}(j\omega) = \varepsilon_{ff}(\omega)$ for the rectangular window

$$f(t) = \Pi_T(t) = u(t+T) - u(t-T).$$

The transform of $f(t)$ is

$$F(j\omega) = 2T \text{Sa}(T\omega).$$

The spectral density is given by

$$\varepsilon_{ff}(\omega) = |F(j\omega)|^2 = 4T^2 \text{Sa}^2(T\omega).$$

The autocorrelation of $f(t)$ is the triangle

$$r_{ff}(t) = (2T - |t|) \Pi_{2t}(t) \triangleq 2T \Lambda_{2T}(t)$$

where, we recall, $\Lambda_x(t)$ is a centered triangle of height unity and total base width $2x$. Its Fourier transform is

$$R_{ff}(j\omega) \triangleq \mathcal{F}[r_{ff}(t)] = \varepsilon_{ff}(\omega).$$

The spectral density and autocorrelation function are shown in Fig. 12.6.

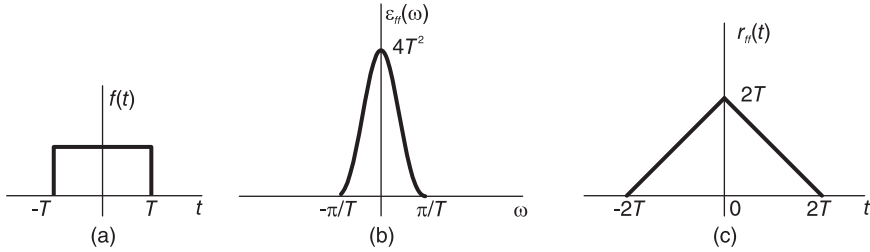


FIGURE 12.6 A rectangle, spectral density and autocorrelation function.

12.6 Energy Signal through Linear System

Let an energy signal $f(t)$ be the input to a linear time invariant (LTI) system of impulse response $h(t)$, as shown in Fig. 12.7.

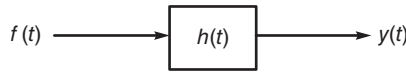


FIGURE 12.7 Linear system with input and output.

Let $r_{ff}(t)$ and $r_{yy}(t)$ be the autocorrelation of $f(t)$ and of $y(t)$, respectively. We have

$$R_{ff}(j\omega) = \mathcal{F}[r_{ff}(t)] = |F(j\omega)|^2 \tag{12.48}$$

$$R_{yy}(j\omega) = \mathcal{F}[r_{yy}(t)] = |Y(j\omega)|^2. \tag{12.49}$$

Now

$$Y(j\omega) = F(j\omega)H(j\omega) \tag{12.50}$$

wherefrom

$$R_{yy}(j\omega) = |F(j\omega)|^2 |H(j\omega)|^2 \tag{12.51}$$

i.e.

$$R_{yy}(j\omega) = R_{ff}(j\omega) |H(j\omega)|^2 = R_{ff}(j\omega) H(j\omega) H^*(j\omega). \tag{12.52}$$

Hence

$$\varepsilon_{yy}(\omega) = \varepsilon_{ff}(\omega) |H(j\omega)|^2. \tag{12.53}$$

Moreover

$$\mathcal{F}^{-1}[H^*(j\omega)] = h(-t) \tag{12.54}$$

we have

$$r_{yy}(t) = r_{ff}(t) * h(t) * h(-t) \tag{12.55}$$

i.e. the autocorrelation of the system response is the convolution of the input signal autocorrelation with the convolution $h(t) * h(-t)$.

12.7 Impulsive and Discrete-Time Energy Signals

Let $f_s(t)$ be a signal formed of equidistant impulses such as the signal

$$f_s(t) = \dots + f[-1] \delta(t+T) + f[0] \delta(t) + f[1] \delta(t-T) + \dots \quad (12.56)$$

$$= \sum_{n=-\infty}^{\infty} f[n] \delta(t-nT) \quad (12.57)$$

shown in Fig. 12.8(a).

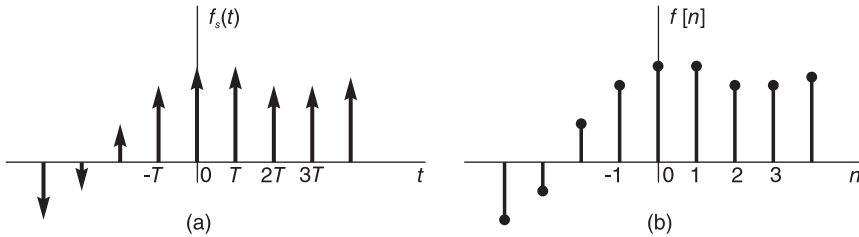


FIGURE 12.8 Signal with equidistant impulses and discrete-time signal counterpart.

We may view the impulsive signal $f_s(t)$ as the result of sampling a continuous-time signal $f_c(t)$ with a sampling interval of T seconds.

$$f_s(t) = f_c(t) \sum_{n=-\infty}^{\infty} \delta(t-nT) = \sum_{n=-\infty}^{\infty} f_c(nT) \delta(t-nT). \quad (12.58)$$

Associated with $f_c(t)$ and $f_s(t)$ we also have a discrete-time function, namely, the sequence $f[n] = f_c(nT)$ shown in Fig. 12.8(b). The energy of the signal $f_s(t)$ as well as that of $f[n]$ are defined by the summation

$$E = \sum_{n=-\infty}^{\infty} |f[n]|^2. \quad (12.59)$$

If the energy is finite then the signal $f_s(t)$ and the sequence $f[n]$ are energy signals. The autocorrelation of the signal $f_s(t)$ can be obtained by evaluating the autocorrelation $r_{ff}[n]$ of the corresponding sequence $f[n]$. In fact the autocorrelation of $f_s(t)$ is given by

$$\begin{aligned}
 r_{f_s f_s}(t) &= \int_{-\infty}^{\infty} f_s(\tau) f_s(t + \tau) d\tau \\
 &= \int_{-\infty}^{\infty} \sum_{m=-\infty}^{\infty} f[m] \delta(\tau - mT) \sum_{i=-\infty}^{\infty} f[i] \delta(t + \tau - iT) d\tau \\
 &= \int_{-\infty}^{\infty} \sum_m \sum_i f[m] f[i] \delta(\tau - mT) \delta(t + \tau - iT) d\tau \\
 &= \sum_m \sum_i f[m] f[i] \int_{-\infty}^{\infty} \delta(\tau - mT) \delta(t + \tau - iT) d\tau \\
 &= \sum_{m=-\infty}^{\infty} \sum_{i=-\infty}^{\infty} f[m] f[i] \delta(t - (i - m)T).
 \end{aligned}$$

Letting $i - m = n$ we have

$$r_{f_s f_s}(t) = \sum_{m=-\infty}^{\infty} \sum_{n=-\infty}^{\infty} f[m] f[m+n] \delta(t - nT). \quad (12.60)$$

Interchanging the order of summations

$$r_{f_s f_s}(t) = \sum_{n=-\infty}^{\infty} \sum_{m=-\infty}^{\infty} f[m] f[m+n] \delta(t - nT) = \sum_{n=-\infty}^{\infty} \rho_n \delta(t - nT) \quad (12.61)$$

where

$$\rho_n = \sum_{m=-\infty}^{\infty} f[m] f[m+n]. \quad (12.62)$$

On the other hand the discrete autocorrelation of the corresponding sequence $f[n]$ is given by

$$r_{ff}[n] = \sum_{m=-\infty}^{\infty} f[m] f[n+m]. \quad (12.63)$$

Hence

$$\rho_n = r_{ff}[n]. \quad (12.64)$$

The autocorrelation $r_{f_s f_s}(t)$ is represented graphically in Fig. 12.9.

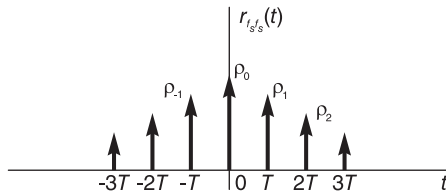


FIGURE 12.9 Autocorrelation of an impulsive signal.

The autocorrelation of the impulsive signal $f_s(t)$ is therefore a one-to-one correspondence to the discrete autocorrelation of the corresponding discrete-time-sequence $f[n]$. It can be

evaluated by simply effecting a discrete autocorrelation of the discrete sequence $f[n]$, followed by converting the resulting sequence $r_{ff}[n]$ into the corresponding impulsive function, which is the autocorrelation function $r_{f_s f_s}(t)$ of the function $f_s(t)$. The same approach can be used for evaluating the cross-correlation of two impulsive functions $f_s(t)$ and $g_s(t)$.

The Fourier transform of $f_s(t)$ is given by

$$F_s(j\omega) = \mathcal{F} \left[\sum_{n=-\infty}^{\infty} f[n] \delta(t - nT) \right] = \frac{1}{T} \sum_{n=-\infty}^{\infty} F_c \left(j\omega + j \frac{2\pi n}{T} \right). \quad (12.65)$$

This is equal to the Fourier transform $F(e^{j\Omega})$ of the discrete-time counterpart, the sequence $f[n]$ with $\Omega = \omega T$.

$$F(e^{j\Omega}) = \sum_{n=-\infty}^{\infty} f[n] e^{-j\Omega n} = F_s(j\omega) \Big|_{\omega=\Omega/T} = F_s \left(j \frac{\Omega}{T} \right). \quad (12.66)$$

The energy density $\varepsilon_{f_s f_s}(\omega)$ of the signal $f_s(t)$ is given by

$$\varepsilon_{f_s f_s}(\omega) = |F_s(j\omega)|^2 \quad (12.67)$$

and is therefore periodic of a period $2\pi/T$. Similarly the energy density of the sequence $f[n]$ is given by

$$\varepsilon_{ff}(\Omega) = |F(e^{j\Omega})|^2 \quad (12.68)$$

and is periodic with a period 2π . The autocorrelation $r_{f_s f_s}(t)$ may be written as the convolution:

$$r_{f_s f_s}(t) = f_s(t) \star f_s(t) = f_s(t) * f_s(-t) \quad (12.69)$$

$$R_{f_s f_s}(j\omega) = F_s(j\omega) F_s^*(j\omega) = |F_s(j\omega)|^2 = \varepsilon_{f_s f_s}(\omega) \quad (12.70)$$

$$r_{ff}[n] = f[n] \star f[n] = f[n] * f[-n] \quad (12.71)$$

$$R_{ff}(e^{j\Omega}) = F(e^{j\Omega}) F(e^{-j\Omega}) = |F(e^{j\Omega})|^2 = \varepsilon_{ff}(\Omega). \quad (12.72)$$

The transform of the energy spectral density is therefore given by

$$\varepsilon_{f_s f_s}(\omega) = R_{f_s f_s}(j\omega) = \mathcal{F} \left[\sum_{n=-\infty}^{\infty} \rho_n \delta(t - nt) \right] = \sum_{n=-\infty}^{\infty} \rho_n e^{-j\omega n T} \quad (12.73)$$

and

$$\varepsilon_{ff}(\Omega) = R_{ff}(e^{j\Omega}) = \sum_{n=-\infty}^{\infty} r_{ff}[n] e^{-j\Omega n}. \quad (12.74)$$

Since $f(t)$ is real we have $r_{ff}[-n] = r_{ff}[n]$ and $r_{f_s f_s}(-t) = r_{f_s f_s}(t)$, i.e., $\rho_{-n} = \rho_n$.

$$\varepsilon_{f_s f_s}(\omega) = \rho_0 + 2 \sum_{n=1}^{\infty} \rho_n \cos nT\omega = r_{ff}[0] + 2 \sum_{n=1}^{\infty} r_{ff}[n] \cos nT\omega \quad (12.75)$$

and

$$\varepsilon_{ff}(\Omega) = r_{ff}[0] + 2 \sum_{n=1}^{\infty} r_{ff}[n] \cos n\Omega. \quad (12.76)$$

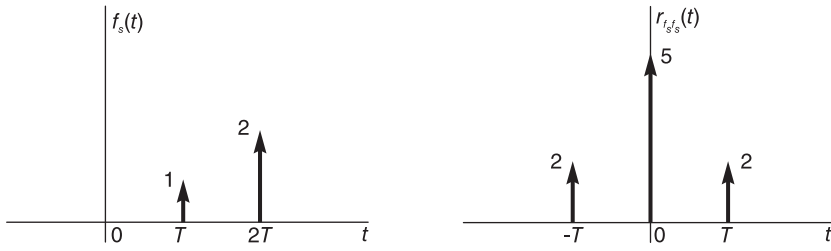


FIGURE 12.10 Impulsive signal and its autocorrelation.

Example 12.4 Let

$$f_s(t) = \delta(t - T) + 2\delta(t - 2T).$$

The signal is shown in Fig. 12.10(a).

Its autocorrelation is shown in Fig. 12.10(b). The autocorrelation may be found by evaluating the autocorrelation of the corresponding sequence $f[n] = \delta[n - 1] + 2\delta[n - 2]$. We have

$$\rho_n = r_{ff}[n] = \sum_{m=-\infty}^{\infty} f[n+m]f[m] = 2\delta[n+1] + 5\delta[n] + 2\delta[n-1].$$

The sequence $f[n]$ and its autocorrelation $r_{ff}[n] = \rho_n$ are shown in Fig. 12.11.

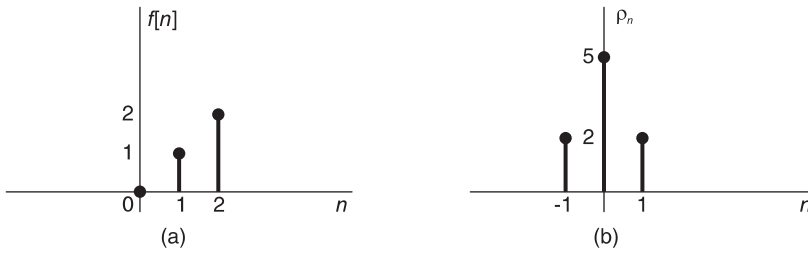


FIGURE 12.11 A sequence and its autocorrelation.

$$r_{f_s f_s}(t) = 5\delta(t) + 2\delta(t+T) + 2\delta(t-T)$$

$$\varepsilon_{f_s f_s}(\omega) = R_{f_s f_s}(j\omega) = 5 + 2e^{j\omega T} + 2e^{-j\omega T} = 5 + 4\cos\omega T.$$

Alternatively, we have

$$F_s(j\omega) = e^{-j\omega t} + 2e^{-j\omega t} = (\cos\omega T + 2\cos 2\omega T) - j(\sin\omega T + 2\sin 2\omega T)$$

$$\varepsilon_{f_s f_s}(\omega) = |F_s(j\omega)|^2.$$

Similarly $\varepsilon_{ff}(\Omega) = R_{ff}(e^{j\Omega}) = 5 + 4\cos\Omega$.

Example 12.5 Let

$$f_c(t) = \begin{cases} t/10, & 0 \leq t \leq 30 \\ 6 - t/10, & 30 \leq t \leq 60. \end{cases}$$

Evaluate the sampled function $f_s(t)$, the discrete-time function $f[n]$ and their autocorrelations, assuming a sampling interval of $T = 10$ sec. We have

$$f_s(t) = \delta(t - T) + 2\delta(t - 2T) + 3\delta(t - 3T) + 2\delta(t - 4T) + \delta(t - 5T)$$

$$f[n] = f_c(nT) = f_c(10n) = \begin{cases} n, & 0 \leq n \leq 3 \\ 6 - n, & 3 \leq n \leq 6 \end{cases}$$

$$\rho_n = r_{ff}[n] = \delta[n + 4] + 4\delta[n + 3] + 10\delta[n + 2] + 16\delta[n + 1] + 19\delta[n] + 16\delta[n - 1] + 10\delta[n - 2] + 4\delta[n - 3] + \delta[n - 4].$$

The sequence $f[n]$ and its autocorrelation $\rho[n] = r_{ff}[n]$ are shown in Fig. 12.12.

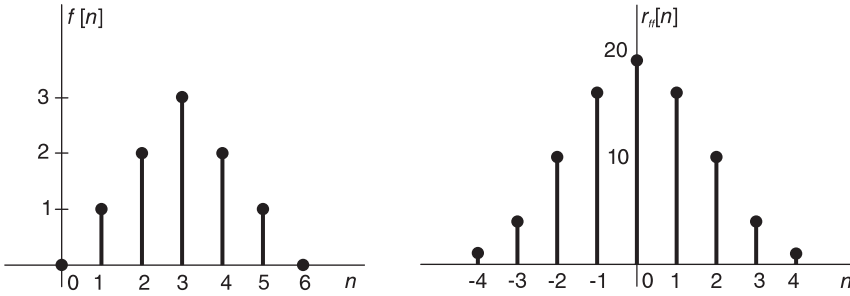


FIGURE 12.12 Sequence $f[n]$ and its autocorrelation.

The corresponding impulsive autocorrelation function $r_{f_s f_s}(t)$ is deduced thereof to be

$$r_{f_s f_s}(t) = \delta(t + 4T) + 4\delta(t + 3T) + 10\delta(t + 2T) + 16\delta(t + T) + 19\delta(t) + 16\delta(t - T) + 10\delta(t - 2T) + 4\delta(t - 3T) + \delta(t - 4T)$$

$$\begin{aligned} \varepsilon_{f_s f_s}(\omega) &= R_{f_s f_s}(j\omega) \\ &= 19 + 32 \cos T\omega + 20 \cos 2T\omega + 8 \cos 3T\omega + 2 \cos 4T\omega \\ &= 19 + 32 \cos 10\omega + 20 \cos 20\omega + 8 \cos 30\omega + 2 \cos 40\omega \end{aligned}$$

$$\varepsilon_{ff}(\Omega) = R_{ff}(e^{i\Omega}) = 19 + 32 \cos \Omega + 20 \cos 2\Omega + 8 \cos 3\Omega + 2 \cos 4\Omega.$$

The energy spectral density $\varepsilon_{ff}(\Omega)$ of the sequence $f[n]$ is shown in Fig. 12.13. Alternatively,

$$\begin{aligned} F_s(j\omega) &= e^{-j\omega T} + 2e^{-j2\omega T} + 3e^{-j3\omega T} + 2e^{-j4\omega T} + e^{-j5\omega T} \\ \varepsilon_{f_s f_s}(\omega) &= |F_s(j\omega)|^2 = F_s(j\omega) F_s^*(j\omega). \end{aligned}$$

Letting

$$z = e^{j\omega T}, \quad z^* = e^{-j\omega T} = z^{-1}.$$

We have, with $z = e^{j\Omega}$,

$$\begin{aligned} \varepsilon_{f_s f_s}(\omega) &= (z^{-1} + 2z^{-2} + 3z^{-3} + 2z^{-4} + z^{-5}) \\ &\quad (z + 2z^2 + 3z^3 + 2z^4 + z^5) \\ &= 19 + 16z^{-1} + 10z^{-2} + 4z^{-3} + z^{-4} + 16z + 10z^2 + 4z^3 + z^4 \\ &= 19 + 32 \cos \omega T + 20 \cos 2\omega T + 8 \cos 3\omega T + 2 \cos 4\omega T = R_{f_s f_s}(j\omega) \\ \varepsilon_{ff}(\Omega) &= 19 + 32 \cos \Omega + 20 \cos 2\Omega + 8 \cos 3\Omega + 2 \cos 4\Omega = R_{ff}(e^{j\Omega}). \end{aligned}$$

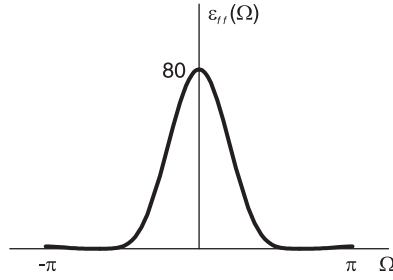


FIGURE 12.13 Energy spectral density.

12.8 Power Signals

We have seen that a power signal has a finite average power

$$0 < \overline{f^2}(t) < \infty, \quad (12.77)$$

where

$$\overline{f^2}(t) = \lim_{T \rightarrow \infty} \frac{1}{2T} \int_{-T}^T |f(t)|^2 dt \quad (12.78)$$

and that a periodic signal is a power signal having an average power evaluated over one period

$$P = \overline{f^2}(t) = \frac{1}{T} \int_{-T/2}^{T/2} |f(t)|^2 dt = \sum_{n=-\infty}^{\infty} |F_n|^2. \quad (12.79)$$

In the following the cross- and autocorrelations of such signals are defined.

12.9 Cross-Correlation

Let $f(t)$ and $g(t)$ be two real power signals. The cross-correlation $r_{fg}(t)$ is given by

$$r_{fg}(t) = \lim_{T \rightarrow \infty} \frac{1}{2T} \int_{-T}^T f(t + \tau) g(\tau) d\tau \quad (12.80)$$

$$r_{fg}(-t) = r_{gf}(t) \quad (12.81)$$

as is the case for energy signals. If $f(t)$ and $g(t)$ are complex then

$$r_{fg}(t) = \lim_{T \rightarrow \infty} \frac{1}{2T} \int_{-T}^T f(t + \tau) g^*(\tau) d\tau \quad (12.82)$$

$$r_{fg}(-t) = r_{gf}^*(t) \quad (12.83)$$

$$r_{ff}(t) = \lim_{T \rightarrow \infty} \frac{1}{2T} \int_{-T}^T f(\tau) f(t + \tau) d\tau \quad (12.84)$$

$$r_{ff}(-t) = r_{ff}(t) \quad (12.85)$$

and

$$r_{ff}(0) = \lim_{T \rightarrow \infty} \frac{1}{2T} \int_{-T}^T |f(t)|^2 dt = \overline{f^2}(t). \tag{12.86}$$

12.9.1 Power Spectral Density

For a real power signal $f(t)$ the power spectral density denoted by $S_{ff}(\omega)$ is by definition the Fourier transform of the autocorrelation function.

$$S_{ff}(\omega) = \mathcal{F}[r_{ff}(t)] = R_{ff}(j\omega). \tag{12.87}$$

and the power is

$$P = \overline{f^2}(t) = \frac{1}{2\pi} \int_{-\infty}^{\infty} S_{ff}(\omega) d\omega. \tag{12.88}$$

Since $r_{ff}(t)$ is real and even its transform $S_{ff}(\omega)$ is real and even. We have

$$S_{ff}(\omega) = 2 \int_0^{\infty} r_{ff}(t) \cos \omega t dt \tag{12.89}$$

and

$$r_{ff}(t) = \frac{1}{\pi} \int_0^{\infty} S_{ff}(\omega) \cos \omega t d\omega. \tag{12.90}$$

Let

$$f_T(t) = f(t) \Pi_T(t) = f(t) \{u(t+T) - u(t-T)\} \tag{12.91}$$

i.e. $f_T(t)$ is a truncation of $f(t)$.

We have

$$F_T(j\omega) = \mathcal{F}[f_T(t)] = \int_{-T}^T f(t) e^{-j\omega t} dt. \tag{12.92}$$

The average power density over the interval $(-T, T)$ is the energy over the interval divided by the duration $2T$. Denoting it by $S_T(\omega)$ we have

$$S_T(\omega) \triangleq \frac{1}{2T} |F_T(j\omega)|^2. \tag{12.93}$$

It can be shown that $S_{ff}(\omega)$ is the limit as T tends to infinity of $S_T(\omega)$

$$S_{ff}(\omega) = \lim_{T \rightarrow \infty} S_T(\omega) = \lim_{T \rightarrow \infty} \frac{1}{2T} |F_T(j\omega)|^2. \tag{12.94}$$

In fact

$$\begin{aligned} S_{ff}(\omega) &= \mathcal{F}[r_{ff}(t)] = \mathcal{F} \left[\lim_{T \rightarrow \infty} \frac{1}{2T} \int_{-T}^T f_T(t+\tau) f_T(\tau) d\tau \right] \\ &= \lim_{T \rightarrow \infty} \frac{1}{2T} \int_{-\infty}^{\infty} \int_{-T}^T f_T(t+\tau) f_T(\tau) d\tau e^{-j\omega t} dt \\ &= \lim_{T \rightarrow \infty} \frac{1}{2T} \int_{-T}^T f_T(\tau) \int_{-\infty}^{\infty} f_T(t+\tau) e^{-j\omega t} dt d\tau. \end{aligned} \tag{12.95}$$

Let

$$t + \tau = x \tag{12.96}$$

$$\begin{aligned}
S_{ff}(\omega) &= \lim_{T \rightarrow \infty} \frac{1}{2T} \int_{-T}^T f_T(\tau) \int_{-\infty}^{\infty} f_T(x) e^{-j\omega(x-\tau)} dx d\tau \\
&= \lim_{T \rightarrow \infty} \frac{1}{2T} \int_{-T}^T f_T(\tau) e^{j\omega\tau} F_T(j\omega) d\tau \\
&= \lim_{T \rightarrow \infty} \frac{1}{2T} F_T(j\omega) \int_{-T}^T f(\tau) e^{j\omega\tau} d\tau = \lim_{T \rightarrow \infty} \frac{1}{2T} F_T(j\omega) F_T^*(j\omega) \\
&= \lim_{T \rightarrow \infty} \frac{1}{2T} |F_T(j\omega)|^2 = \lim_{T \rightarrow \infty} S_T(\omega). \tag{12.97}
\end{aligned}$$

12.10 Power Spectrum Conversion of a Linear System

Let $f(t)$ be a power signal applied to the input of a linear time invariant LTI system the impulse response of which $h(t)$ is an energy signal. The system response may be written

$$y(t) = f(t) * h(t) = \int_{-\infty}^{\infty} f(\tau) h(t - \tau) d\tau. \tag{12.98}$$

Let $r_{ff}(t)$ and $S_{ff}(\omega)$ be the autocorrelation and spectral density respectively of the input $f(t)$. The autocorrelation of the output signal $y(t)$ is given by

$$\begin{aligned}
r_{yy}(t) &= \lim_{T \rightarrow \infty} \frac{1}{2T} \int_{-T}^T y(\tau) y(t + \tau) d\tau \\
&= \lim_{T \rightarrow \infty} \frac{1}{2T} \int_{-T}^T h(u) f(\tau - u) du \int_{-\infty}^{\infty} h(x) f(t + \tau - x) dx dt. \tag{12.99}
\end{aligned}$$

Interchanging the order of integration

$$\begin{aligned}
r_{yy}(t) &= \lim_{T \rightarrow \infty} \frac{1}{2T} \int_{-\infty}^{\infty} h(u) \int_{-\infty}^{\infty} h(x) \int_{-T}^T f(\tau - u) f(t + \tau - x) d\tau dx du \\
&= \lim_{T \rightarrow \infty} \frac{1}{2T} \int_{-\infty}^{\infty} h(u) \int_{-\infty}^{\infty} h(x) \int_{-T-u}^{T-u} f(\alpha) f(\alpha + u + t - x) d\tau dx du \\
&= \int_{-\infty}^{\infty} h(u) \int_{-\infty}^{\infty} h(x) r_{ff}(u + t - x) dx du. \tag{12.100}
\end{aligned}$$

We note that the second integral is a convolution. Writing

$$z(u + t) = \int_{-\infty}^{\infty} h(x) r_{ff}(u + t - x) dx = h(t) * r_{ff}(u + t) \tag{12.101}$$

i.e.

$$z(t) = h(t) * r_{ff}(t) \tag{12.102}$$

we have

$$r_{yy}(t) = \int_{-\infty}^{\infty} h(u) z(u + t) du = r_{zh}(t) = z(t) * h(-t) = r_{ff}(t) * h(t) * h(-t). \tag{12.103}$$

We conclude that the system response $y(t)$ is a power signal the autocorrelation $r_{yy}(t)$ of which is the convolution of the input signal autocorrelation $r_{ff}(t)$ with the function $h(t) * h(-t)$ that is, the convolution of $h(t)$ with its reflection. Moreover,

$$S_{yy}(\omega) = \mathcal{F}[r_{yy}(t)] = \mathcal{F}[r_{ff}(t)] \cdot H(j\omega) H^*(j\omega) = S_{ff}(\omega) |H(j\omega)|^2. \tag{12.104}$$

We conclude that the time domain convolution $y(t) = f(t) * h(t)$ leads to the power spectral density transformation

$$S_{yy}(\omega) = S_{ff}(\omega) |H(j\omega)|^2 \tag{12.105}$$

and that more generally, the convolution $y(t) = f(t) * x(t)$ of a power signal $f(t)$ and an energy signal $x(t)$ leads to the power spectral density transformation

$$S_{yy}(\omega) = S_{ff}(\omega) |X(j\omega)|^2. \tag{12.106}$$

In the case of input white noise, for example

$$S_{ff}(\omega) = 1 \tag{12.107}$$

wherefrom $r_{ff}(t) = \delta(t)$ and $S_{yy}(\omega) = |H(j\omega)|^2$, i.e. the power density of the system response is equal to the energy density of the impulse response $h(t)$.

Example 12.6 Let $f(t) = K$, where K is a constant. The autocorrelation of $f(t)$ given by

$$r_{ff}(t) = \lim_{T \rightarrow \infty} \frac{1}{2T} \int_{-T}^T K^2 dt = K^2$$

is a constant, and

$$S_{ff}(\omega) = \mathcal{F}[r_{ff}(t)] = R_z z j\omega = 2\pi K^2 \delta(\omega)$$

as shown in Fig. 12.14.

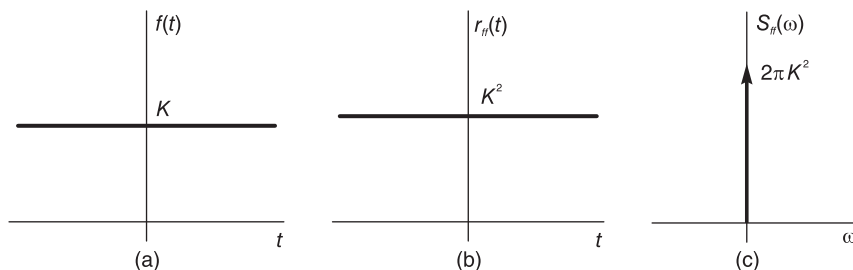


FIGURE 12.14 A constant, autocorrelation and power spectral density.

The power by direct evaluation is $P = K^2$ and, alternatively,

$$P = \overline{f^2}(t) = \frac{1}{2\pi} \int_{-\infty}^{\infty} S_{ff}(\omega) d\omega = K^2.$$

Note that functions that are absolutely integrable such $e^{-t}u(t)$ have finite energy and thus represent energy signals, whereas functions such as the step function and unity represent power signals.

Example 12.7 Evaluate the autocorrelation and spectral density of the signal

$$f(t) = Ku(t).$$

The signal is shown in Fig. 12.15(a).

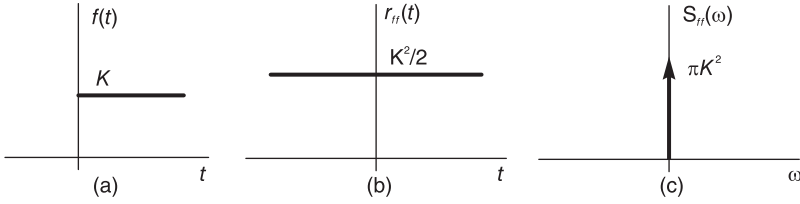


FIGURE 12.15 Unit step function, autocorrelation and power spectral density.

$$r_{ff}(t) = \lim_{T \rightarrow \infty} \frac{K^2}{2T} \int_{-T}^T u(\tau) u(t + \tau) d\tau.$$

Consider the integral

$$I = \int_{-T}^T u(\tau) u(t + \tau) d\tau$$

and the case $t > 0$. We have

$$I = \int_0^T d\tau = T$$

and

$$r_{ff}(t) = \lim_{T \rightarrow \infty} \frac{K^2}{2T} I = \frac{K^2}{2}, \quad t > 0.$$

For $t < 0$ we can use the symmetry property

$$r_{ff}(-t) = r_{ff}(t) = K^2/2$$

wherefrom

$$r_{ff}(t) = K^2/2, \quad \forall t$$

and

$$S_{ff}(\omega) = R_{ff}(j\omega) = \pi K^2 \delta(\omega).$$

The autocorrelation and spectral density are shown in Fig. 12.15(b) and (c), respectively.

12.11 Impulsive and Discrete-Time Power Signals

Let $f(t)$ be the impulsive function

$$f_s(t) = \sum_{n=-\infty}^{\infty} f[n] \delta(t - nT). \quad (12.108)$$

If the average power of $f(t)$ is finite and not zero, that is,

$$0 < \lim_{N \rightarrow \infty} \frac{1}{2N} \sum_{n=-N}^{N-1} |f[n]|^2 < \infty \quad (12.109)$$

then $f(t)$ is a power signal. As noted earlier $f_s(t)$ may be the result of ideal sampling of a continuous-time function $f_c(t)$

$$f_s(t) = \sum_{n=-\infty}^{\infty} f_c(nT) \delta(t - nT). \quad (12.110)$$

The discrete-time representation of the same signal is the sequence $f[n]$ defined by $f[n] = f_c(nT)$. The autocorrelation of $f_s(t)$ is given by

$$r_{f_s f_s}(t) = \lim_{T \rightarrow \infty} \frac{1}{2T} \int_{-T}^T f_s(\tau) f_s(t + \tau) d\tau. \quad (12.111)$$

As in the case of impulsive and discrete-time energy signals it can be shown that

$$r_{f_s f_s}(t) = \sum_{n=-\infty}^{\infty} \rho_n \delta(t - nT) \quad (12.112)$$

where

$$\rho_n = \lim_{M \rightarrow \infty} \frac{1}{2MT} \sum_{m=-M}^{M-1} f[m] f[m+n]. \quad (12.113)$$

The power density is given by

$$\begin{aligned} S_{f_s f_s}(\omega) &= \mathcal{F}[r_{f_s f_s}(t)] \triangleq R_{f_s f_s}(j\omega) = \mathcal{F}\left[\sum_{n=-\infty}^{\infty} \rho_n \delta(t - nT)\right] \\ &= \sum_{n=-\infty}^{\infty} \rho_n e^{-jnT\omega} = \rho_0 + 2 \sum_{n=1}^{\infty} \rho_n \cos nT\omega. \end{aligned} \quad (12.114)$$

For the sequence $f[n]$ the autocorrelation is given by

$$r_{ff}[n] = \lim_{M \rightarrow \infty} \frac{1}{2M} \sum_{m=-M}^{M-1} f[m] f[n+m] \quad (12.115)$$

so that

$$\rho_n = \frac{1}{T} r_{ff}[n] \quad (12.116)$$

$$\begin{aligned} S_{ff}(\Omega) &= \mathcal{F}[r_{ff}[n]] = R_{ff}(e^{j\Omega}) = \sum_{n=-\infty}^{\infty} r_{ff}[n] e^{-j\Omega n} \\ &= r_{ff}[0] + 2 \sum_{n=1}^{\infty} r_{ff}[n] \cos \Omega n. \end{aligned} \quad (12.117)$$

12.12 Periodic Signals

Let a real signal $f(t)$ be periodic of period T . Its autocorrelation $r_{ff}(t)$ is periodic defined by

$$\begin{aligned} r_{ff}(t) &= \frac{1}{T} \int_0^T f(\tau) f(t+\tau) d\tau = \frac{1}{T} \int_0^T f(\tau) \sum_{n=-\infty}^{\infty} F_n e^{jn\omega_0(t+\tau)} d\tau \\ &= \frac{1}{T} \sum_{n=-\infty}^{\infty} F_n e^{jn\omega_0\tau} \int_0^T f(\tau) e^{jn\omega_0\tau} d\tau = \sum_{n=-\infty}^{\infty} F_n e^{jn\omega_0 t} F_n^* \end{aligned} \quad (12.118)$$

i.e.

$$r_{ff}(t) = \sum_{n=-\infty}^{\infty} |F_n|^2 e^{jn\omega_0 t}, \quad \omega_0 = 2\pi/T \quad (12.119)$$

which has the form of a Fourier series expansion having as coefficients $|F_n|^2$. We can therefore write

$$|F_n|^2 = \frac{1}{T} \int r_{ff}(t) e^{-jn\omega_0 t} dt \quad (12.120)$$

$$r_{ff}(t) = \sum_{n=-\infty}^{\infty} |F_n|^2 \cos n\omega_0 t \quad (12.121)$$

$$r_{ff}(t) = |F_0|^2 + 2 \sum_{n=1}^{\infty} |F_n|^2 \cos n\omega_0 t. \quad (12.122)$$

The power spectral density is given by

$$S_{ff}(\omega) = R_{ff}(j\omega) = 2\pi \sum_{n=-\infty}^{\infty} |F_n|^2 \delta(\omega - n\omega_0). \quad (12.123)$$

The average power of $f(t)$ is given by

$$P = \overline{f^2(t)} = r_{ff}(0) = \frac{1}{2\pi} \int_{-\infty}^{\infty} R_{ff}(j\omega) d\omega = \frac{1}{2\pi} \int_{-\infty}^{\infty} S_{ff}(\omega) d\omega. \quad (12.124)$$

Moreover,

$$P = \frac{1}{T} \int_T f^2(t) dt = \sum_{n=-\infty}^{\infty} |F_n|^2. \quad (12.125)$$

Example 12.8 Evaluate the power, the spectral density and autocorrelation function of the signal $f(t) = A \cos \omega_0 t$ where $\omega_0 = 2\pi/T$. We have

$$P = \frac{1}{T} \int_0^T A^2 \cos^2 \omega_0 t dt = \frac{A^2}{T} \times \frac{1}{2} \int_0^T (\cos 2\omega_0 t + 1) dt = A^2/2.$$

The evaluation of the average power of a sinusoid is often needed. It is worthwhile remembering that the average power of a sinusoid of amplitude A is simply $A^2/2$.

We also note that the Fourier series coefficients of the expansion

$$f(t) = \sum_{n=-\infty}^{\infty} F_n e^{jn\omega_0 t}$$

are given by

$$F_n = \begin{cases} A/2, & n = \pm 1 \\ 0, & \text{otherwise} \end{cases}$$

wherefrom

$$P = \overline{f^2(t)} = \sum |F_n|^2 = 2 \times A^2/4 = A^2/2$$

$$S_{ff}(\omega) = 2\pi \sum |F_n|^2 \delta(\omega - n\omega_0) = \pi \frac{A^2}{2} \{ \delta(\omega - \omega_0) + \delta(\omega + \omega_0) \}$$

$$P = \frac{1}{2\pi} \int_{-\infty}^{\infty} \frac{\pi A^2}{2} \{ \delta(\omega - \omega_0) + \delta(\omega + \omega_0) \} d\omega = A^2/2$$

$$r_{ff}(t) = |F_0|^2 + 2 \sum_1^{\infty} |F_n|^2 \cos n \omega_0 t = (A^2/2) \cos \omega_0 t.$$

We note, moreover, that

$$R_{ff}(j\omega) = \frac{\pi A^2}{2} \{ \delta(\omega - \omega_0) + \delta(\omega + \omega_0) \} = S_{ff}(\omega).$$

12.12.1 Response of an LTI System to a Sinusoidal Input

Let $x(t) = \sin(\beta t + \theta)$ be the input to an LTI system. We evaluate the power spectral density at the input and output of the system.

The power spectral density of the input is

$$S_{xx}(\omega) = 2\pi \sum_{n=-\infty}^{\infty} |X_n|^2 \delta(\omega - n\omega_0) \tag{12.126}$$

where $\omega_0 = \beta$. The power spectral density of the output is

$$S_{yy}(\omega) = 2\pi \sum_{n=-\infty}^{\infty} |Y_n|^2 \delta(\omega - n\omega_0) = 2\pi \sum_{n=-\infty}^{\infty} |X_n|^2 |H(jn\beta)|^2 \delta(\omega - n\beta). \tag{12.127}$$

The average power of the input $x(t)$ is

$$P = \overline{x^2(t)} = \sum_{n=-\infty}^{\infty} |X_n|^2 = A^2/2 \tag{12.128}$$

and that of the output is

$$P = \overline{y^2(t)} = \sum_{n=-\infty}^{\infty} |Y_n|^2 = (A^2/2) |H(jn\beta)|^2. \tag{12.129}$$

Example 12.9 The signal $x(t) = A \sin(\beta t)$, with $A = 1$ and $\beta = \pi$, is applied to the input of an LTI system of impulse response $h(t) = \Pi_{0.5}(t)$. Is the system response $y(t)$ an energy or power signal? Evaluate the energy and power, and the spectral density at the system input and output. The input signal $x(t)$ and response $y(t)$ have infinite energy and are hence power signals since their energy is infinite. The spectral densities are

$$S_x(\omega) = (\pi/2)[\delta(\omega - \pi) + \delta(\omega + \pi)]$$

and

$$S_y(\omega) = S_x(\omega)|H(j\omega)|^2 = \frac{\pi}{2}Sa^2(\pi/2)[\delta(\omega - \pi) + \delta(\omega + \pi)] = 0.637[\delta(\omega - \pi) + \delta(\omega + \pi)].$$

The input power is

$$P_x = \overline{x^2(t)} = \frac{1}{2\pi} \int_{-\infty}^{\infty} S_x(\omega)d\omega = 0.5.$$

The output power is

$$P_y = \overline{y^2(t)} = \frac{1}{2\pi} \int_{-\infty}^{\infty} S_y(\omega)d\omega = 0.203.$$

Alternatively, note that the input sinusoid Amplitude is $A = 1$ and its power is $P_x = \overline{x^2(t)} = A^2/2 = 0.5$. The output is $y(t) = A|H(j\pi)| \sin(\beta t + \arg[H(j\pi)]) = B \sin(\pi t + \theta)$, where $B = 0.6366$ and $\theta = -\pi/2$, and its power is $P_y = \overline{y^2(t)} = B^2/2 = 0.203$.

12.13 Power Spectral Density of an Impulse Train

Consider the impulse train shown in Fig. 12.16(a).

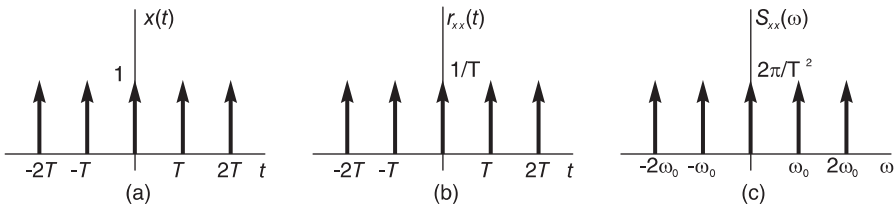


FIGURE 12.16 Impulse train, autocorrelation and power spectral density.

$$x(t) = \rho_T(t) \triangleq \sum_{n=-\infty}^{\infty} \delta(t - nT). \tag{12.130}$$

To evaluate the power spectral density of the impulse train we may proceed by applying the correlation definition directly over one period.

$$r_{xx}(t) = \frac{1}{T} \int_{-T/2}^{T/2} \delta(\tau)\delta(t + \tau) d\tau = \frac{1}{T}\delta(t), \quad -T/2 \leq t \leq T/2 \tag{12.131}$$

that is, $r_{xx}(t)$ is an impulse train of period T and impulses of intensity $1/T$

$$r_{xx}(t) = \frac{1}{T} \sum \delta(t - nT) = \frac{1}{T}\rho_T(t). \tag{12.132}$$

The power spectral density with $\omega_0 = 2\pi/T$ is given by

$$S_{xx}(\omega) = R_{xx}(j\omega) = \frac{1}{T}\omega_0\rho_{\omega_0}(\omega) = \frac{2\pi}{T^2} \sum_{n=-\infty}^{\infty} \delta(\omega - n\omega_0). \tag{12.133}$$

Alternatively, $X_n = 1/T$ and

$$S_{xx}(\omega) = 2\pi \sum_{n=-\infty}^{\infty} |X_n|^2 \delta(\omega - n\omega_0) = \frac{2\pi}{T^2} \sum_{n=-\infty}^{\infty} \delta(\omega - n\omega_0). \quad (12.134)$$

Example 12.10 Let $v(t)$ be the periodic ramp shown in Fig. 12.17. Evaluate the power spectral density.

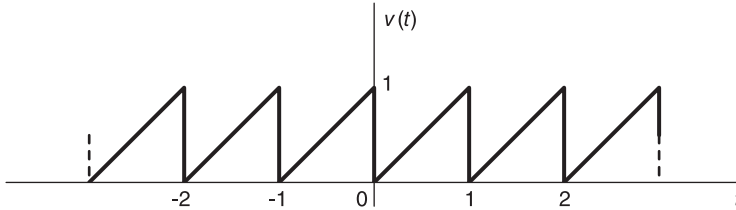


FIGURE 12.17 Periodic ramp.

We have found in Chapter 2 that the Fourier series coefficients are

$$V_n = \begin{cases} A/2, & n = 0 \\ jA/(2\pi n), & n \neq 0 \end{cases}$$

where $A = 1$ and $\omega_0 = 2\pi$. Hence

$$S_{vv}(\omega) = 2\pi \sum_{n=-\infty}^{\infty} |V_n|^2 \delta(\omega - n\omega_0) = (\pi A^2/2) \delta(\omega) + \sum_{\substack{n=-\infty \\ n \neq 0}}^{\infty} \frac{A^2}{2\pi n^2} \delta(\omega - n\omega_0)$$

$$r_{vv}(t) = V_0^2 + 2 \sum_{n=1}^{\infty} |V_n|^2 \cos n\omega_0 t = 1/4 + \sum_{n=1}^{\infty} \left(\frac{1}{2\pi^2 n^2} \right) \cos n\omega_0 t.$$

A direct evaluation of the periodic autocorrelation of the periodic ramp $v(t)$ by the usual shift-multiply-integrate process as shown in Fig. 12.18, we obtain

$$\begin{aligned} r_{vv}(t) &= \int_0^{1-t} (t + \tau) \tau \, d\tau + \int_{1-t}^1 (t + \tau - 1) \tau \, d\tau, \quad 0 < t < 1 \\ &= (1/6) (2 - 3t + 3t^2), \quad 0 < t < 1. \end{aligned}$$

A Fourier series expansion of $r_{vv}(t)$ as a verification produces the trigonometric coefficients

$$a_n = 2 \int_0^1 (1/6) (2 - 3t + 3t^2) \cos n2\pi t \, dt = \frac{1}{2\pi^2 n^2}, \quad n \geq 1$$

and $a_0 = 1/2$ as expected. The functions $S_{vv}(\omega)$ and $r_{vv}(t)$ are shown in Fig. 12.19 and Fig. 12.20, respectively.

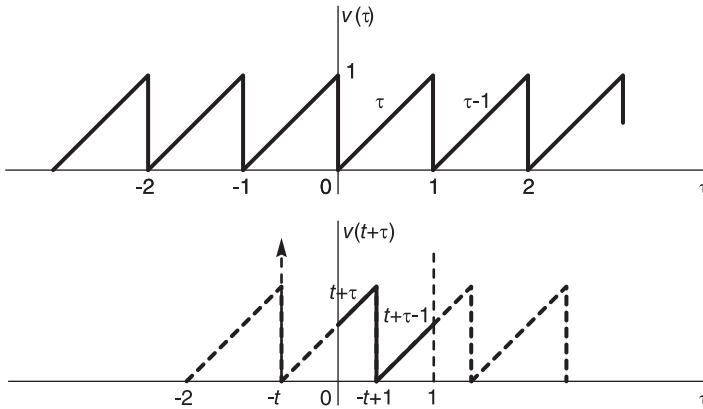


FIGURE 12.18 Periodic ramp and its shifting in time.

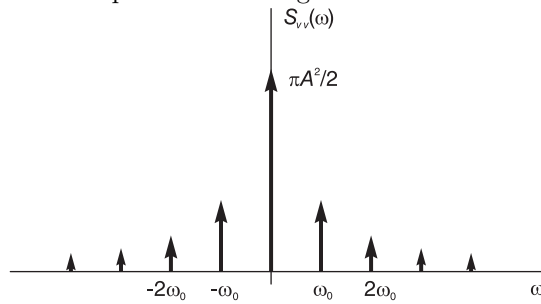


FIGURE 12.19 Power spectral density.

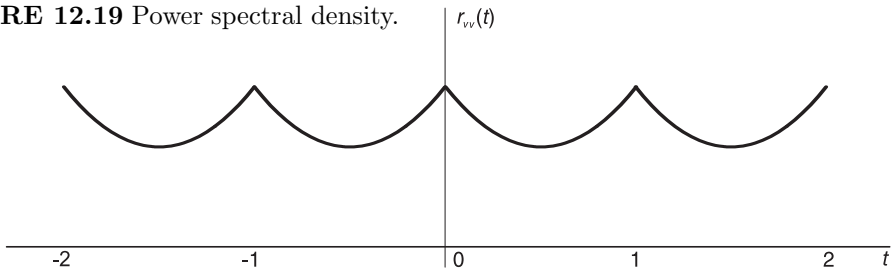


FIGURE 12.20 Autocorrelation of a periodic function.

Example 12.11 Let

$$v(t) = A \cos(m\omega_0 t + \theta), \quad m \text{ integer}$$

where $\omega_0 = 2\pi/T$. Evaluate $S_{vv}(\omega)$ and $r_{vv}(t)$.

We have

$$V_n = \begin{cases} (A/2) e^{j\theta}, & n = \pm m \\ 0, & \text{otherwise} \end{cases}$$

$$\begin{aligned} S_{vv}(\omega) &= 2\pi \left\{ |V_m|^2 \delta(\omega - m\omega_0) + |V_{-m}|^2 \delta(\omega + m\omega_0) \right\} \\ &= \frac{\pi A^2}{2} \left\{ \delta(\omega - m\omega_0) + \delta(\omega + m\omega_0) \right\} \end{aligned}$$

$$r_{vv}(t) = 2 \left\{ (A^2/4) \cos m\omega_0 t \right\} = (A^2/2) \cos m\omega_0 t.$$

12.14 Average, Energy and Power of a Sequence

As noted in Chapter 1 the average value of a sequence $x[n]$ is

$$\overline{x[n]} = \lim_{M \rightarrow \infty} \frac{1}{2M+1} \sum_{n=-M}^M x[n]. \quad (12.135)$$

A real sequence $x[n]$ is an energy sequence if it has a finite energy which can be defined as

$$E = \sum_{n=-\infty}^{\infty} x[n]^2. \quad (12.136)$$

A real aperiodic sequence $x[n]$ is a power sequence if it has a finite average power

$$P = \overline{x[n]^2} = \lim_{M \rightarrow \infty} \frac{1}{2M+1} \sum_{n=-M}^M x[n]^2. \quad (12.137)$$

If the sequence is periodic of period N its average power would be

$$P = \overline{x[n]^2} = \frac{1}{N} \sum_{n=0}^{N-1} x[n]^2. \quad (12.138)$$

Example 12.12 Let the sequence $x[n] = 3^{-n} u[n]$. Evaluate its energy.

$$E = \sum_{n=0}^{\infty} 3^{-2n} u[n] = \sum_{n=0}^{\infty} 9^{-n} u[n] = \frac{1}{1-9^{-1}} = \frac{9}{8}.$$

Example 12.13 Evaluate the power of the signal

$$x[n] = 10 \cos(\pi n/8).$$

The period N is deduced from

$$x[n+N] = x[n]$$

$$10 \cos(\pi n/8) = 10 \cos[\pi(n+N)/8] = 10 \cos(\pi n/8 + \pi N/8).$$

N is the least value satisfying

$$(\pi/8)N = 2\pi, 4\pi, 6\pi, \dots$$

$$N = 16$$

$$\begin{aligned} \bar{P} &= \frac{1}{16} \left\{ 100 \sum_{n=0}^{15} \cos^2(\pi n/8) \right\} = \frac{100}{16} \times 2 \sum_{n=0}^7 \cos^2(\pi n/8) \\ &= \frac{25}{2} (1 + 0.8536 + 0.5 + 0.1464 + 0 + 0.1464 + 0.5 + 0.8536) = 50. \end{aligned}$$

12.15 Energy Spectral Density of a Sequence

The energy of a sequence $x[n]$ is given by

$$E = \sum_{n=-\infty}^{\infty} |x[n]|^2.$$

The energy spectral density is given by $\varepsilon_x(\Omega) = |X(e^{j\Omega})|^2$.

Parseval's relation states that

$$\sum_{n=-\infty}^{\infty} |x[n]|^2 = \frac{1}{2\pi} \int_{-\infty}^{\infty} |X(e^{j\Omega})|^2 d\Omega = \frac{1}{2\pi} \int_{-\infty}^{\infty} \varepsilon_x(\Omega) d\Omega.$$

12.16 Autocorrelation of an Energy Sequence

The autocorrelation of a real energy sequence is given by

$$r_{xx}[n] = \sum_{m=-\infty}^{\infty} x[n+m]x[m] = x[n] * x[-n].$$

Its Fourier transform is

$$R_{xx}(e^{j\Omega}) = X(e^{j\Omega})X^*(e^{j\Omega}) = |X(e^{j\Omega})|^2.$$

12.17 Power Density of a Sequence

The power of a sequence is given by

$$P = \overline{x^2[n]} = \lim_{N \rightarrow \infty} \frac{1}{2N+1} \sum_{n=-N}^N |x[n]|^2.$$

The autocorrelation of a power sequence $x[n]$ is given by

$$r_{xx}[n] = \lim_{N \rightarrow \infty} \frac{1}{2N+1} \sum_{k=-N}^N x[n+k]x[k].$$

The power spectral density is given by

$$S_x(\Omega) = \mathcal{F}[r_{xx}[n]] = R_{xx}(e^{j\Omega}).$$

Parseval's relation takes the form

$$P = \overline{x^2[n]} = \lim_{N \rightarrow \infty} \frac{1}{2N+1} \sum_{n=-N}^N |x[n]|^2 = \frac{1}{2\pi} \int_{-\infty}^{\infty} S_x(\Omega) d\Omega.$$

12.18 Passage through a Linear System

Let $x[n]$ be the input and $y[n]$ the output of a linear time-invariant discrete-time system.

If $x[n]$ is an energy sequence its energy spectral density is $\varepsilon_x(\Omega) = |X(e^{j\Omega})|^2$ and that of the output is

$$\varepsilon_y(\Omega) = |Y(e^{j\Omega})|^2 = |X(e^{j\Omega})|^2 |H(e^{j\Omega})|^2.$$

If $x[n]$ is a power sequence its energy spectral density is $S_x(\Omega)$ and that of the output is

$$S_y(\Omega) = S_x(\Omega) |H(e^{j\Omega})|^2.$$

12.19 Problems

Problem 12.1 A system has the impulse response

$$h(t) = \sin \pi t \Pi_T(t) = \sin \pi t \{u(t) - u(t - T)\}.$$

The system receives the ideal impulse train $\rho_T(t)$ as input

$$x(t) = \rho_T(t) = \sum_{n=-\infty}^{\infty} \delta(t - nT).$$

a) Evaluate the output $y(t)$ of the system if

i) $T = 11$ sec

ii) $T = 12$ sec

Evaluate its Fourier transform $Y(j\omega)$ and its Fourier series expansion with analysis interval T .

b) With $T = 12$ sec evaluate the energy and power spectral densities of $h(t)$ and $y(t)$. Write the expressions describing the autocorrelation of $h(t)$ and $y(t)$ in terms of their spectral densities.

Problem 12.2 A signal $f(t)$ has a Fourier transform

$$F(j\omega) = 14\pi\delta(\omega) + j6\pi\delta(\omega - 2\pi \times 10^3) - j6\pi\delta(\omega + 2\pi \times 10^3) + 2\pi\delta(\omega - 8\pi \times 10^3) + 2\pi\delta(\omega + 8\pi \times 10^3).$$

a) Is the signal $f(t)$ an energy or power signal?

b) Evaluate the spectral density of $f(t)$.

c) What is the average power of $f(t)$?

d) What is the energy of the signal over an interval of 10^{-3} sec?

e) The signal $f(t)$ is filtered by an ideal bandpass filter with a pass-band $1000\pi < |\omega| < 6000\pi$ r/s and gain K . Evaluate the filter output $g(t)$. What is the average power of $g(t)$?

Problem 12.3 Let

$$x(t) = f(t) + g(t)$$

where

$$f(t) = A_1 \sin(\omega_1 t + \theta_1)$$

$$g(t) = A_2 \sin(\omega_2 t + \theta_2)$$

where $\omega_2 > \omega_1$.

- Evaluate $S_x(\omega)$ the power spectral density of $x(t)$.
- What is the average power of the component of $x(t)$ of frequency ω_2 ? A signal $y(t)$ is generated as

$$y(t) = f(t)g(t).$$

- Evaluate the power spectral density $S_y(\omega)$.
- The signal $y(t)$ is fed to a filter of frequency response

$$H(j\omega) = K \Pi_{\omega_2}(\omega).$$

Evaluate the power spectral density at the filter output $z(t)$.

Problem 12.4

- Evaluate the function $f(t)$ that is the inverse Laplace transform of the function

$$F(s) = \left\{ 1 - e^{-(s+1)} \right\} / (s+1).$$

- Evaluate the autocorrelation $r_{ff}(t)$ of the function $f(t)$ and its Fourier transform $R_{ff}(j\omega)$.

c) Can the Fourier transform $F(j\omega)$ of $f(t)$ be evaluated from $F(s)$ by letting $s = j\omega$? Justify your answer.

- Evaluate $|F(j\omega)|^2$ and compare it with $R_{ff}(j\omega)$.

e) Is $f(t)$ a power or energy signal?

Evaluate the energy or power spectral density of $f(t)$. Evaluate the energy / power of $f(t)$.

f) Let $H(s) = F(s)$ be the transfer function of a linear system. Let the input to the system be the signal

$$x(t) = \sum_{n=-\infty}^{\infty} \delta(t-n).$$

Evaluate the power spectral density of the system response $y(t)$. Evaluate the average power of $y(t)$ in the frequency band $0 < f < 1.5$ Hz.

Problem 12.5 Consider a signal $x(t)$ of which the autocorrelation function is given by

$$r_{xx}(t) = e^{-|t|}, \quad -\infty < t < \infty.$$

- Evaluate $\varepsilon_{xx}(\omega)$ the energy spectral density of $x(t)$.
- Evaluate the total energy of $x(t)$.
- The signal $x(t)$ is fed as the input of a filter of frequency response

$$H(j\omega) = \begin{cases} A, & 2 < |\omega| < 4 \\ 0, & \text{otherwise.} \end{cases}$$

Evaluate the total energy of the signal $y(t)$ at the filter output.

Problem 12.6 In the system shown in Fig. 12.21 the transfer function $G(s)$ is that of a causal system and is given by

$$G(s) = 100\pi / (s + 100\pi).$$

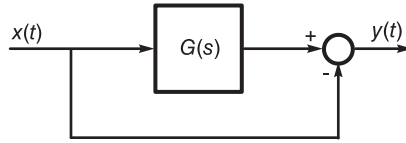


FIGURE 12.21 System block diagram.

- a) Evaluate the system impulse response between the input $x(t)$ and the output $y(t)$
- b) Given that the input is

$$x(t) = 1 + \cos 120\pi t$$

evaluate the average normalized power of the output $y(t)$. Evaluate the power spectral density of $y(t)$.

Problem 12.7 Consider the signals

$$x(t) = \sum_{n=-\infty}^{\infty} \{u(t - 2n) - u(t - 1 - 2n)\}$$

$$y(t) = e^{-t}u(t)$$

which represent voltage potentials in volts as functions of time t in seconds.

a) For each of the two signals evaluate the total normalized energy and the average normalized power.

b) The signals $z(t)$ and $v(t)$ are given by $z(t) = x(t)y(t)$ and $v(t) = x(t) * y(t)$. For each of these signals state whether the signal is an energy or power signal, explaining why.

Problem 12.8 The frequency transformation

$$s \longrightarrow (s^2 + 1)/s$$

is applied to a second order lowpass Butterworth filter prototype.

a) Write down the transfer functions $H_{LP}(s)$ and $H_{BP}(s)$ of the lowpass and bandpass filters.

b) Evaluate the central frequency ω_0 and the low- and high-edge frequencies ω_L and ω_H of the bandpass filter.

c) Rewrite the values of $H_{LP}(s)$ and $H_{BP}(s)$ so that the filter maximal gain be 14 dB. Let the input to this bandpass filter be $x(t) = 10 + 7 \sin \omega_0 t$. Evaluate the average normalized power of the output $y(t)$.

Problem 12.9 For each of the following signals, which are expressed in volts as function of time in seconds, state whether it is an energy or power signal and evaluate its total normalized energy or average normalized power.

a) $v(t) = 3 \sin [1000\pi(t + 0.0025)] + 2 \cos (1500\pi t + \pi/5)$.

b) $w(t) = \begin{cases} 0.25(t - 2), & 2 < t < 6 \\ 0, & \text{otherwise.} \end{cases}$

c) $x(t) = \sum_{n=0}^{10} w(t - 10n)$.

d) $y(t) = \sum_{n=-\infty}^{\infty} w(t - 5n)$.

Problem 12.10 Let $x(t)$ be a function, $X(j\omega)$ its Fourier transform and

$$|X(j\omega)| = 1/\sqrt{1 + \omega^2} + \pi/2 \{ \delta(\omega - \beta) + \delta(\omega + \beta) \}.$$

- What is the average value of $x(t)$?
- Is $x(t)$ periodic? If yes what is its period? If not why?
- The signal $x(t)$ is applied as the input to a filter of frequency response $H(j\omega)$, where

$$|H(j\omega)| = \Pi_{2\beta}(\omega), \quad \arg[H(j\omega)] = -\pi\omega/(4\beta).$$

Sketch the amplitude spectrum $|Y(j\omega)|$ of the filter output $y(t)$.

d) Let $z(t) = x(t) + 0.5 \sin(2.5\beta t) + 0.5$. Sketch the amplitude spectrum $|Z(j\omega)|$ of the signal $z(t)$.

Problem 12.11 For each of the following signals evaluate the signal total energy and the average normalized power and deduce whether it is an energy or power signal:

- $v(t) = A \sin(2000\pi t + \pi/3)$.
- $w(t) = A \sin(2000\pi t + \pi/3) R_{0.001}(t)$, where

$$R_{0.001}(t) = u(t) - u(t - 0.001).$$

- $x(t) = \sum_{n=-\infty}^{\infty} e^{-(t-5n)} \{u(t-5n) - u(t-5-5n)\}$.
- $z(t) = A$.

Problem 12.12 A system of transfer function

$$H(s) = \frac{K}{s+1} \Big|_{s \rightarrow s/\omega_c}$$

receives an input $x(t)$ and produces an output $y(t)$. Assuming $x(t) = A \cos \omega_0 t$, where $A = 5$ volts and $\omega_0 = 2\pi f_0 = 2\pi \times 500$ Hz.

- With $K = 1$ and $\omega_c = 500\pi$ r/s, evaluate the average power of the signal $y(t)$.
- With $K = 1$ find the value of ω_c so that the average power of $y(t)$ be 5 watts.
- With $\omega_c = 1000\pi$ r/s evaluate K so that the average power of $y(t)$ be 5 watts.

Problem 12.13 Given the signals $v(t) = x(t)y(t)$ and $f(t) = x(t) * z(t)$, where

$$x(t) = 5R_3(t) = 5[u(t) - u(t-3)]$$

$$y(t) = 2\Pi_{0.5}(t) = 2[u(t+0.5) - u(t-0.5)]$$

$$z(t) = 1 + \cos(\pi t + \pi/3).$$

a) Evaluate $V(j\omega)$ and $F(j\omega)$, the Fourier transforms of $v(t)$ and $f(t)$ as well as the Fourier series coefficients F_n of $f(t)$.

b) State whether each of the signals $v(t)$ and $f(t)$ is an energy or power signal, evaluating the energy or power spectral density, the total energy or the average normalized power in each case.

Problem 12.14 A signal $f(t)$ of average value $\overline{f(t)} = 15$ is applied to the input of a linear system of impulse response

$$h(t) = 5e^{-7t} \sin 5\pi t u(t).$$

What is the average value $\overline{y(t)}$ of the system output $y(t)$?

Problem 12.15 A signal $x(t)$ has a Fourier transform

$$X(j\omega) = 2\pi \text{Sa}(\omega/400) e^{-j\omega/100} \sum_{n=-\infty}^{\infty} \delta(\omega - 100\pi n).$$

The signal is applied to the input of a filter of frequency response $H(j\omega)$ and output $y(t)$, where

$$|H(j\omega)| = \begin{cases} 1 - [(\omega - 300\pi)/(200\pi)]^2, & 100\pi < |\omega| < 500\pi \\ 0, & \text{otherwise} \end{cases}$$

$$\arg[H(j\omega)] = \begin{cases} -\pi/2, & \omega > 0 \\ \pi/2, & \omega < 0. \end{cases}$$

a) Evaluate the exponential Fourier series coefficients X_n of $x(t)$ with an analysis interval of 0.02 sec.

b) Sketch the frequency response $|H(j\omega)|$.

c) Evaluate the Fourier series coefficients Y_n of the output $y(t)$ over the same analysis period.

d) Evaluate the output $y(t)$ and the normalized average power of each components of $y(t)$.

Problem 12.16 A system receives an input $x(t)$ and produces an output $y(t)$ that is the sum of $x(t)$ and a delayed version $x(t - \tau)$ where $\tau = 0.4 \times 10^{-3}$ sec. The signal $x(t)$ is a sinusoid of amplitude 5 volts and frequency 1 kHz.

a) Draw the block diagram describing the system.

b) Evaluate the impulse response $h(t)$ and frequency response $H(j\omega)$ of the system between its input $x(t)$ and output $y(t)$.

c) Evaluate and sketch the power spectral density $S_x(\omega)$ of the signal $x(t)$, expressed in terms of the Fourier series coefficients X_n of $x(t)$.

d) Evaluate and sketch the power spectral density $S_y(\omega)$ and the average power $\overline{y_2(t)}$ of the output $y(t)$.

Problem 12.17 The signal $x(t) = e^{-7t}u(t)$ is applied to the input of a filter of frequency response $H(j\omega)$ given by

$$H(j\omega) = \begin{cases} 5, & 1.1 \leq |\omega| \leq 3 \\ 0, & \text{otherwise} \end{cases}$$

Evaluate the energy spectral density $\varepsilon_x(\omega)$ of $x(t)$ and $\varepsilon_y(\omega)$ of $y(t)$.

Problem 12.18 A filter of frequency response

$$H(j\omega) = (1 - \omega^2/W^2) \Pi_W(\omega)$$

receives an input $v(t)$ and produces an output $y(t)$.

Assuming that the input $v(t)$ has an autocorrelation $r_{vv}(t) = \cos(Wt/4)$ evaluate the power spectral densities $S_{vv}(\omega)$ and $S_{yy}(\omega)$ of the signals $v(t)$ and $y(t)$, respectively. Evaluate the normalized average power of $y(t)$.

Problem 12.19 Consider the signal

$$v(t) = 10 \sin \beta t \Pi_{T/2}(t)$$

where $\beta = 4\pi/T$.

a) Sketch the signal $v(t)$. Evaluate its energy and normalized average power and corresponding spectral density if any.

b) What is the result of integrating the evaluated spectral density?

Problem 12.20 A signal is given by

$$v(t) = 10 \cos[\beta(t - 1)] + 5 \sin[4\beta(t - 2)] + 8 \cos[10\beta(t - 3)]$$

where $\beta = 2\pi/T$ and $T = 1$ sec.

- Evaluate the exponential Fourier series coefficients of $v(t)$ with an analysis interval of one second.
- Evaluate the signal power spectrum.

Problem 12.21 A spectrum analyzer displays the amplitude spectrum in volts and phase spectrum in degrees as the Fourier series coefficients F_n versus the frequency in Hz of a function $f(t)$ as shown in Table 12.1 and with $F_{-n} = F_n^*$.

TABLE 12.1 Amplitude and phase spectra

Frequency kHz	0	10	20	30	40	≥ 50
$ F_n $ volt	2	2.5	3.5	2	1	0
$\arg[F_n]$ deg.	0	-10	-20	-30	-40	-

- What is the period τ and the average value of the function $f(t)$?
- Write the value of the function $f(t)$ as a sum of real expressions.
- The signal $f(t)$ is fed to a filter of frequency response $H(j\omega)$ where

$$|H(j\omega)| = \Pi_B(\omega)$$

where $B = 50000\pi$ rad/sec, $\arg[H(j\omega)] = -(10^{-3}/180)\omega$ rad/sec and the filter output $g(t)$ is modulated by the carrier $\cos(40000\pi t)$ producing an output $y(t)$. Sketch the Fourier transforms $G(j\omega)$ and $Y(j\omega)$ of $g(t)$ and $y(t)$.

- What is the average power of the output signal $y(t)$?

Problem 12.22 Consider the signal:

$$v(t) = u(t + t_0) - u(t - b + t_0)$$

where $b > t_0 > 0$.

- Evaluate the autocorrelation $r_{vv}(t)$ of $v(t)$.
- Evaluate the Fourier transform $R_{vv}(j\omega)$ of $r_{vv}(t)$.
- Evaluate the Fourier transform $V(j\omega)$, the energy spectral density and deduce therefrom the total energy of $v(t)$. Compare the result with $R_{vv}(j\omega)$.

Problem 12.23 Evaluate the energy spectral density for each of the following signals:

- $x(t) = e^t [u(t) - u(t - 1)]$.
- $y(t) = e^{-t} \sin(t) u(t)$.

Problem 12.24 Given the signal $v(t) = e^{-t} u(t)$

- Evaluate the energy of the signal $v(t)$.
- Evaluate the energy of the signal contained in the frequency range 0 to 1 Hz.

Problem 12.25 Given the signal $v(t) = e^{-t} u(t)$.

- Show that $v(t)$ is an energy signal.
- Evaluate the energy spectral density of $v(t)$.
- Evaluate the normalized energy contained in the frequency range 0 to 1 r/s.
- Evaluate the normalized energy contained in the frequency range 0 to 1 Hz.
- Evaluate the autocorrelation function $r_{vv}(t)$ of $v(t)$.
- Show how from $r_{vv}(t)$ you can deduce the energy spectral density of $v(t)$.

Problem 12.26 The signal $v(t) = 4e^{-2t}u(t)$ is applied to the input of a filter of frequency response $H(j\omega)$.

- What is the total normalized energy E_v of $v(t)$?
- What is the total normalized energy E_y of the signal $y(t)$ at the filter output in the case where the filter is an ideal lowpass filter of unit gain and cut-off frequency 2 r/s?
- What is the total normalized energy E_y of the signal $y(t)$ at the filter output in the case where the filter is an ideal bandpass filter of unit gain and pass-band extending from 1 to 2 Hz?
- What is the total normalized energy E_y of the signal $y(t)$ at the filter output in the case where the filter transfer function is $H(s) = 1/(s+2)$?
- What is the total normalized energy E_y of the signal $y(t)$ at the filter output in the case where the filter frequency response is $H(j\omega) = e^{-j\omega T}$, where T is a constant?

Problem 12.27 Each of the following signals is given in volts as a function of the time t in seconds. For each signal evaluate the total energy if it is an energy signal or the average power if it is a power signal.

- $x_a(t) = 3[u(t - T_a) - u(t - 6T_a)]$, where $T_a > 0$.
- $x_b(t) = x_a(t) \cos(2\pi t/T_b)$, where $T_b = T_a$.
- $x_c(t) = \sum_{n=-\infty}^{+\infty} x_b(t - nT_c)$, where $T_c = 15T_a$.
- $x_d(t) = x_a(t) + 1$.

Problem 12.28 Consider the three signals $x(t)$, $y(t)$ and $z(t)$:

$$x(t) = u(t) - u(t-1), \quad y(t) = u(t+0.5) - u(t-0.5), \quad z(t) = \sin(\pi t).$$

- Is the sum $v(t) = x(t) + y(t)$ an energy or power signal? Depending on the signal type, evaluate the total normalized energy or the average normalized power, respectively.
- Is the convolution $s(t) = x(t) * z(t)$ an energy or power signal? Depending on the signal type, evaluate the energy spectral density or the power spectral density, respectively.

Problem 12.29 Evaluate the power spectral density and the average power of the following periodic signals:

- $v(t) = 5 \cos(2000\pi t) + 3 \sin(500\pi t)$.
- $x(t) = [1 + \sin(100\pi t)] \cos(2000\pi t)$.
- $y(t) = 4 \sin^2(200\pi t) \cos(2000\pi t)$.
- $z(t) = \sum_{n=-\infty}^{+\infty} 10^4 (t - 10^{-3}n) \{u(t - 10^{-3}n) - u(t - 10^{-3}[n+1])\}$.

Problem 12.30 Let $x(t)$ be a periodic signal having a period 5×10^{-2} sec. Its exponential Fourier series expansion with an analysis interval equal to its period has the Fourier series coefficient

$$X_n = \begin{cases} 1, & n = 0, \pm 4 \\ \pm j, & n = \pm 1 \\ 0, & \text{otherwise.} \end{cases}$$

Let $y(t)$, be a signal having the Fourier transform $Y(j\omega) = 150/(125 + j\omega)$.

- Let $z(t)$ be the convolution $z(t) = x(t) * y(t)$. Evaluate the average power $\overline{z^2(t)}$ of $z(t)$.
- Let $v(t) = x(t) + y(t)$. Evaluate the average power $\overline{v^2(t)}$ of $v(t)$.

Problem 12.31 Let $x(t) = 3 \cos(\omega_1 t) + 4 \sin(\omega_2 t)$, where $\omega_1 = 120\pi$ and $\omega_2 = 180\pi$. The signal $x(t)$ is applied to the input of a filter of transfer function $H(s) = 1/(1 + 120\pi/s)$.

Evaluate the power spectral density $S_y(\omega)$ of the signal $y(t)$ at the filter output. Evaluate the average power $\overline{y^2(t)}$ of $y(t)$.

Problem 12.32 A filter that has a transfer function $H(s) = K/(1 + s/\omega_c)$ receives an input signal $x(t) = A \cos(2\pi f_0 t)$, where $A = 5$ volts and $f_0 = 500$ Hz, and produces an output signal $y(t)$.

- Let $K = 1$ and $\omega_c = 500\pi$ r/s. Evaluate the average signal power at the filter output.
- Let $K = 1$. Determine the value of ω_c so that the average power of the output signal $y(t)$ is 5 watts.
- Let $\omega_c = 1000\pi$ r/s. Determine the value of K so that the average power of the output signal $y(t)$ is 5 watts.

Problem 12.33 The periodic signal $v(t) = \sum_{n=-\infty}^{\infty} (-1)^n \Lambda_{T/4}(t - nT/2)$ is applied to the input of filter of frequency response $H(j\omega) = 4\Lambda_{12}(\omega)$ and output $y(t)$. Evaluate

- The average power of the signal $v(t)$
- The average power of $y(t)$ if $T = 2\pi/3$
- The average power of $y(t)$ if $T = \pi/6$

Problem 12.34 A voltage $v_E(t)$ is applied to the input of a first order lowpass RC filter with $RC = 1$, of which the output is $v_S(t)$. For each of the following cases evaluate the average power of the input and output signal $v_E(t)$ and $v_S(t)$, respectively.

- The power spectral density of $v_E(t)$ is $S_{v_E}(\omega) = A[\delta(\omega + 1) + \delta(\omega - 1)]$.
- The power spectral density of $v_E(t)$ is $S_{v_E}(\omega) = u(\omega + 1) - u(\omega - 1)$.
- The power spectral density of $v_E(t)$ is $S_{v_E}(\omega) = A$.

Problem 12.35 The signal $x(t) = \sin(4\pi t)$ is applied to the input of a filter of transfer function $H(s) = 1/(s + 1)$ and output $y(t)$.

- Evaluate the power spectral density $S_x(\omega)$ of the signal $x(t)$.
- Evaluate the average power of the signal $x(t)$.
- Evaluate the normalized energy of one period of the signal $x(t)$.
- Evaluate the power spectral density $S_y(\omega)$ of the signal $y(t)$ at the filter output.
- Evaluate the average power $\overline{y^2(t)}$ of the filter output signal $y(t)$.

Problem 12.36 The signal $v(t) = \sum_{n=-\infty}^{\infty} \delta(t - 12n)$ is applied to the input of a linear system of impulse response $h(t) = \sin(\pi t)[u(t) - u(t - 12)]$. Evaluate the power spectral density of the filter output signal $y(t)$.

Problem 12.37 Let $x(t)$ be a periodic signal of period 5×10^{-3} sec and exponential Fourier series coefficients X_n , evaluated with an analysis interval equal to its period, given by

$$X_n = \begin{cases} 1, & n = \pm 1 \\ \pm j/5, & n = \pm 2 \\ (1 \mp 2j)/10, & n = \pm 4 \\ 0, & \text{otherwise.} \end{cases}$$

The properties of the message $m(t)$ are $\overline{m(t)} = 0$ volt, $\overline{m^2(t)} = 2$ watts, $|m(t)|_{max} = 5$ volts.

$M(f) = 0$ for $|f| > 7.5 \times 10^3$ Hz.

For each of the five possible frequency responses of the bandpass filter, evaluate the maximum amplitude of the modulated signal $y(t)$.

Defining the harmonic distortion rate (HDR) as

$$\text{HDR} = \frac{P_h}{P_T} \times 100\%$$

where P_h is the average power of the signal harmonics other than the fundamental and P_T is the total signal average power.

a) Evaluate the HDR of the signal $x(t)$.

b) The signal $x(t)$ is applied to the input of a filter the transfer function of which is given by

$$H(s) = \frac{1}{s+1} \Big|_{s \rightarrow s/(400\pi)}$$

Evaluate the HDR of the filter output signal $y(t)$.

Problem 12.38 Let $x(t) = v(t) + a v(t - t_0)$, where $v(t)$ is a power signal and t_0 is a constant.

Show that $\overline{x^2(t)} = (1 + a^2) \overline{v^2(t)} + 2a r_v(t_0)$, where $\overline{x^2(t)}$ is the average power of $x(t)$, $\overline{v^2(t)}$ is that of $v(t)$ and $r_v(t_0)$ is the autocorrelation function of $v(t)$ evaluated at $t = t_0$.

12.20 Answers to Selected Problems

Problem 12.1 a)

$$\text{i) } y(t) = \sum_{n=-\infty}^{\infty} \sin \pi(t - 11n) \{u(t - 11n) - u(t - 11n - 11)\}$$

$$\begin{aligned} Y(j\omega) &= 2\pi \sum_{n=-\infty}^{\infty} H_n \delta(\omega - n\omega_0) \\ &= -j\pi \sum_{n=-\infty}^{\infty} [e^{-jn\pi + j\beta T/2} \text{Sa}(n\pi - \beta T/2) - e^{-jn\pi - j\beta T/2} \text{Sa}(n\pi + \beta T/2)] \delta(\omega - n\omega_0) \end{aligned}$$

$$Y(j\omega) = j\pi \sum_{n=-\infty}^{\infty} [e^{-jn\pi + j11\pi/2} \text{Sa}(n\pi - 11\pi/2) - e^{-jn\pi - j11\pi/2} \text{Sa}(n\pi + 11\pi/2)] \delta(\omega - n2\pi/11)$$

$$\text{ii) } Y(j\omega) = -j\pi \{\delta(\omega - \pi) - \delta(\omega + 6)\}$$

$$Y_n = \begin{cases} \mp j/2, & n = \pm 6 \\ 0, & n \neq \pm 6 \end{cases}$$

$$\text{b) } h(t) = \sin \pi t \{u(t) - u(t - 12)\}.$$

$$\varepsilon_h(t) = (T^2/4) |e^{-j(\omega - \pi)T/2} \text{Sa}\{(\omega - \pi)T/2\} - e^{-j(\omega + \pi)T/2} \text{Sa}\{(\omega + \pi)T/2\}|^2$$

$$y(t) = \sin \pi t, \quad S_y(\omega) = (\pi/2) \{\delta(\omega - \pi) + \delta(\omega + \pi)\}.$$

Problem 12.2

- a) The signal, having an impulsive spectrum, is periodic.
- b) $S_f(\omega) = 98\pi\delta(\omega) + 18\pi\{\delta(\omega - 2\pi \times 10^3) + \delta(\omega + 2\pi \times 10^3)\} + 2\pi\{\delta(\omega - 8\pi \times 10^3) + \delta(\omega + 8\pi \times 10^3)\}$.
- c) $P = \overline{f^2(t)} = \sum_{n=-\infty}^{\infty} |F_n|^2 = 49 + 2 \times 9 + 2 \times 1 = 69$.
- d) $P = \frac{1}{T}E$, $E = TP = \frac{2\pi}{\omega_0} \times 69 = 69 \times 10^{-3}$.
- e) $G_n = \begin{cases} \pm j 3 K, & n = \pm 1 \\ 0, & n \neq \pm 1 \end{cases}$, $\overline{g^2(t)} = \sum_{n=-\infty}^{\infty} |G_n|^2 = 2 \times 9 K^2 = 18 K^2$.

Problem 12.5

- a) $\varepsilon_{xx}(\omega) = 2/(1 + \omega^2)$
- b) $E = 1$
- c) $E = 0.4373A^2/\pi$

Problem 12.6

$$Y_n = \begin{cases} \frac{\mp j\beta}{2(100\pi \pm j\beta)}, & n = \pm 1 \\ 0, & \text{otherwise} \end{cases}$$

$$S_y(\omega) = 2\pi \sum_{n=-\infty}^{\infty} |Y_n|^2 \delta(\omega - n\omega_0) = 2\pi \times 0.1475 \{\delta(\omega - \beta) + \delta(\omega + \beta)\}$$

$$\overline{y^2(t)} = 0.295$$

Problem 12.7 See Fig. 12.22

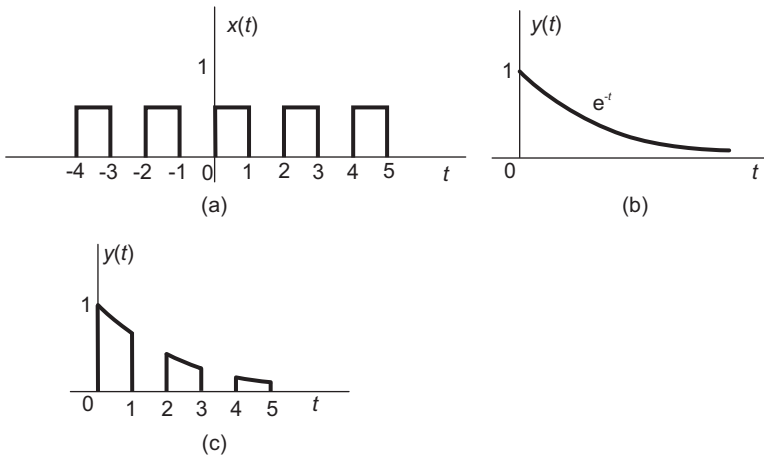


FIGURE 12.22 Figure for Problem 12.7.

- a) $E_x = \infty E_y(t) = 1/2$ joules.
- b) The average normalized powers are $\overline{x^2(t)} = (1/2) \cdot 1 = 1/2$ Watt.
 $\overline{y^2(t)} = 0$.
 $y(t)$ is an energy signal since $E_y < \infty$, $z(t)$ is periodic since $x(t)$ is periodic. The signal $z(t)$ is therefore a power signal.

Problem 12.8

- a) $H_{LP}(s) = \frac{K}{s^2 + 1.4142s + 1}$, $H_{BP}(s) = \frac{Ks^2}{(s^2 + 1)^2 + 1.4142s(s^2 + 1) + s^2}$, $K = 1..$
 b) $\omega_L = 1.6180$
 c) $|H_{BP}(j\omega_0)| = 5.01$
 $y(t)$ a sinusoid of amplitude $A = 35.07$, average normalized power 614.95 watts.

Problem 12.9

- a) $\overline{v^2(t)} = 6.5$ watts.
 b) *Energy signal, being of finite duration
 $E_w = \int_0^4 (t^2/16) dt = 1.333$ joules
 c) $\frac{E_x}{E_w} = 11$ $E_w = 14.63$ joules
 d) $\overline{y^2(t)} = \frac{1}{5}E_w = 0.267$ watts.

Problem 12.10

- a) $x(t) = 0$ since $X(j\omega)$ has no impulse at the origin $\omega = 0$.
 b) $x(t)$ is not periodic. To be periodic the spectrum has to be composed solely of impulses.
 c) See Fig. 12.23

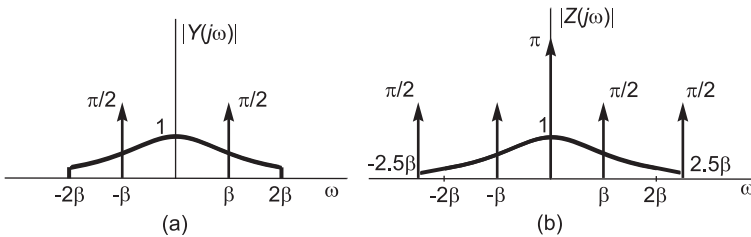


FIGURE 12.23 Figure for Problem 12.10.

Problem 12.11

- a) Total Energy = $A^2/2$ watt. Power signal
 b) Total Energy = $A^2/2000$ joule. Average normalized power = 0. Energy signal [equal to a single period of $v(t)$].
 c) $\overline{x^2(t)} = \frac{1}{6}(1 - e^{-6}) = 0 \cdot 15$. Power signal. Energy = ∞
 d) $\overline{z^2(t)} = A^2$, Power signal. Total Energy = ∞ .

Problem 12.12

- a) $\overline{y^2(t)} = 2.5$ watts.
 b) Note that the average power of a sinusoid of Amplitude A is $A^2/2$ $\omega_c = 2565.1$ r/s.
 c) $K = 0.8944$.

Problem 12.13

- a) $V(j\omega) = 5 \text{Sa}(0.25\omega) e^{-j0.25\omega}$. $F(j\omega) = 30\pi\delta(\omega) - 10e^{-j7\pi/6}\delta(\omega - \pi) + 10e^{j7\pi/6}\delta(\omega + \pi)$.

$$F_n \begin{cases} 15, n = 0 \\ \mp (5/\pi) e^{\mp j7\pi/6}, n = \pm 1 \\ 0, \text{otherwise} \end{cases}$$

- b) $\varepsilon_v(\omega) = |V(j\omega)|^2 = 25 \text{Sa}^2(0.25\omega)$, $P = \overline{f^2(t)} = 230.07$ watts.

Problem 12.14

$$\overline{y(t)} = \overline{f(t)} H(0) = 15 \frac{25\pi}{7^2 + (5\pi)^2} = 3.984.$$

Problem 12.15

- a) $X_n = 1, -0.9, 0.636, -0.301, 0, 0.18$ for $n = 0, \pm 1, \pm 2, \pm 3, \pm 4, \pm 5$ respectively, and $X_n = 0$, otherwise.
 b) See Fig. 12.24.

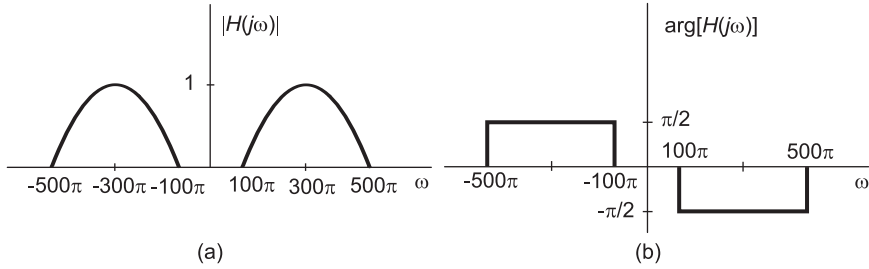


FIGURE 12.24 Amplitude and phase of frequency response, Problem 12.15.

- c) $Y_2 = \mp j0.4775, Y_3 = \pm j0.3001, Y_5 = \mp j0.135, Y_n = 0$, otherwise.
 d) $y(t) = 0.955 \sin 200\pi t - 0.6 \sin 300\pi t + 0.27 \sin 500\pi t$.

Problem 12.16 See Fig. 12.25 and Fig. 12.26.

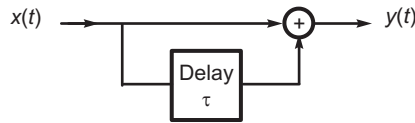


FIGURE 12.25 Figure for Problem 12.16.

- b) $h(t) = \delta(t) + \delta(t - \tau), H(j\omega) = 1 + e^{-j\omega\tau}$.
 c) $S_x(\omega) = 2\pi \{2.5^2\delta(\omega - 2000\pi) + 2.5^2\delta(\omega + 2000\pi)\}$.
 d) $S_y(\omega) = 2\pi \times 2.387 \{\delta(\omega - 2000\pi) + \delta(\omega + 2000\pi)\}, \overline{y^2(t)} = \frac{1}{2\pi} \int_{-\infty}^{\infty} S_y(\omega) d\omega = 2 \times 2.387 = 4.775$ watts.

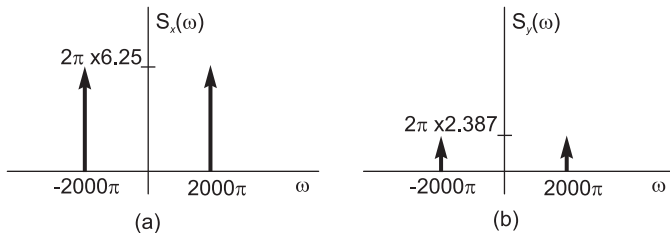


FIGURE 12.26 Figure for Problem 12.16.

Problem 12.17

- a) $\varepsilon_x(\omega) = 1/(\omega^2 + 49)$.

$$b) \quad \varepsilon_y(\omega) = \begin{cases} \frac{25}{\omega^2 + 49}, & 1.1 \leq \omega \leq 1.3 \\ 0, & \text{otherwise} \end{cases}.$$

Problem 12.18

$$S_{vv}(\omega) = \pi [\delta(\omega - W/4) + \delta(\omega + W/4)], \quad S_{yy}(\omega) = (15\pi/16) [\delta(\omega - W/4) + \delta(\omega + W/4)],$$

$$\overline{y^2(t)} = 15/16 = 0.9375 \text{ watt.}$$

Problem 12.19 See Fig. 12.27

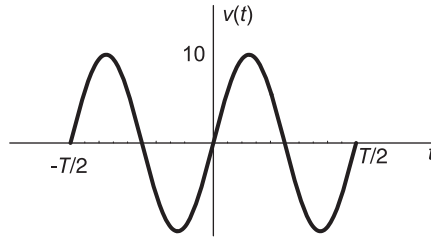


FIGURE 12.27 Figure for Problem 12.19.

$$a) \quad E = 50T, \quad P = 0, \quad \varepsilon_v(\omega) = |V(j\omega)|^2.$$

$$\varepsilon_v(\omega) = 25T^2 \{ Sa^2 [T(\omega - \beta/2)] - 2Sa [T(\omega - \beta/2)] Sa [T(\omega + \beta)/2] \}$$

$$+ 25T^2 \{ Sa^2 [T(\omega + \beta)/2] \}.$$

$$b) \quad 100\pi T$$

Problem 12.20

$$V_n = \begin{cases} 5, & n = \pm 1 \\ \mp j2.5, & n = \pm 4 \\ 4, & n = \pm 10 \end{cases}$$

$$S_n = |V_n|^2 = \begin{cases} 25, & n = \pm 1 \\ 6.25, & n = \pm 4 \\ 16, & n = \pm 10 \end{cases}$$

Problem 12.22

- a) For $-t_0 \leq -t + b - t_0 \leq b - t_0$ i.e. $0 \leq t \leq b$ $r_{vv}(t) = -t + b - t_0 + t_0 = b - t$. For $-t_0 \leq -t - t_0 \leq b - t_0$ i.e. $-b \leq t \leq 0$ $r_{vv}(t) = b - t_0 + t + t_0 = b + t$
- b) $R_{vv}(j\omega) = b^2 Sa^2(b\omega/2)$
- c) $\varepsilon(\omega) = R_{vv}(j\omega)$, $E = b$ joules.

Problem 12.23

- a) $|X(j\omega)|^2 = (1 - 2e \cos(\omega) + e^2) / (1 + \omega^2)$
- b) $|Y(j\omega)|^2 = \frac{1}{\omega^4 + 4}$

Problem 12.24

- a) Energy : $\int_0^{+\infty} (e^{-t})^2 dt = 0.5$.
- b) $V(j\omega) 1/(1 + \omega^2)$
 Energy = $\frac{1}{2\pi} \int_{-2\pi}^{+2\pi} \frac{1}{1 + \omega^2} d\omega = \frac{1}{2\pi} [\tan^{-1}(\omega)]_{-2\pi}^{+2\pi} = 0.45$

Problem 12.25

- a) Energy signal.

- b) The energy spectral density is $1/(1 + \omega^2)$
 c) 0.25.
 d) 0.45.
 e) $r_{vv} = 0.5e^{-t}u(t) + 0.5e^{+t}u(-t)$
 f) $\mathcal{F}\{r_{vv}(t)\} = 1/(1 + \omega^2)$

Problem 12.26

- a) $E_v = 4$
 b) $E_y = 2$
 c) $E_y = 0.383$
 d) $E_y = 0.5$
 e) $E_y = 4$

Problem 12.27

- a) $E = 45T_a$ joules.
 b) $E = 22.5T_a$ joules. $P = 22.5T_a/15T_a = 1.5$ watts
 c) $P = 1$ watts.

Problem 12.28

- a) $E = 0.5 + (4 \times 0.5) + 0.5 = 3$.
 b) $S_s(\omega) = 0.637 [\delta(\omega + \pi) + \delta(\omega - \pi)]$.

Problem 12.29

- a) $P = 17$
 b) $P = 0.75$
 c) $P = 3$
 d) $P = 33.33$.

Problem 12.30

- a) $\overline{z^2(t)} = 3$. b) $\overline{v^2(t)} = 5$.

Problem 12.31

$$S_y(\omega) = 2\pi \times (9/8) [\delta(\omega + 120\pi) + \delta(\omega - 120\pi)] \\
+ 2\pi \times (36/13) [\delta(\omega + 180\pi) + \delta(\omega - 180\pi)] \\
\overline{y^2(t)} = 7.8.$$

Problem 12.32

- a) $\overline{x^2(t)} = 2.5$.
 b) $\overline{y^2(t)} = 0.4$. $\omega_c = 2565$ r/s.
 c) $\overline{y^2(t)} = 0.4$. $K = 0.894$.

13

Introduction to Communication Systems

In this chapter we study the basic principles of some communication systems. We begin by studying different methods of modulation of continuous-time signals. Sampled and discrete-time signal communication systems are subsequently explored.

13.1 Introduction

In a communication system, a signal is normally encoded and emitted by a transmitter, travels across a communication channel, and is detected and decoded by a receiver. The simultaneous communication of a group of signals along the same communication channel may be effected using time-domain or frequency-domain multiplexing. Frequency-domain multiplexing may be obtained using modulation by different carrier frequencies. Signals thus occupy distinct frequency bands and can each be recovered through filtering.

Modulation, moreover, serves another important purpose. Transmission of a signal in free space is effected through radiation by antennas. Such radiation necessitates that the transmitted signal be of a wave length comparable to the antenna dimensions. The relation between the wave length λ and the frequency f is given by

$$\lambda f = c \tag{13.1}$$

where c is the speed of light

$$c \approx 3 \times 10^5 \text{ km/s.} \tag{13.2}$$

For an audio signal of frequency $f = 1$ kHz. The wave length is $\lambda = 300$ m, an impractical length for an antenna. If, on the other hand, the signal is translated to a frequency of 10 MHz the corresponding wave length would be 30 m, an antenna of a few meters length would thus suffice for its radiation. It should also be noted that the effective signal bandwidth is affected by modulation. For example, an audio signal bandwidth may extend from say, 50 Hz to 10 kHz.

The higher frequency limit is therefore 200 times the lower one. If this signal is translated to a frequency of 1 MHz the ratio of these two frequencies is reduced to $1.01/1.00005 \approx 1.01$. An antenna designed for a 1 MHz signal would thus function efficiently for the entire signal bandwidth. In what follows we study different approaches to amplitude modulation, also known as linear modulation and to frequency modulation.

13.2 Amplitude Modulation (AM) of Continuous-Time Signals

Amplitude modulation is commonly used in radio broadcasting. For continuous-time signals, several systems of amplitude modulation are currently in use. Among these can be found double side-band (DSB), single side-band (SSB) and Vestigial Side-Band (VSB) systems.

13.2.1 Double Side-Band (DSB) Modulation

Let $m(t)$ be a signal representing a message to be transmitted. If the signal is multiplied by a carrier $A_c \cos \omega_c t$ the result is a modulated signal $y(t) = A_c m(t) \cos \omega_c t$, having a spectrum

$$Y(j\omega) = 0.5A_c \{M[j(\omega - \omega_c)] + M[j(\omega + \omega_c)]\}. \quad (13.3)$$

Such a DSB signal may thus be transmitted and after reception demodulated by multiplying the received signal by the carrier followed by filtering.

An alternative approach used in practice, which leads to a simpler demodulator, adds a bias to the signal $m(t)$, obtaining the signal $e(t) = 1 + m(t)$ which modulates the carrier. The modulated signal $f_m(t)$ is written

$$f_m(t) = e(t)A_c \cos \omega_c t = A_c [1 + m(t)] \cos \omega_c t. \quad (13.4)$$

We note, therefore, that the carrier is effectively added to the usual modulated signal $A_c m(t) \cos \omega_c t$. A signal thus modulated is shown in Fig. 13.1.

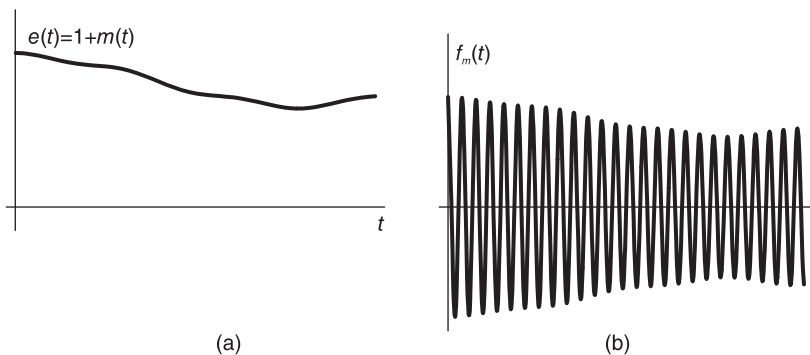


FIGURE 13.1 A signal and its modulation.

The spectrum of $f_m(t)$ is given by

$$F_m(j\omega) = A_c \pi [\delta(\omega - \omega_c) + (\omega + \omega_c)] + \frac{A_c}{2} [M\{j(\omega - \omega_c)\} + M\{j(\omega + \omega_c)\}] \quad (13.5)$$

where

$$M(j\omega) \triangleq \mathcal{F}[m(t)]. \quad (13.6)$$

The demodulation, or *detection*, of the signal $f_m(t)$ may be effected using an electric circuit such as that shown in Fig. 13.2. The circuit output is an approximation of the envelope

$A_c e(t) = A_c [1 + m(t)]$, wherefrom the signal $m(t)$ can be simply recovered. We note that for such a demodulator to function properly the envelope

$$A_c [1 + m(t)] \tag{13.7}$$

must be greater than or equal to zero, i.e. $m(t) \geq -1$. If $m(t)$ is a sinusoid

$$m(t) = A_m \cos \omega_m t \tag{13.8}$$

then this condition implies that $A_m \leq 1$.

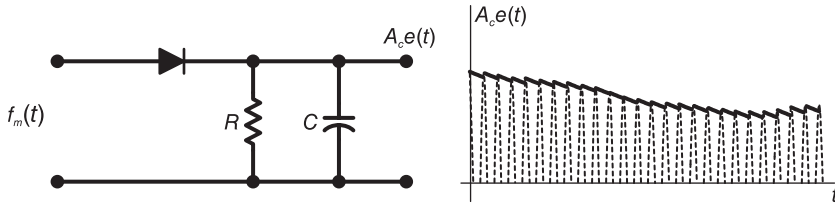


FIGURE 13.2 Demodulation.

13.2.2 Double Side-Band Suppressed Carrier (DSB-SC) Modulation

As just noted, the addition of a bias to the message before modulation leads to a signal that adds the carrier to the modulated signal. If the transmitter’s carrier frequency is reliably stable and if the receiver has an oscillator that generates a stable and precise carrier frequency then there is no need to transmit the carrier together with the modulated signal. A system that eliminated the carrier before transmission is called double side-band suppressed carrier (DSB-SC) system.

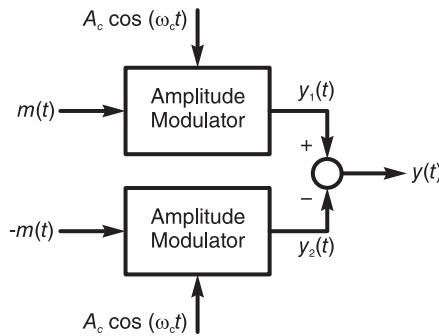


FIGURE 13.3 Double side-band suppressed carrier modulation.

A *balanced modulator*, which suppresses the carrier, is shown in Fig. 13.3. In this figure, the signal $y_1(t)$ at the upper amplitude modulator (AM) output is given by

$$y_1(t) = A_c [1 + m(t)] \cos \omega_c t \tag{13.9}$$

and that of the lower modulator output is

$$y_2(t) = A_c [1 - m(t)] \cos \omega_c t. \tag{13.10}$$

The output of the balanced modulator is given by

$$y(t) = y_1(t) - y_2(t) = 2A_c \cos \omega_c t m(t) \tag{13.11}$$

and with $M(j\omega) = \mathcal{F}[m(t)]$

$$Y(j\omega) = A_c [M\{j(\omega - \omega_c)\} + M\{j(\omega + \omega_c)\}]. \tag{13.12}$$

Note the absence of the carrier. The suppression of the carrier implies less power needed to transmit the signal.

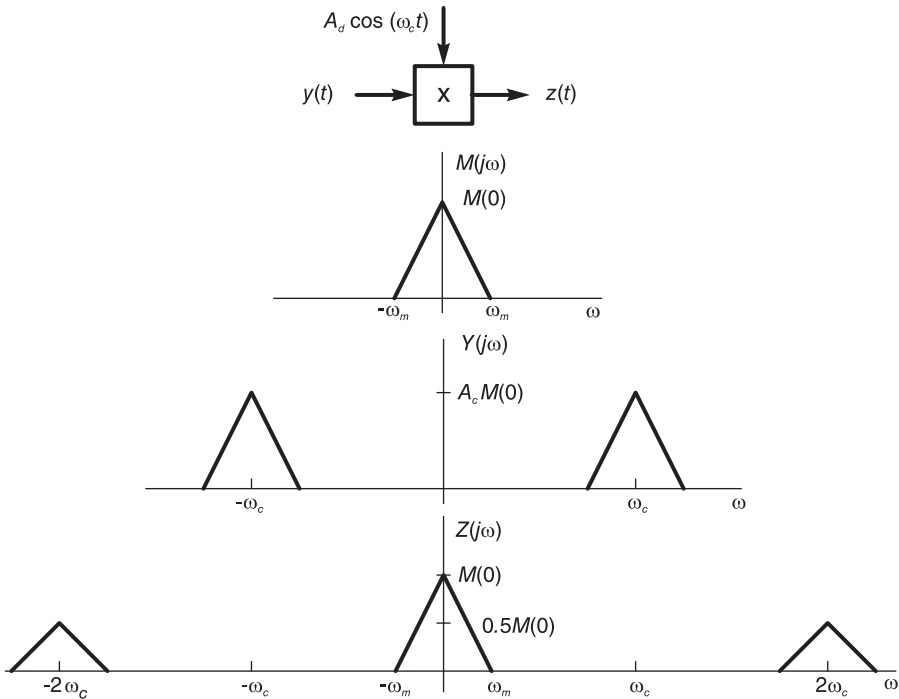


FIGURE 13.4 Modulation and demodulation of a DSB-SC signal.

Demodulating a DSB-SC signal can be implemented by multiplying the modulated signal by a sinusoid, namely, $A_d \cos \omega_c t$, where $A_d = 1/A_c$, as shown in Fig. 13.4. The figure also shows the spectrum $Y(j\omega)$ assuming, for illustration, a message $m(t)$ of a triangular-shaped spectrum $M(j\omega)$. The demodulator output is given by

$$z(t) = y(t) A_d \cos \omega_c t = 2A_c \cos^2 \omega_c t A_d m(t) = (1 + \cos 2\omega_c t) m(t) \tag{13.13}$$

$$Z(j\omega) = M(j\omega) + 1/2 [M\{j(\omega - 2\omega_c)\} + M\{j(\omega + 2\omega_c)\}] \tag{13.14}$$

as shown in the figure. If the signal $m(t)$ is band limited to the frequency $\omega = \omega_m$ r/s then it can be reconstructed from $z(t)$ using an ideal lowpass filter of bandwidth B such that $\omega_m < B < 2\omega_c - \omega_m$. The filter output is then $m(t)$.

It should be noted that such a receiver should employ a carrier oscillator that is well synchronized with that of the transmitter. A constant phase difference between the two oscillator outputs can be accounted for in the demodulation operation. Unpredictable phase variations, on the other hand, would lead to distortion of the received signal.

13.2.3 Single Side-Band (SSB) Modulation

Since the Fourier spectrum of a physical signal $f(t)$ has conjugate symmetry, i.e.,

$$F(-j\omega) = F^*(j\omega) \tag{13.15}$$

the power required for the transmission of a modulated signal may be reduced by suppressing the mirror image of the spectrum. The resulting transmitted signal, in addition, occupies half the bandwidth of the original modulated signal. Such a system is called single side-band (SSB) modulation. The principle is illustrated in Fig. 13.5.

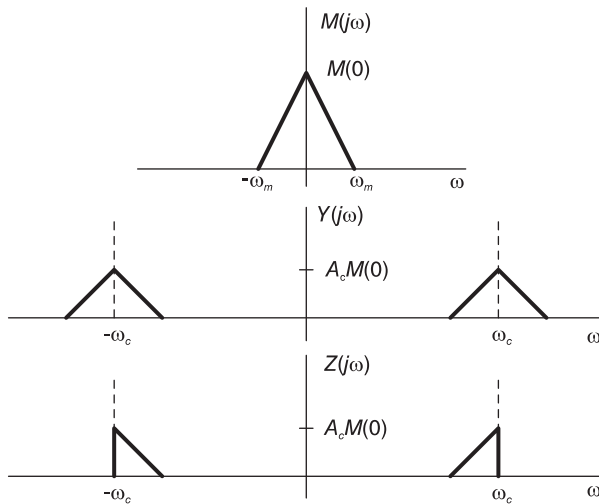


FIGURE 13.5 Single side-band modulation.

The figure shows the spectrum $M(j\omega)$ of a signal, its DSB-SC version and the SSB signal obtained by suppressing the upper-half spectrum. The lower half could be suppressed instead. Let $y(t)$ be the DSB-SC signal as described above.

$$Y(j\omega) = A_c [M\{j(\omega - \omega_c)\} + M\{j(\omega + \omega_c)\}]. \tag{13.16}$$

Let $z(t)$ be the SSB signal. We have

$$\begin{aligned} Z(j\omega) &= \mathcal{F}[z(t)] = Y(j\omega) \Pi_{\omega_c}(\omega) \\ &= A_c [M\{j(\omega - \omega_c)\} + M\{j(\omega + \omega_c)\}] \{u(\omega + \omega_c) - u(\omega - \omega_c)\}. \end{aligned} \tag{13.17}$$

The signal $z(t)$ is thus obtained by filtering the signal $y(t)$ using an ideal lowpass filter of bandwidth ω_c , as shown in Fig. 13.6. In the time domain we can write

$$z(t) = y(t) * h(t) \tag{13.18}$$



FIGURE 13.6 Filtering a DSB-SC signal.

where $h(t)$ is the filter impulse response

$$h(t) = \mathcal{F}^{-1} [\Pi_{\omega_c}(\omega)] = \frac{\omega_c}{2\pi} Sa(\omega_c t). \tag{13.19}$$

The signal $z(t)$ also can be written using the Hilbert transform. In fact, as will be studied in more detail in the next chapter the “Hilbert transformer” imparts a 90° phase lag on sinusoidal signals; hence on all signal frequency components.

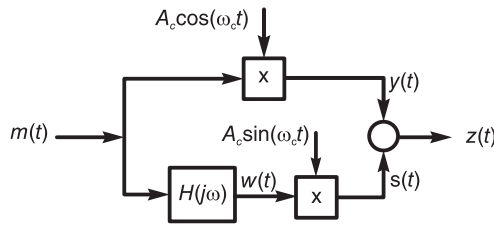


FIGURE 13.7 Generating an SSB-SC signal.

As shown in Fig.13.7, using a Hilbert transformer-type filter of frequency response

$$H(j\omega) = -j \operatorname{sgn}(\omega) = \begin{cases} -j, & \omega > 0 \\ j, & \omega < 0 \end{cases} \tag{13.20}$$

which means an impulse response $h(t) = 1/(\pi t)$, the Hilbert transformer output $w(t)$ has the spectrum

$$W(j\omega) = M(j\omega) H(j\omega) = \begin{cases} -jM(j\omega), & \omega > 0 \\ jM(j\omega), & \omega < 0. \end{cases} \tag{13.21}$$

The transformer is followed by a multiplication by $A_c \sin \omega_c t$, producing a signal $s(t) = w(t)A_c \sin \omega_c t$ and the corresponding spectrum

$$S(j\omega) = -(j/2) A_c \{W[j(\omega - \omega_c)] - W[j(\omega + \omega_c)]\} \tag{13.22}$$

as can be seen in Fig. 13.8. The system total output $z(t) = s(t) + y(t)$ has the spectrum shown in the figure and can be seen to be the required SSB signal.

The demodulation of an SSB signal may be effected by multiplying the received modulated signal by a carrier, followed by filtering, as shown in Fig. 13.9. Let $x(t)$ be the multiplier output. We have

$$x(t) = z(t)A_d \cos \omega_c t \tag{13.23}$$

and

$$X(j\omega) = \frac{A_d}{2} [Z\{j(\omega - \omega_c)\} + Z\{j(\omega + \omega_c)\}] \tag{13.24}$$

as can be seen in the figure. With $v(t)$ denoting the filter output, we have

$$V(j\omega) = \mathcal{F}[v(t)] = X(j\omega) \Pi_{\omega_c}(\omega) = 0.25A_c A_d M(j\omega). \tag{13.25}$$

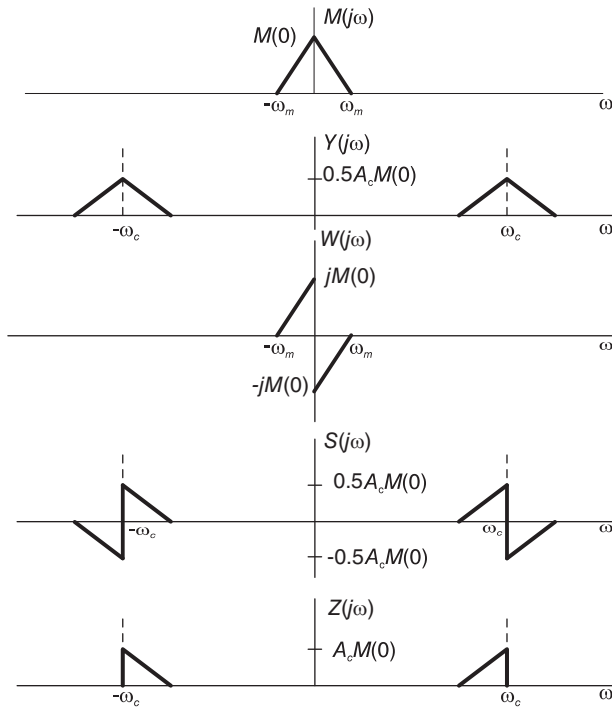


FIGURE 13.8 Generating an SSB-SC signal.

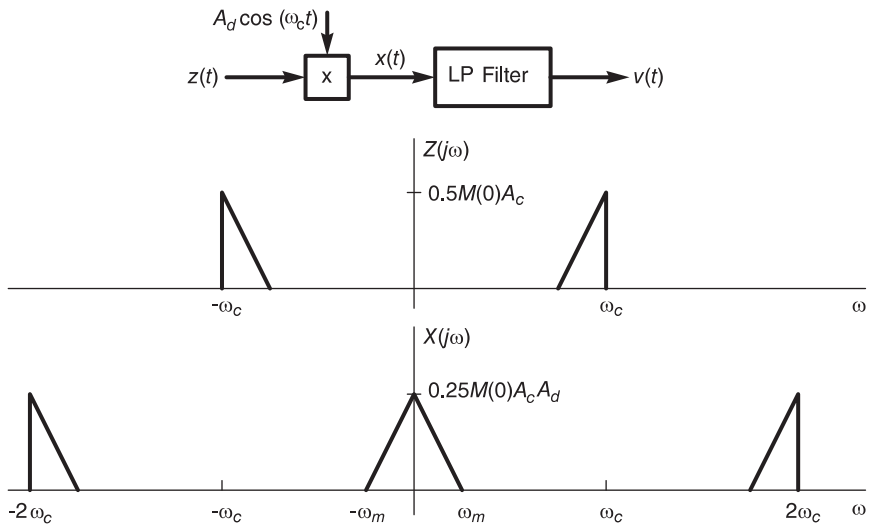


FIGURE 13.9 SSB demodulation.

If $A_d = 4/A_c$ we have the demodulated signal

$$v(t) = m(t). \quad (13.26)$$

13.2.4 Vestigial Side-Band (VSB) Modulation

We have seen that the suppression of the carrier necessitates a synchronization between the carrier generator at the receiver with that at the transmitter. We have also noted that in an SSB modulation system the suppression of one half of the spectrum calls for filtering of the received signal at precisely the carrier frequency ω_c . A slight deviation from this frequency could lead to the loss of part of the signal spectrum.

In the communication of audio signals such requirements are not critical, since the signal spectrum does not extend down to zero frequency. Television signals, on the other hand, extend down to very low frequencies and can thus be adversely affected by such slight frequency deviations. To avoid the need for a synchronous demodulator in every TV receiver a VSB modulation is employed in present-day commercial TV systems. In this approach the half band is gradually attenuated rather than simply cut off at the frequency ω_c . Such VSB-type modulation is illustrated in Fig. 13.10.

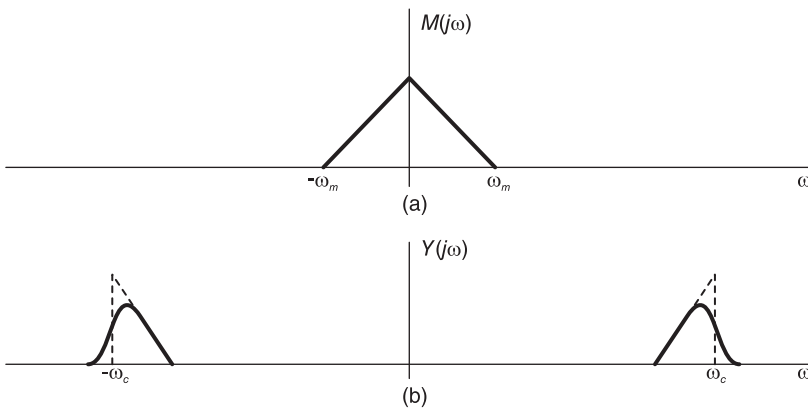


FIGURE 13.10 VSB modulation.

In this figure the spectrum $Y(j\omega)$ of the VSB modulated signal is the result of modulating the signal $m(t)$ by a carrier, and filtering the modulated signal using a lowpass filter with a gradual attenuation to the frequency ω_c .

The VSB modulation and demodulation of a signal is shown in Fig. 13.11.

13.2.5 Frequency Multiplexing

Frequency multiplexing may be used to communicate a set of signals on a single communication channel. The overall communication channel bandwidth is partitioned into frequency bands, which are assigned successively to the signals to be transmitted. Each signal is thus assigned a carrier frequency that corresponds to the frequency band it should occupy. At the receiver a bank of filters is used for demultiplexing the messages.

Such a frequency multiplexing system is shown in Fig. 13.12.

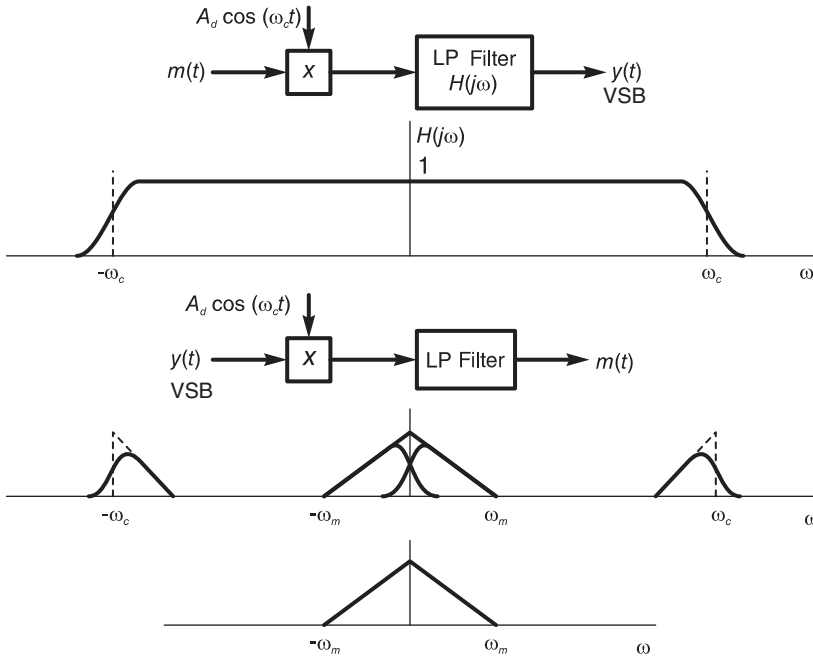


FIGURE 13.11 Modulation and demodulation of a received VSB signal.

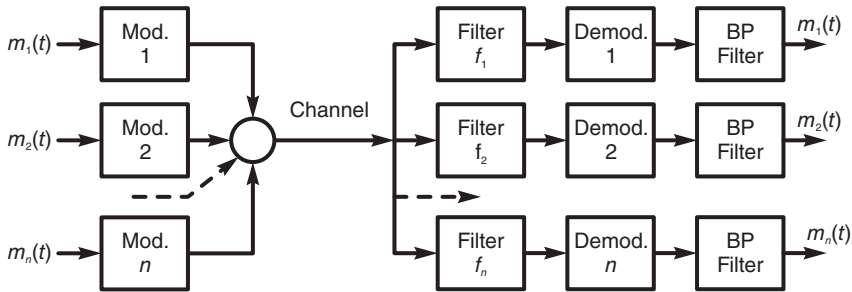


FIGURE 13.12 Frequency multiplexing system.

13.3 Frequency Modulation

Different types of modulation approaches are illustrated in Fig. 13.13. The left side of the figure shows a case where the modulating signal $m(t)$ is a triangle, while the right side shows the case where the modulating signal is a sinusoid. Part (a) of the figure depicts the carrier signal. Part (b) shows the modulating signal $m(t)$. Parts (c), (d) and (e) show the result of amplitude modulation, phase modulation and frequency modulation of the carrier, respectively. In general, frequency modulation is effective in noise suppression at the expense of wider frequency band requirements.

In one of several frequency modulation systems the angle $\phi(t)$ of the sinusoidal carrier

$$f(t) = A \cos \phi(t) \tag{13.27}$$

is modulated by the message signal denoted by $m(t)$.

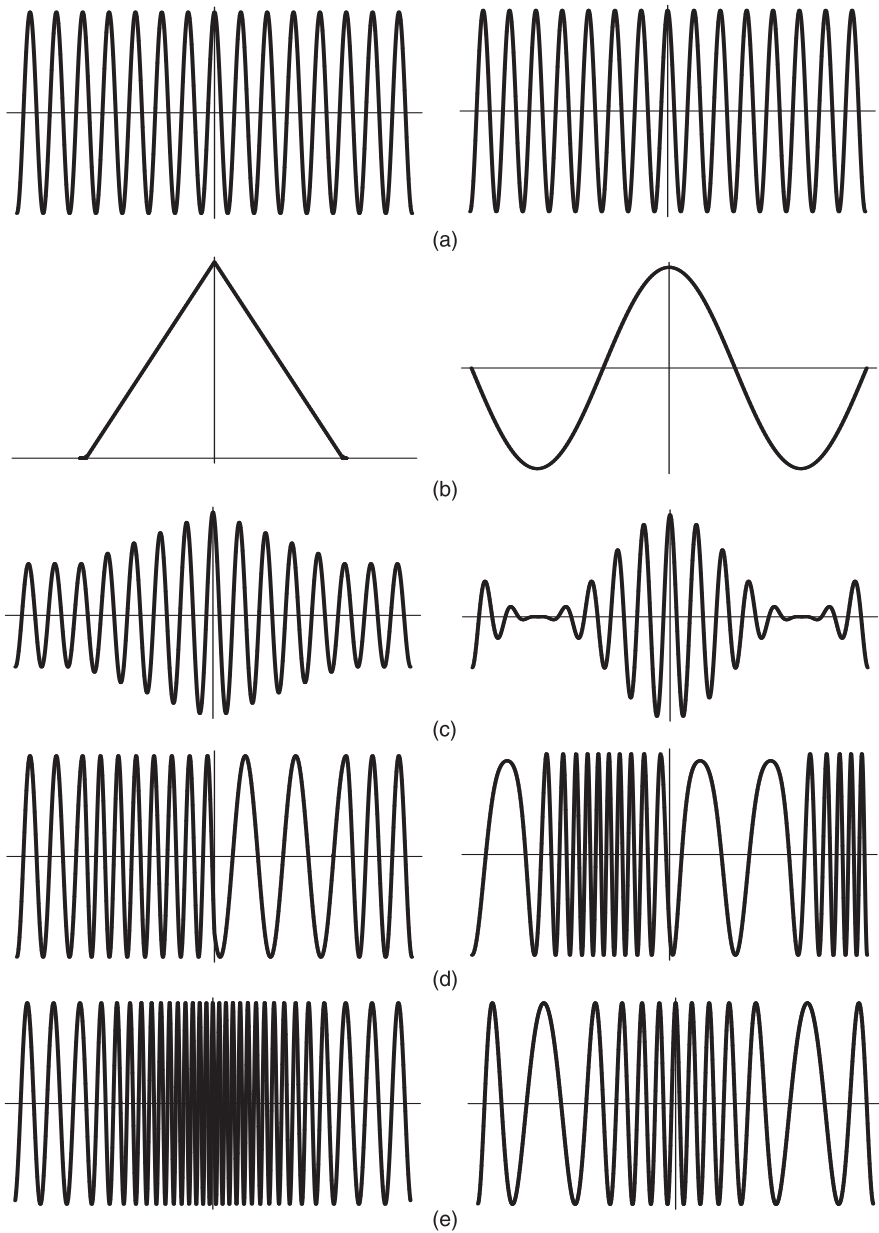


FIGURE 13.13 (a) Carrier, (b) two messages, (c) amplitude modulation, (d) phase modulation, (e) frequency modulation.

In the absence of modulation the carrier is the usual constant frequency pure sinusoid

$$f(t) = A \cos(\omega_c t + \theta). \quad (13.28)$$

Modulation of the carrier angle $\phi(t) = (\omega_c t + \theta)$ is also known as *angle modulation*. If the

phase θ is nil, the function $f(t) = A \cos \omega_c t$ can be written in the form

$$f(t) = \Re [Ae^{j\omega_c t}] \quad (13.29)$$

and may be represented as a vector of length A and angle $\gamma = \omega_c t$, a vector which as t increases rotates around the origin with a speed $\dot{\gamma} = \omega_c$, which is the usual radian frequency of $f(t)$. If the system of coordinates turns with the same speed the vector would appear stationary. If a phase $\theta(t)$ is added and made to vary slowly the vector representing

$$f(t) = \Re [Ae^{j(\omega_c t + \theta(t))}] \quad (13.30)$$

will not remain stationary. Instead, its angle will vary similarly to the phase $\theta(t)$. The angular velocity of the vector is thus modulated and is given by

$$\omega = d[\omega_c t + \theta(t)]/dt \quad (13.31)$$

This is the effective instantaneous angular frequency of the signal $f(t)$. Denoting it by the symbol ω_i we have

$$\omega_i(t) = d\phi(t)/dt \quad (13.32)$$

and conversely,

$$\phi(t) = \int_0^t \omega_i(\tau) d\tau \quad (13.33)$$

and if $\theta(t)$ is a constant then $\omega_i = \omega_c$ as expected. The instantaneous frequency in Hz of $f(t)$ is

$$f_i = \frac{1}{2\pi} \frac{d}{dt} [\omega_c t + \theta(t)] = \frac{\omega_c}{2\pi} + \frac{1}{2\pi} \frac{d\theta}{dt} = f_c + \frac{1}{2\pi} \frac{d\theta}{dt}. \quad (13.34)$$

The carrier phase angle $\theta(t)$ can be rendered proportional to the modulating signal $m(t)$.

$$f(t) = A \cos [\omega_c t + k m(t)]. \quad (13.35)$$

This is phase modulation.

Alternatively, the instantaneous angular frequency ω_i can be made linearly proportional to the message signal $m(t)$, such that

$$\omega_i = \omega_c + k_f m(t). \quad (13.36)$$

where k_f is known as the *modulation constant*. This implies that the carrier angle should equal

$$\phi(t) = \int_0^t \omega_i(\tau) d\tau = \omega_c t + k_f \int_0^t m(\tau) d\tau \quad (13.37)$$

wherefrom

$$f(t) = A \cos \left[\omega_c t + k_f \int_0^t m(t) dt \right]. \quad (13.38)$$

Such direct modulation of the carrier angle is known as frequency modulation.

Frequency modulation is nonlinear, in contrast with amplitude modulation which, being linear, permits the application of the principle of superposition. To evaluate the spectrum of a frequency modulated signal let

$$m(t) = A_m \cos \omega_m t. \quad (13.39)$$

We have

$$\phi(t) = \omega_c t + k_f A_m \int_0^t \cos \omega_m \tau d\tau = \omega_c t + (k_f A_m / \omega_m) \sin \omega_m t \quad (13.40)$$

$$f(t) = A_c \cos(\omega_c t + \beta \sin \omega_m t) \quad (13.41)$$

where $\beta = (k_f A_m / \omega_m)$. We may write

$$f(t) = \Re [x(t) e^{j\omega_c t}] \quad (13.42)$$

where $x(t) = A_c e^{j\beta \sin \omega_m t}$ is the complex envelope of the signal $f(t)$. The value β is thus the maximum phase deviation and is known as the *modulation index*. The signal $x(t)$ is periodic of fundamental frequency ω_m , i.e. of period $2\pi/\omega_m$, since $x\left(t + k\frac{2\pi}{\omega_m}\right) = x(t)$, k integer. We can expand $x(t)$ in a Fourier series

$$x(t) = \sum_{n=-\infty}^{\infty} X_n e^{jn\omega_m t} \quad (13.43)$$

$$X_n = \frac{\omega_m}{2\pi} A_c \int_{-\pi/\omega_m}^{\pi/\omega_m} e^{j\beta \sin \omega_m t} e^{-jn\omega_m t} dt. \quad (13.44)$$

Let

$$\theta = \omega_m t. \quad (13.45)$$

We have

$$X_n = A_c \int_{-\pi}^{\pi} e^{j(\beta \sin \theta - n\theta)} / (2\pi) d\theta. \quad (13.46)$$

The integral on the right-hand side is the n^{th} order Bessel function of the first kind denoted $J_n(\beta)$. We can therefore write $X_n = A_c J_n(\beta)$ and

$$x(t) = A_c \sum_{n=-\infty}^{\infty} J_n(\beta) e^{jn\omega_m t}. \quad (13.47)$$

The Bessel functions $J_n(\beta)$ for different values of n are shown in Fig. 13.14.

Moreover

$$f(t) = \Re \left[A_c \sum_{n=-\infty}^{\infty} J_n(\beta) e^{j(n\omega_m + \omega_c)t} \right] = A_c \sum_{n=-\infty}^{\infty} J_n(\beta) \cos[(n\omega_m + \omega_c)t]. \quad (13.48)$$

The spectrum of $f(t)$ is thus given by

$$F(j\omega) = \pi A_c \sum_{n=-\infty}^{\infty} J_n(\beta) \{ \delta[\omega - \omega_c - n\omega_m] + \delta[\omega + \omega_c + n\omega_m] \}. \quad (13.49)$$

We note that the spectrum of $f(t)$ has spectral lines at ω_c , $\omega_c \pm \omega_m$, $\omega_c \pm 2\omega_m$, ... A single pure sinusoid $\cos \omega_m t$ thus produces an infinite number of spectral lines. Theoretically the transmission of an FM signal thus requires an infinite bandwidth. In practice, a finite bandwidth is utilized while ensuring that the distortion resulting from such bandwidth truncation is within acceptable limits.

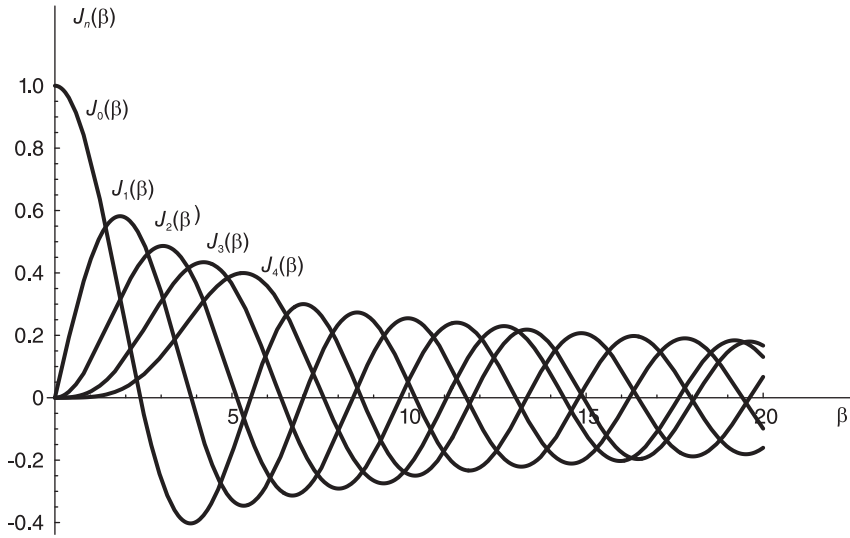


FIGURE 13.14 Bessel functions of different orders.

13.4 Discrete Signals

We have studied in Chapter 4 different sampling systems such as ideal, natural and instantaneous systems. In this section we focus the attention on these and other discrete-time signal communication systems.

13.4.1 Pulse Modulation Systems

The transmission of a set of messages along a single communication channel may be effected by time multiplexing the successive messages. As we shall shortly see, one sample is taken from the first message followed by a sample from the second message and so on until the last message, and the whole process repeated over and over as needed. Ideal, natural and instantaneous sampling systems studied in Chapter 4 are known as pulse amplitude modulation (PAM) systems.

A system represented in Fig. 13.15 employs time multiplexing of PAM produced messages. Such a system is also referred to as a *time division multiplexing* (TDM) system.

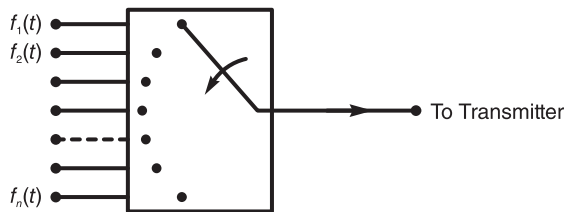


FIGURE 13.15 Time multiplexing of PAM produced messages.

A communication channel of a cut-off frequency $\omega_c = 2\pi f_c$ may be viewed as an ideal filter of bandwidth $B = \omega_c$. The input $f(t)$ to the communication channel can pass through without distortion if the signal cut-off frequency is at most $B = \omega_c$. If the signal $f(t)$ is ideally sampled

$$f_s(t) = f(t) \sum_{n=-\infty}^{\infty} \delta(t - nT) \tag{13.50}$$

its Fourier transform is given by

$$F_s(j\omega) = \frac{1}{T} \sum_{n=-\infty}^{\infty} F \left[j \left(\omega - \frac{2\pi n}{T} \right) \right]. \tag{13.51}$$

If the channel bandwidth is f_c Hz, the bandwidth of each signal should not exceed (f_c/n) . The channel capacity, i.e. the channel bandwidth, has to be n times the bandwidth of an individual channel.

At the receiver end demultiplexing is effected to separate the impulses, thus associating each one successively with its original message. Each demultiplexer output represents therefore a sampled individual message. Each output, successively, is applied to the input of a lowpass filter to reconstruct the original continuous-time signal as shown in Fig. 13.16.

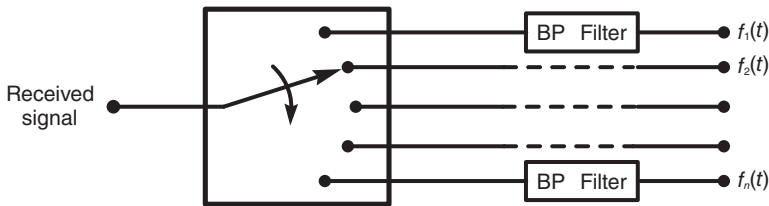


FIGURE 13.16 Demultiplexing received signal.

13.5 Digital Communication Systems

13.5.1 Pulse Code Modulation

In pulse code modulation (PCM) a signal is sampled and the samples are then quantized so that their values are converted to binary (or in general M-ary) code as is the conversion to binary effected by an A/D converter. Parity and other synchronization bits may be added. The bits thus generated are transmitted serially (or in parallel). At the receiving end a D/A conversion is performed, thus generating the original continuous-time signal.

PCM sampling with 3-bit 8-level quantization of a signal is shown in Fig. 13.17. As the figure shows, the 8-level quantization corresponding to a 3-bit code implies that at the sampling instants the signal values are approximated to the nearest integer value between 0 and 7.

For the signal shown in the figures, the successive quantized levels of the successive samples are given by 5, 7, 4, 2, 1. The corresponding 3-bit binary codes are: 101, 111, 100, 010 and 001.

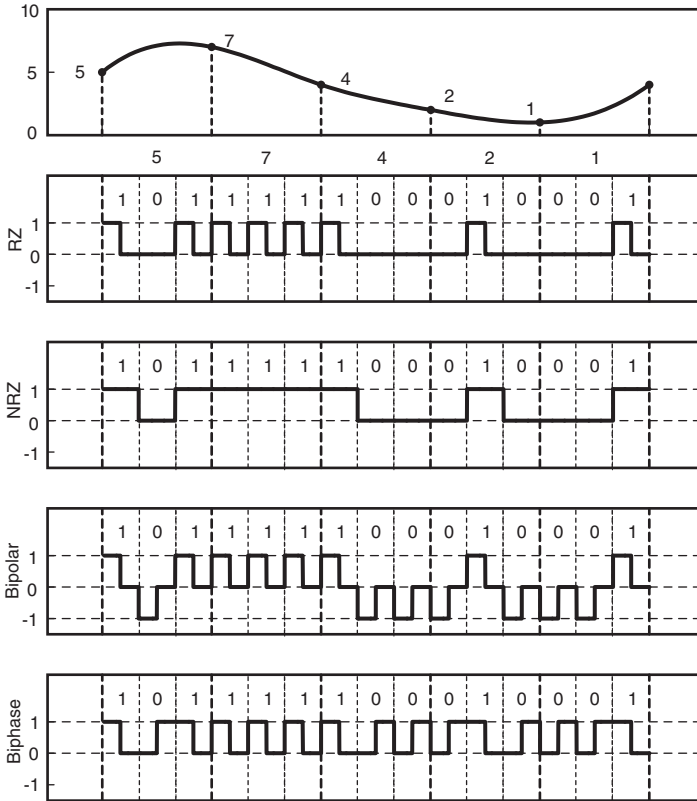


FIGURE 13.17 PCM sampling with 3-bit quantization.

The figure shows three different approaches of coding these binary values by rectangular pulses. In the first, designated *RZ* for *return to zero* code, a binary 1 is a positive pulse, which returns to zero before the generation of the subsequent bit. A binary zero is simply coded by a zero voltage.

In the second system shown in the figure, the *no return to zero (NRZ)* code, binary 1 is coded as a wide rectangle that occupies the whole bit time (bit-slot). As the figure shows, a 1 is coded as a “high” voltage level, a 0 as a “low” voltage level.

The figure shows a third pulse coding scheme which is *bipolar*. In this system a 1 is a positive rectangular pulse; a 0 is a negative pulse.

There are other variations, where for example the 1 is coded as in the *RZ* system we have just seen, but where the zero-bit is coded as the reversal (in time or polarity) of the 1-bit pulse code. This is shown in the figure as an example of a *biphase* pulse code.

Parity bits are added for error detection and correction. TDM is normally used to sample multiple channels, quantize each channel into PCM code and multiplex the signals of the successive channels. A synchronization *framing* bit is transmitted at the beginning of each new cycle where the channels are reaccessed starting with the first and sampled.

Figure 13.18 shows three signals — $f_1(t)$, $f_2(t)$ and $f_3(t)$ — on three channels, and the TDM signal $f_m(t)$ obtained by multiplexing them. The sampling multiplexing operation is represented schematically for a system with four channels in Fig. 13.19.

The samples in $f_m(t)$ are quantized into PCM code as seen above. The figure shows a low-pass filter LPF included in each channel to ensure that the sampled signals are bandlimited,

thus avoiding spectral aliasing.

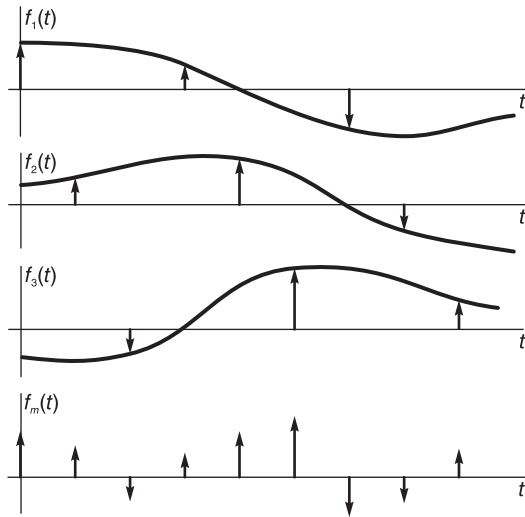


FIGURE 13.18 TDM signal generation.

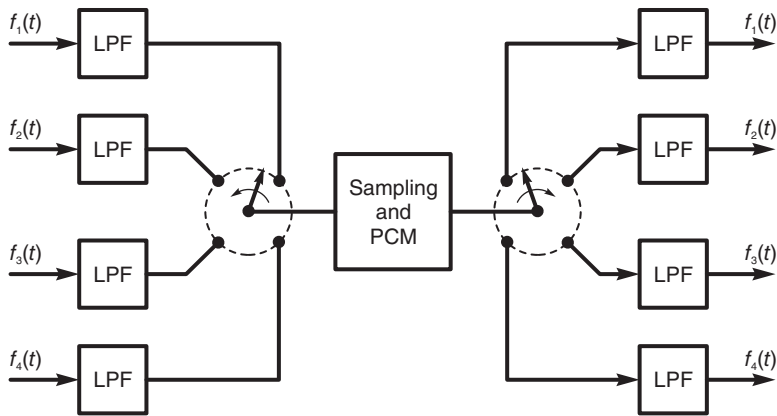


FIGURE 13.19 Sampling multiplexing.

13.5.2 Pulse Duration Modulation

In pulse duration modulation (PDM) also called pulse width modulation (PWM) the continuous-time signal is sampled uniformly and at each sampling interval a rectangular pulse is generated of constant height but of a width that is proportional to the value of the

signal at the sampling instant.

As depicted in Fig. 13.20, this type of modulation can be viewed as starting with an ideal sampling at constant sampling interval T . Each impulse $f(kT)\delta(t - kT)$ at sampling instant $t = kT$ triggers a rectangular pulse of constant height but of width τ_k that is proportional to the intensity $f(kT)$.

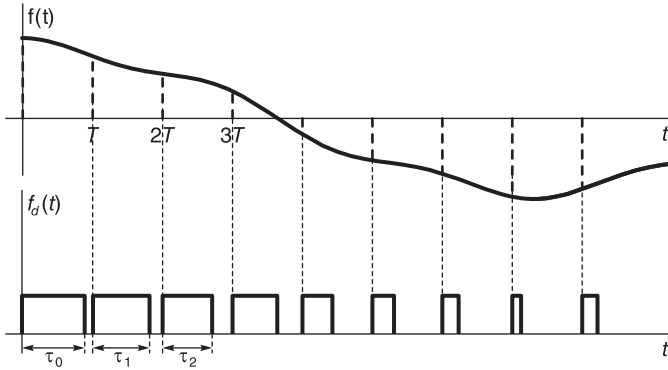


FIGURE 13.20 Pulse duration modulation.

As shown in Fig. 13.21 the modulation system may be modeled as consisting first of an ideal sampling step where the signal $f(t)$ is multiplied by the impulse train $\rho_T(t)$ producing the sampled signal

$$f_s(t) = f(t)\rho_T(t) = \sum_{k=-\infty}^{\infty} f(kT)\delta(t - kT). \tag{13.52}$$

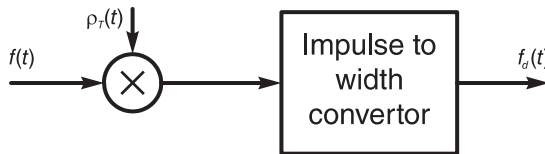


FIGURE 13.21 Model of pulse duration modulation generation.

The sampled signal $f_s(t)$ is then applied to an *impulse intensity to width converter* system which is described in Fig. 13.22.

As shown in the figure, an impulse of intensity A , representing any of the samples of $f_s(t)$ applied as the input $x(t)$ in the figure produces a rectangular pulse of unit height and of a width proportional to A . The output $y(t)$ thus has the form

$$y(t) = R_\tau(t) = u(t) - u(t - \tau) \tag{13.53}$$

where

$$\tau = C(1 + mA). \tag{13.54}$$

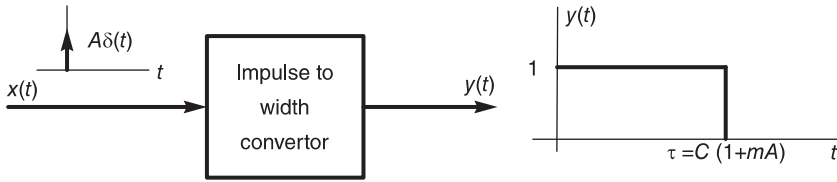


FIGURE 13.22 Impulse intensity to width conversion.

At the instant $t = kT$ the impulse intensity is $f(kT)$ as shown in Fig. 13.20 and the corresponding pulse has a width given by

$$\tau(k) = C[1 + m f(kT)]. \tag{13.55}$$

We note that the constant C is the pulse width at zero modulation, that is, with $f(kT) = 0$. The value m is so chosen that the pulse width is greater than zero and less than the sampling interval T .

13.5.3 Pulse Position Modulation

In pulse position modulation (PPM) represented schematically in Fig. 13.23, the position of a pulse is modulated in proportion to the function value at each sampling interval. The PPM function $f_p(t)$ may be viewed as obtained by first sampling the continuous-time signal $f(t)$ ideally with a sampling interval T . An impulse of intensity A then triggers a unit height constant width narrow pulse which is delayed by an amount given by

$$\tau = C(1 + m A). \tag{13.56}$$

Corresponding to sampling instant $t = kT$ the function value $f(kT)$ is thus used to adjust the pulse delay to

$$\tau(k) = C[1 + m f(kT)]. \tag{13.57}$$

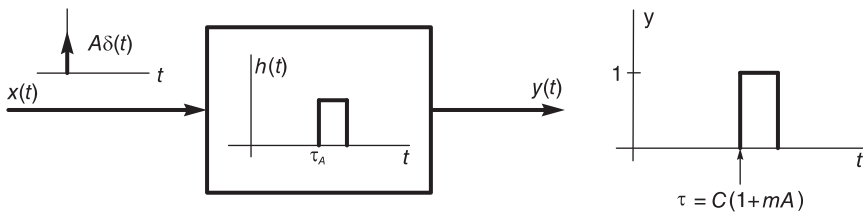


FIGURE 13.23 Pulse position modulation.

We can see the similarity with and slight difference from the PWM system.

13.6 PCM-TDM Systems

Time division multiplexing (TDM) may be used for the communication of a set of PCM signals. Assuming n signals $x_1(t), x_2(t), \dots, x_n(t)$, each signal is sampled and each sample is quantized to m bits, say $m = 8$, which are transmitted serially. The multiplexer accesses successively the n channels, so that each m -bit word that is the quantization of a signal sample is transmitted serially.

The system thus transmits one m -bit word after another, each corresponding to a channel, for a total of $m \times n$ bits in one scan of the multiplexer of the n channels, and the process repeated.

13.7 Frequency Division Multiplexing (FDM)

We have already seen that in pulse modulation time division multiplexing (TDM) samples of different signals are accessed sequentially in time, one sample from each signal at a time, and the cycle repeated. Within one cycle each signal is assigned a time-slot. Frequency division multiplexing (FDM) is a similar concept but where the roles of time and frequency are reversed.

In FDM the spectrum of each signal occupies a specified frequency slot of the overall spectrum through modulation by a distinct frequency. Given n data signals $x_1(t), x_2(t), \dots, x_n(t)$, each signal is modulated by its assigned “subcarrier” frequency. The set of signals is thus modulated by the set of subcarrier frequencies $f_{sc1}, f_{sc2}, \dots, f_{scn}$, as shown in Fig. 13.24.

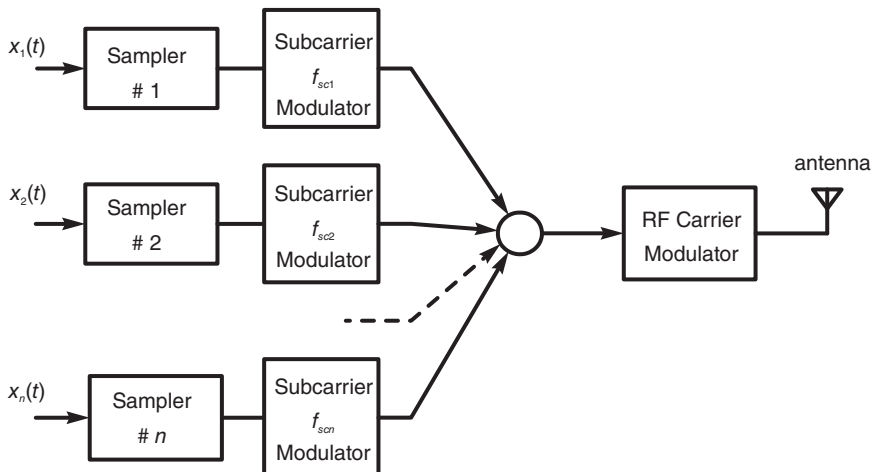


FIGURE 13.24 Modulation by a set of subcarrier frequencies.

The modulated signals thus generated are summed producing the composite signal of

multiplexed spectra. The overall spectrum of the composite signal at the adder output is shown in Fig.13.25.

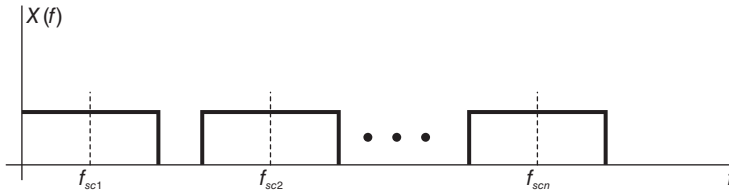


FIGURE 13.25 Composite signal spectrum.

The subcarrier frequencies are so chosen as to leave guard bands between the successive spectra. The composite signal is subsequently radio-transmitted after modulation by a higher frequency radio frequency (RF) carrier suitable for electromagnetic radiation.

At the receiver side shown in Fig. 13.26 the input signal is the RF signal is demodulated by the RF carrier frequency and the result is applied to a bank of bandpass (BP) filters.

The filters' outputs are applied, respectively, to detectors at the subcarrier frequencies $f_{sc1}, f_{sc2}, \dots, f_{scn}$ Hz to recover the original data signals.

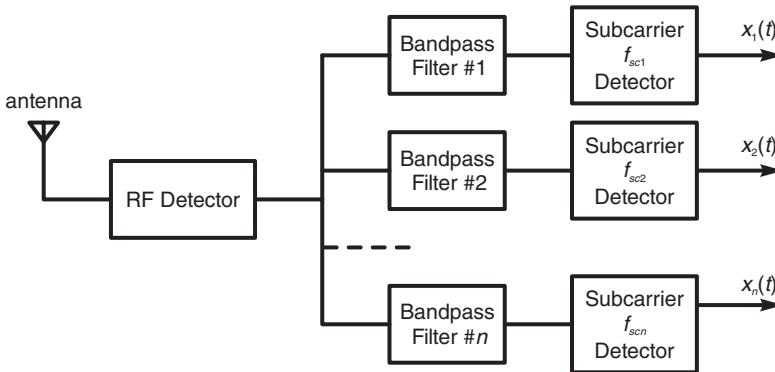


FIGURE 13.26 Demodulation by RF carrier frequency and a filter bank.

13.8 Problems

Problem 13.1 A signal $f(t)$, modulated by a carrier $\cos \omega_c t$, is transmitted. The modulated signal

$$g(t) = f(t) \cos \omega_c t$$

is captured by a receiver and is multiplied by $\cos \omega_c t$. Assuming that the Fourier transform $F(j\omega)$ of $f(t)$ can be approximated as

$$F(j\omega) = \begin{cases} 1, & -B/2 \leq \omega \leq B/2 \\ 2(1 - |\omega|/B), & B/2 \leq |\omega| \leq B \\ 0, & \text{elsewhere.} \end{cases}$$

a) Evaluate and sketch the spectra

$$G(j\omega) = \mathcal{F}[g(t)]$$

and

$$X(j\omega) = \mathcal{F}[x(t)]$$

where

$$x(t) = g(t) \cos \omega_c t.$$

b) Suggest a method of reconstructing the signal $f(t)$ from the signal $x(t)$. Justify your answer. Is there a lower limit of the carrier frequency ω_c for the reconstruction to be possible?

Problem 13.2 A signal $x(t)$ is limited in bandwidth to a frequency B r/s, having the Fourier spectrum

$$X(j\omega) = \begin{cases} 1, & |\omega| \leq B/2 \\ 2 - 2|\omega|/B, & B/2 \leq |\omega| \leq B \\ 0, & |\omega| > B. \end{cases}$$

This signal is modulated by the carrier $\cos \omega_c t$ with $\omega_c = B/2$.

Sketch the spectra $X(j\omega)$ of $x(t)$ and $Y(j\omega)$ at the modulator output.

Problem 13.3 A signal has the Fourier spectrum

$$X(j\omega) = \begin{cases} 1 - |\omega|/2, & |\omega| \leq 2 \\ 0, & |\omega| \geq 2 \end{cases}$$

is the input of an ideal lowpass filter of frequency response

$$H(j\omega) = \Pi_1(\omega) = u(\omega + 1) - u(\omega - 1).$$

- Sketch the frequency response of the filter output $y(t)$.
- The filter output $y(t)$ is modulated by the carrier $\cos t$. Sketch the frequency response of the modulator output $z(t)$.
- Evaluate the energies of the signals $x(t)$ and $z(t)$.

Problem 13.4 In a communication system, two band-limited signals $f_1(t)$ and $f_2(t)$ are modulated by the two carriers $\cos \omega_c t$ and $\sin \omega_c t$, respectively. The sum $g(t)$ of the two modulated signals is transmitted. At the receiver's end the same signal $g(t)$ is applied to the inputs of two separate multipliers where it is multiplied by $\cos \omega_c t$ and $\sin \omega_c t$, respectively. Show that, by filtering, the two signals $f_1(t)$ and $f_2(t)$ can be recovered. Sketch the spectra of the different signals to justify the answer, assuming two abstract but distinct band-limited spectra $F_1(j\omega)$ and $F_2(j\omega)$.

See Fig. 13.27

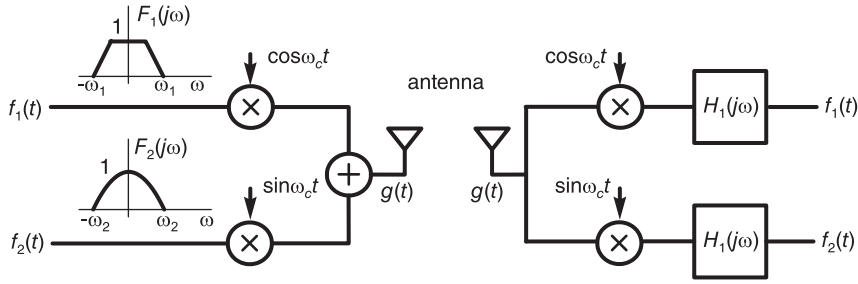


FIGURE 13.27 Communication system.

Problem 13.5 The receiver shown in Fig. 13.28 has as input the signal $s_0(t)$ and produces the output $s_3(t)$ where

$$s_0(t) = [1 + m(t)] \cos 2\pi f_c t$$

$$s_1(t) = s_0(t) \cos [2\pi(f_c + f_i)t]$$

$$s_3(t) = s_2(t) \cos 2\pi f_i t$$

with

$$m(t) = 0.5 \cos 2\pi f_1 t + 0.5 \cos 2\pi f_2 t$$

$$f_c = 10^3 \text{ kHz}, \quad f_i = 455 \text{ kHz}, \quad f_1 = 2 \text{ kHz}, \quad f_2 = 4 \text{ kHz}.$$

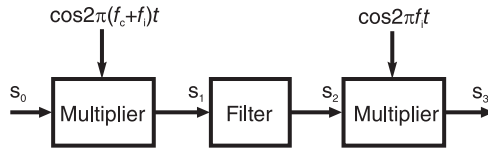


FIGURE 13.28 Component of a communication system.

Assuming the frequency response $H(j\omega)$ shown in Fig. 13.29, evaluate and sketch the spectra of the signal $s_0(t)$, $s_1(t)$, $s_2(t)$ and $s_3(t)$.

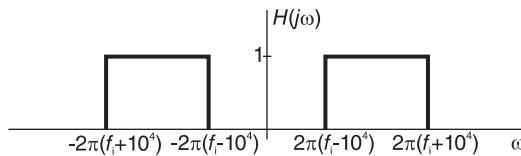


FIGURE 13.29 Ideal bandpass filter response.

Problem 13.6 Let

$$x(t) = \Pi_{\tau/2}(t) = u(t + \tau/2) - u(t - \tau/2)$$

$$y(t) = \sum_{n=-\infty}^{\infty} x(t - nT)$$

where $T > \tau$.

- Evaluate $Y(j\omega)$.
- Let $z(t) = y(t) \cos(2k\pi t/T)$, k integer. Evaluate $Z(j\omega)$.

Problem 13.7 In a communication system the input signal $x(t)$ is modulated by a carrier $\cos \omega_c t$. The result $v_1(t) = x(t) \cos \omega_c t$ is fed to a filter of frequency response $H(j\omega)$. The filter output $v_2(t)$ is modulated by a carrier $\sin \omega_c t$. The result is the signal $v_3(t)$. In a parallel path the same signal $x(t)$ is modulated by the carrier $\sin \omega_c t$ and the resulting signal $w_1(t) = x(t) \sin \omega_c t$ is fed to a filter of the same frequency response $H(j\omega)$. The filter output is modulated by the carrier $\cos \omega_c t$ producing the signal $w_3(t)$. The system output is $y(t) = w_3(t) - v_3(t)$. The filter frequency response $H(j\omega)$ is defined by

$$H(j\omega) = j \operatorname{sgn}(\omega).$$

Evaluate the Fourier transforms of the signals $v_1(t)$, $v_2(t)$, $v_3(t)$, $w_1(t)$, $w_2(t)$, $w_3(t)$ and $y(t)$ as functions of $X(j\omega)$, the transform of $x(t)$. Deduce the value of $y(t)$.

Problem 13.8 An impulse train $\rho_T(t) = \sum_{n=-\infty}^{\infty} \delta(t - nT)$ is modulated by a sinusoid $\sin \beta t$. The modulated impulse train $r(t) = \sin \beta t \rho_T(t)$ is used to sample a signal $x(t)$. The sampled signal $x_s(t) = x(t)r(t)$ is then filtered with the objective of producing a signal $y(t) = x(t) \sin(4\pi/T + \beta)t$. Assuming that the signal $x(t)$ is band-limited to the frequency range $-\beta < \omega < \beta$ and that $2\pi/T > 4\beta$, evaluate and sketch the Fourier transform $X_s(j\omega)$ of $x_s(t)$ and deduce the required filter frequency response $H(j\omega)$. Assume $X(j\omega)$ to be a triangle of base extending from $-\beta$ to β and of height equal to one.

Problem 13.9 A signal $v(t)$ is multiplied by the train of rectangular pulses

$$r(t) = \sum_{n=-\infty}^{\infty} r_0(t - n)$$

where

$$r_0(t) = \Pi_{0.1}(t).$$

The resulting signal $f(t) = v(t)r(t)$ is transmitted. The same signal $f(t)$ is received and fed to a filter by a receiver, the filter having a frequency response $H(j\omega)$ and output $y(t)$.

- Evaluate the Fourier transform $F(j\omega)$ of $f(t)$ as a function of $V(j\omega)$.
- Given that

$$V(j\omega) = (1 - \omega^2/B^2) \Pi_B(\omega)$$

sketch $R(j\omega)$ and $V(j\omega)$. What condition should be satisfied to avoid spectral aliasing and allow the receiver to reconstruct the original signal $v(t)$? Sketch $F(j\omega)$ for the critical condition after which aliasing would occur.

c) Assuming that the condition in part b) is satisfied, ensuring the absence of aliasing, specify the filter frequency response $H(j\omega)$ so that the filter output be given by

$$y(t) = v(t) \sin(4\pi t).$$

Problem 13.10 The signal

$$v(t) = B \text{Sa}(Bt/2)$$

is modulated by the carrier

$$x(t) = \cos Bt.$$

The result

$$v_1(t) = v(t)x(t)$$

is ideally sampled by the impulse train

$$\rho_T(t) = \sum_{n=-\infty}^{\infty} \delta(t - nT)$$

and the sampled signal

$$v_2(t) = v_1(t)\rho_T(t)$$

is fed to a filter of impulse response

$$h(t) = R_T(t) = u(t) - u(t - T).$$

- Plot $v(t)$, $x(t)$ and $v_1(t)$.
- Evaluate and sketch $V(j\omega)$, $V_1(j\omega)$ and $V_2(j\omega)$.
- What is the maximum value T_{\max} of T to avoid spectral aliasing?
- Let $T = 0.25T_{\max}$. Sketch the signals $v_2(t)$ and the filter output $y(t)$. Evaluate and sketch $V_2(j\omega)$ and $|Y(j\omega)|$.

Problem 13.11 In a sampling-communication system four signals $x_i(t)$, $i = 1, 2, 3, 4$, are each sampled by an ideal impulse train

$$\rho_T(t) = \sum_{n=-\infty}^{\infty} \delta(t - nT)$$

and the result $v_i(t)$ is fed to a filter of impulse response $h_i(t)$, $i = 1, 2, 3, 4$, respectively as shown in Fig. 13.30.

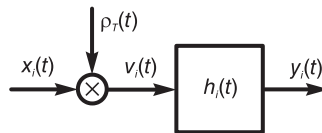


FIGURE 13.30 A sampling system.

The system output is the sum of the four filters outputs $y_i(t)$, $i = 1, 2, 3, 4$. Given that

$$R_T(t) \triangleq u(t) - u(t - T), \quad T = 1/80 \text{ sec}$$

$$h_1(t) = R_T(t), \quad h_2(t) = R_T(t - 0.025),$$

$$h_3(t) = R_T(t - 0.05), \quad h_4(t) = R_T(t - 0.075).$$

a) Sketch the system output $y(t) = \sum_{i=1}^4 y_i(t)$ for $0 \leq t < 0.6$, given that

$$x_1(t) = \cos(4\pi t), \quad x_2(t) = 3, \quad x_3(t) = 0, \quad x_4(t) = 2.$$

b) Explain in a few words the advantage of adopting this approach in the communication of a set of signals.

Problem 13.12 The two signals $v(t) = \sin(200\pi t)$ and $x(t) = \cos(250\pi t)$ are sampled by the two trains of rectangular pulses $p(t)$ and $p(t - 0.5 \times 10^{-3})$, respectively, where

$$p(t) = \sum_{n=-\infty}^{\infty} p_0(t - 10^{-3}n)$$

and

$$p_0(t) = \Pi_{5 \times 10^{-5}}(t).$$

The two thus sampled signals

$$v_s(t) = v(t)p(t) \quad \text{and} \quad x_s(t) = x(t)p(t - 0.5 \times 10^{-3})$$

are added together and the result $y(t)$ are transmitted along a communication channel.

a) Sketch the sampled signal $v_s(t)$ and $x_s(t)$ and the signal $y(t)$.

b) This same system is used to transmit two signals $v(t)$ and $x(t)$ of finite frequency bands extending from 0 to 550 Hz and 300 Hz, respectively. The sum $y(t)$ of the two sampled signals $v_s(t)$ and $x_s(t)$ is transmitted. At the receiving end a demultiplexer is used to separate the two sampled signals.

To reconstruct the original signals $v(t)$ and $x(t)$ the two sampled signals are applied to two lowpass filters of frequency responses $H_1(j\omega)$ and $H_2(j\omega)$, respectively. Specify $H_1(j\omega)$ and $H_2(j\omega)$ if such reconstruction is possible. If not, state the reason.

Problem 13.13 As shown in Fig. 13.31(a), a signal $x(t)$ is modulated by a carrier of frequency $\omega_c = 6000\pi$. The result $y(t)$ is applied to the input of an ideal lowpass filter of frequency response $H(j\omega) = \Pi_{6000\pi}(\omega)$. The filter output $z(t)$ is transmitted. As shown in Fig. 13.31(b), the same signal $z(t)$ arrives at the receiver, is modulated by a carrier of the same frequency ω_c and applied to an ideal lowpass filter of same frequency response and output $v(t)$. Assuming the signal $x(t)$ is a sinusoid of frequency f_0 Hz where $300 < f_0 < 3400$, sketch the spectra $X(j\omega)$, $Y(j\omega)$, $Z(j\omega)$, $W(j\omega)$ and $V(j\omega)$ of $x(t)$, $y(t)$, $z(t)$, $w(t)$ and $v(t)$ respectively. Deduce whether or not the form and frequency of the final output $v(t)$ are the same as those of $x(t)$.

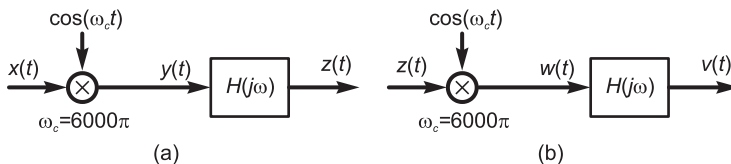


FIGURE 13.31 A communication system.

Problem 13.14 The Fourier transforms of two band-limited signals $f_1(t)$ and $f_2(t)$ may be approximated as the two abstract forms

$$F_1(j\omega) = \Pi_{\omega_1}(\omega) \quad \text{and} \quad F_2(j\omega) = 2(1 - \omega^2/\omega_2^2) \Pi_{\omega_2}(\omega),$$

where ω_1 is greater than ω_2 .

The two signals are modulated by the carriers $\cos\omega_c t$ and $\sin\omega_c t$, respectively. The sum $g(t)$ of the modulated signals is transmitted. At the receiver the same signal

$$g(t) = f_1 \cos\omega_c t + f_2 \sin\omega_c t$$

is received and modulated by the same two carriers. The results

$$y_1(t) = g(t) \cos\omega_c t \quad \text{and} \quad y_2(t) = g(t) \sin\omega_c t$$

are applied to the inputs of two filters of frequency responses $H_1(j\omega)$ and $H_2(j\omega)$, in order to reconstruct the two original signals $f_1(t)$ and $f_2(t)$, respectively.

a) Evaluate $G(j\omega) = \mathcal{F}[g(t)]$, expressed as a function of $F_1(j\omega)$ and $F_2(j\omega)$. Sketch $G(j\omega)$.

b) Evaluate $Y_1(j\omega)$ and $Y_2(j\omega)$, expressed as functions of $F_1(j\omega)$ and $F_2(j\omega)$. Sketch $Y_1(j\omega)$ and $Y_2(j\omega)$.

c) Deduce the frequency responses $H_1(j\omega)$ and $H_2(j\omega)$ needed to reconstruct $f_1(t)$ and $f_2(t)$.

Problem 13.15 The system shown in Fig. 13.32(a) is used for transmitting a stereo audio signal composed of a left signal $x_l(t)$ and a right one $x_r(t)$, limited in frequency to 15 kHz. The stereo coder and decoder are shown in Fig. 13.32(b) and (c), respectively. The following observations were made during a system verification:

The decoder input signal is assumed to be the same as the coder output signal $v(t)$.

The frequency divider of the coder (box marked 'f ÷ 2') is ideal, producing no phase shift, such that an input $\sin(2\pi f_0 t)$ produces an output $\sin(\pi f_0 t)$.

The frequency multiplier (box 'f × 2') produces a phase shift of $\pi/4$ radian such that if the multiplier input signal is $\sin(\pi f_0 t)$ its output is $\sin(2\pi f_0 t - \pi/4)$.

a) Evaluating the decoder outputs $y_l(t)$ and $y_r(t)$ in terms of the coder inputs $x_l(t)$ and $x_r(t)$ deduce the effect of the phase distortion observed at the multiplier output. To this end express the 38 kHz coder sinusoid in the form $\sin(2\pi f_0 t)$, where $f_0 = 38 \times 10^3$.

b) Would it be possible to eliminate the effect of phase distortion by reducing the gain of one of the two decoder's lowpass filters? If yes, state which filter and the required gain; otherwise show why not?

Problem 13.16 The AM modulator shown in Fig 13.33 has weighting coefficients A_1, A_2, A_3, A_4 . It receives the signal $m(t)$ and the carrier $p(t) = \cos(2\pi f_c t)$. The signal $m(t)$ which has a zero average value is band-limited to a frequency f_m , which is much smaller than the carrier frequency f_c .

a) Evaluate the output signal $y_{AM}(t)$ as a function of $m(t)$, f_c , A_1, A_2, A_3 et A_4 .

b) Given that in the output signal the "useful" term that carries the information about the input signal $m(t)$ is that which is proportional to $m(t) \cos(2\pi f_c t)$ evaluate the quality factor of the modulator, defined as $\eta = pu/pt$, where $pu =$ power of the useful component and $pv =$ power of the useful component/total power. Simplify the expression, eliminating any terms that have no influence on the value of η .

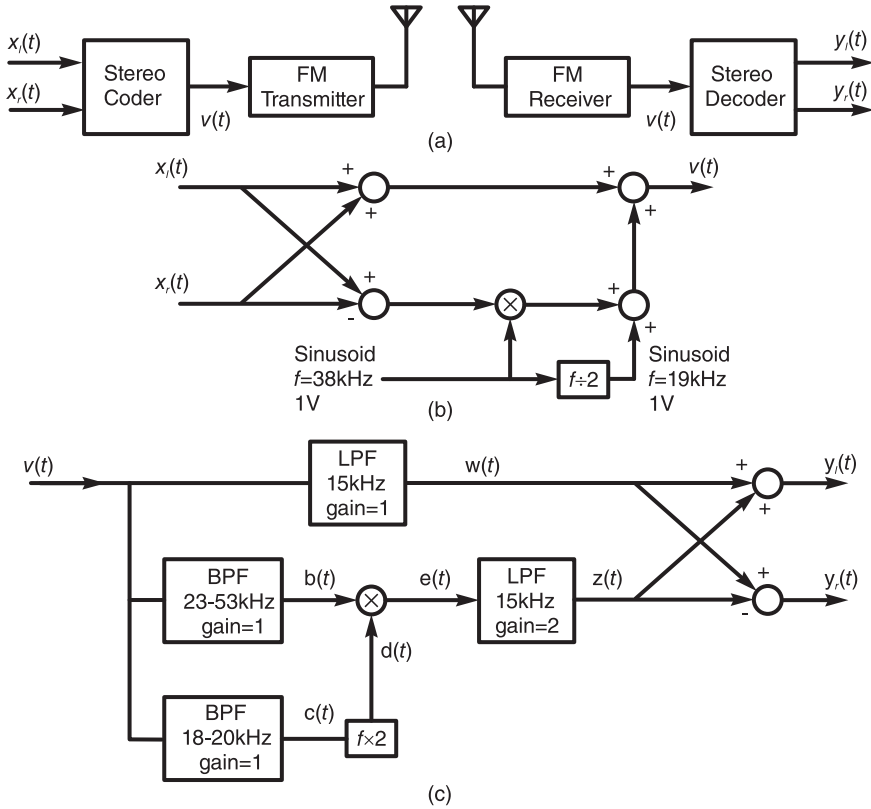


FIGURE 13.32 (a) A stereo signal communication system, (b) coder, (c) decoder.

Problem 13.17 To effect amplitude modulation it is proposed to employ a nonlinear system which generates intermodulation and harmonic distortion.

The message $m(t)$ is band-limited to a frequency of 7 kHz. It has a zero average d-c value and an average power of 2 watts.

Assuming that the output of the nonlinear system shown in Fig. 13.34 is related to its input $x(t)$ by the equation $y(t) = x(t) + 0.2x^2(t)$ deduce the needed linear system S_1 shown in the figure so that a signal $z(t)$ that is an amplitude modulation of $m(t)$ with an average power of 50 watts may be obtained.

Problem 13.18 Two alternative schemes using nonlinearity, shown in Fig. 13.35(a-b), are proposed for demodulating the signal

$$w(t) = m(t) \cos(2\pi f_c t).$$

Assuming that $\overline{m(t)} = 0$ volt, $\overline{m^2(t)} = 0.2$ Watt, $|m(t)|_{MAX} = 1.2$ volts. The Fourier transform as a function of the frequency f of $m(t)$ is such that $M(f) = 0$ for $|f| < 50$ Hz and $|f| > 15 \times 10^3$ Hz (15 kHz). The nonlinear systems are identical. A nonlinear system receiving an input $x(t)$ would produce the output $v(t) = x(t) + 0.2x^2(t)$.

The modulating carrier frequency is $f_c = 20 \times 10^6$ Hz (20 MHz). Verify for both proposed systems if demodulation is properly effected. Justify your conclusion and specify the frequency response of the lowpass filter which should produce the demodulated signal $m(t)$. If you conclude that demodulation is not properly achieved, explain why.

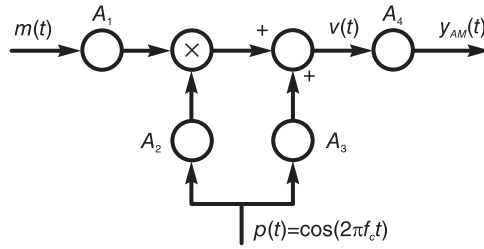


FIGURE 13.33 AM modulator with weighting coefficients.

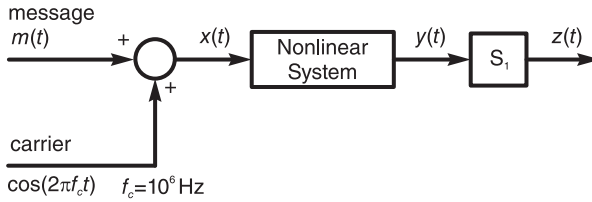


FIGURE 13.34 Proposed modulation using a nonlinear system.

Problem 13.19 You are required to generate a sinusoidal signal of a frequency that varies linearly in time from 1 kHz to 10 kHz in the time interval $t = 0$ to $t = 5$ seconds. The signal should be produced using a frequency modulator, Fig. 13.36, which has the properties

- i) Average output power 12.5 Watt.
- ii) Frequency of the unmodulated carrier 5 kHz.
- a) For $0 \leq t \leq 5$, specify $m(t)$, the signal that needs be applied to the FM modulator.
- b) Evaluate $y(t)$, the signal produced by the FM modulator.

Problem 13.20 The output of an FM modulator denoted $y_{FM}(t)$ is given by

$$y_{FM}(t) = A_c \cos \left(2\pi f_c t + 2\pi k_f \int m(t) dt \right)$$

where $A_c = 7.5$, $f_c = 100$ MHz, $k_f = 17 \times 10^3$ Hz/volt, and $m(t)$ is a sinusoid of amplitude 5 volts and frequency 10 kHz.

Determine the bandwidth of the signal $y_{FM}(t)$ as the width of the signal spectrum after eliminating the components that are below 40 dB relative to the unmodulated carrier.

Problem 13.21 A signal $m(t)$, limited in frequency to 10 kHz, is transmitted as shown in Fig. 13.37.

In the receiver, at the output of the bandpass filter the signal $y(t - t_0)$ is observed, where t_0 is the propagation delay between the transmitter and receiver antennas. The delay may be evaluated by noticing that the distance between them is 7162 m and that wave propagation speed is 3×10^8 m/s. It is noted that the demodulation carrier is out of phase by an angle θ relative to the modulation carrier. The receiver's lowpass filter has a gain of 2 and a cut-off frequency of 10 kHz.

- a) Express the signal $x(t)$ as a function of $m(t)$ and θ (all other parameters have to be evaluated).
- b) In one transmission it is noted that $x(t) \approx 0$. It is proposed to displace the receiver closer or farther away from the transmitter in order to maximize the receiver output signal power. Evaluate the required displacement (within 5 m if possible).

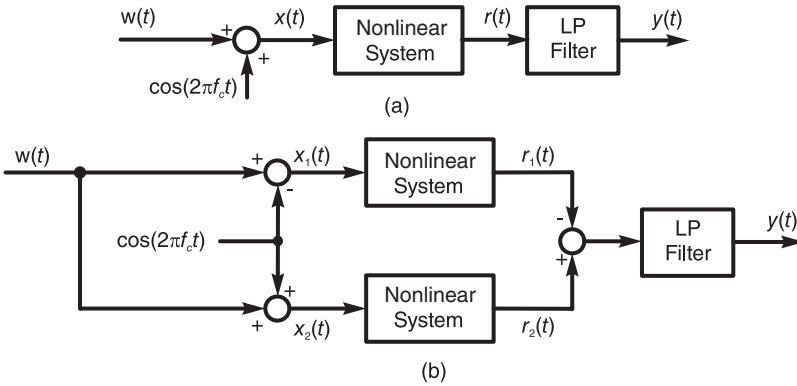


FIGURE 13.35 Two proposed modulation systems.



FIGURE 13.36 An FM modulator.

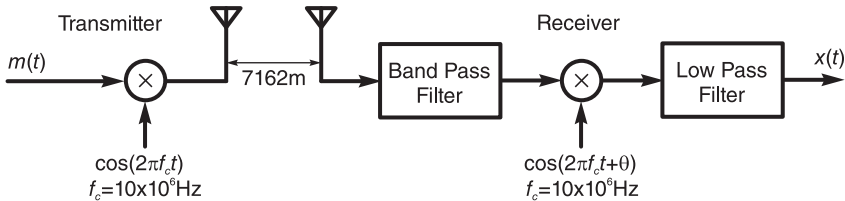


FIGURE 13.37 A communication system.

Problem 13.22 A signal $x(t)$ limited in frequency to 4 MHz should be transmitted by linear modulation over a communication channel wherein a frequency band of 90 MHz (20 MHz to 110 MHz) is assigned to it and no signal trace is allowed outside this frequency band. The modulator is represented in Fig. 13.38.

Specify the allowable values f_0 for the case:

- a) $p(t) = 2 \sin(2\pi f_0 t + \pi/8)$.
- b) $p(t) = 4 \sin(2\pi f_0 t + 3\pi/4) + 3 \sin(6\pi f_0 t - 11\pi/16)$.
- c) $p(t)$ is a periodic triangular signal of frequency f_0 and amplitude 5 volts.

Problem 13.23 The system shown in Fig. 13.39 is used to produce a modulated signal of which the carrier frequency can be fixed by setting the filter's pass-band central frequency to the required value.

The properties of the message $m(t)$ are $\overline{m(t)} = 0$ volt, $\overline{m^2(t)} = 2$ Watt, $|m(t)|_{max} = 5$ volts. $M(f) = 0$ for $|f| > 7.5 \times 10^3$ Hz.

For each of the five possible frequency responses of the bandpass filter evaluate the maximum amplitude of the modulated signal $y(t)$.

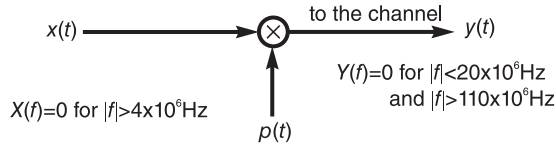


FIGURE 13.38 Modulator.

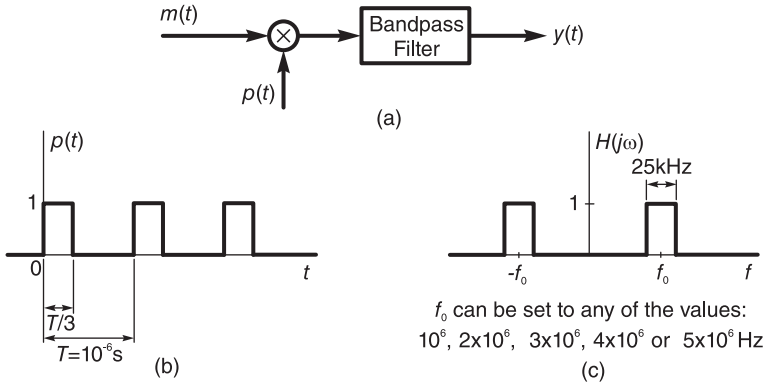


FIGURE 13.39 An AM modulator with weighting coefficients.

13.9 Answers to Selected Problems

Problem 13.1 See Fig. 13.40.

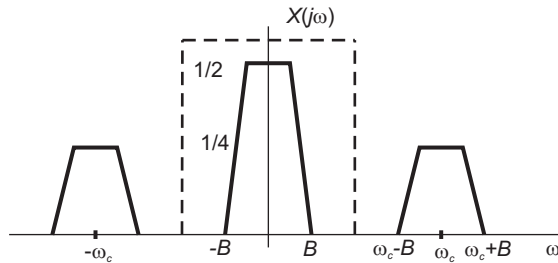


FIGURE 13.40 Figure for Problem 13.1

Problem 13.2 See Fig. 13.41.

Problem 13.3 See Fig. 13.42.

c) For $0 < \omega < 2$, $X(j\omega) = -\frac{1}{2}(\omega - 2)$.

$E_1 = \frac{1}{2\pi} 2 \int_0^2 \frac{1}{4}(\omega - 2)^2 d\omega = \frac{2}{3\pi}$. The energy at the output $z(t)$ is $E_2 = 7/(24\pi)$.

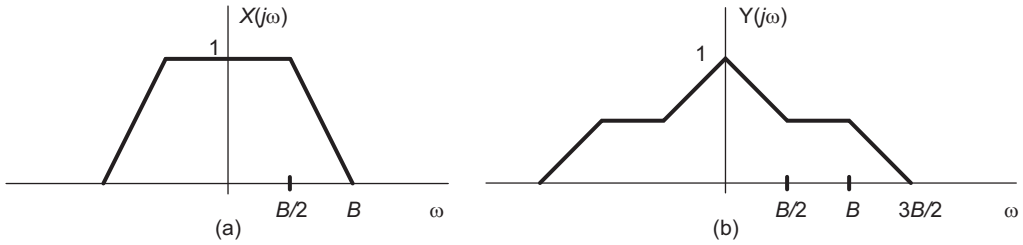


FIGURE 13.41 Figure for Problem 13.2

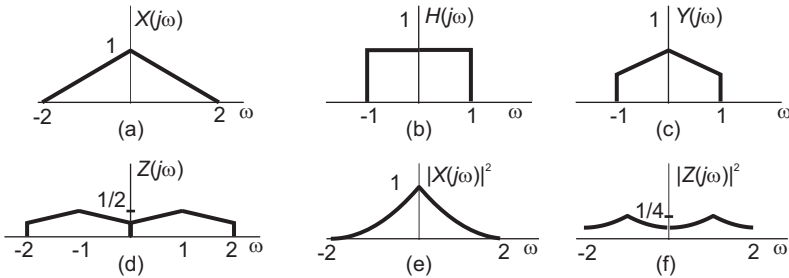


FIGURE 13.42 Figure for Problem 13.3

Problem 13.6

$$Z_n = (0.5\tau/T) \{Sa [(n - K) \pi\tau/T] + Sa [(n + K) \pi\tau/T]\}$$

$$Z(j\omega) = 2\pi \sum_{n=-\infty}^{\infty} Z_n \delta(\omega - 2n\pi/T).$$

Problem 13.9 b) See Fig. 13.43.

Problem 13.11 See Fig. 13.44.

Problem 13.12

$v(t)$ cannot be constructed without distortion. For $x(t)$, reconstruction is possible. One choice is $H_3(j\omega) = \Pi_{1000\pi}(\omega)$. See Fig. 13.45.

Problem 13.13

See Fig. 13.46 and Fig. 13.47. The first figure shows the spectra $X(j\omega)$, $Y(j\omega)$, $Z(j\omega)$, $W(j\omega)$ and $V(j\omega)$ for the case $2\pi \times 300 < \omega_0 < 2\pi \times 3000$. The second figure shows the same spectra for the case $2\pi \times 3000 < \omega_0 < 2\pi \times 3400$. $y(t)$ is a sinusoid of frequency $6000\pi - \omega_0$; $z(t)$ is the same as $y(t)$. $w(t)$ is a sinusoid of frequency ω_0 and $v(t)$ is the same as $w(t)$. In the second case, shown in the second figure, the frequency of $y(t)$ is $\omega_0 - 6000\pi$. The frequency of $z(t)$ is the same. The frequency of $w(t)$ is $12000\pi - \omega_0$ and that of $v(t)$ is the same as that of $w(t)$.

Problem 13.14 See Fig. 13.48.

- a) $G(j\omega) = 0.5 \{F_1 [j(\omega - \omega_c)] + F_1 [j(\omega + \omega_c)]\} - (j/2) \{F_2 [j(\omega - \omega_c)] - F_2 [j(\omega + \omega_c)]\}$. See Fig. 13.49.
- b) See Fig. 13.50.
- c) $H_1(j\omega)$ and $H_2(j\omega)$ are ideal lowpass filters with cut-off frequencies B_1 and B_2 rad/sec, respectively where $\omega_1 < B_1 < 2\omega_c - \omega_1$ and $\omega_2 < B_2 < 2\omega_c - \omega_1$.

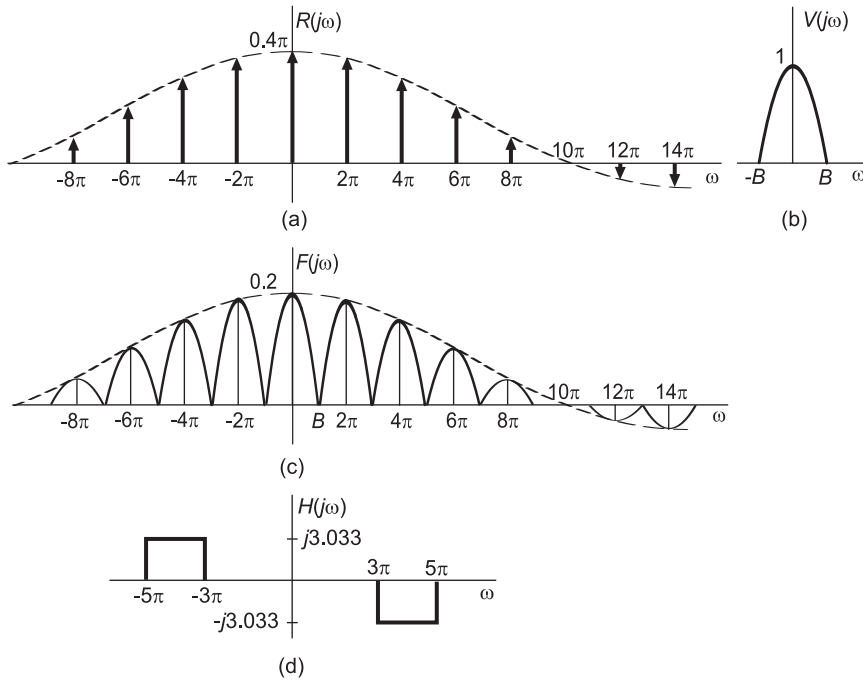


FIGURE 13.43 Figure for Problem 13.9

Problem 13.15

- a) $y_r(t) = x_l(t) [1 - \cos(\pi/4)] + x_r(t) [1 + \cos(\pi/4)]$ Complete signal separation not achieved.
- b) Complete separation.

Problem 13.16

- a) $y_{AM}(t) = A_3 A_4 \cos(2\pi f_c t) + A_1 A_2 A_4 m(t) \cos(2\pi f_c t)$ b)

$$\eta = \frac{A_1^2 A_2^2 \overline{m^2(t)}}{A_3^2 + A_1^2 A_2^2 \overline{m^2(t)}}$$

Problem 13.17

Pass-band width 14 kHz central frequency 1 MHz, gain 8.7.

Problem 13.18

For first system:

$$v(t) = [m(t) + 1] \cos(2\pi f_p t) + 0.1 [m(t) + 1]^2 + 0.1 [m(t) + 1]^2 \cos(4\pi f_p t)$$

The only low frequency term is $0.1 [m(t) + 1]^2$, and is not proportional to $m(t)$. Modulation is thus not correctly obtained.

For the second system:

$$v_3(t) = 0.4m(t)$$

Demodulation is achieved. The lowpass filter should have a gain of 2.5 and a cut-off frequency of 15 kHz.

Problem 13.19

- a) Instantaneous frequency of the FM signal: $f_i(t) = 5000 + 800m(t)$. To obtain the relation $f_i(t) = 1000 + 1800t$ for $0 \leq t \leq 5$, we should set $m(t) = 2.25t - 5$, for $0 \leq t \leq 5$

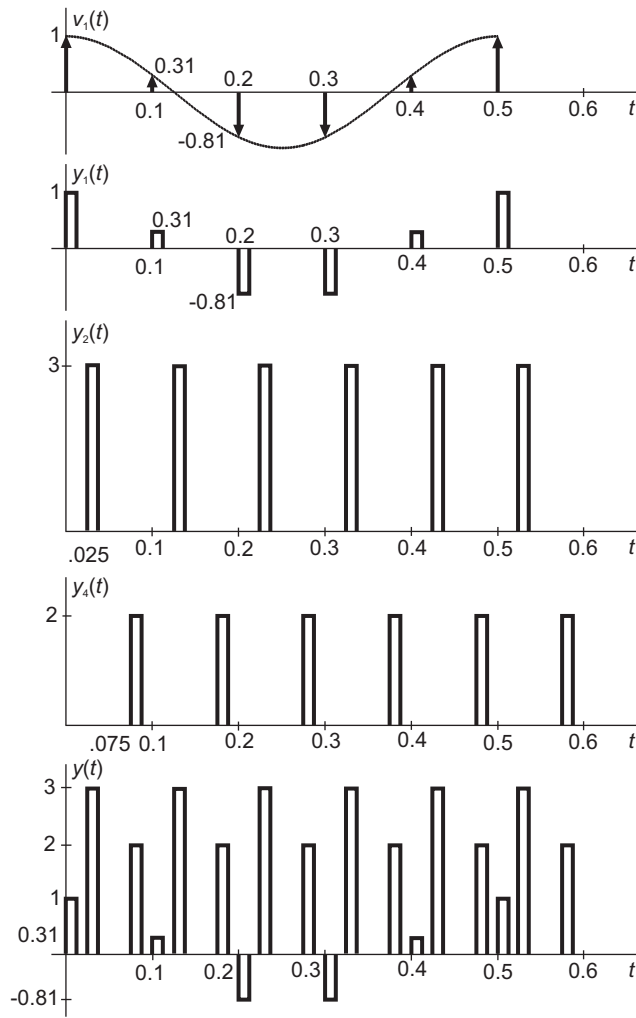


FIGURE 13.44 Figure for Problem 13.11.

b) $y(t) = A_p \cos(2\pi \int [1000 + 1800t] dt)$, where $A_p^2/2 = 12.5$

$$y(t) = 5 \cos(2000\pi t + 1800\pi t^2)$$

Problem 13.20

The bandwidth of the signal $y_{FM}(t)$ is $B = 240$ kHz.

Problem 13.21

a) Bandpass filter output

$$x(t) = m(t - 23.873 \times 10^{-6}) \cos(3000 + \theta)$$

b) Maximum receiver power obtained if the receiver is displaced by the distance 3.75 m farther from, or closer to, the transmitter.

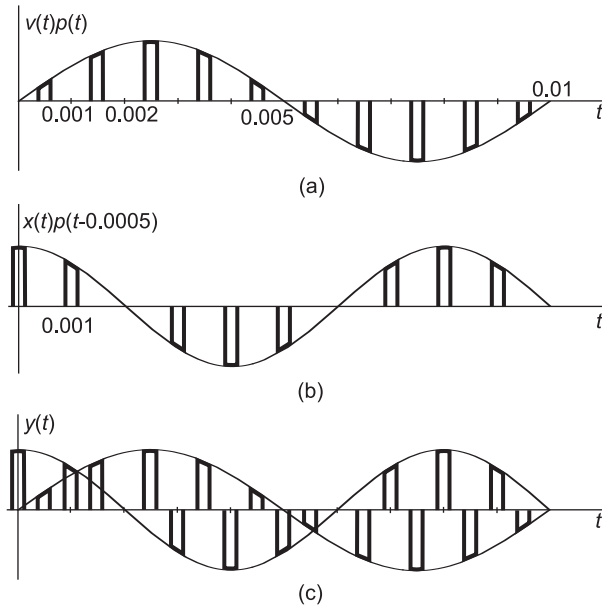


FIGURE 13.45 Figure for Problem 13.12.

Problem 13.22

- a) $24 \times 10^6 \leq f_0 \leq 106 \times 10^6$
- b) $24 \times 10^6 \leq f_0 \leq 35.3 \times 10^6$
- c) No solution exists

Problem 13.23

$$|y(t)|_{\max} = \begin{cases} |(2/3) \text{Sa}(\pi/3)| \times 5 = 2.76 & , \text{ if } f_0 = 10^6 \text{ Hz} \\ |(2/3) \text{Sa}(2\pi/3)| \times 5 = 1.38 & , \text{ if } f_0 = 2 \times 10^6 \text{ Hz} \\ 0 & , \text{ if } f_0 = 3 \times 10^6 \text{ Hz} \\ |(2/3) \text{Sa}(4\pi/3)| \times 5 = 0.689 & , \text{ if } f_0 = 4 \times 10^6 \text{ Hz} \\ |(2/3) \text{Sa}(5\pi/3)| \times 5 = 0.551 & , \text{ if } f_0 = 5 \times 10^6 \text{ Hz} \end{cases}$$

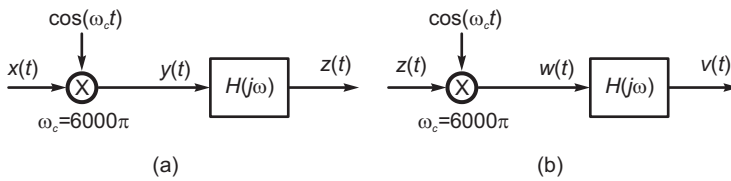


FIGURE 13.46 Figure for Problem 13.13.

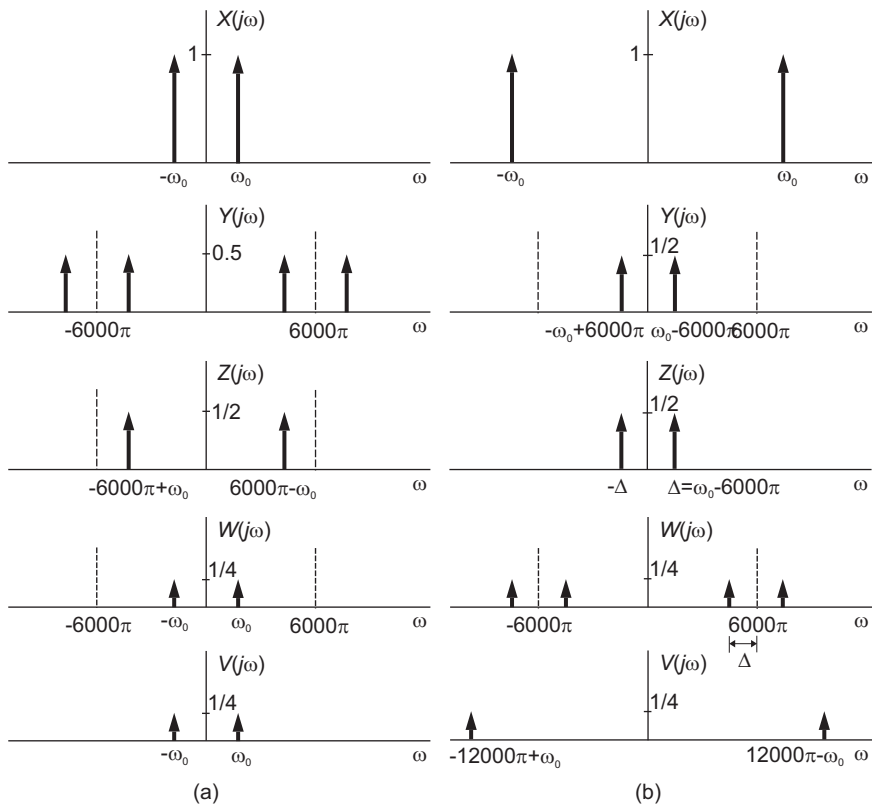


FIGURE 13.47 Figure for Problem 13.13.

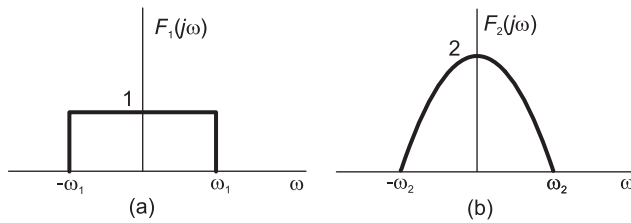


FIGURE 13.48 Figure for Problem 13.14.

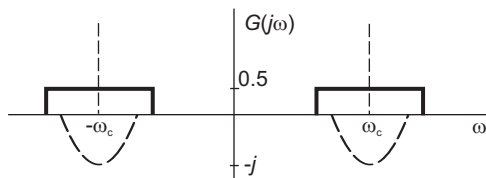


FIGURE 13.49 Figure for Problem 13.14

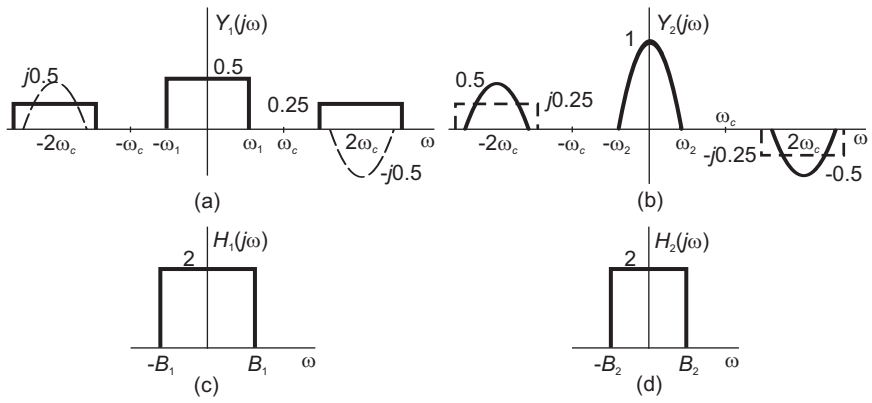


FIGURE 13.50 Figure for Problem 13.14 b)

In this chapter we study Fourier-, Laplace- and z -related transforms, and in particular Walsh, Hilbert, Hartley, Mellin and Hankel transforms.

14.1 Walsh Transform

In what follows, we study the Walsh–Hadamard and generalized Walsh transforms. We start by learning about Walsh functions and related nonsinusoidal orthogonal functions. Subsequently, we focus our attention on the discrete-time domain Walsh transforms.

14.2 Rademacher and Haar Functions

Rademacher functions, introduced in 1922, are an incomplete set of orthogonal functions. The Rademacher function of index m , denoted $rad(m, t)$, is a train of rectangular pulses with 2^{m-1} cycles in the half-open interval $[0, 1)$, alternating between the values $+1$ and -1 . The zero-index function $rad(0, t)$ is a constant of 1 on the same interval as can be seen in Fig. 14.1(a). Outside this interval the Rademacher functions repeat periodically so that

$$rad(m, t) = rad(m, t + 1) \tag{14.1}$$

They can be generated recursively using the relations

$$rad(m, t) = rad(1, 2^{m-1}t)$$

$$rad(1, t) = \begin{cases} 1 & , 0 \leq t < 1/2 \\ -1 & , 1/2 \leq t < 1 \end{cases}$$

Haar functions date back to 1912. Denoted $har(n, m, t)$ they are a periodic and complete set of orthonormal functions. A set of N Haar functions can be generated recursively using the following relations, which apply for $0 \leq t < 1$ and with $N = 2^n$,

$$har(r, m, t) = \begin{cases} 2^{r/2} & , (m - 1)/2^r \leq t < (m - 1/2)/2^r \\ -2^{r/2} & , (m - 1/2)/2^r \leq t < m/2^r \\ 0 & , \text{otherwise} \end{cases}$$

$$har(0, 0, t) = 1,$$

where $0 \leq r < n$ and $1 \leq m \leq 2^r$, as can be seen in as can be seen in Fig. 14.1(b) where $N = 8$. A Haar transform matrix denoted $H^*(n)$ may be constructed by sampling the

successive Haar functions. For example sampling the functions shown in the figure produces the Haar transform matrix.

$$H^*(3) = \begin{bmatrix} 1 & 1 & 1 & 1 & 1 & 1 & 1 & 1 \\ 1 & 1 & 1 & 1 & -1 & -1 & -1 & -1 \\ \sqrt{2} & \sqrt{2} & -\sqrt{2} & -\sqrt{2} & 0 & 0 & 0 & 0 \\ 0 & 0 & 0 & 0 & \sqrt{2} & \sqrt{2} & -\sqrt{2} & -\sqrt{2} \\ 2 & -2 & 0 & 0 & 0 & 0 & 0 & 0 \\ 0 & 0 & 2 & -2 & 0 & 0 & 0 & 0 \\ 0 & 0 & 0 & 0 & 2 & -2 & 0 & 0 \\ 0 & 0 & 0 & 0 & 0 & 0 & 2 & -2 \end{bmatrix}$$

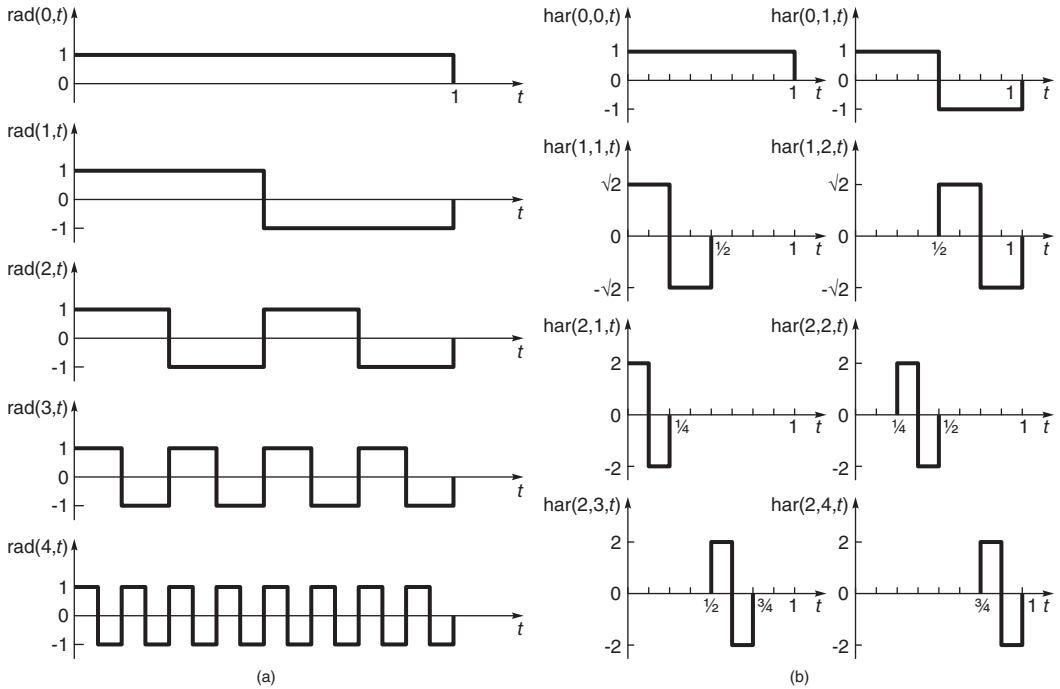


FIGURE 14.1 Orthonormal functions, (a) Rademacher, (b) Haar functions.

14.3 Walsh Functions

The incomplete set of Rademacher functions was completed by J.L. Walsh in 1923. There are three types of ordering of Walsh functions, namely, the *natural* or *Hadamard* ordering, the *dyadic* or *Paley* ordering, and the *sequency* or *Walsh* ordering. We may view each of these orderings by either plotting their forms or, equivalently, by writing the value of their transform matrix which is but a sampling of the waveforms. As an illustration, the $N = 8$

natural ordering Walsh functions are shown in Fig. 14.2(c). Sampling of these waveforms produces the natural-order Hadamard transform matrix.

The name *sequency* is the corresponding term to the word *frequency* used in the Fourier sinusoidal functions domain. Sequency is the number of zero crossings of a waveform. It therefore increases with the number of times that the waveform alternates in sign.

$$H_{8,nat} = \begin{bmatrix} 1 & 1 & 1 & 1 & 1 & 1 & 1 & 1 \\ 1 & -1 & 1 & -1 & 1 & -1 & 1 & -1 \\ 1 & 1 & -1 & -1 & 1 & 1 & -1 & -1 \\ 1 & -1 & -1 & 1 & 1 & -1 & -1 & 1 \\ 1 & 1 & 1 & 1 & -1 & -1 & -1 & -1 \\ 1 & -1 & 1 & -1 & -1 & 1 & -1 & 1 \\ 1 & 1 & -1 & -1 & -1 & -1 & 1 & 1 \\ 1 & -1 & -1 & 1 & -1 & 1 & 1 & -1 \end{bmatrix}$$

14.4 The Walsh (Sequency) Order

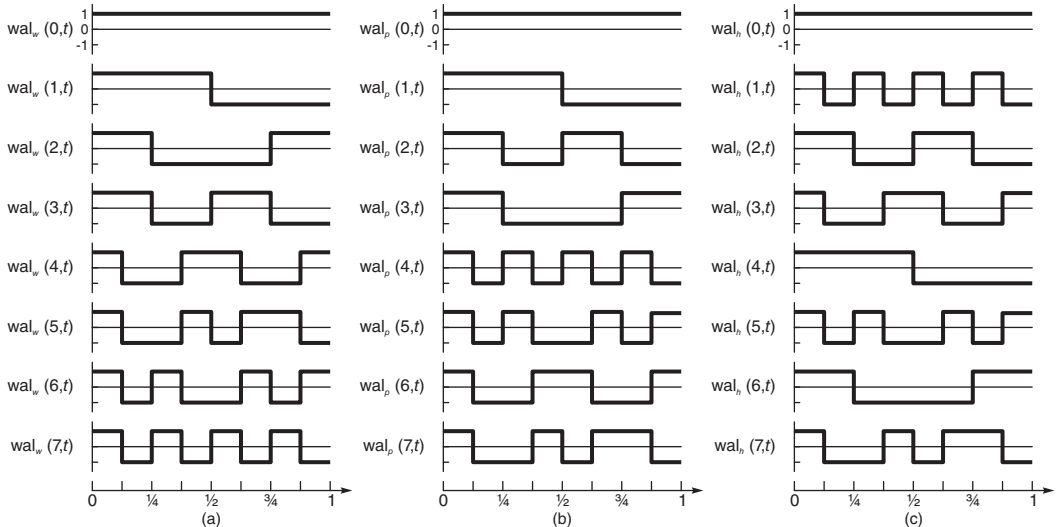


FIGURE 14.2 Walsh–Hadamard functions in (a) Sequency, (b) Paley, (c) Natural orders.

The sequency-ordered (Walsh-ordered) Walsh functions $wal_w(i, t)$ appear as in Fig. 14.2(a) for $N = 8$. We may refer to this set for short as the set S_w where the subscript stands for Walsh-ordered. We write

$$S_w = \{wal_w(i, t), i = 0, 1, \dots, N - 1\} \tag{14.2}$$

where $N = 2^n$, n integer ≥ 1 . The sequency s_i of the waveform $wal_w(i, t)$ is given simply by $s_i = i$. Corresponding to the cos and sin functions we have *cal* and *sal* functions defined

by

$$\begin{aligned} cal(s_i, t) &= wal_w(i, t), i \text{ even} \\ sal(s_i, t) &= wal_w(i, t), i \text{ odd} \end{aligned}$$

14.5 Dyadic (Paley) Order

The dyadic (Paley) ordered Walsh functions $wal_p(i, t)$ appear as in Fig. 14.2(b). We may refer to them as

$$S_p = \{wal_p(i, t), i = 0, 1, \dots, N - 1\} \quad (14.3)$$

The set of Paley-ordered functions are related to the Walsh-ordered ones by the equation

$$wal_p(i, t) = wal_w[b(i), t] \quad (14.4)$$

where $b(i)$ represents the Gray code to binary conversion of i . For $N = 8$, for example, with $i = 0, 1, 2, \dots, 7$ the binary representation being

$$\{000, 001, 010, 011, 100, 101, 110, 111\}, \quad (14.5)$$

the Gray code

$$b(i) = \{000, 001, 011, 010, 111, 110, 100, 101\} \quad (14.6)$$

so that

$$\begin{aligned} wal_p(0, t) &= wal_w(0, t); wal_p(1, t) = wal_w(1, t); \\ wal_p(2, t) &= wal_w(3, t); wal_p(3, t) = wal_w(2, t); \\ wal_p(4, t) &= wal_w(7, t); wal_p(5, t) = wal_w(6, t); \\ wal_p(6, t) &= wal_w(4, t); wal_p(7, t) = wal_w(5, t). \end{aligned}$$

14.6 Natural (Hadamard) Order

The natural (Hadamard) ordered Walsh functions $wal_h(i, t)$ appear as in Fig. 14.2(c). We may refer to them as

$$S_h = \{wal_h(i, t), i = 0, 1, \dots, N - 1\} \quad (14.7)$$

They are related to the Walsh (sequency)-ordered functions by the equation

$$wal_h(i, t) = wal_w[b(\langle i \rangle), t] \quad (14.8)$$

where $\langle i \rangle$ stands for the bit-reversed representation of i and $b(\langle i \rangle)$ is the Gray code to binary conversion of $\langle i \rangle$. For example, for $i = 0, 1, \dots, 7$ we have

$$\langle i \rangle = \{000, 100, 010, 110, 001, 101, 011, 111\} \quad (14.9)$$

and

$$b(\langle i \rangle) = \{000, 111, 011, 100, 001, 110, 010, 101\} \tag{14.10}$$

i.e., in decimal the order is $\{0, 7, 3, 4, 1, 6, 2, 5\}$, so that

$$\begin{aligned} wal_h(0, t) &= wal_w(0, t); wal_h(1, t) = wal_w(7, t); \\ wal_h(2, t) &= wal_w(3, t); wal_h(3, t) = wal_w(4, t); \\ wal_h(4, t) &= wal_w(1, t); wal_h(5, t) = wal_w(6, t); \\ wal_h(6, t) &= wal_w(2, t); wal_h(7, t) = wal_w(5, t). \end{aligned}$$

The Gray code is a reflective binary code wherein two successive values differ in only one bit. The 3-bit Gray code for example has the successive values shown in Fig. 14.3.

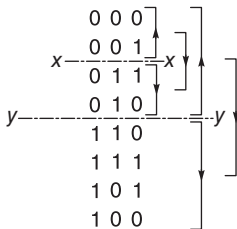


FIGURE 14.3 Gray code showing reflective structure.

Note the reflection of the upper code each time a 1 is added to the left, as seen in crossing the axes $x - - - x$ and $y - - - y$ in the figure. The Gray code is used in labeling the axes of Karnaugh Maps. They have applications in error correction in digital communication such as digital terrestrial television and cable TV systems.

To convert binary code to Gray code, let the binary number be the n -bit word $(b_{n-1} \dots b_1 b_0)$ and the corresponding Gray code be $(g_{n-1} \dots g_1 g_0)$. The bits g_i are given by

$$g_i = b_i \oplus b_{i+1}, \quad g_{n-1} = b_{n-1} \tag{14.11}$$

where \oplus means exclusive OR. With bit b_n set to 0 we can therefore represent the operation graphically as in the example shown in Fig. 14.4, where the binary code (11010110) is converted to the Gray code (10111101).

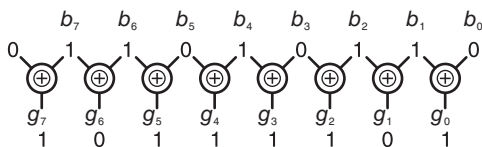


FIGURE 14.4 Binary to Gray code conversion.

The inverse operation, converting from Gray code to binary, is effected by starting at the MSB (at the leftmost bit) and moving to the right toward the LSB setting $b_i = g_i$ if the number of 1's to the left of g_i is even; otherwise set $b_i = \bar{g}_i$. For the above example the

reverse operation produces

$$\begin{matrix} g_7 & g_6 & g_5 & g_4 & g_3 & g_2 & g_1 & g_0 \\ 1 & 0 & 1 & 1 & 1 & 1 & 0 & 1 \\ b_7 & b_6 & b_5 & b_4 & b_3 & b_2 & b_1 & b_0 \\ 1 & 1 & 0 & 1 & 0 & 1 & 1 & 0 \end{matrix}$$

14.7 Discrete Walsh Transform

The Walsh matrices can be evaluated as samples of the Walsh functions in the three orderings. We can also directly evaluate the elements of these matrices. In particular, for the Walsh-ordered (sequency ordered) matrix H_w , the $(rs)^{th}$ element $h_{rs}^{(w)}$ may be directly evaluated. Let r be represented in binary notation as

$$r \simeq (r_{n-1} \dots r_1 r_0) \tag{14.12}$$

that is, r_i is the i^{th} bit of r . Similarly, let

$$s \simeq (s_{n-1} \dots s_1 s_0). \tag{14.13}$$

The element $h_{rs}^{(w)}$ is given by

$$h_{rs}^{(w)} = (-1)^p, \quad r, s = 0, 1, \dots, N - 1 \tag{14.14}$$

where

$$p = \sum_{i=0}^{n-1} \rho_i(r) s_i \tag{14.15}$$

$$\rho_0(r) = r_{n-1}, \quad \rho_1(r) = r_{n-1} + r_{n-2}, \quad \rho_2(r) = r_{n-2} + r_{n-3}, \quad \dots, \quad \rho_{n-1}(r) = r_1 + r_0. \tag{14.16}$$

For example, with $N = 8$, $n = 3$ the elements along row 4 are found by substituting $r = 4 = (100)_2$ and $s = \{000, 001, \dots, 111\}_2$. We obtain

$$p = \rho_0(4)s_0 + \rho_1(4)s_1 + \rho_2(4)s_2 = 1 \times s_0 + 1 \times s_1 + 0 \times s_2 = s_0 + s_1$$

$$h_{4,s}^{(w)} = [1 \ -1 \ -1 \ 1 \ 1 \ -1 \ -1 \ 1]$$

and those along row 7 are

$$h_{7,s}^{(w)} = (-1)^{s_0+2s_1+2s_2} = [1 \ -1 \ 1 \ -1 \ 1 \ -1 \ 1 \ -1]$$

For the dyadic (or Paley) order Walsh matrix, the elements are given by

$$h_{r,s}^{(p)} = (-1)^q, \quad r, s = 0, 1, \dots, N - 1 \tag{14.17}$$

where

$$q = \sum_{i=0}^{n-1} r_{n-1-i} s_i. \tag{14.18}$$

The matrix elements of the natural (or Hadamard) order Walsh matrix are given by

$$h_{rs}^{(h)} = (-1)^{\sum_{i=0}^{n-1} r_i s_i}, \quad r, s = 0, 1, \dots, N - 1. \tag{14.19}$$

We shall see in what follows that the Walsh matrix in the three orders can be alternatively evaluated using the *Kronecker* product of matrices.

14.8 Discrete-Time Walsh Transform

In as much as the discrete Fourier transform (DFT) is a sampling of the continuous-time domain Fourier transform, the discrete Walsh transform (DWT) is a sampling of the continuous-time domain Walsh transform. The base-2 DWT is known as the *Walsh–Hadamard transform* [2]. The general-base Walsh transform is known as the *generalized Walsh transform* [20], [25], [41]. We shall see that the generalized Walsh transform may be viewed as a generalization of the DFT.

14.9 Discrete-Time Walsh–Hadamard Transform

We presently consider the base-2 Walsh transform. This transform operates on $N = 2^n$ -point vectors and will be referred to as the “Walsh–Hadamard” transform. In a following section we study the generalized Walsh transform, which is a generalization to a general base p of this transform and which operates on vectors of length $N = p^n$.

The Walsh–Hadamard core matrix of order 2, denoted H_2 , is the 2×2 DFT matrix, that is, the Fourier transformation matrix for a two-point vector

$$H_2 = \begin{bmatrix} w^0 & w^0 \\ w^0 & w^1 \end{bmatrix} = \begin{bmatrix} 1 & 1 \\ 1 & -1 \end{bmatrix} \tag{14.20}$$

where $w = e^{-j2\pi/2} = -1$. We now consider the three ordering classes of Walsh functions cited above, in the present context of discrete-time functions. We see in particular how to directly generate the Walsh matrices of these three orderings using the Kronecker product of matrices.

14.9.1 Natural (Hadamard) Order

Given an input vector x of four points the Walsh–Hadamard matrix H_4 in natural or Hadamard order is given by the Kronecker product of H_2 by itself, i.e.

$$(H_4)_{\text{nat}} = H_2 \times H_2 = \begin{bmatrix} w^0 & w^0 & w^0 & w^0 \\ w^0 & w^1 & w^0 & w^1 \\ w^0 & w^0 & w^1 & w^1 \\ w^0 & w^1 & w^1 & w^0 \end{bmatrix} = \begin{bmatrix} 1 & 1 & 1 & 1 \\ 1 & -1 & 1 & -1 \\ 1 & 1 & -1 & -1 \\ 1 & -1 & -1 & 1 \end{bmatrix} \begin{matrix} 0 \\ 3 \\ 1 \\ 2 \end{matrix} \tag{14.21}$$

of sign changes

The sequency of each row is the number of sign changes of the elements along the row and is indicated to the right of the matrix. The sequencies are, respectively, 0, 3, 1 and 2. For an eight-point vector x the natural order Walsh transformation matrix is given similarly by

$$(H_8)_{\text{nat}} = (H_4)_{\text{nat}} \times H_2 = H_2 \times H_2 \times H_2 = \begin{bmatrix} 1 & 1 & 1 & 1 & 1 & 1 & 1 & 1 \\ 1 & -1 & 1 & -1 & 1 & -1 & 1 & -1 \\ 1 & 1 & -1 & -1 & 1 & 1 & -1 & -1 \\ 1 & -1 & -1 & 1 & 1 & -1 & -1 & 1 \\ 1 & 1 & 1 & 1 & -1 & -1 & -1 & -1 \\ 1 & -1 & 1 & -1 & -1 & 1 & -1 & 1 \\ 1 & 1 & -1 & -1 & -1 & -1 & 1 & 1 \\ 1 & -1 & -1 & 1 & -1 & 1 & 1 & -1 \end{bmatrix} \begin{matrix} 0 \\ 7 \\ 3 \\ 4 \\ 1 \\ 6 \\ 2 \\ 5 \end{matrix} \quad (14.22)$$

of sign changes

and the sequences of the successive rows can be seen to be given by 0, 7, 3, 4, 1, 6, 2 and 5, respectively. The *natural order* Walsh–Hadamard transform of the vector x is given by

$$X_{\text{nat}} = H_{8,\text{nat}}x \quad (14.23)$$

14.9.2 Dyadic or Paley Order

Premultiplying the naturally ordered Hadamard matrix by the bit-reverse order matrix yields the *dyadic or Paley* ordered matrix. With input vector length $N = 4$ the bit reversed ordering matrix, denoted K_4 selects elements in the order:

$$K_{4,\text{bit-rev}} : (0, 2, 1, 3) \quad (14.24)$$

Hence the dyadic or Paley ordered matrix is given by Hence the dyadic or Paley ordered matrix is given by

$$(H_4)_{\text{dyad}} = \begin{bmatrix} 1 & 1 & 1 & 1 \\ 1 & 1 & -1 & -1 \\ 1 & -1 & 1 & -1 \\ 1 & -1 & -1 & 1 \end{bmatrix} \begin{matrix} 0 \\ 1 \\ 3 \\ 2 \end{matrix} \quad (14.25)$$

of sign changes

With input vector length $N = 8$ the bit reversed ordering matrix, denoted K_8 selects elements in the order:

$$K_8 : (0, 4, 2, 6, 1, 5, 3, 7) \quad (14.26)$$

so that

$$(H_8)_{\text{dyad}} = \begin{bmatrix} 1 & 1 & 1 & 1 & 1 & 1 & 1 & 1 \\ 1 & 1 & 1 & 1 & -1 & -1 & -1 & -1 \\ 1 & 1 & -1 & -1 & 1 & 1 & -1 & -1 \\ 1 & 1 & -1 & -1 & -1 & -1 & 1 & 1 \\ 1 & -1 & 1 & -1 & 1 & -1 & 1 & -1 \\ 1 & -1 & 1 & -1 & -1 & 1 & -1 & 1 \\ 1 & -1 & -1 & 1 & 1 & -1 & -1 & 1 \\ 1 & -1 & -1 & 1 & -1 & 1 & 1 & -1 \end{bmatrix} \begin{matrix} 0 \\ 1 \\ 3 \\ 2 \\ 7 \\ 6 \\ 4 \\ 5 \end{matrix} \quad (14.27)$$

of sign changes

14.9.3 Sequency or Walsh Order

The *dyadic ordered* matrix needs be operated upon by the *Gray code-to-binary conversion matrix* to produce the Sequency or Walsh Order matrix. The conversion from the binary order {00, 01, 10, 11} to Gray code is obtained according to the relation: $b_i \oplus a_{i+1} = a_i$, resulting in the order {00, 01, 11, 10}The sequency (Walsh) ordered matrix for $N = 4$ is therefore

The *dyadic ordered* matrix needs be operated upon by the Gray code-to-binary conversion matrix to produce the Sequency or Walsh Order matrix. The conversion from the binary order {00, 01, 10, 11} to Gray code is obtained according to the relation: $b_i \oplus a_{i+1} = a_i$, resulting in the order {00, 01, 11, 10}The sequency (Walsh) ordered matrix for $N = 4$ is therefore

$$(H_4)_{\text{seq}} = \begin{bmatrix} 1 & 1 & 1 & 1 \\ 1 & 1 & -1 & -1 \\ 1 & -1 & -1 & 1 \\ 1 & -1 & 1 & -1 \end{bmatrix} \begin{matrix} 0 \\ 1 \\ 2 \\ 3 \end{matrix} \tag{14.28}$$

of sign changes

and the sequency ordered matrix for $N = 8$ is given by

$$(H_8)_{\text{seq}} = \begin{bmatrix} 1 & 1 & 1 & 1 & 1 & 1 & 1 & 1 \\ 1 & 1 & 1 & 1 & -1 & -1 & -1 & -1 \\ 1 & 1 & -1 & -1 & -1 & -1 & 1 & 1 \\ 1 & 1 & -1 & -1 & 1 & 1 & -1 & -1 \\ 1 & -1 & -1 & 1 & 1 & -1 & -1 & 1 \\ 1 & -1 & -1 & 1 & -1 & 1 & 1 & -1 \\ 1 & -1 & 1 & -1 & -1 & 1 & -1 & 1 \\ 1 & -1 & 1 & -1 & 1 & -1 & 1 & -1 \end{bmatrix} \begin{matrix} 0 \\ 1 \\ 2 \\ 3 \\ 4 \\ 5 \\ 6 \\ 7 \end{matrix} \tag{14.29}$$

of sign changes

14.10 Natural (Hadamard) Order Fast Walsh–Hadamard Transform

The Hadamard transform for the natural (or Hadamard) ordering is obtained by successive Kronecker multiplication of the core matrix H_2 . Thus

$$H_{N,\text{nat}} = H_{N/2,\text{nat}} \times H_2 = H_{N/4,\text{nat}} \times H_2 \times H_2 = [H_2]^{[n]}, \tag{14.30}$$

where $[.]$ in the exponent means a Kronecker product. In what follows in this section, we shall drop the subscript nat. We may write

$$\begin{aligned} H_N &= \begin{bmatrix} H_{N/2} & H_{N/2} \\ H_{N/2} & -H_{N/2} \end{bmatrix} = \begin{bmatrix} H_{N/2} & \\ & H_{N/2} \end{bmatrix} \begin{bmatrix} I_{N/2} & I_{N/2} \\ I_{N/2} & -I_{N/2} \end{bmatrix} \\ &= (H_{N/2} \times I_2)(I_{N/2} \times H_2). \end{aligned} \tag{14.31}$$

Expressing $H_{N/2}$ in terms of $H_{N/4}$, we have

$$H_{N/2} = (H_{N/4} \times I_2)(I_{N/4} \times H_2). \tag{14.32}$$

In general, if we write $k = 2^i$ ($i = 0, 1, 2, \dots, n-1$), then

$$H_{N/k} = (H_{N/(2k)} \times I_2)(I_{N/(2k)} \times H_2). \quad (14.33)$$

Carrying this iterative procedure to the end,

$$H_N = \{[\dots\{\{[\dots\{\{[(H_2 \times I_2)(I_2 \times H_2)] \times I_2\}(I_4 \times H_2)] \times I_2\} \dots] \times I_2\} \cdot (I_{N/2k} \times H_2)] \times I_2\} \dots (I_{N/4} \times H_2)] \times I_2\}(I_{N/2} \times H_2). \quad (14.34)$$

Using the property

$$(A, B, C, \dots) \times I = (A \times I)(B \times I)(C \times I) \dots \quad (14.35)$$

we obtain

$$H_N = (H_2 \times I_{N/2})(I_2 \times H_2 \times I_{N/4}) \dots (I_{N/2k} \times H_2 \times I_k) \dots \cdot (I_{N/4} \times H_2 \times I_2)(I_{N/2} \times H_2). \quad (14.36)$$

This equation can be written in the form

$$H_N = \prod_{i=1}^n [I_{2^{(i-1)}} \times H_2 \times I_{2^{(n-i)}}]. \quad (14.37)$$

Similarly to the case of the DFT matrix, we express the factorization in terms of the matrix

$$C_N = (I_{N/2} \times H_2) \quad (14.38)$$

using the property

$$P_N^{-k}(I_{N/2} \times H_2)P_N^k = I_{N/2^{k+1}} \times H_2 \times I_{2^k} \quad (14.39)$$

where P_N is the base-2 perfect shuffle matrix for N points. We obtain

$$H_N = \prod_{i=1}^n P_N C_N. \quad (14.40)$$

The matrix $C_N = C$ is the same as the matrix S of the fast Fourier transform (FFT) factorization. It is optimal in the sense that it calls for operating on elements that are farthest apart. In very large scale integrated VLSI design this means the possibility of storing data as long queues in long registers, eliminating the need for addressing. In fact the same wired-in base-2 FFT processor can implement this Walsh transform.

14.11 Dyadic (Paley) Order Fast Walsh–Hadamard Transform

The dyadic-ordered Hadamard matrix $H_{N,D}$ can be obtained from the naturally ordered matrix by permuting the latter with the bit-reversed ordering permutation matrix. This permutation matrix can be expressed using the perfect shuffle matrix, as noted above in connection with the radix-2 FFT factorization,

$$K_N = \prod_{i=1}^n P_{2^{(n-i+1)}} \times I_{2^{(i-1)}} \quad (14.41)$$

i.e.

$$H_{N,D} = \prod_{i=1}^n P_{2^{(n-i+1)}} \times I_{2^{(i-1)}} \prod_{i=1}^n [I_{2^{(i-1)}} \times H_2 \times I_{2^{(n-i)}}]. \tag{14.42}$$

Using the property

$$P_k(A_{k/2} \times I_2)P_k^{-1} = I_2 \times A_{k/2} \tag{14.43}$$

we obtain after some manipulation

$$H_{N,D} = \prod_{i=1}^n (I_{2^{(n-i)}} \times P_{2^i})C_N = \prod_{i=1}^n J_i C_N \tag{14.44}$$

where

$$J_i = (I_{2^{(n-i)}} \times P_{2^i}). \tag{14.45}$$

14.12 Sequency Ordered Fast Walsh–Hadamard Transform

The Sequency or (Walsh) ordered Walsh–Hadamard matrix may be written in the form

$$H_{N,s} = P_N H'_N = P_N \begin{bmatrix} H_{N/2,s} & D_{N/2} H_{N/2,s} \\ H_{N/2,s} & -D_{N/2} H_{N/2,s} \end{bmatrix}. \tag{14.46}$$

The $D_{N/2}$ is a diagonal matrix the elements of which alternate between +1 and -1, for example $D_8 = \text{diag}(1, -1, 1, -1, 1, -1, 1, -1)$. We can write

$$H_{N,s} = P_N (I_{N/2} \times H_2) D'_N (H_{N/2,s} \times I_2) \tag{14.47}$$

where D'_N is a diagonal matrix of which the top left half is the identity matrix $I_{N/2}$ and the lower right half is $D_{N/2}$,

$$D'_N = \begin{bmatrix} I_{N/2} & \\ & D_{N/2} \end{bmatrix} = \text{quasidiag}(I_{N/2}, D_{N/2}). \tag{14.48}$$

We obtain

$$H_{N,s} = P_{2^n} \left\{ \prod_{i=1,2,3,\dots}^n P_{2^{n-1}} r_i C d_i \right\} P_{2^n}^{-1}. \tag{14.49}$$

where

$$r_i = I_{2^{(i-1)}} \times P_{2^{(n-i+1)}} \tag{14.50}$$

$$d_i = I_{2^{(i-1)}} \times D'_{2^{(n-i+1)}}. \tag{14.51}$$

As will be seen in Chapter 15, the same wired-in machine obtained for radix-2 FFT implementation can be used for the implementation of both the natural and dyadic order Walsh–Hadamard transforms. A slight addition in the form of a gating switch needs be added to implement the sequency ordered transform.

14.13 Generalized Walsh Transform

The base- p generalized Walsh transform operates on a vector of $N = p^n$ elements. The generalized Walsh core matrix is the $p \times p$ DFT matrix

$$W_p = \begin{bmatrix} w^0 & w^0 & \dots & w^0 \\ w^0 & w^1 & \dots & w^{p-1} \\ \dots & \dots & \dots & \dots \\ w^0 & w^{p-1} & \dots & w^1 \end{bmatrix} \quad (14.52)$$

where $w = e^{-j2\pi/p}$. In the literature the matrix W_p is sometimes similarly defined but is multiplied by a normalizing factor $1/\sqrt{p}$. To simplify the presentation we start by considering the example of a base $p = 3$ and $N = p^2 = 9$. The core matrix is given by

$$W_3 = \begin{bmatrix} w^0 & w^0 & w^0 \\ w^0 & w^1 & w^2 \\ w^0 & w^2 & w^1 \end{bmatrix} \longleftrightarrow \begin{bmatrix} 0 & 0 & 0 \\ 0 & 1 & 2 \\ 0 & 2 & 1 \end{bmatrix} \quad (14.53)$$

where on the right the matrix is rewritten in exponential notation for abbreviation, so that an element k stands for a true value w^k . In what follows the matrix $P_N^{(p)} = P^{(p)} = P$ stands for the base- p perfect shuffle permutation matrix defined above in Equation (7.220). As with the base-2 Walsh–Hadamard transform there are three orderings associated with the base- p transform. In what follows to simplify the presentation we start by illustrating the transform in the three orderings on an example of $N = 9$ and $p = 3$.

14.14 Natural Order

The natural order base- p generalized Walsh transform of an N -point input vector x , where $N = p^n$, is given by

$$X_{W_{a,\text{nat}}} = W_{N,\text{nat}}x \quad (14.54)$$

where $W_{N,\text{nat}}$ is the base- p generalized Walsh transform matrix formed by the Kronecker product of W_p by itself n times, denoted

$$W_{N,\text{nat}} = W_p \times W_p \times \dots \times W_p \triangleq W_p^{[n]}. \quad (14.55)$$

14.15 Generalized Sequency Order

The generalized sequency is the sum of distances between successive eigen values w^k divided by $(p - 1)$. The distance between w^r and w^s is $s - r$ if $s \geq r$; otherwise it is $p + (s - r)$.

$$W_{3^2} = W_3 \times W_3 = \begin{bmatrix} 0 & 0 & 0 & 0 & 0 & 0 & 0 & 0 \\ 0 & 1 & 2 & 0 & 1 & 2 & 0 & 1 & 2 \\ 0 & 2 & 1 & 0 & 2 & 1 & 0 & 2 & 1 \\ 0 & 0 & 0 & 1 & 1 & 1 & 2 & 2 & 2 \\ 0 & 1 & 2 & 1 & 2 & 0 & 2 & 0 & 1 \\ 0 & 2 & 1 & 1 & 0 & 2 & 2 & 1 & 0 \\ 0 & 0 & 0 & 2 & 2 & 2 & 1 & 1 & 1 \\ 0 & 1 & 2 & 2 & 0 & 1 & 1 & 2 & 0 \\ 0 & 2 & 1 & 2 & 1 & 0 & 1 & 0 & 2 \end{bmatrix} \begin{matrix} 0 \\ 8/2=4 \\ 16/2=8 \\ 2/2=1 \\ 10/2=5 \\ 12/2=6 \\ 4/2=2 \\ 6/2=3 \\ 14/2=7 \end{matrix} \tag{14.56}$$

where the generalized sequencies appear to the right of the matrix.

14.16 Generalized Walsh–Paley (p-adic) Transform

The generalized Walsh–Paley (GWP) matrix is the base- p generalization of the base-2 Walsh–Hadamard dyadic order. The digit-reversed ordering matrix $N = 3^2 = 9$ produces the order

	a_1	a_0	b_1	b_0	
0	0	0	0	0	0
1	0	1	1	0	3
2	0	2	2	0	6
3	1	0	0	1	1
4	1	1	1	1	4
5	1	2	2	1	7
6	2	0	0	2	2
7	2	1	1	2	5
8	2	2	2	2	8

The generalized sequency of the generalized Walsh–Paley is given by:

$$0, 1, 2, 4, 5, 3, 8, 6, 7.$$

14.17 Walsh–Kaczmarz Transform

The generalized Walsh–Kaczmarz (GWK) matrix is the base- p generalization of the Walsh–Hadamard sequency matrix. It is obtained by applying the base- p to Gray code permutation matrix to the generalized Walsh–Paley matrix

The base- p to Gray code conversion is written:

$$k_i \circ a_{i+1} = a_i, \text{ where } \circ = \text{addition mod } p$$

and the inverse is written

Inverse: from g to p

$$p_1 = g_1$$

$$p_0 = g_0 \circ p_1, \quad p_i = g_i \circ p_{i+1}.$$

	a_1	a_0	k_1	k_0	
	p_1	p_0	g_1	g_0	
0	0	0	0	0	0
1	0	1	0	1	1
2	0	2	0	2	2
3	1	0	1	2	5
4	1	1	1	0	3
5	1	2	1	1	4
6	2	0	2	1	7
7	2	1	2	2	8
8	2	2	2	0	6

The generalized sequences of the successive rows of the Walsh–Kaczmarz matrix are as expected:

$$0, 1, 2, 3, 4, 5, 6, 7, 8.$$

Fast generalized Walsh algorithms leading to wired-in or virtually-wired-in parallel general radix processors have been proposed [20] [25]. A general-radix parallel processor for generalized spectral analysis and in particular higher radix FFT and fast generalized Walsh transform has been constructed and referred to in Chapter 15.

14.18 Generalized Walsh Factorizations for Parallel Processing

Three basic forms of the generalized Walsh GW transform in three different orderings are given in what follows [20].

14.19 Generalized Walsh Natural Order GWN Matrix

We have seen that the natural order base- p generalized Walsh transformation matrix for an N -point input vector x , where $N = p^n$, is given by

$$W_{N,nat} = W_p \times W_p \times \dots \times W_p \triangleq W_p^{[n]}. \tag{14.57}$$

In what follows in this section, we shall drop the subscript nat . Similarly to the base-2 transform we obtain

$$W_N = W_{N/p} \times W_p = \begin{bmatrix} W_{N/p} & W_{N/p} & \dots & W_{N/p} \\ W_{N/p} & w^1 W_{N/p} & \dots & w^{p-1} W_{N/p} \\ \dots & \dots & \dots & \dots \\ W_{N/p} & w^{p-1} W_{N/p} & \dots & w^1 W_{N/p} \end{bmatrix} \tag{14.58}$$

where we have used the fact that $w^{(p-1)^2} = w^1$. We may write

$$W_N = (W_{N/p} \times I_p)(I_{N/p} \times W_p). \tag{14.59}$$

Expressing $W_{N/p}$ in terms of $W_{N/(2p)}$, we have

$$W_{N/p} = (W_{N/(2p)} \times I_p)(I_{N/2p} \times W_p). \tag{14.60}$$

In general, if we write $k = p^i$ ($i = 0, 1, 2, \dots, n - 1$), then

$$W_{N/k} = (H_{N/(kp)} \times I_p)(I_{N/(kp)} \times W_p). \tag{14.61}$$

Similarly to the general base FFT as well as the base-2 Walsh matrix factorization we obtain

$$W_N = \prod_{i=1}^n [I_{p^{(i-1)}} \times W_p \times I_{p^{(n-i)}}]. \tag{14.62}$$

Proceeding similarly to the factorization of the DFT matrix, we express the factorization in terms of the matrix

$$C_N = (I_{N/p} \times W_p). \tag{14.63}$$

using the property

$$P_N^{-k}(I_{N/p} \times W_p)P_N^k = I_{p^{n-k-1}} \times W_p \times I_{p^k} \tag{14.64}$$

After some manipulation we obtain

$$T_N = \prod_{i=1}^n P_N C_N. \tag{14.65}$$

The matrix C_N is the same as the matrix S of the general-base FFT factorization. It is optimal in the sense that it calls for operating on elements that are farthest apart for a given data record size $N = p^n$. In VLSI design this means the possibility of storing data as long queues in long registers, eliminating the need for addressing. In fact the same wired-in base- p FFT processor can implement this Walsh transform.

14.20 Generalized Walsh–Paley GWP Transformation Matrix

The generalized Walsh transform in the Walsh–Paley order, which may be reffered to as GWP transform is related to the transform in natural order by a digit-reverse ordering. The general-base digit reverse ordering matrix $K_N^{(p)}$ can be factored using the general-base perfect shuffle permutation matrix $P^{(p)}$ and Kronecker products as seen above in factoring the DFT, Equation (7.267). We may write,

$$K_N^{(p)} = \prod_{i=0}^{n-1} (P_{p^{(n-i)}}^{(p)} \times I_{p^i}). \tag{14.66}$$

The GWP matrix $W_{N,W P}$ can thus be written in the form

$$W_{N,W P} = K_N^{(p)} W_{N,\text{nat}} = \prod_{i=0}^{n-1} (P_{p^{(n-1)}}^{(p)} \times I_{p^i}) \prod_{i=1}^n [I_{p^{(i-1)}} \times W_p \times I_{p^{(n-i)}}]. \tag{14.67}$$

Similarly to the base-2 dyadic Walsh–Hadamard transform we obtain

$$W_{N,W P} = \prod_{i=1}^n (I_{p^{(n-i)}} \times P_{p^i}) C_N = \prod_{i=1}^n J_i^{(p)} C_N \tag{14.68}$$

where

$$J_i^{(p)} = (I_{p^{(n-i)}} \times P_{p^i}). \tag{14.69}$$

14.21 GWK Transformation Matrix

The GWK transformation matrix is related to the GWP matrix through a p -ary to Gray transformation matrix $G_N^{(p)}$.

$$W_{N,WK} = G_N^{(p)} W_{N,WP}. \quad (14.70)$$

Let $P_N \triangleq P_N^{(p)}$. The matrix can be rewritten in the form

$$W_{N,WK} = P_N P_N^{-1} W_{N,WK} = P_N W_N'. \quad (14.71)$$

Similarly to general base FFT matrix, this matrix has a recursive form, namely,

$$W_{N/k} = P_{N/k} (I_{N/(kp)} \times W_p) D'_{N/K} (W_{N/(kp)} \times I_p) \quad (14.72)$$

where for $m = 1, 2, \dots, n$

$$D'_{p^m} = \text{quasidiag} \left(I_{p^{m-1}}, D_{p^{m-1}}, D_{p^{m-1}}^2, \dots, D_{p^{m-1}}^{(p-1)} \right) \quad (14.73)$$

$$D_{p^{m-1}}^i = D_p^i \times I_{p^{m-2}} \quad (14.74)$$

$$D_p = \text{diag} \left(w^0, w^{-1}, w^{-2}, \dots, w^{-(p-1)} \right). \quad (14.75)$$

With some manipulation we obtain

$$W_{N,WK} = \prod_{i=1}^n (P_{p^{n-i+1}} \times I_{p^{i-1}}) (I_{p^{n-i}} \times W_p \times I_p \times I_{p^{i-1}}) (D'_{p^{n-i+1}} \times I_{p^{i-1}}) \quad (14.76)$$

which can be rewritten in terms of the matrix C_N in the form

$$W_{N,WK} = P \left\{ \prod_{i=0}^{n-1} P^{-1} H_i C_N E_i \right\} P^{-1}. \quad (14.77)$$

where

$$H_i = I_{p^i} \times P_{p^{n-i}}, \quad E_i = I_{p^i} \times D'_{p^{n-i}} \quad (14.78)$$

14.22 High Speed Optimal Generalized Walsh Factorizations

As can be seen in [20], using a similar approach to that seen above in relation to the shuffle-free, labeled high speed FFT factorization, the following generalized Walsh factorizations are obtained. The corresponding parallel processor architecture is presented in Chapter 15.

14.23 GWN Optimal Factorization

As seen above, the GWN transformation matrix has the form

$$W_{N,\text{nat}} = \prod_{i=0}^{n-1} P_N C_N = \prod_{i=0}^{n-1} P_N (I_{N/p} \times W_p). \quad (14.79)$$

We can rewrite the matrix in the form

$$W_{N,\text{nat}} = P \left\{ \prod_{n=0}^{n-1} CP \right\} P^{-1} = P \left\{ \prod_{n=0}^{n-1} F \right\} P^{-1} \tag{14.80}$$

$$C \equiv C_N = I_{p^{n-1}} \times W_p \tag{14.81}$$

and $F = CP$.

14.24 GWP Optimal Factorization

The GWP matrix has been factored in the form

$$W_{N,Wp} = \prod_{i=0}^{n-1} J_i C_N \tag{14.82}$$

where

$$J_i = (I_{p^{n-i-1}} \times P_{p^{i+1}}) = H_{n-i-1} \tag{14.83}$$

and $H_k = I_{p^k} \times P_{p^{n-k}}$. Letting

$$Q_i = C_N J_{i+1} = C_N H_{n-i-2}, \quad i = 0, 1, \dots, n-2 \tag{14.84}$$

$$Q_{n-1} = C_N \tag{14.85}$$

we obtain

$$W_{N,Wp} = \prod_{i=0}^{n-1} Q_i \tag{14.86}$$

where each matrix Q_i , $i = 0, 1, \dots, n-2$, is p^2 -optimal, meaning that the minimum distance between data points is N/p^2 , while Q_{n-1} is p -optimal, meaning that the minimum distance is N/p [20].

14.25 GWK Optimal Factorization

The GWK matrix factorization was obtained in the form

$$W_{N,WK} = P \left\{ \prod_{i=0}^{n-1} P^{-1} H_i C_N E_i \right\} P^{-1}. \tag{14.87}$$

We may write

$$W_{N,WK} = P \left\{ \prod_{i=0}^{n-1} P^{-1} H_i G_i \right\} P^{-1} \tag{14.88}$$

where

$$G_i = C_N E_i. \tag{14.89}$$

Letting

$$S_i = P^{-1}H_iP = (I_{p^{i-1}} \times P_{p^{n-i}} \times I_p) \quad (14.90)$$

we have

$$W_{N,WK} = P^2 \left\{ \prod_{i=0}^{n-1} P^{-1}G_iS_{i+1} \right\} P^{-1} \quad (14.91)$$

with

$$S_{n-1} = S_n = I_N. \quad (14.92)$$

The factorization can also be rewritten in the form

$$W_{N,WK} = P \left\{ \prod_{i=0}^{n-1} \Gamma_i \right\} P^{-1} \quad (14.93)$$

where

$$\Gamma_i = P^{-1}G_iS_{i+1} = P^{-1}G_i (I_{p^i} \times P_{p^{n-i-1}} \times I_p), \quad i = 1, 2, \dots, n-1$$

$$\Gamma_0 = G_0S_1.$$

These are optimal shuffle-free constant-topology algorithms for massive parallelism [25]. Constant topology refers to the fact that in all iterations, the data to be operated upon are throughout equidistant, as can be seen in Fig. 14.5 and Fig. 14.6. They can be implemented by massive parallelism processors in a multiprocessing structure. The level of parallelism in processing vectors of length $N = p^n$, where p is the base, in the form of $M = p^m$ base- p processors, can be chosen by varying m between 0 and $n-1$. A base- p operates on p operands simultaneously. The Fast Fourier transform factored to a general base p is but a special case of the class of generalized Walsh transform that are implemented by such processors. This topic will be discussed further in Chapter 15.

14.26 Karhunen Loève Transform

An optimum transform A of a vector x is one which produces a vector y having uncorrelated coefficients. Thus we seek a transform which, applied to the vector x with covariance matrix C_x produced a covariance matrix C_y which is diagonal. Such transformation allows signal extraction from noise using diagonal filters and results in what is called scalar filtering in contrast with vector filtering that is encountered when the matrix C_y contains off diagonal elements.

From matrix theory, we recall that if a nonsingular matrix C has distinct eigenvalues with corresponding eigenvectors written as the columns of a matrix U then $U^{-1}CU$ is a diagonal matrix containing the eigenvalues of C as its elements.

The eigenvalues of the matrix C_x are obtained as the roots of the characteristic equation

$$\det(C_x - \lambda I_N) = 0.$$

Let these eigenvalues be denoted as λ_i , $i = 0, 1, \dots, N-1$. Corresponding to each eigenvalue λ_i there is an eigenvector $v^{(i)}$ which satisfies

$$C_x v^{(i)} = \lambda_i v^{(i)}.$$

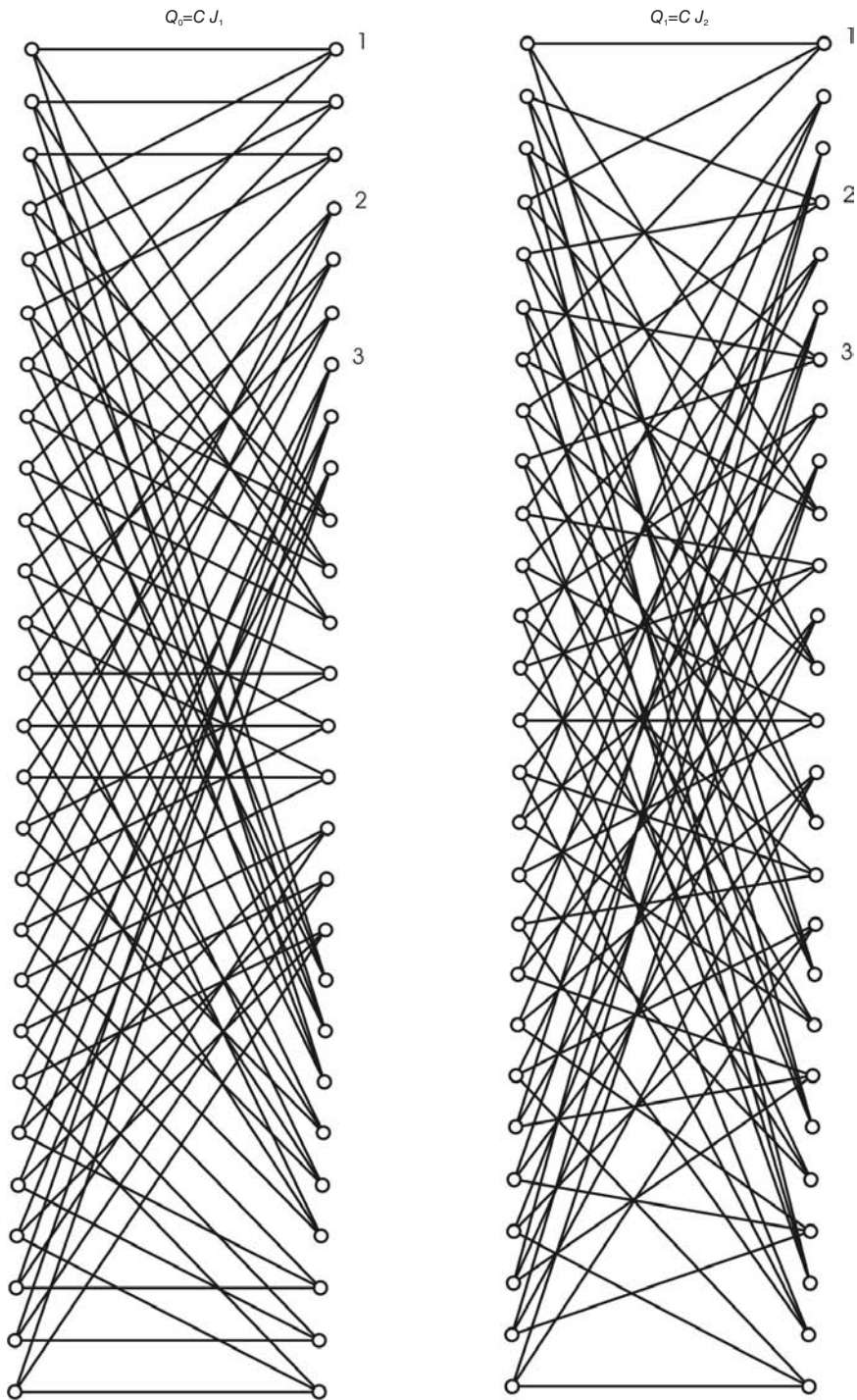


FIGURE 14.5 Generalized Walsh-Paley (GWP) transform two-iterations with $N = 27$ points.

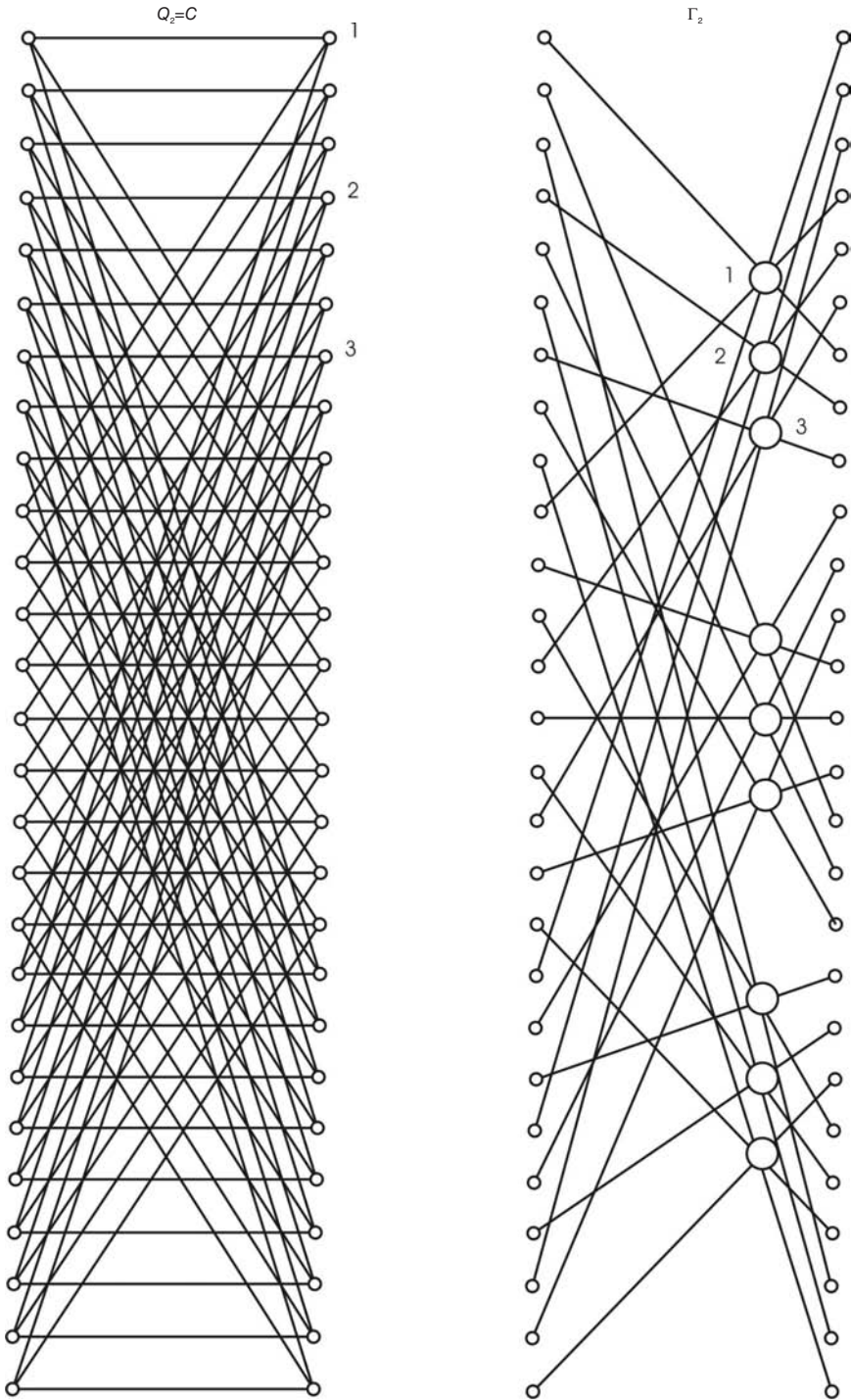


FIGURE 14.6 Generalized Walsh-Paley (GWP) transform third iteration, and a Walsh-Kaczmarz iteration.

Thus if U is the matrix

$$U = [v^{(0)}v^{(1)} \dots v^{(N-1)}]$$

then

$$\begin{aligned} C_x U &= [C_x v^{(0)} C_x v^{(1)} \dots C_x v^{(N-1)}] \\ &= [\lambda_0 v^{(0)} \lambda_1 v^{(1)} \dots \lambda_{N-1} v^{(N-1)}] \\ &= U \Lambda \end{aligned}$$

where

$$\Lambda = \text{diag}(\lambda_0, \lambda_1, \dots, \lambda_{N-1})$$

We thus deduce that

$$U^{-1} C_x U = \Lambda$$

That is, the matrix C_x is diagonalized by the matrix U . Now, since

$$C_y = A C_x A^{*T}$$

we see that for C_y to be diagonal we should have

$$A^{*T} = A^{-1} = U$$

Such an optimal transform is called the Karhunen Loève (KL) transform. Its matrix A is given the symbol K . We thus have

$$K = U^{-1}$$

$$K^{*T} = K^{-1} = U = [v^{(0)}v^{(1)} \dots v^{(N-1)}]$$

i.e.

$$K = [v^{(0)*}v^{(1)*} \dots v^{(N-1)*}]^T$$

That is, the rows of K are the conjugates of the eigenvectors of C_X .

The KL transform is thus an optimal transform that works in general for any class of signal statistics. It is formed from those statistics, however, requiring knowledge of the covariance matrices of the analyzed signals, computation of their eigenvectors, and calls for N^2 multiplication for its direct application to the input vector. It is for these reasons that transforms which are optimal only for a certain class of statistics, and which are known to be asymptotically optimal, such as Fourier and Walsh transforms, are more commonly used for generalized spectral analysis.

14.27 Hilbert Transform

The Hilbert transform of a function $f(t)$ is by convention a function $g(t)$ given by

$$g(t) = \frac{1}{\pi} \int_{-\infty}^{\infty} \frac{f(\tau)}{t - \tau} d\tau. \quad (14.94)$$

The integral divergence at the point $t = \tau$ is avoided by taking the principal value of the integral. We note that the ‘‘Hilbert transform’’ $g(t)$ of a function $f(t)$ is but the convolution of $f(t)$ with the function $1/(\pi t)$

$$g(t) = f(t) * \frac{1}{\pi t}. \quad (14.95)$$

This is a transformation from the time domain to the time domain.

We note that $\text{sgn}(t) \xleftrightarrow{\mathcal{F}} \frac{2}{j\omega}$. Hence by duality $\frac{2}{jt} \xleftrightarrow{\mathcal{F}} 2\pi \text{sgn}(-\omega) = -2\pi \text{sgn}(\omega)$, i.e. $\frac{1}{\pi t} \xleftrightarrow{\mathcal{F}} -j \text{sgn}(\omega)$ and

$$g(t) \xleftrightarrow{\mathcal{F}} G(j\omega) = F(j\omega) \mathcal{F} \left[\frac{1}{\pi t} \right] = -j \text{sgn}(\omega) F(j\omega). \quad (14.96)$$

We can therefore adopt an equivalent representation by stating that the Hilbert transform of a signal $f(t)$ is a transformation from the time domain to the frequency-domain function $G(j\omega) = \mathcal{F}[g(t)] = -j \text{sgn}(\omega) F(j\omega)$.

We may use the notation

$$f(t) \xleftrightarrow{\mathcal{H}_t} g(t) \quad (14.97)$$

and

$$f(t) \xleftrightarrow{\mathcal{H}_\omega} G(j\omega) \quad (14.98)$$

to denote transformation from the time domain to the time domain and to the frequency domain, respectively. Similarly, we write $\mathcal{H}_t[f(t)] = g(t)$ and $\mathcal{H}_\omega[f(t)] = G(j\omega)$.

The Hilbert transform $g(t)$ of a function $f(t)$ may thus be evaluated by effecting the convolution of $f(t)$ with the function $1/(\pi t)$ or by evaluating the inverse Fourier transform of $G(j\omega)$.

Example 14.1 Evaluate the Hilbert transform of $f(t) = \cos \beta t$. We have $F(j\omega) = \pi \{ \delta(\omega - \beta) + \delta(\omega + \beta) \}$

$$G(j\omega) = -j \text{sgn}(\omega) \pi \{ \delta(\omega - \beta) + \delta(\omega + \beta) \} = -j\pi \{ \delta(\omega - \beta) - \delta(\omega + \beta) \}$$

$$g(t) = \sin \beta t.$$

Similarly it can be shown that $\mathcal{H}_t[\sin \beta t] = -\cos \beta t$.

Example 14.2 Evaluate the Hilbert transform of $f(t) = \Pi_T(t)$. We have $g(t) = f(t) * \frac{1}{\pi t}$.

Referring to Fig. 14.7 we have for $t - T > 0$ i.e. $t > T$

$$g(t) = \frac{1}{\pi} \int_{t-T}^{t+T} \frac{d\tau}{\tau} = \frac{1}{\pi} \ln \tau \Big|_{t-T}^{t+T} = \frac{1}{\pi} \ln \frac{t+T}{t-T}.$$

For $t > 0$ and $t - T < 0$ i.e. $0 < t < T$ by symmetry the convolution integral over the interval $t - T < \tau < T - t$ is zero; hence

$$g(t) = \frac{1}{\pi} \int_{T-t}^{t+T} \frac{d\tau}{\tau} = \frac{1}{\pi} \ln \tau \Big|_{T-t}^{t+T} = \frac{1}{\pi} \ln \frac{t+T}{T-t}.$$

We may therefore write for $t > 0$

$$g(t) = \frac{1}{\pi} \ln \frac{t+T}{|t-T|}.$$

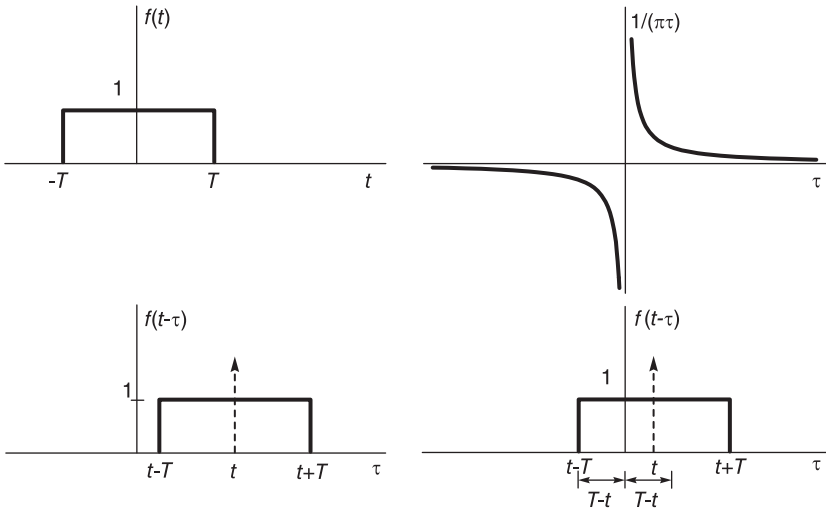


FIGURE 14.7 Hilbert transform of a rectangle through convolution.

By symmetry we have $g(-t) = -g(t)$ so that

$$g(t) = \frac{1}{\pi} \ln \frac{|t + T|}{|t - T|}.$$

See Fig. 14.8 for plot of $\frac{1}{\pi} \ln \frac{|t + T|}{|t - T|}$

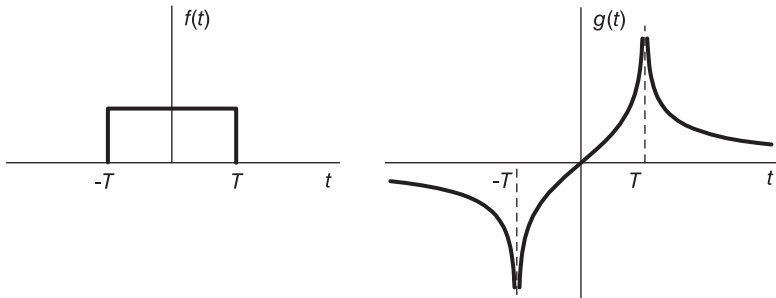


FIGURE 14.8 Plot of a centered rectangle and $\frac{1}{\pi} \ln \frac{|t + T|}{|t - T|}$.

Example 14.3 Evaluate the Hilbert transform of $f(t) = Sa(Bt)$.

We have

$$F(j\omega) = \frac{\pi}{B} \Pi_B(\omega)$$

$$G(j\omega) = -j \operatorname{sgn}(\omega) \frac{\pi}{B} \Pi_B(\omega) = \begin{cases} -j \frac{\pi}{B}, & 0 < \omega < B \\ j \frac{\pi}{B}, & -B < \omega < 0 \\ 0, & |\omega| > B \end{cases}$$

$$= -j \frac{\pi}{B} \Pi_{B/2}(\omega - B/2) + j \frac{\pi}{B} \Pi_{B/2}(\omega + B/2).$$

See Fig. 14.9

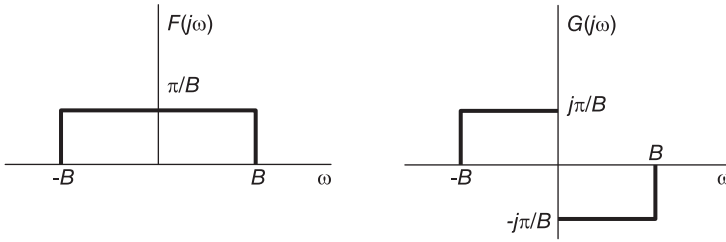


FIGURE 14.9 Spectra $F(j\omega)$ and $G(j\omega)$.

Note that

$$\operatorname{Sa}[(B/2)t] \longleftrightarrow \frac{2\pi}{B} \Pi_{B/2}(\omega)$$

and

$$\operatorname{Sa}[(B/2)t] \sin(B/2)t \longleftrightarrow -j \frac{\pi}{B} [\Pi_{B/2}(\omega - B/2) - \Pi_{B/2}(\omega + B/2)].$$

Hence

$$g(t) = \operatorname{Sa}[(B/2)t] \sin(B/2)t = \frac{\sin^2(B/2)t}{(B/2)t} = \frac{1 - \cos Bt}{Bt}.$$

14.28 Hilbert Transformer

We have found that

$$\cos \beta t \xrightarrow{\mathcal{H}_t} \sin \beta t = \cos(\beta t - \pi/2) \tag{14.99}$$

$$\sin \beta t \xrightarrow{\mathcal{H}_t} -\cos \beta t = \sin(\beta t - \pi/2). \tag{14.100}$$

We conclude that the Hilbert transform imparts a 90° phase lag on sinusoidal signals. A signal $f(t)$ having a Fourier spectrum $F(j\omega)$ is Hilbert transformed to a signal having a spectrum $G(j\omega) = -j \operatorname{sgn} \omega F(j\omega)$. A “Hilbert transformer” is therefore equivalent to a filter of frequency response

$$H(j\omega) = -j \operatorname{sgn} \omega = \begin{cases} -j, & \omega > 0 \\ j, & \omega < 0 \end{cases} \tag{14.101}$$

as depicted in Fig. 14.10.

We note that

$$\arg [H(j\omega)] = \begin{cases} -\pi/2, & \omega > 0 \\ \pi/2, & \omega < 0 \end{cases} \tag{14.102}$$

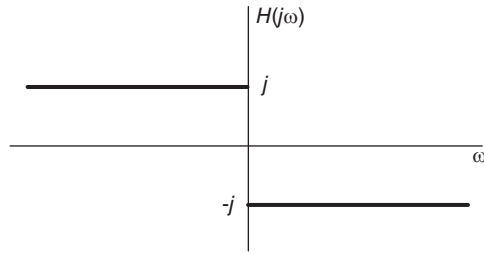


FIGURE 14.10 Hilbert transformer frequency response.

implying a 90° phase lag on input signals’ positive frequencies and a 90° phase lead on negative ones. Referring to Chapter 13, a Hilbert transformer can therefore be employed in producing single side-band (SSB) amplitude modulated signals.

The Hilbert transformer’s impulse response is given by

$$h(t) = \mathcal{F}^{-1} [H(j\omega)] = 1/(\pi t). \tag{14.103}$$

14.29 Discrete Hilbert Transform

Similarly to the continuous-time Hilbert transform, the discrete Hilbert transform of a sequence $x[n]$ is a sequence $y[n]$ given by

$$y[n] = x[n] * h[n] \tag{14.104}$$

where

$$h[n] = \begin{cases} 0, & n \text{ even} \\ \frac{2}{\pi n}, & n \text{ odd.} \end{cases} \tag{14.105}$$

The “discrete Hilbert transformer” has the frequency response

$$H(e^{j\Omega}) = \begin{cases} -j, & 0 < \Omega < \pi \\ j, & -\pi \leq \Omega < 0 \end{cases} \tag{14.106}$$

as depicted in Fig. 14.11

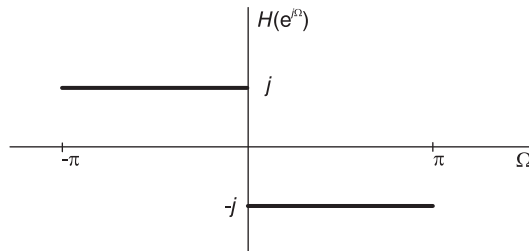


FIGURE 14.11 Discrete Hilbert transformer frequency response.

We note that the inverse transform of the frequency response is the impulse response

$$\begin{aligned} h[n] &= \frac{1}{2\pi} \left\{ \int_{-\pi}^0 j e^{j\Omega n} d\Omega + \int_0^{\pi} -j e^{j\Omega n} d\Omega \right\} = \frac{j}{2\pi} \left\{ \frac{e^{j\Omega n}}{jn} \Big|_{-\pi}^0 - \frac{e^{j\Omega n}}{jn} \Big|_0^{\pi} \right\} \\ &= \frac{1}{2\pi} \left\{ \frac{1 - e^{-j\pi n}}{n} - \frac{e^{j\pi n} - 1}{n} \right\} = \frac{1 - \cos(\pi n)}{\pi n} = \begin{cases} 0, & n \text{ even} \\ \frac{2}{\pi n}, & n \text{ odd} \end{cases} \end{aligned} \quad (14.107)$$

as stated.

14.30 Hartley Transform

Proposed by R.V.L. Hartley in 1942, the Hartley transform is closely related to the Fourier transform. It has the advantage that it transforms real functions into real functions and it is identical to its inverse.

The Hartley transform of a function $f(t)$ which we may denote $F_{Ha}(j\omega)$, being a special type of a Fourier transform and due to a generalization to $F_{Ha}(s)$ in Laplace domain recently proposed, [27], is given by

$$F_{Ha}(j\omega) = \int_{-\infty}^{\infty} f(t) \text{cas}(\omega t) dt \quad (14.108)$$

where

$$\text{cas}(\omega t) = \sin \omega t + \cos \omega t. \quad (14.109)$$

The inverse Hartley transform is given by

$$f(t) = \frac{1}{2\pi} \int_{-\infty}^{\infty} F_{Ha}(j\omega) \text{cas}(\omega t) dt. \quad (14.110)$$

As with Fourier transform, the forward transform may be multiplied by the factor $1/(\sqrt{2\pi})$, in which case the same factor $1/(\sqrt{2\pi})$ would appear in the inverse transform. Such symmetry has the advantage that the forward and inverse transforms have the same form. A particular advantage of the Hartley transform is that the transform of a two-dimensional signal, such as an image, is simply a two-dimensional signal, that is, an image that can be readily visualized. This is in contrast with the Fourier transform, of which only the amplitude or the phase (or the real or the imaginary) spectrum can be displayed, but not the entire combined spectrum as the image of the transform.

We note that if $f(t)$ is an even function i.e. $f(-t) = f(t)$ then the Hartley transform is given by

$$F_{Ha}(j\omega) = \int_{-\infty}^{\infty} f(t) \{\cos \omega t + \sin \omega t\} dt = \int_{-\infty}^{\infty} f(t) \cos \omega t dt \quad (14.111)$$

which is the same as the Fourier transform

$$F(j\omega) = \int_{-\infty}^{\infty} f(t) e^{-j\omega t} dt = \int_{-\infty}^{\infty} f(t) \cos \omega t dt. \quad (14.112)$$

For even functions, therefore, the Hartley transform is equal to the Fourier transform.

If $f(t)$ is an odd function, i.e. $f(-t) = -f(t)$ then

$$F_{Ha}(j\omega) = \int_{-\infty}^{\infty} f(t) \sin \omega t \, dt \tag{14.113}$$

and

$$F(j\omega) = \int_{-\infty}^{\infty} f(t) (-j \sin \omega t) \, dt = -j \int_{-\infty}^{\infty} f(t) \sin \omega t \, dt \tag{14.114}$$

so that

$$F_{Ha}(j\omega) = jF(j\omega). \tag{14.115}$$

The following examples illustrate the evaluation of the Hartley transform.

Example 14.4 Evaluate the Hartley transforms of the functions a) $\delta(t)$, b) 1, c) $\cos \beta t$, d) $\sin \beta t$

a) We have $f(t) = \delta(t)$

$$F_{Ha}(j\omega) = \int_{-\infty}^{\infty} \delta(t) \cos(\omega t) dt = \int_{-\infty}^{\infty} \delta(t) dt = 1$$

which is the same as the Fourier transform as expected since $f(t)$ is even.

b) $f(t) = 1$

$$\begin{aligned} F_{Ha}(j\omega) &= \int_{-\infty}^{\infty} (\cos \omega t + \sin \omega t) \, dt \\ &= \frac{1}{2} \int_{-\infty}^{\infty} [e^{j\omega t} + e^{-j\omega t} - j(e^{j\omega t} - e^{-j\omega t})] \, dt. \end{aligned}$$

Recall that

$$\mathcal{F}[1] = \int_{-\infty}^{\infty} e^{-j\omega t} dt = 2\pi\delta(\omega).$$

We may write

$$F_{Ha}(j\omega) = \frac{1}{2} \{2\pi\delta(-\omega) + 2\pi\delta(\omega) - j2\pi\delta(-\omega) + j2\pi\delta(\omega)\} = 2\pi\delta(\omega) = F(j\omega)$$

as expected

c) $f(t) = \cos \beta t$

$$F_{Ha}(j\omega) = F(j\omega) = \pi \{ \delta(\omega - \beta) + \delta(\omega + \beta) \}.$$

d) $f(t) = \sin \beta t$.

Since $f(t)$ is odd we have

$$F_{Ha}(j\omega) = jF(j\omega) = \pi \{ \delta(\omega - \beta) - \delta(\omega + \beta) \}$$

as shown in Fig. 14.12.

We may also write

$$F_{Ha}(j\omega) = \left\{ \int_{-\infty}^{\infty} f(t) \cos \omega t \, dt + \int_{-\infty}^{\infty} f(t) \sin \omega t \, dt \right\} \tag{14.116}$$

$$F(j\omega) = \int_{-\infty}^{\infty} f(t) \cos \omega t \, dt - j \int_{-\infty}^{\infty} f(t) \sin \omega t \, dt \tag{14.117}$$

i.e.

$$F_{Ha}(j\omega) = \{ \Re[F(j\omega)] - \Im[F(j\omega)] \}. \tag{14.118}$$

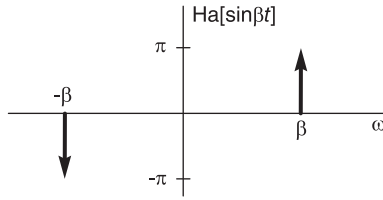


FIGURE 14.12 Hartley transform of $\sin \beta t$.

Example 14.5 Let $f(t) = e^{-\alpha t}u(t)$, $\alpha > 0$

$$F(s) = \frac{1}{s + \alpha}, \quad F(j\omega) = \frac{1}{j\omega + \alpha}$$

$$F(j\omega) = \frac{\alpha - j\omega}{\alpha^2 + \omega^2}$$

$$F_{Ha}(j\omega) = \frac{\alpha}{\alpha^2 + \omega^2} + \frac{\omega}{\alpha^2 + \omega^2} = \frac{\alpha + \omega}{\alpha^2 + \omega^2}.$$

Table 14.1 lists Hartley transform of basic functions.

TABLE 14.1 Hartley transform of some basic functions

$f(t)$	$F_{Ha}(j\omega)$
$\delta(t)$	1
1	$2\pi\delta(\omega)$
$\cos \beta t$	$\pi \{ \delta(\omega - \beta) + \delta(\omega + \beta) \}$
$\sin \beta t$	$\pi \{ \delta(\omega - \beta) - \delta(\omega + \beta) \}$
$\Pi_T(t)$	$2T Sa(T\omega)$
$e^{-\alpha t }$	$2\alpha/(\omega^2 + \alpha^2)$
$sgn(t)$	$2/\omega$
$u(t)$	$\pi\delta(\omega) + 1/\omega$

14.31 Discrete Hartley Transform

The discrete Hartley transform (DHT) was introduced by R. N. Bracewell in 1983. It is related to the continuous-time domain Hartley transform in the same way the DFT is related to the continuous-time domain Fourier transform.

Given a sequence of N values $x[0], x[1], \dots, x[N-1]$ the DHT denoted $X_{Ha}[k]$ is given by

$$X_{Ha}[k] = \sum_{n=0}^{N-1} \text{cas}(kn2\pi/N) x[n] = \sum_{n=0}^{N-1} \{ \cos(kn2\pi/N) + \sin(kn2\pi/N) \} x[n]. \quad (14.119)$$

The inverse DHT is given by

$$x[n] = \frac{1}{N} \sum_{k=0}^{N-1} \text{cas}(kn2\pi/N) X_{Ha}[k]. \tag{14.120}$$

We note that the DFT of $x[n]$ is given by

$$X[k] = \sum_{n=0}^{N-1} e^{-j\frac{2\pi}{N}nk} x[n] = \sum_{n=0}^{N-1} \left\{ \cos\left(\frac{2\pi}{N}nk\right) - j \sin\left(\frac{2\pi}{N}nk\right) \right\} x[n]. \tag{14.121}$$

With $x[n]$ real we may write

$$X_{Ha}[k] = \Re\{X[k]\} - \Im\{X[k]\}. \tag{14.122}$$

If $x[n]$ has even symmetry, i.e.

$$x[N-n] = x[n], \quad n = 1, 2, \dots, N-1. \tag{14.123}$$

then $X[k]$ is real and

$$X_{Ha}[k] = X[k] \tag{14.124}$$

and if $x[n]$ has odd symmetry, i.e. $x[N-n] = -x[n]$, $n = 1, 2, \dots, N-1$ and $x[0] = 0$. then $X[k]$ is pure imaginary and

$$X_{Ha}[k] = jX[k]. \tag{14.125}$$

Example 14.6 Evaluate the DHT of the sequences, where $b = 2\pi m/N$ and m integer.

- a) $\delta[n]$, b) 1, c) $\cos(bn)$, d) $\sin(bn)$.
- a) $x[n] = \delta[n]$ is an even function since $x[N-n] = x[n]$, $n = 1, 2, \dots, N-1$

$$X_{Ha}[k] = X[k] = 1.$$

b) $x[n] = 1$, $X_{Ha}[k] = X[k] = \begin{cases} N, & k = 0 \\ 0, & k = 1, \dots, N-1. \end{cases}$

c) $x[n] = \cos(bn)$, $X_{Ha}[k] = \begin{cases} N/2, & k = m, N-m \\ 0, & \text{otherwise.} \end{cases}$

d) $x[n] = \sin(bn)$, $X[k] = \begin{cases} \mp jN/2, & k = m, N-m \\ 0, & \text{otherwise} \end{cases}$

$$X_{Ha}[k] = \begin{cases} \pm N/2, & k = m, N-m \\ 0, & \text{otherwise.} \end{cases}$$

Evaluating the DHT of a sequence can thus be directly deduced from its DFT.

14.32 Mellin Transform

The Mellin transform of a function is defined by the integral

$$F_{\mathcal{M}}(s) = \int_0^{\infty} f(x)x^{s-1} dx. \tag{14.126}$$

In what follows we shall occasionally refer to the Mellin transform of $f(x)$ as $\mathcal{M}[f(x)]$.

Let

$$x = e^{-t} \quad (14.127)$$

$$dx = -e^{-t} dt \quad (14.128)$$

$$x^{s-1} = e^{-t(s-1)} = e^{-ts} e^t \quad (14.129)$$

$$F_{\mathcal{M}}(s) = - \int_{-\infty}^{\infty} f(e^{-t}) e^{-st} dt = \int_{-\infty}^{\infty} f(e^{-t}) e^{-st} dt = \mathcal{L}[f(e^{-t})]. \quad (14.130)$$

This is a bilateral Laplace transform. We note in passing that in Chapter 18 recent developments are shown to considerably expand the domains of existence of bilateral Laplace and z -transform and consequently Mellin transform.

Example 14.7 *Let*

$$f(x) = u(x - a), \quad a > 0$$

$$\begin{aligned} f(e^{-t}) &= 1 \quad \text{iff. } e^{-t} > a, \text{ i.e. } t < -\ln a \\ &= u(-\ln a - t) \end{aligned}$$

$$\begin{aligned} F_{\mathcal{M}}(s) &= \int_{-\infty}^{\infty} u(-\ln a - t) e^{-st} dt = \int_{-\infty}^{-\ln a} e^{-st} dt = \frac{e^{-st}}{s} \Big|_{-\infty}^{-\ln a} \\ &= \frac{0 - e^{s \ln a}}{s} = \frac{-a^s}{s}, \quad \sigma < 0. \end{aligned}$$

Example 14.8 *For*

$$f(x) = u(a - x), \quad a > 0$$

$$f(e^{-t}) = u(a - e^{-t}) = u(t + \ln a)$$

$$\begin{aligned} F_{\mathcal{M}}(s) &= \int_{-\infty}^{\infty} u(t + \ln a) e^{-st} dt = \int_{-\ln a}^{\infty} e^{-st} dt = \frac{e^{-st}}{s} \Big|_{-\ln a}^{\infty} \\ &= \frac{e^{s \ln a}}{s} = \frac{a^s}{s}, \quad \sigma > 0. \end{aligned}$$

Example 14.9 *Let*

$$f(x) = x^n u(x - a), \quad a > 0$$

$$f(e^{-t}) = e^{-nt} u(e^{-t} - a) = e^{-nt} u(-\ln a - t)$$

$$\begin{aligned} F_{\mathcal{M}}(s) &= \int_{-\infty}^{\infty} e^{-nt} u(-\ln a - t) e^{-st} dt = \int_{-\infty}^{-\ln a} e^{-(s+n)t} dt \\ &= \frac{e^{-(s+n)t}}{(s+n)} \Big|_{-\infty}^{-\ln a} = -\frac{a^{(s+n)}}{s+n}, \quad \sigma < -n. \end{aligned}$$

For the case

$$f(x) = e^{-\alpha x}, \quad \alpha > 0. \quad (14.131)$$

We have, directly,

$$F_{\mathcal{M}}(s) = \int_0^{\infty} f(x) x^{s-1} dx = \int_0^{\infty} e^{-\alpha x} x^{s-1} dx = \alpha^{-s} \Gamma(s), \quad \sigma > 0, \quad \alpha > 0. \quad (14.132)$$

We note the definition of the Gamma Function:

$$\begin{aligned} \Gamma(z) &= \int_0^\infty t^{z-1} e^{-t} dt, \quad \text{Re}[z] > 0 \\ &= k^z \int_0^\infty t^{z-1} e^{-kt} dt, \quad \text{Re}[z] > 0, \quad \text{Re}[k] > 0. \end{aligned} \tag{14.133}$$

Let $f(x) = e^{-x^2}$

$$F_{\mathcal{M}}(s) = \int_0^\infty e^{-x^2} x^{s-1} dx. \tag{14.134}$$

Let $x^2 = v, \quad 2x dx = dv$

$$F_{\mathcal{M}}(s) = \int_0^\infty e^{-v} v^{(1/2)(s-1)} \frac{dv}{2v^{1/2}} = \frac{1}{2} \int_0^\infty e^{-v} v^{(1/2)s-1} dv = \frac{1}{2} \Gamma(s/2). \tag{14.135}$$

14.33 Mellin Transform of e^{jx}

The Mellin transform of $f(x) = e^{jx}$ is given by

$$F_M(s) = \int_0^\infty e^{jx} x^{s-1} dx. \tag{14.136}$$

To evaluate this integral consider the contour integral

$$\oint_C z^{2s-1} e^{jz^2} dz \tag{14.137}$$

where C is the closed contour in the z -plane shown in Fig. 14.13.

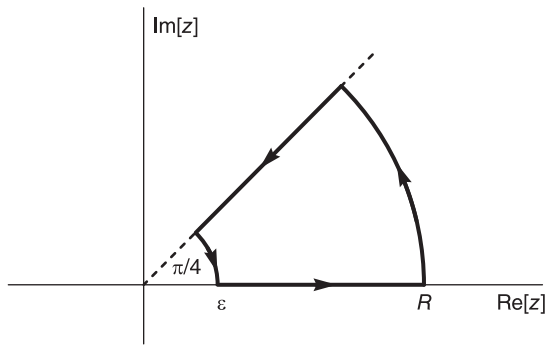


FIGURE 14.13 Contour of integration in z -plane.

The contour is so chosen as to avoid the singularity at $z = 0$. We have

$$I \triangleq \oint_C z^{2s-1} e^{jz^2} dz = 0. \tag{14.138}$$

On the real axis we write $z = x$, $dz = dx$. On the circle of radius R we write $z = R e^{j\theta}$, $dz = R j e^{j\theta} d\theta$. On the line of slope $\pi/4$ we have $z = r e^{j\pi/4}$, $dz = e^{j\pi/4} dr$,

$$\begin{aligned} I &= \int_{\varepsilon}^R x^{2s-1} e^{jx^2} dx + \int_0^{\pi/4} (R e^{j\theta})^{2s-1} e^{jR^2 e^{j2\theta}} R j e^{j\theta} d\theta \\ &\quad + \int_R^{\varepsilon} (r e^{j\pi/4})^{2s-1} e^{-r^2} e^{j\pi/4} dr + \int_{\pi/4}^0 (\varepsilon e^{j\theta})^{2s-1} e^{j\varepsilon^2 e^{j2\theta}} \varepsilon j e^{j\theta} d\theta \\ &= 0 = I_1 + I_2 + I_3 + I_4. \end{aligned} \quad (14.139)$$

Writing $s = \sigma + j\omega$ we note that the fourth integral I_4 has an absolute value of

$$\varepsilon^{2s} e^{-\varepsilon^2 \sin 2\theta} \quad (14.140)$$

which tends to zero as $\varepsilon \rightarrow 0$ if $\sigma > 0$. The second integral I_2 has the absolute value

$$R^{2s} e^{-R^2 \sin 2\theta}. \quad (14.141)$$

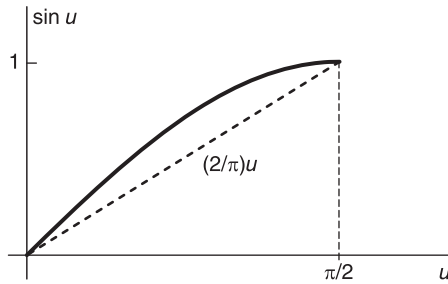


FIGURE 14.14 Inequality of the sine function.

From the well-known inequality illustrated in Fig. 14.14, namely,

$$\sin u \geq (2/\pi) u, \quad 0 \leq u \leq \pi/2 \quad (14.142)$$

we have $u = 2\theta$

$$R^{2s} e^{-R^2 \sin 2\theta} \leq R^{2s} e^{-R^2 (2/\pi) 2\theta}, \quad 0 \leq \theta \leq \pi/4 \quad (14.143)$$

i.e.

$$\begin{aligned} |I_2| &\leq \int_0^{\pi/4} R^{2\sigma} e^{-R^2 \sin 2\theta} d\theta \leq \int_0^{\pi/4} R^{2\sigma} e^{-(4/\pi)R^2 \theta} d\theta \\ &= R^{2\sigma} \frac{e^{-(4R^2/\pi)\theta}}{-4R^2/\pi} \Big|_0^{\pi/4} = \frac{\pi}{4} R^{2\sigma-2} (1 - e^{-R^2}) \end{aligned} \quad (14.144)$$

which tends to zero as $R \rightarrow \infty$ if and only if $\sigma < 1$.

We may therefore write, as $\varepsilon \rightarrow 0$ and $R \rightarrow \infty$,

$$\int_0^{\infty} x^{2s-1} e^{jx^2} dx = e^{j(\pi/2)s} \int_0^{\infty} r^{2s-1} e^{-r^2} dr. \quad (14.145)$$

Letting $x^2 = u$, $2x dx = du$, $r^2 = v$, $2r dr = dv$ we have with $0 < \sigma < 1$

$$\int_0^\infty u^{(2s-1)/2} e^{ju} (1/2) u^{-1/2} du = e^{j(\pi/2)s} \int_0^\infty v^{(2s-1)/2} e^{-v} (1/2) v^{-1/2} dv \quad (14.146)$$

i.e.

$$\int_0^\infty u^{s-1} e^{ju} du = e^{j(\pi/2)s} \int_0^\infty u^{s-1} e^{-v} dv, \quad 0 < \sigma < 1 \quad (14.147)$$

deducing that

$$F_M(s) = e^{j(\pi/2)s} \Gamma(s) = j^s \Gamma(s). \quad (14.148)$$

If $f(x) = e^{j\omega x}$ we let $\omega x = u$ obtaining

$$F_{\mathcal{M}}(s) = e^{j\pi s/2} \omega^{-s} \Gamma(s) \quad (14.149)$$

and thereof

$$\mathcal{M}[e^{-j\omega x}] = e^{-j\pi s/2} \omega^{-s} \Gamma(s).$$

For the case

$$f(x) = \sin x \quad (14.150)$$

$$\begin{aligned} F_{\mathcal{M}}(s) &= \int_0^\infty \sin x x^{s-1} dx = \int_0^\infty \frac{e^{jx} - e^{-jx}}{2j} x^{s-1} dx \\ &= \frac{1}{2j} (\mathcal{M}[e^{jx}] - \mathcal{M}[e^{-jx}]) = -j0.5\Gamma(s) \{e^{+j(\pi/2)s} - e^{-j(\pi/2)s}\} \\ &= \sin[(\pi/2)s]\Gamma(s). \end{aligned} \quad (14.151)$$

Similarly if

$$f(x) = \cos x \quad (14.152)$$

then

$$F_{\mathcal{M}}(s) = \int_0^\infty \cos x x^{s-1} dx = \cos\left(\frac{\pi}{2}s\right) \Gamma(s). \quad (14.153)$$

As will be elaborated upon in Chapter 18, we note that from knowledge of Mellin transforms we can extend Laplace transforms. For example, we know that if $f(x) = e^{-ax}$ then $F_{\mathcal{M}}(s) = a^{-s}\Gamma(s)$.

This implies that $a^{-s}\Gamma(s)$ is the bilateral Laplace transform of $f(e^{-t}) = e^{-ae^{-t}}$. In other words $\mathcal{L}[e^{-ae^{-t}}] = a^{-s}\Gamma(s)$.

If $f(x) = \text{sgn}(-\ln x)$ then $f(e^{-t}) = \text{sgnt}$

$$F_{\mathcal{M}}(s) = \mathcal{L}[\text{sgnt}] = \frac{2}{s}. \quad (14.154)$$

14.34 Hankel Transform

The Hankel transform is suitable for transforming a two-dimensional signal $f(x, y)$ which has symmetry about the origin of the $x - y$ plane so that its value is simply a function of the distance $r = \sqrt{x^2 + y^2}$ from the origin. To obtain perfect symmetry we write the two-dimensional Fourier transform of the signal $f(x, y)$ in the form

$$F(f_1, f_2) = \int_{-\infty}^\infty \int_{-\infty}^\infty f(x, y) e^{-j2\pi(f_1 x + f_2 y)} dx dy. \quad (14.155)$$

so that the inverse transform is given by

$$f(x, y) = \int_{-\infty}^{\infty} \int_{-\infty}^{\infty} F(f_1, f_2) e^{j2\pi(f_1x + f_2y)} df_1 df_2. \quad (14.156)$$

We may write

$$g(r) = f(x, y) \quad (14.157)$$

and, using polar coordinates,

$$x = r \cos \theta, \quad y = r \sin \theta \quad (14.158)$$

and in the transform domain

$$f_1 = \rho \cos \phi, \quad f_2 = \rho \sin \phi \quad (14.159)$$

$$f_1x + f_2y = r\rho \{ \cos \theta \cos \phi + \sin \theta \sin \phi \} = r\rho \cos(\theta - \phi) \quad (14.160)$$

$$dA = dx dy = r dr d\theta \quad (14.161)$$

$$F(f_1, f_2) = \int_0^{2\pi} \int_0^{\infty} g(r) e^{-j2\pi r \rho \cos(\theta - \phi)} r dr d\theta. \quad (14.162)$$

Letting $\theta - \phi = \lambda$ we may write

$$\begin{aligned} \int_0^{2\pi} e^{-j2\pi r \rho \cos(\theta - \phi)} d\theta &= \int_{-\phi}^{-\phi + 2\pi} e^{-j2\pi r \rho \cos \lambda} d\lambda \\ &= \int_0^{2\pi} e^{-j2\pi r \rho \cos \lambda} d\lambda = 2\pi J_0(2\pi r \rho) \end{aligned} \quad (14.163)$$

using the Bessel function integral form [1]

$$J_0(z) = \frac{1}{2\pi} \int_0^{2\pi} e^{-jz \cos \gamma} d\gamma. \quad (14.164)$$

The transform of $g(r)$, denoted $G(\rho)$, is therefore

$$G(\rho) \triangleq F(f_1, f_2) = 2\pi \int_0^{\infty} r g(r) J_0(2\pi r \rho) dr. \quad (14.165)$$

This is known as the Hankel transform, and the inverse transform is given by

$$g(r) = \frac{1}{2\pi} \int_0^{\infty} \rho G(\rho) J_0(2\pi r \rho) d\rho. \quad (14.166)$$

Example 14.10 A circular plateau $g(r)$ of radius a centered at the origin of the $x - y$ plane may be viewed as a rotation about the origin of a rectangle. We may write it in the form

$$g(r) = \Pi_a(r) = \begin{cases} 1, & 0 \leq r < a \\ 0 & r > a. \end{cases}$$

Its Hankel transform is given by

$$G(\rho) = 2\pi \int_0^a r J_0(2\pi r \rho) dr = (a/\rho) J_1(2\pi a \rho)$$

Example 14.11 The Hankel transform of $g(r) = e^{-r}$ is

$$G(\rho) = 2\pi \int_0^\infty r e^{-r} J_0(2\pi r \rho) dr = 2\pi / (4\pi^2 \rho^2 + 1)^{3/2}$$

using the integrals of Bessel functions.

Example 14.12 A ring of radius a formed by the Dirac-delta impulse, namely, $g(r) = \delta(r - a)$ has the Hankel transform

$$G(\rho) = 2\pi \int_0^\infty r \delta(r - a) J_0(2\pi r \rho) dr = 2\pi a J_0(2\pi a \rho).$$

Example 14.13 With $g(r) = 1/r$ we have

$$G(\rho) = 2\pi \int_0^\infty J_0(2\pi r \rho) dr = 1/\rho$$

and with $g(r) = e^{-r}/r$,

$$G(\rho) = 2\pi \int_0^\infty e^{-r} J_0(2\pi r \rho) dr = 2\pi / \sqrt{4\pi^2 \rho^2 + 1}$$

Other transforms are listed in Table 14.2.

TABLE 14.2 Hankel basic transforms

$g(r)$	$G(\rho)$
$\Pi_1(r)$	$J_1(2\pi\rho) / \rho$
$1/r$	$1/\rho$
$\delta(r - a)$	$2\pi a J_0(2\pi a \rho)$
e^{-r}	$2\pi / (4\pi^2 \rho^2 + 1)^{3/2}$
e^{-r}/r	$2\pi / \sqrt{4\pi^2 \rho^2 + 1}$
$1/\sqrt{1 + r^2}$	$e^{-2\pi\rho} / \rho$
$1 / (1 + r^2)^{3/2}$	$2\pi e^{-2\pi\rho}$

14.35 Fourier Cosine Transform

We have studied properties of half-range expansion in Chapter 2. We have noted that if a given function $f(t)$ is reflected about the $t = 0$ axis, the resulting even function has real

spectrum. This same property is the basis of a special form case of the Fourier transform referred to as the Fourier cosine transform (FCT).

Given a one-sided function $f(t)$ defined for $t \geq 0$ if we reflect the function about the $t = 0$ axis we obtain an even function $f_e(t)$ such that

$$f_e(t) = f(|t|) = f(t), \quad t \geq 0 \quad (14.167)$$

$$f_e(-t) = f_e(t) \quad (14.168)$$

and its Fourier transform is given by

$$\begin{aligned} F_e(j\omega) &= \int_{-\infty}^{\infty} f_e(t) e^{-j\omega t} dt = \int_{-\infty}^{\infty} f_e(t) (\cos \omega t - j \sin \omega t) dt \\ &= 2 \int_0^{\infty} f_e(t) \cos \omega t dt = 2 \int_0^{\infty} f(t) \cos \omega t dt. \end{aligned} \quad (14.169)$$

The FCT $F_c(j\omega)$ is by definition

$$F_c(j\omega) = \int_0^{\infty} f(t) \cos \omega t dt, \quad \omega \geq 0 \quad (14.170)$$

which is half the transform of the even function $f_e(t)$

$$F_c(j\omega) = F_e(j\omega) / 2. \quad (14.171)$$

The inverse FCT is given by

$$f(t) = \frac{2}{\pi} \int_0^{\infty} F_c(j\omega) \cos \omega t d\omega, \quad t \geq 0. \quad (14.172)$$

The FCT is preferred in analyzing causal signals and when the evaluation of real expressions is preferred to complex ones.

A Fourier sine transform (FST) is similarly defined by a half range expansion based on an odd reflection of the function about the $t = 0$ axis. In this case the spectrum is purely imaginary.

The FST transform is written

$$F_s(j\omega) = \int_0^{\infty} f(t) \sin \omega t dt, \quad \omega > 0 \quad (14.173)$$

and the inverse transform is

$$f(t) = \frac{2}{\pi} \int_0^{\infty} F_s(j\omega) \sin \omega t d\omega, \quad t \geq 0. \quad (14.174)$$

14.36 Discrete Cosine Transform (DCT)

The discrete cosine transform is the discrete time counterpart of the FCT.

Given the $(2N - 2)$ -elements sequence $x[0], x[1], \dots, x[2N - 3]$, with even symmetry about $n = N - 1$, such as that shown in Fig. 14.15, i.e. $x[1] = x[2N - 3]$, $x[2] = x[2N - 4]$, ..., $x[N - 2] = x[N]$, and of which the elements $x[0]$ and $x[N - 1]$ are unique. We may write

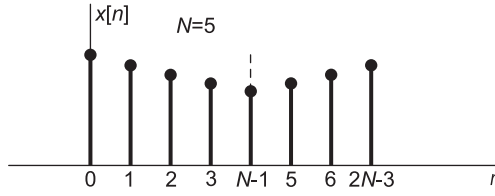


FIGURE 14.15 Even symmetry.

$$\begin{aligned}
 X[k] &= \sum_{n=0}^{2N-3} x[n] e^{-j\frac{2\pi}{2N-2}nk} = \sum_{n=0}^{2N-3} x[n] e^{-j\frac{\pi}{N-1}nk} \\
 &= x[0] + x[N-1] e^{-j\frac{\pi}{N-1}(N-1)k} + \sum_{n=1}^{N-2} x[n] e^{-j\frac{\pi}{N-1}nk} \\
 &= x[0] + (-1)^k x[N-1] + x[1] \left\{ e^{-j\frac{\pi}{N-1}k} + e^{j\frac{\pi}{N-1}k} \right\} \\
 &\quad + x[2] \left\{ e^{-j\frac{\pi}{N-1}2k} + e^{j\frac{\pi}{N-1}2k} \right\} + \dots \\
 &\quad + x[N-2] \left\{ e^{-j\frac{\pi}{N-1}(N-2)k} + e^{j\frac{\pi}{N-1}(N-2)k} \right\} \tag{14.175}
 \end{aligned}$$

$$X[k] = x[0] + (-1)^k x[N-1] + 2 \sum_{n=1}^{N-2} x[n] \cos \frac{\pi}{N-1}nk \tag{14.176}$$

$X[k]$ has the same symmetry as $x[n]$.

$$\begin{aligned}
 x[n] &= \frac{1}{2N-2} \sum_{k=0}^{2N-3} X[k] e^{j\frac{\pi}{N-1}nk} \\
 &= \frac{1}{2(N-1)} \left\{ X[0] + X[N-1] e^{j\frac{\pi}{N-1}(N-1)n} + \sum_{k=1}^{2N-2} X[k] e^{j\frac{\pi}{N-1}nk} \right\} \\
 &= \frac{1}{2(N-1)} \left\{ X[0] + (-1)^n X[N-1] + 2 \sum_{k=1}^{N-2} X[k] \cos \frac{\pi}{N-1}nk \right\} \tag{14.177}
 \end{aligned}$$

Example 14.14 let $x[n] = 3, 2, 1, 2$. We may write

$$\begin{aligned}
 X[k] &= x[0] + (-1)^k x[N-1] + 2 \sum_{n=1}^{N-2} x[n] \cos \frac{\pi}{N-1}nk \\
 &= 3 + (-1)^k \times 1 + 2 \left\{ 2 \cos \frac{\pi}{2}k \right\} = 3 + (-1)^k + 4 \cos \frac{\pi}{2}k
 \end{aligned}$$

$X[0] = 3 + 1 + 4 = 8$, $X[1] = 3 - 1 - 4 \times 0 = 2$, $X[2] = 3 + 1 + 4 \times (-1) = 4 - 4 = 0$,

$$X[3] = 3 - 1 + 4 \cos 3\frac{\pi}{2} = 2 + 0 = 2$$

$$x[n] = \frac{1}{4} \left\{ X[0] + (-1)^n X[N-1] + 2 \sum_{k=1}^{N-2} X[k] \cos \frac{\pi}{N-1}nk \right\}$$

$$\begin{aligned}
 x[0] &= \frac{1}{4} (8 + 0 + 2X[1]) = \frac{8 + 2 \times 2}{4} = 12/4 = 3 \\
 x[1] &= \frac{1}{4} \left(8 - 0 + 2 \times 2 \cos \frac{\pi}{2} \right) = 8/4 = 2 \\
 x[2] &= \frac{1}{4} \left(8 + 0 + 2 \times 2 \cos \frac{\pi}{2} \times 2 \right) = \frac{8 - 4}{4} = 4/4 = 1 \\
 x[3] &= \frac{1}{4} \left(8 - 0 + 2 \times 2 \times \cos \frac{\pi}{2} \times 3 \right) = 8/4 = 2
 \end{aligned}$$

confirming that

$$x[n] = \frac{1}{2(N-1)} \left[X[0] + (-1)^n X[N-1] + 2 \sum_{k=1}^{N-2} X[k] \cos \frac{\pi}{N-1} nk \right].$$

We can equivalently write the DCT in the form

$$X_{DC}[k] = 2 \sum_{n=0}^{N-1} x[n] \xi[n] \cos \frac{\pi}{N-1} nk, \quad k = 0, 1, \dots, N-1$$

where

$$\xi[n] = \begin{cases} 1, & n = 1, 2, \dots, N-2 \\ 1/2, & n = 0, N-1 \end{cases}$$

and the inverse DCT in the form

$$x[n] = \frac{1}{N-1} \sum_{k=0}^{N-1} X_{DC}[k] \xi[k] \cos \frac{\pi}{N-1} nk, \quad n = 0, 1, \dots, N-1.$$

14.37 Fractional Fourier Transform

The fractional Fourier transform is given by

$$F_a(j\omega) = \int_{-\infty}^{\infty} A_\alpha e^{j\pi [\cot \alpha \omega^2 / (4\pi^2) - 2 \csc \alpha (\omega/2\pi)t + \cot \alpha t^2]} f(t) dt \quad (14.178)$$

i.e.

$$F_a(j\omega) = A_\alpha e^{j \cot \alpha \omega^2 / (4\pi)} \int_{-\infty}^{\infty} e^{-j \csc \alpha \omega t + j\pi \cot \alpha t^2} f(t) dt \quad (14.179)$$

where

$$A_\alpha = \sqrt{1 - j \cot \alpha} \quad (14.180)$$

Alternatively, with $\omega = 2\pi f$

$$F_a(f) = A_\alpha e^{j\pi \cot \alpha f^2} \int_{-\infty}^{\infty} e^{-j2\pi \csc \alpha ft + j\pi \cot \alpha t^2} f(t) dt \quad (14.181)$$

If $\alpha = \pi/2$ the fractional transform is the usual Fourier transform.

For example, let $f(t) = 1$. We may write

$$x = \cot \alpha, \quad \xi = \csc \alpha f \quad (14.182)$$

$$F_a(f) = A_\alpha e^{j\pi \cot \alpha f^2} \int_{-\infty}^{\infty} e^{j\pi(xt^2 - 2\xi t)} dt \tag{14.183}$$

$$F_a(f) = \sqrt{1 - j \cot \alpha} e^{j\pi \cot \alpha f^2} \frac{1}{\sqrt{\cot \alpha}} e^{j\pi/4} e^{-j\pi(\csc \alpha)^2 f^2 / \cot \alpha} \tag{14.184}$$

having used the relation

$$\int_{-\infty}^{\infty} e^{j\pi(xu^2 \pm 2\xi u)} du = \frac{1}{\sqrt{x}} e^{j\pi/4} e^{-j\pi\xi^2/x}. \tag{14.185}$$

With

$$\xi \text{ real, } x > 0 \tag{14.186}$$

$$\int e^{-j\pi(xu^2 \pm 2\xi u)} du = \frac{1}{\sqrt{x}} e^{-j\pi/4} e^{j\pi\xi^2/x} \tag{14.187}$$

we have

$$\int_{-\infty}^{\infty} e^{j\pi(xt^2 + 2yt)} dt = \frac{1 + j}{\sqrt{2}} \frac{e^{-j\pi y^2/x}}{\sqrt{x}} \tag{14.188}$$

$$F_a(f) = A_\alpha \int_{-\infty}^{\infty} e^{j\pi(\cot \alpha f^2 - 2 \csc \alpha f t + \cot \alpha t^2)} f(t) dt \tag{14.189}$$

$$A_\alpha = \sqrt{1 - j \cot \alpha} \tag{14.190}$$

$$F_a(f) = A_\alpha e^{j\pi \cot \alpha f^2} \int_{-\infty}^{\infty} e^{j\pi(\cot \alpha t^2 - 2 \csc \alpha f t)} f(t) dt \tag{14.191}$$

$$\begin{aligned} F_a(f) &= A_\alpha e^{j\pi \cot \alpha f^2} \int_{-\infty}^{\infty} e^{j\pi(xt^2 - 2\xi t)} dt \\ &= A_\alpha e^{j\pi \cot \alpha f^2} \frac{1}{\sqrt{\cot \alpha}} e^{j\pi/4} e^{-j\pi(\csc \alpha)^2 f^2 / \cot \alpha} \\ &= \sqrt{\frac{1 - j \cot \alpha}{\cot \alpha}} \sqrt{j} e^{j\theta} = \sqrt{j} \sqrt{\tan \alpha - j} e^{j\theta} = \sqrt{1 + j \tan \alpha} e^{j\theta} \end{aligned} \tag{14.192}$$

$$\theta = \pi \cot \alpha f^2 - \pi \frac{f^2}{\sin^2 \alpha} \frac{\sin \alpha}{\cos \alpha} = -\pi \tan \alpha f^2 \tag{14.193}$$

so that

$$F_a(f) = \sqrt{1 + j \tan \alpha} e^{-j\pi \tan \alpha f^2} \tag{14.194}$$

Example 14.15 With $f(t) = \delta(t - t_0)$

$$\begin{aligned} F_a(f) &= A_\alpha e^{j\pi \cot \alpha f^2} \int_{-\infty}^{\infty} \delta(t - t_0) e^{j\pi(\cot \alpha t^2 - 2 \csc \alpha f t)} dt \\ &= A_\alpha e^{j\pi \cot \alpha f^2} e^{j\pi(\cot \alpha t_0^2 - 2 \csc \alpha f t_0)} \\ &= \sqrt{1 - j \cot \alpha} e^{j\pi \cot \alpha f^2} e^{j\pi(\cot \alpha t_0^2 - 2 \csc \alpha f t_0)} \end{aligned}$$

$$F_a(f) = \sqrt{1 - j \cot \alpha} e^{j\pi(\cot \alpha f^2 - 2 \csc \alpha f t_0 + \cot \alpha t_0^2)}$$

Example 14.16 Consider $f(t) = e^{j\omega_0 t} = e^{j2\pi f_0 t}$

$$\begin{aligned} F_a(f) &= A_\alpha e^{j\pi \cot \alpha f^2} \int_{-\infty}^{\infty} e^{j\pi(\cot \alpha t^2 - 2 \csc \alpha f t + 2f_0 t)} dt \\ &= A_\alpha e^{j\pi \cot \alpha f^2} \int e^{j\pi\{\cot \alpha t^2 + 2(f_0 - \csc \alpha f)t\}} dt \\ &= A_\alpha e^{j\pi \cot \alpha f^2} \frac{1}{\sqrt{\cot \alpha}} \sqrt{j} e^{-j\pi(f_0 - \csc \alpha f)^2 / \cot \alpha} \\ &= \sqrt{\frac{1 - j \cot \alpha}{\cot \alpha}} \sqrt{j} e^{j\theta} = \sqrt{1 + j \tan \alpha} e^{j\theta} \end{aligned}$$

$$\begin{aligned}
 j\theta &= j\pi \{ \cot \alpha f^2 + [2 \csc \alpha f f_0 - f_0^2 - \csc^2 \alpha f^2] / \cot \alpha \} \\
 &= -j\pi \left\{ -\cot \alpha f^2 - 2 \frac{f f_0}{\cos \alpha} + f_0^2 \tan \alpha + \frac{f^2}{\sin \alpha \cos \alpha} \right\} \\
 &= -j\pi \left\{ -\cot \alpha f^2 - 2 \sec \alpha f f_0 + f_0^2 \tan \alpha + \frac{f^2}{\sin \alpha \cos \alpha} \right\} \\
 &= -j\pi \{ C f^2 - 2 \sec \alpha f f_0 + f_0^2 \tan \alpha \}
 \end{aligned}$$

where

$$C = -\cot \alpha + \frac{1}{\sin \alpha \cos \alpha} = \frac{1}{\sin \alpha \cos \alpha} - \frac{\cos \alpha}{\sin \alpha} = \frac{1 - \cos^2 \alpha}{\sin \alpha \cos \alpha} = \frac{\sin^2 \alpha}{\sin \alpha \cos \alpha} = \tan \alpha$$

Hence

$$F_a(f) = \sqrt{1 + j \tan \alpha} e^{-j\pi \{ \tan \alpha f^2 - 2 \sec \alpha f f_0 + f_0^2 \tan \alpha \}}$$

Example 14.17 Consider $f(t) = \cos \beta t = 0.5 (e^{j\beta t} + e^{-j\beta t})$

$$\begin{aligned}
 F_a(f) &= 0.5 \sqrt{1 + j \tan \alpha} \left[e^{-j\pi \{ \tan \alpha f^2 - 2 \sec \alpha f_0 f + f_0^2 \tan \alpha \}} + e^{-j\pi \{ \tan \alpha f^2 + 2 \sec \alpha f_0 f + f_0^2 \tan \alpha \}} \right] \\
 &= 0.5 \sqrt{1 + j \tan \alpha} e^{-j\pi \{ \tan \alpha f^2 + f_0^2 \tan \alpha \}} \{ e^{j2\pi \sec \alpha f_0 f} + e^{-j2\pi \sec \alpha f_0 f} \} \\
 &= \sqrt{1 + j \tan \alpha} e^{-j\pi \tan \alpha (f^2 + f_0^2)} \cos 2\pi f_0 \sec \alpha f.
 \end{aligned}$$

Table 14.3 lists fractional transforms of some basic functions. In deriving the transform of $f(t) = e^{-\pi\gamma t^2}$ use is made of the the relation

$$\int_{-\infty}^{\infty} e^{j\pi(xt^2+2yt)-\pi\gamma t^2} dt = \frac{1}{\sqrt{\gamma - jx}} e^{-j\pi y^2/(x+j\gamma)}. \tag{14.195}$$

14.38 Discrete Fractional Fourier Transform

The discrete fractional Fourier transform is given by

$$X_b[k] = \sum_{n=0}^{N-1} x[n] e^{-j \frac{2\pi}{N} b n k} \tag{14.196}$$

and may be evaluated using *Mathematica*®.

14.39 Two-Dimensional Transforms

Operations on two-dimensional sequences, including z transformation, convolution and correlation have been studied in Chapter 6. We have seen that the concept is a straightforward extension to two variables of the one-dimensional, one-variable transform.

The definitions of several two-dimensional transforms are given in what follows.

TABLE 14.3 Fractional Fourier transforms of some common functions

$f(t)$	$F_\alpha(f)$
$\delta(t)$	$\sqrt{1-j\cot\alpha} e^{j\pi f^2 \cot\alpha}$
$\delta(t-t_0)$	$\sqrt{1-j\cot\alpha} e^{j\pi(f^2 \cot\alpha - 2ft_0 \csc\alpha + t_0^2 \cot\alpha)}$
1	$\sqrt{1+j\tan\alpha} e^{-j\pi f^2 \tan\alpha}$
$e^{j2\pi f_0 t}$	$\sqrt{1+j\tan\alpha} e^{-j\pi(f^2 \tan\alpha - 2f_0 f \sec\alpha + f_0^2 \tan\alpha)}$
$e^{j\pi\gamma t^2}$	$\sqrt{(1+j\tan\alpha)/(1+\gamma\tan\alpha)} e^{j\pi f^2 [\gamma - \tan\alpha]/[1+\gamma\tan\alpha]}$
$e^{j\pi(\gamma t^2 + 2f_0 t)}$	$\sqrt{(1+j\tan\alpha)/(1+\gamma\tan\alpha)}$ $e^{j\pi[f^2(\gamma - \tan\alpha) + 2f_0 f \sec\alpha - f_0^2 \tan\alpha]/[1+\gamma\tan\alpha]}$
$e^{-\pi t^2}$	$e^{-\pi f^2}$
$e^{-\pi\gamma t^2}$	$\sqrt{(1-j\cot\alpha)/(\gamma-j\cot\alpha)} e^{j\pi f^2 [\cot\alpha(\gamma^2-1)]/[\gamma^2+\cot^2\alpha]}$ $e^{-\pi\gamma f^2 \csc^2\alpha/(\gamma^2+\cot^2\alpha)}$
$e^{-\pi(\gamma t^2 + 2f_0 t)}$	$\sqrt{\frac{1-j\cot\alpha}{\gamma-j\cot\alpha}} e^{j\pi \cot\alpha [(\gamma^2-1)f^2 + 2\gamma f_0 \sec\alpha f + f_0^2] / [\gamma^2 + \cot^2\alpha]}$ $e^{-\pi \csc^2\alpha [\gamma f^2 + 2f_0 \cos\alpha f - \gamma f_0^2 \sin^2\alpha] / [\gamma^2 + \cot^2\alpha]}$

14.40 Two-Dimensional Fourier Transform

The 2-D Fourier transform of the two-dimensional function $f(x, y)$ is given by

$$F(j\omega_1, j\omega_2) = \int_{-\infty}^{\infty} \int_{-\infty}^{\infty} f(x, y) e^{-j(\omega_1 x + \omega_2 y)} dx dy. \tag{14.197}$$

The inverse transform is given by

$$f(x, y) = \frac{1}{4\pi^2} \int_{-\infty}^{\infty} \int_{-\infty}^{\infty} F(j\omega_1, j\omega_2) e^{j(\omega_1 x + \omega_2 y)} d\omega_1 d\omega_2. \tag{14.198}$$

As an example, the Fourier transform of the two-dimensional weighted Gaussian function

$$f(x, y) = (xy)^6 e^{-(x^2+y^2)}$$

is given by

$$F(u, v) = e^{-(u^2+v^2)/4} (-120 + 180u^2 - 30u^4 + u^6) (-120 + 180v^2 - 30v^4 + v^6) / 8192.$$

and can be seen in Fig. 14.16.

The Fourier transform of a 2-D sequence $x[m, n]$ is defined by

$$X(e^{j\Omega_1}, e^{j\Omega_2}) = \sum_{m=-\infty}^{\infty} \sum_{n=-\infty}^{\infty} x[m, n] e^{-j(\Omega_1 m + \Omega_2 n)}. \tag{14.199}$$

and the inverse transform is given by

$$x[m, n] = \frac{1}{4\pi^2} \int_{-\pi}^{\pi} \int_{-\pi}^{\pi} X(e^{j\Omega_1}, e^{j\Omega_2}) e^{j(\Omega_1 m + \Omega_2 n)} d\Omega_1 d\Omega_2. \tag{14.200}$$

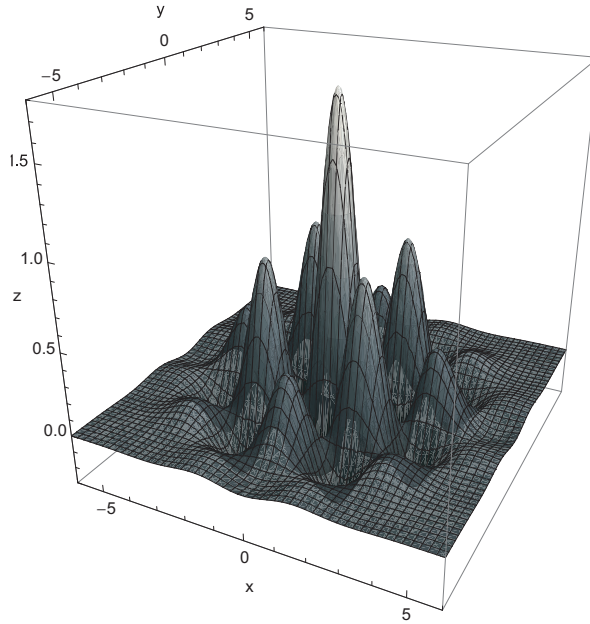


FIGURE 14.16 Fourier transform of a two-dimensional weighted Gaussian function.

Two-Dimensional DFT

The two-dimensional DFT of the $N \times N$ point 2-D sequence $x[m, n]$ is given by

$$X[r, s] = \sum_{m=0}^{N-1} \sum_{n=0}^{N-1} x[m, n] e^{-j(2\pi/N)(rm+sn)} \quad (14.201)$$

$$x[m, n] = (1/N^2) \sum_{r=0}^{N-1} \sum_{s=0}^{N-1} X[r, s] e^{j(2\pi/N)(rm+sn)}. \quad (14.202)$$

The two-dimensional DFT of a matrix representing an image can be found by first evaluating the one-dimensional DFT of each row of the matrix, followed by applying a one-dimensional DFT to each successive column of the resulting matrix. The transform can also be found by transforming the columns followed by transforming the rows of the resulting matrix.

As an example, the two-dimensional DFT amplitude spectrum of the portrait of Niels Henrik Abel (1802-1829), which appears in the biography section of Chapter A, can be seen as an image and as a three-dimensional surface in Fig. 14.17(a) and (b), respectively.

The two-dimensional DCT transform of the same Abel portrait can be seen in Fig. 14.18(a).

The two-dimensional Walsh–Hadamard transform, in natural order, of the same Abel portrait can be seen in Fig. 14.18(b). The function `hadamard(N)` of MATLAB® generates the Walsh–Hadamard matrix in natural order.

The functions `fft2` and `DCT2` of MATLAB evaluate the two-dimensional DFT and DCT of an image, respectively.

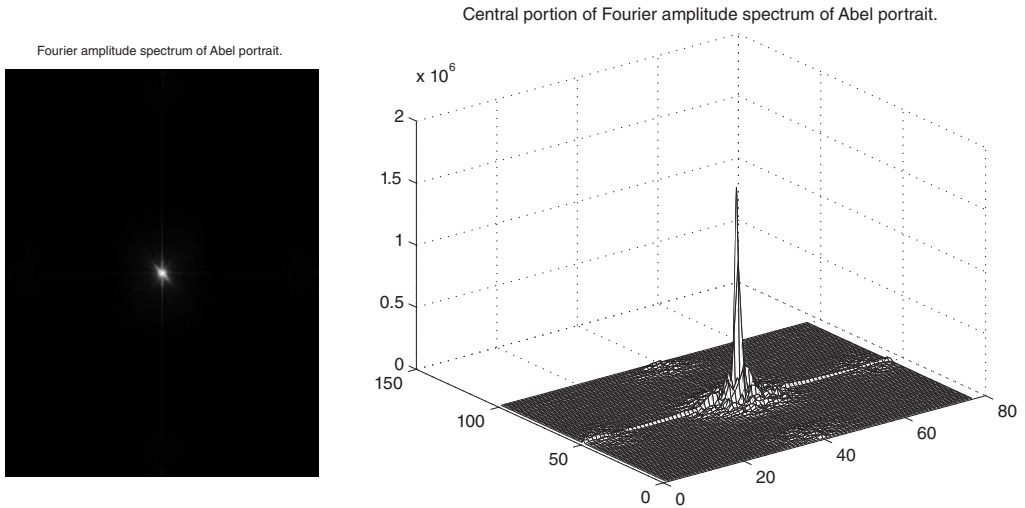


FIGURE 14.17 Amplitude spectrum of Abel’s portrait, a) as an image, and b) as a three-dimensional surface.

14.41 Continuous-Time Domain Hilbert Transform Relations

Let $h(t)$ be a real causal system impulse response. We have

$$H(j\omega) = \mathcal{F}[h(t)] = H_R(j\omega) + jH_I(j\omega) \tag{14.203}$$

$$H(s) = \mathcal{L}[h(t)]. \tag{14.204}$$

In what follows we show that $H(j\omega)$ may be deduced from either $H_R(j\omega)$ or $H_I(j\omega)$. Let $H(j\omega)$ be a rational function. In this case we have

$$H(s) = \frac{N(s)}{D(s)}. \tag{14.205}$$

Since $H(s)$ is analytic there are no poles in the right-half plane, i.e. $D(s)$ has no zeros for $Re(s) > 0$, $D(s)$ is called a “Hurwitz” polynomial. In the following, we study the case where there are no poles on the $j\omega$ axis followed by the case of poles on the axis.

14.42 $H_I(j\omega)$ versus $H_R(j\omega)$ with No Poles on Axis

In what follows we assume a causal impulse response $h(t)$ and no poles of the system function $H(s)$ on the imaginary axis. We show that given $H_R(j\omega)$, we can evaluate $H(s)$ and $H_I(j\omega)$. We may write

$$H(j\omega) = H_R(j\omega) + jH_I(j\omega) \tag{14.206}$$

$$H(-j\omega) = H_R(j\omega) - jH_I(j\omega) \tag{14.207}$$

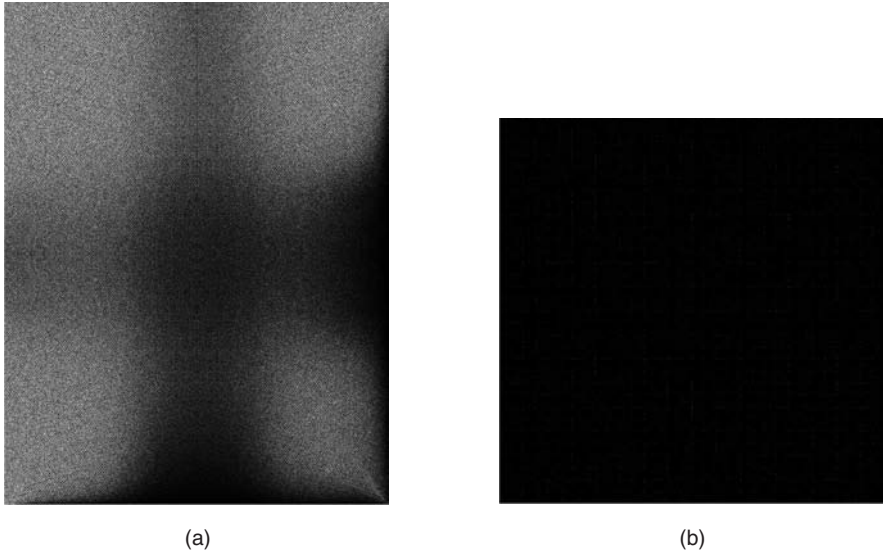


FIGURE 14.18 Two-dimensional transforms: (a) DCT, (b) Walsh–Hadamard.

$$H_R(j\omega) = (1/2) [H(j\omega) + H(-j\omega)] \tag{14.208}$$

$$jH_I(j\omega) = (1/2) [H(j\omega) - H(-j\omega)] \tag{14.209}$$

$$H_R(s) = (1/2) [H(s) + H(-s)] \tag{14.210}$$

$H_R(j\omega)$ being even has only even powers of ω . Hence $H_R(s)$ has even powers of s . Hence we may write

$$H_R(s) = \frac{P(s^2)}{Q(s^2)} = \frac{1}{2} [R(s) + R(-s)] \tag{14.211}$$

where $R(s)$ is a ratio of two polynomials in s , with the numerator polynomial assumed to be of order less than or equal to that of the denominator. Let $s^2 = q$. A partial fraction expansion of $H_R(s)$ leads to the form

$$H_R(s) = \frac{P(q)}{Q(q)} = K + \sum_{i=1}^n \frac{r_i}{q - q_i} \tag{14.212}$$

where q_1, q_2, \dots, q_n are the zeros of $Q(q)$. Now with $q_i = s_i^2$ and s_i the poles in the left half plane, we have

$$\frac{r_i}{q - q_i} = \frac{r_i}{s^2 - s_i^2} = \frac{r_i/(2s_i)}{s - s_i} - \frac{r_i/(2s_i)}{s + s_i} \tag{14.213}$$

$$H_R(s) = \frac{P(s^2)}{Q(s^2)} = \left\{ K/2 + \sum_{i=1}^n \frac{r_i/(2s_i)}{s - s_i} \right\} + \left\{ K/2 + \sum_{i=1}^n \frac{r_i/(2s_i)}{-s - s_i} \right\}. \tag{14.214}$$

We note that the second term is the same as the first with s replaced by $-s$. We conclude that

$$H(s) = K + \sum_{i=1}^n \frac{r_i/(s_i)}{s - s_i}. \tag{14.215}$$

Similarly, if $H_I(j\omega)$ is known we can evaluate $H(s)$. We have

$$jH_I(s) = (1/2)[H(s) - H(-s)]. \tag{14.216}$$

Since this is an odd function we may write

$$jH_I(s) = \frac{sP(s^2)}{Q(s^2)} \tag{14.217}$$

where the order of the polynomial $P(s^2)$ is less than that of the denominator $Q(s)$. With $s^2 = q$ we may write

$$\frac{P(q)}{Q(q)} = \sum_{i=1}^n \frac{\rho_i}{q - q_i} \tag{14.218}$$

$$jH_I(s) = \frac{sP(s^2)}{Q(s^2)} = \sum_{i=1}^n \frac{s\rho_i/(2s_i)}{s - s_i} - \sum_{i=1}^n \frac{(-s)\rho_i/(2s_i)}{-s - s_i} \tag{14.219}$$

where again the second term is the same as the first but with s replaced by $(-s)$. We conclude that

$$H(s) = \sum_{i=1}^n \frac{s\rho_i/s_i}{s - s_i} + C \tag{14.220}$$

where C is an arbitrary constant. Knowing $H_I(j\omega)$ we can therefore evaluate $H(s)$ only within an arbitrary constant. Thus knowing $H_R(j\omega)$ we can evaluate $H(s)$ and thereof $H_I(j\omega)$. Knowing $H_I(j\omega)$ we can evaluate $H(s)$ and $H_R(j\omega)$ within a constant. The following example illustrates the approach.

Example 14.18 *Given*

$$H_R(j\omega) = \frac{-4\omega^4 - 2\omega^2 - 2}{\omega^6 + \omega^4 + \omega^2 + 1}$$

evaluate $H(s)$ and $H_I(j\omega)$.

We write

$$H_R(s) = 0.5 [H(s) + H(-s)] = \frac{4s^4 - 2s^2 + 2}{s^6 - s^4 + s^2 - 1}.$$

Using a partial fraction expansion with the poles given by

$$s_1 = e^{j3\pi/4}, \quad s_2 = -1, \quad s_3 = e^{-j3\pi/4}, \quad s_4 = -s_1, \quad s_5 = -s_2, \quad s_6 = -s_3$$

as seen in Fig. 14.19, we obtain

$$H_R(s) = 0.5 \left[\left\{ \frac{r_1}{s - s_1} + \frac{r_2}{s - s_2} + \frac{r_3}{s - s_3} \right\} + \left\{ \frac{r_1}{-s - s_1} + \frac{r_2}{-s - s_2} + \frac{r_3}{-s - s_3} \right\} \right]$$

where $r_1 = e^{-j3\pi/4} = 1/s_1$, $r_2 = -2 = 2/s_2$, $r_3 = e^{j3\pi/4} = 1/s_3$. Since the poles s_1 , s_2 and s_3 are in the left half of the s plane we have

$$H(s) = \frac{r_1}{s - s_1} + \frac{r_2}{s - s_2} + \frac{r_3}{s - s_3} = \frac{-3.414s^2 - 4.242s - 2}{s^3 + 2.414s^2 + 2.414s + 1}$$

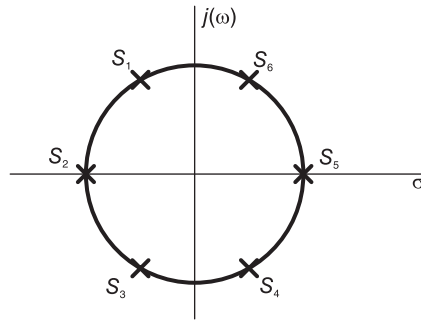


FIGURE 14.19 Poles in s plane.

$$H(j\omega) = \frac{3.414\omega^2 - j4.243\omega - 2}{(j\omega)^3 - 2.414\omega^2 + j2.414\omega + 1}$$

$$H_I(j\omega) = \frac{3.414\omega^5 + 0.585\omega}{\omega^6 + \omega^4 + \omega^2 + 1}$$

Example 14.19 Given that the imaginary part of $H(j\omega)$ is

$$H_I(j\omega) = \frac{3.414\omega^5 + 0.585\omega}{\omega^6 + \omega^4 + \omega^2 + 1}$$

evaluate $H(s)$ and $H_R(j\omega)$.

We have

$$jH_I(s) = (1/2)[H(s) - H(-s)] = \frac{-3.414s^5 - 0.585s}{s^6 - s^4 + s^2 - 1}$$

Using a partial fraction expansion of $jH_I(s)$ we obtain the form

$$jH_I(s) = \sum_{i=1}^3 \frac{r_i}{s - s_i} - \sum_{i=1}^3 \frac{r_i}{-s - s_i}$$

wherefrom

$$H(s) = \sum_{i=1}^3 \frac{r_i}{s - s_i} + K$$

where K is a constant. We obtain

$$H(s) = \frac{-3.414s^2 - 4.242s - 2}{s^3 + 2.414s^2 + 2.414s + 1}$$

as expected, and

$$H(j\omega) = \frac{3.414\omega^2 - j4.243\omega - 2}{-j\omega^3 - 2.414\omega^2 + j2.414\omega + 1}$$

$$H_R(j\omega) = \frac{-4\omega^4 - 2\omega^2 - 2}{\omega^6 + \omega^4 + \omega^2 + 1}$$

14.43 Case of Poles on the Imaginary Axis

We now consider the case where the poles are on the imaginary axis. Let

$$H(s) = \frac{a + jb}{s - j\beta} \tag{14.221}$$

$$h(t) = (a + jb) e^{j\beta t} u(t) \tag{14.222}$$

$$H(j\omega) = a \left\{ \frac{1}{j(\omega - \beta)} + \pi\delta(\omega - \beta) \right\} + jb \left\{ \frac{1}{j(\omega - \beta)} + \pi\delta(\omega - \beta) \right\}$$

$$H_R(j\omega) = \pi a\delta(\omega - \beta) + \frac{b}{\omega - \beta} \tag{14.223}$$

$$H_I(j\omega) = \frac{-a}{\omega - \beta} + b\pi\delta(\omega - \beta). \tag{14.224}$$

We conclude that in the case of poles on the $j\omega$ axis if $H_R(j\omega)$ is given by the first of the these equations we can deduce directly the corresponding term of $H_I(j\omega)$ as in the second equation and vice versa. Moreover, the system function can be directly deduced as

$$H(s) = (a + jb) / (s - j\beta). \tag{14.225}$$

Example 14.20 *Given*

$$H_R(j\omega) = \frac{-6\omega^4 + 42\omega^2 + 84}{(\omega^2 - 1)(\omega^2 - 4)(\omega^2 + 9)}$$

evaluate $H_I(j\omega)$. Using partial fraction expansion we have

$$H_R(j\omega) = \frac{-2}{\omega - 1} + \frac{2}{\omega + 1} + \frac{1}{\omega - 2} - \frac{1}{\omega + 2} - \frac{6}{\omega^2 + 9}.$$

The first four terms lead to impulses in $H_I(j\omega)$ and in particular

$$2[-\pi\delta(\omega - 1) + \pi\delta(\omega + 1)] + [\pi\delta(\omega - 2) - \pi\delta(\omega + 2)].$$

The fifth term which may be denoted $H_{R,2}(j\omega)$ is given by

$$H_{R,2}(j\omega) = \frac{-6}{\omega^2 + 9} = \frac{j}{\omega - j3} - \frac{j}{\omega + j3} = (1/2) [H_2(j\omega) + H_2(-j\omega)]$$

$$H_2(j\omega) = \frac{j^2}{\omega - j3}$$

i.e.

$$H_2(s) = \frac{j^2}{-js - j3} = \frac{-2}{s + 3}$$

and

$$H_2(j\omega) = \frac{j^2(\omega + j3)}{\omega^2 + 9} = \frac{-6 + j2\omega}{\omega^2 + 9}$$

so that its imaginary part is

$$H_{2,I}(j\omega) = \frac{2\omega}{\omega^2 + 9}$$

wherefrom

$$H_I(j\omega) = 2\pi[-\delta(\omega - 1) + \delta(\omega + 1)] + \pi[\delta(\omega - 2) - \delta(\omega + 2)] + \frac{2\omega}{\omega^2 + 9}.$$

14.44 Hilbert Transform Closed Forms

Consider a causal impulse response $h(t)$, having no impulse at $t = 0$. The above relations between the real and imaginary of the spectrum of a causal impulse response can be put into closed forms known as Hilbert transform relations. In fact, the Hilbert transform relations state that

$$H_I(j\omega) = -\frac{1}{\pi} \int_{-\infty}^{\infty} \frac{H_R(jy)}{\omega - y} dy \quad (14.226)$$

$$H_R(j\omega) = \frac{1}{\pi} \int_{-\infty}^{\infty} \frac{H_I(jy)}{\omega - y} dy. \quad (14.227)$$

Proof Let h_e and h_o be the even and odd parts of $h(t)$. Referring to Fig. 14.20,

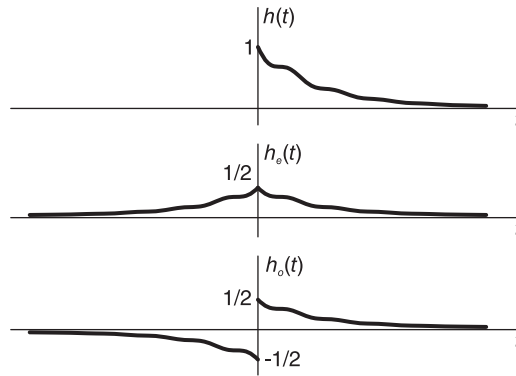


FIGURE 14.20 Even-odd decomposition of a causal function.

$$h(t) = h_e + h_o \quad (14.228)$$

$$h_e = \begin{cases} (1/2)h(t), & t > 0 \\ (1/2)h(-t), & t < 0 \end{cases} \quad (14.229)$$

$$h_o = \begin{cases} (1/2)h(t), & t > 0 \\ -(1/2)h(-t), & t < 0 \end{cases} \quad (14.230)$$

$$h_o(t) = h_e(t) \operatorname{sgn} t \quad (14.231)$$

$$h_e(t) = h_o(t) \operatorname{sgn} t \quad (14.232)$$

wherefrom

$$\begin{aligned} jH_I(j\omega) &= \frac{1}{2\pi} \mathcal{F}[h_e(t)] * \mathcal{F}[\operatorname{sgn} t] = \frac{1}{2\pi} H_R(j\omega) * \frac{2}{j\omega} \\ &= \frac{1}{j\pi} \int_{-\infty}^{\infty} H_R(jy) \times \frac{1}{(\omega - y)} dy \end{aligned} \quad (14.233)$$

as stated. Similarly the second transformation can be verified.

Example 14.21

$$\begin{aligned} H_R(j\omega) &= \delta(\omega) \\ H_I(j\omega) &= \frac{-1}{\pi} \int \delta(y) \frac{1}{\omega - y} dy = \frac{-1}{\pi} \frac{1}{\omega}. \end{aligned}$$

14.45 Wiener–Lee Transforms

Alternative expressions relating the real and imaginary spectral components, referred to as Wiener–Lee transforms, are obtained by writing

$$\omega = -\tan \frac{\Omega}{2} \tag{14.234}$$

$$H(j\omega) = H\left(-j \tan \frac{\Omega}{2}\right) = H_R\left(-j \tan \frac{\Omega}{2}\right) + jH_I\left(-j \tan \frac{\Omega}{2}\right). \tag{14.235}$$

Referring to Fig. 14.21, let $X(\Omega) = H_R(j \tan \Omega/2)$ and $Y(\Omega) = H_I(j \tan \Omega/2)$. We have

$$H(-j \tan \Omega/2) = X(\Omega) - jY(\Omega). \tag{14.236}$$

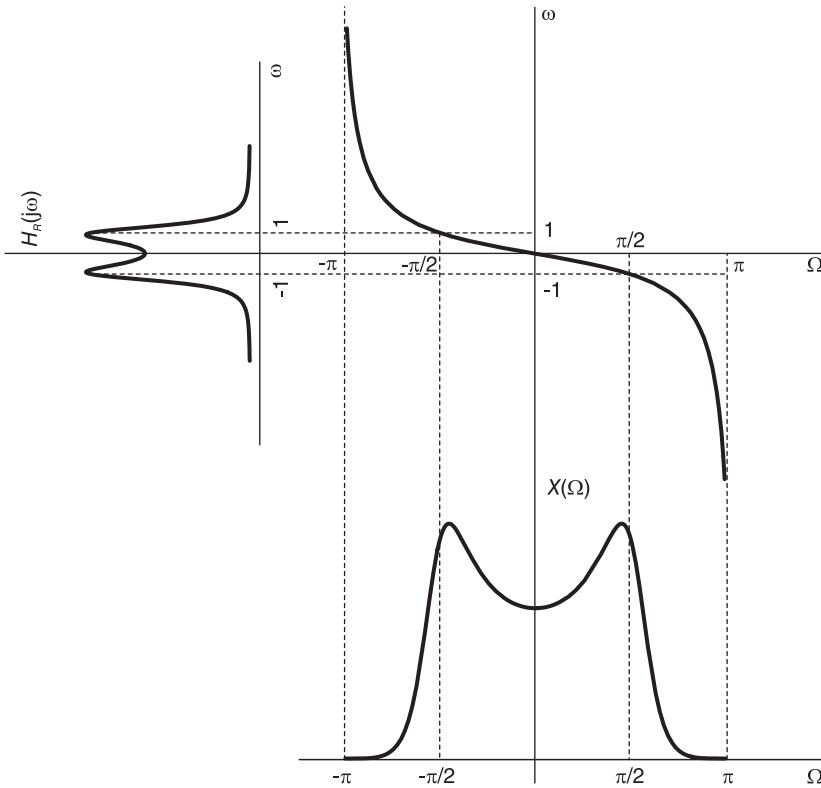


FIGURE 14.21 Wiener–Lee spectral transformation.

Expanding the even function $X(\Omega)$ and the odd function $Y(\Omega)$, of period 2π each into trigonometric Fourier series we have

$$X(\Omega) = a_0 + a_1 \cos \Omega + \dots + a_n \cos n\Omega + \dots \tag{14.237}$$

$$Y(\Omega) = b_1 \sin \Omega + b_2 \sin \Omega + \dots + b_n \sin n\Omega + \dots \tag{14.238}$$

$$a_n = \frac{1}{\pi} \int_{-\pi}^{\pi} X(\Omega) \cos n\Omega \, d\Omega \quad (14.239)$$

$$b_n = \frac{1}{\pi} \int_{-\pi}^{\pi} Y(\Omega) \sin n\Omega \, d\Omega. \quad (14.240)$$

It can be shown that if $h(t)$ is causal then

$$b_n = -a_n \quad (14.241)$$

wherefrom, knowing $H_R(j\omega)$, to evaluate $H_I(j\omega)$ we may find $X(\Omega)$, then its Fourier series coefficients a_n and thence $b_n = -a_n$. The function $Y(\Omega)$ is thus deduced, followed by $H_I(j\omega)$.

If $H_I(j\omega)$ is known we evaluate the coefficients b_n and thence $a_n = -b_n$, except for a_0 which stays as an arbitrary constant. The real component $H_R(j\omega)$ is thus determined within an arbitrary constant.

Example 14.22 Given

$$H_R(j\omega) = \cos(2n \tan^{-1} \omega).$$

Evaluate $H_I(j\omega)$ and $h(t)$.

We have

$$H_R(j\omega) = \cos n\Omega$$

$$X(\Omega) = H_R(j \tan \Omega/2) = H_R(-j\omega) = \cos n\Omega.$$

Hence the Fourier series coefficients of its expansion are given by

$$a_n = \cos n\Omega$$

and those of $Y(\Omega)$ are $b_n = -a_n$ so that

$$Y(\Omega) = H_I(j \tan \Omega/2) = H_I(-j\omega) = -\sin n\Omega$$

i.e.

$$H_I(j\omega) = \sin n\Omega$$

$$H(j\omega) = X(\Omega) - jY(\Omega) = \cos n\Omega + j \sin n\Omega = e^{jn\Omega}.$$

We note that

$$\frac{1 - j\omega}{1 + j\omega} = e^{j2 \tan^{-1} \omega} = e^{j\Omega}.$$

Hence

$$H_I(j\omega) = \left(\frac{1 - j\omega}{1 + j\omega} \right)^n$$

$$H(s) = \left(\frac{1 - s}{1 + s} \right)^n.$$

Using the binomial expansion

$$\begin{aligned} H(s) &= \left(\frac{2}{s+1} - 1 \right)^n = \sum_{k=0}^n \binom{n}{k} \left(\frac{2}{s+1} \right)^k (-1)^{n-k} \\ &= (-1)^n \sum_{k=0}^n \binom{n}{k} \left(\frac{-2}{s+1} \right)^k = (-1)^n \left\{ 1 + \sum_{k=1}^n \binom{n}{k} \frac{(-2)^k}{(s+1)^k} \right\} \end{aligned}$$

$$\frac{1}{s^k} \longleftrightarrow \frac{t^{k-1}}{(k-1)!} u(t)$$

$$h(t) = (-1)^n \left\{ \delta(t) + \sum_{k=1}^n \binom{n}{k} (-2)^k e^{-t} \frac{t^{k-1}}{(k-1)!} u(t) \right\}.$$

14.46 Discrete-Time Domain Hilbert Transform Relations

Similarly, in the discrete-time domain, we can decompose a sequence into even and odd parts

$$h[n] = h_e[n] + h_o[n] \tag{14.242}$$

$$h_e[n] = (1/2)[h[n] + h[-n]] \tag{14.243}$$

$$h_o[n] = (1/2)[h[n] - h[-n]]. \tag{14.244}$$

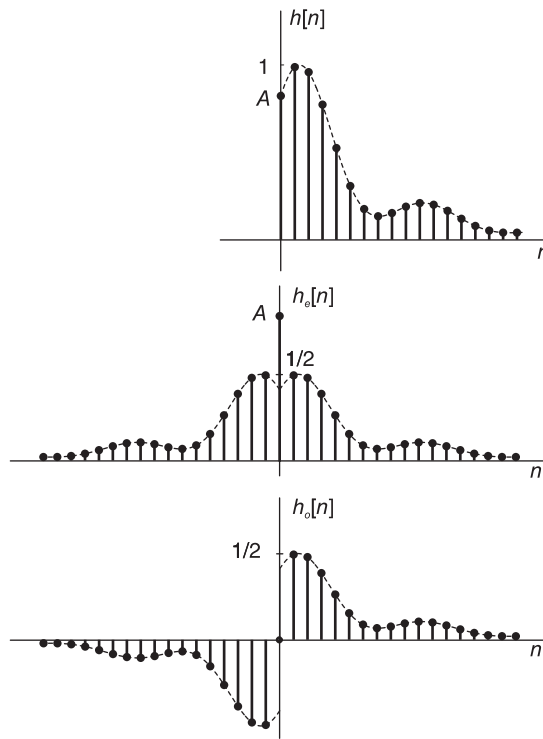


FIGURE 14.22 Even and odd parts of a causal sequence.

If the sequence $h[n]$ is causal, as in Fig. 14.22, we have

$$h_e[0] = (1/2)\{h[0] + h[-0]\} = h[0] \tag{14.245}$$

$$h_e[n] = \begin{cases} (1/2)h[n], & n > 0 \\ (1/2)h[-n], & n < 0 \\ h[0], & n = 0 \end{cases} \tag{14.246}$$

and

$$h[n] = \begin{cases} 2h_e[n], & n > 0 \\ h_e[n], & n = 0 \\ 0, & n < 0 \end{cases} \tag{14.247}$$

and

$$h_o[n] = \begin{cases} (1/2)h[n], & n > 0 \\ -(1/2)h[-n], & n < 0 \\ 0, & n = 0 \end{cases} \quad (14.248)$$

and

$$h[n] = \begin{cases} 2h_o[n], & n > 0 \\ 0, & n < 0 \end{cases} \quad (14.249)$$

$h(0)$ cannot be determined from $h_o(n)$. Fourier transforming the relation $h[n] = h_e[n] + h_o[n]$ we have

$$H(e^{j\Omega}) = \mathcal{F}[h[n]] \triangleq H_R(e^{j\Omega}) + jH_I(e^{j\Omega}) = H_e(e^{j\Omega}) + H_o(e^{j\Omega}) \quad (14.250)$$

where $H_e(e^{j\Omega}) = \mathcal{F}[h_e[n]]$ and $H_o(e^{j\Omega}) = \mathcal{F}[h_o[n]]$, wherefrom

$$H_e(e^{j\Omega}) = H_R(e^{j\Omega}) \quad (14.251)$$

$$H_o(e^{j\Omega}) = jH_I(e^{j\Omega}). \quad (14.252)$$

Knowing $H_R(e^{j\Omega})$ we can therefore deduce $H_I(e^{j\Omega})$. From $H_R(e^{j\Omega}) = H_e(e^{j\Omega})$ we can deduce $h_e[n]$, and thence $h_o[n]$, $H_o(e^{j\Omega})$; hence $H_I(e^{j\Omega})$ or from $h_e[n]$ deduce $h[n]$, wherefrom $H(e^{j\Omega})$. If we know only $H_I(e^{j\Omega})$ we have $H_o(e^{j\Omega})$; hence $h_o[n]$. We need to know $h[0]$ to be able to deduce $h_e[n]$ or $h[n]$. Knowing $h[0]$ we can deduce $H_R(e^{j\Omega})$ from $H_I(e^{j\Omega})$.

For real, causal and stable $h[n]$, knowing $H_R(e^{j\Omega})$ we can evaluate $H(z)$ for $|z| > 1$. Knowing $H_I(e^{j\Omega})$ and $h[0]$ we can deduce $H(z)$ for $|z| > 1$.

We can write

$$h[n] = h_e[n] \{\delta[n] + 2u[n-1]\} \quad (14.253)$$

$$H(z) = \mathcal{Z}[h[n]] = \mathcal{Z}[h_e[n] \{\delta[n] + 2u[n-1]\}] \quad (14.254)$$

which equals the convolution of $H_e(z) \triangleq \mathcal{Z}[h_e[n]]$ with

$$\mathcal{Z}[\{\delta[n] + 2u[n-1]\}] = 1 + \frac{2z^{-1}}{1-z^{-1}} = \frac{1+z^{-1}}{1-z^{-1}}, \quad |z| > 1 \quad (14.255)$$

i.e.

$$\begin{aligned} H(z) &= \frac{1}{2\pi j} \oint H_e(v) \frac{1+(z/v)^{-1}}{1-(z/v)^{-1}} v^{-1} dv \\ &= \frac{1}{2\pi j} \oint H_e(v) \frac{z+v}{z-v} v^{-1} dv, \quad |z| > 1. \end{aligned} \quad (14.256)$$

If the contour of integration is the unit circle $v = e^{j\theta}$ then $H_e(v) = H_R(v)$ so that

$$H(z) = \frac{1}{2\pi j} \oint H_R(v) \frac{z+v}{z-v} v^{-1} dv, \quad |z| > 1. \quad (14.257)$$

Example 14.23 Given

$$H_R(e^{j\Omega}) = \frac{a^2 \cos \Omega - a}{a^2 - 2a \cos \Omega + 1}, \quad |a| > 1,$$

evaluate $H(z)$.

$$H_R(e^{j\Omega}) = \frac{a^2 (e^{j\Omega} + e^{-j\Omega}) / 2 - a}{(ae^{j\Omega} - 1)(ae^{-j\Omega} - 1)}$$

Referring to Fig. 14.23

$$\begin{aligned}
 H(z) &= \frac{1}{2\pi j} \oint \frac{a^2(v+v^{-1})/2 - a}{(av-1)(av^{-1}-1)} \frac{z+v}{z-v} \frac{dv}{v} \\
 &= \frac{1}{2\pi j} \oint \frac{a(v^2+1)/2 - v}{-(v-1/a)(v-a)} \frac{z+v}{z-v} \frac{dv}{v} \\
 &= -\frac{a}{2} + \frac{a(1/a^2+1)/2 - 1/a}{-(1/a-a)} \frac{z+a^{-1}}{z-a^{-1}} a \\
 &= -\frac{a}{2} + \frac{a}{2} \frac{z+a^{-1}}{z-a^{-1}} = \frac{z^{-1}}{1-a^{-1}z^{-1}}.
 \end{aligned}$$

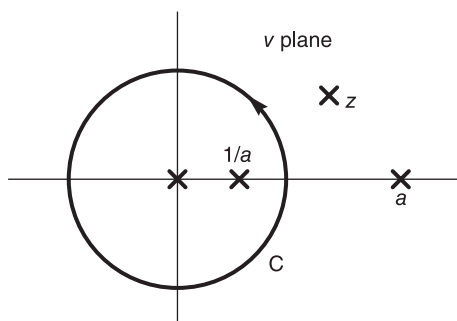


FIGURE 14.23 Evaluation of residues in v plane.

Line integral form:

Letting $v = e^{j\theta}$ we have

$$H(re^{j\Omega}) = \frac{1}{2\pi} \int_{-\pi}^{\pi} H_I(e^{j\theta}) P_r(\theta - \Omega) d\theta + \frac{j}{2\pi} \int_{-\pi}^{\pi} H_R(e^{j\theta}) Q_r(\theta - \Omega) d\theta \quad (14.258)$$

where

$$P_r(\theta) = Re \left[\frac{1+r^{-1}e^{j\theta}}{1-r^{-1}e^{j\theta}} \right] = (1-r^{-2}) / [1-2r^{-1}\cos\theta+r^{-2}] \quad (14.259)$$

$$Q_r(\theta) = Im \left[\frac{1+r^{-1}e^{j\theta}}{1-r^{-1}e^{j\theta}} \right] = 2r^{-1}\sin\theta / [1-2r^{-1}\cos\theta+r^{-2}]. \quad (14.260)$$

The functions $P_r(\theta)$ and $Q_r(\theta)$ are known as the Poisson Kernel and its conjugate, respectively.

$$H_R(re^{j\Omega}) = \frac{1}{2\pi} \int_{-\pi}^{\pi} H_I(e^{j\theta}) P_r(\theta - \Omega) d\theta \quad (14.261)$$

$$H_I(re^{j\Omega}) = \frac{1}{2\pi} \int_{-\pi}^{\pi} H_R(e^{j\theta}) Q_r(\theta - \Omega) d\theta. \quad (14.262)$$

Similarly, we obtain

$$H(z) = \frac{1}{2\pi} \oint_{unit\ circle} \frac{H_I(v)(z+v)}{(z-v)v} dv + h(0), \quad |z| > 1 \quad (14.263)$$

$$H_R(re^{j\Omega}) = -\frac{1}{2\pi} \int_{-\pi}^{\pi} H_I(e^{j\theta}) Q_r(\theta - \Omega) d\theta + h(0) \quad (14.264)$$

$$H_I(re^{j\Omega}) = \frac{1}{2\pi} \int_{-\pi}^{\pi} H_R(e^{j\Omega}) P_r(\theta - \Omega) d\theta, \quad r > 1. \quad (14.265)$$

To obtain a relation between $H_R(e^{j\Omega})$ and $H_I(e^{j\Omega})$ (on the unit circle $r = 1$) the integrals have to be evaluated using the Cauchy principal values since

$$\lim_{r \rightarrow 1} Q_r(\theta) = \frac{2 \sin \theta}{2(1 - \cos \theta)} = \cot(\theta/2) \quad (14.266)$$

wherefrom $Q_r(\theta - \Omega)$ has a singularity at $\theta = \Omega$. The relations take therefore the form:

$$H_I(e^{j\Omega}) = \frac{1}{2\pi} PV \int_{-\pi}^{\pi} H_R(e^{j\theta}) \cot\left(\frac{\theta - \Omega}{2}\right) d\theta \quad (14.267)$$

$$H_R(e^{j\Omega}) = h(0) - \frac{1}{2\pi} PV \int_{-\pi}^{\pi} H_I(e^{j\theta}) \cot\left(\frac{\theta - \Omega}{2}\right) d\theta. \quad (14.268)$$

These are Poisson's formulas, also known as Hilbert transforms.

Example 14.24 Let

$$H_R(e^{j\Omega}) = \frac{\cos \Omega - a}{1 - 2a \cos \Omega + a^2}, \quad a > 0.$$

To find $H(z)$

$$H_R(e^{j\Omega}) = \frac{(e^{j\Omega} + e^{-j\Omega})/2 - a}{(1 - ae^{-j\Omega})(1 - ae^{j\Omega})}.$$

Substituting $e^{j\Omega} = v$ we have

$$\begin{aligned} H(z) &= \frac{1}{2\pi j} \oint \frac{(v + v^{-1})/2 - a}{(1 - av^{-1})(1 - av)} \frac{z + v}{z - v} dv \\ &= \frac{1}{2\pi j} \oint \frac{(v^2 + 1)/2 - av}{(v - a)(1 - av)} \frac{z + v}{z - v} \frac{dv}{v} \\ &= \sum \text{res. at } v = 0 \text{ and } v = a \\ &= \frac{1/2}{-a} + \frac{(a^2 + 1)/2 - a^2}{1 - a^2} \frac{z + a}{z - a} \frac{1}{a} \\ &= \frac{1}{a} \left[-\frac{1}{2} + \frac{a^2/2 + 1/2 - a^2}{1 - a^2} \frac{z + a}{z - a} \right] \\ &= \frac{1}{a} \left[-\frac{1}{2} + \frac{1}{2} \frac{z + a}{z - a} \right] = \frac{1}{z - a}. \end{aligned}$$

14.47 Problems

Problem 14.1 a) With base $p = 5$, a three digit number takes on the successive values 000, 001, 002, 003, 004, 010, 011, 012, ..., 444. Show the corresponding Gray code for the first 27 values, i.e. the values 000, 001, 002, ..., 101.

b) Let $N = 27$ and $p = 3$. Write, in exponential notation, if preferred, the 10^{th} , 11^{th} and 12^{th} row of the generalized Walsh transform in natural order. Evaluate the generalized sequency (GS) of each of the three rows.

c) Let A be a matrix of dimension $N \times N$ where $N = 32 = 2^n$ having the structure

$$A = \begin{bmatrix} a_{0,0} & a_{0,1} & \dots & a_{0,31} \\ a_{1,0} & a_{1,1} & \dots & a_{1,31} \\ \dots & & & \\ a_{31,0} & a_{31,1} & \dots & a_{31,31} \end{bmatrix}.$$

Let

$$B = A \left\{ P^{(2)} \right\}^3$$

where $P^{(2)}$ is the base-2 perfect shuffle permutation matrix.

Evaluate the matrix B , showing its structure. It suffices to show a few elements of the first row/columns as well as the last row/column, to specify the matrix structure.

Problem 14.2 a) For $N = p^n$ with $p = 2$ and $n = 4$ write the Walsh–Hadamard matrices in the three different well-known orders. Show how to obtain each matrix from the one preceding it.

b) Repeat a) with now $p = 3$ and $n = 2$.

c) Write a “fast” factorization for the general case $N = p^n$ of the generalized Walsh transform. It suffices to write and precisely define the component matrices. To justify it suffices to precisely cite the source wherefrom the factorization can be found.

Problem 14.3 Show that the Hilbert transform of $f(t) = 1/(t^2 + 1)$ is $g(t) = t/(t^2 + 1)$.

Problem 14.4 Evaluate the Hilbert transform of $f(t) = \delta(t - 3)$.

Problem 14.5 Given

$$H_R(e^{j\Omega}) = \frac{a^2 - a \cos \Omega}{a^2 - 2a \cos \Omega + 1}, \quad |a| > 1,$$

evaluate $H_I(e^{j\Omega})$.

Problem 14.6 Given

$$H_R(j\omega) = \frac{2\beta}{\omega^2 - \beta^2} + \pi \{ \delta(\omega - \beta) + \delta(\omega + \beta) \},$$

evaluate $H_I(j\omega)$.

Problem 14.7 Given

$$H_R(j\omega) = \frac{1}{1 + \omega^4},$$

evaluate $H_I(j\omega)$.

Problem 14.8 Given

$$H_I(j\omega) = \frac{\omega + \omega^3}{1 + \omega^4},$$

evaluate $H_R(j\omega)$.

Problem 14.9 Evaluate the fractional Fourier transform of $f(t) = e^{-\pi\gamma t^2}$.

Problem 14.10 Let

$$T_3 = \begin{bmatrix} w^0 & w^0 & w^0 \\ w^0 & w^1 & w^2 \\ w^0 & w^2 & w^1 \end{bmatrix}$$

where $w = e^{-j2\pi/3}$, $j = \sqrt{-1}$

a) Evaluate

$$T_9 = T_3 \times T_3$$

where “ \times ” denotes the Kronecker product.

b) Show that T_9 can be written as a simple product of factors containing Kronecker products of only T_3 and the identity matrix I_3 . Show how to subsequently obtain a factorization of T_9 containing only the matrix $C_9 = I_3 \times T_3$ and the perfect shuffle matrix P_9 destined toward a wired-in processor architecture with a minimum of memory partitions.

c) Simplify, with $N = 3^{10}$ and radix $r = 3$,

$$T_N = P_N^4 (I_{3^4} \times T_3 \times I_{3^5}) (I_{3^2} \times T_3 \times I_{3^7}) (T_3 \times I_{3^9}) (I_{3^9} \times T_3) P_N^{-4}$$

to obtain a factorization of T_N as a function of only $C = (I_{3^9} \times T_3)$ and P_N^i ; i integer.

Problem 14.11 a) Write the Walsh–Hadamard (base 2) matrix in natural order for the cases $N = 2$, $N = 4$, $N = 8$ and $N = 16$.

b) For the case $N = 16$ deduce thereof the dyadic and then the sequency transformation matrices, listing on the right of each matrix the number of sign changes (the sequency) of each row.

c) Let A be a matrix of dimension $N \times N$, where $N = 32 = 2^n$ having the structure

$$A = \begin{bmatrix} a_{0,0} & a_{0,1} & \dots & a_{0,31} \\ a_{1,0} & a_{1,1} & \dots & a_{1,31} \\ \dots & & & \\ a_{31,0} & a_{31,1} & \dots & a_{31,31} \end{bmatrix}.$$

Let

$$B = A \left\{ P^{(2)} \right\}^3$$

where $P^{(2)}$ is the perfect shuffle matrix with radix 2. What operation should be applied to the rows or columns of the matrix A to obtain the matrix B ? Evaluate the matrix B by showing its structure in terms of the elements of A . It suffices to show the first four elements of the first four rows/columns of the matrix as well as the last row/column, thus specifying its structure.

Problem 14.12 a) Using the radix $p = 5$, three-digit numbers can be written in the normal ascending order 000, 001, 002, 003, 004, 010, 011, 012, ..., 444. Show the corresponding Gray code order for the first 27 values, i.e. corresponding to the values 000, 001, 002, ..., 101.

b) With a radix $p = 3$ and $N = 9$, write the generalized Walsh matrix in natural order W_9 . With $N = 27$, write the expression which produces W_{27} as a function of W_9 in the same natural order. Write the values of the rows 0, 12, 13 and 14 of the matrix W_{27} in natural order. Evaluate the generalized sequency of each of the four rows.

Problem 14.13 a) A matrix Y is related to a given matrix X of dimension $N \times N$, where $N = 32$, through a permutation operation. With radix $r = 2$ and

$$\rho = I_{r^2} \times P_{N/r^2}^{(r)}$$

$P_N^{(r)}$ being the radix-2 $N \times N$ perfect shuffle matrix, evaluate the matrix Y in the two cases (i) $Y = \rho X$ and (ii) $Z = X \rho$.

b) Let P_{16} be the perfect shuffle matrix of 16 points with radix $r = 2$,

$$T_2 = \begin{bmatrix} 1 & 1 \\ 1 & -1 \end{bmatrix}$$

and

$$S = I_8 \times T_2$$

Evaluate PSP^{-1} , P^2SP^{-2} and P^3SP^{-3} .

Problem 14.14 For $N = 9$ points and radix $p = 3$

- a) Write the generalized Walsh transform matrix in the natural order.
- b) Write the permutation matrix that converts the natural order matrix to the Walsh–Paley order. Write the Walsh–Paley order matrix thus obtained.
- c) Write the permutation matrix that converts the Walsh–Paley order matrix to the Walsh–Kaczmarz order matrix. Write the Walsh–Kaczmarz matrix thus obtained.
- d) For each of these matrices write the closed form of a fast transformation factorization leading to a wired-in processor and sketch the processor structure.

14.48 Answers to Selected Problems

Problem 14.1

a) Gray code $g_i = b_i - b_{i+1}$. See Table 14.4

b)

$$\begin{aligned} W_{3^3} [9] &= 000\ 000\ 000\ 111\ 111\ 111\ 222\ 222\ 222, & G.S. &= 2/2 = 1 \\ W_{3^3} [10] &= 012\ 012\ 012\ 120\ 120\ 120\ 201\ 201\ 201 & G.S. &= 2/2 = 14 \\ W_{3^3} [11] &= 021\ 021\ 021\ 102\ 102\ 102\ 210\ 210\ 210 & G.S. &= 2/2 = 24 \end{aligned}$$

c)

$$\begin{bmatrix} a_{0,0} & a_{0,8} & a_{0,16} & a_{0,24} & a_{0,1} & a_{0,9} & \dots \\ a_{1,0} & a_{1,8} & a_{1,16} & a_{1,24} & a_{1,1} & a_{1,9} & \\ a_{2,0} & a_{2,8} & a_{2,16} & & & & \\ a_{3,0} & a_{3,8} & a_{3,16} & & & & \\ \dots & & & & & & \\ a_{31,0} & a_{31,8} & a_{31,16} & a_{31,24} & a_{31,1} & a_{31,9} & \end{bmatrix}$$

TABLE 14.4 Answer to Problem 14.1

	$p_2p_1p_0$	$g_2g_1g_0$	
0	000	000	0
1	001	001	1
2	002	002	2
3	003	003	3
4	004	004	4
5	010	014	9
6	011	010	5
7	012	011	6
8	013	012	7
9	014	013	8
10	020	023	13
11	021	024	14
12	022	020	10
13	023	021	11
14	024	022	12
1...
32	112	101	26
33	113	102	27
34	114	103	28

Problem 14.2

a)

$$H_8 = \begin{bmatrix} 1 & 1 & 1 & 1 & 1 & 1 & 1 & 1 \\ 1 & -1 & 1 & -1 & 1 & -1 & 1 & -1 \\ 1 & 1 & -1 & -1 & 1 & 1 & -1 & -1 \\ 1 & -1 & -1 & 1 & 1 & -1 & -1 & 1 \\ 1 & 1 & 1 & 1 & -1 & -1 & -1 & -1 \\ 1 & -1 & 1 & -1 & -1 & 1 & -1 & 1 \\ 1 & 1 & -1 & -1 & -1 & -1 & 1 & 1 \\ 1 & -1 & -1 & 1 & -1 & 1 & 1 & -1 \end{bmatrix}$$

The sequencies are: {0, 1, 2, 3, 4, 5, 6, 7, 8, 9, 10, 11, 12, 13, 14, 15}.
 The Gray binary order is {0, 1, 3, 2, 6, 7, 5, 4, 12, 13, 15, 14, 10, 11, 9, 8}, producing the Kaczmarz matrix with sequencies {0, 1, 2, 3, 4, 5, 6, 7, 8, 9, 10, 11, 12, 13, 14, 15}

b)

$$T_9 = \begin{bmatrix} 0 & 0 & 0 & 0 & 0 & 0 & 0 & 0 & 0 \\ 0 & 1 & 2 & 0 & 1 & 2 & 0 & 1 & 2 \\ 0 & 2 & 1 & 0 & 2 & 1 & 0 & 2 & 1 \\ 0 & 0 & 0 & 1 & 1 & 1 & 2 & 2 & 2 \\ 0 & 1 & 2 & 1 & 2 & 0 & 2 & 0 & 1 \\ 0 & 2 & 1 & 1 & 0 & 2 & 2 & 1 & 0 \\ 0 & 0 & 0 & 2 & 2 & 2 & 1 & 1 & 1 \\ 0 & 1 & 2 & 2 & 0 & 1 & 1 & 2 & 0 \\ 0 & 2 & 1 & 2 & 1 & 0 & 1 & 0 & 2 \end{bmatrix} \begin{matrix} 0 \\ 4 \\ 8 \\ 1 \\ 5 \\ 6 \\ 2 \\ 3 \\ 7 \end{matrix}$$

c) For T_9 Walsh–Paley, the generalized sequencies are {0, 1, 2, 4, 5, 3, 8, 6, 7}. The binary Gray code gives the order {00, 01, 02, 12, 10, 11, 21, 22, 20} i.e. the order {0, 1, 2, 5, 3, 4, 7, 8, 6}. The Kaczmarz matrix has the generalized sequencies {0, 1, 2, 3, 4, 5, 6, 7, 8}.

Problem 14.4

$$g(t) = 1/[\pi(t - 3)].$$

Problem 14.5

$$H(z) = \frac{z}{z - a^{-1}}$$

Problem 14.6

$$H_I(j\omega) = \frac{-2\omega}{\omega^2 - \beta^2} + \pi \{ \delta(\omega - \beta) - \delta(\omega + \beta) \}.$$

Problem 14.7

$$H_I(j\omega) = \frac{-(\omega/\sqrt{2})(1 + \omega^2)}{1 + \omega^4}$$

Problem 14.8

$$H_R(j\omega) = \frac{\sqrt{2} \omega^4}{1 + \omega^4} + C$$

If there is a pole on the $j\omega$ axis, say at $s = j\omega_0$ we have

$$H_R(j\omega) = \pi\delta(\omega - \omega_0)$$

$$H(s) = \frac{1}{s - j\omega_0} \quad \text{and} \quad H_I(j\omega) = \frac{1}{\omega_0 - \omega}$$

If $H_I(j\omega) = \pi\delta(\omega - \omega_0)$ then

$$H(s) = \frac{j}{s - j\omega_0} \quad \text{and} \quad H_R(j\omega) = \frac{1}{\omega - \omega_0}$$

Problem 14.10

a) In exponential notation

$$T_9 = \begin{bmatrix} 0 & 0 & 0 & 0 & 0 & 0 & 0 & 0 & 0 \\ 0 & 1 & 2 & 0 & 1 & 2 & 0 & 1 & 2 \\ 0 & 2 & 1 & 0 & 2 & 1 & 0 & 2 & 1 \\ 0 & 0 & 0 & 1 & 1 & 1 & 2 & 2 & 2 \\ 0 & 1 & 2 & 1 & 2 & 0 & 2 & 0 & 1 \\ 0 & 2 & 1 & 1 & 0 & 2 & 2 & 1 & 0 \\ 0 & 0 & 0 & 2 & 2 & 2 & 1 & 1 & 1 \\ 0 & 1 & 2 & 2 & 0 & 1 & 1 & 2 & 0 \\ 0 & 2 & 1 & 2 & 1 & 0 & 1 & 0 & 2 \end{bmatrix}$$

b)

$$T_9 = PS_9PS_9$$

$$S_9 = (I_3 \times T_3)$$

c) With $C = T_3 \times I_{3^9}$

$$T_N = P_N^4 P^4 C P^{-4} P^2 C P^{-2} C P^9 C P^{-9} P^{-4} \\ = P^8 C P^{-2} C P^{-2} C P^9 C P^{-3}.$$

Problem 14.12

a)

B	G	S
000	000	0
001	001	1
002	002	2
003	003	3
004	004	4
010	014	9
...
100	140	45
101	141	46

b)

$$W_9 = W_3 \times W_3 = \begin{bmatrix} 0 & 0 & 0 \\ 0 & 1 & 2 \\ 0 & 2 & 1 \end{bmatrix} \times \begin{bmatrix} 0 & 0 & 0 \\ 0 & 1 & 2 \\ 0 & 2 & 1 \end{bmatrix} = \begin{bmatrix} 0 & 0 & 0 & 0 & 0 & 0 & 0 & 0 & 0 \\ 0 & 1 & 2 & 0 & 1 & 2 & 0 & 1 & 2 \\ 0 & 2 & 1 & 0 & 2 & 1 & 0 & 2 & 1 \\ 0 & 0 & 0 & 1 & 1 & 1 & 2 & 2 & 2 \\ 0 & 1 & 2 & 1 & 2 & 0 & 2 & 0 & 1 \\ 0 & 2 & 1 & 1 & 0 & 2 & 2 & 1 & 0 \\ 0 & 0 & 0 & 2 & 2 & 2 & 1 & 1 & 1 \\ 0 & 1 & 2 & 2 & 0 & 1 & 1 & 2 & 0 \\ 0 & 2 & 1 & 2 & 1 & 0 & 1 & 0 & 2 \end{bmatrix}$$

$$W_{27} = W_3 \times W_9 = \begin{bmatrix} 0 & 0 & 0 \\ 0 & 1 & 2 \\ 0 & 2 & 1 \end{bmatrix} \times \begin{bmatrix} 0 & 0 & 0 & 0 & 0 & 0 & 0 & 0 & 0 \\ 0 & 1 & 2 & 0 & 1 & 2 & 0 & 1 & 2 \\ 0 & 2 & 1 & 0 & 2 & 1 & 0 & 2 & 1 \\ 0 & 0 & 0 & 1 & 1 & 1 & 2 & 2 & 2 \\ 0 & 1 & 2 & 1 & 2 & 0 & 2 & 0 & 1 \\ 0 & 2 & 1 & 1 & 0 & 2 & 2 & 1 & 0 \\ 0 & 0 & 0 & 2 & 2 & 2 & 1 & 1 & 1 \\ 0 & 1 & 2 & 2 & 0 & 1 & 1 & 2 & 0 \\ 0 & 2 & 1 & 2 & 1 & 0 & 1 & 0 & 2 \end{bmatrix}$$

$$W_{27} [13] = [000 \ 111 \ 222 \ 111 \ 222 \ 000 \ 222 \ 000 \ 111]$$

$$W_{27} [14] = [012 \ 120 \ 201 \ 120 \ 201 \ 012 \ 201 \ 012 \ 120]$$

$$W_{27} [15] = [021 \ 102 \ 210 \ 102 \ 210 \ 021 \ 210 \ 021 \ 102]$$

The sequencies of the lines are

$$S [13] = 10/2 = 5 \\ S [14] = 30/2 = 15 \\ S [15] = 38/2 = 19$$

Problem 14.13

a)

$$\rho \longrightarrow \{(0, 1, 2, 3), (16, 17, 18, 19), (4, 5, 6, 7), \\ (20, 21, 22, 23), (8, 9, 10, 11), (24, 25, 26, 27), \\ (12, 13, 14, 15), (28, 29, 30, 31)\}$$

i)

$$Y = \rho X$$

Let x_i be the row vectors of X . The row vectors of Y are

$$\begin{aligned} &x_0, x_1, x_2, x_3 ; \quad x_{16}, x_{17}, x_{18}, x_{19} ; \\ &x_4, x_5, x_6, x_7 ; \quad x_{20}, x_{21}, x_{22}, x_{23} ; \\ &x_8, x_9, x_{10}, x_{11} ; \quad x_{24}, x_{25}, x_{26}, x_{27} ; \\ &x_{12}, x_{13}, x_{14}, x_{15} ; \quad x_{28}, x_{29}, x_{30}, x_{31} ; \end{aligned}$$

ii) Let $Z = X\rho$

$$\rho \longrightarrow \{0, 1, 2, 3 ; \quad 8, 9, 10, 11 ; \quad 16, 17, 18, 19 ; \quad 24, 25, 26, 27 ; \\ 4, 5, 6, 7 ; \quad 12, 13, 14, 15 ; \quad 20, 21, 22, 23 ; \quad 28, 29, 30, 31\}$$

The column vectors of Z are

$$\begin{aligned} &x_0, x_1, x_2, x_3 ; \quad x_8, x_9, x_{10}, x_{11} ; \quad x_{16}, x_{17}, x_{18}, x_{19} ; \\ &x_{24}, x_{25}, x_{26}, x_{27} ; \quad x_4, x_5, x_6, x_7 ; \quad x_{12}, x_{13}, x_{14}, x_{15} ; \\ &x_{20}, x_{21}, x_{22}, x_{23} ; \quad x_{28}, x_{29}, x_{30}, x_{31} \end{aligned}$$

b)

$$\begin{aligned} PSP^{-1} &= (T_2 \times I_8) \\ P^2SP^{-2} &= (I_2 \times T_2 \times I_4) \\ P^3SP^{-3} &= (I_4 \times T_2 \times I_2) \end{aligned}$$

Problem 14.14

c)

$$W_{N, \text{Walsh-Kaczmarz}} = \frac{1}{3} \begin{bmatrix} 0 & 0 & 0 & 0 & 0 & 0 & 0 & 0 & 0 & 0 \\ 0 & 0 & 0 & 1 & 1 & 1 & 2 & 2 & 2 & 2 \\ 0 & 0 & 0 & 2 & 2 & 2 & 2 & 1 & 1 & 1 \\ 0 & 1 & 2 & 2 & 0 & 1 & 1 & 2 & 0 & 0 \\ 0 & 1 & 2 & 0 & 1 & 2 & 0 & 1 & 2 & 0 \\ 0 & 1 & 2 & 1 & 2 & 0 & 2 & 0 & 1 & 0 \\ 0 & 2 & 1 & 1 & 0 & 2 & 2 & 1 & 0 & 0 \\ 0 & 2 & 1 & 2 & 1 & 0 & 1 & 0 & 2 & 0 \\ 0 & 2 & 1 & 0 & 2 & 1 & 0 & 2 & 1 & 0 \end{bmatrix}$$

This page intentionally left blank

15.1 Introduction

The logic of computer arithmetic constitutes the foundation of computer architecture and logic design. In the first part of this chapter we study the fundamentals of digital computer arithmetic. We start by studying some systems of representation of numbers and follow them by methods for effecting basic computer arithmetic operations. Examples of the architectures of parallel processors follow. Texas Instruments TMS320C6713B Floating-Point™ digital signal processor (DSP) is subsequently introduced, and its programming for real-time applications studied in some detail.

15.2 Systems for the Representation of Numbers

A number X can be represented using many possible forms. A basic form that is well established uses a *radix*, or *base*, r and is called *positional notation*. The usual decimal system that we use everyday is a positional notation system using a radix, also referred to as base, $r = 10$. When we write $X = 7294.15$, we implicitly assume that a radix $r = 10$ is used. To denote this explicitly we should write $X = 7294.15_{10}$ or $X = (7294.15)_{10}$ meaning that

$$X = 7 \times 10^3 + 2 \times 10^2 + 9 \times 10^1 + 4 \times 10^0 + 1 \times 10^{-1} + 5 \times 10^{-2}. \quad (15.1)$$

More generally we write a number with a radix r as

$$\begin{aligned} X &= (d_{n-1}d_{n-2} \dots d_1d_0.d_{-1}d_{-2} \dots d_{-m})_r \\ &= d_{n-1} \times r^{n-1} + d_{n-2} \times r^{n-2} + \dots + d_1r + d_0 + d_{-1}r^{-1} + \dots = \sum_{i=-m}^{n-1} d_i r^i. \end{aligned}$$

The digits d_i have values ranging between 0 and $r - 1$; that is, $0 \leq d_i \leq r - 1$. In a decimal system, $r = 10$ and $0 \leq d_i \leq 9$. In a binary system $r = 2$ and $d_i = 0$ or 1, while in a ternary system $r = 3$ and $0 \leq d_i \leq 2$. The ternary number $X = 2101.22_3$ has a value equal to

$$\begin{aligned} X &= 2 \times 3^3 + 1 \times 3^2 + 0 + 1 + 2 \times 3^{-1} + 2 \times 3^{-2} \\ &= 3^{-2} (2 \times 3^5 + 3^4 + 3^2 + 2 \times 3 + 2) = 584/9 = (64.888 \dots)_{10}. \end{aligned} \quad (15.2)$$

Higher radix systems include quaternary ($r = 4$), quinary ($r = 5$), octal ($r = 8$), duodecimal ($r = 12$), hexadecimal ($r = 16$) In a hexadecimal system, ($r = 16$), the digits d_i when

greater than 9 are given alphabetic symbols to avoid the double-digit values 10 to 15. The digits d_i take on the values 0, 1, 2, ..., 9, A, B, C, D, E, F. The digit F thus denotes the value $(15)_{10}$. In what follows the radix subscript appended to a number will be specified when necessary and omitted when clear from the context or when the representation is decimal. The left-most digit of a number is called the most significant digit (MSD). The right-most digit is the least significant digit (LSD).

In a binary system where binary digits are called bits the left- and right-most bits are denoted MSB and LSB respectively. A binary number can be converted readily into an octal or hexadecimal number, respectively. To convert to octal we proceed from the LSB toward the MSB grouping each 3 bits into their octal equivalent. To convert to hexadecimal we do the same but grouping each 4 bits into their hexadecimal equivalent. The binary number $1\ 0111\ 0100\ 1100\ 1110_2$ can thus be written as 272316_8 and $(174CE)_{16}$. A binary coded decimal (BCD) number is one where each decimal digit is coded in binary. The number 7195_{10} is thus coded as $(0111\ 0001\ 1001\ 0101)$, each 4 bits representing the corresponding decimal digit.

15.3 Conversion from Decimal to Binary

Given a decimal number N it may be converted to binary by successive divisions by 2. The successive remainders obtained after each division are the successive bits of the equivalent binary number. For example, with $N = 27$, dividing by 2 we obtain 13 with remainder $r(1) = 1$. Dividing 13 by 2 we obtain 6 and $r(2) = 1$. Dividing 6 by 2 we obtain 3 and $r(3) = 0$. Repeating we obtain $\lfloor 3/2 \rfloor = 1$ and $r(4) = 1$ and finally $\lfloor 1/2 \rfloor = 0$ and $r(5) = 1$.

The value in binary is $\{r(1), r(2), r(3), r(4), r(5)\}$ i.e. $(11011)_2$.

15.4 Integers, Fractions and the Binary Point

Equation (15.1) above describes a decimal number that has an integer part, composed of n digits: d_0, d_1, \dots, d_{n-1} , a decimal point and a fractional part composed of m digits, $d_{-1}, d_{-2}, \dots, d_{-m}$. Similarly, a binary number $(b_{n-1}b_{n-2} \dots b_1b_0.b_{-1}b_{-2} \dots b_{-m})_2$ is composed of an integer part of n bits and a fractional part of m bits, both parts separated by a binary point.

In designing and describing arithmetic operations in a digital computer it is found convenient to view a given number as wholly integer or wholly fractional. A wholly integer number has the form $(b_{n-1}b_{n-2} \dots b_1b_0)_2$ with the binary point located on the right. Such a convention of viewing all numbers as integers is called “integer or integral number representation” (INR). In contrast, “fractional number representation” (FNR) is a convention where all numbers are viewed as fractions, having the form $(.b_{-1}b_{-2} \dots b_{-m})_2$, with the binary point situated on the left of the fractional bits. In the floating point representation of numbers, as we shall see later on, a number is represented by a mantissa and an exponent. In one convention the mantissa is a fraction. The exponent is an integer. It is therefore advisable to be familiar with both types of notation, the integral and fractional representations of numbers.

We note that the fractional number (.101101) has a value $(2^{-1} + 2^{-3} + 2^{-4} + 2^{-6}) = 2^{-6} (2^5 + 2^3 + 2^2 + 2^0) = 45 (2^{-6})$.

This same number in the integer-number representation would be viewed as (101101.), having a value of 45. The fractional value of the number is therefore $2^{-6} \times$ its integer value. This is generally the case: Given a number of k bits, say, its value in fractional representation is the same as its value in integer representation except for a factor of 2^{-k} . We can therefore evaluate the number as an integer (with the binary point on the right) and multiply it by 2^{-k} to give its value in fractional notation.

In what follows, as is usually the convention, the binary point will often be omitted when its position is clear from the context. A number such as 110101101 will thus be understood to have a binary point on its right in the case of integral number representation INR, and on its left in the case of FNR. Having 9 bits the latter representation gives a value for the number equal to $2^{-9} \times$ the value given by the integer representation, that is, $429 (2^{-9})$.

If we multiply the two integers 110010 and 101101 the result is the integer $50 \times 45 = 2250_{10}$. Viewed as fractions the result would be $50 (2^{-6}) \times 45 (2^{-6}) = 2250 \times 2^{-12}$, that is, the same result except with the factor 2^{-12} associated with it. In either case, however, whether numbers are viewed as integers or fractions, the logic circuits are the same. In the literature, some books adopt integer number representation, others adopt fractional representation. Both types of number representation and their formalism are dealt with in this book.

15.5 Representation of Negative Numbers

There are three common approaches to representing negative numbers in binary. These are: (1) *sign and magnitude notation*, (2) *1's complement notation* and (3) *2's complement notation*. We now consider each of these in turn.

15.5.1 Sign and Magnitude Notation

In sign and magnitude notation, the negative number appears identically to the positive number except for a sign bit; which is normally zero for a positive number and one for the corresponding negative number. The representation of a number composed of n magnitude bits would thus occupy $n + 1$ bits, the additional bit being the sign bit.

Assuming integer number representation INR and $n = 5$ magnitude bits, a signed number is stored in a 6-bit register, the left-most bit of which is the sign bit. The decimal value +23 is thus represented as (0, 10111.), while the value -23 is represented as (1, 10111.). We note that the comma, separating the sign bit from the magnitude bits, and the binary point on the right, signifying that the number in question is an integer, are added here only for clarity and are not stored in the register containing the number. The actual content of the register for $+23_{10}$ is 010111, and for -23_{10} is 110111.

We adopt the notation

$$+23 \xrightarrow{S\&M} (0, 10111), \quad -23 \xrightarrow{S\&M} (1, 10111) \quad (15.3)$$

where $S\&M$ denotes sign and magnitude notation.

Consider now the sign and magnitude notation in the context of fractional number representation FNR. Note that in this notation the binary number (10111) has the decimal value $+23 (2^{-5})$. To represent this value and its negation in sign and magnitude notation

we may write

$$+23 (2^{-5}) \xleftrightarrow{S\&M} (0; 10111), \quad -23 (2^{-5}) \xleftrightarrow{S\&M} (1; 10111). \quad (15.4)$$

The semicolon here serves to delimit the sign bit and, meanwhile, indicate that the number is a fraction.

The notation just proposed specifies whether integer or fractional representation is used and meanwhile delimits the sign bit from the other magnitude bits. In what follows, however, we shall at times for the sake of notational simplicity only delimit the sign bit by a point and not indicate explicitly the location of the binary point. We will do this when the binary point location is clear from the context.

15.5.2 1's and 2's Complement Notation

Consider a number $x = (x_{n-1}x_{n-2} \dots x_1x_0 \cdot x_{-1}x_{-2} \dots x_{-m})_r$ of radix r , that is, a number represented with n integer bits and m fraction bits. The r 's complement of x , which will be denoted $x^{[r]}$ is given by

$$x^{[r]} = r^n - x. \quad (15.5)$$

The $(r - 1)$'s complement of x is given by

$$x^{[r-1]} = r^n - x - r^{-m}. \quad (15.6)$$

In a decimal system, $r = 10$, the 10's complement of x is given by

$$x^{[10]} = 10^n - x \quad (15.7)$$

and the 9's complement by

$$x^{[9]} = 10^n - x - 10^{-m}. \quad (15.8)$$

For example, if $x = 937.25$ then $x^{[10]} = 1000 - 937.25 = 62.75$ and $x^{[9]} = 62.75 - 0.01 = 62.74$.

Similarly in the binary system representation the 2's complement of x is given by

$$x^{[2]} = 2^n - x \quad (15.9)$$

and the 1's complement

$$x^{[1]} = 2^n - x - \varepsilon \quad (15.10)$$

where $\varepsilon = 2^{-m}$. Since $m = 0$ in INR and $n = 0$ in FNR the 2's and 1's complement representations in INR are respectively

$$x^{[2]} = 2^n - x \quad (15.11)$$

and

$$x^{[1]} = 2^n - x - 1 \quad (15.12)$$

and in FNR

$$x^{[2]} = 1 - x \quad (15.13)$$

and

$$x^{[1]} = 1 - x - 2^{-m}. \quad (15.14)$$

In what follows we shall also use the notation \bar{x} and $\overline{\bar{x}}$ to denote the 1's and 2's complement respectively. We will focus our attention primarily on binary systems; hence on 1's and 2's complement. We note that in integral (integer) notation, where all numbers are integers,

we have $m = 0$. For example, with $x = 1101011$ we have $n = 7$ and the 2's complement is given by

$$\begin{array}{r} 10000000 \ 2^n \\ - \ 1101011 \ x \\ \hline 0010101 \ \bar{x} \equiv x^{[2]}. \end{array}$$

Similarly, the 1's complement is found by subtracting x from $(2^n - 1)$. Let $M = 2^n - 1$. We note that $M = 1111111$, the maximum possible value that x may have in a 7-bit register.

The 1's complement is thus given by

$$\begin{array}{r} 1111111 \ M = 2^n - 1 \\ - \ 1101011 \ x \\ \hline 0010100 \ \bar{x} \equiv x^{[1]}. \end{array}$$

We note that the 1's complement $x^{[1]}$ of x can be written directly by complementing each bit of x . Moreover, that the 2's complement $x^{[2]}$ can be evaluated by adding 1 to the 1's complement $x^{[1]}$, that is,

$$x^{[2]} = x^{[1]} + 1. \tag{15.15}$$

We can thus deduce $x^{[2]}$ by complementing each bit of x to obtain $x^{[1]}$ and then adding 1 to $x^{[1]}$.

Alternatively, the 2's complement of a number x may be obtained by starting at the right-most bit copying each bit 0 as is, until the first bit 1 is met and copied as is. Thenceforth each bit is complemented to the end of x . For example, given $x = 0110101100$ the 2's complement is $x^{[2]} = 1001010100$.

Now let us consider fractional number representation FNR. In this notation, where numbers are fractions with the binary point on the left, we have $n = 0$ so that the 2's complement of x is given by

$$x^{[2]} = 1 - x \tag{15.16}$$

and the 1's complement by

$$x^{[1]} = 1 - x - \epsilon = 1 - x - 2^{-m}. \tag{15.17}$$

The above example would then read as

$$\begin{array}{r} 1.0000000 \ 1 \\ - \ .1101011 \ x \\ \hline .0010101 \ \bar{x} \equiv x^{[2]} \end{array}$$

and

$$\begin{array}{r} .1111111 \ M = 1 - \epsilon = 1 - 2^{-m} \\ - \ .1101011 \ x \\ \hline .0010100 \ \bar{x} \equiv x^{[1]} \end{array}$$

where the smallest positive number is $\epsilon = 2^{-m}$ and where $M = 1 - \epsilon = (.1111111)$ is the maximum number that can be represented without causing over-flow of the 7-bit register. Henceforth if INR is used, we shall assume that any given positive number A of magnitude a is by default n bits long and written as $a_n.a_{n-1}a_{n-2} \dots a_1a_0$, stored in a register of length $N = n + 1$ bits. The dot serves as a delimiter, separating the sign bit $a_n = 0$ from the magnitude bits. The binary point is implied to be to the right of the LSB a_0 . If FNR is used it will have the form $a_0.a_{-1}a_{-2} \dots a_{-n}$, where the binary point is between the sign bit $a_0 = 0$ and the left-most magnitude bit a_{-1} .

15.6 Integer and Fractional Representation of Signed Numbers

In what follows a signed number will be denoted using an upper case letter and its magnitude using lower case. A number A may be positive or negative, and its absolute value is $a = |A|$. The INR is shown in Fig. 15.1, where an implied binary point is seen on the right.

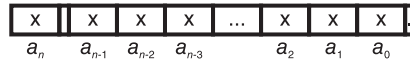


FIGURE 15.1 Integer number representation (INR).

The (FNR) has the form shown in Fig. 15.2, where the implied binary point is seen to be on the left of the most significant of the magnitude bits.

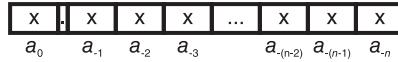


FIGURE 15.2 Fractional number representation (FNR).

As shown in these figures, in integer number representation the bits of the number are a_0 to a_n where a_n is the sign bit, while in FNR the bits of a number are labeled a_0 to a_{-n} , with a_0 the sign bit and the binary point situated between a_0 and a_{-1} .

In INR we write:

$$A = \pm a \xleftrightarrow{S\&M} A^{[0]} = \begin{cases} \sum_{i=0}^{n-1} a_i 2^i \\ 1 + \sum_{i=0}^{n-1} a_i 2^i \end{cases} \tag{15.18}$$

where we write $A^{[0]}$ to imply that the number is represented in $S\&M$ notation.

In FNR we write

$$A = \pm a \xleftrightarrow{S\&M} A^{[0]} = \begin{cases} \sum_{i=1}^n a_{-i} 2^{-i} \\ 1 + \sum_{i=1}^n a_{-i} 2^{-i} \end{cases} \tag{15.19}$$

noting that in INR $a_n = 0$ for $A = +a$ and $a_n = 1$ for $A = -a$ and in FNR $a_0 = 0$ for $A = +a$ and $a_0 = 1$ for $A = -a$.

The representations of numbers $A = 90$ and $A = -90$ in $S\&M$ notation are shown in Fig. 15.3 and Fig. 15.4. The corresponding representations in FNR are shown in Fig. 15.5 and Fig. 15.6, respectively.

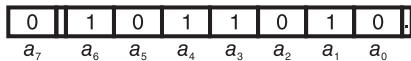


FIGURE 15.3 Positive number in *S&M* INR.

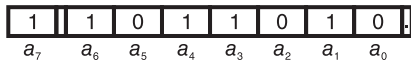


FIGURE 15.4 Negative number in *S&M* INR.

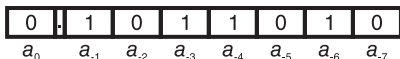


FIGURE 15.5 Positive number in *S&M* FNR.

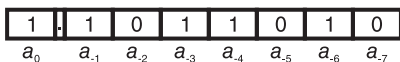


FIGURE 15.6 Negative number in *S&M* FNR.

15.6.1 1’s and 2’s Complement of Signed Numbers

We notice that so far 1’s complement and 2’s complement representations were described in the context of unsigned numbers. Let us now develop these representations for signed numbers using the same register length, $N = n + 1$ bits, as we have just done for *S&M* notation.

In addition to the complemented bits we need to add a sign bit that is zero if the number is positive, and one if negative. The 1’s complement of a signed number $A = \pm a$ will be denoted, in accordance with the above, $A^{[1]}$ or \bar{A} . The 2’s complement of $A = \pm a$ will be denoted $A^{[2]}$ or $\bar{\bar{A}}$. The bits of $A^{[1]}$ will be denoted $A_i^{[1]}$, where in integer notation i varies from 0 to n and in fractional notation i varies from 0 to $-n$. Similarly, the bits of $A^{[2]}$ will be denoted $A_i^{[2]}$. Adding the sign bit to the forms developed above we first notice that all representations are the same for a positive number, since the added sign bit is simply zero. We can therefore write

$$A = +a \longrightarrow A^{[0]} = A^{[1]} = A^{[2]} \tag{15.20}$$

meaning that if $A \geq 0$ then *S&M*, 1’s complement and 2’s complement representations are the same. If $A = -a$, that is, $A < 0$ we write

$$\begin{aligned} A = -a &\xleftarrow{\text{1's complt}} A^{[1]} = 2^{n+1} - a - 1 \text{ (INR)} \\ &= -a \xleftarrow{\text{1's complt}} A^{[1]} = 2 - a - 2^{-n} = 2 - a - \varepsilon \text{ (FNR)}. \end{aligned} \tag{15.21}$$

For example with $A = +45$ we have $a = 45$, $A^{[0]} = A^{[1]} = A^{[2]} = 0,101101$. Now let $A = -45$. The absolute value of A , denoted a is $a = 45 = 0,101101$. We have in sign and magnitude notation $A^{[0]} = 1,101101$ and in the 1’s complement representation $A^{[1]}$ is

given in INR and FNR as follows.

	INR	FNR
10,000000	2^{n+1}	2
- 1	1	ϵ
1,111111	W	W
- 0,101101	a	a
1,010010	$A^{[1]}$	$A^{[1]}$

We note that the INR column is written with the binary point viewed on the right of the number while the FNR column is written with it viewed at the same position as the comma, that is, the sign delimiter. We will follow this convention throughout, listing whenever appropriate both the INR and FNR values for each given number. From this example we note that the value $W = (2^{n+1} - 1)$ is the maximum possible value that can be stored in the $N = n + 1$ -bit register. We also note that $A^{[1]}$ can be obtained from $A^{[0]} = a$ by reversing every bit including the sign bit.

Consider now the case of signed numbers. A sign bit is added and is zero if the number is positive and 1 if it is negative as is the case in the sign and magnitude notation.

In this case the 1's complement may be obtained by inverting all bits, including the sign bit. The 2's complement may be obtained by adding ϵ to the 1's complement, where $\epsilon = 1$ in integer number representation INR and $\epsilon = 2^{-n}$ in fractional number representation FNR. Consider the example dealt with in connection with sign and magnitude notation above. In particular, let $A = +a = +90$. Since the number is positive its representation in an 8-bit register is identical to that in the sign and magnitude notation, as shown in Fig. 15.3.

If instead $A = -a = -90$ its 1's complement representation is obtained by inverting all bits including the sign bit, and is shown in Fig. 15.7 and Fig. 15.8 for INR and FNR, respectively, where in the second case the number represented is $A = -a = -90(2^{-7})$.

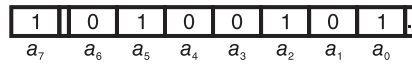


FIGURE 15.7 Representation of -90 in 1's complement INR.

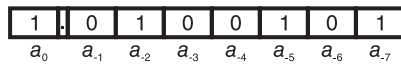


FIGURE 15.8 Representation of -90 in 1's complement FNR.

We can write (with $A < 0$) for 1's complement representation

$$\begin{aligned}
 A &= -a \simeq 2^{n+1} - a - 1 \quad (\text{INR}) \\
 &= -a \simeq 2 - a - \epsilon \quad (\text{FNR})
 \end{aligned}
 \tag{15.22}$$

where $\epsilon = 2^{-n}$.

We may thus write in integer number representation INR

$$A^{[1]} = 2^{n+1} - a - 1
 \tag{15.23}$$

and in fractional number representation FNR

$$A^{[1]} = 2 - a - 2^{-n}. \tag{15.24}$$

2's complement representation may be obtained from 1's complement by adding 1 to 1's complement in INR, or adding $\varepsilon = 2^{-n}$ in FNR. We have for 2's complement representation

$$\begin{aligned} -a &\simeq 2^{n+1} - a \text{ (INR)} \\ -a &\simeq 2 - a \text{ (FNR)} \end{aligned} \tag{15.25}$$

With $A = -90$ we obtain $A^{[2]}$ as the sum

$$\begin{array}{r} 1\ 0100101\ A^{[1]} \\ \underline{\ 1\ \varepsilon} \\ 1\ 0100110\ \Sigma \end{array}$$

with $\varepsilon = 1$ in INR and $\varepsilon = 2^{-n}$ in FNR, as shown in Fig. 15.9 and Fig. 15.10, respectively.

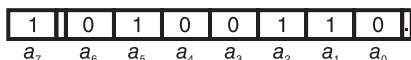


FIGURE 15.9 Representation of -90 in 2's complement INR.

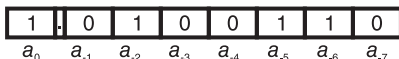


FIGURE 15.10 Representation of -90 in 2's complement FNR.

Given a negative number represented in 2's complement, such as $A^{[2]} = 1.0111$ we can find its absolute decimal value by 2's complementing it, i.e. negating it, obtaining its positive value $a = 0.1001$ i.e. a decimal value of 9 in integral representation INR and $9 \times (2^{-4})$ in FNR. It is interesting to note that there is another way of evaluating the decimal equivalent of a negative number given in 2's complement representation. The approach is to view the sign bit as a magnitude bit, weighted according to its position, but negative valued. For the same example we may rewrite the 2's complement representation of -9 as $\bar{1}.0111$ and consider the representation as the sum of the magnitude part $(0111)_2 = 7_{10}$ and the sign part properly weighted, i.e. $-2^4 = -16$, for a total of -9 as required. Similarly, in FNR we obtain the sum $-1 + (0.0111)_2 = -1 + 7 \times 2^{-4} = -9 (2^{-4})$.

In general therefore we may write the 2's complement representation as the sum of a weighted negative sign and a positive magnitude part, obtaining for INR and FNR, respectively,

$$A_I^{[2]} \longleftrightarrow -2^n + x_I \tag{15.26}$$

$$A_F^{[2]} \longleftrightarrow -1 + x_F. \tag{15.27}$$

The value x_I is the magnitude part of the 2's complement representation, i.e. $x_I = 0111 = 7_{10}$ in the present example. In general it is the 2's complement representation without the

sign bit, i.e.

$$x_I = (2^{n+1} - a_I) - 2^n = 2^n - a_I \quad (15.28)$$

in INR, and

$$x_F = (2 - a_F) - 1 = 1 - a_F \quad (15.29)$$

i.e. $x_F = 1 - 9(2^{-4}) = 7(2^{-4})$ in FNR of the same example.

The significance of this property is that it can be used, as we shall see, in an efficient method for effecting multiplication in 2's complement.

15.7 Addition

In this section we study the addition $A + B$ of two signed numbers A and B , A being called the “augend” and B the “addend,” having absolute values a and b , respectively, in sign and magnitude, 1's complement and 2's complement notation. We assume the absence of overflow OVF. In other words, when the augend A of a magnitude represented by n bits is added to the addend B , also of an n -bit magnitude, the result should occupy n bits. In fractional number representation FNR this means that the result remains a fraction, i.e. less than 1; same as A and B . In INR this means that the result has a magnitude less than 2^n .

In what follows we consider for the different possibilities of the signs of A and B the corresponding sum $A + B$, as given in the different representations, with examples illustrating each case.

To lighten the presentation we shall mainly use FNR. The corresponding representation in INR may be directly deduced by replacing 1 by 2^n and $\varepsilon = 2^{-n}$ by $\varepsilon = 1$.

15.7.1 Addition in Sign and Magnitude Notation

In addition in sign and magnitude notation, we have to consider the following cases:

a) Positive Operands $A \geq 0$, $B \geq 0$.

With positive operands A and B , in all three systems, sign and magnitude, 1's and 2's complement, the result is simply the sum of $a + b$ with a zero, for positive, sign attached.

$$\begin{aligned} C = A + B &\longleftrightarrow a + b; \quad a + b < 1, \quad A, B \geq 0 \quad (\text{FNR}) \\ &= A + B \longleftrightarrow a + b; \quad a + b < 2^n, \quad A, B \geq 0 \quad (\text{INR}). \end{aligned} \quad (15.30)$$

b) Negative Operands $A < 0$, $B < 0$.

Algorithm: To effect the addition add the magnitude bits without the sign. Attach to the result the common sign of A and B , i.e.

$$\begin{aligned} A + B &\longleftrightarrow 1 + a + b; \quad a + b < 1 \quad (\text{FNR}) \\ &\longleftrightarrow 2^n + a + b; \quad a + b < 2^n \quad (\text{INR}). \end{aligned} \quad (15.31)$$

c) Oppositely Signed Operands

(i) The case $a > b$.

Algorithm: Add to the magnitude $a = |A|$ the 1's complement of the magnitude $b = |B|$. Add the “end-around-carry” that results, that is, ignore the carry-out, replacing it by adding ε to the result.

Example 15.1 With $n = 5$ and FNR

$$\begin{array}{r} A : +15 (2^{-5}) \ 0.01111 \\ B : +14 (2^{-5}) \ 0.01110 \\ \hline C : +29 (2^{-5}) \ 0.11101 \end{array}$$

Example 15.2

<i>Augend positive</i>	<i>FNR</i>	<i>INR</i>
$+15(2^{-5})$	0.01111 <i>A</i>	
$-14(2^{-5})$	1.01110 <i>B</i>	
	01111 <i>a</i>	
	10001 $1 - \varepsilon - b$	$2^n - 1 - b$
	00000 Σ	
	$1 \ \varepsilon$	1
	00001	
	<i>result</i> : 0.00001	

<i>Augend negative</i>	<i>FNR</i>	<i>INR</i>
$-15(2^{-5})$	1.01111 <i>A</i>	
$+14(2^{-5})$	0.01110 <i>B</i>	
	01111 <i>a</i>	
	10001 $1 - \varepsilon - b$	$2^n - 1 - b$
	00000 Σ	
	$1 \ \varepsilon$	1
	00001	
	<i>result</i> : 1.00001	

We may therefore write, noticing that the addition of the end-around carry is equivalent to ignoring the carry out bit and adding instead ε , meaning adding $\{-1 + \varepsilon\}$ in FNR, and to adding $|-2^n + 1|$ in INR:

For the case $A \geq 0, B < 0$

$$\begin{aligned} A + B &\longleftrightarrow a + (1 - \varepsilon - b) + \{-1 + \varepsilon\} = a - b \quad (\text{FNR}) \\ &\longleftrightarrow a + (2^n - 1 - b) + \{-2^n + 1\} = a - b \quad (\text{INR}). \end{aligned} \tag{15.32}$$

For the case $A < 0, B \geq 0$ we have in FNR and INR, respectively,

$$\begin{aligned} A + B &\longleftrightarrow 1 + a + (1 - \varepsilon - b) + \{-1 + \varepsilon\} = 1 + a - b \\ &\longleftrightarrow 2^n + a + (2^n - 1 - b) + (-2^n + 1) = 2^n + a - b. \end{aligned} \tag{15.33}$$

(ii) The case $b \geq a$.

Algorithm: Add to the magnitude a the 1's complement of b . Attach to the result the sign of the addend B .

Example 15.3

$$\begin{array}{r|l}
 \text{With } A \geq 0 & \begin{array}{l} \text{FNR} \\ \hline 0.01110 \ A \\ 1.01111 \ B \\ \\ 01110 \ a \\ \underline{10000} \ 1 - \varepsilon - b \\ 11110 \ \Sigma \\ 00001 \ \varepsilon \\ 1.00001 \ C \end{array} & \begin{array}{l} \text{INR} \\ \hline \\ \\ \\ \\ \varepsilon \end{array}
 \end{array}$$

$$\begin{array}{r|l}
 \text{With } A < 0 & \begin{array}{l} \text{FNR} \\ \hline 1.01110 \ A \\ 0.01111 \ B \\ \\ 01110 \ a \\ \underline{10000} \ 1 - \varepsilon - b \\ 11110 \ \Sigma \\ 00001 \ \varepsilon \\ 0.00001 \ C \end{array} & \begin{array}{l} \text{INR} \\ \hline \\ \\ \\ \\ \varepsilon \end{array}
 \end{array}$$

With $b \geq a$ and $A \geq 0, B < 0$ we may therefore write

$$\begin{aligned}
 A + B &\longleftrightarrow 1 + [1 - \varepsilon - \{a + (1 - \varepsilon - b)\}] = 1 + b - a \quad (\text{FNR}) \\
 &\longleftrightarrow 2^n + [2^n - 1 - \{a + (2^n - 1 - b)\}] = 2^n + b - a \quad (\text{INR}).
 \end{aligned} \tag{15.34}$$

With $b \geq a$ and $A < 0, B \geq 0$ we have

$$\begin{aligned}
 A + B &\longleftrightarrow 1 - \varepsilon - \{a + (1 - \varepsilon - b)\} = b - a \quad (\text{FNR}) \\
 &\longleftrightarrow 2^n - 1 - \{a + (2^n - 1 - b)\} = b - a \quad (\text{INR}).
 \end{aligned} \tag{15.35}$$

15.7.2 Addition in 1's Complement Notation

Algorithm : Add the two operands including the sign bit. Add the end-around carry, if any.

a) Two positive operands $A \geq B$ with no OVF.

$$A + B \longleftrightarrow a + b, \quad a + b < 1 \quad (\text{FNR}); \quad a + b < 2^n \quad (\text{INR}). \tag{15.36}$$

b) Two negative operands $A < B, B < 0$. Algorithm: Add the two operands including the sign bit. Add the end-around carry.

Example 15.4

$$\begin{array}{r}
 -15(2^{-5}) : 1.10000 \\
 -14(2^{-5}) : 1.10001 \\
 \hline
 1.00001 \\
 \hline
 1 \\
 \hline
 1.00010 = -29.
 \end{array}$$

We may write

$$\begin{aligned}
 A + B &\longleftrightarrow (2 - \varepsilon - a) + (2 - \varepsilon - b) + \{-2 + \varepsilon\} = 2 - \varepsilon - (a + b) \quad (\text{FNR}) \\
 &\longleftrightarrow 2^n - 1 - (a + b) \quad (\text{INR}).
 \end{aligned} \tag{15.37}$$

c) Oppositely signed numbers:

Algorithm: Add the two numbers including the sign bit. Add end-around-carry if any.

Example 15.5

$$\begin{array}{r}
 -15(2^{-5}) \ 1.10000 \\
 +14(2^{-5}) \ 0.01110 \\
 \hline
 -1 \ 1.11110 \\
 \\
 +15(2^{-5}) \ 0.01111 \\
 -14(2^{-5}) \ 1.10001 \\
 \hline
 0.00000 \\
 \hline
 1 \\
 \hline
 0.00001
 \end{array}$$

As the examples show, we have two cases:

(i) No carry-out generated. This is the case if the negative operand has an absolute value greater than the positive operand, leading to a negative sum: i.e.

$$A < 0, \ B \geq 0, \ a > b \tag{15.38}$$

or

$$B < 0, \ A \geq 0, \ b \geq a. \tag{15.39}$$

For these two cases we have, respectively, (in FNR)

$$\begin{aligned}
 A + B &\longleftrightarrow (2 - \varepsilon - a) + b \\
 &\longleftrightarrow 2 - \varepsilon - (a - b); \quad A < 0, \ B \geq 0, \ a > b
 \end{aligned} \tag{15.40}$$

$$\begin{aligned}
 A + B &\longleftrightarrow (2 - \varepsilon - b) + a \\
 &\longleftrightarrow 2 - \varepsilon - (b - a); \quad B < 0, \ A \geq 0, \ b \geq a
 \end{aligned} \tag{15.41}$$

and a similar expression in INR.

(ii) A carry-out is generated. This is the case if the negative operand is of an absolute value less than the positive operand, leading to a positive result. We have the two cases (in FNR):

For $A < 0, \ B \geq 0, \ b \geq a$:

$$A + B \longleftrightarrow (2 - \varepsilon - a) + b + \{-2 + \varepsilon\} \longleftrightarrow b - a. \tag{15.42}$$

For $B < 0, \ A \geq 0, \ a \geq b$:

$$A + B \longleftrightarrow (2 - \varepsilon - b) + a + \{-2 + \varepsilon\} \longleftrightarrow a - b. \tag{15.43}$$

15.7.3 Addition in 2's Complement Notation

In addition in 2's Complement we have the following cases:

a) Positive operands

Algorithm: Add the two operands signs included.

$$A + B \longleftrightarrow a + b; \quad a + b < 1, \quad A, B \geq 0 \tag{15.44}$$

which is the same as in the sign and magnitude and 1's complement representation.

b) Negative Numbers $A < 0, \ B < 0$, no OVF

Add the two operands, signs included. Neglect any generated carry-out.

Example 15.6

$$\begin{array}{r} -15(2^{-5}) \ 1.10001 \\ -14(2^{-5}) \ 1.10010 \\ \hline 1.00011 \end{array}$$

$$A + B \longleftrightarrow (2 - a) + (2 - b) - 2 = 2 - (a + b).$$

The value -2 represents the neglected output carry.

c) Oppositely signed numbers

Algorithm: Same as above. We have the following cases:

(i) $A \geq 0, a > b$:

$$A + B \longleftrightarrow a + 2 - b - 2 \longleftrightarrow a - b; \quad a > b, \quad A \geq 0, \quad B < 0. \tag{15.45}$$

(ii) $A \geq 0, a < b$:

$$A + B \longleftrightarrow a + 2 - b \longleftrightarrow 2 - (b - a); \quad a < b, \quad A \geq 0, \quad B < 0. \tag{15.46}$$

(iii) $A < 0, a > b$:

$$A + B \longleftrightarrow 2 - a + b \longleftrightarrow 2 - (a - b); \quad a > b, \quad A < 0, \quad B \geq 0. \tag{15.47}$$

(iv) $A < 0, a < b$:

$$A + B \longleftrightarrow 2 - a + b - 2 = b - a; \quad a \leq b, \quad A < 0, \quad B \geq 0. \tag{15.48}$$

Example 15.7

$$\begin{array}{r} +15(2^{-5}) \ 0.01111 \\ -14(2^{-5}) \ 1.10010 \\ \hline 0.00001 \end{array}$$

$$\begin{array}{r} -15(2^{-5}) \ 1.10001 \\ +14(2^{-5}) \ 0.01110 \\ \hline 1.11111 \end{array}$$

$$\begin{array}{r} -14(2^{-5}) \ 1.10010 \\ +15(2^{-5}) \ 0.01111 \\ \hline 0.00001 \end{array}$$

$$\begin{array}{r} +14(2^{-5}) \ 0.01110 \\ -15(2^{-5}) \ 1.10001 \\ \hline 1.11111 \end{array}$$

15.8 Subtraction

We consider the subtraction $C = A - B$, A is called the “minuend,” B the “subtrahend.” They are assumed to be represented by n bits for magnitude and one sign bit. Since the subtraction $C = A - B$ is the same as $C = A + (-B)$, the same approach given above may be used by replacing B by $-B$. The subtraction $C = A - B$ is usually performed by simply reversing the bits of the B operand which produces its 1’s complement, and adding ε , i.e. a bit 1 as a carry-in to the least significant bit, resulting in the 2’s complement of B , which is then added to A . The following assumes that numbers are represented in FNR.

15.8.1 Subtraction in Sign and Magnitude Notation

In subtraction in sign and magnitude notation we have the following cases:

a) Operands of opposite signs

Algorithm: Add the absolute values a and b . Attach to the result the sign of the minuend A .

Example 15.8

$$\begin{array}{r}
 +15(2^{-5}) \ 0.01111 \ A \\
 - [-14(2^{-5})] \ 1.01110 \ B \\
 \hline
 \end{array}
 \tag{15.49}$$

$$\begin{array}{r}
 01111 \ a \\
 01110 \ b \\
 \hline
 \text{result : } 0.11101
 \end{array}$$

$$\begin{array}{r}
 -15(2^{-5}) \ 1.01111 \ A \\
 - [+14(2^{-5})] \ 0.01110 \ B \\
 \hline
 \end{array}
 \tag{15.50}$$

$$\begin{array}{r}
 01111 \ a \\
 01110 \ b \\
 \hline
 11101 \\
 \text{result : } 1.11101
 \end{array}$$

$$\begin{aligned}
 A - B \iff a + b; \quad a + b < 1, \quad A \geq 0, \quad B < 0 \\
 \iff 1 + a + b; \quad a + b < 1, \quad A < 0, \quad B \geq 0.
 \end{aligned}
 \tag{15.51}$$

b) Same sign operands

(i) $a \geq b$.

Algorithm: Add to the absolute value a of A the 1's complement of the absolute value b of B . Add the end-around carry. Attach to the result the sign of A .

Example 15.9

$$\begin{array}{r}
 A, B \geq 0 \quad +15(2^{-5}) \ 0.01111 \ A \\
 - [+14(2^{-5})] \ 0.01110 \ B \\
 \hline
 \end{array}$$

$$\begin{array}{r}
 01111 \\
 10001 \\
 \hline
 00000 \\
 1 \\
 \hline
 00001
 \end{array}$$

result : 0.00001

$$\begin{array}{r}
 A, B < 0 \quad -15(2^{-5}) \ 1.01111 \ A \\
 - [-14(2^{-5})] \ 1.01110 \ B \\
 \hline
 \end{array}$$

$$\begin{array}{r}
 01111 \\
 10001 \\
 \hline
 00000 \\
 1 \\
 \hline
 00001
 \end{array}$$

result : 1.00001

For $A, B \geq 0$

$$A - B \longleftrightarrow [a + (1 - b - \varepsilon) - 1 + \varepsilon] = a - b. \tag{15.52}$$

For $A, B < 0$

$$A - B \longleftrightarrow 1 + [a + (1 - b - \varepsilon) - 1 + \varepsilon] = 1 + (a - b). \tag{15.53}$$

(ii) $b \geq a$.

Algorithm: Add to the absolute value a of A the 1's complement of the absolute value b of B . No carry-out is generated. Complement the result. Attach to the result the complement of the sign bit of A .

$$\begin{array}{r} +14(2^{-5}) \ 0.01110 \ A \\ - [+15(2^{-5})] \ 0.01111 \ B \\ \hline \phantom{+14(2^{-5})} \ 01110 \\ \phantom{+14(2^{-5})} \ 10000 \\ \hline \phantom{+14(2^{-5})} \ 11110 \end{array} \tag{15.54}$$

complement : 00001
result : 1.00001

$$\begin{array}{r} -14(2^{-5}) \ 1.01110 \\ - [-15(2^{-5})] \ 1.01111 \end{array}$$

$$\begin{array}{r} \phantom{-14(2^{-5})} \ 01110 \\ \phantom{-14(2^{-5})} \ 10000 \\ \hline \phantom{-14(2^{-5})} \ 11110 \end{array} \tag{15.55}$$

complement : 00001
result : 0.00001

$A, B > 0, a \leq b$

$$A - B \longleftrightarrow 1 + \{1 - [a + (1 - b - \varepsilon)] - \varepsilon\} = 1 + b - a. \tag{15.56}$$

$A, B < 0, a \leq b$:

$$A - B \longleftrightarrow 1 - [a + (1 - b - \varepsilon)] - \varepsilon = b - a. \tag{15.57}$$

15.8.2 Numbers in 1's Complement Notation

Algorithm: Add to A the 1's complement of B (signs included). Add the end-around carry, if any. No OVF is assumed i.e., in the present FNR presentation, $a + b < 1$

$$\begin{array}{r} +15(2^{-5}) \ 0.01111 \ A \\ - (-14(2^{-5})) \ 1.10001 \ B \\ \hline \phantom{+15(2^{-5})} \ 0.01111 \\ \phantom{+15(2^{-5})} \ 0.01110 \\ \hline \text{result : } \overline{0.11101} \end{array} \tag{15.58}$$

$$\begin{array}{r} -15(2^{-5}) \ 1.10000 \\ - (+14(2^{-5})) \ 0.01110 \end{array}$$

$$\begin{array}{r} \phantom{-15(2^{-5})} \ 1.10000 \\ \phantom{-15(2^{-5})} \ 1.10001 \\ \hline \phantom{-15(2^{-5})} \ 1.00001 \end{array} \tag{15.59}$$

result : $\overline{1.00010}$

(i) $A \geq 0, B < 0:$

$$A - B \longleftrightarrow a + b. \tag{15.60}$$

(ii) $A < 0, B \geq 0:$

$$A - B \longleftrightarrow (2 - a - \varepsilon) + (2 - b - \varepsilon) - 2 + \varepsilon = 2 - (a + b) - \varepsilon. \tag{15.61}$$

(iii) $A \geq 0, B \geq 0, a \geq b:$

$$A - B \longleftrightarrow a + (2 - b - \varepsilon) - 2 + \varepsilon = a - b. \tag{15.62}$$

(iv) $A \geq 0, B \geq 0, a < b:$

$$A - B \longleftrightarrow a + (2 - b - \varepsilon) = 2 - \varepsilon - (b - a). \tag{15.63}$$

(v) $A < 0, B < 0, a \geq b:$

$$A - B \longleftrightarrow (2 - \varepsilon - a) + [2 - \varepsilon - (2 - \varepsilon - b)] = 2 - \varepsilon - a + b. \tag{15.64}$$

(vi) $A < 0, B < 0, a < b:$

$$A - B \longleftrightarrow 2 - \varepsilon - a + [2 - \varepsilon - (2 - \varepsilon - b)] - 2 + \varepsilon = b - a \tag{15.65}$$

Example 15.10 Case (v)

$$\begin{array}{r} -15(2^{-5}) \ 1.10000 \\ -(-14(2^{-5})) \ 1.10001 \\ \hline -15(2^{-5}) \ 1.10000 \\ +14(2^{-5}) \ 0.01110 \\ \hline \text{result : } 1.11110 \end{array}$$

Case (vi)

$$\begin{array}{r} -14(2^{-5}) \ 1.10001 \\ -(-15(2^{-5})) \ 1.10000 \\ \hline -14(2^{-5}) \ 1.10001 \\ +15(2^{-5}) \ 0.01111 \\ \hline 0.00000 \\ \hline 1 \\ \hline 0.00001 \end{array}$$

15.8.3 Subtraction in 2's Complement Notation

Algorithm: Add to A the 2's complement, i.e. the negation, of B .

(i) $A \geq 0, B < 0:$

$$A - B \longleftrightarrow a + \{2 - (2 - b)\} = a + b, \quad a + b < 1. \tag{15.66}$$

(ii) $A < 0, B \geq 0:$

$$A - B \longleftrightarrow (2 - a) + (2 - b) - 2 = 2 - (a + b). \tag{15.67}$$

(iii) $A \geq 0, B \geq 0, a \geq b:$

$$A - B \longleftrightarrow a + 2 - b - 2 = a - b. \tag{15.68}$$

(iv) $A \geq 0, B \geq 0, a < b$:

$$A - B \longleftrightarrow a + 2 - b = 2 - (b - a). \quad (15.69)$$

(v) $A < 0, B < 0, a \geq b$:

$$A - B \longleftrightarrow (2 - a) + \{2 - (2 - b)\} = 2 - a + b. \quad (15.70)$$

(vi) $A < 0, B < 0, a < b$:

$$A - B \longleftrightarrow 2 - a + \{2 - (2 - b)\} - 2 = (b - a). \quad (15.71)$$

Example 15.11 case (iii)

$$\begin{array}{r} +15(2^{-5}) \ 0.01111 \\ - (+14(2^{-5})) \ \underline{0.01110} \\ \hline +15(2^{-5}) \ 0.01111 \\ -14(2^{-5}) \ \underline{1.10010} \\ \hline 0.00001 \end{array}$$

case (iv)

$$\begin{array}{r} +14(2^{-5}) \ 0.01110 \\ - (+15(2^{-5})) \ \underline{0.01111} \\ \hline +14(2^{-5}) \ 0.01110 \\ -15(2^{-5}) \ \underline{1.10001} \\ \hline 1.11111 \end{array}$$

case (vi)

$$\begin{array}{r} -14(2^{-5}) \ 1.10010 \\ - (-15(2^{-5})) \ \underline{1.10001} \\ \hline -14(2^{-5}) \ 1.10010 \\ +15(2^{-5}) \ \underline{0.01111} \\ \hline 0.00001 \end{array}$$

15.9 Full Adder Cell

A full adder (FA) cell receives two bits, a_i and b_i , and a carry-input bit c_{i-1} and produces the sum bit and carry-out bit s_i and c_i respectively.

The sum bit s_i is 1 if and only if the number of 1-bits in the input combination $\{a_i, b_i, c_{i-1}\}$ is odd. We may therefore write

$$s_i = a_i \oplus b_i \oplus c_{i-1}. \quad (15.72)$$

The carry-out bit is 1 if two of the input bits or all three are 1. We may write

$$c_i = a_i b_i + a_i c_{i-1} + b_i c_{i-1}. \quad (15.73)$$

A full adder cell may thus be logically implemented as shown in Fig. 15.11(a) and represented as the FA cell in part (b) of the figure.

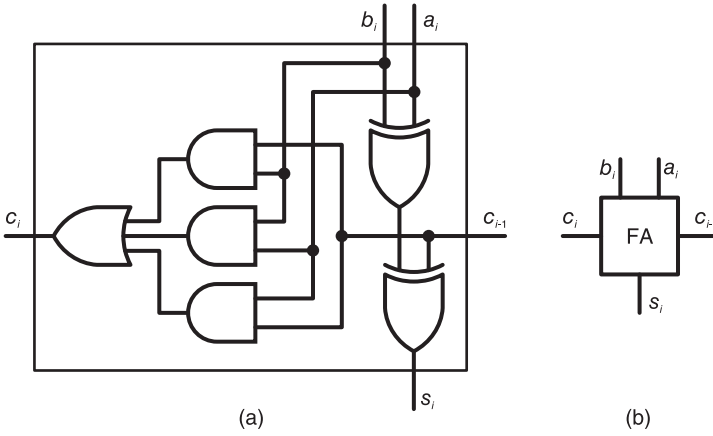


FIGURE 15.11 Full adder cell.

15.10 Addition/Subtraction Implementation in 2's Complement

An implementation of a logical circuit for addition/subtraction of two numbers A and B in 2's complement is shown in Fig. 15.12(a) and in symbolic form in (b).

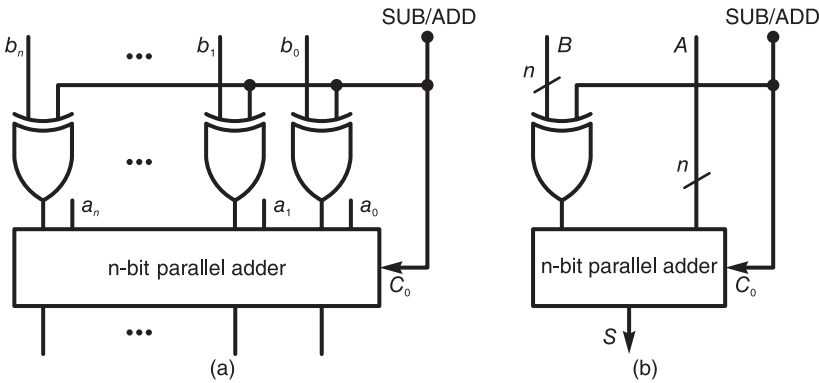


FIGURE 15.12 Addition/subtraction of two numbers in 2's complement.

A control-bit input labeled Sub/Add dictates whether addition or subtraction is to be performed. If it is logic "High," i.e. 1, the unit performs the subtraction $C = A - B$; if it is logic "low" i.e. 0, the addition $C = A + B$ is performed. Subtraction is effected by complementing the bits b_i of the subtrahend B , producing its 1's complement, and applying a carry-in bit c_0 , obtaining the 2's complement, i.e. negation of B , which is added to A .

15.11 Controlled Add/Subtract (CAS) Cell

The 2's complement Addition/Subtraction unit just seen may be redrawn to show the individual FA cells as shown in Fig. 15.13(a).

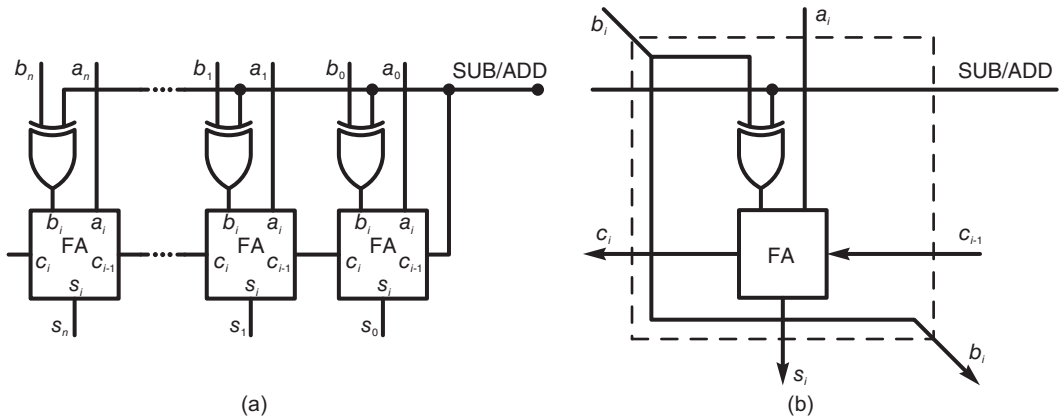


FIGURE 15.13 2's complement n -bit addition/subtraction employing FA cells.

We note that each stage of this implementation contains an FA cell and an exclusive or gate. The combination of the two can be implemented as a controlled add/subtract (CAS) cell, as shown in Fig. 15.13(b). Such a cell is a basic and important component for the implementation of basic operations such as division and square-root evaluation, as we shall see shortly. In such operations it is convenient to pass on the input bit b_i with a shift to neighboring cells, same as the control bit ADD/SUB. These bits are therefore made to enter and exit the CAS cell, to be connected to the neighboring cells, as shown in the figure.

15.12 Multiplication of Unsigned Numbers

Similarly to the paper and pencil method, multiplication is effected by successive add and shift operations. We shall use mainly fractional number representation FNR and occasionally show the corresponding equivalent INR. In FNR, the operands being fractions, their product is also a fraction; hence no overflow can occur. The input operands are the multiplicand A and the multiplier B and are n bits long each. The product is $2n$ bits long. The results of the add-shift operations are partial products which appear in an n -bit accumulator. The following example illustrates the multiplication of two such numbers.

Example 15.12 Evaluate $C = A \times B$ where

$$A = 17 (2^{-5}), \quad B = 25 (2^{-5}).$$

We have, with $n = 5$,

$$ab = a \sum_{i=1}^n b_{-i} 2^{-i} = b_{-1} 2^{-1} a + b_{-2} 2^{-2} a + b_{-3} 2^{-3} a + \dots + b_{-n} 2^{-n} a$$

$$\begin{array}{r}
 17 \ (2^{-5}) : 0.10001 \ A = a \\
 25 \ (2^{-5}) : 0.11001 \ B = b \\
 \hline
 0.0000010001 \ b_{-5} \ (2^{-5} a) \\
 0.0000000000 \ b_{-4} \ (2^{-4} a) \\
 0.0000000000 \ b_{-3} \ (2^{-3} a) \\
 0.0010001000 \ b_{-2} \ (2^{-2} a) \\
 0.0100010000 \ b_{-1} \ (2^{-1} a) \\
 \hline
 0.0110101001 \ \Sigma = 425 \ (2^{-10}).
 \end{array}$$

We can rewrite the procedure by adding each new term $b_{-i} 2^{-i} a$ to the accumulated sum, as follows

0.10001	$A = a$		
0.11001	$B = b$	FNR	INR
<u>0.0000010001</u>	$b_{-5} (2^{-5} a)$	$b_{-5} (2^{-5} a)$	$b_0 a$
0.0000000000	$b_{-4} (2^{-4} a)$	$b_{-4} (2^{-4} a)$	$b_1 2a$
<u>0.0000010001</u>	Σ	Σ	
0.0000000000	$b_{-3} (2^{-3} a)$	$b_{-3} (2^{-3} a)$	$b_2 2^2 a$
<u>0.0000010001</u>	Σ	Σ	
0.0010001000	$b_{-2} (2^{-2} a)$	$b_{-2} (2^{-2} a)$	$b_3 2^3 a$
<u>0.0010011001</u>	Σ	Σ	
0.0100010000	$b_{-1} (2^{-1} a)$	$b_{-1} (2^{-1} a)$	$b_4 2^4 a$
<u>0.0110101001</u>	Σ	Σ	

In INR we write

$$ab = a \sum_{i=0}^{n-1} b_i 2^i = b_0 2^0 a + b_1 2^1 a + b_2 2^2 a + \dots + b_{n-1} 2^{n-1} a.$$

15.13 Multiplier Implementation

Since multiplication consists of shifts and additions, a multiplier may be implemented using FA cells. Consider the 4-bit by 4-bit multiplication of two positive numbers A and B represented as follows

$$\begin{array}{r}
 a_3 \ a_2 \ a_1 \ a_0 \ A \\
 b_3 \ b_2 \ b_1 \ b_0 \ B \\
 \hline
 a_3 b_0 \ a_2 b_0 \ a_1 b_0 \ a_0 b_0 \\
 a_3 b_1 \ a_2 b_1 \ a_1 b_1 \ a_0 b_1 \\
 a_3 b_2 \ a_2 b_2 \ a_1 b_2 \ a_0 b_2 \\
 a_3 b_3 \ a_2 b_3 \ a_1 b_3 \ a_0 b_3 \\
 \hline
 P_7 \ P_6 \ P_5 \ P_4 \ P_3 \ P_2 \ P_1 \ P_0 \ \Sigma
 \end{array}$$

Such operation can be implemented using a cellular structure made up of FA units as shown in Fig. 15.14.

The required additions on each successive column of such products are thus effected, producing the 8-bit multiplication result.

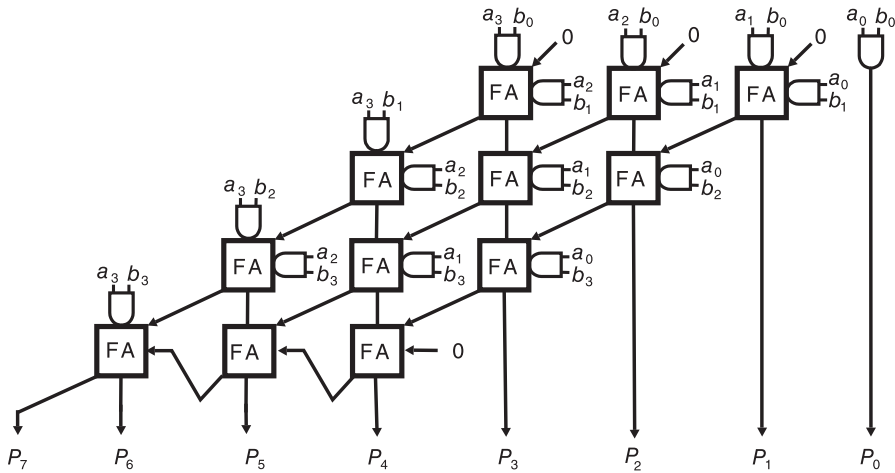


FIGURE 15.14 Cellular 4 bit × 4 bit non-additive multiplier.

It is to be noted, however, that such a multiplier is a stand alone unit that cannot be easily employed as a module to effect multiplications of longer words. If we are to design a multiplier to act as such a module we would need to replace this multiplier by one that can perform not only the multiplication $A \times B$ but, moreover, addition of partial results. It is for this reason that the simple direct multiplier just seen is referred to as a “nonadditive multiplier.” The more versatile building module, referred to as an “additive multiplier,” performs the operation $A \times B + C + D$, where the the operands C and D are in general partial results to be added to the product $A \times B$.

The operation of additive multiplication for the case of 4-bit operands A, B, C and D may be represented in the form

$$\begin{array}{r}
 \begin{array}{cccc}
 a_3 & a_2 & a_1 & a_0 & A \\
 b_3 & b_2 & b_1 & b_0 & B \\
 \hline
 a_3b_0 & a_2b_0 & a_1b_0 & a_0b_0 & \\
 a_3b_1 & a_2b_1 & a_1b_1 & a_0b_1 & \\
 a_3b_2 & a_2b_2 & a_1b_2 & a_0b_2 & \\
 a_3b_3 & a_2b_3 & a_1b_3 & a_0b_3 & \\
 \hline
 & c_3 & c_2 & c_1 & c_0 & C \\
 & d_3 & d_2 & d_1 & d_0 & D \\
 \hline
 P_7 & P_6 & P_5 & P_4 & P_3 & P_2 & P_1 & P_0 & \Sigma
 \end{array}
 \end{array}$$

Multiplication of operands of higher word lengths can be implemented using this additive multiplier employed as a building block. A cellular array type additive multiplier may be realized as shown in Fig. 15.15.

Using the 4 bit × 4 bit additive multiplier consider the realization of two 16-bit operands X and Y . We may write

$$X = X_0 + X_12^4 + X_22^8 + X_32^{12} \tag{15.74}$$

$$Y = Y_0 + Y_12^4 + Y_22^8 + Y_32^{12} \tag{15.75}$$

where the two operands X and Y are partitioned into four 4-bit words X_0, X_1, X_2, X_3 and Y_0, Y_1, Y_2, Y_3 , respectively.

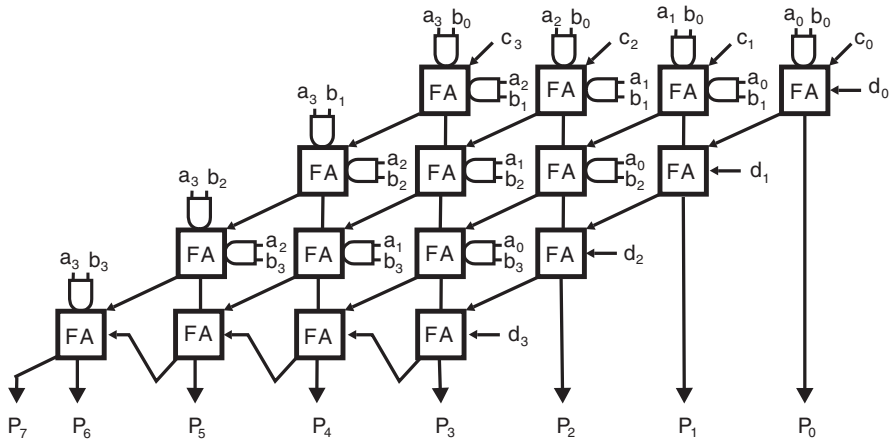


FIGURE 15.15 Cellular array additive multiplier.

The multiplication $Z = X Y$ may thus be effected by evaluating the cross products and adding the partial sums. We write

$$\begin{aligned}
 Z = X Y &= X_0 Y_0 + (X_0 Y_1 + X_1 Y_0) 2^4 + (X_0 Y_2 + X_1 Y_1 + X_2 Y_0) 2^8 \\
 &+ (X_0 Y_3 + X_1 Y_2 + X_2 Y_1 + X_3 Y_0) 2^{12} \\
 &+ (X_1 Y_3 + X_2 Y_2 + X_3 Y_1) 2^{16} + (X_2 Y_3 + X_3 Y_2) 2^{20} + (X_3 Y_3) 2^{24}.
 \end{aligned}
 \tag{15.76}$$

These partial sums are represented graphically in Fig. 15.16 where each such sum is drawn displaced to the left by the number of bits associated with them in this equation. For example the third term in the right-hand side, namely, $(X_0 Y_2 + X_1 Y_1 + X_2 Y_0) 2^8$ implies that the partial results $X_0 Y_2, X_1 Y_1$ and $X_2 Y_0$ should be drawn displaced 8 bits to the left of the least significant bit, as shown in the figure.

Rearranged, the multiplier appears as the diamond-like structure, with reduced carry ripple propagation delay, shown in Fig. 15.17.

15.14 3-D Multiplier

A 3-D structure was proposed in [24] and constructed [28]. This multiplier is shown in Fig. 15.18.

As can be seen the sum bits at the outputs of the 4-bit parallel adders are not propagated in the same plane producing a 2-D structure as in the last figure. Instead a three-dimensional structure and higher processing speed is obtained by propagating the adders' outputs to a new plane. In the new plane each two rows of bits are paired and added together using 4-bit parallel adders again. The resulting sums are propagated to another plane and so on. The multiplier rows are thus added in a structure that is in the form of a binary tree made up of successive parallel planes, as shown in the figure. This multiplier was constructed and used to build complex multipliers as parts of the arithmetic unit of an FFT radix-4 parallel processor [28] [15].

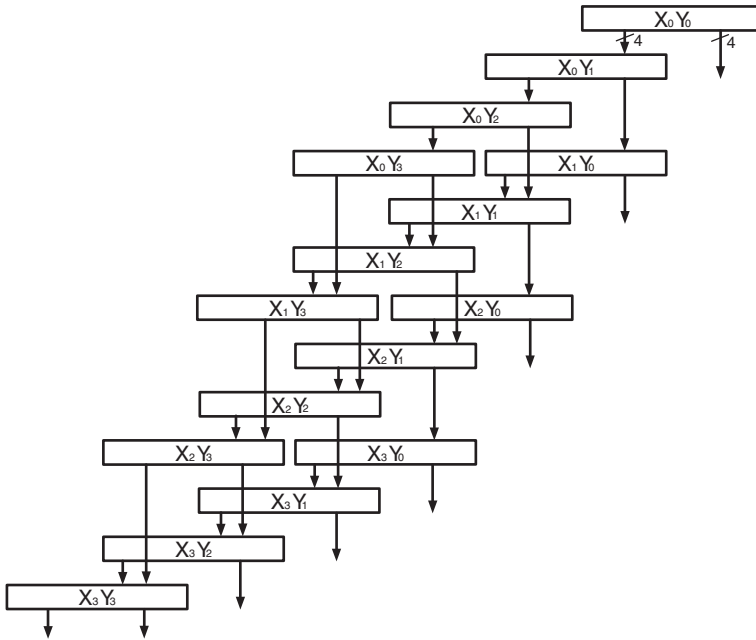


FIGURE 15.16 A 16 bit \times 16 bit multiplier using 4 bit \times 4 bit multipliers.

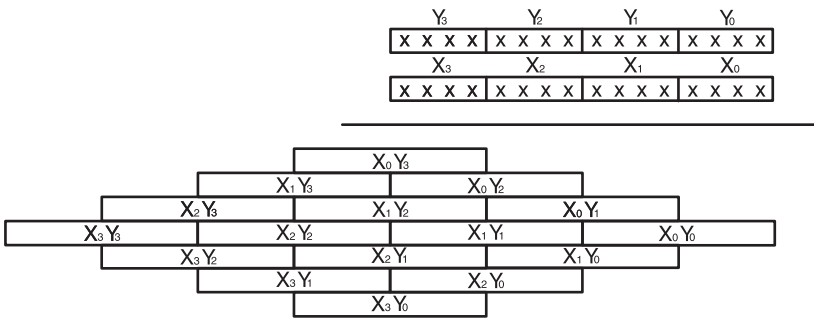


FIGURE 15.17 A 16 bit \times 16 bit multiplier rearranged as a rhombus-like structure.

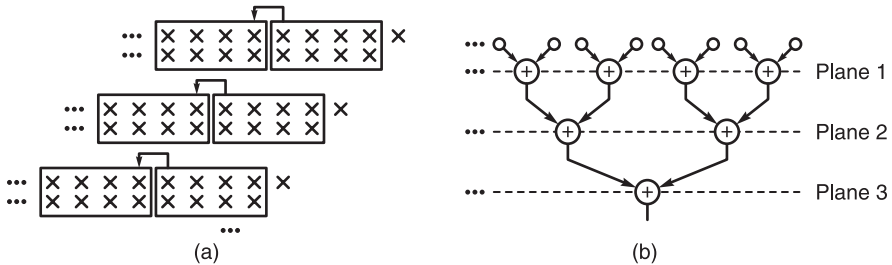


FIGURE 15.18 A 3-D multiplier.

15.14.1 Multiplication in Sign and Magnitude Notation

In sign and magnitude notation the following algorithm may be employed:

a) Positive numbers are multiplied as shown above.

b) Negative numbers: Multiply the numbers without their sign bits $S(A)$ and $S(B)$, respectively, as if the numbers were positive. Attach to the result the sign bit $S(C)$ where $S(C) = S(A) \oplus S(B)$.

15.14.2 Multiplication in 1's Complement Notation

In 1's complement notation we have the following cases:

(i) $B \geq 0, A < 0$, i.e. $B = +b, A = -a$.

Algorithm: For each bit b_{-i} of the multiplier B add the multiplicand A shifted to the right by i bits, performing a "sign-extend" by inserting i bits to the left of the shifted bits of A . Moreover, add 1-bits to the right of the shifted bits of A , up to the end of the $2n$ -bit word length.

Example 15.13

$$\begin{array}{r}
 A = -17 (2^{-5}) \quad 1.01110 \quad 2 - a - \varepsilon \\
 B = +25 (2^{-5}) \quad 0.11001 \quad +b \\
 \hline
 1.1111101110 \quad b_{-5} (2 - \varepsilon^2 - 2^{-5}a) \\
 1.1101110111 \quad b_{-2} (2 - \varepsilon^2 - 2^{-2}a) \\
 \hline
 1.1101100101 \quad \Sigma \\
 \quad 1 \quad \varepsilon^2 \\
 \hline
 1.1101100110 \quad \Sigma \\
 1.1011101111 \quad b_{-1} (2 - \varepsilon^2 - 2^{-1}a) \\
 \hline
 1.1001010101 \quad \Sigma \\
 \quad 1 \quad \varepsilon^2 \\
 \hline
 1.1001010110 = -425 (2^{-10})
 \end{array}$$

$$\begin{aligned}
 A B &\longleftrightarrow \left[\sum_i b_{-i} (2 - \varepsilon^2 - 2^{-i}a - 2 + \varepsilon^2) \right] - \varepsilon^2 + 2 \\
 &= -a \sum_i b_{-i} 2^{-i} - \varepsilon^2 + 2 = 2 - \varepsilon^2 - ab.
 \end{aligned} \tag{15.77}$$

The term $-\varepsilon^2 + 2$ following the term in brackets is added due to the fact that the end around carry operation is performed in all but the first step.

Note that the addition of the 1-bits is due to the fact that A is negative and is effectively shifted to the right within a $2n$ bit register. Hence all zero bits are complemented to 1's, as they should in 1's complement notation.

(ii) $B = -b, A = +a$.

Algorithm: Since the result should be negative, add the 1's complement of the multiplicand A shifted right i bits for each bit $b_{-i} = 0$ of the multiplier B . Add end-around carry. Note that 1-bits are added to the left and to the right of the shifted bits of A as noted above.

Example 15.14

$$\begin{array}{r}
 +25 (2^{-5}) \quad 0.11001 \quad +a \\
 -17 (2^{-5}) \quad 1.01110 \quad 2 - \varepsilon - b \\
 \hline
 1.1111100110 \quad b_{-5} (2 - \varepsilon^2 - 2^{-5}a) \\
 1.1001101111 \quad b_{-1} (2 - \varepsilon^2 - 2^{-1}a) \\
 \hline
 1.1001010101 \\
 \hline
 1 \quad \varepsilon^2 \\
 \hline
 1.1001010110
 \end{array}$$

$$A B \longleftrightarrow \left[\sum_i b_i (2 - \varepsilon^2 - 2^{-i}a - 2 + \varepsilon^2) \right] + 2 - \varepsilon^2 = 2 - \varepsilon^2 - ab. \tag{15.78}$$

(iii) $B = -b, A = -a.$

Algorithm: Add the negation of A , that is, add $+a$ shifted to the right i bits for each bit $b_{-i} = 0$ of B .

Example 15.15

$$\begin{array}{r}
 -17 (2^{-5}) \quad 1.01110 \quad 2 - \varepsilon - a \\
 -25 (2^{-5}) \quad 1.00110 \quad 2 - \varepsilon - b \\
 \hline
 0.0000010001 \quad b_{-5} (2^{-5}a) \\
 0.0010001000 \quad b_{-2} (2^{-2}a) \\
 \hline
 0.0010011001 \quad \Sigma \\
 0.0100010000 \quad b_{-1} (2^{-1}a) \\
 \hline
 0.0110101001 \quad \Sigma
 \end{array}$$

$$A B \longleftrightarrow \sum b_{-i} (2^{-i}a) = ab. \tag{15.79}$$

15.14.3 Numbers in 2’s Complement Notation

With either or both operands negative we have the following cases:

(i) $B = +b, A = -a.$

Algorithm: Add A shifted right for each bit equal to 1 of B . Perform sign extend to the shifted A . Add zeros to the right of the shifted A up to the end of the $2n$ bit word length.

Example 15.16

$$\begin{array}{r}
 -17 (2^{-5}) \quad 1.01111 \quad 2 - a \\
 +25 (2^{-5}) \quad 0.11001 \quad b \\
 \hline
 1.1111101111 \quad b_{-5} (2 - 2^{-5}a) \\
 1.1101111000 \quad b_{-2} (2 - 2^{-2}a) \\
 \hline
 1.1101100111 \\
 1.1011110000 \quad b_{-1} (2 - 2^{-1}a) \\
 \hline
 1.1001010111 \quad 2 - ab
 \end{array}$$

$$A B \longleftrightarrow \sum_i b_{-i} (2 - 2^{-i}a - 2) + 2 = -a \sum_i b_{-i} 2^{-i} + 2 = 2 - ab. \tag{15.80}$$

(ii) $B = -b, A = +a$ (method 2).

Algorithm: 2’s complement B , replacing it by its absolute value b . Add the complement of A shifted for each bit $b_{-i} = 1$. Add zeros to the right of the shifted bits.

Example 15.17

$$\begin{array}{r}
 +25(2^{-5}) \quad 0.11001 \quad a \\
 -17(2^{-5}) \quad 1.01111 \quad 2 - b \\
 \hline
 0.10001 \quad b \\
 \hline
 1.1111100111 \quad b_{-5}(2 - 2^{-5}a) \\
 1.1001110000 \quad b_{-1}(2 - 2^{-1}a) \\
 \hline
 1.1001010111
 \end{array}$$

$$A B \longleftrightarrow \sum b_i (2 - 2^{-i}a - 2 + 2) = 2 - ab. \tag{15.81}$$

Note that it is possible to interchange the multiplicand and the multiplier, thus adding B shifted for each bit of a equal to 1.

It is interesting to note, that as we have seen above in Equations (15.26) and (15.27), a number in 2's complement may be viewed as composed of a weighted sign bit plus the positive value of the magnitude bits. As we shall see in the following section, this property may be used to treat the magnitude bits as a positive operand and deal with the sign bit separately.

Example 15.18 $A < 0, B < 0$

$$A = 1.0110 = -10$$

$$B = 1.1001 = -7$$

$$n = 4, \quad A = -2^n + 6, \quad B = -2^n + 9$$

$$A B = (-2^n + 6) \times (-2^n + 9) = 2^{2n} - 6 \times 2^n - 9 \times 2^n + 6 \times 9$$

$$\begin{array}{r}
 1.0110 \quad A \\
 \underline{1.1001} \quad B \\
 \begin{array}{l}
 0110 \\
 0\ 000 \\
 00\ 00 \\
 011\ 0
 \end{array} \left. \vphantom{\begin{array}{l} 0110 \\ 0\ 000 \\ 00\ 00 \\ 011\ 0 \end{array}} \right\} 6 \times 9 \\
 \begin{array}{l}
 1.1001 \\
 1 \quad b_4
 \end{array} \left. \vphantom{\begin{array}{l} 1.1001 \\ 1 \quad b_4 \end{array}} \right\} -6 \times 2^n \\
 \begin{array}{l}
 1.0110 \\
 1 \quad a_4
 \end{array} \left. \vphantom{\begin{array}{l} 1.0110 \\ 1 \quad a_4 \end{array}} \right\} -9 \times 2^n \\
 \hline
 1 \quad a_4 b_4 = 2^{2n} \\
 \hline
 0.0100\ 0110 \quad \Sigma
 \end{array}$$

Example 15.19 $B = -b, A = -a$

$$\begin{array}{r}
 -17(2^{-5}) \quad 1.01111 \quad 2 - a \\
 -25(2^{-5}) \quad 1.00111 \quad 2 - b \\
 \hline
 1.00111 \quad -1 + x \\
 \hline
 1.1111101111 \\
 1.111101111 \\
 1.11101111 \\
 \hline
 0.10001 \\
 \hline
 0.0110101001 \quad ab
 \end{array} \tag{15.82}$$

We can write $B = -b = -1 + x$

$$\begin{aligned}
 A B &\longleftrightarrow \sum \{x_{-i} (2 - a2^{-i} - 2)\} + 2 + a \pmod{2} = \sum x_{-i} (-a2^{-i}) + a \\
 &= -ax + a = -a(1 - b) + a = ab.
 \end{aligned}
 \tag{15.83}$$

15.15 A Direct Approach to 2's Complement Multiplication

In 2's complement we have seen that the representation of a negative number may be viewed as composed of a negatively weighted sign bit and a positive magnitude part which when added produce the decimal value of the number. In the present context of the multiplication $A \times B$, where the multiplier B is negative, of absolute value b , the 2's complement representation has a decimal value described in INR and FNR respectively by the relations

$$B_I^{[2]} \longleftrightarrow -2^n + x_I \tag{15.84}$$

and

$$B_F^{[2]} \longleftrightarrow -1 + x_F \tag{15.85}$$

where the index I stands for INR and the index F for FNR, As stated earlier, $x_I = 2^n - b_I$ and $x_F = 1 - b_F$.

Let $B \equiv B_I = -9$ in INR and $n = 5$ bit representation, with the corresponding $B \equiv B_F = -9(2^{-5})$ in FNR. We have $x_I = 2^4 - 9 = 7$ and $x_F = 1 - 9(2^{-4}) = 7(2^{-4})$.

$$B_I^{[2]} \longleftrightarrow -2^4 + x_I = -9 \text{ and } B_F^{[2]} \longleftrightarrow -1 + x_F = -9(2^{-4}).$$

Example 15.20

$$\begin{array}{r}
 +13(2^{-4}) \quad 0.1101 \quad a \\
 -9(2^{-4}) \quad 1.0111 \quad B^{[2]} = -1 + x \\
 \hline
 0.00001101 \quad x_{-4} (2^{-4}a) \\
 0.0001101 \quad x_{-3} (2^{-3}a) \\
 \hline
 0.00100111 \quad \Sigma \\
 0.001101 \quad x_{-2} (2^{-2}a) \\
 \hline
 0.01011011 \quad \Sigma \\
 0.00000000 \quad x_{-1} (2^{-1}a) \\
 \hline
 0.01011011 \quad \Sigma \\
 1.0011 \quad 2 - a \\
 \hline
 1.10001011 \quad C = -117.
 \end{array}$$

As the example shows, multiplication in FNR is performed by multiplying the magnitude parts a_F and x_F and the subtraction of a by the addition of its 2's complement. In other words the multiplication takes the form

$$A \times B = a_F \times (-1 + x_F) \longleftrightarrow a_F x_F + (2 - a_F). \tag{15.86}$$

As a verification, replacing x_F by its value we obtain

$$A \times B \longleftrightarrow a_F (1 - b_F) + (2 - a_F) = 2 - a_F b_F \tag{15.87}$$

which is the proper product in 2's complement as required. In INR the corresponding relations are

$$A \times B = a_I \times (-2^n + x_I) = a_I x_I - 2^n a_I \longleftrightarrow a_I x_I + 2^n (2^{n+1} - a_I) \tag{15.88}$$

i.e.

$$A \times B \longleftrightarrow a_I x_I + 2^{2n+1} - 2^n a_I. \tag{15.89}$$

Again, as a verification, replacing x_F by its value we have

$$A \times B \longleftrightarrow a_I (2^n - b_I) + 2^{2n+1} - 2^n a_I = 2^{2n+1} - a_I b_I \tag{15.90}$$

which is the proper result represented in 2's complement and in INR.

This approach of multiplication of numbers in 2's complement may be used as the basis for constructing a cellular multiplier. The cellular multiplier, is known as the Baugh–Wooley multiplier. We may add a slight modification to the Baugh–Wooley multiplier resulting in a reduction of one Full Adder. The result is the structure shown in Fig. 15.19 and which may be referred to as the Modified Baugh–Wooley Multiplier.

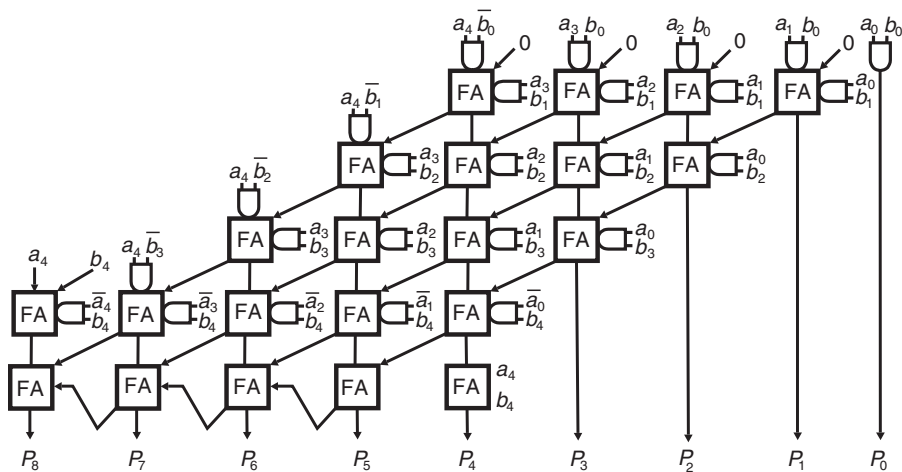


FIGURE 15.19 Modified cellular Baugh–Wooley multiplier.

The cellular array effects the operations described by the following bit layout:

$$\begin{array}{r}
 a_4 \cdot \quad a_3 \quad a_2 \quad a_1 \quad a_0 \\
 b_4 \cdot \quad b_3 \quad b_2 \quad b_1 \quad b_0 \\
 \hline
 \\
 b_0 \\
 a_0 b_0 \\
 a_1 b_1 \quad a_0 b_1 \\
 a_2 b_2 \quad a_1 b_2 \quad a_0 b_2 \\
 a_3 b_3 \quad a_2 b_3 \quad a_1 b_3 \quad a_0 b_3 \\
 b_4 \cdot \quad b_4 \bar{a}_3 \quad b_4 \bar{a}_2 \quad b_4 \bar{a}_1 \quad b_4 \bar{a}_0 \\
 \\
 a_4 \cdot \quad a_4 \bar{b}_3 \quad a_4 \bar{b}_2 \quad a_4 \bar{b}_1 \quad a_4 \bar{b}_0 \\
 \\
 a_4 \\
 \hline
 a_4 b_4 \cdot \\
 P_8 \cdot \quad P_7 \quad P_6 \quad P_5 \quad P_4 \quad P_3 \quad P_2 \quad P_1 \quad P_0 \quad \Sigma
 \end{array}$$

15.16 Division

In the division operation a “dividend” A is divided by a “divisor” D . The result of the division $A \div D$ is a “quotient” Q and a “remainder” R . We write

$$\frac{A}{D} = Q + \frac{R}{D}. \tag{15.91}$$

In what follows we study division and its implementation in the three systems of representation of numbers: sign and magnitude, 1’s complement and 2’s complement notations. We shall use FNR with occasional referencing to the corresponding INR which should by now be easy to deduce. The dividend A is assumed to be in general $2n$ -bits long plus sign, while the divisor is n -bits long plus sign. We may therefore use the representation

$$A : \boxed{\begin{matrix} a_0 & a_{-1} & a_{-2} & \dots & a_{-2n} \end{matrix}} \quad D : \boxed{\begin{matrix} d_0 & d_{-1} & d_{-2} & \dots & d_{-n} \end{matrix}}$$

We start by an example recalling decimal division since in different parts of the world the approach takes different forms.

Example 15.21 Evaluate $753802.392 \div 82.96$.

With $A = 753802392$, and $D = 82960$, the result should be $A/D = Q + R/D$, with $Q = 9086.33\dots$. The long division process is represented in the form

$$\begin{array}{r}
 \begin{matrix} q_1 & q_2 & q_3 & q_4 & q_5 & q_6 \\ 0 & 9 & 0 & 8 & 6 & .3 & 3 & \dots \end{matrix} \\
 \hline
 D = 82960 \overline{) A = 7 \ 5 \ 3 \ 8 \ 0 \ 2 \ 3 \ 9 \ 2} \\
 \begin{matrix} q_1 D & 7 \ 4 \ 6 \ 6 \ 4 \ 0 \\ r_1 & \underline{7 \ 1 \ 6 \ 2 \ 3 \ 9} \\ q_3 D & \underline{6 \ 6 \ 3 \ 6 \ 8 \ 0} \\ r_3 & \underline{5 \ 2 \ 5 \ 5 \ 9 \ 2} \\ q_4 D & \underline{4 \ 9 \ 7 \ 7 \ 6 \ 0} \\ r_4 & \underline{2 \ 7 \ 8 \ 3 \ 2 \ 0} \\ q_5 D & \underline{2 \ 4 \ 8 \ 8 \ 8 \ 0} \\ r_5 & \underline{2 \ 9 \ 4 \ 4 \ 0 \ 0} \\ q_6 D & \underline{2 \ 4 \ 8 \ 8 \ 8 \ 0} \\ r_6 & \underline{4 \ 5 \ 5 \ 2 \ 0} \end{matrix}
 \end{array}$$

As shown, we place the dividend A on the right and the divisor D on the left and proceed to evaluate the quotient Q , which appears above A , one digit at a time. The first step is to take enough digits of A so that when divided by the divisor D the result is an integer. We therefore select the first 6 digits of A and obtain the first quotient digit as $q_1 = 753802/82960 = 9$, as shown above.

We next multiply q_1 times D obtaining $q_1 D = 746640$ and effect a subtraction, obtaining the remainder

$$r_1 = A - q_1 D = 7162$$

Next we repeat the process by annexing to the right of r_1 the next digit “3” of A , obtaining $r'_1 = 71623$. We divide r'_1 by D . The result is $q_2 = 0$. We annex to r'_1 one more digit of A , namely 9, obtaining $r''_1 = 716239$. We divide r''_1 by D . The result is $q_3 = 8$. This process is repeated, as shown above. We obtain $r_3 = r''_1 - q_3 D = 52559$, $q_4 = \lfloor r'_3/D \rfloor =$

$\lfloor 525592/D \rfloor = 6$ and $r_4 = r'_3 - q_4D = 27832$. Since all digits of A have already been used we annex a decimal point and a zero to r_4 obtaining $r'_4 = 27832.0$ and insert the decimal point next to q_4 . We obtain next $q_5 = \lfloor r'_4/D \rfloor = 3$ and $r_5 = r'_4 - q_5D = 2944.0$.

With a zero annexed we have $r'_5 = 2944.00$ and $q_6 = \lfloor r'_5/D \rfloor = 3$. Then $r_6 = r_5 - q_6D = 455.20$. We have thus obtained the quotient $Q = 9086.33$ and the remainder $R = 455.20$ so that the result of the division is given by $A \div D = 9086.33 + 455.20/82960$. The process can be continued if higher precision is required.

15.16.1 Division of Positive Numbers:

Binary division follows the same procedure. It is simpler in the sense that each quotient bit q_i is either 0 or 1. In what follows, since we view all numbers as fractions using the FNR system the result Q of the division has to be a fraction; otherwise overflow occurs. In the formalism and examples to follow therefore the dividend A will be less in absolute value than the divisor, leading to a quotient that is a fraction.

The division of binary positive numbers is illustrated by the following example

$$A = (490 \times 2^{-10}) = 0.0111101010 \tag{15.92}$$

and

$$D = (26 \times 2^{-5})_{10} = 0.11010. \tag{15.93}$$

	$q_{-1}q_{-2}q_{-3}q_{-4}q_{-5}$	
$Q = 0$.1 0 0 1 0	$= 18 \times 2^{-5}$
$D = 0.11010$	0 .0 1 1 1 1 0 1 0 1 0	$= A$
$\equiv d$	1 .1 0 0 1 0 1	$q_{-1} (2 - 2^{-1}d - 2^{-1}\epsilon)$
	0 .0 0 0 0 1 1	Σ
	1	$2^{-1}\epsilon$
	0 .0 0 0 1 0 0 1 0 1	$\Sigma, r_1, r'_1, r''_1, r'''_1$
	1 .1 1 1 1 0 0 1 0 1	$q_{-4} [2 - 2^{-4}(d + \epsilon)]$
	0 .0 0 0 0 0 1 0 1 0	Σ, r_2
	1	$2^{-4}\epsilon$
	0 .0 0 0 0 0 1 0 1 1 0	$r_3, R = 22 \times 2^{-10}$

$$R = r = a - qd. \tag{15.94}$$

Note that the divisor D and the dividend A are positive and are $n = 5$ and $2n = 10$ bits long, respectively. As in decimal division the dividend A is placed on the right, as shown, and the divisor D on the left of the chart. The process consists of attempting to place a 1-bit as q_{-i} in the quotient Q and verifying the remainder obtained by subtracting $q_{-i}D$, shifted by i bits to the right, initially from A and subsequently from the previous remainder.

If the subtraction leads to the same sign as A , positive in this case, a "success" is met, q_{-i} is set to 1 and the subtraction is confirmed. If on the other hand it produces a remainder of opposite sign it is deemed a "failure." In this case q_{-i} is set to zero and the process repeated. As can be seen, the subtractions of the shifted divisor D are performed by adding its 2's complement, effected in fact by adding the 1's complement followed by adding a carry-input, i.e. adding $2^{-i}\epsilon$.

The division starts by attempting to set the first bit q_{-1} of the quotient Q to 1. We then subtract $q_{-1}2^{-1}D$ from A . As shown in the figure this is accomplished by adding to the seven leftmost bits of A , i.e. 0.011110, the 1's complement of the shifted D , i.e. $2 - 2^{-1}d - 2^{-1}\epsilon = 1.100101$ and a carry-in of a value $2^{-1}\epsilon$. The result is given by $r_1 = 0.000100$, as shown in

the figure. The process is repeated by first annexing the next unused bit of A i.e. 1 to the last result, obtaining $r'_1 = 0.0001001$.

We now attempt to place a 1 in the Q register, i.e. set $q_{-2} = 1$. If we evaluate the result of subtracting the shifted D from r'_1 , i.e. the value $r'_1 - q_{-2}(2 - 2^{-2}d - 2^{-2}\varepsilon)$ we would discover that the result is negative, opposite to the sign of A . This means a “failure” is encountered. We reset $q_{-2} = 0$, annex a new bit to r'_1 from A so that $r''_1 = 0.00010010$ and attempt setting $q_{-3} = 1$. Again a failure is encountered. We reset q_{-3} to 0, annex bit to r''_1 from A obtaining $r'''_1 = 0.000100101$. An attempt of setting bit $q_{-4} = 1$ is found to be a “success” confirming its validity. We evaluate $r_2 = r'''_1 - (2 - 2^{-4}d - 2^{-4}\varepsilon)$ and add $2^{-4}\varepsilon$ as shown in the figure. The result is $r_3 = 0.000001011$. We annex the last bit of A to r_3 obtaining $r'_3 = 0.0000010110$. An attempt of setting $q_{-5} = 1$ fails, leading to a change of sign of the new remainder r_4 . We therefore reset q_{-5} to 0, ending the process. The result of the division is $Q = 0.10010$ and $R = 0.0000010110$, i.e. $Q = 18 \times 2^{-5}$ and $R = 22 \times 2^{-10}$. We have obtained

$$R \longleftrightarrow A + \sum_{i=1}^5 q_{-i} \{2 - 2^{-i}(d + \varepsilon) + 2^{-i}\varepsilon - 2\} = a - qd \tag{15.95}$$

which is the proper representation of the remainder.

15.16.2 Division in Sign and Magnitude Notation

Algorithm: Divide the absolute values. Attach the sign to the quotient as the exclusive-or of the signs of A and D , i.e. $S(Q) = S(A) \oplus S(D)$.

15.16.3 Division in 1’s Complement

(i) $A = -a, D = +d$.

Algorithm: Add $D = +d$ shifted right to the dividend A in case of a success, i.e. if the resulting sum has the same sign as A . Throughout, the quotient being negative, a quotient bit 0 is inserted in Q if a success is met, and a 1 otherwise.

$$A = -490 \times 2^{-10}, \quad D = +26 \times 2^{-5} \tag{15.96}$$

$$\begin{array}{r}
 \bar{q}_0 \bar{q}_{-1} \bar{q}_{-2} \bar{q}_{-3} \bar{q}_{-4} \bar{q}_{-5} \\
 1 \ .0 \ 1 \ 1 \ 0 \ 1 \\
 D = 0.11010 \left[\begin{array}{cccccccccccc}
 1 & .1 & 0 & 0 & 0 & 0 & 1 & 0 & 1 & 0 & 1 & A \\
 0 & .0 & 1 & 1 & 0 & 1 & 0 & & & & & q_{-1}2^{-1}d \\
 \hline
 1 & .1 & 1 & 1 & 0 & 1 & 1 & 0 & 1 & 0 & & \Sigma \\
 0 & .0 & 0 & 0 & 0 & 1 & 1 & 0 & 1 & 0 & & q_{-4}2^{-4}d \\
 \hline
 1 & .1 & 1 & 1 & 1 & 1 & 0 & 1 & 0 & 0 & 1 & \Sigma
 \end{array} \right.
 \end{array}$$

$$Q = 1.01101 = -18 \times 2^{-5} \tag{15.97}$$

$$R = -22 \times 2^{-10} \tag{15.98}$$

$$R = (-a) - (-qd) = -a + qd \longleftrightarrow (2 - \varepsilon^2 - a) + \sum q_{-i}2^{-i}d = 2 - \varepsilon^2 - (a - qd). \tag{15.99}$$

(ii) $A = +a, D = -d$.

Algorithm: Add D shifted and set the bit of Q to 0 if success is met.

$$\begin{array}{r}
 \bar{q}_0\bar{q}_{-1}\bar{q}_{-2}\bar{q}_{-3}\bar{q}_{-4}\bar{q}_{-5} \\
 1 \ .0 \ 1 \ 1 \ 0 \ 1 \\
 \hline
 D = 1.00101 \left[\begin{array}{r}
 0 \ .0 \ 1 \ 1 \ 1 \ 1 \ 0 \ 1 \ 0 \ 1 \ 0 \ A = +a \\
 1 \ .1 \ 0 \ 0 \ 1 \ 0 \ 1 \ \qquad \qquad \qquad q_{-1} [2 - 2^{-1}(d + \varepsilon)] \\
 \hline
 0 \ .0 \ 0 \ 0 \ 0 \ 1 \ 1 \ \qquad \qquad \qquad \Sigma \\
 \qquad \qquad \qquad \qquad \qquad \qquad \qquad \qquad 1 \ \qquad \qquad \qquad 2^{-1}\varepsilon \\
 \hline
 0 \ .0 \ 0 \ 0 \ 1 \ 0 \ 0 \ 1 \ 0 \ 1 \ \Sigma \\
 1 \ .1 \ 1 \ 1 \ 1 \ 0 \ 0 \ 1 \ 0 \ 1 \ \qquad \qquad \qquad q_{-4} [2 - 2^{-4}(d + \varepsilon)] \\
 \hline
 0 \ .0 \ 0 \ 0 \ 0 \ 0 \ 1 \ 0 \ 1 \ 0 \ \Sigma \\
 \qquad \qquad \qquad \qquad \qquad \qquad \qquad \qquad \qquad \qquad \qquad \qquad \qquad 1 \ \qquad \qquad \qquad 2^{-4}\varepsilon \\
 \hline
 0 \ .0 \ 0 \ 0 \ 0 \ 0 \ 1 \ 0 \ 1 \ 1 \ 0 \ R
 \end{array} \right.
 \end{array}$$

$$R \longleftrightarrow a + \sum_i q_{-i} [2 - 2^{-i}(d + \varepsilon) + 2^{-i}\varepsilon - 2] = a - qd \quad (15.100)$$

as required.

(iii) $A = -a, D = -d.$

Algorithm: Add the 1's complement, i.e. add d , the negation, of D shifted if success is met.

$$\begin{array}{r}
 \qquad \qquad \qquad q_{-1}q_{-2}q_{-3}q_{-4}q_{-5} \\
 Q = 0 \ .1 \ 0 \ 0 \ 1 \ 0 \\
 D = 1.00101 \left[\begin{array}{r}
 1 \ .1 \ 0 \ 0 \ 0 \ 0 \ 1 \ 0 \ 1 \ 0 \ 1 \ A \longleftrightarrow 2 - \varepsilon^2 - a \\
 0 \ .0 \ 1 \ 1 \ 0 \ 1 \ 0 \ \qquad \qquad \qquad q_{-1}2^{-1}d \\
 \hline
 1 \ .1 \ 1 \ 1 \ 0 \ 1 \ 1 \ 0 \ 1 \ 0 \ \Sigma \\
 0 \ .0 \ 0 \ 0 \ 0 \ 1 \ 1 \ 0 \ 1 \ 0 \ \qquad \qquad \qquad q_{-4}2^{-4}d \\
 \hline
 1 \ .1 \ 1 \ 1 \ 1 \ 1 \ 0 \ 1 \ 0 \ 0 \ 1 \ \Sigma
 \end{array} \right.
 \end{array}$$

$$R \longleftrightarrow A + \sum q_{-i}2^{-i}d = 2 - \varepsilon^2 - a + dq = 2 - \varepsilon^2 - (a - qd). \quad (15.101)$$

15.16.4 Division in 2's Complement

(i) $A = -a, D = +d.$

Algorithm: Proceed as in the 1's complement case, obtaining the quotient in 1's complement. Calling this result G we have to add ε to obtain the required quotient $Q = G + \varepsilon; \varepsilon = 2^{(-5)}.$

In the following example the bits of the 1's complement form G of the quotient are denoted $G_0, G_{-1}, G_{-2}, \dots, G_{-5}.$

$$\begin{array}{r}
 G = 1 \ .0 \ 1 \ 1 \ 0 \ 1 \ \qquad \qquad \qquad + \varepsilon = 1.01110 \longrightarrow Q \\
 D = 0.11010 \left[\begin{array}{r}
 1 \ .1 \ 0 \ 0 \ 0 \ 0 \ 1 \ 0 \ 1 \ 1 \ 0 \ A \\
 0 \ .0 \ 1 \ 1 \ 0 \ 1 \ 0 \ \qquad \qquad \qquad \bar{G}_{-1}2^{-1}d \\
 \hline
 1 \ .1 \ 1 \ 1 \ 0 \ 1 \ 1 \ 0 \ 1 \ 1 \ \Sigma \\
 0 \ .0 \ 0 \ 0 \ 0 \ 1 \ 1 \ 0 \ 1 \ 0 \ \qquad \qquad \qquad \bar{G}_{-4}2^{-4}d \\
 \hline
 1 \ .1 \ 1 \ 1 \ 1 \ 1 \ 0 \ 1 \ 0 \ 1 \ 0
 \end{array} \right.
 \end{array}$$

$$R \longleftrightarrow (2 - a) + \sum \bar{G}_{-i}2^{-i}d = 2 - a + qd \quad (15.102)$$

$$R \longleftrightarrow 2 - a + qd = 2 - (a - qd). \quad (15.103)$$

(ii) $A = +a, D = -d.$

Similarly to the last case we proceed as follows:

$$\begin{array}{r}
 G = 1 \quad .0 \quad 1 \quad 1 \quad 0 \quad 1 \quad \quad \quad + \varepsilon = 1.01110 \\
 D = 1.00110 \left| \begin{array}{cccccccc}
 0 & .0 & 1 & 1 & 1 & 1 & 0 & 1 & 0 & 1 & 0 \\
 1 & .1 & 0 & 0 & 1 & 1 & 0 & & & & \\
 \hline
 0 & .0 & 0 & 0 & 1 & 0 & 0 & 1 & 0 & 1 & \\
 1 & .1 & 1 & 1 & 1 & 0 & 0 & 1 & 1 & 0 & \\
 \hline
 0 & .0 & 0 & 0 & 0 & 0 & 1 & 0 & 1 & 1 & 0
 \end{array} \right. \begin{array}{l}
 A = +a \\
 \overline{G}_{-1} [2 - 2^{-1}d] \\
 \overline{G}_{-4} [2 - 2^{-1}d]
 \end{array}
 \end{array}$$

Note that $\overline{G}_{-i} = q_{-i}$.

$$R \longleftrightarrow a + \sum \overline{G}_{-i} (2 - 2^{-i}d - 2) = a - qd. \tag{15.104}$$

(iii) $A = -a, D = -d$.

Algorithm: Add d , the negation of D , shifted if success is met.

$$\begin{array}{r}
 Q = 0 \quad .1 \quad 0 \quad 0 \quad 1 \quad 0 \\
 D = 1.00110 \left| \begin{array}{cccccccc}
 1 & .1 & 0 & 0 & 0 & 0 & 1 & 0 & 1 & 1 & 0 \\
 0 & .0 & 1 & 1 & 0 & 1 & 0 & & & & \\
 \hline
 1 & .1 & 1 & 1 & 0 & 1 & 1 & 0 & 1 & 1 & \\
 0 & .0 & 0 & 0 & 0 & 1 & 1 & 0 & 1 & 0 & \\
 \hline
 1 & .1 & 1 & 1 & 1 & 1 & 0 & 1 & 0 & 1 & 0
 \end{array} \right. \begin{array}{l}
 A = -a \\
 q_{-1}2^{-1}d \\
 q_{-4}2^{-4}d
 \end{array}
 \end{array}$$

$$R \longleftrightarrow (2 - a) + \sum_i q_{-i}2^{-i}d = 2 - (a - qd). \tag{15.105}$$

A combinatorial approach to construct a divider in sign and magnitude, 1's and 2's complements is depicted in Fig. 15.20. At each step a subtraction of the divisor is performed. If the remainder does not change sign a success is deduced and the quotient bit is thus set. If the remainder changed sign a failure is deduced and restoration is performed using a multiplexer.

15.16.5 Nonrestoring Division

In nonrestoring division $A \div D$ of two positive operands the process starts by subtracting the divisor D from the dividend A by adding the 2's complement of D . The values of the dividend and divisor should be such that no overflow may occur. We assume a dividend A of $2n - 1$ bits plus sign, and a divisor D of n bits plus sign, leading to a quotient and a remainder of n magnitude bits each. If instead the divisor is $2n$ bits long the same approach would yield a quotient and a remainder of $n + 1$ bits each.

To simplify the presentation we consider the example used above for illustrating restoring division, where $A = +a = 490_{10} = (0.111101010)_2$ and $D = +d = 26_{10} = (0.11010)_2$. We use integer number representation INR to lighten the description, noting that fractional number representation FNR can be used instead with little modification.

The process of nonrestoring division is illustrated by the following example:

$$A = 0.111101010 = 490, \quad D = 0.11010 = 26 \tag{15.106}$$

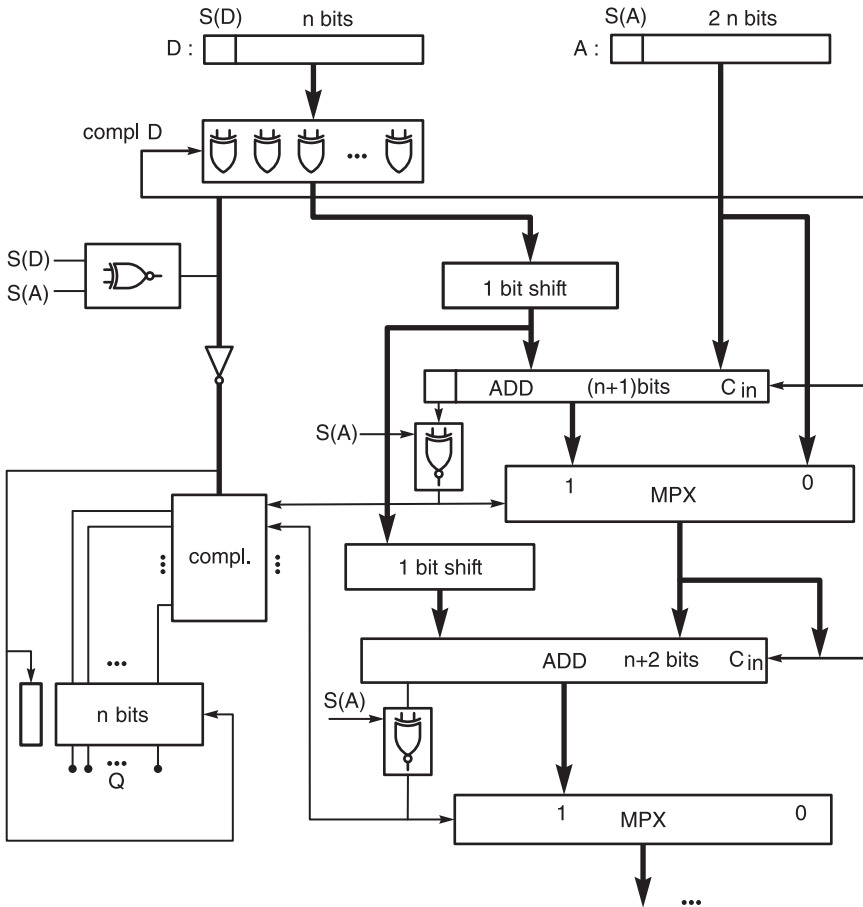


FIGURE 15.20 A combinational sign and magnitude, 1's and 2's complement divider.

$$\begin{array}{r}
 D : 0.11010 \overline{0.111101010} \quad A \\
 -D = 1.00110 \quad 1.00110 \quad -2^4d \\
 \hline
 0.001001010 \quad \Sigma, \quad c_o = 1, \quad q_4 = 1 \\
 1.100110 \quad -2^3d \\
 \hline
 1.101111010 \quad \Sigma, \quad c_o = 0, \quad q_3 = 0 \\
 0.0011010 \quad 2^2d \\
 \hline
 1.111100010 \quad \Sigma, \quad c_o = 0, \quad q_2 = 0 \\
 0.00011010 \quad 2d \\
 \hline
 0.000010110 \quad \Sigma, \quad c_o = 1, \quad q_1 = 1 \\
 1.111100110 \quad -d \\
 \hline
 1.111111100 \quad \Sigma, \quad c_o = 0, \quad q_0 = 0 \\
 0.000011010 \quad +d \quad \text{Restore} \\
 \hline
 0.000010110 \quad \Sigma, \quad R
 \end{array}$$

The positive quotient Q may be denoted in binary $q_5; q_4q_3q_2q_1q_0$ or simply $q_5.q_4q_3q_2q_1q_0$ where $q_5 = 0$ is the sign bit and the binary point is implicitly to the right next to the LSB. The first step consists of subtracting the divisor d shifted four bits to the left so that its MSB is aligned with the MSB of the dividend A . The subtraction is effected by adding the 2's complement of 2^4d , which equals in 2's complement notation $1.001100000 = -416_{10}$.

Since $A = 490$ the result of the addition is the remainder $490 - 416 = 74 = 0.001001010$. The carry-out of this operation, denoted c_o in the figure, is equal to 1, reflecting the fact that the remainder is positive.

Since $c_o = 1$ the quotient bit q_4 is set to 1, and the following step is to subtract the dividend d shifted by 3 bits. This is effected as shown in the figure by adding to the remainder the value -2^3d , which appears as $1.100110 = -208$. The result is the new remainder $r = 74 - 208 = -134 = 1.101111010$ (in 2's complement). This time the carry-out is $c_o = 0$ and, equivalently, the remainder is negative. We set $q_3 = c_o = 0$ and since the remainder is negative an addition instead of a subtraction of the shifted divisor to the remainder is performed next, effectively restoring the value of the remainder.

The rationale is simple. In the nonrestoring division, given a remainder r a subtraction of the dividend is attempted obtaining $r \leftarrow (r - d)$. If the sign of the new remainder is positive, same as the sign of the dividend A , the operation is a "success" and the next step proceeds similarly by evaluating $2r - d$. If on the other hand the sign is negative a 'failure' is declared and we restore by adding d to the result restoring the value of the remainder to $(r - d) + d = r$, and we proceed by evaluating $2r - d$. In the nonrestoring division we start similarly by subtracting the divisor d from the remainder r obtaining the new remainder $r \rightarrow (r - d)$. If the result is positive the process continues as in the corresponding case of the restoring division by evaluating $(2r - d)$. If, on the other hand, the result is negative then instead of a restoration the remainder is shifted right one bit as usual followed now by the *addition* of d . The result of such procedure is therefore a remainder equal to $2(r - d) + d = 2r - d$, which is the same value obtained subsequent to the restoration in the restoring division.

Returning to the example we note that with $C_{\text{out}} = c_o = 0$ in the fifth line, indicating a negative remainder, and q_3 set to $q_3 = 0$ the following step as just stated should be an addition of the shifted remainder. To the remainder is added $2^2d = 0.0011010 = 104$, producing the new remainder $r = -134 + 104 = -30 = 1.11110010$ and $C_{\text{out}} = 0$, hence $q_2 = 0$. In the following steps, as the figure shows, the quotient bits q_2 to q_0 are equal to the corresponding carry-out bits. Each time the carry-out bit is a 1, indicating a positive remainder, the shifted divisor d is subtracted from the remainder. If the carry-out bit is zero, i.e. a negative remainder the shifted divisor is added to the remainder. At the end of the process, if $q_0 = 0$ a final-step restoration is called for to correct the remainder by adding the divisor d as shown in the figure. If $q_0 = 1$ no such final-step restoration is needed. Referring to the figure we may write

$$Q = 0.10010 = 18, \quad R = 0.000010110 = 22$$

$$\begin{aligned} R &\simeq A - 2^4d + q_4(-2^3d) + \bar{q}_3(2^2d) + \bar{q}_2(2d) + q_1(-d) + \bar{q}_0(d) \\ &= A - d\{2^4 + q_42^3 - \bar{q}_32^2 - \bar{q}_22 + q_1 - \bar{q}_0\} \\ &= A - d(2^4 + 2^3 - 2^2 - 2 + 1 - 1) = A - 18d = A - qd. \end{aligned}$$

We now show that in general this process produces the proper quotient and remainder. We shall shortly show in fact that the approach of nonrestoring division may be justified by noticing that a given number can be decomposed using shift-right versions of its magnitude. To this end we note from this example where $n = 5$ that the remainder R , may be written in the form

$$R \simeq A - d[2^4 + \{q_4 - \bar{q}_4\}2^3 + \{q_3 - \bar{q}_3\}2^2 + \{q_2 - \bar{q}_2\}2 + \{q_1 - \bar{q}_1\} - \bar{q}_0]. \quad (15.107)$$

Since the value of the remainder should be $R = A - qd$ we should show that for this example the quantity in the square brackets is in fact equal to the quotient q . We can

visualize this quantity, with the given quotient $q = 10010 = 18$, by writing it in the form

$$\begin{array}{r}
 10000 \ 2^4 \\
 1001 \ q_4 2^3 + q_1 2^0 \equiv q/2 \\
 -0110 \ -(\bar{q}_3 2^2 + \bar{q}_2 2) \equiv -1\text{'s comp of } q/2\text{'s magnitude} = -6 \\
 \underline{\quad -1 \ -\bar{q}_0}
 \end{array} \tag{15.108}$$

$$10010 \ \Sigma = 16 + 9 - 6 - 1 = 18 = q.$$

Note that if instead $q = 19$ a final-step restoration would be applied and since $q_0 = 1$ the last term $-\bar{q}_0 = 0$ leading to a sum of 19 as required.

The fact that the quantity in the squared brackets in the expression of the remainder R is equal to the quotient q may be proved in general as follows.

We may write for q odd:

$$\begin{aligned}
 q &= \lfloor q/2 \rfloor + \lfloor q/2 \rfloor + 1 = \lfloor q/2 \rfloor + \lfloor q/2 \rfloor + 1 + 2^{n-1} - 2^{n-1} \\
 &= \lfloor q/2 \rfloor - (2^{n-1} - 1 - \lfloor q/2 \rfloor) + 2^{n-1}
 \end{aligned} \tag{15.109}$$

and for q even

$$q = \lfloor q/2 \rfloor + \lfloor q/2 \rfloor = \lfloor q/2 \rfloor - (2^{n-1} - 1 - \lfloor q/2 \rfloor) + 2^{n-1} - 1 \tag{15.110}$$

so that for a general n we may write

$$q = 2^{n-1} + \lfloor q/2 \rfloor - (2^{n-1} - 1 - \lfloor q/2 \rfloor) - \bar{q}_0. \tag{15.111}$$

We have thus shown that the quotient q can in general be decomposed as the sum $2^{n+1} + \lfloor q/2 \rfloor - 1$'s complement of the magnitude of $\lfloor q/2 \rfloor - \bar{q}_0$. which is what nonrestoring division effectively applies in evaluating the quotient and remainder values, as we have just noted in the above example.

15.17 Cellular Array for Nonrestoring Division

A possible cellular array realization for nonrestoring division is shown in Fig. 15.21. The cells in this figure are the CAS cell shown in Fig. 15.13(b).

The array is a modification of previously proposed structures with the purpose of permitting the division of a $2n$ -bit dividend with no leading zeros by an n -bit divisor. The CAS cell employed is the same as the one previously described. If the control input to the cell is a 0 it performs addition of the bits at its input, a_i and b_i , otherwise it complements the bit b_i . If the control bit is a 1 a carry-in of 1 is also applied to the least significant CAS cell carry-in pin. The result is that a control bit of 1 produces the subtraction $a - b$ as the output of the row of CAS cells.

In the example of operands shown in the figure the dividend $A = 490$ and $D = 26$. The result should be the quotient $Q = 18$ and remainder $R = A - QD = 22$.

The array depicted in the figure shows the structure of the array divider in this case of $n = 5$, that is, a dividend of 10 magnitude bits and a divisor of 5 magnitude bits.

The successive bits of the dividend $A = 0a_9a_8a_7a_6a_5a_4a_3a_2a_1a_0$ and the divisor $D = 0d_4d_3d_2d_1d_0$ are connected to the "a" and "b" inputs of the CAS cells. As shown in the figure the control bit input to the left-most cell of the first row of cells is set to 1, so that the operation effected by the first row is " $A - D$."

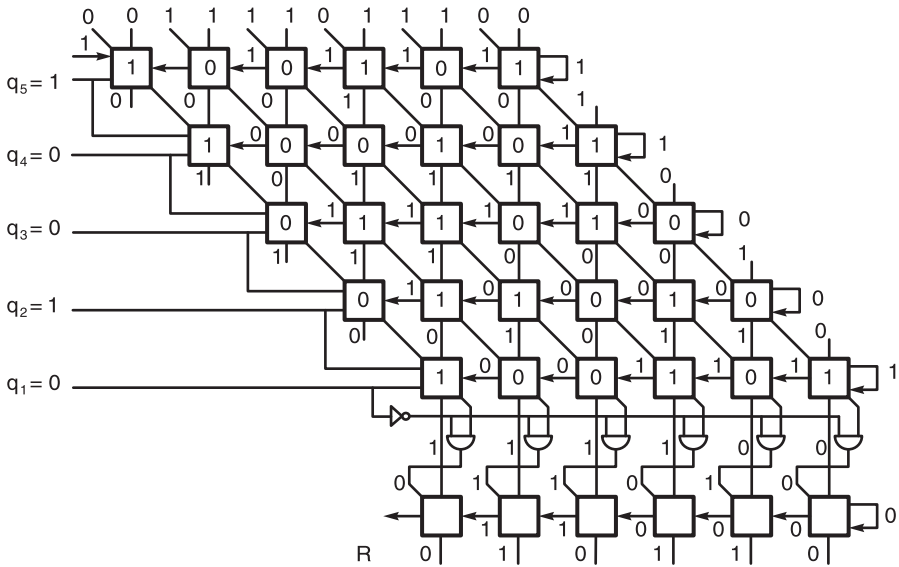


FIGURE 15.21 Cellular array realization for nonrestoring division.

The carry-out of each CAS is fed to the cell on the left and the carry-out c_{out} of the left-most cell, which in fact determines the value of the quotient bit corresponding to the row, is fed as the control input to the following row of cells. As shown in the figure the successive carry-outs of the first to the fifth row are themselves the quotient bits q_4, q_3, q_2, q_1 and q_0 . Following the fifth row a row of AND gates controlled by the bit q_0 are included to effect the final-step restoration, in which the remainder is corrected by adding the divisor D if $q_0 = 0$, and leaves the remainder unchanged by adding zero if $q_0 = 1$.

The values of the input, control, intermediate and output bits of the cellular array are shown in the figure for the case of the last example, where $A = 490 = 0.111101010$ and $D = 0.11010$. The bits $a_0 - a_8$ and $d_0 - d_4$ appear at the inputs of the CAS cells.

In the first (upper) row the control bit applied to the leftmost cell is a “1” meaning a “subtract” command. The effect is to complement the D bits $0, d_4, d_3, d_2, d_1, d_0$. The complemented bits $\bar{d}_4, \bar{d}_3, \bar{d}_2, \bar{d}_1$ and \bar{d}_0 are equal to $1, 0, 0, 1, 0, 1$ as can be seen inside the successive cells of the first row. These bits represent the 1’s complement of the divisor D . The 2’s complement is obtained by applying the same control bit which is equal to “1” into the carry-input of the right-most cell of the first row, as seen in the figure. The first row of cells thus effects the addition:

$$\begin{array}{r}
 011110 \\
 100101 \\
 \hline
 1 \\
 \hline
 1\ 000100
 \end{array}$$

as can be seen at the outputs of the first row of cells and their carry-out bit which is equal to 1. The process is repeated in the following rows and can be seen to be identical to the successive results which we already saw in the numeric example.

15.18 Carry Look Ahead (CLA) Cell

In adding long words, the propagation time of the carry ripple from the LSB stage to the higher stages may be slow down a processor. To accelerate the process of addition we need to shorten carry ripple paths. This is the objective of the carry look-ahead approach. This approach is based on foreseeing the carry that should be injected at each stage without having to wait to receive a carry input from the preceding one.

The addition of a bit a_i with another b_i generates a carry if $a_i = b_i = 1$. This is called a “generate” condition and we write

$$G_i = a_i \wedge b_i \tag{15.112}$$

as shown in Fig. 15.22.

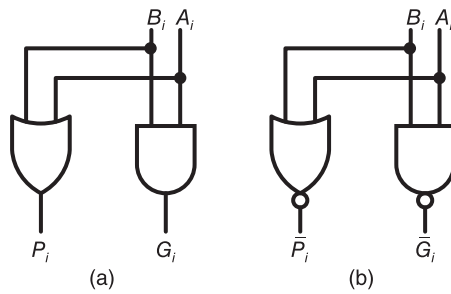


FIGURE 15.22 Generate-bit and propagate-bit logic implementation.

A “propagate” condition exists if either a_i or b_i is equal to 1. We write

$$P_i = a_i \vee b_i \text{ or } P_i = a_i \vee b_i. \tag{15.113}$$

The carry-generate and carry-propagate conditions are used to produce the carry out at any stage of a multiple bit adder. For a 4-bit parallel adder receiving a carry-input c_0 into the least significant bit (LSB) adder the successive carry-out signals from each of the four stages can be written in the form

$$c_1 = G_0 \vee P_0 c_0 \tag{15.114}$$

$$c_2 = G_1 \vee P_1 G_0 \vee P_1 P_0 c_0 \tag{15.115}$$

$$c_3 = G_2 \vee P_2 G_1 \vee P_2 P_1 G_0 \vee P_2 P_1 P_0 c_0 \tag{15.116}$$

$$c_4 = G_3 \vee P_3 G_2 \vee P_3 P_2 G_1 \vee P_3 P_2 P_1 G_0 \vee P_3 P_2 P_1 P_0 c_0 \tag{15.117}$$

with s_1, s_2, s_3, \dots representing the sum bits and c_1, c_2, c_3, \dots the carry bits.

In practice these equations are realized using NOR and Exclusive-OR gates. To this end we may write

$$c_1 = \frac{G_1 + P_1 c_0}{\overline{P_1 + \overline{G_1 C_0}}} = \frac{\overline{\overline{G_1 P_1} + \overline{G_1 C_0}}}{\overline{\overline{G_1 P_1} + G_1 \overline{P_1} + \overline{G_1 C_0}}} \tag{15.118}$$

$$s_2 = P_2 \overline{G_2} \oplus \overline{\overline{P_1 + \overline{G_1 C_0}}} \tag{15.119}$$

$$s_3 = P_3 \overline{G_3} \oplus c_2 \tag{15.120}$$

$$c_2 = \frac{G_2 + P_2G_1 + P_2P_1c_0}{\overline{G_2} \cdot \{\overline{P_2} + \overline{G_1} \cdot (\overline{P_1} + \overline{C_0})\}} = \frac{G_2 + P_2(G_1 + P_1c_0)}{\overline{G_2}\overline{P_2} + \overline{G_2}\overline{G_1}\overline{P_1} + \overline{G_2}\overline{G_1}\overline{C_0}} \tag{15.121}$$

Now

$$G_2\overline{P_2} = 0 \text{ (a don't care condition)} \tag{15.122}$$

and

$$G_1\overline{P_1} = 0. \tag{15.123}$$

Hence

$$c_2 = \frac{\overline{G_2}\overline{P_2} + G_2\overline{P_2} + \overline{G_2}(\overline{G_1}\overline{P_1} + G_1\overline{P_1}) + \overline{G_2}\overline{G_1}\overline{C_0}}{\overline{P_2} + \overline{G_2}\overline{P_1} + \overline{G_2}\overline{G_1}\overline{C_0}} \tag{15.124}$$

$$s_3 = P_3\overline{G_3} \oplus \overline{P_2} + \overline{G_2}\overline{P_1} + \overline{G_2}\overline{G_1}\overline{C_0} \tag{15.125}$$

$$s_4 = P_4\overline{G_4} \oplus c_3 \tag{15.126}$$

$$\begin{aligned} c_3 &= G_3 + P_3G_2 + P_3P_2G_1 + P_3P_2P_1c_0 \\ &= G_3 + P_3[G_2 + P_2\{G_1 + P_1c_0\}] \\ &= \overline{G_3} \cdot [\overline{P_3} + \overline{G_2}\{\overline{P_2} + \overline{G_1} \cdot (\overline{P_1} + \overline{C_0})\}] \\ &= \overline{G_3}\overline{P_3} + \overline{G_3}\overline{G_2}\overline{P_2} + \overline{G_3}\overline{G_2}\overline{G_1}\overline{P_1} + \overline{G_3}\overline{G_2}\overline{G_1}\overline{C_0}. \end{aligned} \tag{15.127}$$

Similarly

$$G_3\overline{P_3} = 0, \quad G_2\overline{P_2} = 0, \quad G_1\overline{P_1} = 0 \tag{15.128}$$

$$c_3 = \frac{(\overline{G_3}\overline{P_3} + G_3\overline{P_3}) + \overline{G_3}(\overline{G_2}\overline{P_2} + G_2\overline{P_2}) + \overline{G_3}\overline{G_2}(\overline{G_1}\overline{P_1} + G_1\overline{P_1})}{\overline{P_3} + \overline{G_3}\overline{P_2} + \overline{G_3}\overline{G_2}\overline{P_1} + \overline{G_3}\overline{G_2}\overline{G_1}\overline{C_0}} \tag{15.129}$$

See Fig. 15.23.

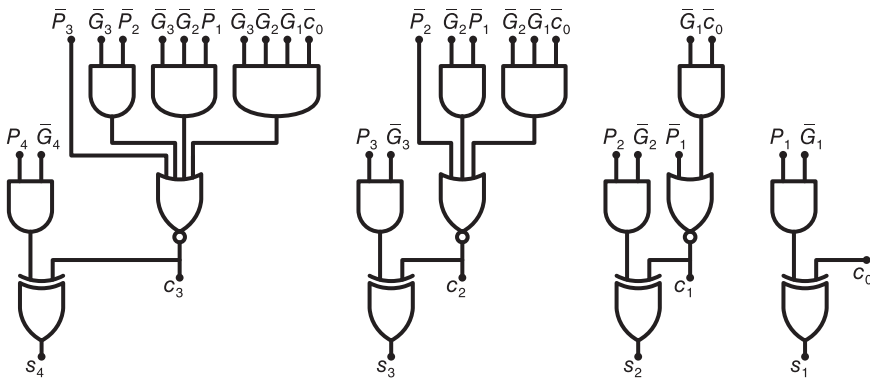


FIGURE 15.23 Sum-bits generation using CLA logic.

In the nonrestoring cellular division array shown in Fig. 15.24 a CLA cell associated with each row of cells is used to generate the carry-input of each of the successive stages as shown in the figure.

The carry bits are thus generated using two levels of logic, the AND and OR levels. This avoids carry-ripple delays, through more logic levels, until the arrival of the proper

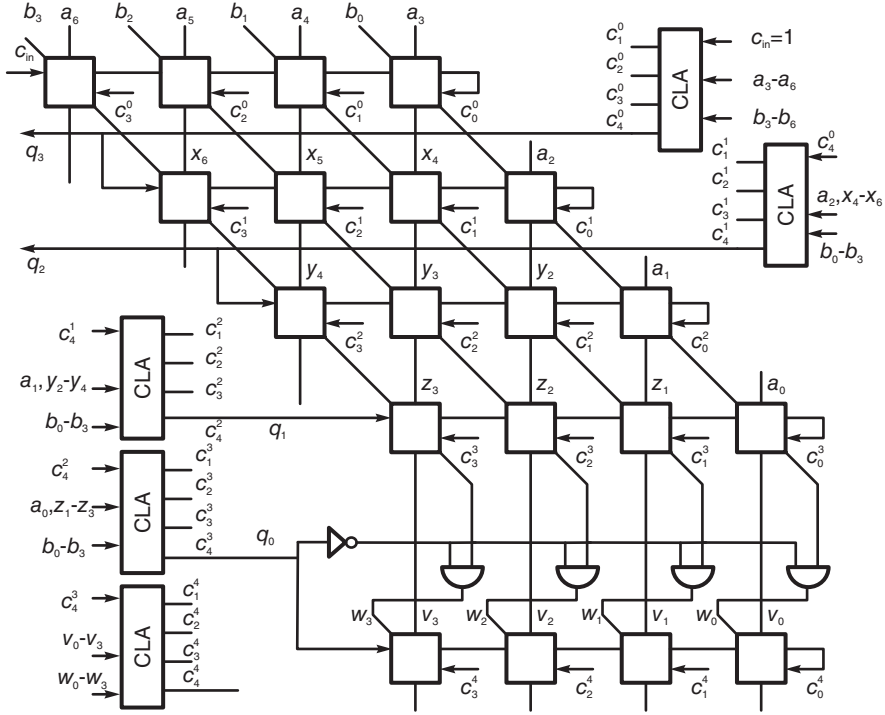


FIGURE 15.24 Nonrestoring cellular division array with CLA blocks.

carry-input to the higher-bits stages. Texas Instruments SN7483 4-bit binary full adder and SN74181 arithmetic logic unit are among the chips that employ the CLA principle for accelerating additions. CLA logic can also be applied to a higher number of bits, not limited to four, leading to even more acceleration of the addition operation. Moreover, second-level CLA has been applied to blocks of bits wherein for each block a block-generate and block-propagate signal are produced. These signals are applied as inputs to next higher blocks, thus accelerating the addition further at a block levels. The principle can be generalized to still higher levels at chips that produce thereof the carry-inputs to the following blocks.

A Lookahead Carry Unit (LCU) is an integrated circuit chip that is used in conjunction with CLAs. A chip such as the Advanced Micro Devices[®] AM2902A can accept four carry-generate signals G_0, G_1, G_2, G_3 , four carry-propagate signals P_0, P_1, P_2, P_3 , and a carry input c_n and produce the carries of the successive stages $c_{n+x}, c_{n+y}, c_{n+z}$, a group-generate signal G and a group-propagate signal P . These signals can be used for higher levels of carry lookahead. The logic equations are similar to the ones used at the basic level. We have

$$c_{n+x} = G_0 + P_0 c_n = \overline{\overline{G_0} \cdot \overline{P_0 c_n}} = \overline{\overline{G_0} \cdot (\overline{P_0} + \overline{C_n})} = \overline{\overline{G_0} \overline{P_0} + \overline{G_0} \overline{C_n}} \quad (15.130)$$

$$\begin{aligned} c_{n+y} &= G_1 + P_1 G_0 + P_1 P_0 c_n = \overline{\overline{G_1 \cdot \overline{P_1 G_0} \cdot \overline{P_1 P_0 c_n}}} \\ &= \overline{\overline{G_1} (\overline{P_1} + \overline{G_0}) (\overline{P_1} + \overline{P_0} + \overline{C_n})} = \overline{\overline{G_1} [P_1 + \overline{G_0} (\overline{P_0} + \overline{C_n})]} \\ &= \overline{\overline{G_1} \overline{P_1} + \overline{G_0} \overline{G_1} \overline{P_0} + \overline{G_0} \overline{G_1} \overline{C_n}} \end{aligned} \quad (15.131)$$

$$\begin{aligned} c_{n+z} &= G_2 + P_2 G_1 + P_2 P_1 G_0 + P_2 P_1 P_0 c_n \\ &= G_2 + P_2 [G_1 + P_1 \{G_0 + P_0 c_n\}] \\ &= \overline{\overline{G_2} \cdot [\overline{P_2} + \overline{G_1} \{\overline{P_1} + \overline{G_0} \cdot (\overline{P_0} + \overline{C_n})\}]} \\ &= \overline{\overline{G_2} \overline{P_2} + \overline{G_1} \overline{G_2} \overline{P_1} + \overline{G_0} \overline{G_1} \overline{G_2} \overline{P_0} + \overline{G_0} \overline{G_1} \overline{G_2} \overline{C_n}} \end{aligned} \quad (15.132)$$

$$\begin{aligned} G &= G_3 + P_3G_2 + P_3P_2G_1 + P_3P_2P_1G_0 \\ &= G_3 + P_3 [G_2 + P_2 \{G_1 + P_1G_0\}] \end{aligned} \tag{15.133}$$

$$\begin{aligned} \overline{G} &= \overline{G_3} \cdot [\overline{P_3} + \{\overline{G_2} \cdot [\overline{P_2} + \overline{G_1} (\overline{P_1} + \overline{G_0})]\}] \\ &= \overline{G_3} \overline{P_3} + \overline{G_2} \overline{G_3} \overline{P_2} + \overline{G_2} \overline{G_3} \overline{G_1} \overline{P_1} + \overline{G_0} \overline{G_1} \overline{G_2} \overline{G_3} \end{aligned} \tag{15.134}$$

$$P = P_3P_2P_1P_0 \tag{15.135}$$

$$\overline{P} = (\overline{P_3} + \overline{P_2} + \overline{P_1} + \overline{P_0}). \tag{15.136}$$

15.19 2's Complement Nonrestoring Division

The following examples illustrate nonrestoring division in 2's complement using the cellular arrays seen above. In the following, as in the above, $c_o \equiv c_{out}$ is the carry-out of the addition operation.

Example 15.22

$$A > 0, \quad D > 0$$

$$A = 0.110110 = 54, \quad D = 0.101 = 5$$

$$\begin{array}{r} -D = 1.011 \quad 0.101 \overline{0.110110} \\ \underline{1.011} \quad -D \\ 1 \quad 0.0011 \quad c_o = 1 \quad q_3 = 1 \\ \quad 0.011 \quad \times 2 \\ \underline{1.011} \quad -D \\ 0 \quad 1.1101 \quad c_o = 0 \quad q_2 = 0 \\ \quad 1.101 \quad \times 2 \\ \quad 0.101 \quad +D \\ \underline{1 \quad 0.0100} \quad c_o = 1 \quad q_1 = 1 \\ \quad 0.100 \quad \times 2 \\ \quad 1.011 \quad -D \\ 0 \quad 1.111 \quad c_o = 0 \quad q_0 = 0 \\ \quad 0.101 \quad +D \quad \text{Restore} \\ \underline{0.100} \end{array}$$

$$Q = (0.1010)_2 = (10)_{10}, \quad R = 0.100 = 4.$$

In the following case the quotient Q is negative and has to be represented in 2's complement. This is performed by first generating the 1's complement of the magnitude q , namely, $\overline{q_3q_2q_1q_0}$ and then adding $\varepsilon = 0001$ and the sign bit to the result.

Example 15.23 $A > 0, D < 0, D = -5$

$$\begin{array}{r}
 c_{in_0} = 0 \quad D : 1.011 \overline{0.110110} \quad c_{in_0} = 0 \\
 \underline{\quad 1.011 \quad} + D \\
 c_{in_1} = 0 \quad c_o = 1 \quad 0.0011 \quad q_3 = c_o = 1 \quad \bar{q}_3 = 0 \\
 \quad \quad \quad 0.011 \quad \times 2 \\
 \quad \quad \quad \underline{\quad 1.011 \quad} + D \\
 c_{in_2} = 1 \quad c_o = 0 \quad 1.1101 \quad q_2 = c_o = 0 \quad \bar{q}_2 = 1 \\
 \quad \quad \quad 1.101 \quad \times 2 \\
 \quad \quad \quad \underline{\quad 0.101 \quad} - D \\
 c_{in_3} = 0 \quad c_o = 1 \quad 0.0100 \quad q_1 = c_o = 1 \quad \bar{q}_1 = 0 \\
 \quad \quad \quad 0.100 \quad \times 2 \\
 \quad \quad \quad \underline{\quad 1.011 \quad} + D \\
 c_{in_4} = 1 \quad c_o = 0 \quad 1.111 \quad q_0 = c_o = 0 \quad \bar{q}_0 = 1 \\
 \quad \quad \quad \underline{\quad 0.101 \quad} - D \quad \text{Restore since } q_0 = 0 \\
 \quad \quad \quad \underline{\quad 0.100 \quad} \\
 \quad \quad \quad 1.100 \quad \text{Complement remainder}
 \end{array}$$

The quotient $Q = -10$ in 2's complement is obtained by adding $\varepsilon = 1$ to the 1's complement representation thus obtained

$$Q \longleftrightarrow 1.\bar{q}_3\bar{q}_2\bar{q}_1\bar{q}_0 + 1 = 1.0101 + 0.0001 = 1.0110 \quad (15.137)$$

The case $A < 0, D > 0$.

Example 15.24 $n = 3$, Dividend $2n = 6$ bits long.

$$\begin{array}{r}
 A = 1.001010 = -54_{10}, \quad D = 0.101 = 5_{10} \\
 0.101 \overline{1.001010} \\
 \underline{\quad 0.101 \quad} + D \quad c_{in,0} = 0 \longrightarrow add D \\
 c_{in,1} = 0 \quad c_o = 0 \quad 1.110010 \quad \bar{q}_3 = c_o = 0 \\
 \quad \quad \quad 1.10010 \quad \times 2 \\
 \quad \quad \quad \underline{\quad 0.101 \quad} + D \\
 c_{in,1} = 1 \quad c_o = 1 \quad 0.00110 \quad \bar{q}_2 = c_o = 1 \\
 \quad \quad \quad 0.0110 \quad \times 2 \\
 \quad \quad \quad \underline{\quad 1.011 \quad} - D \\
 c_{in,1} = 0 \quad c_o = 0 \quad 1.1100 \quad \bar{q}_1 = c_o = 0 \\
 \quad \quad \quad 1.100 \quad \times 2 \\
 \quad \quad \quad \underline{\quad 0.101 \quad} + D \quad \bar{q}_0 = c_o = 1 \\
 c_o = 1 \quad 0.001 \quad \bar{q}_0 = c_o = 1 \\
 \quad \quad \quad \underline{\quad 1.011 \quad} - D \quad \text{Restore since } q_0 = 0 \\
 \quad \quad \quad \underline{\quad 1.100 \quad} R
 \end{array}$$

$$Q \longleftrightarrow 1.\bar{q}_3\bar{q}_2\bar{q}_1\bar{q}_0 + 1 = 1.0101 + 0.0001 = 1.0110 = -10_{10}.$$

No need to complement the remainder. It is already negative in 2's complement.

As the example illustrates start with $c_{in} = 0$. To A thus D is added. If the carry out c_o is 0, set $\bar{q}_3 = c_o = 0$ and $c_{in} = 0$ for next row, leading to the addition of D to the shifted-by-one-bit-left remainder, else if the carry out $c_o = 1$, set $\bar{q}_3 = c_o = 1$ and $c_{in} = 1$ for next row, leading to the addition of $-D$ to the shifted-by-one-bit-left remainder. If the final quotient bit $q_0 = 1$, restore by adding $-D$ to the remainder. Add $\varepsilon = 0.001$ to the quotient to convert it from 1's complement to 2's complement representation.

The case $A > 0, D < 0$.

As the example shows start with input carry $c_{in} = 0$ (to the left of first row of cells). To A thus D is added. If the carry out of the row of cells is $c_o = 1$, set $\bar{q}_3 = \bar{c}_o = 0$ and the carry-in for the next row $c_{in} = \bar{c}_o = 0$, leading to the addition of D to the shifted-by-one-bit-left remainder, else if the carry out $c_o = 0$, set $\bar{q}_3 = \bar{c}_o = 1$ and the carry-in for the next row $c_{in} = \bar{c}_o = 1$, leading to the addition of $-D$ to the shifted-by-one-bit-left remainder. If the final quotient bit $q_0 = 1$ restore by adding $-D$ to the remainder. This produces the correct absolute value of the remainder. To obtain a negative remainder, 2's complement the result.

The case $A < 0, D < 0$.

$$\bar{A} = 1.001010 = -54, \quad D = 1.011 = -5 \tag{15.138}$$

$$c_{in,0} = 1 \longrightarrow \text{To } A \text{ add } -D = 0.101 \tag{15.139}$$

	1.011	1.001010		
		0.101	-D	
$c_{in} = 1$	$c_o = 0$	0 1.1100	$c_o = 0$	$q_3 = 1$
		1.100	$\times 2$	
		0.101	-D	
$c_{in} = 0$	$c_o = 1$	1 0.0011	$c_o = 1$	$q_2 = 0$
		0.011	$\times 2$	
		1.011	+D	
$c_{in} = 1$	$c_o = 0$	0 1.1100	$c_o = 0$	$q_1 = 1$
		1.100	$\times 2$	
		0.101	-D	
$c_o = 1$		1 0.001	$c_o = 1$	$q_0 = 0$
		1.011	+D	Restore since $q_0 = 0$
		1.100		
		0.010		Complement result

The process starts with input carry $c_{in} = 1$. To the dividend A is thus added $-D$. If the carry-out of the row of cells is $c_o = 0$ then set $q_i = \bar{c}_o = 1$ and vice versa. The carry-in to the next row of cells is set equal to $c_{in} = \bar{c}_o$. With $c_{in} = 1$, the value added to the remainder is $-D$. If $c_{in} = 0$ the added value is $+D$. If the final quotient bit, q_0 in this example is equal to 0, restore by adding D . The final remainder thus obtained is equal to $-R$. It needs to be 2's complemented to yield the required positive remainder value R , as shown in this last example.

15.20 Convergence Division

In convergence division instead of attempting to divide the dividend A by the divisor B we evaluate the reciprocal $1/B$ and then multiply the result by A . An effective approach to evaluate the reciprocal is to use of the Newton–Raphson iterative method. This important numerical technique may be used to solve a larger class of problems. In fact, as we shall see in the following section, it can also be used for evaluating the n^{th} root of a number.

The approach is illustrated in Fig. 15.25. To evaluate the reciprocal $1/B$, $B > 0$ we write $f(x) = 1/x - B$. Finding the zero of $f(x)$ we have $f(x) = 1/x - B = 0$, hence $x = 1/B$.

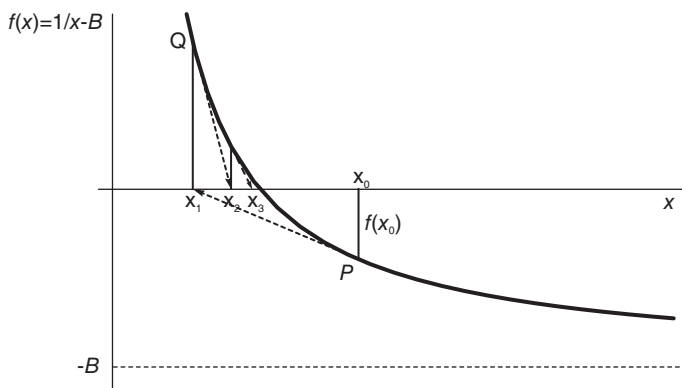


FIGURE 15.25 Conversion division using Newton–Raphson iterative approach.

To find the zero of a function we may use the Newton–Raphson iterative approach illustrated in Fig. 15.25. In this figure x_0 represents an initial guess of the root of $f(x)$. The tangent at point P in the figure intersects the axis x at the new estimate x_1 . As the figure shows if the process is repeated, by drawing the tangent at point Q we obtain the following estimate x_2 . Repeating the process the estimate approaches progressively the zero of $f(x)$.

We can write

$$f'(x) = -1/x^2 \tag{15.140}$$

and from the figure we note that with $x = x_i$ the slope of the curve is given by

$$f'(x_i) = \frac{f(x_i)}{x_i - x_{i+1}} \tag{15.141}$$

We may therefore write

$$x_{i+1} = x_i - \frac{f(x_i)}{f'(x_i)} = x_i - \frac{1/x_i - B}{-1/x_i^2} = 2x_i - Bx_i^2$$

From the figure note that to find the initial estimate x_0 has to be greater than zero. Moreover, all successive estimates x_i must also be greater than zero. In particular we should have $x_1 = 2x_0 - Bx_0^2 > 0$, implying that the condition $0 < x_0 < 2/B$ should be satisfied. To reduce the number of iterations the initial estimate x_0 is normally stored in a read only memory (ROM). The number B is assumed to be a normalized fraction so that $1/2 \leq B < 1$ and $1 < 1/B \leq 2$. A possible ROM would have eight words. It receives as input address the value of B in the form $B = 0.1xxx$, where $xxx = 000, 001, 010, \dots, 111$, and stores at each address the initial estimate of the corresponding value $1/B$. The content of a ROM that stores five bits of the reciprocal initial estimate is shown in following table.

B	$1/B$ estimate
0 0.1000	1.11111
1 0.1001	1.11000
2 0.1010	1.10011
3 0.1011	1.01110
4 0.1100	1.01010
5 0.1101	1.00111
6 0.1110	1.00100
7 0.1111	1.00010

15.21 Evaluation of the n^{th} Root

We consider the problem of evaluating the n^{th} root of a given number A , where n is an integer, using the Newton–Raphson iterative approach. The result sought is $\sqrt[n]{A} = A^{1/n}$, i.e. \sqrt{A} if $n = 2$, $\sqrt[3]{A}$ if $n = 3$, for example.

To illustrate the approach for evaluating the n^{th} root consider first the case $n = 3$ and let

$$f(x) = x^n - A = x^3 - A. \quad (15.142)$$

We note that the zero of $f(x)$ occurs for a value of x given by

$$f(x) = x^3 - A = 0 \quad (15.143)$$

i.e.

$$x = \sqrt[3]{A} = A^{1/3}. \quad (15.144)$$

In other words if the value of x is found such that $f(x) = 0$ then that value is the sought value $\sqrt[3]{A}$. The Newton–Raphson’s iterative technique in this case is illustrated in Fig. 15.26.

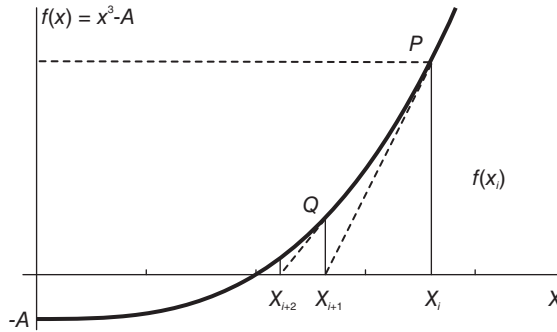


FIGURE 15.26 Newton–Raphson’s zero-locating technique.

In this figure x_i represents an initial guess of the root of $f(x)$. The tangent at point P in the figure intersects the axis x at the new estimate x_{i+1} . As the figure shows if the process is repeated, by drawing the tangent at point Q we obtain the following estimate x_{i+2} . Repeating the process the estimate approaches progressively the zero of $f(x)$.

We have, as seen in the last section,

$$f'(x_i) = \frac{f(x_i)}{x_i - x_{i+1}} \quad (15.145)$$

i.e.

$$3x_i^2 = \frac{x_i^3 - A}{x_i - x_{i+1}} \quad (15.146)$$

$$3x_i^3 - 3x_i^2 x_{i+1} = x_i^3 - A \quad (15.147)$$

$$2x_i^3 - 3x_i^2 x_{i+1} = -A \quad (15.148)$$

$$3x_i^2 x_{i+1} = 2x_i^3 + A \tag{15.149}$$

$$x_{i+1} = \frac{2x_i^3 + A}{3x_i^2} = \frac{2}{3}x_i + \frac{A}{3x_i^2} \tag{15.150}$$

For example let $A = 1253.351$ and assume an initial estimate of $\sqrt[3]{A}$ be $x_0 = 7$. The sequence of improved estimates x_1, x_2, \dots, x_5 is shown in the following table.

i	x_i
1	13.1928639
2	11.1955855
3	10.7968965
4	10.7818119
5	10.7817908

The result $\sqrt[3]{A} = 10.7817908$ agrees with the full-precision floating point evaluation of the cubic root of A .

Consider now the more general problem of evaluating $\sqrt[n]{A}$ where n is an integer. Similarly to the above we write

$$f(x) = x^n - A \tag{15.151}$$

$$f'(x) = nx^{n-1} \tag{15.152}$$

$$f'(x_i) = nx_i^{n-1} = \frac{f(x_i)}{x_i - x_{i+1}} = \frac{x_i^n - A}{x_i - x_{i+1}} \tag{15.153}$$

$$nx_i^n - nx_i^{n-1}x_{i+1} = x_i^n - A \tag{15.154}$$

$$-nx_i^{n-1}x_{i+1} = -A \tag{15.155}$$

$$nx_i^{n-1}x_{i+1} = (n - 1)x_i^n + A \tag{15.156}$$

$$x_{i+1} = \frac{n - 1}{n}x_i + \frac{A}{nx_i^{n-1}} \tag{15.157}$$

The n^{th} root of a given number can thus be evaluated iteratively for any value n . As stated above, to reduce the number of iterations the initial estimate x_0 is normally stored in a read only memory (ROM). To illustrate the approach consider again the case $n = 3$, that is, the problem of evaluating the cubic root $\sqrt[3]{A}$. Using the FNR the number A is assumed to be a fraction. Moreover, as is the case with the floating point number system, we assume the number be to be normalized. This means that if $A \neq 0$ then $A = (0.1xx\dots x)_2$ where x signifies 0 or 1, that is, $0.5 \leq A < 1$, and we may represent A in the form shown in Fig. 15.27.

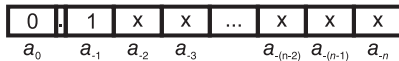


FIGURE 15.27 Normalized number in FNR.

The entries of the ROM that stores the initial estimate of $\sqrt[3]{A}$ may be evaluated as a function of say the three bits a_{-2}, a_{-3} and a_{-4} . There are eight possibilities 000, 001, ..., 111 and the ROM is therefore eight words in size. Since $a_{-1} = 1$ the value of A corresponding to these eight possibilities are 1000, 1001, 1010, 1011, ..., 1111. For each of these respectively the cubic root is evaluated and, assuming that the ROM has words of m

bits each, only m bits of those cubic roots are stored. Assuming $m = 4$, the following table shows a listing of the set of eight 4-bit values of A in the first column, and their cubic roots in decimal, in the second column.

	A	$\sqrt[3]{A}$	$\sqrt[3]{A} \times 64$	$\left(\lfloor 64\sqrt[3]{A} \rfloor\right)_2$
0	0.1000	0.7937	50.79	0.110010
1	0.1001	0.8255	52.83	0.110100
2	0.1010	0.8550	54.71	0.110110
3	0.1011	0.8826	56.48	0.111000
4	0.1100	0.9086	58.14	0.111010
5	0.1101	0.93312	59.72	0.111011
6	0.1110	0.9565	61.21	0.111101
7	0.1111	0.9787	62.63	0.111110

The third column shows these values multiplied by $2^6 = 64$, and the fourth includes the binary equivalent of the integer part of each of these values. Since the left-most two bits in all eight values are both ones they need not be stored in the ROM. Only the right-most four bits are stored. The initial estimate for any given value of A is deduced by reading the ROM content at the address equal to the value of A .

Two 1 bits are then annexed to the left of the value read from the ROM. For example, if the cubic root of a number given in binary as $A = (0.1101xxx\dots)_2 = 13/16 + \dots$, where x stands for either 0 or 1, we may find the initial estimate by setting $A = (0.1101)_2 = 13/16$, which is the sixth value in the table. The following columns show that $\sqrt[3]{A} = 0.93312$, and this value multiplied by 64 is equal to 59.7201. The next column shows the binary equivalent of $\lfloor 59.7201 \rfloor = 59$ which is 0.111011. The sixth word of the ROM, i.e. at the address 101 the word content should be 1011. With the two 1 bits annexed to the left the initial estimate corresponding to $A = (0.1101)_2$ is 0.111011.

15.22 Function Generation by Chebyshev Series Expansion

Chebyshev polynomials may be used in the generation of functions by digital computers. Trigonometric, exponential, hyperbolic and other functions may be expanded into a power series using Chebyshev polynomials which converge faster than other expansions such as Taylor's series [14].

The Chebyshev series expansion of a function $f(x)$ is similar to the Fourier series expansion. The "shifted Chebyshev polynomials" $T_n^*(x)$ are defined by

$$T_n^*(x) = \cos(n\theta), \quad \theta = \cos^{-1}(2x - 1). \quad (15.158)$$

and are suitable for the expansion of functions over the interval $0 \leq x \leq 1$. They are listed in Table 15.1.

Consider the expansion of the function $f(x) = e^x$, $0 \leq x \leq 1$ into the form

$$f(x) = e^x = \frac{a_0}{2} + \sum_{n=1}^{\infty} a_n T_n^*(x) \quad (15.159)$$

We have

$$T_n^*(x) = \cos[n \cos^{-1}(2x - 1)] = \cos n\theta \quad (15.160)$$

TABLE 15.1 Shifted Chebyshev polynomials

n	$T_n^*(x)$
0	1
1	$2x - 1$
2	$8x^2 - 8x + 1$
3	$32x^3 - 48x^2 + 18x - 1$
4	$128x^4 - 256x^3 + 160x^2 - 32x + 1$
5	$512x^5 - 1280x^4 + 1120x^3 - 400x^2 + 50x - 1$
6	$2048x^6 - 6144x^5 + 6912x^4 - 3584x^3 + 840x^2 - 72x + 1$
7	$8192x^7 - 28672x^6 + 39424x^5 - 26880x^4 + 9408x^3 - 1568x^2 + 98x - 1$
8	$32768x^8 - 131072x^7 + 212992x^6 - 180224x^5 + 84480x^4 - 21504x^3 + 2688x^2 - 128x + 1$

$$\theta = \cos^{-1}(2x - 1) \tag{15.161}$$

$$2x - 1 = \cos \theta \tag{15.162}$$

$$x = (1 + \cos \theta) / 2 \tag{15.163}$$

$$f(x) = f[(1 + \cos \theta) / 2] = g(\theta) \tag{15.164}$$

The function $g(\theta)$ is periodic and can be expanded as a Fourier series

$$g(\theta) = \frac{a_0}{2} + \sum_{n=1}^{\infty} a_n \cos n\theta \tag{15.165}$$

so that

$$f(x) = \frac{a_0}{2} + \sum_{n=1}^{\infty} a_n T_n^*(x) \tag{15.166}$$

$$a_n = \frac{2}{\pi} \int_0^{\pi} g(\theta) \cos n\theta \, d\theta \tag{15.167}$$

$$2 \, dx = -\sin \theta \, d\theta, \quad \sin \theta = \sqrt{1 - 4x^2 + 4x - 1} = 2\sqrt{x - x^2} \tag{15.168}$$

$$d\theta = \frac{-2 \, dx}{\sin \theta} = \frac{-2 \, dx}{2\sqrt{x - x^2}} = \frac{-dx}{\sqrt{x - x^2}} \tag{15.169}$$

$$a_n = \frac{-2}{\pi} \int_1^0 \frac{f(x) T_n^*(x)}{\sqrt{x - x^2}} \, dx = \frac{2}{\pi} \int_0^1 \frac{f(x) T_n^*(x)}{\sqrt{x - x^2}} \, dx. \tag{15.170}$$

The same approach may be used in the expansion of the functions $f(x) = e^{-x}$, $\log(1 + x)$ and $\Gamma(1 + x)$, $0 \leq x \leq 1$.

For odd functions such as $\sin \pi x/2$, $\arcsin x$ and $\arctan x$ we may expand instead the even functions $(\sin \pi x/2)/x$, $(\arcsin x)/x$ and $(\arctan x)/x$, respectively. If the given function to be expanded, $f(x)$, is one of the functions $(\sin \pi x/2)/x$, $\cos \pi x/2$ or $(\arctan x)/x$, over the interval $-1 \leq x \leq 1$, it may be expanded as the sum

$$\frac{a_0}{2} + \sum_{n=1}^{\infty} a_n T_n^*(x^2). \tag{15.171}$$

We have

$$T_n^*(x^2) = \cos [n \cos^{-1}(2x^2 - 1)] = \cos(n\phi) \tag{15.172}$$

$$\phi = \cos^{-1}(2x^2 - 1) \tag{15.173}$$

$$x^2 = (1 + \cos \phi) / 2 \quad (15.174)$$

$$f(x) = f\left(\sqrt{(1 + \cos \phi) / 2}\right) = g(\phi) \quad (15.175)$$

$$g(\phi) = \frac{a_0}{2} + \sum_{n=1}^{\infty} a_n \cos n\phi \quad (15.176)$$

so that

$$f(x) = \frac{a_0}{2} + \sum_{n=1}^{\infty} a_n T_n^*(x^2) \quad (15.177)$$

$$a_n = \frac{2}{\pi} \int_0^{\pi} g(\phi) \cos n\phi \, d\phi \quad (15.178)$$

$$4x \, dx = -\sin \phi \, d\phi \quad (15.179)$$

$$d\phi = \frac{-4x \, dx}{\sin \phi} = \frac{-4x \, dx}{2x\sqrt{1-x^2}} = \frac{-2 \, dx}{\sqrt{1-x^2}} \quad (15.180)$$

$$a_n = \frac{-4}{\pi} \int_1^0 \frac{f(x) T_n^*(x^2)}{\sqrt{1-x^2}} dx = \frac{4}{\pi} \int_0^1 \frac{f(x) T_n^*(x^2)}{\sqrt{1-x^2}} dx. \quad (15.181)$$

For $\arcsin x/x$ with $-1/\sqrt{2} \leq x \leq 1/\sqrt{2}$, we use $T_n^*(2x^2)$

$$T_n^*(2x^2) = \cos [n \cos^{-1}(4x^2 - 1)] = \cos n\gamma \quad (15.182)$$

$$\gamma = \cos^{-1}(4x^2 - 1) \quad (15.183)$$

$$x^2 = (1 + \cos \gamma) / 4 \quad (15.184)$$

$$f(x) = f\left(\sqrt{(1 + \cos \gamma) / 2}\right) = g(\gamma) \quad (15.185)$$

$$g(\gamma) = \frac{a_0}{2} + \sum_{n=1}^{\infty} a_n \cos n\gamma \quad (15.186)$$

i.e.

$$f(x) = \frac{a_0}{2} + \sum_{n=1}^{\infty} a_n T_n^*(2x^2) \quad (15.187)$$

$$a_n = \frac{2}{\pi} \int_0^{\pi} g(\gamma) \cos n\gamma \, d\gamma \quad (15.188)$$

$$8x \, dx = -\sin \gamma \, d\gamma, \quad (15.189)$$

$$d\gamma = -\frac{8x \, dx}{\sin \gamma} = -\frac{8x \, dx}{\sqrt{8} x \sqrt{1-2x^2}} = -\sqrt{8} \frac{dx}{\sqrt{1-2x^2}} \quad (15.190)$$

$$a_n = \frac{-2}{\pi} \int_{1/\sqrt{2}}^0 \sqrt{8} \frac{f(x) T_n^*(2x^2)}{\sqrt{1-2x^2}} dx = \frac{4\sqrt{2}}{\pi} \int_0^{1/\sqrt{2}} \frac{f(x) T_n^*(2x^2)}{\sqrt{1-2x^2}} dx \quad (15.191)$$

For $J_0(x)$ and $J_1(x)$, $-10 \leq x \leq 10$ we write

$$T_n^*(x^2/100) = \cos \left[n \cos^{-1} \left(2 \frac{x^2}{100} - 1 \right) \right] = \cos n\psi \quad (15.192)$$

$$\psi = \cos^{-1}(x^2/50 - 1) \quad (15.193)$$

$$x^2 = 50(1 + \cos \psi) \quad (15.194)$$

$$f(x) = f(\sqrt{50(1 + \cos \psi)}) = g(\psi) \tag{15.195}$$

$$g(\psi) = \frac{a_0}{2} + \sum_{n=1}^{\infty} a_n \cos n\psi \tag{15.196}$$

i.e.

$$f(x) = \frac{a_0}{2} + \sum_{n=1}^{\infty} a_n T_n^*(x^2/100) \tag{15.197}$$

$$a_n = \frac{2}{\pi} \int_0^\pi g(\psi) \cos n\psi \, d\psi \tag{15.198}$$

$$2x \, dx = -50 \sin \psi \, d\psi \tag{15.199}$$

$$d\psi = \frac{-2x \, dx}{50 \times \frac{x}{5} \sqrt{1 - x^2/100}} = \frac{-dx}{5\sqrt{1 - x^2/100}} \tag{15.200}$$

$$a_n = \frac{-2}{\pi} \int_{10}^0 \frac{f(x) T_n^*(x^2/100)}{5\sqrt{1 - x^2/100}} dx = \frac{2}{\pi} \int_0^{10} \frac{f(x) T_n^*(x^2/100)}{5\sqrt{1 - x^2/100}} dx \tag{15.201}$$

The coefficients a_n for such trigonometric function expansions are listed in Table 15.2. To summarize

$$\sin(\pi x/2) = x \left(\frac{a_0}{2} + \sum_{n=1}^{\infty} a_n T_n^*(x^2) \right), \quad -1 \leq x \leq 1. \tag{15.202}$$

$$\cos(\pi x/2) = \frac{a_0}{2} + \sum_{n=1}^{\infty} a_n T_n^*(x^2), \quad -1 \leq x \leq 1. \tag{15.203}$$

$$\tan^{-1} x = x \left(\frac{a_0}{2} + \sum_{n=1}^{\infty} a_n T_n^*(x^2) \right), \quad -1 \leq x \leq 1. \tag{15.204}$$

For $|x| > 1$, we may write

$$\tan^{-1} x = \pi/2 - \tan^{-1}(1/x). \tag{15.205}$$

Table 15.3 lists the Chebyshev expansion coefficients of inverse trigonometric and exponential functions.

$$\sin^{-1} x = x \left(\frac{a_0}{2} + \sum_{n=1}^{\infty} a_n T_n^*(2x^2) \right), \quad -1/\sqrt{2} \leq x \leq 1/\sqrt{2} \tag{15.206}$$

TABLE 15.2 Chebyshev expansion coefficients of some trigonometric functions

n	$\sin(\pi x/2)$ a_n	$\cos(\pi x/2)$ a_n	$\tan^{-1} x$ a_n
0	2.552557925	0.9440024315	1.762747174
1	-0.2852615692	-0.4994032583	-0.1058929245
2	0.009118016007	0.022799207962	0.01113584206
3	-0.0001365875135	-0.0005966951965	-0.001381195004
4	$1.184961858 \times 10^{-6}$	$6.704394870 \times 10^{-6}$	0.0001857429733
5	$-6.702791604 \times 10^{-9}$	$-4.653229590 \times 10^{-8}$	-0.00002621519611
6	$2.667278599 \times 10^{-11}$	$2.193457659 \times 10^{-10}$	$3.821036594 \times 10^{-6}$
7	$-7.872922122 \times 10^{-14}$	$-7.481648701 \times 10^{-13}$	$-5.699186167 \times 10^{-7}$

TABLE 15.3 Chebyshev expansion coefficients of inverse trigonometric and exponential functions

n	$\sin^{-1} x, \cos^{-1} x$ a_n	e^x a_n	e^{-x} a_n
0	2.102463918	3.506775309	1.290070541
1	0.05494648722	0.8503916538	-0.3128416064
2	0.004080630393	0.1052086936	0.03870411542
3	0.0004078900685	0.008722104733	-0.003208683015
4	0.00004698536743	0.0005434368312	0.0001999192378
5	$5.880975814 \times 10^{-6}$	0.00002711543491	$-9.975211043 \times 10^{-6}$
6	$7.773231246 \times 10^{-7}$	$1.128132889 \times 10^{-6}$	$4.150168967 \times 10^{-7}$
7	$1.067742334 \times 10^{-7}$	$4.024558230 \times 10^{-8}$	$-1.480552233 \times 10^{-8}$

TABLE 15.4 Chebyshev expansion coefficients of logarithmic and Gamma functions

n	$\log(1+x)$ a_n	$\Gamma(1+x)$ a_n
0	0.7529056258	1.883571196
1	0.3431457505	0.004415381325
2	-0.02943725152	0.05685043682
3	0.003367089256	-0.004219835396
4	-0.0004332758886	0.001326808181
5	0.00005947071199	-0.0001893024530
6	$-8.502967541 \times 10^{-6}$	0.00003606925327
7	$1.250467362 \times 10^{-6}$	$-6.056761904 \times 10^{-6}$

$$\cos^{-1} x = \frac{\pi}{2} - x \left(\frac{a_0}{2} + \sum_{n=1}^{\infty} a_n T_n^*(2x^2) \right), \quad 0 \leq x \leq 1/\sqrt{2}. \tag{15.207}$$

For $1/\sqrt{2} \leq x \leq 1$, we may write

$$\sin^{-1} x = \cos^{-1} \sqrt{1-x^2}, \quad \cos^{-1} x = \sin^{-1} \sqrt{1-x^2}. \tag{15.208}$$

$$e^x = \frac{a_0}{2} + \sum_{n=1}^{\infty} a_n T_n^*(x), \quad 0 \leq x \leq 1. \tag{15.209}$$

$$e^{-x} = \frac{a_0}{2} + \sum_{n=1}^{\infty} a_n T_n^*(x), \quad 0 \leq x \leq 1. \tag{15.210}$$

Chebyshev expansion coefficients of logarithmic and Gamma functions are listed in Table 15.4.

$$\log(1+x) = \frac{a_0}{2} + \sum_{n=1}^{\infty} a_n T_n^*(x), \quad 0 \leq x \leq 1. \tag{15.211}$$

$$\Gamma(1+x) = \frac{a_0}{2} + \sum_{n=1}^{\infty} a_n T_n^*(x), \quad 0 \leq x \leq 1. \tag{15.212}$$

Table 15.5 lists the Chebyshev expansion coefficients of Bessel functions.

$$J_0(x) = \frac{a_0}{2} + \sum_{n=1}^{\infty} a_n T_n^*(x^2/100), \quad -10 \leq x \leq 10. \tag{15.213}$$

TABLE 15.5 Chebyshev expansion coefficients of Bessel functions

n	$J_0(x)$ a_n	$J_1(x)$ a_n
0	0.06308122636	0.1388487046
1	-0.2146161828	-0.1155779057
2	0.004336620108	0.1216794099
3	-0.2662036537	-0.1148840465
4	0.3061255197	0.05779053307
5	-0.1363887697	-0.01692388016
6	0.03434754020	0.003235025204
7	-0.005698082322	-0.0004370608604

$$J_1(x) = x \left(\frac{a_0}{2} + \sum_{n=1}^{\infty} a_n T_n^*(x^2/100) \right), \quad -10 \leq x \leq 10. \tag{15.214}$$

Note that once the coefficients a_n are evaluated as given above, the expansion of the function is rewritten by replacing the Chebyshev polynomials by their values in terms of powers of x . By collecting terms of same powers of x the expansion takes the form of a polynomial, namely,

$$f(x) = \sum_{k=0}^m \alpha_k x^k. \tag{15.215}$$

The coefficients $\alpha_0, \alpha_1, \dots, \alpha_m$ are thus stored in a ROM and used for evaluating $f(x)$ for any given value x .

Example 15.25 Evaluate the coefficients α_k of the powers x^k of x with $n = 6$ terms in the Chebyshev series expansion of $f(x) = \sin(\pi x/2)$.

The expansion has the form

$$\begin{aligned} &x [a_0/2 + a_1(2x^2 - 1) + a_2(8x^4 - 8x^2 + 1) + a_3(32x^6 - 48x^4 + 18x^2 - 1) \\ &+ a_4(128x^8 - 256x^6 + 160x^4 - 32x^2 + 1) \\ &+ a_5(512x^{10} - 1280x^8 + 1120x^6 - 400x^4 + 50x^2 - 1) \\ &+ a_6(2048x^{12} - 6144x^{10} + 6912x^8 - 3584x^6 + 840x^4 - 72x^2 + 1)]. \end{aligned}$$

From the coefficients tables we have

$$\begin{aligned} \sin(\pi x/2) &\simeq x \left\{ \frac{a_0}{2} + \sum_{n=1}^6 a_n T_n^*(x^2) \right\} \\ &= x [2.552557925/2 - 0.2852615692(2x^2 - 1) \\ &\quad + 0.009118016007(8x^4 - 8x^2 + 1) - \dots] \\ &= 1.57079632x - 0.64596409x^3 + 0.07969262612x^5 \\ &\quad - 0.004681753389x^7 + 0.000160439053x^9 \\ &\quad - 3.59570689810^{-6}x^{11} + 5.46258657010^{-8}x^{13}. \end{aligned}$$

The polynomial coefficients

$$\begin{aligned} \alpha_1 &= 1.57079632, \alpha_3 = -0.64596409, \alpha_5 = 0.07969262612, \alpha_7 = -0.004681753389, \\ \alpha_9 &= 0.000160439053, \alpha_{11} = -3.59570689810^{-6}, \alpha_{13} = 5.46258657010^{-8}, \end{aligned}$$

may thus be stored in a ROM and used to approximate the function for any given value x .

15.23 An Alternative Approach to Chebyshev Series Expansion

An alternative approach to the evaluation of the Chebyshev series coefficients is to start by writing down the power series expansion of the given function. For example, the power series expansion of $\cos x$ is given by

$$\cos x = 1 - \frac{x^2}{2!} + \frac{x^4}{4!} - \frac{x^6}{6!} + \dots \quad (15.216)$$

The powers of x can be expressed in terms of the Chebyshev polynomials. In fact from the same Chebyshev polynomials C_n defined in Chapter 9, which are presently denoted T_n , we have the inverse relations

$$1 = T_0(x), \quad x = T_1(x), \quad x^2 = \{T_0(x) + T_2(x)\}/2, \quad (15.217)$$

$$x^3 = \{3T_1(x) + T_3(x)\}/4, \quad x^4 = \{3T_0(x) + 4T_2(x) + T_4(x)\}/8, \quad (15.218)$$

$$x^5 = \{10T_1(x) + 5T_3(x) + T_5(x)\}/16, \quad (15.219)$$

$$x^6 = \{10T_0(x) + 15T_2(x) + 6T_4(x) + T_6(x)\}/32. \quad (15.220)$$

In general

$$x^n = 2^{-n+1} \sum_{k=0}^{\lfloor n/2 \rfloor} \alpha_k T_{n-2k} \quad (15.221)$$

where

$$\alpha_k = \binom{n}{k}. \quad (15.222)$$

By replacing the powers of x in the power series expansion by their values as function of the Chebyshev polynomials we obtain the required expansion to the desired accuracy. For example, substituting in the case of $f(x) = \cos x$ we have

$$\begin{aligned} \cos x &\simeq T_0(x) - \frac{1}{2!} \frac{\{T_0(x) + T_2(x)\}}{2} + \frac{1}{4!} \frac{\{3T_0(x) + 4T_2(x) + T_4(x)\}}{8} \\ &\quad - \frac{1}{6!} \frac{\{10T_0(x) + 15T_2(x) + 6T_4(x) + T_6(x)\}}{32} \\ &\simeq T_0(x) - 0.25 \{T_0(x) + T_2(x)\} \\ &\quad + 0.0052 \{3T_0(x) + 4T_2(x) + T_4(x)\} \\ &\quad - 4.3403 \times 10^{-5} \{10T_0(x) + 15T_2(x) + 6T_4(x) + T_6(x)\} \\ &\simeq 0.765166 T_0(x) - 0.229851 T_2(x) + 0.00493958 T_4(x) \\ &\quad - 0.000043403 T_6(x). \end{aligned} \quad (15.223)$$

Higher accuracy is obtained by incorporating more terms of the power series. The coefficients of the expansion

$$f(x) = \frac{a_0}{2} + \sum_{n=1}^{\infty} a_n T_n(x) \quad (15.224)$$

in the present case are given by

$$a_0 = 1.53033, \quad a_2 = -0.229851, \quad a_4 = 0.00493958, \quad a_6 = -0.000043403 \quad (15.225)$$

$$a_k = 0 \quad \text{for } k \text{ odd.} \quad (15.226)$$

The expansion in powers of x is deduced by replacing the polynomials by their values obtaining

$$\begin{aligned} \cos x \simeq & 0.765166 - 0.229851 (2x^2 - 1) + 0.00493958 (8x^4 - 8x^2 + 1) \\ & - 0.00043403 (32x^6 - 48x^4 + 18x^2 - 1) \simeq 1 - 0.5x^2 + 0.0416x^4 - 0.0013889x^6 \end{aligned}$$

and the coefficients

$$\alpha_0 = 1, \quad \alpha_2 = -0.5, \quad \alpha_4 = 0.0416, \quad \alpha_6 = 0.0013889, \quad \alpha_k = 0 \text{ for } k \text{ odd.} \quad (15.227)$$

The same approach may be used to represent any polynomial of order n

$$p(x) = \sum_{k=0}^n \alpha_k x^k \quad (15.228)$$

and in particular the power series expansion of a given function, into an expansion in terms of other well-known orthogonal polynomials such as Legendre, Laquerre and Hermite polynomials. Chebyshev polynomials have been shown to lead to rapid convergence resulting in a higher accuracy upon truncation of an infinite expansion to a given finite number of terms.

15.24 Floating Point Number Representation

Thanks to breathtaking advances in integrated circuit technology, floating point arithmetic has become increasingly feasible in recent years. In fixed point notation, the addition, or cumulative addition, of numbers may lead to overflow, necessitating a right shift of the operands before or after addition, leading to truncation or round-off errors. In floating point arithmetic the machine simply adjusts the exponent of the result, keeping track of the effects of any required shift operations. Nowadays, fixed point computation is justified only if the range of numbers involved is fairly limited in dynamic range. It should be noted, however, that even today the full potential of floating point arithmetic has not yet been achieved. Only when full parallelism and pipelining combinatorial logic is used to achieve the highest possible speeds will the full potential of floating point arithmetic be attained. As is seen in what follows, apart from normalization operations floating point arithmetic is made up of sequences of fixed point arithmetic operations, such as addition, subtraction, multiplication and division. To achieve highest speed the computer designer should convert, whenever possible, such sequential fixed point operations into operations performed in parallel. Parallel pipelined architecture and as much as possible combinatorial, rather than sequential, logic circuit implementation may require more hardware, but lead potentially to the highest speed of processing.

As in scientific notation of number representation a floating point number a is written in base 2 binary in the form

$$a = m 2^e \quad (15.229)$$

where m is the *mantissa* or *fraction* part and e is the *exponent*.

The IEEE 754 Standard for single precision and double precision floating point representation uses a “biased” exponent e and an implied 1 added to the mantissa m , as seen in what follows. The Standard specifies that, in single precision, eight bits are assigned to the biased exponent e , 23 bits to the mantissa m and one bit to the sign s of the number. In

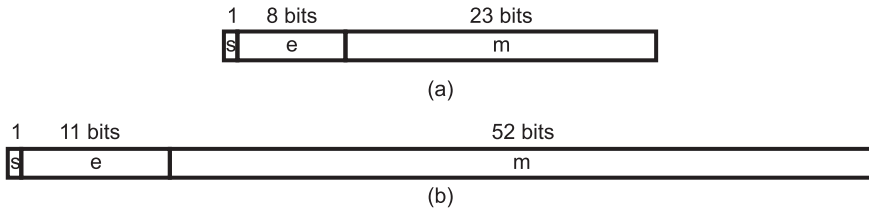


FIGURE 15.28 Floating point representation in (a) single and (b) double precision.

double precision, 11 bits, 52 bits and 1 bit are assigned to the exponent e , the mantissa m and the sign bit, as shown in Fig. 15.28(a) and (b) respectively.

The reason for the bias in the exponent is to avoid the need for positive as well as negative exponents. The biased exponent e is rendered always positive, being the true exponent e_{true} plus $2^{k-1} - 1$ where k is the number of bits of the exponent field. With $k = 8$ we have

$$e = e_{\text{true}} + 2^{k-1} - 1 = e_{\text{true}} + 127. \tag{15.230}$$

The true exponential e_{true} is deduced from a given IEEE standard biased exponential e as

$$e_{\text{true}} = e - 127. \tag{15.231}$$

There is an implied 1 to be added to the mantissa m to obtain scientific notation-like representation. The decimal value of a normalized IEEE standard stored number is thus given by

$$A = (-1)^s (1 + 0.m) 2^{e-127} = (-1)^s (1.m) 2^{e-127}. \tag{15.232}$$

For example the number in IEEE standard

$$0.10011011.101000000000000000000000$$

has $s = 0$, $e = 10011011 = 155$, $m = 2^{-1} + 2^{-3} = 5/8 = 0.625$, so that its decimal value is

$$A = 1.625 \times 2^{155-127} = 1.625 \times 2^{28} = 436207616 \tag{15.233}$$

while the number

$$1.11000101.101011000000000000000000$$

has $s = 1$, $e = 197$, $m = 2^{-1} + 2^{-3} + 2^{-5} + 2^{-6} = 43/64 = 0.6719$ so that

$$A = -1.6719 \times 2^{197-127} = -1.6719 \times 2^{70} = -1.9738 \times 10^{21}. \tag{15.234}$$

In the double-precision IEEE standard format the bias is $2^{11-1} - 1 = 1023$, so that

$$e_{\text{true}} = e - 1023 \tag{15.235}$$

and the value of a stored number is

$$A = \pm 1.m \times 2^{e-1023}. \tag{15.236}$$

Example 15.26 A number before normalization is stored in IEEE single precision format with $s = 1$, $e = 10110000$, $m = .0000010101100\dots0$. Show the number after normalization, state its value and show how it is stored.

We have $e_{true} = 176 - 127 = 49$. Before normalization the value of the number is $A = -(0.00000101011)_2 \times 2^{49}$. Normalization is effected by applying six shift-left steps to the mantissa so that the first 1-bit appears on the left of the binary point. This 1-bit is then omitted as an implied bit to save one bit of storage space. After normalization the mantissa has the form $.0101100\dots 0$ and

$$A = -(1.01011)_2 \times 2^{43}.$$

The number is stored as the three components $s = 1$, $e = 176 - 6 = 170$ and the normalized mantissa $m = .0101100\dots 0$.

The IEEE Standard 754 deals also with the extreme values such as 0 and infinity, overflow and underflow as well as NAN (not a number). Some of these conditions are called exceptions and usually trigger flags or messages signaling their occurrence.

15.24.1 Addition and Subtraction

Addition and subtraction of floating point numbers are effected by aligning the exponents followed by the addition or subtraction of the mantissas, checking for overflow or underflow and a normalization of the result.

Aligning the exponents is effected by shifting right the mantissa bits of the number with the smaller exponent and incrementing its exponent by one for each bit of shift-right. The number of bit shifts is equal to the difference between the exponents. After the shifts, the two exponents having been made equal, the addition/subtraction of the mantissas is performed. The exponent of the result is the common exponent of the numbers after alignment. Normalization of the result is effected by shifting the mantissa bits left until a 1 appears to the left of the binary point as seen above. For each shift-left step the exponent of the result is reduced by one.

In constructing a circuit for addition/subtraction improved accuracy of computation may be achieved by using long registers-accumulators so that the operation of exponent alignment through right shifts does not lead to loss of bits due to a fixed register length. Truncation or round-off of the result is performed only after the addition/subtraction has thus been performed using a temporary longer accumulator-register.

15.24.2 Multiplication

An interesting property of floating point arithmetic is that multiplication is in a way simpler than addition. We have seen that addition requires exponential alignment as well as postnormalization. Multiplication is more straightforward. The product of two numbers

$$A \times B = r_1 2^{e_1} \times r_2 2^{e_2} = r_1 r_2 2^{e_1 + e_2}. \quad (15.237)$$

The mantissas are multiplied as in the usual fixed point multiplication, the exponents are added and 127 is subtracted thereof and the sign attached to the result. Since a normalized number, other than zero, has the form $1.xxxx\dots x$, its value is

$$1 < v < 2 \quad (15.238)$$

and the product of two such numbers has a value

$$1 < v < 4. \quad (15.239)$$

Normalization is therefore easily effected.

15.24.3 Division

In division the exponents are subtracted and 127 is subtracted from the result. The mantissas are divided and the sign attached to the result. Normalization is applied to the result.

15.25 Square Root Evaluation

In this section we recall the paper and pencil method of the decimal evaluation of square roots. Subsequently, binary square root evaluation is considered. Note that, alternatively, as seen earlier the Newton–Raphson method may be used to evaluate the square root and more generally the n^{th} root of a number where n is any positive integer.

15.25.1 The Paper and Pencil Method

We consider the evaluation of $A = \sqrt{B}$. The operand B is referred to as the “radicant,” and the result A as the “quotient.”

Example 15.27 Evaluate

$$A = \sqrt{98924.37}.$$

We group digits in pairs starting from the binary point, and proceed as follows:

$A = \sqrt{B} = \sqrt{09'89'24'.37}$	
$Q^2 : \underline{09}$	$q_1 = 3, \quad Q = q_1 = 3, \quad 2Q = 6$
$r_1 : \quad 00 \ 89$	$\text{Find } q_{2,max} \mid 6q_2 \times q_2 \leq r_1; \quad q_2 = 1$
$6\underline{1} \times 0\underline{1} : \underline{61}$	$Q = q_1q_2 = 31, \quad 2Q = 62$
$r_2 : \quad 28 \ 24$	$\text{Find } q_{3,max} \mid 62q_3 \times q_3 \leq r_2; \quad q_3 = 4$
$62\underline{4} \times 0\underline{4} : \underline{24 \ 96}$	$Q = q_1q_2q_3 = 314, \quad 2Q = 628$
$r_3 : \quad 3 \ 28 \ .37$	$\text{For } q_{4,max} \mid 628.q_4 \times q_4 \leq r_3; \quad q_4 = 5$
$628.5 \times 0.5 : \underline{3 \ 14 \ .25}$	$Q = q_1q_2q_3.q_4 = 314.5, \quad 2Q = 629.0$
$r_4 : \quad 14 \ .12 \ 00$	$q_{5,max} \mid 629.0q_5 \times 0.0q_5 \leq r_4; \quad q_5 = 2$
$629.\underline{02} \times 0.\underline{02} : \underline{12 \ .58 \ 04}$	$Q = q_1q_2q_3.q_4q_5 = 314.52$
$r_5 : \quad 1 \ .53 \ 96 \ \dots$	

The quotient is $A = Q = \sqrt{B} = 314.52$ and the remainder is $R = 1.5396$. The process starts by finding the square root of the two left-most digits; in this case 09. We obtain the first quotient digit $q_1 = 3$. We write $Q = 3$ and retain the value $2Q = 6$. We subtract $Q^2 = 9$ from B and annex the following pair of digits 89 of B obtaining the first remainder $r_1 = 0089$.

We next find the second quotient digit q_2 as the maximum value satisfying $6q_2 \times 0q_2 \leq r_1$, the digit 6 being the value $2Q$. We obtain $q_2 = 1$, so that $Q = q_1q_2 = 31$, $2Q = 62$ and $6q_2 \times 0q_2 = 61 \times 01 = 61$ which is subtracted from r_1 .

To the result $89 - 61 = 28$ we annex the following two digits from B , namely, 24 obtaining the remainder $r_2 = 2824$. The quotient digit q_3 is similarly found as the maximum value satisfying $62q_3 \times 0q_3 \leq r_2$. We find $q_3 = 4$, i.e. $Q = q_1q_2q_3 = 314$ and $2Q = 628$. The process is repeated as shown above leading to improved accuracy as more digits of the fractional part are annexed to the latest remainder.

15.25.2 Binary Square Root Evaluation

The evaluation of the square root in the binary system proceeds in a manner similar to the paper and pencil method. The problem is to evaluate the quotient Q of the radicant A where, in binary,

$$A = 0.a_1a_2 \dots a_{2n} \tag{15.240}$$

$$Q = 0.q_1q_2 \dots q_n \simeq \sqrt{A} \tag{15.241}$$

the left-most bit zero signifying a positive value. The radicant A may be viewed as a fraction with the binary point on the left, or equivalently as an integer with the binary point on the right.

15.25.3 Comparison Approach

In the “comparison” approach, which is identical to the decimal paper and pencil method, a subtraction is performed and the quotient bit is $q_i = 1$ if and only if it leads to a positive result. Consider the case

$$A = 0.00'10'01'00'10'01'11'00'10'01 = 149961_{10} \tag{15.242}$$

which may be written $A = 149961 (2^{-20})$ in FNR, and where the bits are grouped in pairs for better visibility. The process is illustrated by the following chart, where we see that in the first step the left-most two bits $a_1a_2 = 00$ are taken to be the initial remainder.

$\sqrt{A} = \sqrt{.00'10'01'00'10'01'11'00'10'01}$	
<u>00</u>	$q_1 = 0, Q = q_1 = 0$
00 10	r_1
<u>01</u>	$q_2 = 1, Q = q_1q_2 = 01, 2Q = 10$
01 01	r_2
<u>1 01</u>	$q_3 = 1, Q = 011, 2Q = 110$
00 00 00	r_3
<u>00</u>	$q_4 = 0, Q = 0110, 2Q = 1100$
00 10	r_4
<u>00</u>	$q_5 = 0, Q = 01100, 2Q = 11000$
10 01	r_5
<u>00 00</u>	$q_6 = 0, Q = 011000, 2Q = 110000$
10 01 11	r_6
<u>00 00 00</u>	$q_7 = 0, Q = 110000$
10 01 11 00	r_7
<u>00 00 00 00</u>	$q_8 = 0, Q = 1100000$
10 01 11 00 10	r_8
<u>1 10 00 00 01</u>	$q_9 = 1, Q = 11000001$
0 11 11 00 01 01	r_9
<u>11 00 00 01 01</u>	$q_{10} = 1, Q = 110000011$
0 00 11 00 00 00	r_{10}

At each step of the algorithm we subtract 01 from the remainder as long as such subtraction does not produce a negative remainder; otherwise we subtract 00. Since the initial remainder is 00 we can only subtract 00. We therefore set the quotient bit $q_1 = 0$ signifying that a 00 is subtracted with the result 00. To this two new left-most bits, $a_3a_4 = 10$ of A are appended, leading to the new remainder $r_1 = 0010$.

The second step follows, where now we find that we can set $q_2 = 1$, subtracting 01 from r_1 since such subtraction leads to a positive result. To this we annex $a_5a_6 = 01$ obtaining

the new remainder $r_2 = 0101$. The process is repeated as shown in the chart above, with the end result

$$Q = 0.0110000011 = 387 \quad (15.243)$$

$$R = 0.00000000000011000000 = 192 \quad (15.244)$$

$$R = A - Q^2 \quad (15.245)$$

and $Q = 387 (2^{-10})$ and $R = 192 (2^{-20})$ in FNR.

15.25.4 Restoring Approach

As in the case of the evaluation of division the restoring approach of the square root extraction is the same as the comparison approach with the exception that at every step the bit pair 01 is subtracted from the remainder. If the result is positive the quotient bit is set to 1 as before. If it is negative the quotient bit is set to 0 and a restoration is applied by adding 01 to annul the effect of the last subtraction.

15.25.5 Nonrestoring Approach

In the nonrestoring approach the algorithm starts by subtracting $D_0 = 01$ from a_1a_2 . If the remainder r_1 is greater than or equal to zero then the quotient bit $q_1 = 1$, the bits a_3a_4 are annexed to r_1 , so the new remainder is $r_1a_3a_4$, $D_1 = q_101$ and a subtraction is performed producing $r_2 = r_1 - D_1$. If on the other hand the remainder $r_1 < 0$ then the quotient bit $q_1 = 0$, the new remainder is again $r_1a_3a_4$, but $D_1 = q_111$ and an addition is performed producing $r_2 = r_1 + D_1$. In the following step the same process takes place. If the remainder r_2 is greater than or equal to zero then the quotient bit $q_2 = 1$, the bits a_5a_6 are annexed to r_2 , so the new remainder is $r_2a_5a_6$, $D_2 = q_1q_201$ and a subtraction is performed producing $r_3 = r_2 - D_2$. If on the other hand the remainder $r_2 < 0$ then the quotient bit $q_2 = 0$, the new remainder is $r_2a_5a_6$, but $D_2 = q_1q_211$ and an addition is performed producing $r_3 = r_2 + D_2$. This process is repeated so that in general if the quotient bit $q_k = 1$ we set $r_{k+1} = r_k a_{2k+1} a_{2k+2} - q_1 q_2 \dots q_k 01$, and if $q_k = 0$ we set $r_{k+1} = r_k a_{2k+1} a_{2k+2} + q_1 q_2 \dots q_k 11$.

Note that if at any point the remainder is simply zero the implication is that the quotient found so far is an exact square root. The process may be restarted at this point to processor the radicand's remaining bits. Alternatively, the process simply resumes producing the desired number of bits of the quotient.

As an example we consider the case $A = 602_{10} = 0.1001011010$. The following chart shows the process generating 13 bits of quotient

$$Q = 24.5357 = 11000.10001001$$

0.11000.10001 001	
$\sqrt{0.10010\ 11010.00}$	
- 0.01	
0.0101	$r_1 > 0 \longrightarrow q_1 = 1$
- 0 0101	$q_1 01$
0 00000 1	$> 0 \longrightarrow q_2 = 1$
- 110 1	$q_1 q_2 01$
1.11010 010	$< 0 \longrightarrow q_3 = 0$
+ 11 011	$q_1 q_2 q_3 01$
1.11101 10110	$< 0 \longrightarrow q_4 = 0$
+ 1 10011	$q_1 q_2 q_3 q_4 11$
1.11111 01001.00	$< 0 \longrightarrow q_5 = 0$
+ 11000.11	$q_1 q_2 q_3 q_4 q_5 11$
0.00000 00001.1100	$> 0 \longrightarrow q_6 = 1$
- 1100 0101	$q_1 q_2 q_3 q_4 q_5 q_6 01$
1.11111 10101.01110 0	$< 0 \longrightarrow q_7 = 0$
+ 110 00101 1	
1.11111 11011 10011 100	$q_8 = 0$
+ 11 00010 011	
1.11111 11110 10101 11100	$q_9 = 0$
+ 1 10001 00011	
0.00000 00000 00110 11111 00	$q_{10} = 1$
- 11000 10001 01	
1.11111 11111 01110 01101 1100	$q_{11} = 0$
+ 1100 01000 1011	
1.11111 11111 11010 10110 01110 0	$q_{12} = 0$
+ 110 00100 01001 1	
0.00000 00000 00000 11010 10111 100	$q_{13} = 1$

15.26 Cellular Array for Nonrestoring Square Root Extraction

A cellular array for nonrestoring square root extraction is shown in Fig. 15.29. The array is composed of CAS cells as the one described above and used in nonrestoring division.

As an example, Fig. 15.30 shows the operation of extracting the square root of $A = 2822 = (101100000110)_2$, producing the result $Q = 53 = (110101)_2$ and $R = 13 = (1101)_2$.

15.27 Binary Coded Decimal (BCD) Representation

BCD code represents a decimal number in our usual positional decimal notation, with each decimal digit coded in binary. For example, the decimal number 7983_{10} is coded as the BCD number

$$0111\ 1001\ 1000\ 0011$$

occupying four decades, each of which coded in binary.

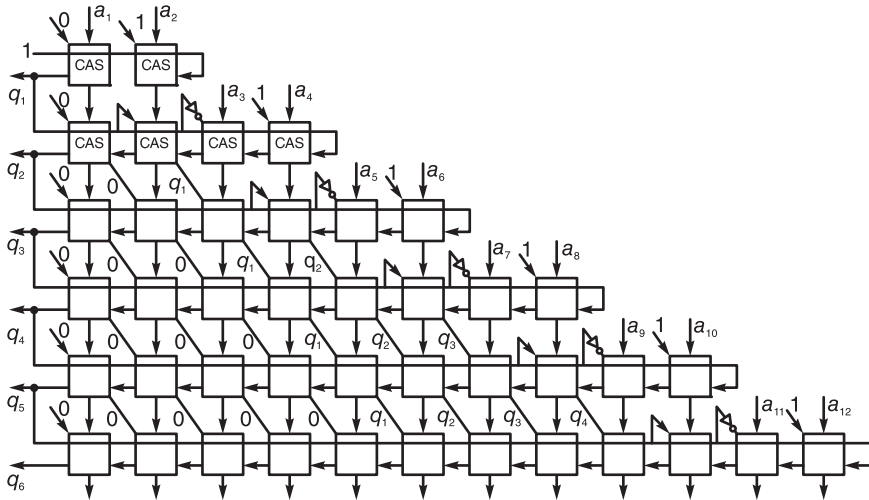


FIGURE 15.29 Nonrestoring square root extraction cellular array.

BCD has the advantage of being a natural way of representing numbers as we usually see them. Moreover, it allows easy conversion to decimal digits for printing or display and natural decimal mathematical operations. Since a decimal digit ranges in value from 0 to 9, BCD representation occupies in general more bits than binary representation. Nevertheless, decimal fixed-point and floating-point representations are used by in financial, commercial, and industrial computing.

Conversion from BCD to binary or from binary to BCD is effected by successive right or left shifts, followed by a conditional restoration after each shift. To view in more detail the process of conversion note that given a decimal number we may obtain the binary equivalent by successive divisions by 2 and retaining each time the fraction part. For example, converting 123_{10} we write $123/2 = 61$ with remainder of 1, then $61/2 = 30$ with remainder of, 1 followed by $30/2 = 15$ with remainder of 0, then $15/2 = 7$ with remainder of 1, followed by $7/2 = 3$ with remainder of 1, then $3/2 = 1$ with remainder of 1, and finally by $1/2 = 0$ with remainder of 1. The series of remainders thus obtained is the set of bit values of the binary representation starting from the LSB up to the MSB. In other words, the binary equivalent is 1111011.

When BCD to binary conversion is performed the same approach is followed. The division by 2 operation is effected by a shift-right operation. However, any time the shift right operation displaces a 1-bit from a decade to the neighboring lower decade, a correction is needed. To see this consider the same number 7983_{10} and its BCD form 0111 1001 1000 0011. A one-bit shift right leads to the code 0011 1100 1100 0001 with a bit of 1 shifted to the right as a remainder. This result is not the true value of the original number divided by two $7983/2 = 3991$. In fact the number as it stands is not a valid BCD code since the middle two decades are 1100, which equals 12. To correct the result we have to subtract 3 from every erroneous decade, that has received a one-bit from its left neighbor due to the shift. By subtracting 3 from the middle decade the correct number 3991 is obtained as the result of the integer division $7983/2 = 3991$.

The logic here is simple. If the LSB of a decade is 1, and if a right shift is applied, the 1-bit becomes the MSB of the lower decade. Relative to the lower decade its value before the shifting is 10, while after the shifting its value is 8, being the MSB of the lower decade.

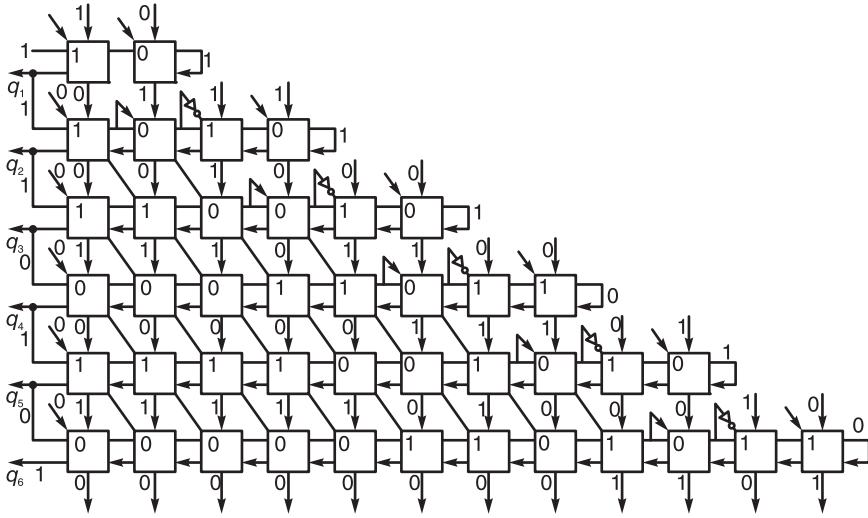


FIGURE 15.30 Example of cellular array square root extraction.

Thus whereas a value of 10 divided by 2 should produce 5, the result after the shifting is 8. To correct the result we need to subtract 3.

We conclude that *if a 1-bit moves to the MSB of a lower decade the lower decade should be reduced by 3. Such restoration has to be applied to all decades wherein the MSB receives a 1 after the right shift.*

Conversely, binary to BCD conversion is accomplished by successive multiplications times 2. This calls for successive left shift operations. Consider the same binary number 1110011. We shift the bits left and assemble successive decades. Note, however, that after three one-bit shifts to the left the lowest order decade contains $(0111)_2 = 7_{10}$ and when shifted one more bit becomes $1110 = (14)_{10}$. In BCD this value 14_{10} should be coded as

$$0001\ 0100$$

which in binary equals 20. We need therefore to add 6 to convert the simply shifted bits in order to convert the result to BCD code. Alternatively, we can add 3 to the binary code before the shift. Adding 3 to 7 produces 10 which after shifting becomes $20_{10} = 1\ 0110$, the proper representation for 14.

Such restoration by the addition of 3 is required any time a decade has the value 5 or more, since multiplication by 2 then exceeds the decade capacity and carries over to a higher decade.

We conclude that *conversion from binary to BCD is accomplished by shifting the bits successively to the left. Any time a formed decade contains a value greater than or equal to 5 it is restored by adding 3 before continuing the shifting operation.*

The design of a logic chip should aim for a structure that allows us to use it as a module or building block to solve bigger problems. The design of a combinatorial logic circuit for the conversion from BCD to binary can be approached as shown in Fig. 15.31.

In part (a) a BCD number of one and a half decade is converted to a six-bit binary number using shifts and two four-bit parallel adders. The drawing of the circuit is simplified by shifting the adders to the left, rather than shifting the bits to the right. Figure 15.31 (a) shows the conversion of the decimal number 39, the maximum allowable, to binary. This unit of conversion may be referred to as a decimal to binary (D/B) converter chip or module which can be used to construct converters of bigger numbers.

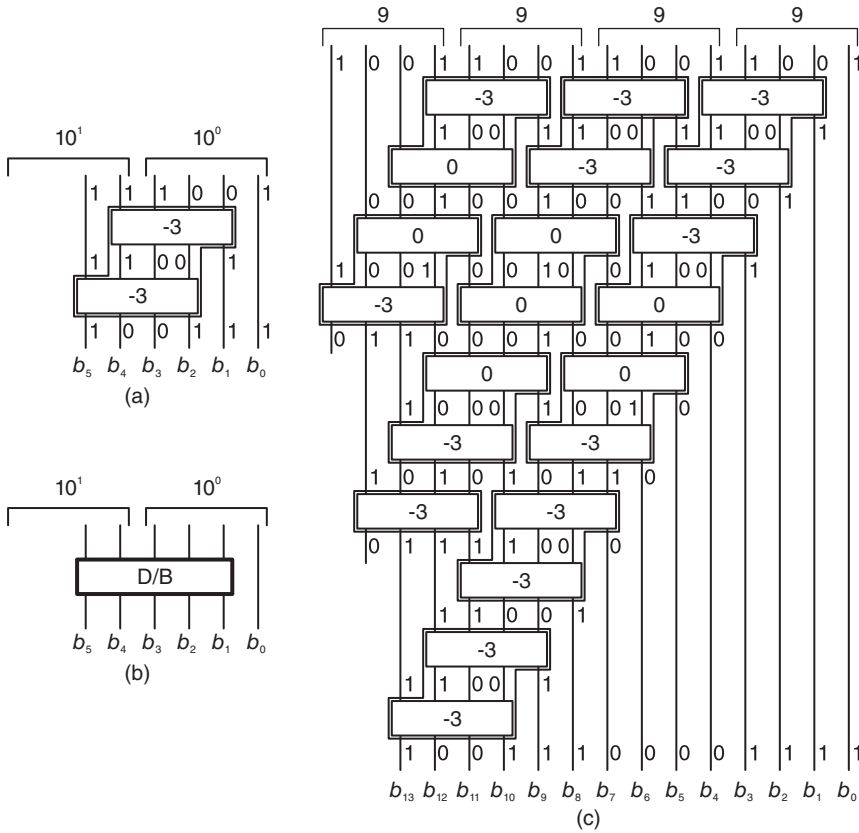


FIGURE 15.31 BCD to Binary conversion using adders.

The chip is sketched in block form in Fig. 15.31 (b). The BCD to binary conversion of a four-decade BCD code to binary may be drawn using adders as shown in Fig. 15.31 (c). The figure also shows the grouping of pairs of adders that would allow each pair to be replaced by the D/B chip. The same converter is then redrawn using the D/B chips as shown in Fig. 15.32.

The same principle of designing a binary to decimal (B/D) conversion chip using four-bit parallel adders is illustrated in Fig.15.33 (a).

Here too, to simplify the drawing, rather than shifting bits to the right the adders are shifted left. The figure shows the conversion the maximum allowable 1 1 1 1 1 to decimal 63 using three adders. The chip is sketched in block form in Fig. 15.33 (b). The binary to BCD conversion of the 12-bit number

$$1\ 1\ 0\ 0\ 0\ 1\ 0\ 1\ 1\ 0\ 1\ 1$$

to the decimal 3063 using adders is shown in Fig. 15.33(c). The figure also shows the grouping of pairs of adders that would allow each pair to be replaced by the B/D chip. The same converter is then redrawn using the B/D chips in Fig. 15.34.

A good approach in designing conversion circuits is to verify the design using the maximum allowable input. In binary this means bits that are all ones; in decimal digits that are all 9's. This provides a quick means of verifying the maximum length that can occupy each number at each step of conversion.

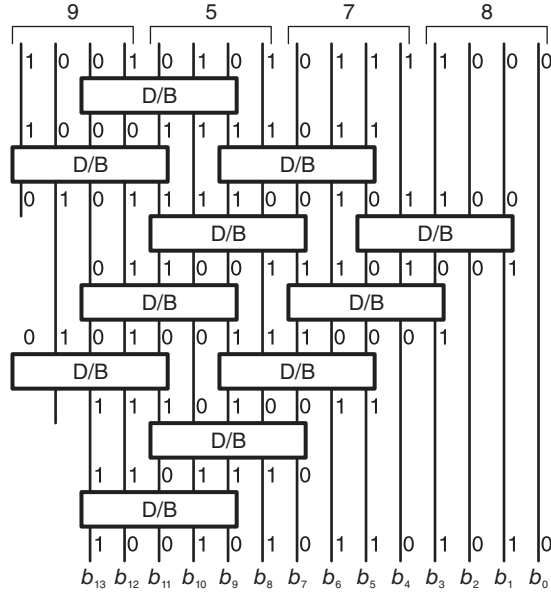


FIGURE 15.32 Four-decade BCD to binary conversion with D/B modules.

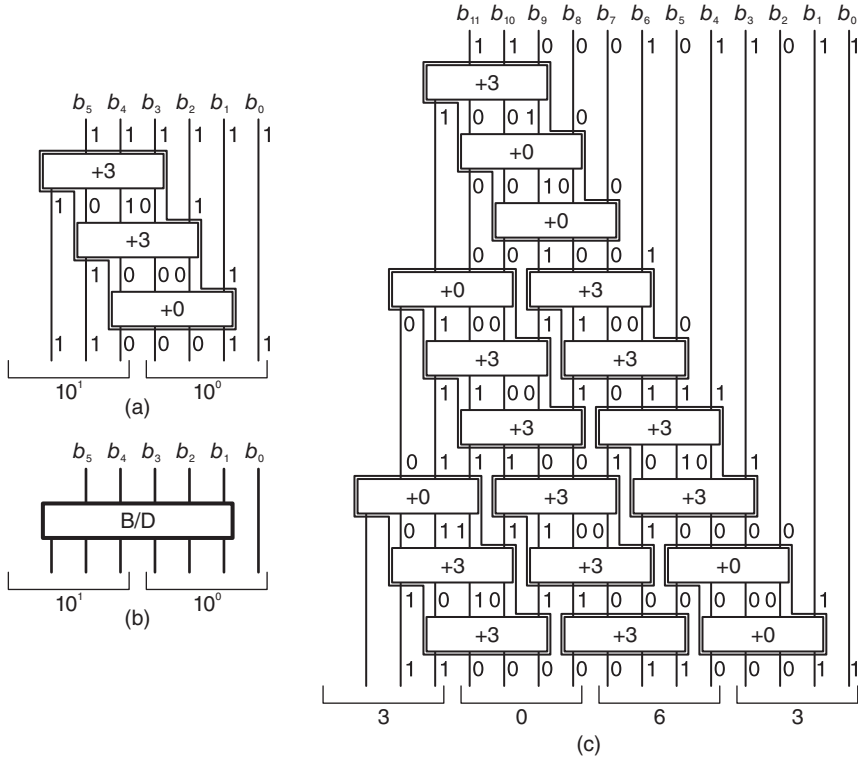


FIGURE 15.33 Binary to BCD conversion array using adders.

15.28 Memory Elements

So far we focused our attention on combinatorial logic circuits. These are characterized by the fact that their outputs at any time are function of present but not past inputs.

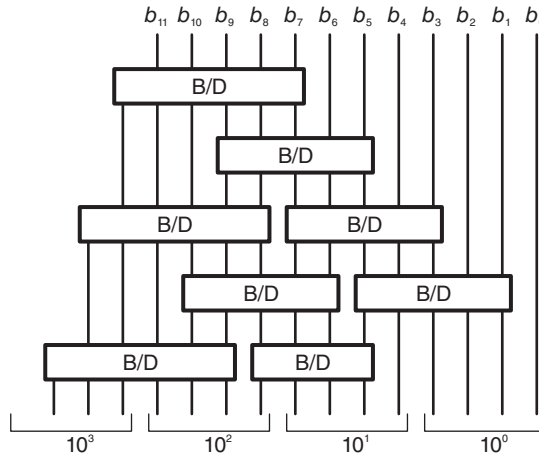


FIGURE 15.34 Binary to BCD conversion array using B/D Modules

Digital signal processors and computers, however, call generally for effecting logical and mathematical operations that are function of preceding, not only present, inputs and operations. Logical circuits capable of storing information are thus called for. These are referred to as *memory elements*, and the logic circuit is called a *sequential circuit* and, more generally, *sequential machines*. The basic memory element is the flip-flop, also called *bistable multi-vibrator*. In what follows we study several kinds of flip-flops.

15.28.1 Set-Reset (SR) Flip-Flop

An SR flip-flop is represented in Fig. 15.35 (a) in block form, and in Fig. 15.35 (b) and (c) using logic gates.

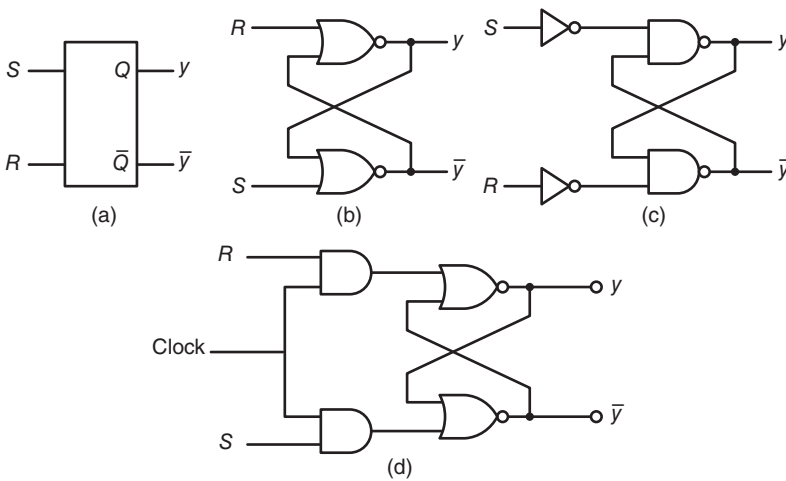


FIGURE 15.35 SR flip-flop: (a) block diagram, (b) using NOR gates, (c) using NAND gates, (d) clocked.

If the input $S = 1$ its output $y = 1$ and the complement $\bar{y} = 0$. If the input $R = 1$ the output $y = 0$ and $\bar{y} = 1$. The inputs R and S cannot be simultaneously equal to 1. The excitation characteristics of the SR flip-flop are listed in Table 15.6, where d means *don't care*. From the Karnaugh map depicted in Fig. 15.36, where ϕ means don't care, we conclude that the next state output

$$Y \equiv y(t + 1) = S + \bar{R}y(t)$$

TABLE 15.6 Excitation characteristics of an SR flip-flop

$y(t)$	$S(t)$	$R(t)$	$y(t+1)$
0	0	0	0
0	0	1	0
0	1	1	d
0	1	0	1
1	1	0	1
1	1	1	d
1	0	1	0
1	0	0	1

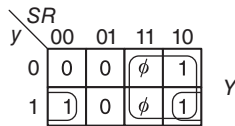


FIGURE 15.36 Karnaugh map for SR flip-flop.

The values of the inputs S and R needed to flip the output or keep it unchanged are listed in Table 15.7. These are the excitation requirements of the SR flip-flop. A clocked

TABLE 15.7 Excitation requirements of an SR flip-flop

$y(t)$	$y(t+1)$	S	R
0	0	0	d
0	1	1	0
1	1	d	0
1	0	0	1

SR flip-flop which has a clock input for the purpose of synchronization is shown in Fig. 15.35 (d). The AND gates serve to synchronize the S and R inputs with the clock.

15.28.2 The Trigger or *T* Flip-Flop

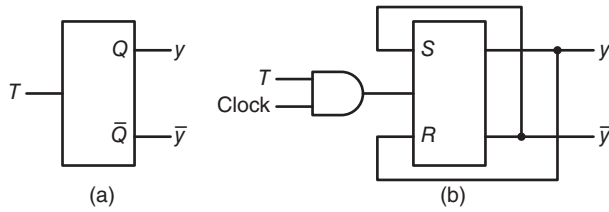


FIGURE 15.37 *T* flip-flop.

The Trigger or *T* flip-flop shown in Fig. 15.37 complements its state upon receiving an input $T = 1$. We may write

$$Y \equiv y(t + 1) = T\bar{y}(t) + T'y(t) = T \oplus y(t)$$

The values of T required to set or reset the *T* flip-flop are summarized in Table .

TABLE 15.8
Excitation requirements of a *T* flip-flop

$y(t)$	$y(t+1)$	T
0	0	0
0	1	1
1	1	0
1	0	1

15.28.3 The *JK* Flip-Flop

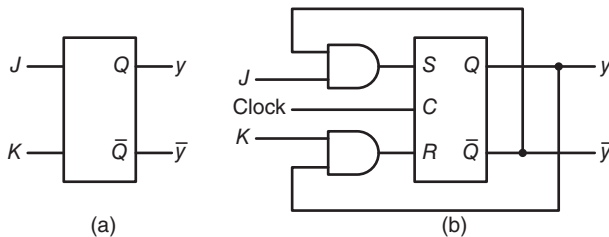


FIGURE 15.38 JK flip-flop, (a) block diagram, (b) using an SR flip flop.

The *JK* flip-flop combines the properties of *SR* and *T* flip-flops. Its J and K inputs act as the S and R inputs of the *SR* flip-flop. If, however, $J = K = 1$, it acts as the *T* flip-flop,

reversing its state. The *JK* flip-flop is represented in block form in Fig. 15.38 (a), and as a logic circuit employing an *SR* flip-flop in Fig. 15.38 (b). Table 15.9 shows the excitation requirements of the *JK* flip-flop.

TABLE 15.9
Excitation requirements of a *JK* flip-flop

$y(t)$	$y(t+1)$	J	K
0	0	0	d
0	1	1	d
1	1	d	0
1	0	d	1

15.28.4 Master-Slave Flip-Flop

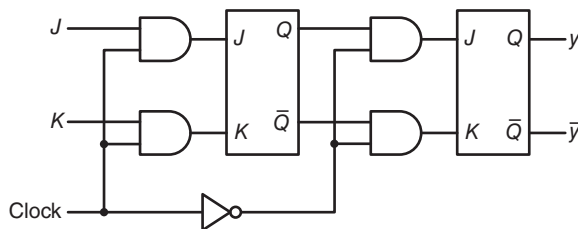


FIGURE 15.39 Master-slave JK flip flop.

An n -bit latch or a shift register is constructed as a set of n flip-flops. An FIR filter such as the one depicted in Chapter 11 Fig. 11.9, for example, employs unit-delay elements referred to in the figure by their transfer function z^{-1} . To construct such a filter using fixed point number representation with say m bits, we would implement each delay element as a latch made up of m flip-flops. At each clock, m input bits are stored into each latch in parallel. Since the latches are connected in series as a chain of memory elements, a latch input is in general the output of the preceding one. The clock pulse should synchronize the data shifting operation so that each flip-flop will transfer its input to its output once during the clock cycle. If the clock pulse lingers, however, flip-flop inputs may change, the preceding stage having changed state. In other words, the clock should ensure that the sampling of the input is done once and at the appropriate time. It should be short enough to sample the input but not so long that the input changes to a new state.

A Master-Slave flip-flop solves this problem by using in fact two flip-flops. The first transfers the input to its output when the clock goes high (1) and the second transfers the output of the first flip-flop to the second when the clock returns to low (0). Such a master-slave flip-flop is shown in Fig. 15.39. A detailed circuit using NAND gates can be seen in Fig. 15.40. The flip-flop has also Clear and Set inputs to override the J and K inputs, with a 0 on the Set input to set the slave to 1 and a 0 on the Clear input to clear it to 0. If

both the Set and Clear inputs are 1 they become transparent letting the flip-flop state be controlled by the J and K flip-flop inputs. The Clear and Set inputs may be used to clear latches or shift registers and to impose a specific state on a counter when needed.

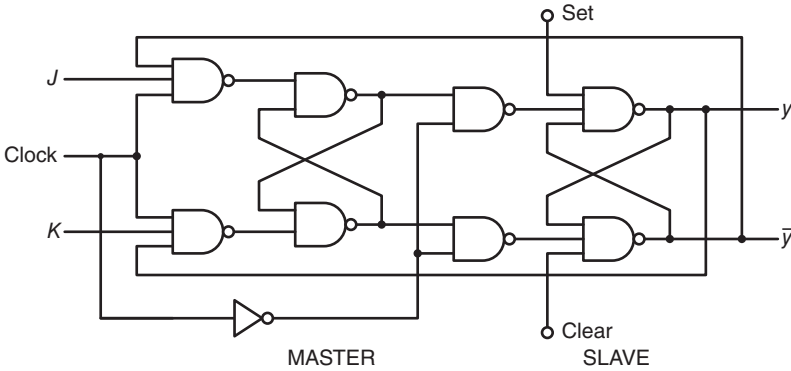


FIGURE 15.40 Master-slave JK flip-flop detailed structure

15.29 Design of Synchronous Sequential Circuits

To design a synchronous sequential circuit for a given application we start by drawing a *state diagram* representing the required sequencing of operations. Consider the state diagram model of a sequential machine (circuit) shown in Fig. 15.41.

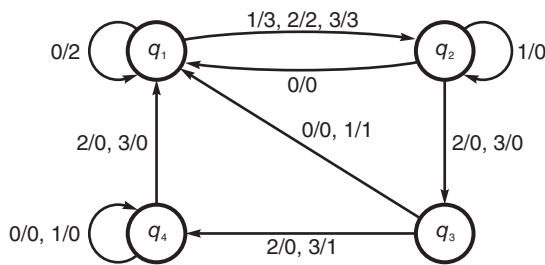


FIGURE 15.41 State diagram of a sequential machine.

Circles in a state diagram represent states of the machine. Directed arcs indicate transitions between states. The labels that appear next to the directed arcs specify the inputs and corresponding outputs. For example, the arc directed from state q_1 to state q_2 has the label $1/3, 2/2, 3/3$. This means that if the input equals 1 the output is 3, if it equals 2 the output is 2 and if it is 3 the output is 3. A sequential circuit can be, alternatively, described by a state table. The sequential circuit in question is described by Table 15.10.

TABLE 15.10 State table of sequential circuit

Present State	Next state, output z			
	$x_1x_2 = 00$	$x_1x_2 = 01$	$x_1x_2 = 11$	$x_1x_2 = 10$
q_1	$q_1, 2$	$q_2, 3$	$q_2, 3$	$q_2, 2$
q_2	$q_1, 0$	$q_2, 0$	$q_3, 0$	$q_3, 0$
q_3	$q_1, 0$	$q_1, 1$	$q_4, 1$	$q_4, 0$
q_4	$q_4, 0$	$q_4, 0$	$q_1, 0$	$q_1, 0$

Since the input values range between 0 and 3, they will be denoted in binary as $x_1x_2 = 00, 01, 10,$ and 11 . The table shows the transitions from each present state $q_1, q_2, q_3,$ or q_4 to the next state and the corresponding output in each transition. Since the circuit has four states, we use two variables, y_1 and y_2 , to denote each one. The state assignment is arbitrary. If, for example, we assign the values $y_2y_1 = \{00, 01, 11, 10\}$ to the states $q_2, q_3, q_1,$ and $q_4,$ respectively, we may construct a state transition table specifying the evolution in time of the state variables y_1 and y_2 and the corresponding outputs, which we may code using two variables z_1 and z_2 . Table 15.11 shows such transitions between states and outputs. In this table, y_1 and y_2 designate the present state variables, while Y_1 and Y_2 designate the next state following the transition.

TABLE 15.11 Transition and output table of sequential circuit

Present State	Next state				Output			
	$x_1x_2 = 00$	01	11	10	00	01	11	10
y_2y_1	Y_2Y_1	Y_2Y_1	Y_2Y_1	Y_2Y_1	z_2z_1	z_2z_1	z_2z_1	z_2z_1
$q_2 : 00$	11	00	01	01	00	00	00	00
$q_3 : 01$	11	11	10	10	00	01	01	00
$q_1 : 11$	11	00	00	00	10	11	11	10
$q_4 : 10$	10	10	11	11	00	00	00	00

From this table we can draw the Karnaugh maps corresponding to the variables $Y_1, Y_2, z_1,$ and z_2 as functions of x_1, x_2, y_1 and y_2 , as can be seen in Fig. 15.42 (a-d), respectively. From these maps we can minimize the required logic functions by grouping zero-cubes to form bigger ones, as can be seen in the figure.

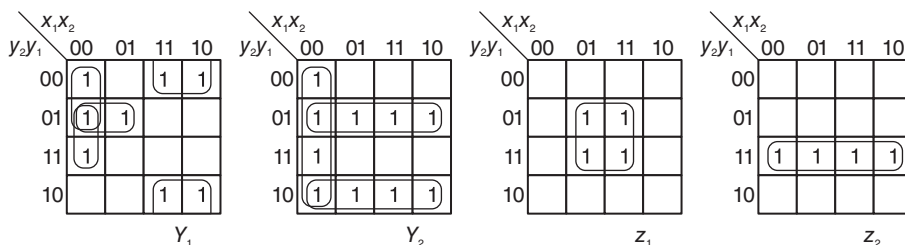


FIGURE 15.42 Karnaugh maps of (a) Y_1 , (b) Y_2 , (c) z_1 and (d) z_2 .

We obtain

$$\begin{aligned}
 Y_1 &= x_1\bar{y}_1 + \bar{x}_1\bar{y}_2y_1 + \bar{x}_1\bar{x}_2\bar{y}_2 + \bar{x}_1\bar{x}_2y_1 \\
 Y_2 &= y_2\bar{y}_1 + \bar{y}_2y_1 + \bar{x}_1\bar{x}_2 = y_1 \oplus y_2 + \bar{x}_1\bar{x}_2 \\
 z_1 &= x_2y_1, \quad z_2 = y_2y_1
 \end{aligned}$$

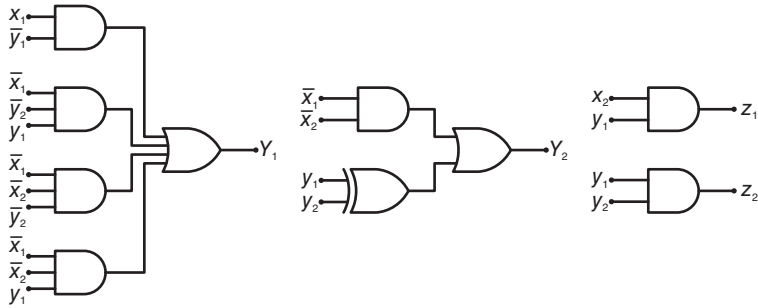


FIGURE 15.43 Combinational circuit evaluating Y_1, Y_2, z_1, z_2 .

The realization of these functions using AND and OR gates is shown in Fig. 15.43. The overall sequential circuit is shown in Fig. 15.44.

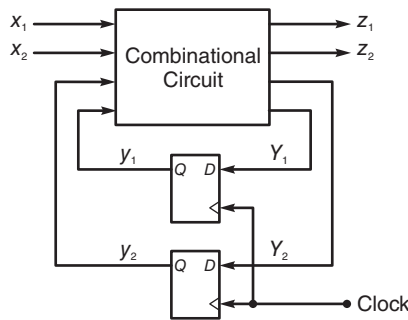


FIGURE 15.44 Sequential machine model.

where D-Type flip-flops are used as memory elements. This figure is typical of a sequential circuit wherein part is combinatorial logic circuit and the other uses memory elements.

The general model of a synchronous sequential machine with m inputs x_1, x_2, \dots, x_m, k outputs z_1, z_2, \dots, z_k and p state variables y_1, y_2, \dots, y_p , is shown in Fig. 15.45. The outputs of the combinatorial logic circuit are the machine outputs z_1, z_2, \dots, z_m and the next state variables Y_1, Y_2, \dots, Y_p , which are registered into the memory elements.

15.29.1 Realization Using SR Flip-Flops

$$S_2 = \bar{y}_2y_1 + \bar{x}_1\bar{x}_2$$

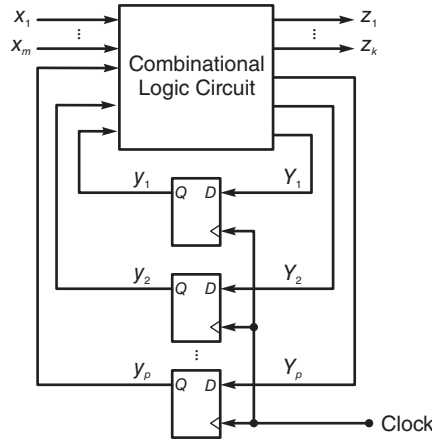


FIGURE 15.45 General Model of a synchronous sequential machine.

$$S_1 = x_1\bar{y}_1 + \bar{x}_2\bar{y}_2\bar{y}_1$$

$$R_2 = x_1y_2y_1 + x_2y_2y_1$$

$$R_1 = x_1y_1 + x_2y_2y_1$$

The excitation table of implementation of the above sequential circuit is obtained using the excitation requirements for *SR* flip-flops to determine the *S* and *R*, namely $S_1, R_1, S_2,$ and R_2 that need to be applied to effect the transition from each present state y_2y_1 to the next one Y_2Y_1 as given in Table 15.12. From this table we draw the Karnaugh maps of $S_2, S_1, R_2,$ and R_1 as seen in Fig. 15.46.

TABLE 15.12 Excitation table using *SR* flip-flops

Present State y_2y_1	Input x_1x_2							
	00		01		11		10	
	S_2R_2	S_1R_1	S_2R_2	S_1R_1	S_2R_2	S_1R_1	S_2R_2	S_1R_1
$q_2 : 00$	10	10	0d	0d	0d	10	0d	10
$q_3 : 01$	10	d0	10	d0	10	01	10	01
$q_1 : 11$	d0	d0	01	01	01	01	01	01
$q_4 : 10$	d0	0d	d0	0d	d0	10	d0	10

15.29.2 Realization Using *JK* Flip-Flops.

The realization using *JK* flip-flops is similarly obtained. Table 15.13 lists the excitation requirements for a *JK* flip-flop. The resulting Karnaugh maps of J_2, J_1, K_2 and k_1 are shown in Fig. 15.47.

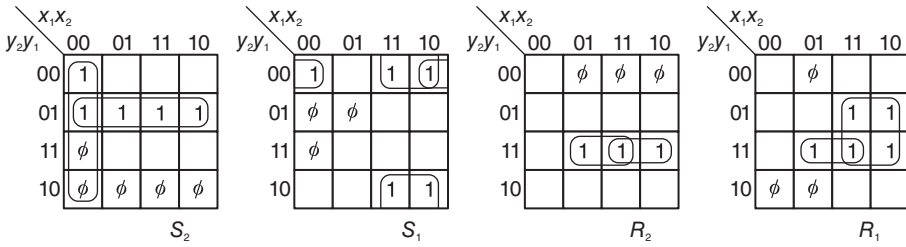


FIGURE 15.46 Karnaugh maps of S_2 , S_1 , R_2 and R_1 .

TABLE 15.13 Excitation table using JK flip-flops

Present State y_2y_1	Input x_1x_2							
	00		01		11		10	
	J_2K_2	J_1K_1	J_2K_2	J_1K_1	J_2K_2	J_1K_1	J_2K_2	J_1K_1
$q_2 : 00$	1d	1d	0d	0d	0d	1d	0d	1d
$q_3 : 01$	1d	d0	1d	d0	1d	d1	1d	d1
$q_1 : 11$	d0	d0	d1	d1	d1	d1	d1	d1
$q_4 : 10$	d0	0d	d0	0d	d0	1d	d0	1d

From these maps we obtain the equations

$$\begin{aligned}
 J_2 &= \bar{x}_1\bar{x}_2 + y_1 \\
 J_1 &= x_1 + \bar{x}_2\bar{y}_2 \\
 K_2 &= x_1y_1 + x_2y_1 \\
 K_1 &= x_1 + x_2y_2y_1
 \end{aligned}$$

15.30 Realization of a Counter Using T Flip-Flops

The control unit of a computer or general digital processor is a sequential machine which, depending on conditions it receives as inputs, will change from the present state to a new one and produce the required output signals. As an illustration of the design of a counter to cycle through predetermined states we consider a 3-bit counter incrementing its binary content with each clock. The state diagram of such a counter is shown in Fig. 15.48.

The states of this counter can be seen in Table 15.14. The corresponding excitation requirements for T flip-flops are listed in Table 15.15.

Drawing the Karnaugh maps for the variables T_1 , T_2 and T_3 we deduce that

$$T_3 = xy_2y_1, \quad T_2 = xy_1, \quad T_1 = x, \quad z = xy_3y_2y_1.$$

15.30.1 Realization Using JK Flip-Flops

The realization using JK flip-flops of the same 3-bit counter leads to the excitation requirements listed in Table 15.16. Drawing the Karnaugh maps for the J and K variables we obtain

$$J_3 = K_3 = xy_2y_1, \quad J_2 = K_2 = xy_1, \quad J_1 = K_1 = x.$$

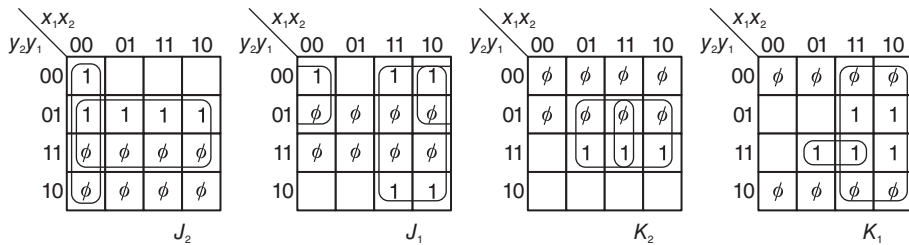


FIGURE 15.47 Karnaugh maps of J_2 , J_1 , K_2 and K_1 .

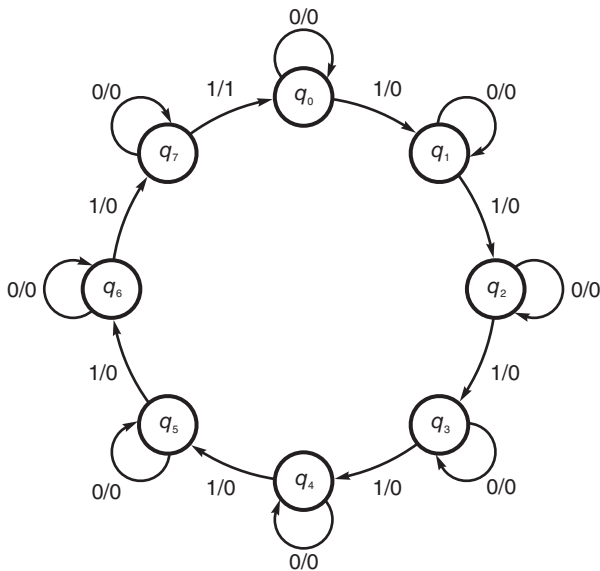


FIGURE 15.48 State diagram of a 3-bit counter.

TABLE 15.14 Transition and output table of 3-bit counter

y_3	y_2	y_1	$x = 0$			$x = 1$			Z
			Y_3	Y_2	Y_1	Y_3	Y_2	Y_1	
0	0	0	0	0	0	0	0	1	0
0	0	1	0	0	1	0	1	0	0
0	1	0	0	1	0	0	1	1	0
0	1	1	0	1	1	1	0	0	0
1	0	0	1	0	0	1	0	1	0
1	0	1	1	0	1	1	1	0	0
1	1	0	1	1	0	1	1	1	0
1	1	1	1	1	1	0	0	0	1

Note that the same approach can be used to design a 3-bit counter that switches between states in any order. For example, we can thus design a counter that follows the Gray code, rather than straight binary. The student is advised to design such a counter.

TABLE 15.15 Excitation table using T flip-flops

y_3	y_2	y_1	$x = 0$			$x = 1$		
			T_3	T_2	T_1	T_3	T_2	T_1
0	0	0	0	0	0	0	0	1
0	0	1	0	0	0	0	1	1
0	1	0	0	0	0	0	0	1
0	1	1	0	0	0	1	1	1
1	0	0	0	0	0	0	0	1
1	0	1	0	0	0	0	1	1
1	1	0	0	0	0	0	0	1
1	1	1	0	0	0	1	1	1

TABLE 15.16 Excitation table using of 3-bit counter using JK flip-flops

y_3	y_2	y_1	$x = 0$			$x = 1$		
			J_3K_3	J_2K_2	J_1K_1	J_3K_3	J_2K_2	J_1K_1
0	0	0	0 d	0 d	0 d	0 d	0 d	1 d
0	0	1	0 d	0 d	d 0	0 d	1 d	d 1
0	1	0	0 d	d 0	0 d	0 d	d 0	1 d
0	1	1	0 d	d 0	d 0	1 d	d 1	d 1
1	0	0	d 0	0 d	0 d	d 0	0 d	1 d
1	0	1	d 0	0 d	d 0	d 0	1 d	d 1
1	1	0	d 0	d 0	0 d	d 0	d 0	1 d
1	1	1	d 0	d 0	d 0	d 1	d 1	d 1

15.31 State Minimization

A sequential machine may have redundant states. A redundant state is one that is equivalent to another state, producing the same output whatever the sequence of inputs. Eliminating redundant states leads to state minimization and, in general, the number of memory elements needed to represent the machine states. We view here briefly an approach to state minimization. The approach starts by grouping together states that have no conflicting outputs for the same input, we thus obtain blocks of states with non-conflicting outputs. Subsequently we separate states which are in the same block but which under any input lead to successor states (next states) that are not in the same block. This operation is repeated until it is found that the no new block partitions are formed.

To illustrate the process consider the machine M_1 described by Table 15.17.

Initially all the states are in the same block

$$P_0 = (ABCDEFGH)$$

Comparing the outputs of these states under the two inputs $x = 0$ and $x = 1$ we construct two blocks, obtaining the new partition

$$P_1 = (ACDGH)(BEF)$$

Now we note that states A , G , and H with input $x = 0$ lead to the successors E and F which are in the same block in P_1 . The same is found if the input is instead $x = 1$. The states (AGH) thus stay in the same block. On the other hand, the successors of states A

TABLE 15.17 State table of Machine M_1

Present State	Next State	
	$x = 0$	$x = 1$
A	E, 1	F, 1
B	E, 0	C, 1
C	D, 1	B, 1
D	H, 1	F, 1
E	F, 0	G, 1
F	E, 0	H, 1
G	F, 1	E, 1
H	E, 1	E, 1

and C with input $x = 0$ are E and D which are in separate blocks. State C has to be removed, therefore, from the $(ACDGH)$ block. Similarly states A and D with $x = 0$ lead to successors E and H which are in different blocks. State D should therefore be also removed from the block $(ACDGH)$. Proceeding similarly we obtain the new partition

$$P_2 = (AGH)(C)(D)(B)(EF)$$

The successors of states A , G , and H are E and F , which are in the same block. Those of E and F are E and F if $x = 0$ and G and H if $x = 1$. Since in both cases the successors are in the same block no further splitting of blocks is need and P_2 is the final equivalence partition. The states A , G and H , being in the same block are equivalent states and can be replaced by one state. Similarly, states E and F are equivalent and can be replaced by one state. Let us call the successive block $\alpha = (AGH)$, $\beta = (C)$, $\gamma = (D)$, $\delta = (B)$ and $\epsilon = (EF)$. These become the new states. We obtain the reduced machine state table shown as Table 15.18.

TABLE 15.18 State table of Machine M_1

Present State	Next State	
	$x = 0$	$x = 1$
α	$\epsilon, 1$	$\epsilon, 1$
β	$\gamma, 1$	$\delta, 1$
γ	$\alpha, 1$	$\epsilon, 1$
δ	$\epsilon, 0$	$\beta, 1$
ϵ	$\epsilon, 0$	$\alpha, 1$

We thus end up with five instead of eight states. They can now be assigned 3-bit codes 000, 001, ... and we may realize the circuit using SR or JK flip-flops, draw the Karnaugh maps and find the S and R or J and K equations, as seen above.

Simplification of incompletely specified machines is obtained by following a similar approach but where compatible, rather than equivalent, state are identified. The approach will be studied in the context of asynchronous sequential machines.

15.32 Asynchronous Sequential Machines

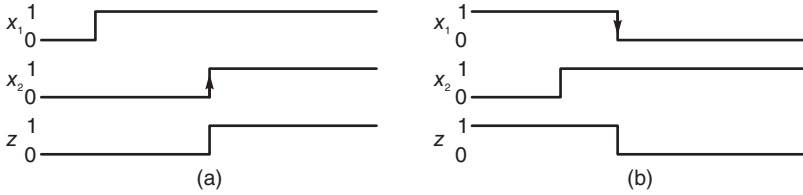


FIGURE 15.49 Waveform description of asynchronous machine requirements.

In many applications, inputs to sequential circuits are not synchronized by a clock. They may occur at any time and the circuit behavior depends on their sequence of values, whenever these values are received. As an example of an asynchronous sequential machine, consider the design of an asynchronous sequential machine which we shall refer to as circuit M_0 . This circuit has two inputs x_1 and x_2 and an output z . The transition of the output z from 0 to 1 and from 1 to 0 depends on the states of the inputs x_1 and x_2 as can be seen in Fig. 15.49 (a) and (b) respectively. Note that the output z should change from 0 to 1 if while input x_1 is 1, input x_2 changes from 0 to 1, and that z should change from 1 to 0 if while input x_2 is 1, input x_1 changes from 1 to 0.

To draw the state diagram of the machine, we may start by representing schematically the output z as a function of different possible values of inputs. This is illustrated in Fig. 15.50. From this figure we note that particular combinations of inputs x_1 and x_2 and output z are possible distinct states of the circuit. As can be seen in the figure, we identify eight such states. We now construct a state table starting from the initial state $x_1 = x_2 = z = 0$. We denote this state by the symbol ①; the circle meaning that it is a stable state.

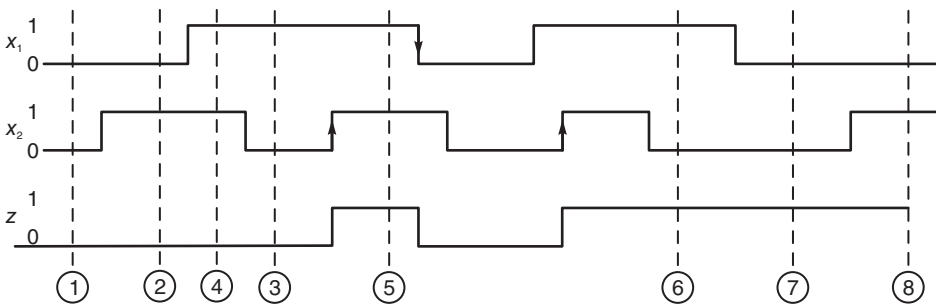


FIGURE 15.50 Waveform of asynchronous machine showing eight possible states.

For an asynchronous sequential circuit to function properly, only one input bit can change at any instant of time. The input x_1x_2 can change from 00 to 01 or from 11 to 01, say, but not from 00 to 11 nor from 10 to 01. The state transition table, referred to as the *primitive flow table*, of the required sequential circuit appears as Table 15.19.

TABLE 15.19 Primitive flow table

Present State	Next state, output			
	$x_1x_2 = 00$	$x_1x_2 = 01$	$x_1x_2 = 11$	$x_1x_2 = 10$
①	①, 0	2	–	3
②	1	②, 0	4	–
③	1	–	5	③, 0
④	–	2	④, 0	3
⑤	–	2	⑤, 1	6
⑥	7	–	5	⑥, 1
⑦	⑦, 1	8	–	6
⑧	7	⑧, 1	5	–

Each line in the table corresponds to a stable state and shows under which input it is stable. For example, state ⑥ is stable under the input 10 and the circuit output should be 1. From state ① an input $x_1x_2 = 10$ leads to unstable state 3 as seen on the first line, which becomes stable state ③ on the third line, with an output $z = 0$. If the circuit is at state ③ and the input changes to $x_1x_2 = 11$, the circuit moves to unstable state 5, ending up in stable state ⑤ and produces $z = 1$, as can be seen on line 5. If the circuit is in stable state ③ and the input changes to $x_1x_2 = 00$ it changes to state 1, ending up in the initial state ① and produces an output $z = 0$.

15.33 State Reduction

Sequential machines are often incompletely specified. Some input transitions are not allowed, such as simultaneous change of more than one bit, and cases where either the input is illegal or the output is not specified. Such don't care conditions may lead to a possible minimization of logic functions and even the number of states of a sequential circuit. There are several approaches to state reduction. One approach is to start by drawing a *merger graph* corresponding to the flow table. The graph has as many vertices as the machine's stable states. To illustrate this approach, consider the same eight-state asynchronous sequential circuit M_0 given above.

The merger graph corresponding to this machine is shown in Fig. 15.51(a).

This graph is used to reveal *compatible states*. These are states which, after transitions following changes of the input, do not lead to states with conflicting outputs when specified. If the machine is stable in state S_1 and upon receiving an input x_0 switches to state S_2 , then S_2 is called the x_0 -successor of S_1 . Two states are compatible if, receiving any input, have compatible successors, i.e. successors that have un-conflicting outputs.

As an illustration, consider the asynchronous machine M_0 . We note that states ① and ② under any of the inputs $x_1x_2 = 00, 01, 11$, and 10 have no conflicting successors as seen by the first two lines of the table. In the merge graph, therefore, vertices 1 and 2 are joined by a solid line. Consider now states ② and ③. As seen in lines 2 and 3 of the table, the successor states under input $x_1x_2 = 11$ are 4 and 5. Whether or not states ② and ③ are compatible depends on whether or not states 4 and 5 under subsequent inputs will lead to compatible successors. In the merger graph, therefore, the arc joining states 2 and 3 is interrupted by the connectivity condition, or *implied pair* (4, 5), implying such dependency on these states for compatibility.

We note further that states ④ and ⑤ are in fact, incompatible, since under input $x_1x_2 =$

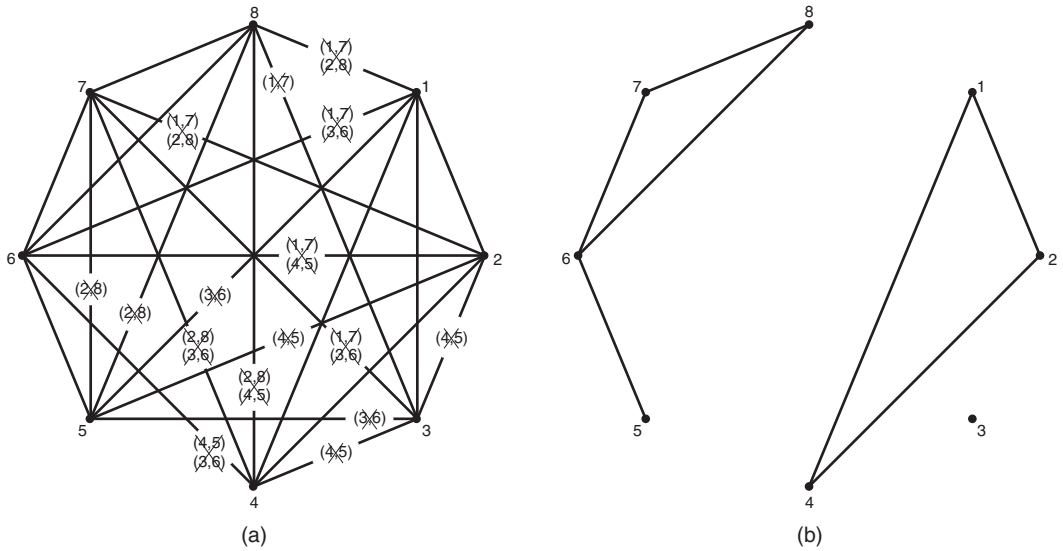


FIGURE 15.51 Merger graph of a sequential machine.

11, their outputs are conflicting. In the merger graph, therefore, states 4 and 5 are not connected. Similarly, the pairs of state ② and ⑧, ① and ⑦, and ③ and ⑥ are incompatible pairs.

The following step is to reduce the merger graph by crossing out any arcs that are interrupted by implied pairs of states that we found to be incompatible. For example, having identified the pair of states ④ and ⑤ to be incompatible, we can remove the arc connecting vertices 2 and 3 that has implied pair (4, 5) interrupting it. Applying this simplification to completion, we obtain the reduced merger graph shown in Fig. 15.51(b).

The following step is to group compatible states into larger sets of mutually compatible states whenever possible. From this figure, we can see that the set of maximal compatibles covering the machine is $\{(1, 2, 4), (3), (5, 6), (6, 7, 8)\}$. Note that states 5 and 6 form a compatible set. However, state 6 is already covered by the set (6, 7, 8), hence a minimum covering is $\{(1, 2, 4), (3), (5), (6, 7, 8)\}$.

An alternative to the merger graph that may be more convenient for larger machines is the *merger table*. For the same machine M_0 , Fig. 15.52 shows the corresponding merger table. This table lists compatible pairs of states and their implied pairs. Each cell in the table shows the compatibility or absence thereof of a pair of states. For an n -state machine, states along the horizontal axis are S_1, S_2, \dots, S_{n-1} . Those on the vertical axis are S_2, S_3, \dots, S_n . A cell at the intersection of S_i of the horizontal axis and S_j of the vertical one describes the compatibility of the two states. The figure shows the compatibilities and implied pairs of each pair of our eight-state machine M_0 . In a similar way to that followed using the merger graph, cells are crossed out if their enclosed implied pairs prove to be incompatible. Thus the cell at the intersection 2 and 3 encloses the implied pair (4, 5). Since this pair is itself incompatible, the cell of intersection 2-3 is crossed out.

Once all incompatible cells have been crossed out, we proceed in the table from the right grouping incompatible pairs, forming larger sets enclosing mutually compatible states whenever possible. We thus obtain the set of maximum compatibles $\{(1, 2, 4), (3), (5, 6), (6, 7, 8)\}$. We conclude that four states suffice to describe this machine. As found above, a minimal covering is $\{(1, 2, 4), (3), (5), (6, 7, 8)\}$. The reduced state table is shown as Table 15.20.

Assigning the codes 00, 01, 11, and 10 to the new states (5), (3), (1, 2, 4), and (6, 7, 8),

2	✓						
3	✓	4,5					
4	✓	✓	4,5				
5	3,6	4,5	3,6	×			
6	3,6 1,7	4,5 1,7	×	4,5 3,6	✓		
7	×	1,7 2,8	3,6 1,7	3,6 2,8	2,8	✓	
8	2,8 1,7	×	1,7	2,8 4,5	2,8	✓	✓
	1	2	3	4	5	6	7

FIGURE 15.52 Merger-Table of a sequential machine.

TABLE 15.20 State table

	00	01	11	10
(5)	–	2, 0	⑤, 1	6, 1
(3)	1, 0	–	5, 1	③, 0
(1, 2, 4)	①, 0	②, 0	④, 0	3, 0
(6, 7, 8)	⑦, 1	⑧, 1	5, 1	⑥, 1

respectively, we obtain the state transition and output table, seen as Table 15.21.

TABLE 15.21 Transition and output table

Present State y_1y_2	Next state, output			
	$x_1x_2 = 00$	$x_1x_2 = 01$	$x_1x_2 = 11$	$x_1x_2 = 10$
00	–	11, 0	00, 1	10, 1
01	11, 0	–	00, 1	01, 0
11	11, 0	11, 0	11, 0	01, 0
10	10, 1	10, 1	00, 1	10, 1

Drawing the Karnaugh maps describing the variables Y_2 , Y_1 , and z we obtain

$$Y_2 = \bar{x}_1 + \bar{x}_2\bar{y}_2 + x_2y_1y_2$$

$$Y_1 = \bar{x}_1\bar{y}_1 + \bar{x}_2y_2 + y_1y_2$$

$$Z = x_1x_2\bar{y}_1 + x_1\bar{y}_2 + y_1\bar{y}_2$$

The circuit realization is shown in Fig. 15.53.

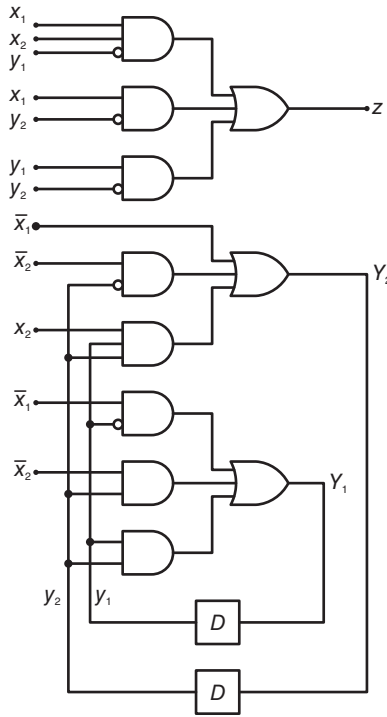


FIGURE 15.53 Logic circuit realization of an asynchronous machine.

15.34 Control Counter Design for Generator of Prime Numbers

As an illustration of the design of a control counter to govern the sequencing of operations in a digital processor we consider the problem of designing a prime numbers generator [13] [52]. The algorithm for generating the first 1024 numbers starts by recognizing the first two prime numbers as $Prime(1) = 2$ and $Prime(2) = 3$. The following prime numbers cannot be even, and a prime number is not divisible by any number except 1 and itself. To test if a number N is prime we effect the division $N/Prime(k)$ with $k = 2$. We write

$$N/Prime(k) = Q + R$$

If $R = 0$ the number N is not prime. If $R \neq 0$ and $Q \leq Prime(k)$ then N is prime; otherwise set $k = k + 1$ and the division $N/Prime(k)$ is effected. This process is repeated until $R = 0$ or else $Q \leq Prime(k)$.

The first step in designing the control unit is to determine the basic components needed to implement the algorithm. These can be seen in Fig. 15.54. We use a prime numbers memory (PNM), with a capacity of 1024 words. This memory has an associated address register AR for storing the value k . Two registers G and P are used for storing indexes j and k , respectively. Register N stores the successive numbers N to be tested. Division A/Q is effected by successive subtractions of the content of register B which contains the divisor $Prime(k)$ from the dividend N which is in register A . The result of subtraction is the difference D and borrow-out bit. We assume a register length of $n = 12$ bits. The least significant bit (LSB) is b_0 and the most significant is b_{n-1} . The borrow-out bit will

be denoted W_n . Division is performed by successively subtracting register B from A and counting, by incrementing register Q , the number of times successful subtractions, i.e. with borrow $W_n = 0$ occur. A one-bit flag register labeled U receives the borrow bit W_n . The figure also shows a control register M connected to a decoder and a combinatorial logic circuit.

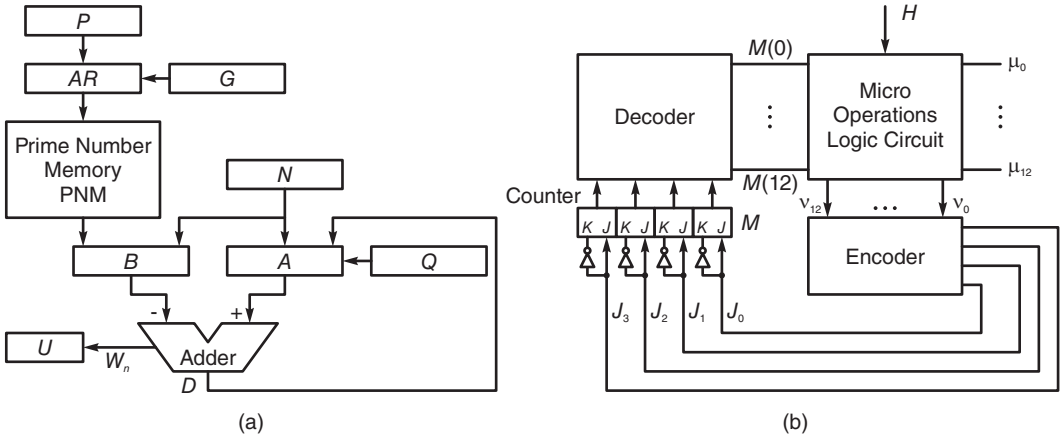


FIGURE 15.54 Prime number generator hardware components.

15.34.1 Micro-operations and States

The processor performs micro-operations μ_1 to μ_{13} . These can be seen in the flowchart of Fig. 15.55. Also shown in the figure are states S_0, S_1, \dots, S_{12} , which can be assigned to the distinct stages of progress during the execution of the algorithm. In addition, we may denote the micro-operations setting the control register to the required state during processing by the symbols $\nu_0, \nu_1, \dots, \nu_{12}$, where the signal ν_i forces the register to state S_i . The control counter M , connected to a one of 16 decoder as seen in Fig. 15.54. When the counter is in state S_i the decoder output $M(i)$ is at logic 1. This is the case for all states, i.e., for $i = 0, 1, 2, \dots, 12$.

The micro-operations μ_1 to μ_{13} can be seen in the flowchart of Fig. 15.55 next to the boxes that include them. As stated D stands for the difference resulting of subtracting B from A and W_n stands for borrow. In fact, we may write for $i = 0, 1, \dots, n - 1$

$$D_i = B_i \bar{A}_i \bar{W}_i + \bar{B}_i \bar{A}_i W_i + B_i A_i W_i + \bar{B}_i A_i \bar{W}_i$$

and

$$W_{i+1} = B_i \bar{A}_i + B_i \bar{W}_i + \bar{A}_i W_i$$

D_i being the difference bit and W_{i+1} the resulting borrow bit. The resulting leftmost borrow bit W_n is transferred to register U indicating a borrow condition when $W_n = 1$.

At any clock time, the states and conditions for branching determine the micro-operations to be performed. Table 15.22 shows such relation between the states S_0 to S_{12} , the results of tests and the micro-operations μ_1 to μ_{13} . These operations are synchronized by the clock labeled H in the figures.

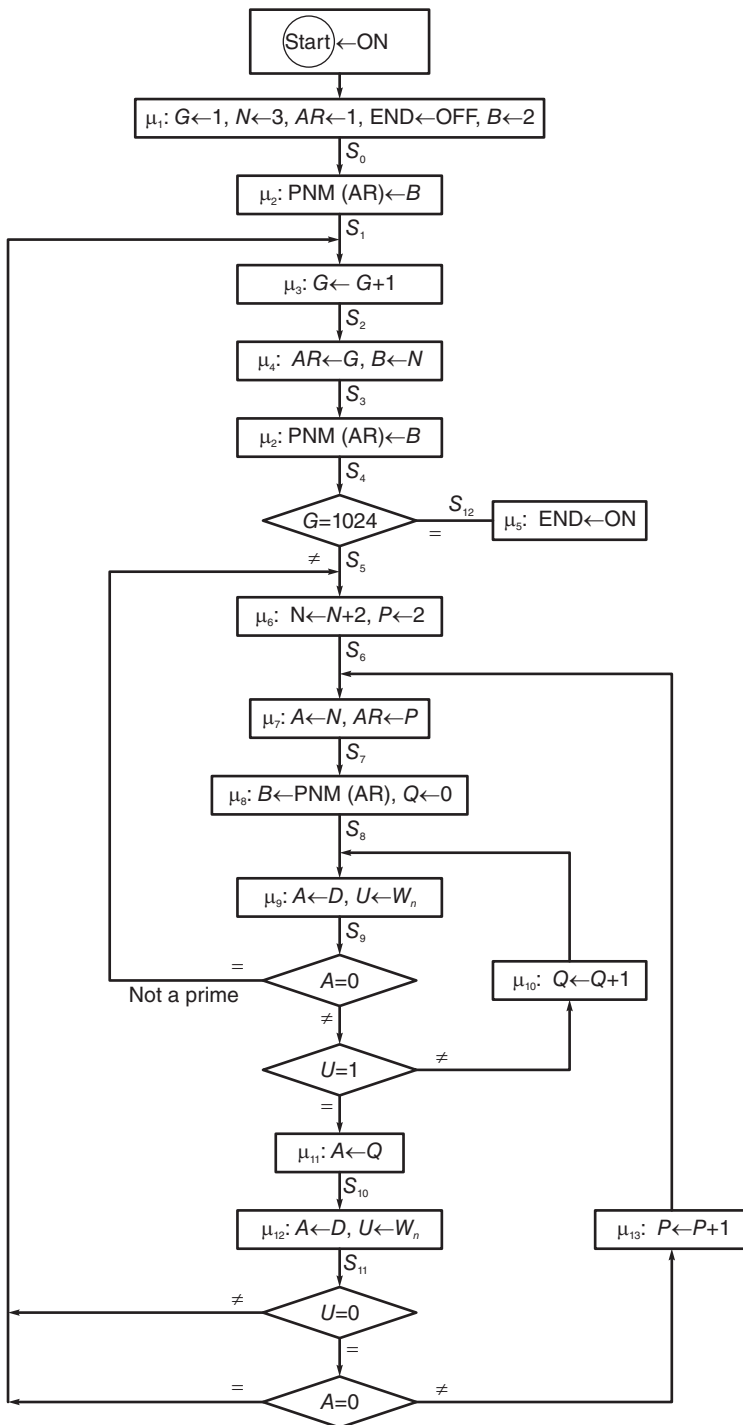


FIGURE 15.55 Prime number generator block diagram.

From the tables we may define the micro-operations as functions of states and conditions. We have

$$\begin{aligned}\mu_1 &= (START \leftarrow ON) \\ \mu_2 &= S_0 + S_3, \mu_3 = S_1, \mu_4 = S_2, \\ \mu_5 &= S_4.GEQ1024 + S_{12}, \mu_6 = S_4.\overline{GEQ1024} + S_5, \\ \mu_7 &= S_6, \mu_8 = S_7, \mu_9 = S_8, \\ \mu_{10} &= S_9.\overline{AEQ0}.\overline{UEQ1}, \mu_{11} = S_9.\overline{AEQ0}.UEQ1, \\ \mu_{12} &= S_{10}.\end{aligned}$$

The counter-setting signals are given by

$$\begin{aligned}\nu_0 &= (START \leftarrow ON), \nu_1 = S_0 + S_{11}.\overline{UEQ0} + S_{11}.AEQ0, \nu_2 = S_1, \nu_3 = S_2, \\ \nu_4 &= S_3, \nu_5 = S_4.\overline{GEQ1024} + S_9.AEQ0 + S_{11}.UEQ0.\overline{AEQ0}, \\ \nu_6 &= S_5, \nu_7 = S_6, \nu_8 = S_7 + S_9.\overline{AEQ0}.\overline{UEQ1}, \nu_9 = S_8, \\ \nu_{10} &= S_9.\overline{AEQ0}.UEQ1, \nu_{11} = S_{10}, \\ \nu_{12} &= S_4.GEQ1024 + S_{12}.\end{aligned}$$

The micro-operation signals μ_1 to μ_{13} are thus generated by a combinatorial circuit, of which the inputs are the signals indicating the states of the counter S_i and the test results, such as $\overline{AEQ0}$, $GEQ1024$, ...

The control register setting signals ν_i are similarly generated using a combination logic circuit of which the inputs are again the signals S_i denoting the states and the test results.

The control register is 4 bits long since it should store 12 states. Receiving an input setting signal ν_i it is set to state S_i . With a register made of JK flip flops, Table 15.24 shows the J and K inputs required to set the counter as desired. A straight forward realization yields

$$\begin{aligned}J_3 &= \nu_8 + \nu_9 + \nu_{10} + \nu_{11} + \nu_{12} \\ J_2 &= \nu_4 + \nu_5 + \nu_6 + \nu_7 + \nu_{12} \\ J_1 &= \nu_2 + \nu_3 + \nu_6 + \nu_7 + \nu_{10} + \nu_{11} \\ J_0 &= \nu_1 + \nu_3 + \nu_5 + \nu_7 + \nu_9 + \nu_{11}\end{aligned}$$

and

$$K_i = \bar{J}_i, \quad i = 1, 2, 3.$$

The logic circuit of the prime numbers generator micro-operations is shown in Fig. 15.56. We may, alternatively, bypass generating the control counter state-setting ν_0 to ν_{12} signals, replacing them by four flip-flop setting signals, to be directly applied to the counter's four flip-flops; thus forcing the new state of the counter at every clock. To this end, let the counter state S_i be coded as $y_3y_2y_1y_0 = (i)_2$. For example, the counter in state S_{10} has the contents $y_3y_2y_1y_0 = 1010$. As can be seen in the flowchart of Fig. 15.55, the counter state will increase by one, i.e. from S_i to S_{i+1} unconditionally for $i = 0, 1, 2, 3$, for example. On the other hand, if the counter is in state S_4 , i.e. 0100 it will change to state S_5 if $MEQ1024 = 0$ and to state S_{12} if $MEQ1024 = 1$. If the counter is in state S_9 , i.e. 1001, it will change to state S_5 if $AEQ0 = 1$, and to state S_{10} i.e. 1010 if $\overline{AEQ0}.UEQ1 = 1$, otherwise it will go to state $S_8 = 1000$ if $\overline{AEQ0}.\overline{UEQ1} = 1$. Moreover, if the counter is in state S_{11} , i.e. 1011, it will change state to S_1 if $(\overline{UEQ0} + AEQ0) = 1$, and to state S_6 i.e. 0110 if $\overline{AEQ0} = 1$.

TABLE 15.24 Control register T states and JK inputs

State	JK inputs			
	J_0K_0	J_1K_1	J_2K_2	J_3K_3
$\nu_0 \implies M \leftarrow 0$	0 1	0 1	0 1	0 1
$\nu_1 \implies M \leftarrow 1$	0 1	0 1	0 1	0 1
$\nu_2 \implies M \leftarrow 2$	0 1	0 1	1 0	0 1
$\nu_3 \implies M \leftarrow 3$	0 1	0 1	1 0	1 0
$\nu_4 \implies M \leftarrow 4$	0 1	1 0	0 1	0 1
$\nu_5 \implies M \leftarrow 5$	0 1	1 0	0 1	1 0
$\nu_6 \implies M \leftarrow 6$	0 1	1 0	1 0	0 1
$\nu_7 \implies M \leftarrow 7$	0 1	1 0	1 0	1 0
$\nu_8 \implies M \leftarrow 8$	1 0	0 1	0 1	0 1
$\nu_9 \implies M \leftarrow 9$	1 0	0 1	0 1	1 0
$\nu_{10} \implies M \leftarrow 10$	1 0	0 1	1 0	0 1
$\nu_{11} \implies M \leftarrow 11$	1 0	0 1	1 0	1 0
$\nu_{12} \implies M \leftarrow 12$	1 0	1 0	0 1	0 1

By drawing the Karnaugh maps of next-state variables Y_3, Y_2, Y_1, Y_0 of the counter, while taking into account the conditions for the state transitions as just observed, and the fact that the states 1101, 1110, 1111 are don't care states that may be used to simplify the logic, we obtain

$$\begin{aligned}
 Y_0 &= y_1\bar{y}_0 + \bar{y}_2\bar{y}_0 + \overline{MEQ1024}\bar{y}_0 + y_3AEQ0 + \overline{UEQ0}y_3y_1 \\
 Y_1 &= y_1\bar{y}_0 + \bar{y}_3\bar{y}_1y_0 + \bar{y}_2y_1\bar{y}_0 + \bar{y}_1y_0.\overline{AEQ0}UEQ1 + y_3y_1.UEQ0.\overline{AEQ0}. \\
 Y_2 &= y_2\bar{y}_1 + y_2\bar{y}_0 + \bar{y}_3\bar{y}_2y_1y_0 + y_3\bar{y}_1y_0 + y_3y_1y_0.UEQ0.\overline{AEQ0}. \\
 Y_3 &= y_2y_1y_0 + y_3\bar{y}_0 + y_3\bar{y}_1.\overline{AEQ0} + y_2\bar{y}_1\bar{y}_0.MEQ1024.
 \end{aligned}$$

These are the counter-setting signals, applied directly to the D input of the counter's D type flip-flops. This approach requires less hardware since it generates directly the four counter state-setting signals, rather than generate first the ν signals followed by their conversion to the four signals required to set the counter's four flip-flops.

15.35 Fast Transform Processors

We shall start with FFT processors followed by generalized Walsh and generalized spectral analysis processors. We have seen in Chapter 7 that an optimal factorization of the FFT wherein all iterations data to be accessed are constantly separated by a fixed maximum distance, thus allowing to store all vectors in maximum length queues leading to wired-in processor architecture. Moreover, we have seen that the ordered input/ordered output (OIOO) factorization

$$F_N = T_N f = \prod_{m=1}^n (p_m \mu_m S) f \tag{15.246}$$

operates on a properly ordered input data vector f and produces a properly ordered set of Fourier coefficients F_N . In what follows we focus our attention on the resulting processor architecture.

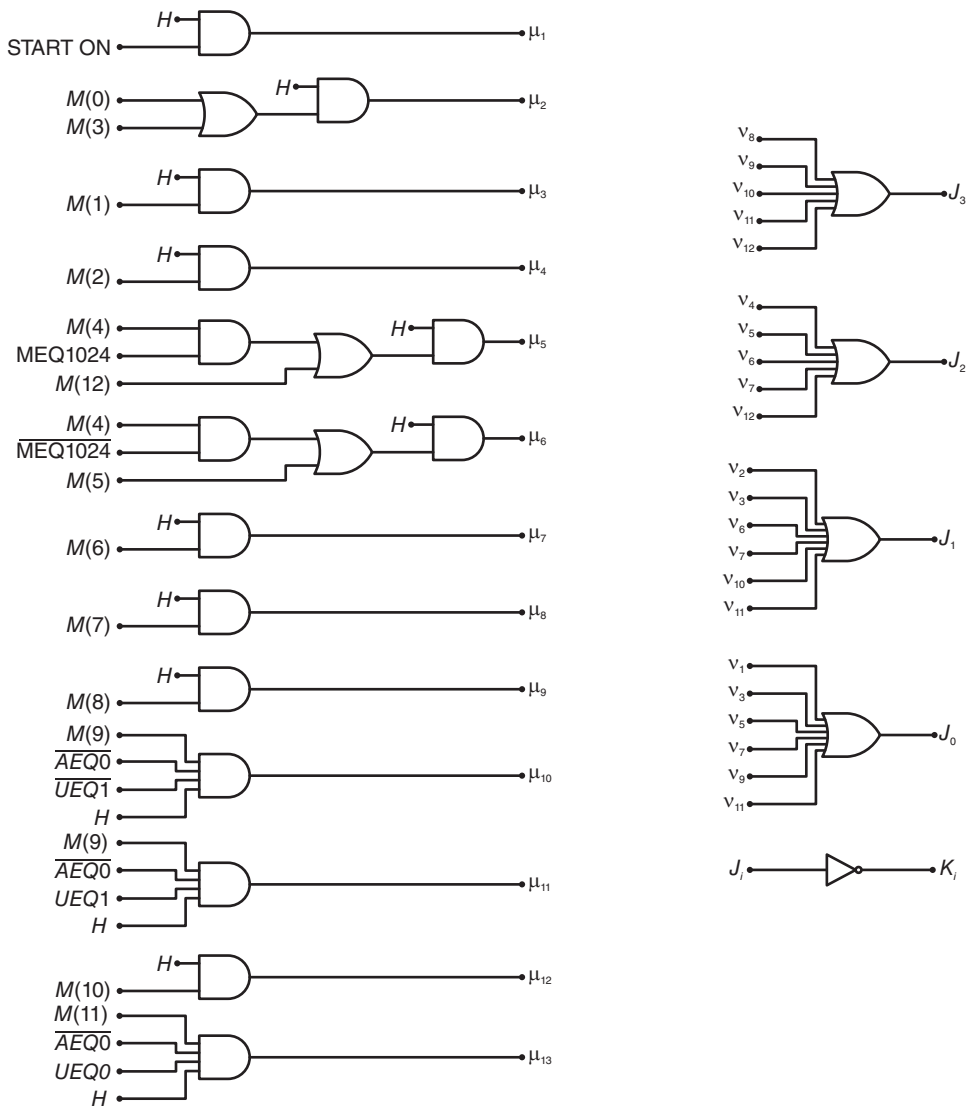


FIGURE 15.56 Logic circuit of prime numbers generator micro-operations.

Figure 15.57 shows the basic radix-2 machine organization for implementing the OIOO machine-oriented algorithm. The set of data points are gated-in in a parallel-bit serial-word form, from the input terminal “In” into the “input memory” which can be in the form of a set of long dynamic shift registers. The input memory is divided into two halves, $N/2$ bits long each. If dynamic registers are used, then each half of the input memory consists of $2W$ such registers, where W is the word length of the real part and that of the imaginary part.

The first step is to apply the addition-subtraction process described by the operator S . Thus the elements f_0 and $f_{N/2}$ are added and subtracted.

The following step is to multiply the result of subtraction by the appropriate weighting coefficient (w^k). This is performed in the wired-in complex multiplier designated by a square box which includes a \times sign in the figure.

The weighting operation corresponding to the element of the matrix μ_n is thus performed.

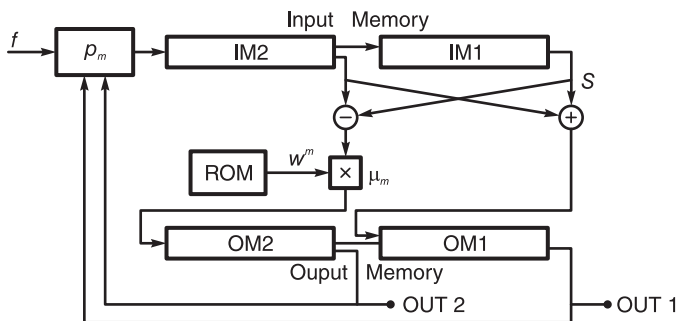


FIGURE 15.57 Radix-2 FFT wired-in processor.

The next step is to store the results of addition and multiplication into the set of output registers “output memory.” The output memory is identical in construction to the input memory and is designated by the two sets “A” and “M” in the figure.

The words in the input memory are then shifted one bit to the right, and the process repeated for the following two words f_1 and $f_{N/2+1}$. The two words are added and subtracted and the result of subtraction is weighted by the appropriate weighting coefficient. The results of addition and multiplication are stored into the output memory and the Process repeated for every successive pair of data (f_i and $f_{i+N/2}$).

The contents of the “A” and “M” memories are then fed back into the input memory. The feedback process is made to include the permutation operations by controlling the sequence in which the outputs of the “A” and “M” memories are gated into the Input Memory. Use is made of the first stage of an n -bit binary counter to alternately gate the contents of the “A” and “M” memories into the input memory. Thus, the permutation operator p_n , which calls for the repeated gating-in of one word of the “A” memory followed by another of the “M” memory, is implemented.

At the end of the feedback process, the “input memory” includes the results of the first iteration. The subsequent iterations are similarly performed by applying the appropriate sets of weighting coefficients using the ROM and performing the appropriate permutations in the feedback process, as controlled by the successive stages of the binary counter.

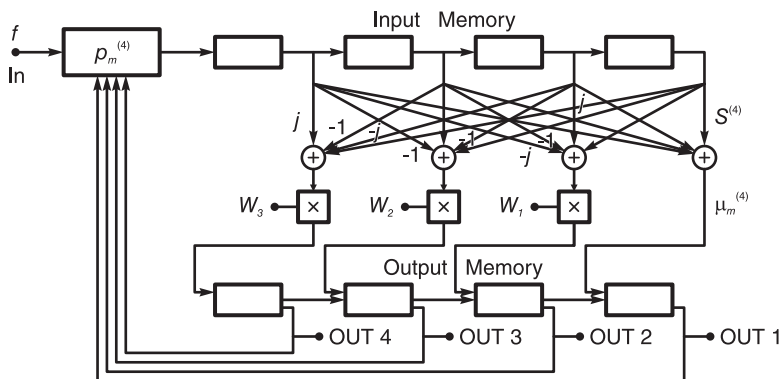


FIGURE 15.58 Parallel radix-4 FFT wired-in processor.

At the end of the n iterations, the output coefficients appear in the proper order. The processor has the advantage of being wired-in, requiring no addressing and is capable of operating in real time with a minimum of control unit requirements. The architecture of a parallel Radix-4 FFT wired-in processor [22] is shown in Fig. 15.58.

The general radix high-speed no feedback algorithm described in Chapter 7 leads to a parallel architecture that is virtually wired-in. This is shown for radix-4 in Fig. 15.59 and is described in detail in [15] [22] [28]. The approach has been applied to optimal massive parallelism of generalized spectral analysis transforms [16] [20]. Real time applications of such parallel high speed processors, as encountered for example in radar signal processing, can be seen in [43].

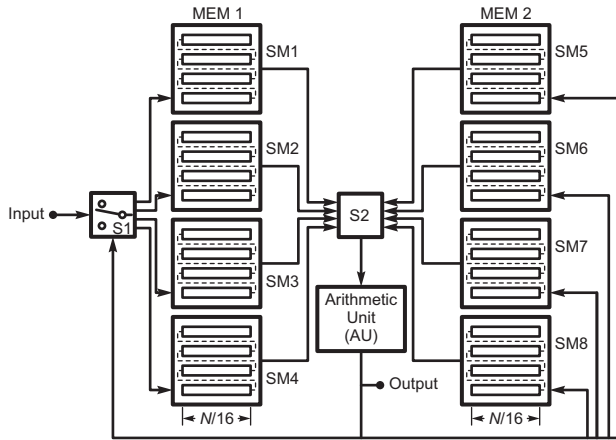


FIGURE 15.59 Parallel radix-4 FFT high speed processor.

15.36 Programmable Logic Arrays (PLAs)

A programmable logic array (PLA) is a semiconductor device that can be programmed to implement logic functions. In configuring a PLA the user needs only program the prime implicants, that is, the necessary products, of the logic functions to be implemented. This is in contrast with programmable read only (PROM) memories, which require programming each and every canonical product term thereof. The PLA has in general a programmable ANDing matrix, of which the outputs are connected to a set of programmable OR gate planes. As an illustration consider the implementation of the three logic functions f_1 , f_2 , and f_3 which are given in terms of four logic variables x_1 , x_2 , x_3 and x_4 by the sum of products logic equations

$$f_1 = x_1 \overline{x_2} x_3 x_4 \vee \overline{x_1} x_2 x_3 \vee \overline{x_1} x_3 \vee \overline{x_3} \overline{x_4}$$

$$f_2 = x_2 \overline{x_3} \vee \overline{x_1} x_2 x_3 \vee x_1 \overline{x_3} \overline{x_4} \vee \overline{x_1} x_3$$

$$f_3 = \overline{x_2} \overline{x_3} \vee x_1 \overline{x_3} \overline{x_4} \vee \overline{x_1} x_2 x_3 \vee \overline{x_3} \overline{x_4}.$$

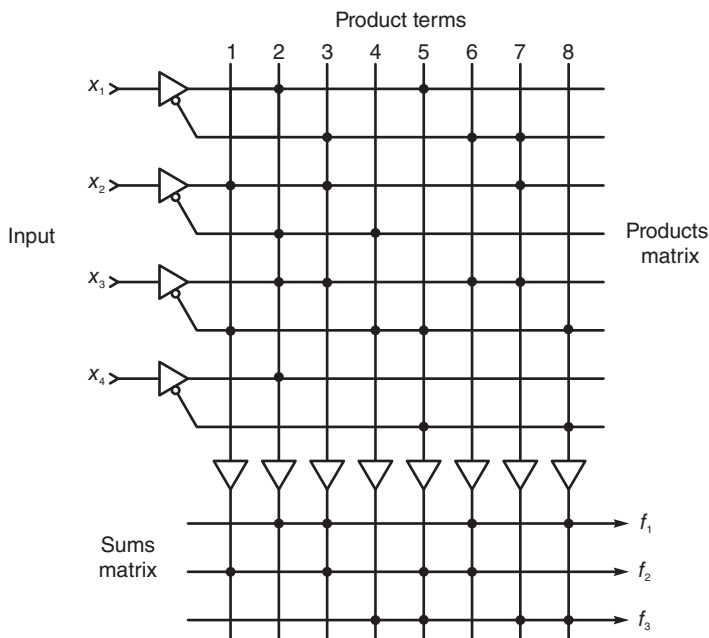


FIGURE 15.60 PLA logic circuit.

The mapping of these functions on a PLA can be seen in Fig. 15.60. For each of the functions, f_1 , f_2 , and f_3 , the dots in the products matrix correspond to the variables that need to be ANDed, and those in the sums section correspond to the terms that need to be ORed, to implement the function. Note the efficiency of such implementation. If a PROM is used, instead, each function would require programming the entire set of sixteen binary values of the set $x_1x_2x_3x_4$, for a total of 48 terms.

Not all PLAs are field-programmable. Many are programmed during manufacture similarly to a mask-programmed ROM. In particular, those PLAs which are embedded in more complex integrated circuits such as microprocessors are mask-programmed during manufacture. Those that can be programmed after manufacture are called FPLA (Field-programmable PLA).

15.37 Field Programmable Gate Arrays (FPGAs)

A field-programmable gate array (FPGA) is a semiconductor chip that can be configured and reconfigured, if need be, by the designer; hence the name “field programmable.” Xilinx® Inc. co-founders, Ross Freeman and Bernard Vonderschmitt, invented the first commercially viable field programmable gate array in 1985.

FPGAs can be used to implement any logic function that an application-specific integrated circuit (ASIC) could perform, but is in addition re-configurable and field-programmable. They contain programmable logic components called *configurable logic blocks* (CLBs), and a hierarchy of reconfigurable interconnects between blocks. A CLB can be configured as simple logic gates, like AND, OR and XOR, or to perform complex combinational functions. In most FPGAs, the CLBs include in addition memory elements, which may be simple

flip-flops or more complete blocks of memory, ROMs and RAMs. On a single chip nowadays, an FPGA includes thousands of CLBs. Moreover, an FPGA chip includes hundreds of *input/output blocks* (IOBs), each equipped with combinatorial logic, multiplexers and memory elements.

Figure 15.61 shows a high-level Altera Inc. Stratix IV GX chip view. Stratix IV GX devices provide up to 32 transceiver channels per device with physical coding sublayer (PCS) and physical medium attachment (PMA) support at data rates between 600 Mbps and 8.5 Gbps. Up to 16 additional channels with PMA-only support at data rates between 600 Mbps and 3.2 Gbps are also available, for a total of up to 48 transceiver channels per device.

Shown in the figure are phase locked loop (PLL) components. Also shown are several units of a Peripheral Component Interconnect (PCI) Express, an expansion card standard. The PCI Express hard intellectual property (IP) block embeds all layers of the PCI Express protocol stack. General-purpose I/O and high-speed low-voltage differential signaling (LVDS) I/O with dynamic phase alignment (DPA) mode, and soft clock data recovery (CDR) mode support is available as indicated in the figure.

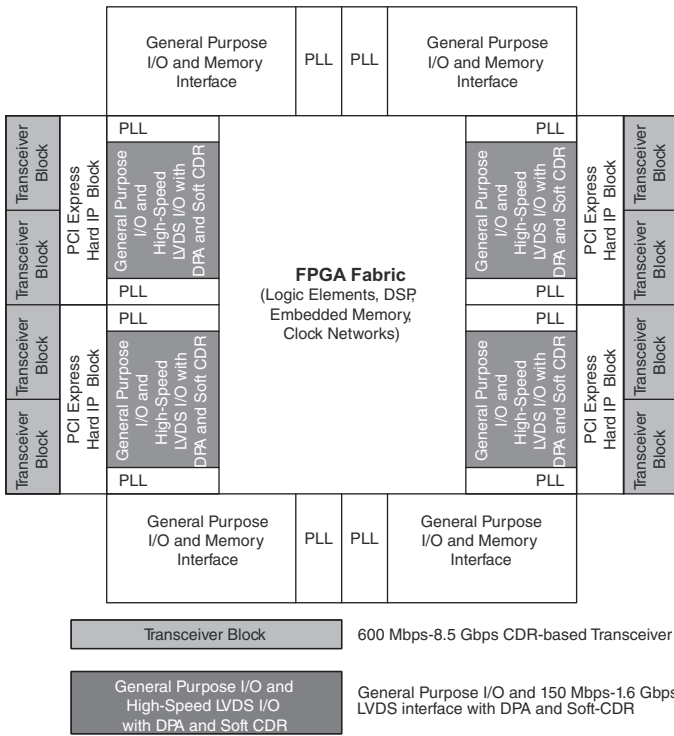


FIGURE 15.61 Altera Stratix-IV-GX Chip.

An FPGA can be programmed by simply drawing a block diagram of the desired architecture, by writing a program in C language, or *ar* source code in a hardware description language (HDL) [66] [74].

An FPGA chip contains several logic-function generators, multiplexers and flip-flops. The designer can thus construct any conceivable processor, be it a combinatorial logic unit, a

sequential machine, a digital filter, a digital signal processor, a microprocessor or a digital computer.

15.38 DSP with Xilinx FPGAs

The following is a brief description in Xilinx literature by Jesse Jenkins, Xilinx engineer, of the evolution of FPGA technology and its increasing popularity among DSP design engineers in recent years.

“Xilinx FPGAs have been around for 25 years. Early products consisted of regular arrays of static-memory based “Look-Up Tables” (LUTs) along with local flip-flops interconnected with a set of segmented connections. The contents of the LUTs and the connections made with the segments offered an extremely versatile framework for designers to create custom tailored logic solutions. Within the first 10 years of manufacture, these devices were discovered by DSP developers, who successfully developed their algorithms exploiting inherent parallel capability not offered by standard DSP processors. This opened a collaborative door between Xilinx FPGA architects and DSP designers.

Initially, improvements were incremental. Xilinx fabric was enhanced to add special circuitry to speed up fast carry operations within the fabric, with specially developed carry chains (fast paths) operating in conjunction with the LUTs. This sped up addition, but did little to improve fabric-based multiplication. Next, a tiny AND gate was married into the LUT arrangement to work in collaboration with the LUTs and carry chains to speed up ‘partial products,’ which now made fabric-based Multiply Accumulates possible. FPGAs became serious candidates as DSP engines at that point.

Xilinx then shifted directions by introducing first the Virtex families, then the Virtex-II families. Virtex parts introduced special blocks of configurable static block RAM (BRAM), which permitted fast load and store operations for data, but also pre-computed partial operations to be loaded in advance, to perform specialty operations. At this point, DSP became a serious market segment for the Virtex families. Virtex-II included fast, larger multipliers into the Virtex framework, making Multiply-Accumulate a building block. Also, Xilinx began serious collaboration with The MathWorks to offer solutions using the computational and simulation resources of MATLAB[®] and Simulink[®] along with Xilinx ISE development tools to form a framework known as System Generator.

Performance focus shifted from multiplication, to the whole calculation of Multiply-Accumulate with the introduction of the Virtex-4 family and its included DSP48 blocks.”

A Xilinx DSP48 tile can be seen in Fig. 15.62. A simplified model of a DSP48 slice can be seen in Fig. 15.63.

“In this simplified version, the DSP48 includes both wide multiplication paths along with high speed addition, and natural feedback and direct cascading paths for operations that can proceed across multiple blocks. It offers a set of instructions to configure the block for a large list of common DSP operations (Add, Subtract, Multiply, MAC, etc.). All operations are 2’s complement and integer based, and a lot of thought has been designed in to handle overflow as well as designer chosen rounding choices. The DSP48 block consists of two identical ‘slices’ and parts exist with varying numbers of the DSP48 blocks.”

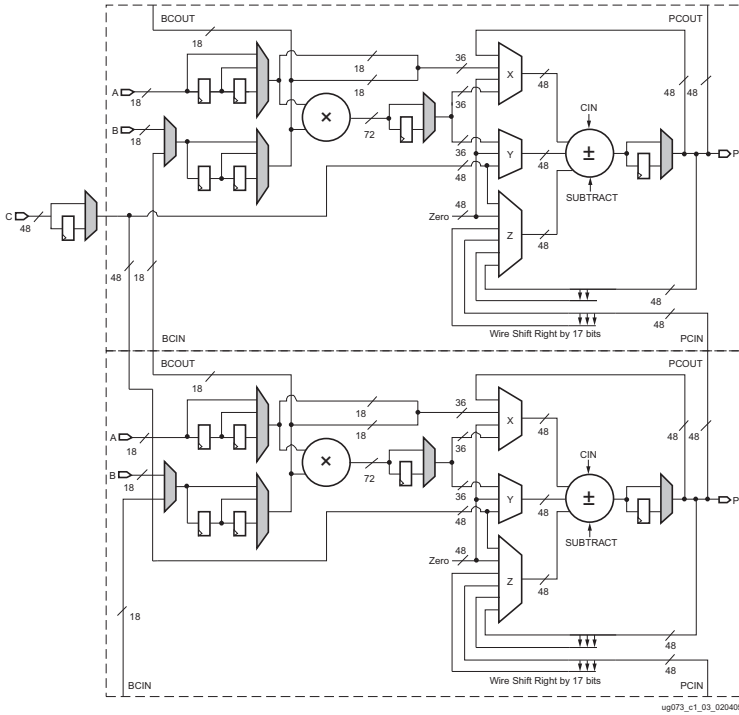


FIGURE 15.62 Xilinx DSP48 tile.

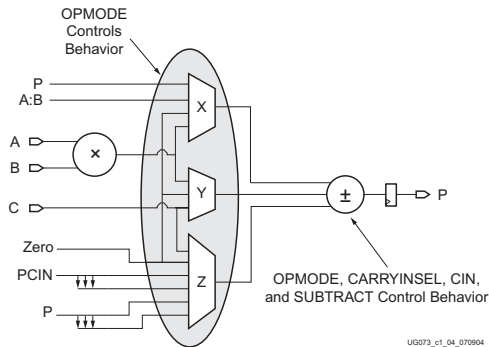


FIGURE 15.63 Simplified DSP48 slice model.

15.39 Texas Instruments TMS320C6713B Floating-Point DSP

In what follows, an overview of a Texas Instruments high performance DSP is presented. We shall view the overall architecture and in particular the central processing unit (CPU) of this DSP chip. The purpose is to allow the student to start by writing a simple program and see the result of real-time processing on the DSP. It may be argued that once capable of writing and executing a simple program, the student should be able to subsequently write any program of whatever complexity and be able to execute and verify it on the same DSP chip.

The following can be readily understood by the student even in the absence of the actual hardware. The presentation is made to help the student understand the system concepts without having to execute the instructions on the DSP itself. Naturally, sooner or later in order to truly appreciate the technology and use it for real-time applications the student would be advised to apply these concepts directly on the TI DSP Starter Kit *DSK*, which is depicted in Fig. 15.64. In this figure the main components, such as the DSP chip, the A/D and D/A conversion Codec unit, memories, JTAG and input and output lines, can be seen.

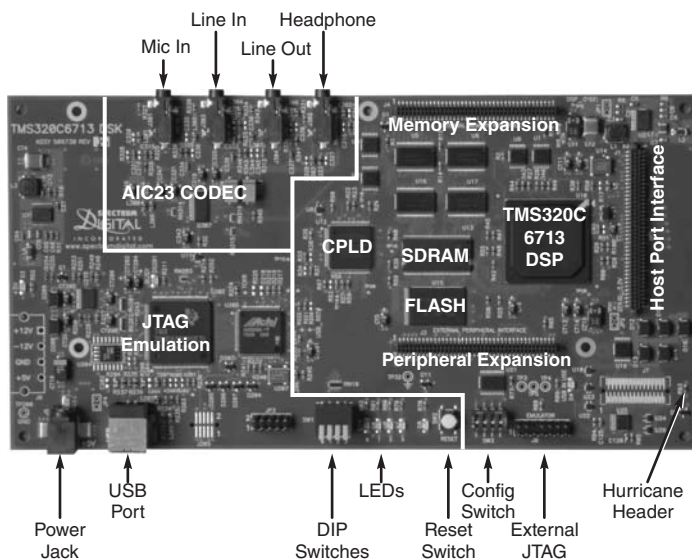


FIGURE 15.64 TMS320C6713 DSP Starter Kit.

What can also be most reassuring to the student and the engineer in general is that, as we shall see, detailed knowledge of the processor architecture and modus operandi is an asset but not absolute necessity for the proper and full utilization of the DSP. Thanks to a collaboration between Texas Instruments Inc. and The MathWorks Corp. it is possible to use Simulink® to draw a block diagram of the desired system. MATLAB would then map the desired system onto the DSP, thus configuring it for real-time processing as if it has been directly applied by the user for the purpose.

The TMS320C67xx, or C67xx for short, family of C6000 DSPs and in particular the TMS320C6713B, represented schematically in Fig. 15.65 uses very long instruction word

(VLIW) architecture and is well suited for multichannel and multifunction applications. The following are extracts from the Texas Instruments data sheets on these devices.

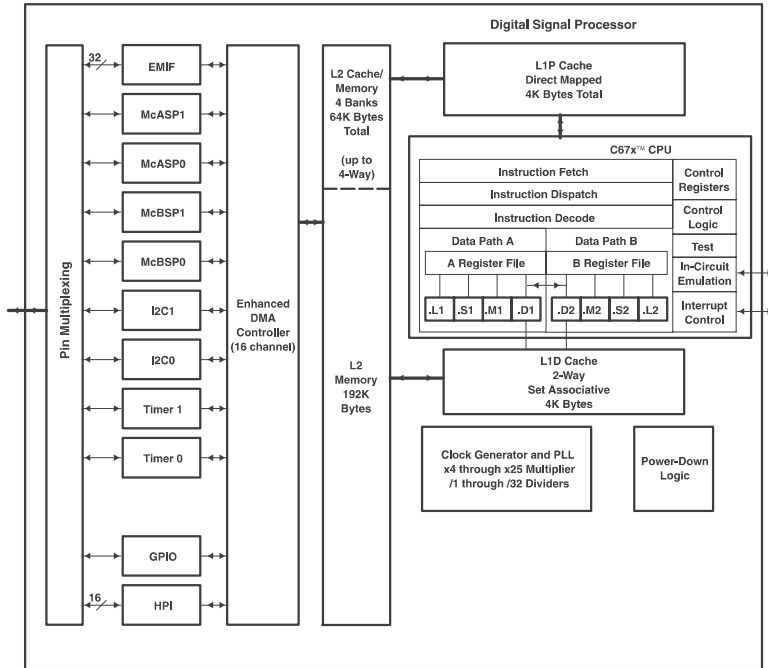


FIGURE 15.65 Texas Instruments TMS320C6713B.

Operating at 300 MHz, the TMS320C6713B delivers up to 1800 million floating-point operations per second (MFLOPS), 2400 million instructions per second (MIPS), and with dual fixed-/floating-point multipliers up to 600 million multiply-accumulate operations per second (MMACS). The DSP is packaged as a 208-pin integrated circuit IC chip.

The C6713B uses a two-level (L1 and L2) cache memory-based architecture. The name “cache memory” refers to fast high speed static RAM (SRAM). The level number reflects the level of proximity to and accessibility by the central processing unit CPU.

The Level 1 **program cache** (L1P) is a 4K-Byte direct-mapped cache and the Level 1 **data cache** (L1D) is a 4K-Byte 2-way set-associative cache. The Level 2 memory/cache (L2) consists of a 256K-Byte memory space that is shared between program and data space. Of these, 64K Bytes can be configured as direct-mapped memory, cache, or combinations of the two. The remaining 192K Bytes in L2 serves as mapped static RAM SRAM.

The C6713B has a large peripheral set that includes two Multi-channel Audio Serial Ports (McASPs), two Multi-channel Buffered Serial Ports (McBSPs), two Inter-Integrated Circuit (I2C) buses, one dedicated General-Purpose Input/Output (GPIO) module, two general-purpose timers, a host-port interface (HPI), and a glueless external memory interface (EMIF) capable of interfacing to SDRAM, to synchronous burst static SBSRAM, and to asynchronous peripherals.

The two I2C ports on the TMS320C6713B allow the DSP to easily control peripheral devices and communicate with a host processor. In addition, the standard multi-channel buffered serial port (McBSP) may be used to communicate with serial peripheral interface

(SPI) mode peripheral devices.

The TMS320C67xx DSP generation is supported by the Texas Instruments eXpressDSP™ set of development tools, including a highly optimizing C/C++ Compiler, the Code Composer Studio™ Integrated Development Environment (IDE), JTAG-based emulation and real-time debugging, and the DSP/BIOS™ kernel.

15.40 Central Processing Unit (CPU)

The CPU of the TMS320C6713B fetches 256 bits long instruction words to supply up to eight 32-bit instructions to the eight *functional units* .L1, .S1, .M1, .D1, .L2, .S2, .M2 and .D2, as can be seen in Fig. 15.66, during every clock cycle. The VLIW supplies instructions to functional units only if they are ready to execute. The first bit of every 32-bit instruction determines if the next instruction belongs to the same *execute packet* as the previous instruction, or whether it should be executed in the following clock as a part of the next execute packet. Fetch packets are always 256 bits wide. However, memory saving is achieved by allowing execute packets to vary in size.

As shown in the figure the eight functional units are divided in two sets, each containing four functional units. With each of the two sets the CPU contains a register file of 16 32-bit registers. As seen in the figure the two sets of functional units, along with their register files, compose two opposite sides, sides *A* and *B* of the CPU. The four functional units on each side of the CPU can freely share access to their 16 registers. Moreover, each side can access the register files on the opposite side.

The CPU executes fixed-point instructions, and six out of eight functional units (.L 1, .S1, .M1, .M2, .S2, and .L2) also execute floating-point instructions. The remaining two functional units (.D1 and .D2) also execute an “LDDW” instruction which loads 64 bits per CPU side for a total of 128 bits per cycle.

All instructions operate on registers (as opposed to data in memory). Data transfers between the register files and memory are effected by the two *data-addressing units* .D1 and .D2. The data address issued by a .D unit allows transferring data addressed by one register file to or from the opposite register file.

The C67x CPU supports a variety of indirect addressing modes using either linear- or circular-addressing with 5- or 15-bit offset. All instructions are conditional, and most can access any one of the 32 registers. Some registers, however, are singled out to support specific addressing or to hold the condition for conditional instructions (if the condition is not automatically “true”).

The two .M functional units are dedicated to multiplication. The two .S and .L functional units perform arithmetic, logical, and branch functions. Instruction processing begins when a 256-bit-wide instruction fetch packet is fetched from a program memory. The 32-bit instructions destined for the individual functional units are “linked” together by “1” bits in the least significant bit (LSB) position of the instructions. The instructions that are thus “chained” together for simultaneous execution (up to eight in total) compose an execute packet. A “0” in the LSB of an instruction breaks the chain, effectively placing the instructions that follow it in the next execute packet. If an execute packet crosses the fetch-packet boundary (256 bits wide), the assembler places it in the next fetch packet, while the remainder of the current fetch packet is padded with No Operation (NOP) instructions.

The number of execute packets within a fetch packet can thus vary from one to eight. Execute packets are dispatched to their respective functional units at the rate of one per

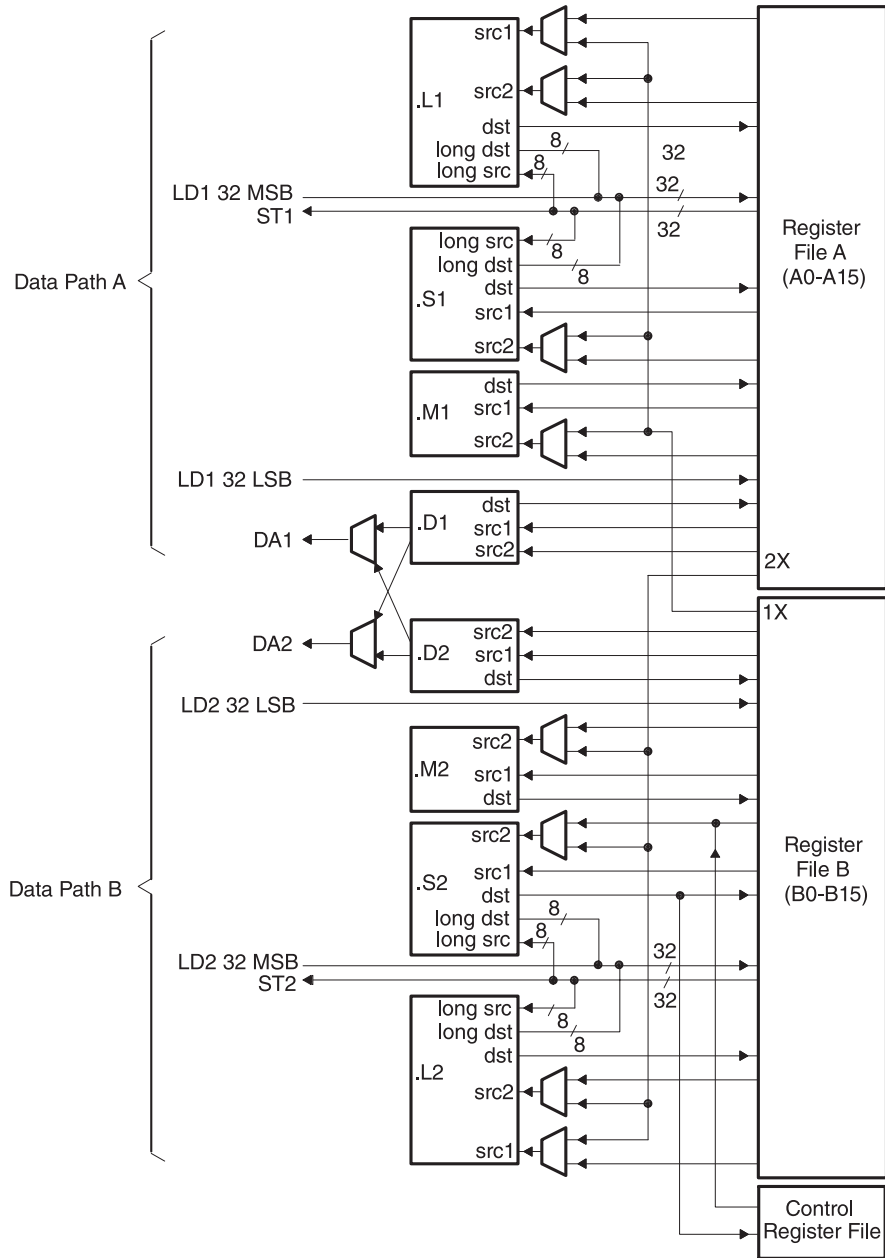


FIGURE 15.66 Texas Instruments TMS320C6713B CPU.

clock cycle and the next 256-bit fetch packet is not fetched until all the execute packets from the current fetch packet have been dispatched. After decoding, the instructions drive simultaneously all active functional units for a maximum execution rate of eight instructions every clock cycle. While most results are stored as words in 32-bit registers, they can also be subsequently moved to memory as bytes or half-words. All load and store instructions are byte-, 16-bit half-word, or word-addressable.

The CPU and Instruction set of the TMS320C6713B DSP are described by the excellent specifications documentation of Texas Instruments. The reader is referred to the *TMS320C6000 CPU and Instruction Set Reference Guide*, TI Literature No. SPRU189F.

The TMS320C6713B DSP has dedicated hardware for single-precision (32-bit) and double-precision (64-bit) IEEE floating-point operations, 32×32 -bit integer multiply with a 32- or 64-bit result, among other multiplications such as four 8×8 bit multiplies every clock cycle.

The TMS320C67x DSP pipeline can dispatch eight parallel instructions every cycle. The pipeline has three main stages, namely, Fetch, Decode and Execute. The Fetch stage has four phases. The Decode stage has two phases. The Execute stage requires a varying number of up to 10 phases, depending on the type of instruction. The Fetch phases of the pipeline are

- PG:** Program address generate
- PS:** Program address send
- PW:** Program access ready wait
- PR:** Program fetch packet receive

The Decode phases of the pipeline are

- DP:** Instruction Dispatch
- DC:** Instruction Decode

The Execute portion of the fixed point pipeline is divided into five phases, while that of the floating-point pipeline is divided into 10 phases.

15.41 CPU Data Paths and Control

The data paths, cross-paths and register files of the TMS320C67xx are shown in Fig. 15.66. The figure shows two general-purpose register files (*A* and *B*), the eight functional units (.L1, .L2, .S1, .S2, .M1, .M2, .D1, and .D2), two load-from-memory data paths (LD1 and LD2), two store-to-memory data paths (ST1 and ST2), two data address paths (DA1 and DA2) and two register file data cross paths (1X and 2X).

15.41.1 General-Purpose Register Files

There are two general-purpose register files (*A* and *B*) in the data paths. Each of these files contains 16 32-bit registers (*A0–A15* for file *A* and *B0–B15* for file *B*). The general-purpose registers can be used for data, data address pointers, or condition registers.

The general purpose register files support data ranging in size from packed 16-bit data through 40-bit fixed-point and 64-bit floating-point data. Values larger than 32 bits, such as 40-bit long and 64-bit float quantities, are stored in register pairs. In these the 32 LSBs of data are placed in an even-numbered register and the remaining 8 or 32 MSBs in the next upper register (which is always an odd-numbered register). Packed data types store either four 8-bit values or two 16-bit values in a single 32-bit register, or four 16-bit values in a 64-

bit register pair. In assembly language syntax, a colon between two register names denotes a register pair, and the odd-numbered register appears on the left, such as in $A13 : A12$.

15.41.2 Functional Units

A table summarizing the the operations performed by the different functional units is shown in Fig. 15.67 and Fig. 15.68, where SP stands for single precision and DP for double precision. Each functional unit has its own 32-bit write port into a general-purpose register file. All units ending in 1 (for example, .L1) write to register file A , and all units ending in 2 write to register file B . Each functional unit has two 32-bit read ports for source operands $src1$ and $src2$. Four units (.L1, .L2, .S1, and .S2) have an extra 8-bit-wide port for 40-bit long writes as well as an 8-bit input for 40-bit long reads. Because each unit has its own 32-bit write port (destination line dst), when performing 32-bit operations all eight units can be used in parallel.

Functional Units and Operations Performed

Functional Unit	Fixed-Point Operations	Floating-Point Operations
.L unit (.L1, .L2)	32/40-bit arithmetic and compare operations 32-bit logical operations Leftmost 1 or 0 counting for 32 bits Normalization count for 32 and 40 bits Byte shifts Data packing/unpacking 5-bit constant generation Dual 16-bit arithmetic operations Quad 8-bit arithmetic operations Dual 16-bit min/max operations Quad 8-bit min/max operations	Arithmetic operations DP → SP, INT → DP, INT → SP conversion operations
.S unit (.S1, .S2)	32-bit arithmetic operations 32/40-bit shifts and 32-bit bit-field operations 32-bit logical operations Branches Constant generation Register transfers to/from control register file (.S2 only) Byte shifts Data packing/unpacking Dual 16-bit compare operations Quad 8-bit compare operations Dual 16-bit shift operations Dual 16-bit saturated arithmetic operations Quad 8-bit saturated arithmetic operations	Compare Reciprocal and reciprocal square-root operations Absolute value operations SP → DP conversion operations

FIGURE 15.67 TMS320C6713B .L and .S functional units and operations performed.

15.41.3 Register File Cross Paths

As represented schematically in Fig. 15.66, each functional unit reads from and writes to the register file within its own data path, that is, the .L1, .S1, .D1, and .M1 units write to register file A and the .L2, .S2, .D2, and .M2 units write to register file B . In addition, the register files are connected to the opposite-side register file’s functional units via the 1X and 2X cross paths. The 1X cross path allows the functional units of data path A to read their source input from register file B , and the 2X cross path allows the functional units of data

Functional Units and Operations Performed (Continued)

Functional Unit	Fixed-Point Operations	Floating-Point Operations
.M unit (.M1, .M2)	16 x 16 multiply operations 16 x 32 multiply operations Quad 8 x 8 multiply operations Dual 16 x 16 multiply operations Dual 16 x 16 multiply with add/subtract operations Quad 8 x 8 multiply with add operation Bit expansion Bit interleaving/de-interleaving Variable shift operations Rotation Galois Field Multiply	32 X 32-bit fixed-point multiply operations Floating-point multiply operations
.D unit (.D1, .D2)	32-bit add, subtract, linear and circular address calculation Loads and stores with 5-bit constant offset Loads and stores with 15-bit constant offset (.D2 only) Load and store double words with 5-bit constant Load and store non-aligned words and double words 5-bit constant generation 32-bit logical operations	Load doubleword with 5-bit constant offset

Note: Fixed-point operations are available on all three devices. Floating-point operations and 32 x 32-bit fixed-point multiply are available only on the C67x. Additional C64x functions are shown in bold.

FIGURE 15.68 TMS320C6713B .M and .D functional units and operations performed.

path *B* to read their source from register file *A*. Six of the eight functional units have access to the register file on the opposite side, via a cross path. As shown in Fig. 15.65, the source input src2 of each of the functional units S1, .M1, .S2, and .M2 are selectable between the same side register file and the cross path. In the case of the units .L1 and .L2, both sources src1 and src2 inputs are selectable between the same-side register file and the cross path.

15.41.4 Memory, Load, and Store Paths

The C67xx has four 32-bit paths for loading data from memory to the register file: two paths LD1 for register file *A*, and two paths LD2 for register file *B*. This allows the double precision LDDW instruction to simultaneously load two 32-bit values into register file *A* and two 32-bit values into register file *B*. For side *A*, LD1a is the load path for the 32 LSBs and LD1b is the load path for the 32 MSBs. For side *B*, LD2a is the load path for the 32 LSBs and LD2b is the load path for the 32 MSBs.

As shown in Fig. 15.65 there are also two 32-bit paths, ST1 and ST2, for storing register values to memory from each register file. On the C6000 architecture, some of the ports for long and double word operands are shared between functional units. This places a constraint on which long or double word operations can be scheduled on a data path in the same execute packet.

15.41.5 Data Address Paths

As shown in Fig. 15.66 the data address paths DA1 and DA2 are each connected to the .D units in both data paths. This allows data addresses generated by any one path to access data to or from any register. The DA1 and DA2 units and their associated data paths are specified as T1 and T2 respectively. T1 consists of the DA1 address path and the LD1 and

ST1 data paths. LD2 is comprised of LD2a and LD2b to support 64-bit loads. The T1 and T2 designations appear in functional unit fields for load and store instructions. For example, the following load instruction uses the .D1 unit to generate the address but is using the LD2 path resource from DA2 to place the data in the *B* register file. The use of the DA2 resource is indicated with the T2 designation LDW .D1T2 *A0[3], B1

15.42 Instruction Syntax

The syntax of an instruction of the TI family of DSPs has the form of an instruction mnemonic followed by the associated functional unit, a source and a destination. For example, the Load a Word from Memory instruction LDW has the syntax **LDW** (.unit) *src*, *dst*, where .unit = .L1, .L2, .S1, .S2, .D1, or .D2. *src* and *dst* mean source and destination, respectively. The (.unit) specifies which functional unit the instruction is mapped to (.L1, .L2, .S1, .S2, .M1, .M2, .D1, or .D2). For each instruction, a table is included in the *Instructions Reference Guide* listing the opcode map fields, that is, the source and destination, the units (.unit) the instruction is mapped to, the types of operands, and the opcode. The **ADD** instruction for example has three opcode map fields: *src1*, *src2*, and *dst*.

Instructions are moreover accompanied by information regarding the details of execution in the CPU pipeline. This is presented in the form of a table which lists the sources, the destinations and the functional unit used during each execution cycle of the instruction.

15.43 TMS320C6000 Control Register File

As can be seen in Fig. 15.66, one functional unit, namely, .S2, can read from and write to the control register file. The components of the control register and their usage are summarized in what follows.

AMR Addressing mode register. Specifies whether to use linear or circular addressing for each of eight registers. Contains, moreover, sizes for circular addressing.

CSR Control status register. Contains the global interrupt enable bit, cache control bits, and other miscellaneous control and status bits.

IFR Interrupt flag register. Displays status of interrupts.

ISR Interrupt set register. Allows manually setting pending interrupts.

ICR Interrupt clear register. Allows manually clearing pending interrupts.

IER Interrupt enable register. Allows enabling/disabling of individual interrupts.

ISTP Interrupt service table pointer. Points to the beginning of the interrupt service table.

IRP Interrupt return pointer. Contains the address to be used to return from a maskable interrupt.

NRP Nonmaskable interrupt return pointer. Contains the address to be used to return from a nonmaskable interrupt.

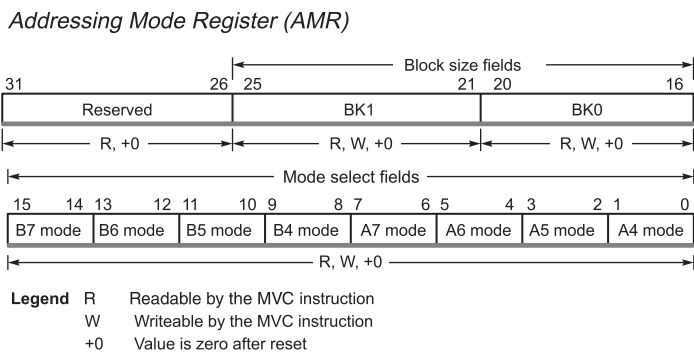
PCE1 Program counter, E1 phase. Contains the address of the fetch packet that is in the E1 pipeline stage.

Each control register is accessed by the Move instruction **MVC**. Some of the control register bits are accessed alternatively. For example, arrival of a maskable interrupt on

an external interrupt pin, INT_m, triggers the setting of flag bit IFR_m. Subsequently, the processing of that interrupt triggers the clearing of IFR_m and the global interrupt enable bit, GIE. Finally, when that interrupt processing is complete, the **B IRP** instruction, in the interrupt service routine, restores the pre-interrupt value of the GIE. Similarly, saturating instructions like **SADD** set the SAT bit in the Control Status Register CSR.

15.44 Addressing Mode Register (AMR)

For each of the eight registers (*A4-A7, B4-B7*) that can perform linear or circular addressing, the AMR specifies the addressing mode. A 2-bit field for each register specifies the address modification mode: linear (the default) or circular mode. With circular addressing, the field also specifies which BK (block size) field to use for a circular buffer. In addition, the buffer must be aligned on a byte boundary equal to the block size. The mode select fields and block size fields, together with the mode select field encoding table are shown in Fig. 15.69.



Addressing Mode Register (AMR) Mode Select Field Encoding

Mode	Description
0 0	Linear modification (default at reset)
0 1	Circular addressing using the BK0 field
1 0	Circular addressing using the BK1 field
1 1	Reserved

FIGURE 15.69 Addressing mode register.

The reserved portion of the AMR is always 0. The block size fields BK0 and BK1 contain 5-bit values used in evaluating block sizes for circular addressing. If the 5-bit value is *N* then *BlockSize* = 2^{*N*+1} bytes. For example, if *N* = 10011₂ = 19₁₀ then *BlockSize* = 2²⁰ = 1048576.

15.44.1 Addressing Modes

All registers can perform linear addressing. Only eight registers can perform circular addressing, namely, *A4-A7* and *B4-B7*.

The load, store add and subtract instructions

LDB(U)/LDH(U)/LDW,STB/STH/STW, ADDAB/ADDAH

/ADDAW/ADDAD, and SUBAB/SUBAH/SUBAW all use the AMR to determine the required type of addressing.

Writing to the AMR Register

The Move instructions **MVK**, **MVKLH** and **MVC** can be used to configure the AMR register in order to perform linear or circular addressing. For example, to use register *A6* for circular addressing with Block BK0 field $N = 9$ implying a block size of $2^{N+1} = 1024$ bytes, the *A6* Mode Select bits, 4 and 5, of the AMR should be set to $M = 01$, as seen above, and the BK0 field, bits 16-20 should be set to the value 9. This can be obtained by loading the lower then upper 16-bit desired codes to a register such as *B2* and then transferring the contents of the *B2* register to the AMR, as shown in the following code segment (values such as 0×0010 are in hexadecimal):

MVK .S2, 0x0010, B2; Move lower 16 bits to *B2*, for *A6* Mode to equal 01

MVKLH .S2 0x0009, B2; Move upper 16 bits to *B2*, to set BK0 = 9

MVC .S2 B2, AMR; Move *B2* contents to AMR

Linear and circular addressing and different kinds of addressing modes using the AMR register are described in more detail in what follows.

15.45 Syntax for Load/Store Address Generation

The instructions of the TMS320C67xx allow in general accessing 32-bit words, 16-bit half-words and 8-bit bytes. Advancing through memory by m words implies advancing by $4m$ bytes while advancing by m half words means advancing by $2m$ bytes. A conversion to number of bytes is effected in decoding instructions as will be seen shortly.

Indirect addressing is used in loading or storing data. In such addressing mode the actual address is the content of a register or its content plus or minus a displacement called an offset. Figure 15.70 shows the syntax of indirect addressing of memory.

Addressing Type	No Modification of Address Register	Preincrement or Pre-decrement of Address Register	Postincrement or Postdecrement of Address Register
Register indirect	*R	*++R *--R	*R++ *R--
Register relative	*+R[ucst5] *-R[ucst5]	*+R[ucst5] *-R[ucst5]	*R++[ucst5] *R--[ucst5]
Register relative with 15-bit constant offset	*+B14/B15[ucst15]	not supported	not supported
Base + index	*+R[offsetR] *-R[offsetR]	*+R[offsetR] *-R[offsetR]	*R++[offsetR] *R--[offsetR]

FIGURE 15.70 Indirect address generation for Load/Store instructions.

The following addressing types are listed:

1. **Register indirect addressing.** Indirect addressing in its simplest form means accessing memory at an address that is the content of one of the CPU 32 registers $A0-A15$, $B0-B15$; the register thus serving as a *pointer* to the required memory location. The syntax is $*R$, as shown in the table. In another form of indirect addressing, the address register R is preincremented and the result is the true memory address to be accessed. In this case the syntax is $*++R$. Alternatively, the register content is used as the memory address to be accessed and, subsequently, the register content is post-incremented in preparation for a subsequent instruction to access the following location. The syntax in this case is $*R++$. As the table shows, pre- and post-increment operations may be replaced by pre- and post-decrement ones, the syntax being $*--R$ and $*R-$, respectively.
2. **Register Relative Addressing.** The syntax $*+R[ucst5]$ calls for accessing the memory location at the address that is the sum of the content of register R , called the *base register* and the unsigned 5-bit constant $ucst5$, called the *displacement* or *offset*. The single $+$ sign implies that the register content itself is not altered, in contrast with the double plus sign $++$ which causes the register content to be altered as stated in the Table column headings. The second form of register relative addressing is the syntax $*++R[ucst5]$. This is a register preincrement mode, meaning that the register content is preincremented by the amount $ucst5$ and the result is the address of memory location to be accessed. The syntax $*R++[ucst5]$ leads to accessing memory at the address contained in the register R and, subsequently, incrementing the register content by adding to it the value $ucst5$. If the single plus sign is replaced by a minus sign then the displacement $ucst5$ is subtracted from rather than added to the register content (R). Similarly, if the double plus sign ($++$) is replaced by a double minus sign ($--$) then the same as above applies except incrementing the register content is replaced by decrementing it.
3. **Register Relative with 15-bit Constant Offset.** If a large offset is required for a load/store the $B14$ or $B15$ register may be used as the base register and a 15-bit constant $ucst15$ as the offset. As shown in the table the syntax $*+B14/B15[ucst15]$ specifies either register $B14$ or $B15$ as the base register, to the content of which the displacement $ucst15$ should be added to obtain the required memory address; without altering the register content itself since only one plus sign is included.
4. **Base + Index Addressing.** This last entry in the table is similar to the Register Relative Addressing except for the fact that the displacement, or offset, here is not a specific constant $ucst$ but, rather, a value that is the content of an offset register referred to as “*offsetR*.”

15.45.1 Linear Addressing Mode

LD/ST Instructions

For load and store instructions, linear mode simply shifts the $offsetR/cst$ operand to the left by 2, 1, or 0 for word, half-word, or byte access, resulting in a multiplication by 4, 2 and 1, respectively, and then performs an add or a subtract of the result to the base register $baseR$, corresponding to a plus or a minus in the instruction syntax, respectively.

ADDA/SUBA Instructions

For integer addition and subtraction instructions, linear mode simply shifts the $src1/cst$ operand to the left by 2, 1, or 0 for word, half word, or byte data sizes, respectively, and then performs the add or subtract specified.

Circular Addressing Mode

As stated above, the BK0 and BK1 fields in the AMR specify block sizes for circular addressing. Consider the load/store instructions **LD**/**ST** in circular addressing mode as they apply to word, half-word or byte length data. After shifting the offsetR/cst to the left by 2, 1, or 0 bits, that is after multiplication by 4, 2 or 1, for **LDW**, **LDH(U)**, or **LDB(U)** instructions, respectively, an add or subtract is to base register baseR is performed with the carry/borrow inhibited between bits N and $N + 1$. Bits $N + 1$ to 31 of baseR remain unchanged. All other carries/borrows propagate as usual. If an offsetR/cst greater than the circular buffer size, 2^{N+1} , is specified, the effective offsetR/cst is modulo the circular buffer size as the following example illustrates. The circular buffer size in the AMR is not scaled; for example, a block size of 4 is 4 bytes, not $4 \times$ the data size that can be in bytes, half-words, words. So, to perform circular addressing on an array of 8 words, a size of 32 should be specified, or $N = 4$.

Example 15.28 Consider a word-type load instruction, in particular, **LDW**, performed with register A4 in circular mode and $BK0 = 4$, i.e. $N = 4$ so the buffer size is $2^{N+1} = 32$ bytes, 16 halfwords, or 8 words. The instruction **MVK** is used to set the proper value in the AMR to 0004 0001h. As seen in Fig. 15.71, the instructions load the address 0000 0104h in A4 and the memory content 1234 5678h at the address 0000 0104h in A4 into A1.

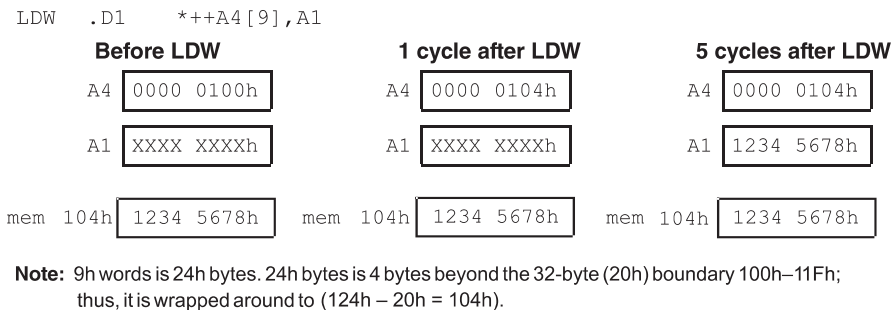


FIGURE 15.71 Circular addressing mode.

15.46 Programming the T.I. DSP

The TMS320C67xx can be programmed using C or C++, using assembly language code or using a MATLAB–Simulink configuration. The objective here is to start with very simple examples, allowing the student to program the DSP for real-time applications in the shortest time possible, and learning that programming it for more complex applications is in fact strikingly as easy as that of the simple ones.

The student will realize at the conclusion of this section that thanks to a collaboration between Texas Instruments and The MathWorks, configuring the TMS320C6xxx DSP to act as a digital IIR filter for example is as easy as drawing a block diagram using Simulink. Once the diagram has been drawn all that is needed is to issue a request to transfer the structure to the DSP. Subsequently the DSP acts in real time as the desired IIR filter.

As just mentioned, one of the approaches to programming the DSP is to use the language C or C++. We shall therefore start by showing how to transfer to the DSP a simple basic program in C and view its conversion into assembly code using the Texas Instruments Code Composer Studio. This allows us to see how the DSP Instruction Set is used to perform the required basic operations. We shall then progressively add lines with basic operations to the C program and observe the corresponding assembly code generated by the **Code Composer Studio**TM (CCS) compiler.

The CCS Debug Tools are part of Texas Instruments' CCS Integrated Development Environment IDE which provides means to program in C/C++ the DSP. It includes software tools for code generation such as a C/C++ compiler, an assembler, a linker and debugging means.

Real-Time Analysis—Code Composer Studio provides real-time analysis capability. Using RTDX technology, DSP/BIOS provides a real-time window into the target system, allowing designers to analyze a system in real-time.

Advanced Data Visualization—The advanced data visualization capability of Code Composer Studio enables DSP developers during the debugging process to view the target signals and data of the execution of an algorithm as images instead of text.

15.47 A Simple C Program

To explore the way a C program is converted into an assembly language code and view properties of the instruction set we start by writing a simple C program which basically states that a, b, c, d, e are integers and $a = 3, b = 4,$

$$c = a + b, \quad d = a - b, \quad e = a * b. \quad (15.247)$$

We add that f, g, h, i, j, k, m are real to effect floating point operations:

$$f = 0.34375, \quad g = 0.21875; \quad (15.248)$$

$$h = f - g, \quad i = f - g, \quad j = f * g, \quad k = -f, \quad m = k * g. \quad (15.249)$$

We now see the result of converting this C Source program into assembly code and the resulting sequence of DSP instructions that effect the successive simple computations. The student should note that it is subsequently possible to increase the C program size and complexity, to do more complex tasks, knowing that the CCS will subsequently simply generate the corresponding assembly code that is required to configure the DSP. The C language listing of the program is shown in Fig. 15.72

As we shall see shortly Code Composer Studio allows the user to view the values of the variables at each step of program execution. For the present program the values of the input and output data are shown in decimal, binary and hexadecimal. As an illustration we note that the values of f and g are given by

$$f = (0.01011)_2 = 1/4 + 1/16 + 1/32 = 11/32 = 0.34375. \quad (15.250)$$

To deduce the floating point form of the variable f we note that its binary representation can be rewritten in the form $f = 1.011 \times 2^{-2}$, which is a form similar to scientific notation, except that it is written here in base 2. In the IEEE format floating point representation, as explained earlier, the 1 to the left of the binary point is omitted as an implicit value.


```

#include <stdio.h>

void main()
{
    int a,b,c,d,e;
    float f,g,h,i,j,k,m;

    //add, sub and mult for integers
    a = 3;
    b = 4;
    c= a + b;
    d= a - b;
    e= a * b;

    //floating point add, sub and mult
    f = 0.34375;
    g = 0.21875;
    h = f + g;
    i = f - g;
    j = f * g;
    k = - f;
    m = k * g;
}

```

FIGURE 15.72 C language program.

The mantissa is therefore given by $m = 0.011$, and the biased exponent is the value of the true exponent of f , namely, $e = -2$ plus the bias 127. The biased exponent is therefore $e_b = -2 + 127 = 125 = (01111101)_2$ so that the floating point representation of f can be written in the form

$$f \longleftrightarrow 0.0111110101100\dots 0 \quad (15.251)$$

and therefore the floating point representation of f as displayed in hexadecimal is $f = 3EB00000$. Similarly, we have $g = (0.00111)_2 = 7/32 = 0.21875$. We write $g = 1.11 \times 2^{-3}$. The mantissa is $m = 0.11$, the exponent is $e = -3$ and the biased exponent is $e_b = -3 + 127 = 124 = (01111100)_2$, so that the representation of the variable g is in hexadecimal code $g = 3E600000$.

The multiplication of f and g produces $j = (7 \times 11) / (32 \times 32) = 0.075195313$, and the representation in binary is deduced by writing $j = 77 \times 2^{-10} = 0.0001001101 = 1.001101 \times 2^{-4}$, so that $m = 0.001101$, $e = -4$, $e_b = 123$ and the representation of the product j is in hexadecimal $j = 3D9A0000$.

With the variable k defined as $k = -f$ we have $k = -0.34375 = BEB0$ and $m = k \times g = -0.075195313 = BD9A00$.

15.48 The Generated Assembly Code

Code Composer Studio (Texas Instruments) allows viewing the C program's successive instructions, each directly followed by the corresponding assembly code. We therefore obtain the mixed mode output code combining each successive C program line and its compilation into assembly code. This is shown in Fig. 15.73, Fig. 15.74 and Fig. 15.75.

```

#include <stdio.h>

void main()
{
000004C0          main:
000004C0 07FFE852          ADDK.S2      -48,SP
    int a,b,c,d,e;
    float f,g,h,i,j,k,m;

    //add, sub and mult for integers
    a = 3;
000004C4 018001A8          MVK.S1      0x0003,A3
000004C8 01BC22F4          STW.D2T1   A3,**SP[0x1]
000004CC 00002000          NOP        2
    b = 4;
000004D0 0200022A          MVK.S2      0x0004,B4
000004D4 023C42F6          STW.D2T2   B4,**SP[0x2]
000004D8 00002000          NOP        2
    c= a + b;
000004DC 02BC42E6          LDW.D2T2   **SP[0x2],B5
000004E0 00006000          NOP        4
000004E4 020CB07A          ADD.L2X    B5,A3,B4
000004E8 023C62F6          STW.D2T2   B4,**SP[0x3]
000004EC 00002000          NOP        2
    d= a - b;
000004F0 021472FA          SUB.L2X    A3,B5,B4
000004F4 023C82F6          STW.D2T2   B4,**SP[0x4]
000004F8 00002000          NOP        2
    e= a * b;
000004FC 02BC42E6          LDW.D2T2   **SP[0x2],B5
00000500 00004000          NOP        3
00000504 020C105A          MV.L2X    A3,B4
00000508 0210A202          MPYI.M2   B5,B4,B4
0000050C 0000E000          NOP        8
00000510 023CA2F6          STW.D2T2   B4,**SP[0x5]
00000514 00002000          NOP        2
    //floating point add, sub and mult
    f = 0.34375;
00000518 018000F8          ZERO.L1    A3
0000051C 019F5868          MVKH.S1    0x3eb00000,A3
00000520 01BCC2F4          STW.D2T1   A3,**SP[0x6]
00000524 00002000          NOP        2
    g = 0.21875;
00000528 020000FA          ZERO.L2    B4
0000052C 021F306A          MVKH.S2    0x3e600000,B4
00000530 023CE2F6          STW.D2T2   B4,**SP[0x7]
00000534 00002000          NOP        2

```

FIGURE 15.73 Result of compilation of C program.

```

h = f + g;
00000538 02BCE2E6          LDW.D2T2      **SP[0x7],B5
0000053C 00006000          NOP          4
00000540 020CB21A          ADDSP.L2X    B5,A3,B4
00000544 00004000          NOP          3
00000548 023D02F6          STW.D2T2    B4,**SP[0x8]
0000054C 00002000          NOP          2
i = f - g;
00000550 021472BA          SUBSP.L2X    A3,B5,B4
00000554 00004000          NOP          3
00000558 023D22F6          STW.D2T2    B4,**SP[0x9]
0000055C 00002000          NOP          2
j = f * g;
00000560 01BCE2E5          LDW.D2T1    **SP[0x7],A3
00000564 020C105A          MV.L2X      A3,B4
00000568 00006000          NOP          4
0000056C 01907E00          MPYSP.M1X   A3,B4,A3
00000570 00004000          NOP          3
00000574 01BD42F4          STW.D2T1    A3,**SP[0xA]
00000578 00002000          NOP          2
k = - f;
0000057C 018000F8          ZERO.L1     A3
00000580 018FFF88          SET.S1      A3,31,31,A3
00000584 020C9DFA          XOR.L2X     B4,A3,B4
00000588 023D62F6          STW.D2T2    B4,**SP[0xB]
0000058C 00002000          NOP          2
m = k * g;
00000590 01BCE2E4          LDW.D2T1    **SP[0x7],A3
00000594 00006000          NOP          4
00000598 01907E00          MPYSP.M1X   A3,B4,A3
0000059C 00004000          NOP          3
000005A0 01BD82F4          STW.D2T1    A3,**SP[0xC]
000005A4 00002000          NOP          2
}
000005A8 07801852          ADDK.S2     48,SP
000005AC 000C0362          B.S2       B3
000005B0 00008000          NOP        5
    
```

FIGURE 15.74 Result of compilation of C program.

Name	Decimal	Binary	Hex
c	7	00000000000000000000000000000011	0x00000007
d	-1	11111111111111111111111111111111	0xFFFFFFFF
e	12	00000000000000000000000000001100	0x0000000C
f	3.4375000e-01	00111110101100000000000000000000	0x3EB00000
g	2.1875000e-01	00111110011000000000000000000000	0x3E600000
h	5.6250000e-01	00111110001000000000000000000000	0x3F100000
i	1.2500000e-01	00111110000000000000000000000000	0x3E000000
j	7.5195313e-02	00111101100110100000000000000000	0x3D9A0000
k	-3.4375000e-01	10111110101100000000000000000000	0xBEB00000
m	-7.5195313e-02	10111101100110100000000000000000	0xBD9A0000

FIGURE 15.75 Result of compilation of C program.

We note that the C source program line $a = 3$; upon compilation generates an assembly code which uses the instructions MVK, STW and NOP, respectively. The first of these, MVK .S1, moves the value 3, denoted 0x0003, that is, hexadecimal 3, to register A3 using the .S1 functional unit. The second instruction, STW, stores the contents of register A3, i.e. the same value 3, to memory at an address given by the contents of the Stack Pointer SP plus 1. The local variable a is thus stored and can subsequently be retrieved from the stack at that address. When no optimization is requested the compiler produces a functional but not optimized assembly code. The instruction No Operation (NOP) is used to add delay slots ensuring that results of one instruction have stabilized before they are used by a subsequent one. The instruction NOP 2 seen following the store instruction in the figure inserts two such delay slots. If optimization of code is requested by the user such NOP instructions are minimized. Only the minimum required is kept in the assembly code.

The following line in the figure, namely, $b = 4$, produces instructions that are seen to move the hexadecimal value 0x0004 to register B4 and stores same in memory at an address given by the stack pointer SP plus 2. The subsequent operation

$$c = a + b \quad (15.252)$$

is seen in the figure to be effected by first loading the value b to register B5 and then adding a and b from registers A3 and B5, putting the result c in register B4. The following STW instruction stores the contents of B4 into the stack at address SP plus 3. The C program line $d = a - b$; produces similar instruction with the exception of a subtraction instead of addition, and the result is stored at (SP) + 4. The multiplication line $e = a * b$ generates a MV instruction which moves the contents of register A3, that is, a to B4. This is followed by the fixed point instruction MPYI which multiplies the contents of B5 and B4 with a destination B4 and the result stored at SP +5. The MPYI instruction is followed by NOP 8 to generate a safeguard NOP of 8 delay slots, as given in the MPYI instruction specifications.

The floating point operations in the rest of the program are similarly compiled into assembly language code. To set the value $f = 0.34375$, the hexadecimal equivalent $f = 3EB00000$, is loaded into register A3 and the same value is stored in memory at the address (SP) + 6.

The operations $h = f + g$; $i = f - g$; are effected using the single precision add and subtract instructions ADDSP and SUBSP, respectively. They are followed by NOP 3, as specified by the number of Delay Slots that they require.

As Fig. 15.73 shows, the line $g = 0.21875$, upon program compilation transfers the hexadecimal equivalent 3E600000 to register B4. The line $j = f * g$; loads the value of g from memory at address (SP) + 7 into register A3, while in parallel, as evidenced by the two vertical strokes, moves the contents of A3, i.e. the value f , to B4. With f in B4 and g in A3, the instruction MPYSP A3, B4, A3 effects the multiplication and stores the product $f * g$ in register A3. Proper pipelining ensures that f , the content of A3, is transferred to B4 before being replaced by the value g . The remaining lines of the C program are similarly related to the corresponding generated assembly code.

15.48.1 Calling an Assembly Language Function

This section presents an easy approach to programming the DSP in Assembly language. Students can thus write assembly language code and verify their understanding of the DSP instruction set. The approach consists of writing the assembly code as an assembly function that is called from a C language main program. The C language program thus performs all input-output operations allowing the programmer to focus attention on the assembly

```

#include <stdio.h>

extern int add_int (int a, int b); //assembly function
extern int mult_int (int a, int b); //assembly function
extern float add_float(float A, float B); //assembly function
extern float mult_float (float A, float B); //assembly function

void main()
{
    int a,b,c,d;
    float A,B,C,D;
    a = 3;
    b = 4;
    A = 2.0;
    B = 5.0;

    c= add_int (a,b); //calling an assembly function
    d= mult_int (a,b); //calling an assembly function
    C= add_float (A,B); //calling an assembly function
    D= mult_float (A,B); //calling an assembly function
}

// add-int function ( c = a + b )
    .def      _add_int
_add_int    ADD      B4,A4,A4 // A4= B4 + A4
            NOP      2 // no operations
            B        B3 //return address of the code
            .end

// mult-int function ( d = a * b )
    .def      _mult_int
_mult_int   MPY      B4,A4,A4 // A4= B4 * A4
            NOP      2 // no operations
            B        B3 //return address of the code
            NOP      3 // no operations
            .end

// add-float function ( C = A + B )
    .def      _add_float
_add_float  ADDSP    B4,A4,A4 // A4= B4 + A4
            NOP      2 // no operations
            B        B3 //return address of the code
            NOP      3 // no operations
            .end

// mult-float function ( C = A * B )
    .def      _mult_float
_mult_float MPYSP    B4,A4,A4 // A4= B4 * A4
            NOP      2 // no operations
            B        B3 //return address of the code
            NOP      3 // no operations
            .end

```

FIGURE 15.76 Main C program calling four basic assembly code functions.

language code. This approach is illustrated by rewriting the last basic C program as a main program which defines the values of the input variables and calls on the assembly function to evaluate the sums and products thereof in fixed and floating point formats.

As will be seen, it is easy subsequently to test more complex examples, by first evaluating them in C, observing the assembly code generated by CCS and then similarly rewriting them as an assembly function called by a main program.

A C main program which calls successively four basic assembly code functions is shown in Fig. 15.76. The functions perform the same basic operations of addition and multiplication in fixed and floating-point formats. The student is encouraged to enter the short program on the TI DSK 2 evaluation kit and observe the results.

We now view a slightly more complex C and C++ Programs. To this end we consider constructing a generator of the Fibonacci series. The series starts with the elements 0 and 1. Each new term is the sum of its last two terms. The third term is thus $0 + 1 = 1$, the fourth is $1 + 1 = 2$, and the following terms are 3, 5, 8, 13, 21, 34, 55, ... Let at any instant x and y denote the last term found and the one before it, respectively.

We can initialize the process by setting $x = 1$; $y = 1$; as the first two terms and the sum is $s = x + y$. We then write $x = y$; $y = s$; and repeat the above, finding successive new terms. The C code is shown in Fig. 15.77. As seen in the figure, a C function is created, accepting as input a number n which is the Fibonacci series term number, and produces the value of that term. The main program chooses a value n and calls the function `fibonacci(n)`, receiving from the function the value of the Fibonacci series n^{th} term. For example, with $n = 10$ the program produces series value 144. The main function then prints that value. The mixed mode output code combining each successive C program line and its compilation into assembly code is shown in Fig. 15.78 and Fig. 15.79.

It is interesting to note that CCS compiles the C program, whatever its complexity, producing the properly functioning assembly code. The user needs not write assembly code. A general knowledge of the instructions set and assembly language of the DSP is preferable for the designer but not essential. CCS can moreover upon request effect an optimization ensuring a highly efficient assembly code making optimal use of the DSP architecture.

```

#include <stdio.h>

int fibonacci (int n)
{
    int x = 1;
    int y = 1;
    int i, sum;

    for (i=1;i<=n;i++)
    {
        sum = x + y;
        x = y;
        y = sum;
    }

    return sum;
}

void main()
{
    int n = 10;                // set value
    int LastTerm;             //result from asm function
    LastTerm = fibonacci (n);

    printf(" term number %d is %d ",n, LastTerm); //print result
}

```

FIGURE 15.77 Generator of the Fibonacci series.

```

#include <stdio.h>

int fibonacci(int n)
{
000066E0          fibonacci:
000066E0 07BF09C2          SUB.D2          SP,0x18,SP
000066E4 023C22F4          STW.D2T1       A4,*+SP[0x1]
000066E8 00002000          NOP            2

    int x = 1;
000066EC 020000AA          MVK.S2         0x0001,B4
000066F0 023C42F6          STW.D2T2       B4,*+SP[0x2]
000066F4 00002000          NOP            2

    int y = 1;
000066F8 018000A8          MVK.S1         0x0001,A3
000066FC 01BC62F4          STW.D2T1       A3,*+SP[0x3]
00006700 00002000          NOP            2

    int i, sum;

    for(i=1;i<=n;i++)
00006704 023C82F6          STW.D2T2       B4,*+SP[0x4]
00006708 00002000          NOP            2
0000670C 02BC82E6          LDW.D2T2       **SP[0x4],B5
00006710 00006000          NOP            4
00006714 0010B8FA          CMPGT.L2X      B5,A4,B0
00006718 20000F90          [ B0] B.S1     DWSLS_fibonacci$2$E
0000671C 00008000          NOP            5
00006720          DWSLS_fibonacci$2$B:
00006754 023C82E6          LDW.D2T2       **SP[0x4],B4
00006758 00006000          NOP            4
0000675C 0210205A          ADD.L2         1,B4,B4
00006760 023C82F6          STW.D2T2       B4,*+SP[0x4]
00006764 00002000          NOP            2
00006768 02BC82E6          LDW.D2T2       **SP[0x4],B5
0000676C 00006000          NOP            4
00006770 0010B8FA          CMPGT.L2X      B5,A4,B0
00006774 3FFF810          [!B0] B.S1     DWSLS_fibonacci$2$B
00006778 00008000          NOP            5

    sum = x + y;
00006720          DWSLS_fibonacci$2$B:
00006720 023C42E6          LDW.D2T2       **SP[0x2],B4
00006724 02BC62E6          LDW.D2T2       **SP[0x3],B5
00006728 00006000          NOP            4
0000672C 0210A07A          ADD.L2         B5,B4,B4
00006730 023CA2F6          STW.D2T2       B4,*+SP[0x5]
00006734 00002000          NOP            2

    x = y;
00006738 0214005A          MV.L2          B5,B4
0000673C 023C42F6          STW.D2T2       B4,*+SP[0x2]
00006740 00002000          NOP            2

    y = sum;
00006744 023CA2E6          LDW.D2T2       **SP[0x5],B4
00006748 00006000          NOP            4
0000674C 023C62F6          STW.D2T2       B4,*+SP[0x3]
00006750 00002000          NOP            2

}

return sum;
0000677C          DWSLS_fibonacci$2$E:
0000677C 023CA2E4          LDW.D2T1       **SP[0x5],A4
00006780 00006000          NOP            4
}

00006784 07800C52          ADDK.S2        24,SP
00006788 000C0362          B.S2           B3
0000678C 00008000          NOP            5

void main()
{
00006790          main:
00006790 01BD14F6          STW.D2T2       B3,*SP--[0x8]
00006794 00002000          NOP            2

    int n = 10;
00006798 01800528          MVK.S1         0x000a,A3
0000679C 01BCA2F4          STW.D2T1       A3,*+SP[0x5]
000067A0 00002000          NOP            2

```

FIGURE 15.78 Generator of the Fibonacci series.

```

int LastTerm;
LastTerm = fibonacci(n);
000067A4 0FFFE810          B.S1          fibonacci
000067A8 01B3DC2A          MVK.S2        0x67b8,B3
000067AC 0180006A          MVKH.S2       0x0000,B3
000067B0 020C0058          MV.L1         A3,A4
000067B4 00002000          NOP           2
000067B8          RL0:
000067B8 023CC2F4          STW.D2T1     A4,**SP[0x6]
000067BC 00002000          NOP           2

printf(" term number %d is %d",n, LastTerm);
000067C0 02BCA2E6          LDW.D2T2     **+SP[0x5],B5
000067C4 0001B410          B.S1          printf
000067C8 0210105B          MV.L2X       A4,B4
000067CC 01C995A8          MVK.S1        0xffff932b,A3
000067D0 023C62F7          STW.D2T2     B4,**+SP[0x3]
000067D4 01800068          MVKH.S1       0x0000,A3
000067D8 01BC22F5          STW.D2T1     A3,**+SP[0x1]
000067DC 00000000          NOP
000067E0 02BC42F7          STW.D2T2     B5,**+SP[0x2]
000067E4 01B3F62A          MVK.S2        0x67ec,B3
000067E8 0180006A          MVKH.S2       0x0000,B3
}
000067EC          RL1:
000067EC 01BD12E6          LDW.D2T2     **+SP[0x8],B3
000067F0 00006000          NOP           4
000067F4 000C0362          B.S2         B3
000067F8 00008000          NOP           5

```

FIGURE 15.79 Generator of the Fibonacci series.

15.49 Fibonacci Series in C Calling Assembly-Language Function

In this example we reconsider generating the Fibonacci series by a main program which accepts a number of terms n and calls the assembly code function which evaluates the corresponding series element. The program is shown in Fig. 15.80. Note that the value n is passed on from the main program to the called function by being stored in register $A4$, by convention. The assembly code program is straightforward. It resembles closely the assembly code generated by the CCS if the whole program were written in C as was seen above.

15.50 Finite Impulse Response (FIR) Filter

As another example we consider configuring the DSP as a FIR filter. As noted above, the DSP can be programmed in C++ and the program is compiled into assembly code using the CCS. The resulting code is then applied to the DSP, configuring it as the required FIR. The FIR filter has a finite impulse response $h[n]$ given by

$$h[n] = a^n R_N[n]$$

where $a = 0.5$, $R_N[n] = u[n] - u[n - N]$ and $N = 16$.

The output $y[n]$ of this filter in response to an input $x[n] = 7 \cos(n\pi/8)R_N[n]$ is given as a function of n as follows.

For $n < 0$, $y[n] = 0$. For $0 \leq n \leq N - 1$, $y[n] = \sum_{k=0}^n x[k]h[n - k]$. For $N - 1 \leq n \leq$


```

#include <stdio.h>
extern int fibonacci(int n)
void main()
{
    int n = 10;           // number of iterations
    int LastTerm;
    LastTerm = fibonacci(n); // calling fibonacci assembly function
}

.def            _fibonacci
_fibonacci
    ZERO        A0
    ADD          A0,1,A0    //x=1
    ZERO        A5
    ADD          A5,1,A5    //y=1
    MV          A4,A1      // move n from A4 to A1
loop    ADD     A0,A5,A3    //sum=x+y
        MV     A5,A0      //x=y
        MV     A3,A5      //y=sum
        SUB     A1,1,A1    // decrement loop counter n
[A1]    B      loop
        NOP
        MV     A5,A4      // return sum
        B      B3
        NOP        4

```

FIGURE 15.80 C main program calling an assembly language function.

$$2N - 2, \quad y[n] = \sum_{k=n-N+1}^{N-1} x[k]h[n-k].$$

A C++ program effecting such computation is shown in Fig. 15.81. Upon compilation the filter input and output signals may be displayed, confirming the expected results. These are shown in Fig. 15.82 (a-b), respectively.

15.51 Infinite Impulse Response (IIR) Filter on the DSP

The next example designs a third order lowpass Chebyshev digital filter. We assume a maximum permissible attenuation of 1 dB in the pass-band. Let ω_c denote the cut-off frequency, that is, the pass-band edge frequency, and let $\omega_s = 2\pi f_s$ r/s be the sampling frequency, where we assume that $f_s = 1/T = 4$ kHz, i.e. the sampling period is $T = 1/4000 = 0.25 \times 10^{-3}$ sec and $\omega_s = 2\pi f_s = 2\pi \times 4000$ r/s.

The objective is to observe the filter response to an input sinusoid of frequency equal to the filter cut-off frequency and compare it with its response to a sinusoid of frequency well beyond the cut-off frequency. Let the filter in the continuous-time domain have a cut-off frequency of 200 Hz, i.e. $\omega_c = 2\pi \times 200$ r/s. The first input to the filter $x_1(t)$ is a causal sinusoid of frequency β_1 r/s which is chosen equal to the cut-off frequency; i.e. $\beta_1 = \omega_c$ and $x_1(t) = \sin \beta_1 t u(t)$. The second input $x_2(t)$ has a frequency that is 1.5 times the cut-off frequency, i.e. $\beta_2 = 1.5\omega_c$ and $x_2(t) = \sin \beta_2 t u(t)$. In the discrete-time domain these frequencies are multiplied by the period T , so that the filter cut-off frequency, denoted Ω_c is equal to $\Omega_c = \omega_c T = 2\pi \times (200/4000) = \pi/10$, the inputs have frequencies $b_1 = \beta_1 T = \Omega_c = \pi/10$ and $b_2 = \beta_2 T = 1.5\Omega_c = 3\pi/20$ and the two input sequences are $x_1[n] = \sin b_1 n u[n]$ and $x_2[n] = \sin b_2 n u[n]$, respectively. We note that MATLAB defines the digital filter normalized cut-off frequency, denoted Wn , as the cut-off frequency ω_c divided by half the sampling frequency, i.e. divided by $\omega_s/2 = \pi/T$, so that

$$Wn = \omega_c / (\omega_s/2) = 2\omega_c / \omega_s. \quad (15.253)$$

```

#include<stdio.h>
#include<math.h>

int main()
{
    float pi=3.141592;
    float a=0.5;
    int n,k;
    int N=16;
    int M=30;
    float x[16];
    float h[16];
    float y[30];
    // Generate Input Sequence x[n]
    for (n=0;n<N;n++)
    {
        x[n]=7*cos(n*pi/8.0);
        printf("input at %d is %f\n ",n,x[n]);
    }
    // Generate Filter Coefficients h[n]
    for (n=0;n<N;n++)
    {
        h[n]=pow(a,n);
        printf(" filter coefficient at %d is %f\n",n,h[n]);
    }
    // Generate FIR Filter Output
    for (n=0;n<N;n++)
    {
        y[n]=0;
        for (k=0;k<=n;k++)
        {
            y[n]=(x[k]*h[n-k])+y[n];
        }
        printf("output at %d is %f\n",n,y[n]);
    }
    for (n=N;n<=M;n++)
    {
        y[n]=0;
        for (k=n-N+1;k<N;k++)
        {
            y[n]=(x[k]*h[n-k])+y[n];
        }
        printf("output at %d is %f\n ",n,y[n]);
    }
}

```

FIGURE 15.81 FIR filter response evaluation C++ program.

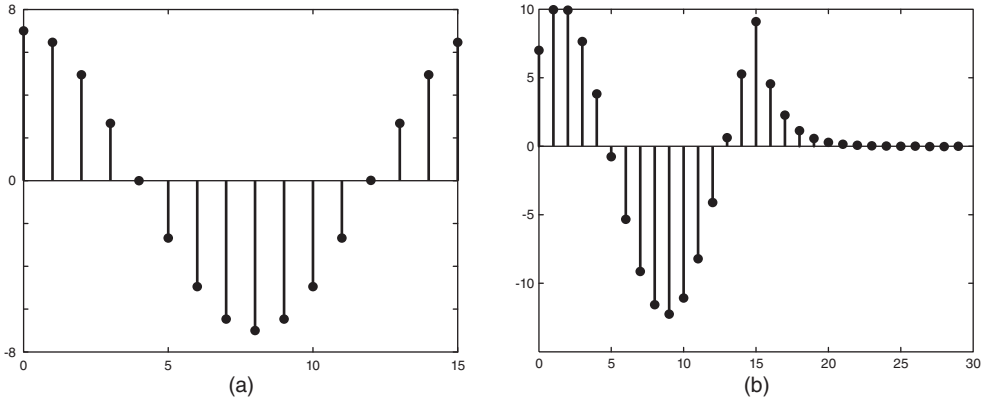


FIGURE 15.82 Sinusoidal FIR filter: (a) input, (b) response.

Equivalently,

$$W_n = \Omega_c / \pi. \quad (15.254)$$

In the present case $W_n = \Omega_c / \pi = 1/10$. We use the MATLAB command

$$[b, a] = \text{cheby1}(N, R, W_n) \quad (15.255)$$

where $N = 3$, $R = 1$ dB and $W_n = 0.1$. MATLAB returns the coefficient vectors b and a , and hence the system function $H(z)$. We then evaluate the filter response to the two sinusoidal inputs $x_1[n]$ and $x_2[n]$. The filter output in response to the first input sequence should be the same sinusoid as its input, except attenuated by 1 dB.

Writing $20 \log_{10} |H| = -1$ dB, we have $|H| = 10^{-0.05} = 0.8913$ which should be the amplitude of the output sinusoid. In response to the second input sinusoid, having a frequency higher than the cut off frequency, the filter output should be further attenuated. The filter transfer function may be written in the form

$$H(z) = \frac{b_1 + b_2 z^{-1} + b_3 z^{-3} + b_4 z^{-4}}{1 + a_2 z^{-1} + a_3 z^{-3} + a_4 z^{-4}} \quad (15.256)$$

where the coefficients of the numerator and denominator are returned by MATLAB as the two vectors

$$b = [0.001641 \ 0.004923 \ 0.004923 \ 0.001641]$$

$$a = [1 \ -2.623 \ 2.369 \ -0.7335]$$

as can be seen in the MATLAB program shown in Fig. 15.83.

The difference equation describing the filter response $y[n]$ to an input sequence $x[n]$ is given by

$$\begin{aligned} y[n] = & -a_2 y[n-1] - a_3 y[n-2] - a_4 y[n-3] + b_1 x[n] + b_2 x[n-1] \\ & + b_3 x[n-2] + b_4 x[n-3] \end{aligned} \quad (15.257)$$

for $n \geq 0$; with the initial conditions $x[n] = y[n] = 0$, $n < 0$.

The same program rewritten in C++ is shown in Fig. 15.84.

The resulting output sequences corresponding to the two input sinusoids are shown in Figs 15.85 (a-b), respectively.

We note that the filter attenuates the second input so that the output amplitude is about 0.2, i.e. 20% of the input sequence amplitude.

```

N=3;
R=1;
Wn=0.1;
[b,a]=cheby1(N,R,Wn)
sys=filt(b,a)
% M= input sequence duration
M=400;
% First input sequence x[n] having frequency at limit of passband
bee1=pi/10
for n=1:M
    x(n)=sin (bee1*(n-1));
end
y(1)=b(1)*x(1);
y(2)=-a(2)*y(1)+b(1)*x(2)+b(2)*x(1);
y(3)=-a(2)*y(2)-a(3)*y(1)+b(1)*x(3)+b(2)*x(2)+b(3)*x(1);
y(4)=-a(2)*y(3)-a(3)*y(2)-a(4)*y(1)+b(1)*x(4)+b(2)*x(3)+b(3)*x(2)+b(4)*x(1);
for n=5:M
    y(n)=-a(2)*y(n-1)-a(3)*y(n-2)-a(4)*y(n-3)+b(1)*x(n)+b(2)*x(n-1)...
        +b(3)*x(n-2)+b(4)*x(n-3);
end
figure(1)
plot(x)
title('first input sequence x1[n]')
figure(2)
plot(y)
title('Response y1[n] to first input sequence x1[n]')
% Second input x[n] with frequency beyond filter cut-off frequency
bee2=3*pi/20
for n=1:M
    x(n)=sin (bee2*(n-1));
end
y(1)=b(1)*x(1);
y(2)=-a(2)*y(1)+b(1)*x(2)+b(2)*x(1);
y(3)=-a(2)*y(2)-a(3)*y(1)+b(1)*x(3)+b(2)*x(2)+b(3)*x(1);
y(4)=-a(2)*y(3)-a(3)*y(2)-a(4)*y(1)+b(1)*x(4)+b(2)*x(3)+b(3)*x(2)+b(4)*x(1);
for n=5:M
    y(n)=-a(2)*y(n-1)-a(3)*y(n-2)-a(4)*y(n-3)+b(1)*x(n)+b(2)*x(n-1)...
        +b(3)*x(n-2)+b(4)*x(n-3);
end
figure(3)
plot(x)
title('Second input sequence x2[n]')
figure(4)
plot(y)
title('Response y2[n] to second input sequence x2[n]')

```

FIGURE 15.83 IIR filter and response MATLAB program.

```

#include<stdio.h>
#include<math.h>
class Computing
{
public:
    void computing_filter_output ( float f )
    {
        float a2=-2.6225,a3=-2.3692,a4=-0.7335;
        float b1=0.0016,b2=0.0049,b3=0.0049,b4=0.0016;
        int n,M=99;
        float x[99],y[99];
        FILE *results;
        results = fopen("results.txt","a+");
        // Generate Input Sequence x1[n]
        for (n=0;n<M;n++)
            { x[n]= sin (f*n);
            }
        // output y[n]
        for (n=0;n<M;n++)
            {
                if(n==0)
                {
                    y[n]=b1*x[n];
                    fprintf (results,"%f\n",y[n]);
                }
                else if(n==1)
                {
                    y[n]=-a2*y[n-1]+b1*x[n]+b2*x[n-1];
                    fprintf (results,"%f\n",y[n]);
                }
                else if(n==2)
                {
                    y[n]=-a2*y[n-1]-a3*y[n-2]+b1*x[n]+b2*x[n-1]+b3*x[n-2];
                    fprintf (results,"%f\n",y[n]);
                }
                else
                {
                    y[n]=-a2*y[n-1]-a3*y[n-2]-a4*y[n-3]+b1*x[n]+b2*x[n-1]+b3*x[n-2]+b4*x[n-3];
                    fprintf (results,"%f\n",y[n]);
                }
            }
        fclose(results);
    }
};
return ;
};
int main()
{
    float f1,f2,f;
    float pi=3.141592;
    f1=pi/10;
    f2=3*pi/20;
    f=f1;
    Computing output1;
    output1.computing_filter_output (f);
    f=f2;
    Computing output2;
    output2.computing_filter_output (f);
    return 0;
}

```

FIGURE 15.84 IIR filter C++ program.

15.52 Real-Time DSP Applications Using MATLAB–Simulink

Using MATLAB's Simulink we can draw a block diagram of the system that we intend to construct. The components of the block diagram may be filters, amplifiers, A/D and D/A converters, oscilloscopes and any of many units that can be chosen from the Simulink library. MATLAB subsequently configures the Texas Instruments DSP identically to the structure of the Simulink block diagram. The block diagram thus replaces the C program. In other words, we have seen how the Assembly language program may be replaced by the simpler C source program. We now see how even the C source program needs not be written. The designer can replace it by the simpler task of connecting a few blocks of his choosing using Simulink.

We consider as an example the problem of designing a digital oscillator which generates

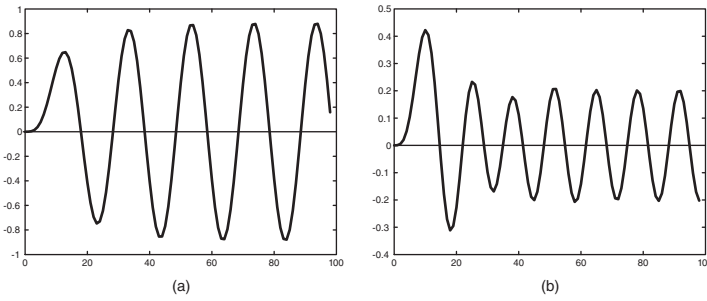


FIGURE 15.85 IIR Filter response: (a) to first sinusoid, (b) to second sinusoid.

a pure sinusoid. To this end we note that we may construct a system which has an impulse response $h[n]$ that is a pure sinusoid. By applying to its input an impulse it would produce the desired sinusoid. Let the filter impulse response be

$$h[n] = \sin \beta n u[n] \tag{15.258}$$

and let us choose its frequency as $\beta = \pi/8$. The filter transfer function is

$$H(z) = \mathcal{Z}[h[n]] = \frac{\sin \beta z^{-1}}{1 - 2 \cos \beta z^{-1} + z^{-2}} \tag{15.259}$$

which has the general form

$$H(z) = \frac{d_0 + d_1 z^{-1}}{1 - c_1 z^{-1} - c_2 z^{-2}} \tag{15.260}$$

with $d_0 = 0$, $d_1 = \sin \beta = \sin \pi/8 = 0.1951$

$$c_1 = 2 \cos \beta = 2 \cos \pi/8, \quad c_2 = 1. \tag{15.261}$$

This “filter” will generate the sinusoid $h[n] = \sin(\pi n/8) u[n]$ as a response to an input impulse $\delta[n]$.

To configure the DSP using Simulink we proceed as follows. Using Simulink Library Browser, with the Menu selection *File* \rightarrow *New* \rightarrow *Model* followed by *Simulation* \rightarrow *Configuration Parameters* with the options *Solver* \rightarrow *Fixed-Step*, the system block diagram shown in Fig. 15.86 is set up. By double clicking on the blocks Discrete Impulse, Discrete Filter and DAC digital to analog converter, the parameters are set up as shown in Fig. 15.87, Fig. 15.88 and Fig. 15.89, respectively. By applying the command *Rebuild All* the system is built on the DSP card. Connecting a loudspeaker, for example, to the output jack of the DSP Starter Kit the oscillator output can be heard.

15.53 Detailed Steps for DSP Programming in C++ and Simulink

The above was written with an emphasis on simplifying the writing of a C, C++, or assembly language program, or constructing a Simulink block configuration, for implementation on the DSP Starter Kit. In what follows we add to the above the important steps to follow in programming the DSP for an application based on a C++ program and another using Simulink.

15.53.1 Steps to Implement a C++ Program on the DSP Card

The steps to implement a C++ program on the DSP card are listed in what follows with reference to the Fibonacci series generation program seen above.

1. Launch the Code Composer Studio (CCStudio).
2. Establish a connection between the CCStudio and the card by clicking in the **Debug**

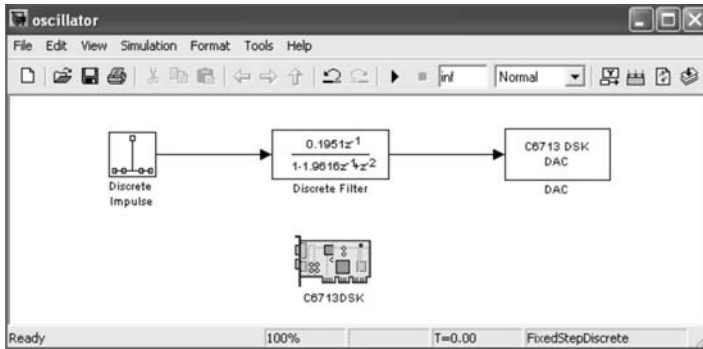


FIGURE 15.86 Digital oscillator on Simulink.

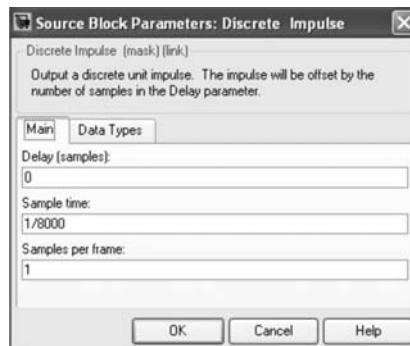


FIGURE 15.87 Discrete impulse system input.

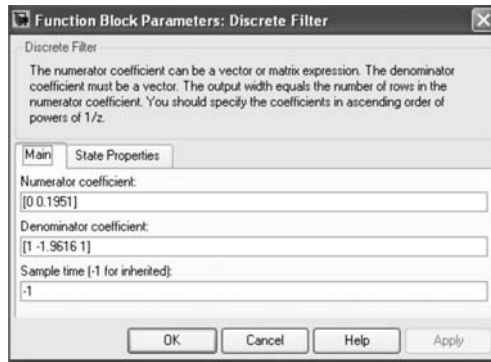


FIGURE 15.88 Oscillator transfer function parameters.

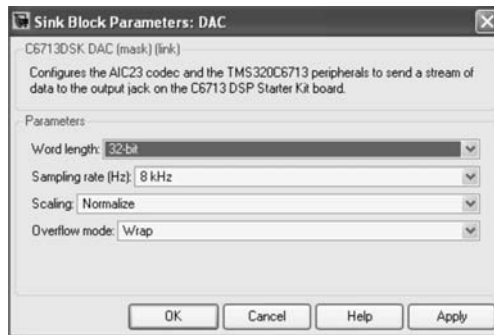


FIGURE 15.89 Digital oscillator output parameters.

menu on “**Connect.**” You can check the status of the connection at the lower left corner of the CCStudio window.

3. Create a new project in which the C program provides its main functionality. From the “**Project**” menu choose “**New.**” In the popped window, shown in Fig. 15.90, enter the *Project Name*, its *Location* on the hard disc, its *Type* (executable (.out) or library (.lib)) and the *Target* card used (C6713).
4. Adding your C and other files to the project:
 - (a) Adding the Source files (.c), for example *Fibonacci.cpp*: Right click on the project name and choose “**Add files to project,**” select your C (or C++) program then click on **Open.**
 - (b) Adding the Linker command files (.cmd, .lcf): The linker command files map sections to memory. Right click on the project name. Choose “**Add files to project,**” and add “volume.cmd” to the project by clicking on **Open.**
Note: you can find the “volume.cmd” file in a tutorial project folder. Go to C:CCStudio_v3.1/tutorial/dsk6713/volume1.
 - (c) Adding the Object and Library files (.o, .l): The library file provides runtime support for the target DSP. Right click on the project name. Choose “**Add files to project.**”
Go to (C:CCStudio_v3.1/C6000/cgtools/lib/rts6700.lib) and click on **Open.**

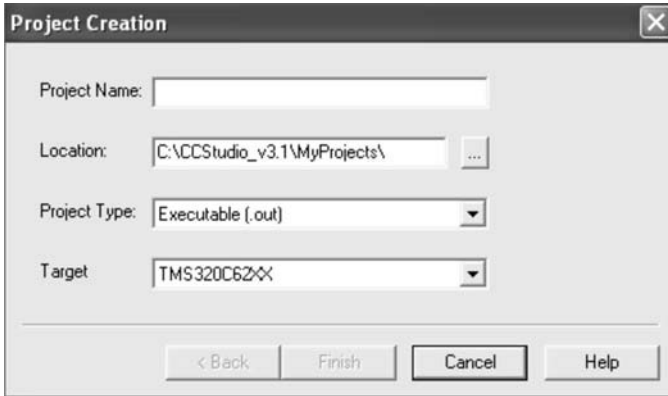


FIGURE 15.90 New project window.

- (d) Adding the include files (.h): Right click on the project name. Choose “**Scan All file dependencies.**” The scan detects and adds automatically all the (.h) files needed.
 - (e) If your C program contains assembly functions, add all the files which contain the functions (.a files). Right click on the project name. Choose “**Add files to project**” and add those files.
5. Compiling the C program: In the project list on the left section of the CCStudio window double-click on the added C program. Then from the “**Project**” menu click on “**Compile File**” or directly use “Ctrl F7.”
 6. Building the project on the target: Select “**Rebuild all**” from the “**Project**” menu. The program recompiles, reassembles, and re-links all the files in the project. The Build frame at the bottom of the window displays messages about this process.
 7. Loading the program: Select “**Load Program**” from the “**File**” menu. Choose *project_name.out* file and click **Open**.
 8. Running the program: From the “**Debug**” menu choose “**Go Main**” then “**Run.**”
 9. To stop the program: From the “**Debug**” menu click on “**Halt.**”

15.53.2 Steps to Implement a Simulink Program on the DSP Card

Configuring the DSP and employing it for real-time processing can be easily effected using Simulink as the following example illustrates.

In Fig. 15.91 Simulink is used to configure the DSP as a filter, which can be programmed as a lowpass, bandpass or highpass filter. A signal generator applies a sinusoid to the DSP card input. The sinusoid is sampled using the A/D converter (ADC). The filter parameters are set to produce a bandpass Chebyshev filter with pass-band edge frequencies 1 and 1.5 kHz. The filtered signal is converted back to analog using the DAC on the card. The card output is connected to a loudspeaker. By varying the frequency of the input sinusoid the effect of attenuation of low and high frequencies are readily noted.

The steps to implement the Simulink program of this IIR bandpass filter on the DSP Card can be summarized as follows:

1. Build the system shown in Fig. 15.91 using Simulink.

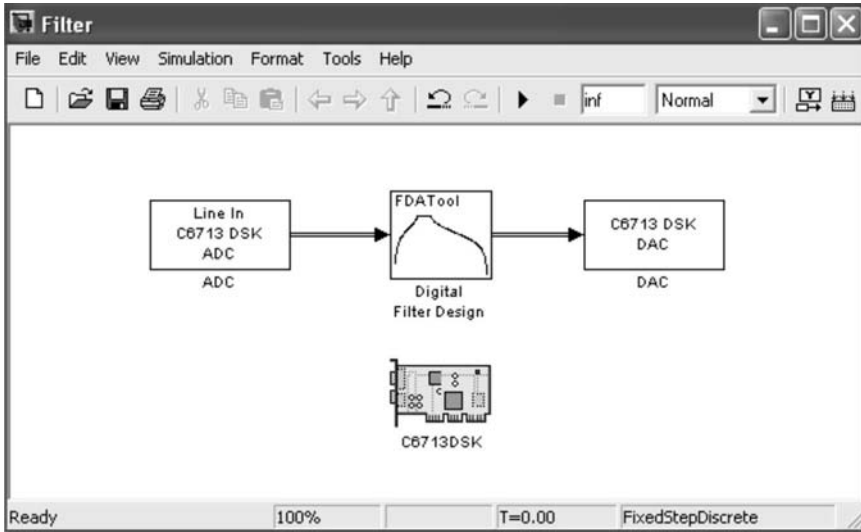


FIGURE 15.91 Simulink block diagram.

2. Launch Code Composer Studio (CCStudio).
3. Generating and charging the code on the DSP target: Go in the Simulink window to “**Simulation**” then “**Configuration Parameters...**” A new window as shown in Fig. 15.92 pops up. In the list which appears on the left, click on “**TIC6000 code generation.**” Deselect “**Incorporate DSP/BIOS.**” In the same list click on “**Real-Time Workshop**”; then on “**Generate Code.**”

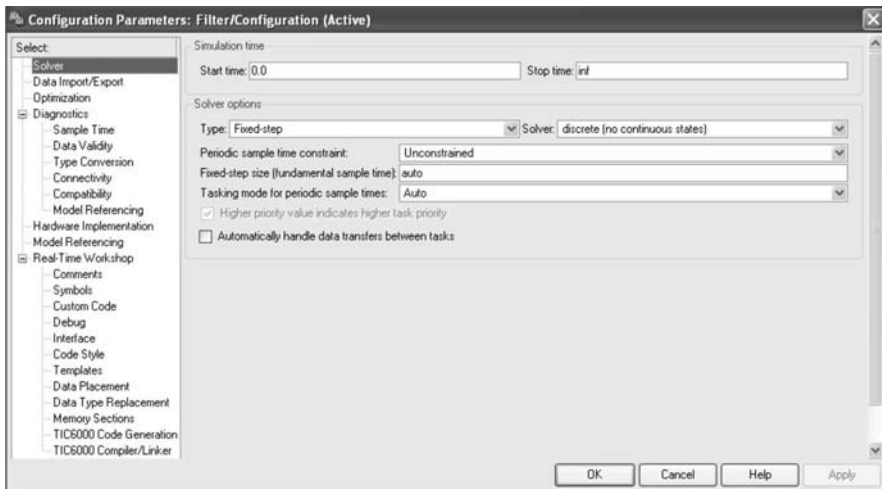


FIGURE 15.92 Configuration parameters window.

Automatically, MATLAB generates the code, establishes a connection with the CC-Studio, transforms the Simulink model to C/C++ files, creates a new project, adds

all the necessary files to the project, builds and loads the program onto the target.

4. Running the program: From the “**Debug**” menu choose “**Go Main**”; then “**Run**.”

Alternatively, an audio input such as speech, music or song is fed to the DSP card input and the effect of altering the filter bandwidth on the signal sound quality may be observed. Similarly, the effect of filtering out the noise in a contaminated signal can be investigated.

15.54 Problems

Problem 15.1 Show the multiplication steps of two numbers represented in FNR, 1’s complement. The two numbers A and B have absolute values $a = 18(2^{-5})$ and $b = 27(2^{-5})$, respectively. Show all four sign combinations. Next to each line of the multiplication process write its value formally in terms of a and b and their bits. Add these values to prove that the result is, as required, the product in 1’s complement.

Problem 15.2 The objective is to verify the direct approach of multiplication in 2’s complement seen in Sec. 15.15.

a) Show the successive steps of the multiplication of the multiplicand A and multiplier B for the cases i) $A = -13, B = 11$, ii) $A = 12, B = -5$, iii) $A = -7, B = -6$, with four bits plus a sign bit.

b) For each one of the same three cases in a) show all values of the input, intermediate and output bits on all the connections of the Modified Baugh–Wooley multiplier, shown in Fig. 15.19.

Problem 15.3 Design a 3-D type multiplier as the one described in Sec. 15.14 for the multiplication of two operands of 12 bits each in sign and magnitude notation, using four-bit parallel adders. Show the adders and how they are connected in each of the multiplier planes. Show the bits at the inputs and outputs of the adders assuming max value for the input and for the output operand.

Problem 15.4 Given $A = (119)_{10}$ and $B = (12)_{10}$, write the bit values at the inputs and outputs of each cell and of the carry-look ahead cells of the nonrestoring division cellular array shown in Fig. 15.24, for the division $A \div B$. Verify whether or not the quotient and remainder are the exact results. If not show any correction needed. Show in a table the values of the propagate and generate bits P_i , and G_i of the carry-look ahead cells for $i = 0, 1, 2, 3$ corresponding to each row of the array.

Problem 15.5 Show the contents of a ROM used to supply the initial estimate of the reciprocal of an operand B for conversion division using the Newton–Raphson iterative approach. The supplied estimate should provide six useful bits of information, meaning that the ROM output should be interpreted as the value $1.xxxxxx$. The ROM should have eight words corresponding to the values $B = 0.1xxx$, where $xxx = 000, 001, 010, \dots, 111$. Using the initial estimate supplied by the ROM evaluate the successive estimates x_1 and x_2 with eight decimal digits for the case $B = 13 \times 2^{-4}$ as produced by the iterative approach.

Problem 15.6 a) Show how to evaluate the fifth root of a given value B using the Newton–Raphson approach. Write the iterative equation which relates the estimate x_{i+1} to the previous one x_i .

b) Consider the case where B is a normalized fraction. Evaluate the estimates x_i , $i = 1, 2, 3$, of the first iterations in evaluating the fifth root of the value $B = (0.75)_{10}$. Suppose an initial estimate $x_0 = B$.

c) Show the contents of the ROM of eight words, which accepts as input $B = (0.1xxx)_2$ and produces the corresponding 5-bit initial estimate of the square root.

Problem 15.7 Design a function generator that produces the exponential function e^{-x} , $0 \leq x \leq 1$ upon receiving an input value x using Chebyshev polynomials.

a) Write the function expansion and its conditions of validity.

b) Write the coefficients of the first five terms in the expansion.

c) Write the expansion in the form of a polynomial in powers of x as used by the function generator. Evaluate the polynomial for $x = 0.4$.

d) Write the contents of a Read Only Memory ROM to be used by the function generator and which stores the coefficients of the powers of x up to x^4 with a word length of 10 bits.

Problem 15.8 Using function generation by Chebyshev series expansion design a processor that evaluates $\ln(1+x)$, $0 \leq x \leq 1$ of any input operand x . Write the expansion of $\ln(1+x)$ in terms of Chebyshev polynomials. Specify the values of the polynomials, for the first four terms, and the successive values of the coefficients in the expansion. Write the reduced form as a polynomial in powers of x , giving the coefficient of each power x^k of x . Write the content of the ROM that supplies to the processor the coefficients to employ. Repeat for the case where the function to be generated is $\Gamma(1+x)$. Verify by evaluating $\Gamma(1.4)$.

Problem 15.9 a) Draw a schematic diagram showing the conversion of a 6-decade BCD coded number to binary using 4-bit parallel adders. Indicate on the connection diagram the value of every bit on every line connecting the adders for the case of maximum value of input.

b) Show the grouping of adders as shown above in Fig. 15.31 (c) as a means of replacing them by the D/B chip shown in Fig. 15.31(a-b). Draw a final schematic diagram of the six-decade BCD to binary converter employing solely the D/B chips. Indicate on the connection diagram the value of every bit on every line connecting the D/B chips for the case of maximum value of input.

Problem 15.10 a) Design a combinatorial BCD to binary converter to convert a BCD number of two decades to binary using 4-bit parallel adders. This unit may be referred to as a D/B99 chip.

b) Draw a schematic diagram showing the conversion of an eight-decade BCD coded number to binary using 4-bit parallel adders. Indicate on the connection diagram the value of every bit on every line connecting the the adders for the case of maximum value of input.

c) Show the grouping of adders as a means of replacing them by the D/B99 chip. Draw a final schematic diagram of the 8-decade BCD to binary converter employing solely D/B99 chips designed in part a). Indicate on the connection diagram the value of every bit on every line connecting the D/B99 chips for the case of maximum value of input.

Problem 15.11 a) Draw a schematic diagram showing the conversion of a 16-bit binary number to BCD using 4-bit parallel adders. Indicate on the connection diagram the value of every bit on every line connecting the adders chips for the case of maximum value of input.

b) Draw a schematic diagram showing the conversion of a 16-bit binary number to BCD using solely B/D chips as the one shown above in Fig. 15.33(a-b).

Problem 15.12 a) Design a seven-bit binary to BCD converter module, employing four-bit parallel adders, as a chip accepting six input bits $b_6b_5\dots b_1$. Indicate on the connection

diagram the value of every bit on every line connecting the adders for the case of maximum value of input; i.e. with each input bit equal to 1. b) Show the structure of a 16-bit binary to BCD converter module, employing four-bit parallel adders, accepting 15 input bits. Indicate on the connection diagram the value of every bit on every line connecting the adders for the case of maximum value of input. c) Show the structure of the 16-bit binary to BCD converter module, employing solely as a building block the seven-bit binary to BCD converter chip you designed in part a). Justify your design by showing the value of every bit on every wire connecting the chips for the same case of maximum value of input.

Problem 15.13 a) Let $N = 32$, $r = 2$, P_K be the base $r = 2$ perfect shuffle permutation matrix of K points. Let x be a column vector having the elements x_0, x_1, \dots, x_{31} , and $y = p_2 x$ where $p_2 = I_{r^2} \times P_{N/r^2}$. Evaluate the vector y .

b) With $P = P_{16}$ the base $r = 2$ perfect shuffle permutation matrix of $K = 16$ points and $T_2 = H_2$ the 2×2 Walsh–Hadamard core matrix given in Equation 14.20, Chapter 14, and $S = I_8 \times T_2$. Evaluate in terms of T_2 and using the Kronecker product and the identity matrix I_k with appropriate values of k the expressions PSP^{-1} , P^2SP^{-2} and P^3SP^{-3} .

Problem 15.14 The objective is to construct an FFT processor using radix $r = 2$ factorization, which should be of a fully wired-in and symmetric architecture, as seen in [17] [24].

Starting from the matrix definition of the discrete Fourier transform show the steps of factorization of the DFT matrix, the resulting factorization in closed form and represent graphically the processor architecture, putting in evidence its symmetry. Sketch the architecture of the corresponding asymmetric processor and describe in a few words the comparative processing speeds of the two realizations.

Problem 15.15 Show the architecture of a radix-3 asymmetric FFT processor implementing the high speed ordered input/ordered output factorization for processing N -point input vectors. Specify the lengths of the processor queues. Describe in a few words the sequence of operations of the processor in the first three iterations.

Problem 15.16 Write a C or MATLAB program which simulates the radix-2 FFT wired-in processor implementing the asymmetric OIOO algorithm for a record length of $N = 256$ data points. Effect the multiplications in floating point assuming that the processor is equipped with floating point multipliers. Verify the processor performance by comparing its output with that produced by the `fft` instruction of MATLAB for the following cases:

i) $x[n] = nR_N[n]$.

ii) $x[n] = ne^{-0.1n}R_N[n]$.

iii) $x[n] = \sin \beta n R_N[n]$, where a) $\beta = 18\pi/N$, b) $\beta = 19\pi/N$.

Evaluate the inverse transform in each case. Evaluate and represent graphically the amplitude and phase spectra for each case as produced by the simulated processor and print their values. For the first case only, show the memory content of each submemory of the two memories following each iteration.

Problem 15.17 For the sequential machine described by Table 15.25, evaluate the partitions of equivalent classes, show the state table of the reduced machine, and show a realization using RS flip-flops.

Problem 15.18 The objective is to design a serial parity-bit generator. The unit receives serially, one clock at a time, four bits, of which the first three constitute a message and the fourth is a space for inserting the parity bit. The unit verifies the number of 1's in the message. If the number is odd it generates a parity bit of 1 which it inserts in the fourth

TABLE 15.25 State table of sequential machine for Problem 15.17

Present State	Next state, output z			
	$x = 0$	$x = 1$	$x = 2$	$x = 3$
a	$e, 0$	$j, 0$	$f, 0$	$a, 0$
b	$e, 0$	$b, 0$	$b, 0$	$e, 0$
c	$e, 0$	$j, 0$	$d, 0$	$e, 0$
d	$h, 1$	$j, 0$	$b, 0$	$e, 0$
e	$e, 0$	$j, 0$	$f, 0$	$e, 0$
f	$e, 0$	$j, 0$	$g, 0$	$e, 0$
g	$h, 1$	$j, 0$	$b, 0$	$e, 0$
h	$k, 1$	$i, 1$	$j, 0$	$a, 0$
i	$k, 1$	$i, 1$	$b, 0$	$e, 0$
j	$e, 0$	$j, 0$	$j, 0$	$e, 0$
k	$k, 1$	$i, 1$	$c, 0$	$e, 0$

bit space, otherwise it inserts a zero. The resulting output stream is the same as the input one except for the parity bit that has been inserted as the fourth bit of each message. Such parity bit is then used for error detection.

- a) Draw a state diagram for the parity-bit generator. Label the states $q_0, q_1, \dots, q_2, \dots$
- b) Show the state table.
- c) Assigning binary code k to state q_k , i.e. the codes 000, 001, 010, 011, 100, 101, ... to states $q_0, q_1, q_2, q_3, q_4, q_5, \dots$, respectively, show the realization of the generator using JK flip-flops.

Problem 15.19 Show the architecture of a radix-3 generalized Walsh fully wired in processor implementing the natural order transform for processing N -point input vectors. Specify the lengths of the processor queues. Describe in a few words the sequence of operations of the processor in the first three iterations.

Problem 15.20 Show the architecture of a radix-3 generalized Walsh fully wired in processor for evaluating the natural, dyadic and sequency order transform for processing $N = 3^n$ -point input vectors. Specify the lengths of the processor queues. Describe in a few words the sequence of operations of the processor in the first three iterations.

Problem 15.21 Show the architecture of a radix-3 asymmetric generalized Walsh processor implementing the “High Speed Ordered Input/Ordered Output” factorization, as seen in the context of FFT processors, for N -point input vectors. Describe in a few words the sequence of operations of the processor in the first three iterations.

15.55 Answers to Selected Problems

Problem 15.3

a) 2’s complement multiplication

- i) $A < 0, B > 0$

$$A = -13 = 1.0011$$

$$B = +11 = 0.1011$$

$$-B = 1.0101$$

	a_4	a_3	a_2	a_1	a_0	
$a :$	1.	0	0	1	1	
$b :$	0.	1	0	1	1	
		0	0	1	1	
		0	0	1	1	
	0	0	0	0		
	0	0	1	1		
<hr style="border-top: 1px solid black;"/>						
	0.	0	0	1	0	0
	0.	0	1	0	1	
<hr style="border-top: 1px solid black;"/>						
	1.	0	1	1	1	0
	1.	0	0	0	0	1

ii) $A > 0, B < 0$

$$A = 12 = 0.1100$$

$$B = -5 = 1.1011$$

$$-B = 5 = 0.0101$$

$$-a = 1.0010$$

	a_4	a_3	a_2	a_1	a_0	
	0.	1	1	0	0	
	1.	1	0	1	1	
		1	1	0	0	
		1	1	0	0	
	0	0	0	0		
	1	1	0	0		
<hr style="border-top: 1px solid black;"/>						
	0.	1	0	0	0	0
	1.	0	1	0	0	
<hr style="border-top: 1px solid black;"/>						
	1.	1	1	0	0	0

iii) $A < 0, B < 0$

$$A = -7 = 1.1001$$

$$B = -6 = 1.1010$$

$$y = 0.1010$$

$$-y = 1.0110$$

$$x = 0.1001$$

$$-x = 1.0111$$

	a_4	a_3	a_2	a_1	a_0	
	1.	1	0	0	1	
	1.	1	0	1	0	
		0	0	0	0	
		1	0	0	1	
	0	0	0	0		
	1	0	0	1		
<hr style="border-top: 1px solid black;"/>						
	0.	0	1	0	1	0
	1.	0	1	1	1	
	1.	0	1	1	0	
	1					
<hr style="border-top: 1px solid black;"/>						
	0.	0	0	1	0	1
	0.	0	1	0	1	0

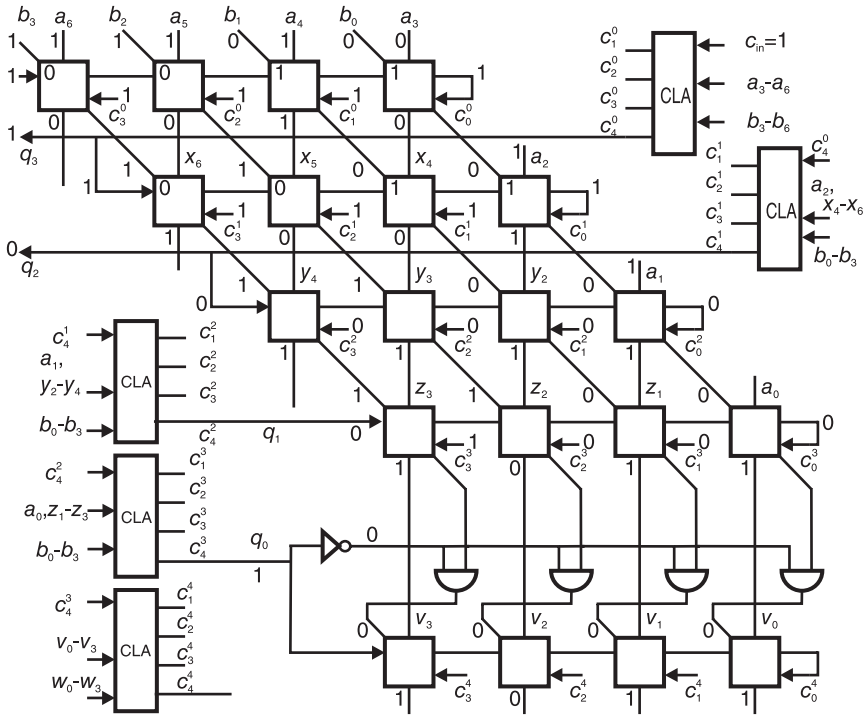


FIGURE 15.93 For Problem 15.4.

Problem 15.4 See Fig. 15.93.

Problem 15.6

a)
$$x_{i+1} = x_i - \frac{x_i^n - B}{nx_i^{n-1}}$$

- b) $x_1 = 1.0741,$
 $x_2 = 0.972,$
 $x_3 = 0.9456, x_4 = 0.9441, x_5 = 0.9441.$
 c) See Table 15.26.

TABLE 15.26 ROM

B binary	B dec.	$\sqrt[5]{B}$ dec.	$\sqrt[5]{B}$ bin.
0, 1000	0.5	0.8706	11011110
0, 1001	0.5625	0.8913	11100100
0, 1010	0.625	0.9103	11101001
0, 1011	0.6875	0.9278	11101101
0, 1100	0.75	0.9441	11110001
0, 1101	0.8125	0.9593	11110101
0, 1110	0.875	0.9736	11111001
0, 1111	0.9375	0.9872	11111100

Problem 15.7

c) $e^{-x} = 0.99999 - 0.99947x + 0.49564x^2 - 0.15386x^3 + 0.02559x^4$

d) $\alpha_i = 0.99999, -0.99947, 0.49564, -0.15386, 0.02559.$

Problem 15.8 $\ln(1+x) = 0.00049 + 0.98248x - 0.39728x^2 + 0.1078x^3.$

Problem 15.13 $PSP^{-1} = T_2 \times I_8, P^2SP^{-2} = I_2 \times T_2 \times I_4, P^3SP^{-3} = I_4 \times T_2 \times I_2.$

Problem 15.17

$P_2 = (ae)(bj)(cf)(dg)(hi)(k).$

Problem 15.18

$J_2 = xy_0 + \bar{x}y_1, K_2 = y_0 + y_1, J_1 = x\bar{y}_0\bar{y}_2 + \bar{x}y_0\bar{y}_2 + \bar{x}\bar{y}_0y_2, K_1 = \bar{x} + y_2$

$J_0 = \bar{x}\bar{y}_2\bar{y}_1 + x\bar{y}_2y_1 + xy_2\bar{y}_1, K_0 = x + y_2, z = y_2y_1\bar{y}_0.$

Random Signal Processing

What we describe mathematically as a pure sinusoid does not exist as a true physical signal. In fact any mathematically defined signal never exists in nature. The complexity of our world, wherein a circle or even a simple straight line exists only in the abstract, in our mind, but never in physical reality, has intrigued philosophers of the past, and in particular Plato, as seen in the Appendix.

In our universe there is virtually an infinite number of elements, from electrons to galaxies, that are in continuous motion and transformation. They influence their neighbors, from atoms to constellations and beyond, causing what may appear to us as mysterious behavior, inexplicable phenomena, sudden expansions, explosions and turmoil.

So erratic appears the behavior of particles and celestial bodies that it is claimed by some, and believed by followers, that in nature there are phenomena which are *purely random*. They state that this has nothing to do with us and our inability to comprehend them. They claim that the behavior of some elements of our universe, whether on the atomic or astronomical level, is *intrinsically* random.

This amounts to saying that there are parts of our universe where the laws of physics do not apply; they are lawless lands, so to speak.

Such contention is preposterous, and risks distorting the views and shaking the confidence of students and young scientists.

In a bowling club, scientists were asked to estimate whether or not the ten pins will be knocked down. They were given all of the information that they asked for and based on that they would evaluate their estimates. The same information was made available to everyone, and each had the same most advanced massively parallel computer in existence. They had already preprogrammed their computers, each scientist employing his or her own advanced probabilistic model of the bowling process. The computers were ready to accept the massive input data from sensors, data that were entered instantly and simultaneously the moment the ball left the hand of the bowler. Data included even those related to that worldwide champion bowler that was expected to knock down all ten pins in one throw.

It was therefore not surprising that all came up with the same estimate; that the ball was on its way to knock down all ten pins; a result that was instantly broadcast, seen by a billion viewers.

The ball hit the pins with determination. Nine pins were swiftly knocked down. Yet, the tenth danced and wobbled, was about to fall but ended up standing upright, refusing to succumb. All scientists have failed. There was a collective gasp and shock all over the world. The scientists were asked to explain their failure.

A young relatively unknown scientist stated jokingly that he was not the Pope, that he will have to take a second look at the required variables, the mathematical models, the equations and the laws of physics behind them.

A top scientist stated that given the state of knowledge at the time it was not surprising that all, including himself, failed. He explained, using complex mathematical equations employing distribution theory, impulsive impacts, quantum mechanics and advanced probabilistic models, that *the problem was in the nature of the problem*.

Few were those who understood what that top scientist meant. The mathematical tools were beyond their means, and even those who were familiar with the scientific notation lacked the time and energy to go over his equations to really comprehend his theory. The general consensus, however, was that what this top scientist meant was that an important previously unknown element in the bowling process was itself *intrinsically* random. That this had nothing to do with our ability or inability to comprehend it. The process itself was random. It was futile to try to mathematically model it. This was not what the top scientist meant. This was what was understood.

A new theory was thus born. Publications *en masse* followed supporting and applying this new scientific wave to other fields from atoms to quasars. Many papers presented highly advanced mathematical analyses proving that *the solution to the problem is that there is no solution*.

Ten years later a scientist published a paper presenting a solution that accepted input variables and evaluated the number of pins that will fall in the bowling process. The solution was a good approximation to physical reality that was valid under usual bowling conditions.

For years thence this solution predicted successfully the number of pins to fall. The metaphor became known as the *bowling process syndrome*. It referred to the fact that the process which was thought to be purely random was fairly predictable. The process itself was not random. Pure randomness was, rather, in the brain of the beholder.

The world has thus learned that if a phenomenon appears to us to be random, unquantifiable, unpredictable, the reason that it so appears is simply due to our ignorance. The more we learn, the more we decipher the universe, the clearer the picture, the less randomness we think we see, and the closer we are to comprehending the scenes as they truly are.

Our theories, the laws of physics as we call them today, will advance, and more of what we see today as purely random, we may see tomorrow as fairly deterministic behavior obeying the law.

Every event related to any element in the universe, from electron to nebula, is a rational, deterministic occurrence. It is governed by the law of causality. No effect is there without a cause. If a phenomenon appears random, if we are unable to find the cause, the fault is in us. The more we learn, the more we refine our laws of physics, the less random the behavior will appear.

However, if we look closer and closer, the behavior of our physical world will always *appear* random. For to be able to evaluate ahead of time, however small that time is, the behavior of any element from the universe as it actually is, deterministic rather than random, we would need to have acquired an infinite amount of knowledge. And that will never happen.

Probability and statistics are powerful tools we use to best model events that we are unable to quantify with certainty. In the following, basic knowledge of the theory of probability and statistics is assumed. Random signals are treated as stationary random processes, having statistics that are invariant to time axis translations. In other words their joint probability density functions are indifferent to translations in time.

A random signal as a function of time will be denoted $x(t)$. It is a single realization of a random process $X(t)$. Given a random process $X(t)$, sampled at time $t = t_i$, the result is a random variable $X_{t_i} = X(t_i)$ which has a probability density function PDF $p(x_{t_i})$. The k^{th} moment of $X(t_i)$ is by definition the expected value of $X^k(t_i)$

$$E[X_{t_i}^k] = \int_{-\infty}^{\infty} x_{t_i}^k p(x_{t_i}) dx_{t_i}. \quad (16.1)$$

If the random process $X(t)$ is sampled at two instants t_1 and t_2 the result is two random variable $X_{t_1} = X(t_1)$ and $X_{t_2} = X(t_2)$. The statistical correlation between $X(t_1)$ and $X(t_2)$

is the joint moment

$$E[X_{t_1}, X_{t_2}] = \int_{-\infty}^{\infty} \int_{-\infty}^{\infty} x_{t_1} x_{t_2} p(x_{t_1}, x_{t_2}) dx_{t_1} dx_{t_2} \tag{16.2}$$

where $p(x_{t_1}, x_{t_2})$ is the joint PDF of x_{t_1} and x_{t_2} . The joint moment is the autocorrelation function denoted $\phi_{xx}(t_1, t_2)$ of the random process $X(t)$ at instants t_1 and t_2 .

If $X(t)$ is a stationary process the joint PDF of $X(t_1)$ and $X(t_2)$ is a function of only the difference $\tau = t_1 - t_2$. The autocorrelation function is thus denoted

$$\phi_{xx}(\tau) = E[X(t_1)X(t_1 + \tau)] \tag{16.3}$$

and we note that, with $t_1 - \tau = \theta$,

$$\phi_{xx}(-\tau) = E[X(t_1)X(t_1 - \tau)] = E[X(\theta + \tau)X(\theta)] = \phi_{xx}(\tau) \tag{16.4}$$

and that $\phi_{xx}(0) = E[X^2(t_1)]$ is the average power of $X(t)$.

The autocovariance function is the same as the autocorrelation function but with the mean values subtracted.

$$\gamma_{xx}(t_1, t_2) = E[\{X(t_1) - m_x(t_1)\} \{X(t_2) - m_x(t_2)\}] = \phi_{xx}(t_1, t_2) - m_x(t_1)m_x(t_2)$$

where $m_x(t_1) = E[X(t_1)]$, $m_x(t_2) = E[X(t_2)]$. If $X(t)$ is stationary, we have, with $\tau = t_1 - t_2$

$$\gamma_{xx}(t_1 - t_2) = \gamma_{xx}(\tau) = \phi_{xx}(\tau) - m_x^2 \tag{16.5}$$

and the variance is $\sigma_x^2 = \gamma_{xx}(0) = \phi_{xx}(0) - m_x^2$.

Consider a random process $X(t)$. Let $\{X(t_i)\}$, $i = 1, 2, \dots, n$, be the random variables at the instants t_i . Let $\{X(t_i + \tau)\}$ be another realization of $X(t)$. If for all values of τ and all values of n the joint probability density functions of the two sets are equal, i.e.

$$p[x(t_1), x(t_2), \dots, x(t_n)] = p[x(t_1 + \tau), x(t_2 + \tau), \dots, x(t_n + \tau)] \tag{16.6}$$

the random process $X(t)$ is known as stationary in the strict sense; otherwise the process is nonstationary. The mean value of the random variable $X_{t_i} = x(t_i)$ is

$$m_x(t_i) = E[X(t_i)] = \int_{-\infty}^{\infty} x_{t_i} p(x_{t_i}) dx_{t_i} \tag{16.7}$$

and the k^{th} moment is

$$E[X^k(t_i)] = \int_{-\infty}^{\infty} x_{t_i}^k p(x_{t_i}) dx_{t_i}. \tag{16.8}$$

For two random variables X_{t_1} and X_{t_2} the autocorrelation is given by

$$\phi_{xx}(t_1, t_2) = E[X_{t_1} X_{t_2}] = \int_{-\infty}^{\infty} \int_{-\infty}^{\infty} x_{t_1} x_{t_2} p(x_{t_1}, x_{t_2}) dx_{t_1} dx_{t_2} \tag{16.9}$$

If the random process is stationary the joint PDF of X_{t_1} and X_{t_2} is the same as that of $X_{t_1+\tau}$ and $X_{t_2+\tau}$ for any time shift τ . In this case the autocorrelation takes the form

$$\phi_{xx}(\tau) = E[X_{t_1} X_{t_1+\tau}] \tag{16.10}$$

In what follows we assume a weaker type of stationarity, referred to as wide-sense stationarity. A wide-sense stationary process is not strictly stationary, yet its first and second

moments are constant, not function of time, and the autocorrelation function depends on only the time difference, i.e. $\phi_{xx}(t_1, t_2) = \phi_{xx}(t_1 - t_2)$.

The cross-correlation is given by

$$\phi_{xy}(\tau) = E[X_{t_1+\tau}Y_{t_1}] \quad (16.11)$$

and the covariance by

$$\gamma_{xy}(\tau) = \phi_{xy}(\tau) - m_x m_y \quad (16.12)$$

16.1 Nonparametric Methods of Power Spectrum Estimation

Stationary random processes, having infinite energy, have no Fourier transform. They have finite average power, however, and can be characterized by a *power spectral density* (PSD). A direct estimate of the (PSD) is known as the *periodogram*, evaluated as the Fourier transform of the autocorrelation function. In what follows we recall first some basic definitions that lead to the definition of the periodogram and related means of PSD estimation.

For continuous-time stationary random signals the PSD is the Fourier transform of the autocorrelation function

$$P_{xx}(\omega) = \Phi_{xx}(j\omega) = \int_{-\infty}^{\infty} \phi_{xx}(\tau) e^{-j\omega\tau} d\tau \quad (16.13)$$

where, for a generally complex random signal $x(t)$, the autocorrelation is

$$\phi_{xx}(\tau) = E[x(t+\tau)x^*(t)]. \quad (16.14)$$

The cross-power spectral density of two jointly stationary random process $x(t)$ and $y(t)$ is by definition

$$P_{xy}(\omega) = \Phi_{xy}(j\omega) = \int_{-\infty}^{\infty} \phi_{xy}(\tau) e^{-j\omega\tau} d\tau. \quad (16.15)$$

In practice we estimate statistical averages by evaluating time averages of single realizations of random processes. Theoretically, a random process for which time averages are asymptotically equal to statistical averages is called *ergodic* [59]. Under such condition

$$\phi_{xx}(\tau) = \lim_{T \rightarrow \infty} r_{xx}(\tau) \quad (16.16)$$

In what follows we assume random signals to be ergodic. The autocorrelation function may therefore be estimated as the time average

$$r_{xx}(\tau) = \frac{1}{2T} \int_{-T}^T x(t+\tau)x^*(t) dt. \quad (16.17)$$

The power spectrum may thus be estimated as the Fourier transform of $r_{xx}(\tau)$

$$\hat{P}_{xx}(\omega) = \int_{-T}^T r_{xx}(\tau) e^{-j\omega\tau} d\tau = \int_{-T}^T \frac{1}{2T} \int_{-T}^T x(t+\tau)x^*(t) dt e^{-j\omega\tau} d\tau$$

Letting $t + \tau = \lambda$ we have

$$\hat{P}_{xx}(\omega) = \frac{1}{2T} \int_{-T}^T x^*(t) \left\{ \int_{-T}^T x(\lambda) e^{-j\omega(\lambda-t)} d\lambda \right\} dt = \frac{1}{2T} |X_T(j\omega)|^2$$

where

$$X_T(j\omega) = \int_{-T}^T x(t)e^{-j\omega t} dt \tag{16.18}$$

The PSD is the expected value of $\hat{P}_{xx}(\omega)$ as T tends to infinity

$$P_{xx}(\omega) = \Phi_{xx}(j\omega) = \lim_{T \rightarrow \infty} E [\hat{P}_{xx}(\omega)] = \lim_{T \rightarrow \infty} E \left[\frac{1}{2T} |X_T(j\omega)|^2 \right]$$

16.2 Correlation of Continuous-Time Random Signals

In this section we study the correlation and power spectral densities of stationary continuous-time domain random signals. Given a generally complex random process $x(t)$ its first moment is the mean

$$m_x = E [x(t)]. \tag{16.19}$$

Its autocorrelation is

$$\phi_{xx}(\tau) = E [x(t + \tau)x^*(t)]. \tag{16.20}$$

Letting $t + \tau = u$ we also have $\phi_{xx}(\tau) = E [x(u)x^*(u - \tau)] = E [x(t)x^*(t - \tau)]$. The joint second moment of two jointly stationary processes $x(t)$ and $y(t)$ is the cross-correlation

$$\phi_{xy}(\tau) = E [x(t + \tau)y^*(t)]. \tag{16.21}$$

Replacing $t + \tau$ by λ and then λ by t we have

$$\phi_{xy}(\tau) = E [x(\lambda)y^*(\lambda - \tau)] = E [x(t)y^*(t - \tau)]. \tag{16.22}$$

We note that $\phi_{xx}(-\tau) = \phi_{xx}^*(\tau)$ and if $x(t)$ is real then $\phi_{xx}(-\tau) = \phi_{xx}(\tau)$. Moreover

$$\phi_{xy}(-\tau) = \phi_{yx}^*(-\tau). \tag{16.23}$$

Subtracting the means we have the cross-covariance

$$\begin{aligned} \gamma_{xy}(\tau) &= E [\{x(t + \tau) - m_x\} \{y^*(t) - m_y^*\}] = \phi_{xy}(\tau) - m_x m_y^* \\ &= \phi_{xy}(\tau) - m_x m_y^*. \end{aligned} \tag{16.24}$$

and the autocovariance

$$\gamma_{xx}(\tau) = E [\{x(t + \tau) - m_x\} \{x^*(t) - m_x^*\}] = \phi_{xx}(\tau) - |m_x|^2. \tag{16.25}$$

If $s(t) = x(t) + y(t)$ then

$$\phi_{ss}(\tau) = \phi_{xx}(\tau) + \phi_{xy}(\tau) + \phi_{yx}(\tau) + \phi_{yy}(\tau). \tag{16.26}$$

If $v(t) = x(t)y(t)$, and if $x(t)$ and $y(t)$ are independent then so are $x(t + \tau)$ and $y(t + \tau)$. We then have

$$\gamma_{vv}(\tau) = E [v(t + \tau)v^*(t)] = E [\{x(t + \tau)x^*(t)\}] E [\{y(t + \tau)y^*(t)\}] = \gamma_{xx}(\tau)\gamma_{yy}(\tau).$$

We note that

$$\phi_{xx}(0) = E [|x(t)|^2] \geq 0 \tag{16.27}$$

and if $x(t)$ is real then

$$E \left[\{x(t + \tau) + x(t)\}^2 \right] = \phi(0) + 2\phi(\tau) + \phi(0) = 2\phi(0) + 2\phi(\tau). \quad (16.28)$$

As stated above, the power spectral density $P_{xx}(\omega)$ or $P_x(\omega)$ of a random process $x(t)$ is the Fourier transform of the autocorrelation function

$$P_{xx}(\omega) = \Phi_{xx}(j\omega) = \int_{-\infty}^{\infty} \phi_{xx}(\tau) e^{-j\omega\tau} d\tau \quad (16.29)$$

and conversely

$$\phi_{xx}(\tau) = \frac{1}{2\pi} \int_{-\infty}^{\infty} P_{xx}(j\omega) e^{j\omega\tau} d\omega \quad (16.30)$$

We note that

$$E \left[|x(t)|^2 \right] = \phi_{xx}(0) = \frac{1}{2\pi} \int_{-\infty}^{\infty} P_{xx}(\omega) d\omega \quad (16.31)$$

and since $\phi_{xx}(-\tau) = \phi_{xx}^*(\tau)$ the transform $P_{xx}(\omega) = \Phi_{xx}(j\omega)$ is real, and we may write

$$P_{xx}(\omega) = \int_{-\infty}^{\infty} \phi_{xx}(\tau) \cos \omega\tau d\tau. \quad (16.32)$$

The power cross-spectral density of two processes $x(t)$ and $y(t)$ is the transform of the cross-correlation

$$P_{xy}(\omega) = \Phi_{xy}(j\omega) = \int_{-\infty}^{\infty} \phi_{xy}(\tau) e^{-j\omega\tau} d\tau \quad (16.33)$$

and conversely

$$\phi_{xy}(\tau) = \frac{1}{2\pi} \int_{-\infty}^{\infty} P_{xy}(\omega) e^{j\omega\tau} d\omega. \quad (16.34)$$

We note that $P_{yx}(\omega) = P_{xy}^*(\omega)$.

Two processes $x(t)$ and $y(t)$ are uncorrelated or “orthogonal” if

$$\phi_{xy}(\tau) = 0 \quad (16.35)$$

then $P_{xy}(\omega) = 0$.

16.3 Passage through an LTI System

Let $x(t)$ be the input and $y(t)$ the output random processes of an LTI system of impulse response $h(t)$. We have

$$y(t) = x(t) * h(t) = \int_{-\infty}^{\infty} h(\tau) x(t - \tau) d\tau. \quad (16.36)$$

The mean value of $y(t)$ is given by

$$m_y = E[y(t)] = E \left[\int_{-\infty}^{\infty} h(\tau) x(t - \tau) d\tau \right] = E[x(t - \tau)] \int_{-\infty}^{\infty} h(\tau) d\tau = H(0)m_x. \quad (16.37)$$

The cross-correlation $\phi_{yx}(\tau)$ relating the system output to its input is found by multiplying both sides of (16.36) by $x^*(t - \tau)$. We have

$$y(t)x^*(t - \tau) = \int_{-\infty}^{\infty} x^*(t - \tau)h(\lambda)x(t - \lambda)d\lambda \tag{16.38}$$

so that

$$\phi_{yx}(\tau) = E[y(t)x^*(t - \tau)] = \int_{-\infty}^{\infty} \phi_{xx}(\tau - \lambda)h(\lambda)d\lambda \tag{16.39}$$

having noted that

$$E[x(t - \lambda)x^*(t - \tau)] = \phi_{xx}[(t - \lambda) - (t - \tau)] = \phi_{xx}(\tau - \lambda) \tag{16.40}$$

or by writing

$$E[x(t - \lambda)x^*(t - \tau)] = E[x(u)x^*(u + \lambda - \tau)] = E[x(t)x^*[t - (\tau - \lambda)]] = \phi_{xx}(\tau - \lambda).$$

Hence

$$\phi_{yx}(\tau) = \phi_{xx}(\tau) * h(\tau) \tag{16.41}$$

We can further write from Equation (16.36)

$$y^*(t) = \int_{-\infty}^{\infty} h^*(\lambda)x^*(t - \lambda)d\lambda \tag{16.42}$$

and multiplying both sides by $y(t + \tau)$ and taking the expectation we have

$$\begin{aligned} E[y(t + \tau)y^*(t)] &= E\left[\int_{-\infty}^{\infty} y(t + \tau)h^*(\lambda)x^*(t - \lambda)d\lambda\right] = \int_{-\infty}^{\infty} h^*(\lambda)E[y(t + \tau)x^*(t - \lambda)]d\lambda \\ \phi_{yy}(\tau) &= \int_{-\infty}^{\infty} \phi_{yx}(\tau + \lambda)h^*(\lambda)d\lambda = \int_{-\infty}^{\infty} \phi_{yx}(u)h^*(u - \tau)du \\ &= \phi_{yx}(\tau) * h^*(-\tau). \end{aligned} \tag{16.43}$$

Similarly, we obtain

$$\begin{aligned} \phi_{xy}(\tau) &= \phi_{xx}(\tau) * h^*(-\tau) \\ \phi_{yy}(\tau) &= \phi_{xy}(\tau) * h(\tau) \\ \phi_{yy}(\tau) &= \phi_{xx}(\tau) * h(\tau) * h^*(-\tau). \end{aligned} \tag{16.44}$$

Taking the Fourier transforms of these relations we obtain corresponding spectral density expressions. In particular we have

$$P_{xy}(\omega) = \Phi_{xy}(j\omega) = \Phi_{xx}(j\omega)H^*(j\omega) = P_{xx}(\omega)H^*(j\omega) \tag{16.45}$$

$$P_{yy}(\omega) = \Phi_{yy}(j\omega) = \Phi_{xy}(j\omega)H(j\omega) = P_{xy}(j\omega)H(j\omega) = P_{xx}(\omega)|H(j\omega)|^2. \tag{16.46}$$

Writing $v(\tau) = h(\tau) * h^*(-\tau) = h(\tau) \star h(\tau)$ we have

$$V(j\omega) = |H(j\omega)|^2 \tag{16.47}$$

$$\phi_{yy}(\tau) = \phi_{xx}(\tau) * v(\tau) \tag{16.48}$$

and

$$\Phi_{yy}(j\omega) = \Phi_{xx}(j\omega)V(j\omega) \tag{16.49}$$

$$P_{yy}(\omega) = P_{xx}(\omega)V(j\omega). \tag{16.50}$$

These relations can be represented in block diagram form as shown in Fig. 16.1.

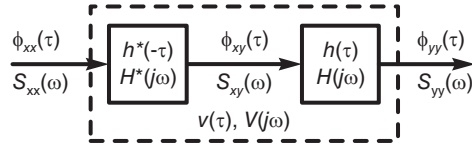


FIGURE 16.1 Linear time invariant (LTI) system input and output correlations.

Example 16.1 Evaluate the power spectral density of the process $x(t)$ for the cases a) $\phi_{xx}(\tau) = e^{-\alpha|\tau|}$, b) $\phi_{xx}(\tau) = e^{-\alpha|\tau|} \cos \beta\tau$

a) We have

$$P_{xx}(\omega) = \Phi_{xx}(j\omega) = \frac{2\alpha}{\alpha^2 + \omega^2} \tag{16.51}$$

b)

$$\begin{aligned} P_{xx}(\omega) &= \mathcal{F} [e^{-\alpha t} \cos \beta t u(t)] + \mathcal{F} [e^{\alpha t} \cos \beta t u(-t)] \\ &= \frac{s + \alpha}{(s + \alpha)^2 + \beta^2} + \frac{-s + \alpha}{(-s + \alpha)^2 + \beta^2} \Big|_{s=j\omega} \\ &= \frac{j\omega + \alpha}{(\alpha + j\omega)^2 + \beta^2} - \frac{j\omega - \alpha}{(\alpha - j\omega)^2 + \beta^2} \end{aligned} \tag{16.52}$$

which can be written in the form

$$P_{xx}(\omega) = \frac{\alpha}{(\omega - \beta)^2 + \alpha^2} + \frac{\alpha}{(\omega + \beta)^2 + \alpha^2}. \tag{16.53}$$

Example 16.2 Given a random process $x(t)$ of autocorrelation $\phi_{xx}(\tau)$ and spectral density $P_{xx}(\omega)$, evaluate the autocorrelation and power spectral density of the random process $y(t)$ defined by

$$y(t) = x(t) * h(t) \tag{16.54}$$

where

$$h(t) = \frac{1}{2T} \Pi_T(t) \tag{16.55}$$

is the impulse response of a smoothing filter.

From the definition, referring to Fig. 16.2 we have

$$y(t) = \int_{-\infty}^{\infty} x(\tau) h(t - \tau) d\tau = \frac{1}{2T} \int_{t-T}^{t+T} x(\tau) d\tau \tag{16.56}$$

$$H(j\omega) = Sa(T\omega) \tag{16.57}$$

$$V(j\omega) = |H(j\omega)|^2 = Sa^2(T\omega) \tag{16.58}$$

$$v(t) = \mathcal{F}^{-1} [Sa^2(T\omega)] = \frac{1}{2T} \{1 - |t|/(2T)\} = \frac{1}{2T} \Lambda_{2T}(t) \tag{16.59}$$

which is depicted in Fig. 16.3.

$$\phi_{yy}(\tau) = \phi_{xx}(\tau) * v(\tau) = \frac{1}{2T} \int_{-2T}^{2T} \Lambda_{2T}(\lambda) \phi_{xx}(\tau - \lambda) d\lambda \tag{16.60}$$

and

$$P_{yy}(\omega) = P_{xx}(\omega) Sa^2(T\omega). \tag{16.61}$$

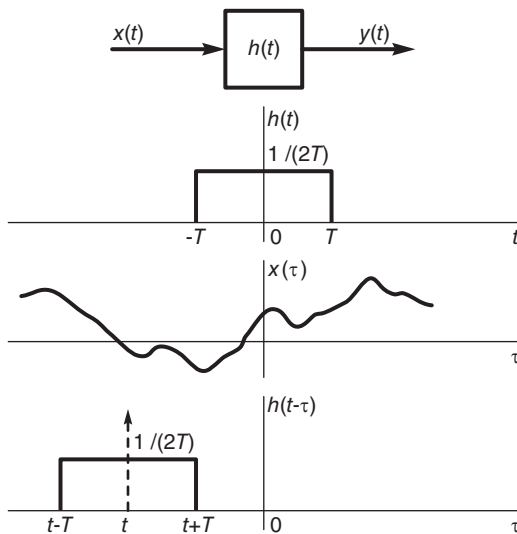


FIGURE 16.2 System response.

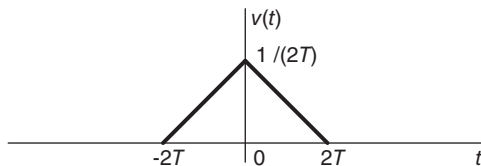


FIGURE 16.3 The function $v(t)$.

16.4 Wiener Filtering in Continuous-Time Domain

Wiener filtering deals with the problem of estimating a signal contaminated by additive noise. Linear mean-square estimation is the basic tool for evaluating an optimal filter impulse response. Consider the problem of estimating a real, for simplicity, random variable v as a weighted sum of n given random variables, or components, u_k

$$\hat{v} = \sum_{k=1}^n a_k u_k \tag{16.62}$$

by minimizing the mean square error

$$e = E \left[(v - \hat{v})^2 \right] = E \left[\left(v - \sum_{k=1}^n a_k u_k \right)^2 \right]. \tag{16.63}$$

To this end we may apply the *orthogonality principle*, which states that the optimum coefficients a_k are those causing the error $(v - \hat{v})$ to be orthogonal to each of the components $\{u_j\}$, $j = 1, 2, \dots, n$, i.e.

$$E[(v - \hat{v}) u_j] = 0, \quad j = 1, 2, \dots, n. \tag{16.64}$$

Indeed, the minimum value of e is such that

$$\frac{\partial e}{\partial a_j} = E \left[-2 \left(v - \sum_{k=1}^n a_k u_k \right) u_j \right] = 0 \quad (16.65)$$

implying that $E[(v - \hat{v}) u_j] = 0$ as stated. The coefficients a_k are thus found by solving the equations

$$E[vu_j] = \sum_{k=1}^n a_k E[u_k u_j], \quad j = 1, 2, \dots, n \quad (16.66)$$

Moreover, since each component u_k of the estimate \hat{v} is orthogonal to the error $(v - \hat{v})$, the estimate \hat{v} is itself orthogonal to $(v - \hat{v})$, i.e. $E[(v - \hat{v}) \hat{v}] = 0$ and $E[v\hat{v}] = E[\hat{v}^2]$. The resulting mean-square error is therefore

$$e_{min} = E[(v - \hat{v})(v - \hat{v})] = E[(v - \hat{v})v] = E[v^2] - E[\hat{v}^2] \quad (16.67)$$

In the Wiener filtering problem we are given a random signal

$$x(t) = v(t) + b(t) \quad (16.68)$$

where $v(t)$ is a stationary random signal to be estimated and $b(t)$ is random noise. The random processes $v(t)$ and $b(t)$ are jointly stationary with known correlations or power spectra. To estimate the signal $v(t)$ we seek a filter of impulse response $h(t)$ which upon receiving the contaminated signal $x(t)$ produces an output

$$y(t) = \int_{-\infty}^{\infty} h(\tau)x(t - \tau)d\tau \quad (16.69)$$

which best approximates $v(t)$ in the minimum mean-square sense. In other words the filter response should be

$$y(t) = \hat{v}(t) = \int_{-\infty}^{\infty} h(\tau)x(t - \tau)d\tau \quad (16.70)$$

and should minimize the error

$$e = E[(v(t) - \hat{v}(t))^2]. \quad (16.71)$$

To obtain the optimum impulse response $h(t)$ we may use the orthogonality principle. We note that the estimate $\hat{v}(t)$ is a weighted sum of the components $x(t - \tau)$ where τ extends in value from $-\infty$ to ∞ .

Drawing on our orthogonality principle results, with the integral limits extending from $-\infty$ to ∞ , we note that the mean square error is minimized if the error $e = (v(t) - \hat{v}(t))$ is orthogonal to the components $x(t - \tau)$

$$E[\{v(t) - \hat{v}(t)\} x(t - \tau)] = 0 \quad (16.72)$$

i.e.

$$E[v(t)x(t - \tau)] = E \left[\int_{-\infty}^{\infty} h(\lambda)x(t - \lambda)d\lambda x(t - \tau) \right] \quad (16.73)$$

or

$$\phi_{vx}(\tau) = \int_{-\infty}^{\infty} h(\lambda)\phi_{xx}(\tau - \lambda)d\lambda \quad (16.74)$$

of which the solution is the optimum impulse response $h(t)$. In terms of power spectral densities this equation, which is a form of the Wiener–Hopf equation, may be put in the form

$$P_{vz}(\omega) = \Phi_{vx}(j\omega) = H(j\omega)\Phi_{xx}(j\omega) = H(j\omega)P_{xx}(\omega) \tag{16.75}$$

$$H(j\omega) = \frac{P_{vx}(\omega)}{P_{xx}(\omega)} \tag{16.76}$$

and since the error $\{v(t) - \hat{v}(t)\}$ is orthogonal to each component $x(t - \tau)$ of $\hat{v}(t)$ we have

$$E [\{v(t) - \hat{v}(t)\} \hat{v}(t)] = 0 \tag{16.77}$$

so that the minimum mean-square error is given by

$$\begin{aligned} e_{min} &= E [\{v(t) - \hat{v}(t)\}^2] = E [\{v(t) - \hat{v}(t)\} v(t)] = \phi_{vv}(0) - E \left[\int_{-\infty}^{\infty} h(\tau)x(t - \tau)d\tau v(t) \right] \\ &= \phi_{vv}(0) - E \left[\int_{-\infty}^{\infty} h(\lambda)x(t - \lambda)d\lambda v(t) \right] = \phi_{vv}(0) - \int_{-\infty}^{\infty} h(\lambda)\phi_{vx}(\lambda)d\lambda. \end{aligned}$$

Using Parseval’s relation we may also write

$$e_{min} = \frac{1}{2\pi} \int_{-\infty}^{\infty} \{P_{vv}(\omega) - P_{vx}(\omega)H(j\omega)\} d\omega. \tag{16.78}$$

If the signal $v(t)$ and noise $b(t)$ are uncorrelated, i.e. $\phi_{vb}(\tau) = E [v(t)b(t - \tau)] = 0$ then the cross-power spectral density

$$P_{vx}(\omega) = P_{vv}(\omega) \tag{16.79}$$

$$P_{xx}(\omega) = P_{vv}(\omega) + P_{bb}(\omega) \tag{16.80}$$

so that

$$H(j\omega) = \frac{P_{vv}(\omega)}{P_{vv}(\omega) + P_{bb}(\omega)} \tag{16.81}$$

$$e = \frac{1}{2\pi} \int_{-\infty}^{\infty} \frac{P_{vv}(\omega)P_{bb}(\omega)}{P_{vv}(\omega) + P_{bb}(\omega)} d\omega \tag{16.82}$$

and if the noise spectral density tends to a value much higher than that of the signal, i.e. $P_{bb}(\omega) \rightarrow B \gg P_{vv}(\omega)$ then

$$H(j\omega) \rightarrow P_{vv}(\omega)/B \tag{16.83}$$

$$h(t) \rightarrow (1/B)\phi_{vv}(t) \tag{16.84}$$

and

$$e \rightarrow \frac{1}{2\pi} \int_{-\infty}^{\infty} P_{vv}(\omega)d\omega = \phi_{vv}(0) = E [v^2(t)]. \tag{16.85}$$

16.5 Causal Wiener Filter

The Wiener filter we have just developed has a two-sided (i.e. noncausal) impulse response. It is therefore not physically realizable. A physically realizable filter has to have a causal impulse response and has available only the past values and present value of the input signal. The estimate of the signal $v(t)$ is thus given by

$$\hat{v}(t) = \int_0^{\infty} h(\tau)x(t-\tau)d\tau \quad (16.86)$$

where τ now takes on all values from 0 to ∞ . Similarly to the above the orthogonality principle states that the mean square estimation error is minimum if

$$E\{[v(t) - \hat{v}(t)]x(t-\tau)\} = 0 \quad \tau > 0. \quad (16.87)$$

Hence the Wiener–Hopf equation takes the form

$$\phi_{vx}(\tau) - \int_0^{\infty} h(\lambda)\phi_{xx}(\tau-\lambda)d\lambda = 0, \quad \tau > 0 \quad (16.88)$$

The optimum impulse response $h(t)$ is obtained by solving this equation.

However, the solution is more elaborate than the previous case of the two-sided Wiener filter where the Wiener–Hopf equation was valid for all τ . Presently we let $f(\tau)$ denote the left-hand side of the equation. We have

$$f(\tau) = \phi_{vx}(\tau) - \int_0^{\infty} h(\lambda)\phi_{xx}(\tau-\lambda)d\lambda \quad (16.89)$$

and note that $f(\tau) = 0$, $\tau > 0$. With $F(s)$ and $H(s)$ the Laplace transforms of $f(\tau)$ of the left-sided $f(\tau)$ and the right-sided $h(\tau)$ we note that their regions of convergence (ROCs) are $\sigma < 0$ and $\sigma > 0$, respectively. Moreover,

$$\phi_{vx}(\tau) \xleftrightarrow{\mathcal{F}} P_{vx}(\omega), \quad \phi_{vx}(\tau) \xleftrightarrow{\mathcal{L}} P_{vx}(-js) \quad (16.90)$$

$$\phi_{xx}(\tau) \xleftrightarrow{\mathcal{F}} P_{xx}(\omega), \quad \phi_{xx}(\tau) \xleftrightarrow{\mathcal{L}} P_{xx}(-js) \quad (16.91)$$

so we may write

$$F(s) = P_{vx}(-js) - P_{xx}(-js)H(s) \quad (16.92)$$

and set out to satisfy this equation in the ROC $\sigma < 0$ of $F(s)$. To this end we may factor the m $P_{xx}(-js)$ into the product

$$P_{xx}(-js) = P^+(s)P^-(s) \quad (16.93)$$

where $P^+(s)$ has a ROC $\sigma > 0$ and is minimum phase, having all its poles and zeros in the left half of the s plane, and $P^-(s)$ has the ROC $\sigma < 0$ and is maximum phase, having all its poles and zeros in the right half of the s plane. Now

$$Y(s) = P_{vx}(-js) - P^+(s)P^-(s)H(s) \quad (16.94)$$

i.e.

$$\frac{Y(s)}{P^-(s)} = \frac{P_{vx}(-js)}{P^-(s)} - P^+(s)H(s). \quad (16.95)$$

We may now decompose the left-hand side into the transform of a causal function plus that of an anticausal one.

$$\frac{Y(s)}{P^-(s)} = Q^+(s) + Q^-(s) \tag{16.96}$$

where $Q^+(s)$ and $Q^-(s)$ are analytic for $\sigma > 0$ and $\sigma < 0$, respectively. The last two equations imply that

$$Q^+(s) + Q^-(s) - P^+(s)H(s) = 0 \tag{16.97}$$

i.e.

$$Q^+(s) = P^+(s)H(s), \sigma > 0 \tag{16.98}$$

or

$$H(s) = Q^+(s)/P^+(s), \sigma > 0 \tag{16.99}$$

and the minimum mean-square error is given similarly to the above by

$$e_{min} = \phi_{vv}(0) - \int_0^\infty h(\lambda)\phi_{vx}(\lambda)d\lambda. \tag{16.100}$$

Example 16.3 We need to approximate the value $x(t + \tau)$ of a stationary random process $x(t)$. Suppose the estimate is $\hat{x}(t + \tau) = \gamma x(t)$. Evaluate the constant γ that leads to minimum mean square error.

The mean square error is given by

$$e_\gamma = E \left[\{x(t + \tau) - \gamma x(t)\}^2 \right] = E \left[x(x + \tau)^2 - 2\gamma x(t)x(t + \tau) + \gamma^2 x^2(t) \right]$$

$$\frac{\partial e_\gamma}{\partial \gamma} = E \left[-2x(t)x(t + \tau) + 2\gamma x^2(t) \right] = 0 \tag{16.102}$$

$$2\phi_{xx}(\tau) = 2\gamma\phi_{xx}(0) \tag{16.103}$$

$$\gamma = \phi_{xx}(\tau)/\phi_{xx}(0). \tag{16.104}$$

The resulting minimum mean square error is

$$\begin{aligned} e_{min} &= E \left[x(t + \tau) \right]^2 - 2\gamma\phi_{xx}(\tau) + \gamma^2\phi_{xx}(0) = \phi_{xx}(0) - 2\gamma^2\phi_{xx}(0) + \gamma^2\phi_{xx}(0) \\ &= \phi_{xx}(0) - \gamma^2\phi_{xx}(0) = \phi_{xx}(0) - \frac{\phi_{xx}^2(\tau)}{\phi_{xx}(0)}. \end{aligned} \tag{16.105}$$

Example 16.4 Evaluate the impulse response $h(t)$ and the minimum mean square error if

$$P_{xx}(\omega) = \frac{5}{\omega^2 + 2}, P_{bb}(\omega) = K$$

assuming that the signal $x(t)$ and the noise $b(t)$ are uncorrelated.

We have

$$H(j\omega) = \frac{P_{xx}(\omega)}{P_{xx}(\omega) + P_{bb}(\omega)}, \quad P_{xb}(\omega) = 0$$

$$H(j\omega) = \frac{\frac{5}{\omega^2 + 2}}{\frac{5}{\omega^2 + 2} + K} = \frac{5}{5 + K(\omega^2 + 2)} = \frac{5/K}{5/K + \omega^2 + 2} = \frac{5/K}{\gamma^2 + \omega^2}$$

$$\gamma^2 = 2 + 5/K$$

$$h(t) = \frac{5}{2K\gamma} e^{-\gamma|t|}$$

$$\begin{aligned} e &= \frac{1}{2\pi} \int_{-\infty}^{\infty} \frac{P_{xx}(\omega)P_{bb}(\omega)}{P_{xx}(\omega) + P_{bb}(\omega)} d\omega = \frac{1}{2\pi} \int_{-\infty}^{\infty} \frac{(5/K)K}{(\gamma^2 + \omega^2)} d\omega \\ &= \frac{5}{2\pi} \int_{-\infty}^{\infty} \frac{d\omega}{\gamma^2 + \omega^2} = \frac{5}{2\gamma}. \end{aligned}$$

16.6 Random Sequences

Similarly to the continuous-time domain, a random process $X[n]$ in the discrete time domain is an ensemble of random sequences $x[n]$ of which the elements have probabilities of occurrence. A sequence $x[n]$, $-\infty < n < \infty$ is one *realization* of the random process and is referred to as a *sample sequence* of the process.

In the discrete-time domain a random signal is often a sampling of a continuous-time random process. The time axis is now a progression of integer values n and the signal is a random variable x_n of which a particular value at time n is $x[n]$. Similarly to the continuous-time domain, the k^{th} moment of $X[n]$ is

$$E[X_n^k] = \int_{-\infty}^{\infty} x_n^k p_{x_n} dx_n \quad (16.106)$$

and the cross-correlation sequence for generally complex sequences X_n and Y_k is by definition

$$\phi_{xy}[n, k] = E[X_n Y_k^*] = \int_{-\infty}^{\infty} \int_{-\infty}^{\infty} x_n y_k^* p(x_n, y_k) dx_n dy_k. \quad (16.107)$$

The autocorrelation is

$$\phi_{xx}[n, k] = E[X_n X_k^*] = \int_{-\infty}^{\infty} \int_{-\infty}^{\infty} x_n x_k^* p(x_n, x_k) dx_n dx_k \quad (16.108)$$

The cross-covariance is

$$\gamma_{xy}[n, k] = E[(X_n - m_{x_n})(Y_k - m_{y_k})^*] = \phi_{xy}[n, k] - m_{x_n} m_{y_k} \quad (16.109)$$

where $m_{x_n} = E[X_n]$ and $m_{y_n} = E[Y_n]$. A random signal, denoted x_n or $x[n]$, are assumed in what follows to be stationary. The mean and variance are constant and we may write the mean, variance and autocorrelation, respectively, as

$$m_x = E[x_n] \quad (16.110)$$

$$\sigma_x^2 = E[(x_n - m_x)^2] \quad (16.111)$$

$$\phi_{xx}[n + m, n] \triangleq \phi_{xx}[m] = E[x_{n+m} x_n^*] \quad (16.112)$$

The cross-correlation $\phi_{xy}[m]$ of random variables x_n and y_n , and of the random sequences $x[n]$ and $y[n]$, respectively, are given by

$$\phi_{xy}[m] = E[x_{n+m} y_n^*] = E[x_n y_{n-m}^*] \quad (16.113)$$

$$\phi_{xy}[m] = E[x[n + m] y[n]^*] = E[x[n] y[n - m]^*] \quad (16.114)$$

and if x_n is real then

$$\phi_{xx}[m] = E[x_{n+m}x_n] \tag{16.115}$$

$$\gamma_{xy}[m] = \phi_{xy}[m] - m_x m_y. \tag{16.116}$$

We note that $\lim_{m \rightarrow \infty} \phi_{xx}[m] = E[x_n^2] = m_x^2$, wherefrom the z -transform $\Phi_{xx}(z)$ of $\phi_{xx}[m]$ exists only if $m_x = 0$, in which case $\Gamma_{xx}(z) = \Phi_{xx}(z)$. The power spectral density is the Fourier transform of the autocorrelation sequence

$$P_{xx}(\Omega) \triangleq \Phi_{xx}(e^{j\Omega}) = \sum_{m=-\infty}^{\infty} \phi_{xx}[m] e^{-j\Omega m} \tag{16.117}$$

and

$$\phi_{xx}[m] = \frac{1}{2\pi} \int_{-\infty}^{\infty} \Phi_{xx}(\Omega) e^{j\Omega m} d\Omega. \tag{16.118}$$

Example 16.5 Let $x[n]$ and $y[n]$ be two zero-mean random processes. Let $v[n] = x[n] - y[n]$. Evaluate the autocovariance sequence of $v[n]$.

The autocovariance sequence of $v[n]$ is given by

$$\gamma_{vv}[m] = \phi_{vv}[m] - m_v^2 \tag{16.119}$$

where

$$m_v = E[v[n]] = E[x[n] - y[n]] = 0 \tag{16.120}$$

so that

$$\gamma_{vv}[m] = \phi_{vv}[m] = E[\{x[n] - y[n]\} \{x[n+m] - y[n+m]\}] \tag{16.121}$$

$$= \phi_{xx}[m] - \phi_{xy}[m] - \phi_{yx}[m] + \phi_{yy}[m]. \tag{16.122}$$

16.7 From Statistical to Time Averages

In practice we do not usually have probability distributions and statistics of a given class of random signals. We often have to evaluate averages from single recordings of finite duration signals. To this end we have to evaluate time averages instead of statistical ones. Assuming the process is ergodic we define an approximation of the mean of a random sequence $x[n]$ as

$$\mu_x = \frac{1}{2N+1} \sum_{n=-N}^N x[n] \tag{16.123}$$

with the implication that as N tends to infinity the time average μ_x will tend to the statistical mean m_x . We note that the time average μ_x is itself a random variable and our approximation would be well justified if its average value is equal to m_x . In this case the estimate μ_x is called *unbiased*. We may also evaluate the variance of the estimate μ_x . The lower the variance the less the deviation there is from the true value m_x .

The time autocorrelation of a real sequence, an approximation of the statistical one, is by definition

$$c_{xx}[m] = \frac{1}{2N+1} \sum_{n=-N}^N x[n+m]x[n] \quad (16.124)$$

and, for any lag m , is a random variable approximating the statistical autocorrelation $\phi_{xx}[m]$.

16.8 Correlation and Covariance in z -Domain

We consider generally complex stationary random processes $\{x_n\}$ and $\{y_n\}$. As noted above the z -transform $\Phi_{xx}(z)$ of the autocorrelation sequence $\phi_{xx}[m]$ exists if and only if $m_x = 0$, in which case $\Gamma_{xx}(z) \triangleq Z[\gamma_{xx}[m]] = \Phi_{xx}(z)$ and $\Gamma_{xy}(z) \triangleq Z[\gamma_{xy}[m]] = \Phi_{xy}(z)$. Moreover, if x and y are linearly independent, i.e. uncorrelated

$$\lim_{m \rightarrow \infty} \phi_{xy}[m] = E[x_n y_n] = m_x m_y \quad (16.125)$$

so that $\Phi_{xy}(z)$ exists if and only if m_x or m_y or both are zero, in which case $\gamma_{xy}[m] = \phi_{xy}[m]$ and $\Gamma_{xy}(z) = \Phi_{xy}(z)$. The following relations can also be inferred.

$$E[x_n^2] \equiv \text{mean - square value} = \phi_{xx}[0] \quad (16.126)$$

$$\sigma_x^2 \equiv \text{variance} = E[(x - m_x)^2] = \gamma_{xx}[0] \quad (16.127)$$

$$\phi_{xx}[m] = \phi_{xx}[-m], \quad \phi_{xy}[m] = \phi_{yx}[-m], \quad (16.128)$$

$$\gamma_{xx}[m] = \gamma_{xx}[-m], \quad \gamma_{xy}[m] = \gamma_{yx}[-m] \quad (16.129)$$

$$|\phi_{xx}[m]| \leq \phi_{xx}[0], \quad \gamma_{xx}[m] \leq \gamma_{xx}[0]. \quad (16.130)$$

$$\lim_{m \rightarrow \infty} \phi_{xx}[m] = E[x_n^2] = \{E[x_n]\}^2 = m_x^2 \quad (16.131)$$

$$\lim_{m \rightarrow \infty} \gamma_{xx}[m] = 0, \quad \lim_{m \rightarrow \infty} \phi_{xy}[m] = m_x m_y, \quad \lim_{m \rightarrow \infty} \phi_{yx}[m] = 0 \quad (16.132)$$

$$\phi_{xx}[m] = \frac{1}{2\pi j} \oint_C \Phi_{xx}(z) z^{m-1} dz \quad (16.133)$$

and

$$\sigma_x^2 = \phi_{xx}[0] = \frac{1}{2\pi j} \oint_C \Phi_{xx}(z) z^{-1} dz \quad (16.134)$$

where C is a closed contour in the ROC of $\Gamma_{xx}(z)$. Moreover, since $\phi_{xx}[m] = \phi_{xx}^*[-m]$ and $\phi_{xy}[m] = \phi_{yx}^*[-m]$

$$\Phi_{xx}(z) = \Phi_{xx}^*(1/z^*) \quad (16.135)$$

and

$$\Phi_{xy}(z) = \Phi_{yx}^*(1/z^*) \quad (16.136)$$

The ROC of $\Gamma_{xx}(z)$ is therefore an annular region $r < |z| < 1/r$ and since $\lim_{m \rightarrow \infty} \gamma_{xx}[m] = 0$ the Fourier transform $\Gamma_{xx}(e^{j\Omega})$ exists; hence the unit circle is within the annular ROC i.e.

$0 < r < 1$. We recall, moreover, that the power spectral density, or power spectrum is by definition

$$P_{xx}(\Omega) = \Phi_{xx}(e^{j\Omega}) \tag{16.137}$$

and we may write

$$\phi_{xx}[m] = \frac{1}{2\pi} \int_{-\pi}^{\pi} \Phi_{xx}(e^{j\Omega}) e^{j\Omega m} d\Omega \tag{16.138}$$

$$\gamma_{xx}[m] = \frac{1}{2\pi} \int_{-\pi}^{\pi} \Gamma_{xx}(e^{j\Omega}) e^{j\Omega m} d\Omega \tag{16.139}$$

and

$$E[|x[n]|^2] = \phi_{xx}[0] = \frac{1}{2\pi} \int_{-\pi}^{\pi} \Phi_{xx}(e^{j\Omega}) d\Omega = \frac{1}{2\pi} \int_{-\pi}^{\pi} P_{xx}(\Omega) d\Omega \tag{16.140}$$

$$\sigma_x^2 = \gamma_{xx}[0] = \frac{1}{2\pi} \int_{-\pi}^{\pi} \Gamma_{xx}(e^{j\Omega}) d\Omega = \frac{1}{2\pi} \int_{-\pi}^{\pi} P_{xx}(\Omega) d\Omega - |m_x|^2 \tag{16.141}$$

16.9 Random Signal Passage through an LTI System

We presently investigate the input–output relations of an LTI system upon applying a real input sequence $x[n]$ that is a realization of a stationary random process. Let $h[n]$ be the system unit pulse response and $H(z)$ its transfer function. The mean value of the system output $y[n]$ is given by

$$m_y = E[y[n]] = E\left[\sum_{k=-\infty}^{\infty} h[k]x[n-k]\right] = \sum_{k=-\infty}^{\infty} h[k]E[x[n-k]] \tag{16.142}$$

$$= m_x \sum_{k=-\infty}^{\infty} h[k] = H(1)m_x. \tag{16.143}$$

The autocorrelation sequence of the output is

$$\begin{aligned} \phi_{yy}[n, n+m] &= E[y[n]y[n+m]] = E\left[\sum_{k=-\infty}^{\infty} h[k]x[n-k] \sum_{i=-\infty}^{\infty} h[i]x[n+m-i]\right] \\ &= E\left[\sum_{k=-\infty}^{\infty} h[k] \sum_{i=-\infty}^{\infty} h[i]x[n-k]x[n+m-i]\right] \\ &= \sum_{k=-\infty}^{\infty} h[k] \sum_{i=-\infty}^{\infty} h[i]E[x[n-k]x[n+m-i]]. \end{aligned}$$

Note however that $x[n]$ is assumed to be stationary. This implies that $E[x[n-k]x[n+m-i]]$ is a function of only the difference $(n+m-i) - (n-k) = m-i+k$, and not a function of n . We may therefore write

$$\phi_{yy}[n, n+m] \triangleq \phi_{yy}[m] = \sum_{k=-\infty}^{\infty} h[k] \sum_{i=-\infty}^{\infty} h[i]\phi_{xx}[m-i+k] \tag{16.144}$$

Letting $r = i - k$ we have

$$\phi_{yy}[m] = \sum_{k=-\infty}^{\infty} h[k] \sum_{r=-\infty}^{\infty} h[r+k] \phi_{xx}[m-r] = \sum_{r=-\infty}^{\infty} \phi_{xx}[m-r] \sum_{k=-\infty}^{\infty} h[k] h[r+k].$$

Letting

$$v[r] = \sum_{k=-\infty}^{\infty} h[k] h[r+k] = h[r] * h[-r] = h[r] * h[-r] \quad (16.145)$$

that is, $v[r]$ is the autocorrelation of the system unit sample response, we have

$$\phi_{yy}[m] = \sum_{r=-\infty}^{\infty} v[r] \phi_{xx}[m-r] \quad (16.146)$$

meaning that the autocorrelation of the system response is equal to the convolution of the input signal autocorrelation with the autocorrelation of the system impulse response. In the z -transform domain we have

$$\Phi_{yy}(z) = V(z) \Phi_{xx}(z) \quad (16.147)$$

and

$$V(z) = H(z)H(z^{-1}) \quad (16.148)$$

so that

$$\Phi_{yy}(z) = H(z)H(z^{-1})\Phi_{xx}(z) \quad (16.149)$$

and if $m_x = 0$ then $m_y = H(1)m_x = 0$, the z -transform exists and $\gamma_{xx}[m] = \phi_{xx}[m]$ so that

$$\Gamma_{yy}(z) = H(z)H(z^{-1})\Gamma_{xx}(z) \quad (16.150)$$

The system output power spectral density is

$$P_{yy}(\Omega) = \Phi_{yy}(e^{j\Omega}) = |H(e^{j\Omega})|^2 \Phi_{xx}(e^{j\Omega}) = |H(e^{j\Omega})|^2 P_{xx}(\Omega). \quad (16.151)$$

The system output-input cross-correlation is given by

$$\phi_{yx}[m] = E[y[n+m]x[n]] = E\left[x[n] \sum_{k=-\infty}^{\infty} h[k]x[n+m-k]\right] \quad (16.152)$$

$$= \sum_{k=-\infty}^{\infty} h[k] \phi_{xx}[m-k] \quad (16.153)$$

that is, equal to the convolution of the impulse response with the input autocorrelation sequence. Again, with $m_x = 0$ the z -transforms exist and

$$\Phi_{yx}(z) = H(z)\Phi_{xx}(z) \quad (16.154)$$

$$P_{yx}(\Omega) = H(e^{j\Omega})P_{xx}(\Omega). \quad (16.155)$$

This is an important relation that can be used for system frequency response evaluation. In particular, if the input sequence $x[n]$ is white noise then

$$\phi_{xx}[m] = \sigma_x^2 \delta[m] \quad (16.156)$$

$$P_{xx}(\Omega) = \Phi_{xx}[e^{j\Omega}] = \sigma_x^2, \quad -\pi \leq \Omega \leq \pi \quad (16.157)$$

so that

$$P_{yx}(\Omega) = \sigma_x^2 H(e^{j\Omega}) \tag{16.158}$$

i.e.

$$H(e^{j\Omega}) = P_{yx}(\Omega)/\sigma_x^2 \tag{16.159}$$

We can thus evaluate the frequency response from knowledge of the input–output power density spectrum $P_{xy}(\Omega)$ and the white noise variance σ_x^2 . Moreover,

$$\phi_{yx}[m] = h[m] * \phi_{xx}[m] = \sigma_x^2 h[m] \tag{16.160}$$

so that the impulse response $h[n]$ can be estimated from knowledge of the input–output cross-correlation sequence $\phi_{xy}[n]$.

Example 16.6 Evaluate the variance of the response $y[n]$ of a linear system if the input to the system $x[n]$ is zero-mean white noise.

The autocorrelation of the input is

$$\phi_{xx}[m] = \sigma_x^2 \delta[m]. \tag{16.161}$$

Now

$$\sigma_y^2 = \frac{1}{2\pi} \int_{-\pi}^{\pi} P_{yy}(\Omega) d\Omega \tag{16.162}$$

and

$$P_{yy}(\Omega) = |H(e^{j\Omega})|^2 P_{xx}(\Omega) = |H(e^{j\Omega})|^2 \Phi_{xx}(e^{j\Omega}) = \sigma_x^2 |H(e^{j\Omega})|^2.$$

Hence

$$\sigma_y^2 = \frac{\sigma_x^2}{2\pi} \int_{-\pi}^{\pi} |H(e^{j\Omega})|^2 d\Omega = \sigma_x^2 \sum_{n=-\infty}^{\infty} h^2[n] \tag{16.163}$$

using Parseval’s relation.

Example 16.7 A linear system has the impulse response $h[n] = 2^{-n}u[n]$. It receives white noise of zero mean and variance σ_x^2 as input. Evaluate the average power of its response.

The average power of the output $y[n]$ is $\phi_{yy}[0]$. We note that

$$\phi_{xx}[m] = E[x[n]x[n+m]] = E[x[n]]E[x[n+m]] \tag{16.164}$$

since the samples of a white-noise random process are statistically independent, i.e.

$$\phi_{xx}[m] = 0, \quad m \neq 0 \tag{16.165}$$

and

$$\phi_{xx}[0] = \sigma_x^2 \tag{16.166}$$

i.e.

$$\phi_{xx}[m] = \sigma_x^2 \delta[m]. \tag{16.167}$$

The average output power is

$$\begin{aligned} \Phi_{yy}[0] &= \frac{1}{2\pi j} \oint_C \Phi_{yy}(z) z^{-1} dz = \frac{1}{2\pi j} \oint_C H(z)H(z^{-1})\Phi_{xx}(z)z^{-1} dz \\ &= \frac{1}{2\pi j} \oint_C \frac{1}{1 - 2^{-1}z^{-1}} \frac{1}{1 - 2^{-1}z} \sigma_x^2 z^{-1} dz = \frac{\sigma_x^2}{2\pi j} \oint_C \frac{1}{z - 0.5} \frac{1}{1 - 0.5z} dz = \frac{4}{3} \sigma_x^2. \end{aligned}$$

Example 16.8 A linear system has an impulse response

$$h[n] = 0.5^n \sin(\pi n/4)u[n] \quad (16.168)$$

It receives a wide-sense stationary random signal $x[n]$ of unit variance. Evaluate the system output autocorrelation sequence, its power density spectrum and its average power.

Let $r = 0.5$, $\Omega_0 = \pi/4$. We have

$$H(z) = \frac{r \sin \Omega_0 z^{-1}}{1 - 2r \cos \Omega_0 z^{-1} + r^2 z^{-2}} \quad (16.169)$$

$$H(z^{-1}) = \frac{r \sin \Omega_0 z^{-1}}{r^2 - 2r \cos \Omega_0 z^{-1} + z^{-2}}. \quad (16.170)$$

Let $G(z) = H(z)H(z^{-1})$.

We have

$$\begin{aligned} \Phi_{yy}(z) &= G(z) = H(z)H(z^{-1}) \\ &= 0.125z^{-2} / (0.25 - 0.8839z^{-1} + 1.563z^{-2} \\ &\quad - 0.8839z^{-3} + 0.25z^{-4}) \end{aligned} \quad (16.171)$$

Evaluating the inverse transform we obtain

$$\phi_{yy}[n] = g[n] = 0.2287(2^n + 0.5^m) \cos(0.7854n - 0.5404)u[n] \quad (16.172)$$

The power spectral density of the system output is

$$P_{yy}(\Omega) = \Phi_{yy}(e^{j\Omega}) \quad (16.173)$$

Now

$$\Phi_{yy}(z) = H(z)H(z^{-1}) = G(z) \quad (16.174)$$

Hence

$$\begin{aligned} P_{yy}(\Omega) &= 0.125e^{-j2\Omega} / (0.25 - 0.8839e^{-j\Omega} \\ &\quad + 1.563e^{-j2\Omega} - 0.8839e^{-j3\Omega} + 0.25e^{-j4\Omega}) \\ &= 0.125 / \{0.5 \cos 2\Omega - 1.7678 \cos \Omega + 1.563\}. \end{aligned} \quad (16.175)$$

The average output power is

$$\Phi_{yy}[0] = 2 \times 0.2287 \times \cos(-0.5404) = 0.3922. \quad (16.176)$$

16.10 PSD Estimation of Discrete-Time Random Sequences

In the discrete-time domain the PSD of a stationary random sequence $x[n]$ is by definition

$$P_{xx}(\Omega) = \Phi_{xx}(e^{j\Omega}) = \sum_{m=-\infty}^{\infty} \phi_{xx}[m]e^{-j\Omega m} \quad (16.177)$$

where $\phi_{xx}[m] = E[x[n+m]x^*[n]]$, and the average power is

$$\phi_{xx}[0] = E[|x[n]|^2] = \frac{1}{2\pi} \int_{-\pi}^{\pi} \Phi_{xx}(e^{j\Omega})d\Omega = \frac{1}{\pi} \int_0^{\pi} P_{xx}(\Omega)d\Omega$$

We shall compare two similar yet distinct estimates of the autocorrelation sequence. Consider an N -point real stationary random sequence $x[n]$, $n = 0, 1, \dots, N - 1$. The autocorrelation of the sequence $x[n]$ may be evaluated by referring to Fig. 16.4.

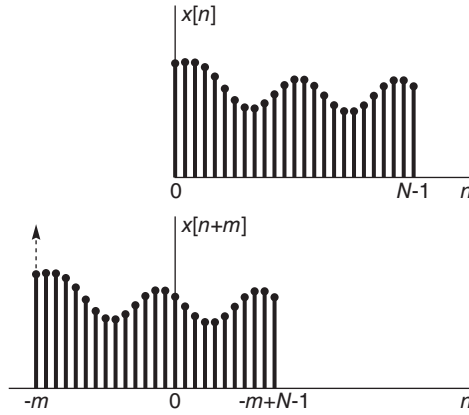


FIGURE 16.4 Autocorrelation of a sequence.

We may write the autocorrelation as

$$c_{xx}[m] = \frac{1}{N} \sum_{n=-\infty}^{\infty} x[n]x[n+m]. \tag{16.178}$$

Note that the roles of m and n are reversed in the figure compared to our usual deterministic signal correlation, and the normalization by the factor $1/N$. As the figure shows, with $0 \leq m \leq N - 1$

$$c_{xx}[m] = \frac{1}{N} \sum_{n=0}^{N-m-1} x[n]x[n+m], \quad m = 0, 1, \dots, N - 1. \tag{16.179}$$

Since the autocorrelation sequence is even-symmetric $c_{xx}[-m] = c_{xx}[m]$ we may write

$$c_{xx}[m] = \frac{1}{N} \sum_{n=0}^{N-|m|-1} x[n]x[n+|m|], \quad m = 0, \pm 1, \pm 2, \dots, \pm(N - 1). \tag{16.180}$$

This is one estimate of the autocorrelation sequence. A closely related estimate is defined as

$$c'_{xx}[m] = \frac{1}{N-m} \sum_{n=0}^{N-m-1} x[n]x[n+m], \quad m = 0, 1, 2, \dots, N - 1. \tag{16.181}$$

where the normalization factor is $1/(N - m)$ instead of the factor $(1/N)$ in $c_{xx}[m]$. The mean value of $c'_{xx}[m]$ is given by

$$E[c'_{xx}[m]] = \frac{1}{N-m} \sum_{n=0}^{N-m-1} E[x[n]x[n+m]] = \frac{1}{N-m} \sum_{n=0}^{N-m-1} \phi_{xx}[m] = \phi_{xx}[m]$$

which is the true statistical autocorrelation sequence. The estimate $c'_{xx}[m]$ is therefore an unbiased estimate of the autocorrelation sequence $\phi_{xx}[m]$. In contrast, the mean value of the estimate $c_{xx}[m]$ is

$$\begin{aligned} E[c_{xx}[m]] &= \frac{1}{N} \sum_{n=0}^{N-m-1} E[x[n]x[n+m]] = \frac{1}{N}(N-m)E[c'_{xx}[m]] \\ &= \frac{N-m}{N}\phi_{xx}[m], \quad m = 0, 1, \dots, N-1 \end{aligned} \quad (16.182)$$

and for $-(N-1) \leq m \leq (N-1)$

$$E[c_{xx}[m]] = \frac{N-|m|}{N}\phi_{xx}[m]. \quad (16.183)$$

This estimate has therefore a bias of $(|m|/N)\phi_{xx}[m]$. It is asymptotically unbiased, however, since as $N \rightarrow \infty$ it tends to the true value $\phi_{xx}[m]$.

Evaluation of the variance of each of these estimates is more complex. An approximation of the variance of $c'_{xx}[m]$ was given by Jenkins and Watts [49] as

$$\text{var}[c'_{xx}[m]] \simeq \frac{N}{|N-m|^2} \sum_{n=-\infty}^{\infty} \{\phi_{xx}^2[n] + \phi_{xx}[n-m]\phi_{xx}[n+m]\} \quad (16.184)$$

an expression that applies if the number of samples N is much larger than m . This variance tends to zero as $N \rightarrow \infty$, as long as the sum $\sum_{n=-\infty}^{\infty} \phi_{xx}^2[n]$ is finite.

Since $E[c'_{xx}[m]] = \phi_{xx}[m]$ and the variance of $c'_{xx}[m]$ tends to zero as $N \rightarrow \infty$ the estimate $c'_{xx}[m]$ is said to be a consistent estimate. On the other hand, for large values of m , and particularly as m approaches the value N , the variance increases progressively in value. The variance of the estimate $c_{xx}[m]$ may similarly be approximated as

$$\text{var}[c_{xx}[m]] \simeq \frac{1}{N} \sum_{n=-\infty}^{\infty} \{\phi_{xx}^2[n] + \phi_{xx}[n-m]\phi_{xx}[n+m]\} \quad (16.185)$$

which tends to zero as $N \rightarrow \infty$.

Since, moreover, $\lim_{N \rightarrow \infty} E[c_{xx}[m]] = \phi_{xx}[m]$, i.e. the estimate $c_{xx}[m]$ is asymptotically unbiased, this estimate is also a consistent estimate of $\phi_{xx}[m]$. Using $c_{xx}[m]$ we have the PSD estimate known as the *periodogram*. It is usually attributed the symbol $I_N(\Omega)$

$$I_N(\Omega) = \sum_{m=-(N-1)}^{N-1} c_{xx}[m]e^{-j\Omega m} \quad (16.186)$$

We note that $c_{xx}[m]$ is the autocorrelation of the N -point sequence $x[n]$ normalized by the factor $(1/N)$. We may write

$$c_{xx}[m] = \{x[m] * x[-m]\} / N \quad (16.187)$$

Hence

$$I_N(\Omega) = c_{xx}(e^{j\Omega}) = (1/N)X(e^{j\Omega})X^*(e^{j\Omega}) = (1/N)|X(e^{j\Omega})|^2.$$

Assuming a zero-mean random process the auto-covariance is equal to the autocorrelation. The mean of the periodogram is given by

$$E[I_N(\Omega)] = \sum_{m=-(N-1)}^{N-1} E[c_{xx}[m]e^{-j\Omega m}] = \sum_{m=-(N-1)}^{N-1} \frac{N-|m|}{N} \phi_{xx}[m]e^{-j\Omega m}$$

which is different from the Fourier transform of $\phi_{xx}[m]$; hence the estimate is biased, relative to the true PSD, $P_{xx}(\Omega)$.

Consider now the second estimate $c'_{xx}[m]$. Its Fourier transform is

$$P_N(\Omega) = \sum_{m=-(N-1)}^{N-1} c'_{xx}[m]e^{-j\Omega m} \tag{16.188}$$

and its mean value is

$$E[P_N(\Omega)] = \sum_{m=-(N-1)}^{N-1} E[c'_{xx}[m]]e^{-j\Omega m} = \sum_{m=-(N-1)}^{N-1} \phi_{xx}[m]e^{-j\Omega m}.$$

Since the limits are finite this too is a biased estimate of $P_{xx}(\Omega)$, even if $c'_{xx}[m]$ is an unbiased estimate of $\phi_{xx}[m]$.

We have just seen that there are two different truncations of the true autocorrelation sequence. The first is the sequence $c_{xx}[m]$, of which the Fourier transform is the periodogram. The expectation

$$E[I_N(\Omega)] = \sum_{m=-(N-1)}^{N-1} \frac{N-|m|}{N} \phi_{xx}[m]e^{-j\Omega m} \tag{16.189}$$

is the Fourier transform of the autocorrelation sequence $\phi_{xx}[m]$ weighted by the triangular Bartlett window

$$w_B[m] = \begin{cases} \frac{N-|m|}{N}, & |m| < N \\ 0, & \text{otherwise} \end{cases} \tag{16.190}$$

of which the Fourier transform is given by

$$W_B(e^{j\Omega}) = \frac{1}{N} Sd_N^2(\Omega/2). \tag{16.191}$$

We may therefore write

$$E[I_N(\Omega)] = \frac{1}{2\pi} \int_{-\pi}^{\pi} P_{xx}(y)W_B(e^{j(\Omega-y)})dy \tag{16.192}$$

In the second truncation, leading to the sequence $c'_{xx}[m]$, the expectation is

$$E[P_N(\Omega)] = \sum_{m=-(N-1)}^{N-1} \phi_{xx}[m]e^{-j\Omega m} \tag{16.193}$$

which implies a truncation of $\phi_{xx}[m]$ by a rectangular window

$$w_R[m] = u[m + (N - 1)] - u[m - (N - 1)] \tag{16.194}$$

of which the Fourier transform is

$$W_R(e^{j\Omega}) = Sd_{2N-1}(\Omega/2). \tag{16.195}$$

Hence we may write

$$E[P_N(\Omega)] = \frac{1}{2\pi} \int_{-\pi}^{\pi} P_{xx}(y) W_R(e^{j(\Omega-y)}) dy \quad (16.196)$$

Similarly to the mean value of the periodogram $E[I_N(\Omega)]$ this mean value $E[P_N(\Omega)]$ is the convolution of the true PSD, $P_{xx}(\Omega) = \Phi_{xx}(e^{j\Omega})$, with the transform of the weighting window. The result is a spectrum that displays spectral leakage accompanied by a reduction in frequency resolution due to the window truncation of the autocorrelation sequence. As $N \rightarrow \infty$, the mean of the periodogram, $E[I_N(\Omega)]$, tends to

$$\lim_{N \rightarrow \infty} E[I_N(\Omega)] = \sum_{m=-\infty}^{\infty} \phi_{xx}[m] e^{-j\Omega m} = \Phi_{xx}(e^{j\Omega}) = P_{xx}(\Omega) \quad (16.197)$$

which is the true value of the PSD, Hence the periodogram is asymptotically unbiased. The Bartlet window, which truncates the autocorrelation sequence, tends to 1 as $N \rightarrow \infty$ leading to no truncation in the limit and hence to the periodogram mean tending to the true PSD.

Windows other than the rectangular and triangular ones may be used in evaluating modified periodograms. It can be shown that the variance of the resulting periodogram is given for large values of N by [49].

$$\text{var}[I_N(\Omega)] = R_w P_{xx}^2(\Omega) \quad (16.198)$$

where R_w is a constant that depends on the window $w[n]$ used. The variance tends to the square of the true PSD rather than the PSD itself $P_{xx}(\Omega)$. As the record length N increases the periodogram displays higher peaks and more rapid fluctuations. It produces in general spectral estimates that are not consistent for different data sequences from the same random process.

Several approaches have been proposed in the literature to provide better estimates of the PSD. In truncating sequences, different windows were applied in an effort to reduce spectral leakage or improve the frequency resolution. A given long data record is divided into nonoverlapping or overlapping segments and the resulting estimates of the power spectral density are averaged over the segments. The averaged periodograms produce in general the same mean value for the different segments while the resulting variance is reduced in proportion to the number of averaged identically distributed segments. For details regarding such approaches to power spectrum estimation the reader is referred to many excellent text books on the subject [39] [55], [59].

16.11 Fast Fourier Transform (FFT) Evaluation of the Periodogram

The periodogram of an N -point random sequence $x[n]$ may be evaluated by sampling the z -plane unit circle uniformly into N points. We may write the result in the form

$$P_{xx}[k] \equiv P_{xx}(2\pi k/N) = \frac{1}{N} \left| \sum_{n=0}^{N-1} x[n] e^{-j2\pi kn/N} \right|^2 = \frac{1}{N} |X[k]|^2, \quad k = 0, 1, \dots, N-1$$

and evaluate the discrete Fourier transform (DFT) $X[k]$ using the FFT.

Interpolation may be performed if finer sampling of the unit circle is desired. If we are given only N samples of $x[n]$ and we need to interpolate between the N samples $X[k]$ of the DFT we should introduce zero padding, thus increasing the length of the data sequence from N points to say L points. We then evaluate the DFT of the resulting L -point sequence $x'[n]$ by sampling the unit circle uniformly into L points. We thus obtain the samples of the spectrum

$$P_{xx}(2\pi k/L) = \frac{1}{N} \left| \sum_{n=0}^{L-1} x'[n] e^{-j2\pi kn/L} \right|^2 = \frac{1}{N} \left| \sum_{n=0}^{N-1} x[n] e^{-j2\pi kn/L} \right|^2, \quad k = 0, 1, \dots, L - 1.$$

It is important to note that interpolation by zero padding allows us to evaluate the same spectrum of the N point sequence $x[n]$ on the unit circle, but with added in-between frequency samples. Zero padding does not, however, add information regarding the sequence $x[n]$ which itself remains the same N -point sequence. The smaller the sampling interval $2\pi/N$ on the unit circle the higher the frequency resolution. To obtain a higher frequency resolution we would need a higher value of N , the number of points of the sequence $x[n]$. The following example illustrates these properties of spectrum sampling and interpolation.

Example 16.9 Given the sequence

$$x[n] = \{\sin(0.0969\pi n + \pi/3) + \sin(0.2031\pi n - \pi/5)\} w[n]$$

where $w[n]$ is the rectangular window $w[n] = R_N[n]$ and $N = 64$.

a) Evaluate the periodogram of $x[n]$. Apply zero padding, evaluating the periodogram with a number of points $L = 2N$ and $16N$.

b) Repeat for the case

$$x[n] = \{\sin(0.0969\pi n + \pi/3) + \sin(0.1219\pi n - \pi/5)\} R_N[n].$$

Observe the failure of the periodogram to reveal the second sinusoid spectral peak, even with the application of zero padding.

c) By doubling the record length of the sequence $x[n]$ defined in part b) so that now $w[n] = R_N[n]$ with $N = 128$, verify that the periodogram reveals the second sinusoid spectral peak.

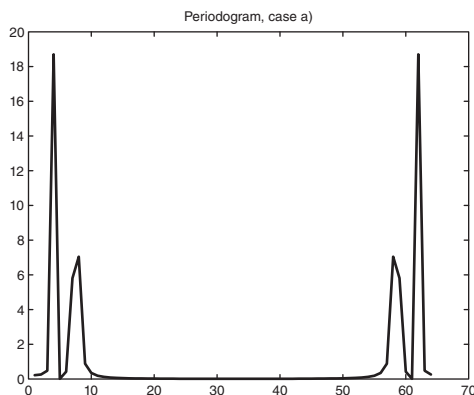


FIGURE 16.5 Periodogram of the sequence $x[n]$.

a) The periodogram is shown in Fig. 16.5. Two spectral peaks correspond to the two sinusoidal components. The results of interpolation by zero padding with $L = 2N$ and $L = 16N$, respectively, are seen in Fig. 16.6(a-b). The resulting spectrum tends toward a continuous curve.

b) The periodogram is shown in Fig. 16.7 for the two cases $L = N$ and with the zero padding case $L = 16N$, respectively.

This time with or without zero padding the periodogram resolution fails to distinguish between the two sinusoids.

c) Doubling the record length N increases the frequency resolution. The periodogram reveals the presence of the two sinusoids as two clear spectral peaks, as seen in Fig. 16.8.

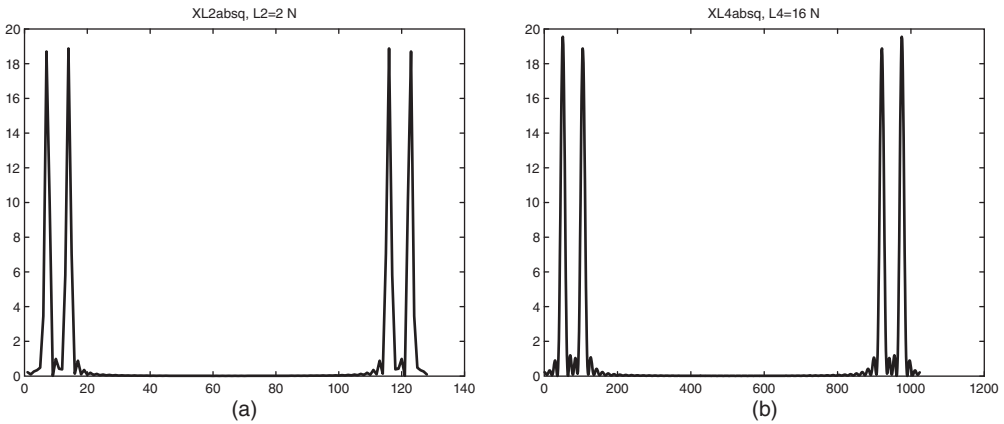


FIGURE 16.6 Periodogram with zero padding of (a) $L = 2N$ and (b) $L = 16N$.

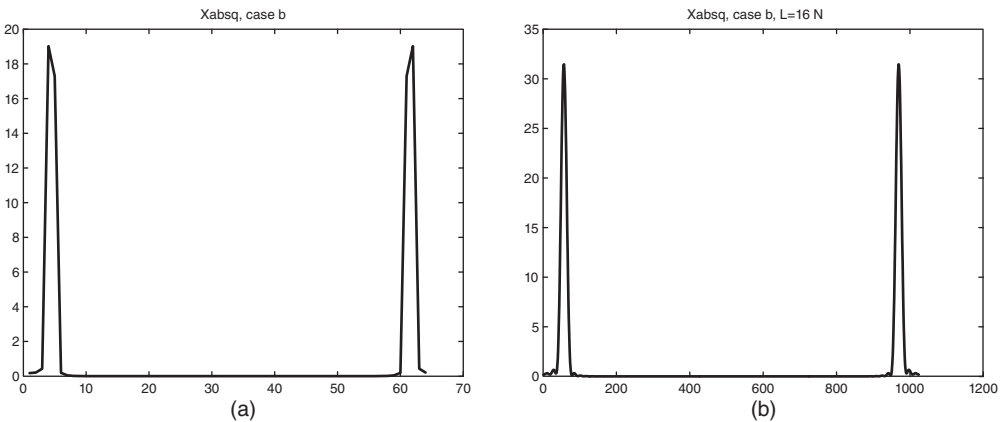


FIGURE 16.7 Periodogram of the sequence $x[n]$ of part (b) with $L = N$ and $L = 16N$, respectively.

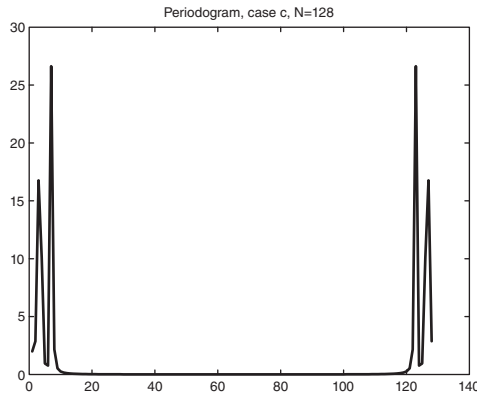


FIGURE 16.8 Periodogram of the sequence $x[n]$ of part (c) with the number of points N doubled.

16.12 Parametric Methods for PSD Estimation

In parametric methods for PSD estimation the stationary random signal $x[n]$ is modeled as the output of a linear system driven by white noise $w[n]$ as input. By estimating the parameters of the system transfer function $H(z)$, the PSD of its output $x[n]$ is readily deduced. Representation of a stationary random process as the response of a causal IIR filter to white noise input is known as *Wold representation*.

As stated earlier the autocorrelation of a white noise process $w[n]$ is

$$\phi_{ww}[m] = \sigma_w^2 \delta[m] \tag{16.199}$$

and its PSD is

$$P_{ww}(\Omega) = \Phi_{ww}(e^{j\Omega}) = \sigma_w^2. \tag{16.200}$$

The PSD of the infinite impulse response (IIR) filter output $x[n]$ is therefore

$$P_{xx}(\Omega) = \Phi_{xx}(e^{j\Omega}) = \Phi_{ww}(e^{j\Omega}) |H(e^{j\Omega})|^2 = \sigma_w^2 |H(e^{j\Omega})|^2. \tag{16.201}$$

More generally, in the z -domain, the PSD is given by

$$\Phi_{xx}(z) = \Phi_{ww}(z)H(z)H(z^{-1}) = \sigma_w^2 H(z)H(z^{-1}), \quad r_1 < |z| < r_2. \tag{16.202}$$

Referring to Fig. 16.9(a) we assume that the system is causal, stable and minimum phase and that its system function $H(z)$ is rational given by

$$H(z) = \frac{X(z)}{W(z)} = \frac{\sum_{k=0}^q b_k z^{-k}}{1 + \sum_{k=1}^p a_k z^{-k}} = \frac{B(z)}{A(z)}, \quad |z| > r_1. \tag{16.203}$$

The PSD of $x[n]$ is therefore also a rational function.

The system inverse, of transfer function $1/H(z)$, Fig. 16.9(b), is thus also a causal, stable and minimum phase filter and if it receives the stationary random process $x[n]$ as input would produce white noise $w[n]$ as output. This filter is referred to as a *whitening* filter

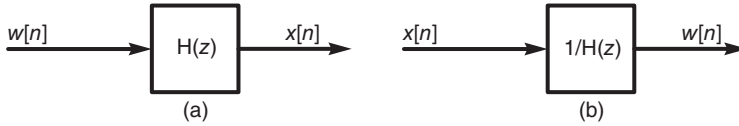


FIGURE 16.9 Parametric modeling: (a) system with white noise as input, (b) inverse system.

and its output $w[n]$ as the *innovation process* associated with the random process $x[n]$. The corresponding linear difference equation is

$$x[n] = - \sum_{k=1}^p a_k x[n-k] + \sum_{k=0}^q b_k w[n-k]. \quad (16.204)$$

This is the general polo-zero model referred to as the autoregressive moving average (ARMA) model for generating an ARMA process. In the special case where $b_0 = 1$ and $b_k = 0, k > 0$, the model is an autoregressive (AR) all-pole filter generating an AR process with the difference equation rewritten as

$$x[n] = - \sum_{k=1}^p a_k x[n-k] + w[n] \quad (16.205)$$

If instead $a_k = 0, k > 0$ the model is a moving average (MA) filter generating and MA process, with the difference equation given by

$$x[n] = \sum_{k=0}^q b_k w[n-k]. \quad (16.206)$$

16.13 The Yule–Walker Equations

We may obtain the relation between the autocorrelation sequence $\phi_{xx}[m]$ and the system transfer function parameters a_k and b_k in the case of ARMA model by multiplying both sides of the difference equation by $x^*[n-m]$ and evaluating their expectations. We have

$$E[x[n]x^*[n-m]] = - \sum_{k=1}^p a_k E[x[n-k]x^*[n-m]] + \sum_{k=0}^q b_k E[w[n-k]x^*[n-m]] \quad (16.207)$$

i.e.

$$\phi_{xx}[m] = - \sum_{k=1}^p a_k \phi_{xx}[m-k] + \sum_{k=0}^q b_k \phi_{wx}[m-k]. \quad (16.208)$$

In this equation the cross-correlation $\phi_{wx}[\cdot]$ is by definition

$$\begin{aligned} \phi_{wx}[m] &= E[w[n+m]x^*[n]] = E[w[n+m] \sum_{k=0}^{\infty} h[k]w^*[n-k]] \\ &= \sum_{k=0}^{\infty} h[k] E[w[n+m]w^*[n-k]] = \sum_{k=0}^{\infty} h[k] \sigma_w^2 \delta[k+m] = h[-m] \sigma_w^2 \end{aligned} \quad (16.209)$$

ans since the system is causal

$$\phi_{wx}[m] = \begin{cases} \sigma_w^2 h[-m], & m \leq 0 \\ 0, & m > 0 \end{cases} \quad (16.210)$$

Now the last term in the difference equation of $\phi_{xx}[m]$ is the sum

$$S = \sum_{k=0}^q b_k \phi_{wx}[m - k] \quad (16.211)$$

and if $m = 0$ we have

$$S = b_0 \sigma_w^2 h[0] + b_1 \sigma_w^2 h[1] + \dots + b_q \sigma_w^2 h[q] \quad (16.212)$$

and more generally if $m = r$ then

$$S = b_r \sigma_w^2 h[0] + b_{r+1} \sigma_w^2 h[1] + \dots + b_q \sigma_w^2 h[q - r] \quad (16.213)$$

wherefrom

$$S = \sigma_w^2 \sum_{k=0}^{q-m} b_{k+m} h[k], \quad 0 \leq m \leq q \quad (16.214)$$

and

$$S = 0 \text{ if } m > q. \quad (16.215)$$

The autocorrelation equation therefore takes the form

$$\phi_{xx}[m] = \begin{cases} - \sum_{k=1}^p a_k \phi_{xx}[m - k] + \sigma_w^2 \sum_{k=0}^{q-m} b_{k+m} h[k], & 0 \leq m \leq q \\ - \sum_{k=1}^p a_k \phi_{xx}[m - k], & m > q \end{cases} \quad (16.216)$$

and for negative values of m we have the symmetry property

$$\phi_{xx}[m] = \phi_{zx}^*[-m]. \quad (16.217)$$

Note that the autocorrelation equation is a nonlinear relation between the autocorrelation $\phi_{xx}[m]$ and the parameters a_k .

If instead of the ARMA model an AR model is used then $q = 0$ and $b_0 = 1$. The equation simplifies to

$$\phi_{xx}[m] = \begin{cases} - \sum_{k=1}^p a_k \phi_{xx}[m - k] + \sigma_w^2, & m = 0 \\ - \sum_{k=1}^p a_k \phi_{xx}[m - k], & m > 0 \end{cases} \quad (16.218)$$

i.e.

$$\sum_{k=0}^p a_k \phi_{xx}^*[k] = \sigma_w^2 \quad (16.219)$$

$$\sum_{k=0}^p a_k \phi_{xx}[m - k] = 0, \quad m = 1, 2, \dots, p \quad (16.220)$$

This linear relationship is known as the Yule–Walker equations. It can be put in the matrix form

$$\begin{bmatrix} \phi_{xx}[0] & \phi_{xx}[-1] & \phi_{xx}[-2] & \cdots & \phi_{xx}[-p] \\ \phi_{xx}[1] & \phi_{xx}[0] & \phi_{xx}[-1] & \cdots & \phi_{xx}[-p+1] \\ \vdots & \vdots & \vdots & \ddots & \vdots \\ \phi_{xx}[p] & \phi_{xx}[p-1] & \phi_{xx}[p-2] & \cdots & \phi_{xx}[0] \end{bmatrix} \begin{bmatrix} 1 \\ a_1 \\ \vdots \\ a_p \end{bmatrix} = \begin{bmatrix} \sigma_w^2 \\ 0 \\ \vdots \\ 0 \end{bmatrix}. \quad (16.221)$$

The matrix of correlations is Toeplitz, a property that can be used to efficiently evaluate its inverse as effected by the Levinson–Durbin algorithm. [53].

The equations simplify, moreover, if the process is an MA one, generated using an MA model. In this all-zero case the model coefficients are $a_k = 0$ for $1 \leq k \leq p$ so that

$$H(z) = \sum_{k=0}^q b_k z^{-k} \quad (16.222)$$

$$h[n] = \sum_{k=0}^q b_k \delta[n-k] \quad (16.223)$$

$$h[k] = b_k, \quad 0 \leq k \leq q \quad (16.224)$$

and

$$\phi_{xx}[m] = \begin{cases} \sigma_w^2 \sum_{k=0}^q b_k b_{k+m}, & 0 \leq m \leq q \\ 0, & m > q \end{cases}. \quad (16.225)$$

16.14 System Modeling for Linear Prediction, Adaptive Filtering and Spectrum Estimation

System modeling, or the identification of a system’s mathematical model, is an important signal processing problem encountered in many applications such as adaptive filtering, adaptive noise cancellation, linear prediction and parametric power spectrum estimation. By adjusting its coefficients in real time, a filter can adapt its response to random variations or nonstationarity accompanying its input signal. In this section we study in particular two main problems of system modeling, namely, the Wiener filtering problem and the least-squares estimation problem. Forward and backward linear prediction filter structures are obtained as applications of these models.

16.15 Wiener and Least-Squares Models

The need often arises to filter a stationary random signal $x[n]$ using a causal finite impulse response (FIR) filter in such a way that the resulting signal approximates a given desired sequence $d[n]$. As shown in Fig. 16.10, the sequence $x[n]$ is applied as the input to the finite impulse response (FIR) filter. The filter impulse response $h[n]$ is p -points long. Its

coefficients are $h_k = h[k]$, $k = 0, 1, \dots, p$. The filter output, denoted $\hat{d}[n]$, is given by

$$\hat{d}[n] = \sum_{k=0}^p h_k x[n - k] \tag{16.226}$$

The system receives as a second input the desired sequence $d[n]$ and compares it with the FIR filter output. The difference $d[n] - \hat{d}[n]$ is the filter estimation error $e[n]$. We may write

$$e[n] = d[n] - \hat{d}[n] = d[n] - \sum_{k=0}^p h_k x[n - k] \tag{16.227}$$

which may be put in the matrix form

$$e[n] = d[n] - [h_0 \ h_1 \ \dots \ h_p] \begin{bmatrix} x[n] \\ x[n-1] \\ \vdots \\ x[n-p] \end{bmatrix} = d[n] - h^T x \tag{16.228}$$

where h and x are column vectors the elements of which are $\{h_k\}$ and $\{x[n - k]\}$, $k = 0, 1, \dots, p$, respectively.

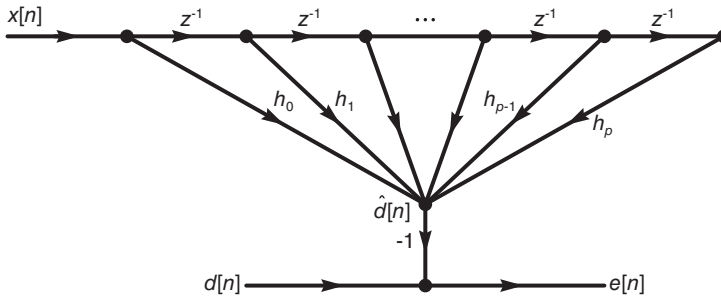


FIGURE 16.10 System modeling by Wiener filtering.

16.16 Wiener Filtering

The objective in the Wiener filtering problem is to evaluate the impulse response vector h that leads to minimization of the magnitude square $|e[n]|^2$ of the error $e[n]$. Such minimization may be carried out statistically by minimizing the mean-square error $E[|e[n]|^2]$, or by using time averages to minimize the sum-square error $\sum_n |e[n]|^2$. These two approaches are referred to as the Wiener filtering problem and the least-squares filtering problem, respectively.

Consider the Wiener filtering approach of minimizing the mean-square error $E[|e[n]|^2]$.

We may write in matrix form

$$\begin{aligned} |e[n]|^2 &= \{d^*[n] - h^{T*}x^*\} \{d[n] - h^T x\} \\ &= d^*[n]d[n] - d^*[n]h^T x - d[n]h^{T*}x^* - h^{T*}x^*h^T x \end{aligned} \quad (16.229)$$

or in direct form

$$\begin{aligned} |e[n]|^2 &= \left\{ d^*[n] - \sum_{k=0}^p h_k^* x^*[n-k] \right\} \left\{ d[n] - \sum_{m=0}^p h_m x[n-m] \right\} \\ &= d^*[n]d[n] - \sum_{m=0}^p h_m d^*[n]x[n-m] - \sum_{k=0}^p h_k^* d[n]x^*[n-k] \\ &\quad + \sum_{k=0}^p \sum_{m=0}^p h_k^* h_m x^*[n-k]x[n-m]. \end{aligned} \quad (16.230)$$

Now $h^T x = x^T h$ so that

$$d^*[n]h^T x = [d^*[n]x[n] \ d^*[n]x[n-1] \ \dots \ d^*[n]x[n-p]] \begin{bmatrix} h_0 \\ h_1 \\ \vdots \\ h_p \end{bmatrix} \quad (16.231)$$

and since by definition

$$E[d[n]x^*[n-m]] = \phi_{dx}[m] \quad (16.232)$$

we have

$$E[d^*[n]h^T x] = [\phi_{dx}^*[0] \ \phi_{dx}^*[1] \ \dots \ \phi_{dx}^*[p]] \begin{bmatrix} h_0 \\ h_1 \\ \vdots \\ h_p \end{bmatrix} \triangleq \phi_{dx}^{*T} h. \quad (16.233)$$

Similarly, $h^{T*}x^* = x^{T*}h^*$ and

$$E[d[n]h^{T*}x^*] = [\phi_{dx}[0] \ \phi_{dx}[1] \ \dots \ \phi_{dx}[p]] \begin{bmatrix} h_0^* \\ h_1^* \\ \vdots \\ h_p^* \end{bmatrix} \triangleq \phi_{dx}^T h^*. \quad (16.234)$$

Moreover $h^{T*}x^*h^T x = h^{T*}x^*x^T h$

i.e.

$$h^{T*}x^*h^T x = [h_0^* \ \dots \ h_p^*] \begin{bmatrix} x^*[n]x[n] & \dots & x^*[n]x[n-p] \\ x^*[n-1]x[n] & \dots & x^*[n-1]x[n-p] \\ \vdots & \ddots & \vdots \\ x^*[n-p]x[n] & \dots & x^*[n-p]x[n-p] \end{bmatrix} \begin{bmatrix} h_0 \\ h_1 \\ \vdots \\ h_p \end{bmatrix} \quad (16.235)$$

and

$$\begin{aligned} E[h^{T*}x^*h^T x] &= [h_0^* \ \dots \ h_p^*] \begin{bmatrix} \phi_{xx}[0] & \phi_{xx}^*[1] & \dots & \phi_{xx}^*[p] \\ \phi_{xx}[1] & \phi_{xx}[0] & \dots & \phi_{xx}^*[p-1] \\ \vdots & \vdots & \ddots & \vdots \\ \phi_{xx}[p] & \phi_{xx}[p-1] & \dots & \phi_{xx}[0] \end{bmatrix} \begin{bmatrix} h_0 \\ h_1 \\ \vdots \\ h_p \end{bmatrix} \\ &= h^{*T} \phi_{xx}^T h \end{aligned} \quad (16.236)$$

where ϕ_{xx} is the matrix

$$\Phi_{xx} = \{\phi_{xx,ij}\} = \{E[x[n-i]x^*[n-j]]\} \quad (16.237)$$

$$\phi_{xx} = \begin{bmatrix} \phi_{xx}[0] & \phi_{xx}[1] & \dots & \phi_{xx}[p] \\ \phi_{xx}^*[1] & \phi_{xx}[0] & \dots & \phi_{xx}[p-1] \\ \vdots & \vdots & \ddots & \vdots \\ \phi_{xx}^*[p] & \phi_{xx}^*[p-1] & \dots & \phi_{xx}[0] \end{bmatrix}. \quad (16.238)$$

We may therefore write the mean-square value of the error in the form

$$E_p \triangleq E[|e[n]|^2] = \phi_{dd}[0] - \phi_{dx}^{*T}h - \phi_{dx}^T h^* + h^{*T} \phi_{xx}^T h \quad (16.239)$$

where $\phi_{dd}[0] = E[d^*[n]d[n]]$. We may also write the same equation in direct form

$$E_p = \phi_{dd}[0] + \sum_{k=0}^p \{h_k \phi_{dx}[k] + h_k^* \phi_{dx}^*[k]\} + \sum_{k=0}^p \sum_{m=0}^p h_k^* h_m \phi_{xx}^*[m-k]. \quad (16.240)$$

The optimal value of the impulse response h is obtained by equating the derivative of E_p with respect to h^* to zero. We have

$$\frac{\partial E_p}{\partial h^*} = 0 - \phi_{dx} + \phi_{xx}^T h = 0 \quad (16.241)$$

$$\phi_{xx}^T h = \phi_{dx}. \quad (16.242)$$

This is known as the *Wiener-Hopf equation* of which the solution is the optimal value of h , the impulse response of the *Wiener filter*

$$h = \{\phi_{xx}^T\}^{-1} \phi_{dx}. \quad (16.243)$$

The corresponding value of the mean-squared error is given by

$$E_{p \min} = \phi_{dd}[0] - \phi_{dx}^{*T} h \quad (16.244)$$

as can be seen by noting that in the expression of E_p we have

$$-\phi_{dx}^{*T} h^* + h^{*T} \phi_{xx}^T h = -h^{*T} \phi_{dx} + h^{*T} \phi_{xx}^T h = h^{*T} \{\phi_{dx} - \phi_{dx}\} = 0 \quad (16.245)$$

We have therefore found that

$$\begin{aligned} E_{min} &= \phi_{dd}[0] - [\phi_{dx}^*[0] \ \phi_{dx}^*[1] \ \dots \ \phi_{dx}^*[p]] \begin{bmatrix} h_0 \\ h_1 \\ \vdots \\ h_p \end{bmatrix} \\ &= \phi_{dd}[0] - \sum_{k=0}^p \phi_{dx}^*[k] h_k \end{aligned} \quad (16.246)$$

where $h = \{h_k\}$ is the optimal impulse response.

We also note that the Wiener-Hopf equation, of which the solution is the optimal vector h , namely,

$$\phi_{dx} = \phi_{xx}^T h \quad (16.247)$$

can be written in the form

$$\phi_{dx}[m] = \sum_{k=0}^p h_k \phi_{xx}[m-k]. \quad (16.248)$$

The orthogonality principle may be used to directly obtain this relation. In particular, since the error sequence is given by

$$e[n] = d[n] - \sum_{k=0}^p h_k x[n-k] \quad (16.249)$$

the orthogonality principle states that the minimum mean-square error is achieved if the error is made orthogonal to each of the elements of the sequence. This implies that

$$E[e[n]x^*[n-m]] = 0, \quad m = 0, 1, \dots, p \quad (16.250)$$

i.e.

$$\phi_{dx}[m] = E[d[n]x^*[n-m] - \sum_{k=0}^p h_k x[n-k]x^*[n-m]] = 0 \quad (16.251)$$

or

$$\phi_{dx}[m] = \sum_{k=0}^p h_k \phi_{xx}[m-k] \quad (16.252)$$

as found above.

16.17 Least-Squares Filtering

In the least-squares approach the optimal filter is found by minimizing the sum of the squares of the error sequence, i.e. minimizing $\sum_n |e[n]|^2$, in contrast with the Wiener filter minimization of the mean square error $E[|e[n]|^2]$. Least-squares filtering is in fact the practical approach where statistical expectations are replaced by deterministic time averages. The same analysis and results obtained in the Wiener filtering problem apply in the least-squares problem where now the correlations are replaced by their time-average approximations. In particular, the correlations $\phi_{dd}[0]$, $\phi_{dx}[m]$ and $\phi_{xx}[m]$ in the Wiener–Hopf equations and Wiener filter solution are replaced respectively by $\sum_n d^*[n]d[n]$, $\sum_n d^*[n]x[n-m]$ and $\sum_n x^*[n]x[n-m]$.

16.18 Forward Linear Prediction

“Forward linear prediction” is better seen as “forward linear approximation.” It is an important problem, closely related to the Wiener and least-squares filtering problems. The one-step forward prediction problem is modeled in Fig. 16.11. As the figure shows an FIR filter of coefficients $\{a_k\}$ disposes of the last p samples $x[n-1]$, $x[n-2]$, \dots , $x[n-p]$ of the

input sequence. Its coefficients $\{a_k\}$ should be adjusted so that the filter's output, that is, the weighted sum of the p samples approximate the value of the following sample $x[n]$. As is the convention in the literature the filter's weighed sum is denoted with a negative sign so that the filter output is $-\hat{x}[n]$. As seen in the figure the approximation error is denoted $f_p[n]$, that is,

$$\hat{x}[n] = - \sum_{k=1}^p a_k x[n-k] \tag{16.253}$$

$$f_p[n] = x[n] - \hat{x}[n] = x[n] + \sum_{k=1}^p a_k x[n-k] \tag{16.254}$$

$$f_p[n] = \sum_{k=0}^p a_k x[n-k], \quad a_0 = 1 \tag{16.255}$$

$$\begin{aligned} |f_p[n]|^2 &= f_p^*[n] f_p[n] = \left\{ x^*[n] + \sum_{k=1}^p a_k^* x^*[n-k] \right\} \left\{ x[n] + \sum_{m=1}^p a_m x[n-m] \right\} \\ &= x^*[n] x[n] + \sum_{k=1}^p \{ a_k x^*[n] x[n-k] + a_k^* x[n] x^*[n-k] \} \\ &\quad + \sum_{k=1}^p \sum_{m=1}^p a_k^* a_m x^*[n-k] x[n-m] \end{aligned} \tag{16.256}$$

$$E_p^f = E \left[|f_p[n]|^2 \right] = \phi_{xx}[0] + \sum_{k=1}^p \{ a_k \phi_{xx}^*[k] + a_k^* \phi_{xx}[k] \} + \sum_{k=1}^p \sum_{m=1}^p a_k^* a_m \phi_{xx}^*[m-k].$$

Similarly to Wiener filtering we have

$$\frac{\partial E_p^f}{\partial a_r^*} = 0 = \phi_{xx}[r] + \sum_{m=1}^p a_m \phi_{xx}^*[m-r], \quad r = 1, \dots, p \tag{16.257}$$

i.e. with r replaced by m and m by k

$$\phi_{xx}[m] = - \sum_{k=1}^p a_k \phi_{xx}^*[k-m] = - \sum_{k=1}^p a_k \phi_{xx}[m-k] \tag{16.258}$$

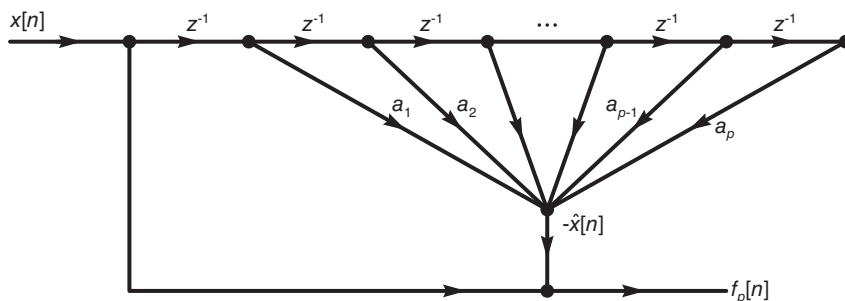


FIGURE 16.11 System modeling by forward prediction.

Note $m = 1, 2, \dots, p$.

The minimum error is given by

$$E_{min}^f = \phi_{xx}[0] + \sum_{k=1}^p \{a_k \phi_{xx}^*[k] + a_k^* \phi_{xx}[k]\} - \sum_{m=1}^p a_m \phi_{xx}^*[m] = \phi_{xx}[0] + \sum_{k=1}^p a_k \phi_{xx}^*[k].$$

We may write, with $a_0 = 1$

$$\sum_{k=0}^p a_k \phi_{xx}[m - k] = 0, \quad m = 1, 2, \dots, p. \quad (16.259)$$

These are called the *normal equations* for the coefficients of the forward linear predictor.

$$E_{min}^f = \sum_{k=0}^p a_k \phi_{xx}^*[k] \quad (16.260)$$

and from Equation (16.221)

$$E_{min}^f = \sigma_w^2. \quad (16.261)$$

In matrix form

$$\begin{bmatrix} \phi_{xx}[1] & \phi_{xx}[0] & \dots & \phi_{xx}[1-p] \\ \phi_{xx}[2] & \phi_{xx}[1] & \dots & \phi_{xx}[2-p] \\ \vdots & \vdots & \ddots & \vdots \\ \phi_{xx}[p] & \phi_{xx}[p-1] & \dots & \phi_{xx}[0] \end{bmatrix} \begin{bmatrix} 1 \\ a_1 \\ \vdots \\ a_p \end{bmatrix} = 0. \quad (16.262)$$

Incorporating into this equation the minimum error equation we may write

$$\begin{bmatrix} \phi_{xx}[0] & \phi_{xx}^*[1] & \dots & \phi_{xx}^*[p] \\ \phi_{xx}[1] & \phi_{xx}[0] & \dots & \phi_{xx}^*[p-1] \\ \phi_{xx}[2] & \phi_{xx}[1] & \dots & \phi_{xx}^*[p-2] \\ \vdots & \vdots & \ddots & \vdots \\ \phi_{xx}[p] & \phi_{xx}[p-1] & \dots & \phi_{xx}[0] \end{bmatrix} \begin{bmatrix} 1 \\ a_1 \\ a_2 \\ \vdots \\ a_p \end{bmatrix} = \begin{bmatrix} E_{min}^f \\ 0 \\ 0 \\ \vdots \\ 0 \end{bmatrix} \quad (16.263)$$

which are referred to as the augmented normal equations. As with Wiener filtering statistical correlations are replaced in practice by the corresponding time average approximations. The Toeplitz property of the matrix of correlations is used to efficiently solve the normal equations by the Levinson–Derbin and the Schur algorithm [39].

16.19 Backward Linear Prediction

Backward Linear Prediction is depicted in Fig. 16.12. We note that in backward prediction the FIR filter has coefficients $\{b_k\}$, $k = 0, 1, \dots, p-1$. It evaluates the weighted sum of the sequence values $x[n], x[n-1], \dots, x[n-p+1]$, producing the estimate

$$-\hat{x}[n-p] = \sum_{k=0}^{p-1} b_k x[n-k] \quad (16.264)$$

so that $\hat{x}[n-p]$ should approximate the value $x[n-p]$. The estimation error is

$$g_p[n] = x[n-p] + \sum_{k=0}^{p-1} b_k x[n-k]. \tag{16.265}$$

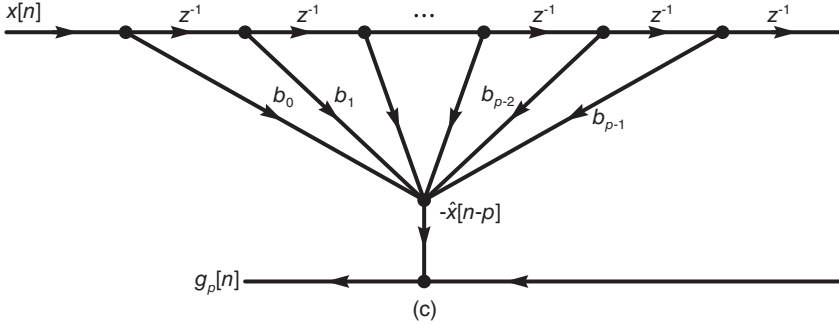


FIGURE 16.12 System modeling by backward prediction.

Similarly to the above we write

$$\begin{aligned} |g_p[n]|^2 &= \left\{ x^*[n-p] + \sum_{k=0}^{p-1} b_k^* x^*[n-k] \right\} \left\{ x[n-p] + \sum_{m=0}^{p-1} b_m x[n-m] \right\} \\ &= x^*[n-p]x[n-p] + \sum_{m=0}^{p-1} b_m x^*[n-p]x[n-m] \\ &\quad + \sum_{k=0}^{p-1} b_k^* x[n-p]x^*[n-k] + \sum_{k=0}^{p-1} \sum_{m=0}^{p-1} b_k^* b_m x^*[n-k]x[n-m]. \end{aligned} \tag{16.266}$$

$$\begin{aligned} E_p^g \triangleq E \left[|g_p[n]|^2 \right] &= \phi_{xx}[0] + \sum_{m=0}^{p-1} b_m = \phi_{xx}^*[m-p] + \sum_{k=0}^{p-1} b_k^* \phi_{xx}[k-p] \\ &\quad + \sum_{k=0}^{p-1} \sum_{m=0}^{p-1} b_k^* b_m \phi_{xx}[k-m] \end{aligned} \tag{16.267}$$

$$\frac{\partial E_p^g}{\partial b_r^*} = \phi_{xx}[r-p] + \sum_{m=0}^{p-1} b_m \phi_{xx}[r-m] \phi_{xx}[m-p] + \sum_{k=0}^{p-1} b_k \phi_{xx}[m-k] = 0 \tag{16.268}$$

i.e. with $b_p = 1$

$$\sum_{k=0}^p b_k \phi_{xx}[m-k] = 0, \quad m = 0, 1, \dots, p-1. \tag{16.269}$$

Consider the 4th term of E_p^g . We may write

$$t_4 = \sum_{k=0}^{p-1} b_k^* \sum_{m=0}^{p-1} b_m \phi_{xx}[k-m] \tag{16.270}$$

$$\sum_{k=0}^{p-1} b_k \phi_{xx}[r-k] = -\phi_{xx}[r-p], \quad \sum_{m=0}^{p-1} b_m \phi_{xx}[r-m] = -\phi_{xx}[r-p]$$

$$t_4 = -\sum_{k=0}^{p-1} b_k^* \phi_{xx}[k-p] \quad (16.271)$$

which cancels the 3rd term. Hence

$$E_{min}^g = \phi_{xx}[0] + \sum_{m=0}^{p-1} b_m \phi_{xx}^*[m-p] = \sum_{m=0}^p b_m \phi_{xx}^*[m-p] = \sum_{m=0}^p b_m \phi_{xx}[p-m].$$

We may therefore write in matrix form

$$\begin{bmatrix} \phi_{xx}[0] & \phi_{xx}^*[1] & \dots & \phi_{xx}^*[p] \\ \phi_{xx}[1] & \phi_{xx}[0] & \dots & \phi_{xx}^*[p-1] \\ \vdots & \vdots & \ddots & \vdots \\ \phi_{xx}[p-1] & \phi_{xx}[p-2] & \dots & \phi_{xx}^*[1] \\ \phi_{xx}[p] & \phi_{xx}[p-1] & \dots & \phi_{xx}[0] \end{bmatrix} \begin{bmatrix} b_0 \\ b_1 \\ \vdots \\ b_{p-1} \\ 1 \end{bmatrix} = \begin{bmatrix} 0 \\ 0 \\ \vdots \\ 0 \\ E_{min}^g \end{bmatrix}. \quad (16.272)$$

From the above we may write

$$\sum_{k=0}^p a_k \phi_{xx}^*[k-m-1] = 0, \quad m = 1, 2, \dots, p \quad (16.273)$$

$$\sum_{k=0}^p a_k \phi_{xx}^*[k] = E_{min}^f \quad (16.274)$$

$$\sum_{k=0}^p b_k \phi_{xx}[p-k-m-1] = 0 \quad (16.275)$$

$$\sum_{k=0}^p b_k \phi_{xx}[p-k] = E_{min}^g. \quad (16.276)$$

Letting $k = p - r$ we have

$$\sum_{r=0}^p a_{p-r} \phi_{xx}^*[p-r-m-1] = 0 \quad (16.277)$$

$$\sum_{r=0}^p a_{p-r}^* \phi_{xx}[p-r-m-1] = 0. \quad (16.278)$$

Hence

$$b_k = a_{p-k}^*, \quad k = 0, 1, \dots, p \quad (16.279)$$

Moreover

$$E_{min}^f = \sum_{k=0}^p a_k \phi_{xx}^*[k] = \sum_{k=0}^p b_{p-k}^* \phi_{xx}^*[k] = \sum_{m=0}^p b_m^* \phi_{xx}^*[p-m] = E_{min}^g. \quad (16.280)$$

16.20 Lattice MA FIR Filter Realization

As we have seen in Chapter 11 an all-zero (MA) FIR filter can be implemented as a lattice-type structure. The result of converting a direct form FIR filter of order p into a lattice filter is shown in Fig. 16.13.

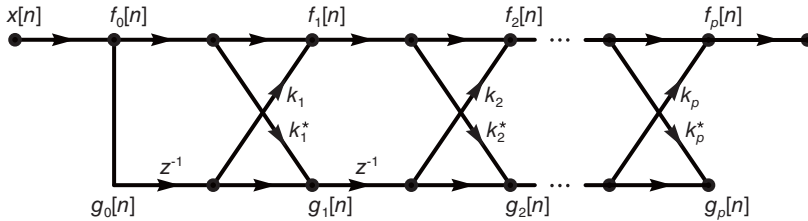


FIGURE 16.13 MA model lattice filter realizations.

The reflection coefficients k_m and k_m^* are deduced from the direct form FIR filter coefficients a_k , which are in fact the samples of the filter impulse response.

At each of the successive p stages of the lattice filter the recursive equations are

$$f_m[n] = f_{m-1}[n] + k_m g_{m-1}[n - 1] \tag{16.281}$$

$$g_m[n] = k_m^* f_{m-1}[n] + g_{m-1}[n - 1] \tag{16.282}$$

where $m = 1, 2, \dots, p$. The initial conditions are

$$f_0[n] = g_0[n] = x[n] \tag{16.283}$$

and $f_m[n]$ and $g_m[n]$ are the forward and backward linear prediction errors at the m^{th} stage of the lattice. To show that this is a proper conversion to the lattice form and to write the resulting z -domain input-output relations we note that since

$$f_p[n] = \sum_{k=0}^p a_k n[n - k] \tag{16.284}$$

we have

$$F_p(z) = \sum_{k=0}^p a_k z^{-k} X(z) = A_p(z) X(z) \tag{16.285}$$

where

$$A_p(z) = \sum_{k=0}^p a_k z^{-k} = (1 + a_1 z^{-1} + \dots + a_p z^{-p}) \tag{16.286}$$

i.e.

$$A_p(z) = \frac{F_p(z)}{X(z)} = \frac{F_p(z)}{F_0(z)} \tag{16.287}$$

This is the filter transfer function from its input to the output $f_p[n]$ of the p^{th} stage. Moreover, we may write

$$g_p[n] = \sum_{k=0}^p b_k n[n-k] \quad (16.288)$$

$$G_p(z) = \sum_{k=0}^p b_k z^{-k} X(z) = B_p(z) X(z) \quad (16.289)$$

$$B_p(z) = \sum_{k=0}^p b_k z^{-k} = \left\{ b_0 + b_1 z^{-1} + \dots + b_{p-1} z^{-(p-1)} + z^{-p} \right\} \quad (16.290)$$

and since, $b_k = a_{p-k}^*$, $k = 0, 1, \dots, p$, we have

$$B_p(z) = \sum_{k=0}^p a_{p-k}^* z^{-k} = \sum_{r=0}^p a_r^* z^{-p+r} = z^{-p} \sum_{r=0}^p a_r^* z^r = z^{-p} A_p^*(1/z^*). \quad (16.291)$$

This is the same relation we encountered in the all-zero lattice filter in Chapter 11. The only difference is that here the coefficients and the input sequence are generally complex. We note that, as expected, if $z = z_0$ is a zero of the polynomial $B_p(z)$ i.e. $B_p(z_0) = 0$ then $z = 1/z_0^*$ is a zero of $A_p(z)$ since $B_p(z_0) = z_0^{-p} A_p^*(1/z_0^*) = 0$. The polynomial $B_p(z)$ is therefore the reciprocal polynomial of $A_p(z)$ as defined in Chapter 11. Note that the polynomial $B_p(z)$ was labeled $\tilde{A}_p(z)$ in Chapter 11, wherein we found that $\tilde{A}_s(z) = z^{-s} A_s(z^{-1})$. Note, moreover, that if $A_p(z)$ is minimum phase then $B_p(z)$ is maximum phase, i.e. its poles and zeros are outside the unit circle.

Proceeding similarly to Chapter 11, we may write the recursive relations

$$F_m(z) = F_{m-1}(z) + k_m z^{-1} G_{m-1}(z) \quad (16.292)$$

$$G_m(z) = k_m^* F_{m-1}(z) + z^{-1} G_{m-1}(z) \quad (16.293)$$

wherefrom

$$A_m(z) = A_{m-1}(z) + k_m z^{-1} B_{m-1}(z) \quad (16.294)$$

$$B_m(z) = k_m^* A_{m-1}(z) + z^{-1} B_{m-1}(z) \quad (16.295)$$

or, in matrix form, where $m = 1, 2, \dots, p$,

$$\begin{bmatrix} A_m(z) \\ B_m(z) \end{bmatrix} = \begin{bmatrix} 1 & k_m z^{-1} \\ k_m^* & z^{-1} \end{bmatrix} \begin{bmatrix} A_{m-1}(z) \\ B_{m-1}(z) \end{bmatrix} \quad (16.296)$$

Note that the coefficients a_k in the polynomial

$$A_p(z) = \sum_{k=0}^p a_k z^{-k} \quad (16.297)$$

are a short-hand notation for $a_k^{(p)}$, the symbol used in Chapter 11. Similarly the coefficients b_k in $B_p(z) = \sum_{k=0}^p b_k z^{-k}$ are short-hand notation for $b_k^{(p)}$. In writing the coefficients of the polynomial $A_m(z)$ and $B_m(z)$, to indicate that the coefficients relate to a lattice filter of m

stages we will use the long notations $a_k^{(m)}$ and $b_k^{(m)}$, i.e.

$$A_m(z) = \sum_{k=0}^m a_k^{(m)} z^{-k} \tag{16.298}$$

$$B_m(z) = \sum_{k=0}^m b_k^{(m)} z^{-k} = \sum_{k=0}^m a_{m-k}^{(m)*} z^{-k} \tag{16.299}$$

We may therefore write

$$\sum_{k=0}^m a_k^{(m)} z^{-k} = \sum_{k=0}^{m-1} a_k^{(m-1)} z^{-k} + k_m z^{-1} \sum_{k=0}^{m-1} a_{m-1-k}^{(m-1)*} z^{-k}. \tag{16.300}$$

Equating the coefficients of the same powers of z^{-1} in both sides of this equation we have

$$\begin{aligned} a_k^{(m)} &= a_k^{(m-1)} + k_m a_m^{(m-1)*} \\ a_m^{(m)} &= k_m. \end{aligned} \tag{16.301}$$

We may also write

$$A_{m-1}(z) = A_m(z) - k_m \{B_m(z) - k_m^* A_{m-1}(z)\} \tag{16.302}$$

wherefrom

$$A_{m-1}(z) = \{A_m(z) - k_m B_m(z)\} / \{1 - |k_m|^2\} \tag{16.303}$$

i.e.

$$a_m^{(m)} = k_m \tag{16.304}$$

and

$$a_k^{(m-1)} = \frac{a_k^{(m)} - k_m b_k^{(m)}}{1 - |k_m|^2} = \frac{a_k^{(m)} - k_m a_{m-k}^{(m)*}}{1 - |k_m|^2} \tag{16.305}$$

which is the step-down recursion as found in Chapter 11. The $\{a_k\}$ and $\{b_k\}$ coefficients can thus be recursively evaluated from the reflection coefficients and vice versa.

The mean-square error $E[|f_m[n]|^2]$ may be directly minimized relative to the lattice filter reflection coefficients k_m . We have

$$f_m[n] = f_{m-1}[n] + k_m g_{m-1}[n-1] \tag{16.306}$$

$$\begin{aligned} |f_m[n]|^2 &= f_{m-1}[n] f_{m-1}^*[n] + k_m^* f_{m-1}[n] g_{m-1}^*[n-1] \\ &\quad + k_m g_{m-1}[n-1] f_{m-1}^*[n] + k_m k_m^* g_{m-1}[n-1] g_{m-1}^*[n-1] \end{aligned} \tag{16.307}$$

$$\frac{\partial E[|f_m[n]|^2]}{\partial k_m^*} = E[f_{m-1}[n] g^*[n-1] + k_m g_{m-1}[n-1] g_{m-1}^*[n-1]] \tag{16.308}$$

$$k_m = \frac{-E[f_{m-1}[n] g_{m-1}^*[n-1]]}{E[|g_{m-1}[n-1]|^2]} \tag{16.309}$$

and we note that $E[|g_{m-1}[n-1]|^2]$ is the minimum prediction error $E_{m-1, min}^g = E_{m-1, min}^f$.

16.21 AR Lattice of Order p

An AR(p) autoregressive stationary random process of order p may be produced by applying white noise of variance σ_w^2 say, to an all-pole IIR filter of transfer function

$$H(z) = \frac{1}{1 + \sum_{k=1}^p a_k z^{-k}}. \tag{16.310}$$

As we have seen in Chapter 11 the all-pole lattice structure is the same as the all-zero structure but with the roles of input and output reversed.

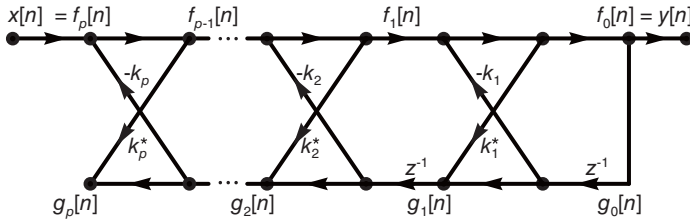


FIGURE 16.14 AR model lattice filter realizations.

The lattice structure is shown in Fig. 16.14. We note that the filter input is

$$x[n] = f_p[n] \tag{16.311}$$

and its output is

$$y[n] = f_0[n] = g_0[n]. \tag{16.312}$$

The recursive relations are

$$f_{m-1}[n] = f_m[n] - k_m g_{m-1}[n-1] \tag{16.313}$$

$$g_m[n] = g_{m-1}[n-1] + k_m^* f_{m-1}[n] \tag{16.314}$$

as we have seen in Chapter 11.

16.22 ARMA(p, q) Process

Similarly, for an ARMA(p, q) process the transfer function is

$$H(z) = \frac{\sum_{k=0}^q b_k z^{-k}}{1 + \sum_{k=1}^p a_k z^{-k}} = \frac{B_q(z)}{A_p(z)}, \tag{16.315}$$

where we assume that $p \geq q$. Receiving, as input, white noise this pole-zero IIR filter generates an ARMA(p, q) process. The lattice structure is shown in Fig. 16.15, based on

the conversion to lattice form development seen in Chapter 11. If the input white noise is of variance σ_w^2 , the ARMA(p, q) process has a power spectral density

$$\Phi_{xx}(e^{j\Omega}) = \sigma_w^2 \frac{|B_q(e^{j\Omega})|^2}{|A_p(e^{j\Omega})|^2}. \tag{16.316}$$

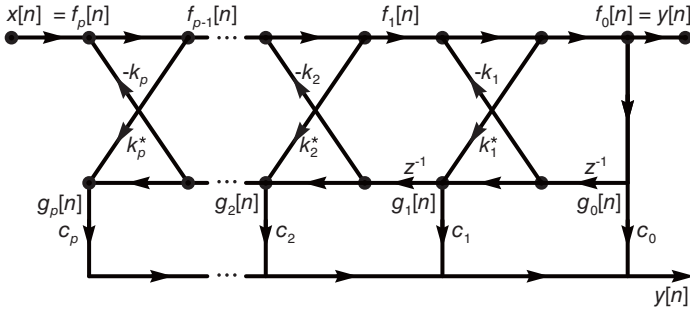


FIGURE 16.15 ARMA model lattice filter realizations.

16.23 Power Spectrum Estimation



FIGURE 16.16 AR process as IIR filter response to white noise.

Referring to Fig. 16.16 and Fig. 16.17, an AR(p) stationary random process $x[n]$ is generated by feeding an all-pole IIR filter with a white noise sequence $w[n]$. We have

$$x[n] + \sum_{k=1}^p a_k x[n - k] = w[n] \tag{16.317}$$

$$X(z) + \sum_{k=1}^p a_k z^{-k} X(z) = W(z) \tag{16.318}$$

$$H(z) = \frac{X(z)}{W(z)} = \frac{1}{1 + \sum_{k=1}^p a_k z^{-k}}. \tag{16.319}$$

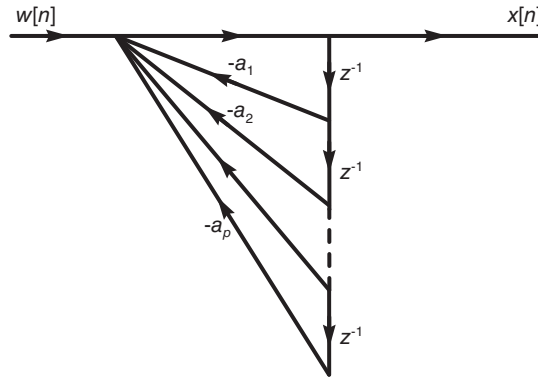


FIGURE 16.17 AR process model for power spectrum estimation.

The white noise is assumed to be of zero mean and of variance σ_w^2 . The power spectral density of the AR(p) process may be estimated by writing

$$\begin{aligned}
 P_x(\Omega) &= \Phi_{xx}(e^{j\Omega}) = \Phi_{ww}(e^{j\Omega}) |H(e^{j\Omega})|^2 = \sigma_w^2 |H(e^{j\Omega})|^2 \\
 &= \frac{\sigma_w^2}{\left| 1 + \sum_{k=1}^p a_k e^{-j\Omega k} \right|^2}.
 \end{aligned}
 \tag{16.320}$$

This is an alternative to the periodogram, and related FFT-based approaches, which has been gaining popularity in some applications calling for narrow-band frequency resolution of limited duration signals. An AR rather than ARMA model is often used in such applications.

16.24 FIR Wiener Filtering of Noisy Signals

We presently focus our attention on the filtering and prediction of a desired signal $s[n]$ contaminated by added noise $w[n]$. We shall see that Wiener filter optimization and filter optimization for prediction lead to practically equivalent results, as found above in the absence of noise.

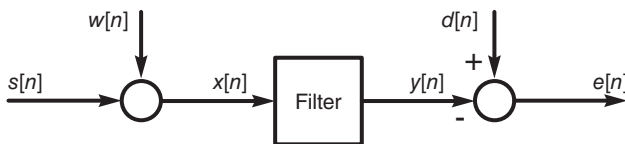


FIGURE 16.18 Wiener filtering and prediction.

The problem of filtering and prediction of a noise-contaminated signal is depicted in Fig. 16.18. As seen in the figure the filter receives as input the sequence

$$x[n] = s[n] + w[n].
 \tag{16.321}$$

Its output $y[n]$ is compared with the desired signal $d[n]$. In the case of (Wiener) filtering the desired signal is the signal before contamination, i.e. $d[n] = s[n]$ and the error is $e[n] = s[n] - y[n]$. In the case of prediction, $d[n] = s[n + K]$, $K \geq 1$.

Assuming that the signal $s[n]$ and noise $w[n]$ are zero-mean stationary random processes which are uncorrelated, the analysis is practically the same as seen above in the case of absence of noise. Optimization of the filter parameters is obtained by minimizing the mean square error $E \left[|e[n]|^2 \right]$ and we presently consider the case of an FIR filter. Similarly to the above we summarize the optimization steps. We have

$$e[n] = d[n] - y[n] \tag{16.322}$$

where

$$y[n] = \sum_{k=0}^{M-1} h[k]x[n-k] \tag{16.323}$$

$\{h[k]\}$ being the M -point samples of the filter impulse response. Note that compared to the above we have $y[n] = -\hat{d}[n]$ leading to a reversal of sign in the result and in matrix form

$$e[n] = d[n] - h^T x. \tag{16.324}$$

The mean-square error is

$$E_M = E \left[\left| d[n] - \sum_{k=0}^{M-1} h[k]x[n-k] \right|^2 \right]. \tag{16.325}$$

Similarly to the above the mean square error E_M is given by

$$E_M = \phi_{dd}[0] - \phi_{xx}^{*T} h - \phi_{dx}^T h^* + h^{*T} \phi_{xx}^T h \tag{16.326}$$

$$\frac{\partial E_M}{\partial h^*} = \phi_{dx} - \phi_{xx}^T h = 0 \tag{16.327}$$

$$\phi_{xx}^T h = \phi_{dx} \tag{16.328}$$

$$h = \{ \phi_{xx}^T \}^{-1} \phi_{dx} \tag{16.329}$$

and the corresponding value of the mean-square error is

$$E_{M \min} = \phi_{dd}[0] - \phi_{dx}^{*T} h = \sigma_d^2 - \phi_{dx}. \tag{16.330}$$

We note that in the case of filtering, with $d[n] = s[n]$ and with $s[n]$ and $w[n]$ uncorrelated we have

$$\phi_{xx} = \phi_{ss} + \phi_{ww} \tag{16.331}$$

$$\phi_{dx} = \phi_{ss} \tag{16.332}$$

while, in the case of prediction,

$$\phi_{dx}[k] = \phi_{ss}[m + K], \quad m = 0, 1, \dots, M - 1. \tag{16.333}$$

Example 16.10 A signal $s[n]$ is an ARMA(p) process with $p = 2$ which is described by the difference equation

$$s[n] = 1.2s[n-1] - 0.35s[n-2] + 3v[n] - 1.7v[n-1] \quad (16.334)$$

where $v[n]$ is a white noise sequence with variance $\sigma_v^2 = 0.49$. Evaluate the power spectral density of $s[n]$. Design a Wiener filter of length $M = 4$ to estimate the signal $s[n]$ from a received signal $x[n] = s[n] + w[n]$ where $w[n]$ is a white noise sequence of variance $\sigma_w^2 = 1$, which is uncorrelated with $s[n]$.

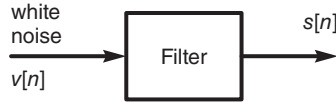


FIGURE 16.19 FIR Wiener filter example.

Referring to Fig. 16.19, the signal $s[n]$ is obtained by applying a white noise signal $v[n]$ to the input of a second order filter. The power spectral density of $s[n]$ is

$$P_{ss}(\Omega) = \Phi_{ss}(e^{j\Omega}) = \sigma_v^2 |H(e^{j\Omega})|^2 \quad (16.335)$$

Now

$$H(z) = \frac{S(z)}{V(z)} = \frac{3 - 1.7z^{-1}}{1 - 1.2z^{-1} + 0.35z^{-2}} = \frac{3 - 1.7z^{-1}}{(1 - 0.5z^{-1})(1 - 0.7z^{-1})} \quad (16.336)$$

$$|H(e^{j\Omega})|^2 = \frac{11.89 - 10.2 \cos \Omega}{2.5625 - 3.24 \cos \Omega + 0.7 \cos 2\Omega} \quad (16.337)$$

The power spectral density of $s[n]$ is

$$P_{ss}(\Omega) = \Phi_{ss}(e^{j\Omega}) = \sigma_v^2 |H(e^{j\Omega})|^2 = \frac{0.49(11.89 - 10.2 \cos \Omega)}{2.5625 - 3.24 \cos \Omega + 0.7 \cos 2\Omega} \quad (16.338)$$

$$\Phi_{ss}(z) = \sigma_v^2 H(z)H(z^{-1}) \quad (16.339)$$

$$\begin{aligned} &= \frac{5.8261 - 2.499z^{-1} - 2.499z}{2.5625 + 0.35z^{-2} - 1.62z^{-1} - 1.62z + 0.35z^2} \\ &= \frac{2.161}{1 - 0.05z^{-1}} - \frac{2.161}{1 - 2z^{-1}} + \frac{5.3508}{1 - 0.7z^{-1}} - \frac{5.3508}{1 - 1.428z^{-1}} \\ \phi_{ss}[m] &= 2.161(0.5)^{|m|} + 5.3508(0.7)^{|m|}. \end{aligned} \quad (16.340)$$

The desired signal is $d[n] = s[n]$ and since $w[n]$ and $s[n]$ are uncorrelated we have

$$\phi_{xx}[k] = \phi_{ss}[k] + \phi_{ww}[k] \quad (16.341)$$

$$\phi_{dx}[k] = \phi_{ss}[k] \quad (16.342)$$

$$\phi_{xx}[0] = \phi_{ss}[0] + \sigma_w^2 = \phi_{ss}[0] + 1 \quad (16.343)$$

$$\phi_{xx}[k] = \phi_{ss}[k], \quad k \neq 0 \quad (16.344)$$

$$\phi_{xx}h = \phi_{ss} \tag{16.345}$$

$$\begin{bmatrix} 8.5118 & 4.82606 & 3.16214 & 2.10545 \\ 4.82606 & 8.5118 & 4.82606 & 3.16214 \\ 3.16214 & 4.82606 & 8.5118 & 4.82606 \\ 2.10545 & 3.16214 & 4.82606 & 8.5118 \end{bmatrix} \begin{bmatrix} h[0] \\ h[1] \\ h[2] \\ h[3] \end{bmatrix} = \begin{bmatrix} 7.5118 \\ 4.82606 \\ 3.16214 \\ 2.10545 \end{bmatrix}. \tag{16.346}$$

Solving we obtain

$$h = \{0.8259, 0.0913, 0.0114, 0.0027\}. \tag{16.347}$$

The minimum mean-square error is

$$\begin{aligned} E_{min} &= \phi_{ss}[0] - \sum_{k=0}^3 \phi_{ss}[k]h_k \\ &= 7.5118 - (7.5118 \times 0.8259 + 4.82606 \times 0.0913 \\ &\quad + 3.16214 \times 0.0114 + 2.10545 \times 0.0027) \\ &= 0.8255. \end{aligned} \tag{16.348}$$

16.25 Two-Sided IIR Wiener Filtering

We consider the case where the optimal Wiener filter has a two-sided impulse response $h[n]$. The filter is therefore not causal and hence not physically realizable. The analysis follows the same steps, where now summations extend from $-\infty$ to ∞ . The filter output is

$$y[n] = \sum_{k=-\infty}^{\infty} h[k]x[n-k]. \tag{16.349}$$

The Wiener-Hopf equation takes the form

$$\sum_{k=-\infty}^{\infty} h[k]\phi_{xx}[m-k] = \phi_{dx}[m], \quad -\infty < m < \infty. \tag{16.350}$$

The left-hand side of this equation being a convolution we have in the z -domain

$$H(z)\Phi_{xx}(z) = \Phi_{dx}(z) \tag{16.351}$$

$$H(z) = \Phi_{dx}(z)/\Phi_{xx}(z) \tag{16.352}$$

The resulting minimum mean square error is

$$E = \sigma_d^2 - \sum_{k=-\infty}^{\infty} h[k]\phi_{dx}^*[k]. \tag{16.353}$$

The minimum mean square error can also be written using Parseval's relation in the form

$$E = \frac{1}{2\pi j} \oint_C \{\Phi_{dd}(z) - H(z)\Phi_{dx}(z^{-1})\} z^{-1} dz. \tag{16.354}$$

Example 16.11 Evaluate the two-sided IIR Wiener filter and the resulting minimum mean square error for the case stated in Example 16.10.

We have

$$\begin{aligned}\Phi_{dx}(z) &= \Phi_{sx}(z) = \Phi_{ss}(z) = \frac{5.8261 - 2.499z^{-1} - 2.499z}{2.5625 - 0.35z^{-2} - 1.62z^{-1} - 1.622z + 0.35z^2} \\ \Phi_{xx}(z) &= \Phi_{ss}(z) + 1 = \frac{0.35 - 4.119z^{-1} + 8.389z^{-2} - 4.119z^{-3} + 0.35z^{-4}}{0.35 - 1.62z^{-1} + 2.563z^{-2} - 1.62z^{-3} + 0.35z^{-4}} \\ H_{opt}(z) &= \frac{\Phi_{dx}(z)}{\Phi_{xx}(z)} = \frac{\Phi_{ss}(z)}{\Phi_{xx}(z)} = 1 - \frac{1}{\Phi_{xx}(z)} \\ H_{opt}(z) &= \frac{-2.499z^{-1} + 5.826z^{-2} - 2.499z^{-3}}{0.35 - 4.119z^{-1} + 8.389z^{-2} - 4.119z^{-3} + 0.35z^{-4}} \\ H_{opt}(z) &= \frac{-0.7732}{1 - 9.3349z^{-1}} - \frac{-0.0041}{1 - 1.7576z^{-1}} + \frac{0.0041}{1 - 0.569z^{-1}} + \frac{0.7732}{1 - 0.1071z^{-1}} \\ h_{opt}[n] &= 0.7732 \times 0.1071^{|n|} + 0.041 \times 0.569^{|n|}.\end{aligned}$$

We note that $\Phi_{dd}(z) = \Phi_{ss}(z)$, $\Phi_{dx}(z) = \Phi_{sx}(z) = \Phi_{ss}(z)$, since $\phi_{sx}[m] = \phi_{ss}[m]$, and $\Phi_{dx}(z^{-1}) = \Phi_{ss}(z^{-1}) = \Phi_{ss}(z)$. The resulting minimum mean square error is

$$E = \frac{1}{2\pi j} \oint_C \{\Phi_{ss}(z) - \Phi_{ss}(z)H_{opt}(z)\} z^{-1} dz$$

$$E = \Sigma \left[\text{residues of } z^{-1}\Phi_{ss}(z)[1 - H_{opt}(z)] \right] = \Sigma \left[\text{residues of } z^{-1} \frac{\Phi_{ss}(z)}{\Phi_{xx}(z)} \right].$$

We may write

$$G(z) = z^{-1} \frac{\Phi_{ss}(z)}{\Phi_{xx}(z)} = -0.714 \frac{(z - 1.7647)(z - 0.5667)}{(z - 9.3349)(z - 1.7576)(z - 0.569)(z - 0.1071)}$$

$$E = \Sigma \left[\text{residues of } G(z) \text{ at the poles } z = 0.569 \text{ and } z = 0.1071 \right]$$

$$E = 0.07732 + 0.000408 = 0.07773.$$

16.26 Causal IIR Wiener Filter

We note that in the case of a causal IIR Wiener filter the Wiener–Hopf equation is valid only for $m \geq 0$. To solve this equation using the z -transform we need to pay attention to the ROC of its transform. We rewrite the Wiener–Hopf equation in the form

$$f[m] = \sum_{k=0}^{\infty} h[k]\phi_{xx}[m-k] - \phi_{dx}[m], \quad m \geq 0. \quad (16.355)$$

Taking its z -transform we have

$$F(z) = \Phi_{dx}(z) - \Phi_{xx}(z)H(z). \quad (16.356)$$

We note that $f[m] = 0, m \geq 0$, i.e. $f[m]$ is left-sided and $F(z)$ is analytic for $|z| < 1$ while $H(z)$ is analytic for $|z| > 1$. Factoring $\Phi_{xx}(z)$ we have

$$\Phi_{xx}(z) = P^+(z)P^-(z) \tag{16.357}$$

where $P^+(z)$ is minimum phase, having all its poles and zeros inside the unit circle, and vice versa for $P^-(z)$. We have

$$F(z) = \Phi_{dx}(z) - P^+(z)P^-(z)H(z) \tag{16.358}$$

$$\frac{F(z)}{P^-(z)} = \frac{\Phi_{dx}(z)}{P^-(z)} - P^+(z)H(z) \tag{16.359}$$

Effecting a decomposition using partial fraction expansion we may write

$$\frac{\Phi_{dx}(z)}{P^-(z)} = Q^+(z) + Q^-(z) \tag{16.360}$$

where $Q^+(z)$ is analytic for $|z| > 1$ and $Q^-(z)$ is analytic for $|z| < 1$. Alternatively we can evaluate $Q^+(z)$ as the transform of the causal part $q[n]u[n]$ of the inverse transform $q[n]$ of $\Phi_{dx}(z)/P^-(z)$. We may write

$$\frac{F(z)}{P^-(z)} = Q^+(z) + Q^-(z) - P^+(z)H(z) \tag{16.361}$$

and for $|z| > 1$ we have

$$Q^+(z) - P^+(z)H(z) = 0 \tag{16.362}$$

so that

$$H(z) = Q^+(z)/P^+(z), |z| > 1. \tag{16.363}$$

Example 16.12 Referring to Example 16.10, design a causal Wiener filter by evaluating its optimal transfer function and impulse response.

$$\Phi_{xx}(z) = \Phi_{ss}(z) + \Phi_{ww}(z) \tag{16.364}$$

$$\phi_{ww}[n] = \sigma_w^2 \delta[n] \tag{16.365}$$

$$\Phi_{xx}(z) = \Phi_{ss}(z) + 1 \tag{16.366}$$

$$\Phi_{xx}(z) = \frac{0.35 - 4.119z^{-1} + 8.389z^{-2} - 4.119z^{-3} + 0.35z^{-4}}{0.35 - 1.62z^{-1} + 2.563z^{-2} - 1.62z^{-3} + 0.35z^{-4}} \tag{16.367}$$

$$\Phi_{xx}(z) = P^+(z)P^-(z) \tag{16.368}$$

$$\Phi_{xx}(z) = \frac{(1 - 0.569z^{-1})(1 - 0.1071z^{-1})(1 - 9.3349z^{-1})(1 - 1.7576z^{-1})}{(1 - 0.5z^{-1})(1 - 0.7z^{-1})(1 - 2z^{-1})(1 - 1.4286z^{-1})} \tag{16.369}$$

$$P^+(z) = \frac{(1 - 0.1071z^{-1})(1 - 0.569z^{-1})}{(1 - 0.5z^{-1})(1 - 0.7z^{-1})} = \frac{1 - 0.6761z^{-1} + 0.061z^{-2}}{1 - 1.2z^{-1} + 0.35z^{-2}} \tag{16.370}$$

$$P^-(z) = \frac{(1 - 1.7576z^{-1})(1 - 9.3349z^{-1})}{(1 - 1.4286z^{-1})(1 - 2z^{-1})} = \frac{1 - 11.09z^{-1} + 16.41z^{-2}}{1 - 3.429z^{-1} + 2.857z^{-2}} \tag{16.371}$$

$$R(z) = \frac{\Phi_{dx}(z)}{P^-(z)} = \frac{\Phi_{ss}(z)}{P^-(z)} \quad (16.372)$$

$$\begin{aligned} R(z) &= \frac{-2.499z^{-1} + 5.8261z^{-2} - 2.499z^{-3}}{0.35 - 1.62z^{-1} + 2.5625z^{-2} - 1.62z^{-3} + 0.35z^{-4}} \\ &\quad \times \frac{(1 - 1.4282z^{-1})(1 - 2z^{-1})}{(1 - 1.7576z^{-1})(1 - 9.3349z^{-1})} \\ &= Q^+(z) + Q^-(z) \end{aligned} \quad (16.373)$$

$$Q^+(z) = \frac{0.8259 - 0.4671z^{-1}}{1 - 1.2z^{-1} + 0.35z^{-2}} \quad (16.374)$$

$$H(z) = \frac{Q^+(z)}{P^+(z)} \quad (16.375)$$

$$\begin{aligned} &= \frac{0.8259 - 1.458z^{-1} + 0.8496z^{-2} - 0.1635z^{-3}}{1 - 1.876z^{-1} + 1.222z^{-2} - 0.3098z^{-3} + 0.02133z^{-4}} \\ &\cong \frac{0.81987}{1 - 0.10712z^{-1}} + \frac{0.005988627}{1 - 0.568955z^{-1}} \\ h[n] &= [0.81987(0.10712)^n + 0.005989(0.56896)^n] u[n] \end{aligned} \quad (16.376)$$

16.27 Wavelet Transform

The wavelet transform was introduced in the 1980s as a means of spectral analysis, over relatively short time periods, of nonstationary signals. In contrast to Fourier and related transforms such as Walsh–Hadamard where the signal is decomposed into the sum of infinite duration sinusoidal or alternating square waves basis functions, the wavelet transform views a short-duration of the signal and evaluates its product with a burst that is typically a fast rising and decaying sinusoid or a few cycles of a square wave. The burst is referred to as a wavelet and, beside being slid along the time axis, it may be stretched or compressed at will, effectively selecting a suitable local frequency resolution, and altering it as desired.

In the continuous-time domain the wavelet transform of a function $f(t)$ is given by

$$F_w(a, \tau) = \frac{1}{\sqrt{a}} \int_{-\infty}^{\infty} f(t) \psi^* \left(\frac{t - \tau}{a} \right) dt. \quad (16.377)$$

Alternatively, we may write

$$F_w(a, \tau) = \int_{-\infty}^{\infty} f(t) \psi_{a, \tau}^*(t) dt \quad (16.378)$$

where

$$\psi_{a, \tau}(t) = \frac{1}{\sqrt{a}} \psi \left(\frac{t - \tau}{a} \right). \quad (16.379)$$

The function $\psi \left(\frac{t - \tau}{a} \right)$ is a shift in time by τ seconds and dilation by a time scale factor a of a wavelet $\psi(t)$ that is a relatively short duration generally oscillating pulse. An example is what is known as the Morlet wavelet given by

$$\psi(t) = e^{-t^2} \cos \left(\pi \sqrt{\frac{2}{\ln 2}} t \right) \quad (16.380)$$

a product of a Gaussian function and a pure sinusoid, seen in Fig. 16.20 a).

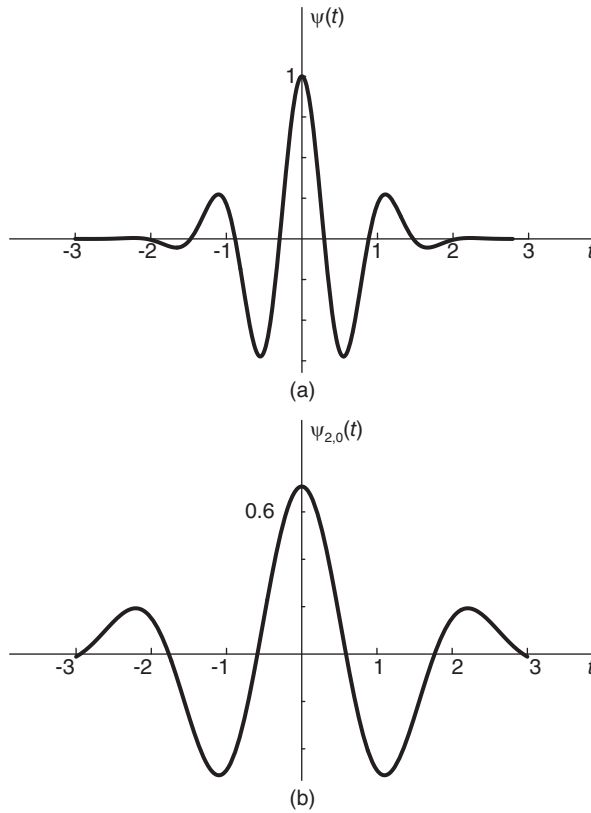


FIGURE 16.20 (a) Morlet wavelet, (b) scaled form.

We note that

$$\psi_{1,0} = \psi(t) \tag{16.381}$$

and that

$$\psi_{a,0} = \frac{1}{\sqrt{a}} \psi\left(\frac{t}{a}\right). \tag{16.382}$$

The dilation of $\psi(t)$ caused by setting $a = 2$ is shown as the function $\psi_{2,0}(t)$ in Fig. 16.20(b).

Another example of the wavelet $\psi(t)$ is the Haar wavelet shown in Fig. 16.21.

$$\psi_{Ha}(t) = \begin{cases} 1, & 0 < t < 0.5 \\ -1, & 0.5 < t < 1 \\ 0, & \text{otherwise.} \end{cases} \tag{16.383}$$

Another example is the Mexican hat introduced by Gabor [40]. It is the second derivative of the Gaussian function $-e^{-t^2/2}$

$$\psi(t) = e^{-t^2/2} (1 - t^2). \tag{16.384}$$

Its Fourier transform is

$$\Psi(j\omega) = -\omega^2 e^{-\omega^2/2} \tag{16.385}$$

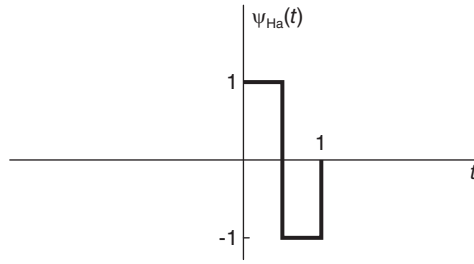


FIGURE 16.21 Haar wavelet.

The Gaussian function has derivatives of all orders, and each on its own qualifies as a wavelet. Its n^{th} order derivative has the Fourier transform

$$\Psi(j\omega) = (j\omega)^n e^{-\omega^2/2} \quad (16.386)$$

By progressively increasing the value of the parameter b the window of the wavelet is made to slide along the time axis. Similarly to short-time Fourier analysis, sliding window spectral analysis and in particular the spectrogram, the resulting wavelet spectrum is a function of time. By choosing a wider wavelet window, lower frequency resolution for slowly varying signal sections can be applied. Higher resolution for fast varying parts of the signal is obtained by applying narrower time-compressed wavelets.

The definition Equation (16.377) implies that the wavelet transform $F_w(a, \tau)$ is a correlation of $f(t)$ with the time-scaled wavelet $\psi^*(t/a)$. The factor $1/\sqrt{a}$ is included in the definition for energy normalization. Moreover, wavelets are in general real, so that the correlation is in fact between $f(t)$ and $\psi(t/a)$. Let

$$\Psi(j\omega) = \mathcal{F}[\psi(t)]. \quad (16.387)$$

We have

$$\mathcal{F}[\psi(t/a)] = a\Psi(ja\omega) \quad (16.388)$$

$$\mathcal{F}[\psi\{(t-\tau)/a\}] = a\Psi(ja\omega)e^{-j\tau\omega} \quad (16.389)$$

so that

$$\psi_{a,\tau}(t) = \frac{1}{\sqrt{a}}\psi\left(\frac{t-\tau}{a}\right) \xleftrightarrow{\mathcal{F}} \sqrt{a}\Psi(ja\omega)e^{-j\tau\omega} \quad (16.390)$$

i.e.

$$\Psi_{a,\tau}(j\omega) = \sqrt{a}\Psi(ja\omega)e^{-j\tau\omega}. \quad (16.391)$$

The Fourier transform of the wavelet transform $F_w f(a, \tau)$ may be written directly since the latter is the correlation of $f(t)$ with $(1/\sqrt{a})\Psi^*(t/a)$. We may write

$$\phi_w(a, j\omega) \triangleq \mathcal{F}[F_w(a, \tau)] = \frac{1}{\sqrt{a}}F(j\omega)a\Psi^*(ja\omega) = \sqrt{a}F(j\omega)\Psi^*(ja\omega) \quad (16.392)$$

and we have the inverse relation

$$F_w(a, \tau) = \frac{\sqrt{a}}{2\pi} \int_{-\infty}^{\infty} F(j\omega)\Psi^*(ja\omega)e^{j\omega\tau} d\omega. \quad (16.393)$$

Similarly to the spectrogram, the wavelet transform is a two-dimensional function of time and frequency. It may be displayed as an image, with the vertical axis being the frequency,

referred to as “scale,” that is, the parameter a , and the horizontal being the time axis, that is, the parameter τ .

In analyzing speech signals, for example for speech recognition, short-time Fourier analysis is a major tool of spectral analysis. The speech signal is in fact a succession of phonemes. To identify such phonemes, be they vowels or consonants, affricate or fricative, the speech signal is divided into sections corresponding generally to distinct phonemes. These are windowed for Fourier analysis, uncluttered by neighboring phonemes. Each phoneme is thus of a relatively short duration. A spectrogram can be displayed as a film strip with the horizontal axis as the time axis and the vertical the frequency axis. At each time interval Δt along the horizontal axis the power spectrum of the windowed section is plotted as a function of frequency in a strip extending along the vertical frequency axis. The succession of such strips, each occupying a time Δt along the horizontal time axis, forms the spectrogram [6].

The wavelet transform leads to a similar time-frequency decomposition. The advantage of the short-time Fourier analysis approach is its classic well-established standard nature, which allows for direct interpretation and comparison of results. The wavelet transform incorporates a decay of the basis function on both sides of the wavelet, effectively applying a sliding short-duration window to the analysis. Its main advantage is to automatically mask out neighboring sections, resulting in a short-time type analysis. New wavelets are proposed in search for an optimal standard. It is therefore that even though wavelets simplify in a way the sectioning of the signal and the application of localized form of spectral analysis, the arbitrariness of wavelet shapes as basis functions introduces some complexity and a wide variety of analysis results.

We note that the scale a is inversely proportional to frequency. The higher the value of the scale a the lower the wavelet frequency and vice versa. In wavelet terminology, “scale” is commonly used, rather than “frequency.”

The Wigner Distribution is one of the oldest approaches for a two-dimensional spectral analysis of one-dimensional functions. The Wigner distribution $W_x(t, f)$ of a function $x(t)$ is given by

$$W_x(t, f) = \int_{-\infty}^{\infty} x(t + \tau/2)x^*(t - \tau/2)e^{-j2\pi f\tau} d\tau \quad (16.394)$$

It is generally free of fuzziness, due to the uncertainty principle, that is commonly associated with wavelet transforms [9].

16.28 Discrete Wavelet Transform

The discrete wavelet transform (DWT) is evaluated by passing the signal through a lowpass and a highpass filter, dividing it into a lower frequency band and an upper band. Each band is subsequently divided into a second level lower and upper bands. The process is repeated, taking the form of a binary, or “dyadic” tree. The lower band is referred to as the “Approximation” and the upper band as the “Detail.” Down sampling by retaining each second sample may be employed to reduce the number of samples at each level of the dyadic tree. The inverse transform is evaluated by doing these steps in reverse, where now upsampling is employed. This is achieved as seen in Chapter 7 by interlacing with zeros.

MATLAB® has a Wavelet Toolbox that greatly simplifies experimentation and application of the wavelet transform to signal analysis. It offers a choice of a reasonably large class

of wavelets, for applying downsampling and upsampling and displaying the time-frequency (scale) spectrogram-like plots.

Example 16.13 *Wavelet DWT*

a) Show the Approximation and Detail parts of the DWT applied to the signal

$$x(t) = \sin(20\pi t + \pi/3) + n(t) \quad (16.395)$$

where $n(t)$ is a zero-mean normally distributed white noise of variance $\sigma^2 = 0.36$. The sampling frequency is $f_s = 1000$ Hz.

b) Observe the effect of doing the same on the signal in the absence of noise.

We write

$Ts = 0.001$ sec, and let $t = (0 : 0.001 : 1)$

$T = \text{size}(t) = 1001$

$x = \sin(20*\text{pi}.* t+\text{pi}/3) + 0.6*\text{randn}(T)$

a) The signal with the added noise, $x(t)$ is shown in Fig. 16.22.

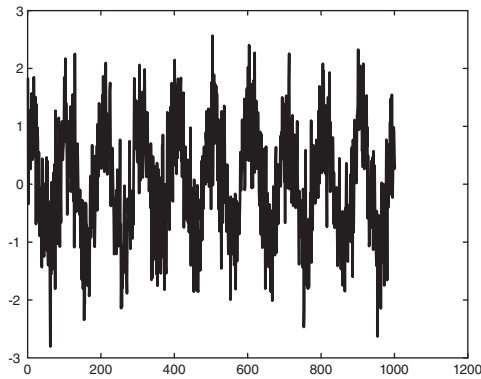


FIGURE 16.22 Noisy signal.

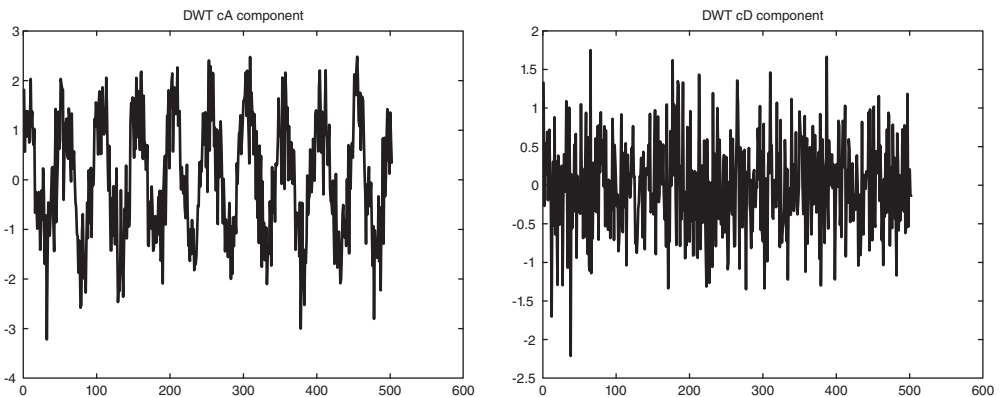


FIGURE 16.23 DWT cA and cD component, respectively, of noisy signal.

The Approximation part *cA* and the Details part *cD*, respectively, are shown in Fig. 16.23. We note that the first shows the lower frequency content revealing the sinusoid and some residual noise after filtering. The Detail part shows the upper frequency content with mainly noise in evidence.

b) In the absence of noise the DWT reveals the sinusoid as seen in the *cA* Approximation part of Fig. 16.24. However, the *cD* Detail part in the same figure includes a residual sinusoid together with spikes at both ends of the Details window.

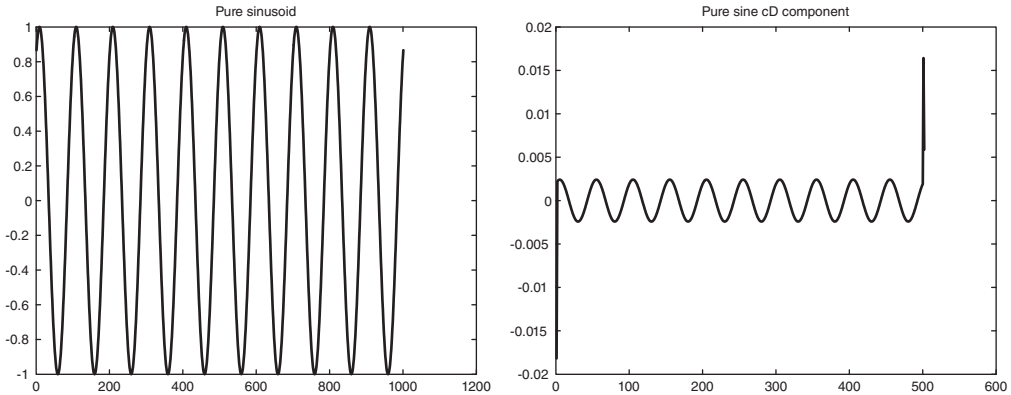


FIGURE 16.24 DWT *cA* and *cD* parts, respectively, of pure sinusoid.

The scale-time plot that wavelet analysis produces is the counterpart of the spectrogram of Fourier analysis. The vertical axis represents the scale, where lower values correspond to time-compressed wavelets, hence higher resolution and, vice versa, higher values correspond to stretched wavelets, hence coarser resolution.

Example 16.14 Show three levels of wavelet transform decomposition for the signal

$$x(t) = \sin(10\pi t - \pi/3) + \sin(50\pi t) + n(t), \quad 0 \leq t \leq 1 \tag{16.396}$$

where $n(t)$ is a zero-mean normally distributed white noise with variance $\sigma^2 = 0.25$.

```
We write
t = 0:0.001:1;
T = size(t)
x = sin(10*pi.*t-pi/3)+sin(50*pi.*t)+0.5*randn(T);
tt= wpdec(x,3,'db2');
fig = plot(tt)
```

The Tree Decomposition is displayed by MATLAB. By clicking on any node of the tree we visualize the resulting filtered component. For example clicking on node (3,0) we obtain the form shown in Fig. 16.25. Clicking on node (3,7) produces the waveform seen in Fig. 16.26.

To visualize the function **db2**, on the Wavelet Toolbox Main Menu click on Display, Wavelet Display and select wavelet: **dB2**.

Example 16.15 Plot the coefficients of the continuous wavelet transform (CWT) as a scale-time diagram for the sinusoid with added noise `noissin` of MATLAB, using the wavelet “`db3`.”

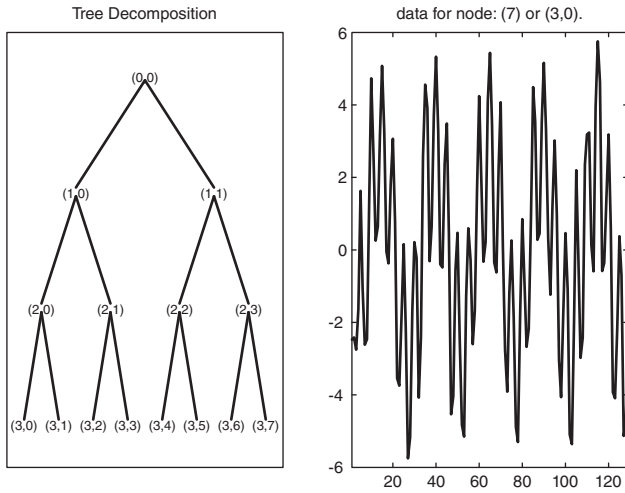


FIGURE 16.25 DWT at node(3,0).

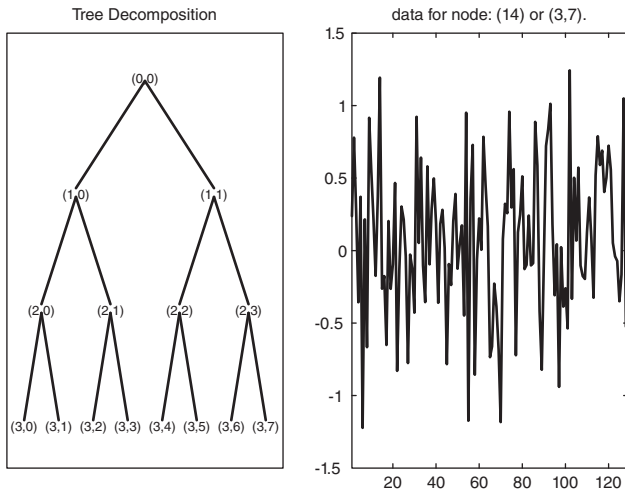


FIGURE 16.26 DWT at node(3,7).

The sinusoid with added noise is generated and the scale-time plot displayed by writing:

`load noissin`

`figure(1)`

`plot(noissin)`

`figure(2)`

`c = cwt(noissin,1:48,'db3','plot')`

These can be seen in Fig. 16.27 and Fig. 16.28, respectively.

The spectrogram of the same signal is generated using the function call `spectrogram(noissin)`. It is shown as a time versus frequency plot in Fig. 16.29.

Example 16.16 For the MATLAB speech sample signal `mtlb`, the sound “MATLAB,” generate the CWT scale-time display and the spectrogram and `specgram` respectively.

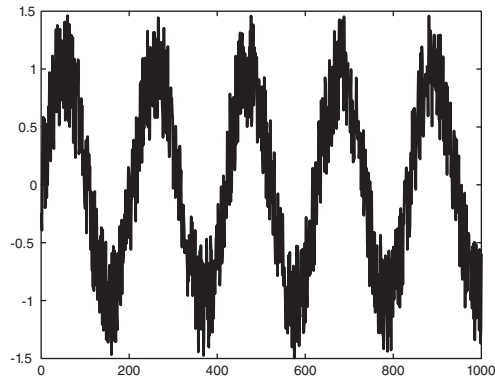


FIGURE 16.27 Noisy sinusoid noissin of MATLAB.

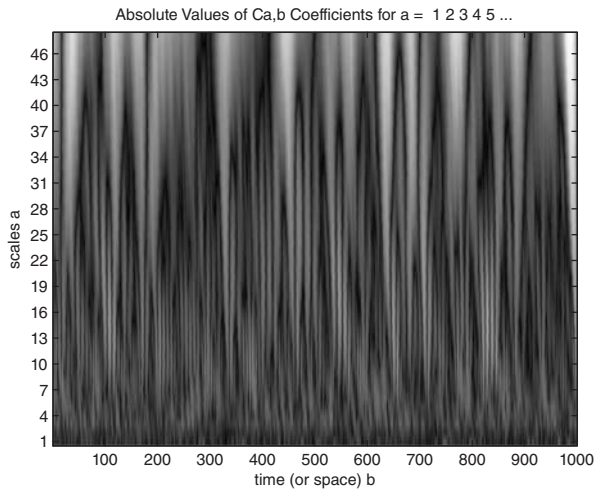


FIGURE 16.28 CWT scale time display.

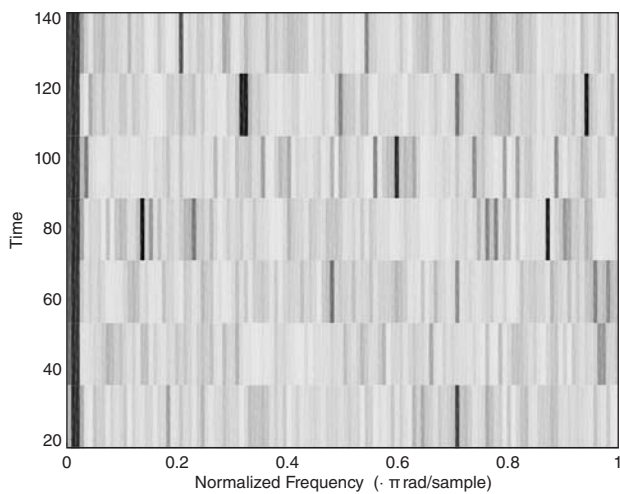


FIGURE 16.29 Spectrogram.

We write:

```
load mtlb
c = cwt(mtlb,1:48,'db3','plot');
spectrogram(mtlb,512,Fs,kaiser(500,5),475)
specgram(mtlb)
```

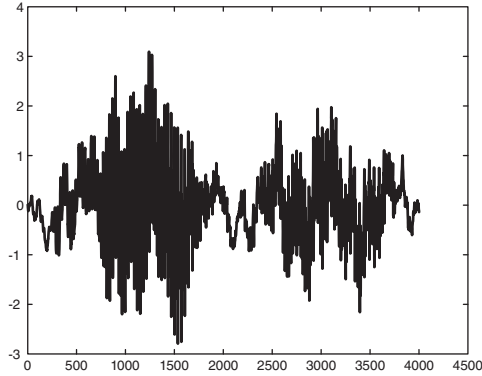


FIGURE 16.30 MATLAB's speech signal "mtlb."

The speech signal *mtlb* is seen in Fig. 16.30. The CWT scale-time plot can be seen in Fig. 16.31.

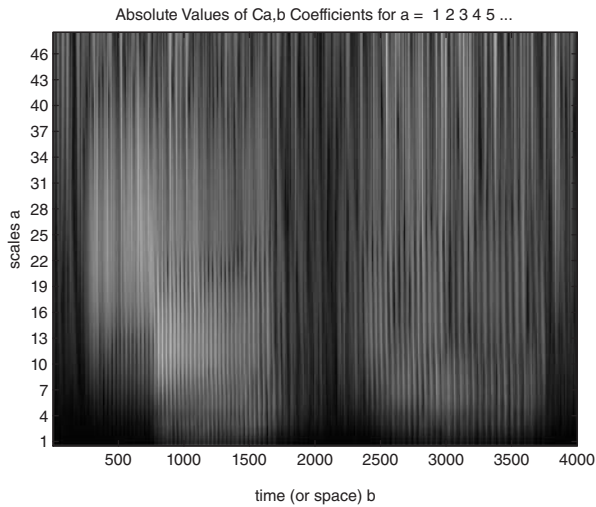


FIGURE 16.31 CWT scale time plot.

The result of the function *spectrogram* of MATLAB can be seen in Fig. 16.32, while that of the function *specgram* is shown in Fig. 16.33.

Each of these plots reveals some properties of the analyzed signal. The last is particularly effective for directly revealing the speech signal formants and their evolution in time.

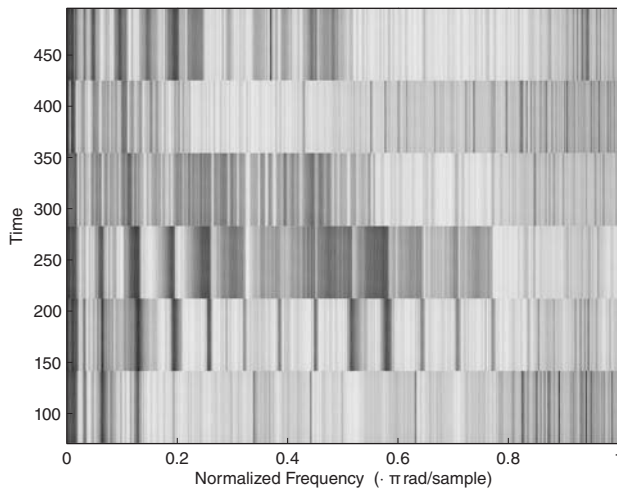


FIGURE 16.32 MATLAB’s **spectrogram** function result.

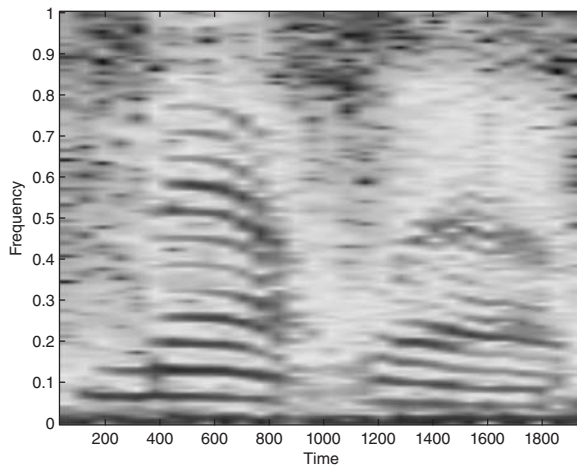


FIGURE 16.33 MATLAB’s **specgram** function result.

Example 16.17 Show the CWT scale-time plot and the short-time Fourier transform spectrogram for a linear swept-frequency sinusoid.

The function **chirp** of MATLAB generates the signal. The swept-frequency signal, its CWT, spectrogram using MATLAB’s function **spectrogram** and that using the function **specgram**, respectively, are shown in Fig. 16.34 to Fig. 16.37. Note that the last the spectrogram reveals directly the frequency sweeping nature of the signal.

The following remarks can be made regarding wavelets [9], [65]. A wavelet has a zero average value. While pure sinusoids, the basis functions of Fourier transformation are perfectly uniform, wavelets tend to be irregular in shape and asymmetric. Wavelets decompose a signal into shifted and scaled versions of the original basic “mother” wavelet. A signal with sudden transition may be better decomposed by short duration wavelets. Note however that the Walsh–Hadaard transform is a highly effective tool for such decomposition.

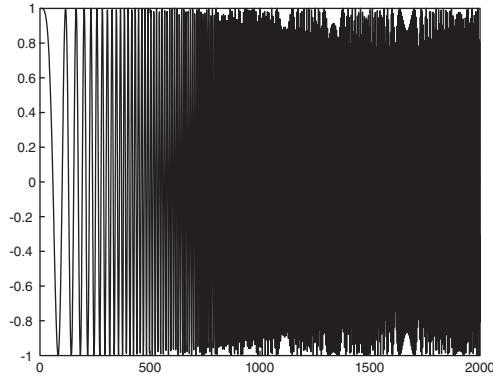


FIGURE 16.34 Swept-frequency signal

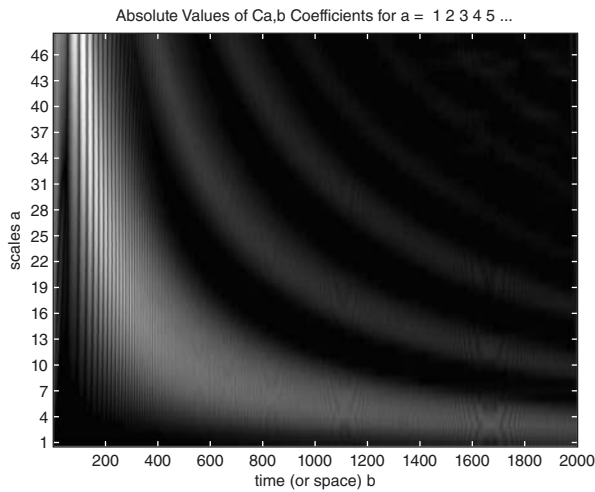


FIGURE 16.35 CWT of swept-frequency signal.

Similarly to Fourier-related transforms wavelet analysis may be applied to images and in general multidimensional signals. The CWT produces a collection of coefficients $F_w(a, \tau)$ which are function of the scale a and position τ . Several scaled versions of wavelets are generated in MATLAB Toolbox.

16.29 Important Signal Processing MATLAB Functions

MATLAB's Signal Processing Toolbox has a family of functions for the efficient execution of statistical signal processing algorithms. Functions such as **xcorr** and **xcov** evaluate the time-averaged approximations of the statistical cross-correlation and covariance functions $\phi_{xx}[m]$ and $\gamma_{xx}[m]$, respectively. The power spectral density and cross-spectral density may be evaluated as averaged periodograms of overlapped, windowed signal sections as in Welch's method, by calling the functions **psd** and **csd**, respectively. The Yule-Walker AR all-pole

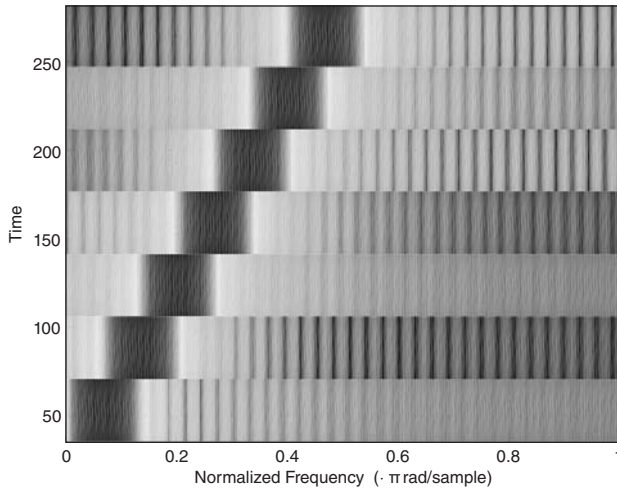


FIGURE 16.36 Spectrogram produced by MATLAB’s function spectrogram.

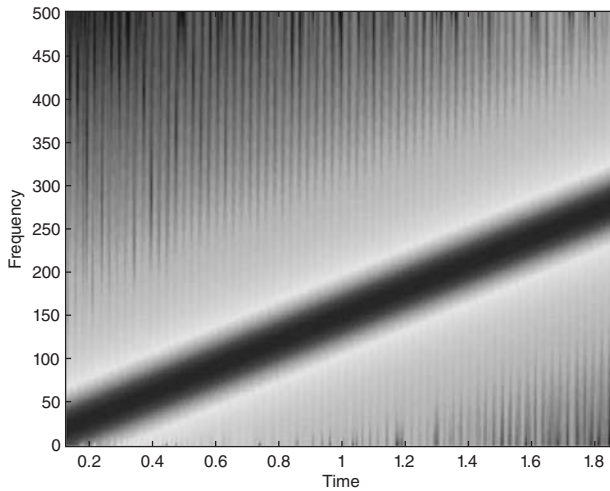


FIGURE 16.37 Spectrogram produced by MATLAB’s function specgram.

model power spectral density estimate is evaluated using the function **pyulear**.

The solution of the general Yule–Walker equation may be obtained by calling **yulewalk**. Several parametric modeling functions are included in MATLAB’s Signal Processing Toolbox. The function **prony** implements Prony’s method and **lpc** effects linear prediction. These are but a few examples of many highly efficient functions included in MATLAB’s Signal Processing Toolbox.

The following MATLAB functions and statements of MATLAB are particularly worth remembering in the context of signal processing. The function **randn** is a random number generator which may be used to simulate normally distributed white noise. To duplicate the results in subsequent function calls it should be initiated using the call `randn(‘seed’,0)`.

sawtooth Generates a periodic ramp.

chirp Generates a linearly swept-frequency sinusoid.

sinc Generates $\text{sinc}(x) = \sin(\pi x)/(\pi x) = Sa(\pi x)$.

diric Generates the Dirichlet function.

$$\text{diric}(x, N) = \begin{cases} \frac{\sin(Nx/2)}{N \sin(x/2)}, & x \neq 2\pi k, k \text{ integer} \\ (-1)^{k(n-1)} & x = 2\pi k, k = 0, \pm 1, \pm 3, \dots \end{cases} \quad (16.397)$$

Note that $\text{diric}(x) = Sd_N(x/2)$.

conv2 Convolution of two-dimensional signal

filter Filters input data with a given IIR or FIR filter.

upfirdn Effects upsampling by an integer factor p by zero insertion between samples, filtering by an FIR filter and downsampling by an integer q .

Multirate Processing

Change the sampling rate from 44.1 KHz to 48 KHz

We write:

$$g = \text{gcd}(48000, 44100) \quad p = 48000/d \quad q = 44100/d \quad y = \text{upfirdn}(x, h, p, q)$$

We obtain $p = 160$, $q = 147$. The output result y is the response of the FIR filter of impulse response h to the input x .

plot(t,x,t,v,'+',t,y,'*') A call for simultaneous plotting of three functions x , v , y versus t .

legend Adds legend of plotted function to a graph.

fftilt For FIR filters, uses sectioning and the overlap add method to filter a long sequence by successive shorter FFTs.

impz Evaluates the impulse response of a discrete-time linear system.

freqz Evaluates the frequency response $H(e^{j\Omega})$ of a given digital filter with transfer function $H(z)$.

unwrap Unwraps the phase to make it continuous across 360° phase transitions by adding $\pm 360^\circ$ when needed.

grpdelay Evaluates the group delay of a filter frequency response.

zplane Plots poles and zeros of a linear system on the z -plane.

roots Evaluates the zeros of a polynomial.

poly Inverse of roots. Evaluates the polynomial given its zeros.

residuez Converts a transfer function to its partial fraction expansion form and vice versa. It is the discrete-time domain function corresponding to the function residue of the continuous-time domain.

zp2sos Factors a transfer function into a product of second order sections, performs pole-zero pairing, section scaling and ordering.

ss2sos Same as zp2sos but in the context of state space models.

tf2latc Evaluates the lattice filter reflection coefficients for an FIR or IIR filter given in polynomial form

latc2tf Evaluates the polynomial coefficients of a filter, given its reflection coefficients.

latcfilt Implements a lattice or lattice-ladder filter given its coefficients.

tf2ss, tf2zp, tf2latc Convert system transfer function to state-space, zero-pole and lattice form respectively.

ss2tf, ss2zp, ss2sos Convert state-space to transfer function, to zero-pole and to second order section forms, respectively.

zp2tf, zp2ss, zp2sos Convert zero-pole form to transfer function, state-space and second order sections, respectively.

sos2tf, sos2ss, sos2zp Convert second order sections model to transfer function, state-space and zero-pole models, respectively.

fft, fftshift Evaluate the FFT and shifted FFT. The latter corresponds to sampling the unit circle from $\Omega = -\pi$ to $\Omega = \pi$.

ifft Evaluates the inverse FFT.

fft2 Evaluates the FFT of two-dimensional signals.

yulewalk Evaluates the IIR filter using least-squares estimation from a given magnitude of frequency response.

16.30 lpc

The function **lpc** of MATLAB evaluates the coefficients of a forward linear prediction FIR filter.

Example 16.18 *Using an eighth order forward predictor estimate the successive samples $\hat{x}[n]$ of a sequence $x[n]$. The sequence $x[n]$ should be the response of an AR process to white noise input.*

We shall choose the AR process transfer function as

$$H(z) = \frac{1}{1 + 0.5z^{-1} + (1/3)z^{-2} + 0.25z^{-3} + 0.2z^{-4}}. \quad (16.398)$$

To generate the white noise we write

```
randn('state',0)
```

```
noise=randn(50000,1)
```

```
% With the white noise applied as input to the AR filter its response is
```

```
x = filter(1,[1 0.5 1/3 0.25], noise)
```

```
% To avoid initial transients we use the last 4096 samples
```

```
x = x(45904:50000)
```

```
% The predictor coefficients are given by
```

```
a = lpc(x,8)
```

```
% Filter x by the FIR predictor filter
```

```
xest = filter([0 -a(2:end)],1,x);
```



```
% Estimation error:
e = x-xest
% Simultaneous plot of x and xest:
plot(1:37,x(4001,4037),1:37,xest(4001,4037),'- -')
```

The predictor coefficients are given by

$$a = \{1, 0.4973, 0.3275, 0.2212, 0.2036, 0.0064, 0.0174, -0.0002, 0.0006\}$$

See Fig. 16.38 depicting a simultaneous plot of the sequence x and its forward linear prediction estimate.

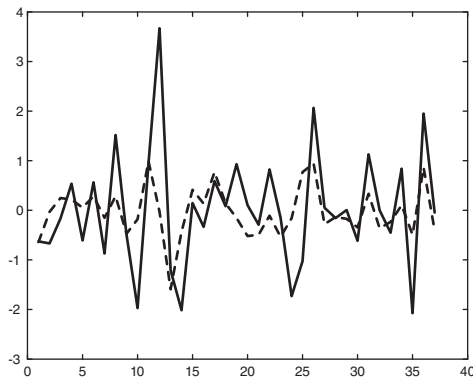


FIGURE 16.38 Signal and lpc estimate.

16.31 Yulewalk

MATLAB's function **Yulewalk** designs an IIR filter of a desired order given samples of a desired magnitude spectrum.

In the function call $[b, a] = \text{yulewalk}(n, f, m)$, n is the filter required order, f is a vector of frequency points ranging in value between 0 and 1 where 1 corresponds to the sampling Nyquist frequency, i.e. to half the sampling frequency and m is the vector of the desired response values at those frequencies.

Example 16.19 Design a tenth order IIR filter using the Yule–Walker least-squares fitting equations having the specification

$$f = [0 \ 0.3 \ 0.3 \ 0.7 \ 0.7 \ 1] \quad (16.399)$$

$$m = [0 \ 0 \ 1 \ 1 \ 0 \ 0] \quad (16.400)$$

Plot the desired and resulting magnitude response.

We write:

```

[b,a] = yulewalk(10,f,m)
[H,w] = freqz(b,a,1024);
Habs = abs(H);
plot (f,m,w/pi,Habs,'.')
legend ('Desired Response','Yule-Walker response')

```

obtaining

$$b = \{0.0827, 0, -0.1877, 0, 0.2458, 0, -0.1983, 0, 0.0954, 0, -0.0061\}$$

$$a = \{1, 0, 0.9306, 0, 1.0145, 0, 0.3901, 0, 0.1433, 0, 0.0216\}$$

The desired response together with the Yule-Walker evaluated filter response can be seen in Fig. 16.39.

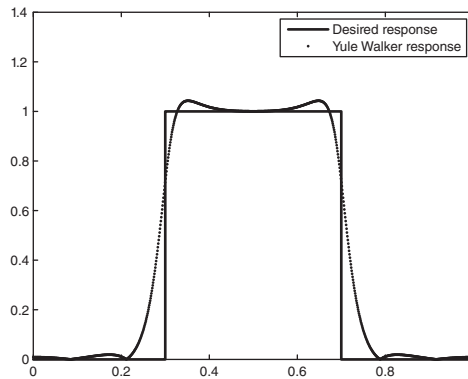


FIGURE 16.39 Desired response and Yule-Walker solution.

16.32 dfilt

dfilt is a discrete-time filter function. $H_d = \mathbf{dfilt.structure}$ returns a discrete-time filter H_d of the structure type specified. For example **dfilt.df1**, **dfilt.df1t**, **dfilt.df2**, **dfilt.df2t** produce filters of structures Direct-form I, Direct-form I transposed, Direct-form II and Direct-form II transposed, respectively.

Similarly, **dfilt.latticear**, **dfilt.latticearma**, **dfilt.latticemamin** produce the structures AR, ARMA and MA minimum phase, respectively. **dfilt.statespace**, **dfilt.cascade** and **dfilt.parallel** produce state space, cascade and parallel filter structures.

16.33 logspace

logspace generates logarithmically spaced elements of a vector. `logspace(x1,x2)` generates a vector of 50 equally spaced points on a logarithmic scale between the decades 10^{x_1} to 10^{x_2} . `logspace(x1,x2,N)` generates N points.

Example 16.20 Generate a semilog and a log-log plot of an elliptic filter of the fifth order with pass-band ripple $R_p = 1\text{dB}$ and stop-band attenuation $R_s = 20\text{dB}$.

We write:

```
[z,p,k] = elliap(7,1,20)
w = logspace(-1,2,10000);
h=freqs(k*poly(z), poly(p), w);
semilogx(w,abs(h)),grid
loglog(w,abs(h)),grid
```

The results appear as seen in Figs. 16.40(a-b) respectively.

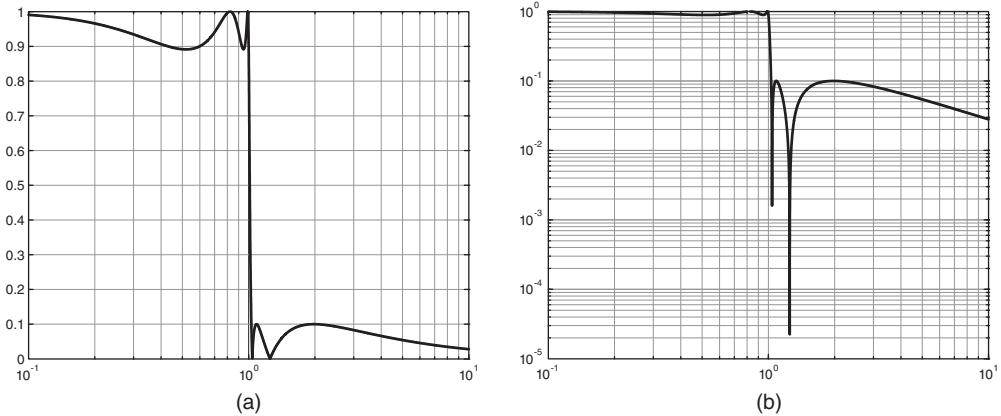


FIGURE 16.40 Elliptic filter (a) semilog magnitude response, (b) loglog magnitude response.

16.34 FIR Filter Design

The MATLAB functions `fir1`, `fir2`, `firls`, `firpm`, \dots , design Types I and II linear phase FIR filters. The functions `firls` and `firpm` design types III and IV FIR linear phase filters when the flag “hilbert” or “differentiator” is appended.

In the windowing method of FIR filter design an ideal lowpass filter is approximated by first evaluating the filter’s infinite impulse response $h[n]$. Since this IIR is not causal, hence not realizable, we multiply it by a truncating window, thus obtaining a finite impulse response of length N say and of even symmetry. This in turn leads to a linear-phase frequency

response. A shift of $N/2$ of the finite impulse response produces a causal filter with a delay of $(N - 1)/2$ samples.

The truncating window may be the rectangular window, in which case the FIR impulse response is the best approximation of the ideal lowpass response in the least-squares sense. To see the effect of applying this window note that the infinite impulse response $h[n]$ of the ideal lowpass filter with cut-off frequency Ω_c given by

$$h[n] = \frac{1}{2\pi} \int_{-\Omega_c}^{\Omega_c} H(e^{j\Omega}) e^{j\Omega n} d\Omega = \frac{\Omega_c}{\pi} \text{Sa}(\Omega_c n). \tag{16.401}$$

Truncating this impulse response by a rectangular window of length N we have the response

$$h_N[n] = h[n]w[n] \tag{16.402}$$

where

$$w[n] = \Pi_{N/2}(n) = u[n + (N - 1)/2] - u[n - (N - 1)/2]. \tag{16.403}$$

The FIR impulse response is the shifted by $(N - 1)/2$ samples sequence

$$h_F[n] = h_N[n - (N - 1)/2]. \tag{16.404}$$

Example 16.21 Plot the IIR of an ideal lowpass filter of cut-off frequency $\Omega_c = \pi/2$. Apply a rectangular window of length $N = 101$. Plot the frequency response of the resulting FIR filter.

We write:

```
h = 0.5*sinc(0.5*(-50:50));
H = freqs(h,1,101)
plot(unwrap(angle(H)),grid)
fplot(h,1)
```

The magnitude-squared frequency response and the unwrapped linear phase response are shown in Fig. 16.41(a-b), respectively.

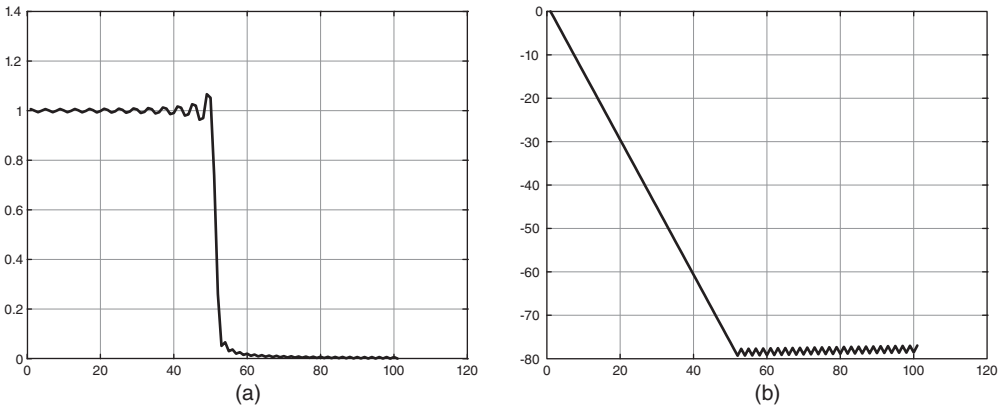


FIGURE 16.41 Rectangular windowing: (a) magnitude-squared and (b) phase response.

An alternative window may be applied to effect smoothing of the spectrum. To apply a Hamming window we write

```
b = h.*hamming(101)';
fvtool(b,1)
```

The reduced ripples, in the magnitude-squared spectrum, at the expense of a wider transition region, may be seen in Fig. 16.42(a).

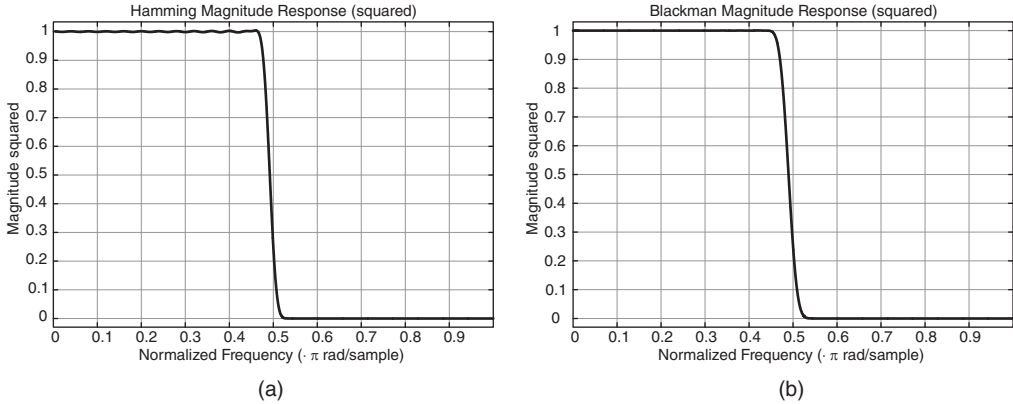


FIGURE 16.42 (a) Hamming, (b) Blackman windowing magnitude-squared response.

The function **fir1** effects the same windowing applying the Hamming window by default. The above is obtained by writing

$$b = \text{fir1}(101, 0.5);$$

The statement

$$b = \text{fir1}(n, Wn, \text{window});$$

applies the window specified in the $(n + 1)$ -element column vector *window* in truncating the impulse response.

For example the Blackman window may be employed by writing

$$\text{win} = \text{window}(@\text{blackman}, 101)$$

$$b = \text{fir1}(100, 0.5, \text{win})$$

The resulting magnitude spectrum is shown in Fig. 16.42(b).

The **window** function is thus called by specifying the function handle as **@blackman**. Other available function handles include **@bartlett**, **@chebwin**, **@gausswin**, **@hann**, **@kaiser**, **@triang**, **@tukeywin**. For windows *chebwin*, *kaiser*, and *tukeywin* the desired window parameter should be specified. For example, the **kaiserord** function estimates the required filter order, cut-off frequency and the β parameter corresponding to given filter specifications.

16.35 fir2

The function `fir2` of MATLAB designs an FIR filter given an arbitrary piecewise linear frequency-magnitude response. The statement

$$b = \text{fir2}(n, f, m)$$

accepts as input the required filter order n , a vector f of frequency points and a vector m of corresponding spectrum magnitude values. It produces the row vector b of $n + 1$ filter coefficients.

Example 16.22 Design an FIR bandpass filter of order $n = 100$ using `fir2`. The magnitude spectrum of the ideal filter should be equal to one in the frequency range $\Omega = 0.3\pi$ to $\Omega = 0.5\pi$ and zero otherwise. Plot the resulting magnitude spectrum approximation and verify the linearity of the FIR filter phase spectrum.

We write:

```
f = [0 0.3 0.3 0.5 0.5 1];
m = [0 0 1 1 0 0];
b = fir2(100,f,m);
[h,w] = freqz(b,1,1024);
plot(f,m,w/pi,abs(h))
legend('desired','approximation')
title('Desired and designed magnitude spectra')
plot(f,m,w/pi,unwrap(angle(h)))
title('phase spectrum')
```

The magnitude and phase spectra are shown in Fig. 16.43(a-b), respectively.

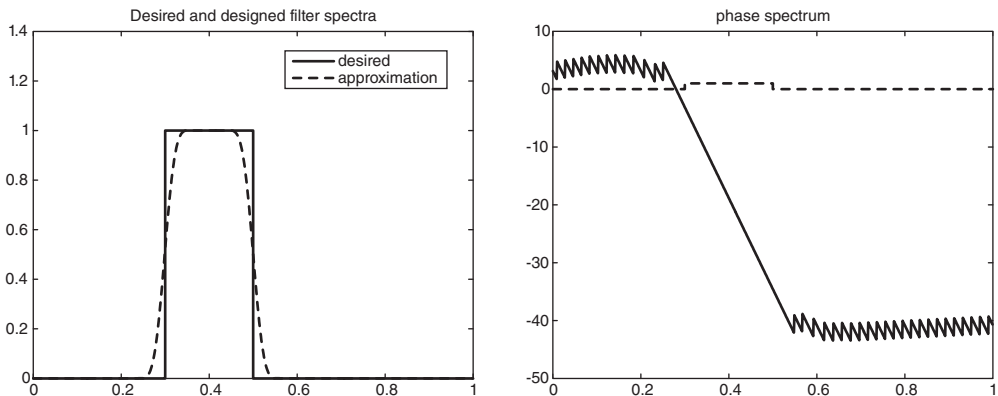


FIGURE 16.43 `fir2`-produced magnitude and phase spectra.

16.36 Power Spectrum Estimation Using MATLAB

MATLAB has nonparametric and parametric spectral estimation functions. The nonparametric approach estimates the power spectrum by direct evaluation of the Fourier transform of the autocorrelation function. As we have seen, the periodogram and modified averaged periodogram obtained by sectioning/overlapping the signal, applying a suitable window and averaging of periodograms are nonparametric methods of spectral estimation. The functions **periodogram**, **spectrum.periodogram**, **pwelch**, **spectrum.welch** are among such highly computationally efficient functions.

MATLAB also has Multitaper functions wherein a combination of multiple orthogonal windows are employed in estimating the power spectrum.

Among the nonparametric spectral estimation methods MATLAB has the Yule–Walker AR estimation functions **pyulear** and **spectrum.yulear**, and the Burg AR linear prediction approach **pburg**, **spectrum.burg**, the Covariance AR spectral estimation by forward and backward linear prediction functions **pcov** and **spectrum.cov**, **pmcov** and **spectrum.mcov**. For signals, composed of sinusoidal components subspace methods perform eigen values and vectors decomposition of the correlation matrix. These function include Multiple signal classification **MUSIC** and eigenvector EV pseudo spectrum estimation ones **pmusic**, **spectrum.music**, **peig** and **spectrum.eigenvector**, respectively.

See *Signal Processing Toolbox User's Guide 6*, The Mathworks, 2008.

16.37 Parametric Modeling Functions

Operating on the impulse or frequency response, parametric modeling functions estimate the system rational transfer function coefficients. These functions are important tools for system identification, as well as the design of FIR and IIR filters.

arcov: The statement $[a, e] = \text{arcov}(x, p)$ estimates the coefficients $\{a\}$ of the AR model of order p , which would produce the sequence x upon receiving white noise as input. The estimation minimizes the forward prediction error in the least-squares sense. The function also evaluates the variance e of the input white noise. The function **armcov** and **arburg** are the same as **arcov** but evaluate a modified covariance by minimizing both the forward and backward prediction errors.

aryule: The statement $a = \text{aryule}(x, p)$ estimates the denominator coefficients $\{a\}$ of an all-pole (AR) model of order p using the Yule–Walker autocorrelation approach. The sequence x is viewed as the output of the AR model upon receiving white noise as input. The statement $[a, e] = \text{aryule}(x, p)$ returns also the variance e of the white noise input. The statement $[a, e, k] = \text{aryule}(x, p)$ returns the vector k of lattice filter realization reflection coefficients. It should be noted that in executing the functions **arcov**, **armcov** and **aryule** we are assuming an all-pole model, rather than an ARMA pole-zero model. Such restriction of the model structure leads to results that are closely tied to the assumed system order p . A judicious choice of the order is thus important in order to produce reliable results.

The Yule–Walker equations, having Toeplitz symmetry, are efficiently solved using the Levinson–Durbin recursion approach. This is effected using the function **levinson**.

16.38 prony

We have seen the basis of Prony's method in Chapter 11. The statement $[b, a] = \text{prony}(h, n, m)$ executes the function **prony** which accepts as input a finite impulse response of an unknown system and estimates the coefficients $\{b\}$ and $\{a\}$ of an IIR(pole-zero) filter that approximates the system and having n and m as the assumed numerator and denominator orders of its transfer function.

stmcb: The **stmcb**(Steiglitz–McBride) function estimates an IIR filter model the output of which upon receiving a given input approximates a given response. The statement $[b, a] = \text{stmcb}(h, nb, na)$ evaluates the filter transfer function's numerator and denominator coefficients $\{b\}$ and $\{a\}$ which approximate the given finite impulse response h . The function attempts to directly minimize the squared error between the impulse response h and the input signal x . The statement $[b, a] = \text{stmcb}(y, x, nb, na)$ evaluates the coefficient vectors b and a of the transfer function which, given x as input, produces an approximation of y as output. Similarly to the AR all-pole modeling functions defined above it is important to specify the correct orders **nb** and **na** in calling the function **stmcb**.

Example 16.23 Evaluate the impulse response of an elliptic filter of the seventh order with pass-band ripple $R_p = 0.5\text{dB}$, stop-band attenuation of at least $R_s = 40\text{dB}$ and pass-band edge frequency of $0.8 \times$ the sampling frequency. Truncate the impulse response to $N = 256$ samples. Apply this finite impulse response h to the function **stmcb**. Evaluate the frequency response obtained in the two cases a) $nb = 7, na = 7$, b) $nb = 6, na = 7$ with the true response of the elliptic filter.

We write:

```
[b,a] = ellip(7,0.5,40,0.4)
impul = [1 zeros(1,256)];
h = filter(b,a,impul);
figure(1)
freqz(b,a,512)
```

a)

```
[b2,a2] = stmcb(h,7,7) fig(2) freqz(b2,a2,512)
```

The true magnitude and phase obtained using the coefficients b and a are shown in Fig. 16.44(a). The estimated spectra are very close to the true spectra.

b)

```
[b3,a3] = stmcb(h,6,7)
freqz(b3,a3,512)
```

The resulting spectra are shown in Fig. 16.44(b). We note the deviation from the true spectra caused by choosing $nb = 6$ instead of $nb = 7$, i.e. six zeros instead of seven.

Example 16.24 Evaluate the impulse response of an elliptic filter of the seventh order with pass-band ripple $R_p = 0.5\text{dB}$, stop-band attenuation of at least $R_s = 40\text{dB}$ and pass-band edge frequency of $0.8 \times$ the sampling frequency. Truncate the impulse response to $N = 256$ samples. Apply this finite impulse response h to the function **stmcb**. Evaluate the frequency response obtained in the two cases a) $nb = 7, na = 7$, b) $nb = 7, na = 6$ with the true response of the elliptic filter.

We write:

```
[b,a] = ellip(7,0.5,40,0.4)
```

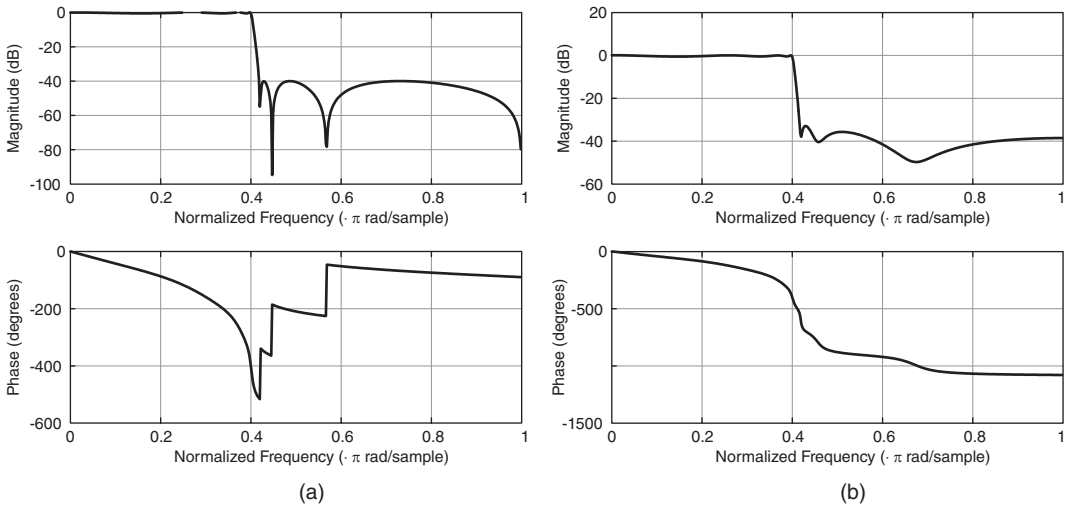



FIGURE 16.44 (a) Elliptic filter impulse response, (b) stmb approximation.

```

impul = [1 zeros(1,256)];
h = filter(b,a,impul);
figure(1)
freqz(b,a,512)

```

16.39 Problems

Problem 16.1 Let $z[n] = x[n] + y[n]$ where $x[n]$ and $y[n]$ are stationary uncorrelated random sequences. Evaluate the mean and variance of $z[n]$ given that those of $x[n]$ and $y[n]$ are m_x , σ_x^2 , m_y and σ_y^2 respectively.

Problem 16.2 Let $z[n] = x[n] + y[n]$, where $x[n]$ and $y[n]$ are zero-mean real stationary uncorrelated random sequences. Evaluate the autocorrelation $\phi_{zz}[n]$ of $z[n]$ given that those of $x[n]$ and $y[n]$ are $\phi_{xx}[n] = a^{|n|}$ and $\phi_{yy}[n] = b^{|n|}$.

Problem 16.3 A zero-mean random signal $x[n]$ is contaminated by a zero-mean white noise sequence $b[n]$, which is linearly independent (uncorrelated) of $x[n]$, producing the sequence $y[n] = b[n]x[n]$. Evaluate the autocorrelation sequence, the variance and the power spectral density of $y[n]$.

Problem 16.4 A zero-mean white noise sequence $x[n]$ of variance σ_x^2 is applied to the input of a causal LTI system of unit sample response

$$h[n] = a^n u[n]$$

with a real, and $0 < a < 1$. Evaluate the autocorrelation of the system output $y[n]$ and the cross correlation $\phi_{yx}[m]$.

Problem 16.5 A random sequence $x[n]$ has an autocorrelation sequence

$$\phi_{xx}[m] = \alpha^{|m|}, \quad 0 < \alpha < 1.$$

Evaluate its power density spectrum.

Problem 16.6 A stationary random sequence $x[n]$ has the autocorrelation $\phi_{xx}[m]$. Given that

$$\Phi_{xx}(z) = \frac{1}{(1 - 0.5z^{-1})(1 - 0.5z)(1 - 0.2z^{-1})(1 - 0.2z)}$$

Evaluate $\phi_{xx}[m]$.

Problem 16.7 A random sequence $x[n]$ has a power spectral density $P_{xx}(\omega) = 4 \sin^2(\Omega/2)$. The sequence is applied to the input of an LTI system of transfer function

$$H(z) = \frac{1}{1 - 0.5z^{-1}}$$

Evaluate the power spectral density $P_{yy}(\Omega)$ of the system output $y[n]$ and the output autocorrelation $\phi_{yy}[n]$.

Problem 16.8 Using time averages to approximate statistical ones, a measurement of N samples of a process $x[n]$ produces the time averaged autocorrelation estimate $C_{xx}[m]$. Evaluate $C_{xx}[0]$ and relate it to the variance of the process.

Problem 16.9 A zero-mean real stationary white noise sequence $x[n]$ is applied to the input of an LTI system of impulse response $h[n]$. Evaluate the input-output cross-correlation $\phi_{xy}[n]$, the output autocorrelation, the average value of the product $x[n]y[n]$ and of $y^2[n]$.

Problem 16.10 A zero-mean real stationary white noise sequence $x[n]$ of variance $\sigma_x^2 = 10$ is applied to the input of an LTI system of transfer function

$$H(z) = \frac{1}{1 - az^{-1}}, \quad a \text{ real}, \quad 0 < a < 1.$$

Evaluate the power spectral density and the variance σ_y^2 of the system response $y[n]$.

Problem 16.11 A real stationary white noise sequence applied to a causal LTI system of transfer function

$$H(z) = \frac{1}{1 - az^{-1}}$$

at an instant $n = M$ is given by $x_i[n] = x[n]u[n - M]$ where $x_i[n]$ is an infinite duration two-sided random sequence. Evaluate the mean and autocorrelation of the output $y[n]$ and their limits as $n \rightarrow \infty$.

Problem 16.12 A real stationary random sequence $x[n]$ with unit variance is applied to the input of an LTI system of the transfer function

$$H(z) = \frac{z^{-2}}{a^2 - 2az^{-1} + z^{-2}}$$

and output $y[n]$. Evaluate the autocorrelation, power spectral density and average power of the output $y[n]$.

Problem 16.13 An AR process is generated by applying a zero-mean stationary white noise $e[n]$ of variance σ_e^2 to the input of a causal LTI system of impulse response $h[n] = a^n u[n]$, where a is real and $a < 1$. Evaluate the autocorrelation of the sequence $x[n]$, the power spectral density of the system output and the mean of $x^2[n]$.

Problem 16.14 The two real zero-mean stationary random signals $x[n]$ and $y[n]$ are applied to the input of an LTI system of the system function $H(z)$ producing the outputs $v[n]$ and $w[n]$ respectively. Assuming knowledge of the autocorrelation and cross-correlation sequences of $x[n]$ and $y[n]$, evaluate the cross-correlation and the cross-power density spectrum of $v[n]$ and $w[n]$.

Problem 16.15 A random signal $x[n]$ is contaminated by additive noise $b[n]$, which is uncorrelated with $x[n]$. The signal $x[n]$ may be modeled as the output of an LTI system of transfer function

$$G(z) = \frac{1}{(1 - az^{-1})}$$

in response to unit variance white noise $w[n]$. The noise contaminated signal $s[n] = x[n] + b[n]$ is applied to the input of a noise reduction filter of impulse response $h[n] = b^n u[n]$.

Assuming that the autocorrelation of the noise $b[n]$ is $\phi_{bb}[n] = \sigma_b^2 \delta[n]$, evaluate the autocorrelation of the signal $\phi_{xx}[n]$, the PSD and deduce thereof the average power of $x[n]$, and the signal to noise ratio

$$SNR_1 = \frac{E[x^2[n]]}{E[b^2[n]]}$$

at the input of the digital filter. With $v[n] = x[n] * h[n]$ and $w[n] = b[n] * h[n]$, evaluate $\phi_{vv}[n]$ and $E[v^2[n]]$. Assuming $a = 0.8$, $b = 0.7$, compare

$$SNR_2 = \frac{E[v^2[n]]}{E[w^2[n]]}$$

with SNR_1 .

Problem 16.16 Given $x[n] = s[n] + w[n]$, where $s[n]$ is an AR(1) random process described by

$$s[n] = 0.7s[n-1] + v[n]$$

$v[n]$ being a white noise sequence of variance $\sigma_v^2 = 0.49$ and $w[n]$ is white noise with variance $\sigma_w^2 = 1$. Design an $M = 5$ -point FIR Wiener filter to estimate $s[n]$. Evaluate the resulting minimum mean square error.

Problem 16.17 A signal $s[n]$ is an ARMA(p) process with $p = 2$ which is described by the difference equation

$$s[n] = 1.4s[n-1] - 0.48s[n-2] + 5v[n] - 3.4v[n-1] \quad (16.405)$$

where $v[n]$ is a white noise sequence with variance $\sigma_v^2 = 0.81$. Evaluate the power spectral density of $s[n]$. Design a Wiener filter of length $M = 3$ to estimate the signal $s[n]$ from a received signal $x[n] = s[n] + w[n]$ where $w[n]$ is a white noise sequence of variance $\sigma_w^2 = 1$, which is uncorrelated with $s[n]$.

Problem 16.18 Evaluate the two-sided IIR Wiener filter and the resulting minimum mean square error for the case of signal contaminated by additive noise stated in Problem 16.17.

Problem 16.19 Referring to Problem 16.17 design a causal Wiener filter by evaluating its optimal transfer function and impulse response.

16.40 Answers to Selected Problems

Problem 16.1

$$m_z = m_x + m_y, \sigma_z^2 = \sigma_x^2 + \sigma_y^2$$

Problem 16.2

$$\phi_{zz}[n] = a^{|n|} + b^{|n|}$$

Problem 16.3

$$P_y(\Omega) = \sigma_b^2 \sigma_x^2$$

Problem 16.4

$$\phi_{yx}[m] = \sigma_x^2 a^m u[m]$$

Problem 16.5

$$P_{xx}(\Omega) = (1 - \alpha^2)/(1 - 2\alpha \cos \Omega + \alpha^2)$$

Problem 16.6

$$\phi_{xx}[m] = 2.469 \times 0.5^{|m|} - 0.776 \times 0.2^{|m|}$$

Problem 16.7

$$\phi_{yy}[n] = 2\delta[n] - (2/3)2^n u[-1 - n] - (2/3)0.5^n u[n]$$

Problem 16.9

$$E[y[n]^2] = \sigma_x^2 \sum_{k=-\infty}^{\infty} h^2[k]$$

Problem 16.10

$$\sigma_y^2 = 10/(1 - a^2)$$

Problem 16.11

$$\phi_{yy}[n_1, n_2] \longrightarrow \sum_{k=0}^{\infty} \sum_{m=0}^{\infty} h[k]h[m]\phi_{xx}[k, m]$$

Problem 16.12

$$\phi_{yy}[0] = (1 + a^2)/(1 - a^2)^3$$

Problem 16.13

$$\phi_{xx}[n] = \sigma_e^2 a^n / (1 - a^2) u[n]$$

Problem 16.14

$$P_{vw}(\Omega) = \Phi_{xy}(e^{j\Omega}) |H(e^{j\Omega})|^2$$

Problem 16.15

$$\text{SNR}_2/\text{SNR}_1 = 5.5 \text{ dB}$$

Problem 16.16

$$h[n] = \{0.4084, 0.1693, 0.0704, 0.0298, 0.0140\}, e[n] = 0.4476$$

Problem 16.17

$$h[n] = \{0.954, 0.0316, 0.0019\}$$

Problem 16.18

$$E = 0.932$$

Problem 16.19

$$h[n] = [0.001 \times 0.6804^n + 0.953 \times 0.0324^n]u[n].$$

This page intentionally left blank

17.1 Introduction

Without the Dirac-delta function, without the theory of generalized functions or distributions, there would be no Fourier transform of the most elementary of functions, such as a simple constant $f(t) = 1$ or a pure sinusoid $f(t) = \cos \beta t$, nor Fourier transform of t , t^k , nor the integral of a two-sided pure sinusoid such as $\cos \beta t$. Such functions, of which the integrals are not absolutely convergent, have no Fourier transform in the ordinary sense. Thanks to the Dirac-delta function and the theory of generalized functions these Fourier transforms exist as distributions, as we have seen in previous chapters. Thanks to distribution theory we can write transforms such as

$$1 \xrightarrow{\mathcal{F}} 2\pi\delta(\omega) \quad (17.1)$$

$$\cos \beta t \longleftrightarrow \pi\{\delta(\omega - \beta) + \delta(\omega + \beta)\}. \quad (17.2)$$

The theory of distributions has its origins in the works of Heaviside, Dirac, Sobolov and Schwartz, among others. It has received its due attention in the literature [3] [5] [7] [8] [9] [10] [29] [30] [33] [35] [36] [37] [44] [45] [46] [50] [51] [54] [61] [67] [68] [72], [75].

This chapter has been placed near the end of this book since a basic knowledge of the family of the Dirac-delta impulse and its derivatives suffices to evaluate the transforms of most common signals. It is thus that with the simple introduction of these basic properties as presented in the first chapters it is possible to evaluate the transforms of such signals without having to refer to the theory of distributions. Now we are more in a position to study this theory.

One objective of this chapter is to equip the student with a simplified presentation of the subject of distributions. It should be valuable to the student who wishes to pursue advanced studies in the area of signals and transforms.

17.2 Distributions as Generalizations of Functions

The process of integration of a continuous function $f(t)$ between the limits $t = a$ and $t = b$ is illustrated in Fig. 17.1. The integral of $f(t)$ is the area under the curve $f(t)$ bounded between a and b . If the interval of integration (a, b) is divided into n subintervals, namely, $t_0, t_1, \dots, t_{n-1}, t_n$ with $t_0 = a$, $t_n = b$, and with a spacing between subintervals equal to Δt_i , $i = 0, 1, \dots, n - 1$ then the surface area may be approximated as the sum

$$A = \sum_{i=0}^{n-1} f(t_i)\Delta t_i. \quad (17.3)$$

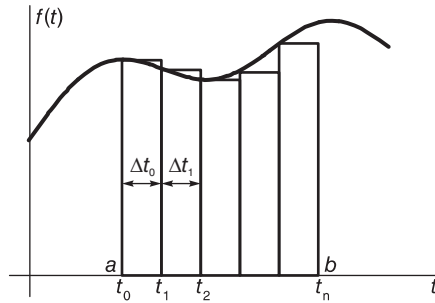


FIGURE 17.1 Integration as a sum of increments.

As the largest time increment $\Delta t_i \rightarrow 0$ the number of slices $n \rightarrow \infty$, the area A approaches the true area under the curve and we can write

$$\int_a^b f(t)dt = \lim_{\Delta t_i \rightarrow 0} \sum_{i=0}^{n-1} f(t_i)\Delta t_i. \quad (17.4)$$

Such interpretation of the integration operation implies that the surface area and hence the value of the integral is not affected if at an isolated point, say $t = \tau$ in the interval of integration, $a < \tau < b$, the value of the function $f(\tau)$ is changed arbitrarily. As long as $f(\tau)$ is finite, and as long as $f(t)$ is the same everywhere else, whether $f(\tau) = 0$ or $f(\tau) = 100$, the value of the integral remains the same. This is due to the fact that the contribution to the area A of such an isolated point such as $t = \tau$ is a strip of height $f(\tau)$ and zero width.

We note that the same applies if the value of the function changes at a set of isolated points. The area remains the same. The integral of a function is thus the same whatever is its value over “a set of measure zero,” that is, a set of isolated points.

Consider now the usual definition of the Dirac-delta impulse:

$$\delta(t) = 0, \quad t \neq 0 \quad (17.5)$$

$$\int_{-\infty}^{\infty} \delta(t)dt = 1. \quad (17.6)$$

The impulse, being nil everywhere except at the isolated point $t = 0$, its integral should be zero since the function is nil almost everywhere and the value of the integral, as just deduced, is unaffected by the value of a function at an isolated point. The fact that it should have a nonzero integral implies that it is not an ordinary function. In fact if its integral is to be other than zero its value $f(0)$ at $t = 0$ cannot be finite.

It is for this reason that the delta function is not an ordinary function and is a main subject of the theory of distributions. In what follows a basic overview of this theory is presented.

17.3 What is a Distribution?

A distribution is a generalized function. It differs from an ordinary function in the fact that whereas a function $f(t)$ is defined for all values of the independent variable t , a distribution $g(t)$ is not defined for any particular value of t . The value of a distribution $g(t)$ is given by

the integral of its product with a test function $\phi(t)$. A test function belongs to a given class C which contains functions that are infinitely smooth, having derivatives of all orders, and decaying more rapidly than any power of t as $|t| \rightarrow \infty$.

A distribution $g(t)$ is in fact a mapping that associates with any test function $\phi(t)$ a value of an integral, which we may call $I_g[\phi(t)]$. This is the value of the integral of the product of the distribution $g(t)$ with the test function $\phi(t)$. We shall use the notation

$$I_g[\phi(t)] = \langle g(t), \phi(t) \rangle = \int_{-\infty}^{\infty} g(t)\phi(t)dt \tag{17.7}$$

assuming that this definite integral, which will be referred to as the defining integral, exists.

For example, the impulse, the Dirac-delta, distribution denoted usually $\delta(t)$, is defined by the property

$$I_{\delta}[\phi(t)] = \langle \delta(t), \phi(t) \rangle = \int_{-\infty}^{\infty} \delta(t)\phi(t)dt = \phi(0) \tag{17.8}$$

and the same property applies even if the test function $\phi(t)$ is replaced by a simple function $f(t)$, as long as it is continuous at $t = 0$ so that $f(0)$ is well defined. We may then write

$$\int_{-\infty}^{\infty} \delta(t)f(t)dt = f(0). \tag{17.9}$$

Beside the Dirac-delta impulse $\delta(t)$, the unit step Heaviside function $u(t)$ and the successive derivatives $\delta'(t)$, $\delta''(t)$, $\delta^{(3)}(t)$, ... are distributions. In the literature the Dirac-delta impulse is sometimes denoted by the symbol $u_0(t)$. Its first derivative $\delta'(t)$ is denoted $u_1(t)$ and its second derivative $\delta''(t)$ is denoted $u_2(t)$. The step function, which we call $u(t)$ is denoted $u_{-1}(t)$, being the integral of the impulse $u_0(t)$. The integral of $u_{-1}(t)$, namely, the function t , where $t > 0$ is denoted by $u_{-2}(t)$ and so on. The index i of $u_i(t)$ thus increases with differentiation and reduces with integration from the central value $i = 0$ corresponding to the Dirac-delta impulse.

Example 17.1 Evaluate the distributions

$$u_i(t), \quad i = -3, -2, -1, 0, 1, 2, 3.$$

We have $u(t) \equiv u_{-1}(t)$,

$$u_0(t) = \delta(t), \quad u_1(t) = \delta'(t), \quad u_2(t) = \delta''(t), \quad u_3(t) = \delta^{(3)}(t)$$

$$u_{-1}(t) = \int_{-\infty}^t u_0(\tau) d\tau = \int_{-\infty}^t \delta(\tau) d\tau = \begin{cases} 1, & t > 0 \\ 0, & t < 0 \end{cases}$$

$$u_{-2}(t) = \int_{-\infty}^t u_{-1}(\tau) d\tau.$$

The integrand $u(\tau)$ is not nil if and only if $\tau > 0$ wherefrom the integral is non-nil if and only if $t > 0$, so that

$$u_{-2}(t) = \left\{ \int_0^t d\tau \right\} u(t) = tu(t).$$

Similarly

$$u_{-3}(t) = \int_{-\infty}^t \tau u(\tau) d\tau = \left\{ \int_0^t \tau d\tau \right\} u(t) = \frac{t^2}{2}u(t).$$

More generally, we can write

$$u_{-n}(t) = \frac{t^{n-1}}{(n-1)!}u_{-1}(t). \tag{17.10}$$

17.4 The Impulse as the Limit of a Sequence

If $g(t) = \delta(t)$, the improper integral defining the Dirac-delta impulse may be replaced by a limit involving a sequence of ordinary functions $\delta_n(t)$ which tend to the impulse. They satisfy the property

$$\lim_{n \rightarrow \infty} \int_{-\infty}^{\infty} \delta_n(t) \phi(t) dt = \int_{-\infty}^{\infty} \delta(t) \phi(t) dt \quad (17.11)$$

which is written symbolically as

$$\delta_n(t) \xrightarrow{n \rightarrow \infty} \delta(t). \quad (17.12)$$

When we write, therefore,

$$I_\delta [\phi(t)] \triangleq \langle \delta, \phi \rangle = \int_{-\infty}^{\infty} \delta(t) \phi(t) dt = \phi(0) \quad (17.13)$$

the integral will be understood to mean the a limit as just defined. Sequences $\delta_n(t)$ having this property will be studied in what follows.

For the distribution $g(t) = u(t)$ we have

$$I_u [\phi(t)] \triangleq \langle u, \phi \rangle = \int_{-\infty}^{\infty} u(t) \phi(t) dt = \int_0^{\infty} \phi(t) dt \quad (17.14)$$

that is, the distribution $u(t)$ is the mapping that assigns to the test function $\phi(t)$ a value that is the area of $\phi(t)$ in the interval $(0, \infty)$.

17.5 Properties of Distributions

In what follows we study the properties of distributions and operations involving distributions.

17.5.1 Linearity

A distribution $g(t)$ is linear. Operating on a sum of test functions it produces the sum of the results of its operations on each function. In particular

$$\begin{aligned} \langle g, a_1 \phi_1 + a_2 \phi_2 \rangle &= \int_{-\infty}^{\infty} g(t) \{a_1 \phi_1(t) + a_2 \phi_2(t)\} dt \\ &= a_1 \int_{-\infty}^{\infty} g(t) \phi_1(t) dt + a_2 \int_{-\infty}^{\infty} g(t) \phi_2(t) dt \\ &= a_1 \langle g, \phi_1 \rangle + a_2 \langle g, \phi_2 \rangle. \end{aligned} \quad (17.15)$$

Moreover, the sum of two distributions is a distribution that assigns to a test function a scalar that is the sum of the scalars assigned by the two distributions. In other words, if $g(t) = g_1(t) + g_2(t)$ then

$$\begin{aligned} \langle g_1 + g_2, \phi \rangle &= \int_{-\infty}^{\infty} \{g_1(t) + g_2(t)\} \phi(t) dt \\ &= \int_{-\infty}^{\infty} g_1(t) \phi(t) dt + \int_{-\infty}^{\infty} g_2(t) \phi(t) dt \\ &= \langle g_1, \phi \rangle + \langle g_2, \phi \rangle \end{aligned} \quad (17.16)$$

or

$$I_g [\phi(t)] = I_{g_1} [\phi(t)] + I_{g_2} [\phi(t)]. \tag{17.17}$$

17.5.2 Time Shift

Given a distribution $g(t)$, its time-shifted version $f(t) = g(t - t_0)$, denoted often by $g_{(t_0)} \triangleq g(t - t_0)$ satisfies

$$\begin{aligned} \langle g(t - t_0), \phi \rangle &\triangleq \int_{-\infty}^{\infty} g(t - t_0)\phi(t)dt \\ &= \int_{-\infty}^{\infty} g(\tau)\phi(\tau + t_0)d\tau = \langle g(t), \phi(t + t_0) \rangle \end{aligned} \tag{17.18}$$

where we have used the substitution $t - t_0 = \tau$ and subsequently replaced τ by t . Applying this property to the Dirac-delta distribution $\delta(t)$ we have

$$\langle \delta(t - t_0), \phi \rangle = \langle \delta, \phi(t + t_0) \rangle = \phi(t_0) \tag{17.19}$$

which can be written in the form

$$\int_{-\infty}^{\infty} \delta(t - t_0)\phi(t)dt = \phi(t_0). \tag{17.20}$$

17.5.3 Time Scaling

Consider the distribution $f(t) = g(\alpha t)$, where α is a scalar. We have, if $\alpha > 0$

$$\langle g(\alpha t), \phi(t) \rangle = \int_{-\infty}^{\infty} g(\alpha t)\phi(t)dt = \frac{1}{\alpha} \int_{-\infty}^{\infty} g(\tau)\phi(\tau/\alpha)d\tau \tag{17.21}$$

having replaced αt by τ .

If $\alpha < 0$ we write $\alpha = -a$ where $a > 0$. Using the substitution $\alpha t = \tau$, i.e. $-at = \tau$

$$\int_{-\infty}^{\infty} g(\alpha t)\phi(t)dt = \frac{-1}{a} \int_{\infty}^{-\infty} g(\tau)\phi\{\tau/(-a)\}d\tau = \frac{1}{a} \int_{-\infty}^{\infty} g(t)\phi(t/\alpha)dt. \tag{17.22}$$

We conclude that for any scalar $\alpha \neq 0$

$$\langle g(\alpha t), \phi(t) \rangle = \frac{1}{|\alpha|} \int_{-\infty}^{\infty} g(t)\phi(t/\alpha)dt = \frac{1}{|\alpha|} \langle g(t), \phi(t/\alpha) \rangle. \tag{17.23}$$

Applying this property to the delta impulse we have

$$\int_{-\infty}^{\infty} \delta(\alpha t)\phi(t)dt = \frac{1}{|\alpha|} \int_{-\infty}^{\infty} \delta(t)\phi(t/\alpha)dt = \frac{1}{|\alpha|}\phi(0). \tag{17.24}$$

We note that the value of $\delta(\alpha t)$ can be deduced from this equation if the right-hand side is rewritten in the form

$$\frac{1}{|\alpha|} \int_{-\infty}^{\infty} \delta(t)\phi(t)dt \tag{17.25}$$

which upon comparison with the left-hand side yields

$$\delta(\alpha t) = \frac{1}{|\alpha|}\delta(t). \tag{17.26}$$

Example 17.2 Evaluate $u(\alpha t)$. Let $g(t) = u(t)$. Applying the property

$$\int_{-\infty}^{\infty} g(\alpha t)\phi(t)dt = \frac{1}{|\alpha|} \int_{-\infty}^{\infty} g(t)\phi(t/\alpha)dt$$

we have

$$\int_{-\infty}^{\infty} u(\alpha t)\phi(t)dt = \frac{1}{|\alpha|} \int_{-\infty}^{\infty} u(t)\phi(t/\alpha)dt = \frac{1}{|\alpha|} \int_0^{\infty} \phi(t/\alpha)dt.$$

If $\alpha > 0$ letting $\tau = t/\alpha$

$$\int_{-\infty}^{\infty} u(\alpha t)\phi(t)dt = \frac{\alpha}{|\alpha|} \int_0^{\infty} \phi(\tau)d\tau = \int_{-\infty}^{\infty} u(t)\phi(t)dt.$$

If $\alpha < 0$ let $\alpha = -a$ where $a > 0$

$$\int_{-\infty}^{\infty} u(\alpha t)\phi(t)dt = \frac{-a}{|\alpha|} \int_0^{-\infty} \phi(\tau)d\tau = \frac{a}{|\alpha|} \int_{-\infty}^0 \phi(\tau)d\tau = \int_{-\infty}^{\infty} u(-t)\phi(t)dt.$$

We deduce that

$$u(\alpha t) = \begin{cases} u(t), & \alpha > 0 \\ u(-t), & \alpha < 0. \end{cases}$$

17.5.4 Product with an Ordinary Function

The product of a distribution and an ordinary function is by definition a distribution. Let $f(t)$ be an ordinary function. The product of a distribution $g(t)$ and the function $f(t)$ can be evaluated by observing its effect on a test function $\phi(t)$. We write

$$I_{gf} = \int_{-\infty}^{\infty} \{g(t)f(t)\} \phi(t)dt = \int_{-\infty}^{\infty} g(t)\{f(t)\phi(t)\}dt. \quad (17.27)$$

We note that the product $f(t)\phi(t)$ should be a test function. For example, if the distribution $g(t)$ is the Dirac-delta impulse $\delta(t)$, the product $f(t)\phi(t)$ should be continuous at $t = 0$.

Example 17.3 Consider the product $x(t) = \delta(t)f(t)$. Evaluate the parameter $I_x[\phi(t)]$ associated with $x(t)$.

We write

$$I_x[\phi(t)] = \int_{-\infty}^{\infty} \delta(t)f(t)\phi(t)dt = f(0)\phi(0) = f(0) \int_{-\infty}^{\infty} \delta(t)\phi(t)dt = \int_{-\infty}^{\infty} f(0)\delta(t)\phi(t)dt.$$

Comparing both sides we have

$$f(t)\delta(t) = f(0)\delta(t).$$

17.5.5 Symmetry

A distribution $g(t)$ is even, i.e., $g(-t) = g(t)$ if

$$\int_{-\infty}^{\infty} g(t)\phi(t)dt = 0 \quad (17.28)$$

for every odd test function $\phi(t)$. Similarly, $g(t)$ is odd if

$$\int_{-\infty}^{\infty} g(t)\phi(t)dt = 0 \quad (17.29)$$

for every even test function $\phi(t)$.

17.5.6 Differentiation

To measure the mapping implied by the derivative $g'(t)$ of a distribution we write

$$\begin{aligned} \langle g', \phi \rangle &= \int_{-\infty}^{\infty} g'(t)\phi(t)dt = g(t)\phi(t)|_{-\infty}^{\infty} - \int_{-\infty}^{\infty} g(t)\phi'(t)dt \\ &= - \int_{-\infty}^{\infty} g(t)\phi'(t)dt = - \langle g, \phi' \rangle \end{aligned} \quad (17.30)$$

where we have integrated by parts and noted that $g(t)\phi(t) \rightarrow 0$ as $t \rightarrow \infty$ and $t \rightarrow -\infty$.

With $g(t) = \delta(t)$ we have

$$\langle \delta', \phi \rangle = \int_{-\infty}^{\infty} \delta'(t)\phi(t)dt = - \int_{-\infty}^{\infty} \delta(t)\phi'(t)dt = -\phi'(0).$$

By differentiating n times we obtain

$$\begin{aligned} \langle g^{(n)}, \phi \rangle &= \int_{-\infty}^{\infty} g^{(n)}(t)\phi(t)dt = (-1)^n \int_{-\infty}^{\infty} g(t)\phi^{(n)}(t)dt \\ &= (-1)^n \langle g, \phi^{(n)} \rangle \end{aligned} \quad (17.31)$$

and with $g(t) = \delta(t)$ we have

$$\langle \delta^{(n)}, \phi \rangle = (-1)^n \langle \delta, \phi^{(n)} \rangle \quad (17.32)$$

i.e.

$$\int_{-\infty}^{\infty} \delta^{(n)}(t)\phi(t)dt = (-1)^n \int_{-\infty}^{\infty} \delta(t)\phi^{(n)}(t)dt = (-1)^n \phi^{(n)}(0). \quad (17.33)$$

17.5.7 Multiplication Times an Ordinary Function

$$\langle gf, \phi \rangle = \int_{-\infty}^{\infty} \{g(t)f(t)\}\phi(t)dt = \int_{-\infty}^{\infty} g(t)\{f(t)\phi(t)\}dt = \langle g, f\phi \rangle \quad (17.34)$$

where $f(t)\phi(t)$ is a test function, i.e. $f(t)$ has derivatives of any order.

17.5.8 Sequence of Distributions

A sequence of distributions $g_n(t)$, $n = 1, 2, 3, \dots$ converges to a distribution $g(t)$ if

$$\lim_{n \rightarrow \infty} \langle g_n, \phi \rangle = \langle g, \phi \rangle \quad (17.35)$$

i.e.,

$$\lim_{n \rightarrow \infty} \int_{-\infty}^{\infty} g_n(t)\phi(t)dt = \int_{-\infty}^{\infty} g(t)\phi(t)dt. \quad (17.36)$$

17.6 Approximating the Impulse

Among the possible sequences $\delta_n(t)$ that tend to the impulse and may thus serve as approximating sequences, we have the centered rectangle of width $\varepsilon = 1/n$

$$\delta_n(t) = \frac{1}{\varepsilon} \Pi_{\varepsilon/2}(t) = n \Pi_{1/(2n)}(t). \quad (17.37)$$

Figure 17.2 shows the effect of increasing n on the approximating rectangle, reducing in width and increasing in height, approaching the shape of the impulse while having an area equal to 1 for any value n .

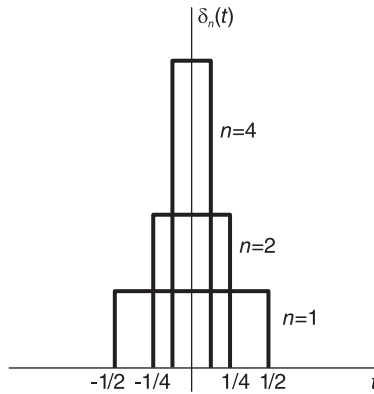


FIGURE 17.2 Rectangles leading to an impulse.

Let $\phi(t)$ be an arbitrary function that is continuous at $t = 0$. We note that as $n \rightarrow \infty$ we have

$$\begin{aligned} \lim_{n \rightarrow \infty} \int_{-\infty}^{\infty} \delta_n(t) \phi(t) dt &= \lim_{n \rightarrow \infty} \int_{-\varepsilon/2}^{\varepsilon/2} \frac{1}{\varepsilon} \phi(t) dt = \lim_{n \rightarrow \infty} \frac{1}{\varepsilon} \phi(0) \varepsilon = \phi(0) \\ &= \int_{-\infty}^{\infty} \delta(t) \phi(t) dt. \end{aligned} \tag{17.38}$$

We deduce that

$$\lim_{n \rightarrow \infty} \delta_n(t) = \delta(t) \tag{17.39}$$

as desired. Another possible approximating function is the Gaussian function shown in Fig. 17.3, namely,

$$\delta_n(t) = \sqrt{\frac{n}{\pi}} e^{-nt^2}. \tag{17.40}$$

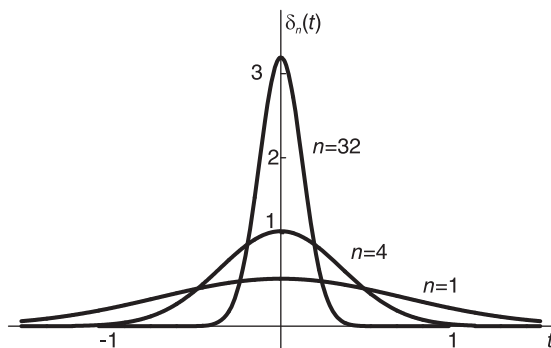


FIGURE 17.3 Gaussian function leading to an impulse.

Following the same reasoning we evaluate

$$\lim_{n \rightarrow \infty} \int_{-\infty}^{\infty} \delta_n(t) \phi(t) dt = \lim_{n \rightarrow \infty} \sqrt{\frac{n}{\pi}} \int_{-\infty}^{\infty} e^{-nt^2} \phi(t) dt. \quad (17.41)$$

As $n \rightarrow \infty$ the Gaussian function becomes increasingly narrower, ultimately sampling $\phi(t)$ at $t = 0$. We can thus write, as $n \rightarrow \infty$,

$$\int_{-\infty}^{\infty} \delta_n(t) \phi(t) dt \rightarrow \sqrt{\frac{n}{\pi}} \phi(0) \int_{-\infty}^{\infty} e^{-nt^2} dt. \quad (17.42)$$

The integral on the right-hand side is well known, given by

$$\int_{-\infty}^{\infty} e^{-\alpha t^2} dt = \sqrt{\frac{\pi}{\alpha}}. \quad (17.43)$$

We thus obtain

$$\lim_{n \rightarrow \infty} \delta_n(t) \phi(t) dt = \phi(0) \quad (17.44)$$

whence

$$\lim_{n \rightarrow \infty} \delta_n(t) = \delta(t) \quad (17.45)$$

as desired.

We can devise another approximating sequence as follows. We note that the Fourier transform of a causal exponential $f(t) = e^{-\alpha t} u(t)$ is given by

$$F(j\omega) = \mathcal{F}[e^{-\alpha t} u(t)] = \frac{1}{\alpha + j\omega}. \quad (17.46)$$

The modulus squared of $F(j\omega)$ is given by

$$|F(j\omega)|^2 = \frac{1}{\alpha^2 + \omega^2} \quad (17.47)$$

and is bell-shaped and a good candidate as an approximating sequence. We also note that by Parseval's theorem

$$\int_{-\infty}^{\infty} f^2(t) dt = \frac{1}{2\pi} \int_{-\infty}^{\infty} |F(j\omega)|^2 d\omega. \quad (17.48)$$

Now

$$\int_{-\infty}^{\infty} f^2(t) dt = \int_0^{\infty} e^{-2\alpha t} dt = \frac{1}{2\alpha} \quad (17.49)$$

wherefrom

$$\int_{-\infty}^{\infty} \frac{1}{\alpha^2 + \omega^2} d\omega = 2\pi \cdot \frac{1}{2\alpha} = \frac{\pi}{\alpha} \quad (17.50)$$

i.e.

$$\int_{-\infty}^{\infty} \frac{\alpha}{\pi} \frac{1}{\alpha^2 + \omega^2} d\omega = 1. \quad (17.51)$$

Letting $\alpha = 1/n$ and replacing ω by t we can thus write the approximating sequence of the impulse in the form

$$\delta_n(t) = \frac{1}{n\pi} \frac{1}{1/n^2 + t^2} = \frac{n}{\pi} \frac{1}{1 + n^2 t^2} \quad (17.52)$$

a sequence of unit area for all values of n as we have just seen and which narrows and increases in height as $n \rightarrow \infty$, ultimately taking the shape of the delta impulse. In Fig. 17.4 we see the narrowing and height increase of this approximating sequence as $n \rightarrow \infty$.

We can, similarly to the above, write

$$\lim_{n \rightarrow \infty} \int_{-\infty}^{\infty} \delta_n(t) \phi(t) dt = \lim_{n \rightarrow \infty} \phi(0) \int_{-\infty}^{\infty} \frac{n}{\pi} \frac{1}{1 + n^2 t^2} dt = \phi(0). \tag{17.53}$$

Hence

$$\lim_{n \rightarrow \infty} \delta_n(t) = \delta(t). \tag{17.54}$$

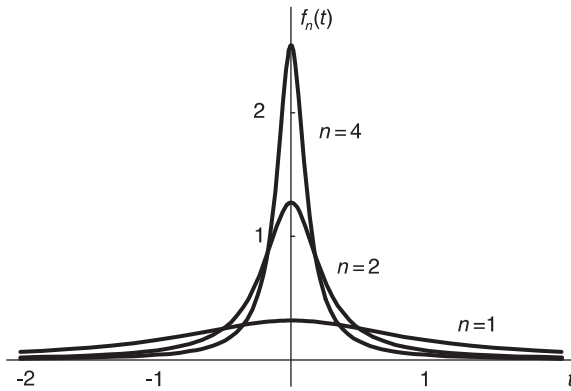


FIGURE 17.4 Impulse approximating sequence.

We conclude from this discussion that one way of verifying if a sequence $\delta_n(t)$ tends or not to $\delta(t)$ is to evaluate the integral

$$\int_{-\infty}^{\infty} \delta_n(t) \phi(t) dt \tag{17.55}$$

and ensure that it tends to $\phi(0)$ as $n \rightarrow \infty$.

17.7 Other Approximating Sequences and Functions of the Impulse

The following are other approximating sequences and functions of the impulse.

Centered triangle, shown in Fig. 17.5(a)

$$\delta(t) = \lim_{\tau \rightarrow 0} \frac{1}{\tau} \left[1 - \frac{|t|}{\tau} \right] \Pi_{\tau}(t) = \lim_{n \rightarrow \infty} n [1 - n|t|] \Pi_{1/n}(t). \tag{17.56}$$

Even exponential, shown in Fig. 17.5(b)

$$\delta(t) = \lim_{\tau \rightarrow 0} \frac{1}{\tau} e^{-2|t|/\tau} = \lim_{n \rightarrow \infty} n e^{-2n|t|}. \tag{17.57}$$

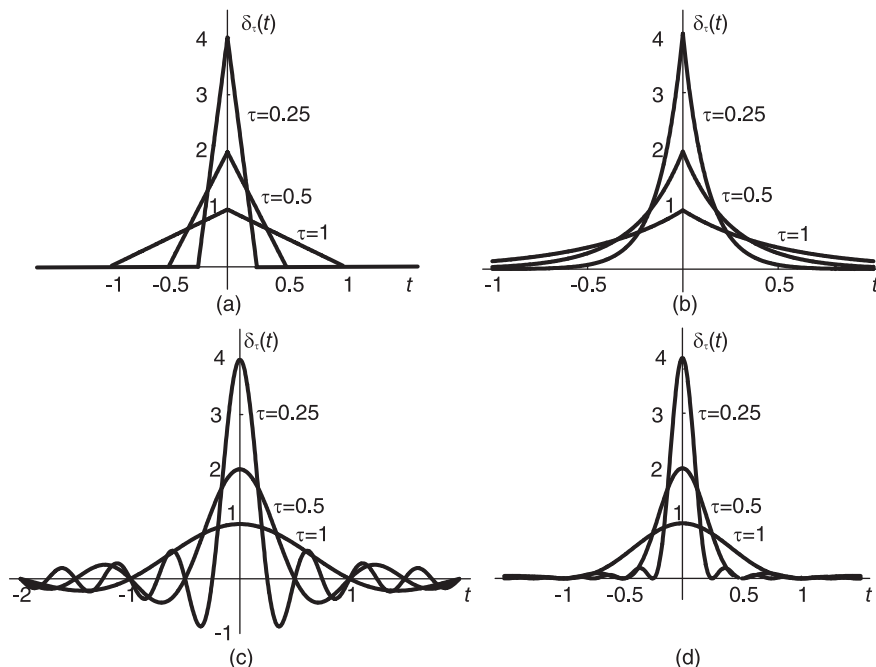


FIGURE 17.5 Impulse approximating sequences.

Sampling function, shown in Fig. 17.5(c)

$$\delta(t) = \lim_{\tau \rightarrow 0} \frac{1}{\tau} Sa(\pi t/\tau). \tag{17.58}$$

Alternatively, we may write

$$\lim_{v \rightarrow \infty} \frac{v}{\pi} Sa(vt) = \delta(t). \tag{17.59}$$

Sampling squared function shown in Fig. 17.5(d)

$$\delta(t) = \lim_{\tau \rightarrow 0} \frac{1}{\tau} Sa^2(\pi t/\tau). \tag{17.60}$$

and, equivalently,

$$\lim_{v \rightarrow \infty} \frac{v}{\pi} Sa^2(vt) = \delta(t). \tag{17.61}$$

17.8 Test Functions

As noted earlier a test function $\phi(t)$ is real-valued. It can be differentiated an arbitrary number of times and is of a finite interval.

Example 17.4 *The function*

$$\phi(t) = e^{\tau^2/(t^2-\tau^2)} \Pi_{\tau}(t)$$

is a test function of finite duration $(-\tau, \tau)$. Its derivative is given by

$$\phi'(t) = e^{\tau^2/(t^2-\tau^2)} \frac{-2\tau^2 t}{(t^2 - \tau^2)^2} \Pi_\tau(t).$$

The function $\phi(t)$ and its derivative $\phi'(t)$ are shown in Fig. 17.6 for the case $\tau = 1$.

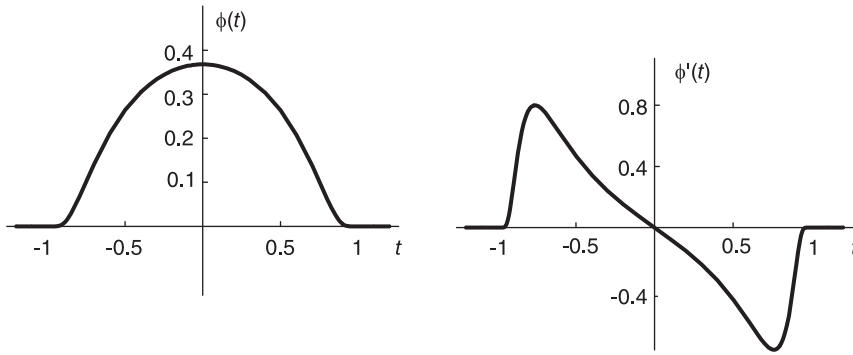


FIGURE 17.6 Test function and its derivative.

If $f(t)$ is a function that can be differentiated an arbitrary number of times then the product $f(t)\phi(t)$ is a test function. If $f(t)$ is a finite duration function its convolution with $\phi(t)$ is a test function $\psi(t)$

$$\psi(t) = \int_{-\infty}^{\infty} f(\tau)\phi(t - \tau)d\tau. \tag{17.62}$$

17.9 Convolution

The convolution of two distributions is given by

$$\begin{aligned} \langle g_1 * g_2, \phi \rangle &= \int_{-\infty}^{\infty} \left\{ \int_{-\infty}^{\infty} g_1(\tau) g_2(t - \tau) d\tau \right\} \phi(t) dt \\ &= \int_{-\infty}^{\infty} g_1(\tau) \left\{ \int_{-\infty}^{\infty} g_2(t - \tau) \phi(t) dt \right\} d\tau \end{aligned} \tag{17.63}$$

through a change of order of integration.

Example 17.5 The convolution of two impulses $g_1(t) = \delta(t - t_0)$ and $g_2(t) = \delta(t - t_1)$ is given by

$$\int_{-\infty}^{\infty} \delta(\tau - t_0)\delta(t - \tau - t_1)d\tau = \delta\{t - (t_0 + t_1)\}.$$

Example 17.6 The derivative $g'_n(t)$ of the sequence

$$g_n(t) = \frac{n/\pi}{(1 + n^2 t^2)}$$

is given by

$$g'_n(t) = \frac{-2n^3t/\pi}{(1+n^2t^2)^2}.$$

The sequence $g_n(t)$ and its derivative $g'_n(t)$ are shown in Fig. 17.7(a-b), respectively.

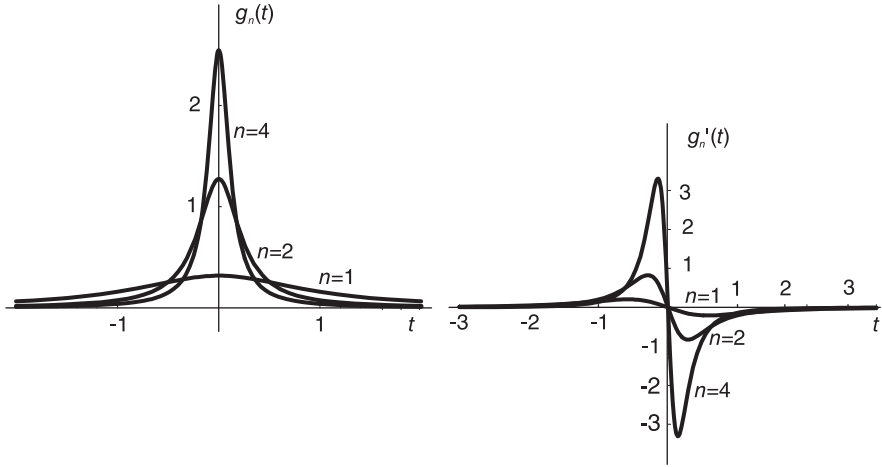


FIGURE 17.7 The sequence $g_n(t)$ and its derivative.

We can write

$$\lim_{n \rightarrow \infty} g'_n(t) = g'(t)$$

i.e.

$$\lim_{n \rightarrow \infty} \left\{ \frac{-2n^3t/\pi}{(1+n^2t^2)^2} \right\} = \delta'(t)$$

and we note that

$$\lim_{n \rightarrow \infty} \langle g'_n, \phi \rangle = \langle g', \phi \rangle = - \langle g, \phi' \rangle$$

wherefrom

$$\langle \delta', \phi \rangle = - \langle \delta, \phi' \rangle = -\phi'(0)$$

i.e.

$$\int_{-\infty}^{\infty} \delta'(t)\phi(t) dt = - \int_{-\infty}^{\infty} \delta(t)\phi'(t) dt = -\phi'(0)$$

as seen above.

17.10 Multiplication by an Impulse Derivative

We set out to prove that

$$f(t)\delta^{(n)}(t) = \sum_{k=0}^n (-1)^k \binom{n}{k} f^{(k)}(0)\delta^{(n-k)}(t) \tag{17.64}$$

where

$$\binom{n}{k} = \frac{n!}{k!(n-k)!} \quad (17.65)$$

Let us first evaluate the product $f(t)\delta'(t)$. We write

$$\langle f\delta', \phi \rangle = \int_{-\infty}^{\infty} f(t)\delta'(t)\phi(t)dt = \int_{-\infty}^{\infty} \{f(t)\phi(t)\}'\delta'(t)dt. \quad (17.66)$$

Integrating by parts we have

$$\begin{aligned} \langle f\delta', \phi \rangle &= f(t)\phi(t)\delta(t)|_{-\infty}^{\infty} - \int_{-\infty}^{\infty} \{f(t)\phi(t)\}'\delta(t)dt \\ &= 0 - \int_{-\infty}^{\infty} \{f(t)\phi'(t) + f'(t)\phi(t)\}\delta(t)dt \\ &= -f(0)\phi'(0) - f'(0)\phi(0). \end{aligned} \quad (17.67)$$

We have established the relation

$$\langle \delta', \phi \rangle = -\phi'(0) \quad (17.68)$$

wherefrom we can write

$$\begin{aligned} \langle f\delta', \phi \rangle &= f(0)\langle \delta', \phi \rangle - f'(0)\langle \delta, \phi \rangle \\ &= \int_{-\infty}^{\infty} f(0)\delta'(t)\phi(t)dt - \int_{-\infty}^{\infty} f'(0)\delta(t)\phi(t)dt. \end{aligned} \quad (17.69)$$

so that

$$f(t)\delta'(t) = f(0)\delta'(t) - f'(0)\delta(t). \quad (17.70)$$

We shall follow basically the same steps to evaluate $f(t)\delta^{(n)}(t)$. We write

$$\langle f\delta^{(n)}, \phi \rangle = \int_{-\infty}^{\infty} f(t)\delta^{(n)}(t)\phi(t)dt = \int_{-\infty}^{\infty} \{f(t)\phi(t)\}'\delta^{(n)}(t)dt. \quad (17.71)$$

Integrating by parts we have

$$\begin{aligned} \langle f\delta^{(n)}, \phi \rangle &= f(t)\phi(t)\delta^{(n-1)}(t)|_{-\infty}^{\infty} - \int_{-\infty}^{\infty} \{f(t)\phi(t)\}'\delta^{(n-1)}(t)dt \\ &= 0 - \int_{-\infty}^{\infty} \{f(t)\phi(t)\}'\delta^{(n-1)}(t)dt. \end{aligned} \quad (17.72)$$

Repeating the process of integration by parts $(n-1)$ times we obtain

$$\langle f\delta^{(n)}, \phi \rangle = (-1)^n \int_{-\infty}^{\infty} \{f(t)\phi(t)\}^{(n)}\delta(t)dt. \quad (17.73)$$

The n^{th} derivative of the product $f(t)\phi(t)$ is given by

$$\{f(t)\phi(t)\}^{(n)} = \sum_{k=0}^n \binom{n}{k} f^{(k)}(t)\phi^{(n-k)}(t) \quad (17.74)$$

wherefrom

$$\begin{aligned} \langle f\delta^{(n)}, \phi \rangle &= (-1)^n \int_{-\infty}^{\infty} \left\{ \sum_{k=0}^n \binom{n}{k} f^{(k)}(t)\phi^{(n-k)}(t) \right\} \delta(t)dt \\ &= (-1)^n \sum_{k=0}^n \binom{n}{k} \int_{-\infty}^{\infty} \delta(t) \{f^{(k)}(t)\phi^{(n-k)}(t)\} dt \\ &= (-1)^n \sum_{k=0}^n \binom{n}{k} f^{(k)}(0)\phi^{(n-k)}(0). \end{aligned} \quad (17.75)$$

Using the property

$$\langle \delta^{(m)}, \phi \rangle = \int_{-\infty}^{\infty} \delta^{(m)}(t) \phi(t) dt = (-1)^m \phi^{(m)}(0) \quad (17.76)$$

so that

$$\phi^{(n-k)}(0) = (-1)^{n-k} \int_{-\infty}^{\infty} \delta^{(n-k)}(t) \phi(t) dt \quad (17.77)$$

and

$$\begin{aligned} \langle f \delta^{(n)}, \phi \rangle &= (-1)^n \sum_{k=0}^n \binom{n}{k} f^{(k)}(0) (-1)^{n-k} \int_{-\infty}^{\infty} \delta^{(n-k)}(t) \phi(t) dt \\ &= \int_{-\infty}^{\infty} \sum_{k=0}^n (-1)^k \binom{n}{k} f^{(k)}(0) \delta^{(n-k)}(t) \phi(t) dt \end{aligned} \quad (17.78)$$

obtaining Equation (17.64) as desired. In particular, the expressions for $f(t)\delta'(t)$ and $f(t)\delta''(t)$ are

$$f(t)\delta'(t) = f''(0)\delta(t) - 2f'(0)\delta'(t) + f(0)\delta''(t) \quad (17.79)$$

$$f(t)\delta''(t) = -f^{(3)}(0)\delta(t) + 3f''(0)\delta'(t) - 3f(0)\delta''(t) + f(0)\delta^{(3)}(t). \quad (17.80)$$

More generally, we have

$$f(t)\delta^{(n)}(t-\tau) = \sum_{k=0}^n (-1)^k \binom{n}{k} f^{(k)}(\tau) \delta^{(n-k)}(t-\tau). \quad (17.81)$$

Example 17.7 Evaluate $e^{\alpha t}\delta'(t)$, $\cos \beta t\delta'(t)$ and $\sin \beta t\delta'(t)$.

We have

$$f(t)\delta'(t) = -f'(0)\delta(t) + f(0)\delta'(t)$$

$$e^{\alpha t}\delta'(t) = -\alpha\delta(t) + \delta'(t)$$

$$\cos \beta t\delta'(t) = \beta \sin \beta t|_{t=0} + \delta'(t) = \delta'(t)$$

$$\sin \beta t\delta'(t) = -\beta \cos \beta t|_{t=0} \delta(t) + 0 = -\beta\delta(t).$$

17.11 The Dirac-Delta Impulse as a Limit of a Gaussian Function

We consider the definition of the impulse as a limit of a Gaussian function.

To show that

$$\lim_{\alpha \rightarrow 0} \frac{e^{-\omega^2/(4\alpha)}}{2\sqrt{\pi\alpha}} = \delta(\omega). \quad (17.82)$$

Let

$$s_{\alpha}(\omega) = e^{-\omega^2/(4\alpha)} / \{2\sqrt{\pi\alpha}\} \quad (17.83)$$

and

$$\langle s_{\alpha}(\omega), \Phi(\omega) \rangle \triangleq \int_{-\infty}^{\infty} \frac{1}{2\sqrt{\pi\alpha}} e^{-\omega^2/(4\alpha)} \Phi(\omega) d\omega. \quad (17.84)$$

We have

$$\begin{aligned} \lim_{\alpha \rightarrow 0} \langle s_\alpha(\omega), \Phi(\omega) \rangle &\simeq \lim_{\alpha \rightarrow 0} \frac{1}{2\sqrt{\pi\alpha}} \Phi(0) \int_{-\infty}^{\infty} e^{-\omega^2/(4\alpha)} d\omega \\ &= \frac{\Phi(0)}{2\sqrt{\pi\alpha}} \sqrt{4\pi\alpha} = \Phi(0) = \langle \delta(\omega), \Phi(\omega) \rangle \end{aligned} \quad (17.85)$$

$$\lim_{\alpha \rightarrow 0} s_\alpha(\omega) = \delta(\omega) \quad (17.86)$$

wherefrom

$$\delta(\omega) = \lim_{\alpha \rightarrow 0} \frac{e^{-\omega^2/(4\alpha)}}{2\sqrt{\pi\alpha}}. \quad (17.87)$$

17.12 Fourier Transform of Unity

We have found the Fourier transform of the Gaussian function, namely,

$$e^{-\alpha t^2} \xleftrightarrow{\mathcal{F}} \sqrt{\pi/\alpha} e^{-\omega^2/(4\alpha)}. \quad (17.88)$$

We deduce that

$$\lim_{\alpha \rightarrow 0} e^{-\alpha t^2} \xleftrightarrow{\mathcal{F}} \lim_{\alpha \rightarrow 0} \sqrt{\pi/\alpha} e^{-\omega^2/(4\alpha)}. \quad (17.89)$$

The left-hand side of this relation is equal to 1. The right-hand side has been found to equal $2\pi\delta(\omega)$, wherefrom

$$1 \xleftrightarrow{\mathcal{F}} 2\pi\delta(\omega). \quad (17.90)$$

Alternatively, consider the function

$$f(t) = \Pi_{\tau/2}(t) = \{u(t + \tau/2) - U(t - \tau/2)\}. \quad (17.91)$$

Its Fourier transform is given by

$$F(j\omega) = \tau Sa[\tau\omega/2]. \quad (17.92)$$

Now

$$\lim_{\omega \rightarrow \infty} \omega \frac{\sin \omega t}{\pi \omega t} = \lim_{\omega \rightarrow \infty} \frac{\omega}{\pi} Sa(\omega t) = \delta(t) \quad (17.93)$$

and with ω replaced by $\tau/2$ and t replaced by ω we have

$$\lim_{\tau \rightarrow \infty} \frac{\tau}{2\pi} Sa(\tau\omega/2) = \delta(\omega) \quad (17.94)$$

wherefrom

$$\lim_{\tau \rightarrow \infty} \Pi_{\tau/2}(t) = 1 \xleftrightarrow{\mathcal{F}} \lim_{\tau \rightarrow \infty} \tau Sa[\tau\omega/2] = 2\pi\delta(\omega). \quad (17.95)$$

17.13 The Impulse of a Function

To show that

$$\delta[f(t)] = \sum_{n=1}^n \frac{\delta(t - t_m)}{|f'(t_m)|} \quad (17.96)$$

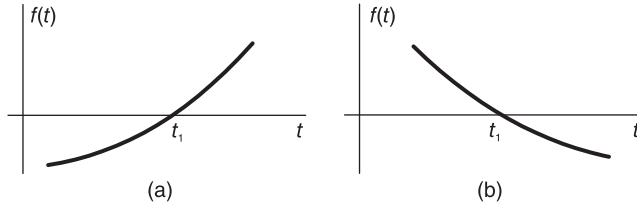


FIGURE 17.8 Functions and their zeros.

where t_m are simple zeros of $f(t)$.

a) assume $f'(t_1) > 0$ as shown in Fig. 17.8(a).

Let t_1 be a zero of $f(t)$, i.e. $f(t_1) = 0$

$$I = \int_{-\infty}^{\infty} \delta[f(t)]\phi(t) dt. \tag{17.97}$$

Writing $y = f(t)$ we have $dy/dt = f'(t)$, i.e. $dt = dy/f'(t) = dy/f'[f^{-1}(y)]$

$$I = \int \delta[f(t)]\phi(t)dt = \int_{-\infty}^{\infty} \delta(y) \frac{\phi[f^{-1}(y)]}{f'[f^{-1}(y)]} dy = \frac{\phi[f^{-1}(0)]}{f'[f^{-1}(0)]} = \frac{\phi(t_1)}{f'(t_1)}. \tag{17.98}$$

We may therefore write

$$I = \left\{ \int_{-\infty}^{\infty} \delta(t - t_1) \phi(t) dt \right\} / f'(t_1). \tag{17.99}$$

Comparing both values of I we have

$$\delta[f(t)] = \frac{\delta(t - t_1)}{f'(t_1)}, \quad f'(t_1) > 0. \tag{17.100}$$

b) For the case $f'(t_1) < 0$, represented in Fig. 17.8(b) we can similarly show that

$$\delta[f(t)] = \frac{\delta(t - t_1)}{-f'(t_1)}, \quad f'(t_1) < 0. \tag{17.101}$$

From cases a) and b) we can write

$$\delta[f(t)] = \frac{\delta(t - t_1)}{|f'(t_1)|}, \quad f'(t_1) \neq 0. \tag{17.102}$$

Now suppose $f(t)$ has two zeros t_1 and t_2 . Let τ be a point between t_1 and t_2

$$t_1 < \tau < t_2. \tag{17.103}$$

We can write

$$I = \int_{-\infty}^{\infty} \delta[f(t)]\phi(t)dt = \int_{-\infty}^{\tau} \delta[f(t)]\phi(t)dt + \int_{\tau}^{\infty} \delta[f(t)]\phi(t)dt. \tag{17.104}$$

Proceeding as above we obtain

$$I = \frac{\phi(t_1)}{|f'(t_1)|} + \frac{\phi(t_2)}{|f'(t_2)|} \tag{17.105}$$

$$I = \frac{\int_{-\infty}^{\infty} \delta(t - t_1)\phi(t)dt}{|f'(t_1)|} + \frac{\int_{-\infty}^{\infty} \delta(t - t_2)\phi(t)dt}{|f'(t_2)|} \quad (17.106)$$

wherefrom

$$\delta[f(t)] = \frac{\delta(t - t_1)}{|f'(t_1)|} + \frac{\delta(t - t_2)}{|f'(t_2)|} \quad (17.107)$$

and in general with $f(t)$ having the zeros t_1, t_2, \dots, t_n we have

$$\delta[f(t)] = \sum_{i=1}^n \frac{\delta(t - t_i)}{|f'(t_i)|}. \quad (17.108)$$

If the zeros are multiple, i.e., if higher order, the distribution $\delta[f(t)]$ is not defined.

Example 17.8 Given the function $f(t) = C_3(t - 1)$ where $C_3(t)$ is the Chebyshev polynomial of the third order as a function of t , evaluate $\delta[f(t)]$.

We have $C_3(t) = 4t^3 - 3t$, so that

$$f(t) = 4(t - 1)^3 - 3(t - 1) = 4t^3 - 12t^2 + 9t - 1$$

which is depicted in Fig. 17.9 The zeros of $f(t)$ are $t_1 = 0.133975$, $t_2 = 1$, $t_3 = 1.86603$.

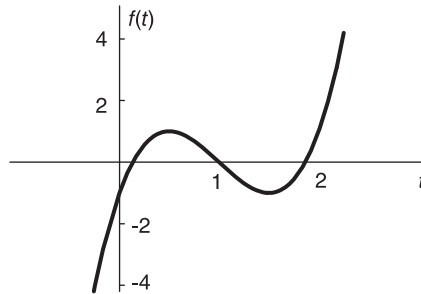


FIGURE 17.9 A function with three zeros.

The derivative of $f(t)$ is $f'(t) = 12t^2 - 24t + 9$, so that $f'(t_1) = 6$, $f'(t_2) = -3$, $f'(t_3) = 6$.

Hence

$$\delta[f(t)] = (1/6)\delta(t - 0.133975) + (1/3)\delta(t - 1) + (1/6)\delta(t - 1.86603).$$

We just found that if $f(t)$ increases monotonically between $t = a$ and $t = b$ and if it has one zero, at $t = \tau$, i.e. $f(\tau) = 0$, where $a < \tau < b$ then

$$\delta[f(t)] = \frac{\delta(t - \tau)}{f'(\tau)}. \quad (17.109)$$

It is interesting to evaluate $\delta'[f(t)]$ where

$$\delta'[f(t)] = \frac{d\delta[f(t)]}{d[f(t)]}. \quad (17.110)$$

Since

$$\frac{d}{dt} \delta[f(t)] = \frac{d\delta[f(t)]}{d[f(t)]} \frac{d}{dt} f(t) \quad (17.111)$$

we have

$$\begin{aligned} \delta' [f(t)] &= \frac{d}{dt} \delta[f(t)] \cdot \frac{1}{f'(t)} = \frac{1}{f'(t)} \frac{d}{dt} \left\{ \frac{\delta(t-\tau)}{f'(\tau)} \right\} \\ &= \frac{1}{f'(t)} \cdot \frac{1}{f'(\tau)} \delta'(t-\tau) = \frac{1}{f'(\tau)} \left\{ \frac{1}{f'(t)} \delta'(t-\tau) \right\}. \end{aligned} \quad (17.112)$$

Using the property

$$g(t)\delta'(t-\tau) = g(\tau)\delta'(t-\tau) - g'(\tau)\delta(t-\tau) \quad (17.113)$$

we have

$$\delta' [f(t)] = \frac{1}{f'(\tau)} \left\{ \frac{1}{f'(\tau)} \delta'(t-\tau) + \frac{f''(\tau)}{|f'(\tau)|^2} \delta(t-\tau) \right\}. \quad (17.114)$$

17.14 Multiplication by t

From the property

$$f(t)\delta(t) = f(0)\delta(t) \quad (17.115)$$

we have

$$t\delta(t) = 0. \quad (17.116)$$

It follows that, if $g_1(t) = g_2(t) + A\delta(t)$ then $tg_1(t) = tg_2(t)$ and vice versa; if $tg_1(t) = tg_2(t)$ we cannot simplify by dividing by t . We have, rather,

$$g_1(t) = g_2(t) + A\delta(t). \quad (17.117)$$

The property

$$f(t)\delta'(t) = f(0)\delta'(t) - f'(0)\delta(t) \quad (17.118)$$

implies that

$$t\delta'(t) = -\delta(t). \quad (17.119)$$

17.15 Time Scaling

If

$$g(t) \xleftrightarrow{\mathcal{F}} G(j\omega) \quad (17.120)$$

then

$$g(at+b) \longleftrightarrow \frac{1}{|a|} G\left(j\frac{\omega}{a}\right) e^{j(b/a)\omega}. \quad (17.121)$$

Example 17.9 Evaluate $\mathcal{F}[\delta(at+b)]$.

Since $\delta(t) \longleftrightarrow 1$ we have

$$\delta(at+b) \longleftrightarrow \frac{1}{|a|} e^{j(b/a)\omega}$$

which is the same as found by applying the property.

17.16 Some Properties of the Dirac-Delta Impulse

The following is a summary of important properties of the Dirac-delta impulse for future reference.

$$f(t)\delta'(t) = f(0)\delta'(t) - f'(0)\delta(t) \quad (17.122)$$

$$\delta(at) = \frac{1}{|a|}\delta(t) \quad (17.123)$$

$$\int_{-\infty}^{\infty} \frac{d^n \delta(t-t_0)}{dt^n} \phi(t) dt = (-1)^n \frac{d^n}{dt^n} \phi(t_0) \quad (17.124)$$

$$\frac{d}{dt} u(t) = \delta(t) \quad (17.125)$$

$$t\delta'(t) = -\delta(t) \quad (17.126)$$

$$\delta^{(n)}(t) = (-1)^n n! t^{-n} \delta(t) \quad (17.127)$$

$$\delta^{(n)}(t) * f(t) = f^{(n)}(t) \quad (17.128)$$

$$\int_{-\infty}^{\infty} t\delta'(t) dt = -1 \quad (17.129)$$

$$\int \delta^{(n)}(t) f(t) dt = (-1)^n f^{(n)}(0) \quad (17.130)$$

$$t^2 \delta'(t) = 0 \quad (17.131)$$

$$t^2 \delta''(t) = 2\delta(t) \quad (17.132)$$

$$t^3 \delta''(t) = 0 \quad (17.133)$$

$$t^n \delta^{(n)}(t) = (-1)^n n! \delta(t) \quad (17.134)$$

If $tg_1(t) = tg_2(t)$ then $g_1(t) = g_2(t) + c\delta(t)$, c constant. (17.135)

$$\int_{-\infty}^{\infty} \delta'(t) \phi(t) dt = -\phi'(0) \quad (17.136)$$

$$\int_{-\infty}^{\infty} \delta^{(m)}(t) dt = 1 \quad \text{iff } m = 0 \quad (17.137)$$

$$\delta'(-t) = -\delta'(t) \quad (17.138)$$

$$\int_{-\infty}^{\infty} \delta''(t) dt = 0 \quad (17.139)$$

$$\delta'(t) * f(t) = f'(t) \quad (17.140)$$

$$\delta^{(n)}(t) * f(t) = f^{(n)}(t) \quad (17.141)$$

$$\delta^{(n)}(\omega) * F(j\omega) = F^{(n)}(j\omega) \quad (17.142)$$

$$\int_{-\infty}^{\infty} \delta(t-t_0) \phi(t) dt = \phi(t_0) \quad (17.143)$$

$$t\delta(t) = 0 \quad (17.144)$$

$$t\delta'(t) = -\delta(t) \quad (17.145)$$

$$t^2 \delta'(t) = 0 \quad (17.146)$$

$$\delta(at) = \frac{1}{|a|} \delta(t) \tag{17.147}$$

$$f(t) \delta'(t) = f(0) \delta'(t) - f'(0) \delta(t) \tag{17.148}$$

$$f(t) \delta''(t) = f(0) \delta''(t) - 2f'(0) \delta'(t) + f''(0) \delta(t) \tag{17.149}$$

$$f(t) \delta'''(t) = f(0) \delta'''(t) - 3f'(0) \delta''(t) + 3f''(0) \delta'(t) - f'''(0) \delta(t) \tag{17.150}$$

$$f(t) \delta^{(n)}(t) = \sum_{k=0}^n (-1)^k \frac{n!}{k!(n-k)!} f^{(k)}(0) \delta^{(n-k)}(t) \tag{17.151}$$

$$\delta(t - t_1) * \delta(t - t_2) = \delta[t - (t_1 + t_2)] \tag{17.152}$$

$$\delta^{(n)}(-t) = \begin{cases} \delta^{(n)}(t), & n \text{ even} \\ -\delta^{(n)}(t), & n \text{ odd} \end{cases} \tag{17.153}$$

17.17 Additional Fourier Transforms

From the transform

$$\text{sgn}(t) \longleftrightarrow \frac{2}{j\omega} \tag{17.154}$$

using the duality property we can write

$$2/jt \longleftrightarrow 2\pi \text{sgn}(-\omega) = -2\pi \text{sgn}(\omega) \tag{17.155}$$

i.e.

$$1/t \longleftrightarrow -j\pi \text{sgn}(\omega). \tag{17.156}$$

Since $(t^{-1})' = -t^{-2}$, $(t^{-2})' = -2t^{-3}$, ... and in general

$$t^{-k} = (-1)^{k-1} \frac{(t^{-1})^{(k-1)}}{(k-1)!} \tag{17.157}$$

we have

$$\mathcal{F}[t^{-k}] = \frac{(-1)^{k-1}}{(k-1)!} (j\omega)^{k-1} \mathcal{F}[t^{-1}] = \frac{(-j)^k \pi}{(k-1)!} \omega^{k-1} \text{sgn}(\omega). \tag{17.158}$$

17.18 Riemann–Lebesgue Lemma

The Riemann–Lebesgue lemma may be stated as follows: If a function $\phi(t)$ is absolutely integrable in an interval (a, b) and if $\psi(t)$ is the same as $\phi(t)$ over the interval (a, b) and is nil elsewhere then the Fourier transform $\Psi(j\omega)$ of $\psi(t)$ tends to zero as $\omega \rightarrow \infty$

$$\lim_{\omega \rightarrow \infty} \Psi(j\omega) = 0 \tag{17.159}$$

where the constants a and b have finite or infinite values. The lemma is easily proved using an integration by parts

$$\begin{aligned}\Psi(j\omega) &= \int_{-\infty}^{\infty} \psi(t)e^{-j\omega t} dt = \int_a^b \phi(t)e^{-j\omega t} dt \\ &= \frac{-1}{j\omega} \{e^{-j\omega b}\phi(b) - e^{-j\omega a}\phi(a)\} + \int_a^b \frac{1}{j\omega} e^{-j\omega t} \phi'(t) dt\end{aligned}\quad (17.160)$$

which tends to zero as $\omega \rightarrow \infty$ as stated.

Using the Riemann–Lebesgue lemma we have as a special case with $a = -\infty$ and $b = \infty$ and $\psi(t)$ a test function

$$\lim_{\omega \rightarrow \infty} \Phi(j\omega) = \lim_{\omega \rightarrow \infty} \int_{-\infty}^{\infty} \phi(t)e^{-j\omega t} dt = 0. \quad (17.161)$$

The function $e^{-j\omega t}$ can be thus seen as a distribution having the property

$$\lim_{\omega \rightarrow \infty} \langle e^{-j\omega t}, \phi(t) \rangle = \lim_{\omega \rightarrow \infty} \int_{-\infty}^{\infty} e^{-j\omega t} \phi(t) dt = 0. \quad (17.162)$$

Hence

$$\lim_{\omega \rightarrow \infty} e^{-j\omega t} = 0. \quad (17.163)$$

Again, this is a limit that makes sense only as a distribution and, in particular, as a generalized limit.

We can write, moreover,

$$\lim_{\omega \rightarrow \infty} (\cos \omega t - j \sin \omega t) = 0 \quad (17.164)$$

$$\lim_{\omega \rightarrow \infty} \cos \omega t = 0 \quad (17.165)$$

$$\lim_{\omega \rightarrow \infty} \sin \omega t = 0. \quad (17.166)$$

Now we can evaluate the improper integral

$$\int_0^{\infty} \cos \omega t dt = \lim_{T \rightarrow \infty} \int_0^T \cos \omega t dt = \lim_{T \rightarrow \infty} \frac{\sin \omega T}{\omega} = 0. \quad (17.167)$$

Similarly

$$\int_0^{\infty} \sin \omega t dt = \lim_{T \rightarrow \infty} \int_0^T \sin \omega t dt = \lim_{T \rightarrow \infty} \frac{1 - \cos \omega T}{\omega} = \frac{1}{\omega}. \quad (17.168)$$

17.19 Generalized Limits

We have already seen that a sequence of distributions $g_n(t)$, $n = 1, 2, 3, \dots$ has as a limit $g(t)$ as $t \rightarrow \infty$ if

$$\lim_{t \rightarrow \infty} \langle g_n, \phi \rangle = \lim_{t \rightarrow \infty} \int_{-\infty}^{\infty} g_n(t)\phi(t) dt = \int_{-\infty}^{\infty} g(t)\phi(t) dt = \langle g, \phi \rangle. \quad (17.169)$$

The same concept of a limit of a distribution sequence applies to the limit of a distribution $g_\beta(t)$ of which the parameter β tends to a limit β_0 . In particular, if for every test function $\phi(t)$

$$\lim_{\beta \rightarrow \beta_0} \langle g_\beta, \phi \rangle = \lim_{\beta \rightarrow \beta_0} \int_{-\infty}^{\infty} g_\beta(t)\phi(t)dt = \int_{-\infty}^{\infty} g_{\beta_0}(t)\phi(t)dt = \langle g_{\beta_0}, \phi \rangle \quad (17.170)$$

then we write

$$g_\beta(t) \longrightarrow g_{\beta_0}(t). \quad (17.171)$$

We use this property to establish a distribution that has as a limit the delta function. Let

$$g_\beta(t) = \frac{\beta}{\pi} Sa(\beta t). \quad (17.172)$$

We consider the limit as $\beta \rightarrow \infty$

$$\lim_{\beta \rightarrow \infty} \langle g_\beta, \phi \rangle = \lim_{\beta \rightarrow \infty} \frac{\beta}{\pi} \int_{-\infty}^{\infty} Sa(\beta t)\phi(t)dt. \quad (17.173)$$

Now

$$\int_{-\infty}^{\infty} Sa(\beta t)\phi(t)dt = \left\{ \int_{-\infty}^{-\varepsilon} + \int_{-\varepsilon}^{\varepsilon} + \int_{\varepsilon}^{\infty} \right\} Sa(\beta t)\phi(t)dt. \quad (17.174)$$

The first integral is given by

$$\frac{1}{\beta} \int_{-\infty}^{\varepsilon} \sin \beta t \frac{\phi(t)}{t} dt. \quad (17.175)$$

Since the function $\{\phi(t)/t\}$ is integrable in the interval of integration $(-\infty, \varepsilon)$ the integral tends to zero according to the Riemann–Lebesgue lemma. Similarly the third integral tends to zero. The second integral is evaluated by noticing that the test function $\phi(t)$ being continuous at $t = 0$ is given approximately by $\phi(0)$ in the interval of integration $(-\varepsilon, \varepsilon)$. We can thus write

$$\int_{-\varepsilon}^{\varepsilon} Sa(\beta t)\phi(t)dt \simeq \phi(0) \int_{-\varepsilon}^{\varepsilon} Sa(\beta t)dt = \frac{\phi(0)}{\beta} \int_{-\beta\varepsilon}^{\beta\varepsilon} Sa(u)du \quad (17.176)$$

having replaced βt by u .

We can therefore write

$$\lim_{\beta \rightarrow \infty} \int_{-\infty}^{\infty} Sa(\beta t)\phi(t)dt = \frac{\phi(0)}{\beta} \int_{-\infty}^{\infty} Sa(u)du = \frac{\pi\phi(0)}{\beta} \quad (17.177)$$

where we have used the well-known integral $\int_{-\infty}^{\infty} Sa(x)dx = \pi$. Hence

$$\lim_{\beta \rightarrow \infty} \langle g_\beta, \phi \rangle = \phi(0) = \langle \delta, \phi \rangle \quad (17.178)$$

wherefrom

$$\lim_{\beta \rightarrow \infty} \frac{\beta}{\pi} Sa(\beta t) = \delta(t). \quad (17.179)$$

This important distribution representing the Dirac-delta impulse may be applied to the evaluation of limits and integrals that do not exist in the ordinary sense. An important integral such as

$$I = \int_{-\infty}^{\infty} e^{j\omega t} d\omega \quad (17.180)$$

is an example of such improper integrals. To evaluate this integral we first note that it can be written in the form

$$I = \int_{-\infty}^{\infty} (\cos \omega t + j \sin \omega t) d\omega = \int_{-\infty}^{\infty} \cos \omega t d\omega \quad (17.181)$$

the imaginary part being an odd function of t . Now

$$\begin{aligned} \int_{-\infty}^{\infty} \cos \omega t d\omega &= \lim_{\beta \rightarrow \infty} \int_{-\beta}^{\beta} \cos \omega t d\omega = \lim_{\beta \rightarrow \infty} \{2 \sin \beta t / t\} \\ &= \lim_{\beta \rightarrow \infty} \{2\beta Sa(\beta t)\} = 2\pi \delta(t) \end{aligned} \quad (17.182)$$

wherefrom

$$\int_{-\infty}^{\infty} \cos \omega t d\omega = 2\pi \delta(t) \quad (17.183)$$

and

$$\int_{-\infty}^{\infty} e^{j\omega t} d\omega = 2\pi \delta(t). \quad (17.184)$$

We thus note how such an improper integral $\int_{-\infty}^{\infty} \cos \omega t d\omega$ that has no meaning in the ordinary sense is assigned a value $2\pi \delta(t)$ when viewed as a distribution. Note that this result is but a statement of the fact that $\mathcal{F}^{-1}[1] = \delta(t)$.

Moreover, replacing ω by t and vice versa we obtain the transform of unity.

$$\int_{-\infty}^{\infty} e^{-j\omega t} dt = 2\pi \delta(\omega) \quad (17.185)$$

i.e.

$$\mathcal{F}[1] = 2\pi \delta(\omega). \quad (17.186)$$

17.20 Fourier Transform of Higher Impulse Derivatives

From the differentiation property of the Fourier transform we know that if $f(t) \longleftrightarrow F(j\omega)$ then $f^{(n)}(t) \longleftrightarrow (j\omega)^n F(j\omega)$. Hence $\delta^{(n)}(t) \longleftrightarrow (j\omega)^n$, and using the duality property we have

$$(jt)^n \longleftrightarrow 2\pi \delta^{(n)}(-\omega) = 2\pi \frac{d^n}{d\omega^n} \delta(-\omega) = 2\pi \frac{d^n}{d\omega^n} \delta(\omega) \quad (17.187)$$

$$t^n \longleftrightarrow 2\pi j^n \delta^{(n)}(\omega). \quad (17.188)$$

17.21 The Distribution t^{-k}

The function t^{-k} is an improper one, being infinite at $t = 0$.

To evaluate the distribution t^{-k} let us first evaluate it for $k = 1$. We write $g(t) = t^{-1}$

$$\langle t^{-1}, \phi \rangle = \int_{-\infty}^{\infty} \frac{\phi(t)}{t} dt. \quad (17.189)$$

Due to the infinite discontinuity jump at $t = 0$, as shown in Fig. 17.10(a), the integral does not exist.

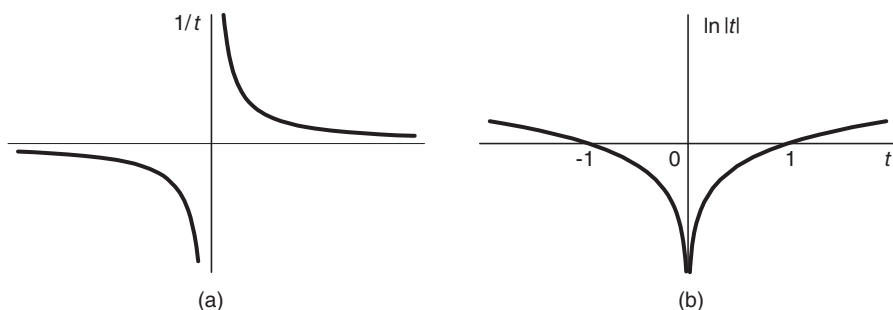


FIGURE 17.10 Functions with infinite discontinuities.

We note however that the integral of $(1/t)$ is the function $\ln|t|$, shown in Fig. 17.10(b), which is itself integrable, even though it is infinite at $t = 0$. We should therefore rewrite the integral in terms of $\ln|t|$ rather than $1/t$. To this end let us write $g'(t) = 1/t$. We now have $g(t) = \ln|t|$, and we may write

$$\langle t^{-1}, \phi \rangle = \int_{-\infty}^{\infty} \frac{\phi(t)}{t} dt = \langle g', \phi \rangle. \quad (17.190)$$

Now applying the distribution property

$$\langle g', \phi \rangle = - \langle g, \phi' \rangle \quad (17.191)$$

we have

$$\langle t^{-1}, \phi \rangle = \int_{-\infty}^{\infty} \frac{\phi(t)}{t} dt = - \int_{-\infty}^{\infty} \ln|t| \phi'(t) dt \quad (17.192)$$

and have thus obtained a definition of the distribution in terms of a convergent integral.

Higher powers k of t^{-k} can be expressed as successive derivatives of $1/t$. The first derivative of $1/t$ is $-1/t^2 = -t^{-2}$, the second derivative is $2t^{-3}$ and so on. We can write

$$\left(\frac{1}{t}\right)^k = \frac{(-1)^{k-1}}{(k-1)!} \left(\frac{1}{t}\right)^{(k-1)} \quad (17.193)$$

where

$$\left(\frac{1}{t}\right)^{(k-1)} = \frac{d^{k-1}}{dt^{k-1}} \left(\frac{1}{t}\right). \quad (17.194)$$

The distribution t^{-k} is thus defined by

$$\begin{aligned} \langle t^{-k}, \phi \rangle &= \int_{-\infty}^{\infty} t^{-k} \phi(t) dt = \frac{(-1)^{k-1}}{(k-1)!} \int_{-\infty}^{\infty} \left(\frac{1}{t}\right)^{(k-1)} \phi(t) dt \\ &= \frac{(-1)^{k-1}}{(k-1)!} \langle (t^{-1})^{(k-1)}, \phi \rangle. \end{aligned} \quad (17.195)$$

Using the property

$$\langle g^{(n)}, \phi \rangle = (-1)^n \langle g, \phi^{(n)} \rangle \quad (17.196)$$

we have

$$\int_{-\infty}^{\infty} \frac{\phi(t)}{t^k} dt = \frac{[(-1)^{k-1}]^2}{(k-1)!} \int_{-\infty}^{\infty} \frac{1}{t} \phi^{(k-1)}(t) dt = \frac{1}{(k-1)!} \int_{-\infty}^{\infty} \frac{1}{t} \phi^{(k-1)}(t) dt \quad (17.197)$$

or

$$\int_{-\infty}^{\infty} \frac{\phi(t)}{t^k} dt = \frac{1}{(k-1)!} \int_{-\infty}^{\infty} \ln |t| \phi^{(k)}(t) dt. \quad (17.198)$$

Example 17.10 Evaluate the integral

$$I = \int_{-\infty}^{\infty} \cos(\beta t) / t^2 dt$$

Using Equation (17.197) or the differentiation property Equation (17.196) we may write

$$I = \int_{-\infty}^{\infty} (1/t) (d \cos \beta t / dt) dt = -\beta \int_{-\infty}^{\infty} (1/t) \sin \beta t dt$$

Since

$$\int_{-\infty}^{\infty} \frac{\sin \tau}{\tau} d\tau = \pi$$

we obtain $I = -|\beta| \pi$.

17.22 Initial Derivatives of the Transform

The Fourier transform $F(j\omega)$ can be expanded in terms of its initial derivatives $F'(0)$, $F''(0)$, $F^{(3)}(0)$, \dots . The expression is instructive for several reasons. We first note that the exponential $e^{-j\omega t}$ in the transform

$$F(j\omega) = \int_{-\infty}^{\infty} f(t) e^{-j\omega t} dt \quad (17.199)$$

can itself be expanded using

$$e^z = 1 + z + \frac{z^2}{2!} + \frac{z^3}{3!} + \dots \quad (17.200)$$

so that

$$e^{-j\omega t} = 1 - j\omega t + \frac{(-j\omega t)^2}{2!} + \frac{(-j\omega t)^3}{3!} + \dots = \sum_{k=0}^{\infty} (-1)^k \frac{(j\omega t)^k}{k!} \quad (17.201)$$

$$F(j\omega) = \int_{-\infty}^{\infty} f(t) \sum_{k=0}^{\infty} \frac{(-j)^k (\omega t)^k}{k!} dt = \sum_{k=0}^{\infty} \frac{(-j)^k \omega^k}{k!} \int_{-\infty}^{\infty} f(t) t^k dt. \quad (17.202)$$

The integral on the right-hand side is known as the k^{th} moment denoted m_k of $f(t)$, so that

$$F(j\omega) = \sum_{k=0}^{\infty} \frac{(-j)^k \omega^k}{k!} m_k. \quad (17.203)$$

Now, using a MacLaurin series expansion we may write

$$F(j\omega) = \sum_{k=0}^{\infty} \frac{\omega^k}{k!} F^{(k)}(0). \quad (17.204)$$

Equating the coefficients of equal power in the last two equations we have

$$F^{(k)}(0) = (-j)^k m_k = (-j)^k \int_{-\infty}^{\infty} t^k f(t) dt \quad (17.205)$$

showing that the k^{th} derivative of $F(j\omega)$ at $\omega = 0$ is equal, apart from a factor, to the k^{th} moment of $f(t)$.

17.23 The Unit Step Function as a Limit

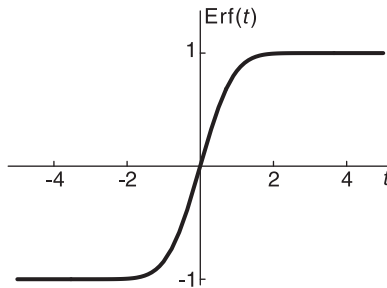


FIGURE 17.11 Error function.

The error function depicted in Fig. 17.11 is by definition the integral of the Gaussian function

$$\operatorname{erf} t = \frac{2}{\sqrt{\pi}} \int_0^t e^{-\tau^2} d\tau. \quad (17.206)$$

The Heaviside unit step function may be written as the limit of a sequence $f_n(t)$ of error functions,

$$f_n(t) = \sqrt{\frac{n}{\pi}} \int_{-\infty}^t e^{-n\tau^2} d\tau \quad (17.207)$$

and is therefore the integral of the scaled Gaussian function $g_n(t) = \sqrt{n/\pi} e^{-n\tau^2}$. The sequences of functions $g(n)$ and its integral $f(n)$ are shown for increasing values of n , namely, $n = 1$, $n = 2$, and $n = 8$, in Fig. 17.12.

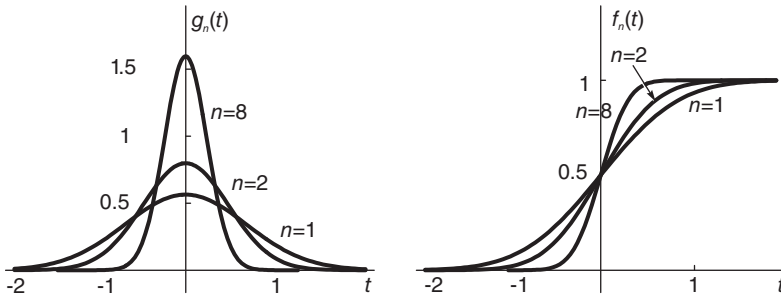


FIGURE 17.12 Gaussian function sequence and integral.

We note that as $n \rightarrow \infty$ the function $g_n(t)$ becomes narrower and higher in value, and $f_n(t)$, approaches the unit step function

$$\lim_{n \rightarrow \infty} f_n(t) = \sqrt{\frac{n}{\pi}} \int_{-\infty}^{\infty} e^{-n\tau^2} d\tau = 1. \quad (17.208)$$

The sequence of functions $f_n(t)$ thus tends to the unit step distribution $u(t)$

$$\lim_{n \rightarrow \infty} f_n(t) = u(t). \quad (17.209)$$

We note, moreover, that

$$u'(t) \triangleq \frac{d}{dt} u(t) = \delta(t) \quad (17.210)$$

and

$$\delta(t) = \int_{-\infty}^t u(t) dt. \quad (17.211)$$

We may also write

$$\lim_{n \rightarrow \infty} \sqrt{\frac{n}{\pi}} \int_{-\infty}^{\infty} e^{-nt^2} \phi(t) dt \simeq \lim_{n \rightarrow \infty} \sqrt{\frac{n}{\pi}} \phi(0) \int_{-\infty}^{\infty} e^{-nt^2} dt = \phi(0) \quad (17.212)$$

i.e.

$$\lim_{n \rightarrow \infty} \int_{-\infty}^{\infty} \sqrt{\frac{n}{\pi}} e^{-nt^2} \phi(t) dt = \phi(0) = \int_{-\infty}^{\infty} \delta(t) \phi(t) dt \quad (17.213)$$

wherefrom

$$\lim_{n \rightarrow \infty} \sqrt{\frac{n}{\pi}} e^{-nt^2} dt = \delta(t) \quad (17.214)$$

and

$$\lim_{n \rightarrow \infty} \int_{-\infty}^t \sqrt{\frac{n}{\pi}} e^{-nt^2} dt = \int_{-\infty}^t \delta(t) dt = u(t). \quad (17.215)$$

17.24 Inverse Fourier Transform and Gibbs Phenomenon

We investigate the inverse Fourier transform and the effect of function discontinuity. We recall from the scaling property that if a function $f(t)$ is compressed in time its spectrum $F(j\omega)$ is spread wider in frequency. A point of discontinuity of a function is the ultimate

in time compression, whereat the function jumps in value in zero time. This is reflected in the frequency domain as an infinitely wide spectrum required to produce in time such rapid transition.

We start by proving the inverse transform formula for continuous functions. We then focus our attention on function discontinuity and the result of applying the inverse transform at a point $t = t_0$ of discontinuity. The inverse transform relation implies that the exact value of the function at the immediate neighboring points $t = t_0^-$ and $t = t_0^+$ of the discontinuity are produced as long as the inverse transform is applied to the infinitely wide spectrum $F(j\omega)$. To view the process of convergence of the inverse transform toward the true function form $f(t)$ in the neighborhood of the discontinuity we investigate the effect of starting from a truncated spectrum and progressively adding spectral components. This leads us to Gibbs phenomenon. From the definition of the Fourier transform $F(j\omega)$ of a function $f(t)$

$$F(j\omega) = \int_{-\infty}^{\infty} f(t)e^{-j\omega t} dt \tag{17.216}$$

we can evaluate the inverse Fourier transform by multiplying both sides by $e^{j\omega\tau}$ and integrating with respect to ω

$$\int_{-\infty}^{\infty} F(j\omega) e^{j\omega\tau} d\omega = \int_{-\infty}^{\infty} \int_{-\infty}^{\infty} f(t) e^{-j\omega t} dt e^{j\omega\tau} d\omega \tag{17.217}$$

$$= \int_{-\infty}^{\infty} f(t) \int_{-\infty}^{\infty} e^{j\omega(\tau-t)} d\omega dt \tag{17.218}$$

using Equation (17.184)

$$\int_{-\infty}^{\infty} e^{j\omega t} d\omega = 2\pi\delta(t) \tag{17.219}$$

$$\int_{-\infty}^{\infty} F(j\omega) e^{j\omega\tau} d\omega = 2\pi \int_{-\infty}^{\infty} f(t)\delta(\tau - t) dt. \tag{17.220}$$

Interchanging t and τ we have

$$\int_{-\infty}^{\infty} F(j\omega) e^{j\omega t} d\omega = 2\pi \int_{-\infty}^{\infty} f(\tau)\delta(t - \tau) d\tau = 2\pi f(t) \tag{17.221}$$

where the last equality holds if and only if the function $f(t)$ is continuous at t . We have thus confirmed that under this condition the inverse transform is given by

$$f(t) = \frac{1}{2\pi} \int_{-\infty}^{\infty} F(j\omega) e^{j\omega t} d\omega. \tag{17.222}$$

We now consider the case where $f(t)$ has a jump discontinuity. Let $F_W(j\omega)$ be a truncation of the true spectrum $F(j\omega)$, as illustrated in Fig. 17.13.

$$F_W(j\omega) = F(j\omega)\Pi_W(\omega) = F(j\omega)[u(\omega + W) - u(\omega - W)]. \tag{17.223}$$

We have

$$\begin{aligned} f_W(t) &= \mathcal{F}^{-1} [F_W(j\omega)] = f(t) * \mathcal{F}^{-1} [\Pi_W(\omega)] = f(t) * \frac{W}{\pi} Sa(Wt) \\ &= \frac{W}{\pi} \int_{-\infty}^{\infty} f(\tau) Sa[W(t - \tau)] d\tau. \end{aligned} \tag{17.224}$$

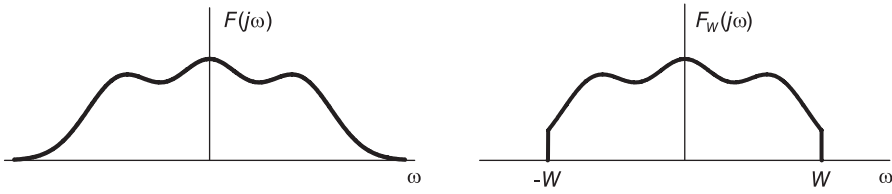


FIGURE 17.13 A spectrum and its truncation.

The function $f_W(t)$ is thus an approximation of $f(t)$ when the Fourier spectrum $F(j\omega)$ is truncated to include only the frequencies $-W < \omega < W$. By increasing W the function $f_W(t)$ tends in the limit to $f(t)$, for all t where $f(t)$ is continuous. Indeed,

$$\lim_{W \rightarrow \infty} f_W(t) = \frac{W}{\pi} \int_{-\infty}^{\infty} f(\tau) \lim_{W \rightarrow \infty} \text{Sa}[W(t - \tau)] d\tau = \int_{-\infty}^{\infty} f(\tau) \delta(t - \tau) d\tau = f(t) \tag{17.225}$$

using Equation (17.59). To show the corresponding relations in the case of a discontinuity, consider a function $f(t)$ that is continuous except for a jump discontinuity at, for simplicity, $t = 0$, as shown in Fig. 17.14. We can write

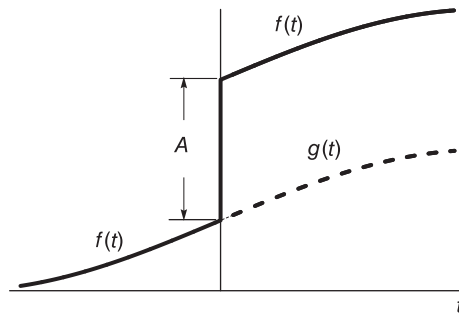


FIGURE 17.14 Function with discontinuity.

$$f(t) = g(t) + Au(t) \tag{17.226}$$

i.e. $f(t) = g(t)$, $t < 0$; $f(t) = g(t) + A$, $t > 0$, where $A = f(0^+) - f(0^-)$. We define $F_W(j\omega)$ as the truncated spectrum

$$F_W(j\omega) = F(j\omega)\Pi_W(\omega) \tag{17.227}$$

and observe the effect of increasing the bandwidth W . We have

$$f_W(t) = \frac{W}{\pi} \int_{-\infty}^{\infty} \left\{ g(\tau)\text{Sa}[W(t - \tau)] + A \int_{-\infty}^{\infty} u(\tau)\text{Sa}[W(t - \tau)] \right\} d\tau. \tag{17.228}$$

Hence

$$\begin{aligned} \lim_{W \rightarrow \infty} f_W(t) &= \int_{-\infty}^{\infty} g(\tau)\delta(t - \tau) d\tau + \lim_{W \rightarrow \infty} \frac{AW}{\pi} \int_0^{\infty} \text{Sa}[W(t - \tau)] d\tau. \\ &= g(t) + A \lim_{W \rightarrow \infty} u_W(t) \end{aligned} \tag{17.229}$$

where we use the notation

$$u_W(t) \triangleq \frac{W}{\pi} \int_0^\infty Sa[W(t - \tau)] d\tau \tag{17.230}$$

since $f_W(t)$ is the approximation of $f(t)$ as given by Equation (17.226). Letting $W(t - \tau) = \lambda$ we have

$$\begin{aligned} u_W(t) &= \frac{1}{\pi} \int_{-\infty}^{Wt} Sa(\lambda) d\lambda = \frac{1}{\pi} \int_{-\infty}^0 Sa(\lambda) d\lambda + \frac{1}{\pi} \int_0^{Wt} Sa(\lambda) d\lambda \\ &= \frac{1}{2} + \frac{1}{\pi} Si(Wt) \end{aligned} \tag{17.231}$$

where $Si(x) = \int_0^x Sa(t) dt$ is the sine integral function. The steeper rise of the approximation $u_W(t)$ as W increases can be seen in Fig. 17.15.

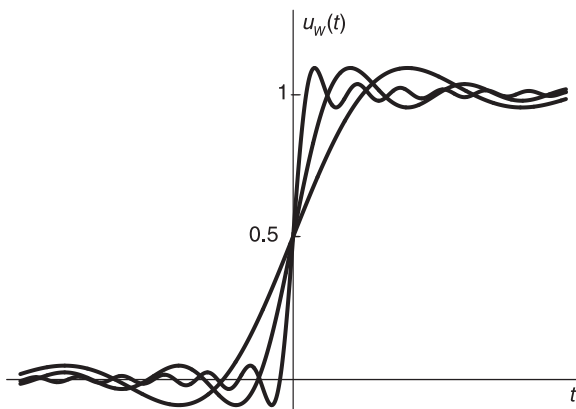


FIGURE 17.15 Unit step approximating sequence.

We conclude that

$$f(t) = \lim_{W \rightarrow \infty} f_w(t) = g(t) + \frac{A}{2} + \frac{A}{\pi} \lim_{W \rightarrow \infty} Si(Wt) \tag{17.232}$$

which at $t = 0$ equals $g(0) + A/2 = f(0^-) + A/2 = \{f(0^-) + f(0^+)\}/2$. The function $f_W(t)$ is sketched schematically in Fig. 17.16. The inverse transform at the point $t = 0$ is therefore equal to the middle value of the discontinuity jump, as stated in connection with Fourier series in Chapter 2. As W increase, however, the approximating function $Si(Wt)$ becomes increasingly more compressed but has the same form with no change in height. The ripples increase in frequency but in height remain the same as long as W remains finite. Only when W becomes infinite do ripples disappear and the inverse transform equals the value as $f(t)$ at all values of t where the function is continuous; including the points 0^- and 0^+ . This is known as Gibbs phenomenon.

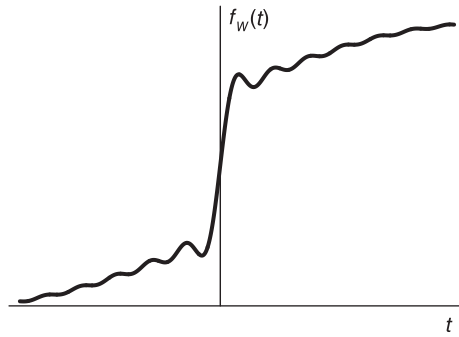


FIGURE 17.16 Convergence to a discontinuity.

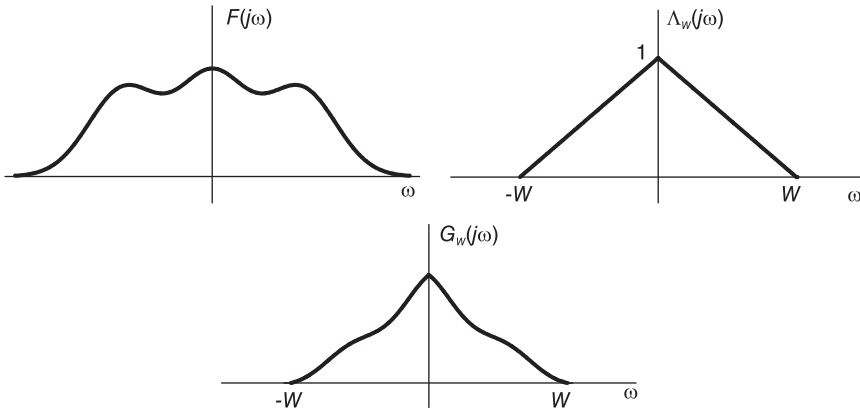


FIGURE 17.17 Spectral multiplication by a triangle.

17.25 Ripple Elimination

We conclude from Gibbs phenomenon that if the spectrum $F(j\omega)$ of a function is truncated to a bandwidth W then in the neighborhoods of a discontinuity the inverse Fourier transform $f_W(t)$ displays ripples near any function discontinuity. We have also noted that the overshoot and ripples are of the same amplitude however large, but finite, the value W . This may be viewed as a *Windowing* problem in the frequency domain. By applying a proper window we may obtain a smoother transition without ripples. For example a transition without overshoot can be obtained if the spectrum $F(j\omega)$ is multiplied by a triangular instead of a rectangular window, of width W , as shown in Fig. 17.17.

$$\Lambda_W(j\omega) = \begin{cases} 1 - \frac{|\omega|}{W}, & |\omega| < W \\ 0, & \text{otherwise.} \end{cases} \tag{17.233}$$

The truncated spectrum denoted by say $F_W(j\omega)$ is given by

$$F_W(j\omega) = F(j\omega)\Lambda_W(j\omega). \tag{17.234}$$

Its inverse transform is

$$\begin{aligned}
 f_W(t) &= f(t) * \mathcal{F}^{-1}[\Lambda_W(j\omega)] = f(t) * \frac{W}{2\pi} Sa^2\left[\frac{W}{2}t\right] \\
 &= \frac{W}{2\pi} \int_{-\infty}^{\infty} f(\tau) Sa^2\left[\frac{W}{2}(t-\tau)\right] d\tau.
 \end{aligned}
 \tag{17.235}$$

The function $f_W(t)$ has the form

$$f_W(t) = \int_{-\infty}^{\infty} f(\tau)x(\tau)d\tau.
 \tag{17.236}$$

The result is a convolution with the square of the sampling function known as the Fejér kernel. Such a convolution with a positive function implies that as a step discontinuity of $f(t)$ is traversed the resulting function $f_W(t)$ converges with no ripple to the value past the discontinuity of $f(t)$; as can be seen in Fig. 17.18.

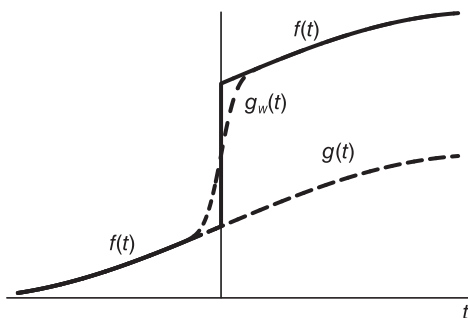


FIGURE 17.18 Ripple elimination at a discontinuity.

We also note that

$$\lim_{W \rightarrow \infty} f_W(t) = \int_{-\infty}^{\infty} f(\tau)\delta(t-\tau)d\tau = f(t)
 \tag{17.237}$$

since, by Equation (17.61)

$$\lim_{W \rightarrow \infty} \frac{W}{2\pi} Sa^2\left[\frac{W}{2}(t-\tau)\right] = \delta(t-\tau)
 \tag{17.238}$$

17.26 Transforms of $|t|$ and $tu(t)$

We have seen in Example 17.10 that

$$\int_{-\infty}^{\infty} \frac{\cos \omega t}{t^2} dt = -\pi|\omega|.
 \tag{17.239}$$

We deduce that

$$\int_{-\infty}^{\infty} \frac{e^{j\omega t}}{t^2} dt = \int_{-\infty}^{\infty} \frac{\cos \omega t}{t^2} dt = -\pi|\omega|
 \tag{17.240}$$

i.e.

$$1/t^2 \longleftrightarrow -\pi|\omega|. \tag{17.241}$$

Using duality we have

$$-\pi|t| \longleftrightarrow 2\pi/\omega^2 \tag{17.242}$$

$$|t| \longleftrightarrow -2/\omega^2. \tag{17.243}$$

We can further write

$$t + |t| = \begin{cases} 2t, & t > 0 \\ 0, & t < 0 \end{cases} = 2tu(t) \tag{17.244}$$

$$tu(t) = \frac{1}{2}(t + |t|) \tag{17.245}$$

$$tu(t) \longleftrightarrow j\pi\delta'(\omega) - 1/\omega^2. \tag{17.246}$$

17.27 The Impulse Train as a Limit

Consider the impulse train of period T shown in Fig. 17.19.

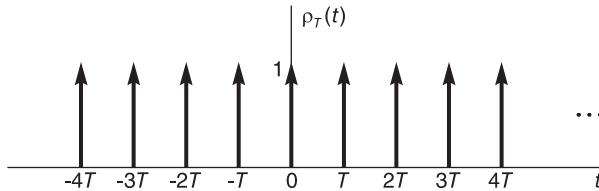


FIGURE 17.19 Impulse train.

$$f(t) = \rho_T(t) \triangleq \sum_{n=-\infty}^{\infty} \delta(t - nT). \tag{17.247}$$

Its Fourier series expansion is

$$\rho_T(t) = \frac{1}{T} \sum_{n=-\infty}^{\infty} e^{jn\omega_0 t} \tag{17.248}$$

and its Fourier transform is

$$\mathcal{F}[\rho_T(t)] = \omega_0 \sum_{n=-\infty}^{\infty} \delta(\omega - n\omega_0). \tag{17.249}$$

It is interesting to note that in as much as the impulse $\delta(t)$ is the limit of a sequence of sampling functions

$$\lim_{w \rightarrow \infty} \frac{w}{\pi} Sa(wt) = \delta(t) \tag{17.250}$$

the impulse train is the limit of a periodic repetition of sampling functions. To this end we consider the truncated sum

$$\rho_N(t) = \frac{1}{T} \sum_{n=-N}^N e^{jn\omega_0 t} \tag{17.251}$$

which is known as the Fourier series kernel, and show that its limit as $N \rightarrow \infty$ is the impulse train. Using the geometric sum

$$\sum_{n=n_1}^{n_2} a^n = a^{n_1} \frac{1 - a^{(n_2 - n_1 + 1)}}{1 - a} \tag{17.252}$$

we have

$$\rho_N(t) = \frac{1}{T} e^{-jN\omega_0 t} \frac{1 - e^{j(2N+1)\omega_0 t}}{1 - e^{j\omega_0 t}} = \frac{\sin[(N + 1/2)\omega_0 t]}{T \sin(\omega_0 t/2)} \tag{17.253}$$

as can be seen in Fig. 17.20.

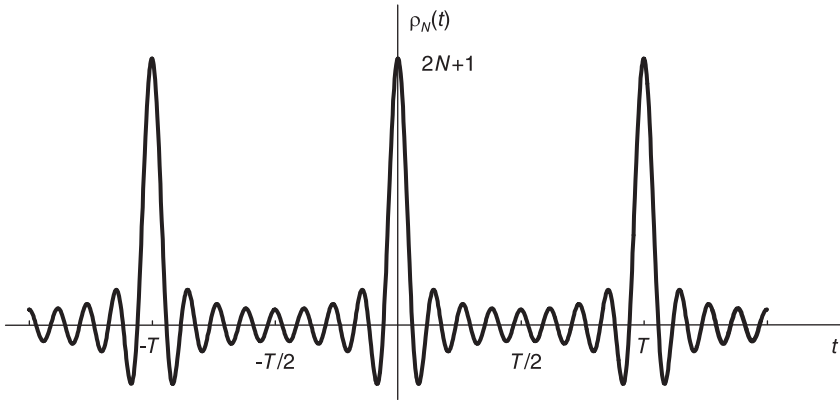


FIGURE 17.20 Periodic sampling function.

We note that $\rho_N(0) = \sum_{n=-N}^N 1 = 2N + 1$ and $\rho_N(t)$ is periodic with period T . We now consider the limit of the period of $\rho_N(t)$ lying between $t = -T/2$ and $t = T/2$. Writing $\rho_N(t)$ in the form

$$\rho_N(t) = \frac{1}{T} Sa[(N + 1/2)\omega_0 t] \frac{(N + 1/2)\omega_0 t}{\sin(\omega_0 t/2)} \tag{17.254}$$

we note that with

$$w = (N + 1/2)\omega_0 \tag{17.255}$$

$$\rho_N(t) = \frac{1}{T} Sa(wt) \frac{wt}{\sin(\omega_0 t/2)}. \tag{17.256}$$

Now $\lim_{w \rightarrow \infty} wSa(wt) = \pi\delta(t)$ so that

$$\begin{aligned} \lim_{N \rightarrow \infty} \rho_N(t) &= \lim_{w \rightarrow \infty} \frac{1}{T} wSa(wt) \frac{t}{\sin(\omega_0 t/2)} = \frac{t}{\sin(\omega_0 t/2)} \frac{\pi}{T} \delta(t) \\ &= \frac{t}{\sin(\omega_0 t/2)} \Big|_{t=0} \frac{\pi}{T} \delta(t). \end{aligned} \tag{17.257}$$

Using L'Hopital's rule we have

$$\lim_{t \rightarrow 0} \frac{t}{\sin(\omega_0 t/2)} = \frac{1}{(\omega_0/2) \cos(\omega_0 t/2)} \Big|_{t=0} = \frac{2}{\omega_0} = \frac{T}{\pi} \quad (17.258)$$

wherefrom

$$\lim_{N \rightarrow \infty} \rho_N(t) = \delta(t), \quad -T/2 \leq t \leq T/2. \quad (17.259)$$

We therefore conclude that the periodic sampling function train $\rho_N(t)$ tends in the limit, as $N \rightarrow \infty$, to the impulse train $\rho_T(t)$

$$\lim_{n \rightarrow \infty} \rho_N(t) = \rho_T(t). \quad (17.260)$$

17.28 Sequence of Distributions

As noted earlier, if a sequence of distributions $g(t)$ tends to a limit such that

$$\lim_{n \rightarrow \infty} \langle g_n, \phi \rangle = \lim_{n \rightarrow \infty} \int_{-\infty}^{\infty} g_n(t) \phi(t) dt = \int_{-\infty}^{\infty} g(t) \phi(t) dt = \langle g, \phi \rangle \quad (17.261)$$

then $g(t)$ is called the limit of $g_n(t)$,

$$g(t) = \lim_{n \rightarrow \infty} g_n(t). \quad (17.262)$$

Example 17.11 *The sequence*

$$g_n(t) = \frac{n}{\pi} \frac{1}{1 + n^2 t^2}$$

satisfies

$$\lim_{n \rightarrow \infty} \langle g_n, \phi \rangle = \lim_{n \rightarrow \infty} \frac{1}{\pi} \int_{-\infty}^{\infty} \frac{n \phi(t)}{1 + n^2 t^2} dt.$$

The right-hand side can be shown to equal $\phi(0)$.

$$\lim_{n \rightarrow \infty} \langle g_n, \phi \rangle = \phi(0) = \langle \delta, \phi \rangle$$

wherefrom

$$\lim_{n \rightarrow \infty} \left\{ \frac{n}{\pi} \frac{1}{1 + n^2 t^2} \right\} = \delta(t).$$

Other sequences that lead in the limit to the delta impulse are

$$g_n(t) = \frac{n}{\sqrt{\pi}} e^{-nt^2} \quad (17.263)$$

and

$$g_n(t) = \frac{n}{\pi} \text{Sa}^2(nt). \quad (17.264)$$

Similarly,

$$\lim_{n \rightarrow \infty} \left\{ \frac{n/\pi}{1 + n^2(t - t_o)^2} \right\} = \delta(t - t_o). \quad (17.265)$$

The limit of the differentiation $g'_n(t)$ is defined by

$$\begin{aligned} \lim_{n \rightarrow \infty} \langle g'_n, \phi \rangle &= \lim_{n \rightarrow \infty} \int_{-\infty}^{\infty} g'_n(t) \phi(t) dt \\ &= \lim_{n \rightarrow \infty} \left\{ g_n(t) \phi(t) \Big|_{-\infty}^{\infty} - \int_{-\infty}^{\infty} g_n(t) \phi'(t) dt \right\} \\ &= - \lim_{n \rightarrow \infty} \left\{ \int_{-\infty}^{\infty} g_n(t) \phi'(t) dt \right\} = - \int_{-\infty}^{\infty} g(t) \phi'(t) dt \\ &= - \langle g, \phi' \rangle. \end{aligned} \tag{17.266}$$

A distribution $g_\alpha(t)$ can also be defined as the limit of a distribution $g_x(t)$ as the parameter x tends to α . We write

$$g_\alpha(t) = \lim_{x \rightarrow \alpha} g_x(t) \tag{17.267}$$

if for every test function $\phi(t)$

$$\lim_{x \rightarrow \alpha} \langle g_x, \phi \rangle = \lim_{x \rightarrow \alpha} \int_{-\infty}^{\infty} g_x(t) \phi(t) dt = \int_{-\infty}^{\infty} g_\alpha(t) \phi(t) dt = \langle g_\alpha, \phi \rangle. \tag{17.268}$$

Example 17.12 *The sequence*

$$g_n(t) = \begin{cases} 1, & t > 1/n \\ n/2, & -1/n < t < 1/n \\ 0, & t < -1/n \end{cases}$$

represents the unit-step Heaviside distribution

$$\lim_{n \rightarrow \infty} g_n(t) = u(t)$$

since

$$\begin{aligned} \lim_{n \rightarrow \infty} \langle g_n, \phi \rangle &= \lim_{n \rightarrow \infty} \int_{-\infty}^{\infty} g_n(t) \phi(t) dt = \int_0^{\infty} \phi(t) dt \\ &= \int_{-\infty}^{\infty} u(t) \phi(t) dt = \langle u, \phi \rangle. \end{aligned}$$

Example 17.13 *The distribution*

$$g_\omega(t) = e^{-j\omega t}$$

has the limit as $\omega \rightarrow \infty$

$$\lim_{\omega \rightarrow \infty} g_\omega(t) = g_\infty(t) = 0$$

since

$$\lim_{\omega \rightarrow \infty} \int_{-\infty}^{\infty} e^{-j\omega t} \phi(t) dt = \lim_{\omega \rightarrow \infty} \Phi(j\omega) = 0$$

by a direct application of Riemann–Lebesgue lemma.

Example 17.14 *Letting*

$$g_\tau(t) = \frac{1}{\tau} \Pi_{\tau/2}(t).$$

We have

$$\lim_{\tau \rightarrow 0} \langle g_\tau, \phi \rangle = \lim_{\tau \rightarrow 0} \int_{-\tau/2}^{\tau/2} (1/\tau) \phi(t) dt = \lim_{\tau \rightarrow 0} \frac{1}{\tau} \phi(0) \int_{-\tau/2}^{\tau/2} dt = \phi(0) = \langle \delta, \phi \rangle$$

wherefrom

$$\lim_{\tau \rightarrow 0} \frac{1}{\tau} \Pi_{\tau/2}(t) = \delta(t).$$

Example 17.15 Let

$$g_\tau(t) = \frac{e^{-t^2/\tau}}{\sqrt{\pi\tau}}.$$

We have

$$\begin{aligned} \lim_{\tau \rightarrow 0} \langle g_\tau, \phi \rangle &= \lim_{\tau \rightarrow 0} \frac{1}{\sqrt{\pi\tau}} \int_{-\infty}^{\infty} e^{-t^2/\tau} \phi(t) dt \cong \frac{1}{\sqrt{\pi\tau}} \phi(0) \int_{-\infty}^{\infty} e^{-t^2/\tau} dt \\ &= \frac{1}{\sqrt{\pi\tau}} \phi(0) \sqrt{\pi\tau} = \phi(0) = \langle \delta, \phi \rangle \end{aligned}$$

so that

$$\lim_{\tau \rightarrow 0} \left\{ \frac{e^{-t^2/\tau}}{\sqrt{\pi\tau}} \right\} = \delta(t).$$

17.29 Poisson's Summation Formula

Let $\phi(t)$ be a real function of Fourier transform $\Phi(j\omega)$. Let $\psi(t)$ be the periodic repetition of $\phi(t)$ with period T , i.e.

$$\psi(t) = \sum_{n=-\infty}^{\infty} \phi(t + nT). \quad (17.269)$$

We can also write $\psi(t) = \phi(t) * \sum_{n=-\infty}^{\infty} \delta(t - nT)$ and its transform

$$\Psi(j\omega) = \Phi(j\omega) \omega_0 \sum_{n=-\infty}^{\infty} \delta(\omega - n\omega_0) = \omega_0 \sum_{n=-\infty}^{\infty} \Phi(jn\omega_0) \delta(\omega - n\omega_0) \quad (17.270)$$

where $\omega_0 = 2\pi/T$.

Taking the inverse transform of both sides we have

$$\sum_{n=-\infty}^{\infty} \phi(t + nT) = \frac{1}{T} \sum_{n=-\infty}^{\infty} \Phi(jn\omega_0) e^{jn\omega_0 t}. \quad (17.271)$$

This is Poisson's summation formula. It also appears in the form

$$\sum_{n=-\infty}^{\infty} \phi(nT) = \frac{1}{T} \sum_{n=-\infty}^{\infty} \Phi(jn\omega_0) \quad (17.272)$$

which is obtained by setting $t = 0$.

Example 17.16

$$f(t) = e^{-\alpha|t|}, \quad \alpha > 0.$$

We have obtained

$$F(j\omega) = \frac{2/\alpha}{1 + \omega^2}.$$

In particular

$$e^{-|t|} \longleftrightarrow \frac{2}{1 + \omega^2}.$$

From the Poisson summation formula we have

$$\begin{aligned} \sum_{m=-\infty}^{\infty} e^{-|mT|} &= \frac{1}{T} \sum_{k=-\infty}^{\infty} \frac{2}{1 + (k\omega_0)^2}, \quad \omega_0 = 2\pi/T \\ &= 2 \sum_{k=-\infty}^{\infty} \frac{T}{T^2 + 4\pi^2 k^2} \end{aligned}$$

and both sides being even functions, we have

$$\frac{1}{2} + \sum_{m=1}^{\infty} e^{-mT} = \frac{1}{T} + 2 \sum_{k=1}^{\infty} \frac{T}{T^2 + 4\pi^2 k^2}.$$

Note that the left-hand side is given by

$$\begin{aligned} \frac{1}{2} + e^{-T} \frac{1}{1 - e^{-T}} &= \frac{1 - e^{-T} + 2e^{-T}}{2(1 - e^{-T})} = \frac{1 + e^{-T}}{2(1 - e^{-T})} = \frac{1}{2} \frac{e^{T/2} + e^{-T/2}}{e^{T/2} - e^{-T/2}} \\ &= \frac{1}{2} \coth(T/2). \end{aligned}$$

We have thus obtained the series sum

$$1 + 2 \sum_{k=1}^{\infty} \frac{T^2}{T^2 + 4\pi^2 k^2} = \frac{T}{2} \coth\left(\frac{T}{2}\right).$$

The Poisson summation formula leads often to a simple expression for series sums.

17.30 Moving Average

An approach to time domain smoothing of a function $f(t)$ which produces its average over a time window that slides with t . The smoothed function denoted by $\bar{f}(t)$ may be written in the form

$$\bar{f}(t) = \frac{1}{2T} f(t) * \Pi_T(t) = \frac{1}{2T} \int_{t-T}^{t+T} f(\tau) d\tau. \tag{17.273}$$

To see the effect of the moving average on smoothing a discontinuity consider the step function $f(t) = u(t)$. The convolution of $f(t)$ with $\{\Pi_T(t)/(2T)\}$ is performed as shown in Fig. 17.21(a). The resulting averaged function $\bar{f}(t)$ is shown in Fig. 17.21(b). The transform of $\bar{f}(t)$ is given by

$$\bar{F}(j\omega) = F(j\omega) Sa(T\omega). \tag{17.274}$$

Suppose now we truncate the spectrum $\bar{F}(j\omega)$ above a frequency $|\omega| = B$ obtaining

$$\bar{F}_B(j\omega) = \bar{F}(j\omega) \Pi_B(\omega) \tag{17.275}$$

$$\bar{f}_B(t) = \bar{f}(t) * (B/\pi) Sa(Bt) = \frac{B}{\pi} \int_{-\infty}^{\infty} \bar{f}(\tau) Sa[B(t - \tau)] d\tau. \tag{17.276}$$

which is the weighted average of $\bar{f}(t)$, with the Fourier kernel $(B/\pi) Sa[B(t - \tau)]$ as the weighting function. As $B \rightarrow \infty$ this kernel tends to $\delta(t - \tau)$, so that

$$\lim_{B \rightarrow \infty} \bar{f}_B(t) = \int_{-\infty}^{\infty} \bar{f}(\tau) \delta(t - \tau) d\tau = \bar{f}(t) * \delta(t) = \bar{f}(t). \tag{17.277}$$

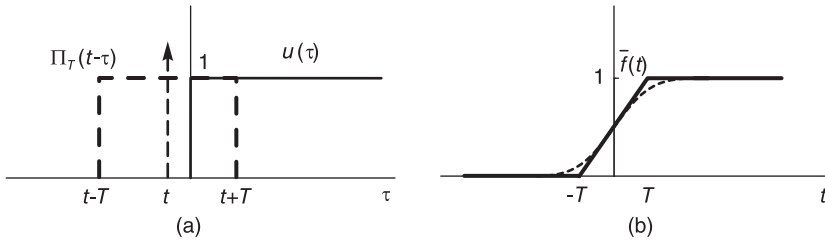


FIGURE 17.21 Moving average evaluation.

In other words, for a large enough value B the function $\bar{f}_B(t)$ is a good approximation, and since $\bar{f}(t)$ is continuous for all t the approximation has no overshoot, as represented by the dashed curve seen in Fig. 17.21(b).

17.31 Problems

Problem 17.1 Show that $\delta(t)$ is even.

Problem 17.2 Evaluate the distribution $f(t)$ if $tf(t) = 0$.

Problem 17.3 Evaluate $u^{(k)} = \frac{d^k}{dt^k}u(t)$, where $u(t)$ is the Heaviside unit step function.

Problem 17.4 Show that $\langle \delta_n, f \rangle \xrightarrow{n \rightarrow \infty} \langle \delta, f \rangle = f(0)$, where $\delta_n(t) = n\Pi_{1/(2n)}(t)$.

Problem 17.5 Reduce the expressions

- $\delta(-t - 5)$.
- $(t - t_0)\delta(t - t_0)$.
- $\int_{-\infty}^{\infty} \delta'(t - t_0)\phi(t)dt$.
- $\int_{-\infty}^{\infty} \delta''(t - t_0)\phi(t)dt$.
- $\int_{-\infty}^{\infty} \delta^{(n)}(t - t_0)\phi(t)dt$.

Problem 17.6 Evaluate the distribution

- $\int_{-\infty}^{\infty} \delta'(t - t_0)f(t)\phi(t)dt$.
- $f(t)\delta'(t)$.
- $f(t)\delta''(t)$.
- $f(t)\delta^{(3)}(t)$.
- $f(t)\delta^{(n)}(t)$.
- $t\delta'(t)$.

Problem 17.7 Evaluate the distribution

- $\int_{-\infty}^{\infty} \delta'(t)dt$.
- $\delta(t^2 - 4)$.
- $\delta(\cos t)$.
- $\delta(\sin t)$.

Problem 17.8 Evaluate the distribution

$$\int_{-\infty}^{\infty} e^{j\omega t}d\omega.$$

Problem 17.9 Evaluate the distribution

- a) $(\sin 2t - 2 \cos 3t)\delta t$.
 b) $\int_{-\infty}^{\infty} (t + 5)^2 e^{3t} \cos(2t)\delta(t)dt$.
 c) $\int_{-\infty}^{\infty} t^3 \sum_{n=1}^m \delta(t - n)dt$.

Problem 17.10 Evaluate the distribution

- a) $\frac{d}{dt} [u(-1 - t) - 2u(t - 1)]$.
 b) $\frac{d}{dt} [\sin 2t \{1 - 2u(t - 1)\}]$.

Problem 17.11 Evaluate the distribution

$$\frac{d}{dt} \{[2u(t - t_0) - u(2t_0 - t)] \cos 2t\} \quad ; \quad t_0 = \pi/2.$$

Problem 17.12 Evaluate the distribution

$$\int_{-\infty}^{\infty} 8 \cos 4\pi t \delta(t^2 - 4)dt.$$

Problem 17.13 Evaluate the distribution

$$\int_{-\pi}^{\pi} e^t \delta(\cos t)dt.$$

Problem 17.14 Evaluate the distribution

- a) $\int_{-\infty}^{\infty} \cos 3t \delta(3t - \pi)dt$.
 b) $\int_0^2 \cosh 2t \delta(3 - 2t)dt$.

Problem 17.15 Evaluate the distribution $\int_{-\infty}^{\infty} \cos t \delta(\sin t)dt$.

Problem 17.16 Evaluate the distribution

- a) $\int_{-\infty}^{\infty} \{t^2 + 3e^t \sin 2t\} \delta'(t)dt$.
 b) $\int_{-\infty}^{\infty} \sin 2t \delta''(t - 3\pi/4)dt$.

Problem 17.17 Deduce the derivative of the product of the distribution $\gamma(t)$ and an ordinary function $f(t)$ by evaluating $\langle (\gamma f)', \phi \rangle$.

Problem 17.18 With $u_{-1}(t) = u(t)$ and $u_0(t) = \delta(t)$, evaluate $u_{-2}(t)$, $u_{-3}(t)$, ..., $u_{-k}(t)$.

Problem 17.19 With $u_{-1}(t) = u(t)$ and $u_0(t) = \delta(t)$, evaluate $u_1(t)$, $u_2(t)$, ..., $u_k(t)$.

Problem 17.20 Show that $\delta'(t) = -\delta(t)/t$.

Problem 17.21 Evaluate $\langle \delta', \phi \rangle$, $\langle \delta'(t - \tau), \phi \rangle$.

Problem 17.22 Show that if $y(t) = \int_{-\infty}^{\infty} f(\tau)g(t - \tau)d\tau = f * g$ then

$$y(t - t_0) = f * g(t - t_0) = f(t - t_0) * g.$$

Problem 17.23 Show that if $y(t) = f * g$ then

$$y'(t) = f * g'(t) = f'(t) * g.$$

Problem 17.24 Evaluate $y'(t)$ if $y = f * \delta$.

Problem 17.25 Evaluate

- a) $u_{-1} * u_{-1}$.
 b) $u_{-1}(t) * u_{-k}(t)$.
 c) $u_{-2}(t) * u_{-k}(t)$.
 d) Deduce $u_{-m}(t) * u_{-k}(t)$, $m, k > 0$.

Problem 17.26 Evaluate $u_k * u_m$ where $u_k = \delta^{(k)}$; $k, m \geq 0$.

Problem 17.27 Show that

$$f(t) * g(t) = y(t) \longrightarrow f(t - t_1) * g(t - t_2) = y[t - (t_1 + t_2)].$$

17.32 Answers to Selected Problems

Problem 17.1

$$\delta(at) = \frac{1}{|a|}\delta(t) \Rightarrow \delta(-t) = \delta(t).$$

Problem 17.3

$$\langle u^{(k)}, \phi \rangle = \langle \delta^{(k-1)}, \phi \rangle = (-1)^{k-1} \phi^{(k-1)}(0).$$

Problem 17.5

- $\delta(-t-5) = \delta(t+5)$
- $(t-t_0)\delta(t-t_0) = 0$
- $\int_{-\infty}^{+\infty} \delta'(t-t_0)\phi(t)dt = -\phi'(t_0)$
- $\int_{-\infty}^{+\infty} \delta''(t-t_0)\phi(t)dt = \phi''(t_0)$
- $\int_{-\infty}^{+\infty} \delta^{(n)}(t-t_0)\phi(t)dt = (-1)^n \phi^{(n)}(t_0)$

Problem 17.6

- $\int_{-\infty}^{\infty} \delta'(t-t_0)f(t)\phi(t)dt = -f(0)\phi'(0) - f'(0)\phi(0)$
- $f(t)\delta'(t) = -f'(0)\delta(t) + f(0)\delta'(t)$
- $f(t)\delta''(t) = f(0)\delta''(t) - 2f'(0)\delta'(t) + f''(0)\delta(t)$
- $f(t)\delta^{(3)}(t) = f(0)\delta^{(3)}(t) - 3f'(0)\delta''(t) + 3f''(0)\delta'(t) - f^{(3)}(0)\delta(t)$
- $f(t)\delta^{(n)}(t) = \sum_{k=0}^n (-1)^k \frac{n!}{k!(n-k)!} f^{(k)}(0)\delta^{(n-k)}(t)$
- $t\delta'(t) = -\delta(t)$

Problem 17.7

- $\int_{-\infty}^{\infty} \delta'(t)dt = 0$
- $\delta(t^2-4) = 1/4[\delta(t-2) + \delta(t+2)]$
- $\delta(\cos t) = \sum_{n=-\infty}^{\infty} \delta[t - (2n+1)\pi/2] = \sum_{n=\text{odd}} \delta(t - n\pi/2)$
- $\delta(\sin t) = \sum_{n=-\infty}^{\infty} \delta(t - n\pi)$

Problem 17.8 $\int_{-\infty}^{+\infty} e^{j\omega t} d\omega = 2\pi\delta(t)$

Problem 17.9

- $(\sin 2t - 2\cos 3t)\delta t = -2$
- $\int_{-\infty}^{\infty} (t+5)^2 e^{3t} \cos(2t)\delta(t)dt = \int_{-\infty}^{\infty} 25\delta(t)dt = 25$
- $\int_{-\infty}^{\infty} t^3 \sum_{n=1}^m \delta(t-n)dt = \sum_{n=1}^m n^3 = m^2(m+1)^2/4$

Problem 17.10

- $(d/dt)[u(-1-t) - 2u(t-1)] = -\delta(-1-t) - 2\delta(t-1)$
- $(d/dt)[\sin 2t\{1 - 2u(t-1)\}] = 2\cos 2t - 2\sin 2t\delta(t-1) - 4\cos 2tu(t-1)$

Problem 17.11

$$\{[2u(t-t_0) - u(2t_0-t)]\cos 2t\}' = -2\sin 2t[2u(t-\pi/2) - u(\pi-t)] - 2\delta(t-\pi/2) + \delta(t-\pi)$$

Problem 17.12

$$\int_{-\infty}^{\infty} 8 \cos 4\pi t \delta(t^2 - 4) dt = 4$$

Problem 17.13

$$\int_{-\pi}^{\pi} e^t \delta(\cos t) dt = \cosh(\pi/2)$$

Problem 17.14

- a) $\int_{-\infty}^{\infty} \cos 3t \delta(3t - \pi) dt = -1/3$
 b) $\int_0^{\infty} \cosh 2t \delta(3 - 2t) dt = (1/2) \cosh 3.$

Problem 17.15

$$\int_{-\infty}^{\infty} \cos t \delta(\sin t) dt = \sum_{n=-\infty}^{\infty} (-1)^n \delta(t - n\pi)$$

Problem 17.16

- a) $\int_{-\infty}^{\infty} \{t^2 + 3e^t \sin 2t\} \delta'(t) dt = -6.$
 b) $\int_{-\infty}^{\infty} \sin 2t \delta''(t - 3\pi/4) dt = 4.$

Problem 17.18

$$u_{-2} = tu_{-1}(t), \quad u_{-3}(t) = \frac{t^2}{2} u_{-1}(t), \quad u_{-4}(t) = \frac{t^3}{6} u_{-1}(t), \quad u_{-k}(t) = \frac{t^{k-1}}{(k-1)!} u_{-1}(t).$$

Problem 17.19

$$u_0(t) = \frac{d}{dt} u_{-1}(t), \quad u_1(t) = \frac{d}{dt} u_0(t) = \delta'(t), \quad u_2(t) = \frac{d}{dt} u_1(t) = \delta''(t), \quad u_k(t) = \delta^{(k)}(t).$$

Problem 17.21

$$\begin{aligned} \langle \delta', \phi \rangle &= -\langle \delta, \phi' \rangle = -\phi'(0) \\ \langle \delta'(t - \tau), \phi \rangle &= -\langle \delta(t - \tau), \phi' \rangle = -\phi'(\tau) \end{aligned}$$

Problem 17.23

$$\begin{aligned} y'(t) &= \frac{d}{dt} \int_{-\infty}^{\infty} f(\tau) g(t - \tau) d\tau \\ &= \int_{-\infty}^{\infty} f(\tau) g'(t - \tau) d\tau \\ &= f * g' \end{aligned}$$

Problem 17.24

$$\begin{aligned} y &= f \quad y' = f' \\ y' &= f * \delta' = f' * \delta \\ \Rightarrow f * \delta' &= f' * \delta = f' \end{aligned}$$

Problem 17.25

- a) $u_{-1} * u_{-1} = u_{-2}(t)$
 b) $u_{-1}(t) * u_{-k}(t) = u_{-(k+1)}(t)$
 c) $u_{-2}(t) * u_{-k}(t) = u_{-(k+2)}(t).$

Problem 17.26

$$u_n * u_k = u_{n+k} = \delta^{(n+k)}.$$

This page intentionally left blank

Generalization of Distributions Theory, Extending Laplace-, z - and Fourier-Related Transforms

18.1 Introduction

This chapter summarizes the results of a recently proposed generalization of the Dirac-delta impulse and the theory of distributions. The generalization leads to a considerable expansion of the domains of existence of Laplace, z - and Fourier-related transforms, such as Hilbert, Hartley and Mellin transforms.

The question may be asked as to why present such topics near the end, rather than the beginning, of this book? The answer to this question is that presenting such new “radical” concepts to a student who is learning the basics of the subject of signals, systems and transforms would be asking too much too soon. The concepts would be better appreciated if the student learned the classical approach, was able to compare what is presented with similar coverage in other books in the literature and, possibly, discovered himself the need for improvement.

It is for this reason that in this book a choice was made to present the subject as it is presented in the literature and, now that the student has been fortified with solid knowledge of the domain, reveal such important new developments that should lead to the rewriting of the transforms.

In recent papers [21] [23] and [27], such a generalization of distribution theory was proposed. New transforms are introduced and some basic transforms are rewritten. The generalization of distribution theory starts with the introduction of generalized Dirac-delta impulses and their families of integrals and derivatives in Laplace and z -transform domains. The purpose of this chapter is to present a simplified summary of these recent developments.

18.2 An Anomaly

A review of the state of art in the literature on transforms, would reveal that whereas for a large class of basic infinite duration two-sided functions and sequences such as a constant or a simple pure sinusoid the Fourier transform exists, the more general Laplace and z -transform do not [1] [39] [42] [56] [58] [62] [63] [64] [70] [73]. The fact that for some functions the Fourier transform exists whereas the more general Laplace and z -transforms do not may be viewed as an anomaly. The effect of such anomaly is that in contrast with the Fourier transform, the literature dealing with Laplace and z -transform show transforms of right-sided or left-sided functions or sums thereof, but no true two-sided infinite duration function. In what follows we summarize the recent generalizations, rewrite some important

transforms and introduce the new extended Laplace and z -transforms which were hitherto nonexistent.

18.3 Generalized Distributions for Continuous-Time Functions

A generalized distribution $G(s)$, associated with the continuous-time domain and transforms such as Laplace, is a generalized function of a complex variable $s = \sigma + j\omega$, which may be defined as an integral along a straight line contour in the s plane extending from a point $s = \sigma - j\infty$ to $s = \sigma + j\infty$ of the product of $G(s)$ with a test function $\Phi(s)$. For convenience we refer to this integral by the symbol $I_G[\Phi(s)]$, or simply $I_G[\Phi]$, and use the shorthand notation

$$I_G[\Phi(s)] = \langle G(s), \Phi(s) \rangle_{\Re[s]=\sigma} = \int_{\sigma-j\infty}^{\sigma+j\infty} G(s) \Phi(s) ds. \quad (18.1)$$

The test function $\Phi(s)$ has derivatives of any order along such a contour line in the s plane, and tends to zero more rapidly than any power of $|s|$. In what follows to lighten the notation we will sometimes write $\langle G(s), \Phi(s) \rangle$, meaning $\langle G(s), \Phi(s) \rangle_{\Re[s]=\sigma}$.

As proposed in [21] and [23], the Dirac-delta impulse may be generalized, leading to a distribution that is a generalized function of a complex variable. The generalized impulse may be denoted $\xi(s)$ being a function of the complex variable s . We may define such a generalized Dirac-delta impulse by writing

$$I_G[\Phi(s)] = \langle \xi(s), \Phi(s) \rangle_{\Re[s]=\sigma} = \int_{\sigma-j\infty}^{\sigma+j\infty} \xi(s) \Phi(s) ds = \begin{cases} j\Phi(0), & \sigma = 0 \\ 0, & \sigma \neq 0. \end{cases} \quad (18.2)$$

18.3.1 Properties of Generalized Distributions in s Domain

The following properties are generalizations of properties of the usual real-variable distributions, and can be proven similarly to the corresponding proofs of the well-known theory of generalized functions.

18.3.2 Linearity

$$\langle G(s), a_1\Phi_1(s) + a_2\Phi_2(s) \rangle = a_1 \langle G(s), \Phi_1(s) \rangle + a_2 \langle G(s), \Phi_2(s) \rangle \quad (18.3)$$

$$\langle G_1(s) + G_2(s), \Phi(s) \rangle = \langle G_1(s), \Phi(s) \rangle + \langle G_2(s), \Phi(s) \rangle. \quad (18.4)$$

18.3.3 Shift in s

Consider the generalized distribution $G(s - s_0)$. We can write

$$\langle G(s - s_0), \Phi(s) \rangle_{\Re[s]=\sigma} = \int_{\sigma-j\infty}^{\sigma+j\infty} G(s - s_0) \Phi(s) ds. \quad (18.5)$$

Let $s - s_0 = y$, $ds = dy$ we obtain

$$\langle G(s - s_0), \Phi(s) \rangle_{\Re[s]=\sigma} = \langle G(y), \Phi(y + s_0) \rangle_{\Re[y]=\sigma - s_0}. \quad (18.6)$$

18.3.4 Scaling

Let $\gamma \neq 0$ be a real constant. We can write

$$\langle G(\gamma s), \Phi(s) \rangle_{\Re[s]=\sigma} = \int_{\sigma-j\infty}^{\sigma+j\infty} G(\gamma s)\Phi(s) ds. \tag{18.7}$$

Letting $\gamma s = y, \gamma ds = dy$ we obtain

$$\begin{aligned} \langle G(\gamma s), \Phi(s) \rangle_{\Re[s]=\sigma} &= \int_{\gamma\sigma-j\infty}^{\gamma\sigma+j\infty} G(y)\Phi(y/\gamma) dy/\gamma \\ &= \frac{1}{|\gamma|} \langle G(y), \Phi(y/\gamma) \rangle_{\Re[y]=\gamma\sigma}. \end{aligned} \tag{18.8}$$

Consider the product $G(s)F(s)$. We can write

$$\langle G(s)F(s), \Phi(s) \rangle_{\Re[s]=\sigma} = \langle G(s), F(s)\Phi(s) \rangle_{\Re[s]=\sigma} \tag{18.9}$$

if $F(s)\Phi(s) \in C$, the class of test functions.

18.3.5 Convolution

Denoting by $G_1(s)*G_2(s)$ the convolution of two generalized distributions, with $y = \Sigma + j\Omega$, we may write

$$\begin{aligned} &\langle G_1(s) * G_2(s), \Phi(s) \rangle_{\Re[s]=\sigma} \\ &= \langle \int_{\Sigma-j\infty}^{\Sigma+j\infty} G_1(y)G_2(s-y) dy, \Phi(s) \rangle_{\Re[s]=\sigma} \\ &= \langle G_1(y), \int_{\sigma-j\infty}^{\sigma+j\infty} G_2(s-y)\Phi(s) ds \rangle_{\Re[y]=\Sigma} \end{aligned}$$

the integral on the right, being in the form of a convolution with a test function, belongs to the class of test functions.

18.3.6 Differentiation

$$\langle G'(s), \Phi(s) \rangle_{\Re[s]=\sigma} = \int_{\sigma-j\infty}^{\sigma+j\infty} G'(s)\Phi(s) ds. \tag{18.10}$$

Integrating by parts we obtain

$$\begin{aligned} \langle G'(s), \Phi(s) \rangle_{\Re[s]=\sigma} &= G(s)\Phi(s)|_{\sigma-j\infty}^{\sigma+j\infty} - \int_{\sigma-j\infty}^{\sigma+j\infty} G(s)\Phi'(s) ds \\ &= - \langle G(s), \Phi'(s) \rangle_{\Re[s]=\sigma} \end{aligned} \tag{18.11}$$

and, by repeated differentiation,

$$\langle G^{(n)}(s), \Phi(s) \rangle_{\Re[s]=\sigma} = (-1)^n \langle G(s), \Phi^{(n)}(s) \rangle_{\Re[s]=\sigma}. \tag{18.12}$$

18.3.7 Multiplication of Derivative by an Ordinary Function

Consider the product $G'(s)F(s)$. We can write

$$\langle G'(s)F(s), \Phi(s) \rangle_{\Re[s]=\sigma} = \int_{\sigma-j\infty}^{\sigma+j\infty} G'(s)F(s)\Phi(s) ds. \quad (18.13)$$

Integrating by parts we obtain

$$\langle G'(s)F(s), \Phi(s) \rangle = - \langle G(s), F(s)\Phi'(s) \rangle - \langle G(s), F'(s)\Phi(s) \rangle. \quad (18.14)$$

18.4 Properties of the Generalized Impulse in s Domain

The following properties of the generalized Dirac-delta impulse are easily established [21] [23].

$$\langle \xi(\gamma s), \Phi(s) \rangle_{\Re[s]=\sigma} = \frac{1}{|\gamma|} \langle \xi(y), \Phi(y/\gamma) \rangle_{\Re[y]=\gamma\sigma} \quad (18.15)$$

$$\langle \xi(\gamma s), \Phi(s) \rangle = \begin{cases} \frac{1}{|\gamma|} \int_{\gamma\sigma-j\infty}^{\gamma\sigma+j\infty} \xi(y) \Phi(y/\gamma) dy = \frac{j}{|\gamma|} \Phi(0), & \sigma = 0 \\ 0, & \sigma \neq 0 \end{cases} \quad (18.16)$$

wherefrom

$$\xi(\gamma s) = \frac{1}{|\gamma|} \xi(s). \quad (18.17)$$

18.4.1 Shifted Generalized Impulse

We can write

$$\begin{aligned} \langle \xi(s-s_0), \Phi(s) \rangle_{\Re[s]=\sigma} &= \langle \xi(y), \Phi(y+s_0) \rangle_{\Re[y]=\sigma-s_0} \\ &= \begin{cases} j\Phi(s_0), & \sigma = \sigma_0 \\ 0, & \sigma \neq \sigma_0. \end{cases} \end{aligned} \quad (18.18)$$

18.4.2 Differentiation

Applying the differentiation property obtained in Equation (18.12) above, with $G(s) = \xi(s)$, we have

$$\begin{aligned} \langle \xi^{(n)}(s-s_0), \Phi(s) \rangle_{\Re[s]=\sigma} &= (-1)^n \langle \xi(s-s_0), \Phi^{(n)}(s) \rangle_{\Re[s]=\sigma} \\ &= \begin{cases} (-1)^n j^n \Phi^{(n)}(s_0), & \sigma = \sigma_0 \\ 0, & \sigma \neq \sigma_0. \end{cases} \end{aligned} \quad (18.19)$$

18.4.3 Convolution

Let $G_1(s) = \xi(s-a)$ and $G_2(s) = \xi(s-b)$, where $a = a_r + ja_i$ and $b = b_r + jb_i$.

Applying the convolution property we have

$$\begin{aligned}
 I &= \langle \xi(s-a) * \xi(s-b), \Phi(s) \rangle_{\Re[s]=\sigma} \\
 &= \langle \xi(y-a), \int_{\sigma-j\infty}^{\sigma+j\infty} \xi(s-y-b)\Phi(s) ds \rangle_{\Re[y]=\Sigma} \\
 &= \begin{cases} \langle \xi(y-a), j\Phi(y+b) \rangle_{\Re[y]=\Sigma}, & \sigma = \Re[y+b] = \Sigma + b_r \\ 0, & \sigma \neq \Sigma + b_r \end{cases} \quad (18.20) \\
 &= \begin{cases} -\Phi(a+b), & \sigma = a_r + b_r \\ 0, & \sigma \neq a_r + b_r \end{cases}
 \end{aligned}$$

i.e. $I = j \langle \xi[s - (a + b)], \Phi(s) \rangle_{\Re[s]=\sigma}$ wherefrom

$$\xi(s-a) * \xi(s-b) = j\xi[s - (a + b)]. \quad (18.21)$$

Two generalized impulses and their convolution are represented graphically in Fig. 18.1.

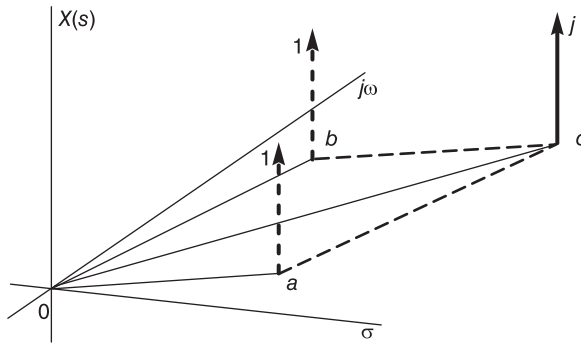


FIGURE 18.1 Convolution of two generalized impulses.

18.4.4 Convolution with an Ordinary Function

Consider the convolution of $G_1(s) = \xi(s - s_0)$ with an ordinary function $F(s)$. Writing, with $s_0 = \sigma_0 + j\omega_0$

$$\begin{aligned}
 &\langle \xi(s - s_0) * F(s), \Phi(s) \rangle_{\Re[s]=\sigma} \\
 &= \int_{\sigma-j\infty}^{\sigma+j\infty} \int_{\Sigma-j\infty}^{\Sigma+j\infty} F(y)\xi(s-y-s_0)dy\Phi(s) ds \\
 &= \int_{\Sigma-j\infty}^{\Sigma+j\infty} F(y) \int_{\sigma-j\infty}^{\sigma+j\infty} \xi(s-y-s_0)\Phi(s) ds dy.
 \end{aligned}$$

From Equation (18.18) the value of this integral is

$$I = \begin{cases} j \int_{\Sigma-j\infty}^{\Sigma+j\infty} F(y)\Phi(y+s_0) dy, & \sigma = \Re[y+s_0] = \Sigma + \sigma_0 \\ 0, & \sigma \neq \Sigma + \sigma_0 \end{cases} \quad (18.22)$$

i.e.

$$I = j \int_{\sigma-j\infty}^{\sigma+j\infty} F(s-s_0)\Phi(s) ds = j \langle F(s-s_0), \Phi(s) \rangle_{\Re[s]=\sigma} \quad (18.23)$$

wherefrom

$$\xi(s-s_0) * F(s) = jF(s-s_0). \quad (18.24)$$

18.4.5 Multiplication of an Impulse Times an Ordinary Function

We can write

$$\begin{aligned} \langle \xi(s-a)F(s), \Phi(s) \rangle_{\Re[s]=\sigma} &= \langle \xi(s-a), F(s)\Phi(s) \rangle_{\Re[s]=\sigma} \\ &= \begin{cases} jF(a)\Phi(a), & \sigma = a_r \\ 0, & \sigma \neq a_r \end{cases} \end{aligned} \quad (18.25)$$

$$\langle \xi(s-a)F(s), \Phi(s) \rangle_{\Re[s]=\sigma} = \langle F(a)\xi(s-a), \Phi(s) \rangle_{\Re[s]=\sigma} \quad (18.26)$$

$$\xi(s-a)F(s) = F(a)\xi(s-a). \quad (18.27)$$

18.4.6 Multiplication by Higher Derivatives of the Impulse

Applying the property of the derivative times an ordinary function we obtain

$$\xi'(s)F(s) = F(0)\xi'(s) - F'(0)\xi(s). \quad (18.28)$$

More generally we obtain

$$F(s)\xi^{(n)}(s) = \sum_{k=0}^n (-1)^k \binom{n}{k} F^{(k)}(0)\xi^{(n-k)}(s). \quad (18.29)$$

Basic properties of Laplace-domain generalized functions of a complex variable are listed in Table 18.1.

18.5 Additional Generalized Impulse Properties

The following are properties of the generalized impulse in the s domain.

$$\xi^{(n)}(j\omega) = \frac{1}{j^n} \delta^{(n)}(\omega) \quad (18.30)$$

$$\xi^{(n)}(s) * \frac{1}{s} = (-1)^n \frac{n!}{s^{n+1}} \quad (18.31)$$

$$\frac{d^n}{d\Omega^n} \psi(z) = \psi^{(n)}(z) j^n e^{j\Omega} \quad (18.32)$$

$$\frac{d^n}{d\Omega^n} \psi(z) = j^n \sum_{m=1}^n S_n^{(m)} \psi^{(m)}(e^{j\Omega}) e^{jm\Omega} \quad (18.33)$$

where

$$\psi^{(m)}(e^{j\Omega}) = \left. \frac{d^m}{dz^m} \psi(z) \right|_{z=e^{j\Omega}} \quad (18.34)$$

TABLE 18.1 Properties of Laplace-domain generalized functions of a complex variable

Linearity 1	$\langle G(s), a_1\Phi_1(s) + a_2\Phi_2(s) \rangle$ $= a_1 \langle G(s), \Phi_1(s) \rangle + a_2 \langle G(s), \Phi_2(s) \rangle$
Linearity 2	$\langle G_1(s) + G_2(s), \Phi(s) \rangle$ $= \langle G_1(s), \Phi(s) \rangle + \langle G_2(s), \Phi(s) \rangle$
Shift in s Plane	$\langle G(s - s_0), \Phi(s) \rangle_{\Re[s]=\sigma}$ $= \langle G(y), \Phi(y + s_0) \rangle_{\Re[y]=\sigma - s_0}$
Scaling	$\langle G(\gamma s), \Phi(s) \rangle_{\Re[s]=\sigma}$ $= \frac{1}{ \gamma } \langle G(y), \Phi(y/\gamma) \rangle_{\Re[y]=\gamma\sigma}$
Impulse-Scaling	$\xi(\gamma s) = \frac{1}{ \gamma } \xi(s)$
Product	$\langle G(s)F(s), \Phi(s) \rangle = \langle G(s), F(s)\Phi(s) \rangle$
Convolution	$\langle \int_{\sigma-j\infty}^{\sigma+j\infty} G_1(y)G_2(s-y)dy, \Phi(s) \rangle$ $= \langle G_1(y), \int_{\sigma-j\infty}^{\sigma+j\infty} G_2(s-y)\Phi(s)ds \rangle$
Differentiation	$\langle G^{(n)}(s), \Phi(s) \rangle = (-1)^n \langle G(s), \Phi^{(n)}(s) \rangle$
Modulation	$L[f(t) \cos \beta t] = (1/2)\{F(s - j\beta) + F(s + j\beta)\}$
Convolution of two impulses	$\xi(s - a) * \xi(s - b) = j\xi[s - (a + b)]$
Sampling the n^{th} derivative	$\int_{s_0-j\infty}^{s_0+j\infty} \frac{d^n}{ds^n} \Phi(s)\xi(s - s_0)ds = (-1)^n j \frac{d^n}{ds^n} \Phi(s_0)$
Multiplication by the n^{th} derivative $\xi^{(n)}(s)$	$F(s)\xi^{(n)}(s) = \sum_{k=0}^n (-1)^k \binom{n}{k} F^{(k)}(0)\xi^{(n-k)}(s)$

$$\frac{d^n}{d\Omega^n} \psi(z) = j^n \sum_{m=1}^n S_n^{(m)} (-1)^r \binom{m}{r} j^r m^r \delta^{(m-r)}(\Omega), \quad -\pi \leq \Omega \leq \pi \tag{18.35}$$

$$\frac{d^n}{d\Omega^n} \psi(z) = j^n \sum_{m=1}^n S_n^{(m)} \sum_{k=-\infty}^{\infty} \sum_{r=0}^m (-1)^r \binom{m}{r} j^r m^r \delta^{(m-r)}(\Omega + 2k\pi) \tag{18.36}$$

$$\frac{d}{d\Omega} \psi(e^{j\Omega}) = \sum_{k=-\infty}^{\infty} \delta'(\Omega + 2k\pi) \tag{18.37}$$

$$\frac{d^2}{d\Omega^2} \psi(e^{j\Omega}) = \sum_{k=-\infty}^{\infty} \delta''(\Omega + 2k\pi) \tag{18.38}$$

$$\frac{d^n}{d\Omega^n} \psi(e^{j\Omega}) = \sum_{k=-\infty}^{\infty} \delta^{(n)}(\Omega + 2k\pi) \tag{18.39}$$

$$\frac{d^n}{d\Omega^n} \psi(r_0^{-1} e^{-j\beta} z) \Big|_{z=r_0 e^{j\Omega}} = \sum_{k=-\infty}^{\infty} \delta^{(n)}(\Omega - \beta + 2k\pi). \tag{18.40}$$

Table 18.2 lists basic properties of the continuous-time domain generalized Dirac-delta impulse $\xi(s)$. In this table the symbol $s(n, k)$ stands for the Striling Numbers of the First Kind, defined in the Appendix.

18.6 Generalized Impulse as a Limit of a Three-Dimensional Sequence

The Dirac-delta impulse may viewed as the limit of a sequence of functions that becomes progressively narrower and of increasing height as a parameter as $\varepsilon \rightarrow 0$, such as a rectangle. In the complex s -plane we can generalize rectangular sequences leading to impulses into three-dimensional solids. A cylinder may be introduced as the form of one such sequence. We may write

$$X_\varepsilon(s) = \begin{cases} 1/\varepsilon, & |s| < \varepsilon/2 \\ 0, & |s| > \varepsilon/2 \end{cases} \tag{18.41}$$

which is represented graphically in Fig. 18.2.

Another sequence leading to the Dirac-delta impulse is the Gaussian sequence shown in Fig. 18.3.

$$v(t) = e^{-t^2/\varepsilon} / \sqrt{\pi\varepsilon}. \tag{18.42}$$

A rotation, about the complex s -plane origin, of this Gaussian sequence would produce a 3-D solid defined by

$$X_\varepsilon(s) = e^{-|s|^2/\varepsilon} / \sqrt{\varepsilon\pi}. \tag{18.43}$$

We can write

$$\begin{aligned} \lim_{\varepsilon \rightarrow 0} \langle X_\varepsilon(s), \Phi(s) \rangle_{\Re[s]=\sigma} &= \frac{1}{\sqrt{\varepsilon\pi}} \lim_{\varepsilon \rightarrow 0} \int_{-j\infty}^{j\infty} e^{-|s|^2/\varepsilon} \Phi(s) ds \\ &= \frac{j}{\sqrt{\varepsilon\pi}} \lim_{\varepsilon \rightarrow 0} \int_{-\infty}^{\infty} e^{-\omega^2/\varepsilon} \Phi(j\omega) d\omega, \quad \sigma = 0 \end{aligned} \tag{18.44}$$

TABLE 18.2 Properties of the ξ impulse

Relation to δ	$\xi(jy) = \delta(y)$
Time scaling	$\xi(\gamma s) = \frac{1}{ \gamma } \xi(s)$
Multiplication	$F(s)\xi(s - a) = F(a)\xi(s - a)$
Sampling property	$\int_{Re[a]-j\infty}^{Re[a]+j\infty} F(s)\xi(s - a)ds = jF(a)$
Complex plane convolution	$\xi^{(n)}(s) \otimes F(s) = F^{(n)}(s)$
Modulation	$L[f(t) \cos \beta t] = (1/2)\{F(s - j\beta) + F(s + j\beta)\}$
Convolution of two impulses	$\xi(s - a) \otimes \xi(s - b) = j\xi[s - (a + b)]$
Sampling the n^{th} derivative	$\int_{s_0-j\infty}^{s_0+j\infty} \frac{d^n}{ds^n} \Phi(s)\xi(s - s_0)ds = (-1)^n j \frac{d^n}{ds^n} \Phi(s_0)$
Multiplication by the n^{th} derivative $\xi^{(n)}(s)$	$F(s)\xi^{(n)}(s) = \sum_{k=0}^n (-1)^k \binom{n}{k} F^{(k)}(0)\xi^{(n-k)}(s)$
Sampling the n^{th} derivative	$\int_{s_0-j\infty}^{s_0+j\infty} \frac{d^n}{ds^n} \xi(s - s_0)\Phi(s)ds = (-1)^n j \frac{d^n}{ds^n} \Phi(s_0)$
Symmetry	$\xi^{(n)}(-s) = (-1)^n \xi^{(n)}(s)$

i.e.

$$\lim_{\epsilon \rightarrow 0} \langle X_\epsilon(s), \Phi(s) \rangle = \begin{cases} \frac{j}{\sqrt{\epsilon\pi}} \Phi(0) \int_{-\infty}^{\infty} e^{-\omega^2/\epsilon} d\omega = j\Phi(0), & \sigma = 0 \\ 0, & \sigma \neq 0 \end{cases} \tag{18.45}$$

wherefrom $\lim_{\epsilon \rightarrow 0} \langle X_\epsilon(s), \Phi(s) \rangle_{\Re[s]=\sigma} = \langle \xi(s), \Phi(s) \rangle_{\Re[s]=\sigma}$ and

$$\xi(s) = \lim_{\epsilon \rightarrow 0} X_\epsilon(s). \tag{18.46}$$

A generalized Gaussian sequence is shown in Fig. 18.4.

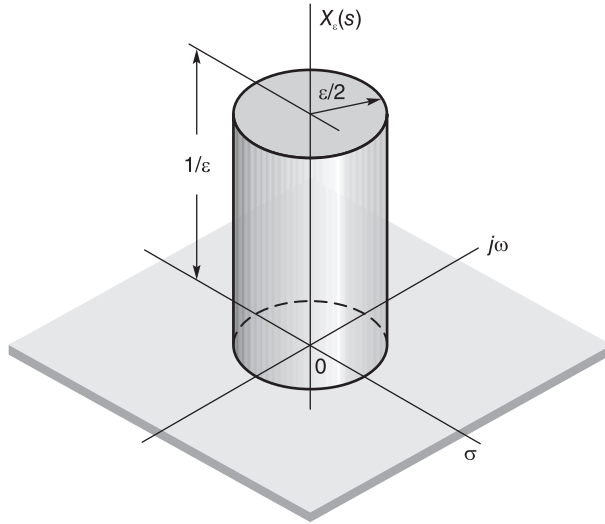


FIGURE 18.2 A cylindrical sequence leading to $\xi(s)$.

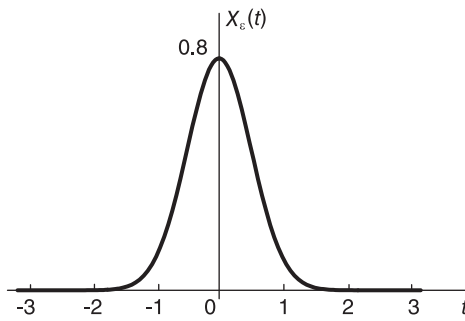


FIGURE 18.3 Gaussian sequence tending to Dirac-delta impulse as $\epsilon \rightarrow 0$.

18.7 Discrete-Time Domain

A distribution $G(z)$ may be defined as the value of the integral, denoted $I_G[\Phi(z)]$, of its product with a test function $\Phi(z)$. Symbolically, we write

$$I_G[\Phi(z)] = \langle G(z), \Phi(z) \rangle_{|z|=r} = \oint_{|z|=r} G(z) \Phi(z) dz \tag{18.47}$$

where the contour of integration is a circle of radius $r = |z|$ centered at the origin in the z -plane.

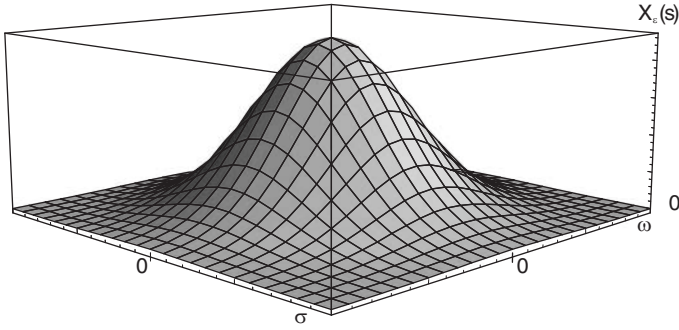


FIGURE 18.4 A 3-D generalized Gaussian sequence.

18.8 3-D Test Function as a Possible Generalization

A 3-D solid resembling a possible generalization of a test function which reduces to the usual test function along the unit circle can be defined as the function $\Phi(z)$ given by

$$\Phi(z) = \begin{cases} e^{\frac{1}{|z-1|^2-1}}, & |1-z| < 1 \\ 0, & |1-z| \geq 1 \end{cases} \quad (18.48)$$

shown in Fig. 18.5.

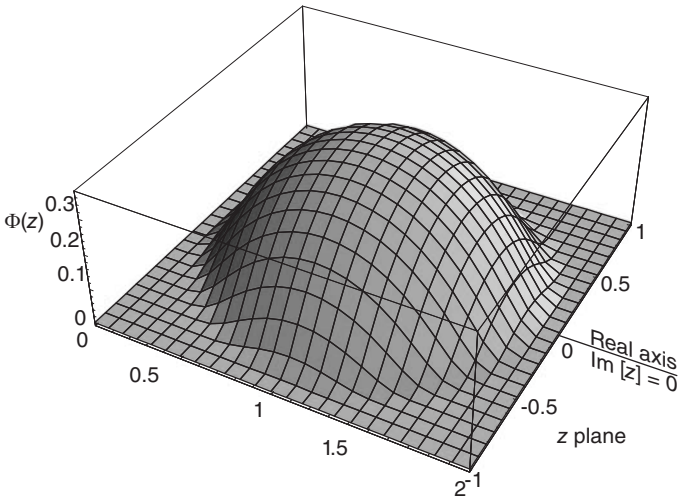


FIGURE 18.5 A 3-D test function in z-domain.

The test function $\Phi(e^{j\Omega})$ as it appears along the unit circle is shown in Fig. 18.6.

18.8.1 Properties of Generalized Distributions in z-Domain

The following properties of generalized distributions are readily established.

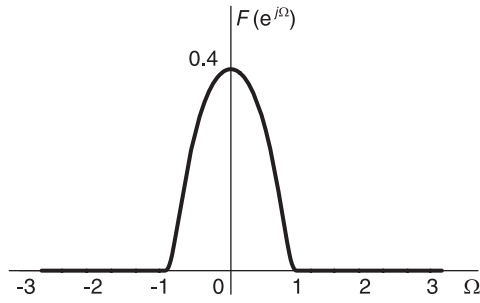


FIGURE 18.6 Test function on unit circle.

18.8.2 Linearity

$$\langle G(z), a_1\Phi(z) + a_2\Phi_2(z) \rangle = a_1 \langle G(z), \Phi_1(z) \rangle + a_2 \langle G(z), \Phi_2(z) \rangle \quad (18.49)$$

$$\langle G_1(z) + G_2(z), \Phi(z) \rangle = \langle G_1(z), \Phi(z) \rangle + \langle G_2(z), \Phi(z) \rangle. \quad (18.50)$$

18.8.3 Scaling in z -Domain

$$\langle G(z/z_0), \Phi(z) \rangle_{|z|=r} = \oint_{|z|=r} G(z/z_0) \Phi(z) dz. \quad (18.51)$$

Letting $z/z_0 = w$ and $w = \rho e^{j\phi}$ we have

$$\langle G(z/z_0), \Phi(z) \rangle_{|z|=r} = \oint_{|w|=\rho} G(w) \Phi(z_0 w) z_0 dw = \langle z_0 G(w), \Phi(z_0 w) \rangle_{|w|=\rho=r/|z_0|}. \quad (18.52)$$

18.8.4 Differentiation

Let

$$I = \langle G'(z), \Phi(z) \rangle_{|z|=r} = \oint_{|z|=r} G'(z) \Phi(z) dz. \quad (18.53)$$

Writing $z = re^{j\Omega}$, $dz = jr e^{j\Omega} d\Omega$, we have

$$\langle G'(z), \Phi(z) \rangle_{|z|=r} = jr \int_{-\pi}^{\pi} G'(re^{j\Omega}) \Phi(re^{j\Omega}) e^{j\Omega} d\Omega. \quad (18.54)$$

Integrating by parts

$$u' = G'(re^{j\Omega}) jr e^{j\Omega}, \quad v = \Phi(re^{j\Omega}) \quad (18.55)$$

$$\begin{aligned} I &= G(re^{j\Omega}) \Phi(re^{j\Omega}) \Big|_{-\pi}^{\pi} - \int_{-\pi}^{\pi} G(re^{j\Omega}) jr \Phi'(re^{j\Omega}) e^{j\Omega} d\Omega \\ &= - \int_{-\pi}^{\pi} G(re^{j\Omega}) jr \Phi'(re^{j\Omega}) e^{j\Omega} d\Omega = - \langle G(z), \Phi'(z) \rangle_{|z|=r}. \end{aligned} \quad (18.56)$$

More generally

$$\langle G^{(n)}(z), \Phi(z) \rangle_{|z|=r} = (-1)^n \langle G(z), \Phi^{(n)}(z) \rangle_{|z|=r}. \quad (18.57)$$

18.8.5 Convolution

The convolution $G_1(z) * G_2(z)$ of two generalized distributions may be written

$$\langle G_1(z) * G_2(z), \Phi(z) \rangle_{|z|=r} = \oint_{|z|=r} \oint_{|y|=\rho} G_1(y)G_2(z/y)y^{-1}dy\Phi(z)dz. \tag{18.58}$$

Interchanging the order of integrations we can write

$$\begin{aligned} \langle G_1(z) * G_2(z), \Phi(z) \rangle_{|z|=r} &= \oint_{|y|=\rho} G_1(y) \oint_{|z|=r} G_2(z/y)\Phi(z)dz y^{-1}dy \\ &= \langle G_1(y)/y, \oint_{|z|=r} G_2(z/y)\Phi(z)dz \rangle_{|y|=\rho}. \end{aligned} \tag{18.59}$$

18.9 Properties of the Generalized Impulse in z -Domain

The discrete-time domain generalized impulse will be denoted by the symbol $\psi(z)$ as in [23], and is equivalent to the symbol $\zeta(z-1)$ proposed in [21], that is,

$$\psi(z) = \zeta(z-1) \tag{18.60}$$

$$\langle \psi(z), \Phi(z) \rangle_{|z|=r} = \begin{cases} j\Phi(1), & r = 1 \\ 0, & r \neq 1 \end{cases} \tag{18.61}$$

having the property

$$\psi(re^{j\Omega}) = \begin{cases} \sum_{k=-\infty}^{\infty} \delta(\Omega + 2k\pi), & r = 1 \\ 0, & r \neq 1. \end{cases} \tag{18.62}$$

18.9.1 Differentiation

Let $G(z) = \psi(z)$

$$\begin{aligned} \langle G'(z), \Phi(z) \rangle_{|z|=r} &= \langle \psi'(z), \Phi(z) \rangle_{|z|=r} \\ &= - \langle \psi(z), \Phi'(z) \rangle_{|z|=r} \\ &= \begin{cases} -j\Phi'(1), & r = 1 \\ 0, & r \neq 1 \end{cases} \end{aligned} \tag{18.63}$$

$$\langle G^{(n)}(z), \Phi(z) \rangle = \langle \psi^{(n)}(z), \Phi(z) \rangle = (-1)^n \langle \psi(z), \Phi^{(n)}(z) \rangle \tag{18.64}$$

$$\langle \psi^{(n)}(z), \Phi(z) \rangle_{|z|=r} = \begin{cases} j(-1)^n \Phi^{(n)}(1), & r = 1 \\ 0, & r \neq 1. \end{cases} \tag{18.65}$$

Let

$$G(z) = \psi(z/z_0) \tag{18.66}$$

$$I = \langle \psi(z/z_0), \Phi(z) \rangle_{|z|=r} = \langle z_0\psi(w), \Phi(z_0w) \rangle_{|w|=r/|z_0|} \tag{18.67}$$

$I \neq 0$ if and only if $r = |z_0|$, i.e. $w = e^{j\phi}$,

TABLE 18.3 Properties of z -domain generalized functions of a complex variable

Linearity	$\begin{aligned} &< G(z), a_1\Phi(z) + a_2\Phi_2(z) > \\ &= a_1 < G(z), \Phi_1(z) > + a_2 < G(z), \Phi_2(z) > \\ &< G_1(z) + G_2(z), \Phi(z) > \\ &= < G_1(z), \Phi(z) > + < G_2(z), \Phi(z) > \end{aligned}$
Differentiation	$< G^{(n)}(z), \Phi(z) > = (-1)^n < G(z), \Phi^{(n)}(z) >$
Impulse-differentiation	$< \psi^{(n)}(z), \Phi(z) > = j(-1)^n \Phi^{(n)}(1)$
Convolution	$F(z) * \psi(z/a) = jF(z/a)$
Convolution of two impulses	$\psi(z/a) * \psi(z/b) = j\psi[z/(ab)]$
The n^{th} derivative	$\psi^{(n)}(z) = \frac{d^n}{dz^n} \psi(z) = \sum_{k=1}^n \frac{s(n, k)}{j^k z^n} \frac{d^k}{d\Omega^k} \psi(z)$
Sampling by the n^{th} derivative $\psi^{(n)}(z)$	$\oint \psi^{(n)}(z) \Phi(z) dz = j(-1)^n \Phi^{(n)}(1)$
The value of the integral $I = \oint F(z) \psi^{(n)}(z) \Phi(z) dz$	$I = \sum_{k=0}^n (-1)^k \binom{n}{k} F^{(k)}(1) \psi^{(n-k)}(z) \Phi(z) dz$
Multiplication by the n^{th} derivative	$F(z) \psi^{(n)}(z) = \sum_{k=0}^n (-1)^k \binom{n}{k} F^{(k)}(1) \psi^{(n-k)}(z)$

$$\begin{aligned} &< \psi(z/z_0), \Phi(z) >_{|z|=r} \\ &= \begin{cases} \int_{-\pi}^{\pi} z_0 \psi(e^{j\phi}) \Phi(z_0 e^{j\phi}) j e^{j\phi} d\phi = j z_0 \Phi(z_0), & r = |z_0| \\ 0, & r \neq |z_0|. \end{cases} \end{aligned}$$

Table 18.3 lists basic properties of z -domain generalized functions of a complex variable.

18.10 Generalized Impulse as Limit of a 3-D Sequence

In the z -plane a cylinder, again, may be proposed as a generalization to a three-dimensional solid of the rectangular sequence leading to impulses. We may write

$$X_{\varepsilon}(z) = \begin{cases} 1/\varepsilon, & |z - 1| < \varepsilon/2 \\ 0, & |z - 1| > \varepsilon/2 \end{cases} \tag{18.68}$$

as represented graphically in Fig. 18.7.

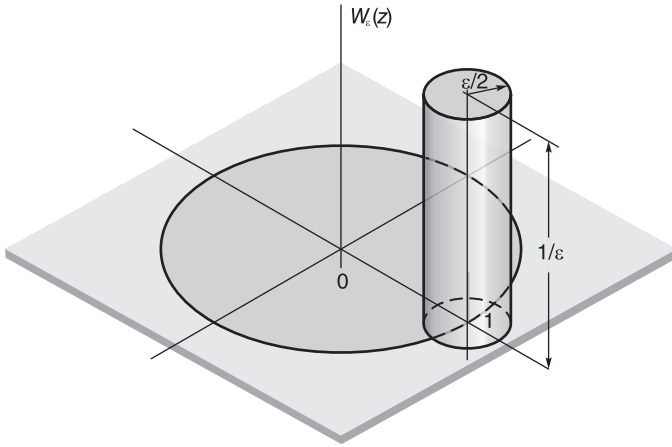


FIGURE 18.7 A cylindrical sequence leading to the generalized impulse $\psi(z)$.

A possible three-dimensional solid generalizing the Gaussian sequence may be defined as the sequence

$$W_\varepsilon(z) = \frac{1}{\sqrt{\pi\varepsilon}} e^{-|z-1|^2/\varepsilon} \tag{18.69}$$

which with $z = e^{j\Omega}$ is equal to

$$W_\varepsilon(e^{j\Omega}) = e^{-4 \sin^2(\Omega/2)/\varepsilon} / \sqrt{\pi\varepsilon} \tag{18.70}$$

$$\begin{aligned} I &= \langle \psi(z), \Phi(z) \rangle_{|z|=1} = \lim_{\varepsilon \rightarrow 0} \langle W_\varepsilon(z), \Phi(z) \rangle_{|z|=1} \\ &= \lim_{\varepsilon \rightarrow 0} \frac{1}{\sqrt{\pi\varepsilon}} \Phi(z) dz = \lim_{\varepsilon \rightarrow 0} \frac{1}{\sqrt{\pi\varepsilon}} \int_{-\pi}^{\pi} e^{-(4/\varepsilon) \sin^2(\Omega/2)} \Phi(e^{j\Omega}) j d\Omega. \end{aligned} \tag{18.71}$$

Letting $\Omega = 2\theta$ the integral I may be approximated as

$$I \simeq \lim_{\varepsilon \rightarrow 0} \frac{j2}{\sqrt{\pi\varepsilon}} \int_{-\pi/2}^{\pi/2} e^{-(4 \sin^2 \theta)/\varepsilon} \Phi(1) d\theta. \tag{18.72}$$

With $u = \sin \theta$, $d\theta = du / \sqrt{1-u^2}$

$$I \simeq \lim_{\varepsilon \rightarrow 0} \frac{j2\Phi(1)}{\sqrt{\pi\varepsilon}} \int_{-1}^1 \frac{e^{-4u^2/\varepsilon}}{\sqrt{1-u^2}} du \tag{18.73}$$

and with $u = \sqrt{\varepsilon}v$

$$\begin{aligned} I &\simeq \lim_{\varepsilon \rightarrow 0} \frac{j2\Phi(1)}{\sqrt{\pi\varepsilon}} \int_{-1/\sqrt{\varepsilon}}^{1/\sqrt{\varepsilon}} \frac{e^{-4v^2}}{\sqrt{1-\varepsilon v^2}} \sqrt{\varepsilon} dv = \frac{j2\Phi(1)}{\sqrt{\pi}} \int_{-\infty}^{\infty} e^{-4v^2} dv \\ &= \frac{j\Phi(1)}{\sqrt{\pi}} \int_{-\infty}^{\infty} e^{-x^2} dx = j\Phi(1). \end{aligned} \tag{18.74}$$

Since

$$\int_{-\pi}^{\pi} \sum_{k=-\infty}^{\infty} \delta(\Omega + 2k\pi) \Phi(e^{j\Omega}) j e^{j\Omega} d\Omega = j\Phi(1) \tag{18.75}$$

we have

$$\psi(e^{j\Omega}) = \sum_{k=-\infty}^{\infty} \delta(\Omega + 2k\pi) \tag{18.76}$$

confirming the validity of the property of the generalized impulse stated above.

We have thus established that the limit of the 3-D Gaussian sequence of ordinary functions tends to the generalized impulse

$$\lim_{\epsilon \rightarrow 0} \langle W_{\epsilon}(z), \Phi(z) \rangle = \langle \psi(z), \Phi(z) \rangle \tag{18.77}$$

$$\psi(z) = \lim_{\epsilon \rightarrow 0} W_{\epsilon}(z). \tag{18.78}$$

The Gaussian sequence $W_{\epsilon}(z)$ of which the limit is the generalized impulse is shown in Fig. 18.8.

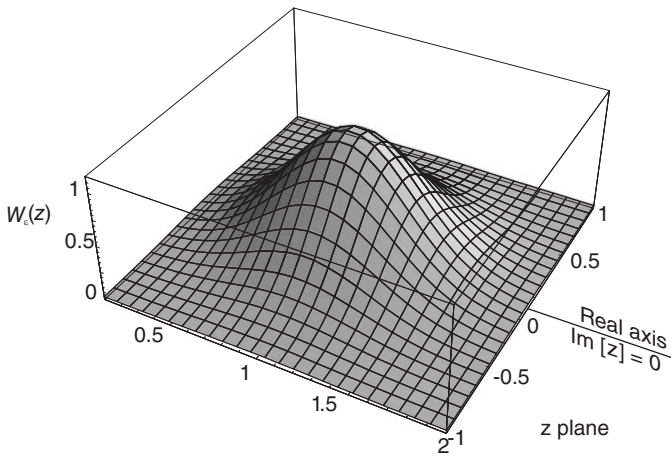


FIGURE 18.8 A 3-D Gaussian sequence leading to $\psi(z)$.

18.10.1 Convolution of Generalized Impulses

Let $G_1(z) = \psi(z/a)$, $G_2(z) = \psi(z/b)$.

We can write

$$I = \langle \psi(z/a) * \psi(z/b), \Phi(z) \rangle_{|z|=r} = \oint_{|z|=r} \oint_{|y|=\rho} \psi(y/a) \psi[z/(yb)] y^{-1} dy \Phi(z) dz \tag{18.79}$$

$$I = \oint_{|y|=\rho} \psi(y/a) \oint_{|z|=r} \psi[z/(yb)] \Phi(z) dz y^{-1} dy. \tag{18.80}$$

Let

$$I_1 = \oint_{|z|=r} \psi[z/(yb)] \Phi(z) dz. \tag{18.81}$$

With $z = ybe^{j\Omega}$ we have

$$I_1 = \int_{-\pi}^{\pi} \psi(e^{j\Omega}) \Phi(ybe^{j\Omega}) j y b e^{j\Omega} d\Omega = j y b \Phi(yb), \quad r = \rho |b| \tag{18.82}$$

$$I = \oint_{|y|=r/|b|} \psi(y/a) j b \Phi(y) dy. \tag{18.83}$$

With $y = ae^{j\phi}$, i.e. $r = |ab|$

$$I = \int_{-\pi}^{\pi} \psi(e^{j\phi}) j b \Phi(a b e^{j\phi}) j a e^{j\phi} d\phi = -ab \Phi(ab), \quad r = |ab| \tag{18.84}$$

i.e.

$$I = \langle j\psi[z/(ab)], \Phi(z) \rangle_{|z|=r} \tag{18.85}$$

wherefrom

$$\psi(z/a) * \psi(z/b) = j\psi[z/(ab)] \tag{18.86}$$

an operation illustrated in Fig. 18.9.

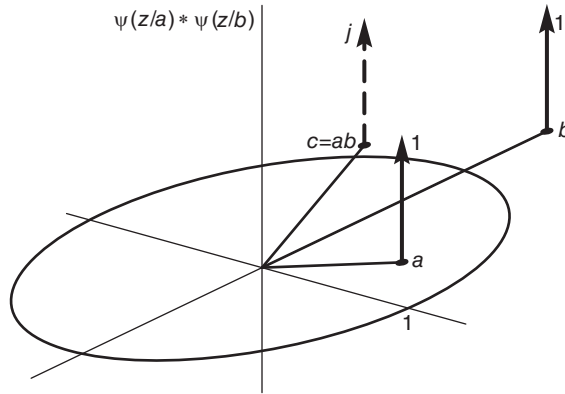


FIGURE 18.9 Convolution of impulses on z-plane.

18.10.2 Convolution with an Ordinary Function

Consider

$$I = \langle \psi(z/a) * F(z), \Phi(z) \rangle_{|z|=r} = \oint_{|z|=r} \oint_{|y|=\rho} F(y) \psi[z/(ay)] y^{-1} dy \Phi(z) dz$$

$$I = \oint_{|y|=\rho} F(y) \oint_{|z|=r} \psi[z/(ay)] \Phi(z) dz y^{-1} dy = \oint_{|y|=\rho} F(y) I_1(y) y^{-1} dy.$$

With $z = aye^{j\Omega}$, i.e. $r = |ay| = \rho|a|$

$$I_1 = \int_{-\pi}^{\pi} \psi(e^{j\Omega}) \Phi(aye^{j\Omega}) jaye^{j\Omega} d\Omega = jay\Phi(ay), \quad r = \rho|a| \quad (18.87)$$

$$\begin{aligned} I &= \oint_{|y|=r/|a|} F(y) ja\Phi(ay) dy = ja \oint_{|z|=r} F(z/a)\Phi(z)a^{-1} dz \\ &= \langle jF(z/a), \Phi(z) \rangle_{|z|=r} \end{aligned} \quad (18.88)$$

wherefrom

$$\psi(z/a) * F(z) = jF(z/a). \quad (18.89)$$

Consider

$$I = \langle \psi(z/a) * F(z), \Phi(z) \rangle_{|z|=r} = \int \int F(y) \psi[z/(ay)] y^{-1} dy \Phi(z) dz \quad (18.90)$$

$$I = \int F(y) \int \psi[z/(ay)] \Phi(z) dz y^{-1} dy = \int F(y) I_1(y) y^{-1} dy. \quad (18.91)$$

With $z = aye^{j\Omega}$, i.e. $r = |ay| = \rho|a|$

$$I_1 = \int_{-\pi}^{\pi} \psi(e^{j\Omega}) \Phi(aye^{j\Omega}) jaye^{j\Omega} d\Omega = jay\Phi(ay), \quad r = \rho|a| \quad (18.92)$$

$$\begin{aligned} I &= \int F(y) ja\Phi(ay) dy = ja \int F(z/a)\Phi(z)a^{-1} dz \\ &= \langle jF(z/a), \Phi(z) \rangle_{|z|=r} \end{aligned} \quad (18.93)$$

wherefrom

$$\psi(z/a) * F(z) = jF(z/a). \quad (18.94)$$

18.11 Extended Laplace and z -Transforms

Some basic new Laplace transforms resulting from the generalization of the distributions and in particular the generalization of the Dirac-delta impulse are listed in Table 18.4. New extended-domain z -transforms are listed in Table 18.5 [21] [23] [27]. In this table the symbol $S(n, m)$ stands for the Strling Numbers of the Second Kind, defined in the Appendix.

Moreover, the z -transform of the sequence $4 \cos \gamma n \cosh \alpha n \times \{1 + (-1)^n\}$ is shown in Fig. 18.10. The z -transform of the exponentially rising impulse train

$$x[n] = \sum_{k=-\infty}^{\infty} a^{kN} \delta[n - kN], \quad N = 16$$

is shown in Fig. 18.11.

18.12 Generalization of Fourier-, Laplace- and z -Related Transforms

We have just seen how the newly introduced generalized Dirac-delta impulses enhance considerably the powers of bilateral Laplace and z -transforms. The existence of these bilateral

TABLE 18.4 New Laplace transforms

$x_c(t)$	Extended ξ-Transform $X_c(s)$
1	$2\pi\xi(s)$
e^{at}	$2\pi \xi(s - a)$
$\cosh(at)$	$\pi\{\xi[s - a] + \xi[s + a]\}$
$\cosh(j\beta t)$	$\pi\{\delta[\omega - \beta] + \xi[\omega + \beta]\}$
$u(t)$	$1/s + \pi\xi(s)$
$e^{at}u(t)$	$1/(s - a) + \pi\xi(s - a)$
$e^{\alpha t} \cos(\beta t)$	$\pi\{\xi[s - (\alpha + j\beta)] + \xi[s - (\alpha - j\beta)]\}$
$e^{\alpha t} \cos \beta t u(t)$	$\frac{s - \alpha}{(s - \alpha)^2 + \beta^2} + \frac{\pi}{2}\{\xi[s - (\alpha + j\beta)] + \xi[s - (\alpha - j\beta)]\}$
t	$-2\pi d\xi(s)/ds$
t^n	$(-1)^n 2\pi\xi^{(n)}(s)$
$t^n u(t)$	$n!/s^{n+1} + (-1)^n \pi\xi^{(n)}(s)$
$t^n e^{at}u(t)$	$\frac{n!}{(s - a)^{n+1}} + (-1)^n \pi\xi^{(n)}(s - a)$
$1/(jt) + \pi\delta(t)$	$2\pi\nu(-s)$
$4 \cos \beta t \cosh \alpha t$	$2\pi\{\xi(s - a) + \xi(s - a^*) + \xi(s + a) + \xi(s + a^*)\}$
$(-t)^n$	$2\pi\xi^{(n)}(s)$
$-tu(-t)$	$1/s^2 + \pi\xi'(s)$
$t^n e^{\alpha t}u(t)$	$\frac{n!}{(s - \alpha)^{n+1}} + (-1)^n \pi\xi^{(n)}(s - \alpha)$
$(-t)^n e^{-\alpha t}u(-t)$	$\frac{n!}{(-1)^{n+1}(s + \alpha)^{n+1}} + \pi\xi^{(n)}(s + \alpha)$

TABLE 18.5 New z -transforms

$x[n]$	Extended z -transform $X(z)$
1	$2\pi\psi(z)$
a^n	$2\pi\psi(z/a)$
$4 \cos \gamma n \cosh \alpha n \{1 + (-1)^n\}$	$2\pi\{\psi(z/a) + \psi(z/a^*) + \psi(z/a^{-1}) + \psi(z/a^{-1*}) + \psi(-z/a) + \psi(-z/a^*) + \psi(-z/a^{-1}) + \psi(-z/a^{-1*})\}$
$a^n \cos(\Omega_0 n)$	$\pi \{ \psi [z / (ae^{j\Omega_0})] + \psi [z / (ae^{-j\Omega_0})] \}$
$u[n]$	$1/(1 - z^{-1}) + \pi\psi(z)$
$a^n u[n]$	$1/(1 - az^{-1}) + \pi\psi(z/a)$
$na^n u[n]$	$\frac{-az^{-1}}{(1 - az^{-1})^2} + \pi\psi'(a^{-1}z)$
$(n + 1)a^n u[n]$	$\frac{1}{(1 - az^{-1})^2} + \pi[z\psi'(a^{-1}z) - \psi(a^{-1}z)]$
$a^{n-n_0} u[n - n_0]$	$z^{-n_0} \left\{ \frac{1}{1 - az^{-1}} + \pi\psi(z/a) \right\}$
$a^n b^n u[n]$	$\frac{1}{1 - abz^{-1}} + \pi\psi \{z/(ab)\}$
$\cos[\Omega_0 n + \phi]$	$\pi[e^{j\phi}\psi(z/e^{j\Omega_0}) + e^{-j\phi}\psi(z/e^{-j\Omega_0})]$
$n^r u[n]$	$(-1)^r \sum_{i=1}^r S(r, i) \frac{(-1)^i i!}{(z-1)^{i+1}} z^i + \pi \sum_{i=1}^{r+1} (-1)^{i+1} S(r+1, i) \psi^{(i-1)}(z)$
$n^r u[-n]$	$\sum_{i=1}^r S(r, i) \frac{(-1)^i i!}{(z^{-1}-1)^{i+1}} z^{-i} + \pi \sum_{i=1}^{r+1} (-1)^{i+r+1} S(r+1, i) \psi^{(i-1)}(z^{-1})$
n^r	$2\pi \sum_{i=1}^{r+1} (-1)^{i+1} S(r+1, i) \psi^{(i-1)}(z)$

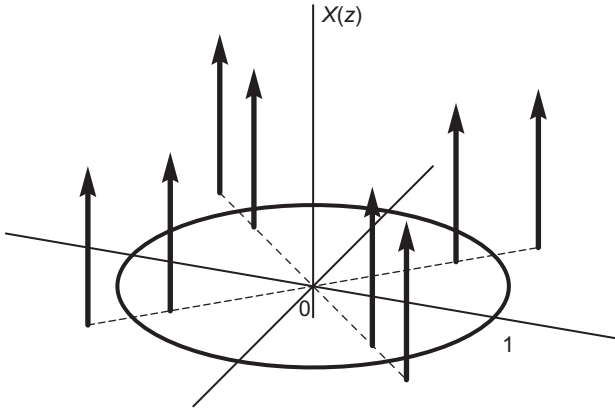


FIGURE 18.10 z -transform of the sequence $4 \cos \gamma n \cosh \alpha n \times \{1 + (-1)^n\}$.

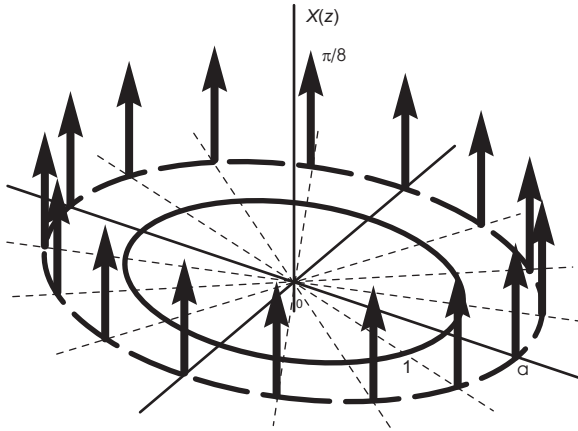


FIGURE 18.11 z -transform of an exponentially rising impulse train.

transforms for a large new class of functions opens the doors to generalizations of several Fourier, Laplace and z -related transforms such as Hilbert, Hartley, Mellin transforms among others, as we see in what follows.

18.13 Hilbert Transform Generalization

As we have seen in Chapter 14 the Hilbert transform of a function $f(t)$ may be defined as a transformation from the time domain to the time domain, producing a function $f_{Hi}(t)$, such that

$$f_{Hi}(t) = \frac{1}{\pi} \int_{-\infty}^{\infty} \frac{f(\tau)}{t - \tau} d\tau = f(t) * h(t) \tag{18.95}$$

where $h(t) = 1/(\pi t)$. Equivalently, we may consider the Hilbert transform as a transformation from the time domain to Fourier frequency domain

$$F_{Hi}(j\omega) = F[j\omega] H[j\omega] \tag{18.96}$$

where

$$H(j\omega) = \mathcal{F}[1/(\pi t)] = -j \operatorname{sgn}(\omega).$$

The generalization of the Hilbert transform would be a transformation from the time domain to the bilateral Laplace transform domain. We may write

$$G(s) = H(s) F(s) \tag{18.98}$$

$$H(s) = \mathcal{L}[1/(\pi t)] = -j \operatorname{sgn}(-js).$$

The signum function of a complex variable $\operatorname{sgn}(s)$ would have to be defined. We may write $\operatorname{sgn}(w) = \operatorname{sgn}(\Re[w])$ so that $\operatorname{sgn}(-js) = \operatorname{sgn}(\omega - j\sigma) = \operatorname{sgn}(\omega)$, $H(s) = -j \operatorname{sgn}(\Im[s])$.

Example Given $f(t) = \cos(\beta t)$ we have

$$F(s) = \pi \{ \xi(s - j\beta) + \xi(s + j\beta) \} \tag{18.100}$$

$$F_{Hi}(s) = -j\pi \operatorname{sgn}(\Im[s]) \{ \xi(s - j\beta) + \xi(s + j\beta) \} = -j\pi \{ \xi(s - j\beta) - \xi(s + j\beta) \} \tag{18.101}$$

$$f_{Hi}(t) = \sin(\beta t) \tag{18.102}$$

Example Given $f(t) = \Pi_T(t)$ we write $F(s) = 2T \operatorname{Sa}(-jTs) = 2T \operatorname{Sah}(Ts)$. Hence

$$F_{Hi}(s) = -j \operatorname{sgn}(\Im[s]) 2T \operatorname{Sah}(Ts) = \begin{cases} -j2T \operatorname{Sah}(Ts), & \Im[s] > 0 \\ j2T \operatorname{Sah}(Ts), & \Im[s] < 0 \end{cases} \tag{18.103}$$

Table 18.6 lists basic generalized Hilbert transforms.

TABLE 18.6 New generalized Hilbert transforms

$f(t)$	$f_{Hi}(t)$	$F_{Hi}(s)$
e^{jt}	$-je^{jt}$	$-j2\pi\xi(s - j)$
$\cos \beta t$	$\sin \beta t$	$-j\pi \{ \xi(s - j\beta) - \xi(s + j\beta) \}$
$\Pi_T(t)$	$\frac{1}{\pi} \ln \left \frac{t+T}{t-T} \right $	$\begin{cases} -j2T \operatorname{Sah}(sT), & \Im[s] > 0 \\ j2T \operatorname{Sah}(sT), & \Im[s] < 0 \end{cases}$
$\frac{1}{t^2 + 1}$	$\frac{t}{t^2 + 1}$	$\begin{cases} -j\pi e^{- s }, & \Im[s] > 0 \\ j\pi e^{- s }, & \Im[s] < 0 \end{cases}$
$\delta(t)$	$1/(\pi t)$	$-j \operatorname{sgn}(\Im[s])$

18.14 Generalizing the Discrete Hilbert Transform

In the discrete-time domain Hilbert transformer may be viewed as a filter of transfer function

$$H(e^{j\Omega}) = \begin{cases} -j, & 0 < \Omega < \pi \\ j, & -\pi < \Omega < 0 \end{cases} \tag{18.104}$$

To generalize the discrete Hilbert transform we may write

$$\text{sgn}[n] = 2u[n] - 1 \tag{18.105}$$

$$\text{sgn}[n] \xleftrightarrow{\mathcal{Z}} 2 \left\{ \frac{1}{1-z^{-1}} + \pi\psi(z) \right\} - 2\pi\psi(z) = \frac{2}{1-z^{-1}} \tag{18.106}$$

The filter impulse response is

$$h[n] = \frac{1}{2\pi} \left\{ \int_{-\pi}^0 j e^{j\Omega n} d\Omega + \int_0^{\pi} -j e^{j\Omega n} d\Omega \right\} = \frac{1}{2\pi} \left\{ \frac{1 - e^{-j\pi n}}{n} - \frac{e^{j\pi n} - 1}{n} \right\} \tag{18.107}$$

$$h[n] = \frac{1}{2n\pi} \{2 - 2\cos(\pi n)\} = \frac{1 - \cos(\pi n)}{\pi n} = \begin{cases} 0, & n \text{ even} \\ \frac{2}{\pi n}, & n \text{ odd} \end{cases} \tag{18.108}$$

$$H(z) = -j \text{sgn}(-j \ln z) \tag{18.109}$$

In other words, if $z = re^{jb}$, $H(z) = -j \text{sgn}(b - j \ln r) = -j \text{sgn}(b)$. Given a sequence $x[n]$ its Hilbert transform in the z -domain is therefore

$$X_{Hi}(z) = -j \text{sgn}(-j \ln z) X(z) \tag{18.110}$$

and in the time domain is $x_{Hi}[n] = x[n] * h[n]$

Example With $x[n] = \cos(bn)$, $X(z) = \pi \{ \psi(e^{-jb}z) + \psi(e^{jb}z) \}$

$$X_{Hi}(z) = -j \text{sgn}(-j \ln z) X(z) = -j\pi \text{sgn}(-j \ln z) \{ \psi(e^{-jb}z) + \psi(e^{jb}z) \} \tag{18.111}$$

Hence $X_{Hi}(z) = -j\pi \{ \psi(e^{-jb}z) - \psi(e^{jb}z) \}$ and $x_{Hi}[n] = \sin(bn)$.

Table 18.7 lists basic generalized discrete Hilbert transforms.

18.15 Generalized Hartley Transform

The Hartley transform, defined above in Chapter 14, may be generalized by an extension in Laplace plane. We may write

$$\begin{aligned} F_{Ha}(s) &= \frac{1}{2} \int_{-\infty}^{\infty} f(t) \{ e^{st} + e^{-st} - j(e^{st} - e^{-st}) \} dt \\ &= \frac{1}{2} \int_{-\infty}^{\infty} f(t) \{ 2 \cosh st - j2 \sinh st \} dt \end{aligned} \tag{18.112}$$

$$F_{Ha}(s) = \int_{-\infty}^{\infty} f(t) \{ \cosh st - j \sinh st \} dt. \tag{18.113}$$

TABLE 18.7 Generalized discrete Hilbert transforms

$x[n]$	$x_{Hi}[n]$	$X_{Hi}(z)$
$\delta[n]$	$\frac{1 - \cos(\pi n)}{\pi n}$	$-j \operatorname{sgn}(-j \ln z)$
$\cos bn$	$\sin(bn)$	$-j\pi \{ \psi(z/e^{jb}) - \psi(z/e^{-jb}) \}$
$u[n]$	$u[n] * \frac{1 - \cos(\pi n)}{\pi n}$	$\begin{cases} \frac{-j}{1 - z^{-1}}, \Im[z] > 0 \\ \frac{j}{1 - z^{-1}}, \Im[z] < 0 \end{cases}$
$\operatorname{sgn}[n]$	$\operatorname{sgn}[n] * \frac{1 - \cos(\pi n)}{\pi n}$	$\begin{cases} \frac{-j2}{1 - z^{-1}}, \Im[z] > 0 \\ \frac{j2}{1 - z^{-1}}, \Im[z] < 0 \end{cases}$

The inverse transform is given by

$$f(t) = \frac{1}{4\pi j} \int_{\sigma-j\infty}^{\sigma+j\infty} F_{Ha}(s) \{e^{st} + e^{-st} - j(e^{st} - e^{-st})\} ds \tag{18.114}$$

$$= \frac{1}{4\pi j} \int_{\sigma-j\infty}^{\sigma+j\infty} F_{Ha}(s) \{2 \cosh st - j2 \sinh st\} ds$$

$$f(t) = \frac{1}{2\pi j} \int_{\sigma-j\infty}^{\sigma+j\infty} F_{Ha}(s) \{ \cosh st - j \sinh st \} ds \tag{18.115}$$

Example

With $f(t) = e^{\alpha t}$

$$F_{Ha}(s) = \int_{-\infty}^{\infty} e^{\alpha t} \{ \cosh st - j \sinh st \} dt = \int_{-\infty}^{\infty} e^{\alpha t} \left(\frac{e^{st} + e^{-st}}{2} - j \frac{e^{st} - e^{-st}}{2} \right) dt \tag{18.116}$$

$$= \frac{1}{2} \int_{-\infty}^{\infty} e^{(s+\alpha)t} + e^{-(s-\alpha)t} - j e^{(s+\alpha)t} + j e^{-(s-\alpha)t} dt$$

$$= \frac{1}{2} \{ 2\pi\xi(-s-\alpha) + 2\pi\xi(s-\alpha) - j2\pi\xi(-s-\alpha) + j2\pi\xi(s-\alpha) \} \tag{18.117}$$

$$= \pi \{ (1-j)\xi(s+\alpha) + (1+j)\xi(s-\alpha) \} \tag{18.118}$$

Table 18.8 lists basic generalized Hartley transforms.

18.16 Generalized Discrete Hartley Transform

A generalized Hartley transform extending the transform over the complex z -plane may be written in the form

$$X_{Ha}(z) = \frac{1}{2} \sum_{n=-\infty}^{\infty} x[n] \{ (1+j)z^{-n} + (1-j)z^n \} = \frac{1}{2} \{ (1+j)X(z) + (1-j)X(z^{-1}) \} \tag{18.119}$$

TABLE 18.8 Generalized Hartley transforms

$f(t)$	$F_{Ha}(s)$
1	$2\pi\xi(s)$
$e^{\gamma t}$	$\pi \{(1-j)\xi(s+\gamma) + (1+j)\xi(s-\gamma)\}$
$\cos \beta t$	$\pi \{\xi(s+j\beta) + \xi(s-j\beta)\}$
$\sin \beta t$	$\pi \{\xi(s-j\beta) - \xi(s+j\beta)\}$
$e^{\alpha t} \cos \beta t$	$(\pi/2) \{(1-j)[\xi(s+\alpha+j\beta) + \xi(s+\alpha-j\beta)] + (1+j)[\xi(s-\alpha-j\beta) + \xi(s-\alpha+j\beta)]\}$
$u(t)$	$j2/s + 2\pi\xi(s)$
$sgnt$	$j2/s$
$\delta(t)$	1

Examples

Let $x[n] = 1$, $X(z) = 2\pi\psi(z)$

$$X_{Ha}(z) = \frac{1}{2} \{(1+j)2\pi\psi(z) + (1-j)2\pi\psi(z^{-1})\} = 2\pi\psi(z) = X(z) \tag{18.120}$$

Let $x[n] = a^n$, $X(z) = 2\pi\psi(a^{-1}z)$,

$$X_{Ha}(z) = \frac{1}{2} \{(1+j)2\pi\psi(a^{-1}z) + (1-j)2\pi\psi(a^{-1}z^{-1})\} \tag{18.121}$$

i.e. $X_{Ha}(z) = \pi \{\psi(a^{-1}z) + \psi(az) + j[\psi(a^{-1}z) - \psi(az)]\}$.

Table 18.9 lists extended discrete Hartley transforms in z -domain.

18.17 Generalization of the Mellin Transform

The Mellin transform of a causal function $f(x)$ is written in the form

$$F_{\mathcal{M}}(s) = \int_0^{\infty} f(x)x^{s-1}dx. \tag{18.122}$$

Let $x = e^{-t}$, $dx = -e^{-t}dt$, $x^{s-1} = e^{-t(s-1)} = e^{-ts}e^t$

$$F_{\mathcal{M}}(s) = - \int_{\infty}^{-\infty} f(e^{-t})e^{-st}dt = \int_{-\infty}^{\infty} f(e^{-t})e^{-st}dt = \mathcal{L}[f(e^{-t})] \tag{18.123}$$

As noted in Chapter 14 the Mellin transform of the function $f(x)$ is the bilateral Laplace transform of the function $f(e^{-t})$. Since the bilateral Laplace transform of the most basic of

TABLE 18.9 Generalized discrete Hartley transforms

$x[n]$	$X_{Ha}(z)$
1	$2\pi\psi(z)$
a^n	$\pi \{ \psi(a^{-1}z) + \psi(az) + j [\psi(a^{-1}z) - \psi(az)] \}$
$\cos bn$	$\pi \{ \psi(e^{-jb}z) + \psi(e^{jb}z) \}$
$\sin bn$	$\pi \{ \psi(e^{-jb}z) - \psi(e^{jb}z) \}$
$u[n]$	$\frac{2 - (z + z^{-1}) - j(z - z^{-1})}{4 - 2(z + z^{-1})} + \pi\psi(z)$
$a^n u[n]$	$\frac{2 - a(z + z^{-1}) - ja(z - z^{-1})}{2(1 - az)(1 - az^{-1})} + \pi\psi(a^{-1}z)$

functions do not exist a great barrier has hitherto blocked the way to evaluating the Mellin transform of a large class of functions. Now, with the introduction of the generalized distributions and generalized Dirac-delta impulse, bilateral Laplace transforms of most functions can be readily obtained. The effect is opening the doors to the expansion of the domains of existence of the Mellin transform.

Example

Given $f(x) = x^{j\beta}$ we have

$$f(e^{-t}) = e^{-j\beta t} \tag{18.124}$$

$$F_{\mathcal{M}}(s) = \mathcal{L}[e^{-j\beta t}] = 2\pi\xi(s + j\beta) \tag{18.125}$$

with $f(x) = x^{-j\beta}$

$$F_{\mathcal{M}}(s) = \mathcal{L}[e^{j\beta t}] = 2\pi\xi(s - j\beta) \tag{18.126}$$

with $f(x) = x^{j\beta} + x^{-j\beta}$

$$F_{\mathcal{M}}(s) = 2\pi \{ \xi(s + j\beta) + \xi(s - j\beta) \} \tag{18.127}$$

with $f(x) = x^{j\beta} - x^{-j\beta}$

$$F_{\mathcal{M}}(s) = 2\pi \{ \xi(s + j\beta) - \xi(s - j\beta) \} \tag{18.128}$$

Table 18.10 lists new basic Mellin transforms obtained thanks to the expansion of the domain of existence of bilateral Laplace transform.

From knowledge of Mellin transforms we can obtain additional new bilateral Laplace transforms as can be seen in Table 18.11.

TABLE 18.10 New Mellin transforms

$f(x)$	$F_{\mathcal{M}}(s)$
x^γ	$2\pi\xi(s + \gamma)$
$x^\gamma + x^{\gamma^*}$	$2\pi\{\xi(s + \gamma) + \xi(s + \gamma^*)\}$
$u(-\ln x)$	$1/s + \pi\xi(s)$
$x^\alpha u(-\ln x)$	$1/(s + \alpha) + \pi\xi(s + \alpha)$
$\text{sgn}(-\ln x)$	$2/s$
$\ln x$	$2\pi d\xi(s)/ds$
$(\ln x)^n$	$2\pi\xi^{(n)}(s)$
$(\ln x)^n u(-\ln x)$	$\frac{(-1)^n n!}{s^{n+1}} + \pi\xi^{(n)}(s)$

18.18 Multidimensional Signals and the Solution of Differential Equations

The extended generalized transforms are applicable to the transformation of multidimensional signals. As an example of such applications, Table 18.12 lists new extended two-dimensional bilateral z -transforms of some basic sequences.

$$S(n, m) \equiv S_n^{(m)} = \frac{1}{m!} \sum_{k=0}^m (-1)^{m-k} \binom{m}{k} k^n.$$

As an example of the application of extended transforms to partial differential equations we consider the solution of the heat equation

$$\frac{\partial u(x, t)}{\partial t} - \frac{\partial^2 u(x, t)}{\partial x^2} = te^{\alpha t} \tag{18.129}$$

with the boundary conditions $u(0, t) = u(1, t) = 0$ and the initial condition $u(x, 0) = 0$. Laplace transforming both sides of the partial differential equation we have

$$\frac{d^2 U}{dx^2}(x, s) - sU(x, s) = -2\pi\xi'(s - \alpha) \tag{18.130}$$

The particular solution has the form $U_p(x, s) = A_0$ which upon substitution in the equation implies that $-sA_0 = -2\pi\xi'(s - \alpha)$, i.e.

$$A_0 = 2\pi\xi'(s - \alpha) / s = (2\pi/\alpha)\xi'(s - \alpha) + (2\pi/\alpha^2)\xi(s - \alpha) \tag{18.131}$$

and the general solution has the form

$$U(x, s) = k_1 \cosh \sqrt{s}x + k_2 \sinh \sqrt{s}x + \frac{2\pi}{\alpha}\xi'(s - \alpha) + \frac{2\pi}{\alpha^2}\xi(s - \alpha) \tag{18.132}$$

TABLE 18.11 Additional new bilateral Laplace transforms

$f(t)$	$F(s)$
$e^{-a} e^{-t}$	$a^{-s} \Gamma(s)$, $Re[a] > 0$, $\sigma > 0$
$e^{-e^{-2t}}$	$\frac{1}{2} \Gamma(s/2)$
$\sin e^{-t}$	$\Gamma(s) \sin(\pi s/2)$, $-1 < \sigma < 1$
$\cos e^{-t}$	$\Gamma(s) \sin(\pi s/2)$, $0 < \sigma < 1$
$\frac{1}{1+e^{-t}}$	$\pi \operatorname{cosec} \pi s$
$\frac{1}{1-e^{-t}}$	$b\pi \cot \pi s$
$\frac{1}{(1+e^{-t})^a}$	$\frac{\Gamma(s)\Gamma(a-s)}{\Gamma(a)}$, $Re[a] > 0$
$\frac{1}{1+e^{-2t}}$	$(\pi/2) \operatorname{cosec}(\pi s/2)$
$(1-e^{-t})^{a-1} u(t)$	$\frac{\Gamma(s)\Gamma(a)}{\Gamma(s+a)}$, $Re[a] > 0$
$(e^{-t}-1)^a u(-t)$	$\frac{\Gamma(a-s)\Gamma(1-a)}{\Gamma(1-s)}$, $0 < Re[a] < 1$
$\ln(1+e^{-t})$	$(\pi/s) \operatorname{cosec} \pi s$, $-1 < \sigma < 0$
$\pi/2 - \tan^{-1} e^{-t}$	$\frac{\pi}{2s} \sec(s/2)$
$\Lambda(e^{-t}-1)$	$\begin{cases} \frac{2(2^s-1)}{s(s+1)}, & s \neq 0, \sigma > -1 \\ 2 \ln 2, & s \neq 0, \sigma > -1 \end{cases}$
$\operatorname{erfc} e^{-t}$	$[\Gamma(s/2+1/2)] / (\pi^2 s)$, $\sigma > 0$
$\operatorname{Si} e^{-t}$	$-\{\Gamma(s) \sin(\pi s/2)\} / s$, $-1 < \sigma < 0$

TABLE 18.12 New two-dimensional bilateral z -transforms

$x [n_1, n_2]$	$X (z_1, z_2)$
1	$4\pi^2\psi (z_1) \psi (z_2)$
$a^{n_1}b^{n_2}$	$4\pi^2\psi (a^{-1}z_1) \psi (b^{-1}z_2)$
$u [n_1, n_2]$	$\frac{1}{(1 - z_1^{-1}) (1 - z_2^{-1})} + \frac{\pi\psi (z_1)}{1 - z_2^{-1}} + \frac{\pi\psi (z_2)}{1 - z_1^{-1}} + \pi^2\psi (z_1) \psi (z_2)$
$\cos \beta_1 n_1 \cos \beta_2 n_2$	$\pi^2 \{ \psi (e^{-j\beta_1} z_1) + \psi (e^{j\beta_1} z_1) \} \{ \psi (e^{-j\beta_2} z_2) + \psi (e^{j\beta_2} z_2) \}$
$n_1 n_2$	$4\pi^2 z_1 z_2 \psi' (z_1) \psi' (z_2)$
$n_1^{r_1} n_2^{r_2}$	$4\pi^2 \left\{ \sum_{i=1}^{r_1+1} (-1)^{i+1} S (r_1 + 1, i) \psi^{(i-1)} (z_1) \right\} \times \left\{ \sum_{k=1}^{r_2+1} (-1)^{k+1} S (r_2 + 1, k) \psi^{(k-1)} (z_2) \right\}$

Using the initial condition $U(0, s) = U(1, s) = 0$ and $U(1, s) = 0$ we have

$$k_1 = -\frac{2\pi}{\alpha} \xi'(s - \alpha) - \frac{2\pi}{\alpha^2} \xi(s - \alpha) \tag{18.133}$$

$$k_1 \cosh \sqrt{s} + k_2 \sinh \sqrt{s} + \frac{2\pi}{\alpha} \xi'(s - \alpha) + \frac{2\pi}{\alpha^2} \xi(s - \alpha) = 0 \tag{18.134}$$

$$k_2 = \left[-k_1 \cosh \sqrt{s} - \frac{2\pi}{\alpha} \xi'(s - \alpha) - \frac{2\pi}{\alpha^2} \xi(s - \alpha) \right] / \sinh \sqrt{s} \tag{18.135}$$

We obtain

$$U(x, s) = (2\pi/\alpha) F(x, s)\xi'(s - \alpha) + (2\pi/\alpha^2) F(x, \alpha)\xi(s - \alpha) \tag{18.136}$$

where

$$F(x, s) = 1 + \coth \sqrt{s} \sinh \sqrt{s}x - \sinh \sqrt{s}x / \sinh \sqrt{s} - \cosh \sqrt{s}x \tag{18.137}$$

Since in general

$$F(s)\xi'(s - \alpha) = F(\alpha)\xi'(s - \alpha) - F'(\alpha)\xi(s - \alpha) \tag{18.138}$$

we may write

$$U(x, s) = (2\pi/\alpha) F(x, \alpha)\xi'(s - \alpha) - (2\pi/\alpha) \{F'(x, \alpha) - F(x, \alpha)/\alpha\} \xi(s - \alpha) \tag{18.139}$$

which can be written in the form

$$U(x, s) = (2\pi/\alpha) F(x, \alpha)\xi'(s - \alpha) - (2\pi/\alpha) G(x, \alpha)\xi(s - \alpha) \tag{18.140}$$

with

$$G(x, \alpha) = F'(x, \alpha) - F(x, \alpha)/\alpha \tag{18.141}$$

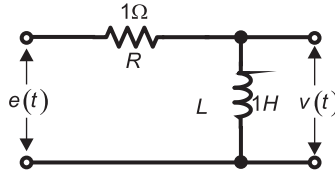


FIGURE 18.12 R-L circuit, Problem 3.7.

After some algebraic manipulation we obtain

$$G(x, \alpha) = \frac{-1}{4\alpha} \{ \operatorname{sech}^2(\sqrt{\alpha}/2) [2 + 2 \cosh \sqrt{\alpha} - 2 \cosh(\sqrt{\alpha}x - \sqrt{\alpha}) - 2 \cosh \sqrt{\alpha}x + \sqrt{\alpha}x \sinh(\sqrt{\alpha}x - \sqrt{\alpha}) - \sqrt{\alpha} \sinh \sqrt{\alpha}x + \sqrt{\alpha}x \sinh \sqrt{\alpha}x] \}$$

wherefrom the solution

$$u(x, t) = \frac{-F(x, \alpha)}{\alpha} t e^{\alpha t} - \frac{1}{\alpha} G(x, \alpha) e^{\alpha t}.$$

18.19 Problems

Problem 18.1 For the circuit shown in Fig.18.12,

- evaluate the transfer function $H(s)$ between the input $e(t)$ and output $v(t)$
- evaluate the system impulse response.
- evaluate the response of the circuit to the inputs

$$i) e_1(t) = \sum_{n=-\infty}^{\infty} \delta(t-n)$$

$$ii) e_2(t) = \sum_{n=0}^{\infty} \delta(t-n)$$

Problem 18.2 Let $x(t) = x_1(t) + x_2(t)$, $v(t) = v_1(t) + v_2(t)$ where $x_1(t) = u(t)$, $x_2(t) = u(-t)$

$$v_1(t) = \sin \beta t u(t), \quad v_2(t) = \sin \beta t u(-t).$$

Evaluate Laplace and Fourier transform of $x(t)$ and $v(t)$ if they exist, stating the regions of convergence and the reason if non-existent.

Problem 18.3 For each of the following signals evaluate the Laplace transform, the poles with the region of convergence, and state whether or not the Fourier transform exists.

$$a) v_1(t) = \sum_{i=1}^P A_i e^{-a_i t} \cos(b_i t + \theta_i) u(t) + \sum_{i=1}^P B_i e^{c_i t} \cos(d_i t + \phi_i) u(-t)$$

where the a_i , b_i and c_i are distinct and $b_i > 0$, $d_i > 0$, $a_i > 0$, $c_i > 0$, $\forall i$.

b) The same function $v_1(t)$ but with the conditions:

$$b_i > 0, \quad d_i > 0, \quad a_i > 0, \quad c_i < 0, \quad \forall i.$$

c) The same function $v_1(t)$ but with the conditions:

$$b_i > 0, \quad a_i = 0, \quad B_i = 0, \quad \forall i.$$

d) $v_2(t) = A \cos(bt + \theta)$, $-\infty < t < \infty$.

e) $v_3(t) = A e^{-t}$, $-\infty < t < \infty$.

18.20 Answers to Selected Problems

Problem 18.1

a) $H(s) = \frac{sL}{R+sL} = \frac{s}{s+1} = 1 - \frac{1}{s+1}$

b) $h(t) = \delta(t) - e^{-t}u(t)$

c)

i)

$$\begin{aligned} V_1(s) &= E_1(s) H(s) = 2\pi \sum_{n=-\infty}^{\infty} \xi(s - jn2\pi) \frac{s}{s+1} \\ &= 2\pi \sum_{n=-\infty}^{\infty} \frac{j2n\pi}{j2n\pi + 1} \xi(s - j2n\pi) \end{aligned}$$

ii)

$$\begin{aligned} E_2(j\omega) &= 0.5 + \sum_{n=-\infty}^{\infty} \frac{1}{j\omega - jn2\pi} + \pi \sum_{n=-\infty}^{\infty} \delta(\omega - n2\pi) \\ V_2(s) &= \frac{s}{(1 - e^{-s})(s+1)}, \quad \sigma > 0. \end{aligned}$$

Problem 18.2

$$\begin{aligned} V_1(j\omega) &= \beta / (\beta^2 - \omega^2) + [\pi / (2j)] \{ \delta(\omega - \beta) - \delta(\omega + \beta) \} \\ V_2(j\omega) &= -\beta / (\beta^2 - \omega^2) - [\pi / (2j)] \{ \delta(\omega + \beta) - \delta(\omega - \beta) \} \end{aligned}$$

$$V(j\omega) = V_1(j\omega) + V_2(j\omega) = (\pi/j) \{ \delta(\omega - \beta) - \delta(\omega + \beta) \} = \mathcal{F}[\sin \beta t].$$

Problem 18.3

c)

$$\begin{aligned} V_1(s) &= \sum_{i=1}^P A_i \cos \theta_i \left[\frac{s}{s^2 + b_i^2} + \frac{\pi}{2} \{ \xi(s - jb_i) + \xi(s + jb_i) \} \right] \\ &\quad - A_i \sin \theta_i \left[\frac{b_i}{s^2 + b_i^2} - \frac{j\pi}{2} \{ \xi(s - jb_i) - \xi(s + jb_i) \} \right] \\ V_1(j\omega) &= \sum_{i=1}^P A_i \cos \theta_i \left[\frac{j\omega}{b_i^2 - \omega^2} + \frac{\pi}{2} \{ \delta(\omega - b_i) + \delta(\omega + b_i) \} \right] \\ &\quad - A_i \sin \theta_i \left[\frac{b_i}{b_i^2 - \omega^2} - \frac{j\pi}{2} \{ \delta(\omega - b_i) - \delta(\omega + b_i) \} \right]. \end{aligned}$$

d)

$$\begin{aligned} V_2(s) &= A\pi [\cos \theta \{ \xi(s - jb) + \xi(s + jb) \} + j \sin \theta \{ \xi(s - jb) - \xi(s + jb) \}] \\ V_2(j\omega) &= A\pi [\cos \theta \{ \delta(\omega - b) + \delta(\omega + b) \} + j \sin \theta \{ \delta(\omega - b) - \delta(\omega + b) \}] \end{aligned}$$

This page intentionally left blank

A

Appendix

A.1 Symbols

The following symbols are adopted:

x^* : Conjugate of x ; $*$: Convolution \star : Correlation.

$\Pi_T(t)$ Centered rectangle of total width $2T$; $\Pi_T(t) = u(t+T) - u(t-T)$.

$\Lambda_T(t)$ Centered triangle of height 1 and total width $2T$.

$R_T(t)$ Rectangle of width T starting at $t = 0$,
 $R_T(t) = u(t) - u(t-T)$.

These functions are represented graphically in Fig. 1.1 of Chapter 1. The figure also shows the usual graphical representation of the Dirac-delta impulse $\delta(t)$, a representation of its derivative $\delta'(t)$ and the impulse train $\rho_T(t)$ of period T ,

$$\rho_T(t) = \sum_{n=-\infty}^{\infty} \delta(t - nT)$$

\triangleq : Equals by definition; $s \longrightarrow y$: s replaced by y

$\xi(s)$ Generalized delta impulse in s domain; $\psi(z)$ Generalized delta impulse in z domain.

The function $Sah(x) \equiv Sh(x)$ is the hyperbolic generalization of the usual (trigonometric) sampling function $Sa(x)$ [26] [18]. $Sah(x) \equiv Sh(x) = \sinh(x)/x$. The function $Sd_N(\Omega)$ is the discrete counterpart of the sampling function. It is related to the transform of a rectangle and is given by [26]

$$Sd_N(\Omega) = \sin(N\Omega)/\sin(\Omega). \tag{A.1}$$

which is depicted together with its modulus in Fig. A.1. We can adopt other generalizations of the sampling function $Sa(x)$, namely, $Ca(x) = \cos(x)/x$, $Ta(x) = \tan(x)/x$, $Sah(x) \equiv Sh(x) = \sinh(x)/x$, $Cah(x) = \cosh(x)/x$, $Tah(x) = \tanh(x)/x$, ... [18] [26].

A.2 Frequently Needed Expansions

General property of differentiation of a product

$$(ab)^{(n)} = \sum_{m=0}^n \binom{n}{m} a^{(n-m)} b^{(m)} \tag{A.2}$$

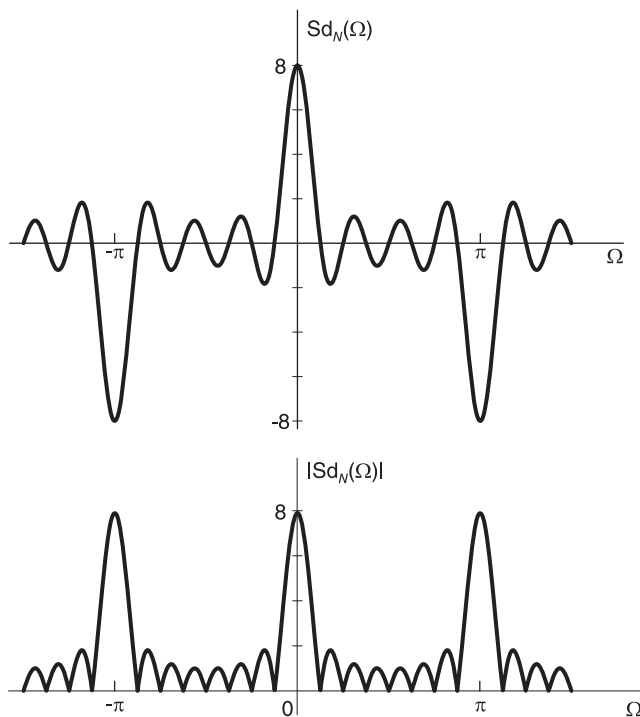


FIGURE A.1 The Sd function and its modulus.

Taylor’s Series

$$f(x) = f(a) + f'(a)(x - a) + \frac{f''(a)(x - a)^2}{2!} + \dots + \frac{f^{(n-1)}(a)(x - a)^{n-1}}{(n - 1)!} + \dots \quad (\text{A.3})$$

Binomial Expansion

$$(x + y)^n = \sum_{k=0}^n \binom{n}{k} x^{n-k} y^k \quad (\text{A.4})$$

$$(1 + x)^{-1/2} = 1 - \frac{1}{2}x + \frac{1 \cdot 3}{2 \cdot 4}x^2 - \frac{1 \cdot 3 \cdot 5}{2 \cdot 4 \cdot 6}x^3 + \dots, \quad -1 < x \leq 1. \quad (\text{A.5})$$

$$(x_1 + x_2 + \dots + x_p)^n = \sum \frac{n!}{n_1!n_2! \dots n_p!} x_1^{n_1} x_2^{n_2} \dots x_p^{n_p} \quad (\text{A.6})$$

$$\left(\frac{1}{\omega}\right)^{(n)} = \frac{(-1)^n n!}{\omega^{n+1}} \quad (\text{A.7})$$

Stirling Number First Kind

$$s(n, m) \equiv s_n^m = \sum_{k=0}^{n-m} (-1)^k \binom{n-1+k}{n-m+k} \binom{2n-m}{n-m-k} s(n-m+k, k) \quad (\text{A.8})$$

Stirling Number Second Kind

$$S_n^{(m)} \equiv S(n, m) = \frac{1}{m!} \sum_{k=0}^m (-1)^{m-k} \binom{m}{k} k^n \quad (\text{A.9})$$

A.3 Important Trigonometric Relations

We have

$$1 + e^{j\theta} = e^{j\theta/2}(e^{-j\theta/2} + e^{j\theta/2}) = 2e^{j\theta/2} \cos(\theta/2) \quad (\text{A.10})$$

$$|1 + e^{j\theta}| = 2 |\cos(\theta/2)| = 2 \cos(\theta/2), \quad 0 < \theta < \pi \quad (\text{A.11})$$

$$\cos \theta = \frac{1}{2} |1 + e^{j2\theta}|, \quad 0 < \theta < \pi/2 \quad (\text{A.12})$$

Similarly

$$1 - e^{j\theta} = e^{j\theta/2}(e^{-j\theta/2} - e^{j\theta/2}) = -2je^{j\theta/2} \sin(\theta/2) \quad (\text{A.13})$$

$$|1 - e^{j\theta}| = 2 |\sin(\theta/2)| = 2 \sin(\theta/2), \quad 0 < \theta < 2\pi \quad (\text{A.14})$$

$$\sin \theta = \frac{1}{2} |1 - e^{j2\theta}|, \quad 0 < \theta < \pi. \quad (\text{A.15})$$

A.4 Orthogonality Relations

The trigonometric and complex exponential functions satisfy the following important orthogonality relations.

With k , m and n integers we have

$$\int_{2\pi} e^{jkt} e^{jmt} dt = \begin{cases} 0, & k \neq -m \\ 2\pi, & k = -m \end{cases}$$

$$\int_{2\pi} \cos kt \sin mt dt = 0$$

$$\int_{2\pi} \cos kt \cos mt dt = \begin{cases} 0, & k \neq m, \quad k \geq 0, \quad m \geq 0 \\ \pi, & k = m > 0 \\ 2\pi, & k = m = 0 \end{cases}$$

$$\int_{2\pi} \sin kt \sin mt dt = \begin{cases} 0, & k \neq m, \quad k \geq 0, \quad m \geq 0 \\ \pi, & k = m > 0 \\ 0, & k = m = 0. \end{cases}$$

From Equation (17.207) with $k + m = n$

$$\int_{2\pi} \cos nt dt + j \sin nt dt = \begin{cases} 0, & n \neq 0 \\ 2\pi, & n = 0 \end{cases}$$

wherefrom

$$\int_{2\pi} \cos nt dt = \begin{cases} 0, & n \neq 0 \\ 2\pi, & n = 0 \end{cases}$$

$$\int_{2\pi} \sin nt dt = 0.$$

Using the substitution $\tau = \frac{2\pi}{T_0} t$, i.e. $d\tau = \frac{2\pi}{T_0} dt$ we obtain with $\omega_0 = \frac{2\pi}{T_0}$

$$\int_{T_0} e^{j(k+m)\omega_0 t} dt = \frac{T_0}{2\pi} \int_{2\pi} e^{j(k+m)\tau} d\tau = \begin{cases} 0, & k \neq -m \\ T_0, & k = -m \end{cases}$$

Similarly we obtain

$$\int_{T_0} \cos k\omega_0 t \sin m\omega_0 t dt = 0$$

$$\int_{T_0} \cos k\omega_0 t \cos m\omega_0 t dt = \begin{cases} 0, & k \neq m, \quad k \geq 0, \quad m \geq 0 \\ T_0/2, & k = m > 0 \\ T_0, & k = m = 0 \end{cases}$$

$$\int_{T_0} \sin k\omega_0 t \sin m\omega_0 t dt = \begin{cases} 0, & k \neq m, \quad k \geq 0, \quad m \geq 0 \\ T_0/2, & k = m > 0 \\ 0, & k = m = 0 \end{cases}$$

$$\int_{T_0} \cos n\omega_0 t dt = \begin{cases} 0, & n \neq 0 \\ T_0, & n = 0 \end{cases}$$

$$\int_{T_0} \sin n\omega_0 t dt = 0$$

A.5 Frequently Encountered Functions

Error Function

$$\operatorname{erf}(t) = \frac{2}{\sqrt{\pi}} \int_0^t e^{-u^2} du. \quad (\text{A.16})$$

Complementary Error Function

$$\operatorname{erfc}(t) = 1 - \operatorname{erf}(t) = \frac{2}{\sqrt{\pi}} \int_t^\infty e^{-u^2} du. \quad (\text{A.17})$$

Exponential Integral

$$\operatorname{Ei}(t) = \int_t^\infty \frac{e^{-u}}{u} du. \quad (\text{A.18})$$

Sine Integral

$$\operatorname{Si}(t) = \int_0^t \frac{\sin u}{u} du. \quad (\text{A.19})$$

Cosine Integral

$$\operatorname{Ci}(t) = \int_t^\infty \frac{\cos u}{u} du. \quad (\text{A.20})$$

A.6 Mathematical Formulae

$$\alpha \sum_{k=0}^{n-1} r^k = \alpha + \alpha r + \alpha r^2 + \alpha r^3 + \dots + \alpha r^{n-1} = \frac{\alpha(1-r^n)}{1-r} = \frac{\alpha - r^n \alpha}{1-r} \quad (\text{A.21})$$

where $-1 < r < 1$. If $-1 < r < 1$, then

$$\alpha \sum_{k=0}^{\infty} r^k = \alpha + \alpha r + \alpha r^2 + \alpha r^3 + \dots = \frac{\alpha}{1-r} \quad (\text{A.22})$$

A.7 Frequently Encountered Series Sums

$$\alpha + (\alpha + d)r + (\alpha + 2d)r^2 + \dots + (\alpha + (n - 1)d)r^{n-1} = \frac{\alpha(1 - r^n)}{1 - r} + \frac{rd\{1 - nr^{n-1} + (n - 1)r^n\}}{(1 - r)^2} \tag{A.23}$$

where $r \neq 1$. If $-1 < r < 1$, then

$$\alpha + (\alpha + d)r + (\alpha + 2d)r^2 + \dots = \frac{\alpha}{1 - r} + \frac{rd}{(1 - r)^2} \tag{A.24}$$

In evaluating z -transforms, convolutions and correlations the sum of a geometric series, or variations thereof, are usually encountered. The following sums are worthwhile remembering.

$$\sum_{n=n_1}^{n_2} a^n = a^{n_1} \frac{1 - a^{n_2 - n_1 + 1}}{1 - a} \tag{A.25}$$

$$\sum_{n=0}^{\infty} a^n = \frac{1}{1 - a}, \quad |a| < 1.$$

Sums such as $\sum na^n$ can be deduced through differentiation.

Differentiating both sides we have

$$\sum_{n=0}^{\infty} na^{n-1} = \frac{1}{(1 - a)^2} \tag{A.26}$$

i.e.

$$\sum_{n=0}^{\infty} na^n = \frac{a}{(1 - a)^2}. \tag{A.27}$$

The Sum of the Weighted Geometric Series $\sum_{k=n_1}^{n_2} ka^k$ is often encountered in evaluating convolutions, correlations and z -transform. It is worthwhile obtaining a closed form that may be subsequently used whenever the need arises. We shall use the notation

$$\mathcal{S}(a, n_1, n_2) \triangleq \sum_{k=n_1}^{n_2} ka^k \tag{A.28}$$

To evaluate the sum we first recall the sum of the geometric series

$$\sum_{k=n_1}^{n_2} a^k = a^{n_1} \frac{1 - a^{n_2 - n_1 + 1}}{1 - a} = \frac{a^{n_1} - a^{n_2 + 1}}{1 - a} \tag{A.29}$$

Differentiating both sides of this equation we have

$$\sum_{k=n_1}^{n_2} ka^{k-1} = \frac{(1 - a)\{n_1 a^{n_1 - 1} - (n_2 + 1)a^{n_2}\} + (a^{n_1} - a^{n_2 + 1})}{(1 - a)^2} \tag{A.30}$$

Hence

$$\mathcal{S}(a, n_1, n_2) \triangleq \sum_{k=n_1}^{n_2} ka^k = \frac{(1 - a)\{n_1 a^{n_1} - (n_2 + 1)a^{n_2 + 1}\} + (a^{n_1 + 1} - a^{n_2 + 2})}{(1 - a)^2} \tag{A.31}$$

This sum of a weighted geometric series can now be coded as a MATLAB® function. The following MATLAB function can subsequently be used to evaluate expressions containing such a sum:

```
function [summ] = wtdsum(a,n1,n2)
sum=0;
for k=n1:n2
sum = sum + k.*ak;
end
summ=sum;
```

A.8 Biographies of Pioneering Scientists

Due to space limitation the following is a snapshot of the lives of only a few of the scientists who laid the foundations of the subjects studied in this book.

A.9 Plato (428 BC–347 BC)

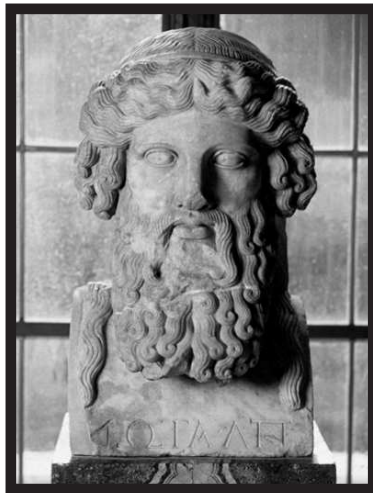


FIGURE A.2 Plato, (Museus Capitolinos, Roma). Photograph courtesy of Corbis Corp.

Plato was born in Athens, Greece, around 428 BC. He is known as one of the earliest and most famous philosophers. His original name was Aristocles, and nicknamed Plato meaning broad-shouldered. He was the son of Ariston and Perictione. His father Ariston is believed to be descendant of the king of Athens, Codrus, and the king of Messenia, Melanthus. His

mother Perictione was related to the famous Athenian legislator and lyric poet Solon. She was sister of Charmides, a close friend of Socrates (c. 469 BC–399 BC), and niece of Critias, both leaders of the Thirty Tyrants, the brief oligarchic regime that rose upon the collapse of Athens at the end of the Peloponnesian War.

This war was fought between Athens and Sparta between 431 BC and 404 BC. Plato was enlisted in military service from 409 BC to 404 BC. At the end of the war he was urged to join in the leadership of the Thirty Tyrants but was repulsed by their violent measures. Plato and his two older brothers became students of Socrates. Socrates advocated questioning irrational dogmas and skepticism in the face of unsubstantiated ideas based on sheer belief. Such revolutionary messages did not endear him to authorities.

After the reign of the Thirty Tyrants which lasted only eight months there was a restoration of democracy in Athens and Plato considered playing a role in its politics. However, Socrates' association with opponents of the democratic regime let an Athenian jury lay charges of corrupting the youth and interfering with the religion of the state. Socrates was convicted and sentenced to death in 399 B.C. Accepting this outcome with remarkable grace, Socrates drank hemlock and died in the company of his friends and disciples. The sentencing to death of Socrates had a profound effect on Plato, and he decided that he would have nothing further to do with politics in Athens.

Plato traveled to Egypt, Sicily and Italy. In Egypt he learnt of a water clock, *clepsydra*, in Greek, and had a role in its existence in Greece. While in Italy he studied the work of Pythagoras (born between 580 and 572 BC, died between 500 and 490 BC) and became enamored with mathematics. Plato acquired knowledge from the disciples of Pythagoras, which helped him form his own idea "... that the reality which scientific thought is seeking must be expressible in mathematical terms, mathematics being the most precise and definite kind of thinking of which we are capable. The significance of this idea for the development of science from the first beginnings to the present day has been immense." [1].

Following another war, during which period he served again in the military, Plato began writing his dialogues. He returned to Athens and founded his Academy, in about 387 BC. It was built in a grove sacred to the demigod Academus; whence the name academy that we use today. The Academy was, in effect, a university of higher learning, which included

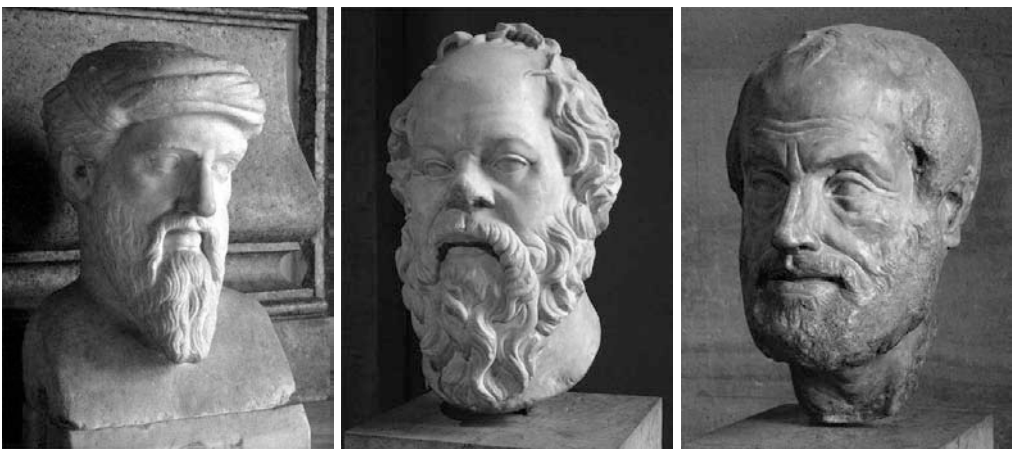


FIGURE A.3 (a) Pythagoras (c.580–500 BC) www.en.wikipedia.org/wiki/Pythagoras
 (b) Socrates (c. 469–399 BC). www.en.wikipedia.org/wiki/Image:Socrates_Louvre.jpg
 (c) Aristoteles (384–322 BC). www.en.wikipedia.org/wiki/Image:Aristoteles_Louvre.jpg

physical science, astronomy, mathematics and philosophy. Aristoteles (384–322 BC) was a student and then teacher at the Academy. He is referred to often as Aristotle. However the true name in Greek is Aristoteles.

Plato's main contributions are in philosophy, mathematics and science. He compared the precise mathematical abstract concept with our attempts to reproduce it. A drawing will never produce a true circle, an isosceles triangle, a right angle, or even a simple straight line as we know them in the abstract.

“Platonic solids” are named after Plato. In his “Timaeus” there is a mathematical construction of the elements that make up the elements of the universe, earth, fire, air, and water, wherein the cube, tetrahedron, octahedron, and icosahedron are the shapes of the atoms of earth, fire, air, and water. The fifth Platonic solid, the dodecahedron, is Plato's model for the whole universe.

Following the death of Dionysius I the ruler of Syracuse, Italy, his brother-in-law, Dion, persuaded Plato to tutor Dionysius II, the new ruler. Plato went to Syracuse, Italy, in 367 BC. Dion and Archytas of Tarentum believed that if Dionysius II was trained in science and philosophy he would become a ruler capable of protecting Sicily from invasion by Carthage. However, Dionysius II expelled Dion out of Syracuse and the plan of educating Dionysius II fell apart. Plato returned to Athens, but went back to Syracuse again in 361 BC, hoping to reconcile Dionysius II and Dion. He did not succeed in his attempts and returned to Athens in 360 BC. Dion attacked Syracuse in a coup in 357 BC. He gained control of the city; but was murdered in 354 BC.

Plato believed that the stars, the planets, the Sun and Moon move round the Earth in crystalline spheres. The sphere of the Moon was closest to Earth, followed by the sphere of the Sun, then Mercury, Venus, Mars, Jupiter, Saturn and, farther away, was the sphere of the stars. He believed that the Moon shines by reflected sunlight. Plato presided over the Academy where he gave lectures, dedicating to it the rest of his life. The Academy lasted until 529 AD when it was closed down by the Christian Emperor Justinian, accusing it of being a pagan institution. Having lasted for close to a millennium, it is the longest surviving university known.

Plato died in 347 BC, at about the age of eighty.

References:

[1] G. C. Field, *The Philosophy of Plato*, Oxford, 1956.

<http://library.thinkquest.org/18775/plato/biop.htm>

Article by: J. J. O'Connor and E. F. Robertson, <http://www-groups.dcs.st-and.ac.uk/history/Biographies/Plato.html>

Wikipedia, the free encyclopedia, <http://en.wikipedia.org/wiki/Plato>

<http://plato-dialogues.org/life.htm>

A.10 Ptolemy (circa 90–168 AD)

Ptolemy was the most influential astronomer, geographer, and mathematician of ancient times. He was a Greek who lived in Alexandria, in Roman Egypt which was a major center of knowledge of the ancient Mediterranean. He promoted the (geocentric) idea that the Earth was the center of the Universe and that all things revolved around it. This theory prevailed for the next 1400 years. The writings of Ptolemy include names and outlines of 48 constellations that are still in use today. He was the author of several scientific treatises including his treatise on astronomy known as the *Almagest*, *The Mathematical Treatise* or



FIGURE A.4 Ptolemy

The Great Treatise, his treatise *Geography*, which is a thorough overview of the geography of the Greco-Roman world, and his astrological treatise known in Greek as the *Apotelesmatika* or the *Tetrabiblos* (“Four books”), in which he proposed ways to reconcile astrology with Aristotelian natural philosophy.

Reference:

<http://en.wikipedia.org/wiki/Ptolemy>

A.11 Euclid (circa 300 BC)



FIGURE A.5 Euclid.

Euclid was a Greek mathematician who lived and taught in Alexandria, Egypt, circa 300 BC. He is considered the most prominent mathematician of antiquity, best known for *The*

Elements, his treatise on mathematics.

Euclid's *Elements* is a mathematical treatise on geometry consisting of thirteen books. It comprises a collection of axioms, theorems and constructions, followed by mathematical proofs of the theorems.

The thirteen books cover what came to be known as Euclidean geometry, and the ancient Greek version of number theory. With the exception of Autolycus *On the Moving Sphere*, *Elements* is one of the oldest extant Greek mathematical treatises and it is the oldest extant axiomatic deductive treatment of mathematics. It laid the foundations of logic and modern science.

Euclid's *Elements* is considered the most successful and influential textbook ever written. It is one of the very earliest mathematical works to be printed, being first set in type in Venice in 1482, after the invention of the printing press. It is second only to the Bible in the number of editions published, with the number surpassing 1,000. It has been used as the basic text on geometry throughout the world for about 2,000 years. For centuries, when the quadrivium was included in the curriculum of university students, knowledge of at least part of Euclid's *Elements* was an absolute requirement.

References:

Bulmer-Thomas, J. E. Murdoch, *Biography in Dictionary of Scientific Biography* (New York 1970–1990).

T. L. Heath, *A History of Greek Mathematics 1* (Oxford, 1931).

Also J. J. O'Connor and E F Robertson,

<http://www-groups.dcs.st-and.ac.uk/history/Mathematicians/Euclid.html>

<http://en.wikipedia.org/wiki/Euclid>

A.12 Abu Ja'far Muhammad ibn Musa Al-Khwarizmi (780–850 AD)



FIGURE A.6 Abu Ja'far Muhammad ibn Musa Al-Khwarizmi.

Born: About 780 in Baghdad (now in Iraq); **died:** About 850

Not much is known about Abu Ja'far Muhammad ibn Musa al-Khwarizmi's life. Within years of al-Khwarizmi's birth, on September 14, 786, the famous conqueror Harun al-Rashid (March 17, 763–March 24, 809 born in Rayy near Tehran, Iran) became the fifth Caliph of the Abbasid dynasty. Harun ruled, from his court in the capital city of Baghdad, over the Islam empire which stretched from the Mediterranean to India. He brought culture to his court. His time was marked by scientific, cultural, and religious prosperity, and he tried to establish intellectual disciplines which he felt were lagging behind in the Arabic world. Art, literature, and music flourished significantly during his reign.

Harun al-Rashid had two sons, the elder al-Amin, the younger al-Mamun. Harun died in 809 and there followed an armed conflict between the two brothers. Al-Mamun prevailed and al-Amin was killed in 813.

Al-Mamun became Caliph and ruled the empire from Baghdad. He continued the cultural patronage started by his father and founded an academy called the House of Wisdom *Bayt al-Hikma* where Greek philosophical and scientific works were translated.

He also constituted a library of manuscripts, the first major library set up since the famous one in Alexandria, collecting important works from Byzantium. In addition, al-Mamun set up observatories in which Muslim astronomers could build on the knowledge acquired by earlier world astronomers.

Under the patronage of Al-Mamun, al-Khwarizmi and his colleagues the Banu Musa brothers were scholars at the Bayt al-Hikma in Baghdad. They worked on translation of Greek scientific manuscripts and studied, and wrote on, algebra, geometry and astronomy.

Al-Khwarizmi dedicated two of his texts to the Caliph. These were a treatise on algebra and the other on astronomy. The algebra treatise *Hisab al-jabr w'al-muqabala* was to be the most famous and important of all of al-Khwarizmi's works. It is the word "al-jabr" in the title that gave the Western world the word "algebra," and in a sense it is the first book to be written on algebra. Al-Khwarizmi wrote that the purpose of the book was to teach "what is easiest and most useful in arithmetic, such as men constantly require in cases of inheritance, legacies, partition, lawsuits, and trade, and in all their dealings with one another, or where the measuring of lands, the digging of canals, geometrical computations, and other objects of various sorts and kinds are concerned."

This may not resemble the algebra of today. However it should be noted that the book was intended to be a practical guide and that algebra was introduced to solve problems of everyday life in the Islamic empire at that time.

Early in the book al-Khwarizmi introduces natural numbers. He then introduces linear and quadratic equations and their solutions.

Al-Khwarizmi employs only words instead of symbols to denote his variables, in contrast to earlier treatises on mathematics. Equation simplification and thence solution is effected using the two operations of al-jabr and al-muqabala. Here "al-jabr" may be interpreted as restoration, wherein terms are moved from one side of the equation to the other to remove negative terms. The term "al-muqabala" means encounter, wherein terms of equal powers of the unknown variable are joined together.

Al-Khwarizmi then shows how to solve six standard types of equations. He uses both algebraic and geometric methods of solution. According to historians the geometrical proofs point to unfamiliarity with Euclid's *Elements*. Yet, while al-Khwarizmi was a young man, al-Hajjaj had translated Euclid's *Elements* into Arabic, and al-Hajjaj was one of al-Khwarizmi's colleagues in the *Bayt al-Hikma* House of Wisdom. According to Toomer [1] "... in his introductory section al-Khwarizmi uses geometrical figures to explain equations, which surely argues for a familiarity with Book II of Euclid's *Elements*."

Rashed [2] on the other hand writes that al-Khwarizmi's "... treatment was very probably inspired by recent knowledge of the *Elements*." However, Gandz in [3] argues that "*Euclid's Elements in structure and deductive reasoning are absent in the geometrical proofs.*"

The next part of al-Khwarizmi's book deals with formulas on the area of geometric figures such as the circle and the volume of solids such as the sphere, cone, and pyramid. This section on mensuration has more in common with Hindu and Hebrew texts than it does with any Greek work.

The final part of the book deals with the complicated Islamic rules for inheritance but requires little from the earlier algebra beyond solving linear equations.

Al-Khwarizmi then wrote a treatise on Hindu-Arabic numerals. The Arabic text is lost but a Latin translation, *Algoritmi de numero Indorum*, or *Al-Khwarizmi on the Hindu Art of Reckoning* gave rise to the word "algorithm" derived from his name in the title. Unfortunately the Latin translation is known to be much changed from al-Khwarizmi's original text (of which even the title is unknown). The work describes the Hindu positional notation system of numerals based on the digits 1, 2, 3, 4, 5, 6, 7, 8, 9, and 0. The first use of zero as a place holder in positional base notation was probably due to al-Khwarizmi in this work.

Methods for arithmetical calculation are given, and a method to find square roots is known to have been in the Arabic original although it is missing from the Latin version. Toomer writes [1] "... the decimal place-value system was a fairly recent arrival from India and ... al-Khwarizmi's work was the first to expound it systematically. Thus, although elementary, it was of seminal importance."

Far from elementary, the decimal positional notation replaced the Latin numerical system and has to date become the universally adopted system of number representation.

Al-Khwarizmi also wrote a book titled *Sindhind zij* on astronomy. It was based on Indian astronomical works [4] "... as opposed to most later Islamic astronomical handbooks, which utilised the Greek planetary models laid out in Ptolemy's *Almagest*..."

Al-Khwarizmi wrote, moreover, a major work on geography. It lists latitudes and longitudes for 2,402 localities on a world map. It was based on Ptolemy's *Geography*. It lists latitudes and longitudes of cities, seas, islands, geographical regions, mountains and rivers. The manuscript contained maps which were on the whole more accurate than Ptolemy's. Wherever al-Khwarizmi could access more advanced information, such as the regions of Islam, Africa and the Far East, his work is considerably more accurate than that of Ptolemy, but for Europe al-Khwarizmi seems to have used Ptolemy's data.

Al-Khwarizmi is a symbol, the tip of the iceberg, of the vast historic contributions of the Arabs and more generally Islamic nations to the world. Here is one mathematician, astronomer, who gave the world the name "Algebra" after the word "al-jabr" in his book title, the word "algorithm," derived from a Latin translation of his own name "Al-Khwarizmi" and thanks to him the Hindu-Arabic system of decimal numbers and positional notation became our basis of number representation and computation. A feast for one man.

References

- [1] G. J. Toomer, *Biography in Dictionary of Scientific Biography* (New York 1970-1990).
- [2] R. Rashed, *The Development of Arabic Mathematics: Between Arithmetic and Algebra* (London, 1994).
- [3] S. Gandz (ed.), *The Geometry of al-Khwarizmi* (Berlin, 1932).
- [4] Z. K. Sokolovskaya, The "pretelescopic" period of the history of astronomical instruments. al-Khwarizmi in the development of precision instruments in the Near and Middle East (Russian), in *The Great Medieval Scientist al-Khwarizmi* (Tashkent, 1985), 165-178.

See article by: J. J. O'Connor and E. F. Robertson (July 1999), MacTutor History of Mathematics <http://www-history.mcs.st-andrews.ac.uk/Biographies/Al-Khwarizmi.htm>

A.13 Nicolaus Copernicus (1473–1543)



FIGURE A.7 Nicolaus Copernicus. (Painting by Jan Matejko. Reproduced by permission of the Museum in Frombork. <http://www.frombork.art.pl/>)

Born: February 19, 1473 in Torun, Poland; died: May 24, 1543 in Frauenburg (now Frombork), Poland

The Polish astronomer Nicolaus Copernicus pioneered the heliocentric ordering of the planets. He was born on Feb. 19, 1473, in Torun about 100 miles south of Danzig. The name Nicolaus Copernicus is the Latin version he chose in place of his original name *Nikolaj Kopernik* or *Nicolaus Koppernigk*. His father, also *Nikolaj Kopernik*, was from Krakow and moved to Torun where he had a copper trading business. The father was active politically; a civic leader in Torun and a magistrate. In 1463 his father married Barbara Watzenrode, and Nicolaus Copernicus was the youngest of their four children

Father *Nikolaj* died when young Nicolaus was 10 years old. His uncle Lucas Watzenrode, a canon at Frauenburg Cathedral, became guardian to Nicolaus and his two sisters and brother. Nicolaus and his brother Andreas continued their elementary education in Torun. In 1488 his uncle Lucas sent Nicolaus to the cathedral school of Wloclawek where he studied humanities. Three years later, Andreas and Nicolaus enrolled in the University of Krakow, at a time when Krakow was in the capital of Poland. Originally founded as *Akademia Krakowska* in 1364 by Casimir III the Great, it is one of the oldest universities in Europe. (It was renamed as the Jagiellonian university in 1817 to commemorate the Jagiellonian dynasty of Polish kings.)

Nicolaus's uncle became Bishop of Ermland and he sought a church career for Nicolaus and Andreas. Nicolaus studied Latin, mathematics, geography, astronomy, and philosophy. The astronomy was based on *Tractatus de Sphaera Mundi*, or *Treatise on the Sphere of the Cosmos*. Written by the English astronomer Johannes de Sacrobosco in 1230, it was based heavily on Ptolemy's *Almagest*, and drawing additional ideas from Islamic astronomy and was one of the most influential works at the time.

Nicolaus was taught Aristoteles' and Ptolemy's views of the universe as means of understanding the calendar, calculating the dates of holy days and navigating the seas. He studied on his own the Latin translation of Euclid's *Elements* published in Venice in 1482, the second edition of the Alfonsine Tables, on planetary theory and eclipses, printed in Venice in 1492; and Regiomontanus's Tables of Directions, on spherical astronomy, published in Augsburg in 1490. Remarkably Copernicus' copies of these works, signed by him, are still preserved.

The world of Latin he now lived through his readings made him choose to use henceforth *Copernicus* as his name, instead of Kopernik or Koppernigk. He returned to Torun after four years of study at the university of Krakow but, as was common at the time, did not graduate with a degree.

With his uncle's urging Copernicus decided to enroll at the university of Bologna to study canon law. In the autumn of 1496 he traveled to Italy, entering the university of Bologna to start three years of study. Meanwhile, his uncle put his name forward for the position of canon at Frauenburg Cathedral. On October 20, 1497, while in Bologna, Copernicus received official notification of his appointment as a canon.

At Bologna university Copernicus studied Greek, mathematics and astronomy, in addition to his official course of canon law. He rented rooms at the house of the astronomy professor Domenico Maria de Novara and began to contribute to his research by making observations. On March 9, 1497 he observed the Moon eclipse the star Aldebaran.

In 1500 Copernicus visited Rome to celebrate the great jubilee. While in Rome he observed an eclipse of the Moon which took place on November 6, 1500. He returned to Frauenburg, also known as Frombork, in 1501 and became officially a canon of the Ermland Chapter on July 27. He asked his uncle for permission to return to Italy both to take a law degree and to study medicine. The Cathedral Chapter liked his proposal to study medicine and provided the necessary funds. He went to Padua where he studied both medicine and astronomy. Astronomy was essentially astrology and considered of value in medicine since physicians made use of astrology.

Copernicus moved to Padua and from there he went to the university of Ferrara, where he obtained the degree of doctor in canon law in 1503. He now could study medicine, which he did in Padua until 1506.

Upon returning to Ermland, Copernicus lived in his uncle's castle at Heilsberg and became his personal physician and secretary. Copernicus' love for the arts and humanities beside mathematics and astronomy, led him to translate from Greek into Latin the 85 poems of the Greek poet and Byzantine historian Theophylactus Simacotta, who was born in Egypt in the seventh century. The work was printed in Krakow in 1509.

He now spent much time reflecting on the movements of heavenly bodies and in particular the heliocentric system. He put in writing his reflections in a short manuscript titled *Commentariolus*, or small commentary, which he completed about 1512. He referred to it as "Sketch of Hypotheses Made by Nicolaus Copernicus on the Heavenly Motions" and sent copies of it to his friends. It proposed a list of seven axioms, each of which stated a feature specific to the heliocentric system.

The third axiom in particular stated that "All the spheres revolve about the sun as their midpoint, and therefore the sun is the center of the universe." The rest of the manuscript presented his proposition that in the new system only 34 circles were needed to explain the motion of planets. The *Commentariolus* was communicated to others by his friends. It produced no reaction whether in print or in letters, but astronomers became aware of Copernicus as a new star on the horizon. Two years later he was invited to attend the Fifth Lateran Council, one of whose aims was the reform of the calendar. He declined the invitation to attend, writing that he felt that the motions of heavenly bodies was still not understood with sufficient precision to allow reformation of the calendar. His reluctance to

informally and freely divulge his ideas seemed to add to his enigma and reputation. In 1522 the secretary to the King of Poland asked Copernicus to comment on *De Motu Octavae Sphaerae*, or On the Motion of the Eighth Sphere, just published by Johann Werner, a mathematician of some renown. He answered in writing expressing a rejection of the value of the work. He added that he intended to set forth elsewhere his own opinion about the motion of the stars, citing his extensive studies of which parts were already in print at that time.

Copernicus as a canon was occupied with administrative, financial, legal and medical affairs. The *Commentariolus* received praise but also condemnation. Martin Luther (1483–1546) denounced him as “the fool who will turn the whole science of astronomy upside down.” In 1531 a satirical play heaping ridicule on his ideas was produced in Elbing, Prussia, by a schoolmaster.

In Rome, however, there was no condemnation; at least so far. In 1533 John Widmanstad, a papal secretary, lectured on Copernicus’ theory before Pope Clement VII and several cardinals. Cardinal Schönberg wrote from Rome to Copernicus in 1536 urging him to publish his theories on the universe.

Georg Joachim (Rheticus), a young scholar from Wittenberg, arrived in Frauenburg in the spring of 1539. He was the catalyst that led eventually to the publishing of Copernicus’ long-awaited masterpiece. When Rheticus returned to Wittenberg, he had printed an account, known as the *Narratio prima*, of Copernicus’ almost-ready book. Rheticus initiated the printing of Copernicus’ book in Nuremberg, which was deposited in the care of Andrew Osiander, a Lutheran clergyman. He probably gave the work its title, *De Revolutionibus Orbium Coelestium*, which is not in the manuscript.

The physics of Copernicus was still Aristotelian and added only 27 observations, a negligible amount, to the data he took over uncritically from Ptolemy and from already published astronomical tables. The accuracy of predicting celestial phenomena on the basis of his system did not exceed that achieved by Ptolemy. Nor did Copernicus give proof for the phases of Mercury and Venus in support of his own theory.

The main thrust of Copernicus’ work was in its appeal to simplicity. The rotation of the earth demystified the daily revolution of thousands of stars. The orbital motion of the earth fitted perfectly, together with its period of 365 days, into the sequence set by the periods of other planets. In the tenth chapter of the first book Copernicus stated unequivocally: “In the center there is the sun. For who would place this lamp of a very beautiful temple in another or better place than the center, wherefrom it can illuminate everything at the same time.”

The book was reprinted only three times prior to the 20th century. No other “masterpiece” of Western scientific or philosophical history was less sought than Copernicus’ *Revolutions*. Yet, it is the book that has more recently been recognized as the cornerstone of modern astronomy.

Copernicus received a copy of his published book, about 200 pages long, in Latin, hours before he died on May 24, 1543, of a cerebral haemorrhage.

Reference:

Encyclopedia of World Biography on Nicolaus Copernicus,
<http://www.bookrags.com/biography/nicolaus-copernicus/>

A.14 Galileo Galilei (1564–1642)

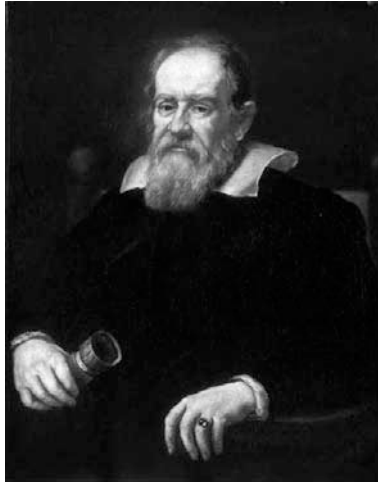


FIGURE A.8 Galileo Galilei.

Galileo Galilei was born February 15, 1564 in Pisa, Italy, into a family of Florentine patricians. In 1581 he was enrolled to study medicine in the university of Pisa but would soon study passionately mathematics and philosophy.

He left Pisa without graduating but would be appointed to the chair of mathematics at the same university of Pisa in July 1589. In 1592 he occupied the prestigious chair of mathematics at the university of Padua.

Galileo's invention of the telescope in 1609 and 1610 put him at the forefront of world scientists. He was appointed as chief mathematician and philosopher at the Florentine Court, to the Grand Duke of Tuscany, Cosimo de Medici II.

Galileo's astronomical discoveries were published in his 1610 book *Sidereus Nuncius*. They questioned and revised age-old Ptolemaic/Aristotelian cosmology theories. His observations of the Moon's surface revealed valleys and mountains, contradicting the smooth spherical surface postulated by Aristoteles. His observations of multitudes of faint stars supported Copernicus' claim that the universe was much larger than was believed at the time. His discovery that there were four moons orbiting Jupiter, effectively refuted the Aristoteles' claim that the Earth was the center of the universe, around which revolved all heavenly bodies. Delving into such radical reflections, however, was viewed as blasphemy by the church.

In the following two years Galileo made two more radical discoveries. These concerned the phases of Venus and the the existence of sunspots. Galileo published his views on the latter in three letters to Mark Wesler, as a follow up of three earlier letters to Wesler by Christoph Scheiner.

Conflict over priority of discovery of sunspots erupted, making to the end bitter enemies out of Scheiner and Galileo.

In 1616 a decree was issued, suspending as belief revisionism Copernicus' *De Revolutionibus*. Galileo was served with an injunction by Cardinal Roberto Bellarmino not to hold, cite

or defend the Copernican doctrine. Galileo, to avoid further wrath of the church, studied oceanic tides and their relations to positions of the moon and the sun. Risking alienation of the church, Galileo published in 1632 *Dialogue* concerning the two chief world systems which effectively embraced the Copernican doctrine.



FIGURE A.9 (a) Christoph Scheiner (1573-1650); (b) Johannes Kepler (1571-1630). (Copy of a lost portrait, painted in 1610, which had been conserved at the Benedictines of Krems).

The Roman ecclesiastic authorities found the book in violation of the 1616 decree. Galileo was put on trial in Rome by the Inquisition. On June 22, 1633 Galileo was forced to kneel in front of the Roman Inquisition and recant his beliefs in the Copernican doctrine and the motion of the Earth. He was sentenced to life imprisonment, commuted to perpetual house arrest without visitors. Galileo's book *Dialogue* was put on the Index of Prohibited Books, added to Copernicus' *De Revolutionibus* and the book of Kepler (1571–1630) dealing with planetary theory.

Outcries for Galileo's release by many of the world's top scientists and statesmen failed to secure his freedom. Galileo lost his sight in 1637. Yet in 1638 he produced another masterpiece, *Discourses on Two New Sciences*, which laid the foundations for the modern mechanics. The manuscript had to be smuggled out of Italy and was published in Holland.

Galileo died on January 8, 1642. The Roman ecclesiastic authorities opposed a public funeral and honor proposed by the Florentine state. His books, together with those of Copernicus and Kepler, were deleted from the Index of Prohibited Books in 1835, and only in 1992 did the Roman Catholic Church formally admit to its historic error in its condemnation of Galileo.

Reference

http://en.wikipedia.org/wiki/Galileo_Galilei

<http://gardenofpraise.com/ibdgilil.htm>

A.15 Sir Isaac Newton (1643–1727)

Born: January 4, 1643 in Woolsthorpe, Lincolnshire, England; **died:** March 31, 1727 in London, England

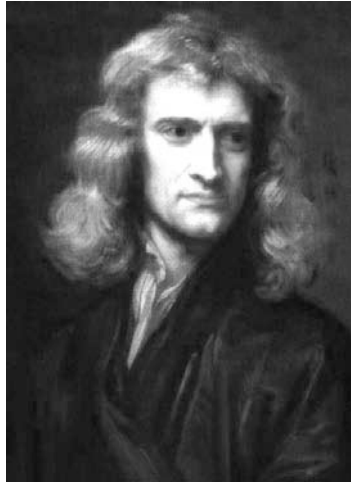


FIGURE A.10 Isaac Newton.

Isaac Newton was born in a family of farmers on Christmas Day 1642 (according to Julian Calendar, Old Style) which translates to the fourth of January, 1643 (New Style), a fatherless child in Woolsthorpe, near Grantham in Lincolnshire, his father, also Isaac Newton, died two months before his birth. When he was barely three years old his mother Hanna (Ayscough) married Barnabas Smith, a wealthy church minister from nearby North Witham, and left Isaac in the care of her elderly parents. Newton had a sad life from the outset and could not stand the sight of his stepfather. Following the death of Barnabas in 1653 his mother returned to Woolsthorpe. Two years later Isaac was placed in a boarding school in Grantham, where he spent four years, returning to Woolsthorpe in 1659.

Newton was asked to manage his late father's farm, but proved not to be well disposed for the job. Thanks to the advice of the headmaster of Stokes grammar school at Grantham as well as that of Hanna's brother, who had graduated with an MA from Cambridge, he was prepared for university education. In 1661 he left Woolsthorpe and enrolled in Trinity College, Cambridge as an undergraduate.

Newton would spend many years at Trinity College in an intense pursuit of knowledge, as a student, a Fellow, and a professor. Newton prepared for a degree in law. In 1664 Isaac Barrow, Lucasian Professor of Mathematics at Cambridge, found marked weakness in Newton's knowledge of Euclid. Newton in fact spent extensive time reading works by René Descartes, Pierre Gassendi, Thomas Hobbes, and other contemporary figures.

He was fascinated by Copernican astronomy of Galileo, who had died less than a year before his own birth. He also studied Kepler's theories on optics. He recorded his thoughts in a book dated 1664, to which he gave the title *Quaestiones Quaedam Philosophicae* (Certain Philosophical Questions) adding at the outset in Latin the words: "Plato is my friend, Aristoteles is my friend, but my best friend is truth." He was 21.

He read Barrow's *Euclid's Elements*, Oughtred's *Clavis Mathematica*, Descartes' *La Géométrie*, Frans van Schooten's edition of Viète's collected works published in 1646 and the newly published major work by van Schooten *Geometria a Renato Des Cartes* which appeared in two volumes in 1659 and 1661. In 1665 Newton obtained his bachelor's degree at Cambridge with no mention of excellence or distinction.

Cambridge university had to close its doors in the summer of 1665 and Newton returned home to Lincolnshire. Within two years Newton was projected to the stratosphere, among the world's top scientists. He was not yet 25 years old, yet he now introduced vast advances in mathematics, physics, optics and astronomy. He constructed the fundamentals of differential and integral calculus, years before its independent discovery by Leibniz, laid the foundations of theories on light and color and established the basis of those on planetary motion. These led in 1687 to his publication of his masterpiece volume *Principia*.



FIGURE A.11 (a) Gottfried Wilhelm Leibniz (1646–1716); (b) Robert Hooke (1635–1703). This portrait is the only one believed to be authentic and was discovered recently.

He wrote *De Methodis Serierum et Fluxionum* in 1671 but could not have it accepted for publication. It was not published in his lifetime. In fact it had to wait until 1736 to be published, translated to English, by John Colson. He returned in 1667 to Cambridge with the end of the plague. With reluctance Cambridge elected him minor fellow at Trinity. He then acquired the MA degree and was elected senior fellow.

In 1669 Isaac Barrow resigned the Lucasian chair to devote himself to divinity and recommended Newton, who was only 27 years old, to replace him. Newton taught a course on optics in January 1670. He made observations that while every scientist since Aristoteles believed that white light was a basic single entity, the chromatic lines seen in a lens, point to otherwise. He illustrated his point by directing a thin beam of sunlight at a glass prism and showed the diffracted spectrum of colors that emerged. Soon he gave his first talk on the nature of color. It was received with acclaim as well as skepticism.

In 1672 he was elected fellow of the Royal Society, having donated a reflecting telescope. In the same year he published his first scientific paper. It was on light and color and was published in the *Philosophical Transactions of the Royal Society*.

The paper was generally well received but the Royal Society's celebrated scientist Robert



FIGURE A.12 King James II by unknown artist; oil on canvas, circa 1690. National Portrait Gallery, London.

Hooke (1635–1703) and Huygens objected to Newton’s attempt to prove, by experiment alone, that light consists of the motion of small particles rather than waves. This was the first among several confrontations with other scientists.

He clashed with Hooke regarding relations to Hooke’s own work. The controversy lasted until 1678. In 1675 with his submission of another paper there were charges of plagiarism from Hooke’s work. It was a totally unfounded accusation. Newton retreated and withdrew from the Royal Society which he associated with Hooke as one of its leaders.

In 1678 Newton suffered an emotional breakdown. His mother died the following year and he withdrew further into his own world, venturing into alchemical experimentation. Such interest was scoffed at and embarrassed fellow scientists. Yet his intense efforts to measure the unseen forces led him to investigate forces between matter as particles and to the role that gravitational force plays.

A famous story has it that in 1666 Newton, sitting in his garden at Woolsthorpe under an apple tree, was hit on his head by an apple that fell. Newton later recalled “In the same year I began to think of gravity extending to the orb of the Moon.” Since Newton formulated his laws of gravitational forces 20 years later, some have wondered if Newton’s memory failed him. They questioned if Newton did extrapolate from the tree to the moon in 1666. They felt rather that he came up with his breakthrough on the laws of gravitation only in 1686.

It is however quite conceivable that Newton knew what he was talking about. The force of gravity woke up an inspiration in him when he was 23 years old in 1666. The idea fomented in his head. Transforming an intuitive inspiration into a mathematical theory takes reflection, investigation, analysis, verification and finally formulation. Newton may have desired to look more into such a force that acted on the apple and whether a similar one acts on the moon and the planets. But he had to find the time, the energy and the serenity to take his idea seriously, to verify if it had not been already proposed to start transforming it from a fleeting thought to a mathematical theory.

Newton published his *De Motu Corporum in Gyrum* (On the motion of bodies in an orbit) in 1684. In the years 1679 to 1684 Newton had corresponded with Hooke and Halley regarding planetary movements and the forces that govern them. Newton arrived at a proof of Kepler’s Areal law based on his own laws of motion and his law of universal gravitation.

Halley urged Newton to publish a thorough treatment of his theories on the laws of physics

and their applications to planetary movements. In 1687 Newton published the *Philosophiæ Naturalis Principia Mathematica*, usually referred to simply as Newton's *Principia*. It is considered one of the most important books published in the history of science. But if the *Principia* was Newton's brainchild, Hooke and Halley were the catalysts that made it happen.

The publication of *Principia* led to more conflict with Hooke who claimed that his letters of correspondence with Newton in the two years 1679 and 1680 were enough proof that Newton was publishing ideas that were Hooke's. Newton's animosity toward Hooke had no limit. He in fact withheld his publication of his *Opticks* until 1704, and stopped all interaction with the Royal Society, returning to it only after Hooke's death in 1703.

In 1669 James II converted to Catholicism. In 1685 he became king of Great Britain having the support of Anglicans as well as Catholics. He began, however, to distrust Protestants and appoint Roman Catholic officers of the state and the army, the judiciary and even the universities such as Cambridge and Oxford. Newton, a zealous Protestant, opposed such an intrusion in his university affairs.

William of Orange received the call from many leaders to bring his army to England and depose the Catholic James. William landed in November 1688 and James, realizing that Protestants abandoned his army, fled to France. Cambridge university, grateful for Newton's defense of academic freedom against James, elected him as one of their two members to the Convention Parliament on January 15, 1689.



FIGURE A.13 William III of Orange (1650–1702).

The Parliament declared that James had abdicated and in February 1689 offered the crown of England, Scotland and Ireland to William of Orange and Mary II. Newton was seen as one of the world's most reputable scientists. He started to see that there is life after research and university and liked living in London. Yet, in 1693, he suffered a severe nervous breakdown, similar to the one that afflicted him in the period 1677 to 1678. Shortly after his recovery, in 1696, Newton was appointed Warden, then Master, of the Mint. He thus left Cambridge for London without regret.

After Hooke's death in 1703, Newton was elected president of the Royal Society and was subsequently elected annually until his death. His tenure as president was seen as autocratic,

if not tyrannical, and his control over the lives and careers of younger disciples was all but absolute. In 1704 he published his second major work, the *Opticks*, based largely on work completed decades earlier. He was knighted in 1705.

In the end, the transactions of the Royal Society were little more than extensions of Newton's will, and until his death he dominated the landscape of science without a rival. He died in London on March 20, 1727 (March 31, New Style).

References:

<http://www-history.mcs.st-andrews.ac.uk/Mathematicians/Newton.html>

<http://books.google.ca/books?id=3wIzvqzfUXkC>

MacTutor History of Mathematics

<http://www-history.mcs.st-andrews.ac.uk/Biographies/Newton.html>

A.16 Guillaume-François-Antoine de L'Hôpital (1661–1704)



FIGURE A.14 Guillaume-François-Antoine de L'Hôpital.

Born: 1661 in Paris, France, died: February 2, 1704 in Paris, France

Marquis de Sainte-Mesme and Comte d'Entremont, Guillaume-François-Antoine de L'Hôpital was the son of the lieutenant-general of the king's armies. He was intended for a military career but soon discovered a passion for mathematics. By the age of 15 he had solved problems proposed by Pascal, and as an army officer, he studied mathematics in his tent. He was forced to resign due to near-sightedness and thenceforth devoted his life to mathematics.

In 1692 he became acquainted with Jean Bernoulli, one of few scientists who were familiar with the new methods of differential calculus. He invited Bernoulli to his estate of Oucques near Vendôme, studying for four months with him and learning from him this relatively new branch of the science of numbers.

He was elected honorary member of the French Academy of Sciences of Paris in 1693 and

soon was cited on a par with Newton, Huyghens, Leibniz, and the Bernoullis as the world-wide top experts of calculus. His work on infinitesimal analysis for the study of curves was published in 1696 and was received with acclaim by many who were in search of solutions for advanced problems of calculus, finding in the book clear and precise statements of the problems and proposed solutions.

L'Hôpital established his reputation by publishing his book *Analyse des Infiniment Petits pour l'Intelligence des Lignes Courbes* in 1696. It was the first textbook to deal with differential calculus. In the introduction L'Hôpital acknowledges his indebtedness to Leibniz, Jacob Bernoulli and Johann Bernoulli.

He is famous for his rule on the evaluation of the limit of a rational function, of which the numerator and denominator each have a limit of zero. His wife is said to have contributed to his work. His published works are: *Analyse des Infiniment Petits pour l'Intelligence des Lignes Courbes* (Paris, 1696; last ed. by Lefèvre, Paris, 1781); *Traité Analytique des Sections Coniques* (Paris, 1707; 2nd ed., 1720); several memoirs and notes inserted in the *Recueil de l'Académie des Sciences* (Paris, 1699–1701), and in *Acta Eruditorum* (Leipzig, 1693–1699).

In the literature, including the French literature dating back to his time, his name is written either L'Hôpital or L'Hospital.

References

MacTutor History of Mathematics

<http://www-history.mcs.st-andrews.ac.uk/Biographies/DeL'Hopital.html>

http://en.wikipedia.org/wiki/Guillaume_de_L'Hopital

A.17 Pierre-Simon Laplace (1749–1827)

Born: March 23, 1749; died: March 5, 1827



FIGURE A.15 Pierre-Simon Laplace

Pierre-Simon Laplace was born in Normandie at Beaumont-en-Auge to a family with prop-

erty in the cider trade. Between the ages of 7 and 16 he was being prepared for the priesthood at a Benedictine priory school, where students were usually destined to a life in the Church or the army. From the age of 16 to 18 Laplace attended Caen university. He studied theology, but before long became progressively absorbed by a passion for mathematics.

At the age of 17 his mathematical talents were already noticed and he became mathematics teacher at the *École Militaire* of Beaumont-en-Auge. Having procured a letter of introduction to Jean le Rond d'Alembert, who was already a renowned scientist for his studies of astronomical physics and mathematics, Laplace left for Paris at the age of 19. With the help of d'Alembert, Laplace is soon appointed professor of mathematics at *École Militaire* of Paris.

In the years 1770 to 1773 Laplace presented papers to the *Académie des Sciences* in Paris on areas ranging from improvements on Lagrange's search for maxima/minima, the calculus of integrals, finite differences to differential and difference equations; pointing to their importance in physics, mechanics and astronomy. He investigated the motions of planets of the solar system, the inclinations of their orbits and the effect of gravitation forces of their moons.

His first paper was in Latin on integral calculus, published at Leipzig in the *Nova acta eruditorum* in 1771. That year, Laplace started one of several attempts to gain election to the *Académie des Science*, but had to wait two years and present more than 10 papers before being elected Adjoint of the *Académie des Sciences*.

During the 1780s Laplace's research results established him as one of the most influential scientists the world has seen.

It was not achieved, however, with good relationships with his colleagues. Although d'Alembert had been proud to have considered Laplace as his protégé, he certainly began to feel that Laplace was rapidly making much of his own life's work obsolete and this did nothing to improve the relation. It does appear that Laplace was not modest about his abilities and achievements, and he probably failed to recognise the effect of his attitude on his colleagues. Lexell visited the Académie des Sciences in Paris in 1780-81 and reported that Laplace let it be known widely that he considered himself the best mathematician in France [1].

About 1782 Laplace conducted research on specific heat and calorimeters with the known chemist Antoine Lavoisier (1743-1794), enhancing his reputation among physicists and chemists.

In 1784, Laplace was appointed by Louis XIV as Examiner of the Royal Artillery Corps, and in this role in 1785, he examined and passed the 16-year-old Napoléon Bonaparte. Through that position he became well known to the ministers of the government and others in positions of power in France. Laplace was shrewd, however, able to navigate well in politics; thus avoiding the guillotine during the French Revolution (1789-1799) and the Reign of Terror (1793-1794). In contrast, Lavoisier who was born to a well-to-do bourgeois family, occupied at the time a position as a tax collection government administrator, which made him a target of hatred by the revolutionaries. After being barred from his laboratory, Lavoisier fled his home but was arrested a few months later. When he protested that he was a scientist, not a tax man, he was told: "The Republic has no need of scientists." Lavoisier was charged with ridiculous crimes. Testifying against him was an age-old enemy, Jean-Paul Marat (1743-1793), whom Lavoisier had prevented, with good reason, from joining the Academy of Sciences. Eager for revenge, Marat accused Lavoisier of diluting commercial tobacco and cutting off Paris's air supply by building a defensive wall around the city. On May 8, 1794, Lavoisier was sentenced to death and guillotined.

Laplace's research in the field of mathematical astronomy culminated in his masterpiece on the dynamic stability of the solar system viewed as a collection of rigid bodies moving in



FIGURE A.16 Antoine Laurent Lavoisier (1743-1794).

a vacuum. He independently formulated the nebular hypothesis and was among the pioneers to postulate the existence of black holes and universal gravitational collapse.

Laplace became a founding member of the Société d'Arcueil about 1805, together with the chemist Berthollet. Among the mathematicians who were members of this active group of scientists were Biot and Poisson. This marks the height of Laplace's influence, dominant in the Institute and on the École Polytechnique of Paris and the courses followed by its students.

Laplace was an opportunist. His political allegiance shifted easily as expediency required; the successive revolutionary governments, the republic, the empire, and the Bourbon restoration rewarded his servility with numerous honors. Napoléon made him a count (comte), and Louis XVII made him a marquis.

References

- [1] J. J. O'Connor and E.F. Robertson, MacTutor History of Mathematics,
<http://www-history.mcs.st-andrews.ac.uk/Biographies/Laplace.html>
<http://www-groups.dcs.st-and.ac.uk/history/Biographies/Laplace.html>
<http://www-groups.dcs.st-and.ac.uk/~history/Mathematicians/Laplace.html>
<http://www.bookrags.com/Pierre-Simon.Laplace>
<http://www.bookrags.com/biography/antoine-laurent-lavoisier-wsd/>
<http://www.normandieweb.org/culture/sciences/laplace/index.html>

A.18 Gaspard Clair François Marie, Baron Riche de Prony (1755–1839)

Born: July 22, 1755; died: July 29, 1839

Gaspard Clair François Marie Riche de Prony was born July 22, 1755 in Chamelet, Beaujolais, France, the son of Gaspard Marie Riche de Prony, a noble ex-magistrate, member of parliament of Dombes and Claudine Jacquet. He was enrolled at the college of Les



FIGURE A.17 Baron Riche de Prony.

Bénédictins de Thoissey, Ain, northeast of Lyon. In 1773, having terminated his schooling, he lived in Lyon, where his father worked as a lawyer.

In 1776 he lived in Paris, and was admitted to engineering studies at the *École des Ponts et Chaussées* (School of Bridges and Causeways). He graduated in 1779 at the top of his class, highly praised for his dedication and brilliance by Perronet, referred to as “First Engineer of the King and Director of *École*” (des Ponts et Chaussées) and known for his construction of the bridge Pont de Neuilly.

From 1780 de Prony worked as an engineer at Bourges, Argenton, Dourdan and Livry. However, in 1783 he received the call to return to Paris from Perronet, to assist de Chézy in the direction of L’*École des Ponts et Chaussées*.

In 1785 de Prony was sent on a mission to England to perform accurate measurements on the geographical-temporal relative positions of the Greenwich Observatory and the Paris Observatory. He was promoted in 1787 to inspector at the *École des Ponts et Chaussées*. Meanwhile he served under the supervision of Demoustier as one of the engineers responsible for the construction of the Louis XVI bridge, until this day a marvel of Paris monuments, known as the Pont de la Concorde. He was also associated later on with the construction of the Sainte-Maxence Bridge. It was at that time that he published his first major work in the *Académie des Sciences* on the forces on arches, motivated by observations of displacements that accompanied the construction of the Pont de Neuilly. The paper confirmed to scientists such as Monge that de Prony was a brilliant young scientist with a great potential.

The French Revolution

The French Revolution lasted from 1789 to 1799. It was a bloody period of political and social turmoil, which sought to put an end to absolute monarchy, with its feudal privileges for the aristocracy and the Catholic clergy. Proclaiming new noble causes of justice, liberty, equality and fraternity it went on to implement them by violence, institutional terrorism, mock trials and executions. It was the era of the Reign of Terror, repression and bloodshed, triggering warfare with every other major European power. The Imperial and Prussian armies threatened retaliation on France if it were to resist their advance or the reinstatement of the monarchy. This cast suspicion on the king Louis XVI as one conspiring with the enemy.

January 17, 1793 saw the king condemned to death for “conspiracy against the public liberty and the general safety.” The January 21 execution led to more wars with other European countries. Louis XVI’s Austrian-born queen, Marie Antoinette, would follow him to the guillotine on October 16.



FIGURE A.18 (a) Louis XVI www.commons.wikimedia.org/wiki/Image:Louis16-1775.jpg
(b) Marie-Antoinette www.commons.wikimedia.org/wiki/Marie-Antoinette

Napoléon Bonaparte

Napoléon Bonaparte (August 15, 1769 – May, 5 1821) was a general who rose to prominence during the French Revolution. He led successful campaigns against Coalitions arrayed against France to stop it from achieving the stated objective of exporting its revolution to its neighbors.



FIGURE A.19 Napoléon Bonaparte, painting by Jacques-Louis David (1748-1825).

In 1798, Bonaparte, now a popular general, proposed a military expedition to invade

Egypt, then part of the Ottoman Empire, as a means of protecting French trade interests and to block Britain's passage to India. To distance him from the center of power the government approved the mission, in spite of its shaky foundation, its risks and a cost it could hardly afford. In May, Napoléon was elected a member of the French Academy of Sciences. His Egyptian expedition included a group of 167 scientists: mathematicians, naturalists, chemists and geodesic scientists among them. They included Fourier, Monge and Malus. Their discoveries included the Rosetta Stone and their work was published in the *Description de l'Égypte* in 1809.

The ships that had landed Bonaparte and his army sailed back to France, while a fleet of ships remained to support the army along the coast. On August 1, 1798, the British fleet under Horatio Nelson destroyed all but two French vessels in the Battle of the Nile. With Bonaparte landbound, his goal of a strengthened French position in the Mediterranean Sea came to an end, even if his army had temporarily succeeded in the consolidation of French power in Egypt.

On August 24, 1799, informed of a departure of British ships from France's ports, he set sail for France, despite the fact he received no approval from Paris. Back in France, he staged a coup d'état and installed himself as First Consul. Five years later he crowned himself Emperor of France. He now attacked every major European power and dominated continental Europe through a series of military victories. The French invasion of Russia in 1812, however, marked a turning point in Napoléon's fate. His army was decimated in Russia's vast lands and harsh winter conditions. In 1813 his army was defeated at Leipzig. France was invaded and Napoléon exiled to the island of Elba. Less than a year later, he returned but was defeated again at the Battle of Waterloo in June 1815. He spent the last six years of his life a prisoner under British supervision on the island of Saint Helena where he died in 1821.

In 1790 de Prony started work on a novel hydraulic architecture which he published as the *Hydraulic Architecture of Bélidor*, in 1796. In 1791, de Prony was appointed Chief Engineer *Ingénieur en Chef des Pyrénées Orientales* at Perpignan, but shortly after he moved to Paris, and was named director of the Cadastres by Chaumont de la Millière, following its creation by the national assembly. He was then assigned the responsibility of generating the logarithmic and trigonometric tables for the Geodesic Service, assisted by Legendre, Carnot and other mathematicians, as well as close to 100 assistants. The work was extensive and lasted many years and finally accomplished in 1801. The tables were vast, spanning 17 folio volumes. It would have taken many more years to compile were it not for the ingenuity of de Prony in developing novel methods for simultaneous processing by the young assistants. It has been told that many of these were wig-makers, who became unemployed due to the suppression of powder and the simpler hairdos of the new republicans.

The École Centrale des Travaux Publiques was founded in 1794 by Carnot and Monge, and de Prony became one of its first professors of Mathematical Sciences, where he stayed as chair until 1815 when he became examiner at the school. The school was renamed École Polytechnique in 1795. In 1796 de Prony was appointed Secretary of the Sciences section of l'Institut Polytechnique. In 1798 de Prony declined Napoléon's invitation to accompany his expedition to Egypt, in contrast to Fourier, Monge and Malus who accepted the invitation. Napoléon's anger at the slight led to his depriving de Prony from the honors that he deserved. His punishment might have gone farther had de Prony's wife not been a close friend of Joséphine.

In the same year he succeeded de Chezy as the Director of the École des Ponts et Chaussées, a position he had longed for and which may have been the reason for his declining Napoléon's invitation. In 1804, in spite of his refusal to join the Egyptian Expedition,

de Prony received from Napoléon the “légion d’honneur” for the publication of part of his results on trigonometric and logarithmic tables.

He published a number of important contributions on mathematical physics, among which, in 1810 and 1811, the two major texts *Leçons de Mécanique Analytique* and *Sommaire des Leçons du Cours de Mécanique* from his lectures at École Polytechnique. Becoming a member of the Bureau de Longitude, de Prony remained the Chair of Analysis and Mechanics at École Polytechnique until 1815 when he became an examiner.

In 1818 he was named Fellow of the Royal Society of London. Years later, to compensate de Prony for the absence of well-deserved awards by Napoléon, successive governments bestowed on him several honors; the title baron as well as *Pair de France* conferred to him by King Louis-Philippe in 1835.

De Prony died on July 28, 1839, having spent 40 years as the Director of École des Ponts et Chaussées, where he spent a good part of his life perfecting its teaching. The school has a portrait and a bust of de Prony, as well as a library donated by de Prony’s niece, Mme de Corancez.

De Prony was an affable character who had many friends. He was passionate about the arts, and published in fact a treatise on musical intervals. One of de Prony’s well-known contributions was a brake named after him, which he invented in 1821 to measure machine performance. It was an improvement on an approach by Pierre Girard of two years earlier, based on concepts of Hachette.

References:

J. J. O’Connor and E. F. Robertson MacTutor History of Mathematics (December 1996)

http://www-history.mcs.st-andrews.ac.uk/Biographies/De_Prony.html

<http://www.newadvent.org/cathen/07469a.htm>

See also:

<http://www.anales.org/archives/x/prony.html>

<http://www.allbiographies.com/biography-barondePronyGaspardFranccedilois-26019.html>

http://www-groups.dcs.st-and.ac.uk/history/Printonly/De_Prony.html

Extrait des Biographies des ingénieurs des Ponts et chaussées.

http://www.geneawiki.com/index.php/RICHE_de_PRONY_Gaspard_Clair_Marie

A.19 Jean Baptiste Joseph Fourier (1768–1830)

Born: March 21, 1768 in Auxerre, Bourgogne, France; **died:** May 16, 1830 in Paris, France

Jean Baptiste Joseph Fourier’s father was a tailor in Auxerre, France. Both parents died when Joseph Fourier was 10 years of age, and he was placed in École Royale Militaire of Auxerre. He studied with ease French and Latin but became progressively more inclined toward mathematics. By the age of 14 he had completed a study of the six volumes of *Cours de Mathématiques of Bézout*. A year later he received the first prize for his study of Bossut’s *Mécanique en Général*. In 1787 he was admitted to the Benedictine abbey of Saint-Benoît-sur-Loire in preparation for the priesthood. Fourier submitted a paper on algebra to Montucla in Paris and corresponded with Professor Bonard of Auxerre. He then left the abbey and presented a paper in 1789 on the numerical solution of algebraic equations at the Royal Academy of Sciences in Paris and became a teacher at his old school at Auxerre. It was the beginning of the French Revolution (1789-1799).



FIGURE A.20 Portrait de J.B.J. Fourier par Claude Gautherot. Droits réservés, musées d'Auxerre(France).

For the following 75 years France would alternate between republic, empire and monarchy. But after the French Revolution, the course of history of France, Europe and Western civilization as a whole had drastically changed forever.

Fourier committed the grievous error of delving into politics and the affairs of a local revolutionary committee at Auxerre. In an incident he defended a cause to the consternation of a rival faction in Orléans in 1793. He was arrested in 1794, fearing he would lose his head by the guillotine, but after Robespierre himself went to the guillotine, political winds changed and he was freed.

In 1794 a central teachers' college, *École Normale Supérieure* was established in Paris, and Fourier became one of its first students where he was taught by Lagrange and Laplace, among others. Before long, Fourier was promoted to its faculty as a lecturer.

Fourier then received an appointment to the newly founded *École Polytechnique*, where he first served as chief lecturer on fortifications and later as professor of mathematical analysis.

Later in 1794 Fourier was admitted to the *École Normale* in Paris which was founded as a model for teacher-training schools. The school opened its doors in January 1795 and Fourier was certainly one of its most brilliant students. He was taught by Lagrange, who Fourier described as *the first among European men of science*, and also by Laplace, who Fourier rated less highly, and by Monge who Fourier described as *having a loud voice and is active, ingenious and very learned*.

Fourier began teaching at the *Collège de France* and, having excellent relations with Lagrange, Laplace and Monge, began further mathematical research. He was appointed to a position at the *École Centrale des Travaux Publics*, which was soon to be renamed *École Polytechnique*. However, repercussions of his earlier arrest remained and he was arrested again and imprisoned. His release has been attributed to a variety of causes such as pleas by his pupils, pleas by Lagrange, Laplace or Monge or a change in the political climate.

Napoléon Bonaparte requested that Fourier who was 30 years of age, participate in 1798 as scientific adviser on an expedition to Egypt.

Napoléon's expedition was at first a great success. Malta was occupied on June 10, 1798, Alexandria taken by storm on July 1, and the delta of the Nile quickly taken.

However, on August 1, 1798, the British surprised 14 of the French ships moored in Aboukir Bay, sinking or capturing them and setting a blaze that triggered a devastating explosion of the flagship of the French fleet, the *Orient*. The conquest established Horatio Nelson as one of Britain's greatest heroes, and Napoléon was left stranded on the Egyptian desert without naval support.

This was the Battle of the Nile. Napoléon had to remain confined to the land that he was occupying. Fourier occupied a high post of Diplomat, General Secretary of l'Institut d'Égypte, wrote the Introduction to the extensive volume published by this Institute, helped establish educational facilities and administered archaeological explorations.

An incredible archeological discovery took place and its significance was deeply felt by not only Napoléon and Fourier but the whole French intelligentsia in Egypt. This was the Rosetta stone.



FIGURE A.21 The Rosetta stone.

The Rosetta stone may be regarded as the most important discovery the world has ever seen. The famous stone, presently one of the most precious treasures of the British Museum, contained same royal edicts of Ptolemy V in three languages.

The first script was Hieroglyphic, the script used for religious documents and other formal edicts. The second was Demotic Egyptian, which was the common script of Egypt. The third was Classical Greek, which was the language of the post-Alexander rulers of Egypt at that time.

Captain Pierre-François Bouchard discovered the stone on July 15, 1799, near the Egyptian port city of Rosetta (present-day Rashid). The stone was sent to the *Institut de l'Égypte*. The French newspaper *Courrier d'Égypte* published by the Institute announced the find in September 1799.

In March 1801 the British landed on Aboukir Bay. The French troops in Cairo capitulated on June 22 and in Alexandria on August 30. After great resistance from the French the Rosetta stone was taken to Britain wherein it remains to date in the British Museum.

Fourier's papers, published in the *Décade* and the *Courrier d'Égypte*, treated subjects ranging from the general solution of algebraic equations to irrigation projects.

Napoléon returned to Paris in 1799. He soon retained absolute power. Upon returning to

France in 1801 Fourier was appointed by Napoléon prefect of Isère, a position he occupied until 1814. It was during those years that he found time and motivation to advance his mathematical research.

The result was his writing the mathematical theory of heat conduction, which he submitted to the academy in 1807. Its publication in 1808 had a marked impact, recognized as a unique mathematical breakthrough. Napoléon was happy with his protégé's brilliant contribution and made him a baron.

A second, expanded version titled *Théorie des mouvements de la chaleur dans les corps solides*, received the award of the French Academy in 1812.

In 1815 Napoléon escapes the Isle of Elba and returns with a great army to France. As prefect of Isère through which Napoléon would make his return, Fourier receives orders from the king and dictates that Napoléon's return should be blocked. He succeeds however to avoid the wrath of Napoléon who upon acceding to power appoints him prefect of the Rhône. Political events intervene, however, and he is elected to the reformed *Académie des Sciences*.

From 1815 Fourier served as director of the Bureau of Statistics in Paris. In the eyes of the new, royalist regime, Fourier's long service under Napoléon was offset by his opposition to Napoléon upon the latter's return from Elba. In 1817 he became a member of the Academy of Sciences. In 1822 he became secretary of the mathematics section, helping young promising mathematicians such as Dirichlet and Sturm.

The first part of his award-winning paper *Théorie des mouvements de la chaleur dans les corps solides* was printed in book form in 1822 under the title *Théorie Analytique de la Chaleur*. It was received as a masterpiece and remained thenceforth a historical breakthrough, becoming the basis of today's special branch of mathematics, namely, Fourier analysis and Fourier integrals.

The overture of his 1822 masterpiece *Théorie Analytique de la Chaleur* Fourier cites a dictum by Plato, which he translates into the Latin words

Et ignem regunt numeri

An English translation may read

Thus Fire by numbers ruled.

The corresponding cited Greek text is part of Plato's *Timaeus* dialogue [1].

ὅτε ὁ ἐπεχειρεῖτο κοσμεῖσθαι τὸ πᾶν, πῦρ πρῶτον καὶ γῆν καὶ ἀέρα καὶ ὕδωρ.....
 διεσχηματίσατο [ὁ θεὸς] εἶδεν τε καὶ ἀριθμοῖς.

FIGURE A.22 Plato's *Timaeus* text.

Near the end of his life he put a lot of effort adding precisions to his discoveries and in long exchanges with his contemporaries, notably Biot and Poisson who were contesting priority of his discoveries.

Fourier's fortunes rose and fell with those of Napoléon, and after Napoléon's defeat at Waterloo, Fourier for a while fell out of favor. Late in life, Fourier was infirm due to complications from diseases he had contracted while in Egypt; possibly The Curse of the Pharaohs. He died in May of 1830.

References:

- [1] <http://en.wikipedia.org/wiki/Timaios>
http://fr.wikipedia.org/wiki/Joseph_Fourier
http://www.bookrags.com/Joseph_Fourier
<http://www.bibmath.net/bios/index.php3?action=affiche&quoi=fourier> :
-

A.20 Johann Carl Friedrich Gauss (1777–1855)

FIGURE A.23 Johann Carl Friedrich Gauss.

Born: April 30, 1777 in Brunswick, Duchy of Brunswick (now Germany);
died: February 23, 1855 in Göttingen, Hanover (now Germany)

Carl Friedrich Gauss was a child prodigy. He was the son of an artisan father, but felt closer to his mother Dorothea Benz to whom he attributed his mental prowess. According to a story he would tell years later, the instructor at school, to keep the children busy for a while, asks them to calculate the sum of the hundred first integers, 1 to 100. Expecting the pupils would be busy for some time he was surprised to hear within seconds Carl Friedrich's response. He said the sum is $(1+100) + (2+99) + (3+98) + \dots$ till $(50+51)$, that is, 50 terms each equal to 101, hence 5050. He was 10 years old! Gauss enrolled in the Gymnasium in Brunswick, where he excelled in ancient languages and mathematics. After receiving a stipend from the Duke of Brunswick-Wolfenbüttel, Gauss entered Brunswick Collegium Carolinum in 1792. At the academy, by the age of 17 he had already formulated many fundamental mathematical theories covering the span of Bode's law, the binomial theorem, the arithmetic-geometric mean, the law of quadratic reciprocity and the prime number theorem.

In 1795 Gauss left Brunswick to study at Göttingen university. Gauss left Göttingen in 1798 without a diploma, but by this time he had made one of his most important discoveries: the construction of a regular 17-gon (heptadecagon) by ruler and compasses. This is

considered to be the greatest advance in this field since the time of Greek mathematics. It was published as Section VII of Gauss' famous work, *Disquisitiones Arithmeticae*.

Gauss received his doctorate in 1799 at the age of 22 from the university of Helmstedt. In his thesis he developed the concept of complex numbers and proved the fundamental theorem of algebra. Two years later, Gauss published his theory of numbers, considered one of the most brilliant discoveries in the history of mathematics.

On the first of January 1801 **Giuseppe Piazzi** (1746–1826) discovered a small planet, to be called Ceres, between the orbits of Mars and Jupiter. It soon disappeared from telescopes and could not be found. Gauss then developed a least-squares approach to estimate the most probable trajectory of the asteroid. At the end of 1801 Ceres is found at the exact location predicted by Gauss. A new approach applying mathematics to astronomy is thus born.

Gauss married Johanna Ostoff on October 9, 1805. Despite having a happy personal life for the first time, his benefactor, the Duke of Brunswick, was killed fighting for the Prussian army.

In 1807 he was appointed professor of astronomy and director of the observatory at the university of Göttingen, a position he occupied for the rest of his life.

In 1808 his father died, and a year later Gauss' wife Johanna died after giving birth to their second son, who was to die soon after her. Gauss was shattered and wrote to Olbers asking him to give him a home for a few weeks.

Gauss was married for a second time the next year, to Minna, Johanna's best friend, and they had three children.

Gauss devised a new approach to evaluating the orbits of asteroids and the theory of squares. He studied the size and form of the Earth and introduced what became known as the Gaussian error curve. He was a pioneer in applying mathematics to electricity and magnetism and developing the underlying potential theory as well as number theory and solid geometry.

References:

J. J. O'Connor and E. F. Robertson

December 1996

MacTutor History of Mathematics

[<http://www-history.mcs.st-andrews.ac.uk/Biographies/Gauss.html>]

Encyclopaedia Britannica

Bertrand Hauchecorne and Daniel Suratteau, "Des Mathematiciens de A a Z", ellipses, edition marketing S. A. 1996.

A.21 Friedrich Wilhelm Bessel (1784–1846)

Born: July 22, 1784 in Minden, Westphalia (now Germany); died: March 17, 1846 in Königsberg, Prussia (now Kaliningrad, Russia)

Born in Westphalia, now part of Germany, Friedrich Wilhelm Bessel was the son of a modest government employee. He attended school in Minden for four years but found little motivation, leaving school in 1799 at the age of 14 to become an apprentice in the import/export firm of Kulenkamp in Bremen. Longing to travel he developed a passion for navigation and consequently astronomy and mathematics.

In 1804 he wrote a paper on Halley's Comet evaluating its orbit from observations dating back to 1607. He sent his paper to the astronomer Wilhelm Olbers who was greatly impressed, ensuring its publication in the same year in *Monatliche Correspondenz*. He rec-

ommended the appointment of Bessel at the Lilienthal observatory of the famed lunar observer J. H. Schroeter.



FIGURE A.24 Friedrich Wilhelm Bessel.

After four years at that post Bessel was charged by the Prussian government with the construction of the first big German observatory at Königsberg. Bessel received a doctorate from the university of Göttingen on the recommendation of Gauss, who had met Bessel in Bremen in 1807 and had high regard for his contributions.

In 1810 Bessel was appointed professor of astronomy at the university of Königsberg where he taught and put much thought on formulating the science of astronomical observation. He was director of the observatory from the date of its completion, and for the rest of his life. Bessel's reputation was established internationally and he was honored with the award of the Lalande Prize of the Institut de France for his refraction tables based on Bradley's observations. He was elected in 1812 to the Berlin Academy.

Bessel's contributions included the precise evaluation, hence the correction, of the length of the seconds pendulum in 1826, attaining the desired period of the swing of exactly one second.

He conducted geodetic measurements of the meridian arcs in East Prussia in 1831 and 1832. In 1841 he evaluated the degree of ellipticity, that is, the deviation from a perfect sphere, of the Earth as $1/299$. He was among the first to obtain highly accurate measurements of the diameter of the Sun using a heliometer. Bessel also performed statistical analysis of errors of measuring instruments and formulated the statistical bias of measurements characteristic of the observer.

Using his statistical bias corrections he presented his own astronomical measurements which surpassed in accuracy those of his predecessors and his methods became the standard in the field.

He was able to obtain highly accurate measurements of the positions and movements of the stars by applying his techniques of correction of imperfections in telescopes and atmospheric disturbances.

He compiled with corrections the observations of the English astronomer James Bradley (1742–1762) accounting for instrumental errors in the mean positions of 3,222 stars, publish-

ing the results in *Fundamenta Astronomiae* in 1818. He has thus laid down the foundations of modern position astronomy. Although the Observatory at Königsberg was still under construction, Bessel took up his new post on May 10, 1810. He continued to work on Bradley's observations while work continued on the observatory from 1810 to 1813.

Bessel undertook his monumental task in Königsberg of evaluating the positions and movements of over 50,000 stars which led to his identification in 1838 of the parallax of 61 Cygni.

Bessel had two sons who died early and three daughters. His health was fragile and deteriorated with time. In 1842 he visited England to participate in the Congress of the British Association in Manchester. His encounters with important English scientists and Herschel in particular motivated him to pursue further and publish his recent research, in a series of papers written in spite of his ailing health condition. Two years later, on March 17, 1846 Bessel died of cancer in Königsberg.

Bessel was honored by the Royal Astronomical Society of London among many others.

References:

<http://www-groups.dcs.st-and.ac.uk/history/Biographies/Bessel.html>

http://en.wikipedia.org/wiki/Friedrich_Wilhelm_Bessel

<http://www.bookrags.com/biography/friedrich-bessel-wsd/>

A.22 Augustin-Louis Cauchy (1789–1857)



FIGURE A.25 Augustin-Louis Cauchy.

Born: August 21, 1789 in Paris, France; **died:** May 23, 1857 in Sceaux (near Paris), France.

Augustin-Louis Cauchy was born in the first days of the eruption of the French Revolution (1789-1799). His father Louis François Cauchy, was a lawyer, a classics scholar, royalist, and had a position in the Prefect of Paris Police. Fearing for his family's life of

the repercussions of the revolution he moved his family to Arcueil. He took personal charge of his son's education before returning to Paris. There, Laplace and Lagrange were among his friends who noticed Augustin-Louis' mathematical gifts. Lagrange's advice was, however, to give attention to the study of languages before the pursuit of mathematics. Cauchy was enrolled between 1802 and 1804 at the École Centrale du Panthéon where he studied classical languages.

He then focused progressively on mathematics and in 1805 wrote the entrance examination for the École Polytechnique, was examined by Biot, placed second and attended courses by Lacroix, de Prony and Hachette, with Ampère as his analysis tutor.

Upon graduation from École Polytechnique in 1807 Cauchy was admitted to the highly sought engineering school École des Ponts et Chaussées. He was appointed to the Ourcq Canal project under the supervision of Pierre Girard.

In 1810, appointed junior engineer at Cherbourg, he contributed to Napoléon's English invasion fleet project by working on the construction of the port of Cherbourg. Meanwhile he avidly studied mathematics, inspired by the work of Laplace and Lagrange. He explored the properties of polygons and polyhedra and submitted papers in 1811 and 1812 on his discoveries, with the support of Legendre and Malus.

In Cherbourg Cauchy worked hard on his mathematics research in addition to the long hours spent on his engineering work. In 1812 he returned to Paris to live with his parents, suffering from a severe state of depression.

In Paris he submitted a thesis on symmetric functions which was published in the *Journal of the École Polytechnique* in 1815. His applications for an academic position were not successful, however, and he had to settle for a return to his Ourcq Canal project.

Cauchy was a devout Catholic and his attitude to his religion alienated him from his colleagues. His aim was for an academic career but he was often turned down. A position he applied for at the Bureau des Longitudes went to Legendre. Another at the geometry section went Poinot. Another position went in 1814 to Ampère, and a mechanics vacancy which followed Napoléon's abdication in April, went to Molard. In this last election Cauchy did not receive a single one of the 53 votes cast. In the same year, however, he published a memoir on definite integrals that became the foundation of his theory of complex functions.

With the fall of Napoléon's Empire in 1814 the royalist Cauchy finds valuable support from protectors who acceded to power. Their influence helped his appointment to assistant professor of analysis, responsible for the second year course, at École Polytechnique.

The following year life smiled on Cauchy at last. He received the Grand Prix of the French Academy of Sciences for his research results on waves. His fame was definitely established, however, when he submitted a paper to the Institute solving one of Fermat's claims on polygonal numbers. He was admitted in 1816 to the Academy of Sciences, when political currents led to the dismissal of Carnot and Monge and Cauchy filled one of their positions.

Cauchy soon married Aloïse de Bure, of a family of reputable Parisian librarians, and they had two daughters.

In 1817 Cauchy filled a position at the College de France left vacant by Biot's expedition to Scotland. He lectured on methods of integration where he presented with rigorous analysis the conditions of convergence of infinite series and his definition of an integral. His cours d'Analyse on the development of basic theorems of calculus as precisely as possible, was designed for the students of École Polytechnique. In 1826 he presented *Sur un nouveau genre de calcul analogue au calcul infinitesimal* on the foundations of his famous theorem of residues, and in 1829 in *Lecons sur le Calcul Différentiel* he defined for the first time a complex function of a complex variable.

The analysis course given by Cauchy is decried by his students as well as his colleagues. It is this same course, however, which was published in 1821 and 1823, to become the reference on analysis of the 19th century, replacing intuition by analytical rigor. Pioneering precise

definitions are given to notions such as limits, continuity and series convergence. Some false conclusions such as his proof that the limit of a series of continuous functions is continuous attest to his pioneering effort in exploring an unknown new domain.

The French Revolution of 1830, also known as the July Revolution, saw the overthrow of King Charles X, the French Bourbon monarch, and the ascension to the throne of his cousin Louis Philippe, the Duc d'Orléans, who himself, after 18 precarious years on the throne, would in turn be overthrown.

Such political turmoil in Paris and the years of strife and hard work made Cauchy, a staunch loyalist to the House of Bourbon, decide to absent himself for a while from France. He left Paris in September 1830 and spent a short time in Switzerland, leaving behind in Paris his wife and two daughters. There he was an enthusiastic helper in setting up the Académie Helvétique but the project collapsed due to political conflicts.

The July Revolution in France required that Cauchy swear an oath of allegiance to the new regime and, when he failed to return to Paris to do so, he lost all his positions.

In Turin during 1831 he accepted an offer from the King of Piedmont for a chair of theoretical physics. He taught in Turin and Menbrea who attended his courses, commented, "very confused, skipping suddenly from one idea to another, from one formula to the next, with no attempt to give a connection between them. His presentations were obscure clouds, illuminated from time to time by flashes of pure genius ... of the 30 who enrolled with me, I was the only one to see through it."

In 1833 Cauchy moved from Turin to Prague in order to tutor the grandson of Charles X. However, the prince showed very little interest in mathematics. Cauchy became annoyed and screamed and yelled. The queen sometimes said to him, "too loud, not so loud."

Cauchy moved back to Paris in 1838 and regained his position at the Academy. However, he did not regain his teaching positions having refused to take the oath. Later in 1839 a position at the Bureau Des Longitudes became vacant. Although Cauchy was elected, he was not allowed to attend any meetings or receive a salary, again because of his refusal to take the oath. The mathematics chair at Collège de France became vacant in 1843. Cauchy should have easily won on account of his exceptional scientific profile, but apparently due to his religious and political views he was not chosen. Henceforth, Cauchy's mathematical contributions declined.

Cauchy made landmark contributions to mathematical physics, mathematical astronomy, and differential equations. His four volume text *Exercices d'Analyse et de Physique Mathématique* was published between 1840 and 1847. He stubbornly stuck to his religious and political views to the dismay of colleagues.

Cauchy never took an administrative post and was disrespectful and condescending toward some young scientists such as Abel and Galois, disregarding and even losing theses of great scientific value. His colleagues begrudged him the political influence that led to his admission to the Academy and resented his intransigence and religious bigotry.

He was disliked, regarded as arrogant, recognizing no one else's contribution. Abel wrote of him after his visit to the Institute in 1826, "Cauchy is mad and there is nothing that can be done about him, although, right now, he is the only one who knows how mathematics should be done."

He was accused by his colleagues of liberally copying without citation the results of others. They referred to Cauchy as *cochon*. In the last few years of his life he had a dispute with Duhamel regarding a result on inelastic shocks. Cauchy claimed to be the first to give the results in 1832, but Poncelet referred to his own work on the subject in 1826. Even though Cauchy was proved wrong he would never admit it.

Cauchy died on May 27, 1857. His last words were "Men pass away, but their deeds abide." Many terms in mathematics bear his name, the Cauchy integral theorem, in the theory of complex functions, the Cauchy–Kovalevskaya existence theorem for the solution

of partial differential equations, the Cauchy–Riemann equations, and the Cauchy sequences. A book of his collective works entitled *Oeuvres complètes d’Augustin Cauchy* (1882–1870) was published in 27 volumes.

References:

J. J. O’Connor and E. F. Robertson, January 1997, MacTutor History of Mathematics

<http://www-history.mcs.st-andrews.ac.uk/Biographies/Cauchy.html>

<http://www.bibmath.net/bios/index.php3?action=affiche&quoi=cauchy>

A.23 Niels Henrik Abel (1802–1829)

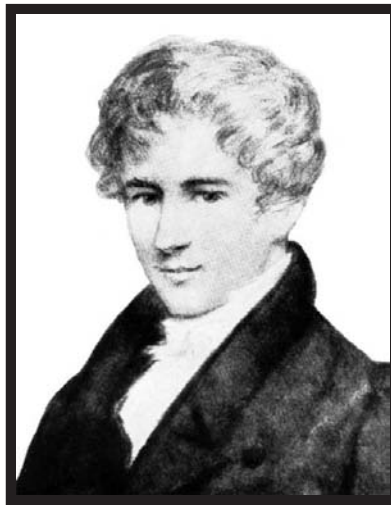


FIGURE A.26 Niels Henrik Abel (www.commonswikimedia.org/wiki/Image:Niels_Henrik_Abel.jpg).

Born: August, 1802 in Frindoe, Norway; died: April 6, 1829 in Froland, Norway.

Niels Henrik Abel was a Norwegian mathematician who in a short life span of 26 years became a pioneer who advanced modern mathematics of his time by leaps and bounds. He was born, one of seven children, in the small village of Frindoe, near Stavanger, Norway, where his father was a poor Protestant minister in the diocese of Christiansand. Abel’s life was spent in poverty. In 1815 he studied at the Cathedral School in Christiania. In 1817 the mathematics teacher Bernt Holmboe, newly arrived at the school, was impressed by the young Abel’s mathematical talent. Soon, Abel began to study university level mathematics texts and, within a year, Abel was reading the works of Euler, Newton, Lagrange, Laplace and Gauss. In 1820 Abel’s father died, and he had to support his mother and family.

Thanks to Holmboe’s help Abel received a scholarship to remain at his school and was able to enter the university of Christiania (Oslo) in 1821. Holmboe, moreover, collected contributions from his colleagues enabling Abel to pursue his studies at the university. At the university of Christiania, Christopher Hansteen, professor of astronomy, provided Abel

with both financial and moral support.

Abel obtained a preliminary degree from the university in 1822 and continued his research independently, with further subsidies obtained by Holmboe. While in his final year at school, Abel had begun working on the solution of quintic equations (of the fifth order) by radicals.

He published papers in 1823 in the new periodical *Magazin for Naturvidenskaberne*, edited by Hanseen, on functional equations and integrals.

In his paper, *Solutions of some problems by means of definite integrals* he gave the first solution of an integral equation.

Abel was given a small grant allowing him to visit Degen and other mathematicians in Copenhagen. There he met Christine Kemp who soon became his fiancée.

Upon his return to the university of Christiania, his friends urged the Norwegian government to grant him a fellowship to study in Germany and France. While awaiting the royal decree, in 1824, he published his proof as a pamphlet at his own expense that no algebraic solution exists for the general quintic equation. He sent the pamphlet to Gauss, whom he intended to visit in Göttingen while on his travels. Gauss disregarded it, failing to recognize its true value.

In August 1825 Abel received the fellowship from the Norwegian government allowing him to travel abroad and he set out with four friends, visiting first mathematicians in Norway and Denmark. In Copenhagen he was given a letter of introduction to August Leopold Crelle. He spent the winter of 1825 to 1826 with his Norwegian friends in Berlin, where Crelle, a civil engineer and avid mathematician, became his close friend and mentor.

With Abel's enthusiastic support, Crelle published the *Journal fur die Reine und Angewandte Mathematik* ("Journal for pure and applied mathematics"). Its first volume appeared in 1826 and contained an article elaborating on his results of the quintic equation titled *Recherches sur les fonctions elliptiques*, together with six other papers by Abel on equation theory, functional equations, integration in finite forms and theoretical mechanics.

Abel had planned to visit Gauss in Göttingen on the way to Paris. However, learning that Gauss was displeased to receive his work on the the general quintic equation, he decided to cancel his trip to Göttingen. He arrived in Paris in 1826 where he sought the most renowned mathematicians and continued work on transcendental and elliptic functions. He developed what was to be known as Abel's theorem on the integrals of algebraic functions. This theorem was the foundation of the later theory of Abelian integrals and Abelian functions. His presentations did not evoke in Paris the enthusiasm he had hoped for, for he was a new unknown entity on the scene.

He showed his treatise on a class of transcendental functions to Cauchy who brushed the young man aside with disdain.

Abel submitted his memoir to the Academy of Sciences on the sum of integrals of a given algebraic function, which is a generalization of Euler's relation on elliptic integrals, hoping to make known his recent discoveries. He waited in vain for a response. Meanwhile he was diagnosed as having tuberculosis.

Heavily in debt, Abel returned to Norway. To subsist he tutored schoolchildren, received a small grant from his university and obtained a substitute teaching position. In spite of his illness and poverty he produced several papers on the theory of equations, later to be referred to as the theory of Abelian equations with Abelian groups. In a short time he developed the theory of elliptic functions independently of the work of Karl Gustav Jacobi.

Legendre saw the new ideas in the papers that Abel and Jacobi were writing and said "Through these works you two will be placed in the class of the foremost analysts of our times."

By now his fame had spread over all mathematics centers. A group from the French Academy submitted a request to grant him a suitable position to King Bernadotte of

Norway-Sweden. Meanwhile Crelle worked on securing for him a position of professor in Berlin.

In the fall of 1828 Abel's health took a turn for the worst, and a trip on a sled to visit his fiancée at Froland near Christmastime aggravated his condition. Crelle persisted more intensely in his efforts to obtain an appointment for Abel in Berlin. He succeeded and wrote to Abel on April 8, 1829 that his dream had come true. It was too late; Abel had died on April 6, at the age of 26.

References:

<http://www-groups.dcs.st-and.ac.uk/history/Biographies/Abel.html>

<http://www-groups.dcs.st-and.ac.uk/history/Mathematicians/Abel.html>

A.24 Johann Peter Gustav Lejeune Dirichlet (1805–1859)



FIGURE A.27 Johann Peter Gustav Lejeune Dirichlet.

Born: February 13, 1805 in Düren, French Empire (now Germany), **died:** May 5, 1859 in Göttingen, Hanover (now Germany)

Lejeune Dirichlet was born in Düren (now in Germany). His grandfather lived in the town of Richelette in Belgium, whence the name “Lejeune Dirichlet” (*“le jeune de Richelette”*) (the young one from Richelette). His father was the postmaster of Düren, situated about halfway between Aachen and Cologne. After two years at the Gymnasium he attended the Jesuit College in Cologne and there he had the good fortune to be taught by Georg Ohm.

His first paper to the Paris Academy in July 1825 established instantly his reputation since it tackled the famous Fermat's last theorem. The theorem claimed that for $n > 2$ there are no nonzero integers x, y, z such that $x^n + y^n = z^n$. The cases $n = 3$ and $n = 4$ had been proved by Euler and Fermat. Dirichlet's paper presented a partial proof for the case $n = 5$, which was completed by Legendre who was one of the referees. Dirichlet also completed his own proof almost at the same time, presenting at a later date a full proof for

the case $n = 14$.

Dirichlet studied mathematics at Göttingen university where he was a student of Karl Gauss and Karl Jacobi. He also studied briefly in Paris where he benefited considerably from his contacts with Fourier, Biot, Laplace, Lacroix, Legendre, and Poisson. Joseph Fourier greatly motivated his interest in expansions using trigonometric series. In 1826 he returned to Germany and taught at Breslau and later at the Military Academy in Berlin. He then moved to the university of Berlin to stay for 27 years before returning to Göttingen university to fill the chair left vacant by Gauss' death.

Dirichlet's work on number theory was an extension of Gauss' developments, and Dirichlet's book, the *Vorlesungen über Zahlentheorie* (1863; Lectures on Number Theory), is comparable in its depth and extent to Gauss' *Disquisitiones*. Dirichlet made many significant discoveries in number theory and his solution of a problem related to primes was a pioneering effort in applying analytical techniques to solve problems in number theory.

In 1829 Dirichlet was able to define the sufficient conditions for the existence of Fourier series to converge. Fourier also initiated the interest of Dirichlet in mathematical physics, motivating his interest in multiple integrals and the boundary-value problem, which came to be known as the *Dirichlet problem*, concerning the formulation and solution of those partial differential equations occurring in the study of heat flow and electrostatics. These are of great importance in many other areas of physics. The growth of a more rigorous understanding of analysis owes to Dirichlet what is essentially the modern definition of the concept of a function.

In 1831, Dirichlet married Rebecca Henriette Mendelssohn Bartholdy, who came from a distinguished family, being a granddaughter of the philosopher Moses Mendelssohn and a sister of the composer Felix Mendelssohn.

Jacobi, who taught at Königsberg, was one of Dirichlet's lifelong friends, and they had great respect for each other's contribution, in particular in number theory.

Ferdinand Eisenstein, Leopold Kronecker, and Rudolf Lipschitz were Dirichlet's students. After his death on May 5, 1859 in Göttingen, Dirichlet's lectures and landmark results in number theory were collected, edited and published by his friend and fellow mathematician Richard Dedekind under the title *Vorlesungen über Zahlentheorie* (*Lectures on Number Theory*).

References:

http://en.wikipedia.org/wiki/Johann_Peter_Gustav_Lejeune_Dirichlet

<http://www-groups.dcs.st-and.ac.uk/history/Biographies/Dirichlet.html>

<http://www.bookrags.com/biography/johann-peter-gustav-lejeune-dirichlet-wom/>

A.25 Pafnuty Lvovich Chebyshev (1821–1894)

Born: May 16, 1821 in Okatovo, Russia; **died:** December 8, 1894 in St. Petersburg, Russia

Pafnuty Lvovich Chebyshev was born in Okatovo, a village west of Moscow. He was one of nine children of Lev Pavlovich Chebyshev and Agrafena Ivanovna Chebysheva. His father was a wealthy landowner who in his earlier military career had fought as an officer against Napoléon's invading armies. Pafnuty Lvovich had a physical handicap with one limb weaker than the other, causing him to limp and he had to walk with a stick. He was thus unable



FIGURE A.28 Pafnuty Lvovich Chebyshev.

to pursue an officer's career and early on replaced child's play and sports with a passion for constructing mechanisms. He was tutored at home by his mother, his cousin Avdotia Kvintillianovna Soukhareva and a music teacher whom he later acknowledged for teaching him the importance of analysis, precision and harmony. From his mother he learned the basic skills of reading and writing, while his cousin acting as a governess taught him French and arithmetic. Later in life his fluency in French helped him in his publications and in his visits to France. French at the time was a natural language for formulating mathematics and communicating with European mathematicians.

In 1832, the family moved to Moscow mainly to attend to the education of their sons. He was tutored at home; his mathematics and physics lessons were given by P. N. Pogorelski, one of the most renowned teachers in Moscow. In 1837, Chebyshev began his studies of mathematics at Moscow university. In courses on mechanics his professor was Nikolai Dmetrievich Brashman, who taught a wide range of subjects covering applied mechanics, mechanical engineering, hydraulics and probability theory. Later Chebyshev would cite the great influence Brashman had on developing his areas of research.

In 1841 Chebyshev was awarded the silver medal for his work "Calculation of the roots of equations." In this contribution Chebyshev proposed an approximation for the solution of algebraic equations of the n th degree based on Newton's algorithm. Chebyshev proceeded to a master's degree program under Brashman's supervision. In 1843 he published a paper on multiple integrals in French in Liouville's journal. In 1846 he received his master's degree upon defending his thesis "An Attempt to an Elementary Analysis of Probabilistic Theory." In 1847 Chebyshev became assistant professor of mathematics at St. Petersburg university. In 1849 he defended his theory of congruences results in his doctorate dissertation and became professor at St. Petersburg university in 1860. The Paris academy elected him corresponding member in the same year, and full foreign member in 1874.

In 1872, after 25 years of teaching at St. Petersburg university, he became professor emeritus. In 1882 he left the university to devote his life to research. In 1893, he was elected honorable member of the St. Petersburg Mathematical Society. He died November 26, 1894, in St Petersburg.

References:

- <http://www-history.mcs.st-andrews.ac.uk/Biographies/Chebyshev.html>
- http://en.wikipedia.org/wiki/Pafnuty_Chebyshev

<http://www.britannica.com/eb/article-9022729/Pafnuty-Lvovich-Chebyshev>

<http://www.bibmath.net/bios/index.php3>.

A.26 Paul A.M. Dirac

The Nobel Prize in Physics 1933

The following is a reproduction, with gratitude and acknowledgment for the permission granted by the Nobel Foundation, of the Foundation's official biography on the life of Paul A.M. Dirac, as it appears on the site:

http://nobelprize.org/nobel_prizes/physics/laureates/1933/dirac-bio.html



FIGURE A.29 Paul A.M. Dirac (www.commonswiki.org/wiki/Paul_A.M._Dirac)

Paul Adrien Maurice Dirac was born on 8th August, 1902, at Bristol, England, his father being Swiss and his mother English. He was educated at the Merchant Venturer's Secondary School, Bristol, then went on to Bristol university. Here, he studied electrical engineering, obtaining the B.Sc. (Engineering) degree in 1921. He then studied mathematics for two years at Bristol university, later going on to St.John's College, Cambridge, as a research student in mathematics. He received his Ph.D. degree in 1926. The following year he became a Fellow of St.John's College and, in 1932, Lucasian Professor of Mathematics at Cambridge.

Dirac's work has been concerned with the mathematical and theoretical aspects of quantum mechanics. He began work on the new quantum mechanics as soon as it was introduced by Heisenberg in 1928 — independently producing a mathematical equivalent which consisted essentially of a noncommutative algebra for calculating atomic properties — and wrote a series of papers on the subject, published mainly in the Proceedings of the Royal Society, leading up to his relativistic theory of the electron (1928) and the theory of holes (1930). This latter theory required the existence of a positive particle having the same mass and charge as the known (negative) electron. This, the positron was discovered experimentally at a later date (1932) by C. D. Anderson, while its existence was likewise proved by

Blackett and Occhialini (1933) in the phenomena of “pair production” and “annihilation.”

The importance of Dirac’s work lies essentially in his famous wave equation, which introduced special relativity into Schrödinger’s equation. Taking into account the fact that, mathematically speaking, relativity theory and quantum theory are not only distinct from each other, but also oppose each other, Dirac’s work could be considered a fruitful reconciliation between the two theories.

Dirac’s publications include the books *Quantum Theory of the Electron* (1928) and *The Principles of Quantum Mechanics* (1930; 3rd ed. 1947).

He was elected a Fellow of the Royal Society in 1930, being awarded the Society’s Royal Medal and the Copley Medal. He was elected a member of the Pontifical Academy of Sciences in 1961.

Dirac has travelled extensively and studied at various foreign universities, including Copenhagen, Göttingen, Leyden, Wisconsin, Michigan, and Princeton (in 1934, as Visiting Professor). In 1929, after having spent five months in America, he went round the world, visiting Japan together with Heisenberg, and then returned across Siberia.

In 1937 he married Margit Wigner, of Budapest.

Paul A.M. Dirac died on October 20, 1984.

From *Nobel Lectures, Physics 1922-1941*, Elsevier Publishing Company, Amsterdam, 1965. This biography was first published in the book series *Les Prix Nobel*. It was later edited and republished in *Nobel Lectures*.

Copyright © The Nobel Foundation 1933.

This page intentionally left blank

References

- [1] M. ABRAMOWITZ and Editors STEGUN, M. *Handbook of Mathematical Functions*. Dover, New York, 1964.
- [2] N. AHMED and K. R. RAO. *Orthogonal Transforms for Digital Signal Processing*. Springer Verlag, Berlin, 1975.
- [3] J. ARSAC. *Transformation de Fourier et Théorie des Distributions*. Dunod, Paris, 1961.
- [4] B. GOLD and C. M. RADER. *Digital Processing of Signals*. Lincoln Laboratory Publications, McGraw-Hill Book Company, 1969.
- [5] J. BARROS-NETO. *An Introduction to the Theory of Distributions*. Marcel Dekker, Inc., New York, 1973.
- [6] J. BENESTY, Y. SONDHI, M. M. HUANG, and Editors. *Springer Handbook of Speech Processing*. Springer, Berlin, 2008.
- [7] J.M. BONY. *Théorie des Distributions et Analyse de Fourier*. École Polytechnique, Paris, 1996.
- [8] M. BOUX. *Les Fonctions Généralisées ou Distributions*. Masson, Paris, 1964.
- [9] R.N. BRACEWELL. *The Fourier Transform and Its Applications*. McGraw Hill, New York, 2000.
- [10] H. BREMERMAN. *Distributions, Complex Variables and Fourier Transforms*. Addison Wesley, Reading, Mass., 1965.
- [11] R.H. CANON. Jr. *Dynamics of Physical Systems*. McGraw-Hill, New York, 1967.
- [12] W.K. CHEN. *Passive and Active Filters*. J. Wiley & Sons, New York, 1996.
- [13] Y. CHU. *Computer Organization and Microprogramming*. Prentice Hall, Englewood Cliffs, NJ, 1972.
- [14] C.W. CLENSHAW. Chebyshev series for mathematical functions. *Mathematical Tables of the National Physics Laboratory, HM Stationary Office, London*, 5:143–147, June 1962.
- [15] M. CORINTHIOS. High Speed Signal Processor for Vector Transformation. U.S. Patent, No. 3,754,128, Canada No. 949 216:1–43, 21 Aug. 1973.
- [16] M. CORINTHIOS. General Base State Assignment for Optimal Massive Parallelism. U.S. Patent, No. 6,401,189:1–40, June 4, 2002.
- [17] M. CORINTHIOS. A time series analyzer. In *Computer Processing in Communication, MRI Symposia Series; New York, Polytechnic Press*, 19:47–60, January 1969.
- [18] M. CORINTHIOS. Laplace spectrum for exponential decomposition and pole-zero estimation. In *IEE Proceedings on Vision Image and Signal Processing*, 148(5):305–314, October 2001.

- [19] M. CORINTHIOS. Extending Laplace and z -transform domains. *European Signal Processing Conference EUSIPCO, Sep 4-8, 2006 Florence, Italy*, 1–5, 2006.
- [20] M. CORINTHIOS. Optimal parallel and pipelined processing through a new class of matrices with application to generalized spectral analysis. *IEEE Trans. Comput.*, (4):443–459, April 1994.
- [21] M. CORINTHIOS. Generalisation of the Dirac-delta impulse extending Laplace and z -transform domains. *IEE Proc. Vision, Image and Signal Processing*, 150(2):69–81, April 2003.
- [22] M. CORINTHIOS. A fast Fourier transform for high speed signal processing. *IEEE Trans. Comput.*, C 20:843–846, Aug. 1971.
- [23] M. CORINTHIOS. Complex-variable distribution theory for Laplace and z -transforms. *IEE Proc. Vision, Image and Signal Processing*, 152(1):97–106, Feb. 2005.
- [24] M. CORINTHIOS. The design of a class of fast Fourier transform computers. *IEEE Trans. Computers*, C 20:617–623, June 1971.
- [25] M. CORINTHIOS. Generalised transform factorisation for massive parallelism. *IEE Proceedings, Vision, image and signal processing*, 151(3):153–163, June 2004.
- [26] M. CORINTHIOS. A weighted z -spectrum, parallel algorithm and processors for mathematical model estimation. *IEEE Trans. Comput.*, 45(5):513–528, May 1996.
- [27] M. CORINTHIOS. New Laplace, z and Fourier-related transforms. *Proceedings of the Royal Society A: Mathematical, Physical and Engineering Sciences, UK, Proc. Roy. Soc. A*, 463:1179–1198, May 2007.
- [28] M. CORINTHIOS, K.C. SMITH, and J.L. YEN. A parallel radix 4 fast Fourier transform computer. *IEEE Trans. Computers*, C 24(1):80–92, Januray 1975.
- [29] R. CRISTESCU and G. MARINESCU. *Applications of the Theory of Distributions*. Editura Academiei, John Wiley, London, 1973.
- [30] B. DAVIES. *Integral Transforms and Their Applications*. Springer, Verlag, New York, 1985.
- [31] H.F. DAVIS. *Fourier Series and Orthogonal Functions*. Dover, New York, 1989.
- [32] T. DELYIANNIS. High- q factor circuit with reduced sensitivity. *Electronic Letters*, 4: 577, 1968.
- [33] W.F. DONOGHUE. Jr. *Distributions and Fourier Transforms*. Academic Press, New York, 1969.
- [34] R.C. DORF and R.H. BISHOP. *Modern Control Systems*. Prentice Hall, Englewood Cliffs, NJ, 2001.
- [35] J. DUPRAZ. *La Théorie des Distributions et ses Applications*. Cepadues Éditions, Paris, 1977.
- [36] F.G. FRIEDLANDER and M. JOSHI. *Introduction to the Theory of Distributions*. Cambridge University Press, Cambridge, U.K., 1998.
- [37] B. FRIEDMAN. *Lectures on Applications Oriented Mathematics*. Holden Day, San Francisco, CA, 1969.
- [38] J.J. FRIEND, C.A. HARRIES, and D. HILBERMAN. Star: An active biquadratic filter section. *IEEE Trans. Circuits and Systems*, CAS-22:115–121, 1975.

- [39] J.G. PROAKIS and D.G. MANOLAKIS. *Digital Signal Processing*. Prentice Hall, Englewood Cliffs, NJ, 1996.
- [40] D. GABOR. Theory of communication. *J.I.E.E.*, 93, Part III: 429–444, 1946.
- [41] Y. GEADAH and M. CORINTHIOS. Natural, dyadic and sequency ordered algorithms and processors for the Walsh–Hadamard transform. *IEEE Trans. Computers*, C 26(5):435–442, May 1977.
- [42] I.S. GRADSHTEYN and I.M. RYZHIK. *Table of Integrals, Series, and Products*. Academic Press, Orlando, FL, 1979.
- [43] P.M. GRANT and J.H. COLLINS. Introduction to electronic warfare. *IEEE Proc.*, Vol. 129, Pt. F, (3):113–132, June 1982.
- [44] I.M. GUELFAND and G.E. CHILOV. *Les Distributions*. Dunod, Paris, 1962.
- [45] P.B. GUEST. *Laplace Transforms and Introduction to Distributions*. Ellis Horwood, New York, 1991.
- [46] I. HALPERIN. *Introduction to the Theory of Distributions*. University of Toronto Press, Toronto, Ontario, 1952.
- [47] S. HAYKIN and B. VAN VEEN. *Signals and Systems*. John Wiley & Sons, New York, 1999.
- [48] L.P. HUELSMAN and P.E. ALLEN. *Introduction to the Theory and Design of Active Filters*. University of Illinois, McGraw-Hill Book Company, 1980.
- [49] G.M. JENKINS and D.G. WATTS. *Spectral Analysis and Its Applications*. Holden-Day, San Fransisco, 1968.
- [50] D.S. JONES. *The Theory of Generalized Functions*. Cambridge, London, 1982.
- [51] R.P. KANWAL, *Generalized Functions: Theory and Technique*. Academic Press, New York, 1983.
- [52] E. KNUTH, D. *The Art of Computer Programming*. Vol. 2 Addison-Wesley, Reading, Massachusetts., 1968.
- [53] N. LEVINSON. The Wiener rms error criterion in filter design and prediction. *J. Math. Phys.*, 25: 261–278, June 1947.
- [54] M.J. LIGHTHILL. *Introduction to Fourier Analysis and Generalized Functions*. Cambridge University Press, Cambridge, U.K., 1958.
- [55] A.V. OPPENHEIM and R.W. SCHAFER. *Digital Signal Processing*. Prentice Hall, Englewood Cliffs, NJ, 1978.
- [56] A.V. OPPENHEIM and R.W. SCHAFER. *Discrete-Time Signal Processing*. Prentice Hall, Englewood Cliffs, NJ, 1999.
- [57] A.V. OPPENHEIM and A.S. WILLSKY. *Signals and Systems*. Prentice Hall, Englewood Cliffs, NJ, 1992.
- [58] A. PAPOULIS. *The Fourier Integral and Its Applications*. McGraw Hill, New York, 1962.
- [59] A. PAPOULIS. *Probability, Random Variables and Stochastic Processes*. 2nd Ed., McGraw Hill, New York, 1984.

- [60] T.W. PARKS and C.S. BURRUS. *Digital Filter Design*. John Wiley & Sons, New York, 1987.
- [61] R. PETIT. *L'outil Mathématique*. Masson, Paris, 1987.
- [62] A. POULARIKAS and S. SEELY. *Signals and Systems*. PWS-KENT, Boston, 1991.
- [63] A. POULARIKAS. *The Transforms and Applications Handbook*. CRC Press, IEEE Press, Boca Raton, FL, 2000.
- [64] W.R. LEPAGE. *Complex Variables and the Laplace Transform for Engineers*. Dover, New York, 1961.
- [65] R.M. RAO and A.S. BOPARDIKAR. *Wavelet Transforms*. Addison Wesley, Reading, MA, 1998.
- [66] S. BROWN and Z. VRANESIC *The Fundamentals of Digital Logic with VHDL Design*. McGraw Hill, New York, 2000.
- [67] T. SCHUKER. *Distributions, Fourier Transforms and Some Applications to Physics*. World Scientific, Singapore, 1991.
- [68] L. SCHWARTZ. *Théorie des Distributions*. Hermann, Paris, 1966.
- [69] H. SLOATE. Matrix representations for sorting and the fast fourier transform. *IEEE Trans. Circuits and Systems*, Vol. CAS-21, No. 1:109–116, January 1974.
- [70] M.R. SPIEGEL. *Laplace Transform*. Schaum's Outline of Theory and Problems, Schaum Publication Co., New York, 1963.
- [71] M.R. SPIEGEL. *Fourier Analysis*. Schaum's Outline of Theory and Problems, Schaum Publication Co., New York, 1974.
- [72] R. STRICHARTZ. *A Guide to Distribution Theory and Fourier Transforms*. CRC Press Boca Raton, Boca Raton, FL, 1996.
- [73] N.S. TZANNES. *Communication and Radar Systems*. Prentice Hall, Englewood Cliffs, NJ, 1985.
- [74] J.F. WAKERLY. *Digital Design Principles and Practices*. Prentice Hall, Upper Saddle River, NJ, 2001.
- [75] A.H. ZEMANIAN. *Distribution Theory and Transform Analysis*. McGraw-Hill, New York, 1965.

Index

- 3D Multiplier, 995
- A Speed-Control System, 239
- A/D conversion
 - quantization error, 403
- Active filter realization, 713
- Allpass systems, 275, 281
- Asymptotic frequency response, 261
- Asynchronous sequential machines, 1050
 - state reduction, 1051
- Average, 25, 838, 859

- Bandpass filter impulse response, 190
- Bessel filter passive networks, 693
- Bilateral Laplace transform, 105
- Binary Coded Decimal (BCD) representation, 1033
- Binomial Expansion, 1258
- Biographies of Scientists
 - Abel, 1295
 - Al-Khwarizmi, 1266
 - Bessel, 1290
 - Bonaparte, 1283
 - Cauchy, 1292
 - Chebyshev, 1298
 - Copernicus, 1269
 - Dirac, 1300
 - Dirichlet, 1297
 - Euclid, 1265
 - Fourier, 1285
 - Galileo, 1272
 - Gauss, 1289
 - King James II, 1276
 - L'Hôpital, 1278
 - Laplace, 1279
 - Lavoisier, 1281
 - Leibniz, 1275
 - Louis XVI and Marie-Antoinette, 1283
 - Newton, 1274
 - Plato, 1262
 - Prony, 1281
 - Ptolemy, 1264
 - Rosetta stone, 1287
 - Scheiner, 1273
 - Socrates, 1263
 - William III of Orange, 1277
- Biquadratic transfer function realization, 723
- Biquadratic transfer functions, 714
- Block diagram reduction, 233
- Bode plot of a composite system, 267

- C/D and D/C conversion, 406
- Carry Look Ahead CLA cells, 1011
- Cauchy's Residue Theorem, 125
- Causal system response, 256
- Circular Shift, 448
- Comb filters, 351
- Communication systems
 - amplitude modulation, 876
 - digital communication systems, 888
 - discrete signals, 887
 - Double Side-Band (DSB) modulation, 876
 - frequency division multiplexing, 893
 - PCM-TDM Systems, 893
 - pulse duration modulation, 890
 - pulse position modulation, 892
- Composite sinusoid period, 86
- Computer arithmetic
 - 1's and 2's complement notation, 976
 - addition, 982
 - addition in 1's complement notation, 984
 - addition in 2's complement notation, 985
 - addition in sign and magnitude notation, 982
 - addition/subtraction implementation, 991
 - conversion from decimal to binary, 974
 - division, 1002
 - floating point addition/subtraction, 1029
 - floating point division, 1030
 - floating point multiplication, 1029
 - floating point number representation, 1027

- integer and fractional number representation, 978
- integers, fractions and the binary point, 974
- representation of negative numbers, 975
- sign and magnitude notation, 975
- signed numbers in 1's and 2's complement notation, 979
- square root evaluation, 1030
- subtraction, 986
- subtraction in 1's complement notation, 988
- subtraction in 2's complement notation, 989
- subtraction in sign and magnitude notation, 987
- systems for representation of numbers, 973
- Continuous-time filters
 - poles of $H(s)$, 589
 - the case $\varepsilon \neq 1$, 552
 - the value ε as function of ripple, 564
 - Bessel delay plots of frequency normalized form, 634
 - Bessel filter denormalization and deviation from ideal response, 622
 - Bessel filter frequency normalized form, 633
 - Bessel filter nomograph, 639
 - Bessel filter poles and zeros, 634
 - Bessel filter's Butterworth asymptotic form, 626
 - Bessel magnitude and delay, 626
 - Bessel quality factor and natural frequency, 618
 - Bessel's constant delay filters, 611
 - Besselfilter delay and magnitude, 622
 - Butterworth approximation, 544
 - Butterworth asymptotic form Bessel delay plots, 629
 - Butterworth filter gain, 547
 - Butterworth filter order formula, 553
 - Chebyshev approximation, 556
 - Chebyshev filter gain, 564
 - Chebyshev filter nomograph, 575
 - Chebyshev filter order, 567
 - Chebyshev's Second form, 571
 - continued fraction expansion, 612
 - delay of Bessel-Butterworth asymptotic form filter, 628
 - denormalization, 547, 568
 - Elliptic filter nomograph, 592
 - Elliptic filters, 576
 - filter delay evaluation, 617
 - frequency normalized form Bessel filter transformation, 635
 - frequency transformations, 639
 - Hamming window, 664
 - Hanning window, 663
 - lowpass to bandpass transformation, 641
 - lowpass to bandstop transformation, 651
 - lowpass to highpass transformation, 653
 - maxima and minima of response, 563
 - maximal flatness of Bessel and Butterworth response, 619
 - nomographs, 554
 - pass-band ripple, 560
 - points of maxima/minima, 591
 - pole zero alignment of Elliptic filter, 584
 - properties of the sn function, 577
 - Rectangular window, 662
 - response rate of decay, 572
 - tables of Chebyshev filter, 565
 - tables of Elliptic filters, 599
 - Triangle (Bartlett) window, 663
 - Windows, 661
 - zeros and poles of $G(\omega)$, 591
 - zeros maxima/minima of spectrum, 591
- Control counter
 - generator of prime numbers, 1054
 - micro-operations and states, 1055
- Controlled add/subtract CAS cell, 992
- Convergence division, 1016
- Conversion
 - A/D D/A, 400
 - continuous to discrete, 400
 - digital to analog, 424
- Convolution, 15
 - as multiplication, 360
 - circular, 443
 - circular using DFT, 445
 - in 2D, 366
 - of impulse and derivatives, 21
 - periodic, 441
- Correlation, 15
 - as multiplication, 360
 - function, 22
 - images, 370
 - in 2D, 366
 - two-dimensional signals, 370

- D-C Motor, 237
- D/A conversion, 404
- Decibels octaves decades, 260
- Design of doubly terminated passive LC ladder networks, 695
- dfilt, 1169
- DFT vs DFS, 438
- Difference equations, 324
- Digital filters
 - all-pole filter, 769
 - allpass filter lattice filter, 781
 - backward-rectangular approximation, 747
 - Bilinear transform, 751
 - cascaded form, 738
 - comparison of windows, 805
 - conversion of continuous-time to digital filter, 743
 - finite impulse response FIR filters, 740
 - FIR all-zero lattice structures, 760
 - first Canonical form, 734
 - first order all-zero lattice filter, 761
 - first order one-pole lattice filter, 770
 - forward rectangular, trapezoidal approximations, 749
 - frequency transformations, 783
 - general order all-pole filter, 772
 - general order all-zero lattice filter, 764
 - Hamming window, 803
 - Hanning window, 802
 - IIR filter models, 374, 734
 - impulse invariance approach, 743
 - impulse response of ideal filters, 798
 - lattice filters, 760
 - linear phase FIR filters, 741
 - matrix representation, 739
 - parallel form, 739
 - pole-zero IIR lattice filter, 775
 - Rectangular window, 801
 - Schur-Cohn stability criterion, 782
 - second Canonical form, 736
 - second Canonical form transposition, 737
 - second order all-pole lattice filter, 771
 - second order all-zero lattice filter, 762
 - short-cut impulse invariance, 746
 - signal flow graphs, 733
 - spectral leakage, 800
 - structures based on poles and zeros, 738
 - transposition, 734
 - Triangular window, 804
 - Windows, 801
- Digital signal processors
 - a simple C program, 1079
 - ADDA/SUBA instructions, 1077
 - Addressing Mode Register (AMR), 1075
 - addressing modes, 1076
 - C++ program on the DSP card, 1094
 - calling an assembly language function, 1083
 - central processing unit, 1069
 - circular addressing mode, 1078
 - computer arithmetic, 973
 - CPU data paths and control, 1071
 - Data Address paths, 1073
 - DSP programming in C++ and Simulink, 1094
 - Fibonacci in C calling assembly-language, 1087
 - Finite Impulse Response (FIR) filter, 1087
 - functional units, 1072
 - general-purpose register files, 1071
 - generated assembly code, 1080
 - IIR filter on the DSP, 1088
 - instruction syntax, 1074
 - linear addressing mode, 1077
 - Memory, Load, and Store paths, 1073
 - programming the T.I. DSP, 1078
 - real-time DSP using MATLAB–Simulink, 1092
 - register file cross paths, 1072
 - Simulink program on the DSP card, 1096
 - syntax for Load/Store address generation, 1076
 - Texas Instruments floating-point DSP, 1067
 - TMS320C6000 control register file, 1074
- Dirac-delta impulse, 7
 - properties, 8, 1200
- Discrete Fourier series, 433
 - duality, 440
 - linearity, 439
 - properties, 439
 - shift in frequency, 439
 - shift in time, 439
 - table of properties, 447
- Discrete Fourier transform, 429
 - duality, 440
 - linearity, 439
 - properties, 439
 - shift in frequency, 439
 - shift in time, 439
 - table of properties, 447

- to z -Transform, 436
 - zero padding, 450
- Discrete Fractional Fourier transform, 950
- Discrete Hartley transform, 938
- Discrete Hilbert transform, 935
 - generalization, 1247
- Discrete impulse, 27
- Discrete systems
 - correlation in 1D, 357
- Discrete Walsh transform, 916
 - Dyadic or Paley order, 918
 - Natural (Hadamard) Order, 917
 - Sequency or Walsh order, 919
- Discrete Wavelet transform, 1157
- Discrete z -transform, 453
- Discrete-time convolution, correlation, 355
- Discrete-time Fourier transform
 - Fourier series duality, 426
 - Parseval's theorem, 425
 - periodic sequence, 419
 - table of properties, 425
 - table of transforms, 420
 - vs Laplace, z -transform, 395
- Discrete-Time system
 - inverse system, 378
 - minimum-phase, 378
- Discrete-time system
 - allpass, 375
 - causality, stability, 30, 353
 - difference equations, 28
 - group delay, 354
 - periodicity, 27
 - stability, 425
- Distributions, 1181
 - additional Fourier transforms, 1201
 - approximating sequences and functions
 - of the impulse, 1190
 - approximating the impulse, 1187
 - convolution, 1192
 - differentiation, 1187
 - Dirac-delta impulse as a limit of Gaussian function, 1195
 - Fourier transform of higher impulse derivatives, 1204
 - Fourier transform of unity, 1196
 - generalized limits, 1202
 - Gibbs Phenomenon, 1208
 - impulse as limit of a sequence, 1184
 - impulse of a function, 1196
 - initial derivatives of the transform, 1206
 - linearity, 1184
 - moving average, 1219
 - multiplication by t , 1199
 - multiplication by an impulse derivative, 1193
 - multiplication by ordinary function, 1187
 - Poisson's Summation Formula, 1218
 - product with an ordinary function, 1186
 - properties of distributions, 1184
 - Reimann-Lebesgue Lemma, 1201
 - ripple elimination, 1212
 - scaling, 1199
 - sequence, 1187
 - sequence of distributions, 1187, 1216
 - symmetry, 1186
 - test functions, 1191
 - the distribution t^{-k} , 1204
 - time scaling, 1185
 - time shift, 1185
 - transform of an impulse train, 1214
 - unit step function as a limit, 1207
 - what is a distribution?, 1182
- Distributions-Generalization
 - convolution, 1227, 1228, 1237
 - convolution of Generalized impulses, 1240
 - convolution with an ordinary function, 1229, 1241
 - differentiation, 1227, 1228, 1236, 1237
 - discrete domain linearity linearity, 1236
 - discrete domain scaling, 1236
 - discrete-time domain, 1234
 - Extended Laplace and z -transforms, 1242
 - Extended Laplace transform of basic functions, 1242
 - generalization of Distribution theory, 1225
 - generalization of Fourier, Laplace and z -related transforms, 1242
 - Generalized distributions for continuous-time functions, 1226
 - Generalized impulse as a limit of a 3D sequence, 1232
 - Generalized impulse as limit of 3D sequence, 1238
 - Generalized impulse properties, 1230
 - linearity, 1226
 - multiplication by higher derivatives of impulse, 1230
 - multiplication derivative and ordinary function, 1228
 - multiplication of impulse times ordinary function, 1230
 - properties, 1226, 1235

- properties Generalized Delta impulse in z , 1237
- properties of the Generalized Dirac-delta impulse in the s domain, 1228
- rewriting Laplace, z and related transforms, 1225
- scaling, 1227
- shift in s , 1226
- shifted Generalized impulse, 1228
- three-dimensional discrete-time domain test functions, 1235
- Division
 - cellular nonrestoring array, 1009, 1014
 - in 1's complement, 1004
 - in 2's complement, 1005
 - in sign and magnitude notation, 1004
 - nonrestoring, 1006
 - of positive numbers, 1003
- Double Side-Band Suppressed Carrier (DSB-SC) Modulation, 877
- Doubly terminated passive networks
 - input impedance evaluation, 695
- DSP with Xilinx FPGAs, 1065
- Eigenvalues, eigenvectors, 497
- Element replacement for frequency transformation, 709
- Elliptic filter approximation, 580
- Elliptic filter as passive network, 706
- Elliptic integral, 576
- Elliptic LC ladder circuit elements, 707
- Energy
 - energy sequences, 29
 - power sequences, 29
- Energy and Power spectral density, 363
- Energy/Power spectral densities
 - autocorrelation of an energy sequence, 860
 - autocorrelation of energy signals, 840
 - cross-correlation, 848
 - discrete-time signals, 839
 - energy and power signals, 25, 838
 - energy signal through linear system, 842
 - energy signals, 840
 - energy spectral density, 835
 - energy spectral density of a sequence, 860
 - impulsive and discrete-time energy signals, 843
 - impulsive and discrete-time power signals, 852
 - passage through a linear system, 861
 - periodic signals, 854
 - power density of a sequence, 860
 - power sequences, 859
 - power spectral density, 849
 - power spectral density of impulse train, 856
 - power spectrum conversion of a linear system, 850
 - powers signals, 848
 - response to a sinusoidal input, 855
- Error minimization in Prony's method, 790
- Even and odd parts of a function, 6
- Even-odd decomposition, 28
- Expansions, 1257
- Fast Fourier transform, 455
 - feedback elimination, 470
 - higher radix, 466
 - Ordered-Input Ordered-Output, 465
 - wired-in processor, 462
- Fast transform processors, 1059
- FFT
 - Ordered-Input Ordered-Output general radix, 469
 - Post-Permutation Algorithm, 464
- Field Programmable Gate Array (FPGA), 1063
- FIR filter design, 1170
 - even order, even symmetry, 815
 - even- and odd-symmetric, 808
 - impulse response evaluation, 814
 - linear phase, 810
 - sampling the unit circle, 810
- FIR inverse filter design, 794
- fir2, 1173
- First order filter realization, 721
- First order system, 264
- Fourier series
 - analysis interval vs period, 55
 - analysis section, 48
 - by power series expansion, 90
 - coefficients, 53
 - convolution in time, 75
 - differentiation property, 72
 - Dirichlet conditions, 53
 - discrete spectrum, 56
 - double symmetry, 67
 - exponential, 48
 - exponential coefficients, 85
 - impulse train, 77

- integration, 75
- inverse, 91
- multiplication in time, 74
- odd function, 65
- Parseval's relations, 89
- passage through system, 88
- periodicity, 51
- properties, 58
- reflection property, 61
- sine and cosine, 78
- symmetry, 64
- time scaling, 70
- trigonometric, 47
- truncated sinusoid, 83
- Fourier transform
 - as function of f , 155
 - case of poles on imaginary axis, 175
 - causal real functions, 168
 - convolution in frequency, 178
 - convolution in time, 176
 - correlation function, 189
 - differentiation in frequency, 164
 - differentiation in time, 164
 - duality property, 160
 - energy spectral density, 179
 - even-odd decomposition, 167
 - frequency shift, 161
 - Gaussian function, 186
 - Gibbs Phenomenon, 1208
 - impulse train, 182
 - initial frequency value, 163
 - initial value, 163
 - integration in time, 164
 - inverse by series expansion, 187
 - of a train of rectangles, 184
 - of causal sinusoid, 172
 - of complex exponential and sinusoid, 169
 - of Dirac-delta impulse, 169
 - Parseval's Theorem, 178
 - periodic functions, 181
 - powers of time, 182
 - properties in ω and f , 188
 - reflection, 161
 - Sign function, 171
 - symmetry, 166
 - table of properties, 158
 - table of transforms, 172
 - Table transforms in ω and f , 188
 - time and frequency sampling, 191
 - time scaling, 161
 - time shift, 161
 - truncated sinusoid, 185
 - unit step function, 172
 - versus Fourier series, 156
 - versus Laplace transform, 174
 - versus periodic function series, 184
- Fourier/Laplace/ z -related transforms
 - $H_I(j\omega)$ vs $H_R(j\omega)$ with no poles on axis, 953
 - case of poles on the imaginary axis, 957
 - continuous-time Hilbert transform relations, 953
 - Discrete Cosine transform DCT, 946
 - Discrete Fractional Fourier transform, 950
 - Discrete Hartley transform, 938
 - Discrete Hilbert transform, 935
 - Discrete Walsh transform, 917
 - Discrete-time domain Hilbert transform relations, 961
 - Dyadic-ordered fast Walsh-Hadamard transform, 920
 - Fourier Cosine transform, 945
 - Fractional Fourier transform, 948
 - generalized Walsh transform, 922
 - Hankel transform, 943
 - Hartley transform, 936
 - Hilbert transform, 931
 - Hilbert transform closed forms, 958
 - Mellin transform, 939
 - Mellin transform of e^{jx} , 941
 - Natural order fast Walsh-Hadamard transform, 919
 - Sequency-ordered fast Walsh-Hadamard transform, 921
 - two-dimensional Fourier transform, 951
 - two-dimensional transforms, 950
 - Walsh-Hadamard transform, 917
 - Wiener-Lee transforms, 959
- Fractional Fourier transform, 948
- Frequency Modulation, 883
- Frequency Multiplexing, 882
- Frequency response, 349
 - geometric evaluation, 349
- Frequency response plots, 260
- Frequently encountered functions, 1260
- Full Adder cell, 990
- Function generation
 - alternative approach, 1026
 - by Chebyshev series, 1020

- Galvanometer, 234
- Gamma function, 138
- General Biquad realization, 716
- General Jordan Canonical Form, 507
- Generalized Discrete Hartley Transform, 1248
- Generalized Hartley Transform, 1247
- Generalized Walsh transform
 - factorizations for parallel processing, 924
 - Generalized Sequency order, 923
 - Generalized Walsh natural order GWN matrix, 924
 - Generalized Walsh–Paley (p-adic) transform, 923
 - Generalized Walsh–Paley GWP transformation matrix, 925
 - GWK optimal factorization, 927
 - GWK transformation matrix, 926
 - GWN optimal factorization, 926
 - GWP optimal factorization, 927
 - High Speed optimal factorizations, 926
 - Natural order, 922
 - Walsh–Kaczmarz transform, 923
- Geometric series
 - weighted, 1261
- Gibbs Phenomenon, 1208
- Graphical representation of a system function, 268

- Hankel transform, 943
- Hartley transform, 936
- Hilbert transform, 931
- Hilbert transform generalization, 1245
- Hilbert transformer, 934
- Homologies, 245

- Ideal filter impulse response, 190
- Ideal highpass filter, 191
- IIR and FIR Digital Filters, 374
- Important trigonometric relations, 1259
- Input impedance single-resistance network, 683
- Interlacing with zeros, 407

- Karhunen Loève transform, 928

- Ladder components evaluation, 684
- Laplace transform
 - anticausal functions, 120
 - Bilateral, 105
 - causal periodic function, 123
 - convolution in frequency, 124
 - convolution in time, 117
 - differentiation in time, 116, 135
 - division by time, 137
 - final value theorem, 119
 - Heaviside Expansion theorem, 131
 - initial and final value, 137
 - initial value theorem, 119
 - integration in time, 117, 137
 - inverse, 128
 - multiplication by exponential, 118
 - multiplication by time powers, 116
 - reflection, 119
 - ROC, 112
 - shift in time, 121
 - table of anticausal functions, 121
 - table of properties, 115
 - table of transforms, 141
 - table of transforms of common functions, 111
 - time scaling, 118
 - Unilateral, 134
- Least squares digital filter design, 786
- Linear differential equations with constant coefficients, 285
- Linear system
 - causality and stability, 12
 - Fourier series, 88
 - frequency response, 14, 166
 - input–output relation, 177
 - mechanical, 13
 - response to sinusoidal input, 183
 - response with initial conditions, 489
 - stability, 183
 - step response, 248
 - transfer function, 14, 233, 488
 - transient and steady-state response, 247
- Linear-phase FIR filter design using windows, 807
- logspace, 1170
- Lowpass to bandpass transformation, 710
- Lowpass to bandstop transformation, 711
- Lowpass to highpass transformation, 711
- lpc, 1167
- LTI system input/output correlation sequences, 362

- Mathematical formulae, 1260
- MATLAB
 - arcov, 1174
 - aryule, 1174
 - important functions, 1164

- parametric modeling functions, 1174
- power spectrum estimation, 1174
- prony, 1175
- Matrix diagonalization, 498
- Matrix evaluation of input impedance, 689
- Mechanical system, 252
- Mellin transform, 939
 - of e^{jx} , 941
- Memory elements, 1037
 - JK flip-Flop, 1040
 - Master-Slave flip-Flop, 1041
 - Set-Reset (SR) flip-Flop, 1038
 - Trigger or T flip-Flop, 1040
- Minimum phase systems, 280
- Modulation theorem, 162
- Multiplication
 - direct approach in 2's complement, 1000
 - implementation, 993
 - in 1's complement notation, 997
 - in 2's complement notation, 998
 - in Sign and Magnitude notation, 997
 - of unsigned numbers, 992
- Orthogonality relations, 1259
- Overshoot evaluation, 255
- Padé approximation, 786
- Partial differential equations, 291
 - transformation, 293
- Passive double-resistance networks
 - table of component values, 701
- Passive ladder lowpass filters, 677
- Passive/Active filters
 - Bessel filter passive networks, 693
 - Biquadratic transfer functions, 714
 - Elliptic filter as passive network, 706
 - first order filter realization, 721
 - general Biquad realization, 716
 - general order active filter realization, 713
 - general order passive ladder network, 680
 - inverting integrator, 713
 - ladder network components, 684
 - matrix evaluation of input impedance, 689
 - passive filters, 677
 - passive ladder lowpass filters, 677
 - Sallen Key circuit, 725
 - table of elliptic filter components, 709
 - tables of passive ladder components, 694
- Passive/Double-Resistance terminated networks
 - closed forms for circuit element components, 703
- perfect-shuffle-matrix, 462
- Periodic convolution, 441
- Periodic functions, 3
 - correlation, 25
- Poles, zeros, 349
- Programmable Logic Array (PLA), 1062
- Properties of the impulse, 11
- Pulse Code Modulation, 888
- Pulse Modulation Systems, 887
- Rademacher and Haar functions, 911
- Random Signal
 - AR lattice, 1146
 - ARMA(p, q) Process, 1146
 - backward linear prediction, 1140
 - causal IIR Wiener filter, 1152
 - continuous-time causal Wiener filter, 1116
 - continuous-time correlation, 1109
 - continuous-time Wiener filtering, 1113
 - correlation covariance in z , 1120
 - discrete-time PSD estimation, 1124
 - forward linear prediction, 1138
 - lattice MA FIR filter, 1143
 - least-squares filtering, 1138
 - nonparametric power spectrum estimation, 1108
 - Parametric PSD estimation, 1131
 - passage through an LTI system, 1110, 1121
 - Periodogram evaluation, 1128
 - power spectrum estimation, 1147
 - random sequences, 1118
 - statistical to time averages, 1119
 - system modeling and prediction, 1134
 - two-sided IIR Wiener filter, 1151
 - Wiener and Least-Squares models, 1134
 - Wiener filtering, 1135
 - Wiener filtering and prediction, 1148
 - Yule-Walker equations, 1132
- Response of a discrete-time linear system to a sinusoid, 361
- Response to causal periodic input, 257
- Response to causal sinusoidal input, 259
- Root evaluation
 - n^{th} root, 1018
 - binary, 1031
- Rotational mechanical system, 253

- Sallen Key circuit, 725
- Sampling
 - arbitrary signal, 201
 - bandpass signal, 200
 - Ideal, 191
 - Instantaneous, 197
 - Natural, 195
 - reconstruction from a sampled signal, 193
 - the Fourier transform, 203
 - the Spectrum, 446
 - time and frequency, 191
- Sampling rate
 - alteration, 417
 - increase, 414
 - reduction, 410
- Sampling rate conversion, 409
- Second order system, 264
- Second order system frequency response, 253
- Second order system model, 249
- Series sums, 1261
- Settling time, 250
- Signal generation, 283
- Single Side-Band (SSB) Modulation, 879
- Sinusoidal signal
 - DFT, 434
- Solution of differential equations, 284
- Square root evaluation
 - cellular nonrestoring array, 1033
 - comparison approach, 1031
 - nonrestoring approach, 1032
 - restoring approach, 1032
 - square root paper and pencil method, 1030
- State space equations
 - solution, 501
- State space model, 484
 - change of variables, 529
 - circuit analysis, 509
 - discrete state equations solution, 528
 - discrete-time systems, 522
 - Jordan form, 490
 - second canonical form, 531
 - second order system, 515
 - trajectories, 513
 - transfer function, 528
 - transformation to Jordan Form, 499
- Stirling Number First Kind, 1258
- Stirling Number Second Kind, 1258
- Symbols, 1, 1257
- Synchronous sequential circuits, 1042
 - counter using JK flip-flops, 1046
 - counter using T flip-flops, 1046
 - state minimization, 1048
 - using JK flip-flops, 1045
 - using SR flip-flops, 1044
- Table
 - z -transform properties, 340
 - z -transforms, 340
 - additional Laplace transforms, 141
 - additional Laplace transforms contd, 142
 - Bessel delay normalized model denominator coefficients, 617
 - Bessel filter coefficients and poles, 617
 - Bessel polynomials, 615
 - Bessel–Butterworth asymptotic form coefficients, 627
 - Bessel–Thomson passive ladder components, 694
 - Butterworth filter coefficients, 545
 - Butterworth filter poles and residues, 546
 - Butterworth passive ladder components, 694
 - Chebyshev coefficients of trigonometric functions, 1023
 - Chebyshev filter, 565
 - Chebyshev filter poles and residues, 566
 - Chebyshev filter polynomial coefficients, 565
 - Chebyshev passive ladder components, 694
 - continued fraction expansion, 688, 692
 - DFT properties, 449
 - Discrete Fourier series properties, 447
 - discrete-time Fourier transform properties, 425
 - Discrete-time Fourier transforms, 420
 - double-resistance ladder components, 701
 - Elliptic filter coefficients poles zeros, 599
 - Elliptic filter components, 709
 - Elliptic filters, 599
 - Fourier transform properties, 158
 - Fourier transform properties in ω and f , 188
 - Fourier transforms, 172
 - Fourier transforms in ω and f , 189
 - Fractional Fourier transforms of some common functions, 950
 - frequency normalized form Bessel filter coefficients, 634

- frequency transformations of a lowpass filter, 784
- Hankel basic transforms, 945
- Hartley transform of some basic functions, 938
- Laplace transform properties, 115
- Laplace transforms of anticausal functions, 121
- Laplace transforms of common functions, 111
- LC components of Butterworth, Chebyshev, and Bessel filter, 703
- matrix of correlations, 796
- properties of Fourier series, 58
- properties of windows, 805
- Shifted Chebyshev polynomials, 1021
- single-resistance ladder components, 694
- Taylor's series, 1258
- Transformation of trajectories between planes, 519
- Two-Dimensional signals, 363
- Uniform convergence, 47
- Unit sample sequence, 27
- Unit step function, 4
- Unit step sequence, 26
- Units and dimensions, 1
- Vectorial evaluation of frequency response, 273
- Vectorial evaluation of residues, 269
- Vestigial Side-Band (VSB) Modulation, 882
- Walsh (Sequency) Order, 913
- Walsh functions, 912
- Walsh transform, 911
 - Dyadic (Paley) Order, 914
 - Natural (Hadamard) Order, 914
- Wavelet transform, 1154
- Yulewalk, 1168
- z-transform, 325
 - conjugate sequence, 340
 - convergence, 327
 - convolution in frequency, 344
 - convolution in time, 344
 - final value theorem, 347
 - frequency translation, 348
 - initial value, 341
 - inverse, 330
 - inverse by long division, 337
 - inverse by partial fraction expansion, 336
 - inverse by power series expansion, 338
 - multiplication by n , 349
 - multiplication by an exponential, 348
 - Parseval's Relation, 347
 - properties, 340
 - reflection property, 349
 - time shift, 340
 - unilateral, 381
 - unilateral, time shift property, 383